This document was produced
by scanning the original publication.

Ce document est le produit d'une
numérisation par balayage
de la publication originale.

Geological Survey of Canada
Commission géologique du Canada

PAPER
ÉTUDE 87-1A

CURRENT RESEARCH PART A
RECHERCHES EN COURS PARTIE A



(Pages 1-498)

Canada

1987

Notice to Librarians and Indexers

The Geological Survey's twice-yearly *Current Research* series contains many reports comparable in scope and subject matter to those appearing in scientific journals and other serials. All contributions to Current Research include an abstract and bibliographic citation. It is hoped that these will assist you in cataloguing and indexing these reports and that this will result in a still wider dissemination of the results of the Geological Survey's research activities.

Avis aux bibliothécaires et préparateurs d'index

La série *Recherches en cours* de la Commission géologique paraît deux fois par année; elle contient plusieurs rapports dont la portée et la nature sont comparables à ceux qui paraissent dans les revues scientifiques et autres périodiques. Tous les articles publiés dans les Recherches en cours sont accompagnés d'un résumé et d'une bibliographie, ce qui vous permettra, nous l'espérons, de cataloguer et d'indexer ces rapports, d'où une meilleure diffusion des résultats de recherche de la Commission géologique.



GEOLOGICAL SURVEY OF CANADA
PAPER 87-1A

COMMISSION GÉOLOGIQUE DU CANADA
ÉTUDE 87-1A

CURRENT RESEARCH
PART A

RECHERCHES EN COURS
PARTIE A

Issued in two sections/Publiée en deux volumes:
pages 1-498 and/et pages 499-946

1987

© Minister of Supply and Services Canada 1987

Available in Canada through

authorized bookstore agents
and other bookstores

or by mail from

Canadian Government Publishing Centre
Supply and Services Canada
Ottawa, Ontario, Canada K1A 0S9

and from

Geological Survey of Canada offices:

601 Booth Street
Ottawa, Canada K1A 0E8

3303-33rd Street N.W.,
Calgary, Alberta T2L 2A7

100 West Pender Street
Vancouver, British Columbia V6B 1R8

A deposit copy of this publication is also available
for reference in public libraries across Canada

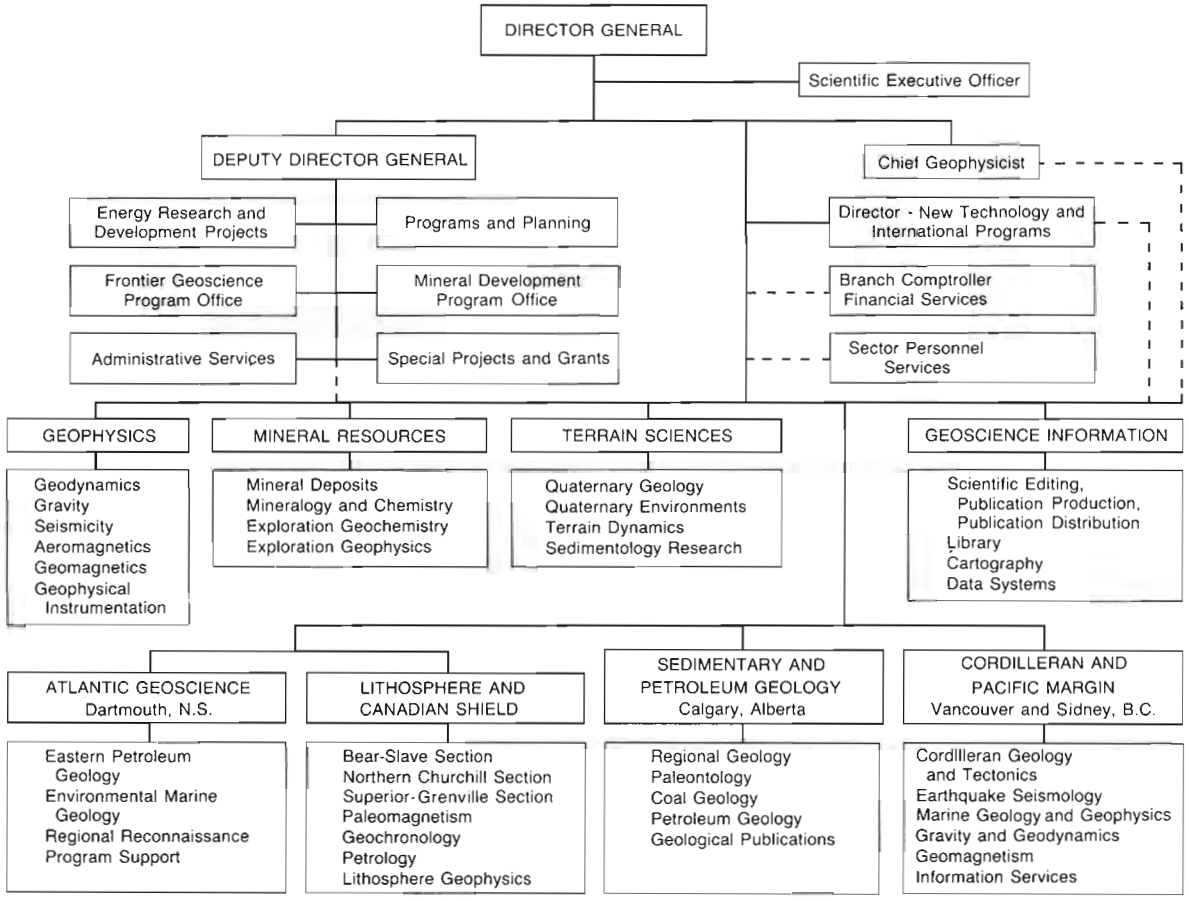
Cat. No. M44-87/1AE Canada: $20.00
ISBN 0-660-53707-9 Other countries: $24.00

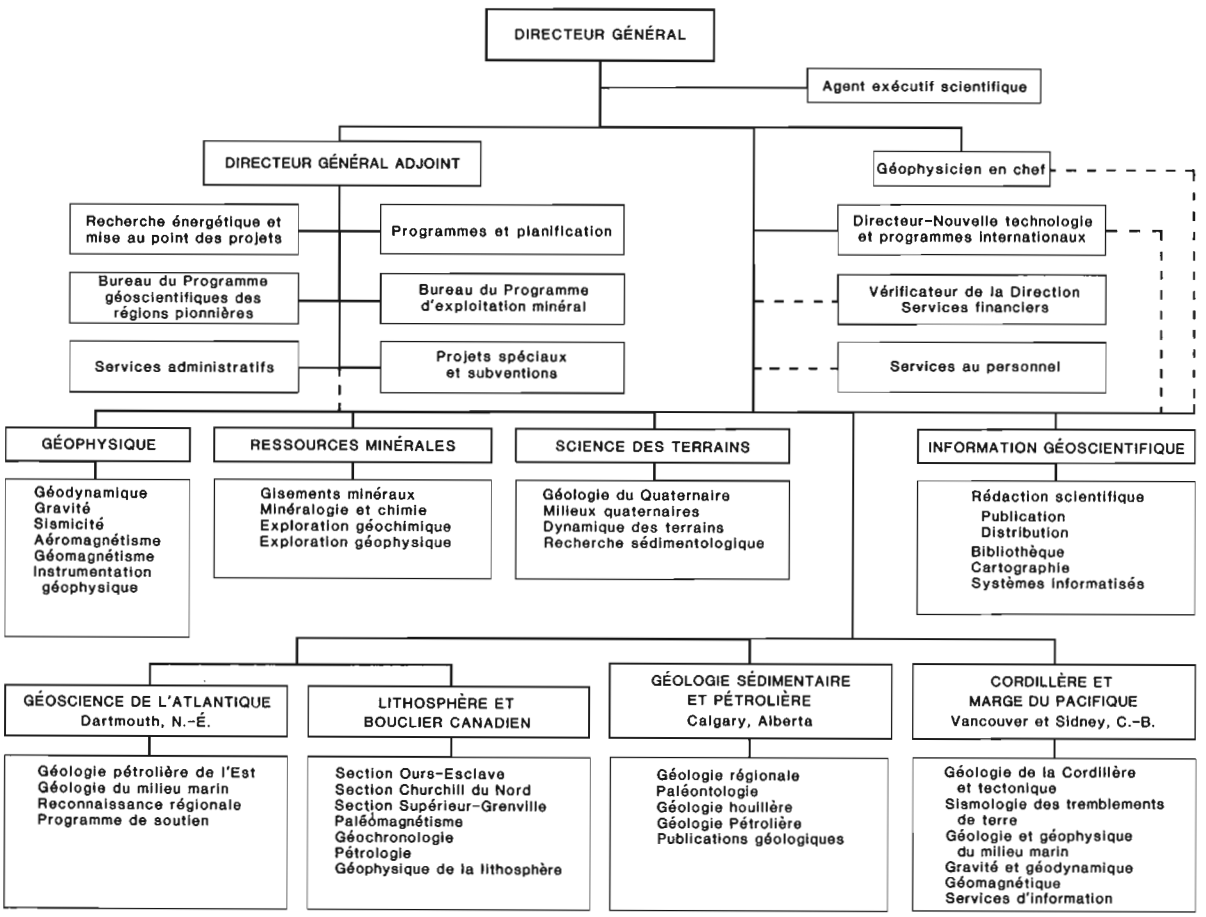
Price subject to change without notice

Sold in sets

Cover
Exhumed Pleistocene valley at the Bullion Mine; view towards the northwest. See Report 18 (p. 177-180) for further details.

Couverture
Vallée pléistocène exhumée, mine Bullion; vue vers le nord-ouest. Pour plus de détails, voir le rapport 18 (p. 177-180).


DIRECTOR GENERAL
Scientific Executive Officer
DEPUTY DIRECTOR GENERAL
Chief Geophysicist
Energy Research and Development Projects
Programs and Planning
Director - New Technology and International Programs
Frontier Geoscience Program Office
Mineral Development Program Office
Branch Comptroller Financial Services
Administrative Services
Special Projects and Grants
Sector Personnel Services
GEOPHYSICS
MINERAL RESOURCES
TERRAIN SCIENCES
GEOSCIENCE INFORMATION
Geodynamics
Gravity
Seismicity
Aeromagnetics
Geomagnetics
Geophysical Instrumentation
Mineral Deposits
Mineralogy and Chemistry
Exploration Geochemistry
Exploration Geophysics
Quaternary Geology
Quaternary Environments
Terrain Dynamics
Sedimentology Research
Scientific Editing, Publication Production, Publication Distribution
Library
Cartography
Data Systems
ATLANTIC GEOSCIENCE Dartmouth, N.S.
LITHOSPHERE AND CANADIAN SHIELD
SEDIMENTARY AND PETROLEUM GEOLOGY Calgary, Alberta
CORDILLERAN AND PACIFIC MARGIN Vancouver and Sidney, B.C.
Eastern Petroleum Geology
Environmental Marine Geology
Regional Reconnaissance
Program Support
Bear-Slave Section
Northern Churchill Section
Superior-Grenville Section
Paleomagnetism
Geochronology
Petrology
Lithosphere Geophysics
Regional Geology
Paleontology
Coal Geology
Petroleum Geology
Geological Publications
Cordilleran Geology and Tectonics
Earthquake Seismology
Marine Geology and Geophysics
Gravity and Geodynamics
Geomagnetism
Information Services


DIRECTEUR GÉNÉRAL
Agent exécutif scientifique
DIRECTEUR GÉNÉRAL ADJOINT
Géophysicien en chef
Recherche énergétique et mise au point des projets
Programmes et planification
Directeur–Nouvelle technologie et programmes internationaux
Bureau du Programme géoscientifiques des régions pionnières
Bureau du Programme d'exploitation minéral
Vérificateur de la Direction Services financiers
Services administratifs
Projets spéciaux et subventions
Services au personnel
GÉOPHYSIQUE
RESSOURCES MINÉRALES
SCIENCE DES TERRAINS
INFORMATION GÉOSCIENTIFIQUE
Géodynamique
Gravité
Sismicité
Aéromagnétisme
Géomagnétisme
Instrumentation géophysique
Gisements minéraux
Minéralogie et chimie
Exploration géochimique
Exploration géophysique
Géologie du Quaternaire
Milieux quaternaires
Dynamique des terrains
Recherche sédimentologique
Rédaction scientifique
Publication
Distribution
Bibliothèque
Cartographie
Systèmes informatisés
GÉOSCIENCE DE L'ATLANTIQUE Dartmouth, N.-É.
LITHOSPHÈRE ET BOUCLIER CANADIEN
GÉOLOGIE SÉDIMENTAIRE ET PÉTROLIÈRE Calgary, Alberta
CORDILLÈRE ET MARGE DU PACIFIQUE Vancouver et Sidney, C.-B.
Géologie pétrolière de l'Est
Géologie du milieu marin
Reconnaissance régionale
Programme de soutien
Section Ours–Esclave
Section Churchill du Nord
Section Supérieur–Grenville
Paléomagnétisme
Géochronologie
Pétrologie
Géophysique de la lithosphère
Géologie régionale
Paléontologie
Géologie houillère
Géologie Pétrolière
Publications géologiques
Géologie de la Cordillère et tectonique
Sismologie des tremblements de terre
Géologie et géophysique du milieu marin
Gravité et géodynamique
Géomagnétique
Services d'information

Separates

A limited number of separates of the papers that appear in this volume are available by direct request to the individual authors. The addresses of the Geological Survey of Canada offices follow:

601 Booth Street,
OTTAWA, Ontario
K1A 0E8

Institute of Sedimentary and Petroleum Geology,
3303-3rd Street N.W.,
CALGARY, Alberta
T2L 2A7

Cordilleran and Pacific Margin Division,
100 West Pender Street,
VANCOUVER, B.C.
V6B 1R8

Pacific Geoscience Centre
P.O. Box 6000,
9860 Saanich Road,
SIDNEY, B.C.
V8L 4B2

Atlantic Geoscience Centre,
Bedford Institute of Oceanography,
P.O. Box 1006,
DARTMOUTH, N.S.
B2Y 4A2

When no location accompanies an author's name in the title of a paper, the Ottawa address should be used.

Tirés à part

On peut obtenir un nombre limité de "tirés à part" des articles qui paraissent dans cette publication en s'adressant directement à chaque auteur. Les adresses des différents bureaux de la Commission géologique du Canada sont les suivantes :

601, rue Booth
OTTAWA, Ontario
K1A 0E8

Institut de géologie sédimentaire et pétrolière
3303-3rd St. N.W.,
CALGARY, Alberta
T2L 2A7

Division de la Cordillère et marge du Pacifique
100 West Pender Street,
VANCOUVER, Colombie-Britannique
V6B 1R8

Centre géoscientifique du Pacific
B.P. 6000,
9860 Saanich Road,
SIDNEY, Colombie-Britannique
V8L 4B2

Centre géoscientifique de l'Atlantique
Institut océanographique de Bedford
B.P. 1006,
DARTMOUTH, Nouvelle-Ecosse
B2Y 4A2

Lorsque l'adresse de l'auteur ne figure pas sous le titre d'un document, on doit alors utiliser l'adresse d'Ottawa.

SCIENTIFIC AND TECHNICAL REPORTS
RAPPORTS SCIENTIFIQUES ET TECHNIQUES

ECONOMIC GEOLOGY/GÉOLOGIE ÉCONOMIQUE

J.J. CLAGUE: A placer gold exploration target in the Cariboo district, British Columbia 177

V. RUZICKA and G.M. LECHEMINANT: Uranium investigations in Canada, 1986 249

L.M. MACKENZIE and D.H.C. WILTON: Uranium, molybdenum and base metal sulphide mineralization: three different styles of ore formation in the Burnt Lake area, central Labrador 467

R.D. THOMAS and C.F. GLEESON: Metallogeny of the Woodstock area, New Brunswick 489

E.L. PROCYSHYN: Wall rock alteration mineral assemblages associated with the E-Zone ore bodies at Mines Gaspé, Murdochville, Quebec 499

A.D. PAKTUNC: Nickel, copper, platinum and palladium relations in Ni-Cu deposits of the St. Stephen intrusion, New Brunswick 543

I.R. JONASSON, O.R. ECKSTRAND, and D.H. WATKINSON: Preliminary investigations of the abundance of platinum, palladium and gold in some samples of Canadian copper-nickel ores 835

GEOCHEMISTRY/GÉOCHIMIE

B. BLAISE and B.D. BORNHOLD: Geochemistry of northern Juan de Fuca Ridge sediments, northeast Pacific 127

E.M. CAMERON and W.J. CARRIGAN: Oxygen fugacity of Archean felsic magmas: relationship to gold mineralization 281

G.E.M. HALL, K.N. DE SILVA, J.C. PELCHAT, and J.E. VAIVE: Advances in analytical methods based on atomic absorption spectrometry in the Geochemistry Laboratories of the Geological Survey of Canada 477

J.L. BOUVIER and G.E.M. HALL: A preliminary investigation of the application of microwave radiation for the dissolution of geological materials 485

C.D. ANGLIN, J.M. FRANKLIN, I.R. JONASSON, K. BELL, and E. HOFFMAN: Geochemistry of scheelites associated with Archean gold deposits: implications for their direct age determination 591

J. DAVID and C. GARIÉPY: Rare-earth element geochemistry of sedimentary sequences from the Lower St-Lawrence, Quebec Appalachians 633

GEOCHRONOLOGY/GÉOCHRONOLOGIE

J.B. WHALEN and J.C.M. RODDICK: K-Ar geochronology of the McGerrigle plutonic complex, Gaspésie Peninsula, Quebec 375

J.K. MORTENSEN: Preliminary U-Pb zircon ages for volcanic and plutonic rocks of the Noranda-Lac Abitibi area, Abitibi Subprovince, Quebec 581

O. VAN BREEMEN, J.B. HENDERSON, W.D. LOVERIDGE, and P.H. THOMPSON: U-Pb zircon and monazite geochronology and zircon morphology of granulites and granite from the Thelon Tectonic Zone, Healey Lake and Artillery Lake map areas, N.W.T. 783

GEOPHYSICS/GÉOPHYSIQUES

P.T. LAFLÈCHE, A.S. JUDGE, and J.A. PILON: Ground probing radar in the investigation of the competency of frozen tailings pond dams 191

L.W. SOBCZAK and J.R. WEBER: Gravity and bathymetry taken along seismic refraction lines from the Canadian Ice Island during 1985 and 1986 299

E.J. SCHWARZ and N. WRIGHT: Buried placers in Chaudière River sediments indicated by ground magnetometer survey, Eastern Townships, Quebec 423

D. REAL and M.D. THOMAS: Gravity models within the southern Central Metasedimentary Belt, Grenville Province, Ontario 763

J.M. CODERRE, M.D. THOMAS, R.A. GIBB, and S.L. FOGARASI: In situ density determinations by gravity measurements in the Underground Research Laboratory shaft, Lac du Bonnet granite batholith, Manitoba 815

MARINE GEOSCIENCE/ÉTUDES GÉOSCIENTIFIQUES DU MILIEU MARIN

A. DE VERNAL et H. JETTÉ: Analyses palynologiques de sédiments holocènes du lac Bras d'Or (carotte 85-036-016P), île du Cap-Breton, Nouvelle-Écosse 11

A. MUCCI and P. PAGÉ: The water chemistry of cruise 85-036 on Bras d'Or Lake, Cape Breton Island, Nova Scotia 17

R.A. KOSTASCHUK and J.L. LUTERNAUER: Large-scale sedimentary processes in a trained, high-energy, sand-rich estuary: Fraser River delta, British Columbia 727

C.F.M. LEWIS and D.R. PARROTT: Iceberg scouring rate studies, Grand Banks of Newfoundland 825

D. PRAEG, B. MACLEAN, D.J.W. PIPER, and A.N. SHOR: Study of iceberg scours across the continental shelf and slope off southeast Baffin Island using the **Sea MARC I** midrange sidescan sonar 847

C. HILLAIRE-MARCEL: Composition isotopique du carbone organique des carottes du forage 85-036-016 dans le lac Bras d'Or, île du Cap-Breton, Nouvelle-Écosse 859

R. MACNAB, J. VERHOEF, and J. WOODSIDE: Techniques for the display and editing of marine potential field data 865

G.V. SONNICHSEN and G. VILKS: A small boat seismic reflection survey of the Lougheed Island Basin–Cameron Island Rise–Desbarats Strait region of the Arctic Island channels using open water leads 877

G. LORTIE: Diatomées et évolution holocène du lac Bras d'Or, Nouvelle-Écosse: résultats préliminaires 889

PALEONTOLOGY/PALÉONTOLOGIE

F. GOODARZI and L.D. STASIUK: Graptolite preparation for reflected light microscopy – a technical note 317

M. LABONTÉ and F. GOODARZI: The relationship between dendographs and Pearson product-moment correlation coefficients 353

PETROLEUM GEOLOGY AND COAL/GÉOLOGIE PÉTROLIÈRE ET LE CHARBON

P.W. BROOKS, K.G. OSADETZ, and L.R. SNOWDON: Origin of compositional differences amongst oils from the Hummingbird Field (Paleozoic), southeast Saskatchewan 331

F. GOODARZI and L.D. STASIUK: Amorphous kerogen: bituminite in the Second White Speckled Shale, southern Saskatchewan 349

QUATERNARY GEOLOGY/GÉOLOGIE DU QUATERNAIRE

Mapping, geomorphological studies, and sedimentology/Cartographie, études géomorphologiques et sédimentologie

J.R. MACKAY and R.V. LESLIE: A simple probe for the measurement of frost heave within frozen ground in a permafrost environment 37

D.A. ST-ONGE and I. MCMARTIN: Morphosedimentary zones in the Bluenose Lake region, District of Mackenzie 89

T. BELL, R.J. ROGERSON, R.A. KLASSEN, and A. DYER: Acoustic survey and glacial history of Adams Lake, outer Nachvak Fiord, northern Labrador 101

R.W. KLASSEN and W.J. VREEKEN: The nature and chronological implications of surface tills and post-till sediments in the Cypress Lake area, Saskatchewan 111

D.E. KERR: Preliminary interpretation of the stratigraphy of the marine offlap sequence in the Clifton Point area, District of Mackenzie 153

S.G. EVANS: Surface displacement and massive toppling on the northeast ridge of Mount Currie, British Columbia 181

H.F.L. WILLIAMS and M.C. ROBERTS: Mid-Holocene paleosurfaces in vertical accretion deposits, Fraser River delta, British Columbia 757

Exploration technology and glacial dispersal studies/Techniques d'exploration et études de la dispersion glaciaire

A.M. BOLDUC, R.A. KLASSEN, and E.B. EVENSON: Cobble lithologies in eskers of central Labrador 43

S.L. SMITH and R.H. RAINBIRD: Soft-sediment deformation structures in overburden drill core, Quebec 53

R.A. KLASSEN and F.J. THOMPSON: Ice flow history and glacial dispersal in the Labrador Trough 61

S.L. SMITH and W.W. SHILTS: Quaternary stratigraphy of Noire River cores, Beauceville area, Quebec 159

Paleoenvironmental studies and geochronology/Étude des paléoenvironnements et géochronologie

J.V. MATTHEWS, JR.: Plant macrofossils from the Neogene Beaufort Formation on Banks and Meighen islands, District of Franklin 73

J.V. MATTHEWS, JR., S.L. SMITH, and R.J. MOTT: Plant macrofossils, pollen, and insect fossils of arctic affinity from Wisconsinan sediments in Chaudière Valley, southern Quebec 165

REGIONAL GEOLOGY/GÉOLOGIE RÉGIONALE

Appalachian region/Région des appalaches

S.M. BARR, R.P. RAESIDE, C.E. WHITE, and W. YAOWANOIYOTHIN: Geology of the northeastern and central Cape Breton Highlands, Nova Scotia 199

J.B. WHALEN: Geology of a northern portion of the Central Plutonic Belt, New Brunswick 209

C. PAYETTE and R.F. MARTIN: The Welsford igneous complex, southern New Brunswick: rift-related Acadian magmatism 239

S.M. BARR: Field relations, petrology and age of plutonic and associated metavolcanic and metasedimentary rocks, Fundy National Park area, New Brunswick 263

J.V. OWEN and D.C. MACHIN: Petrography and geochemistry of some mafic dykes in the Long Range Inlier, western Newfoundland 305

H.S. SWINDEN: Geology and mineral occurrences in the central and northern parts of the Roberts Arm Group, central Newfoundland 381

M.A.J. PIASECKI: Possible basement-cover relationships in the Fleur de Lys terrane, western Newfoundland 391

J.T. VAN BERKEL: Geology of the Dashwoods Pond, St. Fintan's and Main Gut map areas, southwest Newfoundland 399

J.W.F. WALDRON and M. GRAVES: Preliminary report on sedimentology of sandstones, slates, and bioclastic carbonate material in the Meguma Group, Mahone Bay, Nova Scotia 409

J.D. HILL: Geology of the Guysborough-Country Harbour area, Nova Scotia 415

J.R. HILL: A preliminary report on geology and on mineral occurrences in Precambrian carbonate rocks, Cape Breton Island, Nova Scotia 533

M.F. JUSTINO and A.L. SANGSTER: Geology in the vicinity of the Lime Hill zinc occurrence, southwestern Cape Breton Island, Nova Scotia 555

G. PE-PIPER: The Late Hydrynian Jeffers Group, western Cobequid Hills, Nova Scotia 573

J.V. OWEN, J.E.M. CAMPBELL, and F.A.R. DENNIS: Geology of the Lake Michel area, Long Range Inlier, western Newfoundland 643

K.L. CURRIE: A preliminary account of the geology of Harrys River map area, southern Long Range of Newfoundland 653

K.L. CURRIE: Late Precambrian igneous activity and its tectonic implications, Musquash-Loch Alva region, southern New Brunswick 663

Arctic Islands/Archipel Arctique

H.P. TRETTIN: Investigations of Paleozoic geology, northern Axel Heiberg and northwestern Ellesmere islands 357

B.D. RICKETTS: Preliminary structural cross-sections across Fosheim Peninsula and Axel Heiberg Island, Arctic Archipelago 369

Cordilleran region/Région de la Cordillère

D.A. BROWN: Hazelton-Bowser Lake Group stratigraphy and structure in the vicinity of the Silbak Premier Mine, northwestern British Columbia 143

R.G. ANDERSON: Plutonic rocks in the Dawson map area, Yukon Territory 689

L.D. CURRIE and P.S. SIMONY: Geology of the Alan Creek area, southeastern Cariboo Mountains, British Columbia 713

C.A. EVENCHICK: Stratigraphy and structure of the northeast margin of the Bowser Basin, Spatsizi map area, north-central British Columbia 719

D.C. MURPHY: Kaza Group, eastern Wells Gray Park, British Columbia 735

M.J. ORCHARD: Conodont biostratigraphy and correlation of the Harper Ranch Group (Devonian–Permian), Ashcroft map area, southern British Columbia 743

J.H. SEVIGNY: Field and stratigraphic relations of amphibolites in the late Proterozoic Horsethief Creek Group, northern Adams River area, British Columbia 751

Canadian Shield/Bouclier canadien

J.A. PERCIVAL: Geology of the Ashuanipi granulite complex in the Schefferville area, Quebec 1

S. TELLA and I.R. ANNESLEY: Precambrian geology of parts of Chesterfield Inlet map area, District of Keewatin 25

J.P. GROTZINGER, D.S. McCORMICK, and S.M. PELECHATY: Progress report on the stratigraphy, sedimentology, and significance of the Kimerot and Bear Creek groups, Kilohigok Basin, District of Mackenzie 219

T. FRISCH, M.R. DIGEL, and E.J. WILLIAMS: Precambrian Shield of the Boothia Uplift, southern Somerset Island and northern Boothia Peninsula, District of Franklin 429

J. VAN GOOL, T. CALON, and T. RIVERS: Preliminary report on the Grenville Front Tectonic Zone, Bruce Lake area, western Labrador

H.H. BOSTOCK: Geology of the south half of the Taltson Lake map area, District of Mackenzie 443

C.S. MACDOUGALL and D.H.C. WILTON: Middle Proterozoic granite-related mineralization in the Round Pond area, Labrador 457

J.E. KING, P.D. BARRETTE, and C.D. RELF: Contrasting styles of basement deformation and longitudinal extension in the metamorphic-internal zone of Wopmay Orogen, N.W.T. 515

T.W. NEEDHAM: Geological setting of two metagabbroic bodies, central Britt domain, southwestern Grenville Province, Ontario 597

M.B. LAMBERT and C.R. VAN STAAL: Archean granite-greenstone boundary relationships in the Beaulieu River volcanic belt, Slave Province, N.W.T. 605

M.R. ST-ONGE, S.B. LUCAS, D.J. SCOTT, and N.J. BÉGIN: Tectono-stratigraphy and structure of the Lac Watts–Lac Cross–Rivière Déception area, central Cape Smith Belt, northern Québec 619

M.B. LAMBERT and R.E. ERNST: Archean mafic dyke swarm, Beaulieu River volcanic belt, Slave Province, N.W.T. 673

R.I. MACFIE: The Clinton-Colden hornblende gabbro-anorthosite intrusion, Artillery Lake map area, District of Mackenzie 681

R.S. HILDEBRAND, S.A. BOWRING, K.P.E. ANDREW, S.F. GIBBINS, and G.C. SQUIRES: Geological investigations in Calder River map area, central Wopmay Orogen, District of Mackenzie 699

A.N. LECHEMINANT, J.C. RODDICK, A.C. TESSIER, and K.M. BETHUNE: Geology and U-Pb ages of early Proterozoic calc-alkaline plutons northwest of Water Bay, District of Keewatin 773

J.B. HENDERSON, P.H. MCGRATH, D.T. JAMES, and R.I. MACFIE: An integrated geological, gravity and magnetic study of the Artillery Lake area and the Thelon Tectonic Zone, District of Mackenzie 803

Interior Plains/Plaines Intérieures

I. BANERJEE: Interpretation of dipmeter logs of the Lower Cretaceous Cutbank Sandstone, Mannville Group, southern Alberta 337

STRATIGRAPHY/STRATIGRAPHIE

A.I. ZOLNAI: Structure and stratigraphy, Mount Bryant area, eastern Rocky Mountain Front Ranges, Alberta 323

C.W. JEFFERSON and S.M. HAMILTON: Structure and stratigraphy of the Paleozoic-Precambrian contact zone on White and Southampton islands, District of Keewatin 451

K. DEWING P. COPPER, and S. HAMILTON: Preliminary report on the stratigraphic position of oil shales in the Lower Paleozoic of Southampton Island, District of Keewatin 883

STRUCTURAL GEOLOGY/GÉOLOGIE STRUCTURALE

S.K. HANMER: Granulite facies mylonites: a brief structural reconnaissance north of Stony Rapids, northern Saskatchewan 563

SCIENTIFIC AND TECHNICAL NOTES
NOTES SCIENTIFIQUES ET TECHNIQUES

L. CORRIVEAU and M. GORTON: Potential economic significance of Precambrian potassic plutons in the Central Metasedimentary Belt, Grenville Province of western Quebec 897

G.W. BERGER and J.L. LUTERNAUER: Preliminary fieldwork for thermoluminescence dating studies at the Fraser River delta, British Columbia 901

S.E. PULLAN, J.A. HUNTER, R.M. GAGNÉ, and R.L. GOOD: Delineation of bedrock topography at Val Gagné, Ontario, using seismic reflection techniques 905

S.R. DALLIMORE and J.L. DAVIS: Ground probing radar investigations of massive ground ice and near surface geology in continuous permafrost 913

G.T. MCKENNA and J.L. LUTERNAUER: First documented large failure at the Fraser River delta front, British Columbia 919

B.E.B. CAMERON: Significance of Lower Jurassic hydrocarbon source rocks in the Cumshewa Inlet area, Queen Charlotte Islands, British Columbia 925

S.G. EVANS: A rock avalanche from the peak of Mount Meager, British Columbia 929

P. HOOD and D.J. TESKEY: Helicopter-borne aeromagnetic gradiometer surveys: a progress report 935

P.J. KURFURST: Cone penetration tests of the nearshore zone sediments off Richards Island, Northwest Territories 939

Author Index/Index des auteurs 498a

SCIENTIFIC AND TECHNICAL REPORTS
RAPPORTS SCIENTIFIQUES ET TECHNIQUES

Geology of the Ashuanipi granulite complex in the Schefferville area, Quebec

Project 860003

J.A. Percival
Lithosphere and Canadian Shield Division

Percival, J.A., Geology of the Ashuanipi granulite complex in the Schefferville area, Quebec; in Current Research, Part A, Geological Survey of Canada, Paper 87-1A, p. 1-10, 1987.

Abstract

A subcircular, 300-km-diameter region of high-grade metamorphic rocks, the Ashuanipi complex, occurs in the southeastern corner of the Superior Province. Older migmatitic gneisses and younger homogeneous granitoids are recognized. The migmatites consist of an older sequence of metasedimentary and rare, probably metavolcanic mafic rocks. Variably migmatitic tonalite occurs as sheets of 1-2000 m width within the supracrustal sequence. The migmatites are cut by both foliated and massive tonalites and by the most abundant rock type, garnet-orthopyroxene-biotite diatexite. Later intrusions include orthopyroxene-biotite diatexite, granite and syenite, the latter locally with nepheline.

Structures trend dominantly northwest and have moderate to steep northeasterly dips suggesting regional homoclinal geometry. Folds of migmatitic layering, involving at least some of the diatexites, are open and upright, with gentle to moderate plunge. Several large, inward-dipping oval structures may either be fold interference structures or deformed magma chambers.

Assemblages of garnet-orthopyroxene-biotite-plagioclase-K-feldspar-quartz occur throughout the region indicating uniform granulite facies conditions. With the exception of some late granites and syenites, all rock types contain orthopyroxene.

Encouraging gold assays were obtained from a sulphide-rich schist at the contact between metasedimentary and mafic gneisses.

Résumé

Au coin sud-est de la province du lac Supérieur, le complexe d'Ashuanipi constitué de roches très métamorphiques occupe une région d'à peu près 300 km de diamètre. Le complexe comprend des gneiss migmatitiques anciens et des roches granitiques homogènes tardives. Les migmatites correspondent à une séquence ancienne de roches métasédimentaires et de rares roches mafiques d'origine métavolcanique probable. La tonalite variablement migmatisée se présente en couches d'une épaisseur passant de 1-2000 m dans la séquence supracrustale. Les migmatites sont coupées par des tonalites foliées et massives et par des diatexites à grenat-orthopyroxène-biotite, cette dernière représentant la lithologie la plus abondante de la région. Des intrusions tardives comprennent une diatexite à orthopyroxène-biotite, du granite et de la syénite, localement avec de la néphéline.

Une structure monoclinale régionale est indiquée par des directions nord-ouest dominantes avec pendages moyens à forts. Les plis du litage migmatitique sont ouverts et droits avec des inclinaisons moyennes à faibles. Les plis déforment au moins quelques unes des masses de diatexite. Plusieurs grandes structures ovales avec pendage vers l'intérieur sont peut-être des plis replissés ou des chambres magmatiques déformées.

Les minéraux à grenat-orthopyroxène-biotite-plagioclase-feldspath potassique-quartz trouvés partout dans la région, indiquent un faciès granulitique uniforme. Toutes les unitées, moins quelques granites et syénites tardives, contiennent de l'orthopyroxène.

Un schiste enrichi en sulphides au contact des gneiss mafiques et métasédimentaires a donné des résultats encourageants pour l'or.

INTRODUCTION

"Massif" granulite terranes are large regions underlain by normal crustal thickness, characterized by high-grade metamorphism which commonly occurred at 800 MPa (8 kbar) (Newton and Perkins, 1982). As 25-30 km of cover has been removed by erosion and the present crustal thickness is some 35 km, massif granulites may mark the site of overthickened crust, perhaps ancient continent-continent collisional orogens. Although features characteristic of such an environment may be difficult to recognize at high metamorphic grade, it is important to know the lithological character of the granulites in order to correlate with or distinguish from units in adjacent lower-grade terranes.

In the southeastern Superior Province, the Ashuanipi granulite complex underlies a circular region of some 100 000 km^2 (Fig. 1.1) (Herd, 1978; Card and Ciesielski, 1986). East-west-trending lithological belts of the southern Superior Province intersect the granulite complex, but lithological correlations have not been carried through into the high-grade region and the relationship of the granulites to the rest of the Superior Province is unclear. The question of whether they represent the high-grade equivalent of the western Superior Province belts, or a basement to those, remains to be answered.

As existing mapping is inadequate to resolve this and other questions of regional significance, a program of 1:250 000 mapping was initiated in 1986, in the Schefferville area (NTS 23J) (Stevenson, 1963; Frarey, 1961), on the eastern side of the complex. This region was chosen because the geology is apparently typical of the complex and it straddles the height of land, providing excellent bedrock exposure.

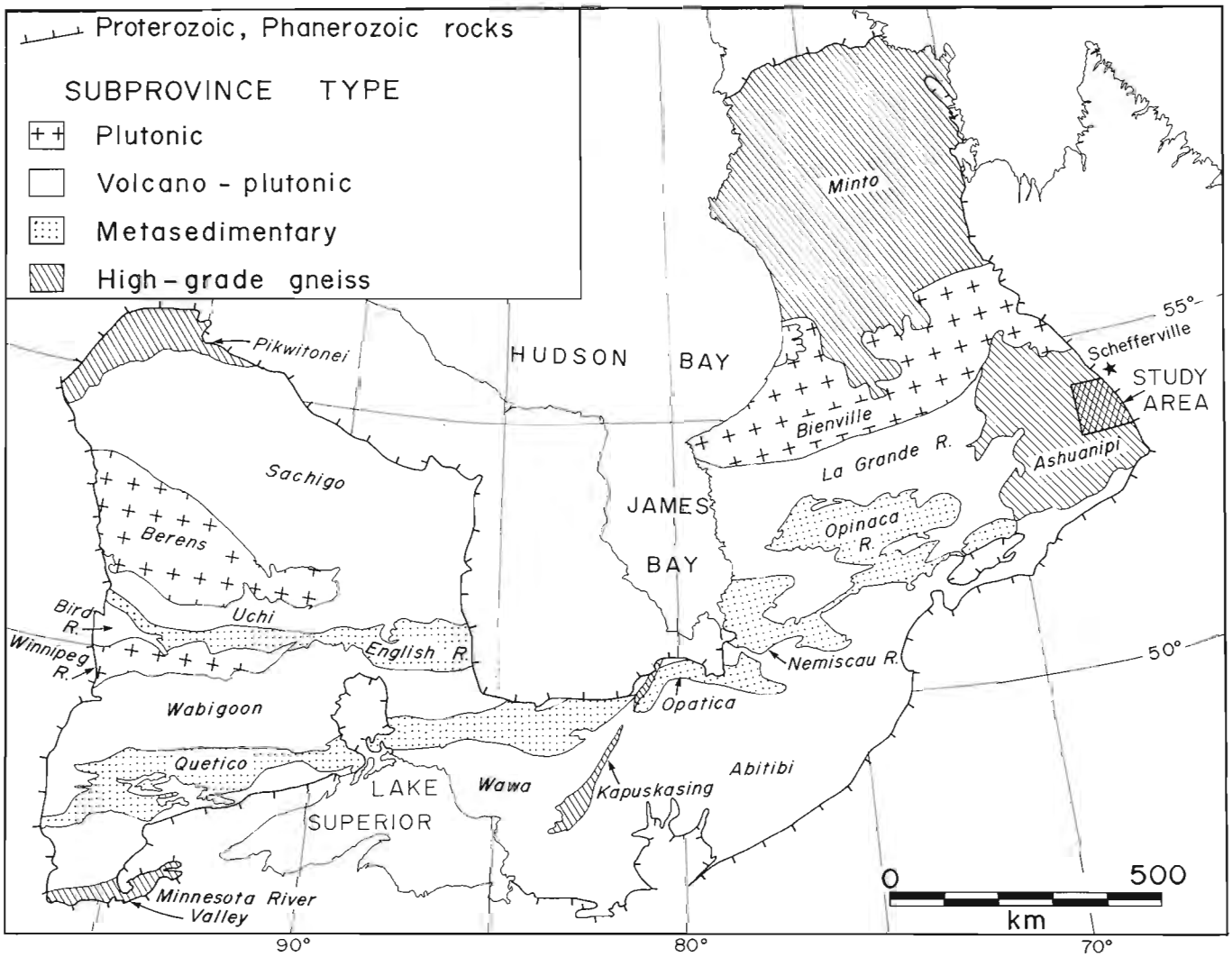


Figure 1.1: Location map showing the Ashuanipi complex in relation to other subprovinces of the Superior Province (after Card and Ciesielski, 1986).

Parts of the area to the west have been mapped by Eade (1966) and Sharma and Dube (1980). The complex is overlain unconformably by rocks of the Kaniapiskau Supergroup in the Labrador Trough to the east.

LITHOLOGY

Mappable units (Fig. 1.2) are defined on the basis of texture and mineralogy and are readily distinguished despite the uniformly high regional metamorphic grade. Two groups of rocks are recognized: 1) migmatitic and gneissic rocks, including paragneiss, tonalitic orthogneiss and mafic gneiss; and 2) homogeneous intrusive rocks, including diatexite, tonalite, granodiorite-granite, and syenite.

Migmatitic rocks

Migmatite terminology follows definitions proposed by Brown (1973): migmatite "is a megascopically composite rock comprising alternating layers or lenses of granitoid and schist or gneiss" (p. 377). Metatexite "is a rock produced by metatexis and in which the migmatitic banding is evident." "Metatexis is the process of segregation (usually of quartz and feldspar) by metamorphic differentiation and partial fusion." (p. 374). Diatexite "is a rock produced by diatexis and in which there is no continuous migmatitic banding." "Diatexis is high-grade anatexis in which fusion may be complete" (p. 375).

Garnet-orthopyroxene-biotite metatexite (paragneiss) These migmatitic rocks are layered on milimetre to centimetre scale with dark grey, medium- to fine-grained, foliated paleosome layers of garnet-orthopyroxene-biotite-plagioclase-quartz, and 5-50% medium- to coarse-grained leucosome of quartz-plagioclase-K-feldspar ± orthopyroxene ± garnet ± biotite. Concordant and discordant white pegmatites are commonly associated. Sillimanite occurs at one location, in association with mauve garnet. Primary compositional layering (Fig. 1.3) at an oblique angle to migmatitic layering was identified at one locality. The unit is inferred to be derived from a clastic sedimentary precursor.

Orthopyroxene-biotite metatexite (tonalitic orthogneiss). This lithological unit varies widely in texture over short distances. In their least altered form, the rocks are homogeneous, medium grained orthopyroxene-biotite tonalite, with spongy, ragged orthopyroxene oikocrysts or poikiloblasts to 1 cm (Fig. 1.4). In its migmatitic state, it consists of layers of dark grey, medium grained orthopyroxene-biotite tonalite, with 5-30% white, medium- to coarse-grained leucosome which may contain garnet. The rocks occur in lenses and layers, generally interlayered with paragneiss on metre to kilometre scale. The igneous texture is best preserved in the interior of large bodies. Near garnet-bearing metatexite, leucosome is more abundant and rosette-shaped garnet porphyroblasts up to 1 cm may occur in paleosome. This garnet-bearing variety is distinguishable from paragneiss only if the characteristic large inclusion-rich orthopyroxene is present. Preservation of igneous features is generally better in the northern two-thirds of the area than in the south.

East of Desliens Lake (Fig. 1.2), well preserved diorite, gabbro and pyroxenite with characteristic coarse orthopyroxene texture occur in minor proportions in association with tonalite and paragneiss. The more mafic rock types occur in the core zone of a 7 km-wide inward-dipping oval structure.

The intimate association of tonalite and paragneiss suggests that the tonalites were probably sills within a sedimentary succession. The origin of the characteristic coarse orthopyroxene is problematic. Its presence in relatively massive, homogeneous rocks and absence from migmatitic varieties suggests a preserved igneous origin, although metamorphic growth is also possible, judging from the metamorphic orthopyroxene present in adjacent rock types. Petrological study is underway by P.N. Nagerl as part of a B.Sc. thesis project.

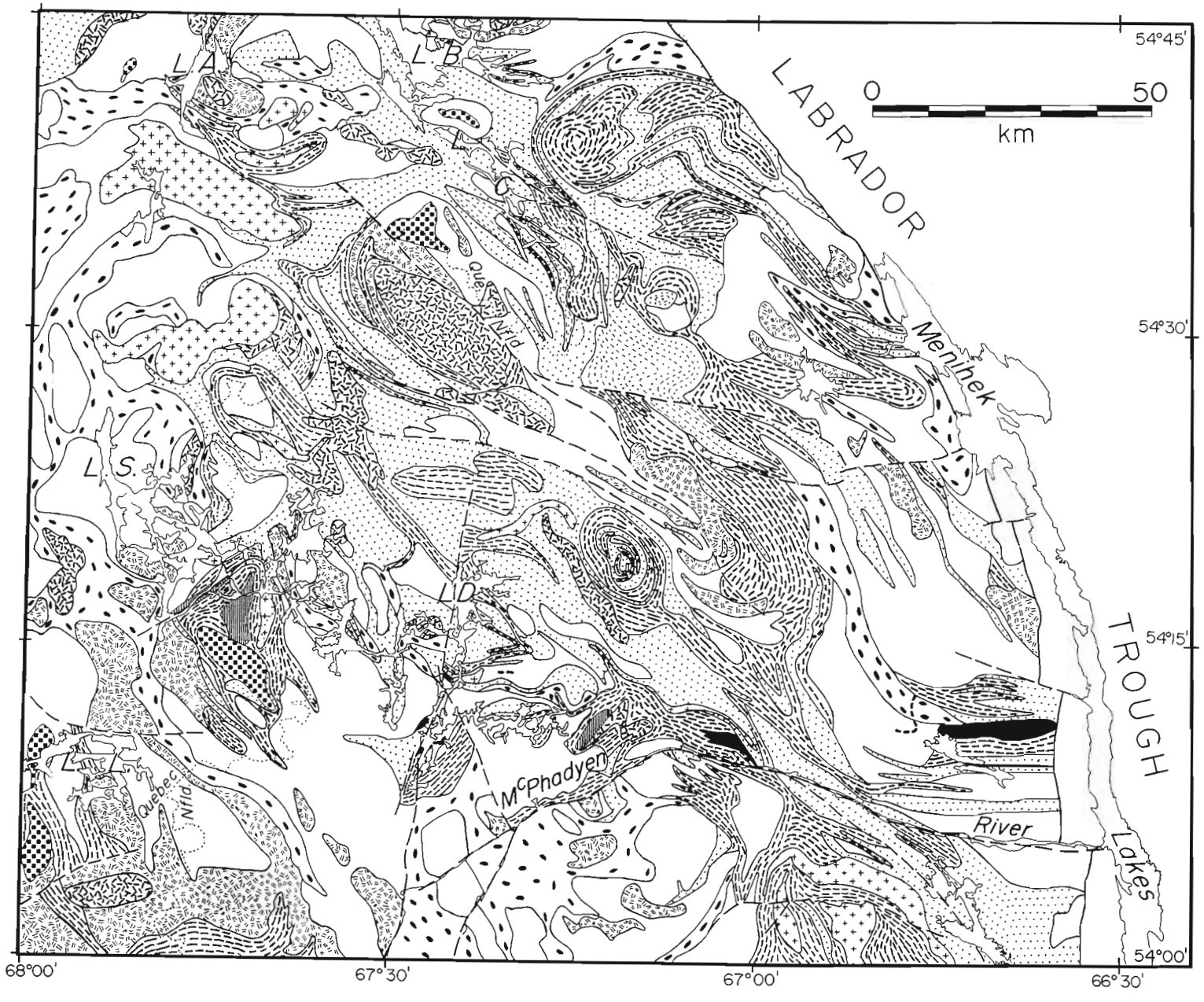
Interlayered metatexites. Parts of the area are underlain by metatexites interlayered on 1-1000 m scale, too fine to be resolved at the present scale of mapping. Within the interlayered sequence, the textural-mineralogical distinction between units cannot be made in places where abundant garnet-bearing tonalitic rocks closely resemble paragneiss.

Mafic gneiss Several small bodies of mafic gneiss, up to 2 km thick, occur dominantly within paragneiss sequences. These are strongly foliated to migmatitic, medium grained orthopyroxene-clinopyroxene-hornblende-plagioclase ± quartz rocks. Some belts are characterized by wispy, discontinuous hornblende-rich layers on the 1-2 cm scale, suggestive of protolith heterogeneities (Fig. 1.5). Rocks of intermediate composition are also present locally. Zones rich in sulphides are associated with some mafic gneiss-paragneiss contacts. Other small mafic belts, dominantly in orthogneiss, are homogeneous and resemble metagabbro.

Homogeneous intrusive rocks

Pyroxenite Homogeneous, massive to foliated pyroxenite consisting of medium to coarse pyroxene and some amphibole, occurs as pods and layers less than 100 m thick. Igneous texture is preserved in one body where clinopyroxene oikocrysts up to 15 cm are present in massive pyroxenite. Granitic dykes cutting this body have 2 cm thick monomineralic biotite selvages. Pyroxenite occurs within metatexite sequences as well as in diatexite where it may be present as inclusions.

Garnet-orthopyroxene-biotite diatexite occurs as intrusive bodies ranging in size from dykes less than 1 m thick in metatexite, to batholiths tens of kilometres wide. It is a medium- to coarse-grained rock with phenocrysts of garnet, orthopyroxene and/or white alkali feldspar up to 1.5 cm (Fig. 1.6). Mafic constituents (10-25%) may define a foliation or wispy layering in these generally granodioritic rocks. Metatexite, particularly garnet-bearing varieties, occurs as 10-200 cm inclusions in variable proportions. Diatexites with less than 25% inclusions are termed homogeneous and those with more than 25% as inhomogeneous (Fig. 1.2). White, garnet-, orthopyroxene-, biotite-bearing leucogranite pegmatites are commonly associated with garnet-bearing diatexite.


54°45'
54°30'
54°15'
54°00'
68°00'
67°30'
67°00'
66°30'
0
50
km
LABRADOR
TROUGH
L.A.
L.B.
L.C.
L.D.
L.S.
Que.
Nfld
Quebec
Nfld
Menihek
McPhadyen
River
Lakes

Dykes of diatexite cut metatexite and metatexite occurs as inclusions in diatexite. Contacts are generally sharp and there is little evidence of gradation between the two rock types. Based on the similarity in mineralogy and composition of garnet-bearing diatexites to garnet-bearing metatexites, the diatexites appear to be derived by anatexis of metatexites.

Orthopyroxene – biotite diatexite generally occurs as small (1-5 km scale) ovoid bodies with positive aeromagnetic anomalies, within garnet-bearing diatexite. It is medium- to coarse-grained, with phenocrysts of orthopyroxene and white alkali feldspar (Fig. 1.7). Mafic minerals, making up 15-25% of the rock, form a foliation or subtle layering. Metatexite inclusions are common although less abundant than in garnet-bearing diatexite.

Figure 1.2: Geological map of the Ashuanipi complex in the Schefferville (23J) area. Structural data is represented in Figure 1.9. L.A.: Avezac Lake; L.B: Bazil Lake; L.C: Clugny Lake; L.D: Desliens Lake; L.L: Lasservolle Lake; L.M: LaMilleraye Lake; L.S: du Sable Lake.

Figure 1.3: Primary compositional layering (bedding) at an oblique angle to migmatite layering in garnet-orthopyroxene-biotite metatexite (paragneiss). (15 km southeast of Clugny Lake).

Figure 1.4: Characteristic large, ragged, inclusion-rich orthopyroxene in well-preserved tonalitic precursor to orthopyroxene-biotite metatexite. The texture may represent preserved igneous oikocrysts or metamorphic poikiloblasts. (10 km east of Desliens Lake).

Tonalite occurs as massive to strongly foliated bodies of various dimensions (Fig. 1.2). The rocks are commonly homogeneous, medium to coarse-grained, and contain 10-20% combined orthopyroxene and biotite in addition to quartz and plagioclase. Inclusions of foliated tonalite are rare in diatexite. Pink, magnetite-bearing leucogranite pegmatites are commonly associated with tonalites. Although commonly foliated, tonalite is rarely migmatitic and thus is readily distinguished from early, tonalitic metatexite.

Three small bodies consisting of *quartz diorite, diorite and mafic tonalite* occur in the southwestern part of the map area. These homogeneous, medium-grained, massive to foliated rocks consist of two pyroxenes, hornblende, biotite, magnetite, plagioclase and 0-10% quartz. The bodies are associated with distinct positive aeromagnetic anomalies.

Granite and *granodiorite* occur as distinct large plutons as well as in small pegmatite pods and dykes. The plutons have individual lithological character: the Lasservolle Lake body is a massive, medium- to coarse-grained, clinopyroxene-biotite-magnetite, quartz-poor granite with a distinct positive aeromagnetic signature. Small bodies of similar composition occur in the same vicinity. To the south, a body of similar size is massive biotite leucogranite. In the southeastern part of the area, a crescent-shaped body is composed of massive clinopyroxene-magnetite-biotite granodiorite (Fig. 1.2). To the south is a body of foliated, homogeneous, medium-grained orthopyroxene-biotite ± magnetite granite with locally abundant pegmatite and inclusions of orthopyroxene-biotite metatexite.

Syenite occurs in several small bodies in the western part of the map-area. Two bodies with positive aeromagnetic anomalies in the La Milleraye Lake area are leucocratic biotite syenite cut by abundant quartz-bearing pegmatite and aplite. A lenticular body southeast of du Sable Lake has a prominent magnetic anomaly and consists of a core of nepheline-bearing syenite (Fig. 1.8) and a marginal nepheline-free zone. Both pink and white coarse-grained biotite-magnetite-clinopyroxene syenite, with flow-aligned K-feldspar (Fig. 1.8), are present within the body. Southwest of Clugny Lake, a body of medium-grained clinopyroxene-hornblende biotite syenite is associated with a moderate positive aeromagnetic anomaly. To the north, a small body of similar composition contains pods of magnetite up to 10 cm thick, possibly accounting for its strong magnetic signature.

A total of some 15 diabase dykes, all less than 30 m wide, and generally trending northerly, were observed. They are fresh, medium-grained diabase of probable tholeiitic composition with well-developed chill margins.

STRUCTURE

Northwesterly structural trends, defined by lithological contacts and migmatitic layering, predominate in the region; these vary to westerly in the southeast. Dips are generally steep to the northeast, indicating an overall northeast homocline. Many small folds, long-wavelengh warps and interference effects of intrusive bodies complicate the general structural pattern. No pervasive linear structural element is present, although macroscopic folds of layering occur locally, generally in association with megascopic folds.

A major northwest-trending, northeast-dipping belt of metatexite occupies the central part of the map area and is bounded to the east and west by intrusive rocks, mainly diatexite. Within the metatexite sequence are several upright folds with horizontal to gentle plunges (Fig. 1.9). In addition, three major oval structures are present within the metatexite belt. Two are basins and the other is a dome (Fig. 1.9).

In the Desliens Lake area, concentric topographic features define an oval structure some 7 km in diameter. Topographic expression is caused by 5-1000 m interlayered relatively high-standing orthopyroxene-biotite metatexite and recessive garnet-orthopyroxene metatexite. Migmatitic



Figure 1.5: Mafic gneiss with discontinuous hornblende-rich layers and heterogenities, suggestive of supracrustal features (deformed pillow selvedges ?) (13 km northwest of mouth of McPhadyen River).

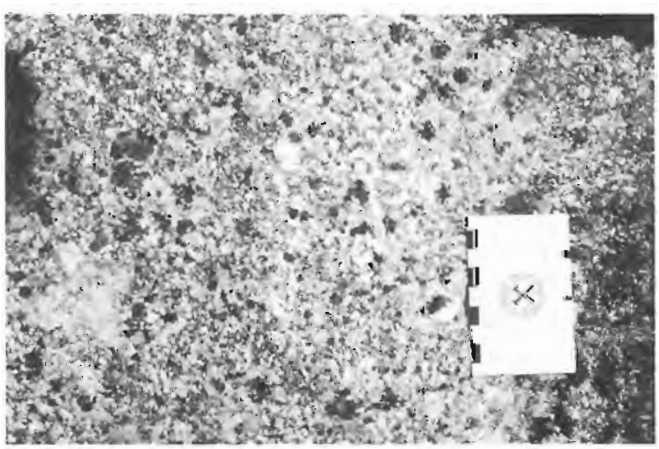


Figure 1.6: Homogeneous garnet – orthopyroxene – biotite diatexite showing prominent phenocrysts of white alkali feldspar, garnet (anhedral) and orthopyroxene (blocky, subhedral).

layering, parallel to lithological contacts, defines an inward-dipping structure, with steep (70° dip) margins and sub-horizontal interior. In the interior, well-preserved meta-igneous rocks including tonalite, diorite, gabbro and pyroxenite with characteristic orthopyroxene poikiloblasts, are interlayered on various scales with garnet-orthopyroxene metatexite. The orthopyroxene-biotite rocks can be traced from the oval structure to the southeast, where they form a synformal belt. It is thus possible that the cone-shaped structure is a type I interference structure at the junction of northwesterly and northeasterly trending synforms. There is no independent evidence for the existence of the latter structure. Alternatively, the mafic meta-igneous rocks in the centre of the structure, dense with respect to the surrounding rocks, could have induced an anti-diapiric sag. Based on the minor amount of mafic rock exposed, this seems unlikely in light of the regional extent of the structure. A further possibility is that the structure represents the basal part of a magma chamber, modified by deformation.



Figure 1.7: Homogeneous orthopyroxene-biotite diatexite with alkali feldspar and orthopyroxene phenocrysts.

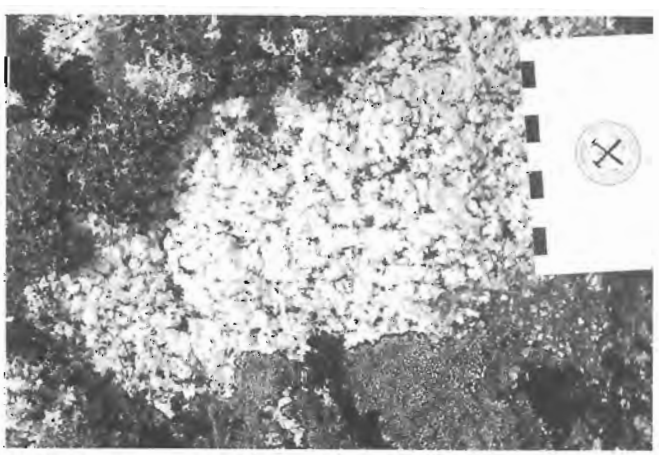


Figure 1.8: Nephiline-bearing syenite showing coarse flow-aligned alkali feldspar (5 km southeast of du Sable Lake).

A second inward-dipping structure is northeast of Clugny Lake. Curvilinear lakes and rivers define a 10 × 15 km northeasterly-elongate ellipse. The margins are interlayered garnet-orthopyroxene and orthopyroxene-biotite metatexite whereas the interior is orthopyroxene-biotite metatexite, giving way to well-preserved tonalite toward the centre. Layering dips inward at 45° over the margins and steepens to 70° toward the interior. The core was not observed. As with the Desliens Lake structure, the origin is enigmatic.

An outward-dipping oval structure occurs within the metatexite belt southwest of Clugny Lake. The core is a composite of intrusive rock types, including a central homogeneous tonalite body, itself with outward dipping foliation, diatexite and syenite. It is surrounded by garnet-orthopyroxene metatexite. Layering wraps around the northwest and southeast ends of the 30-km-long structure to form a bulge, convex to the northeast, in the homoclinal geometry. It is not clear whether this shape is the result of "ballooning" by intrusion of the igneous bodies or of material flow around early, structurally resistant intrusive bodies.

A moderately southeast-plunging, map-scale "Z" fold of interlayered metatexites is present south of Clugny Lake. The association of this and other megascopic structures with metatexites interlayered on 1-2000 m scale suggests that this lithologic package contains competency contrasts which induced folds.

The relative age of diatexite with respect to deformation is ambiguous. Some large bodies are massive but have contacts parallel to regional structural trends and contain aligned inclusion trains. These bodies are probably late to syntectonic. Other sill-like bodies are concordant to and folded with layering, as at Bazil Lake. These may be slightly earlier with respect to deformation.

All of the structures discussed above are defined by variation in orientation of migmatitic layering. Structures which formed prior to production of this layering have not been recognized. Aside from the one locality previously noted (Fig. 1.3), bedding is not preserved in metatexite and lithological contacts are in general parallel to migmatitic layering.

Fault-related structures were noted at several locations. A narrow zone of north-south striking mylonite is associated with a prominent valley south of Clugny Lake. Both mylonite and cataclasite-series fault rocks are developed in a 2 km-wide zone adjacent to the McPhadyen River. At its eastern end, some 3 km of brittle, apparent sinistral movement can be documented by offset of the Proterozoic unconformity. Total displacement on the fault is probably much greater, judging from the discontinuity of units across the river. Mylonitic rocks with similar trend are also present in a 30-50 m wide zone south of McPhadyen River.

A set of prominent northerly faults is present in the Desliens Lake area. Cataclasites and mylonite are associated with quartz stockwork systems, hematitic alteration and chlorite-epidote development (Fig. 1.9). Locally well-developed shear bands suggest dextral movement. Sheared quartz

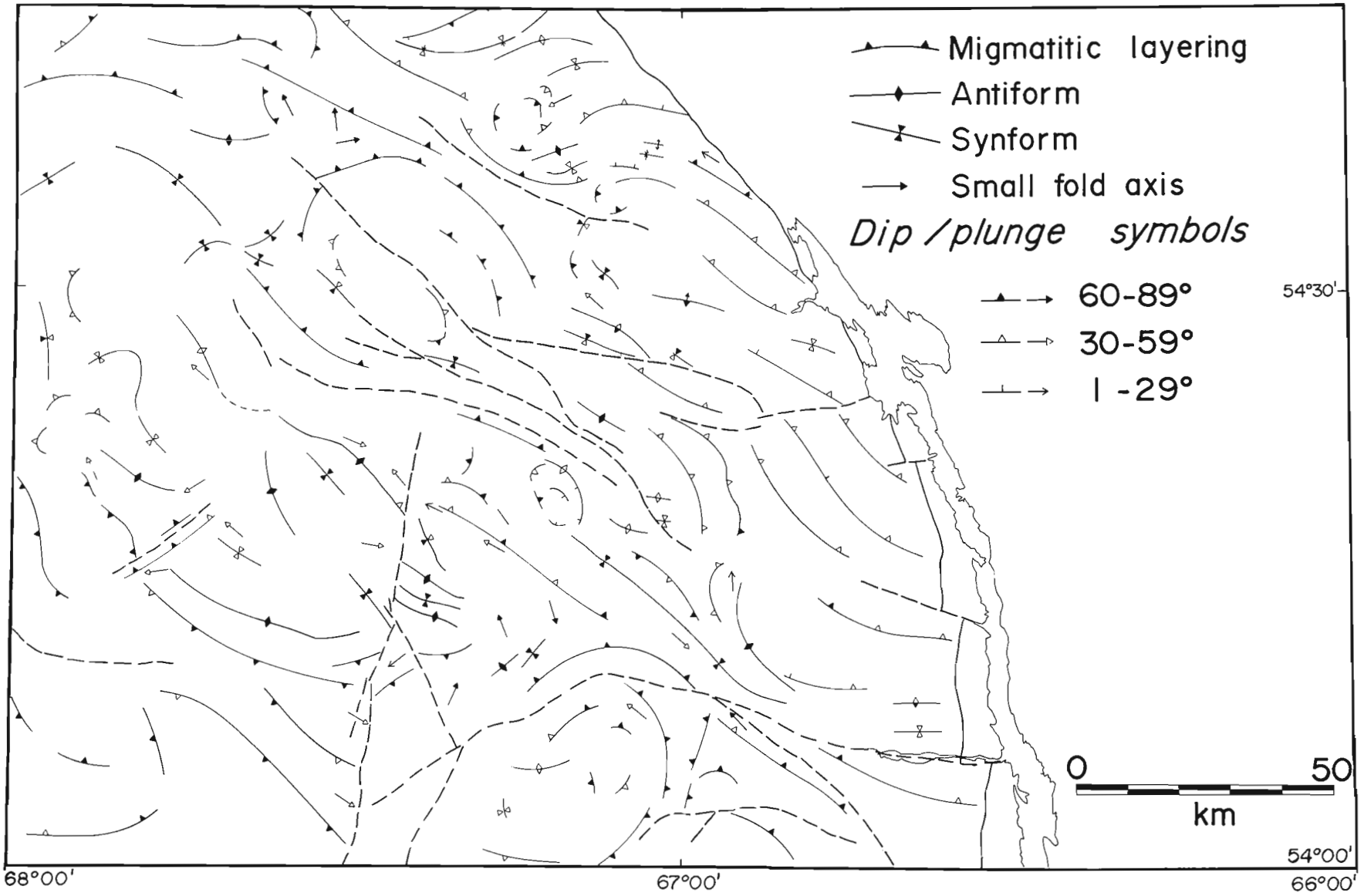


Figure 1.9. Summary map of structural elements in the Schefferville area. Note dominant northwesterly structural grain.

veins from this environment yield analyses of less than 1 ppb Au. A set of prominent northwesterly faults in the central part of the area is associated with topographic lineaments, lithological contrasts and at least local cataclasite development.

METAMORPHISM

Orthopyroxene is present in all rock types with the exception of the syenites, some granites and some leucopegmatites. It is everywhere associated with biotite, plagioclase and quartz, and very commonly with garnet and K-feldspar. It occurs in both the paleosome and leucosome of metatexites, as well as in diatexites, tonalites, some granites and pegmatites. The volume of orthopyroxene in metatexite is least in the north, in the Bazil Lake area but there is no obvious modal variation throughout the remainder of the area. Orthopyroxene and garnet appear fresh, even in the felsic igneous rocks.

The coexistence of orthopyroxene and a granitic melt, inferred from the presence of leucosome in metatexite, indicates crystallization temperatures above about 750°C, assuming a pressure of about 5 kbar (Bohlen et al., 1983). This estimate also applies to orthopyroxene-bearing diatexites, which although attaining coarse grain size, must have been relatively dry (low water activity) to avoid back-reaction of orthopyroxene to biotite-quartz during crystallization.

Metatexite contains milimetre-scale leucosome layers and pods, many of which appear to be *in situ* products of anatectic melting. A melt phase of granodioritic composition implies a minimum metamorphic temperature of about 700°C. Under any normal geothermal gradient, higher temperatures and more thorough melting would occur at deeper structural levels. Thus the diatexites, intrusive at the exposed level, are inferred to be derived from metatexite sources at depth within the crust.

A single occurrence of sillimanite in association with pale mauve garnet at Clugny Lake constrains metamorphic pressure at 750°C, to less than 8 kbar.

Minor retrograde metamorphism to greenschist facies is associated with cataclastic deformation at several localities. Both features imply development at shallow crustal levels.

CHRONOLOGY

Based on cross-cutting relationships and intensity of development of foliation, a relative chronology may be constructed. Supracrustal rocks appear to be oldest. This includes the major metasedimentary units and very minor mafic rocks of probable metavolcanic origin. Interlayered orthopyroxene-biotite metatexites probably represent early sills that were partly migmatized during the high-grade metamorphism. However, it is possible that some orthopyroxene-biotite metatexites represent felsic metavolcanic rocks. For example, south of McPhadyen River, mafic gneiss is interlayered with orthopyroxene-biotite metatexite and rare deformed, metamorphosed mafic dykes cut metatexite. This is an uncommon lithological association to the north, where metatexite precursors are better preserved.

At least two ages of homogeneous tonalite are present: older foliated bodies, which occur locally as inclusions in diatexite, and younger, massive types. Three ages of diatexite may be present: older garnet-bearing varieties, folded with migmatitic layering, younger garnet-bearing varieties; and still younger orthopyroxene-biotite diatexite. Orthopyroxene-bearing pegmatites and aplites cut the preceding units, as well as some syenites and granites suggesting persistence of granulite facies conditions to late in the magmatic history. Massive syenites and granites are the youngest felsic bodies, having no cross-cutting granitic dykes. Mafic dykes cut pegmatites and are probably Proterozoic in age. Based on the variation in trend, more than one set of dykes may be present. The relative ages of dykes and faults could not be determined from the available data.

ECONOMIC GEOLOGY

The Ashuanipi complex has some potential as a source of gold. In the Pailleraut Lake area, 60 km north of the present area, grab samples of rusty paragneiss associated with quartz-magnetite iron formation yielded analyses of up to 18.9 g/tonne (Lapointe, 1986).

In the present map area, several gossans in paragneiss show gold values above background (A. Thomas, personal communication, 1986). In particular, the sulphide-rich contact zone between a small belt of mafic gneiss west of Menihek Lake and structurally overlying paragneiss yields assays of up to 750 ppb Au (A. Thomas, personal communication, 1986). Although mafic gneiss is a minor unit in the region, contacts with paragneiss could be a favourable environment for syngenetic gold mineralization.

Quartz veins associated with shear zones in the southern Desliens Lake area were assayed for gold. The results are not encouraging; two samples gave values of less than 1 ppb Au.

DISCUSSION

According to Card and Ciesielski (1986) the Ashuanipi complex is a high- grade gneiss subprovince of the Superior Province. The uniformly high metamorphic grade in the Schefferville area confirms this classification. The predominance of rocks of metasedimentary derivation, both gneisses and granitoids, suggests a lithological kinship with the lower-grade metasedimentary belts of the western Superior Province, such as the English River and Opinaca River belts, although there appears to be no direct lithological link (Card and Ciesielski, 1986). Alternatively, the Ashuanipi complex could be a continuation of the high-grade Minto subprovince to the northwest, separated from it by the Bienville plutonic belt (Card and Ciesielski, 1986). The main evidence for this correlation is the northwesterly structural trend in the Schefferville area, similar to the structural grain within the Minto subprovince. U-Pb zircon geochronology, underway in collaboration with J.K. Mortenson, will enable comparisons with the well-dated western Superior Province. However, age comparison with the Minto subprovince must await geochronological studies in that area.

A major lithological component of the granulites is paragneiss of supracrustal origin. If one accepts the inference that garnet-bearing diatexites are anatectic derivatives of garnet-bearing paragneiss, then supracrustal rocks are also present at some depth below the present erosion level. The mechanism of emplacement of supracrustal rocks in the deep crust has intrigued petrologists for many years; tectonic burial by an overriding continental slab which is subsequently removed isostatically, is currently a commonly accepted explanation. If the Ashuanipi rocks correlate with belts of the western Superior Province, then it would be inappropriate to consider the complex as an isolated block with a history distinct from that of the remainder of the Province. Small regions at granulite facies are present sporadically throughout the metasedimentary terranes to the west; the Ashuanipi complex may simply be a larger example. Its origin may thus be linked to processes which shaped the entire Superior Province.

Preliminary geobarometry of granulites from 30 km west of the area indicates pressures on the order of 500 MPa (5 kbar), implying removal of some 20 km of cover. Assuming a present crustal thickness of 35 km and no underplating, this would suggest a 55-km-thick crust during metamorphism. The nature of the process which caused the chain of events from overthickening and burial of supracrustal rocks to over 20 km, to granulite metamorphism, to uplift, is not understood. One clear conclusion from the mapping is that low-angle, ductile, high-strain zones, symptomatic of crustal stacking in the Grenville Province (e.g. Davidson, 1984), are not present. Major crustal thickening thus occurred prior to the high-grade metamorphism and plutonism. A possible environment of formation of thick crust of dominantly sedimentary character is an accretionary wedge. Subsequent heating of what normally become belts of high-pressure metamorphic rocks would be necessary to explain the high-temperature metamorphism.

CONCLUSIONS

In the Schefferville area, the Ashuanipi complex consists of an older sequence of interlayered paragneissic and orthogneissic units, younger tonalite and diatexite intrusions derived from the gneissic units, and still younger granite and syenite bodies. Structural trends are dominantly northwest and dips mainly steep to the northeast. Folds of migmatitic layering are upright and open, with gentle to moderate plunge. The origin of several inward-dipping, cone-shaped oval structures is not understood.

The assemblage garnet-orthopyroxene-biotite-quartz-plagioclase-K-feldspar is present throughout the region and is present in rock types including gneisses, diatexites, tonalites, pegmatite and some granite. Granulite-facies conditions persisted throughout most of the magmatic history.

Several small belts of mafic gneiss in the southeast have heterogeneities suggesting a supracrustal origin. A sulphide-rich schist at a mafic gneiss-paragneiss contact yields assays of up to 750 ppb Au.

ACKNOWLEDGMENTS

Capable field assistance was cheerfully provided, often under trying working conditions, by E. Clark (McGill), S. Trepanier (Laurentian), P. Nagerl and L. Harnois (Carleton). Luc Harnois is responsible for approximately half of the mapping. J. Prud'homme (Cargair Ltée) is thanked for expediting and logistic support. Logistic support provided by A. Thomas (Newfoundland Department of Mines and Energy) greatly facilitated helicopter time-sharing and work based in Schefferville. Helicopter set-outs by F. Thompson (G.S.C.) are gratefully acknowledged. Iron Ore Company of Canada is thanked for use of facilities at Menihek. Helpful comments by K.E. Eade and A. Davidson are appreciated.

REFERENCES

Bohlen, S.R., Boettcher, A.L. Wall, V.J. and Clemens, J.D.
1983: Stability of phlogopite-quartz and sanidine quartz: a model for melting in the lower crust; Contributions to Mineralogy and Petrology, v. 83, p. 270-277.

Brown, M.
1973: The definition of metatexis, diatexis and migmatite; Proceedings of the Geological Association, v. 84, p. 371-382.

Card, K.D. and Ciesielski, A.
1986: Subdivisions of the Superior Province of the Canadian Shield; Geoscience Canada, v. 13, p. 5-13.

Davidson, A.
1984: Tectonic boundaries within the Grenville Province of the Canadian Shield; Journal of Geodynamics, v. 1, p. 433-444.

Eade, K.E.
1966: Fort George River and Kaniapiskau River (west half) map-areas, New Quebec; Geological Survey of Canada. Memoir 339, 84 p.

Frarey, M.J.
1961: Geology, Menihek Lakes, Newfoundland and Quebec; Geological Survey of Canada Map 1087A, scale: 1:253 440.

Herd, R.K.
1978: Notes on metamorphism in New Quebec *in* Metamorphism in the Canadian Shield; Geological Survey of Canada Paper 78-10, p. 79-83.

Lapointe, B.
1986: Reconnaissance geologique de la région du lac Pailleraut, Territoire du Nouveau Quebec; Ministere de l'Energie et des Ressources du Quebec MB85-73, 10 p.

Newton, R.C. and Perkins, D.
1982: Thermodynamic calibration of geobarometers based on the assemblage garnet-plagioclase-orthopyroxene (clinopyroxene)-quartz; American Mineralogist, v. 67, p. 203-222.

Stevenson, I.M.
1963: Lac Bazil, Québec; Geological Survey of Canada Paper 62-37, 4 p.

Sharma, K.N.M. and Dube C-Y
1980: Region des Lacs Caniapiscau-Clairambault; Ministère de l'Energie et des Ressources DPV-755, 13 p.

Analyses palynologiques de sédiments holocènes du lac Bras d'Or (carotte 85-036-016P), île du Cap-Breton, Nouvelle-Écosse

Project 730072, 690064

A. de Vernal[1] et H. Jetté[2]
Centre géoscientifique de l'Atlantique, Dartmouth

de Vernal A., et Jetté, H., Analyses palynologiques de sédiments holocènes du lac Bras d'Or (carotte 85-036-016P), île du Cap-Breton, Nouvelle-Écosse dans Recherches en cours, Partie A, Commission géologique du Canada, Étude 87-1A, p. 11-15, 1987.

Résumé

Le lac Bras d'Or qui s'étend au centre de l'île du Cap-Breton a été affecté par des variations du niveau relatif de la mer depuis la déglaciation. L'analyse palynologique de la carotte 85-036-016P révèle en effet d'importants changements microfloristiques liés à diverses conditions paléohydrologiques. Trois principales étapes de l'évolution du milieu aquatique sont distinguées: 1) la première (survenue il y a environ 9000 à 10 000 ans) se caractérise par une productivité primaire limitée et correspond à une phase de sédimentation rapide; 2) un milieu lacustre dulcicole, favorable à l'implantation d'une importante vie algaire, l'a remplacée; 3) la pénétration des eaux nord-atlantiques dans le bassin, par le chenal Great Bras d'Or (profondeur de 8 m), a par la suite favorisé la prolifération d'une microflore marine. À en juger par la palynostratigraphie régionale holocène, la transition de milieu lacustre à milieu marin aurait eu lieu il y a environ 4000 ou 5000 ans. On peut ainsi calculer un taux moyen de submersion de l'ordre de 16 à 20 cm par siècle, au cours de l'Holocène supérieur.

Abstract

Lake Bras d'Or, in central Cape-Breton Island, has been influenced by postglacial relative sea level changes, as demonstrated by the palynological analysis of core 85-036-016P, which revealed microfloral variations related to various paleohydrological conditions. Three main stages in the evolution of the aquatic environment are distinguished: (1) the first (from ca. 10 000 to 9 000 B P) is characterized by a low phytoplanktonic productivity and corresponds to an episode of high sedimentation rate; (2) it was succeeded by a lacustrine fresh water environment, favourable to algal productivity; (3) finally, the penetration of North Atlantic water, throughout the Great Bras D'Or channel (presently 8 m deep), allowed the development of a rich marine microflora. According to the regional palynostratigraphy, the fresh water/marine transition can be dated at ca. 5000/4000 B P. A mean submergence rate of ca. 16 to 20 cm/century may therefore be inferred during the late Holocene.

[1]Laboratoire de géochimie isotopique et de géochronologie (GEOTOP), Université du Québec à Montréal, C.P. 8888, succursale «A», Montréal (Québec), H3C 3P8.
[2]Commission géologique du Canada, 601, rue Booth, Ottawa (Ontario), K1A 0E8.

INTRODUCTION

Dans les provinces atlantiques du Canada, des rajustements géoïdaux d'origine glacio-isostatique ont engendré, à l'Holocène, une remontée du niveau relatif de la mer (p. ex. Grant, 1977; Scott et coll., 1981; Quinlan et Beaumont, 1981; Miller et coll., 1982; de Vernal et coll., 1985). Compte tenu du caractère quelque peu marginal du lac Bras d'Or, ce dernier a certainement été affecté par les fluctuations du niveau relatif de la mer. En effet, le lac Bras d'Or, vaste bassin s'étendant au centre de l'île du Cap-Breton (fig. 2.1), est relié à l'Atlantique nord par quelques chenaux, principalement celui de Great Bras d'Or, dont le seuil se situe 8 m sous le niveau actuel de la mer. Les masses d'eau y enregistrent aujourd'hui une salinité de l'ordre de 24,5 à 29 ‰ (Mucci et Pagé, 1987). La faible salinité des eaux favorise la formation d'une couche de glace continue pendant la saison hivernale.

La carotte 85-036-016P a été prélevée sous une tranche d'eau de 31 m dans le secteur est du chenal Great Bras d'Or (baie East, fig. 1) au cours d'une mission du CSS Dawson. La pénétration du carottier a été interrompue à une profondeur de 3,4 m, soit au niveau d'un dépôt silto-graveleux de couleur rougeâtre, associé au till du Wisconsinien supérieur. La séquence sédimentaire représente donc l'ensemble du postglaciaire. Les dépôts consistent en boues stratifiées de couleur grise à brunâtre et renferment une quantité relativement abondante de matière organique (2,3 à 6,3 %; voir Hillaire-Marcel, 1987), à l'exception de la partie basale de la carotte (3,4 à 2,6 m). À des fins d'études microfloristiques, on a prélevé des échantillons dans ces sédiments à des intervalles de 20 cm. Les analyses sporo-polliniques fournissent une image régionale de la végétation et favorisent l'établissement de corrélations stratigraphiques approximatives; l'analyse de la microflore organique (dinokystes et *Pediastrum* essentiellement) permet la reconstitution des paléomilieux aquatiques.

LA PALYNOSTRATIGRAPHIE

Dans son ensemble, la palynostratigraphie de la carotte 85-036-016P (fig. 2.2) est conforme à celle que l'on observe au cours de l'Holocène, dans les provinces atlantiques du Canada: elle se caractérise par un assemblage de zone mixte (à *Picea, Betula*, arbustes et herbes), puis par l'augmentation de *Pinus*, suivie d'un maximum de *Tsuga* auquel succède un assemblage à *Betula*. Quelques corrélations chronostratigraphiques peuvent ainsi être établies en fonction de la palynostratigraphie régionale:

1) La base de la carotte (2,4 à 3,4 m) semble postérieure à l'oscillation climatique du tardiglaciaire qui a pris fin il y a environ 10 000 (voir Mott et coll., 1986); elle s'inscrit plutôt dans la zone à *Picea* et *Betula* qui marque le début de l'Holocène (Anderson, 1985).

2) L'augmentation de *Pinus*, essence identifiée entre 2,4 et 2,6 m dans la carotte 85-036-016P, aurait eu lieu il y a environ 8000 à 9500 ans, selon les régions: environ 9500 ans au Nouveau-Brunswick (Mott, 1975); plus de 9600 ans en Nouvelle-Écosse (Livingstone, 1968); environ 8000 ans sur l'Île-du-Prince-Édouard (Anderson, 1980);

3) *Tsuga* est un élément caractéristique de l'Holocène moyen: dans les provinces atlantiques son maximum de représentation correspond à une période survenue il y a environ 5000 à 7000 ans (Anderson, 1985). On a remarqué qu'il y a environ 4500 à 5000 ans, une augmentation de *Betula* a généralement accompagné le déclin de *Tsuga*. L'intervalle compris entre 1,7 et 1,9 m dans la carotte 85-036-016P daterait donc d'il y a environ 4500 à 5000 ans.

Dans la mesure où ces corrélations palynostratigraphiques sont exactes, la base de la carotte (2,4 à 3,4 m) représenterait un intervalle de temps relativement bref: des taux élevés de sédimentation paraissent en effet probables, compte tenu du caractère minéral du dépôt (voir Hillaire-Marcel, 1987) et des faibles concentrations polliniques. Par ailleurs, l'abondance des spores trilètes d'âge mississipien milite en faveur d'une certaine érosion des roches sédimentaires du groupe de Windsor qui affleurent autour du lac Bras d'Or (p. ex. Weeks et Guernsey, 1954). La forte proportion d'éléments arbustifs (*Alnus, Salix, Myrica* et *Ericaceae*) et herbacés (Gramineae, Cyperaceae et Asteraceae) à la base de la carotte permet d'évoquer l'existence d'un paysage forestier régional ouvert; elle peut aussi traduire l'occupation des milieux ripariens et riverains proximaux par une végétation essentiellement herbacée et arbustive.

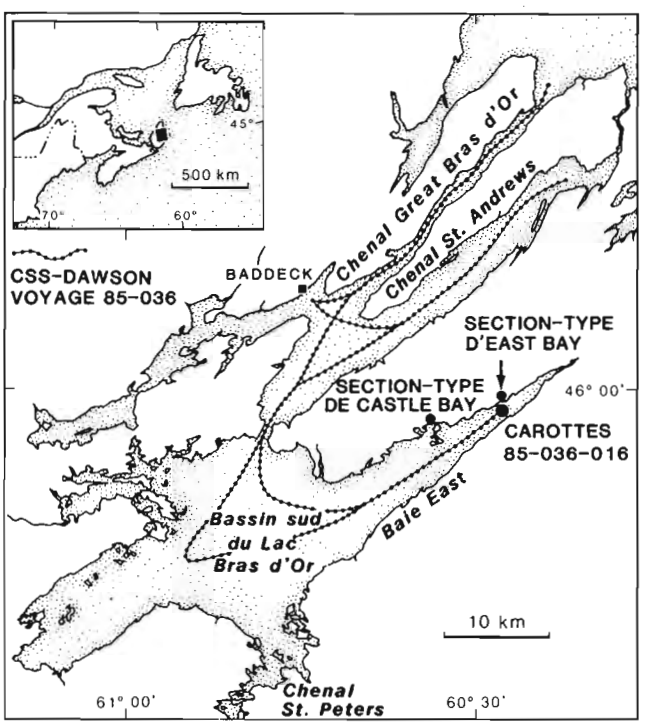


Figure 2.1 Carte de localisation.

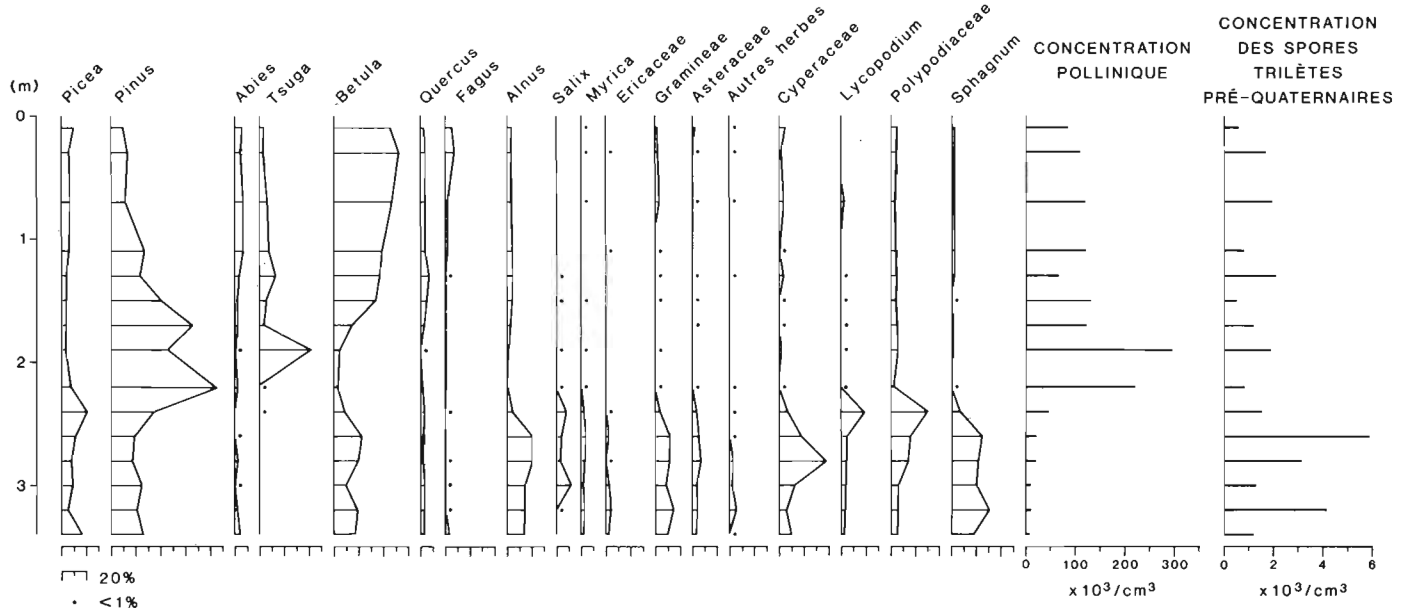


Figure 2.2 Diagramme pollinique de pourcentages. Les cypéracées, les spores de ptéridophytes et de sphaigne sont exclues de la somme pollinique

LA PALYNOFLORE AQUATIQUE

Les sédiments de la carotte 85-036-016P renferment une palynoflore aquatique (fig. 2.3) relativement riche et diversifiée. L'abondance des dinokystes dulcicoles et marins ainsi que celle des algues coloniales du genre *Pediastrum* reflètent une importante productivité primaire au cours de la majeur partie de l'Holocène. Des variations importantes de la concentration de la microflore et de la nature des assemblages sont enregistrées: elles répondent à des changements importants dans les conditions environnementales du milieu aquatique proprement dit. Trois principales zones d'assemblage peuvent être distinguées:

Zone I (2,4 à 3,4 m de profondeur)

La base de la carotte se caractérise par une microflore aquatique mixte, comprenant à la fois des éléments marins (*Operculodinium centrocarpum, Spiniferites* et *Brigantedinium*) et dulcicoles (*Pediastrum, Peridinium* et spores d'*Isoetes*). Leurs concentrations sont relativement faibles, phénomène que l'on peut probablement attribuer à une productivité primaire limitée et à un taux de sédimentation élevé. Le caractère mixte de la palynoflore peut s'expliquer de deux façons, soit par l'existence d'un milieu lacustre dulcicole marqué toutefois par une pénétration épisodique d'eaux marines à la faveur de hautes marées atteignant le seuil du chenal Great Bras d'Or, soit par le remaniement de sédiments fossilifères.

Zone II (1,5 à 2,4 m de profondeur)

Elle se singularise par la richesse de sa palynoflore aquatique et son caractère dulcicole. L'abondance des dinokystes et de *Pediastrum* témoigne d'une productivité algaire très importante. Le grand nombre de spores d'*Isoetes* révèle par ailleurs l'existence très répandue d'une flore aquatique riparienne.

Parmi les dinokystes, le genre *Peridinium* est bien représenté. On compte, au nombre des principales espèces identifiées, *P. limbatum* (Kyste type A; voir Norris et McAndrews, 1970) et *P. wisconsinense* (Kyste type B; voir Norris et McAndrews, 1970). Des travaux minutieux sont nécessaires afin de préciser la nature taxonomique de l'ensemble des assemblages de dinokystes lacustres. Parmi les algues du genre *Pediastrum, P. boryanum* constitue l'élément dominant.

En dépit d'une riche microflore dulcicole, quelques dinokystes marins (*Spiniferites* et *Brigantedinium*) se manifestent à 1,7 m de profondeur: ils témoignent probablement de relations épisodiques avec la mer. Le niveau des hautes marées atteignait sans doute alors le seuil du chenal Great Bras d'Or.

Zone III (0 à 1,5 m de profondeur)

À 1,5 m de profondeur, une transition brutale est observée. Les éléments dulcicoles disparaissent, en effet presque totalement, au profit des dinokystes marins. Entre 0 et 1,5 m de profondeur, la palynoflore évoque donc l'existence d'un milieu marin. Des variations de la représentation des différents taxons sont enregistrées: elles reflètent sans doute des changements au niveau des conditions de salinité et de température dans les masses d'eau superficielles.

À la base de la zone III (1,5 m), *Spiniferites* (essentiellement *S. cf. bentori**) constitue un assemblage presque monospécifique. La présence de *S. bentori*, espèce souvent observée dans les baies fermées (Reid, 1974), témoignerait de

* Il s'agit d'un kyste à processus se rejoignant pour former des trabécules parallèles. L'espèce observée dans les sédiments du lac Bras d'Or diffère de *N. labyrinthea* par un nombre réduit de processus et par sa structure plus rigide.

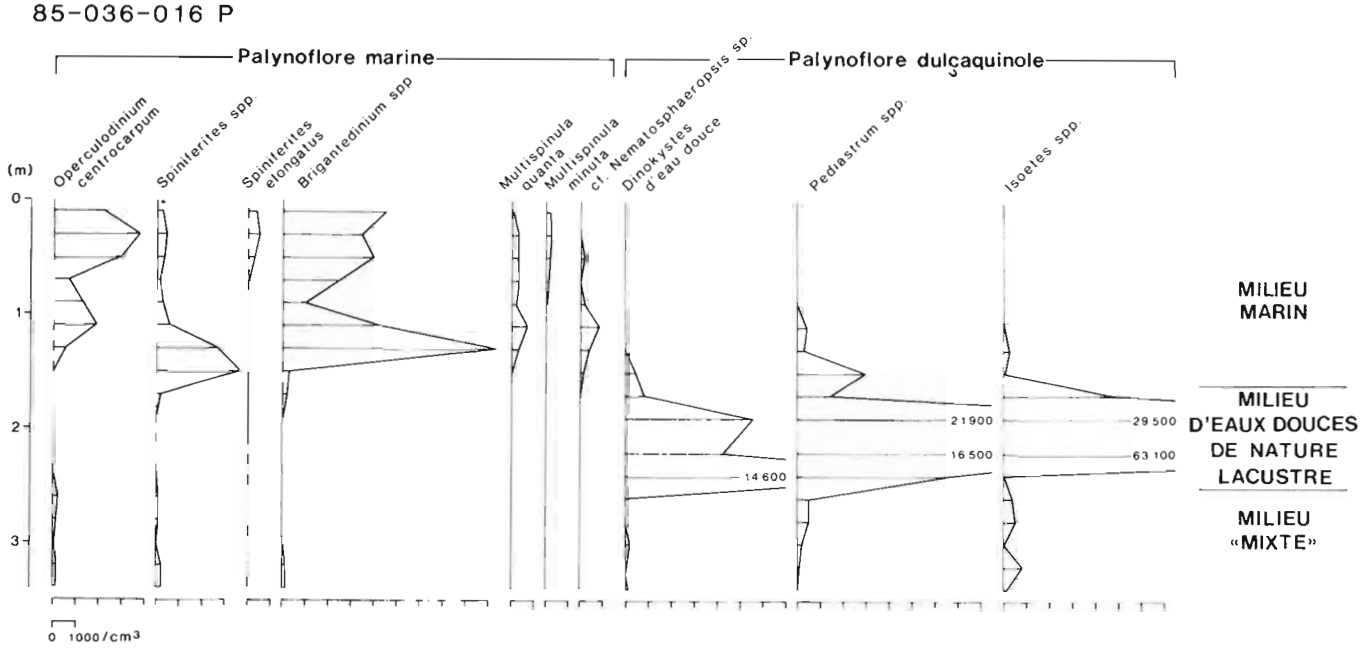


Figure 2.3 Diagramme de concentration de la palynoflore squatique.

l'existence d'un milieu néritique estuarien à caractère tempéré, sinon tempéré chaud (Wall et coll., 1977).

Entre 1,7 à 0,9 m de profondeur, on observe une augmentation de la diversité taxonomique: *Brigantedinium* (notamment *B. simplex*) est abondant; *Multispinula quanta, Operculodinium centrocarpum* et *Spiniferites cf. bentori* sont bien représentés; une espèce non identifiée appartenant probablement au genre *Nematosphaeropsis** est présente. Cet assemblage de dinokystes témoigne de l'existence de conditions néritiques et tempérées (p. ex. Wall et coll. 1977; Harland 1983). Une salinité inférieure à 30 ‰ peut être déduite de l'abondance de *B. simplex* (voir Mudie et Short, 1985).

Le sommet de la carotte (0,70 à 0 m de profondeur) se distingue par l'augmentation d'*Operculodinium centrocarpum*, le déclin de *Spiniferites spp.* et de *cf. Nematosphaeropsis sp.* ainsi que l'apparition de *Spiniferites elongatus* et de *Multispinula minuta*. La présence de ces deux derniers taxons est très intéressante; il s'agit en effet d'espèces associées généralement à des milieux arctiques ou subarctiques (voir Harland et coll., 1980; Mudie et Short, 1985). La concentration (plusieurs centaines d'individus par cm^3) de *M. minuta* et de *S. elongatus* est suffisamment élevée pour indiquer une prolifération locale. La présence de ces taxons, en dehors de leur aire de répartition habituelle, peut s'expliquer par le caractère marginal du bassin où l'effet de saisonnalité (par exemple la formation d'une couche de glace en hiver) est amplifié en raison d'une basse salinité et de la faible épaisseur de la tranche d'eau. Le fait que *M. minuta* et *S. elongatus* se manifestent dans le lac Bras d'Or est probablement lié à leur implantation à la suite d'un transport de formes thécales ou enkystrées par le courant du Labrador. L'implantation et la prolifération de ces Dinoflagellés, à l'Holocène supérieur, s'expliqueraient donc par une influence accrue du courant du Labrador à l'Holocène supérieur (voir Fillon, 1976; Scott et coll., 1984; Schafer et coll., 1985) le long des côtes de la Nouvelle-Écosse et rendrait compte, par ailleurs, d'un certain refroidissement des masses d'eau superficielles régionales.

CONCLUSION

La palynologie de la carotte 85-036-016P révèle que le lac Bras d'Or a connu d'importants changements de ses conditions paléohydrologiques depuis la déglaciation. Trois étapes principales de l'évolution du paléomilieu sont ainsi distinguées:

1) Une phase de sédimentation rapide (survenue il y a entre 9000 et 10 000 ans) qui a très probablement constitué une réponse aux changements paléogéographiques qui se sont produits après la fonte des dernières glaces wisconsiniennes dans le bassin du lac Bras d'Or (Grant, 1977).

2) Un milieu lacustre dulcicole s'est par la suite instauré dans le lac Bras d'Or. Il a certainement favorisé une productivité algaire considérable (dinoflagellés et *Pediatrum*) et le développement d'une végétation aquatique riparienne (*Isoetes*). Le bassin semble avoir conservé un caractère dulcicole tout au long de la période s'étendant d'il y a 4500 à 9000 ans environ.

3) Par la suite, les masses d'eau du las Bras d'Or ont connu des conditions marines estuariennes à caractère tempéré. Les premiers éléments marins apparaissent après le

* Les specimens attribuées à *S. cf. bentori* présentent d'importantes variations morphologiques, concernant notamment la longueur et le développement des processus. Des études plus détaillées permettront d'établir une plus grande précision taxonomique.

déclin de *Tsuga* (il y a environ 4000 à 5000 ans). Connaissant la profondeur du seuil du chenal Great Bras d'Or (environ 8 m), on peut donc calculer, depuis cette transition, un taux moyen de remontée du niveau relatif de la mer de l'ordre de 16 à 20 cm par siècle. L'apparition de dinokystes «arctiques» à l'Holocène supérieur est attribuée à une intensification du courant du Labrador le long de la côte sud de la Nouvelle-Écosse.

REMERCIEMENTS

Les auteurs remercient sincèrement le Centre géoscientifique de l'Atlantique pour son appui logistique et, notamment, M. D. Piper (responsable scientifique de la mission en mer) et M. P.J. Mudie. Le CRSNG (subvention A-9156) et le Fonds FCAR du Québec (Équipe 492) ont contribué aux travaux entrepris dans le cadre du présent rapport par leur soutien financier.

BIBLIOGRAPHIE

Anderson, T.W.
1985: Late-Quaternary pollen records from eastern Ontario, Quebec, and Atlantic Canada, dans: Pollen Records of Late-Quaternary North American Sediments, AASP Foundation, p. 281-326.
1980: Holocene vegetation and climatic history of Prince Edward Island, Canada, Canadian Journal of Earth Sciences, 17, p. 1152-1165.

de Vernal, A., Lortie, G., Larouche, A., Scott, D.B. et Richard, P.J.H.
1985: Évolution d'un milieu littoral et remontée du niveau relatif de la mer à l'Holocène supérieur au nord de l'île du Cap-Breton, Nouvelle-Écosse; Journal canadien des sciences de la Terre, 22, p. 315-323.

Fillon, R.H.
1976: Hamilton Bank, Labrador Shelf: Postglacial sediment dynamics and paleo-oceanography, Marine Geology, 20, p. 7-25.

Grant, R.J.
1977: Glacial styles and ice limits, the Quaternary stratigraphic record and changes of land and ocean level in the Atlantic Provinces, Canada, Géographie physique et Quaternaire, 31, p. 247-260.
1980: Quaternary sea-level changes in Atlantic Canada as an indication of crustal delevelling, in Earth Rheology, Isostasy and Eustasy, N.A. Möner (editor), J. Wiley & Sons, New York, p. 201-214.

Harland, R.
1983: Distribution maps of recent dinoflagellate cysts in bottom sediments from the North Atlantic Ocean and adjacent seas, Palaeontology, 26, p. 321-387.

Harland, R., Reid, P.C., Dobell, P. and Norris, G.
1980: Recent and subrecent dinoflagellate cysts from the Beaufort Sea, Canadian Arctic, Grana, 19, p. 211-225.

Hillaire-Marcel, C.
1987: Composition isotopique du carbone organique des carottes du forage 85-036-016 dans le lac Bras d'Or, île du Cap-Breton, Nouvelle-Écosse; dans Recherches en cours, Partie A, Commission géologique du Canada, Étude 87-1A, nº 89.

Livingstone, D.A.
1968: Some interstadial and postglacial pollen diagrams from eastern Canada, Ecological monographs, 38, p. 87-125.

Miller, A.A.L., Mudie, P.J. and Scott, D.B.
1982: Holocene history of Bedford Basin, Nova Scotia: foraminifera, dinoflagellate and pollen records, Canadian Journal of Earth Sciences, 19, p. 2342-2367.

Mott, R.J.
1975: Palynological studies of lake sediment profiles from southwestern New Brunswick, Canadian Journal of Earth Sciences, 12, p. 273-288.

Mott, R.J., Grant, D.R., Stea, R. et Occhietti, S.
1986: Late glacial climatic oscillation in Atlantic Canada equivalent to the Alleröd/Younger Dryas event, Nature, 323, p. 247-250.

Mucci, A. and Pagé, P.
1987: Bras d'Or Lake cruise No. 85-036: the water chemistry, in Current Research, Part A, Geological Survey of Canada, Paper 87-1A, no. 3.

Mudie, P.J. and Short, S.K.
1985: Marine palynology of Baffin Bay, dans Quaternary environments, eastern Canadian Arctic, Baffin Bay and Western Greenland, J.T. Andrews (editor), Allen & Unwin, London, p. 263-307.

Norris, G. and McAndrews, J.H.
1970: Dinoflagellate cysts from post-glacial lake muds, Minessota (USA), Review of Paleobotany and Palynology, 10, p. 131-156.

Quinlan, G. and Beaumont, C.
1981: A comparison of observed and theoretical postglacial sea level in Atlantic Canada, Canadian Journal of Earth Sciences, 18, p. 1146-1163.

Reid, P.C.
1974: Gonyaulacacean dinoflagellate cysts from the British Isles, Nova Hedwigia, 25, p. 579-637.

Scott, D.B., Mudie, P.J., Vilks, G. and Younger, D.C.
1984: Latest Pleistocene-Holocene paleoceanographic trends on the continental margin of eastern Canada: foraminiferal, dinoflagellate and pollen evidence, Marine Micropaleontology, 9, p. 181-218.

Scott, D.B., Williamson, M.A. and Duffett, T.E.
1981: March foraminifera of Prince Edward Island: their recent distribution and application for former sea-level studies, Maritime Sediments and Atlantic Geology, 17, p. 98-129.

Schafer, C.T., Tan, F.C., Williams, D.F. and Smith J.N.
1985: Late glacial to recent stratigraphy, paleontology and sedimentary processes: Newfoundland continental slope and rise, Canadian Journal of Earth Sciences, 22, p. 266-282.

Wall, D., Dale, B., Lohmann, G.P. and Smith, W.K.
1977: Environmental and climatic distribution of dinoflagellate cysts in modern marine sediments from regions in the North and South Atlantic ocean and adjacent seas, Marine Micropaleontology, 2, p. 121-200.

Weeks, L.J. and Guernsey, T.D.
1954: Geology, Grand Narrows, Nova Scotia, Geological Survey of Canada, Map 1040A.

The water chemistry of cruise 85-036 on Bras d'Or Lake, Cape Breton Island, Nova Scotia

Project 730072

Alfonso Mucci[1] and Pierre Pagé[2]
Atlantic Geoscience Centre, Dartmouth

Mucci, A., and Pagé, P., The water chemistry of cruise 85-036 on Bras d'Or Lake, Cape Breton Island, Nova Scotia; in Current Research, Part A, Geological Survey of Canada, Paper 87-1A, p. 17-24, 1987.

Abstract

Bras d'Or Lake water samples were collected during the CSS Dawson 85-036 cruise in November 1985. Surface water samples were taken at various stations along the cruise track, while subsurface water samples were collected from selected deep basins. The salinity, temperature, total alkalinity, calcium concentration, pH and $^{18}O:^{16}O$ ratio were determined for each sample. The specific alkalinity and $\delta^{18}O$ measurements indicate that the lake waters are composed of a conservative mixture of seawater, typical of the Northwest Atlantic Ocean, and fresh water of mostly meteoric origin (direct precipitation). Groundwater from land drainage, whose composition should reflect the bedrock geology around the lake, is not an important component of the lake water mixture.

Résumé

Des échantillons d'eau du lac Bras d'Or ont été prélevés lors d'une mission (#85-036) à bord du CSS Dawson en novembre 1986. Des eaux de surface ont été échantillonnées en plusieurs points tout au long du parcours, tandis qu'un nombre d'échantillons ont été prélevés dans certains bassins profonds. La salinité, la température, l'alcalinité totale, la concentration en calcium, le pH et le rapport $^{18}O:^{16}O$ ont été déterminés pour chacun des échantillons. L'alcalinité specifique et le $\delta^{18}O$ indiquent que les eaux du lac sont composées d'un mélange raisonnable d'eau de mer typique du nord-ouest de l'ocean Atlantique et d'une eau douce d'origine principalement météorique (précipitation directe sur le bassin). L'eau souterraine provenant du lessivage des sols et dont la composition devrait refléter la géologie de la roche en place ne constitue pas une composante importante des eaux du lac.

[1]Department of Geological Sciences, McGill University, 3450 University Street, Montreal, Quebec, H3A 2A7
[2]Département des Sciences de la Terre, Université du Québec à Montréal, Case postale 8888, succursale A, Montréal, Québec, H3C 3P8

INTRODUCTION

Semi-enclosed bodies of seawater function as estuaries in which the flushing time is determined by the physical ability of outlets to drain the fresh water fraction. Bras d'Or Lake, on Cape Breton Island, is such a body of water and is partially isolated from the open ocean by long and narrow channels. The lake waters were sampled during the *CSS Dawson* 85-036 cruise, in November 1985, in order to assess, using chemical and isotopic tracers, the identity of the water mixture. Objectives were to determine the hydrological components of the lake waters with the help of conservative properties (alkalinity, isotope ratio) and examine the vertical structure of the water column over topographic troughs or basins in the deepest parts of the lake.

SAMPLING

Surface water was taken with a plastic bucket attached to a nylon rope over the side of the ship at various stations along the cruise track (Fig. 3.1). At selected stations, subsurface water samples were collected with 100/L Go-Flo bottles. Upon recovery, the temperature of the water was measured using a mercury thermometer. A 60 mL polypropylene bottle was promptly filled with the water and capped, leaving no headspace gas. This subsample was used to measure the pH of the water. Another 60 mL of water was filtered through a 0.45 μm Millipore filter and stored for later analysis of the calcium concentration and titration alkalinity.

Finally, for each station and depth, a 1 L plastic bottle was filled with water for ^{18}O:^{16}O and ^{2}H:^{1}H analyses, together with a 125 mL plastic bottle to which were added a few drops of $HgCl_2$, for later ^{13}C:^{12}C determinations.

ANALYSIS

The pH of the water samples was measured onboard at 25°C following thermal equilibration in a constant temperature bath. An Orion Research Ross combination electrode fitted with a piece of Tygon and Parafilm was inserted in the neck of the bottle, forming an airtight seal. This procedure was adopted to minimize CO_2 exchange with the atmosphere. The electrode was calibrated using NBS buffer solutions, before and after every 5 measurements. The precision of the pH measurements, once corrected for temperature (Harvey, 1963), was estimated to be better than ± 0.01 pH units.

The salinity of the water samples was determined from conductivity measurements using a Guildline 8400A salinometer. Calibration of the salinometer was done with IAPSO standard seawater. Total alkalinities, A_t, were determined by potentiometric titration with a dilute HCl solution to the second equivalence point corresponding to the neutralization of bicarbonate ions using the method described by Mucci (in press). Reproducibility of these measurements was better than 0.4% using a Na_2CO_3 solution for standardization of the acid.

Calcium concentrations were determined potentiometrically with EGTA using the method described by Lebel and Poisson (1976). The titrant solution was standardized with IAPSO standard seawater. The precision of these measurements was better than 0.5%.

Isotope measurements (^{18}O:^{16}O) were performed at the GEOTOP laboratory using the standard equilibration method, on a triple collector VG Micromass spectrometer. Results are given in δ notation with respect to SMOW, with a precision of ± 0.2‰.

RESULTS

Results of the analyses described above are presented in Table 3.1, along with the position and depth at which each sample was collected.

The specific alkalinity, A_t/Cl‰, and $[Ca^{2+}]$/Cl‰ ratio were calculated for each sample in order to verify if the various bodies of water sampled were subjected to compositional variations other than conservation mixing between continental freshwater and seawater. Chlorinity was calculated from the salinity according to the following relationship (UNESCO, 1966):

$$Cl‰ = S‰ / 1.80655 \quad (1)$$

Results of these calculations are presented in Table 3.2.

The $[Ca^{2+}][CO_3^{2-}]$ ion concentration product of the water samples was calculated to determine their saturation

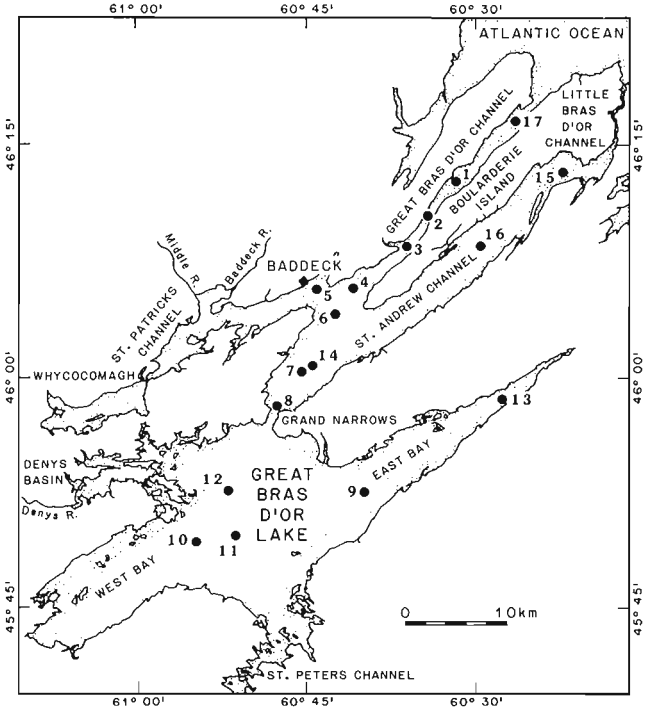


Figure 3.1. Location of water stations in Bras d'Or Lake.

Table 3.1 Measured physical and chemical parameters of water samples collected from Bras d'Or Lake in November 1985

Station	Position Lat°N	Position Long°W	Depth (m)	Temp. (°C)	S (‰)	pH 25°C	$[Ca^{2+}]$ (m mole kg^{-1})	A_t (meq kg^{-1})	$\delta^{18}O_{smow}$ (‰)
1.1	461219	603238	0	9	26.596	7.956	7.18	1.736	−2.53
2.1	461039	603436	0	9.5	26.537	7.949	7.13	1.746	−3.16
3.1	460843	603610	0	9.5	26.537	7.951	7.15	1.730	−2.68
4.1	460673	603871	0	9	26.518	7.959	7.10	1.736	−3.37
5.1	460580	604400	0	9	26.544	7.963	7.12	1.751	−3.00
6.1	460400	604242	0	9	26.254	7.955	7.00	1.709	−3.14
7.1	460082	604525	0	9	25.797	7.938	6.70	1.680	−2.78
8.1	455752	604790	0	9	25.226	7.918	6.82	1.653	−2.83
9.1	455218	604004	0	9	24.870	7.944	6.62	1.639	−2.99
10.1	454885	605520	0	9	25.174	7.908	6.68	1.643	−3.43
11.1	454919	605111	145	5	25.782	7.664	6.84	1.652	−3.39
11.2	454919	605111	90	6	25.782	7.725	6.82	1.662	−3.26
11.3	454919	605111	20	9	25.174	7.894	6.70	1.637	−2.85
11.4	454919	605111	0	9	25.174	7.907	6.64	1.636	−3.45
12.1	455203	605211	0	9	25.266	7.898	6.67	1.640	−3.38
13.1			0	9	24.563	7.852	6.46	1.617	−3.06
14.1	460120	604463	200	2	28.170	7.731	7.68	1.831	−2.77
14.2	460120	604463	100	4	27.875	7.764	7.55	1.823	−2.96
14.3	460120	604463	50	8.5	27.875	7.923	7.39	1.800	−2.31
14.4	460120	604463	0	9	25.782	7.913	6.86	1.686	−3.38
15.1	461334	602212	0	9	26.685	7.933	7.17	1.745	−3.12
16.1	460863	603008	255	0.8	27.875	7.663	7.57	1.809	−2.92
16.2	460863	603008	150	1.0	27.580	7.669	7.48	1.806	−2.97
16.3	460863	603008	75	3.5	27.579	7.720	7.51	1.813	−2.30
16.4	460863	603008	25	9	26.685	7.912	7.19	1.763	−3.03
16.5	460863	603008	0	9	26.685	7.941	7.10	1.746	−3.25
17.1	461663	602640	0	9	28.758	—	7.92	1.885	−2.84

state with respect to calcite. Carbonate ion concentrations were calculated from the in situ pH and carbonate alkalinity of the sample, A_c, according to the following equation:

$$[CO_3^{2-}] = \frac{Ac}{2 + (10^{-pH}/K'_2)} \quad (2)$$

where K'_2 is the second apparent dissociation constant of carbonic acid in seawater. Values determined by Mehrbach et al. (1973) as refitted by Millero (1979) were used in this study. The carbonate alkalinity was calculated from the total alkalinity according to:

$$A_c = A_t - [B(OH)_4^-] \quad (3)$$

where $[B(OH)_4^-]$ is the product of the first dissociation of boric acid. The boric acid contribution to the total alkalinity was estimated from the total boric acid content of the sample ($\Sigma B = 1.17 \times 10^{-5} \times S‰$) and the following relationship.

$$[B(OH)_4^-] = \frac{K'_B \times \Sigma B}{(K'_B \times 10^{-pH})} \quad (4)$$

where K'_B is the first apparent dissociation constant of boric acid. The apparent dissociation constants determined by Lyman (1957) were used for this calculation.

The saturation state or omega of the water samples with respect to calcite was calculated from the $[Ca^{2+}]$ $[CO_3^{2-}]$ ion concentration product of the sample and the stoichiometric solubility of calcite, K^*_c, at the appropriate temperature and salinity (Mucci, 1983) according to the following equation:

$$\Omega = \frac{[Ca^{2+}]\,[CO_3^{2-}]}{K^*_c} \quad (5)$$

Results of these calculations are presented in Table 3.2.

The CO_2 partial pressure, P_{CO_2}, in equilibrium with the water was also calculated from the in situ pH and carbonate alkalinity using the first and second apparent dissociation constants of carbonic acid determined by Merhbach et al. (1973) as refitted by Millero (1979) and the solubility constants of CO_2 in seawater determined from the equation of Weiss (1974) which is based on the measurements of Murray and Riley (1971). Calculated P_{CO_2}'s are presented in Table 3.2 and Figures 3.2C, 3.3C and 3.4C.

Isotope ratios given in Table 3.1 were corrected in Figure 3.5 for nonlinerarity with respect to salinity, owing to the definition itself of this parameter. In fact, there is (1 – S) kg of pure water (solvent) in 1 kg of seawater (solution); the solvent being characterized by a given isoptope concentration. Thus, the notation $\triangle$ is used in Figure 3.5, and defined following the theoretical considerations of Paren and Potter (1984) as:

$$\triangle = (1 - S)\,\delta^{18}O \quad (6)$$

In Figure 3.5, linearity between $\triangle$ and S is indicative of the conservative mixing behaviour of two end-member components.

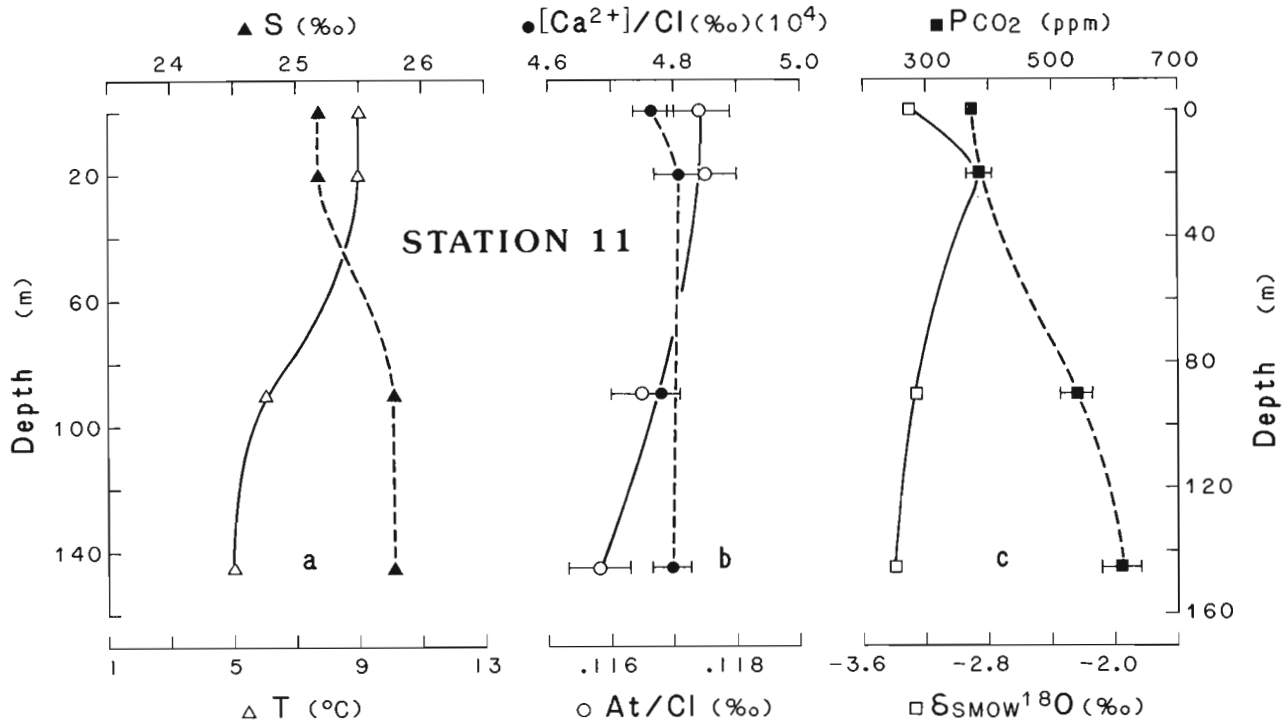


Figure 3.2. Depth profiles at station 11

Table 3.2 Results of chlorinity calculated from the salinity, the saturation state of the water samples with respect to calcite, and calculated P_{CO_2}.

Station	Cl (‰)	$[Ca^{2+}]$Cl‰ (10^4) ±0.25	At/Cl‰ ± .0005	$pH^{in\text{-}situ}$ ±0.01	A_c (meq kg^{-1})	$[Ca^{2+}]$ $[CO_3^{2-}]$ (mole^2 $kg^{-2} \times 10^7$)	Ω_C	PCO^2 (ppm) ±3%
1.1	14.722	4.877	.1179	8.134	1.691	7.18	1.81	338
2.1	14.689	4.854	.1189	8.121	1.702	7.13	1.79	353
3.1	14.689	4.867	.1178	8.123	1.686	7.15	1.79	348
4.1	14.679	4.840	.1183	8.137	1.691	7.10	1.81	335
5.1	14.693	4.846	.1192	8.141	1.706	7.12	1.84	335
6.1	14.533	4.820	.1176	8.133	1.665	7.00	1.74	335
7.1	14.280	4.692	.1176	8.116	1.639	6.70	1.59	345
8.1	13.964	4.884	.1184	8.096	1.615	6.82	1.55	360
9.1	13.767	4.809	.1191	8.122	1.600	6.62	1.58	336
10.1	13.935	4.794	.1179	8.097	1.606	6.68	1.46	374
11.1	14.271	4.793	.1158	7.864	1.629	6.84	0.82	611
11.2	14.271	4.779	.1165	7.923	1.635	6.82	0.97	538
11.3	13.935	4.808	.1175	8.067	1.601	6.70	1.42	384
11.4	13.935	4.765	.1174	8.080	1.599	6.64	1.44	371
12.1	13.986	4.769	.1173	8.071	1.603	6.67	1.42	380
13.1	13.597	4.751	.1190	8.025	1.585	6.46	1.25	424
14.1	15.593	4.925	.1174	7.966	1.800	3.67	1.10	501
14.2	15.430	4.893	.1181	7.982	1.791	3.98	1.20	490
14.3	15.430	4.789	.1166	8.105	1.755	5.81	1.76	370
14.4	14.271	4.807	.1181	8.089	1.647	4.69	1.55	371
15.1	14.771	4.854	.1181	8.109	1.702	5.42	1.72	362
16.1	15.430	4.906	.1172	7.913	1.783	3.02	0.91	559
16.2	15.267	4.900	.1183	7.914	1.780	2.99	0.91	559
16.3	15.266	4.919	.1188	7.939	1.784	3.50	1.07	541
16.4	14.771	4.868	.1194	8.088	1.722	5.27	1.67	386
16.5	14.771	4.868	.1194	8.088	1.702	5.46	1.73	354
17.1	15.919	4.975	.1184	—	—	—	—	—

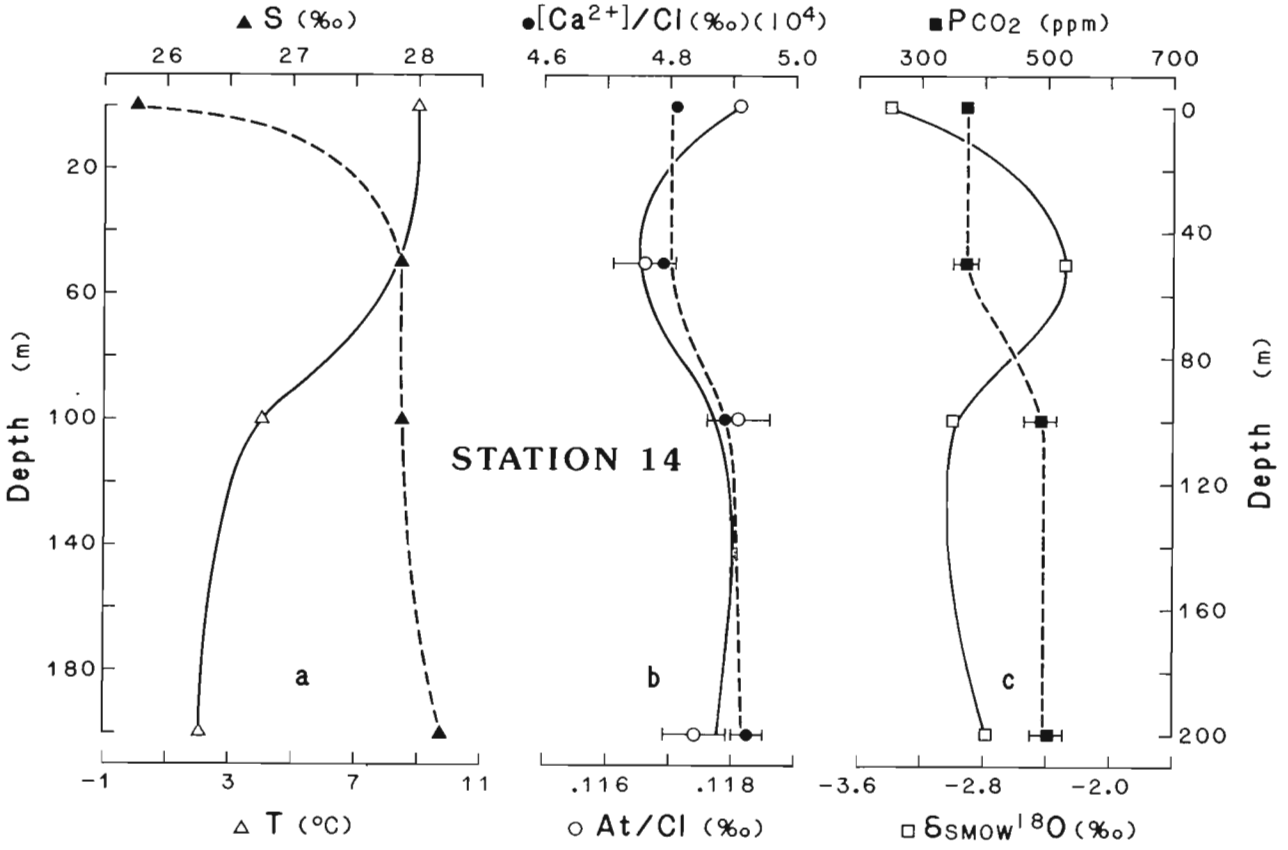


Figure 3.3. Depth profiles at station 14

DISCUSSION

Salinity distribution and stratification

As expected from the configuration of the lake (Fig. 3.1), the salinity of surface waters decreases regularly from 28.76 ‰ at the entrance of Great Bras d'Or Channel to 24.56 ‰ at the end of East Bay in the Great Bras d'Or Lake. An opening to the Atlantic Ocean through Little Bras d'Or Channel is responsible for the slight increase in the surficial salinity of water collected in St-Andrew's Channel. Mass balance calculations indicate that fresh water accounts for 20 to 30% of the surface water mixture.

The only important continental inflows to the lake are located in sub basins on the north-western side of Great Bras d'Or Lake. They are the Middle and Baddeck rivers which flow into the St-Patricks Channel and the Denys River which runs into the Denys Basin. Many short brooks also drain the highlands around the lake and one might expect a relatively small land drainage component to the lake waters.

Figures 3.2a, 3.3a and 3.4a indicate that stratification of the water column is characterized by a halocline situated between 40 and 60 m depth. The lifetime of this halocline is unknown as data from other seasons are unavailable. However, as the lake is known to freeze in winter, the stratification is probably destroyed during this season and re-established during the summer. Similarly, Vilks (1967) noted that deep basins, such as the ones we sampled (Stations 11, 14, and 16), contain cold water all summer but that water in shallower localities may undergo extensive changes in temperature during the seasons.

Alkalinity-chlorinity relationship

Figure 3.6 shows the results of the alkalinity titrations as a function of chlorinity for each collected sample. All the data are grouped around a straight line with a slope of 0.1175 (meq/kg)/Cl‰. This is indicative of the conservative mixing behaviour of the total alkalinity in this lake. The lake waters would have obtained their present composition from the mixing of a fresh water source of negligible alkalinity (about 6 μeq/kg) and seawater typical of the Northwest Atlantic at this latitude. The GEOSECS station situated closest to the latitude of the lake is Station 26 (44° 57.6'N/42° 0.4.6'W). Surface waters (4 m) collected at Station 26 during the GEOSECS expedition had a salinity of 35.754‰ (or Cl‰ = 19.791) and a total alkalinity of 2.331 meq/kg (Bainbridge, 1981). This datum point is presented in Figure 3.6 and clearly demonstrates the conservative mixing of the two water masses to form the lake waters. In fact, nearly all the water

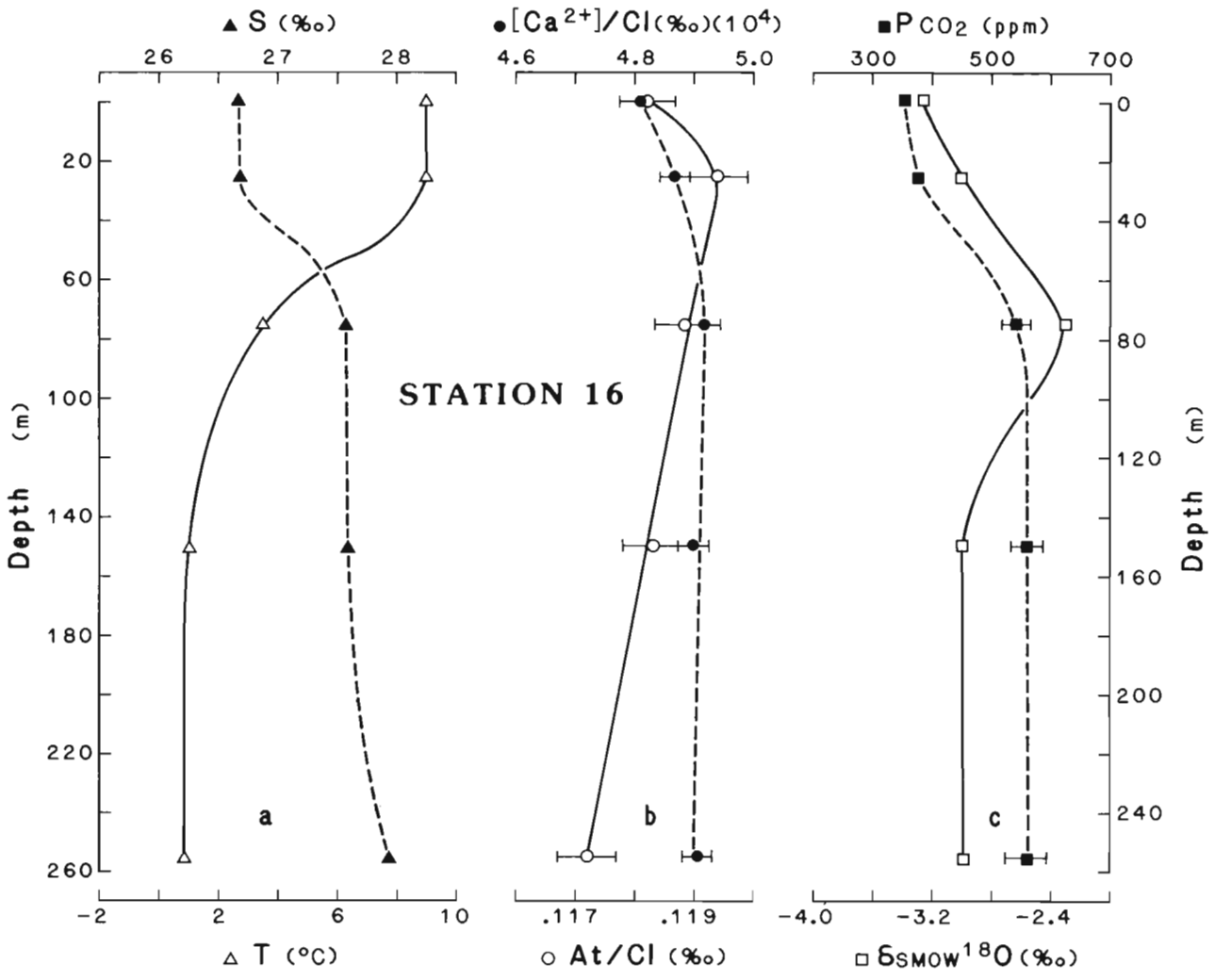


Figure 3.4. Depth profiles at station 16

samples collected in the lake possess a specific alkalinity (see Table 3.2) equal to the Northwest Atlantic Ocean water value (0.1178 ± .0005).

However, the $[Ca^{2+}]/Cl‰$ ratios of all the lake water samples (Table 3.2) are significantly lower than the value for standard seawater (5.31×10^{-5} (mole/kg)(Cl‰). The value of 4.98×10^{-5} determined for surface waters collected at Station 17, which is situated closest to the open sea channel, was the highest one measured in the lake. Lowered $[Ca^{2+}]/Cl‰$ ratios are most often associated with productivity of calcium sequestring organisms in surface waters. The $[Ca^{2+}]/Cl‰$ ratios are smaller in surface waters than at depth (Fig. 3.2b, 3.3b, 3.4b) which would support the hypothesis that biological activity is responsible for the low $[Ca^{2+}]/Cl‰$ ratios in the lake water. Even bottom waters however, at Stations 11, 14 and 16 have lower $[Ca^{2+}]/Cl‰$ ratios than standard seawater or surface waters at Station 17. Furthermore, no significant deviations of the specific alkalinity are associated with the surface $[Ca^{2+}]/Cl‰$ minima. This appears to rule out the possibility of important biogenic calcium carbonate production as calcium carbonate frustules would be expected to dissolve and increase the $[Ca^{2+}]/Cl‰$ in the deep basin waters of the lake since these are often undersaturated with respect to calcite (Table 3.2).

CO_2 partial pressure-depth relationship

The CO_2 partial pressures calculated from in situ pH and carbonate alkalinity indicate that surface waters are close to equilibrium with the atmosphere. Surface water values vary between 335 and 424 ppm with an average of 358 ± 23 ppm.

The deep waters of the lake (Fig. 3.2c, 3.3c and 3.4c) are characterized by high P_{CO_2} values (about 600 ppm). This accumulation of CO_2 is most probably due to the oxidation of organic matter at depth and the limited exchange of these waters with the surface as a consequence of the stratification

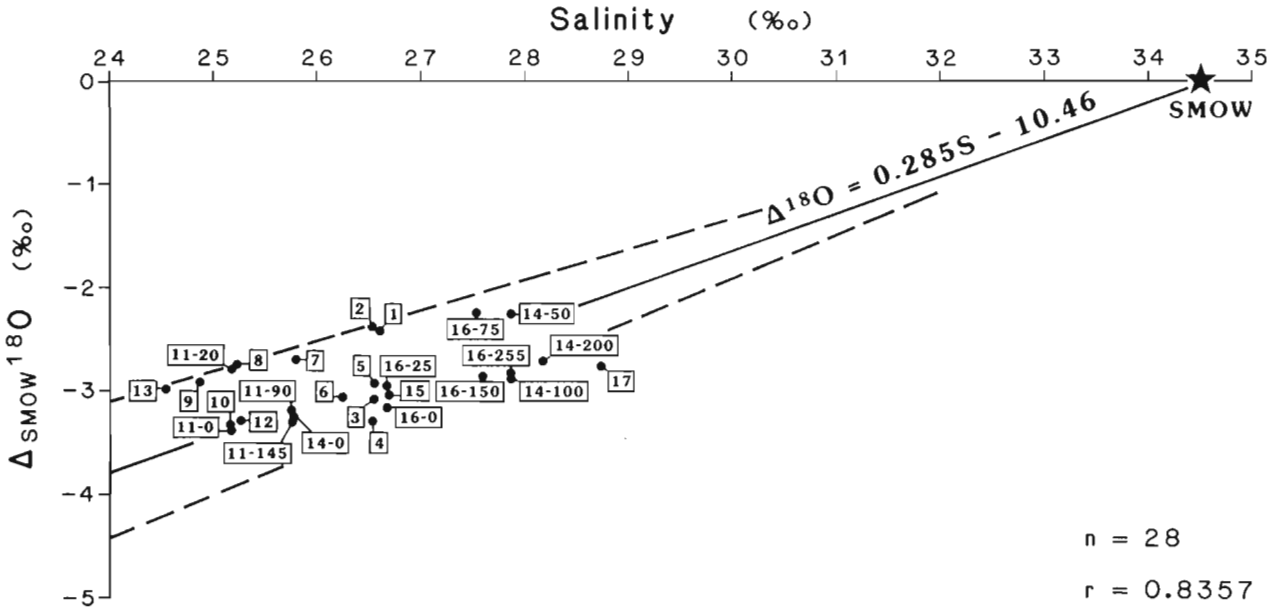


Figure 3.5. ^{18}O:^{16}O isotope ratios as a function of salinities.

over the summer and fall seasons. The increased CO_2 content of the deeper waters is responsible for the decrease in pH with depth as the carbonate alkalinity does not change significantly. This results in the deeper waters being undersaturated with respect to calcite ($\Omega < 1$).

Oxygen isotope-salinity relationship

Surficial water isotopic ratios do not show a trend similiar to salinity. Low values are found irregularly along the sampling track, either in the Great Bras d'Or Channel or Great Bras d'Or Lake, suggesting complex mixing between seawater and fresh water of variable isotopic composition. The relationship between mean annual $\delta^{18}O$ in precipitation and latitude (Yurtsever and Gat, 1981) indicates that precipitation over Cape Breton Island should reach a value of $-10‰$. Taken altogether, the data fit a regression line with an intercept of -10.46 (Fig. 3.5). All the data are bracketed between mixing lines which intercept the $\Delta^{18}O$ axis at $-10‰$ and $-14‰$ when linearly extrapolated to zero salinity.

Since seawater flowing through the northern channels originates from the Labrador Current, it must be diluted by meteoric waters collected around the Gulf of St-Lawrence or the Labrador coast where the precipitation exhibits lower $\delta^{18}O$ values than on Cape Breton Island. Supporting this view, waters collected at Stations 15, 16, and 17 which are closest to the oceanic inlets give $\delta^{18}O$ values near the lower mixing line. In addition, most of the deep water samples, and in particular those collected in St-Andrew's Channel below 90 m (Stations 14 and 16), are close to that lower line (they fit the following regression line: $\Delta^{18}O‰ = 0.398\ S - 13.91$). The salinity of these waters (>27.58‰) is also close to the salinity of waters entering the channel and indicates that they have not been influenced significantly by dilution from local precipitation. On the other hand, surficial and shallow waters fall in between, or even near the upper mixing line in Figure 3.5, indicating that local precipitation intervenes in the mixing. This pattern is clearly visible in the depth profiles (Fig. 3.2, 3.3 and 3.4). Salinity increases slightly below the halocline, while $\delta^{18}O$ values decrease slowly due to a fresh water contribution depleted in heavy isotope.

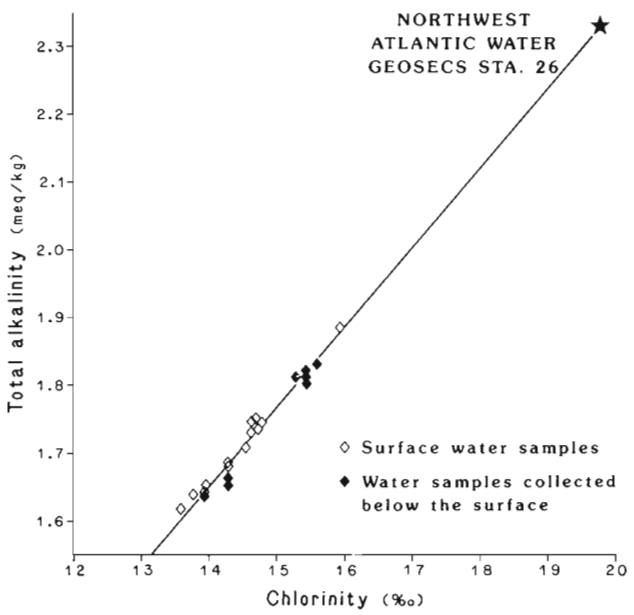


Figure 3.6. Conservative mixing in surficial and deep waters.

The seasonal precipitation could also explain the span of $\triangle^{18}O$ values. Winter snow and rain have lower isotopic ratios than summer rain since fractionation is thermodependent. Sinking and storage of cold isotopically lighter waters at depth would also result in depth profiles similar to those observed. The importance of this factor is determined by the flushing time of the fresh water fraction and is reflected by a more or less homogenized meteoric signal approximating the annual $\delta^{18}O$ value.

CONCLUSIONS

Bras d'Or Lake is a dominantly marine body of water possessing a slight longitudinal and vertical salinity gradient. The lake waters are composed of a nearly conservative mixture of seawater typical of the northwest Atlantic Ocean and fresh water. The fresh water end member is characterized by a very low alkalinity and a normal $\delta^{18}O$ value partly influenced by an allochthonous meteoric signal originating from the dilution of oceanic waters at higher latitudes.

It appears that fresh water from the deep underground drainage, which should have been mineralized following contact with the lithologies of this geological subprovince (for instance, dolomite, gypsum and limestone of the Carboniferous Windsor Group outcrop in the Middle and Baddeck river watersheds: Kelley, 1967), is not an important component of the lake water mixture. The presence of proximal runoff waters or even direct precipitation on the lake surface is supported by the fact that the $[Ca^{2+}]/Cl‰$ ratio of the lake water is always lower than the standard seawater value or even the maximum value measured in the lake at Station 17. The influence of the surrounding geology on the lake water composition is only slightly noticeable from the higher specific alkalinity of surficial waters at Stations 2, 5, 13 and 16 which are situated near outcrops of the Windsor Group.

The water column in the lake is stratified below approximately 60m, particularly in deep basins. The stratification is most likely destroyed during winter since the lake is known to freeze. The temporary stratification is responsible for limiting the exchange of gases in the deeper waters with the atmosphere. This results in an accumulation of CO_2 in the deeper portions of the lake following the degradation of organic matter at or near the sediment-water interface. As a consequence of the increased CO_2 concentration, bottom waters (>80m depth) are undersaturated with respect to calcite.

REFERENCES

Bainbridge A. E.
1981: GEOSECS: Atlantic Expedition, v. 1, Hydrographic Data; U.S. Government Printing Office, Washington D.C., 121 p.

Harvey H.W.
1963: The Chemistry and Fertility of Sea Waters; Cambridge University Press, London, 240 p.

Kelley D.G.
1967: Baddeck and Whycocomagh map areas; Geological Survey of Canada, Memoir 351, 65 p.

Lebel J. and Poisson A.
1976: Potentiometric determination of calcium and magnesium in seawater; Marine Chemistry, v. 4, p. 321-332.

Lyman J.
1957: Buffer mechanism of seawater; unpublished Ph. D. dissertation, University of California, Los Angeles, 196 p.

Mehrbach C., Culberson C. H., Hawley J. E., and Pytkowicz R. M.
1973: Measurements of the apparent dissociation constants of carbonic acid in seawater at atmospheric pressure; Limnology and Oceanography, v. 18, 897-907.

Millero F. J.
1979: The thermodynamics of the carbonate system in seawater; Geochimica et Cosmochimica, Acta, v. 43, p. 1651-1661.

Mucci A.
1983: The solubility of calcite and aragonite in seawater at various salinities, temperatures, and one atmosphere total pressure; American Journal of Science, v. 283, p. 780-799.
—: Growth kinetics and composition of magnesian calcite overgrowths precipitated from seawater: Quantitative influence of orthophosphate ions; Geochimica et Cosmochemica Acta, v. 50 (in press).

Murray C.N. and Riley J.P.
1971: The solubility of gases in distilled water and seawater. IV. Carbon dioxide; Deep-Sea Research, v. 18, p. 533-541.

Paren J.G. and Potter, J.R.
1984: Isotopic tracers in polar seas and glacier ice; Journal Geophysical Research, v. 89, p. 749-750.

UNESCO
1966: Second report of the joint panel on Oceanographic Tables and Standards; UNESCO Technical, Paper on Marine Science, no. 4, 9 p.

Vilks G.
1967: Quantitative analysis of foraminifera in Bras d'Or lakes; Bedford Institute of Oceanography, Report, 67-1, 84 p.

Weiss R.F.
1974: Carbon dioxide in water and seawater: the solubility of a non-ideal gas; Marine Chemistry v. 2, p. 203-215.

Yurtsever, Y. and Gat, J.R.
1981: Atmospheric waters, In Gat, J.R. and Gonfiantini, R. (eds.), Stable Isotopic Hydrology – Deuterium and Oxygen = 18 in the Water Cycle, J.R. Crat and R. Goufiantini (ed); International Atomic Energy Agency, Technical Report no. 210, Vienna, p. 103-142.

- 4 -

Precambrian geology of parts of Chesterfield Inlet map area, District of Keewatin

Project 850002

Subhas Tella and I.R. Annesley[1]
Lithosphere and Canadian Shield Division

Tella, S. and Annesley, I.R., Precambrian geology of parts of Chesterfield Inlet map area, District of Keewatin; in Current Research, Part A, Geological Survey of Canada, Paper 87-1A, p. 25-36, 1987.

Abstract

The central part of the map area is underlain by ?Archean lithologies dominated by polydeformed orthogneiss, migmatite and weakly deformed granitoid plutons, and to a lesser extent by pelitic gneiss, amphibolite and banded quartz-magnetite iron-formation. To the south, a 15-km-wide west-northwest-trending and south-dipping paragneiss belt, consisting of garnet-biotite + staurolite + kyanite ± sillimanite + muscovite assemblages, overlies the central gneiss region. Two-pyroxene granulites occur to the northeast, north of the settlement of Chesterfield Inlet. An apparent increase in metamorphic grade from amphibolite to granulite facies occurs from south to north, and a tilted structural cross-section with progressively deeper-crustal levels towards the north, is exposed in the Chesterfield Inlet region. The age of metamorphism and deformation is considered to be Archean.

An approximately 5-km-wide, ENE-trending ductile shear zone occurs within the gneiss terrane north of Chesterfield Inlet. Asymmetrical pull-apart structures, and ENE-trending pervasive mineral-stretching lineations within the shear zone suggest shallow oblique, dextral displacement of unknown magnitude.

Résumé

La partie centrale de la région levée repose sur des formations rocheuses ?archéennes composées principalement d'orthogneiss à déformations multiples, de migmatite et de plutons granitoïdes peu déformés, avec de petites quantités de gneiss pélitique, d'amphibolite et de formation ferrifère rubanée à quartz et à magnétite. Vers le sud, une zone de paragneiss à orientation ouest-nord-ouest et à pendage sud, ayant une largeur de 15 km et composée d'assemblages de grenat-biotite + staurolite + cyanite ± sillimanite + muscovite, repose sur la partie centrale de la zone de gneiss. Des granulites à deux pyroxènes se trouvent au nord-est, au nord de Chesterfield Inlet. Le degré de métamorphisme semble augmenter du sud vers le nord, passant du faciès des amphibolites à celui des granulites. Une coupe transversalle structurale inclinée affleure dans la région de Chesterfield Inlet; on y voit des niveaux structuraux progressivement plus profonds à mesure que l'on s'avance vers le nord. Le métamorphisme et la déformation dateraient de l'Archéen.

Une zone de cisaillement ductile à orientation est-nord-est, d'une largeur de près de 5 km, se trouve à l'intérieur du terrane gneissique, au nord de Chesterfield Inlet. La présence, dans la zone cisaillée, de structures asymétriques formées par étirement et déchirement et de linéations minérales omniprésentes à orientation est-nord-est porte à croire qu'un déplacement dextre oblique peu profond, d'ampleur inconnue, a eu lieu dans cette zone.

[1]Department of Geology, University of Ottawa, Ottawa, Ontario, K1N 6N5

INTRODUCTION

Bedrock mapping in the southern two-thirds of Chesterfield Inlet map area (550Ø), at a scale of 1:250 000, was completed during the 1986 field season; the remainder is scheduled for completion in 1987. This paper summarizes preliminary results. The map area is part of a region previously mapped by Lord (1953) and Wright (1955, 1967), at a scale of one inch to eight miles. The earliest geological explanation was by Bell (1885, 1887). Results of most-recent bedrock mapping in adjoining parts to the south, the Rankin Inlet-Marble Island region (parts of 55K and 55J), were previously reported by Tella et al. (1986).

Acknowledgments

We thank our field assistants T.W. Needham, S.G. Digel, and D.C. Robinson for their excellent support during the summer. Thanks are due to Polar Continental Shelf Project for generous rotary-wing support during a part of the field season, and to Jim Aspinall and Orest Anhel of Quasar Helicopters on contract to the Polar Continental Shelf Project for their excellent support. Brian Zawadski of L&C Enterprises Ltd., and Bob Bissett of Nippisar Enterprises provided expediting services at Chesterfield Inlet and Rankin Inlet respectively. J.H. Maley of Lithosphere and Canadian Shield Division, Geological Survey of Canada, helped with the computer pro-

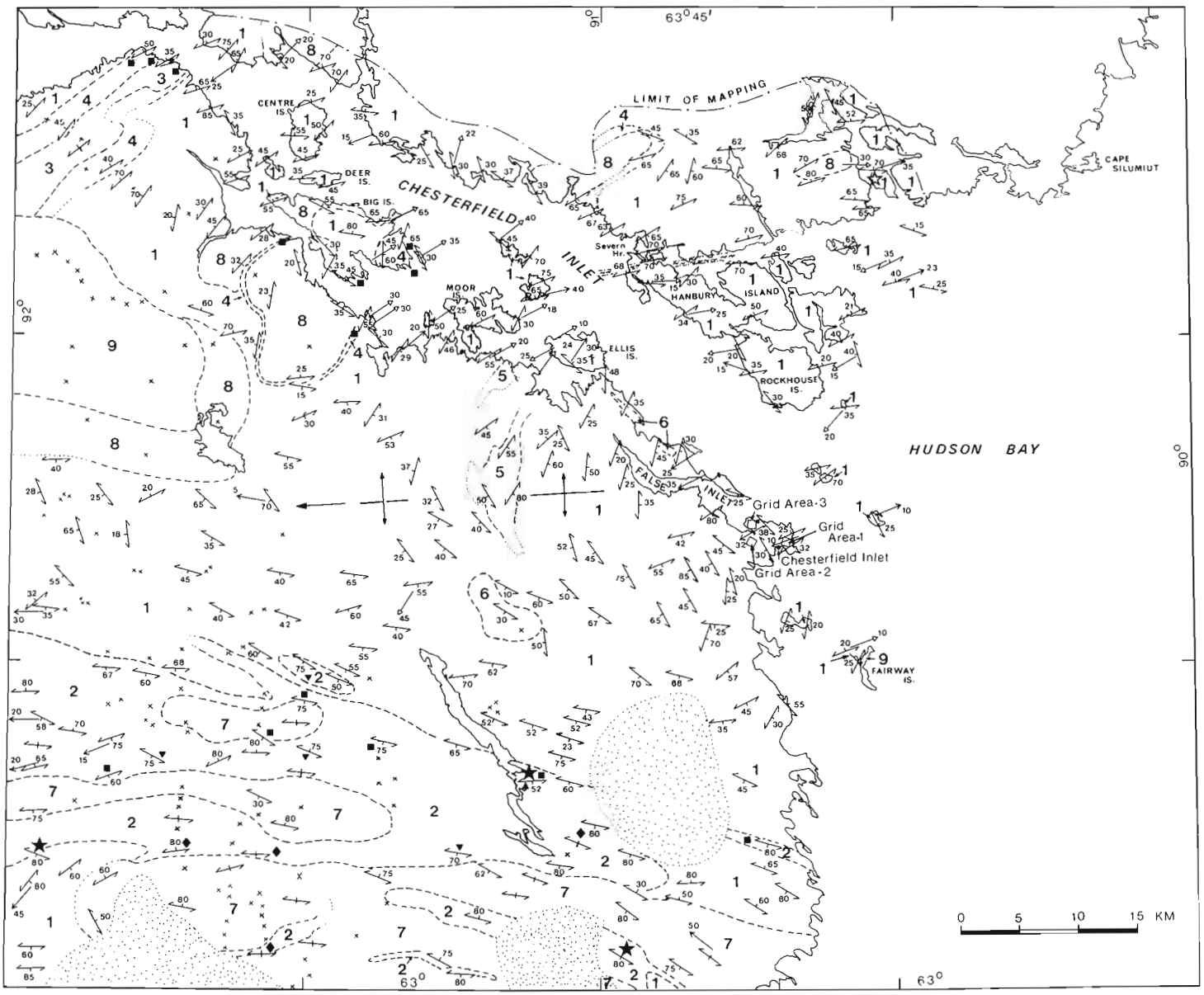


Figure 4.1. Geological sketch map of parts of Chesterfield Inlet map area, District of Keewatin.

cessing of field data. K.E. Eade and D.C. Kamineni reviewed the manuscript.

LITHOLOGY

General statement

The distribution of rock units in the Chesterfield Inlet map-area is shown in Figure 4.1. The area is predominantly underlain by polydeformed ?Archean layered orthogneiss, migmatite, amphibolite and pelitic gneiss (units 1 to 4) and to a lesser extent by weakly deformed gabbro and granitoid plutons (units 5 to 8). Undeformed Helikian fluorite-granite (unit 9) and biotite lamprophyre dykes (unit 10, not shown in Fig. 4.1) are sporadically distributed in the central region.

LEGEND

HELIKIAN

10 BIOTITE LAMPROPHYRE DYKES (NOT SHOWN IN FIGURE-1)

9 GRANITE: MASSIVE TO WEAKLY CLEAVED, PINK, EQUIGRANULAR TO PORPHYRITIC; IN PART FLUORITE-BEARING, AND CONTAINS CHALCOPYRITE AND SPECULARITE ON FAIRWAY ISLAND

ARCHEAN AND/OR LOWER PROTEROZOIC

8 QUARTZ DIORITE TO GRANITE PLUTONS; MASSIVE TO WEAKLY FOLIATED CENTRES AND WELL FOLIATED MIGMATITIC MARGINS

7 BIOTITE-MUSCOVITE LEUCOGRANITE, IN PART CONTAINS XENOCRYSTIC GARNETS; INTRUDES LAYERED GNEISS AND PARAGNEISS (UNITS 1 AND 2)

6 GABBRO: MASSIVE TO WEAKLY FOLIATED, COARSE GRAINED; LOCALLY CUT BY PINK PEGMATITE DYKES

5 MEGACRYSTIC (K-FELDSPAR) GRANITE: COARSE GRIANED, WELL FOLIATED

4 GARNET-BIOTITE PARAGNEISS; IN PART CONTAINS MIGMATITIC GNEISS, CUT BY YOUNGER GRANITIC INTRUSIONS

3 AMPHIBOLITE; MINOR METAVOLCANIC ROCKS AND GARNET-BIOTITE SCHIST

2 GARNET + BIOTITE + KYANITE + SILLIMANITE + STAUROLITE + MUSCOVITE PARAGNEISS; METAMORPHOSED QUARTZ-MAGNETITE BANDED IRON-FORMATION, AMPHIBOLITE; CONTAINS SMALL METAGABBRO INTRUSIONS

1 LAYERED TO BANDED HORNBLENDE-BIOTITE (GREY) ORTHOGNEISS, MIGMATITE, QUARTZO-BIOTITE SCHIST; INCLUDES MINOR PROPORTIONS OF METAMORPHOSED IRON-FORMATION, GARNET + BIOTITE + SILLIMANITE PARAGNEISS, AND TWO-PYROXENE GRANULITE (MOSTLY NORTHEAST OF HANBURY ISLAND), IN PART CONTAINS XENOLITHS OF METAMAFIC ROCKS (GARNET AMPHIBOLITE, PYROXENITE), AND RAFTS OF MAGNETITE-RICH CORONITE GABBRO; CUT BY PEGMATITE, LAMPROPHYRE AND DIABASE DYKES, AND QUARTZ-SYENITE PLUGS

NOTE: RELATIVE AGES OF UNITS 3 TO 8 ARE FOR THE MOST PART UNCERTAIN AND NO STRATIGRAPHIC ORDER IS IMPLIED

DRIFT COVERED AREA

GEOLOGICAL BOUNDARY (APPROXIMATE, ASSUMED)

70 FOLIATION, GNEISSOSITY (INCLINED, VERTICAL, DIP UNKNOWN)

35 MINOR FOLD AXIS (TREND AND PLUNGE)

32 MINERAL STRETCHING LINEATION (TREND AND PLUNGE)

AXIAL TRACE OF MAJOR ANTIFORM, SHOWING DIRECTION OF PLUNGE

FAULT, SHEAR ZONE

BANDED IRON-FORMATION

METAMORPHIC MINERAL OCCURRENCES IN PARAGNEISS BELTS
- GARNET + BIOTITE
- GARNET + BIOTITE + KYANITE + SILLIMANITE + MUSCOVITE
- GARNET + BIOTITE + KYANITE + STAUROLITE + MUSCOVITE
- GARNET + BIOTITE + KYANITE + MUSCOVITE
- GARNET + GRUNERITE
- GARNET + BIOTITE + Al_2SiO_5 + CLINOPYROXENE + ORTHOPYROXENE

Description of rock units:

Rocks within unit 1 (Fig. 4.1) consist of polydeformed, well layered to banded hornblende-biotite (grey) orthogneiss (Fig. 4.2), migmatite, and biotite schist. They include minor proportions of rusty weathering, iron-rich metasediments that contain garnet-biotite-sillimanite-quartz assemblages, garnetiferous amphibolites, and bands of grunerite-bearing iron formation. The orthogneiss is fine- to medium-grained, light- to dark-grey to pink, well banded to well layered rock consisting of several distinct compositional phases that range from granite to tonalite. The gneissic layers contain varying proportions of quartz (25-30%) + plagioclase (45-50%) + K-feldspar (commonly microcline, 4-5%) + biotite (12-15%) + hornblende (2-5%). Epidote, sphene, muscovite and chlorite are present in minor proportions. Accessories include

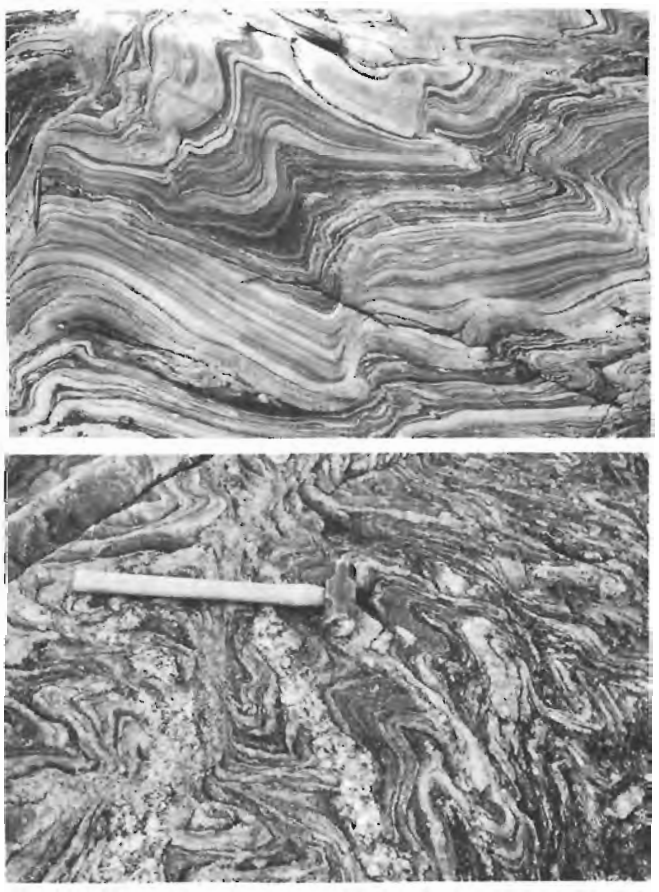


Figure 4.2. A & B. Ductilely deformed layered orthogneiss, unit 1. GSC 204039-U,V.

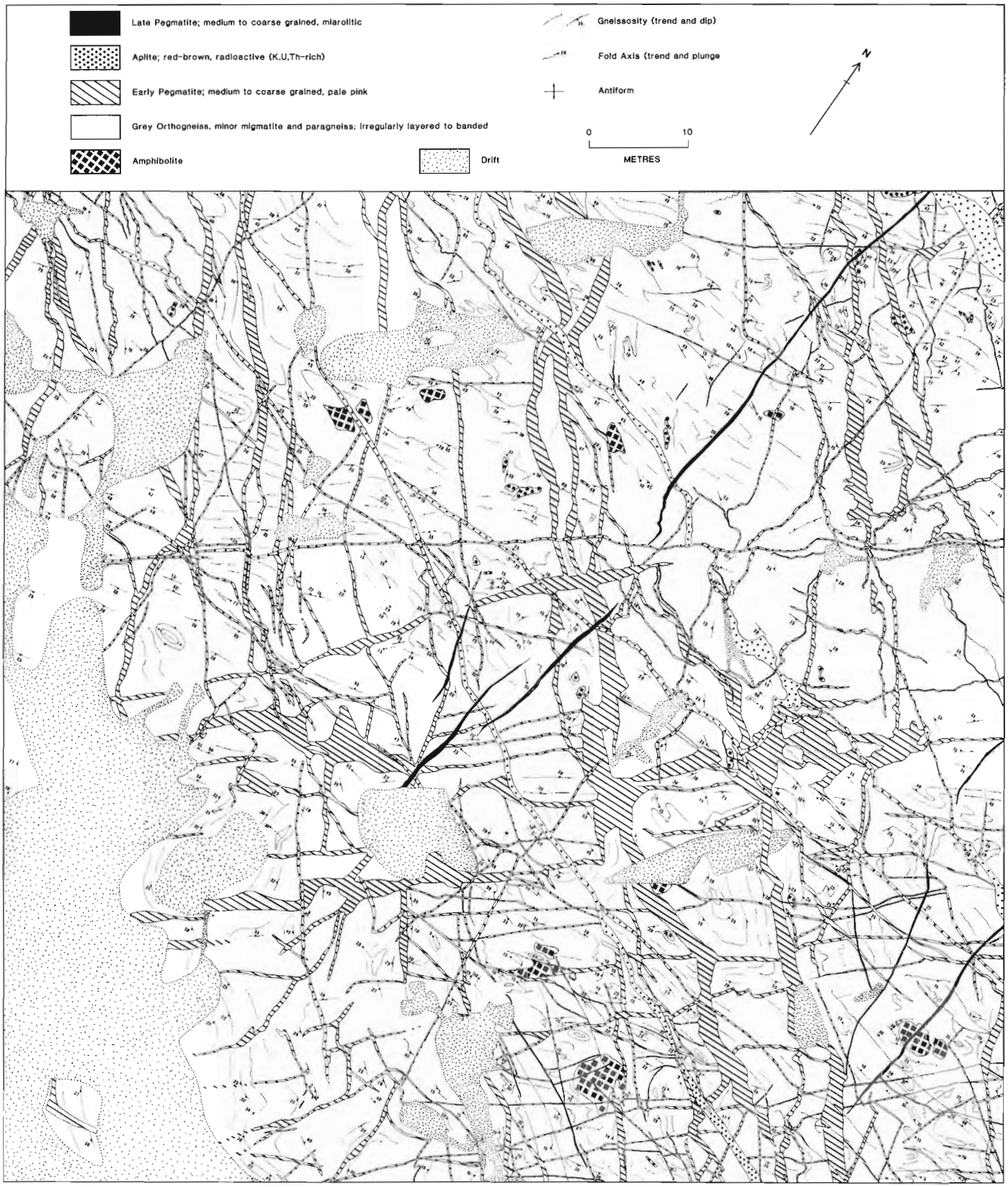


Figure 4.3. Map (grid area-1, Fig. 4.1) showing the distribution of several generations of pegmatite dykes and the complex structural pattern within unit 1.

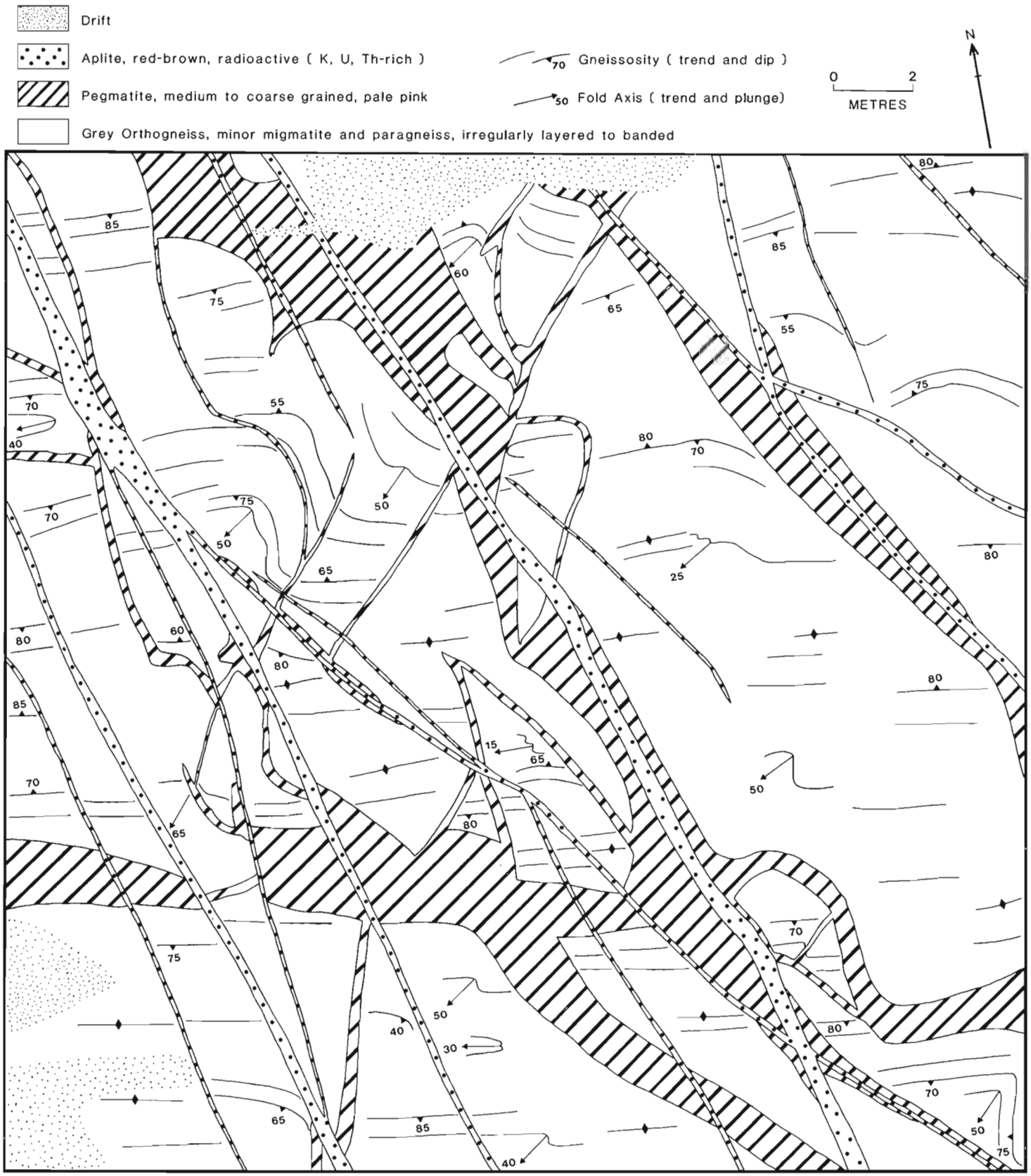


Figure 4.4. Grid area 2 (Fig. 4.1) showing the distribution of different generations of pegmatite and aplite dykes in unit 1.

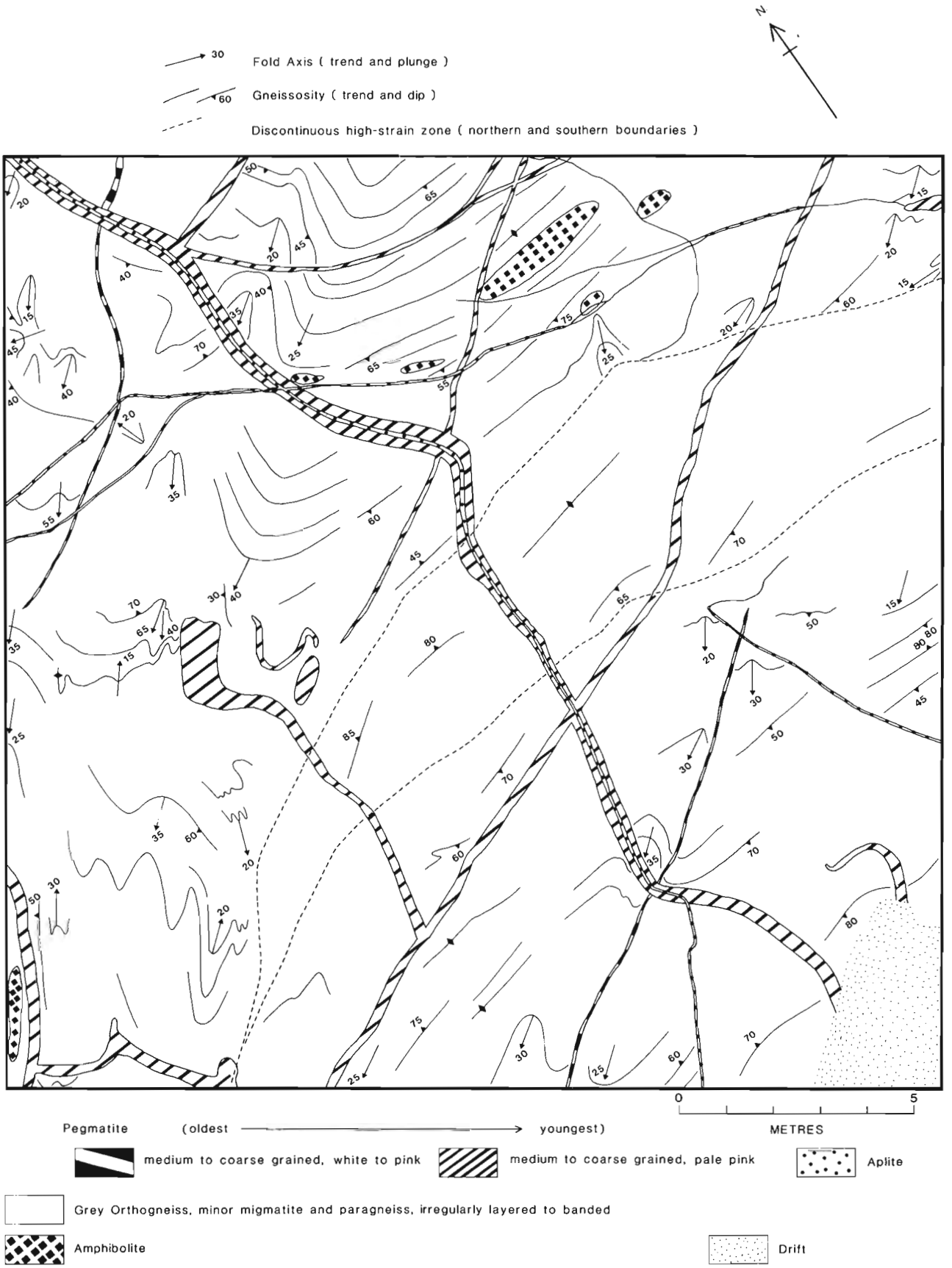


Figure 4.5. Grid area 3 (Fig. 4.1) showing the distribution of different generations of pegmatite and aplite dykes in unit 1.

apatite, zircon, and leucoxene. Less deformed megacrystic (K-feldspar) portions of granite occur within the gneiss with gradational contacts that may represent a protolith for the orthogneiss. The layered gneissic rocks contain abundant xenoliths of metamafic rocks consisting of garnet-hornblende-clinopyroxene assemblages, and rafts of magnetite-rich coronite gabbro. Discontinuous agmatite layers are present within the gneiss. Incipient migmatization is noted locally in the central region near the settlement of Chesterfield Inlet. The migmatitic aspect of the gneiss is more pronounced in the region north and northeast of Hanbury Island (Fig. 4.1).

North of Chesterfield Inlet, rusty paragneiss, and quartz-magnetite iron-formation occur as discontinuous bands within unit 1. They are commonly massive to weakly foliated, and contain quartz-plagioclase-hornblende-biotite ± garnet ± clinopyroxene assemblages. Layering is obscure. The anomalous aeromagnetic signature (Geological Survey of Canada, 1966a) of this region is, in part, a reflection of the underlying magnetite-rich rusty paragneiss and iron-formation.

Sillimanite bearing paragneiss layers, and two-pyroxene granulites are also sporadically distributed in the region north and northeast of Hanbury Island between Severn Harbour and Cape Silumiut (Fig. 4.1). These rocks form a part of the layered gneiss (unit 1). Some dense mafic bands associated with the above metapelites may represent metavolcanic inclusions in a metasedimentary sequence.

Several generations of pegmatite and aplite intrude the layered gneissic rocks near the settlement of Chesterfield Inlet. The distribution of complex anastomosing dyke swarms with cross-cutting relations is shown in Figures 4.3, 4.4, and 4.5 which represent three grid-areas near the settlement (see Fig. 4.1 for location of the grids). The plan views of the three grids represent subhorizontal to horizontal erosional surfaces. Early pegmatite dykes (grid areas 1 and 2, Figs. 4.3, 4.4, 4.6, and 4.7) are commonly medium- to coarse-grained, pink granite that show relatively coarser granophyric margins essentially composed of pink feldspar and quartz. They are cut by cherry red-brown aplite dykes (Fig. 4.6) which are highly radioactive (K-U-Th-rich; with readings: T_1 – 14000 cps; T_2 – 600 cps; T_3 – 270 cps on McPhar TV-1A Scintillometer). The aplite dykes are in turn cut by late coarse grained, red-brown, relatively less radioactive (T_1 – 7000 cps; T_2 – 300 cps; T_3 – 80 cps) pegmatite dykes (Figs. 4.3 and 4.6). In grid area 3 (Fig. 4.5) a set of pre-early pegmatite dykes (Fig. 4.3) are present. They are white to pale pink, coarse grained, and least radioactive of all (T_1 – 4000 cps; T_2 – 150 cps; T_3 – 40 cps). Most dykes, in each generation, are composite dykes that contain pegmatite and aplite phases. Most show high-angle intersections with little or no offsets due to dilation. Lack of offsets in some obliquely intersecting dykes suggest either a replacement origin for some of the younger dykes, or emplacement during ductile deformation of the country rocks. Early pegmatite dykes have been deformed prior to the emplacement of younger aplite and later coarse grained pegmatite. The highly radioactive aplite dykes appear to be related to the fluorite-granite intrusions (unit 9, Fig. 4.1) that are exposed on Fairway Islands and at the western margin of the map area. Zircon geochronology of the various dyke-sets is planned to establish their absolute ages.

A series of west-northwest trending and moderately to steep, south dipping paragneiss belts (unit 2, Fig. 4.1) consisting of garnet ± staurolite ± kyanite ± sillimanite + biotite + muscovite assemblages, structurally overlie the central gneiss region in the southern parts of the map area. These belts have a composite width of approximately 15 km. Gneissosity in paragneiss is commonly concordant with the gneissic layering in layered gneiss (unit 1) for the most part, but locally sheared contact zones are present at a few places. The rocks in this unit are commonly fine- to medium-grained iron-rich pelites that are compositionally and texturally well banded and layered with quartz-rich, quartzofeldspathic, and garnet-biotite-kyanite rich layers. Abundant porphyroblasts of kyanite as blades up to 5 cm long, staurolite, and garnet are widespread throughout the entire length of the belts (see Fig. 4.1 for the distribution of these minerals). Garnet and staurolite porphyroblasts contain an internal metamorphic fabric that is discordant to the external regional biotite fabric. Several interlayers of metamorphosed banded iron-formation, consisting of quartz-magnetite-garnet-grunerite, form an integral part of the paragneiss belts. The distribution of iron-formation is shown by linear magnetic anomalies on an aeromagnatic map (Geological Survey of Canada, 1966a). The iron-formation is finely banded on a millimetre to centimetre scale, and seldom exceeds more than a few tens of centimetres in thickness. Some of the multiple bands may represent the same stratigraphic levels repeated by tight isoclinal folds commonly present in the paragneiss. Along the entire length of the belts the paragneiss-iron formation (unit 2) is extensively intruded by large deformed masses, elongate sheets, intrusive plugs, and lit-par-lit injections of two-mica leucogranite (unit 7) that form topographically high resistant ridges.

A northeast trending belt (unit 3) consisting of amphibolite, minor metavolcanic rocks, and garnet-biotite schist is exposed in the northwestern part of the region south of Chesterfield Inlet (Fig. 4.1). The rocks are in part intermixed with grey gneiss and biotite paragneiss (units 1 and 4) and are in turn intruded by younger granitic and pegmatitic rocks (units 8 and 9). The rocks within the belt display a distinctive aeromagnetic expression (Geological Survey of Canada 1966b) which extends southwesterly into Gibson Lake map area (55N).

Several discontinuous belts of garnet-biotite paragneiss (unit 4) occur in the northwest corner of the map area, on Moor Island, and northeast of Chesterfield Inlet (Fig. 4.1). Narrow belts, 100-200 m thick, of paragneiss are also distributed throughout the region within the layered gneisses (unit 1). The paragneiss belts are commonly rusty weathering, fine- to medium-grained, and contain garnet-biotite-plagioclase-quartz assemblages. Garnet porphyroblasts are characteristically translucent pink, and range in size from less than 1 mm to up to 3 cm in diameter. Sillimanite is noted in a few places (on Moor Island and northeast of Chesterfield Inlet) adjacent to granitoid plutons and appears to have resulted from contact metamorphism.

Megacrystic (K-feldspar) and well foliated granite (unit 5) intrudes the layered gneiss complex (unit 1) in the central part of the gneiss region, south of Chesterfield Inlet (Fig. 4.1). For the most part, the granite is highly deformed subsequent to its emplacement into the gneiss but relatively undeformed megacrystic portions of the protolith are locally preserved within the mass. The granite shows an arcuate magnetic expression on the aeromagnetic map (Geological Survey of Canada – 1966a); the expression of a broad, west-plunging, open antiform. Granitic sheets that parallel the gneissic layering are common along the margins of this granite.

Massive to weakly foliated intrusions of gabbro (unit 6) are sporadically distributed throughout the region. They are undoubtedly of different generations as some are deformed and metamorphosed subsequent to their intrusion and others are massive. Two plugs of gabbro, exposed along the southern shore of Chesterfield Inlet and north of False Inlet (Fig. 4.1), contain abundant garnet with corona textures. The gabbro intrudes the gneiss (unit 1), and in turn is cut by younger, coarse grained pink pegmatite dykes. Isolated outcrops of gabbro also occur within the layered and paragneiss units (1 and 2) southwest of Chesterfield Inlet. They are relatively undeformed, contain garnets, and display excellent ophitic and subophitic textures. Northeast of Hanbury Island, rafts of coronite leucogabbro (not shown in Fig. 4.1) with high concentrations of magnetite occur within a mylonitized gneiss. They are interpreted as post-intrusion remnants within a ductile shear zone.

Coarse- to medium-grained, grey- to white-weathering weakly- to well-foliated biotite-muscovite leucogranite (unit 7) is extensively exposed in the southern parts of the map area (Fig. 4.1) and extends southeasterly into Marble Island map area (Tella et al., 1986). The granite forms west-northwest trending elongate masses that intrude the paragneiss belts (unit 2). The regional foliation within the granite trends west-northwest and dips steeply (70°-80°) to the south, although local reversals to the north are common. The granite cores are generally less deformed compared to the margins. The granite is composed of biotite (5%), muscovite (10%), quartz (30-35%), potash feldspar (mostly microcline, 20%), plagioclase (30%) and rare amphibole. Well rounded garnet xenocrysts with internal fabric, and large books of muscovite xenocrysts are abundant. Accessory minerals include apatite, tourmaline, zircon, and sphene. Abundant inclusions of layered gneiss and paragneiss (units 1 and 2), and minor portions of garnetiferous metagabbro are also present within the granite. Textural and mineralogical characteristics of this granite are suggestive of an S-type origin.

A number of granitoid plutons intruding the layered gneiss and biotite paragneiss (units 1 and 4) are distributed in a northeasterly trend in the northwestern portions of the map area (Fig. 4.1). Although individual plutons are compositionally homogeneous, they range in composition from granite in the southwestern parts through to quartz diorite northeast of Chesterfield Inlet. Southwest of Chesterfield Inlet they contain abundant inclusions, rafts, and roof-pendants of layered gneiss and paragneiss. Related pegmatite and aplite dykes are widespread throughout the region and extend as far east as the settlement of Chesterfield Inlet. The plutonic rocks are commonly undeformed at the cores, but have a well developed foliation at the margins, as well as migmatitic aureoles (approximately 100-200 m thick) and gradational contacts with the host gneisses. The above field relations suggest that regional metamorphism of the gneisses was probably contemporaneous with plutonic migmatization and syntectonic emplacement of granitic rocks. These observations are consistent with those noted by Reinhardt and Chandler (1973) and Reinhardt et al. (1980) in the Gibson-MacQuoid Lake map-area to the west. North of Chesterfield Inlet the plutonic rocks are coarse grained, equigranular, light- to dark-grey, homogeneous masses of granodiorite to quartz diorite. They also contain inclusions of paragneiss and layered gneiss, and are foliated at the margins. Sillimanite, a contact metamorphic mineral, is noted at one locality northwest of Hanbury Island (Fig. 4.1) in the biotite paragneiss (unit 4) adjacent to one of the plutons. Although all of the above plutonic rocks are grouped into a single rock unit (8) they may not necessarily be coeval. Geochronological studies are planned to determine their absolute ages.

Massive- to weakly-cleaved, and equigranular to porphyritic, in part miarolitic, pink granite (unit 9) plutons are exposed in the northwestern part of the region and on Fairway Island in Hudson Bay (Fig. 4.1). Smaller satellite plugs of similar composition are sporadically distributed in the central region between the western boundary of the map area and the settlement of Chesterfield Inlet. The granite shows a well developed granophyric and myrmekitic texture and contain numerous inclusions of older gneissic rocks (unit 1) as schlieren and rafts, especially within the large pluton at the western margin of the map (Fig. 4.1). Mafic minerals, mostly biotite, make up less than 2 per cent of the rock, and accessory minerals include fluorite, apatite, sphene, zircon, and magnetite. On Fairway Island the granite is radioactive (K, Th, U-rich) and contains abundant fluorite, chalcopyrite and specularite. Aplite dyking, related to these granite intrusions, is widespread along the west coast of Hudson Bay (Fig. 4.1), west of Fairway Island. There cherry red-brown aplite dykes are highly radioactive. Granites of unit 9 are texturally and compositionally similar to the late Aphebian to Helikian alkaline intrusions that are widely distributed in the Baker Lake region to the west, and may be of similar age.

Northwest-trending, dark grey to black, biotite lamprophyre dykes (unit 10, not shown in Fig. 4.1) are sporadically distributed in the Chesterfield Inlet region. The dykes range in thickness from less than a metre to up to 2 metres thick. They are compositionally similar to the lamprophyre dykes described from the Rankin Inlet region to the south (Tella et al., 1986) where they are considered to be of Helikian age.

STRUCTURE AND METAMORPHISM

For comparison and discussion of fabrics and metamorphism in respective regions, the Chesterfield Inlet map area (Fig. 4.1) is subdivided into four geographic regions – southern, central, northern (north of Chesterfield Inlet and northwest of Hanbury Island), and northeastern (north and northeast of Hanbury Island). The subdivisions also reflect lithological contrasts which have been described in the previous section. Figures 4.8 and 4.9 show the orientation of various fabric elements (foliations, fold axes, lineations) in



Figure 4.6. Intersecting pegmatite and aplite dykes showing relative ages (grid area-1, Fig. 4.1). GSC 204040-M.



Figure 4.7. Biotite lamprophyre dyke cutting two intersecting pegmatite dykes, and in turn cut by a later coarse pegmatite. Location: approximately 1 km south- southeast of grid area-1, Fig. 4.1. GSC 204039-Y.

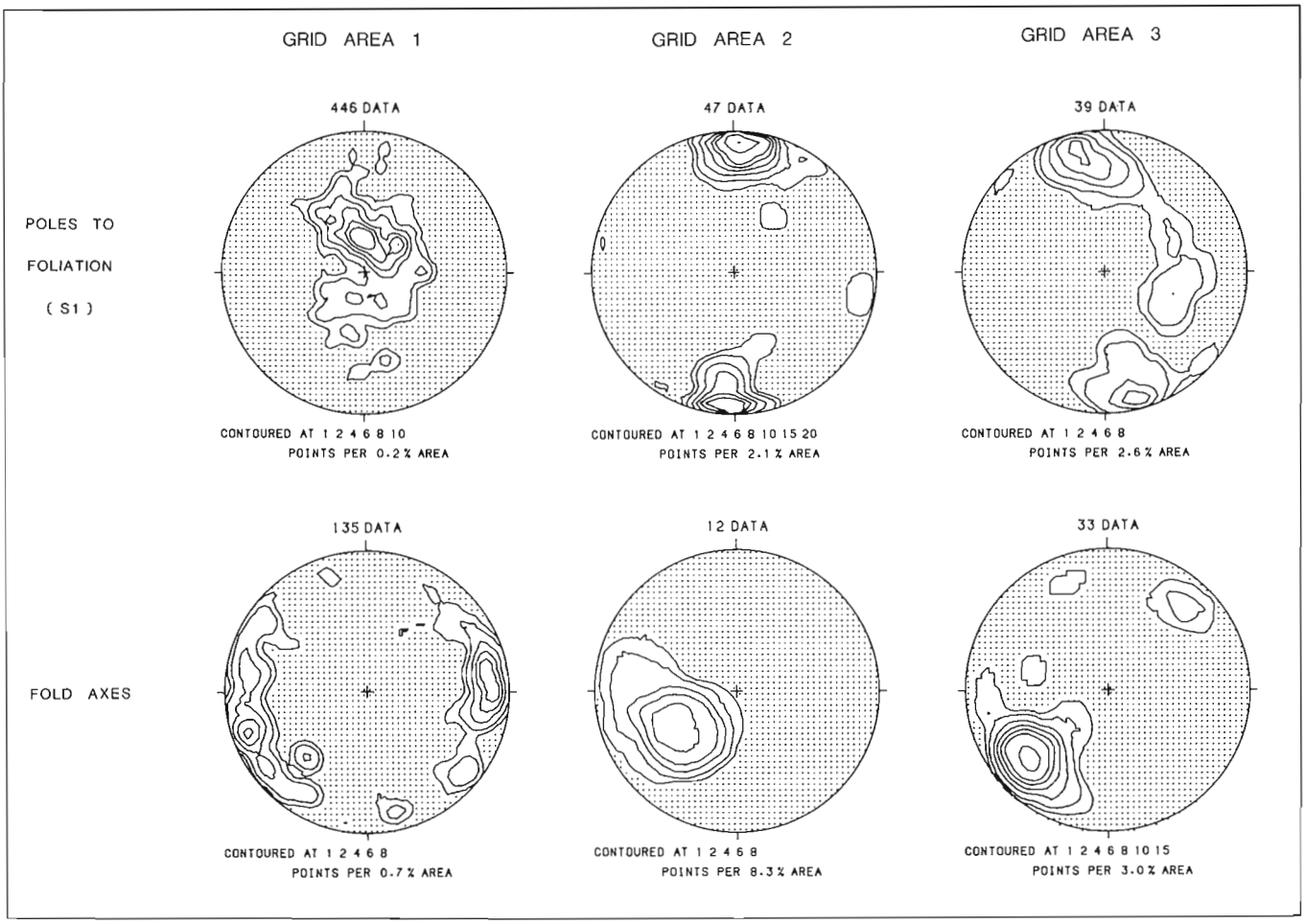


Figure 4.8. Stereonet plots of fabric elements from grid areas 1, 2, and 3; contoured according to the method of Starkey (1969, 1977).

these regions. The orientation data are contoured according to the method proposed by Starkey (1969, 1977). The data in Figure 4.8 correspond to the structures observed in the gneissic rocks (unit 1) from the three grid areas (Figs. 4.3 to 4.5). It is obvious from these plots that the regional pattern shown by the planar and linear fabrics in the central region (Fig. 4.9) is reflected in the orientation of mesoscopic structures noted in the grid areas (Fig. 4.8).

All rocks in the Chesterfield Inlet map-area, with the exception of units 8 to 10, have been polydeformed and regionally metamorphosed under amphibolite to granulite facies conditions. The age of deformation and metamorphism

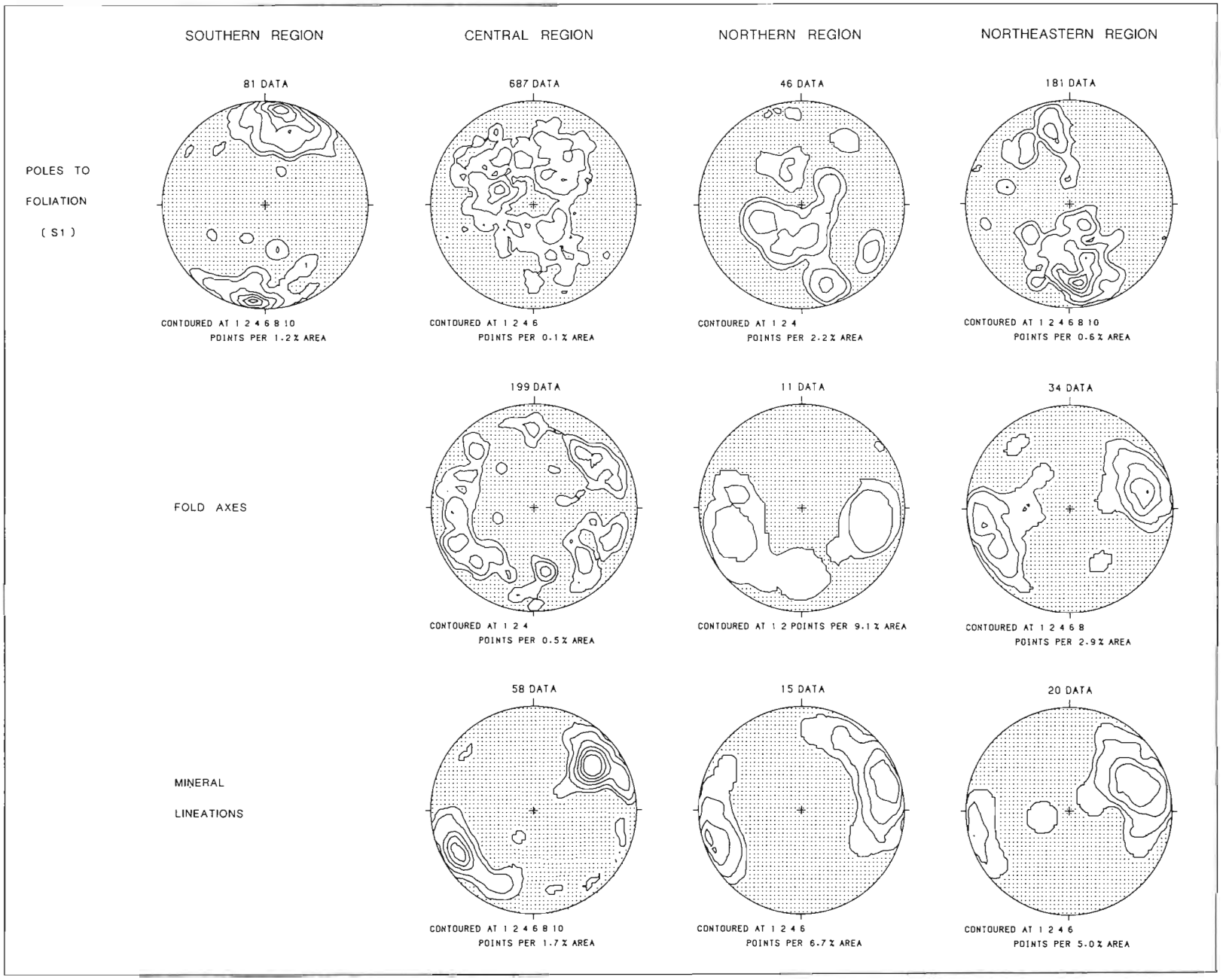


Figure 4.9. Stereonet plots of fabric elements from the Chesterfield Inlet map area; contoured according to the method of Starkey (1969, 1977).

is believed to be Archean, but definitive geochronology is required to establish temporal relationships between metamorphism, deformation and plutonism, and to document constraints with certainty. The following observations are made with regards to structure and metamorphism of the Chesterfield Inlet region:

1. At least four sets of folds are present within the layered gneiss (unit 1). The first two sets commonly occur as coaxially refolded, recumbent intrafolial folds that have been modified by later, west plunging, open F_3-folds. Local plunge reversals of F_3-fold axes towards east and east-northeast are present near the settlement of Chesterfield Inlet. The regional distribution of rock units is largely controlled by a major, moderately west-plunging (30°), open, upright F_3-fold. The distribution of fold axes shown in Figure 4.9 largely reflects F_3-fold pattern somewhat modified by a later, northwest to north-northwest trending upright open fold-set. Type I and III interference fold patterns (Ramsay, 1967) are present in the rocks of unit 1 throughout the region.

2. In the central, northern, and northeastern regions pervasive mineral stretching lineations (quartz/feldspar rodding, hornblende; Figs. 4.9 and 4.11) are commonly restricted to a zone (approximately 5 km wide) of high ductile-strain that extends east-northeasterly from Moor Island through Severn Harbour to Cape Silimiut (Fig. 4.1).

3. Garnet-biotite ± staurolite ± kyanite ± sillimanite ± muscovite assemblages in pelitic gneiss (unit 2) indicate amphibolite facies conditions of metamorphism in the southern region. Garnet, kyanite and sillimanite coexist with staurolite and muscovite in one thin section. Porphyroblasts of garnet with internally rotated inclusion trails of quartz and feldspar are wrapped and partially flattened by an external biotite fabric. Porphyroblasts of kyanite and partially altered staurolite are commonly aligned in the planes of biotite fabric. Random chlorite overgrowths across the regional biotite fabric are noted in a few thin sections. Minor kinks in chlorite record a post-chlorite deformation event in these pelitic gneisses. Polymetamorphic textures are evident from the mineral assemblages.

4. The metamorphic grade in the central, quartzofeldspathic gneiss region (unit 1, Fig. 4.1) is less clear because of lack of critical metamorphic mineral assemblages. However, some rusty paragneiss inclusions within the grey gneiss locally contain sillimanite, K-feldspar, muscovite assemblages, and an incipient migmatization character of the gneissic rocks is noted in the coastal bedrock-exposures near the settlement of Chesterfield Inlet.

5. Two-pyroxene granulites with aluminium silicate polymorph, possibly sillimanite, and quartz occur in the region north and northeast of Hanbury Island, which indicate granulite facies conditions of metamorphism. Migmatitic aspect of the rocks is more pronounced in this region.



Figure 4.11. Quartz and feldspar rodding lineation in mylonitic gneiss, northeast of Hanbury Island. GSC 204039-T.



Figure 4.10. Mylonitic layering in orthogneiss, unit 1. Northeast of Hanbury Island. GSC 204040-K.



Figure 4.12. Boudinaged amphibolite layer within the shear zone north of Hanbury Island. GSC 204040-F.

6. Most granitoid plutons (unit 8) contain abundant inclusions of layered rocks (units 1, 2 and 4) and well-foliated migmatitic margins, and commonly show gradational contacts with the country rock suggesting that the regional metamorphism was probably contemporaneous with plutonic migmatization and syntectonic emplacement of granitoid rocks.

The above observations, based on field relations and preliminary petrographic data, suggest an apparent increase in metamorphic grade from south to north and that an oblique or tilted structural cross-section with progressively deeper-crustal levels towards the north is represented in the Chesterfield Inlet region. In the adjoining area to the south, greenschist to amphibolite facies grade metavolcanic and metasedimentary rocks of the Rankin Inlet Group (Tella et al., 1986) overlie the gneissic rocks (units 1 and 2), with an apparent conformable relationship; thus exposing a still higher crustal-level in the Rankin Inlet region.

An approximately 5 km wide, east-northeast trending and steep to vertically dipping ductile, dextral shear zone (Fig. 4.10) is exposed within the gneiss terrain (unit 1) north of Hanbury Island between Severn Harbour and Cape Silumiut (Fig. 4.1). Mylonite rocks characterize this zone. The mylonitic layering contains abundant, highly disrupted and boudinaged amphibolite layers (mafic dykes) (Fig. 4.12). Asymmetrical pull-apart structures (Hanmer, 1986) in amphibolite layers (Fig. 4.13) together with subhorizontal, shallow-plunging (10°-30°) mineral stretching lineations (Fig. 4.11) suggest shallow oblique dextral displacement of unknown magnitude. C- and S-fabrics (Berthé et al., 1979) within the zone are indistinguishable for the most part but the regional S-fabric outside the mylonite zone defines a large scale 'discrete dextral shear'. The southwesterly extension of the zone can be traced across Chesterfield Inlet through Moor Island (Fig. 4.1) where the rocks, marked by high ductile strain, are well lineated. Further detailed mapping is necessary to delineate the southwestern limits of this shear zone.



Figure 4.13. Asymmetrical pull-apart structures in amphibolite layer showing dextral sense of shear in mylonite. GSC 204040-L.

REFERENCES

Bell, Robert

1885: Observations on the geology, mineralogy, zoology and botany of the Labrador coast, Hudson's Strait and Bay, made in 1885; Geological Survey of Canada, Annual Report, Part DD, p. 1-20.

1887: Marble Island and the northwest coast of Hudson's Bay; *in* Proceedings of Canadian Institute, 3rd Series, v. 4, 1885-86, p. 192-204.

Berthé, D., Choukroune, P., and Jegouzo, P.

1979: Orthogneiss, mylonite and non-coaxial deformation of granites: the example of the South Armorican Shear Zone; Journal of Structural Geology, v. 1, p. 31-42.

Geological Survey of Canada

1966a: Chesterfield Inlet; Geophysical Series (Aeromagnetic) Map 7298G.

1966b: Gibson Lake; Geophysical Series (Aeromagnetic) Map 7299G.

Hanmer, Simon

1986: Asymmetrical pull-aparts and foliation fish as kinematic indicators. Journal of Structural Geology, v. 8, no. 2, p. 111-122.

Lord, C.S.

1953: Geological Notes on Southern District of Keewatin, Northwest Territories. Geological Survey of Canada Paper 53-22, 11 p.

Ramsay, J.G.

1967: Folding and Fracturing of rocks. McGraw Hill, New York.

Reinhardt, E.W. and Chandler, F.W.

1973: Gibson-MacQuoid Lake Map Area, District of Keewatin; *in* Report of Activities, Part A, Geological Survey of Canada Paper 73-1A, p. 162-165.

Reinhardt, E.W., Chandler, F.W., and Skippen, G.B.

1980: Geological Map of the MacQuoid Lake (NTS 55M, E1/2) and Gibson Lake (NTS 55N, W1/2) Map Area, District of Keewatin, Geological Survey of Canada, Open File Map No. 703, June 1980; compiled by G.B. Skippen.

Starkey, J.

1969: A computer program to prepare orientation diagrams; *in* Experimental and Natural Rock Deformation. Editor: P. Paulitsch. Springer-Verlag, New York, p. 51-74.

1977: The contouring of orientation data represented in spherical projection. Canadian Journal of Earth Sciences, v. 14, p. 268-277.

Tella, Subhas, Annesley, I.R., Borradaile, G.J., and Henderson, J.R.

1986: Precambrian geology of parts of Tavani, Marble Island and Chesterfield Inlet map area, District of Keewatin, N.W.T., Geological Survey of Canada Paper 86-13, 20 p.

Wright, G.M.

1955: Geological notes on central District of Keewatin, Northwest Territories; Geological Survey of Canada Paper 55-17.

1967: Geology of the southeastern barren grounds, Parts of the District of Mackenzie and Keewatin; Geological Survey of Canada, Memoir 350.

- 5 -

A simple probe for the measurement of frost heave within frozen ground in a permafrost environment

Project 680047

J. Ross Mackay[1] and R.V. Leslie[1]
Terrain Sciences Division

Mackay, J.R. and Leslie, R.V., A simple probe for the measurement of frost heave within frozen ground in a permafrost environment; in Current Research, Part A, Geological Survey of Canada, Paper 87-1A, p. 37-41, 1987.

Abstract

Laboratory experiments have shown that unfrozen water in a frozen soil can move under a temperature gradient from warmer to colder areas. Field experiments have demonstrated that unfrozen water in frozen ground in a permafrost environment may move upward and downward in an annual cycle, in both the frozen active layer and the top of permafrost. A simple magnet probe for the field measurement of heave within frozen ground and settlement of thawing soil is described. Results of three years of field trials at Inuvik and Illisarvik, Northwest Territories show a resolution of 1 mm and general agreement with other methods.

Résumé

Des expériences en laboratoire ont démontré que de l'eau non gelée dans un gélisol peut se déplacer, sous un gradient de température, d'une zone plus chaude à zone plus froide. Par ailleurs, d'autres expériences, réalisées cette fois sur le terrain, ont révélé qu'en milieu de pergélisol, l'eau non gelée dans un gélisol peut monter et descendre suivant un cycle annuel, tant dans la couche active que dans le sommet du pergélisol. Les auteurs décrivent une sonde magnétique simple, qui sert à mesurer sur le terrain le soulèvement d'un sol gelé et le tassement provoqué par le dégel. Les résultats de trois ans d'essais réalisés sur le terrain à Inuvik et Illisarvik, dans les Territoires du Nord-Ouest, montrent qu'il est possible d'obtenir des mesures précises à 1 mm près et concordent généralement avec les résultats obtenus au moyen d'autres méthodes.

[1]Department of Geography, University of British Columbia, Vancouver, B.C. V6T 1W5

INTRODUCTION

It is well known that frozen soils have varying amounts of both ice and unfrozen water with the amount of unfrozen water being dependent upon the temperature, soil, and past freeze-thaw conditions. Numerous laboratory experiments (e.g. Williams, 1984) have shown that water can move in frozen soil under a temperature gradient from a warmer to a colder site. In a permafrost environment the frozen active layer is colder than the top of permafrost from freeze-back to mid-winter but becomes warmer in late winter and summer. Therefore, some unfrozen water may move upward in the active layer in early and mid-winter and downward in late winter, especially during the snowmelt period, and in early summer in response to reversals in the temperature gradient. The amount of flow would depend upon time, temperature, and soil conditions.

Numerous techniques are available for the measurement of the ground surface heave in winter and thaw settlement in summer (James, 1971) but the measurement of in situ frost heave within frozen ground and thaw settlement in thawing soil is a much more difficult problem. This report 1) reviews briefly the evidence for frost heave of frozen ground and 2) discusses a simple magnet probe for the field measurement of heave within frozen ground and thaw settlement of thawing soil in a permafrost environment.

EVIDENCE FOR FROST HEAVE IN FROZEN GROUND

During the past decade, field data derived independently in China, North America, and the USSR demonstrate that unfrozen water can move within frozen ground both upwards in winter and downwards in summer in the top of permafrost and in the frozen active layer above it (Mackay, 1983). Field methods that have been used to study the movement of unfrozen water in frozen ground include the following types of measurements: 1) vertical changes in water content with neutron probes (Cheng, 1982; Wright, 1983; Chen, 1984; Smith, 1985); 2) differential movement of telescoping tubes, markers, and bench marks in frozen ground (Mackay et al., 1979; Mackay, 1981, 1983; Mackay and Lewis, 1981; Muir, 1983; Smith, 1985); 3) changes in water content in frozen ground from repetitive sampling in areas of homogeneous frozen ground (Parmuzina, 1977, 1978; Lagov and Parmuzina, 1978); 4) horizontal movement of water from a vertical water-filled hole into adjacent frozen ground (Parmuzina, 1979); 5) the downward movement of tritium into permafrost (Chizhov et al., 1983; Mackay, 1983); 6) seasonal changes as registered by soil pressure cells in frozen ground (Mackay and MacKay, 1976; Mackay, 1983); and 7) temperature changes (probably induced by the water transport of sensible and latent heat) within frozen ground during the summer thaw period (McGaw et al., 1978; Mackay, 1983).

In view of the considerable field evidence for the movement of water in frozen ground, a simple magnet probe has been designed and field tested for the purpose of estimating frost heave in frozen ground and thaw settlement in thawed ground.

MAGNET PROBE

The general principle of the magnet probe has been used in a variety of position detecting devices for many years. The magnet probe discussed here consists of three elements: 1) a vertical access tube (Fig. 5.1) inserted into a hole augered into the ground; 2) an array of ring magnets, stacked one above the other in the augured and backfilled hole, with the magnets coaxial (Fig. 5.1) with the access tube; and 3) a reed switch probe (Fig. 5.2) that produces an audible signal when it enters the magnetic field of a ring magnet.

ACCESS TUBES

The access tubes used in the field tests are of stainless steel, 0.250 inch (6.4 mm) diameter with a wall thickness of 0.035 inches (0.9 mm), and with a 2 cm diameter disk welded on the bottom end to prevent frost heave of the tube. The tubes are inserted into vertically augered holes about 2.5 cm in diameter. The tops of the tubes, if installed in summer, are left protruding sufficiently high above ground level if there is winter frost heave. A plug (e.g., snug fitting nail) is inserted into the top of the access tube and then the above-ground part is capped with a protective outer cover to prevent snowmelt and rain from entering the access tube. The protective cover should not be pushed into the ground in summer because it will then be frozen in place at freeze-back and so will be difficult to uncover in winter.

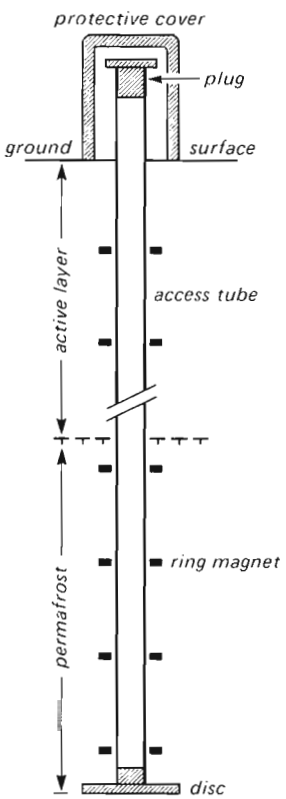


Figure 5.1. An access tube installed in a back-filled hole.

MAGNETS

The magnets, which are used as floating markers in the ground, are ceramic permanent ring magnets, 0.5 inch (12.7 mm) diameter, 1/8 inch (3.2 mm) thick, with a centre hole of 0.27 inch (6.9 mm) diameter. For installation, the lowest magnet is centred and dropped over the access tube at the desired bottom depth, and the hole partially back filled with soil and tamped. The process is then repeated for each successively higher magnet. The magnets should not be spaced closer than 3 or 4 cm in order to avoid confusion in identifying magnet signals with the probe. A rigid plastic tube with a diameter slightly greater than that of the access tube has been found helpful in pushing each magnet down to the desired depth and in compacting the soil. Water can be added to assist in compaction

PROBE

The rigid part of the magnet probe is made of a stainless steel tube, 1/8 inch (3.2mm) diameter and 0.029 inch (0.7mm) wall thickness. The steel tube should be at least 10 cm longer than the access tubes. The sensing part of the probe is a miniature reed switch (MMR2 or similar) which is soldered onto two insulated wires inserted through the steel tube and attached at the top to a coaxial cable (RG176 or similar) whose length depends upon the depth to be measured. The cable must be securely attached to the stainless steel tube for stress relief. The reed switch is then potted and firmly attached to the bottom of the probe. The free end of the cable can then be connected to a buzzer (e.g., Mallory SC6) which gives an audible signal when the reed switch is closed by the magnetic field of the magnet. As care must be taken to limit the current through the reed switch, the switch is operated at 1.5 V to produce an audible signal with a current of only 2 mA. The probe should be accurately marked at 25 cm intervals from the bottom end upwards.

FIELD MEASUREMENTS

In order to take a set of readings, the probe is first inserted through a small clamping ring (Fig. 5.2), which can be finger screw tightened, and then the magnet probe is pushed slowly down the access tube until the first audible "beep" is heard. The probe is then moved slightly up and down until the depth at which the least possible movement will produce a "beep" is located. Care should be taken to measure, consistently, either the first "beep" of the probe as it enters the magnetic field above a magnet or the second "beep" at the bottom of the magnet. Preferably, the first "beep" should be used. The camping ring is then finger tightened to mark the length of the probe inserted below the top of the access tube (Fig. 5.3). The distance between the clamping ring and the first scale mark below it is measured with a pocket tape or othe device, depending upon the accuracy required. With a little practice most observers can replicate measurements to considerably better than 0.5 mm and two observers rarely differ by as much as 0.5 mm in their readings. The same procedure is used for all the other magnets present at depth. The magnets should be spaced at least several centimeters apart to avoid confusion in the recognition of the audible signals from closely spaced magnets. If the access tube is firmly anchored in permafrost (i.e, the tube does not frost heave), then the readings give the locations of the magnets with respect to the top of the access tube, which is a stable datum. If the access tube heaves, or if it is entirely in the active layer and thus heaves in winter and settles in summer, then the differences in the separation of the magnets are a measure of differential frost heave and thaw settlement.

The question can be raised as to whether the magnets can move freely with reference to the access tube in response to frost heave and thaw settlement. So far, the evidence suggests that the magnets, with an average clearance of about 0.5 mm, move like a pebble with the soil. Heat conduction along the access tube seems unimportant in summer, as suggested by probing the depth of the active layer close to and remote from the access tube.

DISCUSSION

During the 1983 to 1986 period, measurements have been taken of magnet probes installed at Inuvik, Northwest Ter-

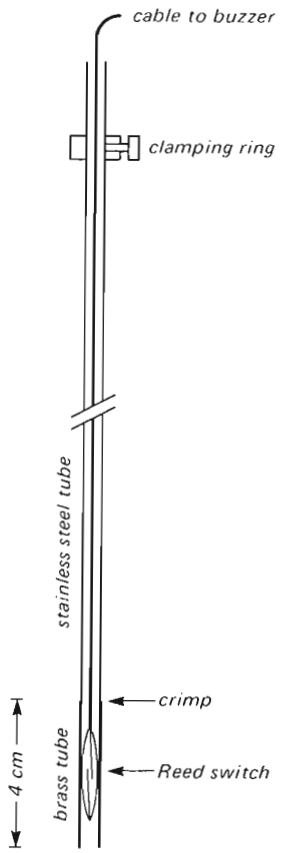


Figure 5.2. Magnet probe that is pushed down the access tube (Fig. 5.1) to locate the positions of each ring magnet relative to the top of the access tube.

ritories and at "Illisarvik" (unofficial name for an artificially drained lake experimental site) at the north end of Richards Island, Northwest Territories about 150 m north of Inuvik. Figure 5.4 shows the change in separation of two pairs of magnets installed in early June 1983 at two sites 500 m apart at Illisarvik, Northwest Territories. Site "a" was in a bare area on the bottom of a drained lake (Fig. 5.3); the material is a sandy organic-rich silt. The active layer exceeds 80 cm. The upper magnet was installed at 55 cm below ground level and the lower magnet 17 cm below the upper magnet. Thaw settlement occurred during the summer of 1983. No measurements were taken in the freeze-back period of 1983. On 8 April 1984 the separation of the two magnets was 10.6 cm and by 30 May 1984 the separation had increased to 12.2 cm for an increase of 1.6 cm (Fig. 5.4). On 30 May the depth of thaw was 18 cm deep so the upper magnet was 37 cm below the 0°C isotherm. The temperature was below −1°C judging from nearby ground temperatures. Therefore, the separation of the two magnets increased 1.6 cm when ground temperatures were probably well below −1°C. The 1.6 cm change in separation of the magnets from 8 April to 30 May 1984 cannot be attributed solely to the infiltration of snowmelt and the freezing of pore water, because a 9% volume expansion from pore water in a soil column 12 cm thick could not result in a 1.6 cm heave. On the other hand, the downward temperature-induced migration and freezing of unfrozen pore water in discrete ice lenses would require the addition of only a 1.45 cm-thick layer of water. Attention should be drawn to the fact that the zone of heaving was between the two magnets because the depth of a third magnet below the second magnet remained constant with reference to the top of the access tube. As the frost table deepened in summer, the upper magnet underwent thaw settlement (Fig. 5.4). In support of the preceding, measurements with a heavemeter located only 1 m from site "a" showed a heave of 0.3 cm from early January to 6 April 1981 with a further heave of 0.3 cm from 6 April to 7 August 1981 (Mackay, 1983).

Site "b" (Fig. 5.4) was 500 m from site "a" in an area of tundra-covered earth hummocks. The access tube was installed in early June 1983 in the middle of an earth hummock. The upper magnet was 40 cm below ground level and the lower magnet was 58 cm. The active layer was about 70 cm thick. From 8 April to 30 May 1984 the separation of the two magnets increased 1.25 cm. On 30 May 1984 the depth of thaw was only 7 cm deep, so both the upper and lower magnets were still in frozen ground well below 0°C as suggested by temperature measurements. Therefore, the 1.25 cm increase in separation took place when both magnets were in frozen ground at temperatures will below 0°C. The same pattern of late winter separation increase was also observed for probes at Inuvik, 150 km to the south where previous studies using other methods (Mackay et al., 1979; Mackay and Lewis, 1981; Smith, 1985) had shown similar heaves in frozen ground. Thus, because four independent methods used at the Inuvik and Illisarvik sites, namely data from the survey of heaves of dowels, differential heaves of heavemeters, neutron probe density measurements, and magnet probe separation measurements have detected a late winter heave, the magnet probe method, which provides results similar to the others, appears to be a promising method of estimating in situ frost heave in frozen ground.



Figure 5.3. The magnet probe in use. The person's right hand is holding the clamping ring which is at the top of the access tube; the left hand is holding the probe; and the buzzer is on the board. The wooden rod is used as a site marker when the access tube is covered by snow.

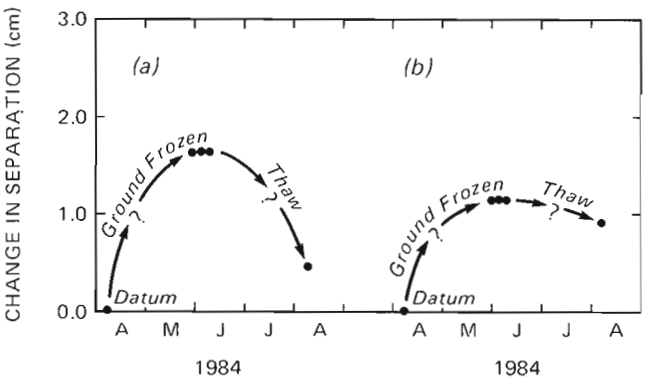


Figure 5.4. The two graphs (a) and (b) show change in magnet separations for two pairs of magnets from April to August 1984. Site "a" is shown in Fig. 5.4 (see text).

SUMMARY AND CONCLUSION

The magnet probe is a simple, inexpensive, manually operated device that can be used in a permafrost environment to estimate in situ frost heave and thaw settlement in the active layer and top of permafrost. The resolution is much better than 1 mm. The accuracy is unknown but the general pattern and amount of heave are in agreement with heave measurements obtained by other methods. Tests have been carried out with the magnets for three years (1983 to 1986). During this three-year period the amount of late winter and early summer heave has shown considerable year to year variation although, in any given year, the heaves at different sites tended to show the same pattern. This suggests that the heave is sensitive to year-to-year variations in factors such as available soil moisture at freeze-back, the winter snow cover, and spring snowmelt conditions.

The magnet probe lends itself to a variety of improvements, depending upon the needs of the users, and it seems amenable to the measurement of numerous field problems.

ACKNOWLEDGMENTS

The field work has been supported by the Geological Survey of Canada; the Polar Continental shelf Project; the Inuvik Scientific Resource Centre, Inuvik, Northwest Territories; and the Natural Sciences and Engineering Research Council of Canada. S. Irwin, G. Lougheed, and G. Thompson have carried out many of the field measurements.

REFERENCES

Chen, X.
1984: Current developments in China on frost-heave processes in soil; Permafrost, Fourth International Conference, Final Proceedings, July 17-22, 1983, National Academy Press, Washington, D.C., p. 55-60.

Cheng, G.
1982: The forming process of thick layered ground ice; Scientia Sinica (Series B), v. 25, p. 777-788.

Chizhov, A.B., Chizhova, N.I., Morkovkina, I.K., and Romanov, V.V.
1983: Tritium in permafrost and in ground ice; Permafrost, Fourth International Conference, Proceedings, July 17-22, 1983, National Academy Press, Washington, D.C., p. 147-151.

James, P.A.
1971: The measurement of soil frost-heave in the field; British Geomorphological Research Group, Technical Bulletin No. 8, GeoAbstracts, University of East Anglia, Norwich, England, 43 p.

Lagov, P.A. and Parmuzina, O. Yu.
1978: Ice formation in the seasonally thawing layer (field observations at the Ust'-Yenisey Research Station) (in Russian); in General Geocryology, P.I. Melnikov (ed.); Nauka, Novosibirsk, USSR, p. 56-59.

Mackay, J.R.
1981: Active layer slope movement in a continuous permafrost environment, Garry Island, Northwest Territories, Canada; Canadian Journal of Earth Sciences, v. 18, p. 1666-1680.
1983: Downward water movement into frozen ground, western Arctic coast, Canada; Canadian Journal of Earth Sciences, v. 20, p. 120-134.

Mackay, J.R. and Lewis, C.P.
1981: Frost heave at Inuvik, N.W.T.; 4th Canadian Permafrost Conference 2-6 March 1981, Calgary, Alberta, Abstracts, p. 116-117.

Mackay, J.R. and MacKay, D.K.
1976: Cryostatic pressures in nonsorted circles (mud hummocks), Inuvik, Northwest Territories; Canadian Journal of Earth Sciences, v. 13, p. 889-897.

Mackay, J.R., Ostrick, J., Lewis, C.P., and MacKay, D.K.
1979: Frost heave at ground temperatures below 0°C, Inuvik, Northwest Territories; in Current Research, Part A, Geological Survey of Canada, Paper 79-1A, p. 403-405.

McGraw, R.W., Outcalt, S.I. and Ng, E.
1978: Thermal properties and regime of wet tundra soils at Barrow, Alaska; Proceedings, 3rd International Conference on Permafrost, 10-13 July 1978, Edmonton, Alberta, National Research Council of Canada, v. 1, p. 47-53.

Muir, M.P.
1983: The role of pe-existing, corrugated topography in the development of stone stripes; Permafrost, Fourth International Conference, Proceedings, July 17-22, 1983, National Academy Press, Washington, D.C., p. 877-882.

Parmuzina, O. Yu
1977: the dynamics of the cryogenic structure of the soils in the active layer (in Russian); Herald of Moscow University, Geography Series No. 6, p. 91-94.
1978: Cryogenic texture and some characteristics of ice formation in the active layer (in Russian); in Problems of Cryolithology, Volume 7, A.I. Popov (ed.); Moscow University Press, Moscow, USSR, p. 141-164; translated in Polar Geography and Geology, July-Sept. 1980, p. 131-152.
1979: An approach to the question of redistribution of moisture in frozen soil (according to full-scale observations) (in Russian); in Problems of Cryolithology, Volume 8, A.I. Popov (ed.); Moscow University Press, Moscow, USSR, p. 194-197.

Smith, M.W.
1985: Observations of soil freezing and frost heave at Inuvik, Northwest Territories, Canada; Canadian Journal of Earth Sciences, v. 22, p. 283-290.

Williams, P.J.
1984: Moisture migration in frozen soils; Permafrost, Fourth International Conference, Final Proceedings, July 17-22, 1983, National Academy Press, Washington, D.C., p. 64-66.

Wright, R.K.
1983: Relationships between runoff generation and active layer development near Schefferville, Quebec; Permafrost, Fourth International Conference, Proceedings, July 17-22, 1983, National Academy Press, Washington, D.C., p. 1412-1417.

- 6 -

Cobble lithologies in eskers of central Labrador[1]

Project 820039

A.M. Bolduc[2], R.A. Klassen, and E.B. Evenson[2]
Terrain Sciences Division

Bolduc, A.M., Klassen, R.A., and Evenson, E.B., Cobble lithologies in eskers of central Labrador; in Current Research, Part A, Geological Survey of Canada, Paper 87-1A, p. 43-51, 1987.

Abstract

Cobble lithology work on the Gabbro esker and the Ossokmanuan esker in central Labrador shows that the eskers are essentially a three-component system – crystalline, sedimentary, and volcanic rocks, with volcanic rocks a minor component. The contents of crystalline and sedimentary rocks have a mirror image behaviour, with concentrations of sedimentary rocks decreasing down-esker and those of crystalline rocks increasing. Tributary eskers can have a dramatic influence on the lithologies of trunk systems for a short distance (≤ 10 km) down-esker from esker junctions. First appearance of a particular bedrock lithology and the peak abundance of the lithology in the esker are not at the same place, but occur some distance down-esker from the first contact with that bedrock type.

Résumé

L'étude pétrographique des galets des eskers Gabbro et Ossokmanuan dans le centre du Labrador montrent que ces remblais sont fondamentalement des systèmes à trois composantes : roches cristallines, sédimentaires et volcaniques, ces dernières en faibles concentrations. Les concentrations en roches cristallines et sédimentaires se présentent un peu comme l'image d'un miroir; celles des roches sédimentaires diminuent en direction descendante du versant de l'esker, tandis que celles de roches cristallines augmentent en sens contraire. Les eskers tributaires peuvent avoir une influence considérable sur la composition des eskers principaux; cette influence s'exerce cependant sur une courte distance (10 km et moins) mesurée en direction descendante à partir du point de confluence. L'abondance d'un type de roche en place donné dans l'esker atteint son maximum non pas au premier contact de la roche, mais à une certaine distance mesurée vers le bas de ce premier contact.

[1]Contribution to Canada-Newfoundland Mineral Development Agreement 1984-1989. Project carried by Geological Survey of Canada
[2]Lehigh University, Bethleham, PA, U.S.A.

INTRODUCTION

Two large esker systems in central Labrador were studied in the summer of 1986 to determine the history of debris transport within glacial and glaciofluvial systems and the origin and development of eskers. The two systems are located west of the town of Churchill Falls. The eskers, informally here named the "Gabbro" and "Ossokmanuan" eskers, were chosen for their accessibility (Fig. 6.1) and for the variety of bedrock units crossed along their lengths, especially within the Labrador Trough (Fig. 6.2). The marked variation in bedrock allows the use of indicator lithologies as a means of studying where and how debris is entrained, transported, and deposited within esker systems. This report presents a preliminary account of field work and results of lithological analysis of the cobble fraction. The work represents a contribution to an ongoing study of drift prospecting techniques in Labrador, funded by the Canada-Newfoundland Mineral Development Agreement, and is part of a Ph.D. thesis by A.M. Bolduc (E.B. Evenson, supervisor).

PREVIOUS WORK

There has been little previous work done on the extensive esker systems of central Labrador. Kirby (1961), based on the regular patterns of eskers and meltwater channels, postulated that the esker systems formed within a stagnant ice sheet during deglaciation. Edwards (1972) studied lithologies and grain size distributions in the Gabbro esker and, based on published curves of grain size distribution for various modern river systems, he postulated deposition of esker sediments within a high energy, river-like environment. The lag in composition between the first crossing of a bedrock unit by an esker and the first appearance of that lithology in the cobble and pebble fraction of the esker led him to conclude that the glaciofluvial sediments were derived from underlying till and debris in and on the ice rather than directly from bedrock.

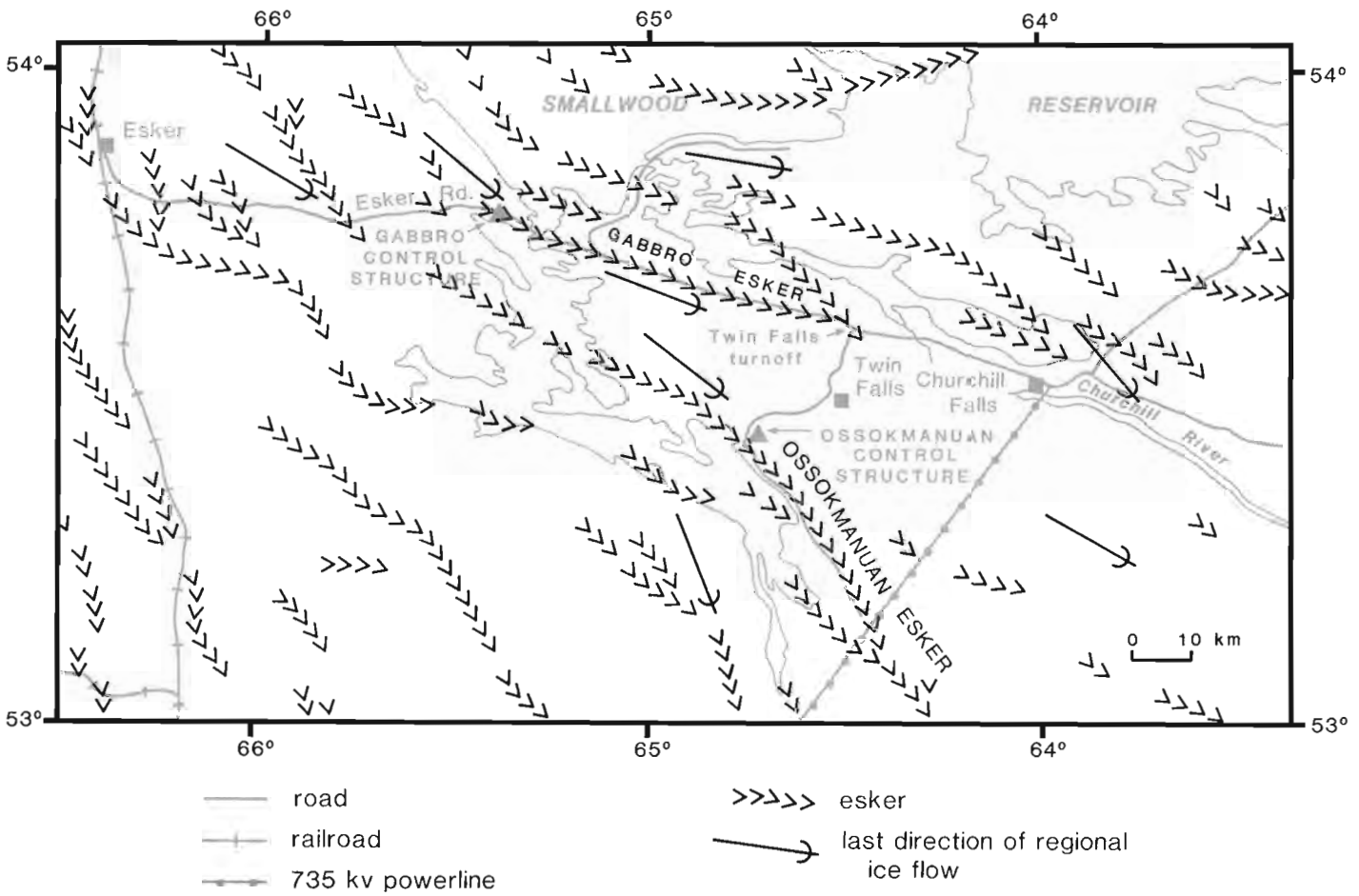


Figure 6.1. Location map showing esker systems studied and regional ice flow directions.

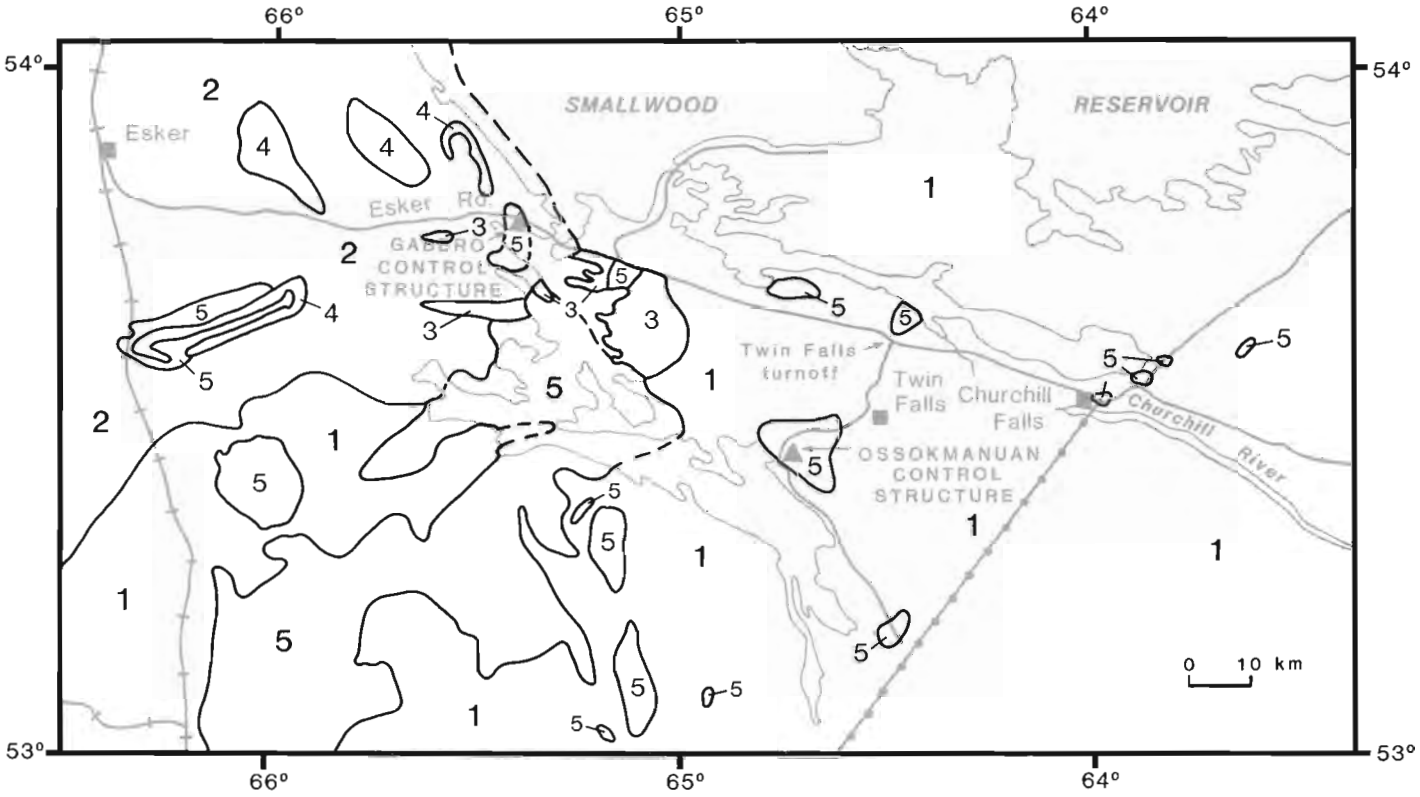
GEOLOGICAL AND PHYSIOGRAPHIC SETTING

The study area lies within the Lake Plateau physiographic region of central Labrador (Hare, 1959). Terrain is generally characterized by low rolling hills having a relief of approximately 175 m, and is deeply dissected by canyon-like river valleys (e.g., the Churchill). To the west, high hills, locally known as the Sims Mountains, have a relief of up to 425 m.

The western half of the study area is located within the Labrador Trough, and is underlain by red and green argillites, arkoses, quartzites, slates, and volcanic rocks (Greene, 1970; Wardle and Rivers; 1985; Fig. 6.2). The eastern half is located in the Grenville Province (Wardle, 1985), and the bedrock includes gneisses and various intrusive suites which are monzonitic and gabbroic in composition (Fig. 6.2). Rocks of the Labrador Trough can be readily identified in cobble size, and because the outcrop area of some lithologies is restricted, they provide indicators of transport within glacial and glaciofluvial systems. The most important indicators are volcanic rocks of the Blueberry Lake Group and quartzites of the Sims Formation. Most of the crystalline rocks cannot be readily distinguished in cobble size, and their outcrop area is usually fairly large, making them poor indicators in most cases.

The area has generally a discontinuous till cover with local areas characterized by drumlins or ribbed (Rogen) moraine. The last ice flow direction, as recorded by glacially streamlined landforms and striations, was towards 120°-140° over most of the area, and varies to 170° in the south-central part of the area (Fig. 6.1). Striations also indicate an earlier phase of flow towards the northeast (40°) across the entire area (Klassen and Bolduc, 1984; Bolduc, 1985).

There are numerous eskers that vary in length from <1 km to hundreds of kilometres, although the longest ones



1. Grenville Province: undifferentiated granitoid to gneissic rocks
2. Labrador Trough: metasedimentary rocks and volcanic rocks
3. Blueberry Lake Group: felsic volcanic rocks
4. Sims Formation: quartzite and arkose
5. Gabbroid rocks

Figure 6.2. Generalized bedrock geology (from Greene, 1970; Wardle and Rivers, 1985).

are discontinuous. Heights range from a few metres to 15 m and widths range from 50 to 100 m for the esker ridge, although the largest eskers may also have an apron of glaciofluvial sediments on their sides which may be up to 1 km wide. The esker systems are oriented parallel to the last ice flow direction. Flow within the eskers, as indicated by the transport directions of indicator erratics, was to the southeast.

The Gabbro esker (Fig. 6.1) is approximately 70 km long, discontinuous, and has two tributary eskers merging with it on its north side. One tributary joins it approximately 20 km downstream from its head while the other joins it less than 10 km from its terminus, near the Twin Falls turnoff. The 'upper' part of the esker lies within Labrador Trough (0-34 km), and the 'lower' part traverses crystalline bedrock. The esker has been cut open and planed off during the construction of the Esker Road and Smallwood Reservoir, but where the original ridge is still present it displays a sharp crest and fairly steep sides. It stands 5 to 15 m above the adjacent terrain. The Gabbro esker connects with Valley River valley, which represents a westward extension of Churchill River. Churchill River has been interpreted as one of the major meltwater channels active during deglaciation (Bolduc, 1985).

The Ossokmanuan esker is close to 200 km long, discontinuous, and has three fairly large eskers merging with it, one near its head, which joins from the east, and two near its end which join from the west (Fig. 6.1). The esker originates in the Labrador Trough (0-110 km), although most of the sampled section overlies crystalline bedrock. It varies from sharply crested to fairly broad and has steep sides; in numerous places it has multiple ridges and kettle holes. The esker stands 3 to 12 m above the adjacent terrain.

METHODS AND DATA

The Gabbro esker is easily accessible along 70 km of the Esker Road from a point located 6 km west of the Gabbro Control Structure to the Twin Falls turnoff (Fig. 6.1). The

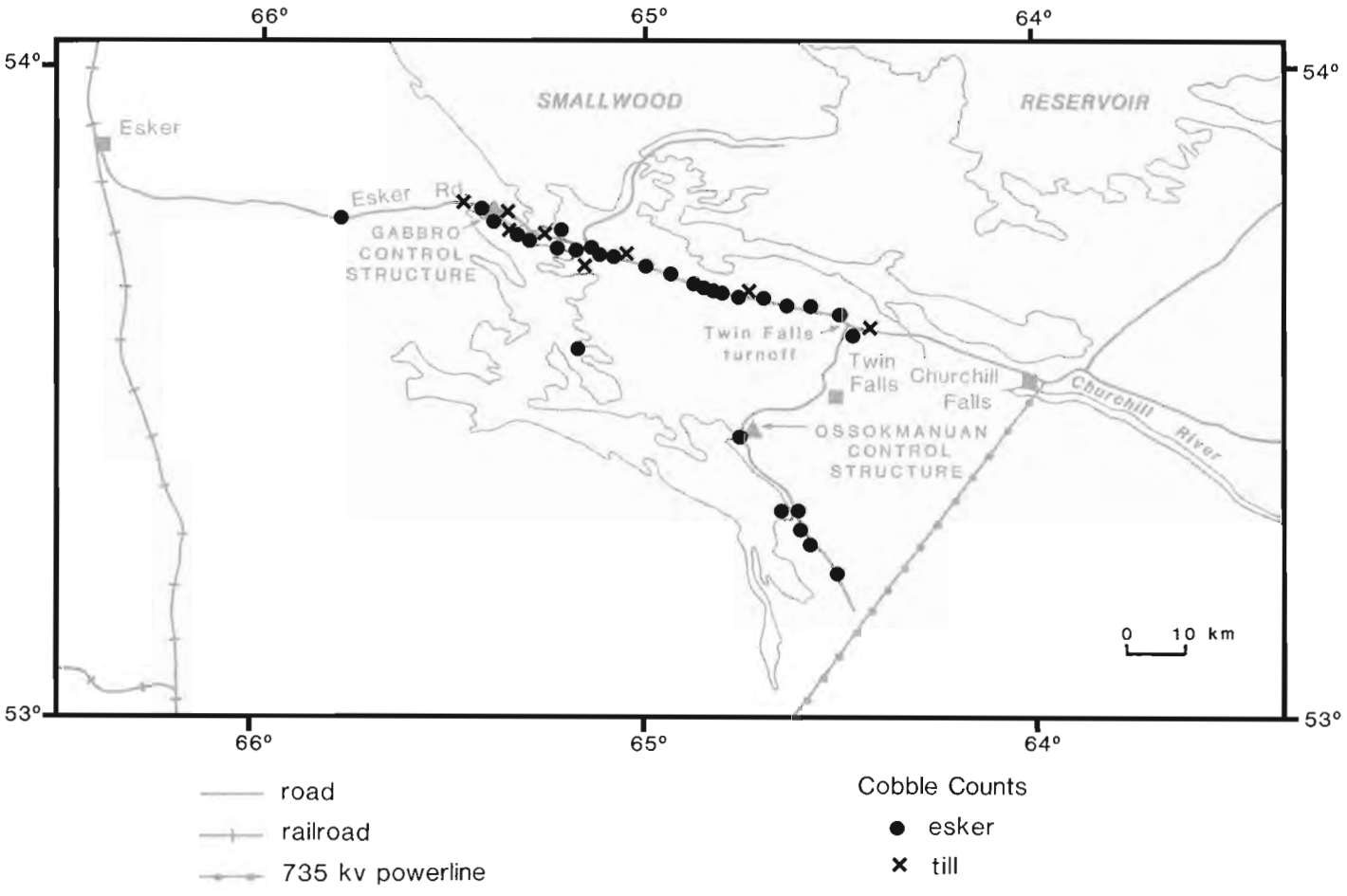


Figure 6.3. Sites of cobble counts in Gabbro esker, Ossokmanuan esker, and till.

Ossokmanuan esker is accessible along the Ossokmanuan road from the Ossokmanuan Control Structure, and over a distance of 31 km from a point located 17 km south of the structure to the 735 kV power line. Borrow pits along Esker and Ossokmanuan roads provided easy access to esker sediments and permitted cobble counts to be made at regular intervals along Gabbro esker and the part of Ossokmanuan esker accessible by road. Other comparatively minor eskers were trenched at their intersection with Esker Road west of the Gabbro esker and with Orma Lake road, northeast of Churchill Falls. The exceptionally low level of Smallwood Reservoir during the 1986 field season also provided opportunities to do cobble counts on strandlines along some eskers.

Cobble counts (100 to 200 cobbles each; clast size ranging from 5 to 20 cm) were performed at 28 sites (Fig. 6.3). At selected sites, duplicate counts provided a measure of the counting variability: the maximum variation was ±3%. Plots of per cent crystalline, sedimentary, and volcanic rocks were made for the Gabbro esker (Fig. 6.4) and Ossokmanuan esker (Fig. 6.5). For Gabbro esker, the crystalline category was further subdivided into gneissic, gabbroic, and "other crystalline" rocks, most of which are granitic in composition (Fig. 6.6). Sedimentary rocks were subdivided into black mudstone, arkose, and Sims quartzite (Fig. 6.7, 6.8). Other lithological types, such as feldspar porphyry, jasper conglomerate, iron formation, and chert breccia occur in minor amounts (<1%) and are not reported here. To facilitate compilation, the distance reported between each count along an individual esker (Fig. 6.4 to 6.8) is a straight line distance rather than along the esker ridge. This may mean a certain amount of distortion in the plots, but it is not believed to have much significance at the scale reported. Distance measurements originate (0 km) at the estimated head of the esker systems. The position of bedrock contacts is indicated on the plots. At eight sites along the Gabbro esker, cobbles in till adjacent to the esker systems were also counted (Fig. 6.9).

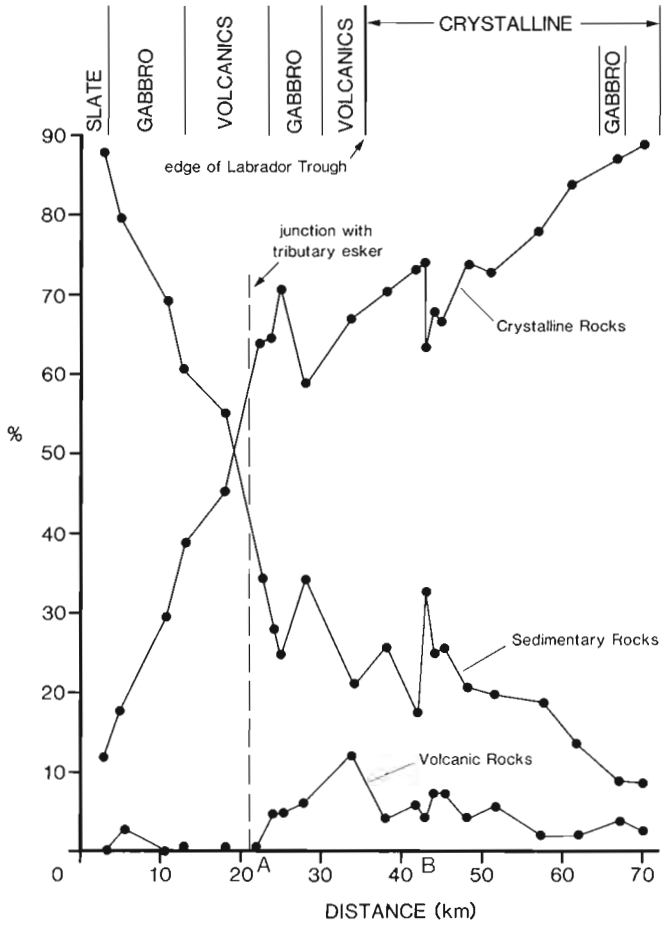


Figure 6.4. Variation in the concentration of crystalline, sedimentary, and volcanic rocks in Gabbro esker; bedrock crossed by the esker is indicated.

RESULTS AND DISCUSSION

Gabbro esker

In the Gabbro esker, the abundance of crystalline rocks (gneissic, gabbroic, and granitic) increases from ≤12% at the head to 89% at the toe, with minor variations of 10-15% (Fig. 6.4). Because volcanic rocks make up only about 10% of the cobbles and because this is a three-component system, the crystalline curve is mirrored by a corresponding decrease (from 88% at the head to 9% at the toe) in the percentage of sedimentary rocks from the Labrador Trough. A perturbation in the crystalline and sedimentary curves corresponds to the junction with a tributary esker at km 21.5, although a second one, at km 43, does not correspond to a junction (Fig. 6.4, A, B, respectively). Volcanic rocks are generally a minor component of the cobbles (0-12%) with a high of 12% occurring at km 34, approximately 20 km down-esker from the first contact with volcanic bedrock at km 14, and then declining to approximately 5% at km 38. Up to 3% volcanic rocks occurs in samples taken before the esker crosses Blueberry Lake Group (volcanic rocks) at km 14; the volcanic rocks are likely derived from glacial transport of volcanic debris from elsewhere in the Labrador Trough.

Within the Labrador Trough, the down-esker increase in the abundance of crystalline rocks, from 10 to 60%, is due primarily to granitic clasts, which increase from 3 to 37% in the first 26 km (Fig. 6.6). The crystalline debris is assumed to have been reworked from till, and this interpretation is supported by the high percentage of crystalline debris in till in the southern part of the Labrador Trough (Fig. 6.9). The presence of this debris is surprising, not only because there is no underlying or up-esker bedrock source of crystalline rock, but also because the last phase of regional ice flow was directed out of the Labrador Trough and could not have transported granitic rocks to the area. Although Edwards (1972) explained these high percentages by local ice movements around Sims Mountains, bringing granitic debris into the area, he did not provide evidence for this interpretation. Recent field work by Klassen and Thompson (1987) documents a strong phase of eastward ice flow across crystalline

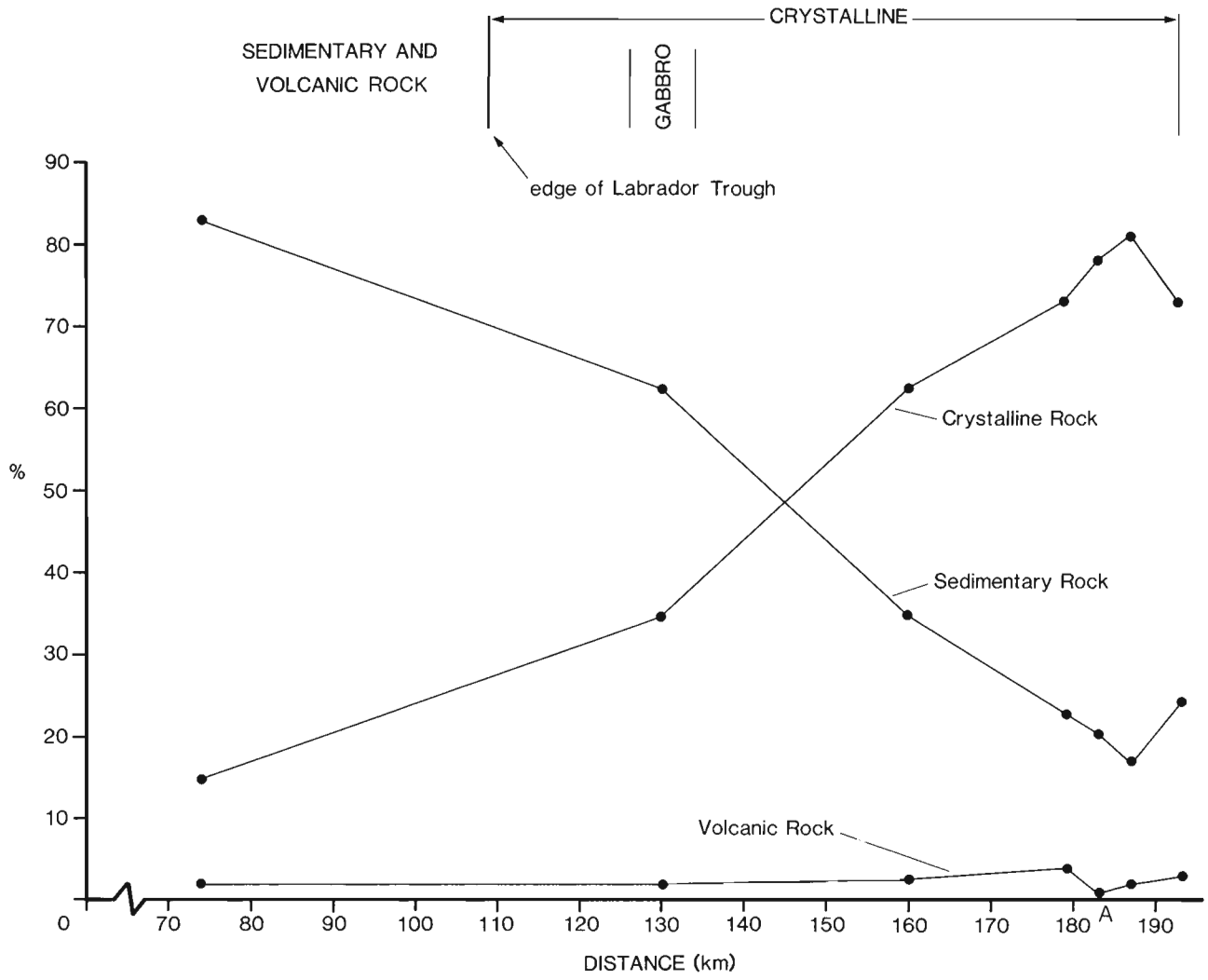


Figure 6.5. Variation in the concentration of crystalline, sedimentary, and volcanic rocks in Ossokmanuan esker; bedrock crossed by the esker is indicated.

highlands west of Labrador Trough and transport of crystalline debris into the trough. In addition, pre-Late Wisconsinan northeast glacial transport has been demonstrated across central Labrador (Klassen and Bolduc, 1984; Bolduc, 1985; Thompson and Klassen, 1986) that could also have brought crystalline debris into the area. Transport during either of these phases of flow, rather than local ice movement, may be resposible for the crystalline debris in this area of the Labrador Trough.

The peak of abundance in gneissic rocks, which is located within the Labrador Trough at km 22 (A of Fig. 6.4 and 6.6), corresponds to the area where a minor esker merges with the Gabbro esker from the north. The minor esker (approximately 7 km in length) runs, in its upper part, over gneisses and appears to have brought a significant amount of gneissic debris to the Gabbro esker. The influence of the tributary esker input lasts for approximately 6 km until km 28, where the percentage of gneiss returns to 18%. This is believed to be a minimum estimate for the length of the glaciofluvial system active at that time.

Outside the Labrador Trough (km 354-70), the crystalline curve (Fig. 6.6) shows increase in the percentage of gneissic rocks as the esker runs over gneissic bedrock, while granitic rock percentages fluctuate. Because different granitic plutons in central Labrador have similar characteristics and can be gneissic in places (Wardle, 1985), further interpretation of the crystalline curves is difficult and will not be attempted here. Gabbroic rocks occur in bedrock throughout the area and account for up to 11% of the cobbles in the esker (Fig. 6.6). Although, it is difficult to assign individual peaks of abundance to specific bedrock sources, there seems to be a broad correlation between gabbroic bedrock and compositional "peaks" which occur approximately 9 km down-esker from the source.

Within the Labrador Trough, concentrations of sedimentary rocks decrease from 88% to 21% (Fig. 6.4, 6.7), either as a result of input of crystalline rock, which dilutes the sedimentary rocks, or breakage of the less resistant sedimentary rocks in the size fraction studied, or both. Quartzites of the Sims Formation, which were found by Edwards (1972) to be

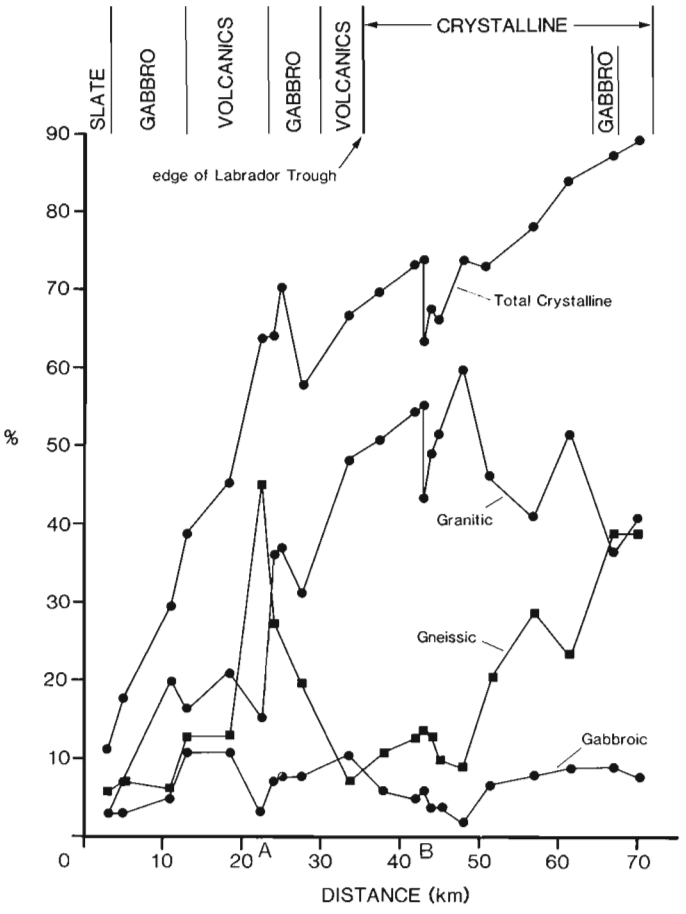


Figure 6.6. Variation in the concentration of granitic, gneissic, and gabbroic rocks, which comprise the crystalline rock fraction, in Gabbro esker.

the least susceptible to breakage, decrease in abundance from 23% to 6% in the first 34 km of the esker (Fig. 6.7), suggesting that dilution maybe an important process. Along the esker, arkose decreases in abundance from 13% at the head to 1% at the toe, although it is generally about 4% outside the Labrador Trough. Black musdtones, which are more fragile, decrease in abundance from 36% to 3%. Other sedimentary rocks account for less than 1% of the cobbles, and their "spotty" occurrence was not plotted.

Cobble lithologies in till adjacent to Gabbro esker (Fig. 6.9) appear to reflect change in underlying bedrock more readily than the esker, an observation used by Edwards (1972) and Van Beever (1971) to conclude that eskers are derived largely from reworked till and not directly from bedrock. Pebble lithologies (4-6 mm fraction) in the till, however, can show the strong influence of bedrock sources up-ice by the glacial transport of significant amounts of Proterozoic sedimentary rocks from the Labrador Trough over crystalline terrane (Bolduc, 1985).

Ossokmanuan esker

In the Ossokmanuan esker, the first cobble count was done 73 km down-esker from its head (Fig. 6.5) and the last one 20 km from its toe. Levels of crystalline rocks increase from 15% to a maximum of 81% at km 187 and then decrease to 73% at the last sample site at km 194. As in the Gabbro esker, the shape of the crystalline curve of the Ossokmanuan esker is mirrored by a corresponding decrease in the percentage of sedimentary rocks (83% to 17%) derived from the Labrador Trough, with an increase to 24% on the last count. Volcanic rock contents range from 1-4% along the Ossokmanuan esker.

The long intervals between the cobble counts in the upper part of the Ossokmanuan esker preclude detailed interpretation of the system (Fig. 6.5, 6.8). Down-esker from a tributary esker, however, a significant increase in black mudstone was registered (A of Fig. 6.8). The tributary esker contains 11% black mudstone, 4% arkose, and 5% quartzite, in comparison with the Ossokmanuan esker, which has 4% black mudstone, 8% arkose, and 9% quartzite just above the junction. The tributary esker leaves the Labrador Trough 50 km to the northwest of the junction, whereas Ossokmanuan esker traverses crystalline bedrock for more than 85 km. It is not clear from the data what length of Ossokmanuan esker is

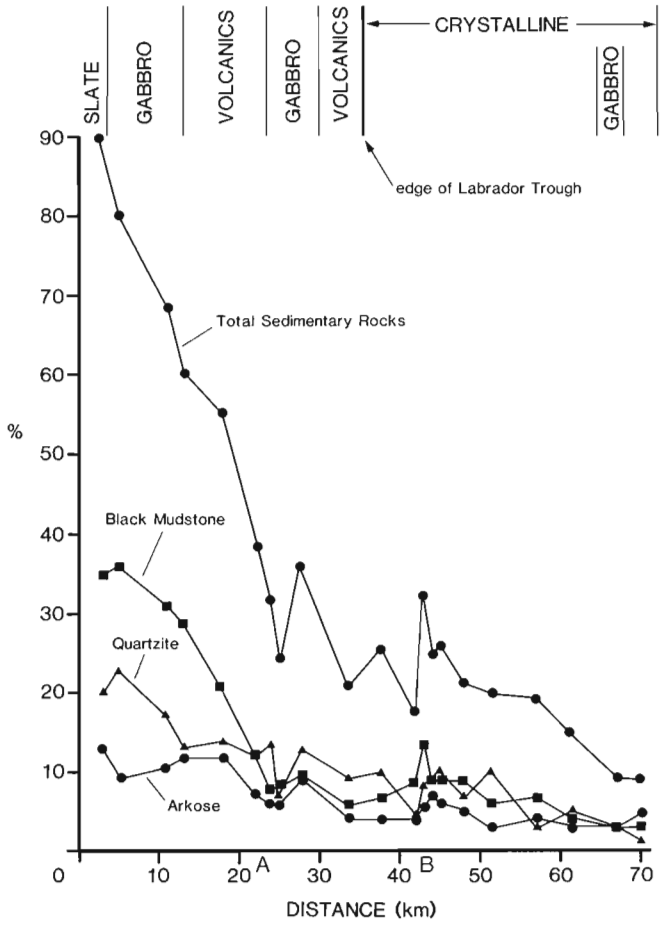


Figure 6.7. Variation in the concentration of mudstone, arkose, and quartzite, which comprise the sedimentary rock fraction, in Gabbro esker.

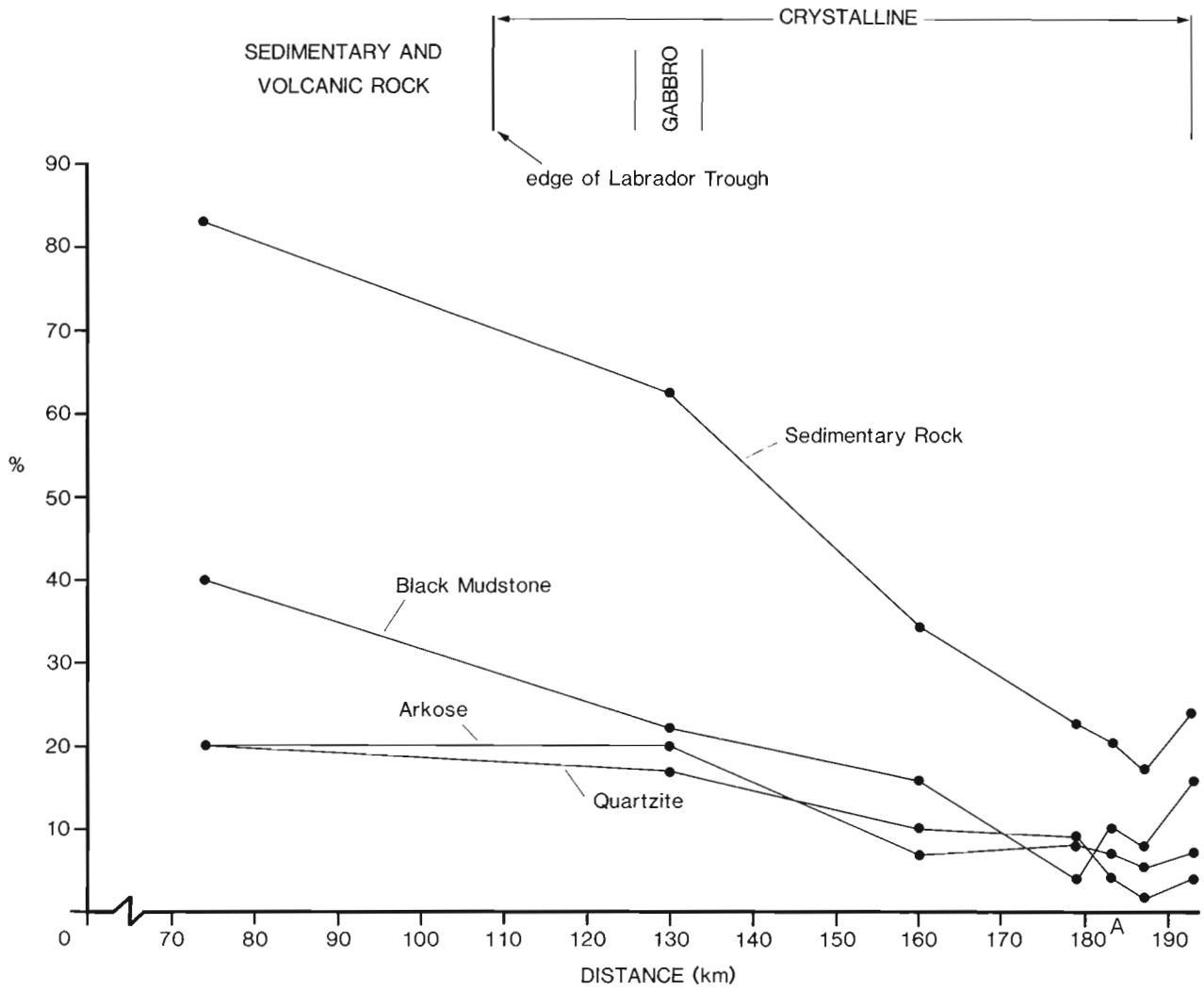


Figure 6.8. Variation in the concentration of mudstone, arkose, and quartzite, which comprise the sedimentary rock fraction, in Ossokmanuan esker.

compositionally influenced by the tributary below the junction, but it is believed to be fairly short, probably in the same order as the Gabbro esker, approximately 6 km.

In both the Gabbro and Ossokmanuan eskers, a significant increase in the abundance of sedimentary rocks (17 to 33% in the Gabbro esker, Fig. 6.4; 17 to 24% in the Ossokmanuan esker, Fig. 6.5) was registered in an area of crystalline rock long after the eskers leave the Labrador Trough (B of Fig. 6.4; A of Fig. 6.5). In both cases, the increase corresponds to the presence of a tall ridge (at least 14 m high in the case of the Gabbro esker) following down-esker from an area of fluvioglacial sediments with no esker ridge development. The compositional peak is due to an increase in concentration of all three major sedimentary rock types, but most particularly arkoses and Sims Formation quartzites in the case of the Gabbro esker, and black mudstones in the case of the Ossokmanuan esker.

CONCLUSION

The study of cobble lithologies of central Labrador esker systems may provide insight into esker genesis and dynamics of glaciofluvial sedimentation. To date, this study has demonstrated that first appearance and peak percentage of certain rock types (e.g. volcanic rocks of the Blueberry Lake Group) do not occur at the same point in the esker, and that both occur some distance down-esker from where the esker first crossed that bedrock type. This "lag" in appearance has been noted by others such as Lee (1965) and Hellaakoski (1931). We can also demonstrate that even minor tributary eskers can have a dramatic influence on the composition of a major esker system for a short distance ($\leq$10 km) down-esker. More work needs to be done in order to explain some aspects of the curves presented and to postulate a comprehensive model for esker sedimentation which could then be of use to the mineral exploration industry.

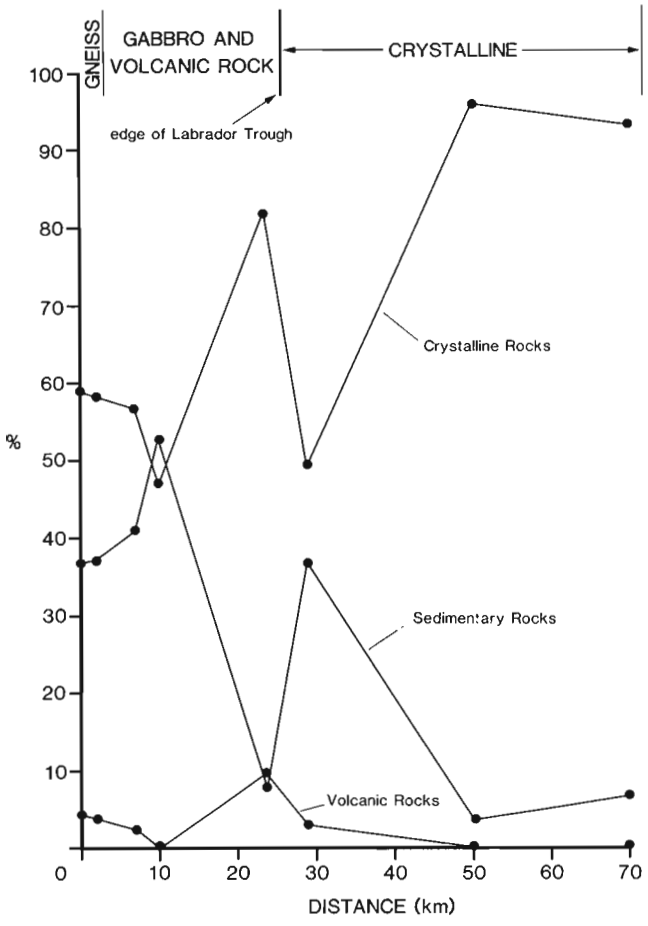


Figure 6.9. Variation in the concentration of crystalline sedimentary and volcanic rocks in till adjacent to Gabbro esker.

ACKNOWLEDGMENTS

Ms. M. Rogers is thanked for her extremely helpful assistance during field work. The Churchill Falls (Labrador) Corporation allowed use of their roads and facilities; both the Corporation and the people of the town of Churchill Falls are thanked for their help during the course of this study. F.J. Thompson provided ice flow directions in the area of the Sims Mountains.

REFERENCES

Bolduc, A.M.
1985: The Quaternary history of the Churchill Falls area, Labrador; unpublished M.Sc. thesis, Carleton University, Ottawa, Ontario, 95 p.

Edwards, W.A.D.
1972: A study of Gabbro Esker, Labrador; unpublished B.Sc. thesis, Brock University, St. Catharines, Ontario, 46 p.

Greene, B.A.
1970: Geological map of Labrador; Department of Mines, Agriculture and Resources, Province of Newfoundland and Labrador, scale 1:100 000.

Hare, F.K.
1959: A photo reconnaissance survey of Labrador-Ungava; Department of Mines and Technical Surveys, Geographical Branch, Memoir 6, 83 p.

Hellaakoski, A.
1931: On the transportation of materials in the esker of Lattila; Fennia, v. 52, no. 7; 41 p.

Kirby, R.P.
1961: Movement of ice in Central Labrador-Ungava; Cahiers de géographie de Québec, v. 10, p. 205-218.

Klassen, R.A. and Bolduc, A.
1984: Ice flow directions and drift composition, Churchill Falls, Labrador; in Current Research, Part A, Geological Survey of Canada, Paper 84-1A, p. 255-258.

Klassen, R.A. and Thompson, F.J.
1987: Ice flow history and glacial dispersal in the Labrador Trough; in Current Research, Part A, Geological Survey of Canada, Paper 87-1A, report 8.

Lee, H.A.
1965: Investigation of eskers for mineral exploration; Geological Survey of Canada, Paper 65-14, p. 1-17.

Thompson, F.J. and Klassen, R.A.
1986: Ice flow directions and drift composition, central Labrador; in Current Research, Part A, Geological Survey of Canada, Paper 86-1A, p. 713-717.

Van Beever, H.G.
1971: The significance of the distribution of clasts within the Great Pond esker and adjacent till; unpublished M.Sc. thesis, University of Maine, Orono, Maine, 62 p.

Wardle, R.J.
1985: Geology of the Churchill Falls area; Mineral Development Division, Department of Mines and Energy, Government of Newfoundland and Labrador, Report 85-2, 70 p.

Wardle, R.J. and Rivers, T.
1985: Geology of the Gabbro Lake area, Labrador (23 H NW); Mineral Development Division, Department of Mines and Energy, Government of Newfoundland and Labrador, Map 85-26, scale 1:100 000.

- 7 -

Soft-sediment deformation structures in overburden drill core, Quebec[1]

Project 690095

S.L. Smith and R.H. Rainbird[2]
Terrain Sciences Division

Smith, S.L. and Rainbird, R.H., Soft-sediment deformation structures in overburden drill core, Quebec; in Current Research, Part A, Geological Survey of Canada, Paper 87-1A, p. 53-60, 1987.

Abstract

Soft-sediment deformation structures in overburden drill core, recovered using the Rotasonic method, can be ascribed to both primary (synsedimentary) and secondary (drill-induced) origins. Liquefaction and hydroplastic deformation, usually resulting from stresses developed during and shortly after deposition, can also be caused by the high-frequency vibration and rotation used to core the sample.

In order to interpret observed sedimentary structures correctly, secondary structures induced by the drilling process are distinguished based on the following criteria: a) truncation or overprinting of primary features; b) downwarping of previously planar layers along the edge of the core; c) symmetry of fold axes about the axis of the drill core; d) symmetry of faults exhibiting opposing sense of reverse displacement; e) rotation of cohesive fragments with associated remobilization of interstitial sediment; f) presence of décollement surfaces in compacted diamictons exhibiting a concentric shear pattern symmetric about the core axis, and g) indication from on-site notes of intervals that would most likely exhibit drill-induced deformation.

Résumé

Les structures de déformation observées dans des sédiments meubles prélevés par carottage Rotasonic peuvent être attribuées à des causes primaires (contemporaines de la sédimentation) et secondaires (provoquées par le forage). La liquéfaction et la déformation hydroplastique, qui résultent habituellement de contraintes ayant pris naissance pendant et peu après la sédimentation, peuvent aussi avoir été causée par les hautes fréquences émises par la vibration et la rotation de l'outil de carottage.

Pour interpréter correctement les structures sédimentaires observées dans les échantillons, il faut distinguer les déformations secondaires provoquées par le forage. On les reconnaît aux indices suivants : a) érosion de structures manifestement primaires, ou déformations secondaires reprises à des déformations primaires; b) affaissement de couches antérieurement planes en bordure de la carotte; c) symétrie des axes de pli autour de l'axe de la carotte; d) présence de failles inverses où le déplacement des lèvres s'est fait dans des directions opposées de part et d'autre de l'axe de la carotte; e) rotation de fragments cohésifs avec remobilisation des sédiments interstitiels; f) présence de surfaces de décollement dans des diamictons compactés montrant des figures de cisaillement concentriques disposées symétriquement autour de l'axe de la carotte; et g) indication, d'après les observations faites sur place, de la présence d'intervalles qui présentent des problèmes de prélèvement, une déformation externe ou ce qui est très probablement une déformation de sédiments meubles provoquée par le carottage.

[1]Contribution to Federal Asbestos Initiatives, Geoscience Research Program 1984-1987. Project carried by Geological Survey of Canada.
[2]University of Western Ontario, London, Ontario N6A 3K7

INTRODUCTION

A major overburden drilling project was undertaken during 1984-85 (Shilts and Smith, 1986) to recover intact, large-diameter core for stratigraphic studies and geochemical sampling. Excellent core recovery was achieved, in most sediments, using the high-frequency vibration Rotasonic drill operated by Midwest Drilling of Winnipeg, Manitoba. The core was "logged" in detail including description of recognizable primary sedimentary structures.

Resonant vibration and rotation used to core the sample has caused selective liquefaction, fluidization, or hydroplastic deformation (terminology of Allen, 1984) of susceptible sediments, producing distinct structures. Evidence from the drill core, documented by photographs, indicates that the secondary soft-sediment deformation imposed by the drilling process, may obscure or modify primary (synsedimentary) structures. This overprinting is common in unconsolidated deformable sediments and usually is difficult to distinguish from primary features. It is important to make this distinction because primary structures are indicative of a particular depositional mechanism. For example, convolute bedding associated with turbidites is indicative of a gravitationally unstable density gradient produced by high sedimentation rates on unstable slopes. Criteria are described in this paper to identify primary versus secondary structures in Quaternary sediments to aid workers using this drilling method. All the photographs are oriented with the top of the core segment upward.

ROTASONIC DRILLING

The Rotasonic method produces intact, large-diameter overburden drill core for stratigraphic interpretation and geochemical sampling. The system utilizes an oscillator head manufactured by Hawker Siddeley Canada Limited and developed by Midwest Drilling of Winnipeg, Manitoba (Fig. 7.1). High frequency (averaging 5000 rpm) resonant vibration and rotation are used to core the sample and, after retrieval of the interval, used to extrude it, in 5 foot lengths[1], into plastic sleeves (Fig. 7.2).

Sediments are cored with tungsten carbide fronted bits into 4½ inch diameter core barrels over an interval of 20 feet. Casing is sunk alongside to prevent collapse of the borehole walls and then the core barrels are pulled up using drill rods. Each drill "run" was restricted to 20 feet because longer runs usually caused extension of soft sediment into the narrower rods resulting in core much longer than the actual interval drilled, not to mention unwanted secondary deformation. Some length distortion is inherent in the system because the volume of metal in the casing and core barrels must displace an equivalent volume of sediment in the borehole. Detailed description of Rotasonic equipment and techniques is given by Averill et al. (1986).

In general, compact diamictons and cohesive muds afforded the best recovery rate and least amount of length distortion whereas cohesionless sands and gravels and saturated or "quick" clays had the poorest recovery rate. Loose sands tended to push outward in the hole, away from the pressure of the drill bit, and fall out the core barrel during retrieval, resulting in loss of sample. Some water-saturated clays liquefied and were difficult to sample. Deformation from core extension or squeezing is strongest at the top and bottom of individual drill runs. The ground around the drill site vibrates noticeably during drilling.

Drilling fluid or "mud" other than water is not required. Water is used to flush the sample out of the core barrel and is pumped down the hole prior to sinking the casing. In some cases water was injected into the plastic sample sleeve and may have washed or disaggregated coarse grained sediments. On-site notes of core recovery recorded obvious water-disturbed intervals where sediments may have been fluidized. The core was labelled on-site, placed in a 5 foot box, and then moved to a convenient local storage site to be logged. Detailed lithological description was undertaken in Ottawa during relogging to take more geochemical samples and confirm preliminary interpretations of borehole stratigraphy.

To log the core, originally sealed to prevent desiccation and contamination, the plastic sleeve was slit open along its length. Lithologies were described after scraping off the outer 5 mm inch of core which is typically highly disturbed and contaminated by drilling. Sedimentary features were best observed by cutting down through cohesive core to create a flat face, which was sprayed with water from a hand-held atomiser to enhance structures and textural variations and to wash off clay coatings on clasts.

SEDIMENTARY STRUCTURES

Soft-sediment deformation structures form either during deposition or after burial by the processes of liquefaction or hydroplastic deformation, associated with the earliest stages of consolidation when pore fluid is being rapidly expelled. Allen (1984) differentiated between liquefaction and fluidization, both components of the broader term liquidization.

Liquefaction, characterized by negligible yield strength and variable effective viscosity, is common in cohesionless sands or coarse silts that are loosely packed. The framework of interconnected grains is easily transformed by stresses to grains suspended in a fluid matrix that has little resistance to flow. Fluidization is a similar process but implies an addition to the system of water or gas from an external source or confining stratum. Drill core sediments can be locally fluidized by the introduction of water used in the coring or retrieval of sample.

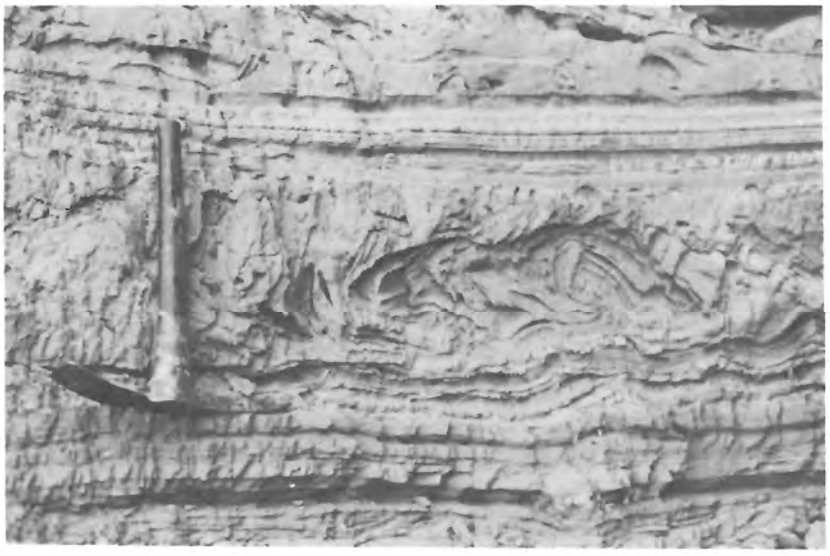
Significant yield strength, or liquid limit, and effective viscosity produces a contorted but not ruptured framework that characterizes hydroplastic deformation. Excellent preservation of deformed laminae contrasts with the apparent lack of preservation of laminae after liquefaction (Lowe, 1975).

Deformation structures usually yield more information about the consolidation history of sediments than their depositional environment (Allen, 1984), but rapid sedimentation

[1]Drilling equipment dimensions and therefore depth are measured in imperial units, which are used in this report where appropriate.



7.1



7.3

Figure 7.1. Rotasonic drilling set-up. 204410-W

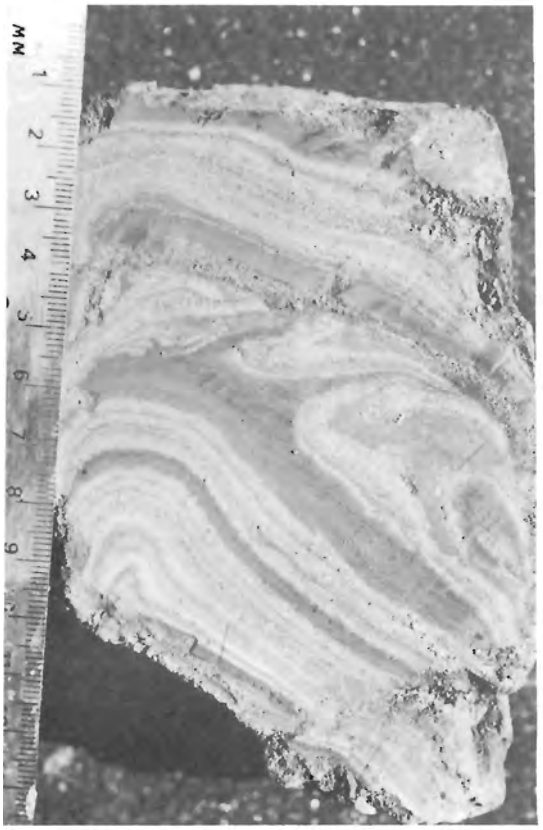
Figure 7.2. Close-up of core being extruded from core barrel into plastic sleeve. 204319

Figure 7.3. Chaotic folding and convolute lamination in a slumped sand-silt horizon. Note that bounding strata are relatively undeformed suggesting a synsedimentary origin for the structure. Length of pick is about 35 cm. 204319-Z

Figure 7.4. Primary flame-like convolute lamination. Note the truncation of the top of the folds by a coarser grained planar bed. 204319-U



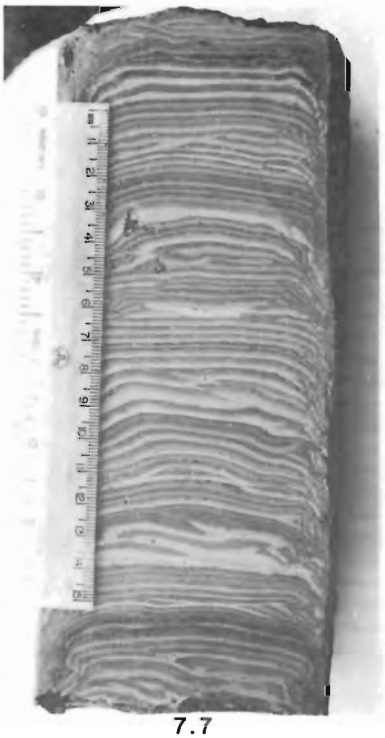
7.2

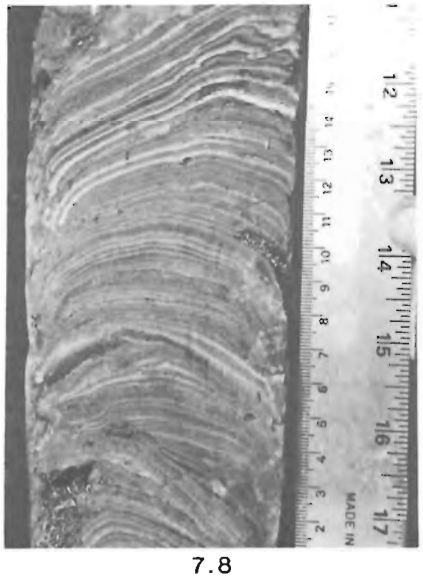


7.4


7.5


7.6


7.7


7.8


7.9

Figure 7.5. Primary brecciated unit overlying undeformed laminated silt. 204319-O

Figure 7.6. Syngenetic brecciated lake sediments, perhaps produced by slumping, unconformably overlying glacial diamict. 204319-H

Figure 7.7. Thinly laminated, color banded, graded rhythmites with edges of the laminae warped downward in the direction of the drilling. Note also microfaulting caused by drill-induced lateral compression. 204319-J

Figure 7.8. Thinly laminated graded rhythmites more pervasively deformed than those shown in Figure 7.7, suggesting that the sediment was less cohesive. 204410-R

Figure 7.9. Graded rhythmite with marked bed-thickness variation and microfaulting of problematic origin. 204410-J

rates occurring in ice-proximal deltaic or glaciolacustrine environments suggest that stresses initiating deformation can be common during initial sedimentation. These stresses are listed by Allen (1984) as: 1) gravitationally unstable vertical profiles of bulk density; 2) non-uniform confining loads; 3) presence of the sediment on a slope; and 4) fluid flow, either at the sediment-fluid interface or internally. Post-depositional stress from glacial overriding, can be invoked to explain localized expulsion of pore water from a rapidly accumulated bed resulting in convolute lamination, diapirs, or other recognizable disruptions (Shilts, 1981). Dionne (1971) described various contorted structures in unconsolidated Quaternary deposits in parts of Quebec.

Sediment gravity flows (turbidites) associated with slumped bedding is developed where high sedimentation rates have promoted loose packing of sands and silts on unstable slopes. Large scale (averaging 50-100 cm thick) slumped beds (Fig. 7.3) sandwiched between undeformed strata, can occur in the glacial environment, perhaps triggered by seismic shock on oversteepened slopes, or the migration of pore water resulting from a build up of pore-fluid pressure. Associated with turbidites, slump structures, and other gravitationally unstable layered sequences, are ball-and-pillow and flame structures, generally attributed to stress caused by non-uniform confining loads. Bogacz et al. (1968) experimentally produced axially symmetric structures resembling ball-and-pillow structures by applying a shock to unconsolidated multilayers.

Strata containing convolute laminae (Fig. 7.3, 7.4), brecciated horizons (Fig. 7.5, 7.6), slump folds, and loading phenomena, which are overlain and underlain by relatively undeformed layers, is considered convincing evidence of synsedimentary origin. Examples of syndepositional faulting, associated with slump structures, were not observed in the drill cores, although could be expected.

Due to the nature of the Rotasonic drilling method, it is hypothesized that high-frequency vibrations produced in the core barrel and drill bit, as well as related compressive stresses, could initiate both hydroplastic deformation and "dynamic" liquefaction. Dynamic liquefaction results from the "single application to a mass of a sufficiently large impulse or load" and depends on events of a more local character than earthquakes or storms (Allen, 1984). The induced vibrations are short-lived and stresses may be related to compression rather than shear. In some cases, this deformation has overprinted primary sedimentary structures and may be difficult or impossible to distinguish based on examination of the drill core. However, some vibration-induced disturbance can be readily recognized.

The most common manifestation of secondary (drill-induced) deformation is downwarping at the edge of the core of previously planar features, causing folding of cohesive silt/clay layers and production of microfaults related to brittle deformation (Fig. 7.7). The depth of penetration of this deformation within a segment of core is probably related to the cohesiveness of the sediment prior to drilling (Fig. 7.8). For example, noncohesive or saturated sediment is more likely to be pervasively deformed. The degree to which an interval of core retains its shape after extrusion is a subjective measure of its cohesiveness.

Grain size variations in laminated sequences result in differing styles of deformation. For example, the silt layer in a graded bed may flow after dynamic liquefaction has been initiated, producing marked bed thickness variation (Fig. 7.9). In the same graded sequence the clay-rich cohesive layers have deformed plastically or brittly.

Loading features such as ball-and-pillow (Fig. 7.10) and flame structures may also result from liquefaction of less cohesive sediments during drilling. Rotated inclusions, such as clay balls (Fig. 7.11) and laminated mud/silt clasts (Fig. 7.12), are common and suggest that at least some of the surrounding material was liquefied and then remobilized to fill interstices.

Further evidence for drill-induced deformation is provided by features such as folds and faults which display structural symmetry about the core axis. Fold axes of primary (gravity-induced) slump folds tend to be flattened towards the original plane of bedding. Also, it would be a rare circumstance where the drill bit would intersect the fold head-on and where the wave length happened to coincide with the core diameter (Fig. 7.13). A similar relationship is seen in Figure 7.14 except that the fold pattern is doubled about the core axis. This symmetry may be analogous to that produced experimentally by Bogacz (1968). Symmetry of faults that display opposing sense of reverse displacement indicates compression probably initiated by the coring process (Fig. 7.15, 7.16). Similar internal disruption can also be expected where the core diameter has obviously been increased by compressional buckling or stretched (thinned) during extrusion. Secondary convolutions can be identified based on axial symmetry and the fact that fold limbs are confined within the core margins (Fig. 7.17).

Lenses of relatively well sorted, fine grained material within a poorly sorted diamict are locally developed, particularly in overconsolidated (extremely compact) tills. The lenses are smaller in size than might be expected for primary structures and are bounded by shear or décollement surfaces developed by the drilling. The presence of décollements or internal shear planes on which the core sheared off and mechanically ground or "sorted" this finer material during rotation, is particularly common in very compacted material (Fig. 7.18). The shear planes are curved down-ward at the edges, as described for laminated sequences (Fig. 7.19). This structure is analogous to brittle deformation in bedrock in which cleavage roughly perpendicular to the drill bit can be selectively ground up along the weaker planes.

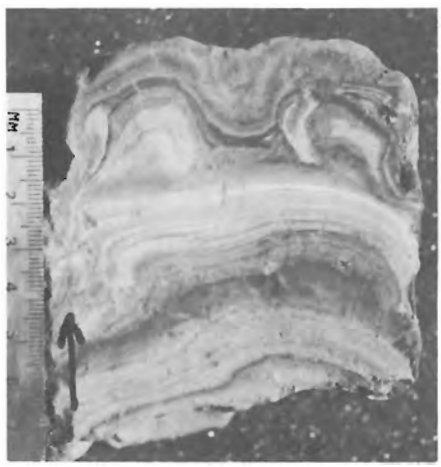
Figure 7.20 illustrates post-drilling secondary deformation induced by a sampling tool, which superficially produces a structure resembling pillar-type water escape structures described by Lowe (1975). Other postdrilling disruption could be caused by vibration of the core during transport and handling.



7.10



7.12



7.14

Figure 7.10. Thick rhythmites displaying primary Bouma divisions associated with turbidites (note the cross-laminations at the top). The superimposed fold near the bottom is probably secondary because it is symmetric about the core axis. 204410-C



7.11



7.13

Figure 7.11. Massive to faintly laminated silty clay containing a rounded clay rip-up clast that has been reoriented parallel to the core axis with resultant concentric laminations in the soft remobilized matrix. 204319-L

Figure 7.12. Graded clay-silt couplets separated along a bedding plane with subsequent infilling by liquefied interstitial material. 204319-G

Figure 7.13. Drill-induced fold with the fold axis parallel to the core axis and fold limbs asymptotic to the edge of the core. 204319-M

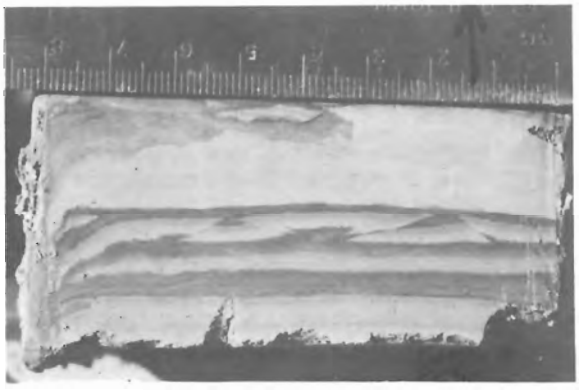
Figure 7.14. Probable secondary folds doubled about the core axis. 204319-R



7.15



7.17



7.16



7.18

Figure 7.15. Micro reverse faults displaying reverse sense of displacement resulting from lateral compression during drilling. 204319-V

Figure 7.16. Multiple reverse faults due to lateral compression during drilling. 204410-A

Figure 7.17. Possible drill-induced convolutions that display some axial symmetry with the core are confined and continuous within the core (i.e., not truncated by the drill), and overprint primary structures evident in the lower half of the photo. 204410

Figure 7.18. Separation of core along a shear plane with concentric structures resulting from rotation along the plane of separation. 204410-X

CONCLUSIONS

The Rotasonic drill proved ideal, in most sediments, for recovery of intact, large-diameter core for stratigraphic studies. However, abundant evidence indicates that secondary, drill-induced deformation may overprint existing primary features or create what initially appears to be synsedimentary structures. The reason for distinguishing between primary and drill-induced disturbance is to ensure correct interpretation of depositional environments.

Deformation of soft sediment normally occurs when sediments are stressed during or shortly after deposition and results in liquefaction, fluidization, or hydroplastic deformation. The presence of a gravitationally unstable density profile, non-uniform confining loads, or gravity-induced downslope shear are responsible for common primary structures

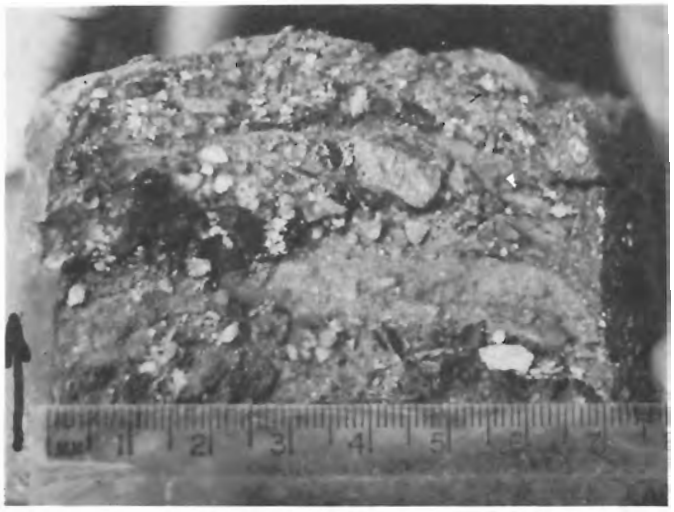


Figure 7.19. Secondary shear bands with downwarped edges in massive diamict. GSC photo 204319-F

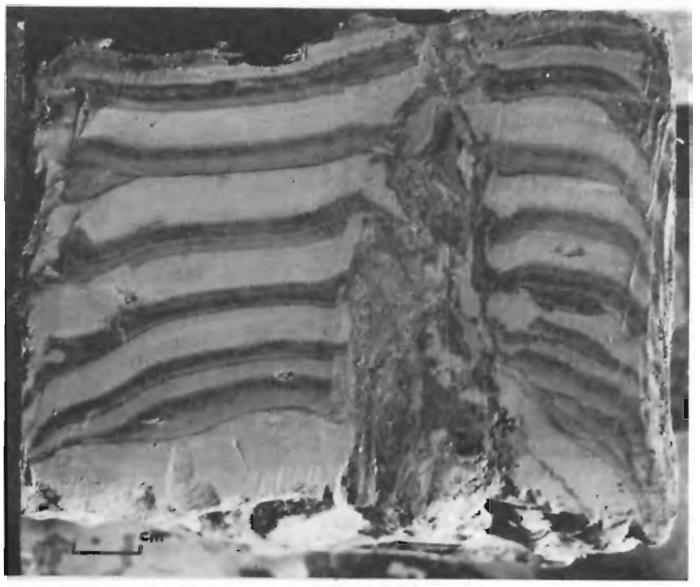


Figure 7.20. Local deformation, caused by postdrilling sampling device, that produced a structure resembling pillar-type dewatering structures of Lowe (1975). 204410-U

such as convolute lamination, ball-and-pillow structures, flame structures, slump structures, and soft-sediment faults. Deformation features associated with defined sedimentation units such as sediment gravity flows, and structures bounded by undeformed strata, are taken as evidence for synsedimentary origin.

In general, the outer 1 cm of drill core has been highly distorted and remobilized during drilling. In addition, the vibratory nature of the coring process caused dynamic liquefaction or hydroplastic deformation in subsceptible material, producing sedimentary structures such as convolute lamination, brecciation, rotated inclusions, and slump structures. Microfaults, resulting from failure of more competent layers, are also common. Identification of these secondary features is made on the basis of: a) truncation or overprinting of obviously primary sedimentary structures, b) downwarping of previously planar layers along the edge of the core, c) symmetry of fold axes about the axis of the drill core, d) symmetry of faults exhibiting opposing sense of reverse displacement due to compression, e) rotation of clay balls or cohesive fragments with associated remobilization of interstitial sediment, f) presence of décollement surfaces and shear bands in compacted diamictons, and g) indication from either on-site notes or during logging of intervals of highly distorted length or sample recovery problems that would most likely exhibit drill-induced soft-sediment deformation.

ACKNOWLEDGMENTS

We would like to thank Jennifer Smith and Joanne Paul for their invaluable help in relogging the drill core and looking for, documenting, and photographing the sedimentary structures. Special thanks to W.W. Shilts for critically reviewing this manuscript.

REFERENCES

Allen, J.R.L.
1984: Sedimentary structures, their character and physical basis; Developments in Sedimentology, v. 30, Elesvier, Amsterdam.

Averill, S.A., MacNeil, K.A., Hueault, R.G., and Baker, C.L.
1986: Rotasonic drilling operations (1984) and overburden heavy mineral studies, Matheson, area, District of Cochrane; Ontario Geological Survey, Open File Report 5569, 61 p.

Bogacz, K., Dzulynski, S., Gradsinski, R., and Kostecka, A.
1968: Origin of crumpled limestone in the Middle Triassic of Poland; Annales de la Société Géologique de Pologne, v. 38, p. 385-394.

Dionne, J-C.
1971: Contorted structures in unconsolidated Quaternary deposits, Lake Saint-Jean and Saguenay regions, Quebec; La Revue de Géographie de Montréal, v. XXV, no. 1, p. 5-33.

Lowe, D.R.
1975: Water escape structures in coarse-grained sediments; Sedimentology, v. 22, p. 157-204.

Shilts, W.W.
1981: Surficial geology of the Lac Mégantic area, Quebec; Geological Survey of Canada, Memoir 397, 102 p.

Shilts, W.W. and Smith, S.L.
1986: Stratigraphy of placer gold deposits; overburden drilling in Chaudière Valley, Quebec; in Current Research, Part A, Geological Survey of Canada, Paper 86-1A, p. 703-712.

- 8 -

Ice flow history and glacial dispersal in the Labrador Trough[1]

Project 820039

R.A. Klassen and F.J. Thompson
Terrain Sciences Division

Klassen, R.A. and Thompson, F.J., Ice flow history and glacial dispersal in the Labrador Trough; in Current Research, Part A, Geological Survey of Canada, Paper 87-1A, p. 61-71, 1987.

Abstract

Five phases of ice flow have been identified in the Schefferville region of western Labrador, based on examination of striae and distribution of indicator erratics. Phase I, the oldest ice movement identified, records flow to the northeast and southwest from one or more important dispersal centres either in or near to the Labrador Trough. Phase II records north directed flow on the Archean highlands and Lake Wakuach area of the trough. Phase III records flow to the northwest and southeast from a dispersal centre in the Schefferville-Attikamagen Lake area, the location of which appears to have shifted southward with time. Phase IV records strong eastward flow across the Archean highlands into the trough and may be related to an ice stream. Phase V records northeast flow across the trough and is considered to be relatively minor. This complex history of ice flow is recorded by patterns of glacial dispersal, which can be fan-shaped to radial, and by till stratigraphy.

Résumé

On a reconnu cinq phases d'écoulement glaciaire dans la région de Schefferville, dans l'ouest du Labrador, d'après un examen des stries et de la répartition des blocs erratiques servant d'indicateurs. Dans la première phase, qui correspond au mouvement le plus ancien, la glace s'est déplacée vers le nord-est et le sud-ouest à partir d'un ou de plusieurs centres de dispersion importants qui se trouvaient soit dans la fosse du Labrador, soit à proximité. Dans un deuxième temps, l'écoulement glaciaire s'est fait vers le nord, sur les hautes-terres archéennes et dans la région du lac Wakuach. Dans la troisième phase, la glace s'est déplacée vers le nord-ouest et le sud-est à partir d'un centre de dispersion situé dans la région de Schefferville-lac Attikamagen, dont la position semble avoir dérivée vers le sud avec le temps. La quatrième phase correspond à un net mouvement en direction est à travers les hautes-terres archéennes et jusque dans la fosse, et peut être apparentée à une langue glaciaire. Dans la cinquième phase, l'écoulement s'est effectué vers le nord-est à travers la fosse labradorienne, et son importance est jugée secondaire. Cette histoire complexe de l'écoulement glaciaire nous est révélée par les figures de dispersion en éventail et radiales, et par la stratigraphie du till.

[1]Contribution to Canada-Newfoundland Mineral Development Agreement 1984-1989. Project carried by Geological Survey of Canada.

INTRODUCTION

This report is a preliminary interpretation of the results of Quaternary studies conducted in western Labrador (Fig. 8.1) during the 1986 field season as part of the Canada-Newfoundland Mineral Development Agreement. The major objectives of the study are to determine history of ice movement and composition of glacial drift as a basis for developing techniques for drift prospecting. Most of the work was carried out in map areas 23 I, 23 J, and 23 O. Geochemical analysis of till samples collected during 1986 is in progress.

PREVIOUS WORK

Several Quaternary studies have been conducted in the Schefferville region that collectively document a complex history of ice flow associated with migration of dispersal centres during the course of glaciation, flow from a large-scale U-shaped ice divide, and late glacial flow associated with a decaying ice sheet. Low (1896) postulated radial flow from an ice sheet that was centred initially near 51°N and 70°W and shifted northward to a position west and northwest of Caniapiscau Lake (west of the study area) and finally northwest to

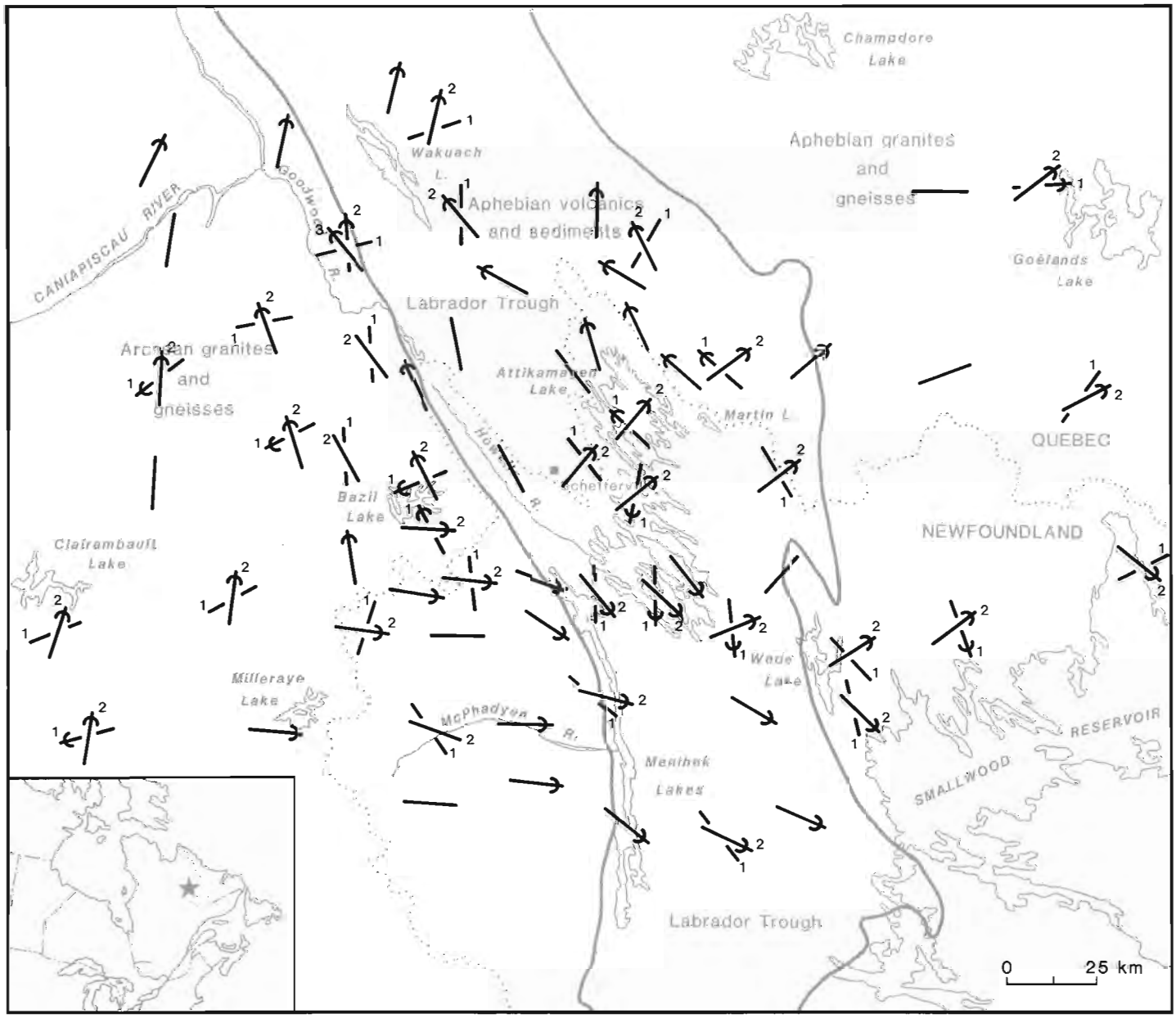


Figure 8.1. Generalized geology and glacial striae, showing direction and relative ages of ice movement (1, oldest).

55° or 56°N. Harrison (1952) recorded that within a few miles of Schefferville movement was in turn to the southeast, northwest, and finally northeast. Henderson (1959) showed the oldest flow to the south and southeast from a centre located north of Lake Wakuach and noted younger northeast flow from a centre located west of Schefferville. Henderson suggested that late northward flow in the Lake Wakuach area may be contemporaneous with the younger northeast flow. He attributed easterly flow in the McPhadyen River area to a late glacial, local phase. Kirby (1961, 1966) indicated that east and northeast directed flow across the Schefferville area predates ice movement to the north-northwest and south-southeast from an ice centre located 40 km northwest Schefferville. Hughes (1964), from work in the western part of the study area, suggested an initial ice movement radially from a disperal centre over or east of the Labrador Trough and late ice movement to the north in the Caniapiscau River area and to the east in the McPhadyen River area. The various ice flow trends noted by these early workers are summarized on the Glacial Map of Canada (Prest et al., 1968), although details concerning the age sequence of flow trends are lacking.

The most prominent flow patterns in the study area are associated collectively with the last regional phase of ice flow, and they describe the southern part of a U-shaped ice divide – the Labrador-Quebec Ice Divide – that extends southward from northwestern Quebec through the Schefferville area and northward to northeastern Labrador. North of the divide, flow trends are convergent towards Ungava Bay, and south of the divide they are divergent, directed towards the Labrador Sea in the east, Lawrence River in the south, and Hudson Bay and James Bay in the west.

METHODS

A helicopter was used for field transportation and in the Schefferville area roads were used for more detailed sampling and access to Quaternary sections exposed in open pit mines. At each observation site, striae and clast lithology were routinely noted and till was sampled for geochemical and lithological analyses in the laboratory. The work was concentrated in areas of Labrador with the greatest mineral potential but was extended to adjoining areas of Quebec and areas of lesser mineral potential in Labrador to provide a more complete understanding of the history of ice flow and of regional variation in drift composition. Sample densities varied from 1 to 7 per 100 km^2. Sampling sites are located preferentially on hilltops because valleys provide few landing sites or till sampling sites due to swamp and forest cover. Where more detailed work was desired, swamps were used as landing sites to permit access on foot to tree covered areas. Pits were dug by shovel to depths of 30-70 cm, depending on depth to bedrock and on difficulties in penetrating stony till. Samples were collected from the least oxidized and most organic-free section of the modern soil profile near the base of the pit. In areas of tundra vegetation on hilltops, pits were dug in mudboils where soil zonation was absent or poorly developed due to periglacial churning (Shilts, 1977).

BEDROCK GEOLOGY AND PHYSIOGRAPHY

The central part of the study area is underlain by Aphebian supracrustal volcanic rocks and sediments of the Labrador Trough which forms an 80 km-wide belt trending northwest-southeast. The trough is sandwiched between Archean granites and gneisses to the west and Aphebian granites and gneisses to the east (Fig. 8.1; Greene, 1970; Wardle, 1982; Avramtchev, 1985). The more resistant quartzites, iron formation, and volcanics of the Labrador Trough produce northwest-southeast trending bedrock ridges and the softer shales produce swamp and lake filled valleys. The southern part of the Labrador Trough and of the Aphebian granites and gneisses is swampy flat land which is now in part flooded by the Smallwood Reservoir. The Archean and northern part of the Aphebian granites and gneisses form rugged bedrock highlands with no distinct topographic trend or grain.

Exploration activity has, in the past, been concentrated in the Labrador Trough which has produced several iron mines which are now abandoned due to high production costs and low metal prices. Showings of Cu, and of Cu, Pb, Zn occur in shales and slates in the Attikamagen and Martin lakes area. The mafic and ultramafic rocks of the eastern Labrador Trough are considered to have potential for base, precious and platinum group metals (T. Birkett, personal communication, 1986). The recent discoveries of anomalous levels of Zn in lake sediments over Archean rocks west of Howells Valley (M. Beaumier, personal communication, 1986) and of economic levels of gold in Archean iron formation along Goodwood River have sparked exploration activity in the Archean area.

SURFICIAL GEOLOGY

Till, the most widespread glacial deposit is generally thin (<2 m) to discontinuous in highland areas and locally thicker (2 to >10 m) in valleys. The nature of the till is commonly dependent on that of the underlying bedrock. On bedrock units resistant to glacial erosion, such as the granites and gneisses, till is thin and has little fine grained matrix component. In the Labrador Trough, sedimentary and volcanic bedrock is softer and more easily comminuted to fines and as a result overlying till is generally thicker, has a greater component of silt and clay, and a colour which reflects that of the bedrock. Red and grey tills are associated with the iron formation and sedimentary rocks of the western Labrador Trough and grey-green tills are associated with volcanics and mafic intrusives of the eastern Labrador Trough.

ICE FLOW TRENDS

Most of the more than 300 striae observations were made on exposed surfaces on hilltops (Fig. 8.1). The youngest striae are generally consistent with the moulding of the outcrop, show little evidence that ice movement was controlled by topography, and consequently appear to reflect a major phase

of ice flow. The sense of flow was determined from the streamlined aspect of the outcrop and from small crag-and-tail features. The relative age of ice flow trends has been established by careful examinations of outcrop where multiple trends are recorded. Oldest striae are recorded on the most protected lee faces and youngest on the most exposed stoss faces (Klassen and Bolduc, 1984). It should be emphasized that age relations and trends described here were found to be consistent throughout the area and are based on observations at literally hundreds of sites.

The last-formed striae in the Labrador Trough indicate flow to the northeast, south, and southeast from the immediate Schefferville area. On the Archean highlands, to the west of the trough, youngest striae indicate ice flow to the east in the McPhadyen River area and to the north in the Lake Clairambault area. In the Lake Goélands area, to the east of Labrador Trough, last-formed striae indicate flow to the east-northeast. Older striae indicate that north directed ice flow occurred in the Lake Wakuach area prior to northeast flow. In the Lake Bazil area northwest flow predates eastward flow. South of Schefferville, flow to the south predates flow to the southeast. On the Archean highlands flow to the southwest predates all other ice flow trends. In the Wade Lake-Attikamagen Lake area, northeast trending striae postdate moulding of the outcrop.

DISTRIBUTION OF GLACIAL ERRATICS

The lithologies and relative abundances of clasts were noted for most sample sites to help define the history of ice movement by recognition of the distance and direction of glacial transport and overall shape of glacial dispersal trains. Till is generally derived primarily from the underlying and immediately up-ice bedrock. Clasts that have undergone transport of more than 50 km commonly comprise less than 3% of the coarse fraction.

Erratics derived from the Labrador Trough, commonly iron formation and sedimentary rock, occur in till more than 100 km both to the east and west of the trough – a distribution which is inconsistent with younger regional flows, which carried material only towards the north and northwest and south and southeast. Outside the trough, erratics derived from the trough commonly comprise trace to 3% of the pebble size fraction but relatively large volumes occur on the Archean highlands west of Howells River and Goodwood River valleys where Labrador Trough debris comprises 5-30% of the pebble size fraction and up to 70% of the finer fraction (C. Wang, personal communication, 1986). In this area of crystalline bedrock the till is commonly red, similar in colour to till in the western part of the Labrador Trough. The large volumes of trough debris and the difference in composition between the fine and coarse fraction of the till may reflect that the rocks of the Labrador Trough are more easily incorporated and comminuted to fines by glaciers than the Archean granites and gneisses.

Three small intrusive bodies of nepheline syenite, which outcrop north of Schefferville (Fumerton and Barry, 1984), and red porphyritic volcanic rock, which outcrops only in the Martin Lake area (R. Wardle, personal communication, 1986), were used as bedrock sources of indicator erratics to define patterns of glacial dispersal at local scales (tens of kilometres) (Fig. 8.2). Erratics of nepheline syenite occur in till up to 70 km north and 30 km southwest of their known source and define a broad fan opening to the northwest through an arc of more than 120°. This distribution cannot be fully explained by ice flow only to the northwest as recorded by the youngest striae and appears to be the composite product of flow in directions between north-northeast and southwest, based on the fan margins. Although erratics of porphyritic volcanic rock are distributed in all directions about the known source, a prominent train defined by relatively abundant volcanic erratics extends more than 60 km northwest from the source. Only northwest transport would be predicted on the basis of the last-formed striae. The distribution of glacial erratics from the two sources indicates a history of shifting ice dispersal centres and demonstrates that the composition of the till is a product of more than one phase of ice flow. The shape of the glacial dispersal train is dependent on the position of the source relative to the Labrador-Quebec Ice Divide.

STRATIGRAPHY

In the Schefferville area of the Labrador Trough several till units were recorded in sections located at open pit iron mines and along roads. Based on strong colour contrasts, the tills are considered to be lithologically distinct and to represent significant changes in the directions of glacial transport. This stratigraphic succession has not been, to our knowledge, previously recognized.

Throughout the area, red till is common at the surface and is considered to be associated with the last phase of regional ice flow, which is generally to the northwest and southeast along the axis of the trough. The till, which is commonly 1-3 m thick, varies from red to red-brown. In some sections a red-brown till appears to overlie a red till and in others they appear interbedded; the stratigraphic significance of this is not known. The red surface till overlies a grey-brown till, which in turn overlies a dark grey till. Although the lithological origins of the colour differences are not well known, the dark grey colour may reflect erosion of shale units. At one site the dark grey till overlies an indurated brown till. The till stratigraphy appears to be the product of ice flow both along and across the axis of the Labrador Trough.

At one site, fluvial (coarse grained, stratified) sediments lie stratigraphically between the red surface till and an underlying grey-brown till. The stratigraphic significance of the section is not fully understood. The stratified sediments could indicate ice-free conditions between glacial phases; alternatively the surface 'till' could have been deposited by mass flow during late glacial conditions. A similar stratigraphic sequence was encountered by overburden drilling in the Labrador Trough (Granberg and Krishnam, 1984), and organic materials reported by them within the stratified sediments support an interpretation of nonglacial conditions.

HISTORY OF THE ICE FLOW MOVEMENTS

A history of ice flow can be interpreted from striae orientation and relative ages and from the distribution of glacial erratics; it is summarized in Figures 8.3 to 8.7 and is discussed from oldest to youngest. The glacial events are considered by the authors to reflect changes in the configuration of the ice sheet, based on the widespread occurrence of striae associated with each phase and on the significant (>50 km) distances of glacial transport shown by indicator erratics. The actual ages of the different phases of ice flow, in contrast to their relative ages, are not known, although geological evidence may be found by detailed examination of stratigraphic sections. Because the ice flow features recorded on outcrop surfaces do not show differential weathering, the phases described below appear to have been produced during a period of continuous ice cover and may represent changes during one or more stadials of Wisconsin Glaciation. It is emphasized that the following is an *interpretation* of geological evidence collected throughout the area; no single part of the area records evidence of the five phases of flow presented here.

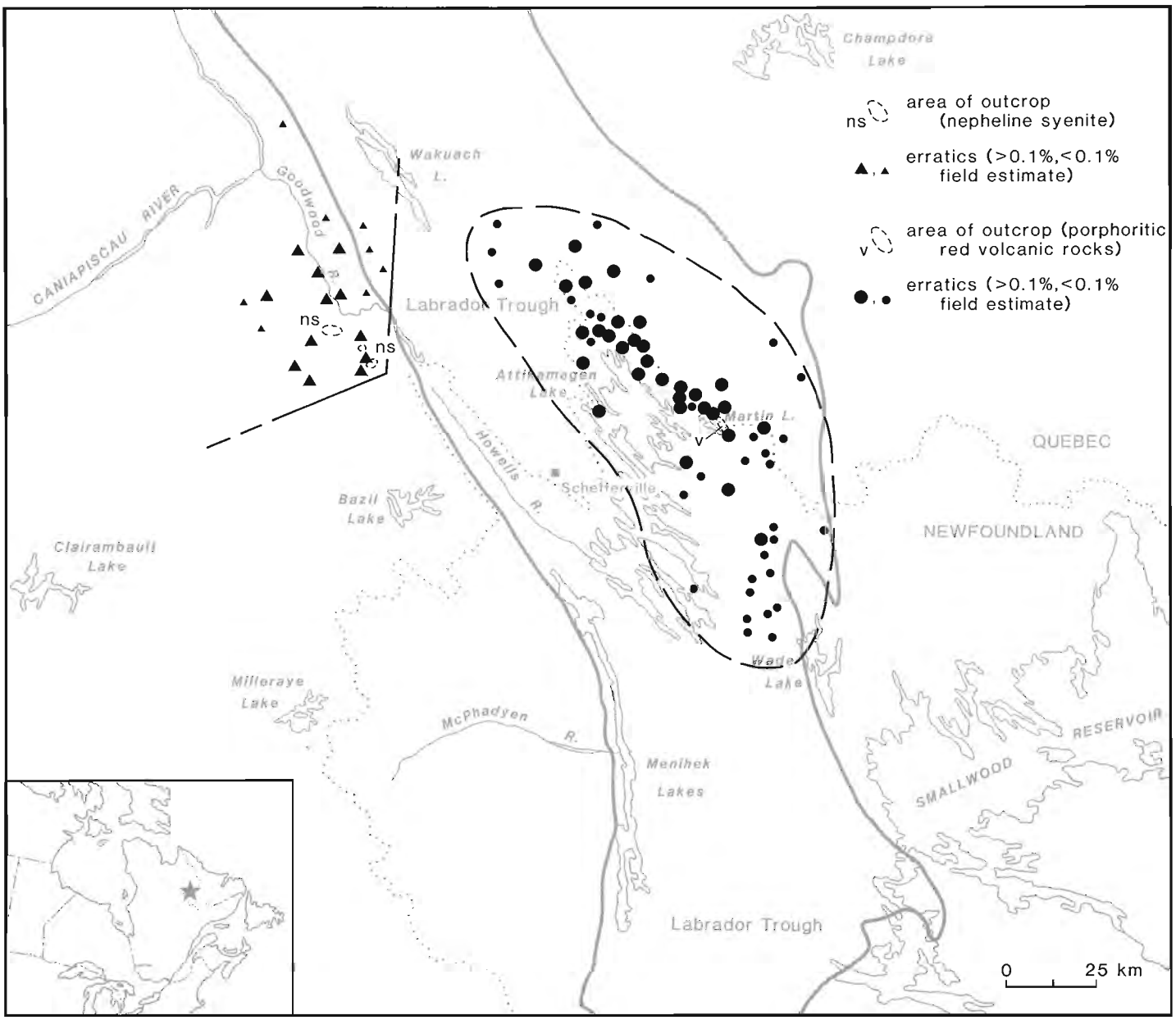


Figure 8.2. Glacial dispersal of nepheline syenite and of porphyritic red volcanic rocks.

Phase I

The oldest glacial event recorded in the study area is southwest ice movement across the Archean highlands and northeast ice movement east of the trough (Fig. 8.3). The southwest trending striae are consistent with glacially moulded outcrop surfaces truncated by later ice flow and they appear to be the product of a major phase of flow. The presence of large volumes of Labrador Trough erratics on the Archean highlands to the west and of nepheline syenite southwest of its source is consistent with transport during this phase of ice flow and indicates that later glacial events did not completely remove this debris. The authors agree with the conclusion drawn by Hughes (1964) that ice moved across the area from a dispersal centre over or east of the Labrador Trough. The presence of Labrador Trough erratics more than 400 km east of the Labrador Trough (unpublished data) suggests that the dispersal centre was also, at some time, located west of the trough.

Phase II

North to north-northeast directed ice flow (Fig. 8.4) is recorded across the Archean highlands in the Lake Clairam-

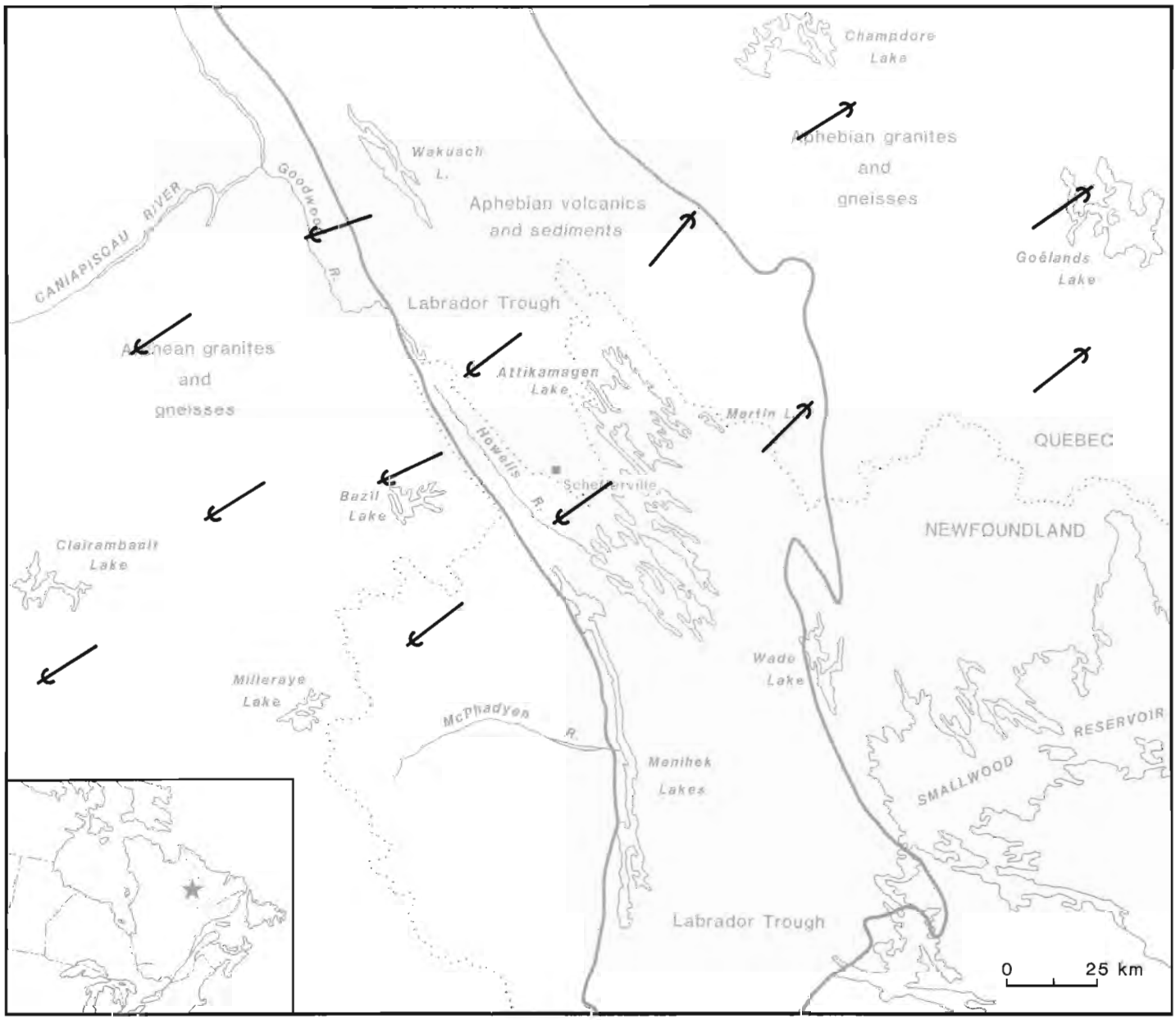


Figure 8.3. Ice flow trends during Phase I.

bault-Caniapiscau River area and into the Labrador Trough in the Lake Wakuach area. Flow trends of Phase II crosscut those of Phase I on the Archean highlands and in the trough north of Schefferville. The northward transport of nepheline syenite is consistent with this phase of flow.

Phase III

Most of the ice flow events recorded in the Labrador Trough (Fig. 8.5) are ascribed to a dispersal centre in the Labrador Trough with northwest flow north of the centre, and south to southeast flow south of the centre. Phase III is distinguished from Phases I and II by evidence of three distinct directions and ages of ice flow seen on outcrops in the Goodwood River-Lake Wakuach area, and its regional context is shown by association of similar flow trends elsewhere. The prominent northwest transport of red porphyritic volcanic rock is consistent with a dispersal centre located southeast of Attikamagen Lake. However, opposing flow trends in the immediate Shefferville area and radial dispersal of porphyritic volcanics suggests a southward migrating ice centre that could, at one stage have been located in the Schefferville-Attikamagen

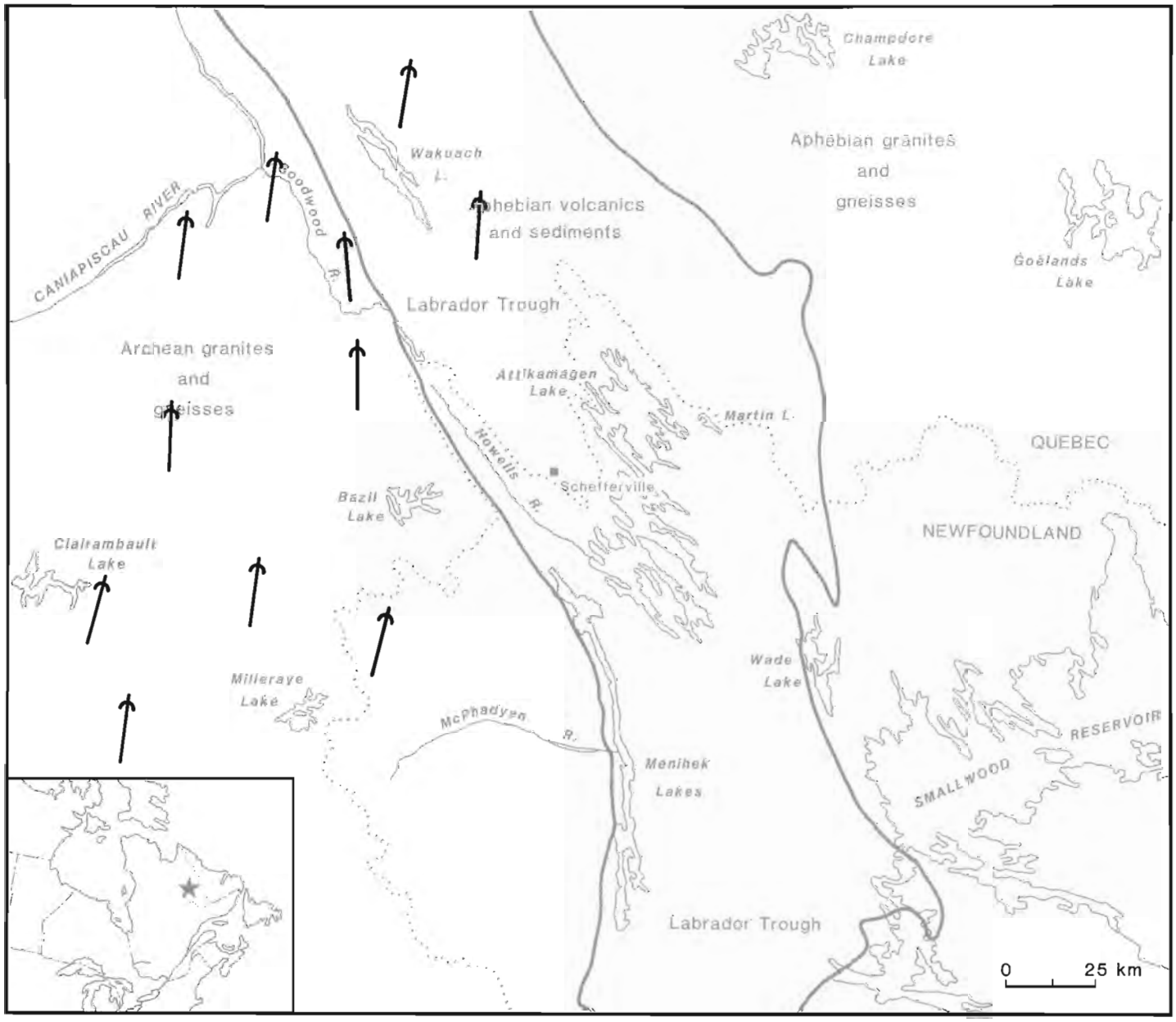


Figure 8.4. Ice flow trends during Phase II.

Lake area. The southeast flow direction recorded north of Schefferville by earlier workers was not noted in the course of the present study but would also be consistent with a shifting ice centre.

Phase IV

East directed ice flow in the McPhadyen River Milleraye Lake area and east-southeast flow in the southern part of the trough (Fig. 8.6) reflect one phase of flow subsequent to Phase II, as shown by crosscutting striae. The area influenced by Phase IV flow is marked by a significant decrease in abundance of Labrador Trough debris on the highlands and a corresponding increase in crystalline debris in the Labrador Trough compared with areas to the north. The compositional evidence, along with age relations shown elsewhere by striae, indicates that Phase IV occurred after transport of Labrador Trough debris onto the highlands during Phase I, and after flow within the trough during Phase III. The well developed glacial streamlining of the Archean bedrock indicates that this was a significant phase of flow. Because in a regional context Phase IV appears to be narrow, elongate, and has no

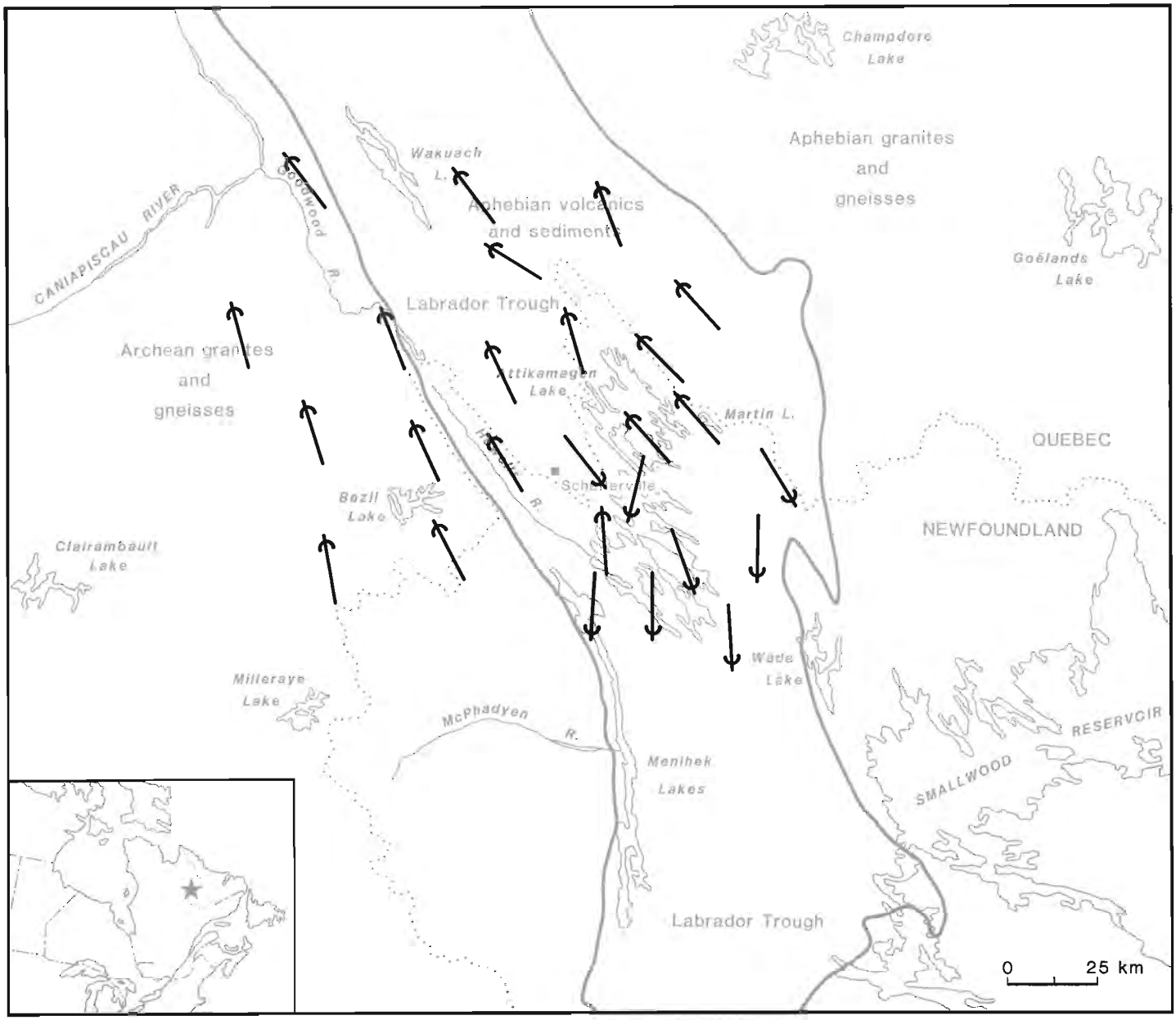


Figure 8.5. Ice flow trends during Phase III.

west flow counterpart, it may be associated with development of an ice stream within the ice sheet.

Phase V

A late glacial and relatively short-lived phase of flow (Fig. 8.7) is recorded by northeast trending striae that crosscut all others in the Labrador Trough. Although the striae trend across regional topographic trends and occur on hilltops, they are weakly developed and ice does not appear to have accomplished significant erosion of outcrops. There is insufficient data to determine if this phase extends east of the Labrador Trough. The east-northeast flow trends in the Lake Goélands area reflect a major phase of flow and are not considered to be contemporaneous with this movement. Red porphyritic volcanic rock could have been transported northeast during either this phase of flow or an earlier phase, possibly Phase I.

IMPLICATIONS FOR GLACIAL HISTORY

The work reported here represents important evidence for the glacial history of the region. Despite the preliminary nature of the work, the following points can be noted:

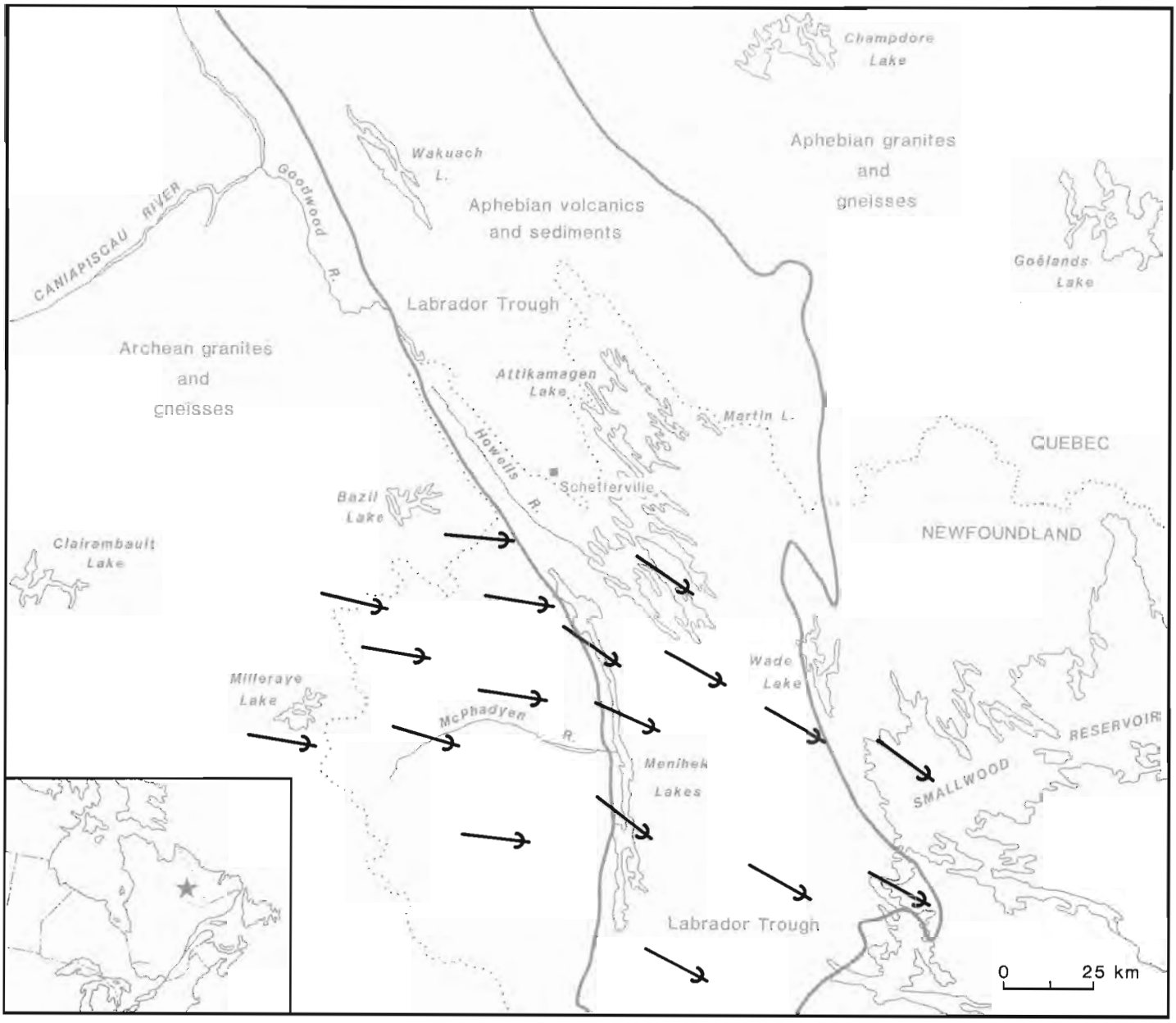


Figure 8.6. Ice flow trends during Phase IV.

1. The complex patterns of ice flow recorded in western Labrador are the product of several distinct dispersal centres and of flow during deglaciation. Based on glacial transport of iron formation to the northeast and to the southwest, and to the southeast over distances of more than 400 km, ice flow during Phase I, and likely during Phase III, is from one or more large-scale dispersal centres within the Labrador Sector of the Laurentide Ice Sheet.
2. The study area straddles the southernmost part of the Labrador-Quebec Ice Divide, which can be recognized by overall flow trends shown on the Glacial Map of Canada (Prest et al., 1968). Our work suggests that the regional patterns that define the divide could be the product of flow of different ages.
3. Our work appears to resolve an apparent contradiction between Henderson (1959) and Kirby (1961) concerning the relative age and importance of northeast ice flow across the Labrador Trough. Northeast flow can be associated with both an older dominant phase (Phase I) and minor late glacial phase (Phase V).
4. Stratigraphic sections present some evidence of a non-glacial interval between deposition of till units and pro-

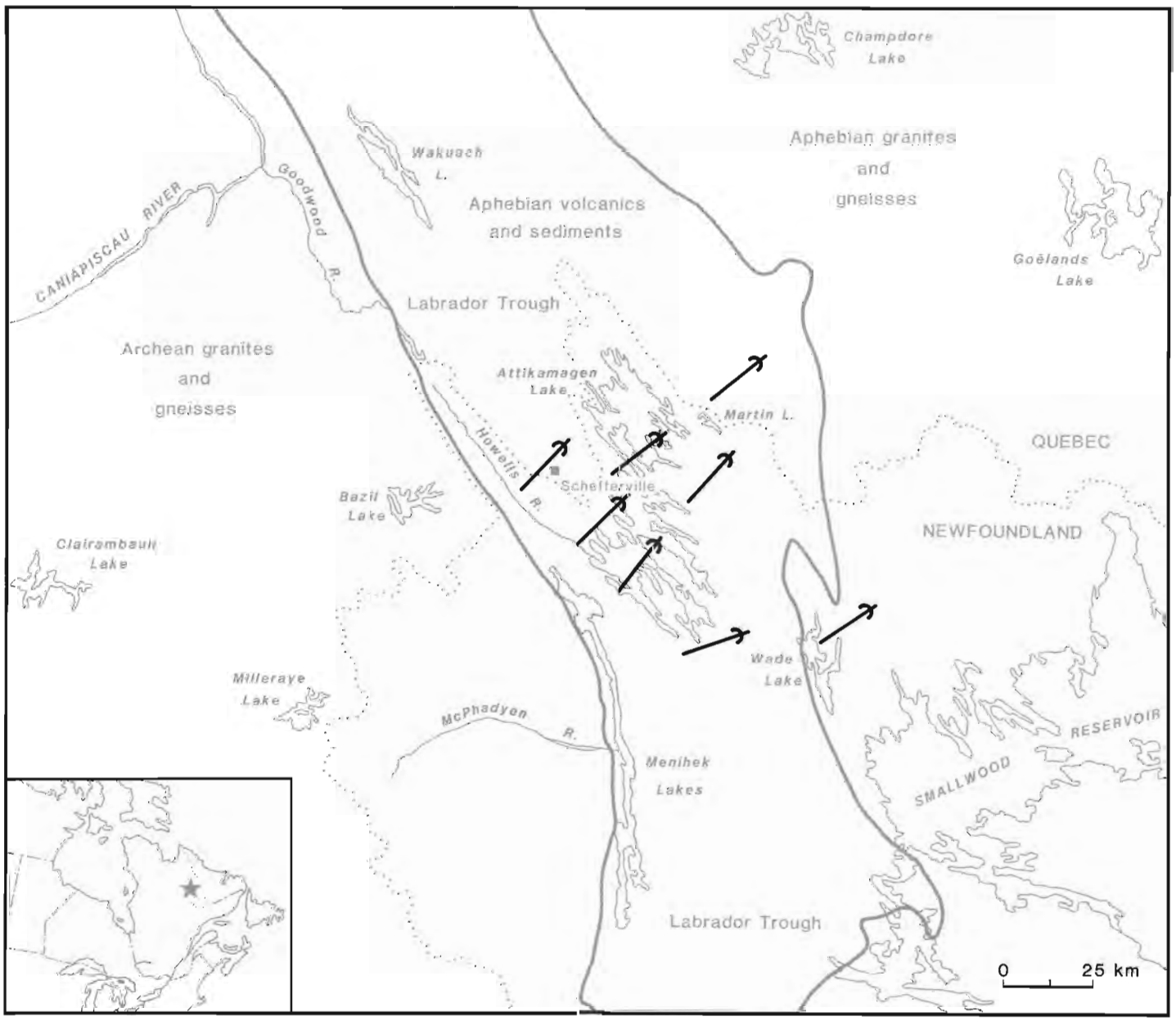


Figure 8.7. Ice flow trends during Phase V.

vide evidence supportive of drillhole stratigraphy described by Granberg and Krishnam (1984).

IMPLICATIONS FOR DRIFT PROSPECTING

Mineral exploration in western Labrador should be based on an understanding of the the complex history of ice movement. Glacial erratics can be traced for several tens of kilometres from bedrock source, but the overall direction of transport and composition of the drift may reflect one or more phases of ice flow other than that most recently recorded. For example, the composition of drift on the Archean highlands west of Howells and Goodwood River valleys reflects transport primarily by an older southwest ice flow (Phase I), and not by the later northwest flow (Phase III). Anomalous levels of Zn recorded in lake sediments in this area may reflect geochemistry of the Labrador Trough and not the Archean bedrock. Lake sediment studies have shown the Labrador Trough to be relatively enriched geochemically (McConnell, 1984).

Although only one till was found at the surface at most sites, in some locations two till units were encountered during sample collection. Based on colour differences, the tills could have different glacial transport histories as well as distinct lithological and geochemical characteristics. Programs of drift prospecting would be required to recognize and accommodate these differences during the course of fieldwork.

ACKNOWLEDGMENTS

The authors would like to acknowledge the keen and enthusiastic field assistance of D. DesRivières, B. Lane, G. McKenna, and P. Rossi. J. Archibald's (Glanford Aviation) flying skills and resourceful assistance were gratefully appreciated during long days and cold weather. J-S. Vincent is thanked for critical review and suggestions that improved the manuscript.

REFERENCES

Avramtchev, L.
1985: Carte géologique du Québec; Gouvernement du Québec, Ministère de l'Énergie et des Ressources, Carte n° 2000 du DV84-02.

Fumerton, S.L. and Barry, A.P.
1984: Probable Archean nepheline syenite plutons in the Superior Province adjacent to the Labrador Trough; Canadian Journal of Earth Sciences, v. 21, p. 615-618.

Granberg, H.B. and Krishnam, T.K.
1984: Wood remnants 24 250 years old in central Labrador (abstract); 5th Congress, AQQUA, Sherbrooke, p. 30.

Greene, B.A.
1970: Geological map of Labrador; Department of Mines, Agriculture and Resources, Province of Newfoundland and Labrador, scale 1:1 000 000.

Harrison, J.M.
1952: The Quebec-Labrador iron belt, Quebec and Newfoundland, in Geological Survey of Canada, Paper 52-20.

Henderson, E.
1959: A glacial study of central Quebec-Labrador; Geological Survey of Canada, Paper 71-26, 37 p.

Hughes, O.L.
1964: Surficial geology, Nichicun-Kaniapiskau map-area, Quebec; Geological Survey of Canada, Bulletin 106, 20 p.

Kirby, R.P.
1961: Deglaciation in central Labrador-Ungava as interpreted from glacial deposits; Geographical Bulletin, no. 16.
1966: Movements of ice in central Labrador-Ungava; in Ten years (1954-1969) of field research in Labrador-Ungava; McGill Sub-Arctic Research Paper no. 20, Department of Geography, McGill University, Montreal, p. 160-171.

Klassen, R.A. anb Bolduc, A.M.
1984: Ice flow directions and drift composition, Churchill Falls, Labrador; in Current Research, Part A, Geological Survey of Canada, Paper 84-1A; p. 255-258.

Low, A.P.
1896: Report on explorations in the Labrador peninsula along the Eastman, Koksoak, Hamilton, Manikuagan and portions of other rivers in 1892-93-94-95; Geological Survey of Canada, Annual Report, v. 8, Part L.

McConnell, J.
1984: Reconnaissance and detailed geochemical surveys of base metals in Labrador; Department of Mines and Energy, Government of Newfoundland and Labrador, Report 82-2, 113 p.

Prest, V.K., Grant, D.R., and Rampton, V.N.
1968: Glacial Map of Canada; Geological Survey of Canada, Map 1253A, scale 1:5 000 000.

Shilts, W.W.
1977: Geochemistry of till in perennially frozen terrain of the Canadian Shield – application to prospecting; Boreas, v. 5, p. 203-212.

Thompson, F.J. and Klassen, R.A.
1986: Ice flow directions and drift composition, central Labrador; in Current Research, Part A, Geological Survey of Canada, Paper 86-1A, p. 713-717.

Wardle, R.J.
1982: Geology of the south-central Labrador Trough; Mineral Development Division, Newfoundland Department of Mines and Energy, Map 82-5.

- 9 -

Plant macrofossils from the Neogene Beaufort Formation on Banks and Meighen islands, District of Franklin

Project 730027

John V. Matthews, Jr.
Terrain Sciences Division

Matthews, J.V., Jr., Plant macrofossils from the Neogene Beaufort Formation on Banks and Meighen islands, District of Franklin; in Current Research, Part A, Geological Survey of Canada, Paper 87-1A, p. 73-87, 1987.

Abstract

This report lists plant macrofossils, representing at least 95 vascular species, from the Neogene Beaufort Formation on Banks and Meighen Islands. Among the specimens are those such as Epipremnum and Aracispermum that have not previously been reported from North America and many others (e.g., Cleome, Polanisia, Teucrium, Physocarpus) that presently occur far to the south of the Northwest Territories.

On Meighen Island at approximately 80°N, the Beaufort Formation is probably no younger than early Pliocene and may be as old as middle Miocene, yet its content of plants, such as Saxifraga oppositifolia, Oxyria digyna and Dryas integrifolia, plus other characteristics of the flora and insect fauna show that it represents a forest-tundra environment. If so, some form of tundra probably existed around the Arctic basin for much of the Pliocene. This has implications for the evolution of the existing lowland arctic flora and fauna.

Résumé

Ce rapport établit une liste de macrofossiles végétaux qui représentent au moins 95 espèces vasculaires et qui ont été identifiés dans la formation néogène de Beaufort, sur les îles Banks et Meighen. Certains des spécimens, comme Epipremnum et Aracispermum, sont attestés pour la première fois en Amérique du Nord et beaucoup d'autres, comme Cleome, Polanisia, Teucrium et Physocarpus, se rencontrent actuellement bien au sud des Territoires du Nord-Ouest.

Dans l'île Meighen, à environ 80°N, la formation de Beaufort remonte probablement au début du Pliocène et pourrait même dater du Miocène moyen; pourtant, les végétaux qu'on y rencontre, comme Saxifraga oppositifolia, Oxyria digyna et Dryas integrifolia, et d'autres caractéristiques de sa flore et de sa population d'insectes, la situent dans un environnement de forêt-toundra. Si tel est le cas, une quelconque forme de toundra a probablement existé autour du bassin arctique pendant une bonne partie du Pliocène. Cette révélation jette une lumière nouvelle sur l'évolution de la flore et de la faune dans les basses-terres de l'Arctique.

INTRODUCTION

The Neogene Beaufort Formation is well known for its content of wood and other types of organic materials, including cones, seeds, leaves, mosses, and insects (Hills, 1975; Hills and Ogilvie, 1970; Kuc and Hills, 1971; Roy and Hills, 1972; Hills et al., 1974; Hills and Matthews, 1974; Hills, 1975; Matthews, 1976, 1977). It occurs primarily on the western Queen Elizabeth Islands from Meighen Island in the north (Thorsteinsson, 1961) to Prince Patrick Island in the south where it was first formally recognized (Tozer, 1956) as well as on Banks Island (Miall, 1979) and at the surface and in the subsurface in wells from the Mackenzie Delta/Anderson Plain region (Young and McNeil, 1984; Dietrich et al., 1985; Fig. 9.1). Eastern outliers occur on Melville Island (Tozer, 1970) and possibly Boothia Peninsula (Dyke and Matthews, in press), although one such presumed Beaufort locality on eastern Axel Heiberg Island (Hills and Bustin, 1976) has recently been shown to be much older (Ricketts and McIntyre, 1986).

Hills and Matthews (1974) published a preliminary list of plant macrofossils from the Beaufort Formation on Meighen Island. This report updates that list and also includes fossils from two well known Beaufort Formation localities on Banks Island – Duck Hawk Bluffs on the southwestern tip of the island and Ballast Brook near the northwest coast (Fig. 9.1). More than 95 species of vascular plants are listed, some of them recorded here for the first time in North America. The fossils have paleoenvironmental and phytogeographic implications.

SITES AND STRATIGRAPHY

In various publications (Hills, 1969, 1970; Hills and Ogilvie, 1970; Hills et al., 1974; Kuc and Hills, 1971), Hills has stated that the Beaufort Formation contains two or three lithological units, each separated by erosional unconformities. The upper two are sometimes grouped into one informally defined "upper member" and correspond to the Beaufort Formation as originally defined on Prince Patrick Island (Tozer, 1956; Hills, 1970).

On Meighen Island, the Beaufort Formation, all of which presumably represents the upper member, consists of approximately 220 m of unconsolidated sand, silt, and clay. The clay is concentrated in a marine tongue that approaches 100 m a.s.l. on the southern part of the island. The plant fossils discussed here were collected in that area (approximately 79°50′N) near the western coast in 1973 and 1975. All but one of the collecting sites are stratigraphically above the marine tongue.

The Beaufort Formation in the Ballast Brook area of northern Banks Island (Fig. 9.1) consists of fine to medium sand, clay, and woody detrital peat. It is the type locality for *Picea banksii* Hills and Ogilvie (1970) and the bryophyte flora discussed by Kuc and Hills (1971). The plant fossils discussed below come from four samples within a 19 m interval in the upper part of the upper unit at Geological Survey of Canada locality C-5552 (Kuc and Hills, 1971) and from a single sample located 10 m below the upland surface at an exposure on the opposite side of the Ballast Brook valley from locality C-5552.

Duck Hawk Bluffs on southwestern Banks Island (Fig. 9.1) consists of a series of coastal bluffs that variously expose Cretaceous (Kanguk Formation), Tertiary (Beaufort Formation), and several Quaternary units, including the preglacial Worth Point Formation (Vincent et al.,1983; Matthews et al., 1986). Two units of the Beaufort Formation are seen there. The lower one, which is thought to be equivalent to the lower member at Ballast Brook, consists of 12-30 m of grey sand and gravel with large concentrations of wood and other organics. The upper Beaufort unit, separated from the main Beaufort unit by a disconformity and formerly thought to be part of the post-Beaufort Worth Point Formation, was first recognized as being of Beaufort age in 1985 on the basis of fossils at one exposure (Matthews et al., 1986). It may correspond with part of the upper member at Ballast Brook.

COMMENTS ON SELECTED PLANT FOSSILS

Table 9.1 lists newly discovered vascular plant macrofossils from the three localities mentioned above as well as those taxa listed previously in Hills and Ogilvie (1970), Hills et al. (1974), and Hills and Matthews (1974). More than 95 species are represented by the fossils. Although the fossils in each area come from multiple samples, some of which may differ in age by thousands of years, the individual sample assemblages are quite similar in composition. Thus in Table 9.1 fossils from each locality are pooled.

Identifications are based on comparison with reference material in the Geological Survey of Canada collection of seeds and fruits and/or by comparison with illustrations in publications on the Neogene floras of Siberia and Europe (Reid and Reid, 1915; Reid, 1927; Szafer, 1946; Kirchheimer, 1957; Dorofeev, 1963; Mai, 1964; Baranova et al., 1976; Friis, 1979, 1985). In table 9.1 the only fossils positively assigned to extant species are those representing taxa that are morphologically unique (e.g. leaves of *Saxifraga oppositifolia*) and/or refer to monotypic genera (e.g., *Oxyria digyna*).

Plates 9.1, 9.2, and 9.3 and Figures 9.2 and 9.3 present SEM micrographs and camera lucida outline drawings of selected fossils. The following comments refer to some of the illustrated specimens.

Epipremnum cf. crassum Reid and Reid (Plate 9.1, fig. 1, 2)

The fossils match in almost every detail Reid and Reid's (1915) description and illustrations of specimens from the Dutch Reuverian. Although reported in a number of Palaearctic floras, *Epipremnum* seeds have not been noted previously in North America. In addition to the Ballast Brook record, *E. crassum* type seeds have also been found in a lignite of possible Pliocene age at a section in the Bluefish Basin of the Northern Yukon (Fig. 9.1; McCourt, 1982;

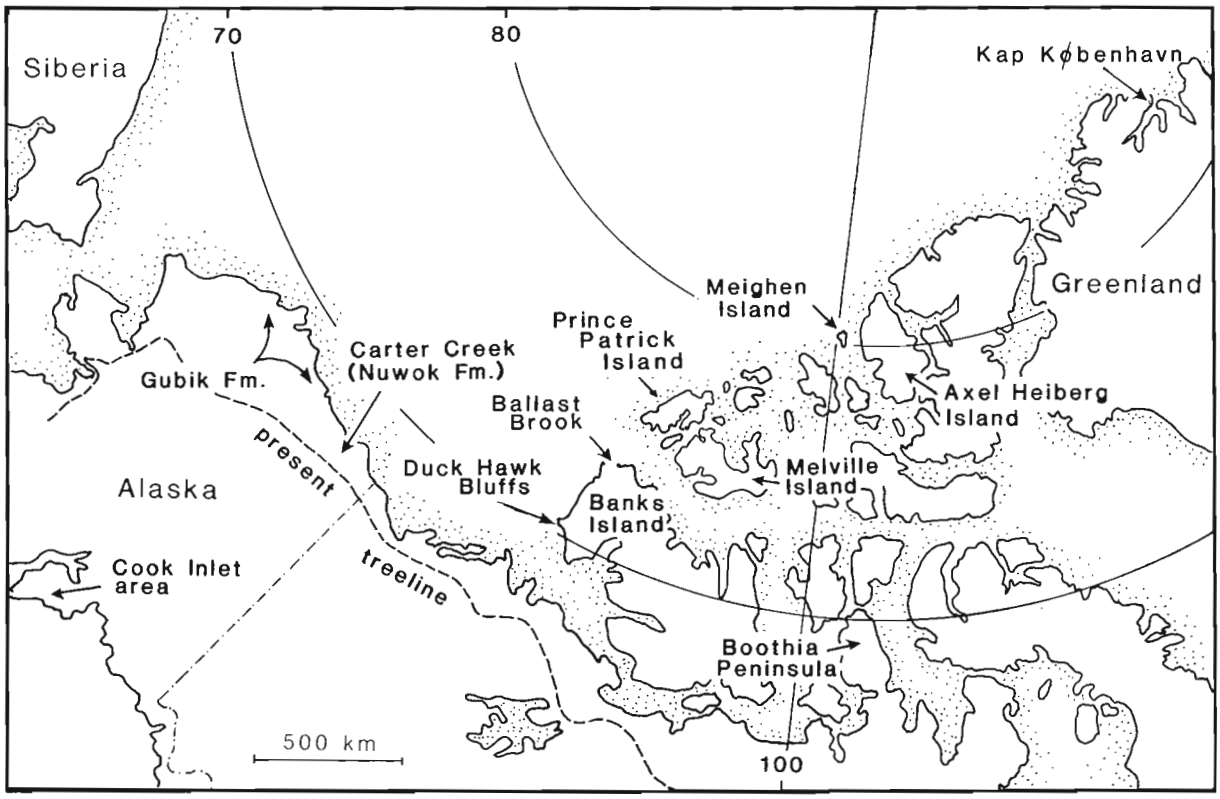


Fig. 9.1 Location map showing the three Beaufort Formation localities from which fossils reported here come plus other localities or sites mentioned in the text.

W.S. Hopkins, unpublished GSC Palynology Report T-02-WSH-1976; J.V. Matthews,Jr., unpublished data).

In a review of modern and fossil taxa of the tribe Monstereae, Madison and Tiffney (1976) show that the genus *Epipremnum* ranges from the Oligocene to the Pliocene (Reuverian) in Europe and Asia. However, they question the identity of fossils that are associated with temperate to boreal taxa because *Epipremnum* is presently restricted to the tropics and subtropics. *E. crassum* is one of the species that they suspect of being erroneously placed.

The fossils cited here are definitely associated with plants typical of a rich boreal forest environment, but rather than being cause for rejection of the *E. crassum* identification, I believe it only indicates that the genus once included a species that had autecological requirements and a distribution much different from the extant *Epipremnum* species. *E. crassum* was probably not a liana, like the modern species; instead it may have been an emergent aquatic (Reid and Reid, 1915).

Aracispermum sp. (Plate 9.1, fig. 3, 4)

Several of the samples from Meighen Island and Ballast Brook contain the distinctive fruits of *Aracispermum*, a genus tentatively referred to the family Araceae (Dorofeev, 1963; Baranova et al., 1976, but see also Madison and Tiffney, 1976).

The Beaufort Formation fossils are similar to illustrations of *Aracispermum Johnstrupii* (Hartz)Nikitin and *A. ovale* Dorofeev (Lancucka-Srodoniowa,1966, Fig. 24; Dorofeev 1963). The fruits are approximately 1.5 mm in length, globular, and have a smooth brown pericarp which is usually completely or partially eroded to expose the thick mesocarp. They possess an opening at one end, which is often somewhat oval in shape due to postmortal deformation. Although superficially similar to *Hippuris*, and once referred to that genus (*H. globosa* in Reid and Reid, 1915), the shape of the internal cavity is not at all like that of *Hippuris* fruits.

This is apparently the first report of *Aracispermum* in North America. The genus is represented by several species in the late Neogene of Germany, Poland, the Netherlands (e.g. *Hippuris globosa* Reid and *Aracites*: Reid and Reid, 1915), and Siberia (Dorofeev, 1963; Mai, 1964; Lancucka-Srodoniowa, 1966; Baranova et al., 1976). Strangely *Aracispermum* also occurs in interglacial floras from the Ukraine and other central European sites (Lancucka-Srodoniowa, 1966), which opens the possibility that it also might have survived into the Quaternary of North America.

Myrica and Comptonia (Plate 9.2, fig. 1-4)

Nuts resembling those of *Myrica gale* L. are abundant in Meighen Island and Ballast Brook samples, and well preserved leaves of the *Myrica gale* type also occur on Meighen Island (L.V. Hills, personal communication, 1975). Some of

Table 9.1 Beaufort Formation plants (excluding bryophtes, pollen, and wood)

Taxa	Duck Bluffs Lower	Hawk Bluffs Upper	Ballast Brook	Meighen Is.
Actinorhizal nodules				+
Selaginellaceae				
Selaginella selaginoides (L.)Link				mg
Pinaceae				
Abies cf. grandis (Dougl.)Lindl.	nd			
*Abies sp.			?nd	
Larix sp.	nd		nd	nd
*(L. cf. omoloica Dorof.)	cn			
Pinus sp.			?nd	nd
*Pinus palaeodensiflora Dorof.	cn			
*Pinus cf. funebris Kom.	cn			cn
Pinus 5-needle type	+			nd
*(P. itelmenorum Vassk.)				cn
*(Pinus cf. albicaulis Engelm.)				nd
Picea sp.	nd	nd	+ nd	+ nd
*(P. banksii Hills&Ogilvie)	cn		cn	cn
Tsuga sp.	nd			
Taxodiaceae				
Metasequoia sp.	+ nd			
*(M. disticha (Heer)Miki)	+ cn			
Cupressaceae				
Thuja sp.			nd	+ nd
*(T. cf. occidentalis L.)				nd
Sparganiaceae				
*Sparganium cf. hyperboreum Laest.		+	+	+
Potamogetonaceae				
Potamogeton spp.	+	+	+	+
Potamogeton cf. epihydrus Raf.			+	
Potamogeton cf. filiformis Pers.			+	+
Juncaginaceae				
Triglochin cf. maritimum L.			+	
Alismaceae				
Sagittaria sp.	?			
Gramineae				
Glyceria type			+	+
genus?				+
Cyperaceae				
*Carex sp.	+	+	+	+
Carex sect. Acutae				+
Carex sect. Chordorrhizae				+
Dulichium sp.			+	
Eleocharis palustris/uniglumis type				+
Scirpus sp.	+		+	
Araceae				
Epipremnum cf. crassum Reid&Reid			+	
Aracispermum sp.			+ +	+
Juncaceae				
Juncus sp.				+
Salicaceae				
*Populus sp.				lf,bd
*Salix sp.			cp	lf,bd
Myricaceae				
*Myrica cf. gale L.			+	+ lf
Comptonia cf. peregrina (L.)Coult.			+	
Comptonia sp.A			+	+ +
Juglandaceae				
*Juglans eocineria Hills & Klovan	+			
Betulaceae				
Alnus (Alnobetula) sp.	+			+
Alnus cf. incana (L.)Moench	+		+	+
Alnus cf. tertiaria Dorof.				+
*Betula (low shrub type)			+	+ lf
*Betula (arboreal type)	+		+	+
Betula cf. apoda/rhomboidea	+		+	
Polygonaceae				
Oxyria digyna (L.)Hill				+
Polygonum sp.			+	
Rumex sp.			+	+
Chenopodiaceae				
Chenopodium cf gigantospermum Aellen			+	
Chenopodium sp.			+	+
Portulacaceae				
Claytonia sp.				+
Caryophyllaceae				
Genus (at least 2)				+
Nymphaeaceae				
*Nuphar sp.			+	+
Nymphaea sp.			+	
Ranunculaceae				
Caltha sp.				?
Ranunculus spp.				+
Ranunculus cf. hyperboreus Rottb.			+	
Ranunculus cf. lapponicus L.			+	+
Ranunculus Macounii/pensylvanicus type			?	
Ranunculus cf. sceleratus L.				+
Ranunculus (Batrachium) type		+		+
Papaveraceae				

Table 9.1 (cont.)

Taxa	Duck Hawk Bluffs Lower	Duck Hawk Bluffs Upper	Ballast Brook	Meighen Is.
Papaver sp.				+
Capparidaceae				
Cleome sp.			+	
Polanisia sp.	+	+		
Cruciferae				
Rorippa sp.				+
Genus?	+			+
Crassulaceae				
Sedum sp.	+			
Saxifragaceae				
Saxifraga oppositifolia L.				+ lf
Rosaceae				
Dryas sp.				?
Dryas integrifolia Vahl				+ lf
Physocarpus sp.			+	+
*Potentilla cf. palustris (L.)Scop.			+	+
Potentilla cf. norvegica L.			+	+
Potentilla sp.		+	+	+
Rubus sp.	+		+	
Rubus cf. idaeus L.				+
Leguminosae				
*Hedysarum sp.				?
Callitrichaceae				
Callitriche sp.	+			?
Aquifoliaceae				
Ilex sp.				+
Hypericaceae				
Hypericum sp.	+	+		
Violaceae				
Viola sp.			+	+
Lythraceae				
Decodon spp.	+	+	+	
cf. Mneme	+		+	
Haloragaceae				
Myriophyllum sp.			+	
Hippuris sp.		+	+	+
Araliaceae				
Aralia sp.	+	?		
Empetraceae				
Empetrum cf. nigrum L.				+
Ericaceae				
*Ledum cf. palustre L.				lf
*Cassiope cf. tetragona (L.)D.Don				lf
Andromeda polifolia L.		+	+	+
Chamaedaphne sp.			+	+
*Vaccinium sp.				+ lf
Oxycoccus sp.				+ lf
Cornaceae				
Cornus spp.			+	+
Gentianaceae				
*Menyanthes trifoliata L.			+	+
Menyanthes sp.A			+	
Verbenaceae				
Verbena sp.			?	
Labiatae				
Teucrium sp.	+			
Solanaceae				
Genus?		?		
Caprifoliaceae				
Sambucus sp.		+	+	
Compositae				
Bidens	?			

+ = presence of seed, fruit, achene or related structure; cn = cone; nd = needle or needle fragments; lf = other leaf fragments; bd = bud scale of fragment; cp = capsule; mg = megaspore; cf. signifies that fossil taxon is near, but possibly not conspecific with named taxon; ? indicates either specimen too poorly preserved for more positive determination or that specimen has some similarity to named taxon.

* indicates taxa that have been reported before in Hills and Matthews (1974), Hills and Ogilvie (1970), and Hills et al. (1974). Taxon shown in parentheses is the one to which the fossils named on the above line probably belong. For example the isolated spruce needles reported here could not be referred to any particular species, but they probably belong to Picea banksii Hills and Ogilvie, which has been identified on basis of its cones.

Most fossils are shown by the "cf." desigantion to be close to the named taxon, but possibly representing an extinct species. Further study of such specimens may show that the fossils are actually conspecific with the named taxon. Finally, a "?" indicates the lowest level of confidence in the determination, usually because of poor preservation of the fossils or lack of diagnostic characters.

the nuts of *M.* cf. *gale* retain the inflated adnate scales and resin nodules that are typical of the species.

A single nut (endocarp) that is similar to those of the extant North American species, *Comptonia peregrina*, occurs in one of the Ballast Brook samples (Plate 9.2, fig. 1, 2). Numerous specimens of another type, here designated as *Comptonia* sp. A (Plate 9.2, fig. 3,4), occur at both Meighen Island and Ballast Brook sites. A similar form also occurs at the Tertiary age Cone Bluff locality in Alaska (Fig. 9.1) on Henderson Slough of Porcupine River (J.V. Matthews,Jr., unpublished data).

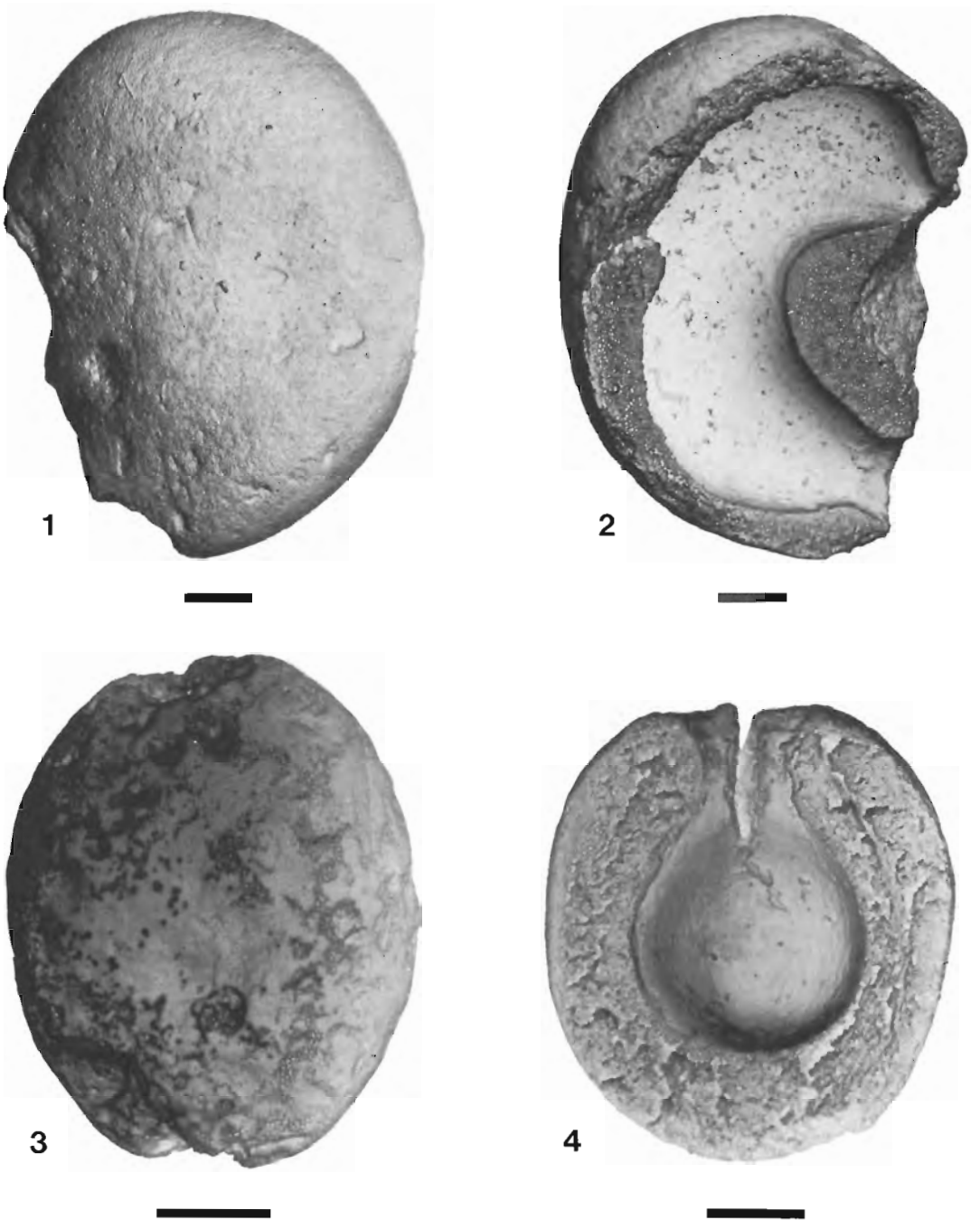
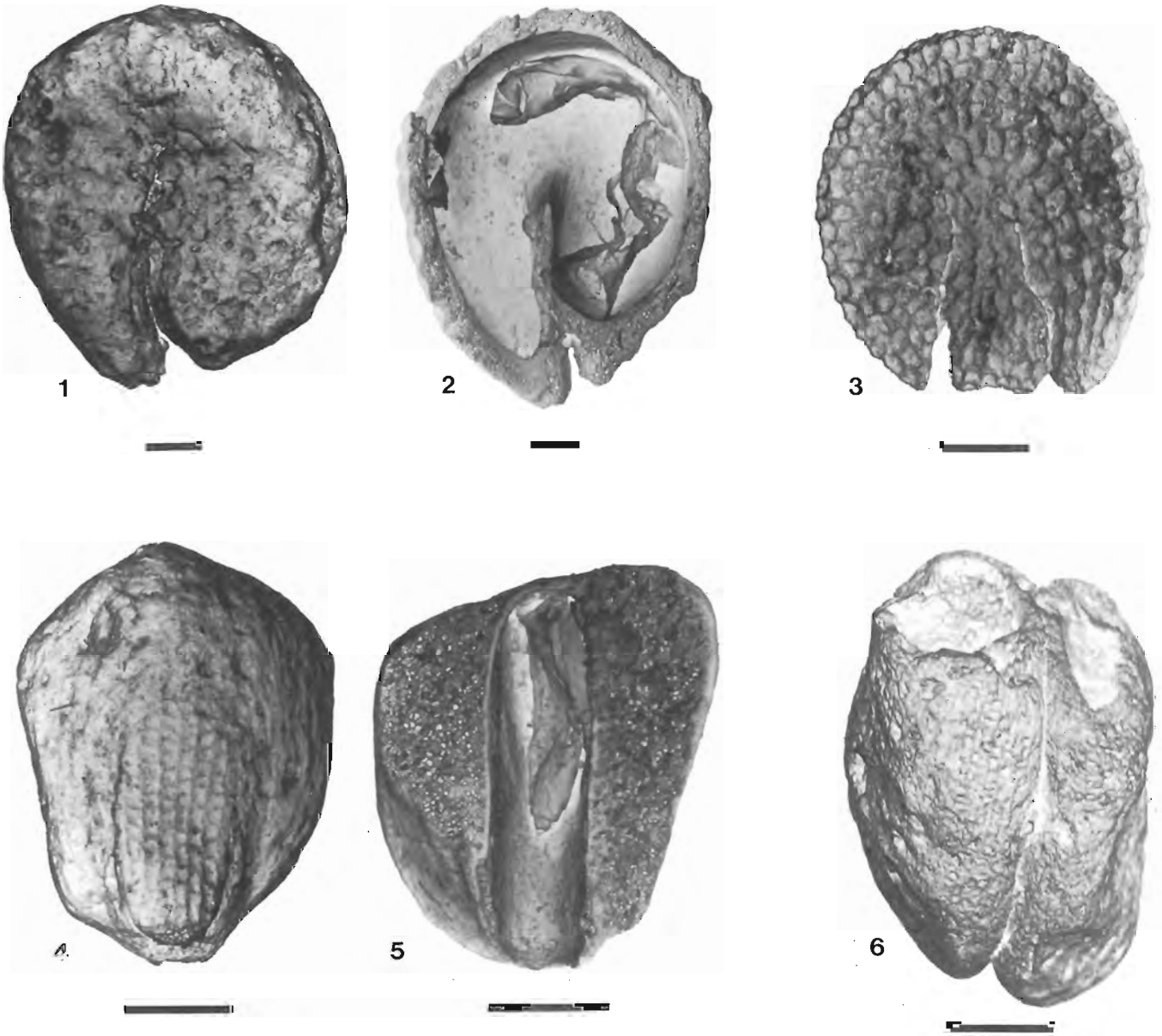


Plate 9.1 SEM micrographs: fig. 1. *Epipremnum* cf. *crassum* Reid & Reid, GSC-85358, Banks Island, Ballast Brook sample JVM3-73, external view; fig. 2. *Epipremnum* cf. *crassum* Reid & Reid, GSC-85359, Banks Island, Ballast Brook sample JVM3-73, internal view of sectioned nut, note thick testa which Reid and Reid (1915) noted as one of the features that distinguishes this species from *E. pinnatum*, the only extant species that occurs north of the tropics; fig. 3. *Aracispermum* sp., GSC-85366, Ballast Brook, Sample JVM3-73; fig. 4. *Aracispermum* sp., GSC-85367, sectioned specimen showing interior cavity, Ballast Brook, Sample JVM3-73.



Plate 9.2 SEM micrographs: fig. 1. *Comptonia* cf. *peregrina* (L.)Coult., GSC-85370, Banks Island sample JVM1-73, external view; fig. 2. *Comptonia* cf. *peregrina* (L.)Coult., GSC-85371, Banks Island sample JVM1-73, internal view of other half of specimen in fig. 1; fig. 3. *Comptonia* sp. A, GSC-85368, Meighen Island, Sample MRA7-25-75-5; external view of nut, note costae; fig. 4. *Comptonia* sp. A, GSC-85369, Meighen Island MRA7-28-75-1, internal view of sectioned nut.



scale bar = 0.3mm

Plate 9.3 SEM micrographs: fig. 1. *Cleome* sp., GSC-85361, Banks Island, Ballast Brook sample JVM3-73, external view; fig. 2. *Cleome* sp., GSC-85362, Banks Island, Ballast Brook sample JVM1-73, internal view of sectioned "seed"; fig. 3. *Polanisia* sp., GSC-85363, Banks Island, Duck Hawk Bluffs sample MRA7-24-85-5; fig. 4. cf. *Mneme*, GSC-85364, Duck Hawk Bluffs, Sample MRA7-24-85-5; fig. 5. cf. *Mneme*, GSC-85365, section showing interior cavity, Duck Hawk Bluffs, Sample MRA7-23-85-2; fig. 6. Unknown seed, GSC-85360, Banks Island, Ballast Brook sample JVM4-73;

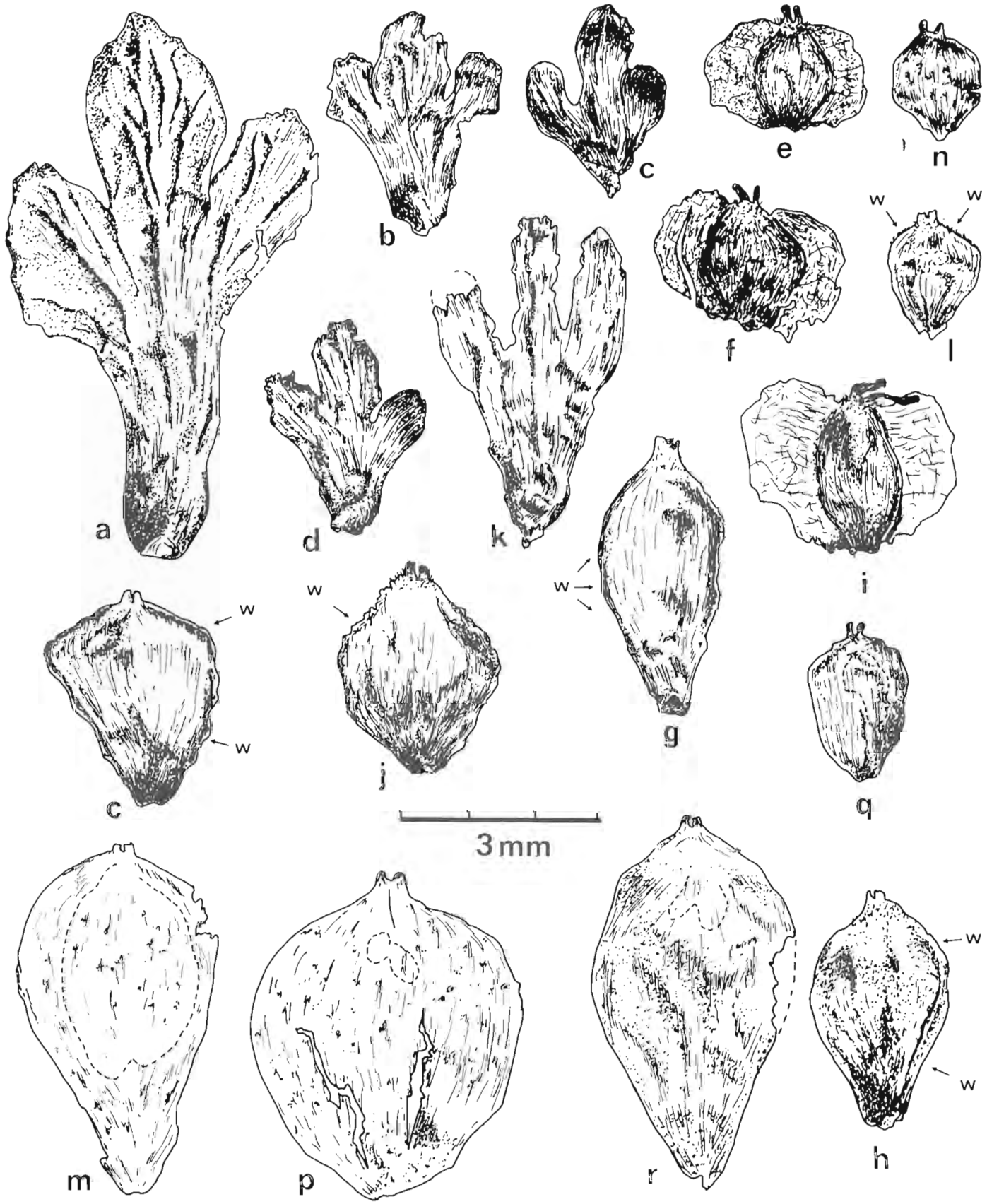


Fig. 9.2 Camera lucida drawings of *Betula* macrofossils from Beaufort Formation Localities on Meighen Island, Ballast Brook (northern Banks Island), and Duck Hawk Bluffs (southern Banks Island). Note that all fossils are shown at the same scale. "w" indicates remnants of wings visible. a. Bractlet, GSC-85372, Meighen Island, Sample JVM5b-73; b. Bractlet, GSC-85373, Meighen Island, Sample JVM5a-73; c. Bractlet, GSC-85374, Meighen Island, Sample JVM5a-73; d. Bractlet, GSC-85375, Meighen Island, Sample JVM9-73; e. Winged nutlet (samara), GSC-85377, Meighen Island, Sample JVM5a-73; f. Winged nutlet (samara), GSC-85376, Meighen Island, Sample JVM5a-73; g. Nutlet, GSC-85378, Meighen Island, Sample JVM5b-73; h. Nutlet, GSC-85379, Meighen Island, Sample JVM5-73; i. Winged nutlet (samara), GSC-85380, Meighen Island, Sample JVM5a-73; j. Nutlet, GSC-85381, Meighen Island, Sample JVM5-73; k. Bractlet, GSC-85382, Ballast Brook, Banks Island, Sample JVM3-73; l. Nutlet, GSC-85383, Ballast Brook, Banks Island, Sample JVM3-73; m. Nutlet, GSC-85384, Ballast Brook, Banks Island, Sample JVM4-73; n. Nutlet, GSC-85385, Ballast Brook, Banks Island, Sample JVM3-73; o. Nutlet, GSC-85386, Ballast Brook, Banks Island, Sample JVM3-73; p. Nutlet, GSC-85387, Duck Hawk Bluffs, Sample MRA7-24-85-5; q. Nutlet, GSC-85388, Duck Hawk Bluffs, Sample MRA7-24-85-5; r. Nutlet, GSC-85389, Duck Hawk Bluffs, Sample MRA7-24-85-5;

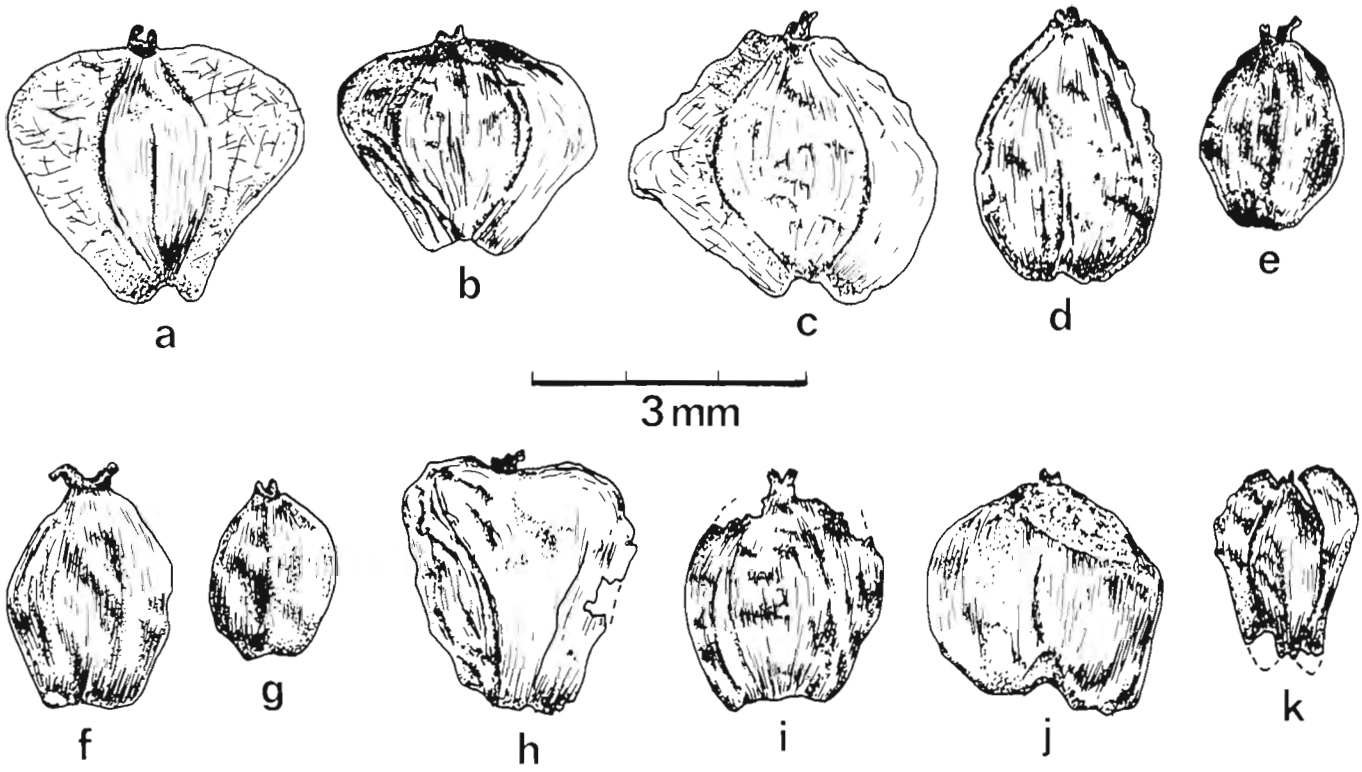


Fig. 9.3 Camera lucida drawings of Alnus nutlets from Beaufort Formation Localities on Meighen Island, Ballast Brook (northern Banks Island), and Duck Hawk Bluffs (southern Banks Island). Note that all fossils are shown at the same scale. a. Alnus (Alnobetula) sp., GSC-85390, Meighen Island, Sample JVM5-73; b. Alnus (Alnobetula) sp., GSC-85391, Meighen Island, Sample JVM5a-73; c. Alnus (Alnobetula) sp., GSC-85392, Meighen Island, Sample JVM5-73; d. Alnus cf. tertiaria Dorof., GSC-85394, Meighen Island, Sample JVM9-73; e. Alnus cf. tertiaria Dorof., GSC-85395, Meighen Island, Sample JVM9-73; f. Alnus cf. tertiaria Dorof., GSC-85396, Meighen Island, Sample JVM5a-73; g. Alnus cf. tertiaria Dorof., GSC-85397, Meighen Island, Sample JVM14-73; h. Alnus cf. incana (L.)Moench, GSC-85393, Meighen Island, Sample JVM5b-73; i. Alnus cf. incana (L.)Moench, GSC-85398, Ballast Brook, Banks Island, Sample JVM3-73; j. Alnus cf. incana (L.)Moench, GSC-85339, Duck Hawk Bluffs, Bank Island, Sample MRA7-23-85-2; k. Alnus (Alnobetula) sp., GSC-85400, Duck Hawk Bluffs, Bank Island, Sample MRA7-23-85-5.

Endocarps of *Comptonia* sp. A are relatively large and vary considerably in shape and development of ribs. Until such time as this variation is better understood and type material of other fossil species described from endocarps is examined, the specific relationships of *Comptonia* sp. A will remain unknown.

In Siberia *Myrica gale* fossils are characteristic of the lowland equivalents of the Miocene/Pliocene Clamgulchian Stage of Alaska (Biske, 1974). A fossil species, *M. eogale* Nikitin (Baranova et al., 1976), which is apparently closely related to *M. gale*, occurs in the mid-Miocene (Seldovian: Biske, 1974) Mamontova Gora Suite near Aldan River in eastern Siberia (Baranova et al., 1976).

The genus *Comptonia* today contains only the single eastern North American species, *C. peregrina* (L.)Coult., but during the Tertiary it was evidently more diverse taxonomically (at least twelve types from the Mamontova Gora Suite alone: Baranova et al., 1976) and distributed across Europe and Asia as well as North America (Lamotte, 1952; Friis, 1979). Whereas the Old World records are based on fossils of both the distinctive foliage and endocarps, only foliar remains have been found in North America and many of those fossils may be incorrectly identified (Wolfe, 1973).

Betula spp. (Fig. 9.2)

Nutlets and bractlets of *Betula* occur in samples from all three sites. Meighen Island deposits have also yielded well preserved leaf fossils (L.V. Hills, personal communication, 1976). Camera lucida drawings of bractlets, nutlets and samaras are shown in Figure 9.2. Some of the nutlets from Meighen Island still possess complete wings, and many retain the pubescence typical of the stigmatal end of the nutlet. A few of the fossils resemble bracts and nutlets of the dwarf shrub species *Betula glandulosa* (Fig. 9.2, b-f), but

none of the latter have wings quite as small as those of typical *B. glandulosa* samaras. Other fossils (e.g., Fig. 9.2, g-j) are similar in size to those of the extant tree *Betula papyrifera* and undoubtedly represent one or more arboreal species.

Birch fossils are neither as abundant nor as well preserved at Ballast Brook. None of the nutlets examined have complete wings, though on many of them remnants of the wings can be seen on the lateral margins. Their size alone allies most of the nutlets with arboreal type birches. Bractlets and nutlets of the shrub birch type (Fig. 9.2, k,l) are also present, however, not in the numbers seen in Meighen Island samples.

One birch nutlet from Ballast Brook (Fig. 9.2, m) stands out because of its large size. It evidently represents the same type that is abundant in the lower unit at Duck Hawk Bluffs (Fig. 9.2, p,r). None of these very large nutlets show remnants of wings and they may have been wingless. In size and shape they resemble the fossil species *Betula apoda* Dorofeev and *Betula rhomboidea* Dorofeev from the Miocene of western Siberia (Dorofeev, 1963), but as in the case for the *Comptonia* fossils, a more detailed statement of affinity must await examination of type material.

Alnus spp. (Fig. 9.3)

Figure 9.3 presents camera lucida drawings of typical *Alnus* nutlets. At least two types appear to occur in the lower member at Duck Hawk Bluffs. One has well developed membranous wings like species of the subgenus *Alnobetula*, which includes the common northern species, *Alnus crispa* (Furlow, 1979). The other is wingless and resembles the extant species *Alnus incana*. *Alnus incana* type nutlets are also present at Ballast Brook and both *Alnobetula* and *Alnus incana* in Meighen Island samples. The latter area has also yielded a third unusual type which is similar in shape, size, and by its lack of wings to the fossil species *Alnus tertiaria* Dorofeev from western Siberia (Dorofeev, 1963).

Capparidaceae: Cleome and Polanisia (Plate 9.3 fig. 1-3).

Seeds of *Polanisia* occur at Duck Hawk Bluffs and *Cleome* is abundant in a few of the samples at Ballast Brook samples. Both taxa occur in Neogene deposits of western and eastern Siberia (Dorofeev, 1963; Baranova et al., 1976). They currently grow in southern Canada (Iltis, 1957) well south of the Northwest Territories (Matthews et al., in press). This is probably the first report of either from Tertiary deposits in North America.

Lythraceae

A few seeds of *Decodon*, possibly representing two different species, occur in samples from both southern and northern Banks Island, and as such represent the first report of the genus from the North American Tertiary (Tiffney, 1981). Also seen at both sites are several small seeds (e.g., Plate 9.3, fig. 4, 5) that undoubtedly belong with the Lythraceae but are quite different from *Decodon*. They have a quadrate shape with much of the seed buried in thick spongy lateral wings. A germination valve, possessing less than ten distinct rows of puctures occupies the apical half of the ventral face. The dorsal face (opposite the germination valve) is flat and possesses neither grooves or folds as do some fossil genera. Tiffney (1981) provided a key to the four genera found as fossils: *Alatospermum*, *Decodon*, *Mneme* (=*Diclidocarya*), and *Microdiptera*. The fossils shown in Plate 9.3 (fig. 4, 5) share characteristics with each of these, but are closest to *Microdiptera* and *Mneme*, which may in fact be variants of a single genus (Tiffney, 1981). In Table 9.1 they are listed as cf. *Mneme*.

The only other record of a related taxon from North America are the seeds of *Microdiptera* in the Oligocene Brandon Lignite (Tiffney, 1981). *Microdiptera* and *Mneme* have been found at a number of European and Asian sites in deposits ranging in age from Oligocene to Pliocene (Tiffney, 1981).

Undetermined fossils

At each of the areas discussed here, but especially the Banks Island sites, there remains a small but potentially significant group of fossils that cannot as yet be referred to a particular genus or family. An example of one of the more peculiar unknowns is illustrated in Plate 9.3 (fig. 6). It appears superficially like two joined specimens of *Hippuris*; however, hundreds of *Hippuris* fruits occur in some of the samples and none of them exhibit the condition seen in the illustrated specimen. Though somewhat smaller, the fossil in Plate 9.3, figure 6 is similar to the specimen of Carpolithus sp. 1 in Mai's (1964: Table IV) treatment of brown-coal floras of Germany.

DISCUSSION

Table 9.1 presents only vascular plants, hence this report is at best merely a progress report on the Beaufort Formation floras. Nevertheless, these new data do allow some comments on paleoenvironments and phytogeography. Unfortunately they provide little new information on one of the most perplexing problems of the Beaufort Formation – its age. Previous estimates of mid to late Miocene (Hill and Matthews, 1974; Hills, 1975) were based partly on assumptions as to what northern (Beaufort) counterparts of the well established Cook Inlet floras (Seldovian, Homerian and Clamgulchian: Wolfe, 1972, 1980) might contain or on the content of key species, such as *Picea banksii*. The first method is fraught with circular reasoning and the second has lead to erroneous conclusions (e.g., cf. Hills and Bustin, 1976 with Ricketts and McIntyre, 1986). Better estimates of the age of the Beaufort Formation will come from study of the marine deposits interbedded with Beaufort sediments or from comparison with other floras that are independently dated by intertonguing marine deposits or other methods.

Table 9.2 Beaufort Formation plants according to habitat type

Taxa	Duck Bluffs Lower	Duck Bluffs Upper	Hawk Ballast Brook	Meighen Is.
AQUATIC AND SHORELINE				
Selaginella selaginoides				+
Potamogeton sp.	+	+	+	+
Potamogeton epihydrus			+	
Potamogeton filiformis			+	+
Nuphar sp.			+	+
Nymphaea sp.			+	
Ranunculus (Batrachium)		+		+
Callitriche sp.	+		?	
Mryiophyllum sp.			+	
Sparganium hyperboreum		+	+	+
Triglochin maritimum			+	
Sagittaria sp.	?			
Glyceria sp.			+	+
Carex sect. Acutae				+
Carex sect. Chordorrhiza				+
Dulichium sp.			+	
Eleocharis sp.				+
Scirpus sp.	+		+	
Juncus sp.				+
Potentilla palustris			+	+
Potentilla norvegica			+	+
Hippuris sp.		+	+ +	+ +
HEATH AND TUNDRA				
Betula (low shrub type)				+
Oxyria digyna				+
Saxifraga oppositifolia				+
Dryas integrifolia				+
Empetrum nigrum				+
Ledum palustre				+
Cassiope tetragona				+
Andromeda polifolia		+	+	+
Chamaedaphne sp.			+	+
Vaccinium sp.				+
Oxycoccus sp.				+
WET LOWLANDS AND FLOODPLAIN				
Populus sp.				+
Salix sp.			+	+
Myrica gale			+	+
Alnus incana	+		+	+
Chenopodium gigantospermum			+	
Chenopodium sp.			+	+
Claytonia sp.				+
WET LOWLANDS (Cont.)				
Ranunculus hyperboreus			+	
Ranunculus lapponicus			+	+
Ranunculus sceleratus				+
Rorippa				+
Sedum sp.	+			
Physocarpus sp.			+	+
Hedysarum sp.				?
Viola sp.			+	+
Decodon sp.	+	+	+ +	
Andromeda polifolia		+	+	+
Menyanthes trifoliata			+ +	+ +
Verbena sp.			?	
Bidens sp.	?			
FOREST AND WOODLAND				
Abies grandis	+ +			
Abies sp.			?	
Larix sp.	+		+	+
Pinus sp.			?	+
Pinus 5-needle type	+			+
Picea sp.	+	+	+	+
Tsuga sp.	+			
Metasequoia sp.	+			
Thuja sp.			+	+
Populus sp.				+
Juglans eocineria	+			
Betula arboreal type	+		+	+
Rubus idaeus				+
Aralia sp.	+	?		
Ilex sp.				+
Viola sp.			+	+
Oxycoccus sp.				+
Cornus sp.				?
Teucrium sp.	+			
Sambucus sp.		+	+	
OPEN UPLANDS				
Betula (low shrub type)			+	+
Papaver sp.				+
Cleome sp.			+ +	
Polanisia sp.	+	+		
Hedysarum sp.				?
Hypericum sp.	+	+		
Verbena sp.			?	

Reliably dated late Pliocene floras occur in the Kap København Formation, in northern Greenland (Funder et al., 1985) and in the Gubik Formation from northern Alaska (Nelson and Carter, 1985; J.V. Matthews,Jr. unpublished GSC Plant Macrofossil Reports 85-11, 86-3; Fig. 9.1). The Kap København flora comes from about the same latitude as the Meighen Island flora and by all accounts represents similar forest-tundra type vegetation (see below). However, Meighen Island has yielded several taxa apparently not found at Kap Kobenhavn (e.g., *Pinus*, *Physocarpus*, *Comptonia*, *Aracispermum*) or in the Gubik Formation; in contrast to the Kap København conifer fossils, all those from Meighen Island appear to refer to extinct species. These distinctions probably mean that the Beaufort Formation on Meighen Island is significantly older than the late Pliocene.

This conclusion is supported by occurrence of fossils of the mollusc *Arctica* in the marine tongue on Meighen Island (L. Marincovich and K. McDougall, personal communication, 1980). *Arctica* is an Atlantic genus, and its presence in the Arctic Basin probably predates the opening of Bering Strait at about 3 Ma because after that event Arctic basin molluscan faunas were dominated by Pacific taxa (e.g., the Gubik Formation molluscs are all of Pacific origin: Carter et al., 1986). A fossil species similar to the Meighen Island *Arctica* species also occurs in the Nuwok Formation at Carter Creek in northern Alaska (Fig. 9.1; L. Marincovich and K. McDougall, personal communication, 1980), which is variously dated at mid-Miocene (Seldovian: Wolfe, 1980; T. Ager, personal communication, 1986) to early Pliocene (L. Maricovich and K. McDougall, personal communication, 1986; E. Brouwers, personal communication, 1986). Further study of the Nuwok Formation and its probable equivalent, the marine tongue on Meighen Island, should have high priority in any future research plans for the Beaufort Formation. Until then, the best estimate of the age of the Meighen Island Beaufort Formation flora is that it is no younger than early Pliocene and possibly as old as mid-Miocene.

Neogene environments in the high arctic

Table 9.2 groups plant taxa listed in Table 9.1 according to their autecology. The most interesting feature of the table is the diversity of heath and tundra plants on Meighen Island. Several of them, such as *Saxifraga oppositifolia*, *Dryas integrifolia*, and *Oxyria digyna*, are typical of lowland tundra sites, and they show more clearly than was evident before that Meighen Island supported some type of tundra environment. Support for this conclusion comes from the content of the insect fauna, which consists of many species that represent or are closely related to extant obligate or facultative tundra species (Matthews, 1976). According to Table 9.2, forests also existed on Meighen Island, but even though they were more diverse taxonomically than modern northern boreal forest, the small size of most of the wood from Meighen Island suggests that they represented stunted forests similar to those currently found near treeline.

It could be argued that both the tundra plants and insects from Meighen Island represent only a narrow fringe of coastal tundra, created by proximity to a cold ocean, and it is true that most fossil collecting localities are near what would have been the former position of the coast. However, one explanation for the anomalously low alle/Ile ratios on fossils of *Arctica* from the marine tongue (J. Brigham-Grette, personal communication, 1986) is that ground temperatures dropped well below 0°C shortly after deposition of the marine unit. If so, this implies a permafrost regime and the type of regional climate that exists at present treeline. Furthermore, if regional treeline existed on Meighen Island, then it represents one of the oldest Northern Hemisphere records of lowland tundra – significantly older than the tundra existing at the time of deposition of the Siberian Kutuyakh Suite (Wolfe, 1985).

Somewhat similar conditions are suggested for Kap København in northern Greenland (Funder et al., 1985). Taken together, the Kap København and Meighen Island floras suggest existence of a type of nascent tundra around the Arctic Basin for nearly all the Pliocene. This span of more than 3.5 Ma would have been ample time for the evolution of obligate tundra plants and insects. Furthermore, it is possible that it was during this long interval that alpine environments and their biota first merged with northern lowland tundra. If so, the late Pliocene floras and faunas should contain more taxa that have relatives in the present alpine zone or montane regions than the earlier Meighen Island floras and faunas. In this regard it is interesting that the lower Gubik Formation and Kap København Formation have both yielded fossils that have current North American montane affinities (Funder et al., 1985; J.V. Matthews,Jr., unpublished data), but some of the insects and plants from Meighen Island also have such links.

Phytogeographic implications

Some of the new finds reported here have potential phytogeographic implications, especially for taxa that are suspected of being remnants of an early Tertiary amphi-Atlantic flora or that are presumed to have dispersed across a North Atlantic land bridge. For example, Tiffney (1981) has suggested that the extant eastern North American *Decodon* is a relict of just such an early Tertiary North Atlantic connection. *Microdiptera* (which may be synonomous with *Mneme* – see Table 9.1) from the Oligocene Brandon Lignite is viewed in similar terms except that it is presently extinct (Tiffney, 1981).

The fossils of *Decodon* and cf. *Mneme* reported here show that dispersal of these two genera between the Old and New Worlds probably continued into the Neogene, and that the route was most likely through Beringia (Matthews, 1979) rather than across a North Atlantic land bridge.

Madison and Tiffney (1976) in their discussion of the Monstereae, the tribe to which *Epipremnum* belongs, state: "If future work reveals North American fossil material, then the similarities of the African and South American forms

could be ascribed to common derivation from a Paleogene Boreotropical flora, in keeping with Wolfe's (1975) hypothesis." The data presented here suggest that *Epipremnum* did occur in the New World (it does not today), but during the Neogene rather than the Paleogene, and as a member of a boreal rather than a tropical flora. It will be interesting to see if fossils representing *Epipremnum* or another genus within the Monstereae are found in the Paleogene forest beds recently discovered in the Canadian Arctic (Lemonick, 1986), but if they are, they too will be members of a flora that was dominantly coniferous and therefore not like the environment in which extant Monstereae occur (Madison and Tiffney, 1976).

ACKNOWLEDGMENTS

I wish to thank S.A. Edlund, S. Cevallos, and R. Stockey for their comments on various parts of this manuscript and L. Barton and A. Telka for their technical help. L. Hills, A. Segouin, T. Sutcliffe, and L. Leclerc helped in collection of the fossils and D. Walker and the staff of the GSC SEM lab recorded the SEM micrographs

Thanks are also extended to the staff at the National Herbarium, National Museums of Canada, and Plant Science Unit at Biosystematics Research Centre, Agriculture Canada for their continuing willingness to provide modern reference material.

REFERENCES

Baranova, Ju.P., Il'jinskaja, I.A., Nikitin, V.P., Pneva, G.P., Fradkina, A.F., and Schvareva, N.Ya.
1976: The Miocene of the Mamontova Gora (Stratigraphy and Paleoflora), "NAUKA", Moscow, 284 p. (in Russian).

Biske, S.F.
1974: Correlation of Tertiary nonmarine deposits in Alaska and northeastern Asia; in Arctic Geology, M.G. Pitcher (ed.); American Association of Petroleum Geologists, Memoir 19, p. 239-245. Carter, L.D., Brigham-Grette, J., Marincovich, L. Jr, Pease, V.L., and Hillhouse, J.W. 1986: Late Cenozoic Arctic Ocean sea ice and terrestrial paleoclimate; Geology, v. 14, p. 675-678.

Dietrich, J.R., Dixon, J., and McNeil, D.H.
1985: Sequence analysis and nomenclature of Upper Cretaceous to Holocene strata in the Beaufort-Mackenzie Basin; in Current Research, Part A, Geological Survey of Canada, Paper 85-1A, p. 613-628.

Dorofeev, P.I.
1963: Tertiary Floras of Western Siberia; U.S.S.R. Academy of Sciences, Komarov Botanical Institute. 345 p. (in Russian)

Dyke, A.S. and Matthews, J.V.,Jr.
Stratigraphy and paleoecology of Quaternary sediments exposed along Pasley River, Boothia Peninsula, Central Canadian Arctic; Géographie physique et Quaternaire (in press).

Friis, E.M.
1979: The Damgaard flora: a new Middle Miocene flora from Denmark; Bulletin of the Geological Society of Denmark, v. 27, p. 117-142.
1985: Angiosperm fruits and seeds from the Middle Miocene of Jutland (Denmark); Det Kongelige Danske Videnskaberne Selskab Biologiske Skrifter, v. 24:3, 165 p.

Funder, S., Abrahamsen, N., Bennike, O., and Feyling-Hanssen, R.W.
1985: Forested arctic: evidence from North Greenland; Geology, v. 13, p. 542-546.

Furlow, J.J.
1979: The systematics of the American species of Alnus (Betulaceae), Rhodora, v. 81, p. 1-121, 151-248.

Hills, L.V.
1969: Beaufort Formation, northwestern Banks Island, District of Franklin; in Report of Activities, Part A, Geological Survey of Canada, Paper 69-1A, p. 204-207.
1970: Stratigraphy of the Beaufort Formation along western margin of Canadian Arctic Islands; American Association of Petroleum Geologists, Bulletin, v. 54, p. 2486 (abstract).
1975: Late Tertiary floras Arctic Canada: an interpretation; Proceedings of Circumpolar Conference on Northern Ecology, National Research Council of Canada, p. I(65)-I(71).

Hills, L.V. and Bustin, R.M.
1976: Picea banksii Hills & Ogilvie from Axel Heiberg Island, District of Franklin; in Report of Activities, Part B, Geological Survey of Canada, Paper 76-1B, p. 61-63.

Hills, L.V. and Matthews, J.V.,Jr.
1974: A preliminary list of fossil plants from the Beaufort Formation, Meighen Island; in Report of Activities, Part B, Geolical Survey of Canada, Paper 74-1B, p. 224-226.

Hills, L.V. and Ogilvie, R.T.
1970: Picea banksii n.sp., Beaufort Formation (Tertiary), northwestern Banks Island, Arctic Canada; Canadian Journal of Botany, v. 48, p. 457-464.

Hills, L.V., Klovan, J.E., and Sweet, A.R.
1974: Juglans eocinerea n., Beaufort Formation (Tertiary) southwestern Banks Island, Arctic Canada; Canadian Journal of Botany, v. 52, p. 65-90.

Iltis, H.H.
1957: Studies in the Capparidaceae. III. Evolution and Phylogeny of the western North American Cleomoideae; Annals of the Missouri Botanical Garden, v. 44, p. 77-119.

Kirchheimer, F.
1957: Die Laubgewachse der Braunkohlenzeit; Veb Wilhelm Knapp Verlag, Halle (Salle), 783 p.

Kuc, M. and Hills, L.V.
1971: Fossil mosses, Beaufort Formation (Tertiary), northwestern Banks Island, western Canada Arctic; Canadian Journal of Botany, v. 49, p. 1098-1094.

Lamotte, R.S.
1952: Catalogue of the Cenozoic plants of North America through 1950; Geological Society of America, Memoir 51, 381 p.

Lancucka-Srodoniowa, M.
1966: Tortonian flora from the "Gdow Bay" in the south of Poland; ACTA Paleobotanica, v. 7, no. 1, 135 p.

Lemonick, M.D.
1986: Unearthing a frozen forest; Time, Sept. 22, p. 84.

McCourt, G.H.
1982: Quaternary palynology of the Bluefish Basin, northern Yukon Territory; unpublished MSc thesis, University of Alberta, Edmonton, 165 p.

Madison, M. and Tiffney, B.H.
1976: The seeds of the Monstereae: their morphology and fossil record; Journal of the Arnold Arboretum, v. 57, p. 185-201, 3 plates.

Mai, D.H.
1964: Die Mastixioideen-Floren im Tertiar der Oberlausitz; Palaontologische Abhandlungen, Ab B, Palaobotanik, Band II, Heft 1, 192 p.

Matthews, J.V., Jr.
1976: Insect fossils from the Beaufort Formation: geological and biological significance; in Report of Activities, Part B, Geological Survey of Canada, Paper 74-1B, p. 217-227.
1977: Tertiary Coleoptera fossils from the North American Arctic; The Coleopterists Bulletin, v. 31, no.??. p. 297-308.
1979: Tertiary and Quaternary environments: historical background for an analysis of the Canadian insect fauna; in Canada and its Insect Fauna, H.V. Danks (ed.); Entomological Society of Canada Memoir 108, p. 31-86.

Matthews, J.V.,Jr., Mott, R.J., and Vincent, J-S.
1986: Preglacial and interglacial environments of Banks Island: Pollen and macrofossils from Duck Hawk Bluffs and related sites; Géographie physique and Quaternaire (in press).

Miall, A.D.
1979: Mesozoic and Tertiary geology of Banks Island, Arctic Canada: The history of an unstable craton margin; Geological Survey of Canada Memoir 387, 235 p.

Nelson, R.E. and Carter, L.D.
1985: Pollen analysis of a Late Pliocene and Early Pleistocene section from the Gubik Formation of Arctic Alaska; Quaternary Research, v. 24, p. 295-306.

Reid, C. and Reid, E.M.
1915: The Pliocene floras of the Dutch-Prussian border; Mededeelingen van de Rijksopsporing van Delfstoffen, no. 6, 178 p., 20 plates.

Reid, E.M.
1927: A new species of Diclidocarya Reid from the Senftenberg Brown-Coal; Journal of Botany, v. 65, p. 1-4.

Ricketts, B.D. and McIntyre, D.J.
1986: The Eureka Sound Group of eastern Axel Heiberg Island: new data on the Eurekan Orogeny; in Current Research, Part B, Geological Survey of Canada, Paper 86-1B, p. 405-410.

Roy, S.K. and Hills, L.V.
1972: Fossil woods from the Beaufort Formation (Tertiary), northwestern Banks Island, Canada; Canadian Journal of Botany, v. 50, p. 2637-2648.

Szafer, W.
1946: The Pliocene Flora of Kroscienko in Poland, II. Descriptive Part; Polska Akademia Umiejetnosci; Rozprawy wydzialu Matematyczno-Przyrodniczego, Tom 72, Dzial B, No. 2, 213 p.

Thorsteinsson, R.
1961: History and geology of Meighen Island; Geological Survey of Canada, Bulletin 75.

Tiffney, B.H.
1981: Fruits and seeds of the Brandon Lignite, VI. Microdiptera (Lythraceae); Journal of the Arnold Arboretum, v. 62, p. 487-516.

Tozer, E.T.
1956: Geological reconnaissance Prince Patrick, Eglinton and western Melville Islands, Arctic Archipelago, Northwest Territories; Geological Survey of Canada, Paper 55-5.
1970: Mesozoic and Cenozoic; in Geology and Economic Minerals of Canada, R.J.W. Douglas (ed.); Geological Survey of Canada, Economic Geology Report No. 1, p. 574-589.

Vincent, J-S., Occhietti, S., Rutter, N., Lortie, G., Guilbault, J-P., and de Boutray, B.
1983: The late Tertiary-Quaternary stratigraphic record of the Duck Hawk Bluffs, Banks Island, Canadian Arctic Archipelago; Canadian Journal of Earth Sciences, v. 20, no. 11, p. 1694-1712.

Wolfe, J.A.
1972: An interpretation of Alaskan Tertiary floras; in Floristics and Paleofloristics of Asia and Eastern North America, A. Graham (ed.); Elsevier, Amsterdam, p. 201-233.
1973: Fossil forms of Amentiferae; Brittonia, v. 25, p. 334-355.
1975: Some aspects of plant geography of the Northern Hemisphere during the Late Cretaceous and Tertiary; Annals of the Missouri Botanical Garden, v. 62, p. 264-279.
1980: The Miocene Seldovia Point Flora from the Kenai Group, Alaska; U.S. Geological Survey, Professional Paper 1105, 52 p.
1981: A chronologic framework for Cenozoic megafossil floras of northwestern North America and its relation to marine geochronology; Geological Society of America, Special Paper 184, p. 39-47.
1985: Distribution of major vegetational types during the Tertiary, in The carbon cycle and atmospheric CO_2: natural variations, Archean to present, E.T. Sondquist and W.A. Broecker (ed.); American Geophysical Union, Monograph 32, p. 357-375.

Young, F.G. and McNeil, D.H.
1984: Cenozoic stratigraphy of the Mackenzie Delta, Northwest Territories; Geological Survey of Canada, Bulletin 336, 63 p.

- 10 -

Morphosedimentary zones in the Bluenose Lake region, District of Mackenzie

Project 840002

Denis A. St-Onge and Isabelle McMartin[1]
Terrain Sciences Division

St-Onge, D.A. and McMartin, I., Morphosedimentary zones in the Bluenose Lake region, District of Mackenzie; in Current Research, Part A, Geological Survey of Canada, Paper 87-1A, p. 89-100, 1987.

Abstract

Using landforms and dominant sediment types, the Bluenose Lake area, northern District of Mackenzie, has been divided into six morphosedimentary zones: A, Felsenmeer, kames, and silt mounds complex; B, Bluenose Lake moraine complex; C, Inman River drumlin field; D, Upper Harding River moraine complex; E, Rae River glacial lakes sequence; F, Marine offlap area. Systematic mapping north of 68°N to the coast and between 116°30′ and 120°W shows that each of these distinct zones was defined mostly by the nature and activity of glacier ice. Zone A was covered by a thin layer of ice but not modified by glacial movement; it marks the limit of Wisconsinan ice advance in this area. Zone B was an area of massive deposition of glacial, glaciofluvial, and glaciolacustrine sediments at the margin of an active ice mass. Zone C, composed of long drumlins on flat-lying dolomite bedrock, reflects active ice flow from the south-southeast between the Bluenose Lake moraine complex and the morainic complex in the upper reaches of Harding River. Zone D is defined by sinuous morainic ridges with extensive areas of boulder fields and hummocky till; the ridges indicate complex lobation at the margin of the retreating ice mass. Zone E is an area of washed till, beach ridges, and at lower elevations, sandy silt and clay rhythmites. These features record the presence, during early deglaciation, of a sequence of overlapping lakes marginal to an ice lobe in the basin of the Rae and Richardson rivers. Zone F is that part of the coast that was covered by the postglacial sea; the limit of submergence varied from approximately 45 m a.s.l. to 120 m a.s.l.

Résumé

En se basant sur les formes de relief et sur les principaux types de sédiment la région du lac Bluenose, dans la partie nord du district du Mackenzie, a été divisée en six zones morphosédimentaires: (A), complexe de felsenmeer, de kames et de monticules de silt; (B), complexe morainique du lac Bluenose; (C), champ de drumlin de la rivière Inman; (D), complexe morainique du cours supérieur de la rivière Harding; (E), la séquence glaciolacustre de la rivière Rae; (F), région de régression marine. La cartographie systématique au nord du 68°N de latitude nord jusqu'à la côte et entre 116°30′ et 120°W démontre que chacune de ces zones résulte principalement de l'activité des glaciers. La zone A a été recouverte par une mince couche de glace mais ne fut pas modelée par l'avancée glaciaire – elle marque la limite de l'avancée de la glace du Wisconsinien dans cette région. La zone B est une région de mise en place massive de sédiments glaciaires, fluvioglaciaires et glaciolacustres à la marge d'une masse de glace active. La zone C composée de longs drumlins reposant sur des assises de dolomie en lits horizontaux traduit un écoulement de glace depuis le sud sud-est entre le complexe morainique du lac Bluenose et le complexe morainique de la rivière Harding supérieure. La zone D est caractérisée par des crêtes morainiques au tracé sinueux et par d'importantes surfaces de champ de blocs et par du till bosselé, ces crêtes réflètent l'activité de nombreux petits lobes à la marge du glacier en retrait. La zone E comprend des régions de till délavé, des lignes de plage et, dans les parties plus basses du bassin, des rythmites de silt sableux et d'argile – ces formes sont liées à la présence, tôt au fini glaciaire d'une séquence de lacs en marge d'un lobe de glace qui occupait le bassin des rivières Rae et Richardson. La zone F comprend la marge côtière qui a été recouverte par la mer postglaciaire; la limite de submersion varie d'environ 45 m a.n.m. et 120 m a.n.m.

[1]Department de géologie, Université Laval, Québec, Québec G1K 7P4

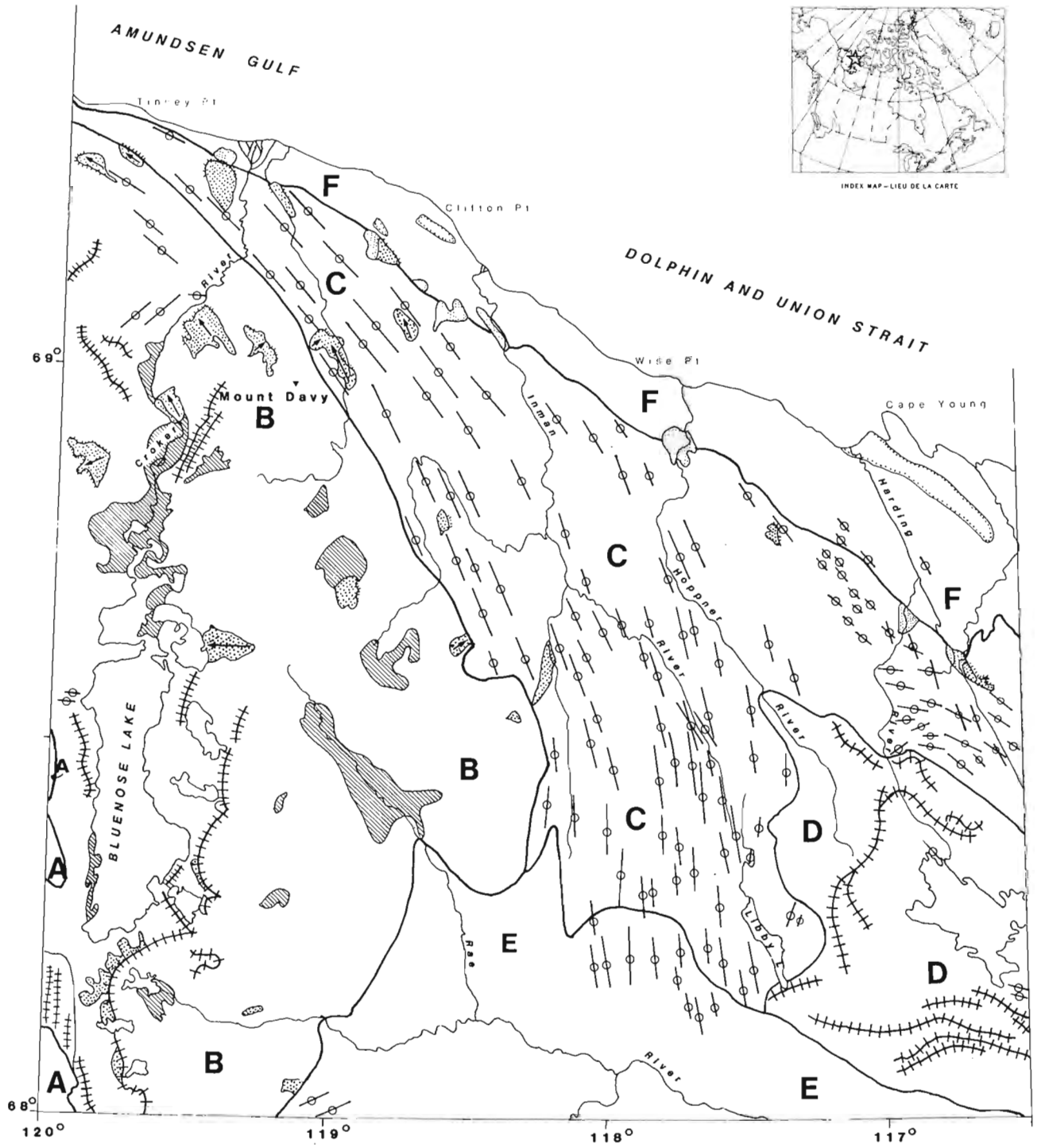


Figure 10.1. Morphosedimentary zones of the Bluenose Lake region, northern District of Mackenzie, Northwest Territories.

MORPHOSEDIMENTARY ZONES,

BLUENOSE LAKE REGION, NORTHWEST TERRITORIES

A Felsenmeer, Kame and Silt Mound Complex: Blocks of dolomite and rare erratics of granite, gneiss gabbro and red sandstone; steep sided conical kames of bouldery gravel 5 to 15 m high surrounded by or adjacent to silt mounds 3-5 m high and 100 to 500 m across.

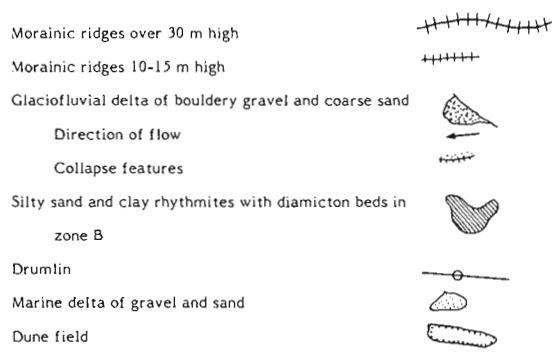
B Bluenose Lake Moraine Complex: Bouldery gravel with a silty sand matrix forming massive north-south ridges and mounds up to 100 m high; bouldery gravel and/or sand in glaciofluvial deltas; sandy silt and clay rhythmites interbedded with bouldery diamicton in glaciolacustrine basins.

C Inman River Drumlin Field: Clasts in a sand-silt matrix, underlying drumlins 10-15 m high and commonly 5 to 8 km long oriented north to northwest and developed on flat lying dolomite bedrock; glaciofluvial deltas of bouldery gravel with collapse features towards the northeast.

D Upper Harding River Moraine System: Bouldery gravel sand and silt forming sinuous ridges up to 50 m high; extensive areas of shattered bedrock surfaces between ridges; locally hummocky till.

E Rae River Glacial Lakes Sequence: Boulders and gravel lag left on till by the washing action of overlapping ice marginal lakes, beached drumlins and other till deposits at higher elevations; silty sand and clay rhythmites up to 10 m thick along the Rae River.

F Marine Offlap area: Buff coloured sandy silt and clay rhythmites with abundant marine shells underlying extensive plain areas; till surfaces washed and modified by wave actions; flights of pebble and gravel beaches; very large blow out sand dune complexes oriented NW-SE. Large deltas of bouldery gravel grading downstream to sand mark the limit of the postglacial marine transgression which increases in elevation from approximately 50 m a.s.l. at the west margin of the map area to 120 m a.s.l. at the east margin.



INTRODUCTION

The Bluenose Lake study area (Fig. 10.1) comprises the drainage basin areas of Croker River, which includes Bluenose Lake, Inman, Hoppner, and Harding rivers, as well as the upper reaches of Rae River which drains the southern part of the map area. The whole region, except for parts of the Rae River basin, is part of the Horton Plain of the Interior Plains region (Bostock, 1970). Based on drift thickness and topography, the Bluenose Lake region can be divided into two parts: The Croker River Hills (zones A and B, Fig. 10.1) and the Inman River Plateau (zones C to F, Fig. 10.1).

The Croker River Hills region is characterized by hills and ridges of drift generally over 30 m thick and above 300 m a.s.l. The predominant material is a sandy silt till with large boulders. The Inman River Plateau is generally below 300 m a.s.l.; it comprises broad expanses of nearly flat to gently undulating topography underlain by flat-lying Lower Palaeozoic dolomites (Fraser et al., 1960); outcrops are common and drift is usually less than 15 m thick.

Few geologists have worked in this remote region so that our prior knowledge of the Quaternary history was fragmentary. John Richardson, a member of Franklin's second overland expedition to the Arctic Coast, explored the coastline between the Mackenzie Delta and the mouth of Coppermine River. Most of the geographical names along the coast were assigned by Richardson. "His detailed and precise notes on the flora, fauna, ice conditions, Eskimo and so forth have contributed substantially to the scientific knowledge of the north" (Mackay, 1958, p. 13). O'Neill (1924), a member of the 1913-1918 Canadian Arctic Expedition, made numerous and detailed observations of the "Pleistocene" all along the coastline; he also collected shells in raised marine sediments and measured the orientation of glacial striae and grooves. More recently, Craig (1960), a member of the Geological Survey of Canada's "Operation Coppermine", mapped major glacial landforms such as drumlins, morainic ridges, and eskers and measured striae. He also collected marine shells which provided the first age estimate for deglaciation. On his map the approximate limit of marine submergence is shown.

Morphosedimentary zones

A. Felsenmeer, kames, and silt mounds complex

The southwest corner of the map area (Fig. 10.1) is part of the southern flank of a broad bedrock plateau to the west of Bluenose Lake, which rises to over 700 m a.s.l. It is underlain mostly by dolomitic rocks of the Lower Paleozoic (Fraser et al., 1960). The generally flat to gently rolling surface is mantled by boulders of dolomite and sparse granite and gabbro erratics. Speckled on this surface are numerous steep sided conical hills of bouldery gravel, 5-15 m high, interpreted as moulin kames. Around or adjacent to these are low mounds of sandy silt 3-5 m high. Outwash sand and gravel cover a small part of this area; this 1 to 3 m-thick deposit has steep slopes to the southeast and to the east which show evidence of collapse (Fig. 10.2).

The presence of erratics, kames, and associated glaciolacustrine sediments and outwash leaves no doubt that zone A was covered by glacial ice. However, the sediments and associated landforms strongly suggest that the last ice to cover this area was inactive. Gravel and sand outwash deposited at the margin of the ice and numerous moulin kames resting on shattered bedrock and a few erratics support the hypothesis of a cover of glacier ice too thin to imprint signs of active movement (Fig. 10.3A). The association of mounds of sandy silt with kames is interpreted as resulting from sedimentation in a water body occupying a depression in the ice that formed as a result of collapse around a moulin. The present subdued relief associated with these fine grained sediments is likely the result of collapse and solifluction following ice melt rather than a reflection of original sedimentation surface.

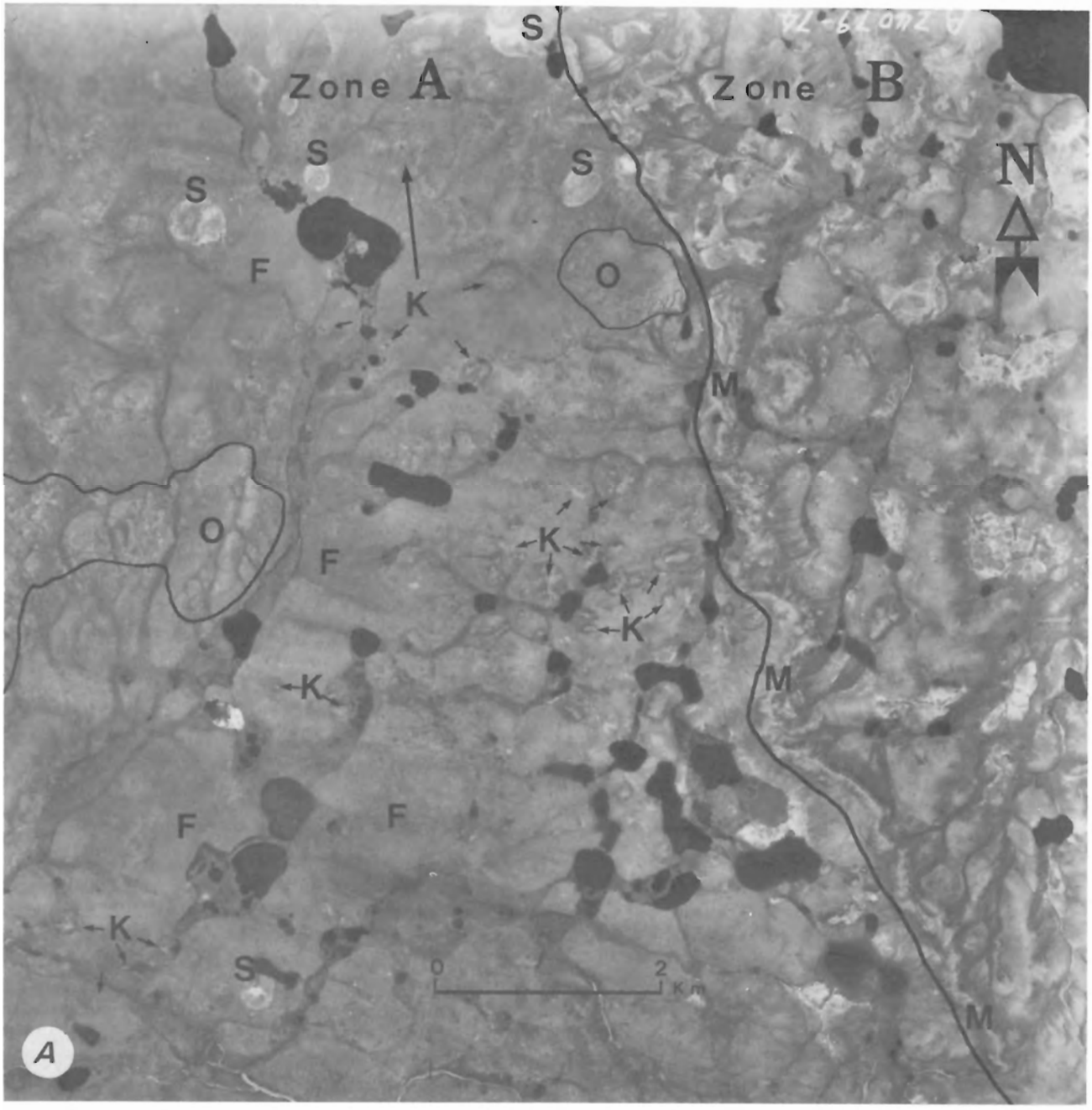


Figure 10.2. Felsenmeer, kame and silt mounds complex (zone A, Fig. 10.1) southwest of Bluenose Lake. A. Outwash sand and gravel (O), kame and silt mounds (S), and kames (K) rest on bouldery debris (F) containing sparse erratics which mantles bedrock. A steep sided moraine ridge (M) marks the approximate western limit of active ice during the last glacial maximum.

B. Bluenose Lake moraine complex

In the southwestern part of the map area, the limit between zones A and B (Fig. 10.1) is marked by a steep sided ridge of bouldery gravel and sand 20-30 m high with an east facing slope that is systematically steeper than the west (Fig. 10.2). The interpretation is that the ridge was deposited by meltwaters and debris flows which dumped englacial and supraglacial debris in a trench that developed within the ice. The trench is thought to correspond to zones of weakness along thrust planes which marked the margin of active ice (Fig. 10.3B).

All of zone B is covered by thick layers, in some places over 100 m, of glacial, glaciofluvial, and glaciolacustrine debris. The till is a bouldery diamicton, is more than 3 m thick, has a sandy to sandy silt matrix, and is often prone to mudflows (Fig. 10.4).

The most common landforms are boulder-covered steep sided hills, up to 60 m high, and hummocks interspersed with numerous lakes. This massive "hummocky moraine" (Prest, 1967, p. 11), which forms a 20-30 km-wide arcuate belt to the west and north of Bluenose Lake, marks the in situ disintegration of a debris-laden ice frontal zone.

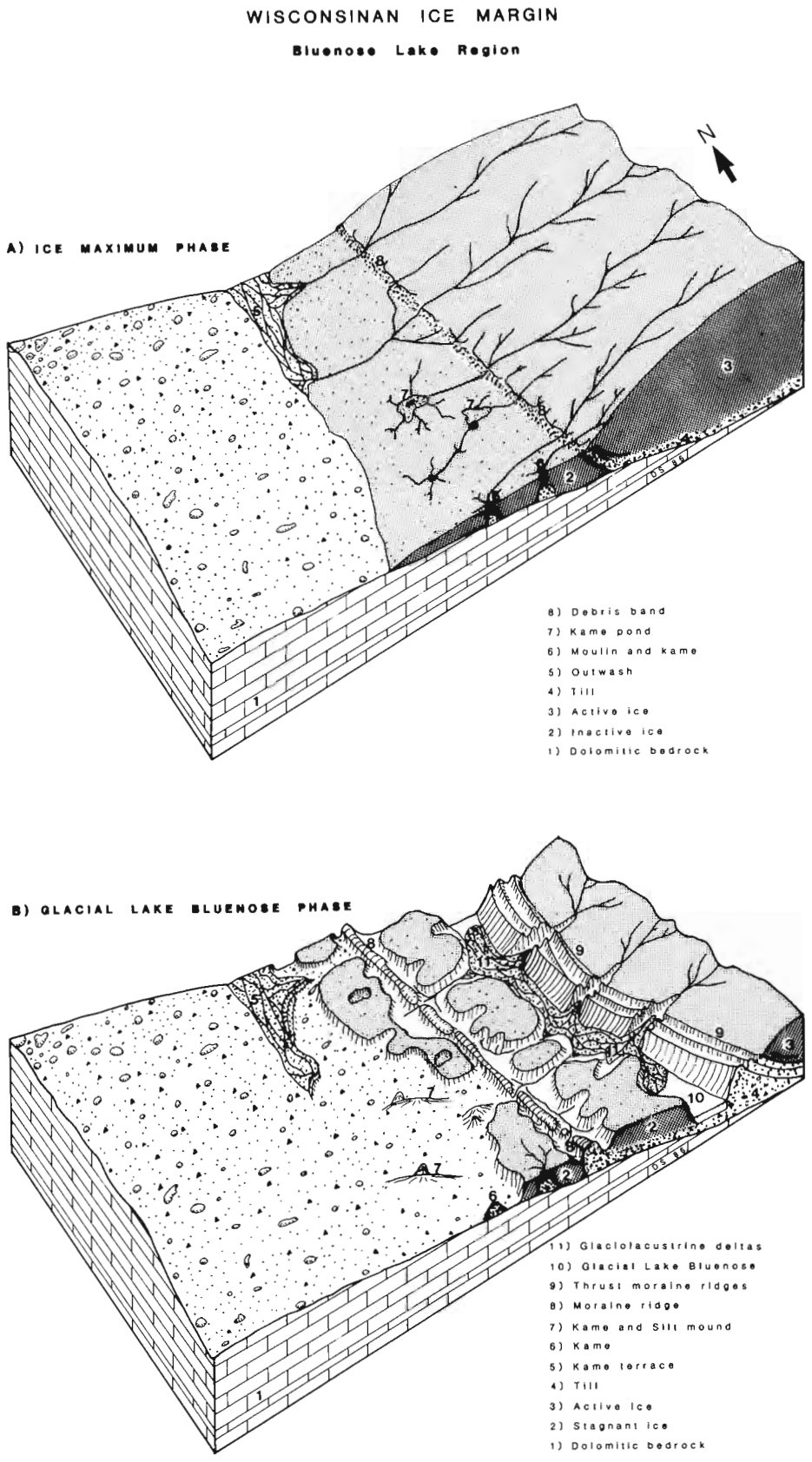
At the western edge of this zone to the east of Bluenose Lake, massive ridges, up to 100 m high, of bouldery till mark the limit of a generally north-south active ice frontal position. Major ridges are either massive or composed of numerous linear ridges at their crest (Fig. 10.5). This gives the appearance of steeply dipping stacked layers of coarse bouldery diamicton which could be explained by extensive thrusting up of basal material at the ice margin. During stagnation the debris was redistributed to the point that linear patterns reflecting thrusting planes were nearly obliterated, except in the case of the outermost ridges. When these ridges were being constructed, meltwater flowing to the west from the active ice mass deposited large loads of sediments in bodies of water which were dammed between masses of stagnant ice located in the depression now occupied by Bluenose Lake. Large "marginal deltas" (Lundqvist, 1979) were thus built on the western slope of the moraine ridges. All are pitted with numerous kettles which are bordered by collapsed slopes. The outer limits of the deltas show ubiquitous evidence of postdepositional collapse (Fig. 10.5). The most northerly of these deltas is located on the east side of a large unnamed lake near the northeast end of Bluenose Lake. The material in this delta (sandy gravel) is generally finer than that (bouldery gravel) of deltas farther south. It is bounded on the north by a moraine ridge and kettles with associated collapse features. Its southern margin is also marked by large kettles and collapse features.

These deltas, constructed by westerly flowing waters, are present over a 70 km distance east and southeast of Bluenose Lake. Their surface is always between 160 and 170 m a.s.l. Rhythmically bedded sandy silt and clay deposits, 2-4 m thick, are found at elevations below the delta surfaces; the deposits, which blanket irregular surfaces around Bluenose Lake, are commonly pitted by kettles and distorted where exposed in sections.

All the above evidence supports the hypothesis of rapid sedimentation from an ice front into a water body occupying a



B. Ground view of silt mounds and associated kames.



A. At the last (?Late Wisconsinan) glacial maximum an apron of inactive ice rests on felsenmeer-covered bedrock. In the early stages of ice retreat the limit of active ice is marked by thrusting which builds a moraine ridge (M, Fig. 10.2); outwash is deposited at the ice margin and within moulins; small ponds occupying depressions resulting from ice collapse around moulin kames fill with silty sand.

B. As a result of increased melting, the active ice front is located farther east where intense ice thrusting is constructing part of a moraine ridge of the Bluenose Lake moraine complex (Fig. 10.1). Ice contact features emplaced during phase A are now exposed. Meltwater streams are rapidly building large bouldery gravel deltas in a part of glacial Lake Bluenose which is clogged with masses of stagnant ice.

Figure 10.3. Block diagrams of Zone A (felsenmeer, kame, and silt mounds complex) and zone B (Bluenose Lake moraine complex), southwest of Bluenose Lake (Fig. 10.1).

depression which was extensively clogged with dead ice masses. The water plane of this lake was 40-50 m above present day Bluenose Lake and is herein named glacial Lake Bluenose. The areal extent of fine grained sediment is limited because of the amount of stagnant ice that was present in the basin. Lakes, kettle holes, and collapse structures (St-Onge, 1984, p. 276) below the level of the deltas all support this hypothesis. The outlet of glacial Lake Bluenose has not yet been identified.

Within the Bluenose Lake moraine complex there are several small basins, 50-100 km^2, in which glacial meltwaters were held by the easterly retreating ice front. In these ice-dammed lakes sandy silt and clay rhythmites accumulated to measured thicknesses of 20 m. Beds of bouldery diamicton, 20-80 cm thick, are commonly interbedded with the silty clay rhythmites (Fig. 10.6). These are interpreted as debris flow diamictons and, because clasts provide high resistance to wind or sheet wash erosion, they commonly form the capping beds of this sequence.

For the first 30 km of its course Croker River, which drains Bluenose Lake, occupies a valley that predates the last glaciation. The present river has exposed sections up to 48 m high which show a complete glacial cycle starting with the pre-last glaciation river alluvium at the base (Fig. 10.7). The alluvial deposits are overlain by sand grading to silt to sandy silt rhythmites deposited in a proglacial lake formed when the advancing ice blocked drainage to the north. The rhythmites are in turn overlain by a massive diamicton containing large boulders of dolomite, gabbro, quartzitic red sandstone, and various types of gneiss. This is believed to be a lodgment till deposited at the base of the last ice sheet when it overrode the glaciolacustrine sediments. Thin silty clay and clay rhythmites and 20-30 cm-thick gravelly diamicton beds rest on the till and represent the early phase of a glacial lake. Massive sedimentation in this basin is represented by sandy foreset beds of an advancing delta which in turn are covered by coarse gravel delta surface sediments. Although bedrock was not seen at the base of the section illustrated in Figure 10.7, it is visible in several other exposures so that there is no doubt that the coarse alluvial gravel at the base of the section is in fact the lowermost unit of the sequence resting on bedrock.

The Bluenose Lake moraine complex with its system of north-south trending ridges and associated high level deltas, along with numerous ice dammed lakes on its eastern flank, represents a major ice frontal position where a westerly trending ice mass piled large amounts of glaciogenic materials. Spatial and stratigraphic relationships suggest that this is a Wisconsinan terminal moraine. Vincent (1984b, p. 94, 96) suggested that it is part of an Early Wisconsinan glacial limit, with Late Wisconsinan ice being limited to elevations below 300 m a.s.l. We have discovered no evidence to support or reject this hypothesis.

C. Inman River drumlin field

The Inman River drumlin field forms a belt 5-45 km wide which starts just north of Rae River in the south and then forms a broad, northwesterly trending arc between the Bluenose Lake moraine complex (zone A) and the marine offlap area (zone F) fringing Amundsen Gulf and Dolphin and Union Strait (Fig. 10.1). The field is composed of long linear ridges up to 8 km long and 10-15 m high with the intervening



Figure 10.4. Retrogressive thaw slump in a silty sand and boulder diamicton of the Bluenose Lake Moraine complex. Note the sharp contact between the exposed ice rich permafrost layer and the overlying material of the active layer.

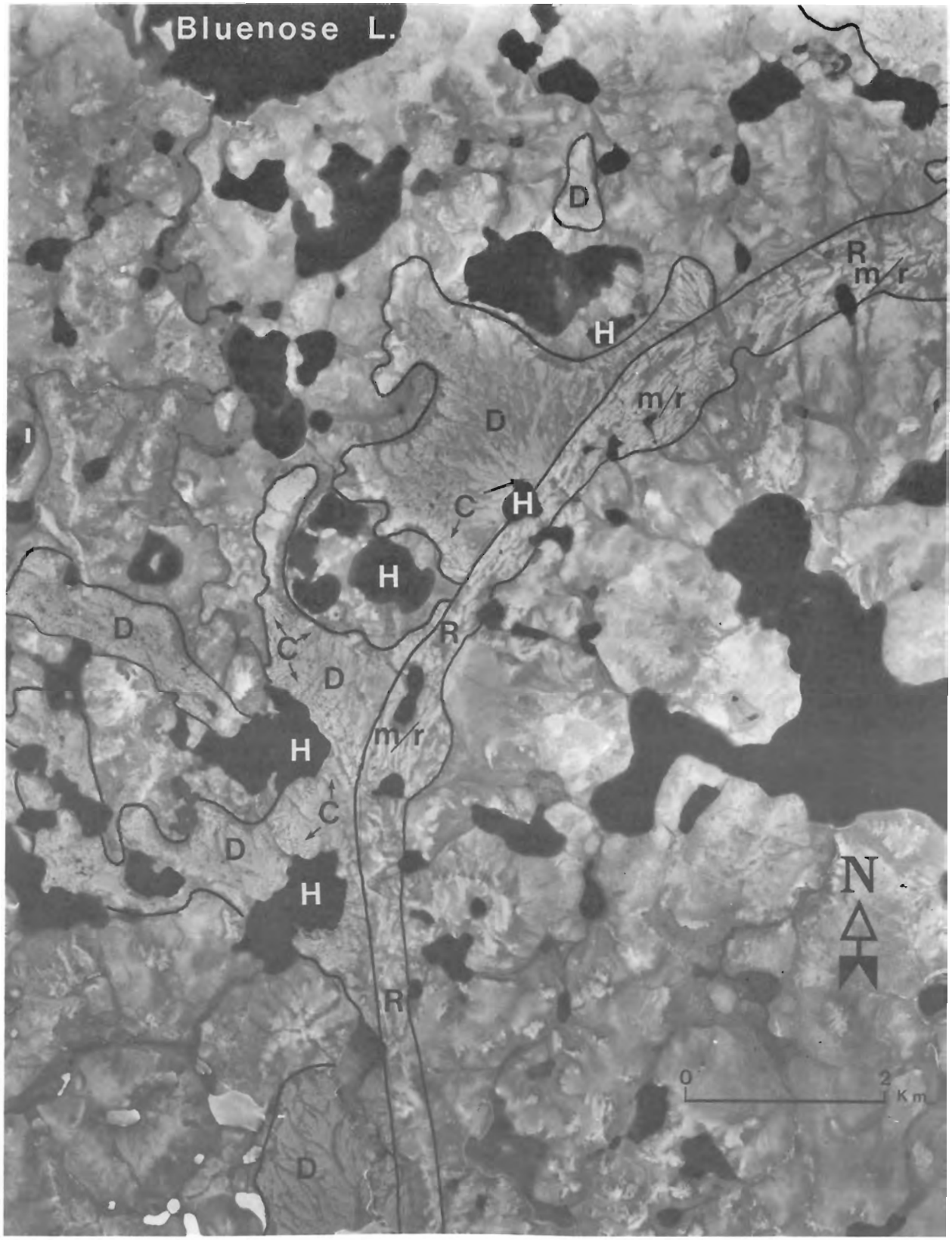


Figure 10.5. Zone B (Fig. 10.1) south of Bluenose Lake. To the west of a large complex moraine ridge (R), large deltas (D) are pitted by numerous kettle holes, and (H) rimmed by collapse (C) ridges and associated fracture zones. Multiple minor ridges (m/r) on main moraine ridge are thought to identify the location of thrust plates (Fig. 10.3B).

swales occupied by narrow lakes or streams. Dolomitic bedrock commonly outcrops between drumlins. Although no sections were found exposing the core of a drumlin, surface exposures and shallow sections show a diamicton with generally well rounded clasts of various lithology in a silty sand matrix. Larger erratics are dominantly of gabbro and granites. Available information suggests that the whole field is composed of moulded till resting on an essentially flat dolomite rock platform.

Outwash sand and gravel bodies are common and occur as dissected terraces irregularly spaced along the course of all major rivers. They commonly form deltas with a steep east or northeast facing slope scarred by slump features. This indicates that in its waning stages the lobe responsible for moulding the drumlin field was shrinking towards the east and northeast allowing streams flowing from the Bluenose Lake moraine complex to deposit coarse sediments in contact with the retreating ice margin at progressively lower elevations.

In the headwater region of Hoppner River, drumlins parallel to the main north-northwest flow direction have been partly remoulded by a more westerly flow as is the case in that part of the drumlin field along Harding River between zones F and D (Fig. 10.1). The implication of this late ice movement is not yet fully understood and will have to await further studies in the region to the east of the study area.

D. Upper Harding River moraine system

Harding River originates in a large unnamed lake in the southeast part of the map area (Fig. 10.1). To the north, west, and south of the lake, several sinuous morainic ridges occur, averaging 20 m high but in places rising to 50 m above the surrounding surface. They are interpreted to represent the frontal position of small ice lobes originating from a glacier to the east. These lobes advanced after the ice responsible for the formation of the Inman River drumlin field had become stagnant.

Drumlins associated with the northernmost ridge indicate that it was built at the front of a lobe which moved westerly and then southwesterly across an older set of drumlins trending SSE-NNW as pointed out above. The middle set of ridges, east of Libby Lake, are associated with a lobe advancing southeast-northwest.

To the southeast of Libby Lake several massive morainic ridges trend east-west. They were formed at the northern margin of a lobe which occupied the basin of Rae River (Fig. 10.1) and Richardson River, immediately south of the study area. They rise up to 270 m a.s.l. and show no sign of modification by wave action which indicates that this area was still under ice when higher level ice marginal lakes formed strandlines farther west at elevations up to 550 m a.s.l. (see zone E below).

E. Rae River glacial lake sequence

During the early phases of deglaciation small glacial lakes were formed within the Bluenose Lake moraine complex, particularly in small basins in the headwater regions of Rae River. Associated with these small glacial lake basins are numerous strandlines southeast of Bluenose Lake. The high-

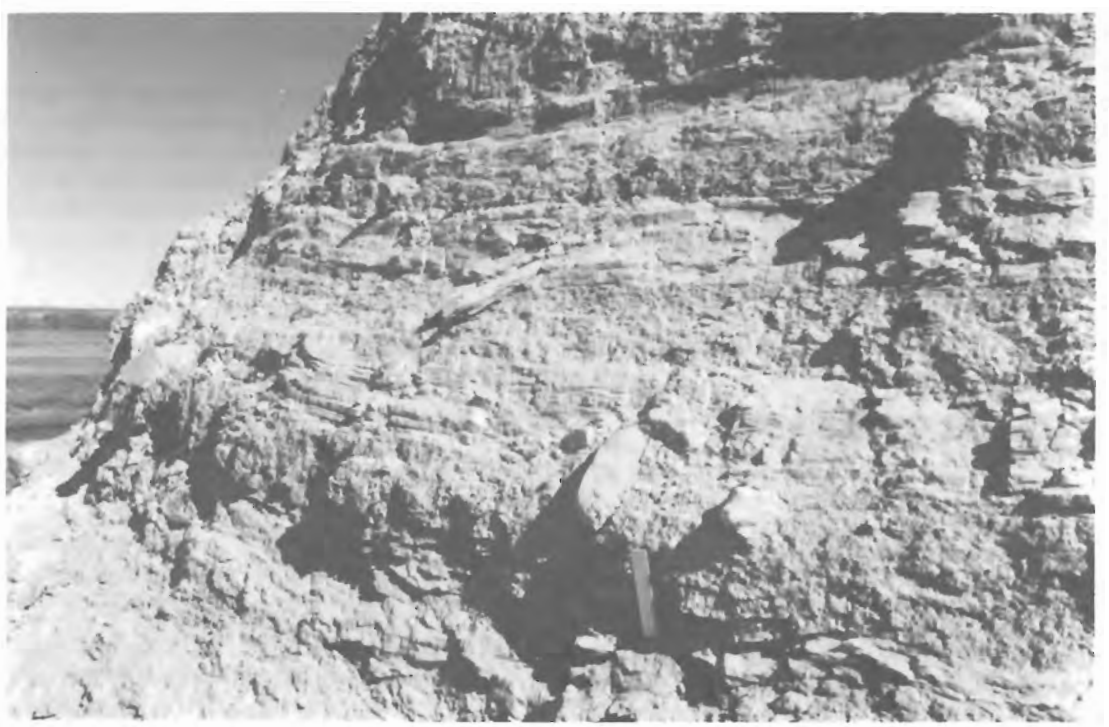


Figure 10.6. Debris flow diamicton interbedded with silty rhythmites form a typical sequence of sediment deposited in ice contact lakes within the Bluenose Lake Moraine complex.

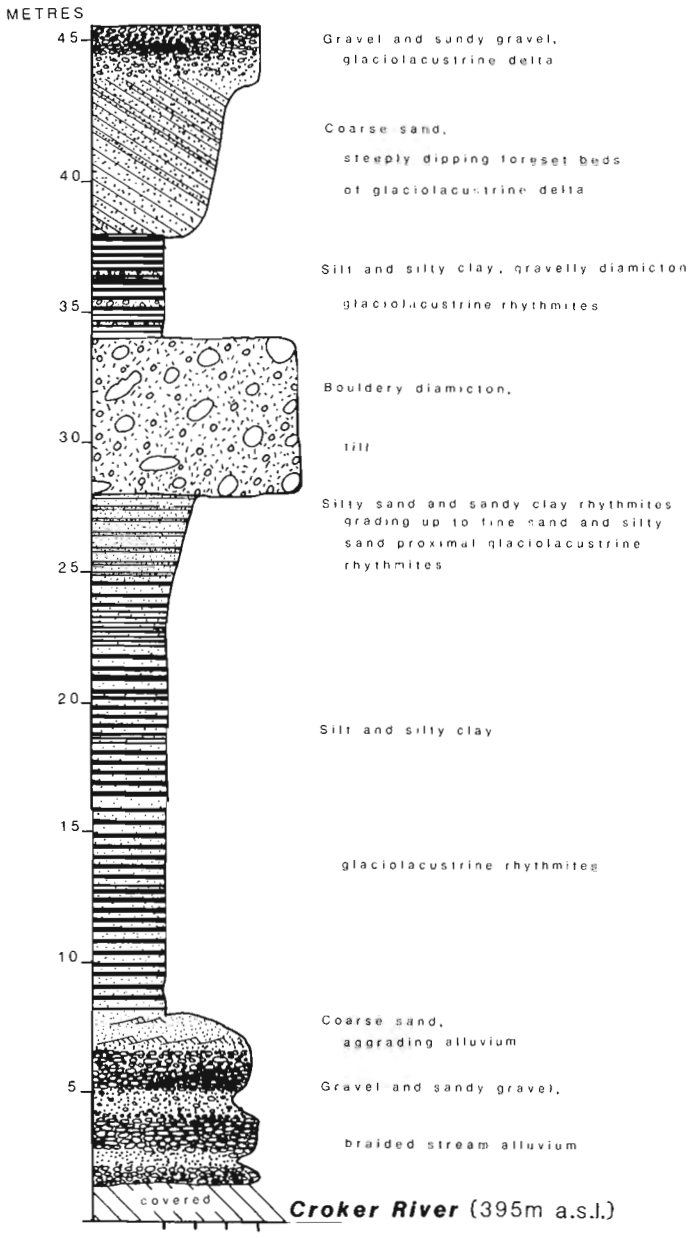


Figure 10.7. Section exposed along the east side of Crocker River, 68°56′58″N, 119°37′36″W. The sediments exposed in this section result from a complete glacial cycle: gravel and coarse sand alluvium at the base emplaced in an environment similar to the present when river flow was not impeded by glacier ice; coarse sand with climbing ripples mark the beginning of aggradation as a result of ice blocking the lower course of the river; silt and clay rhythmites deposited in a glacial lake which occupied the ice dammed valley; sandy silt and silt proximal rhythmites reflect encroaching ice mass; till emplaced by overriding glacier; silty rhythmites and debris flow diamicton deposited in a glacial lake during ice retreat and, at the top, the sand and gravel of a glaciolacustrine delta.

est of these is at 550 m a.s.l.; others occur at lower elevations of 520, 500, 470, 450, 420, 400, 380, 350, 220 m. South of Libby Lake a strandline occurs at 200 m a.s.l.

Deltas of bouldery gravel are associated with the strandlines and the steep outer slope of all of them shows evidence of collapse. Above 200 m glaciolacustrine sediments are generally thin (1-3 m) with abundant diamicton beds; however, as mentioned above, in some small basins thicknesses can be up to 20 m. All this evidence suggests that these features are related to narrow ice marginal lakes along a large lobe occupying the basin of Rae and Richardson rivers. This interpretation differs from the hypothesis of Mercier (1984) in which he proposed various levels of a large glacial lake maintained by an ice front to the east. Mercier's hypothesis does not take into account the ubiquitous collapse structures on all glaciolacustrine deltas or the absence of fine sediments downstream from coarse bouldery gravel deltas. Both can be readily explained by deltaic sedimentation in a narrow ice marginal lake where the outer part of the delta front is in contact with and partly on top of ice which then collapses upon melting of the ice. In narrow water bodies at the margin of the ice, water flow velocities would be sufficient to remove all sediments finer than coarse sands. This readily explains the apparent contradiction presented by large coarse deltas standing above till bodies or bare bedrock, a common occurrence in the upper reaches of Rae River basin.

Below 200 m a.s.l. glaciolacustrine rhythmites of silt and clay mantle the surface to a thickness of 2 m or more. South of Libby Lake, however, this mantle of glaciolacustrine sediments is found only below 140 m a.s.l., again suggesting a lowering sequence of lakes marginal to a shrinking ice lobe.

F. Marine offlap area

Along the south coast of Amundsen Gulf and of Dolphin and Union Strait a belt of postglacial marine offlap sequence occurs (Kerr, 1987) which widens and increases in elevation towards the east. Approximately 1 km wide and reaching elevations of 45 m a.s.l. at the margin of the map area west of Tinney Point, it widens to 30 km and reaches elevations of 120 m a.s.l. south of Cape Young.

A typical sequence from marine limit to the present day shoreline exposes the following units:

1. A bouldery gravel delta deposited at marine limit. Numerous well preserved abandoned channels mark its surface. The marine delta is commonly cut into an excessively bouldery kame deposit 10-15 m higher which is scarred by numerous collapse features.
2. The material in the marine delta rapidly becomes finer downstream, grading from bouldery gravel near the apex of the delta to sand and silty sand on the delta front.
3. Material farther out in the basin is silt and clay size and commonly rhythmically bedded. This unit is composed of buff coloured sandy silt beds and brown sticky clay laminae. Except in bedrock valleys which predate the last

glaciation, the thickness of this unit seldom exceeds 2 m. Numerous inliers of bedrock and till (drumlins) protrude through the marine material. Some areas, where the material is sandier, have been extensively modified by an eolian activity which is responsible for large blowout dunes indicating an effective wind direction from 305°.

4. Flights of beaches of pebbly gravel lead to the modern shoreline. These raised beaches form an irregular belt from a few tens of metres to over 3 km wide.
5. The modern beach, strewn with driftwood, is a 30-50 m-wide strip of sandy pebbly gravel.

Although the relative importance of any given unit may vary greatly, the sedimentary succession described above can be found along a transect across any part of the marine offlap sequence.

One of the striking aspects of this sequence is that deltas of bouldery gravel are confined to marine limit and do not occur at lower elevations. The implication is that following the initial flush of sediments carried to the sea by powerful meltwater streams, inland ice had disappeared to the point where rivers were no longer sufficiently fed by melting ice to enable them to transport coarse sediment. As is the case today, they carried material in the clay to coarse sand size range which was redistributed by wave action and shore currents.

The fact that most of these deltas are in part carved into bodies of kame gravel deposited at the margin of an ice mass occupying Amundsen Gulf and Dolphin and Union Strait indicates that the sedimentation of coarse clastics was continuous from ice marginal to marine environments. The implication is that marine invasion initially occurred along a corridor at the margin of a shrinking ice lobe.

DISCUSSION

The morphosedimentary zones described for the Bluenose Lake study area result, to a large degree, from the activity of the last glacier ice which occupied the region. The topography of the predominantly dolomitic bedrock affected flow patterns and, indirectly, the deposition of unconsolidated sediments, but only to a limited extent.

The last ice mass to affect the study area is certainly Late Wisconsinan, but whether or not it occupied the area for all or only part of Wisconsinan time is not known. At its margin along the south and east slope of a high bedrock plateau west of Bluenose Lake it was too thin to be active and did not modify the landscape. During deglaciation, however, coarse gravel and silty sand were deposited in ice- walled cavities to form kames and glaciolacustrine silt clay mounds.

Extensive ice thrusting from the east built massive moraine ridges extending for 100 km in a north-south direction east of Croker River and Bluenose Lake. Meltwater flowing west across gaps in these ridges built large bouldery gravel deltas in glacial Lake Bluenose which was choked with masses of stagnant ice. As the ice front retreated easterly, numerous lakes were formed in depressions, usually valley heads, sloping to the east. These depressions were partly filled with sandy silt/silty clay rhythmites interbedded with diamicton layers emplaced by debris flows.

At some stage during ice retreat the dominantly east-west ice movement reponsible for the construction of the Bluenose Lake moraine complex was replaced by a strong south-north movement which curved to the northwest and west near the present coast. This strong ice flow moulded drift into large drumlins – here named the Inman River drumlin field.

Further shrinking of the ice mass resulted in two large lobes, one in the basins of the Rae and Richardson rivers and the other in the channel of Amundsen Gulf and Dolphin and Union Strait. These two lobes originated from the same ice mass to the east. Morainic ridges to the east and northeast of Libby Lake result from advances of small lobes from the southeast. South and southeast of Libby Lake a series of large morainic ridges marks the shrinking of the northern margin of the glacier lobe which occupied Rae and Richardson river basins. At the western terminus of this lobe the former presence of a sequence of ice marginal lakes is marked by strandlines, by bouldery deltas with their fronts deformed by ice collapse, and by fine sediments which become progressively thicker towards the east.

The southern margin of the ice lobe that flowed west in the depression of Dolphin and Union Strait and Amundsen Gulf is marked by ice contact sediments deposited by north flowing rivers fed by melting dead ice masses inland. The shrinking of the lobe allowed the sea to invade the land from the west along the ice margin. Continuing rapid sedimentation of coarse material resulted in the construction of numerous large deltas, usually built in part within the collapse kame deposits. The elevation of these deltas and their associated marine offlap sequence show that marine limit rises towards the east southeast from 45 m to 120 m a.s.l. from the west to the east margin of the study area (45 cm/km). The absence of gravel deltas below the maximum limit of submergence indicates that melting ice masses, which were feeding the high energy streams flowing to the sea, disappeared early after marine transgression so that only coarse sand and smaller grain size sediments were transported.

SUMMARY AND CONCLUSIONS

Results of systematic mapping during July and August 1986 show that:

1. The Bluenose Lake moraine complies lies at the western limit of the last (Late Wisconsinan?) ice advance. Sparse erratics indicate that an older glaciation of unknown age extended farther west.
2. During the early phases of ice retreat, the Bluenose Lake depression was occupied by glacial lake waters and by large masses of dead ice. The upper limit of "glacial Lake Bluenose" is marked by numerous, large deltas which commonly display ice collapse features.

3. Thick accumulation of drift, commonly more than 30 m, in the Bluenose Lake moraine complex is probably the result of thrusting at the margin of an active ice mass.
4. Small ice-dammed lakes occupied several depressions within the moraine complex. Commonly these depressions are in the uppermost valley sections of easterly flowing streams which were blocked by the ice mass responsible for moulding the Inman River drumlin field.
5. Although the ridges in the Bluenose Lake moraine complex result from ice thrusting from the east, the Inman River drumlin field was moulded by ice moving from the south, i.e. from the basin of the Rae and Richardson River and curving to the northwest in the vicinity of Amundsen Gulf.
6. Deltas, strandlines, and marginal moraines show that a sequence of lowering glacial lakes occupied the headwaters of Rae River in contact with a retreating ice lobe in the basin of Rae and Richardson rivers.
7. Marine limit, which is defined by the presence of deltas and a clear upper washing limit, rises towards the southeast (approximately 45 cm/km) – 45 m a.s.l. at the western limit of the study area to 120 m south of Cape Young.

Sediment and landform associations in the Bluenose Lake area record the recent geological history related mostly to the initial retreat of part of the Keewatin Sector of the Laurentide Ice Sheet from its Wisconsinan (Late?) limit. Dating of these events must await the results of analyses onTHsamples being processed in the ^{14}C dating laboratory. Detailed studies of marine sediments, eolian processes, and marine offlap sequence are the subject of four different ongoing theses by students who assisted in the 1986 fieldwork.

Results so far confirm that present processes such as erosion by rivers, wind and mass movement do little to modify the landscape inherited from late glacial time.

ACKNOWLEDGMENTS

We are particularly grateful to the following student assistants for their dedicated and enthusiastic contribution in the field: D. Kerr, R. Avery, M. Potschin, and H. Beaudet. Martin Irving provided expert expediting and radio communications from Yellowknife. He was outstanding during a difficult 30 hours when a plane was missing and knows how deeply grateful we are. We take pleasure in thanking Polar Continental Shelf Project for its co-operation in providing air support. The competent co-operation of fixed wing and helicopter pilots and engineer was much appreciated and the welcome extended them at YSO (Clifton Point) camp testified to that.

REFERENCES

Bostock, H.S.
1970: Physiographic regons of Canada; Geological Survey of Canada, Map 1254A, scale 1:5 000 000.

Craig, B.G.
1960: Surficial geology of north-central District of Mackenzie, Northwest territories; Geological Survey of Canada, Paper 60-18, 8 p.

Fraser, J.A., Craig, B.G., Davison, W.L., Fulton, R.J., Heywood, W.W., and Irvine, T.N.
1960: Geology, north-central District of Mackenzie, Northwest Territories; Geological Survey of Canada, Map 18-1960.

Kerr, D.
1987: Stratigraphy of the marine offlap sequence in the Clifton Point area, District of Mackenzie: Preliminary interpretation; *in* Current Research, Part A, Geological Survey of Canada, Paper 87-1A.

Lundqvist, J.
1979: Morphogenetic classification of glaciofluvial deposits; Sveriges Geologiska Undersokring, serie C, Nr 767, 72 p.

Mackay, J.R.
1958: The Anderson River map-area, N.W.T.; Geographical Branch, Memoir 5, 137 p.

Mercier, A.L.
1984: Glacial lakes in the Richardson and Rae River basin, District of Mackenzie, Northwest Territories; Géographie physique et Quaternaire, v. 38, no. 1, p. 75-80.

O'Neill, J.S.
1924: Report of the Canadian Arctic Expedition 1913-18, v. 11, Geology and Geography; King's Printer, Ottawa.

Prest, V.K.
1967: Nomenclature of moraines and ice-flow features as applied to the Glacial Map of Canada; Geological Survey of Canada, Paper 67-57, 32 p.

St-Onge, D.A.
1984: Surficial deposits of the Redrock Lake area, District of Mackenzie; *in* Current Research, Part A, Geological Survey of Canada, Paper 84-1A, p. 271-278.

Vincent, J-S.
1984: Quaternary stratigraphy of the western Canadian Arctic Archipelago; *in* Quaternary Stratigraphy of Canada – A Canadian Contribution to IGCP Project 24, R.J. Fulton (ed.); Geological Survey of Canada, Paper 84-10, p. 87-100.

Acoustic survey and glacial history of Adams Lake, outer Nachvak Fiord, northern Labrador[1]

Project 820039

T. Bell[2], R.J. Rogerson[2], R.A. Klassen, and A. Dyer[2]
Terrain Sciences Division

Bell, T., Rogerson, R.J., Klassen, R.A., and Dyer, A., Acoustic survey and glacial history of Adams Lake, outer Nachvak Fiord, northern Labrador; in Current Research, Part A, Geological Survey of Canada, Paper 87-1A, p. 101-110, 1987.

Abstract

Adams Lake is a 3.9 km-long by 300 m-wide finger lake occupying a glacially overdeepened valley, oriented east-west parallel to Nachvak Fiord, northern Labrador. It is characterized by three basins ranging from 12 to 21 m in depth, separated by distinct barriers between 3 and 6 m below lake level. The most westerly barrier is likely the subaqueous extension of the Tinutyarvik moraine. Analysis of the 3.5 kHz acoustic record of lake sediments reveals three acoustic units which are tentatively interpreted as representing sedimentary facies related to a glacial/deglacial cycle. Unit A, the lowermost unit, is characterized by a massive structure and reflector-free image and may comprise drift or bedrock. Unit B is acoustically stratified and is interpreted as a proglacial deposit ranging in depositional environment from ice-proximal to ice-distal, towards the east. Subunit B2, interpreted as a coarse clastic deposit, is tentatively related to the draining of a nearby moraine-dammed lake. Unit C, an acoustically transparent unit with a uniform thickness of approximately 1.5 m, is interpreted as a postglacial lacustrine sediment.

Résumé

Le lac Adams est un lac digitiforme de 3,9 km de longueur sur 300 m de largeur qui occupe une vallée surcreusée par un glacier, dont l'orientation est-ouest est parallèle au fjord Nachvak, dans le nord du Labrador. Il renferme trois bassins de profondeur variant entre 12 et 21 m, séparés par des barrières distinctes surmontées d'une colonne d'eau de 3 à 6 m. La barrière la plus à l'ouest est probablement le prolongement subaquatique de la moraine Tinytyarvik. L'analyse d'un sondage acoustique à 3,5 kHz des sédiments lacustres fait ressortir trois unités acoustiques que l'on interprète provisoirement comme représentant des faciès sédimentaires associés à un cycle de glaciation/déglaciation. L'unité A, la plus basse, se caractérise par une structure massive et une image sans réflecteur; elle pourrait renfermer des matériaux de transport glaciaire ou de la roche en place. L'unité B est acoustiquement stratifiée, et on l'interprète comme un sédiment proglaciaire dont le milieu de dépôt par rapport au glacier varie entre proximal et distal, vers l'est. La sous-unité B2, qui correspondrait à un dépôt clastique grossier, est provisoirement associée à l'assèchement d'un lac voisin endigué par des moraines. L'unité C, caractérisée par sa transparence acoustique et par une épaisseur uniforme d'environ 1,5 m, est interprétée comme un sédiment lacustre postglaciaire.

[1]Contribution to Canada-Newfoundland Mineral Development Agreement 1984-1989. Project carried by Geological Survey of Canada.
[2]Department of Geography, Memorial University of Newfoundland, St. John's, Newfoundland A1B 3X9

INTRODUCTION

In the summer of 1985 a 3.5 kHz acoustic survey and coring program was carried out on Adams Lake in the Torngat Mountains of northern Labrador. The lake is situated 6 km south of Nachvak Fiord and was chosen because it may be located close to the margin of regional Laurentide ice at the Late Wisconsinan maximum (Fig. 11.1). This report describes the acoustic stratigraphy of the lake sediments and correlates interpreted lake sedimentary facies with a local glacial chronology. Research carried out over the last five years in the Torngat Mountains and on the Labrador Shelf has produced conflicting accounts on the maximum extent of Late Wisconsinan ice in the region. Rogerson, Evans, and Bell suggest limited ice cover, possibly restricted to the basin of Nachvak Fiord, based on geological investigation of the fiord and outer coast (Rogerson and Evans, 1984; Evans and Rogerson, 1986, Rogerson and Bell, 1986). Josenhans and Clark prefer ice extending to the Labrador Shelf during the maximum, based on the interpretation of Labrador Shelf acoustic units as Late Wisconsinan tills and the reconstruction of an extensive ice shelf from moraine segments in the Torngat region (Clark et al., 1985; Clark et al., 1986; Josenhans, 1986).

On the basis of moraines dated by soil development, Evans and Rogerson (1986) tentatively suggested that ice terminated in the outer fiord during the Nachvak phase of glaciation, between 23 and 17 ka, but did not reach the Labrador Shelf. Subsequently a large moraine was identified near Tinutyarvik Cove from analysis of a 3.5 kHz acoustic record of fiord sediments (Rogerson et al., 1986). This moraine is compatible with the limits of the Nachvak phase, although Rogerson and Bell (1986) suggested that Late Wisconsinan maximum ice in the fiord may have terminated farther east in Nachvak Bay, and presented tentative evidence that ice abandoned the area west of Tinutyarvik Cove, as late as 9 ka.

LOCATION AND DESCRIPTION

Physiographic setting

Adams Lake is situated approximately 6 km south of Nachvak Fiord among the Torngat Mountains, which comprise the peninsula of northern Labrador (Fig. 11.1). The lake occupies the western part of a glacially overdeepened valley which opens into Delabarre Bay, 3 km east; 1 km west of the lake, Tinutyarvik valley leads north to Nachvak Fiord. Similarly, Naksaluk valley connects the fiord with Adams Lake valley, although it appears as a hanging valley, approximately 44 km above lake level. Adams Lake valley has been eroded on one or more occasions by glacier ice from Nachvak Fiord moving eastwards from Tinutyarvik valley. The fiord is a major trough which held ice streaming from the interior of Labrador to the Labrador Sea. Evidence of glacier flow directions is found in the form of striations (Fig. 11.1) and from pebble lithology (Bell and Rogerson, 1985).

Adams Lake is narrow and linear, and is 36 m above sea level, 3.9 km in length, and is oriented in an east-west direction (Fig. 11.2). It varies in width from 100 to 400 m and is bounded by steep valley walls (400-500 m high) along most of its central portion. The lake drainage basin comprises the sparsely vegetated valley sides and a poorly defined part of Tinutyarvik valley. Alluvial fans, which occur along the lower slopes, are virtually inactive during the summer, although they may be relatively important sediment sources during spring runoff. There are no inflowing streams of significant size; there is only one stream outlet, which is located in the southeast corner.

Geological setting

The Adams Lake region lies within the Churchill Border structural zone of northern Labrador. This zone is underlain by granitoid gneiss intruded by late Archean dykes and is overlain by Proterozoic supercrustal sedimentary rocks (Wardle, 1983; Fig. 11.3). Adams Lake basin is situated within a sedimentary series of the Lower Proterozoic Ramah Group. The lake threshold (eastern margin) is located on a fault which marks the unconformity between the lowest quartzite member of the Rowsell Harbour Formation and the local Archean gneisses. Nachvak Fiord Thrust, 600 m west of Adams Lake, delimits the western extent of the Ramah Group. It is not known if the lake is underlain by Proterozoic sediments and/or Archean gneiss. Within the Ramah Group are diabase sills which outcrop normal to the east-west orientation of the lake basin.

Quaternary geology

At the head of Tinutyarvik valley is a large end moraine feature (Quartzite moraine) at 130 m above high tide (aht) (Fig. 11.1). At the western end of Adams Lake valley is a second moraine (Tinutyarvik moraine) at 106 m aht which appears to cut across Adams Lake. At the eastern end of the lake, Adams Lake moraine lies along the southern valley margin and is a lateral moraine formed by ice which terminated farther east, possibly as far as "Valley of the Flies" where a terminal moraine is evident (Fig. 11.1).

Marine limit is 73.1 ± 0.5 m aht east of Adam Lake moraine, whereas it is 66 ± 1 m aht west of the moraine. Marine limit in Tinutyarvik valley is recorded at 55-58 ± 1 m aht – the most westerly extent of relict shorelines higher than approximately 40 m aht.

The existence of a former proglacial lake dammed by Quartzite moraine is suggested by shorelines in a valley south of the moraine, at 120 m aht, and by a large alluvial fan which appears to originate from a deep gully through the moraine and which may have formed as the moraine was breached and the lake emptied (Fig. 11.4).

3.5 KHZ ACOUSTIC RECORD

The Adams Lake acoustic survey was carried out from a rubber Zodiac using a Raytheon RTT 1000 system, with 3.5 kHz and 200 kHz acoustic signals. A 12 volt battery was used as an energy source for the equipment. The Zodiac was maintained at a constant speed and direction within the

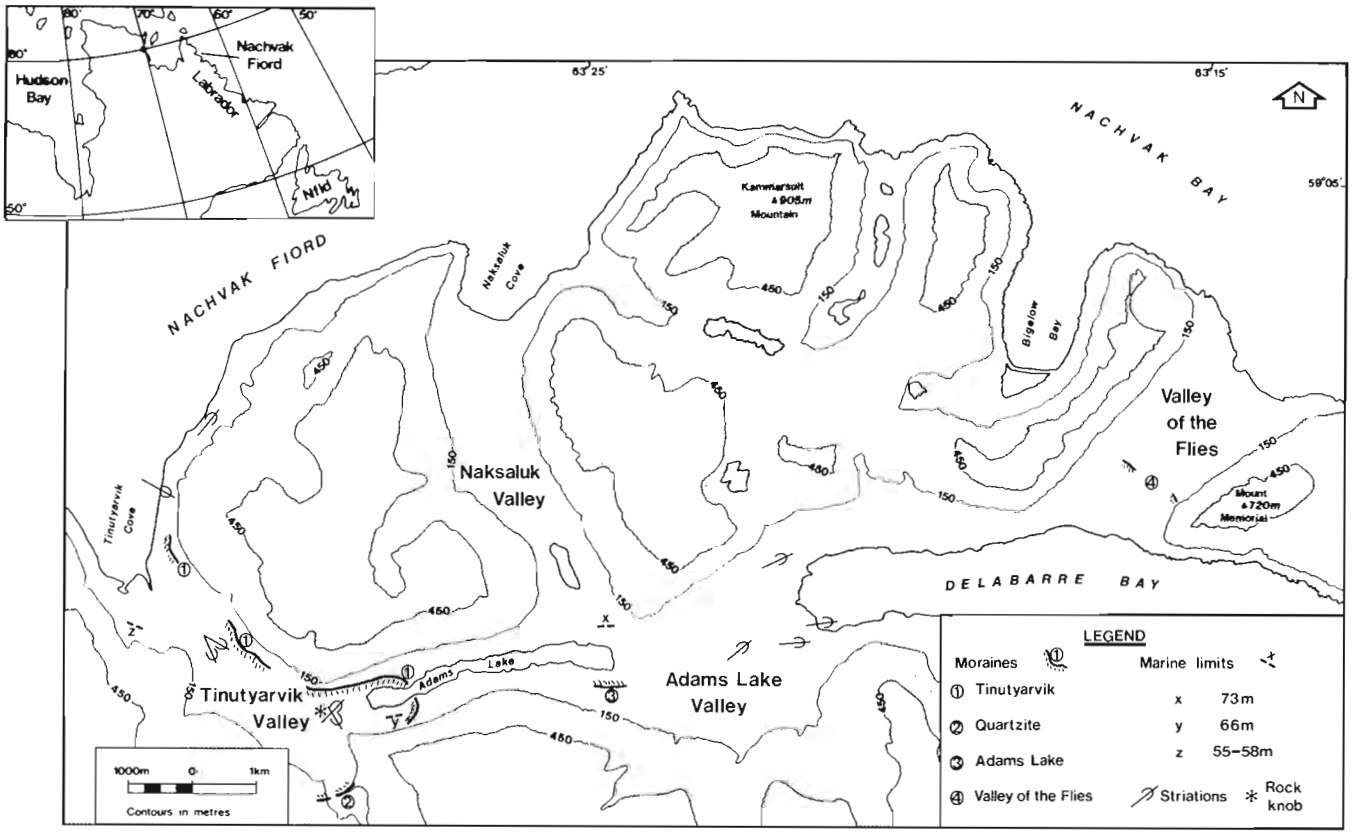


Figure 11.1. Outer Nachvak Fiord showing location of Adams Lake and moraines, marine limits, and striae discussed in the text.

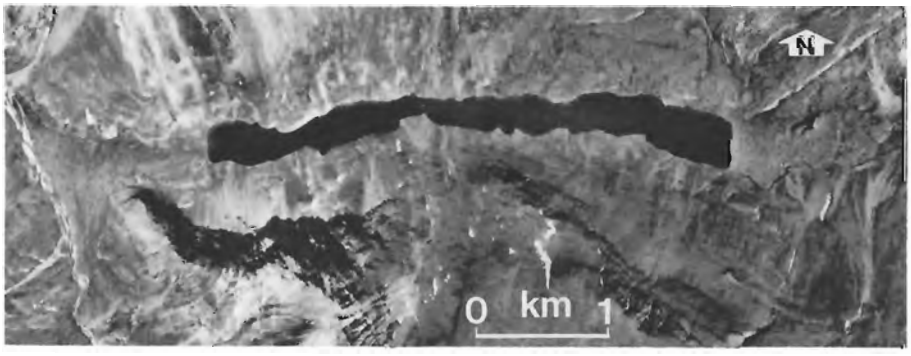


Figure 11.2. Adams Lake Valley and the southeastern margin of Tinutyarvik Valley.

constraints of field conditions. Orientation and location of acoustic transect were recorded using a magnetic compass and through identification of specific shoreline features. Accuracy of the portrayed lines in Figure 11.5 is suggested to be ±25 m. Following examination of the acoustic record, core sites were selected and marked using floats.

Adams Lake is characterized by a series of basins separated by relatively shallow barriers (Fig. 11.5, 11.6). The basins, denoted X, Y, and Z, are progressively deeper towards the east, attaining maximum depths of 12, 19, and 21 m, respectively. Basin Z contains a smaller basin along its eastern margin, which will not be treated as a separate basin

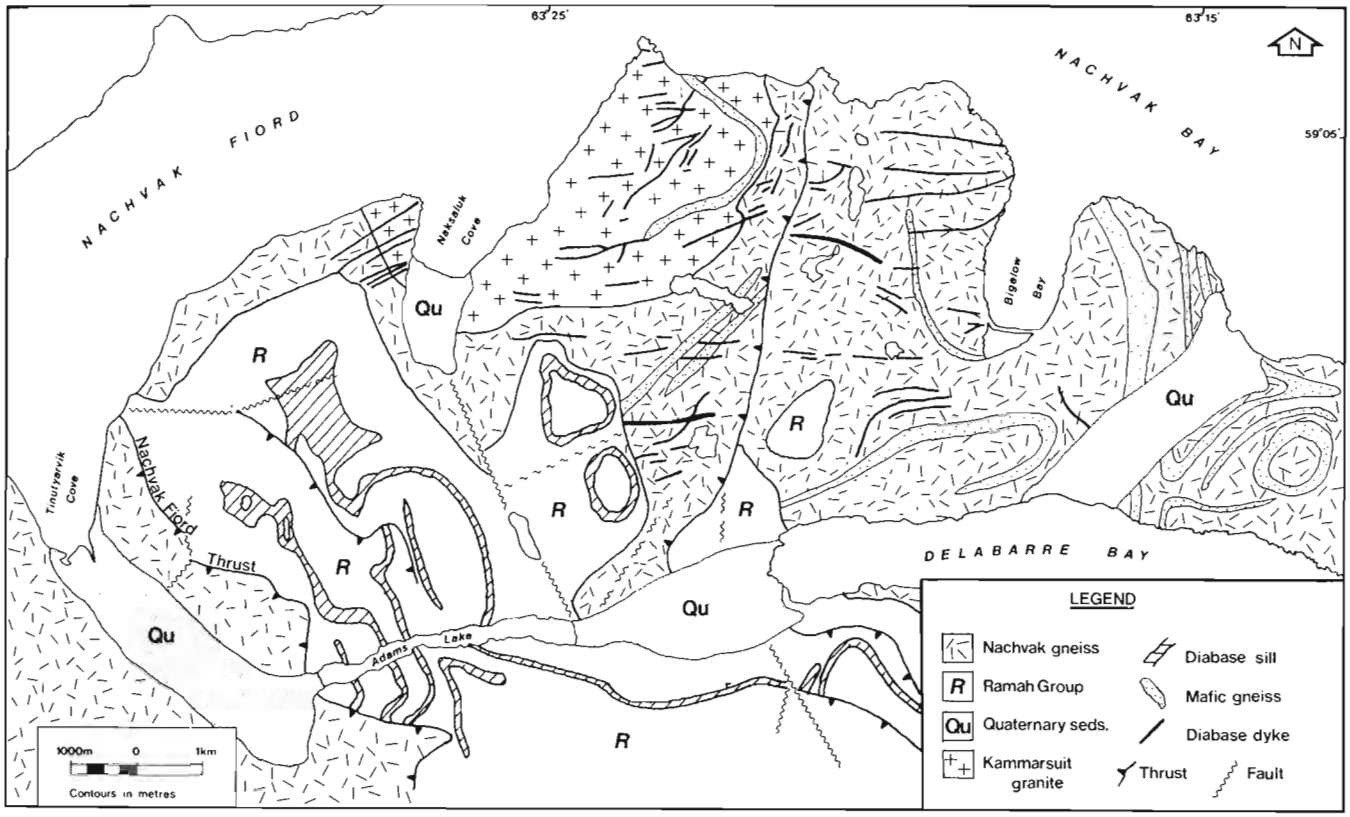


Figure 11.3. Generalized geology of the outer Nachvak Fiord area (after Morgan, 1975; Wardle, 1983).

in this report. The Barriers U, V, and W, separating the basins, are distinct features between 3 and 6 m below lake level. Barriers V and W are separated by another small basin, but in the context of this report, the Barrier complex VW will be regarded as a single barrier except in discussion of its origin and significance. The lake basin has an asymmetric U-shaped cross-section with steeper slopes on its southern margin and gentle or stepped slopes along its northern edge (Fig. 11.7).

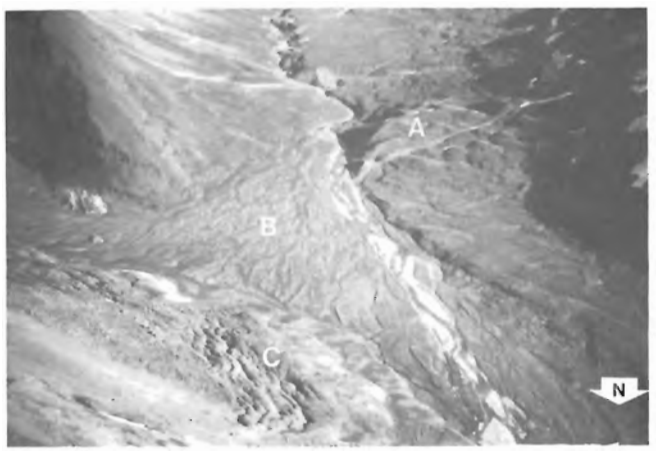


Figure 11.4. Southern Tinutyarvik Valley. A. Quartzite moraine; B. Alluvial fan associated with the draining of a lake dammed by Quartzite moraine; C. Tinutyarvik moraine, displaying the effects of solifluction and mass movement.

Stratigraphic units: description and facies interpretation

Three major units are recognized based on their 3.5 kHz acoustic signature. These units, which may represent facies, are further subdivided based on their acoustically defined properties and stratigraphical relationships within the lake basin (Fig. 11.6).

Unit A, the lowermost unit, is acoustically massive, without internal structure. Penetration of this unit in the profiles is limited. The surface morphology is variable and irregular and defines the basins in which the overlying units are recorded. Unit A is interpreted as either bedrock or till. Both media are considered likely to have an upper surface that could act as a strong reflector, and because of the limited penetration by the acoustic signals, no attempt is made here to distinguish between bedrock and till on the record. During seismic reflection studies of sediments under Lake Superior, Landmesser et al. (1982) reported problems in distinguishing till

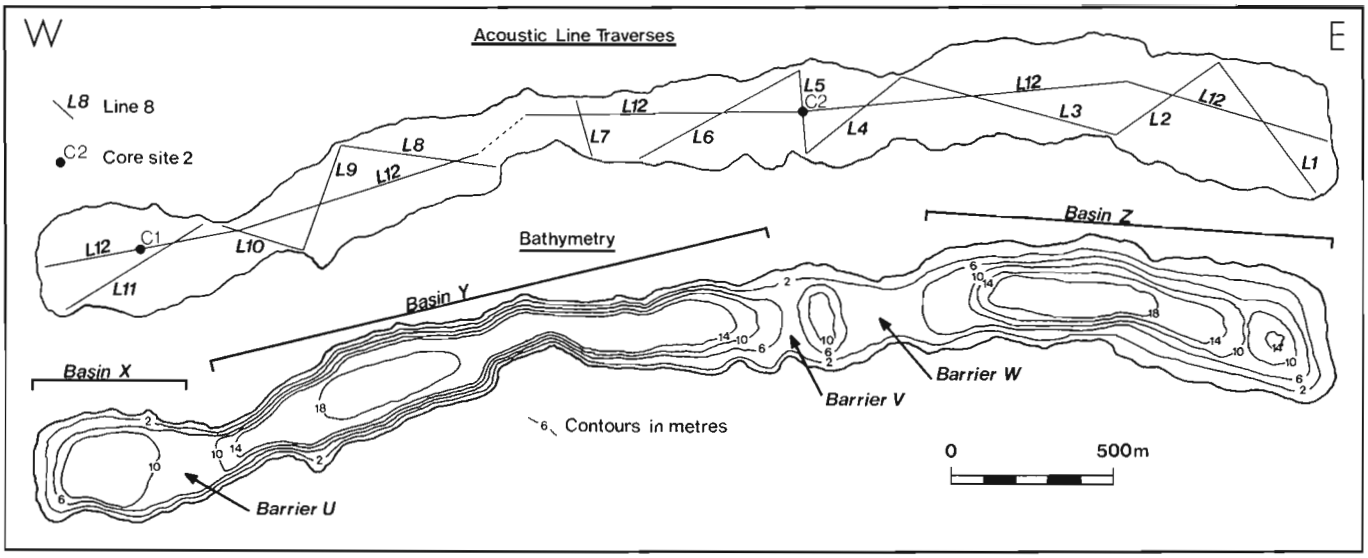


Figure 11.5. Adams Lake bathymetry with location of acoustic line traverses and core sites.

from bedrock, especially when the till was present only as a thin veneer. Diabase sills in the vicinity of Barriers V and W would suggest that unit A represents bedrock in those locations (Fig. 11.3). Barrier U has a pronounced asymmetric shape and steeper distal (eastern) slope, characteristic of an end moraine feature, and its position corresponds to the location of Tinutyarvik moraine. It is suggested that Barrier U and the end moraine are geomorphically associated and that Unit A comprises morainic drift/till in this locality.

Unit B is an acoustically stratified unit which is divided into subunits on acoustic stratigraphical relationships within the lake basin. Subunit B1 occurs in Basins X, Y, and Z. It may be classified as a basin-fill deposit, showing an onlap relationship with Unit A in Basins Y and Z, but having a poorly defined lower acoustic boundary in Basin X. Stratification in subunit B1 varies from well defined in Basins X and Z and eastern Basin Y to discontinuous with internal deformation in western Basin Y. This subunit has infilled a large basinal depression in the centre of Basin Y and is at least 10 m thick in this locality; elsewhere it is approximately 2-3 m thick. The upper boundary of subunit B1 marked by a strong reflector, subunit B2, in Basins X and Y and is the uppermost internal reflector in Basin Z.

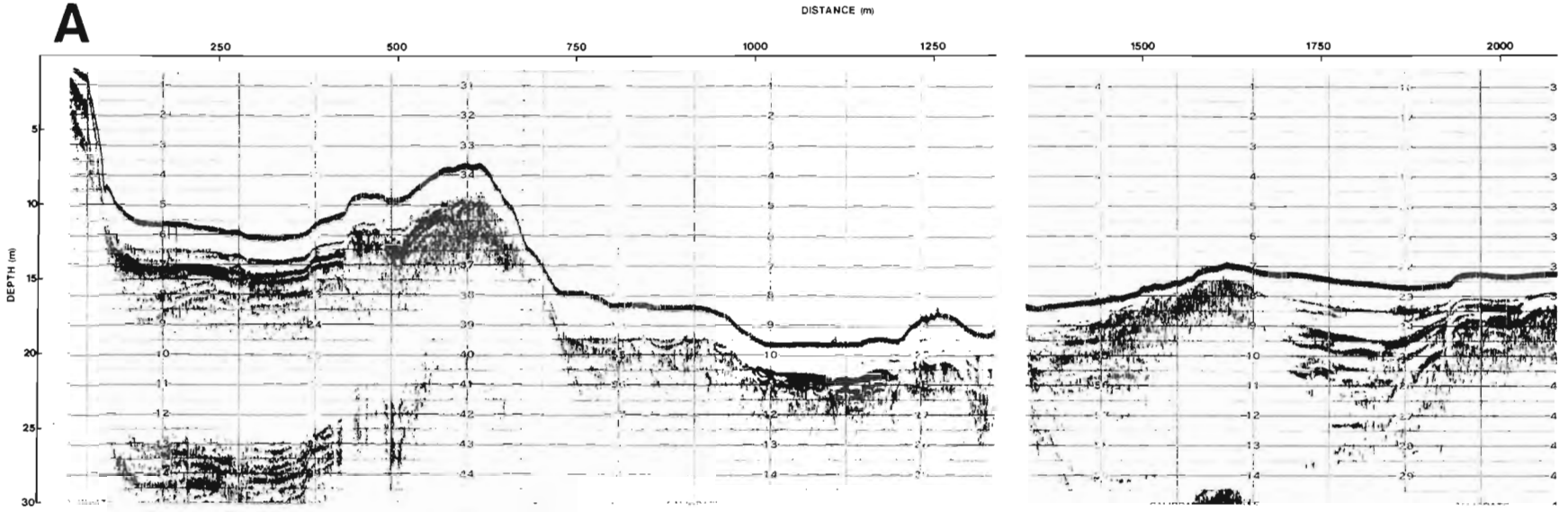
Subunit B2 is approximately 0.5-1.0 m thick (Fig. 11.8) and occurs in the bottom of Basins X and Y, pinching out along the basin margins. It is a strong, well defined reflector which suggests that it contains a greater component of coarse clastic debris than the rest of unit B. The strength of the acoustic signal varies but the subunit generally appears conformable with the stratification and upper surface of the underlying subunit B1.

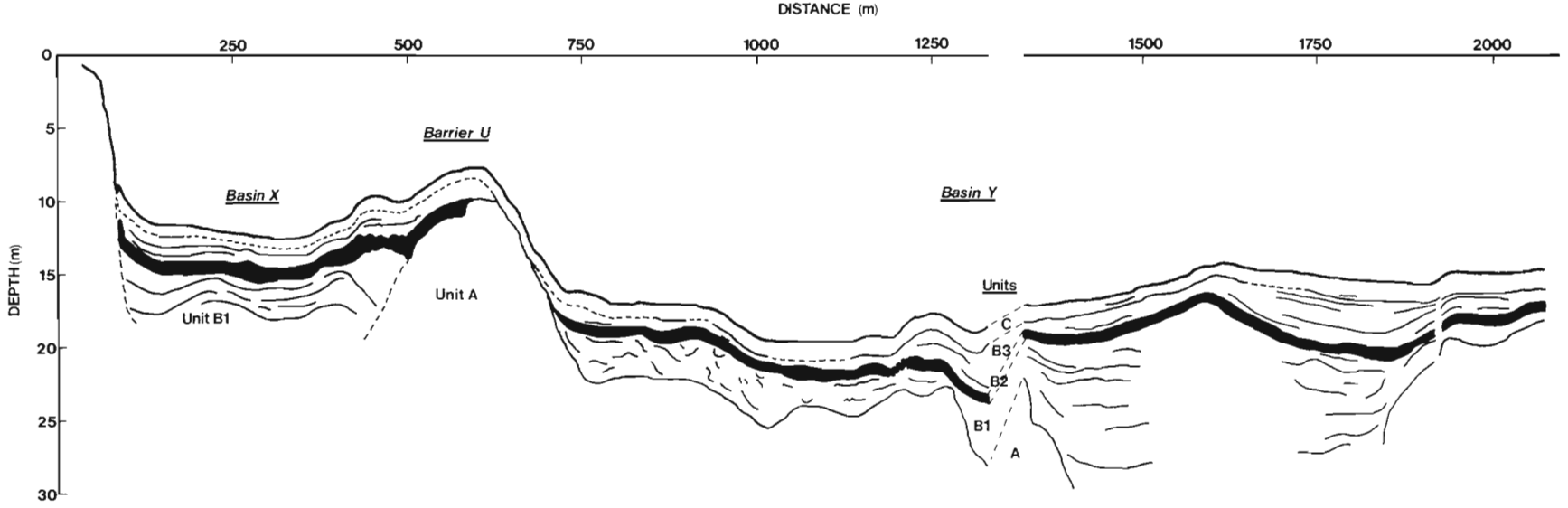
Subunit B3 occurs in Basins X and Y and conformably overlies subunit B2 (Fig. 11.8). Its upper boundary is marked by the uppermost reflector in both basins. It is predominantly an acoustically stratified unit although towards the upper boundary the unit becomes more transparent. For the most part it is a basin fill deposit pinching out along the lower slopes of the basins. The unit varies from 0.5-3 m in thickness and is thickest in the centre of Basin Y.

Unit B is interpreted as a proglacial sedimentary sequence, deposited in the semi-isolated basins of Adams Lake. Thickest accumulations of Unit B sediments occur in the western basins, suggesting that density currents, derived from local glacial drainage systems in the west, settled out in Basins X and Y, while Barrier complex VW prevented large scale sediment transport eastwards to Basin Z. The semi-isolated nature of the basins as 'settling ponds' obscures the probable diachronous deposition within this unit, particularly subunit B1 in Basin X which may only have formed following the recession of ice from Tinutyarvik moraine.

Drainage of the glacial lake dammed by Quartzite moraine and downcutting of the moraine may be recorded by the strong acoustic signal of subunit B2 which may be the record of a significant input of coarse clastic debris. Faulting of the Unit B stratified sequence near to the eastern margin of Basin Y (Fig. 11.6A) may have resulted from the meltout of buried ice.

Unit C, the uppermost unit in the acoustic record, appears draped over the sediment package beneath. It is an acoustically transparent to semi-transparent unit which can contain single, well defined internal reflectors. It is recorded in all basins and on the tops of barriers, and it has a uniform thickness of approximately 1.5 m on the floors of basins (Fig. 11.8). Unit C is interpreted as a relatively homogeneous, fine grained sedimentary unit deposited postglacially, under low sediment influx rates, in a lacustrine environment.


A
DISTANCE (m)
250
500
750
1000
1250
1500
1750
2000
DEPTH (m)


DISTANCE (m)
250
500
750
1000
1250
1500
1750
2000
DEPTH (m)
Barrier U
Basin X
Basin Y
Unit A
Unit B1
Units
C
B3
B2
B1
A

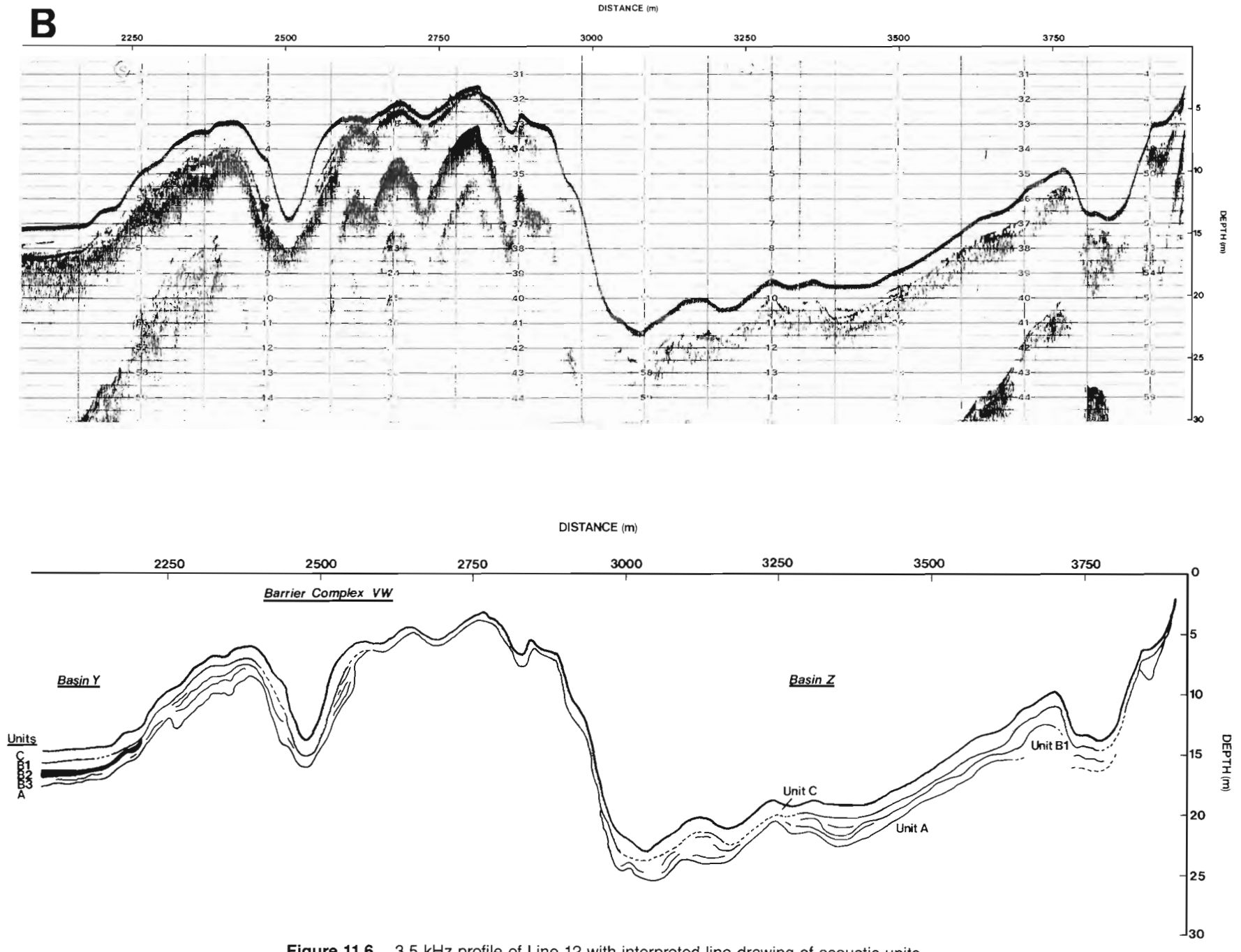


Figure 11.6. 3.5 kHz profile of Line 12 with interpreted line drawing of acoustic units.

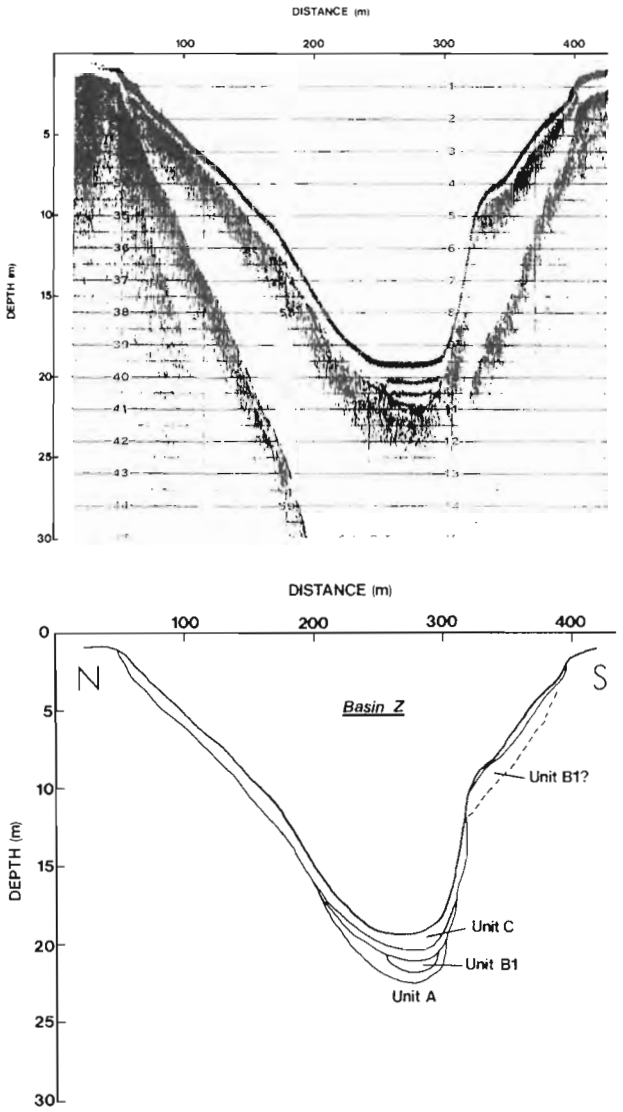


Figure 11.7. 3.5 kHz profile of Line 2 with interpreted line drawing of acoustic units.

REGIONAL INTERPRETATION

Interpretation of acoustic units in terms of facies and depositional environments is tentative, and is presented along with terrestrial evidence of glacial and deglacial events. Drift pebble lithologies for Tinutyarvik and Adams Lake valleys show a marked change in composition across Tinutyarvik moraine (Bell and Rogerson, 1985). To the west of the moraine, local Ramah Group lithologies predominate. The marked change in drift pebble lithologies between the western and eastern ends of Adams Lake suggests that during the last glacial phase, ice from Nachvak Fiord did not pass along the lake to Delabarre Bay, but terminated at some point along the lake. The point of termination would appear to be marked by Tinutyarvik moraine, and its subaqueous continuation, Barrier U.

Marine limit similarly suggests that ice stood still at some point along Adams Lake during formation of Adams Lake moraine since it is higher at the eastern end (73 m aht) than at the western end (66 m aht), despite the fact that lower raised beaches in Adams Lake valley are tilted up to the west (Rogerson and Bell, 1986). Marine limit in Tinutyarvik valley was recorded at 55 to 58 m aht, significantly lower than that at Adams Lake, suggesting that the Tinutyarvik valley was deglaciated later.

Barriers V and W may be either bedrock or moraines which formed during an earlier glacial phase when ice was more extensive. Adams Lake moraine at the eastern end of Adams Lake is evidence of a further eastward extent of ice that predates Tinutyarvik moraine. Ice probably extended as far east as "Valley of the Flies" where glaciomarine diamictons and related sandy units contain shells dated 33 700 ± 710 BP (GSC-3950), 37 800 ± 1610 BP (GSC-4189), 38 900 ± 1420 BP (GSC-4204-OF) (GSC-4204), and 40 600 ± 1640 BP (GSC-4204-IF), suggesting either mid Wisconsinan or early-Late Wisconsinan age for the Valley of the Flies phase. The difference in till composition suggests that the Tinutyarvik moraine/Barrier U phase was not merely a recessional stage of the ice that formed Adams Lake moraine, but the limit of a separate, later glacier advance. A relative age difference may also be apparent in the degree of soil development evident on the moraines. The mean depth of solum to the base of the B horizon, on a section of the Adams Lake moraine above marine limit (approximately 78 m aht) was 36 cm, while soil depths on Quartzite moraine (130 m aht) averaged 28 cm. Factors other than age, such as elevation or sediment type, may also be responsible for this difference. From the reconstruction, there is a reasonable possibility that Tinutyarvik moraine may have been formed at the limit of the Nachvak phase, the last major advance of ice down Nachvak Fiord, and may be Late Wisconsinan in age.

There is abundant evidence for the northwards draining of a lake formerly dammed by Quartzite moraine. A trench cuts through the moraine and feeds a major multichannelled alluvial fan spreading towards Adams Lake (Fig. 11.4). Farther down Tinutyarvik valley, a gorge-like scour through drift cuts across the higher raised beaches. The acoustic properties of subunit B2 are consistent with an interpretation of input from a glacial lake draining outwards through unconsoli dated sediment. Since the alluvial fan appears to have been formed subaerially and was necessarily formed after Tinutyarvik valley was deglaciated and the development of marine beaches, its deposition may be close to the time when Adams Lake changed from an inlet of the sea to a freshwater lake. Thus Unit C may represent a lacustrine environment which developed after sea level had fallen below 36 m aht. This possibility will be tested when 2 m-long cores (C1 and C2, Fig. 11.5), taken in 1985, are closely examined.

ACKNOWLEDGMENTS

Fieldwork was financed partly by Natural Sciences Engineering Research Council Operating Grants to, and Energy Mines and Resources Research Agreements with R.J. Rogerson, and

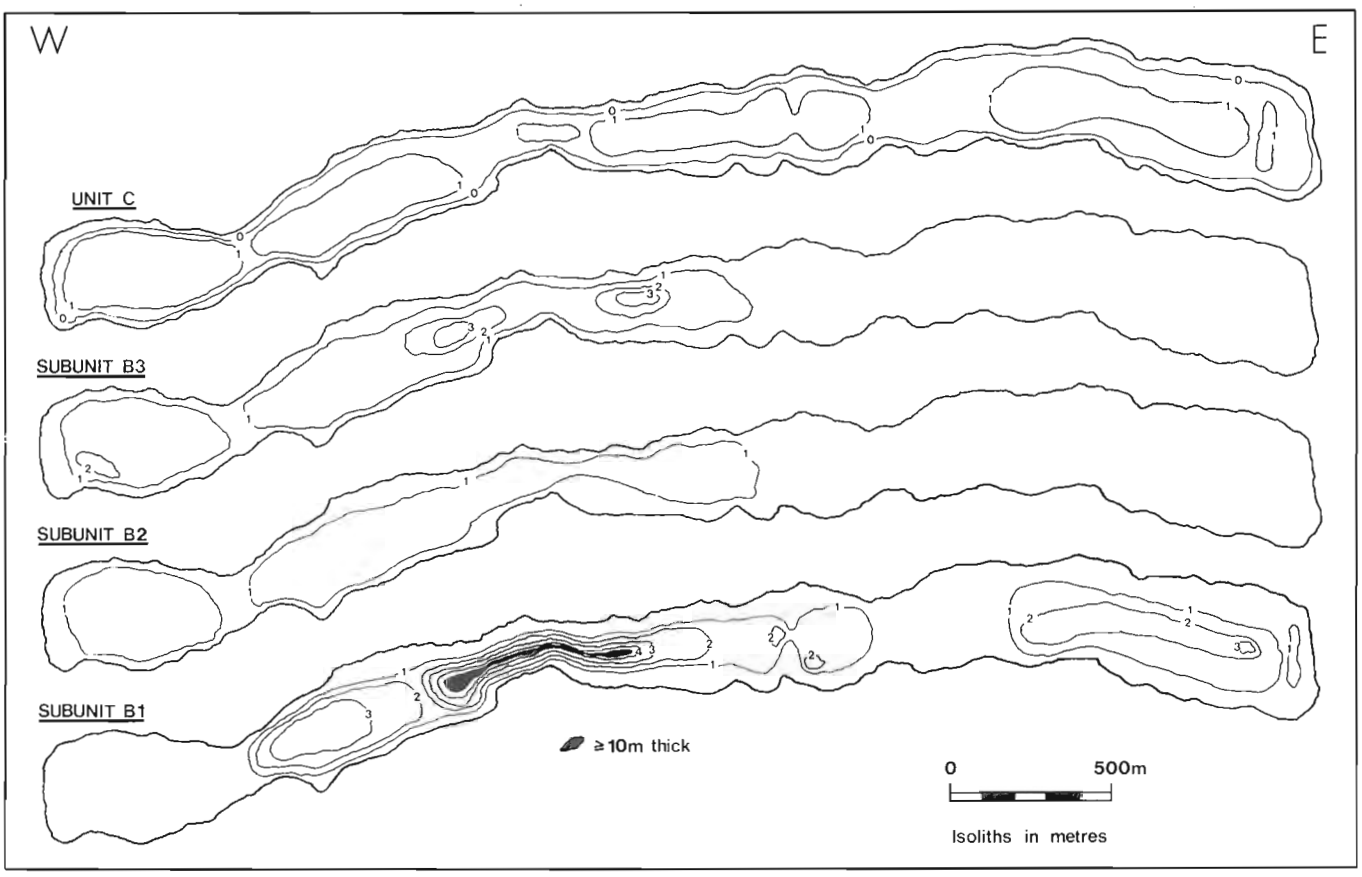


Figure 11.8. Isopach maps of subunits B1, B2, and B3, and Unit C.

a Department of Indian Affairs and Northern Development Northern Science Training Grant to A. Dyer. The Captain and crew of the **CCGS Sir John Franklin** are acknowledged for their help in establishing the camp, T. Bell and A. Dyer were financed in St. John's by Memorial University fellowships and bursaries. W. Blake, Jr. obtained the four radiocarbon dates, and MUN Cartographic Laboratory assisted in the preparation of illustrations.

REFERENCES

Bell, T. and Rogerson, R.J.
1985: Drift pebble lithology and glaciation of Gulch Peninsula, Nachvak Fiord, northern Labrador (abstract); 1985 Annual Meeting, Canadian Association of Geographers, Université de Trois-Rivières, Quebec, p. 29.

Clark, P., Josenhans, H.W., and McCoy, W.D.
1985: Correlation of Late Quaternary events: Torngat Mountains and Labrador Shelf (abstract); 14th Arctic Workshop, Bedford Institute of Oceanography, Dartmouth, Nova Scotia, p. 131.

Clark, P., Andrews, J.T., Short, S., and Williams, K.
1986: Late-glacial and Holocene paleoenvironmental record from Square Lake, Torngat Mountains, Labrador (abstract); 15th Annual Arctic Workshop, Institute of Arctic and Alpine Research (INSTAAR), Boulder, Colorado, p. 9.

Evans, D.J.A. and Rogerson, R.J.
1986: Glacial geomorphology and chronology in the Selamiut Range — Nachvak Fiord area, Torngat Mountains, Labrador; Canadian Journal of Earth Sciences, v. 23 p. 66-76.

Josenhans, H.W.
1986: The Quaternary stratigraphy of Nachvak Fjord and the adjacent Continental Shelf (abstract), 15th Annual Arctic Workshop, Institute of Arctic and Alpine Research (INSTAAR), Boulder, Colorado, p. 33.

Landmesser, C.W., Johnson, T.C., and Wold, R.J.
1982: Seismic reflection study of recessional moraines beneath Lake Superior and their relationship to regional deglaciation; Quaternary Research, v. 17, p. 173-190.

Morgan, W.C.
1975: Geology Map 1469A, Nachvak Fiord-Ramah Bay, Newfoundland-Quebec Geological Survey of Canada, Ottawa.

Rogerson, R.J. and Bell, T.
1986: The Late-Wisconsin maximum in the Nachvak Fiord area of northern Labrador (abstract); 15th Annual

Arctic Workshop, Institute of Arctic and Alpine Research (INSTAAR), Boulder, Colorado, p. 57.

Rogerson, R.J. and Evans, D.J.A.
1984: Glaciation of the northern Selamiut Range and part of Nachvak Fiord, Torngat Mountains, northern Labrador (abstract); 13th Annual Arctic Workshop, Institute of Arctic and Alpine Research (INSTAAR), Boulder, Colorado, p. 49.

Rogerson, R.J., Josenhans, H.W., and Bell, T.
1986: A 3.5 kHz acoustic survey of Nachvak Fiord, northern Labrador; in Current Research, Part A, Geological Survey of Canada, Paper 86-1A, p. 221-228.

Wardle, R.J.
1983: Nain-Churchill province cross section, Nachvak Fiord, northern Labrador; in Government of Newfoundland and Labrador, Department of Mines and Energy, Report 83-1, p. 68-90.

- 12 -

The nature and chronological implications of surface tills and post-till sediments in the Cypress Lake area, Saskatchewan

Project 830024

R.W. Klassen and W.J. Vreeken[1]
Terrain Sciences Division, Calgary

Klassen, R.W. and Vreeken, W.J., The nature and chronological implications of surface tills and post-till sediments in the Cypress Lake area, Saskatchewan; in Current Research, Part A, Geological Survey of Canada, Paper 87-1A, p. 111-125, 1987.

Abstract

Two tills commonly seen in stream cuts and identified in shallow borehole sediments in the Cypress Lake area, Saskatchewan appear to be lodgment and melt-out tills deposited by Late Wisconsinan ice lobes. The suggested till origin has its basis in the following observations: 1) The lower till is compact, jointed, high in clay and local bedrock clasts, whereas the upper unit is looser and contains sand lenses and a higher proportion of erratic clasts. 2) The contact between the tills is typically gradational and lacks evidence of subaerial weathering and biota. 3) The upper unit, typically several metres thick over the till plains, is absent in places and either the lower till or Tertiary gravel forms the surface.

The Late Wisconsinan age is suggested because of the similar nature and thicknesses of post-till sediments studied in back-hoe excavations and boreholes at seven selected sites and several radiocarbon dates obtained at three of the sites. The oldest dates were from two sites in hummocky moraines in the south-central part near the International Boundary where a basal peat dated at ca. 14 ka and shells from a moraine plateau dated at ca. 12 ka.

Résumé

Deux tills généralement visibles dans des cours d'eau et qu'on retrouve dans des sédiments traversés par des trous de sondes peu profonds dans la région de Cypress Lake, en Saskatchewan, semblent être des tills de fond et de fonte déposés par les lobes glaciaires du Wisconsin supérieur. L'origine présumée de ces tills est fondée sur les observations qui suivent: 1) le till inférieur est compact, diaclasé, contenant beaucoup d'argiles et un grand nombre de clastes du socle local, alors que l'unité supérieure est plus meuble et renferme des lentilles de sable ainsi qu'une proportion plus élevée de clastes erratiques; 2) le contact entre les tills est typiquement progressif et ne montre aucune altération subaérienne et aucun biote; 3) l'unité supérieure est puissante de plusieurs mètres dans les plaines de tills, elle est absente par endroits et la surface est alors formée soit par le till inférieur soit que du gravier tertiaire.

On suppose un âge wisconsinien supérieur en raison de la nature et des épaisseurs similaires des sédiments postérieurs au till étudiés dans des excavations effectuées à la pelle mécanique et dans des trous de sonde à sept endroits choisis; plusieurs datations au radiocarbone ont été obtenues dans trois de ces sites. Les dates les plus anciennes ont été obtenues en deux sites à l'intérieur de moraines bosselées de la partie centre-sud, à proximité de la frontière internationale où une tourbe de base avait un âge de 14 ka environ et des coquilles provenant d'un plateau de moraine âgé de 12 ka environ.

[1]Department of Geology, Queen's University, Kingston, Ontario K7L 3N6

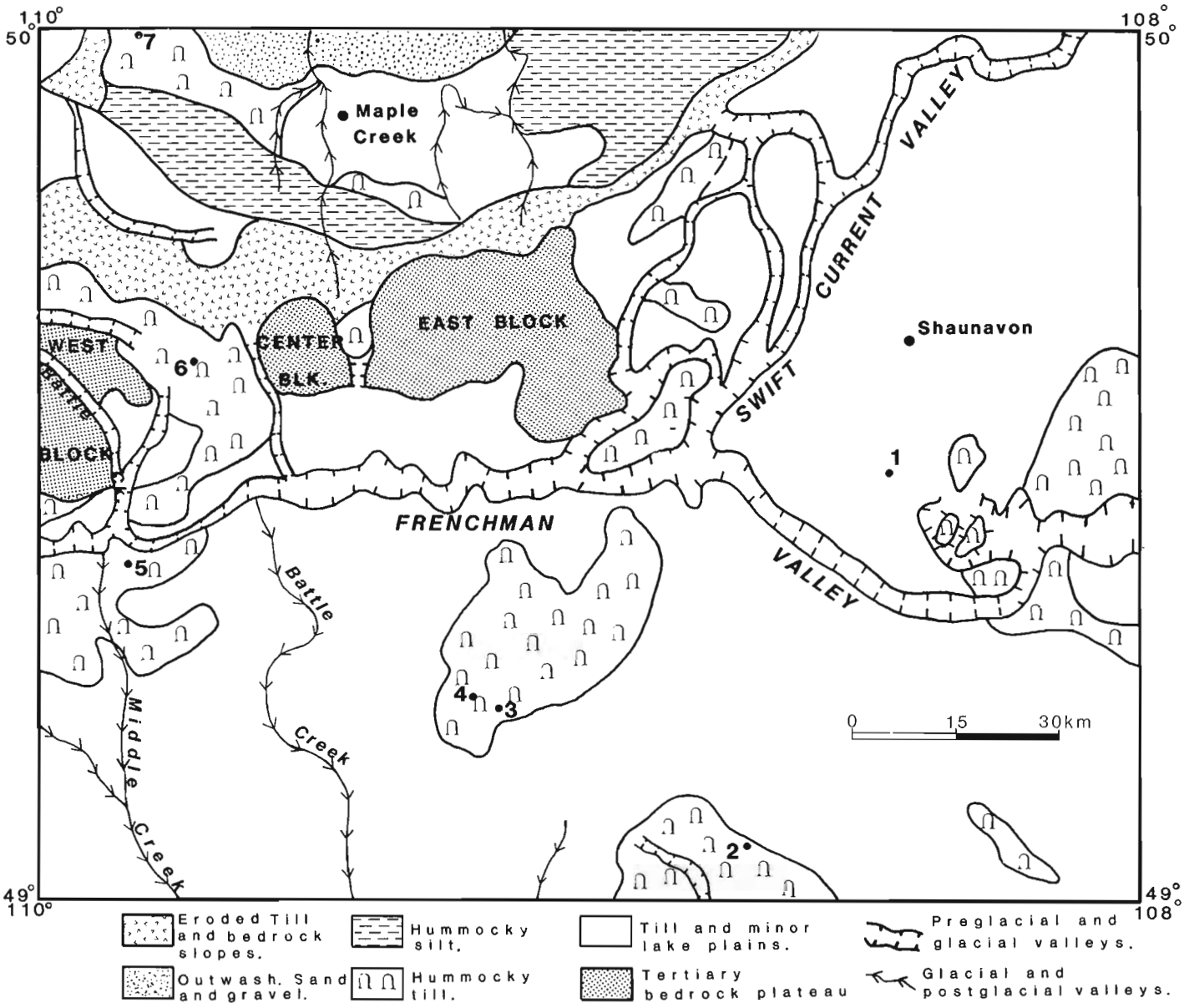


Figure 12.1. Generalized surficial geology of the Cypress Lake area (72F). Numbers identify sites described in the text.

INTRODUCTION

This report deals with the nature and age of surface tills and post-till sediments in the Cypress Lake area (72 F) in southwestern Saskatchewan. It is based largely on 1985-86 fieldwork and on laboratory analysis and studies of materials collected at selected back-hoe excavations, drill sites, and natural exposures. The preliminary results of detailed studies of back-hoe excavations, mainly within hummocky moraine belts, make up most of this report. These studies are part of a surficial geology mapping project in southwestern Saskatchewan begun in 1983.

Fieldwork included the drilling of 48 boreholes at 10 to 12 m depth using a truck-mounted auger, and back-hoe trenching from 4 to 6 m depth at 10 sites. Textural and carbonate analyses of about 200 till samples from borehole sediments, trenches, roadcuts, and natural exposures were completed in the Geological Survey of Canada sedimentology laboratory in Ottawa.

A particular focus of this study is to determine relative and absolute age differences of glaciated terrain in this region. Tentative proposals concerning the age of surfaces were made on the basis of results of fieldwork in 1983 and 1984 (Klassen, 1984; Klassen and Vreeken, 1985). Initially, these supported the concept of extensive ice free areas in the study area and adjacent parts of Alberta and Montana during the Late Wisconsinan maximum; but more detailed studies of the tills and post-till sediments, particularly radiocarbon dates obtained from several sites, suggest that most of the glacial deposits in the map area are of Late Wisconsinan age.

NATURE AND STRATIGRAPHY OF THE TILLS

Till[1] forms the bulk of the drift that generally is between 10 and 25 m thick with maximum thicknesses of about 60 m in buried valleys (Whitaker, 1976). The thicker driftforms the hummocky terrain whereas the Tertiary gravel pediments flanking the upland and Cretaceous bedrock surfaces beyond have a patchy veneer or blanket of thin till mapped as till plains (Fig. 12.1). The tills throughout the area are composed of roughly equal parts of sand, silt, and clay and minor gravel consisting of a variable mix of Tertiary quartzites and igneous and carbonate rocks of "eastern" provenance.

The most obvious differences in the physical properties of two tills underlying the till plains seen in stream banks and evident from sample analyses are as follows:

1. The lower till has well developed joint patterns reflected as vertical columnar structures that terminate along a recessive upper zone formed by a somewhat looser, sandier upper till 2 to 4 m thick (Fig. 12.2, 12.3).



Figure 12.2. Two tills exposed along Lyons Creek near the International Boundary (NW sec. 24, tp. 1, rge. 25, W 3 mer.; 49°03'N, 109°15') south of the Cypress Hills. Till bluffs, approximately 20 m high, marked by vertical columns typical of the lower till form the east wall of the creek valley. To the right of centre is the transition from the lower jointed till (dark) to the upper massive till (light). Light colour here reflects the surface wash of silt and sand from within and overlying the till. ISPG 2626-106

2. The ratio of quartzite pebbles to erratic pebbles is substantially higher in the jointed lower till than in the looser upper till.
3. The carbonate content of the silt fraction of the upper unit is higher than in the lower unit; also, the carbonate contents in the tills of the hummocky moraine are higher than in the adjacent till plains and are highest in the northernmost part of the area (Fig. 12.4).

The tills are mostly dark greyish brown (25Y 4/2)[2] to olive brown (25Y 4/4), although the lower till very dark greyish brown (25Y 3/2) at depths near the contact with Cretaceous shale. Although the lower till generally has a stronger preferred orientation of elongate pebbles than does the overlying till, the ice flow directions indicated more or less correspond to the directions of striations on faceted boulders in the tills.

The evidence available from the tills and their stratigraphic relationships with other sediments in the Cypress Lake area suggest that they are mostly lodgment and melt-out tills as defined by Dreimanis and Lundquist (1984) and were deposited during the last glaciation. The physical differences noted in the tills can, in a general way, be accounted for on the basis of a depositional model where erratic materials carried higher in the ice are concentrated in the melt-out sediments (Shield rocks and eastern carbonates); local materials are concentrated in the lodgment sediments (quartzite and clays). The columnar structures of the lower unit probably reflect greater glacial compaction and a somewhat higher clay content. Also, relatively clean ice conditions are indicated in areas where the jointed till forms extensive tracts of the

[1]The term till is herein used as defined by Dreimanis and Lundquist (1984): "a sediment that has been transported and is subsequently deposited by or from glacier ice, with little or no sorting by water."

[2]Munsell colour chart (moist)

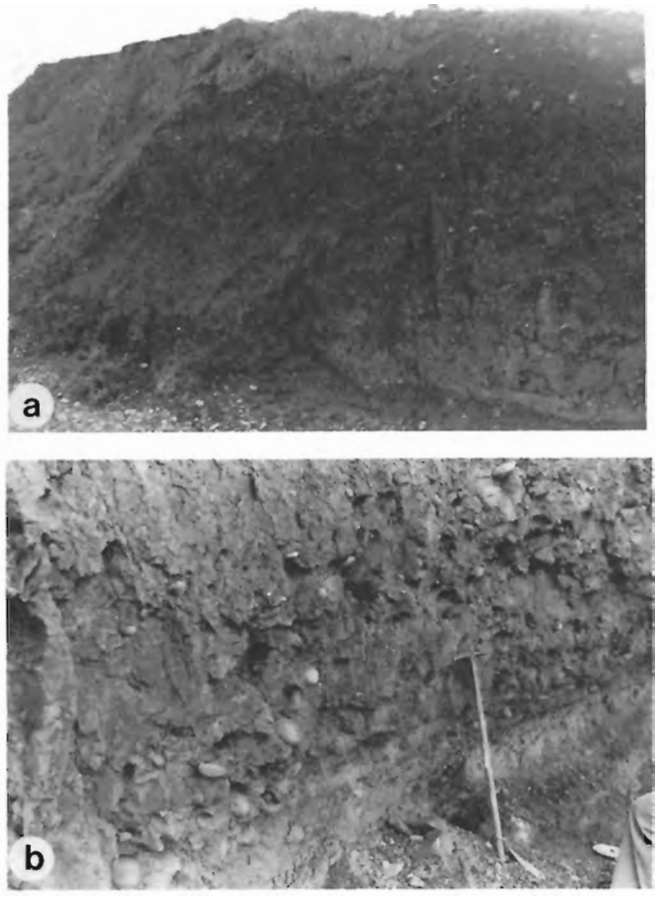


Figure 12.3. Two tills exposed along the north bank of Gap Creek (NW sec. 19, tp. 9, rge. 27, W 3 mer.; 49°45'N, 109°39'W) near the foot of the north-facing slope of the Cypress Hills. A. Bluff, approximately 15 m high, exposes a lower jointed till, transitional upwards to a somewhat stonier and sandier till, about 4 m thick with tongue-like inclusions of the lower till. ISPG-2626-134 B. Sharp contact between lower jointed till and Cretaceous shale. Rounded pebbles in the till are locally derived quartzite pebbles. ISPG 2626-133

surface such as ones found within the "eroded till" belt between hummocky terrain on the upland and across the northwest part of the map area (Fig. 12.1).

Deposition of the hummocky silt belt and ice retreat from the eroded (jointed) till surfaces north of the Cypress Hills (Fig. 12.1) apparently were part of the same event as suggested by conformable stratigraphic relationships between the jointed till and overlying hummocky silt seen in several exposures. Near contemporaneity of ice lobes north and south of the Cypress Hills is also requisite to explaining the truncation of a meltwater channel by the till plain south of the hummocky moraine between the Centre Block and East Block and, on the other hand, the dissection by meltwater channels of the western continuation of the same till plain between the Centre Block and West Block (Fig. 12.1). Finally, the evidence crucial to demonstrating the deposition of the two tills by separate glaciations – weathered and/or organic material between them – was not found.

The substantial difference in the carbonate content of the surface tills (Fig. 12.4) in the northwestern part of the map area (more than 15%) and in the southwestern part (less than 5%) most likely reflects differences in till provenance rather than other factors. Surface assemblages of erratic boulders in these parts also differ significantly; the northwest part has, along with the typical Shield erratics found everywhere, abundant eastern carbonate erratics; in the southwest, only scattered erratics of eastern carbonates occur along with scattered carbonates and quartzite boulders of western provenance not found elsewhere in the map area. Thus, the till in the northwest part appears to reflect ice flow from the northeast, and till in the southwest part, ice flow from the northwest.

NATURE AND STRATIGRAPHY OF POST-TILL SEDIMENTS

Mappable occurrences of stratified glacial deposits are restricted to the northwest part of the map area. Here they occur as belts of hummocky to gently irregular glaciolacustrine silt and clay, in places up to 25 m thick, over till and gently irregular to flat outwash plains underlain by sand and gravel typically somewhat thinner than the finer sediments (Fig. 12.1). Most of the glaciated surfaces elsewhere in the area are underlain by till that forms the extensive plains and belts of hummocky moraine, although local deposits of glaciolacustrine clay and silt occur, the most distinctive being the varved sediments beneath moraine plateau surfaces in hummocky moraine south of the Cypress Hills. Holocene silt and clay deposits, some 1 to 4 m thick, occur in low swales and shallow depressions on the till plains and are typically 4 to 6 m thick in the myriads of depressions within hummocky moraine throughout the area. These sediments appear to have been deposited by a combination of lacustrine, eolian, and slope processes, with lacustrine and slope processes dominant within the hummocky moraine belts. The bottoms of spillways and meltwater channels are underlain mostly by silt, sand, and gravel deposited by alluvial and mass wasting processes. Valley fill thicknesses of almost 30 m were recorded in two boreholes in Frenchman River valley and one in Conglomerate Creek valley near the confluence with the former. Thicknesses of fills in former spillways, such as the valley of Swift Current Creek, and modern valleys, such as Middle and Battle creeks, are likely in the 5 to 15 m range.

The absolute chronology for late glacial and Holocene events in this area is restricted to organic material from stratified sediments over till at several sites included in the detailed descriptions that follow. A radiocarbon date of 12 630 ± 80 BP (TO-216; see description of Ham site) from freshwater shells in a moraine plateau (site 2, Fig. 12.1) and a date of 14 340 ± 100 BP (TO-310; see description of Horseman site) from basal peat in a depression in hummocky moraine (site 3, Fig. 12.1) are the oldest obtained. A valuable stratigraphic marker for Holocene deposits in the western part of the map area is a widespread pinkish grey (7.5Y 5/2,

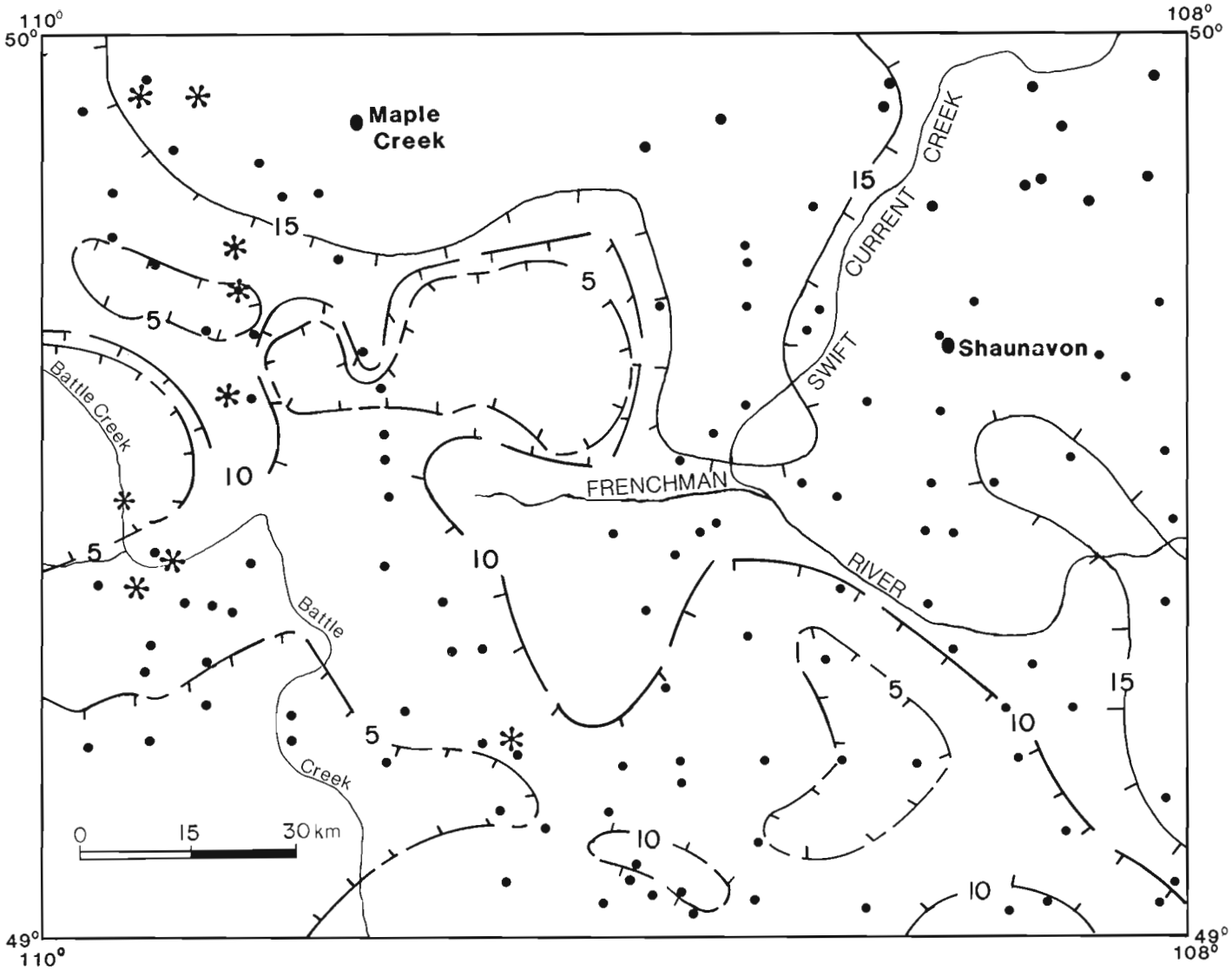


Figure 12.4. Contours of carbonate content of the silt fraction of surface tills in the Cypress Lake area. Dots are till sample sites; stars are volcanic ash (Mazama?) localities.

moist Munsell colour) volcanic ash approximately 2 to 5 cm thick, in a bed from 1 to 3 m below the surface (Fig. 12.4). The ash has been identified as Mazama at one site and was initially dated from deposits in Washington State as 6.6 ka (Fryxell, 1965; Westgate et al., 1969).

WILKINS SITE (1, FIG. 12.1)

The Wilkins site, about 17 km south of Shaunavon, is in a transition zone between a gently irregular till plain and hummocky moraine. Local relief is about 8 m and surfaces are at about 1000 m elevation. Several trenches were excavated to 3 m depth along a line from the crest of a low rise into an adjacent depression (SW 1/4 sec. 26, tp. 6, rge. 19, W 3 mer.; 49°29′48″N, 108°27′30″W). The surface materials were previously described from fresh roadcuts (Klassen, 1984). The tentative interpretations warranted further studies conducted by Vreeken in 1985. The following discussion is based on a more detailed unpublished report by Vreeken (entitled "Quaternary soil-geomorphology of southwestern Saskatchewan").

Sediments and environmental implications

Three main stratigraphic units consisting of diamicton (till), overlain by loess and colluvium were identified in the exposures (Fig. 12.5). The diamicton can be separated into a lower zone composed of an olive brown (2.5Y 4/4), calcareous (~13% carbonates),[1] sandy brown till including mostly local quartzite clasts along with Shield and eastern carbonate clasts (lower till of Fig. 12.5B) and an upper zone similar in composition but with a blocky pseudopedogenicstructure (upper

[1]Per cent of the silt fraction

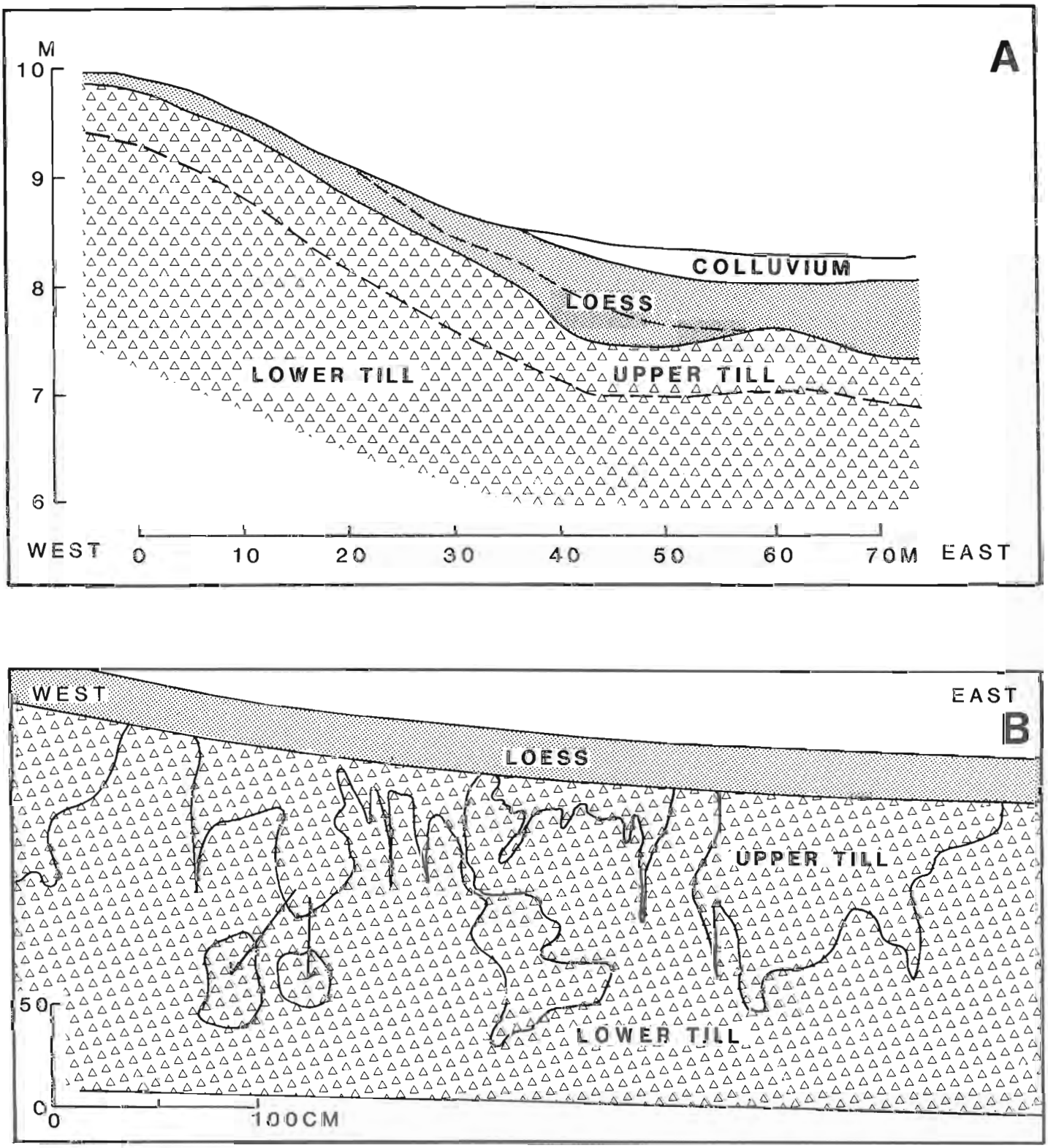


Figure 12.5. Stratigraphic relationships of sediments exposed at the Wilkins site. A. Generalized stratigraphic relationships of till and overlying sediments. B. Nature of the contact of the lower and upper till along part of exposure studied.

till of Fig. 12.5B). The upper zone is discontinuous on the highest partof the slope (Fig. 12.5B) and has a more variable texture than the lower zone. The contact between the tills is marked by a highly irregular stoneline that dips downslope.

A weakly bedded, olive brown (2.5Y 4/4) silt loam overlies the till along a sharp, slightly undulating contact. It thickens from about 0.2 m at the ridge crest to 0.9 m at the toe of the slope. This unit is designated as loess because of its distribution and the size fraction of its constituents; however, small amounts of fine gravel within it suggest that some is reworked material. Surface soil profiles on the crest and higher part of the slope are developed in the loess; however farther downslope, a wedge of hillslope colluvium separates the soil into a buried and subaerial component. The buried, loess-derived paleosol has a strongly developed A horizon and weak B horizon. The silt is leached to a depth just below the paleosol and the lower limit of the B horizon marks the limit of decalcification. An olive brown (2.5Y 4/4) silty loam forms a colluvial wedge up to 0.3 m thick along the lower part of the slope. It overlies the paleosol in loess along a sharp, even contact. This unit appears to be composed of detritus derived from soils farther upslope.

The cursory observations made in 1983 (Klassen, 1984) suggested evidence of polycyclical, postglacial soil-landscape evolution in the following manner: phase 1: emplacement of glacial till; phase 2: soil development; phase 3: hillslope erosion and deposition, resulting in partial stripping of the paleosolic mantle and in formation of a subaerial stoneline, penecontemporaneously mantled by hillslope sediments; phase 4: cryoturbatic convolution of the buried stoneline and paleosol; phase 5: hillslope erosion and deposition resulting in smoothing of the pre-existing surface; phase 6: eolian deposition of loess-like silt loam; phase 7: soil development; and phase 8: localized hillslope erosion and colluviation. These inferences were based largely on interpretation of the subangular blocky structure of the lower diamicton as being of pedogenic origin, and of the stoneline between the diamictons as being of subaerial origin.

Reassessment in the field and analytical data no longer support the idea that a paleosol formed prior to loess deposition; in other words, there is no evidence to support the occurrence of phase 2. Stonelines can be formed as a result of various mechanisms. In absence of paleopedogenic evidence, a biogenic origin of this stoneline, such as could result from selective removal of fine particles by earthworms, ants or termites, can be discarded. Stonelines can form as a result of selective dissolution of certain rock constituents, which can leave behind a weathering residuum composed of resistant lithologies. The presence of abundant carbonates, both above and beneath this stoneline, precludes applicability of this model; besides, this again would require evidence of paleopedogenesis, which is absent. Subaerial stonelines also can result from purely physical, selective removal of fine particles by wind action or by surface wash. In the former case, the gravel lag normally includes ventifacts and is locally overlain by sorted windblown sands. No such evidence was found at the Wilkins site. Stonelines that result from surface wash normally are overlain in part by redeposited hillslope sediments and certainly so when they occur within enclosed landscapes. Such slope sediments are sorted, that is, devoid of coarse clasts and progressively finer textured both in the downslope and in the upward direction. In addition, such sediments within enclosed hillslope systems are distributed in the form of a downslope thickening clastic wedge. No such features are unambiguously represented along the Wilkins hillslope transect.

The nature of this stoneline, therefore, must be assessed in relation to the nature of the two tills (or two zones), because their genesis may be related. There is no doubt that the diamictons are of glacial origin. The distorted nature of the stoneline, that is, the contact between the till units, is associated with distortion features within the diamictons which are evident from local sand lenses. Also, at one spot along the sloping part of a trench, material from the lower unit occurred above the stoneline in the form of a small diapiric feature; together with the features at the hillslope crest (Fig. 12.5B), this suggests that the materials were distorted while in a supersaturated underconsolidated state and that the mechanism for distortion was subsidence as the underlying stagnant ice melted. Because the stoneline shows evidence of vertical subsidence at the crest location and also evidence of an additional lateral stress component at backslope locations, it may be concluded that the greater mass of stagnant ice largely corresponded with the extent of the present day landscape depression. Indeed, this suggests that the till originated from melt-out of a stagnant decaying ice sheet. This explanation is somewhat similar to that offered by Shaw (1982) for till in the Edmonton area.

The presence of sorted sand lenses within the lower unit, of the stoneline, and of discontinuous layers of sorted sand within the upper unit seems to support the above explanation. These would reflect an alternation of conditions of mass movement resulting in the diamictons and of conditions of flowing water, enabling sand deposition and winnowing of sediment to form a gravel lag. This alternative explanation does away with phases 3 and 5 from the previous interpretation for the Wilkins site.

The deformed nature of the stoneline was initially attributed to cryoturbatic convolution or solifluction of sediments that were oversaturated as a result of thaw. This was based on observations on soliflucted deposits in The Netherlands (Vreeken, 1984). The physical prerequisite for solifluction is essentially the same as for subsidence and flow during melt-out. As there is no evidence of subaerial exposure associated with the formation of the stoneline, the solifluction model is therefore rejected. This does away with phase 4 from the previous interpretation. In short, phases 2 to 5, inclusive, from the earlier interpretation are replaced with a modified view on phase 1.

The only datable material identified at this site is organic carbon from the paleosol. The stratigraphic relationships, however, suggest that the paleosol has a late Holocene or modern age. The occurrence of Mazama ash in association

with a Holocene paleosol in other parts of the area (Fig. 12.1, 12.4) suggests its possible occurrence in these sediments. Further laboratory analyses may prove this, although this is unlikely because the ash can generally be recognized in fresh exposures.

HAM SITE (2, FIG. 12.1)

The Ham site is within a hummocky moraine belt that straddles the International Boundary in the south-central part of the map area (Fig. 12.1). Moraine plateaus of various shapes and sizes occur within this belt; many are distinctive circular to oval-shaped in plan, some 200 to 400 m across, and outlined by "fresh-looking" rim ridges (Fig. 12.6). The local relief ranges from about 8 to 25 m at elevations of about 1000 m. This site (NW sec. 28, tp. 1, rge. 21, W 3 mer.; 49°04′05″N, 108°45′35″W) is along a 140 m transect from the outer edge of a rimless moraine plateau to the central part of an adjacent depression (Fig. 12.7). Eight trenches were excavated to depths between 2 or 4 m, with the deepest located on the plateau edge and in the central part of the depression flat.

Sediments and environmental implications

The main types of sediments exposed were till underlying either thinly bedded sequences of lacustrine and ice contact silt, sand, and gravelly diamicton along the plateau edge, silty hillslope detritus including loess and paleosols, or pond sediments consisting primarily of clay beneath the depression flat (Fig. 12.8). The till is composed of a light brownish grey (2.5Y 6/2) to olive brown (2.5Y 4/4) sandy loam matrix (~9% carbonates) with scattered pebbles of mainly quartzite along with Shield and eastern carbonate rock types.



Figure 12.7. View east from edge of the moraine plateau (foreground) across the depression flat at the Ham site. ISPG 2482-26

Sediments exposed along the edge of the moraine plateau consist of a light yellowish brown (2.5Y 6/4) diamicton in the lower 1 m of a trench beneath an interbedded unit of silt, sand, and fine gravel about 3 m thick. Scattered bivalve shells (*Pisidium* sp.) occur in the silt and sand beds at 2 to 2.5 m depth; the shells were a radiocarbon date at 12 630 ± 80 BP (TO-216). Ostracods from the same zone indicate that the lower part was deposited in the nearshore littoral zone of a shallow lake and that the upper part was deposited in deeper water of a larger lake (L.D. Delorme, unpublished report[1], 1986). The climatic implications are that conditions were cooler and moister than those at present and that a change to

[1]Unpublished Technical Note AED-86-4, National Water Research Institute, Burlington.

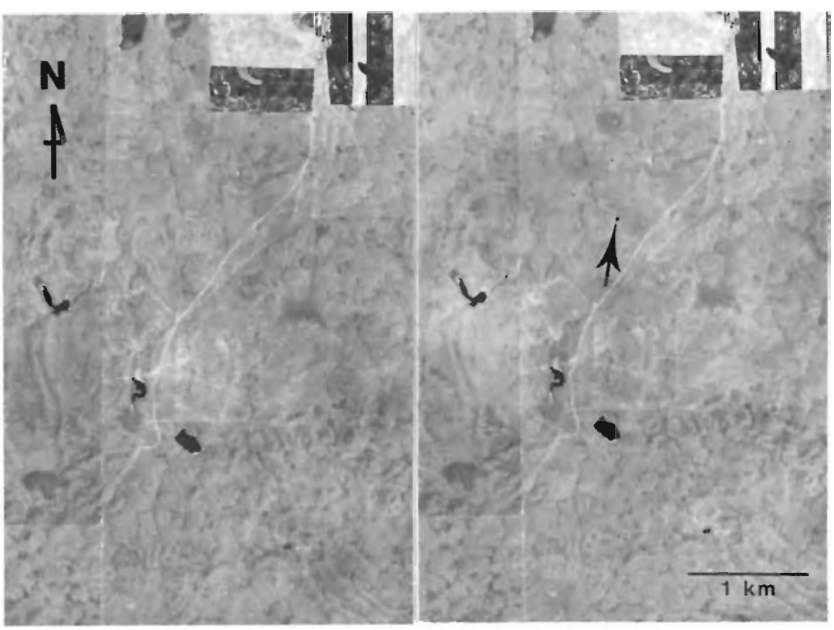


Figure 12.6. Hummocky moraine surrounding the Ham site; arrow indicates site location. CSMA 80181-03-168, 170

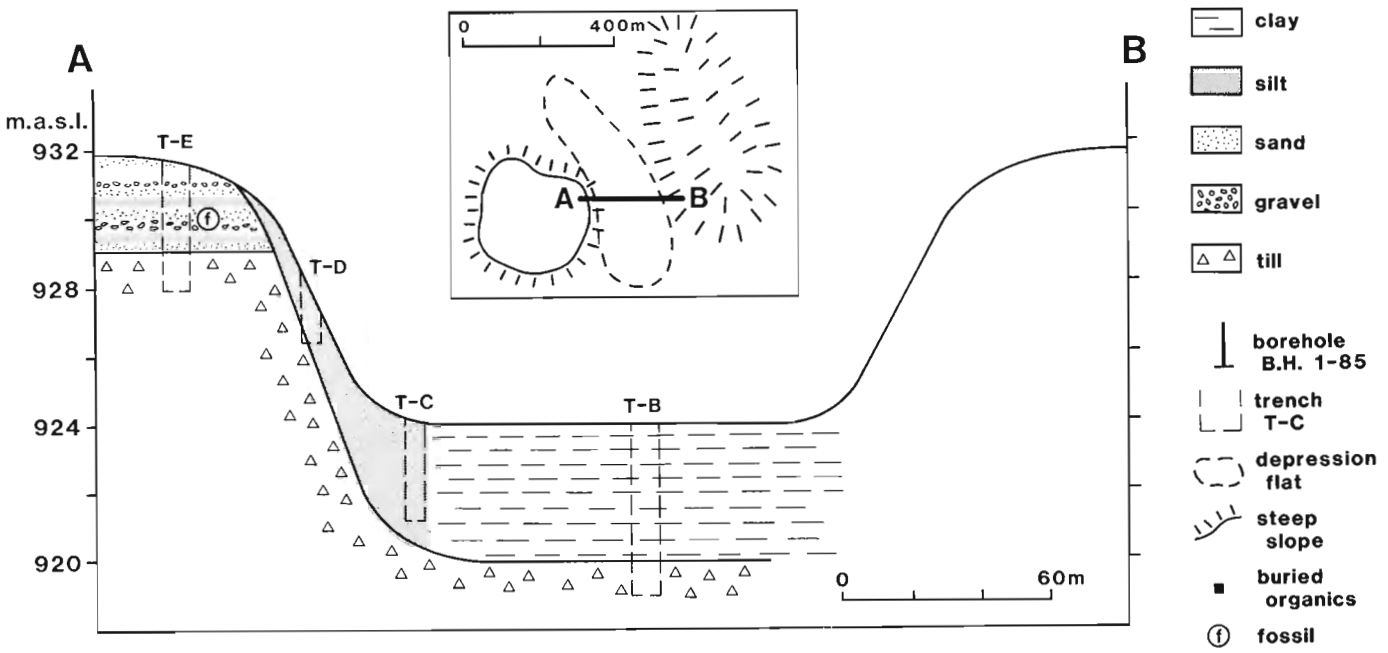


Figure 12.8. Stratigraphic cross-section of the Ham site. Shells from the fossil locality were radiocarbon dated as 12 630 ± 80 BP. Index map shows the location of the site in the local topographic setting.

yet warmer and moister conditions is reflected by fossils in the upper zone. The corresponding vegetational changes may have been from a subboreal broadleaved forest to open parkland (L.D. Delorme, unpublished report, 1986).

The sediments beneath the 10° slope between moraine edge and depression margin consist of poorly sorted silt, sand, and gravel overlain by a veneer of silt (Fig. 12.8). These materials are hillslope sediments covered by loess. Periods of slope stability are reflected by weakly developed paleosols.

The sediments in the central part of the depression include a light brownish grey (2.5Y 6/2) till with a calcareous (~8% carbonates) sandy loam matrix. The till is overlain by a massive, very dark greyish brown (2.5Y 4/2) clay about 3 m thick. It is mostly noncalcareous except in a middle zone where volcanic ash shards (Mazama?) were noted at 1.4 m depth.

The radiocarbon date and paleoclimatic implications of the ostracods are evidence that stagnant ice conditions prevailed at this site about 12.6 ka. The position of the dated sediments along the moraine plateau margin reflects formation along the edge of an ice-walled lake. The slope sediments and clays beneath the depression flat are Holocene sediments that accumulated after the remnant ice that occupied the depression had melted. Should the volcanic ash be identified as Mazama, then about half of the clays were deposited by 6.6 ka.

HORSEMAN SITE (3, FIG. 12.1)

The Horseman site about 17 km south and 8 km east of Robsart is within a patch of low relief hummocky moraine about 4 km^2 marked by subdued knolls and depressions with 5 to 15 m local relief. The area, at about 1000 m elevation, is separated from surrounding, somewhat higher, more distinctive hummocky moraine by a discontinuous ice contact ridge (Fig. 12.9).

The site is located between hummocks in a channel that opens into a depression flat (SW sec. 2, tp. 3, rge. 24, W 3 mer.; 49°13′20″N, 109°10′40″W).

Sediments and environmental implications

A trench excavated to 4 m depth across the channel and a power-auger hole to 12 m depth indicate that the regional till is here overlain by a succession consisting of 3 m of gravel, 2 m of silt and peat, and about 3 m of silty clay (Fig. 12.10).

The till is dark grey (5Y 4/1) to olive grey (5Y 4/2) with a slightly stony sandy loam matrix. It is slightly calcareous (~3% carbonates) to noncalcareous, and rock types are mainly quartzite with scattered Shield types and carbonates of eastern and western provenance. Gravel overlying the till consists mainly of local quartzite pebbles and cobbles along with minor Shield and eastern carbonate types.

Organic-rich silt overlying the gravel includes a mid-zone of about 1 m of silty fossiliferous peat. The peat contains a variety of plant and animal remains including bits of wood[1], insect parts, and small shells. A radiocarbon date on the wood yielded an age of 9560 ± 80 BP (GSC-4098), and organic material from the lower silty unit provided a radiocarbon date

[1]Identified as *Salix* sp. by H. Jetté, unpublished GSC Wood Identification Report No. 85-71

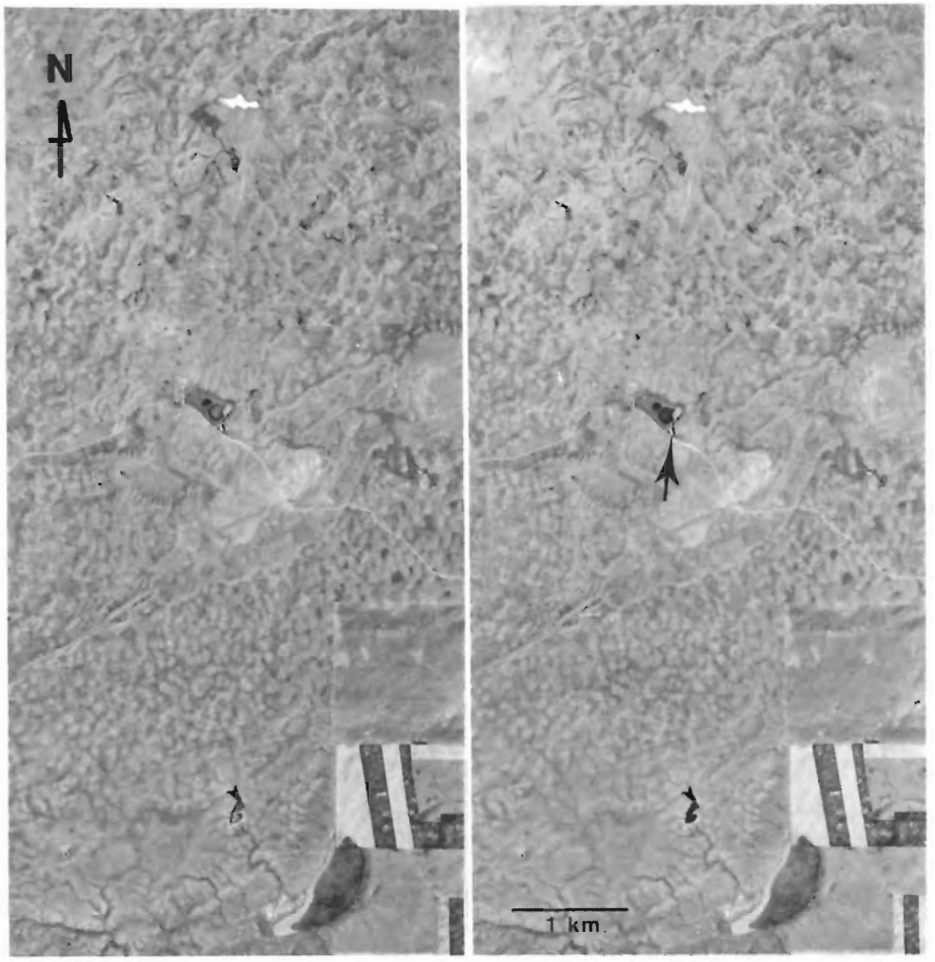


Figure 12.9. Hummocky moraine surrounding the Horseman site; arrow indicates site location. CSMA 80181-02-26, 28

of 14 340 ± 100 BP (TO-310). Pollen analysis of the peat bed indicates open vegetation dominated by sage and grasses (G.M. MacDonald, McMaster University, personal communication, 1986). Study of the ostracods in this unit (L.D. Delorme, unpublished report, 1986) indicates deposition in a permanent pond under climatic conditions similar to but cooler than the present.

The uppermost beds of clay and silt are dark grey (5Y 4/1) to olive grey (5Y 4/3) in the lower 2 m and mostly olive brown (2.5Y 4/4) in the upper part. A distinctive bed of volcanic ash (Mazama?) 10 cm thick separates the upper and lower parts. Ostracods from the lower part indicate a change to a cooler and drier climate than that during deposition of the organic-rich unit (L.D. Delorme, unpublished report, 1986). Delorme suggested that the climate was suitable for development of an aspen parkland type vegetation in the vicinity.

The sedimentary record above the till indicates that fluvial activity, most likely associatedwith ice stagnation, followed deposition of the till. The change to permanent pond conditions marked by the deposition of the peaty unit andupward transition to the relatively thin surface unit above the ash, appears to record much of the Holocene sedimentary succession. The absence of a pollen record of the early postglacial boreal forest assemblage recognized elsewhere in western Canada (Ritchie and Yarranton, 1978) and its occurrence at the nearby Rangeview site, however, suggests that the earliest part of the Holocene succession is missing.

RANGEVIEW SITE (4, FIG. 12.1)

The Rangeview site is about 3 km west of the Horseman site within the same belt of hummocky moraine. Sediments were studied in a fresh dug-out excavation, about 4 m deep, in a depression flat at about 1000 m elevation (Fig. 12.11), and in a nearby power-auger hole to 18 m depth (SW sec. 20, tp. 3, rge. 24, W 3 mer.; 49°13′20″N, 109°12′38″W). The depression lies between flat-topped moraine plateaus marked by minor gullies eroded downslope from the plateau rims. The latter are erosional features common to the hummocky moraines south of Frenchman Valley (Fig. 12.9) but not to those in the north.

Sediments and environmental implications

The sedimentary succession consists of till with a distinctive paleosol preserved in the upper 40 cm and an overlying unit

of massive clay about 2.5 m thick. The till consists of a lower unoxidized unit more than 12 m thick and an upper oxidized unit about 2 m thick. The lower unit has a very dark grey (2.5Y N/3) to dark olive grey (5Y 3/2), slightly calcareous clayey loam matrix, whereas the upper unit is dark greyish brown (2.5Y 4/2) to olive brown (2.5Y 4/4) with a calcareous (~8% carbonates) silty loam matrix. The tills are slightly stony with the typical mix of quartzites, Shield stones, and eastern carbonates although the proportion of quartzites is higher in the lower unit.

A paleosol with a distinctive A horizon and weakly developed B horizon occurs in the upper 40 cm of the till. Soil structures are evident in the upper horizon which is also leached. The overlying unit is a dark greyish brown (2.5Y 4/2) clay. Scattered fragile shells within it and the geomorphic setting indicate that it consists mostly of pond sediments although fine slopewash sediments are likely included. Samples taken at 10 cm intervals from the base of the paleosol to the surface were submitted to J.C. Ritchie (University of Toronto) for pollen analysis and to L.D. Delorme (Canada Centre for Inland Waters, Burlington) for ostracod analysis. Pollen counts indicate that Picea sp. pollen occurs throughout the units and is particularly abundant within the paleosol (J.C. Ritchie, personal communication, 1985). Ostracods were not identified in significant numbers in these units (L.D. Delorme, personal communication, 1985). R.W. Barendregt (University of Lethbridge) conducted paleomagnetic analysis of samples from a depth of 1 m in the till upward through the overlying units. The till shows a strong trend towards reversed polarity (R. Barendregt, personal communication, 1985) but sampling at greater depth is required to confirm a reversal. Excursions from normal polarity were not detected in the overlying sediments.

The paleosol developed on the till surface indicates that an interval of subaerial exposure followed deglaciation and subsequent deposition of the overlying clay. The similarity of the pollen assemblage within the paleosol and overlying clay (J.C. Ritchie, personal communication, 1985) suggests that significant climatic changes did not occur during the formation of these units. This locality probably records the boreal forest vegetation recognized elsewhere in the western interior

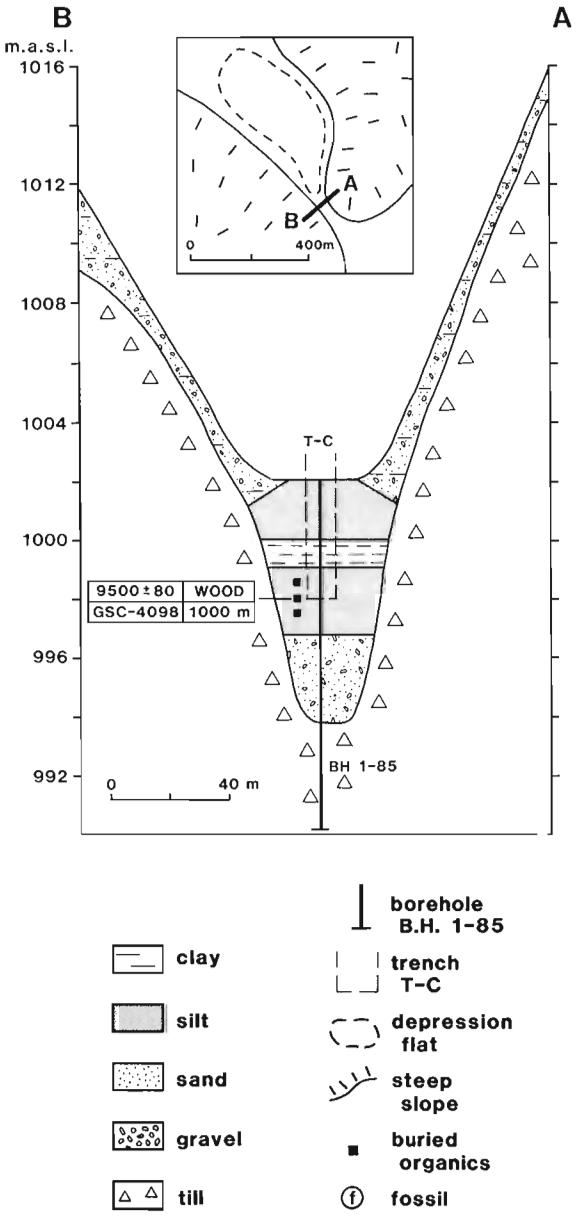


Figure 12.10. Stratigraphic cross-section of the Horseman site; index map shows the location of the site in the local topographic setting.

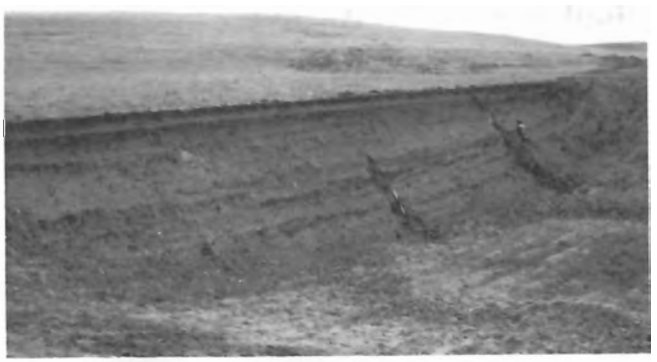


Figure 12.11. Setting of the Rangeview site. South wall of a dug-out in a depression flat within hummocky moraine; Till is overlain by massive clay; the person's feet are at the position of the till-clay contact. ISPG 2332-9

(Ritchie and Yarranton, 1978). Should the occurrence of a paleomagnetic reversal in the till be confirmed by further study, then the till and paleosol must predate the Late Wisconsinan glaciation.

GAFF SITE (5, FIG. 12.1)

The Gaff site is within a belt of hummocky moraine immediately south of a broad shallow trench occupied by Battle Creek that marks the western continuation of Frenchman Valley. This belt includes numerous moraine plateaus marked by gullied sides and depressions which lack the closure common in the "fresher" looking hummocky moraine. Local relief is between 5 and 20 m and elevations are about 1000 m. This site is about 4.5 km south of the former hamlet of Battle Creek (SW sec. 23, tp. 5, rge. 22, W 3 mer.; 49°23′30″N, 109°50′00″ W). Sediments were described from and sampled in a trench excavated to 6 m depth and a nearby auger-hole to 12 m depth.

Sediments and environmental implications

The regional till is here overlain by about 6 m of silt and clay including a volcanic ash bed. The till is a dark greyish brown (2.5Y 4/2) to olive (2.5Y 4/3), oxidized, calcareous (~11% carbonates), slightly stony clay loam. Silt and clay beds from 0.5 to 2 m thick, containing scattered fragile shells and a volcanic ash (Mazama?), overlie till. The ash occurs at a depth of 1.3 m and lies on a weakly developed paleosol.

Ostracods were identified only in the lowermost silt unit, from 4 to 6 m depth, and in silt above the volcanic ash (L.D. Delorme, unpublished report, 1986). Assemblages from both suggest a climate that may have supported an aspen parkland type vegetation with a strong grassland component in the upper silt. The ostracod assemblages suggest that there were no significant climatic changes during the deposition of the post-till sediments.

BLACK SITE (6, FIG. 12.1)

This site is within a belt of hummocky moraine that includes end moraine ridges at about 1265 m – the highest elevation of glacial deposits in the area. It is along the Cypress Hills road (NW sec. 3, tp. 8, rge. 28, W 3 mer.; 49°37′00″N, 109°43′05″W) across "The Gap" between the West Block and Centre Block where local relief is between 5 and 10 m and the elevation about 1130 m. Moraine plateaus are not developed in this terrain. Sediments were studied in cores from a line of 6 shallow borings up to 6 m depth along a transect of a depression about 36 m across.

Sediments and environmental implications

The sediments beneath the central part of the depression consist of interbedded sand, silt, and clay more than 6 m thick (Fig. 12.12). The regional till was not penetrated here; however a power-auger hole in a similar setting nearby reached till at a depth of 7 m suggesting most of the post-till sedimentary succession was penetrated.

Roadcuts in adjacent hummocks expose a dark greyish brown (2.5Y 4/2) till with a calcareous (~11% carbonates), slightly stony, silty loam matrix. Clasts are mainly quartzites along with Shield and eastern carbonate rock types. Vreeken (Klassen and Vreeken, 1985) described the sedimentary successions here as follows: "The basal increment of this sequence consists of interbedded fine sands and coarse silts, followed by 75 cm of well sorted medium sands. The middle increment measures about 265 cm; it includes materials ranging from gravel to clay loam in texture, whereas the coarser materials are confied to the lower 125 cm. At the base of this increment, several thin (<0.5 cm), black, clay-like intercalations occur within a sandy unit. These intercalations may well consist of colloidal organic matter. Gastropod shells occur throughout the middle increment. A distinct zone of organic enrichment extends to 50 cm below the top, and another one surmounts the top of the increment. Both zones can be correlated with equivalent zones at Station 7, where they were sampled for the purpose of radiocarbon dating. The upper increment at Station 6 consists of 220 cm of dark-coloured clay loams. These are separated by several buried soils and by one layer of light-coloured volcanic ash."

Gastropod shells from 3 to 3.3 m depth, including *Pisidium*, *Fossaria* sp., *Bakerilymnaea bulimoides*, *Gyraulus* (or *Promentus* sp.), *Armiger crista* (Linaeus, 1758), were radiocarbon dated 8590 ± 100 BP (TO-201) and the ash bed was identified as Mazama (unpublished data).

The nature and thickness of the sediments at this site, the absolute chronology of the dated horizon of 8.5 ka, and the 6.6 ka age of the Mazama ash suggest a Holocene age for the entire succession pentrated. A Late Wisconsinan age, therefore, appears likely for this belt of hummocky moraine.

SHOCK SITE (7, FIG. 12.1)

This site is within the youngest belt of hummocky moraine in the area that was previously thought to mark the maximum position of the Late Wisconsinan ice margin (Klassen and Vreeken, 1985). The terrain is broadly hilly to hummocky, has 10 to 30 m local relief, and lacks the distinctive moraine plateaus common to the hummocky moraine south of the Cypress Hills. The site is a depression flat about 60 by 150 m where several pits were excavated from 2 to 5 m depth and an auger-hole drilled to 12 m depth, about 7 km west of Kincorth (SW1/4 sec. 18, tp. 12, rge. 28, W 3 mer.; 49°59′45″N, 109°49′35″W).

Sediments and environmental implications

Massive clay, about 5 m thick, overlies a till which is dark greyish brown (2.5Y 4/2) in the upper 3 m to very dark grey (5Y 3/1) below. It has a sandy loam, calcareous (~17% carbonates) matrix and is moderately stony. Pebbles include a significantly higher proportion of eastern carbonates than found in the tills to the south. The overlying sediments are essentially massive olive grey (5Y 4/2) to dark greyish brown (2.5Y 4/2) clays that can be separated into three units of about equal thickness, marked by weakly developed partings. The lower and upper units contain scattered shell fragments

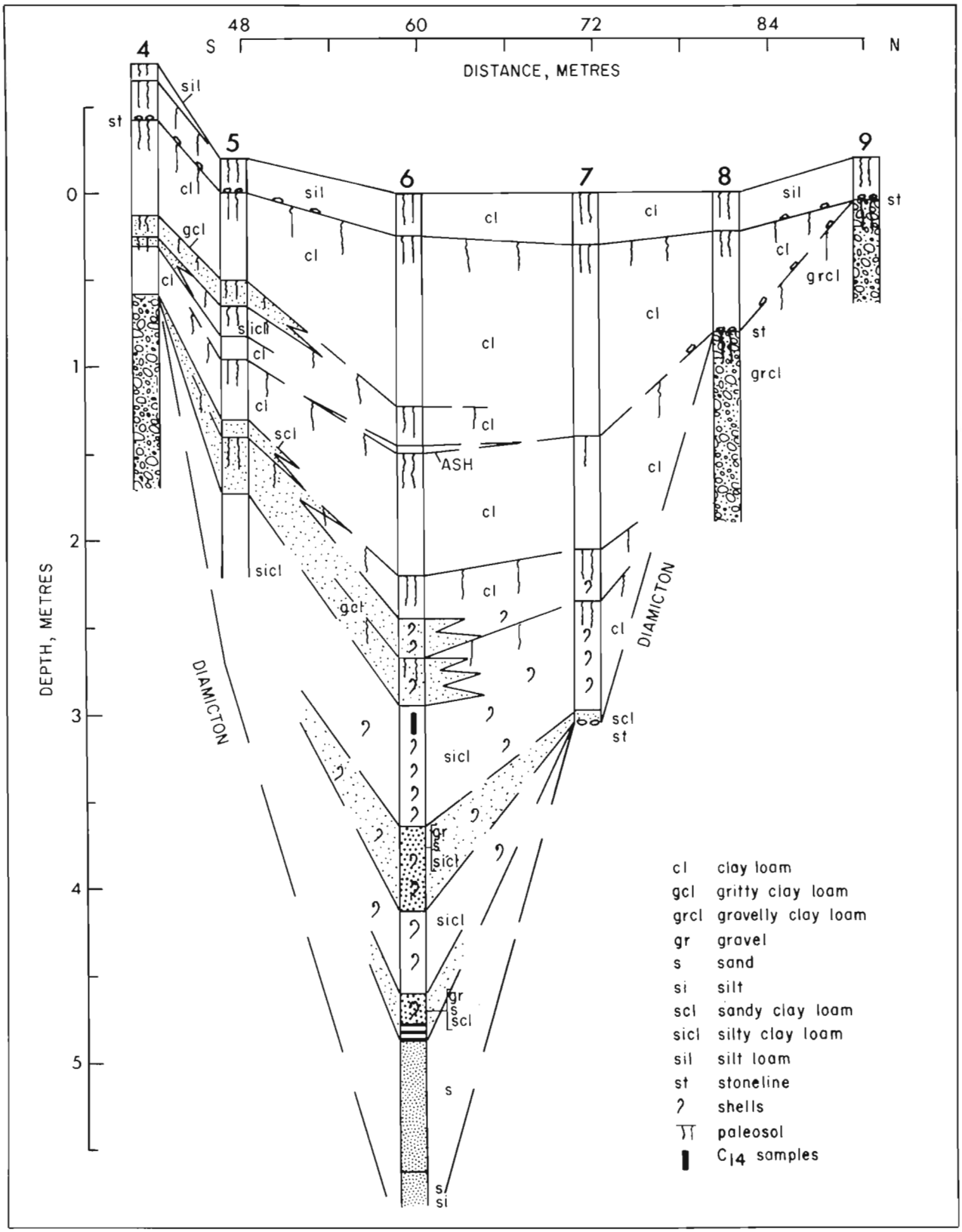


Figure 12.12. Stratigraphic cross-section of sediments beneath a depression in hummocky moraine at the Black site (after Fig. 25-2, Klassen and Vreeken, 1985).

whereas the middle unit is virtually barren. Ostracods were found only in the upper unit. L.D. Delorme (unpublished report, 1986) suggested a climate tolerable to an aspen parkland vegetation may be inferred from the ostracod assemblages. Volcanic glass (Mazama?) was not detected in the pits but occurs in the sand fraction of samples from about 1.1 m depth.

The nature and thickness of the sediments here are similar to those of sediments in the older hummocky moraine belts south of the Cypress Hills. The uniformly fine textured sediments and absence of any evidence of marked change in sedimentation suggest that deposition processes and climatic conditions were relatively uniform throughout formation of these sediments and that the entire sequence is Holocene.

CONCLUSIONS

The nature and origin of the tills and overlying sediments in the study area can be best explained in terms of Late Wisconsinan glaciation and Holocene deposition. Local differences in the physical properties of two tills commonly exposed in stream banks appear to reflect mainly the distribution of local versus far travelled detritus within a glacier rather than multiple glaciation. Differences in the carbonate content of tills north of Frenchman Valley and tills south of the valley are likely in part the result of separate ice streams in the area. The northern part was covered by southward flowing ice, whereas ice flowing northeastward around the Cypress Hills covered the southernmost part. Advances and retreats of separate ice lobes were not wholly synchronous; however they occurred within the Late Wisconsinan time frame of initial advance some 20 ka and final deglaciation about 12 ka. During the Late Wisconsinan maximum much of the glaciated terrain in the study area was likely ice covered.

These conclusions are rather simplistic interpretations based on the evidence obtained primarily from the tills and overlying sediments. There clearly are marked differences in the degree of erosion of similar surface features, weathering of glacial erratics, and soil development (Klassen, 1984; Klassen and Vreeken, 1985) within the map area that imply significant age differences. The absolute chronology and similarity of post-till sedimentation, however, does not support the concept of extensive pre-Late Wisconsinan age glaciated surfaces in this area.

The results of this study to date therefore support the concept of extensive Late Wisconsinan glaciation of the southern prairies and Montana as proposed by Christiansen (1979), Clayton and Moran (1982), Mickelson et al. (1983), and Shetsen (1984), rather than a more restricted glaciation as suggested by Reeves (1973), Stalker (1977), Jackson (1979), Rutter (1980), and Mott and Jackson (1982). Nevertheless, the "ice-free" concept is supported by a considerable body of evidence including absolute age chronology and presents an enigma that will likely be resolved when more absolute dating control is established.

ACKNOWLEDGMENTS

The initial results of special studies of sediments made available to the authors by R.W. Barendregt (paleomagnetism), L.D. Delorme (ostracods), G.M. MacDonald and J.C. Ritchie (pollen) provided valuable data and are gratefully acknowledged. Field studies were greatly facilitated through assistance and independent field work by Mark Pawson (1984) and Victor Levson (1986) and field assistance by Bryon Bahnsen (1984, 1985) and Lawrence Smith (1986).

REFERENCES

Christiansen, E.A.
1979: The Wisconsinan glaciation of southern Saskatchewan and adjacent areas; Canadian Journal of Earth Sciences, v. 16, p. 913-938.

Clayton, L. and Moran, S.R.
1982: Chronology of Late Wisconsinan glaciation in middle North America; Quarternary Science Reviews, v. 1, p. 55-82.

Dreimanis, A. and Lundquist, J.
1984: What should be called till? – in Ten Years at Nordic Till Research, L.K. Konigsson (ed.); Striae, v. 20, p. 5-10.

Fryxell, R.
1965: Mazama and Glacier Peak volcanic ash layers: relative ages; Science, v. 147, p. 1288-1290.

Jackson, L.E.
1979: Glacial history and stratigraphy of the Alberta portion of the Kananaskis Lakes map area; Canadian Journal of Earth Sciences, v. 17, p. 459-477.

Klassen, R.W.
1984: Quaternary geology of southwestern Saskatchewan; in Current Research, Part A, Geological Survey of Canada, Paper 84-1A, p. 641-642.

Klassen, R.W. and Vreeken, W.J.
1985: Quaternary geology of southwestern Saskatchewan; in Current Research, Part A, Geological Survey of Canada, Paper 85-1A, p. 187-192.

Mickelson, D.M., Clayton, L., Fullerton, D.S., and Barnes, H.W.
1983: The Late Wisconsinan glacial record of the Laurentide ice sheet in the United States; in Late-Quaternary Environments of the United States, H.E. Wright, Jr. (ed.); Volume 1, The Late Pleistocene, J.C. Porter (ed.); University of Minnesota Press, Minneapolis, p. 3-37.

Mott, R.J. and Jackson, L.E., Jr.
1982: 18 000 year palynological record from the southern Alberta segment of the classical Wisconsinan "Ice-free Corridor"; Canadian Journal of Earth Sciences, v. 19, no. 3, p. 504-513.

Reeves, B.D.K.
1973: The nature and age of the contact between the Laurentide and Cordilleran ice sheets in the western interior of North America; Arctic and Alpine Research, v. 5, no. 1, p. 1-16.

Ritchie, J.C. and Yarranton, G.A.
1978: Patterns of change in the late-Quaternary vegetation of the Western Interior in Canada; Canadian Journal of Botany, v. 56, no. 17, p. 2177-2183.

Rutter, N.W.
1980: Late Pleistocene history of the western Canadian ice-free corridor; in The ice-free corridor and peopling of the New World, N.W. Rutter and C.E. Schwager (ed.); Canadian Journal of Anthropology, v. 1, p. 1-8.

Shaw, J.
1982: Melt-out till in the Edmonton area, Alberta, Canada; Canadian Journal of Earth Sciences, v. 19, p. 1548-1569.

Shetsen, I.
1984: Application of till pebble lithology to the differentiation of glacial lobes in southern Alberta; Canadian Journal of Earth Sciences, v. 21, no. 8, p. 920-933.

Stalker, A.MacS.
1977: The probable extent of classical Wisconsin ice in southern and central Alberta; Canadian Journal of Earth Sciences, v. 14, p. 2614-2619.

Vreeken, W.J.
1984: Re-deposition of loess in southern Limbourg, The Netherlands; 3. Field evidence for conditions of deposition of middle and upper silt loam complexes; Earth Surface Processes and Landforms, v. 9, p. 1-18.

Westgate, J.A., Smith, A.G.W., and Nichols, H.
1969: Late Quaternary pyroclastic layers in the Edmonton area, Alberta; in Pedology and Quaternary Research, Symposium Proceedings, University of Alberta, p. 179-186.

Whitaker, S.H.
1976: Geology and groundwater resources of the Cypress area (72F), Saskatchewan; Saskatchewan Research Council, Geology Division, Map No. 22.

- 13 -

Geochemistry of northern Juan de Fuca Ridge sediments, northeast Pacific

Project 750108

B. Blaise and B.D. Bornhold
Cordilleran and Pacific Margin Division, Sidney, B.C.

Blaise, B. and Bornhold, B.D., Geochemistry of northern Juan de Fuca Ridge sediments, northeast Pacific; in Current Research, Part A, Geological Survey of Canada, Paper 87-1A, p. 127-142, 1987.

Abstract

Sedimentological and geochemical studies of cores from the Juan de Fuca Ridge identified various types of sediment: hydrothermal; pure detrital hemipelagic; and diagenetically and/or hydrothermally altered sediments. The data allow us to establish a mixing curve to determine the percentage of hydrothermal and terrigenous material in the Juan de Fuca Ridge area.

The sulphide sediments show a high hydrothermal contribution in the coarse fraction compared to the finer material. The inverse is true for the sediment which contains less than 8% hydrothermal material.

An authigenic clay (iron-rich smectite) is found with both a hydrothermal, and basaltic and/or biogenic origin.

These data show clearly that, in a high terrigenous supply area the hydrothermal impact on the sediment is low and very local. As,S, Cu, Ba, Zn, Pb, MgO, Fe_2O_3, P_2O_5, V and Sr are clearly related to the hydrothermal system.

Résumé

A partir d'analyses sédimentologiques et géochimiques, issues de sédiments de la dorsale de Juan de Fuca, différents dépôts peuvent être identifiés: des dépôts hydrothermaux; des sédiments hémipélagiques à composante terrigène très importante; et des sédiments hémipélagiques ayant subis une influence diagénétique et hydrothermale ou les deux à la fois. Ces données permettent de construire une courbe de mélange type pour des dépôts hydrothermaux et terrigènes de la région de la dorsale de Juan de Fuca.

Les sédiments hydrothermaux présentent une contribution hydrothermale plus importante pour les fractions grossières par rapport aux fractions fines. Pour les sédiments contenant moins de 8% de matériel hydrothermal l'inverse est observé.

On a fait la découverte d'un smectite authigénique riche en fer. Elle est issue de l'altération de verre volcanique et l'effet hyhothermal d'organismes siliceux ou de l'action des deux phénomènes ainsi que de l'effet hydrothermal.

Ces donnees montrent clairement que, dans une région à apports terrigènes important, l'influence de l'effet hydrothermal sur le sédiment est faible et très local ou les deux à la fois. As, S, Cu, Ba, Zn, Pb, MgO, Fe2O3, P2O5, V et Sr sont clairement relié au système hydrothermal.

INTRODUCTION

The Juan de Fuca Ridge is of considerable interest due to the recent discovery of several sulphide deposits along its various segments (e.g., Normark et al., 1983; Kadko et al., 1985; Canadian American Seamount Expedition, 1985; Davis et al., in press). During a September 1985 cruise of the *C.S.S. PARIZEAU* an intensive coring program resulted in the recovery of 43 cores (up to 11 m long, using boomerang, gravity and piston corers) from Northern Explorer Ridge, West and Middle Valley and the Endeavour Segment of Juan de Fuca Ridge System (Fig. 13.1).

Macroscopic descriptions made on board show at least six different types of sediment: (a) olive-grey hemipelagic muds; (b) black sulphides; (c) brown muds overlying sulphides; (d) brown muds; interlayered in (e) semi-granular olive-grey muds; and (f) olive-green granular muds with volcanic glass. This paper describes the general geochemical aspects of the sediments from the upper parts of ten cores and the sources of these sediments.

GEOLOGICAL SETTING

The Juan de Fuca Ridge system is located a few hundred kilometres off the Washington and British Columbia coast. Over most of its length, spreading takes place at a rate of about 60 mm per year. The ridgecrest morphology is typical of a medium- to fast-spreading ridge. Rifting takes place at the top of the high volcanic ridge and sometimes in deep axial valleys with lower spreading rates.

The geographical location, close to the continent, and the relief of these deep valleys have resulted in a large volume of turbidite sediments which have buried the spreading axis along parts of the northern Juan de Fuca Ridge (Davis et al., in press). In the Middle Valley area, several mounds have been recognized by Sea-Marc I and II imagery (Davis et al., 1985, in press; Currie et al., 1985). These were seen to be up to a few hundred metres across with up to 60 m of local relief above the smooth flat-lying sediment surface. The cores sampled were obtained mainly in this area (Table 13.1).

METHODS

After being freeze-dried, sand and mud were separated under distilled water with a 63 μm sieve. The clay fraction was separated by sedimentation. The grain size analyses were performed using a Sedigraph 5000 D and a 2 m long settling tube. CaCO3 content was determined by HCl leaching (N/5). The less-than-two-micron fraction clay mineralogy was estimated using oriented smear-slides using a PW1130 generator with a PW1050/85 vertical goniometer and PM8210 Printing Recorder controlled by a PW1710 microprocessor. The X-ray

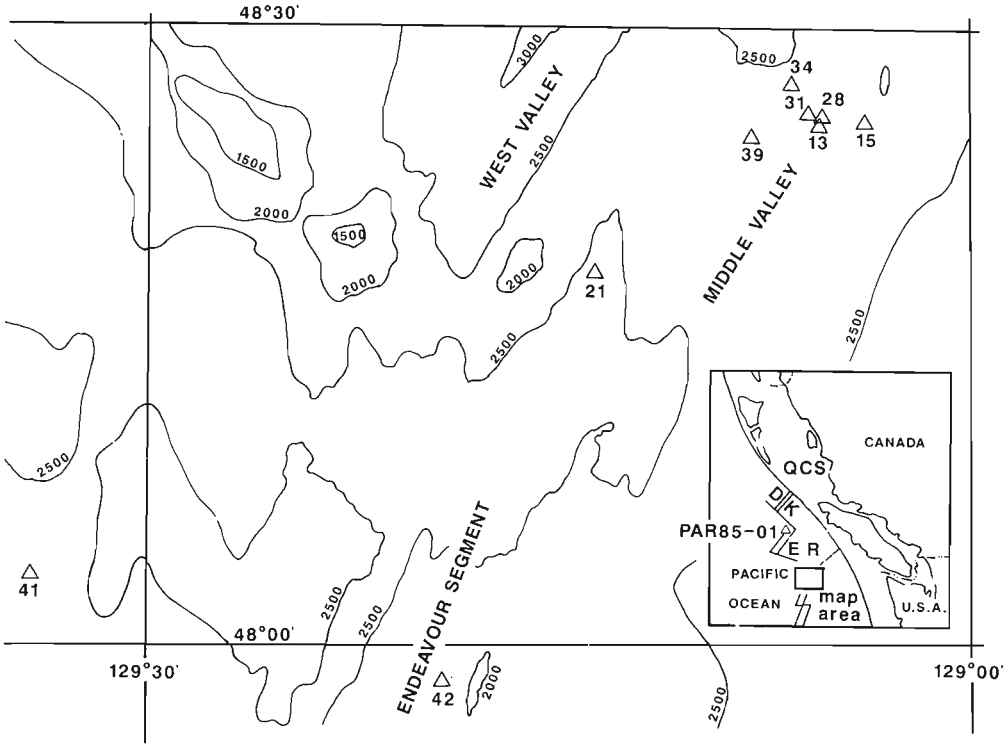


Figure 13.1. Study area on the northern Juan de Fuca Ridge showing some of the locations of cores obtained in 1985. QCS: Queen Charlotte Sound, DK: Dellwood Knolls, ER: Explorer Ridge. Depth in metres.

Table 13.1. Core location data for the northern Juan de Fuca Ridge.

Number	Core	Sample Depth (cm)	Length Core (cm)	Lat. N.	Long W.	Depth (m)	Locality
01	PAR 85-01	00-12	1142	49° 52.44'	130° 27.51'	2390	Explorer Ridge
13a	PAR 85-13	00-12	343	48° 26.14'	128° 40.74'	2460	Middley Valley (sulphide mound)
13b	PAR 85-13	28-35	343	48° 26.14'	128° 40.74'	2460	Middley Valley (sulphide mound)
15	PAR 85-15	00-11	165	48° 26.06'	128° 37.43'	2400	East of Middle Valley
21	PAR 85-21	00-15	102	48° 18.72'	128° 56.23'	2700	near West Valley
28	PAR 85-28	10-24	420	48° 26.11'	128° 40.84'	2507	Middley Valley (sulphide mound)
31	PAR 85-31	00-20	767	48° 26.25'	128° 40.87'	2445	Middley Valley (sulphide mound)
34	PAR 85-34	00-15	960	48° 27.39'	128° 42.61'	2442	Middle Valley high heat flow station
39	PAR 85-39	03-15	992	48° 25.19'	128° 42.64'	2442	Middle Valley
41a	PAR 85-41	00-12	166	48° 02.95'	129° 40.75'	2795	Endeavour Segment
41b	PAR 85-41	12-14	166	48° 02.95'	129° 40.75'	2795	Endeavour Segment
42	PAR 85-42	Catcher	11	47° 58.69'	129° 08.32'	2387	Endeavour Segment

source was a normal focus Cu tube with a Ni filter. The detector was a sealed proportional counter PW1711/10. These X-ray traces were made on carbonate-free sediment for each sample: (1) air dried (2) glycolated for 24 h with ethylene glycol (3) heated at 500°C (15°C) for 2 hours. The geochemical analyses were done by inductively coupled plasma analysis for all elements except Pb and As (atomic absorption) and FeO, H_2OT, CO_2, C, S and LOI (chemical methods).

RESULTS

The analyzed samples are mainly composed of hemipelagic mud except core PAR85-13 which contains brown and massive black sulphides (Davis et al., in press).

The carbonate contents are between 4.7 and 15.5% in the bulk sediment and between 0.6 and 8.4% in the mud fraction (Table 13.2). The sand fraction is less than 2.13% in all samples except PAR 85-42(5.6%) and PAR 85-13(34 to 44%) (Table 13.3). In these two samples the sand fraction comprises, respectively, volcanic ash and sulphides. In other samples, biogenic components (up to 94%) dominate this fraction, with minor quartz, feldspar and fecal pellets. The less-than-two-micron fraction is made up of smectite, chlorite, illite and irregular mixed-layer minerals associated with minor quartz, feldspar and amphibole. The percentages are everywhere similar except for PAR 85-42 which has a very high smectite content (65%) (Tables 13.2 and 13.3).

Geochemistry results given in Table 13.4 include analyses from (1) the Dellwood Knolls area for terrigenous comparison (Blaise, 1985; Blaise et al., 1985), (2) Queen Charlotte Sound for inter-laboratory comparison (Blaise, 1985) and (3) Juan de Fuca Ridge System (this study). Comparison between bulk sediment, washed sediment, mud and clay samples for all cores except PAR 85-13 and PAR 85-41-12/14cm (41B) shows that compared to bulk samples

Table 13.2. Lithology, texture and carbonate content of samples used in this study.

Sample number	Macroscopic description	Colour	Carbonate content %		Texture %			
			Bulk sediment	mud fraction	Sand	Silt	Clay <4μm	Clay <2μm
PAR85-01-00/12 cm (pilot)	hemipelagic mud	dark olive grey 5Y 4/1	9.93	4.85	1.4	22.83	75.78	54.63
PAR85-13-00/12 cm (13a)	coarse sandy sulphides	brown 7.5 YR 3/2	4.73	1.83	44.43	19.89	35.68	23.62
PAR85-13-25/38 cm (13b)	coarse blocky sulphides	black 5Y2.5/1	12.88	4.06	34.98	43.43	21.59	10.81
PAR85-15-00/11 cm	hemipelagic mud	dark olive grey 5Y3/2	11.87	6.56	1.56	22.38	76.05	56.67
PAR85-21-00/15 cm	hemipelagic mud	dark olive grey 5Y4/1	11.65	4.34	0.34	21.72	77.94	56.67
PAR85-28-10/24 cm	hemipelagic mud	dark olive grey 5Y4/1	12.62	8.37	1.7	26.67	71.63	52.79
PAR85-31-00/20 cm (pilot)	hemipelagic mud	olive grey 5Y4/2	12.01	6.48	2.13	33.22	64.65	49.38
PAR85-34-00/15 cm (pilot)	hemipelagic mud	dark olive grey 5Y4/1	5.31	0.64	0.83	22.52	76.65	56.69
PAR85-39-03/15 cm	hemipelagic mud	olive grey 5Y4/2	10.99	8.32				
PAR85-41-00/09 cm (41a)	semi-granular hemipelagic mud	olive grey 5Y4/2	13.63		1.56	22.97	75.46	48.66
PAR85-41-12/14 cm (41b)	brown mud	dark reddish brown 5YR3/3	15.59					
PAR85-42-catcher	granular brownish green olive mud	light olive 5Y5/6	10.04	7.43	5.6	19.11	75.29	54.69
PAR85-42-catcher	granular green olive mud	olive 5Y4/4	10.03	1.1				

Table 13.3. (a) Sand fraction composition and (b) clay mineralogy of samples used in this study.

Sample	Sand analyses (% of particles)								
	diatoms	foraminifera	radiolaria	other biogenics	fecal pelets	quartz	other minerals	volcanic glass	sulphides
PAR81-01	7.3	2.18	16.4	2.61	1.6	-	4.06	-	-
-13a	9.35	0.38	5.73	2.86	-	-	-	-	81.68
-13b									100
-15	45.74	9.69	28.68	9.30	0.78	0.78	5.04		
-21	51.92	7.05	17.31	0.64	17.95	-	5.13		
-28	7.61	56.52	24.64	3.62	2.54	1.45	3.62		
-31	10.23	76.14	7.95	-	5.68	-	-		
-34	39.52	2.82	43.15	5.24	3.23	-	6.05		
-39	2.9	57.68	23.24	2.49	2.49	4.98	6.22		
-41a	53.49	4.65	30.23	3.10	-	1.16	7.36		
-41b	32.53	9.95	10.48	19.35	5.91	-	21.77		
-42	1.81	3.17	22.17	4.07	0.45	23.08	5.88	39.37	
-42	1.25	5.83	21.67	7.08	3.83	18.75	1.25	40.83	

Sample	Less-than-two-microns fraction Clay minerals (%)							Associated minerals		
	chlorite	illite	irregular mixed-layers (10-14s)	(10-14v)	(14-14)	kaolinite	smectite	quartz	amphibole	feldspar
PAR81-01	30	17	0	5	5	0	43	trace	trace	+
-13a	32	17	5	5	5	2	34	trace	trace	+
-13b	33	19	4	8	6	0	30	trace	trace	+
-15	-	-	-	-	-	-				
-21	26	19	3	2	5	0	45	trace	-	++
-28	30	23	5	0	5	0	37	++	++	+++
-31	30	23	0	5	5	0	37	trace	trace	++
-34	29	14	0	3	7	2	45	++	trace	++
-39	31	20	2	2	6	0	39	+	+	++
-41a	27	18	3	2	5	0	45	-	-	+
-41b										
-42	15	8	5	0	5	2	65	trace	+	+
-42	17	7	0	3	7	2	64	trace	+	++

Legend: - : absent; + common; ++ : abundant; +++ very abundant.

the washed samples show a decrease in Na_2O (salt), S, Ba (barite?), Pb and As. Salt and barite dissolution could explain the Na_2O, S and Ba decrease; the Pb and As decrease and their elationship to other possible phases are still being investigated. The trace elements are, in general, more abundant in the mud and clay fractions compared to the bulk samples (especially for Pb, Cu, Zn, Sr, Yb, La, Be and Co; Fig. 13.2). Only an increase in Ba, As and S in the mud fraction compared to the clay fraction is apparent. The following discussion will not be made on a carbonate-free basis because of the low amount of $CaCO_3$.

To classify the sediment by sedimentological and geochemical analyses two common diagrams have been chosen from the literature (Fig. 13.3). On

$$\log \left[\frac{\text{Mn sample}}{\text{Mn shale}} \quad \frac{\text{Fe sample}}{\text{Fe shale}} \right]$$

versus Al/(Al + Fe + Mn) (Mn* versus D*), Mn* reflects both volcanic influences on sedimentation and oxidation-reduction potential and D* gives an indication of the detrital input (values greater than 0.63 indicate a high terrigenous influence). Samples from cores 28, 31 and 39 are close to the shale average while cores 01, 15 and 34, core 21 and samples PAR 85-41-00/12cm (41a), PAR 85-41-12/14cm (41b), PAR 85-13-00/12cm (13a) and PAR 85-13-28/35cm (13b) show an increase in volcanogenic and hydrothermal influence. Sand

Table 13.4a. Geochemical data for the uppermost sedimentary unit near the Dellwood Knolls.

		01-1-12/14 cm	01-1-52/54 cm	06-05/07 cm	06-35/37 cm	06-50/52 cm	08-04/06 cm	08-34/36 cm	08-64/66 cm	09-04/06 cm	09-24/26 cm	09-54/56 cm	10-04/06 cm	10-34/36 cm
SiO_2	%	56.70	57.10	56.30	56.40	55.10	56.60	56.10	53.40	55.30	56.50	55.00	55.10	55.40
TiO_2	%	0.72	0.66	0.68	0.69	0.68	0.66	0.70	0.73	0.73	0.67	0.64	0.76	0.67
Al_2O_3	%	13.82	14.25	13.86	15.03	15.12	14.18	15.15	15.31	13.77	13.67	14.27	13.91	14.35
Fe_2O_3T	%	5.64	6.21	5.87	6.40	6.21	5.79	6.23	7.21	5.69	6.67	6.27	5.92	6.25
Mn	%	0.05	0.05	0.05	0.06	0.06	0.05	0.06	0.06	0.08	0.06	0.07	0.05	0.07
MnO	%	0.06	0.06	0.06	0.07	0.08	0.07	0.08	0.08	0.10	0.08	0.09	0.07	0.09
MgO	%	2.89	2.97	2.99	3.13	3.24	3.00	3.22	3.36	2.96	3.09	3.12	3.04	3.06
CaO	%	3.13	2.73	2.46	2.86	3.12	3.10	2.98	3.59	2.55	2.70	3.40	2.44	3.22
Na_2O	%	5.80	4.55	5.24	5.42	4.22	5.23	5.23	4.98	5.03	5.01	4.85	5.93	7.05
K_2O	%	1.71	1.86	1.86	1.97	1.98	1.80	1.94	1.99	1.86	1.77	1.92	1.78	1.91
Co	p.p.m.	15	16	17	18	20	17	18	19	15	16	19	16	19
Cr	p.p.m.	74	67	68	56	62	61	67	69	73	68	61	87	60
Cu	p.p.m.	59	58	69	65	63	66	60	65	68	66	69	68	60
Ni	p.p.m.	55	57	64	62	68	70	62	67	69	76	81	67	72
Pb	p.p.m.	55	35	19	22	23	28	21	22	29	26	27	26	17
V	p.p.m.	110	130	100	130	140	120	130	150	130	120	120	130	130
Zn	p.p.m.	184	184	210	278	210	173	189	220	220	368	257	184	199
Sr	p.p.m.	263	273	268	268	278	284	299	362	257	268	273	273	247

		11-11/13 cm	11-41/43 cm	15-00/02 cm	15-10/12 cm	21-00/02 cm	21-30/32 cm	21-60/62 cm	23-00/02 cm	23-30/32 cm	23-60/62 cm	23-80/82 cm	29-00/02 cm
SiO_2	%	56.00	55.30	55.90	55.20	57.10	55.30	57.00	53.30	55.50	55.00	55.60	55.70
TiO_2	%	0.64	0.63	0.69	0.67	0.73	0.70	0.74	0.69	0.66	0.77	0.77	0.70
Al_2O_3	%	14.19	15.13	13.41	14.04	13.93	13.65	14.05	13.63	13.57	14.20	14.25	13.74
Fe_2O_3T	%	6.23	6.57	5.17	5.63	6.86	6.26	6.47	6.14	6.28	6.31	6.74	5.42
Mn	%	0.06	0.07	0.06	0.07	0.06	0.08	0.07	0.05	0.06	0.06	0.10	0.04
MnO	%	0.08	0.09	0.08	0.09	0.08	0.10	0.09	0.07	0.08	0.08	0.13	0.05
MgO	%	3.05	3.23	2.90	3.07	3.15	3.06	3.12	2.98	2.97	3.06	3.11	2.83
CaO	%	3.19	3.43	2.31	2.79	3.00	2.87	2.69	3.36	3.21	3.73	3.81	2.03
Na_2O	%	4.96	4.54	6.80	4.21	4.40	4.39	4.24	5.89	5.49	4.65	5.80	5.00
K_2O	%	1.93	2.05	1.80	1.93	1.87	1.83	1.78	1.80	1.80	1.86	1.83	1.81
Co	p.p.m.	22	23	17	21	16	15	17	14	16	17	18	11
Cr	p.p.m.	63	62	54	62	71	61	84	59	64	89	92	60
Cu	p.p.m.	72	75	62	65	67	71	67	65	68	75	73	57
Ni	p.p.m.	94	92	68	75	65	68	69	58	63	59	60	53
Pb	p.p.m.	24	22	14	18	29	23	27	28	27	32	34	16
V	p.p.m.	110	120	130	140	130	120	130	120	120	120	130	110
Zn	p.p.m.	252	236	247	189	278	215	220	199	231	205	247	215
Sr	p.p.m.	299	294	231	241	315	268	278	289	263	263	263	231

		29-30/32 cm	MEAN	STD.	MAX	MIN
SiO_2	%	54.70	55.64	0.96	57.10	53.30
TiO_2	%	0.71	0.70	0.04	0.77	0.63
Al_2O_3	%	14.37	14.19	0.53	15.31	13.41
Fe_2O_3T	%	5.68	6.16	0.46	7.21	5.17
Mn	%	0.04	0.06	0.01	0.10	0.04
MnO	%	0.06	0.08	0.02	0.13	0.05
MgO	%	2.96	3.06	0.12	3.36	2.83
CaO	%	2.15	2.96	0.46	3.81	2.03
Na_2O	%	4.57	5.13	0.73	7.05	4.21
K_2O	%	1.95	1.87	0.08	2.05	1.71
Co	p.p.m.	12	17	2.69	23	11
Cr	p.p.m.	72	68	9.94	92	54
Cu	p.p.m.	58	66	5.05	75	57
Ni	p.p.m.	56	67	9.95	94	53
Pb	p.p.m.	16	25	8.02	55	14
V	p.p.m.	120	125	10.46	150	100
Zn	p.p.m.	294	227	42.25	368	173
Sr	p.p.m.	236	272	27.21	362	231

Table 13.4b. Interlaboratory comparison of 7 samples from Queen Charlotte Sound analysed by the University of Lille and the Geological Survey of Canada.

		08/10 cm	18/20 cm	108/110 cm	245/247 cm	278/280 cm	730/732 cm	770/772 cm
SiO_2	%	56.9	56.2	54.4	59.9	61.9	55	55.9
TiO_2	%	0.58	0.58	0.67	0.71	0.62	0.67	0.73
Al_2O_3	%	14.14	14.1	15.2	15.72	16.52	16.38	16.34
Fe_2O_3T	%	5.48	5.62	6.82	5.72	5.96	6.7	7.11
MnO	%	0.08	0.08	0.10	0.10	0.10	0.13	0.12
MgO	%	2.39	2.51	2.98	2.44	2.63	3.18	3.28
CaO	%	5.81	5.99	5.44	5.48	5.8	5.26	6.01
Na_2O	%	3.1	5.49	4.97	4.81	3.72	3.97	4.17
K_2O	%	1.33	1.47	1.51	1.39	1.43	1.62	1.79
Co	p.p.m.	11	11	18	13	14	19	18
Cr	p.p.m.	54	56	66	24	30	47	53
Cu	p.p.m.	20	20	21	14	18	27	27
Ni	p.p.m.	35	36	35	22	22	28	27
Pb	p.p.m.	27	27	25	23	23	27	27
V	p.p.m.	110	110	130	120	120	130	130
Zn	p.p.m.	132						
Sr	p.p.m.	463	463	463	537	547	489	515

		08/10 cm	18/20 cm	108/110 cm	245/247 cm	278/280 cm	730/732 cm	770/772 cm
SiO_2	%	56.5	56.2	56.1	59.8	59.4	56.7	56.4
TiO_2	%	0.67	0.67	0.74	0.75	0.71	0.78	0.77
Al_2O_3	%	13.3	13.3	14.2	14.8	15	15.1	15.5
Fe_2O_3T	%	5.5	5.52	6.29	5.82	5.74	6.67	6.94
Fe_2O_3	%				1.3	2	1.7	1.9
FeO	%				4.1	3.4	4.5	4.5
MnO	%	0.08	0.08	0.1	0.1	0.1	0.12	0.12
MgO	%	2.46	2.54	2.94	2.53	2.53	3.2	3.27
CaO	%	5.79	6.04	5.34	5.65	6.46	5.24	5.15
Na_2O	%	3.8	3.82	3.82	3.8	3.6	3.81	3.61
K_2O	%	1.52	1.45	1.6	1.42	1.46	1.85	1.83
LOI	%	8.8	8.7	6.9	3.5	3.4	4.7	4.8
CO_2T	%	6.5	6.3	3.7	1.6	1.1	1.6	1.6
P_2O_5	%	0.2	0.19	0.2	0.22	0.22	0.26	0.25
S	%	0.99	0.87	0.86	0.28	0.21	0.24	0.42
Ba	p.p.m.	430	420	480	490	520	590	610
Be	p.p.m.	1.1	1.1	1.1	1.1.	1.1	1.2	1.2
Co	p.p.m.	12	12	14	13	15	18	18
Cr	p.p.m.	52	53	54	48	47	47	45
Cu	p.p.m.	22	20	26	16	22	28	26
La	p.p.m.	12	12	11	16	14	12	12
Ni	p.p.m.	43	42	42	36	37	43	43
Pb	p.p.m.	16	20	21	19	16	16	16
V	p.p.m.	110	110	120	120	120	130	130
Yb	p.p.m.	1.2	1.2	1.3	1.4	1.4	1.3	1.3
Zn	p.p.m.	75	75	90	67	81	86	93
As	p.p.m.	6.7	5.1	4.3	3.6	3.1	3.3	4.3
Sr	p.p.m.	370	374	375	445	457	406	389

Table 13.4c. Geochemical data for samples from the northern Juan de Fuca Ridge.

Bulk Sediment

		42-cat.b	42-cat.g	13-0/12	13-25/3801-00/1231-00/2034-00/1528-10/24					41-00/0941-12/1415-00/1139-03/1521-00/05				
SiO_2	%	45.3	46	47.8	21.6	50.3	50.3	51.6	48.3	46.1	44.2	51.5	50.7	50.4
TiO_2	%	0.53	0.56	0.37	0.21	0.69	0.79	0.73	0.68	0.59	0.57	0.65	0.69	0.68
Al_2O_3	%	9.02	9.6	7.1	4.05	12.9	14.2	14.2	13.5	11.3	10.6	12.1	13.5	12.9
Fe_2O_3	%	11.7	11.7	12.2	35.4	6.82	6.47	7.21	6.29	6.88	6.31	6.16	7.01	6.88
Fe_2O_3	%	9.5	9.4			3.5	3.1	2	2.8	4.3	5.9	3.3	3	3.4
FeO	%	2	2.1			3	3	4.7	3.1	2.3	0.4	2.6	3.6	3.1
MnO	%	0.1	0.1	0.4	0.07	0.1	0.09	0.1	0.09	0.33	2.85	0.09	0.1	0.18
MgO	%	3.56	3.63	8.9	4.8	3.22	3.1	3.57	3.25	3.42	3.09	3.08	3.39	3.57
CaO	%	4.58	3.4	1.28	0.75	3.8	5.94	2.07	5.78	4.8	4.57	3.37	4.61	2.76
Na_2O	%	3.76	3.86	2.53	2.11	3.87	2.96	3.51	3.29	3.96	4.05	3.77	3.77	4.09
K_2O	%	1.96	2.06	1.23	0.85	2.06	2.26	2.19	2.07	1.98	1.87	2.08	1.99	2.12
LOI	%	16.4	15	12.8	22.1	12.8	10.9	11.6	12.9	16.3	18.1	15.1	12.5	13.9
CO_2T	%	6.2	5.2	3.9	3.6	5.4	5.7	4.6	6.9	6.3	6.7	6.9	5.9	5.6
P_2O_5	%	0.16	0.16	0.34	0.23	0.17	0.2	0.19	0.18	0.18	0.2	0.17	0.19	0.17
S	%	0.1	0.13	0.87	21.8	0.1	0.02	0.56	0.02	0.05	0.05	0.02	0.08	0.05
Ba	p.p.m.	2600	2400	17000	6500	2700	1100	4700	1500	4600	5200	2700	1500	2500
Be	p.p.m.	1.2	1.3	1.1	1.3	1.4	1.7	1.5	1.5	1.5	1.4	1.4	1.3	1.5
Co	p.p.m.	19	20	12	10	20	19	22	20	33	45	18	18	23
Cr	p.p.m.	72	76	52	16	65	64	78	70	64	47	65	71	72
Cu	p.p.m.	150	160	680	9800	80	43	100	59	130	140	56	56	74
La	p.p.m.	18	19	10	7	16	20	16	17	21	15	14	15	17
Ni	p.p.m.	160	160	62	72	160	78	190	120	280	320	150	120	170
Pb	p.p.m.	55	68	180	590	30	34	43	46	49	45	35	26	28
V	p.p.m.	160	210	140	250	150	130	150	150	150	110	120	140	150
Yb	p.p.m.	2	2	1	0	1.7	1.8	1.6	1.5	2.2	2.1	1.4	1.5	1.7
Zn	p.p.m.	200	220	1200	26000	250	120	220	190	360	320	200	160	240
As	p.p.m.	4	5	44.8	347.1	5.8	3	7.7	1.9	2.2	7.5	1.7	2	3.4
Sr	p.p.m.	254	220	484	274	279	271	299	300	327	368	254	267	235

Mud Fraction
(<63 um)

		42-cat.b	42-cat.g	13-0/12	13-25/2801-00/1231-00/2034-00/1528-10/24					41-00/0941-12/1415-00/1139-03/1521-00/05				
SiO_2	%		50.8	51.6	30.3	55.6	53.2	56.1	54.3	52.7	50.2	56.2	54.2	54.6
TiO_2	%		0.58	0.69	0.4	0.75	0.83	0.79	0.76	0.68	0.65	0.72	0.75	0.73
Al_2O_3	%		10.4	13	7.59	14	15.6	14.9	15	12.9	12.2	13.1	14.5	14.1
Fe_2O_3	%		13.3	11.2	29.6	7.36	7.69	7.72	7.07	7.96	7.32	6.71	7.75	7.61
Fe_2O_3	%		10.9			4	4	2.5	3.3	5.9	7.1	3.8	4.1	4.2
FeO	%	1.9	2.2			3	3.3	4.7	3.4	1.9	0.2	2.6	3.3	3.1
MnO	%		0.11	0.65	0.1	0.1	0.11	0.1	0.1	0.39	3.3	0.1	0.12	0.2
MgO	%		3.81	3.33	3.11	3.3	3.62	3.72	3.57	3.72	3.22	3.27	3.65	3.8
CaO	%		3.6	1.73	1.03	4.02	4.63	2.13	5.92	5.05	4.78	3.5	4.79	2.86
Na_2O	%		1.33	1.49	0.79	1.81	1.69	1.84	1.9	1.54	1.64	1.42	1.95	1.63
K_2O	%		1.8	1.76	0.97	1.9	2.58	2.25	2.43	2.16	1.97	1.98	2.12	2.22
LOI	%		12	11.5	17.7	9.7	9.4	9.8	9.6	11.3	13.9	11.4	10.4	11.4
CO_2T	%	7.2	5.8	5	5.5	5.3	5.3	4.8	6.4	6.7	6.9	7.3	6.5	7.3
P_2O_5	%		0.16	0.27	0.24	0.18	0.21	0.18	0.19	0.19	0.2	0.16	0.19	0.16
S	%	0.11	0.13	0.66	15.3	0.11	0.03	0.49	0.05	0.14	0.13	0.09	0.07	0.09
Ba	p.p.m		2600	5600	7200	3100	1100	4500	1500	4900	6800	3100	1700	3100
Be	p.p.m	1.4	1.4	1.6	2	1.5	1.9	1.7	1.7	1.6	1.6	1.6	1.5	1.6
Co	p.p.m		23	25	14	22	24	24	23	37	53	22	23	22
Cr	p.p.m		87	82	60	72	75	90	81	70	62	81	82	81
Cu	p.p.m		190	530	14000	170	60	190	110	160	890	71	88	71
La	p.p.m		23	23	19	18	24	20	21	25	23	20	18	20
Ni	p.p.m		190	170	88	160	95	170	120	290	370	170	130	170
Pb	p.p.m		100	160	840	150	43	95	50	47	220	36	37	36
V	p.p.m		180	150	360	130	130	150	140	140	120	120	140	120
Yb	p.p.m		2.5	2.1	1.1	2	2.1	2.1	2	2.6	2.6	1.9	1.9	1.9
Zn	p.p.m		290	1300	29000	280	150	280	200	420	630	260	190	260
As	p.p.m		4.7	25.9	113.4	1.5	3.6	6.3	7.6	2.8	1.9	1.7	2.5	2.5
Sr	p.p.m	315	275	389	414	332	285	342	360	384	447	306	323	278

Table 13.4c. (cont.)

Clay Fraction
(< 2 um)

		42-cat.b	42-cat.g	13-0/12	13-25/28	01-00/12	31-00/20	34-00/15	28-10/24	41-00/09	15-00/11	39-03/15	21-00/05
SiO_2	%	48.6		50.2	40.9	50	49.9	51.3	48.3	48.2	53	49.2	52.1
TiO_2	%	0.51		0.72	0.56	0.74	0.76	0.78	0.72	0.61	0.7	0.71	0.7
Al_2O_3	%	9.7		14.2	11.6	14.4	16.5	15.8	15.7	12.8	13.7	14.8	14.6
Fe_2O_3	%	13.2		10.4	18.8	8.73	8.23	8.87	8.2	8.21	7.96	9.12	8.8
Fe_2O_3	%	11.3		9.3	5.7	5.3	4.8	4.7	4.4	6	4.9	5.2	5.1
FeO	%	1.7		1	11.8	3.1	3.1	3.8	3.4	2	2.8	3.5	3.3
MnO	%	0.13		0.85	0.09	0.12	0.12	0.11	0.11	0.42	0.11	0.13	0.24
MgO	%	3.83		3.85	3.49	3.93	3.98	4.27	4.14	3.82	3.65	4.13	4.31
CaO	%	4.2		1.37	1.07	3.41	4.08	1.57	4.77	5.46	3.18	4.73	2.75
Na_2O	%	0.78		0.95	0.77	1	1.21	1.04	1.16	0.87	1.02	1.33	1.2
K_2O	%	1.75		2.03	1.59	1.91	2.56	2.12	2.28	1.79	1.77	1.96	2.02
LOI	%	16.4		14.4	16.2	13.7	11.9	13	13.1	15.3	15.2	13.9	14
CO_2T	%	8.1		6.5	8	6.7	5.4	6	7.3	7.9	8.7	7.9	7.3
P_2O_5	%	0.23		0.22	0.25	0.17	0.21	0.19	0.17	0.18	0.21	0.2	0.19
S	%			0.1		0.06	0.03	0.16	0.04	0.04	0.08	0.04	0.08
Ba	p.p.m	2800		3500	3500	2400	1200	2900	1500	4400	2800	1600	2300
Be	p.p.m			1.7		1.7	2.1	1.8	1.8			1.6	1.8
Co	p.p.m			28		26	27	27	28			25	30
Cr	p.p.m			95		81	85	84	93			86	81
Cu	p.p.m			400		240	76	220	160			120	120
La	p.p.m			22		19	24	19	21			18	21
Ni	p.p.m			170		180	110	180	150			150	190
Pb	p.p.m			170		160	39	110	50			46	41
V	p.p.m			160		160	140	180	160			160	150
Yb	p.p.m			2.2		2.3	2.2	2	2			2	2.2
Zn	p.p.m			530		370	170	350	250			230	340
As	p.p.m	2.1		18	102	2.2	3	3.9	2.2	1.2	1.8	2.1	2.3
Sr	p.p.m			299		273	272	238	315			290	239

Washed Bulk Sediment

		31-00/20	34-00/15	28-10/24	28-10/24
SiO_2	%	52.2	54.6	51.7	51.9
TiO_2	%	0.82	0.77	0.72	0.73
Al_2O_3	%	14.6	14.7	14.1	14.3
Fe_2O_3	%	6.75	7.55	6.7	6.74
Fe_2O_3	%	3.4	2.3	2.9	3.1
FeO	%	3	4.7	3.4	3.3
MnO	%	0.09	0.1	0.09	0.09
MgO	%	3.11	3.62	3.29	3.36
CaO	%	6.14	2.07	5.81	5.97
Na_2O	%	1.84	1.85	2.04	2.02
K_2O	%	2.32	2.05	2.09	2.1
LOI	%	10.1	9.9	11.4	11.4
CO_2T	%	5.8	4.7	7	7.1
P_2O_5	%	0.18	0.19	0.18	0.18
S	%	0.04	0.55	0.07	0.01
Ba	p.p.m.	1000	4800	1700	1600
Be	p.p.m.	1.8	1.6	1.5	1.5
Co	p.p.m.	21	24	19	18
Cr	p.p.m.	71	81	69	72
Cu	p.p.m.	51	120	59	59
La	p.p.m.	25	21	17	16
Ni	p.p.m.	82	200	120	120
Pb	p.p.m.	34	43	35	32
V	p.p.m.	130	150	150	150
Yb	p.p.m.	2.1	2.1	1.5	1.5
Zn	p.p.m.	120	240	160	160
As	p.p.m.	2.5	6.6	1.8	1.9
Sr	p.p.m.	327	356	301	302

Sand Fraction

		13-0/12	13-25/28
SiO_2	%	50.9	15.3
TiO_2	%	0.03	0.04
Al_2O_3	%	1.13	1.08
Fe_2O_3	%	12.9	44.3
Fe_2O_3	%		
FeO	%		
MnO	%	0.13	0.08
MgO	%	16.6	6.13
CaO	%	0.82	0.45
Na_2O	%	0.04	0.01
K_2O	%	0.18	0.16
LOI	%	9.3	24.2
CO_2T	%	2.9	2.1
P_2O_5	%	0.43	0.26
S	%	2.19	31.5
Ba	p.p.m.	37000	11000
Be	p.p.m.	0.7	0.8
Co	p.p.m.	5	10
Cr	p.p.m.	30	0
Cu	p.p.m.	890	7400
La	p.p.m.	5	6
Ni	p.p.m.	25	76
Pb	p.p.m.	140	430
V	p.p.m.	110	160
Yb	p.p.m.	0.6	0
Zn	p.p.m.	1500	26000
As	p.p.m.	57	447.7
Sr	p.p.m.	769	339

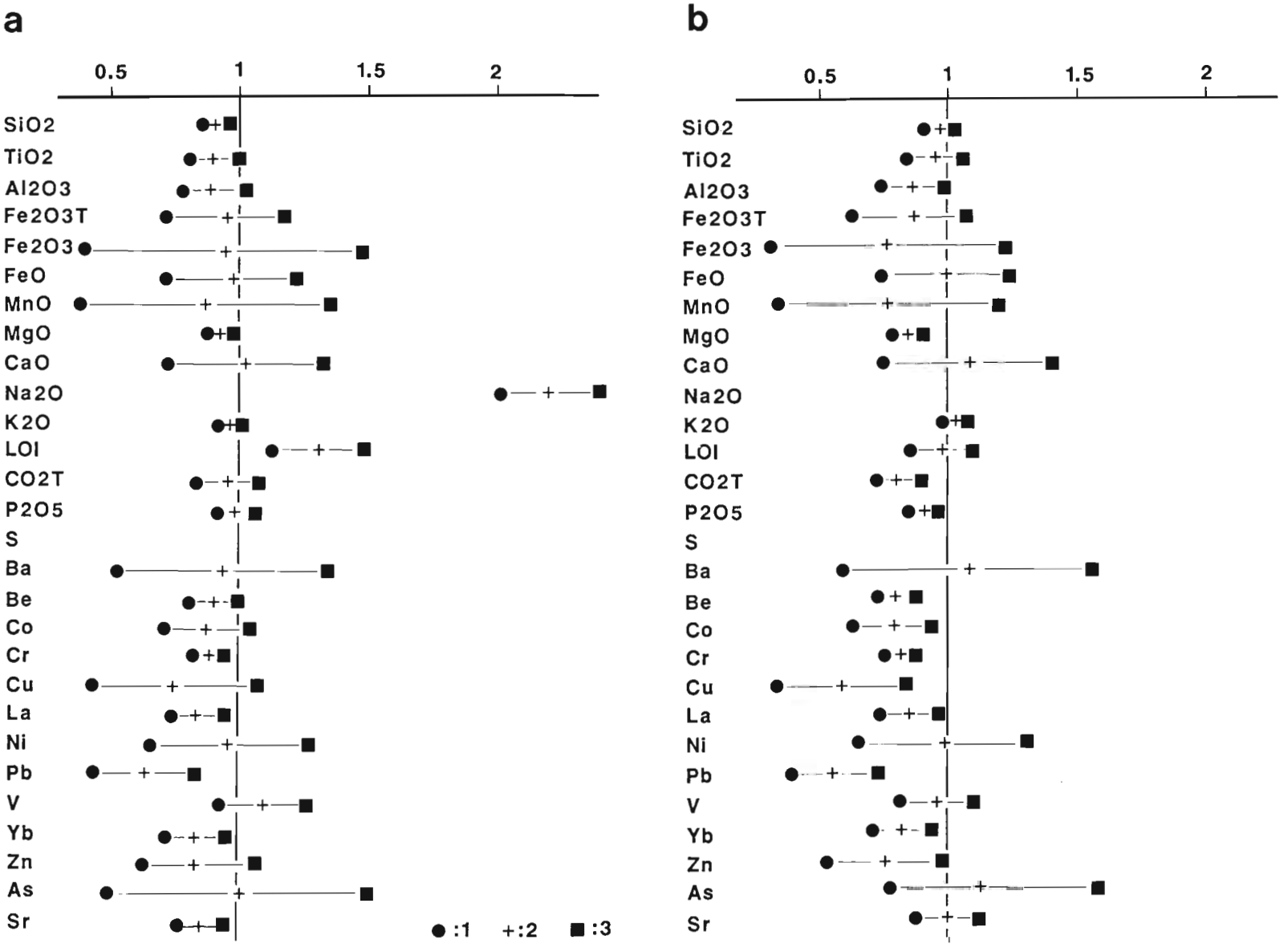


Figure 13.2. Comparison of mud, clay and bulk sediment geochemistry. The values comprise all the analyses for each fraction except those from core 13 and 41-12/14 cm; (1) mean-standard deviation/mean. (2) mean/mean; (3) mean + standard deviation/mean. (a) ratio of bulk sediment to mud fraction; (b) ratio of bulk sediment to clay fraction.

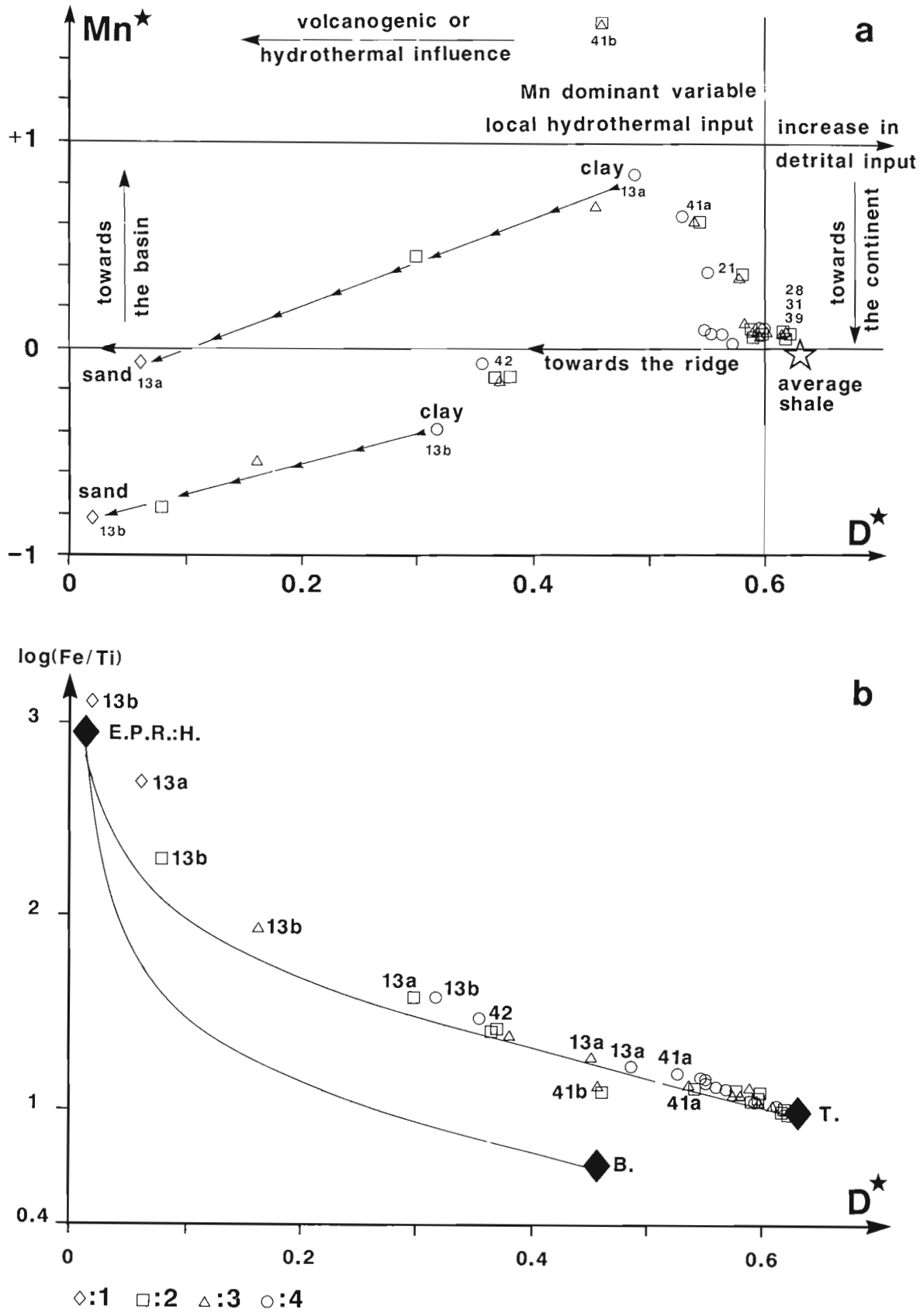


Figure 13.3. (a) Mn* versus D* plot (see text) for northern Juan de Fuca Ridge sediments (after Debrabant and Foulon, 1979); (b) log (Fe/Ti) versus D* plot (see text) for northern Juan de Fuca Ridge sediments (after Bostrom. 1973); (1): sand fraction; (2): bulk sediment; (3): mud fraction ((4): clay fraction (<2 um).

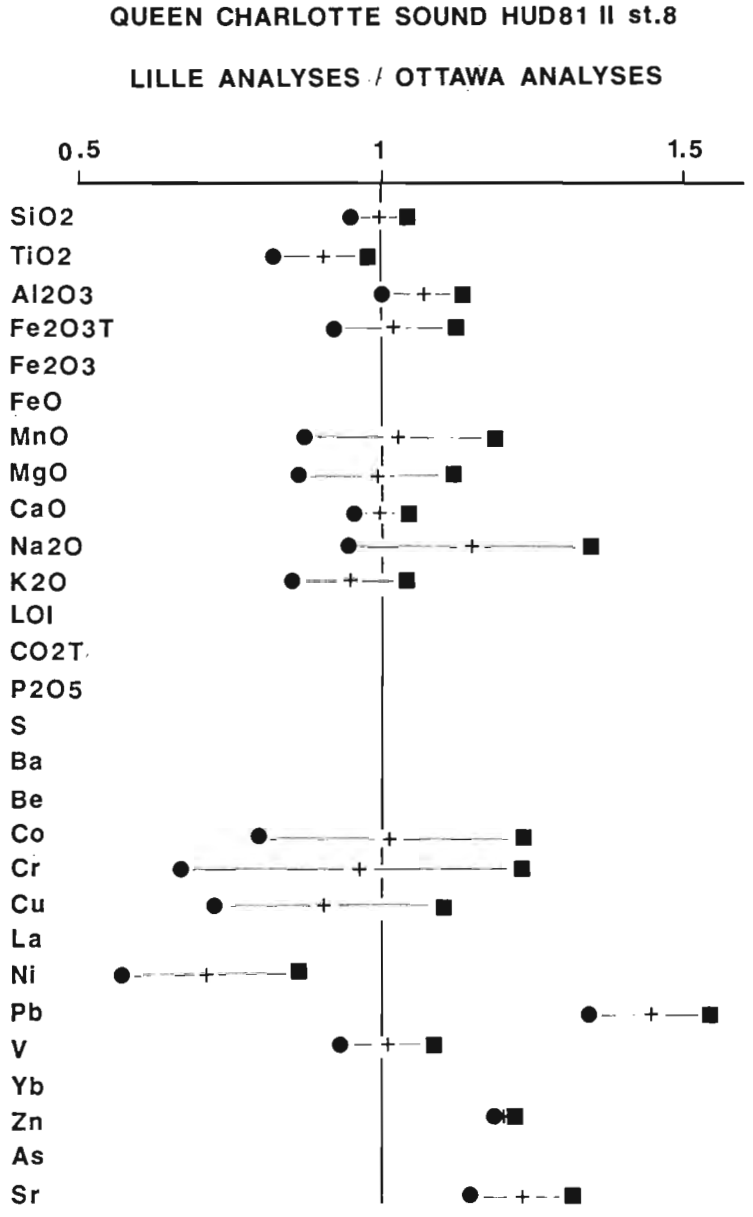


Figure 13.4. Interlaboratory comparison for 7 samples from Queen Charlotte Sound. (Core Hud 81 II st.8; (*see* legend Fig. 13.2).

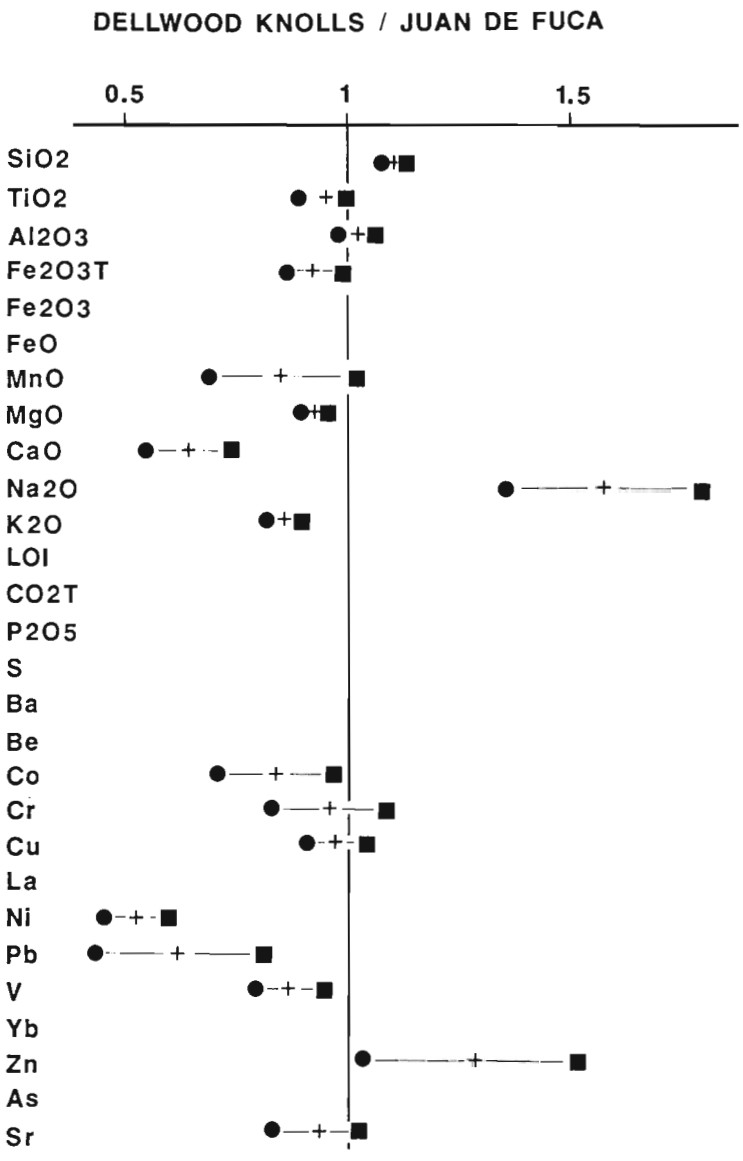


Figure 13.5. Comparison of Dellwood Knolls sediment analyses and those from the northern Juan de Fuca Ridge (*see* legend Fig. 13.2).

fractions of core 13 have the highest hydrothermal influence while sample 41B shows a greater hydrogenous influence than hydrothermal. On the diagram log (Fe/Ti) versus D*, the same trend is evident with all the points falling on a mixing curve between terrigenous (T.) and hydrothermal (H.) end-members (after Bostrom, 1973). On the two plots, except for core 13, the coarse fractions are always closer to T. and the finer to H.; the inverse is true for core 13. To confirm the terrigenous origin of the sediment in core 28, 31 and 39 a comparison was made with analyses from the Dellwood Knolls area (Fig 13.1; Table 13.4). In fact, to compare the analyses an interlaboratory comparison was necessary to understand the source of the variation. This was done on 7 analyses from Queen Charlotte Sound (Fig 13.1), both analyzed at the University of Lille (France), Laboratoire de Dynamique Sedimentaire et Structurale and at the Geological Survey of Canada (Ottawa), Mineralogy and Chemistry Subdivision, Economic Geology and Mineralogy division. Figure 13.4 shows an underestimate for Na_2O, Pb and Sr and an overestimate for Ni relative to Lille results. These differences are small though, and thus the two sets of data appear comparable.

Using the same kind of diagram, Dellwood Knolls and Juan de Fuca analyses are compared (Fig. 13.5). Only CaO, Pb and Zn concentrations change if we remove the laboratory variations. CaO, Pb and Ni increase and Zn decreases near the Juan de Fuca Ridge relative to the Dellwood Knolls area. In this case samples 8, 31 and 39 show evidence of a strong terrigenous influence; other calculations and comparisons will be made on this basis. Figure 13.6 shows variations between anomalous sediments and the hemipelagic sediment from cores 28, 31 and 39. In bulk sediments, the hydrothermal system is represented by black sulphides rich in S, As, Cu, Ba, Zn, Pb, MgO, Fe_2O_3(T),P_2O_5, V and Sr, and poor in CaO, Cr, TiO_2, Al_2O_3 La, K_2O, Co, CO_2(T), Na_2O, Ni and MnO compared to hemipelagic sediments. Brown mud 13a overlying the black sulphides shows an increase in MnO. Brown mud 41b shows a low content of FeO and very high concentration of MnO and lesser concentrations of Ba, As, Ni, Cu, Co, Zn, Fe_2O_3, Pb, Yb and Sr. For other samples, 42 (green granular mud), 41a and cores 15, 21, 01 and 34, the differences are smaller but still significant for S, As, Ba, Zn, Ni, Co, MnO, Cu, Pb and Fe. For the mud and clay fraction geochemical trends parallel those of the coarser fraction. Only As and S in the clay-size fraction and, in the mud fraction, sometimes As, appear to be associated with FeO, and do not follow the above trends.

DISCUSSION

Comparison of sand and clay fractions from this study and those of sediments from the Dellwood Knolls area shows a high input of terrigenous material (Blaise et al., 1985) on the northern Juan de Fuca Ridge except for the sulphide core and the green granular muds.

Hydrothermal systems are in general enriched in Mn, Fe, Zn, Cu, As, Cr, V, P and B (Marchig et al., 1986). Ba, S, Ni and Co occur in high concentrations near hydrothermal vents due either to enrichment in hydrothermal fluids (e.g. Adshead et al., 1986) or to diagenetic alteration effects (e.g. Marchig et al., 1986). High MnO content could also be the result of diagenetic processes (Campbell, 1985). Arsenic seems to be more correlated with hydrothermal deposits than diagenetic effects (Marchig et al., 1982). In Middle Valley, the sulphides show significant interaction with underlying sediments compared to sulphide deposits occurring directly on basalts in other ridge areas (Davis et al., in press).

The hemipelagic sediments, although mostly of terrigenous origin could also show some of these other influences. To determine these, mixing curves of Figure 13.3 have been constructed with end-member analyses exclusively from the northern Juan de Fuca area: (a) from cores 28, 31 and 39 for T.; (b) from sand of sample 13B for H.; (c) and from 25 basalt glass microprobe analyses from core 42 (Blaise, unpublished data). Relative percentages of each end-member were estimated from the curve H. - T. and H - B. (Fig. 13.7). The black sulphide sand is of 100% hydrothermal origin, 75% for the bulk sample, 55% for the mud and 30% for the clay size fraction. The brown mud overlying the black sulphide is composed of 85, 30, 12 and 10% hydrothermal material for sand, bulk sediment, mud and clay fraction, respectively. Samples 42 and 41b also show hydrothermal influences although somewhat different. Hydrothermal input for the other samples is less than 8% but is higher in the finer fraction.

Ba, S, As are commonly associated with hydrothermal input; they represent direct or secondary hydrothermal effects. In all of the samples with high terrigenous content, these elements are associated with Co and Ni. In samples with a low As content, a diagenetic influence is certainly involved; arsenic has a relationship to FeO that could result from a pyrite-arsenic association due to diagenetic mobilization (Belzile and Lebel, 1986). In sample 41b, As content is not low (three times the hemipelagic content) but MnO, Ni and Co are very high. On a Fe-Mn-Al diagram (not shown), these sediments are close to Bauer Deep sediments. They are certainly metalliferous with an early hydrothermal source. The location of this core, on the western side of the Endeavour segment, could explain the lack of terrigenous supply and account for these metalliferous sediments. Stratigraphic studies could resolve whether such sediments are a result of significant concentration due to slow sedimentation (hydrogenous) or due to rapid deposition from a nearby hydrothermal source.

Core PAR 85-42 contains the only clear authigenic clay in the area (Blaise and Bornhold, in press). The iron-rich smectite is a new mineral with a rosette-shape (S.E.M. study) of hydrothermal and basaltic and/or biogenic silica origin (op. cit.).

Sediments from cores 01, 15, 21, 34 and 41a show a low but identifiable hydrothermal input (primary or secondary). They are from different locations around Middle Valley including a very high heat flow station (PAR 85-34, Davis et al., in press). From the sulphide mound, cores 28 and 31 show no

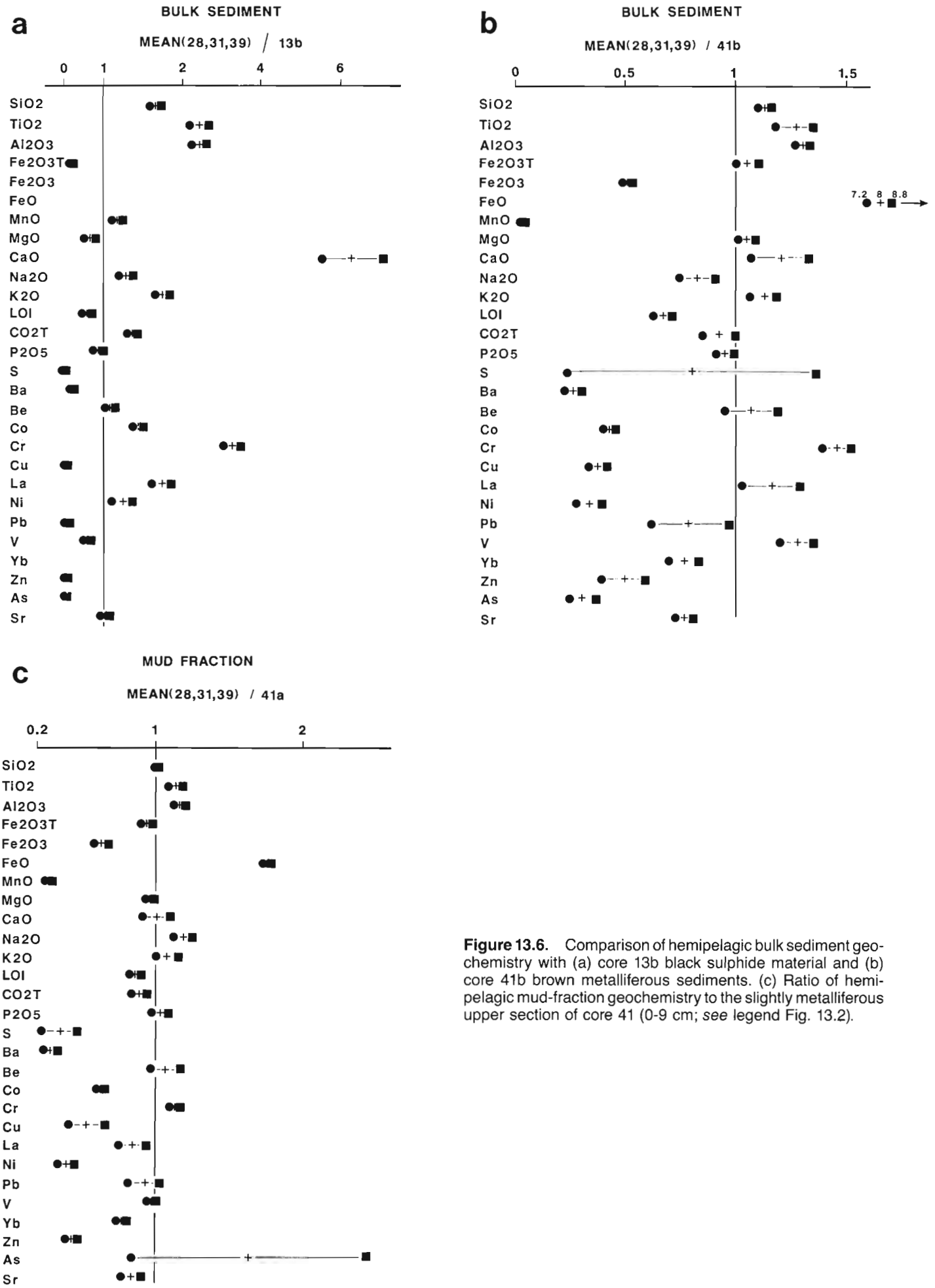


Figure 13.6. Comparison of hemipelagic bulk sediment geochemistry with (a) core 13b black sulphide material and (b) core 41b brown metalliferous sediments. (c) Ratio of hemipelagic mud-fraction geochemistry to the slightly metalliferous upper section of core 41 (0-9 cm; *see* legend Fig. 13.2).

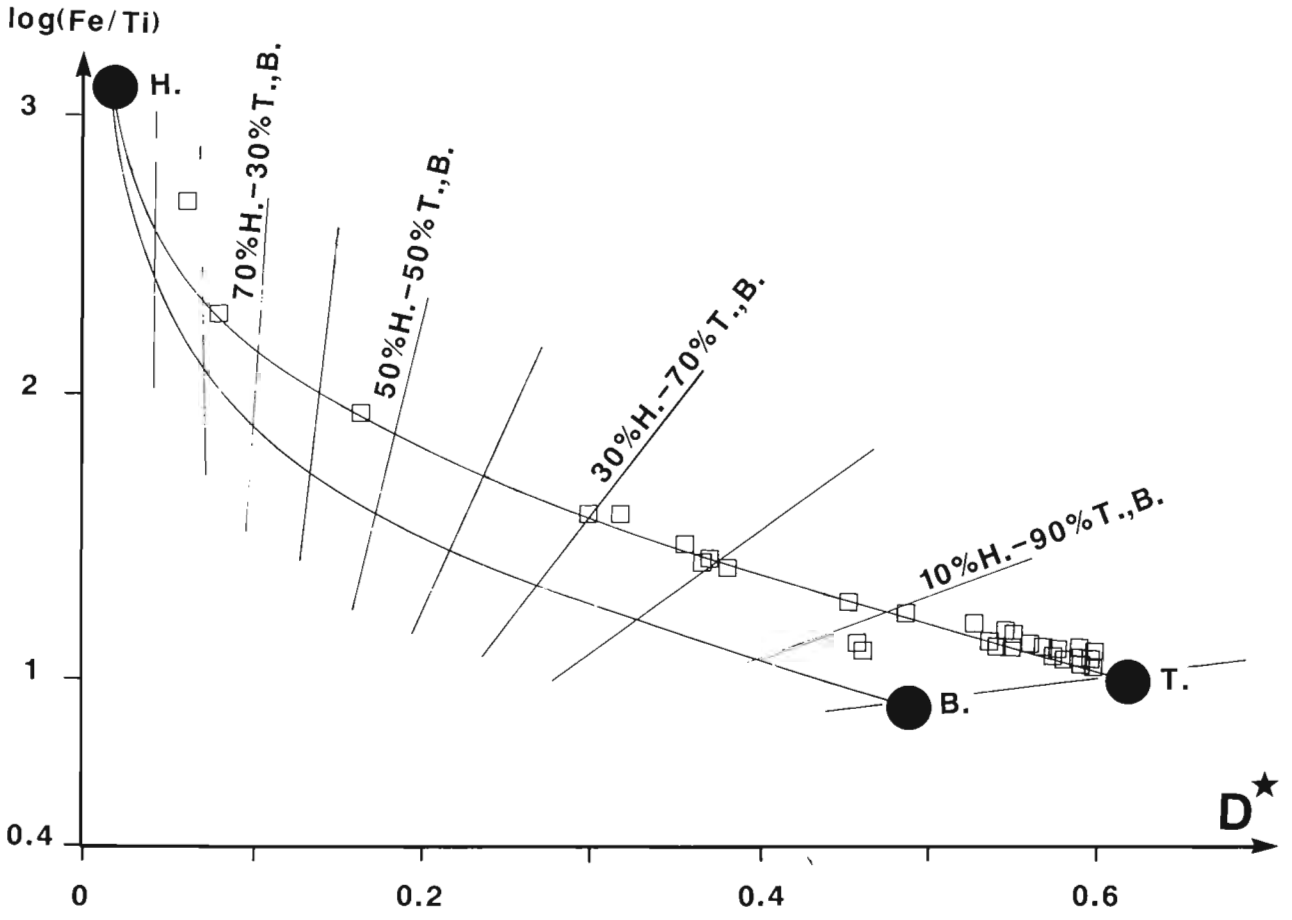


Figure 13.7. Theoretical mixing curve for hydrothermal, terrigenous and basaltic end-members on the northern Juan de Fuca Ridge. T – terrigenous; B – volcanic glass; H – hydrothermal. Data from Figure 13.3b. (after Boström, 1973).

evidence of hydrothermal influence. Thus the geographic impact of the hydrothermal system was very localized and/or the terrigenous sedimentation was extremely high. The other cores with a slight hydrothermal input, are probably located very close to hydrothermal vents or alternatively the rates of sedimentation during the late Quaternary have changed significantly.

CONCLUSIONS

Based on different sediment types from the northern part of the Juan de Fuca Ridge, mixing curves were constructed to determine the relative contributions of hydrothermal and terrigenous sources to a sediment. The association S, Cu, Zn, As, Pb, Fe_2O_3, T, Ba, V and MgO appear to be related to a primary hydrothermal system, whereas S, Cu, Zn, As and Ba, associated with MnO, Ni and Co indicate the influence of diagenetic processes.

This study also shows clearly the relationship between sediment texture and minor and trace element abundances in hydrothermal sediments and normal hemipelagic sediments. A strong hydrothermal influence is associated with coarser sediments whereas in normal hemipelagic sediments higher minor and trace elements occur in finer sediments.

ACKNOWLEDGMENTS

We especially thank the Captain and the Crew of the *C.S.S. PARIZEAU* for their help and cooperation. We thank T. Forbes, K. Conway and R. Smith for laboratory assistance, G. Le Cheminant for the X-ray data, G. Lachance and P. Belanger for the geochemistry.

REFERENCES

Adshead, J.D., Bornhold B.D. and Davis E.E.
1986: Indurated deposits and possible plume bands in a hydrothermal mound, northeast Pacific; in Current Research, Part A, Geological Survey of Canada, Paper 86-1A, p. 737-748.

Belzile, N. and Lebel J.
1986: Capture of arsenic by pyrite in near-shore marine sediments; Chemical Geology, v. 54, p. 279-281.

Blaise, B.
1985: Sédimentation et paléoenvironnements plio-quaternaires sur la bordure Nord-Est de l'Océan Pacifique; Université des Sciences et techniques de Lille, France; Thèse 3 eme Cycle, 227 p.

Blaise, B. and Bornhold, B.C.
Different sources for iron-rich smectite; EOS Transactions, American Geophysical Union. (in press)

Blaise, B. Bornhold, B.D., Maillot, H., and Chamley, H.
1985: Observations sur les environnements recents au Nord de la dorsale de Juan de Fuca (Pacifique Nord-Est); Revue de Géologie Dynamique et de Geographie Physique, v 26, p. 201-213.

Boström, K.
1973: The origin and fate of ferromanganoan active ridge sediments; Stockholm Contributions in Geology, v. 27, p. 149-243.

Campbell, A.C.
1985: Sediment geochemistry in the Guaymas Basin geothermal system; in Genesis of Stratiform Sediment-hosted Pb-Zn Deposits, M. Cinandi and B. Turner, (ed.). Stanford, U.S.A., p. 26-28.

Canadian American Seamount Expedition
1985: Hydrothermal vents on an axis seamount of the Juan de Fuca Ridge; Nature, v. 313, p. 212-214.

Currie, R.G., Davis, E.E., Riddihough, R.P. and Sawyer, B.S.
1985: Juan de Fuca Ridge Atlas: Preliminary Seabeam Bathymetry; Geological Survey of Canada, Open File 1143.

Davis, E.E., Currie, R.G., Sawyer, B., and Riddihough, R.
1985: Juan de Fuca Ridge Atlas: Seamarc II Acoustic image mosaic (Wilson and Dellwood Knolls); Geological Survey of Canada, Open File 1144.

Davis, E.E., Goodfellow, W.D., Bornhold, B.D., Adshead, J., Blaise, B., Villinger, H. and Le Cheminant, G.M.
Massive sulfides in a sedimented rift valley, northern Juan de Fuca Ridge; Earth and Planetary Science Letters. (in press)

Debrabant, P. and Foulon, J.
1979: Expression géochimique des variations du paléoenvironnement depuis le Jurassique Supérieur sur les marges Nord-Atlantiques; Oceanologica Acta, v. 2, p. 469-476.

Kadko, D., Koski, R., Tatsumoto, M. and Bouse, R.
1985: An estimate of hydrothermal fluid residence times and vent chimney growth rates based on 210 Pb/Pb ratios and mineralogic studies of sulfides dredged from the Juan de Fuca Ridge; Earth and Planetary Sciences Letters; v. 76, p. 35-44.

Marchig, V., Gundlach, H., Moller, P., and Schley, F.
1982: Some geochemical indicators for discrimination between diagenetic and hydrothermal metalliferous sediments; Marine Geology, v. 50, p. 241-256.

Marchig, V., Erzinger, J., and Heinze, P.M.
1986: Sediment in the black smoker area of the East Pacific Rise (18.5oS); Earth and Planetary Sciences Letters, v. 79; p. 93-106.

Normark, R.W., Morton, J.L., Randolph, A.K., and Clague, D.A.
1983: Active hydrothermal vents and sulfide deposits on the southern Juan de Fuca Ridge; Geology, v. 11, p. 158-163.

- 14 -

Hazelton-Bowser Lake Group stratigraphy and structure in the vicinity of the Silbak Premier Mine, northwestern British Columbia

Project 840046

Derek A. Brown[1]
Cordilleran and Pacific Margin Division,
Vancouver

Brown, D.A., Hazelton-Bowser Lake Group stratigraphy and structure in the vicinity of the Silbak Premier Mine, northwestern British Columbia; in Current Research, Part A, Geological Survey of Canada, Paper 87-1A, p. 143-151, 1987.

Abstract

Silbak Premier, a major past gold-silver producer, occurs within Lower Jurassic Hazelton Group calc-alkaline volcanics and cogenetic porphyry intrusions. Minor limestone and thinly bedded siliceous sediment overlie the volcanics and mark the end of volcanism and marine transgression during the Toarcian. Unmetamorphosed Bowser Lake Group argillite, siltstone and shale cap the sequence. Hazelton Group volcanics and Bowser Lake Group sediments exhibit fabrics produced from at least two phases of pre-Cenozoic deformation. A significant detachment surface at the Hazelton-Bowser Lake Group contact separates distinct structural styles. Tertiary transtensional features include brittle faulting and Eocene extensional dyke swarms.

Résumé

Silbak Premier, ancien important producteur d'or et d'argent, se trouve dans des roches volcaniques calcaro-alcalines et dans des intrusions porphyriques cogénétiques du groupe de Hazelton du Jurassique inférieur. Un calcaire secondaire et des sédiments siliceux finement lités recouvrent les roches volcaniques et marquent la fin du volcanisme et de la transgression marine au Toarcien. De l'argilite, du siltstone et des argiles litées du groupe de Bowser Lake, non métamorphiques, recouvrent cette séquence. Des roches volcaniques du groupe de Hazelton et des sédiments du groupe de Bowser Lake montrent des textures produites par au moins deux phases de déformation pré-cénozoïques. Une surface importante de décollement au contact du groupe de Hazelton et du groupe de Bowser Lake sépare des styles structuraux distincts. Parmi les éléments de transtension du Tertiaire, on note la présence de failles fragiles et de systèmes de dykes d'extension de l'Éocène.

[1]Department of Geological Sciences, University of British Columbia, Vancouver, B.C. V6T 2B4

INTRODUCTION

Silbak Premier, historically British Columbia's second largest total gold producer after Bralorne, is 22 km north of Stewart, British Columbia (NTS 104B/1, 104A/4). Mineralization is hosted in Late Triassic to Early Jurassic Hazelton Group calc-alkaline volcanics and cogenetic intrusions.

Stratigraphy and structure of a 60 km2 area extending south from Long Lake to Silbak Premier (Fig. 14.1) was mapped during August, 1984 and June to August, 1985. Those data and previous work were compiled at map scales of 1:5000, 1:2500 and 1:500, as part of a M.Sc. thesis currently underway at the University of British Columbia, supervised by R.L. Armstrong, R.G. Anderson and P.J. Wojdak.

STRATIGRAPHY

The Hazelton Group stratigraphic succession (Figs. 14.2 and 14.3) comprises a thick accumulation of greenschist-grade meta-andesite, tuff and breccia overlain by alternating green and maroon volcaniclastics. Meta-andesite is intruded by dacitic porphyry intrusions which are overlain by more differentiated felsic to rhyolitic breccia and welded tuff. The felsic rocks mark the cessation of volcanism; limestone and/or siliceous (cherty), thinly bedded sediment deposition followed. Finely laminated, unmetamorphosed argillite, siltstone and shale of the Bowser Lake Group cap the sequence and indicate marine transgression in the Late Jurassic.

HAZELTON GROUP

Unit 1: Meta-andesite, tuff and breccia

Meta-andesite, tuff and breccia of Unit 1 outcrop along the Granduc road at Silbak Premier (Fig. 14.2) and is at least 1000 m thick.

Most of the green to dark green weathering andesite is fine grained, massive and monotonous greenstone. Local fragmental lithologies include tuff, lapilli tuff and monolithic breccia which indicate the unit's extrusive origin. Angular fragments (up to 50 cm long) are the same composition as the matrix.

Preliminary zircon U-Pb isotopic age determinations obtained by the author, with the guidance and assistance of P. van der Heyden, indicate a Late Triassic age (about 210 Ma) for the andesite.

Within the andesite is a sedimentary member of intensely folded and fractured argillite, siltstone and minor quartz sandstone exposed 1250 m south of the Westmin camp and also along the Granduc road northwest of Indian Mine (Fig. 14.2) (P. McQuigan, personal communication, Sept. 1985).

Unit 2: Green and maroon dacitic volcaniclastics

Dacitic volcaniclastics of Unit 2 outcrop from Mount Dilworth outh through Silver Lakes, on west side of Slate Mountain, above Silbak Premier and along Bear River Ridge. Massive volcaniclastics overly Unit 1 with local unconformity indicated by boulder conglomerate; elsewhere, the contact is obscure. Total thickness of the volcaniclastics is less than 1750 m.

The dacitic volcaniclastics weather pale green, maroon and purple. Lithologies include varieties of ash tuff to coarse volcanic breccia and conglomerate. Fragments are predominantly feldspar porphyry similar to Unit 6 with minor andesite and fine grained volcanic material.

Unit 3: Black tuff

Outcrops of Unit 3 extend from the south end of Mount Dilworth to the southern edge of Slate Mountain, the unit is up to 200 m thick and is assumed to be conformable with Unit 2. Black to dark grey weathering, massive crystal-lithic

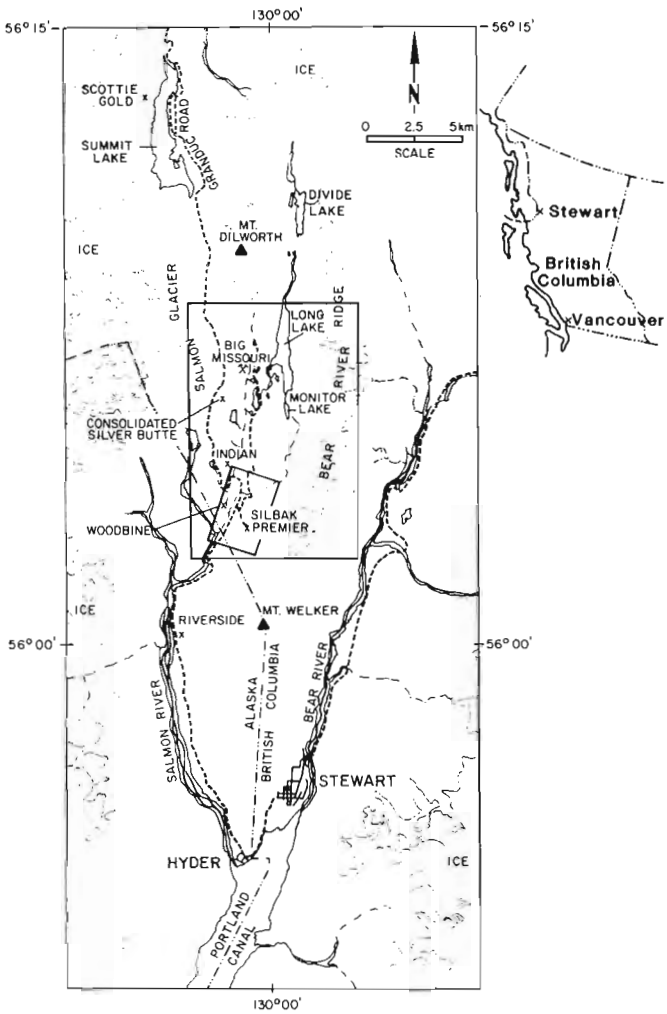


Figure 14.1. Location map for regional mapping and compilation (large rectangle), and detailed study area (inclined rectangle) and abandoned mines and mineral deposits.

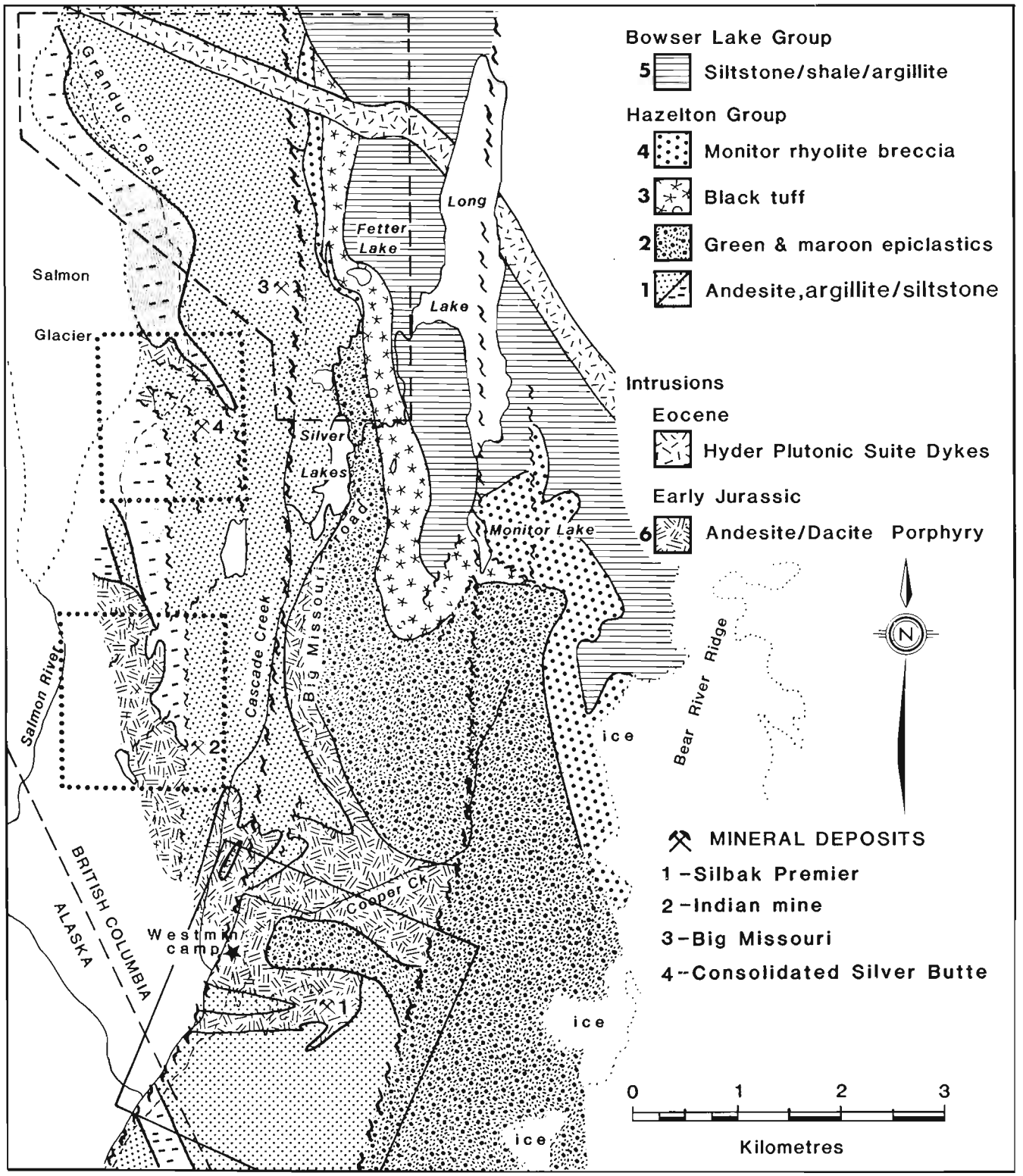


Figure 14.2. Regional geology with inclined rectangle indicating detailed study area. Numbers beside rock units refer to units described in text. Dashed and dotted outlined areas are compiled from Westmin Resources Ltd. and Esso Minerals Canada respectively.

tuff and lapilli tuff are characteristic. Predominant biotite and white plagioclase phyric fragments are set in a black carbonaceous matrix. Lithic fragments include aphanitic, dark grey volcanic material.

Unit 4: Monitor Lake/Mount Dilworth rhyolite breccia

Unit 4 is a regionally extensive siliceous volcaniclastic marker horizon well exposed at Monitor Lake and Mount Dilworth. It attains a maximum thickness of 200 m at Monitor Lake. Contact with Unit 3 is believed to be conformable. The unit consists of rhyolitic tuff, welded tuff and breccia with silicic to felsic angular fragments up to 25 cm long. At Monitor Lake are rare accidental subrounded limestone fragments. Exposures on the south end of Fetter Lake on Big Missouri claims have well preserved fiamme. The Monitor Lake outcrops weather pale grey to buff. Farther south, rhyolite is pale waxy green with irregular maroon to red (hematitic) patches.

On Mount Dilworth rhyolite breccia contains fragments of limestone and is overlain by fossiliferous (belemnite- and *Welya*-bearing) buff limestone which is regionally correlated with other mid-Toarcian localities.

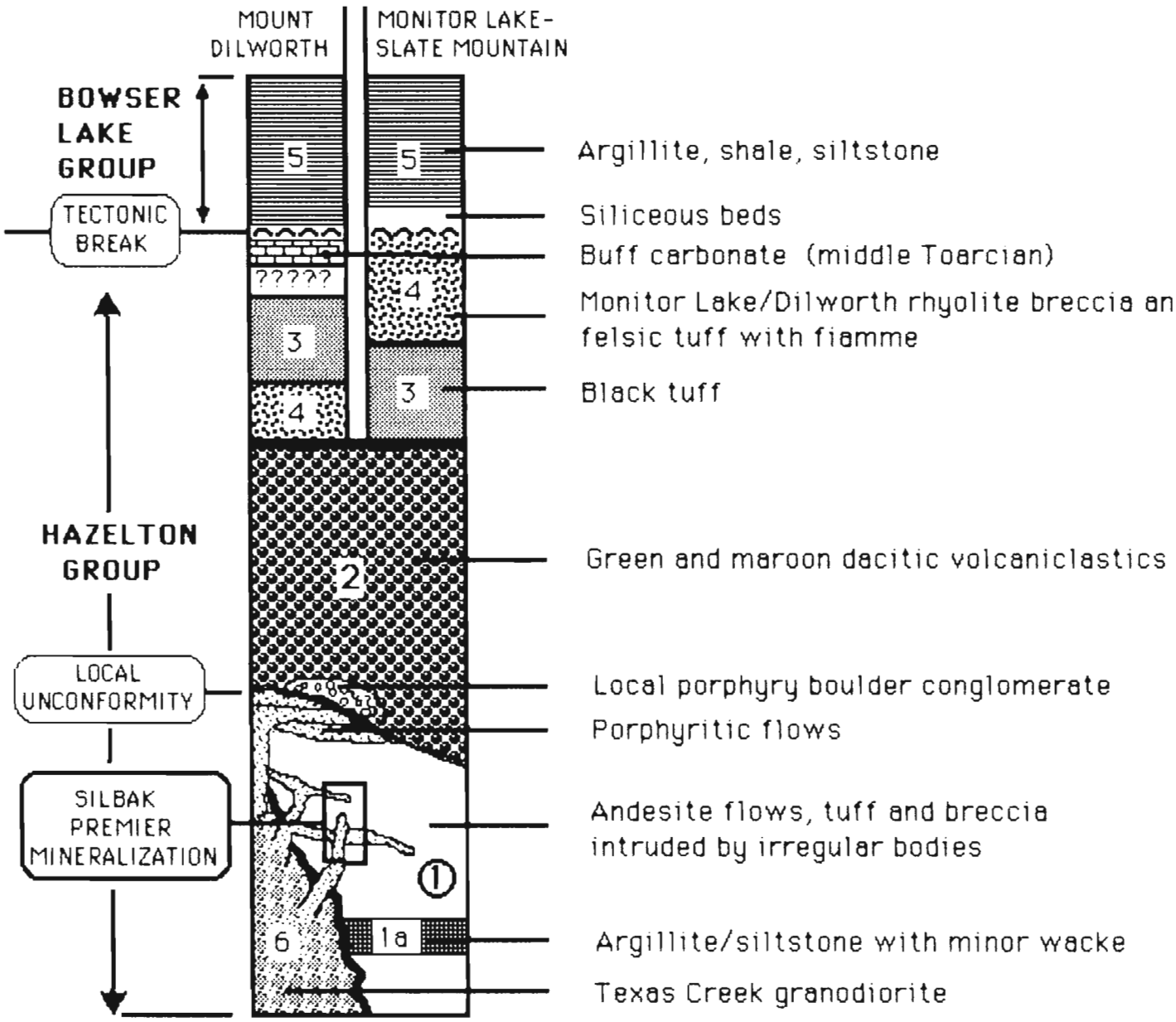


Figure 14.3. Schematic stratigraphy of Silbak Premier-Slate Mountain area, partly based on Alldrick (1985).

BOWSER LAKE GROUP

Unit 5: Argillite, shale and siltstone

Argillite, shale and siltstone of Unit 5 underlie the shore of Long Lake, Slate Mountain and Mount Dilworth. At Mount Dilworth, Units 3 and 5 are separated by a bedding plane fault which dips steeply to the east. Southeast of Monitor Lake Bowser Lake Group bedding is subparallel to rhyolite tuff of Unit 4, but the contact is a fault. On Slate Mountain Unit 4 is absent and there is a marked structural discordance between Unit 3 black tuff and nit 5 sedimentary rocks.

The unit weathers from light to dark grey. Siltstone is well bedded and characterized by fine laminations whereas shale is massive or intensely cleaved. Siltstone contains rare chert pebbles. Rare limy beds, centimetre-scale buff carbonate concretions in shale, and dismembered, brown iron-carbonate pods in siltstone are characteristic.

Well-bedded siliceous (cherty) rocks outcrop at the base of the Bowser Lake Group in the "Monitor Lake-Slate Mountain" stratigraphic section. They form alternating light (siliceous) and dark grey (argillaceous) layers. In thin sections of siliceous beds, spherical outlines less than 0.1 mm in diameter are interpreted to be relict radiolaria. Elsewhere thin cracks in siliceous beds are believed to be pipe vesicles as proposed by Grove (1971). They are concentrated in the upper portion of beds but do not cross beds. These pipe vesicles suggest the siliceous beds correlate with the Monitor rhyolite breccia rather than the Bowser Lake Group.

INTRUSIONS

Unit 6: Dacitic feldspar porphyry

Dacitic feldspar porphyry, abundant at Silbak Premier between 6- and 110-level (250 and 640 m elevation ASL), intrudes Unit 1 but not Unit 2.

The porphyry weathers shades of green except adjacent to mineralization where it is commonly bleached grey, or locally maroon at higher structural levels. The porphyritic rocks vary from tabular bodies to irregular lenses. They intrude Unit 1 below 2-level at Silbak Premier, but at structurally higher levels they may be extrusive (Fig. 14.2 and 14.3).

Three varieties of porphyry are distinguished at 1:2500 scale mapping: (1) potassium feldspar porphyry ("Premier porphyry"), (2) hornblende-plagioclase porphyry, and (3) maroon porphyry, possibly an extrusive equivalent of (1).

The term "Premier porphyry" has been used historically for a potassium feldspar-quartz-hornblende-plagioclase porphyry spatially associated with mineralization at Silbak Premier but its use has been inconsistent. Schofield and Hanson (1922) used "Premier sills" synonymously for "Premier porphyry" because of the porphyry's sill-like character. Inconsistent use of the term "Premier porphyry" derives from the rock's wide textural and compositional variability. The abundance of potassium feldspar phenocrysts can change abruptly from nil to several percent. Feldspar alteration is also variable. Locally, potassium feldspar phenocrysts are fresh and prominent but elsewhere both potassium feldspar and plagioclase are replaced by carbonate and ericite which obscure them in altered rocks. "Premier porphyry" is not unique to the mine area; similar porphyry occurs regionally. More confusion arises when the name "Premier dykes" (Grove, 1971) is used. These dykes are part of the Eocene Hyder plutonic suite which crosscut "Premier porphyry" (*sensu stricto*). Therefore potassium feldspar porphyry (or K-feldspar porphyry) will be used herein for "Premier porphyry".

The K-feldspar porphyry contains phenocrysts of K-feldspar (0.1-10%), quartz (<5%), hornblende (2-8%) and plagioclase (25-35%) in a fine-grained, altered groundmass. Megacrysts of K-feldspar (<5 cm long) are variably altered to carbonate and/or sericite and commonly weather out leaving euhedral pits.

Quartz is equant, commonly resorbed and unstrained in thin section. Prismatic hornblende averages 3 mm long and is up to 6 mm long. In thin section hornblende is completely altered to chlorite ± pyrite ± leucoxene (?). Plagioclase phenocrysts are altered to carbonate and sericite. Relict crystal outlines suggest that biotite may also have been present.

The second porphyry variety, hornblende-plagioclase porphyry, is texturally similar to K-feldspar porphyry but devoid of K-feldspar phenocrysts. Quartz phenocrysts are rare or absent.

Maroon porphyry, the third porphyry variety, is equivalent to the K-feldspar porphyry except that it has a distinctive maroon to purple (hematitic) groundmass alteration which differs from that in the green porphyritic units. It is believed to be extrusive, at least in part, due to its intimate association with a veneer of maroon epiclastics (Unit 2). In addition, the pervasive groundmass oxidation suggests possible subaerial extrusion. Rare fragmental textures are found locally.

The porphyritic rocks are cogenetic with the Texas Creek granodiorite, a 189-195 Ma (concordant zircon U-Pb; Alldrick et al., 1986) batholith exposed along the western edge of the map area. Similar zircon U-Pb results were obtained by the author and P. van der Heyden.

METAMORPHISM

Units 1 and 6 are greenschist-grade meta-andesite and dacite with preserved primary textures. Secondary minerals include chlorite, carbonate, pyrite, sericite, epidote, ± leucoxene(?). Chlorite, sericite and quartz have grown in pressure shadows around euhedral pyrite crystals. Local curved sericite-chlorite crystals suggest syndeformational mineral growth.

Metamorphic grade of the volcaniclastics (Unit 2) decreases from greenschist low in the section, to essentially unmetamorphosed up section and to the east. Phyllosilicate growth occurs in phyllitic, finer grained tuff. Units 3 to 5 are essentially unmetamorphosed.

Potassium feldspar (adularia), sericite, quartz, carbonate, chlorite and pyrite are hydrothermal alteration products genetically and spatially related to mineralization at Silbak

Premier. Intense propylitic alteration of Unit 1 meta-andesite results in ubiquitous and abundant secondary chlorite and carbonate.

STRUCTURE

Regional stratigraphy strikes north and is northeast facing. Structures are divided into post-Middle Jurassic to Cretaceous ductile-brittle deformation and Cenozoic brittle deformation. Hazelton volcanics and Bowser Lake sediments exhibit fabrics produced by at least two phases of pre-Cenozoic deformation. Tertiary transtensional features include brittle faulting and Eocene extensional dyke swarms.

Post-Middle Jurassic-Cretaceous (?) deformation:

Lithology-dependent Jura-Cretaceous fabrics vary from ductile shear zones and folds to brittle fracture cleavage. Bowser Lake Group sediments and shale- argillite-siltstone in the Hazelton volcanics are isoclinally to tightly, disharmonically folded with prominent fracture and slaty cleavages. In contrast, competent Hazelton volcanics and intrusive rocks are openly folded on a larger scale, locally with discrete, steep, highly strained zones.

Southeast-verging and northwest-dipping fabrics

Asymmetric chevron folds in siliceous sediments of Unit 5 (Fig. 14.4) and folds in Unit 1 argillite are southeast verging. Nappe structures described by Grove (1971) also indicate southeast vergence. Meta-andesite volcanics (Unit 1) have a variably developed moderate northwest-dipping phyllosilicate foliation. The foliation, concentrated in narrow (100 m) zones, is formed by chlorite-sericite phyllite to chlorite-sericite schist. Porphyritic dacite (Unit 6) can be traced into a 100 m-wide zone of chlorite-sericite schist. This high-strain zone may be a shear zone or thrust.

The northwest-dipping foliation is axial planar to asymmetric folds with southeast vergence. Therefore, both folds and foliation are related to components of southeasterly-directed compression. The foliation is syn-metamorphic and both metamorphism and deformation are believed to be Late Jurassic or Cretaceous.

Strained epiclastics

Narrow, west to northwest-dipping zones of strained epiclastics in Unit 2 (Fig. 14.5) are exposed on the Big Missouri oad at Cooper Creek. Elongated fragments have length to width ratios of 6:1 to 10:1. The elongation direction is coaxial with the pencil lineation (260°/45°W). Fragment asymmetry indicates elements of southeastward transport (southeast verging, hanging wall over footwall, i.e. northwest over southeast). Although the foliation and southeastward vergence are geometrically similar elements, the orientation and lineation is more east-west.

Folds in Bowser Lake Group rocks and Monitor Lake rhyolite breccia

An important detachment surface exists at the Bowser Lake-Hazelton Group contact. Disharmonic folding of interbedded argillite, siltstone, shale, limy beds and siliceous sediments relative to open folds in the volcanics is characteristic. Flexural slip and flow mechanisms are proposed to explain structures in interbedded sediments of high competency contrast (Fig. 14.6).

Recumbent folds in Unit 5 siltstone beds along the penstock from Long Lake Dam to Big Missouri powerhouse have fold amplitudes and wavelengths of about 2 m and 0.5 m, respectively.

Isoclinally folded cleavage on Slate Mountain indicates a second phase of deformation. Axial planes are 265°/15°NW and fold axes plunge 265°/15°W.



Figure 14.4. View northeast to southeast-verging chevron folds in Unit 5 siliceous sediments.

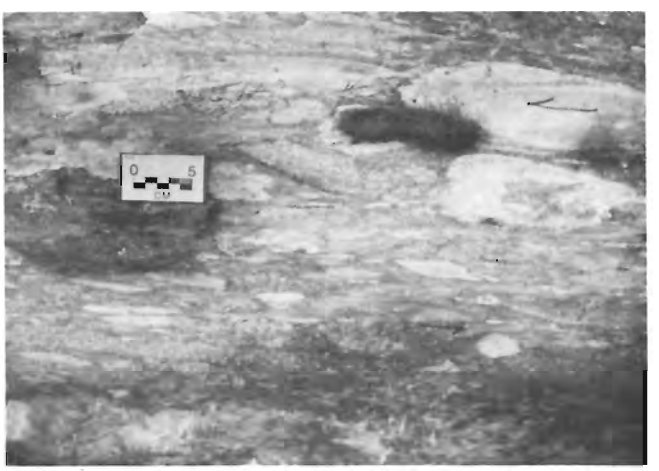


Figure 14.5. Strained epiclastics in Unit 2.

Open folds in rhyolite (Unit 4) 1.5 km southeast of Monitor Lake plunge gently to the north-northwest with steep axial planes. These minor folds are on the limb of a large anticline-syncline pair (Dilworth syncline-American Creek anticline) involving Hazelton Group and Bowser Lake Group rocks.

East-west planar fabrics

Tight to isoclinal folds in phyllitic argillite (Unit 1) plunge gently to the east or west with moderate to steep south-dipping axial planes. Fold amplitudes are up to 10 m. Tops as determined by flame structures, cut and fill, and load casts indicate bedding is overturned to the southeast. These structures are exposed on the Granduc road 1250 m south of the Westmin camp and below Consolidated Silver Butte.

Two parallel mylonite zones, in the Texas Creek granodiorite exposed around the Riverside Mine, 12 km north of Hyder, Alaska (Smith, 1977) dip steeply south. Highly strained maroon epiclastics (Fig. 14.7, an L-S tectonite) along Bear River Ridge also exhibit an east-west flattening fabric normal to bedding.

Sulphide-rich veins are layered at 6-level, 2-level and Glory Hole with a consistent vertical dip and east strike. Some base-metal quartz veins, siliceous breccia zones, strike-slip faults, hornblende-plagioclase foliation and cleavages at Silbak Premier also have this east-west attitude.

East-west lineations

The most prominent and consistent feature of the area is the pencil lineation. This lineation (260°/45°W) in Hazelton Group and Bowser Lake Group rocks is the intersection of two S-surfaces (cleavage and/or chlorite-sericite foliation; Fig. 14.8 and 14.9). Elongation axes in strained siliceous fragments in the Monitor ake rhyolite breccia (Unit 4), and epiclastic clasts (Unit 2) are coaxial with the pencil lineation.



Figure 14.6. Flexural slip and flow mechanisms within folded siliceous siltstone and impure carbonate beds (Unit 5).



Figure 14.7. View east to east-west flattening fabric in maroon epiclastics, Bear River Ridge.



Figure 14.8. View west to pencil lineation produced by intersecting cleavages in Unit 5 siltstone, Long Lake area.



Figure 14.9. Pencil lineation developed in Unit 1 andesite, Silbak Premier Mine.

Chlorite and biotite aligned along this 260°/45°W lineation form steep dipping, east-west mylonitic foliation in the Texas Creek granodiorite 1 km south of Riverside Mine on the Granduc road.

Crenulation-cleavage fold axes are coaxial with this west-plunging lineation in schistose rocks.

Extensional quartz veins

Crystalline, milky quartz veins up to 1 m thick cut the meta-andesite (Unit 1). The veins and parallel joints are planar with consistent 150-165o/50-70oNE attitudes. Quartz crystals are oriented perpendicular to vein walls. No country rock fragments are present within the veins. The veins are classified as syntaxial growth type (Durney and Ramsay, 1973), and possibly are synmetamorphic with dewatering of the andesite. The veins are approximately perpendicular to the pencil lineation and elongation direction and are assumed to have formed in the same deformational event.

Locally, relative timing of deformation is suggested where an older closely spaced fracture and slaty cleavage (130-150°/25-80°NE) is cut by a more widely spaced cleavage (165-180°/50-65°SW). A subordinate fracture cleavage at 130-140°/30-50°SW is locally developed.

Mineralization at Silbak Premier occurs in K-feldspar porphyry and adjacent meta-andesite. Ore is discordant to lithologic contacts and appears to be structurally controlled. Two distinct ore zone trends are: (1) steeply dipping to vertical, northwest trending, and (2) en echelon, moderate northwest dipping, northeast trending (Hanson, 1935). The northeast-trending group consists of two or more subparallel zones (stopes) displaced regularly to the northwest. It is not clear whether this left-lateral offset is due to faulting or is the original mineralization geometry.

Cenozoic deformation

Numerous and widespread brittle fault systems are related to a Tertiary transtensional stress regime. Faults are characterized by clay gouge zones less than 4 cm thick, fault breccia less than 1 m wide and limonite staining.

Physiography and drainage (i.e. Long Lake-Fish Creek, Cascade Creek and possibly Salmon River) are controlled by steeply dipping, north-south striking (170-190°/75-90°W) faults. Slickensides suggest both horizontal and dip-slip motion. Smith (1977) proposed a 5-km dextral offset since the Jurassic, with 1 km displacement occurring in the Tertiary. At Silbak Premier, the Tertiary Hyder-plutonic-suite dyke swarms do not appear to be significantly offset. Fractures and minor faults cut the dykes with lateral movement limited to a few metres. Mineralization atSilbak Premier is locally right-laterally displaced more than 10 m across these faults.

Faults oriented at 150-165°/35-70°SW are cut by the steeper north-south set. Secondary drainage and gullies follow these moderate dipping structures. Coplanar fracture and slaty cleavage suggest some of these faults are reactivated cleavage planes.

Less defined fault attitudes are 090°/90° (some sinistral strike-slip as indicated by offset quartz veins and horizontal slickensides), 30°/55-65°NW and 170°/45-75°NE (dip-slip suggested by down dip slickensides).

Eocene crustal extension is manifested by Hyder plutonic suite dyke swarms. The granodiorite and quartz phyric rhyolite dykes with consistent attitude (135°/75°SW) at Silbak Premier indicate northeast-southwest extension. The Portland Canal dyke swarm (Grove, 1971), approximately 1 km wide, at the Salmon glacier exhibits more than 30 per cent extension filled by leucogranite and microdiorite dykes. The Silbak Premier dyke swarm indicates similar extension.

The dyke-swarm orientation suggests the extension is not related to dextral strike-slip faulting.

CONCLUSION

Silbak Premier Mine is hosted by Hazelton Group meta-andesites intruded by coeval dacitic porphyries related to the Texas Creek granodiorite. Mineralization is spatially associated with K-feldspar porphyry and adjacent meta-andesites. Distribution of ore is controlled by: (1) en echelon structures that strike northeast and dip moderately northwest, and (2) a steep to vertical dipping, northwest-striking structure.

Bowser Lake Group sediments are disharmonically and isoclinally folded, whereas the structurally underlying Hazelton volcanics are broadly folded. The Bowser Lake-Hazelton Group contact is a tectonic break which also represents a regional unconformity. The pervasive northwest-dipping foliation formed axial-planar to southeast-verging folds. A younger deformational event produced the east-west fabrics. Alternatively, southeast-verging structures are related to southeast-directed thrusts and the east-west fabrics were developed on ramps. During the Tertiary faults and dykes cut the region.

ACKNOWLEDGMENTS

Westmin Resources Ltd. provided summer employment and generous field support during this research. Geological Survey of Canada provided logistical support for the regional part of the study under project 840046. Dani Alldrick, Paul McQuigan and Paul Wodjak shared information and ideas freely and are gratefully acknowledged and appreciated. Particular thanks are due to Bob Anderson for his patient advice throughout this study.

REFERENCES

Alldrick, D.J.
1985: Stratigraphy and petrology of the Stewart Mining Camp (104B/1); British Columbia Ministry of Energy, Mines and Petroleum Resources, Geological Fieldwork, 1984, Paper 1985-1, p. 316-341.

Alldrick, D.J., Mortenson, J.K., and Armstrong, R.L.
1986: Uranium/Lead age determinations in the Stewart area (104B/1); British Columbia Ministry of Energy, Mines and Petroleum Resources, Geological Fieldwork, 1985, Paper 1986-1, p. 217-218.

Durney, D.W. and Ramsay, J.G.
1973: Incremental strains measured by syntectonic crystal growths: in Gravity and Tectonics, De Jong, K.A. and Scholten, R. (eds.), John Wiley, New York, p. 67-96.

Grove, E.W.
1971: Geology and mineral deposits of the Stewart area, B.C.; British Columbia Ministry of Energy, Mines and Petroleum Resources, Bulletin 58, 229 p.

Hanson, G.
1935: Portland Canal area, British Columbia; Geological Survey of Canada, Memoir 175, 179 p.

Schofield, S.J. and Hanson, G.
1922: Geology and ore deposits of the Salmon River District, B.C.; Geological Survey of Canada, Memoir 132, 81 p.

Smith, J.G.
1977: Geology of the Ketchikan D-1 and Bradfield Canal A-1 Quadrangles, Southeastern Alaska; U.S. Geological Survey, Bulletin 1425, 49 p.

- 15 -

Preliminary interpretation of the stratigraphy of the marine offlap sequence in the Clifton Point area, District of Mackenzie

Project 840002

Daniel E. Kerr[1]
Terrain Sciences Division

Kerr, D.E., Preliminary interpretation of the stratigraphy of the marine offlap sequence in the Clifton Point area, District of Mackenzie; in Current Research, Part A, Geological Survey of Canada, Paper 87-1A, p. 153-157, 1987.

Abstract

The stratigraphic study of several river bank sections in the Clifton Point area, Northwest Territories has made it possible to reconstruct late glacial glaciomarine and postglacial marine environments of deposition. In the early stages of deglaciation when the ice front terminated in the sea, sequences of massive to well stratified diamicton, subaqueous outwash deposits, and silty clay rhythmites were deposited close to their glacial source. As the deglaciation of the coastal area took place, the sea contemporaneously invaded the isostatically depressed coastal lowlands. Regions in the vicinity of sediment laden deltaic waters experienced an important rhythmic sedimentation giving rise to marine rhythmites. Sedimentation in deeper areas of the sea, which remained relatively unaffected by high sediment input, resulted in the deposition of massive silty clay. These sediments were overlain by deltaic or beach sediments, typical of an offlap phase.

Résumé

L'étude de nombreuses coupes exposées dans la région de Clifton Point, Territoires du Nord-Ouest, a permis de reconstituer les environnements de déposition du tardi glaciaire et du posglaciaire de la région. Au début de la déglaciation alors que la glore aboutissait dans la mer, vs faciès sédimentaires suivants ont été mis in place: diamicton massif à bien stratifie, épandage de sable fluvie-glaciaire sub-aquatigous et rythmites silto-argileuses. Suite au retrait du glacier de la zone côtière, la mer a envahi les basses terres déprimées par glacio-isostasie. Dans les régions ou aboutissaien des rivières transportant d'énormes quantités de sédiments de trés grénds obtens fuent constuits et, dans des zones depots les dépôts de silt et d'argile forment des rythmites moins. La sédimentation marine ou dans les régions plus profondes et plus éloignées de grandes sources de sédiments est représentée par des dépôts massifs silto-argileux. Ces sédiments ont été recouverts par des dépôts de delta ou de plage, faisant partie d'une séquence sédimentaire inverse typgin d'une mer en régression.

[1]Department of Geology, University of Alberta, Edmonton, Alberta

INTRODUCTION

The stratigraphic record along 80 km of the mainland coast of the Northwest Territories in the area of Clifton Point (Fig. 15.1) was studied during the summer of 1986. Sections include a sequence of glacial, glaciomarine and marine sediments that were deposited during the Late Quaternary; these have not been studied previously in detail. Five stratigraphic sections are discussed (Fig. 15.2) which are considered to be representative of Quaternary sequences in the Clifton Point area.

Investigations by O'Neill (1924), Mackay (1958), and Craig (1960) refer only briefly to the marine stratigraphy. Craig (1960) also initially identified the approximate limit of marine submergence in the north-central District of Mackenzie. The area lies within morphosedimentary zone F (St-Onge and McMartin, 1987) which is characterized by bouldery gravel and coarse sand deltas that mark the differential character of the marine limit from 61 to 100 m a.s.l. (Fig. 15.1). Below this level are also found thick sequences of silty clay rhythmites, hills of bedrock and washed till, as well as raised gravel beaches.

The area was glaciated during the last ice advance by a lobe moving from the south with curved to the northwest roughly parallel to the present-day coastline (Craig, 1960). As ice receded towards the southeast during deglaciation, the shrinking of the lobe permitted the sea to invade the land from the west along the ice margin (St-Onge and McMartin, 1987).

STRATIGRAPHY

Sediments of glacial and proglacial origins

A diamicton occurs commonly at the base of stratigraphic sections and represents the oldest unconsolidated deposit in the study area. The unit is a silt to silty sand containing well rounded to angular clasts of dolomite, diabase, granite, and red and green sandstone which can be up to 2 m in diameter. These clasts are derived predominantly from outcrops to the south and east, suggesting a glacial transport direction towards the northwest. Clasts may be striated (Fig. 15.3) and appear to have no preferred orientation. Locally, where the unit can be seen directly overlying bedrock, the majority of the clasts are angular and of the same lithology as the underlying bedrock. The unit may appear massive but commonly exhibits poor to well defined stratification. More rarely a crude stratification is defined by a thin layer of gravels and cobbles concentrated at the contacts between diamicton beds. Overall thickness varies from less than 1 m to more than 20 m. The diamicton, interpreted as till, is associated with the last glaciation and the massive to poorly bedded units were deposited during deglaciation either at or near the ice-sea interface. It is not known whether sedimentation took place beneath a grounded ice sheet, beneath a floating ice shelf, or seaward from the ice margin.

In some areas (Section 2, Fig. 15.2) diamicton beds are interbedded with waterlain sediments that range from fine sand and silt to coarse sand and gravel. The sediment can be massive or be characterized by planar crossbedding and type A crosslaminations with no preservation of stoss-side laminae (Jopling and Walker, 1968), type B crosslaminations with complete preservation of stoss-side laminae, and sinusoidal crosslaminations. Climbing ripples are commonly inter bedded with planar-bedded fine sand and silt laminae with thin clay-draped horizons. Paleocurrent directions obtained from rippled sands indicate deposition from currents flowing in a northwesterly to northeasterly direction. The sediments are believed to be subaqueous outwash deposits and derived from meltwater streams entering the sea from the southeasterly retreating ice margin. Because they are interbedded with the diamicton units (Fig. 15.4), the introduction of sand and gravel appears to have been sporadic. Units of subaqueous outwash vary from 0.3 to 5 m or more in thickness and have sharp upper and lower boundaries.

The sandy outwash sequence grades upwards into thinly bedded to finely laminated sand, silt, and clay rhythmites (Fig. 15.5), although the rhythmites may also be found directly overlying the diamicton unit. Rhythmites vary considerably from one location to another with respect to the thickness of individual beds, grain size, nature of the boundaries, and sedimentary structures.

When the lower parts of the rhythmites directly overlie outwash deposits, they are commonly 30 to 50 cm thick, representing a graded bed of medium sand to silty clay with internal laminae of sandier or clay-rich horizons, 0.1 to 1 cm thick. Boundaries are planar and gradational, and only rarely sharp and erosional. Thicker rhythmites may in places contain thin sequences of type A and B climbing ripples. Where rhythmites are found overlying till, their characteristics are considerably different. The thickness of individual laminae ranges from 1 to 5 mm, rarely exceeding 1 cm (Fig. 15.6). Each lamination consists of sand, silty sand, or silty clay, separated by either sharp or gradational contacts. The colour of each lamination is also variable, accentuating the well laminated structure of these sediments.

Rhythmites may exhibit soft-sediment deformation, i.e., convolute bedding and dewatering structures, and in places contain dropstones and diamicton pods or balls, less than 5 cm in diameter. In general, the rhythmites overlying outwash deposits become progressively thinner and finer grained towards the top of sections; those overlying till show no readily visible trend. Rhythmite sequences commonly grade upwards into sublittoral sand and deltaic sediments. They can, however, be overlain by massive silty clay which in turn grades up into sandy littoral deposits.

Sediments of marine sublittoral, littoral and deltaic origin

The marine regression, resulting from isostatic uplift, is represented by several different sedimentary sequences. The variations (Fig. 15.2) are the result of changes in the environment of deposition, the sedimentary processes, the length of time that areas were submerged, and the amount of uplift a region experienced. In areas where relatively little uplift

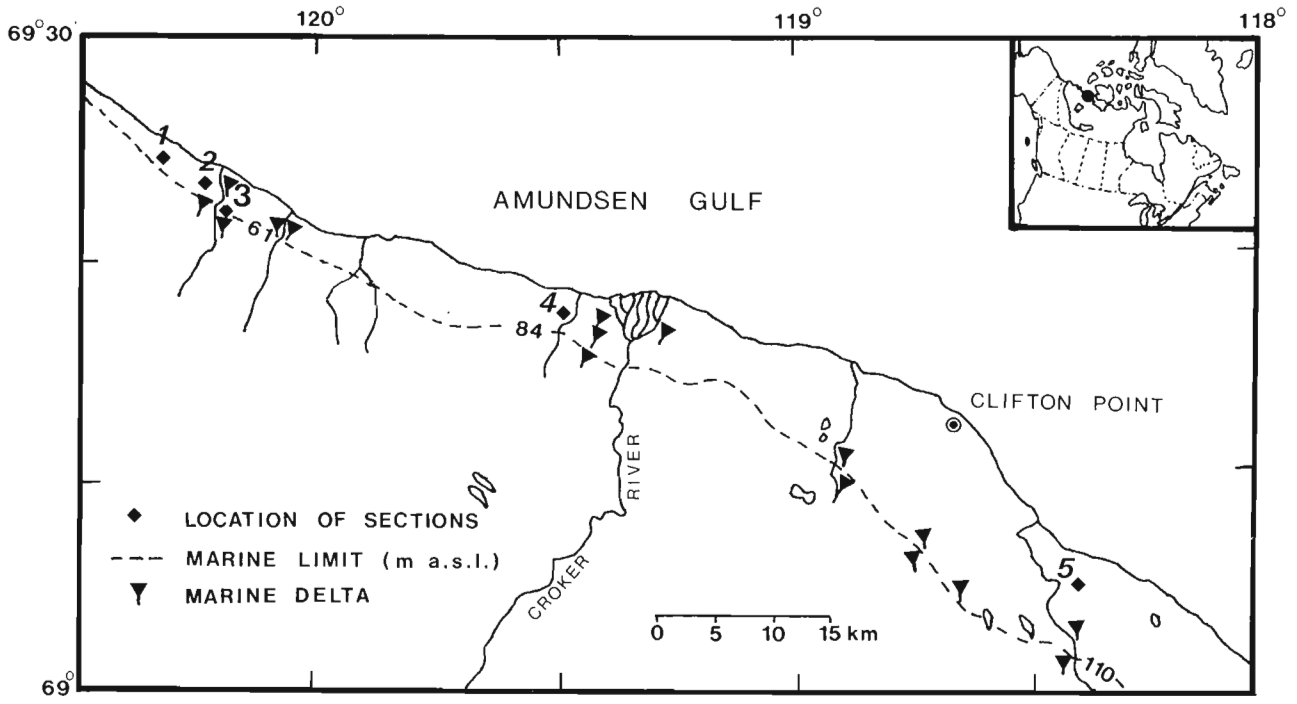


Figure 15.1. Location map showing the elevation of marine limit and locations of marine deltas and sections described in Figure 15.2.

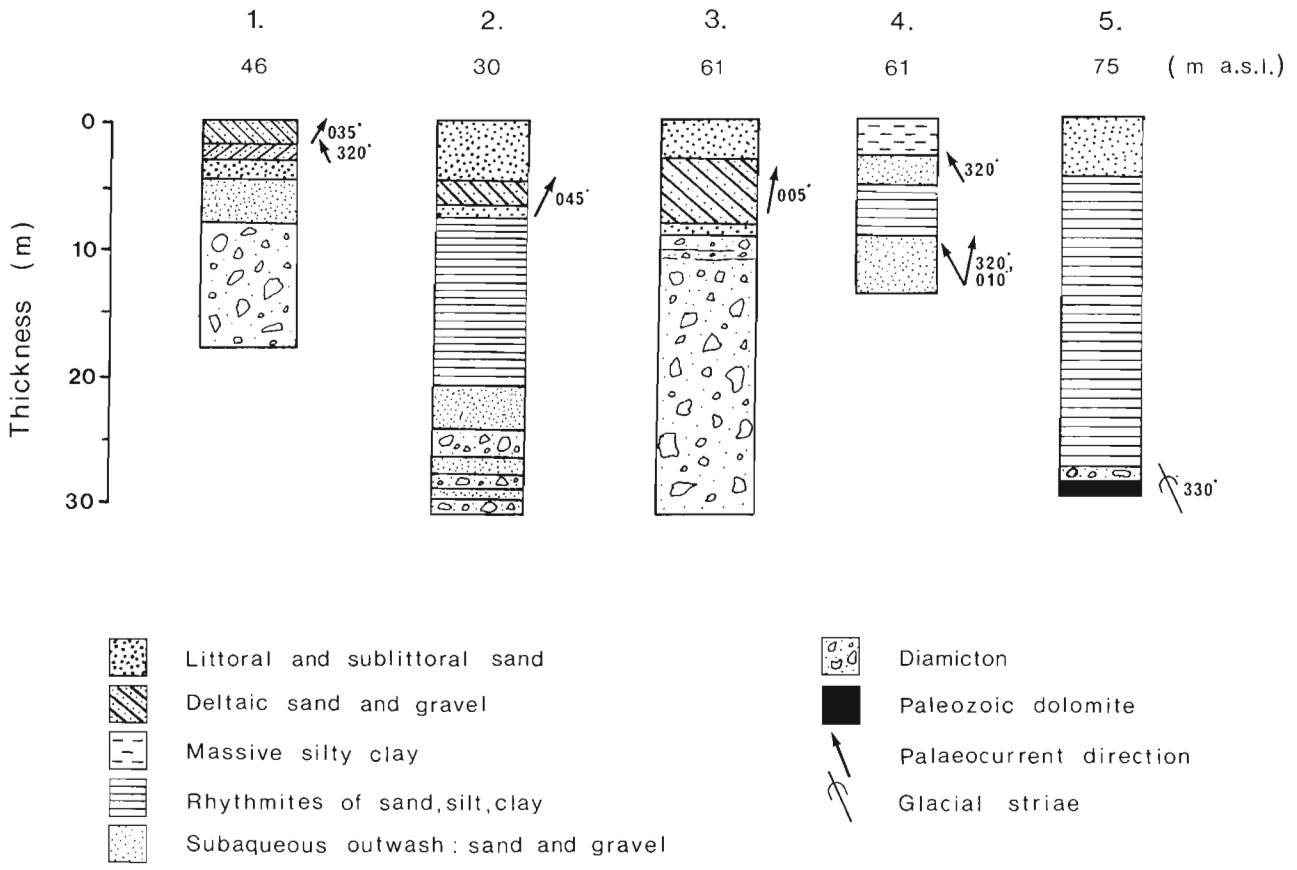


Figure 15.2. Sediments exposed in sections within the marine offlap area along the south coast of Amundsen Gulf (cf. Fig. 15.1).



Figure 15.3. Striated clast in massive diamicton unit.



Figure 15.4. Laminated sandy unit between poorly bedded diamicton layers.

occurred (Section 1, Fig. 15.2) only coarser grained marine sublittoral and deltaic sediments are found overlying deposits of glacial origin. Elsewhere, similar environments existed at the marine limit where isostatic uplift was somewhat greater (Section 3, Fig. 15.2). In areas submerged by ten's of metres of water, two sedimentary successions are recorded. In the first, glaciomarine rhythmites appear to grade into marine rhythmites with no apparent change in structure. These in turn are overlain by a coarsening upwards sequence consisting of bottomset, foreset, and topset deltaic sediments, or littoral sediments containing marine micro and macrofossils (Sections 2 and 5).

The second sedimentary succession is characterized by glaciomarine rhythmites overlain by a structureless silty clay unit (Section 4) containing marine fossils, which also forms part of a coarsening upwards sequence of either deltaic or littoral marine sands.

DISCUSSION

The sediments record ice retreat when glacial sediments were being deposited in the sea, through to the postglacial marine regression, from relatively deep water to littoral sedimentary facies. Various sedimentary processes appear to have been active along the ice front, as evidenced by the presence of massive to bedded deformation units, sequences of subaqueous outwash, successions of interbedded diamicton and outwash, as well as thick sequences of well laminated to thinly bedded sandy clay rhythmites. These rhythmites are believed to have been deposited by subglacial turbidity currents issuing from the ice front. Variations in thickness and structure within the rhythmic deposits may be the result of proximity to the ice front, the availability and abundance of sediment supplied by meltwater, as well as fluctuations in the strength of bottom-water turbidity currents; the introduction of sediment by overflows and interflows is also possible, contributing sediment from other sources within different parts of the glacier.

Large amounts of meltwater flowed into the sea during the early phases of deglaciation, constructing bouldery gravel deltas at marine limit. At lower elevations, deltaic sediments did not exceed coarse sand size. During this period of initial marine regression, large inland rivers draining the uplands farther south carried a sufficiently high sediment load to overcome the buoyant effect of seawater (Gilbert, 1983) and deposited graded beds of sediment along the sea bottom.

Areas with no major source of sediment represent more open marine environments, which were not directly influenced by large rivers. These sections are characterized by glaciomarine rhythmites which are overlain by massive silty clay which settled out of suspension in a more tranquil environment, away from high-sediment input sites. Marine micro and macrofossil studies presently being carried out will provide paleoenvironmental data which may contribute to a



Figure 15.5. Sandy sediments (?subaqueous outwash) grading into proximal glaciomarine rhythmites.

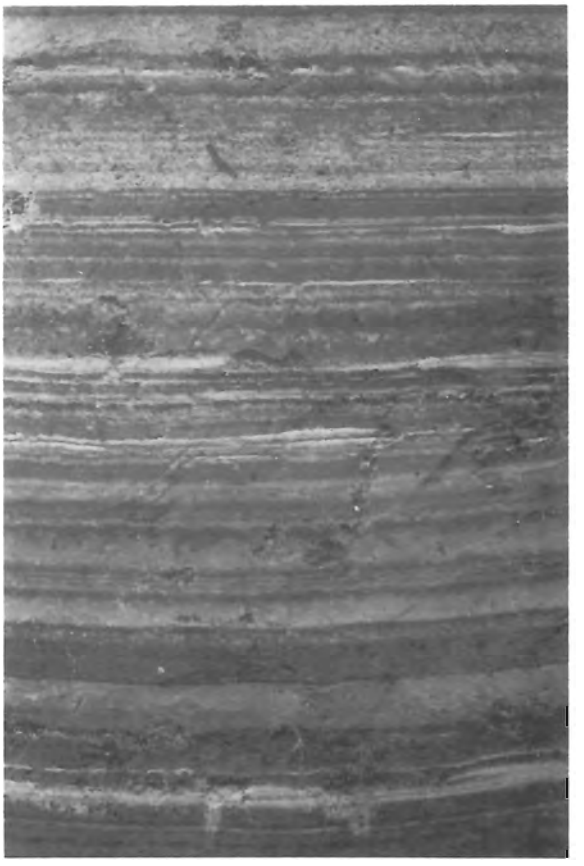


Figure 15.6. Finely laminated glaciomarine rhythmite; thickest lamination is 1 cm.

better understanding of water depth, salinity, and the general paleogeographic reconstruction. Similarly, radiocarbon dates of marine bivalves will help elucidate the temporal framework of the marine regression.

ACKNOWLEDGMENTS

This study is part of a continuing Ph.D. research project investigating the stratigraphy of the glaciomarine and marine sediments along the mainland coast of the Northwest Territories. Field work was made possible by the logistical and financial support of D.A. St-Onge, Geological Survey of Canada, W.A. Padgham, Department of Indian and Northern Affairs, Polar Continental Shelf Project, and Lakeland-Maple Leaf Helicopters. Additional research grants from the Boreal Institute for Northern Studies, in addition to the field assistance provided by R. Avery, M. Beaudet, I. McMartin, and M. Potschin are also gratefully acknowledged.

REFERENCES

Craig, B.G.
1960: Surficial geology of north-central District of Mackenzie, Northwest Territories; Geological Survey of Canada, Paper 60-18.

Gilbert, R.
1983: Sedimentary processes in Canadian Arctic Fjords; Sedimentary Geology, v. 36, p. 147-175.

Jopling, A. and Walker, R.
1968: Morphology and origin of ripple-drift cross-laminations, with examples from the Pleistocene of Massachusetts; Journal of Sedimentary Petrology, v. 38, p. 971-984.

Mackay, J.R.
1958: The Anderson River map-area, N.W.T.; Geographical Branch, Memoir 5, Department of Mines and Technical Surveys.

O'Neill, J.J.
1924: The geology of the Arctic Coast of Canada west of Kent Peninsula; Report of the Canadian Arctic Expedition 1913-18, v. XI, Geology and Geography, Part A.

St-Onge, D.A. and McMartin, I.
1987: Morphosedimentary zones in the Blue Nose Lake region, District of Mackenzie; in Current Research, Part A, Geological Survey of Canada, Paper 87-1A.

- 16 -

Quaternary stratigraphy of Noire River cores, Beauceville area, Quebec[1]

Project 690095

S.L. Smith and W.W. Shilts
Terrain Sciences Division

Smith, S.L. and Shilts, W.W., Quaternary stratigraphy of Noire River cores, Beauceville area, Quebec; in Current Research, Part A, Geological Survey of Canada, Paper 87-1A, p. 159-164, 1987.

Abstract

Potentially gold-bearing sediments in buried valleys in the Beauceville area have been sampled and studied using stratigraphic drilling techniques. These investigations show that river orientation transverse to dominant ice flow directions, the relationships of preglacial and glacial sediments, oxidation at depth, brown colour in till, and distinctive geochemical data for Ni all provide important clues useful for evaluating the potential for gold mineralization.

Three drill cores from Noire River reveal unique stratigraphy and are tentatively correlated with sections and boreholes on nearby Plante and Gilbert rivers. The similarity of the stratigraphic succession at Noire River to stratigraphy at Gilbert River suggests that conditions for gold mineralization may also be favourable in Noire Valley.

Résumé

Une nouvelle méthode d'exploration de sédiments aurifères dans des vallées enfouies de la région de Beauceville est fondée sur la reconnaissance de certaines caractéristiques. Ces paramètres comprennent: l'orientation des rivières perpendiculaires aux directions dominantes de l'écoulement de la glace, le relief structural, la stratigraphie des sédiments anté-glaciaires et du Wisconsinien inférieur à moyen, l'oxydation en profondeur, la couleur brune des tills et les données géochimiques distinctives du Ni.

Trois carottages de forage prises dans la rivière Noire révèlent une stratigraphie unique et peuvent être corrélées provisoirement avec des coupes transversales et des trous de sonde effectués dans les rivières avoisinantes Plante et Gilbert. Ces caractéristiques, conjointement avec les renseignements sur le forage et la sismique, indiquent qu'il y aurait lieu d'effectuer d'autres travaux d'exploration sur la rivière Noire.

[1]Contribution to Federal Asbestos Initiatives, Geoscience Research Program 1984-1987. Project carried by Geological Survey of Canada

INTRODUCTION

As a component of a field program to examine glacial stratigraphy in relation to gold placer deposits in preglacial (Tertiary), interglacial or interstadial, and postglacial sediments in the Eastern Townships, 45 boreholes were drilled through overburden to bedrock from 1984-1986 (Shilts and Smith, 1986a) in Chaudière River valley and its tributaries.

From drilling and seismic surveys, it is evident that many modern rivers in the region are suspended above their preglacial bedrock floors. Even though they may have cut down through as much as 30-40 m of glacial fill, further downcutting has been prevented by the stream striking bedrock of the preglacial valley sides. Using seismic refraction data, boreholes were sited on the axes of these paleovalleys on the assumptions that: 1) preglacial materials are most likely to be preserved there if at all and 2) complete sequences of Quaternary sediment might be recovered. For example, the gold-bearing (Tertiary?) sediment of Gilbert River is preserved only in the deepest part of the old bedrock channel where it is overlain by several glacial stratigraphic units. It is hypothesized that by examining certain physiographic, goechemical, and mineralogical parameters, it may be possible to locate other buried valleys that also preserve potentially gold-bearing sediments at depth. On this basis, we selected Noire River[1] for exploratory drilling.

The presence of a buried valley beneath Noire River was determined using seismic refraction techniques. The decision to drill three boreholes in a line along the river was made when it became evident, during core recovery from the exploratory hole, that complex stratigraphy existed at depth (Fig. 16.1). The spacing of the sites 150 m apart permitted the interpretation of lateral continuity of the stratigraphic units. Siting of the drill was controlled by limited access for the equipment.

TECHNIQUE

Intact, large-diameter drillcore was retrieved using a Rotasonic drill that utilized high-frequency vibration and rotation to core the sediments. Core was extruded in 5-foot lengths into a plastic sleeve and placed in core boxes to be moved to the logging facility. An objective approach to describing the physical characteristics of unconsolidated sediments was developed based on the lithofacies code proposed by Eyles et al. (1983). The modifications, shown in the legend of Figure 16.2, make better provision for grain size variations within the gross subdivisions of D (diamict), G (gravel), S (sand), and F (fine-grained lithologies). Genetic interpretations were made after the core logging was completed, and stratigraphic interpretations were developed from observations of compositional characteristics.

Correlation of detailed logs of cored sediment with regional glacial stratigraphy was based on characteristics such as clast lithology, texture, clast:matrix ratio, colour (related to weathering as well as provenance), and geochemical data. Fluvial and lacustrine sediments were correlated on the basis of relative stratigraphic position, similar lithology, or the presence of organic material.

QUATERNARY STRATIGRAPHY

No evidence has yet come to light through the regional drilling program, of any stratigraphic units not already known from previous studies (McDonald and Shilts, 1971; Shilts, 1978, 1981). Many buried valleys, however, contain thick fine- to coarse-grained waterlain sediments and debris flows deposited in depressions in the floors of proglacial lakes during advance or retreat of ice fronts representing one or more of the three glacial events recognized from the region.

Johnville, Chaudière, and Lennoxville tills represent the three major, documented advances of Wisconsinan ice sheets

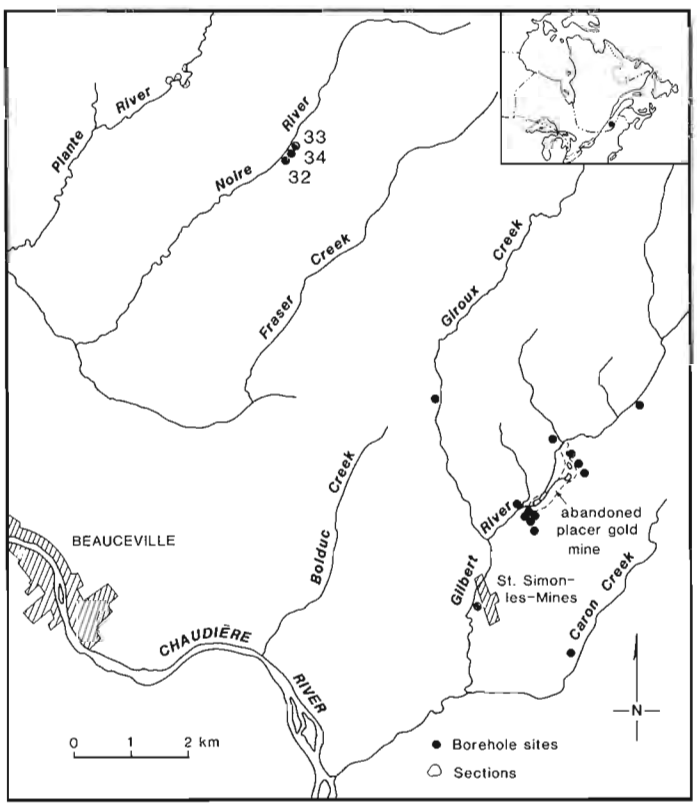


Figure 16.1. Location map of Noire River boreholes in relation to Gilbert River boreholes and Plante River sections.

[1]Noire River should not be confused with a river of the same name which flows through Valcourt and l'Enfant Jesus-d'Ely about 20 km west of Sherbrooke. Important glacial sequences are exposed on that river (P. LaSalle, pers. comm., 1986) and will be discussed soon in the literature.

over the region. The Johnville Glaciation was preceded and followed by periods of free drainage, inferred from fluvial sediments below and above the till at Grande Coulée River (Shilts, 1981). Fabric and clast lithology data indicate a Laurentide source for the southeastward flowing Johnville glacier. At the few sites where Johnville Till is exposed, it is oxidized in its upper part, attesting to the period of free drainage, subaerial weathering, and ice-free conditions during the subsequent Massawippi Interstade.

The Massawippi Formation has been tentatively correlated with the St. Pierre interstadial, peat-bearing deposits of the St. Lawrence Lowlands (Gadd, 1971; McDonald and Shilts, 1971; Matthews et al., 1987). Fluvial gravels and sand, overbank flood deposits, laminated proglacial lake sediments, and rare disseminated organic material or discrete peaty lenses comprise Massawippi Formation sediments.

Westward or southwestward flowing glaciers advanced from an Appalachian centre of outflow at the beginning of the Chaudière Glaciation but were subsequently overwhelmed by a Laurentide glacier flowing southeastward. Parameters that reflect the shift in dominant ice flow direction, such as composition and fabric, have been recorded from most natural exposures of Chaudière Till in the region (Shilts, 1978). Contrasts in compositional parameters are particularly pronounced between Chaudière Till and overlying and underlying tills of northwest provenance on Plante, Noire, and Gilbert Rivers, all of which are located a short distance southeast of major ultramafic outcrops. Although Lennoxville and Johnville tills, deposited by southeastward flowing glaciers, contain abundant nickel, chromium, and minerals and erratics originating exclusively within the ultramafic belt, Chaudière Till, deposited initially by westerly or southwesterly flowing ice, contains few of these components.

Relatively brief retreat of the Chaudière glacier to the front of the Appalachian Mountains south of the St. Lawrence River, ponded drainage of north-flowing Chaudière River, producing a large proglacial lake into which locally thick glaciolacustrine or deltaic sediments of the Gayhurst Formation were deposited. Boreholes have intersected Gayhurst interstadial sequences up to 60 m thick in upper Chaudière Valley.

The last regional Wisconsinan ice advance deposited Lennoxville Till, the surface till of the region. During the waning phase of the Lennoxville Glaciation, an ice divide extended roughly northeast-southwest through the north-central part of the Eastern Townships (Lamarche, 1971; Gadd et al., 1972), documented by northward or northeastward striae north of the divide.

DESCRIPTION OF SEDIMENTS

Three boreholes drilled in a profile along the axis of the buried valley of Noire River have been interpreted in context of the regional Quaternary stratigraphy (Fig. 16.2). They are located between the large, intensively studied exposures on Plante River (Shilts and Smith, 1986b) and boreholes in the gold placer mining area of Gilbert River (Fig. 16.1) and contain sediments with similar stratigraphic relationships.

The Plante River sections expose the most complete record of Quaternary units recorded at any one place within the Appalachians (Shilts and Smith, 1986b). The Noire River borehole sediments similarly reveal a remarkably complete stratigraphic record for the area but also intersect a lower oxidized unit that bears a strong resemblance to the lower gold-bearing unit at Gilbert River. The basal stratum at Gilbert River is brownish yellow (strongly oxidized and Fe-rich), clast supported, depleted in Ni, contains clay minerals indicative of long and/or intense weathering, exhibits heterolithic clasts of strictly local lithologies, and contains perfect iron oxide pseudomorphs of pyrite (Shilts and Smith, 1986b).

As shown in the borehole logs (Fig. 16.2), the general stratigraphy of Noire River comprises a grey till in contact with a lower brown till complex, which in turn overlies laminated silty clay with diamict lenses. This glacial sequence overlies an extremely oxidized diamict, similar in many aspects to that at the base of Gilbert River boreholes.

The buried basal unit at Noire River is characterized by orange-brown colour, matrix supported to almost clast supported framework, abundant clasts of local black shales, Ni content depleted below background levels for the region, and inclusions of pink clay. Results of gold analyses and clay mineralogy are anticipated by the time this report is published.

The high degree of oxidation of the lower parts of each drillcore is unusual and has been encountered only rarely in boreholes from Chaudière Valley. Iron concentrations of about 8-10% are typical in the lowermost highly oxidized stratum. Overlying brown glacial sediments contain about 6% Fe on average, compared to 4% in the clay size fraction ($<\mu m$) for fresh grey tills. The iron-rich, brown nonglacial sediments are preserved directly below clayey laminated sediment that itself lies under a brown diamict complex of uncertain stratigraphic rank. The brown colour of the diamict is caused by reworking of the basal oxidized nonglacial unit as at Gilbert River. The stratigraphic significance of the alternating enrichment and depletion of ultramafic components in this unit must await further detailed study of the core. The sharp decrease in nickel in the upper part of the Lennoxville Till is also presently unexplained (Fig. 16.3).

In the Plante River sections, the Chaudière and Johnville tills are inter calated through a complex system of thrusting caused by glacial drag. The thrust complex is overlain with sharp angular unconformity by the Gayhurst Formation and Lennoxville Till. Although there is no evidence of laminated Gayburst Formation in the Noire River sequence, perhaps the sharp lithological break between the upper grey till and the brown till complex represents a similar contact.

Such a model could account for the variation in nickel concentrations in the brown till complex (Fig. 16.3). Alternatively, a subtle lithological break between Chaudière, (Ni-poor) and Johnville (Ni-rich) tills may have been missed in the preliminary logging.

CRITERIA FOR RECOGNIZING BURIED PLACER POTENTIAL

A number of criteria can be identified in the Beauceville area that may lead to discovery of further buried placer deposits.

Valleys oriented northeast-southwest, approximately at right angles to the regional ice flow directions during Johnville and Lennoxvile glaciations, appear to provide the best setting for preservation of potentially gold-bearing preglacial colluvium and alluvium. If significant amounts of fine grained, proglacial laminated sediment was deposited in lakes ponded in front of the first glacier to traverse the valley, the potential for preservation of the paleocolluvium/alluvium is even further enhanced. Except on Plante River, the lower part of these laminae in the Beauceville area are distinctive in that they are as impoverished as the underlying colluvium in Ni which originates exclusively in the ultramafic belt.

The preglacial colluvium can be distinguished from other oxidized sediments within the overlying Quaternary sequence by its composition. The glacial sediments contain erratics and are enriched in nickel compared to the colluvium, allowing easy differentiation. Elsewhere in the

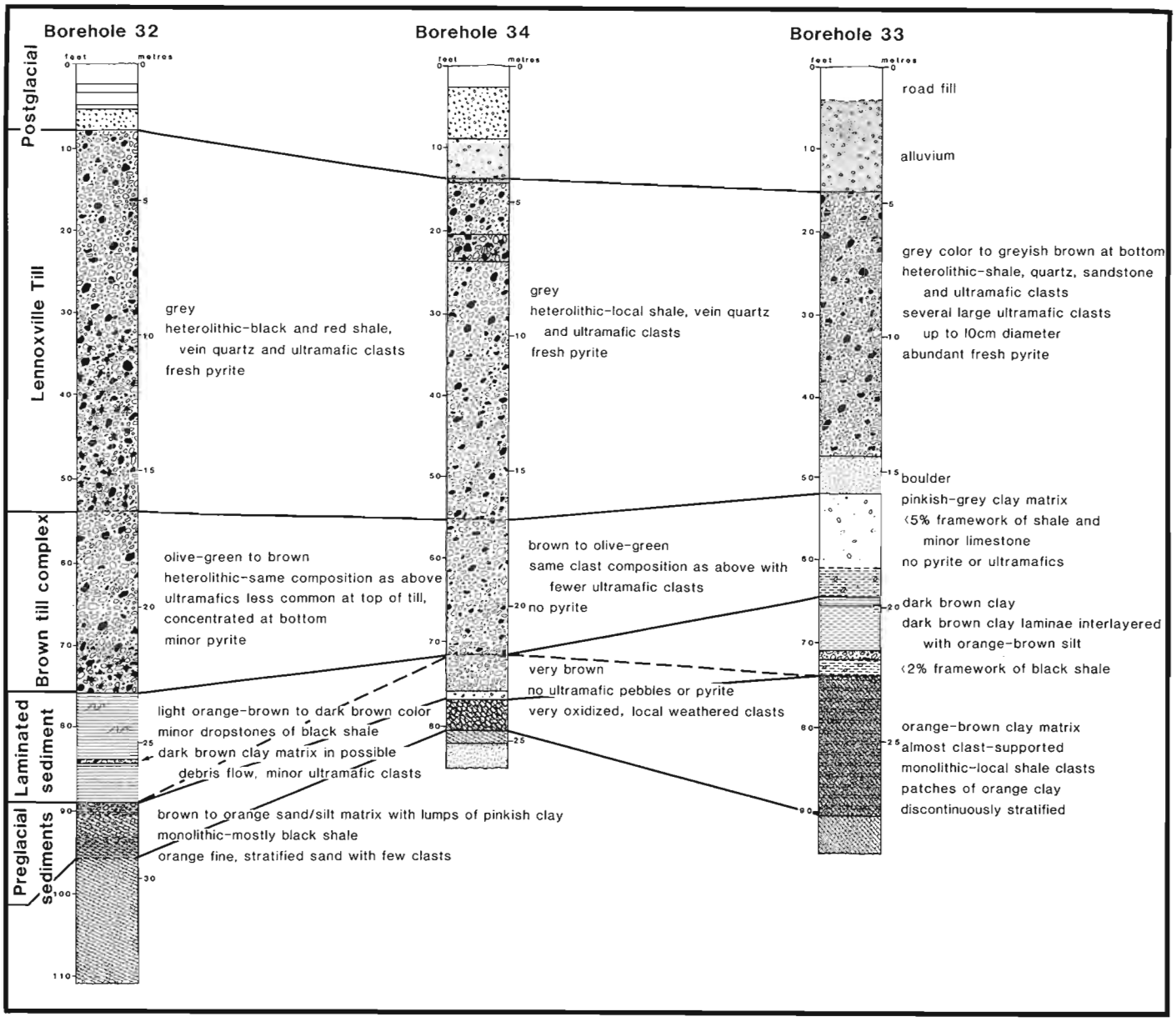
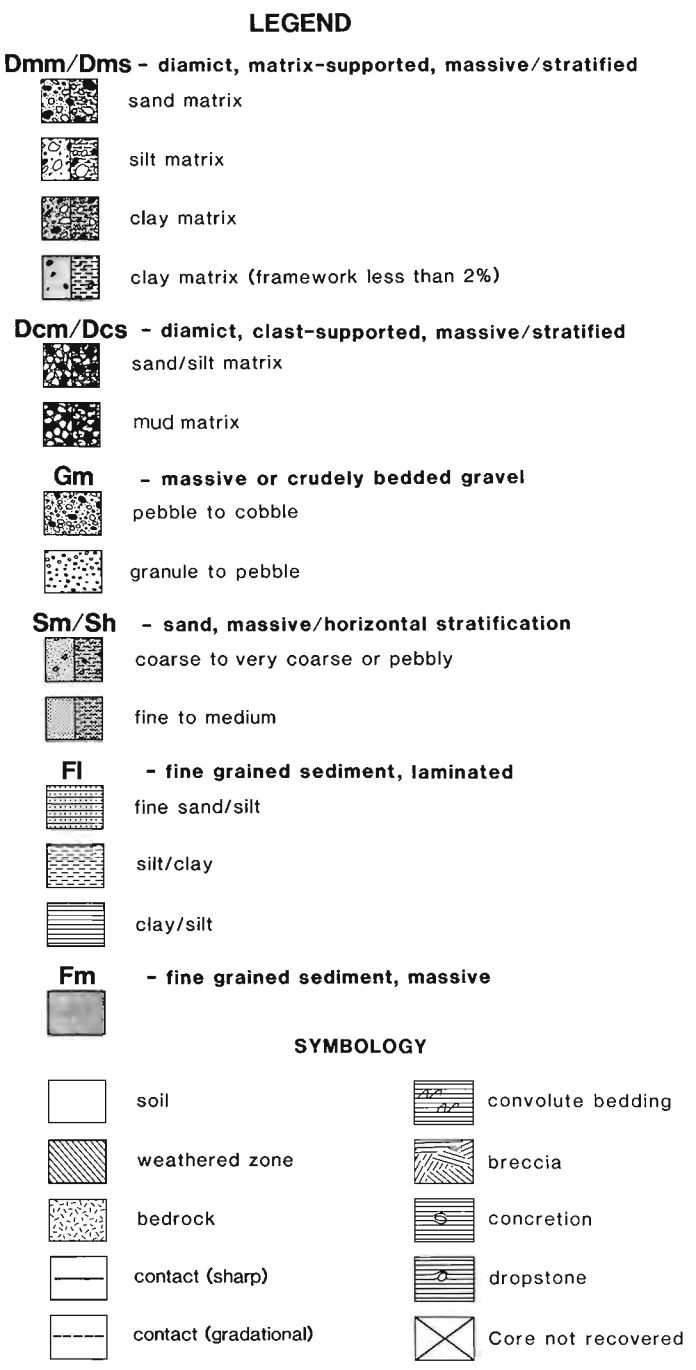


Figure 16.2. Profiles of Noire River cores lithostratigraphy.

Appalachians, where the ultramafic influence is not so great, this compositional pecularity is not likely to be as useful.

The paleocolluvium is very rich in kaolin, a clay mineral rarely encountered in glaciated terrains of the Appalachians (C. De Kimpe, personal communication, 1986). This compositional parameter should be definitive for the paleocolluvium and can be considered as a "pathfinder" in tills containing material reworked from colluvial deposits. This component can be recovered only if appropriate drilling techniques are employed to recover the fine (clay-sized) fractions of the unconsolidated sediments. If kaolin could be identified confidently in the clay fractions of surface or older tills collected from natural or man-made exposures or from boreholes, kaolin dispersal trains could be mapped, presumeably trailing from buried deposits with gold potential.

Finally, the iron concentration in paleocolluvium is very high, up to 12% in the clay (<μm) fraction, relative to the 6% or less Fe encountered in the clay fractions of tills in the Appalachians. The iron enrichment should allow preglacial colluvium to be differentiated from diamicts of similar colour due to oxidation or reworking within the overlying glacial stratigraphic succession.



CONCLUSIONS

To summarize, drilling on buried valley targets defined by prior seismic surveys is necessary to evaluate the potential for finding new occurrences of buried gold placers in Chaudière River valley and adjacent areas. Drilling techniques should provide intact pieces of the unconsolidated cover so that clay mineralogy and geochemistry can be evaluated.

Presence of kaolin is considered as definitive of preglacial colluvial deposits thought to have the highest potential for association with buried placer gold, as well as for tills reworked from them, based on our experience in the Gilbert River area. Kaolin-bearing tills could provide dispersal trains that might indicate location of unknown paleocolluvial deposits. Unfortunately kaolin is difficult to identify without special equipment in the presence of chlorite which dominates the clay fractions of Appalachian tills.

In the Beauceville region, ultramafic components such as Ni and serpentinized ultramafic erratics are useful for differentiating deposits formed preglacially in situ from glacially transported sediments. These compositional pecularities may be useful to a greater of lesser extent eastward and southeastward from the ophiolitic belt, depending on local details of ultramafic dispersal.

Finally, Noire River has all the requisite physiographic and stratigraphic conditions that are thought to indicate a favourable environment for preservation of buried deposits with high potential for gold enrichment. If the experience and methodology we have employed here is applied to similar valleys in the region, other favourable gold environments may be located.

ACKNOWLEDGMENTS

We would like to express our thanks to the crew of Midwest Drilling of Winnipeg, Manitoba for producing the drill-core. Joanne Paul, Tanya Howes, Liana Melchiorre, and Isabelle Poliquin worked diligently at logging and sampling the cores described here, and with Andrée Blais provided capable assistance during the drilling and sampling carried out in 1986. R.N.W. DiLabio critically reviewed the manuscript.

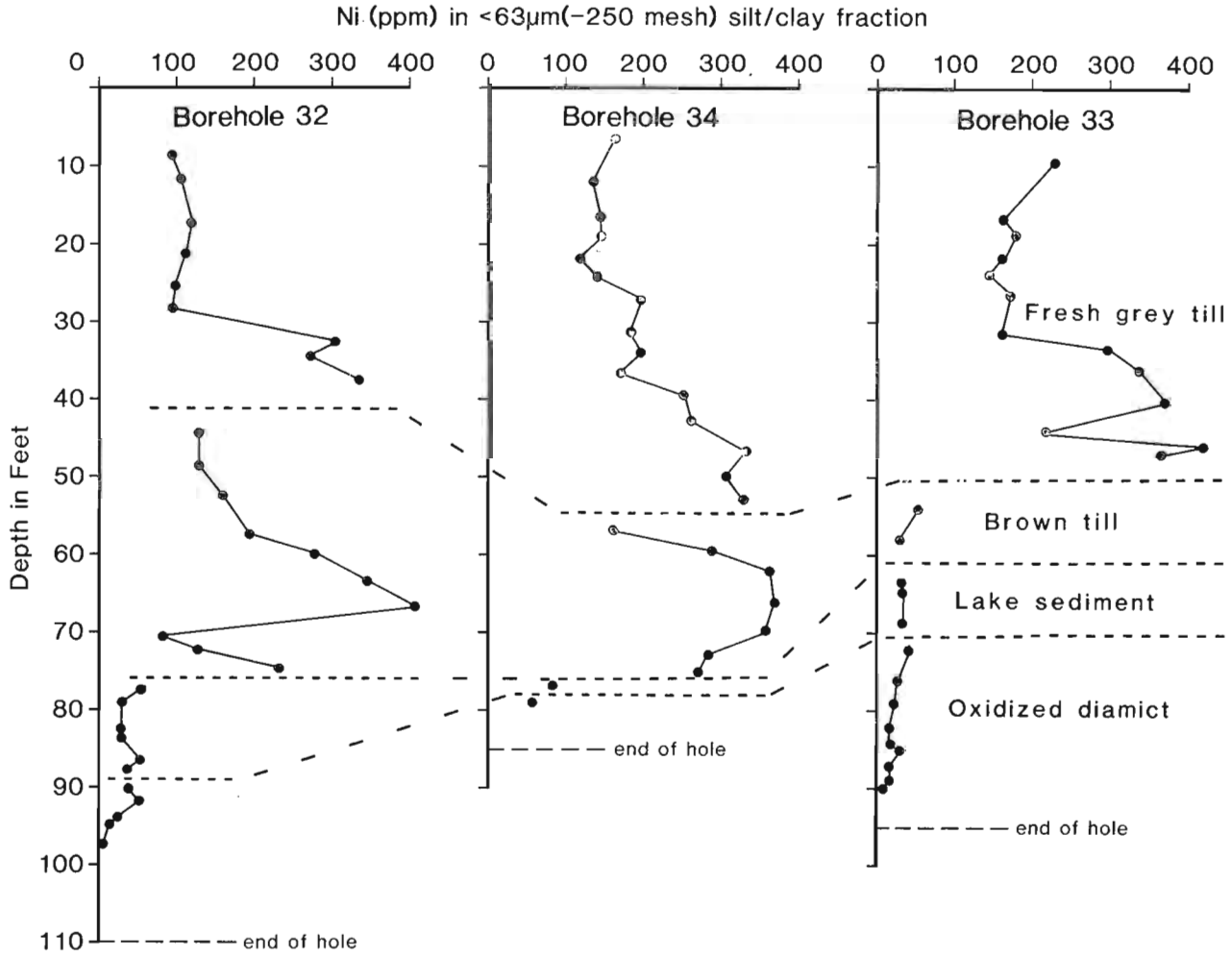


Figure 16.3. Nickel concentration in borehole sediments.

REFERENCES

Eyles, N., Eyles, C.H., and Miall, A.D.
1983: Lithofacies types and vertical profile models; an alternative approach to the description and environmental interpretation of glacial diamict and diamictite sequences; Sedimentology, v. 30, p. 393-410.

Gadd, N.R.
1971: Pleistocene geology of the central St. Lawrence Lowland (with selected passages from an unpublished manuscript "The St. Lawrence Lowlands", by J.W. Goldthwait); Geological Survey of Canada, Memoir 359, 153 p.

Gadd, N.R., McDonald, B.C., and Shilts, W.W.
1972: Deglaciation of southern Quebec; Geological Survey of Canada, Paper 71-47, 19 p.

Lamarche, R.Y.
1971: Northward moving ice in the Thetford Mines area of southern Quebec; American Journal of Science, v. 271, p. 383-388.

Matthews, J.V., Smith, S.L., and Mott, R.J.
1987: Plant macrofossils, pollen and insect fossils of arctic affinity from Wisconsinan sediments in Chaudière Valley, southern Quebec; in Current Research, Part A, Geological Survey of Canada, Paper 87-1A.

McDonald, B.C. and Shilts, W.W.
1971: Quaternary stratigraphy and events in southeastern Quebec; Geological Society of America Bulletin, v. 82, p. 683-698.

Shilts, W.W.
1978: Detailed sedimentological study of till sheets in a stratigraphic section, Samson River, Quebec; Geological Survey of Canada, Bulletin, 285, 30 p.
1981: Surficial geology of the Lac Mégantic area, Quebec; Geological Survey of Canada, Memoir 397, 102 p.

Shilts, W.W. and Smith, S.L.
1986a: Stratigraphy of placer gold deposits; overburden drilling in Chaudière Valley, Quebec; in Current Research, Part A, Geological Survey of Canada, Paper 86-1A, p. 703-712.
1986b: Stratigraphic setting of buried gold-bearing sediments, Beauceville area, Quebec; in Current Research, Part B, Geological Survey of Canada, Paper 86-1B, p. 271-278.

Plant macrofossils, pollen, and insect fossils of arctic affinity from Wisconsinan sediments in Chaudière Valley, southern Quebec[1]

Projects 730027, 690095, 690064

J.V. Matthews, Jr., S.L. Smith, and R.J. Mott
Terrain Sciences Division

Matthews, J.V., Jr., Smith, S.L., and Mott, R.J.; Plant macrofossils, pollen, and insect fossils of arctic affinity from Wisconsinan sediments in Chaudière Valley, southern Quebec; in Current Research, Part A, Geological Survey of Canada, Paper 87-1A, p. 165-175, 1987.

Abstract

Three overburden boreholes in southeastern Quebec contain organic-bearing strata. Based on their relative stratigraphic position, the intervals containing disseminated organic material are assigned to the Massawippi Formation.

Pollen, plant macrofossils, and insect fossils from the organic zones point to an arctic environment, like that of present day northernmost Quebec, at the time of deposition. This paleoclimatic interpretation of these Massawippi Formation sediments contrasts with climatic implications of the St. Pierre interval peat beds in the St. Lawrence Lowlands.

Résumé

Trois sondages forés dans des morts-terrains du sud-est du Québec renferment des couches riches en matières organiques. La position stratigraphique relative des intervalles renfermant des matières organiques disséminées permet d'attribuer ces derniers à la formation de Massawippi.

Du pollen, des macrofossiles de plantes et des fossiles d'insectes provenant de ces zones organiques témoignent de l'existence, au moment de la sédimentation, d'un milieu arctique semblable au milieu actuel des régions les plus septentrionales du Québec. Cette interprétation paléoclimatique concernant ces sédiments de la formation de Massawippi ne concorde pas avec les conditions climatiques observées à partir des lits de tourbe de l'intervalle de Saint-Pierre des basse terres du Saint-Laurent.

[1]Contribution to Federal Asbestos Initiatives, Geoscience Research Program 1984-1987. Project carried by Geological Survey of Canada

INTRODUCTION

In the region of the Chaudière River and its tributaries between Saint-Joseph-de-Beauce and Woburn, Quebec (Fig. 17.1) thick accumulations of glacial sediment fill bedrock paleovalleys. From 1985 to 1986, 45 overburden boreholes were drilled in these valleys for the purpose of examining the stratigraphy of Quaternary and locally preserved Tertiary sediments (Shilts and Smith, 1986a).

Seismic reflection and refraction profiles of bedrock topography were utilized to site the boreholes at the axes of buried valleys where the thickest and possibly most complete stratigraphic sections were expected to occur. In upper Chaudière Valley, south of Saint-Martin, up to 120 m of glacial fill has been documented by drilling, but much thinner sections exist in the Beauce County region (Shilts and Smith, 1986a).

This report discusses pollen and macrofossils found in samples from three boreholes, BP-F1, BP-15 and BP-9, located in the valleys of Grande Coulée, Abenakis, and Moulin Rivers respectively (Fig. 17.1). Pollen preservation was poor and macrofossils were rare; nevertheless, the fossils indicate a cold arctic environment that presumably existed during the latter part of the Massawippi interstade, just prior to the advance of Middle Wisconsinan ice into the area.

SAMPLING AND PROCESSING METHODS

The drillcores were logged using a version of the lithofacies code of Eyles et al. (1983), modified to make better provision for grain size variation within the gross subdivisions of D (diamict), G (gravel), S (sand) and F (fine grained lithologies) (Fig. 17.2). Genetic interpretation was made after the cores were logged. Correlation of the sedimentary units with regional exposures was based on clast lithology, texture, clast:matrix ratio, colour (associated with weathering as well as provenance), and geochemical data from analyses of clay (<2 μm) and silt/clay (<63μm) size fractions and heavy mineral separates of tills. Because radiometric or other types of dates were not available, the fluvial and lacustrine interstadial sediments were correlated on the basis of their relative stratigraphic position.

Of 45 drillcores, only three contain noticeable organic material. These organics were best observed by cutting through the core to create a flat face. Water sprayed on the face from a hand held atomiser quickly revealed whether or not organics were present, because they float.

Intervals containing organic-bearing sediment from the Abenakis and Moulin river boreholes (Fig. 17.3,17.4) were sampled in consecutive 30 cm increments after splitting each increment into two halves. Each analyzed half consisted of approximately 1500 ml of sediment. The Grande Coulée River core contained only two closely spaced organic horizons at the 47.5 m Level. All of the samples from this level were studied for fossils.

For pollen analysis a measured volume (2 mL) of sediment, to which a standardized Eucalyptus pollen aliquot was added, was subjected to a modified acetolysis treatment involving digestion in HCl, HF, KOH, dilute HNO_3, and acetolysis mixture. The residue was suspended in silicon oil for counting.

Plant and animal macrofossils were isolated by sieving the sediments with 80-40 mesh/inch (0.180-0.425 mm opening) sieves and then examining all of the remaining residue, which usually amounted to as little as 1/1000 of the original sediment volume. All picked fossils are stored in alcohol or mounted for microscopic examination.

REGIONAL SETTING

Glacial Events

At least three glacial units have been recorded from Chaudière Valley, represented from oldest to youngest by the Johnville, Chaudière, and Lennoxville tills (McDonald and Shilts, 1971; Shilts, 1978, 1981; Occhietti et al., 1982; LaSalle, 1984. The dominant ice flow direction during the Johnville and Lennoxville glaciations was to the southeast from a Laurentide source northwest of the region. Ice moved to the south-southwest from a possible Maritimes source during the initial phase of the Chaudière glaciation and was later overwhelmed by ice that advanced again from a Laurentide dispersal centre (Shilts, 1978, 1981).

Sediments separating these Wisconsinan tills comprise the Massawippi Formation which postdates the Johnville glaciation, and the Gayhurst Formation which represents a relatively brief retreat of the Laurentide Chaudière glacier to south of St. Lawrence River and subsequent readvance of the Lennoxville ice front.

Massawippi Formation and the St. Pierre interval

Sediments representing the Massawippi Formation and St. Pierre interval have been reported from the Eastern Townships and the St. Lawrence Lowlands, respectively. In the Eastern Townships, sections at Ascot, Samson, Grand Coulée, and Plante rivers (Fig. 17.1) expose sediments of the interstadial Massawippi Formation (McDonald and Shilts, 1971; Shilts, 1978, 1981; Shilts and Smith, 1986b). In cores, Massawippi sediments comprise rounded coarse gravel interstratified with sandy or silty layers (Shilts and Smith, 1986a). In river bluff sections, the gravel is imbricated and oxidized. Bedded and crossbedded sand and associated silty overbank flood deposits are exposed, and at Plante River grade laterally into a facies equivalent slump deposit of stony diamict containing peat beds or disseminated organic material. Locally overlying this fluvial sequence is 5 m of maroon, laminated, graded, lacustrine silt and clay that formed when the advancing ice front of the Chaudière glacier ponded drainage.

Detailed work is continuing on the organic material at the Plante River sections but preliminary fossil analyses (pollen and macrofossils; Matthews and Mott, unpublished data)

indicate a boreal to subarctic climate. Other recent discoveries of organic sites in southern Quebec include a section near Bethanie (LaSalle et al., 1986) and another at Vallee-Jonction (LaSalle et al., 1979; Fig. 17.1). The first has yielded boreal to subarctic insects, plant macrofossils and pollen, the latter a subarctic to arctic type flora.

The St. Pierre interval is defined by organic-bearing sediments occurring at several exposures in the St. Lawrence Lowlands (Terasmae, 1958; Gadd, 1960). St. Pierre sediments comprise well sorted, bedded, fluvial sand and pebble or cobble size gravel that is locally cemented and interstratified with autochthonous peat beds or sediments containing disseminated organic material. The peaty facies of the St. Pierre sequence occurs most commonly in abandoned channels that represent former meandering streams (Gadd, 1971). Detailed descriptions of St. Pierre peat beds are given by Gadd (1955) and Terasmae (1955).

According to the pollen and macrofossil data, the St. Pierre sediments record a complete climatic cycle that took place between the Bécancour and Gentilly glaciations. After retreat of the Bécancour glacier, mean annual temperature in the St. Lawrence Lowlands rose to within 3 to 5°F of present values (Terasmae, 1958) before declining to a cold, subarctic level prior to onset of the Gentilly Stade.

Similarities of relative stratigraphic position suggest correlation between the Massawippi Formation in Chaudière Valley and the St. Pierre interstadial sediments of the St. Lawrence Lowlands (Gadd, 1960, 1971; McDonald and Shilts, 1971; LaSalle et al., 1979; LaSalle, 1984).

Correlations based on radiometric dates or environmental interpretation of organic material, however, are not definitive because most dates on the Massawippi Formation and the St. Pierre interval are nonfinite. Occhietti (1982) has reported a date of >54,000 BP (Y-1683) for the Massawippi sediments and a finite date of $74{,}700^{+2700}_{-2000}$ has been obtained on wood from one of the classical St. Pierre localities (QL-198; Stuiver et al., 1978). Although several options remain open for the age of the St. Pierre interval, it probably dates from some time between stage 3 (Mid Wisconsinan) and stage 5a of the marine isotopic record.

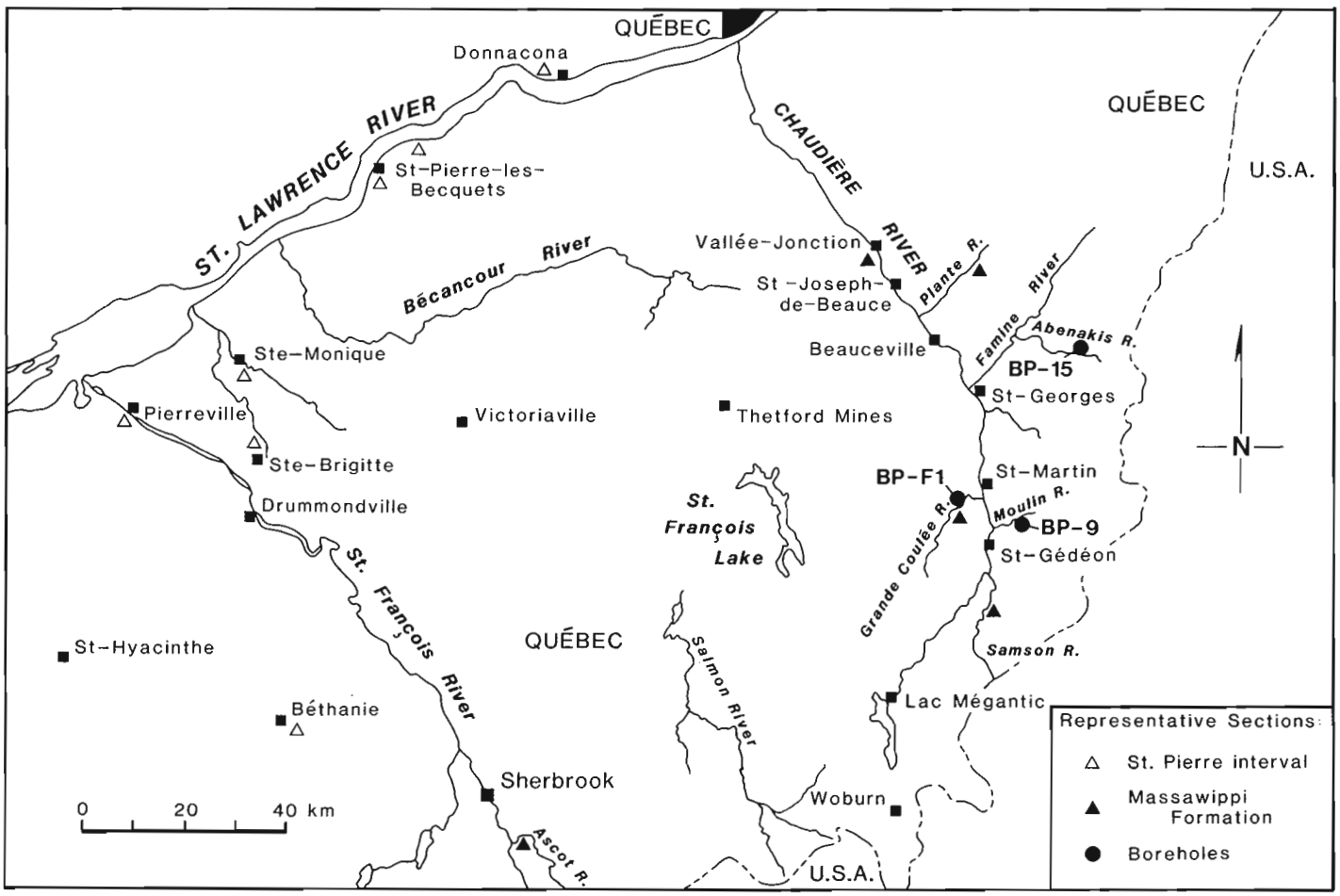
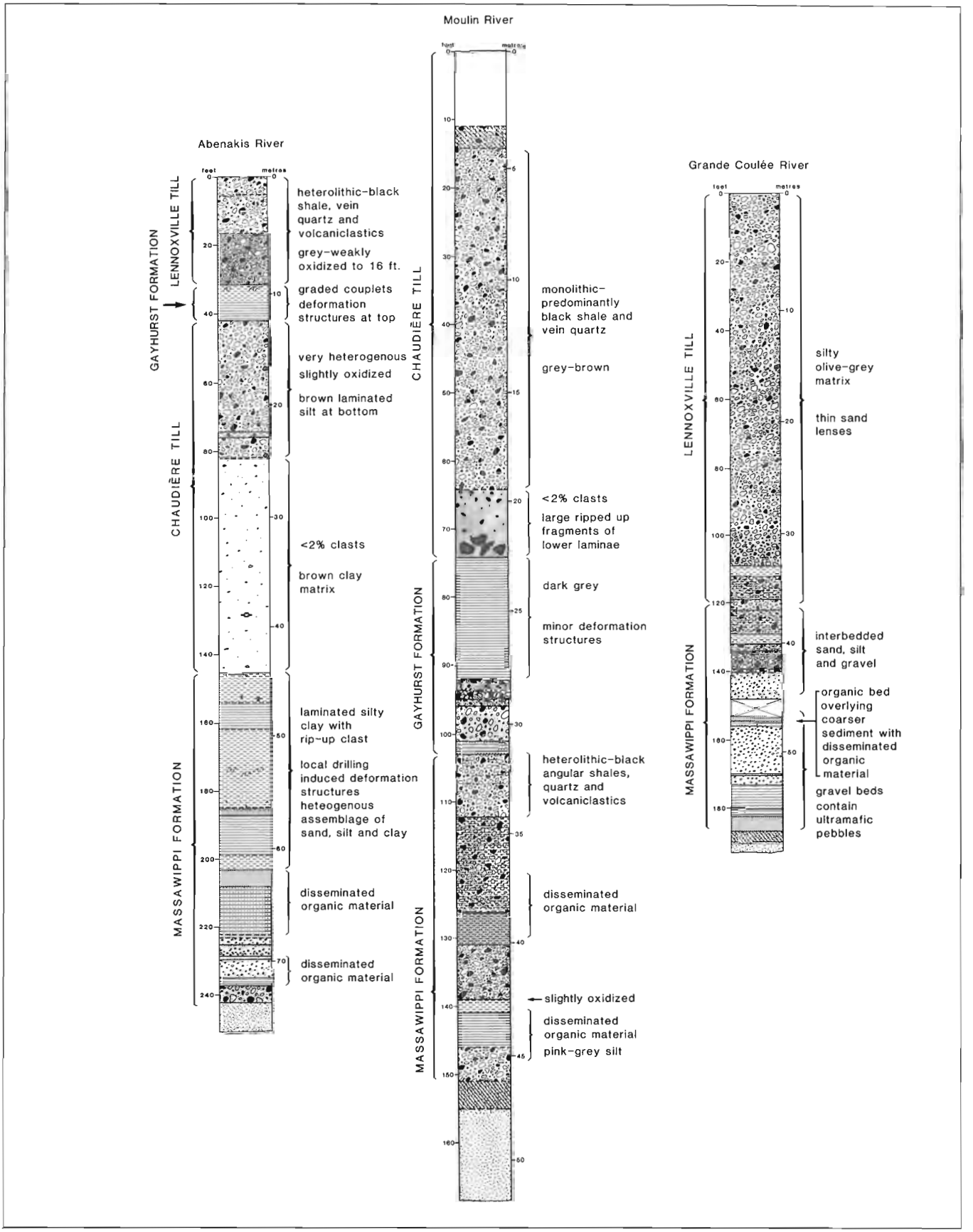


Fig. 17.1. Map showing well documented St. Pierre and Massawippi sites and location of boreholes BP-F1 (Grande Coulée River), BP-9 (Moulin River), and BP-15 (Abenakis River).


Abenakis River
feet
metres
GAYHURST FORMATION
LENNOXVILLE TILL
heterolithic-black shale, vein quartz and volcaniclastics
grey-weakly oxidized to 16 ft.
graded couplets deformation structures at top
CHAUDIÈRE TILL
very heterogenous slightly oxidized
brown laminated silt at bottom
<2% clasts
brown clay matrix
MASSAWIPPI FORMATION
laminated silty clay with rip-up clast
local drilling induced deformation structures heteogenous assemblage of sand, silt and clay
disseminated organic material
disseminated organic material
Moulin River
CHAUDIÈRE TILL
monolithic-predominantly black shale and vein quartz
grey-brown
<2% clasts
large ripped up fragments of lower laminae
GAYHURST FORMATION
dark grey
minor deformation structures
MASSAWIPPI FORMATION
heterolithic-black angular shales, quartz and volcaniclastics
disseminated organic material
slightly oxidized
disseminated organic material
pink-grey silt
Grande Coulée River
LENNOXVILLE TILL
silty olive-grey matrix
thin sand lenses
MASSAWIPPI FORMATION
interbedded sand, silt and gravel
organic bed overlying coarser sediment with disseminated organic material
gravel beds contain ultramafic pebbles

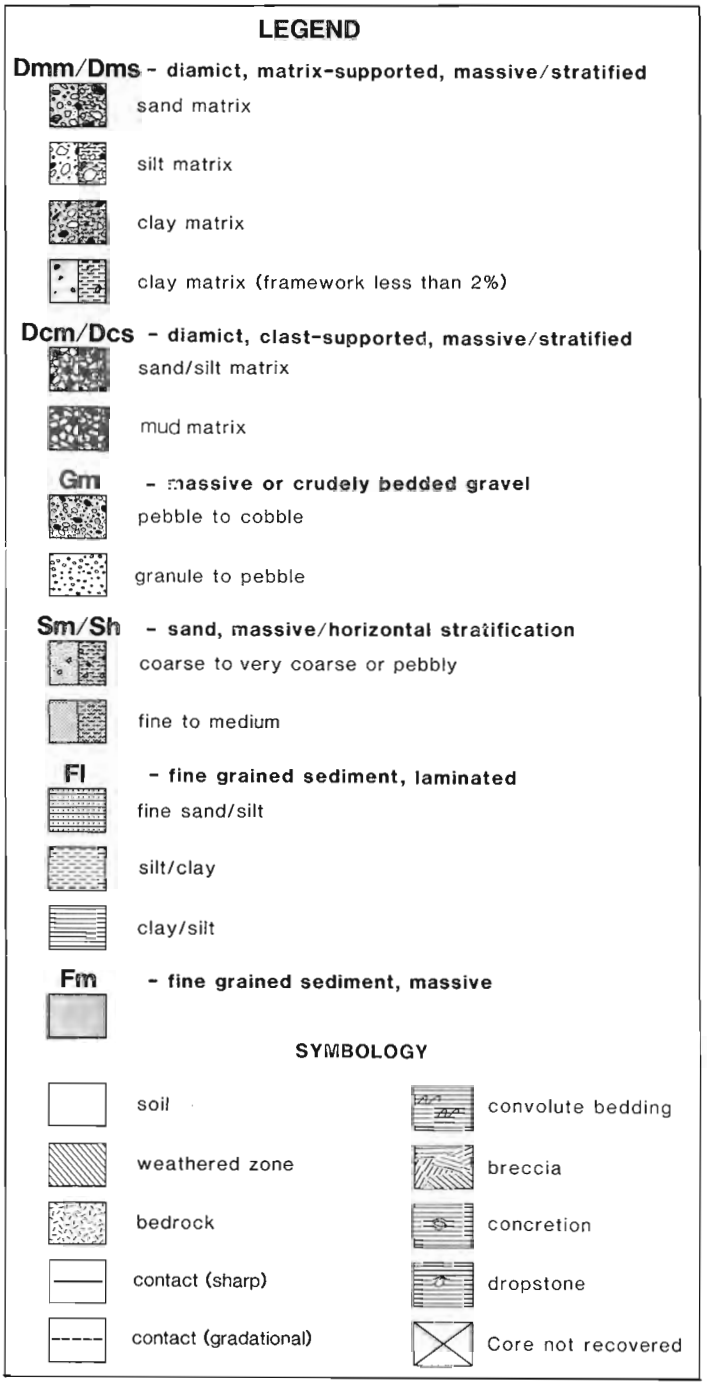


Fig. 17.2. Lithological logs of borehole sediments including descriptive notes and position of the organic bearing core sediments.



Fig. 17.3. Core segment of BP-9 (Moulin River), showing organic layers along thin clay laminae. 204319-C

POLLEN ANALYSES

Pollen analyses were conducted on selected samples from the more organic-rich intervals in each of the three cores. No attempt was made to process and count all samples collected for analyses because it was obvious that many of them were barren or contained pollen too poorly preserved to count. Results are listed in Table 17.1 as percentage values based on the sum of palynomorphs exclusive of aquatics and spores.

In all samples the pollen grains were corroded or degraded to a considerable degree, making identification difficult as can be seen in the relatively large amounts of unidentified grains. Pollen concentrations were variable with largest values (approximately 120 000) occurring in Abenakis level 67.36 m 1) and the lowest (approximately 2400) in Moulin River level 38.25 m (Table 17.1). A few other samples were virtually barren of pollen. Because pollen concentrations are relative values that are dependent on the sedimentation rate, they cannot be used in an absolute sense to indicate vegetation cover.

It is readily apparent (Table 17.1) that all of the spectra are variations on the same theme. Gramineae (grass) pollen is the most or second most abundant taxon in all samples. *Pinus*

Table 17.1 Selected pollen analyses from Chaudière Valley cores

	Moulin R.					Abenakis R.			G. Coulée R.	
Taxa	36.8	38.25	39.3	43.58	44.9	67.2	67.36	67.51	A	B
Picea	3.2	8.0	9.9	8.6	7.5	4.6	5.9	5.1	2.4	11.3
Pinus	10.8	21.6	20.6	21.7	11.6	28.3	25.7	30.1	33.8	39.6
Abies	0.5	–	–	0.4	–	–	–	–	–	–
Larix	–	–	–	–	–	–	–	–	1.2	–
Betula	1.4	5.7	0.9	9.6	9.7	23.8	21.0	11.3	3.6	5.7
Tilia	–	–	–	–	0.4	–	–	–	–	–
Carya	–	–	–	–	–	0.4	–	–	–	–
Juniperus (?)	0.5	–	–	–	–	–	–	–	–	–
Alnus	1.4	2.3	1.7	0.9	1.9	3.3	5.1	2.5	–	–
Salix	0.9	–	0.4	–	0.4	0.4	–	–	–	1.9
Corylus (?)	0.5	–	–	–	–	–	–	–	–	–
Shepherdia canadensis	0.5	–	–	–	–	–	–	–	–	–
Myrica	–	–	–	–	–	0.4	–	0.6	–	–
Nemopanthus/Ilex	–	–	–	–	–	–	0.9	–	–	–
Ericaceae	–	–	–	0.4	–	–	–	–	1.2	–
Gramineae	61.3	54.5	50.6+	39.3	53.4	25.4	29.3	34.9	40.5	22.6+
Tubuliflorae	0.9	–	1.3	2.5	2.2	5.8	4.1	5.1	2.4	–
Ambrosieae	–	–	–	–	–	0.4	0.3	0.6	–	–
Artemisia	0.9	–	1.3	2.5	0.4	1.2	0.9	0.8	–	1.9
Chenopodiineae	–	–	0.4	–	–	0.4	0.9	0.3	–	–
Sanguisorba canadensis ?	–	–	–	–	–	–	–	0.8	–	–
Dryas (?)	–	–	0.4	–	–	–	–	0.3	–	–
Caryophyllaceae	4.1	2.3	3.4	6.8	5.6	2.1	1.8	3.7	3.6	–
Ranunculaceae	–	–	–	0.4	–	0.8	–	0.3	–	–
Thalictrum	0.9	–	–	0.4	0.7	0.4	0.9	0.6	2.4	5.7
Cruciferae (?)	–	–	–	–	–	–	–	0.3	–	–
Saxifragaceae	0.9	–	–	0.4	0.4	–	–	–	–	–
Rumex/Oxyria	1.8	–	2.6	–	–	–	–	–	–	1.9
Koenigia islandica	–	–	–	–	–	–	–	0.3	–	–
Polygonum	–	–	–	–	0.7	–	–	–	3.6	–
Leguminosae	–	–	–	–	–	–	–	–	1.2	–
Polemonium	–	–	–	–	0.4	–	–	–	–	–
Rubus chamaemorus	–	–	–	–	–	–	0.3	–	–	–
Unidentified	9.9	3.4	6.4	4.6	3.0	2.1	3.0	2.5	4.8	9.4
included in pollen sum										
excluded from pollen sum										
Lycopodium	0.9	–	1.3	0.7	1.9	2.1	0.3	0.3	1.2	–
Selaginella selaginoides	0.5	–	–	–	–	–	–	–	–	–
Pteridophyta	0.5	–	–	–	–	0.4	0.3	–	–	–
Polypodiaceae	0.9	2.3	0.9	0.7	0.4	–	0.6	0.8	1.2	–
Osmunda	–	1.2	–	–	0.7	–	0.3	–	–	–
Cyperaceae	14.9	31.8	17.2	17.9	9.7	22.1	24.0	23.9	26.2	39.6
Sphagnum	2.7	5.7	5.2	0.4	3.0	2.1	1.8	1.7	6.2	11.3
Isoetes	–	–	–	–	0.4	–	–	–	–	–
wood fragments	+	+	+						+	

Numbers at head of each column refer to level (in metres) in the borehole (see Fig. 17.2). Numbers in each column represent the percentages.



Fig. 17.4. Core sediment from BP-15 (Abenakis River), showing visible organic fragments. 204319-S

(pine), Cyperaceae (sedge), and *Betula* (birch) are the next most prominent components. *Alnus* (alder) is a consistently represented shrub taxon, but in very low amounts. *Salix* (willow) pollen is sparse or absent. A variety of herbaceous types are represented with Caryophyllaceae (pink family), Tubuliflorae (composite subfamily) and *Artemisia* being consistently present. The Abenakis River core spectra differ somewhat from the other spectra in that they have much higher *Betula* values. A mixture of sizes and morphological differences suggest that both shrub and tree birch may be represented.

The dominance of Gramineae and Cyperaceae pollen and the variety of open-ground indicators with tundra affinities indicate that the area was tundra like. Despite the abundance of *Pinus* and *Picea* pollen, spruce and pine trees were probably not present in the area. Tundra spectra typically contain large numbers of *Pinus* and *Picea* pollen as well as *Alnus* and *Betula* (Lichti-Federovich and Ritchie, 1968; Farley-Gill, 1980) that have been blown into tundra areas from a considerable distance and are relatively abundant because of the low pollen production of local tundra vegetation. The *Betula* pollen in the Abenakis River samples and in other samples as well, represents, at least in part, shrub birch which may have been present locally. Arboreal birch species probably did not occur in the area.

MACROFOSSILS

Macrofossils recovered from the sediments of the three boreholes are listed in Table 17.2. The identifiable plant remains include 'seeds', capsules, and leaf fragments. Insect fossils comprise isolated unidentifiable fragments plus a few diagnostic pronota, elytra, and heads of Coleoptera (beetles). Although a number of individual core increments were studied, the fossils from each core were pooled, because fossils from individual samples were so rare that there appeared to be no consistent differences between the samples.

In all the cores, preservation of plant remains was rather poor, but this is typical of alluvium (Fig. 17.3, 17.4). Insect fossils were rarer than those of plants, but relatively better preserved. Figures 17.5 and 17.6 show the present distribution of some of the plants and insects that were found as fossils. Figure 17.6a also shows the present limit of forests in Quebec.

Even though the insect fossils are rare in the sediments from the three boreholes, almost all of those that could be identified represent species that do not occur in the lowlands of southern Quebec today. One of the most notable of these is the ground beetle *Amara alpina* from the Moulin River core (Fig. 17.6b). This species is typical of dry tundra sites across North America and its southern distribution limit corresponds closely with the forest/tundra boundary and the 10°C mean July isotherm (Lindroth, 1963a). As with some of the other insect taxa and several of the plants, it does occur at a few southern Canadian localities, but only in alpine areas that mimic the climate much farther north. Thus, the *Amara alpina* fossils call for a climate much colder than at present during deposition of the organics in the Moulin River borehole. At that time large areas of the Appalachians must have been essentially treeless.

A similar conclusion is suggested by the fossils of the staphylinid beetle *Olophrum latum* from the Moulin River core and the hydrophilid beetle *Helophorus parasplendidus* from the Abenakis River core. Furthermore, unlike some of the other insects listed in the table, these two have not been found east of Hudson Bay (Campbell, 1983; Smetana, 1985). Fossils of the ground beetles *Bembidion hasti* and *Elaphrus lapponicus* were found in the Grande Coulée River borehole sediments. The former presently resides "on barren gravelly banks and shores, usually along rivers, but also at lakes and pools on the tundra" (Lindroth, 1963b, p. 298). Its distribution in Quebec is strictly arctic (Larochelle, 1975; Fig. 17.6b). *Elaphrus lapponicus* has been collected at only a few localities in Quebec and Labrador (Larochelle, 1975; Fig. 17.6a). It is more common west of Hudson Bay but, unlike some of the other species in the table, is more likely to be found in subarctic than arctic areas. According to Goulet (1983), adults can be collected near cold waters of ponds and lakes, among mosses, but in open sunny areas where trees are scattered.

All three boreholes yielded fragments referred with various degrees of confidence to the subgenus *Cryobius* of the ground beetle genus *Pterostichus*. The subgenus contains a number of morphologically similar species that are difficult to separate on the basis of fossils, but nearly all of them are northern boreal or strictly arctic in distribution. Only three species occur in Quebec and all of these in the northern part of the province except at isolated alpine sites in the south (Ball, 1966; Lindroth, 1966; Larochelle, 1975; Fig. 17.6c).

Table 17.2 Animal (mainly Insecta) and plant macrofossils from Chaudière Valley cores

ANIMALS				PLANTS			
Taxa	Moulin R.	Abenakis R.	G. Coulée R.	Taxa	Moulin R.	Abenakis R.	G. Coulée R.
BRYOZOA				Fungal Sclerotia	+		+
Cristatella mucedo L.	+			Bryophytes	+		
ARTHROPODA				Selaginellaceae			
INSECTA				*Selaginella selaginoides* (L.)Link		+	
HEMIPTERA				Isoetaceae			
Saldidae				*Isoetes* sp.	+		+
Genus?	+			Gramineae			
COLEOPTERA				Genus?	+	+	+
Carabidae				Cyperaceae			
Notiophilus sp.	+	+		*Carex* sp.	+	+	+
Dyschirius sp.		+		*Kobresia* sp.	+		
Elaphrus lapponicus Gyll.	+		+	Juncaceae			
Bembidion hasti Sahlb.			+	*Juncus* sp.	+		+
Bembidion sp.	+			*Juncus/Luzula* type	+	+	
Pterostichus sp.	+			Salicaceae			
Pterostichus (Cryobius) sp.	+			*Salix* sp.	+		+
P. (Cryobius) arcticola Chaud.		+		Polygonaceae			
P. (Cryobius) pinguedineus Eschz.	+			*Oxyria digyna* (L.)Hill	+	+	+
P. (Cryobius) ventricosus Eschz.		?	?	*Rumex* sp.	+		
Amara alpina Payk.	+			Ranunculaceae			
Hydrophilidae				*Ranunculus hyperboreus* type	+		
Helophorus parasplendidus Angus		+		*Ranunculus pedatifidus* Sm.		+	
Staphylinidae				*Thalictrum alpinum* L.			+
Stenus sp.	+	+	+	Portulacaceae			
Olophrum latum Makl.	+			*Claytonia* sp.			+
Olophrum boreale (Payk.)			+	Caryophyllaceae			
Arpedium/Eucnecosum type			+	*Cerastium* sp.	+		
Aleocharinae	+			*C. Beeringianum* Cham.Schlecht.	+		
Genus?	+			*Melandrium* sp.		+	
Byrrhidae				*Minuartia yukonensis* type		+	
Simplocaria sp.	+			*Silene Menziesii* type	+		
genus?	+			*Stellaria* sp.	+		
Chrysomelidae				Papaveraceae			
Chrysolina sp.	+			*Papaver* sp.	+	+	
Curculionidae				Cruciferae			
Rhynchaenus sp.	+			*Draba* sp.	+	+	+
Genus?	+	+		*Erysimum* type		+	+
DIPTERA				Saxifragaceae			
Chironomidae				*Saxifraga aizoides* type	+	+	+
Genus?	+			*S. caespitosa/flagellaris* type	+		
Xylophagidae				*S. oppositifolia* L.		+	
Xylophagus sp.	+			Rosaceae			
Family	+	+		*Potentilla* sp.	+	+	
HYMENOPTERA				*Dryas integrifolia* Vahl.			+
Ichneumonoidea	+			*Dryas* sp.	+		
Undet.	+			Primulaceae			
ARACHNIDA				*Androsace* sp.			?
Araneae				Scrophulariaceae			
Erigonidae				*Castilleja* sp.			+
Erigone sp.	+			Lobeliaceae			
Acari				*Lobelia* sp.			+
Oribatei				Compositae			
Undet.	+	+		Genus?			+

Fossils labelled Moulin R. come from between 36.8 and 44.8 m level from a borehole (86-BP-9) located approximately 4 km NE of Saint-Gédéon, Quebec (45°52.83′N; 70°36.75′W: see text and Fig. 17.1).

Fossils labelled Abenakis R. come from between 63 and 67 m and 69-73.5 m depth from a borehole (86-BP-15) located 16 km NE of Saint-Georges (46°12.83′N; 70°32.42′W: see text and Fig. 17.1).

Fossils labelled G. Coulée R. come from two organic zones at approximately the 45.7 m depth from a borehole (86-BP-F1) located 8 km SW of Saint-Martin (45°54.67′N; 70°45′W: see text and Fig. 17.1).

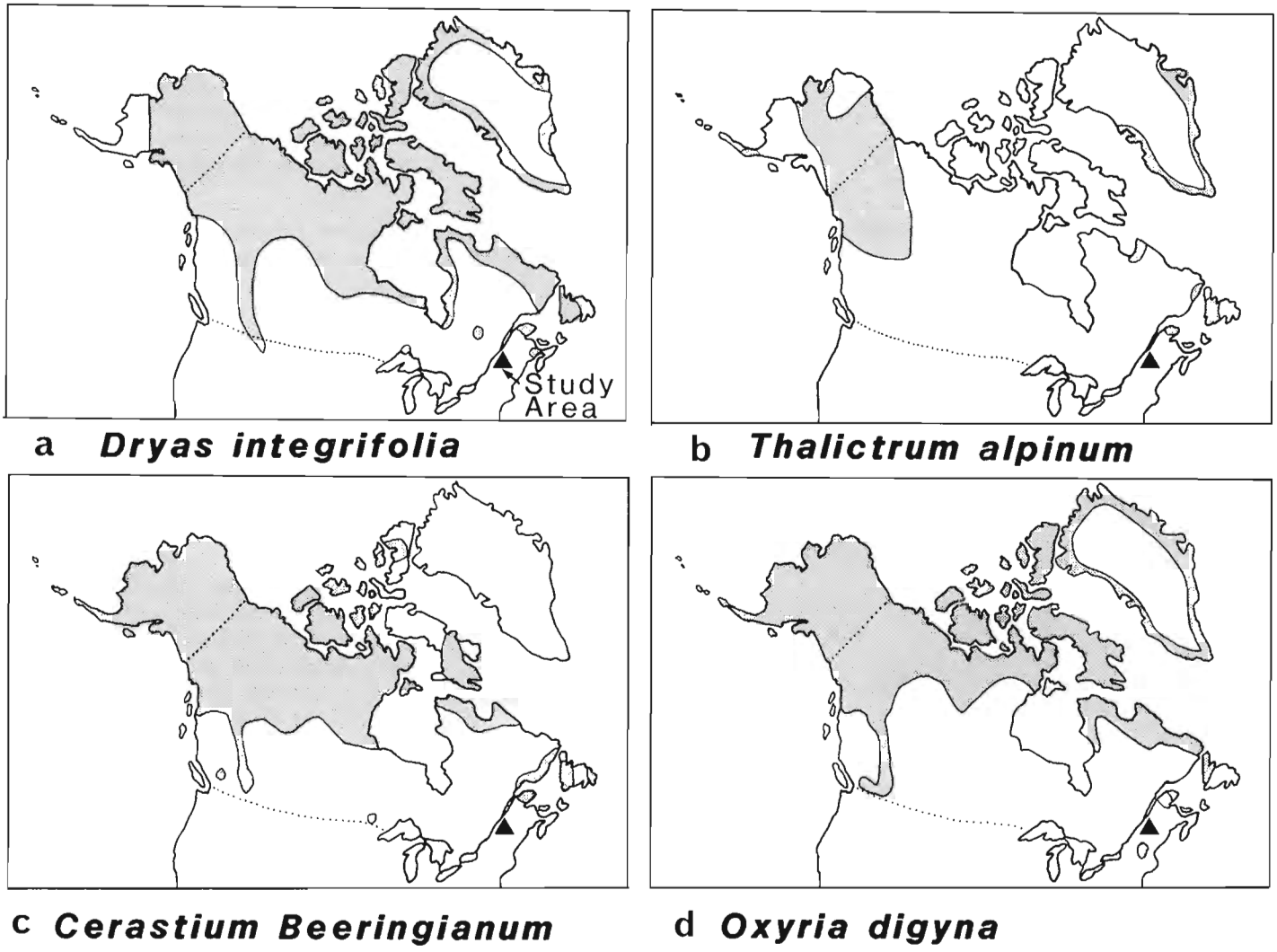


Fig. 17.5. Present distribution (generalized) of selected plant species listed in Table 17.2 (after Porsild and Cody, 1980).

Thus the presence of *Cryobius* fossils, regardless of their identity, also suggests much colder climate than at present in the lowlands of southern Quebec.

Plant macrofossils from the Grande Coulée River core clearly indicate arctic conditions. *Thalictrum alpinum*, for example, is typical of well vegetated tundra sites (Fig. 17.5b), and the assemblage also contains leaf fragments of *Dryas integrifolia* and seeds of *Oxyria digyna*, both of which occur on the tundra, and occupy dry, open sites when they are found within treeline (Fig. 17.5,a,d). *Saxifraga oppositifolia* from the Abenakis River borehole calls for similar conditions. *Selaginella selaginoides* is not often found beyond treeline, but there are many localities recorded within the subarctic region of northern Canada (Porsild and Cody, 1980).

All three cores, but particularly the one from the Abenakis River site, contained an abundance of Caryophyllaceae seeds. "Caryoph" seeds are difficult enough to identify when well preserved, and most of those from the boreholes were poorly preserved. The number of Caryophyllaceae taxa in Table 17.2 is greater than for other families listed there. This tendency would undoubtedly be accentuated if more of the fossils could be identified.

Conifer needles are easily transported and very resistant to degredation with the result that whenever conifers exist in a region, even if only in upland and interfluve areas, their needles become incorporated in local alluvial sediments. There are no conifer needles in any of the borehole samples, hence conifers were likely to have been rare or even absent from the region at the time of deposition. Similarly, none of the fossil assemblages contain macroremains of shrub birch and alder, even though both taxa are usually well represented in the vegetation of low arctic tundra sites. Shrub birch was obviously rare, in contrast with typical low arctic tundra, but according to the pollen evidence it was probably growing somewhere in the region.

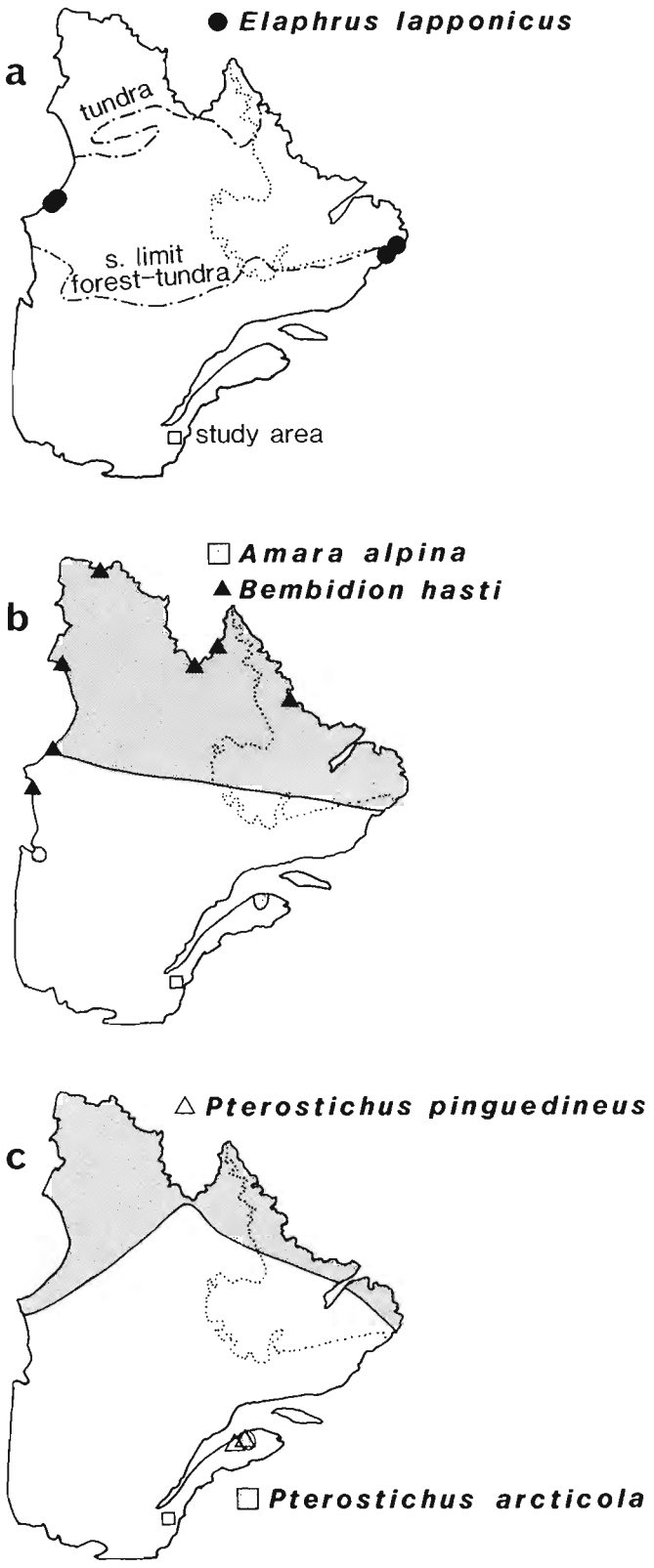


Fig. 17.6. Present distribution of selected beetle species listed in Table 17.2 (after Larochelle, 1975). Major vegetation zones in Quebec today are indicated in "a".

DISCUSSION

Pollen and macrofossils from all three boreholes show clearly that tundra prevailed in the lowlands of Chaudière Valley at the time of deposition of the organic sediments. If the entire area was treeless, then mean July temperatures were no warmer than 10°C, which is much colder than at present in the area.

None of the plants or insects represented by macrofossils are restricted to forested areas. Note, however, that at least one of the insect species and one of the plant species recorded from the borehole sediments have contemporary ranges that are more subarctic than arctic, and many of the pollen samples show nearly 10% spruce pollen. These facts hint that treeline may not have been far removed from Chaudière Valley. Minor amounts of shrub birch may have been present at suitable sites in the region but, according to the macrofossils, not on the former floodplain of Chaudière River. Instead, the local floodplain vegetation was dominated by herbs such as grasses, sedges, and various species of Caryophyllaceae.

The results presented here deviate considerably from the boreal forest indicators commonly encountered in St. Pierre interstadial peats (Terasmae, 1958; LaSalle et al., 1986) that indicate conditions only slightly cooler than at present in the St. Lawrence Lowlands. Any one of three alternatives may reconcile this paradox: 1) The St. Pierre and Massawippi Formations may actually represent different intervals despite the stratigraphic constraints apparent from section and borehole data. 2) They may represent different parts of the same interval; the St. Pierre representing the warmest part of the interval and the Massawippi the cooler part at the begining of the interval, or more likely, the colder waning phase prior to the onset of glaciation. 3) The St. Pierre spectra may typify conditions in the St. Lawrence Lowlands, whereas the Massawippi reflects conditions at higher elevations in tributary valleys flowing from the Appalachian Highlands.

Although the available fossil evidence from the three cores is somewhat limited, we believe it reflects a cold period of the Massawippi immediately before the onset of the Chaudiere glaciation. Studies presently in progress on organics from the Plante River section may help to define the character of the warmer phases of the Massawippi interstade. It will be interesting to compare such conclusions with those derived from study of macrofossils and pollen at the St. Pierre localities in the St. Lawrence Lowlands. We feel strongly, however, that correlation of such units should be based on physical stratigraphic relationships or isotopic and other types of absolute dating, rather than on the fossil content of organic deposits.

ACKNOWLEDGMENTS

Rob Rainbird, Jennifer Smith, and Joanne Paul relogged these cores, in the process discovering and sampling the organic-bearing intervals. T. W. Anderson critically reviewed the manuscript.

REFERENCES

Ball, G.E.
1966: A revision of the North American species of the subgenus *Cryobius* Chaudoir (*Pterostichus*, Carabidae, Coleoptera); Opuscula Entomologica, Supplementum XXVIII, 166 p.

Campbell, J.M.
1983: A revision of the North American Omaliinae (Coleoptera: Staphylinidae), the genus *Olophrum* Erichson; The Canadian Entomologist, v. 115, p. 577-622.

Eyles, N., Eyles, C.H., and Miall, A.D.
1983: Lithofacies types and vertical profile models; an alternative approach to the description and environmental interpretation of glacial diamict and diamictite sequences; Sedimentology, v. 30, p. 393-410.

Farley-Gill, L.D.
1980: Contemporary pollen spectra in the James Bay Lowland, Canada, and comparison with other forest-tundra assemblages; Géographie physique et Quaternaire, v. 34, p. 321-334.

Gadd, N.R.
1955: Pleistocene geology of the Bécancour map-area, Quebec; unpublished PhD thesis, University of Illinois, Urbana.
1960: Surficial geology of the Bécancour map-area, Quebec; Geological Survey of Canada, Paper 59-8, Map 42-1959.
1971: Pleistocene geology of the central St. Lawrence Lowland (with selected passages from an unpublished manuscript "The St. Lawrence Lowlands", by J.W. Goldthwait); Geological Survey of Canada Memoir 359, 153 p.

Goulet, H.
1983: The genera of Holarctic Elaphrini and species of *Elaphrus* Fabricius (Coleoptera: Carabidae): classification, phylogeny and zoogeography; Quaestiones Entomologicae, v. 19, p. 219-482.

Larochelle, A.
1975: Les Carabidae du Quebec et du Labrador; Departement de Biologie du College Bourget, Rigaud, Bulletin 1, 255 p.

LaSalle, P.
1984: Quaternary stratigraphy of Quebec: a review; in Quaternary Stratigraphy of Canada – A Canadian contribution to IGCP Project 24, R.J. Fulton (ed.); Geological Survey of Canada, Paper 84-10, p. 155-171.

LaSalle, P., Martineau, G. and Chauvin, L.
1979: Lits de bryophytes du Wisconsin Moyen, Vallee-Jonction, Quebec; Journal canadien des sciences de la terre, vol. 16, p. 593-598.

LaSalle, P., Matthews, J.V.,Jr., and Mott, R.J.
1986: Stratigraphy and paleoenvironmental conditions from a section near Bethanie, Quebec, Canada (abstract); 9th biennial meeting, American Quaternary Association, 2-4 June, 1986, abstract volume, p. 144.

Lichti-Federovich, S. and Ritchie, J.C.
1968: Recent pollen assemblages from the western interior of Canada; Review of Paleobotany and Palynology, v. 7, p.297-344.

Lindroth, C.H.
1963a: The faunal history of Newfoundland; Opuscula Entomologica, Supplementum XXIII, 112 p.
1963b: The ground-beetles of Canada and Alaska, part 3; Opuscula Entomologica, Supplementum XXIV, p. 201-406.
1966: The ground-beetles of Canada and Alaska, part 4; Opuscula Entomologica, Supplementum XXIX, p. 409-648.

McDonald, B.C. and Shilts, W.W.
1971: Quaternary stratigraphy and events in southeastern Quebec; Geological Society of America Bulletin, v. 82, p.683-698.

Occhietti, S.
1982: Synthèse lithostratigraphique et paléoenvironnements du Quaternaire au Québec méridional. Hypothèse d'un centre d'englacement wisconsinien au Nouveau-Québec; Géographie physique et Quaternaire, vol. 36, p. 15-39.

Occhietti, S., David, P.P., Gadd, N.R., and Shilts, W.W.
1982: Fiches des principales unités lithostratigraphiques quaternaires du Québec méridional; Géographie physique et Quaternaire, vol. 36, p. 40-49.

Porsild, A.E. and Cody, W.J.
1980: Vascular Plants of Continental Northwest Territories, Canada; National Museums of Canada, Ottawa, 667 p.

Shilts, W.W.
1978: Detailed sedimentological study of till sheets in a stratigraphic section, Samson River, Quebec; Geological Survey of Canada, Bulletin 285, 30 p.
1981: Surficial geology of the Lac Mégantic area, Québec; Geological Survey of Canada, Memoir 397, 102 pp.

Shilts, W.W. and Smith, S.L.
1986a: Stratigraphy of placer gold deposits; overburden drilling in Chaudière Valley, Quebec; in Current Research, Part A, Geological Survey of Canada, Paper 86-1A, p. 703-712.
1986b: Stratigraphic setting of buried gold-bearing sediments, Beauceville area, Quebec; in Current Research, Part B, Geological Survey of Canada, Paper 86-1B, p. 271-278.

Smetana, A.
1985: Revision of the subfamily Helophorinae of the Nearctic region (Coleoptera: Hydrophilidae); Memoirs of the Entomological Society of Canada, no. 131, 154 p.

Stuiver, M., Heusser, C.J., and In Che Yang
1978: North American glacial history extended to 75 000 years ago; Science, v. 200, p. 16-21.

Terasmae, J.
1955: Palynological study relating to Toronto Formation, Ontario, and the Pleistocene deposits in the St. Lawrence Lowlands, Quebec; unpublished PhD thesis, McMaster University, Hamilton, Ontario.
1958: Contributions to Canadian palynology, Part 2; nonglacial deposits in the St. Lawrence Lowlands, Quebec; Geological Survey of Canada, Bulletin 46, p. 13-28. .bp

- 18 -

A placer gold exploration target in the Cariboo district, British Columbia

Project 810006

John J. Clague
Terrain Sciences Division, Vancouver

Clague, J.J., A placer gold exploration target in the Cariboo district, British Columbia; in Current Research, Part A, Geological Survey of Canada, Paper 87-1A, p. 177-180, 1987.

Abstract

A previously unknown, buried Quaternary valley has been found in the Cariboo district, central British Columbia. This valley, located 3 km south of Cariboo Lake, is similar in form to the nearby Bullion valley which has yielded over 120 000 ounces of placer gold since it was discovered in the late 1800s. Holocene river terraces in the vicinity of the buried valley contain placer gold. In addition, Keithley Creek, one of the richest placer streams in the Cariboo, is located only 6 km to the north. These observations suggest that the buried valley may itself contain placer gold and thus should be considered a priority mineral exploration target.

Résumé

Une vallée enfouie du Quaternaire, auparavant inconnue, a été découverte dans le district de Cariboo, au centre de la Colombie-Britannique. Cette vallée, située à 3 km au sud du lac Cariboo, a une forme similaire à la vallée avoisinante de Bullion qui a produit plus de 120 000 onces d'or alluvionnaire depuis sa découverte à la fin des années 1800. Des terrasses fluviales de l'Holocène, à proximité de la vallée enfouie, renferment de l'or alluvionnaire. En outre, le ruisseau Keithley, un des cours d'eau les plus riches en placers dans le district de Cariboo, se situe à 6 km au nord. Ces observations semblent indiquer que la vallée enfouie peut elle-même renfermer de l'or alluvionnaire et devrait alors faire l'objet de travaux d'exploration minérale de toute première importance.

INTRODUCTION

The Cariboo district of British Columbia has yielded more than 2.5 million ounces of placer gold since the first discoveries along Quesnel River and its tributaries almost 130 years ago (Boyle, 1979). It thus ranks as the premier placer gold district in the province. Although the richest placers are now nearly exhausted, there still are numerous small-scale mining operations in the region, and some gold continues to be recovered from deposits that have been mined one or more times in the past.

The main source of placer gold in the Cariboo is auriferous quartz veins which occur in metasedimentary rocks of the Cariboo Group (Johnston and Uglow, 1926). This gold probably was released from its host rocks during a lengthy period of Tertiary weathering and denudation. Subsequently, during late Tertiary time, much of the gold was concentrated in valleys as rejuvenated streams dissected a landscape of low to moderate relief.

During the Quaternary, streams and glaciers removed most late Tertiary auriferous gravels. The gold within these gravels, however, was recycled into fluvial and glaciofluvial deposits and tills. In detail, during Quaternary nonglacial periods, streams degraded their valleys or were at equilibrium, and gold was washed from older Quaternary and Tertiary sediments and concentrated in channels. Much of the placer gold in the Cariboo may have been recycled many times in this manner. The youngest gold-bearing channel deposits underlie 1) the beds of present-day streams and 2) fluvial terraces which formed during a period of fluvial incision following the last (Fraser = Late Wisconsinan) glaciation. These deposits generally are thin and are not covered by younger sediments, consequently pay streaks are shallow. In contrast, some older fluvial deposits are buried beneath thick Quaternary sediments, and the channels in which they occur have little or no surface expression.

During the growth and decay phases of Pleistocene glaciations, large amounts of coarse stratified drift were deposited locally in valleys in the Cariboo region. Some of these drift bodies are auriferous; however, the gold generally is highly disseminated and fine grained, and thus most deposits are not economic. At glacial maxima, many placers were eroded by ice flowing from the Cariboo Mountains to the east. Much of the gold eroded and transported by glaciers was deposited subglacially in till. During and following deglaciation, some of this gold was released from till and concentrated in valleys by fluvial and mass wasting processes.

It is clear from the above that gold in the Cariboo district occurs in a variety of sediments of different ages. Most surface (i.e., Holocene) placers have been mined, although some gold continues to be extracted from old workings. Significant new finds probably will be limited to Pleistocene and late Tertiary (?) buried valleys. Although the richest of these were exploited long ago, some buried valleys undoubtedly await discovery. In addition, auriferous deposits in a few known buried valleys (i.e., Bullion Mine; see below) have not been completely exhausted.

The purpose of this report is to alert the mining community to new possibilities for placer gold production in the Cariboo district. Specifically, a previously unknown buried valley south of Cariboo Lake is identified and compared with a similar valley near Likely which has yielded more than 120 000 ounces of gold. It may be possible to find other buried valleys in this region through the use of geomorphic analysis and various ground-based geophysical techniques.

BULLION MINE

The buried valley fill at the Bullion Mine, 4 km west of Likely (Fig. 18.1), has been mined periodically for over 100 years, with a peak production of about 60 000 ounces of gold between 1894 and 1905 (Sharpe, 1939). Much of the thick sediment fill at the Bullion Mine was removed in massive hydraulic operations during the late nineteenth and early twentieth centuries. In the course of these operations, part of the old buried valley was exhumed (Fig. 18.2, 18.3). The exhumed part of the valley is 300-500 m south of, and parallel to, Quesnel River; it is more than 1 km long, 300-450 m wide at the rim, and has an average depth of 120 m (Fig. 18.4). The valley walls are steep, in places >45°. The floor of the valley slopes gently (0.5-1°) to the northwest and lies about 50 m above the level of Quesnel River.

The Bullion valley fill comprises drift of two glaciations and underlying nonglacial or proglacial fluvial deposits. Gold is most common on the bedrock floor of the valley and in fluvial (or glaciofluvial) gravel at the base of the Quaternary succession. Some gold also is present higher in the succession in stratified gravelly drift units deposited at the end of the

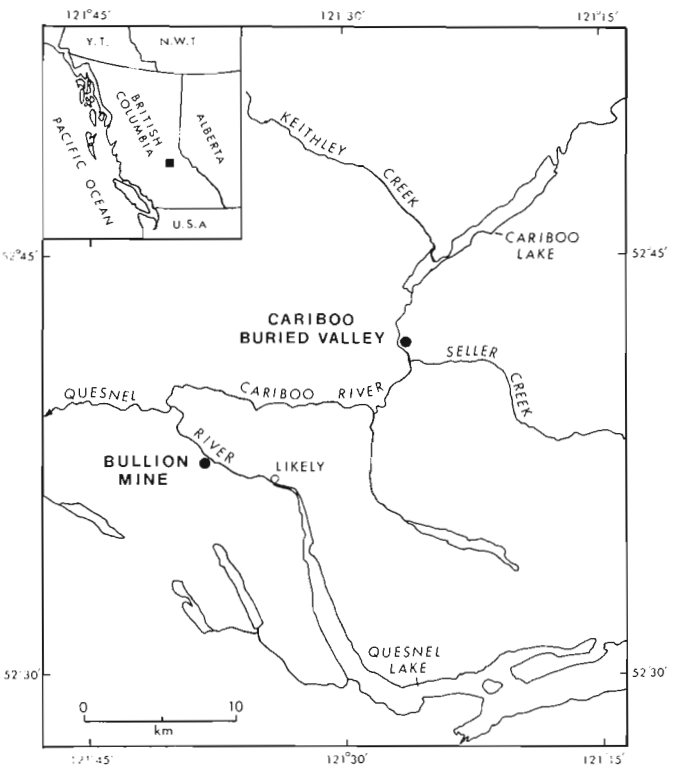


Figure 18.1. Locality index map.

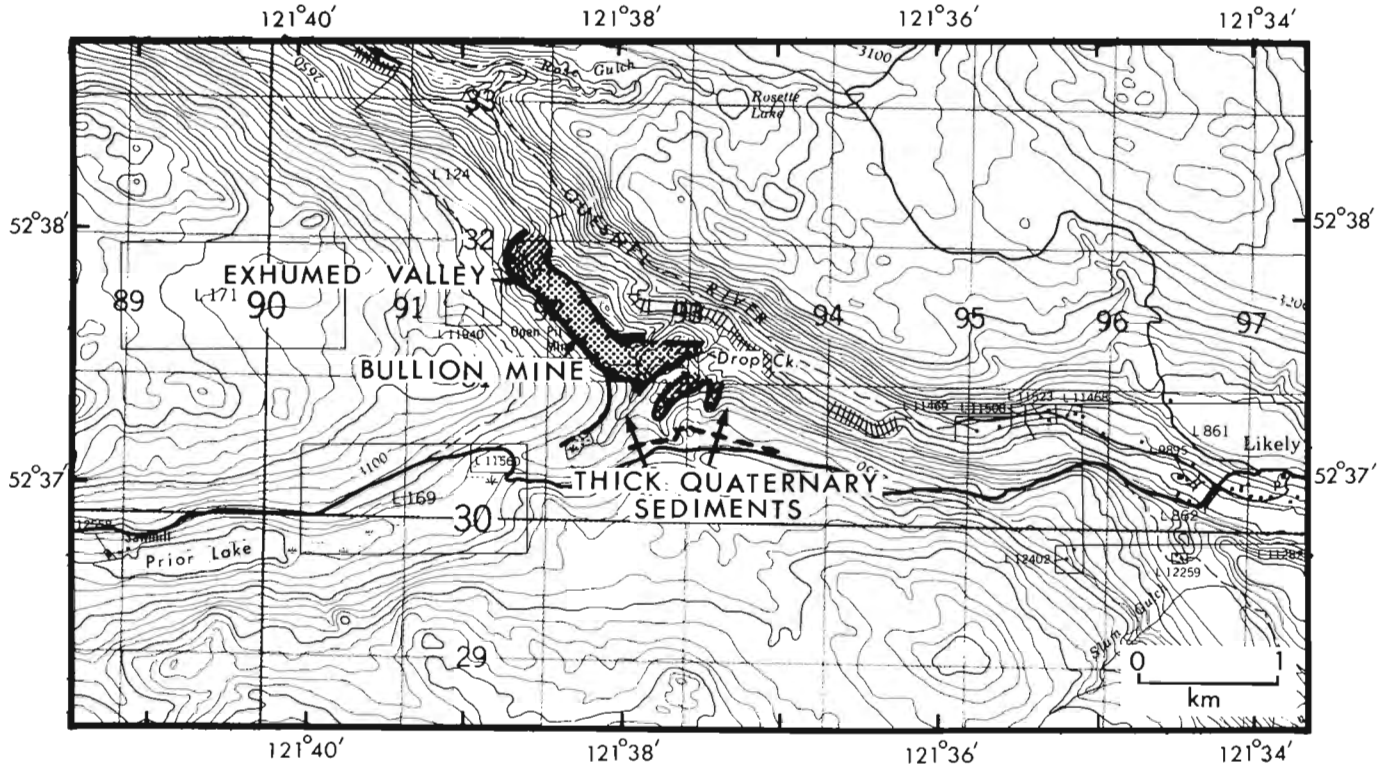


Figure 18.2. Location and setting of the Bullion Mine; area of hydraulic mining during the late nineteenth and early twentieth centuries is stippled. Contour interval is 50 feet.

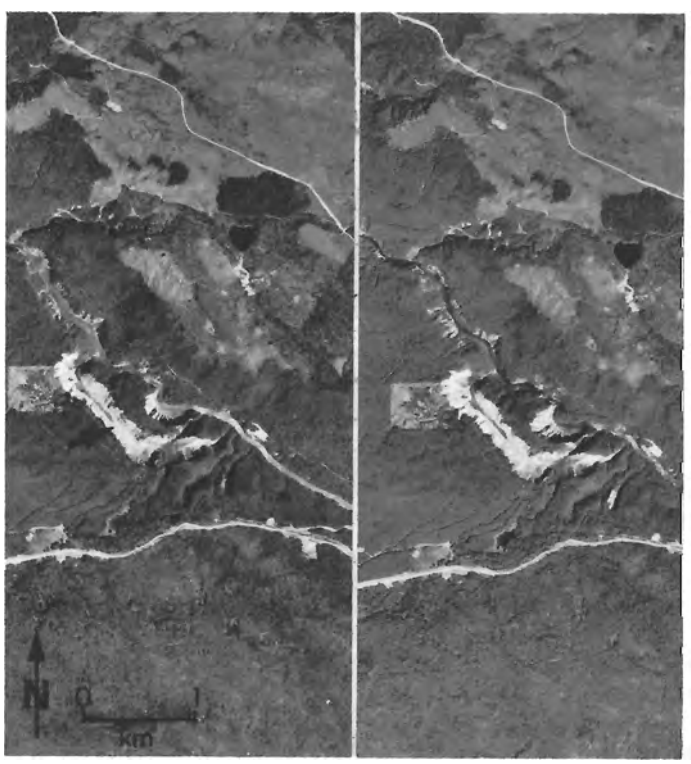


Figure 18.3. Photostereogram of the Bullion Mine (arrow) and surrounding area. BC82026-173, 174.

penultimate Pleistocene glaciation (Early Wisconsinan?) and during the advance phase of the Fraser Glaciation.

Bullion valley was cut some time before the penultimate glaciation and thus is at least 100 000 years old; it may, in fact, be middle or early Pleistocene in age. The valley at one time carried the flow of a major stream, probably a precursor of present-day Quesnel River. Almost the entire fill in the central and northern parts of the valley has been removed by hydraulic mining, but a significant fill is still present in the vicinity of Drop Creek (Fig. 18.2). The exact form and extent of the buried valley in this area is uncertain, although thick Quaternary sediments extend some distance southwest from Drop Creek towards Prior Lake and east from Drop Creek towards Quesnel River. It is possible that the lower part of this remnant fill contains a large amount of gold. The economics of exploiting this fill are questionable, however, considering the great thickness of low-grade glacial deposits above the old valley floor and the difficulties in disposing large volumes of tailings in this area.

BURIED VALLEY, CARIBOO RIVER

An inconspicuous, buried Quaternary valley is present just east of Cariboo River, 3 km south of the south end of Cariboo Lake (Fig. 18.1, 18.5). This valley is about 1 km long and 150-200 m wide; it is separated from Cariboo River by a bedrock ridge. The top of the valley fill is about 40-50 m above the level of Cariboo River.

Sediments within the buried valley have not yet been investigated, but colluviated till and thin glaciolacustrine



Figure 18.4. Exhumed Pleistocene valley at the Bullion Mine; view towards the northwest.

sediments are present in exposures along the logging road directly to the east. Because this valley was cut by Cariboo River, there is a good possibility that fluvial gravel may be present at depth in the fill. Any such gravel, as well as the bedrock floor of the valley, is likely to be gold-bearing for the following reasons:

1. The similarity in form of the buried valley discussed here to Bullion valley and others which have yielded placer gold is striking. Past experience indicates that buried river valleys in this region are likely to contain gold.
2. Cariboo River is an important placer gold stream. Large amounts of gold have been recovered from fluvial terraces bordering Cariboo River between Cariboo Lake and Quesnel River. Low terraces directly north of the buried valley have yielded some gold.
3. The Cariboo River buried valley is situated only 6 km south of the mouth of Keithley Creek (Fig. 18.1), the fourth richest placer stream in the Cariboo (Haggen, 1924). Gold has been recovered in large quantities from Pleistocene (?) buried valley fills and Holocene gravelly alluvium in the Keithley Creek basin. The gold apparently was reworked repeatedly by streams and glaciers following its release from bedrock during the Tertiary. Some gold undoubtedly was transported out of the basin into Cariboo Valley at various times during the Quaternary Period. Since the end of the Fraser Glaciation, for example, gold has accumulated in the large fan-delta at the mouth of Keithley Creek. Southerly transport of Keithley Creek gold during the Pleistocene by the ancestral Cariboo River and glaciers may have produced placer deposits in Cariboo Valley south of Cariboo Lake.

In view of the foregoing, further exploration of the Cariboo River buried valley is warranted. Geophysical investigations (e.g., seismic reflection, resistivity) may help to document the three-dimensional form and stratigraphy of the valley fill, but drilling will be required to determine whether or not significant gold is actually present at this site.

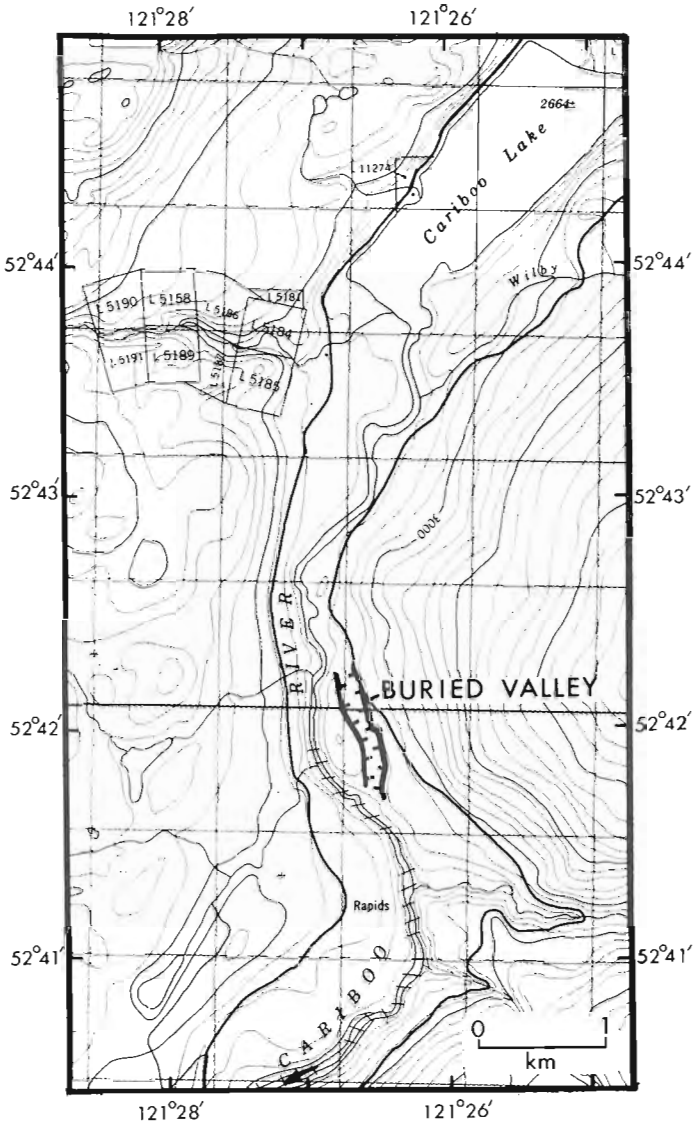


Figure 18.5. Location and setting of the buried valley south of Cariboo Lake. Contour interval is 100 feet.

REFERENCES

Boyle, R.W.
1979: The geochemistry of gold and its deposits (together with a chapter on geochemical prospecting for the element); Geological Survey of Canada, Bulletin 280, 584 p.

Haggen, E.A.
1924: Keithley Creek; Mining and Engineering Record, v. 28, no. 1, p. 44-47.

Johnston, W.A. and Uglow, W.L.
1926: Placer and vein gold deposits of Barkerville, Cariboo district, British Columbia; Geological Survey of Canada, Memoir 149, 246 p.

Sharpe, R.F.
1939: The Bullion hydraulic mine; The Miner, v. 12, no. 1, p. 37-40.

Surface displacement and massive toppling on the northeast ridge of Mount Currie, British Columbia

Project 830016

S.G. Evans
Terrain Sciences Division

Evans, S.G., Surface displacement and massive toppling on the northeast ridge of Mount Currie, British Columbia; in Current Research, Part A, Geological Survey of Canada, Paper 87-1A, p. 181-189, 1987.

Abstract

Mount Currie dominates Lillooet Valley near Pemberton in the southern Coast Mountains of British Columbia. Surface displacement features on the northeast ridge of Mount Currie, involving gneissic rocks of the Pemberton dioritic complex, have been examined and their relationship to rock mass structure determined. The structure of the rock mass is dominated by three planar elements viz., near vertical gneissic foliation (D1), near vertical joints (D2), and near horizontal joints (D3). The major surface linear on Mount Currie is due to dip-slip displacement along element D2 and at least part of this displacement results from slope movement. The rock mass which has undergone slope movement exhibits gaping tension cracks. In addition, within this area massive toppling of the gneissic foliation is taking place. The observations raise the question of the catastrophic potential which is presented by the existence of a disrupted rock mass high above a populated valley.

Résumé

Le mont Currie (2549 m) surplombe la vallée de Lillooet à proximité de Pemberton dans la partie sud de la chaîne Côtière de la Colombie-Britannique. On a étudié les caractéristiques des déplacements superficiels sur la crête nord-est du mont Currie des roches gneissiques du complexe dioritique de Pemberton et on a déterminé leur relation avec la structure de la masse rocheuse. Cette structure est dominée par trois éléments planaires à savoir : la foliation gneissique presque verticale (de type D1), les joints presque verticaux (de type D2) et les joints presque horizontaux (de type D3). Le plus important linéament superficiel du mont Currie a comme origine un déplacement normal le long de l'élément de type D2 et une partie au moins de ce déplacement résulte d'un mouvement de pente. La masse rocheuse qui a subi ce mouvement de pente présente des fissures d'extension ouvertes. En outre, au sein de cette zone, il se produit un éboulement massif de la foliation gneissique. Ces observations soulèvent la question des risques de catastrophe que présente ici l'existence d'une masse rocheuse disloguée, surplombant une vallée peuplée.

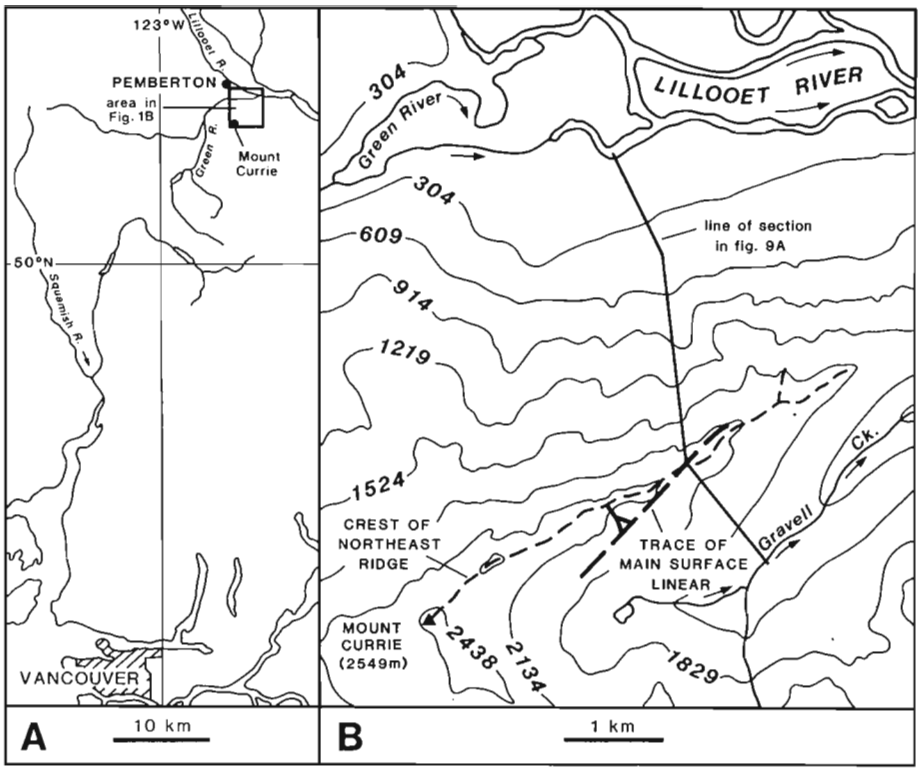


Figure 19.1. A. Location of Mount Currie. B. Location of linear feature on northeast ridge of Mount Currie.



Figure 19.2. Oblique view to the southeast of the north face of Mount Currie. Surface displacement has taken place along linear (arrows). Toppling is taking place in light toned area (T). Tension crack shown in Figure 19.8 is located at C and toppled block shown in Figure 19.10 is located at B. 204 247-V

INTRODUCTION

Lillooet Valley in the vicinity of Pemberton, British Columbia is dominated by the towering north face of Mount Currie (2549 m) (Fig. 19.1) which rises 2.3 km in a horizontal distance of only 4.25 km. Surface displacement features on the northeast ridge of Mount Currie, previously noted by Eisbacher (1983), have been examined in detail and form part of a group of problematical slope movement features which are currently under study in the southern Coast Mountains. This report presents a preliminary interpretation of the Mount Currie features and the slope movements associated with them based on fieldwork carried out in August 1986. It is apparent that an area of surface displacement exists on the ridge, part of which is related to slope movement, and within this area massive toppling is presently active along part of the ridge crest. The report addresses the problematic origin of the displacement features, their relationship to rock mass structure, and raises the question of the catastrophic potential which is presented by a large disrupted rock mass located high above a populated valley.

GEOLOGICAL SETTING AND ROCK MASS STRUCTURE

The area of the northeast ridge under discussion is shown in Figure 19.1 and 19.2. The relief of the mountain slope varies along the northeast ridge between 1650 and 2300 m and the upper 1000 m has an average slope approaching 45°. The ridge is made up of rocks of the Pemberton dioritic complex (Roddick and Hutchison, 1973; Woodsworth, 1977; Price et al., 1985). According to Woodsworth (1977) and Price et al. (1985) greenstones of the Upper Triassic Pemberton Belt are present towards the northeast end of the ridge but these were not encountered in traverses undertaken in this work. The complex is a heterogeneous unit in which the rock is commonly banded and gneissic with abundant epidote stringers. Outcrops are characterized by well developed northwest trending foliation with vertical or steep northeast dips.

Structural measurements were taken in an attempt to characterize the rock mass fabric on the ridge. As seen in Figure 19.3 the rock mass fabric consists of three planar

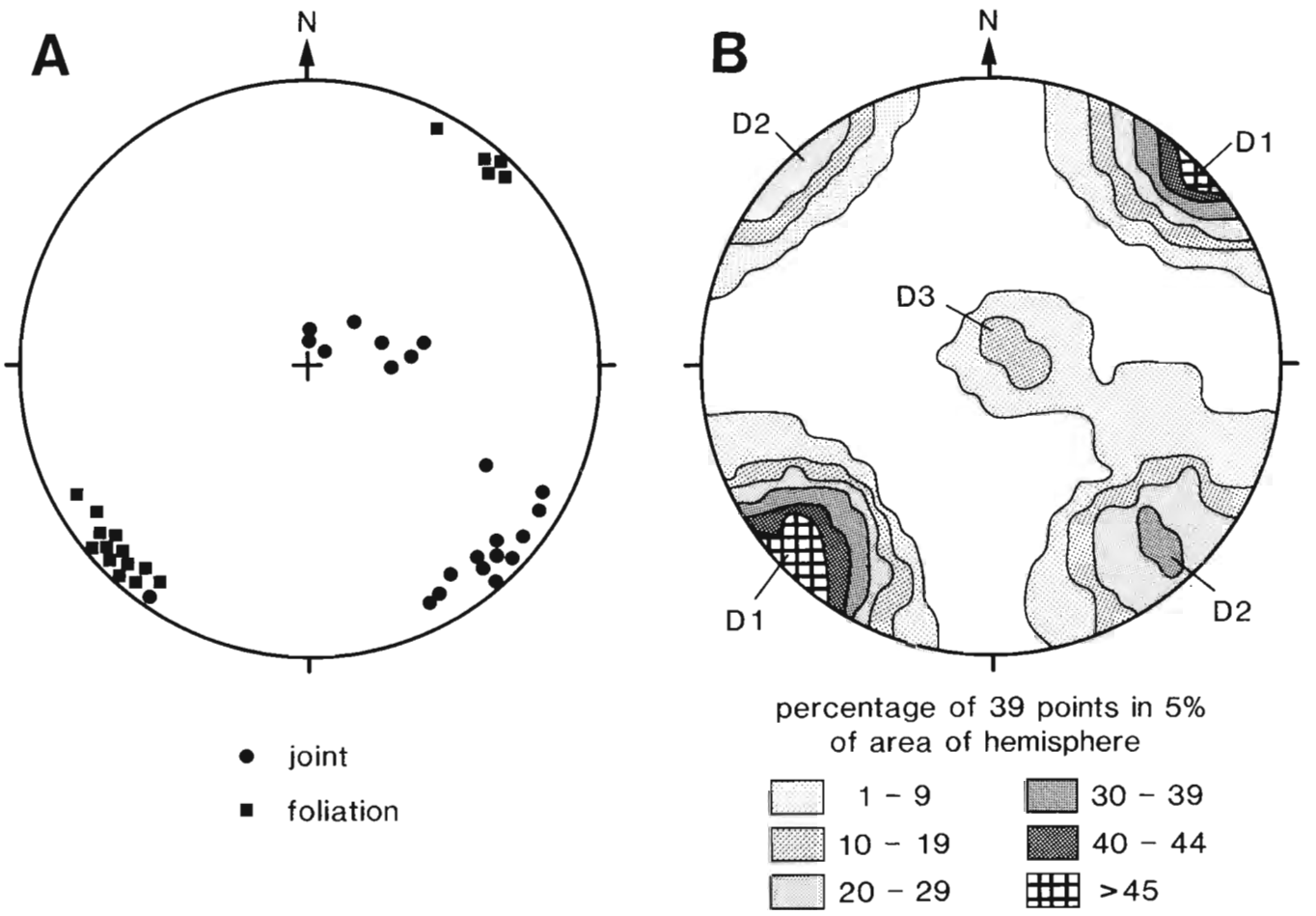


Figure 19.3. Rock mass fabric within displaced area on the northeast ridge of Mount Currie. A. Poles to discontinuities plotted on lower hemisphere of equal area projection. B. Densities of poles shown in A. Key to pole concentrations; D1 = gneissic foliation, D2 = high angle joints, D3 = low angle joints. Lower hemisphere of equal area projection.



Figure 19.4. Oblique view, to the east, of the upper part of the north face of Mount Currie. Near vertical gneissic foliation is evident in rock slopes to the right of the arrow. Note north to northeasterly dipping planar structures in the face. The rubble and the light tone of the slope to the left of the vertical arrow are produced by toppling as described in the text. 204 207-M

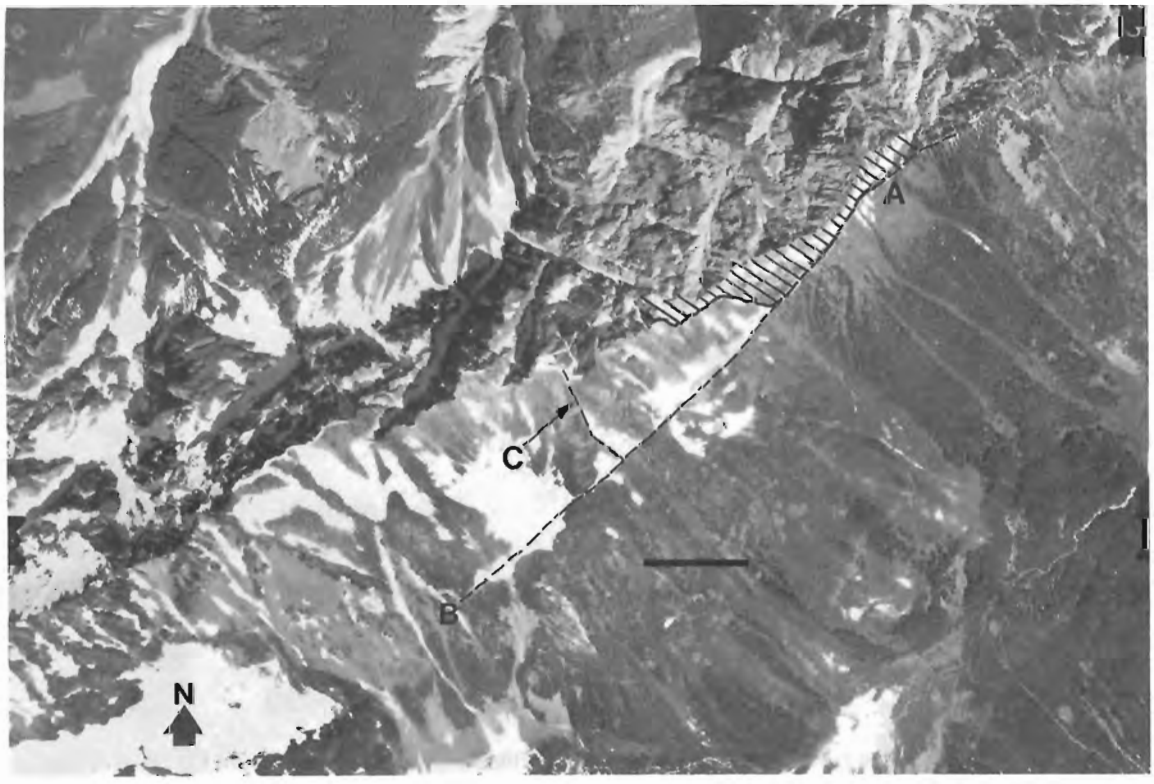


Figure 19.5. Aerial photograph of linear feature (A-B) on Mount Currie. C is trace of the secondary linear feature shown in Figure 19.7 which defines the slope movement on the northeast ridge within which area of toppling (outlined by hachuring) occurs. Scale bar represents approximately 280 m. BC 7478-207

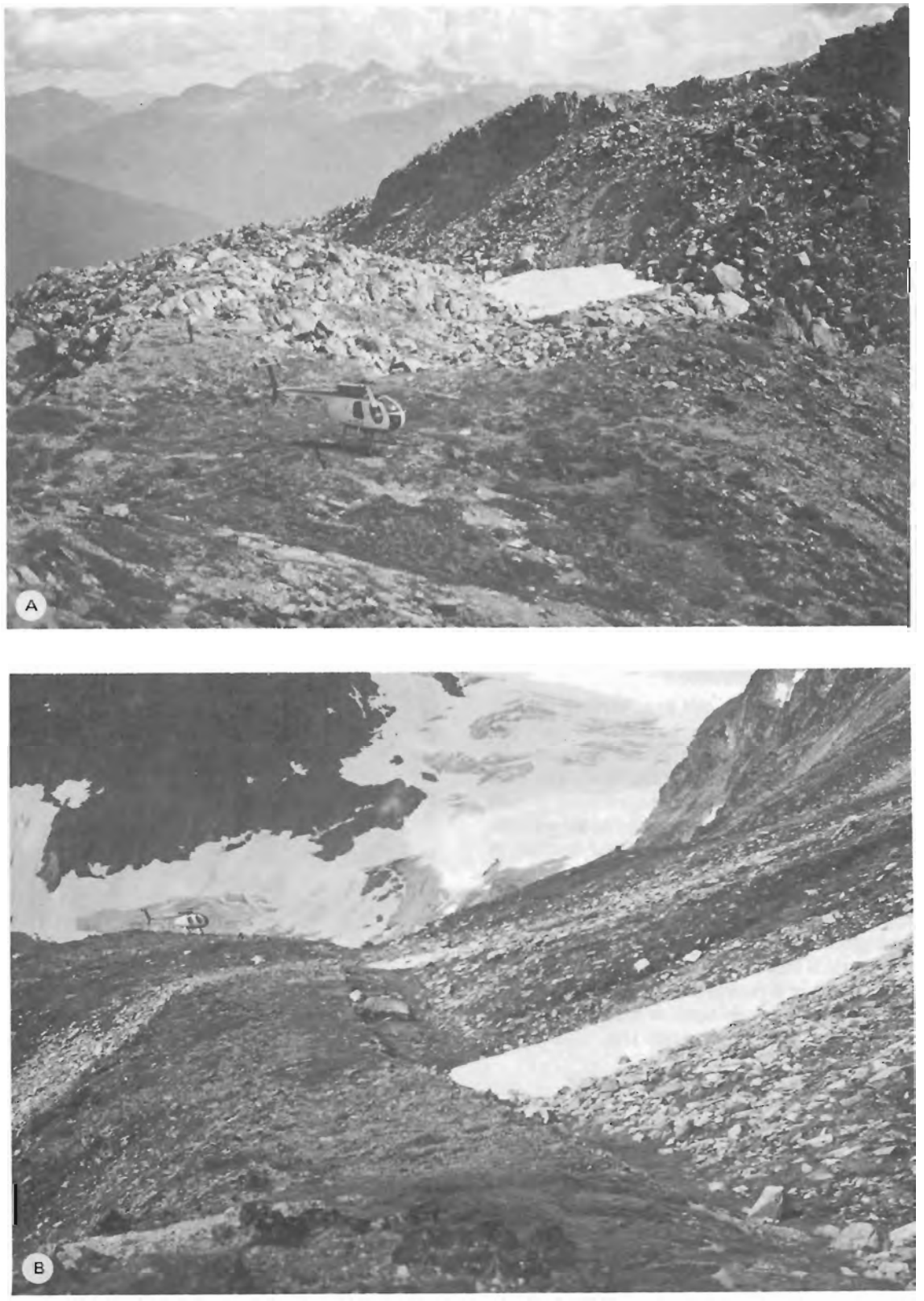


Figure 19.6. A. Scarp at northeast end of ridge. Downslope direction in relation to the north face of Mount Currie is behind the camera position. Maximum displacement at right hand of photograph is approximately 25 m. Helicopter is parked on part of the toppled mass. B. Linear feature near the southwest limit of its trace. Downslope direction in relation to the north face of Mount Currie is to the right. Note helicopter for scale. 204 247-E, 204 247-K



Figure 19.7. Splayed tension crack defining slope movement on northeast ridge. Main surface linear is visible in foreground across photograph. 204 247-B

elements. The major element is the near vertical gneissic foliation (D1) which is oriented between 040° and 050°. The foliation consists of well developed planar surfaces with spacing varying between 0.5 and 2.0 m (Fig. 19.4). Along the ridge the epidote layering is parallel to this element. A well developed joint set (D2) exists at right angles to the gneissic foliation trending 130°-140° which is also near vertical. A third fabric element (D3) consists of low angle joints dipping within 30° of the horizontal trending 132°. The foregoing description of rock mass fabric is based upon traverses of the surface of the northeast ridge only, since the precipitous north face of Mount Currie is inaccessible. From aerial inspections of the north face, however, it is clear that other fabric elements exist in the slope which include north or northeasterly dipping planar structures of unknown origin (Fig. 19.4).

SURFACE DISPLACEMENT ON THE NORTHEAST RIDGE

A major linear feature is evident on the surface of the northeast ridge of Mount Currie (A-B, Fig. 19.5). It has an orientation of 043° and is approximately 1750 m in length. Differential vertical movement is evident along the linear forming a scarp. Movement has been greatest at the northeast end where displacement is in the order of 20-30 m (Fig. 19.6A). The height of the scarp decreases to the southwest (Fig. 19.6B) until it becomes imperceptible in the vicinity of B in Figure 19.5. The lack of uniform displacement along the linear feature is suggestive of a downward hinge-type movement about an axis oriented 313°. The surface displacement which the linear represents has taken place along a steeply dipping joint set identified as D2 in Figure 19.3 and the joint surfaces are clearly exposed in the scarp at numerous places along it.



Figure 19.8. Gaping tension crack trending 040° parallel to discontinuity set D2 in banded gneiss within displaced area (see Fig. 19.2 for location). 204 207-S

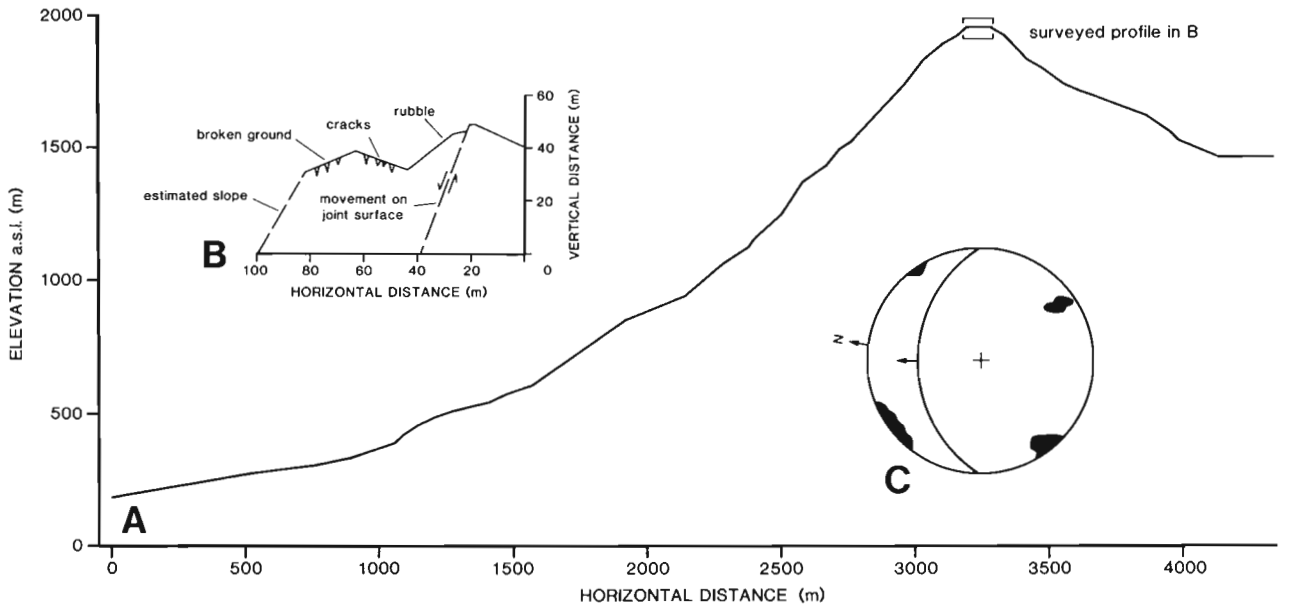


Figure 19.9. A. Topographic profile of northeast ridge of Mount Currie. B. Topography of scarp surveyed at top of ridge. C. Pole concentrations of discontinuities in untoppled rock mass in displaced area plotted on equal area projection, lower hemisphere. The great circle represents the slope of the north face.

Eisbacher (1983) has suggested that the linear feature described above is an earthquake generated fault scarp and went as far as to calculate the Richter magnitude of the generating event based on scarp height. However, a tension crack at C in Figure 19.5 obviously defines an area of the ridge that has undergone downslope movement towards Lillooet Valley (Fig. 19.7). The existence of gaping tension cracks throughout this area (Fig. 19.8) indicates the extent to which the rock mass has undergone disruption; these cracks appeared remarkably fresh in August 1986. Therefore, at least part of the displacement represented by the scarp between A and C in Figure 19.5 is downslope movement of the ridge in a northwest direction. The linear between C and B takes on the character of a linear depression (Fig. 19.6B) and its relation to possible slope movement remains problematical. It is significant that the area that has undergone slope movement is located at the unconfined end of a ridge, a common location for landslides, since shear resistance along one movement margin is nonexistent.

The kinematics of the movement are difficult to rationalize on the basis of rock mass characteristics measured on the ridge since discontinuity patterns within the slope do not appear to provide surfaces along which slope movement in the 352° direction is possible (Fig. 19.9). Limited downslope movement along joint set D2 could be accommodated by dilation of the rock mass without the necessity for structural planes to intersect the slope of the north face. Alternatively, the limited movement may have been possible on other structures in the slope, such as these noted in Figure 19.4, in a wedge or planar failure.



Figure 19.10. Toppled block within toppled area of northeast ridge of Mount Currie. Note figure for scale. 204 247-Q

TOPPLING ON THE NORTHEAST RIDGE

An area of massive toppling occurs within that part of the northeast ridge that has undergone downslope movement and is outlined in Figure 19.5. Toppling involves the forward rotation or overturning of units about a hinge line and involves a forward tilting without collapse taking place (Varnes, 1978). On Mount Currie the toppling units are defined by the gneissic foliation (D1, Fig. 19.3).



Figure 19.11. Fresh cracking along slope edge within toppled area. Note rock mass behind and to the right of the figure has almost completely overturned to a near horizontal position as a result of toppling towards camera position.

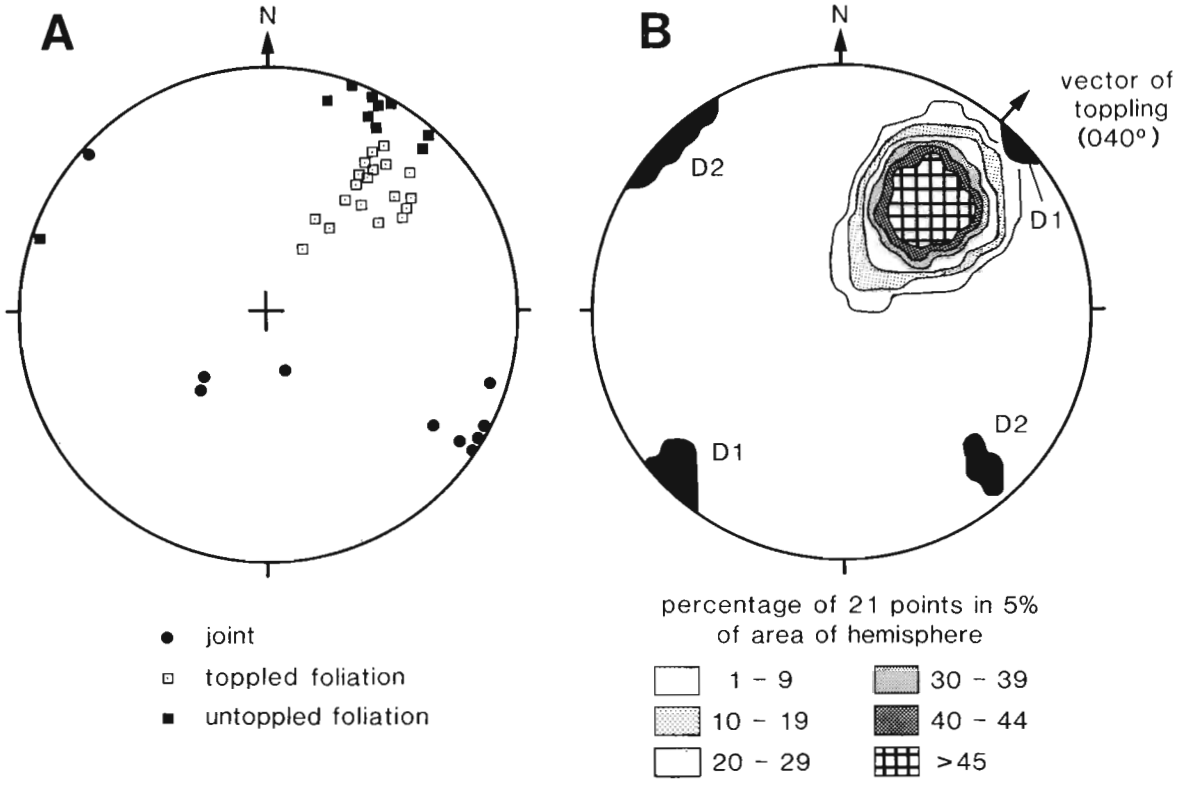


Figure 19.12. Toppled fabric on northeast ridge of Mount Currie. A. Poles to untoppled and toppled discontinuities plotted on equal area projection lower hemisphere. B. Densities of poles to toppled discontinuities shown in A in relation to pole concentrations of untoppled discontinuities in Figure 19.3B plotted on equal area projection, lower hemisphere. D1 is gneissic foliation and D2 is a joint set.

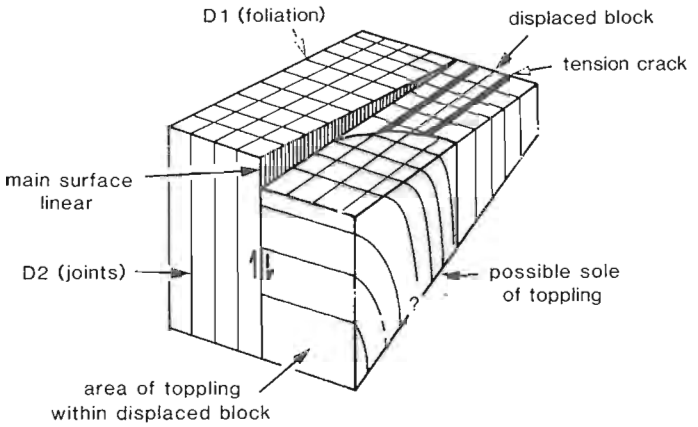


Figure 19.13. Suggested mode of complex slope movements on the northeast ridge of Mount Currie (see text).

A traverse was made over the area affected by toppling movement. Large toppled blocks are common (Fig. 19.10) and fresh cracking (Fig. 19.11) is widespread suggesting that toppling is presently active. In places the overturning of the gneissic foliation is almost complete and its attitude approaches the horizontal (Fig. 19.11). As the toppling has developed, large masses of rock have become disaggregated which results in the rubbly appearance of the northeastern part of the ridge (Fig. 19.4). Rock fragments breaking away from the toppling masses are actively feeding debris chutes and talus slopes below the ridge.

Structural measurements were carried out on the gneissic foliation in the toppled blocks and were compared with untoppled fabric at the margin of the toppled area (Fig. 19.12). From Figure 19.12 it is clear that toppling is not taking place in the downslope direction (352°), i.e. the direction of greatest stress gradient, but in a northeasterly direction oblique to the slope (040°), perpendicular to the strike of the gneissic foliation, and towards the free end of the northeast ridge.

An examination of the north face of Mount Currie was made from a helicopter and overturning of layering was noted to at least 300 m below the crest of the ridge. Further, planar structures dipping east or northeast were observed which are thought to be the sole of the toppling movement.

DISCUSSION AND CONCLUSIONS

This report presents a preliminary interpretation of a complex slope movement on the summit ridge of Mount Currie where massive toppling has been documented within a larger area that has undergone downslope movement. It is possible that the two movements are related in a manner suggested in Figure 19.13 since the orientation of the axis around which the differential movement of the area of displacement has taken place corresponds to the axis around which overturning is taking place in the toppling movement. Further, the sense of movement corresponds in both cases. It is also noted that the direction of both movements are controlled by planar elements of the rock mass fabric.

Note has been made above of the presence of apparently fresh cracking both within the displaced area and in the toppled mass. This observation raises the question of the future behaviour of the northeast ridge and in particular the potential for catastrophic detachment. The existence of such a large volume of displaced material located high above a populated valley is a significant ground failure hazard that should be taken into consideration in future development in this part of Lillooet Valley. Additional detailed mapping on the north face of Mount Currie is required to fully evaluate this hazard.

ACKNOWLEDGMENTS

I am grateful to Eldon Talbot (Pemberton Helicopters Ltd.) for his expert flying onto and off the northeast ridge of Mount Currie, to Karen Bertrand for her excellent assistance in the field, and to Rosanna Von Sacken for the processing of structural data.

REFERENCES

Eisbacher, G.H.
1983: Slope stability and mountain torrents, Fraser Lowlands and southern Coast Mountains, British Columbia; Field Trip Guidebook, Trip 15, Geological Association of Canada, Mineralogical Association of Canada, Canadian Geophysical Union, Joint Annual Meeting, Victoria, B.C., 46 p.

Price, R.A., Monger, J.W.H. and Roddick, J.A.
1985: Cordilleran Cross-Section: Calgary to Vancouver, Trip 3; in Field Guide to Geology and Mineral Deposits in the Southern Canadian Cordillera, D. Tempelman-Kluit (ed.); Geological Society of America, Cordillera Section Meeting, Vancouver, B.C., p. 3-1 to 3-85.

Roddick, J.A. and Hutchison, W.W.
1973: Pemberton (east half) map-area, British Columbia; Geological Survey of Canada, Paper 73-17.

Varnes, D.J.
1978: Slope movement types and processes; in Landslides, analysis and control, R.L. Schuster and R.J. Krizek (ed.); Transportation Research Board, National Research Council, Special Report 176, p. 11-33.

Woodsworth, G.J.
1977: Geology, Pemberton (92 J) map-area; Geological Survey of Canada Open File 482.

Ground probing radar in the investigation of the competency of frozen tailings pond dams

Project 62501

P.T. LaFlèche, A.S. Judge, and J.A. Pilon
Terrain Sciences Division

LaFleche, P.T., Judge, A.S., and Pilon, J.A., Ground probing radar in the investigation of the competency of frozen tailings pond dams; in Current Research, Part A, Geological Survey of Canada, Paper 87-1A, p. 191-197, 1987.

Abstract

Frozen core containment dams are relatively new to North America. The tailings pond facility at the Echo Bay Mines Ltd. Lupin site, near Contwoyto Lake, Northwest Territories, employs several such dams to enclose a small watershed for the purpose of retaining tailings fluid. The frozen nature of the dam interior and the underlying subsurface creates an impermeable barrier to fluid flow.

Ground probing radar (GPR) surveys were conducted during the summer of 1986 over two of the dams which had shown previous evidence of leaking tailings water into the surrounding environment. The ability of GPR to image the subsurface to 50 m in some cases allows resolution of the dam structures, subdam overburden conditions, bedrock topography, and depth of thaw; and to locate unfrozen zones (taliks) within the subsurface.

Résumé

Les barrages qui utilisent le principe du gel du noyau central pour retenir les eaux usée en région de pergélisol sont relativement nouveaux en Amérique du Nord. La mine Lupin de la compagnie Echo Bay Ltée utilise plusieurs de ces barrages pour fermer un petit bassin de drainage près du lac Contoyto, T.N.-O. afin d'y créer un bassin de sédimentation pour y contenir les résidus toxiques provenant du traitement du minerai. Le gel du noyau central du barrage lié au pérgelisol de la région créent ensemble une barrière imperméable aux fuites liquides.

A l'été 1986 nous avons effectués des levés géoradars sur deux des barrages de la mine Lupin qui avaient montrés des siqnes de fuites à l'été 1985. Le géoradar est un instrument géophysique capable d'imager les matériaux à la surface du globe jusqu'à une profondeur de 50 m dans certain cas. Cette capacité nous permet d'étudier les structures intérieures des barrages, les matérieux meubles sous les barrages, la topographie de la roche en place ainsi que de localiser la couche active et les zones dégelées sous la surface.

INTRODUCTION

During June and late September of 1986 several ground probing radar (GPR) surveys were undertaken over tailings pond dams at the Lupin Mine site of Echo Bay Mines Ltd. The Lupin site is located in the Northwest Territories, on the northwest side of Contwoyto Lake, about 480 km east of Great Bear Lake. The area is underlain by several hundred metres of permafrost: over 500 m of frozen ground were intersected in the development of the mine shaft. The tailings pond at the site (Figure 20.1) was created by damming off a small watershed to create an enclosed storage basin. The basin was designed to hold the tailings output of the mine for several years. Decantation into the natural environment would occur after treatment has reduced the contaminant content to an acceptable level. The containment dams were constructed from locally derived sand and gravel or crushed tailings sand. Some of the dams were lined with an impermeable liner. Typically each dam site was scraped clean of organic material before construction of the dams began (Holubec et al., 1982, unpublished report entitled "Earthfill dam design and construction in cold permafrost at Contwoyto Lake, N.W.T."). The frozen nature of the dams and the underlying overburden and bedrock should preclude any transportation of fluid through or beneath the structures.

Despite the precautions taken in the design and construction of the dams, leakage of tailings water has been known to occur during the thaw season at several of the dams. The purpose of the GPR surveys was to establish if a high resolution geophysical technique, such as ground probing radar (GPR), could detect unfrozen zones (taliks) within or below the dams and so reveal a picture of the dam and overburden conditions. Unfrozen zones were thought to be the cause of fluid transport from the tailings pond into the surrounding environment. In addition to the radar surveys, a ground temperature monitoring program has been carried out at the site since 1982. Thermistors are installed in boreholes through four of the dams. Reliable ground temperature data are available from June 1, 1985 to the present date. Temperature data are collected several times per month.

GROUND PROBING RADAR

Ground probing radar is a fairly new geophysical tool, the first model being commercially available in the mid 1970s. GPR works similarly to conventional navigational radar in that a short pulse of electromagnetic energy is emitted by a transmitter antenna, reflects off a distant electrical boundary and the reflection is picked up by a receiver antenna (Davis et al., 1984, unpublished report entitled "Surface and borehole ground penetration radar surveys for mapping geological structure"). The time taken for the pulse to travel from the transmitter to receiver antenna via the reflector is measured. Provided the velocity of the pulse is known, the distance to a reflector can be calculated. In air, the pulse, typically in the MHz or GHz frequency range, travels with the speed of light (0.3 m/ns). In the subsurface the pulse travels with a velocity which is dependent upon the electrical properties of the material traversed. This velocity will be some appreciable fraction of the speed of light. In addition, the ability of the radar to resolve closely spaced reflectors in a material will increase as the velocity decreases. Spatial resolution is inversely proportional to the product of pulse velocity and pulse width. In moderately conductive materials a decrease in velocity will be counterbalanced by an increase in the pulse width arising from pulse dispersion. Contrasts in the dielectric permittivity or electrical conductivity of the subsurface due to changes in the material content will show up as distinct reflecting events. Common causes of subsurface reflections are material interfaces (overburden-rock, gravel-sand), water table limits, boundaries between frozen and unfrozen water, and ice lenses. A large dielectric contrast exists between water and most natural geological materials. As such, the presence or absence of water to a large degree controls the subsurface propagation characteristics of the radar pulse. The ability of a material to retain water within its pore spaces is an important determiner of its bulk electrical properties. The depth to which a radar pulse will effectively "penetrate" is dependent upon the electromagnetic absorption characteristics of the subsurface. In a general sense, this depth will decrease with increasing water content.

The analog ground probing radars currently available commercially have suffered from a limited potential depth

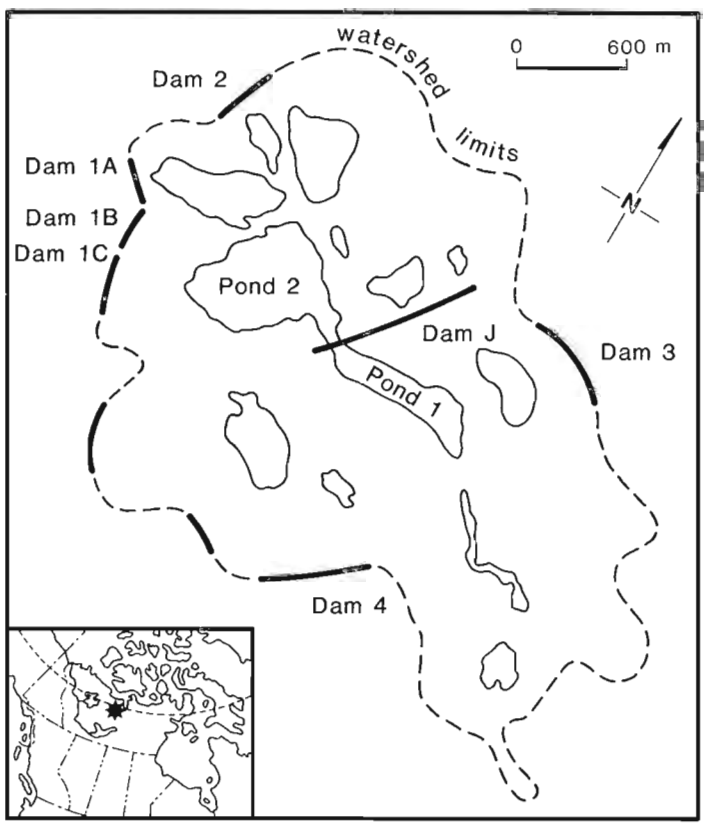


Figure 20.1 The Lupin Mine tailings facility.

penetration and crude data display and manipulation techniques. These drawbacks have severely limited the widespread application of the GPR technique. The Permafrost Research Section of Terrain Sciences Division has recently developed, through A-Cubed Ltd. of Mississauga, a fully digital radar (PulseEKKO III) which incorporates signal stacking and digital data processing. The section is at present testing a prototype of this unit under a variety of field conditions with a view towards evaluating its potential for solving a number of research and engineering problems and establishing survey procedures. The PulseEKKO III system is shown in Figure 20.2. Applications include permafrost, groundwater and overburden delineation; and void, channel, fracture, pipe and cable detection. The Lupin site is an excellent test facility as it provides a site where a good degree of ground truth is available from construction, drilling and temperature logging activities.

DAM SITE INVESTIGATIONS

Two dam sites were initially surveyed in June of 1986: dams 2 and J (Fig. 20.1, 20.3, 20.4). Both of these dams currently have or have experienced associated groundwater leakage. Borehole temperature data are available for Dam 2. Dam J was recently constructed in 1985, thus only the details of the construction plans are available. It was built to seal off the main tailings pond, Pond 2, from the decantation pond, Pond 1. Pond 1 serves as a temporary holding basin before decantation into the environment. The water is treated to remove contaminants during decantation from Pond 2 to Pond 1.

Dam 2

Dam 2 (Figure 20.3) was surveyed with the object of mapping the sub-dam bedrock and overburden competency. Leakage had been observed to occur around the south end of the dam abutment, near 310 m on the radar profile (Fig. 20.5, 20.6), during previous summer seasons. The core extracted from a drillhole at 356 m, 36 m beyond the end of the profile, had shown indication of substantial fracturing through the first 5 m of bedrock. The source of water transport was thought to be due to the melting, during the thaw season, of ice infilling these fractures. Temperature data indicate that the ground temperature could rise as high as 0°C at 7 m depth during the period of maximum thaw.

The dam was profiled from north to south using the PulseEKKO III radar equipped with 50 MHz antennas. The transmitter and receiver antennas were separated by 4 m and the station spacing was 4 m. The radar profiles are shown in Figures 20.5 and 20.6. The horizontal axis represents the distance (m) along the dam, while the vertical axis represents travel time (ns) to a particular event. Figure 20.6 shows only the top section of the time plot with an expanded time scale. As stated in the introduction above, travel time can be directly related to depth below the surface if the subsurface material velocity distribution is known. There was no common depth point (CDP) sounding taken at Dam 2 because of overall time constraints and the importance of surveying Dam J. CDP soundings are standardly taken along with the radar profile in order to determine the subsurface radio frequency velocity distribution and depths to specific reflectors (Annan and Davis, 1976). It is essentially the same technique as used in seismic surveys in that the source and receiver elements are incrementally spread apart. Subsurface velocities to different interfaces are calculated from a plot of separation versus travel time. A 100 MHz CDP sounding on Dam 1A is available from a subsequent survey in September of 1986. Dams 1A and 2 are identical in terms of their construction so top layer velocities should be roughly equivalent. The calculated velocity should be identical at 50 and 100 MHz for all practical purposes. The velocity calculated for the topmost layer is 0.0939 m/ns. This estimated velocity can be used to calculate the depths to reflectors 1, 2, and 3 indicated on Fig. 26.6. As a check on the velocity, the time gap between the air and ground wave arrivals on the profile was used to estimate a surface layer velocity. This is not as reliable a method as the character and separation of these events on a record can be affected by the processing options chosen. Specifically, the WOW correction, which corrects for receiver amplifier saturation, can affect the resultant velocity determination. The velocity calculated using this technique is about 0.110 m/ns, agreeing well with the CDP derived velocity.

Reflector 1 is at a depth of about 2 m and combines the boundary between the new and old dam material and the depth of the active layer. The latter should reside between 2 and 3 m as indicated by the temperature data from thermistors D2-5 and D2-6. Since both interfaces could be roughly coincident at this time of year, it would be difficult to resolve them as separate events. It can, however, be observed that in many places reflector 1 is represented by a broad double pulse. The new dam fill, which is believed to be gravelly sand, should retain much less moisture than the



Figure 20.2 The PulseEKKO III ground probing radar system on Dam 1A, Lupin Mine site. The system consists of a transmitter and receiver antenna package and a central control unit lying on the sled. The various units are connected by fiber optic cables.

original silty sand. Such an interface should provide a good electrical contrast as indicated by reflector 1.

Reflector 2 is at a depth of about 4.2 m and represents the interface of the silty sand dam fill with the natural silty sand overburden. The natural overburden should contain considerably more frozen water than the dam fill resulting in a strong electrical contrast. The dam fill material was obtained by drying excavated natural overburden material to substantially reduce its water content.

Reflector 3 varies considerably in depth along the profile. It represents the top of the bedrock. A substantial (5 m) dip in the bedrock topography is observed near the middle of the dam (110-222 m). Drillholes D2-6 and D2-7 indicate bedrock depths of 4.1 and 10.4 m, respectively. The depths calculated at D2-6 and D2-7 from the radar profile are 5.9 and 9.5 m, respectively. The discrepency arises from our ignorance of the true velocity profile. Figure 20.3 illustrates the dam profile as we believe it now exists. Each layer possesses its own radar velocity and thickness and these should be taken into account when calculating the depth to bedrock.

Strong reflections are observed to depth within the bedrock. These most likely represent included ice within the phyllite. The ice could be present either along cleavage planes or in fractures and joints. The limit of the reflections at depth

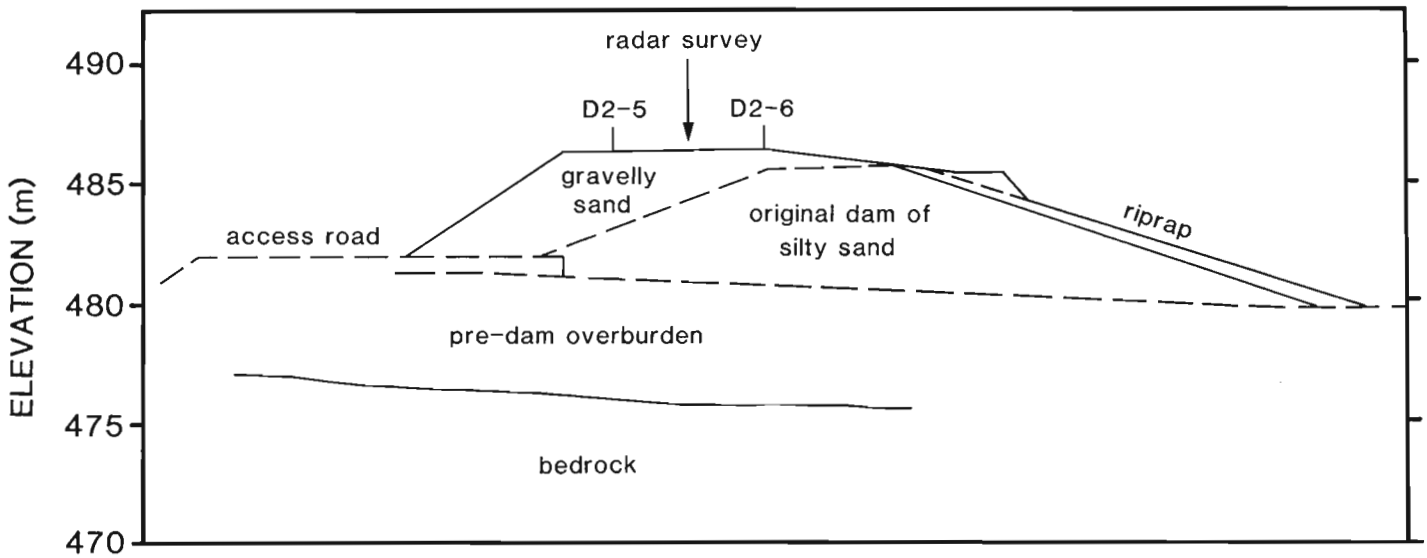


Figure 20.3 Cross-section of Dam 2, as reconstructed in June of 1986.

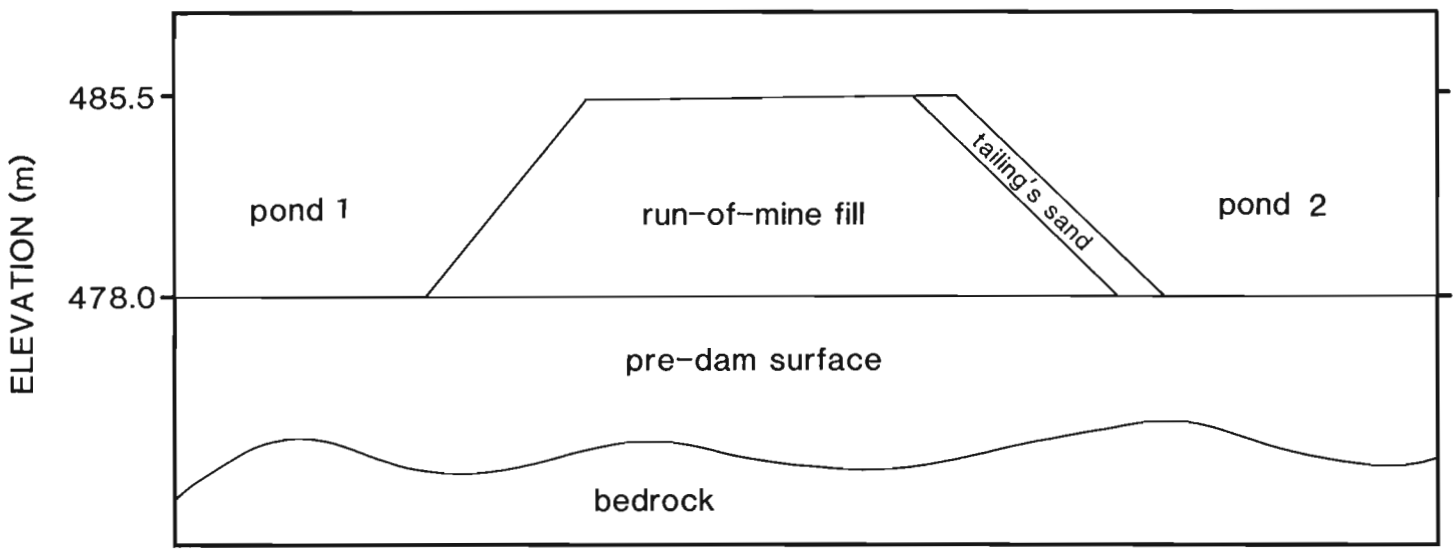


Figure 20.4 Cross-section of Dam J, as constructed in June of 1986.

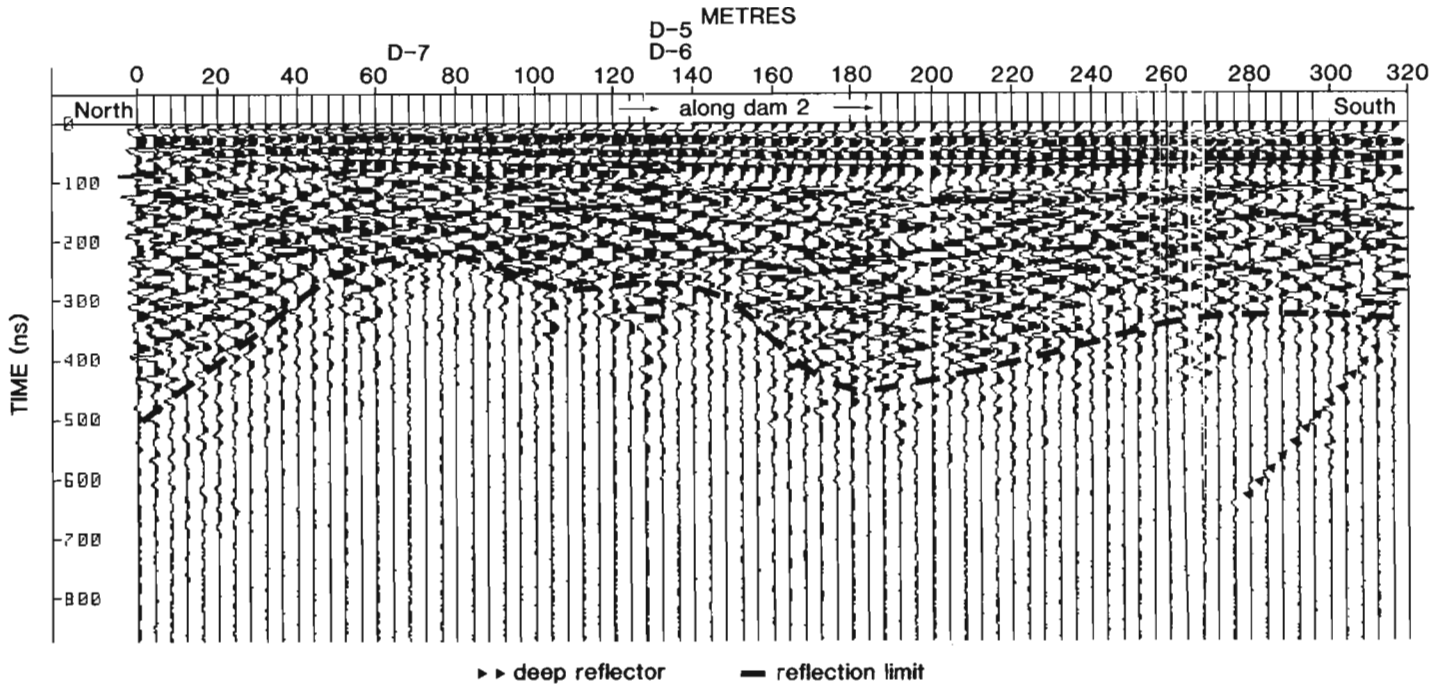


Figure 20.5 A 50 MHz radar profile across Dam 2. R represents subsurface reflectors.

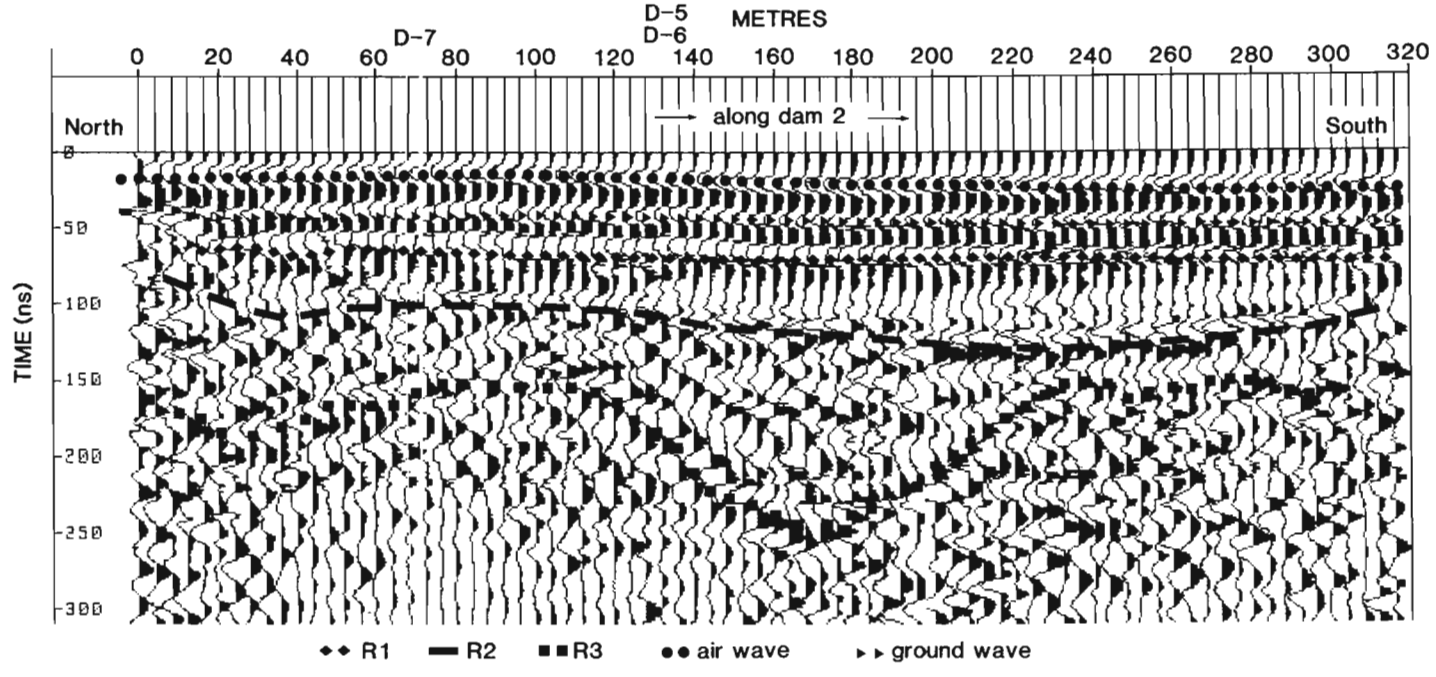


Figure 20.6 A expanded time-scale 50 MHz radar profile across Dam 2. R represents subsurface reflectors.

(Figure 20.5) is a function of the gain level, the absorptive characteristics of the subsurface materials, and the detection threshold of the instrumentation. Increasing or decreasing the gain in processing will move this apparent boundary either downward or upward. The apparent dip in the base of these reflections is an artifact of the increased thickness of overburden in the central area of the dam. The bedrock material should possess a higher radar velocity than the natural silty sand overburden. The addition of an increased thickness of lower velocity material stretches out the traces in this area yielding a false image of the deep structure.

The strong reflector observed at late times on Figure 20.5 (288-310 m) could either be a real subsurface feature or reflector on the surface. Given the pulse propagation velocity in air, a surface reflector would have to be between 45 and 100 m away. The vicinity of the survey site was, however, visibly barren of surface reflectors. The reflector is near the drillhole which indicated that the first several metres of bedrock was highly fractured. The reflection could indicate a large ice filled fracture or some other strong reflector buried at shallow depth within the bedrock below the dam.

Dam J

Dam J (Figure 20.4) was surveyed with the object of detecting a possible area of leakage through either the dam iself or its base. The dam was profiled with the PulseEKKO III radar using the 50 MHz antennas. The transmitter-receiver separation and the station spacing were 4 m. A CDP sounding was taken near the north end of the dam. The radar profile over the dam is shown in Figure 20.7. The CDP was centred about station 188 m which unfortunately was located too close to the north end of the main dam section. The subsurface in this area is substantially different in character from the central dam area. Some of the ground was originally above water and thus well frozen, also less dam fill was used to reach the desired dam height. In short, this particular area was not the best place in which to conduct the CDP sounding. Ideally, it should have been centred about 130 m. The presence of vehicles and diving equipment at the centre of the dam directed the final choice of location. Despite the fact that the subsurface structure is more complicated under the CDP centrepoint, the calculated ground wave velocity (.171 m/ns) should still be valid as the top-layer dam fill material does not change across the structure. A CDP taken over the center of the dam using the 100 MHz antennas yields a top layer velocity of 0.155 m/ns. This is consistent with the velocity determined using the lower frequency antennas. The ground wave velocity is high enough that at a 4 m transmitter-receiver separation, the air and ground waves are seen to

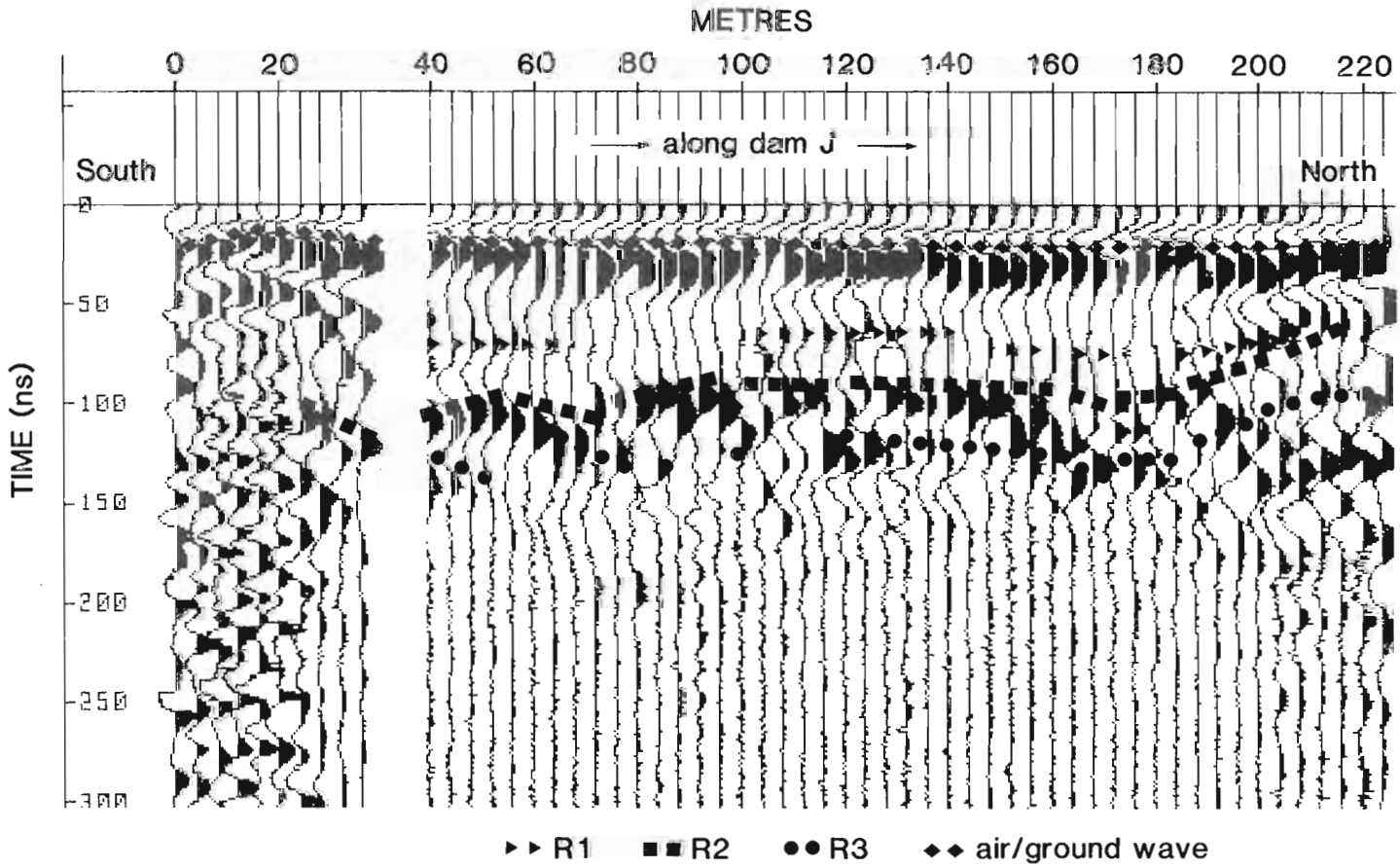


Figure 20.7 A 50 MHz radar profile across Dam J. R represents subsurface reflectors.

arrive almost simultaneously. This is quite evident in the profile (Figure 20.7) in the form of a long or double initial pulse. Note that the traces immediately south of the dam, in the undisturbed frozen environment, are more representative in character of the conditions found below Dam 2 (Figure 20.6).

Three reflectors, labelled R1, R2, and R3 have been identified on the Dam J profile. Reflector R1 has an average calculated depth of 5.2 m in the central portion of the dam. It is discontinuous across the dam profile. Given that the top of the dam is at 485.5 m (Figure 20.4), this reflector is located at elevation 480.3. The dam should be entirely filled with run of mill (ROM) material to its base (Golder Associates, 1986, unpublished "Draft report on tailings impoundment area, Contwoyto Lake, N.W.T." to Echo Bay Mines Ltd.). The impermeable sand liner is found only on the upstream side of the dam. This means we should not encounter any layering or large reflectors within the dam itself. We see several possible explanations for this reflector. First, it could represent the top of the frozen material. This is, however, a little deep for the depth of the active layer and it is doubtful that the dam, which was built in 1985, could have frozen to depth so quickly. Second, the reflector could represent the presence of ice included in the dam construction phase. This would explain satisfactorily the rather diverse nature of the reflector across the dam. Third, it could represent void areas that have been created from the melting out of included ice. Given the velocity of the dam material, isolated voids of less than 1 m in cross-section should not be detectable. This means that the void would have to be significant in size and could only result from the sublimation or melting out of included ice. Subsequent water infiltration of the voids from Pond 1 is possible. Fourth, the reflections could represent the water table level. Water should enter the dam from Pond 1 as the ROM material is relatively permeable and no sand liner seals the downstream side of the dam. The presence of water in the ROM material should be detectable as there will be a substantial electrical contrast with the dry ROM fill above the pond height. The height of Pond 1 during July of 1986 was approximately 482.5 m (Geocon Inc., 1986, unpublished interm data Report No. 40906-1-04 to Earth Physics Branch, Energy, Mines and Resources).

Reflector 2 is located at a depth of about 7 m. This is coincident with the boundary between the dike fill material and the previously existing ground surface. The surface ground wave velocity should yield an accurate depth estimate as the dam material is fairly uniform to its base.

Reflector 3, at a depth of 9.6 m, denotes either the bedrock-natural overburden interface or a layering within the overburden. Most likely it is the latter. It is probably slightly shallower than indicated as the slower velocity in the natural channel bottom sediments should be considered in any depth calculation.

Most of the central portion of the dam foundation was originally covered by water. This resulted in the material immediately under the central portion of the dam being unfrozen. The high water content and unfrozen nature of the overburden under the dam limits the penetration of the radar pulse. Note that the rather clean radar traces directly under Dam J are in direct contrast to the profile presented under Dam 2 where strong reflections are indicated to depth. The traces at either end of Dam J, that is in the areas not originally submerged, exhibit the latter character.

Several possible causes of leakage from Pond 2 to Pond 1 are envisaged. These are:

1) Leakage could be occurring directly through the rather thin tailings sand liner.

2) Leakage could be aided by the melting of lake ice included with the ROM material during winter dam construction period. Reflector 1, discussed above, indicates the possible location of included ice or voids.

3) Fluid could be transported through the natural overburden or lake bottom base which seems to be possibly unfrozen or at least low in ice content relative to the surrounding material.

CONCLUSION

The ground probing radar surveys were able to yield considerable information on the dam and sub-dam conditions. This information corresponded well to the subsurface conditions as determined by the dam construction procedures and subsequent drill coring. The radar has also served to extend our knowledge of the subsurface to areas where little is currently known. Radar surveys should be a powerful technique for preconstruction site investigation and for monitoring both before and after dam construction. Problems, such as those encountered at Dam 2 with the poor quality of bedrock, could be detected in advance and designed around in the construction phase.

Given the changing ground conditions associated with the yearly freeze-thaw cycle, it would be advantageous to monitor the dam conditions with the radar at several times during the year. This, in conjunction with the on-going temperature monitoring program, would allow us to determine the nature of any long term changes at the site. A combined geophysical and thermal history of these sites will be important when considering future developments of this type on permafrost.

ACKNOWLEDGMENTS

The authors wish to express their gratitude to Echo Bay Mines Ltd. for providing logistic assistance, in particular, Bob Gilroy, Hugh Wilson, and Ed Wong. The thermal monitoring program, funded through the Northern Environmental Directorate of Indian and Northern Affairs, is conducted under contract by Geocon Inc. for Energy, Mines and Resources.

REFERENCES

Annan, A.P., and Davis, J.L.,
1976: Impulse radar sounding in permafrost; Radio Science, v. 11, p. 383-394.

Geology of the northeastern and central Cape Breton Highlands, Nova Scotia[1]

Contract 27ST.23233-5-0009

Sandra M. Barr[2], Robert P. Raeside[2], Chris E. White[2], and Winai Yaowanoiyothin[2]

Barr, S.M., Raeside, R.P., White, C.E. and Yaowanoiyothin, W., Geology of the northeastern and central Cape Breton Highlands, Nova Scotia; in Current Research, Part A, Geological Survey of Canada, Paper 87-1A, p. 199-207, 1987.

Abstract

Northeastern and central Cape Breton Highlands consist of three lithological zones. Northwest of the Wilkie Brook fault system are Grenville-aged anorthosite and gneisses of the Blair River Complex.

To the southeast lie younger gneisses of the Cape North Group and predominantly metasedimentary units southeast of the Aspy Fault. The latter include quartzofeldspathic gneisses, mafic and pelitic schists, semipelitic gnesisses and subordinate orthogneiss. These units are intruded by undated gneissic plutons and a distinctive, probably Devonian, suite of granitic plutons. These plutonic rocks include abundant xenoliths and septa, many derived from the metasedimentary units to the west.

Separated from this central area by mylonite, a southeastern zone includes a regionally continuous amphibolite layer, felsic to intermediate volcanic and volcaniclastic rocks and slates. The, probably late Ordovician to early Silurian, megacrystic Cameron Brook Pluton intrudes this zone. The Devono-Carboniferous, megacrystic, Margaree Pluton forms the western margin of the area in the west-central Highlands.

Résumé

Les parties nord-est et centrale des hautes-terres du Cap-Breton se composent de trois zones lithologiques. L'anorthosite et les gneiss grenvilliens du complexe de Blair River se trouvent au nord-ouest du champ de failles de Wilkie Brook.

Au sud-est, on trouve des gneiss plus récents du groupe de Cape North et des unités surtout métasédimentaires au sud-est de la faille d'Aspy. Ces unités métasédimentaires se composent de gneiss quartzofeldspathiques, de schistes pélitiques et mafiques, de gneiss semipélitiques et d'orthogneiss secondaire. Ces unités sont recoupés par des plutons gneissiques non datés et par une suite distinctive de plutons granitiques vraisemblablement d'âge dévonien. Ces roches plutoniques contiennent de nombreux xénolites et septa, dont bon nombre sont dérivés d'unités métasédimentaires situées plus à l'ouest.

Cette zone centrale est séparée d'une zone sud-est par de la mylonite; la zone sud-est comprend une couche d'amphibolite qui est continue à l'échelle régionale, ainsi que des roches et des schistes ardoisiers volcaniques et volcano-détritiques felsiques et intermédiaires. Le pluton macrocristallin de Cameron Brook, qui date vraisemblablement de la fin de l'Ordovicien ou du début du Silurien, a fait intrusion dans cette zone. Le pluton macrocristallin de Margaree, d'âge dévonien-carbonifère, forme la marge ouest de la région dans la partie centrale ouest des hautes-terres.

[1]Contribution to Canada-Nova Scotia Mineral Development Agreement 1984-1989. Project carried by Geological Survey of Canada, Lithosphere and Canadian Shield Division.

[2]Department of Geology, Acadia University, Wolfville, Nova Scotia B0P 1X0

INTRODUCTION

During the 1986 field season, mapping in the central and eastern Cape Breton Highlands resulted in the compilation of a 1:50 000 scale geological map, a reduced version of which is shown in Figure 21.1. Previous regional maps of this area are of a reconnaissance nature (McLaren, 1956a, b; Neale 1963a, b) and provide only an outline of the major rock types. More detailed studies in the map area have been of limited extent (Wiebe, 1972, 1975; Barr et al., 1982; Smith and Macdonald, 1983).

This map completes the current phase of geological mapping of the Cape Breton Highlands, previous results of which were presented by Jamieson (1981), Barr et al. (1982), Jamieson and Craw (1983), Jamieson and Doucet (1983), Raeside et al. (1984), Barr et al. (1985a, b), Raeside et al. (1986), and Plint et al. (1986).

The Cape Breton Highlands form a dissected peneplain which gradually drops in elevation from 530 m in the central part of the map area to about 200 m in the northeast. Drainage is generally radial, although there is a prominent linearity to the drainage system in the east which appears to be related to tilting of the peneplain as there is no apparent bedrock or structural control. Outcrop is good in stream beds and on valley walls, but is patchy on top of the peneplain; in the eastern part of the map area good outcrop occurs on unforested ridges and knobs, especially where these are underlain by granite, but in the west outcrop is very limited over large areas where schistose lithologies are deeply weathered and there is extensive development of bog. Coastal exposures are excellent from White Point to Ingonish.

Access can be made to the northwestern and eastern parts of the map area by means of the Cabot Trail, and a maintained network of hiking trails and disused fire access tracks in the Cape Breton Highlands National Park. The southwestern and central parts of the area are best reached by helicopter.

OVERVIEW

The map area can be divided into three distinct zones on the basis of metamorphic lithologies. In the northwest is the southerly extension of the Grenvillian Blair River Complex, separated from rocks to the south and southeast by the Wilkie Brook and Red River fault systems, as described by Raeside et al. (1986) and Barr et al. (in press). The central part of the map area is underlain by varied schists and gneisses which are tentatively correlated in part with the Cape North and Money Point groups (Macdonald and Smith, 1980; Raeside et al., 1986) and the Cheticamp Lake gneiss (Raeside et al., 1984; Raeside and Barr, in press). The southeastern corner of the map area includes mainly low-grade metavolcanic and metasedimentary rocks, probably correlative with the McMillan Flowage Formation (Raeside and Barr, in press) to the south. In addition to these lithologies, abundant granitoid units occur, dominant of which are the Margaree Pluton forming the western margin of the map area, the Middle Aspy and Glasgow Brook plutons in the north, the White Point-Black Brook-Warren Brook-Clyburn Brook plutonic suite in the east, and the Cemeron Brook Pluton in the southeast. Overlying these metamorphic and plutonic lithologies are Carboniferous conglomerates, sandstones, limestones and evaporites in the Cape North, Ingonish and Ingonish Beach areas.

Cape North Group and Big Southwest Brook gneiss

The small portion of the Cape North Group exposed between the Wilkie Brook fault system and the Aspy Fault consists of semipelitic and pelitic gneisses with thin layers of kyanite schist and marble which serve as marker horizons.

Immediately adjacent to the Aspy Fault, and extending to the east for 1500 m in an arcuate belt is a unit characterized by quartzofeldspathic gneisses, calc-silicate schists and amphibolites (Big Southwest Brook gneiss). Marble has also been reported in Big Southwest Brook (Neale, 1963a) but was not observed in this study. The quartzofeldspathic gneisses are typically coarse grained, leucocratic gneisses with minor biotite. A variety with scarce nematoblastic crystals of hornblende and biotite (both commonly chloritized) and sparse garnet metacrysts appears to be particularly diagnostic of this unit. Calc-silicate layers are concordant with layering in the gneisses, and are present on scales ranging from millimetres to tens of centimetres. Amphibolites appear to occur both as concordant and cross-cutting bodies representing metamorphosed mafic intrusions. Many amphibolites are garnetiferous.

The Big Southwest Brook gneiss bears many lithologic similarities to the Cape North Group and is tentatively correlated with it. In particular, the predominance of semipelitic compositions, the leucocratic gneiss, the thin marble and calc-silicate layers, and the amphibolite dykes are common to both units.

North Aspy River schist

This extensive series of stratified rocks extends in an arcuate belt from the Aspy Fault east and south to the headwaters of the Aspy and Cheticamp rivers. The dominant lithologies are hornblende-biotite schists and gneisses, biotite schists, calc-silicate rocks, and minor amphibolites. Hornblende-biotite schists are particularly common and diagnostic of this unit – typically the hornblende and biotite occur as medium to coarse grained crystals and each comprises 15 to 25 % of the rock, the remainder being plagioclase, quartz and accessory sphene and apatite. Some samples also contain scarce large metacrysts of garnet, with complex inclusion patterns. Biotite schists and garnet-biotite schists are also common in this unit; these tend to show well developed compositional layering with biotite-rich, garnet-rich and quartzofeldspathic layers. Calc-silicate rocks also show compositional layering on a millimetre to centimetre scale with biotite schists and hornblende-biotite schists. Calc-silicate layers include hornblende-diopside-plagioclase, diopside-biotite-plagioclase ± quartz, and scapolite-hornblende-clinozoisite-plagioclase assemblages. Amphibolites are less common in this unit and

are probably restricted to metamorphosed mafic dykes. Mafic schists and gneisses in the Cheticamp River may be a southern extension of this unit.

BLAIR RIVER COMPLEX

The Blair River Complex in the map area includes the southern part of the Red River Anorthosite and gneisses of the Polletts Cove Brook Group (Raeside et al., 1986; Barr et al., 1986). The eastern margin of the Blair River Complex is the Wilkie Brook fault system, a series of anastomosing mylonite zones, up to 1000 m across, involving rocks of the Polletts Cove Brook Group and the adjacent Cape North Group (Smith and Macdonald, 1983). The degree of deformation in the fault system ranges from pervasive chloritization and mild shearing to intense mylonitization. The southwestern margin of the Blair River Complex, the Red River mylonite zone, projects into the extreme northwestern margin of the map area but is cut off by the Margaree Pluton. However, strong shearing in the pluton (described below) indicates some post-intrusion movement on the fault zone.

In the south, the Blair River Complex and the mylonite zones are truncated by the Aspy Fault, implying that the main phase of movement on the fault was during the Carboniferous, between the late Devonian-early Carboniferous emplacement of the Margaree Pluton (O'Beirne-Ryan et al., 1986) and the Mississippian deposition of the Horton Group in the Aspy Lowlands. Deformed lithologies associated with the Aspy Fault are well exposed in the North Aspy River – these are typically chloritic schists showing relatively brittle deformation structures, mainly brecciation, and limited mylonite development. In contrast to the Wilkie Brook fault system, the effects of the Aspy Fault are limited to a zone no wider than 50 to 100 m.

CENTRAL METAMORPHIC UNITS

In addition to a small portion of the Cape North Group (Macdonald and Smith, 1980; Smith and Macdonald 1983) exposed between the Wilkie Brook and Aspy faults, five metamorphic units occur in the central part of the map area. Adjacent to the Aspy Fault is a series of gneisses and calc-silicate rocks (Big Southwest Brook gneiss). The most extensive unit is the North Aspy River schist, a thick sequence of mafic and pelitic schists and subordinate calc-silicate rocks which occur east of the Big Southwest Brook gneiss. A third unit (South Aspy River schist) consisting of a similar series of mafic and pelitic schists with minor calcareous and amphibolitic rocks occurs in the northern part of the map area south of Cape North Village, separated from the North Aspy River schist by orthogneissic plutons. The fourth unit consists mainly of felsic gneisses (some of which may be orthogneisses) and extends through the central part of the area. These in part are the Cheticamp Lake gneisses of Raeside et al. (1984) and Raeside and Barr (in press).

The predominance of mafic lithologies and the interlayering with pelitic lithologies in this unit are similar to features observed in the Money Point Group (Macdonald and Smith, 1980; Raeside et al., 1986) and in the Jumping Brook metamorphic suite in the western Highlands (R.A. Jamieson, personal communication, 1986).

South Aspy River schist

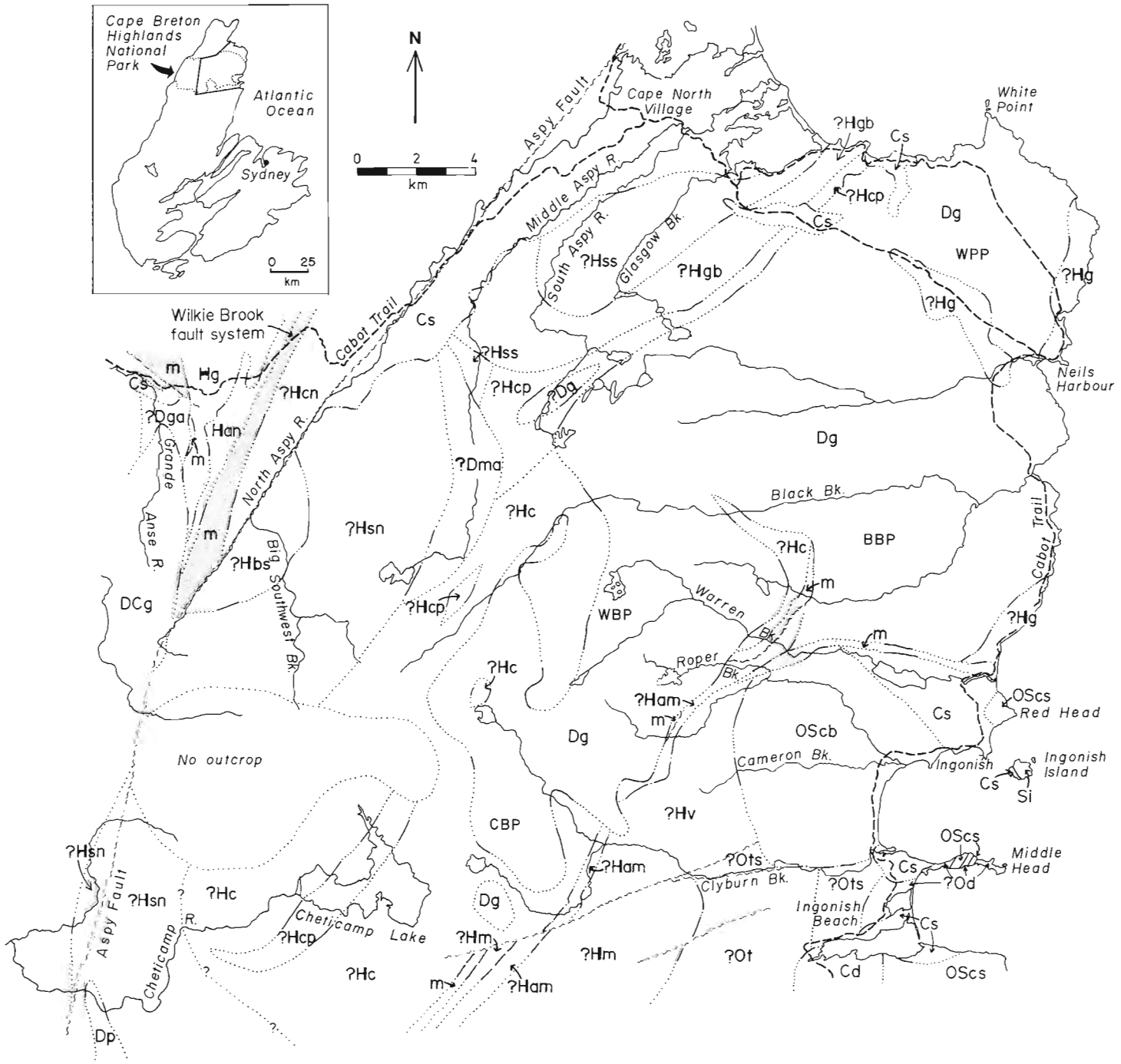
Two areas of predominantly schistose lithologies occur south of Cape North Village, in the valleys of the South and Middle Aspy rivers. The main outcrop area of the South Aspy River is isolated from other stratified units by the Glasgow Brook Pluton, a biotite orthogneiss. The small area of biotite schist and amphibolite in the Middle Aspy River is probably correlative with the South Aspy River schist, and is in turn isolated from the North Aspy River schist by the Middle Aspy biotite orthogneiss.

Biotite, muscovite-biotite and hornblende-biotite schists are common, but there are numerous amphibolite layers and some marble horizons. The hornblende-biotite schists in particular are similar to those exposed in the North Aspy River schist, and support correlation with that unit. Minor differences, however, also exist: muscovite-rich schists appear to be more abundant, amphibolites are more widespread, marbles are present, and calc-silicate rocks appear to be lacking in the South Aspy River schist. The marbles occur as layers (up to 80 cm thick) in association with amphibolites. Two outcrops were noted in South Aspy River, one containing three marble layers, the other two.

Cheticamp Lake gneiss

To the east of the hornblende-biotite schist unit in the North Aspy River schist is a series of semipelitic gneisses, with interlayered schists, granitic orthogneisses and rare amphibolites. This unit outcrops in the headwaters of a number of streams and on the Highlands plateau but is generally poorly exposed. A number of large xenoliths or isolated blocks of gneiss which are surrounded by the granites of the eastern plutonic belt are considered to be remnants of the Cheticamp Lake gneiss. Biotite- and biotite-muscovite schists and gneisses are typical; some also contain garnet. Outcrops tend to be massive, with poorly preserved or developed compositional layering, although there are some very distinctive 5 to 20 cm wide micaceous layers which are made up of over 80 % biotite and muscovite. Approximately 20 % of the outcrops in this area are orthogneissic in appearance, with very uniform, leucocratic aspect, or with possible xenolithic inclusions. These orthogneisses and semipelitic gneisses are similar to and geographically adjacent to the Cheticamp Lake gneiss described by Raeside et al. (1984) and Raeside and Barr (in press), and are considered as a northerly extension of the Cheticamp Lake gneiss.

Throughout the Cheticamp Lake gneiss as well as the North and South Aspy River schists are numerous pegmatitic and granitic dykes and veins. These increase in concentration to the east, adjacent to the eastern granitic belt, where the boundary between the metamorphosed stratified units and the plutonic units is drawn on the basis of predominance of one or


Cape Breton Highlands National Park
Atlantic Ocean
Sydney
0 25 km
N
0 2 4 km
Aspy Fault
Cape North Village
White Point
?Hgb
Cs
?Hcp
Dg
WPP
?Hg
Middle Aspy R.
South Aspy R.
Glasgow Bk.
?Hss
?Hgb
Cabot Trail
Wilkie Brook fault system
Cs
m
Hg
?Hcn
?Dga
Han
Grande
Anse R.
North Aspy R.
?Hss
?Hcp
?Dg
Dg
Neils Harbour
?Dma
?Hc
?Hsn
?Hbs
Big Southwest Bk.
DCg
Black Bk.
BBP
Warren Bk.
WBP
Roper Bk.
?Ham
OScs
Red Head
OScb
Cs
Dg
No outcrop
Cameron Bk.
Ingonish
Ingonish Island
Si
CBP
?Hv
?Ots
Clyburn Bk.
Middle Head
?Od
Ingonish Beach
Cheticamp R.
Cheticamp Lake
?Hcp
?Hm
?Ot
Cd
Aspy Fault
Dp

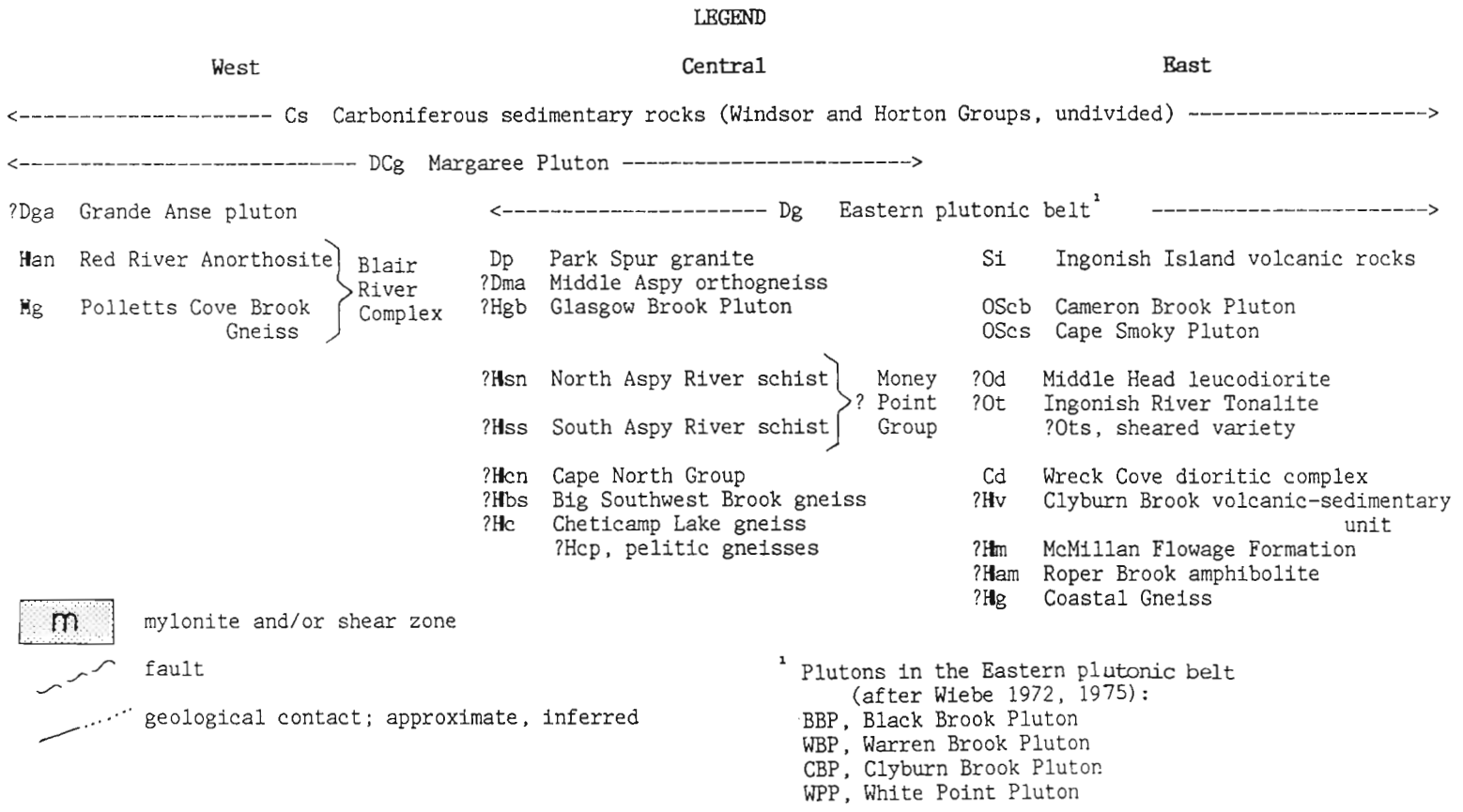


Figure 21.1 Geological map of the northeastern and central Cape Breton Highlands.

the other lithology. Correspondingly, numerous metasedimentary xenoliths, screens and septa, which are lithologically similar to the semipelitic gneisses, occur in the plutons of the granitic belt near their western margins and are probably disrupted pieces of the Cheticamp Lake gneiss.

The eastern limit of Cheticamp Lake gneisses and related rocks appears to be a major mylonite zone, here termed the Eastern Highlands mylonite. South of the present map area, this mylonite zone is up to 600 m wide (Raeside et al., 1984), although its width is variable. North of Clyburn Brook, the mylonite zone is exposed in Warren Brook, and extends to the north where it is cut off by granitic rocks of the eastern plutonic belt.

The regional structure of the North Aspy River schists and Cheticamp Lake gneiss is apparently simple. Foliations in all the units generally describe a semicircular arcuate feature, focused on the Aspy Fault. Farther away from the focal point, the regularity of the structure is less obvious. In detail, however, the structure is more complex. Minor fold trends are extremely variable, and many outcrops showing evidence of repeated foliation development (metacrysts with relict inclusion trails, crenulation cleavages, and mineral lineations).

SOUTHEASTERN ZONE

Coastal gneiss

Heterogeneous gneissic rocks (Coastal gneisses of Wiebe, 1972) occur east of the eastern plutonic belt and as abundant xenoliths in the granites. They are mainly granodioritic orthogneisses, locally porphyroblastic with microcline megacrysts. The latter are similar to the Cameron Brook Pluton, described below. Screens of biotite schist occur locally within the gneisses, and dykes of granite and pegmatite from the adjacent plutons are abundant. A Rb-Sr isochron reported by Cormier (1972) indicates a late Precambrian to Cambrian age for these gneisses.

Roper Brook amphibolite

A regionally continuous amphibolite layer ranging in outcrop thickness from 400 to 700 m extends along the southeastern margin of the Black Brook Pluton, the northwestern margin of the Cameron Brook Pluton, and southwest to the area mapped by Raeside et al. (1984). The total strike length is about 35 km. Typically the rock is a massive to moderately foliated, mesocratic epidote amphibolite. Some specimens contain large metamict allanite(?) grains, which acted as nuclei for the further growth of epidote, and medium to coarse grained magnetite and ilmenite, the latter partly replaced by sphene.

The western margin of the amphibolite has been truncated in Roper Brook by the intrusion of the Black Brook Pluton, but farther to the north, and to the south in the area mapped by Raeside et al. (1984) it includes hornblende schists and mafic hornblende-biotite schists which grade into massive amphibolite to the southeast. The schistose nature of these rocks appears to be the result of deformation at the margin of the Eastern Highlands mylonite which separates the amphibolite from the Cheticamp Lake gneiss, to the west.

Clyburn Brook volcanic-sedimentary unit

A suite of metamorphosed volcanic, volcaniclastic and sedimentary rocks is exposed in Clyburn Brook and in a number of streams draining into Clyburn Brook from the north. Metamorphic grade in this area is uniformly low, and the main rock types are green and grey slates, green phyllites and metasiltstones. Volcaniclastic rocks appear to be the most abundant including volcaniclastic breccias, crystal and lithic tuffs and sheared varieties of these. Volcanic rocks include aphanitic and porphyritic types, with phenocrysts of plagioclase (some albitized, others with An_{25-45}), quartz (deeply embayed and corroded) and less commonly sanidine. The volcanic and volcaniclastic rocks are predominantly felsic, with chlorite and epidote rarely comprising more than 30 % of the rock. Interlayered with the eruptive rocks are black slates, phyllites and siltstones. In Clyburn Brook, these show the development of sericitic foliation (slates) and decussate muscovite (siltstones). Closer to the Cameron Brook Pluton, the slates have developed first biotite, and within 400 m of the contact, microscopic garnet.

Ingonish Island volcanic rocks

Most of Ingonish Island is underlain by lightly metamorphosed flow-banded rhyolites. In places these are moderately cleaved, with the development of chlorite; more typically phenocrysts of plagioclase and alkali feldspar are preserved in a fine grained recrystallized groundmass of feldspar and muscovite. Sparse volcaniclastic rocks include strongly flattened chloritic tuffs and breccias. The volcanic and volcaniclastic rocks are cut by pink porphyritic rhyolite dykes, which are similar to feldspar porphyry dykes in the Cameron Brook Pluton and the Clyburn Brook volcanic-sedimentary unit. A Rb-Sr whole-rock isochron has suggested a late Silurian age for the Ingonish Island volcanic rocks (J.D. Keppie, personal communication, 1986).

PLUTONIC ROCKS

Margaree Pluton

The Margaree Pluton (Currie, 1975) forms the western margin of the map area, extending from the Red River mylonite zone in the north across the Cheticamp River in the south. It is strongly sheared along its northeastern margin, probably by late movement along the Red River mylonite zone, and along its eastern margin by the Aspy Fault. However, the eastern contact is not everywhere faulted, as an intrusive contact is exposed in the Cheticamp River where the Aspy Fault apparently lies farther east within the North Aspy River metamorphic sequence. On its western side, the Margaree Pluton has an intrusive relationship with the Pleasant Bay Gneiss (Plint et al., 1986).

The Margaree Pluton in the map area consists of distinctive coarse grained megacrystic biotite-hornblende monzogranite similar to that described by O'Beirne-Ryan et al. (1986) from the southern extension of the pluton in the west-central Cape Breton Highlands. It is cut by fine grained syenogranite dykes similar in composition to the Salmon Pool granite to the west. The Margaree Pluton has given a Rb-Sr whole-rock isochron age of 343 ± 17 Ma but this may be too young, the actual age being similar to the age of the Salmon Pool granite (about 365 Ma) as discussed by O'Beirne-Ryan et al. (1986).

Glasgow Brook Pluton

The Glasgow Brook Pluton (Wiebe, 1972) is an elongate orthogneissic intrusion in the northeastern part of the map area. It consists of strongly foliated medium grained hornblende-biotite tonalite to granodiorite. Dioritic xenoliths are locally abundant, and combined with the relatively homogeneity of the body confirm its igneous origin. However, the rock is gneissic in appearance, with biotite and hornblende concentrated on foliation planes separated by quartzofeldspathic layers with augen of feldspar and quartz.

The age of the Glasgow Brook Pluton is not known. However it intruded and was deformed with the adjacent South Aspy River schist and is of probable early Paleozoic or late Precambrian age.

Middle Aspy biotite orthogneiss

A small body of orthogneiss separates metamorphic rocks of the North and South Aspy River schists and the Cheticamp Lake gneiss in the central part of the map area. It consists of strongly foliated fine to medium grained biotite granodiorite, similar to that of the eastern plutonic belt except much more strongly foliated. On the basis of the latter, it is considered to be a separate older(?) map unit.

Eastern plutonic belt

The eastern half of the map area is dominated by distinctive granodioritic to granitic rocks forming a large intrusion, lobes of which Wiebe (1972, 1975) named (from north to south) the White Point, Black Brook, Warren Brook, and Clyburn Brook plutons. Metamorphic xenoliths are locally very abundant in these units, and granitic rocks are very abundant in the adjacent schist and gneiss units, so the positions of the margins of these plutons are rather arbitrarily placed. Abundant granitoid rocks of this type also occur to the west across the Highlands to the Pleasant Bay area, and south to include the Park Spur granite (R.A. Jamieson, personal communication, 1986), a small part of which extends into the Cheticamp River (Fig. 21.1). However, as also recognized by Wiebe (1975), they do not extend southeast of a line in the southeastern part of the map area which is here identified as a major mylonitic fault zone (the Eastern Highlands mylonite).

The plutons and related dykes of the eastern granitoid belt consist mainly of pale pink to grey biotite granite gradational to granodiorite. Locally the rocks contain muscovite and garnet. Associated pegmatite and aplite are common, both within the plutons and in adjacent metamorphic rocks. Foliation varies from moderate to absent, and locally the rocks are strongly sheared. Preliminary petrological studies of these rocks were reported by Wiebe (1975); Barr et al. (1982) and Barr and Pride (1986) have described the petrology of the White Point Pluton in more detail. These granitoid rocks are interpreted to have been derived from metasedimentary source rocks and emplaced at relatively deep crustal levels.

On the basis of Rb-Sr whole-rock isochrons (Cormier, 1972; R.F. Cormier, personal communication, 1980), these granitoid rocks are interpreted to be Devonian in age and hence a widespread Devonian thermal event in the northern Highlands.

Cameron Brook Pluton

The Cameron Brook Pluton is a nearly circular intrusion south of the eastern granitoid belt. It was originally described and named by Wiebe (1972), who interpreted it to be late Precambrian in age. Raeside et al. (1984) mapped the southern margin of the pluton where it has intruded gneissic and tonalitic rocks, and suggested that it might be Devonian. O'Beirne-Ryan et al. (1986), however, reported a Rb-Sr whole rock isochron indicating an Ordovician to Silurian age of 445 ±16 Ma. The present mapping essentially confirmed the boundaries of the pluton shown by Wiebe (1972).

The Cameron Brook Pluton consists of equigranular and megacrystic biotite (± hornblende) granite grading to granodiorite. Colour varies from red to pink, and grain size from medium to coarse. Major minerals are plagioclase, microcline, quartz and biotite. Hornblende occurs in minor amounts in some samples. Accessory minerals include opaque oxides, sphene and apatite. Where megacrysts are present, they are generally subhedral and consist predominantly of plagioclase with less abundant microcline. The pluton is cut by abundant feldspar porphyry dykes.

The pluton intruded of the Clyburn Brook volcanic-sedimentary unit on the west and xenoliths of both metavolcanic and metasedimentary composition are abundant. A contact metamorphic aureole is developed in the volcanic and sedimentary rocks adjacent to the pluton.

On the south the pluton is chilled against tonalite and tonalitic gneiss of the Ingonish River Tonalite (Wiebe, 1972; Raeside et al., 1984). However, the pluton appears not to have been affected by mylonitic fault zones in Clyburn Brook (Raeside et al., 1984). On the north, the Cameron Brook Pluton is separated by a shear zone from the Black Brook Pluton. However, xenoliths of gneissic megacrystic granite similar to the Cameron Brook Pluton are common in the southern part of the Black Brook Pluton, and parts of the Coastal Gneisses are also similar.

OTHER ROCK UNITS

Coarse grained granite of presumed Devonian age (Grande Anse granite of Plint et al., 1986) occurs in the northwestern part of the map area, and is similar to other relatively young granites along the Red River, Wilkie Brook and Aspy faults (Raeside et al., 1986).

In the southeastern part of the map area, several igneous units occur which are extensions or correlatives of those to the south described by Raeside et al. (1984). Also present throughout the map area are varied mafic, lamprophyric and felsic dykes.

Conglomerate and sandstone of the Horton Group and limestone, siltstone and gypsum of the Windsor Group occur locally at the periphery of the map area. These units were not included in the present study and their distribution was shown by previous workers (Neale, 1963a, b; McLaren, 1956b).

DISCUSSION

The oldest sequence recognized in the map area is probably the Polletts Cove Brook Gneiss, which has been intruded by anorthosite and, to the north of the present map area, by syenite, the latter having yielded a U-Pb zircon age of 1040^{+10}_{-40} Ma (Barr et al., in press). These units make up much of the Grenvillian Blair River Complex which is bounded by mylonitic zones on its eastern and southern margins. It is unlikely that any lithologies can be correlated across these mylonite zones, and the Blair River Complex is considered to be a fragment of the Grenville Province incorporated into the Appalachian Orogen.

The age of metamorphic units in the central part of the map area between the Wilkie Brook fault system and the Eastern Highlands mylonite zone is poorly constrained. Based on its higher metamorphic grade, the Cheticamp Lake gneiss is tentatively considered to lie below the hornblende-biotite schists and quartzofeldspathic gneisses, although nowhere is the boundary between these units clearly exposed. Prominent changes in foliation orientation between the Cheticamp Lake gneiss and the hornblende-biotite schists might indicate that the gneiss has a more protracted deformational history. The hornblende-biotite schists appear compositionally similar to, and may be correlable with, the Money Point Group to the north (Macdonald and Smith, 1980) and at least parts of the Jumping Brook metamorphic suite to the south (R.A. Jamieson, personal communication, 1986). Similarly, the quartzofeldspathic gneisses of the Big Southwest Brook unit may be correlated to the Cape North Group, west of Aspy Fault.

Prior to a major phase of deformation and foliation development, the stratified units were intruded by the Middle Aspy and Glasgow Brook Pluton and other smaller granitoid plutons which are now exposed as orthogneisses.

East of the Eastern Highlands shear zone, the volcanic-sedimentary section and the Roper Brook amphibolite are tentatively correlated with rocks of the McMillan Flowage Formation (Raeside and Barr, in press). The amphibolite in particular is regionally continuous, begin offset 2 km by the Clyburn Brook fault. The extensive volcanic and volcaniclastic lithologies of the Clyburn Brook unit north of the fault contrasts with predominance of clastic sedimentary units to the south, and if the correlation is correct, may represent either a lateral facies variation in the Middle Clastic Division or a separate previously unrecognized division in the McMillan Flowage Formation. In either case, the Clyburn Brook unit was intruded by the apparently Ordovician to Silurian Cameron Brook Pluton, prior to movement on the Eastern Highlands mylonite zone. The mylonite zone is cut off by the extensive apparently Devonian granitic plutons of the eastern plutonic belt, which also display mild to moderately intense pervasive syntectonic foliation.

In the western part of the area, the Devono-Carboniferous Margaree Pluton intruded both the Blair River Complex and the metasedimentary lithologies of the central Highlands, but was itself affected by Mississippian movement on the Aspy Fault.

Deposition of conglomerates and sandstones (Horton Group) and limestones, siltstones and evaporites (Windsor Group) occurred during the Mississippian, and these units are not affected by movement on the Aspy Fault.

ACKNOWLEDGMENTS

We gratefully acknowledge financial support from the Department of Energy, Mines and Resources, Geological Survey of Canada, and the Natural Sciences and Engineering Research Council of Canada. We are also very appreciative of the co-operation of Parks Canada, and the wardens at Ingonish Beach, Neils Harbour and Big Intervale.

REFERENCES

Barr, S.M. and Pride, C.R.
1986: Petrogenesis of two contrasting Devonian granitic plutons, Cape Breton Island, Nova Scotia; Canadian Mineralogist, v. 24, p. 137-146.

Barr, S.M., Jamieson, R.A. and Raeside, R.P.
1985a: Igneous and metamorphic geology of the Cape Breton Highlands; Geological Association of Canada/Mineralogical Association of Canada Excursion Guide 10, Fredericton, New Brunswick, 48 p.

Barr, S.M., O'Reilly, G.A. and O'Beirne, A.M.
1982: Geology and geochemistry of selected granitoid plutons of Cape Breton Island; Nova Scotia Department of Mines and Energy, Paper 82-1, 176 p.

Barr, S.M., Raeside, R.P. and Macdonald, A.S.
1985b: Geology of the southeastern Cape Breton Highlands, Nova Scotia; in Current Research, Part B, Geological Survey of Canada, Paper 85-1B, p. 103-109.

Barr, S.M., Raeside, R.P. and Van Breeman, O.
in press: Grenvillian basement in the northern Cape Breton Highlands, Nova Scotia; Canadian Journal of Earth Sciences.

Cormier, R.F.
1972: Radiometric ages of granitic rocks, Cape Breton Island, Nova Scotia; Canadian Journal of Earth Sciences, v. 9, p. 1074-1086.

Currie, K.L.
1975: Studies of granitoid rocks in the Canadian Appalachians; in Report of Activities, Part A; Geological Survey of Canada, Paper 75-1A, p. 265-268.

Jamieson, R.A.
1981: The geology of the Crowdis Mountain volcanics, southern Cape Breton Highlands; in Current Research, Part C, Geological Survey of Canada, Paper 81-1C, p. 77-81.

Jamieson, R.A. and Craw, D.
1983: Reconnaissance mapping of the southern Cape Breton Highlands – a preliminary report; in Current Research, Part A, Geological Survey of Canada, Paper 83-1A, p. 263-268.

Jamieson, R.A. and Doucet, P.
1983: The Middle River-Crowdis Mountain area, southern Cape Breton Highlands; in Current Research, Part A, Geological Survey of Canada, Paper 83-1A, p. 269-275.

Macdonald, A.M. and Smith, P.K.
1980: Geology of the Cape North area, northern Cape Breton Island, Nova Scotia; Nova Scotia Department of Mines and Energy, Paper 80-1, 60 p.

McLaren, A.S.
1956a: Cheticamp River; Geological Survey of Canada, Preliminary Map 55-36.

McLaren, A.S.
1956b: Ingonish; Geological Survey of Canada, Preliminary Map 55-35.

Neale, E.R.W.
1963a: Geology, Pleasant Bay, Cape Breton Island, Nova Scotia; Geological Survey of Canada, Map 1119A.

Neale, E.R.W.
1963b: Geology, Dingwall, Cape Breton Island, Nova Scotia; Geological Survey of Canada, Map 1124A.

O'Beirne-Ryan, A.M., Barr, S.M., and Jamieson, R.A.
1986: Contrasting petrology and age of two megacrystic granitoid plutons, Cape Breton Island, Nova Scotia; in Current Research, Part B, Geological Survey of Canada, Paper 86-1B, p. 179-190.

Plint, H.E., Connors, K.A., and Jamieson, R.A.
1986: Geology and mineral occurrences of the Jumping Brook Complex, Cheticamp-Pleasant Bay area, Cape Breton Island, Nova Scotia; in Current Research, Part B, Geological Survey of Canada, Paper 86-1B, p. 557-566.

Raeside, R.P. and Barr, S.M.
in press: Stratigraphy and structure of the southeastern Cape Breton Highlands, Nova Scotia; Maritime Sediments and Atlantic Geology.

Raeside, R.P., Barr, S.M., and Jong, W.
1984: Geology of the Ingonish River–Wreck Cove area, Cape Breton Island, Nova Scotia; Nova Scotia Department of Mines and Energy, Report 84-1, p. 249-258.

Raeside, R.P., Barr, S.M., White, C.E., and Dennis, F.A.R.
1986: Geology of the northernmost Cape Breton Highlands, Nova Scotia; in Current Research, Part A, Geological Survey of Canada, Paper 86-1A, p. 291-296.

Smith, P.K. and Macdonald, A.S.
1983: Red River Anorthosite Complex; Nova Scotia Department of Mines and Energy, Map 83-4.

Wiebe, R.A.
1972: Igneous and tectonic events in northeastern Cape Breton Island, Nova Scotia; Canadian Journal of Earth Sciences, v. 9, p. 1262-1277.
1975: Origin and emplacement of Acadian granitic rocks, northern Cape Breton Island; Canadian Journal of Earth Sciences, v. 12, p. 252-262.

Geology of a northern portion of the Central Plutonic Belt, New Brunswick[1]

Project 850019

J.B. Whalen
Lithosphere and Canadian Shield Division

Whalen, J.B., Geology of a northern portion of the Central Plutonic Belt, New Brunswick; in Current Research, Part A, Geological Survey of Canada, Paper 87-1A, p. 209-217, 1987.

Abstract

In the northern part of the Central Plutonic Belt, deformed Ordovician intrusive rocks have been subdivided into five muscovite +/− garnet-bearing (S-type granite ?) units and one amphibole-bearing (I-type granite) unit. These intrusive rocks are probably consanguinous with felsic volcanics of the upper Tetagouche Group. The undeformed Devonian Mount Elizabeth intrusive complex contains mafic intrusive, alkaline (A-type) granitic, and peraluminous granitic suites, all thought to be contemporaneous. The undeformed North Pole granite contains biotite granodiorite, biotite granite and muscovite-biotite-cordierite granite. Intrusive rocks in the area, like the Tetagouche Group volcanic rocks, are bimodal in composition, with felsic rocks greatly exceeding mafic rocks in abundance. Available data suggest that the Miramichi Massif is underlain by continental crust and that the plutonic rocks formed in a within-plate rift or back-arc basin.

Résumé

Les roches intrusives ordoviciennes déformées de la partie nord de la zone plutonique centrale se subdivisent en cinq unités à muscovite, plus ou moins grenatifères (granite de type S ?), et en une unité à amphibole (granite de type I). Ces roches intrusives se sont probablement formées à partir du même magma que les roches volcaniques felsiques du groupe supérieur de tétagouche. Le complex intrusif dévonien non déformé Mount Elizabeth contient des suites granitiques alcalines (de type A) intrusives ainsi que des suites granitiques hyper alumineuses qui seraient toutes contemporaines. Le granite de North Pole, non déformé, se compose de granodiorite à biotite, de granite à biotite et de granite à muscovite, à biotite, et à cordiérite. Les roches intrusives de la région, telles que les roches volcaniques du groupe de Tétagouche, ont une composition bimodale, les roches felsiques étant beaucoup plus abondantes que les roches mafiques. Les données disponibles portent à croire que le massif de Miramichi repose sur la croûte continentale et que les roches plutoniques se sont formées dans un fossé d'effondrement à l'intérieur de la plaque ou dans un bassin d'arrière-arc.

[1]Contribution to the Canada-New Brunswick Mineral Development Agreement 1984-1989. Project carried by Geological Survey of Canada.

INTRODUCTION

New Brunswick can be subdivided, from southeast to northwest, into five tectonostratigraphic zones (Fig. 22.1): the Avalonian Platform, the Fredericton Trough, the Miramichi Massif, the Imtree Inlier and the Matapedia Basin (Ruitenburg et al., 1977). The Central Plutonic Belt is found mainly within the Miramichi Massif and includes both Silurian-Devonian and Ordovician intrusive rocks (Fyffe et al., 1981). These intrusive rocks have received relatively little attention in the past. However, explaining their petrogenesis is a fundamental requirement of tectonic models for the New Brunswick Applalachians. Detailed petrographic, geochemical and isotopic (U/Pb zircon, Rb/Sr, and common Pb (M.L. Bevier, personal communication)) work is in progress. A northern portion of this belt in which A-type granites were recognized (Whalen, 1986a) was mapped at a scale of 1:25000 during 1986. This report describes the geology of this area (Fig. 22.2) and briefly discusses the implications of this work.

GENERAL GEOLOGY

Even though recent logging has greatly improved access, the study area is heavily forested, covered by a variable thickness of glacial drift, and characterized by relatively poor outcrop. The oldest rocks exposed in the area are part of the lower Tetagouche Group, a thick sequence of shale, greywacke and quartzite, which has been interpreted as quartzose turbidites (Skinner, 1974; Rast and Stringer, 1974; Fyffe, 1982) deposited on a continental rise (Ruitenburg et al., 1977). An Arenig shallow water, shelly fauna (Fyffe, 1976b) and conodonts (Nowlan, 1981) from metasediments just below the felsic volcanics of the Bathurst camp indicate a pre-Middle Ordovician age for the lower Tetagouche Group. These lower Tetagouche Group rocks were intruded by a suite of granitic rocks generally considered to be Ordovician (eg. Fyffe et al., 1981) prior to regional metamorphism and polydeformation. The age of deformation of the Tetagouche Group is still a matter of debate (see Fyffe, 1982; van Staal, in press). Subsequently, Devonian clastic sediments and bimodal volcanics, which underlie the northwestern part of the map area, were deposited. All these rocks were intruded by a number of suites of Acadian plutonic rocks ranging in composition from mafic to felsic.

DESCRIPTION OF UNITS

The lowest part of the Tetagouche Group (unit 1) in the investigated field area (Fig. 22.2) consists mainly of dark grey to black shaley siltstone. It also includes areas of argillaceous quartzite and some mafic and felsic volcanic rocks. Outcrop is commonly somewhat broken-up, making structural data difficult to obtain. In the Tetagouche Group to the north and east of Popple Depot, Helmstaedt (1970) recognized three generations of folds,at least two of which were interpreted to be pre-Late Silurian. Clearly defined metamorphic aureoles in Tetagouche Group rocks adjacent to either deformed "Ordovician" or Acadian intrusives are rare. Northeast of Big Bald Mountain, there is a well exposed contact between Tetagouche Group metabasalt and a marginal quartz-feldspar porphyry phase of the North Pole Granite. The hornfelsed basalt contains garnets up to 2 cm in diameter and fine vuggy fracture-filling garnets, both of which postdate the main penetrative fabric in the basalts. The North Pole granite and, by correlation, the other Acadian granites postdate at least the main phase of deformation of the Tetagouche Group (F1) and probably also the later phases of deformation (F2 and F3). However, work on the Pabineau granite near Bathurst (van Staal, in press), suggests this "Acadian" granite is pre- or syntectonic with the later phases of Tetagouche Group deformation.

The older granites in the area have been subdivided into six units, most of which trend in a northwest to southeast direction, parallel to regional structural trends. Their width to length ratios suggest they have undergone extensive flattening. The older granites (unit 2) will be described from north to south:

Popple Depot granite (unit 2a)

This granite, which outcrops mainly in the form of talus on the slopes north and northeast of Popple Depot, has been called the Popple Depot granite. It is a reddish pink to beige, finegrained, mafic-poor biotite granite. Deformation is quite variable and generally not intense for delicate primary

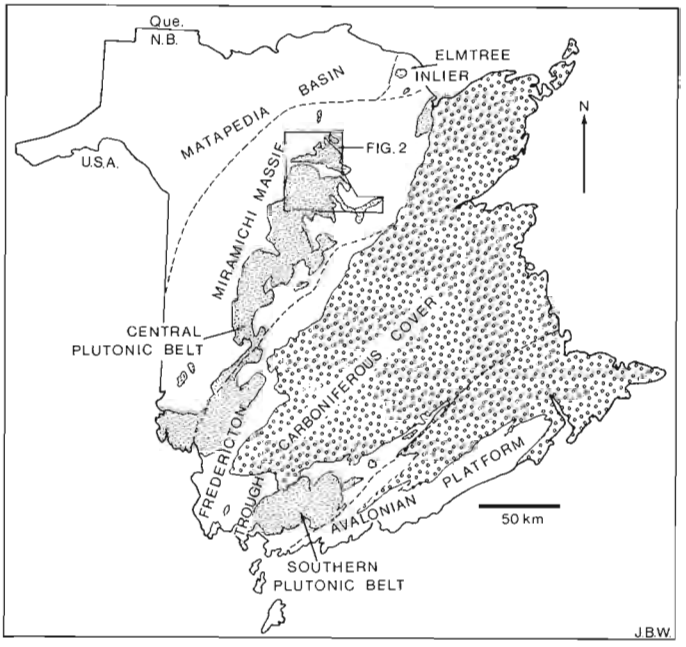


Figure 22.1 Map of New Brunswick showing the locations of the different tectonostratigraphic zones of Ruitenberg et al.(1977), the central and southern plutonic belts and the study area (Fig 22.2)

granophyric textures are preserved. The finegrained nature, the presence of abundant granophyric textures and pegmatitic clots suggest that this is a high level intrusive.

Mount Johnson granite (unit 2b)

South of Tilley Ridge and east of Mount Mitchell a reddish brown to grey, finegrained, strongly foliated granite has been given the new name, the Mount Johnson granite. It contains recrystallized quartz and feldspar, clotty biotite plus amphibole and opaque aggregates and accessory allanite and zircon. Included in this unit are some exposures of deformed mafic igneous and metasedimentary inclusion-rich granodiorite to tonalite along the West Branch of the South Branch of the Nepisiguit River.

Meridian Brook granite (unit 2c)

Bordering the Mount Johnson granite to the south and extending 22 km to the west, is an orange to beige, medium- to coarse-grained, equigranular, biotite-muscovite granite which has been given the new name Meridian Brook granite. Muscovite is concentrated along foliation planes and is probably not primary, at least in its present state. Although it is compositionally homogeneous over a large area, deformation is heterogeneously distributed throughout the granite. Weakly foliated portions, generally not near contacts, occur beside strongly mylonitized parts characterized by a reduction in grain size.

Sweat Hill granite (unit 2d)

Separated from the Meridian Brook granite by a screen of metasediments is a similar sized body of quartz and feldspar-porphyritic, biotite-muscovite granite. Portions of this granite have clotty patches of tourmaline. Muscovite, in the Sweat Hill granite, is a texturally late phase. Degree of deformation in the granite is quite variable. At its west end, only a weak foliation is present. Primary textural variations ranging from a coarsegrained, nearly equigranular granite to a high-level porphyry have been mapped. In contrast, there is a gradational change from a nearly massive coarse-grained granite to a chloritic feldspar-augen schist, along a 5 km, north to south running road that transects the eastern end of the body. A lithologically similar granite in the southeastern part of the map area is thought to be part of this unit.

Serpentine River granite (unit 2e)

Separated from the Sweat Hill granite by a screen of metasediments is a medium- to coarse-grained, dark pink to beige, biotite-muscovite granite, which has been given the new name Serpentine River granite. Going from north to south along a road which transects the west end of the body, the granite changes from being very weakly to quite strongly foliated, increases in grain size from medium- to coarse-grained and changes from being equigranular into a feldspar-porphyroblastic phase.

Mullin Stream Lake granite (unit 2f)

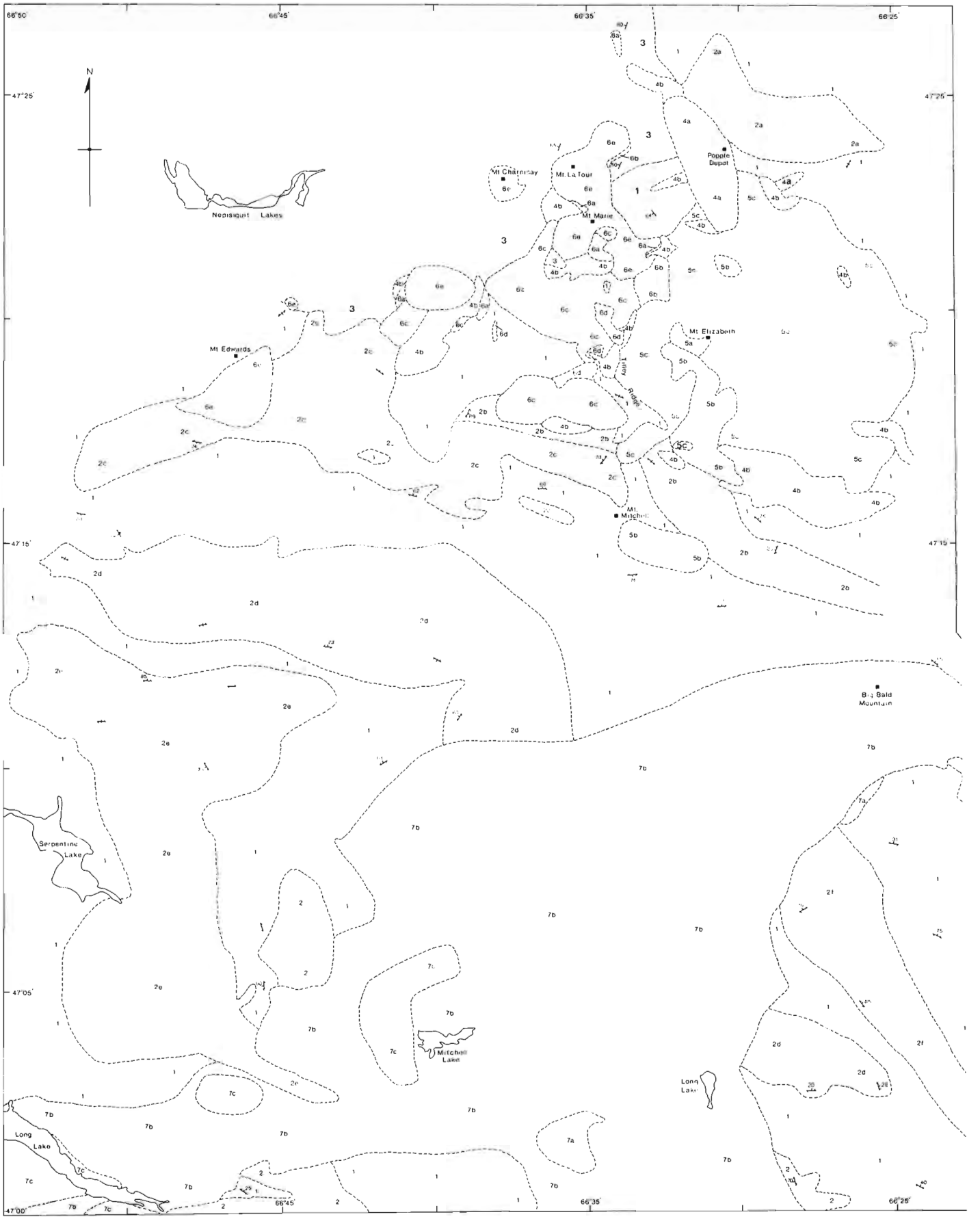
This granite extends northwest and northeast of Mullin Stream Lake and has a trend parallel to the regional structure in the host lower Tetagoughe Group sediments. It is a pink to orange, medium- to coarse-grained, weakly to strongly foliated biotite-muscovite granite. Much of the muscovite is probably metamorphic, but the presence of garnet in some samples suggests a primary peraluminous character for this granite. Muscovite may be a rimary phase which has been modified by deformation and metamorphism. The northeast portion of the body varies from granitic to quartz monzonitic in composition, has finer grained portions and is more strongly deformed. The northwestern portion of the body, where it is in close proximity to the North Pole granite, is cut by quartz veins and displays fracture related alteration. A close lithological resemblance between Mullin Stream Lake and the Meridian Brook (unit 2c) granites suggests they may be parts of the same intrusive unit. If so, the unit is about 63 km long versus only about 3-4 km wide (length to width ratio of at least 15 to 1).

The northwestern portion of the map area is underlain by a sequence of northeast to southwest striking, sedimentary and bimodal volcanic rocks of Devonian age (unit 3). The sediments include quartzites, fine to coarse, poorly sorted, conglomerates, siltstones and shales. The basalts are amygdaloidal with epidote filled vesicules and fractures. The felsic volcanics include flow-banded to massive, beige, brown and red rhyolites and fragmental tuffs. The western portion of the Mount Elizabeth intrusive complex clearly intrudes this sequence. However, granite grades to high-level, subvolcanic porphyry adjacent to rhyolites on Mount Charnisay and there are rhyolites in the area which look like possible volcanic equivalents of this granite.

Based on this study, it seems appropriate to rename the Mount Elizabeth granite (Fyffe et al., 1981), the Mount Elizabeth intrusive complex, for it includes a number of apparently contemporaneous igneous suites. These have been grouped into a mafic suite (unit 4) and eastern (unit 5) and western (unit 6) granitic suites. Chemical data in Fyffe et al.(1981) indicate that the eastern portion of the suite is peraluminous and the western portion is alkaline.

Mafic suite (unit 4)

The mafic suite includes one substantial troctolite body, the Portage Brook troctolite (unit 4a), and many other small to medium sized diabase to gabbro bodies (unit 4b). The troctolite contains plagioclase, olivine, two pyroxenes, brown amphibole, opaques and apatite, and has locally well-developed banding. This banding, which reflects slight compositional differences, probably represents igneous flow banding rather than cumulate layering. Other than variation in grain size from medium- to coarse-grained and in degree of development of banding, the troctolite is remarkably homogeneous over its outcrop area. Contact relationships between this gabbro and other mafic and felsic intrusive phases have not been observed.


66°50'
66°45'
66°35'
66°25'
47°25'
47°15'
47°05'
47°00'
N
Nepisiguit Lakes
Mt Chamberlain
Mt La Tour
Mt Marie
Poppie Depot
Mt Edwards
Mt Elizabeth
Tilley Ridge
Mt Mitchell
Big Bald Mountain
Serpentine Lake
Mitchell Lake
Long Lake
Long Lake

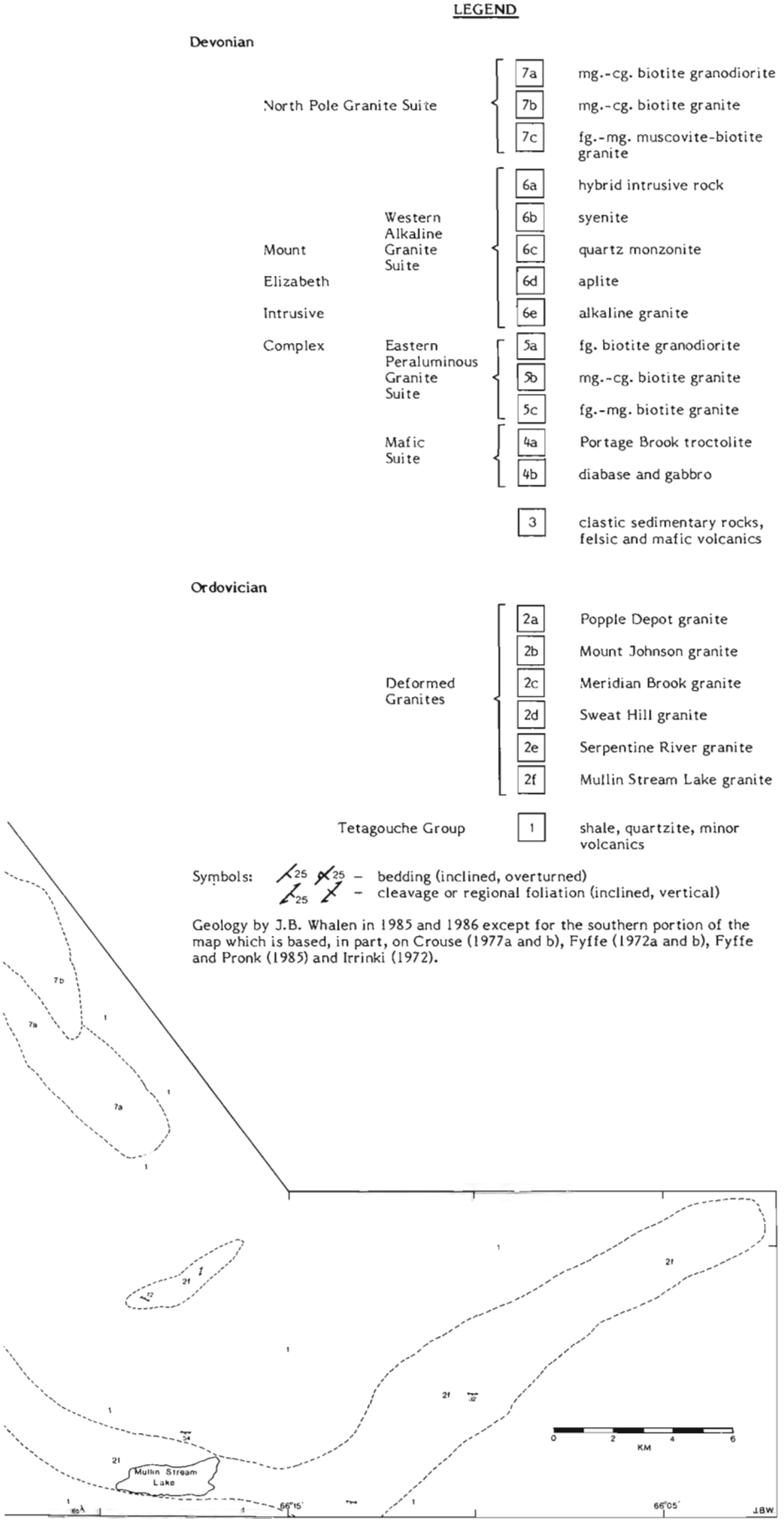


Figure 22.2 Preliminary geological map of a northern portion of the Central Plutonic Belt.

The other mafic intrusive rocks (unit 4b) are texturally and also probably compositionally quite variable. They include fine-to medium- grained, plagioclase porphyritic and equigranular ophitic textured diabase, medium- to coarse-grained amphibole-clinopyroxene-biotite gabbro and minor areas of diorite to quartz diorite adjacent to granitic intrusions.

Field relationships between the younger granitic rocks (units 5 and 6) and the mafic intrusive rocks suggest that they are contemporaneous. Such features as cuspated, irregular contacts with chilled margins of mafic against felsic rocks, pillowed mafic rock in granitic rock and evidence of interaction between the two different composition melts to produce intermediate or hybrid composition rocks have been interpreted at other locations (Whalen and Currie, 1984; Whalen, 1985a) as reflecting magma-mixing. A few felsic dykes have been noted cutting gabbroic rocks, but no mafic dykes have been observed to cut granitic rocks.

Eastern Peraluminous Granitic suite (unit 5)

The eastern portion of the Mount Elizabeth complex consists of a compositionally and texturally homogeneous, pink and white, equigranular, biotite granite which contains traces of muscovite. A small body of K-feldspar porphyritic biotite granite occuring to the south of Mount Mitchell appears to be compositionally similar. Also, there is a restricted area adjacent to Mount Elizabeth where the granite is more biotite rich (granodiorite, unit 5a). Though, medium- to coarse-grained portions (unit 5b) have been subdivided from finer grained portions (unit 5c) of this granite, contacts are thought to be mainly gradational. The remarkably finegrained and compositionally homogeneous nature of this granite over almost all its outcrop area may reflect a high level of intrusion under quiescent conditions.

It did not prove possible to locate contacts between the eastern and western granitic suites. Where they were observed at their closest proximity, at the north end of Tilley Ridge, they are separated by a screen of gabbroic rocks. As already noted, relationships between the mafic and felsic intrusive rocks suggest they are contemporaneous. As similar relationships exist between the mafic intrusive rocks and both the eastern and western granitic suites, and if there is only one age of mafic intrusion, then both the granitic suites are of a similar age.

Western Alkaline Granitic suite (unit 6)

The western ortion of the Mount Elizabeth intrusive complex contains a spectrum of compositions and is characterized by an apparent close genetic relationship between mafic and felsic intrusive rocks. Though some areas are quite homogeneous, it appears, from both restricted outcrop and float, that portions of this suite are remarkably heterogeneous. A diversity of compositional, from mafic to felsic, and textural variations appears to be present in the area south of Mt. Marie, similar to that documented in the northern half of the McGerrigle intrusive complex, Gaspe, Quebec (Whalen, 1985a; Whalen and Gariepy, 1986). Contacts between the various phases have not been observed but they are all tentatively considered to be of similar age. The intrusive phases will be discussed in order of increasing silica content.

Hybrid intrusive rocks (unit 6a)

There are areas adjacent to mafic intrusive rocks where probable interaction between coexisting mafic and felsic magmas has produced hybrid or intermediate compositions. Most of these are truly mixed rocks in that they are characterized by partially digested mafic igneous inclusions in a dioritic to granitic composition matrix.

Syenite (unit 6b)

A dark blue-green, red brown weathering syenite defines a small body in the middle of the complex and occurs as a marginal phase of the alkaline granite on Mount La Tour. It contains quartz, plagioclase, alkali feldspar, fayalite, hedenbergite, zircon, apatite and opaque minerals.

Quartz monzonite (unit 6c)

A beige grey to orange, fine- to medium-grained biotite-amphibole quartz monzonite is a major intrusive phase of the western suite. A notable feature of this rock is euhedral white plagioclase grains which are prominent on weathered surfaces. On the northwest slope of Tilley Ridge, there are a number of zones or dykes of glassy, flow-banded, grey to beige rhyolitic intrusive rocks which appear to be late offshoots of the quartz monzonite.

Aplite (unit 6d)

Closely associated with the quartz monzonite, are a number of areas of dark pink to red, very felsic aplite. Some portions have spherulitic textures and contain texturally-late interstitial blue amphibole but no biotite. Other portions consist of equigranular, biotite-bearing aplite which lacks amphibole. This phase could represent a finer grained equivalent of the quartz monzonite but it lacks the distinctive plagioclase grains and appears to be more felsic.

Alkaline granite (unit 6e)

The most abundant phase of the western suite is a scarlet red, medium- to coarse-grained, equigranular granite. Most of this phase contains only one feldspar (ie. hypersolvus granite) and is amphibole-bearing. However, there are two feldspar bearing portions east of Mt. Marie. Red brown biotite aggregates in some samples may be pseudomorphs after fayalite rather than amphibole. On Mount Charnisay, this granite varies to fine- grained miarolitic granite and rhyolitic porphyry.

North Pole Granite suite (unit 7)

One of the largest intrusive bodies in the Central Plutonic Belt, the North Pole granite (unit 7), is more appropriately called an intrusive suite because of its composite nature. The main intrusive phase is a medium- to coarse-grained, equigranular to K-feldspar porphyritic, white and pink biotite granite (unit 7b). In the region of Big Bald Mountain, this phase is very deeply weathered. To the south of Big Bald Mountain, there is a body of grey and black, biotite granodiorite (unit 7a) which contains abundant, highly digested metasedimentary inclusions. It is cut by white felic dykes which may be offshoots of the main phase of biotite granite. An area of pre-unit 7b, amphibole-bearing tonalite in the middle of the North Pole granite has been included in unit 7a. Cutting the biotite granite (unit 7b) are bodies of fine- to medium-grained, white, muscovite-biotite granite (unit 7c). Some samples of this phase contain muscovite pseudomorphs after and some relict cordierite.

ECONOMIC GEOLOGY

A number of areas with potential for gold mineralization have been recognized: (1) zones of extensive quartz veining and dyking occur in Tetagouche Group rocks incorporated in roof pendants in the Mount Elizabeth intrusive complex; (2) along their contact with the alkaline granite suite (unit 6e), Devonian felsic volcanic rocks (unit 3) contain disseminated and fracture-filling pyritic zones; (3) deformed granites north of Serpentine Lake (unit 2e) are cut by sulphide-bearing veins with associated alteration haloes; and (4) all the deformed granites are cut by major shear zones which could have acted as conduits for gold-bearing fluids. Also, a greissen alteration zone containing molybdenite was recognized in the eastern biotite granite (unit 5c) of the Mount Elizabeth complex and a brecciated and silicified zone was identified in the body of alkaline granite (unit 6e) south of Mount Edwards.

DISCUSSION AND REGIONAL IMPLICATIONS

In the northern part of the Central Plutonic Belt, most of the granites are quite felsic. The cordierite-bearing phases of the North Pole granite and also the muscovite +/− garnet-bearing deformed intrusives are S-type granites while the lone amphibole-bearing deformed intrusive, the Mount Johnson granite, is an I-type granite (Chappell and White, 1974). The western portion of the Mount Elizabeth complex is an A-type (Whalen, 1986a). Many of the granites in the area, such as the felsic biotite granites of the Mount Elizabeth and North Pole suites require chemical data to resolve their classification.

A-type granites are thought to be derived from remelting of lower crustal source rocks from which an orogenic granite magma has been previously extracted (ie. felsic granulite) (Collins et al. 1982). The source of the western portion of the Mount Elizabeth may be the same source from which the deformed granites in the area were derived. This suite bears a close resemblance to the McGerrigle plutonic complex, Gaspesie (Whalen, 1985a; Whalen and Gariepy, 1986), a complex which is thought to be underlain at depth by Grenville basement. Comparison of chemical and isotopic data from the two suites should be very informative. If this western A-type suite is consanguinous with Devonian felsic volcanics in the area, then there should be A-type volcanics present, similar to those associated with the Topsails A-type suite in Newfoundland (Whalen, 1986b).

A notable feature of the deformed and undeformed intrusive rocks in the Central Plutonic Belt is their bimodal character (Fyffe et al.,1981). Mafic igneous rocks are subordinate in abundance to felsic igneous rocks and the felsic intrusives appear to be mainly peraluminous in composition. This is in marked contrast to the range of plutonic rock compositions present at destructive plate margins such as the Cordillera of British Columbia (Roddick and Hutchinson, 1974) or in island arcs (Kesler et al., 1975; Whalen, 1985b). The Tetagouche Group volcanic rocks have a similar bimodal character (van Staal, in press) and may be consanguinous with the deformed granites. Evidence which supports this is: (1) the paucity of deformed intrusive rocks cutting upper portions of the Tetagouche Group versus lower portions of the group; (2) similarities in petrography and deformation for felsic intrusive and volcanic rocks (C.R. van Staal, personal communication); and (3) gradations to high-level porphyries and the presence of granophyric and aplitic textures in some deformed intrusives indicate a high-level of emplacement. The abundance of felsic volcanic rocks and associated pervasively deformed granites is thought to indicate that continental crust underlies the area (Fyffe et al., 1981).

Tectonic models for the Miramichi Massif, which attempt to xplain the Tetagouche Group sedimentary and volcanic rocks, include an island- arc setting (Rast and Stringer, 1974; Pajari et al., 1977), a basin- and-range intracontinental setting (Janes, 1976), an off-axis rift environment (Whitehead and Goodfellow, 1978) and a marginal sea or back-arc basin setting (van Staal, in press). Chemical and isotopic work on the plutonic rocks will help determine the age of deformation of the Tetagouche Group and the nature and age of lower crustal source rocks for the granites. This information could substantiate or refute the proposed tectonic models for this area. Also, the possibility has been suggested that large scale detachments (ie. thrusts) exist between cover and basement in the northern Appalachians in general (Karlstrom, 1983; Coleman-Sadd and Swinden, 1984) and northern New Brunswick in particular (van Staal, in press). As the deformed granites predate much of the deformation of the Tetagouche Group and the younger granites postdate at least the main deformation (F1), contrasting the sources of the older versus the younger granites could help determine the applicability of such models to the Miramichi Massif. Presently available data suggest that the area was, at least in part, underlain by continental crust and supports either a within- plate rift model or a back-arc basin model (van Staal, in press) for the Central Plutonic Belt.

ACKNOWLEDGMENTS

I thank P. Neelands for able field assistance, M.L. Bevier, L. Fyffe and K.L. Currie for helpful discussions and C. van Staal for discussions and critical reading of the manuscript.

REFERENCES

Bird, J.M.and Dewey, J.F.
1970: Lithosphere plate-continental margin tectonics and the evolution of the Appalachian Orogen; Geological Society of America Bulletin, v.81, p.1031-1060.

Chappell, B.W. and White, A.J.R.
1974: Two contrasting granite types; Pacific Geology, v.8, p.173-174.

Colman-Sadd, S.P. and Swinden, H.S.
1984: A tectonic window in central Newfoundland? – geological evidence that the Appalachian Dunnage Zone may be allocthonous; Canadian Journal of Earth Sciences, v.21, p.1349-1367.

Collins, W.J., Beams, S.D., White, A.J.R., and Chappell, B.W.
1982: Nature and origin of A-type granites with particular reference to southeastern Australia; Contributions to Mineralogy and Petrology, v. 80, p. 189-200.

Crouse, G.
1977a: Geology of North Pole and Vandine Brooks; Mineral Resources Division, New Brunswick Department of Natural Resources, Map L-10.
1977b: Geology of Grover, Mitchell and Logan Lakes; Mineral Resources Division, New Brunswick Department of Natural Resources, Map L-11.

Fyffe, L.R.
1972a: Geology of Lower North Branch Little S.W. Miramichi River; Mineral Resources Division, New Brunswick Department of Natural Resources, Map M-10.
1972b: Geology of part of North Pole Brook and Lower North Branch Little S.W. Miramichi River; Mineral Resources Division, New Brunswick Department of Natural Resources, Map M-11.
1976a: Comparison of some tectonostatigraphic zones in the Appalachians of Newfoundland and New Brunswick: Discussion; Canadian Journal of Earth Sciences, v.14, p.1468-1469.
1976b: Correlation of geology in the southeastern and northern parts of the Miramichi zone; in 139th Annual Report of the Department of Natural Resources of New Brunswick, p.137-141.
1982: Taconian and Acadian structural trends in central and northern New Brunswick; in Major Structural Zones and Faults of the Northern Appalachians, ed. P. St.Julien and J. Beland Geological Association of Canada, Special Paper 24, p.117-129.

Fyffe, L. R. and Pronk, A.G.
1985: Bedrock and surficial geology - rock and till geochemistry in the Trousers Lake area, Victoria County, New Brunswick; Mineral Resources Division, New Brunswick Department of Natural Resources, Report of Investigation 20, 74p.

Fyffe, L.R., Pajari, G.E., and Cherry, M.E.
1981: The Acadian plutonic rocks of New Brunswick; Maritime Sediments and Atlantic Geology, v.17, p.23-36.

Helmstaedt, H.
1970: Geology of map area O-6: Head of Middle River and Wildcat Brook, map series 70-1; Mineral Resources Branch, Department of Natural Resources, New Brunswick, 18p.
1971: Structural geology of Portage Lakes area, athurst-Newcastle district, New Brunswick; Geological Survey of Canada, Paper 70-28, 42p.

Irrinki, R.R.
1972: Geology of Gaugus and Mullin Stream Lakes; Mineral Resources Division, New Brunswick Department of Natural Resources,Map N-11.

Janes, P.A.
1976: Geochemistry of the altered volcanic and intrusive rocks of the Bathurst district, New Brunswick; unpublished M.Sc. thesis, University of Montreal, 110 p.

Karlstrom, K.E.
1983: Reinterpretation of Newfoundland gravity data and arguments for an allochthonous Dunnage Zone; Geology, v.11, p.263-266.

Kesler, S.E., Jones, L.M. and Walker, R.L.
1975: Intrusive rocks associated with porphyry copper mineralization in island-arc areas; Economic Geology, v.70, p.515-526.

Nowlan, G.S.
1981: Some Ordovician conodont faunules from the Miramichi Anticlinorium, New Brunswick; Geological Survey of Canada Bulletin 345, 35p.

Pajari, G.E., Rast, N. and Stringer, P.
1977: Paleozoic volcanicity along the Bathurst-Dalhousie geotraverse, New Brunswick and its relation to structure; in Volcanic Regimes in Canada, W.R.A. Baragar, L.C. Coleman and J.M. Hall, ed., Geological Association of Canada, Special Paper 16, p.111-124.

Rast, N. and Stringer, P.
1974: Recent advances and the interpretation of the geological structure of New Brunswick; Geoscience Canada, v.1, p.15-25.

Roddick, J.A. and Hutchison, W.W.
1974: Setting of the Coast Plutonic Complex; Pacific Geology, v.8, p.91-108.

Ruitenberg, A.A., Fyffe, L.R., McCutcheon, S.R., St.Peter, C.J., Irrinki, R.R. and Venugopal, D.V.
1977: Evolution of pre-Carboniferous tectonostratigraphic zones in the New Brunswick Appalachians; Geoscience Canada, v.4, p.171-181.

Skinner, R.
1974: Geology of the Tuadook Lake map-area, New Brunswick (21J/15); Geological Survey of Canada, Paper 74-33.

van Staal, C.R.
in press: Tectonic setting of the Tetagouche Group in northern New Brunswick: implications for plate tectonic models of the Northern Appalachians; Canadian Journal of Earth Sciences

Whalen, J.B.

1985a: The McGerrigle plutonic complex, Gaspe, Quebec: evidence of magma mixing and hybridization; in Current Research, Part A, Geological Survey of Canada, Paper 85-1A, p.795-800.

1985b: Geochemistry of an island-arc plutonic suite: the Uasilau-Yau Yau intrusive complex, New Britain, P.N.G.; Journal of Petrology, v.26, p.603-632.

1986a: A-type granites in New Brunswick; in Current Research, Part A, Geological Survey of Canada, Paper 86-1A, p.297-300.

1986b: Geochemistry of the mafic and volcanic components of the Topsails igneous suite, western Newfoundland; in Current Research, Part B, Geological Survey of Canada, Paper 86-1B, p.121-130.

Whalen, J.B. and Currie, K.L.

1984: The Topsails igneous terrane, Western Newfoundland: evidence for magma mixing; Contributions to Mineralogy and Petrology, v.87, p.319-327.

Whalen, J.B. and Gariepy, C.

1986: Petrogenesis of the McGerrigle plutonic complex, Gaspe, Quebec: a preliminary report; in Current Research, Part A, Geological Survey of Canada, Paper 86-1A, p. 265-274.

Whitehead, R.E.S. and Goodfellow, W.D.

1978: Geochemistry of volcanic rocks from the Tetagouche Group, Bathurst, New Brunswick, Canada; Canadian Journal of Earth Sciences, v.15, p.207-219.

Williams, H.

1979: The Appalachian orogen in Canada; Canadian Journal of Earth Sciences, v.16, p.792-807.

- 23 -

Progress report on the stratigraphy, sedimentology and significance of the Kimerot and Bear Creek groups, Kilohigok Basin, District of Mackenzie

Project 810021

J.P. Grotzinger[1], D.S. McCormick[1], and S.M. Pelechaty[2]
Lithosphere and Canadian Shield Division

Grotzinger, J.P., McCormick, D.S. and Pelechaty, S.M., Progress report on the stratigraphy, sedimentology and significance of the Kimerot and Bear Creek groups, Kilohigok Basin, District of Mackenzie; in Current Research, Part A, Geological Survey of Canada, Paper 87-1A, p. 219-238, 1987.

Abstract

Some results of ongoing field investigations of the Kimerot and Bear Creek groups are summarized as they pertain to several topics, including: (1) revision of stratigraphic nomenclature for Kilohigok Basin; (2) vertical and lateral distribution of facies/fabrics of disconformities developed in the lower Bear Creek group; (3) stratigraphy and sedimentology of the Beechey Formation; (4) diagenesis studies of the Peg Formation (new name); and (5) constraints on the stratigraphy, sedimentology, and provenance of the Burnside Formation.

Résumé

Des résultats de travaux de terrain en cours sur les groupes Kimerot et Bear Creek sont colligés et comprennent les sujets d'études suivants: 1) une revision de la nomenclature stratigraphique du basin de Kilohigok; 2) la distribution latérale et verticale des faciès et des textures des discordances générées dans la partie la plus basse du groupe de Bear Creek; 3) la stratigraphie et la sédimentologie de la formation de Beechey; 4) les études de la diagenèse de la formation de Peg (nouveau nom); 5) les effets de contraintes en stratigraphie et sédimentologie et la provenance de la formation de Burnside.

[1]Lamont-Doherty Geological Observatory, Palisades, NY 10964 USA
[2]Department of Geology, Brandon University, Brandon, Manitoba R7A 6A9

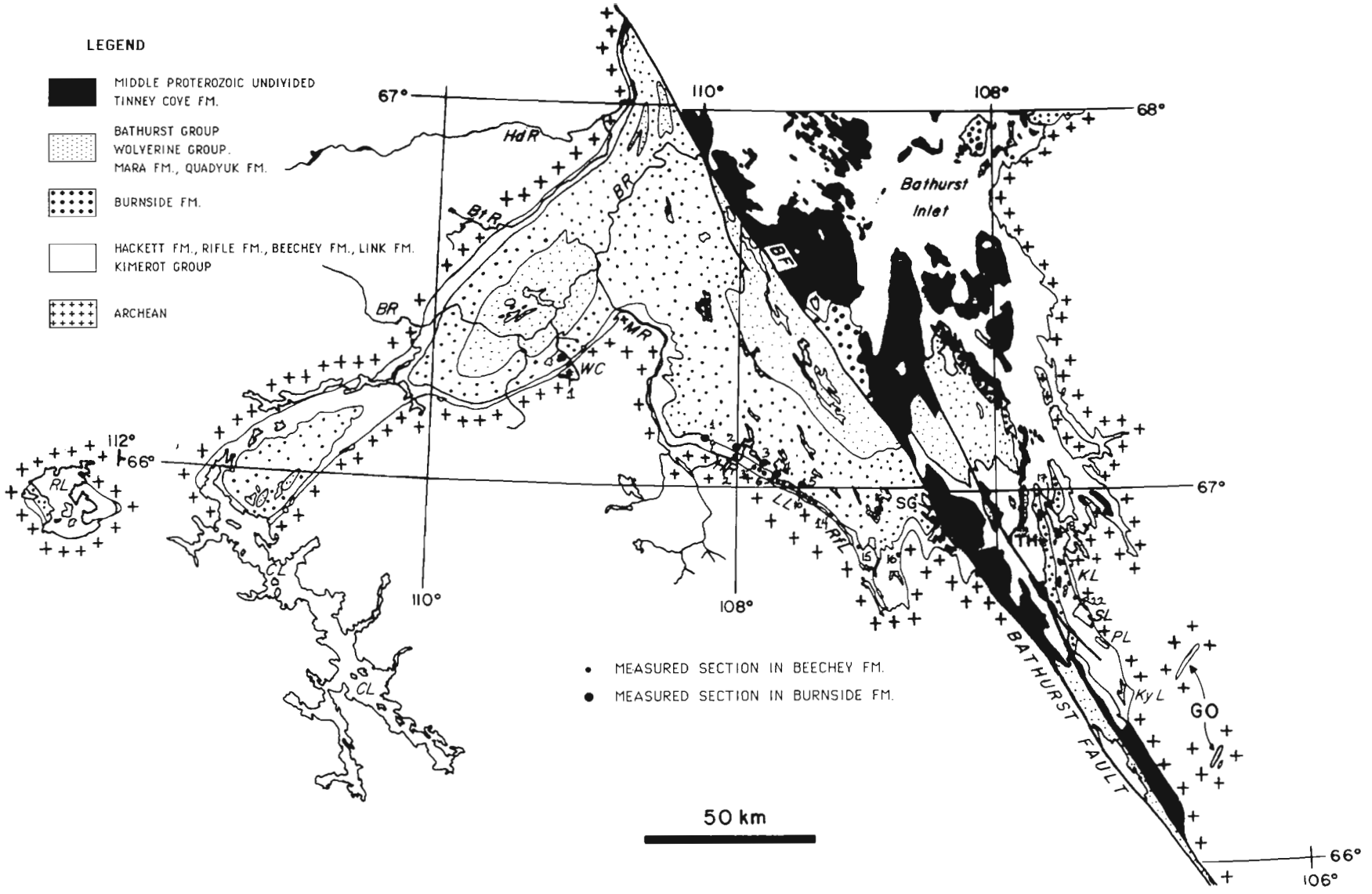


Figure 23.1 Palinspastic base map of Kilohigok Basin based on restoration of 135 km of left-lateral slip on the Bathurst Fault as recommended by Tirrul (1985). Includes location of measured sections in Beechey and Burnside formations and geographic features referred to in the text. *Note:* measured sections are intermittently numbered from northwest to southeast; numbers for unlabeled sections can be directly interpolated. *RL*, Rockinghorse Lake; *CL*, Contwoyto Lake; *BR*, Burnside River, *BtR*, Booth River; *HdR*, Hood River; *WC*, Wolverine Canyon; *MR*, Mara River; *HR*, Hackett River; *LL*, Link Lake; *RfL*, Rifle Lake; *KyI*, Kenyon Lake; *SL*, Starvin Lake; *KL*, Kathleen Lake; *PL*, Peg Lake; *SG*, Straight Gorge; TH, Tinney Hills. GO, Outliers of Goulburn Supergroup (Kimerot Group).

INTRODUCTION

Detailed stratigraphic studies of the early Proterozoic (circa 1.9 Ga) Kilohigok Basin are continuing in order to exploit the unusually advantageous circumstance that the basin fill is exposed continuously for over 250 km transverse to its depositional strike. During the field season of 1986, investigations of the Kimerot and Bear Creek groups (new names) were continued in the Beechey Lake (76G), Mara River (76K), and Tinney Hills (76J) map areas (Fig. 23.1). Work concentrated on 1:50 000 scale mapping of individual stratigraphic units (JPG, DSM), and detailed topical studies were initiated related to the nature and extent of intraformational disconformities (JPG), the stratigraphy and sedimentology of the Beechey Formation (new name) (SMP), and the stratigraphy, sedimentology and provenance of the Burnside Formation (DSM). In addition, carbonate facies and cements of the Kimerot Platform were sampled as part of a geochemical study of Peg Formation carbonate precipitation and diagenesis, including dolomitization. Studies of the Burnside Formation (DSM) will form the basis for a Ph.D. dissertation, and studies of the Beechey (SMP) Formation will form the basis for a B.Sc. thesis.

Results reported here support the tentative conclusion of Grotzinger and Gall (1986) that the Kilohigok Basin subsided in response to flexure of the lithosphere, probably associated with convergence and crustal loading along the Thelon Tectonic Zone. Stratigraphic trends in thickness and facies on the group scale were delineated during earlier work (Tirrul, 1985; Grotzinger and Gall, 1986) and indicated that downwarping of the most deeply subsiding parts of the basin was concommitant with flexure and uparching of the foreland. Similar trends can now be independently recognized on the formation scale and are discussed below. In addition, the occurrence of stratigraphic disconformities bounding individual sequences (formations) has been confirmed and indicates that although eustasy may have been the dominant control on foreland stratigraphy, formation thickness and extent of erosion of formations along sequence boundaries was localized by intrabasinal arching which persisted through all of Bear Creek Group time.

REVISION OF STRATIGRAPHIC NOMENCLATURE

The stratigraphic nomenclature of units within the Kilohigok Basin has been subjected to numerous revisions in the past as a function of increasing scales of mapping as new projects were initiated and completed. Ongoing 1:50 000 scale mapping and detailed topical stratigraphic studies form the basis for the current project and require a more refined stratigraphic nomenclature. Consequently, several new formations are proposed, and these additions, along with most of the existing formations, are organized into new groups (see Fig. 23.2). The previous Goulburn Group is elevated to supergroup status and the name Goulburn is retained. The new revisions are discussed briefly below only as they specifically pertain to units discussed in this report. A more comprehensive summary is planned for a future report designed for that purpose.

Kimerot Group. The name Kimerot Group is proposed for the units previously designated as belonging to the "Kimerot Platform" (c.f. Campbell and Cecil 1981; Tirrul 1985; Grotzinger and Gall, 1986) of the lower Western River Formation. The name Western River Formation is discarded here, and does not occur in the new nomenclature. The Kimerot Group contains two new formations, the lower Kenyon Formation and the overlying Peg Formation. These new formations correspond to the lower "siliciclastic part" and the upper "carbonate part" of the old Kimerot Platform (c.f. Grotzinger and Gall, 1986). The type areas for the Kenyon and Peg formations are in the vicinity of Peg Lake and Kenyon Lake (see Fig. 23.1 for locations), where both are well exposed.

Bear Creek Group. The name Bear Creek Group is proposed for the units previously assigned to the Western River Formation above the Kimerot Platform, plus the Burnside Formation, the Mara Formation, and the Quadyuk Formation. All those formation names are retained with the exception of Western River Formation which is abandoned. The new formations proposed all occur within the stratigraphic assemblage previously regarded as the Western River Formation above the Kimerot Platform. The four new formations approximately coincide with the previous four members of the Western River Formation described in Campbell and Cecile (1981). The new Hackett Formation, the lowest of the four, is equivalent to the old Lower member of the Western River Formation, and its type area is in the vicinity of Hackett River where it is well-developed (see Fig. 23.1 for location). The Hackett Formation consists of a lower siltstone member and an upper quartzite member.

The Rifle Formation (new name) overlies the Hackett Formation and is equivalent to the Red Siltstone member (old name) of the Western River Formation. The type area for the Rifle Formation is in the vicinity of Rifle Lake where it is best exposed (see Fig. 23.1 for location). The Rifle Formation consists almost exclusively of monotonous maroon siltstone in its type area, with uncommon sequences of disconformity-bounded(?) quartzites at its top.

The Beechey Formation (new name) overlies the Rifle Formation and is approximately equivalent to the previous Quartzite member of the Western River Formation. The type area for the Beechey Formation is between Rifle Lake and Hackett River where it is well-exposed. The Beechey Formation is a heterogeneous mixture of carbonates, quartzites, and siltstones, and is described in more detail below.

The Link Formation (new name) overlies the Beechey Formation and is approximately equivalent to the previous Upper Argillite member of the Western River Formation. The type area for the Link Formation is in the vicinity of Link Lake where it is well exposed (see Fig. 23.1 for location). The Link Formation consists of interbedded siltstones and quartztites.

Wolverine Group. The name Wolverine Group is proposed to embrace the previously defined (Campbell and Cecile, 1981) Peacock Hills and Kuuvik formations. The

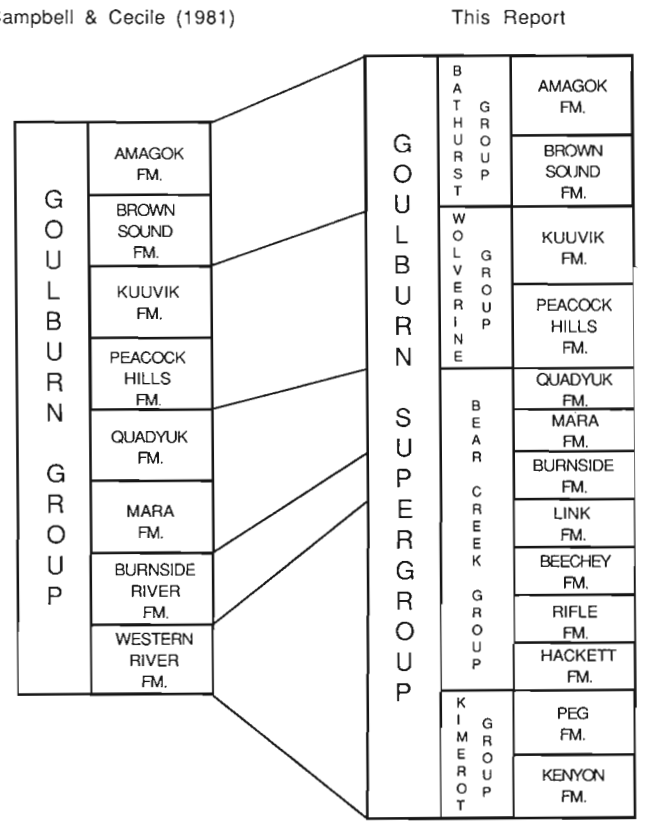


Figure 23.2 Revised Early Proterozoic stratigraphic nomenclature for Kilohigok Basin.

Wolverine Group is well-exposed in the vicinity of Wolverine Canyon (see Fig. 23.1 for location).

Bathurst Group. The name Bathurst Group is proposed to embrace the previously defined (Campbell and Cecile, 1981) Brown Sound and Amagok formations. The Bathurst Group is best-exposed along the southeastern margin of Bathurst Inlet.

DISCONFORMITIES OF THE LOWER BEAR CREEK GROUP

Vertical and lateral distribution

Disconformities exist at several different stratigraphic levels within the Bear Creek Group (see Fig. 23.2 for review of stratigraphic nomenclature). They occur on both sides of the Bathurst Fault, but are best developed west of the fault, in the southwest part of the basin within the Beechey Lake map area. The stratigraphically lowest disconformity is developed at the top of the Kimerot Group (new name) as discussed in Grotzinger and Gall (1986). Beneath this disconformity (here termed the "sub-Hackett disconformity"), each unit of the Kimerot Group is progressively truncated from southeast to northwest. Truncation of uppermost units first occurs in the vicinity of Gordon Bay, along the east side of the Bathurst Fault, and continues down through the remaining part of the section along the outcrop belt exposed in the Beechey Lake map area, west of Bathurst Fault. The lowest units of the platform are finally truncated in the southern parts of the large basement-involved synclines of the Beechey Lake map area. In the northern parts of the synclines, and along the rest of the outcrop belt to the northwest, the Kimerot Group is absent and the overlying Hackett Formation of the Bear Creek Group sits directly on Archean basement.

The distribution of basal conglomerate and/or regolith developed along the Archean/Proterozoic unconformity directly relates to the presence or absence of the Kimerot Group. Where the Kimerot Group is preserved, the Archean/Proterozoic unconformity is characterized by a well-developed basal conglomerate and poorly-developed or absent regolith (Fig. 23.3a). Conversely, where the Kimerot Group is absent, the Archean/Proterozoic unconformity is marked by a thick (several metres locally), carbonate-matrix regolith, and absent or poorly developed basal conglomerate (Fig. 23.3b). This correlation between the absence of Kimerot units and presence of carbonate-matrix regolith along the Archean/Proterozoic unconformity indicates that the regolith is most likely of post-Kimerot age and was produced following truncation of the Kimerot Group and subsequent re-exposure of the Archean basement surface. This relationship is important in that a method is now available to assess the width of the Gordon Bay Arch that was active during erosion of the Kimerot Group. Even though the Kimerot Group was eroded down to the level of the Archean basement, the area of basement that was exposed above sea level during sub-Hackett disconformity time can be directly estimated by evaluating the distribution of carbonate-matrix regolith that occurs to the northwest of where the sub-Hackett disconformity intercepts and becomes part of the Archean/Proterozoic unconformity. Preliminary reconnaissance data indicate that in the area of Wolverine Canyon, where the entire Bear Creek Group section thickens again after thinning in the Beechey Lake map area, the Archean/Proterozoic unconformity is devoid of any carbonate-matrix regolith and is overlain by quartzites that may be time-equivalent to the Kenyon Formation (Kimerot Group). Thus the "crest" of the Gordon Bay Arch during sub-Hackett disconformity time probably occurred near the northwest corner of the Beechey Lake map area. The trend of the arch was previously delineated by Grotzinger and Gall (1986) as running to the northeast.

A stratigraphic disconformity is also developed at the top of the Hackett Formation which overlies the Kimerot Group in the southeast part of the basin (palinspastic), and overlies Archean basement in the northwest areas where Kimerot sediments are absent. The Hackett Formation is a shallowing-upward, siltstone-to-quartzite sequence; the basal siltstone member progressively overlies (onlaps) stratigraphically lower formations of the Kimerot Group and then rests directly on basement to the northwest. The upper quartzite member is separated from the overlying Rifle Formation by a disconformity (here termed the sub-Rifle disconformity) which becomes more pronounced to the northwest, in the vicinity of the Hackett River (Fig. 23.3c,d). The contact between the

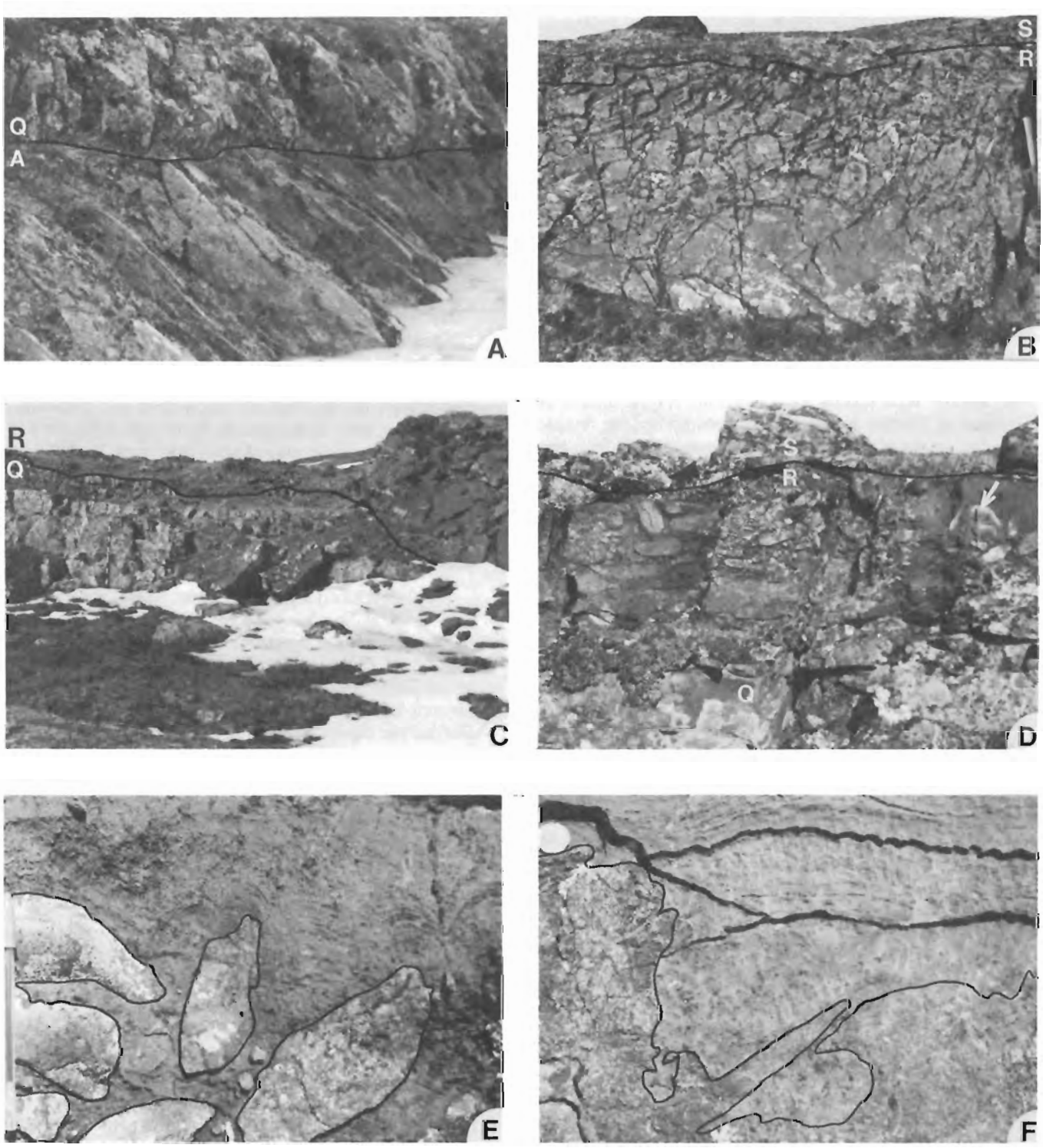


Figure 23.3 Disconformable surfaces and regoliths of Kimerot and Bear Creek Groups A) Contact between steeply-dipping Archean meta-greywacke (A) and flat-lying quartzites and basal conglomerate (Q) of Kenyon Formation (Kimerot Group). Note lack of regolith or brecciation below contact. Day-pack for scale. B) Contact between brecciated Archean meta-greywacke (R) and overlying flat-lying siltstones (S) of Hackett Formation. Note extensive brecciation of Archean meta-greywacke; breccias have well-developed "fitted" fabrics and are filled with carbonate matrix. Hammer for scale. C) Contact between quartzites (Q) of upper Hackett Formation and overlying siltstones of Rifle Formation. A thick regolith (R) is developed along the contact. Jacobs staff is 1.5 m long. D) Close-up of regolith (R) developed on Hackett Formation quartzites (Q); regolith is overlain by siltstones (S) of Rifle Formation. Arrow points to pen for scale. E) Close-up of D. Note encrustation of breccia blocks and scalloped hard-rock platform by digitate tufa. F) Similar to D. Digitate tufas were precipitated on scalloped hard-rock surfaces, possibly in the splash-zone during the early phases of transgression of the regolith surface. As such, they are analogous to the pelagosite crusts of Shark Bay.

Hackett Formation and Rifle Formation shows no evidence of disconformity east of the Bathurst Fault. Although the upper surface of the quartzite member of the Hackett Formation is locally karstic and up to several metres of section are missing, the quartzite member as a whole is regionally continuous and does not appear to be systematically truncated as is the underlying Kimerot Group.

The upper contact of the Rifle Formation is also a disconformity (here termed the sub-Beechey disconformity). The surface is conformable at the southern end of the outcrop belt east of the Bathurst Fault, becoming disconformable to the north-northwest where it truncates upper units (thick quartzites) of the Rifle Formation. Along the Beechey Lake outcrop belt to the west of the Bathurst Fault, the upper quartzite units are missing, and siltstones of the lower Beechey Formation sit directly on siltstones of the lower Rifle Formation, separated by a thick (locally several metres) sequence of pisolite and sand-rich breccia.Mapping revealed local remnants of the upper quartzite units of the Rifle Formation beneath the sub-Beechey disconformity, indicating that a significant amount of section has been removed (at least several metres). The juxtaposition of deep-water siltstones (subwave-base) of the Beechey surface that deletes a significant thickness of strata, suggests that this is perhaps the most important disconformity in the lower Bear Creek Group. Significantly, siltstones of the Rifle Formation can be traced at least as far as Wolverine Canyon where they become concretionary; this unit may correlate with the lower member of the Odjick Formation (Coronation Supergroup) in Wopmay Orogen.

A major disconformity also occurs at the top of the Beechey Formation (here termed the sub-Link disconformity). This surface is conformable at the south end of the outcrop belt, east of the Bathurst Fault, becoming disconformable to the north-northwest. Along the Beechey Lake outcrop belt, west of the Bathurst Fault, uppermost units of the Beechey Fromation are truncated to the northwest and remnants of an upper stromatolitic unit are locally present. Northwest of Link Lake the upper quartzite unit is also cut out and siltstones of the lower Link Formation sit directly on the main stromatolite unit of the Beechey Formation. This relationship suggests that the sub-Link disconformity is also important.

Detailed mapping and stratigraphic studies define a distinct zone of maximum stratigraphic truncation along each disconformity in the region of the southwest part of the "basin", extending from the area of Rifle Lakenorthwest to the Mara River. In this zone, all formations thin significantly as a result of both facies changes and erosion of upper units, and fabrics indicative of subaerial exposure and erosion are best developed. Northwest of this region, in the vicinity of Wolverine Canyon, formations are thicker, additional units are present beneath disconformities, and disconformity-related fabrics are less well developed. These relationships provide evidence for continued, perhaps episodic, influence of the Gordon Bay Arch on the stratigraphy of the lower Bear Creek Group.

Facies and fabrics associated with disconformities

The sub-Hackett disconformity and those of the lower Bear Creek Group contain unique assemblages of diagnostic facies and/or fabrics that can be considered as important evidence of prolonged subaerial exposure of the underlying sequence and development of paleosols. These facies and fabrics comprise a continuum of regoliths ranging from incipient alteration of underlying facies (eg. "blotchy: carbonate cementation of quartzites) to extensive brecciation, dissolution, replacement and erosion of underlying facies. Some of these features are illustrated in Figure 23.3. In advanced stages of development, regoliths become vertically zoned with distinct facies that warrants their classification as true paleosols.

Regoliths associated with disconformities range in thickness from a few decimetres to several meters depending on degree of development (Fig. 23.3b,c,d). To a certain degree this reflects the duration of exposure of any particular sequence, but also must relate to lateral variability on a local basis in that well-developed regoliths can be traced within a few metres or tens of metres into "incipient" regoliths, and then back into pronounced regoliths. Consequently, suspected disconformable surfaces must be traced over considerable distances (tens of kilometres) in order to determine how important the disconformity is.

Well-developed regoliths (paleosols) are characterized by brecciation and/or dissolution of the underlying parent material to form angular breccias (Fig. 23.3b) or rounded blocks (Fig. 23.3d,e). Where the parent material consists of siltstone or mudstone, large tepee structures are generally developed beneath breccias. Disaggregated blocks generally fill irregular, karstic depressions up to 3 or 4 m thick. Blocks are both clast- and matrix-supported, and cavities associated with clast-constructed frameworks are generally filled with geopetal sediment including laminated dolomitic muds and pisolite. Roofs of cavities may also contain downward projecting, laminated conical structures interpreted as paleostalactites. Pisolitic units generally overlie breccias and are less than 1 m thick, although occasionally up to several metres thick; units are commonly sheets, thickening into karstic depressions and are associated with continuous layers of dolomitic fibrous cement crusts. Reverse grading may be developed.

Fibrous cement crusts consist of superimposed, isopachous layers of laminar cements, as well as upward-diverging mammillate or botryoidal structures. Individual botryoidal fans are up to 15 cm high and are defined by radiating arrays of crystal fibers up to 1 or 2 mm wide with blunt terminations. Preliminary petrographic observations suggest that these crusts may have been originally aragonitic. Individual pisoliths, as well as cement crusts, characteristically are iron-rich and contain peloids of hematite and possibly other iron-rich sedimentary minerals. These peloids also occur in local concentrations with carbonate cement.

Breccias, related cavities, and layers of pisolite show evidence for multiple generations of fracturing and renewed

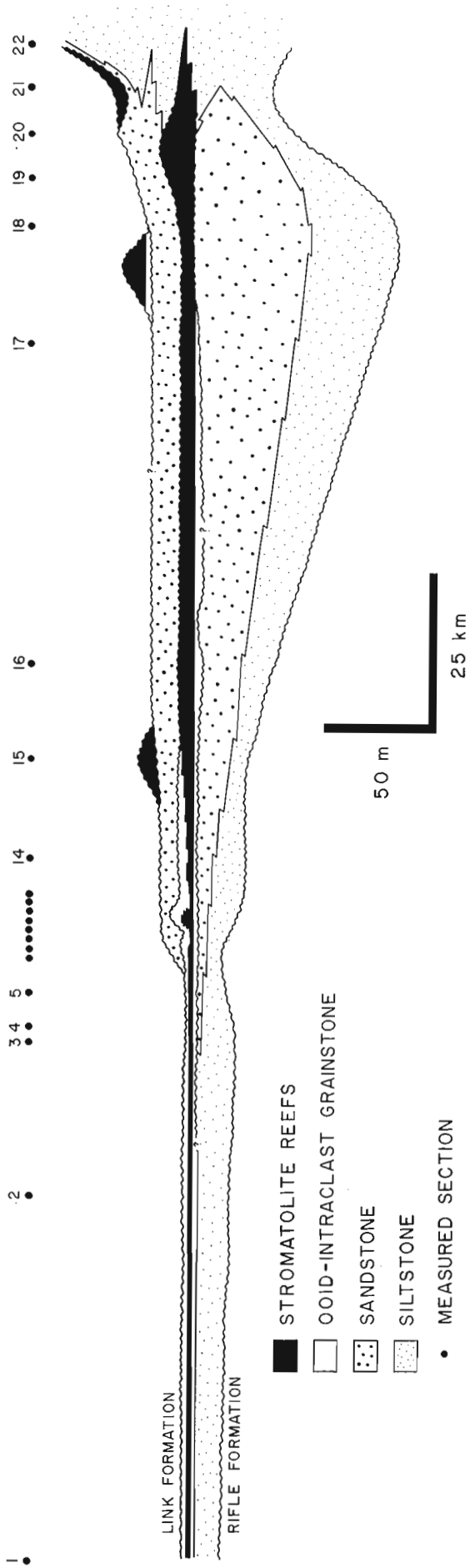


Figure 23.4 Palinspastic cross-section of Beechey Formation. Note prominent NW-SE thickening and apparent paleohigh beneath sections 19-21. Section locations on Figure 23.1.

precipitation of cements and accumulation of geopetal sediments in fracture voids. Replacement of all lithologies by jasper is typical as one of the latest stages of fabric development related to exposure. This is generally associated with formation of crusts of laminated jasper silcrete which coat breccia blocks.

The last stage of fabric development commonly involves precipitation of dolomitic, colloform to digitate tufas as isophachous coatings that drape irregularities on the upper surfaces of regoliths (Fig. 23.3e,f). Although morphologically and petrographically similar to the tidal flat tufas described by Grotzinger and Read (1983) and Grotzinger (1986), these tufas are distinctly iron-rich and contain abundant hematite. In this respect they are very similar to the hematitic stromatolites and cement fans described by Grotzinger and Hoffman (1983) and Hofmann and Grotzinger (1985). This facies locally occurs capping regoliths associated with the Kimerot disconformity and overlying disconformities of the lower Bear Creek Group. Preliminary investigations reveal that similar facies also characterize parts of the Mara pisolite (Campbell and Cecile, 1981) which is related to development of a major disconformity at the top of the Mara Formation (upper Bear Creek Group). Furthermore, small digitate stromatolites and associated ferruginous pisolite interpreted as part of a paleosol has been reported from the Gibraltar Formation (Great Slave Supergroup) by Hoffman (1969). Finally, similar iron-rich peloidal pisolites occur along the contacts between shelf quartzites and overlying siltstones of some sequences in the Wilson Island Group (Great Slave Supergroup) (B. Johnson, pers. comm., 1985). Thus, it can be concluded that the distribution of this particular suite of facies (paleosols) is process-related, and independent of time. Consequently, recognition of these facies in other Proterozoic basins constitutes a method for identification of stratigraphic disconformities related to relative changes in sea level. Furthermore, the spatial distribution of such paleosols may define paleogeographic patterns useful in evaluating the relative importance of tectonic (e.g. flexure) versus eustatic effects on basin stratigraphy. If eustatic, disconformities have the added importance of being valid time markers for use in intra- and interbasinal lithostratigraphic correlation.

STRATIGRAPHY AND SEDIMENTOLOGY OF THE BEECHEY FORMATION

The Beechey Formation (Fig. 23.4,5,6a,b) was studied in the outcrop belt extending from Wolverine Canyon to Straight Gorge along the west side of Bathurst Fault, and along the Tinney Hills east of the Bathurst Fault. The study supplements initial work by Campbell and Cecile (1981) by providing new information concerning the lateral extent and diversity of carbonate facies and significance of related quartzites and disconformities. The Beechey Formation forms a shallowing-upward siltstone-to-quartzite sequence, and comprises four major lithofacies.

Siltstone lithofacies. Maroon to greyish green siltstones consist of finely- to thickly-interlaminated mudstone layers and "streaky" siltstone and very fine sandstone layers. Fine sandstones may also form ripples, and occasionally hummocky cross-laminae. Concretions and discontinuous carbo-

BEECHY FORMATION - SECTION 11

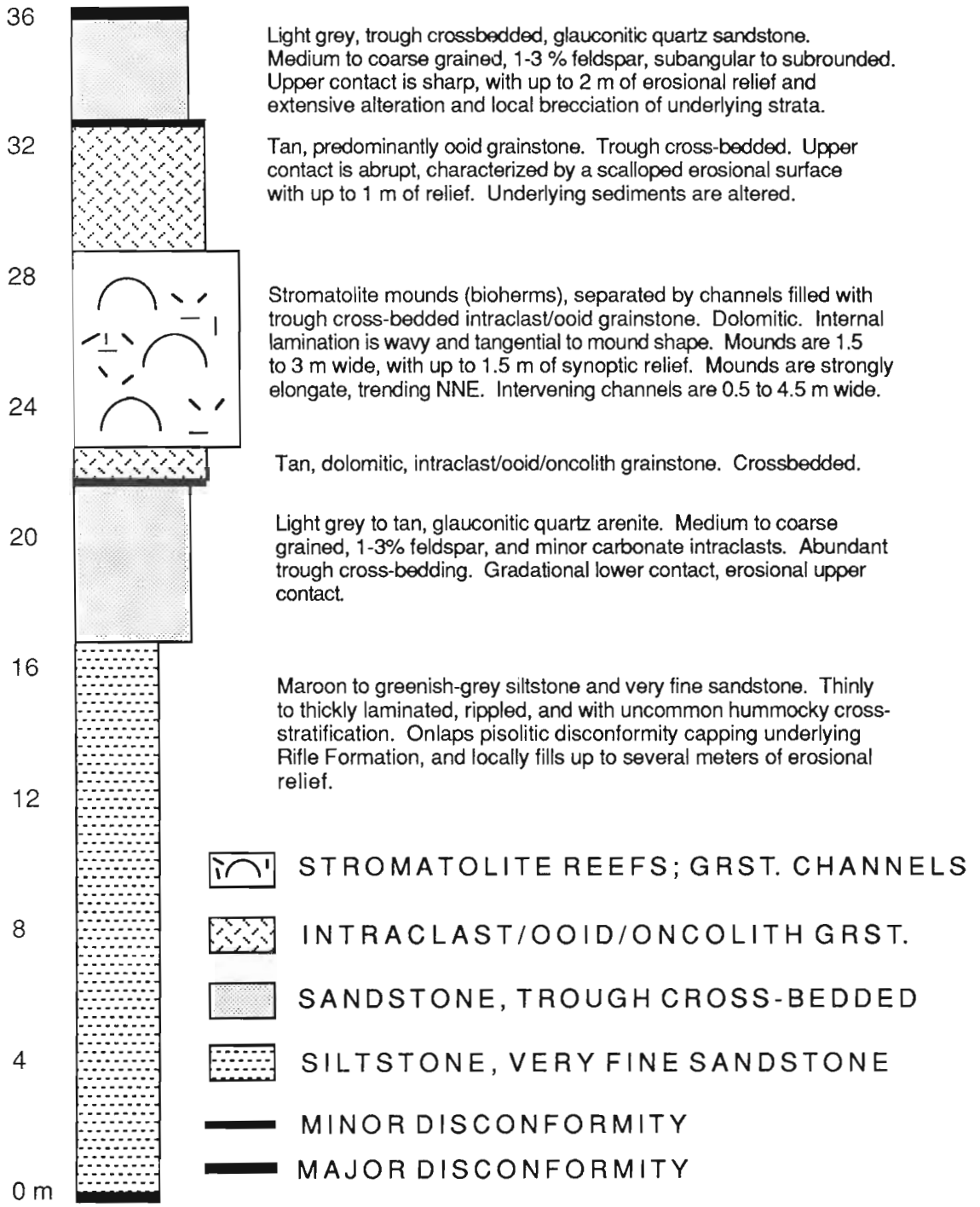


Figure 23.5 Representative measured section from type area of Beechey Formation.

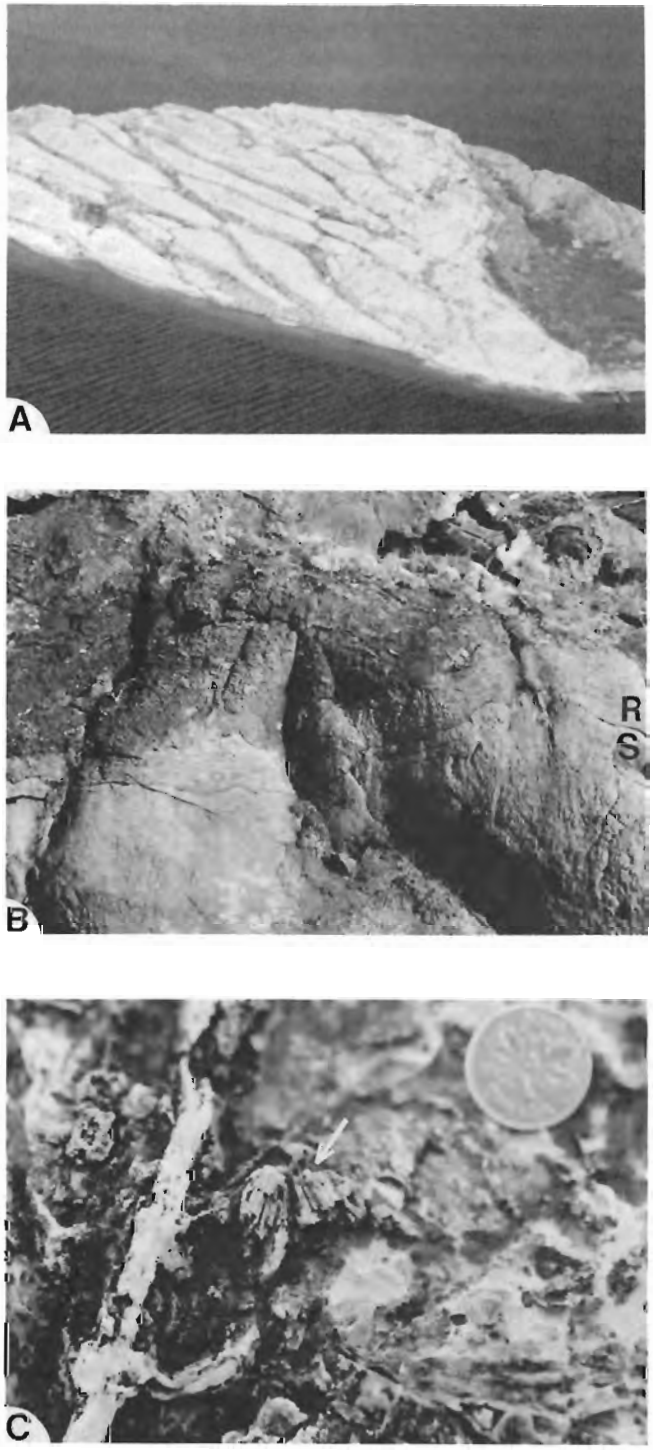


Figure 23.6 A) Stromatolitic bioherms of Beechey Formation. Note prominent elongation of bioherms and development of intervening channels. Aircraft for scale in lower right. B) Disconformity at top of main stromatolite unit (S) in Beechey Formation. Note well-developed scalloped erosional surface, overlain by intraclastic breccia and regolith (R). Day-pack at top for scale. C) Silica pseudomorphs after radial-fibrous precursor cements, probably aragonite. Pseudomorphs occur in cement-filled fractures associated with breccias in reefal facies at top of Peg Formation (Kimerot Group).

nate layers are present in southeasterly exposures. In places, mud cracks are developed near the tops of siltstone sequences.

Siltstones were probably formed in relatively deep subtidal shelf settings, perhaps near storm wave-base. They are developed as the lowermost member of the Beechey Formation and grade upward into quartzite facies. This overall transition probably reflects initial transgression of the exposure surface at the top of the Rifle Formation (sub-Beechey disconformity), followed by deepening and deposition of the siltstone facies. This was followed by progressive fall of relative sea level over the shelf to form overlying shallower-water quartzite facies.

Quartzite lithofacies. Medium- to coarse-grained quartzites occur as sheets up 50 m thick, thinning northwestward, and extending for up to 150 km. Quartzites are composed of beds up to 1m thick, generally 20-50 cm thick, and with scoured bases. Beds pinch and swell locally, and contain trough crossbedding and uncommon planar crossbedding. Grains are generally quartz-cemented, but carbonate cements are common near disconformable surfaces. Grains are 95% quartz, with a few percent feldspar, glauconite, and opaques.

Quartzites probably represent shallow-marine sheet sands deposited during lowering of relative sea level, associated with decreasing rates of tectonic subsidence or eustatic lowering of sea level.

Ooid-intraclast grainstone facies. Carbonate (dolomitic) grainstones occur at several different stratigraphic levels within the Beechey Formation. They consist of beds 10 to 30 cm thick, which generally form sheets up to several metres thick that extend in some examples for several tens of kilometres. Other grainstones form lenses between stromatolite bioherms. Many grainstones are cross-stratified and contain oncoliths and scattered quartz grains.

Grainstones probably accumulated in shallow subtidal environments as blankets of shoal sediments that formed during periods of diminished siliciclastic influx, or as channel deposits between stromatolite biostromes. Sheet deposits are generally coarsest and thickest in the vicinity of the best-developed stromatolite biostromes suggesting that much sediment was supplied by degradation of stromatolites.

Stromatolite reef facies. Stromatolite biostromes and bioherms are best-developed at one stratigraphic interval in the Beechey Formation. However, remnants of what may have been another major stromatolitic unit are locally present beneath the sub-Link disconformity; these units were probably largely removed by erosion, although the possibility of depositional discontinuity cannot be discounted. Reefal facies consist of stromatolite mounds up to 1.5 m thick, characterized by either tangential or columnar internal structure. Component columnar stromatolites range from a few cm up to several decimeters in width. Bioherms are up to 3 m wide and separated by channels up to several metres wide (Fig. 23.6a). Both mounds and component stromatolites are elongate NNE-SSW. The main stromatolitic interval can be traced the entire distance of the Beechey Formation studied so far

(Starvin Lake to Wolverine Canyon), although it thins and passes laterally into concretionary siltstones south of Starvin Lake (off-shelf direction).

Reefal facies formed predominantly in shallow subtidal conditions, although it is not yet certain whether they developed diachronously by sheet progradation, or synchronously by vertical aggradation.

Regional stratigraphic relationships

Figure 23.4 illustrates the regional stratigraphy of the Beechey Formation. The same southeast-thickening trend observed for the entire Bear Creek Group (Grotzinger and Gall, 1976, Fig. 12.6) is displayed in the Beechey Formation. Similarly, shallow-water facies pass laterally into deeper-water facies to the southeast. Finally, individual stratigraphic units are generally bounded by erosional disconformities (Fig. 23.6b) that are best developed between sections 3 and 16, the same region inferred to represent the crest of the Gordon Bay Arch during erosional truncation of the Kimerot Group. This strongly suggests that processes influencing basin geometry and stratigraphy were probably operative on the time scale of individual formations, and that further detailed studies of other relatively thin units are warranted in that they can potentially provide important information on the subsidence and/or sea level history of the basin.

One particularly interesting feature that may have exerted a strong control on Beechey Formation stratigraphy is the apparent erosional high on top of the underlying Rifle Formation at sections 20, 21, and 22, which coincides with the shelf-to-basin transition zone. This feature has been carefully examined and all relevent contacts are well exposed. Evidence for disconformity along this surface includes brecciation of underlying siltstone, and development of autogenic pisolite, microdigitate tufa, and chert. Thus it seems likely that this surface represents an erosional high that influenced the thickness of the overlying siltstone and lower quartzite members of the Beechey Formation, consequently limiting their progradation to the southeast by restricting sediment dispersal. In turn, this probably restricted the southeastward expansion of the Beechey reefal sequence.

DIAGENETIC STUDIES OF THE PEG FORMATION, KIMEROT GROUP

Geochemical and petrographic studies of the Peg Formation, which forms the upper carbonate platform of the Kimerot Group (Grotzinger and Gall, 1986), will be undertaken by R. Creswell as part of a Ph.D. dissertation at the University of Toronto. Over 100 samples were collected from various facies of the Peg Formation including dololutites, dolarenites, cryptalgalaminites, stromatolites, tufas, and dolomitic quartzites. These facies formed in a variety of depositional settings ranging from subtidal open marine to peritidal restricted (Grotzinger and Gall, 1986). The upper part of the Peg Formation was subaerially exposed and eroded to the northwest beneath the sub-Hackett disconformity, and was locally brecciated. Breccias are filled with dolomite and silica pseudomorphs after probably aragonite (Fig. 23.6c). Thus, a range of possible diagenetic environments may have existed during sedimentation and burial of the Peg Formation. Samples will be analyzed for information pertaining to the diagenetic history of the platform, particularly the timing of dolomitization and source of dolomitizing fluids.

CONSTRAINTS ON STRATIGRAPHY, SEDIMENTOLOGY, AND PROVENANCE OF THE BURNSIDE FORMATION

The Burnside Formation (formerly Burnside River Formation) forms a thick (<1500 m) mostly nonmarine fluvial cap to the coarsening-upwards Bear Creek Group. It is underlain by green, shallow marine siltstones and sandstones of the Link Formation. It is abruptly overlain by finer-grained silty brown sandstone of the Mara Formation to the northwest, while there is a gradational, interfingering contact with stromatolites of the Quadyuk Formation to the southeast. The Burnside Formation has been interpreted as a braided stream deposit (Campbell and Cecile, 1981). The Burnside Formation is currently being studied in detail to: (1) investigate the significance of prolonged flucial sedimentation in the subsidence history of the Kilohigok Basin, (2) determine the provenance of the Burnside Formation, (3) document regional sedimentary facies mosaics within an Early Proterozoic fluvial sequence, and (4) provide more detailed correlation of tectonic and sedimentary events between Kilohigok Basin and Wopmay Orogen.

In this section, the Burnside Formation will be characterized by lithofacies and their representative sequences. Several aspects of the Burnside Formation have stratigraphic and tectonic significance. These include the lateral variability of the lower contact, the significance and lateral facies variability in the Bd dolarenite unit, the variation of composition and lithofacies of conglomerates. Plans for future research and economic considerations are summarized at the end.

Lithofacies of the Burnside Formation

Sedimentation units within the Burnside Formation can be divided into a series of end-member lithofacies (Table 23.1) based on grain size and sedimentary structures following an interpretive classification scheme developed by Miall (1977, 1978a) and Rust (1978). Sequences of certain lithofacies repeated over hundreds of metres in the Burnside Formation suggest a hierarchy of fluvial cycles regulated by both autocyclic and allocyclic controls. These characteristic sequences allow the Burnside Formation to be divided into several mappable members.

On the largest scale (hundreds of metres), the Burnside Formation records uplift events in a southeastern source area, and changes in lithofacies sequences across depositional strike demonstrate proximal-to-distal transitions in the fluvial regime from southeast to northwest. Campbell and Cecile (1981, p. 111-115) presented a series of qualitative facies

Table 23.1 Lithofacies of Burnside Formation.

Facies Code	Lithofacies	Sedimentary Structures	Interpretation
Fm	silty (vf-f) sand silt, mud	massive to laminated, small rpls.,mudcracks	waning flow deposits
Fl	silty (vf-f) sand, silt	fine lamination, small ripples	waning flow deposits
Sr	(vf-c) sand	ripple marks	ripples (lower flow regime)
Sh	(vf-vc) sand, may be pebbly	bedding-parallel lamination	plane bed flow (l. and u. flow regime)
St	(f-vc) sand, may be pebbly	trough cross-beds	migrating dunes (cm-dm)
Sp	(f-vc) sand, may be pebbly	planar cross-beds	lingoid bars (lower flow regime)
Ss	(f-c) sand, may be pebbly	broad, shallow scours with downlapping x-strata	scour fills
Gm	gravel, massive or crudely-stratified	horizontal bedding	lag deposits, longitudinal bars

Classification scheme after Miall (1977, 1978) and Rust (1978).

successions for the Burnside Formation, but did not constrain their spatial distribution. Additional lithofacies have also been interpreted. These differences are shown in measured sections and cross-sections (Fig. 23.7, 8, 9, 10).

Gm lithofacies. This lithofacies consists of massive- or horizontally-bedded clast-supported conglomerate. Bed geometry is commonly sheet-like and individual horizons can be traced laterally at least 20 km in the Tinney Hills (Fig. 23.1). Clasts are pebble to cobble size and commonly well-rounded. Matrix sand is medium to very coarse size. Basal contacts are commonly scoured <10 cm, but rarely may downcut 0.5-3 m in very coarse units. Gm units range in thickness from single clast lags to amalgamated beds up about 2 m thick. Amalgamated beds pass laterally and vertically to interbedded Gm and St lithofacies with 30-50 cm of Gm facies at the base of beds. Single clast layers are interpreted as traction carpet lags. Thicker decimetre-scale and amalgamated beds are interpreted as sheet-flood gravels, longitudinal bars, and rare channel fills.

Clasts are composed of mostly vein quartz with minor amounts of probably Archean basement lithologies and

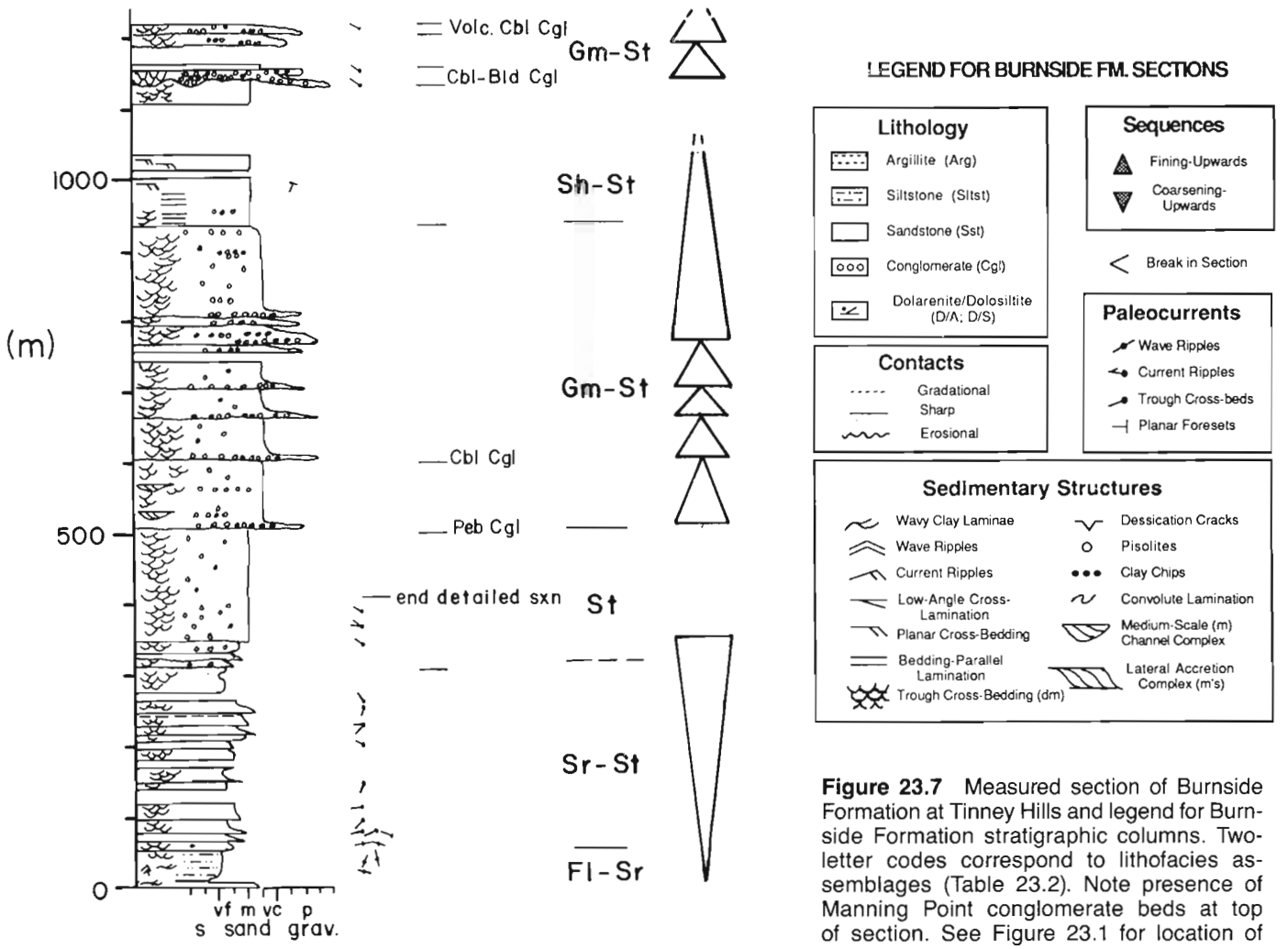


Figure 23.7 Measured section of Burnside Formation at Tinney Hills and legend for Burnside Formation stratigraphic columns. Two-letter codes correspond to lithofacies assemblages (Table 23.2). Note presence of Manning Point conglomerate beds at top of section. See Figure 23.1 for location of sections.

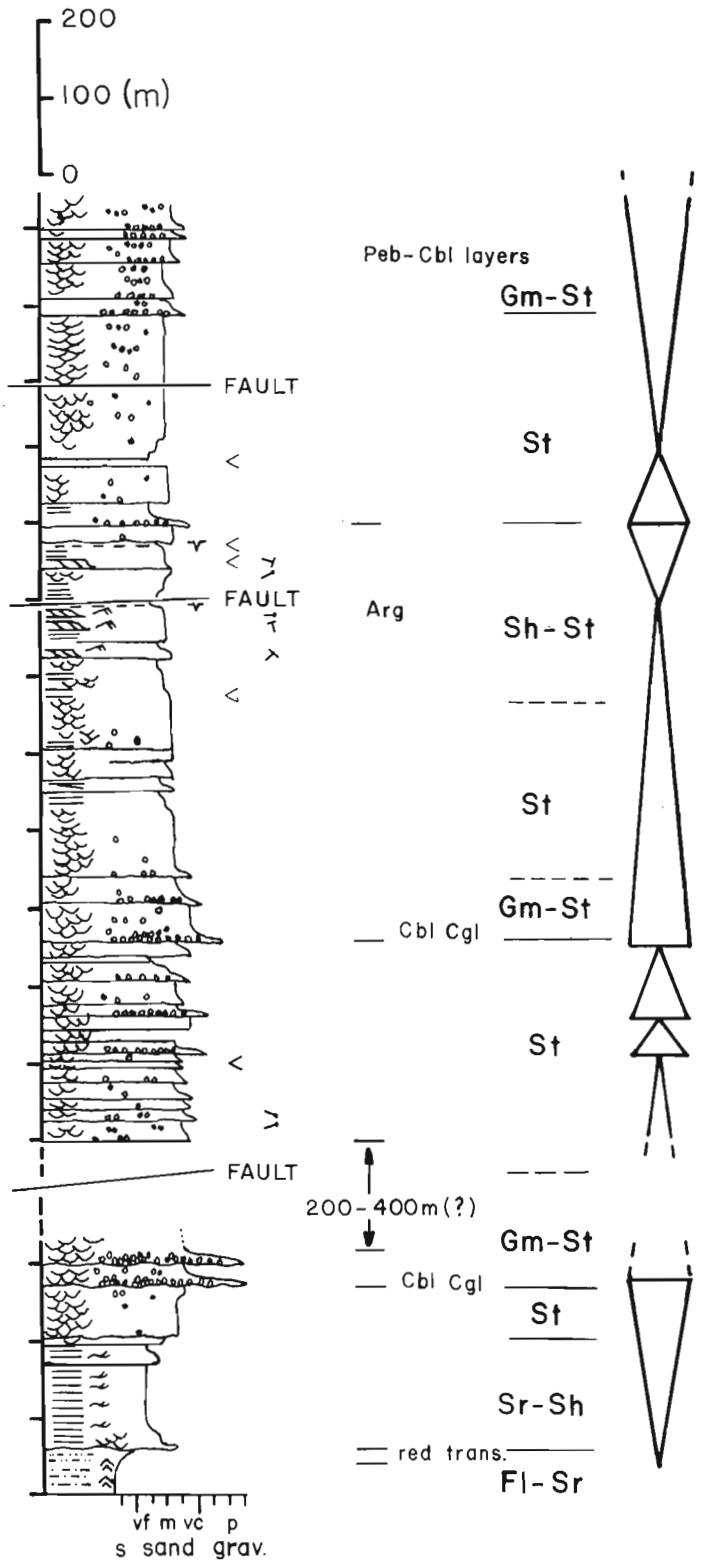


Figure 23.8 Measured section of Burnside Formation at Straight Gorge.

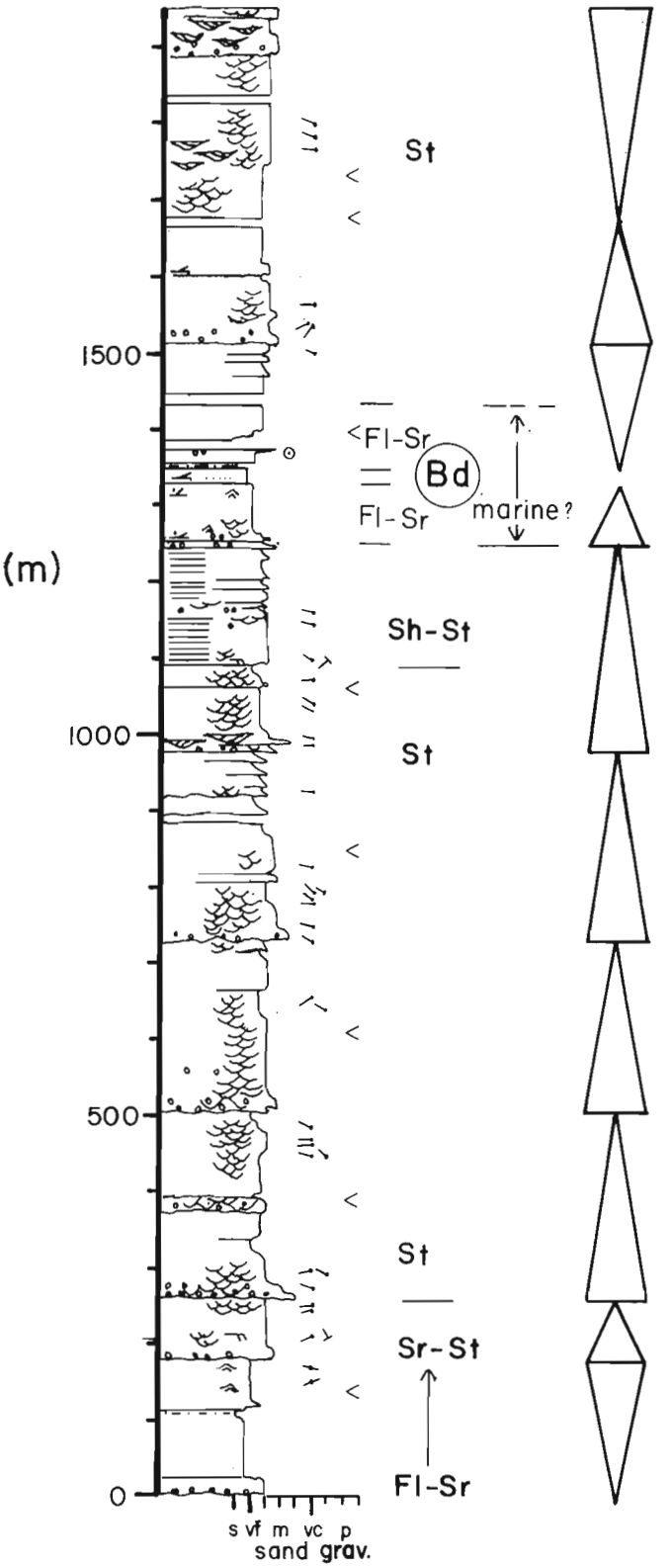


Figure 23.9 Measured section of Burnside Formation at Wolverine Canyon. Note Bd dolarenite unit and surrounding fine grained siliciclastic rocks which probably represent a marine incursion.

Lower Goulburn Supergroup clasts of jasper and sandstone. Intraformational Burnside clasts appear about two-thirds through the longer measured sections (Fig. 23.7, 8, 9).

The thickness, frequency, and maximun clast size of the Gm facies decrease to the northwest, subparallel to the predominant paleocurrent direction. Pebble to cobble conglomerate is common in the Tinney Hills and Straight Gorge areas (Fig. 23.1), whereas only granules to pebbles are found farther northwest. Individual cobbly conglomerate beds in the Tinney Hills can be mapped laterally for more than 20 km. A unique set of two Gm horizons 35 m apart are found at Manning Point at the northwest end of the Tinney Hills. Conglomerate beds contain well-rounded, boulders of intraformational Burnside clasts up to 100 cm and vein quartz up to 45 cm. The second unit consists of cobbly Gm and St lithofacies containing a large proportion of undeformed felsic volcanic clasts similar to ones described by Campbell and Cecile (1981) in the Amagok Formation. The significance of these conglomerates is discussed below.

Ss lithofacies. Ss is a minor lithofacies characterized by broad scours 60-150 cm deep and 1-5 m wide. Ss lithofacies is developed in successions with medium to very coarse sandstone. Ss is associated with St lithofacies which laps onto the scour surface. These are interpreted as scour-and-fill channels created during rising flood stage.

In the Straight Gorge section three large-scale lateral accretion complexes were identified (Fig. 23.1, 8). These are characterized by beds with sigmoidal foresets 1.5-3.0 m thick. Foreset dip directions are nearly orthogonal to the northwest-directed trough transport azimuths. One 3 m thick unit can be traced at least 200 m, the length of outcrop. These complexes are developed at the top of a gross fining-upwards cycle in fine- to medium-grained sandstone. These lateral accretion surfaces are interpreted as point bars in broad channels that may migrate across a braidplain.

St lithofacies. This lithofacies forms the majority of the Burnside Formation. It consists of fine- to very coarse-grained trough cross bedded sandstone which locally contains granules or pebbles along cross-strata and near the base of beds. Crossbed sets range from 10-80 cm thick, but are generally less than 40 cm. Thicker, coarser sets are commonly associated with Gm lithofacies, while thinner, finer sets commonly pass into Sh lithofacies. St crossbeds are generally the same scale within a given bed and bedset. The St lithofacies is interpreted as the product of migrating sinuous-crested or lignoid subaqueous dunes.

Sh lithofacies. Horizontally-laminated very fine to coarse sandstone is common. Laminae are generally 0.5-2.0 mm thick, with size differences of less than 2 phi units between laminae. Beds with Sh are commonly tabular and laterally continuous over the scale of outcrops (tens of metres). Sh is commonly associated with smaller-scale finer St lithofacies sandstone. Sh is developed in the lower transtitional units and towards the top of gross (hundreds of metres) fining-upwards successions. Sh increases in abundance in more distal sections. Sh is interpreted as a lower flow regime planar bedform as it is not commonly associated with thicker, coarser St beds. It may also represent unchannellized sheet-flow deposits on low-gradient, distal alluvial plains.

Sp lithofacies. Planar crossbedded fine to coarse sandstone is a very minor component of Burnside Formation silicastic rocks. The occurance of Sp is typically restricted to single sets 10-25 cm thick. Paleocurrents in this facies are mostly at a large angle to trough transport azimuths (see Fig. 23.7, 8, 9, 10). Sp is associated with Sh and finer St lithofacies. Due to small size of sets, occurrence with Sh and St, and oblique paleocurrent trends, Sp is interpreted as the product of migrating lingoid or transverse bars in the lower flow regime.

Sr lithofacies. This facies forms a minor part of the Burnside Formation. Thin (<10 cm) successions of very fine to medium sandstone with current ripples and rare wave ripples are seen. Ripples commonly have amplitudes of <2 cm and wavelengths <20 cm. They are very rarely dessication cracked. Where recognized, Sr caps Sh and St sets. It is more common in distal sections. These are interpreted as lower flow regime migrating ripples.

Fl lithofacies. This lithofacies consists of silty, very fine- to fine-grained sandstone and rare siltstone. It is commonly a pale-greenish colour. Sedimentary structures are thin (mm) parallel to wavy laminae and small ripples with wavelengths <10 cm and amplitudes <1 cm; commonly laminae drape underlying structures. This facies rarely exceeds a few centimetres in thickness. The Fl facies forms the caps of crossbed sets and beds. Aside from clay chips, Fl is the only fine grained material in much of the Burnside Formation. It is interpreted as a waning flow deposit.

Fm lithofacies. This rarely-developed lithofacies consists of massive to laminated, reddish to purplish siltstone and argillite with mudcracks and small ripples. The thickest succession in which Fm occurs is in the middle of the Burnside Formation underlying the Bd unit (see below) in the Hackett River-Link Lake area in the southwest part of the basin. This corresponds to the Bm member mapped by Campbell and Cecile (1976, 1981); it appears to be absent from stratigraphic sections in either direction (WC and SG sections, Fig. 23.8, 9). This rarely preserved lithofacies is interpreted as a low-gradient distal fan-fringe which possibly interfingers with shallow marine siltstones to the northwest.

Lithofacies assemblages and sedimentary regimes

Five characteristic sets of lithofacies assemblages are derived from measured sections of the Burnside Formation. These are summarized in Table 23.2 and measured sections are annotated with these designations. It appears that facies assemblages persisist over many tens to hundreds of kilometres through the basin. Fluvial deposits of the Burnside Formation extend a minimum of 150 km across-depositional strike as inferred from paleocurrent trends, suggesting that the alluvial plain was very extensive. In this respect, it is comparable to the scale of the paleo-braidplains documented from the middle Proterozoic Belt Supergroup of the northwest U.S.A. (cf. Winston, 1978).

Table 23.2 Lithofacies assemblages of Burnside Formation.

Major Facies	Minor Facies	Environmental Interpretation
Sr-St	Sh, Sp, Fl, Fm	fan-flat on low gradient distal alluvial plain
Sr-Sh	St, Fl	sheet-floods on distal alluvial plain
Sh-St	Sp, Sr, Fl, Fm + point bar	distal alluvial plain
St	Gm, Ss, Sp, Sh, Fl	shallow braid-plain channels
Gm-St	Sp, Sh	distal sheet-flow gravel and shallow channels on alluvial plain

Classification scheme after Miall (1977, 1978) and Rust (1978).

Sr-St assemblage. The lower contact of the formation is everywhere transitional from wave-rippled siltstones of the Link Formation. The contact does not appear erosionally disconformable as interpreted by Campbell and Cecile (1981). In the southeast part of the basin lower units consist of red Sr and St lithofacies with Sr decreasing upwards. Minor lithofacies include Sh, Sp, Fl, and rare Fm. This transitional unit thins from 300+ m in the northern Tinney Hills to 17 m at the Straight Gorge area to about 1 m in the Link Lake area (Fig. 23.8, 9, 10, 11). This sequence is interpreted as the transitional marine to fluvial unit of the Burnside Formation probably deposited on the distal part of a low-gradient alluvial plain with shallow channels and migrating dunes.

Southwest-directed paleocurrent trends in the transitional unit within the southeastern axial zone parallel trends recorded in underlying lower Bear Creek Group submarine fan turbidites and shelf deposits (Grotzinger and Gall, 1986). These paleocurrent trends shift abruptly to the northwest at the base of the overlying pink or buff-coloured St sequence. This suggests that in the axial zone the lower transitional Sr-St sequence initially developed a paleodrainage system parallel to the inferred trend of the basin axis and the Gordon Bay Arch, and probably the trend of the uplifted source terrane. Commonly, the initial phases of molasse show longitudinal dispersal patterns confined to a moat parallel to the mountain front (Miall, 1978b; 1981). However, to the northwest, initial paleocurrent trends at base of the Burnside Formation are entirely northwest-directed, suggesting that at the onset of Burnside deposition west of the Bathurst Fault, sediment dispersal was transverse to the mountain front, unrestricted, and reflects regional paleoslope. This can be extended to infer that in the axial zone, the Gordon Bay Arch influenced sedimentation by constricting paleodrainage in lingitudinal systems. In contrast, to the northwest of the axial zone, initial fluvial sedimentation occurred directly over the Gordon Bay Arch which thereby could not modify dispersal patterns.

Northwestward onto the craton, Sr-St sequences of the lower transitional unit pass laterally into green silty sandstone characterized by Fl-Sr-Sh assemblage with common wave ripples (Fig. 23.8, 11) which coarsen upwards to a reddish Sr-St sequence. This silty sandstone probably represents a wave-dominated shallow-marine shelf environment, but detailed interpretion requires further study. This facies change probably indicates that the transitional unit passes laterally from distal fan-fringe alluvial facies into a marine shelf facies reflecting proximal-to-distal expression of the initial diachronous phase of Burnside progradation. This diachroneity is also suggested by the differing thickness from the lower contact of the Burnside to the first occurrence of conglomerates in the Hackett River/Link Lake area (Fig. 23.10). Overlying nonmarine sequences comprising the majority of the Burnside Formation form a blanket extending up to 150 km to the northwest. The lower transitional unit may be correlative with the "Bg" green siltstone member of Campbell and Cecil (1976) reported only in the Rockinghorse Lake area (Fig. 23.1).

Sr-Sh assemblage. In most sections the first sandstone free of silt is a buff- or pink-coloured unit characterized by an association of St at the base, with overlying Sh-Sr with sparse wavy green clay laminae and clay chips. This facies grouping probably represents unconfined shallow sheet-flow deposits on a distal alluvial plain. As mentioned above, this facies group is laterally and vertically gradational with the red and green silty sandstone facies with increasing Sr and Fl to the northwest.

St assemblage. The most common facies group consists of almost entirely St with minor thin Gm, Ss, Sh, Sp, Sr, and Fl. Multiple crossbed sets are common. Fining-upwards cycles are developed on the scale of tens to hundreds of m. This grouping is commonly seen above the lower transistional Sr-St group. This association is interpreted as a sandy braided stream environment dominated by migrating dunes. The abundance of conglomerate layers tends to increase upwards at the base of all long sections as well as the top few hundred metres. This probably represents progradation of coarser sediment into the basin in response to uplift in the source area (Heward, 1978).

Gm-St assemblage. In the lower part of the Tinney Hills and Straight Gorge, the St group is commonly abruptly overlain by the Gm-St group. Minor lithofacies include Ss, Sh, Sp, Sr, and Fl. Thin- to thick-bedded Gm lithofacies fines upwards to large-scale St with gravel content decreasing upwards. As noted before, conglomerate beds rarely exceed 30-50 cm in thickness. In the Tinney Hills section at least five distinct pebbly to cobbly conglomerate horizons can be traced over 20 km. Similar mappable Gm-St groups are seen at Straight Gorge. These intervals probably represent distal gravelly rivers reflecting increased uplift in the source area. The lack of thick (metres to tens of metres) channelized conglomeratic intervals, their sheet-like geometry, and their lateral extent over many kilometres suggests that the area presumed to be closest to source (i.e. Tinney Hills) was always on the distal reaches of an alluvial plain subjected to sheet floods, rather than an alluvial fan or proximal alluvial plain (Andrews-Speed, 1986). The repetition of conglomeratic horizons at 50-100 m intervals could represent either discrete uplift and erosional events in the source area (allocyclic process) or the return of the focus of sedimenta-

tion which migrates over an alluvial plain (autocyclic process). The wide lateral extent of conglomerates in the Tinney Hills suggests that allocyclic control predominated.

Sh-St assemblage. Commonly St facies grades upwards over tens to hundreds of metres to a Sh-Sh association with concommitant decrease in grain size and disappearance of gravel. The scale of bedding decreases, but its lateral continuity increases. Minor lithofacies include Sp, Sr, Fl, and rare Fm. Lateral accretion complexes are found in this assemblage at Straight Gorge. In the Tinney Hills this group locally contains heavy mineral laminae along trough crossbeds. The Sh-St group probably represents a distal alluvial plain environment. However, the tabular, more continuous nature of bedding, finer grain size, and the presence of local heavy mineral laminae and interbedded stromatolites in a similar assemblage in the uppermost Burnside Formation at Tinney Cove, suggest that Sh-St may represent a shallow-marine environment as well. The vertical gradation and fining-upwards over 300-500 m from Gm-St and St assemblages suggests that the alluvial plain may have aggraded. This aggradation probably represents long-term denudation of the source area with little or no uplift (Heward, 1978).

At Wolverine Canyon a locally-developed assemblage of lithofacies brackets the Bd dolarenite unit (Fig. 23.9). This distinctly brown-coloured assemblage abruptly overlies a section of Sh-St. This lower unit (80 m) is characterized by Fl-Sr lithofacies with abundant wave ripples and minor dolomitic sandstone and thin (tens of centimetres) dolarenite horizons. The upper unit (about 50 m) contains a basal brown siltstone (4 m) with decimetres scale fining upward cycles. Cycles are based by intraclastic carbonate lags derived from underlying Bd dolarenite plus quartz and jasper granules. Overlying siltstones coarsen upwards to sandstone with a gradation from Fl-Sr to Fl-Sr-St assemblage. A probable pisolite horizon is present in the middle of the upper unit.

The presence in the lower unit of dolarenite resembling the overlying Bd dolarenite, finer grain size, thinner bedding and structures, and abundance of wave ripples suggests that this unit represents a shallow marine environment. As ex-

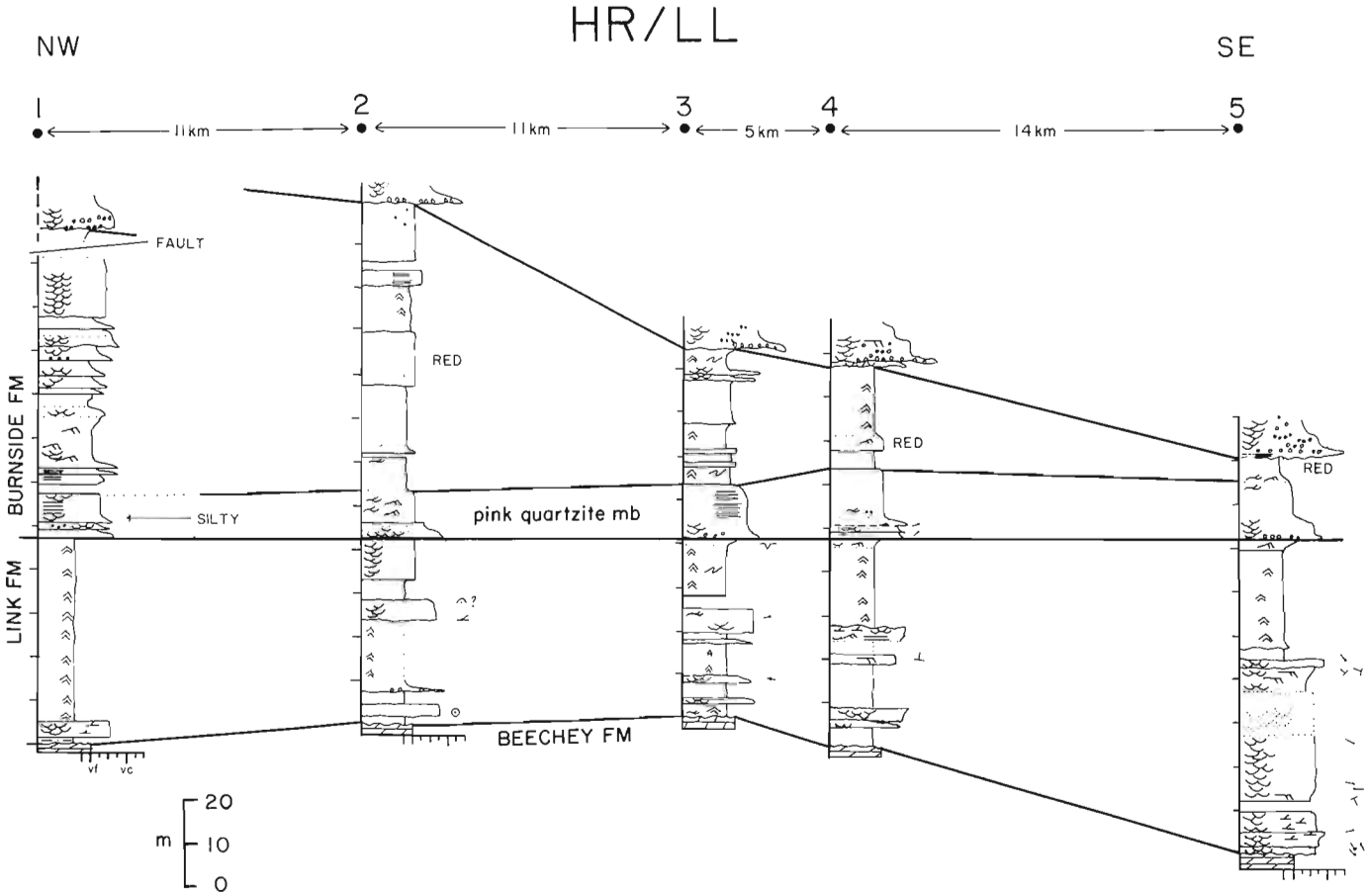


Figure 23.10 Measured sections and stratigraphic cross-section of the interval from top of the Beechey Formation through the basal Burnside Formation in the Hackett River/Link Lake area. See Figure 23.1 for location of sections. Note the fining and thinning of "pink quartzite" to the northwest and thickening of the interval to the onset of conglomerate deposition. Datum is the base of the Burnside Formation.

plained below, if the Bd unit represents a eustatic rise in sea level, the effect on the Burnside Formation should be to cause a back-stepping of fluvial facies towards the source area. This suggests that the silty to muddy Bm member of the Burnside Formation that underlies the Bd unit northeast of Hackett River may be the nonmarine facies equivalent to dolomitic sandstones underlying the Bd at Wolverine Canyon. The Bm could then represent a distal alluvial flat environment. This would discount the interpretation of Campbell and Cecile (1981) that the Bm member represents a lake environment. If such a back-stepping of fluvial facies belt did occur, then an additional allocyclic mechanism, eustasy, exerted control on the patterns of Burnside Formation sedimentation in distal areas.

Future petrographic analysis will allow more refined description of sandstone texture and composition associated with different lithofacies assemblages. Furthermore, the possible identification of petrographic trends and marker phases may provide more detailed correlation between widely separated sections. In particular, heavy-mineral bearing sandstone samples collected in 1985 near the top of the Tinney Hills section were inspected for the presence of detrital zircons. Initial results indicate that a significant population of very euhedral, probable first-erosional-cycle, detrital zircons are present (S.A. Bowring, pers. comm., 1986). Therefore, the possibility exists for detailed cross-basin correlation based on the presence, trends, and first occurrence of different zircon populations.

In every thick measured section a charateristic pattern of vertical lithofacies assemblages is observed. The first phase of sedimentation is characterized by a coarsening upwards from shallow-marine siltstones of the Link Formation to the first occurance of conglomerates or gravels. This phase corresponds to progradation of the siliciclastic sediments from the source area. The next phase consists of several hundred metres of fining-upwards cycles. These may represent a series of uplift events that shed coarser detritus to the alluvial plains; progressive erosion probably aggraded the alluvial plain. They also may represent autocyclic meandering of the focus of sedimentation across the alluvial plain during a time of relatively steady uplift. In the distal Wolverine Canyon section (Fig. 23.9) a fining- then coarsening-upwards cycle is seen which corresponds to the Bd dolarenite and surrounding finer siliciclastic beds. This probably represents a marine incursion into the basin. The more proximal sections do not appear to have a similar pattern. The final phase of sedimentation is represented by a coarsening-upwards sequence at Straight Gorge and Wolverine Canyon (Fig. 23.8, 9). This probably reflects a second large uplift event in the source area. Interestingly, gravels seen in this coarsening upward sequence contain the first Burnside Formation intraformational clasts, suggesting that synorogenic sediments were being deformed in the hinterland. Future study of the Mara and Quadyuk formations will document the waning stages of sedimentation.

Description and significance of the Bd dolarenite unit

On the western margin of the Kilohigok Basin, a distinct westward-thickening interval of brown dolarenite and dolosiltite is developed (Campbell and Cecile, 1976, 1981). This interval is 21 m thick at Wolverine Canyon. It consists of cycles a few decimetres thick with basal intraclast lags of ripped-up doloarenite clasts overlain by wave-rippled dolosilite grading up to dolarenite with common siliciclastic silt, sand, and rare granules. Cycles are capped by laminated dolomitic siltstone which may be brecciated. The abundance of wave ripples, clastic-textured dolomite, upward coarsening cycles, and evidence of brecciation suggest that this unit represents a subtidal to intertidal facies. The Bd unit at Wolverine Canyon resembles the shallowing-upwards lagoonal facies of the Rocknest Formation (Grotzinger, 1986). Hoffman et al. (1984) and Grotzinger (1985) have correlated the Bd unit with an interval of the Rocknest Formation in Wopmay Orogen to the west. Grotzinger (1985, 1986) postulated that the correlative Rocknest Formation interval (intraclastic member, middle non-cyclic interval) represented a eustatic rise in sea level. This suggests that the thinly-bedded, wave-rippled, silty, dolomitic units bracketing the Bd may represent a marine tongue that prograded into the predominantly fluvial succession. Thus, allocyclic sea level changes may have influenced Burnside sedimentation in the distal areas of the basin.

The Bd unit was also briefly examined in an area about 10 km northeast of Hackett River. At this location the Bd unit exhibits significantly different characteristics. The unit is underlain by several tens of metres of red silty sandstone and minor siltstone (the Bm unit of Campbell and Cecile, 1976). The Bd in the Hackett River area consists of about 1.5 m of possible caliche with a sharp upper boundary. The unit contains pink and white intraclastic carbonate cut internally by subvertical to subhorizontal cracks 1-10 cm wide which flare upward and form roughly polygonal plan patterns up to 1 m across. Probable primary carbonate material with intraclastic texture is preserved locally. At least three generations of cement-filled fractures appear to crosscut intraclastic layers and previous fractures until all continuity of bedding is lost upwards. The first two generations of cement form fibrous, isopachous linings subparallel to walls of cracks. The last generation appears to be coarse, void-filling dolomite spar. Convex-downward, concentric botryoidal carbonate fabrics are also present. The unit is capped by a few centimetres of pisolite with crudely-developed inverse grading. The unit immediately overlying consists of brown siltstone with common sand to pebble layers with intraclastic carbonate granules at the base of fining-upwards cycles.

These fabrics suggest that in the Hackett River area the Bd is a caliche, a weathering horizon subjected to vadose diagenesis in a semi-arid evironment (Read, 1976; Retallack, 1981; Retallack et al., 1984; Calvet and Julia, 1983). If so, it represents the only such horizon identified in the Burnside

Formation. If it is truly correlative with the Bd dolarenite horizon at Wolverine Canyon, it implies that the northwestern part of the basin was submerged while to the east it was exposed, or at least, received little sediment at that time.

Establishing whether these two Bd units correlate and identifying their lateral equivalents is important for two reasons. According to arguments outlined above, both Bd horizons would be roughly time planes tracable through siliciclastic deposits. Lithostratigraphic correlation, which is presumably diachronous (e.g. Fig. 23.10), is the only method currently applied to the Burnside Formation. Second, if eustatic submergence occured synchronously with exposure, an apparent paradox exists. This may be explained by a tectonic effect superimposed on the presumed eustatic effect. If this is the case, further constraints could be placed on the location of the Gordon Bay Arch and perhaps show if it migrated laterally through time. This would be an expected effect in a foreland basin where frontal deformation advances episodically toward the foreland through time (Beaumont, 1981). Thus the Bd unit could provide a good method for testing if flexure of the basin occurred during Burnside sedimentation.

Composition and significance of conglomerates

Gravel-size material is present throughout the basin, usually as isolated layers and sheet-like beds. As indicated, in the areas examined conglomerate clast size, frequency, and bed thickness decrease to the northwest, roughly parallel to paleocurrent trends. Campbell and Cecile (1981) reported that the majority of conglomerate clasts in the Burnside Formation are vein quartz plus intraformational quartzite. The remaining small proportion (<10%) of clasts were identified as "quartzite of unknown origin, and granitoid or gneissic rocks". Lithologies identified to date comprise a suite of possibly Archean basement-derived and Lower Goulburn Supergroup clasts. Tentatively-identified basement lithologies include meta-greywacke, banded iron formation (jasper plus magnetite), jasper plus chert, mylonites, and rare feldspathic and amphibolite gneisses. Goulburn clasts include jasper with detrital quartz grains probably derived from silicified disconformity surfaces within the lower Bear Creek Group. Other Goulburn clasts include white sandstones probably derived from the Kenyon Formation and sandy members in the Rifle and Link formations, and red siltstones and sandstones from the upper Link and lower Burnside formations. Clast lithologies will be identified by petrographic thin-section study during 1987.

A distinctive set of conglomerate outcrops occurs at Manning Point on the northwest end of the Tinney Hills (Fig. 23.1). The lower horizon (5-20 m thick) contains cobble to boulder size clasts in channels which down-cut up to 3 m. Intraformational Burnside clasts reach 100 cm in size (mean size locally 30-40 cm) while vein quartz clasts reach 45 cm (mean size locally 15-20 cm). Other lithologies rarely exceed 10 cm. The sharp lower contact of this unit varies up to 15 m within 50 m laterally, whereas the upper contact is planar and sharp. Two pebble counts indicate that clast populations are composed of 52-57% vein quartz, 26-27% pink intraformational Burnside clasts, 6-11% red siltstone and sandstone, and 2-3% Goulburn jasper, and minor amounts of above-mentioned Archean lithologies.

The second conglomerate unit present at Manning Point (15 m exposed) contains a significantly different clast population. Clast size does not exceed 10 cm. Most notable is the presence of a high proportion of undeformed felsic volcanic clasts. These clasts appear to be similar to red to brown crystal-rich tuffs described by Campbell and Cecile (1981) in the Amagok Formation at the top of the Goulburn Supergroup. Identical volcanic clasts were found in the upper Burnside Formation just below the contact with the Quadyuk and Peacock Hills formations at Tinney Cove 23 km to the south. Two pebble counts indicate that volcanic clasts make up 26-44% of all clasts in this conglomerate unit; vein quartz are 43-57% and Burnside intraclasts are 6-8%. The presence of the undeformed volcanic clasts in the Burnside Formation indicate that unroofing of a magmatic terrane younger than deformed Archean basement began much earlier in the Goulburn Supergroup than previously assumed. Volcanic clast samples were collected and sent to S.A. Bowring for zircon U/Pb age-dating.

It is notable that a few of the vein quartz clasts seen at Manning Point contain pegmatitic muscovite. Campbell and Cecile (1981) ascribed the origin of voluminous vein quartz clasts in the Burnside Formation to silcrete formation on alluvial plains. Vein quartz production was inferred to result from fracturing of an early-cemented flood plain associated with fluvial avulsion. If this were the case then Burnside intraformational clasts would be expected to appear in the first conglomerate layer. The first occurance of intraformational Burnside clasts is about two-thirds through longer sections measured to date. Furthermore, the extreme bimodal size distribution of clasts in the Manning Point conglomerates and abrupt contact with finer sandstones suggests a proximal source for the larger clasts and a rapid uplift event. The introduction of intraformational clasts high in stratigraphic sections is a common feature of prograding molasse basins in which earlier deposited sediments are incorporated and uplifted in foreland-propagating thrust sheets; older parts of the formation are thereby reworked, recycled and deposited near the top of the section (Bally et al., 1966; Miall, 1978b, 1981).

Finally, none of the vein quartz clasts examined to date display any fabric or composition indicative of silcrete, such as isopachous coatings of chert or jasper around detrital quartz grains, or radial-fibrous growths of chalcedony. Vein quartz seen in the Burnside clasts appears to be uniform megacrystalline quartz, too coarse to be silcrete (cf. Summerfield, 1983; Ross and Chiarenzelli, 1985).

The conglomerates in the Burnside Formation thus provide the best indication of the unroofing history of the source area. Although no single attribute of the conglomerates is diagnostic of tectonic setting, when considered collectively, several features support a foreland basin setting for the Burnside Formation. These include the unimodal, low dispersion paleoccurrent trends away from the source area; a general coarsening upwards through the entire Burnside Formation; the presence of intraformational clasts high in the stratigraphic section; and the great thickness of the formation at a distal location from the source area. Furthermore, Burnside deposits clearly prograded over and away from the zone of maximum basin subsidence (Campbell and Cecile, 1981; Grotzinger and Gall, 1986; this paper). This observation is most consistant with a foreland basin model, and argues strongly against other basin models, especially rifts and transpressional strike-slip basins in which sediment dispersal of fluvial units is almost exclusively directed away from the basin margins and into the basin center (cf. Miall, 1981; Christie-Blick and Biddle, 1985; Nilsen and McLaughlin, 1985).

ECONOMIC POTENTIAL

Disconformities of the Bear Creek Group were traversed by total-count scintillometers and measurements were taken at 1-5 km spacings. Readings appreciably greater than background were found only in one area, adjacent to the sub-Beechey disconformity. The area is located at 65° 57′N and 107° 26°W and readings of up to 50 times background were recorded.

Several Precambrian fluvial deposits contain economic concentrations of minerals, most notably detrital gold and uraninite (e.g. Witswatersrand, South Africa: Minter, 1978). The Archean basement rocks from which Burnside sediments were derived are known to contain gold, so the potential exists for remobilization and concentration of placer minerals. However, the Burnside Formation appears to lack key features associated with placer deposits. The vast majority of Burnside Formation congomerate horizons have a thin, unchannellized sheet-like geometry (cf. Minter, 1978; Andrews-Speed, 1986). The unimodal, low-dispersion paleocurrent trends in all facies suggest that the Burnside Formation was deposited on a distal alluvial plain, not an alluvial fan. There is no indication of angular unconformities at conglomerate horizons. There are few heavy mineral laminae in sandstones. There is only one interval that indicates a possible marine transgression into the basin, i.e. the Bd dolarenite, and this occurrs at the most distal location with no indication of transgressive reworking of underlying beds.

The only channelized conglomerate horizons occur at Manning Point, but these beds have an outcrop length of only a few hundred metres. Sandstones underlying these conglomerates do contain heavy mineral laminae (Sh-St assemblage), and these were beds which yielded euhedral detrital zircons. These appear to be the most promising prospects.

Perhaps another potentially more interesting prospect would be the sand-rich regoliths associated with the sub-Hackett disconformity. As discussed above,the Archean weathering surface along the trend of the Gordon Bay Arch was exposed during flexure and erosion of the Kimerot Group. This would create a situation for reworking of earlier-formed winnowed lags, allowing for further concentration of heavy minerals. Furthermore, the Gordon Bay Arch was developed over a major iron formation in the underlying Archean rocks of the Beechey Lake area. Carbonate-matrix regolith is now developed over much of the iron formation indicating that it underwent erosion during development of the sub-Hackett disconformity. Any concentration of heavy minerals derived from the Archean during this event might be preserved in regoliths that flank the crest of the Gordon Bay Arch.

CONCLUSIONS

Investigations during the 1986 field season lead to several conclusions.

1) Formations of the Bear Creek Group are bounded by laterally continuous disconformities characterized by well-developed regoliths. Regoliths exhibit distinct suites of facies that may ultimately permit enhanced intrabasinal correlation.

2) The Beechey Formation is a shallowing-upward sequence of siltstones, quartzites, and carbonates that extends for over 150 km perpendicular to depositional strike. Its internal stratigraphy reflects the same processes that control overall basin stratigraphy.

3) Lithofacies patterns interpreted from the Burnside Formation suggest that fluvial deposition occurred on a distal alluvial plain largely in response to allocyclic controls. Proximal areas were effected by tectonic controls, whereas more distal areas may have been effected by changes in sea level. Two major phases of source-area uplift are interpreted to have created two large-scale coarsening-upwards sequences. The second phase probably records the reworking of synorogenic material. These results are consistent with the interpretation of Grotzinger and Gall (1986) that the Bear Creek Group was deposited in a foreland basin and that the Burnside Formation is a culminating molasse.

ACKNOWLEDGMENTS

We gratefully acknowledge the Geological Survey of Canada for logistical support and the opportunity to work in Kilohigok Basin. Sarah Bohan, Richard Cresswell, and Kurt Roggensack are thanked for field assistance. Martin Irving provided excellent expediting services. E. Buhlmann, S. Fraser, R. Johnson, C. Stargaard are thanked for stimulating discussions. Critical reviews by P. Hoffman and R. Hildebrand helped improve earlier versions of the manuscript.

REFERENCES

Andrews-Speed, C.P.

1986: Gold-bearing fluvial and associated tidal marine sediments of Proterozoic age in the Mporokoso Basin, northern Zambia. Sedimentary Geology, v. 48, p. 193-222.

Bally, A.W., Gordy, P.L., and Stewary, G.A.
1966: Structure, seismic data and orogenic evolution of southern Canadian Rockies. Bulletin Canadian Petroleum Geology, v. 14, p. 337-381.

Beaumont, C.
1981: Foreland basins. Geophysical Journal, Royal Astronomical Society, v. 65, p. 471-498.

Calvet, F. and Julia, R.
1983: Pisoids in the caliche profiles of Tarragona (N.E. Spain), in, T.M. Peryt (ed.), *Coated Grains*. Springer-Verlag (Berlin), p. 456-473.

Campbell, F.H.A., and Cecile, M.P.
1976: Geology of the Kilohigok Basin. Geological Survey of Canada, Open File Map 332, 1:500,000 Scale.
1981: Evolution of the Early Proterozoic Kilohigok Basin, Bathust Inlet-Victoria Island, Northwest Territories, in, F.H.A. Campbell, ed., *Proterozoic Basins of Canada*. Geological Survey of Canada Paper 81-10, p. 103-131.

Christie-Blick, N., and Biddle, K.T.
1986: Deformation and basin formation along strike-slip faults, in, K.T. Biddle and N. Christie-Blick (eds.) *Strike-Slip Deformation, Basin Formation, and Sedimentation*, Society of Economic Paleontologists and Mineralogists (Tulsa, OK, USA), Spec. Pub. No. 37, p. 1-34.

Grotzinger, J.P.
1985: Evolution of Early Proterozoic passive-margin carbonate platform, Rocknest Formation, Wopmay Orogen, N.W.T., Canada. Unpublished PhD. Thesis, Virginia Polytechnic Institute and State University (Blacksburg, VA).
1986: Cyclicity and paleoenvironmental dynamics, Rocknest platform, northwest Canada, Geological Society of America Bulletin, v. 97, p. 1208-1231.

Grotzinger, J.P., and Gall, Q.
1986: Preliminary investigations of Early Proterozoic Western River and Burnside River Formations: evidence for foredeep origin of Kilohigok Basin, N.W.T., Canada, in, Current Research, Part A. Geological Survey of Canada, Paper 86-A, p. 95-106.

Grotzinger, J.P. and Hoffman, P.F.
1983: Aspects of the Rocknest Formation, Asiak fold-thrust belt, Wopmay Orogen, District of Mackenzie, in, Current Research, part B. Geological Survey of Canada Paper 83-1B, pp. 83-92.

Grotzinger, J.P. and Read, J.F.
1983: Evidence for primary aragonite precipitation, lower Proterozoic (1.9 Ga) Rocknest dolomite, Wopmay orogen, northwest Canada, Geology, v. 11, p. 710-713.

Heward, A.P.
1978: Alluvial fan sequence and megasequence models: with examples from the Westphalian D – Stephanian B coalfields, northern Spain, in, A.D. Miall (ed.), *Fluvial Sedimentology*, Canadian Society of Petroleum Geologists Memoir 5, p. 669-702.

Hoffman, P.F.
1973: Evolution of an Early Proterozoic continental margin: The Coronation geosyncline and associated aulacogens of the northwestern Canadian shield. Royal Society London, Philosophical Transactions, Series A, v. 273, p. 547-581.

Hoffman, P.F.
1969: Proterozoic paleocurrents and depositional history of the East Arm fold belt, Great Slave Lake, Northwest Territories, Canadian Journal of Earth Sciences, 6, p. 441-462.

Hoffman, P.F., Tirrul, R., Grotzinger, J.P., Lucas, S.B., and Eriksson, K.A.
1984: The Externides of Wopmay Orogen, Takijuk Lake and Kikerk Lake map areas, District of Mackenzie, in, Current Research, Part A. Geological Survey of Canada, Paper 84-1A, p. 383-395.

Hofmann, H.J.
1985: Shelf-facies microbiotas from the Odjick and Rocknest formations (Epworth Group; 1.89 Ga), northwestern Canada, Canadian Journal of Earth Sciences, v. 22, p. 1781-1792.

Miall, A.D.
1977: A review of the braided-river depositional environment, Earth Science Reviews, v. 13, p. 1-62.
1978a: Lithofacies types and vertical profile models in braided river deposits: a summary, in, A.D. Miall (ed.), *Fluvial Sedimentology*. Canadian Society of Petroleum Geologists Memoir 5, p. 597-604.
1978b: Tectonic setting and syndepositional deformation of molasse and other nonmarine-paralic sedimentary basins, Canadian Journal of Earth Sciences, v. 15, p. 1613-1632.
1981: Alluvial sedimentary basins: tectonic setting and basin architecture, in, A.D. Miall (ed.), *Sedimentation and Tectonics in Alluvial Basins*. Geological Association of Canada, Special Paper 23, p. 1-34.

Minter, W.E.L.
1978: A sedimentologic sythesis of placer gold, uraninite and pyrite concentrations in Proterozoic Witswatersrand sediments, in, A.D. Miall (ed.), *Fluvial Sedimentology*, Canadian Society of Petroleum Geologists Memoir 5, p. 801-830.

Nilsen, T.H., and McLaughlin, R.J.
1986: Comparison of tectonic framework and depositonal patterns of the Hornelen strike-slip basin of Norway and the Ridge and Little Sulphur Creek strike-slip basins of California, in, K.T. Biddle and N. Christie-Blick (eds.) *Strike-Slip Deformation, Basin Formation, and Sedimentation*, Society of Economic Paleontologists and Mineralogists (Tulsa, OK, USA), Spec. Pub. No. 37, p. 79-104.

Read, J.F.
1976: Calcretes and their distinction from stromatolites, in, M.R. Walter (ed.) *Stromatolites*, Developments in Sedimentology 20, Elsevier (New York), p. 55-71.

Retallack, G.J.
1981: Fossil soils: indicators of ancient terrestrial environments, in, K.J. Niklas (ed.), *Paleobotany, Paleoecology, and Evolution*. Praeger (New York), p. 55-102.

Retallack, G.J., Grandstaff, D.E., and Kimberley, M.M.
1984: The promise and problems of Precambrian paleosols. Episodes, v. 7, no. 2, p. 8-12.

Ross, G.M., and Chiarenzelli, J.R.
1985: Paleoclimate significance of widespread Proterozoic silcretes in the Bear and Churchill Provinces of northwestern Canadian Shield, Journal of Sedimentary Petrology, v. 55, no. 2, p. 196-204.

Rust, B.R.
1978: Depositional models for braided alluvium, in, A.D. Miall (ed.), *Fluvial Sedimentology*, Canadian Society of Petroleum Geologists Memoir 5, p. 605-625.

Summerfield, M.A.
1983: Petrography and diagenesis of silcrete from the Kalahari Basin and Cape Coastal Zone, southern Africa, Journal of Sedimentary Petrology, v. 53, no. 3, p. 895-909.

Tirrul, R.
1985: Nappes in the Kilohigok Basin and their relationship to the Thelon Tectonic Zone, District of Mackenzie, in, Current Research, Part A. Geological Survey of Canada, Paper 85-1A, p. 407-420.

Winston, D.
1978: Fluvial systems of the Precambrian Belt Supergroup, Montana and Idaho, U.S.A., in, A.D. Miall (ed.), *Fluvial Sedimentology*, Canadian Society of Petroleum Geologists Memoir 5, p. 343-359.

- 24 -

The Welsford igneous complex, southern New Brunswick: rift-related Acadian magmatism[1]

Contract 27ST.23233-5-0010

Christine Payette[2] and Robert F. Martin[2]

Payette, C. and Martin, R.F., The Welsford igneous complex, southern New Brunswick: rift-related Acadian magmatism; in Current Research, Part A, Geological Survey of Canada, Paper 87-1A, p. 239-248, 1987.

Abstract

The Welsford igneous complex contains the association quartz syenite, alkali granite, porphyritic granite and granophyre. Minor quantities of hybrid and more basic rocks are also exposed. Mineralogical and geochemical data indicate that the suite is anorogenic and has not been reheated since its emplacement. The granite is peralkaline and locally enriched in Zr, Nb, Y and Rb. The suite is considered to be Early Devonian and associated with Late Silurian ignimbritic felsic volcanic rocks that share some geochemical indications of a peralkaline ancestry. A Late Silurian-Early Devonian period of rift-related igneous activity may have followed a cycle of crustal shortening in the area.

Résumé

Le complexe igné de Welsford contient l'association de syénite quartzifère, granite alcalin, granite porphyritique et granophyre. Leurs sont associées des roches hybrides et d'autres plus mafiques, en quantités moins importantes. Les données minéralogiques et géochimiques montrent que ces roches constituent une suite anorogénique qui n'a pas été réchauffée depuis sa mise en place. Le granite est hyperalcalin et localement enrichi en Zr, Nb, Y et Rb. Le complexe aurait été mis en place au début du Dévonian et serait associé à des roches volcaniques felsiques ignimbritiques qui partagent certains indices d'une filiation hyperalcaline. Une période d'extension qui s'étend du Silurien supérieur au Dévonien inférieur pourrait avoir suivi un épisode de compression dans cette région.

[1]Contribution to the Canada-New Brunswick Mineral Development Agreement, 1984-1989.
[2]Department of Geological Sciences, McGill University, 3450 University Street, Montreal, Quebec H3A 2A7.

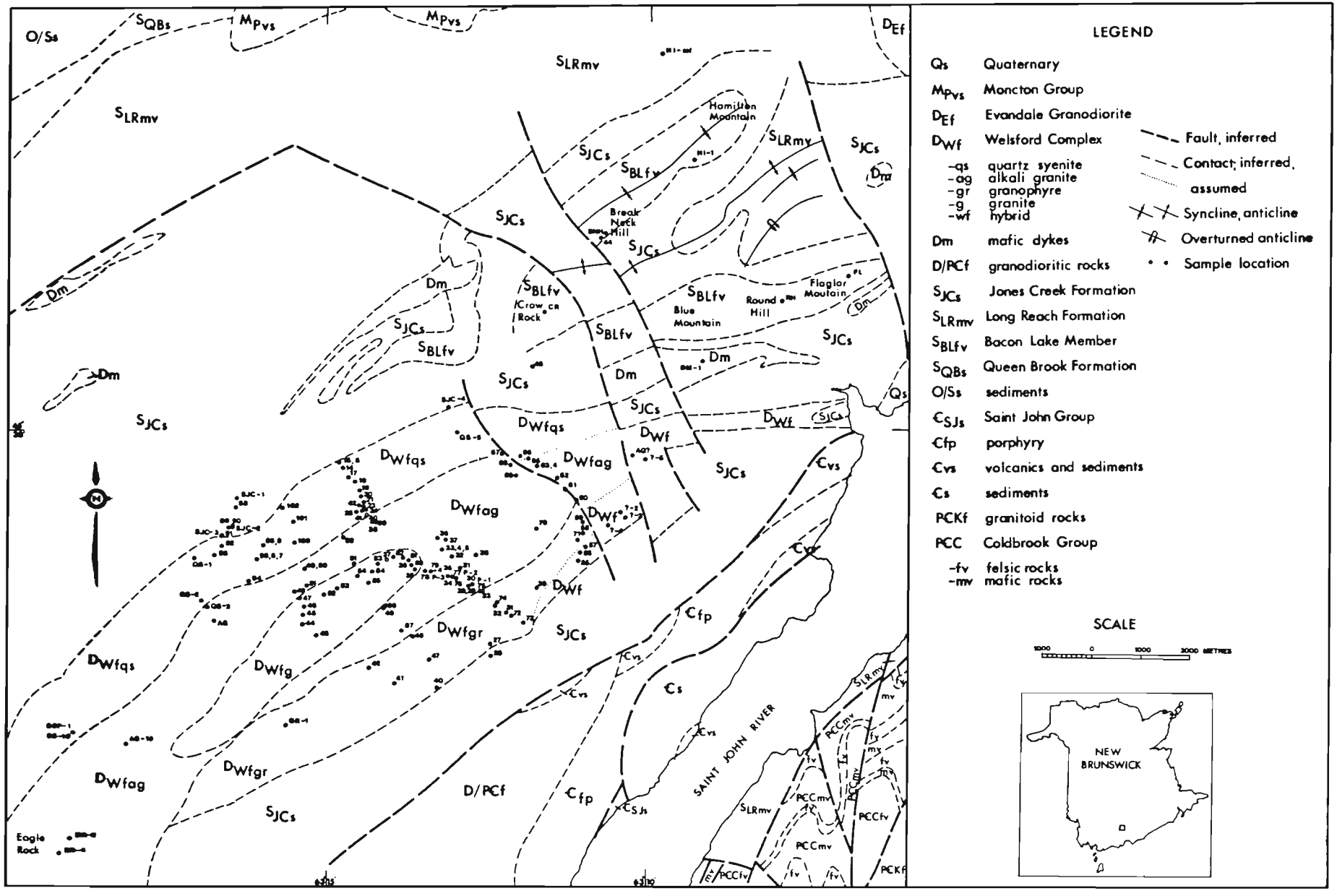


Figure 24.1 Sample location map, Welsford complex and adjoining areas in southern New Brunswick. The definition of the various units follows that of McCutcheon and Ruitenberg (in press), and is explained in the text.

INTRODUCTION

The Welsford igneous complex, southern New Brunswick, has been interpreted as an elongate northeasterly trending protrusion of the St. George granitic batholith (Fig. 24.1). Alcock (1941) considered it Middle Devonian, as do McCutcheon and Ruitenberg (in press); it intrudes locally fossiliferous rocks of the Silurian Jones Creek Formation. Preliminary Rb-Sr geochronological data (R.F. Cormier, personal communication, 1986) indicate an age of emplacement in the Earliest Devonian (Gedinnian). As the eastern half of the St. George batholith is now known to be Early Carboniferous (Visean; R.F. Cormier, personal communication, 1986), the Welsford complex can no longer be viewed as an appendage of the St. George (*cf.* Cherry, 1976).

The Welsford complex differs from the eastern part of the St. George not only in age, but also in lithology. Both contain granitic rocks, but those in the Welsford complex are dominantly of alkaline affinity, whereas those in the eastern portion of the St. George are mildly peraluminous. In addition, the Welsford suite contains more basic rocks (e.g., syenite, diorite, gabbro), whereas the St. George batholith is predominantly granitic in its eastern part. This paper presents information that clearly establishes the Welsford complex as anorogenic and rift-related.

The area was recently remapped by S.R. McCutcheon and A.A. Ruitenberg (in press) who build on the earlier work of Sharpe (1958) and MacKenzie (1964a, b). We have retained their five-fold subdivision: from north to south, in three bands roughly parallel to the outer contacts, (1) alkali quartz syenite and alkali syenite (DWfqs), (2) alkali granite and alkali quartz syenite (DWfag), and (3) granophyric and fine grained alkali granite (DWfgr). Also mapped are smaller bodies of porphyritic granite (DWfg, 4) and hybrid and more basic rocks (DWf, 5).

THE VOLCANIC ENVELOPE

The plutonic rocks of the Welsford complex crosscut Silurian rocks, primarily of the Jones Creek Formation (Fig. 24.1). These rocks consist mostly of laminated siltstone and fine grained sandstone. The Bacon Lake Member, however, is volcanic and occurs in two roughly linear belts: (1) Break Neck Hill (BNH), Crow Rock (CR) and Hamilton Mountain (HI), and (2) Blue Mountain, Round Hill (RH) and Flaglor Mountain (FL). These localities were sampled because we consider them genetically related to the plutonic rocks mentioned above. Specifically, they seem to consist dominantly of pyroclastic (ignimbritic) felsic volcanic material into which the plutonic suite was emplaced, shortly after the evacuation of the water-saturated upper portion of the Welsford magma reservoir. Isotopic data will be sought, to test this hypothesis. Here we report bulk-composition data on the volcanic envelope and the granitic and syenitic rocks that strongly suggest that the Welsford suite should be considered to include the felsic volcanic rocks.

CHEMICAL COMPOSITION OF THE WELSFORD ROCKS

The bulk chemical composition of the granitic and syenitic plutonic rocks sampled has been determined by standard X-ray fluorescence techniques. The data define an almost continuous population in a triangular plot of normative quartz, albite and orthoclase (Fig. 24.2). The distribution of points corresponds to the low temperature though on the liquidus in the water-saturated haplogranite system at low confining pressures (Tuttle and Bowen, 1958). Along this trend, Ca and Mg are uniformly very low, so that the points are in fact close to the plane of the projection. One can tentatively conclude, from the distribution of data points, that magma differentiated efficiently in the upper crust to produce evolved granitic compositions. The presence of pegmatitic pods and miarolitic cavities in the granites suggest that the granitic liquids achieved water saturation during their crystallization. The proximity of many points to the cotectic curve relative to a confining pressure of 1 kilobar in the water-saturated system is consistent with this proposal.

The same data are shown in a portion of the diagram $SiO_2 - Al_2O_3 - (Na_2O + K_2O)$ (Fig. 24.3). The vertical line in this plot reflects the equality $(Na + K) = Al$. It is immediately apparent that the syenitic bulk compositions straddle the line, but the granitic compositions are markedly peralkaline. The data points are scattered and do not define a single vector into the peralkaline field, as could have been expected if a marginally peralkaline syenitic luquid were fractionating alkali feldspar (in which $Na + K = Al$). This scatter may indicate that the peralkalinity in the granites is acquired at an early postmagmatic stage via a gas phase of magmatic derivation (e.g., Ike et al., 1984). Perhaps an even more likely hypothesis is that both statements are true, i.e., peralkalinity is a property that characterized the granitic liquids that evolved by fractionation at Welsford, but the magmatic vapour phase that separated upon crystallization "back-reacted" with the hot silicates to enhance their alkalinity in many instances. This could also account for the marginally subalkaline (metaluminous) compositions of some members of the suite.

CHEMICAL COMPOSITION OF THE VOLCANIC ROCKS

McCutcheon and Ruitenberg (in press) considered the volcanic rocks of the Bacon Lake Member to be dominantly composed of flow-banded dacite and compositionally similar flow breccia. Our field evidence, petrographic studies and chemical data (Table 24.1) show that the dominant lithology is ignimbritic and rhyolitic (BNH, CR) or rhyodacitic (RH, FL, HI) in composition. These tuffs are devitrified, and their texture varies from eutaxitic (BNH) to granophyric (RH). The dominant phenocryst phase is alkali feldspar (originally sanidine, now presumably orthoclase perthite), and quartz is present only in the devitrified, aphanitic groundmass.

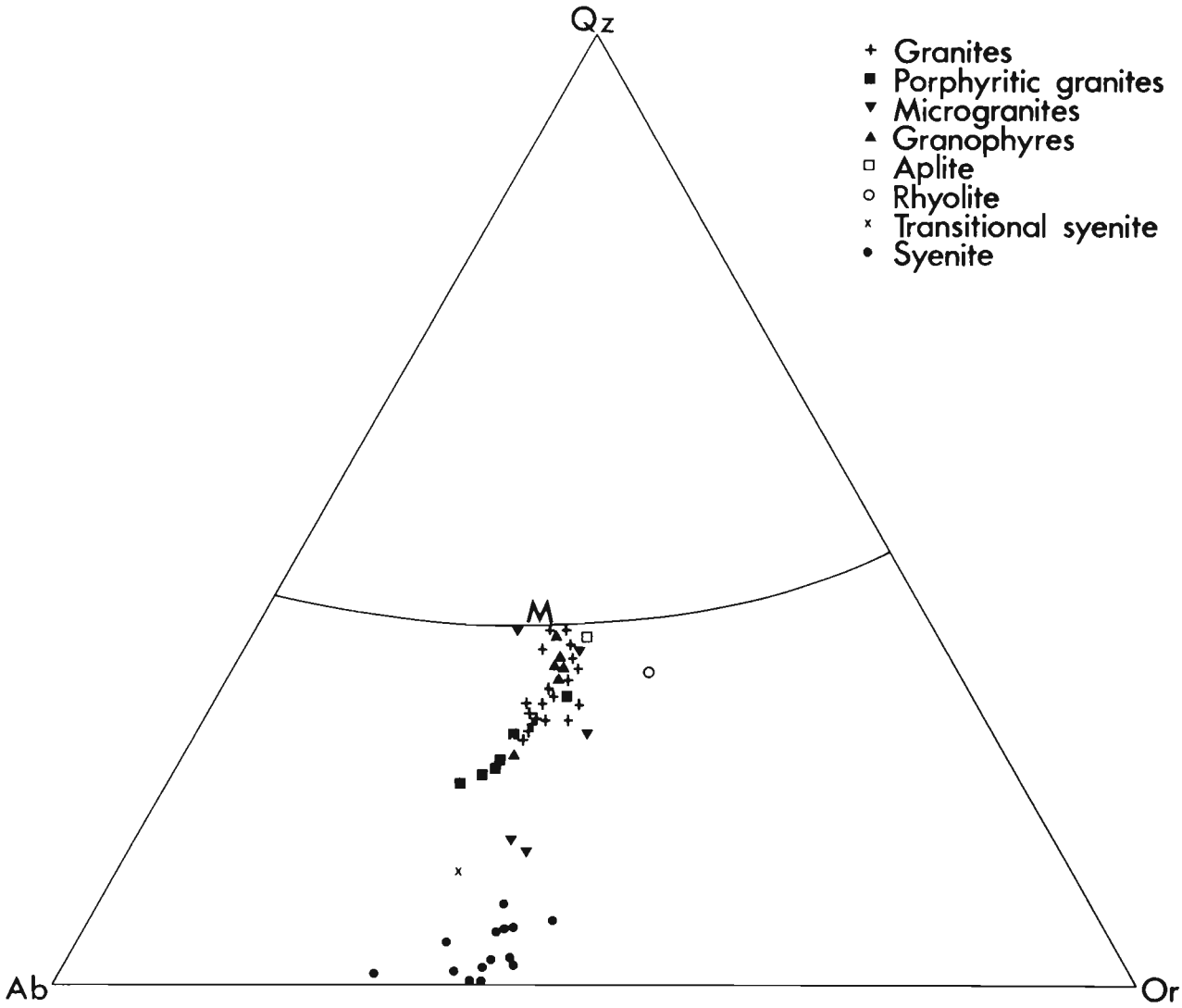


Figure 24.2 Bulk composition of representative samples of the various map units in the Welsford igneous complex, plotted in terms of the normative constituents quartz, albite and orthoclase. The letter M represents the pseudo-ternary minimum along the cotectic separating the primary fields of quartz and alkali feldspar. The points conform to the thermal trough on the liquidus, and suggest that the bulk compositions are, *gross modo*, representative of the liquids from which they crystallized.

The chemical composition of the felsic volcanic rocks is not peralkaline; the agpaitic index (Na + K)/Al ranges from 0.92 to 0.97. However, the rocks contain between 550 and 744 ppm Zr and approximately 20 ppm Nb and 115 ppm Y (Table 24.1). These concentrations are high, and characteristic of peralkaline felsic volcanic rocks. A hypothesis that will be tested with more complete information would attribute the marginally subalkaline bulk compositions to net loss of some Na and K during the devitrification of these volcanic rocks. Note that the representative bulk composition of peralkaline Welsford granite in Table 24.1 (agpaitic index 1.25) contains 612 ppm Zr, 53 ppm Nb and 26 ppm Y.

MINERALOGY OF SELECTED PLUTONIC ROCKS

The quartz syenite (DWfqs) is dominated by brownish orthoclase mesopherthite (see below). Oligoclase (An_{81}) occurs as a xenocrystic phase. Less than 10% of the volume of the rock consists of complicated clusters of mafic minerals: fayalite, ferroaugite, ferro-edenite and ferro-hornblende, the amphibole commonly as a rim. Biotite may also be present as an accessory. Representative data are provided in Table 24.2. The fayalite is very close to the end member, and is commonly partly oxidized to hematite and replaced by "iddingsite".

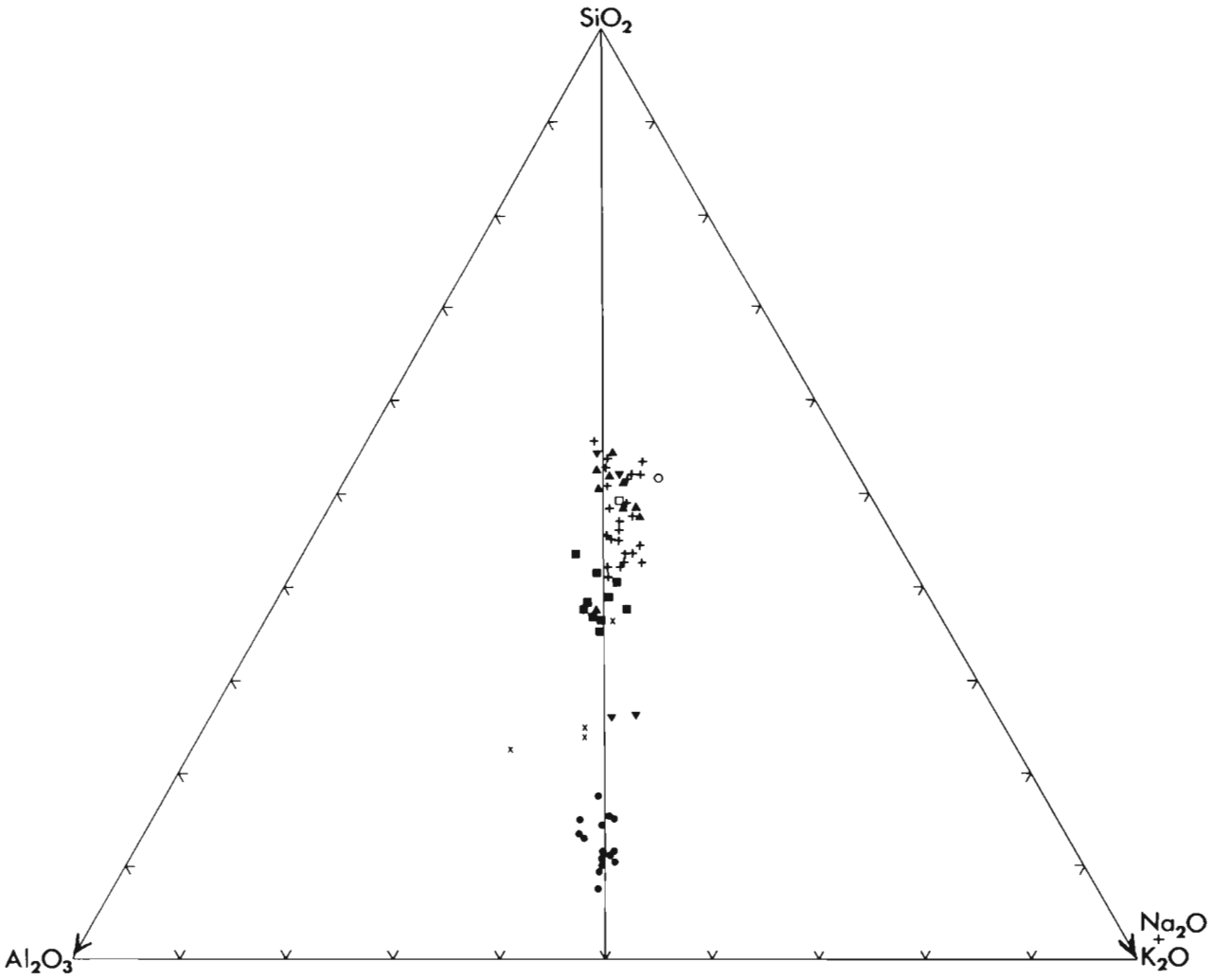


Figure 24.3 The same bulk compositions as shown in Figure 24.2 are here plotted in terms of molar proportions of SiO_2, Al_2O_3 and $Na_2O + K_2O$. The feldspars $NaAlSi_3O_8$ and $KAlSi_3O_8$ plot at the intersection of the base of the diagram with the vertical line, along which $Na + K = Al$. Note that most granitic rocks in the Welsford suite are peralkaline.

Also present are granules of ilmenite, needles of apatite and very coarse grains of zircon.

Pegmatitic pockets are also developed in more basic rocks of hybrid origin. Table 24.3 contains electron microprobe data relevant to such a pocket in specimen QSP-1. The pocket is devoid of olivine, but does contain augite and magnesio-hornblende rimmed by ferro-actinolite. Accessory phases include ilmenite, titanite, two varieties of apatite, chlorine-rich (included in amphibole) and fluorine-rich (intergranular position), and abundant Fe-rich prehnite (Zolotukhin et al., 1965) and epidote.

The alkali granite (DWfag) contains numerous pegmatite pockets, which are dominantly composed of cream microcline perthite and interstitial amphibole. A dominant composition for the amphibole is titanian arfvedsonite that is relatively fluorine-rich (Table 24.4). Sodian hedenbergite is also present as a primary phase. Clinopyroxene is also found as a rim on the amphibole, and ranges from aegirine-augite to aegirine. Preliminary microprobe work on the accessory minerals reveals the presence of apatite, zircon, aenigmatite, rare astrophyllite (Table 24.4). The astrophyllite occurs as prismatic orange to yellow crystals that are compositionally highly variable; in particular, uranium is not uniformly distributed in the crystals (concentrated in the yellow portions, absent in the orange portions). Uranium is not usually found in astrophyllite, and levels of titanium are not usually so high (Macdonald and Saunders, 1973). At least three different

Table 24.1 Average chemical composition* of the different members of the Welsford intrusive complex and associated rocks.

	SJC (3)	BNH (4)	CR (1)	RH (1)	FL (1)	HI (1)	HI-mf (1)	DM (1)	QS (4)	QS-10 (2)	MQS (1)	AG (1)	G (1)	?-2 (1)
SiO_2	62.63	72.72	73.81	69.25	70.91	69.25	59.66	46.56	63.14	47.68	55.75	74.61	72.72	74.52
TiO_2	0.92	0.21	0.21	0.29	0.22	0.32	1.22	1.91	0.61	2.86	2.02	0.16	0.26	0.23
Al_2O_3	17.69	12.61	13.05	13.56	13.27	13.19	15.10	16.35	16.72	13.54	14.48	10.21	13.14	11.62
Fe_2O_3**	7.24	3.22	2.85	4.94	3.78	5.30	10.21	12.63	5.25	15.00	11.07	5.27	2.61	3.32
MnO	0.09	0.06	0.04	0.12	0.09	0.12	0.18	0.19	0.12	0.20	0.16	0.09	0.04	0.06
MgO	2.43	0.14	0.01	0.07	0.04	0.09	1.72	7.13	0.37	5.65	3.15	0.00	0.27	0.00
CaO	1.09	0.86	0.61	1.15	0.93	1.48	3.22	9.45	1.73	9.61	6.22	0.08	0.86	0.23
Na_2O	1.59	4.36	5.91	4.93	5.23	4.74	5.55	3.18	5.50	3.32	4.76	5.04	4.63	4.46
K_2O	3.81	4.36	2.66	4.08	3.89	4.01	1.30	0.72	5.89	1.12	1.92	4.09	4.76	4.65
P_2O_5	0.10	0.02	0.01	0.04	0.02	0.04	0.53	0.23	0.16	0.30	0.25	0.01	0.04	0.02
L.O.I.	2.60	0.95	0.74	1.25	1.08	0.84	1.57	2.47	0.47	1.35	0.42	0.37	0.48	0.49
Total	100.20	99.51	99.95	99.75	99.46	99.49	100.29	100.91	99.96	100.64	100.23	99.88	99.85	99.57
Trace elements (ppm)														
Ba	357	703	491	683	635	641	116	321	511	117	80	0	253	39
V	108	5	0	6	0	0	42	288	17	445	257	0	32	11
Cr	108	0	159	0	0	2	36	0	0	127	26	0	0	0
Ni	82	2	61	16	0	48	98	0	0	64	9	0	0	0
Nb	20	20	20	17	17	19	20	10	18	23	27	53	25	67
Zr	218	550	577	744	602	607	390	123	507	321	418	612	355	886
Y	38	117	112	119	122	104	86	35	48	56	65	26	60	97
Sr	136	87	75	94	52	227	350	386	107	249	219	4	48	7
Rb	158	124	70	134	125	95	55	32	12	20	17	18	22	21
Th	9	12	11	9	10	7	2	0	1	2	3	7	22	17
U	6	6	10	5	3	8	11	13	8	12	10	0	1	3
Na_2O/K_2O	0.65	1-3.9	3.38	1.84	2.04	1.80	6.49	6.72	1.46	4.53	3.77	1.87	1.48	1.46
Na + K/Al	0.38	0.94	0.97	0.92	0.97	0.92	0.70	0.37	0.92	0.49	0.68	1.25	0.97	1.07

SJC – Jones Creek Formation
BNH – Break Neck Hill
CR – Crow Rock
RH – Round Hill
FL – Flaglor Mountain
HI – Hamilton Mountain
HI-mf – Hamilton Mountain, mafic volcanics,
DM – Devonian mafics
QS, QS-10, MQS – quartz syenite
AG – alkali granite
G – granite
?-2 – hydrid unit (see Fig. 24.1).

*Chemical composition obtained by X-ray fluorescence.
**Fe total as Fe_2O_3.
Numbers in brackets = number of analyses

niobium- and tantalum-bearing rare-earth minerals have been found, but as yet are not fully characterized owing to incomplete analyses by electron microprobe. However, pyrochlore and chevkinite are tentatively identified. Rutile has been mentioned as an accessory by McCutcheon and Ruitenberg (in press), but has not been found in the sections studied by microprobe. Elpidite has been confirmed as a secondary phase filling miarolitic cavities in the alkali granite (X-ray diffraction study).

FELDSPAR MINERALOGY OF THE WELSFORD ROCKS

Preliminary information is provided in terms of a plot of the cell dimensions *b* versus *c* (Fig. 24.4). The five samples of syenite considered are hypersolvus rocks, and contain orthoclase mesoperthite. In contrast, the five samples of alkali granite, also good examples of the hypersolvus texture, contain intermediate microcline. In one case, the microcline coexists with orthoclase (tie line in Fig. 24.4). Two of the granite samples contain microcline that plots outside the *b-c* quadrilateral. Three samples of granophyre and one of porphyritic granite also contain intermediate microcline. All the samples examined contain a K-rich feldspar that is very close to the end member composition, to judge from the proximity of the data points to the HS-LM sideline.

The feldspar mineralogy of the samples examined so far indicates that the complex has not been affected by any important thermal event after its cooling. Such reheating would have eliminated the metastable forms of K-feldspar recorded here at the expense of low microcline (absent at Welsford). The orthoclase that is typical of the syenite is a

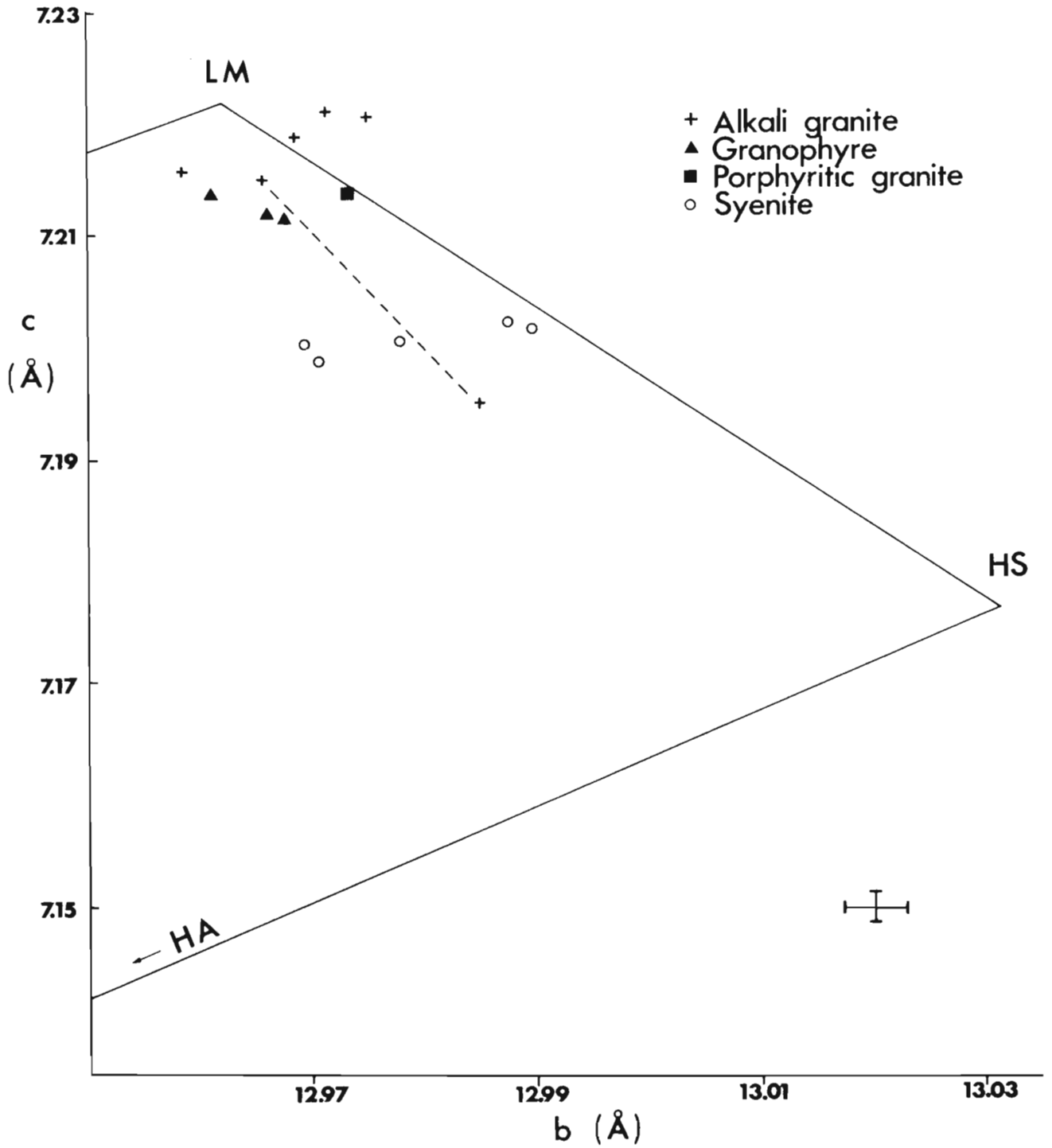


Figure 24.4 Mineralogy of the K-rich feldspar in selected granitic and syenitic rocks at Welsford, as determined by relative position of the data points in a plot of *b* versus *c*. Symbols: LM low microcline, HS high sanidine, HA high albite.

Table 24.2 Chemical composition of the major and accessory minerals in the quartz syenite (QS-5).

	Px (4)	Amp 1 (3)	Amp 2 (3)	Fa (2)	Oli (2)	Bio (2)	Ilm (3)	Ap (4)	Zir (2)
SiO_2	50.13	47.55	43.06	30.82	65.60	33.85	—	0.32	33.46
TiO_2	0.26	0.46	1.91	0.09	0.02	4.75	53.47	0.07	0.06
Al_2O_3	0.55	3.94	6.90	0.01	22.04	11.56	0.00	0.00	0.00
Fe_2O_3	0.04	6.84	2.08	—	0.17	0.00	0.10	—	—
FeO	20.64	24.23	24.94	62.72	—	33.46	45.58	0.19	0.00
MgO	5.89	4.46	4.67	3.18	0.00	2.20	0.04	0.00	0.01
MnO	0.65	0.67	0.50	2.24	—	0.17	1.78	0.07	0.00
CaO	20.70	10.19	10.60	0.09	3.34	0.08	—	55.43	0.01
Na_2O	0.33	1.17	2.06	0.02	9.12	0.07	—	0.14	0.00
K_2O	—	0.53	1.11	0.00	0.47	8.95	—	0.00	0.00
P_2O_5	—	—	—	—	—	—	—	42.58	—
ZrO_2	—	—	—	—	—	—	—	—	65.78
F	—	0.11	0.24	—	—	0.08	—	2.88	—
Cl	—	0.41	0.61	—	—	0.89	—	0.17	—
O = F, Cl	—	0.14	0.24	—	—	0.23	—	1.25	—
Total	99.18	99.74	98.24	99.17	100.76	95.83	100.97	100.60	99.32
Ab					80.89				
Or					2.76				
An					16.35				

Px – ferroaugite
Ampl – ferrohornblende
Amp 2 – ferroedenite (Leake, 1978)
Fa – fayalite
Oli – oligoclase
Bio – biotite
Members in brackets = number of samples
Ilm – ilmenite
Ap – apatite
Zir – zircon
All analyses by electron microprobe
— not determined

product of the Al-Si ordering and exsolution of a magmatic (disordered) sanidine solid-solution. As the orthoclase entered the field of microcline, below 400°C or so, it failed to invert. We contend that this failure is due to the relative shortage of magmatically derived water in the syenitic liquids, and to the relative unimportance of infiltration of meteoric water into this unit. Such an observation is consistent with the preservation of fayalite in the syenites. In the case of the granites, crystallized from liquids that did contain a higher amount of dissolved water and that commonly did achieve water saturation during their crystallization, the conversion to microcline did occur, although vestiges of the orthoclase are still present. The water, which likely was largely of magmatic derivation, did catalyze the extremely sluggish ordering reaction, but complete conversion to low microcline was not achieved. The intermediate microcline that characterizes these rocks is viewed as a metastable intermediate product. Most likely, the length of time at which the assemblage could react with water was not sufficiently long.

In some very evolved granites, the buildup of rubidium concentrations is held responsible for the expansion of *b* and *c*, so that points plot outside the quadilateral. The same rocks are expected to also contain the highest concentrations of the incompatible elements.

TECTONIC IMPLICATIONS

The alkali granite characteristic of the Welsford suite is mildly to strongly peralkaline. Associated granophyric rocks and the felsic volcanic suite are at present subalkaline in most instances, but from concentrations of Zr, Nb and Y, they are inferred to have been peralkaline and to have lost Na and K, probably during devitrification and deuteric adjustments affecting these fine grained assemblages. Clearly, more work needs to be done concerning the detailed geochemistry of the volcanic members of the association, to firmly establish their petrological affiliation.

Although a considerable body of literature exists on the age of emplacement and petrochemistry of granitic rocks in New Brunswick (e.g., Fyffe et al., 1981; Ruitenberg and Fyffe, 1982), appropriate tectonic reconstructions using these data, consistent with findings in tectonically less complicated terranes, do not seem to have been made. The Welsford suite is characteristically anorogenic. By analogy with petrologically similar suites (Black et al., 1985), in Niger and Nigeria, for example (Bowden and Turner, 1974), we contend that the tectonic setting at the time of emplacement, considered to have been in the Late Silurian to Early Devonian, was one of distension. Unlike the Nigerian magmatic centres,

Table 24.3 Chemical composition of the major and accessory minerals in the diorite pocket pegmatite (QSP-5).

	Ab (4)	Ampl (6)	Amp2 (9)	Ilm (5)	Tita (3)	Epi (3)	Preh (5)	Apl (1)	Ap2 (4)	Px (1)
SiO_2	70.85	48.89	49.25	—	30.74	38.31	42.96	0.18	0.12	51.80
TiO_2	0.00	1.42	0.07	51.48	40.92	0.03	0.05	0.01	0.03	1.04
Al_2O_3	19.42	4.73	3.50	0.01	0.75	22.36	19.84	0.01	0.01	2.41
Fe_2O_3	0.04	5.60	0.71	1.40	—	—	—	—	—	0.00
FeO	—	13.39	24.11	43.92	0.62	12.06	6.96	0.29	0.05	8.12
MgO	0.00	11.19	6.54	0.06	0.00	0.00	0.08	0.00	0.00	13.78
MnO	0.00	0.36	0.26	1.45	0.01	0.03	0.09	0.14	0.02	0.30
CaO	0.07	10.44	11.67	0.00	27.75	22.67	24.29	52.72	55.03	21.12
Na_2O	10.43	1.27	0.57	0.00	0.00	0.00	0.01	0.17	0.01	0.55
K_2O	0.04	0.47	0.36	0.00	0.00	0.00	0.01	0.00	0.00	—
P_2O_5	—	—	—	—	0.09	0.03	0.03	40.80	42.58	—
F	—	0.06	0.03	—	0.06	0.00	—	1.13	1.98	—
Cl	—	0.33	0.52	—	0.00	0.00	—	2.53	0.40	—
O = F, Cl	—	0.10	0.13	—	0.03	0.00	—	1.06	0.92	—
Total	100.85	97.49	97.46	98.32	100.91	95.49	94.34	96.92	99.31	99.12
Ab	99.36									
Or	0.26									
An	0.38									

Ab – albite
Ampl – magnesiohornblende
Amp 2 – ferroactinolite
Ilm – ilmenite
Tita – titanite
Epi – epidote
Preh – Fe-rich prehnite
Apl – Cl-apatite
Ap 2 – F-apatite
Px – augite
All analyses by electron microprobe
— not determined
Members in brackets = number of samples

Table 24.4 Chemical composition of the major and accessory minerals in an alkali granite pocket pegmatite (AG-P1).

	Ab[1] (1)	Or (1)	Amp (7)	Pxl (4)	Px2 (4)	Px3 (2)	Zir (2)	Ast (1)	Aen (1)
SiO_2	69.84	66.12	50.22	49.52	52.08	50.62	31.97	35.57	41.24
TiO_2	0.00	0.00	2.09	0.37	1.23	0.31	0.02	12.47	9.71
Al_2O_3	19.14	17.77	0.77	0.16	0.18	0.44	0.00	1.02	0.59
Fe_2O_3	—	—	0.9	4.3	24.4	15.5	—	—	—
FeO	0.52	0.46	32.18	25.36	6.68	14.00	0.05	35.06	40.67
MgO	0.00	0.00	0.29	0.90	0.08	0.75	0.00	0.04	0.03
MnO	0.00	0.00	0.87	0.92	0.34	0.69	0.00	2.08	1.28
CaO	0.00	0.00	1.78	16.79	4.74	11.49	0.00	1.42	0.17
Na_2O	10.50	0.94	7.94	2.20	10.94	6.51	0.01	1.92	7.85
K_2O	0.10	15.66	1.48	0.00	0.00	0.00	0.00	5.62	0.01
P_2O_5	0.00	0.01	—	—	—	—	0.23	0.01	—
ZrO_2	—	—	0.14	0.06	1.00	0.18	58.34	0.59	0.04
UO_2	—	—	—	—	—	—	—	3.03	—
F	—	—	0.88	—	—	—	—	0.71	0.01
Cl	—	—	0.01	—	—	—	—	0.00	0.00
O = F, Cl	—	—	0.37	—	—	—	—	0.29	0.00
Total	100.10	100.96	99.10	100.56	101.63	100.47	90.62	99.25	101.60
Ab	99.38	8.36							
Or	0.00	91.64							
An	0.00	0.00							

Ab – albite
Or – orthoclase
Amp – titanian arfvedsonite (Leake, 1978)
Pxl – Sodian ferro-hedenbergite
Px2,3 – aegirine-augite (Deer et al., 1978)
Zir – zircon
Ast – astrophyllite
Aen – aenigmatite.
— not determined
Members in brackets = number of samples

whose surface expressions are isolated or nested ring complexes, the Welsford magmatic centre seems to have been controlled by a graben. Along strike of the Welsford complex are the Evandale granitic pluton and the Stewarton gabbro-diorite complex, both assigned to the "mafic-felsic association" by Fyffe et al. (1981). Both are considered coeval, and seem to have been emplaced at a shallow level in the crust during an episode of regional extension in southern New Brunswick.

The period of extension indicated by the occurrence of alkaline magmatism may represent a time of relaxation soon after an episode of crustal compression. The Acadian Orogeny, which caused deformation in the host rocks in the area, must have been relatively brief and must have waned by the time of the intrusion into the crust of mantle-derived alkaline basic magmas that ultimately differentiated to give the Welsford suite. An accurate determination of the age of the complex, which, according to feldspar mineralogy, has not been reheated since its crystallization, clearly should be sought to provide a constraint on the timing of the inception of rifting in this area. An environment of rifting is widely accepted for the formation of the thick clastic wedges of Upper Devonian and Carboniferous age in this area. The hypothesis that rifting was in fact locally important in late Silurian time, as seems indicated by the igneous rocks described in this paper, requires a re-evaluation of the true nature of the Acadian event in this region. Certainly, not all "so-called" Acadian granites are of calc-alkaline affiliation.

ACKNOWLEDGMENTS

We are grateful to the officers of Range Control, Camp Gagetown, for access to the northern part of the Welsford igneous complex. Farid Shahzada provided able field assistance. S.R. McCutcheon, of the New Brunswick Department of Natural Resources, provided excerpts from the Annidale-Nerepis report in advance of publication.

REFERENCES

Alcock, F.J.
1941: The geology of Long Reach, King's County, New Brunswick; Trans. Royal Society of Canada, Transactions, v. 4, p. 17-24.

Black, R., Lameyre, J., and Bonin, B.
1985: The structural setting of alkaline complexes; Journal of African Earth Sciences, v. 3, p. 5-16.

Bowden, P. and Turner, D.C.
1974: Peralkaline and associated ring-complexes in the Nigeria–Niger province, West Africa; in the Alkaline Rocks H. Sorensen (ed.), J. Wiley & Sons, London.

Cherry, M.E.
1976: The petrogenesis of granites in the St. George Batholith, southwestern New Brunswick, Canada; unpublished Ph.D. thesis, University of New Brunswick, Fredericton, N.B.

Deer, W.A., Howie, R.A., and Zussman, J.
1978: Rock-Formating Minerals, v. 2A. Single-Chain Silicates (2nd edition). Longman, London.

Fyffe, L.R., Pajari, G.E., Jr., and Cherry, M.E.
1981: The Acadian plutonic rocks of New Brunswick; Maritime Sediments and Atlantic Geology, v. 17, p. 23-36.

Ike, E.C., Bowden, P., and Martin, R.F.
1984: Fayalite and clinopyroxene in the porphyries of the Tibchi anorogenic ring-complex, Nigeria: postmagmatic initiation of a peralkaline trend; Canadian Mineralogist, v. 22, p. 401-409.

Leake, B.E.
1978: Nomenclature of amphiboles; Canadian Mineralogist, v. 16, p. 501-520.

Macdonald, R. and Saunders, M.J.
1973: Chemical variation in minerals of the astrophyllite group; Mineralogist Magazine, v. 39, p. 97-111.

MacKenzie, G.S.
1964a: Geology of the Saint John map-area, New Brunswick; Geological Survey of Canada, Map 1113A.
1964b: Geology of the Hampstead map-area, New Brunswick; Geological Survey of Canada, Map 1114A.

McCutcheon, S.R. and Ruitenberg, A.A.
— Geology and mineral deposits of the Annidale-Nerepis area; New Brunswick Department of Natural Resources, Report (in press).

Pajari, G.E., Jr., Trembath, L.T., Cormier, R.F., and Fyffe, L.R.
1974: The age of the Acadian deformation in southwestern New Brunswick; Canadian Journal of Earth Sciences, v. 11, p. 1309-1313.

Ruitenberg, A.A. and Fyffe, L.R.
1982: Mineral deposits associated with granitoid intrusions and related subvolcanic stocks in New Brunswick and their relationship to Appalachian tectonic evolution; Canadian Institute of Mining and Metallurgy, Bulletin, v. 75(842), p. 83-97.

Sharpe, J.I.
1958: The Welsford Igneous Complex; unpublished M.Sc. thesis, University of New Brunswick, Fredericton, N.B.

Tuttle, D.F. and Bowen, N.L.
1958: Origin of granite in the light of experimental studies in the system $NaAlSi_3O_8$–$KAlSi_3O_8$–SiO_2–H_2O; Geological Society of America, Memoir 74.

Zolotukhin, V.V., Vasil'yev, Y.R., and Zyuzin, N.J.
1965: Iron-rich modification of prehnite and a new diagram for prehnites; Doklady Akademiia Nauk SSSR, v. 164, p. 138-141.

- 25 -

Uranium investigations in Canada, 1986

Project 750010

V. Ruzicka and G.M. LeCheminant
Mineral Resources Division

Ruzicka, V. and LeCheminant, G.M., Uranium investigations in Canada, 1986; in Current Research, Part A, Geological Survey of Canada, Paper 87-1A, p. 249-262, 1987.

Abstract

In the course of regional uranium resource assessment, key areas and deposits were studied. Some results of these studies are presented in this paper.

The Cigar Lake deposit, Saskatchewan, is a typical representative of deposits associated with the sub-Athabasca unconformity. The uranium and uranium-polymetallic ores of this deposit formed as a re-mobilized concentration of uranium and associated metals. Distribution of uranium minerals of the Eagle Point and Dominique-Peter deposits in the Collins Bay area and the Carswell Structure, respectively, is structurally controlled by major faults and/or mylonite zones. These deposits are representatives of vein-like mineralization indirectly associated with unconformities.

Uranium-titanium aggregates and presence of kerogen in Huronian uraniferous conglomerates support the idea of placer-type mineral concentration and subsequent diagenetic modification.

The newly discovered uranium occurrences in the Appalachian Orogen are associated with Devonian and Mississippian intrusive rocks and with euxinic sedimentary rocks.

Résumé

Des zones et des gisements clés ont été étudiés au cours d'une évaluation régionale des ressources d'uranium. Ce rapport présente quelques-uns des résultats de ces études.

Le gisement de Cigar Lake, en Saskatchewan, est caractéristique des gisements associés à la discordance trouvée sous la formation d'Athabasca. L'uranium et les minerais uranifères polymétalliques du gisement se sont accumulés sous forme de concentrations remises en mouvement d'uranium et de métaux associés. La répartition des minéraux uranifères du gisement d'Eagle Point près de Collins Bay et du gisement Dominique-Peter dans la structure de Carswell, est contrôlée par la présence de failles majeures, de zones mylonitiques ou les deux. Ces gisements sont caractéristiques de la minéralisation en filons qui est indirectement associée aux discordances.

La présence de kérogène et d'aggrégats d'uranium et de titanium dans les conglomérats uranifères huroniens porte à croire que les minéraux se sont concentrés sous forme de placer et qu'ils ont ensuite été modifiés par diagénèse.

Les venues d'uranium nouvellement découvertes dans l'orogène des Appalaches sont associées à des roches intrusives mississippiennes et dévoniennes et à des roches sédimentaires euxiniques.

INTRODUCTION

In 1986 studies of Canadian uranium resources focussed on producing mines, deposits under development and on recently discovered occurrences.

In 1986 Canada continued as the world's leading producer and exporter of uranium, maintaining the level of 1985 production of about 11 000 tonnes of uranium in concentrates. The mining centres are at Elliot Lake, Ontario, and at Key Lake, Rabbit Lake – Collins Bay and Cluff Lake, Saskatchewan. The recoverable resources of uranium in these deposits in measured, indicated and inferred categories are 545 000 tonnes of uranium metal as of 1 January 1986 (Energy, Mines and Resources, 1986).

During 1986 several deposits were under development, namely the Deilmann orebody at Key Lake; the Collins Bay 'B' zone; the Cigar Lake, the world's largest high grade uranium-polymetallic deposit; and some of the Dominique-Peter zones at Cluff Lake, all in Saskatchewan.

Exploration for uranium during the year was principally oriented to areas favourable for uranium and uranium-polymetallic deposits associated with Proterozoic unconformities as well as to extensions of identified deposits. The centres of exploration activity were the Athabasca Basin region in northern Saskatchewan, the Baker Lake-Thelon Basin region in the District of Keewatin, and some areas in the District of Mackenzie. In New Brunswick investigations under the Federal-Provincial Mineral Development Agreement were conducted.

In the course of regional mineral resource assessment, key deposits and areas were selected for detailed study. Some results are presented in this paper. Locations of the deposits and prospects examined are shown in Figure 25.1.

URANIUM AND URANIUM-POLYMETALLIC DEPOSITS ASSOCIATED WITH UNCONFORMITIES

At present more than one fifth of the western world's Reasonably Assured Resources of uranium recoverable at up to $US 130/kg U is attributed to deposits associated with Proterozoic unconformities. The present annual uranium output from these deposits amounts to about a quarter of the total world production. Annual production from the Key Lake mine alone represents about ten per cent of the world output. There are two areas with producing deposits associated with Proterozoic unconformities: the Athabasca Basin region in Canada and the Pine Creek Geosyncline in Australia. Other areas with similar mineralization, but without mines, are: Baker Lake-Thelon, NWT, and Otish Basin, Quebec.

The Bertholene deposit in the Rodez area, France, which is under exploration, is the only deposit in Phanerozoic rocks with features similar to those of ones associated with Proterozoic unconformities (Fig. 25.2).

The uranium and uranium-polymetallic deposits associated with Proterozoic unconformities typically contain high grade ores (e.g. the Cigar Lake deposit, the world's highest grade large uranium deposit, contains ore averaging 120

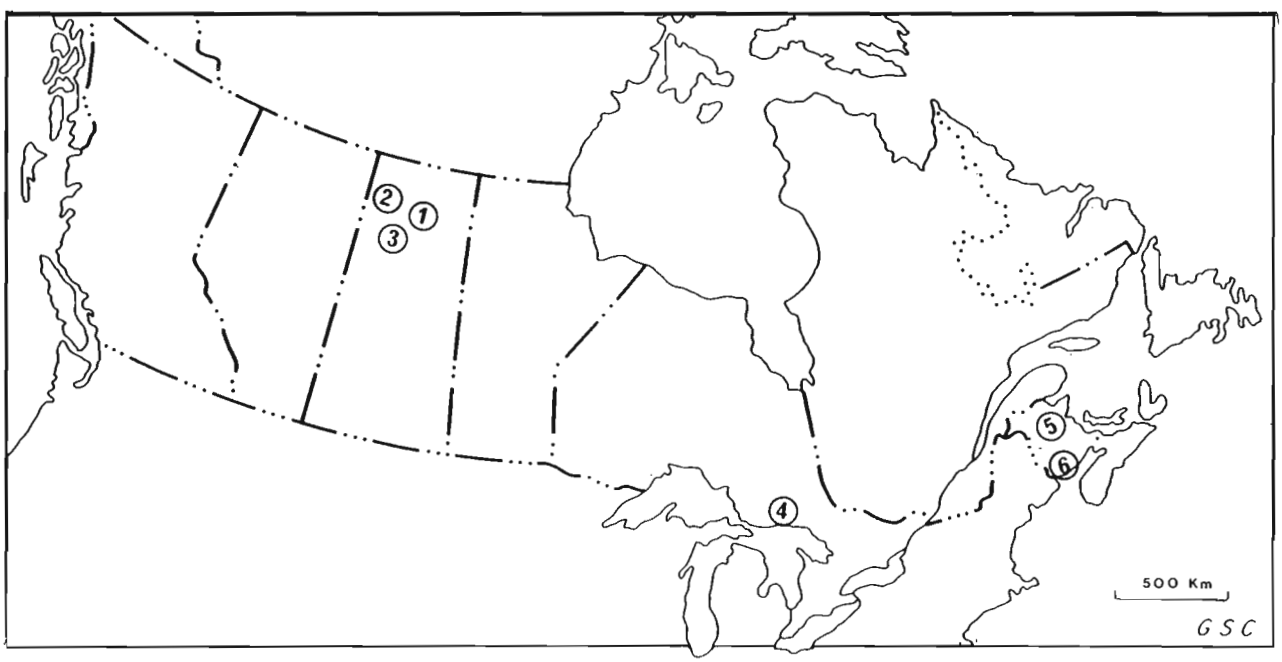


Figure 25.1. Producing centres and main exploration targets in Canada, 1986: (1) Collins Bay – Cigar Lake, Saskatchewan; (2) Carswell Structure, Saskatchewan; (3) Key Lake, Saskatchewan; (4) Elliot Lake, Ontario; (5) Bathurst and Rocky Brook areas, New Brunswick; (6) St. George area, New Brunswick.

times higher grade than the economic deposits in quartz-pebble conglomerates at Elliot Lake). The grade and tonnage relationships in the deposits related to unconformities differ substantially, from 0.16%U / 60.9 thousand tonnes U in the Ranger III deposit to 12.2%U / 110 thousand tonnes U in the Cigar Lake deposit (Table 25.1; Fig. 25.3).

The deposits are either monometallic, consisting of pitchblende, coffinite and locally of secondary uranium minerals, or polymetallic, containing, in addition to several generations of pitchblende and coffinite, arsenides and sulpharsenides of nickel and cobalt, sulphides of nickel, copper, lead, molybdenum, iron and zinc, oxides and hydroxides of iron and native metals, such as gold and bismuth, in various proportions.

These deposits were formed during several mineralizing episodes (Fig. 25.4).

The regional geochemical cycle of uranium was initiated by the introduction of uranium by granitoid magmatism during Kenoran Orogeny at about 2.5 Ga. Uranium was subsequently concentrated in pegmatitic mobilizates (about 1870 Ma) and in some sedimentary rocks of the Tazin Group. The first major epigenetic concentration of uranium, associated with the Hudsonian Orogeny (at about 1740 Ma), led to formation of the pitchblende-brannerite deposits in the Beaverlodge area.

The second major period of uranium mobilization and epigenetic ore deposition, was associated with diagenetic processes that affected the Athabasca Group rocks and with the thermal events related to emplacement of diabase dykes. During this period (between 1.3 and 0.8 Ga) uranium and uranium-polymetallic deposits spatially related to the sub-Athabasca unconformity formed. This mineralization was rejuvenated in at least two later periods (at about 300 to 200 Ma and at about 80 Ma), as indicated by pitchblende U-Pb data.

CIGAR LAKE DEPOSIT

Studies of the ore-forming and associated minerals in the Cigar Lake deposit have indicated that the uranium occurs in mineralogically distinct zones (Ruzicka, 1984; Ruzicka and LeCheminant, 1984, 1985). The polymetallic assemblages tend to occur at the base of the orebodies, whereas the monometallic mineralization tends to be localized in the peripheral parts of the orebodies and in the so-called "perched" (Fouques et al., 1986) or satellitic zones. Similar patterns were reported for the Key Lake deposit by von Pechmann (1985), who observed that nickel extends to greater depths than the uranium. He attributed this zoning to "non-simultaneous" deposition of nickel and uranium.

Fouques et al. (1986) compared the uranium-polymetallic assemblages of the Cigar Lake deposit with the assemblages of the Key Lake and Cluff Lake deposits. They distinguished three main stages in the mineralization and attributed them to polyphased hydrothermal processes.

Results of our preliminary studies agree with their conclusions. The oldest stage is a polymetallic mineral assemblage consisting of pitchblende and of arsenide-sulpharsenide-sulphide minerals of nickel, cobalt, iron, copper and lead; the second stage contains predominantly pitchblende with some sulphide minerals of iron, copper and lead; coffinite and pitchblende prevail in the third stage (Fig. 25.5).

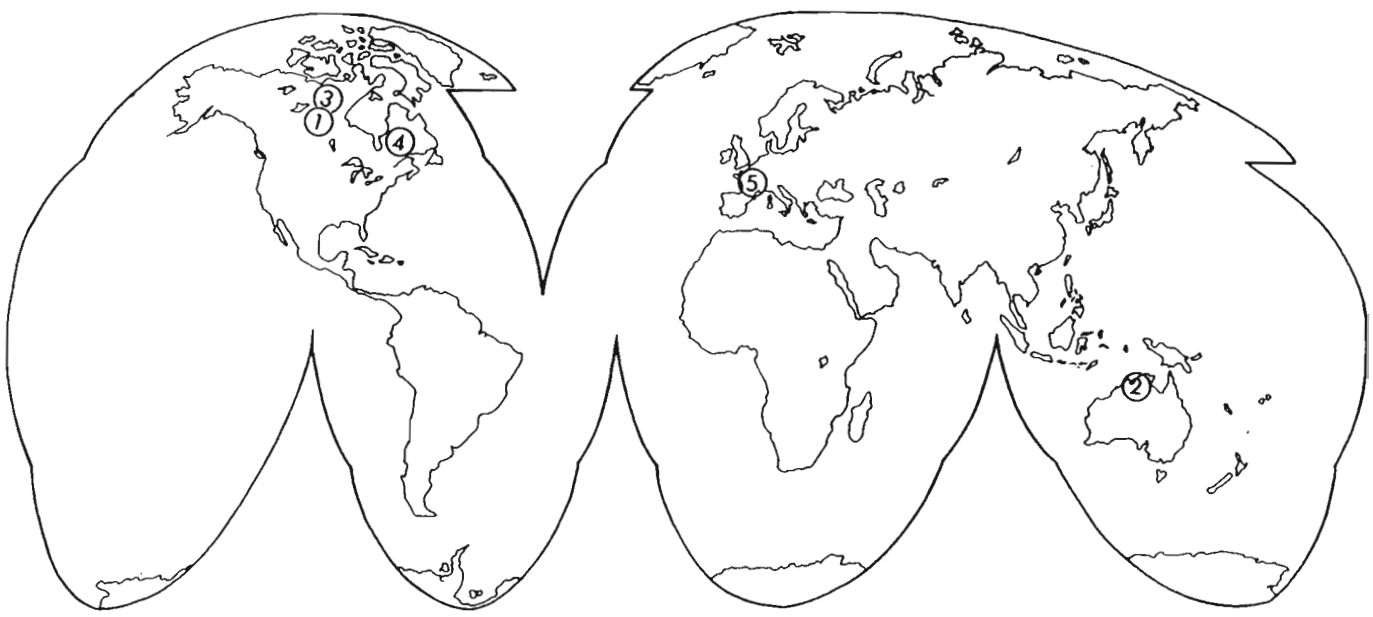


Figure 25.2. Areas with uranium and uranium-polymetallic deposits associated with unconformities: (1) Athabasca Basin; (2) Pine Creek Geosyncline; (3) Baker Lake-Thelon Basin; (4) Otish Basin; (5) Rodez.

Table 25.1. Uranium production, Reasonably assured and estimated additional resources I in selected deposits associated with unconformities as of 1986; (compiled from various sources, mainly publications of the International Atomic Energy Agency and GSC files).

Country Deposit	Ore Megatonnes	Grade %U	U Metal Kilotonnes	Remark
CANADA				
Key Lake	3.50	1.99	70.20	Producing
Rabbit Lake	5.70	0.34	19.20	Depleted in 1984
Collins Bay 'B'	3.00	0.38	11.40	Producing
Collins Bay 'A'	0.07	9.68	6.50	Under development
Cluff Lake 'D'	0.11	3.79	4.20	Depleted in 1980
Midwest Lake	1.20	1.60	19.30	Dormant
McClean Lake	0.40	1.53	5.40	Dormant
Cigar Lake	0.90	12.20	110.00	Under development
AUSTRALIA				
Nabarlek	0.55	1.56	8.70	Depleted in 1979
Ranger I	18.60	0.24	44.80	Dormant
Ranger III	38.30	0.16	60.90	Producing
Koongarra	6.10	0.22	13.20	Dormant
Jabiluka I	1.40	0.21	2.90	Dormant
Jabiluka II	52.30	0.33	173.00	Dormant

In the first stage pitchblende is typically intimately intergrown with sulphides, arsenides or sulpharsenides (Fig. 25.6); it is in some cases replaced by them (Fig. 25.7); and it occurs in places in fragments cemented by a mixture of them and by associated mica or clay minerals (Fig. 25.8). Ore minerals show evidence of redistribution into veins, mutual replacement or crosscutting relationships. A gradual sulphidization of arsenides and an increase in the proportion of sulphides during mineralization occurred at the Cigar Lake (Fig. 25.9) and Key Lake deposits (von Pechmann, 1985). The concentration of metallic elements apparently occurred independently of each other, as indicated by different distribution patterns of uranium, nickel, arsenic, copper, cobalt and molybdenum (Fig. 25.10) and textures of ore minerals.

The Cigar Lake deposit is surrounded by a wide alteration halo, consisting of illite, chlorite and kaolinite in various proportions. The halo extends locally from the unconformity to as much as 200 m up into the sandstone and 100 m down into basement rocks. The extent of the alteration halo is proportional to the size of uranium ore bodies at the unconformity (Fouques et al., 1986). Alteration products occur also as a matrix within the ores. In addition to illite, chlorite and kaolinite, celadonite and montmorillonite are present locally in the matrix (Fig. 25.11). The alteration exhibits features indicative of hydrothermal processes, namely an increase in the K/Al ratio, increase in magnesium content, introduction of carbonates (calcite, siderite), phosphates (goyazite) and dravite (Fouques et al., 1986). The reactive hydrothermal solutions, which invaded the depositional environment in several pulses and contained abundant Fe-oxides, caused corrosion of quartz and pitchblende (Fig. 25.12). The solutions also mobilized and deposited kerogen, which occurs typically in the alteration haloes as dendrites or globules. Ionization effects of radiation apparently enhanced these processes.

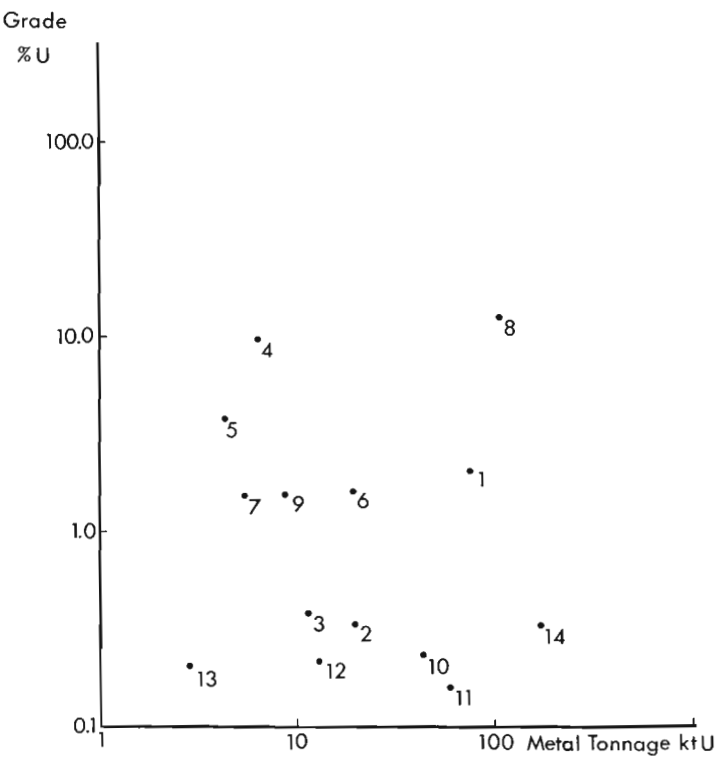


Figure 25.3. Grade/Tonnage relationships in uranium deposits associated with Proterozoic unconformities. Compiled from various sources.

1 – Key Lake; 8 – Cigar Lake;
2 – Rabbit Lake; 9 – Nabarlek;
3 – Collins Bay 'B'; 10 – Ranger I;
4 – Collins Bay 'A'; 11 – Ranger III;
5 – Cluff Lake 'D'; 12 – Koongarra;
6 – Midwest Lake; 13 – Jabiluka I;
7 – McClean Lake; 14 – Jabiluka II.

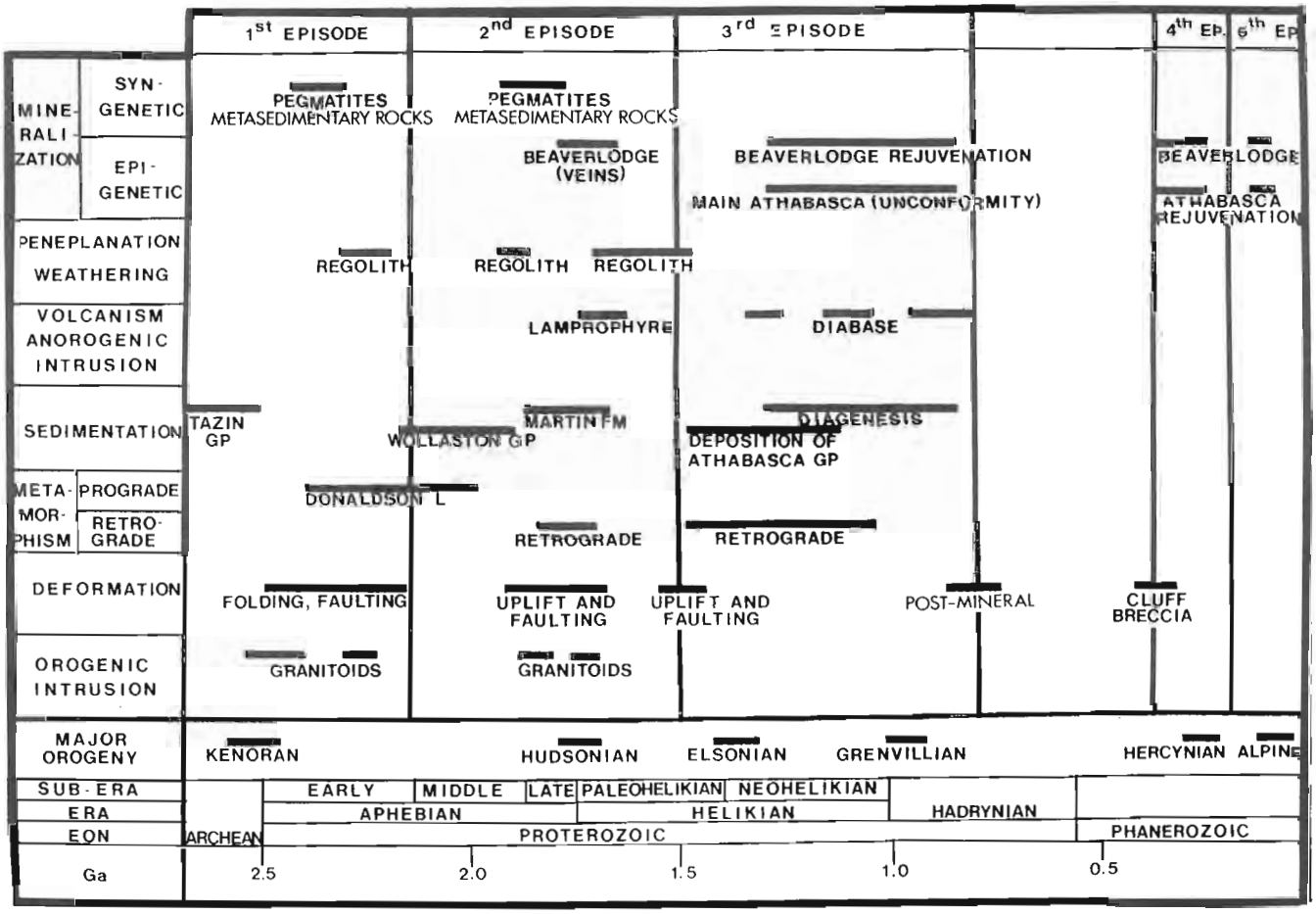


Figure 25.4. Uranium metallogenic periods and geological events in northern Saskatchewan. A conceptual model compiled from various sources.

EAGLE POINT DEPOSIT

The Eagle Point deposit, which occurs about 11 km to the northeast of Rabbit Lake, was tested recently by drilling to a depth exceeding 400 m.

The deposit occurs in lenses, as fault and fracture fillings, breccias and as impregnations. The predominant host rocks are moderately to strongly altered paragneisses, which are locally graphitic, and pegmatoids. The known mineralization is localized between the Collins Bay and Eagle Point faults. The orebodies trend generally 080° and plunge 40° to the east-northeast. The Eagle Point deposit, as outlined by exploration during the summer of 1986, is about 1130 m long, 180 to 400 m wide and more than 400 m deep. The mineralization, consisting of pitchblende lenses in alteration zones, was still under exploration in 1986.

The mineralization consists of several generations of uraninite and pitchblende. The euhedral variety of pitchblende (Fig. 25.13) is similar to the crystalline species of the Key Lake and Cigar Lake deposits (Ruzicka, 1977; Ruzicka and Littlejohn, 1982; Ruzicka and LeCheminant, 1985; von Pechmann, 1985; Fouques et al., 1986). Uranium in minor amounts occurs also in boltwoodite, coffinite and uranophane. Small amounts of galena, native copper, marcasite, chalcopyrite, bornite, covellite, digenite and bravoite in places are associated with the uranium minerals. However, unlike in the Key Lake, Cigar Lake and other uranium-polymetallic deposits of the Athabasca Basin region, nickel and cobalt minerals have not been detected in the Eagle Point deposit.

Nickel, cobalt, arsenic and zinc contents in the high grade uranium ore are very low (Table 25.1). On the other hand iron, magnesium and aluminum contents are high. The hydrothermal solutions altered the host rocks and micas, chlorite and clay minerals which surround the pitchblende (Fig. 25.14).

Relatively high values of Loss of Ignition (LOI) in some samples are indicative of organic matter in the ores (Table 25.1, samples 6, 7, 8 and 9). Core of drillhole ES 249A contains globules of kerogen in altered pegmatite and a vein or uranoan anthraxolite at 374.3; another vein, about 5 cm

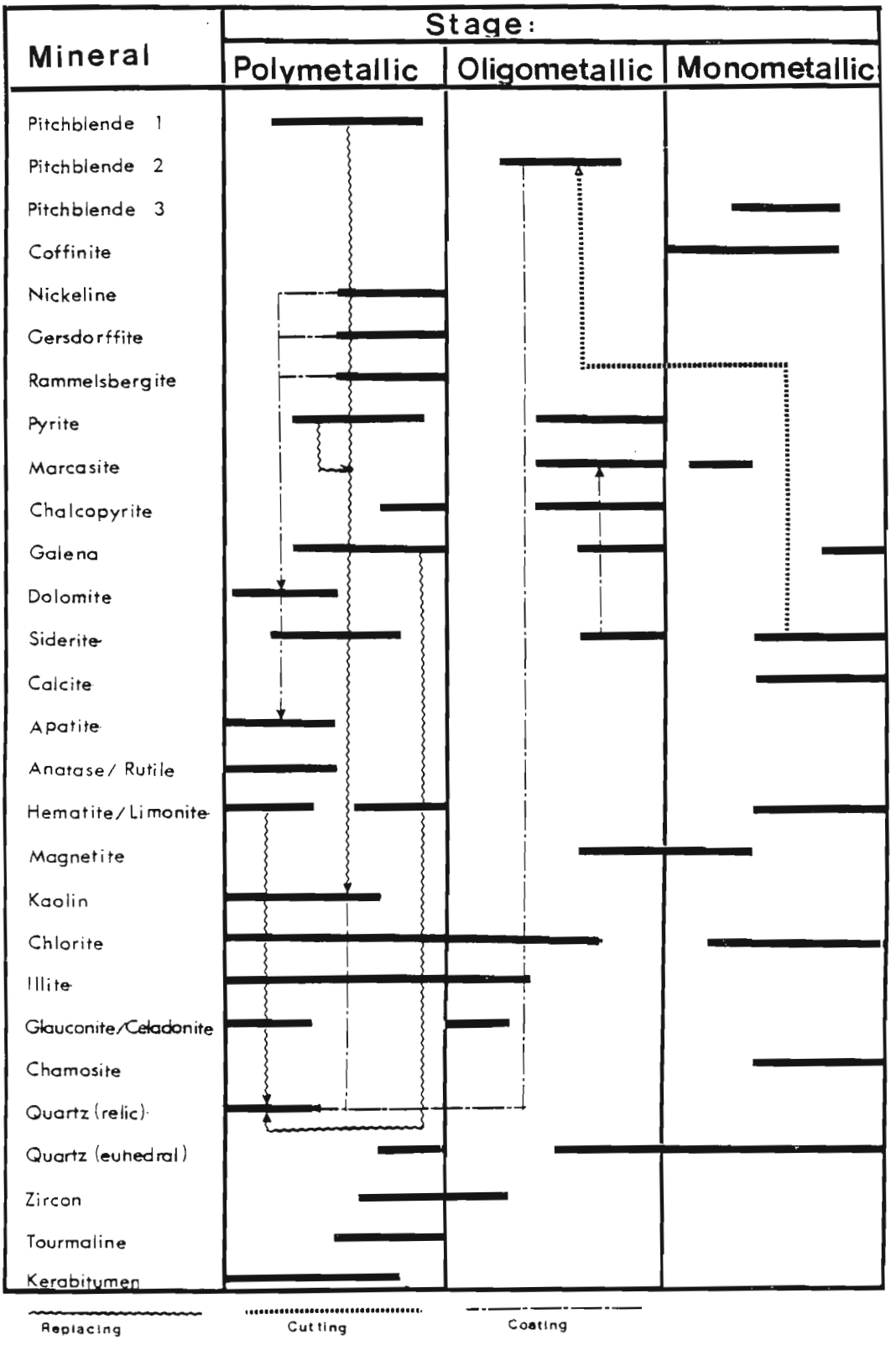


Figure 25.5. Mineral paragenesis of the Cigar Lake deposit, Saskatchewan.

Table 25.2. Selected constituents in ore samples, Eagle Point deposit, Saskatchewan. The low totals of samples 2, 3, 4 and 5 are apparently attributed to organic matter.

Constituent	Sample No: 1	2	3	4	5	6	7	8	9
SiO_2	21.400	32.100	32.100	>42.8	>42.8	25.900	21.100	51.000	37.600
TiO_2	0.250	1.170	0.330	0.050	0.050	0.120	0.180	0.220	0.640
Al_2O_3	9.500	9.500	9.500	13.200	18.900	14.700	13.200	13.800	18.400
Fe_2O_3	10.000	10.000	4.300	4.300	0.400	19.800	4.570	5.280	1.430
MnO	0.130	0.190	0.190	0.060	0.030	0.070	0.160	0.150	1.140
MgO	0.830	2.490	4.970	0.330	0.830	2.450	3.740	2.260	4.310
CaO	2.100	4.200	2.100	0.420	0.210	1.390	2.110	1.420	10.500
Na_2O	NA	NA	NA	<0.04	<0.04	0.250	0.340	0.170	0.180
K_2O	NA	NA	NA	NA	NA	3.880	1.940	3.060	3.840
LOI	NA	NA	NA	NA	NA	11.000	8.000	8.700	17.600
P_2O_5	NF	NF	NF	<0.2	<0.2	0.090	0.040	0.070	0.070
S	NA	NA	NA	NA	NA	0.020	0.150	0.020	0.040
Ag	NA	NA	NA	NF	NF	0.000	0.007	<0.001	0.001
As	<0.1	<0.1	<0.1	<0.1	0.050	NA	NA	NA	NA
Ba	0.020	0.050	0.050	0.020	0.030	0.041	0.063	0.031	0.078
Be	<0.001	0.001	0.002	<0.001	0.001	0.004	0.002	0.001	0.002
Co	NA	NA	NA	0.002	<0.001	0.004	0.023	<0.001	0.002
Cr	<0.001	<0.001	<0.001	0.002	0.003	<0.001	0.001	0.002	0.003
Cu	0.100	0.030	0.070	0.002	0.002	0.010	0.117	0.004	0.076
La	NF	NF	NF	NF	0.005	0.026	0.009	0.006	0.003
Ni	NA	NA	NA	0.002	0.002	0.003	0.019	0.002	0.006
Pb	5.000	2.000	2.000	0.050	0.050	0.260	2.400	0.260	0.300
U	43.300	27.500	21.600	3.390	1.690	18.900	33.200	12.900	3.100
V	0.030	0.030	0.070	0.030	0.050	0.012	0.049	0.059	0.040
Yb	0.015	0.007	0.003	<0.001	<0.001	0.006	0.007	0.002	0.002
Zn	NA	NA	NA	NF	NF	0.003	0.005	0.001	0.002
Totals	92.777	89.369	77.386	65.000	65.345	98.939	91.432	99.418	99.365

All analyses in per cent
Analytical methods: U: delayed neutron activation (Atomic Energy Canada Limited)
All other elements in smaples 1 to 5: spectrochemical optical method (GSC)
All analyses of samples 6 to 9 except Fe,S and LOI: ICP (GSC)
Fe, S, LOI in samples 6 to 9: chemical methods
Sample location: 1: drillhole EP78/251.5 m; 2: drillhole EP78/206.7 m; 3: drillhole EP82/176.2 m; 4: drillhole ES2/71.9 m; 5: drillhole ES2/75.6 m; 6: drillhole EP164/250.0 m; 7: drillhole EP164/169 m; 8: drillhole EP62/320.0 m; 9: drillhole EP155/158.0 m

wide, of uranoan anthraxolite was identified in strongly kaolinized graphic pegmatite at 377.3 m. The drillhole intersected the orebodies at the same depth in the southern segment of the deposit. The disseminations of kerogen and the anthraxolite veins occur in the vicinity of pitchblende mineralization. The disseminations of kerogen resemble closely those in the Cigar Lake deposit (Ruzicka and LeCheminant, 1986).

DOMINIQUE-PETER DEPOSIT, CLUFF LAKE AREA

Geological features of the Dominique-Peter deposit have been described by Tona et al. (1985), Ruhlmann (1985), Blaise and Koning (1985) and Laine (1986). Our observations are complementary to those of the above mentioned authors.

The deposit contains the largest uranium resources in the Carswell Structure. It occurs adjacent to a basement granitic domal structure, the Dominique-Peter Dome, which has distinct gravity and magnetic signatures. The uranium mineralization occurs entirely in the basement gneisses, is controlled structurally by a mylonite zone and steep faults and lithologically by Peter River gneisses. The deposit is surrounded by a chloritic and illitic alteration halo. The structural and morphological features of the Dominique-Peter deposit resemble those of the Eagle Point deposit in the Collins Bay area.

Ruhlmann (1985) and Laine (1986) distinguished several stages of uranium deposition: uraninite with sulphides, pitchblende with carbonates, and coffinite with sulphides. Within the uraninite-sulphide stage they distinguished two mineral assemblages: the uraninite-selenide-sulphide assemblage, which is characterized by the presence of galena, and the uraninite-sulphide assemblage, which contains molybdenite as a dominant sulphidic phase. The uraninite-selenide-sulphide assemblage was dated 1050 Ma, the uraninite-sulphide assemblage 900 Ma and the pitchblende-carbonate assemblage 300 Ma by the U-Pb method by Bell (1985).

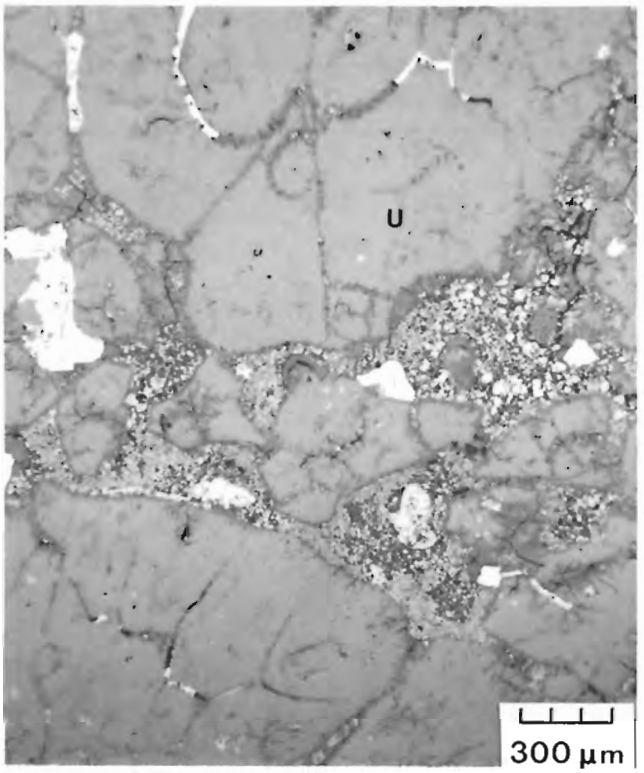


Figure 25.6. Pitchblende(U) in large globular clusters with gersdorffite, chalcopyrite, pyrite and rutile in a clay matrix. Cigar Lake deposit, Saskatchewan; drillhole 154/436m.

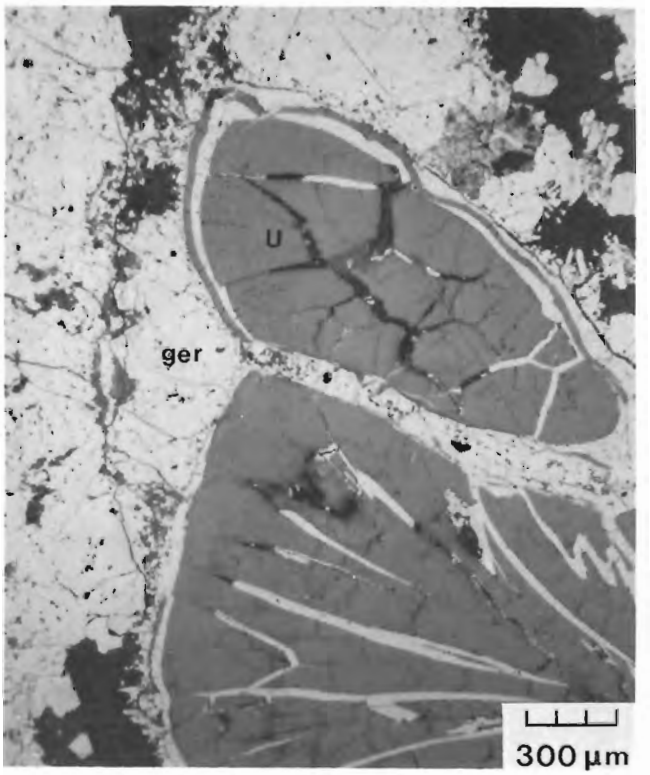


Figure 25.7. Pitchblende(U) locally replaced by gersdorffite(ger). Cigar Lake deposit, Saskatchewan; drillhole 145/3m below the unconformity.

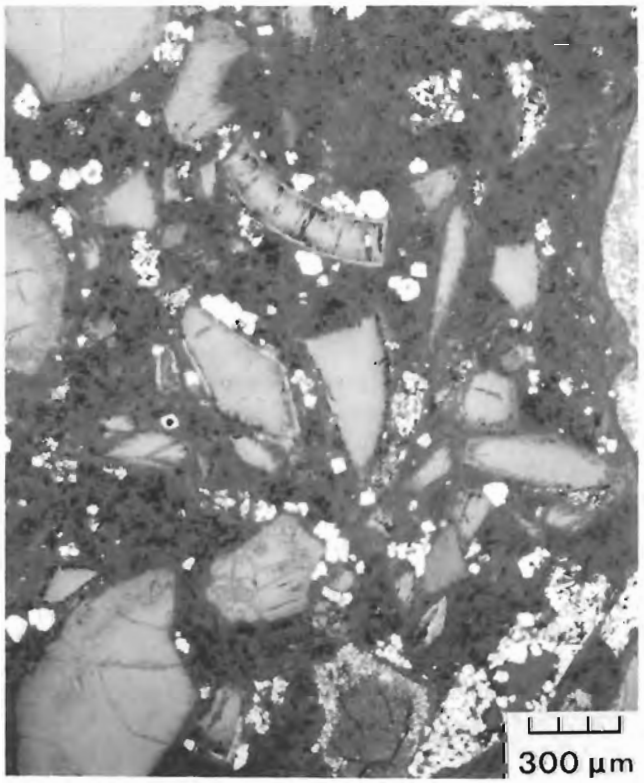


Figure 25.8. Broken "shards" of pitchblende(grey), associated with smaller subhedral grains of gersdorffite(light grey) and chalcopyrite(white), in micaceous matrix. Cigar Lake deposit, Saskatchewan; drillhole 145/3m below the unconformity.

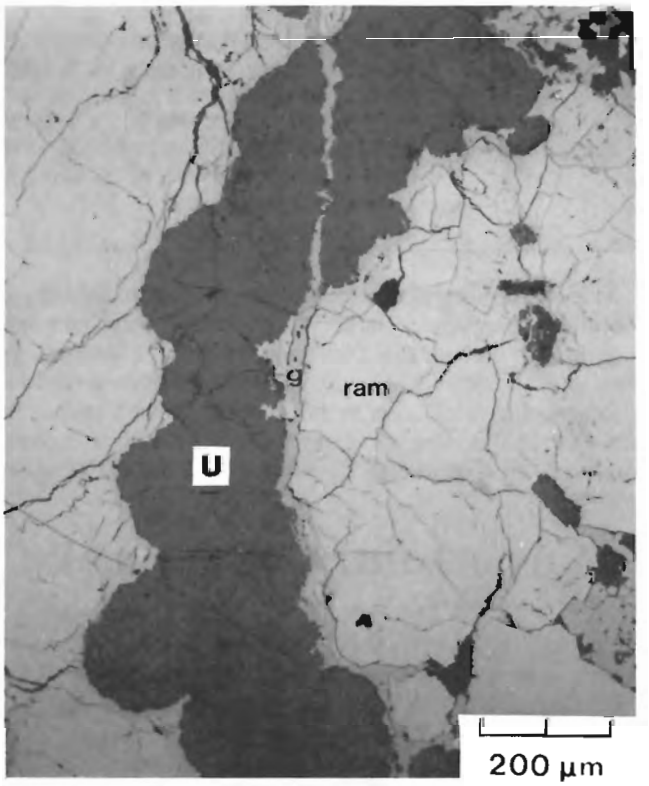


Figure 25.9. A narrow vein of gersdorffite(g) crossing pitchblende(U) and rammelsbergite(ram). Cigar Lake deposit, Saskatchewan; drillhole 154/439.5m.

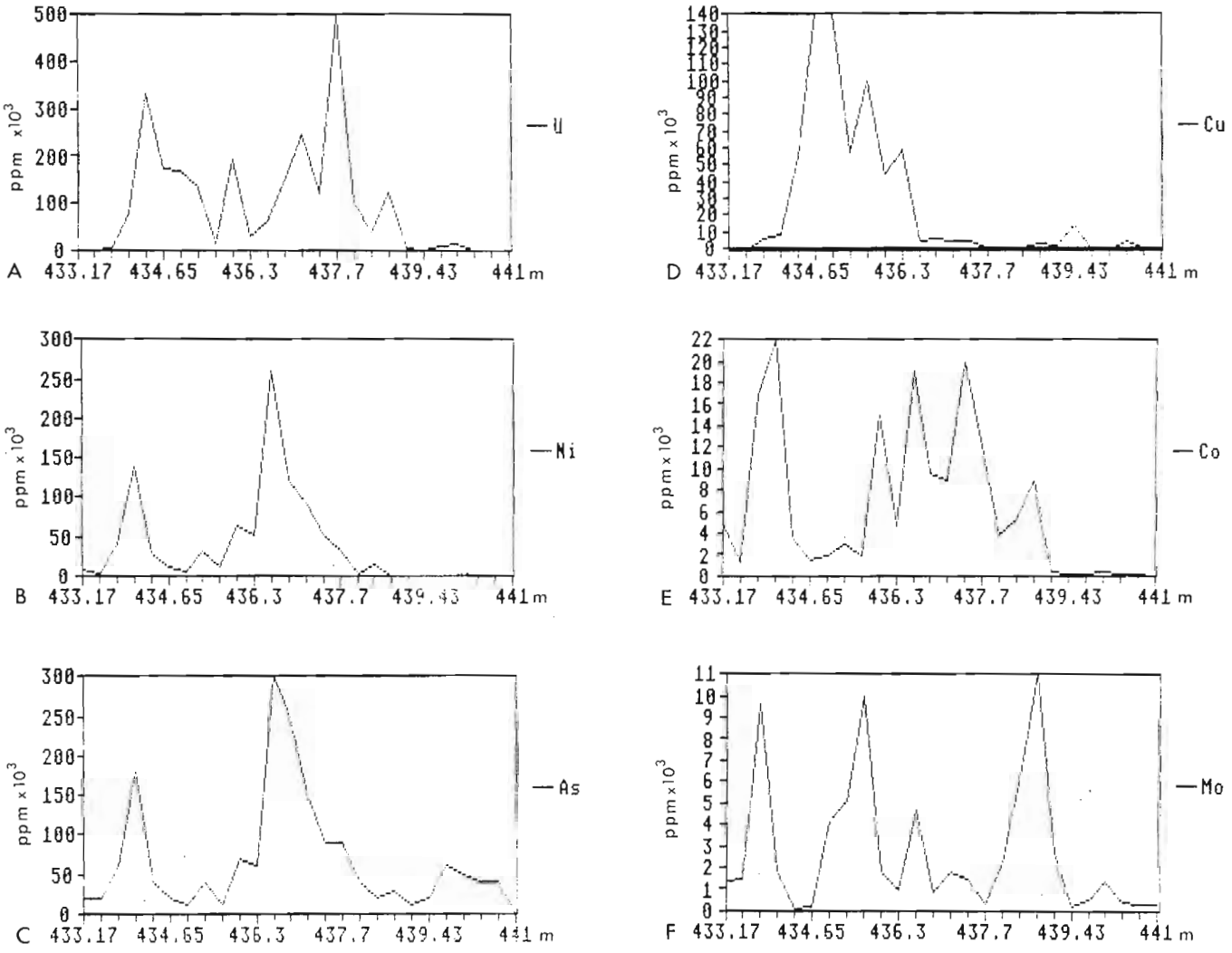


Figure 25.10. Vertical distribution of selected elements in the central part (drillhole 38) of the Cigar Lake deposit, Saskatchewan. From data supplied by Cogema Canada Limited.

Our observations on samples collected from the core of drillhole DP 483 indicate that some of the massive uranium mineralization is essentially clusters of small grains of 'crystalline' uraninite, which have coalesced into anhedral mass or seams (Fig. 25.15). According to a microprobe analysis the matrix surrounding the cluster of uraninite (U) is a very fine grained felted mass of mica containing a K, Al, Si, (Mg, Fe) elemental assemblage. A few small grains of clausthalite and one inclusion of gold [Au(Ag)] occur in the massive cluster of uraninite. An aggregate of the 'crystalline' uraninite, embedded in fine grained muscovite was observed at the periphery of the ore concentration.

In contrast one sample collected from core of the same drillhole contained small disseminated grains of uraninite associated with molybdenite in a matrix consisting of a mixture of muscovite and chlorite (Fig. 25.16). Chalcopyrite and galena in a muscovite matrix associated with kerogen was identified in a core sample collected at a slightly greater depth in the hole (Fig. 25.17).

U-Ti AGGREGATES AND CARBON FROM THE MATINENDA FORMATION, ELLIOT LAKE, ONTARIO

Occurrences of brannerite and U-Ti aggregates from the Matinenda Formation have been studied by several authors, e.g. by Ramdohr (1957, 1958), Roscoe (1969) and Theis (1979). Two groups of brannerite are generally distinguished: (i) the allogenic brannerite and (ii) the authigenic brannerite and the so-called Ti-U grain-aggregates.

The allogenic (detrital), i.e. stoichiometrically true brannerite in the conglomerate of the Matinenda Formation is rare (Ramdohr, 1958). On the other hand the authigenic brannerite and the titanium-uranium grain-aggregates are common. Theis (1979) observed that the amounts of uranium contained in the composite grain-aggregates show a relationship with the proximity to uraninite grains and that their composition, according to electron microprobe analyses, is consistent with a low temperature in situ formation. Both Ramdohr and Theis

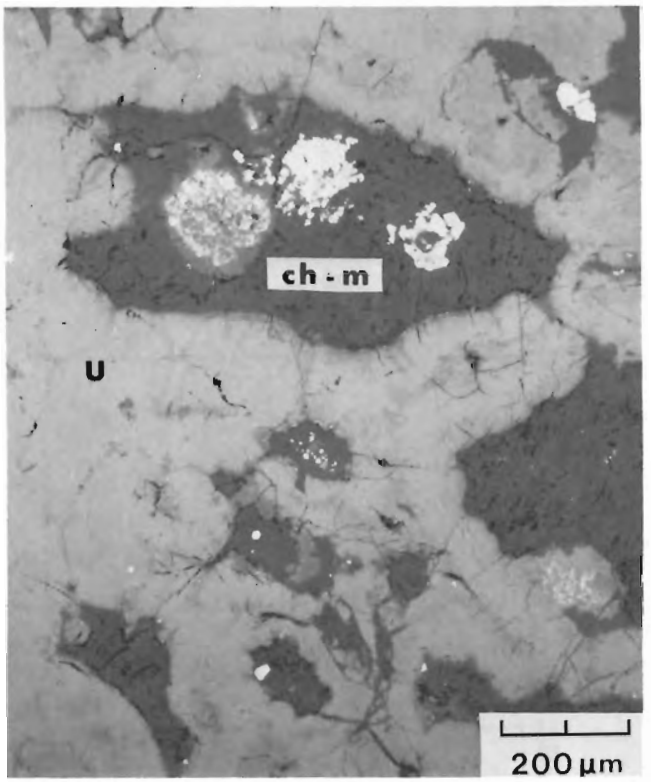


Figure 25.11. Pitchblende(U) enclosing chlorite and montmorillonite (ch-m) surrounding sulphides and arsenides. Cigar Lake deposit, Saskatchewan, drillhole 154/436m.

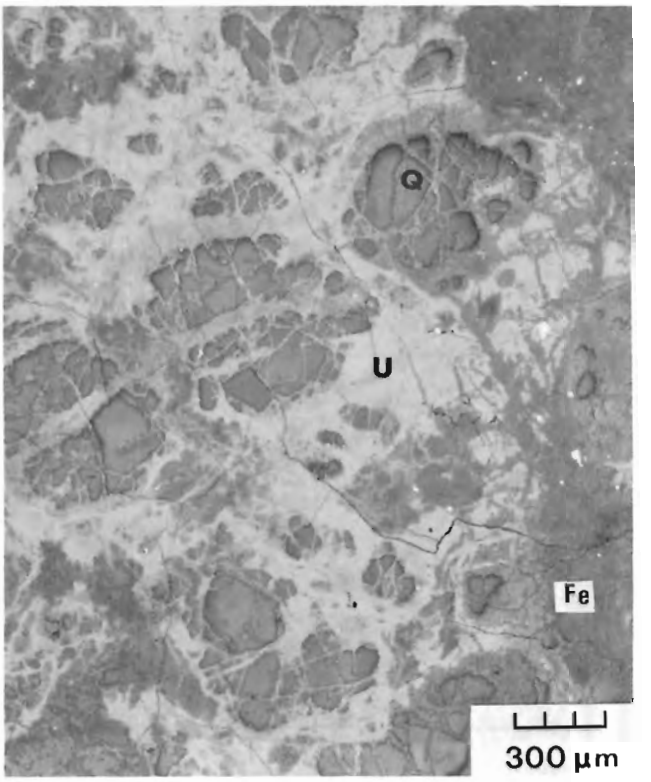


Figure 25.12. A mixture of Fe oxides(Fe) invading pitchblende(U) and corroding quartz grains(Q). Cigar Lake deposit, Saskatchewan; drillhole 78.

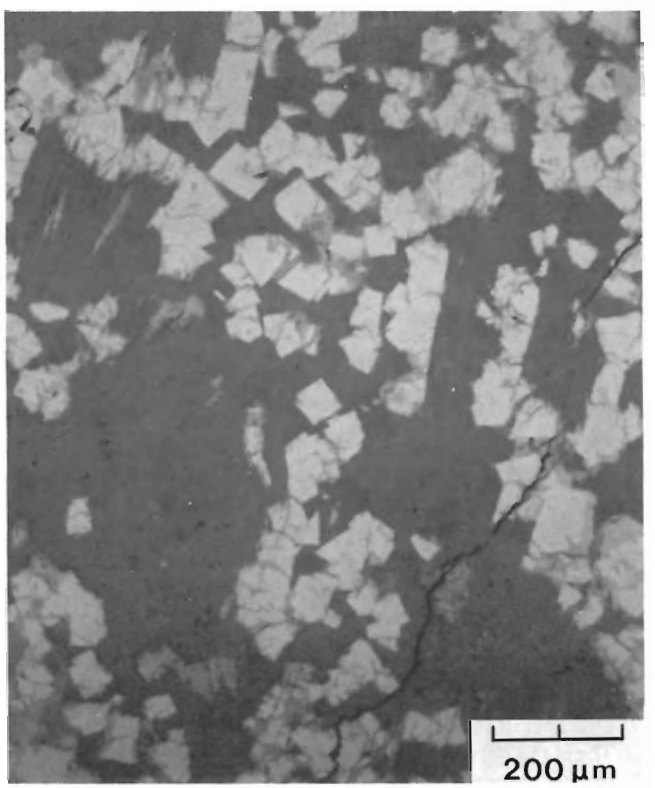


Figure 25.13. Euhedral pitchblende (thorium-free uraninite) in a micaceous matrix. Eagle Point deposit, Saskatchewan; drillhole EP 222/205.2m.

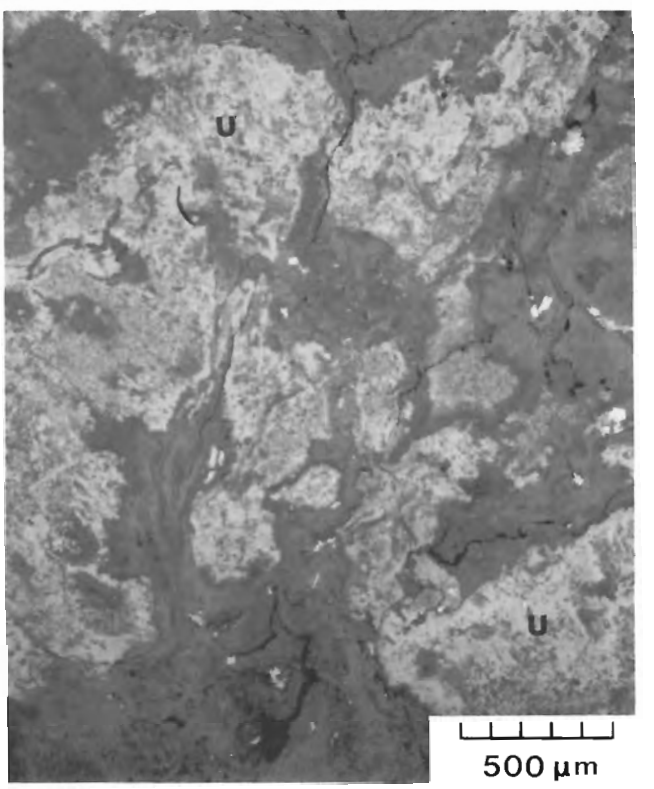


Figure 25.14. Dusty, irregular mass of pitchblende(U) in a micaceous matrix. Quartz is present in the matrix as dusty chalcedony. Some chlorite and minor calcite are intergrown with the mica. Eagle Point deposit, Saskatchewan; drillhole EP 222/204.8m.

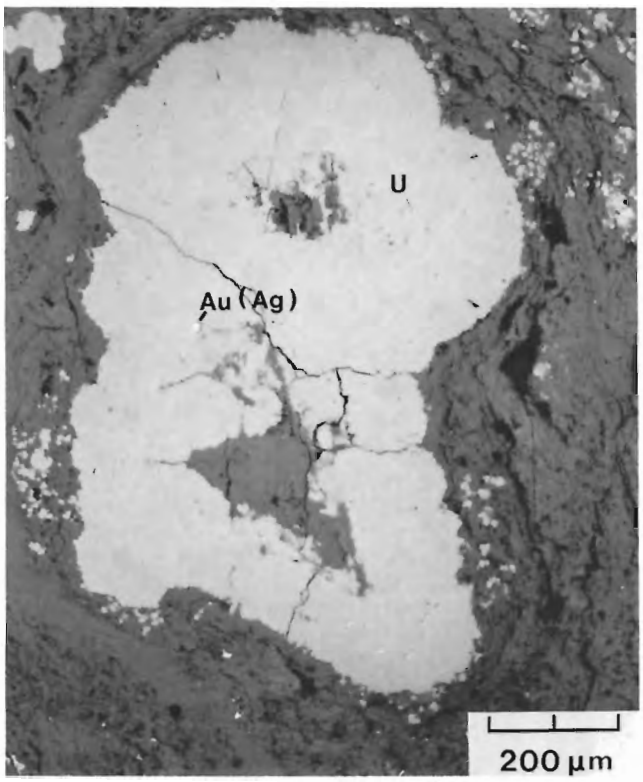


Figure 25.15. A cluster of anhedral uraninite crystals(U). The cluster contains specks of clausthalite and one inclusion of gold with traces of silver[Au(Ag)]. The matrix is very fine grained felted mica. Dominique-Peter deposit, Saskatchewan; drillhole DP 483/49.4m.

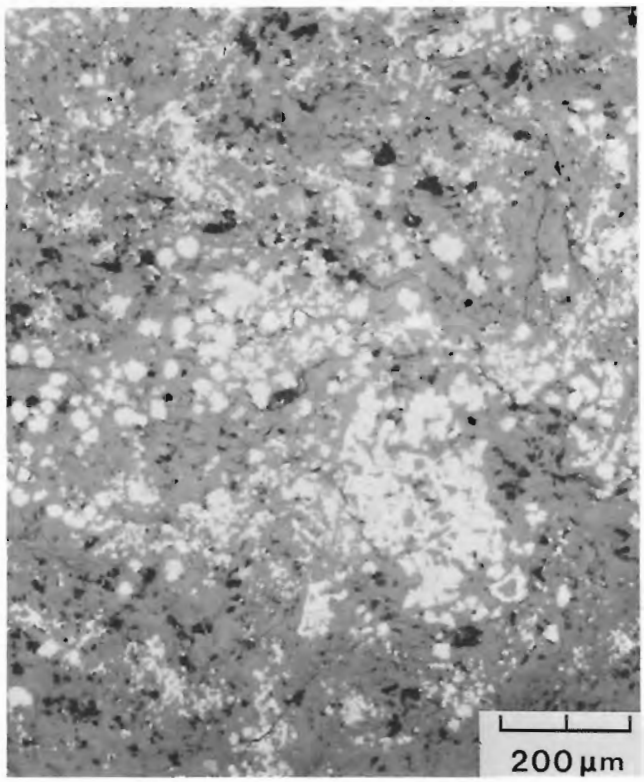


Figure 25.16. A mylonite containing large fragments of felted mica, chlorite and opaque minerals. Small dusty uraninite inclusions are disseminated within the micaceous matrix. The white specks are molybdenite. Dominique-Peter deposit, Saskatchewan; drillhole DP 483/41.1m.



Figure 25.17. A globule of kerogen (black) surrounded by small grains of chalcopyrite and galena in fine grained mica. Dominique-Peter deposit, Saskatchewan; drillhole DP 483/51.0 m.

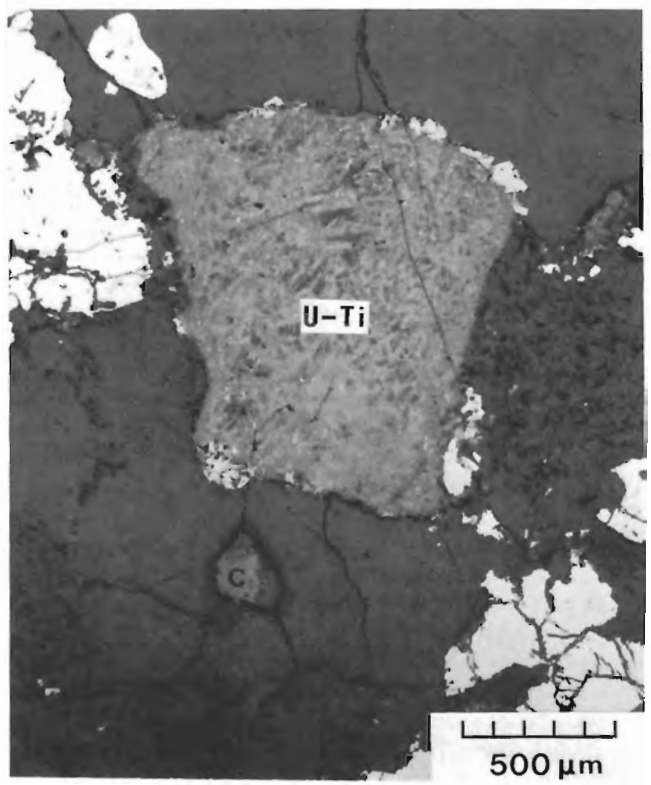


Figure 25.18. A mottled grain-aggregate(U-Ti), consisting of variable amounts of uraninite and rutile, and granular kerogen (C) as interstitial components in a specimen of quartz-pebble conglomerate from the Quirke mine, Elliot Lake, Ontario.

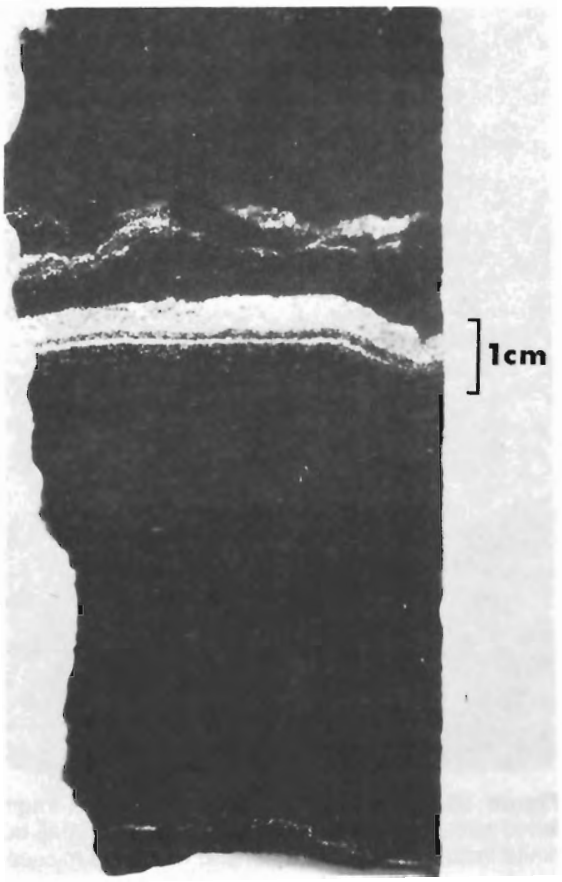


Figure 25.19. Autoradiograph of an ore sample containing the carbonaceous layer, details of which are shown in Figure 25.20. 'C' reef, Quirke mine, Elliot Lake, Ontario. Positive image, 1 hour exposure.

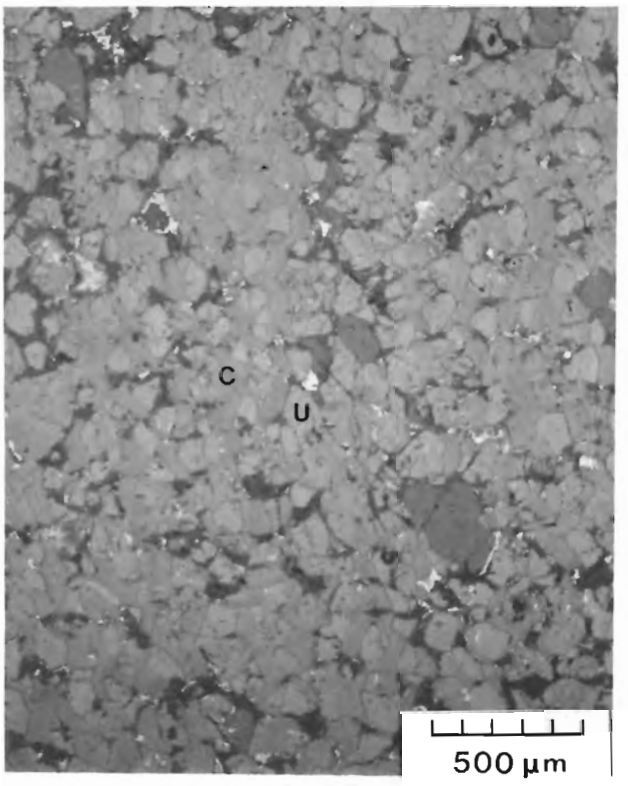


Figure 25.20. Sub-angular grains of uraninite(U) embedded in kerogen(C) from a layer (see Fig. 25.19) in the conglomerate of the Matinenda Formation, Quirke mine, Elliot Lake, Ontario.

considered that the authigenic brannerite and the U-Ti grain-aggregates formed during diagenesis of the conglomerate.

A sample collected from a uraniferous conglomerate bed of the Matinenda Formation at the Quirke mine, Elliot Lake, Ontario, contained several uranium-titanium grain-aggregates. The grains were analyzed by optical, electron microprobe and X-ray diffraction methods. The electron microprobe analyses indicated that the uranium and titanium contents of the grain-aggregates (Fig. 25.18), varied greatly even within one aggregate. The X-ray diffraction pattern of the grain-aggregate shown in Figure 25.18 indicated the presence of uraninite rather than brannerite. Taking into account these features as well as the grain structure, as shown in the photomicrograph (Fig. 25.18), such aggregates were interpreted by us as mixtures of UO_2 and TiO_2 grains, which formed prior to their deposition as heavy mineral grains in a paleoplacer. We suggest that at least some of the grain-aggregates in the conglomerate of the Matinenda Formation were formed before the diagenesis. The presence of the sulphur-bearing carbon in the form of interstitial inclusions (Fig. 25.18), representing apparently relicts of original algal mats, which were trapped in the detritus, supports this conclusion.

A layer of sulphur-bearing carbon was found in the same area. The carbon layer is highly radioactive (Fig. 25.19) and contains about 45% of carbon, 40% of sub-angular grains of uraninite, 5% monazite grains, 5% quartz clasts and 5% sericite (Fig. 25.20). Along the top of the layer are coarse grains of galena that contain native bismuth and are associated with ordinary pyrrhotite as well as silver- and nickel-bearing pyrrhotite (Fig. 25.21). As demonstrated by Willingham et al. (1985) for a similar layer from the Denison mine at Elliot Lake (GSC sample RAD 74-11, collected by VR), the carbon layers contain kerogen, which was derived apparently from algal mats, as postulated by Ruzicka and Steacy (1975) and Ruzicka (1981). The mineral grains within the layer are, apparently, allogenic and represent a fraction of the detritus that was enclosed in the algal material during its transport and deposition. On the other hand the mineral assemblage on the top of the layer, which was associated with galena, was formed authigenically. This assemblage includes both products of the radiogenic decay (galena, native bismuth) as well as minerals (pyrrhotite and Ni- and Ag-pyrrhotite) derived from connate solutions. Crystallization of these minerals took place during the diagenesis of the conglomerate and during the polymerization of the carbon. This interpretation supports the idea that the Huronian uraniferous conglomerate deposits represent paleoplacer concentrations modified during the diagenesis.

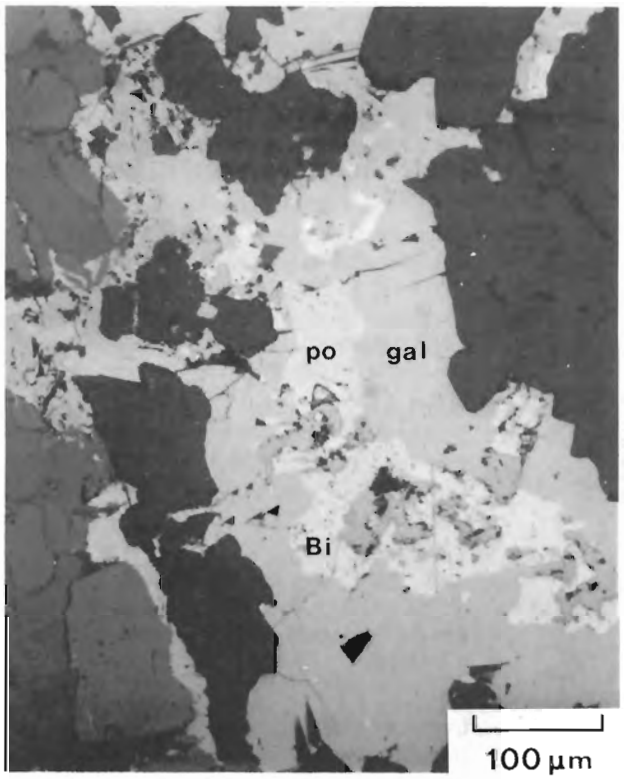


Figure 25.21. Coarse grained galena(gal) containing native bismuth(Bi) associated with pyrrhotite and Ag-Ni-bearing pyrrhotite(po) formed authigenically along the top of the uraninite-kerogen layer shown in Figure 25.19.

NEW DISCOVERIES OF URANIUM MINERALIZATION IN NEW BRUNSWICK

During a reconnaissance survey for uranium mineralization in New Brunswick in 1986 by the first author (VR) and N. Prasad several occurrences of uranium were discovered.

In the Miramichi Anticlinorium three fractures filled with radioactive material were discovered in Devonian granitic rocks in the vicinity of their contacts with Ordovician sedimentary and volcanic rocks and a Mississippian granitic pluton. The occurrences are in the Miramichi River area, about 40 km northwest of Boiestown (46°37′20″ N and 66°37′13″ W). The occurrences are about 4 km to the south along the road from the Rocky Brook occurrence, which was explored by the former Aquitaine Company of Canada Limited and reported to the New Brunswick Department of Natural Resources by Grant (1978) and Wilson (1978). The general strike of the fractures is 105 to 110 degrees, dip subvertical to vertical and width from 1 to 5 cm. The fractures are exposed for lengths from 5 to 20 m. Alteration zones, up to 0.5 m wide, surround the fractures. The fracture filling consists mainly of quartz and radioactive material containing about 0.008%eU.

Total radioactivity amounting to about 2.5 times background values was detected in carbonaceous argillite from the older metasedimentary unit of the Tetagouche Group in the Bathurst area. This unit consists mainly of schists, quartzites, greywackes and argillites with carbonaceous (graphitic) facies, which contains locally disseminated pyrite and pyrrhotite (Luff, 1977, van Staal et al., 1983).

During a follow-up of the Canada-New Brunswick airborne radiometric surveys and the New Brunswick reconnaissance ground gamma-ray radiometric surveys (Chandra and Wallace, 1979) a uranium occurrence with 0.013%eU was found in silicified and feldspathized argillite along the highway 760, 1.15 km southwest of Lily Lake and west-northwest of St. George, Charlotte County (40°10′10″N, 66°55′10″W). The occurrence is spatially related to the intrusive contact between the Devonian granitic rocks and Devonian volcanic and sedimentary rocks.

Studies of the metallogeny of the uranium and uranium-polymetallic occurrences of the Miramichi Anticlinorium, which started under the Canada-New Brunswick Mineral Development Agreement in 1985 (Ruzicka and LeCheminant, 1986), continued in 1986 with the analyses of the Long Lake area data. The studies indicate a coincidence of a distinct negative gravity anomaly with elevated concentrations of the uranium-polymetallic mineralization.

ACKNOWLEDGMENTS

Continuing excellent co-operation of geological and managerial personnel of the following organizations is sincerely acknowledged: R. Laine and J.F. Chaveau of Amok/Cluff Mining Limited and Amok Limited, G. Peebles of Cigar Lake Mining Corporation, A. Coste of Cogema Canada Limited, R. Gunning and A. McEackern of Denison Mines Limited, the late W.E. Hale of Ecological and Resources Consultants Limited, D. Ward and F. Hamilton-Tode of Eldorado Resources Limited, A. deCarle of Key Lake Mining Corporation, D. Sprague of Rio Algom Limited, E. Parviainen of the Saskatchewan Mining Development Corporation, A. Gracie of the Saskatchewan Geological Survey, K. Lehnert-Thiel of Uranerz Exploration and Mining Limited and M. Stuart and W. Hilger of Urangesellschaft Canada Limited. Critical reading of the manuscript by R.I. Thorpe and R.V. Kirkham is appreciated.

REFERENCES

Bell, K.
1985: Geochronology of the Carswell area, northern Saskatchewan; in The Carswell Structure Uranium Deposits, Saskatchewan, ed. R. Laine, D. Alonso and M. Svab; Geological Association of Canada, Special Paper 29, p. 33-46.

Blaise, J.R. and Koning, E.
1985: Mineralogical and structural aspects of the Dominique-Peter uranium deposit; in The Carswell Structure Uranium Deposits, Saskatchewan, ed. R. Laine, D. Alonso and M. Svab; Geological Association of Canada, Special Paper 29, p. 139-151.

Chandra, J. and Wallace, J.
1979: Reconnaissance ground investigation of the Digdeguash radiometric (airborne) anomaly, Digdeguash, Charlotte Co., N.B.; New Brunswick Mineral Resources Branch, Open File Report 79-23, 50 p.

Energy, Mines and Resources
1986: Canada continues as world's leading uranium producer; News Release 86/138, September 3, 1986

Fouques, J.P., Fowler, M., Knipping, H.D. and Schimann, K.
1986: The Cigar Lake uranium deposit: discovery and geological characteristics; in Uranium Deposits of Canada, ed. E.L. Evans; The Canadian Institute of Mining and Metallurgy, Special Volume 33, p. 218-229.

Grant, D.B.
1978: Rocky Brook Claims, Aquitaine Company of Canada Ltd.; New Brunswick Department of Natural Resources, Assessment Report 472461.

Laine, R.
1986: Uranium deposits of the Carswell Structure; in Uranium Deposits of Canada, ed. E.L. Evans, The Canadian Institute of Mining and Metallurgy, Special Volume 33, p. 155-169.

Luff, W.M.
1977: Geology of Brunswick No. 12 Mine; The Canadian Mining and Metallurgical Bulletin, June, 1977, 11 p.

Ramdohr, P.
1957: Die "Pronto-Reaktion"; Neues Jahrbuch fuer Mineralogie Monatshefte, p. 217-222.
1958: Die Uran- und Goldlagerstätten Witwatersrand – Blind River District – Dominion Reef – Serra de Jacobina: Erzmikroskopische Untersuchungen und ein geologischer Vergleich; Abhandlungen der Deutschen Akademie der Wissenschaften zu Berlin, Klasse fuer Chemie und Biologie, Jahrgang 1958, Nr. 3, 35 p.

Roscoe, S.M.
1969: Huronian rocks and uraniferous conglomerates in the Canadian Shield; Geological Survey of Canada, Paper 68-40, 205 p.

Ruhlmann, F.
1985: Mineralogy and metallogeny of uraniferous occurrences in the Carswell Structure; in The Carswell Structure Uranium Deposits, Saskatchewan, ed. R. Laine, D. Alonso and M. Svab; Geological Association of Canada, Special Paper 29, p. 105-120.

Ruzicka, V.
1977: Assessment of selected uranium occurrences and areas favourable for uranium mineralization in Canada; in Report of Activities, Part A, Geological Survey of Canada, Paper 77-1A, p. 27-29.
1981: Some metallogenic features of the Huronian and Post-Huronian uraniferous conglomerates; in Genesis of Uranium- and Gold-bearing Precambrian Quartz-Pebble Conglomerates, ed. F.A. Armstrong; United States Geological Survey, Professional Paper 1161-V, p. V1-V8.
1984: Unconformity-related uranium deposits in the Athabasca Basin region, Saskatchewan; in Proterozoic Unconformity and Stratabound Uranium Deposits, ed. J. Ferguson; A Technical Document IAEA-TEC-DOC-315 issued by the International Atomic Energy Agency, Vienna, 1984, p. 219-267.

Ruzicka, V. and LeCheminant, G.M.
1984: Uranium deposit research, 1983; in Current Research, Part A, Geological Survey of Canada, Paper 84-1A, p. 39-51.
1985: Summary on uranium in Canada, 1984; in Current Research, Part A, Geological Survey of Canada, Paper 85-1A, p. 15-22.
1986: Developments in uranium geology in Canada, 1985; in Current Research, Part A, Geological Survey of Canada, Paper 86-1A, p. 531-540.

Ruzicka, V. and Littlejohn, A.L.
1982: Notes on mineralogy of various types of uranium deposits and genetic implications; in Current Research, Part A, Geological Survey of Canada, Paper 82-1A, p. 341-349.

Ruzicka, V. and Steacy, H.R.
1975: Some sedimentary features of conglomerate uranium ore from Elliot Lake, Ontario; in Report of Activities, Part A, Geological Survey of Canada, Paper 76-1A, p. 343-346.

Theis, N.J.
1979: Uranium-bearing and associated minerals in their geochemical and sedimentological context, Elliot Lake, Ontario; Geological Survey of Canada, Bulletin 304, 50 p.

Tona, F., Alonso, D. and Svab, M.
1985: Geology and mineralization in the Carswell Structure – a general approach; in The Carswell Structure Uranium Deposits, Saskatchewan, ed. R. Laine, D. Alonso and M. Svab; Geological Association of Canada, Special Paper 29, p. 1-18.

van Staal, C., Luff, W. and Williams, P.F.
1983: Brunswick Mining and Smelting Corporation No. 12 and No. 6 mines; in Field Trip Guidebook to Stratabound Sulphide Deposits, Bathurst Area, N.B., Canada and West-Central New England, U.S.A., ed. D.F. Sangster; Geological Survey of Canada, Miscellaneous Report 36, p. 7-15.

von Pechmann, E.
1985: Mineralogy of the Key Lake U-Ni orebodies, Saskatchewan, Canada: evidence for their formation by hypogene hydrothermal processes; in Geology of Uranium Deposits, ed. T.I.I. Sibbald and W. Petruk; The Canadian Institute of Mining and Metallurgy, Special Volume 32, p. 27-37.

Willingham, T.D., Nagy, B., Nagy, L.N., Krinsley, D.H. and Mossmann, D.J.
1985: Uranium-bearing stratiform organic matter of the Lower Huronian Supergroup, Elliot Lake – Blind River region, Canada; Canadian Journal of Earth Sciences, v. 22, p. 1930-1944.

Wilson, A.J.
1978: Rocky Brook Claims; Aquitaine Company of Canada Ltd.; New Brunswick Department of Natural Resources, Assessment Report 472237.

- 26 -

Field relations, petrology and age of plutonic and associated metavolcanic and metasedimentary rocks, Fundy National Park area, New Brunswick[1]

Contract OTT84-92309 B-72

Sandra M. Barr[2]

Barr, S.M., Field relations, petrology and age of plutonic and associated metavolcanic and metasedimentary rocks, Fundy National Park area, New Brunswick; in Current Research, Part A, Geological Survey of Canada, Paper 87-1A, p. 263-280, 1987.

Abstract

Geological mapping and petrological studies of the Fortyfive River pluton and associated metavolcanic, metasedimentary and intrusive rocks in southeastern New Brunswick indicate that all of these units formed in a volcanic arc environment. The Fortyfive River pluton and other granitoid rocks in the map area have characteristics typical of I-type intrusions. Most of the rock units were subsequently multiply deformed and metamorphosed to lower greenschist facies. A Rb-Sr whole-rock isochron age of 597 ± 18 Ma for the Fortyfive River pluton and a K-Ar age of 598 ± 27 Ma for the hornblende from diorite of the nearby Alma pluton are interpreted to be minimum ages for these units. These ages confirm a Precambrian age for the host metavolcanic and metasedimentary units.

Résumé

Le levé géologique et l'étude pétrologique du pluton de Fortyfive River et des roches métavolcaniques, métasédimentaires et intrusives associées dans le sud-est du Nouveau-Brunswick révèle que ces unités se sont toutes formées dans un arc volcanique. Le pluton de Fortyfive River et les autres roches granitoïdes de la région levée présentent des caractéristiques d'intrusions de type I. La plupart des unités rocheuses ont par la suite subi de multiples déformations et ont été métamorphisées jusqu'au faciès inférieur des schistes verts. La datation de roches tirées du pluton de Fortyfive River par la méthode au strontium donne un âge de 597±18 Ma tandis que la datation par la méthode à l'argon d'une hornblende tirée d'une diorite provenant du pluton voisin d'Alma donne un âge de 598±27 Ma; ces chiffres représenteraient l'âge minimal des unités et confirment que les unités métasédimentaires et métavolcaniques encaissantes datent du Précambrien.

[1]Contribution to the Canada-New Brunswick Mineral Development Agreement, 1984-89. Project carried by Geological Survey of Canada, Lithosphere and Canadian Shield Division, Project 730044

[2]Department of Geology, Acadia University, Wolfville, Nova Scotia, B0P 1X0

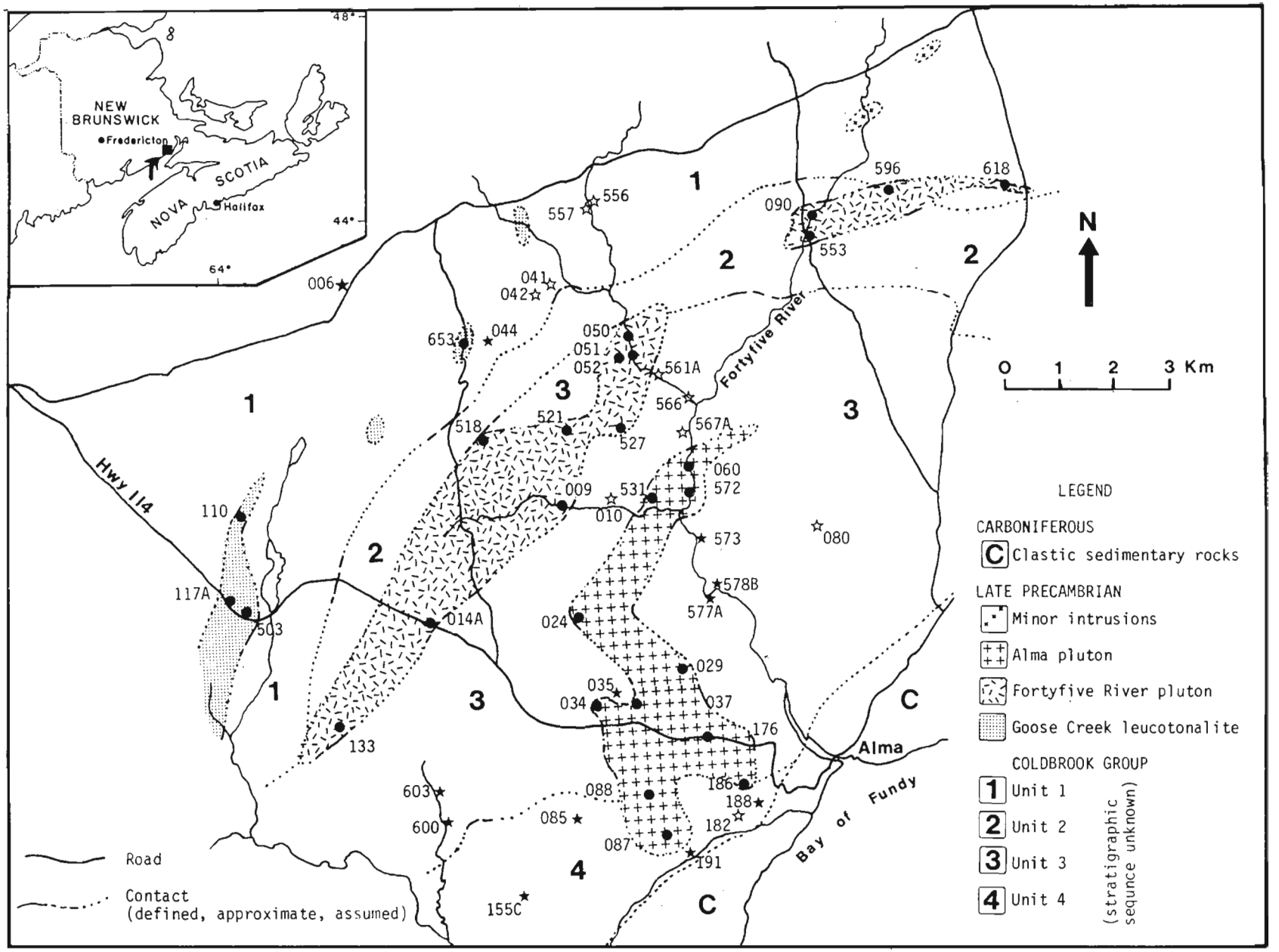


Figure 26.1. Distribution of major rock units in the Fortyfive River map area. Numbered circles, black stars, and open stars indicate locations of analyzed samples in plutonic rocks, volcanic rocks, and sills/dykes, respectively. Map units are described in the text.

INTRODUCTION

Much of the Caledonian Highlands of southern New Brunswick is underlain by metavolcanic and metasedimentary rocks of the Coldbrook Group (Kindle, 1962; Ruitenberg et al., 1977, 1979; Giles and Ruitenberg, 1977). These rocks are considered to be late Precambrian in age and correlative with similar units in southeastern Cape Breton Island, eastern Newfoundland and elsewhere in the Avalon Terrane of the Appalachian Orogen (e.g. Williams, 1979; O'Brien et al., 1983; Rast and Skehan, 1983; Williams and Hatcher, 1983). They are intruded by various granitoid plutons of uncertain ages which range from dioritic to granitic in composition (e.g. Ruitenberg et al., 1979).

The Caledonian Highlands have been previously mapped on a reconnaissance scale by Ruitenberg et al. (1979) and earlier workers, and locally on a more detailed scale (e.g. McLeod, 1983), but no detailed petrological studies have been done. Hence the present study was undertaken to describe and interpret field relations, petrology and age of plutonic and associated metavolcanic rocks in the area of the Fortyfive River pluton north of Alma (Fig. 26.1). This is the first phase of a continuing study of field relations and petrology of igneous rocks in the eastern Caledonian Highlands.

An area of approximately 160 km^2 was mapped in four weeks during the summer of 1985 using 1:10 000 scale orthophoto maps as base maps. A final map was compiled at a scale of 1:20 000, a simplified version of which is shown in Figure 26.1. Over 300 samples were collected; most were slabbed and stained for potassium feldspar and about 165 were examined in thin section. On this basis, 30 plutonic and 22 volcanic and associated sill/dyke samples were selected for major and trace element analyses. Samples were also chosen for Rb-Sr and K-Ar age dating and for mineral analysis by electron microprobe.

This report summarizes the results and conclusions from these studies, with emphasis on the granitoid rocks.

Acknowledgments

The author is grateful to her enthusiastic field assistant, Chris White. She also thanks Kevin Cameron and Juta Cabilio for analytical work, R. McKay for assistance with microprobe analyses. J. Blenkinsop for Rb-Sr dating, and H. Conley for typing the draft manuscript.

METAVOLCANIC AND METASEDIMENTARY ROCKS

Introduction

In areas of good outcrop, the metavolcanic and metasedimentary rocks in the study area can be seen to be extremely varied. However, detailed mapping is hampered by poor exposure except in the larger stream and river valleys. Consequently very broad map units have been defined and numbered arbitrarily from north to south (Fig. 26.1). Further subdivision of these units will probably be possible as mapping is extended beyond the present map area.

The original igneous and sedimentary features of the rocks have been overprinted, and in many places obliterated, by subsequent metamorphism and deformation. Mineral assemblages are now dominated by albite, epidote, and chlorite. No primary igneous minerals remain (except in some mafic rocks interpreted to be younger sills and dykes). The assemblages are indicative of the chlorite zone of the greenschist facies of regional metamorphism. Biotite and amphibole were not observed (except locally in a contact metamorphic aureole), nor were prehnite, pumpellyite or zeolite minerals.

Structural features

Most of the rocks are strongly foliated – many are most accurately termed phyllites or phyllonites. In the relatively few outcrops where identifiable primary layering (S_0) is present, it is parallel to foliation (S_1). However, a strong cataclastic or tectonic overprint has affected most rocks, and has resulted in movements parallel to the S_1 foliation. Such transposition may have obscured any minor folds; no major or minor F_1 folds have as yet been identified.

The S_1 foliation strikes essentially northeast and dips northwest but commonly deviates towards northerly and easterly trends. Such deviations are attributed to later refolding and (or) shearing. The fine-grained metasedimentary phyllites and slates display a variety of minor structures, presumably partly reflecting these later events. Crenulations (L_2) plunging gently northeast and southwest and related steep crenulation cleavage (S_2) striking northeasterly are thought to represent a second weak phase of folding (F_2), approximately coaxial with the presumed F_1 phase of folding which created the main penetrative foliation. More obvious are a group of upright folds (F_3) and related lineations (L_3) which plunge at low to moderate angles towards the northwest. Large scale representatives of these folds certainly cause many of the observed deviations in strike of the S_1 foliation. Conjugate sets of east-west kink bands (F_4) are also a common feature. These plunge westerly at low to moderate angles and have steep east-west kink planes. If large scale kink-style folds exist, these too could contribute to deviations in strike of the S_1 foliation. As an east-west shear foliation (S_4?) is locally present in the granitoid rocks, kinking could also be related to a late shearing event transecting the main northeasterly structural trend.

Although faults may be a major control of the distribution of map units (as suggested by Ruitenberg et al., 1979), they are omitted from Figure 26.1 because of a lack of direct field evidence for their location.

Unit 1

Unit 1, the northernmost unit in the map area, is dominantly a pyroclastic unit in which the most abundant rock types are varied grey phyllitic tuffs generally of intermediate composition. Also present are lithic crystal tuffs, andesitic to dacitic

flows, welded dacitic to rhyolitic tuffs and flows and a variety of other volcanic lithologies. Sedimentary units are locally abundant and include slate and phyllite in which colour varies from pale grey to green, maroon and black, and less commonly medium-to fine-grained meta-arkose. None of these lithologies could be traced as continuous mappable units with the available outcrop distribution.

The mineralogical composition of these rocks is consistent with lower greenschist facies matamorphism. Albite, chlorite, epidote, and quartz are the dominant minerals. White mica is also abundant in metasedimentary rocks. Most samples are strongly foliated, and relict igneous textures, other than crystals and rarely lithic fragments, are not preserved.

Unit 2

Unit 2 is a distinctive arkosic unit which was informally termed the "Fortyfive River arkose" by Ruitenberg et al. (1979). It varies from coarse-grained and pebbly to medium-grained equigranular. Quartz is the dominant component of clasts, which are typically angular and poorly sorted. Most samples are foliated, sheared, and cataclased so that the original texture is difficult to interpret. Variable amounts (up to 15%) of potassium feldspar and albite clasts are also present. Lithic fragments are mainly quartzitic.

The groundmass consists almost entirely of sericite, together with some coarser grained muscovite, epidote, chlorite and accessory minerals. It displays a strong foliation in many samples.

The relationship between the arkose and the dominantly metavolcanic units to the north and south is not known. However, the arkose unit appears to predate the Fortyfive River granodiorite, sheets of which occur within the arkose in the northeastern part of the map area. Also present locally in unit 2 are small mafic and felsite dykes.

Unit 3

Unit 3 is a dominantly volcanic rock package which lacks the abundant phyllitic tuffs, phyllites and slates of unit 1 to the north. Although unit 3 contains several distinctive rock types, limited outcrop prevented subdivision into mappable lithologies. The most abundant rock type is medium-grained crystal tuff containing 20-50% plagioclase (now albite) crystals in a fine-grained groundmass dominated by sericite, feldspar and quartz. A second characteristic rock type is a grey pyritic felsite consisting of very fine grained quartz and sericite with minor albite. Also present locally are banded rhyolites and ignimbrites, basaltic to andesitic flows, and many mafic and felsic porphyry sills and dykes. The basaltic flows locally contain large (up to 1 cm) amygdales.

Unit 4

Unit 4 includes abundant mafic volcanic rocks, locally with amygdales up to 1 cm or more in maximum diameter. The amygdales are typically elongate parallel to the foliation which is generally approximately east-west. Plagioclase (now albite) is the most abundant mineral; in some samples it exhibits flow(?) alignment. Other abundant minerals are epidote and chlorite. Carbonate is common in amygdales.

Interlayered with the volcanic rocks are varied metasedimentary rocks, mainly maroon and grey phyllites and slates but locally marble and possibly chert. Mafic dykes are also present.

Although mafic volcanic rocks, in places amygdaloidal, also occur in unit 3, those of unit 4 differ in their association with abundant sedimentary rocks. Crystal tuffs, a dominant component of unit 3, are largely absent from unit 4. Some of the maroon phyllites and slates of unit 4 resemble those of unit 1, but the associated volcanic rocks differ.

Sills and dykes

Mafic sills and dykes are common, especially in the metavolcanic sequences. Most are less than 2 m in width and are conformable with layering and/or foliation in the host rocks. Some are porphyritic with plagioclase phenocrysts. Thin section study indicated that these intrusions are of two types, one containing relict clinopyroxene and the other lacking primary igneous mafic minerals. The clinopyroxene-bearing rocks have subophitic textures. Plagioclase is partially saussuritized but retains compositions of labradorite to andesine. One pyroxene-bearing sill is lamprophyric, containing relict olivine and brown hornblende as well as pyroxene.

The intrusions containing pyroxene are interpreted to be younger than those which lack pyroxene. The latter consist of plagioclase (now albite) with abundant chlorite and epidote. Their mineralogy is similar to that in the host volcanic rocks, and these sills/dykes are interpreted to have been deformed and metamorphosed together with the host rocks, with which they could be comagmatic.

Also present are less abundant felsic sills/dykes including felsite and quartz-feldspar porphyry. These may also be comagmatic with the host volcanic rocks.

Geochemistry

Twenty-two samples were analyzed for major and trace elements (Table 26.1), including both flows and sills/dykes from map units 1, 3 and 4 (Fig. 26.1).

Alteration is reflected in fairly high loss on ignition values, especially in the mafic rocks, ranging up to 4 per cent. It is also probably the cause of much of the variation in the more mobile elements such as Na_2O, K_2O, Rb and Sr. Hence interpretations of the chemistry are based primarily on elements which are normally less mobile during alteration and low-grade metamorphism.

The analyzed volcanic samples are mainly basaltic and rhyolitic, and hence appear bimodal. However, most of the pyroclastic rocks in the map area are andesitic to dacitic in composition; hence to term the volcanic package bimodal on

Table 26.1 Chemical analyses* of volcanic rocks and sills/dykes.

	Unit 1		Unit 3						Unit 4			
	006	044	577A	578B	603	035	573	600	085	155C	188	191
SiO_2	57.38	56.84	50.66	47.15	57.58	75.30	68.50	74.0	51.84	47.50	47.61	48.09
TiO_2	1.18	1.51	1.45	1.45	1.24	0.30	0.83	0.3	2.07	1.59	1.31	1.79
Al_2O_3	15.09	15.06	17.09	18.95	17.02	13.16	15.92	14.1	16.05	16.89	17.15	16.89
Fe_2O_3t	9.24	10.28	9.67	10.43	10.40	1.75	3.84	1.9	13.08	12.67	10.18	13.51
MnO	0.15	0.23	0.19	0.20	0.09	0.05	0.10	0.0	0.22	0.20	0.19	0.21
MgO	3.07	4.34	4.34	7.25	1.63	0.00	0.49	0.0	4.81	6.86	7.65	5.80
CaO	4.53	3.75	8.08	4.14	2.97	5.19	3.71	4.8	2.53	4.14	7.09	4.14
Na_2O	4.57	5.32	4.44	4.97	6.32	5.19	3.71	4.8	5.95	5.31	3.17	5.45
K_2O	0.19	0.24	0.14	0.47	0.91	1.51	2.16	2.6	0.13	0.54	1.54	0.68
P_2O_5	0.38	0.40	0.52	0.55	0.24	0.05	0.10	0.0	0.40	0.34	0.38	0.35
LOI	4.12	2.31	3.48	4.16	1.39	0.76	2.52	0.7	2.91	3.88	3.42	3.12
Total	99.90	100.28	100.06	99.69	99.79	99.48	97.92	99.6	99.99	99.90	99.69	100.03
Ba	39	127	133	177	314	290	583	828	85	268	787	368
Rb	3	2	0	6	28	37	61	61	1	10	32	13
Sr	196	141	510	232	369	249	298	130	194	136	336	291
Y	33	36	28	32	27	14	50	17	40	27	26	33
Zr	204	107	149	165	126	185	248	180	145	104	129	127
Nb	13	5	8	10	7	11	10	8	8	6	8	7
Cu	85	12	239	38	15	8	4	0	30	7	15	11
Pb	5	7	5	10	9	8	11	16	11	7	12	10
Zn	114	99	126	156	69	31	92	42	165	141	191	195
Ni	12	18	14	27	4	0	19	7	10	37	59	18
Cr	10	86	51	105	18	29	15	31	10	88	219	37
V	244	160	275	258	270	8	49	4	449	290	275	433
Ga	20	22	24	22	17	15	20	16	24	18	21	22
Th	13	0	0	0	1	4	2	8	0	0	2	2

	Mafic Dykes/Sills							Felsic Sill	Porphyry Sills	
	010	041	042	182	556	557	567A	566	080	561A
SiO_2	47.44	46.32	52.39	47.91	46.80	45.84	46.82	70.79	77.50	70.08
TiO_2	1.14	1.12	1.64	1.71	1.02	1.53	1.12	0.39	0.23	0.43
Al_2O_3	15.93	16.56	14.11	16.64	16.26	15.85	15.89	14.52	11.52	14.73
Fe_2O_3t	11.01	12.12	12.62	10.91	12.09	13.49	10.63	1.72	1.57	2.86
MnO	0.18	0.20	0.21	0.19	0.21	0.26	0.17	0.07	0.04	0.07
MgO	8.05	8.18	5.52	6.92	7.61	7.29	8.39	0.34	0.00	0.76
CaO	10.18	9.74	7.32	7.31	10.17	8.71	10.32	2.71	0.14	2.77
Na_2O	1.90	2.00	3.14	3.17	1.75	2.12	1.72	4.10	4.59	4.44
K_2O	0.67	0.67	0.88	1.76	0.72	0.98	0.95	3.52	3.14	2.32
P_2O_5	0.12	0.15	0.33	0.33	0.13	0.32	0.12	0.07	0.03	0.09
LOI	3.35	2.55	2.33	3.03	2.74	3.01	3.11	0.99	0.47	0.91
Total	99.97	99.61	100.49	99.88	99.37	99.27	99.08	99.22	99.23	99.45
Ba	180	215	262	516	115	287	167	1186	683	766
Rb	18	28	25	41	20	29	26	51	58	35
Sr	141	230	176	341	177	324	130	348	56	336
Y	27	20	36	30	26	32	24	15	39	17
Zr	77	53	115	147	57	95	64	182	164	159
Nb	6	3	7	9	3	7	5	9	12	9
Cu	76	83	53	7	81	55	70	28	0	3
Pb	6	4	1	9	7	9	9	29	13	2
Zn	98	98	111	131	110	135	87	44	46	30
Ni	82	86	26	79	75	64	92	3	14	4
Cr	295	139	32	280	92	75	254	32	30	13
V	277	260	324	245	248	291	228	41	0	35
Ga	15	21	23	20	19	20	18	16	14	16
Th	0	0	0	0	0	0	2	6	5	0

*Major element analyses by atomic absorption spectrometry, Acadia University; analyst J. Cabilio. LOI = loss on ignition. Fe_2O_3t = total iron expressed as Fe_2O_3. Trace element analyses by X-ray fluorescence, St. Mary's University; analyst K. Cameron.

the basis of the analyzed samples would be misleading, because pyroclastic rocks are not represented.

The analyzed samples are clearly subalkaline (Fig. 26.2). They appear to be tholelitic rather than calc-alkalic (Fig. 26.3). They do not display a decrease in V with increasing Cr and FeO^t/MgO, criteria suggested by Miyashiro and Shido for identification of calc-alkalic suites. A plate margin tectonic setting is indicated (Fig. 26.4). These geochemical indicators are consistent with the abundance of pyroclastic rocks which is also indicative of a volcanic arc environment.

The mafic sills/dykes are generally chemically similar to their host rocks (Fig. 26.2, 26.3, 26.4), and also appear to have formed in a volcanic arc environment. The clinopyroxene-bearing dykes are not significantly different from the other mafic dykes, although their less metamorphic mineralogy suggests that they may be younger.

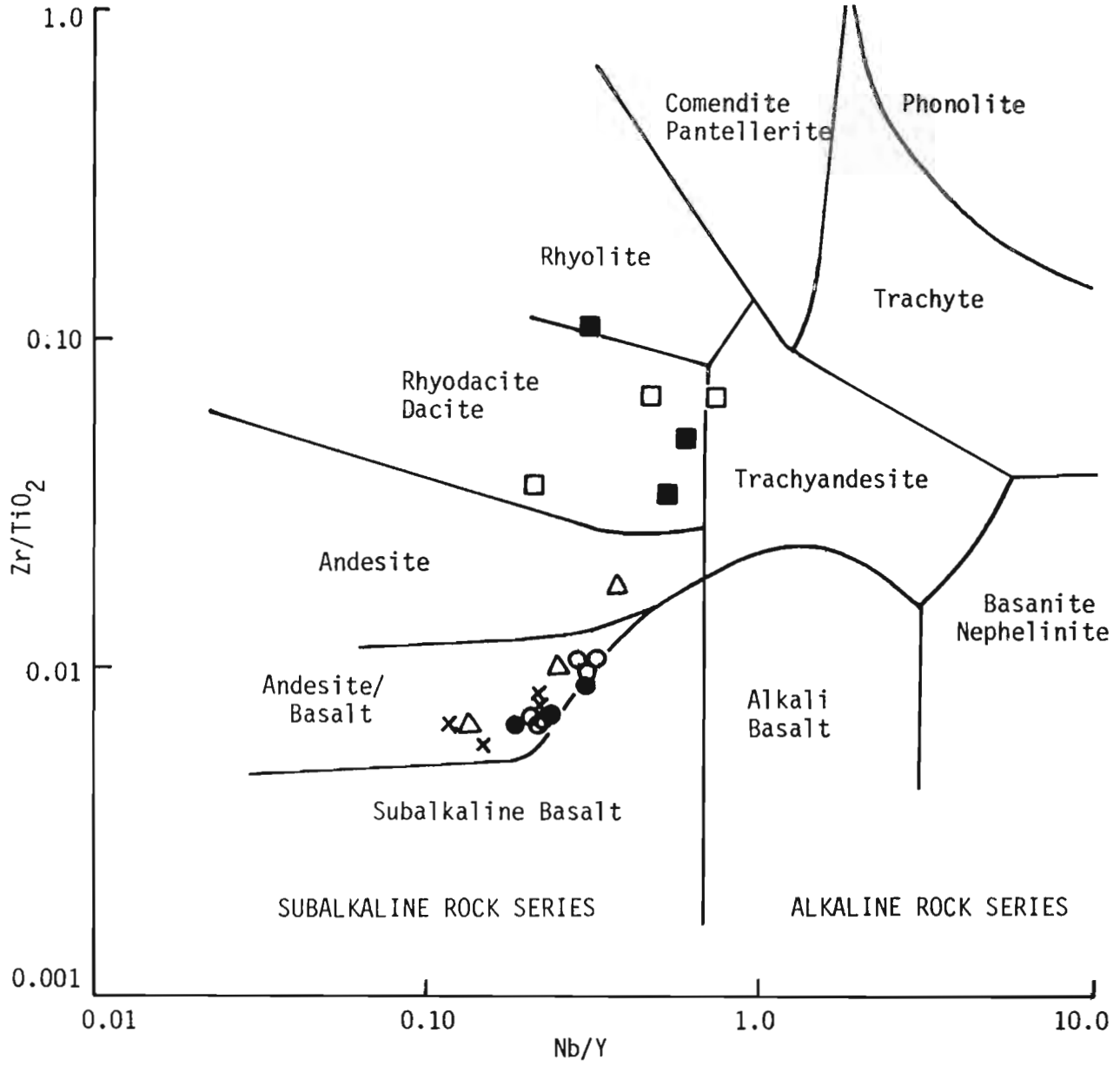


Figure 26.2. Plot of Zr/TiO_2 against Nb/Y for metavolcanic rocks (open circles = basalt, open triangles = andesites, open squares = felsic flows) and sill/dykes (black circles = pyroxene-free, crosses = pyroxene-bearing, black squares = felsic rocks). Fields from Winchester and Floyd (1977).

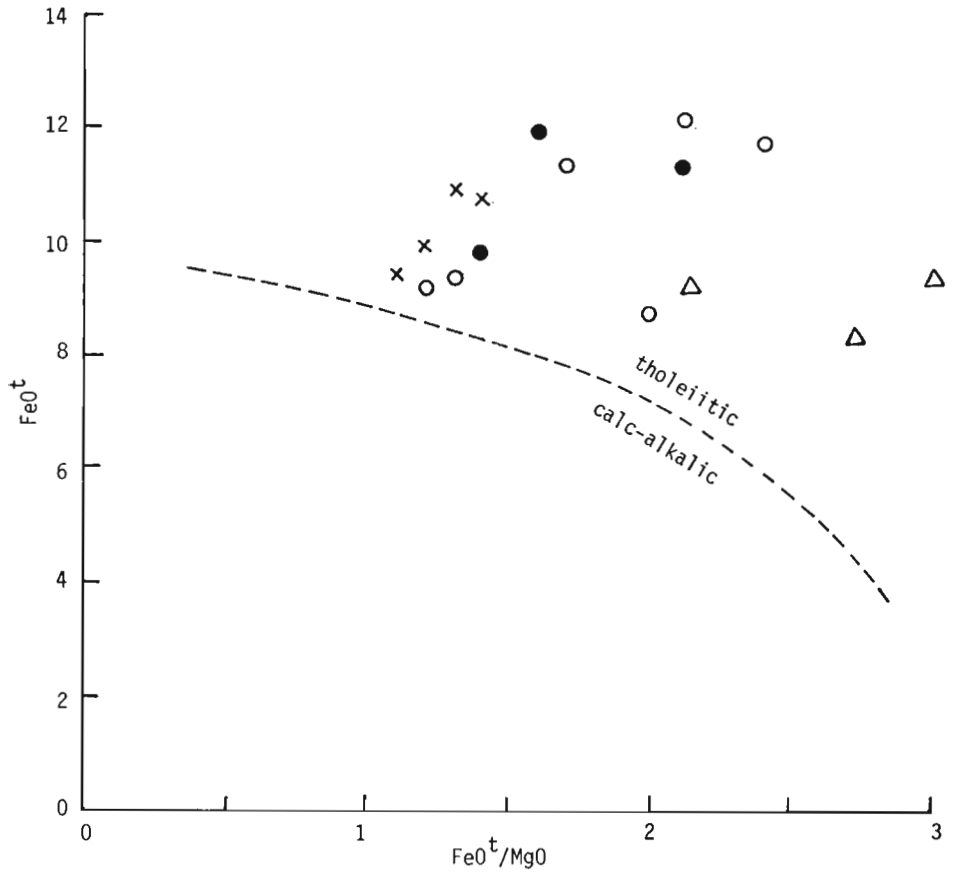


Figure 26.3. Plot of FeO^t against FeO^t/MgO. Symbols as in Figure 26.2. Calc-alkali and tholeiitic dividing line from Miyashiro (1974).

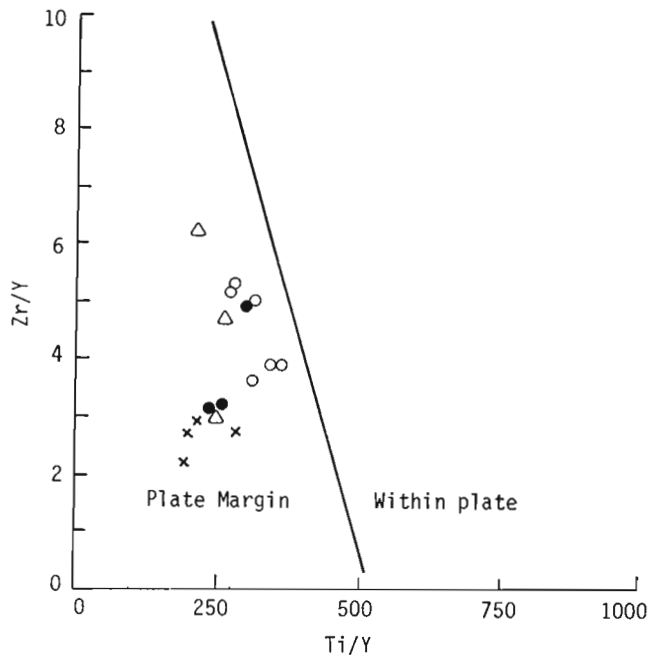


Figure 26.4. Plot of Zr/Y against Ti/Y. Symbols as in Figure 26.2. Within plate and plate margin dividing line from Pearce and Gale (1977).

PLUTONIC ROCKS

Introduction

Previous workers named three intrusions in the map area – the Alma Stock, Fortyfive River Sill, and Goose Creek Sill (Ruitenberg et al., 1979) and these names are retained with some modification. The Alma Stock, herein referred to as the Alma pluton, is the best exposed intrusion, and its boundaries are little changed from Ruitenberg et al. (1979). The Fortyfive River "sill" is referred to as the Fortyfive River pluton and interpreted to consist of two separate bodies (eastern and western). The Goose Creek "sill" is re-interpreted in the study area as a series of small intrusions (Fig. 26.1), which are collectively referred to as the Goose Creek leucotonalite.

In addition, various granitoid dykes/sills and minor intrusive bodies were noted. Most appear to be similar in composition to the larger plutons noted above. However, small isolated bodies of pyroxene-bearing diorite and tonalite in the northeastern corner of the map area and rare granitic dykes/sills in units 1, 3, and 4 appear distinctly different from the major plutons described below. Detailed petrological descriptions of these minor intrusions are beyond the scope of this report.

Foliations in the plutonic rocks are essentially shear foliations which have produced locally pervasive cataclasis. Strike orientations of these foliations are mainly northeast-southwest, north-northwesterly, and east-west, corresponding geometrically, and probably genetically, to the S_{2-4} foliations recognized in the country rocks. More than one foliation may be present in one pluton; e.g., in the Alma pluton east-west foliation predominates in the central part whereas more northerly foliation(s) are found at the southern end.

Fortyfive River pluton

Field relations and petrography

The Fortyfive River pluton consists of distinctive medium-grained, greenish granodiorite. The elongate eastern and western parts of the pluton are grossly concordant with their metasedimentary and metavolcanic host rocks. However, in places the contacts appear to be strongly discordant, and outcrops of granodiorite, interpreted to be dykes or sheets are common in the metasedimentary unit adjacent to the eastern pluton and in the metavolcanic unit southeast of the western pluton. Nonetheless, no actual intrusive contacts were observed, and the role of faulting in controlling the form and distribution of the plutonic rocks may be considerable.

Locally strong and pervasive foliation in the pluton is the result of shearing and cataclasis. Where least deformed the plutonic rocks have subporphyritic hypidiomorphic inequigranular texture consisting of subhedral plagioclase in a groundmass of quartz, potassium feldspar and mafic minerals. The plagioclase is almost completely altered to saussurite, a mixture of opidote, albite, sericite and other secondary minerals. Microprobe analyses in samples 051, 090, and 553 yielded albitic compositions (Ab_{97-99}). Potassium feldspar, occurring interstitially with quartz, is much less altered,

Table 26.2 Representative microprobe analyses* of amphiboles.

	Alma Pluton			Fortyfive River Pluton		
	060		531	051		553
SiO_2	44.22	44.54	48.71	47.28	51.77	53.35
TiO_2	2.77	2.21	1.43	1.73	0.55	0.10
Al_2O_3	11.33	10.58	6.66	7.01	3.47	2.72
FeO	12.49	13.83	13.32	12.54	13.71	13.02
MnO	0.18	0.21	0.29	0.20	0.60	0.22
MgO	13.86	13.57	15.04	15.21	15.08	15.50
CaO	11.53	11.47	11.26	11.52	11.90	12.46
Na_2O	1.82	1.67	1.13	1.63	0.84	0.29
K_2O	0.03	0.02	0.04	0.44	0.16	0.04
H_2O	2.06	2.04	2.06	2.05	2.07	2.08
Total	100.29	100.14	99.94	99.61	100.15	99.78
Number of cations on the basis of 24 oxygen, 2 hydrogen.						
Si	6.44	6.53	7.08	6.92	7.51	7.69
Al	1.56	1.48	0.92	1.08	0.49	0.31
Al	0.38	0.35	0.22	0.13	0.10	0.16
Ti	0.30	0.24	0.16	0.19	0.06	0.01
Fe	1.52	1.69	1.62	1.54	1.66	1.57
Mn	0.02	0.03	0.04	0.03	0.07	0.03
Mg	3.01	2.96	3.26	3.32	3.26	3.33
Ca	1.80	1.80	1.75	1.81	1.85	1.93
Na	0.51	0.47	0.32	0.46	0.24	0.08
K	0.01	0.00	0.01	0.08	0.03	0.01

* Using Cambridge Instruments Microscan 5 with Ortec Energy Dispersive system at Dalhousie University, Department of Geology.

and locally displays patchy microperthitic exsolution blebs. Microprobe analyses indicated compositions of about Or_{95-97}. A relatively low 2V (50-60°) and lack of grid twinning suggest that the potassium feldspar is orthoclase.

The mafic minerals are almost entirely replaced by chlorite, epidote, actinolite and opaque minerals. Only a few samples contain what may be a primary magnesio-hornblende, and this survives only as cores in large grains which are actinolitic (Table 26.2). Based on crystal form, some chlorite and epidote appear to have replaced biotite. Scattered magnetite grains are also present, as well as veinlets of epidote and carbonate.

Because of the alteration in these rocks, accurate modal analyses are not possible. However, an estimate based on the least altered samples is plagioclase (45%), potassium feldspar (10%), quartz (15%), and mafic minerals (30%). The present mineralogy indicates that, like its host rocks, the Fortyfive River pluton has experienced lower greenschist facies metamorphism.

Geochemistry

Silica contents in 13 samples from the Fortyfive River pluton range from 61 to 69% (Table 26.3). The two highest SiO_2 samples (553 and 618) are both from the eastern part of the pluton (Fig. 26.1) and contain more quartz and K-feldspar compared to the other samples. In spite of the extremely altered nature of many of the samples, geochemical data are not widely scattered and TiO_2, Al_2O_3, $Fe_2O_3^t$, MnO, MgO, CaO and P_2O_5 all show reasonable negative correlation with SiO_2 (Fig. 26.5). However, CaO is variable, and Na_2O and K_2O are also scattered and show no significant correlation with SiO_2. Ba, Rb, and Sr show similar patterns (Fig. 26.6). Although scattered, U and Th show some positive correlation with SiO_2 (Fig. 26.7) and V displays negative correlation (Fig. 26.8), whereas the other trace elements show little systematic variation.

A plot of normative mineralogy (Fig. 26.9) confirms the grandioritic composition of the samples. Most contain normative diopside or small amounts of normative corundum

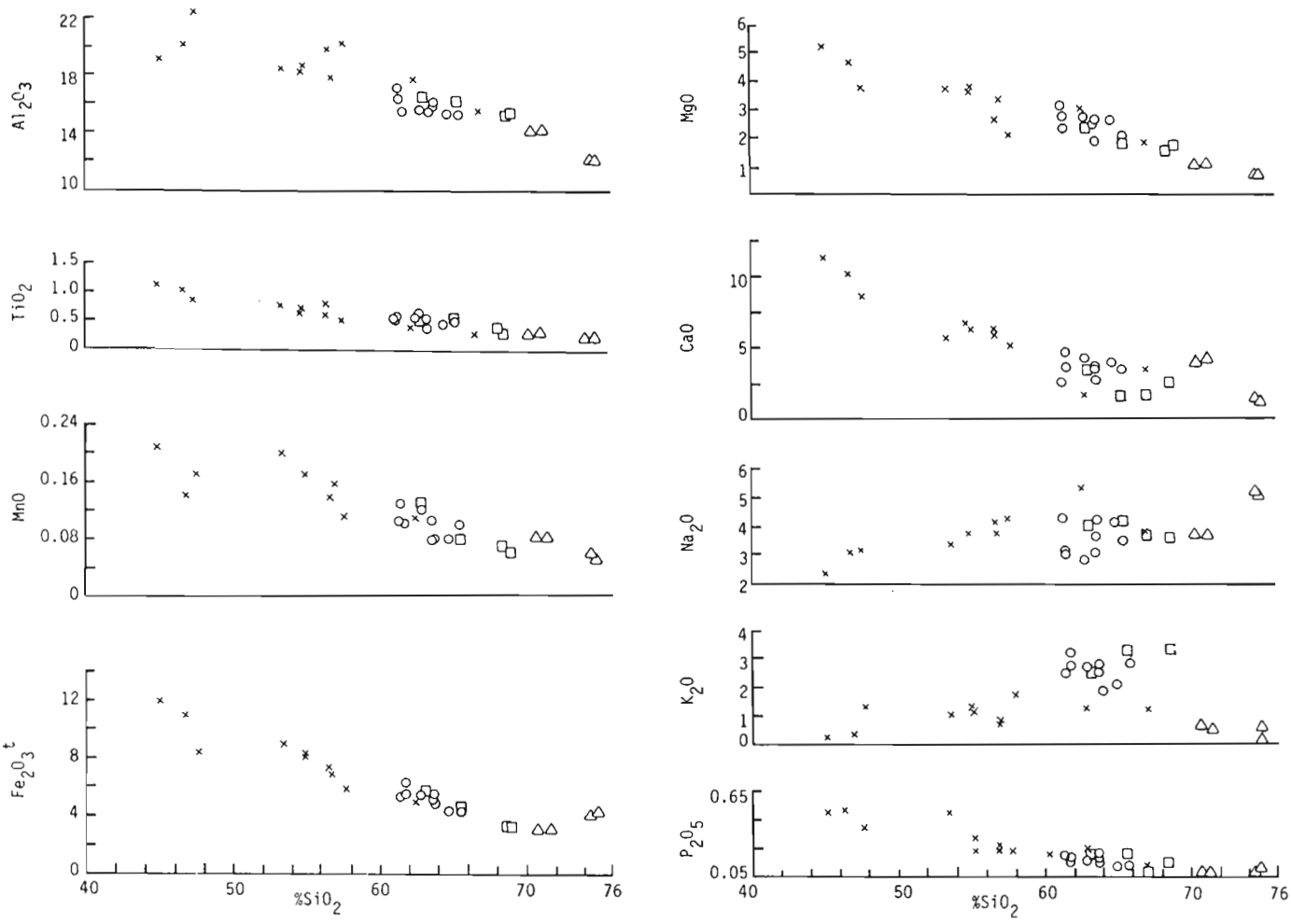


Figure 26.5. Silica variation diagram for major element oxides in samples from the Fortyfive River pluton (open circles west half; open squares east half), Alma pluton (crosses), and Goose Creek leucotonalite (triangles).

Table 26.3 Geochemical data* and CIPW normative mineralogy for samples from the Fortyfive River pluton.

	Western									Eastern			
	009	014A	133	518	521	527	050c	051	052	090	553	596	618
SiO_2	64.71	63.88	61.28	63.49	65.60	63.47	62.89	61.48	61.61	65.37	68.29	63.00	68.93
TiO_2	0.50	0.62	0.67	0.48	0.52	0.72	0.64	0.64	0.60	0.54	0.45	0.66	0.39
Al_2O_3	14.94	16.11	17.03	15.66	15.42	15.99	15.84	16.37	15.41	16.26	15.10	16.57	15.15
$Fe_2O_3^t$	4.54	4.94	5.74	4.26	4.71	5.40	5.95	6.03	5.70	4.49	3.57	5.42	3.59
MnO	0.08	0.08	0.11	0.08	0.10	0.11	0.12	0.13	0.10	0.08	0.07	0.13	0.06
MgO	2.29	2.30	3.22	1.91	2.02	2.59	2.80	2.82	2.49	1.88	1.59	2.47	1.71
CaO	4.00	2.98	2.79	3.86	3.51	3.40	4.35	4.81	3.70	1.55	2.52	3.40	1.73
Na_2O	4.23	4.29	4.47	3.72	3.64	3.12	2.91	3.29	3.04	4.31	3.65	4.01	3.86
K_2O	2.06	1.91	2.54	2.59	2.98	2.91	2.77	2.71	3.28	3.33	3.46	2.67	3.35
P_2O_5	0.14	0.20	0.20	0.17	0.14	0.16	0.16	0.16	0.15	0.18	0.15	0.19	0.11
LOI	2.70	2.90	2.10	2.30	1.50	2.10	1.90	1.60	2.30	1.70	1.40	1.70	1.30
Total	100.17	100.21	100.16	98.53	100.13	99.98	100.33	100.06	98.39	99.71	100.26	100.20	100.18
CIPW Normative Mineralogy													
Q	19.49	20.52	12.65	19.90	20.66	21.11	19.63	15.20	17.86	20.06	25.01	16.52	26.24
C	0.00	2.14	2.40	0.14	0.14	1.97	0.58	0.00	0.51	3.25	1.17	1.40	2.34
Or	12.55	11.61	15.41	15.99	17.95	17.65	16.68	16.32	20.31	20.14	20.72	16.11	20.06
Ab	36.79	37.39	38.70	32.76	31.36	27.16	25.08	28.44	26.92	37.39	31.36	34.53	33.07
An	16.19	13.92	12.85	18.84	16.87	16.28	20.93	22.40	18.18	6.69	11.65	15.94	8.00
Di	1.53	0.00	0.00	0.00	0.00	0.00	0.00	0.40	0.00	--	--	--	--
En	5.17	5.89	8.20	4.94	5.10	6.64	7.10	6.97	6.46	4.80	4.02	6.25	4.32
Il	0.98	1.22	1.31	0.95	0.99	1.00	1.24	1.24	1.19	1.03	0.85	1.28	0.75
Mt	0.87	0.94	1.10	0.83	0.89	1.03	1.13	1.14	1.11	0.86	0.68	1.04	0.66
Ap	0.31	0.48	0.48	0.39	0.31	0.38	0.38	0.38	0.36	0.40	0.35	0.45	0.24
ppm													
Ba	610	548	1073	735	755	776	842	806	923	1063	692	913	770
Rb	34	60	46	58	76	71	73	65	77	98	101	64	79
Sr	300	450	261	444	406	433	427	443	346	272	294	446	322
Y	21	22	23	19	24	24	25	24	26	23	22	21	20
Nb	8	9	9	10	9	9	123	138	139	146	141	145	128
Cu	20	73	16	11	20	26	8	8	8	10	10	9	9
Pb	6	11	5	8	8	6	14	13	95	27	9	24	6
Zn	52	66	89	41	53	66	101	74	55	68	55	63	41
Ni	11	8	8	8	10	10	11	7	10	7	10	8	9
Cr	23	26	21	20	26	22	10	17	21	28	23	21	24
V	89	110	117	73	101	104	126	135	120	76	58	116	66
Ga	15	19	18	19	17	17	18	18	16	18	18	19	20
Th	3	5	2	7	4	3	3	5	0	8	8	2	12
U	2.3	2.2	1.9	3.0	2.1	2.8	2.2	1.8	1.8	2.2	2.5	1.7	3.3
Li	10	9	11	13	6	14	13	11	12	8	9	12	14

* Analyses by X-Ray Fluorescence, St. Mary's University; analyst K. Cameron.
Normative mineralogy calculated with $Fe^{3+}/Fe^{2+} = 0.15$.

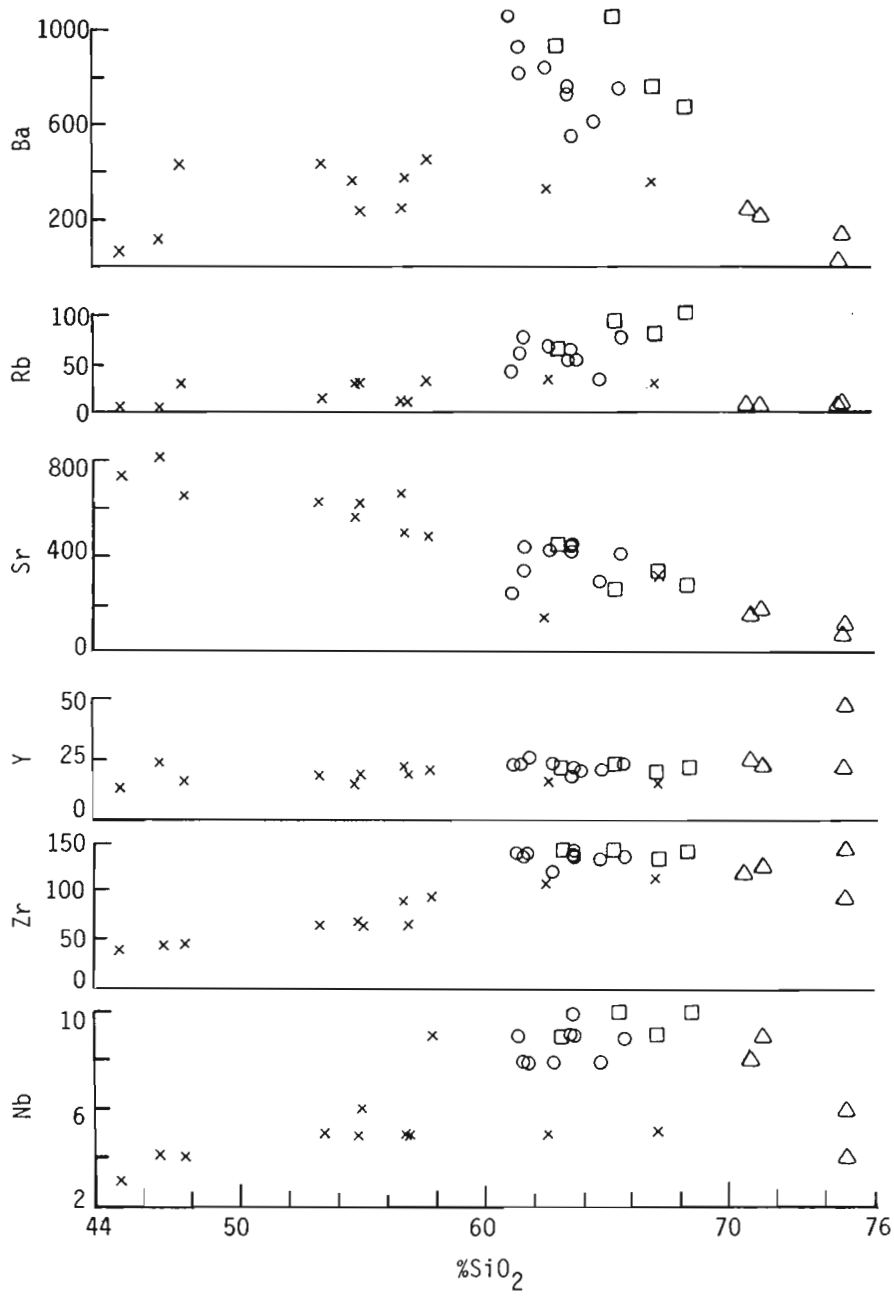


Figure 26.6. Silica variation diagrams for Ba, Rb, Sr, Y, Zr, and Nb. Symbols as in Figure 26.5.

(Table 26.3). On the basis of mineralogical and chemical criteria, the pluton is "I-type" (Chappell and White, 1974, 1983) and the low Rb and Y + Nb, even in the high SiO_2 samples, clearly indicate formation in a volcanic arc tectonic environment (Pearce et al., 1984).

Alma pluton

Field relations and petrography

Varied dioritic rocks are the main components of the Alma pluton, located northwest of the village of Alma (Fig. 26.1). Unlike the other plutons to the north, the lobate Alma intrusion is elongate north-south, and hence largely discordant with regional structural trends (Fig. 26.1).

The pluton ranges from diorite through quartz diorite to tonalite. These lithologies are interlayered and gradational in some areas, but elsewhere appear to have intrusive contacts. The rocks are typically medium-grained with hypidiomorphic granular texture consisting of plagioclase, amphibole, variable amounts of quartz, and secondary minerals.

In most samples, the plagioclase is almost completely saussuritized, consisting of a mixture of albite, epidote, sericite, zoisite and other secondary minerals. Microprobe

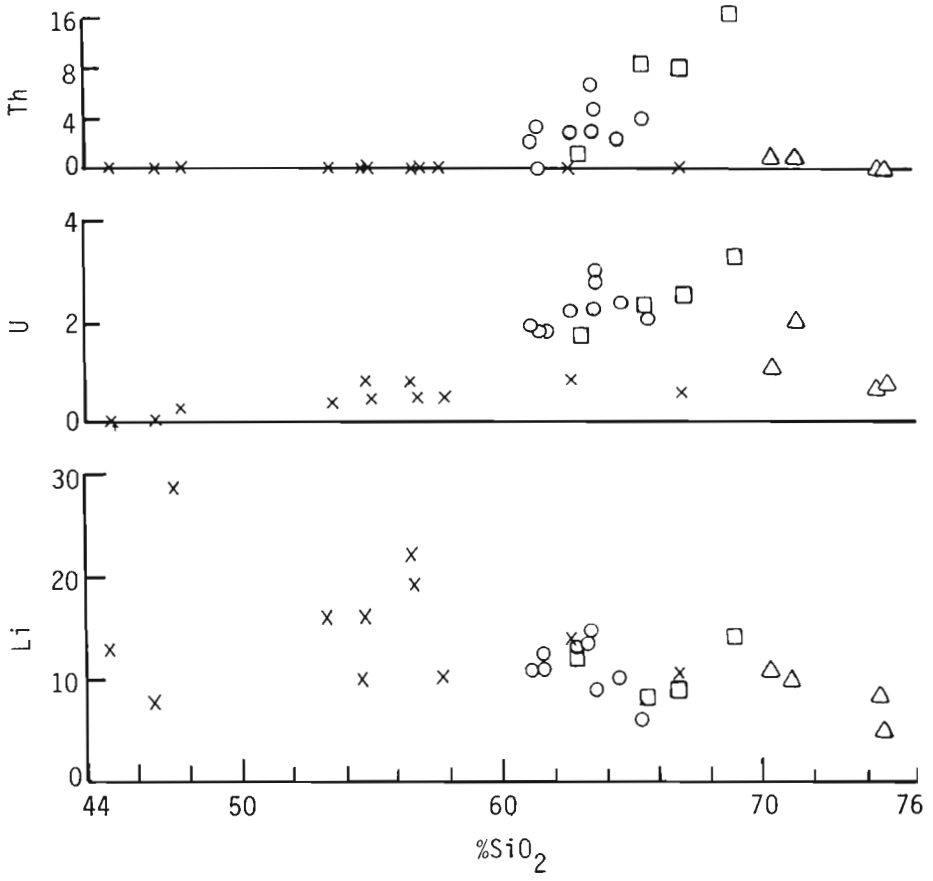


Figure 26.7. Silica variation diagrams for Th, U, and Li. Symbols as in Figure 26.5.

analyses of plagioclase in two of the latest altered samples indicated zoned labradorite compositions in sample 060 (diorite) and labradorite to oligoclase in sample 531 (quartz diorite).

Relict amphibole is present in some samples, but in many it has been altered to Mg-Fe chlorite and other secondary minerals. Where present, it displays olive green to green to colourless pleochroism and has a subophitic relation to plagioclase. Microprobe analyses (Table 26.2) indicate that the amphiboles are magnesio-hornblendes (Leake, 1978). However, amphibole in sample 060 has higher alumina and lower silica and borders on tschermakitic hornblende. In quartz diorite and tonalite samples, some of the chlorite appears to have replaced biotite rather than amphibole, indicating the former presence of both mafic minerals.

Where present, quartz is medium grained, anhedral and interstitial to plagioclase. Granulation, subgrain boundaries and undulatory extinction are typically developed. Accessory minerals include apatite, magnetite, and pyrite.

Geochemistry

The silica content in eleven analyzed samples from the Alma pluton ranges from about 45 to 67% (Table 26.4). This variation is reflected in the amount of quartz in the samples. The three samples with lowest SiO_2 are diorites, with less than 1% interstitial quartz. The intermediate-silica samples are representative of the quartz diorite which is the most abundant lithology in the pluton. The two high-silica samples are tonalites.

Major element contents (e.g. high Al_2O_3) are generally correlative with the abundance of plagioclase in these samples. Although there is considerable scatter, TiO_2, Al_2O_3, $Fe_2O_3^t$, MnO, MgO, CaO, and P_2O_5 display negative correlation with SiO_2, whereas Na_2O generally increases (Fig. 26.5). The three diorite and quartz diorite samples with high P_2O_5 contain relatively abundant coarse granular apatite. K_2O varies little through the range of SiO_2; its slightly higher abundance in diorite sample 037 is reflected in the presence of minor K-fledspar in the rock. The low K_2O level in the tonalites contrasts with K_2O contents in the Fortyfive River granodiorite which has similar SiO_2 abundances. Other major elements in the two tonalite samples are generally similar to those in the Fortyfive River grandiorite. A typical calc-alkalic trend is apparent between the dioritic rocks and the Fortyfive River granodiorite (Fig. 26.10).

Ba and Rb contents are relatively low and patterns are very similar to that of K_2O, with no regular trend with increasing SiO_2 (Fig. 26.6). Similarly, Sr follows CaO. Y and Nb show little systematic variation, whereas Zr increases with SiO_2 (Fig. 26.6).

The elements Cu, Pb, Zn, Ni, and Li are scattered and show little correlation with SiO_2 (Fig. 26.7, 26.8). V and Ga

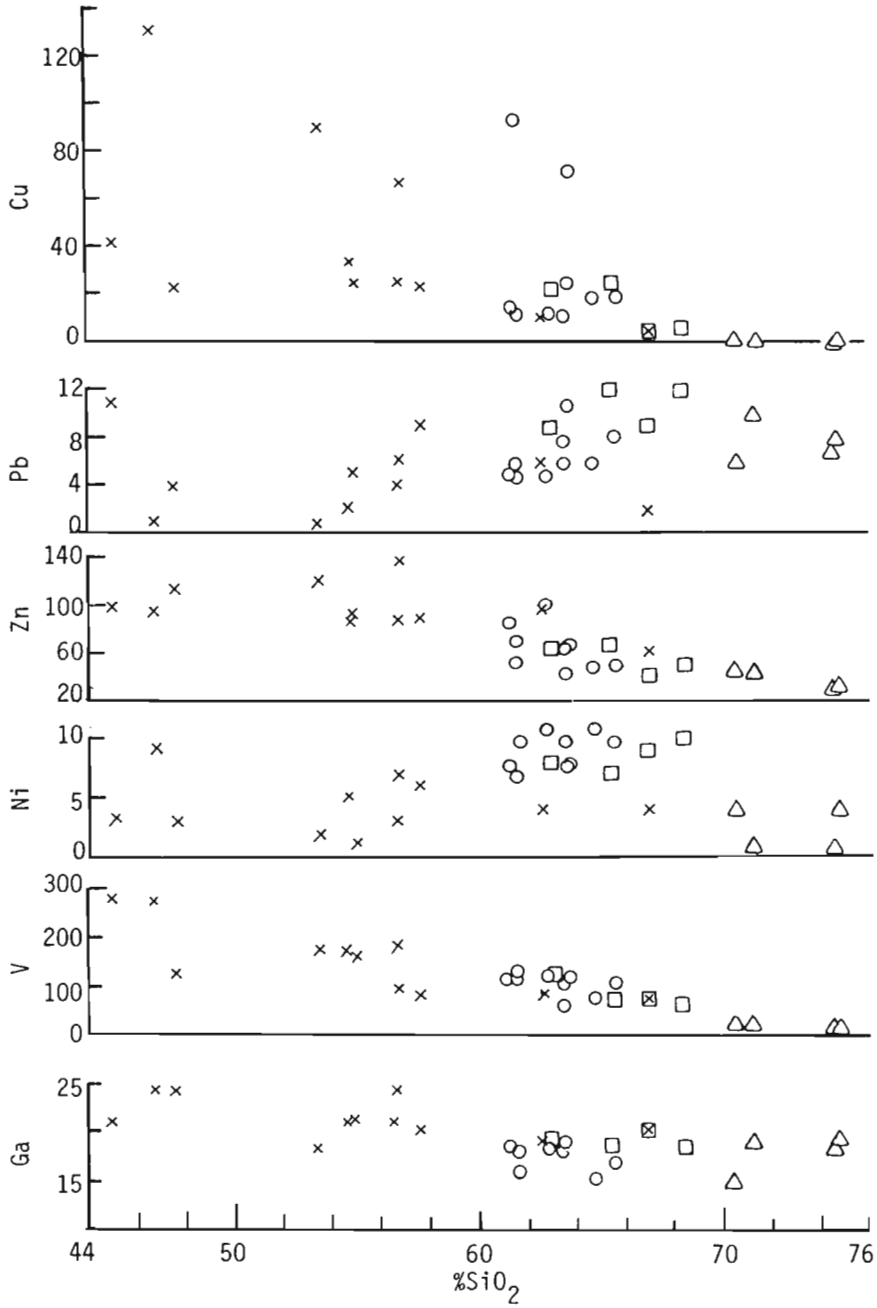


Figure 26.8. Silica variation diagrams for Cu, Pb, Zn, Ni, V, and Ga. Symbols as in Figure 26.5.

display negative correlation with SiO_2 but Th is essentially O in all eleven samples. The low U in particular contrasts with values in the Fortyfive River granodiorite.

The normative mineralogy is consistent with dioritic to tonalitic compositions (Fig. 26.9).

Goose Creek leucotonalite

Field relations and petrography

The Goose Creek leucotonalite is a distinctive greyish-white leucocratic rock which lacks potassium feldspar. It apparently extends southwest of the study area as a major map unit (Ruitenberg et al., 1979; McLeod, 1983) but within the study area it is interpreted to occur in four separate bodies. However, outcrop is very limited, and these bodies could be more (or less) extensive than shown.

The leucotonalite consists mainly of quartz and plagioclase. The plagioclase now appears to be entirely of albite composition, as confirmed by microprobe analyses of one sample which yielded compositions of Ab_{97} to Ab_{99}. Granophyre-like intergrowths, consisting of quartz and albite, form up to 30 per cent of some samples. Non-granophyric samples are fine- to medium-grained and allotriomorphic granular. Secondary minerals include epidote in abundant, small, interstitial grains and rare coarse clusters, and much

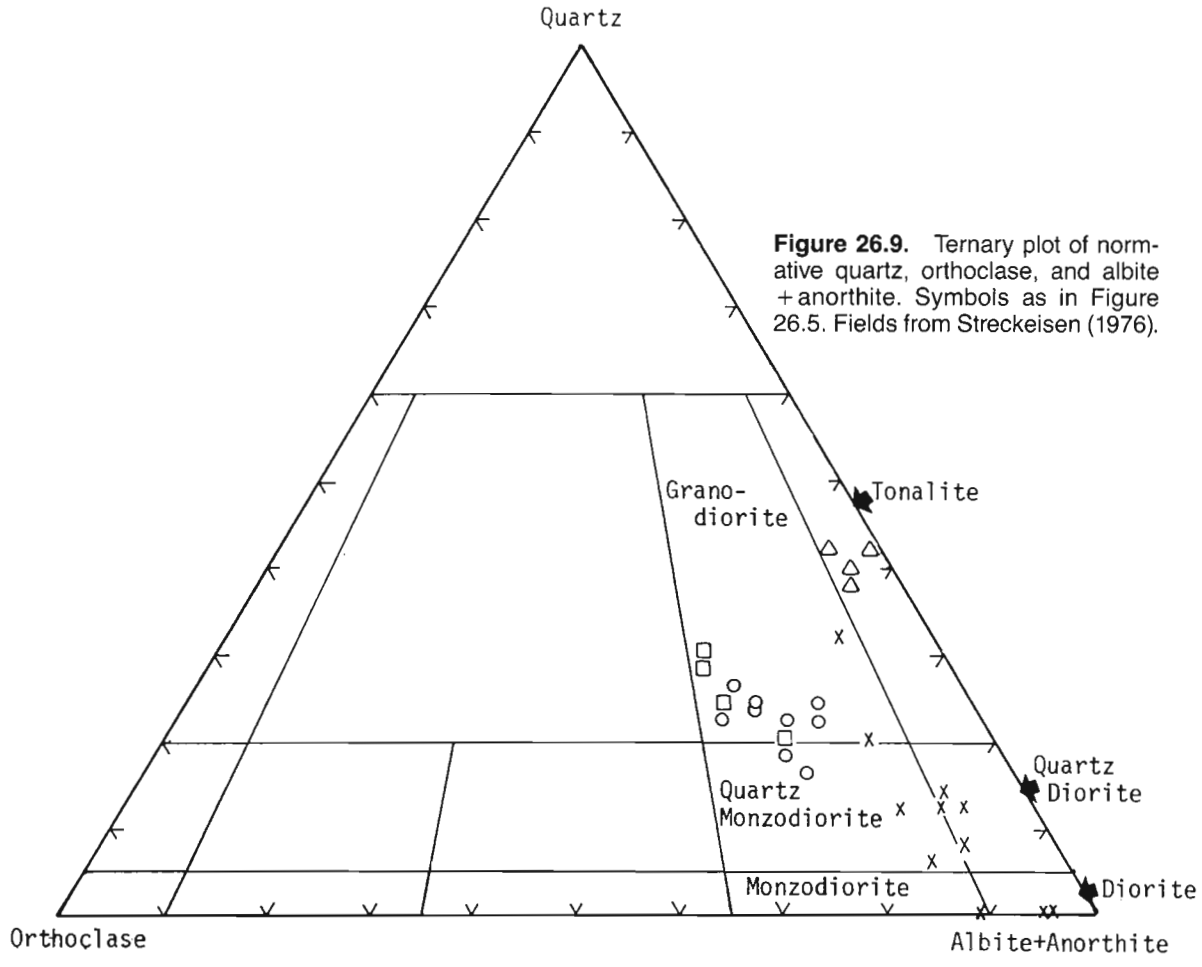


Figure 26.9. Ternary plot of normative quartz, orthoclase, and albite + anorthite. Symbols as in Figure 26.5. Fields from Streckeisen (1976).

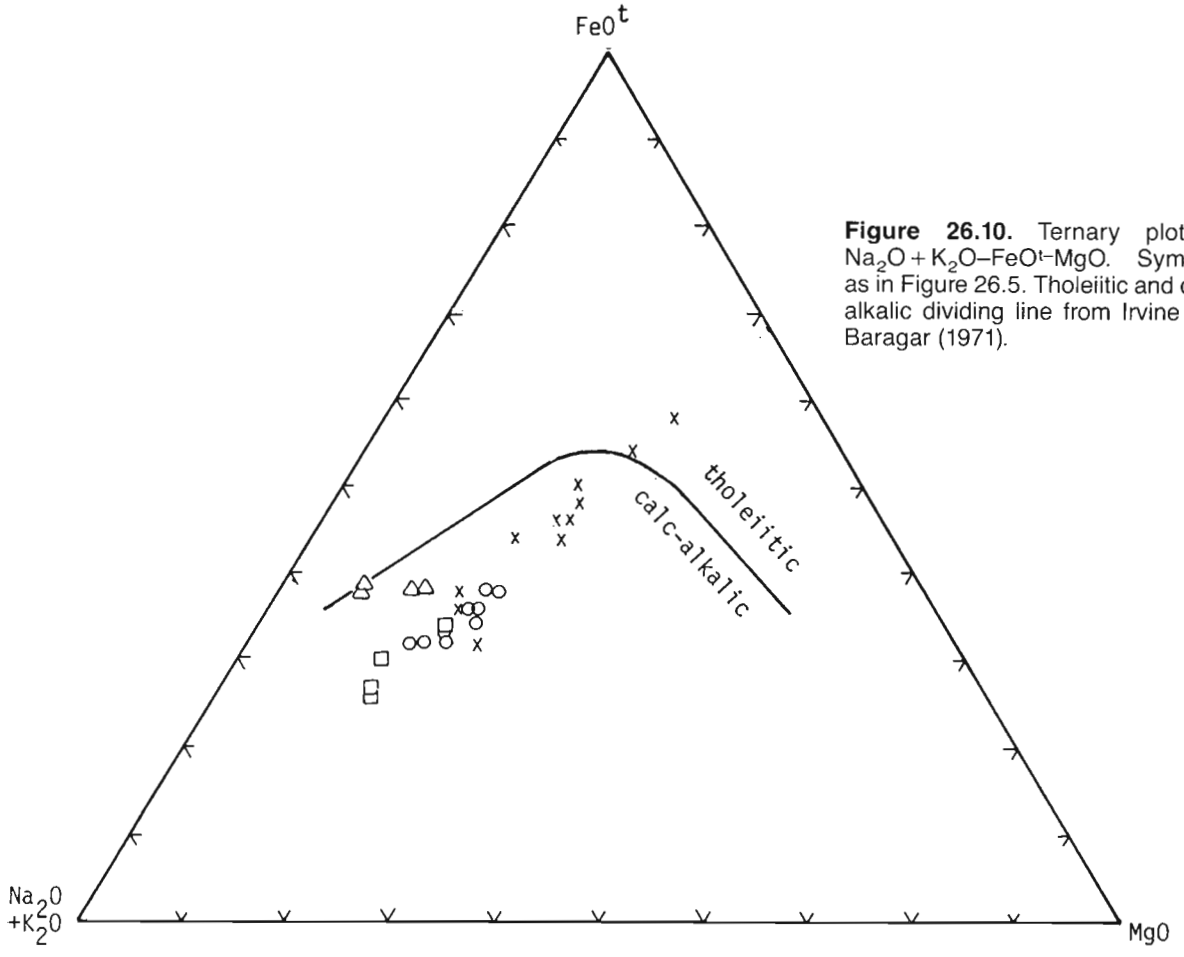


Figure 26.10. Ternary plot of $Na_2O + K_2O$–FeO^t–MgO. Symbols as in Figure 26.5. Tholeiitic and calc-alkalic dividing line from Irvine and Baragar (1971).

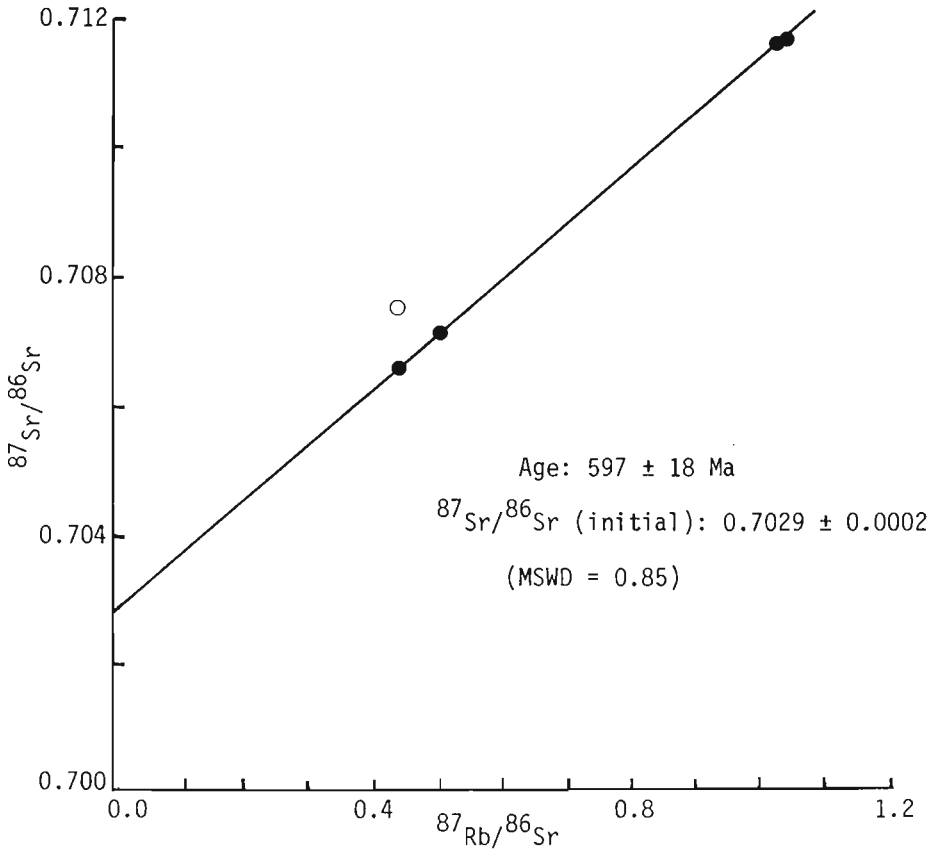


Figure 26.11. Rb-Sr isochron plot for samples from the Fortyfive River pluton. Open symbol is sample 596 which was excluded from the age calculation. Uncertainties quoted are based on the method of York (1969).

less abundant chlorite. No relict mafic minerals are present. Cataclastic deformation ranges from moderate to intense, and the most deformed samples are difficult to recognize as granitoid.

Geochemistry

Four analyzed samples from the leucotonalite have compositions consistent with its leucocratic composition (Table 26.4). Two samples have silica contents of about 71% whereas the other two have nearly 75% SiO_2. Petrographically this difference correlates with more abundant modal quartz in the high silica samples. All four samples are relatively low in TiO_2, Al_2O_3, $Fe_2O_3{}^t$, MnO, MgO, and P_2O_5, with lower concentrations in the high-silica samples than in the low-silica samples, except in the case of $Fe_2O_3{}^t$ (Fig. 26.5). The low-silica samples are notably high in CaO and the high-silica samples high in Na_2O compared with chemical trends in the Fortyfive River granodiorite suite. Most anomalous compared to the latter suite is the very low K_2O content in the Goose Creek leucotonalite, even compared to the Alma tonalite.

These major element patterns are accompanied by generally low minor and trace element abundances. Ba and Rb are exceptionally low (Fig. 26.6), consistent with the low K_2O.

Low K_2O results in the samples plotting close to the quartz-albite + anorthite join on the normative Q-Or-Ab + An triangle (Fig. 26.9). The samples contain small amounts of normative corundum.

AGE DATING

The Fortyfive River pluton was assigned an Ordovician or older age by Ruitenberg et al. (1979), and the Alma and Goose Creek bodies were assigned to the Mississippian or older. As part of the present study, five samples of the Fortyfive River granodiorite were selected for Rb-Sr dating (Table 26.5). Four of these define a whole-rock Rb-Sr isochron indicating an age of 597 ± 18Ma. However, the fifth sample (596) does not lie on this isochron, although no reason for this discrepancy is apparent from the petrography, chemistry, or field relations. Although less affected than most other samples from the pluton, all five samples exhibit the alteration and deformational effects which are pervasive throughout the Fortyfive River pluton. Hence the age is likely to be a minimum age of the intrusion. It is similar to ages obtained from granitoid plutons elsewhere in areas considered to be part of the Avalon Terrane (see Discussion). The very low initial $^{87}Sr/^{86}Sr$ ratio is also a typical feature of these Avalonian plutons (e.g. Cormier, 1972; O'Brien et al., 1983).

Table 26.4 Geochemical data* and CIPW normative mineralogy for samples from the Alma pluton and Goose Creek leucotonalite.

	Alma Pluton											Goose Creek Leucotonalite			
	024	029	034	037	060	087	088	176	186	531	572	110	117A	503	653
SiO_2	45.07	56.65	54.84	47.74	46.81	56.80	53.44	57.87	62.57	54.98	66.97	74.76	71.32	70.47	74.64
TiO_2	1.10	0.59	0.71	0.90	1.03	0.83	0.79	0.52	0.47	0.71	0.39	0.34	0.40	0.40	0.31
Al_2O_3	19.15	19.88	18.29	22.56	20.34	17.78	18.49	20.05	17.63	18.63	15.59	12.16	14.26	14.20	12.50
Fe_2O_3t	12.07	6.40	8.09	8.39	10.69	7.23	9.29	5.55	5.08	8.06	4.64	4.51	3.65	3.62	4.26
MnO	0.21	0.14	0.16	0.17	0.14	0.16	0.20	0.11	0.11	0.17	0.08	0.05	0.08	0.08	0.06
MgO	5.23	2.66	3.72	3.89	4.68	3.47	3.74	2.15	3.10	3.82	1.95	0.69	1.18	1.09	0.75
CaO	11.22	6.33	6.67	8.80	10.12	5.66	5.85	5.20	1.65	6.29	3.46	1.15	4.01	3.95	1.39
Na_2O	2.39	4.20	3.68	3.20	3.10	3.80	3.46	4.40	5.44	3.84	3.99	5.10	3.69	3.75	5.35
K_2O	0.26	0.79	1.44	1.26	0.41	0.88	1.03	1.69	1.37	1.09	1.26	0.64	0.51	0.63	0.11
P_2O_5	0.49	0.26	0.33	0.37	0.54	0.22	0.51	0.21	0.20	0.23	0.13	0.07	0.08	0.08	0.06
LOI	2.70	2.50	2.30	3.20	1.20	2.80	2.80	2.10	2.00	2.30	2.00	0.70	1.00	1.00	0.40
Total	99.82	100.39	100.22	100.46	99.06	99.60	99.60	99.84	99.61	100.12	100.45	100.18	100.18	99.29	99.82
CIPW Normative Mineralogy															
Q	0.00	9.17	5.09	0.00	0.00	11.27	7.89	9.27	15.86	5.66	27.01	37.22	36.33	35.17	37.22
C	0.00	1.26	0.00	0.83	0.00	0.86	2.39	2.09	4.85	0.27	1.73	1.18	0.57	0.37	1.24
Or	1.54	4.74	8.71	7.66	2.50	5.36	6.35	10.22	8.29	6.64	7.55	3.82	3.05	3.75	0.60
Ab	21.04	36.45	32.04	28.06	26.99	33.37	30.43	38.30	47.31	33.47	34.36	43.48	31.51	32.40	45.62
An	42.42	30.60	29.99	42.80	41.72	27.74	26.72	25.15	7.03	30.55	16.67	5.31	19.55	19.48	8.57
Di	5.10	0.00	0.77	0.00	2.76	0.00	0.00	0.00	0.00	0.00	0.00	--	--	--	--
En	2.95	6.79	9.15	2.56	2.54	8.97	9.68	5.51	7.93	9.77	4.96	1.74	2.95	2.77	1.89
Il	2.17	1.13	1.39	1.75	2.02	1.58	1.54	1.00	0.92	1.39	0.76	0.63	0.77	0.78	0.60
Mt	2.34	1.22	1.55	1.62	2.05	1.40	1.80	1.07	0.97	1.55	0.87	0.85	0.69	0.68	0.81
Ap	1.18	0.60	0.79	0.87	1.27	0.51	1.23	0.48	0.48	0.55	0.28	0.14	0.19	0.19	0.14
ppm															
Ba	73	244	379	422	109	391	438	450	339	255	386	143	202	264	45
Rb	3	11	26	27	4	13	18	32	31	26	26	15	9	12	0
Sr	741	656	567	656	803	500	604	499	149	604	349	106	190	169	76
Y	13	21	17	16	23	20	19	21	18	19	15	21	21	24	48
Zr	34	81	74	45	41	65	69	95	107	61	114	94	125	124	144
Nb	3	5	5	4	4	5	5	5	5	6	5	4	9	8	6
Cu	41	25	34	21	131	69	90	24	11	25	6	2	7	2	0
Pb	11	6	2	4	1	4	1	9	6	5	2	8	10	6	7
Zn	99	88	86	117	94	138	120	90	99	91	63	33	42	45	27
Ni	3	3	5	3	9	7	2	6	4	1	4	4	1	4	1
Cr	24	18	20	11	14	18	28	16	16	14	27	33	31	25	42
V	266	95	170	137	264	184	164	85	79	160	72	0	33	32	0
Ga	21	24	21	24	24	21	18	20	19	22	20	19	18	15	17
Th	0	0	0	0	0	0	0	0	0	0	0	0	1	1	0
U	0.2	0.7	0.8	0.3	0.2	0.5	0.4	0.5	0.8	0.5	0.8	0.7	2.0	1.2	0.6
Li	12	22	10	29	8	19	16	10	14	16	10	5	10	11	8

* Data as in Table 26.3

Table 26.5 Rb-Sr data* for the Fortyfive River pluton.

Sample	Rb	Sr	$^{87}Rb/^{86}Sr$	$^{87}Sr/^{86}Sr$
051	75	490	0.438	0.70658
090	110	305	1.037	0.71160
527	82	475	0.499	0.70711
553	115	325	1.028	0.71168
596	73	480	0.439	0.70748

*Error limits are: Rb and Sr, ± 5%; $^{87}Rb/^{86}Sr$, ±2%; $^{87}Sr/^{86}Sr$, ±0.006%. $\lambda Rb = 1.42 \times 10^{-11}\ y^{-1}$. Analyses by J. Blenkinsop, Carleton University. Rb, Sr, and Rb-Sr ratios were determined by X-ray Fluorescence. Sr was separated from the samples by conventional ion exchange techniques. Sr isotope ratios were measured in static mode on a Finnigan-MAT 261 multi-collector mass spectrometer.

Table 26.6 K-Ar data** for sample 060, Alma pluton.

K%	^{40}K ppm	$^{40}Ar^*$ ppm	$^{40}Ar^*/^{40}Ar$	$^{40}Ar^*/^{40}K$	Age (Ma)
0.146	0.174	0.007152	0.718	0.04120	598 ± 27

* Radiogenic ^{40}Ar

** Amphibole concentrate, -80/+20 mesh, treated with dilute HF and HNO_3 to remove alteration. Analyzed by Krueger Enterprises, Inc., Geochron Laboratories Division, Cambridge, Massachusetts. Constants used: $\lambda_\beta = 4.962 \times 10^{-10}$/year; $\lambda e = 0.581 \times 10^{-10}$/year; $^{40}K/K = 1.193 \times 10^{-4}$ g/g.

For comparison with the Rb-Sr age, hornblende from a diorite sample from the Alma pluton was dated by the K-Ar method (Table 26.6). The age of 598 ± 27 Ma is essentially identical to the Rb-Sr age, and is similarly interpreted to be a minimum age of intrusion and cooling of the Alma pluton.

DISCUSSION

Although in detail the stratigraphy of the metavolcanic and metasedimentary rocks in the study area is complex, the overall assemblage of lithologies, in particular the abundance of tuffaceous rocks, indicates a volcanic arc environment. This is further supported by the geochemical data which show that the volcanic (and related intrusive) rocks are tholeiitic. If these data are representative, then it is likely that the rocks formed in a relatively primitive subduction zone environment (Miyashiro 1974; Pearce et al., 1984).

The lithologies and chemical compositions of the plutonic rocks in the study area are also consistent with this tectonic environment. The Fortyfive River and Alma plutons are similar in composition to plutons of similar age in southeastern Cape Breton Island (Barr et al., 1982; Barr and Setter, in press), and elsewhere in the Avalon Terrane (e.g. O'Brien et al., 1983). Low Rb contents and low initial $^{87}Sr/^{86}Sr$ ratios are particularly characteristic (Cormier, 1972). Plutons like the Goose Creek leucotonalite are not known to be typical of these other areas, but such rocks are found in more primitive (M-type) granitoid suites (Pitcher, 1983; Pearce et al., 1984) and hence this may indicate that the tectonic environment in the study area involved less evolved (continental) crust than, for example, in southeastern Cape Breton Island. However, additional mapping and petrological studies of the leucotonalite are necessary in order to determine its significance.

Rocks formed in the postulated tectonic environment should have potential for porphyry-type Cu-Mo-Au mineralization; however, no strong indication for the presence of such mineralization is apparent in the geochemical results from this study.

The Goose Creek leucotonalite and the Fortyfive River pluton are more affected by metamorphism and deformation than the Alma pluton. The latter may be a younger intrusion, or it may be that the intensity of deformation and metamorphism decrease to the south across the study area. Some support for the latter interpretation is also seen in the adjacent metavolcanic and metasedimentary rocks, which appear to retain more primary igneous features in the southern part of the map area.

Continued mapping and petrological studies in areas adjacent to the present map area should lead to more detailed understanding of the petrogenesis of the igneous rocks units and their subsequent metamorphic and tectonic history.

REFERENCES

Barr, S.M., O'Reilly, G.A. and O'Beirne, A.M.
1982: Geology and geochemistry of selected granitoid plutons of Cape Breton Island. Nova Scotia Department of Mines and Energy, Paper 82-1, 176 p.

Barr, S.M. and Setter, J.R.D.
1984: Petrology of granitoid rocks of the Boisdale Hills, central Cape Breton Island, Nova Scotia. Nova Scotia Department of Mines and Energy. Paper 84-1, in press.

Chappell, B.W. and White, A.J.R.
1974: Two contrasting granite types. Pacific Geology, v. 8, p. 173-174.

Chappell, B.W. and White, A.J.R.
1983: Granitoid types and their distribution in the Lachlan Fold Belt, southeastern Australia. In R.D. Hatcher, Jr. and H. Williams and I. Zietz (eds.). Contributions to the tectonics and geophysics of mountain chains. Geological Society of America, Memoir 158, p. 33-53.

Cormier, R.F.
1972: Radiometric ages of granitic rocks, Cape Breton Island, Nova Scotia. Canadian Journal of Earth Sciences, v. 9, p. 1074-1086.

Giles, P.S. and Ruitenberg, A.A.
1977: Stratigraphy, paleogeography and tectonic setting of the Coldbrook Group in the Caledonia Highlands of southern New Brunswick. Canadian Journal of Earth Sciences, v. 14, No. 6, p. 1263-1275.

Irvine, T.N. and Baragar, W.R.A.
1971: A Guide to the chemical classification of the common volcanic rocks. Canadian Journal of Earth Sciences, v. 8, p. 523-548.

Kindle, E.D.
1962: Point Wolfe Sheet (21H/11E). Geological Survey of Canada, Map 1109A.

Leake, B.E.
1978: Nomenclature of amphiboles. Canadian Mineralogist, v. 16, p. 501-520.

McLeod, M.
1983: Geology of S-26, S-27, and T-26 (parts of 21H/11 and 21H/6), Plates 83-34, 83-35 and 83-36. New Brunswick Department of Natural Resources, Mineral Resources Division.

Miyashiro, A.
1974: Volcanic rock series in island arcs and active continental margins. American Journal of Science, v. 274, p. 321-355.

O'Brien, S.J., Wardle, R.J. and King, A.F.
1983: The Avalon Zone: a Pan-African terrane in the Appalachian orogen of Canada. Geological Journal, v. 18, p 195-222.

Pearce, J.A. and Gale, G.H.
1977: Identification of ore-deposition environment from trace element geochemistry of associated igneous host rocks. In Volcanic Processes in Ore Genesis, Geological Society of London, Publication 7, p. 14-24.

Pearce, J.A., Harris, N.B.W. and Tindle, A.G.
1984: Trace element discrimination diagrams for the tectonic interpretation of granitic rocks. Journal of Petrology, v. 25, p. 956-983.

Pitcher, W.S.
1982: Granite type and tectonic environment. In Hsü, K.J. (ed.) Mountain Building Processes, Academic Press, London.

Rast, N. and Skehan, J.W.
1983: The evolution of the Avalonian Plate. Tectonophysics, v. 100, p. 257-286.

Ruitenberg, A.A., Fyffe, L.R., McCutcheon, S.R., St. Peter, C.J., Irrinki, R.R. and Venugopal, D.V.
1977: Evolution of pre-Carboniferous tectonostratigraphic zones in the New Brunswick Appalachians. Geoscience Canada, v. 4, p. 171-181.

Ruitenberg, A.A., Giles, P.S., Venugopal, D.V., Buttimer, S.M., McCutcheon, S.R. and Chandra, J.
1979: Geology and Mineral Deposits Caledonia area. New Brunswick Department of Natural Resources, Memoir 1, 165 p.

Streikeisen, A.
1976: To each plutonic rock its proper name. Earth Science Reviews, v. 12, p. 1-13.

Williams, H.
1979: Appalachian Orogen of Canada. Canadian Journal of Earth Sciences, v. 16, p. 792-807.

Williams, H. and Hatcher, R.D. Jr.
1983: Appalachian suspect terranes. In R.D. Hatcher Jr., H. Williams and I. Zietz (eds.). Contributions to the tectonics and geophysics of mountain chains. Geological Society of America Memoir 158, p. 33-53.

Winchester, J.A. and Floyd, P.A.
1977: Geochemical discrimination of different magma series and their differentiation products using immobile elements. Chemical Geology, v. 20, p 321-355.

York, D.
1969: Least-squares fitting of a straight line with correlative errors. Earth and Planetary Science Letters, v. 5, p. 320-324.

Oxygen fugacity of Archean felsic magmas: relationship to gold mineralization

Project 800030

E.M. Cameron[1] and W.J. Carrigan[1]
Mineral Resources Division

Cameron E.M. and Carrigan W.J., Oxygen fugacity of Archean felsic magmas: relationship to gold mineralization; in Current Research, Part A, Geological Survey of Canada, Paper 87-1A, p. 281-298, 1987.

Abstract

Recent studies show that several Archean gold deposits, including some of the largest, were derived from oxidized hydrothermal fluids. Consideration of possible magmatic, metamorphic or meteoric sources suggests that the fluids were derived from relatively oxidized, felsic magmas. For this to be a viable hypothesis, magmas of this type are required to be in temporal and spatial association with the mineralization. There is a dearth of data on the oxidation state of Archean felsic magmas; moreover, the mantle, the ultimate source for the magmas, is thought to have been more reduced in Archean time.

We have attempted to estimate the oxygen fugacity (f_{O_2}) of magmas that produced felsic intrusions associated with gold mineralization in the Kirkland Lake and Matachewan camps and the Canadian Arrow and Hemlo deposits. Most of the intrusions are altered. Nonetheless, the data indicate f_{O_2}'s between the nickel-nickel oxide and hematite-magnetite buffers, consistent with magmas that might produce an oxidized aqueous phase. Furthermore, the intrusions at Kirkland Lake, Matachewan and Canadian Arrow record subsolidus alteration, including oxidation, e.g. magnetite to hematite, that suggests equilibration with an oxidized, CO_2-rich, aqueous phase. In addition to this pervasive alteration, wall rocks around gold-bearing veins show more intense carbonatization and oxidation.

Résumé

Les résultats d'études récentes indiquent que plusieurs gisements aurifères archéens, y compris certains des plus vastes, sont dérivés de solutions hydrothermales oxydées. L'étude des diverses sources possibles (météoriques, métamorphiques ou magmatiques) des solutions hydrothermales suggère que ces dernières se sont formées à partir de magmas felsiques plus ou moins oxydés. Pour que cette hypothèse soit viable, il aurait fallu que des magmas de ce genre aient existés en même temps et au même endroit que la minéralisation. Toutefois, les données sur l'état d'oxydation des magmas felsiques archéens sont peu nombreuses; en outre, le manteau, qui est la source ultime des magmas, aurait été plus réduit au cours de l'Archéen.

Pour vérifier cette hypothèse, les auteurs ont tenté d'évaluer la fugacité de l'oxygène (O_2) dans les magmas qui ont produit les intrusions felsiques associées à la minéralisation aurifère dans les gisements de Kirkland Lake et de Matachewan et ceux de Canadian Arrow et Hemlo. Cependant, cette évaluation est plutôt difficile à faire puisque la plupart des intrusions ont été altérées. Néanmoins, les données indiquent que dans le cas des tampons nickel-oxyde de nickel et hématite-magnétite, l'oxygène serait conforme à celle de magmas pouvant donner une phase aqueuse oxydée. En outre, les intrusions à Kirkland Lake, à Matachewan et à Canadian Arrow font voir une altération dans la zone subsolidus, y compris l'oxydation (par exemple, transformation de la magnétite en hématite) qui porte à croire qu'il y avait équilibre avec une phase aqueuse oxydée riche en CO_2. En plus de cette altération envahissante, les roches encaissantes des filons aurifères ont subi une carbonatation et une oxydation plus intenses.

[1]Derry Laboratories, Department of Geology, University of Ottawa

INTRODUCTION

For much of this century, it was widely held that Archean gold mineralization is of magmatic origin. Only in the 1970s and 1980s has there been a swing in opinion to a metamorphic source, an hypothesis supported by the CO_2-rich, low salinity nature of the ore-forming fluids, similar to common metamorphic fluids. And the most familiar locus of this mineralization is metamorphic rocks; more specifically, within shear zones that are an expression of tectonism associated with regional metamorphism.

The composition of ore-forming fluids is the principal guide to the source of the mineralization. Recently, we have drawn attention to the unusual abundance of sulphate minerals associated with some Archean gold deposits, compared to the paucity of these and other oxidized mineral species elsewhere in the Archean record (Hattori and Cameron, 1986a). A significant number of Archean gold deposits, including some of the largest, appear to be linked to relatively oxidizing hydrothermal fluids, which are expressed in the presence of sulphates and/or isotopically fractionated sulphides and/or hematite in close association with the gold. On the basis of a variety of geological and isotopic evidence, Cameron and Hattori (in press) concluded that these fluids are most similar to the aqueous phase of an oxidized, felsic magma.

The oxygen fugacity (f_{O_2}) of a magma and its contained aqueous fluids are both mainly buffered by Fe^{2+}/Fe^{3+} in the melt. During cooling, magmas and their fluids tend to follow temperature vs f_{O_2} curves that parallel the major oxidation-reduction buffers (Mathez, 1984), such as the fayalite-magnetite-quartz (FMQ) or hematite-magnetite (HM) (Fig. 27.1). Some deviation from this parallelism can be caused by the loss of oxidized or reduced solid or gaseous species from the melt. For example, the precipitation of Fe^{2+}-bearing minerals can cause the f_{O_2} of the remaining melt and aqueous fluid to increase. However, for most felsic melts, where the bulk of crystallization occurs within a few degrees of the vapour-saturated solidus, the effect of this will be minor (Candela, 1986). Degassing of reduced species, e.g., H_2, causes oxidation of the aqueous fluid, while release of an oxidized species, e.g., SO_2, will cause its reduction. Because of its high diffusivity, selective loss of H_2 has been implicated in the oxidation of magmatic fluids (Sato and Wright, 1966). On account of the high buffering capacity of the Fe^{2+}/Fe^{3+} system, this will only have a major effect on melts with low total Fe contents (Candela, 1986) or in subsolidus conditions.

The hypothesis that the oxidized ore-forming fluids for certain Archean gold deposits are of magmatic origin is contingent on their being magmas of suitably high f_{O_2} with a close spatial and temporal relationship to this mineralization. During review of the manuscript of Cameron and Hattori (in press), the question was raised whether such magmas existed in Archean time. This is a reasonable query. To our knowledge there have been no determinations of the f_{O_2} of Archean felsic magmas. Moreover, such magmas are derived, either directly or indirectly, from the mantle, which is generally regarded as being more reduced in Archean time. The latter was suggested by Haggerty and Tompkins (1983) on the evidence that diamonds are of Archean age, irrespective of the age of the host intrusion (Kramers, 1979), and that these contain inclusions of Ni-poor metallic iron (Sobolev et al., 1981). A similar conclusion was reached by D. Walker (in Holland, 1984) and by Arculus (1985) based on higher contents of Cr in Archean basaltic melts, which may have been facilitated by the presence of Cr^{2+} in addition to Cr^{3+}. Jones and Drake (1986) indicate that all models for core formation in the earth require that the mantle became more oxidized with time.

This brief project was undertaken in the summer of 1986 to obtain estimates of magmatic f_{O_2} for intrusions spatially associated with some gold deposits in the Abitibi belt that seemingly formed from oxidized hydrothermal fluids. Esti-

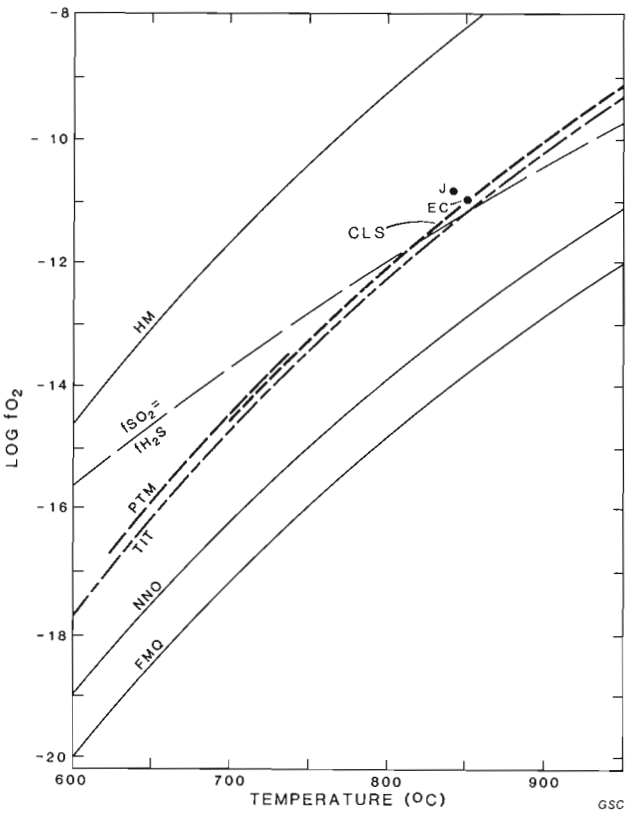


Figure 27.1. Log f_{O_2} - temperature diagram showing: CLS, hypothetical cooling curve for Cedar Lake stock, based on f_{O_2} estimates from biotite analysis; PTM, plot of titanite-bearing members of the Paintbrush and Timber Mountain Tuffs, southern Nevada, (Lipman, 1971); TIT, curve for titanite-magnetite-quartz- amphibole equilibria (Noyes et al., 1983); J, Julcani volcanic rocks, Peru (Drexler and Munoz, 1985; Whitney, 1984); EC, El Chichon volcanic rocks, Mexico (Luhr et al., 1984; Whitney, 1984); HM, hematite-magnetite equilibria (Chou, 1978); NNO, Ni-NiO equilibria (Heubner and Sato, 1970); FMQ, fayalite-magnetite-quartz equilibria (Hewitt, 1978).

mating f_{O_2} from this population of igneous rocks presents difficulties. First, most fugacity estimates have been made on unaltered, fast-cooling volcanic rocks, i.e., pyroclastic rocks, where the minerals most closely reflect magmatic equilibria. Plutonic rocks are more subject to subsolidus reactions. Second, igneous rocks associated with Archean gold mineralization are frequently altered. In many cases, e.g., the Hemlo area, this alteration seems to be more severe for the pyroclastic rocks than for the felsic intrusions.

There are a variety of ways of estimating the f_{O_2} of a melt. The most widely used method (which is also a geothermometer) is based on the compositions of coexisting titanomagnetite and ilmentite (Buddington and Lindsley, 1964; Spencer and Lindsley, 1981). Unfortunately, Fe-Ti oxides in plutons frequently re-equilibrate during slow cooling below the solidus (Czamanske and Mihalik, 1972; Czamanske et al., 1981), vitiating their use as a estimator of magmatic f_{O_2}. Another commonly used method is based on the atomic proportions of Fe^{2+}, Fe^{3+}, and Mg in biotites (Wones and Eugster, 1965; Speer, 1984). A more general indicator is the magnetite content, used by Ishihara (1981) as the primary criterion for distinguishing between his magnetite series (oxidized) and ilmenite series (reduced) granitoids. The former contains abundant magnetite, contrasting with <0.1 vol % opaque oxide minerals in the ilmenite series, giving the magnetite series a magnetic susceptibility $>1 \times 10^{-4}$emu/g and a bulk Fe_2O_3/FeO ratio >0.5. Another indicator mineral is titanite, which requires a relatively high f_{O_2} for its formation (Verhoogen, 1962; Carmichael and Nicholls, 1967).

SAMPLING AND GEOLOGY

Kirkland Lake

At Kirkland Lake, major gold mineralization is associated with augite syenite, felsic syenite, and porphyritic syenite, all intruded along the axis of a major fault zone, the Kirkland Lake fault. Two-thirds of the ore is found within or near the contacts of the youngest phase, the porphyritic syenite (Thomson et al., 1950). Oxidized hydrothermal fluids are indicated by strongly ^{34}S-depleted pyrite in the ore, hematitization of host syenites near ore, and remobilized sulphate minerals in late veins cutting the ore (Hattori and Cameron, 1986a; Cameron and Hattori, in press).

The syenites have a pervasive regional alteration, including carbonatization. In the coarse-grained augite syenite, augite is generally altered to actinolite, chlorite and carbonates. Primary oligoclase is largely replaced by fine grained orthoclase. The felsic syenite is mainly orthoclase, with small amounts of oligoclase. Biotite in this rock has been replaced by chlorite, carbonates and leucoxene. In the porphyritic syenite oligoclase/albite is the dominant phenocryst, with lesser orthoclase. Biotite and hornblende have been variably altered to chlorite, magnetite, carbonate and leucoxene. There is accessory magnetite and apatite in all three rock types. Superimposed on the regional alteration, there is alteration around the gold-bearing veins and stockworks, consisting of carbonatization, silicification, sericitization and pyritization. Most of the syenites developed a reddish coloration from the formation of hematite.

Samples of syenite were obtained from outcrop near Kirkland Lake and Swastika and drill core from the Lake Shore Mine. Although an effort was made to collect only the freshest material, all samples show at least moderate alteration. The analyses given in Table 27.1 are for some of the least altered samples of porphyritic and augite syenite. The content of CO_2 is an crude index of the degree of alteration.

Canadian Arrow

This minor deposit is in the southwest portion of Hislop Township, near Matheson, Ontario. Gold-bearing veins occur in fractures within and immediately adjacent to a trondhjemite stock that intrudes tholeiitic basalts (Moore, 1936; Prest, 1957; Cherry, 1983; McNeil and Kerrich, 1986). The medium-grained trondhjemite consists of sericitized albite with hornblende and biotite largely replaced by chlorite, carbonate, Fe-oxides and orthoclase. Magnetite is relatively abundant as an accessory, with titanite, apatite, carbonate and pyrite. Both the ore and the intrusion contain strongly 34S-depleted pyrite (Schwarcz and Rees, 1985; Cameron and Hattori, in press). Other evidence of oxidized fluids is the hematitization of wall rocks about the gold-bearing veins. This is a brick-red colour from fine grained inclusions of hematite in K-feldspar (Cherry, 1983; McNeil and Kerrich, 1986). Lamprophyre dykes with a similar orientation to these veins are intruded into the trondhjemite (McNeil and Kerrich, 1986) and are also altered. Samples from the least altered trondhjemite were collected from near the open pit, which is now filled with water. Analyses for two of these samples are given in Table 27.1.

Matachewan

Syenitic intrusions are common in this area, the largest being the Cairo stock (Fig. 27.2). This is mainly hornblende syenite, consisting of 70-80 vol.% orthoclase, 10-15 vol.% hornblende and 5-10 vol.% albite, with minor quartz, biotite, magnetite and titanite (Sinclair, 1982). Lovell (1967) notes the relative abundance of magnetite in the intrusions, a typical mafic syenite containing 5% of this mineral. Gold mineralization is associated with the syenites, mostly within or near the margins of small stocks. The principal deposits are the Matachewan Consolidated and Young-Davidson, 1 km apart in a small stock of trachytic syenite, mainly composed of microcline with some sodic feldspar. This is brecciated and fractured, with pyritic, carbonatite and hematitic alteration. Gold is mostly dispersed in a pyritic, highly fractured phase of the syenite that is a cherry-red colour from disseminated hematite. It is this hematite that is the principal indicator of the involvement of oxidized fluids in the formation of these deposits (Cameron and Hattori, in press). Dyer (1936) observed barite, but it must be relatively minor in amount. There is only moderate isotopic fractionation of the sulphides

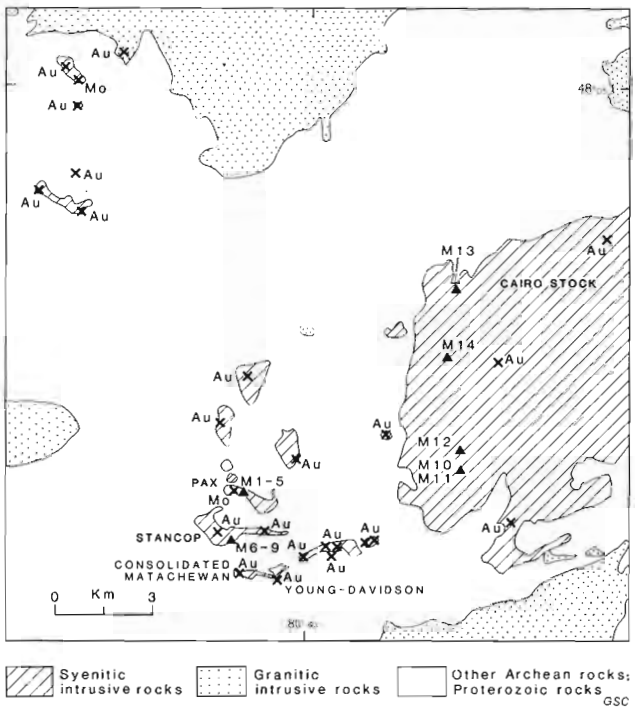


Figure 27.2. Map showing relationship of gold and of molybdenum mineralization to syenitic intrusions, Matachewan area, Ontario. Geology after Lovell (1967). Some sample sites shown, other samples collected near Consolidated Matachewan and Young-Davidson mines.

around 0‰ (Cameron and Hattori, in press). Elsewhere in the Matachewan area gold can occur in quartz and quartz-carbonate veins, the wall rocks of which are in places red-stained with hematite (Lovell, 1967). Several porphyry copper- molybdenum deposits are present near Matachewan, also hosted by syenite (Sinclair, 1982).

Since the syenite hosting the Matachewan Consolidated and Young-Davidson deposits is highly altered, sampling also included the less altered portions of the Cairo stock. However, even these show moderate alteration, including carbonatization, as is shown by the analytical data (Table 27.1).

Hemlo

The mineralization within the above three areas is reasonably typical of Archean lode deposits, where gold is associated with quartz or quartz-carbonate veins. The Hemlo area is different, since gold is disseminated through thick ore zones comprised of pyritic, sericite schist and baritic rock; carbonate alteration is essentially absent. The element assemblage, which includes Sb, Tl, As, Hg, Mo and V, is more typical of younger epithermal deposits (Cameron and Hattori, 1985) and, unlike the other areas, ore does not occur within an intrusion.

Mineralization is within the Heron Bay Group, comprising metamorphosed felsic pyroclastic deposits, sedimentary rocks and felsic subvolcanic intrusions, all cut by Kenoran plutons. The deposit is near a transition between footwall

Table 27.1. Analyses (in percent) of whole rock samples from intrusions

LOCATION	Kirkland Lake				Canadian Arrow		Cairo Stock		Cedar Lake Stock		
ROCK TYPE	Porphyritic Syenite		Augite Syenite		Trondhjemite		Syenite		Gradodiorite		
SAMPLE	K-14	812-096	K-10	812-108	CA-5	CA-6	M10	M12	NBG-1-190	NBG-1-495	NBG-1-1300
SiO_2*	62.6	65.3	52.6	51.1	64.6	65.2	64.7	61.4	69.3	69.4	68.7
TiO_2*	0.40	0.40	0.92	0.90	0.24	0.25	0.30	0.36	0.35	0.37	0.38
Al_2O_3*	14.3	14.9	15.4	14.7	17.2	17.8	15.7	15.4	15.8	16.2	15.7
Fe_2O_3+	1.6	1.9	3.5	4.5	0.6	1.1	2.0	2.9	0.9	0.9	1.1
FeO+	2.1	1.6	4.8	4.5	1.4	1.4	1.0	1.7	1.1	1.1	1.1
MnO*	0.07	0.06	0.14	0.09	0.05	0.03	0.05	0.09	0.03	0.02	0.03
MgO*	2.72	1.74	4.13	5.82	1.06	1.04	1.19	2.33	0.76	0.77	0.80
CaO*	3.56	2.74	5.22	4.28	2.81	1.63	1.82	2.73	2.55	2.46	2.61
Na_2O*	5.06	4.90	3.83	3.55	6.71	6.90	4.74	4.70	5.58	5.46	5.30
K_2O*	2.35	3.31	3.84	4.65	2.08	2.40	5.70	6.49	2.42	2.46	2.40
BaO*	0.53	0.34	0.27	0.26	0.10	0.07	0.27	0.34	0.10	0.10	0.12
H_2O+	1.1	1.2	2.1	2.3	0.8	0.9	0.4	0.5	0.4	0.5	0.5
CO_2+	2.5	1.7	2.5	2.5	1.3	0.8	0.9	1.0	0.2	0.2	0.2
P_2O_5*	0.30	0.21	0.55	0.65	0.11	0.11	0.15	0.30	0.13	0.15	0.14
S+	0.09	0.06	0.04	0.04	0.11	0.03	0.03	0.04	0.03	0.00	0.04
Total	99.3	100.4	99.8	99.8	99.2	99.7	99.0	100.3	99.7	100.1	99.1
Fe_2O_3/FeO	0.76	1.2	0.73	1.0	0.43	0.79	2.0	1.7	0.82	0.82	1.0

*By Inductively Coupled Plasma Spectrometry
+ By Wet Chemistry

pyroclastic rocks, derived from the west and epiclastic rocks in the hanging wall that thicken eastwards (Muir, 1982). The transition is also along a major zone of shearing. Several tabular orebodies are concordant to the regional stratigraphy and to the structural lineation, the main ore zone being up to 45 m thick. In addition to barite, evidence for oxidized hydrothermal fluids is given by strongly fractionated pyrite. A linkage between the ore-forming process and the redox reactions responsible for this isotopic fractionation is indicated by a correlation between gold grades and the isotopic composition of the pyrite (Cameron and Hattori, 1985).

Mapping by Muir (1982) identified the Cedar Lake pluton as a large body of hornblende-biotite granodiorite north of the Hemlo deposit. The southwestern portion of the pluton is now recognized as a separate intrusion, referred to as the Cedar Lake stock, with distinctively high magnetic relief (see colour aeromagnetic map, Canadian Mining Journal, January, 1986). A preliminary U-Pb zircon age for a felsic volcanic rock near the deposit is ~2.77 Ga and for the Cedar Lake pluton ~2.69 Ga (Corfu and Muir, 1986).

Recently, a deep drill hole passed through the Cedar Lake stock to test for the extension of the Hemlo deposit at depth (Fig. 27.3). It is this drill hole, NBG-1, that we sampled. The stock is a uniform, medium grained equigranular biotite granodiorite, with major quartz, microcline, sodic plagioclase and biotite and lesser amounts of hornblende, epidote, titanite and magnetite. The uniformity of the stock is emphasized by the chemical data (Table 27.1). In this and subsequent tables the last digits of the sample number give the depth in the hole in meters. In contrast to the other intrusions sampled, thin sections of the Cedar Lake stock show only minor alteration. This is further expressed by the CO_2 values (Table 27.1), which are in the normal range for granitic rocks, significantly lower than for the other intrusions.

MINERALOGY AND GEOCHEMISTRY OF THE IRON-TITANIUM OXIDES

We have examined the opaque oxides in sections from all the intrusions. Complementary microprobe analyses are given in Table 27.2. Magnetite is a relatively abundant constituent of most of the samples. We have identified only very minor amounts of ilmenite. The method of Buddington and Lindsley (1964) and Spencer and Lindsley (1981) permits the estimation of f_{O_2} and temperature from the intersection of compositional curves for magnetite and ilmenite solid solution pairs in f_{O_2}-temperature space. In the absence of ilmenite, the Ti content of magnetite (usually in the percent range) allows an approximation to the f_{O_2}.

In the Cedar Lake, Canadian Arrow and Cairo stocks, there is a consistent pattern of sphenitization of the magnetites. (Note: following recent convention, we have used titanite over sphene; we have, however, retained the term sphenitization, as the most frequently used and euphoneous expression of this process). In sphenitization, Ti is removed from the magnetite-ulvospinel solid solution to form coronas or partial coronas of titanite around magnetite grains (Fig. 27.4-27.6), leaving the magnetite essentially free of Ti (Table 27.2). Coronas of titanite around magnetite are not uncommon in plutonic rocks and are interpreted as due to sub-solidus oxidation (Carmichael and Nicholls, 1967). Sphenitization may have occurred concurrently with the alteration of the silicate minerals, when Ca and Si was available. The loss of Ti from the magnetite structure precludes the estimation of magmatic f_{O_2}.

Sphenitization of magnetites seems less common in samples of syenite from Kirkland Lake, although it is present (Fig. 27.7). The Ti contents of Fe-Ti oxide grains in these syenites are in the percent range, but are highly variable from grain to grain (Table 27.2). These grains are inhomogeneous on a very fine scale (Fig. 27.8), and it appears that the Ti is not present as a solid solution impurity, but rather as a discrete Ti-bearing phase. In addition to Ti, substantial amounts of Mn and Cr are present in some of the oxide grains from Kirkland Lake.

Magnetite in the Canadian Arrow trondhjemite, and the syenites at Matachewan and Kirkland Lake show variable degrees of conversion to hematite (Fig. 27.9-27.11), but this has not been observed in sections from the Cedar Lake stock. Most frequently this oxidation has taken place preferentially along the margins and fractures in magnetite grains. Less commonly, oxidation is along (111) spinel planes (Fig. 27.5, 27.10). Typical sections show sphenitization of all magnetite grains, but variable hematitization of the magnetite, with

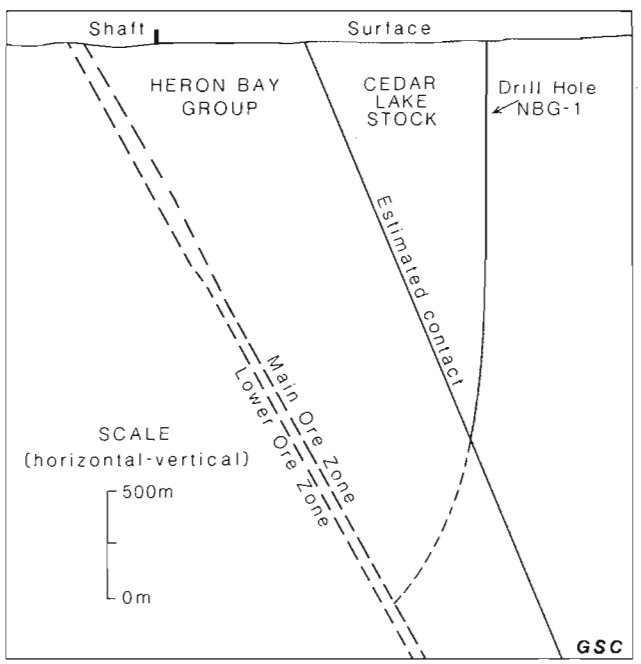


Figure 27.3. Section showing spatial relationship of Cedar Lake stock to the Hemlo gold deposit near Marathon, Ontario, and the location of drill hole NBG-1. Modified from a section supplied by Noranda Mines, Hemlo Division.

Table 27.2 Microprobe analyses (in percent) of magnetite. Total Fe reported as FeO.

LOCATION	CEDAR LAKE STOCK			CANADIAN ARROW		
SAMPLE NO.	NBG-1-190	NBG-1-495	NBG-1-825	CA-1	CA-5	CA-6
ANALYSES	2	5	2	3	3	2
FeO	93.59	93.57	92.90	94.12	91.98	93.54
TiO_2	0.03	0.01	0.04	0.05	0.04	0.04
MnO	0.18	0.14	0.13	0.10	0.12	0.04
Al_2O_3	0.02	0.03	0.05	0.04	0.02	0.05
Cr_2O_3	0.08	0.04	0.02	0.05	0.09	0.17
MgO	0.00	0.02	0.03	0.00	0.03	0.03
SiO_2	0.03	0.04	0.02	0.04	0.04	0.04
V_2O_3	0.17	0.19	0.14	0.33	0.32	0.35
ZnO	0.03	0.04	0.06	0.04	0.01	0.02
CaO	0.00	0.02	0.01	0.00	0.01	0.01
TOTAL	94.13	94.10	93.40	94.77	92.66	94.29

LOCATION	CAIRO STOCK			KIRKLAND LAKE		
SAMPLE NO.	M10	M12	M14	K14		
ANALYSES	2	5	2	INDIVIDUAL ANALYSES		
FeO	93.65	92.53	93.35	87.67	93.02	88.09
TiO_2	0.02	0.07	0.14	3.00	0.54	6.00
MnO	0.08	0.09	0.10	0.07	0.05	0.07
Al_2O_3	0.02	0.03	0.01	0.04	0.06	0.00
Cr_2O_3	0.42	0.41	0.42	3.57	0.03	0.09
MgO	0.06	0.00	0.04	0.04	0.03	0.00
SiO_2	0.04	0.06	0.09	0.12	0.27	0.11
U_2O_3	0.20	0.16	0.20	0.09	0.07	0.18
ZnO	0.05	0.02	0.05	0.05	0.00	0.00
CaO	0.02	0.06	0.01	0.00	0.11	0.01
TOTAL	94.56	93.43	94.41	94.65	94.18	94.55

some grains free of hematite. The spatial distribution of hematite within magnetite grains is seemingly unrelated to the distribution of titanite. These observations suggest that sphenitization preceded the oxidation of magnetite to hematite. Some samples show the complete oxidation of Fe-oxides to hematite. This is notable within the small syenite stocks associated with Au and Mo mineralization near Matachewan and for some samples from Kirkland Lake. Where there has been alteration of ferromagnesian minerals, the Fe lost from the silicate structure has also formed hematite.

Magnetite is the principal magnetic mineral of rocks and as such is conveniently measured by the magnetic susceptibility of a sample. Ishihara (1981) and others have utilized the magnetic susceptibility of granitoid rocks as an index of the Fe^{2+}/Fe^{3+} ratio or oxidation state of the parent magma. A susceptibility value of $\sim 2.5 \times 10^{-4}$ emu/cc is used by Ishihara to separate the "magnetite series" granitoids from the "ilmenite series". In as much as the susceptibility is an indirect measure of the primary oxidation state, its significance needs to be carefully evaluated for each geological unit.

In the magnetite - ulvospinel series, the magnetic susceptibility increases towards the magnetite, i.e., low-Ti, end member. As Buddington and Lindsley (1964) have shown, the Ti content of the series decreases as the f_{O_2} increases. Thus in this respect, magnetic susceptibility is a better measure of the oxidation state of the magma than the absolute content of

Figure 27.4. Subhedral to anhedral magnetite (light) with titanite as partial coronas around the magnetite (TC) or as grains within the magnetite and silicates (IT). Sample NBG-1-1300, Cedar Lake Stock, reflected light.

Figure 27.5. Corona of titanite (TC) around grain of magnetite (medium grey). Magnetite oxidizing to hematite (light) along (111) spinel planes. Trondhjemite sample CA-4, Canadian Arrow stock, reflected light.

Figure 27.6. Grains of magnetite (M), with partial coronas of titanite (TC). Euhedral crystal of pyrite (PY). Trondhjemite sample CA-6, Canadian Arrow stock, reflected light.

Figure 27.7. Partial coronas of titanite (TC) around magnetite. Magnetite grain is inhomogeneous on a very fine scale. Augite syenite sample 812-108, drill core Lake Shore Mine, Kirkland Lake, reflected light.



Figure 27.4

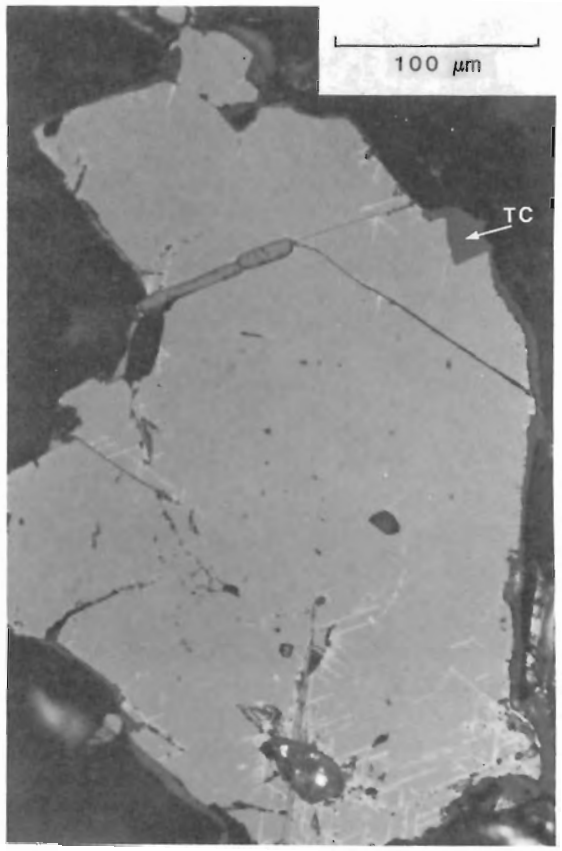


Figure 27.5

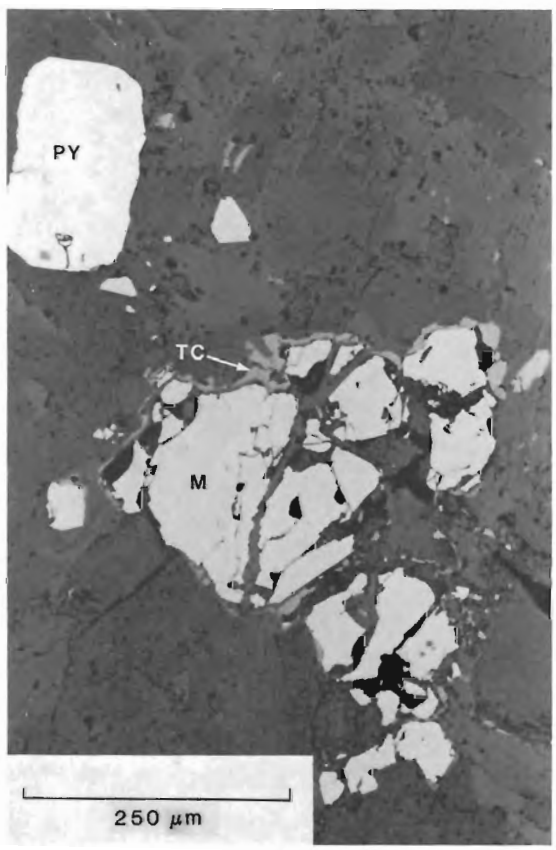


Figure 27.6

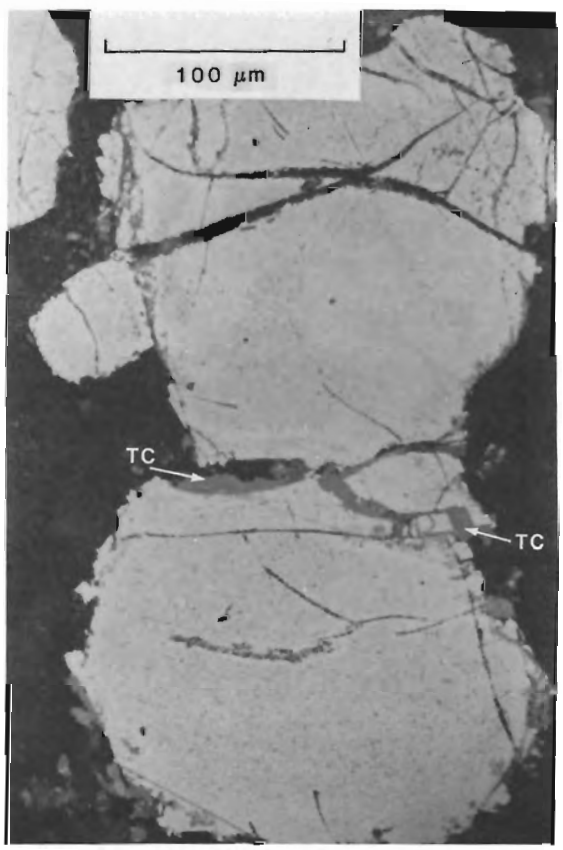


Figure 27.7

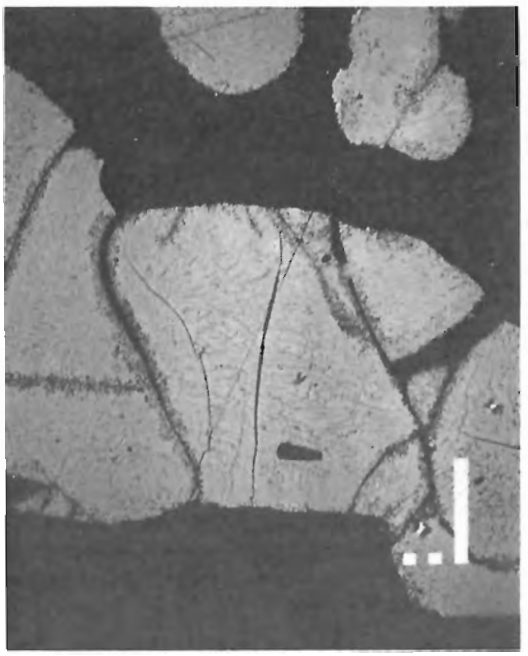


Figure 27.8

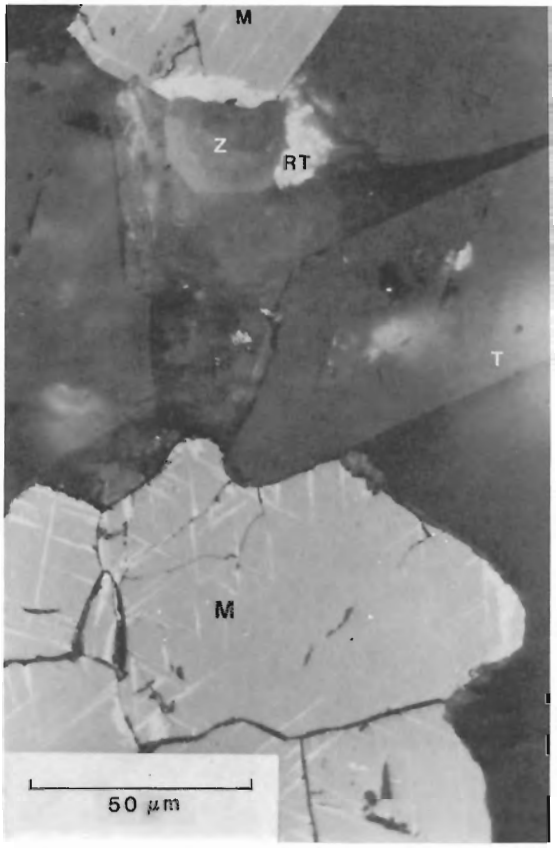


Figure 27.10

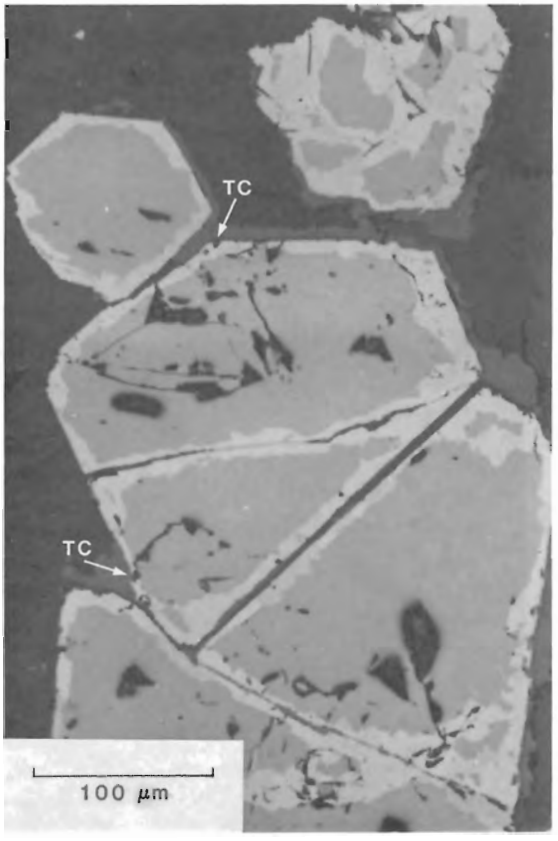


Figure 27.9

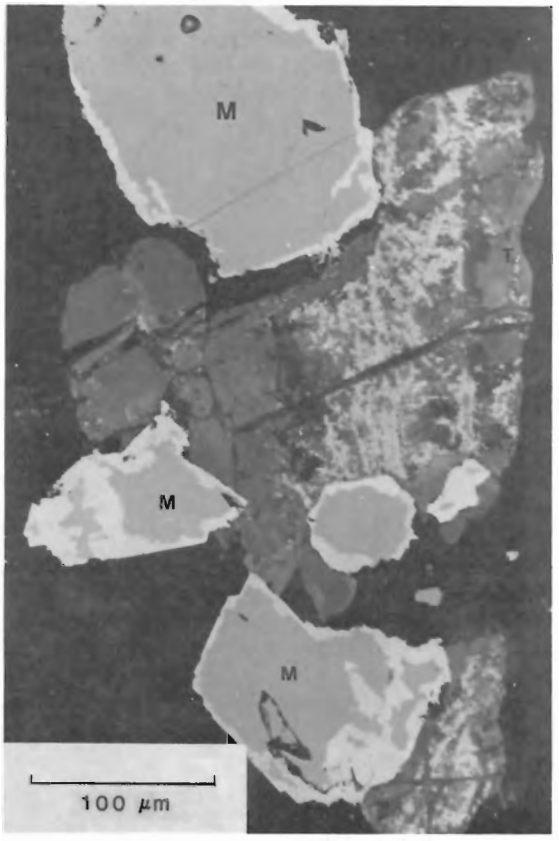


Figure 27.11

magnetite. The amount of magnetite precipitated from a magma is not only dependent on the ratio Fe^{2+}/Fe^{3+}, but also on the absolute content of Fe in the magma. Thus basic rocks tend to have higher magnetite contents than felsic rocks.

There have been a number of post-crystallization influences on the magnetic susceptibility of the rocks described here. Some magnetite has been produced by the alteration of ferromagnesian minerals. While in most samples this is less in amount than the content of apparent "primary" magnetite, it does produce a net gain in the susceptibility. Second, all Ti has been lost from the magnetite lattice to form either titanite or, in the Kirkland Lake samples, a very fine grained Ti mineral. Loss of Ti from the magnetite structure results in a net gain in susceptibility. Thirdly, a loss in magnetic susceptibility accompanies the oxidation of magnetite to hematite.

In Figure 27.12 we show the magnetic susceptibility of representative samples from the three areas studied. These values fall into two groups. In the first group, with high susceptibilities, are samples from the Cedar Lake, Canadian Arrow and Cairo stocks and most samples of syenite from Kirkland Lake. The second group, consisting of some samples of felsic syenite from Kirkland Lake and most samples from the small mineralized bodies of syenite west of the Cairo stock (Fig. 27.2) have low susceptibilities. For samples from group 1, susceptibilities have been enhanced by the partial alteration of ferromagnesian minerals to magnetite and by the loss of Ti from the magnetite structure. In all cases but the Cedar Lake stock, this has been offset by the partial oxidation of magnetite to hematite. It is not possible to quantitatively evaluate these varying influences. Since the majority of the samples in this group are well within the range of Ishihara's "magnetite series", it is unlikely that this classification has been influenced by post-crystallization events. Thus, in these terms the rocks are from relatively oxidized magmas. For group 2, polished section examination shows that the low susceptibility values are due to the oxidation of much or all of the magnetite to hematite. Prior to oxidation these samples likely had a magnetite content similar to those of group 1. Note that the Kirkland Lake samples included in Figure 27.12 do not include material from near the ore zones. Measurements on a large number of such samples were made after completion of the figure. These, almost invariably, have very low susceptibilities.

Representative Fe_2O_3/FeO values for the different intrusions are given in Table 27.1. These samples are among the least altered and do not include vein-related alteration. In most cases the ratios are high, well within the range of Ishihara's magnetite series granitoids, with values >0.5. Note, however, that in all cases save the Cedar Lake stock, the ratios will have been influenced by the partial conversion of magnetite to hematite and are thus unlikely to represent magmatic Fe^{3+}/Fe^{2+}.

Figure 27.8. Electron backscattered image of magnetite grain. Sample K-8, porphyritic syenite, syenite, Kirkland Lake. Vertical scale, 100 microns. The light reflected from the field increases with the atomic number of the element scanned. Photograph illustrates the small scale inhomogeneity of the grains.

Figure 27.9. Subhedral grains of magnetite (grey), showing oxidation to hematite (light) along the margins and fractures. Also coronas of titanite (TC). Syenite sample M14, Matachewan, reflected light.

Figure 27.10. Subhedral grains of magnetite (M), showing partial oxidation to hematite (light) along (111) spinel planes and along margins. Titanite (T) present as euhedral grains and in minor amounts along margins of magnetite. Also zircon (Z). Syenite sample M-10, Matachewan, reflected light.

Figure 27.11. Grains of magnetite (M) partially altered to hematite (light). Grain of titanite (T) partly altered to rutile (medium light). Syenite sample M-12, Matachewan, reflected light.

MINERALOGY AND GEOCHEMISTRY OF BIOTITE

Following Wones and Eugster (1965), a qualitative estimate of f_{O_2} can be obtained from ternary plots of atomic Fe^{3+}, Fe^{2+}, and Mg in biotite. Much of the data published has been reviewed by Speer (1984). Within some granitoid suites, biotite analyses plot parallel to the major buffers (e.g., Sierra Nevada trend, Fig. 27.13), indicating a relatively constant oxidation status during crystallization. In other instances buffers are crossed by the biotite trend, indicating changing f_{O_2}. For the present study, compositions of biotites were obtained by electron microprobe analysis, supplemented by analysis of biotite separates for Fe^{2+} and Fe^{3+}. Biotite is present in samples from all four areas studied. Only in the case of the Cedar Lake stock is this mineral unaltered; for the other locales biotite is partially or completely altered to chlorite. Biotite in samples from Canadian Arrow, Matachewan and Kirkland Lake are too chloritized to permit separation for chemical determination of Fe^{2+} and Fe^{3+}. As will be apparent from Figure 27.13, the estimation of f_{O_2} is quite sensitive to small variations in the Fe^{3+} content of the biotites, and would be affected by chlorite contamination. However, W.D. Sinclair provided a clean biotite separate (KA 3185) from a small syenite stock on the west bank of the Montreal River, 0.75 km north of Matachewan. Immediately south of Kirkland Lake we have sampled the Lebel syenite and have obtained clean biotite separates. Although this intrusion is broadly related, both temporally and compositionally, to the syenites along the Kirkland Lake fault, the precise relationship is not known. For sample KA 3185 and those from the Lebel syenite, Fe^{2+}, Fe^{3+}, and Mg were all determined chemically.

Analyses of the six biotites from the Cedar Lake stock are given in Table 27.3 and the atomic proportions Fe^{2+}-Fe^{3+}-Mg are shown in a ternary plot (Fig. 27.13). This defines a tight grouping midway between the HM and nickel-nickel oxide (NNO) buffers, indicative of a relatively high and uniform f_{O_2} at the time of crystallization. One of the more

extensive studies of biotite compositions is for the Sierra Nevada batholith by Dodge et al. (1969). The Cedar Lake biotites plot at the Mg-rich end of the Sierra Nevada trend. For Japanese granitoids, the NNO buffer is the approximate boundary between biotites from magnetite and ilmenite series rocks (Ishihara, 1977). Biotite KA 3185 and the two samples from the Lebel stock also plot between the NNO and HM buffers.

MINERALOGY AND GEOCHEMISTRY OF AMPHIBOLE

Like biotite, the composition of amphibole reflects the fO^2 of the environment at the time of formation. However, for amphibole this relationship seems more complex and is less well defined. Dodge and Ross (1971) compared the compositions of coexisting biotite and hornblende from a number of granitoid intrusions on Fe^{2+}-Fe^{3+}-Mg ternary plots. These showed a variety of relationships between the two minerals. For samples from the Sierra Nevada batholith, hornblende was more Mg-rich and tie lines between pairs parallel the oxygen buffers, such as NNO. This indicated to Dodge and Ross that relative f_{O_2} was constant during crystallization of both minerals. For granitoids from near the San Andreas fault, tie lines run roughly normal to the buffers, the hornblende having a higher proportion of Fe^{3+}. This was interpreted as indicating a declining relative f_{O_2} during crystallization, with the hornblende probably having formed first. In general, hornblende formed at high f_{O_2} is enriched in Mg and Fe^{3+} (Czamanske and Wones, 1973; Czamanske et al., 1981), which has been confirmed experimentally (Spear, 1981).

For hornblende Fe^{2+} and Fe^{3+} reported in Table 27.4 and Figure 27.14 were calculated from microprobe data, since only one clean separate was obtained. The program by G.J. Pringle follows the method of computing total cations to 13, exclusive of K, Na and Ca, discussed by Robinson et al. (1982). For sample M-12, amphibole was separated and analyzed chemically. The measured results of 8.4% FeO and 5.5% Fe_2O_3 compare with computed values of 7.4% FeO and 6.1% Fe_2O_3. The Fe^{2+}-Fe^{3+}-Mg ternary plot (Fig. 27.14) shows that amphiboles from the Cedar Creek stock (Fig. 27.15) have a higher proportion of Fe^{3+} than coexisting biotites.

The amphiboles from Canadian Arrow and the Cairo stock are Mg- and Fe^{3+}-rich and seem to have formed under oxidizing conditions near the HM buffer (Fig. 27.14). Apart from higher Fe^{3+}, their composition is broadly similar to hornblende reported from oxidized phases of the Finnmarka complex (Czamanske and Wones, 1973). The indicated high f_{O_2} may more closely reflect a late-stage magmatic environment, since amphibole readily recrystallizes (Czamanske et al., 1981). The altered nature of the rocks support this possibility.

MINERALOGY AND CHEMISTRY OF TITANITE

A further useful method for estimating the redox state of a magma is based on the presence or absence of primary titanite. Verhoogen (1962) first showed that this mineral required relatively oxidized conditions for its formation and Carmichael and Nicholls (1967) calculated limits in f_{O_2}-temperature space for the formation of titanite. Lipman (1971) investigated the f_{O_2} and temperature of crystallization of a series of ash-flow sheets in southern Nevada. In some of the members ilmenite phenocrysts were abundant, but they lacked titanite, while the reverse was the case for other members. These differing associations may be represented by the following reaction:

$$3\ FeTiO_3 + 3\ CaSiO_3 + \tfrac{1}{2}O_2 = 3\ CaTiSiO_5 + Fe_3O_4$$

The units lacking titanite appeared to have formed at somewhat lower f_{O_2} than those in which this mineral was abundant. In Figure 27.1 we have plotted the curve defining f_{O_2} and temperature for the major group of Lipman's titanite-bearing samples. A curve calculated from thermodynamic data for the assemblage titanite-magnetite-quartz-amphibole by Noyes et al. (1983) is also shown in Figure 27.1. It lies close to the curve based on Lipman's data. These curves should only be considered as approximate indicators of the minimum f_{O_2} required for titanite formation, since the conditions that control its equilibrium are several and include pressure (Spear, 1981). Magmas sufficiently oxidized to precipitate primary anhydrite also contain titanite, e.g. El Chichon, Mexico (Luhr et al., 1984): Julcani, Peru (Drexler and Munoz, 1985).

Euhedral titanite, apparently of primary origin, is abundant in many of the samples discussed in this report. In the Cedar Lake stock two representative slides gave point count estimates of 1.2% and 1.1% titanite (samples NBG-1-825 and NBG-1-1300). Titanite present as coronas around magnetite was not included in this estimate. Comparative values for rocks derived from relatively oxidized magmas are: Julcani volcanics, 0.1 vol.% (Drexler and Munoz, 1985); El Chichon pumices, 0.2 wt.% (Luhr et al., 1984); Finnmarka (Norway) granodiorite, 1.2 vol.% and granite, 0.2 vol.% (Czamanske and Mihalik, 1972); and Red Lake and Eagle Lake plutons, Nevada, 0.3 to 1.0 vol.% (Noyes et al., 1983). The crystals in the Cedar Lake stock can be relatively large, up to 0.4 mm, and were formed at an early stage, since they are included within crystals of feldspar (Fig. 27.16) or quartz. Noyes (1978) considered certain rocks from the Sierra Nevada batholith to be intrinsically oxidized because early-formed magnetite and titanite grains are enclosed in plagioclase and hornblende. Microprobe analyses of euhedral titanite and secondary titanite (as coronas around magnetite grains) from the Cedar Lake stock (Table 27.5) indicates that the compositions of the two are similar.

Syenite from the Cairo stock contain large crystals of titanite, that may exceed 1 mm in length, again often enclosed in feldspar or quartz. These titanites are variably altered to rutile, and K-feldspar (Fig. 27.17). Point count estimates of sample M14 gave 0.7% titanite. Analyses of unaltered, euhedral titanite from the Cairo stock (Table 27.5) give low totals, presumably because they contain significant amounts of elements that were not determined. This does not apply to the secondary titanite from this intrusion.

Titanite is also present in the Canadian Arrow intrusion, but at 0.5 vol.% in sample CA-4 is somewhat less abundant than in the other listed samples, has a smaller grain size, and is usually present interstitially. Many of the crystals are altered. In the syenites from Kirkland Lake we have identified relicts of euhedral titanite crystals and this is confirmed by reports of titanite in these rocks by Thomson et al. (1950). We have also identified abundant euhedral titanite in the Lebel syenite.

DISCUSSION

The intrusions hosting the deposits at Kirkland Lake, Matachewan and Canadian Arrow have a good deal in common. These plutons are altered throughout, which includes carbonatization and the partial oxidation of magnetite to hematite. The same type of alteration is maintained close to the veins, but here it is more intense, and in some instances has caused the complete oxidation of Fe present in magnetite

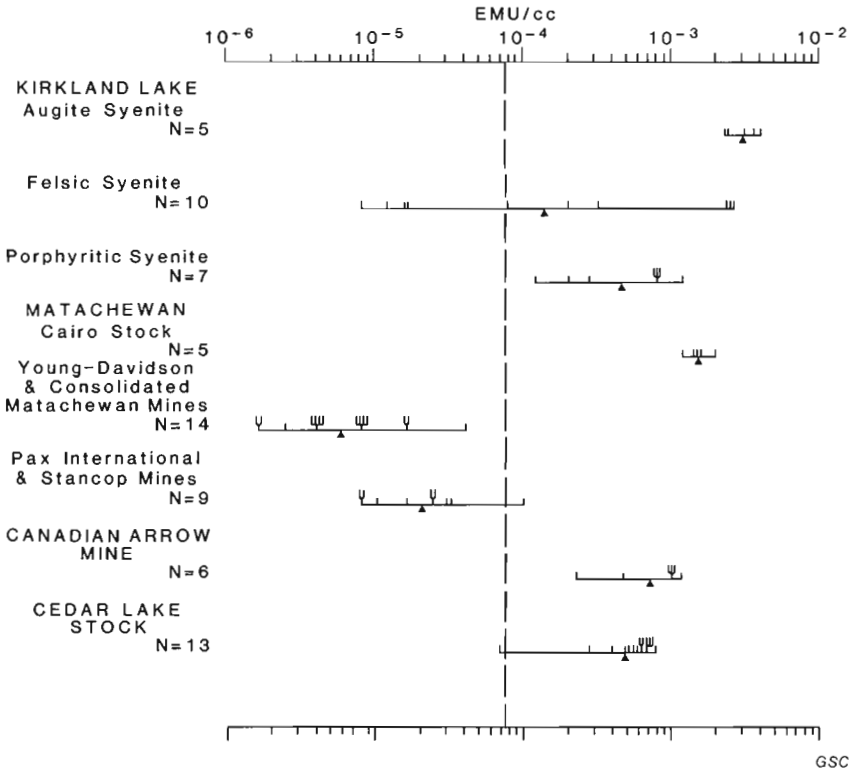


Figure 27.12. Magnetic susceptibility of samples from intrusions.

Table 27.3. Microprobe analyses (in percent) of biotite from Cedar Lake stock, Hemlo

SAMPLE NO. ANALYSES	NBG-1-190 6	NBG-1-345 6	NBG-1-495 3	NBG-1-520 3	NBG-1-825 3	NBG-1-1300 4
SiO_2	37.63	37.88	37.91	37.33	37.90	38.06
Al_2O_3*	14.77	14.69	14.80	14.37	14.85	14.06
Fe_2O_3*	3.39	3.83	3.93	3.48	3.36	3.40
FeO	15.80	15.34	15.25	16.34	16.10	16.65
MgO	12.13	12.35	12.88	11.79	12.37	12.52
MnO	0.36	0.40	0.38	0.36	0.28	0.31
TiO_2	1.75	1.70	1.42	2.04	1.30	1.29
CaO	0.10	0.12	0.01	0.13	0.00	0.06
K_2O	9.77	9.49	9.52	9.72	9.40	9.49
Na_2O	0.28	0.06	0.09	0.34	0.07	0.13
Cr_2O_3	0.03	0.02	0.02	0.06	0.05	0.07
TOTAL	96.01	95.88	96.21	95.96	95.68	96.04

*Chemical determinations

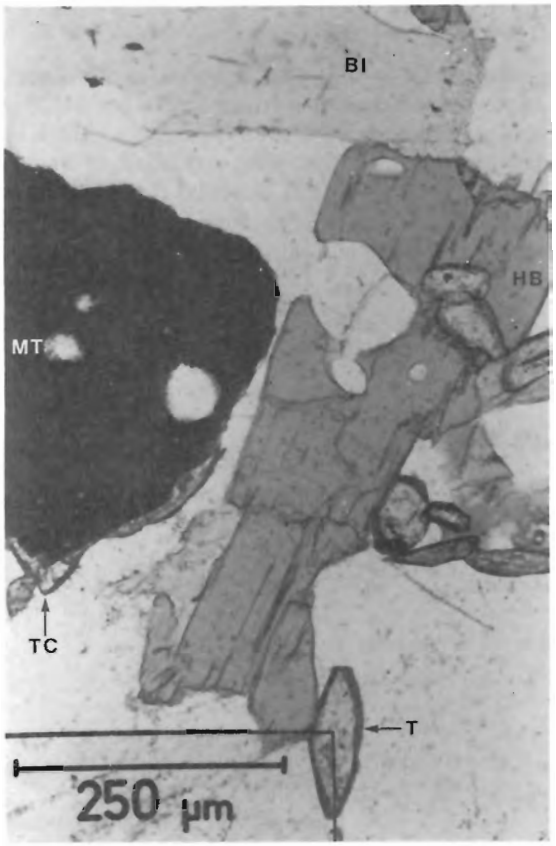


Figure 27.15

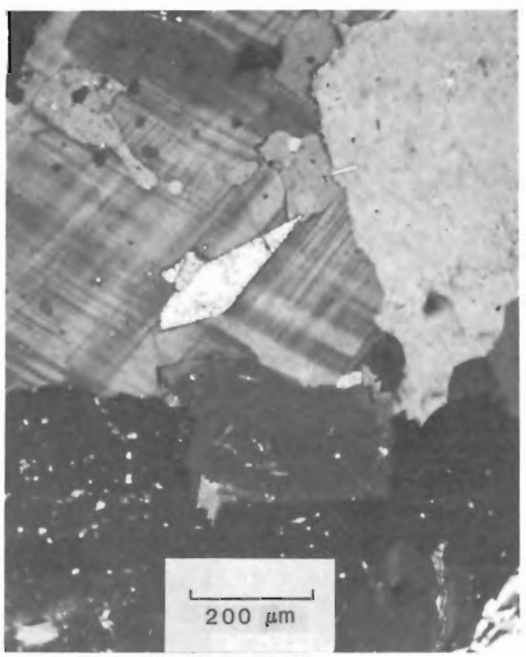


Figure 27.16



Figure 27.17

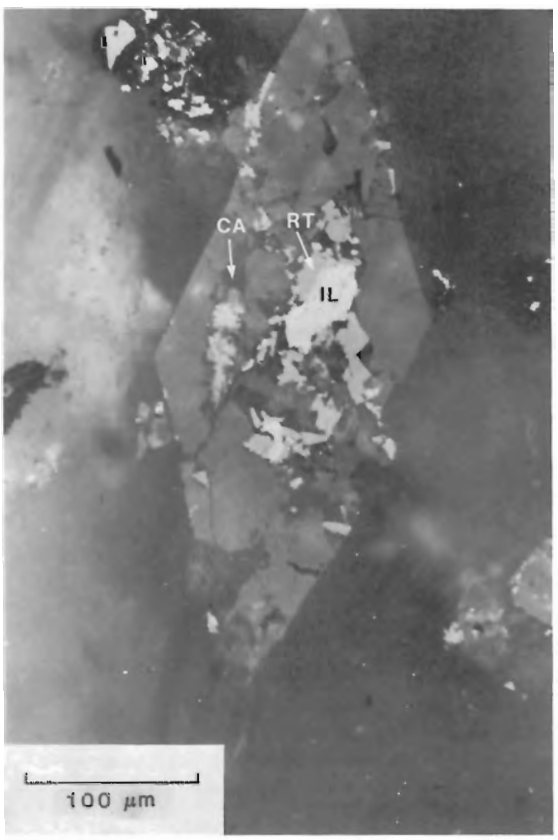


Figure 27.18

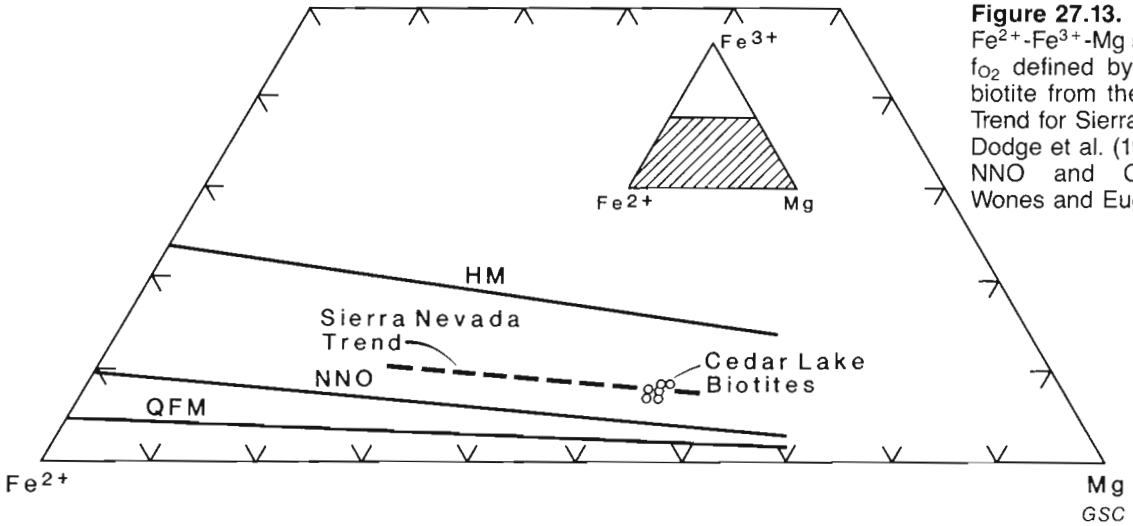


Figure 27.13. Ternary plot of Fe^{2+}-Fe^{3+}-Mg showing approximate f_{O_2} defined by the composition of biotite from the Cedar Lake stock. Trend for Sierra Nevada biotite from Dodge et al. (1969). Position of HM, NNO and QFM buffers from Wones and Eugster (1965).

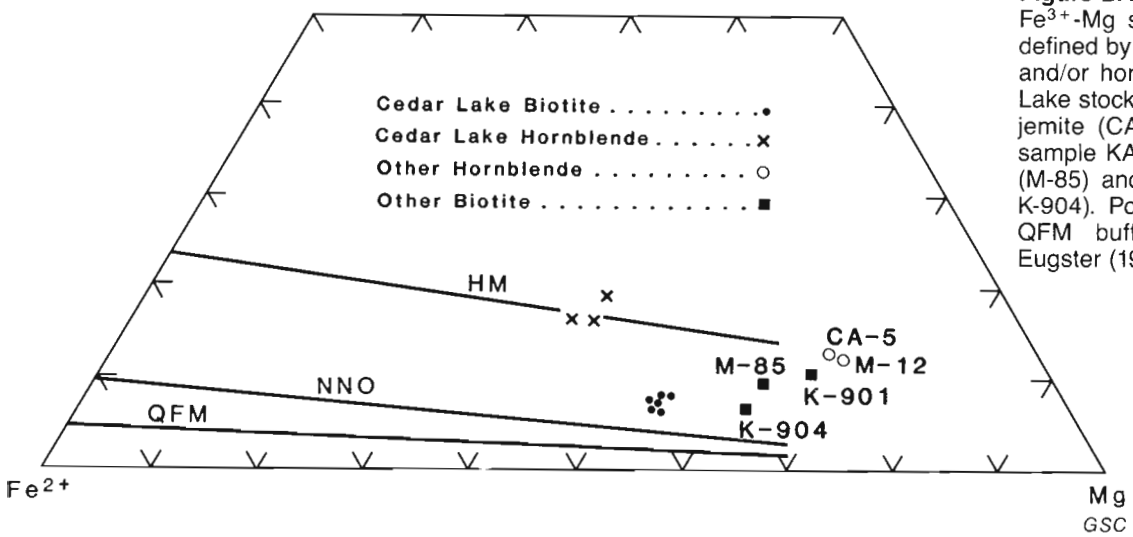


Figure 27.14. Ternary plot of Fe^{2+}-Fe^{3+}-Mg showing approximate f_{O_2} defined by the composition of biotite and/or hornblende from the Cedar Lake stock, Canadian Arrow trondhjemite (CA-5), Cairo stock (M-12), sample KA 3185, near Matachewan (M-85) and the Lebel stock K-901, K-904). Position of HM, NNO and QFM buffers from Wones and Eugster (1965).

Figure 27.15. Biotite (BI), hornblende (HB), magnetite, with two generations of titanite, euhedral to subhedral crystals (T) and partial coronas of titanite around magnetite (TC). Sample NBG-1-335, Cedar Lake stock, transmitted light.

Figure 27.16. Euhedral crystal of titanite in microcline. Sample NBG-1-1300, Cedar Lake stock, transmitted light, cross nichols.

Figure 27.17. Euhedral crystal of titanite partly altered to rutile (dark) and K-feldspar. Syenite sample 41P850008, Young-Davidson mine, transmitted light.

Figure 27.18. Euhedral crystal of titanite partly altered to rutile (RT), calcite (CA) and ilmenite (IL). Trondhjemite sample CA-2, Canadian Arrow stock, reflected light.

and silicates to hematite. Pyritization of the wall rocks is omnipresent. While this has sometimes been taken to indicate a reduced fluid, it is not necessarily the case. Figure 27.19 shows a plot of Fe species in f_{O_2}-f_{S_2} space. Given a moderately high f_{S_2}, pyrite is stable in rather oxidized fluids. The preponderance of pyrite over pyrrhotite in Archean gold mineralization suggests that f_{S_2} was generally high in the ore-forming fluids.

Despite the alteration of these intrusions, some evidence remains of magmatic f_{O_2}. For the Matachewan syenites, the few analyses of biotite and amphibole, together with the early formation of titanite, and the high contents of magnetite indicate a relatively oxidized magma. Information is more sparse for the Canadian Arrow stock, but again, what information there is from primary titanite and the moderately high magnetite contents, indicates that the magma was oxidized. It is only from Kirkland Lake that the regional alteration has been so intense as to destroy most of the evidence relevant to the oxidation state of the magma. However, the relict titanite

Table 27.4. Microprobe analyses (in percent) of hornblende

LOCATION	CEDAR LAKE STOCK			CANADIAN ARROW	CAIRO STOCK
SAMPLE	NBG-1-190	NBG-1-345	NBG-1-520	CA-5	M-12
NO. ANALYSES	6	4	5	9	6
SiO_2	42.09	41.83	41.72	50.99	52.17
Al_2O_3	9.23	9.34	9.38	3.20	2.45
Fe_2O_3	8.40	7.36	7.43	6.28	6.06
FeO	14.13	15.11	15.57	7.57	7.41
MgO	9.20	9.03	8.59	15.76	16.19
MnO	0.42	0.40	0.42	0.80	0.45
TiO_2	0.48	0.48	0.43	0.48	0.85
CaO	11.54	11.55	11.44	11.52	8.09
K_2O	1.27	1.29	1.30	0.36	1.03
Na^{2O}	1.64	1.93	1.91	1.38	4.24
Cr_2O_3	0.05	0.10	0.10	0.07	0.02
TOTAL	98.45	98.42	98.29	98.41	98.96

Table 27.5. Microprobe analyses (in percent) of titanite. E = euhedral titanite; S = secondary titanite rimming magnetite grains. Total Fe reported as FeO.

LOCATION	CEDAR LAKE STOCK				CANADIAN ARROW				CAIRO STOCK			
SAMPLE	NBG-1-190	NBG-1-495		NBG-1-825	CA-1	CA-5		CA-6	MIO	M12		M14
TYPE	S	E	S	E	S	E	S	E	E	E	S	S
NO. ANALYSES	2	4	2	3	1	3	2	2	1	4	1	1
FeO	1.53	1.44	1.83	1.08	2.85	1.41	1.77	1.66	3.06	2.61	1.76	2.96
TiO_2	36.97	36.76	36.12	36.73	37.11	37.36	37.80	36.00	35.47	36.50	38.32	37.17
MnO	0.08	0.09	0.08	0.11	0.26	0.17	0.24	0.21	0.20	0.11	0.09	0.19
Al_2O_3	1.64	2.15	2.16	2.17	0.86	1.34	1.19	2.16	0.74	0.42	0.23	0.34
Cr_2O_3	0.03	0.01	0.04	0.02	0.00	0.01	0.02	0.00	0.01	0.03	0.01	0.07
MgO	0.00	0.00	0.00	0.00	0.00	0.00	0.00	0.00	0.00	0.00	0.00	0.00
SiO_2	30.44	29.76	30.47	28.80	30.92	28.82	29.43	29.15	29.44	29.05	29.52	30.42
V_2O_3	0.23	0.25	0.26	0.22	0.33	0.29	0.35	0.25	0.28	0.24	0.17	0.32
ZnO	0.00	0.01	0.00	0.00	0.02	0.01	0.04	0.03	0.00	0.01	0.00	0.00
CaO	28.33	28.73	28.85	29.01	28.49	28.22	28.94	28.15	26.30	26.80	28.10	27.68
TOTAL	99.25	99.20	99.81	98.14	100.84	97.63	99.78	97.61	95.50	95.77	98.20	99.15

and the high magnetite contents suggest an oxidized magma. The biotite data from the Lebel syenite and the presence of primary titanite in this intrusion also indicate that high f_{O_2} syenitic magmas were present in this district broadly contemporaneously with the intrusion of the syenites that host the gold mineralization.

These intrusions record a consistent pattern of intrinsically oxidized magmas producing plutonic rocks that were then altered in subsolidus conditions in the presence of a more oxidized fluid. A similar magmatic history has been documented in detail by Lalonde and Martin (1983a, 1983b) for units within the Baie-des-Moutons syenite complex in the St. Lawrence graben of Quebec. Units forming from more oxidized magmatic phases are a pink colour from hematite in fluid inclusions within K-feldspar. The oxidized magma favoured incorporation of Fe into primary oxide phases, so that ferromagnesian minerals, such as pyroxene and biotite are Mg-rich. Hematite in feldspar formed during post-magmatic recrystallization of this feldspar, the Fe coming from the alteration of ferro magnesian minerals. Further similarities to some of the rocks discussed in the present paper are recrystallization of titanomagnetite to a low-Ti variety and the presence of calcite as an alteration product of pyroxene. One of the most significant findings of Lalonde and Martin was to identify the source of late, oxidized fluids. Meteoric water has frequently been postulated as the cause for subsolidus oxidation. In this case it is only the units derived from intrinsically oxidized magma phases that show the effects of post-magmatic oxidation. Adjacent units are not affected, precluding the involment of meteoric water. That the fluids are of magmatic origin is confirmed by δ 18O analyses.

The Cedar Lake stock differs from the other intrusions studied here in that it does not directly host the mineralization. This granodiorite is relatively unaltered, there being no carbonatization and no oxidation of magnetite to hematite. This lack of alteration permits reasonable estimates to be made of f_{O_2} Biotite compositions, abundant and early crystallization of titanite, and a moderately high magnetite content denote a relatively oxidized magma with f_{O_2}'s between the NNO and HM buffers. In Figure 27.1 is plotted in f_{O_2}-temperature space a hypothetical cooling curve for the Cedar Lake stock based on the f_{O_2} estimates obtained from the biotite analyses and assuming that this curve parallels the major oxygen buffers. Its position is consistent with the curve for minimum estimated f_{O_2} required for titanite formation, also shown in this figure. These curves are in the same general range of f_{O_2} as the magmas at El Chichon and Julcani, from which anhydrite precipitated.

As discussed earlier, fluids in contact with the melt will usually be buffered by Fe^{2+}/Fe^{3+} and on cooling will follow curves that parallel the major buffers. Should they separate from the melt, or in subsolidus conditions, the fluids are free from this control and will be buffered mainly by sulphur in those systems that are relatively rich in this element. For example, a fluid in equilibrium with the melt and with f_{O_2} midway between the HM and FMQ buffers will initially cool along the path A-B (Fig. 20). If it were then to separate from the melt it will tend to follow a different path, buffered by sulphur. This path, which will parallel the $f_{O_2} = f_{H_2S}$ curve (Fig. 27.20), will take the fluid into f_{O_2}-temperature conditions where hematite may be stable and where significant isotopic fractionation can take place between oxidized and reduced sulphur species (Fig. 27.20). While this is a general tendency, the precise path that the fluid takes on leaving the melt is conditional on the loss of oxidized species, such as SO_2 and SO_4^{2+}, relative to losses of reduced species, such as H_2, H_2S and S^{2+}. The rate and direction of change in f_{O_2} will be strongly influenced by the environment into which the fluids pass. Thus oxidized magmatic fluids penetrating supracrustal rocks rich in Fe^{2+} and C will experience a rapid decline in f_{O_2} as they react with the wall rock. By contrast, this will not occur for fluids passing through a felsic intrusion derived from an oxidized magma. This explains why hematitization of the wall rocks of gold-bearing veins is much more extensive within the felsic intrusion than outside.

What makes a relatively oxidized, CO_2-rich felsic magma seemingly so suitable for releasing gold-bearing aqueous phases? This has been discussed by Cameron and Hattori (in press), although major aspects are poorly constrained by high temperature experimental data. As shown in Figure 27.21, S is more soluble in oxidized melts and the S species present in aqueous phases in equilibrium with such melts is predominantly SO_2. This favours the dissolution of sulphides and, presumably, gold associated with the sulphides during partial melting and inhibits their precipitation in dispersed form as the magma rises to the surface. In lower temperature, low salinity aqueous fluids, the solubility of gold as the bisulphide complex is strongly influenced by f_{O_2}. It is most soluble in relatively oxidized fluids near the pyrite/hematite boundary (Fig. 27.22).

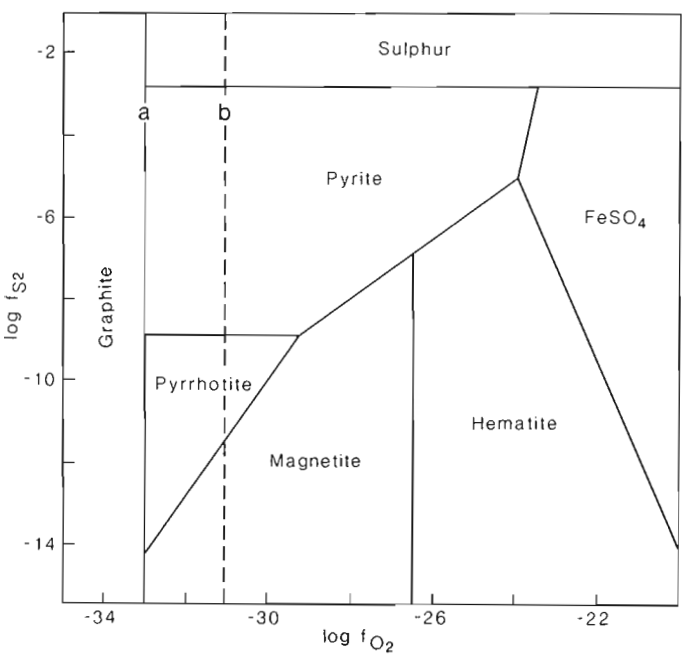


Figure 27.19. Stability of iron minerals in log f_{S_2}-log f_{O_2} space at 350°C and fH_2O = 165 atm. (a) is graphite boundary if fCO_2 is = 1 atm.; (b) is graphite boundary if fCO_2 = 100 atm. From Cameron and Hattori (1987).

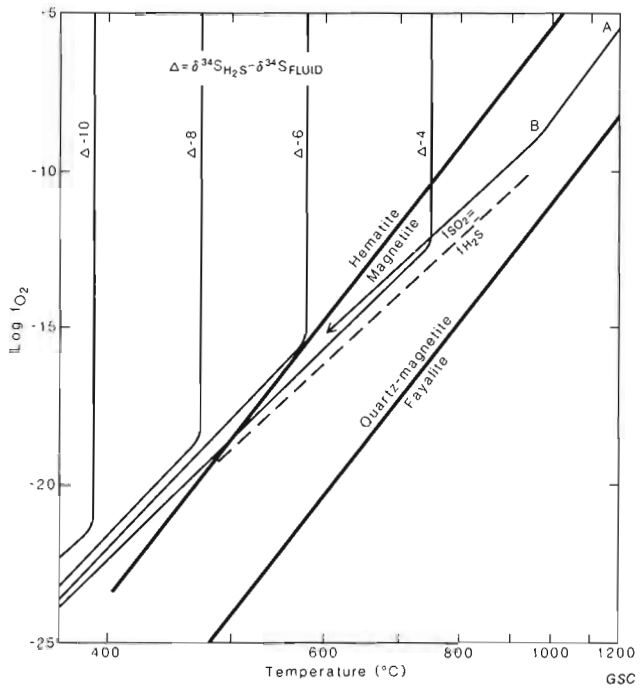


Figure 27.20. Log f_{O_2} – temperature diagram showing cooling path of a hypothetic magmatic aqueous fluid. Isotopic fractionation curves derived from Ohmoto and Rye (1979).

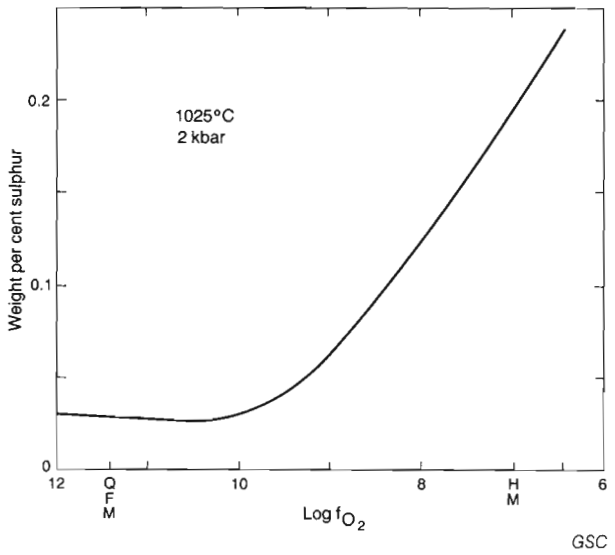


Figure 27.21. Solubility of sulphur in silicate melts with varying f_{O_2}. From Carroll and Rutherford (1985).

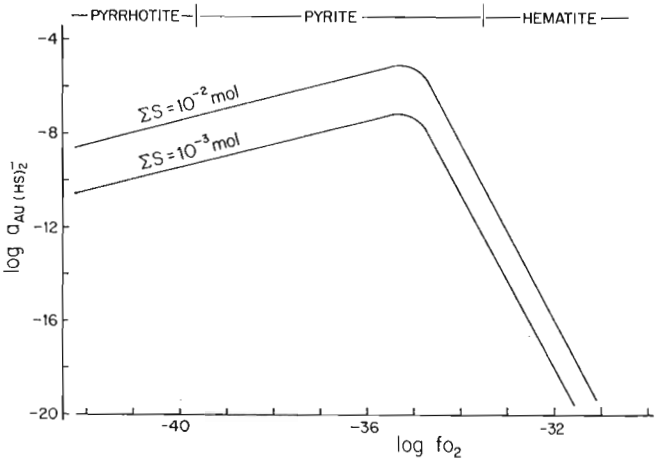


Figure 27.22. Variation in the solubility of gold with change in oxidation conditions at 250°C and pH 6. Curves constructed for dissolved sulphur concentrations of 0.001 and 0.01 mole/l. Although the position of the solubility curve for gold varies with pH, temperature and dissolved sulphur content, the relationship to f_{O_2} remains essentially the same. From Hattori and Cameron (1986b).

For most felsic magmas the solubility of H_2O is only exceeded at near-surface pressures, such that an aqueous phase can only develop at relatively shallow depth. Thus porphyry copper mineralization is mostly formed near surface. CO_2 is much less soluble in silicate melts and the solubility is a linear function of pressure, rather than the square root of pressure in the case of H_2O. Thus partial melts are more readily saturated with CO_2, which separates continuously as the magma rises. Since water partitions into this phase, even if it is undersaturated in the melt, this permits the separation of an aqueous phase from the melt at greater depth than for a CO_2-absent melt. This is important if, as generally believed, Archean vein gold mineralization is of deeper origin than porphyry copper mineralization. Further the addition of CO_2 to the system H_2O-NaCl permits the partitioning of an aqueous fluid into immiscible saline and non-saline phases at greater pressure and temperature than otherwise. Archean gold mineralization is associated predominantly with low salinity aqueous fluids.

CONCLUSIONS

Examination of certain Archean gold deposits, including some of the largest, suggests that these were derived from oxidized hydrothermal fluids. This is expressed by a close association between gold and isotopically fractionated pyrite and/or sulphate minerals and/or hematite. Consideration of possible magmatic, metamorphic or meteoric origins for these fluids, indicates that relatively oxidized magmas are the likeliest general source. There are data to suggest that an oxidized, CO_2-rich magma is particularly suited for evolving gold-bearing aqueous fluids. We have here examined whether magmas of suitable type existed in close spatial and temporal proximity to the formation of four examples of Archean gold mineralization.

Three of the area studied – at Kirkland Lake, Matachewan, and Canadian Arrow – are typical of Archean quartz and quartz-carbonate vein deposits. In each case oxidized fluids were involved in the formation of gold-bearing veins either within or in close proximity to felsic intrusions. Host intrusions and mineralization from the three areas have much in common. In every case the entire intrusion or group of intrusions is altered, including carbonatization and the partial oxidation of magnetite to hematite. In the vicinity of the veins there is more intense alteration, which may include complete oxidation of oxide and silicate iron to hematite, accompanied by pyritization of wall rock. Although often taken to indicate a reduced ore-forming fluid, pyrite may be formed in high f_{O_2}, high f_{S_2} conditions. Alteration of the intrusions precludes precise determination of magmatic f_{O_2}'s, but sufficient evidence remains to indicate that these were relatively oxidizing.

The Hemlo deposit is different. Gold is disseminated through thick tabular orebodies which closely parallel the regional stratigraphy and structural lineation within a metamorphosed volcanic — sedimentary sequence. The element assemblage is more typical of younger epithermal deposits. Deposition from oxidized hydrothermal fluids is indicated by strongly fractionated pyrite and abundant barite. We have previously suggested that the fluids may have been derived either directly or indirectly (via a restricted basin) from an oxidized felsic magma. The Cedar Lake stock intrudes the supracrustal sequence within a few hundred metres of the deposit. This biotite granodiorite is very uniform and much less altered than the intrusions noted above, with no car-

bonatization nor oxidation of magnetite to hematite. Relative lack of alteration permits estimation of magmatic f_{O_2}, which is midway between the hematite-magnetite and nickel-nickel oxide buffers.

Thus all four areas contained magmas capable of producing oxidized hydrothermal fluids and which are broadly contemporaneous with the gold mineralization. We do not suggest that the specific pulse of magma that formed the sampled intrusions was necessarily the source of these fluids. Indeed, in several cases this seems unlikely. For example, at Kirkland Lake there has been significant faulting of the host intrusions prior to mineralization. In the general case it is more likely that fluids exsolved from melts at greater depth. While we have emphasized in this paper the similarities of the ore fluids to the aqueous phase of an oxidized felsic magma, the complex structural setting of Archean gold deposits should be recognized. These occur along major structural breaks which were, almost certainly, the focus for the movement of magmas and of fluids of magmatic, mantle and metamorphic origin (Cameron and Hattori, in press). Indeed CO_2-rich fluids of mantle and metamorphic origin may have been intimately involved in magma genesis (Newton et al., 1980; Allen et al., 1986). Thus strict categorization of the nature of ore-forming fluids is inappropriate.

ACKNOWLEDGMENTS

We are most grateful to Peter Cooper of Noranda Mines, Hemlo Division, who permitted sampling drill core and provided a geological section and to Frank Ploeger of Lac Minerals, Lake Shore Division, who permitted sampling of drill core. David Sinclair kindly provided a biotite sample.

This project would not have been possible without the generous cooperation of members of the Mineralogy and Chemistry subdivision of the GSC who carried out the analytical work. We are particularly grateful to Don Harris, Peter Belanger, M. Bonardi, Jean Louis Bouvier, Ken Church, Bob Delabio, Pat Lavergne, Gina LeCheminant, George Plant and David Walker. Richard Lancaster kindly provided petrographic equipment and Kevin Hicks (University of Ottawa) facilitated examination of samples from the Lake Shore mine. Joanne Belec typed the manuscript.

We are further grateful to Don Harris and to Andre Lalonde and Keiko Hattori (University of Ottawa) for carefully reviewing a draft of the manuscript.

REFERENCES

Allen, P., Condie, K., and Bowling, G.P.
1986: Geochemical characteristics and possible origins of the southern Closepet batholith, South India; Journal of Geology, v. 94, p. 283-299.

Arculus, R.J.
1985: Oxidation status of the mantle; Annual Reviews Earth Planetary Science, v. 13, p. 75-95.

Buddington, A.F., and Lindsley, D.H.
1964: Iron-titanium oxide minerals and synthetic equivalents; Journal of Petrology, v. 5, p. 310-357.

Cameron, E.M., and Hattori, K.
1985: The Hemlo gold deposit, Ontario: a geochemical and isotopic study; Geochimica et Cosmochimica Acta, v. 49, p. 2041-2050.
1986: Archean sulphur cycle: evidence from sulphate minerals and isotopically fractionated sulphides in Superior Province, Canada; submitted to Isotope Geoscience.
in press: Archean gold mineralization and oxidized hydrothermal fluids; Economic Geology;

Candela, P.A.
1986: The evolution of aqueous vapor from silicate melts: effect of oxygen fugacity; Geochimica et Cosmochimica Acta, v. 50, p. 1205-1211.

Carmichael, I.S.E., and Nicholls, J.
1967: Iron-titanium oxides and oxygen fugacities in volcanic rocks; Journal of Geophysical Research, v. 72, p. 4665-4687.

Carroll, M.R., and Rutherford, M.J.
1985: Sulfide and sulfate saturation in hydrous silicate melts; Journal of Geophysical Research, v. 90 (supplement), p. C601-C612.

Cherry, M.E.
1983: The association of gold and felsic intrusions - examples from the Abitibi Belt; Ontario Geological Survey Miscellaneous Paper, v. 110, p. 48-55.

Chou, I-Ming
1978: Calibration of oxygen buffers at elevated P and T using the hydrogen fugacity sensor; American Mineralogist, v. 63, p. 690-703.

Corfu, F., and Muir, T.L.
1986: Preliminary U-Pb ages from the Hemlo area, northwestern Ontario; Geological Association Canada, Mineralogical Association Canada, Canadian Geophysics Union, Annual Meeting, Abstract Volume, p. 59.

Czamanske, G.K., and Mihalik, P.
1972: Oxidation during magmatic differentiation, Finnmarka complex, Oslo area, Norway; 1, The mafic silicates; Journal of Petrology, v. 13, p. 493-509.

Czamanske, G.K., and Wones, D.R.
1973: Oxidation during magmatic differentation, Finnmarka complex, Oslo area, Norway; 2, The mafic silicates; Journal of Petrology, v. 14, p. 349-380.

Czamanske, G.K., Ishihara, S., and Atkin, S.A.
1981: Chemistry of rock-forming minerals of the Cretaceous-Paleocene Batholith in southwestern Japan and implications for magma genesis; Journal of Geophysics Research, v. 86, B11, p. 10431-10469.

Dodge, F.C.W., and Ross, C.D.
1971: Coexisting hornblendes and biotites from granitic rocks near the San Andreas fault, California; Journal of Geology, v. 79, p. 158-172.

Dodge, F.C.W., Smith, V.C., and Mays, R.E.
1969: Biotites from granitic rocks of the central Sierra Nevada batholith; Journal of Petrology, v. 10, p. 250-271.

Drexler, J.W., and Munoz, J.L.
1985: Highly oxidized, pyrrhotite-anhydrite bearing silicic magmas from the Julcani Ag-Cu-Bi-Pb-Au-W district, Peru: physiochemical conditions of a productive magma; in Petrogenesis and Tectonic Setting, ed. R.P. Taylor and D.F. Strong; Canadian Institute Mining Metallurgy Conference, Halifax, Nova Scotia, p. 87-100.

Dyer, W.S.
1936: Geology and ore deposits of the Matachewan – Kenogami area; Ontario Department Mines Annual Report, Part 2, v. 44, 69 p.

Haggerty, S.E., and Tompkins, L.A.
1983: Redox state of Earth's upper mantle from kimberlitic ilmenites; Nature, v. 303, p. 295-300.

Hattori, K., and Cameron, E.M.
1986a: Archean magmatic sulphate; Nature, v. 319, p. 45-47.
1986b: Pyrite of distinctive isotopic composition from the Hemlo deposit: A potential tool to identify this type of gold mineralization in Archean terrain; Journal of Geochemical Exploration (in press).

Heubner, J.S., and Sato, M.
1970: The oxygen fugacity temperature relationship of manganese oxide and nickel oxide buffers; American Mineralogist, v. 55, p. 934-952.

Hewitt, D.A.
1978: A redetermination of the fayalite-magnetite-quartz equilibrium between 650° and 850°C; American Journal of Science, v. 278, p. 715-724.

Holland, H.D.
1984: The chemical evolution of the atmosphere and oceans; Princeton University Press, Princeton, New Jersey, 582 p.

Ishihara, S.
1977: The magnetite-series and ilmentite-series granitic rocks; Mining Geology, v. 27, p. 293-305.
1981: The granitoid series and mineralization; Economic Geology, 75th Anniversary Volume, p. 458-484.

Jones, J.H., and Drake, M.J.
1986: Geochemical constraints on core formation in the Earth; Nature, v. 322, p. 221-228.

Kramers, J.D.
1979: Lead, uranium, strontium, potassium and rubidium in inclusion-bearing diamonds and mantle-derived xenoliths from southern Africa; Earth and Planetary Science Letters, v. 42, p. 58-70.

Lalonde, A.E., and Martin, R.F.
1983a: The Baie-des-Moutons syenitic complex, La Tabatiere, Quebec 1. Petrography and feldspar mineralogy; Canadian Mineralogist, v. 21, p. 65-79.
1983b: The Baie-des-Moutons syenitic complex, La Tabatiere, Quebec 2. The ferromagnesian minerals; Canadian Mineralogist, v. 21, p. 81-91.

Lipman, P.W.
1971: Iron-titanium oxide phenocrysts in compositionally zones ash-flow sheets from southern Nevada; Journal of Geology, v. 79, p. 438-456.

Lovell, H.L.
1967: Geology of the Matachewan area; Ontario Department of Mines, Geology Report 51, 61 p.

Luhr, J., Carmichael, I.S.E., and Varekamp, J.C.
1982: The 1982 eruptions of El Chichon volcano, Chiapas, Mexico: mineralogy and petrology of the anhydrite-bearing pumices; Journal of Volcanology and Geothermal Research, v. 23, p. 69-108.

Mathez, E.A.
1984: Influence of degassing on oxidation states of basaltic magmas; Nature, v. 310, p. 371-375.

McNeil, A.M., and Kerrich, R.
1986: Archean lamprophyre dykes and gold mineralization, Matheson, Ontario: the conjunction of LILE-enriched mafic magmas, deep crustal structures, and Au concentration; Canadian Journal of Earth Science, v. 23, p. 324-343.

Moore, E.S.
1936: Geology and ore deposits of the Ramore area; Ontario Department Mines Annual Report, Part 6, v. 45, p. 1-37.

Muir, T.L.
1982: Geology of the Hemlo area, District of Thunder Bay; Ontario Geology Survey Report 217, p. 65.

Newton, R.C., Smith, J.V., and Windley, B.F.
1980: Carbonic metamorphism, granulties and crustal growth; Nature, v. 288, p. 45-50.

Noyes, H.J.
1978: Petrogenesis of Sierran plutons: a petrologic and geochemical investigation into the origin and differentiation of granodioritic plutons in the central Sierra Nevada batholith, California; unpublished Ph.D thesis, Massachusettes Institute of Technology.

Noyes, H.J., Wones, D.R., and Frey, F.A.
1983: A tale of two plutons: petrographic and mineralogic constrints on the petrogenesis of the Red Lake and Eagle Lake plutons, central Sierra Nevada, California; Journal of Geology, v. 91, p. 353-379.

Ohmoto, H., and Rye, R.O.
1983: Isotopes of sulfur and carbon; in Geochemistry of Hydrothermal Ore Deposits, ed. H.L. Barnes, John Wiley and Sons, New York, p. 509-567.

Prest, V.K.
1957: Geology of Hislop Township; Ontario Department Mines Annual Report, Part 5, v. 65, 48 p.

Robinson, P., Spear, F.S., Schumacher, J.C., Laird, J., Klein, C., Evans, B.W., and Doolan, B.L.
1982: Phase relations of metamorphic amphiboles: Natural occurrence and theory; in Reviews in Mineralogy, Volume 9B, Amphiboles: Petrology and Experimental Phase Relations, eds. D.R. Veblen and P.H. Ribbe, Mineralogical Society of America, p. 1-227.

Sato, M., and Wright, T.C.
1966: Oxygen fugacities directly measured in magmatic gases; Science, v. 153, p. 1103-1105.

Schwarcz, H.P., and Rees, C.E.
1985: S-34 in pyrite from gold deposits; in Ontario Geological Survey Miscellaneous Paper 127, ed. V.G. Milne, p. 151-156.

Sinclair, W.D.
1982: Gold deposits of the Matachewan area, Ontario; in Geology of Canadian Gold Deposits, ed. R.W. Hodder and W. Petruk, Canadian Institute Mining Metallurgy, Special Volume 24, p. 83-93.

Sobolev, N.V., Efimova, E.S., and Pospelova, L.N.
1981: Native iron in diamonds of Yakutiya and its paragenesis; Soviet Geology Geophysics, v. 22, p. 18-21.

Spear, F.S.
1981: An experimental study of hornblende stability and compositional variability in amphibolite; American Journal of Science, v. 281, p. 697-734.

Speer, J.A.
1984: Micas in igneous rocks; in Reviews in Mineralogy, ed. S.W. Bailey, v. 13, p. 299-356.

Spencer, K.J., and Lindsley, D.H.
1981: A solution model for coexisting iron-titanium oxides; American Mineralogist, v. 66, p. 1189-1201.

Thomson, J.E., Charlewood, G.H., Griffin, K., Hawley, J.E., Hopkins, H., MacIntosh, C.G., Ogrizlo, S.P., Perry, O.S., and Ward, W.
1950: Geology of the main ore zone at Kirkland Lake; Ontario Department Mines Annual Report, Part 5, v. 57, p. 54-188.

Verhoogen, J.
1962: Distribution of titanium between silicates and oxides in igneous rocks; American Journal of Science, v. 260, p. 211-220.

Whitney, J.
1984: Fugacities of sulfurous gases in pyrrhotite-bearing silicic magmas; American Mineralogist, v. 69, p. 69-78.

Wones, D.R., and Eugster, H.P.
1965: Stability of biotite, experiment, theory, and application; American Mineralogist, v. 50, p. 1228-1272.

Gravity and bathymetry taken along seismic refraction lines from the Canadian Ice Island during 1985 and 1986[1]

L.W. Sobczak[2] and J.R. Weber[3]

Sobczak, L.W., and Weber, J.R., Gravity and bathymetry taken along seismic refraction lines from the Canadian Ice Island during 1985 and 1986; in Current Research, Part A, Geological Survey of Canada, Paper 87-1A, p. 299-304, 1987.

Abstract

As part of the Frontier Geoscience Program a combined gravity – bathymetry survey along four seismic refraction lines was carried out during the spring of 1985 and 1986 from the Canadian Ice Island base camp located on the Arctic Ocean about 30 to 40 km northwest of Axel Heiberg Island, N.W.T. A total of 140 gravity observations and 124 water depth measurements were made along two lines parallel, and two lines perpendicular to the coastline of the Queen Elizabeth Islands.

Water depth measurements from these surveys combined with previous data indicate two hitherto unmapped ridges and valleys striking perpendicular to the trend of the Queen Elizabeth Shelf.

Gravity measurements indicate an elongated coastal Bouguer anomaly "high", subparallel to the coastline, with accompanying landward trending spurs. These anomalies overlie the northeastern end of the Sverdrup Rim at the northwestern end of Ellesmere Island where the Bourne Complex and Unnamed Formation, consisting of volcanic basalt flows with dense mafic intrusions, are exposed.

Résumé

Au printemps de 1985 et de 1986, dans le cadre du Programme géoscientifique des régions pionnières, un relevé combiné de gravité-bathymétrie a été effectué le long de quatre lignes de sismique réfraction à partir du camp de base de la Canadian Ice Island située dans l'océan Arctique à environ 30 ou 40 km au nord-ouest de l'île Axel-Heiberg (T.N.-O.). Au total, 140 observations gravimétriques et 124 mesures de bathymétrie ont été recueillies le long de 2 lignes parallèles et de 2 lignes perpendiculaires à la côte des îles Reine Elizabeth.

Les relevés bathymétriques annexés aux données antérieures montrent l'existence de deux crêtes et de deux vallées jusqu'ici inconnues, d'orientation perpendiculaire à la direction générale du plateau continental Reine Elizabeth.

Les mesures gravimétriques indiquent l'existence d'une anomalie de Bouguer positive subparallèle à la côte et avec des ramifications dans la direction de cette dernière. Cette anomalie coïncide avec l'extrémité nord-est du bassin de Sverdrup et l'extrémité nord-ouest de l'île Ellesmere où sont exposés le complexe de Bourne et la formation Sans Nom constitués de coulées volcaniques de basalte et d'intrusions mafiques denses.

[1]Ice Island Contribution no. 10
[2]Lithosphere and Canadian Shield Division
[3]Geophysics Division

INTRODUCTION

During April, 1985 and April to May, 1986, 140 gravity and 124 water depth measurements were made along seismic refraction lines (Fig. 28.1) in support of the seismic refraction program (The Refraction Team, 1986). The Polar Continental Shelf Project (PCSP) camp on the Canadian Ice Island (CII) was used as a base.

Gravity observations were made with Lacoste-Romberg G gravimeters on the ice surface at about 5 km intervals at the locations of the seismic recording sites and shot points. Water depths were determined at the same sites using seismic water depth sounders.

This report discusses primarily the new gravity and bathymetry data obtained in 1985 and 1986. Field procedures

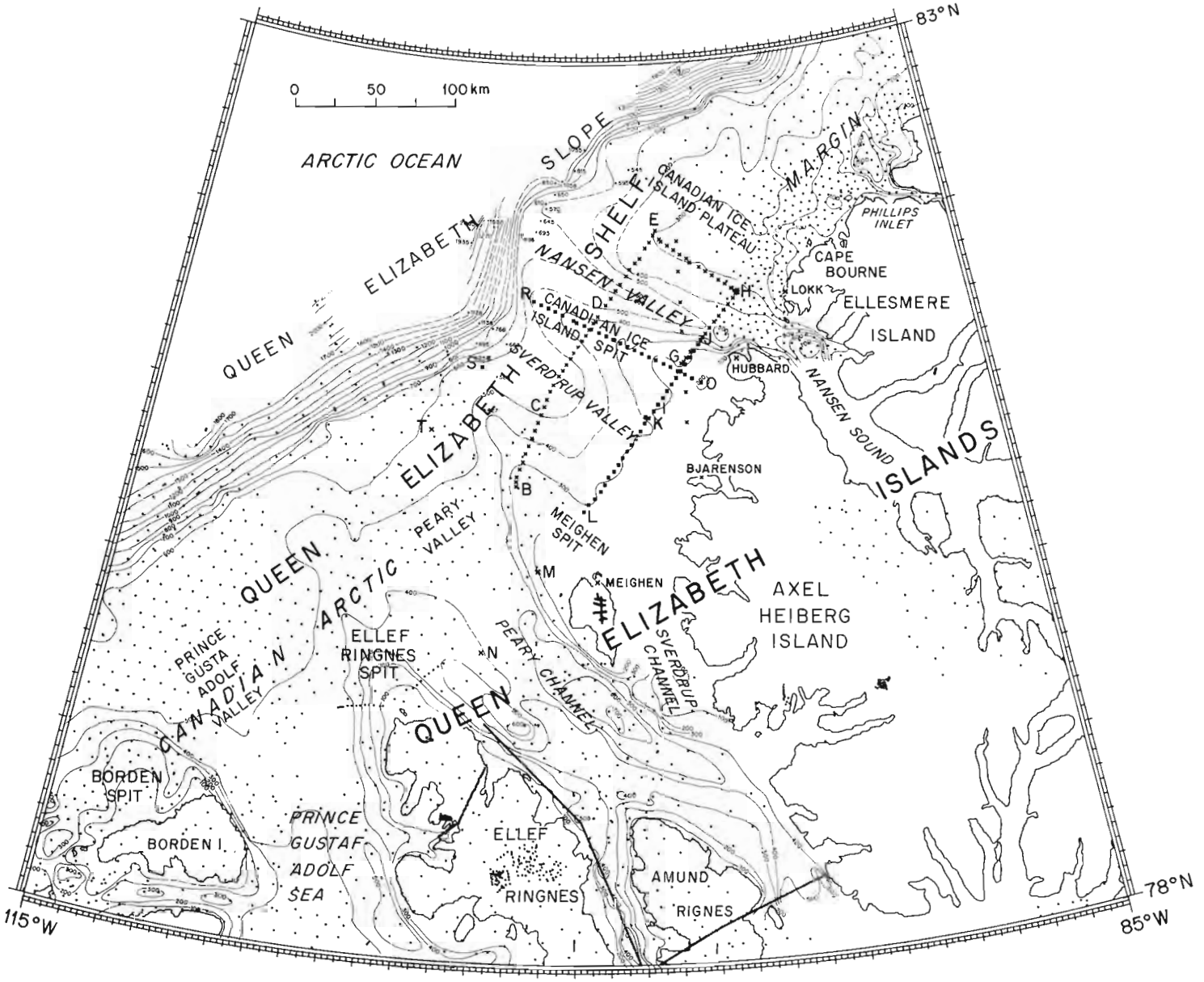


Figure 28.1. Location of gravity and water depth measurements are shown by dots prior to 1985, crosses for 1985 and squares for 1986. The shot points are lettered. Water depths are in metres corrected for temperature and salinity using Matthews' velocity – depth relationship (Matthews, 1939). Depth contours are at 100 m intervals (dashed contours show regions of poor control). The Syledis transmitters are located at Lokk, Hubbard, Bjarenson, Meighen and the Ice Island (I).

and instrumentation have been discussed elsewhere by Sobczak and Schmidt (1985), Sobczak and Weber (1986) and Weber and Sobczak (1986).

THE SURVEY

Navigation was provided by a Syledis UHF positioning system, loaned and operated by the Canadian Hydrographic Survey, Department of Fisheries and Oceans at the Bedford Institute of Oceangraphy. Five unmanned transmitter stations were situated at Lokk, Hubbard, Bjarnason, Meighen and on the CII, which was located near shot point H in 1985 and near point I in 1986 (Fig. 28.1). The stations were positioned by means of a model T14100 Global Positioning System (GPS) to an accuracy of ±40 m absolute (J. Popelar, personal communication, 1986). The helicopters used for the survey were equipped with Syledis UHF as well as Omega VLF receivers. The positioning accuracy of the Syledis system depends on the distance from the transmitters, on the geometrical configuration of transmitters and on the accuracy of the transmitter antennae locations. Comparison of the Syledis and GPS positions on the CII indicated a difference of less than 20 m.

Water depths were determined by a seismic reflection method using 0.5 to 1 kg charges of geogel (Weber and Sobczak, 1986). The seismic recorder determined two-way travel time to an accuracy of ± 0.5 ms, corresponding to a ± 0.7 m of water depth. Travel time was converted to water depth using Mathew's velocity – depth relationship (Sobczak et al., 1973).

The gravity difference between the CII and the gravity control station in Resolute Bay was determined with the two LaCoste-Romberg gravimeters, G75 and G498, during deployment and again at evacuation. During the survey period G75 was used as a base monitor housed in a temperature-controlled environment while G498 was used on traverse. The CII did not move significantly between deployment and evacuation. The accuracy of individual gravity measurements are estimated at ± 0.1 mGal (1 mGal = 10 $\mu m/s^2$). Gravity measurements were reduced to free-air and Bouguer anomalies by the method described by Tanner and Buck (1964) using the International Gravity Standardization Net, 1971 (1974) and the Geodetic Reference System, 1967 (1971).

RESULTS

Bathymetry, including new names proposed for undersea features, free-air and Bouguer anomalies are discussed below and shown in Figures 28.1 to 28.3. The new names have been submitted for approval to the Advisory Committee on Undersea Feature Names.

Bathymetry

Water depths taken along the seismic refraction lines during 1985 and 1986 combined with data from earlier surveys (Sobczak et al., 1963; Weber, 1963; Weber and Sweeney, 1985) and the twenty-six water depths taken from the Arctic Geophysical Review (Sobczak and Sweeney, 1978) although sparse, show a corrugated morphology in the area of the refraction lines. There is evidence for two, previously unmapped, valleys striking northwest from the mouth of Nansen Sound and the Sverdrup Channel across the Queen Elizabeth Shelf. These valleys will be referred to in this discussion as *Nansen Valley* and *Sverdrup Valley* respectively. Nansen Valley is flanked to the northeast by a prominent plateau which is about 250 to 400 m higher than the valley floor and about 100 m higher than the adjacent shelf to the northeast. During the winter months of 1985 the Canadian Ice Island was stationary over this plateau, and thus it will be referred to here as the *Canadian Ice Island Plateau*. Between the valleys there is evidence for an underwater spit that plunges seaward and, because the Canadian Ice Island was stationary over this feature in 1986, it is referred to here as the *Canadian Ice Island Spit*. Similar spit features are observed trending northwest from the islands of the Queen Elizabeth Islands and are named after the adjacent islands as *Meighen Spit, Ellef Ringnes Spit* and *Borden Spit*.

Based on the limited data, it seems that Nansen Valley differs in shape and depth from Sverdrup Valley, but has characteristics similar to Peary Channel. It is deeper than Sverdrup Valley, more V-shaped with deep pockets right into the mouth of Nansen Sound (maximum depth of 730 m). The 300 m contour of the Sverdrup Valley meanders along the southern refraction line, whereas in Nansen Valley it is located on steep valley walls that extend landward into Nansen Sound.

The Canadian Ice Island Spit protrudes from the northwestern part of Axel Heiberg Island as a narrow crest that plunges seaward from a depth of 144 m along the southern seismic refraction line to possibly 700 m, where it merges with the Queen Elizabeth Slope. Similarly Meighen Spit extends seaward from Meighen Island, is a little wider, and is not as pronounced as the Canadian Ice Island Spit in intercepting the slope.

Free-air anomalies

Gravity anomalies observed prior to 1985 within the area of Figure 28.2 have been discussed previously by Sobczak (1963), Weber (1963), Sobczak et al. (1963), Sobczak and Weber (1970, 1973), Sobczak and Overton (1984), Sweeney et al. (1984), Sweeney et al. (1987), and Sobczak et al. (1987). The discussion of free-air anomalies in this report is restricted to anomalies shown along the seismic refraction lines completed in 1985 and 1986.

Generally, higher gravity values are noted over the plateau and spits and lower values over the valleys, but not in a one to one relationship. Differences between the gravity – bathymetry relationship indicate an anomalous behavior of the gravity field. The free-air gravity high over the Canadian Ice Island Plateau (maximum value + 36 mGal) is localized over the southeastern end of the plateau, trends parallel to the coastline and extends over the eastern flank of Nansen Valley.

To the east, an east-west low centered on Phillips Inlet (minimum value −52 mGal) crosses the seaward end of the Canadian Ice Island Plateau and appears to merge with a northwestward trending belt of lows along Nansen Valley.

Gravity lows along Nansen Valley are normal in some places and anomalous in others. At the eastern end of Nansen Valley, a low is localized over an area with greatest water depths, whereas the low to northeast of Hubbard, although centred over Nansen Channel, does not overlie the deepest portion which lies about 20 km to the west. This low trends northwards across the southeastern end of the Canadian Ice Island Plateau and also extends seaward along Nansen Channel but disappears between points D and E, where Nansen Valley is quite prominent.

The gravity high over the Canadian Ice Island Spit is not centred over the crest but is shifted to the west about 16 km over its western flank.

A very broad low overlies the seaward end of Sverdrup Valley and does not appear to go much farther southeastward than the most southern refraction line. A minor relative gravity high overlies Meighen Spit.

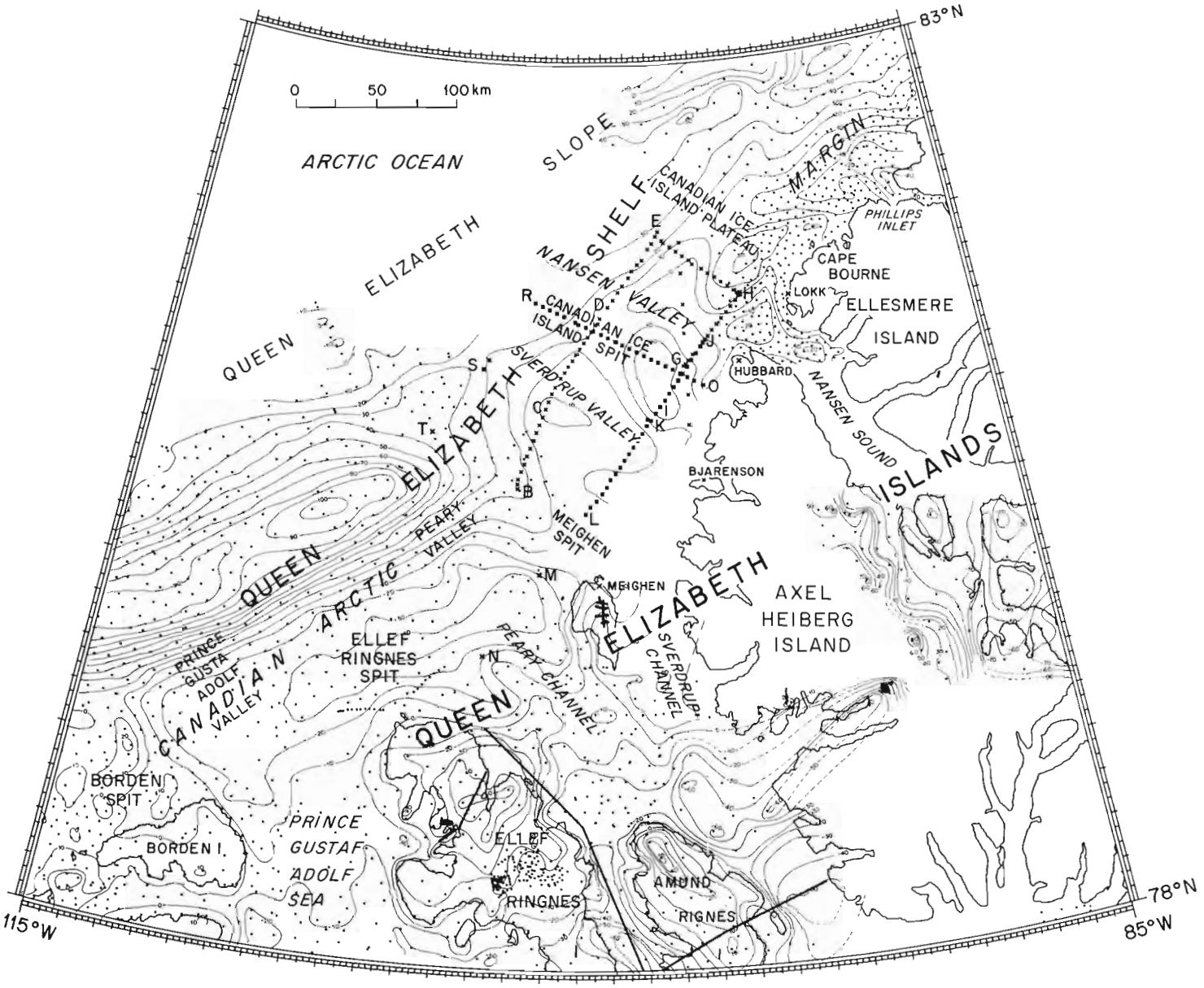


Figure 28.2. Free-air anomalies are shown in contours at 10 mGal intervals.

Bouguer anomalies

Bouguer anomalies (Fig. 28.3) within the vicinity of the seismic refraction lines indicate a large elliptical anomaly overlying the Canadian Ice Island Plateau and Canadian Ice Island Spit. The strike of this anomaly is parallel to the coast. Above the 30 mGal contour the anomaly is not well defined as there are no gravity observations across Nansen Valley. From the southern flank of this elliptical anomaly, a spur of positive values extends across Nansen Valley towards Hubbard. Also, on the southern side of the eastern end of this anomaly, a spur of positive anomalies crosses Cape Bourne and overlies the eastern end of Nansen Valley. Between these spurs lies a relative low which overlies and crosses Nansen Valley from the Hubbard area towards Lokk. No prominent high overlies Meighen Spit.

To the east of the elliptical high lies an extensive low that curves around the northern flank of the high and crosses the northern sides of the Canadian Ice Island Plateau and the Canadian Ice Island Spit. Normally, gravity lows occur along or just seaward of the coastline, often reflecting a seaward thickening of low density sediments (Fig. 4, Sobczak et al., 1986).

The high over the Canadian Ice Island plateau and spit, with accompanying landward trending spurs, is anomalous to the shelf area. It has a steep gravity gradient, which probably indicates a shallow dense mafic rock complex, similar to the multi-layered intrusions drilled and modelled in the vicinity of northern Ellef Ringnes Island (Sobczak, 1963; Sobczak and Overton, 1984, Sweeney et al., 1984; Sobczak et al., 1986). In addition, the adjoining north-south trending high, which crosses Cape Bourne and overlies the mouth of Nansen

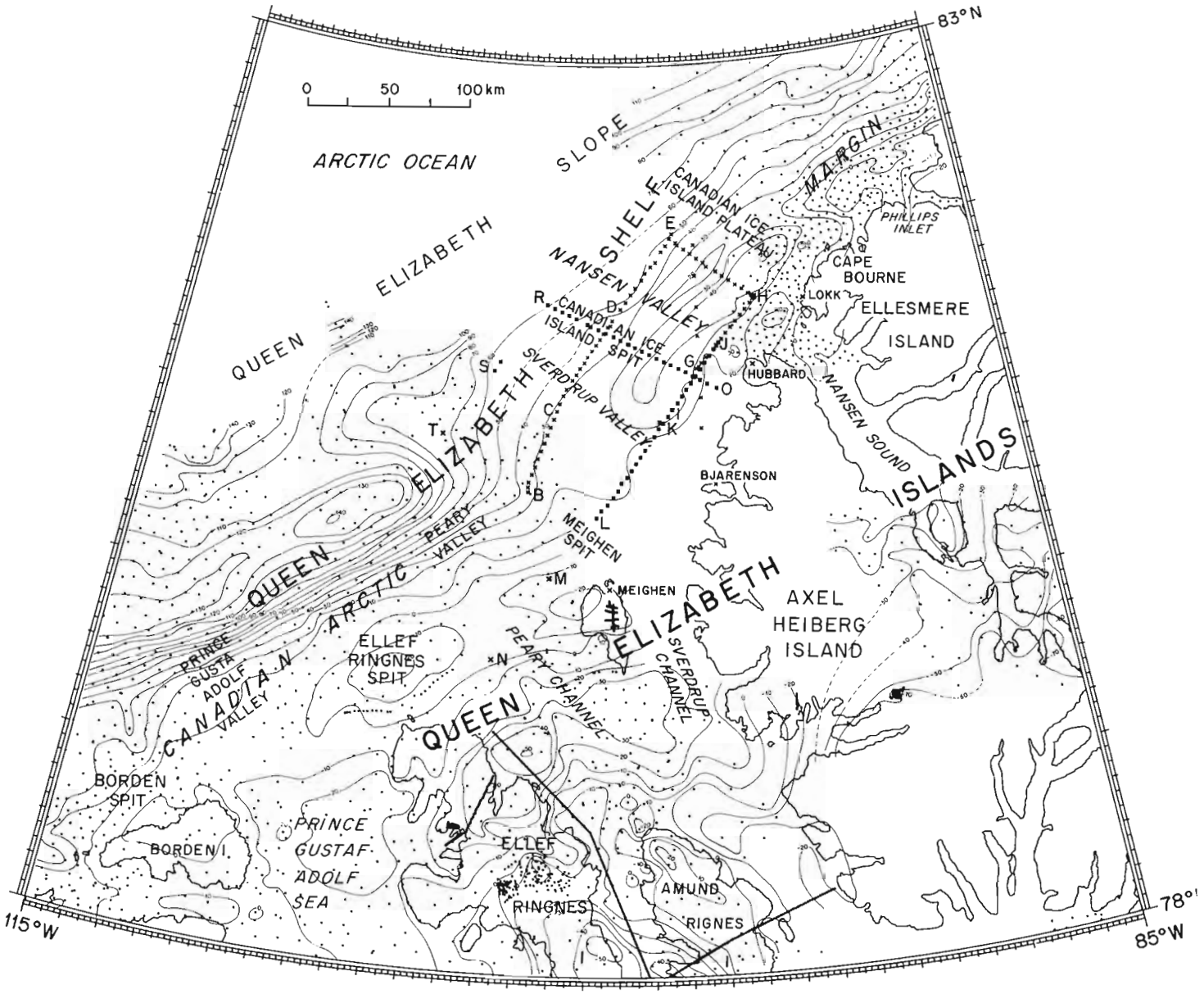


Figure 28.3. Bouguer anomalies are shown in contours at 10 mGal intervals and the density used in data reduction is $\rho = 2.67$ Mg/m^3.

Sound, may be related to the exposed rocks of the Bourne Complex along the northwestern coast of Ellesmere Island and the Unnamed Formation exposed on the peninsula southeast of Lokk (Thornsteinsson and Trettin, 1972). The Bourne Complex, a hybrid terrane, includes volcanic flows with abundant diabase intrusions of unknown age and the Unnamed Formation includes volcanic basalt flows also of unknown age. Mafic intrusions and flows are usually dense (greater than 3.00 Mg/m^3) and are generally distributed within low-density sedimentary rocks. These probable zones of mafic rocks, as depicted by the gravity highs, lie at the northeastern extension of the Sverdrup Rim and northwestern edge of the Sverdrup Basin (Sobczak et al., 1986, Fig. 1).

ACKNOWLEDGMENTS

We would like to thank the following people for their support and assistance: Jack Davison and Morley Wright for instructions on the use of Syledis equipment and Edo echo Sounders; Mike Schmidt and Don White for making some of the gravity and bathymetric determinations in 1985; George Hobson, Barry Hough and their staff for financial and logistical support; Jack Thomas for modifications to the seismic sounding equipment; Lyman Warren and his personnel for drafting; Dave Haliday for computer processing of gravity data; Brian Hearty for plotting of the data; to Jean Pilon, Richard Bastien and Patrick Morel for translation of abstract and to Malcolm Drury and Dave Forsyth for comments on this paper.

REFERENCES

Geodetic Reference System
1967,
1971: International Association of Geodesy. Publication Special Number 3, Paris. 116 p.

Matthews, D.J.
1939: Tables of the velocity of sound in pure water and sea water for use in echo-sounding and sound ranging; Admiralty Table HD 282, F.I.C., 2nd edition.

Morelli, C., Gantar, C., Honkasalo, T., McConnell, R.K., Tanner, J.G., Szabo, B., Uotila, U. and Whalen, C.T.
1974: The International Gravity Standardization Net 1971 (I.G.S.N. 71): The International Association of Geodesy; Special Publication No. 4. 194 p.

Sobczak, L.W.
1963: Regional gravity survey of the Sverdrup Islands and vicinity with map; Dominion Observatory, Department of Energy, Mines and Resources, Ottawa, Canada. Gravity Map Series No. 11, 19 p.

Sobczak, L.W. and Overton, A.
1984: Shallow and deep crustal structure of the western Sverdrup Basin; Canadian Journal of Earth Sciences, v. 21, p. 902-919.

Sobczak, L.W. and Schmidt, M.
1985: Gravity survey along the seismic refraction line from Ice Island, N.W.T.; Canada, Department of Energy, Mines and Resources, Earth Physics Branch; Internal Report No. 85-15. Ice Island Contribution No. 3, 5p.

Sobczak, L.W. and Sweeney, J.F.
1978: Bathymetry of the Arctic Ocean in Arctic Geophysical Review. Ed. J.F. Sweeney; Canada, Department of Energy, Mines and Resources, Publication of the Earth Physics Branch, v. 45 (4), p. 7-14.

Sobczak, L.W. and Weber, J.R.
1970: Gravity measurements in the Queen Elizabeth Islands with maps; Canada, Department of Energy, Mines and Resources, Earth Physics Branch, Gravity Map Series, No. 115-116, 14 p.

Sobczak, L.W. and Weber, J.R.
1973: Crustal structure of the Queen Elizabeth Islands and polar continental margin; in Arctic Geology. Edited by M.G. Pitcher. American Association of Petroleum Geology, Memoir 19, p. 517-525.

Sobczak, L.W. and Weber, J.R.
1986: Gravity and bathymetry along seismic refraction lines, Canadian Ice Island, N.W.T., April 18 – May 2, 1986. Geological Survey of Canada, Geophysics Division, Internal Report No. 86-13. Ice Island Contribution No. 4, 14 p.

Sobczak, L.W., Hearty, D.B., Forsberg, R., Kristofferson, Y., Eldholm, O. and May, S.D.
1987: Gravity from 64°N to the North Pole in Grantz, A., Johnson, L., and Sweeney, J.F., eds., the Arctic Regions: The Geology of North America, Geological Society of America. v. L (in press).

Sobczak, L.W., Mayr, U. and Sweeney, J.F.
1986: Crustal section across the Polar continent-ocean transition in Canada from Somerset Island to the Canada Basin; Canadian Journal of Earth Sciences, v. 23, (4), p. 608-621.

Sobczak, L.W., Stephens, L.E., Winter, P.J. and Hearty, D.B.
1973: Gravity measurements over the Beaufort Sea, Banks Island and Mackenzie Delta. Canada, Department of Energy, Mines and Resources, Earth Physics Branch, Gravity Map Series, No. 151, 16 p.

Sobczak, L.W., Weber, J.R., Goodacre, A.K. and Bisson, J.L.
1963: Preliminary results of gravity surveys in the Queen Elizabeth Islands with maps. Canada, Department of Energy, Mines and Resources, Dominion Observatory, Gravity Map Series Nos. 12-15, 2 p.

Sweeney, J.F., Balkwill, H., Franklin, R., Mayr, U., McGrath, P., Snow, E., Sobczak, L.W. and Wetmiller, R.J.
1984: North American Continent-Ocean Transect Program Corridor G Somerset Island to Canada Basin; Geological Survey of Canada, Open File 1093.

Sweeney, J.F., Mayr, R., Sobczak, L.W. and Balkwill, H.R.
1987: The Polar Continent-Ocean Transition in Canada (1987) (Corridor G) in Speed, R.C., ed., Phanerozoic evolution of North American continent/ocean transitions; Geological Society of America, Centennial Continent/Ocean Transect Volume CTV-1 (in press).

Tanner, J.G. and Buck, R.J.
1964: A computer oriented system for the reduction of gravity data; Canada, Department of Mines and Technical Surveys, Publications of the Dominion Observatory, v. 31, p. 57-65.

The Refraction Team
1986: Ice Island seismic refraction report; Geological Survey of Canada, Ice Island Contribution No. 7, 7p.

Thornsteinsson, R. and Trettin, H.P.
1972: Cape Stallworthy, Geological Survey of Canada, Map 1305 A.

Weber, J.R.
1963: Gravity anomalies over the polar continental shelf; Canada, Department of Mines and Technical Surveys, Contribution No. 12 of the Dominion Observatory, Ottawa, v. 5, no. 17, p. 1-10.

Weber, J.R. and Sobczak, L.W.
1986: Arctic Ocean bathymetry using the seismic sounding method. Geological Survey of Canada, Ice Island Contribution No. 4, Geophysics Division Internal Report No. 86-13.

Weber, J.R. and Sweeney, J.F.
1985: Reinterpretation of morphology and crustal structure in the central Arctic Ocean Basin; Journal of Geophysical Research, v. 90, p. 663-677.

- 29 -

Petrography and geochemistry of some mafic dykes in the Long Range Inlier, western Newfoundland[1]

Project 840024

J. Victor Owen[2] and David C. Machin[3]
Lithosphere and Canadian Shield Division

Owen, J.V. and Machin, D.C., Petrography and geochemistry of some mafic dykes in the Long Range Inlier, western Newfoundland; in Current Research, Part A, Geological Survey of Canada, Paper 87-1A, p. 305-316, 1987.

Abstract

Rectiplanar mafic dykes in the southern part of the Long Range Inlier are narrower, less abundant, and show a wider range of orientations than the Long Range mafic dykes in the northern part of the inlier. The dykes from both areas are hypersthene normative, within-plate subalkaline basalts. The similarity of their major and trace element geochemistry suggests that the Long Range swarm extends the length of the inlier, but is more conspicuous in the north, where the dykes form prominent ridges. Amphiboles record the polymetamorphic history of the dykes. The earliest metamorphic event in the southern part of the inlier involved the crystallization of high Ti/Al tschermakitic hornblende at relatively low pressure conditions. Low Ti/Al magnesio-hornblende subsequently developed at higher (but indeterminate) pressures attributed to the burial of parts of the inlier by Cambro-Ordovician platformal rocks thrust westward during the Taconic Orogeny. Some of the dykes contain actinolite±chlorite±epidote. This greenschist facies imprint may record late Taconic uplift or, more likely in light of geochronological data, a thermal event accompanied by regional granite plutonism during the Acadian Orogeny.

Résumé

Les filons mafiques plans dans la partie sud de la fenêtre de Long Range sont plus étroits et moins nombreux et ont une plus vaste gamme d'orientations que les dykes mafiques de Long Range dans la partie nord de la fenêtre. Les dykes deux régions sont des basaltes subalcalins à hypersthène standard formés à l'intérieur de la plaque. La similarité de la géochimie des éléments majeurs et des éléments à l'état de trace suggère que le groupe de dykes de Long Range se prolonge tout au long de la fenêtre, bien qu'ils soit plus évident au nord, où les dykes forment des crêtes proéminentes. Les amphiboles ont enregistré l'histoire polymétamorphique des dykes. Dans la partie sud de la fenêtre, le phénomène métamorphique le plus ancien serait la cristallisation, à une pression relativement faible, de hornblende tschermakitique à rapport Ti/Al élevé. La formation subséquente de hornblende magnésien à faible rapport Ti/Al à des pressions indéterminées mais plus élevées est attribuée à l'enfouissement de certaines parties de la fenêtre par des roches cambro-ordoviciennes de plate-forme qui ont été poussées vers l'ouest durant l'orogenèse du Taconique. Certains dykes contiennent des quantités plus ou moins variables d'actinolite, de chlorite et d'épidote. Cette impression du faciès des schistes verts pourrait avoir enregistré un soulèvement tardi-taconique ou, ce qui est plus probable vu les données géochronologiques, un événement thermique accompagné par l'intrusion, à l'échelle régionale, de plutons granitiques durant l'orogenèse acadienne.

[1]Contribution to Canada-Newfoundland Mineral Development Agreement 1984-1989. Project carried by Geological Survey of Canada
[2]Department of Mines and Energy, 95 Bonaventure Ave., St. John's, Newfoundland A1C 5T7
[3]Department of Earth Sciences, Memorial University of Newfoundland, St. John's, Newfoundland A1B 3X5

INTRODUCTION

Mafic dykes with an overall northeastern trend are a conspicuous feature of the eastern Grenville Province of Labrador and the Long Range Inlier of western Newfoundland. The dykes in the Long Range Inlier and in southeastern Labrador are tholeiitic (Strong, 1974) and appear to have acted as feeders for plateau basalts of the Lighthouse Cove Formation (Williams and Stevens, 1969) which directly overlies "Grenvillian" crystalline basement rocks. Northeast-trending mafic dykes in the northern part of the inlier form prominent ridges. The dykes are up to about 50 m thick and are steeply dipping. Dykes of the Long Range swarm in this area have been reported to show a greenschist facies overprint near the eastern margin of the inlier, but are better preserved farther west, where they typically contain a well preserved igneous mineralogy, including zoned plagioclase phenocrysts, and clinopyroxene, locally with serpentinized olivine (Strong, 1974).

The Long Range dykes have yielded K/Ar (whole rock) ages ranging from 334±100 Ma (Clifford, 1965) to 805±35 Ma (Pringle et al., 1971). This may indicate the presence of several generations of dykes, or may be attributed to variable alteration (metamorphism) of the dykes, or may be due to the presence of excess radiogenic argon in the dykes. On the basis of a $^{40}Ar/^{39}Ar$ study of the dykes, Stukas and Reynolds (1974) interpreted the relatively old isotopic ages to be the result of excess argon, and proposed an isochron age of 605±10 Ma. The Lighthouse Cove Formation yielded K/Ar (whole rock) ages of 375-427 Ma (Wanless et al., 1965; Wanless et al., 1974), which overlaps a K/Ar age of 434±18 Ma determined for biotite from the basement gneiss. These anomalously young ages have been interpreted to record crustal uplift (Bostock, 1983). The age of intrusion of the Long Range dykes and their extrusive equivalents is interpreted to be latest Hadrynian.

Dykes of the Long Range swarm in insular Newfoundland have been documented only in the northern part of the Great Northern Peninsula, where Bostock (1983) conducted the first comprehensive mapping project of the Long Range Inlier. This report presents new petrographic and geochemical data on similarly oriented but thinner and less abundant mafic dykes from the Silver Mountain area (NTS 12H/11), in the southern part of the Long Range Inlier. A comparison of these data with descriptions of the Long Range dykes from the literature indicates that these dykes are exposed along the length of the Long Range Inlier. This paper examines both primary (igneous) and secondary (metamorphic) features of the mafic dykes. We compare the geochemistry of dykes from the southern and northern parts of the inlier, and expand on the model involving west-directed thrusting of Cambro-Ordovician schists over the inlier previously suggested by Owen and Erdmer (1986) to account for evidence of early, low pressure metamorphism and later, relatively high pressure recrystallization of the dykes.

Acknowledgments

Gert Andrews (Memorial University of Newfoundland) performed the major element analyses. We are indebted to D.F. Strong for providing the Cloud Mountain samples. Flemming Mengel made available his amphibole recalculation program. We thank Ken Currie, John Greenough and George Jenner for their constructive reviews of the manuscript.

Geological setting

The geology of the southern part of Long Range Inlier has been described by Erdmer (1986) and Owen (1986). Rectiplanar mafic dykes in this area cut west- to northwest-trending, high grade gneisses dated at ca. 1250 Ma (U/Pb, zircon; Erdmer, 1986) and a similarly oriented, regional schistosity developed in both the gneisses and in Grenvillian plutonic rocks (ca. 1042 Ma; Erdmer, 1986). Since the regional west- to northwest-trending schistosity developed prior to emplacement of the Long Range dykes, but postdates the emplacement of Grenvillian granites, it is inferred to be a late Grenvillian feature (Owen and Erdmer, 1986).

The mafic dykes described here show a range of orientations from north-northwest to northeast. In order to evaluate possible east-to-west variations in the degree of metamorphic imprint in the dykes as noted farther to the north by Bostock (1983), dykes were sampled westward across the study area (Fig. 29.1). The dykes in the Silver Mountain area show a greater range of orientations than the Long Range dykes farther to the north. It is noteworthy in this regard that dykes cutting the Taylor Brook gabbro complex (TBGC; Fig. 29.1), rheologically the most homogeneous major rock unit in the study area, show the smallest range of orientations, and closely coincide with the northeast-orientation of the Long Range dykes in the northern part of the inlier. We tentatively attribute the variable orientation of dykes outside the Taylor Brook gabbro complex to rheological differences in the sequence of gneisses and granitoid rocks which likely influenced the distribution of fracture patterns developed during regional extension prior to or during emplacement of the dykes. We nonetheless acknowledge the possibility that markedly different orientations of rectiplanar dykes in the area may signify diachronous intrusive events.

The dykes are narrow (typically ≤ 1m) and generally have well preserved chilled margins. A minority of the dykes contain a primary (igneous) mineralogy, since most have been metamorphosed to amphibolite grade, with a variably developed, greenschist facies overprint.

Samples from 12 dykes have been selected for petrographic and geochemical investigation. Field data pertinent to the dykes are presented in Appendix 29.1; their mineralogy is listed in Table 29.1. Several of the samples preserve an igneous texture (subophitic texture; rare quench textures) despite an extensive metamorphic overprint. These samples are from dykes which cut gneissic or schistose fabrics generally present in the country rocks (except for the Taylor Brook gabbro complex). Three samples are from north-northwest- to northeast-trending dykes which contain a tectonic fabric paralleling the schistosity (or gneissosity) in the host rock. Primary (igneous) textures are obliterated in these dykes. Although their age relative to the discordant dykes is unknown from field observations, their mineralogy

Table 29.1. Mineralogy of mafic dykes from the Silver Mountain area. The samples are listed according to their location from east to west across the study area.

VO-85-	Amphibole				Pyroxene		Plag. (%AN)	Bi	Ilm.	Other
	Brown hbl	Green hbl	act	cum	cpx	opx				
841-2	X	X		X	X	X	65-47*		X	
678	X	X					46	X	X	chl
655	X	X	X				61-49*	X	X	chl
155	X	X	X			X	70	X	X	chl;ep
641-2	X			X	X	X	51	X	X	
383			X		X		63-59		X	
363-2		X					31-25	X	X	
409		X					24	X	X	ep?;qz
541-2		X					25	X	X	ep;chl;qz
538-3		X	X				59-53*	X	X	ep
505			X		X		60			ep;sph?
568-2	X	X					47	X	X	ct;chl

*normal zoning hbl = hornblende; chl = chlorite; ep = epidote; ct = carbonate; sph = sphene; cum = cummingtonitic amphibole

indicates a similar metamorphic history. Both groups of dykes will be described since together they serve as important indicators of metamorphism from high- and low-strain domains in the southern part of the Long Range Inlier.

Five samples of the Long Range dykes from the Cloud Mountain area (Fig. 29.1, inset) were analyzed to provide a means of comparing the geochemistry of dykes from the northern and southern extremities of the inlier. The Cloud Mountain samples are from north- to northeast-trending dykes some 12 to 15 m wide. The dykes are characterized by well developed chilled margins, and preserve igneous assemblages comprising plagioclase, clinopyroxene, opaques, and locally with serpentinized olivine (Strong, 1974).

PETROGRAPHY AND MINERAL CHEMISTRY

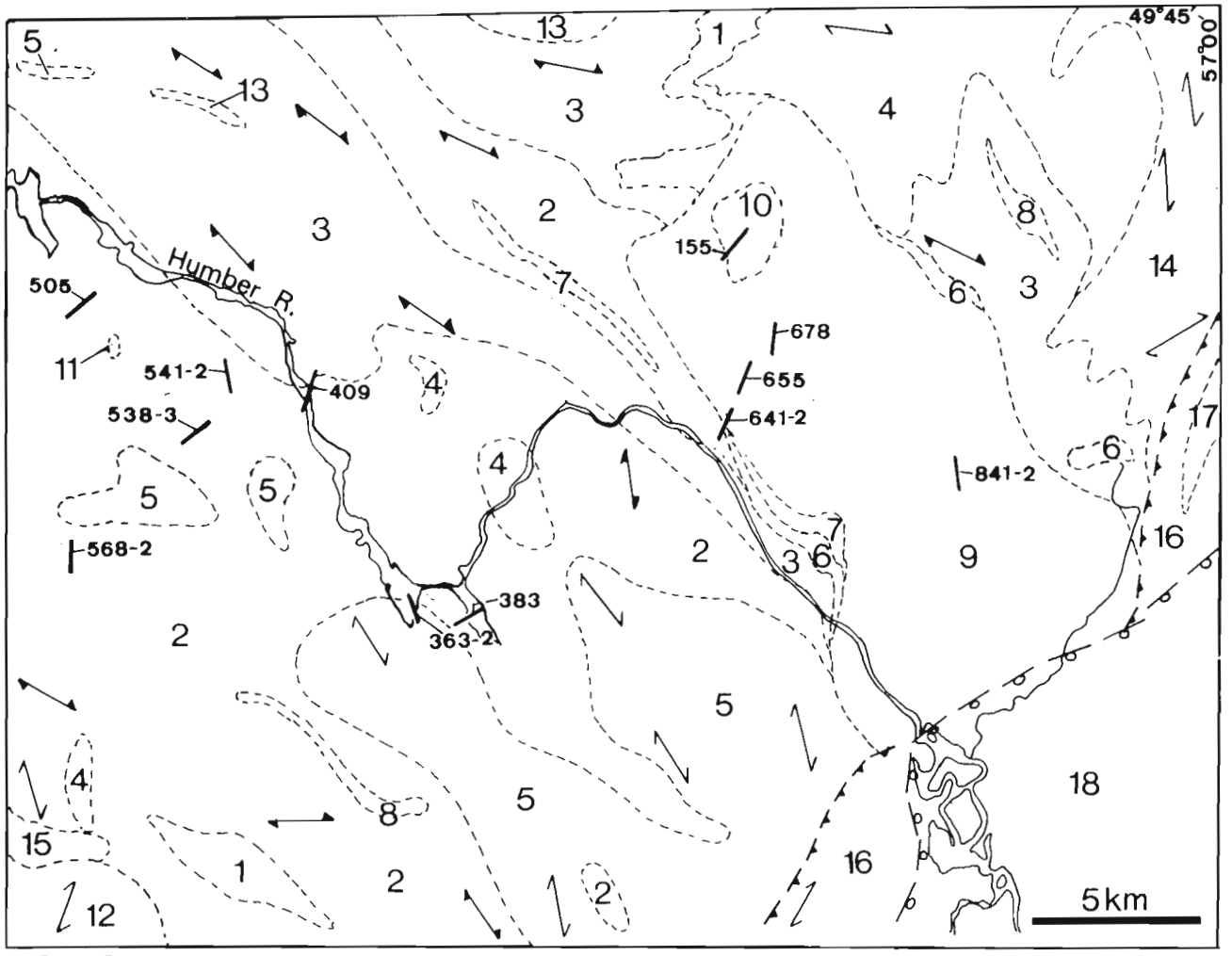
Methods of study

Polished thin sections were prepared for the 12 dyke samples from the Silver Mountain area. Mineral compositions were determined using a fully automated JEOL JXA-50A wavelength dispersive electron microprobe. The microprobe was operated with a beam current of 22 nanoamps and an accelerating voltage of 15kV. Counts were made for 30s or to a maximum of 60 000. Analyses were performed using calibrations based on appropriate natural and synthetic standards; Bence-Albee corrections were employed in data reduction. Precision and accuracy of the microprobe data were tested by repeated analysis of natural clinopyroxene standards FCPX and ACPX (for standard data, see Owen and Erdmer, 1986). Mineral analyses are presented in Table 29.2. Pyroxene analyses are recalculated to 6 oxygens; trivalent iron has been estimated by the method of Papike et al. (1974). Amphiboles have been recalculated to 23 oxygens, and normalized to 13 cations in the M1 site excluding Ca, Na and K. Ferric iron was then determined by charge balancing (see Robinson et al., 1982). We adopt the amphibole nomenclature scheme of Leake (1978).

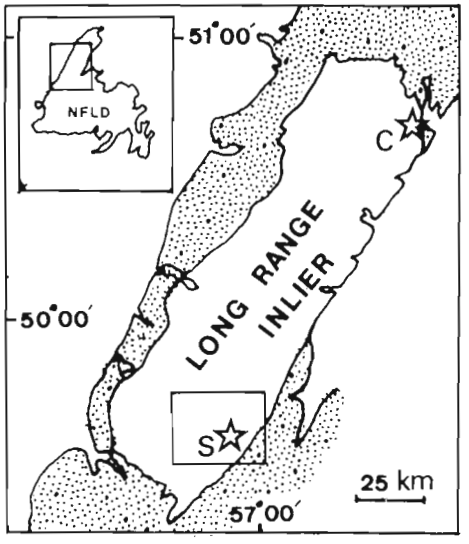
Petrography of mafic dykes in the Silver Mountain area

The discordant dykes typically have well preserved chilled margins, and subophitic textures which in places are pseudomorphed by amphibole. Despite relict primary textures, the distinction of igneous from metamorphic minerals in the dykes is problematic. Although amphibole, chlorite and epidote (and possibly ilmenite and biotite) may be attributed to the metamorphic overprint, the significance of pyroxene and different textural occurrences of plagioclase spanning a range of compositions in the dykes is more equivocal.

Plagioclase may occur as phenocrysts and(or) as groundmass laths defining (together with mafic minerals) a subophitic texture in many of the dykes. In one sample (VO-85-505), groundmass plagioclase microlites preserve a primary quenched texture (swallowtail terminations; Fig. 29.2). Megacrysts and groundmass laths of plagioclase have similar compositions; subgrains and new grains formed on the edge of larger plagioclase porphyroclasts apparently record partial recrystallization of the earlier, calcic plagioclase. Plagioclase ranges in composition from ca. An_{46-70} in the best preserved samples (e.g. those containing pyroxenes of inferred igneous origin). Subgrains forming from partly recrystallized plagioclase porphyroclasts coincide with the more sodic composition similar to the rim compositions of normally zoned plagioclase crystals. The textures and compositions thus suggest that the bulk of the plagioclase in the discordant dykes is a relict primary phase. Subgrains and newgrains of plagioclase, however, may be attributed to a metamorphic overprint.



SAMPLE PREFIX = VO-85-___



= thrust = unconformity

= schistosity = gneissosity

PHANEROZOIC

18 Conglomerate (Deer Lake Basin)
17 Felsic porphyry
16 Metasedimentary schist (Coney Arm Group?)

MIDDLE PROTEROZOIC OR YOUNGER

15 Biotite granite-granodiorite
14 Ksp-megacrystic granite
13 Ksp-megacrystic granodiorite-granite
12 Biotite + hornblende granodiorite
11 Subophitic metagabbro
10 Pegmatitic leucogabbro (TBGC)
9 Pyroxene + olivine gabbro (TBGC)
8 Quartz, quartzite
7 Pelitic gneiss
6 Marble, calc-silicate rock
5 Biotite granite, minor granitic gneiss
4 Amphibolite, dioritic gneiss
3 Granitic-granodioritic gneiss
2 Quartz dioritic-granodioritic gneiss
1 Quartz dioritic-tonalitic gneiss

Figure 29.1. Geological sketch map of the Silver Mountain area showing the location of north- to nort. east-trending mafic dykes described in the text. Dimensions of individual dykes are greatly exaggerated. Inde . map shows the location of the Silver Mountain area (S) and the Cloud Mountain area (C).

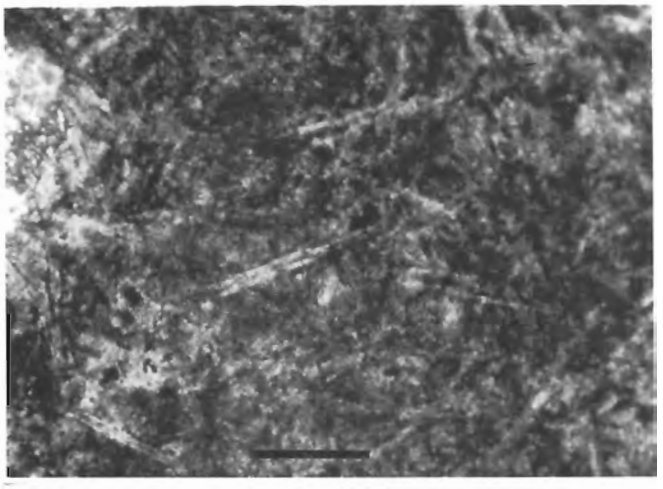


Figure 29.2. "Quenched" plagioclase microlites showing swallowtail terminations in the groundmass of dyke sample VO-85-505. Plane polarized light; bar = 0.2 mm.

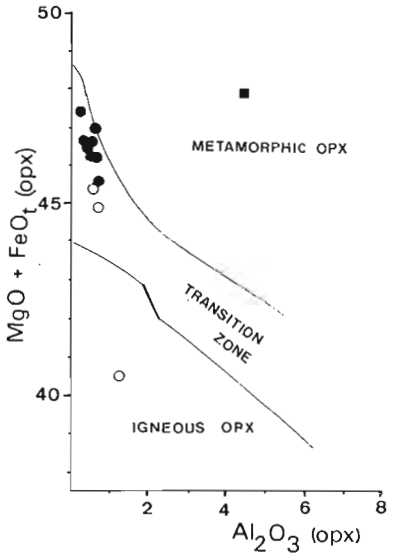


Figure 29.3. Comparison of the compositions of orthopyroxenes from mafic dykes (open circles) with orthopyroxenes from orthogneiss (black dots) and garnetiferous pelitic gneiss (square) in the Silver Mountain area. Field boundaries are from Rietmeijer (1983).

Clinopyroxene is present in five of the nine discordant dyke samples; orthopyroxene occurs in three of the samples (including two, two-pyroxene assemblages). The clinopyroxenes are augites with compositions of Wo34-45, En41-51, and Fs12-16; the orthopyroxenes are hypersthenes with an Mg number (= Mg/(Mg + Fe)) of 0.61 to 0.66.

The preservation of subophitic textures by amphibole which in other samples encloses pyroxene suggests that the former mineral is of metamorphic origin, while the latter is a relict igneous phase. Textural and compositional features of the dyke pyroxenes do not, however, unequivocally support this interpretation. Pyroxenes in the sample suite typically occur as xenomorphic or subidiomorphic crystals defining a granoblastic rather than subophitic texture. The composition of orthopyroxene in the two-pyroxene assemblages falls in the transition zone of Rietmeijer's (1983) discrimination diagram along with metamorphic orthopyroxene from orthogneiss in the area (Fig. 29.3); only hypersthene from VO-85-155 clearly plots in the igneous field. Furthermore, the compositions of clinopyroxene from the two-pyroxene assemblages yield divergent temperature estimates. Clinopyroxene compositions plotted against Kretz's (1982) isotherms yield a crystallization temperature of ca. 1150-1200°C in sample VO-85-641-2 but an anomalously low temperature of ca. 850°C in VO-85-841-2; both samples yield temperatures of ca. 870-900°C using Lindsley's (1983) isotherms. Numeric calibrations of the two-pyroxene geothermometer yield similarly low, "metamorphic-range" temperatures; the Wood and Banno (1973), Wells (1977) and Powell (1978) calibrations yield temperatures of 873°, 891° and 812°C for VO-85-641-2, respectively, and 883°, 907° and 868°C for VO-85-841-2. It is not known whether this reflects the subsolidus reequilibration of pyroxene compositions or inaccuracies in the two-pyroxene geothermometer.

The condordant mafic "dykes" are characterized by a granoblastic texture and a penetrative schistosity defined by a preferred dimensional orientation of green hornblende. The absence of relict igneous pyroxene and the relatively sodic composition of plagioclase (An_{25}) in the deformed dykes demonstrate thorough recrystallization under amphibolite facies conditions.

MAJOR AND TRACE ELEMENT GEOCHEMISTRY

Methods of study

Both the discordant and concordant dykes were analysed for major and trace elements (Table 29.3). Five samples of Long Range dykes from the Cloud Mountain area (Strong and Williams, 1972; Strong, 1974; Fig. 29.1) were also analyzed for comparative purposes. Major element analyses were obtained by atomic absorption spectrometry using a Perkin-Elmer digitized spectrometer housed in the Department of Earth Sciences, Memorial University of Newfoundland. FeO was determined by cold dissolution and titration methods. Trace element analyses were performed using a Phillips 1450 X-ray fluorescence spectrometer autocalibrated against international rock standards G2 and PCC-1.

Comparison with data from the literature

The geochemistry of the Long Range dykes from Labrador and the northern portion of the Long Range inlier indicates that the Long Range swarm comprises within-plate tholeiites emplaced in an extensional tectonic setting (Strong, 1974; Gower, personal communication 1986). We have employed a

Table 29.2. Compositions of selected minerals from mafic dykes from the southern Long Range Inlier. Amphiboles are normalized to 13 cations in the M1 site exclusive of Ca, Na and K, unless otherwise indicated.

	VO-85-568-2		VO-85-655		VO-85-678		VO-85-841-2		VO-85-383	VO-85-505	VO-85-538-3		Amphiboles in Schistose "Dyke" VO-85-409		
	Brown hbl	Green hbl	Brown hbl	Green hbl	Brown hbl	Green hbl	Brown hbl	Green hbl	Act hbl	Act hbl	Green hbl	Act hbl	Hbl P'blast*	Fabric-forming hbl	Hbl oblique to fabric
SiO_2	51.85	47.43	43.77	42.55	42.50	47.75	42.75	48.38	52.58	54.79	45.23	50.24	43.63	42.64	42.85
TiO_2	2.42	1.60	3.34	.56	2.86	.57	2.97	1.22	.26	1.00	.25	.75	.48	.80	.58
Al_2O_3	5.29	8.59	11.49	14.48	12.86	9.48	10.97	7.02	4.51	3.77	12.33	5.85	12.79	12.26	13.04
Cr_2O_3	.00	.04	.00	.08	.01	.00	.03	.02	.02	.22	.01	.28	.05	.03	.08
FeO	12.42	13.40	12.27	16.59	16.08	13.57	13.59	12.29	14.25	9.65	17.17	13.17	20.58	20.82	20.15
MnO	.14	.13	.19	.28	.15	.25	.12	.21	.19	.20	.18	.24	.22	.25	.20
MgO	13.66	14.51	13.40	9.04	10.77	13.16	12.45	15.17	14.83	17.71	9.84	14.46	7.97	7.63	8.00
CaO	12.64	11.77	10.90	10.31	11.14	10.93	11.56	11.86	12.02	12.35	11.34	12.06	10.88	10.93	10.99
Na_2O	.58	1.11	1.92	2.93	1.70	1.59	2.04	1.07	.62	.32	1.55	.70	1.52	1.20	1.48
K_2O	.07	.82	.51	.12	.63	.11	.82	.46	.20	.06	.54	.13	.57	.61	.61
Total	99.07	99.43	97.79	96.94	97.70	97.41	97.30	97.70	99.48	100.07	98.44	97.88	98.69	97.17	97.98
Si	7.375*	6.720	6.307	6.308	6.235	6.857	6.318	6.938	7.407	7.514	6.596	7.202	6.417	6.393	6.354
Aliv	.625	1.280	1.693	1.692	1.765	1.143	1.682	1.062	.593	.486	1.404	.798	1.460	1.607	1.646
Alvi	.262	.155	.259	.839	.459	.462	.229	.125	.155	.123	.716	.190	.635	.559	.634
Ti	.259	.170	.362	.062	.316	.062	.330	.132	.028	.103	.027	.081	.053	.090	.065
Cr	.000	.008	.000	.009	.001	.000	.004	.002	.002	.024	.001	.032	.006	.004	.009
Fe^{3+}	-	.750	.715	.578	.569	.731	.388	.646	.547	.407	.548	.491	.866	.887	.840
Fe^{2+}	1.477	.838	.764	1.479	1.281	.898	1.292	.828	1.132	.699	1.546	1.087	1.666	1.723	1.659
Mn	.017	.016	.023	.035	.019	.030	.015	.026	.023	.023	.022	.029	.027	.032	.025
Mg	2.896	3.064	2.878	1.997	2.355	2.816	2.742	3.242	3.113	3.620	2.139	3.089	1.747	1.705	1.768
Ca	1.927	1.787	1.683	1.638	1.751	1.682	1.831	1.822	1.814	1.815	1.772	1.852	1.715	1.756	1.746
Na	.160	.305	.538	.842	.484	.443	.584	.298	.169	.085	.438	.195	.148	.105	.426
K	.013	.148	.094	.023	.118	.020	.155	.084	.036	.010	.100	.024	.433	.349	.115

* total charge >46; all Fe as Fe2+ *P'blast = porphyroblast

number of discrimination diagrams to (1) determine whether dykes from the study area are geochemically similar to the Long Range swarm, and thus should be considered to be part of the same intrusive suite, and (2) constrain the most plausible tectonic setting of dyke emplacement. We have chosen discrimination diagrams comprising relatively immobile elements (e.g. Nb, Y, Ti, Al, P; Pearce and Cann, 1973; Floyd and Winchester, 1975, 1978; Winchester and Floyd, 1976, 1977) which reflect the primary igneous geochemistry of the dykes rather than features of the metamorphic overprint.

The dykes from the Silver Mountain area are geochemically similar to the Long Range dykes from the north part of the inlier, both in their major (Fig. 29.4) and trace (see Machin, 1986) element compositions. We therefore conclude that the Silver Mountain samples are part of the Long Range dyke swarm despite the wider range of orientations north-northwest to northeast of these dykes.

Samples from the Silver Mountain and Cloud Mountain areas are hypersthene normative (CIPW norms) and thus are tholeiites by definition (Cox et al., 1979). Two of the samples (VO-541-2, -568-2) plot in the alkaline field on the alkalis versus silica diagram of Irvine and Baragar (1971) (Fig. 29.5). Although this may be attributed to the mobility of alkalis during metamorphism of the dykes (i.e. Winchester and Floyd, 1976), both samples plot in the overlap area between the alkaline and tholeiite fields on the Nb/Y versus Zr/P205 diagram (Winchester and Floyd, 1976) (Fig. 29.6). We conclude that although the bulk of the Silver Mountain samples are tholeiites, some samples have transitional affinities.

The Silver Mountain and Cloud Mountain samples plot in the within-plate basalt field on Pearce and Cann's (1973) discrimination diagram (Fig. 29.7). Relations between the Lighthouse Cove Formation and the Long Range dykes suggest that the dykes are continental basalts. The trace element geochemistry of the Silver Mountain samples is consistent with this interpretation; most of the samples plot in the continental basalt field on Floyd and Winchester's (1975) TiO_2 versus Y/Nb discrimination diagram (Fig. 29.8). The samples plotting outside the continental basalt field (s.s.) are oceanic tholeiites; their Y/Nb ratios (<2) characterize them as transitional basalts. The remaining dykes from the Silver Mountain and Cloud Mountain areas are continental tholeiites.

Petrogenetic modelling by Machin (1986) reveals that the chemistry of the dykes, particularly with regard to immobile trace elements, may record the influence of polybaric, partial

Pyroxenes						
VO-85-641-2		VO-85-841-2		VO-85-505	VO-85-155	VO-85-383
Cpx	Opx	Cpx	Opx	Cpx	Opx	Cpx
52.78	54.26	52.41	52.72	52.20	55.02	53.27
.11	.10	.23	.15	.80	.03	.48
1.34	.87	1.43	.83	3.16	1.41	3.26
.00	.04	.01	.00	.13	.05	.32
8.51	22.12	8.13	22.40	9.33	21.46	7.03
.23	.58	.28	.60	.25	.83	.19
14.52	22.77	14.57	22.97	17.11	19.04	17.98
22.67	.47	21.83	.68	17.80	.43	19.67
.26	.01	.52	.12	.30	.04	.32
.01	.02	.06	.03	.01	.00	.01
100.43	101.24	99.47	100.50	101.09	98.31	102.53
1.960	1.988	1.960	1.958	1.907	2.061	1.907
.040	.012	.040	.042	.093	-	.093
.018	.026	.022	-	.043	.123	.044
.003	.002	.005	.003	.022	.001	.013
.000	.000	.000	.000	.004	.001	.009
.035	.000	.045	.044	.023	-	.036
.229	.677	.208	.651	.262	.672	.174
.007	.017	.008	.060	.008	.026	.006
.804	1.243	.811	1.271	.932	1.063	.959
.902	.018	.874	.026	.697	.017	.754
.019	.001	.037	.008	.021	.003	.022
.000	.000	.002	.001	.000	.000	.000

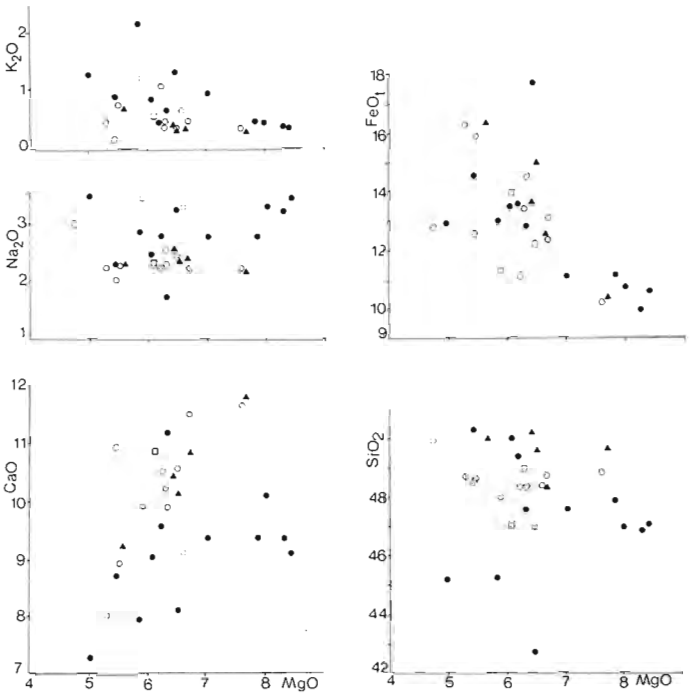


Figure 29.4. Comparison of the major element geochemistry of dyke samples from the study area (black dots) with analyses of the Long Range dykes from the literature (open circles: Strong and Williams, 1972; square: average of 14 samples, Strong, 1974) and new analyses of dykes from the Cloud Mountain area (triangles).

modal melting of a garnet lherzolite mantle source rock, as well as subsequent fractional crystallization of the Long Range basaltic magma.

METAMORPHISM

The polymetamorphic history of the Long Range dykes in the study area is chiefly recorded by coexisting amphibole and relatively sodic plagioclase (oligoclase-andesine, contrasting with zoned, igneous labradorite present in some samples). Three generations of compositionally distinct calcic amphibole have been identified. Each generation occurs in a distinct textural association, and the apparent relative ages of the amphiboles, as inferred from corona and local crosscutting structures, is consistent within and between samples. The three compositional groups in their inferred, relative chronologic sequence area: (1) High Ti/Al tschermakitic hornblende (Ti/Al = 0.15-0.29, mean = 0.18, n = 8); (2) low Ti/Al magnesio-hornblende (to tschermakitic hornblende) (Ti/Al = 0.01-0.12, mean = 0.05, n = 12); (3) actinolite-actinolitic hornblende. A fourth generation of amphibole is present in two of the dykes (samples VO-85-641-2, -841-2). It is a clinoamphibole of cummingtonitic composition which appears to replace orthopyroxene; its age relative to calcic amphibole in the dykes is unknown.

High Ti/Al hornblende occurs as brown, subidiomorphic crystals, typically enclosed by green, low Ti/Al hornblende (Fig. 29.9). Both hornblendic amphiboles coexist in five of the discordant, north-northwest- to northeast-trending dykes. We discount the likelihood (but acknowledge the possibility) that the high Ti/Al hornblende is a late magmatic phase since compositionally similar brown hornblende (Ti/Al = 0.203 in one sample) occurs in the Taylor Brook gabbro complex, a fortuitous coincidence if the amphibole is interpreted as a primary feature of both suites of mafic rocks.

Actinolite (or actinolitic hornblende) is present in five of the dykes. It has three typical textural modes of occurrence: (1) as 0.1-1.0 mm ovoid patches of clear or pale green fibroradial crystals (Fig. 29.10) overprinting the relict igneous textures locally pseudomorphed by hornblendic amphibole; (2) in veins cutting pseudomorphed primary textures in the dykes; and (3) as fine grained mats of crystals enclosing pyroxene. Textural features (1) and (2) indicate that actinolite is the youngest calcic amphibole in the mafic dykes.

The actinolite typically coexists with chlorite and(or) epidote although these minerals also occur with hornblendic amphibole in the absence of actinolite (Table 29.1). It is emphasized that albite has not been identified in any of the samples; in some specimens, subgrains of metamorphic plagioclase (andesine) have formed along the recrystallized margins of more calcic plagioclase (typically labradorite). It coexists either with clinopyroxene of inferred igneous origin or with hornblendic amphibole.

Table 29.3. Major and trace element geochemistry of mafic dykes from the Silver Mountain area. Major elements are expressed in weight %; trace elements in ppm.

	Cloud Mountain Samples					Silver Mountain Samples VO-85-____									
	277	279	283	296	300	383	409	505	538	541	568	641	655	678	841
SiO_2	48.4	49.7	49.7	50.0	50.2	50.1	51.4	49.4	49.1	47.1	48.6	49.0	48.0	47.9	47.9
TiO_2	2.06	1.22	2.42	2.88	2.33	1.27	2.78	2.16	2.19	3.13	3.14	2.21	1.83	1.92	1.92
Al_2O_3	16.3	16.4	13.2	12.2	13.4	14.4	12.8	14.1	16.1	15.8	15.2	16.0	17.4	17.0	16.7
FeO	9.98	8.18	11.84	12.79	11.53	8.97	10.25	10.10	8.68	10.23	10.87	7.62	8.08	8.64	7.57
Fe_2O_3	2.58	2.17	3.04	3.57	2.18	2.80	4.56	3.18	2.71	3.32	3.02	3.75	2.65	1.51	3.30
MnO	.20	.17	.23	.24	.22	.21	.21	.22	.17	.21	.18	.18	.17	.18	.17
MgO	6.68	7.74	6.51	5.64	6.46	8.13	5.67	5.56	7.26	6.09	5.38	8.02	8.58	8.47	8.16
CaO	10.83	11.80	10.12	9.16	10.44	11.41	8.89	11.57	9.64	8.29	7.85	9.58	8.58	8.47	8.16
Na_2O	2.49	2.23	2.34	2.29	2.57	2.22	2.33	1.76	2.84	2.94	3.74	2.81	3.24	3.24	3.29
K_2O	.32	.29	.35	.75	.42	.42	.90	.65	.94	2.28	1.32	.47	.33	.38	.44
P_2O_5	.25	.09	.26	.44	.27	.12	.35	.24	.31	.59	.69	.36	.33	.38	.29
Total	100.01	100.09	99.99	100.01	99.96	100.05	100.14	99.94	99.94	99.98	99.99	100.00	100.00	99.05	100.01
LOI	1.33	1.25	1.21	1.43	1.08	1.44	1.61	1.86	1.66	2.52	6.04	2.07	2.07	1.99	1.31
Ba	105	73	92	256	115	61	41	54	68	59	42	78	80	69	49
Rb	17	15	13	24	23	18	38	21	21	69	27	12	5	16	16
Sr	232	227	188	186	223	164	227	198	435	334	535	419	373	358	430
Y	38	22	44	57	38	26	49	38	28	37	37	37	35	37	36
Zr	146	63	152	235	158	72	230	161	195	223	220	147	148	161	170
Nb	16	6	13	20	16	8	20	13	22	32	28	8	8	7	14
Ga	16	13	11	12	13	12	16	14	15	18	18	16	17	19	15
Zn	74	54	96	123	158	67	111	88	89	129	137	75	63	68	65
Cu	78	87	192	283	148	114	220	165	32	4	18	39	40	82	32
Ni	77	68	56	44	45	130	392	135	275	504	527	532	172	160	250
V	309	273	407	476	346	314	437	397	246	283	265	256	225	271	271
Cr	143	157	95	54	76	165	70	88	41	17	2	144	60	76	75

Samples from the three concordant "dykes" (VO-85-363-2, -409, -541-2) contain a schistose fabric defined by green hornblendic amphibole and oligoclase with accessory biotite±ilmenite±chlorite±epidote. The lower amphibolite facies mineralogy of these metabasites is similar to narrow, north- to northeast-trending, high-strain zones which locally transect the country rock (Owen and Erdmer, 1986), and may coincide with the crystallization of the low Ti/Al hornblende in the unstrained, discordant mafic dykes.

Interpretation

Few conclusive statements can be made concerning the distribution of amphibole (and other metamorphic minerals; see Table 29.1) in the dykes sampled westward across the study area. Although high Ti/Al tschermakitic hornblende preferentially occurs in the easternmost samples (e.g. in dykes cutting the TBGC), it is also present in the westernmost sample (VO-85-568-2). Noteworthy in the regional context is the sporadic occurrence of both pyroxene and actinolite in dykes across the study area. This contrasts with the observation from the Long Range dykes from the north part of the inlier (Bostock, 1983; Strong, 1974) that greenschist-facies assemblages are more common in east, while primary assemblages (i.e. including pyroxene) are better preserved farther to the west.

The presence of three generations of calcic amphibole in the discordant dykes in the southern part of the inlier is significant since their contrasting compositions reflect changing metamorphic P-T conditions during burial and subsequent uplift of the dykes. The influence of metamorphic environment on amphibole compositions has been evaluated by a number of workers. There is not, however, consensus on which compositional parameters are most sensitive to changing P-T conditions, and a variety of formula proportion diagrams purported to reveal changes in metamorphic conditions have been proposed. Among the most useful for calcic amphiboles are the formula proportion diagrams presented by Hynes (1982) and Laird and Albee (1981). Hynes (1982) determined that amphiboles from low pressure metabasites have higher Ti/Al(total) ratios than amphiboles from medium pressure metabasites. The early, brown, tschermakitic hornblende has a markedly higher Ti/Al ratio than the younger, green, magnesio-hornblende (Fig. 29.11A); it is thus inferred to have crystallized at relatively low pressure.

Compositional differences between the two hornblendic amphiboles are not as pronounced on the remaining formula proportion diagrams (Fig. 29.11B to E). Only the Aliv versus Alvi + trivalent Fe + Ti + Cr plot (Fig. 29.11E) distinguishes the high Ti/Al tschermakitic hornblende as being compositionally distinct. These plots are constructed such

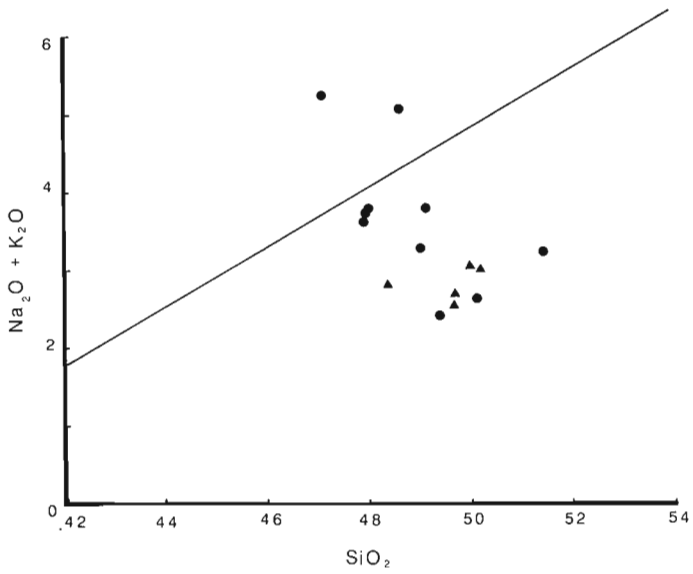


Figure 29.5. Alkali versus silica diagram for mafic dykes from the Silver Mountain (dots) and Cloud Mountain (triangles) areas. Alkaline and subalkaline field boundary after Irvine and Baragar (1971).

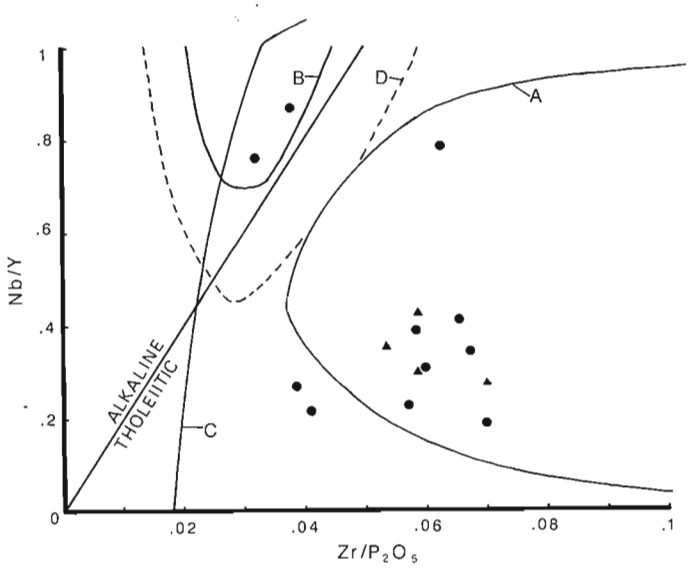


Figure 29.6. Nb/Y versus Zr/P_2O_5 discrimination diagram. Symbols as in Figure 29.5. Field A–oceanic basalts, B–oceanic alkali basalts, C–continental tholeiitic basalts, D–continental alkali basalts, from Floyd and Winchester (1975). Alkaline/tholeiitic basalt line (extrapolated to origin) is from Winchester and Floyd (1976).

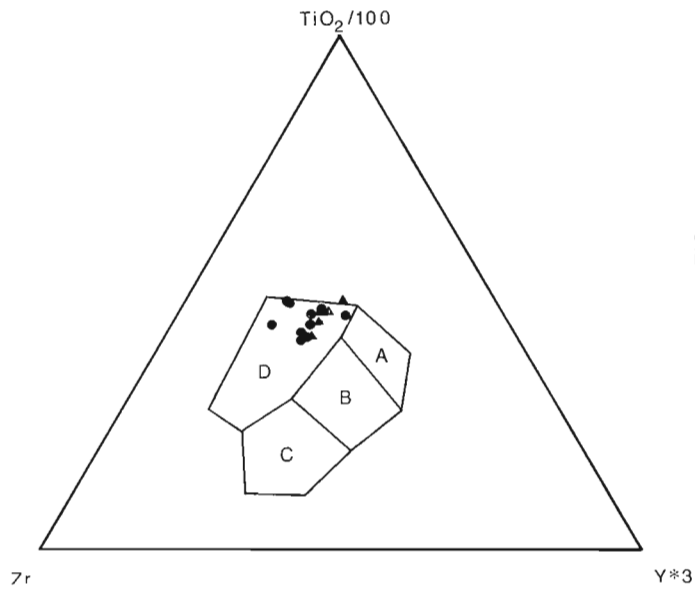


Figure 29.7. TiO_2/100-3Y-Zr discrimination diagram (Pearce and Cann, 1973). Fields A + B–low K tholeiites, C + B–calc-alkali basalts, B–ocean floor basalts, D–within plate basalts. Symbols as in Figure 29.5.

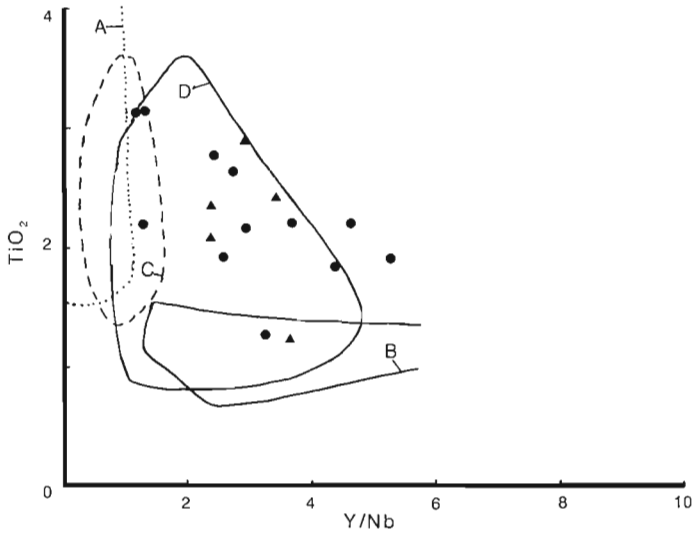


Figure 29.8. TiO_2 versus Y/Nb discrimination diagram (Floyd and Winchester, 1975). Field A–oceanic alkali basalts, B–oceanic alkaline basalts, C–continental tholeiitic basalts, D–continental basalts. Symbols as in Figure 29.5.

that higher grade (e.g. higher P-T) amphiboles plot progressively farther away from the origin. Although the overlapping compositions for the high- and low-Ti/Al hornblendes may be an artifact of the normalization scheme employed here, two other possibilities should also be considered: (1) the hornblendes crystallized under similar metamorphic conditions, or (2) the resolution of these diagrams is insufficient for distinguishing the P-T series represented by these amphiboles. Given the distinct compositional fields defined for the hornblendes in the Ti versus Al plot, we favour the latter interpretation.

The compositions of amphibole from north to northeast-trending, discordant mafic dykes in the southern part of the

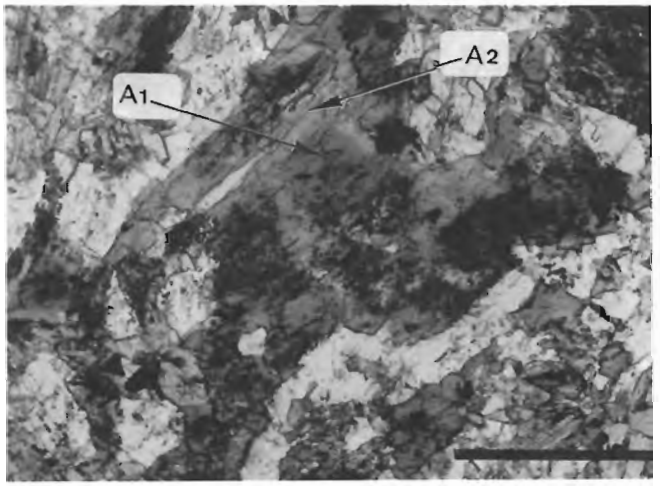


Figure 29.9. Photomicrograph showing brown tschermakitic hornblende (A1) enclosed by green magnesio-hornblende (A2) in dyke sample VO-85-678. Plane polarized light; bar = 0.5 mm.

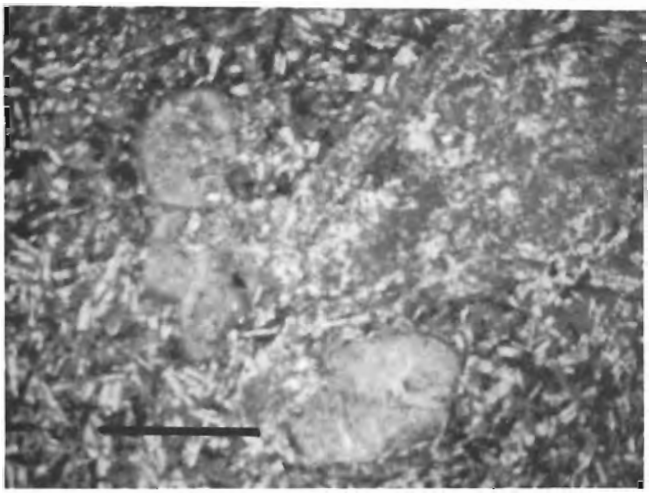


Figure 29.10. Pods of fibroradial actinolite set in a subophitic groundmass of tschermakitic- and magnesio-hornblende and plagioclase. Sample VO-85-538-3; plane polarized light; bar = 1.0 mm.

Long Range Inlier thus record a polymetamorphic history embracing early, low pressure, medium grade metamorphism, followed by a higher pressure event, and finally a variable, greenschist facies overprint. It is noteworthy that evidence for early, low pressure metamorphism (e.g. high Ti/Al hornblende) is present only in low strain, discordant dykes; the mineralogy of the schistose dykes records only the higher pressure metamorphic event. Presumably the schistose dykes were sufficiently recrystallized during the development of their north-northwest to northeast trending fabric to obliterate earlier metamorphic mineral assemblages.

The significance of early, low pressure metamorphism followed by a higher pressure event becomes apparent when considering the structural setting of the Long Range Inlier and its envelope of Cambro-Ordovician supracrustal rocks. Owen (1986) noted the local presence of C-S fabrics in deformed felsic porphyry associated with Cambro-Ordovician metasedimentary schists immediately to the east of the inlier (units 16 and 17, Fig. 29.1). The geometry of the C-S fabrics indicates west-directed thrusting of the schists over the inlier. This observation provides the basis for a working hypothesis to account for evidence of increasing metamorphic pressure in the inlier following regional extension and intrusion of the Long Range dykes at ca. 605 Ma. We suggest that high Ti/Al tschermakitic hornblende in the dykes crystallized prior to the thrusting of Cambro-Ordovician rocks over the inlier. The thrusting event itself may be attributed to the Taconic Orogeny, since low grade, north- to northeast-trending fabrics in both the Paleozoic rocks and in quartzfeldspathic rocks along the eastern edge of the inlier are cut by a massive Acadian granite within the inlier (Devil's Room granite; ca. 398 Ma, Erdmer, 1986). Burial of the inlier by Cambro-Ordovician rocks during the Taconic Orogeny provides a plausible mechanism for developing the relatively high pressure (low Ti/Al) hornblende enclosing the low pressure (high Ti/Al) hornblende in the dykes. The preservation of primary igneous textures in most of the dykes despite the polyphase metamorphic overprint is consistent with burial metamorphism instigated by thrust tectonics; most of the strain was probably accomodated along narrow zones at higher structural levels. The mineralogy of narrow, north- to northeast-trending high strain zones occurring locally in the inlier is indicative of lower amphibolite (to greenschist) facies. The kinematic significance of these high strain zones in a regional, thrust-tectonics framework is uncertain, however it is noteworthy that the mineralogy of these high strain zones is consistent with similarly oriented, amphibolite facies fabrics present in the deformed mafic "dykes".

It is difficult to attribute the late, passive, greenschist facies overprint to a specific metamorphic event on the basis of field and petrographic data alone. U-Pb (zircon, sphene) dating of diverse granitoid rocks undertaken by Erdmer (1986) is pertinent in this regard. The zircons record the primary intrusive ages of both Grenvillian and Acadian granites, but the sphenes uniformly yield an age of ca. 400 Ma, indicating an early Acadian thermal event accompanied by regional granite plutonism. This is supported by Stukas and Reynolds' (1974) isotopic study, which indicates that the Long Range dykes were degassed at ca. 380 Ma. We thus attribute the greenschist facies overprint to the Acadian Orogeny.

CONCLUSIONS

Interpretation of aspects of the petrography and geochemistry of rectiplanar mafic dykes from the Silver Mountain and Cloud Mountain areas of the Long Range Inlier permit the following conclusions:

1) The Silver Mountain samples are part of the ca. 605 Ma Long Range mafic dyke swarm

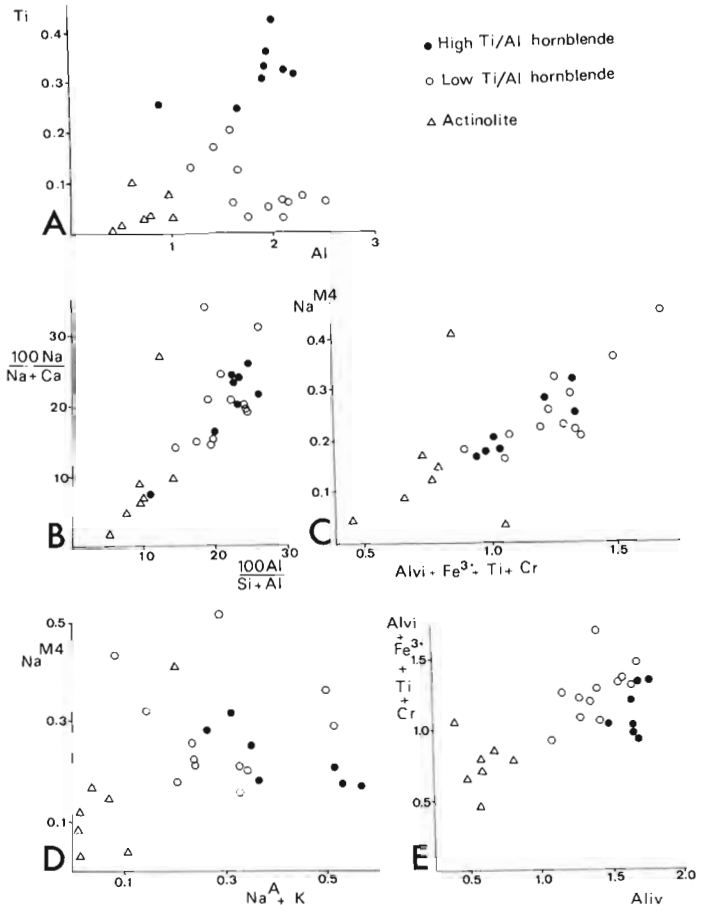


Figure 29.11. Cation formula proportion diagrams for metamorphic amphiboles from mafic dykes in the Silver Mountain area. One analysis of brown tschermakitic hornblende for which the 13exCa,Na,K recalculation scheme was not possible is excluded in the normalization dependent diagrams.

2) The dykes are within-plate tholeiites or transitional basalts emplaced in an extensional tectonic environment

3) Calcic amphiboles in the dykes record a polymetamorphic history, spanning an early, low pressure event, followed by higher pressure metamorphism possibly instigated by west-directed thrusting of Cambro-Ordovician platformal rocks over the inlier during the Taconic Orogeny, and finally a greenschist facies imprint attributed to regional heating during the Acadian Orogeny.

REFERENCES

Bostock, H.H.
1983: Geology of the Strait of Belle Isle area, northwestern insular Newfoundland, southern Labrador, and adjacent Quebec. Part 1. Precambrian rocks of the Strait of Belle Isle area; Geological Survey of Canada Memoir 400, p. 1-73.

Clifford, P.M.
1965: Paleozoic flood basalts in northern Newfoundland and Labrador; Canadian Journal of Earth Sciences, v. 2, p. 183-187.

Cox, K.G., Bell, J.D., and Pankhurst, R.J.
1979: The Interpretation of Igneous Rocks; George Allen and Unwin, London, 450 p.

Erdmer, P.
1986: Geology of the Long Range Inlier in the Sandy Lake map area, western Newfoundland; in Current Research, Part B, Geological Survey of Canada, Paper 86-1B, p. 19-27.

Floyd, P.A. and Winchester, J.A.
1975: Magma type and tectonic setting using immobile elements; Earth and Planetary Science Letters, v. 27, p. 211-218.

Floyd, P.A. and Winchester, J.A.
1978: Identification and discrimination of altered and metamorphosed volcanic rocks using immobile elements; Chemical Geology; v. 21, p. 291-306.

Hynes, A.
1982: A comparison of amphiboles from medium- and low-pressure metabasites; Contributions to Mineralogy and Petrology, v. 81, p. 119-125.

Irvine, T.N. and Baragar, W.R.A.
1971: A guide to the chemical identification of the common volcanic rocks. Canadian Journal of Earth Sciences, v. 8, p. 523-548.

Kretz, R.
1982: Transfer and exchange equilibria in a portion of the pyroxene quadrilateral as deduced from natural and experimental data; Geochimica et Cosmochimica Acta, v. 46, p. 411-421.

Laird, J. and Albee, A.L.
1981: Pressure, temperature and time indicators in mafic schist from northern Vermont; American Journal of Science. v. 281, p. 97-126.

Leake, B.E.
1978: Nomenclature of amphiboles; American Mineralogist, v. 63, p. 1023-1052.

Lindsley, D.H.
1983: Pyroxene thermometry; American Mineralogist, v. 68, p. 477-493.

Machin, D.C.
1986: The petrography and petrogenesis of the Long Range dykes; Grenvillian inlier, western Newfoundland. Unpublished B.Sc. thesis, Memorial University of Newfoundland, St. John's, Newfoundland, 51 p.

Owen, J.V.
1986: Geology of the Silver Mountain area, western Newfoundland; in Current Research, Part A. Geological Survey of Canada, Paper 86-1A, p. 515-522.

Owen, J.V., and Erdmer, P.
1986: Precambrian and Paleozoic metamorphism in the Long Range Inlier, western Newfoundland; in Current Research, Part B. Geological Survey of Canada, Paper 86-1B, p. 29-38.

Papike, J.J., Cameron, K.L., and Baldwin, K.
1974: Amphiboles and pyroxenes: Characterization of OTHER than quadrilateral components and estimation of ferric iron from microprobe data (abstract); Geological Society of America, Abstracts with Programs, 6, p. 1053-1054.

Pearce, J.A. and Cann, J.R.
1973: Tectonic setting of basic volcanic rocks determined using trace element analyses; Earth and Planetary Science letters, v. 19,. p. 290-300.

Powell, R.
1978: The thermodynamics of pyroxene geotherms; Philosophical Transactions of the Royal Society of London, v. A283, p. 457-469.

Pringle, I.R., Miller, J.A., and Warrell, D.M.
1971: Radiometric age determinations from the Long Range Mountains, Newfoundland. Canadian Jounral of Earth Sciences, v. 8, p. 1325-1330.

Rietmeijer, F.J.M.
1983: Chemical distinction between igneous and metamorphic orthopyroxenes especially those coexisting with Ca-rich clinopyroxenes: a re-evaluation; Mineralogical Magazine, v. 47, p. 143-151.

Robinson, P., Spear, F.S., Schumacker, J.C., Laird, J., Klein, C., Evans, B.W., and Doolan, B.L.
1982: Phase relations of metamorphic amphiboles: natural occurrence and theory; in D.R. Veblen and P.H. Ribbe (eds.). Amphiboles: Petrology and experimental phase relations, Mineralogical Society of America, Reviews in Mineralogy, v. 9B, p. 1-227.

Strong, D.F.
1974: Plateau lavas and diabase dikes of northwestern Newfoundland; Geological Magazine v. 111, p. 501-514.

Strong, D.F. and Williams, H.
1972: Early Paleozoic flood basalts of northwestern Newfoundland: their petrology and tectonic significance; Proceedings of the Geological Association of Canada, v. 24, p. 43-53.

Stukas, V. and Reynolds, P.H.
1974: 40Ar/39Ar dating of the Long Range dikes, Newfoundland; Earth and Planetary Science Letters, v. 22, p. 256-266.

Thompson, R.N., Morrison, M.A., Hendry, G.L. and Parry, S.J.
1984: An assessment of the relative roles of crust and mantle in magma genesis: an elemental approach; Philosophical Transactions of the Royal Society of London, Series A, v. 310, p. 111-152.

Wanless, R.K., Stevens, R.D., Lachance, G.R. and Rimsaite, J.Y.H.
1965: Age determinations and geological studies, K-Ar isotopic ages, Report 5; Geological Survey of Canada, Paper 64-17.

Wanless, R.K., Stevens, R.D., Lachance, G.R. and Delabio, R.N.
1974: Age determinations and geological studies, K-Ar isotopic ages, report 12; Geological Survey of Canada, Paper 74-2.

Wells, P.R.A.
1977: Pyroxene thermometry in simple and complex systems; Contributions to Mineralogy and Petrology, v. 62, p. 129-139.

Williams, H. and Stevens, R.K.
1969: Geology of the Belle Isle-northern extremity of the deformed Appalachian miogeosynclinal belt; Canadian Journal of Earth Sciences, v. 6, p. 1145-1157.

Winchester, J.A. and Floyd, P.A.
1976: Geochemical magma type discrimination: application to altered and metamorphosed basic igneous rocks; Earth and Planetary Science Letters, v. 28, p. 459-469.

Winchester, J.A. and Floyd, P.A.
1977: Geochemical discrimination of different magma series and their differentiation products using immobile elements; Chemical Geology, v. 20, p. 325-343.

Wood, B.J. and Banno, S.
1973: Garnet-orthopyroxene and orthopyroxene-clinopyroxene relationships in simple and complex systems; Contributions to Mineralogy and Petrology, v. 42, p. 109-124.

Appendix 29.1. Field data for mafic dykes in the Silver Mountain area. All dykes are discordant to tectonic fabrics (where present) in the country rock unless otherwise indicated.

Sample VO-85-	Orientation	Width (cm)	Comments
841-2	353	60	plagioclase phenocrysts
678	7	25	
655	22	40	
155	40	12	
641-2	25	150	
383	60	>2000	
363-2	340	<100	concordant to schistosity*
409	18	>400	concordant to gneissosity; crenulated
541-2	350	35	concordant to schistosity; crenulated
538-3	50	25	chilled margins are plagioclase-phyric; dyke core is aphyric
505	50	25	
568-2	2	100	

*fabric in country rock

- 30 -

Graptolite preparation for reflected light microscopy – a technical note

Project 820048

F. Goodarzi and L.D. Stasiuk[1]
Institute of Sedimentary and Petroleum Geology, Calgary

Goodarzi, F. and Stasiuk, L.D., Graptolite preparation for reflected light microscopy – a technical note; in Current Research, Part A, Geological Survey of Canada, Paper 87-1A, p. 317-322, 1987.

Abstract

The optical properties of organic fossils such as graptolites have recently been investigated for their applicability in assessing thermal maturation and source rock potential of sedimentary rocks. The sample preparation and polishing of graptolites is briefly reviewed. Substandard technical preparation of graptolites for reflected light microscopy will produce high-relief surfaces, significantly altering optical properties, including air and oil reflectance, bireflectance and reflectance dispersion. Subsequent thermal history interpretations based on graptolite optical properties will be incorrect.

Résumé

On a récemment examiné les propriétés optiques de fossiles organiques tels que les graptolites, et l'on étudie les possibilités d'application de ces propriétés à l'évaluation de la maturation thermique et du potentiel des roches sédimentaires comme sources de matières premières. On traite brièvement de la préparation des échantillons et du polissage des graptolites. Une préparation technique insuffisante des graptolites en vue de la microscopie en lumière réfléchie, donne des surfaces de relief prononcé, ce qui altère nettement les propriétés optiques, y compris la réflectance dans l'air et dans l'huile, la biréflectance et la dispersion par réflectance. De ce fait, l'interprétation de l'évolution thermique d'après les propriétés optiques des graptolites serait incorrecte.

[1]Department of Geology – Energy Research Unit, University of Regina, Saskatchewan, S4S 0A2.

INTRODUCTION

The feasibility of using the optical properties of organic constituents to assess the thermal maturity level of potential hydrocarbon source rocks has been known for several years. Quantitative reflected light microscopy techniques (i.e. per cent reflectance in oil) were used as early as 1958 by Teichmüller to approximate the degree of diagenetic alteration or coalification of vitrinite-like inclusions in both hydrocarbon reservoir and source rocks. Vitrinite or type III kerogen (Brooks, 1981) reflectance studies have since become a valuable component in many hydrocarbon exploration programs, particularly in frontier geological basins.

Assessing the thermal maturation of Pre-Devonian sedimentary sequences using reflected light microscopy is hindered by the rarity or complete absence of vitrinite in sedimentary rocks of Lower Paleozoic age. Using the optical properties of other organic constituents common to Paleozoic sediments (e.g. graptolites, chitinozoans, acritarchs, scolecodonts) as thermal maturation indices has recently been investigated by several authors (Teichmüller, 1978; Clausen and Teichmüller, 1982; Goodarzi, 1984; Goodarzi and Norford, 1985; Goodarzi et al., 1985; Goodarzi and Higgins, in press).

The development and ultimate perfection of a technical procedure for the attainment of a polished surface on organic fossils such as graptolites is essential in order to determine the true reflectance and other optical measurements. The surface of any type of organic matter on which reflectance measurements are to be made must be free of any influence of relief or other inhomogeneities such as fine scratches or minute mineral inclusions. Imperfections in the polished surface can artificially increase or decrease the reflectance, initiating subsequent errors in geological interpretations.

This technical note will compare and contrast two methods experimented with in the preparation of graptolites for reflected light microscopy.

A flat, relief-free surface is essential to ensure accurate quantitative measure ments; the deviation of results (from correct readings) obtained from graptolite surfaces affected by relief will be briefly compared.

SAMPLE PREPARATION

Graptolite remains are macroscopically identified on the bedding plane of a shale; the sample is then cut to size with a rock saw to provide workable dimensions for the subsequent grinding and polishing stages (perhaps 2 cm × 2 cm).

Shales frequently become unconsolidated upon handling and especially upon wetting. To prevent this, the sized blocks are coated with an extremely thin film of epoxy. This also impregnates the porous and fissured regions of the specimen and prevents loss of the more labile constituents (graptolites) during grinding and polishing.

GRINDING

After the epoxy has cured, the bedding plane surface is gently ground on a piece of plate glass (approximately 30 × 30 × 0.5 cm) flooded with a slurry of 600 grit silicon carbide powder and alcohol or water. Isopropyl alcohol is generally used as a lubricant if there are clay minerals in the shale as these would become hydrated if saturated with water.

During the process of grinding away the epoxy to expose a portion of a graptolite, one must be extremely patient. A process of grinding gently in a circular fashion for 20 to 30 seconds, rinsing the sample, and examining the surface must be repeated frequently; once the epoxy covering a graptolite is removed, the extremely thin, film-like organic remains might be ground away unless frequent examination of the surface is maintained.

Gentle grinding is even more important when the graptolite becomes exposed. If excessive pressure is used, scratches will become deeply entrenched in the graptolite, making their removal difficult, if not impossible, during the polishing stage. It is also critical to prevent deep scratches because they greatly accentuate even the lowest degree of relief in an organic particle.

Exposing an area of graptolite approximately 2 to 3 mm in length and 1 to <1 mm in width is satisfactory. Any attempt to enlarge the exposure generally results in destruction of the initial graptolite surface uncovered. The sample is then thoroughly rinsed under a stream of water to remove silicon carbide or any mineral matter clinging to the surface. Immediate drying using pressurized air prevents hydration of clay minerals during the rinsing stage.

POLISHING

The particular suite of graptolites used for this study are relatively soft and in many situations are associated with significantly harder, massive to high concentrations of disseminated pyrite. When an exposed graptolite is associated with concentrations of sulphide minerals (Fig. 30.1a), it is recommended that this particular exposure be ground away and another graptolite, isolated from sulphides, be exposed. Obtaining a quality, relief-free, polished surface on juxtaposed sulphide/graptolites is extremely difficult.

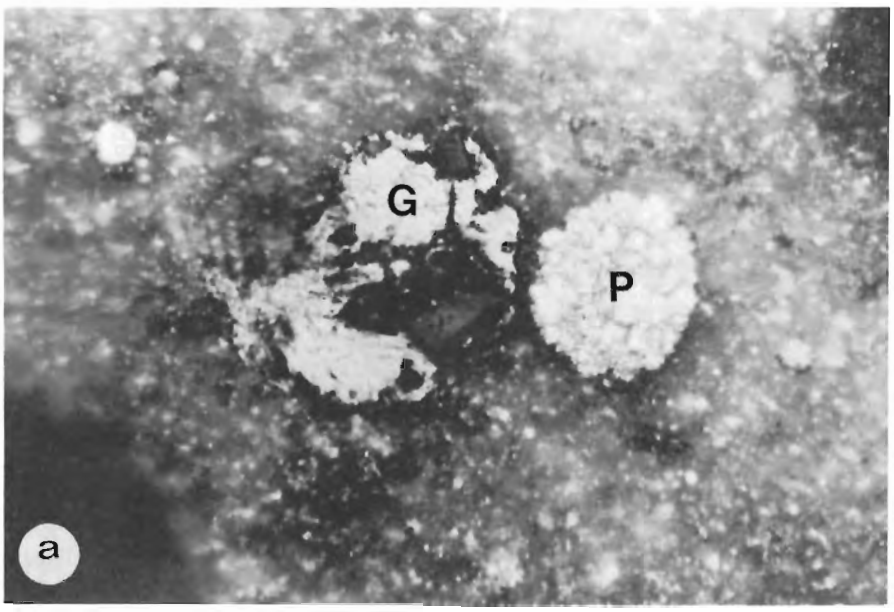
Several polishing methods were experimented with in order to produce a relief-free, graptolite surface. The polishing technique most commonly used by coal petrologists was first applied:

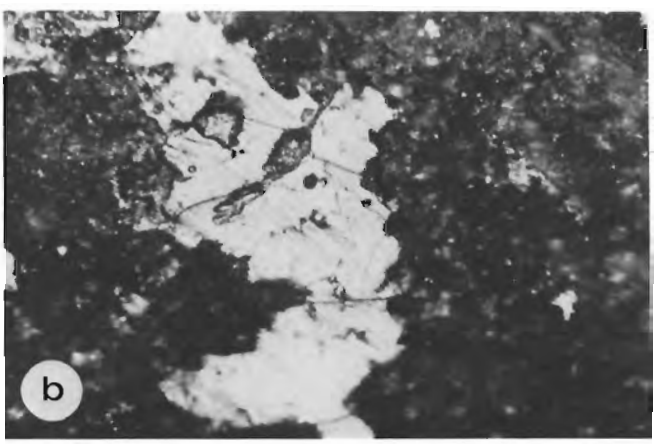
1. Hand polish the specimen in a circular motion on a stationary lap covered with selvyt cloth, Texmet paper or any other similar material; the polishing lubricant is a slurry of 0.3μ alumina and alcohol.
   RINSE THOROUGHLY UNDER A STREAM OF WATER AND DRY UNDER PRESSURIZED AIR.

2. Hand polish, as above, on a lap covered in silk cloth using 0.05μ alumina and alcohol as the polishing lubricant. RINSE UNDER A STREAM OF WATER AND DRY USING PRESSURIZED AIR.

The coal petrology polishing technique was found to produce a graptolite surface with very high relief (Fig. 30.1b), even when the sample was polished for a maximum of 10 to 15 seconds in each stage.

The second technique applied is that used by Teichmüller (pers. comm.) and briefly described by Goodarzi and Norford (1985). Two pieces of wood are substituted for the laps and cloths used in coal sample preparation. The wood must be soaked in water (or alcohol) for several minutes in order to soften or swell the grain. The following polishing procedure is recommended for producing relief-free graptolite surfaces (Fig. 30.1c):





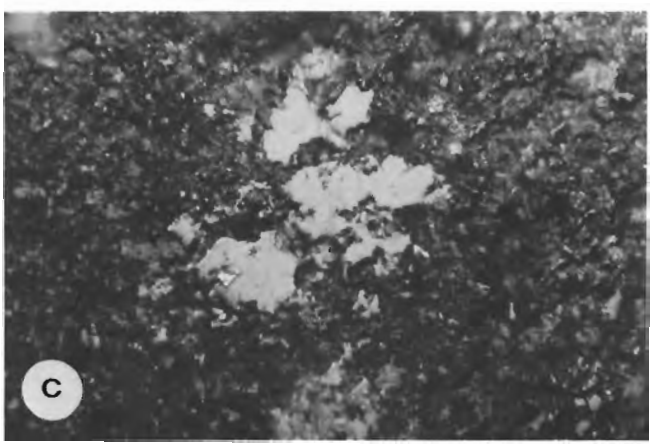


Figure 30.1. Photomicrographs x400, oil immersion, partially crossed polars.
a. Graptolite (G) intimately associated with sulphide minerals (P).
b. High-relief surface of graptolite polished using coal petrological techniques.
c. Relief-free surface of graptolite polished using modified polishing technique.

1. Flood a grain-smooth area of the wood with a slurry of 0.3μ alumina and alcohol. Polish the sample in 10 to 15 small revolutions, applying a moderate amount of pressure.
   RINSE THOROUGHLY UNDER A JET OF WATER; DRY IMMEDIATELY WITH PRESSURIZED AIR.
2. On a second piece of wood, flood a grain-smooth area with a slurry of 0.05μ alumina and alcohol. Polish the sample, using a maximum of 10 revolutions, and applying slightly less pressure than in the previous stage.
   RINSE THOROUGHLY AND DRY USING PRESSURIZED AIR.

During any of the stages, and in particular the grinding stage, mount the graptolite specimen and observe it under the microscope at low magnification (150-250X) using reflected light and an air objective. Progress in polishing the delicate graptolite can be monitored by frequent microscopic examination, and technical procedures may be adjusted accordingly. For example, during the grinding stage, it is difficult to determine with the naked eye or hand lens whether or not the graptolite has been exposed. Frequent microscopic examination will eventually reveal exposure.

EFFECT OF POLISHING ON GRAPTOLITE OPTICAL PROPERTIES

Polished high-relief and relief-free graptolite surfaces were microscopically examined and measured for per cent reflectance.

OPTICAL EQUIPMENT

Reflected light microscopy

A Zeiss MPM II microscope fitted with white (halogen) and fluorescent (HBO) light sources and attached to a Zonax microcomputer was used for optical data collection. A motorized monochromator attachment facilitated spectral scanning (400-700 nm). The maximum and minimum reflectance values for the graptolites were determined in air (N.A. 0.85/X 40) and under oil (n = 1.518) immersion objectives (N.A. 0.90/X 40).

RESULTS AND DISCUSSION

The quality of a polished surface is very important in determining the optical properties of the material (Piller, 1977). The important flaws on polished surfaces of organic material (coal macerals, graptolites, bitumens) are fine scratches, pits, smears, adhering of polishing powder, and relief (Goodarzi, 1975; Juckes and Pitt, 1977). Lengthy polishing of coal leads to the formation of relief and thus to the deterioration of polished surfaces (Murchison and Boult, 1961).

Reliefs due to polishing are either positive, for fragments harder than the imbedding media, for example, pyrofusinite; or negative, for material softer than the imbedding media, for example, bitumen.

Piller (1977) stated that focusing above the plane of a polished surface results in more light reaching the photomultiplier than would be the case if the focused plane were the polished surface (Fig. 30.2a). The reverse is true when the plane of focus is below the polished surface (Fig. 30.2b).

Positive relief on a specimen creates a situation where, in many cases, the plane of focus is slightly above the polished surface; negative relief is similar to focusing below the polished surface. The positive relief is accompanied by an increase in reflectance, whereas negative relief may decrease the true reflectance.

A considerable difference is evident in reflectance data collected from high- relief and relief-free graptolite surfaces. Table I presents some typical discrepancies in reflectance data from properly and poorly polished samples. The per cent reflectance in both air and oil, and the bireflectance are significantly greater for high relief, polished surfaces. In general, relief artificially increased Rair max by 2 to 3 per cent, and Roil by as much as 5 per cent. The values of Roil max tend to decrease between 1 and 2 per cent following elimination of polishing relief.

Graptolite reflectance can be used in assessing the thermal maturation level of a sedimentary sequence, with respect to hydrocarbon generation. Artificially increased or decreased graptolite reflectance resulting from undetected inferior sample preparation may lead to severe errors in maturation interpretations. Figure 30.3A shows incorrect and

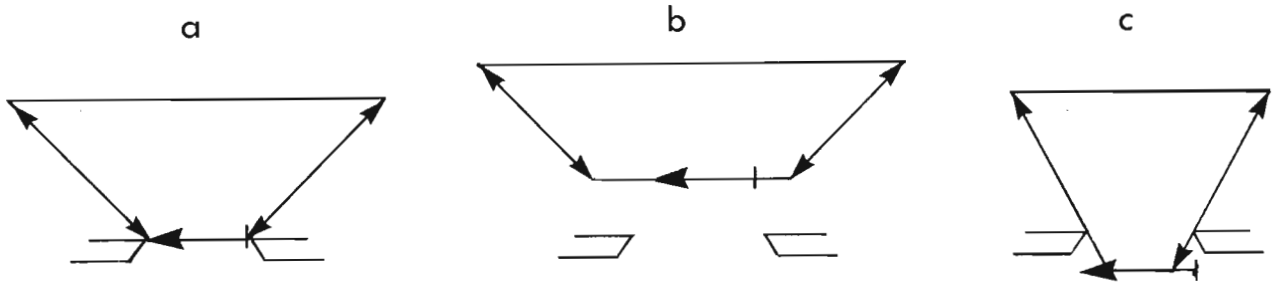


Figure 30.2. A schematic area under focus a) relief-free surface, b) surface with positive relief and c) surface with negative relief.

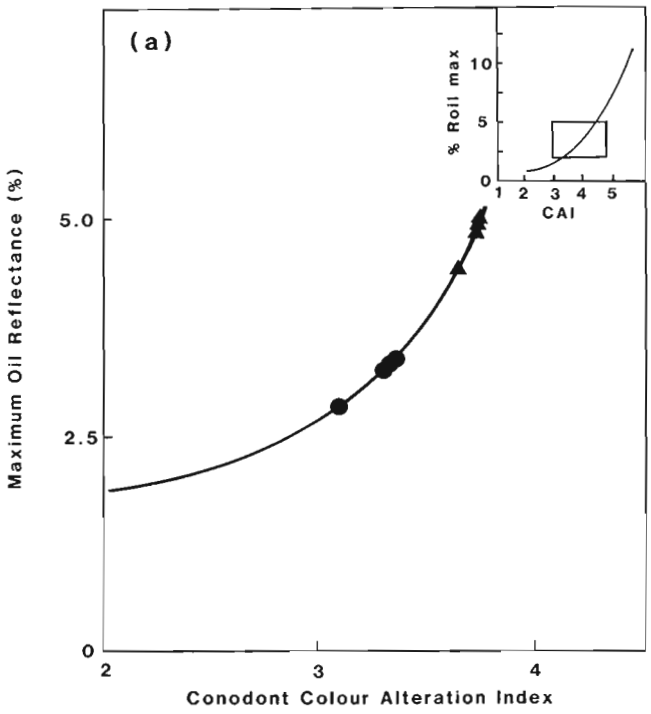


Figure 30.3a. Per cent maximum oil reflectance of graptolites from Table 1 plotted on the %Roil max-CAI diagram of Goodarzi and Norford (1985). Note the difference in corresponding CAI for %Roil max of high-relief graptolite surface (▲) and relief-free graptolite surface (●).

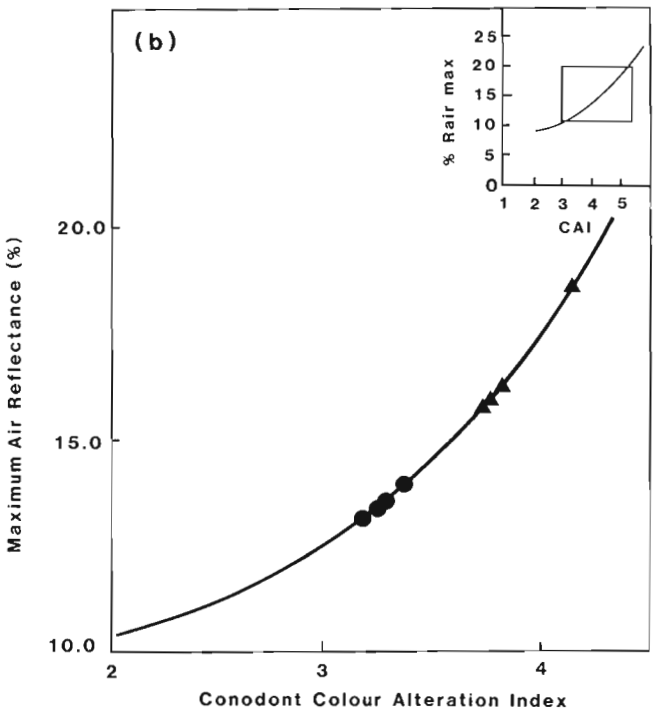


Figure 30.3b. Per cent maximum air reflectance of graptolites from Table 1 plotted on the %Rair max-CAI diagram of Goodarzi and Norford (1985). Note the difference in corresponding CAI for %Rair max of high-relief graptolite surface (▲) and relief-free graptolite surface (●).

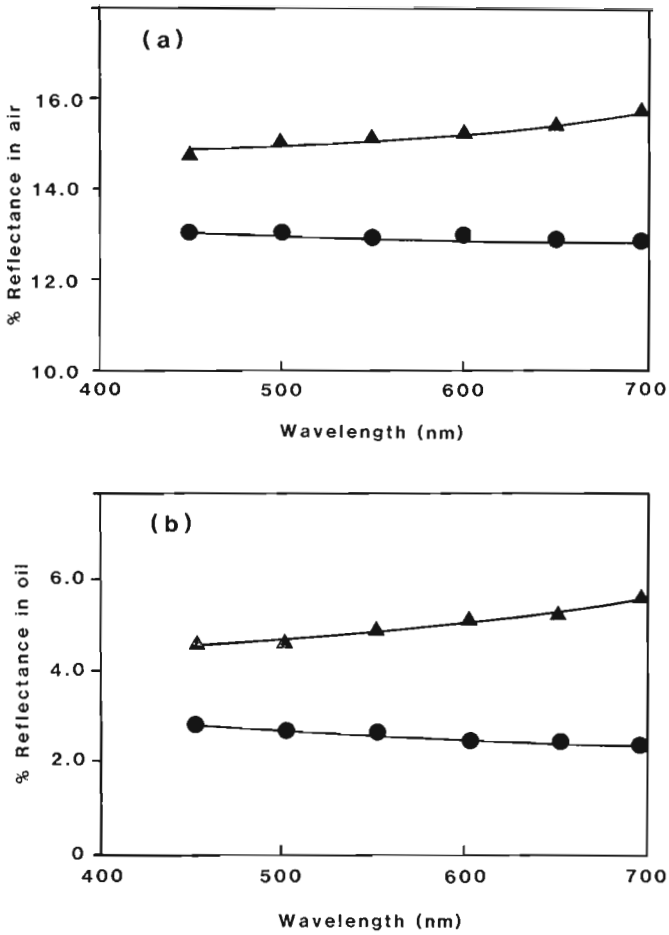


Figure 30.4a. Per cent reflectance dispersion in air of high-relief graptolite surfaces (▲) and relief-free graptolite surfaces (●). (b) Per cent reflectance dispersion in oil of high-relief graptolite surfaces (▲) and relief-free graptolite surfaces (●).

correct reflectance data from Table 30.1, plotted on the graptolite % R max - conodont Colour Alteration Index (CAI) diagram of Goodarzi and Norford (1985). The initial incorrect data would correlate with a CAI of 4 rather than the true CAI of 3, generating misleading conclusions regarding the stage of hydrocarbon generation.

Reflectance dispersion is altered by polishing imperfections. Figure 30.4 shows graptolite reflectance dispersion in air and oil (between 400 and 700 nm) for a sample prior to and after attaining a relief-free polished surface. The reflectance dispersion patterns of carbon-rich material (e.g. bitumen, vitrinite, graptolite) can be used in determining the relative amount of ordered to amorphous carbon (Marshal and Murchison, 1971; Khavari-Khorasani and Murchison, 1977; Goodarzi, 1985). Relatively immature organic matter exhibits patterns decreasing in reflectance from the blue to the red region of the visible spectrum. With increasing maturation and increasing amount of ordered to amorphous carbon, the pattern displays an increase in reflectance from the blue to the red region. Comparison of dispersion patterns for high-relief and relief-free graptolites (Fig. 30.4), illustrates the

Table 30.1 A comparison of the reflectance (% Rair and % Roil) and bireflectance data for improperly polished graptolites with a high-relief surface (values in parenthesis) and properly polished graptolites with a relief-free surface.

	Rair			Roil		
Sample	max	min	birefl.	max	min	birefl.
Ws	13.19	11.84	1.35	2.86	2.58	0.28
	(15.82)	(13.99)	(1.83)	(4.59)	(1.87)	(2.72)
Qs	13.40	12.69	0.71	3.27	2.91	0.36
	(18.70)	(14.80)	(3.90)	(4.80)	(2.09)	(2.71)
As	13.62	12.73	0.89	3.48	2.88	0.60
	(15.29)	(14.01)	(1.28)	(4.60)	(2.34)	(2.26)
Bs	13.97	12.90	1.07	3.65	2.93	0.72
	(16.13)	(14.69)	(1.44)	(4.37)	(2.58)	(1.79)

hazard of using improperly polished graptolite surfaces for maturation interpretation.

CONCLUSIONS

1. The technique used in preparing graptolite-bearing shales for reflected light microscopy has a pronounced effect on the optical properties of graptolite periderms.
2. Reflectance data (% Roil and % Rair) are artificially increased when obtained from improperly polished, high-relief graptolite surfaces.
3. Dispersion of graptolite reflectance (400-700 nm), tends to rise from the blue to the red region of the spectrum for high-relief surfaces, whereas relief-free graptolites produce a horizontal pattern of dispersion.

REFERENCES

Brooks, J.
1981: Organic maturation of sedimentary organic matter and petroleum exploration: a review; in Organic maturation studies and fossil fuel exploration, J. Brooks (ed.); Academic Press, London, p. 1-38.

Clausen, C.D. and Teichmüller, M.
1982: Die Bedeutung der groptolithen fragmente in palaozoikum von Soest Erwitte f'ur Stratigraphie and Inkohlung; Fortschritte in der Geologie von Rheinland und Westfalen, v. 30, p. 145-167.

Goodarzi, F.
1975: Some factors influencing the behaviour of the optical properties of carbonised maceral; Ph.d thesis, University of Newcastle-Upon-Tyne, England, 349 p.
1984: Organic petrography of graptolite fragments from Turkey; Marine and Petroleum Geology, v. 1, p. 202-210.
1985: Dispersion of optical properties of graptolite epiderms with increased maturity in early Paleozoic organic rich sediments; Fuel, v. 64, p. 1735-1740.

Goodarzi, F. and Norford, B.S.
1985: Graptolites as indicators of the temperature histories of rocks; Journal of the Geological Society, London, v. 142, p. 1089-1099.

Goodarzi, F., Snowdon, L.R., Gunther, P.R., and Jenkins, W.A.M.
1985: Preliminary organic petrography of Palaeozoic rocks from the Grand Banks, Newfoundland; Marine and Petroleum Geology, v. 2, p. 254-259.

Goodarzi, F. and Higgins, A.C.
in press: Optical properties of scolecodonts and their use as indicators of thermal maturity; Marine and Petroleum Geology.

Jukes, L.M. and Pitt, G.J.
1977: The standardization of petrographic analysis of coal; Journal of Microscopy, v. 104, Pt. 1, p. 13-21.

Khavari-Khorasani, G. and Murchison, D.G.
1977: Application of light microscopy in structural studies of bitumen; International Committee for Coal Petrology, Essen, Federal Republic of Germany.

Marshal, R.G. and Murchison, D.G.
1971: Dispersion of the optical properties of carbonized vitrinites; Fuel, v. 50, p. 4-22.

Murchison, D.G. and Boult, E.
1961: Polished surface of coal macerals; Fuel, v. 40, p. 386-406.

Piller, H.
1977: Microscope photometry; Springer Verlag, Berlin. 251 p.

Teichmüller, M.
1958: Métamorphisme du charbon et prospection du pétrole; Revue de l'Industrie Minérale Num. Spéc., Paris, p. 99-113.
1978: Nachweis Von Graptolithen – periderm in geschieferten Gesteinen mit Hilfe Kohlen petrologischer Methoden; Montashefte, Neues Jahrbuch f'ur Geologie und Païaontologie, v. 7, p. 430-447.

Structure and stratigraphy, Mount Bryant area, eastern Rocky Mountain Front Ranges, Alberta

Contract OSG85-00013

A.I. Zolnai[1]
Institute of Sedimentary and Petroleum Geology, Calgary

Zolnai, A.I., Structure and stratigraphy, Mount Bryant area, eastern Rocky Mountain Front Ranges, Alberta; in Current Research, Part A, Geological Survey of Canada, Paper 87-1A, p. 323-330, 1987.

Abstract

In the eastern Front Ranges of the southern Rocky Mountains southwest of Calgary, Alberta, middle Cambrian, upper Devonian and Mississippian strata are imbricated and complexly folded in the McConnell, Kananaskis and Lac des Arcs thrust sheets (east to west in ascending order of structural stacking). The Fullerton Tear, south of Mount Bryant, cuts obliquely across the McConnell thrust sheet, within which it juxtaposes structures of contrasting complexity, and marks the southern termination of the Kananaskis thrust sheet, but does not appear to affect the overlying Lac des Arcs sheet or strata beneath the McConnell Thrust.

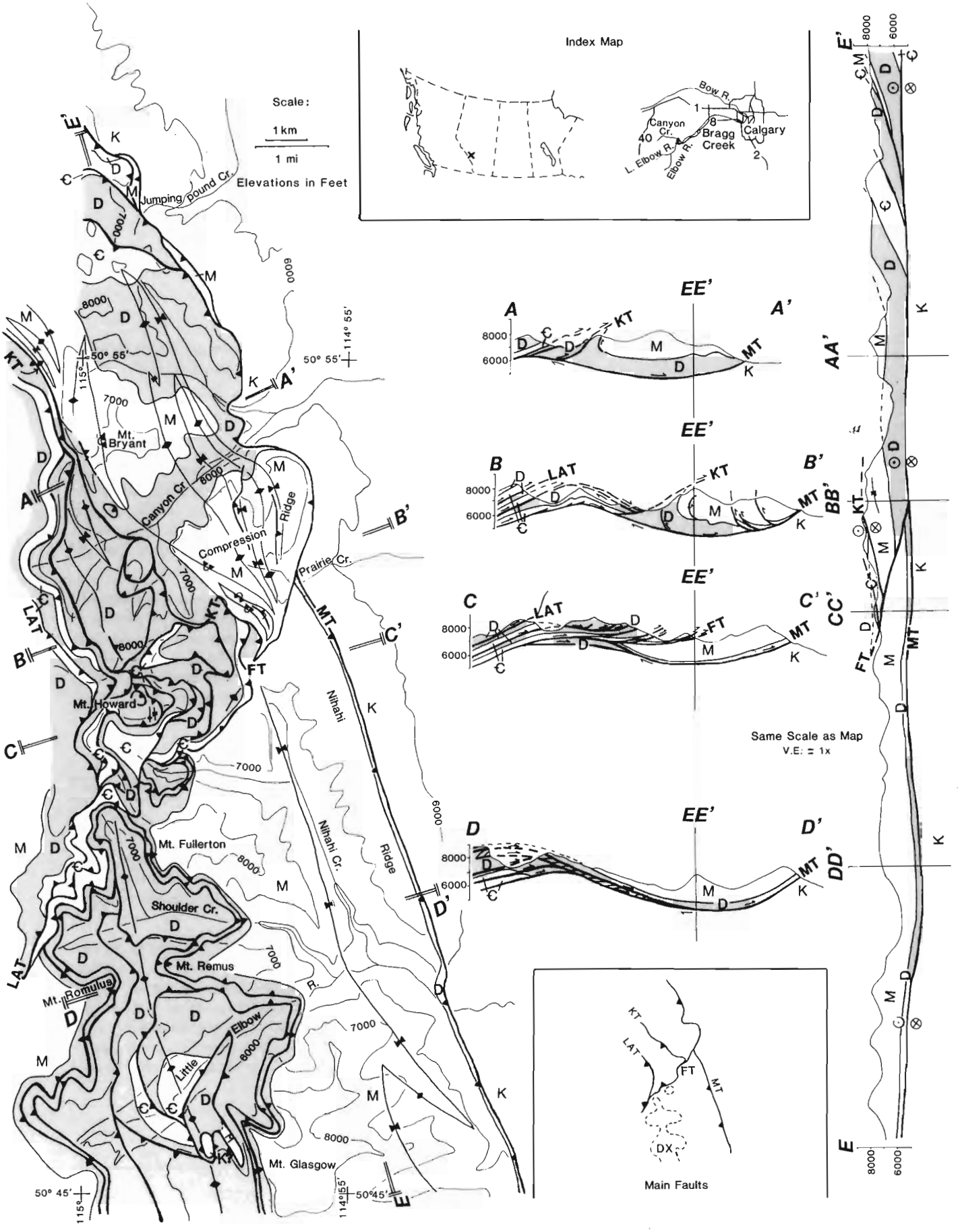
The role of the Fullerton Tear is interpreted as follows: the tear fault acted as an oblique ramp between the McConnell and Lac des Arcs thrusts; folds and faults north of it were accentuated as they were transported over a footwall ramp and anticlinorium-synclinorium pair located to the south of it. The tear fault also separates two structural levels; displacement of imbricate structures of the Kananaskis thrust sheet north of the tear is transferred to the Lac des Arcs Thrust. The duplex fault zone within Palliser strata to the south plunges underneath the tear, and connects with the McConnell Thrust to the east.

Résumé

Dans la partie est des Front Ranges du sud des Rocheuses, au sud-ouest de Calgary en Alberta, les strates du Cambrien moyen, du Dévonien supérieur et du Mississippien, sont imbriquées et plissées de façon complexe dans les nappes de charriage de McConnell, de Kananaskis et de Lac-des-Arcs (d'est en ouest suivant un ordre ascendant d'empilement structural). Au sud du mont Bryant, le décrochement de Fullerton traverse obliquement la nappe de charriage de McConnell, à l'intérieur de laquelle il juxtapose des structures de complexité contrastée, et marque la limite sud de la nappe de charriage de Kananaskis, et ne semble pas modifier la nappe sus-jacente de Lac-des-Arcs, ou les strates situées sous le charriage de McConnell.

On a interprété le rôle du décrochement de Fullerton de la façon suivante : la faille de déchirement s'est comportée comme une rampe oblique entre les charriages de McConnell et de Lac-des-Arcs; les plis et failles apparus au nord de celle-ci ont été accentués, lorsqu'ils ont été transportés par-dessus une rampe constituée par la lèvre inférieure de la faille, et un couple anticlinorium-synclinorium situé au sud de celle-ci. Le décrochement a aussi séparé deux niveaux structuraux; le mouvement des structures imbriquées de la nappe de charriage de Kananaskis, au nord de la faille de décrochement, a été transmis au charriage de Lac-des-Arcs. La zone faillée doubel située à l'intérieur des strates de Palliser au sud, plonge sous le décrochement et rejoint le charriage de McConnell à l'est.

[1]36 Cedardale Mews S.W., Calgary, Alberta, T2W 5G4.


Index Map
Bow R.
Canyon Cr.
Bragg Creek
Calgary
L. Elbow R.
Elbow R.
Scale:
1 km
1 mi
Elevations in Feet
Jumping Pound Cr.
Mt. Bryant
Canyon Cr.
Compression Ridge
Prairie Cr.
Nihahi Ridge
Nihahi Cr.
Mt. Howard
Mt. Fullerton
Shoulder Cr.
Mt. Remus
Mt. Romulus
Elbow R.
Little Elbow R.
Mt. Glasgow
50° 55'
50° 45'
114° 55'
115°
Same Scale as Map
V.E.: = 1x
Main Faults
DX

INTRODUCTION

The Mount Bryant area lies in the Front Ranges of the southern Alberta Rocky Mountains, 50 km west of Calgary and 20 km south of the Trans-Canada Highway, in the eastern Kananaskis Country west of Moose Mountain (Fig. 31.1). The Front Ranges are bordered to the east by the McConnell Thrust, which places Cambrian through Mississippian strata on top of the Jura-Cretaceous rocks of the Foothills. In this area, the main thrusts exposed west of the McConnell Thrust are the Kananaskis Thrust (marked as Exshaw Thrust [Bielenstein et al., 1971]: there exists a displacement transferon the north shore of Barrier Lake to the north of this area, between Exshaw Thrust to the north and Kananaskis Thrust to the south [Maurel, 1986]), terminated southward by the Fullerton Tear; and Lac des Arcs Thrust, which merges with the Fullerton Tear farther south.

ACKNOWLEDGMENTS

The area mapped in July, 1985 by the author, while under contract to the Geological Survey of Canada, covers 115 km2 in the southwest corner (about 1/6) of the Bragg Creek map area (NTS 82 J/15). Field advice was provided by M.E. McMechan (Institute of Sedimentary and Petroleum Geology), field assistance by J. Greggs, S. Hada (Kochi University, Kochi, Japan), R. Stachko and D. Redgate (Alberta Forestry Service). Discussions with I.S.P.G. staff were beneficial to the study. L. Maurel (University of Calgary) provided data from the north end of the map area. N.C. Ollerenshaw (I.S.P.G.) and R.A. Price (Geological Survey of Canada) supplied unpublished data pertaining to the area from their files.

STRATIGRAPHY

Strata of Cambrian to Cretaceous age are exposed in the area. Distinctive features of the stratigraphy, primarily recorded in Aitken (1981), Bamber et al. (1981), Bielenstein et al. (1971), Mountjoy and Geldsetzer (1981), Ollerenshaw (1975) and Richards et al. (1984), are described below (Table 31.1, Figure 31.2).

Middle Cambrian

Rocks of the Cathedral and Stephen formations are exposed only at the northern end of the map area. Strata of the overlying Eldon Formation outcrop in the western part of the study area, in the immediate hanging wall of numerous imbricate structures, suggesting that the underlying shale (Stephen Formation) is a major bedding glide plane.

Middle Cambrian-Upper Devonian

Strata of the middle Cambrian Arctomys Formation and upper Devonian Yahatinda Formation form noticeable outcrops of variegated, recessive shale and siltstone. They conspicuously outline structural repetitions in the dark grey strata of the overlying Fairholme Group, and form the hanging walls of these faults. These recessive shales and siltstones appear to constitute another bedding glide horizon.

Upper Devonian

The area lies within the Fairholme reef complex of Frasnian age (McLean, 1986; Mountjoy and Geldsetzer, 1981). The Cairn Formation consists of three distinct but discontinuous members, seen as far north as Mount Yamnuska (H.H.J. Geldsetzer, pers. comm., 1985). The Yellow (middle) member, unreported in literature to the author's knowledge, is similar to older rocks of the Pika and Yahatinda formations (Table 31.1) and thus is an important clue in explaining the history of the imbricate structures in the study area. A lesser source of confusion lies in the dolostone bioherms also found in the area, visually similar to but lithologically distinct from calcitised breccia zones along fault planes (R.H. Workum, pers. comm., 1985).

The Palliser Formation is uniform throughout the area (Geldsetzer et al., 1986), except for an upper member of thin bedded, silty limestone weathering into a platy talus, which is present in lieu of the Costigan Member in the McConnell thrust sheet only. It contrasts with the underlying Morro Member, a thick, massive, cliff forming limestone with rare breccia beds and a thick, dark interval of strata between two light ones (Figure 31.3a, outlines small repeats in the duplex fault zone discussed below).

Mississippian

Contrasts in stratigraphy of Carboniferous rocks east and west of the McConnell Thrust have been documented elsewhere (Bamber et al., 1981; Richards et al., 1984). Strata underlying the area comprise the Banff Formation (three members), the Livingstone Formation (one distinctive thin marker bed 50 m from top), and the Mount Head Formation (alternating resistant and recessive members), as outlined in Table 31.1. The disappearance of the middle member of the Banff Formation in the Lac des Arcs thrust sheet west of the McConnell thrust sheet is worthy of note.

STRUCTURAL GEOLOGY

The McConnell, Kananaskis and Lac des Arcs thrusts and the Fullerton Tear separate the structural domains of the area (intervening thrust sheets are named after their respective floor thrusts). The structure of the area is interpreted

Figure 31.1. Simplified geology and cross-sections, southwest corner of the Bragg Creek map area (82J/15), after present work and Bielenstein et al. (1971), Maurel (1986 and pers. comm., 1985), Ollerenshaw (1975 and pers. comm., 1985), and Price (unpub. data, pers. comm., 1985). ∈:Cambrian; D: Devonian; M: Mississippian; K: Cretaceous; DX: duplex fault zone; KT: Kananaskis Thrust; FT: Fullerton Tear; LAT: Lac des Arcs Thrust; MT: McConnell Thrust.

schematically in serial cross-sections (Figure 31.1, AA'-DD') and a longitudinal section (EE'). They are very localised, lack control in the subsurface and surface to the east and west, and are not intended to balance.

Lac des Arcs thrust sheet

The western limit of the map area (Figure 31.1, left) is the eastern limit of the Lac des Arcs thrust sheet, which carries Cambrian through Cretaceous rocks beneath the Rundle Thrust farther west. The Rundle Thrust overlies the Mount Allan Syncline at the top of the Lac des Arcs thrust sheet in the Kananaskis Valley (Bielenstein et al., 1971; Ollerenshaw, 1975).

Kananaskis thrust sheet

The Kananaskis Thrust is the lowest of numerous small imbricate structures of Cambrian and Devonian strata in the Mount Howard area (Figure 31.1, center; Figure 31.3b, left). These northwest-striking faults terminate in a complex imbricate structure west of Mount Fullerton at the Fullerton Tear, which strikes southwestward between the McConnell and Lac des Arcs thrusts without apparently offsetting their traces or cutting out substantial amounts of stratigraphy (Figure 31.1, EE').

McConnell thrust sheet north of Fullerton Tear

Strata exposed north of Compression Ridge range in age from Cambrian to Mississippian, the oldest (Cathedral Formation) and youngest (Etherington Formation) in this area (Table 31.1). The northernmost structures are splays off the McConnell Thrust, the southern portion of the Barrier Peak thrust stack (Maurel, 1986). The overturned Mount Bryant Syncline (Figure 31.1, top, AA'; Figure 31.3b, right) is akin to the Mount Allan Syncline, which is overturned beneath the Rundle Thrust farther west. A convergence point near the Fullerton

Table 31.1

Stratigraphy			
System or Stage	Formation	Thickness	Lithology
Jura-Cretaceous	Kootenay	Thickness unknown, imbricated	Sandstone, coal, shale
Mississippian	Etherington	(>50 m)	Dolostone: microcrystalline; grading up into resistant, chert lime wackestone and grainstone
	Mount Head	(members; ~80 m)	Alternating resistant, medium to very thick bedded grainstone and packstone; and recessive, medium bedded silty dolostone and cherty wackestone to grainstone
	Livingstone	(~150 m)	Lime grainstone to dolomitic lime packstone and wackestone: thick to very thick bedded, commonly crossbedded one third of the way down from top; brown recessive shaly interval
	Banff	(<150 m)	Skeletal lime wackestone and packstone: dark grey, cherty, dolomitic
	Upper member		
	Middle member	(20 m)	Cherty lime grainstone and packstone: medium grey, medium to very thick bedded, local large-scale crossbedding
	Lower member	(<150 m)	Shale: dark grey, greyish orange weathering, laminated to thin bedded; argillaceous to silty limestone and dolostone; local slump folds
	Exshaw		Siltstone (<2 m): medium to dark grey; basal bituminous black shale (<10 m)
Upper Devonian	Palliser	(~50 m)	Limestone: dark grey to yellowish, thin bedded, platy, silty, thin, recessive
	Upper member		
	Morro Member	(150 m?, usually faulted)	Limestone: medium to light grey, massive; dolomitic near base with rare breccia
	Alexo	(<10 m)	Silty dolostone to dolomudstone with reddish siltstone: yellow, thin bedded; recessive
	Southesk	(~50 m)	Dolomudstone: light grey, thick bedded to laminated, massive coral/brachiopod debris wackestone and grainstone
	Arcs Member		

Tear at Compression Ridge (Figure 31.1, center), imparts a flower-like map pattern seen near other tear faults in thrust faulted terranes (Douglas, 1974; Douglas and Norris, 1976).

The inferred steeper attitude of the tear (~45° NW) between Mount Fullerton and Compression Ridge (west and east of which it merges, respectively, with the Lac des Arcs and McConnell thrusts) is in marked contrast to shallower dipping (<30° SW) and folded imbricate structures. The tear separates structures of contrasting complexity within the McConnell thrust sheet without affecting strata above and below that sheet, and marks the southern limit of the Kananaskis thrust sheet. In this way the Fullerton Tear differs from other tear faults of the Front Ranges (Moffat, 1981), which are near vertical and disrupt strata with no appreciable variation in structural style within the affected sheets.

McConnell thrust sheet south of Fullerton Tear

Strata south of Compression Ridge are gently folded into a broad anticlinorium- synclinorium pair in uppermost Devonian (Palliser) through Mississippian strata (Figure 31.1, bottom, DD'). The fold pair appears to be grossly cylindrical and, contrary to strata north of the Fullerton Tear, abuts the latter with no apparent increase in complexity of structures. The northeast-striking tear fault may have acted as an oblique ramp, accentuating northwest-striking folds and faults in the hanging wall of the northeast-striking tear fault (McConnell sheet north of Fullerton Tear) as they were carried over a footwall ramp and the northwest-striking anticlinorium-synclinorium pair (McConnell sheet south of Fullerton Tear).

The anticlinorium is cored with imbricate structures of Cambrian to Devonian strata. An outcrop of Jura-Cretaceous Kootenay sands and coal (Figure 31.1, bottom) may be a horse among other imbricate structures if the McConnell Thrust is folded, as are the surrounding structures, but remains in the subsurface (Section B, Gordy and Frey, 1975; Figure 31.1, DD'). Alternatively, the Kootenay strata may be a window, provided that a footwall drop and a lateral hanging wall ramp exist between the Cambrian strata in the Little

Table 31.1 (cont.)

Stratigraphy			
System or Stage	Formation	Thickness	Lithology
	Grotto Member	(<50 m)	Dolomudstone: dark grey, thin bedded, recessive
	Peechee Member	(~50 m)	Dolomudstone to amphipora/brachiopod/coral wackestone: light grey, laminated to thick bedded, moderately resistant
	Cairn Upper member	(~30 m)	Amphipora dolo-wackestone to mudstone: dark grey, medium bedded; flaggy weathering
	Yellow member	(<100 m)	Dolomitic siltstone: yellow, thin, thin bedded, recessive
	Lower member	(<100 m)	Dolo-wackestone to mudstone: dark grey to brown, irregularly thick to medium bedded, massive, flaggy weathering, amphipora-and bulbous stromatoporoid-bearing; bioherms; light grey, laterally discontinuous (thick, rapidly pinching out to zero thickness), massive, massively leached with up to one metre long vugs, totally dolomitized, amorphous
	Yahatinda	(<15 m)	Dolomitic siltstone: variegated (red, yellow, green, variably thick (lens-shaped outcrops) and thin bedded; desiccation cracks
Middle Cambrian	Arctomys	(<50 m?)	Silty dolostone and dolomitic mudstone: yellow, medium bedded to laminated, massive
	Pika	(<50 m)	Cyclic silty dolostone (grey) and dolosiltstone (brown): mottled brown and grey, wavy bedded, laminated, recessive, dolosiltstone dominant down-section with trilobite hash
	Eldon	(>150 m?, usually faulted)	Limestone: light grey, medium to thin bedded, massive, extensive brownish dolomitic mottling
	Stephen	(<30 m, usually sheared)	Shale: dark grey, thin, fissile; limestone: thin, flaggy; conglomerate: silty, glauconitic; trilobite hash
	Cathedral	(150 m?, faulted)	Limestone: dark grey, medium to thick bedded, flaggy; dolomitic limestone: brownish medium grey, dolomitic mottling

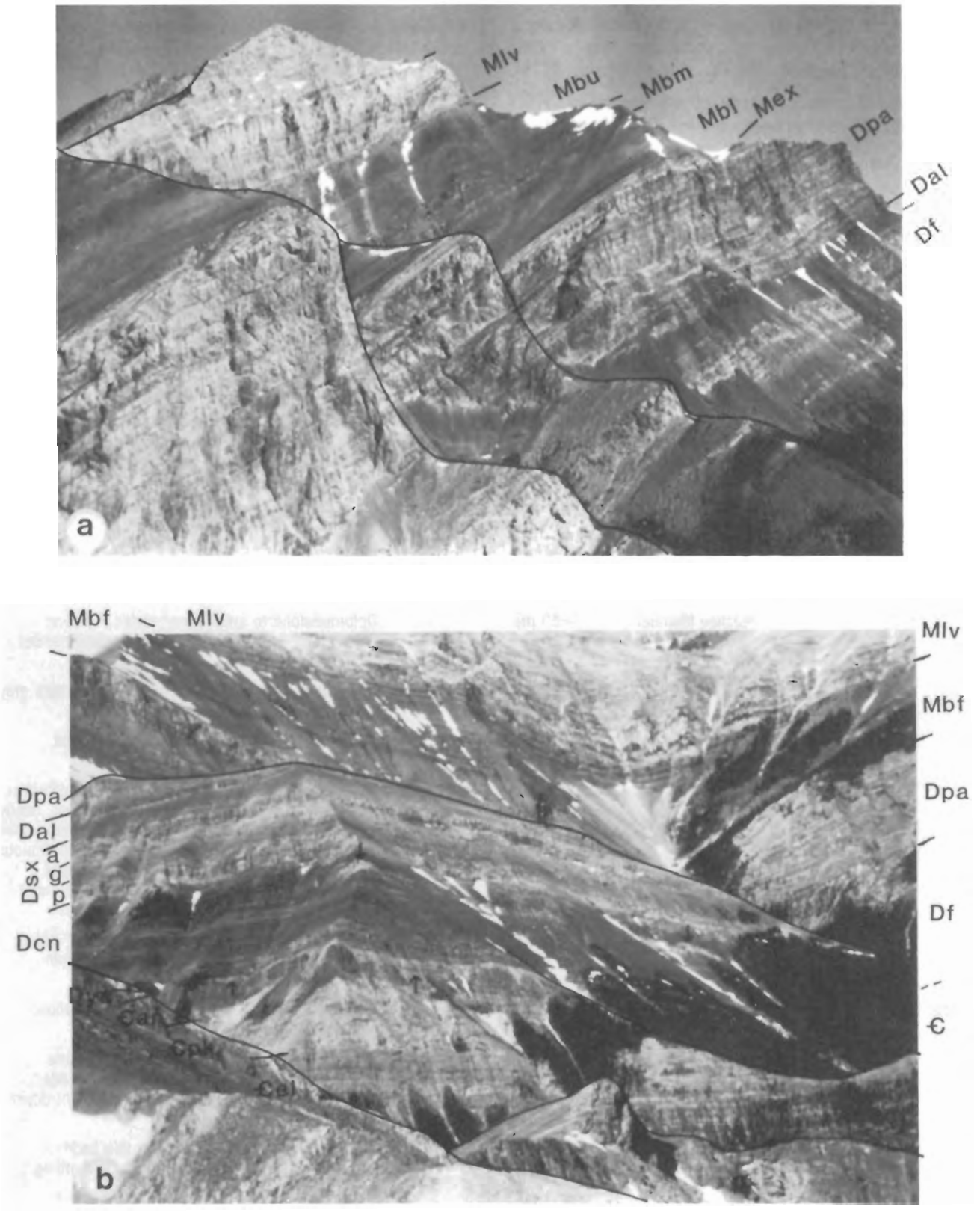


Figure 31.2. Stratigraphy a) looking northwest, b) looking west toward Fisher Peak west of Mount Howard in Lac des Arcs thrust sheet; lines indicate middle ground ridges and spurs. ϵel: Eldon Formation; ϵpk: Pika Formation; ϵar: Arctomys Formation; Dya: Yahatinda Formation (arrows: sub-Devonian unconformity); Dcn: Cairn Formation (arrows: bioherms); Dsx: Southesk Formation (members: p: Peechee; g: Grotto; a: Arcs); Dal: Alexo Formation; Dpa: Palliser Formation; Df: Fairholme Group; Mex: Exshaw Formation; Mbf: Banff Formation (members: Mbl: lower; Mbm: thin middle; Mbu: upper); Mlv: Livingstone Formation (tick: shaly interval); Mount Head and Etherington formations behind skyline.

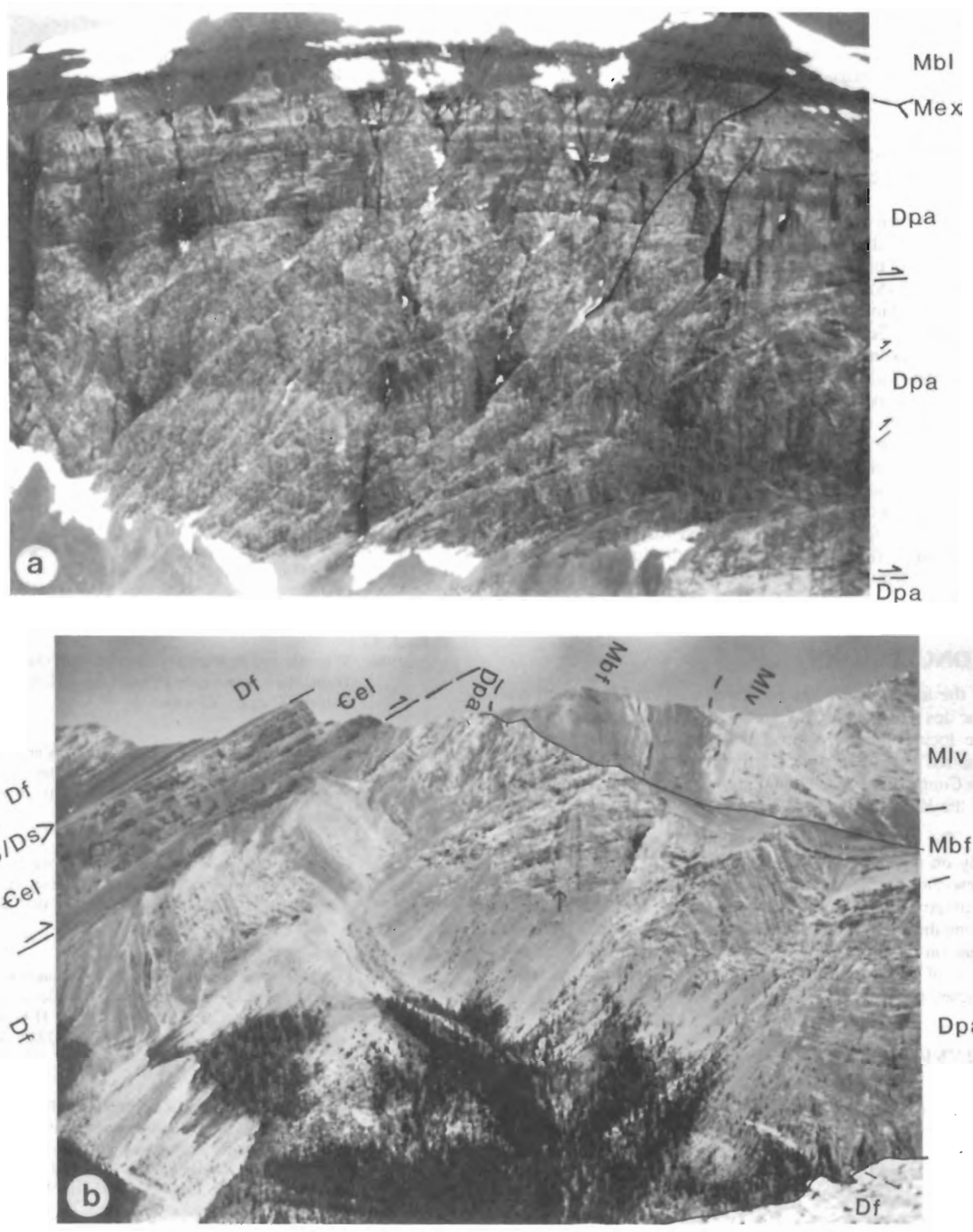


Figure 31.3. Structures a) Duplex fault zone in the Morro Member of the Palliser Formation looking north at the south slope of Mount Glasgow, cliff height approximately 200 m (photo courtesy M.E. McMechan); b) Darker Cambro-Devonian strata of Kananaskis thrust sheet (left), lighter Devono-Mississippian strata in overturned Mount Bryant Syncline of McConnell sheet (arrow: horse of horizontal Palliser Formation in overturned limb of same), looking north toward Mount Bryant. Abbreviations as in Figure 31.2, as well as: €/DS: Pika-Yahatinda formations.

Elbow River valley and Devonian strata above another window of Jura-Cretaceous rocks in the Elbow River Valley south of Mount Glasgow (Bielenstein et al., 1971; Ollerenshaw, 1975; R.A. Price, pers. comm., 1985).

Another structural peculiarity is found in the Palliser Formation. Repetition of different coloured limestones between poorly distinguishable, tightly spaced faults (best viewed when at the same altitude, on Mounts Romulus, Remus and Glasgow; Figure 31.3a) form a duplex fault zone below a roof thrust approximately 50 to 100 m below the top of the cliff (Morro Member), and above a floor thrust most often buried in scree at the cliff base, but above the yellowish, platy Alexo Formation (approximately 200 m below the top of the thickened Morro Member). The thickness of strata above the roof thrust of the duplex is comparable to that of the incomplete top of the Palliser Formation in the immediate hanging wall of the McConnell Thrust south of Compression Ridge (Figure 31.1, center), and of other sheets farther south (Geldsetzer et al., 1986). There thus exists an enigmatic plane of weakness (possibly relict evaporite horizons) regionally developed within the massive Palliser limestone. The duplex fault zone is presumed to connect with the McConnell Thrust farther east, and to plunge beneath the Fullerton Tear and Lac des Arcs Thrust to the north and west, respectively.

CONCLUSIONS

In the area between the northwest-striking McConnell and Lac des Arcs thrusts, the northeast-striking Fullerton Tear is the locus of important variations in structural style. It is inferred that it separates different structural levels in the McConnell thrust sheet, and marks the southern termination of the Kananaskis thrust sheet.

The detailed examination of the Mississippian stratigraphy on the north slope of Mount Fullerton, the Cambrian-Devonian stratigraphy on the east slope of Fisher Peak, of the geometry of the duplex fault zone and the McConnell Thrust along the Little Elbow and Elbow rivers, and of the Fullerton Tear on Compression Ridge, south of Mount Howard and west of Mount Fullerton, are some of the areas meriting further work.

REFERENCES

Aitken, J.D.
1981: The Cambrian System in the Southern Canadian Rocky Mountains, Alberta and B.C.; Guidebook for field trip no. 2, compiled by J.D. Aitken, edited by M.E. Taylor, 2nd International Symposium on the Cambrian System, Denver.

Bamber, E.W., Macqueen, R.W., and Ollerenshaw, N.C.
1981: Mississippian stratigraphy and sedimentation, Canyon Creek (Moose Mtn.), Alberta; in Field Guide to Geology and Mineral Deposits, R.I. Thompson and D.G. Cook (eds.); Calgary '81 Annual Meeting, GAC, MAC, CGU, p. 177-194.

Bielenstein, H.U., Price, R.A. and Jones, P.B.
1971: Geology of the Seebe-Kananaskis area; in A Geological Guide of the Canadian Cordillera along the Trans-Canada Highway between Calgary and Revelstoke, I.A.R. Halladay and D.H. Matthewson (eds.); American Society of Petroleum Geologists, Canadian Exploration Frontiers Symposium Guidebook.

Douglas, R.J.W.
1974: Dahadinni map area, District of Mackenzie (95N); Geological Survey of Canada, Map 1374A.

Douglas, R.J.W. and Norris, D.K.
1976: Virginia Falls map area, District of Mackenzie (95F); Geological Survey of Canada, Map 1378A.

Gordy, P.L. and Frey, F.R.
1975: Structural cross-section through the Foothills west of Calgary; in Structural Geology of the Foothills between Savanna Creek and Panther River, southwest Alberta, Canada, H.J. Evers and J.E. Thorpe (eds.); Canadian Society of Petroleum Geologists, Exploration Update '75 Guidebook, Plate 2.

Geldsetzer, H., de Mille, G., Sangster, D.F., Chung, C.F., McDonald, J.A. and Jonasson, I.R.
1986: The Upper Devonian Palliser Formation, Rocky Mountains, British Columbia and Alberta: Geochemistry and General Geology; Geological Survey of Canada, Open File 1021.

Maurel, L.
1986: Structure and stratigraphy, Barrier Peak (Mt. Boldy) Thrust stack; unpublished Ph. D. thesis, University of Calgary, Calgary, Alberta.

McLean, R.A.
1986: The rugose coral Pachyphyllum Edwards and Haime in the Frasnian (Upper Devonian) of Western Canada; in Current Research, Part B, Geological Survey of Canada, Paper 86-1B, p. 443-455.

Moffat, I.W.
1981: Geometry and mechanisms of transverse faulting, Rocky Mountain Front Ranges, Canmore, Alberta; unpublished M.Sc. thesis, University of Calgary, Calgary, Alberta, 178 p.

Mountjoy, E.W. and Geldsetzer, H.H.J.
1981: Devonian stratigraphy and sedimentation, southern Rocky Mountains; in Field Guide to Geology and Mineral Deposits, R.I. Thompson and D.G. Cook (eds.); Calgary '81 Annual Meeting, GAC, MAC, CGU, p. 195-224.

Ollerenshaw, N.C.
1975: Geological Map of the Rocky Mountain Foothills and Front Ranges, Calgary region; in Structural Geology of the Foothills between Savanna Creek and Panther River, southwest Alberta, Canada, H.J. Evers and J.E. Thorpe (eds.); Canadian Society of Petroleum Geologists, Exploration Update '75 Guidebook, Plate 1.

Richards, B.C., Styan, W., and Harrison, R.S.
1984: Paleozoic carbonate reservoir units and facies distribution; Canadian Society of Petroleum Geologists and Canadian Society of Exploration Geophysicists, Exploration Update '84, Field Trip B1 Guidebook, 23 p.

Origin of compositional differences amongst oils from the Hummingbird Field (Paleozoic), southeast Saskatchewan

Projects 780003 and 730062

P.W. Brooks, K.G. Osadetz, and L.R. Snowdon
Institute of Sedimentary and Petroleum Geology, Calgary

Brooks, P.W., Osadetz, K.G., and Snowdon, L.R., Origin of compositional differences amongst oils from the Hummingbird Field (Paleozoic), southeast Saskatchewan; in Current Research, Part A, Geological Survey of Canada, Paper 87-1A, p. 331-336, 1987.

Abstract

Hummingbird Field is a multiple pay zone field in southeast Saskatchewan with production from the Mission Canyon (Ratcliffe zone), Bakken and Birdbear formations. The field is structural, formed by stratigraphic inversion associated with multiple stage solution of the Prairie Formation salt. The oil in the Mission Canyon Formation zone is distinguished by its low pristane/phytane ratio and a low ratio of rearranged/regular steranes. The oils in the Bakken and Birdbear formations have higher pristane/phytane ratios and abundant diasteranes. These characteristics indicate the contribution of oil from at least two distinct source rocks. The ratio of tricyclic/pentacyclic terpanes distinguishes the oil of the Bakken Formation from that of the Birdbear Formation. The Birdbear oil may be the result of a mixing of oils resembling those in Ordovician reservoirs and those oils similar to the Bakken Formation in the Hummingbird Field.

Résumé

Le champ pétrolifère de Hummingbird est une zone productive multiple du sud-est de la Saskatchewan, dans laquelle les formations productives sont les formations de Mission Canyon (zone de Ratcliffe), et les formations de Bakken et Birdbear. Le champ est de type structural, et formé par une inversion stratigraphique associée à des solutions stratifiées issues des dépôts salins de la formation de Prairie. Le pétrole provenant de la zone de la formation de Mission Canyon se distingue par son faible rapport pristane/phytane, et son faible rapport stéranes reconstitués/ordinaires. Les pétroles des formations de Bakken et Birdbear sont caractérisés par des rapports plus élevés pristane/phytane et des quantités abondantes de diastéranes. Ces caractéristiques indiquent qu'une partie du pétrole provient d'au moins deux roches-mères distinctes. Le rapport terpanes tricycliques/pentacycliques différencie le pétorle de la formation de Bakken de celui de la formation de Birdbear. Il est possible que le pétrole de Birdbear soit le résultat d'un mélange de pétroles semblables à ceux des réservoirs d'âge Ordovicien et de pétroles semblables à ceux de la formation de Bakken, dans le champ pétrolifère de Hummingbird.

INTRODUCTION

Hummingbird Field is located approximately 70 km southwest of Weyburn in southeast Saskatchewan. The pool occurs in the vicinity of Township 2, Range 19, west of the second meridian. It was discovered in September, 1966, with the drilling of the Miami-Hudson Bay Hummingbird 10-26-002-19W2 well, and represented the initial discovery of oil in Devonian carbonate reservoirs in Saskatchewan. There are three producing zones. The lowest zone is in the Birdbear Formation (Upper Devonian). It originally contained approximately 1.173 million cubic metres of 823 Kg/m3 oil in-place (Saskatchewan Energy and Mines, 1983). The highest zone produces from a completion in the Ratcliffe Beds of the Mission Canyon Formation (Carboniferous) and produces 869 Kg/m3 oil from an initial in-place reserve of 4.115 million cubic metres (ibid.). There is miscellaneous production from the Bakken Formation (Upper Devonian and Carboniferous).

The Hummingbird Field is structurally controlled (Fuzesy, 1973; Smith and Pullen, 1967). The field lies in a structural depression, the Hummingbird Trough, which resulted from solution of the Middle Devonian Prairie Formation salts. The feature controlling the oilfield is a structural inversion. In Devonian time, progressive solution of Prairie Formation salts resulted in local thickening of several overlying Devonian formations. Subsequent regional solution of the surrounding salt in late Jurassic and early Cretaceous times resulted in the locally thickened Devonian strata occurring as structurally positive elements (Smith and Pullen, 1967).

Oil was originally produced from the Mission Canyon and Birdbear formations. The physical properties of the oils produced from the two formations are distinctive. Oil produced from the Birdbear zone is of low density, with larger volumes of solution gas than those in the medium density crude produced from the Mission Canyon zone. In the course of a regional investigation of geochemistry of Saskatchewan crude oils, oils from the three currently producing zones in the Hummingbird Field were examined. The geochemistry of these three oils indicates that the differences in physical properties of these oils is not the result of the biodegradation. Instead, at least two and possibly three distinctive sources have provided oils for these pools.

FAMILIES OF OILS IN SOUTHEAST SASKATCHEWAN

Brooks et al. (in progress) recognize three families of oils in southeast Saskatchewan. The first family of oils is restricted to Ordovician reservoirs. These oils, Group A, are generally characterized by a virtual absence of pristane and phytane, an odd carbon number predominance of the n-alkanes in the range C9-C19, and a predominance of rearranged steranes relative to regular steranes. The Group B oils, which occur in Devonian and Carboniferous reservoirs, are primarily characterized by pristane/phytane ratios between one and two, and abundant diasteranes. Within Group B, two subgroups are distinguished on the basis of the C23/C30 terpane ratio. Low values of the tricyclic terpane/pentacyclic terpane ratio distinguish oils in Group Bi, and may reflect a mixture of oils derived from Group A and Group Bii sources. Group C oils have pristane/phytane ratios of generally less than one, a predominance of even over odd numbered n-alkanes, and a low abundance of diasteranes (ibid.). Other features are also characteristic of each of the families of oils.

The geochemistry of these families of oils suggests a distinctive source for each of the three major groups. The presence of diasteranes in Group A and Group B oils suggests the presence of clay minerals in the source rock, and the pristane/phytane ratios of Group B are consistent with deposition of the source rock at the base of an oxidized water column. In contrast, the source rocks of Group C oils were deposited in a setting virtually devoid of clay minerals, lying at the base of an anoxic water column.

OILS FROM THE HUMMINGBIRD FIELD

Three oil samples from different producing zones in the Hummingbird Field were examined (Table 32.1). Sample numbers 556, 553, and 551 are from the Mission Canyon (Ratcliffe Beds), Bakken and Birdbear formations, respectively. Both the saturate and aromatic hydrocarbon fractions of the oils with boiling points greater than 210°C were examined by capillary column gas chromatography (GC) and gas chromatography — mass spectometry (GC-MS). Significant characteristics of the oils are listed in Table 32.2. Saturate fraction gas chromatograms (Figure 32.1) and mass to charge (M/Z)" 217 cross scans of the steroidal alkanes (Figure 32.2, Table 32.3) accompany Table 32.2.

The gas chromatograms of the normal alkane fractions of all three oils (Figure 32.1) show that the complete range of carbon number compounds are present in normal relative abundances, indicating that none are biodegraded to any great extent. The differences in density and solution gas ratio that characterize the physical properties of these oils mirror variations in the composition of the oils through a broad range of compounds.

The oil from the Ratcliffe zone, sample number 556, is distinguished from the two other oils by its low pristane/phytane and high nC17/pristane ratios (Table 32.2). A similar distinction is apparent in the ratio of rearranged steranes to regular steranes (Tables 32.2 and 32.3, Figure 32.2). The oils from the two lower zones, sample numbers 553 and 551, have high pristane/phytane ratios and lower nC17/pristane ratios; however, the Birdbear zone oil has a distinctive predominance of odd numbered n-alkanes in comparison to a slight even number predominance exhibited by the Bakken zone oil. A distinction between the Birdbear and Bakken zone oils is also indicated by the ratios of rearranged to regular steranes and the 20S/20R ratio, and clearly displayed by the ratio of tricyclic to pentacyclic terpanes.

The carbon number distribution amongst the steranes is similar for all three oils; there is a slight predominance of C29 steranes over the C27.

Table 32.1 Oil samples from Hummingbird Field, southeast Saskatchewan

Lab #	Location	Producing Depth	Producing Zone
556	11-26R-002-19W2	1876 – 1904 m	Mission Canyon (Ratcliffe Beds)
553	05-26B-002-19W2	2223 – 2229 m	Bakken
551	10-26B-002-19W2	2309 – 2318 m	Birdbear

Table 32.2 Composition and character of oils from GC and GC-MS

	#556	#553	#551
Pristane/Phytane	0.72	1.03	1.20
nC_{17}/Pristine	2.26	1.31	1.34
Even-Odd Predominance (n-alkanes)	even	slightly even	odd
$\%C_{27}$ sterane[1]	39	30	35
$\%C_{28}$ sterane[1]	15	20	16
$\%C_{29}$ sterane[1]	45	50	49
rations of diasteranes[2] to regular steranes	0.37	0.77	1.51
20S/20R steranes[3]	1.09	0.83	1.01
ratio of tricyclic to pentacyclic terpanes[4]	0.41	0.21	0.08
Oil Group	"C"	"Bil"	"Bi"

[1] ratio of peaks 14:17:23 (Fig. 2, Table 3)
[2] ratio of peak 6:13 (Fig. 2 Table 3)
[3] ratio of peak 20:23 (Fig. 2, Table 3)
[4] ratio of C_{23} tricyclic terpane to 17α(H)-hopane (from m/z 191 chromatograms by GC-MS, not illustrated in this paper).

Table 32.3 Peaks identified in m/z 217 traces (Fig. 32.2)

2	C_{21} sterane
3	C_{21} sterane
5	C_{22} sterane
6	13β(H), 17α(H)-diacholestane (20S)
7	13β(H), 17α(H)-diacholestane (20R)
10	5α(H), 14α(H), 17α(H)-cholestane (20S)
11	5α(H), 14α(H), 17α(H)-cholestane (20R)
12	24-ethyl-13β(H), 17α(H)-diacholestane (20S)
13	5α(H), 14β(H), 17β(H)-cholestane (20S)
14	5α(H), 14α(H), 17α(H)-cholestane (20R)
15	24-ethyl-13β(H), 17α(H)-diacholestane (20R)
16	24-methyl-5α(H), 14α(H), 17α(H)-cholestane (20S)
17	24-methyl-5α(H), 14β(H), 17β(H)-cholestane (20R)
18	24-methyl-5α(H), 14α(H), 17α(H)-cholestane (20S)
19	24-methyl-5α(H), 14α(H), 17α(H)-cholestane (20R)
20	24-ethyl-5α(H), 14α(H), 17α(H)-cholestane (20S)
21	24-ethyl-5α(H), 14β(H), 17β(H)-cholestane (20R)
22	24-ethyl-5α(H), 14β(H), 17β(H)-cholestane (20S)
23	24-ethyl-5α(H), 14α(H), 17α(H)-cholestane (20R)

INTERPRETATION

Following the grouping of families of oils proposed by Brooks et al. (in progress), the three oils produced from the Hummingbird Field can be assigned to Groups B and C. The oil from the Mission Canyon zone, sample number 556, is assigned to Group C and the other two oils to Group B. This distinction is evident in the pristane/phytane ratios of the two groups and consistent with the other geochemical characteristics of the oils from these pools. The low pristane/phytane ratio of the Ratcliffe zone oil suggests that this oil is the product of a source rock deposited at the base of an anoxic water column. The pristane/phytane ratios of the Bakken and Birdbear oils suggest that the dominant contribution to these oils is from a source, or sources, deposited at the base of a more oxidized water column, or, since these values are still relatively low, that the environment of deposition varied from oxidizing to reducing. The pristane/phytane values of the Bakken and Birdbear oils are also completely consistent with a fully mature oil.

The ratios of rearranged to regular steranes are controlled by the presence of clays in the depositional environment of the source rock. The extent to which the diasterane rearrangement reaction proceeds is inferred to be controlled by acid clay catalysis (Rubinstein et al., 1975; Sieskind et al., 1979). The low ratio of this parameter for the Mission Canyon Formation zone oil suggests the virtual absence of clays from the depositional environment of the source rock for these oils. The other two oils have more abundant diasteranes, indicating a greater abundance of clays in the depositional environment of their sources.

The ratio of 20S/20R steranes for all three oils is near unity. This suggests that all three oils are thermally mature (Mackenzie et al., 1980). The carbon number distribution of the steranes for all three oils implies that all are derived from sources composed of Type II marine organic matter (Huang and Meinschein, 1979).

Although the oils from the Bakken and Birdbear zones are generally similar, they are distinguished by the ratio of tricyclic to pentacyclic terpanes. Brooks et al. (in progress) observe that low values of this ratio occur in all oils from Group A (Ordovician reservoirs) and some oils from Group B (oils in Devonian and Carboniferous reservoirs with pristane/phytane greater than one). Group B oils with low

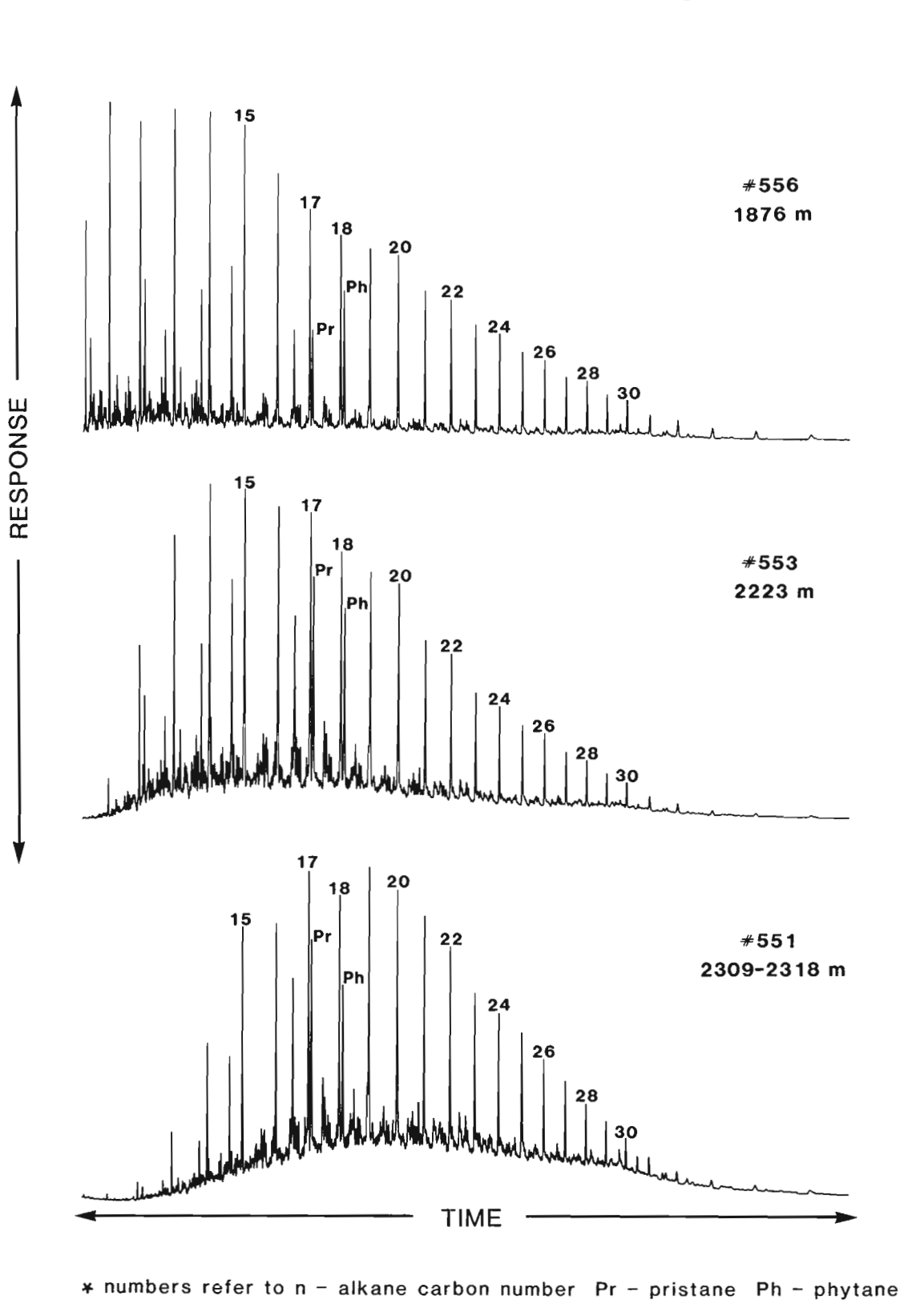
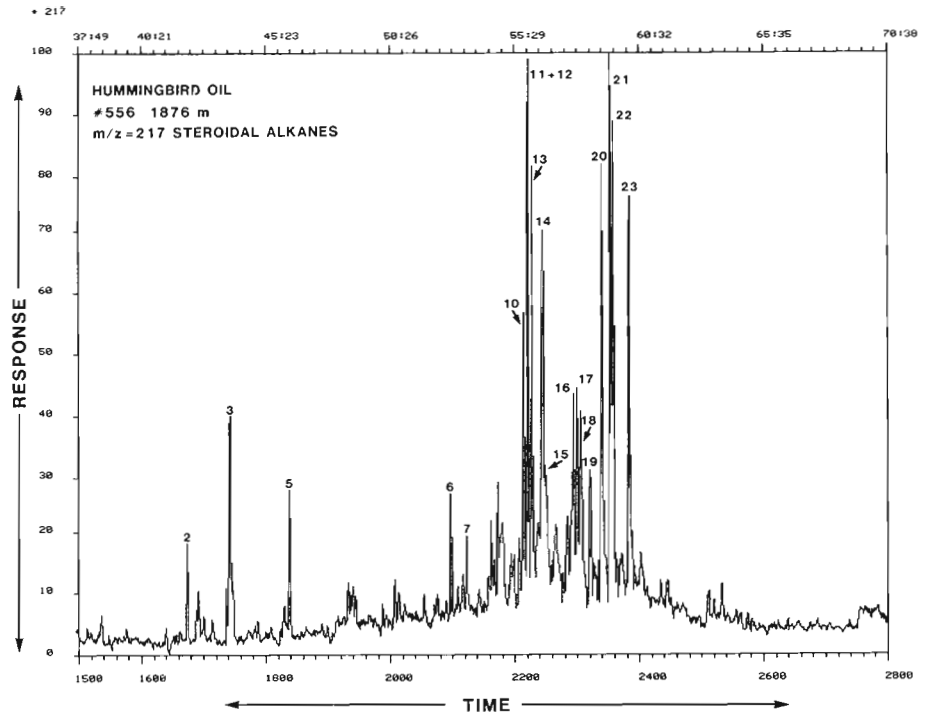
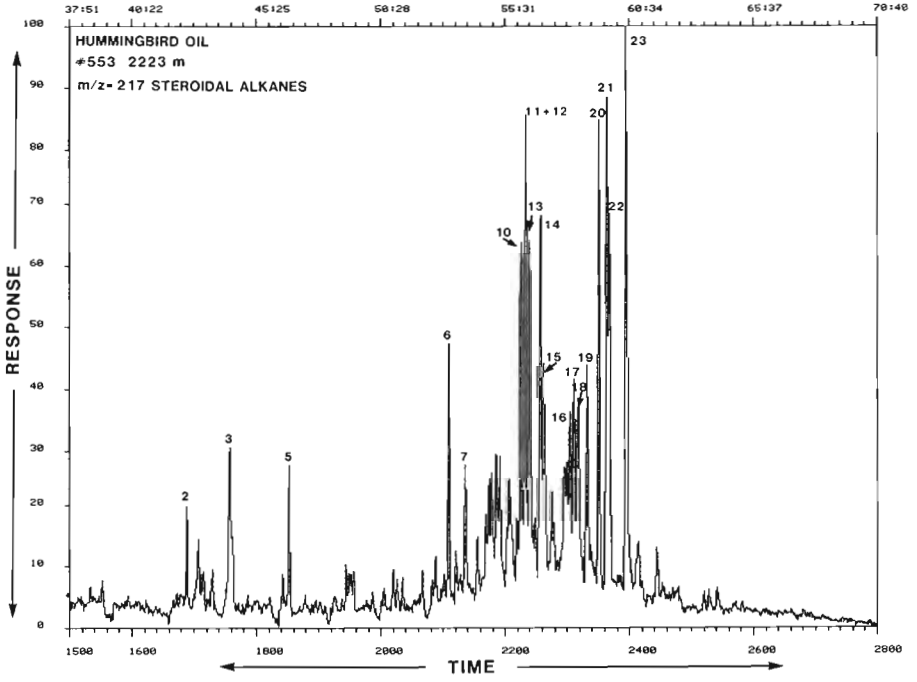


Figure 32.1. Saturate fraction gas chromatograms for oils from the Hummingbird Field.





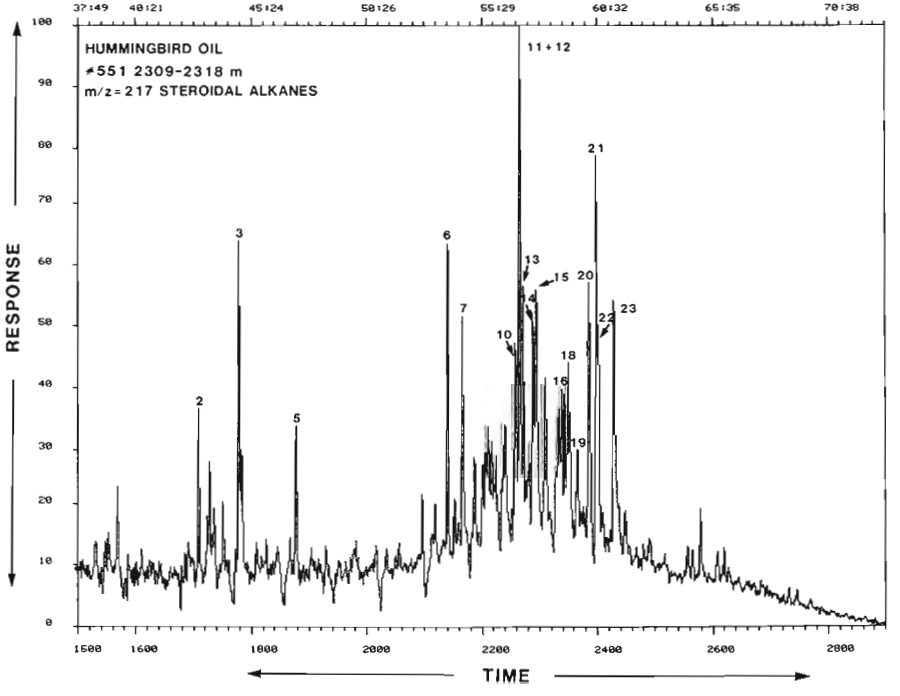


Figure 32.2. Mass chromatograms for Steordal alkanes (m/2 217) by GC-MS analysis of the oils from the Hummingbird Field. Peak identifications are given in Table 32.3.

values of the terpane ratio were assigned to a subgroup Bi. The Birdbear zone oil belongs to this group, and the Bakken zone oil belongs to subgroup Bii (Table 32.2).

The compositional distinctions amongst the three families of oils in the Hummingbird Field are significant and are largely attributable to profound differences in the depositional environment of the source rocks for each family of oils. The distinctions between the Group B and Group C oils, for example, are so great that it is clear that separate sources were responsible for each group of oils. Group C oils were derived from a clay poor, "carbonate", source deposited at the base of an anoxic water column. The source rocks of Group B oils contain significant clay minerals deposited under less reducing conditions. Brooks et al. (in progress) suggest that Group Bi oils may be the result of a possible mixture of oils from Group Bii and Group A because of their low tricyclic to pentacyclic terpane ratios, and that oils in this group may represent a mixture of Group Bii and Group A oils. However, if this were the case, it would be expected that the n-C17/ pristane values of Group Bi oils would be lower than those observed. Thus, a separate source for Group Bi oils cannot at this time be excluded.

Two and possibly three sources have contributed to the oils in the Hummingbird Field, a conclusion generally consistent with those of Williams (1974) and Meissner, et al. (1984) who suggest that potential source rocks in the Winnipeg (Ordovician), Bakken (Devonian and Carboniferous) and Tyler (Carboniferous) formations are the most significant potential sources for oils in the Williston Basin. Oils examined for this study have yet to be definitively correlated to source rocks. Potential sources may be among those previously attributed source rock potential by Osadetz and Snowdon (1986a, b). However, the character of the oils in the Hummingbird Field allows some comment regarding the potential source rocks that have been identified to date. All of the potential source rocks mentioned above are fine clastic rocks in which clay minerals are abundant. Such sources would be expected to produce oils with high ratios of rearranged steranes to regular steranes. This possibly precludes these sources from consideration as a source of the Mission Canyon Formation zone oil. The other oils in the Hummingbird Field could be derived from clastic source rocks, though the actual source also remains to be identified.

CONCLUSIONS

Three producing zones are present in Carboniferous and Devonian strata of the Hummingbird Field in southeast Saskatchewan. None of the oils are biodegraded, and observed differences in the composition and physical properties of these oils are a reflection of their derivation from two and possibly three source rocks of distinctive composition and differing depositional environment. Although the source rocks of these oils remain to be identified, it is clear that the composition of the oils in the Ratcliffe beds of the Hummingbird Field makes it unlikely that they originated in the shales commonly considered to be the source rocks of oils in southeast Saskatchewan.

ACKNOWLEDGMENTS

The authors appreciate the collection and donation of oils from southeast Saskatchewan for this study by the Saskatchewan Geological Survey, and thank J. Christopher and L. Kim Kreis for arranging their delivery. This project was set up under the guidance of the O.E.R.D. 6.1.1., Government-Industry Review Committee, and the authors are grateful for this assistance.

REFERENCES

Fuzesy, L.M.
1973: The Geology of the Mississippian Ratcliffe Beds in south-central Saskatchewan; Saskatchewan Department of Mineral Resources, Report no. 163, p. 63.

Huang, W.Y. and Meinschein W.G.
1979: Sterols as ecological indicators; Geochimica and Cosmochimica Acta, v. 43, p. 739-745.

Mackenzie, A.S., Patience, R.L., Maxwell, J.R., Vandenbrouke, M. and Durand, B.
1980: Molecular parameters of maturation in the Toarcian shales, Paris Basin, France – 1. changes in the configuration of acyclic isoprenoid alkanes, steranes and triterpanes; Geochimica and Cosmochimica Acta, v. 44, p. 1709-1721.

Meissner, F.F., Woodward, J., and Clayton, J.L.
1984: Stratigraphic relationships and distribution of source rocks in the greater Rocky Mountain region; in Hydrocarbon source rocks of the greater Rocky Mountain region, J. Woodward, and J.L. Clayton (eds.); Rocky Mountain Association of Geologists, Denver, p. 1-34.

Osadetz, K.G. and Snowdon, L.R.
1986a: Petroleum source rock reconnaissance of southern Saskatchewan; in Current Research, Part A, Geological Survey of Canada, Paper 86-1A, p. 609-617.
1986b: Speculation on the petroleum source rock potential of portions of the Lodgepole Formation (Mississippian) of southern Saskatchewan; in Current Research, Part B, Geological Survey of Canada, Paper 86-1B, p. 647-651.

Rubinstein, I., Sieskind, O. and Albrect, P.
1975: Rearranged sterenes in a shale: occurrence of simulated formation; Journal of the Chemical Society, Perkin Transactions I, p. 1833-1835.

Sieskind, O., Joly, G. and Albrecht, P.
1979: Simulation of the geochemical transformation of sterols: superacid effect of clay minerals; Geochimica and Cosmochimica Acta, v. 43, p. 1675-1679.

Saskatchewan Energy and Mines
1983: Reservoir Annual 1982; Saskatchewan Energy and Mines, Petroleum and Natural Gas, Miscellaneous Report 83-1.

Smith, D.G. and Pullen, J.R.
1967: Hummingbird structure of southeast Saskatchewan; Bulletin of Canadian Petroleum Geology, v. 15, no. 4, p. 468-482.

Williams, J.A.
1974: Characterization of oil types in Williston Basin; American Association of Petroleum Geologists, Bulletin, v. 58, no. 7, p. 1243-1252.

Interpretation of dipmeter logs of the Lower Cretaceous Cutbank Sandstone, Mannville Group, southern Alberta

Project 820033

Indranil Banerjee
Institute of Sedimentary and Petroleum Geology, Calgary

Banerjee, I., Interpretation of dipmeter logs of the Lower Cretaceous Cutbank Sandstone, Mannville Group, southern Alberta; in Current Research, Part A, Geological Survey of Canada, Paper 87-1A, p. 337-348, 1987.

Abstract

In a small area in southern Alberta (Townships 2 to 6, Ranges 16 to 19 W4) nine dipmeter logs of the crossbedded Cutbank Sandstone, the basal unit of the Lower Cretaceous Mannville Group, have been interpreted in terms of stratification types based on a model constructed from a study of thirty cores of the sandstone in the area.

Validity of the model was demonstrated in two cored wells with dipmeter logs. In an uncored well, stratification types inferred from dipmeter patterns corresponded well with those in a cored well 3.1 km away. Azimuths from arrow plots of the nine logs were used to construct rose diagrams from which paleocurrent directions were obtained. Implications of this paleocurrent pattern in terms of the existing sedimentation model (north-flowing braided stream) of the Cutbank Sandstone have been discussed. The validity of the method used in this study should be further tested in future studies involving dipmeter interpretation of crossbedded sandstones.

Résumé

On a interprété neuf diagraphies réalisées avec un pendagemètre dans une région de petite étendue du sud de l'Alberta (cantons 2 à 6, rangs 16 à 19 WA) à l'intérieur du grès de Cutbank, à stratification oblique, qui constitue l'unité basale du groupe de Mannville (Crétacé inférieur), en fonction des types de stratification qu'indique un modèle élaboré d'après l'étude de trente carottes de forage obtenues dans le grès de la même région.

On a démontré la validité du modèle grâce à des prélèvements de carottes dans deux puits de sondage, et à des diagraphies avec pendagemètre. Dans un autre puits où l'on n'a prélevé aucune carotte de sondage, les types de stratification déduits de la configuration indiquée par le pendagemètre correspondaient bien à ceux observés dans un autre puits exploré par carottage situé à 3,1 km de distance. On a employé les azimuts indiqués par les représentations sagittales des neuf diagraphies pour construire des roses de fréquences, d'après lesquelles on a évalué les directions des paléocourants. On a discuté des implications que pouvait avoir la configuration des paléocourants pour le modèle existant de sédimentation du grès de Cutbank (cours d'eau anastomosé s'écoulant vers le nord). On doit mettre encore à l'épreuve la validité de la méthode employée dans cette étude, lors d'études futures basées sur l'interprétation des mesures faites avec le pendagemètre dans des grès à stratification oblique.

INTRODUCTION

In subsurface studies, dipmeter logs may be used in undeformed areas as sedimentological tools for the interpretation of facies and paleocurrent patterns (Selley, 1978; Schlumberger Limited, 1981). Care must be taken to determine the nature of the planar surfaces measured by the dipmeter. In areas of good core control, the nature of various stratification types found in the formation to be studied should be investigated in detail prior to any dipmeter interpretation. Dipmeter logs of cored intervals are also necessary to show which dipmeter pattern corresponds to which stratification type, so that all interpretations can be made with reasonable confidence.

Such an exercise is presented in this paper. Nine dipmeter logs of the Cutbank Sandstone (also called Taber Sandstone) in southern Alberta form the basis of the study. In two wells, cores of the required interval are also available and a third well can be precisely correlated with a nearby (3.1 km away) cored well. The study area covers twenty townships (Fig. 33.1) and thirty cores of the Cutbank Sandstone in this area have been examined for a basic understanding of the stratification in this formation.

There are no published reports of dipmeter interpretations of the Cutbank Sandstone. However, in northeastern Alberta, in the Fort McMurray area, Muwais (1985) made environmental interpretations, using dipmeter data, of the stratigraphically equivalent McMurray Formation. Muwais' was a broader study because the Cutbank Sandstone is thinner (10-35 m) and environmentally more simple (fluvial) than the McMurray Formation (50 m thick; tidal channel, intertidal mud flats, prograding shoreline). The emphasis of this study, therefore, is on the recognition of individual stratification types rather than on migration and stacking of channels.

FACIES OF THE CUTBANK SANDSTONE

The stratigraphy of the study area is illustrated in Figure 33.2. The Cutbank Sandstone is a 10 to 35 m thick, regionally extensive stratigraphic unit that extends from Montana in the U.S.A. (Glaister, 1959; Hopkins, 1985) to southern Alberta in Canada (Hayes, 1986) where it constitutes the basal unit of the Lower Cretaceous Mannville

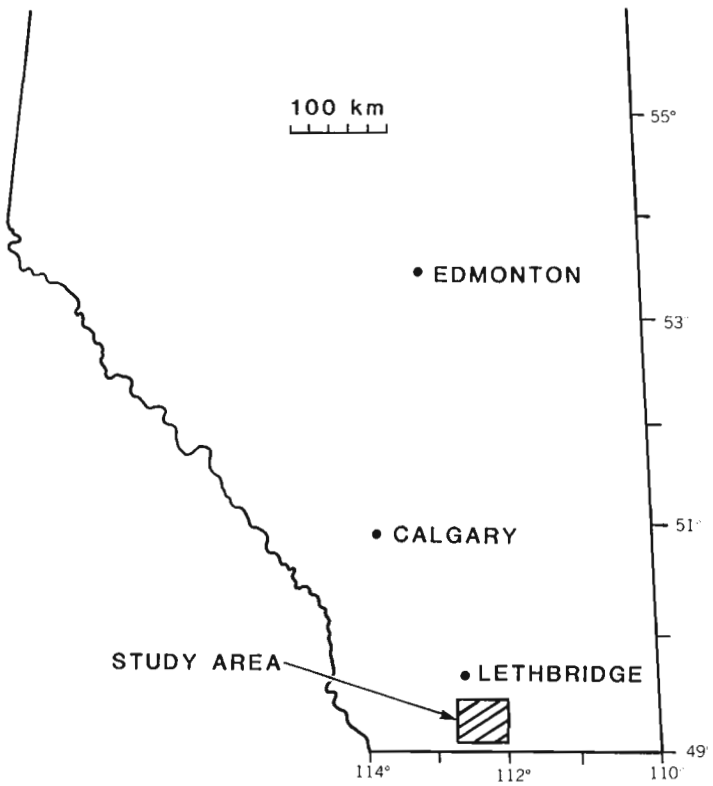


Figure 33.1. Location of the study area. The nine dipmeter logs studied come from Townships 2, 3, 6 and Ranges 16, 17, 18, and 19, west of the fourth meridian.

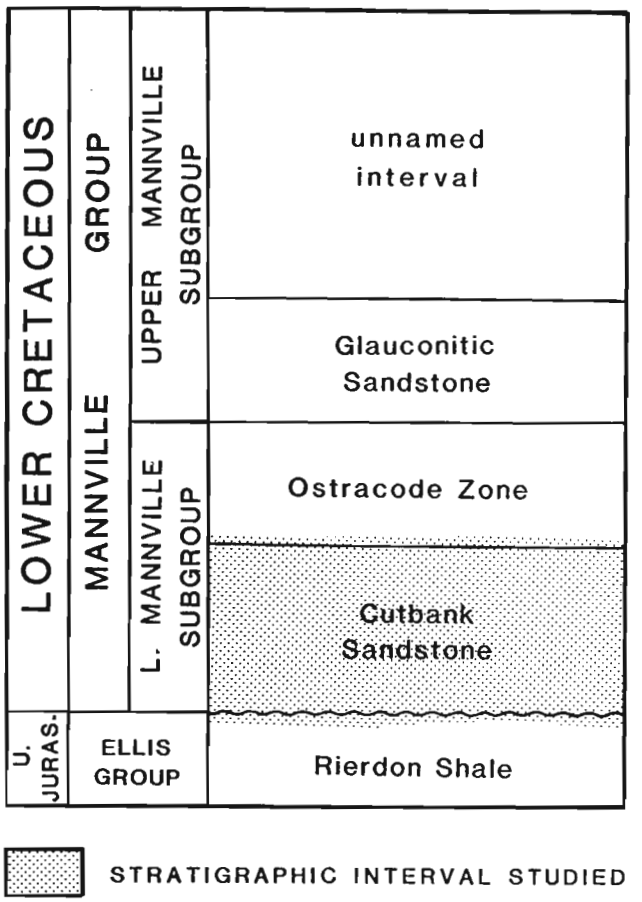


Figure 33.2. Stratigraphy of the study area. Dipmeter patterns of the two units adjacent to the Cutbank Sandstone have been examined only briefly to emphasize their differences from it.

Group. It overlies a regional unconformity at the base of the Mannville. The Rierdon Shale, an Upper Jurassic marine shale unit, lies below the unconformity in the study area (Fig. 33.2). Regional facies analysis of the Cutbank Sandstone has revealed the existence of two contrasting facies (Banerjee, in press):

1. Channel Facies: This is a sandstone unit, 10 to 35 m thick, dominated by a medium grained, crossbedded sandstone containing several shale-pebble conglomerates. There is an overall trend of upward decrease in grain size and a decrease in the scale of cross-stratification. Individual sedimentary units recognized both from gamma-ray log patterns and core lithology are 2 to 3 m thick, scour-based sandstones, with a basal parallel-bedded mudclast layer overlain by cross-stratified units decreasing in set thickness from 30 to 35 cm at the base to 5 to 6 cm at the top (Fig. 33.3). This facies occupies north-, or north-northwest-trending, 10 to 20 km wide linear zones.

2. Interchannel Facies: Between belts of channel facies occur extensive areas of fine grained, sandstone/mudstone facies. The sandstone is ripple-laminated, contorted, bioturbated or structureless. Primary structures have been affected by bioturbation and liquefaction, either destroying them completely or leaving isolated lenses of ripple-laminated sandstones.

Dipmeter logs studied here have all been chosen from the channel facies of the Cutbank Sandstone because only this facies contains well-defined primary stratification.

BASIC STRATIFICATION TYPES

From a study of 30 cores located within the study area or closely adjacent to it, the following summary of various stratification types in the Cutbank channel facies has been prepared.

Genetically, the stratification types belong to three categories of bedforms: ripples (small-scale cross-stratification measured in centimetres), megaripples (large- scale cross-stratification measured in decimetres), and flat beds (parallel stratification). Ripples are either climbing, descending or truncated by stoss side erosion (Fig. 33.3a, b, c). Megaripples are truncated by erosional planes (Fig. 33.3d). Flat beds are marked either by parallel stratification (F in Fig. 33.3e) in medium to coarse grained sandstone (rare) or by concentration of parallel-aligned (P in Fig. 33.3e) discoidal mudclasts (common).

Because dipmeter logs record true dip angles, an effective way of grouping the stratification types is according to their steepness. Such a classification into three groups of inclination (1. 0°-10°; 2. 11°-20°; and 3. 21°-35°) is shown in Figure 33.4, which also lists the origin of each stratification type and its value as a paleocurrent indicator. Group 1 is not a paleocurrent indicator; Group 2 is a fair one (only the erosional truncation planes within this group could possibly be steeper than 10° but none has been encountered in this study); and Group 3 is an excellent one.

LOG EXPRESSION OF STRATIFICATION

A dipmeter detects planar discontinuities in a rock unit by continuous conductivity measurements at closed intervals (0.2 inches apart). The channel facies of the Cutbank Sandstone studied here contains little clay. Possible causes of minute conductivity contrasts between strata in the otherwise homogeneous Cutbank Sandstone unit have been surmised from a study of cores. These are:

1. Concentration of flat-lying mudclasts on subhorizontal scoured surfaces (Fig. 33.3e).
2. Mud clasts aligned parallel to lee slope, in megaripples (Fig. 33.3d).
3. Thin muddy or organic-rich layer along stoss or lee slopes in ripples (s, l in Figure 33.3a, b).
4. Grain size variation along slip faces of megaripples (G in Figure 33.3d) producing subhorizontal layers.
5. Differences in packing of grains and consequently of porosities in different avalanched layers in the slip faces of megaripples (Hunter, 1977; Fig. 33.3d).

Features 1 and 3 are illustrated in core photographs a, b and e in Figure 33.5. Feature 5 is dramatically illustrated by colour banding of oil-soaked and oil-free sands defining high and low porosity cross-strata in Figure 33.5d.

Another major constraint in the dipmeter recording of cross-strata is the thinness (~ 20 cm) of cross-stratified units in the Cutbank. The normal "correlation length" (vertical interval over which conductivity logs are matched to identify bedding planes) used is greater than 2 ft (60 cm). Therefore, a typical "blue" pattern (Schlumberger Limited, 1981), namely, a flattening of dips with depth in a concave- upward cross-stratified unit (see Figure 33.3d) will be missed by the instrument. "Blue" patterns, therefore, are not common in the dipmeter logs of the Cutbank Sandstone. Those present are spurious and are caused by some other feature, such as an unconformity.

DIPMETER LOGS

Stratigraphic zonation

Patterns in dipmeter logs may also define different stratigraphic units. A sharp contrast between the "green" pattern (dip remaining constant with depth) of low (2°-6°) northwesterly or northeasterly dips (reflecting the regional structural dip) exhibited by the Rierdon Shale contrasts sharply with the variable dip patterns of the crossbedded Cutbank Sandstone (Figs. 33.6, 33.8). The Ostracode Zone does not show a consistent dipmeter pattern. It may show a "green" pattern with low dips (probably shale as in Figure 33.7) or an anomalous thin zone of high dips (probably a single crossbedded sandstone) as in Figures 33.6 and 33.8.

In Figure 33.6, a 1.5 m thick "blue" pattern zone occurs at the base of the Cutbank, defining a weathered zone on the unconformity surface. The same "blue" pattern defining the unconformity surface occurs in several other logs and is useful in locating the unconformity.

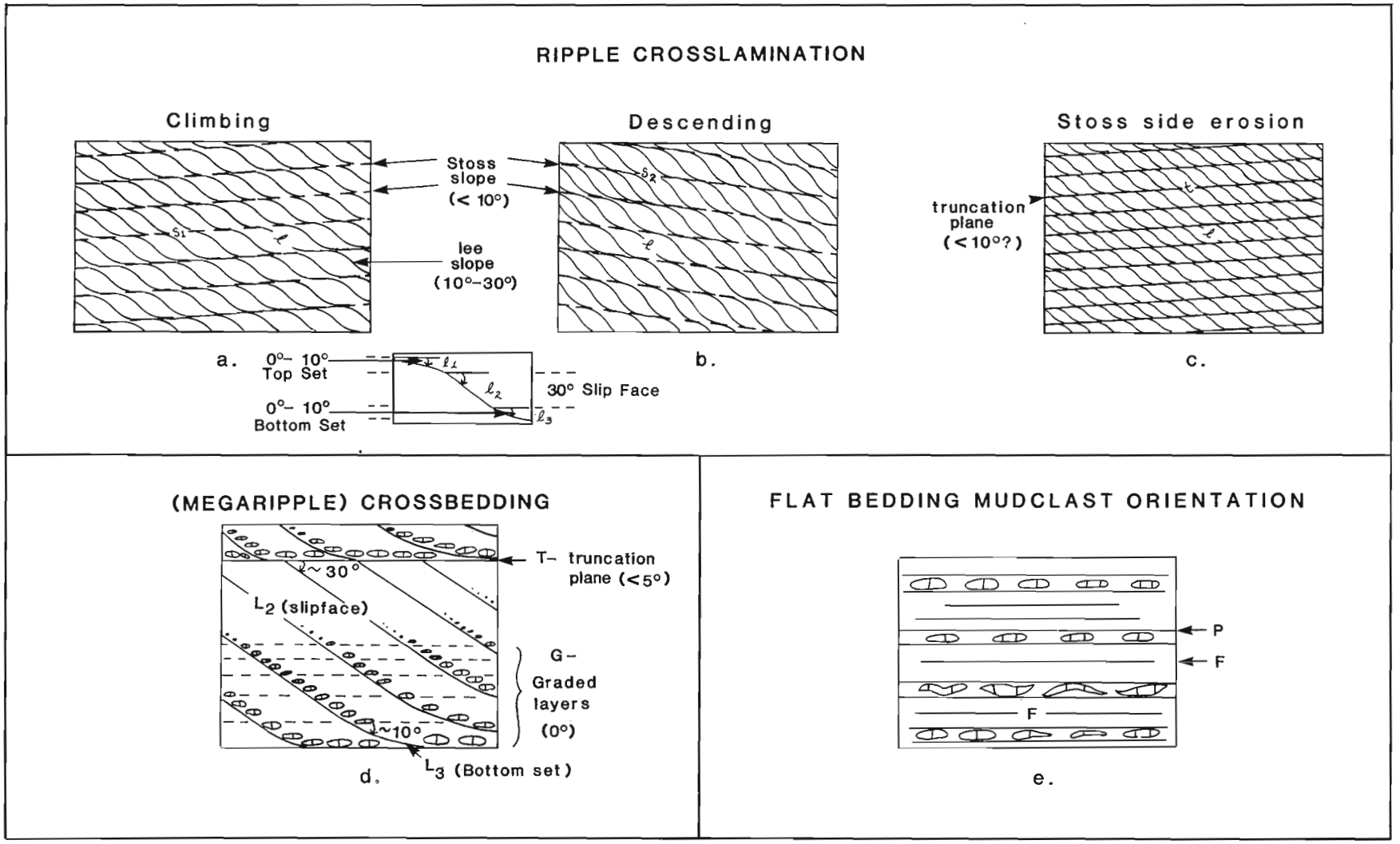


Figure 33.3. Common types of stratification in the Cutbank Sandstone. See explanation in text.

	Inclination	Origin	Paleocurrent Indicator
Group 1	0-10°	Erosional truncation planes (T,t)	NO
	0-2°	Grain-size variation across cross-stratification (G)	NO
	0-2°	Mudclast layers (P)	NO
	0-2°	Upper flow regime flat bed (rare) (F)	NO
	0-10°	Bottomset of ripple (ℓ_3) or megaripple (L_3)	YES
	5-10°	Stoss slope of ripples — climbing (s_1)	YES (upcurrent)
		Stoss slope of ripples — descending (s_2)	YES
Group 2	11-20°	Upper and lower part of ripple foreset (ℓ_1, ℓ_3)	YES
	11-20°	Lower part of megaripple foreset (L_3)	YES
	11-20°	Erosional truncation planes (rare) (t,T)	NO
Group 3	21-35°	Slipface in the middle of ripple foreset (ℓ_2)	YES
		Slipface near the top of megaripple foreset (L_2)	YES

Figure 33.4. Classification of stratification according to inclination, origin and value as paleocurrent indicator. Letters t, T . . etc. refer to those in Figure 33.3.

Dipmeter logs with cored intervals

Figure 33.6 shows a dipmeter log of the Cutbank Sandstone together with the lithology of the cored interval. Matching each dipmeter pattern with a stratification type identified in the core, five zones were erected, each typified by a stratification type (coded by a symbol used in Figure 33.3) and an azimuth. Overall, the unit shows a "fining-upward" trend and an upward decrease in the scale of cross-stratification. A persistent southeasterly dipmeter reading is recognized.

Figure 33.7 illustrates a short cored interval of another well (11-6-6-16W4). The crossbedded zone in this core (zone 2, Fig. 33.7) has 10 to 20 cm thick sets of cross- strata with an average inclination of 18° to 20°, but the dipmeter has only recorded dips of up to 12°. The broad 'red pattern' or steepening of dips with depth shown by zone 2 is probably spurious, consisting in fact, of short segments of both "blue" and "red" patterns.

The well (12-19-6-16W4) shown in Figure 33.8 does not have a cored interval but can be correlated with a cored well (8-35-6-16W4) 3.1 km north-northeast of it. The detailed correlation shown in Figure 33.8 has been done with the help of gamma-ray, resistivity and dipmeter logs as well as core lithology. Basic sedimentation units seen in Figure 33.8 (left), which typify the Cutbank Channel facies, are 2 to 3 m thick, cross-bedded sandstones with a basal mudclast layer overlying a scoured surface. Figure 33.8 (right), indicates paleocurrents that were oriented between the northeast and north-northwest.

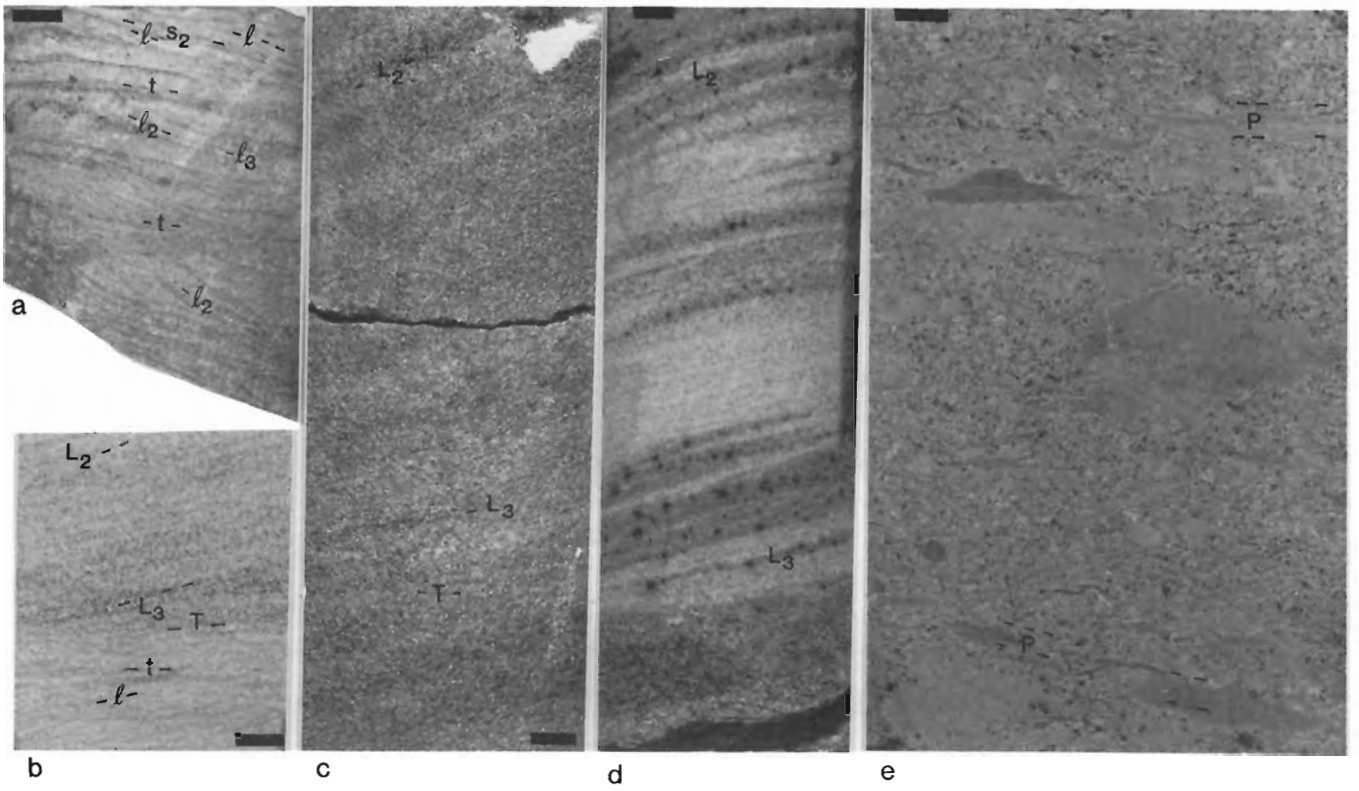


Figure 33.5. Core photographs illustrating different stratification types in the Cutbank Sandstone. Bar represents 1 cm.

a) Ripple crosslamination (descending and stoss side erosion). Letters s, l, t . . . refer to stratification types illustrated in Figure 33.3. Compare with Figure 33.3b, c. Location of photograph shown in Figure 33.6.

b) Crossbedding overlying ripple crosslamination. Grain size variation along foresets has produced a graded bed (subhorizontal). Note flattening of foresets (from L2 to L3) toward the base. Location of photograph shown in Figure 33.8 (left).

c) Crossbedding showing flattening of foresets (L_2 to L_3) toward the base. Location of photograph shown in Figure 33.6.

d) Crossbedding emphasized by oil-stained (dark) and oil-free foresets indicating differences in porosity between layers. Location of photograph shown in Figure 33.8 (left).

e) Stratification caused by alignment of flat mudclasts (see Fig. 33.3e). Inclination varies from 1° to 10°. Location of photograph shown in Figure 33.7.

Dipmeter logs without cored interval

With the background information obtained from the cored wells, the gamma-ray and dipmeter logs in a well without cores have been interpreted in terms of basic lithology or stratification types (Fig. 33.9). A reconstructed lithology column shown on the right of the gamma-ray log illustrates the interpretation. An anomalously high dip (marked X) may represent a fracture zone. Data from this log suggest three major paleocurrent directions — north, southeast and southwest. Data from five more dipmeter logs of uncored wells were utilized in paleocurrent studies to be discussed next.

PALEOCURRENT AND PALEOGEOGRAPHY

The Cutbank Sandstone has been interpreted as a braided river deposit (Hradsky and Griffin, 1984; Hopkins, 1985; Hayes, 1986; Ryer et al., 1983) deposited by a system of north-flowing streams. The various paleocurrent directions suggested by the dipmeter logs of the cross-stratification may now be integrated to see how much of the data is consistent with this regional paleogeography. Data from the four wells shown in Figures 33.6, 33.7, 33.8 and 33.9 have been used to construct the rose diagrams shown in Figure 33.10, and data from five more wells are shown in Figure 33.11. Stratification types of Groups 2 and 3 are paleocurrent indicators. Azimuths of these two groups from all wells are presented in Figure 33.12a. The pattern shown in Figure 33.12a is approximately trimodal with modes toward the north, southeast and south. A similar pattern was obtained from fifty measurements in the outcrops of the stratigraphically equivalent Cadomin and Lower Gladstone formations in the southern Foothills of Alberta (Fig. 33.12b).

A general paleogeographic reconstruction of the area, based on a facies map to be presented by the author in a

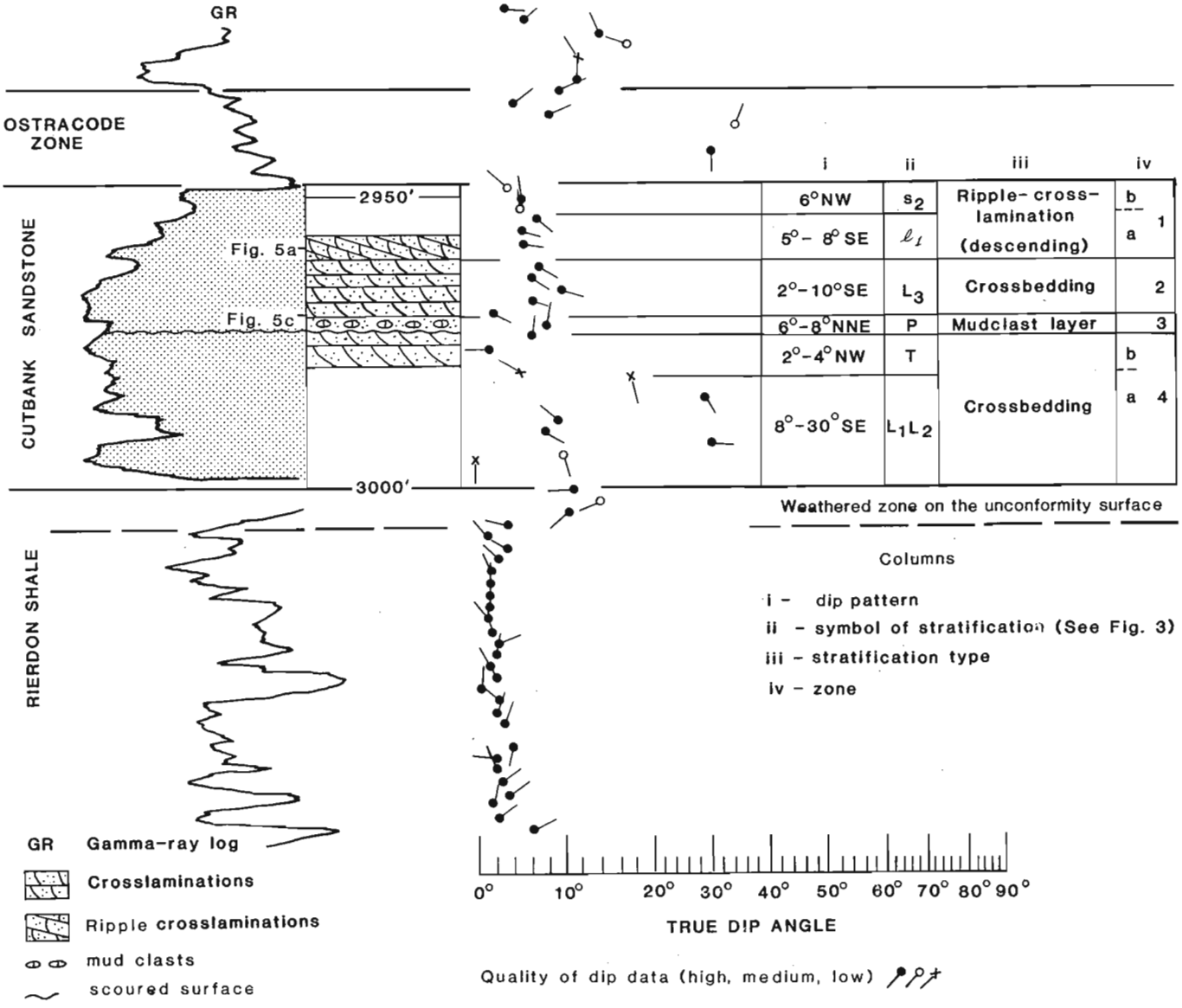


Figure 33.6. Dipmeter log. Gamma-ray log and lithology of the cored interval in well 1-13-3-17W4.

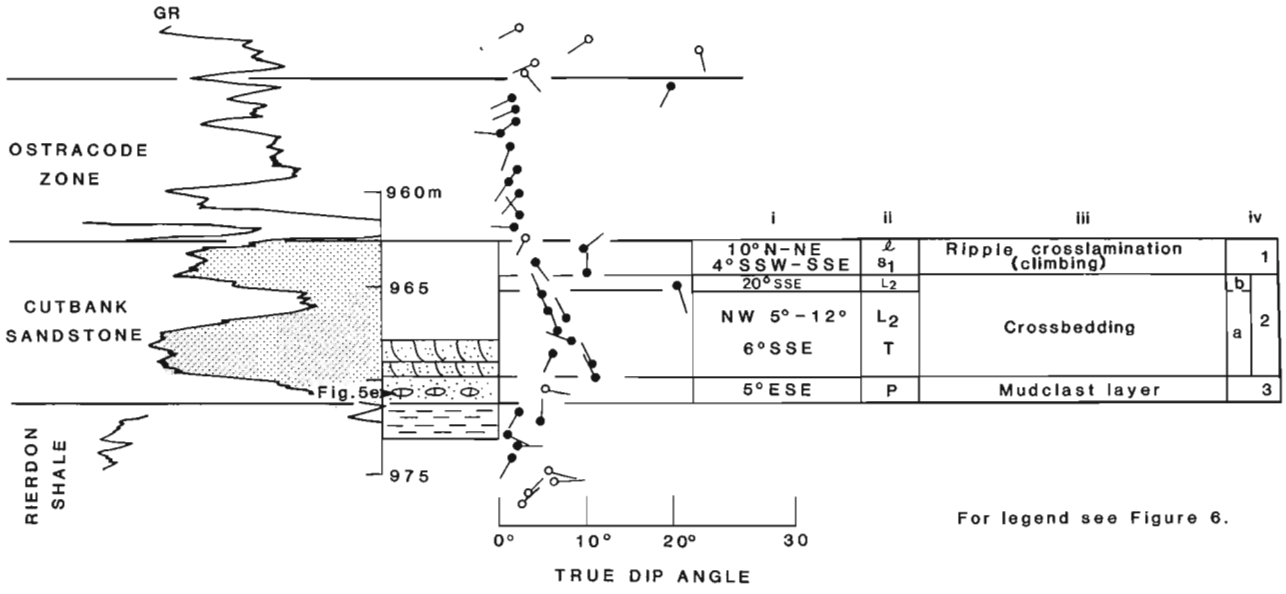


Figure 33.7. Dipmeter log. Gamma-ray log and lithology of the cored interval in well 11-6-6-16W4.

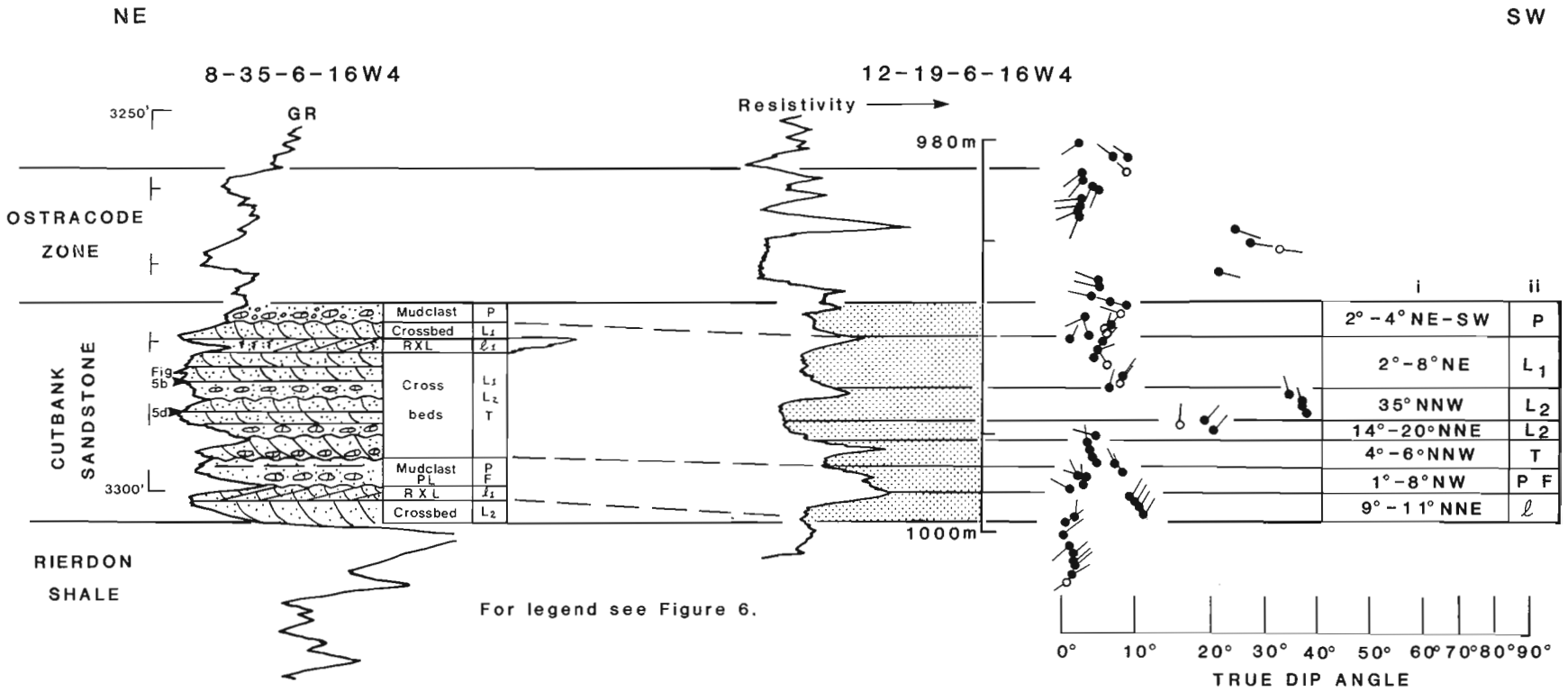


Figure 33.8. Correlation at the sedimentation unit level between a cored and an uncored well.
Right: Resistivity log of well 12-19-6-16W4. 1, 2, 3 . . . basic sedimentation units recognized in the resistivity as well as the dipmeter log.
Left: Gamma-ray log and core lithology of a well 8-35-6-16W4, 3.1 km away from well 12-19-6-16W4. Sedimentation units with different stratification types found in this well can be correlated with those of well 12-19-6-16W4 defined on the basis of dipmeter patterns.

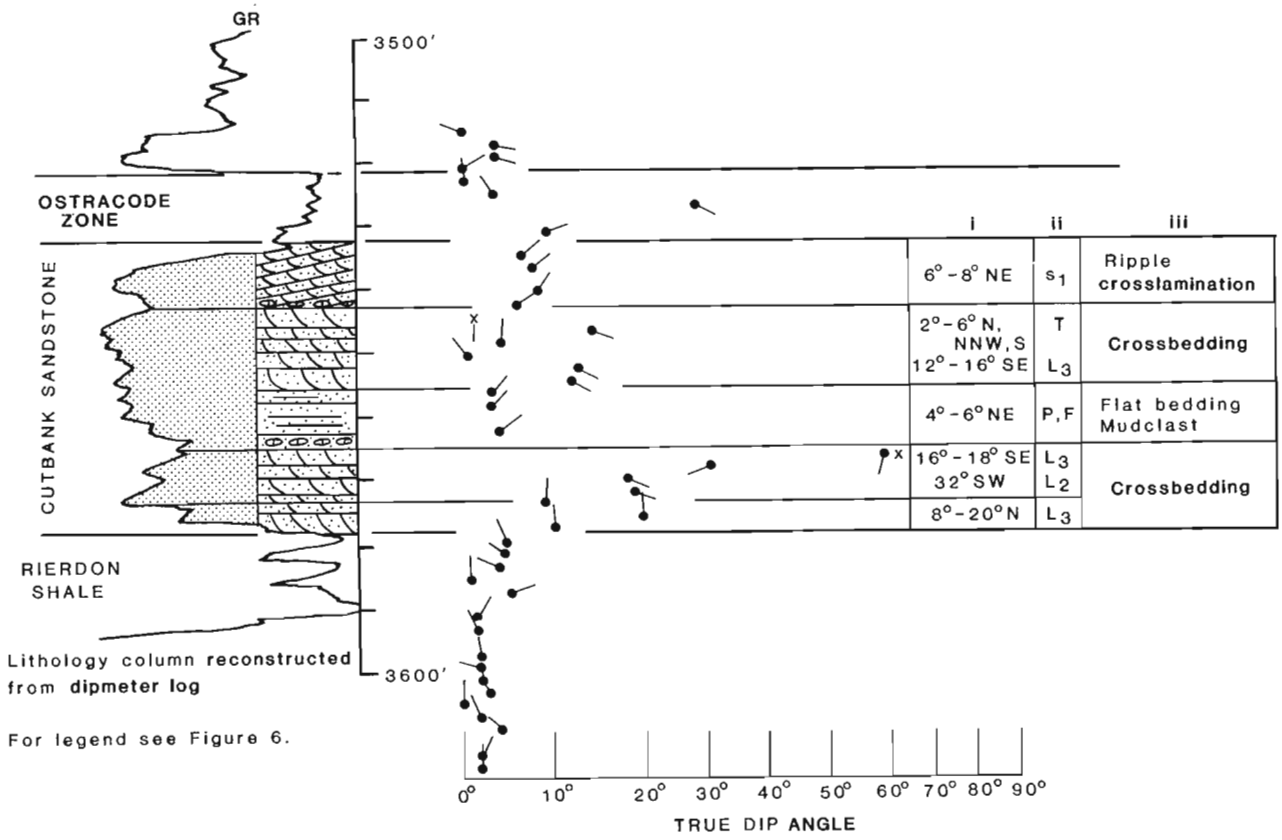


Figure 33.9. Gamma-ray and dipmeter logs of well 14-3-2-19W4 (no cored interval). Zones with distinctive dipmeter patterns coincide with basic sedimentation units 1, 2, 3 . . . recognized in the gamma-ray log.

forthcoming publication (Banerjee, in press) on the stratigraphy and sedimentology of the Cutbank Sandstone, is shown in Figure 33.13. A valley axis has been obtained from subcrop patterns on the paleogeological map of the surface below the Pre-Cutbank unconformity. Facies belts of the channel facies were outlined from core studies. These two sources of information define the course of an ancient river. Paleocurrent modes from four wells (Fig. 33.10) are plotted on this map (Fig. 33.13) to show their relationship with the reconstructed channel pattern. The northerly modes are consistent with the paleogeography but the east-southeast and southeasterly modes are anomalous. There could be several explanations for this:

1. The facies belt consists, not of a single northerly stream, but of a series of coalescing alluvial fans, each with a radial paleocurrent pattern.
2. The southeasterly paleocurrents represent tributaries. This however, seems unlikely, as the acute angle made by such a tributary with the master stream would face upstream (south) instead of downstream as is the usual case here.
3. The presence of variable scale bedforms. At least two hierarchies of bedforms — megaripples and ripples — have been recognized. Smaller bedforms superimposed on a larger one may migrate obliquely, downslope, upslope or alongslope on the lee surface, thus causing a great apparent divergence in paleocurrent directions.

Explanation 2 seems unlikely and explanation 1 lacks two vital pieces of evidence. Firstly, pebbles are rare, and when present, are well rounded, well sorted, and small in size. Secondly, there is no debris-flow deposit. Therefore, the presence of a variable scale of bedforms is a very likely explanation for the divergence in the paleocurrent pattern.

SUMMARY AND CONCLUSIONS

1. In a small area in southern Alberta covering twenty townships, nine dipmeter logs of the Cutbank Sandstone of the Lower Cretaceous Mannville Group have been interpreted in terms of several types of stratification and cross-stratification.
2. A model for these types was erected on the basis of a study of 30 cores of the Cutbank Sandstone.
3. In two wells with cores, dipmeter patterns were verified against stratification types. From these results, stratification types have been inferred from dipmeter patterns in uncored wells.

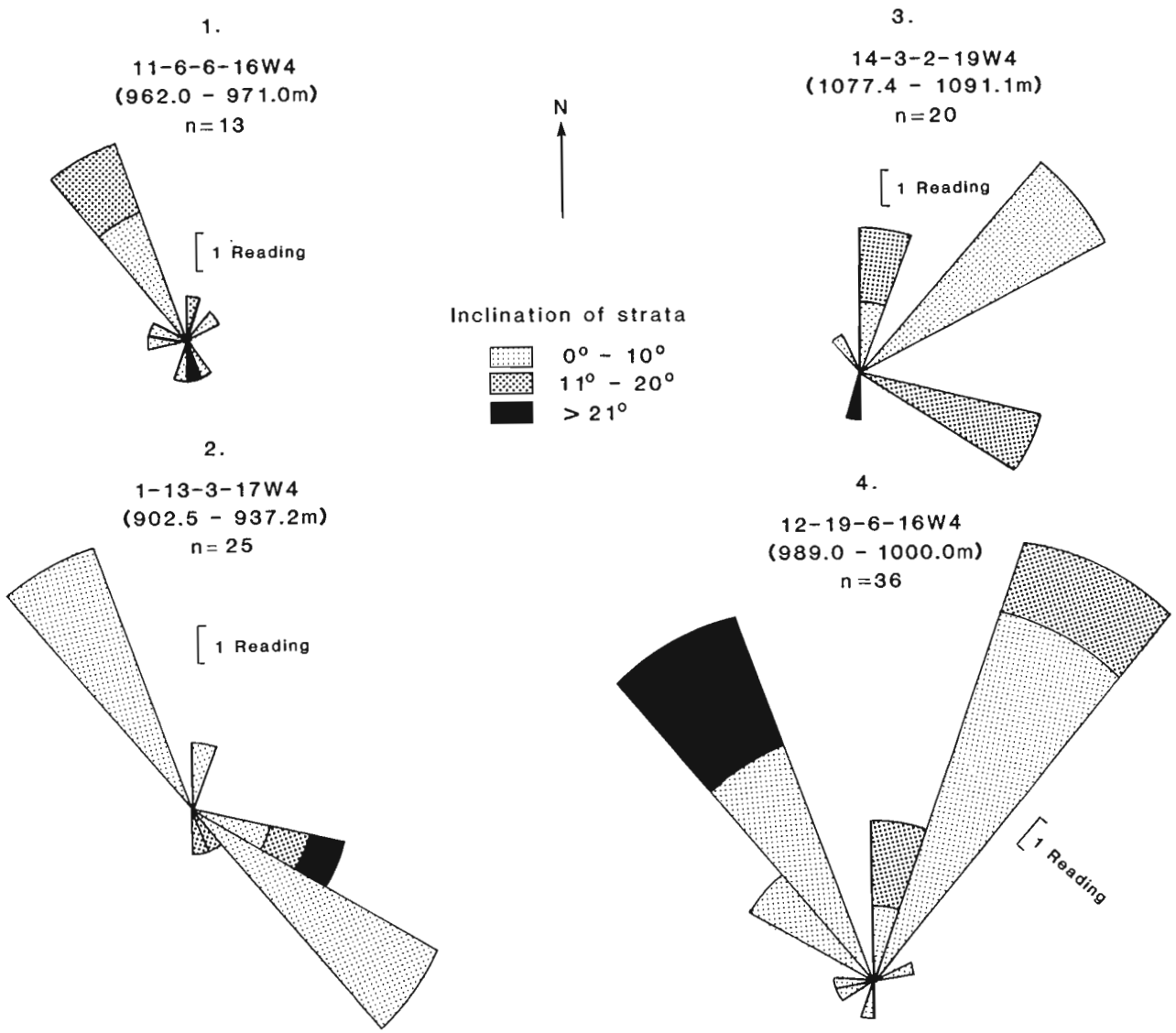
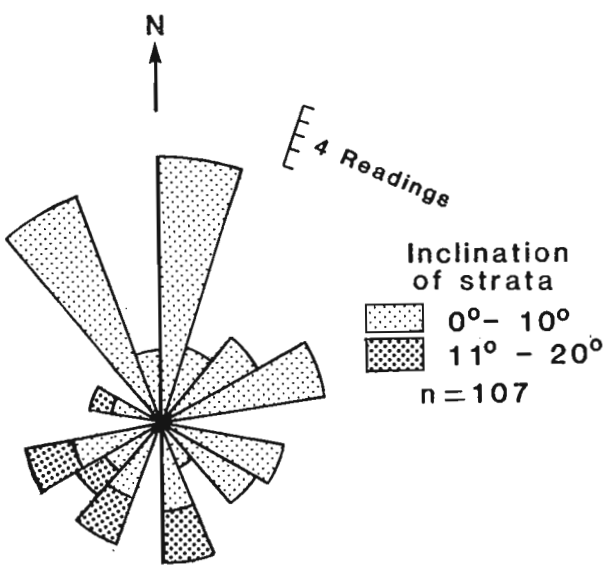


Figure 33.10. Rose diagram of dipmeter arrows in four wells illustrated in Figures 33.6, 33.7, 33.8 and 33.9.



5. 11-18-6-16W4 925 - 930 m
6. 13-19-6-16W4 989 - 1000 m
7. 1-24-6-16W4 937 - 947 m
8. 7-24-6-16W4 967 - 978 m
9. 4-30-6-16W4 991 - 1002 m

Figure 33.11. Rose diagram of combined data of dipmeter arrows from five wells.

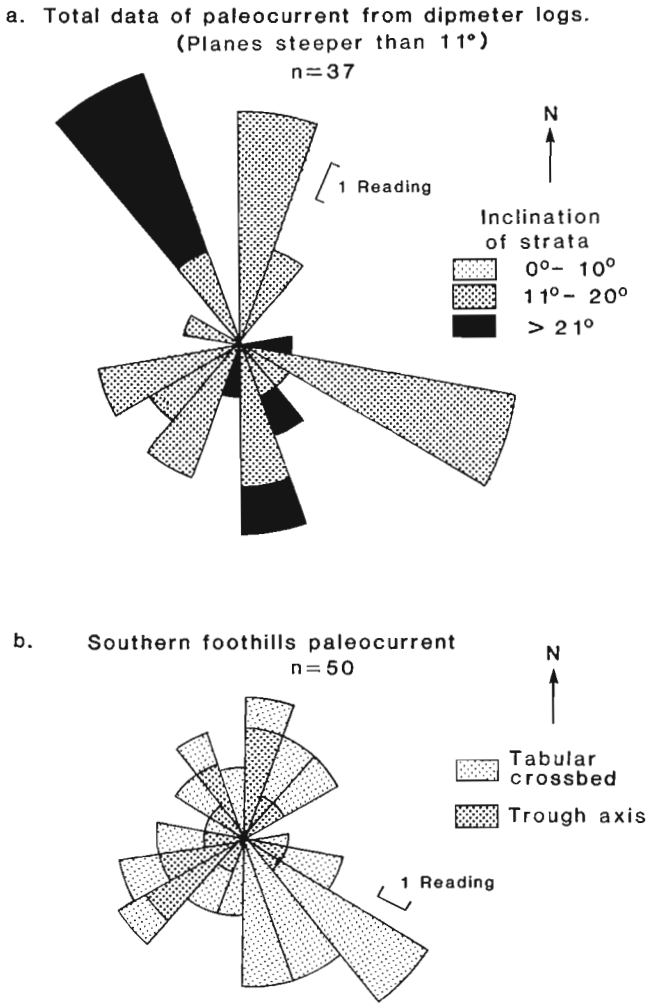


Figure 33.12. a) Rose diagram of paleocurrent indicators (stratification steeper then 10°) from all nine wells. b) Rose diagram for tabular and trough crossbeds in the southern foothills.

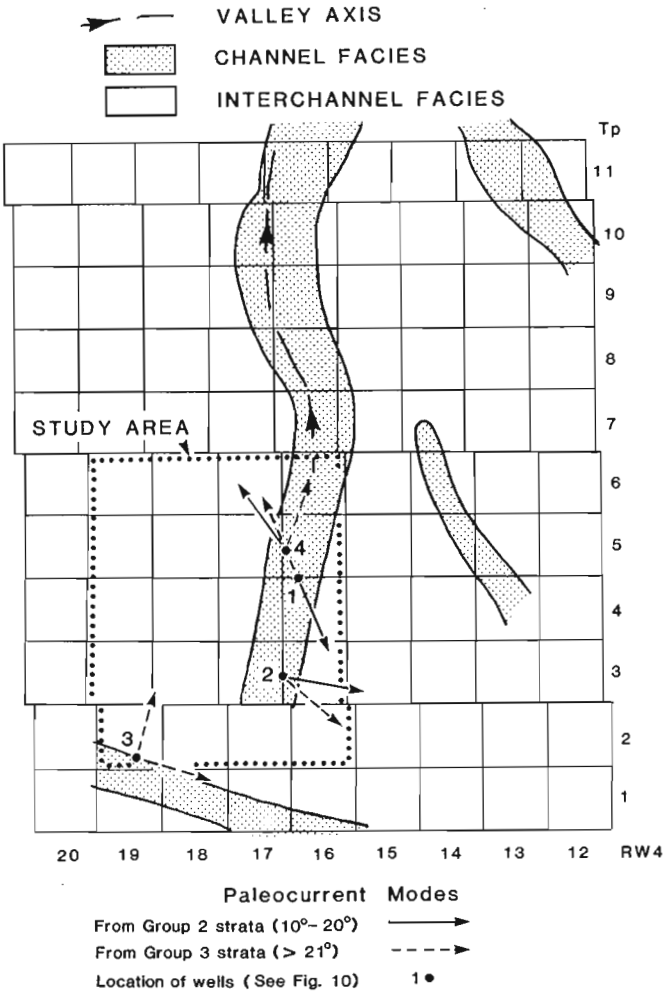


Figure 33.13. Paleocurrent directions derived from dipmeter logs and the facies map of the Cutbank Sandstone in the study area.

4. The scale of cross-stratification in the Cutbank is less than 30 cm, so that the typical "blue" pattern of cross-strata cannot be detected by the dipmeter and should not be present in the dipmeter log. Any "blue" pattern in the dipmeter log, therefore, must be due to some other cause (e.g. unconformity) or may be treated as spurious.
5. Inferred paleocurrents from the dipmeter interpretation have been used for paleogeographic analysis.
6. The methodology used in this study may be followed in similar subsurface studies of crossbedded sandstones.

REFERENCES

Banerjee, I.
in press: Lower Mannville sedimentation in southeastern Alberta; Geological Survey of Canada, Paper 85-99.

Glaister, R.P.
1959: Lower Cretaceous of southern Alberta and adjoining areas; American Association of Petroleum Geologists, Bulletin, v. 43, p. 590-640.

Hayes, B.J.R.
1986: Stratigraphy of the Basal Cretaceous Lower Mannville Formation, southern Alberta and north-central Montana; Canadian Society of Petroleum Geologists, Bulletin, v. 34, p. 30-48.

Hopkins, J.C.
1985: Channel-fill deposits formed by aggradation in deeply scoured, superimposed distributories of the Lower Kootenai Formation (Cretaceous); Journal of Sedimentary Petrology, v. 55, p. 42-51.

Hradsky, M. and Griffin, M.
1984: Sandstone body geometry, reservoir quality and hydrocarbon trapping mechansims in Lower Cretaceous

Mannville Group, Taber/Turin area, southern Alberta; in The Mesozoic of Middle North America, D.F. Stott and D.J. Glass (eds.); Canadian Society of Petroleum Geologists, Memoir 9, p. 401-411.

Hunter, R.E.
1977: Basic types of stratification in small eolian dunes; Sedimentology, v. 24, p. 361-388.

Muwais, W.K.
1985: Application of dipmeter measurements for interpreting McMurray Formation depositional environments (abs.); *in* General Programme, 36th Annual Technical Meeting; The Petroleum Society of Canadian Institute of Mining and the Canadian Society of Petroleum Geology. Edmonton, June 1985, p. 70.

Ryer, T.A., Horne, J.C., and Hayes, M.O.
1983: Aggradational valley-fill model for strata of Cretaceous Lower Mannville Formation, south-central Alberta (abs.); in The Mesozoic of Middle North America, D.F. Stott and D.J. Glass (eds.); Canadian Society of Petroleum Geologists, Memoir 9, p. 562.

Schlumberger Limited
1981: Dipmeter Interpretation Volume 1 - Fundamentals; Schlumberger Limited, New York, 61 p.

Selley, R.C.
1978: Concepts and methods of subsurface facies analysis; Education Course Notes Series, No. 9; American Association of Petroleum Geologists, 85 p.

Amorphous kerogen: bituminite in the Second White Speckled Shale, southern Saskatchewan

Project 780003

F. Goodarzi and L.D. Stasiuk[1]
Institute of Sedimentary and Petroleum Geology, Calgary

Goodarzi, F. and Stasiuk, L.D., Amorphous kerogen: bituminite in the Second White Speckled Shale, southern Saskatchewan; in Current Research, Part A, Geological Survey of Canada, Paper 87-1A, p. 349-352, 1987.

Abstract

Bituminite is a common component of the amorphous kerogen fraction in the Upper Cretaceous Second White Speckled Shale, southern Saskatchewan. Reflectance in oil of bituminite varies considerably and ranges from approximately 0.10 per cent to 1.2 per cent. Frequency distribution of bituminite reflectance is skewed toward the high reflectance region for samples from a borehole from southwest Saskatchewan; whereas the frequency distribution for samples from a borehole from southeast Saskatchewan is skewed toward the low reflectance region. Type III kerogen or vitrinite reflectance for samples from both boreholes is near 0.27% Roil, suggesting that the shale interval is thermally immature. The variation in bituminite reflectance is probably related to depositional or very early diagenetic processes rather than thermal degradation. Preliminary results also suggest that the predominance of a high reflecting bituminite population tends to coincide geographically with areas of natural gas production (i.e. southwest Saskatchewan).

Résumé

La bituminite est un constituant courant de la fraction kérogène amorphe contenue dans le schiste argileux secondaire mouchetée de blanc (Crétacé supérieur) que l'on rencontre dans le sud de la Saskatchewan. Dans le pétrole, la réflectance de la bituminite varie considérablement, et se situe approximativement entre 0,10 % et 1,2 %. La distribution de fréquence que montre la réflectance de la bibuminite est biaisée vers la région des hautes réflectances, dans le cas d'échantillons provenant d'un trou de sondage pratiqué dans le sud-ouest de la Saskatchewan; tandis que la distribution de fréquence, dans le cas d'échantillons provenant d'un trou de sondage du sud-est de la Saskatchewan, est biaisée vers la région des basses réflectances. La réflectance du kérogène de type III ou de la vitrinite dans le cas d'échantillons prélevés dans les deux trous de sondage, se rapproche de 0,27 % Roil, ce qui suggère que l'intervalle de l'argile litée est caractérisé par une immaturité thermique. La variation de la réflectance de la bituminite est probablement liée aux processus de sédimentation ou de diagenèse initiale, plutôt qu'à la dégradation thermique. Les résultats préliminaires suggèrent aussi que la prédominance d'une population de bituminite à forte réflectance tend à coïncider géographiquement avec les zones de production de gaz naturel (par exemple, dans le sud-ouest de la Saskatchewan).

[1]Department of Geology – Energy Research Unit, University of Regina, Regina, Saskatchewan S4S 0A2

INTRODUCTION

Exploration for hydrocarbon accumulations using geological, geophysical and geochemical data has been supplemented in recent years with organic petrology studies of stratigraphically and structurally associated potential source rocks. Using methods such as vitrinite (Type III kerogen) reflectance, and fluorescent spectral analysis defining λ max and red/green quotient (Q), organic petrologists are able to determine the thermal maturity of a potential hydrocarbon source rock. The level of thermal maturity combined with optical analysis defining the type of organic matter provide an insight as to whether a potential source rock is prone to liquid or gas hydrocarbon generation.

Thermal maturity levels equivalent to Type III kerogen reflectance between 0.50% and 1.30% Roil are considered to be within the liquid hydrocarbon generation stage or "oil window" for hydrogen-rich organic matter (Monnier et al., 1981; Teichmüller, 1982). A Type III kerogen reflectance of 1.30% to 1.40% Roil and the extinction of visible kerogen Type I and II fluorescence indicate the beginning of condensate and gas generation. Snowdon and Powell (1982) have recognized significant thermogenic gas generation from sediments with Type III kerogen reflectance levels as low as 0.60% Roil. Gas generation ceases between reflectances of approximately 2.0% to 3.0% Roil (Robert, 1971; 1980).

The kerogen or dispersed organic components of sedimentary rocks are characterized by organic petrologists on the basis of optical properties such as fluorescence under ultraviolet light, per cent reflectance under normal white light, and morphology. Generally, kerogen can be classified into four types (Table 34.1).

Within each type category variations exist, and thus further subdivisions of each kerogen type can be made. One example is amorphous kerogen, which is a common component of organic-rich sediments such as oil shales.

The origin of amorphous kerogen is generally assumed to be biodegraded phytoplanktonic, zooplanktonic and in some instances humic and liptinitic components (Mukhopadhyay et al., 1985a). Mukhopadhyay et al. (1985b) determined through chemical analysis that bituminite in Tertiary sediments of offshore India was derived from microbially degraded algae or from the bacterial bodies themselves.

ACKNOWLEDGMENTS

Appreciation is extended to T.H. Gentzic, L.R. Snowdon and K.G. Osadetz, Institute of Sedimentary and Petroleum Geology, for project collaboration and for critically reviewing the manuscript. Thanks are extended to J. Potter and L.W. Vigrass, Energy Research Unit, University of Regina, and N.J. McMillan, Institute of Sedimentary and Petroleum Geology, for initiating the study of organic petrology in the Mesozoic of Saskatchewan.

Table 34.1. The four main kerogen types, related terminologies and origin (from Brooks, 1981, Fig. 7).

Origin	Terminologies					
Aquatic	Liptinite	Type I	Algal / Amorphous (Sapropel)	Amorphous	Amorphous debris	Exinite
Terrestrial	Exinite	Type II	Herbaceous		Structured Plant Debris	Vitrinite
	Vitrinite	Type III	Woody	Humic		
	Inertinite	Type IV	Coaly / Inertinite			Inertinite

CURRENT INVESTIGATION

A recent study of the organic petrology and thermal maturation of Mesozoic sediments in Saskatchewan has encountered abundant amorphous kerogen in the Upper Cretaceous Second White Speckled Shale. The organic-rich nature of this shale was first noted by Tyrrell (1892) in the region of the Manitoba escarpment. Goodman (1951) described the shale as including flattened bituminous streaks, insoluble in ordinary solvents, but susceptible to distillation upon heating.

Several recent studies have centered around assessing the potential of the Second White Speckled Shale as an oil shale resource (Macauley, 1984a, 1984b; Macauley, Snowdon and Ball, 1985).

A common amorphous component in the Second White Speckled Shale has been identified and defined as bituminite Type III. This type of kerogen was first described by Teichmüller and Ottenjann (1977) from the Posidonia shale of West Germany. In the Second White Speckled Shale, bituminite commonly comprises the dominant organic component (trace – 15% of the volume). It is generally wispy and elongate, with a granular to pitted, moderately homogeneous surface exhibiting a reflectance of 0.10 per cent to 1.20 per cent (Fig. 34.1a, b). This type of bituminite rarely shows fluorescence under ultraviolet excitation. Uncommonly, low reflecting varieties (<0.20% Roil) of bituminite fluoresce brown to dark brown with λ max ranging from 580 to 600 nm and R/G quotients of 0.80 to 1.0 (Fig. 34.2). Lack of a specific morphology, and 'Schlieren' type autochthonous bedding are characteristic features of bituminite in the Second White Speckled Shale. In samples where foraminifera are present, a close association between the bituminite and the nannoplankton is evident.

A single sample of the shale can contain forms of bituminite with highly variable reflectances (i.e. 0.10-1.20% Roil), but, as a rule, a single population of either very low reflecting (<0.40% Roil), or high reflecting (0.60-1.20% Roil) bituminite is dominant. This situation is illustrated by the histograms in Figure 34.3. High reflecting bituminite is dominant in samples from borehole 1-1-5-25W3 in southwest Saskatchewan, whereas the low reflecting variety is dominant in samples from borehole 14-7-3-3W2 in southeast Saskatchewan (Fig. 34.4).

The reflectance in oil of kerogen Type III from the Second White Speckled Shale is 0.27 per cent at a depth of 820 to 856 m in borehole 14-7-3-3W2, and 0.26 per cent at a depth of 889 m to 915 m in borehole 1-1-5-25W3. The level of thermal maturity is far below that conventionally required for the onset of oil generation. Considering the low level of thermal maturity of the Second White Speckled Shale in both boreholes, the variation of % Roil of bituminite and the predominance of either a low reflecting population or high reflecting population (Fig. 34.3) must result from a depositional or very early diagenetic process rather than thermal degradation associated with hydrocarbon generation. The low reflecting bituminite III variety may represent the precursor to a more severely biogenically altered, higher reflecting bituminite III.

Preliminary results suggest that the predominance of a high reflecting bituminite population (0.60-1.2% Roil) in the Second White Speckled Shale tends to coincide geographically with areas of natural gas production (i.e. southwest Saskatchewan). Further investigation into the genesis of the variable varieties of bituminite Type III may establish a relationship between the occurrence of biogenic methane and high reflecting bituminite Type III.

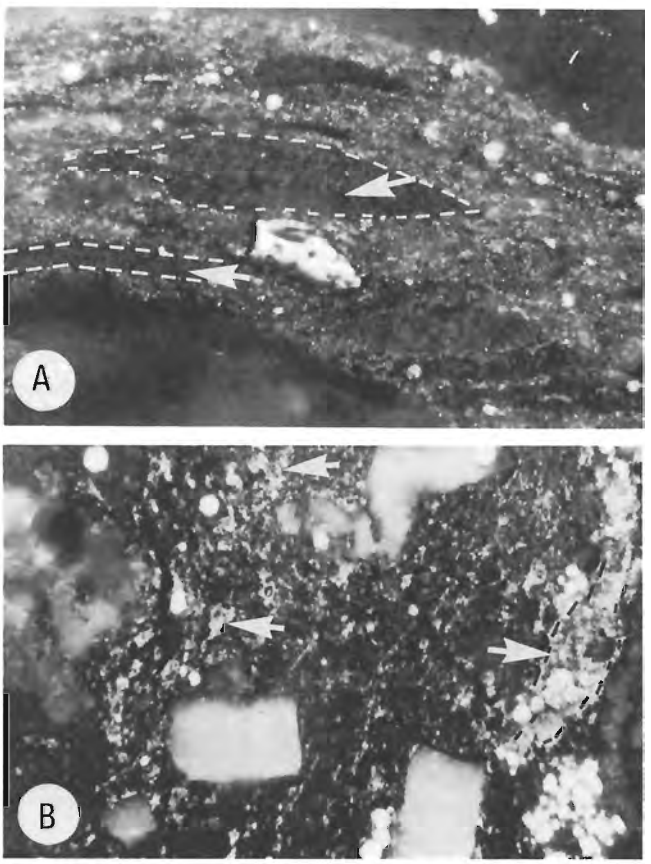


Figure 34.1. Photomicrographs of bituminite Type III; oil immersion, reflected white light, x500.
A. Low reflecting variety of bituminite Type III (indicated by arrow); reflectance in oil, 0.10-0.18%.
B. High reflecting variety of bituminite Type III (indicated by arrow); reflectance in oil, 0.80-1.0%.

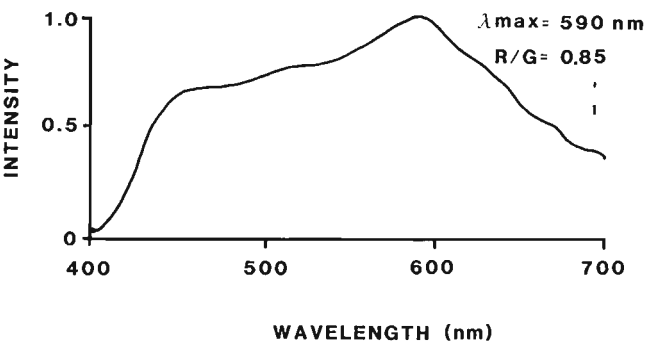


Figure 34.2. Fluorescence spectra of brown fluorescing bituminite Type III.

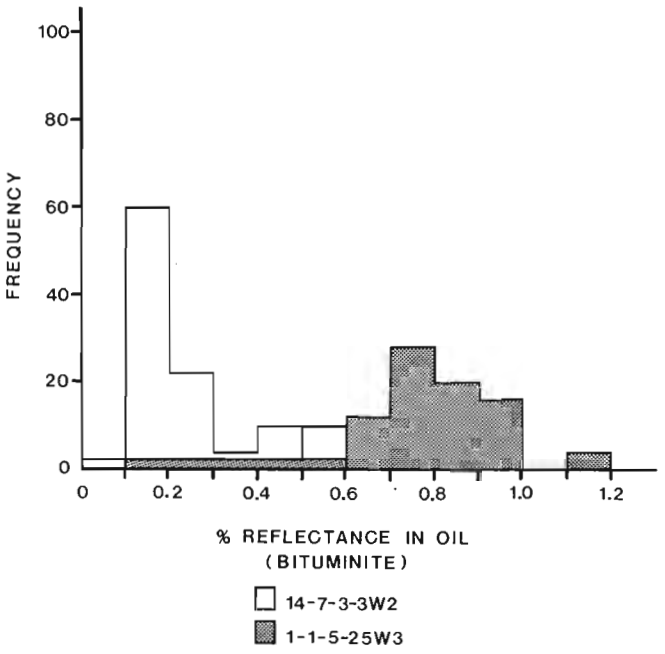


Figure 34.3. Histogram illustrating the frequency distribution of per cent reflectance of bituminite Type III in samples from boreholes 14-7-3-3W2 and 1-1-5-25W3.

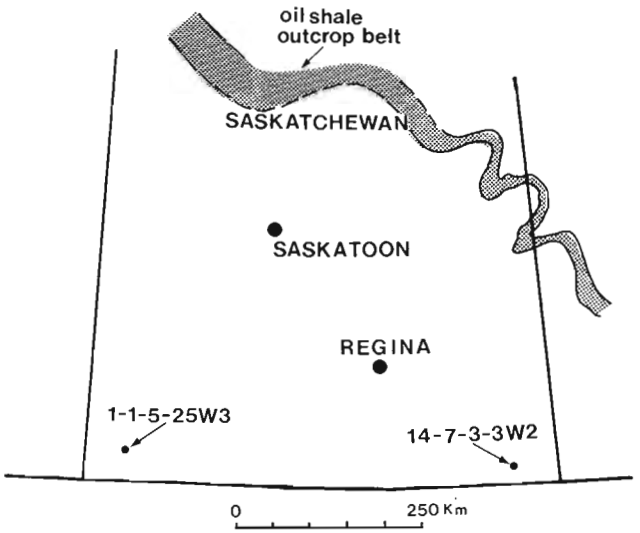


Figure 34.4. Location map of the two boreholes in southern Saskatchewan from which bituminite Type III was observed in the Second White Speckled Shale.

REFERENCES

Brooks, J.
1981: Organic maturation of sedimentary organic matter and petroleum exploration – a review; in Organic maturation studies and fossil fuel exploration, J. Brooks (ed.); Academic Press, London, p. 1-38.

Goodman, A.J.
1951: White specks in Colorado shale; American Association of Petroleum Geologists, Bulletin, v. 35, p. 2427-2433.

Macauley, G.
1984a: Cretaceous oil shale potential of the Prairie provinces, Canada; Geological Survey of Canada, Open File Report no. 977, 61 p.
1984b: Geology of the oil shale deposits of Canada; Geological Survey of Canada, Paper 81-25, 65 p.

Macauley, G., Snowdon, L.R., and Ball, F.D.
1985: Geochemistry and geological factors governing exploitation of selected Canadian oil shale deposits; Geological Survey of Canada, Paper 85-13, 65 p.

Monnier, F., Powell, T.G., and Snowdon, L.R.
1981: Qualitative and quantitative aspects of gas generation during maturation of sedimentary organic matter. Examples from Canadian frontier basins; in Advances in Organic Geochemistry 1981, M. Bjorøy et al. (eds.); John Wiley and Sons Ltd., p. 487-495.

Mukhopadhyay, P.K., Hagemann, H.W., and Gormly, J.R.
1985a: Characterization of kerogens as seen under the aspect of maturation and hydrocarbon generation; Erdól und Kohle, v. 38, p. 7-18.

Mukhopadhyay, P.K., Samanta, U., and Jassal, J.K.
1985b: Origin of oil in a lagoon environment: desmocollinite/bituminite source-rock concept; in Proceedings of 11th International Congress of Carboniferous Stratigraphy and Geology, Illinois, 1979, v. 4, Southern Illinois University Press, p. 753-763.

Robert, P.
1971: Étude pétrographique des matieres organiques insolubles par la mesure de leur pouvoir réflecteur; Contribution à l'exploration pétroliere et à la connaissance des bassins sédimentaires; Revue de l'Institut français du pétrole et annales des combustibles liqûides, v. 26, p. 105-135.
1980: The optical evolution of kerogen and geothermal histories applied to oil and gas exploration; in Kerogen, B. Durand (ed.); Technip, Paris, p. 385-414.

Snowdon, L.R. and Powell, T.G.
1982: Immature oil and condensate – modification of hydrocarbon generation model for terrestrial organic matter; American Association of Petroleum Geologists, Bulletin, v. 66, p. 775-788.

Teichmüller, M.
1982: Stach's textbook of Coal Petrology; E. Stach et al. (eds.); Gebrúder Borntraeger, Berlin, p. 381-413.

Teichmüller, M. and Ottenjann, K.
1977: Art und iagneese von Liptiniten and lipoiden stoffen in eimem Erdölmuttergestein auf Grund fluoreszenzmikroskopisher untersuchangen, Erdöl und Kohle, v. 30, p. 397-398.

Tyrrell, J.B.
1892: North-western Manitoba with portions of the districts of Assiniboia and Saskatchewan; Geological Survey of Canada, Annual Report, 1890-1891, v. 5, pt. 1, Report E.

- 35 -

The relationship between dendographs and Pearson product-moment correlation coefficients

Project 780006

M. Labonté and F. Goodarzi
Institute of Sedimentary and Petroleum Geology, Calgary

Labonté, M. and Goodarzi, F., The relationship between dendographs and Pearson product-moment correlation coefficients; in Current Research, Part A, Geological Survey of Canada, Paper 87-1A, p. 353-356, 1987.

Abstract

The usefulness of the dendograph for representing the results of the comparison of many objects (usually variables) contained in a multivariate data-set is reviewed. This comparison is often conducted by using the formula known as the Pearson product-moment correlation coefficient. The information contained in a correlation coefficient is usually difficult to decipher and thus, in the multivariate situation, a pattern recognition method known as an indexed ascending hierarchical classification such as the dendograph is often used. The graphical depiction produced by the dendograph method permits comparison of a large number of correlation coefficients. These may also be presented in the form of a triangular matrix, and a natural extension of the dendograph method is to plot this triangular matrix under the dendograph itself, an idea originally presented by Valentine and Peddicord (1967).

Résumé

On examine dans quelle mesure l'emploi d'un dendrogramme est utile pour représenter les résultats de la comparaison de nombreux objets (habituellement variables) contenus dans un ensemble de données multivariées. On effectue souvent cette comparaison en employant la formule connue sous le nom de coefficient de corrélation entre le produit de Pearson et le moment. L'information contenue dans un coefficient de corrélation est habituellement difficile à déchiffrer; par conséquent, dans la situation où l'on dispose d'un ensemble de données multivariées, on emploi souvent une méthode de reconnaissance des configurations connue sous le nom de classification hiérarchique ascendante indexée, ou dendrogramme. L'image graphique obtenue par la méthode du dendrogramme permet de comparer un grand nombre de coefficients de corrélation. On peut les présenter sous forme de matrice triangulaire, et une extension naturelle de la méthode du dendrogramme consiste à représenter cette matrice triangulaire au-dessous du dendrogramme lui-même, conception initialement proposée par Valentine et Peddicord (1967).

INTRODUCTION

The "Pearson product-moment correlation coefficient" is a measure of the linear relationship between two observed random variables, X and Y. Variables in a multi-variable situation must therefore be treated in pairs. The results define a square matrix in which the number of rows or columns equals the number of comparisons.

Since comparison of variable A with variable B yields the same results as comparison of B with A, and total colinearity occurs when A and B are identical, the correlation coefficient matrix is symmetrical and the diagonal elements are equal to unity. Thus, both the upper and the lower triangular portions each contain all results.

When we are faced with a large array or correlation matrix, as defined above, we need a way to obtain an overall view. It is not sufficient to examine every correlation coefficient individually and try to deduce the information contained, because a correlation coefficient is not related to the cause of the linear relationship between the two variables being considered; it merely expresses the colinearity between the two variables.

The correlation coefficient can vary between + 1 and -1, the + 1 value indicating a totally positive linear relationship, the -1 a totally negative linear relationship. Numbers between these two extremes, for example zero, cannot be taken to mean that there is no inherent relationship between the two variables — they merely indicate that this relationship is not linear. The correlation coefficient is actually a property of the underlying bivariate distribution.

The correlation coefficient can also be defined as a measure of similarity between two (random) variables. This

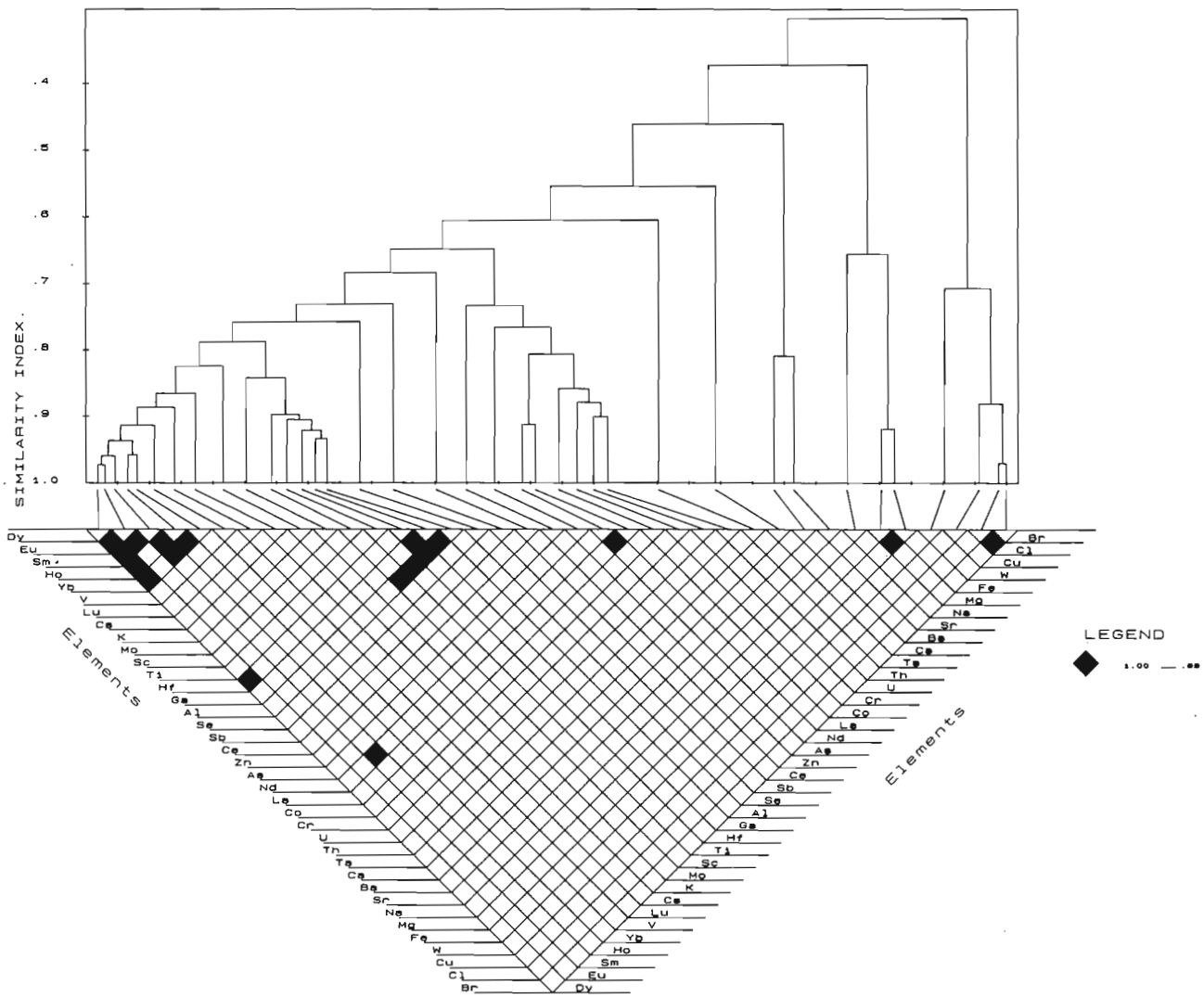


Figure 35.1. Correlation between dendograph and Pearson products for 37 elements in coals.

measure is not a metric (or a distance between two variables) since then two absolutely similar variables would be measuring (no distance) zero instead of unity.

The following two considerations have led us to use the dendograph program:

1. the "non-causality" nature of the correlation coefficient, and
2. the similarity measure approach of the correlation coefficient.

The dendograph is a picture of the process of coalescing progressively less similar objects, which uses as input the presence or absence of similarity between the objects compared in pairs (Labonté and Goodarzi, 1985). The fact that the picture left by the coalescing process in the dendograph program is in turn a cluster analysis leads us to appreciate the importance of the presence and absence of similarity between objects (variables).

The dendograph shows the relationship between elements (Labonté and Goodarzi, (1985)); for example, that of Cesium and Potassium (Cesium is a dispersed element in Potassium-bearing minerals [Mason and Moore, 1985] such as clay). A similar relationship is apparent in coefficient of correlations variables (Fig. 35.1). However, because of the "non-causality" nature of the correlation coefficient, the relationship is expressed in a global fashion involving all the relationships at our disposal, that is, the dendograph.

It is evident that the dendograph is a type of cluster analysis classifying the entire set of variables (or elements), and thus may facilitate the discovery of other relationships. It is in this sense that a dendograph may help resolve the geochemical relationships between a set of elements or, ultimately, the geology of the problem itself (or the geological aspects of it).

Nature of refinements present in the dendograph method

The definition of the dendograph starts with the definition of the dendogram. The dendogram is a tree-like depiction of the results of a clustering process. This 'tree' is plotted on a two dimensional surface. The object names (variables or samples) are spaced evenly along the x axis. The clustering process is based on the magnitude of similarity, starting with the highest order and ending with the lowest. Fusion of objects occurs at levels shown on the y axis, which constitutes a similarity index and which also has annotations that the user can utilize as a reference level to ascertain how many clusters are contained in the dendogram. Thus, the dendogram is cut at a certain level. The dendogram contains only one dimension of information, the y axis, which indicates the level at which objects coalesce or fuse. The dendograph, however, preserves the previous information dimension but also depicts similarities between groups as well as within groups of objects by presenting a group spacing instead of a constant object spacing as is the case in the dendogram method. Thus it achieves another information dimension.

Extension

The dendograph program by R. McCammon (from an article by Valentine and Peddicord (1967)) is complemented by the drawing of the similarity matrix that was used by the program (dendograph) to construct the dendograph.

The extension of the dendograph display to include a subjacent triangular diagram depicting the re-ordered similarity matrix makes obvious the associations (or relationships) of elements utilized to produce the dendograph. Plots of the different correlation values, when ordered by the dendograph method, reveal more patterns in trace-element data (Fig. 35.2).

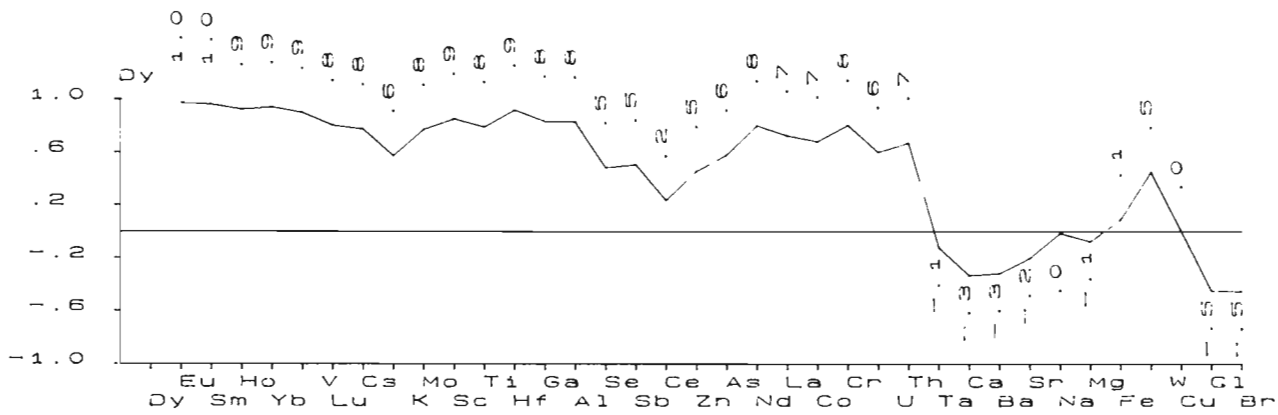


Figure 35.2. Example of correlation plot showing the individual Pearson product-moment correlation coefficient values for all elements present in an input data-file. Notice the rather smooth aspect of the curve.

The method has helped fuel scientists to ascertain the groupings (as relationships) that produce a given dendograph. The correlation plots complete the information on the patterns highlighted by the dendograph-triangle method.

REFERENCES

Labonté, M. and Goodarzi, F.
1985: Use of the dendograph for data processing in fuel science; Fuel, v. 64, p. 1177-1179.

Mason, B. and Moore, C.N.
1985: Principles of geochemistry, John Wiley and Sons, New York.

Valentine, J.W. and Peddicord, R.C.
1967: Evaluation of fossil assemblages by cluster analysis, University of California, Davis; Journal of Paleontology, v. 41, no. 13, p. 502-507.

- 36 -

Investigations of Paleozoic geology, northern Axel Heiberg and northwestern Ellesmere islands

Project 860007

H.P. Trettin
Institute of Sedimentary and Petroleum Geology, Calgary

Trettin, H.P., Investigations of Paleozoic geology, northern Axel Heiberg and northwestern Ellesmere islands; in Current Research, Part A, Geological Survey of Canada, Paper 87-1A, p. 357-367, 1987.

Abstract

The Rens Fiord Complex of Axel Heiberg Island is divided into: 1. interstratified basalt and carbonate of Early Cambrian or Hadrynian age; 2. dolostone and minor limestone of probable Early Cambrian age (facies equivalent of Ella Bay Formation?); 3. the Grant Land Formation (Lower Cambrian); and 4. the Hazen Formation (Lower Cambrian to Lower Silurian). The Svartevaeg Formation probably is a thrust-faulted facies equivalent of the Silurian Lands Lokk Formation. The basal Carboniferous succession includes a thin volcanic unit.

Steeply inclined to subhorizontal thrusts in northern Axel Heiberg Island, directed both to the northeast and the southwest, are attributed to deformations of Late Silurian – Early Devonian, and post-Early Devonian to pre-Visean ages.

On northwestern Ellesmere Island, the sandy and argillaceous member C of the Lands Lokk Formation represents a submarine fan facies that ranges in age from latest Llandovery or Wenlock to Ludlow. The chert-rich sediments are comparable to formations of northeastern Greenland and may have been affected by sinistral strike slip.

Résumé

Le complexe de Rens Fiord dans l'île Axel Heiberg se subdivise de la façon suivante: 1) basaltes et carbonates interstratifiés d'âge Cambrien inférieur ou Hadrynien; 2) dolomie détritique et quantités mineures de calcaire, probablement d'âge Cambrien inférieur (faciès équivalent à la formation d'Ella Bay?); 3) formation de Grant Land (Cambrien inférieur); et 4) formation de Hazen (Cambrien inférieur à Silurien inférieur). La formation de Svartevaeg est probablement un faciès avec failles chevauchantes, équivalent à celui de la formation silurienne de Lands Lokk. La succession basale du Carbonifère comprend une mince unité volcanique.

On attribue des charriages fortement inclinés à subhorizontaux, présents dans le nord de l'île Axel Heiberg, dirigés vers le nord-est et le sud-ouest, à des déformations survenues du Silurien supérieur au Dévonien inférieur, et durant une autre préiode, ultérieure au Dévonien inférieur et antérieure au Viséen.

Dans le nord-ouest de l'île Ellesmere, le membre sableux et argileux de la formation de Lands Lokk correspond à un faciès de cône alluvial sous-marin, dont l'âge se situe entre le sommet du Llandovérien ou le Wenlockein, et le Ludlovien. Les sédiments cherteux sont comparables aux formations du nord-ouest du Groenland, et ont peut-être subi un décrochement sénestre.

INTRODUCTION

The purpose of fieldwork in 1986 was to update the information on the pre- Carboniferous geology of northern Axel Heiberg Island and northwestern Ellesmere Island obtained from 1955 through 1962 (in chronological order) by E.F. Roots, R. Thorsteinsson, P.E. Fricker, and the author (Trettin, 1969). Stratigraphic and structural studies in northern Axel Heiberg Island, from three camps south of Rens Fiord and from one camp northeast of Rens Fiord (Fig. 36.1), were concerned mainly with the lower Paleozoic rocks, but also included a newly discovered volcanic unit in the basal part of the Carboniferous succession. On Ellesmere Island, stratigraphic and sedimentological studies of the Silurian Lands Lokk Formation were made from two camps, south and southeast of Emma Fiord, respectively.

The writer is indebted to the officers and pilots of the Polar Continental Shelf Project for transport in the field and courtesies. Gordon Check, student assistant from Dalhousie University, is thanked for his excellent work and companionship. The graptolite identifications were made by R. Thorsteinsson and B.S. Norford and the chemical analyses of volcanic rocks collected earlier, were carried out by the Analytical Chemistry Section of the Geological Survey under the supervision of G.R. Lachance.

PRE-CARBONIFEROUS GEOLOGY, NORTHERN AXEL HEIBERG ISLAND

Stratigraphy

The unfosssiliferous and severely deformed Ordovician and/or older strata of northern Axel Heiberg Island were originally assigned to four lithological units of uncertain stratigraphic order, collectively referred to as the Rens Fiord Complex. They are now reassigned to two informal units of Early Cambrian and(?) older age (Jaeger Lake assemblage and Aurland Fiord beds), and to two formations of the Franklinian deep-water basin established on northern Ellesmere Island — the Lower Cambrian Grant Land Formation, and the Cambrian to Lower Silurian Hazen Formation.

The fossiliferous Silurian-Devonian succession was divided into three formal stratigraphic units: the Lands Lokk Formation, established on Ellesmere Island (see below); the Lower Devonian Stallworthy Formation; and the Svartevaeg Formation of presumed Early and/or Middle Devonian age. The last now is interpreted as Silurian in age and correlative, to some extent, with the Lands Lokk Formation. Only those parts of the Lands Lokk Formation exposed southwest of Aurland Fiord were restudied in 1986; the summaries of the other units are based on more detailed descriptions in Trettin (1969) with some reinterpretation.

Lower Cambrian and (?) older

The original volcanic and carbonate units of the Rens Fiord Complex now are regarded as informal units of formational rank, provisionally named Jaeger Lake assemblage and Aurland Fiord beds, respectively. Their age and stratigraphic order are uncertain because they are unfossiliferous, bounded by faults, and not in stratigraphic or structural contact with each other. However, the fact that both have been thrust over the Grant Land Formation suggests that they are older than that unit and hence Early Cambrian and/or Hadrynian in age. The Aurland Fiord beds are tentatively correlated with the Lower Cambrian Ella Bay Formation of central Eastern Ellesmere Island. If this correlation is correct, then the Aurland Fiord beds underlie the Grant Land Formation in a stratigraphic sense and the Jaeger Lake assemblage is the oldest exposed unit in this area.

The **Jaeger Lake assemblage** occurs as small fault blocks in the central part of the study area and as thrust sheets in a narrow belt extending from east of Rens Fiord to southeast of Cape Thomas Hubbard (Fig. 36.2A). A 426 m thick stratigraphic section east of Jaeger Lake (Trettin, 1969, p. 9) comprises nearly equal proportions of volcanic and carbonate rocks, occurring in three units each. The volcanic rocks are original flows and tuffs, metamorphosed in the greenschist facies and pervasively altered by calcite and quartz. The ratios of immobile trace elements (Zr/TiO_2 vs. Nb/Y according to Winchester and Floyd [1977, Fig. 6]) in three specimens analyzed indicate that they are subalkaline basalts, probably of within-plate origin (Pearce and Cann, 1973, Fig. 3; and Holm, 1982). The carbonate rocks are dolostones and recrystallized limestones (marbles) that locally contain stromatolites.

The Jaeger Lake assemblage is comparable to the Yelverton assemblage of northwestern Ellesmere Island (south of Phillips Inlet to east of the head of Yelverton Inlet), which consists of interstratified, variably metamorphosed tholeiitic tuff, flows and sills, limestone, dolostone, mudrock, and chert, with an estimated total thickness of more than 1 km. This unit also has been thrust over the Grant Land Formation.

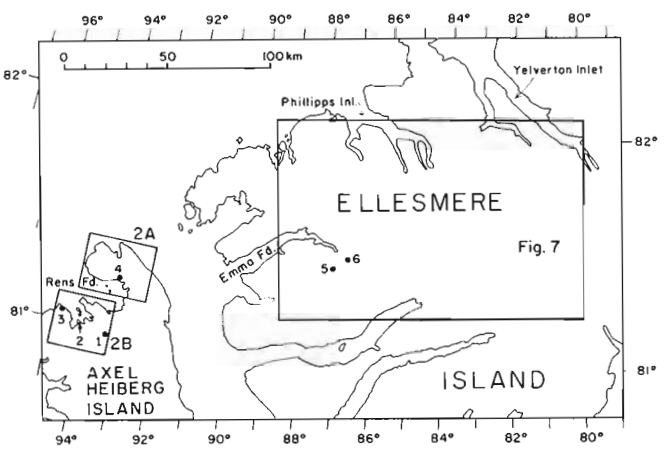


Figure 36.1. Index for Figures 36.2A, 36.2B and 36.7, and location of camp sites (numbered 1-6).

Both may be correlative with Hadrynian basalt on Victoria Island (Natkusiak Formation), which has yielded a K-Ar isochron age of 635 Ma (recalculated from Palmer and Hayatsu (1975) using present constants) and the related Franklin dyke swarms, but the possibility that they are Early Cambrian in age cannot be dismissed.

The **Aurland Fiord beds** are widely distributed in the vicinity of Aurland Fiord (Fig. 36.2B) and also occur north and east of Rens Fiord. The stratigraphic thickness of the various fault slices and blocks varies from a few metres to about 1.3 km, attained in a steeply dipping block west of Aurland Fiord. The unit consists mainly of flat- laminated dolostone and related dolomitic intraformational conglomerate with lesser proportions of nonlaminated dolostone, microcrystalline limestone, and dolomitic grainstone, pisolite, and solution (?) breccia. Recrystallized argillaceous and cherty sediments are interbedded with dolostone near the base of a major thrust sheet 8.4 km southeast of central Aurland Fiord. Quartz veins and chert replacement are ubiquitous.

The abundant laminated dolostone is tentatively interpreted as an original "peri-platform ooze" deposited in outer shelf – upper slope settings, but differs from typical sediments of this type by a lack of interstratified mudrock; the grainstones, accordingly, would represent high-energy shoals on the shelf margin. The unit may represent a facies intermediate in water depth between the shelf sediments of the Lower Cambrian Ella Bay Formation of central Ellesmere Island (Long, 1985; and unpublished manuscript), and the correlative deep-water carbonate sediments of the southern Grant Land Mountains (Nesmith beds, Trettin, unpublished manuscript) and northeastern Greenland (Paradisfjeld Formation, Friderichsen et al., 1982). If so, the Aurland Fiord beds, like the Nesmith beds, would underlie the Grant Land Formation stratigraphically. However, neither the Ella Bay Formation nor the Nesmith beds are exposed on Axel Heiberg Island and western Ellesmere Island, so that this assignment is speculative.

Grant Land Formation

The Grant Land Formation was established in the southern Grant Land Mountains of northern Ellesmere Island (Trettin, 1971, and unpublished manuscript) where it lies stratigraphically between resedimented carbonates of Early Cambrian age (Nesmith beds) and the Hazen Formation (see below). At this location, it comprises an estimated 2 km of clastic sediments, mainly variably feldspathic quartzite and multicoloured phyllite or slate with small proportions of pebble conglomerate and intraformational mudrock-clast conglomerate. The unfossiliferous formation is considered to be middle to late Early Cambrian in age on the basis of regional stratigraphic relationships. It is similar to the Polkorridoren Group of northeastern Greenland (Friderichsen et al., 1982) and correlative with the Ellesmere Group of central Ellesmere Island. It appears to be a submarine fan deposit, (although classical turbidites [Bouma sequences] are rare on Ellesmere Island) and evidently was derived from the North American craton (Trettin et al., in press).

The original sandstone unit of the Rens Fiord Complex, and a large proportion of the rocks originally designated as "argillaceous and cherty strata", now are assigned to the Grant Land Formation on the basis of lithological and petrographic similarity. On Axel Heiberg Island, the formation consists mainly of fine to coarse grained quartzite and dark grey, greenish grey or purplish red slate and phyllite with small amounts of granule conglomerate. The thickness of the formation cannot be established here because of complex folding and faulting but appears to be considerable (i.e. probably greater than 1 km) because of its wide distribution.

Hazen Formation

In the Hazen Plateau region of northern Ellesmere Island the Hazen Formation is a condensed succession of deep water carbonate, radiolarian chert, mudrock and minor sandstone of late Early Cambrian to Early Silurian age that lies stratigraphically between the Grant Land Formation and flysch of the Imina Formation (Trettin, 1971, and unpublished manuscript). Its thickness decreases from probably more than 1 km near the Franklinian shelf to about 250 m in the northwesternmost exposures. The lower part is dominated by resedimented carbonate and the upper part by radiolarian chert, but the contact between the carbonate and chert members is diachronous, ranging in age from Arenig in the northeast to middle Landovery in the southwest. In some areas, the carbonates and mudrocks have been replaced by chert.

On northern Axel Heiberg Island, three major and a few minor outcrop areas of this formation have been recognized south of Rens Fiord and east and west of Aurland Fiord. North of Rens Fiord, only a few small outcrop areas have been mapped, but others may be present within the northern part of the outcrop area of the Grant Land Formation, which was not traversed in 1986.

In a syncline south of central Aurland Fiord, the Grant Land Formation is overlain by more than 60 m of carbonate and minor mudrock that must represent the basal part of the formation if the concealed contact between the two units is not faulted. The carbonate rocks include: 1. laminated, variably argillaceous dolostone; 2. graded dolsiltite and dolarenite; and 3. dolomitic intraformational conglomerate that appears to have originated by sliding of carbonate boudins in a submarine slope environment. The carbonate member of the Hazen Formation is probably also represented by dolomitic strata associated with dark grey mudrock and chert in small outcrop areas southwest and southeast of Aurland Fiord.

Silurian sedimentary and volcanic strata

The Silurian sedimentary and volcanic rocks are discussed below in terms of the two units to which they were assigned originally – the Lands Lokk and Svartevaeg formations – but a revision of that usage is advisable. The stratigraphy of the

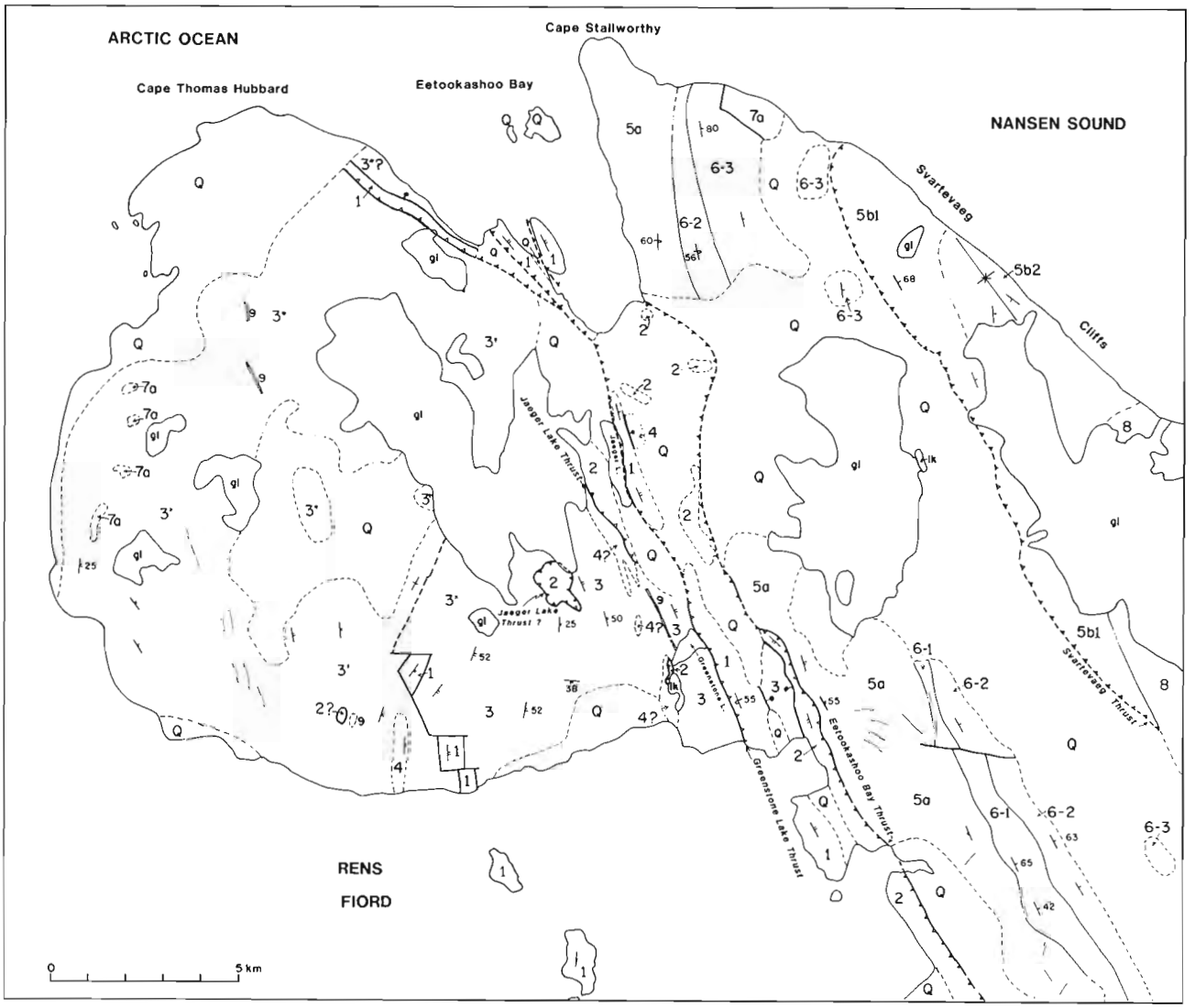


Figure 36.2. Geology of northern Axel Heiberg Island; 36.2A: area north of Rens Fiord; 36.2B: area south of Rens Fiord.

LEGEND, FIGURES 36.2A and 36.2B

Q QUATERNARY
sand, gravel, mud

CRETACEOUS and/or OLDER

9 diabase

CARBONIFEROUS and PERMIAN

8 undifferentiated

8-3 limestone, dolostone, minor sandstone

8-2 volcanics

8-1 sandstone etc.

DEVONIAN and (?) YOUNGER
felsic to intermediate intrusions

7a quartz diorite, tonalite, granodiorite (Devonian)

7b diorite (Devonian or Cretaceous)

7c felsic porphyry (Devonian or Cretaceous)

LOWER DEVONIAN
Stallworthy Formation

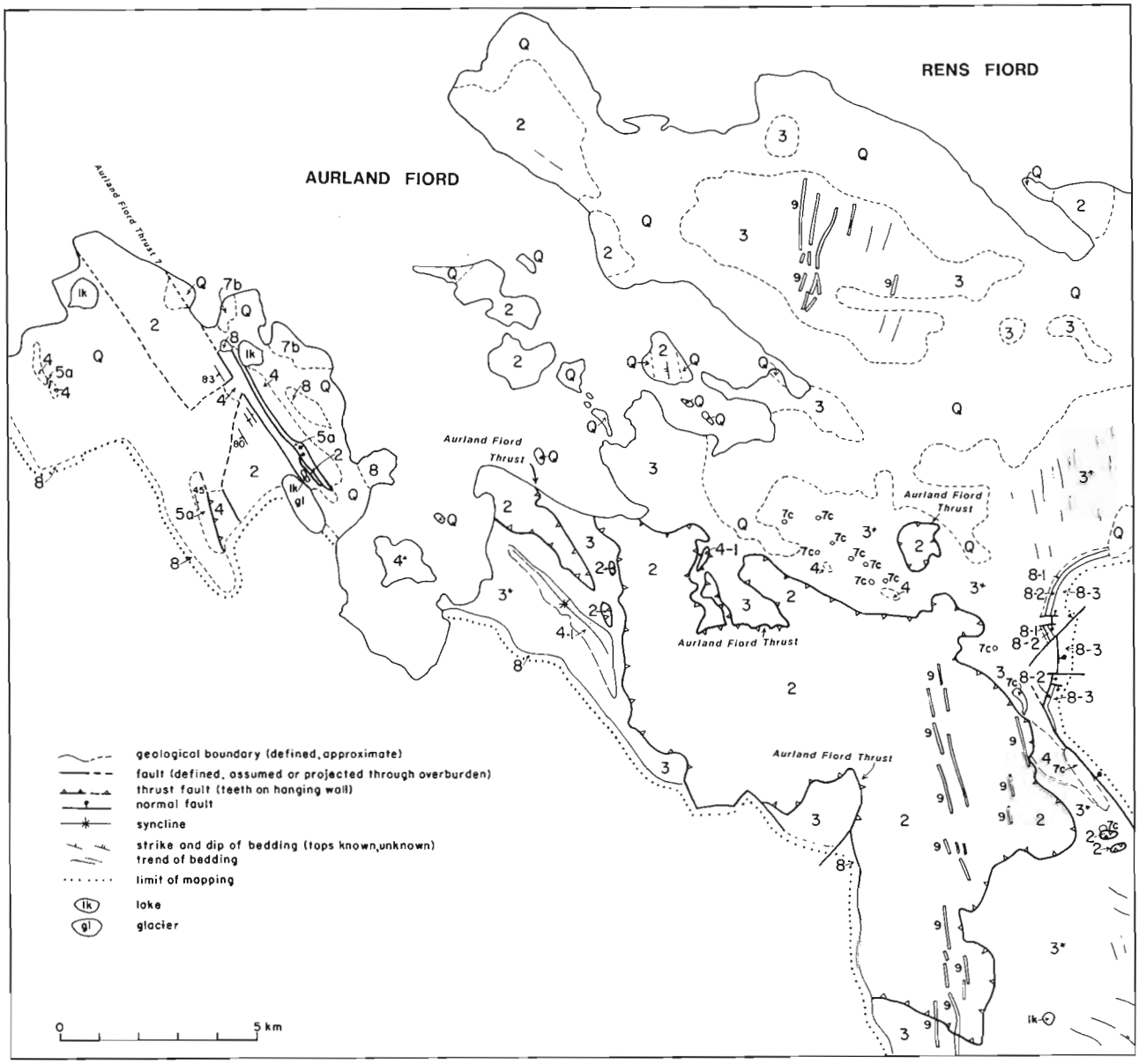
6-3 Member C
multicoloured mudrock, minor sandstone, conglomerate

6-2 Member B
sandstone, conglomerate, breccia, mudrock (mainly red)

6-1 Member A
red mudrock, minor sandstone, conglomerate

SILURIAN
upper Llandovery (?), Wenlock, and (?) Ludlow

5a **Lands Lokk Formation**
north of Rens Fiord:
slate, minor sandstone, volcanogenic sandstone, tuff, conglomerate
south of Aurland Fiord:
volcanogenic sandstone, slate, minor conglomerate



Svartevaeg Formation

5b-2 Member B
volcanogenic sandstone, minor slate, tuff, conglomerate, breccia, volcanic flows (including basalt)

5b-1 Member A
tuff, volcanic flows (including andesite), volcanogenic sandstone, minor slate

UPPER LOWER CAMBRIAN TO LOWER SILURIAN

4 **Hazen Formation (undifferentiated)**
chert, slate, phyllite, dolostone, limestone
4*: may include Grant Land and/or Lands Lokk formations

4-1 Carbonate Member
dolostone, minor slate

LOWER CAMBRIAN

3 **Grant Land Formation**
quartzite, slate, phyllite, very rare conglomerate
3*: may include minor outcrop areas of Hazen Formation and Aurland Fiord beds

LOWER CAMBRIAN (?)

2 **Aurland Fiord beds**
dolostone, minor limestone, rare phyllite

LOWER CAMBRIAN or HADRYNIAN

1 **Jaeger Lake assemblage**
metamorphosed basaltic flows and tuff, dolostone, limestone

Lands Lokk Formation in its type area on northwestern Ellesmere Island is reviewed in a later part of this report.

Lands Lokk Formation

The main outcrop belt of the Lands Lokk Formation extends from east of Rens Fiord to east of Eetookashoo Bay. This intensely deformed belt is overthrust on the southwest by the Aurland Fiord beds and unconformably overlain on the northeast by the Stallworthy Formation. The Lands Lokk Formation here consists mainly of medium to dark grey slaty mudrock, lesser proportions of lithic and tuffaceous sandstone and tuff, and of at least one carbonate conglomerate of pebble to cobble grade. The volcanic fraction in the tuffs and sandstones comprises rock fragments of intermediate to siliceous composition, feldspar, chlorite, and volcanic quartz; the sedimentary fraction of the sandstones consists mainly of nonvolcanic quartz, chert and carbonate fragments. The occurrence of graded bedding indicates that these rocks represent sediment gravity flows (including turbidites); the carbonate conglomerate appears to be a subaqueous debris flow.

Benthonic fossils in the carbonate clasts of the conglomerate are of Llandovery or Wenlock, perhaps late Llandovery age. Graptolites near the top of the unit are probably late Wenlock in age.

Outcrops of similar, but coarser grained rocks, in fault contact with the Hazen Formation, occur in three small areas southwest of Aurland Fiord. The strata consist mainly of sandstone with lesser proportions of slate and small proportions of pebble conglomerate. Both Bouma sequences, and thick massive beds deposited by concentrated sediment gravity flows, are present. The sandstones are composed of volcanic material of intermediate to siliceous composition and of sedimentary quartz and chert. The chert is reminiscent of that in the Hazen Formation because of the presence of lamination and "ghosts" of radiolarians.

Svartevaeg Formation

The name Svartevaeg Formation (originally Svartevaeg Group) was introduced by Fricker and Trettin (1962) for a thick succession of volcanogenic sediments and volcanic rocks that overlies the Stallworthy Formation in a structural sense; the contact between the two units is covered and its nature is subject to interpretation. The Svartevaeg is overlain by the Emma Fiord Formation of Visean (late Early Carboniferous) age with angular unconformity.

The Svartevaeg Formation consists primarily of sediment gravity flows that are composed mainly of volcanogenic (tuffaceous ?) sandstone with lesser amounts of siltstone and breccia or conglomerate; a minor proportion of the formation consists of tuff and volcanic flows. The proportion of volcanic rocks and mudrock versus sandstone is greater in the lower part (member A) than in the upper part (member B). The sandstones consist mostly of volcanic rock fragments of siliceous to mafic, predominantly intermediate (andesitic) composition, with lesser proportions of feldspar, carbonate and chlorite. A chemically analyzed tuff from member A is classified as calc-alkaline andesite and a flow from the upper part of member B as calc-alkaline basalt, both on the basis of major elements (cf. Trettin et al., 1972, p. 104, analyses 6 and 7). The plagioclase in the sedimentary rocks studied and in the andesitic tuff mentioned (but not in the basalt) has been altered to albite to a large extent.

The formation contains several limestone breccias with benthonic fossils. The most diagnostic faunule, from a slide block of limestone about 60 m above the base of the exposures, is late Llandovery or Wenlock in age. Basaltic breccia near the top of the formation contains Silurian pentamerids.

The age assignment for this unit depends on the interpretation of its stratigraphic-structural relationship with the Stallworthy Formation. In the 1960's, when the lower Paleozoic geology of the northern regions was poorly known, this boundary was cautiously interpreted as a normal stratigraphic contact. The following considerations, however, strongly suggest that it is a thrust fault:

1. Thrust faults are common in northern Axel Heiberg Island (see below).
2. The Svartevaeg Formation is comparable in lithology and origin to the volcanogenic components of the Lands Lokk Formation both in northern Axel Heiberg Island and northwestern Ellesmere Island. Differences in the proportion and clast size of the volcanic material can be explained by a facies change, telescoped by thrust faulting. On the other hand, no evidence has come to light indicating that deep-water and arc-type conditions existed in the region in late Early or Middle Devonian time.
3. On Ellesmere Island, as far as is known, the shelf-derived fossils in Ordovician to Devonian deep water sediments all are of about the same age as the enclosing strata. Inclusion of Silurian fossils in sediment gravity flows and volcanic rocks of Early or Middle Devonian age would be anomalous and difficult to explain.

If the present interpretation is true, then the formation must be, at least in part, late Llandovery in age. Considering the great thickness of these deposits, their overall age range could extend from late Llandovery to early Ludlow, the same age as volcanic member B of the Lands Lokk Formation in adjacent northwestern Ellesmere Island.

Stallworthy Formation

The Stallworthy Formation, divisible into three members, comprises 3 to 4 km of sandstone, multicoloured mudrock, and conglomerate that overlie the Lands Lokk Formation with angular unconformity. Its upper boundary, as mentioned, is now interpreted as a fault. The unit was not re-examined in 1986 and the reader is referred to Trettin (1969) for detailed information. Ostracoderms, found about 1 km below the top of the formation, now are regarded as mid-Early Devonian (late Lochkovian or early Pragian) in age (R. Thorsteinsson and H.P. Schultze, pers. comm., 1985). The formation is

interpreted as a syntectonic and post-tectonic deposit derived from uplands to the southwest, in which the Hazen and Grant Land formations were exposed, providing detrital chert and quartz, respectively. Its lower part (members A and B) was deposited in alluvial fan and braided river environments; its upper part (member C) mainly in brackish delta environments.

Granitic intrusions

Granitic intrusions north of Rens Fiord are in the compositional field of granodiorite - tonalite - quartz diorite. They include a fault-bounded pluton southeast of Cape Stallworthy, and four aligned plugs southwest of Cape Thomas Hubbard, one of which has yielded a K-Ar age of 367 ± 25 Ma (recalculated from Lowdon et al. (1963), according to present standards). These rocks are probably no younger than early Late Devonian and may be correlative with a granitic pluton in northwestern Ellesmere Island, which has yielded a U-Pb (sphene) age of 390 ± 10 Ma (Trettin et al., in press).

Granitic intrusions in the region south and southwest of Rens Fiord comprise: 1. felsic porphyry dykes and plugs, and 2. a diorite pluton. It is uncertain whether they also are Devonian in age or whether they belong to the Late Cretaceous bimodal suite reported recently from northern Ellesmere Island (Trettin and Parrish, in press). These intrusions were reinvestigated in 1986 and sampled for isotopic age determination.

Felsic porphyry

A linear, northwesterly trending belt of porphyritic felsite dykes and plugs, more than 11 km long and up to about 0.7 km wide, occurs within the Grant Land Formation south of central Rens Fiord. The intrusions range in length from a few metres to about 2 km. The rocks are uniform in composition and appearance. Phenocrysts, mainly of plagioclase (zoned from sodic andesine to sodic labradorite or altered to albite) with small proportions of K-feldspar and biotite, variably replaced by chlorite, are set in a pale brown to pale red groundmass of feldspar with minor biotite, chlorite and quartz.

Diorite southwest of Aurland Fiord

This intrusion, exposed in two areas, probably has an overall extent of 3 by 2 km and appears to intrude the Hazen Formation although its contacts are covered. It consists of feldspar (mainly zoned andesine, a little K-feldspar), pyroxene, hornblende, and biotite (partly replaced by chlorite), and minor quartz.

STRUCTURAL GEOLOGY

Structural trends are northwest, almost at right angles to those in northwestern Ellesmere Island, but parallel or subparallel to trends in central and southern Axel Heiberg Island. The area lies at the northwestern end of the southeast-plunging Princess Margaret Arch of Tertiary age and represents a structural high, named Rens Fiord Uplift, that is marked by extensive outcrops of Lower Cambrian strata. The margins of the high are characterized by complex thrust faults, some of which were investigated in 1986.

Thrust faults at the northeastern margin of Rens Fiord Uplift

The Aurland Fiord beds have been displaced northeastward onto the Lands Lokk formation along the Eetookashoo Bay Thrust. The dip of this fault is apparent only in the area immediately north of Rens Fiord. A short distance to the southwest, the Jaeger Lake assemblage has been thrust southwestward over the Grant Land Formation along the Greenstone Lake Thrust, which splays into three thrusts southeast of Cape Thomas Hubbard. The area of poor exposure between the Aurland Fiord beds and the Jaeger Lake assemblage, underlain by the Grant Land and Hazen formations, is interpreted as a graben.

Farther west, the Jaeger Lake Thrust places the Aurland Fiord beds onto dark grey chert that is tentatively assigned to the Hazen Formation but could represent older strata. A subhorizontal thrust sheet of the Aurland Fiord beds lying on the Grant Land Formation about 2 km to the west is interpreted as a klippe related to the Jaeger Lake Thrust.

Southwestern Margin of Rens Fiord Uplift

South of central Rens Fiord and southeast of Aurland Fiord, subhorizontal sheets of the Aurland Fiord beds lie on tightly folded, generally steeply dipping strata of the Grant Land Formation and, locally, the Hazen Formation. This relationship was recognized earlier but it was uncertain whether it indicated an angular unconformity or a flat thrust fault. The absence of clastic sediments and presence of tectonic breccia at the base of the dolomitic Aurland Fiord beds support the



Figure 36.3. Aurland Fiord beds, southwest of Aurland Fiord: laminated dolostone showing intraformational deformation.

second alternative. The various subhorizontal outcrops of the Aurland Fiord beds evidently are erosional remnants (klippen) of a single thrust sheet no less than 20 km long and 10 km wide. About 1.75 km southeast of Aurland Fiord, the Aurland Fiord thrust sheet lies on a parallel thrust sheet of the Grant Land Formation, which, in turn, overlies the carbonate member of the Hazen Formation (Fig. 36.4). Minor folds in the Hazen Formation suggest relative motion of the Grant Land strata toward the northeast.

West of Aurland Fiord, two steeply dipping blocks of the Aurland Fiord beds are in fault contact with the Hazen Formation. The northeastern fault bounding these blocks may represent the root of the Aurland Fiord Thrust but appears to have been affected by a later (Tertiary ?) event of block faulting. If it is the root, then the thrust had no less than 12 km of northeastward horizontal displacement.

Age of structures

The regional stratigraphic-structural record indicates that northern Axel Heiberg Island was affected by three major periods of deformation:

1. The oldest event is indicated by the angular unconformity between the Lands Lokk and Stallworthy formations. Its age range is bracketed by fossils of late Wenlock age below the unconformity and of late Lochkovian – early Pragian age some distance above it, but it must have been more restricted. It now is thought to have occurred in latest Silurian (Pridoli) – earliest Devonian time, probably simultaneously with compressive deformation of the Boothia Uplift (Thorsteinsson, 1980; Okulitch et al., 1986) and northern Ellesmere Island (Trettin, in press).
2. The second deformational period is indicated by the angular unconformity between the Stallworthy and Emma Fiord formations of Early Devonian and Visean age, respectively. This interval includes the main phase of the Ellesmerian Orogeny of latest Devonian and/or earliest Carboniferous age.
3. The third event is the Eurekan Orogeny of latest Cretaceous to early Tertiary age.

The tight and complex folds in the Silurian and older rocks differ markedly in style from the open folds in the Carboniferous and younger strata, and therefore are almost certainly related to the two earlier phases of deformation. The same probably applies to major faults such as the Svartevaeg, Eetookashoo Bay and Jaeger Lake thrusts, the southeastward projections of which (under Quaternary cover) do not seem to have affected the Carboniferous and younger rocks (cf. Thorsteinsson and Trettin, 1972). The Aurland Fiord thrust sheet and the structurally underlying Grant Land Formation are both cut by mafic dykes (Fig. 36.2B) that are Late Cretaceous or older in age (younger swarms are not known in the region); the Aurland Fiord Thrust, therefore, is also older than the Eurekan Orogeny.



Figure 36.4. Stacked thrust sheets of carbonate member of Hazen Formation (4-1), Grant Land Formation (3), and Aurland Fiord beds (2) about 1.75 km southeast of central Aurland Fiord. Minor folds in Hazen Formation (lower left) suggest northeastward motion of overlying sheet.

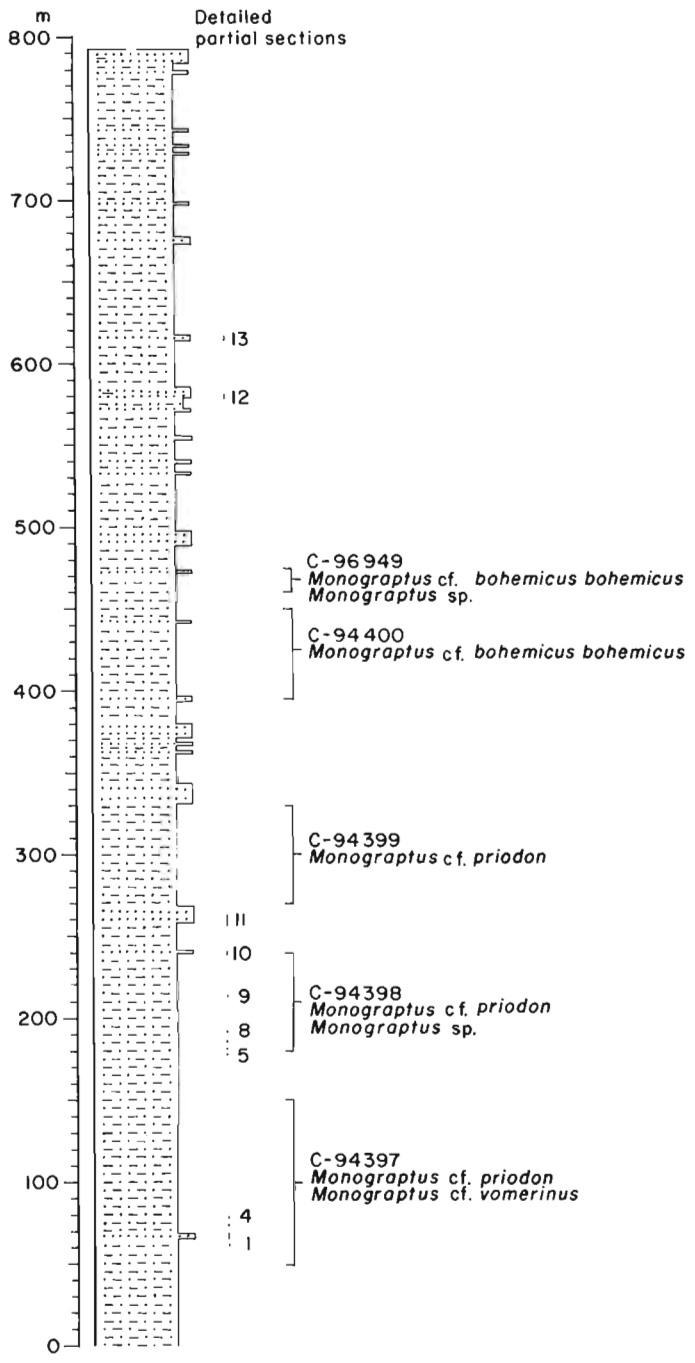


Figure 36.5. Generalized stratigraphy of member C of the Lands Lokk Formation south of Emma Fiord (locality 5 of Figure 36.1).

The postulated Svartevaeg Thrust is the only structure that can be attributed with some assurance to the Middle Devonian – Early Carboniferous deformation; elsewhere, distinction between the first and second phases is impossible at present. However, differences in structural style between the Stallworthy Formation on the one hand and the Lands Lokk Formation and older units on the other hand, suggest that the Late Silurian – Early Devonian deformation was a major compressional event, characterized by tight and complex folding and thrust faulting in spite of the fact that the angular discordance is relatively small where best exposed (Trettin, 1962, Fig. 3.).

MEMBER C OF THE LANDS LOKK FORMATION IN NORTHWESTERN ELLESMERE ISLAND

In northwestern Ellesmere Island, the Lands Lokk Formation conformably overlies a tongue of the lower Imina Formation, and is overlain by the Upper Carboniferous Borup Fiord Formation with angular unconformity. Three members have been distinguished in this region (Trettin, 1969). Member A, probably more than 1.5 km thick locally, consists mainly of mudrock with small proportions of quartzose and tuffaceous sandstone and small amounts of tuff. Graptolites indicate a late Llandovery to early Ludlow age range. Member B, restricted to the immediate vicinity of Emma Fiord, consists of mudrock, tuff and volcanic flows of siliceous to intermediate, calc-alkaline composition (Trettin et al., 1972, p. 104, analysis #5) and small amounts of limestone. At Fire Bay, Emma Fiord, member B seems to overlie strata of member A containing graptolites of early Ludlow age. Member C is exposed south and southeast of Emma Fiord, where it overlies member A. The latter exposures, examined only very briefly in 1962, were re-investigated in 1986.

Member C has a minimum thickness of 1 km southeast of Emma Fiord (east of locality 6, Figure 36.1) and the lower 800 m are well exposed on the northern limb of a syncline south of Emma Fiord (locality 5, Fig. 36.1). There it can be divided into two assemblages: 1. thinly interstratified mudrock and sandstone, commonly forming Bouma sequences a few centimetres to a few decimetres in thickness; and 2. units composed of sandstone, with or without small proportions of mudrock and very small proportions of pebble conglomerate (Fig. 36.5). The sandstone units are 0.8 to 13.5 m thick (mean: 3.6 m) and constitute about 11 per cent of the succession. The sandstones occur in Bouma sequences (Fig. 36.6) and as thick, structureless beds that show an upward decrease in grain size only in the uppermost part. Individual sandstone beds commonly have convex parting surfaces at the base that indicate shallow minor channels, probably within broader channels of the mid-fan environment.

Graptolites of undifferentiated latest Llandovery-Wenlock age (*Monograptus* ex gr. *priodon* (Bronn) and *Monograptus* sp. cf. *M. vomerinus* (Nicholson)) occur about 50 to 330 m above the base of the formation, and graptolites of Ludlow age (*Monograptus* sp. cf. *M. bohemicus bohemicus* Barrande) 395 to 473 m above the base of the formation at locality 5 (Fig. 36.1). The contact between members A and C is probably a highly diachronous facies boundary, member C representing submarine fan environments and member A basin plain environments.

The provenance and paleocurrent directions of these strata are important for interpretation of the regional tectonic history. The sandstone consists mainly of chert and quartz with smaller amounts of carbonate, feldspar, chlorite and white mica. The chert was evidently derived from deep water sediments (Hazen Formation or equivalents in Greenland) because it contains "ghosts" of radiolarians.

It had earlier been inferred (Trettin, 1969) that the sediments were derived from northern Axel Heiberg Island because they are comparable in composition to those of the Stallworthy Formation, and this conclusion seemed to be supported by northeastward paleocurrent determinations from the Kulutingwak Fiord - Yelverton Inlet area (Trettin, 1976). However, a total of 129 paleocurrent determinations at two localities south and southeast of Emma Fiord indicate northwestward transport in this area (Fig. 36.7). The determinations are based on the angle between paleocurrent indicators (mainly flute casts, minor tool marks) and local strike measured on the underside of beds. Structural plunge, established on local folds, has been taken into consideration in the conversion of these angles to azimuths. Sediment derivation from Axel Heiberg Island also is contradicted by the fact that the Wenlock strata of member C on Ellesmere Island are older than the uplift of northern Axel Heiberg Island, which probably did not occur before Ludlow time (see above). The significance of the paleocurrent directions is difficult to evaluate. Compositionally, the sediments of the Lands Lokk Formation are more closely related to the chert-rich Lauge Koch and Nordkronen formations of northeastern Greenland (Hurst and Surlyk, 1982) than to the correlative, carbonate-rich Imina Formation of central Ellesmere Island (Trettin, 1979), and it is possible that the Lands Lokk Formation has been affected by the sinistral strike slip inferred for the Pearya Terrrane of northernmost Ellesmere Island, (Trettin, in press). The anomalous directions may have been inherited from that region (Hurst and Surlyk, 1982, Fig. 124) and may also have been affected by counterclockwise rotation during the postulated transcurrent motion.



Figure 36.6. Bouma sequence (divisions A-D) in member C of Lands Lokk Formation with undulating lower surface (detailed interval 12 of Figure 36.4; scale in cm on hammer handle).

CARBONIFEROUS VOLCANICS, NORTHERN AXEL HEIBERG ISLAND

Carboniferous volcanics are exposed south of central Rens Fiord in a narrow belt about 5 km long (Fig. 36.2B). The outcrop belt is terminated by a fault in the south and by overburden in the northeast. The volcanic rocks are flows of

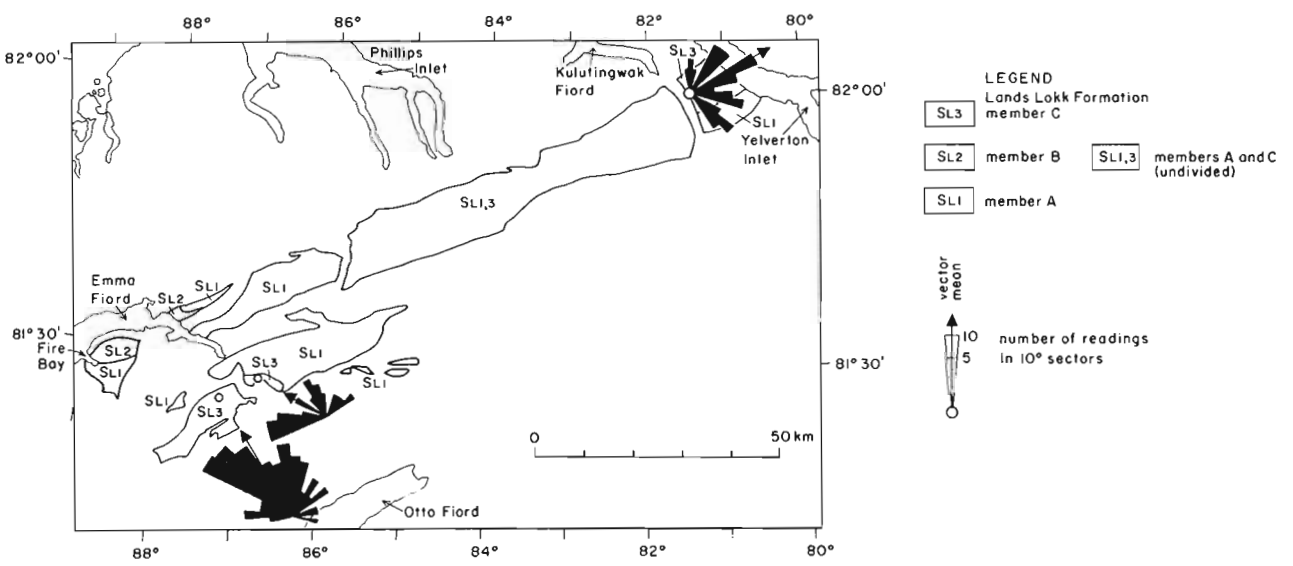


Figure 36.7. Paleocurrent directions in member C of Lands Lokk Formation.

basaltic aspect, and occur 26.8 to 48.5 m above the angular unconformity that separates red sandstone of the Borup Fiord Formation from quartzite of the Grant Land Formation, but only the lowermost 5 m of the Borup Fiord Formation are exposed. The volcanics are separated from overlying sandstone, dolostone and limestone, presumably of the Nansen Formation, by a covered interval 15.5 m thick. They either represent the Audhild Formation, so far known only from northwestern Ellesmere Island (Thorsteinsson, 1974), or are part of the Borup Fiord Formation.

REFERENCES

Fricker, P.E. and Trettin, H.P.
1962: Pre-Mississippian succession of northernmost Axel Heiberg Island, District of Franklin; Geological Survey of Canada, Paper 62-18.

Friderichsen, J.D., Higgins, A.K., Hurst, J.M., Pedersen, S.A.S., Soper, N.J. and Surlyk, F.
1982: Lithostratigraphic framework of the Upper Proterozoic and Lower Paleozoic deep water clastic deposits of North Greenland; The Geological Survey of Greenland, Report No. 107.

Holm, P.E.
1982: Non-recognition of continental tholeiites using the Ti-Y-Zr diagram; Contributions to Mineralogy and Petrology; v. 79, p. 308-310.

Hurst, J.M. and Surlyk, F.
1982: Stratigraphy of the Silurian turbidite sequence of North Greenland; Grønlands Geologiske Undersøgelse, Bulletin No. 145.

Long, D.G.F.
1985: Early evolution of a lower Paleozoic passive margin: the lower Lower Cambrian history of the Franklinian sequence, northeast Ellesmere Island, Arctic Canada; Geological Association of Canada, Mineralogical Association of Canada, Annual Meeting, Program with Abstracts, v. 10, p. A35.

Lowdon, J.A., Stockwell, C.H., Tipper, H.W., and Wanless, R.K.
1963: Age determinations and geological studies; Geological Survey of Canada, Paper 62-17.

Okulitch, A.V., Packard, J.J., and Zolnai, A.I.
1986: Evolution of the Boothia Uplift, arctic Canada; Canadian Journal of Earth Sciences, v. 23, p. 350-358.

Palmer, H.C. and Hayatsu, A.
1975: Paleomagnetism and K-Ar dating of some Franklin lavas and diabases, Victoria Island; Canadian Journal of Earth Sciences, vol. 12, p. 1439-1447.

Pearce, J.A. and Cann, J.R.
1973: Petrogenetic implications of Ti, Zr, Y and Nb variations in volcanic rocks; Contributions to Mineralogy and Petrology, v. 69, p. 33-47.

Thorsteinsson, R.
1974: Carboniferous and Permian stratigraphy of Axel Heiberg Island and western Ellesmere Island, Canadian Arctic Archipelago; Geological Survey of Canada, Bulletin 224.
1980: Part I. Contributions to stratigraphy (with contributions by T.T. Uyeno); in Stratigraphy and conodonts of Upper Silurian and Lower Devonian rocks in the environs of the Boothia Uplift, Canadian Arctic Archipelago; Geological Survey of Canada, Bulletin 282, p. 1-38.

Thorsteinsson, R. and Trettin, H.P.
1972: Geology, Cape Stallworthy, District of Franklin (scale 1:250 000); Geological Survey of Canada, Map 1305 A.

Trettin, H.P.
1969: Pre-Mississippian geology of northern Axel Heiberg and northwestern Ellesmere islands, Arctic Archipelago; Geological Survey of Canada, Bulletin 171.
1971: Geology of lower Paleozoic formations, Hazen Plateau and southern Grant Land Mountains, Ellesmere Island, Arctic Archipelago; Geological Survey of Canada, Bulletin 203.

Trettin, H.P.
1976: Reconnaissance of lower Paleozoic geology, Agassiz Ice Cap to Yelverton Bay, northern Ellesmere Island; in Current Research, Part A, Geological Survey of Canada, Paper 76-1A, p. 431-444.
1979: Middle Ordovician to Lower Devonian deep-water succession at southeastern margin of Hazen Trough, Canon Fiord, Ellesmere Island; Geological Survey of Canada, Bulletin 272.
in press: Pearya: a composite terrane with Caledonian affinities in northern Ellesmere Island; Canadian Journal of Earth Sciences.

Trettin, H.P., Frisch, T.O., Sobczak, L.W., Weber, J.R., Niblett, E.R., Law, L.K., DeLaurier, J.M., and Witham, K.
1972: The Innuitian Province; in Variations in tectonic styles in Canada, R.A. Price and R.J.W. Douglas (eds.), Geological Association of Canada, Special Paper 11, p. 83-179.

Trettin, H.P. and Parrish, R.
in press: Late Cretaceous bimodal magmatism, northern Ellesmere Island: isotopic age and origin; Canadian Journal of Earth Sciences.

Trettin, H.P., Parrish, R. and Loveridge, W.D.
in press: U-Pb age determinations on Proterozoic to Devonian rocks from northern Ellesmere Island, Arctic Canada; Canadian Journal of Earth Sciences.

Winchester, J.A. and Floyd, P.A.
1977: Geochemical discrimination of different magma series and their products using immobile elements; Chemical Geology, vol. 20, p. 325-343.

Preliminary structural cross-sections across Fosheim Peninsula and Axel Heiberg Island, Arctic Archipelago

Project 850043

B.D. Ricketts
Institute of Sedimentary and Petroleum Geology, Calgary

Ricketts, B.D., Preliminary structural cross-sections across Fosheim Peninsula and Axel Heiberg Island, Arctic Archipelago; in Current Research, Part A, Geological Survey of Canada, Paper 87-1A, p. 369-374, 1987.

Abstract

Partially balanced structure cross-sections have been drawn through the Eurekan orogen of west-central Ellesmere Island (Fosheim Peninsula) and central Axel Heiberg Island. Most of the horizontal shortening depicted in the cross-sections is taken up by slip along the Otto Fiord Formation detachment (evaporites); about 55 km (25-30%) of shortening occurs between Parrish Glacier Thrust and the hanging wall of the Stolz Fault Zone. A pair of ramps beneath Princess Margaret Range is inferred to explain the transfer of slip from an Ordovician detachment to the Otto Fiord detachment. The effect of Eurekan deformation on the lower Paleozoic Franklinian strata beneath Axel Heiberg Island and the northern half of Fosheim Peninsula is unknown.

Résumé

On a tracé des coupes structurals epartiellement équilibrées à travers l'orogène eurékien de la partie ouest-centrale de l'île Ellesmere (péninsule de Fosheim), et la partie centrale de l'île Axel Heiberg. La majeure partie du rétrécissement horizontal apparaissant dans les coupes de terrain est due à un glissement le long du décollement de la formation d'Otto Fiord (évaporites); on observe un rétrécissement d'environ 55 km (25-30 %) entre le charriage de Parrish Glacier et la lèvre supérieure de la zone faillée de Stolz. Pour expliquer la propagation du mouvement de glissement, à partir du décollement de strates ordoviciennes jusqu'au décollement des strates d'Otto Fiord, on a suggéré qu'il existait un couple de rampes au-dessous du chaînon Princess Margaret. On ignore l'effet de la déformation eurékienne sur les strates franklinienes du Paléozoïque inférieure au-dessous de l'île Axel Heiberg et de la moitié nord de la péninsule de Fosheim.

INTRODUCTION

Complete analysis of sedimentary basins requires that the paleogeographic limits of depositional sites, facies and sediment source areas be palinspastically restored. Structural cross-sections have been constructed for Fosheim Peninsula, and from Fosheim Peninsula to west Axel Heiberg Island (Fig. 37.1), as part of an ongoing study of the evolution of the Eureka Sound Group basins. Upper Cretaceous and Paleogene strata of the Eureka Sound Group (Ricketts, 1986; Miall, 1986) represent the last phase of sedimentation in Sverdrup Basin and upon adjacent Franklinian bedrock. In a general way, Eureka Sound Group sedimentation can be viewed as taking place in two distinct phases: deposition of deltaic, shallow marine, estuarine and related facies prior to the principal tectonic events of the Eurekan Orogeny; and deposition in orogenic foredeeps during folding and thrusting, the main phase of deformation occurring from Middle to Late Eocene, possibly extending into the early part of the Oligocene (Ricketts and McIntyre, 1986). Thus, palinspastic reconstructions are a necessary prerequisite to establishing basin limits and changing sediment source areas during the different stages of foredeep evolution. The structural sections presented here (Figs. 37.2, 37.3) are a first attempt to solve

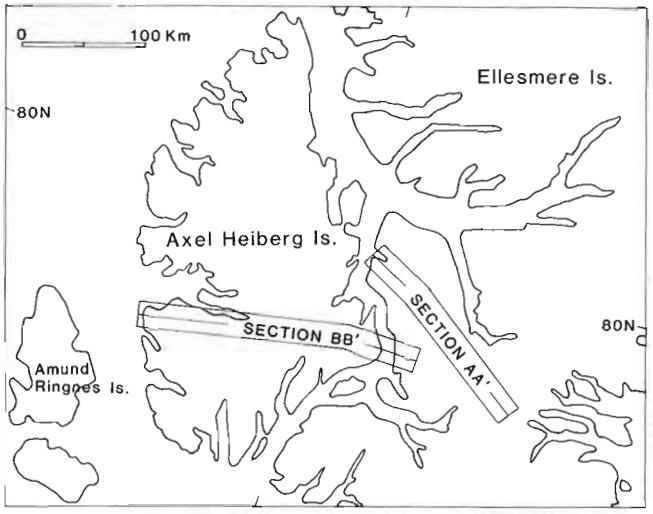


Figure 37.1. Index map of Ellesmere and Axel Heiberg islands showing locations of map strips and lines of section.

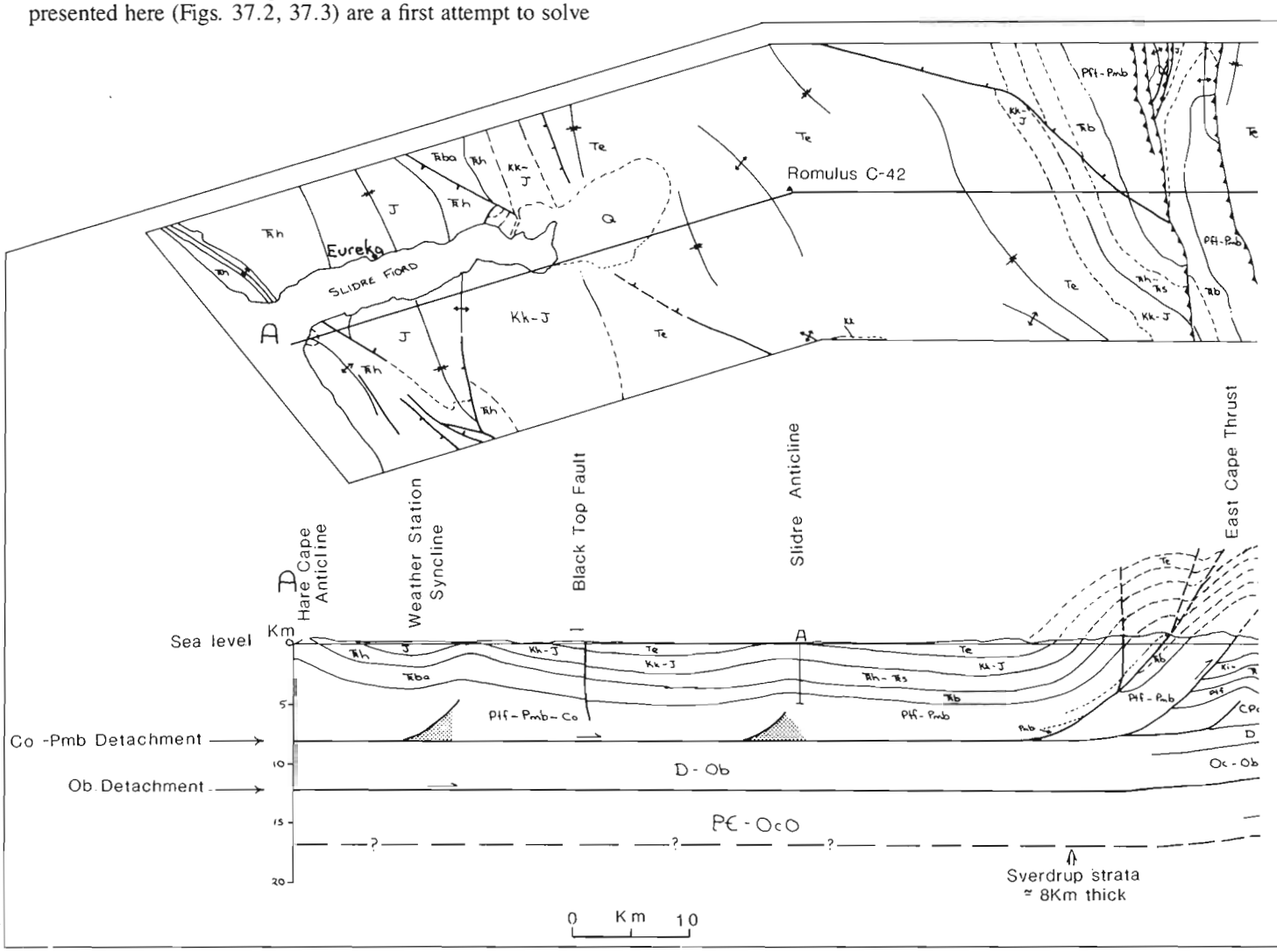
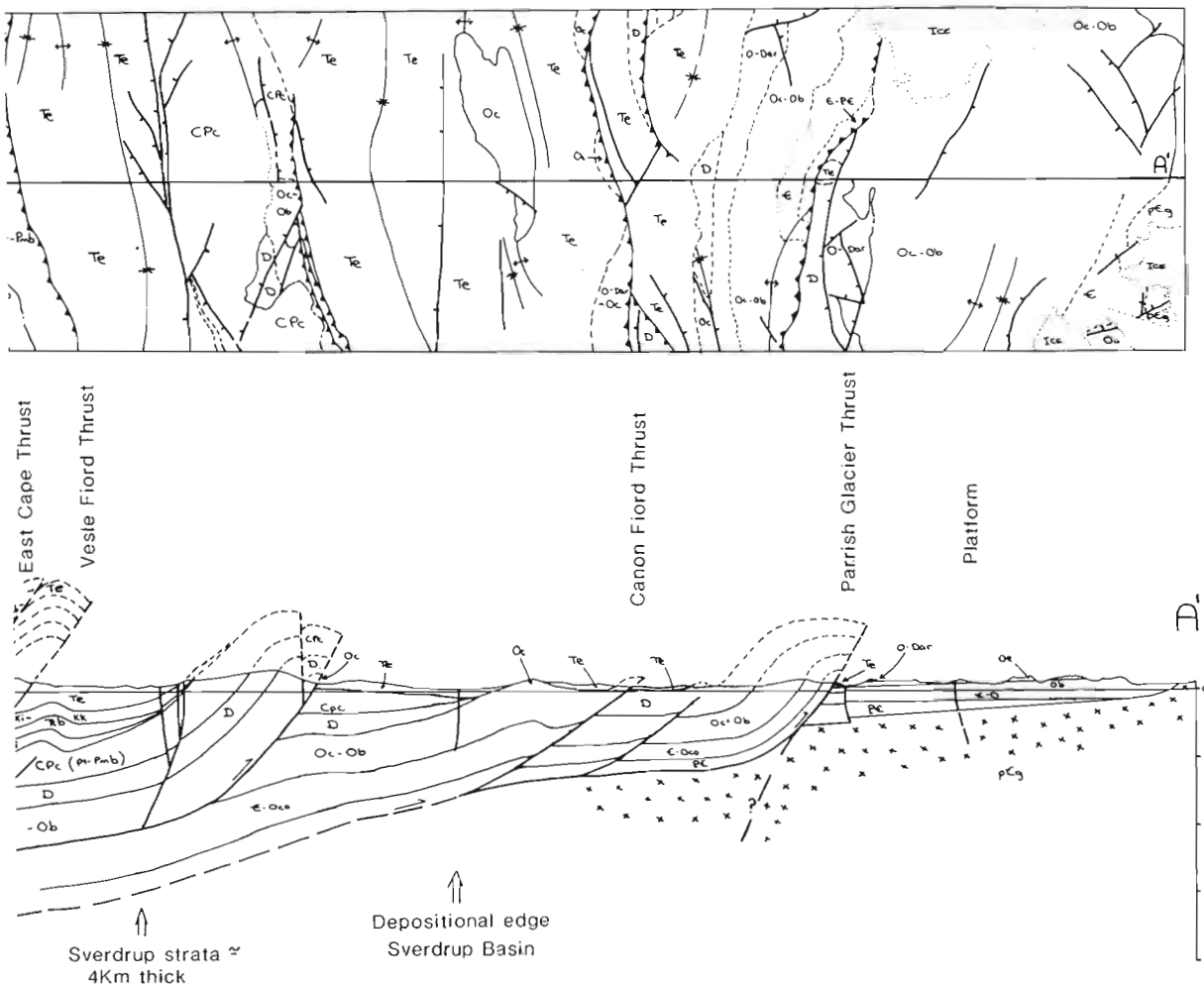


Figure 37.2. Structural cross-section AA' and geology of map strip through Fosheim Peninsula. Geology from Thorsteinsson (1971d; 1972a; 1972c); and unpublished data. Stippled pattern represents region of (Otto Fiord Formation) evaporite addition and doming, possibly associated with blind thrusts. However, the temporal relationship between thrusting and diapirism is uncertain. No vertical exaggeration in scale.

Stratigraphic designations are as follows:

Te	= Eureka Sound Group	D	= Devonian undivided
Kk-J	= Kanguk Fm. (Kk), Hassel Fm. (Kh), Christopher Fm. (Kc), Isachsen Fm. (Ki), Jurassic undivided (J)	O-Dar	= Ordovician to Lower Devonian undivided
		Oc-Ob	= Cornwallis Group to Baumann Fiord Fm.
		Oe	= Eleanor River Fm.
Trh-Trs	= Heiberg Fm. to Savik Fm.	ϵ-OcO	= Cambrian to Copes Bay Fm.
Trb-Trba	= Bjorne Fm. to Blaa Mountain Group	ϵ-Pϵ	= Cambrian to Upper Precambrian
Ptf-Pmb	= Trold Fiord Fm. to Mount Bayley Fm. (includes Assistance and Tanquary fms.)	Pϵ-OcO	= Upper Precambrian to Copes Bay Fm. undivided
CPc	= Upper Carboniferous to Permian undivided	Pϵ-g	= Gneissic basement



some of these problems, and provide a starting point for regional interpretations. Conclusions regarding structural style, structural shortening and levels of detachment for example, are likely to change as new studies are undertaken.

ACKNOWLEDGMENTS

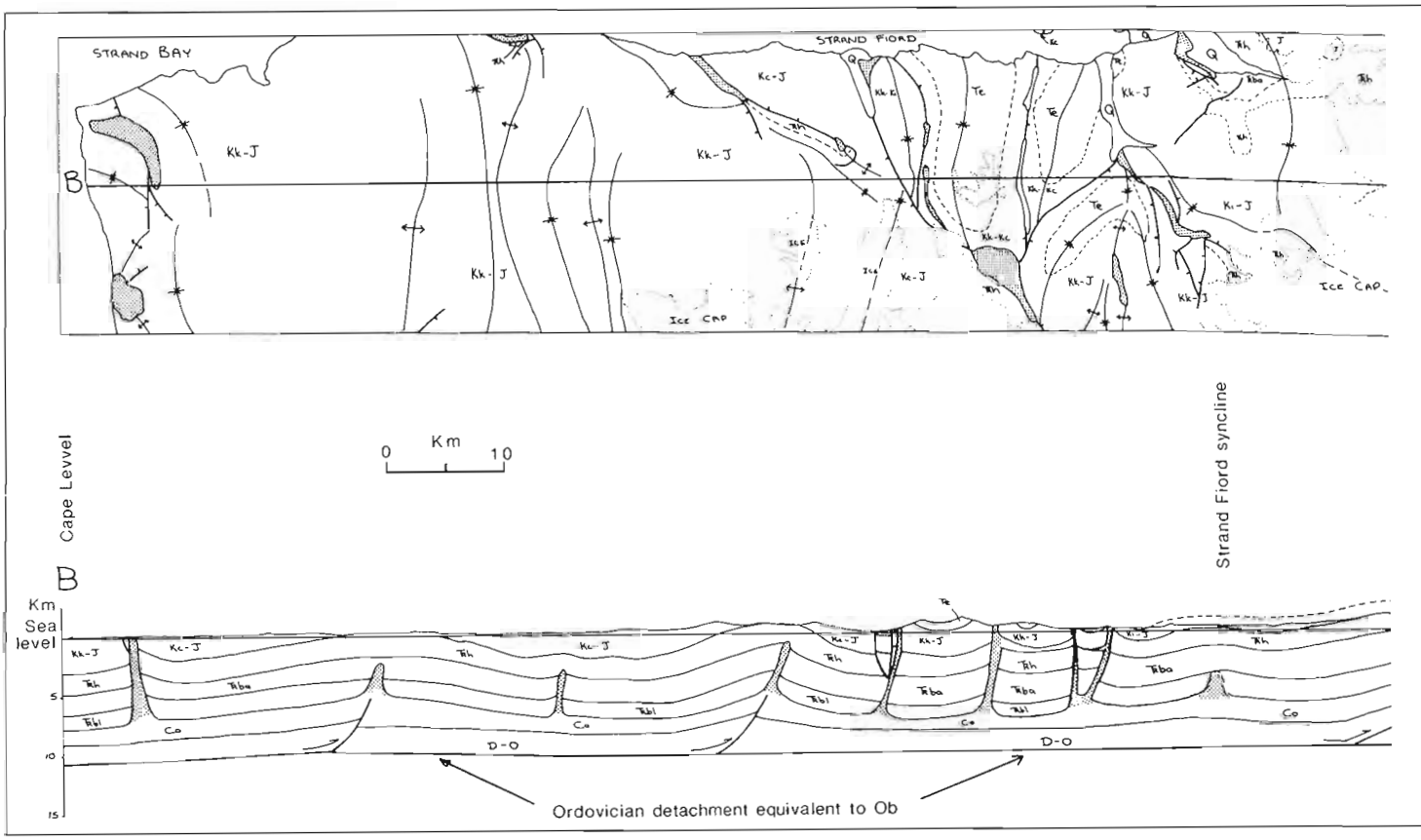
I have benefitted considerably from discussions with my colleagues. In this regard I would like to thank D.K. Norris, D.G. Cook, M.P. Cecile and K.G. Osadetz, all of the Institute of Sedimentary and Petroleum Geology. D.G. Cook, M. McMechan and A. Zolnai provided constructive criticism of the manuscript, and pointed out many of the problems inherent in the balancing of structural sections.

CONSTRAINTS

The lower Paleozoic platform and Precambrian basement southeast of Parrish Glacier Thrust are regarded as fixed relative to the thrust and fold belt in section AA' (through Fosheim Peninsula, Figure 37.2). Although Precambrian gneisses are exposed between Bache Peninsula and Bay Fiord, the depth to this basement elsewhere on Fosheim Peninsula and Axel Heiberg Island is unknown. Furthermore, the thickness of lower Paleozoic strata west and northwest of Vesle Fiord Thrust is also unknown.

Only some of the Ellesmerian structures in the Franklinian rocks have been included in section AA'; the most obvious example is the broad, antiformal structure immediately northwest of Canon Fiord Thrust, where Eureka Sound strata (Expedition Formation – in this area mostly Lower Paleocene, possibly as old as Maastrichtian) overlap eroded Cornwallis Group rocks (Ordovician). Furthermore, Ellesmerian folds (and possibly faults) in Devonian and Ordovician strata probably occur in the footwall of the Canon Fiord thrust and also are overlain by the Eureka Sound Group. Some of the Eurekan thrusts may represent reactivated Ellesmerian faults. For example, "A" Canon Fiord Thrust (Fig. 37.2) is an Ellesmerian structure which placed Ordovician Cornwallis Group on Devonian strata. It was rejuvinated during the Eurekan Orogeny, thrusting Ordovician strata over Tertiary. For the purpose of calculating shortening in the Franklinian rocks resulting from Eurekan deformation, only those structures between Parrish Glacier and Vesle Fiord thrusts have been taken into account (Fig. 37.2). Elsewhere in the two sections, the effect of Eurekan deformation on lower Paleozoic rocks is unknown.

Most of the shortening occurs as a result of thrusts and associated folds. Doming of Sverdrup Basin strata because of salt intrusion is known to have taken place sporadically since the Late Carboniferous (Balkwill, 1978). Several of the anticlinal structures on western Ellesmere and central Axel Heiberg islands are cored by evaporites (Otto Fiord Formation); for example, the Mokka Fiord, Depot Point and Fosheim anticlines. Jackson and Halls (1985) have demonstrated, in the case of Mokka Fiord, that doming occurred prior to the



main phase of Eurekan deformation. However, for the purpose of this investigation, the amount of horizontal shortening is not considered to be great. In fact, some extension might be expected where the diapirs have breached the anticlines.

DISCUSSION

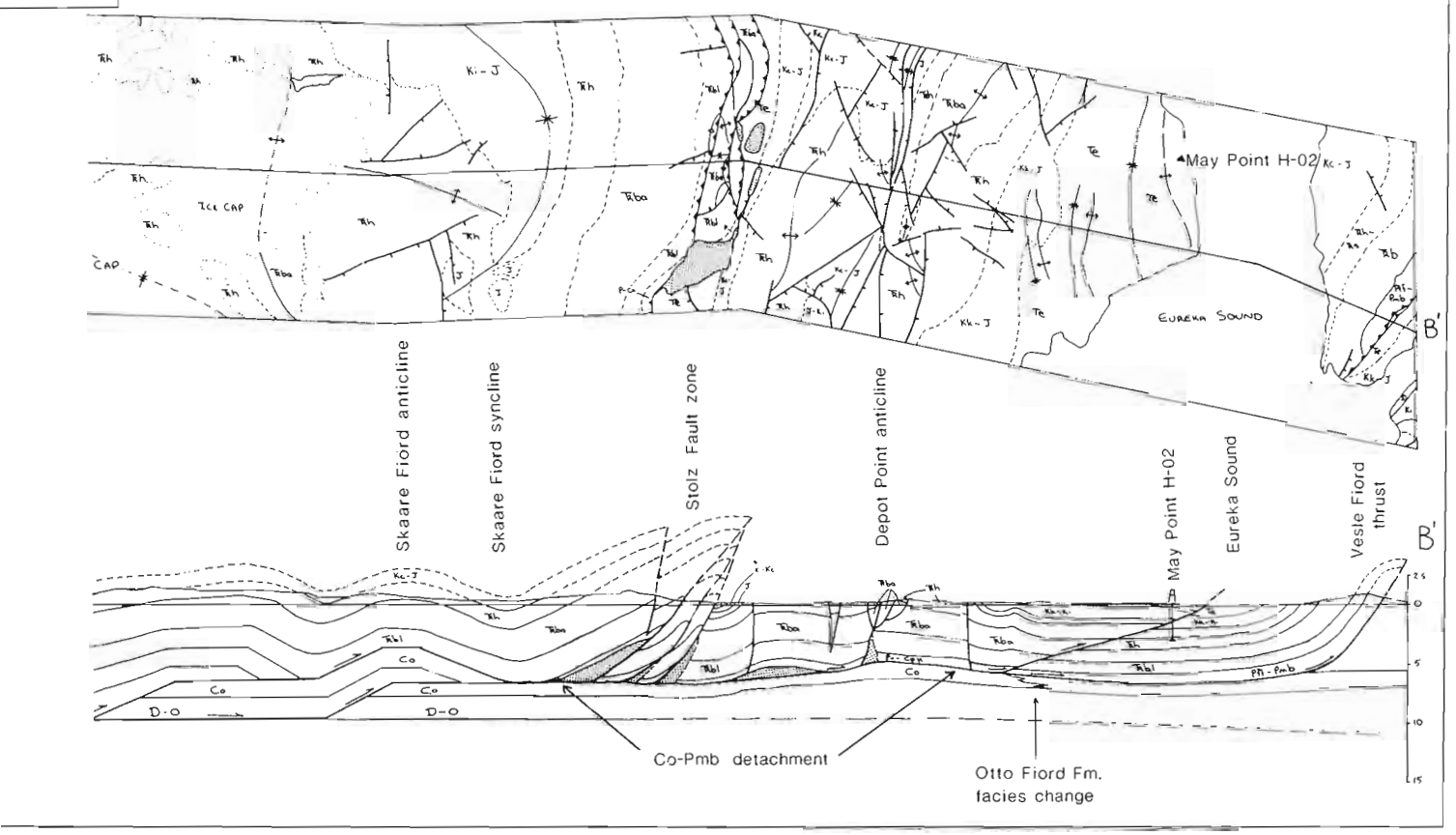
The sections have been constructed showing three levels of detachment.

1. A basement detachment exposes Upper Precambrian-Cambrian strata in the hanging wall of the Parrish Glacier Thrust. The thrust surfaces approximately at the lower Paleozoic platform – shelf margin (Trettin and Balkwill, 1979), and may reflect reactivation of an older basement structure. There appears to be a considerable change in stratigraphic thickness in the lower Paleozoic sequence across this fault. The depth to basement along Fosheim Peninsula, assuming constant thickness of lower Paleozoic and upper Precambrian strata, is about 15 to 18 km, and corresponds reasonably well to depths calculated along a transect through Devon and Ringnes islands on the basis of geophysical parameters (Sobczak et al., 1986).
2. A major detachment occurs in the Lower Ordovician Baumann Fiord Formation evaporites, and is found locally in the hanging wall of an unnamed thrust between Canon Fiord and Vesle Fiord thrusts, as well as in the Canon Fiord Thrust. Beneath western Axel Heiberg Island, this detachment is assumed to occur in stratigraphically equivalent basin shale (Fig. 37.3).

Figure 37.3. Structural cross-section BB' and geology of map strip from Vesle Fiord Thrust, due west across central Axel Heiberg Island. Geology from Thorsteinsson (1971a; 1971b; 1971c; 1972a; 1972b; 1972c); van Berkel et al. (1984); unpublished data. Stippled areas represent Otto Fiord evaporites that have been added to the section as diapirs or domal thickenings. No vertical exaggeration in scale.

Stratigraphic designations are as follows:

Te	= Eureka Sound Group	Trba	= Blaa Mountain Group
Kk-J	= Kanguk Fm. (Kk), Hassel Fm. (Kh), Christopher Fm. (Kc), Isachsen Fm. (Ki), Jurassic undivided (J)	Trbl	= Blind Fiord Fm.
		Ptf-Pmb	= Trold Fiord Fm. to Mount Bayley Fm.
		Co	= Otto Fiord Fm.
Trh	= Heiberg Fm.	D-O	= Devonian to Ordovician undivided



3. The third and uppermost detachment is here drawn at the contact between the Lower Triassic Blind Fiord Formation and Upper Carboniferous Otto Fiord evaporites. Most of the shortening illustrated in Figures 37.2 and 37.3 takes place along this detachment. At its eastern limit near Vesle Fiord Thrust, this detachment occurs in the slightly younger Mount Bayley Formation (Lower Permian). A facies change occurs in the Carboniferous strata approximately between Depot Point anticline and May Point (section BB'), where Otto Fiord evaporites grade into nonevaporitic rocks (see Nassichuk and Davies, 1980, Figure 11). At section BB, slip along the detachment is transferred to the Lower Permian Mount Bayley Formation, which occurs locally in the hanging wall of Vesle Fiord Thrust.

In considering the transfer of slip from the Otto Fiord to the Ordovician detachment beneath Axel Heiberg Island, two possible scenarios are suggested. In the first, the upper detachment (Co = Otto Fiord evaporites) continues west of Axel Heiberg Island with a ramp to the Ordovician detachment (above D-0) located somewhere offshore. The alternative scenario, depicted in Figure 37.3, shows a pair of ramps beneath the Princess Margaret Range, coinciding with an anticline – syncline fold pair in the hanging wall of the Stolz Fault Zone. One problem with this explanation is the possible requirement for a lateral ramp from the Otto Fiord detachment to the Ordovician detachment between sections AA' and BB'.

SHORTENING

The sections have been balanced only to the upper (Otto Fiord) detachment level by comparing lengths of units (the top of the Blind Fiord Formation was used here). The volume of evaporite in the Otto Fiord Formation cannot be assumed to be constant because of salt withdrawal from some areas and addition to halokinetic structures in others. The temporal relationship between thrusting and diapirism remains uncertain. Most of the Sverdrup Basin strata also thin along the lines of section, from the basin depocentre near Strand Fiord to the basin margin east of Vesle Fiord Thrust (see Figure 37.2). Particularly noticeable is the rapid thinning of units like the Blaa Mountain Formation and Blind Fiord Formation east of the Stolz Fault Zone in Figure 37.3 (BB'), and east of Vesle Fiord Thrust in Figure 37.2 (AA').

Shortening along the Ordovician detachment and basal detachment between Vesle Fiord Thrust and the Franklinian platform is about 14.5 km. Elsewhere along these surfaces, the amount of shortening due to Eurekan deformation is unknown. About 10 km (40%) of shortening has taken place at Stolz Fault Zone. The total amount of shortening between the Paleozoic platform and the hanging wall of Stolz Thrust is about 55 km, or 30 per cent. Vergence is to the east and southeast, that is, toward the craton. Between 25 and 50 per cent shortening was estimated by Okulitch (1982) for sections constructed along southern Ellesmere Island, although this value includes both Ellesmerian and Eurekan structures.

REFERENCES

Balkwill, H.R.
1978: Evolution of Sverdrup Basin, Arctic Canada; American Association of Petroleum Geologists, Bulletin, v. 62, p. 1004-1028.

Jackson, K.C. and Halls, H.C.
1985: The age of the north Mokka Anticline, Axel Heiberg Island, Canadian Arctic Archipelago: an application of the paleomagnetic fold test; Bulletin of Canadian Petroleum Geology, v. 33, p. 227-235.

Miall, A.D.
1986: The Eureka Sound Group (Upper Cretaceous-Oligocene), Canadian Arctic Islands; Bulletin of Canadian Petroleum Geology, v. 34, p. 240-270.

Nassichuk, W.W. and Davies, G.R.
1980: Stratigraphy and sedimentation of the Otto Fiord Formation - a major Mississippian-Pennsylvanian evaporite of subaqueous origin in the Canadian Arctic Archipelago; Geological Survey of Canada, Bulletin 286.

Okulitch, A.V.
1982: Preliminary structure sections, southern Ellesmere Island, District of Franklin; in Current Research, Part A, Geological Survey of Canada, Paper 82-1A, p. 55-62.

Ricketts, B.D.
1986: New formations in the Eureka Sound Group, Canadian Arctic Islands; in Current Research, Part B, Geological Survey of Canada, Paper 86-1B, p. 363-374.

Ricketts, B.D. and McIntyre, D.J.
1986: The Eureka Sound Group of eastern Axel Heiberg Island: new data on the Eurekan Orogeny; in Current Research, Part B, Geological Survey of Canada, Paper 86-1B, p. 405-410.

Sobczak, L.W., Mayr, U., and Sweeny, J.F.
1986: Crustal section across the polar continent – ocean transition in Canada; Canadian Journal of Earth Sciences, v. 23, p. 608-621.

Thorsteinsson, R.
1971a: Middle Fiord; Geological Survey of Canada Map 1299A.
1971b: Strand Fiord; Geological Survey of Canada Map 1301A.
1971c: Haig-Thomas Island; Geological Survey of Canada Map 1303A.
1971d: Greely Fiord West; Geological Survey of Canada Map 1311A.
1972a: Eureka Sound North; Geological Survey of Canada Map 1302A.
1972b: Glacier Fiord; Geological Survey of Canada Map 1304A.
1972c: Canon Fiord; Geological Survey of Canada Map 1308A.

Trettin H.P. and Balkwill, H.R.
1979: Contributions to the tectonic history of the Innuitian Province, Arctic Canada; Canadian Journal of Earth Sciences, v. 16, p. 748-769.

van Berkel, J.T., Schwerdtner, W.M., and Torrance, J.G.
1984: Wall-and-basin structure: an intriguing tectonic prototype in the central Sverdrup Basin, Canadian Arctic Archipelago; Bulletin of Canadian Petroleum Geology, v. 32, p. 343-358.

K-Ar geochronology of the McGerrigle plutonic complex, Gaspésie Peninsula, Quebec[1]

Project 840021

J.B. Whalen and J.C.M. Roddick
Lithosphere and Canadian Shield Division

Whalen, J.B. and Roddick, J.C.M., K-Ar geochronology of the McGerrigle plutonic complex, Gaspésie Peninsula, Quebec; in Current Research, Part A, Geological Survey of Canada, Paper 87-1A, p. 375-380, 1987.

Abstract

The McGerrigle plutonic complex consists of a compositionally diverse (gabbro to granite) hybrid suite and a relatively homogeneous granite suite. Recent Rb-Sr whole-rock ages from the complex indicate two distinct periods of intrusion separated by at least 7 Ma. 18 new K-Ar mineral ages overlap in the range 370 to 390 Ma. Though field evidence suggests the granite suite is contemporaneous with, or slightly younger than, the hybrid suite, the K- Ar ages from the granite suite are older. This can be explained by a mafic-felsic magma-mixing model for the hybrid suite. The granite at the south end of the complex cooled quickly, whereas high temperature (550 C) mixing and hybridization continued over a period of time at the north end of the pluton. The significance of younger whole-rock Rb-Sr ages obtained from the granite suite remains unresolved.

Résume

Le complexe plutonique de McGerrigle comprend une suite hybride à composition variée (du gabbro au granite) et une suite granitique relativement homogène. La datation par la méthode du strontium de roches tirées du complexe révèle qu'il y a eu deux périodes distinctés d'intrusion à au moins 7. La datation au K-Ar de minéraux donne dix-huit âges nouveaux variant de 370 à 390 Ma. Même si les données recueillies sur le terrain portent à croire que la suite granitique est du même âge ou légèrement plus récente que la suite hybride, la datation au K-Ar de la suite granitique donne des âges plus anciens. On peut expliquer cet écart en supposant que la suite hybride ait été formée à partir d'un mélange de magmas mafiques et felsiques. Le granite à l'extrémité sud du complexe s'est refroidi rapidement, tandis que la mixtion et l'hybridation à haute température (>550°C) se sont poursuivies pendant une certaine période de temps à l'extrémité nord du pluton. L'importance des âges plus récents obtenus par datation au Rb-Sr de roches provenant de la suite granitique n'a pas encore été établie.

[1]Contribution to the "Plan de development economique Canada/Gaspesie et Bas Saint-Laurent".

INTRODUCTION

The McGerrigle plutonic complex covers an area of about 100 sq km in the Gaspé segment of the north-central Appalachian orogenic belt (Fig. 38.1). Geological work (Whalen, 1985; 1986) and geochemical studies (Whalen and Gariépy, 1986) have documented the complex nature of this suite and have indicated possible models for its petrogenesis. The most plausible of these is that all the various intrusive phases in the complex are essentially contemporaneous products of interaction between at least one acid and one mafic magma. K/Ar mineral ages were determined on various phases to clarify age relationships in the suite. Whole-rock Rb-Sr isotopic work, in progress at the time of initiation of this project, has just been completed (Larocque, 1986), and suggests the existence of a number of ages of intrusive rocks in the complex.

ACKNOWLEDGMENTS

We would like to thank G. Wallace and C. Gariépy for mineral separation work and C. Larocque for permiting us to quote her Rb/Sr work on the McGerrigle complex.

GENERAL GEOLOGY

The simplified geological map of the McGerrigle plutonic complex, Figure 38.1, and the following summary of the geology are based on the 1:25,000 scale map and marginal notes of Whalen (1986). The complex can be roughly subdivided into granite and hybrid suites. The bulk of the granite suite occurs in the southern portion of the pluton. The hybrid suite, though mainly restricted to the northern half of the pluton, outcrops to the north and southeast of Mount Richardson and to the east of Les Cones. The hybrid suite includes a component lithologically identical to the granite suite rocks but the contact relationships between the hydrid and granite suites are ambiguous: contacts appear to be gradational in many areas, being marked by the appearance of mafic inclusions in the granite. There are, however, also examples of sharp intrusive relationships between younger granite and hydrid suite rocks. Based on their outcrop area, granitic rocks form about 75% of the complex, basaltic rocks about 5% and hybrid rocks (dioritic to syenitic composition) about 20%.

The compositionally relatively homogeneous granite suite has been subdivided into different intrusive phases on the basis of grain size, feldspar mineralogy and equigranular or porphyritic character. Contacts between these phases, which are not shown in Figure 38.1, appear to be mainly gradational. The granitic rocks vary in colour from scarlet red to white and their main mafic mineral is biotite with local hornblende +/− pyroxene. Magnetite, apatite, zircon, titanite and allanite are minor accessory phases.

The hybrid suite consists of compositionally diverse mixtures of gabbro, diorite, quartz diorite, granodiorite, monzodiorite, quartz monzonite, syenite and granite. Although some portions of the hybrid suite have been subdivided into homogeneous intrusive units on a map scale, the most striking feature of the bulk of the suite is its heterogeneity on both map and outcrop scale. Variations in texture and composition commonly occur over such a short distance that it is often difficult to decide whether such variants represent large inclusions or contemporaneous or younger intrusions. In the case of mafic-felsic mixtures, contact relationships described byhalen (1985) such as chilled margins on mafic inclusions, pillow-like structures of chilled basaltic rock in granite and broken-up mafic dykes cutting granite, indicate the coexistence of mafic and felsic magmas. On an outcrop scale, there is evidence for intermediate or hybrid rocks produced by mixing, but the field relationships are complex and indicate multiple injection and hybridization.

The mafic portion of the hybrid suite ranges in grain size from fine- to coarse-grained and forms small bodies scattered over the northern half of the pluton. In some areas mafic rocks form abundant inclusions in more felsic hybrid suite rocks. The finer grained variants often occur in close proximity to felsic rocks and exhibit evidence of potassium metasomatism in the form of fine-grained secondary biotite. The mineralogy is titanaugite, plagioclase (labradorite), kaersutitic amphibole, biotite, apatite, ilmenite, magnetite and sulphides. A significant feature which distinquishes felsic portions of the hybrid suite from the granite suite is a lower quartz content (<20%) and the presence of patchy mafic mineral aggregates derived from partially digested mafic xenoliths. Such aggregates vary in colour from grey to reddish, are fine- to medium-grained and range in texture from hypidiomorphic granular to porphyritic. Mafic mineral content ranges to as high as 30%, the main phase being hornblende, commonly with salitic clinopyroxene cores, and less abundant biotite. Opaques, zircon, titanite, apatite and allanite are common accessory phases. Associated with the two southern areas of hybrid suite rocks are metasomatized gabbros which vary from fine- to coarse-grained and form areas up to 0.5 km across. Primary calcic plagioclase has been replaced by untwinned plagioclase and the mafic minerals are pseudomorphed by diopside plus rutile and titanite.

In the northern portion of the pluton, there are a number of pod-shaped bodies of miaskitic nepheline syenite which have irregular, probably gradational contacts with hybrid suite rocks. They are porphyritic with perthitic alkali feldspar, biotite and aegerine-augite phenocrysts in a trachytic textured matrix of similar mineralogy plus nepheline, apatite, titanite, zircon and oxides. Field relationships suggest that this undersaturated magma was contemporaneous with the magmas that produced the hybrid suite. Also, cutting hybrid suite rocks in the northern part of the pluton, are rare, thin (up to 3 m wide) peralkaline nepheline syenite dykes or sills which contain trachytic textured alkali feldspar, nepheline, sodalite, aegerine, arfvedsonite, aenigmatite and accessory minerals.

GEOCHRONOLOGY

Analytical techniques and background

Mineral separates were obtained by standard magnetic and heavy liquid techniques followed by hand-picking to obtain

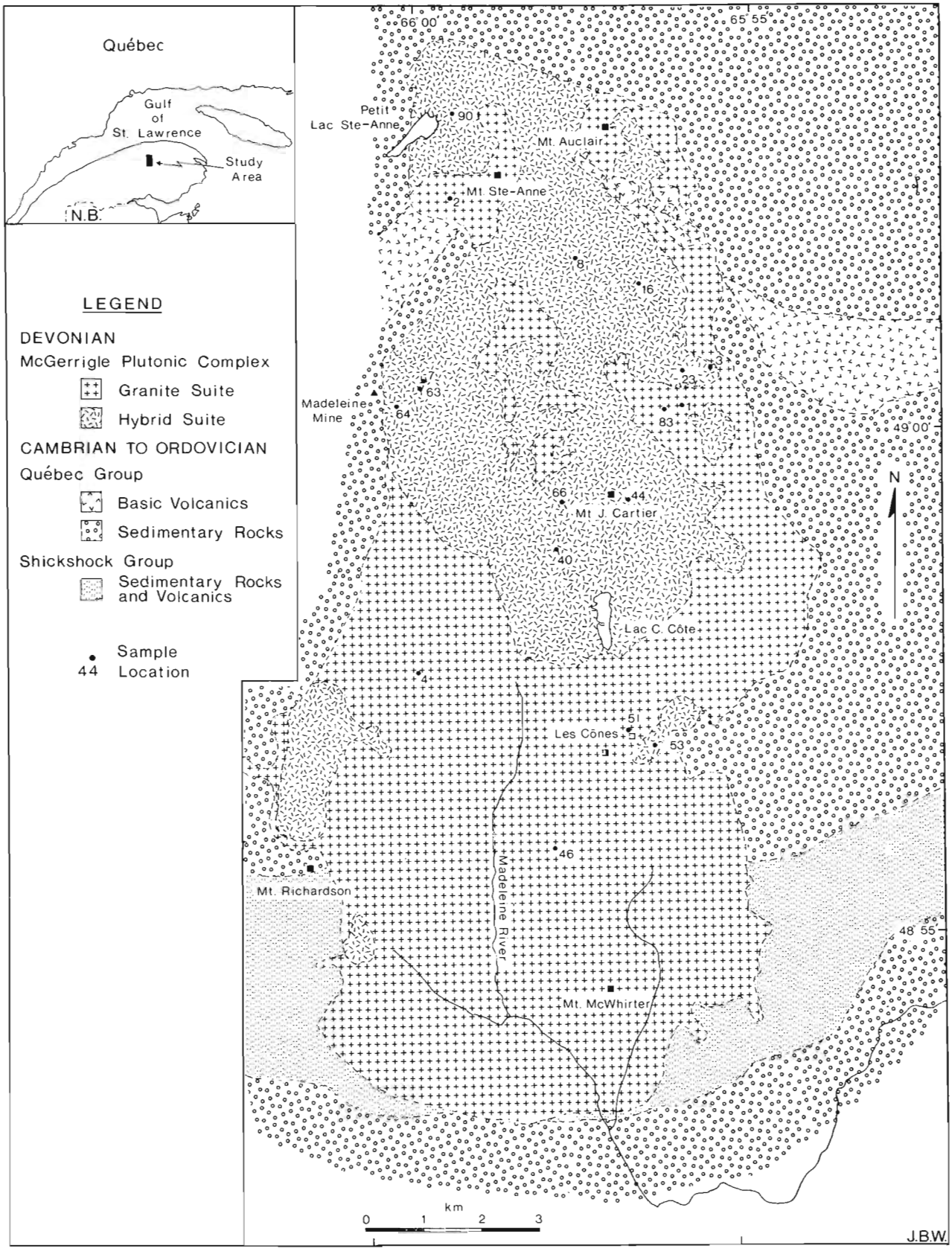


Figure 38.1. Location of the McGerrigle plutonic complex, Gaspésie, Quebec and a generalized geological map of the area after Whalen (1986). The sites of K-Ar ages are given, numbers 1 to 4 and 7 are samples of de Romer (1974) while the other samples are those of this study (WXMG prefix omitted).

better than 99% purity. The concentration of potassium in theamples was determined by atomic absorption spectrometry on multiple aliquots of duplicate sample dissolutions. Analytical precision was usually 0.4 to 1.0 % (1 sigma) but a few ranged up to 2.0 %. Multiple analyses of a biotite (LP-6) and a syenite (SY-2) standard were run as references with the samples.

Extraction of argon from the samples involved radio-frequency induction heating to fuse the sample in a vacuum. A precisely determined quantity of enriched argon-38 was added to the liberated gas which was then purified by passage through cold-traps, and over titanium sponge getters. Isotopic analyses were carried out in modified A.E.I. MS-10 mass spectrometers operated in static mode. Precision on argon concentrations are 0.6 (1 sigma). The ages were calculated using the decay constants recommended by Steiger and Jager (1977) and errors at the two sigma level were assigned to them based on the accumulated errors from the potassium and argon analyses (Table 38.1).

A K-Ar mineral age records the time since a mineral became a closed system with respect to argon and is dependent on the closure temperature (diffusion threshhold) of individual minerals. Continuous diffusion of argon after crystallization will result in an age which is too young. Estimates by Harrison and McDougall (1980) of the temperatures at which hornblende and biotite are effectively closed with respect to radiogenic argon are $530+/-40$ and $280+/-40$ C, respectively. Since cooling of intrusive rocks may extend over millions of years, plutonic rock K-Ar ages may significantly post-date the time of intrusion and crystallization of the rock. Because of their difference in blocking temperatures, discordant ages from coexisting hornblende-biotite pairs can be interpreted either as reflecting a cooling history or a superimposed thermal event which has reset biotite to a greater extent than hornblende. Concordant ages indicate rapid cooling and K-Ar ages which closely approximate intrusion ages.

Previous work

All ages of previous workers have been recalculated using decay constants of Steiger and Jager (1977). A Siluian K-Ar biotite age of 427 Ma was obtained from a coarse-grained red granite from the west side of the McGerrigle pluton by Leech et al. (1963) (sample 4 in Fig. 38.1). This age, which was viewed with suspicion by workers in the area, proved to be erroneous. A rerun of the same biotite concentrate gave an age of $365+/-16$ Ma (Wanless et al., 1973). De Romer (1974), in an attempt to substantiate a Devonian age for the pluton, obtained three whole rock K-Ar determinations from the pluton: a porphyritic granite (sample 1) ($363+/-11$ Ma), a biotite granodiorite (sample 2) ($352+/-10$ Ma),and a hornblende-biotite diorite (sample 3) ($325+/-10$ Ma). In addition, de Romer collected a quartz diorite (sample 7) from which Wanless et al. (1973) obtained a hornblende K-Ar age of $348+/-14$ Ma. All these K-Ar agesverlap within the estimated errors, except for the $325+/-10$ Ma age and indicate a Devonian age for the complex. Whole rock K-Ar ages are often undependable due to argon loss so the younger diorite age is readily explained. As part of a whole rock Rb-Sr isotopic study on igneous rocks in Gaspésie, Larocque (1986) analyzed samples of the McGerrigle intrusive complex. This work indicated the presence of two distinct intrusive ages

Table 38.1 K-Ar ages from the McGerrigle plutonic complex

Suite	Sample No. (WXMG-)	Rock % SiO2 (wt. %)	Lithology	Mineral	K (wt. %)	Radiogenic Ar ($\times 10^{-7}$ cc/gm)	% Atmospheric Ar	Calculated Age (Ma.)±2 s.e.
	64	47.93	gabbro	Biot	6.27	1016	0.7	375±12
	90	53.06	diorite	Biot	7.85	1269	0.6	374±8
	23	55.32	syenodiorite	Biot	7.24	1185	0.5	378±8
	53	56.23	diorite	Hbl	0.530	86.22	5.3	376±11
				Biot	7.13	1155	0.5	375±6
Hybrid Suite	16	61.22	nepheline syenite	Biot	7.67	1250	1.3	377±9
	40	63.88	quartz monzonite	Hbl	0.567	92.89	4.8	379±6
	8	64.90	syenite	Hbl	0.586	90.48	11.0	359±12
	44	66.78	syenite	Hbl	0.672	107.6	3.1	371±6
	63	67.48	quartz monzonite	Hbl	0.374	60.68	7.4	376±11
	66	67.89	quartz monzonite	Hbl	0.501	86.02	6.1	395±22
				Biot	6.17	1029	1.7	385±5
	46	72.49	porphyritic granite	Hbl	0.524	89.19	7.8	392±5
				Biot	6.92	1172	0.6	391±7
Granite Suite	51	72.70	porphyritic granite	Hbl	0.747	127.3	4.4	392±17
				Biot	7.14	1158	0.5	375±7
	83	73.78	porphyritic granite	Hbl	0.672	113.3	4.2	389±8
				Biot	5.64	893.4	0.9	368±5

Constants employed: $\lambda_\beta = 4.962 \times 10^{-10} a^{-1}$; $\lambda_\epsilon + \lambda_\epsilon = 0.581 \times 10^{-10}$; $^{40}K/K = 0.1167$ atom%
Abbreviations: Hbl = hornblende; Biot = biotite

in the complex: the hybrid suite from around Lac Riffou, 1.5 km southeast of Madeleine Mine, yielded an isochron of 382 +/− 8 Ma and granitic suite isochrons of 356 +/− 8 Ma and 362 +/− 5 Ma were obtained from the Madeleine River and Mont McWhirter areas at the southern margin of the complex. The granitic suite isochrons have significantly higher initial ratios of about 0.71 versus a ratio of 0.704 for the hybrid suite.

Discussion of results

The 18 new K-Ar mineral ages from the Mount McGerrigle plutonic complex, presented in Table 38.1 and diagrammatically depicted in Figure 38.2, are subdivided on the basis of rock type. The major aim of this study was to try to establish whether there are intrusions of different ages present in the complex. There is some variation in the K-Ar mineral ages, but most of the ages overlap in the range 370 to 390 Ma. Though the K-Ar ages represent cooling ages, most are within the error of the hybrid suite Rb-Sr whole-rock age (382 +/− 8 Ma) of Larocque (1986).

Based on field relationships, the granite suite is contemporaneous with (Whalen, 1985, 1986) or younger than (de Romer, 1977) the hybrid suite. However, ages from the granite suite are older (average amphibole age of 391 Ma) than those from the hybrid suite (average amphibole age of 376 Ma) and there is a spread of ages from the hybrid suite. This is not readily explained as reflecting a protracted cooling history. Biotite and hornblende ages from the same samples have the same ages within error limits in four out of five cases. This indicates rapid cooling of the intrusive rocks, so differences in hornblende ages suggest differences in solidification ages for the granite and hybrid suites. While this may represent different times of intrusion, another explanation is provided by the magma-mixing model for petrogenesis of the hybrid suite (Whalen, 1985; Whalen and Gariépy, 1986). Interaction between a hot (1200 C), low viscosity, mafic magma and a cooler (700 C), viscous, felsic magma can be a very complex process involving remelting and superheating of the felsic magma, double diffusive convection and turbulent mafic magma injections or fountains into the felsic magma (see summary of Turner and Campbell, 1986). An extended period of multiple injection, mixing and hybridization is supported by the complexity of the hybrid suite. The north-end of the pluton, which is dominated by hybrid suite rocks, could have been characterized by quite high temperatures (550 C) over an extended period of time compared to the south end of the pluton dominated by the granitic suitehich cooled quickly through the closure temperatures of hornblende and biotite. The older ages from the granite suite would be the best estimate of intrusion age, whereas the ages from the hybrid suite would reflect the end of the mixing process by solidification. The apparent variation in ages from the hybrid suite may record real differences in the time when mixing and cooling ceased at different locations. A granite suite sample collected in close proximity to the hybrid suite (WXMG-83; Fig. 38.1), contains an age gap between hornblende and biotite. The youger biotite age may reflect thermal effects of

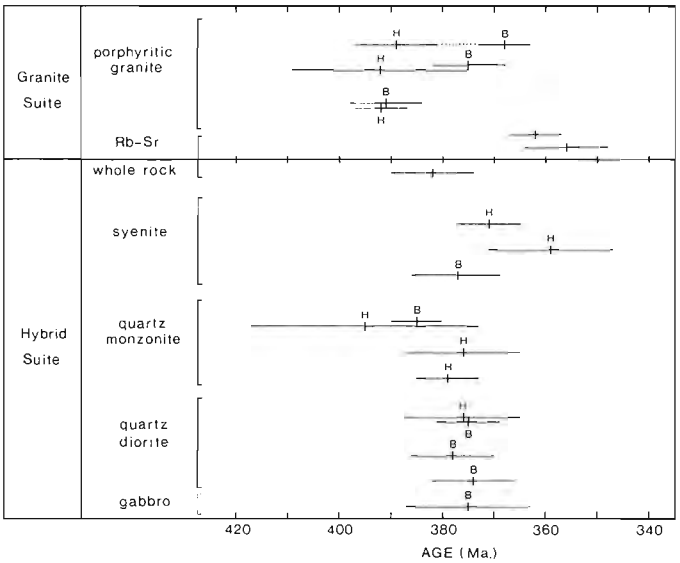


Figure 38.2. Diagrammatic presentation of K-Ar mineral ages from the McGerrigle plutonic complex and , for comparison purposes, the whole rock Rb-Sr ages of Larocque (1986). The samples are subdivided according to rock type. Ages from Table 1 are plotted together with error bars (2 sigma), biotite-hornblende pairs are joined. Abbreviations: biotite = B; hornblende = H.

the still molten hybrid suite. Support for higher heat flux from the hybrid suite is given by regional illite crystallinity work (Islam et al., 1982; Hesse, unpublished data). At the north-end of the complex, there is a 16-20 km wide epimetamorphic halo which decreases in width southward to only about 1 km at the south end of the intrusion.

The K-Ar ages of the granitic suite are distinctly older than the whole rock Rb-Sr ages of Larocque (1986) for similar rocks (Fig. 38.2). As the hornblende-biotite K-Ar ages are essentially concordant, this suggests that the Rb-Sr ages are not simply isochrons but may also represent the mixing of rocks with different initial ratios. Previously, Roddick and Compston (1977) detailed similar relationships for apparently homogeneous granitic intrusions. Rb-Sr mineral isochrons may resolve this anomaly.

In summary, the new K-Ar ages, in combination with the Rb-Sr work on the hybrid suite (Larocque, 1986), indicate that the hybrid suite is about 382 Ma old and is apparently 10 Ma younger than the granitic suite located in the southern portion of the plutonic complex. While this suggests later intrusion of the hybrid suite, the field relationships suggest they are contemporaneous (Whalen, 1985, 1986). This anomaly may be resolved if the production of the hybrid suite involved a protracted interaction and cooling history between a granitic and a high temperature mafic magma, both emplaced at similar times. The miaskitic nepheline syenite probably formed a third component in a magma-mixing process that produced the hybrid suite (Whalen and Gariepy, 1986).

REFERENCES

de Romer, H.S.

1974: Geology and age of some plutons in north-central Gaspé, Canada; Canadian Journal of Earth Sciences, v.11, p.570-582.

1977: McGerrigle Mountains area; Quebec Ministry of Natural Resources, Geological Report 174, 233 p.

Harrison, T.M. and McDougall, I.

1980: Investigations of an intrusive contact, northwest Nelson, New Zealand. 1. Thermal, chronological and isotopic constraints; Geochimica et Cosmochimica Acta, v. 44, p. 1985-2003.

Islam, S., Hesse, R. and Chagnon, A.

1982: Zonation of diagenesis and low-grade metamorphism in Cambro- Ordovician flysch of Gaspe Peninsula, Quebec Applalachians; Canadian Mineralogist, v. 20, p. 155-167.

Larocque, C.

1986: Geochronology and petrology of north-central Gaspé igneous rocks, Quebec; unpublished M.Sc. thesis, McGill University.

Leech, G.B., Lowdon, J.A., Stockwell, C.H., and Wanless, R.K.

1963: Age determinations and geological studies; Geological Survey of Canada, Paper 63-17.

Roddick, J.C.M. and Compston, W.

1977: Strontium isotopic equilibrium: a solution to a paradox; Earth and Planetary Science Letters, v.34, p.238-246.

Steiger, R.H., and Jager, E.

1977: Subcommission on geochronology: convention on the use of decay constants in geo- and cosmochronology; Earth and Planetary Science Letters, v.36, p.359-362.

Turner, J.S. and Campbell, I.H.

1986: Convection and mixing in magma chambers; Earth Science Reviews, v.23, p.255-352.

Wanless, R.K., Stevens, R.D., Lachance, G.R., and Delabio, R.N.

1973: Age determinations and geological studies, K-Ar isotopic ages, report 11; Geological Survey of Canada, Paper 73-2.

Whalen, J.B.

1985: The McGerrigle plutonic complex, Gaspé, Quebec: evidence of magma mixing and hybridization; in Current Research, Part A, Geological Survey of Canada, Paper 85-1A, p. 795-800.

1986: Geology of the McGerrigle Mountains plutonic complex, Gaspé, Quebec: 1:25,000 scale map and marginal notes; Geological Survey of Canada, Open File 1284.

Whalen, J.B. and Gariépy, C.

1986: Petrogenesis of the McGerrigle plutonic complex, Gaspé, Quebec: a preliminary report; in Current Research, Part A, Geological Survey of Canada, Paper 86-1A, p. 265-274.

Geology and mineral occurrences in the central and northern parts of the Roberts Arm Group, central Newfoundland

Project 840059

H. Scott Swinden[1]
Mineral Resources Division

Swinden, H.S., Geology and mineral occurrences in the central and northern parts of the Roberts Arm Group, central Newfoundland; in Current Research, Part A, Geological Survey of Canada, Paper 87-1A, p. 381-390, 1987.

Abstract

The stratigraphic continuity of the Roberts Arm Group has been established from Highway 380 south to the Handcamp Prospect. The Roberts Arm Group is structurally juxtaposed to the west with the mafic and intermediate dominantly intrusive rocks of the Hall Hill Complex, which passes to the north into the coeval Mansfield Cove Complex of plagiogranite with lesser mafic intrusive rock. These units were probably a fragment of oceanic crust.

Showings of volcanogenic mineralization near Roberts Arm and Sunday Cove Island, hosted by mafic, calc-alkaline volcanic rocks, have patterns of wall rock alteration similar to those of the nearby, statigraphically approximately equivalent, Pilley's Island Mine. Stratigraphically lower base metal-bearing tension veins, near Crescent Lake, also considered volcanogenic, may represent a deeper level of the Pilley's Island hydrothermal cell. In the Rust Pond and Round Pound areas, pyritic stockworks in high-Ti tholeiites carry minor base metals.

Résumé

La continuité stratigraphique du groupe de Roberts Arm a été établie depuis la route 380 vers le sud jusqu'à la zone d'intérêt de Handcamp. Le groupe de Roberts Arm est structuralement juxtaposé à l'ouest aux roches mafiques et neutres d'origine surtout intrusive du complexe de Hall Hill qui devient, plus au nord, le complexe contemporain de Mansfield Cove. Ce dernier se compose de plagiogranite et de petites quantités de roches intrusives mafiques. Ces unités représentent probablement un fragment de la croûte océanique.

Des minéralisations d'origine volcanique se manifestent dans des roches volcaniques mafiques de nature calco-alcaline aux alentours de Robert's Arm et de l'île Sunday Cove; l'altération de la roche encaissante produit un motif similaire à celui observé dans les roches encaissantes de la mine voisine, plus ou moins stratigraphiquement équivalente, de Pilley's Island. Près du lac Crescent, des filons d'extension situés stratigraphiquement plus bas contiennent des métaux communs et auraient également une origine volcanique; ces filons pourraient représenter un niveau plus profond de la cellule hydrothermale de Pilley's Island. Aux alentours des étangs Rust et Round, des tholéiites riches en Ti contiennent des stockwerks pyriteux, lesquels renferment de faibles concentrations de métaux communs.

[1]Department of Mines and Energy, P.O. Box 4750, St. John's, Newfoundland A1C 5T7.

INTRODUCTION

This report summarizes the results of field work in the second year of a project designed to investigate the metallogeny of the "Buchans-Robert's Arm belt", an early Ordovician volcanic, subvolcanic and volcaniclastic sequence in the north central part of the Dunnage Zone, central Newfoundland (Fig. 39.1). Swinden and Sacks (1986) summarized the initial results of this project, outlining the stratigraphic succession and providing a stratigraphic framework for volcanogenic mineralization in the southern part of the Robert's Arm Group. Field mapping during 1986, concentrated in the central part of the Robert's Arm Group, was aimed at tracing geological units from the limit of 1985 mapping northward to the southern limit of Bostock's (1978) mapping of the northern part of the Robert's Arm Group. Particular attention was paid to the western side of this area between Hall Hill and Halls Bay in an attempt to reconcile geological relationships portrayed by Currie (1975, 1976) and Bostock et al. (1979) in this area with those of Dean and Strong (1976) and Kean et al (1981).

Swinden and Sacks (1986) summarized most of the previous work and development of stratigraphic nomenclature in the southern Robert's Arm Group and adjacent rocks. The earliest mapping in the central part of the Robert's Arm Group was that of Hayes (1951) and Kalliokoski (1953) who traced volcanic and sedimentary rocks north from the Gull Pond area and assigned volcanic and volcaniclastic rocks in this area to the Bader Bay Series following the work of Espenshade (1938) to the north. Volcanic rocks were assigned to the Robert's Arm Formation and underlying felsic tuff and chert to the Crescent Lake Formation. Kalliokoski (1953) was the first to map intrusive rocks of mafic and intermediate composition in the area of South Pond immediately west of the Robert's Arm Group which he interpreted as younger than and intrusive into the Robert's Arm Group volcanic rocks. He noted that there were many fine and medium grained, relatively featureless, mafic rocks in this area for which an intrusive or extrusive origin could not be definitely established. Kalliokoski (1953) was the first to recognize granitic rocks west of the Robert's Arm Group near Halls Bay (the Mansfield Cove Complex in present nomenclature, see below) although he only mapped a small outlier of these rocks northwest of Loon Pond.

Dean and Strong (1976) and Kean et al. (1981) followed Kalliokoski's (1953) interpretation of the distribution of rock units with relatively minor revisions. They interpreted mafic rocks which underlie the area from Hall Hill to Halls Bay to be volcanic rocks of the Robert's Arm Group, and suggested that these were intruded from the west by Devonian intermediate and felsic plutonic rocks. Granitoid rocks on the shore of Halls Bay (which they termed the "Halls Bay Pluton") were likewise interpreted as Devonian, intrusive into the Robert's Arm Group.

A somewhat different interpretation of this geology was presented by Currie (1975, 1976) and Bostock et al. (1979) who suggested that much of the area between Hall Hill and Halls Bay was in fact underlain by an older, dominantly mafic intrusive suite which Currie (1976) termed the Hall Hill Complex. They further showed that granitoid rocks on the shores of Halls Bay, which they termed the "Mansfield Cove Complex", consisted dominantly of tonalite similar to oceanic plagiogranite and were likewise older than the Robert's Arm Group. They interpreted the Hall Hill Complex and the Mansfield Cove Complex as fragments of the ocean floor and the contact between them and the Robert's Arm Group to be, at least in part, a fault (see also Bostock, 1978). Recognizing that some mafic dykes in the Mansfield Cove Complex were similar to subvolcanic dykes in the Robert's Arm Group, they suggested that the Mansfield Cove and Hall Hill Complexes probably were basement to the Robert's Arm Group during the early Ordovician volcanic activity.

The present mapping was intended to address the disparity between these interpretations and to define the limits of the Robert's Arm Group in this area.

Following completion of the mapping, examination of mineral occurrences in the central and northern parts of the Robert's Arm Group was carried out with the aim of documenting their geological relationships and sampling them for geochemical analysis. The best known deposits in this area are at Pilley's Island where a complex hydrothermal alteration and massive sulphide system is associated with an extrusive dacite dome. The massive sulphides were mined for pyrite around the turn of the century. Several minor occurrences between Pilley's Island and Sunday Cove Island were examined in detail to compare them with the Pilley's Island deposits and investigate the relationship if any between them. In addition, numerous minor occurrences previously reported in the area southwest and west of Crescent Lake were visited, their geological setting documented and samples taken for base and precious metal analyses.

REGIONAL GEOLOGY

Mapping in the central part of the Robert's Arm Group (Fig. 39.2) has shown that the Robert's Arm Group can be traced continuously from the south end of Bostock's (1978) mapping to the northern end of Swinden and Sacks' (1986) mapping near the Handcamp prospect. However, as shown by Currie (1976) and Bostock et al. (1979), much of what Kalliokoski (1953), Dean and Strong (1976) and Kean et al. (1981) considered as the western part of the Robert's Arm Group in fact consists dominantly of mafic to intermediate intrusive rocks (the Hall Hill Complex, Currie, 1976). The individual geological units in this area are described briefly below.

Hall Hill and Mansfield Cove complexes

For the most part, the Hall Hill Complex consists of fine to medium grained intrusive rocks. In the area immediately south of Highway 380, fine to medium grained gabbro and diorite prevail. Although these are generally equigranular, it is not uncommon to see very coarse grained pegmatitic gabbro, with individual plagioclase and pyroxene crystals up to 3 cm long, forming pods and dykes within the country

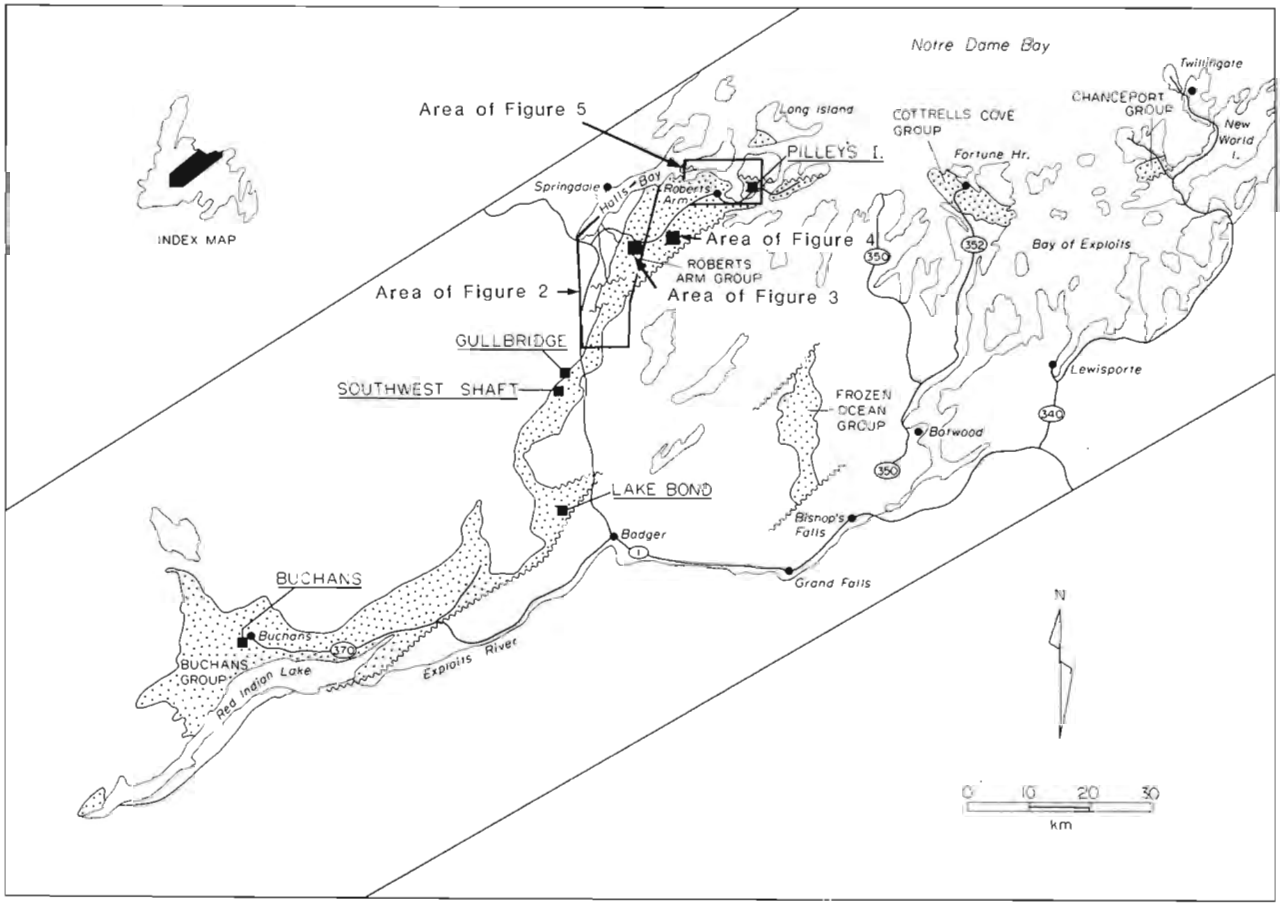


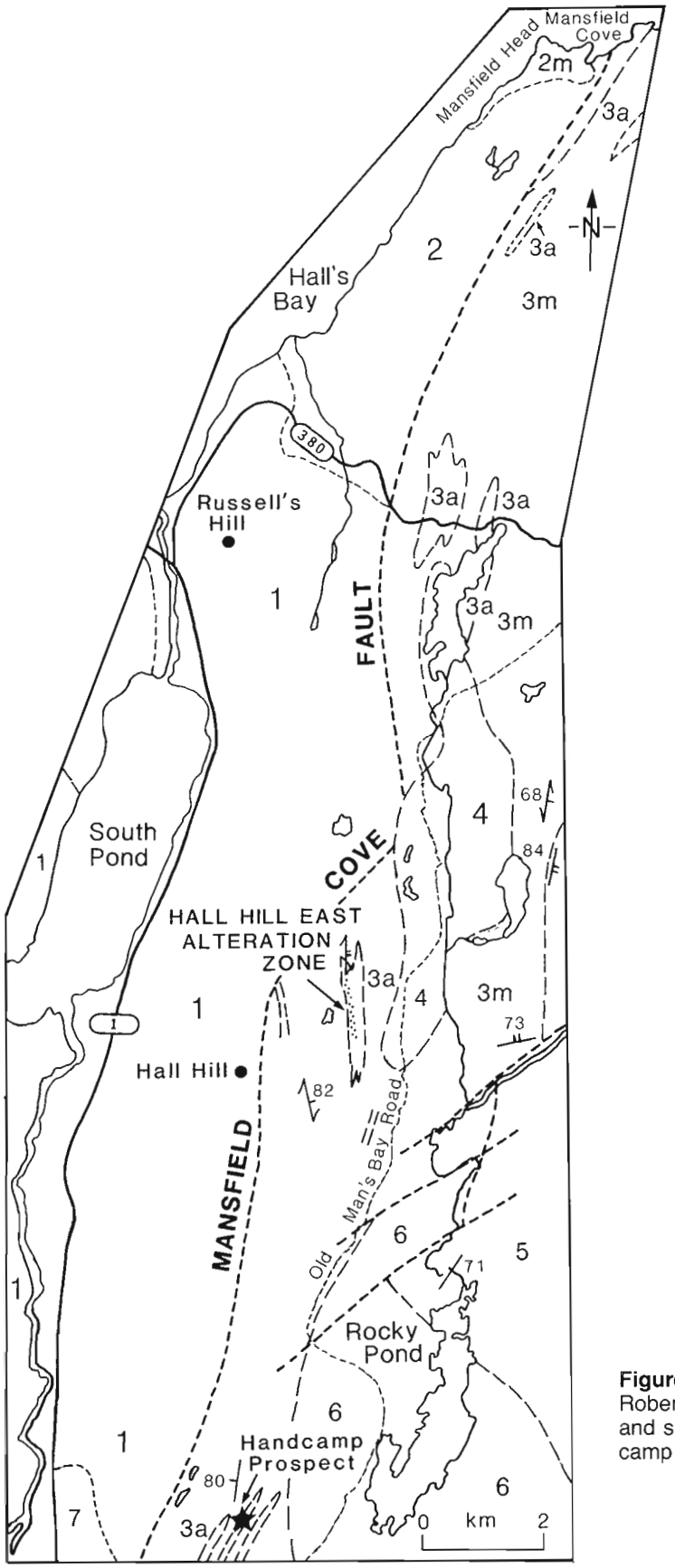
Figure 39.1. Location of the Buchans – Roberts Arm Belt (stippled). Major volcanogenic sulphide deposits indicated by solid squares.

rocks, and feldspar porphyritic diabase is locally abundant. Most outcrops contain two or more phases and intrusive relationships are complex. Outcrops on Rowsell's Hill expose what appears to be part of a sheeted dyke complex, consisting of parallel, 2 cm to 2 m wide dykes of equigranular gabbro, diorite and diabase and feldspar-phyric diabase. In general, the dykes trend slightly east of north and dip steeply to the east. Screens of pillow lava up to 10 m wide and tens of metres long are locally present; the pillows are generally small (<5 m), epidotized and moderately flattened. Plagiogranite occurs as crosscutting, generally relatively late dykes and as pods (inclusions) in the mafic rocks. Plagiogranite abundance declines southward although sparse dykes can be found almost as far south as Hall Hill.

The Mansfield Cove Complex (Bostock et al., 1979), otherwise referred to as the Mansfield Cove pluton (Currie, 1975, 1976; Bostock, 1978) or the Halls Bay pluton (Dean and Strong, 1976; Kean et al., 1981), consists dominantly of plagiogranite, which generally has abundant distinctive large quartz eyes. Lesser granodiorite and local patches of alaskite (Currie, 1976) are present. It is cut by abundant dykes of gabbro and diabase similar to those in the Hall Hill Complex. Near Mansfield Head, a large inlier of mafic intrusive rocks outcrops along the shore. Although previously mapped as volcanic rocks, these appear to be dominantly intrusive, including much finer grained diabase, but also many coarser intrusive lithologies. The dykes are locally intruded in parallel swarms like those on Rowsell's Hill.

The relationship between the Hall Hill and Mansfield Cove complexes is inferred from crosscutting observations. Plagiogranite both cuts and is included in mafic dykes in the northern part of the Hall Hill Complex. Likewise, on the Halls Bay shore, fine grained gabbro and diabase like that in the Hall Hill Complex both cut and elsewhere are cut by plagiogranite. Magmatic activity recorded by the two complexes appears to have occurred simultaneously and in fact, they should perhaps be redefined as a single complex. This is not to suggest they are necessarily petrogenetically related; detailed geochemical studies are needed to test this possibility.

The contact between the Mansfield Cove Complex and the Robert's Arm Group is a fault, exposed on the shoreline east of Mansfield Head (Bostock, (1978). Although the eastern contact of the Hall Hill Complex with the Robert's Arm Group does not outcrop, it is interpreted as a fault based on



LEGEND AND SYMBOLS FOR FIGURE 39.2

DEVONIAN AND YOUNGER

7 Granitoid rocks. 7s–South Pond pluton

6 Mafic to intermediate plutonic rocks, probably related to the Twin Lakes Complex

ORDOVICIAN TO SILURIAN

5 Sansom Greywacke: greywacke and fine grained conglomerate with volcanic provenance

4 Loon Pond pluton: fine to medium grained granite, syenite

EARLY ORDOVICIAN AND OLDER(?)

3 Roberts Arm Group: 3a–dominantly felsic volcanic rocks, quartz-sericite schist; 3m–dominantly mafic volcanic rocks; 3c–Crescent Lake Fomation, fine grained volcaniclastic rocks, red chert and mudstone

2 Mansfield Cove Complex: dominantly plagiogranite, lesser granodiorite, alaskite, mafic dykes. 2m–dominantly fine grained mafic intrusive rocks, lesser gabbro

1 Hall Hill Complex: Dominantly mafic and intermediate intrusive rocks. Includes minor pegmatitic gabbro, pillow lava, pyroxenite and plagiogranite

SYMBOLS

- approximate geological contact
- fault (assumed)
- strike and dip of bedding
- strike and dip of principal foliation
- volcanogenic alteration zone

Figure 39.2. General geology of the central part of the Roberts Arm Group. The northeastern corner is compiled and simplified after Bostock (1978). Location of the Handcamp Prospect is indicated by a star.

observed relationships between the related Mansfield Cove Complex and the Robert's Arm Group (Bostock, 1978; see below). The Hall Hill Complex is intruded by the Loon Pond granite.

Bostock et al. (1979) emphasized the similarity of the Mansfield Cove plagiogranite to typical oceanic plagiogranite and suggested that it represented magmatism at a spreading centre related to the late Hadrynian opening of Iapetus, intruded into ocean floor represented in part by the Hall Hill Complex. This remains the preferred interpretation although recent radiometric dating has demonstrated that the rocks are considerably younger than previously thought (Dunning et al., in press). The interpretation of the Hall Hill Complex as a fragment of ocean floor is strengthened by the recognition of sheeted dykes with pillow lava screens, pegmatitic gabbro phases and local dykes of pyroxenite and plagiogranite, all typical of the middle to upper levels of ophiolitic plutonic suites. This interpretation requires further documentation through detailed mapping, petrochemical studies and regional correlation along strike.

Dunning and Chorlton (1985) have described similar intrusive rocks and geological relationships along strike to the southwest in southwestern Newfoundland. In this area, ophiolitic fragments are engulfed in tonalite and they consider this to reflect arc-related magmatism in the roots of an island arc or in the arc-trench gap. Such an interpretation is also possible in the Mansfield Cove–Hall Hill complexes but intrusive relationships seem to require that ocean floor and arc-related magmatism be closely related in time and space.

A further topic for petrochemical investigation is the relationship between vesicular dykes in the Mansfield Cove Complex and the Robert's Arm Group. The interpretation of a basement-cover relationship between these units hinges on whether the dykes in the former are the subvolcanic dykes related to mafic volcanism in the latter. At present, the only evidence for this relationship is lithological similarity which cannot be considered definitive. Detailed petrochemical studies are needed to test this hypothesis.

Robert's Arm Group

The Robert's Arm Group is poorly exposed in the area immediately north of the Handcamp Prospect, which precludes tracing the stratigraphy in detail to the area of more abundant outcrop northeast of Rocky Pond.

East of Hall Hill, the Robert's Arm Group comprises dominantly mafic volcanic rocks which are generally quite schistose. Pillows are not commonly recognized but interbedded silicic tuff, chert and volcaniclastic greywacke locally confirm the stratified nature of the rocks. Silicic volcanic rocks are prevalent in this region; where relatively undeformed, they comprise quartz- and quartz-feldspar crystal-bearing tuffs but are more commonly altered quartz-sericite schists. Disseminated pyrite, which locally forms 7-10% of the rock but averages less than 2%, gives many outcrops a distinctive rusty appearance. The felsic lithologies generally comprise up to 60% of individual outcrops and are interbedded with fine grained chloritic schists. These rocks are identical lithologically and structurally to deformed and mineralized rocks of the Gullbridge felsic volcanics further south (Swinden and Sacks, 1986), particularly those near the Southwest Shaft prospect and in the alteration zones near Starkes' Pond.

North of the Tommy's Arm River at the eastern edge of the map area, volcaniclastic rocks, mainly fine grained tuffaceous rocks with a few beds of red to wine-coloured ferruginous chert, are lithologically similar to the Gull Hill sediments of Swinden and Sacks (1986) and appear to occupy a similar stratigraphic position. If this correlation is correct, the basalts immediately to the west probably correlate with the Burnt Island basalt of Swinden and Sacks (1986). The volcaniclastic rocks are also on strike with units to the northeast assigned to the Crescent Lake Formation (Espenshade, 1938; Bostock, 1978). More detailed correlations await petrochemical studies of the volcanic rocks now in progress.

Sansom greywacke

The Sansom Greywacke in north-central Newfoundland, represents post-Caradocian flysch that is interpreted to have blanketed the area following the cessation of active volcanism in the middle Ordovician (Dean, 1978; Kean et al., 1981). Sedimentary rocks exposed along the Tommy's Arm River north of Rocky Pond are assigned to this unit, following Dean and Strong (1976), based on the presence of rare, fine grained polylithic conglomerate beds and the lack of cherty or fine tuffaceous horizons. The contact with the Robert's Arm Group is not exposed but because the latter is thought to be northwest facing in this area, it is assumed to be a fault. More detailed mapping is required to confirm the classification of the rocks and document the contact relationships.

Younger intrusive rocks

Granodiorite, diorite and gabbro intrude the Robert's Arm Group and the Sansom Greywacke near Rocky Pond. These rocks were not examined in detail during the present program. They were interpreted by Dean and Strong (1976) to be related to the nearby Twin Lakes Complex.

West of the north end of South Pond, a post-tectonic granite, termed the South Brook pluton by Currie (1975), intrudes the Hall Hill Complex and the Springdale Group. Dean and Strong (1976) correlated this body with the Topsails Intrusive Suite.

MINERAL OCCURRENCES

There are in excess of 50 mineral occurrences in the central and northern parts of the Robert's Arm Group according to the Newfoundland Department of Mines and Energy mineral inventory files, most of which occur within Bostock's (1978) calc-alkaline suite of mafic to felsic volcanics which form the top of the Robert's Arm Group. Many are isolated occurrences of minor pyrite + chalcopyrite in pillow lava. However, in five areas, termed the Hall Hill East, Loon Pond, Rust Pond

– Fourth Pond, Crescent Lake Mine and Pilley's Island – Sunday Cove Island areas (Fig. 39.1), mineralization is relatively concentrated and may attain some regional economic significance.

Hall Hill East

Several small showings of pyrite and very minor chalcopyrite are exposed in outcrops along a strike length of approximately 1 km northeast of Hall Hill. As previously noted, these showings closely resemble pyritic alteration zones in the Gullbridge felsic volcanics southwest of Great Gull Pond which Swinden and Sacks (1986) have interpreted as deformed and transposed volcanogenic stockworks. A similar interpretation is applied here. These rocks are approximately along strike with the previously mapped northern extent of the Gullbridge volcanics.

Loon Pond

There are several pyrite and minor base metal occurrences in the immediate vicinity of Loon Pond, hosted by moderately to strongly altered felsic tuff (Fig. 39.3). Alteration is dominantly quartz-sericite although minor chloritic zones are present. Pervasively altered zones up to 2 m wide contain 2 to 10% disseminated pyrite and locally a little chalcopyrite. Mineralization in some cases is concentrated on randomly oriented fractures which have narrow alteration haloes. Very minor veinlets carrying sphalerite and galena have been reported by exploration companies although none was seen during the present investigations. These showings are interpreted as relatively lean volcanogenic stockworks. They are probably genetically similar to showings in the Hall Hill East area but have not undergone the same degree of deformation.

Rust Pond – Ghost Pond area

These showings are the only significant mineralization to occur in the high-Ti basalts of Bostock (1978). Mineralization outcrops in two significant areas: near the south end of Rust Pond and at the north end of Round Pond (Fig. 39.4). Mineralized boulders have been discovered at several locations between these two areas.

The Rust Pond showing occupies a large outcrop in a bog immediately south of Rust Pond. The rocks are intensely hydrothermally altered but clear pillow shapes on the outcrop attest to the mafic volcanic protolith. The dominant and pervasive alteration is chloritic with disseminated pyrite (generally less than 3%). There are several, apparently cross cutting zones of quartz-sericite alteration which contain considerably more disseminated pyrite, massive pyrite stringers up to several millimetres wide and minor chalcopyrite as well. This alteration facies displays more deformation than the pervasive chlorite facies. Contrary to previous descriptions of the mineralization, there do not appear to be any felsic volcanic rocks near the showing; silicic rocks previously interpreted as felsic volcanics are actually pillow lavas which have been silicified by the hydrothermal alteration. Diamond drilling of this showing in the early 1960s yielded a best intersection of approximately 1.6 m of 2.1% Cu.

Similar alteration and mineralization outcrops on the shoreline near the north end of Round Pond. The lateral extent of this mineralization has been tested by several trenches to the northeast of the pond but none currently expose either mineralization or alteration.

As previous workers (e.g. MacQuarrie, 1976; Fryer, 1981) have noted, the mineralization at Rust Pond and Round Pond is probably volcanogenic. The showings are on strike with each other and with mineralized boulders discovered between them in the Ghost Pond area (Fig. 39.4) and may therefore represent the surface expression of a widespread volcanogenic alteration system. There is as yet no indication of exhalative activity related to this alteration.

Pilley's Island – Sunday Cove Tickle

There are more than 20 individual prospects along the northern edge of the Robert's Arm Group (Fig. 39.5). The best

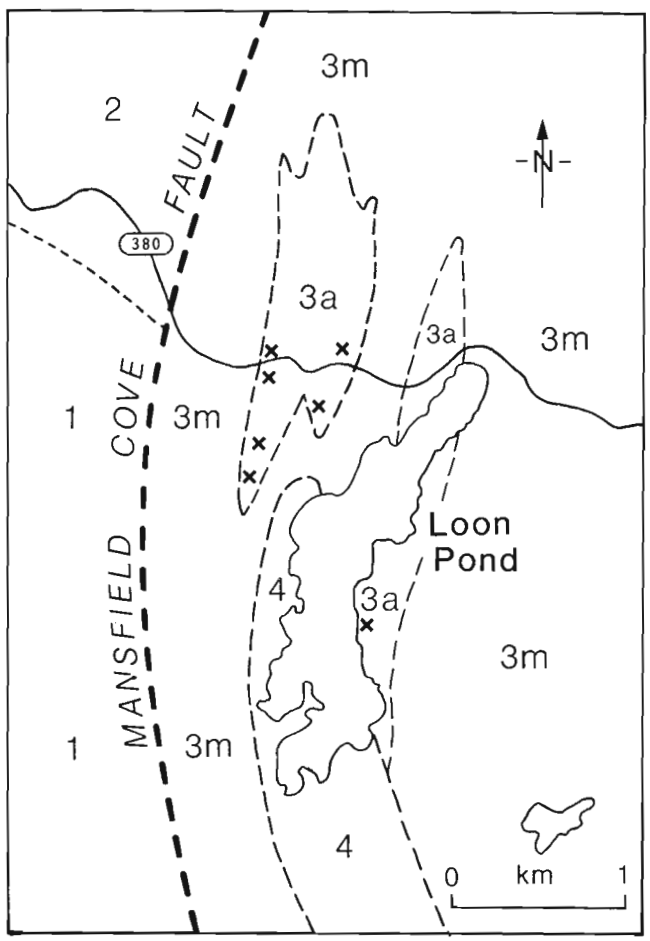


Figure 39.3. Mineral occurrences near Loon Pond (marked by "x"). Legend is the same as Figure 39.2.

known of these are the deposits on Pilley's Island (Espenshade, 1938; Strong, 1974; Appleyard and Bowes, 1978; Tuach, 1984) where approximately 450 000 tonnes of pyritic ore was mined at the turn of the century from a total reserves of close to 2 000 000 t of massive sulphide. Detailed studies of alteration and distribution of the mineralization by Appleyard and Bowes (1978) and Tuach (1984) have shown that the mineralization is related to a hydrothermal alteration zone associated with an extrusive dacitic dome. Tuach (1984) identified two main areas of alteration, the main zone in the village of Pilley's Island and a second zone at Spencer's Dock to the east (Fig. 39.5) and he presented an integrated model for the sequence of events leading up to the mineralization.

Several showings are reported along the shore between Flat Rock Tickle and Robert's Arm (Fig. 39.5). The most intense mineralization is in Tilley Cove where four separate showings include pyrite-galena-bearing quartz veins, relatively restricted (~10 m^2) pyritic alteration zones in mafic volcanics and semi-massive pyrite veins and pods in a 1-2 m wide band of ferruginous chert. The host rocks are not pervasively altered away from the mineralization but the style of mineralization and the alteration patterns close to it suggest that the showings are probably volcanogenic. It seems likely that these may represent a relatively distal facies of the Pilley's Island alteration zone, perhaps reflecting the escape of metalliferous fluids from the immediate area of the alteration zones and subsequent precipitation in fractures away from the main centre of activity.

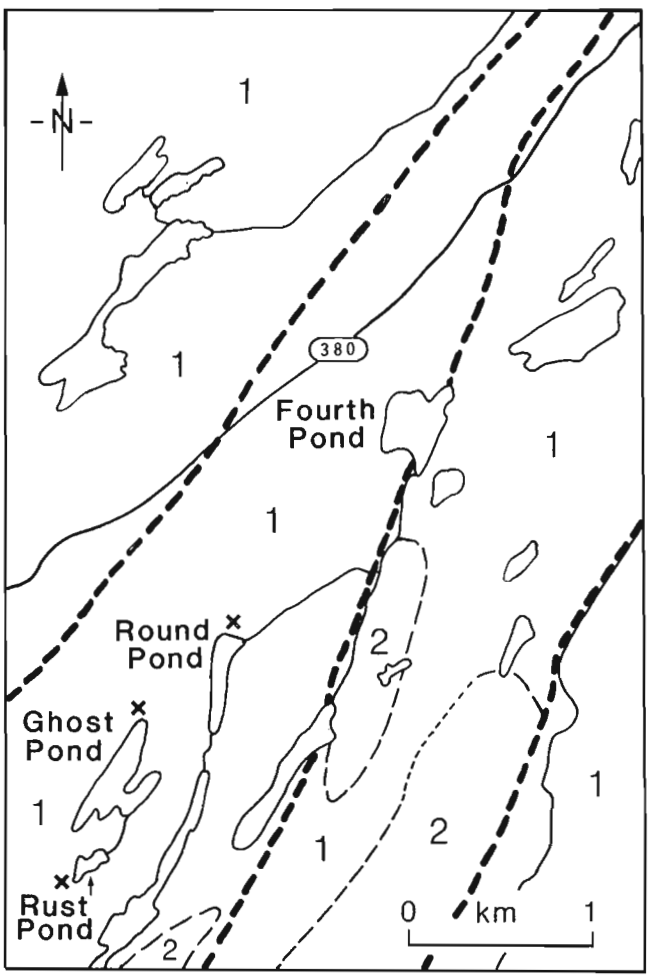


Figure 39.4. General geology and mineral occurrences (marked by "x") in the Rust Pond–Round Pond area. Geology after MacQuarrie (1976) and Bostock (1978). Legend as in Figure 39.2.

Farther east, some of the showings in Measles Cove and Hammer Cove comprise disseminated pyrite in carbonated faults zones and may not be related to volcanogenic processes.

Other than Pilley's Island, the most widespread and intense volcanogenic alteration is found along the shores of Sunday Cove Tickle on the south shore of Sunday Cove Island (Fig. 39.5). The alteration, which underlies an area of 200-300 m^2, is exposed in several roadcuts and open cut trenches immediately north of the causeway on Sunday Cove Island. It is strongly pyritic but contains little base metal sulphide other than scattered grains of chalcopyrite. The host rock is dominantly pillow lava although there are dykes of granitic rock related to the Sunday Cove pluton which have also been altered and mineralized.

There are several styles of alteration and mineralization in the Sunday Cove Tickle area although in the absence of three dimensional information, a regular zoning pattern cannot be recognized. The most intense sulphide mineralization is associated with zones of quartz-sericite alteration. These appear to be the most altered rocks, in the sense that most original features in the rock have been destroyed. Many of these zones have undergone intense shearing as well, presumably because of their relative incompetence due to the alteration. Pyrite occurs as disseminations (up to 10%) in an anastamosing veinlets from 10 to 50 mm wide that can locally be traced for tens of metres on the outcrop face.

Away from the quartz-sericite zones, the basalt is pervasively but less intensely altered and retains some of its original characteristics (e.g. pillow shapes, vesicles). Epidote characterizes this alteration facies, occurring both as a pervasive alteration and in epidote (±quartz) veins which locally form up to 40% of the rock. Pyrite and lesser chalcopyrite is concentrated in the epidote-bearing veins in these areas. Pervasive black chloritic alteration, typical of volcanogenic alteration elsewhere in the belt, is not widely developed in this area.

The relationship between this alteration zone and that at Pilley's Island is not obvious. Both occupy approximately the same stratigraphic level in the volcanic pile and are presumably roughly coeval. The most intense and heavily mineralized rocks at Pilley's Island are felsic volcanics although locally there are recognizable altered and mineralized pillow lavas which underlie the mineralized dacite extrusive (e.g. on the shore of Bumble Bee Bight). There is no prominent altered feslic volcanic dome in the Sunday Cove Tickle area. The presence of altered granitic dykes in the mineralized zone

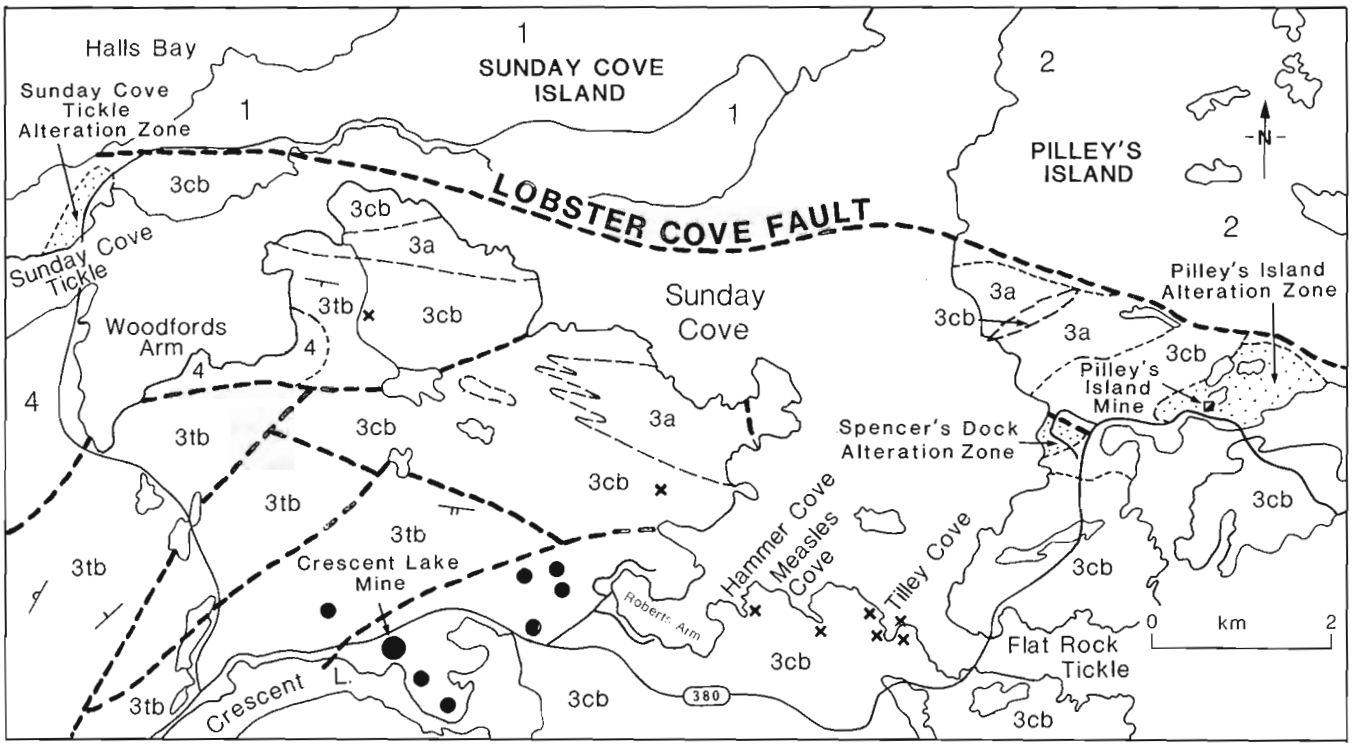


Figure 39.5. Mineral occurrences in the Pilley's Island – Sunday Cove Tickle and Crescent Lake areas. Volcanogenic alteration zones are shown in heavy stipple (after Tuach, 1984, on Pilley's Island). Mineral occurrences are shown by "x" except those of the Crescent Lake Mine type which are shown by solid dots. Geology simplified after Bostock (1978). Symbols as in Figure 39.3.

LEGEND FOR FIGURE 39.5

SILURIAN

5 Springdale Group: red conglomerate, sandstone

EARLY ORDOVICIAN

4 Sunday Cove Pluton: granodiortie, quartz-monzonite

3 Roberts Arm Group: 3a–felsic volcanic rocks; 3cb–dominantly mafic volcanic rocks of calc-alkaline affinity; 3tb–dominantly mafic volcanic rocks of tholeiitic affinity

2 Dominantly mafic and intermediate volcaniclastic and pyroclastic rocks; probably equivalent to Cutwell and/or Western Arm Groups (Kean, 1984)

1 Lushs Bight Group: Mafic pillow lavas, sheeted dykes

which are related to the Sunday Cove Pluton suggests that this subvolcanic intrusion may be related to the mineralization, perhaps marking the focus of a second hydrothermal system, near to but separate from that developed at Pilley's Island.

Crescent Lake Mine area

Several showings near the east end of Crescent Lake are associated with quartz-epidote veining and host rock alteration. The best exposed and most extensively explored is the Crescent Lake Mine deposit, a composite quartz vein up to 3 m wide containing disseminated pyrite, chalcopyrite, sphalerite and galena. Silver values averaging approximately 10 to 20 g/t have been reported from the dumps (Howse and McArthur, 1977). In the late 1800s, 1269 tons of material grading 28% Cu was mined from this deposit and in 1924 and 1926, further mining took place although production figures are not known.

The Crescent Lake deposit is well exposed in several outcrops and small open cuts near highway 380 east of Robert's Arm. The mineralization is hosted by quartz veins which are commonly sheeted suggesting repeated opening and filling of the veins. The veins locally brecciate the adjacent wall rocks. Base metal sulphides are apparently restricted to the quartz veins and locally comprise up to 15% of them, although averaging considerably less. There is a widespread wallrock alteration associated with the veins in which the host basalt is generally highly chloritized and locally has quartz-sericite alteration as well.

The pattern of mineralization is similar to, although considerably more intense than, the smaller showings nearby (Fig. 39.5). The nature of these small showings is best illustrated by a roadside outcrop at the west end of Robert's Arm across the street from the village hall where quartz-epidote veins carry pyrite and minor chalcopyrite are associated with relatively restricted host rock alteration consisting of quartz-sericite and lesser chloritization.

The relationship between the showings in the Crescent Lake Mine area and those at Pilley's Island is not clear.

Wallrock alteration associated with the Crescent Lake veins is mineralogically similar to that at Pilley's Island and suggests the operation of a sub-seafloor hydrothermal system in a volcanic environment. It is therefore reasonable to suggest that mineral occurrences in the two areas are related. The Pilley's Island deposits include syngenetic massive sulphides and therefore were generated quite close to the ocean floor. The mineralization at the Crescent Lake Mine is quite different in style and alteration patterns to the Pilley's Island area and also occurs relatively deeper in the stratigraphy. It is possible that the Crescent Lake area deposits represent a deeper level of the hydrothermal cell which formed the Pilley's Island deposits.

CONCLUSIONS

1) The Robert's Arm Group can be traced continuously from the southern limit of Bostock's (1978) mapping to the area of the Handcamp Prospect. Outcrop is not sufficiently abundant to trace the southern Robert's Arm Group stratigraphy through this area although elements of this stratigraphy can be recognized locally.

2) The Hall Hill Complex (Currie, 1976) can be traced from Halls Bay to the area northwest of Great Gull Pond and elements typical of ophiolitic plutonic sequences elsewhere in Newfoundland have been recognized within it. It is believed to be approximately coeval with the Mansfield Cove Complex to the north and the two together apparently represent oceanic crust somewhat older than the Robert's Arm Group.

3) Volcanogenic mineralization in the central and northern part of the Robert's Arm Group is mainly concentrated in the calc-alkaline volcanic series of Bostock (1978). Mineralization immediately west of Pilley's Island is interpreted as a distal expression of the hydrothermal system exposed there. However, the relatively intense alteration and mineralization at Sunday Cove Tickle may be a separate although temporally related hydrothermal cell. Mineralized vein systems in the Crescent Lake area are interpreted as a deeper-level manifestation of the Pilley's Island hydrothermal cell. Lean pyritic stockwork associated with quartz-sericite alteration of pillow basalt in the Rust Pond–Round Pond area is the only significant volcanogenic mineralization hosted by High-Ti basalts (Bostock, 1978).

ACKNOWLEDGMENTS

Lorne Garnier provided capable field assistance during the field work. Discussions with Baxter Kean, Geoff Thurlow and Greg Dunning have been helpful in appreciating the regional aspects of the mapping. Two traverses in the southern part of the area which are reported as part of this work were mapped by Paul E. Sacks during the 1985 field season.

The manuscropt has benefitted from the critical reading of Baxter Kean and Steve Colman-Sadd.

REFERENCES

Appleyard, E.C. and Bowes, E.G.
1978: The geology of the West Mine, Pilley's Island, Newfoundland; in Report of Activities, Part A, Geological Survey of Canada, Paper 78-1A, p 199-203.

Bostock, H.H.
1978: The Robert's Arm Group, Newfoundland: geological notes on a Middle or Upper Ordovician island arc environment; Geological Survey of Canada, Paper 78-15, 21 p.

Bostock, H.H., Currie, K.L. and Wanless, R.K.
1979: The age of the Robert's Arm Group, north-central Newfoundland; Canadian Journal of Earth Sciences, v. 16, p. 599-606.

Currie, K.L.
1975: Studies of granitoid rocks in the Canadian Appalachians; in Report of Activities, Geological Survey of Canada, Paper 75-1A, p. 265-270.

Currie, K.L.
1976: Studies of granitoid rocks in the Canadian Appalachians: Part 2; in Report of Activities, Part A, Geological Survey of Canada, Paper 76-1A, p. 155-163.

Dean, P.L. and Strong, D.F.
1976: Geological compilation maps of the Notre Dame Bay area, Central Newfoundland with explanatory notes; Newfoundland Department of Mines and Energy, Mineral Development Division, Open File 979.

Dunning, G.R. and Chorlton, L.B.
1985: The Annieopsquotch Belt of Southwest Newfoundland: Geology and tectonic significance; Geological Society of America Bulletin, v. 96, p. 1466-1476.

Dunning, G.R., Thurlow, J.G., Kean, B.F. and Swinden, H.S.
in press: Geochronology of the Buchans, Robert's Arm and Victoria Lake Groups and the Mansfield Cove Complex, Newfoundland; Canadian Journal of Earth Sciences.

Espenshade, G.H.
1938: Geology and mineral deposits of the Pilley's Island area; Newfoundland Department of Natural Resources, Geological Section, Bulletin 6, 56 p.

Fryer, B.J.
1981: Report on the geology and mineral potential of the Rust Pond to South Pond area, Green Bay district, Newfoundland; unpublished company report.

Hayes, J.J.
1951: Marks Lake, Newfoundland; Geological Survey of Canada, Paper 51-20, preliminary map with marginal notes.

Howse, A.F. and McArthur, J.G.
1977: Preliminary report and proposal for crown properties; Newfoundland Department of Mines and Energy, Mineral Development Division, unpublished internal report.

Kalliokoski, J.
1953: Preliminary map, Springdale, Newfoundland; Geological Survey of Canada, Paper 54-4, map with marginal notes.

Kean, B.F., Dean, P.L. and Strong, D.F.
1981: Regional geology of the Central Volcanic Belt of Newfoundland; Geological Association of Canada, Special Paper 22, p. 65-78.

MacQuarrie, R.
1976: Halls Bay South (Nfld.) Summary Report, 1976; unpublished report to Texasgulf Inc.

Strong, D.F.
1974: Mineral occurrences of the Pilley's Island area; in Metallogeny and Plate Tectonics – A Guidebook to Newfoundland Mineral Deposits. NATO Advanced Studies Institue, St. John's, Newfoundland, p. 87-94.

Swinden, H.S. and Sacks, P.E.
1986: Stratigraphy and economic geology of the southern part of the Robert's Arm Group, central Newfoundland; in Current Research, Part A, Geological Survey of Canada, Paper 86-1A, p. 213-220.

Tuach, J.
1984: Geology and volcanogenic sulphide mineralization in the Robert's Arm Group on Pilley's Island, Central Newfoundland; in Mineral Deposits of Newfoundland – a 1984 perspective, Newfoundland Department of Mines and Energy, Mineral Development Division, Report 84-3, p. 117-130.

Possible basement-cover relationships in the Fleur de Lys terrane, western Newfoundland[1]

Project 850017

M.A.J. Piasecki[2]
Lithosphere and Canadian Shield Division

Piasecki, M.A.J., Possible basement-cover relationships in the Fleur de Lys terrane, western Newfoundland; in Current Research, Part A, Geological Survey of Canada, Paper 87-1A, p. 391-397, 1987.

Abstract

Detailed structural, petrographic and chemical examination of the Middle Arm metaconglomerate of the East Pond Metamorphic Suite indicates that it does not rest on an old basement of granitic gneiss. Rather the metaconglomeratic rocks have been locally transformed into gneisses by migmatization. The East Pond Metamorphic Suite, thought to be the structural base of the Fleur de Lys Supergroup, is separated from the Fleur de Lys by a complex ductile shear zone about 1 km thick.

Résumé

Une étude de la structure, de la pétrographie et de la chimie détaillée du métaconglomérat de Middle Arm, dans l'ensemble métamorphique d'East Pond, révèle que le conglomérat ne repose pas sur un socle ancien de gneiss granitique. Les roches conglomératiques métamorphiques ont plutôt été migmatitisées localement en gneiss. L'ensemble métamorphique d'East Pond, qui serait la base structurale du supergroupe de Fleur de Lys, est séparé du super-groupe par une zone de cisaillement ductile complex de puissance d'environ 1 km.

[1]Contribution to Canada-Newfoundland Mineral Development Agreement 1984-1989. Project carried by Geological Survey of Canada.
[2]Department of Geology, University of Hull, Hull HU6 7RX, England

INTRODUCTION

The Southern Long Range region of Newfoundland is currently being investigated and remapped (van Berkel et al., 1986). In this region, the relationships between gneisses and schists are complex, and commonly obscured by voluminous granitoids, and as a consequence, different opinions have been expressed regarding the possible presence of an older basement underneath a metasedimentary cover (cf. Herd and Dunning, 1979, with Chorlton 1980, 1983). Some of the schists have been compared with the rocks of the Fleur de Lys Supergroup. To establish criteria for separating basement from cover in a complex region (Piasecki, 1980), it is useful to examine in detail an area in which the presence of basement has been generally accepted, in this case, the Fleur de Lys terrane. This paper reports the results of a study at the structural base of the Fleur de Lys Supergroup.

DESCRIPTION OF OCCURRENCES

The Fleur de Lys Supergroup of probable Late Hadrynian to early Ordovician age, overlies antiformal(?) cores of structurally more complex schists, the East Pond metamorphic suite, which is generally regarded as a probable structural basement to the Fleur de Lys Supergroup (Fig. 40.1; de Wit, 1972). A detailed description and review can be found in Hibbard (1983). This suite consists of psammitic and semipelitic schists, a metaconglomerate (the Middle Arm metaconglomerate), and rarer, but important developments of migmatites and granitic gneisses. Its metaconglomerate member has been described as a possible Eocambrian(?) tillite (Church, 1969; Harland, 1969), as a conglomerate deposited unconformably on a remobilized Grenville(?) complex (the migmatites, gneisses and the schists, de Wit, 1974, 1980), and as a conglomeratic facies within the schists, the latter resting unconformably on Grenville basement (the migmatites and granitic gneisses, Hibbard, 1983). The contacts between the rocks of the East Pond Metamorphic Suite and the Fleur de Lys Superground are marked by shear zones 500 m to 1 km wide.

The eastern flank of the Middle Arm metaconglomerate is exposed in two large new roadcuts along the Westport road (roadcuts 1 and 2 in Fig. 40.1), where it is closely associated with migmatitic paragneisses. These and other exposures mentioned by Hibbard (1983) along the Bear Cove road and

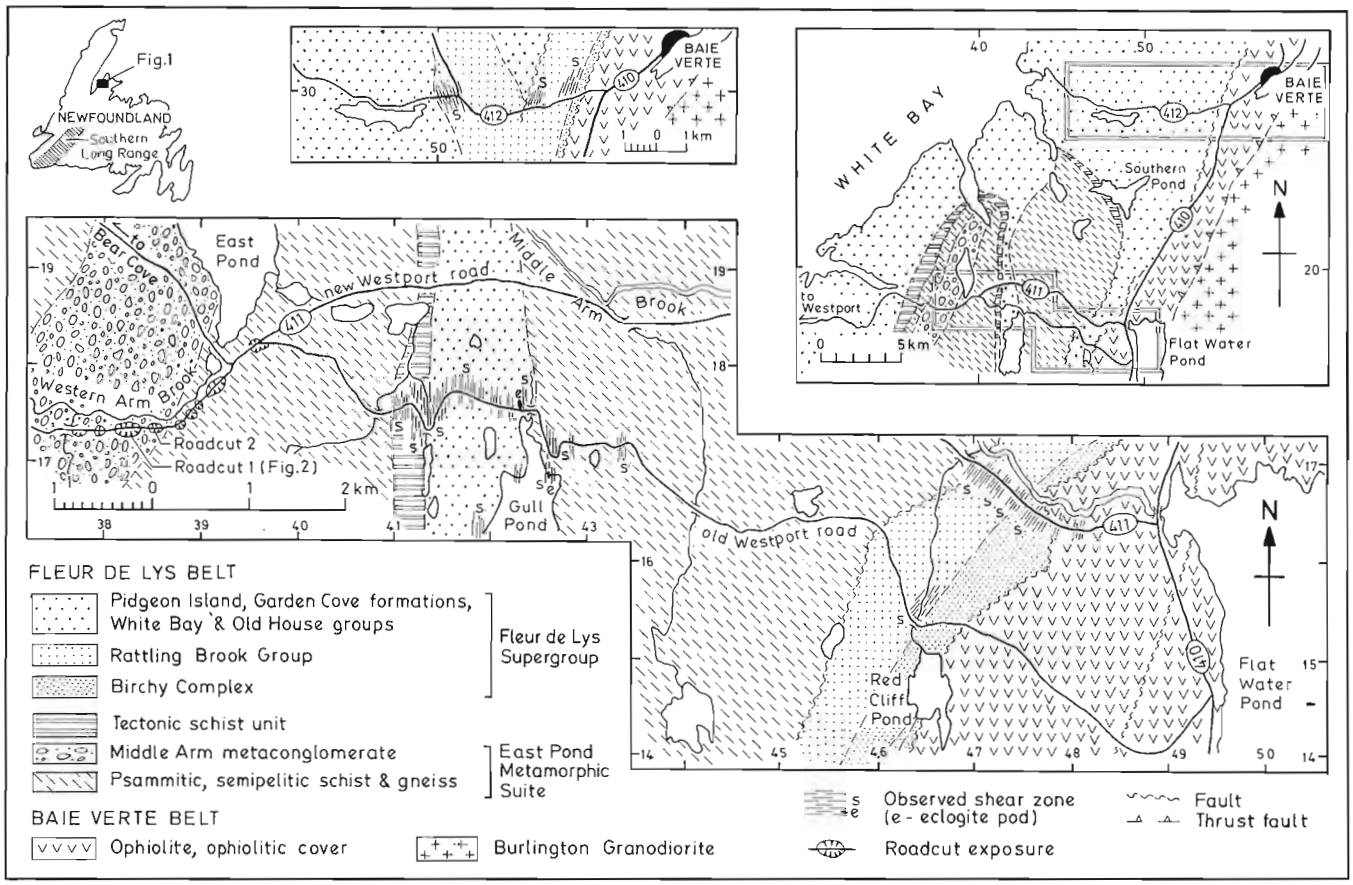


Figure 40.1 Localities examined in the Fleur de Lys belt on the Baie Verte peninsula. Inset at top right shows the areas examined in their regional geological setting. Geology simplified after Hibbard (1983).

on the western shore of East Pond have been studied to test the cover-basement model for the East Pond Metamorphic Suite. The rocks featured by him as banded gneiss (Plate 4-5 in Hibbard, 1983) exposed 1.3 km east along the road from Gull Pond bridge, were also studied, and are believed to be schists of the East Pond Metamorphic Suite, highly strained and attenuated in the vicinity of a wide shear zone.

In the field the metaconglomerate is a massive to schistose, siliceous to quartzofeldspathic rock with matrix supported clasts (Fig. 40.2, at 0-40 m) and with local developments of semipelitic bands. The most common clasts are pebbles of quartzite and semipelitic schists (Fig. 40.3a). These do not appear to contain fabrics older than those present in the matrix. There are rarer clasts of granite, and also apparently of granitic gneiss (Fig. 40.3b) which at first sight appear to suggest derivation from an older, eroded basement complex (see also Hibbard, 1983). Much of the metaconglomerate is migmatitized to varying degrees (Fig. 40.3a, b). The form of the migmatitic neosome varies from individual feldspar porphyroblasts (Fig. 40.3c), through lit-par-lit layers, to developments which could be mistaken for pebbles of gneiss. With progressive migmatization, the rocks coarsen from an average grain size of below 0.1 mm to 0.2 mm and more, and take on a more gneissic aspect (Fig. 40.2 at 95 m; Fig 40.3c, d). With more recrystallization and more strain, they then appear to pass into migmatitic granitic gneisses (Fig. 40.3 d, e; Fig. 40.2 at 150-170 m), locally garnetiferous (Fig. 40.2, at 75 m). However, the coarse granitic neosome of the gneisses locally overprints the dominant foliation of the rocks (Fig. 40.3c). In between the coarse neosomes, the matrix is commonly as fine in grain size as in some of the less migmatized metaconglomerates. In all the studied exposures, the granitic gneisses repeatedly grade imperceptibly into recognizable migmatitic psammite, sometimes with pebbly clasts (Fig. 40.2, at 40-70 m). Subconcordant amphibolites are common in the metaconglomerate and in the gneissic rocks (Fig. 40.2, at 100-130 m).

On their field relationships alone, the rocks may be at first sight interpreted either as a mobilized basement injected into a cover conglomerate and the two subsequently metamorphosed, migmatized and deformed together; or, as one continuous series of sediments metamorphosed, migmatized and deformed to different degrees.

PETROGRAPHIC, MINERALOGICAL AND MICROSTRUCTURAL OBSERVATIONS

For petrographic, mineralogical and microstructural studies, 68 thin sections were made from 12 samples of the metaconglomerate, 18 samples of the migmatitic rocks and the gneisses, and 12 "clasts" of gneiss separated from the metaconglomerate.

The least migmatized samples of the metaconglomerate are fine grained psammites in which biotite, epidote, muscovite, opaque ore, sphene and occasionally garnet occur in well separated, discontinuous bands (Fig. 40.4a, b, d, e). Several small clasts of quartzite and semipelite within the metaconglomerate also contain features typical of their

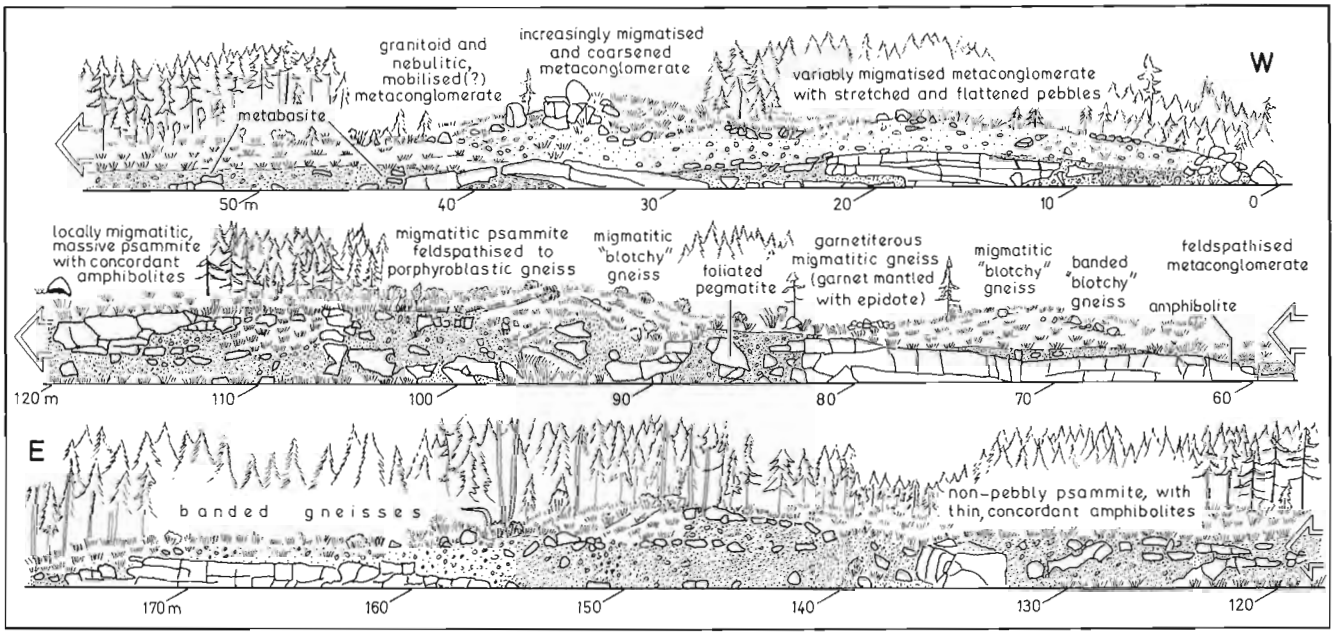


Figure 40.2 Profile of the exposure at the south side of roadcut 1 (location shown in Fig. 40.1, centre left), showing the location of transitions from metaconglomerate and semipsammite into gneiss. Further explanation in text.

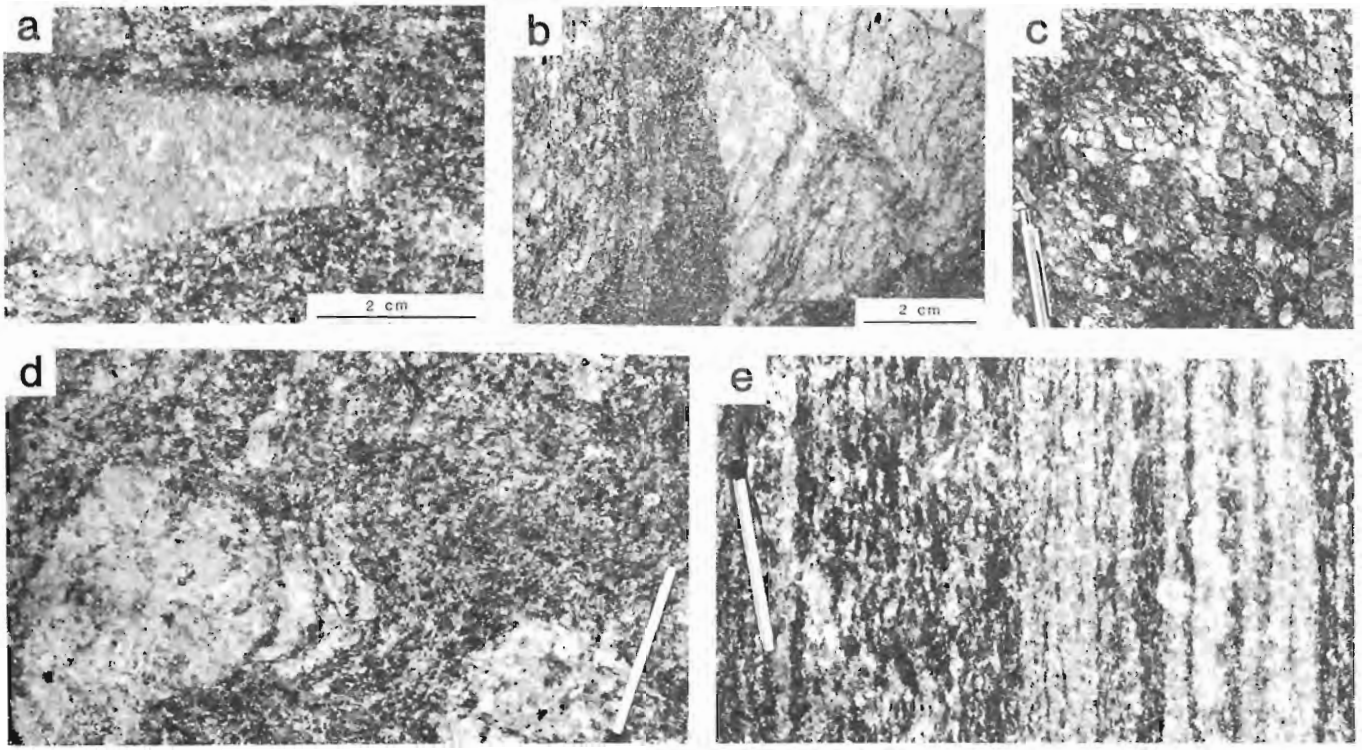


Figure 40.3 Rocks of the East Pond Metamorphic Suite.
a Pebble of quartzite in migmatized, recrystalized matrix of the Middle arm metaconglomerate. Roadcut 1.
b An apparent pebble granitic (basement?) gneiss, in strongly migmatized metaconglomerate matrix (centre left). Roadcut 2.
c Extensively feldspathized, "dents-de-cheval" migmatite after the metacongloemrte, which passes laterally into a granitic nebulite. Roadcut 1.
d Migmatitic gneiss with "blotchy" neosome. Roadcut 1, north side.
e Banded granitic gneiss. Photomicrographs shown in fig. 40.4 c, d. Roadcut 1, at 160-170 m.

Figure 40.4 Salient mineralogical and textural characteritistics of rocks from the East Pond Metamorphic Sutie. Abbreviations on photomicrographs: (b) biotite, (e) epidote, (e) iron-rich epidote, (g) garnet, (m) muscovite, (mi) microcline, (o) orthite, (q) quartz, (s) sphene, (z) zircon.
a, b Typical biotite-rich bands in the semipsammitic matrix of the metaconglomerate, showing the substantial amount of epidote and sphene in the rocks. Most of the biotite appears black. Roadcut 1, at 0-20 m.
c Typical biotite-rich band in the banded gneiss of Figure 40.3e, again showing the substantial amount of epidote and sphene in the rock. The zoned epidote surrounding a core of orthite (centre) is also typical of the matrices of all sectioned metaconglomerates, and even occurs in some of the psammitic pebbles.
d Garnet mantled with epidote, biotite and sphene (right of label). Mantles around other garnet contain more epidote. From the same banded gneiss as in c, but also developed in migmatized psammites.
e A mantle of epidote and sphene around a core of iron-rich epidote. Matrix of metaconglomerate in roadcut 2, but equally typical of the gneiss, and also developed inside some psammite pebbles in the metaconglomerate.
f An epidote mantle around sphene intergrown with biotite and plagioclase. Migmatitic, garnetiferous granitic gneiss from roadcut 1, at 75 m. Again, such mantles are common in migmatities and metaconglomerate.
g Ductile mylonite fabric in migmatitic psammite: a quartz plate formed of elongate quartz grains (centre) with even more elongate grains of plagioclase (above and below) which replace the matrix of the rock, and are charged with inclusions of quartz, biotite, etc. Roadcut 1.
h Same rock as in g, showing quartz plates (centre and bottom), and a highly elongate, strained microcline (top). Note elongate sphene (centre right). In g and h, the feldspars appear to have nucleated together with the quartz plates, i.e. during a phase of shearing.

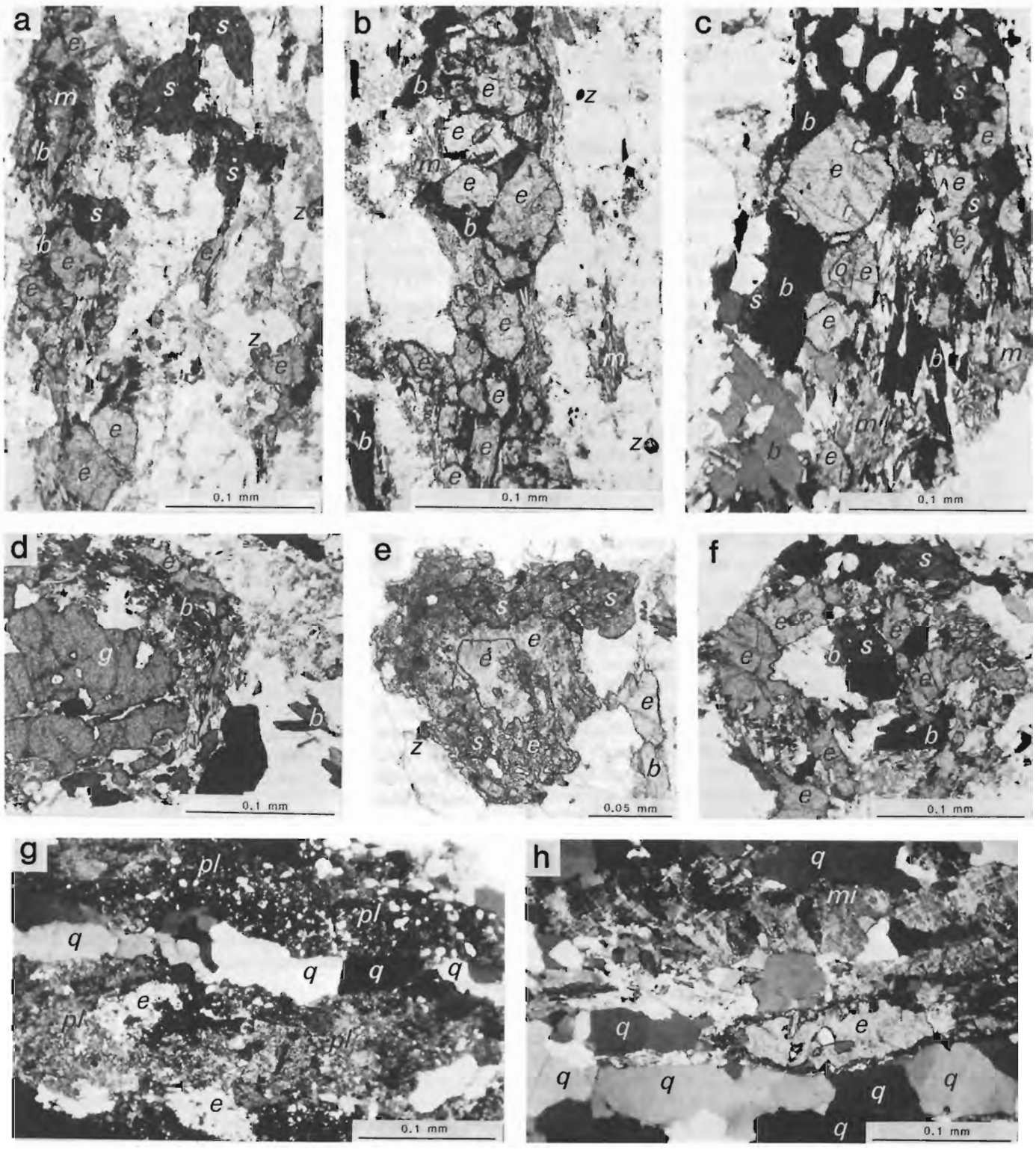


Figure 40.4

matrix, such as magnetite mantled by sphene, epidote, and zoned epidote cored by allanite, suggesting that these clasts may be intraformational.

Thin sections of the metaconglomerate show the presence of a polyphase sequence of metamorphic-structural events. The earliest visible event (D1) was the development of a penetrative, layer-parallel schistosity. The grade of the accompanying metamorphism is uncertain, but is likely to have reached at least the amphibolite facies.

The second event (D2) was marked by amphibolite facies metamorphism, by repeated feldspathization, and a schistosity (S2) which paralleled and enhanced S1. D2 resulted in an almost complete recrystallization of the rocks, and in the overprinting of the D1 schistosity by feldspar porphyroblasts which are often cloudy and contain inclusions of ferromagnesian minerals and of matrix quartz (Fig. 40.4g). In biotite-rich bands, epidote occurs as large grains and in substantial quantities, suggesting a calcareous nature to the initial sediment (Fig. 40.4a, b). It is commonly zoned, with cores of orthite or Fe-rich epidote (Fig. 40.4e). Grains of magnetite are mantled by coronas of granular sphene, suggesting retrogression of primary ilmenite. The presence of concentric intergrowths of epidote and sphene and/or the early plagioclase porphyroblasts (Fig. 40.4f) associated with large, radiating grains of biotite also suggest the recrystallization of previous, higher grade minerals, which may have been related to the D1 event, or an earlier phase of D2. Garnets are characteristically mantled by epidote and biotite (Fig. 40.4d). Earliest (D1?) plagioclase grains are strongly epidotized.

Outside the metaconglomerate, along the contracts between the East Pond Metamorphic Suite and the rocks of the Fleur de Lys Supergroup at Gull Pond and Southern Pond, the D2 metamorphic and structural history involved probably two phases of ductile shearing under amphibolite facies conditions. Each phase of shearing was accompanied by the nucleation of swarms of quartz veins and of small pegmatites, and of porphyroblasts of feldspar and muscovite in the mylonites (Piasecki, 1984; Piasecki and van Breemen 1983). In this shear zone, belts of coarse, mylonitic schists anastomose within a zone about 1 km thick, their S-C fabrics (Berthe et al., 1979) indicating a dextral (northerly) sense of movements. This and other shear zones in the Fleur de Lys terrane are described elsewhere. As the metaconglomerate occurs outside these belts of shearing, it contains only very minor shear zones (Fig 40.4 g, h) and intense D2 strain is very inhomogeneously distributed. The metaconglomerate shows a complex sequence of feldspathization events. Following and overlaping the early D2 migmatization and growth of pagioclase porphyroblasts, two more phases of feldspathization contributed further to the general coarsening and recrystallization of the rocks. One resulted in the partial replacement of the early D2 plagioclase porphyroblasts and of the matrix of the rocks by microcline containing inclusions of quartz (c.f. Fig. 40.4h). The other was a partial replacement of that microcline by a sodic plagioclase with the formation of myrmekite. Muscovite is generally late, replacing biotite and microcline, often forming unoriented porphyroblasts. Events later than D2 were essentially retrogressive, probably related to later, sinistral movements in nearly shear zones and to faulting.

The migmatitic rocks and the granitic gneisses all reveal mineralogies strikingly similar to those of the metaconglomerates, with remarkably similar proportions of the minerals present and similar textural characteristics. Thin sections of the migmatic gneisses differ only in that they are coarser grained (Fig. 40.4a, b, c) and provide spectacular examples of feldspathization. In several localities, such as in the northern face of the roadcut illustrated in figure 40.2, it can be demonstrated that, with locally extensive D2 formation (most likely related to movements on the nearby shear zones), the migmatitic rocks with recognizable clasts pass into "granitic gneisses" indistinguishable from those forming "pebbles" in the metaconglomerate.

Such striking mineralogical similarities, taken together with a notable absence from the gneisses of older fabrics than those present in the metaconglomerate, appear to rule out the concept that the gneiss might form a basement to the metaconglomerate.

Thin sections cut from clasts of granitic gneiss separated from the metaconglomerate show the same mineralogical characteristics as the migmatized and gneissic rocks described above. They also show more intense developments of deformation microfabrics (grain granulation, recovery and recrystallization) than other samples of the gneisses. Several samples which showed rounded, pebble-like forms in two-dimensional exposure surfaces were broken up into a three-dimensional configuration, revealing transitions from the pebble form into discordant veins of migmatitic neosome in the metaconglomerate. Taken together, these features are more consistent with the origin of the "clasts" being due to deformation of "patchy" migmatitic neosome, rather than by derivation from a pre-existing gneissose basement. A less favoured alternative would be that some basement derived pebbles had undergone partial melting with local mobilization and injection of some of the melt into the host metaconglomerate.

The 12 samples representing the metaconglomerate, the migmatites and gneisses, were analyzed for their major and trace element content, in an attempt to test for possible chemical differences between the rocks. Even though this number of samples is insufficient for statistical assessment, the mineralogical and textural similarities outlined above are reflected by a monotonous similarity in the composition of all the rocks.

CONCLUSIONS

As a result of this study, the metaconglomerate, the migmatitic rocks and the gneisses as exposed in the Westport road section and in the region of East Pond are interpreted as one continuous metasedimentary sequence which includes a conglomeratic facies. This has been subsequently migmatized, coarsened and deformed into rocks resembling banded

granitic gneisses. In view of the finding that at least some of the "gneiss clasts" may not represent boulders derived from an older gneiss provenance, the clast content of the metaconglomerate warrants a detailed study. The absence of cover-basement relationships across the Middle Arm metaconglomerate does not invalidate the concept of a (Grenville?) basement to the Fleur de Lys Supergroup; such a basement may lie below the present level of exposure, or, it may be in part represented by the East Pond Metamorphic Suite itself, the age of which is not yet known. The presence of a shear zone between the East Pond Metamorphic Suite and the Fleur de Lys Supergroup at Gull Pond and Southern Pond makes it now more likely that the entire base of the Fleur de Lys Supergroup may be tectonic.

ACKNOWLEDGMENTS

I am endebted to K.L. Currie for introducing me to the Canadian Caledonides and Newfoundland, J. van Berkel and again K.L. Currie for their help and support in the field, to the Geological Survey of Canada for financial support in Canada, chemical analyses and thin-sections of samples, and to the Geological Society of London for a Joseph Burr Tyrrell travel grant during the 1985 season.

REFERENCES

1986: A preliminary report on the geology of the southern Long Range, southwest Newfoundland (Project 850017); in Current Research, Part B, Geological Survey of Canada, Paper 86-1B, Report 19.

Berthé, D., Choukroune, P. and Jegouzo, P. 1979.
1979: Orthogneiss, mylonite and non coaxial deformation of granites: the example of the South Amorican Shear Zone; Journal of Structural Geology, v. 1, p. 31-42.

Chorlton, L.
1980: Geology of the La Poile River area (110/16), Newfoundland; Newfoundland Department of Mines and Energy, Mineral Development Division, Report 80-3, 96 p.

Chorlton, L.
1983: Geology of the Grandys Lake area (110/15), Newfoundland; Newfoundland Department of Mines and Energy, Mineral Development Division, Report 83-7, Part 1, 116 p.

Church, W.R.
1969: Metamorphic rocks of Burlington Peninsula and adjoining areas of Newfoundland and their bearing on continental drift in the North Atlantic; in North Atlantic Geology and Continental Drift, ed. M. Kay, American Association of petroleum Geologiss, Memoir 12, p. 212-233.

de Wit, M.J.
1972: The geology around Bear cove, eastern White Bay, Newfoundland; Ph.D. thesis, Cambridge University, England, 232 p.
1974: On the origin and deformation of the Fleur de Lys metaconglomerate, Appalachian fold belt, northwest Newfoundland, Canadian Journal of Earth Sciences, v. 11, p. 1168-1180.
1980: Structural and metamorphic relationships of pre-Fleur de Lys and Fleur de Lys rocks of the Baie Verte Peninsula, Newfoundland; Canadian Journal of Earth Sciences, v. 17, p. 1559-1575.

Harland, W.B.
1969: Fleur de Lys "Tilloid"; in North Atlantic Geology and Continental Drift, ed. M. Kay, American Association of Petroleum Geologists, Memoir 12, p. 234-235.

Herd, R.K., and Dunning, G.R.
1979: Geology of the Puddle Pond map area, southwestern Newfoundland; in Current Research, Part A, Geological Survey of Canada, Paper 79-1A, p. 305-310.

Hibbard, J.
1983: Geology of the Baie Verte Peninsula, Newfoundland; Memoir 2, Mineral Development Division, Department of Mines and Energy, Government of Newfoundland and Labrador, Memoir 2, 279 p.

Piasecki, M.A.J.
1980: New light on the Moine rocks of the Central Highlands of Scotland; Geological Society of London, Journal, v. 137, p. 41-59.

Piasecki, M.A.J.
1984: Ductile thrusts as time markers in orogenic evolution: an example from the Scottish Caledonides; in First European Geotraverse Workshop: the Northern Segment; ed. D.A. Galson, and S. Mueller, European Science Foundation Publication, Strasbourg, p. 109-14.

Piasecki, M.A.J. and van Breemen, O.
1983: Field and isotopic evidence for a c.750 Ma tectonothermal event in the Moine rocks in the Central Highland region of the Scottish Caledonides; Transactions of the Royal Society of Edinburgh, Earth Sciences, v. 73, 119-34.

- 41 -

Geology of the Dashwoods Pond, St. Fintan's and Main Gut map areas, southwest Newfoundland[1]

Project 850017

J.T. van Berkel
Lithosphere and Canadian Shield Division

van Berkel, J.T., Geology of the Dashwoods Pond, St. Fintan's and Main Gut map areas, southwest Newfoundland; in Current Research, Part A, Geological Survey of Canada, Paper 87-1A, p. 399-408, 1987.

Abstract

A strip of Grenvillian gneisses with a low grade metamorphic overprint lies along both sides of the entire mapped length of the Long Range Fault. A Grenvillian massif-type anorthosite with minor facies of norite and quartz diorite – tonalite occurs northwest of the Long Range Fault. Early Ordovician regional deformation associated with medium- to high-grade metamorphism formed a stack of thrust slices composed of late Proterozoic to Cambrian quartzofeldspathic rocks and metasediments, locally interleaved by highly tectonized layers and inclusions of ophiolite. Biotite leucogranite intruded during the regional deformation. Three diabase (-gabbro) plutons with well preserved igneous textures are emplaced at a late stage of regional deformation. All these rocks are invaded and partially assimilated by large plutons of late tectonic biotite granite, porphyritic granite and hornblende-biotite granodiorite. Small plutons of post-tectonic homogeneous leucogranite are found southeast of the Long Range Fault. Undeformed diorite intrusions occur as small bodies throught the map area.

Résumé

Une bande de gneiss grenvilliens faiblement métamorphisés longe les deux côtés de la partie cartographiée de la faille de Long Range. Une anorthosite grenvillienne contenant des faciès peu importants de norite et de diorite quartzotonalite se présente sous forme de massif au nord-ouest de la faille de Long Range. Au début de l'Ordovicien, une déformation régionale associée à un métamorphisme moyen ou prononcé a formé une pile de lambeaux de poussée composés de roches quartzo-feldspathiques et de métasédiments du Protérozoïque inférieur ou du Cambrien avec par endroits des couches fortement tectonisées et des inclusions d'ophiolite. Un leucogranite à biotite a fait intrusion au cours de la déformation régionale. Trois plutons de diabase (-gabbro) contenant des structures ignées bien conservées ont été mis en place vers la fin de la période la déformation régionale. Toutes ces roche sont coupées et partiellement assimilées par de gros plutons de granite à biotite, de granite porphyrique et de granodiorite à hornblende et à biotite tardi-tectoniques. On trouve de petits plutons de leucogranite homogène post-tectonique au sud-est de la faille de Long Range et des petites masses intrusives non déformées de diorite partout dans la région levée.

[1]Contribution to the Canada-Newfoundland Mineral Development Agreement 1984-1989. Project carried by Geological Survey of Canada.

INTRODUCTION

The study area is located in southwest Newfoundland between Stephenville and Port aux Basques, east of the Trans-Canada Highway. It is bounded by 58° and 58°48′ west longitudes and 48° and 48°30′ north latitudes.

The Trans Canada Highway (Route 1), the Burgeo Road (Route 480) which connects the town of Burgeo on the south coast of Newfoundland with the Trans-Canada Highway, and some privately owned logging roads provide access to portions of the western and northern part of the area. The greater portion of the area is accessible only by helicopter.

The topography is dominated by the Long Range uplands, a gently rolling surface with an elevation between 300 and 650 m, which is deeply dissected by rivers and streams. Forest cover is rare above an elevation of 300 to 350 m, except a more or less dense growth of stunted spruce ("tuckamore") and the area is characterized by bogs between barren peaks and ridges. The degree of bedrock exposure is high in the barren uplands, although exposure in areas underlain by granite is restricted to the top of large rounded hills. Except in streams, exposure is poor to non-existent in the wooded valleys.

Large portions in the south of map area (12B/1) are covered by bouldery till. All of the area has been glaciated, with ice movements dominantly to the northwest.

The area was previously covered by 1:250 000 reconnaissance mapping (Riley, 1962). In the 1985 field season most of the present area and the adjacent map sheets to the east and north were mapped on a 1:100 000 scale (van Berkel et al., 1986; van Berkel and Currie, 1986). During the 1986 field season the area was mapped on a 1:50 000 scale and key areas were studied in detail. The adjacent southern (Grandys Lake, 110/15, and La Poile River, 110/16) and eastern areas (King George IV, 12A/4) were mapped on a 1:50 000 scale by Chorlton (1980, 1983) and Kean (1983) respectively. The adjacent northern area (Harrys River, 12B/9) is described by Currie (1987).

Acknowledgments

The author is indebted to the following persons for field mapping assistance and stimulating discussions: K.L. Currie and M.A.J. Piasecki in 1985, 1986, T. Rivers, D. Fox, T. van Nostrand, D. Machin and G. Goucher in 1986, and H.P. Johnson, J.C. Martin and S. Dawson in 1985. The manuscript was reviewed by K.L. Currie, S.P. Colman-Sadd, S.J. O'Brien, B. O'Brien and P.A. Cawood. Viking Helicopter of Pasadena supplied and moved the field parties efficiently. I thank the Forest Research Station, Environment Canada, for supplying base camp space and logistical help. I thank Kruger Inc. and Abitibi-Price Ltd. for permission to use woods roads.

GENERAL GEOLOGY

The boundary between the Humber and Dunnage tectonostratigraphic zones (Williams, 1979) crosses the map area (Fig. 41.1). The Humber Zone contains a Grenville basement with a late Proterozoic to early Paleozoic sedimentary cover. Locally, early Paleozoic ophiolitic allochthons derived from the Dunnage Zone rest on the sediments. Some recent workers (Chorlton, 1983; Kean, 1983) have abandoned the term Dunnage Zone and have returned to the old nomenclature of "Central Mobile Belt" (Williams, 1964) for these rocks because the subdivision by Williams (1979) into Dunnage and Gander Zone was found to be oversimplified. The Central Mobile Belt consists of felsic to mafic volcanics, clastic sediments and ophiolite rocks, all cut by granite and granodiorite ranging in age from Ordovician to Devonian.

The Long Range Fault (Fig. 41.1) forms the boundary between the Humber Zone and the Central Mobile Belt. Along the entire length of the Long Range Fault granitic to intermediate gneisses (unit P3) form a continuous strip of Grenville basement(?) across the area. The gneisses (unit P3) continue southwestwards into the Grandys Lake area. (110/15; see Chorlton, 1983). The dominant rock type northwest of the Long Range Fault is anorthosite (Steel Mountain anorthosite, unit P1) which contains minor facies of norite (unit P2a) and meta quartz-diorite to tonalite (unit P2b). Carboniferous sedimentary rocks (unit C; Knight, 1983) unconformably overlie or are in fault contact with the anorthositic rocks (unit P1) and intermediate to granitic gneisses (unit P3).

Southeast of the Long Range Fault, medium- to high-grade metamorphic quartzofeldspathic rocks of the Cormacks Lake Complex (unit Pє1; Herd and Dunning, 1979) and metamorphosed clastic sediments (unit Pє2) are invaded by syntectonic granite (unit 02). They are all intruded by large late-tectonic plutons of granite (units 06a and b) and granodiorite (unit 06c), and smaller post-tectonic plutons of biotite leuco granite (unit 07). The metasediments (unit Pє2) contain numerous inclusions and strips of serpentinite and metamorphosed ultramafic rocks (unit O1a), and metagabbro (unit 01b). Well-preserved diabase (-gabbro) (units 03, 04 and 05) occurs in three different bodies. Several, generally small, bodies of post-tectonic diorite (unit 08) were found throughout the region.

DESCRIPTION OF ROCK UNITS

Upper Proterozoic (Grenvillian) rocks

Anorthosite of the Steel Mountain complex (Fig. 41.1, unit P1) dominates the Grenvillian rock. Anorthositic rocks terminate in the adjacent northern map sheet (Currie, this volume). Much of the anorthosite now has massive partly recrystallized, medium-grained (up to 10 cm long) feldspar

and even larger (up to 3 m) pyroxene crystals. Pyroxene is altered to hornblende and may have a rim of biotite. Layered igneous textures are rare. Most anorthositic rocks have a colour index of less than 5 but locally gabbroic anorthosite (CI = 10-30) and norite (CI = 50) (unit P2a) are present. Pockets and layers of titaniferous magnetite locally up to a few hundred metres across are common (Baird, 1943, 1954). Brittle faults and fracture zones are widespread. Narrow ductile shear zones have been observed in a few outcrops but probably have a limited extent. Epidotization has been observed in many exposures along the Burgeo Road (Route 480). Amphibolite dykes are uncommon and may be correlative to the 600 Ma Long Range dyke swarm (Stukas and Reynolds, 1974) of the Great Northern Peninsula (Long Range Inlier; Owen 1986, Erdmer, 1986). The Steel Mountain anorthosite is a massif-type anorthosite (Simmons and Hanson, 1978; Emslie, 1978) and can be correlated with the Grenvillian Indian Head anorthosite (Walthier, 1949; Heyl

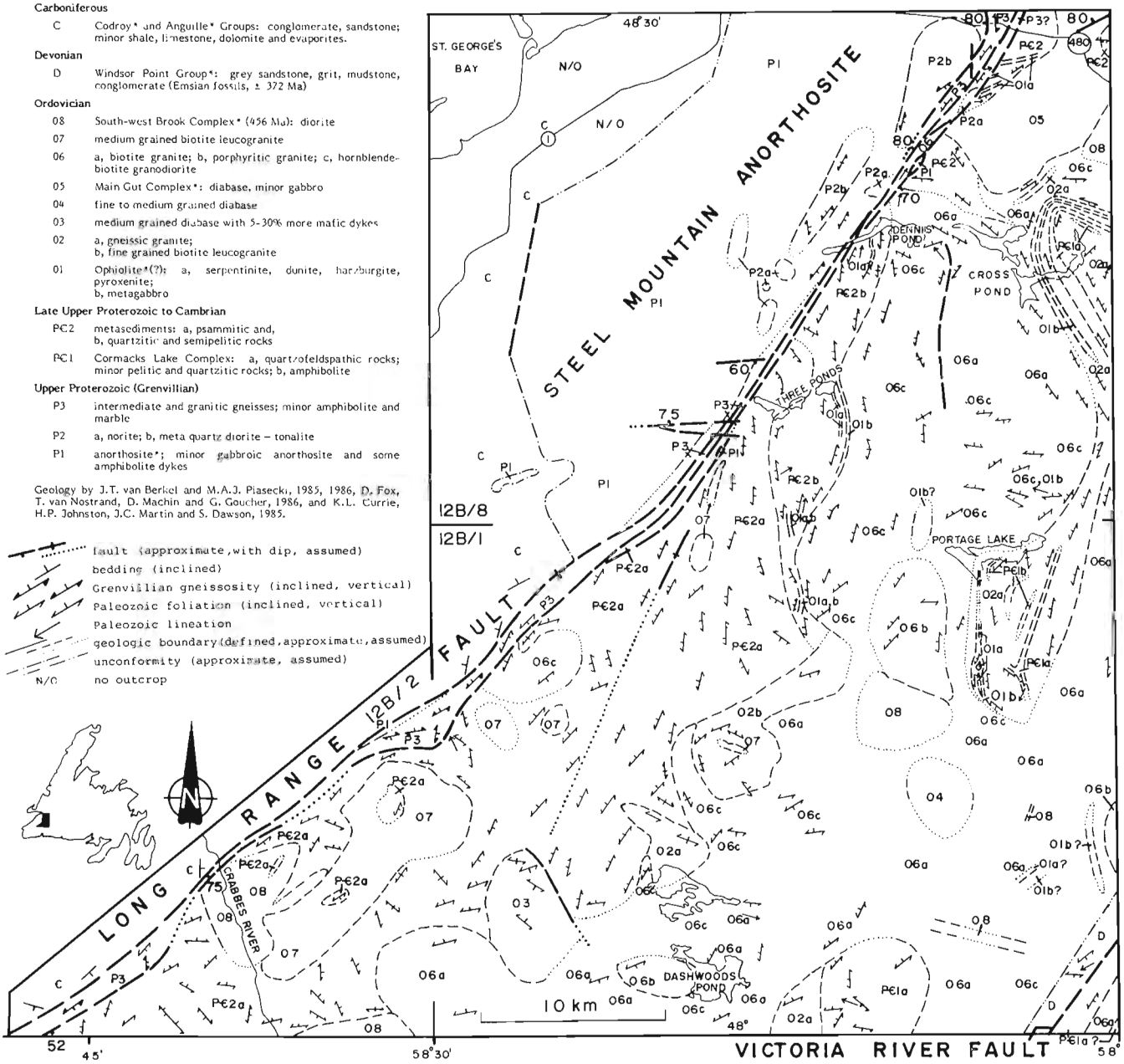


Figure 41.1. Generalized geological map of the Dashwoods Pond (12B/1), St. Fintan's (12B/2) and Main Gut (12B/8) map areas, southwest Newfoundland. An asterisk indicates that the age of the unit is reasonably well known. All other age assignments are speculative.

and Ronan, 1954; Colman-Sadd, 1974) located some 15 km to the west, east of Stephenville.

Several very coarse grained norite bodies (unit P2a) up to one kilometre across are more mafic facies of the Steel Mountain anorthosite. Poorly foliated quartz diorite-tonalite (unit P2b) is present along the eastern margin of the Steel Mountain anorthosite and has intrusive contacts unlike the intermediate and granitic gneisses (unit P3).

A strip of intermediate and granitic gneisses (unit P3) occur between the Long Range Fault and the Steel Mountain anorthosite, and continues to the southwest. This strip contains inclusions and large bodies of amphibolite. A small occurrence of anorthosite was found in this strip about 14 km southwest of the Steel Mountain anorthosite, just inside the St. Fintan's map sheet (12B/2). To the east, inside the Dashwoods Pond map sheet (12B/1), a 1.5-m-thick layer of marble was observed between amphibolite and granitic gneiss (Fig. 41.2). A low-grade metamorphic overprint is common and the orientation is parallel to the trace of the Long Range Fault. Southwest of the Steel Mountain anorthosite the gneisses (unit P3) are bounded by the brittle Long Range Fault to the northwest and by a minor, probably related brittle fault to the southeast. The intermediate and granitic gneisses (unit P3) are identical to the composite gneiss complex in the Harrys River map area (12B/9; see Currie, 1987), and are assumed to be Grenvillian on the basis of composition, structural style and high grade metamor phic textures.

Late Upper Proterozoic to Cambrian rocks

Across the Long Range Fault rock types change dramatically. Basement seems to be absent on the east side and the oldest rocks in this area form two north- south trending belts, one with quartzofeldspathic rocks (unit Pє1) of unknown origin and one with metasedimentary rocks (unit Pє2). They are separated by late-tectonic granite and granodiorite (unit 06).

Quartzofeldspathic rocks of the Cormacks Lake Complex (unit Pє1; Herd and Dunning, 1979) contain minor amounts of quartzitic to pelitic rocks and amphibo lite. Locally gedrite which develops characteristic sheafs, is present. Large bodies of amphibolite (unit Pє1b) are grouped with the Cormacks Lake Complex (unit Pє1) but may represent metamorphosed equivalents of the ophiolitic rocks (unit 01). The unit (Pє1) extends in to the adjacent eastern Puddle Pond (12A/5; Herd and Dunning, 1979) and King George IV (12A/4; Kean, 1983) map sheets, and into the adjacent southern La Poile River map sheet (110/16; Chorlton, 1980). East of the Victoria River Fault quartzofeldspathic gneisses containing elongated bodies of biotite granite (unit 06a; Kean, 1983), resemble those of the Cormacks Lake Complex (unit Pє1), and are tentatively classified with this unit.

The metasedimentary rocks (unit Pє2) can be subdivided into a western portion dominated by psammitic sediments and a much smaller eastern portion of quartzitic and semipelitic sediments. All were deformed and metamorphosed during medium- to high-grade metamorphism. The psammitic sediments (unit Pє2a) exhibit a medium-grained granoblastic texture with abundant feldspar porphyroblasts that obliterated primary sedimentary features. Amphibolite inclusions are common and locally large bodies of amphibolite are present. Trains of amphibolite inclusions may be highly deformed and disrupted dykes.

Quartzitic and semipelitic metasediments (unit Pє2b) form a narrow zone along the eastern edge of the metasedimentary belt (unit Pє2). They are lithologically monotonous (e.g. van Berkel et al., 1986) but contain strips and inclusions of tectonized serpentinized dunite and other metamorphosed ultramafic rocks (unit 01a), and gabbro (unit 01b). It has been proposed that they form part of a tectonic mélange zone (van Berkel et al., 1986) and that the host rocks have undergone severe deformation. Microstructural evidence for strong deformation is obliterated by recrystallization but numerous foliation-parallel quartz veins and lenses (Fig. 41.3) are preserved in certain zones and probably formed in shear zones by tectonic segregation (Piasecki, 1980; Temperley, in press). An alternative hypo

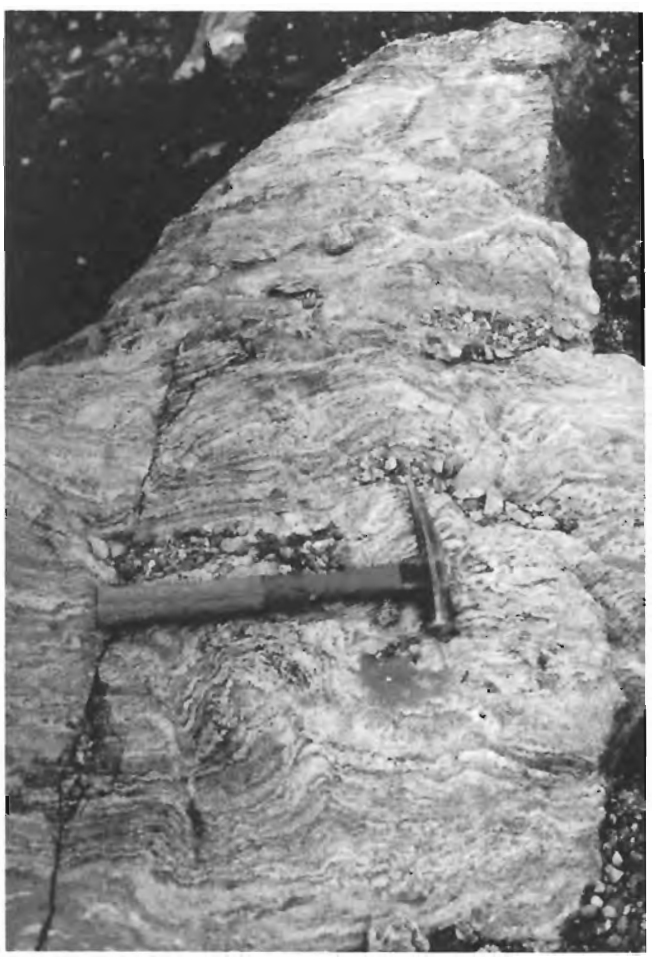


Figure 41.2. Grenvillian migmatitic granite gneiss (unit P3). GSC-204243-V

thesis of a sedimentary mélange with ophiolite blocks (e.g. Williams, 1977) was not considered by van Berkel et al. (1986). Deformation of such a sedimentary mélange during severe regional deformation could give similar field relations. A detailed study of this unit (Pє2b) and the ultramafic-mafic rocks (unit 01) was initiated in the 1986 field season (D. Fox, M.Sc. Thesis Project, Memorial University). The nature of the contact between the two metasedimentary units (Pє2a and b) is not well established. It seems to be a gradual change over a distance of a few hundred metres. Evidence for a tectonic contact was not observed. Serpentinite is apparently absent in the psammitic unit (Pє2a) but some of the amphibolite inclusions in this unit could be the amphibolitized equivalent of the serpentine.

The quartzitic and semipelitic metasediments (unit Pє2b) could be the medium to high metamorphic grade equivalents of the quartzite and pelitic schists around the southwest tip of Grand Lake in the Harrys River map area (12B/9; Currie, 1987) which have been correlated with the Fleur de Lys Supergroup (Knapp et al., 1979; Kennedy, 1981; Hibbard, 1983 a, b; Williams, 1985).



Figure 41.3. Foliation-parallel quartz veins and lenses in quartzitic and semipelitic metasediments (unit PC2b). Location south of Three Ponds. GSC-204460

Ordovician rocks

Mafic and ultramafic rocks of possible ophiolitic affinities (unit 01) not only occur in the metasediments (unit Pє2) but also as enclaves in gneissic granite (unit 02a). Metagabbro (unit 01b) is generally altered to amphibolite and variably epidotized, but locally, moderately strained, coarse-grained original textures are preserved, e.g. south of Portage Lake (Fig. 41.4) and northeast of Cross Pond. Dunite, harzburgite and pyroxenite (unit 01b) are well preserved in a large outcrop south of Portage Lake where moderately to highly strained metagabbro encloses a large (300 by 200 m) tectonic sliver of partially serpentinized dunite, harzburgite and pyroxenite. From southeast to northwest dunite with minor hazburgite passes abruptly into pyroxenite veined by harzburgite. Other tectonic slivers enclosed by metagabbro (unit 01b) in this region contain harzburgite and pyroxenite. Small amounts of chromite are found as dispersed euhedral crystals in dunite south of Portage Lake, and also as thin seams in serpentinite inclusions and layers in the metasedimentary rocks (unit Pє2; see van Berkel et al., 1986, Fig. 19.7).

Syn tectonic biotite granite (unit 02) invaded the quartzofeldspathic (unit Pє1), metasedimentary (unit Pє2) and ophiolitic rocks (unit 01). The field relations are well exposed around Cross Pond. Quartzofeldspathic rocks



Figure 41.4. Deformed relict igneous texture in metagabbro (unit 01b) of the ophiolitic rocks. GSC-204311-Z

(unit Pϵl) and complexly folded metagabbro (unit 01b) form enclaves within structurally less complex gneissic granite (unit 02a). Inclusions composed of fine grained biotite- plagioclase and amphibolite are common around Cross Pond (Fig. 41.5). The fine-grained biotite-plagioclase rock appears to be metasomatised amphibolite. Some of the better preserved amphibolites in this exposure contain recognizable dykes, are less consumed by the granite and could represent synplutonic dykes. The gneissosity in the granite is best developed where the granite contains numerous enclaves. In many exposures away from the enclave zones a poorly foliated medium grained texture is visible. Close to the ultramafic ophiolitic rocks of Portage Lake (unit 01a) structural complexity increases in the gneissic granite (unit 02a) and xenoliths of the ophiolitic rocks are common (Fig. 41.6). Fine-grained biotite leucogranite (unit 02b) which rarely shows a gneissic banding is classified with the gneissic granite (unit 02a).

Bodies with fine- to medium-grained mafic rocks (units 03, 04 and 05) have been termed diabase complexes because they generally exhibit a well-preserved subophitic texture. West of Dashwoods Pond a large diabase complex (unit 03) contains rather leucocratic (CI = 40) medium-grained rocks composed of plagioclase with minor orthopyroxene and even less hornblende. They are cut by more mafic dykes (CI = 60) which generally trend between northeast and southwest, and comprise between 5 to 30 per cent of individual exposures. Besides plagioclase the mafic dykes have significant amounts of hornblende and minor orthopyroxene. Plagio clase and orthopyroxene crystals are locally seen to form fine-grained cumulus crystals surrounded by much coarser grained intercumulus of hornblende. The rocks generally have a weak metamorphic fabric and contain secondary actinolite, epidote and mica. Fine to medium grained diabase (unit 04) was found in a poorly exposed area 13 km south of Portage Lake. Boulder mapping suggests a fairly large body. The Main Gut Complex (unit 05) in the northeastern corner of the area consists of fine- and medium-grained diabase. At the eastern edge of the complex coarse grained gabbro is developed which locally exhibits an igneous layering rich in magnetite. Zircon dating (Dunning, personal communication, 1985) and K-Ar determinations (R.K. Herd, *in* Stevens et al., 1982, p. 46, 47) indicates an lowermost Upper Ordovician age for this body.



Figure 41.5. Gneissic granite (unit 02a) with numerous mafic inclusions and a broken up mafic dyke. GSC-204243-U

Late-tectonic, massive to weakly foliated plutons composed of a variety of granitic rocks (unit 06) invade the previously described rock units. Dominant rock types are medium-grained biotite granite (unit 06a), porphyritic biotite granite (unit 06b) with K-feldspar crystals up to 3 cm long in a medium-grained matrix, and medium- to coarse-grained hornblende-biotite granodiorite (unit 06c). Rare meso cratic hornblende granodiorite and leucocratic granite with less than 1 per cent biotite appear as phases of the other granitic rocks. Offshoots of the granitic rocks (unit 06) into the country rocks, generally composed of a medium grained biotite leucogranite, are common in the area around Cross Pond. Hornblende-biotite granodiorite (unit 06c) often contains amphibolite inclusions, expecially in the region between Portage Lake and Cross Pond where inclusions form 5 to 30 per cent of individual exposures.

Medium-grained, massive homogeneous biotite leucogranite (unit 07) occurs as one large and a number of small plutons and dykes in the middle and southwestern part of the area. Felsic porphyry dykes were also found in this region.

Small, massive diorite plutons (unit 08) are widespread. Around Crabbes River the diorite contains numerous mafic inclusions. These massive diorites are thought to be correlative with diorite-tonalite of the South west Brook Complex (Herd and Dunning, 1979).

Devonian and Carboniferous rocks

One exposure in the area contains a felsic to intermediate altered volcanic rock thought to form part of the Windsor Point Group. The age of these rocks is uncertain. Kean (1983) and Chorlton (1983) considered them to be Devonian on the basis of fossils from grey sandstone but Chandler and

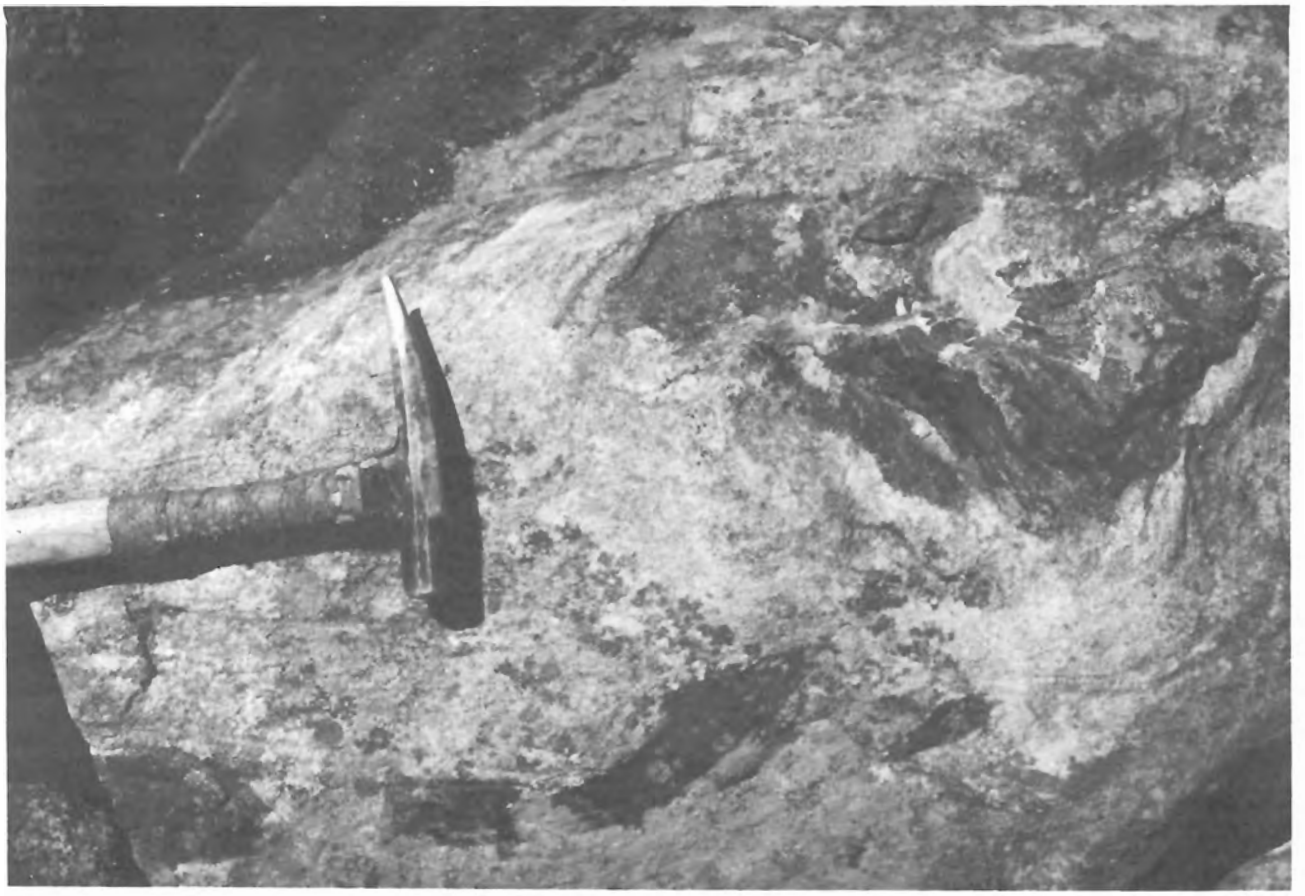


Figure 41.6. Ophiolitic mafic inclusions (unit 01) in gneissic granite (unit 02a). GSC-204243-R

Dunning (1983) showed that the fossiliferous sandstone unconformably overlies a red bed – acid volcanic sequence which gave a tightly defined Silurian radiometric age (431 ± 5 Ma).

Carboniferous sediments of the Bay St. George Subbasin (C) occupy the western edge of the area. These rocks have been described in detail by Knight (1983) and were not mapped by the author. They unconformably overlie the Steel Mountain anorthosite (unit P1) to the southwest but are in fault contact along the northwest margin. Southwest of the Steel Mountain anorthosite they are separated from the strip of Grenvillian gneisses by the Long Range Fault. Here, they mainly consist of sandstone and conglomerate.

ECONOMIC GEOLOGY OF ULTRAMAFIC ROCKS

Several rock samples of the ultramafic body (unit 01a) south of Portage Lake were analyzed for Au, Pd and Pt (Table 41.1). Pyroxenite in the northwestern portion of the ultramafic body contains numerous harzburgite veins and both (samples 6VM62-71) harzburgite and pyroxenite (samples 6VM62-71) have relatively high values of Pd (up to 100 ppb) and Pt (up to 130 ppb) but no detectable Au (less than 1 ppb). Closer to the dunite-pyroxenite contact Au content increases for harzburgite (up to 12 ppb; samples 6VM72A and B, 6VM73 and 6VM74) but the Pd and Pt content decreases dramatically (Fig. 41.7). Harzburgite pods (sample 6VM79) in the dunite portion (sample 6VM80) of the ultramafic body has similar low values.

TECTONIC EVOLUTION

The oldest rocks (units P1, P2 and P3) are assumed to be Grenville basement on the basis of composition, high-grade metamorphic textures and structural style. A low-grade metamorphic overprint was observed in much of the intermediate and granitic gneisses (unit P3) and is thought to represent early Paleozoic deformation and metamorphism. The Steel Mountain anorthosite is only partially statically recrystallized and contains a few minor shear zones. It therefore behaved as a fairly rigid block during the proposed early Paleozoic deformation.

East of the Long Range Fault Paleozoic regional metamorphism increases to medium and high-grade in the presumably late Proterozoic to Cambrian quartzo feldspathic

Table 41.1. Au, Pd and Pt analyses (in ppb) of ultramafic rocks 5 km south of Portage lake. Analyses by X-Ray Assay Laboratories Limited, Toronto. Method fire assay/DC plasma.

Sample number	Element (in ppb) Au	Pd	Pt	Rock type
6VM62	<1	13	30	pyroxenite
6VM64	<1	34	70	harzburgite
6VM65	<1	45	90	harzburgite
6VM66	<1	32	50	harzburgite
6VM67	<1	98	120	pyroxenite
6VM68A	<1	99	100	harzburgite
6VM68B	<1	100	100	same sample
6VM69	<1	97	130	harzburgite
6VM70A	<1	56	60	dunite
6VM70B	6	60	60	same sample
6VM71	<1	17	30	dunite
6VM72A	12	18	<10	harzburgite
6VM72B	12	12	<10	same sample
6VM73	2	10	20	harzburgite
6VM74	5	5	20	harzburgite
6VM75	<1	39	60	pyroxenite
6VM76	4	5	<10	pyroxenite
6VM77	<1	15	30	dunite
6VM78	<1	5	<10	dunite
6VM79	6	4	<10	harzburgite
6VM80	<1	9	30	dunite

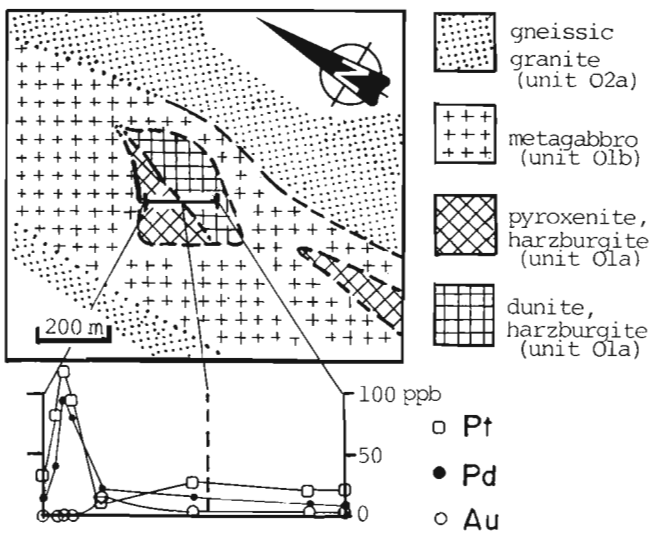


Figure 41.7. Detailed map of the ultramafic ophiolite sliver south of Portage Lake. Diagram displays average values for Au, Pd and Pt in each locality.

rocks (unit Pε1) and metasediments (unit Pε2). The quartzofeldspathic rocks may represent continental rift felsic volcanics and the psammitic, quartzitic and pelitic metasediments are possibly part of the Fleur de Lys Supergroup. Thrust slices of these rocks are locally interleaved by highly tectonized layers and inclusions of mafic to ultramafic rocks, interpreted as ophiolitic remnants (cf. Dewey and Shackleton, 1984). This period of deformation is thought to be of Lower Ordovician age. A zone characterized by highly deformed mafic and ultramafic rocks (unit 01) runs from south of Portage Lake to north of Cross Pond and separates the quartzofeldspathic rocks (unit Pε1) from the metasediments (Pε2). It is proposed that this zone forms a major thrust fault separating continental rift felsic volcanics from continental shelf metasediments. Both ultramafic and mafic rocks are interpreted as ophiolitic rocks sitting in a tectonic mélange zone.

Biotite granite (unit 02) was intruded during regional deformation and metamorphism, and together with the older rocks folded about northwest to southeast-trending fold axes. The granite (unit 02) contains numerous, partly assimilated amphibolite xenoliths (unit Pε1b and/or unit 01b) and enclave zones of the quartzo feldspathic rocks (unit Pε1) and metasediments (unit Pε2). Diabase (-gabbro) complexes have well-preserved and only partially altered igneous textures unlike the mafic to ultramafic ophiolitic rocks. They were emplaced at a very late stage of regional deformation and metamorphism. Large plutons of late-tectonic biotite granite (unit 06a), porphyritic granite (unit 06b) and hornblende-biotite granodiorite (unit 06c) invaded all the previously described rocks. Numerous amphibolite xenoliths and enclaves in the hornblende-biotite granodiorite and its composition suggest that a substantial portion of the invaded and assimilated rocks consist of mafic to ultramafic rocks. Metasedimentary inclusions (e.g. quartzite) were found north of Portage Lake but are rare.

Zircon dating (Dunning, personal communication, 1985) and K-Ar age deter minations (Herd, *in* Stevens et al., 1982, p. 46, 47) of the late-tectonic Main Gut Complex (unit 05) and tonalite-diorite of the post-tectonic Southwest Brook Complex (unit 08; Herd and Dunning, 1979) suggest that around the lowermost Upper Ordovician regional deformation and metamorphism has stopped. There is no evidence for Acadian regional metamorphism. Homogeneous biotite leuco granite (unit 07), tentatively assumed to be Upper Ordovician in age, and porphyry dykes may be correlated with high level Silurian granitoid intrusions of the Topsails Terrane (Whalen and Currie, 1983a and b; Whalen et al., in press). These rocks only occur in the middle to southwestern part of the area. On the other hand more heterogeneous syntectonic hornblende- biotite granodiorite (unit 06c) was mainly found in the central region and syntec tonic biotite granite (unit 06a) in the southern and eastern parts of the area.

Ductile shear zones and brittle faults generally strike northeast southwest. Ductile shear zones have been observed in some of the younger Ordovician intrusive rocks like the late-tectonic granites (unit 06) and tonalite-diorite of the Southwest Brook Complex (unit 08). An upper age limit can be inferred from Silurian redbeds occurring east of the map area (Chandler and Dunning, 1983) because these rocks never developed a metamorphic fabric (Chandler, 1982; Kean, 1983). Ductile shear zones must therefore have been active in the late Ordovician and possibly also earlier. Brittle faults cut Carboniferous rocks (unit C) and have a major displacement in this period. Most of the ductile shear zones and brittle faults have a limited extent. Only the Long Range Fault and Victoria River Fault are crustal scale ductile shear zones and both have a major brittle component.

REFERENCES

Baird, D.M.

1943: Titaniferous magnetites in anorthosite, east of St. Georges, Newfoundland; unpublished M.Sc. thesis, University of Rochester, Rochester, New York, U.S.A., 102 p.

1954: The magnetite and gypsum deposits of the Sheep Brook-Lookout area. Geological Survey of Canada, Bulletin 27, p. 20-41.

Chandler, F.W.

1982: Sedimentology of two middle Paleozoic terrestrial sequences, King George IV Lake area, Newfoundland and some comments on regional paleoclimate; *in* Current Research, Part A, Geological Survey of Canada, Paper 82-1A, p. 213-219.

Chandler, F.W. and Dunning, G.R.

1983: Fourfold significance of an early Silurian U-Pb zircon age from rhyolite in redbeds, southwest Newfoundland, NTS 12A/4; in Current Research, Part B, Geological Survey of Canada, Paper 83-1B, p. 419-421.

Chorlton, L.

1980: Geology of the La Poile River area (110/16), Newfoundland; Newfoundland Department of Mines and Energy, Mineral Development Division, Report 80-3, 86 p.

1983: Geology of the Grandys Lake area (110/15), Newfoundland; Newfoundland Department of Mines and Energy, Mineral Development Division, Report 83-7, Part 1, 116 p.

Colman-Sadd, S.P.

1974: Iron deposits of the Indian Head Range; in Metallogeny and Plate Tectonics. A Guidebook to Newfoundland Mineral Deposits (edited by D.F. Strong). NATO Advanced Studies Institute, p. 150-158.

Currie, K.L.

1987: A preliminary account of the geology of Harrys Run map area, southern Long Range, Newfoundland; in Current Research, Part A, Geological Survey of Canada, Paper 87-1A, Report 68.

Dewey, J.F. and Shackleton, R.M.

1984: A model for the evolution of the Grampian tract in early Caledonides and Appalachians; Nature, v. 312, p. 115-121.

Emslie, R.F.

1978: Anorthosite massifs, rapakivi granites, and late Proterozoic rifting of North America, Precambrian Research, v. 7, p. 61-98.

Erdmer, P.

1986: Geology of the Long Range Inlier in the Sandy Lake map area, western Newfoundland; in Current Research, Part B, Geological Survey of Canada, Paper 86-1B, p. 19-27.

Herd, R.K. and Dunning, G.R.

1979: Geology of Puddle Pond map area, southwestern Newfoundland; in Current Research, Part A, Geological Survey of Canada, Paper 79-1A, p. 305-310.

Heyl, A.V. and Ronan, J.J.

1954: The iron deposits of Indian Head area; in Contributions to the Economic Geology of Western Newfoundland, Geological Survey of Canada, Bulletin 27, p. 42-62.

Hibbard, J.

1983a: Notes on the metamorphic rocks in the Corner Brook area (12A/13) and regional correlation of the Fleur de Lys Belt, western Newfoundland; in Current Research, Newfoundland Department of Mines and Energy, Mineral Development Divison, Report 83-1, p. 41-50.

1983b: Geology of the Island of Newfoundland; Newfoundland Department of Mines and Energy, Mineral Development Division, Map 83-106.

Kean, B.F.

1983: Geology of the King George IV Lake map area (12A/4); Newfoundland Department of Mines and Energy, Mineral Development Division, Report 83-4, 67 p.

Kennedy, D.P.

1981: Geology of the Corner Brook Lake area, western Newfoundland; unpublished M.Sc. thesis, Memorial University of Newfoundland, 370 p.

Knapp, D.A., Kennedy, D.P., and Martineau, Y.A.
1979: Stratigraphy, structure and regional correlation or rocks at Grand Lake, western Newfoundland; *in* Current Research, Part A, Geological Survey of Canada, Paper 79-1A, p. 317-325.

Knight, I.
1983: Geology of the Carboniferous Bay St. George Subbasin, western Newfoundland; Newfoundland Department of Mines and Energy, Mineral Development Division, Memoir 1, 358 p.

Martineau, Y.A.
1980: The relationships among rock groups between the Grand Lake Thrust and Cabot Fault, western Newfoundland; unpublished M.Sc. thesis, Memorial University of Newfoundland, 150 p.

Owen, J.V.
1986: Geology of the Silver Mountain area, western Newfoundland; in Current Research, Part A, Geological Survey of Canada, Paper 86-1A, p. 515-522.

Piasecki, M.A.J.
1980: New light on the Moine rocks of the Central Highlands of Scotland, Journal of the Geological Society of London, v. 137, p. 41-59.

Riley, G.C.
1962: Stephenville map area, Newfoundland; Geological Survey of Canada, Memoir 323, 72 p.

Simmons, E.C. and Hanson, G.N.
1978: Geochemistry and origin of massif-type anorthosites, Contributions to Mineralogy and Petrology, v. 66, p. 119-135.

Stevens, R.D., Delabio, R.N., and Lachance, G.R.
1982: Age determinations and geological studies, K-Ar isotopic ages, Report 16, Geological Survey of Canada, Paper 82-2, 56 p.

Stukas, V. and Reynolds, P.H.
1974: $^{40}AR/^{39}AR$ dating of the Long Range dykes of Newfoundland, Earth and Planetary Science Letters, v. 22, p. 256-266.

Temperley, S.
(in press) Vein systems and porphyroblasts in high temperature high strain zones: their bearing on the nature of shearing. Journal of Structural Geology.

Van Berkel & Currie, K.L.
1986: Geology of the southern Long Range, southwest Newfoundland (12B/1, 12B/8, 12B/9, 12A/4, 12A/5, 12A/2); Geological Survey of Canada, Open File 1328.

Van Berkel, J.T., Johnston, H.P. and Currie, K.L.
1986: A preliminary report on the geology of the southern Long Range, southwest Newfoundland; in Current Research, Part B, Geological Survey of Canada, Paper 86-1b, p. 157 to 170.

Walthier, T.N.
1949: Geology and mineral deposits of the area between Corner Brook and Stephenville, western Newfoundland; Newfoundland Geological Survey, Bulletin 35, Part I.

Whalen, J.B. and Currie, K.L.
1983a: The Topsails igneous terrane of western Newfoundland; in Current Research, Part A, Geological Survey of Canada, Paper 83-1A, p. 15-23.
1983b: Geology of the Topsails igneous terrane; Geological Survey of Canada, Open File Report 923 (1:100 000 map with marginal notes).

Whalen, J.B., Currie, K.L., and van Breemen, O.
(in press) Episodic Ordovician-Silurian plutonism in the Topsails igneous terrane, western Newfoundland. Canadian Journal of Earth Sciences.
1964: The Appalachians in northeastern Newfoundland – A two-sided symmetrical system. American Journal of Science, v. 262, p. 1137-1158.
1977: Ophiolitic mélange and its significance in the Fleur de Lys Supergroup, northern Appalachians, Canadian Journal of Earth Sciences, v. 14, p. 987-1003.
1979: Appalachian Orogen in Canada; Canadian Journal of Earth Sciences, v. 16, p. 792-807.
1985: Geology, Stephenville map area, Newfoundland; Geological Survey of Canada, Map 1579A (scale 1:100 000 with marginal notes).

- 42 -

Preliminary report on sedimentology of sandstones, slates, and bioclastic carbonate material in the Meguma Group, Mahone Bay, Nova Scotia[1]

DSS Contract 27 ST. 23233-6-0052

John W.F. Waldron[2] and Milton Graves[3]

Waldron, J.W.F. and Graves, M., Preliminary report on sedimentology of sandstones, slates, and bioclastic carbonate material in the Meguma Group, Mahone Bay, Nova Scotia in Current Research, Part A, Geological Survey of Canada, Paper 87-1A, p. 409-414, 1987.

Abstract

Within the Cambro-Ordovician Meguma Group of Nova Scotia, there is a complex transition zone between the Goldenville Formation and the overlying Halifax Formation. In the transition zone, two members are well exposed in the Tancook Island area of Mahone Bay. The lower, Tancook member, contains two intervals of interbedded turbiditic sandstone and slate, separated by an interval of laminated and bioturbated manganiferous slate. A sandy bioclastic limestone horizon near the top of the member contains shell and echinoderm debris. The overlying Mosher's Island Member consists mostly of hemipelagic laminated manganiferous slate. The transition zone records a progressive reduction in the supply of sand to the area by turbidity currents, and a concurrent decrease in the supply of dissolved oxygen at the sediment-water interface.

Résumé

Une zone de transition complexe sépare la formation de Goldenville de la formation susjacente de Halifax dans le groupe cambro-ordovicien de Méguma, en Nouvelle-Écosse. Deux termes affleurent dans la zone de transition aux alentours de l'île Tancook, dans la baie Mahone. Le terme inférieur, celui de Tancook, contient deux intervalles de grès turbiditique et de schiste ardoisier interstratifiés, séparés l'un de l'autre par un intervalle de schiste ardoisier manganifère laminé et bioturbé. Un niveau de calcaire bioclastique sableux trouvé près du sommet du terme contient des débris de coquilles et d'échinodermes. Le terme susjacent de Mosher's Island se compose surtout de schiste ardoisier manganifère, laminé, hémipélagique. La zone de transition montre qu'il y a eu réduction progressive de la quantité de sable transporté par les courants de turbidité et en même temps, diminution de la quantité d'oxygène dissous à l'interface eau-sédiment.

[1]Contribution to the Canada-Nova Scotia Mineral Development Agreement 1984-1989. Project carried by Geological Survey of Canada, Lithosphere and Canadian Shield Division, Project 760027

[2]Geology Department, Saint Mary's University, Halifax, Nova Scotia B3H 3C3

[3]Cuesta Research Ltd., Dartmouth, Nova Scotia

INTRODUCTION

The Cambro-Ordovician Meguma Group of southern mainland Nova Scotia is well exposed on the shores of Mahone Bay, Nova Scotia (Figure 42.1). The group was divided in this area by Faribault (1908, 1924, 1929) into two formations: the lower, Goldenville Formation consists mainly of metamorphosed turbiditic sandstones ("quartzites" or "quartz wackes"), with subordinate slates; whereas the upper, Halifax Formation, consists predominantly of slate with lesser amounts of sandstones. The majority of the Halifax slates are black and pyrite-bearing; slates in the Goldenville Formation are green and generally lack pyrite. Tremadocian graptolites were recorded from the Halifax Formation elsewhere in Nova Scotia by Smitheringale (1960) and Crosby (1962), but the Goldenville Formation has hitherto been regarded as unfossiliferous. Both formations are metamorphosed at low greenshist facies in the Mahone Bay area. In a more detailed investigation of the geology of Mahone Bay, O'Brien (1986) demonstrated that the Goldenville-Halifax transition is more complex than was recognized by Faribault. (op cit.) O'Brien recognized a number of distinct members in the transition (Table 42.1), and showed that Faribault's Goldenville-Halifax boundary had been mapped at varying levels within this succession of members. In this report we discuss sedimentary features of the transition zone in particularly good exposures on the coasts of Big and Little Tancook islands and on the corresponding mainland coast at Blandford; we also report on the discovery of a horizon of transported bioclastic limestone in one of these sections.

STRATIGRAPHY

Table 42.1 illustrates the lithostratigraphic succession mapped by O'Brien (1986) in the Mahone Bay area. O'Brien informally defined the Green Bay Formation to include the units in the transition zone that had previously been mapped inconsistently as Goldenville or Halifax. The lowest member recognized, the New Harbour Member of the Goldenville Formation, consists of extremely thickly bedded (up to 20m) sandstones with very minor slate. It is overlain in the Mahone Bay area by the Tancook Member, consisting of subequal proportions of slate and generally thinly to thickly bedded sandstone. The overlying Mosher's Island Member consists of grey-green manganiferous slate and argillite. This passes up into black carbonaceous slates and thinly to very thinly bedded siltstones of the Cunard Member of the Halifax Formation; both slates and siltstones in the Cunard Member contain abundant pyrite.

Tancook Member

The Tancook Member is exposed most completely on the east coast of Tancook Island; figure 42.2 summarizes the stratigraphy of this section. The upper part of the Member is also well displayed on the west coast of Little Tancook Island. Neither island shows good exposure of the base of the member; incompletely exposed near-horizontal strata at the anticline axis on Big Tancook Island (Figure 42.1) may include the top few metres of the underlying New Harbour Member. However the lower contact is best located on the mainland

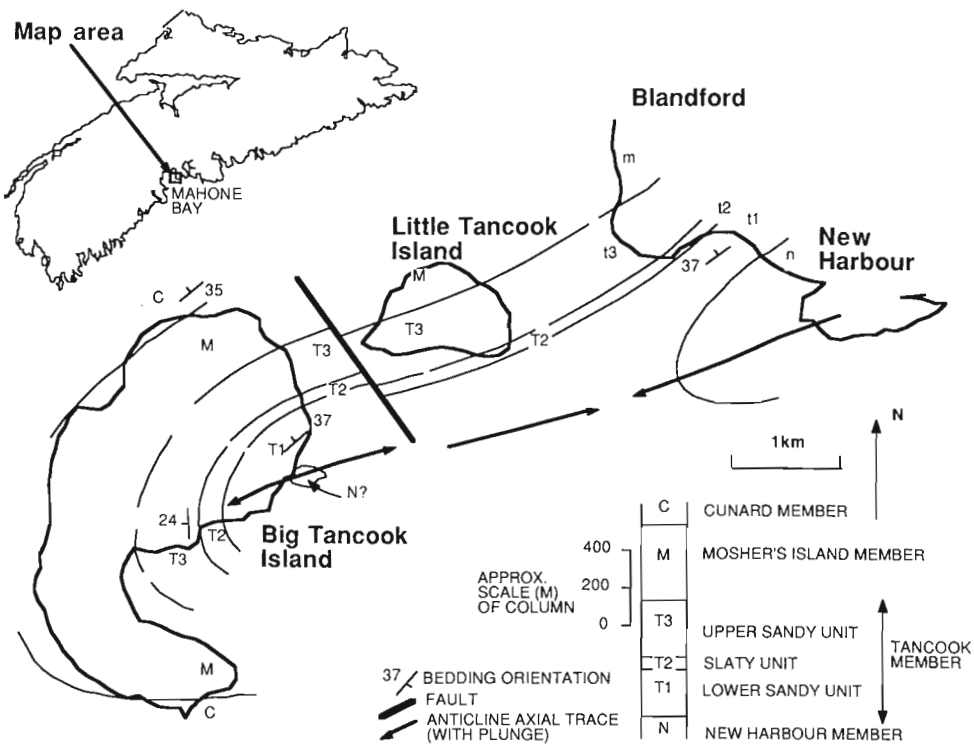


Figure 42.1 Geological map of Big and Little Tancook islands and the adjacent shore of Mahone Bay showing the outcrop of the Goldenville-Halifax transition.

shore north of New Harbour (Figure 42.1), although even here the section is interrupted by a few metres of boulder beach.

The Tancook Member can be subdivided into three easily mappable units: a lower sandy unit, a slaty unit, and an upper sandy unit. In the lower sandy unit, thinly to medium bedded, fine to very fine sandstones are interbedded with generally subordinate amounts of laminated to unlaminated green silty slate. Sand beds are typically graded and show partial or complete Bouma sequences, characteristic of deposition from dilute turbidity currents. Sole marks include flute and groove casts, and bed-parallel burrows and trails. Rare vertical burrows resembling *Skolithus* were noted. Occasional packages of thicker-bedded sandstone occur within this unit; these contain internal scours, dewatering pipes and sheet structures, and are probably deposits of high-concentration turbidity currents (Lowe, 1982). Carbonate concretions occur sporadically within this unit, but are particularly abundant at the top, where they are manganiferous and weather reddish brown. The uppermost of several thick sandstone beds at the top of the lower sandy unit shows intense bioturbation by steep burrows with internal "meniscus" laminations, and passes gradationally up into almost homogeneous slates of the overlying unit.

The slaty unit of the Tancook member is almost devoid of sand, consisting of slates that alternate irregularly between well laminated and poorly laminated to mottled facies. High concentrations of manganese are indicated by black-weathering laminations and concreations, and by black films on joint and cleavage surfaces. Elsewhere fine laminations are absent, but a gross stratification is defined by thin mottled brown-weathering beds which are lenticular when traced along strike over distances of metres. Short (3-10cm) burrows are preserved in some intervals by conspicuous fills of black concretionary material rich in pyrite. The mottled appearance of some of the slates is also interpreted as a product of intense bioturbation.

The base of the upper sandy unit is marked by a return of thin bedded sandstones. In general the upper sandy unit is more variable than the lower. It is characterized by sandstone beds ranging in thickness from 1cm to over 3m. The thicker beds are clustered in packages, separated by thinly bedded intervals, suggesting that two distinct facies associations are present. Sandstones in thickly bedded intervals are generally laminated to massive or internally scoured, and closely resemble those described from the Goldenville Formation of the Nova Scotia Eastern Shore by Waldron and Jensen (1985), where they were interpreted as deposits of high-concentration turbidity currents. The thickly bedded packages contain only minor amounts (less than 10%) of laminated to cross-laminated green slate. Thinly bedded intervals contain up to about 50% slate. The thin sandstone beds are generally graded and in places show partial Bouma sequences suggesting deposition by more dilute turbidity currents. Elsewhere in the sequence, however, they have homogeneous structureless tops; in some cases steep spreite burrows resembling *Teichichnus* are visible, suggesting that homogenization was due to bioturbaton. Figure 42.3 shows both thickly bedded and thinly bedded sandstone intervals in the upper sandy unit of the Tancook Member.

Table 42.1 Lithostratigraphic units recognized by previous workers in Tancook Island area of Mahone Bay.

Faribault (1909)	O'Brien (1986)	
Halifax Formation	Feltzen Member	Halifax Formation
	Cunard Member	
	Mosher's Island Member	Green Bay Formation
	Tancook Member	
Goldenville Formation	New Harbour Member	Goldenville Formation

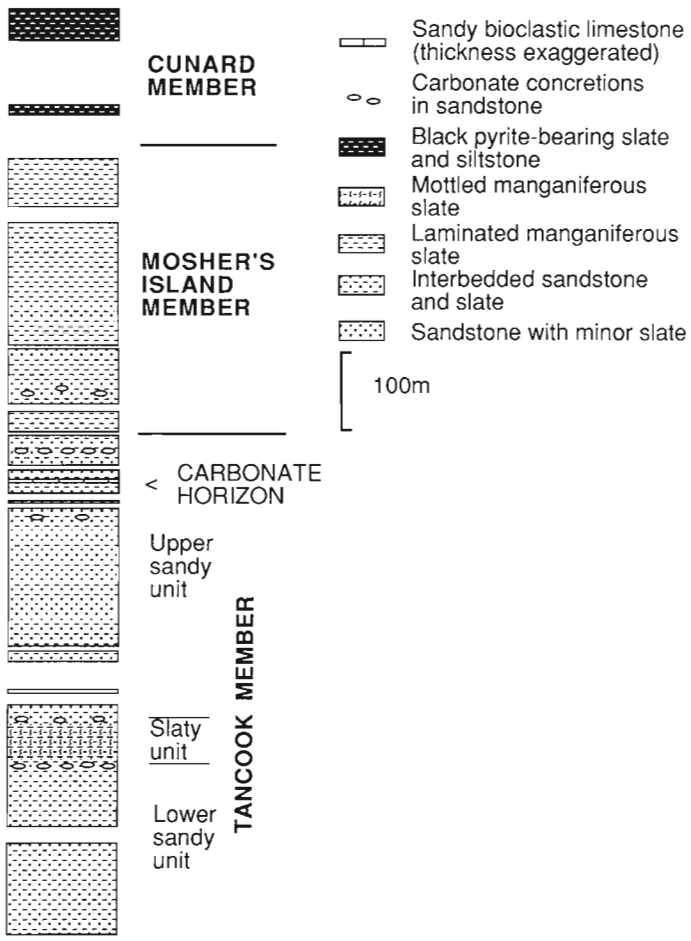


Figure 42.2 Schematic stratigraphic column representing section on northeast coast of Big Tancook Island.

Bioclastic carbonate horizon

About 60m below the top of the upper sandy unit on Tancook Island a 44cm bed of brown-weathering limestone and calcareous sandstone is present. The section in Figure 42.3 includes this horizon. The bed is laminated and in outcrop is seen to contain numerous generally bed-parallel brown-weathering flakes up to about 10mm in diameter. The flakes impart a strong fissility to the rock. In thin section (Fig. 42.4a) the flakes are seen to be shell fragments consisting of prismatic calcite crystals with a strong preferred orientation. Under crossed polars, the extinction direction varies smoothly within each flake. The flakes are, however, too recrystallized to be identified even by phylum at this stage. More characteristic are single crystals of calcite having a reticulate pattern of inclusions characteristic of echinoderm skeltons. These vary in shape, but include typical circular cross sections of crinoid ossicles (Fig. 42.4b). The shell and echinoderm fragments are well sorted and mixed with sand; they are obviously highly transported, and indicate derivation from a carbonate-producing shelf area. Probe analyses of carbonate material in this bed show that it now contains up to 3.6% by weight of MnO, presumably as a result of interaction with Mn-rich pore waters from which the carbonate concretions were deposited.

Concretionary carbonate material becomes more abundant up-section from the bioclastic layer, and the sand/shale ratio decreases. Many sandstone beds in this uppermost part of the Tancook member are bioturbated by *Teichichnus*-type spreite burrows. Hexagonal *Paleodictyon* networks have also been observed on one in situ bedding surface and on several loose boulders from this part of the shore.

Mosher's Island Member

The Mosher's Island Member is dominated by slate, though occasional packages of thinly to medium bedded sandstone are present in the lower 160 m of section. With the exception of the lowermost sandstone package, in which spreite burrows are spectacularly developed, the sandstones are not bioturbated; they show well developed parallel laminations and current-ripple cross-laminations.

In the slates the only common primary sedimentary structures are parallel laminations, together with occasional low-amplitude starved ripples and wavy laminations; a few horizons show soft-sediment deformation structures (pseudonodules), but these do not have any consistent sense of asymmetry that would suggest formation on a slope. Colour variations visible in the field, especially on weathered cleavage surfaces, are probably due to original variations in organic carbon content; dark grey laminae tend to be well cleaved and fissile, whereas the more abundant grey-green slates are relatively massive. Carbonate beds, laminae, and concretion horizons weather yellow in outcrops in the intertidal zone, but brown elsewhere, and are rich in manganese (up to 14.2% MnO in preliminary analytical results). Abundant disseminated metamorphic garnets (probably spessartines) are visible in thin section in both the concretion horizons and the

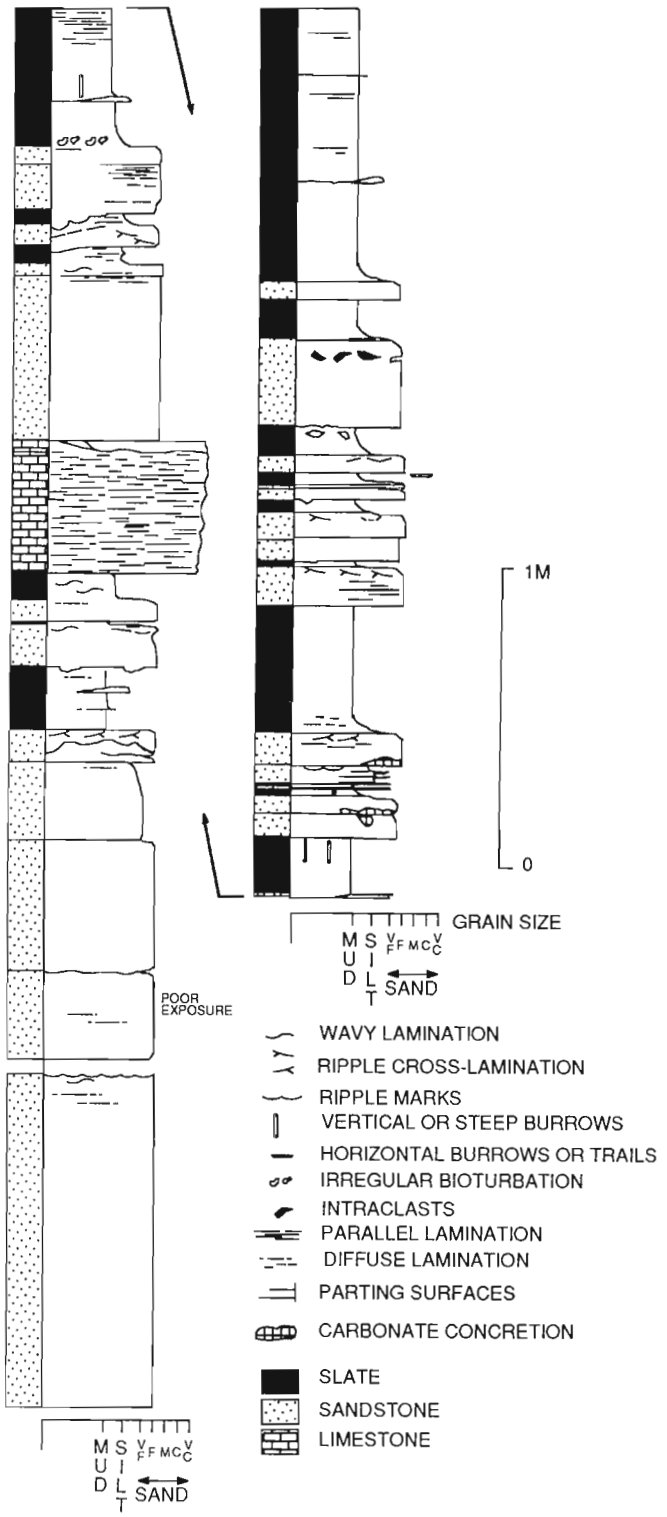


Figure 42.3 Detailed measured section including carbonate horizon near top of Tancook Member on northeast coast of Big Tancook Island.

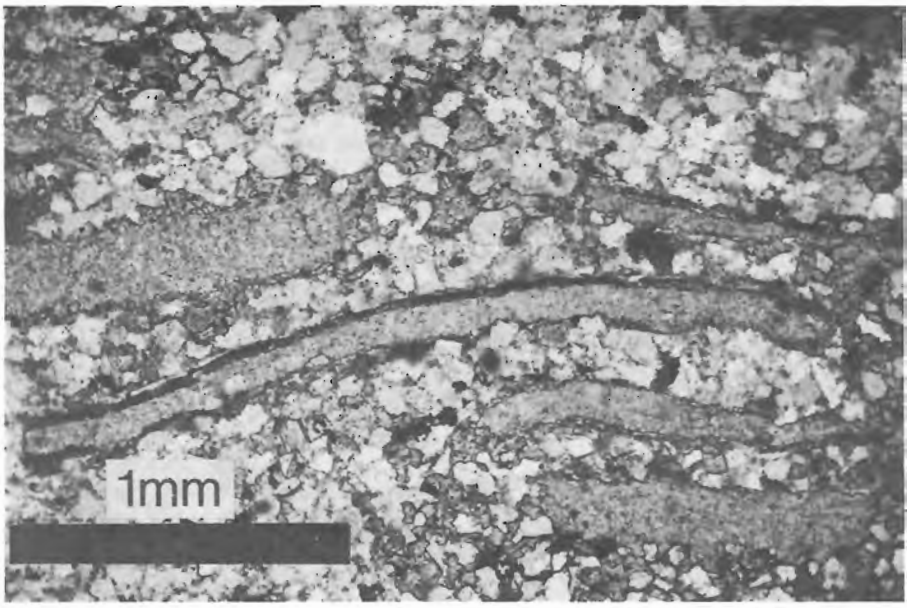


Figure 42.4a Photomicrograph of shell fragments from sandy carbonate horizon in Tancook Member: plane polarized light.

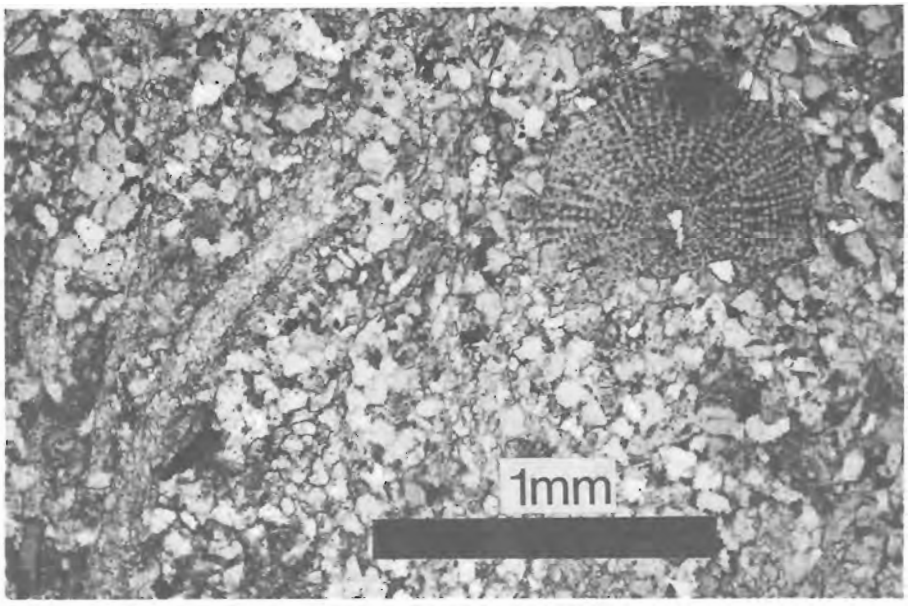


Figure 42.4b Sample from same horizon showing echinoderm fragment, probably a crinoid ossicle (upper right): plane polarized light.

green slates. The garnets impart a sandy appearance to the member in the field and hand specimen, which led O'Brien to describe this unit as sandstone. However the extremely fine grain-size of other components seen in thin-section, and the generally finely laminated nature of the sediment, indicate that the member was originally very fine grained hemipelagic mud. The transition into the overlying black slates of the Cunard Member is exposed, though slightly faulted, on the south coast of Big Tancook Island. Manganiferous and pyrite-bearing lithologies alternate throughout an interval of about 3m. Above this, only black pyrite-rich slates and siltstones occur.

CONCLUSIONS

A number of distinct changes in sedimentary environment or source area were responsible for the development of a com-

plex Goldenville-Halifax transition in the Mahone Bay area. The first to take effect was a reduction in sediment supply. This might have been due to tectonic or eustatic events affecting the source area, or to a rearrangmeent in the geometry of the submarine fan in which the Goldenville sediments were deposited. The reduced rate of sedimentation led to establishment of a larger bottom fauna, producing more thorough bioturbation. Subsequently, a final shut-off of the sand supply, and a probable reduction in dissolved oxygen at the sediment-water interface, led to deposition of laminated non-bioturbated slates of the Mosher's Island Member. Finally, an increase in organic productivity or establishment of fully anoxic conditions led to deposition of black slates of the Cunard Member, typical of the Halifax Formation.

ACKNOWLEDGMENTS

We acknowledge useful discussions with B. O'Brien, M. Zentilli, P. Schenk and F. Chandler. J.A. burns assisted in the field.

REFERENCES

Crosby, D.G.
1962: Wolfville map area, Nova Scotia: Geological Survey of Canada, Memoir 325, 67 p.

Faribault, E.R.
1908: Aspotogan; Geological Survey of Canada, Map 70.
1924: Chester Basin; Geological Survey of Canada, Map 87.
1929: Mahone Bay; Geological Survey of Canada, Map 88.

Lowe, D.R.
1982: Sediment gravity flows: II. Depositional models with special reference to the deposits of high density turbidity currents; Journal of Sedimentary Petrology, v. 52, p. 279-297.

O'Brien, B.F.
1986: Preliminary report on the geology of the Mahone Bay area, Nova Scotia; in Current Research Part A: Geological Survey of Canada, Paper 86-1A, p. 439-444.

Smitheringale, W.C.
1960: Geology of the Nictaux – Torbrook Map area Annapolis and Kings Counties, Nova Scotia; Geological Survey of Canada, Paper 60-13.

Waldron, J.W.F., and Jensen, L.R.
1985: Sedimentology of the Goldenville Formation, Eastern Shore, Nova Scotia: Geological Survey of Canada, Paper 85-15, 31 p.

Geology of the Guysborough-Country Harbour area, Nova Scotia[1]

Project 850016

J.D. Hill
Lithosphere and Canadian Shield Division

Hill, J.D., Geology of the Guysborough-Country Harbour area, Nova Scotia; in Current Research, Part A, Geological Survey of Canada, Paper 87-1A, p. 415-422, 1987.

Abstract

Regional mapping at 1:10 000 scale indicates that the Country Harbour-Guysborough area is underlain by Meguma Group strata intruded by granite, tonalite and pegmatite. The Goldenville Formation could not be subdivided. The Halifax Formation is composed of graphitic schist stratigraphically overlain by quartz-muscovite schist containing a few thin coticule beds.

Seven granitic plutons were outlined, ranging from medium grained muscovite-biotite granite to aplitic muscovite leucogranite. Six small bodies of biotite tonalite, three of which contain abundant hornblende, are exposed along the margins of the granitic plutons. The age relationships between the plutonic rocks were not determined.

The area has been affected by two main phases of ductile deformation, separated by a period of porphyroblast growth and granitoid emplacement, and followed by major transcurrent faulting.

Résumé

La cartographie régionale à l'échelle de 1/10 000 révèle que la région de Country Harbour – Guysborough repose sur des couches du groupe de Méguma dans lequelles ont fait intrusion du granite, de la tonalite et de la pegmatite. La formation de Goldenville ne peut pas être subdivisée. La formation de Halifax se compose d'un schiste graphitique sous-jacent à un schiste à quartz et à muscovite qui contient quelques minces couches de coticule.

Sept plutons granitiques ont été étudiés; leur composition varie d'un granite à deux micas, à grain fin, à un leucogranite à muscovite aplitique. Six petites masses de tonalite à biotite, trois desquelles contiennent d'abondantes quantités de hornblende, affleurent en bordure des plutons granitiques. Aucun lien chronologique n'a été établie entre les diverses roches plutoniques.

La région a subi deux phases principales de déformation ductile séparées par une période de formation de porphyroblastes et d'intrusion granitoïde et suivies par la formation de grands décrochements.

[1]Contribution to Canada-Nova Scotia Mineral Development Agreement 1984-1989. Project carried by Geological Survey of Canada

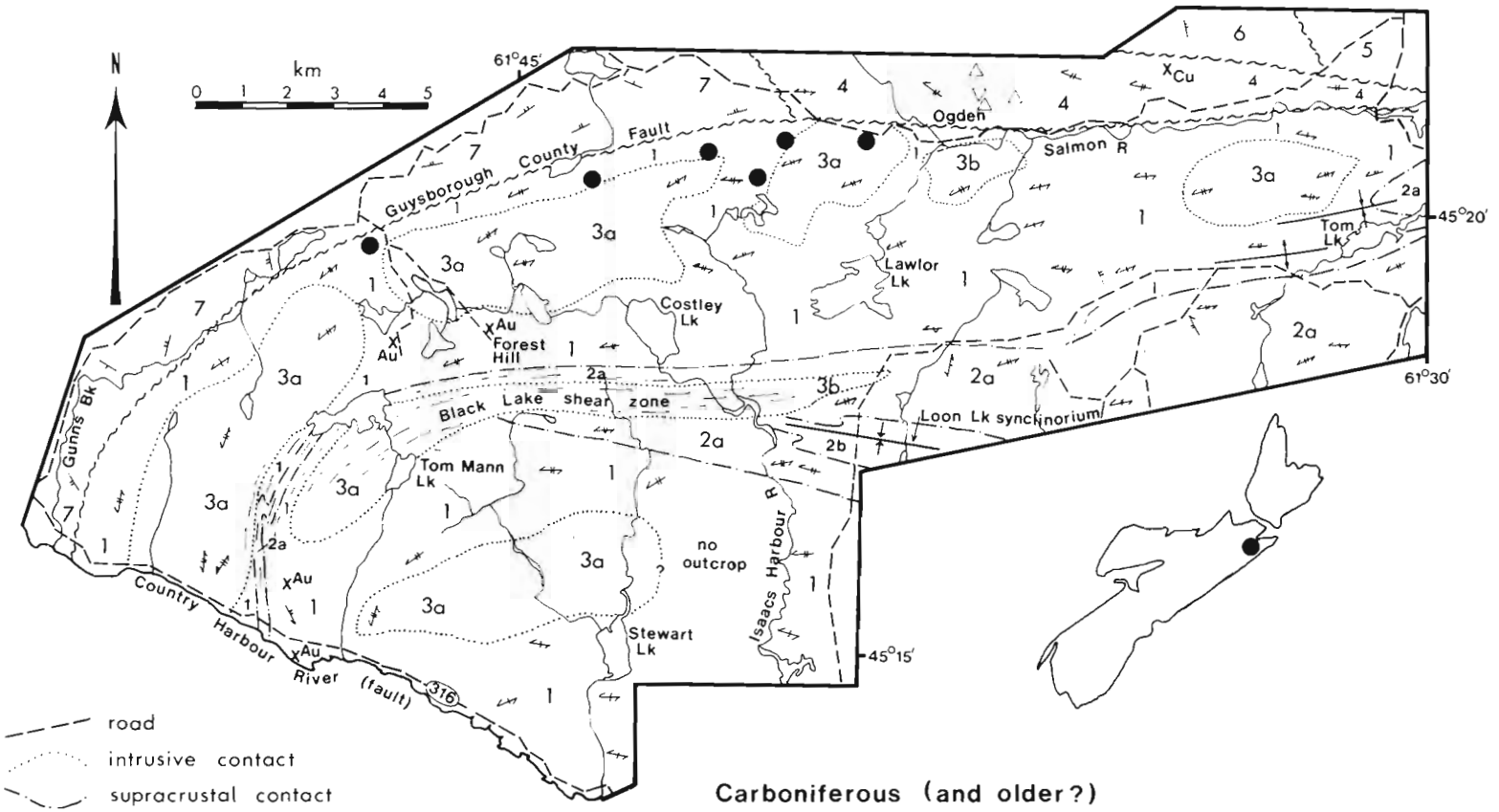


Figure 43.1. Preliminary geology map of the Guysborough–Country Harbour area.

INTRODUCTION

This report summarizes data collected during the second field season of a multi-year mapping and petrological project on granitoid plutons in the eastern Meguma terrane. The initial phase of the study centred on the area between Whitehead and Canso (Hill, 1986a,b). The latest work involved 1:10 000 scale mapping of an area of about 330 km^2 between Country Harbour and the town of Guysborough during the summer of 1986. Outcrops were found mainly along streams and roads. In addition, some exposures were located on old trails, around lakeshores and on wooded and barren ridges. Outcrops are particularly lacking in the southern part of the map area.

The area has been mapped previously by Faribault (1893a,b) and Schiller (1961), the latter's work forming the basis of a PhD thesis (Schiller, 1963). The Goldenville terrain has received considerable attention since the late 1800s by companies exploring for gold. Several mines have operated at various times and places near Forest Hill and Country Harbour Mines. Currently, Seabright Resources is actively exploring for gold at Forest Hill, and Louisburg Property Holdings and Bartex Developments have recently completed an evaluation of the Triangle Lake area, 2 km west of Forest Hill. McKenzie and MacGillivary (1974) briefly described and sampled two granitoid plutons south of Salmon River. Ford and Ballantyne (1983) studied the lithogeochemistry and U-Th distribution patterns in granitoid plutons throughout the eastern Meguma terrane. A structural analysis of the Goldenville Formation around Triangle Lake has been completed by Haynes et al. (1986). Harmeson (1986) studied the relationship between geology and lineaments defined by Landsat and aeromagnetic images.

Acknowledgments

The project is part of the Canada-Nova Scotia Mineral Development Agreement. B.G. Eddy of Acadia University provided able assistance in the field. The manuscript was reviewed by G.M. Yeo.

GEOLOGICAL SETTING

The map area is mainly underlain by metasedimentary rocks of the Cambro-Ordovician Meguma Group which are intruded by several granitoid plutons of probable Devonian age (Fig. 43.1). Small bodies of hornblende-bearing tonalite were found at six localities. Although these rocks are complexly deformed and several ages of tectonic structures can be recognized locally, only two periods of ductile deformation appear to have regional significance. These include folding and metamorphism of probable Acadian age that developed prior to granite emplacement, and a post-intrusive period of intense dextral shearing. Major transcurrent faulting followed the shearing event, with the Guysborough County Fault separating the Meguma terrane from the Avalon terrane farther north.

To determine the relationships between the Guysborough County Fault and its adjacent rocks, mapping was extended 1-2 km north and west of the fault into the eastward extension of the St. Mary's River graben. However, correlation of these rocks with those in adjacent map sheets is hindered by the scarcity of outcrop and the small size of the area examined.

MEGUMA GROUP (UNITS 1 AND 2)

The Goldenville Formation (unit 1) is composed of a rather monotonous assemblage of psammitic and minor pelitic metasedimentary rocks. It is locally intruded by numerous sills and irregular lenses of muscovite leucogranite pegmatite, particularly along the Guysborough County Fault and in zones adjacent to granitoid plutons. Quartz veins up to 2 m thick are typically oriented parallel to bedding (and S_1) and carry accessory graphite, muscovite, feldspar, chlorite, pyrite, arsenopyrite and tourmaline.

Unit 1 ranges from relatively massive metawacke and meta-arenite to thinly bedded metawacke intercalated with pelitic schist. All variations between these two end-members exist and the unit could not be subdivided at map scale due to lack of lithologic continuity along strike. The more massive lithology, which dominates the area, consists of quartz with up to 30% each of feldspar, biotite (locally altered to chlorite) and muscovite. It is typically structureless to slightly platy with blocky fracturing. Beds range from 10 cm to 5 m thick where observed, being shown by faint differences in colour or weathering and by the local presence of 1-20 cm thick layers of schist or calc-silicate material. The calc-silicate beds are commonly discontinuous and lensoid in shape, although planar layers up to 100 m long and 15 cm thick were observed in exploration trenches at Forest Hill. They consist of quartz, amphibole and biotite with accessory garnet, plagioclase and sphene, and are compositionally zoned in some places.

The thinly bedded variant of unit 1 is best developed between Lawlor Lake and Forest Hill where it may represent a transition to the younger Halifax Formation. Beds are 1 cm to 1 m thick and are commonly laminated. Cross-lamination and grading, typically distorted by deformation, are visible locally. Interbedded schist and semischist form up to 50% of the rock but much smaller proportions are more common. Calc-silicate layers and a few thin beds of pink-weathering coticule are present at Forest Hill. The mineralogy is the same as that described above for the more massive variety except that small porphyroblasts of garnet, staurolite and cordierite are locally developed in the more pelitic beds (Fig. 43.2).

The Halifax Formation occupies the core of a large synclinorium exposed in the southeastern part of the map area (Fig. 43.1). The unit is subdivided into an older member of graphitic schist (unit 2a) and a younger member of quartz-muscovite schist (unit 2b). The only evidence for their relative ages is a single younging determination south of Lawlor Lake and their structural positions in the synclinorium.

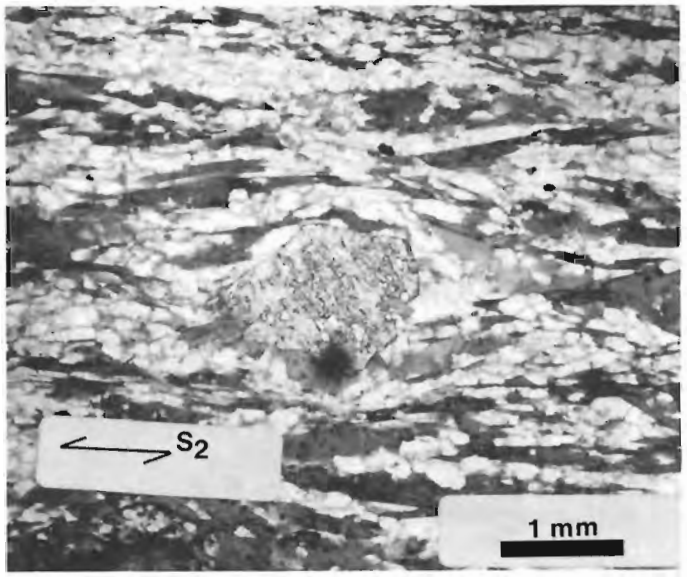


Figure 43.2. Quartz-biotite-muscovite semischist containing staurolite porphyroblasts, Goldenville Formation, Forest Hill. Porphyroblast, enveloped by S_2 schistosity, contains internal inclusion trail interpreted to represent S_1. Oblique nicols.

Unit 2a is mainly composed of grey to black, rusty, graphitic schist (Fig. 43.3) that is typically porphyroblastic. Beds are 1-30 cm thick and are locally laminated. Minor amounts of quartz-mica schist lacking graphite and 1-5 cm thick beds of fine grained metawacke occur in some outcrops. Due to their relative competence, the metawacke beds are commonly boudinaged. Quartz veins up to 30 cm thick are present in many exposures. They are usually oriented parallel to bedding (and S_1). Quartz, muscovite and biotite (locally altered to chlorite) are the dominant constituents, with graphite, pyrite, pyrrhotite and garnet occurring as accessory phases. Porphyroblasts of pink andalusite up to 4 cm long characterize most outcrops, although small porphyroblasts of biotite and cordierite are abundant in some places.

Unit 2b was only observed in five exposures. It is composed of grey, laminated quartz-muscovite schist carrying accessory biotite and garnet as well as porphyroblasts of andalusite and cordierite. A few 0.1 to 2 cm thick beds of pink coticule are usually present.

GRANITOID PLUTONS (UNIT 3)

Seven granitoid plutons were distinguished in the map area, although the two large bodies north and west of Forest Hill may form a single intrusion. In addition, small masses of tonalite occur near the edges of the granitic plutons. The margins of the granitoid intrusions are commonly migmatitic, containing numerous lenses of Goldenville metawacke and injections of pegmatite. The pegmatite is muscovite-bearing and carries accessory garnet, tourmaline and biotite. Schiller (1963) has reported the presence of minor andalusite in pegmatite south of Costley Lake. Except for those in the Stewart Lake area, all of the plutonic rocks are mylonitic to varying degrees, but igneous terminology is used for simplicity.

Two main types of granitic rocks were identified. The more abundant is medium grained granodiorite to granite (Fig. 43.4) containing variable amounts of biotite and muscovite (unit 3a). The most leucocratic pluton in unit 3a, with about 5-10% muscovite and 2-4% biotite occurs northwest of

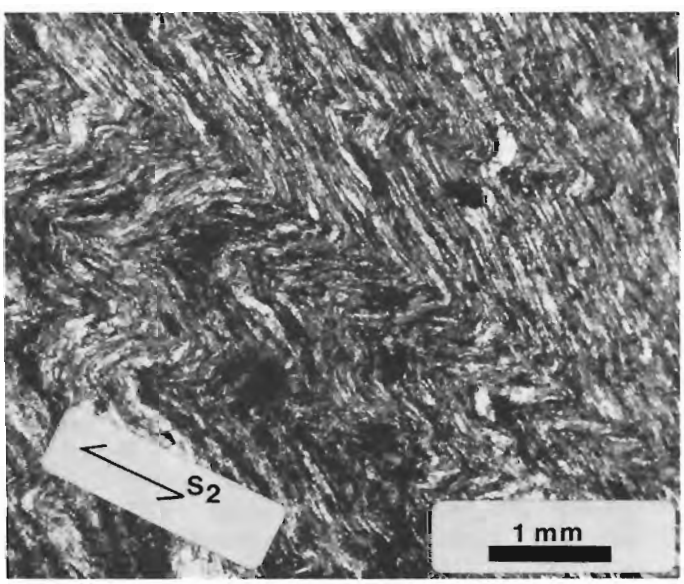


Figure 43.3. Graphitic schist (unit 2a) with S_1 schistosity crenulated by S_2. Oblique nicols.

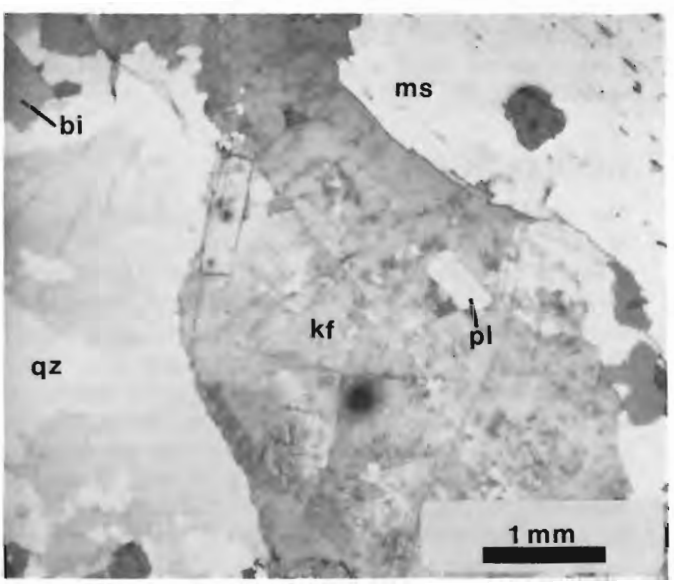


Figure 43.4. Medium grained muscovite-biotite granite (unit 3a) from a relatively undeformed pluton. Oblique nicols.

Tom Lake. In contrast, the pluton north of Lawlor Lake is the most mafic, having approximately 6-10% biotite and 1-5% muscovite. The remaining intrusions in unit 3a have subequal but variable proportions of the two micas. Unit 3b consists of aplitic leucogranite with 7-12% muscovite and less than 2% biotite. It forms the small pluton northeast of Lawlor Lake and the eastern tip of the elongate body south of Lawlor Lake.

Six separate occurrences of fine to medium grained tonalite occur within the Meguma terrane in close proximity to the Guysborough County Fault and along the margins of larger granitic plutons. The tonalite contains 15-25% biotite and 0-10% hornblende, the latter occurring in three of the bodies. In addition, the tonalite contains accessory clinopyroxene, sphene, apatite and Fe-Ti oxides. Curiously, the tonalite is only slightly deformed despite its proximity to the Guysborough County Fault. In fact, the body lying 1 km west of Ogden is only about 400 m south of the fault but is virtually undeformed (Fig. 43.5). In contrast, granitic rocks in the same area are quite mylonitic. Similar hornblende-bearing tonalite has also been reported to occur about 15 km west of the map area (S. Edmonds, personal communication, 1986).

Contact relationships between the various granitic and tonalitic rocks were not observed. Pegmatite, which is commonly gradational with unit 3, intrudes all of the igneous rocks in the Meguma terrane. Masses of aplite, similar in composition to unit 3b, appear to intrude the two large plutons north and west of Forest Hill.

ROCKS OUTSIDE THE MEGUMA TERRANE (UNITS 4 TO 7)

Rocks north of the Meguma terrane are divided into four units that appear to be separated by faults. They are believed to be correlative, at least in part, with the early Carboniferous Horton Group. This interpretation is supported by occurrences of early Mississippian fossils in rocks similar to units 4 and 7 north and west of the map area (Schiller, 1963). Although Schiller (1963) favoured a pre-Horton age for the altered andesites of unit 5, Stevenson (1964) has described an occurrence of purple amygdaloidal basalt intercalated with Horton strata at Bigby Head, about 2 km east of the map area. The relative ages of units 4 to 7 are uncertain.

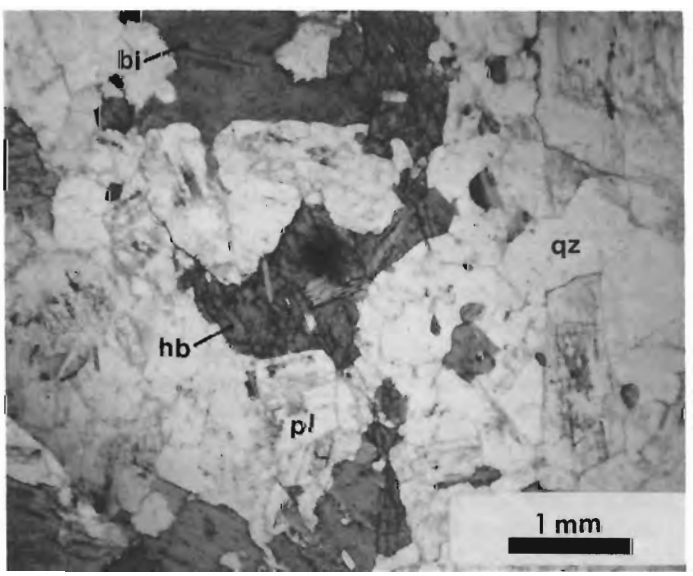


Figure 43.5. Hornblende-biotite tonalite. Oblique nicols.

Three small inliers of mylonite containing scattered porphyroclasts of plagioclase, garnet and quartz lie within unit 4 near Ogden. An outcrop of light-weathering conglomerate (outlier?) containing unmetamorphosed clastic sedimentary pebbles occurs in the same area. The relationships of these rocks to unit 4 are unknown.

Unit 4 consists of grey to grey-black, slightly graphitic slate and phyllite locally interbedded with minor fine grained meta-arenite. Quartz, biotite, muscovite and chlorite are the dominant minerals, with graphite present in minor amounts. Lamination in the pelitic beds is caused by discontinuous quartz-rich streaks. Although these rocks are metamorphosed to greenschist grade and isoclinally folded, Schiller (1963) stated that they become less deformed and metamorphosed northward away from the Guysborough County Fault. The unit appears to be correlative with the Strathlorne Formation of the Horton Group mapped by Schiller (1963) and Benson (1974).

Altered andesite flows (unit 5) are only exposed in a few outcrops and numerous boulders in the northeast corner of the map area. The andesite is characterized by a dark maroon colour and up to 30% each of plagioclase phenocrysts and vesicles. The vesicles are commonly flattened and many are filled with calcite, quartz, chlorophaeite and stilbite(?). The plagioclase phenocrysts are euhedral, up 5 mm long, and locally define an irregular flow foliation. Despite considerable hydrothermal alteration to chlorite, epidote, hematite, sericite, calcite and tremolite, primary clinopyroxene and olivine can be recognized in a few places. The rocks are highly fractured and crosscut by veinlets of quartz, epidote, calcite and specular hematite. Most of the outcrops and boulders examined contain vein-like fracture fillings of hematitic mudstone and siltstone. In addition, conglomerate boulders just north of the map area contain pebbles of andesite identical to unit 5 in a red sandstone matrix. These features suggest an unconformity exists between units 5 and 6. The fact that veinlets in the andesite do not penetrate the fracture fillings of clastic material suggests that unit 6 was only deposited after the andesite flows had cooled and degassed.

Unit 6 is composed of red to buff, hematitic, quartzose sandstone and siltstone and minor maroon conglomerate containing unmetamorphosed volcanic (not similar to unit 5) and sedimentary pebbles. The sandstone is typically well sorted and massive, although lamination occurs locally. The unit appears to lie unconformably on unit 5, although the present boundaries in the map area are fault-controlled.

Unmetamorphosed, immature sandstone and conglomerate (unit 7) occupy the east end of the St. Mary's River graben in the western side of the map area. The dominant lithology is a poorly sorted, flaggy, feldspathic to lithic wacke, but quartz wacke occurs locally. Detrital muscovite flakes are abundant along bedding planes. The sandstone is brown to green-grey, although oxidation to a red-brown colour along subhorizontal fractures is a common feature. Conglomerate increases in abundance toward the Guysborough County Fault. It appears to form shoestring-shaped deposits up to 3 m high and 5 m wide within the sandstone. A few thin beds of carbonaceous shale occur farther away from the fault. Metre-scale festoon crossbeds and asymmetric ripples are relatively common. Abundant root casts were found in two places. Although Schiller (1963) referred to these rocks as the Gum Brook Member of the Horton Group, they appear to be correlative with the Ainslie Formation of Benson (1974) farther west. Obvious cobbles of Goldenville metawacke up to 1 m long and pebbles of Halifax graphitic schist are concentrated in conglomerate and lithic sandstone at several places close to the fault. No fragments of Acadian granite or porphyroblastic Halifax schist were found. However, Keppie (1985) has noted the presence of andalusite schist clasts near Salmon River Lake and Benson (1974) found granite fragments in conglomerate west of Melrose.

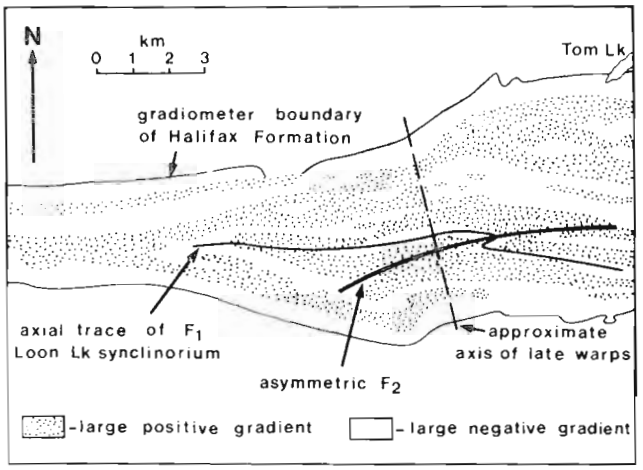


Figure 43.6. Sketch of the aeromagnetic vertical gradient map (Geological Survey of Canada, 1985, Map C40099) of the area underlain by the Halifax Formation in the core of the Loon Lake synclinorium. Inferred fold axial traces are indicated.

DEFORMATION AND METAMORPHISM

The Meguma terrane has been affected by two main periods of ductile deformation, separated in time by amphibolite-grade metamorphism and granite emplacement. In addition, major transcurrent faulting and events of restricted significance that produced local minor structures of several ages have affected the area. North of the Guysborough County Fault, only unit 4 is recognizably deformed and metamorphosed, although the volcanic rocks in unit 5 are badly altered to greenschist mineral assemblages.

The first main phase of ductile deformation (D_1) is represented by widespread development of cleavage (S_1) that is typically oriented subparallel bedding. S_1 is a weak pressure solution cleavage in the more competent rocks of the Goldenville Formation, where it is commonly the dominant fabric element, and a schistosity defined by biotite and muscovite in more pelitic rocks. No mesoscopic F_1 folds were recognized. However, based on stratigraphic considerations, a large F_1 synclinorium, here termed the Loon Lake synclinorium, is inferred to exist in the central part of the map area (Fig. 43.1). Its shape is accurately shown on the aeromagnetic vertical gradient map for the area (Fig. 43.6). The narrowing of the structure westward suggests an overall eastward plunge, a feature that is supported by a stereonet plot of bedding for the eastern third of the map area (Fig. 43.7).

Porphyroblasts of staurolite, garnet, cordierite, andalusite and biotite appear to overprint S_1 in the more pelitic rocks. They probably formed during a period of static metamorphism that may be temporally related to granitoid plutonism (Keppie, 1983). These porphyroblasts are ubiquitous in rocks of appropriate composition in the Meguma Group within the map area, occurring as much as 4 km from the nearest granitoid pluton. Considering the small sizes of the plutons, it is unlikely that the porphyroblasts grew in direct response to contact metamorphism, unless the intrusions are merely cupolas of a much larger near-surface batholith. Sillimanite was found in two samples of Goldenville metawacke just west of Ogden. Its origin is uncertain, although the presence of numerous sills of granite in that area suggests it may be related to localized contact metamorphism. Sillimanite has also been found by Haynes et al. (1986) in similar rocks south of Tom Mann Lake.

The second main phase of deformation (D_2) is characterized by numerous mesoscopic Z-shaped folds (F_2) in pelitic rocks and a penetrative cleavage (S_2) developed in both the Meguma Group and granitoid plutons. D_2 has largely obliterated the effects of contact metamorphism and caused considerable transposition of earlier structures. The mesofolds are tight to isoclinal and plunge gently ENE and WSW, although moderate to steep plunges occur locally (Fig. 43.7). Macrofolds inferred from aeromagnetic vertical gradient data (Fig. 43.6) lie just south of the map area and affect both limbs of the core of the Loon Lake synclinorium. S_2 is a variably developed schistosity, defined by muscovite and biotite and commonly accompanied by a gently plunging intersection lineation. It typically trends 10-30° counterclockwise from S_0-S_1, envelops and deforms porphyroblasts (Fig. 43.2) and is attendant to F_2 mesofolds where it crenulates S_1 (Fig. 43.3). It is defined by a grain flattening foliation in granitoid rocks. Although confined to a 10-15 km wide zone in the Meguma terrane adjacent to the Guysborough County Fault, the intensity of D_2 deformation is variable and does not gradually increase northward toward the fault as has been suggested by Haynes et al. (1986). Rather, it is most intense in a narrow belt in the central part of the map area, here termed

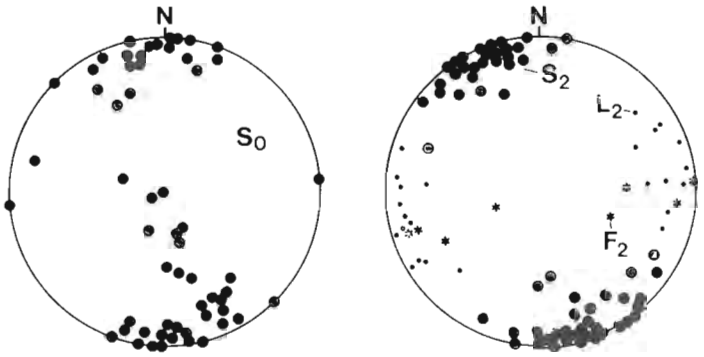


Figure 43.7. Equal-area steronet plots of poles to bedding (left) and poles to S_2, L_2 mineral lineations, slickensides and intersection lineation, and F_2 mesofold axes (right).

the Black Lake shear zone (Fig. 43.1). There, the rocks are strongly mylonitic and S-C fabrics are well developed, both in granitic (Fig. 43.8) and locally in metasedimentary rocks. A subhorizontal mineral lineation and slickensides are visible on cleavage surfaces (Fig. 43.7). These structures are consistent with significant subhorizontal dextral movement in an east-west direction. Strain appears to have been concentrated along the Black Lake shear zone due to the presence of a narrow band of highly incompetent graphitic schist. D_2 structures appear to be related to a widespread ductile shearing event interpreted by Keppie (1983) to have been associated with right-lateral displacement along the Minas Geofracture during the Devonian.

Prior to deposition of the Horton Group, major transcurrent faulting occurred, possibly as a brittle culmination of D_2 dextral shearing. Within 800 m of the Guysborough County Fault, breccias and cataclasites are sporadically developed (Fig. 43.9). Rocks tend to be highly fractured, and biotite, which is the dominant mafic mineral farther south, is supplanted by chlorite. Subhorizontal and rare subvertical slickensides are present on numerous polished fracture surfaces. The presence of a 3 m wide zone of breccia and discontinuous pseudotachylite veins parallel bedding at Forest Hill suggests that similar and possibly related faults may occur within the Meguma terrane. Sinistral displacement along the County Harbour Fault is interpreted to have caused the swing in D_2 structures from east-west in the east to north-south in the west (Keppie, 1983). Normal movement along the Guysborough County Fault is believed to be responsible for the deposition of the Horton Group in the St. Mary's River graben.

North of the Guysborough County Fault, centimetre-scale isoclinal folds with gentle westward plunges were recognized in several places in unit 4. A slaty cleavage defined by muscovite, biotite and chlorite is associated with the folds. Although the data are inconclusive, these structures may be related to D_2 in the Meguma terrane. The slaty cleavage is locally crenulated in at least two directions.

MINERALIZATION

Gold-bearing quartz veins in the Goldenville Formation have been mined at several localities in the past. Pyrite and coarse crystals of arsenopyrite are common constituents of the veins. Although no mineralization of economic importance was

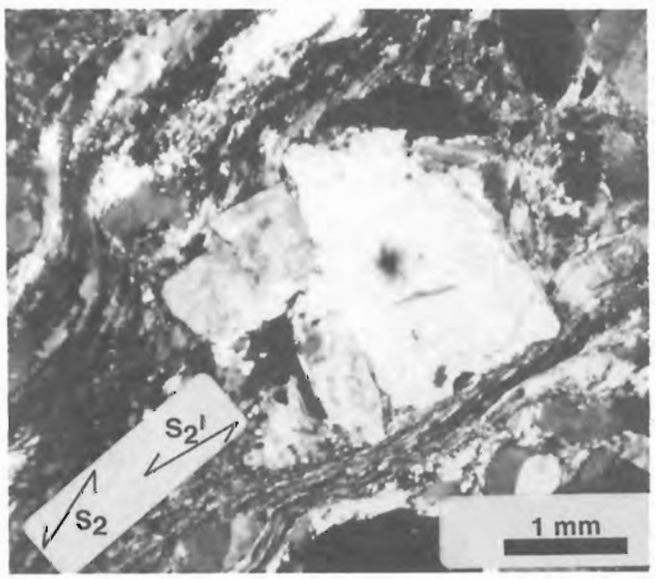


Figure 43.8. Mylonitic granite with well developed S-C fabric. Grain flattening foliation defined by ribbon quartz and fine grained mica (S_2) is dextrally deformed along discrete shear planes (S_2'). Horizontal section, oblique nicols.

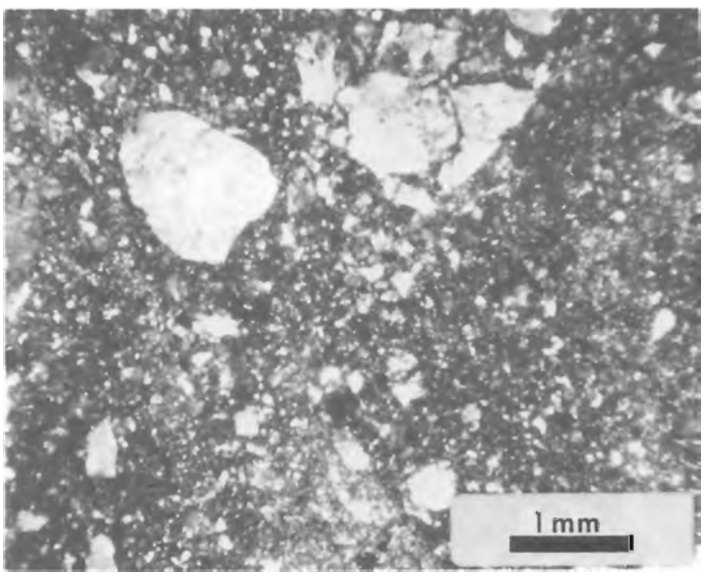


Figure 43.9. Cataclasite developed within the Guysborough County Fault from granite. Angular porphyroclasts are feldspar. Oblique nicols.

found in the Halifax Formation, pyrite and pyrrhotite are ubiquitous accessories in the graphitic schist.

The granitoid intrusions appear to be relatively barren. A high eU/eTh ratio for the pluton northwest of Tom Lake, determined by an airborne radiometric survey (Ford and Ballantyne, 1983), appears to be related to an unusually high muscovite content for unit 3a. Schiller (1963) used a berylometer to find a small amount of beryl in pegmatite 2 km west of Forest Hill. Geologists of Seabright Resources reported minor beryl and wolframite (?) in pegmatite float north of Forest Hill (K. Adams, personal communication, 1986).

A small amount of pyrite and chalcopyrite was found in laminated phyllite of unit 4 east of Ogden. Specular hematite occurs as rare veinlets crosscutting altered andesite in unit 5.

REFERENCES

Benson, D.G.
1974: Geology of the Antigonish Highlands, Nova Scotia; Geological Survey of Canada, Memoir 376, 92 p.

Faribault, E.R.
1893a: Guysborough Town sheet; Geological Survey of Canada, Sheet No. 25.
1893b: Country Harbour sheet; Geological Survey of Canada, Sheet No. 30.

Ford, K.L. and Ballantyne, S.B.
1983: Uranium and thorium distribution patterns and lithogeochemistry of Devonian granites in the Chedabucto Bay area, Nova Scotia; in Current Research, Part A, Geological Survey of Canada, Paper 83-1A, p. 109-119.

Harmeson, B.
1986: Integration of Landsat and aeromagnetic digital imagery: Meguma terrane, Guysborough County, Nova Scotia; unpublished diploma report, Nova Scotia College of Geographic Sciences, Lawrencetown, Nova Scotia, 93 p.

Haynes, S.J., Reilly, B.A. and Kiely, L.A.
1986: Structural setting of the Mile Lake gold prospect, Guysborough County, Nova Scotia; in Current Research, Part A, Geological Survey of Canada, Paper 86-1A, p. 141-150.

Hill, J.D.
1896a: Granitoid plutons in the Canso area, Nova Scotia; in Current Research, Part A, Geological Survey of Canada, Paper 86-1A, p. 185-192.
1986b: Geological map of Cape Canso, Nova Scotia; Geological Survey of Canada, Open File 1276.

Keppie, J.D.
1983: Geological history of the Isaacs Harbour area, parts of 11F/3 and 11F/4, Guysborough County, Nova Scotia; in Report of Activities, Nova Scotia Department of Mines and Energy, Report 83-1, p. 109-143.
1985: Geology and tectonics of Nova Scotia: in Appalachians Geotraverse (Canadian Mainland), Geological and Mineralogical Associations of Canada Annual Meeting, guidebook to excursion 1, p. 23-108.

McKenzie, C. and MacGillivary, J.
1974: Eastern Nova Scotia granites project: unpublished internal report, Dalhousie University, Halifax, Nova Scotia.

Schiller, E.A.
1961: Guysborough, Nova Scotia; Geological Survey of Canada, Map 27-1961.
1963: Mineralogy and geology of the Guysborough area, Nova Scotia, Canada; PhD thesis, University of Utah, 162 p.

Stevenson, I.M.
1964: Geology, Chedabucto Bay, Nova Scotia; Geological Survey of Canada, Map 1156A.

Buried placers in Chaudière River sediments indicated by ground magnetometer survey, Eastern Townships, Quebec[1]

Project 840057

Erik J. Schwarz and Norrie Wright
Lithosphere and Canadian Shield Division

Schwarz, E.J. and Wright, N., Buried placers in Chaudière River sediments indicated by ground magnetometer survey, Eastern Townships, Quebec; in Current Research, Part A, Geological Survey of Canada, Paper 87-1A, p. 423-428, 1987.

Abstract

Ground magnetic surveys using a 0.1 nT sensitivity proton precession magnetometer in both the total field and its vertical gradient mode were carried out on terraces along the Chaudière River at Vallée-Jonction and 30 km upstream, at Notre-Dame-des-Pins. Station interval was 1 m and line spacing 10 or 15 m. These spacings were selected on the basis of computer modelling of the magnetic effects of 10-m-wide, 0.5- to 1-m-thick, elongated plate-shaped enrichment of magnetite (0.5 to 1.0% by volume) at 10 m depth. The resulting total field and "gradient" (difference reading of two magnetometer sensors one vertical metre apart) show well defined variations with wavelengths from somewhat less than 10 to over 100 m along profile lines about 200 m long. Line to line correlations were made for both the total field and the gradient data, and contour maps were prepared. These maps reveal that the anomalies are elongated in the valley or river direction (northwest to north) indicating that the magnetic sources are situated within the river sediments. The northeast trend of the underlying bedrock is borne out by aeromagnetic maps (1:50 000), the higher frequency anomalies, such as those represented by the fine structure of the terrace ground profiles, not being present. Areas of prime interest in the exploration for placers containing heavy minerals can be selected from the contour maps.

Résumé

Des levés magnétiques terrestres ont été effectués dans des terrasses le long de la rivière Chaudière à Vallée Jonction et à 30 km en amont, à Notre-Dame des Pins. Un magnétomètre à précession nucléaire d'une sensiblité de 0,1 nT a été utilisé pour mesurer la valeur du champ total et du gradient vertical. Les stations étaient espacées de 1 m et les cheminements, de 10 ou 15 m. Cet intervalle a été choise en fonction de modèles établis par ordinateur de l'effet magnétique d'un zone riche en magnétite (de 0,5 à 1,0 % par volume) située à un profondeur de 10 m et ayant une largeur de 10 m, une épaisseur de 0,5 à 1 m et une forme plane allongée. La valeur du champ total et le gradient (différence entre les résultats affichés par deux capteurs de magnétomètre, espacés verticalement d'un mètre) font voir des variations bien définies, les longueurs d'onde allant de moins de 10 m à plus de 100 m le long de lignes ayant près de 200 m de longueur. La corrélation entre des valeurs du champ total et du gradient vertical a permis d'établir des cartes d'isogrammes. Ces cartes révèlent que les anomalies sont allongées parallèlement à la vallée ou à la rivière (nord-ouest à nord), ce qui indique que les sources magnétiques, se situent à l'intérieur des sédiments fluviatiles. Les cartes aéromagnétiques à l'échelle de 1/50 000 permettent de voir l'orientation nord-est du socle sous-jacent; les anomalies trouvées à plus haute fréquence, telles que celles qui sont représentées par la structure fine des profils terrestres de la terrasse, y sont absentes. Les cartes d'isogrammes peuvent être utilisées pour choisir des zones d'intérêt où l'on pourrant trouver des placers contenant des minéraux lourds.

[1]Contribution to Federal Asbestos Initiatives, Geoscience Research Program 1984-1987

INTRODUCTION

Placers are mineral deposits formed by mechanical action involving running water during the break-down of a rock by weathering. Concentrations of valuable minerals may thus occur as residues where minerals are left in situ or after transportation of mineral grains over some distance and subsequent sedimentation has taken place in favourable localities in a stream. As a result, an alluvial pile may contain a three-dimensional irregular distribution of mostly buried, lens-like placer deposits enriched in one or more valuable minerals. The problem is to find these placers from the surface using an inexpensive method rather than drilling without much guidance as to how to select the most promising areas of a river terrace.

The association of gold, uranium and other economic heavy minerals with magnetite (the so-called black sands) in many placer deposits was known to early prospectors. This association suggested the use of the magnetic exploration method. In a recent study, Adler and Adler (1985) show the correlation of positive magnetic total field anomalies with gold content in pay channels in the Keithley Creek and other areas in British Columbia and Alaska. However, a systematic study has not yet been carried out to distinguish magnetic sources within the alluvium and those in the underlying bedrock from the magnetic anomaly pattern observed at the surface. Without such a study the potential of the magnetic exploration method, using modern high sensitivity magnetometers in both the total field and vertical gradient modes in the detection of buried placers cannot be evaluated.

The Chaudière River sediments were selected for the present study. The Chaudière Valley and those of some tributaries were prolific placer gold producers nearly a century ago. The river system cuts a variety of rocks, sedimentary, plutonic, and volcanic, so that conditions such as average magnetite content probably are representative and the results are therefore expected to be of general interest. The Chaudière Valley placers have been described in detail by LaSalle (1980). The survey localities are shown on Figure 44.1. The thickness of the Quaternary alluvium is about 100 m but large variations are known to occur locally.

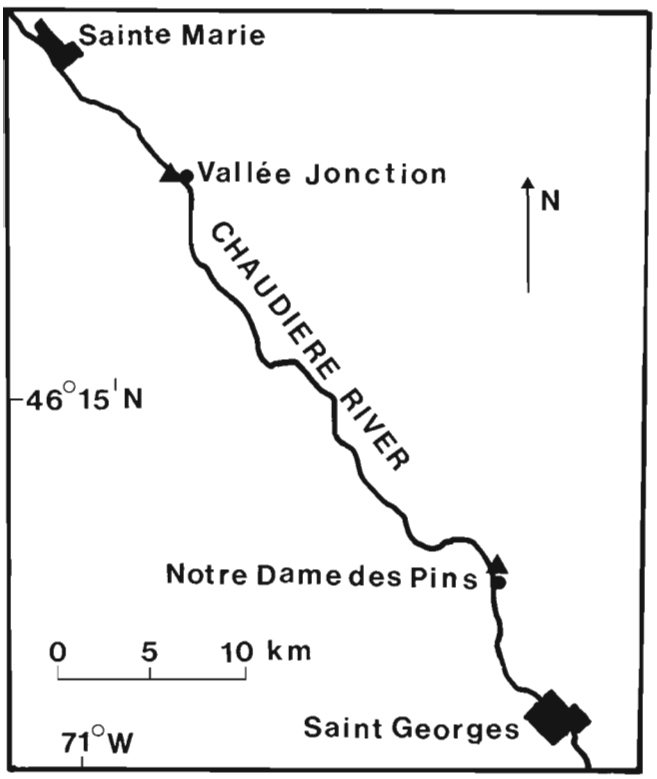


Figure 44.1. Location of survey sites (black triangles) along the Chaudière River, Eastern Townships, Quebec.

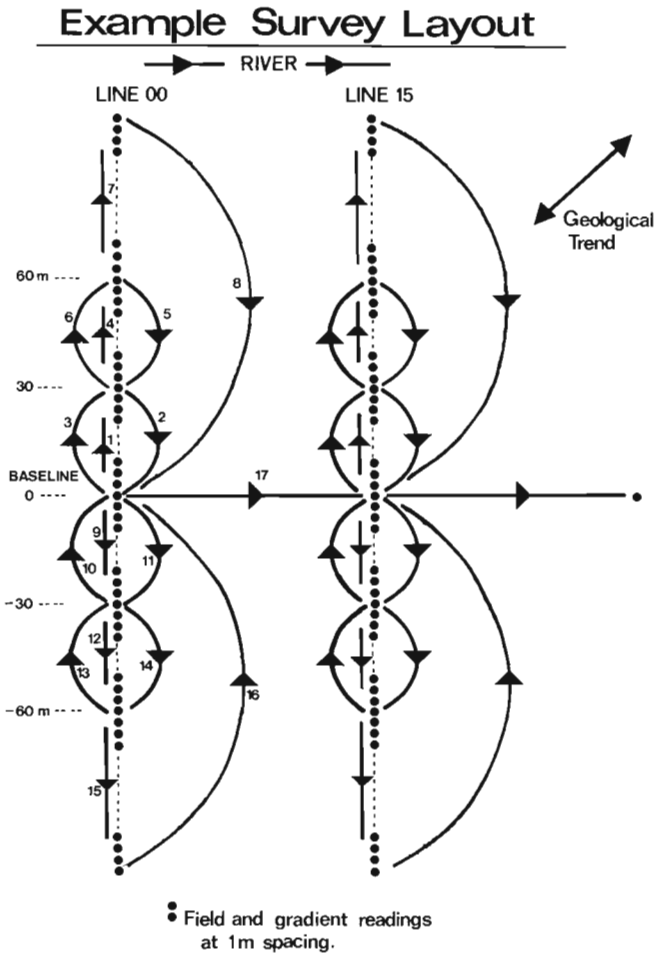


Figure 44.2. Example of design of a ground magnetometer survey schematically showing orientation of base line and profile lines in relation to river direction and predominant geological trend of underlying bedrock as borne out by both aeromagnetic and geological maps.

FIELD SURVEY

An EDA OMNI IV proton precession magnetometer with a sensitivity of 0.1 nT was selected for the survey. It was used in both the total field and vertical gradient modes. The vertical "gradient" reading was taken automatically by the instrument by computation of the difference in the total field readings of a sensor placed at 2 m above ground and another sensor 3 m above ground. Both sensors were attached to a vertical pole and energized at the same time so that any diurnal effect is strongly minimized. Two mutually perpendicular carpenter's levels (non-magnetic) were attached to the pole so that the sensor pole could, with negligible error, be held vertically during the reading. The instrument records total field and gradient readings, time of reading, and station locality as programmed prior to the survey. Diurnal corrections were calculated using software built into the instrument and the results were dumped onto soft discs using a microcomputer following the recipe provided by the manufacturer. A single operator can take well over a thousand readings per day on flat river terraces.

The survey layout was generally of the type shown on Figure 44.2. The base or control line was in the general valley or river direction. At distances between 10 and 15 m along the base line, lines were laid out for measurements at 1 m distance. This small station spacing was selected on the basis of computer model experiments on the magnetic response of 10 m wide elongated plates of thickness 0.5 to 1 m and effective susceptibility contrast of 1.10^{-3} to 5.10^{-4} cgs (multiply by 4π for SI units). Every 30th station was visited at least twice to allow correction for diurnal effects of each

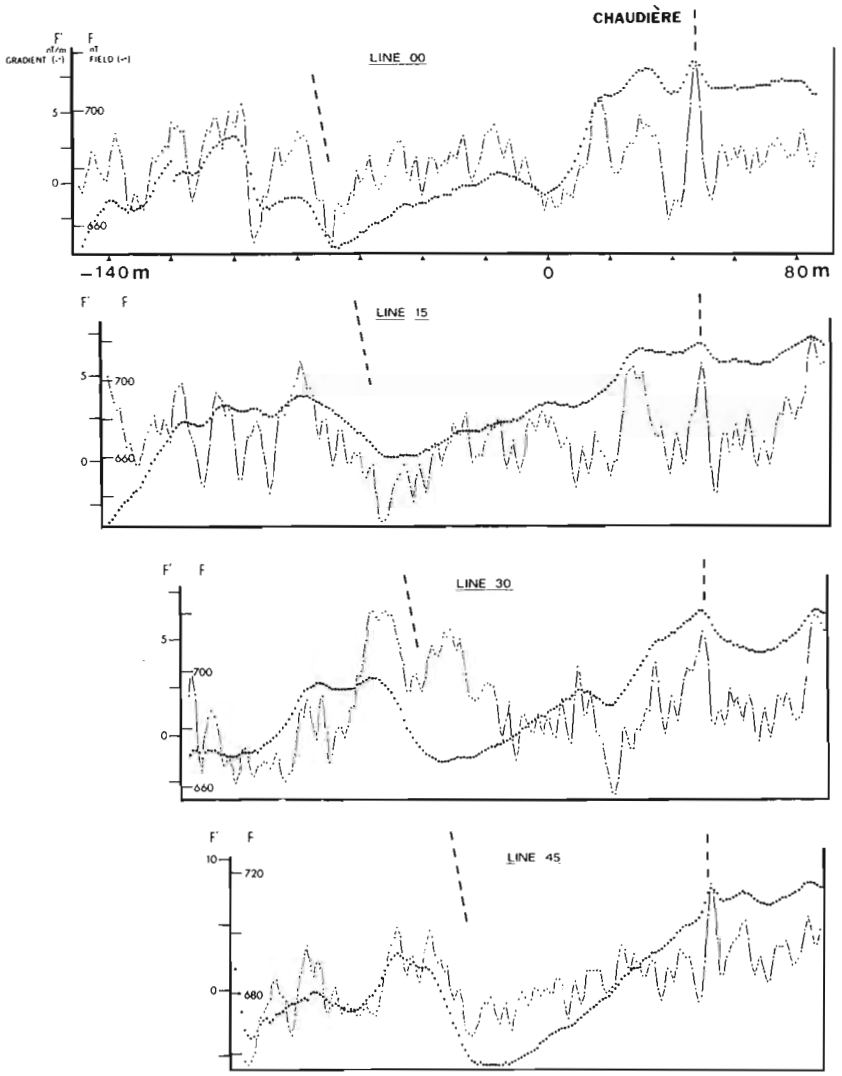


Figure 44.3. Unsmoothed total field (after diurnal correction) and vertical "gradient" data collected on a Chaudière River terrace just North of Jonction Vallée (west bank). Distance between lines is 15 m and station spacing is 1 m. Dashed lines indicate line to line correlations.

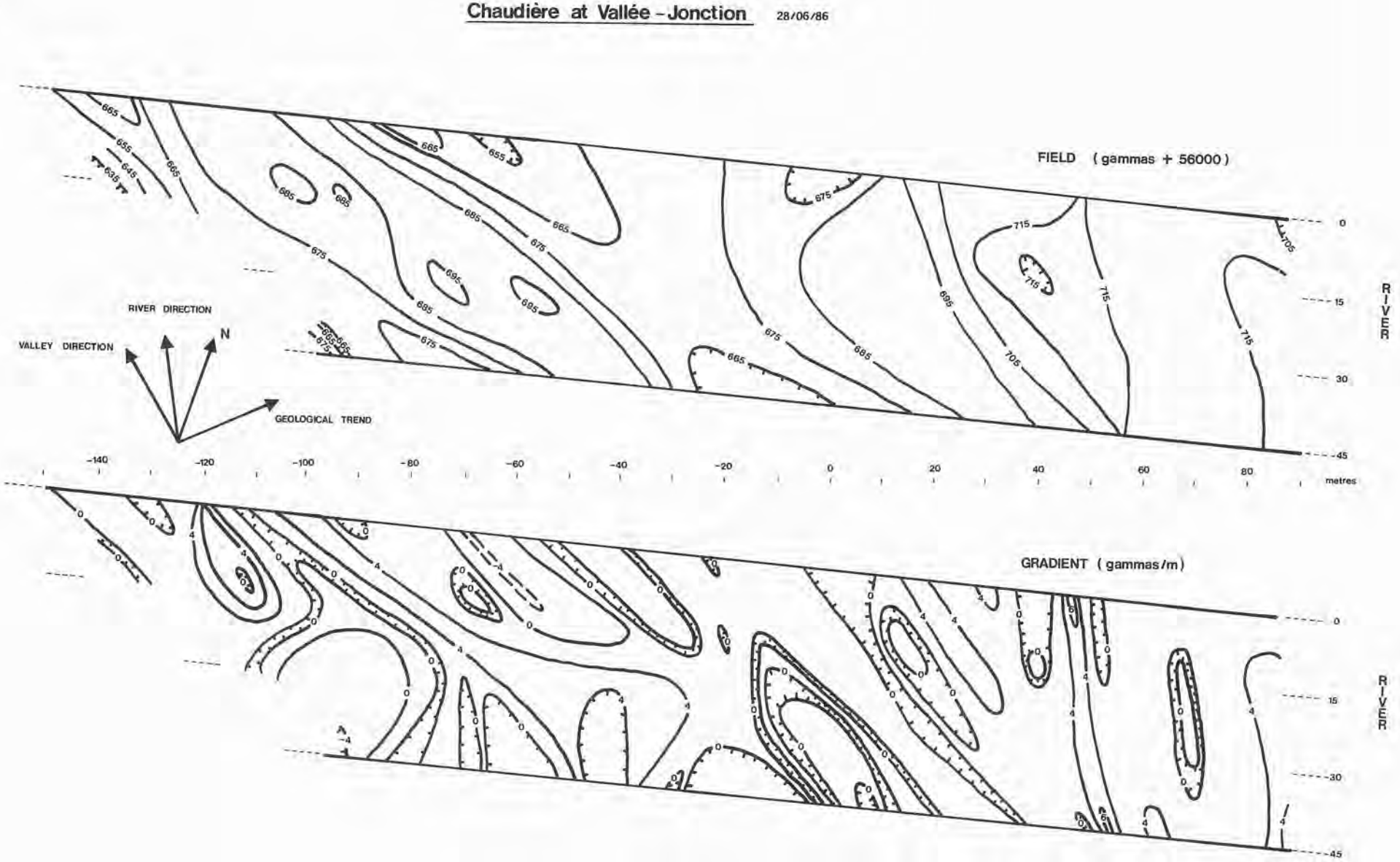


Figure 44.4. Hand drawn contour map obtained from the data shown on Figure 44.3. Contours are approximate but show that anomaly axes are aligned in the general valley and river direction but do not follow the bedrock trend. This means that the anomaly sources are elongated in the river direction and therefore are lens-like bodies parallel to the river within the river sediments.

group of 30 stations visited in the intervening time (about 20 minutes). The layout was such that the profiles were directed approximately perpendicular to the river and on the other hand made a large angle with the magnetic trend of the underlying bedrock as shown by aeromagnetic maps (e.g. Geological Survey of Canada, 1954). This magnetic trend conforms to the bedrock trend shown by geological maps (e.g. Harro, 1976).

EXPERIMENTAL RESULTS

Total field and vertical "gradient" data after diurnal corrections are shown on Figure 44.3 for the Valleé-Jonction site surveyed along the Chaudière River. As expected the total field curves are much smoother than the gradient curves. Shortest wavelengths in the total field data are somewhat less than 10 m and wavelengths over 100 m can also be observed. Correlation between lines at 15 m spacing on the basis of these long wavelength components is easy. Line to line correlations based on the gradient data are more difficult. Long wavelength variation in the gradient profile is expected to follow the total field most closely and therefore correlate in a similar way as these variations would tend to be due to deeper sources. This is indeed generally observed but a substantial deviation is shown along line 30. Individual high amplitude short wavelength variations correlate well in some cases (i.e. positive at about -50 m) but not at all in other cases. Both total field and gradient curves indicate correlations on both sides of the base line intersection (zero on horizontal distance axis).

The data presented in Figure 44.3 are contoured and therefore smoothed resulting in the total field and vertical "gradient" maps shown on Figure 44.4 for the same survey area. The anomaly axes are seen to rotate from northwest farthest away from the river to a more northerly direction near the river bank. This conforms to a rotation of the axes from the general valley direction to the present river direction going towards the river. Furthermore, there is no indication, not even in the total field map, of an appreciable contribution of bedrock sources in the spatial frequency range represented by these results. Such a contribution would be expected to trend northeast which is the general strike of the underlying steeply folded Hadrynian schists (Harron, 1976). Thus, the important conclusion is reached that the anomaly pattern of Figure 44.4 is produced by magnetic sources *within* the river sediments without noticeable bedrock interference.

Model studies show that a magnetite enriched plate within the alluvium will show up as a positive anomaly of the total field with a negative on the North side as well as a positive anomaly flanked by smaller negatives in the gradient data (Fig. 44.5). In practice, in particular the gradient will be much more complicated because of the enhanced response of even minor magnetite variations near each station. However, the contour maps indicate that the most promising areas for buried placer exploration are between 40 and 60 m east of the base line (distance 0) and also between about 40 and 110 m west of the base line.

Figure 44.6 shows the results of a survey along the Chaudière River at Notre-Dame-des-Pins about 30 km upstream

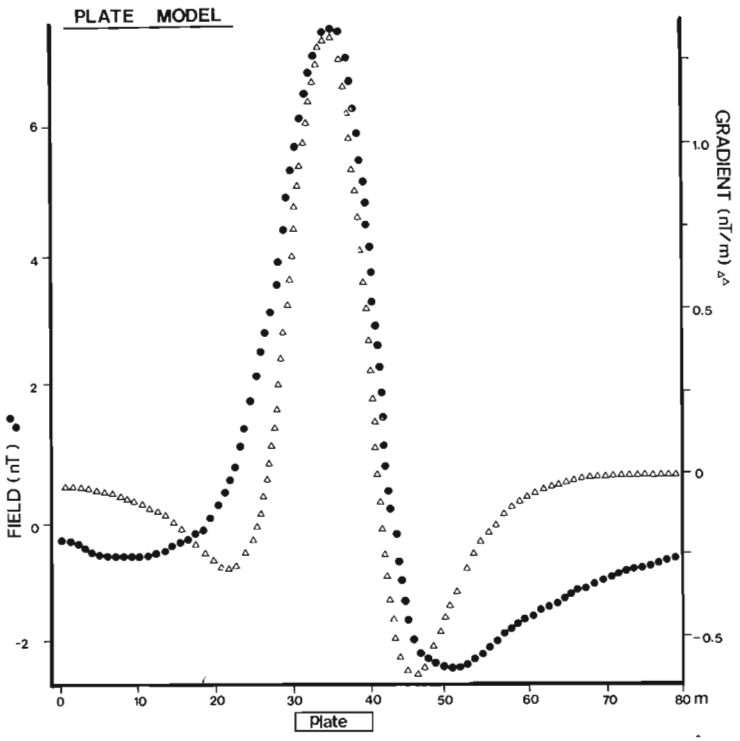


Figure 44.5. Total magnetic field and its vertical gradient over a 10 m wide, 1 m thick, 100 m long and 10 m deep plate. The susceptibility contrast is 1×10^{-3} cgs ($\times 4\pi$ SI), the field intensity is 56,000 nT and the field inclination is 65°. The plate is oriented 30° off magnetic North.

from Vallée-Jonction. Total field and gradient anomaly variation is much smaller at Notre-Dame-des-Pins. The gradient has been contoured at 1 nT/m and it appears likely that much of the minor variation is noise. However, again, the imporant observation can be made that the anomaly trend is related to the valley and river direction. As before near Vallée-Jonction, this indicates that the anomalies are due to magnetite enrichment in lenses elongated in the river and valley direction but not to magnetic sources in underlying bedrock. The combined total field and gradient data indicate that this surveyed area is of minor interest in buried placer exploration.

CONCLUSIONS

1. Model studies show that relatively narrow, thin and elongated buried volumes with slightly higher magnetite contents than the surrounding alluvium can be detected in a detailed ground magnetic survey using a sensitive magnetometer. In the few areas surveyed in this preliminary study, the total field appears to yield the most useful result the gradient showing much more variation probably due to the additive effect of small magnetic sources near the sensors. However, the use of both total field and its vertical "gradient" enhances the possibility of selecting areas within the area surveyed which are of prime interest in the search for buried placers.

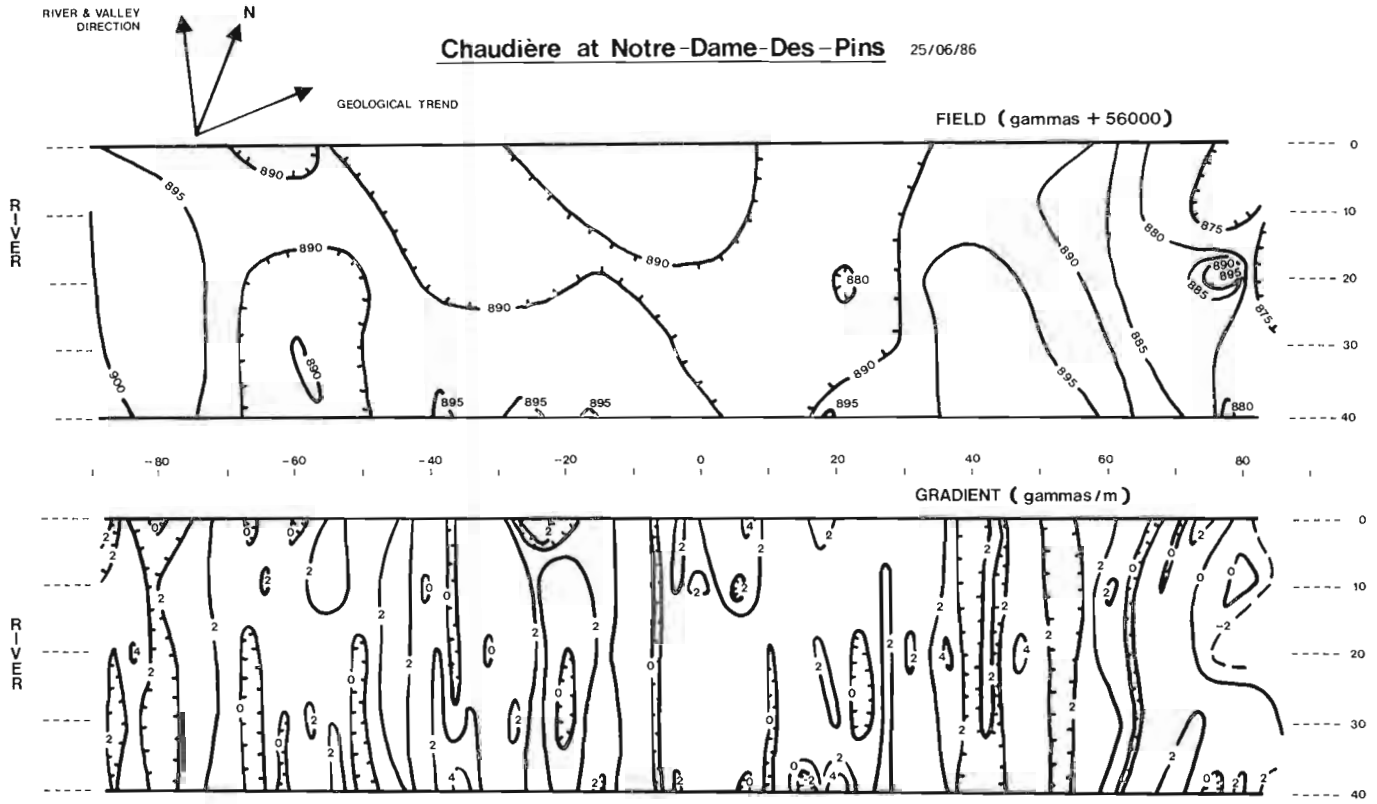


Figure 44.6. A similar map obtained by contouring data obtained on a Chaudière River terrace just north of Notre Dame des Pins, east bank. Note the small gradient contour interval of 1 nT/m.

2. Total field and also gradient profiles show well defined variations when the measurements are carried out every metre. Profile to profile correlations were easy for line spacings of 10 to 15 m. The number of measurements per day is in excess of 1000.

3. The line-to-line correlations reveal anomaly axes which are aligned in the local river and/or valley directions rather than in the structural trend of the underlying bedrock. This is strong evidence that the magnetic sources causing the observed anomalies are situated within the river sediments. The contour maps reveal areas of prime interest in the exploration for buried placers containing relatively high concentrations of magnetite and other heavy and economic minerals.

4. The method to detect buried placers proposed in this preliminary study relies heavily on identifying areas where the river and valley directions differ substantially in order to ensure that the measured anomalies are indeed due to magnetite concentrations within the alluvium. However, where this is not so or where deeper, within-bedrock sources are also of interest, an examination of different frequency components in the survey results may allow a separation of magnetic effects due to sources (1) within the Quaternary sediments, (2) represented by bedrock topography below the alluvium, and (3) within the bedrock. One specific application is detailed quantitative modelling of the magnetic sources within the river sediments where the stratigraphy is only locally known from a few percussion drill holes or dug pits as is the case in the Atlin area of British Columbia. Another application is detecting relatively magnetite- and gold-rich, locally derived, detritus filling bedrock depressions below a till blanket in the Hemlo area of Ontario.

ACKNOWLEDGMENTS

Peter McGrath's comments on the original manuscript improved the presentation of the results, and landowners in the Beauce area kindly allowed the surveys to be carried out on their fields. Dr. W. Shilts and his field crew in Saint Georges provided background geological information.

REFERENCES

Adler, Kevin P. and Adler, James E.
1985: Placer magnetics for the large and small operator; Proceedings of the Seventh Annual Conference on Alaskan Placer Mining, James A. Madonna, Editor, p. 17-22.

Geological Survey of Canada
1954: Aeromagnetic map 151 G, Beauceville, Quebec.

Harron, Gerald A.
1976: Metallogeny of sulphide deposits in the Eastern Townships; Ministère des Richesses Naturelles, Québec, 42 p.

Lasalle, P.
1980: L'or dans les sédiments meubles: Formation des placers, extraction et occurrences dans le sud-est du Québec; Ministère de l'Énergie et des Ressources, Québec, 26 p.

- 45 -

Precambrian Shield of the Boothia Uplift, southern Somerset Island and northern Boothia Peninsula, District of Franklin

Project 860001

Thomas Frisch, Mark R. Digel[1] and E. Joy Williams[2]
Lithosphere and Canadian Shield Division

Frisch, T., Digel, M.R., and Williams, E.J., Precambrian Shield of the Boothia Uplift, southern Somerset Island and northern Boothia Peninsula, District of Franklin; in Current Research, Part A, Geological Survey of Canada, Paper 87-1A, p. 429-434, 1987.

Abstract

The crystalline core of the Boothia Uplift between 71 and 73°N comprises a north-trending belt of orthopyroxene-bearing granitoid gneisses flanked by metasediments consisting chiefly of garnet-sillimanite(-cordierite-biotite) gneiss and garnet-biotite gneiss. Diopside-calcite marble and garnet-orthopyroxene gneiss occur among both the metasediments and the granitoid gneisses, suggesting that the latter are in part of supracrustal origin. Pre- or syntectonic intrusive rocks include two-pyroxene amphibolite, ultramafite and syenite.

Three phases of folding were recognized. Evidence for the first is confined to relict isoclines preserved in hinge zones of later folds. Second phase folds (F_2) show up mainly in domes and basins generated by interference between east-west, open F_2 folding and north-south folding of the third and dominant phase (F_3). F_3 folds range from open and concentric to tight and similar, are largely upright and generally plunge north.

The crystalline terrane is cut by five major ENE-trending faults, each showing right-lateral displacement of about 2 km.

Résumé

Le noyau cristallin du soulèvement de boothia que se situe entre 71° et 73° de latitude nord se compose d'une zone à orientation nord de gneiss granitoïdes à orthopyroxène flanquée par des métasédiments composés surtout de gneiss à grenat et à sillimanite (et peut-être à cordiérite et à biotite) et de gneiss à grenat et à biotite. On trouve du marbre à diopside-calcite et du gneiss à grenat-orthopyroxène parmis les métasédiments et les gneiss granitoïdes, ce qui porte à croire que ces derniers ont une origine au moins en partie supracrustale. Les roches intrusives prétectoniques ou syntectoniques comprennent une amphibolite à deux pyroxènes, une ultramafite et une syénite.

Trois phases de plissement sont reconnues. Le première phase est représentée uniquement par des plis isoclinaux résiduels trouvés dans les charnières des plis plus récents. Les plis de la deuxième phase (F_2) se trouvent surtout dans les dômes et les bassins produits par l'interférence des plis ouverts F_2, à orientation est-ouest, et des plis orientés nord-sud de la troisième phase (F_3), soit la phase dominante. Les plis F_3 varient des plis ouverts et concentriques aux plis fermés et semblables; ces plis sont en grande partie à plongement vers le nord.

Le terrane cristallin est recoupé par cinq grandes failles à orientation est-nord-est, qui ont un rejet latéral droit d'environ 2 km.

[1]Department of Geology, University of Ottawa, Ottawa, Ont. K1N 6N5
[2]c/o F.E. Myshrall, R.R. 4, Fredericton, N.B. E3B 4X5

INTRODUCTION

The Boothia Uplift extends 800 km north from southern Boothia Peninsula to northwesternmost Devon Island. It is cored by high grade metamorphic and igneous rocks of the Churchill Structural Province of the Canadian Shield and flanked by Helikian to Devonian sediments more than 4000 m thick. The major tectonism that produced the uplift occurred in Silurian-Devonian time. Accounts of the Boothia Uplift have been given by, among others, Kerr (1977) and Okulitch et al. (1986). Geological maps (scale 1:250 000) of Somerset Island and Boothia Peninsula north of 70° 25′ N, showing the sedimentary cover rocks subdivided but the basement as a single unit, have been compiled by Stewart and Kerr (1984).

The present study is concerned with the basement rocks between latitudes 71 and 73° N, a belt that includes the best exposures of the Precambrian Shield in the Boothia Uplift. Field work in 1986 – the first year of the project – was confined to the Shield terranes between 73° N and Amituryouak Lake and west of Wrottesley River (Fig. 45.1).

Work on the basement rocks prior to 1986 includes: reconnaissance mapping on Somerset Island and Boothia Peninsula by the Geological Survey of Canada in 1962 (Blackadar, 1967); relatively detailed work in selected localities on Somerset Island by Brown et al. (1969) and Giguère (1968); and comprehensive, but largely unpublished, mapping on Somerset Island by C.D.S. de Vries (Kerr and de Vries, 1976, 1977). These investigations showed that the basement consists mainly of north-trending ortho- and paragneisses, was metamorphosed in the granulite-upper amphibolite facies and underwent three phases of folding. The only radiometric data available from the basement of the Boothia Uplift are three K-Ar ages falling between 1600 and 1700 Ma, determined on biotite from gneisses and granite (Blackadar, 1967).

LITHOLOGY

The bulk of the crystalline terrane can be subdivided into three map units: granitoid gneiss, metasedimentary gneiss rich in garnet, and marble/calc-silicate. These rocks were intruded by syenitic and mafic bodies prior to penetrative deformation and by diabase dykes following metamorphism.

Granitoid gneiss

Gneisses of granitoid composition, commonly with pyroxene or pseudomorphs thereof, are the most common rock type in the map area and dominate the lithology of the central region (Fig. 45.1). Seen from a distance, they present a somewhat nondescript homogeneous appearance. Weathering colour is dark and generally brown, less commonly grey. Up close, the gneisses are seen to be medium grained, strongly gneissic, and greenish on fresh surfaces. Orthopyroxene and biotite are the chief mafic minerals and are locally accompanied by hornblende and clinopyroxene; garnet is uncommon. Gneissic texture is commonly defined by the parallel arrangement of platy quartz, as well as mafic minerals, which can be seen in favourable exposures to cut across compositional layering and early minor folds (Brown et al., 1969).

K-feldspar augen gneiss locally forms extensive layers in more equigranular gneiss. Severe deformation causing flattening, however, commonly obscures the augen texture.

Hornblende-rich mafic schieren, lenses and layers, typically garnet free and isoclinally folded, are characteristic of many of the granitoid gneisses. Also common, particularly in retrograde gneiss, are broadly concordant granitic and pegmatitic sheets and veins but migmatitic structure is not as well developed as in the metasedimentary gneisses. Rocks south of Amituryouak Lake tend to be more retrograded than their equivalents farther north but their granulite facies heritage is invariably recognizable.

Although many of the granitoid gneisses are of metaigneous aspect, they can by no means be considered as entirely of intrusive origin. Intimate association with metasediments – expressed by features such as the interlayering of granitoid and aluminous gneisses, the occurrence of kilometre-long marble layers in homogeneous granitoid gneiss, and the presence of graphite – suggest a supracrustal origin for a significant proportion of the granitoid gneisses (see also Blackadar, 1967).

Garnetiferous metasedimentary gneiss

This map unit can generally be easily distinguished from the granitoid gneisses by its variegated appearance and an abundance of recessively weathered, rusty rock. Rocks of the unit occur throughout the crystalline terrane but are especially abundant in tracts on either side of the central granitoid gneiss belt in northern Boothia Peninsula and southern Somerset Island.

The major rock types are graphitic garnet-sillimanite (-cordierite-biotite) gneiss and garnet-biotite gneiss, very well layered and migmatitic. Rusty layers and schistose rocks abound. Also common in the metasediments are ultramafic and mafic pods and calc-silicate layers. Subordinate members of the metasedimentary sequences include felsic garnet-orthopyroxene gneiss, granitoid gneiss (described above), quartzite and, at one locality, garnet-magnetite iron-formation. The major occurrences of marble are associated with the garnetiferous gneisses.

Sillimanite is the only aluminosilicate mineral so far recognized and occurs in well crystallized prisms up to 2 mm thick. Cordierite is considerably more common than the results of Blackadar's (1967) and Brown et al.'s (1969) work imply and, along with the regionally developed orthopyroxene, characterizes the Boothia-Somerset basement as a transitional granulite terrane.

Marble and calc-silicate rock

Although easily eroded, marble outcrops remarkably persistently, if discontinuously, over distances of many tens of kilometres in several parts of the crystalline terrane. The marble typically is white, medium grained, calcitic and rich

in diopside. Wollastonite has been identified in the field at several localities. Marble beds commonly are no more than a few tens of metres thick but flowage into axial zones of folds has produced major bodies several hundreds of metres thick in the area between Macgregor Laird Lake and Fitz Roy Inlet.

Calc-silicate rock is represented by calcareous diopside- and hornblende-rich gneiss, generally, but not exclusively, associated with marble.

Metamorphosed mafic and ultramafic rocks

Metamafite bodies occur throughout the area and range from thin lenses and layers to sheets more than 100 m thick. They generally are rich in hornblende and some of the larger bodies consist of coarse, plagioclase-poor amphibolite bordered by finer grained pyroxene (clino ± orthopyroxene)-plagioclase rock. Garnet is rarely present. An intrusive origin is indicated by locally preserved apophyses into, and discordant contacts with, surrounding gneiss.

Ultramafic rocks form yellowish green or brown weathering bodies 20-50 m across and 50 to 200 m long, typically associated with metasedimentary gneiss. The bodies consist primarily of heavily serpentinized metaperidotite and subordinate coarse grained orthopyroxenite; metagabbro occurs in some of the larger bodies.

In what may be a unique occurrence in the area – on the east slope of Mount Walker on Somerset Island at the eastern end of Bellot Strait – an ultramafic mass has recrystallized to an orthoamphibole rock and a reaction zone, rich in sapphirine, phlogopite and garnet, has developed against the bordering aluminous gneiss.

Another ultramafic body of unusual interest underlies the western part of Arcedeckne Island, a small (1 km^2) island off the west coast of Boothia Peninsula (Fig. 45.1). It consists of a gently dipping sheet, in concordant contact with garnet-sillimanite gneiss, made up essentially of layers of garnetite and garnet-peridotite (field identification, to be confirmed in the laboratory). The garnet is commonly intergrown with, or rimmed by, dark green hornblende.

Intrusive syenitic rocks

Syenitic rock of two varieties and probably two ages of intrusion have been found.

One type forms a crudely gneissic body, 3 km × 2 km, at Cape Bird, west of Macgregor Laird Lake. It weathers brownish, carries orthopyroxene and perthite as the chief feldspar, and, despite a variable, if low, quartz content, is a broadly homogeneous rock. Overall mineralogical monotony and the occurrence of what appears to be a screen of supracrustal gneiss at its northern end suggest that the body is an intrusion, which was subsequently metamorphosed. According to Kerr and de Vries (1977), the same rock type is concordantly infolded in gneisses to the east.

The other variety of syenite is a dull red, very felsic rock with a weakly gneissic texture expressed by roughly aligned hornblende crystals or clots. The syenite forms two bodies, 3-4 km long and up to 2 km wide, on Boothia Peninsula. One body, which occupies the core of an antiformal dome, has preserved evidence of its intrusive origin in the form of sheet-like inclusions of country rock concordant with the contact. Insofar as the red syenite appears to be less deformed, it may be younger than the orthopyroxene syenite but was nevertheless involved in the last major folding event.

Diabase dykes

Unmetamorphosed diabase dykes traverse the crystalline rocks in several directions but do not cut Paleozoic strata. A few dykes outcrop essentially continuously for distances up to 15 km but most dykes are only intermittently exposed.

Three main dyke trends are northwest, north-northwest and west-northwest. These trends follow lineaments that probably represent late fractures of the crystalline terrane. However, no dyke swarms parallel any of the east-northeast trending fault valleys of Somerset Island and Boothia Peninsula.

Age relations of the dykes in the map area are not known but both Mackenzie (Neohelikian) and Franklin (Hadrynian) diabase dykes are present in northern Somerset Island (Okulitch et al., 1986).

STRUCTURAL GEOLOGY

The crystalline terrane is characterized by strong northerly structural trends and steeply dipping foliations. This "grain" is largely due to pervasive, north-south, mainly upright folding, which followed two earlier folding events.

The earliest folds recognizable (F_1) are very tight to isoclinal structures outlined most commonly by mafic layers preserved in quartzofeldspathic gneiss in hinge zones of the major north-south folds (F_3). The original orientation of F_1 folds is unknown but, because of the evidence for them throughout the Boothia-Somerset area (Kerr and de Vries, 1977), F_1 structures probably once predominated in the map area.

Second period folds (F_2) are generally apparent from north-south trending dome and basin interference structures, which are found in southern Somerset Island (Kerr and de Vries, 1977) and in northern Boothia Peninsula. F_2 folds are east-west trending and open and have steep axial planes. One example that is not part of an interference structure occurs southwest of Stanwell-Fletcher Lake. Beautifully exposed domes and basins, resulting from interference of F_2 and F_3 folds, occur in western Somerset Island (Kerr and de Vries, 1977) and in northern Boothia Peninsula. The shape of these structures is determined by the tightness of the F_3 folds (Kerr and de Vries, 1977). A roughly circular dome, outlined by marble and 4 km across, is exposed southwest of Stanwell-Fletcher Lake; an elongate basin, 13 km long and 3 wide, lies west of Nudlukta Lake (Fig. 45.1). Most of the interference structures are oval and no more than a few kilometres long, e.g. the basins between False Strait and Fitz Roy Inlet.

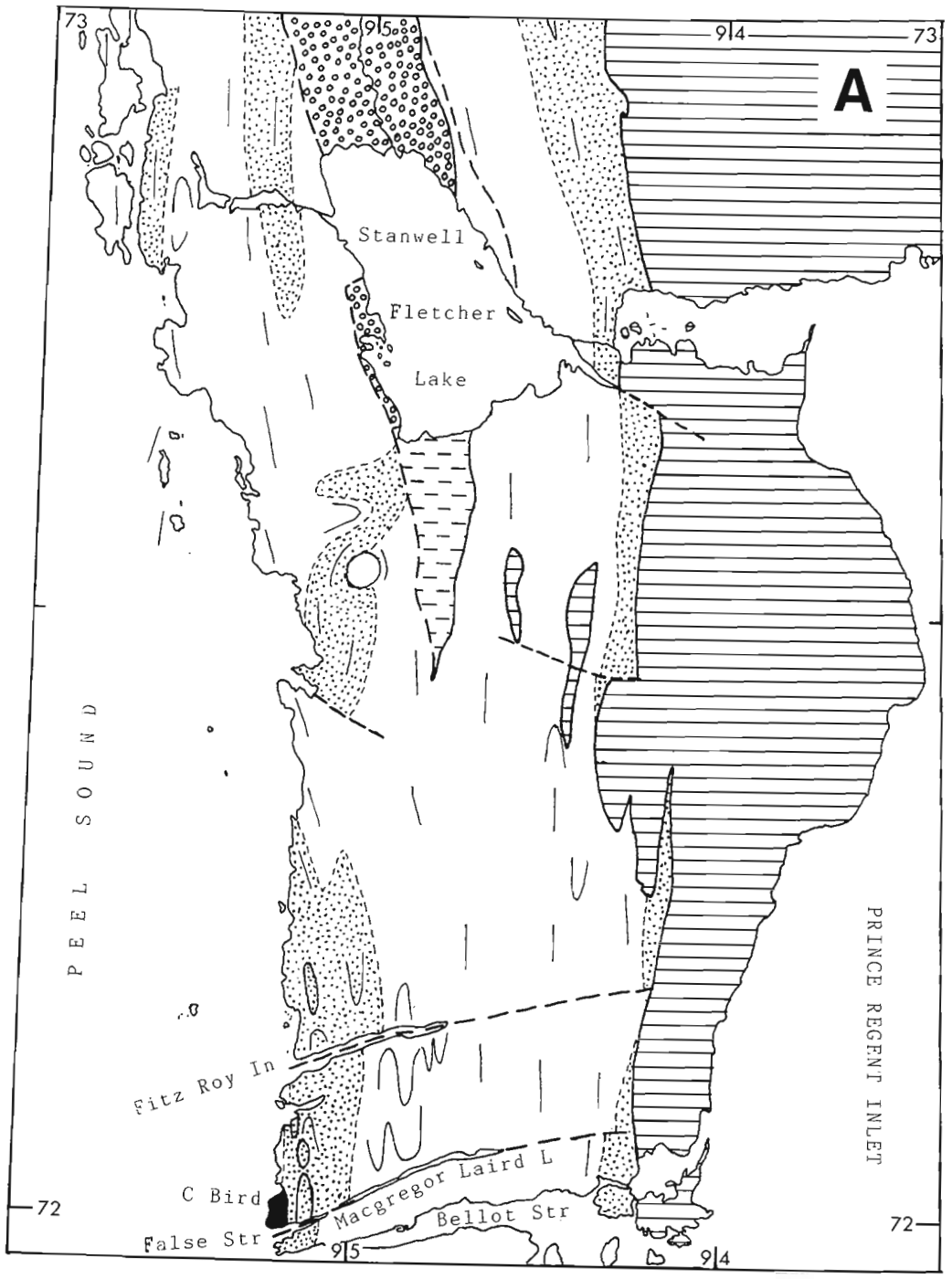
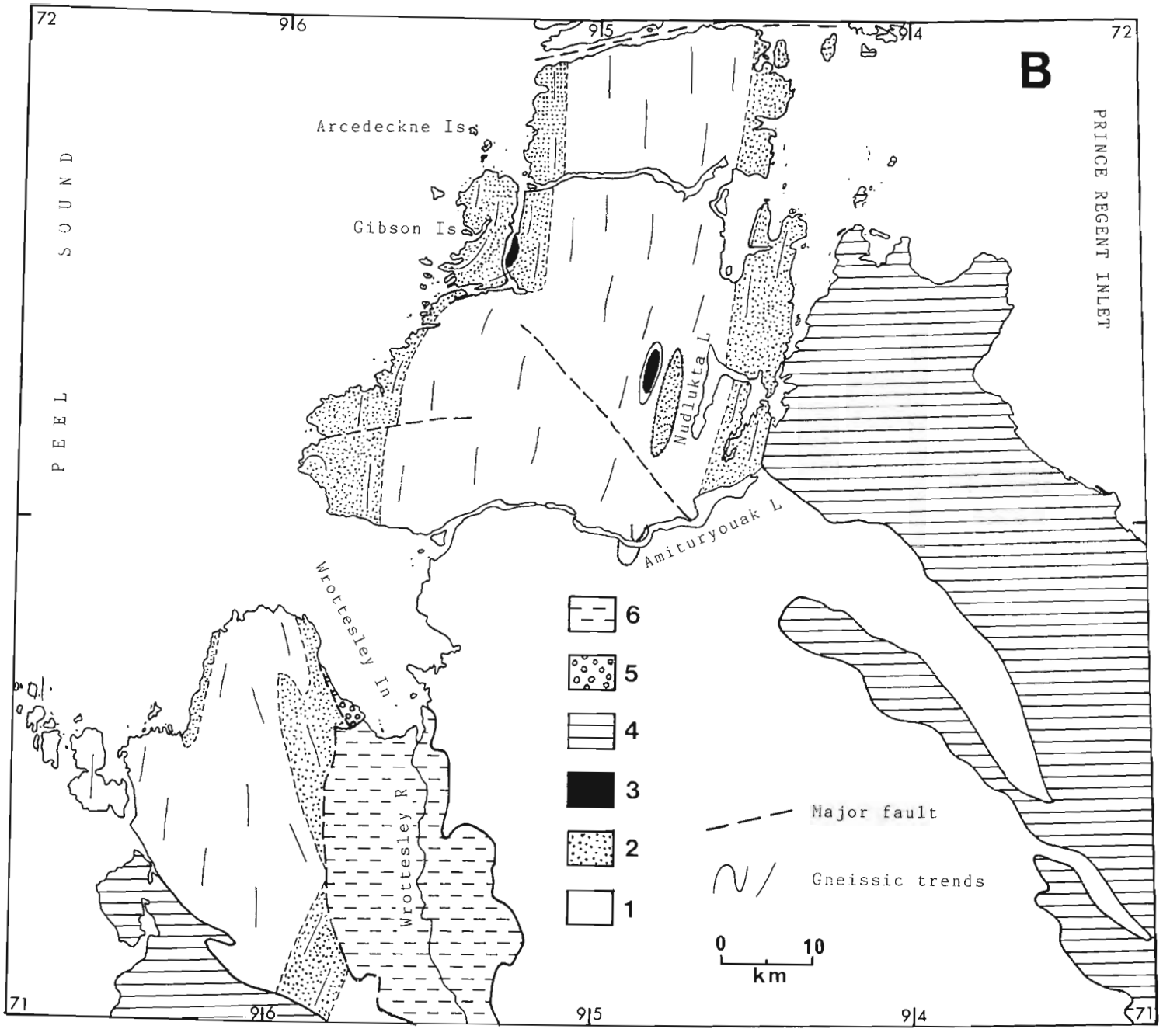


Figure 45.1. Sketch map of the geology, greatly simplified, of southern Somerset Island (A) and northern Boothia Peninsula (B). Key to units: 1 – Orthopyroxene-bearing granitoid gneiss; subordinate garnetiferous metasediment. 2 – Garnetiferous metasediment and marble; subordinate granitoid gneiss. 3 – Metamorphosed intrusive syenitic rock. 4 – Paleozoic. 5 – Tertiary. 6 – Quaternary (underlain chiefly by Precambrian crystalline rocks).


72
916
915
914
72
B
Arcedeckne Is
Gibson Is
PEEL SOUND
PRINCE REGENT INLET
Nudlukta L
Amituryouak L
Wrottesley In
Wrottesley R
6
5
4
3
2
1
Major fault
Gneissic trends
0
10
km
71
916
915
914
71

As recognized by earlier workers (Brown et al., 1969; Kerr and de Vries, 1976, 1977), the dominant fold structures are the north-south trending folds (F_3), readily apparent from the air – particularly north and south of Bellot Strait – and in aerial photographs. They range from open and concentric to tight and similar and, while axial planes are generally steeply dipping or vertical, moderately overturned F_3 folds occur in northernmost Boothia Peninsula. F_3 folds in the northern part of the map area are, on average, tighter than those farther south. Fold axes plunge 10° to 30° north, except in the doubly-plunging dome and basin structures.

It is the F_3 folding that is responsible for the platy quartz foliation so prevalent in the quartzofeldspathic gneiss. In the vast majority of mesoscopic folds, the quartz plates parallel the F_3 axial surfaces. Kerr and de Vries (1977) did, however, find an F_1 quartz foliation preserved alongside an F_3 quartz foliation in the hinges of some F_3 folds.

The crystalline terrane is cut by major east-northeast trending faults, marked by the topographic depressions of Fitz Roy Inlet, Macgregor Laird Lake, Bellot Strait, the unnamed inlet east of northern Gibson Island, and Amituryouak Lake. Correlation of lithologic markers and axial traces of folds across these structures indicates right-lateral displacement, generally in the order of 2 km (see also Kerr and de Vries, 1977). Significant movement on these faults appears to have been confined to Precambrian time as Paleozoic strata lying on the fault traces are essentially undisturbed.

Northwesterly trending faults are basically normal faults with some left-lateral movement. These faults displace Paleozoic, as well as Precambrian, rocks.

As discussed in more detail by Kerr and de Vries (1977), the north-northwesterly trending normal faults bounding the grabens filled by Tertiary clastics at Stanwell-Fletcher Lake and south of Wrottesley Inlet are probably rejuvenated older structures. The western sides of the grabens are marked by prominent scarps, which appear to truncate metasedimentary belts in the gneisses.

ECONOMIC GEOLOGY

Although rusty layers and zones are abundant and prominent in metasedimentary and, to a lesser extent, in quartzofeldspathic gneisses, no metallic mineral showings of significant economic interest were found. The rusty zones result from the weathering of pyritiferous rock.

Pyrrhotite was found in metamorphosed ultramafic rock at two localities, invariably in disseminated form.

Accessory graphite is a characteristic constituent of garnet-sillimanite gneiss but is also present locally in orthopyroxene-bearing granitoid gneiss. Locally in garnet-sillimanite gneiss, graphite is concentrated in centimetre-thick layers several tens of metres long.

ACKNOWLEDGMENTS

Grateful thanks for assistance and support go to: L.H. Adamitz and A.M. Sasso (field assistants), S. Arlidge (cook) G.S. Suthern (helicopter pilot) and R. Benson and R.W. Bell (helicopter engineers). We are also indebted to R.K. Herd for assistance and petrological expertise during a brief visit.

Twin Otter flying time, accommodation at Resolute Bay and assistance in numerous other ways were generously provided by the Polar Continental Shelf Project. The helicopter used was under charter to PCSP.

REFERENCES

Blackadar, R.G.
1967: Precambrian geology of Boothia Peninsula, Somerset Island, and Prince of Wales Island, District of Franklin; Geological Survey of Canada, Bulletin 151, 62 p.

Brown, R.L., Dalziel, I.W.D. and Rust, B.R.
1969: The structure, metamorphism, and development of the Boothia Arch, Arctic Canada; Canadian Journal of Earth Sciences, v. 6, p. 525-543.

Giguère, J.F.
1968: Element distribution in coexisting pyroxenes from granulite rocks of southeast Stanwell-Fletcher Lake area, Somerset Island, District of Franklin, N.W.T.; M.Sc. thesis, University of Ottawa, 126 p.

Kerr, J.Wm
1977: Cornwallis Fold Belt and the mechanism of basement uplift; Canadian Journal of Earth Sciences, v. 14, p. 1374-1401.

Kerr, J.Wm. and de Vries, C.D.S.
1976: Structural geology of Somerset Island, District of Franklin; in Report of Activities, Part A, Geological Survey of Canada, Paper 76-1A, p. 493-495.
1977: Structural geology of Somerset Island and Boothia Peninsula, District of Franklin; in Report of Activities, Part A, Geological Survey of Canada, Paper 77-1A, p. 107-111.

Okulitch, A.V., Packard, J.J. and Zolnai, A.I.
1986: Evolution of the Boothia Uplift, arctic Canada; Canadian Journal of Earth Sciences, v. 23, p. 350-358.

Stewart, W.D. and Kerr, J.Wm.
1984: Geology of Somerset Island North, Somerset Island South, Boothia Peninsula North, and Central Boothia Peninsula, District of Franklin; Geological Survey of Canada, Maps 1595A, 1596A, 1597A, 1598A, scale 1:250 000.

Preliminary report on the Grenville Front Tectonic Zone, Bruce Lake area, western Labrador[1]

Project 840059
DSS Contract 23233-6-0580/01-ST

J. van Gool[2], T. Calon[2], and T. Rivers[2]

van Gool, J., Calon, T., and Rivers, T., Preliminary report on the Grenville Front Tectonic Zone, Bruce Lake area, western Labrador; in Current Research, Part A, Geological Survey of Canada, Paper 87-1A, p. 435-442, 1987.

Abstract

During the Grenvillian Orogeny the gneissic and migmatitic basement rocks of the Superior Province and the Aphebian supracrustal rocks of the Knob Lake Group were metamorphosed and deformed in a fold and thrust belt.

An oldest Grenvillian deformation phase (D_1), mainly thrusting, was followed by two events, mainly folding. During D_1, NW directed thrusting on shallow, SE dipping shear zones caused development of thin-skinned thrust slices. Both basement and supracrustal rocks were involved in the thrusting. In large parts of the area the rocks contain a pervasive L-S fabric. Large scale NW-verging folds developed during the second deformation phase. These highly noncylindrical structures originated in several folding generations, since F_2 structures overprint each other. A third deformation phase caused open folding on a large scale. Interference of F_2 and F_3 structures resulted in an irregular dome and basin map pattern.

The Grenvillian metamorphism was of greenschist facies. The peak of the metamorphism is syn-kinematic with respect to D_1 and the temperature seems to have been still high during D_2.

Extensive beds of iron-formation might have economic significance as possible future iron resources.

Résumé

La région de Bruce Lake se situe dans la zone tectonique du front de Grenville, dans l'ouest du Labrador. Au cours de l'orogénèse grenvillien, le socle migmatitique et gneissique de la province du lac-Supérieur et les roches supracrustales aphébiennes du groupe de Knob Lake ont été métamorphisés et déformés dans une zone orogénique.

La phase de déformation grenvillienne la plus ancienne (D_1), qui comportait surtout du charriage, a été suivi par deux phases surtout de plissement. Au cours de la phase D_1, le charriage vers le nord-ouest dans des zones cisaillées peu profondes, à pendage sud-est, a produit des lambeaux de poussée peu épais. Le charriage a touché les roches du socle et les roches supracrustales. Dans une bonne partie de la région, les roches présentent une texture L-S envahissante. Il y a eu formation de grands plis à vergence nord-ouest au cours de la deuxième phase de déformation. Ces structures non cylindriques se sont formées au cours de plusieurs générations de plissement, puisque les structures F_2 sont superposées les unes sur les autres. Une troisième phase de déformation a produit de grands plis ouverts. L'interférence des structures F_2 et F_3 a produit un modelé irrégulier en dômes et en bassins.

Le métamorphisme grenvillien a atteint le faciès des schistes verts. Le métamorphisme le plus avancé était syntectonique par rapport à D_1 et la température aurait encore été élevée au cours de D_2.

Des couches de formation ferrifère de grande étendue pourraient constituer une source rentable de fer.

[1]Contribution to the Canada-Newfoundland Mineral Development Agreement 1984-1989. Project carried by Geological Survey of Canada, Mineral Resources Division

[2]Centre for Earth Resources Research, Department of Earth Sciences, Memorial University of Newfoundland, St. John's, Newfoundland A1B 3X5

INTRODUCTION

The western boundary of the Grenville Province against the Superior Province is the Grenville Front Tectonic Zone, a fold and thrust belt 10 to 50 km wide. This NE-trending structure, delineates the western margin of Grenvillian deformation and metamorphism. The Grenville Front Tectonic Zone (CFTZ) is characterized by intensive thrusting and an increase of the thickness of the crust by 5 to 8 km. L-S tectonites dominate the zone.

The Bruce Lake area is in the CFTZ, about 25 to 40 km north of Labrador City, Western Labrador (Fig. 46.1, 46.2) and is part of the parautochthon zone as defined by Rivers and Nunn (1985). The area contains Aphebian supracrustal rocks of the Grenville Province, which are in thrust contact with the gneisses of the Superior Province foreland, known as the Ashuanipi Metamorphic Complex (AMC). Both basement and previously undeformed supracrustal rocks possess a strong Grenvillian L-S fabric in the vicinity of the thrust faults. The AMC rocks exhibit mylonitic and protomylonitic microstructures. The whole sequence is folded into a dome and basin interference pattern, similar to that of the Wabush/ Labrador City area (Rivers, 1983a). Figures 46.2 and 46.3 are form surface maps of the area that highlight the structural style. At least some of the structures are related to the northwestward thrust movement of Grenville Province rocks.

Metamorphism in the GFTZ is generally of high grade, with kyanite reported in several places (Wynne Edwards, 1972). The study area, however, is situated mainly in the muscovite-chlorite-biotite zone defined by Rivers (1983b), where progressive metamorphism to greenschist facies affected the supracrustal rocks. In zones of intense Grenvillian deformation, the Archean gneisses of the Superior basement show intense retrogression from the granulity(?) facies. The low grade of metamorphism indicates that the area represents a high level in the GFTZ.

Regional mapping in the area was done by Fahrig (1967) and Rivers (1980 a,b) and Rivers (1983 a,b) constructed by a regional tectonic and metamorphic framework which is well applicable to the Bruce Lake area.

The present study was initiated because a thorough knowledge of the structural geometry of this area may be of long-term economic benefit, as both iron formation, which is successfully exploited in the mining area to the south, as well as minor base metal showings, related to thrust faults, are present in the area. A study of the GFTZ in the Bruce Lake area may also enable construction of a kinematic model for the Grenville Province in Western Labrador and Eastern Quebec.

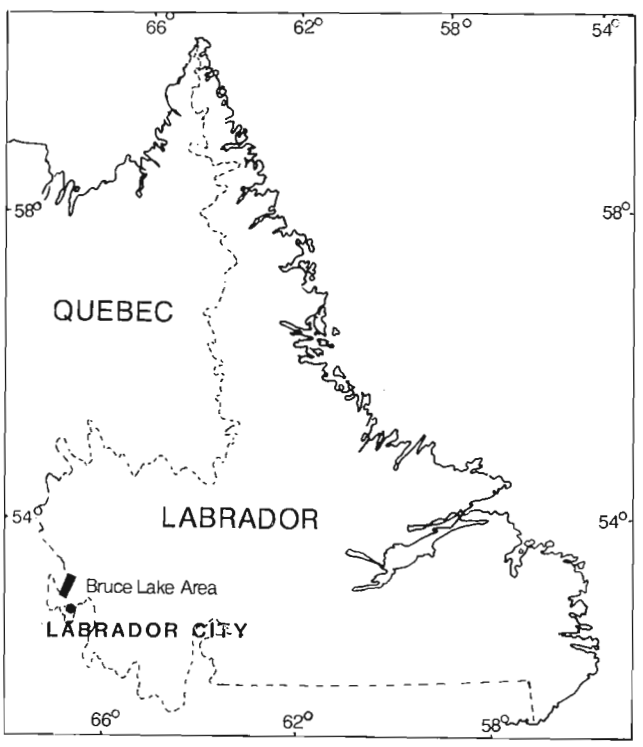


Fig. 46.1 Location of the Bruce Lake area in western Labrador.

LITHOLOGIES

Dominant rock types in the study area are Archean gneisses and migmatites, Proterozoic iron-formations and graphitic phyllites, whereas felsic schists and gabbroic intrusions are minor.

The Ashuanipi Metamorphic Complex (AMC) of the Superior Province is a complex of migmatitic and gneissic rock types. In the field separation of the rocks of the complex into dark, fine to medium grained ferromagnesian gneissic restites and leucocratic, medium to coarse grained granitoid neosomes is convenient. The neosomes are typically orthopyroxene-bearing. The metamorphism is of the granulite facies grade and of Kenoran age (Rivers, 1983b).

The AMC formed the crystalline basement for sedimentation of the Aphebian rocks of the Knob Lake Group. The oldest unit of these Aphebian supracrustals, the Attikamagen Formation, is exposed in beds several metres thick only in the area southeast of Bruce Lake. It consists of quartz-ofeldspathic schists in which coarse feldspar clasts and granitic pods are common. In zones of high shear strain, both the Archean gneisses and the felsic schists of the Attikamagen Formation form phyllitic rocks with feldspar porphyroclasts, which makes discrimination between the two impossible in the field. If orthopyroxene occurs in a rock, a positive determination as Archean gneiss is possible. If microscopic or chemical analysis allows distinction, a reassesment of the rock types might change the map pattern considerably.

The Sokoman Formation overlies the Attikamagen schists. This Formation, the best exposed in the area, consists of carbonate and quartzitic iron-formations. Quartz, Fecarbonates, Fe-Ca-amphiboles, hematite and magnetite are common minerals, with siderite commonly forming millimetre to

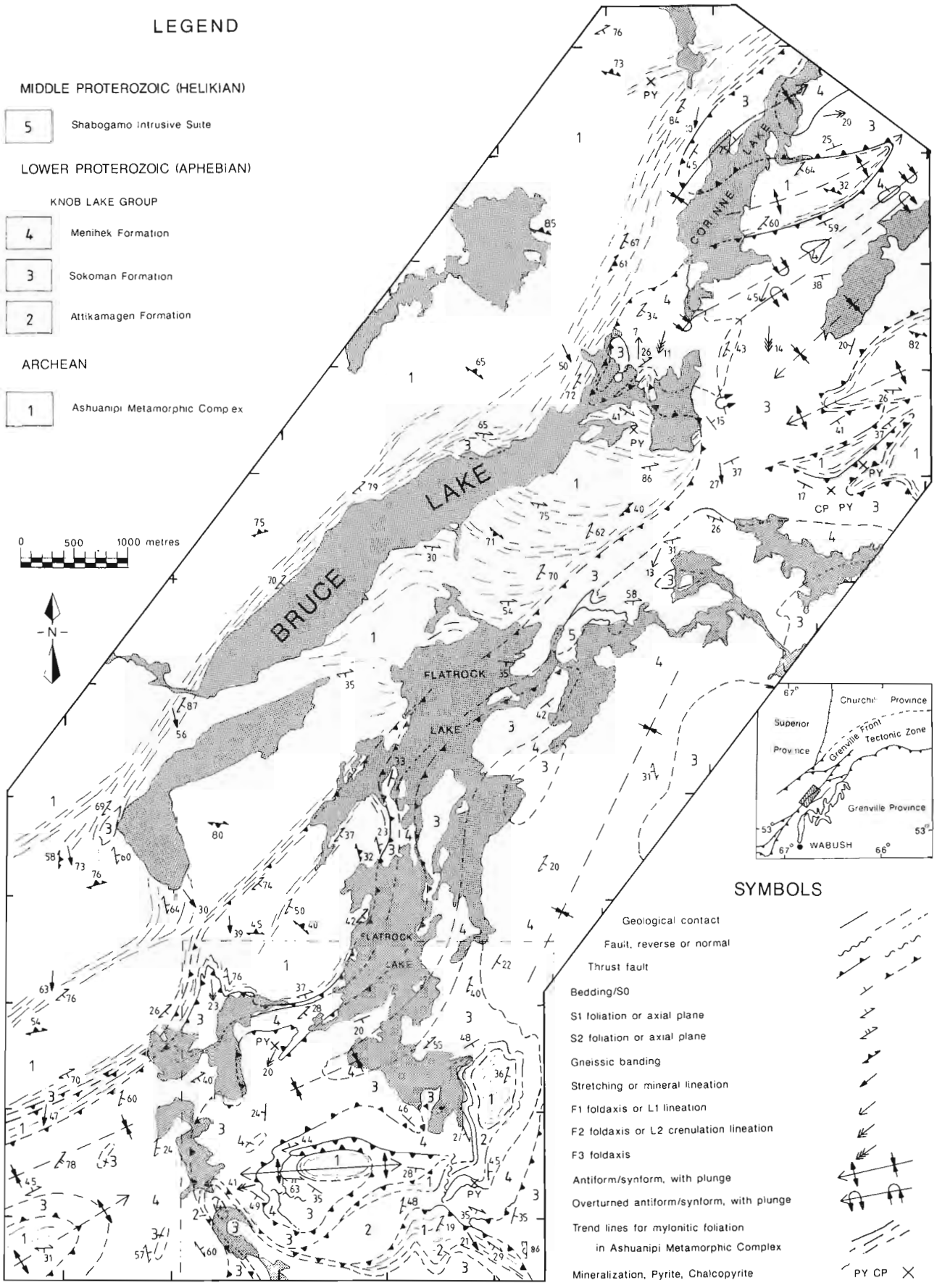


Fig. 46.2 Synoptic map of the Bruce Lake area. The map is compiled from the recent detailed mapping and maps by Rivers (1980a, b). The inset shows the position with respect to the Superior Province and the Churchill Province. In the south, the location of Figure 46.3 outlined.

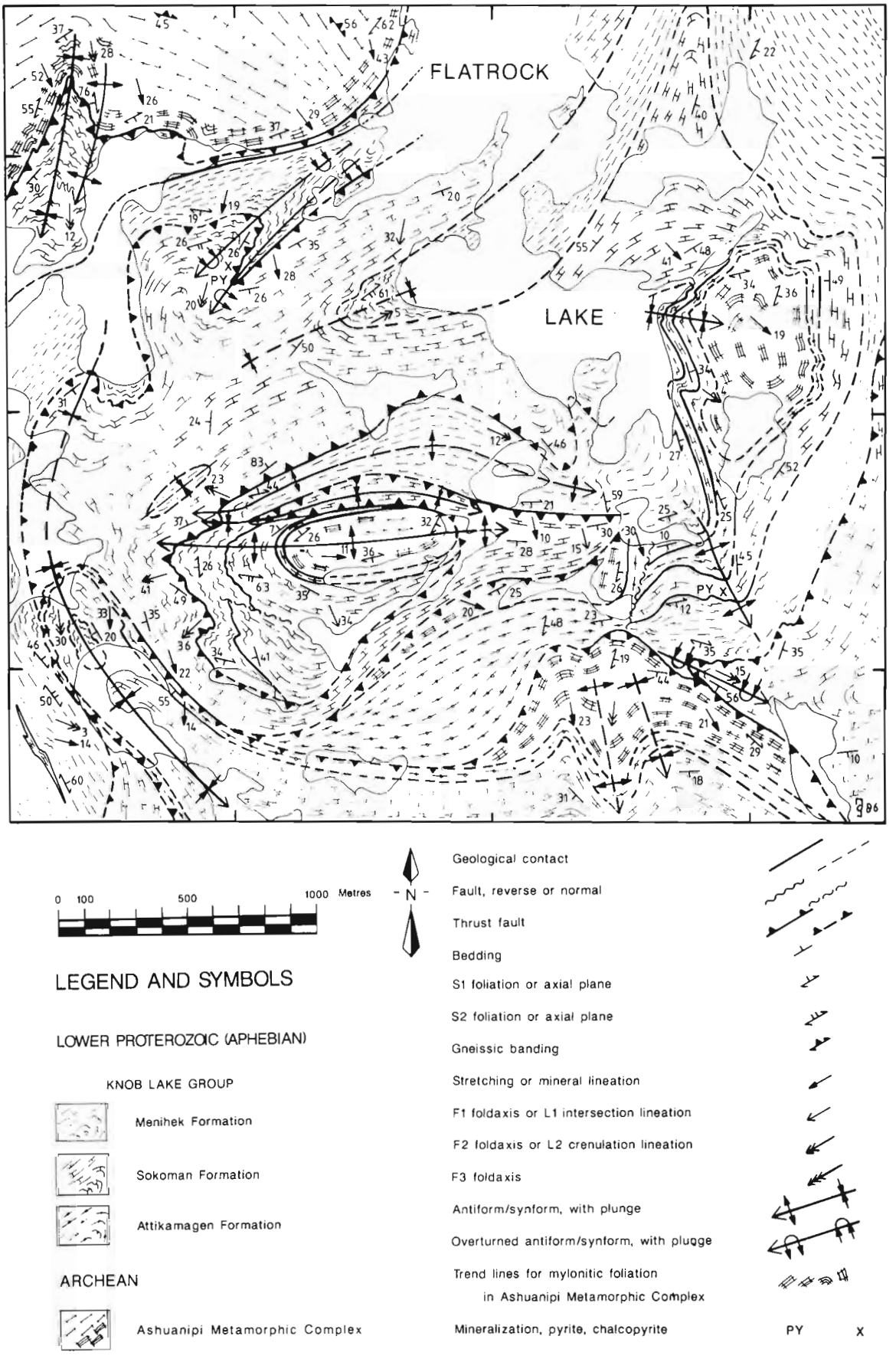


Fig. 46.3 Form surface map of the southern part of the Bruce Lake area. Location is shown in Figure 46.2

centimetre sized porphyroblasts in the carbonate bands. Compositional banding is on centimetre to metre scale. Although consistent stratigraphy within this formation is not established, the quartzitic oxide component commonly forms the base of the tectonic units. The top of the sequence in the study area the fine grained phyllites of the Menihek Formation. This is a very homogeneous rocktype, in which the original sedimentary layering is only locally observed.

Helikian rocks of the Shabogamo intrusive suite form dykes in the Knob Lake Group supracrustal rocks. These fine to medium grained intrusions form minor bodies in this area, are of predominantly gabbroic composition, and rarely form amphibolites.

SMALL SCALE STRUCTURES

Using overprinting relationships, three Grenvilliam deformation phases were distinguished, affecting the previously undeformed supracrustal rocks of the Knob Lake Group as well as in the Archean gneisses where these are intensely sheared. Each deformation phase can have different manifestations in the various lithologies.

D_1 deformation

During the first deformation phase thrusting and folding occurred. F_1 folds, which are not common in the area, are mainly intrafolial and isoclinal (Fig. 46.4) with a well developed axial plane schistosity S_1. The main foliation S_1, well developed in the whole area, is predominantly (sub-)parallel with the sedimentary layering S_0. In carbonate units in the Sokoman Formation, S_1 is mainly defined by oriented amphiboles and flattened siderite porphyroblasts (Fig. 46.5). Other carbonate minerals, specular hematite and elongate quartz grains can also form an S_1 schistosity. Micas mainly delineate the S_1 schistosity in the other units. The lineation L_1, formed by the intersection of S_0 and S_1, is parallel with the F_1 fold axis and has a general plunge towards the southeast, which is down dip in the S_1 plane.

Shear zones developed not only on the contact between the Archean basement and the supracrustal rocks but also within either of the two rock types. The thrusting caused the development of a stretching lineaton (Fig. 46.6) which is consistantly southeast plunging (cf. Owen et al., in press). The thrust planes and shear zones were all southeast-dipping originally, but were folded during younger deformation phases. S-C mylonites (Lister and Snoke, 1984) and phyllonites are developed in the Archean gneisses and the felsic schists in zones of high shear strain. Ribbon quartz and tailed feldspar porphyroclasts are typical for these zones, in which shear bands are also common (Fig. 46.7). Well foliated rocks, characterized by a stretching lineation, delineate the shear zones within the iron-formation. Boundinaged carbonate layers in a matrix of more quartz rich layers indicate extension during D_1 throughout the rock mass (Fig. 46.8). Shearband cleavage and a strong grainsize reduction characterize the shear zones in the Menihek Formation (Fig. 46.9). The orientation of S and C planes (Berthé et al., 1979) in mylonites and the asymmetry of tailed feldspar porphyroblasts indicates, that the movement direction during the thrusting was towards the northwest.

Few Archean gneisses in the study area show no signs of Grenvillian deformation. Even at a distance of over a kilometre away from the shear zones, the gneisses still reveal a Grenvillian schistosity, although very weakly developed. Closer to the shear zones these rocks are well foliated, with micas and elongate quartz grains defining the Grenvillan fabric.

D_2 deformation

Mesoscopic folds of the second generation are the most prominent structures at the outcrop scale. They have a wide variety of morphologies, from open to almost isoclinal with angular to rounded hinges, depending on the rock type in which they developed. Generally no axial plane schistosity developed locally however, an S_2 axial plane schistosity, similar to the S_1 indicates that the folds might not all have developed contemporaneously under identical metamorphic conditions. The Menihek phyllites possess an S_2 crenulation cleavage in zones of high D_2 strain, which is then the dominant foliation. A crenulation lineation subparallel with the F_2 fold axis is common. The folds are mainly asymmetric as shown in Figure 46.10, have shallow southeast-dipping axial planes and a west to northwest vergence is dominant. F_2 fold axes plunge south to southwest but in the south of the area they show a wide dispersion which is caused by overprinting of the D_2 structures on older ones and by later refolding during the youngest deformation phase.

D_3 deformation

The third deformation phase, dominated by open northeast-trending folds, formed mainly structures on a large scale (tens to hundreds of metres). Only in the north of the area can F_3 folds be observed on an outcrop scale.



Fig. 46.4 Isoclinal intrafolial F_1 fold in the Sokoman Formation.

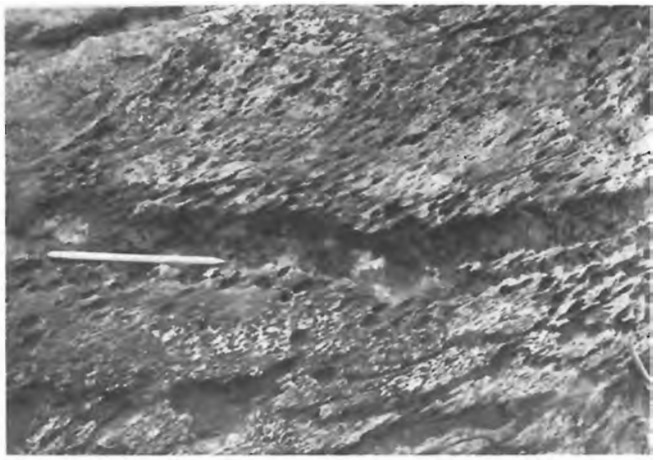


Fig. 46.5 S_1 in the Sokoman Formation developed at an angle to the sedimentary layering which is parallel with the pencil. S_1 is defined by flattened siderite porphyroblasts and oriented amphiboles.



Fig. 46.6 Stretching lineation in a D_1 shear zone, developed during the northwest thrusting. The photo shows stretched quartz in the quartzitic part of the Sokoman Formation.

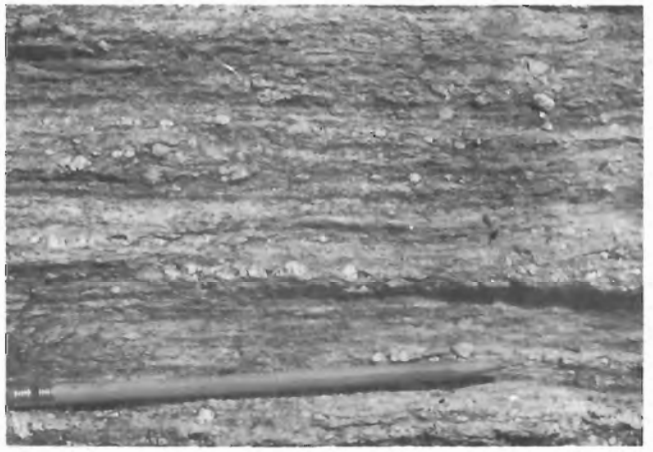


Fig. 46.7 Mylonite in the Archean gneisses with feldspar porphyroclasts. Those porphyroclasts that are tailed can serve as kinematic indicators.



Figure 46.8 Boudins in the Sokoman Formation indicate flattening during D_1. The boudins consist of carbonate material and are surrounded by a quartzitic matrix.



Fig. 46.9 Granitic pod in a mylonite in the Attikamagen Formation. A mylonitic foliation parallel to the slip plane has developed. It is cross cut by shear bands, which in the photo are about parallel to the pencil.

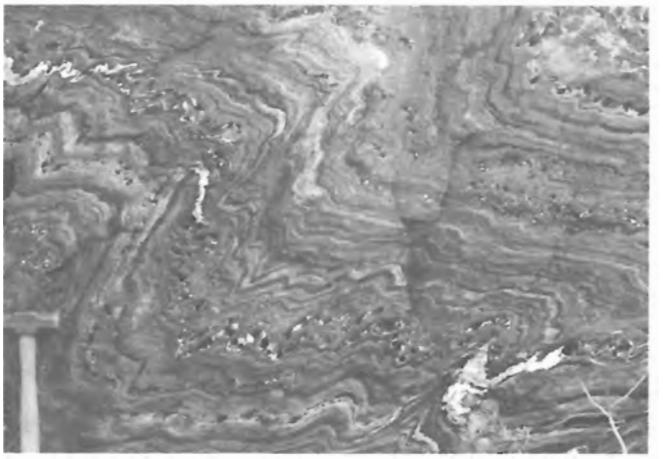


Fig. 46.10 Asymmetric F_2 folds in the Sokoman Formation.

LARGE SCALE STRUCTURES

By tracing marker horizons and fold asymmetries, several large scale folds were mapped. The geometry of these structures is indicated Figures 46.2 and 46.3. Since mesoscopic F_1 folds are scarce, F_1 structures are hard to reconstruct. Repetition of stratigraphy can therefore often be attributed to either isoclinal folding or thrusting during D_1. Although its configuration is not yet clearly understood, the structure in the eastern part of Figure 46.3 seems to be an isoclinal F_1 fold with an overturned lower limb.

F_2 folds, which dominate the map pattern, form structures on the scale of tens of metres to several hundreds of metres. On a large scale the frontal thrust between Archean basement and the Knob Lake Group has been folded, as well as the thrusts in the higher nappes. The asymmetries of the mesoscopic F_2 folds, however, show that some large folds, especially those in the front thrust, are not F_2 structures because the F_2 small scale asymmetry does not change over them. Since the orientation of these structures is not in agreement with the orientation of F_3 structures, it is most probable that *they are original highs and lows in the basement*. The basement rocks here do not reveal any evidence for Grenvillian folding so we assume that the folds in the thrusts originated from movement over these irregularities in the basement.

During D_2 the area was refolded in gentle large scale folds, with axial planes that are subvertical and trend northwest. An irregular dome and basin structure results, resembling the one reported by Rivers (1983a) southeast of the area, farther away from the Grenville Front. This caused large variations of the F_2 fold axis orientations in the area.

Detailed mapping showed that the area is dominated by thin-skinned thrust tectonics, as shown in Figures 46.2 and 46.3. The thrust slices range from some tens of metres up to several hundred metres in true thickness. It appears that the basement rocks of the AMC not only form the rigid footwall of the nappe system, but also are actively involved in the thrusting. In the higher nappes these rocks appear in duplex structures, as for example in the extreme southeast part of the area.

In the west of the area, several large scale, steeply dipping shear zones are developed in the Archean gneisses. One, west of Bruce and Corinne Lakes (Fig. 46.2), can be traced for over 12 km in the map area and probably even more outside the area. These major fault zones ranging from 200 to about 500 m wide form an en echelon pattern. The movement pattern is oblique slip with a large downdip (normal) component, in contrast with the reverse movement on all other shear zones. At several places in the shear zones slices of the Sokoman Formation were found, extending for at most 200 m, except in the extreme southwest where a slice of over a kilometre in length is found.

We have no control on the exact amount of displacement on the shear zones. Most of the thrusts, except the floor thrust, are considered to have minor displacements. (cf Rivers, 1983b). Towards the south they seem to 'die out' and to change into large overturned folds as found in the mining area west of Wabush Lake.

METAMORPHISM

The Knob Lake Group rocks, unmetamorphosed prior to the Grenvillian orogeny, were affected by a single prograde greenschist facies metamorphism. The main part of the area is situated in the muscovite-chlorite-biotite zone as defined by Rivers (1983b). In the northwest the biotite isograd cuts through the area, separating the main part from the muscovite-chlorite zone. In the pelitic rock types (Menihek Formation) the mineral assemblages quartz-muscovite-biotite-K-feldspar and quartz-muscovite-chlorite (-K-feldspar) are the most common in the two zones, respectively.

Field observations of the mineralogy of the iron-formation give no exact information on the metamorphic grade. Microprobe analyses of mineral assemblages in these rock types will ultimately be used to infer a metamorphic grade. The gneisses of the AMC are originally of granulite facies grade. In the shear zones complete retrogression of the gneisses to greenschist facies assemblages occurs. In the less strained rocks, orthopyroxenes are replaced by actinolite and chlorite or biotite. In thin sections, the plagioclase is sericitized or replaced by epidote. Rivers (1983b) reported a temperature of at least 325°C in the muscovite-chlorite zone northwest of the area. Generally the metamorphic grade increases towards the internal part of the orogen to the southeast.

The (peak) metamorphic minerals define the S_1 schistosity, which indicates that D_1 deformation was contemporaneous with the metamorphism. Recrystallized minerals related to F_2 structures show that the temperature during the second deformation phase remained high.

ECONOMIC GEOLOGY

In the Wabush – Labrador City mining area iron ore has been successfully recovered from the Sokoman Formation. This same Formation, which is also widely exposed in the Bruce Lake area, contains significant quantities of ferrugenous minerals. Almost pure hematite layers up to several centimetres thick are not uncommon in these rocks. Hematite and magnetite are mainly concentrated in the quartzitic rock types, whereas the carbonate sequences only contain minor quantities of these minerals and of goethite.

The carbonate iron-formation and the gabbros locally contain minor pyrite. Quartz lenses, which develop in dilation sites in and near shear zones, contain chlorite and calcite, and minor pyrite, pyrrhotite, and chalcopyrite. Showings of manganiferous minerals, which were expected in the area, were not observed.

DISCUSSION

Thin-skinned thrust tectonics and younger folding obviously dominate the Grenvillian orogeny in the Bruce Lake area, occurring on a much smaller scale than previously reported.

Intense shearing and flattening in the tectonic front are indicators for a regional simple shear deformation, which is related to the northwest movement of the nappe system. Thin skinned thrusting, typical for situations involving unmetamorphosed rocks, and internal deformation of the thrust slices are combined in this area. Both basement and cover rocks are involved in the formation of duplex structures that form the thrust slices. A *complicated ramp configuration* and folding during the younger deformation phases cause a *complicated map pattern*.

The second generation deformation structures indicate that northwest movement continued after the first deformation event, causing folding by movement of the thrust slices over irregularities in the subsurface. A good indication of post F_1 thrust movement is the F_2 overturned synform (in the extreme southeast corner of Fig. 46.3) which is truncated by a thrust. The map also shows that F_2 structures have a more complicated morphology than the overturned northeast-trending folds reported by Rivers (1983a). Basement relief, rotation of the fold axes towards the northwest as a result of stretching and fold overprinting produced this complexity. The F_2 structures overprint each other, as can be seen in the synform in the southwest corner of Figure 46.3, which is refolded in the dome structure that dominates the area just below the centre of the map. This indicates the complexity of F_2 folding.

The origin of the normal/oblique slip fault zone in the west of the area is not yet clearly understood. A possible model is the development of an extensional stress regime at the trailing edge of a thrust nappe. Another possibility is a late episode of extensional tectonics in the area. Except for some gentle folds, which may also be interpreted as anastomosing shear foliation, the fault zone is not affected by F_2 and F_3 folding. Large scale folds in the frontal thrust are absent in this fault zone, making a late origin of this shear zone plausible. A transtensional regime would explain this type of structure. A careful study of the kinematic indicators through out the area should result in a detailed reconstruction of the kinematics of the Grenville Front.

Grenvillian metamorphism is synkinematic with D_1 and D_2. Thin section studies should give a more detailed picture of deformation-crystallization relationships, and document movement of a metamorphic front with respect to the deformation front. Geobarometry and geothermometry on suitable mineral assamblages should highlight the deformaton-metamorphism relationships. These data will assist construction of a detailed movement and burial/stacking history of the rocks in this part of the Grenville Front Tectonic Zone.

ACKNOWLEDGMENTS

This work was carried out under contract with the Geological Survey of Canada. G. Blackwood assisted in the field, and T. Birkett provided field and logistical advice and support. Critical Reviews by D. Richardson, T. Birkett and H. Poulsen of the GSC improved the text.

REFERENCES

Berthé, D., Choukroune, P. and Jegouzo, P.
1979: Orthogneiss, mylonite and non coaxial deformation of granites: the example of the South American Shearzone; Journal of Structural Geology, v. 1, p. 31-32.

Fahrig, W.F.
1967: Shabogamo Lake map area, Newfoundland-Labrador and Quebec: 23G (east half); Geological Survey of Canada, Memoir 354, 23 pp.

Lister, G.S. and Snoke, A.W.
1984: S-C mylonites; Journal of Structural Geology, v. 6, p. 617-638.

Owen, J.V., Calon, T. and Rivers, T.
in press: The significance of reclined folds and the evolution of the Grenville Front zone in Labrador; Canadian Journal of Earth Sciences.

Rivers, T.
1980a: Wabush Lake, NTS23G/2; Mineral Development Devision, Newfoundland Department of Mines and Energy, Map 80-1, 1:50,000 scale with marginal notes.

Rivers, T.
1980b: Sawbill Lake, NTS23G/7; Mineral Development Devision, Newfoundland Department of Mines and Energy, Map 80-2, 1:50,000 scale with marginal notes.

Rivers, T.
1983a: The northern margin of the Grenville Province in Western Labrador – Anatomy of an ancient orogenic front; Precambrian Research, v. 22, p. 41-73.

Rivers, T.
1983b: Progressive metamorphism of pelitic and quartzofeldspathic rocks in the Grenville Province of western Labrador – tectonic implications of bathozone 6 assemblages; Canadian Journal of Earth Sciences, v. 20, no. 12, p. 1791-1804.

Rivers, T. and Nunn, G.A.G.
1985: A reassesment of the Grenvillian orogeny in Western Labrador; in: The deep Proterozoic crust in the North Atlantic Provinces, ed. A.C. Tobi and J.L.R. Touret, D. Riedel Publishing Company, p. 163-174.

Wynne – Edwards, H.R.
1972: The Grenville Province; in: Variations in tectonic styles in Canada, ed. R.A. Price and R.J.W. Douglas, Geological Association of Canada, Special Paper 11, p. 263-334.

Geology of the south half of the Taltson Lake map area, District of Mackenzie

Project 850005

H.H. Bostock

Bostock, H.H., Geology of the south half of the Taltson Lake map area, District of Mackenzie; in Current Research, Part A, Geological Survey of Canada, Paper 87-1A, p. 443-450, 1987.

Abstract

In western and central parts of the area metasedimentary and metavolcanic gneiss have been intruded in succession by plutons of Middle Proterozoic granodiorite, monzogranite and syenogranite. Minor dioritic rocks are engulfed within these plutons.

Mixed gneisses in the east were derived from lithologies similar to those in the west, but are intruded by syntectonic mafic dykes and late tectonic granite, and have been subject to variable northerly trending shear. Local plagioclase-hornblende-rich gneisses are of unknonwn origin.

The Nonacho Group, including monomict conglomerate, shale, siltstone, sandstone and polymict conglomerate, overlies the mixed gneiss. Although large lenses of basal monomict conglomerate are unconformable upon the gneiss, the structural relationships between basal conglomerate and the younger sediments is not clear.

The mixed gneisses are locally intruded by northeasterly trending diorite- granodiorite dykes that are weakly foliated along their margins. Northwesterly trending diabase dykes of the Sparrow dyke swarm, which are locally brecciated and altered, cut all units. Two small, white, unaltered, unfoliated quartz latite dykes intrude the mixed gneisses.

Lead, zinc, copper, tungsten, boron and beryllium mineralization has been observed.

Résumé

Dans les parties ouest et centrale de la région des plutons de granodiorite, de monzogranite et de syénogranite du Protérozoïque moyen, contenant de faibles quantités de roches dioritiques, ont recoupé successivement des gneiss métavolcaniques et métasédimentaires.

À l'est, les gneiss mélangés sont dérivés d'une lithologie similaire à celle de l'ouest, mais ils sont recoupés par des dykes mafiques syntectoniques et par un granique tardi-tectonique; ils ont été soumis à un cisaillement variable à orientation nord. L'origine des gneiss locaux à plagioclase et à hornblende est inconnue.

Le groupe de Nonacho, qui se compose de conglomérat monogénique, d'aleurolite ardoisière, de grès et de conglomérat polygénique, repose sur le gneiss mélangé. Bien que de grosses lentilles de conglomérat monogénique basal reposent en discordance sur le gneiss, les liens structuraux entre le conglomérat basal et les sédiments plus récents ne sont pas évidents.

Les gneiss mélangés sont par endroits recoupés par des dykes de diorite-granodiorite à orientation nord-est, dont les marges sont faiblement feuilletées. Des dykes de diabase à orientation nord-ouest du groupe de dykes de Sparrow ont été localement bréchifiés et altérés et recoupent toutes les unités. Deux petits dykes de latite quartzique blanche, non altérée et non feuilletée, ont fait intrusion dans les gneiss mélangés.

On y trouve des minéralisations de plomb, de zinc, de cuivre, de tungstène, de bore et de béryllium.

INTRODUCTION

Reconnaissance (1:250 000 scale) mapping of the south half of the Taltson Lake area (NTS75E) was initiated in summer 1986 using three independent mapping teams supported by boat transport. Camps were moved on a weekly basis by float plane. In this manner the map area will be covered in two years, and parts inaccessible by this means will be completed in a third summer. This account is therefore a preliminary report on the first year's work with interpretation extended between the more widely spaced lakes where the data available appear to permit. The major pluton contacts have been delineated but a number of smaller bodies of gneiss remain incompletely mapped and many are too small to show on Figure 47.1.

For purposes of this report granite with a prominent plagioclase phase is called monzogranite, and granite with a subordinate or no recognizeable plagioclase phase is called syenogranite.

GENERAL GEOLOGY

Paragneiss and metavolcanics

The oldest rocks, based on local intrusive relationships, recognized within the map area are a widespread suite of metasediments and metavolcanics (units 1 and 2, Fig. 47.1). Amphibolites with rare preserved pillows are most extensive immediately east of O'Connor Lake, but individual pillowed flows up to a few metres thick, with associated banded amphibolite, have also been found south of Rutledge River near 111° west longitude. Minor bands of silicate iron-formation up to 0.5 m thick are associated with these latter volcanics along strike. Amphibolites at O'Connor Lake are part of a more extensive belt of presumably largely metavolcanic amphibolites preserved about Thubun Lakes to the north of the map area, and remnants of similar rocks are common as inclusions within the granodiorite complex. A minor fine- to medium-grained, serpentinized ultramafic body about 80% pyroxene, 10% hornblende and 10% serpentine, and 10 m or more in width, is apparently conformable within metavolcanics east of O'Connor Lake.

Metasediments of this suite are predominantly semipelitic and pelitic gneisses with local bands of calc-silicate and common quartz-rich beds. Small tabular bodies of fine grained, grey to white plagioclase-rich rocks occur mostly within or along the margins of the major granitic plutons. Some of these bodies are clearly intruded by granitic rocks and appear to form gneissic layers within supracrustal rocks of unit 1. Others are medium grained, contain inclusions of more mafic gneiss, and may be of intrusive origin. Graded beds, preserved in least deformed rocks, suggest deposition by turbidity flow. Metamorphic grade over much of the area has reached upper amphibolite-lower granulite facies as indicated by the presence of sillimanite-cordierite-potassium feldspar assemblages in pelitic gneiss, and the occurrence of hypersthene locally in more calcareous bands. Locally, however, andalusite is a prominent constituent of these gneisses.

Gneisses of unknown origin occur within unit 1 near O'Connor Lake. Mostly these are highly deformed biotite-rich gneisses and schists, but some are breccias. In large part they are probably derived from metasediments but some may initially have been granitic or volcanic rocks. Rocks of unit 1 are intruded in widely varying proportion by plutonic rocks which reach up to 50% granite along the margins of the unit.

The absolute age of these rocks (unit 1) is unknown. Similar metasedimentary rocks far to the south in Alberta have been assigned an Archean age on the basis of Rb-Sr dating of cross cutting pegmatite (Baadsgaard and Godfrey, 1972).

Dioritic plutonic rocks

Medium- to fine-grained biotite-bearing foliated dioritic rocks (unit 3), which are locally garnet-bearing, have been engulfed along with supracrustal gneisses (unit 1) in the syenogranite within the central part of the map area. They have been folded and are clearly intruded by the enclosing granite, but their age relative to the supracrustal rocks in not known. A possibly related body of foliated, biotite- plagioclase-rich gneiss occurs largely within paragneiss of unit 1 immediately northeast of O'Connor Lake.

Granodiorite-granite complex

Granodioritic to granitic rocks (unit 4) containing abundant inclusions of supracrustal gneisses, which extends westward to the Paleozoic overlap (Bostock, 1986), projects into the map area south of Thubun Lakes. Xenoliths of amphibolite are substantially more common than those of metasediments but the proportions of both to the plutonic rocks vary widely. The granodioritic phase of this complex is medium grained and weakly foliated with biotite and commonly hornblende contributing to a colour index about 15. Large, typically subhedral pink microcline porphyroblasts are commonly present. Granodiorite west of the map area is characterized by accessory sphene and absence of aluminous minerals, garnet and cordierite, which are widely present in the plutonic rocks to the east. The granodiorite grades into less mafic granitic rocks and is commonly intruded by finer grained pink granular granite dykes bearing a little biotite. The eastern contact of the granodiorite south of Thubun Lakes is not precisely known but is marked by a deformed zone containing two medium grained granitic phases.

Monzogranite

Medium- to fine-grained mostly equigranular, biotite monzogranite (unit 5), containing variable proportions of small to large remnants of metasedimentary rocks and local amphibolite xenoliths, lies to the east of the granodiorite complex. East of a north-south line approximately through O'Connor Lake the monzogranite commonly contains garnet or cordierite, or both, especially where paragneiss remnants are present. Similar rocks occur in the southern part of the map area near the 111th meridian and in the eastern part about

Rutledge Lake. Commonly the monzogranite is moderately to strongly foliated and/or lineated but parts are only slightly foliated. A broad lenticular zone containing a complex mixture of syenogranite, monzogranite and included supracrustal rocks (unit 5a) follows much of the western contact between the monzogranite and succeeding syenogranite. Where the zone is narrow, veins of syenogranite penetrate the monzogranite more or less parallel to the contact zone. Preliminary zircon U-Pb age determinations (Van Breemen, personal communication, 1986) suggest that the monzogranite is younger than the granodiorite complex.

Syenogranite batholith and possibly related plutons

A major batholith (unit 6) of megacrystic syenogranite (unit 6a) characterized by euhedral to rounded or augen shaped megacrysts of submesoperthitic k-feldspar, commonly 2.5 cm in length, occupies the central part of the area. The western two thirds of the batholith contain irregularly distributed cordierite and garnet, both more or less altered to biotite and chlorite. Megascopic plagioclase is subordinate or absent. Strength of foliation and lineation vary widely.

Along the east margin of the batholith an extensive north-south zone of granite penetrates monzogranite and the eastern mixed gneisses. Within this zone the granite is variably sheared, some parts of the zone displaying fine grained quartz in ribbons wrapped about rounded k-feldspar megacrysts. In other parts the megacrysts occur in a fine grained matrix that appears little sheared, and elsewhere (unit 6b) the granite is fine grained, megacrysts are rare to absent, and equigranular white weathering feldspar, believed to be plagioclase, is present in small amounts. Mafic minerals are biotite, chlorite and locally magnetite. Garnet and cordierite are absent. Although apparently emplaced under different conditions than were rocks of the main part of the syenogranite batholith to the west, these granites locally appear to grade into it and have been mapped as part of it.

Still farther east megacrystic granitic rocks occur as smaller isolated plutons (unit 6c) some of which are too small to be shown on the map. Most of these are deformed with megacrysts more or less crushed and granulated forming clumps of cleavage fragments within amorphous masses of fine grained feldspar. In places these clumps are linear and elsewhere they are disc-shaped. The matrix usually contains biotite-chlorite of coarser grain size than is present in the batholith to the west, and a brown vitreous mineral tentatively identified as sphene is visible in some hand specimens.

Within the area occupied by the small megacrystic plutons (east of the megacrystic syenogranite batholith) the gneisses are intruded by many dykes and small bodies of weakly to unfoliated, pink to white, fine- to medium-grained granite. Fine grained pink granite locally grades to pink to white, medium grained granite that commonly shows monzogranitic composition but may contain a few scattered k-feldspar megacrysts up to 3 cm in length. The largest of these bodies (unit 6d) is only partly mapped immediately west of Borrowes Lake. Weakly foliated conformable lenses of fine grained pink granite similar to fine grained granite above, occur locally within the small megacrystic plutons but sharp crosscutting relations were not seen. On the other hand no megacrystic rocks were seen to intrude the biotite granite. It is possible therefore that the biotite-chlorite granite is younger than the more deformed small megacrystic plutons.

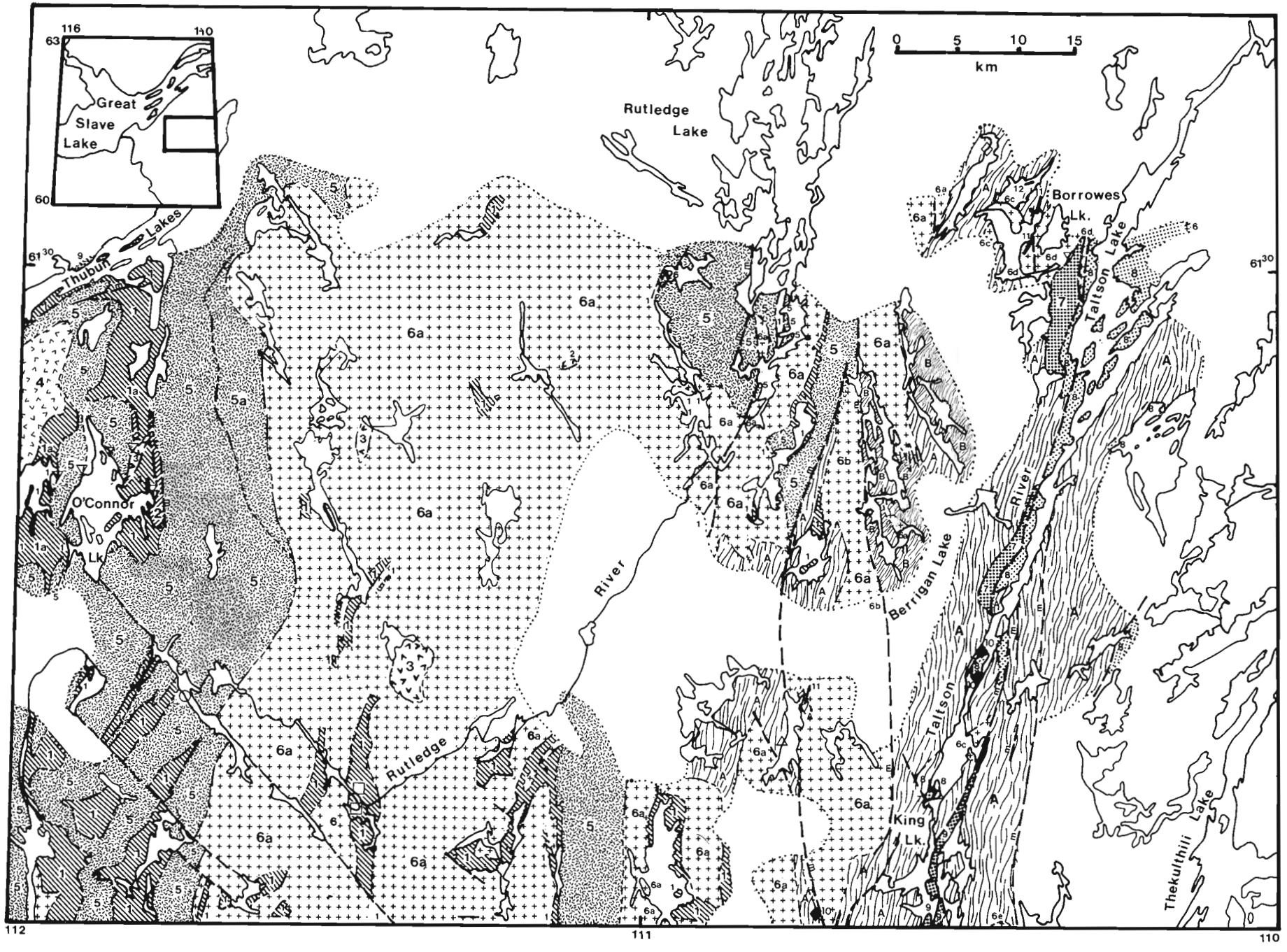
One oval shaped pluton (unit 6e), present in the southeast corner of the area mapped, and examined only south of the 61st parallel, is undeformed. It comprises syenogranite (rich in k-feldspar) but is mostly coarse grained rather than megacrystic. Fragments of mylonite are included in a western megacrystic phase of this granite.

Crosscutting relations indicate that the megacrystic syenogranite batholith is younger than the monzogranite, and it is inferred to be younger than the western granodiorite complex. Small megacrystic plutons east of the batholith are tentatively correlated with it. Biotite-chlorite granite may be younger than the small megacrystic plutons but this temporal relation also remains to be confirmed. Of all these granitic rocks the one which most clearly contributes cobbles to the overlying Nonacho basal conglomerate is the coarse white phase of the biotite- chlorite granite.

Eastern mixed gneisses

Mixed plutonic rocks and gneisses (unit A) occur mostly in the eastern third of the map area. These rocks comprise remnants of biotite gneiss, hornblende-biotite gneiss, amphibolite, some pelitic gneiss and locally mafic plutonic rocks intruded in variable proportion by a less mafic, commonly grey to white granite. In places the rocks have an agmatitic structure with more or less angular inclusions separated by little foliated granitic matrix. Elsewhere the included phase is more or less deformed or forms schlieren within the granite. Some exposures comprise gneiss with little or no plutonic phase. The granite may be foliated or unfoliated. In places amphibolite dykes are clearly intrusive into these rocks, but more commonly amphibolite bands showing boudinage are conformable with local banding or foliation. Small bodies of massive to weakly foliated pink to white, fine- to medium-grained biotite-chlorite granite and of megacrystic granite locally intrude the gneisses. Rarely dark green inclusions consisting mostly of pyroxene and garnet were observed. The mixed gneisses include rocks possibly equivalent to units 1 to 6.

At Berrigan Lake and along the large lake immediately to the east, lenticularly banded gneisses (unit B) made up of fine grained, hornblende-rich and plagioclase-rich bands are present. Xenoliths of amphibolite are common and locally xenoliths mostly composed of fine grained plagioclase were observed. Near the west margin of this unit a zone of medium grained plagioclase-rich gneiss with patches or bands rich in amphibole resembles gabbroic anorthosite. Interleaved with these gneisses are bands of intensely sheared megacrystic granite- protomylonite which coalesce northward to form a major body north of Berrigan Lake.


116
140
63
60
Great
Slave
Lake
0
5
10
15
km
Rutledge
Lake
Borrowes
Lk.
Tallson Lake
Lakes
Thubun
61 30
O'Connor
Lk.
River
Berrigan Lake
Tallson
River
King
Lk.
Rutledge
Thekulthili
Lake
112
111
110

LEGEND

13 — quartz latite.

(12) — diabase dykes (not shown).

11 — fine-grained granodiorite-diorite.

10 — felsite.

9 — mylonite, some schist.

7 8 — NONACHO GROUP
7. basal monomict conglomerate.
8. slate, siltstone, sandstone, polymict conglomerate.

6 — MEGACRYSTIC GRANITE & RELATED PLUTONS
a. megacrystic granite
b. fine- to medium-grained syenogranite-monzogranite.
c. small megacrystic granite plutons.
d. medium-grained biotite-chlorite granite.
e. coarse-grained to megacrystic syenogranite.

5 — MONZOGRANITE
5a. mixed monzogranite with units 1,2 & 6.

4 — GRANODIORITE COMPLEX
granodiorite-granite with included units 2 & 1.

3 — foliated biotite diorite-granodiorite.

1 2 — SUPRACRUSTAL GNEISSES
1. semipelitic & pelitic gneiss, biotite gneiss, quartz-rich gneiss: some calcsilicate gneiss, minor amphibolite. 1a schist, some breccia, mylonite. (Intruded in widely varying proportions by granitic rocks.)
2. amphibolite.

A B — MIXED GNEISSES
A. biotite gneiss, hornblende gneiss, some amphibolite, and minor pelitic gneiss engulfed in granitic plutonic rocks & locally intruded by late pink granite.
B. fine- to medium-grained, lenticularly banded hornblende- and plagioclase-rich gneiss locally intruded by granitic rocks.

SYMBOLS

geological contacts: defined, approximate.

fault, fault with mylonite. (m)

limits of mapping.

MINERAL OCCURRENCES

beryl	○	galena (with sphalerite about O'Connor Lake)	▽
scheelite	□		
malachite	△	tourmaline-muscovite zoned pegmatite	◇

Figure 47.1. Geological map of the Taltson Lake area, south half, District of Mackenzie.

Nonacho Group

Nonacho Group (units 7 and 8) clastic sediments have been examined mainly along and adjacent to Taltson and King lakes, but the major part of the Nonacho basin lies to the east (see Aspler, 1985). These sediments comprise a basal monomict conglomerate (unit 7); and younger clastic sediments (unit 8) which include shale with local siltstone and some fine sandstone interbeds, polymict conglomerate, and bedded sandstone/siltstone.

The basal conglomerate comprises close packed rounded clasts of granitic rocks up to a metre or more in diameter, some gneiss and amphibolite, and minor vein quartz in a matrix of sand of granite composition. Clasts are commonly variably red-stained, but in places fresh pink-white granite cobbles, similar to the coarser biotite-chlorite granite in the immediately subjacent basement, are present. The basal contact is locally faulted but in several places the conglomerate appears to grade into granite through increase in angularity and size of clasts, suggesting that the contact is an unconformity. Gently dipping (20° east) sandy beds at the east margin of the largest conglomerate lens and the character of the basal contact suggest that the conglomerate lenses are not overturned. Between the uppermost sandy beds of the basal conglomerate and Taltson Lake is a belt of folded and more steeply dipping slatly shales with local siltstone interbeds. Farther south on the west side of Taltson Lake moderately to steeply dipping polymict paraconglomerate, bearing clasts of sedimentary and locally of intermediate volcanic rocks in addition to granite and gneiss, is faulted against both granite basement and basal conglomerate. Similar polymict conglomerates on the islands in central Taltson Lake show gently east-plunging slickensides on minor fault planes, possibly reflecting east or westward thrusting. Interbedded sandstone and siltstone occur on the eastern islands of central Taltson Lake. Farther north, between the two arms of Taltson Lake, similar sandstone with minor polymict conglomerate interbeds appears to overlie polymict conglomerate with unusually high granite clast content. An isolated exposure of megacrystic granite near the crest of the peninsula is surrounded on three sides by sandstone. It is not clear whether the contact there is faulted or unconformable. An approximate minimum for the Nonacho Group is provided by the age of crosscutting Sparrow mafic dykes (1700 Ma; McGlynn et al., 1974).

Mylonite

Northerly trending mylonite belts (unit 9) or faults accompanied by lesser zones of mylonite cut most of the major rock units. The main mylonite belt, which is extensive west of Lady Grey Lake in the Fort Smith area to the south, narrows northward where it draws abreast of King and Taltson lakes, and deformation appears to become more brittle. Farther west and north, ductile shear is evident in zones within the megacrystic granite, but extensive unmapped terrane in this region precludes their correlation. Lineations associated with the mylonites are mostly shallow plunging suggesting strike slip movement. Along the east margin of the megacrystic syenogranite batholith, kinematic indicators (mainly shear bands) indicating sinistral strike slip have been widely observed in the northward trending gneisses and along the margins of some mylonite within the granite. Dextral shear bands appear to be most common in local northerly trending shear zones within the megacrystic syenogranite.

Mylonite and schist examined on the islands and northwest shore of southern Thubun Lakes, are part of a southwest-trending mylonite belt which extends across granodioritic terrane to the Paleozoic overlap. Local schists, breccia and minor mylonite have been found along the west margin of the map area, mostly within supracrustal gneisses (unit 1a). These zones may be related to displacements along the Warren Fault Zone (Godfrey and Langenberg, 1978) or to shearing evident in the valley of Deskenatlata Lake south of the map area (Bostock, 1981).

Felsite

Grey to purple flinty aphanitic felsite (unit 10), intrusive into Nonacho sandstone near the east rapids at the south end of Taltson Lake, forms a body several tens of metres across. Irregular, altered, dyke-like bodies containing minute phenocrysts penetrate plutonic rocks near the north end of the west rapids. Flinty, aphyric felsite also occurs on an island along a fault zone near the south boundary of the area some 8 km west of King Lake. The body is at least 100 m across. Megacrystic granite and gneisses nearby are severely brecciated and show greenish alteration zones reminiscent of alteration in some submarine felsite flows in spilitic suites.

Small grey, flinty pseudotachylyte breccia veins are locally prominent in monzogranite along a narrow shear zone separating monzogranite from volcanic rocks east of O'Connor Lake. Their presence may be related to changes in strike of the shear zone. Similar breccia veins were observed in syenogranite along minor shears near northwestward-trending faults in the southwest corner of the map area. A single vein, up to 20 cm thick, containing abundant country rock fragments in a black glassy matrix, cuts syenogranite near the west contact of the batholith 9 km east of O'Connor Lake. The vein strikes 120°, dips about 80° southwest and was observed for 30 m along strike. Two dykes, one of pegmatite and the other of fine grained mafic syenogranite cutting the batholith show an apparent dextral offset of 3 m along the vein.

Diorite-granodiorite dykes

Two dykes of fine-to medium-grained, equigranular to porphyritic diorite to granodiorite (Unit 11) occur near the northwest end of the large lake 10 km west of King Lake, and about 300 m west of Borrowes Lake. Both dykes have somewhat irregular contacts and variable but generally north-northeasterly trends with steep dips. Weak foliation near contacts is subparallel to contacts in both. The southern dyke is 10 m thick and at least 0.25 km long. Dextral bending of gneissosity in enclosing gneiss bands is evident at the southeastern contact. The dyke intrudes both mixed gneiss

(unit A) and a band of sheared megacrystic granite (unit 6a). The northern dyke is at least 150 m wide and a small body found to the north of the main exposure suggests that it may have a strike length in excess of 9 km. Grain size reaches up to 1.5 mm but phenocrysts of hornblende are locally up to 2.5 to 3 mm. Some parts of the dyke contain scattered feldspar phenocrysts reaching 2 cm. Feldspar, hornblende, chlorite and locally quartz are evident in the matrix. Angular inclusions of amphibolite up to 1 mm diameter are widespread, inclusions of hornblende gabbro are present locally and fragments of medium grained granite and coarse grained hornblendite were seen at some exposures. Local 1 to 3 m scale bodies of fine grained pink granite with smooth contacts in contrast to those of inclusions, occur within the dyke locally. These are ovoid to complex lenticular, like small apophyses in plan, but similar bodies seen at the top of a small bluff appear to be rootless, suggesting globs of immiscible liquid. Small irregular bodies of similar fine grained dioritic intrusive appear within gneisses and megacrystic granite on islands surrounding the dyke. If the included bodies of fine grained, pink, chlorite-biotite granite were liquid during emplacement of these dykes, then either the two are about the same age or the granite represents a remelted fraction from the country rock at depth.

Sparrow dykes

Northwesterly trending, aphanitic to medium grained diabase dykes (not shown in Fig. 47.1), reaching about 40 m in thickness but mostly less than 1 m, are wide spread through the map area, but are particularly abundant in the southern part. Dykes tend to occur in swarms of several small dykes, and such swarms are common along the margins of major dykes in the southwest corner of the map area. Chilled margins are evident on most dykes and the contacts in detail tend to be irregular being slightly offset along joints. Along Taltson River valley similar dykes trend more northerly and are more severely chloritized and brecciated. Crosscutting fresh dykes were not seen in this area so it is not known whether these dykes represent a distinct swarm or are part of the Sparrow dyke swarm that has been more severely altered. Northwesterly trending Sparrow dykes intrusive into sediments of the Nonacho Group have been dated at about 1700 Ma (McGlynn et al., 1974).

The largest northwesterly trending Sparrow dykes occupy fault valleys in the southwest corner of, and along the west margin of, the map area. Offset of contacts along these valleys suggests sinistral displacements of 1-2 km. One such dyke, with felsic veins intruded perpendicular to its margins during dyke emplacement, has fractures parallel to its contacts showing sinistral displacement of veins. This indicates that at least some of the sinistral faulting took place after emplacement of the Sparrow dykes.

Quartz latite dykes

Two small irregular bodies of grey to white aphanitic to fine grained porphyritic quartz latite (unit 13) intrude biotite gneiss on adjacent islands northwest of Borrowes Lake. These bodies have irregular chilled margins, contain bipyramidal quartz, plagioclase and biotite phenocrysts up to 2 to 3 mm in diameter and are unfoliated and apparently unaltered.

ECONOMIC GEOLOGY

Sphalerite, galena, pyrite and minor chalcopyrite are present in northwesterly trending quartz-carbonate breccia veins at the O'Connor Lake Mine and in the surrounding area (Irwin and Prusti, 1955). Trace galena and pyrite occur in a minor quartz vein cutting basal Nonacho conglomerate west of Taltson Lake. Similar quartz veins are present cutting all the principal gneiss and granitic units within the map area but most are barren of sulphides. Locally, similar veins appear to penetrate the diabase dykes and base metal mineralization may therefore be younger than 1700 Ma diabase intrusion (McGlynn et al., 1974).

Very minor copper stain (malachite) was observed near the west shore of King Lake and near the west shore of the large lake 13 km east of King Lake.

Scheelite occurs as minute fracture fillings and as fine grained disseminations within individual gneiss bands near Rutledge River in the southwestern part of the map area (Bostock, 1986; Bostock and Thompson, 1983).

A single crystal of beryl was found in a small irregular pegmatite intruding monzogranite on Rutledge River in the southwestern part of the map area.

Two generations of pegmatite intrude the gneisses along the east margin of the major western body of syenogranite west of Borrowes Lake. The earlier pegmatites, which are commonly small irregular bodies, locally contain a black glassy mineral in ovoid masses up to 5 cm in diameter with a distinctive blue weathered surface. The metamict mineral grains, which are surrounded by extensive expansion cracks due to destruction of the mineral lattice by radioactive disintegration, are likely allanite. The younger pegmatites are concentrated near the contact of the syenogranite. These locally contain tourmaline and muscovite. One such pegmatite some 15 m across contains a succession of fine- and coarse- grained zones with muscovite and 10% tourmaline in the fine grained zones.

DISCUSSION

Reconnaissance mapping of the tectonic zone (hereafter called the southern tectonic zone), which extends along the west margin of the Churchill Province from the Great Slave Lake Shear Zone (Hanmer and Lucas, 1985) in the north into northern Alberta in the south, (Godfrey and Langenberg, 1978; Langenberg, 1983) is well advanced. Geochronological investigations based on Rb-Sr isotopic determinations (Baadsgaard and Godfrey, 1972;Nielsen et al., 1981) and preliminary U-Pb determinations by the Geological Survey (Van Breemen, personal communication,

1986) indicate that this zone is of Middle Proterozoic age. Granitic plutonism in the zone correlates broadly with that in the Thelon Tectonic Zone (Van Breemen et al., 1987). It is not as yet known, however, whether the Slave Province, which lies at the west boundary of the Thelon Tectonic Zone, has a correlative structural province west of the southern tectonic zone, or whether rocks of a different type form the basement to the west of the Paleozoic overlap.

Shearing along the east margin of the southern tectonic zone began before plutonism was completed. Present data suggest two or more periods of shear characterized by sinistral and dextral strike slip at least in their later stages. Preservation of high grade mineral assemblages in the central part of the zone may also reflect uplift of this region. Two or possibly 3 episodes of posttectonic hypabyssal intrusion occurred, one widespread and the other two of local significance as presently understood.

Continued study of the southern orogenic zone northward to its confluence with Great Slave Lake Shear Zone, and geochronological investigation of rocks which bracket the interval of shearing should provide a better understanding of interactions between these two zones. In so doing it will make possible a more detailed correlation between Middle Proterozoic events along the west margin of Churchill Province and those recently described along the margins of Slave Province.

REFERENCES

Aspler, L.B.
1985: Geology of Nonacho Basin (Early Proterozoic) N.W.T.; unpublished, Ph.D. Thesis, Carleton University, 384 p.

Baadsgaard, H. and Godfrey, J.D.
1972: Geochronology of the Canadian Shield in northeastern Alberta, II: Charles-Andrew-Collins Lakes area; Canadian Journal of Earth Sciences, v. 9, p. 863-881.

Bostock, H.H.
1981: A granitic diapir of batholithic dimensions at the west margin of the Churchill Province, in Current Research, Part B, Geological Survey of Canada, Paper 81-1B, p. 73-82.

1986: Reconnaissance geology of Precambrian rocks of the Fort Resolution, Taltson Lake, and Fort Smith areas, District of Mackenzie; in Current Research, Part A, Geological Survey of Canada, Paper 86-1A, p. 35-42.

Bostock, H.H. and Thompson, D.L.
1983: Fluorescent minerals from the Fort Smith area, District of Mackenzie, N.W.T.; in Current Research, Part B, Geological Survey of Canada, Paper 83-1A, p. 401-402.

Godfrey, J.D. and Langenberg, C.W.
1978: Metamorphism in the Canadian Shield of northwestern Alberta; in Metamorphism in the Canadian Shield, Geological Survey of Canada, Paper 78-10, p. 129-138.

Hanmer, S. and Lucas, S.B.
1985: Anatomy of a ductile transcurrent shear; the Great Slave Lake Shear Zone, District of Mackenzie; in Current Research, Part B, Geological Survey of Canada, Paper 85-1B, p. 7-22.

Irwin, A.B. and Prusti, B.D.
1955: O'Connor Lake (west half), District of Mackenzie, Northwest Territories, Geological Survey of Canada, Paper 55-9.

Langenberg, C.W.
1983: Polyphase deformation in the Canadian Shield of northeastern Alberta; Alberta Research Council Natural Resources Division, Bulletin 45, p. 1-33.

McGlynn, J.C., Hanson, G.N., Irving, E., and Park, J.K.
1974: Paleomagnetism and age of Nonacho Group sandstones and associated Sparrow dykes, District of Mackenzie; Canadian Journal of Earth Sciences, v. 11, p. 30-42.

Nielsen, P.A., Langenberg, C.W., Baadsgaard, H., and Godfrey, J.D.
1981: Precambrian metamorphic conditions and crustal evolution, northeastern Alberta, Canada; Precambrian Research, v. 16, p. 171-193.

Van Breemen, O, Henderson, J.B., Loveridge, W.D., and Thompson, P.H.
1987: U-Pb zircon and monazite geochronology and zircon unorphology of granulites and granite from the Thelon Tectonic Zone, Healey Lake and Artillery Lake map areas, N.W.T.; in Current Research, Part A, Geological Survey of Canada, Paper 87-1A report 83.

Structure and stratigraphy of the Paleozoic-Precambrian contact zone on White and Southampton islands, District of Keewatin

Project 840003

C.W. Jefferson and S.M. Hamilton[1]
Mineral Resources Division

Jefferson, C.W. and Hamilton, S.M., Structure and stratigraphy of the Paleozoic-Precambrian contact zone on White and Southampton islands, District of Keewatin; in Current Research, Part A, Geological Survey of Canada, Paper 87-1A, p. 451-455, 1987.

Abstract

The lowermost 10 m of Paleozoic strata on White Island are very recessive-weathering, intercalated friable sands and muds that unconformably overlie Precambrian gneisses and are conformably overlain by fossiliferous limestones of the Bad Cache Rapids Group. The unconformity overlain by this sequence dips gently to the southwest, as exposed on southwesterly facing slopes. The depositional contacts are offset by westerly to southerly trending, steeply dipping faults. Some faults have normal offsets. Other faults are high-angle reverse, with movement directed east-northeasterly. One of these is exposed on a steep east-facing slope. The reverse faults are interpreted to be compressive features tied into the evolution of the Boothia- Bell Arch, and related to distal continental margin plate tectonics of post-Early Silurian age.

Résumé

Les 10 mètres inférieurs de couches paléozoïques dans l'île White se composent de sables friables et de boues intercalés à altération récessive, qui reposent en discordance sur des gneiss précambriens et qui sont recouverts en concordance par des calcaires fossilifères du groupe de Bad Cache Rapids. La discordance sous-jacente à cette séquence est légèrement inclinée vers le sud-ouest et affleure sur les pentes sud-ouest. Les contacts synsédimentaires sont décalés par des failles à pendage abrupte, à orientation ouest ou sud. Certaines failles ont des rejets normaux. D'autres sont des failles inverses à fort pendage dont le mouvement était orienté est-nord-est. Une de ces failles est visible sur une pente est abrupte. Les failles inverses auraient été formées par compression au cours de l'évolution de l'arche de Boothia-Bell et seraient reliées à une marge continentale distale de la fin du Silurien inférieur soumise aux effets de la tectonique des plaques.

[1]Geology Department, Laurentian University, Sudbury, Ontario P3E 2C6

INTRODUCTION

The Paleozoic-Precambrian contact on the west side of White Island was examined in early July 1986 because of its potential for mineralization near faults that might have been active before, during and after deposition of the limestones. . This is one aspect of the non-renewable resource assessment of the Wager Bay- Southampton Island area which is being considered for a national park (Parks Canada, 1978). White Island has relatively good exposures of the Paleozoic-Precambrian contact which continues to the south on Southampton Island (Fig. 48.1). This contact and Ordovician-Silurian bioherms have potential for base metal and hydrocarbon resources (Sangster, 1970; Sanford, 1970). White Island was mapped at reconnaissance scales by Heywood (1967) and looked at only briefly by Sanford (in Heywood and Sanford, 1976). Revisions to lower Paleozoic stratigraphy proposed by Dewing et al. (1987) for Southampton Island are briefly discussed here.

The faults noted by Heywood (1967) and Heywood and Sanford (1976) trend both parallel and at high angles to the Paleozoic-Precambrian contact. On Southampton Island they appear to be responsible for rapid westward thickening of the Paleozoic strata (Sanford, in Heywood and Sanford, 1976). This paper will describe the nature of similar faults on White Island, provide some detailed information on the stratigraphy, and discuss related aspects of the non-renewable resource potential of White and Southampton islands.

STRATIGRAPHY

Precambrian rocks are dominantly migmatitic and mylonitic gneisses (unit 3) which were described by Heywood (1967) and Heywood (in Heywood and Sanford, 1976). These gneisses are also very much like those described by Henderson et al.(1986) around Wager Bay. The main additional feature noted on White Island is the common occurrence of retrogressed granulite facies rocks - greasy green leucocratic gneisses with milky quartz and rarely preserved orthopyroxenes. This metamorphic facies was not observed north of the Wager Bay Shear Zone although it is present south of the shear zone.

Few supracrustal rocks (unit 1) of Precambrian age were seen on White Island. One narrow unit on the west side of 358 Lake comprises abundant large garnets and sillimanite in a biotite-hornblende-quartz-feldspar gneiss, and minor magnetite iron-formation. Another band south of 358 Lake is truncated by the basal Paleozoic unconformity to the southeast and by a steeply dipping fault to the northeast. The northwest contact of the supracrustal band with the grey gneisses is a straight granitic mylonite with C and S fabric suggesting northwest-side- down extensional shear. The supracrustal unit is typically recessive; it includes garnet-biotite rich semipelites and calc-silicates. The southeastern part of the supracrustal belt includes unit 2 (amphibolite and ultramafic gneisses) as well as relict granulite facies leucogneisses containing relict orthopyroxenes.

The basal Paleozoic unconformity is well exposed above the supracrustal band and at the measured section ("S" on Fig. 48.1). Spheroidal weathering is well developed in the retrogressed granulites. A basal clastic sequence exposed at only one locality (S, Fig. 1) is 11 m thick but very recessive weathering and underlies the most extensive raised beach platform on White Island. It is mapped with unit 4. Sanford (in Heywood and Sanford, 1976) previously encountered at most 2 feet (0.6 m) of orthoquartzitic sandstone overlying the Precambrian gneisses.

The basal 4 m of the clastic sequence on White Island comprise friable to calcite-cemented granule conglomeratic quartzarenites 0-0.5 m thick, intercalated with unlithified rusty pyritic and sandy grey mud. The succeeding 6 m consist of brown-grey unlithified mud, the upper half containing hematite-coated sand and microfossil grains. The mud grades through about 1 m of thinly bedded calcareous shale and shaly fossiliferous limestone to medium bedded highly fossiliferous limestone of the lower Bad Cache Rapids Group.

Descriptions of the upper Bad Cache Rapids Group (unit 4), Churchill River Group (unit 5), Red Head Rapids Formation (unit 6) and Severn River Formation (unit 7) are given by Sanford (in Heywood and Sanford, 1976) with suggested revisions of stratigraphic and age relationships by Dewing et al. (1987). Briefly, the Bad Cache Rapids Group (unit 4) is an abundantly fossiliferous grey limestone of Middle Ordovician age. The age of the overlying Boas River oil shale (not found on White Island) is Late Ordovician. Dewing et al. (1987) described 90 cm of fossiliferous micrite at the base of the Boas River Shale, then stated that the contact between the Boas River Shale and the underlying Bad Cache River Groupo was not exposed. In actuality Sanford (in Heywood and Sanford, 1976 and personal communication, 1986) includes the 90 cm of fossiliferous micrite in the Bad Cache River Group and therefore the contact is exposed.

The Churchill River Group (unit 5) is an abundantly fossiliferous, brown, fine grained limestone not recognised on White Island but possibly present on the west side of 358 Lake (Fig. 48.1, detailed section C-D within A-B). Elsewhere on White Island the Churchill River Group and the upper part of the Bad Cache Rapids Group are interpreted to have been either not deposited or removed at an unconformity beneath the Red Head Rapids Formation (unit 6). Such an unconformity might be related to local uplift during the Ordovician (B.V. Sanford, personnal communication, 1986).

The Ordovician to possibly Silurian (Dewing et al., 1987) Red Head Rapids Formation (unit 6) consists of three units on Southampton Island which were described by Sanford (in Heywood and Sanford, 1976): (A) thin bedded, fine grained, orange-brown dolomite, (B) massive, thick bedded stromatolitic dolomite, and (C) stromatolite bioherms hosted by dolomitic algal laminite. The top of the Red Head Rapids Formation includes a discontinuous, thin, petroliferous, black shale known as the 16-Mile Brook Shale. (Dewing et al., 1987).

On the west side of 358 Lake, unit 6A in Figure 48.1 comprises reddish tan weathering, thin bedded to finely laminated unfossiliferous dolostones that overlie the Bad Cache Rapids Group. The Red Head Rapids Formation had not been

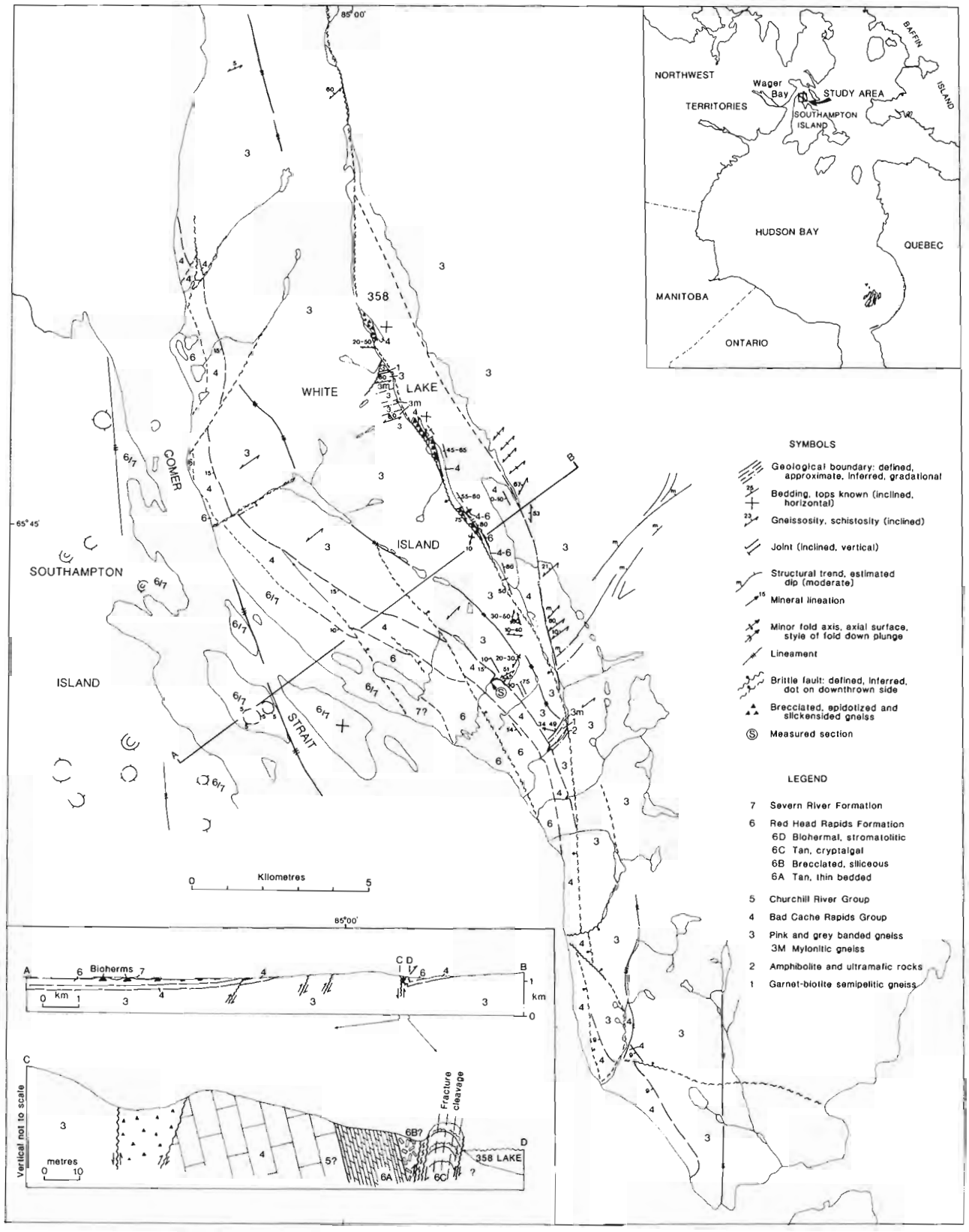


Figure 48.1 Location and geological sketch map of western White Island area. Cross-section A-B and map are at the same scale; C-D shows detail on west side of 358 Lake with vertical exaggeration not to scale.

previously been mapped here. On section C-D unit 6B is a brecciated vuggy limestone with minor chert; unit 6C is pale tan coloured, interbedded planar laminated and cryptalgal laminated limestone with some hemispherical stromatolites 5 to 10 cm in diameter.

On the west side of White Island the upper part of the Bad Cache Rapids Group is poorly exposed, and the base of Unit 6 was placed stratigraphically beneath a linear zone of algal bioherms that range in diameter from decimetres to more than 100 m. The outcrop consists mostly of vuggy reef core material: light grey finely crystalline limestone with vugs ranging in size from 0.1 to 5 cm. Lateral portions of the bioherms are brecciated and veined by coarse sparry calcite. Very poorly exposed dolomitic limestones beneath the bioherms are finely laminated.

The Severn River Formation (unit 7) is a yellow-brown particulate to abundantly fossiliferous dolostone of early Silurian age. Stratigraphic relationships with the underlying Red Head Rapids Formation are described by Sanford (in Heywood and Sanford, 1976) and by Dewing et al. (1987) (see Discussion, below). The lower beaches of western White Island are mono- lithologic gravels and appear to represent the immediately underlying bedrock. Areas mapped as unit 6/7 on the coast and on the small islands in Comer Strait (Figure 48.1) are underlain by dolostone comprising three interbedded components: (1) fine, planar to undulatory cryptalgal laminae; (2) crinoid hash with trilobites, brachiopods, small favosites and algal laminae; and (3) abundant ostracods with rare small trilobites in ex-micrite. All are now saccharoidal in texture and some beds have a faint petroliferous odour when broken.

The circular structures indicated on the westernmost small island are clearly visible on air photographs and have been described as "biohermal structures in unit 3 of Red Head Rapids Formation" by Sanford (in Heywood and Sanford, 1976, Plate 25). The lithology of the outcrop, however, includes the three components listed above, suggesting assignment to the Severn River Formation as described by Sanford (in Heywood and Sanford, 1976, p.25). Depositional dips are low, less than 5 degrees, and vuggy cores like those described above were not observed, therefore the domes may be the result of compactional drape over underlying bioherms of the Red Head Rapids Formation. Sanford (in Heywood and Sanford, 1976, p. 22) has noted that many such bioherms "occur in Middle Silurian terrane where they project upwards through the Severn River Formation."

STRUCTURE

Both depositional and fault contacts were observed between the Paleozoic and Precambrian rocks on White Island. The contact exposed at "S" (Figure 48.1) is depositional – granule conglomerate infills small irregularities on the peneplaned gneiss surface. The muddy part of the basal clastic sequence exposed at "S" is virtually unlithified and fault movements might be localized here. The mud is nevertheless interpreted to be a depositional undeformed unit because of the lack of shear, fold or cleavage structures and because of parallelism of bedding in the Bad Cache Rapids Group with that of the underlying sandstone units.

Similar depositional contacts are inferred to the north along the western side of White Island, and along the east side of 358 Lake. Shallowing of bedding from about 16 degrees southwesterly at the basal contact to subhorizontal on the islands in Comer Strait may be a result of faulting, but no lineaments or breccia were observed which could account for faults. Because the basement unconformity is tilted, basement deformation appears to have been involved, with Paleozoic cover as a passive rider.

Steeply dipping faults offset the Paleozoic-Precambrian contact described above. Some of these trend at high angles to the strike of the contact, and appear to be normal in offset. Many however trend obliquely or parallel to the contact. The curvature of their traces suggest that they are steeply dipping reverse faults.

Evidence of reverse faulting is best exposed along the west side of 358 Lake. The contact comprises the following components from west to east as shown in Figure 48.1: granitoid gneiss with structures trending southwesterly; crackle brecciated, epidotized and slickensided gneiss; tilted Paleozoic carbonates of the Bad Cache Rapids Group and Red Head Rapids Formation; and folded and fracture cleaved Red Head Rapids Formation bounded by fault gouged limestone. Dips in the tilted Paleozoic rocks range from subhorizontal to steep to the west and east. Slickensides suggest high-angle reverse movement on faults within the limestones that dip about 80 degrees to the west.

Segments of the reverse-fault structural sequence are offset by steeply dipping southwest-trending faults that do not affect the main mass of basement gneisses, and are truncated along a northerly trending major fault. This major fault extends along the length of White Island. To the south of 358 Lake it truncates the supracrustal and mylonite band described earlier. This band was not found in gneisses on the other side of the fault, suggesting strike-slip movement. Continuing south, the same fault separates southwesterly dipping Paleozoic strata and gneisses and appears to be a west-side-down normal fault. This major normal fault appears to post date reverse (and strike-slip?) movement recorded by the other faults.

DISCUSSION

The Paleozoic-Precambrian contact on the west side of White Island was examined because of its potential for base metal mineralization near faults that were active before, during and after deposition of the limestones. We were specifically looking for karst features, coarse vuggy secondary dolomite, unconformities, conglomerates, facies changes, and base metal sulphides. We found no direct evidence of pre- or syn-Paleozoic movement on the faults we examined, for example the limestones preserved around 358 Lake are similar in lithology to those along the coast of White Island. Field tests

for zinc were negative, and lithogeochemical and till samples are still being processed. Unconformities have been inferred from the lack of recognition of the Churchill River Group. The reefs might be restricted to specific fault-controlled zones such as Sanford et al. (1985) recognized in southern Ontario. These suppositions could not be confirmed on the scale that we were able to examine.

Dewing et al. (1987) suggested that the upper Red Head Rapids Formation is a restricted hypersaline facies of the lower Severn River Formation. Interfingering of the two formations could also be inferred from the interlayering of diversely fossiliferous (Severn River) and sparsely fossiliferous to ostracod-rich (Red Head Rapids?) facies in the Comer Strait area. These interpretations must be reconciled with observations by Sanford (in Heywood and Sanford, 1976, p. 21-23) that "the Red Head Rapids Formation is a consistent lithologic unit . . . in abrupt and disconformable contact with the succeeding Middle Silurian Severn River Formation . . . two samples submitted for conodont analysis yielded faunas that confirm a . . . Late Ordovician age". Two reconciliations are possible: (A) The disconformable contacts observed by Sanford might be in areas where marginal uplift caused erosion during the early Silurian, whereas the Hansine Lake (Dewing et al., 1987) and Comer Strait areas preserved more of the section; or (B) some units within the Severn River Formation look remarkably like units in the Red Head Rapids Formation, suggesting local restricted sedimentation during deposition of the Severn River Formation. In either case, the lower part of the Red Head Rapids Formation is Late Ordovician.

The faults examined here are similar to those described by Heywood and Sanford (1976). Who related development of the faults to a "post-Middle Silurian epeirogeny". Sanford et al. (1985) have related these faults to continent-wide patterns propagated from more intense deformation on the margins of North America related to plate tectonics. White and Southampton islands lie on the Bell Arch which is a continuation of the Boothia Arch.

Development of the Boothia Uplift has also been related to distant plate tectonic events by Okulitch et al. (1985). They specifically related post-Silurian unconformities, westward-directed folds and thrust faults involving the basement to compression during plate convergence recorded by the Caledonian Orogeny in Greenland. One problem with interpretation of the White Island structures is their northeasterly vergence. Perhaps the faults along the west side of 358 Lake were originally normal and east-side down, related to development of extensional half- graben structures. Subsequent compression may have been enough to cause folding but not to reverse the movement on the faults.

ACKNOWLEDGMENTS

This field study was jointly supported by Parks Canada, DIAND and EMR (both Polar Continental Shelf Project and Mineral Resources Division, GSC). Mikkel Schau kindly loaned us his helicopter while ours was unserviceable. D.C. Findlay, R.F.J. Scoates, W.A. Spirito and J.E.M. Smith contributed to the mapping and R. Lancaster provided expeditious technical support. This note benefited from critical reviews by B.V. Sanford and D.F. Sangster.

REFERENCES

Dewing, K., Copper, P. and Hamilton, S.
1987: Preliminary report on the stratigraphic position of oil shales in the lower Paleozoic of Southampton Island, District of Keewatin; in Current Research, Part A, Geological Survey of Canada, Paper 87-1, p. 000-000.

Henderson, J.R., LeCheminant, A.N., Jefferson, C.W., Coe, K. and Henderson, M.N.
1986: Preliminary account of the geology around Wager Bay, District of Keewatin; in Current Research, Part A, Geological Survey of Canada, Paper 86-1A, p. 159-176.

Heywood, W.W.
1967: Geological notes, northeastern District of Keewatin and southern Melville Peninsula, District of Franklin, Northwest Territories (Parts of 46, 47, 56, 57); Geological Survey of Canada, Paper 66-40, 20 p.

Heywood, W.W. and Sanford, B.V.
1976: Geology of Southampton, Coats, and Mansel islands, District of Keewatin, Northwest Territories; Geological Survey of Canada, Memoir 382, 35p.

Okulitch, A.V., Packard, J.J. and A.I. Zolnai
1985: Evolution of the Boothia Uplift, arctic Canada; Canadian Journal of Earth Sciences, V. 23, p. 350-358.

Parks Canada
1978: Wager Bay – A Natural area of Canadian significance; Parks Canada, 13 p.

Sangster, D.F.
1970: Geological exploration guides for Canadian lead-zinc deposits in carbonate rocks; in Guidelines to prospecting and mineral exploration, Proceedings of the Prospectors and Developers Association, 38th Annual Meeting, Canadian Mining Journal, v. 91, no. 4 (April), p. 49-51.

Sanford, B.V.
1970: Paleozoic stratigraphy of Southampton, Coats and Mansell Islands, District of Keewatin; in Report of Activities, Part A; Geological Survey of Canada, Paper 70-1A, p. 236-237.

Sanford, B.V., Thompson, F.J. and McFall, G.H.
1985: Plate tectonics – a possible controlling mechanism in the development of hydrocarbon traps in southwestern Ontario. Bulletin of Canadian Petroleum Geology, v. 33, no. 1, p. 52-71.

Middle Proterozoic granite-related mineralization in the Round Pond area, Labrador[1]

DSS Contract 27ST.23233-5-0062

Craig S. MacDougall[2] and Derek H.C. Wilton[2]

MacDougall, C.S. and Wilton, D.H.C., Middle Proterozoic granite-related mineralization in the Round Pond area, Labrador; in Current Research, Part A, Geological Survey of Canada, Paper 87-1A, p. 457-466, 1987.

Abstract

The Round Pond area is underlain by felsic volcanic and sedimentary rocks of the Early Proterozoic Upper Aillik Group, which were folded and intruded by post-tectonic granitic stocks. The area is characterized by numerous, widely distributed, pyritiferous gossans, magmatic-hydrothermal veins hosting ore mineral assemblages of Mo-(W)-Cu-Zn-Pb-U-F-Ba with minor enrichments of Co, Ag, Bi, Te, and Au, and stratabound radioactive zones. A crude ore mineral zonation is developed outwards from one of the intrusive stocks, from proximal Mo-(W)-Cu, to distal Mo-Zn, and Zn-U.

Alteration associated with the mineralized hydrothermal veins is dominated by the calc-silicate minerals diopside-hedenbergite, and andradite-grossularite, characteristic of a calcic skarn type alteration assemblage. Abundant quartz, fluorite, calcite, and lesser sphene, epidote, actinolite and biotite also occur.

The mineralization is epigenetic, related to the activity of shallow, post-tectonic granitic intrusions, and thus represents a significant departure from the style of mineralization that occurs inland in the Central Mineral Belt.

Résumé

La région de Round Pond repose sur des roches sédimentaires et volcaniques felsiques du groupe d'Upper Aillik du Protérozoïque inférieur. Ces roches sont plissées et recoupées par des petits massifs intrusifs granitiques post-tectoniques. La région se caractérise par la présence de nombreux chapeaux de fer pyriteux, de filons magmatiques-hydrothermaux contenant des cortèges de minéraux inétalliques (Mo-(W)-Cu-Zn-Pb-U-F-Ba) et de petites zones riches en cobalt, en argent, en bismuth, en tellure et en or, ainsi que des zones radioactives adhérant aux strates. Il y a zonation grossière des minéraux métalliques autour d'un des petits massifs, les minéraux dans la partie proximale étant riches en Mo-(W)-Cu, et dans la partie distale, en Mo-Zn et en Zn-U.

L'altération associée aux filons hydrothermaux minéralisés a surtout produit du diopside et de l'hédenbergite, ainsi que de l'andradite et du grossulaire, minéraux calco-silicatés caractéristiques d'un cortège formé par altération dans un skarn calcaire. On y trouve également beaucoup de quartz, de fluorite et de calcite ainsi que des quantités moins abondantes de sphène, d'épidote, d'actinote et de biotite.

La minéralisation épigénique est reliée à l'activité d'intrusions granitiques post-tectoniques peu profondes; elle est donc très différente du type de minéralisation trouvée à l'intérieur des terres, dans la zone minérale centrale.

[1]Contribution to the Canada–Newfoundland Mineral Development Agreement 1984-1989. Project carried by Geological Survey of Canada, Mineral Resources Division

[2]Department of Earth Sciences, Memorial University of Newfoundland, St. John's, Newfoundland A1B 3X5

LOCATION AND PHYSIOGRAPHY

The Round Pond area is within the northern coastal region of the Central Mineral Belt (CMB) of Labrador (Fig. 49.1), approximately 2 km south-southeast of the village of Makkovik. Round Pond is situated in a narrow north-northeast-trending valley, and is flanked to the east and west by low, rounded, exposed ridges with elevations ranging between 400 and 200 m respectively. Situated 1-2 km to the south and southeast of Round Pond is a rugged, poorly drained plateau consisting of discontinuous, subparallel, marshy draws with numerous small scattered ponds. This area contains numerous mineralized showings. Falls Lake is located approximately 5 km south of Round Pond, and drains northward into Round Pond through the Makkovik Brook, a turbulent river with numerous waterfalls and rapids.

Outcrop exposure is generally excellent in elevated ridge areas, approaching nearly 100%, but is very poor in the central valley region directly south of Round Pond.

PREVIOUS WORK

Numerous regional surveys have been carried out in coastal Labrador since the late 1800s. These early studies were based largely on descriptions of coastal outcrops (Lieber, 1860; Packard, 1891; Daly, 1902; Kranck, 1939, 1953). In more recent times, mineral exploration programs, as well as a number of petrologic, geochronological, and geochemical research studies have been carried out through the Central Mineral Belt. A detailed discussion of previous investigations has been given by Gower et al. (1982).

The discovery of uranium mineralization in 1954, 15 km south of Makkovik by M.J. Piloski (Piloski, 1955) working for Brinex Ltd., initiated extensive mineral exploration activity in the belt that spanned roughly 25 years. The most intensive exploration was carried out in the late 1960s by Brinex Ltd. and by Placer Development Ltd. in the late 1970s. Information on the exploration work is contained in unpublished exploration company reports (i.e. Brinex, Brinex-Cominco, Brinex-Urangeseschaft, Placer, etc.); a large number of reports remain confidential. Information concerning the regional, as well as local geological features associated with the widespread uranium and molybdenite mineralization within the Central Mineral Belt have been published by Beaven (1958), Gandhi et al. (1969), Gandhi (1978, 1986), and Gower et al. (1982). In addition, several undergraduate and graduate theses have been completed, generally in concert with mineral exploration activity. Those specifically related to the Round Pond area include studies by Sampson (1966), Barua (1969), and the structural work by Clark (1970, 1973).

The present investigation is a detailed metallogenic study of the mineralization hosted in the felsic volcanic rocks of the Upper Aillik Group in the Round Pond area undertaken as the basis of a M.Sc. program currently in progress by the first author at Memorial University of Newfoundland. The observations and conclusions presented within this report are preliminary and are based on work carried out during the 1985 field season, and subsequent research completed during the past academic year.

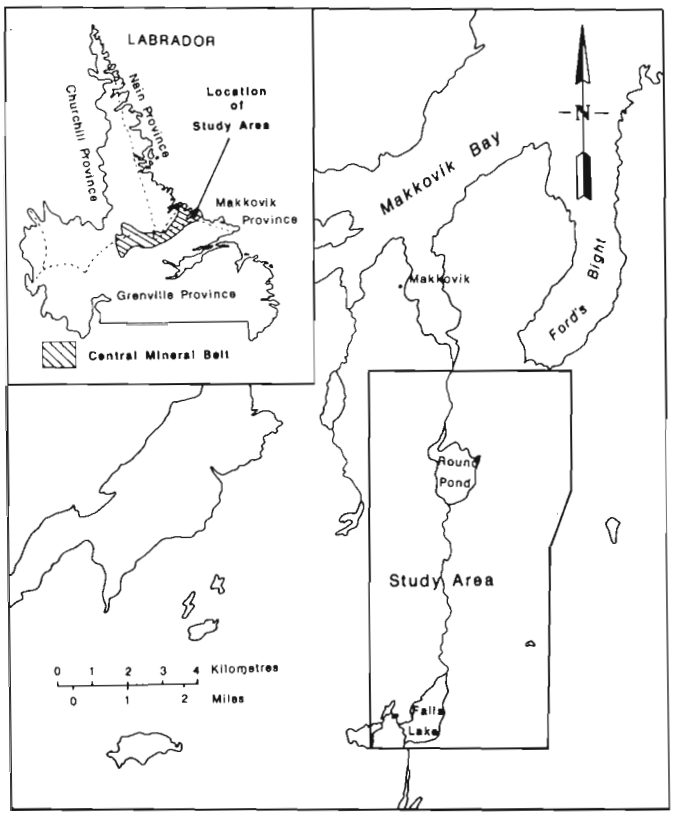


Figure 49.1. Location of the Round Pond study area, Central Mineral Belt, Labrador.

GENERAL GEOLOGY

The Round Pond area was mapped in the course of this investigation at a scale of 1:25 000, and the geology of the area is illustrated in Figure 49.2. The general stratigraphic sequence of the Upper Aillik Group in this area is shown in Figure 49.3, which also indicates the preferential association of mineral assemblages with certain host lithologies. The oldest rocks in the area (unit 1) are in the core of a major antiformal structure, and the units young towards the fold limbs.

The Upper Aillik Group is a thick pile of felsic volcanic rocks (rhyolites, tuffs and their subvolcanic equivalents), intermixed with felsic volcanic conglomerates/agglomerates, and amphibolitized basaltic volcanic rocks. Total thickness of the group was estimated by Gandhi et al. (1969) to be 7620 m. Recent geochronological work (Scharer, personal communication), on zircons obtained from rhyolites within the Upper Aillik near Makkovik, indicate an age of 1860 Ma.

The group was deformed and metamorphosed during the Hudsonian orogeny around 1600 Ma (Gandhi et al., 1969).

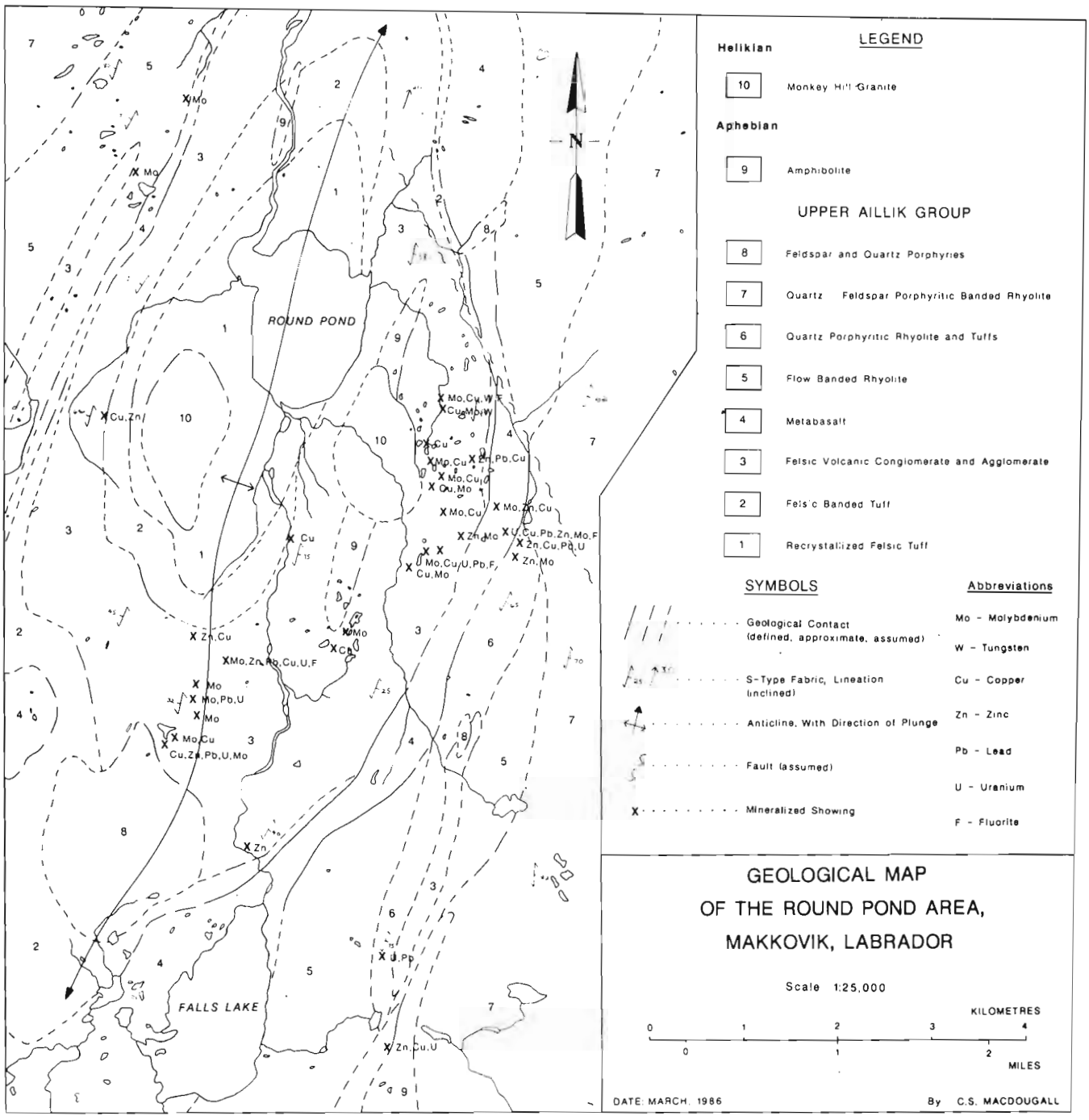


Figure 49.2. Geology and mineral occurrences of the Round Pond area, Makkovik, Labrador.

Metamorphism is of the upper greenschist/lower amphibolite facies, and is best defined by metabasaltic rocks. Complex polyphase deformational features have been interpreted by Clark (1973) to indicate at least four phases of deformation during the Hudsonian Orogeny. One of these phases was a major event which was responsible for the dominant north-northeast-trending structures and fabrics developed within the lithologies in the coastal regions. Structurally, the Round Pond area has been interpreted by previous workers (Gandhi et al., 1969; Clark, 1973) as a broad, open, northeast-trending, doubly plunging, antiformal structure, with a vertical axial plane, and a 40-60° dip on the fold limbs.

Within the Round Pond map area, two small, high level, post-tectonic, granitic stocks intrude the rocks of the Upper Aillik Group. The intrusions belong to the regionally extensive Monkey Hill Granite, which has been dated by K-Ar methods on biotite at 1620±60 Ma (Wanless et al., 1970),

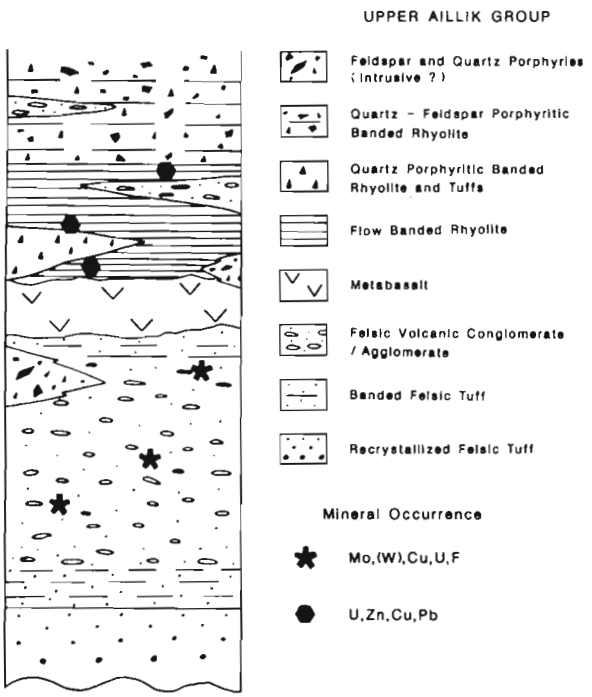


Figure 49.3. Simplified stratigraphic section of the Upper Aillik Group at Round Pond.

and thus related to the Hudsonian Orogeny. Contact metamorphic effects of the stocks are only locally developed. The Upper Aillik Group is also cut by a number of pre- to post-tectonic amphibolite and diabase dykes in the study area.

Previous workers have had some difficulty in interpreting unit 1. Gandhi et al. (1969) mapped this unit as a granoblastic feldspathic quartzite, whereas Clark (1973) favoured a plutonic origin and mapped it as a granodiorite. Gower et al. (1982) questioned Clark's interpretation, but lacked sufficient data to provide an equivocal interpretation of the unit. The lack of intrusive contact features, the presence of occasional quartz phenocrysts and felsic clasts, and the general similarity of this lithology to other felsic volcanic rocks in the area, suggests a volcanic origin, thus the unit is herein described as a recrystallized felsic tuff.

MONKEY HILL GRANITE

The Monkey Hill Granite is a homogenous, white to pink, fine to medium grained, equigranular, leucogranite. Its two stocks in the Round Pond area are small (<2 km in diameter) and elliptical in plan, elongated parallel to the fold axis of the dominant antiformal structure. Previous workers (e.g. Clark, 1973; Gower et al., 1982) also mapped a third smaller plug due south of Round Pond. Field work completed for this present study failed to verify this plug, although numerous pegamatitic dykes were observed.

Associated with the granitic intrusions are numerous granitic, pegmatitic, and aplitic dykes, which contain minor pyrite, fluorite, and molybdenite mineralization.

Field relations suggest that the stocks in the Round Pond area are shallow, epizonal intrusions. The granite-country rock contact is generally covered by overburden, but it is exposed on the northeast margin of the eastern stock. There the contact can be traced discontinuously for several hundred metres, and appears as a sharp discordant, intrusive contact, with the country rock only weakly contact metamorphosed.

Although the Monkey Hill intrusions are commonly referred to as "granite", their major mineral proportions of 30-40% quartz, 30-40% albite, 20-30% microcline, would classify them as "monzogranite" according to the I.U.G.S. modal classification scheme for granitic rocks (after Streckeisen, 1976). Granophyric and perthitic textures are extensively developed. Biotite, chlorite, and fluorite are the most abundant accessory minerals. Previous workers (Gandhi et al., 1969; Clark, 1973; Gower et al., 1982) also observed hornblende, sphene, epidote, and apatite as accessories within the granite, and pyrite, arsenopyrite, and molybdenite in associated veins. In the course of this investigation, magnetite, pyrite, and very rare flakes of molybdenite have been observed within the granite.

Chemical analyses (Table 49.1) reveal that Monkey Hill Granite is a highly differentiated, mildly peraluminous, corundum normative, granitic intrusion. The granite is high in silica, soda, potash, and alumina (averaging 75.7, 4.14, 4.63 and 13.1 wt. , respectively) and low in CaO (averaging 0.54 wt %). Combined Fe_2O_3, and MgO average 1.05 wt %. Trace element abundances (Table 49.1) are typical of evolved granites, with enrichments in Rb, Zr, Nb, Y, and U, average to low Sr, and low Ba contents compared to the compiled average for low Ca granites (Turekian and Wedepohl, 1961). Rb/Sr ratios vary from 0.77 to 12.6, but average around 3.3. Fluorine values, however, average 435 ppm, and are significantly below average for low Ca granites. This is apparently contradictory in view of the highly differentiated nature of the granite, the occurrence of fluorite as an accessory mineral, and the abundance of mineralized fluorite veins in the immediate area. But as Bailey (1977) has pointed out, during differentiation towards more siliceous melts, there is an increasing loss of F to the vapour phase. In the case of the Monkey Hill Granite, such a phase escaped to form various hydrothermal fluorite veins, leaving the crystallizing granite low in F. This interpretation is also consistent with F-zoned granite intrusions listed by Bailey (1977), which consist of a F-rich residual granite that exhibits degassed margins containing only 400-600 ppm F.

Rare earth elements from the Monkey Hill Granite show typical fractionated patterns, with HREE depleted relative to LREE (see Fig. 49.4). With increasing SiO_2 (i.e. differentiation) the overall REE contents decrease, and the REE profiles become flatter. This is a common observation (Hansen, 1980), and is probably due to fractional crystallization of accessory minerals such as allanite or monazite that contain high abundances of REE (Cullers and Graf, 1984). However,

Table 49.1 Geochemical analyses of the Monkey Hill Granite stock at Round Pond

	18	19	28	39	53	56	121	122	171	171A	180	181
SiO_2 wt%	76.4	76.4	73.5	75.4	77.4	76.1	77.8	73.8	72.4	75.8	76.6	76.6
TiO_2	0.08	0.08	0.12	0.04	0.00	0.04	0.00	0.08	0.08	0.04	0.04	0.04
Al203	12.8	12.5	13.6	13.2	12.5	13.3	12.7	14.1	14.1	13.1	12.7	13.0
Fe203 (total Fe)	0.58	0.67	1.53	0.95	0.63	0.71	0.39	1.65	1.60	0.81	0.61	0.61
MnO	0.01	0.01	0.04	0.01	0.00	0.01	0.01	0.06	0.06	0.02	0.01	0.01
MgO	0.05	0.04	0.36	0.21	0.04	0.08	0.04	0.40	0.40	0.14	0.06	0.06
CaO	0.38	0.18	0.82	0.64	0.32	0.54	0.34	0.32	1.08	0.52	0.40	0.40
Na20	3.96	3.80	4.39	3.88	4.19	4.16	4.34	4.39	4.34	3.99	3.98	3.98
K20	4.79	5.06	4.58	5.20	4.40	4.50	4.28	4.49	4.56	4.87	4.63	4.63
P205	0.01	0.02	0.03	0.02	0.00	0.00	0.00	0.03	0.02	0.01	0.00	0.00
LOI	0.41	0.53	0.76	0.66	0.42	0.39	0.32	0.44	0.90	0.54	0.30	0.30
F g/t	90	140	580	610	400	160	540	540	750	970	110	140
Pb	20	24	22	22	68	39	34	30	33	23	28	30
U	9	7	1	1	4	10	11	7	8	4	0	3
Th	22	9	17	15	32	10	19	10	24	22	14	16
Rb	175	177	184	184	200	176	214	174	183	188	175	170
Sr	53	103	197	136	22	87	17	227	212	62	73	62
Y	11	12	22	15	17	15	16	29	29	23	11	17
Zr	71	92	121	101	82	68	86	124	132	88	77	56
Nb	15	12	16	13	19	12	18	18	20	12	12	8
Ga	19	17	21	19	22	20	22	20	19	19	19	19
Zn	0	0	8	–	59	0	0	34	11	0	0	0
Cu	6	11	5	27	38	12	12	5	6	17	6	5
La	0	0	2	7	0	0	0	23	20	2	0	0
Ce	38	0	63	36	65	16	48	99	31	84	50	74
Ba	66	333	438	307	0	185	0	482	466	133	75	48
Ni	0	0	0	0	0	0	0	0	0	0	0	0
V	0	1	0	0	0	0	0	0	3	0	0	0
Cr	0	0	0	0	0	0	0	0	0	0	0	0

Note: Samples 53 and 121 taken from west granite stock, all others from east granite stock in Round Pond area.

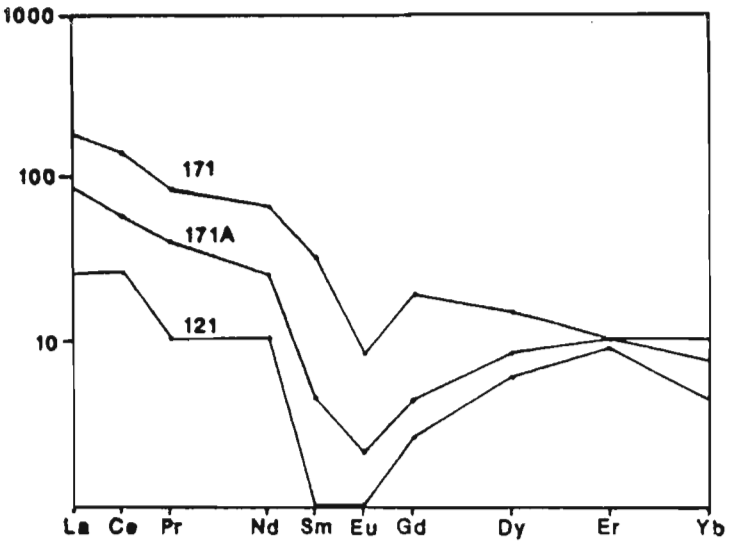


Figure 49.4. Chondrite-normalized REE patterns for the Monkey Hill Granite. SiO_2 content increases from sample 171 through 171A to 121 (see text). Normalized to the chondrite values of Taylor and Gorton (1977).

increasing SiO_2 is also marked by significant depletions in Sm and Gd, which together with the typically low Eu, suggests a fractionation of the MREE with differentiation. This may be due to crystallization of apatite which could remove the middle REE. A decrease in P_2O_5 with increasing SiO_2 (see Table 49.1) seems to support this.

The above data suggest that the stocks in the Round Pond area are highly differentiated, apical portions of a large granitic batholith present at depth. Kerr (1986) has reached similar conclusions based on the preliminary results of his regional granite study. Such intrusions are considered to be favourable sites for the accumulation of metal-bearing, volatile-rich phases (Mutschler et al., 1978; Stemprok, 1980), which can ultimately result in the formation of mineral deposits. The occurrence of mineralized hydrothermal fluorite veins in the Round Pond area, that are commonly associated with shallow seated plutons, clearly lends support to this interpretation.

MINERALIZATION

General features

The Round Pond area was extensively explored from 1963-1969 (see summary in Gower et al., 1982), and numerous Mo-Cu showings were discovered. Several linear radioactive zones were also reported near Falls Lake. Although the mineralization is widely distributed (Fig. 49.2), there appears to be a dominant lithological control with respect to the localization of mineralization (Fig. 49.3). Mo-base metal-U-F-(W) showings are heavily concentrated around the contact zone of the east stock of Monkey Hill Granite. The mineralization is hosted in the felsic volcanic conglomerate, and appears to be associated with fractures and shear zones, probably related to the intrusion of the granitic stock. A similar intrusive stock to the west intrudes a recrystallized felsic tuff unit, and does not appear to be associated with any significant mineralization. This suggests that the felsic volcanic conglomerate was a favourable lithologic unit for the localization of mineralization, probably related to a greater permeability due to structural weakness, compared to other lithologies in the Round Pond area. Similar mineralization northwest of Falls Lake is also hosted in the felsic volcanic conglomerate. Linear radioactive zones in contrast, are predominantly restricted to the rhyolite units.

Types of mineralization

1) Granite-hosted mineralization

Disseminated pyrite, fluorite, and very rare flakes of molybdenite occur within the Monkey Hill Granite, and associated pegmatitic, granitic, and aplitic dykes. Although the mineralization is of limited economic importance, it provides an important genetic link regarding the source of the mineralization in the Round Pond area. The potential exists for mineralization hosted within unexposed portions of the Monkey Hill plutons.

2) Pyritiferous gossan zones

Rusty pyritiferous gossan zones hosted in felsic tuffs, rhyolites, and volcanic conglomerates represent the most abundant type of mineralization in the Round Pond area. The gossans appear as lightly to moderately rusted, linear zones up to a kilometre in length. Mineralization is dominated by disseminated pyrite, with traces of molybdenite, chalcopyrite, sphalerite, fluorite, and rare galena. Where gossan zones are intruded by diabase dykes, mineralization appears to be concentrated towards the intrusive contacts. The dykes themselves are unmineralized, suggesting that the concentration represents a secondary redistribution of mineralization within the gossan zones.

3) Stockwork mineralization

Finely disseminated pyrite-molybdenite in the anastomozing siliceous matrix of a brecciated porphyroblastic metabasalt was observed at only one location, but represents a previously unrecognized style of mineralization. The showing occurs at the base of metabasalt (unit 4), distal from the main concentration of showings around the east stock of Monkey Hill Granite. Trace element analysis (Wilton et al., in press) indicate a significant enrichment in Zn and Ag.

4) Carbonate vein-hosted Zn(Pb)

Significant sphalerite (with minor pyrite, galena, fluorite and chalcopyrite) hosted in a carbonate breccia zone represents a significant new showing in the Round Pond area. The showing occurs distally from the east granitic stock, in a brecciated talus slope along a ridge, and appears to be fault controlled. Unfortunately, the extent of mineralization was not fully determined. Microprobe analysis (Wilton et al., in press) indicates that the sphalerite has very low Fe contents, suggesting a low temperature of formation for the sphalerite.

5) Hydrothermal veins

Discordant hydrothermal veins in the Upper Aillik Group represent the most significant mineralization in the Round Pond area. Most occur proximal to the eastern stock of Monkey Hill Granite, but one vein system occurs northwest of Falls Lake, and may be related to the large intrusive body of Monkey Hill Granite that occurs west of the study area. The vein systems are small, ranging from tens of centimetres to several metres wide, with lengths up to 100 m. Often veins disappear under low, swampy, grassy areas, suggesting that they might extend farther along strike. The vein systems appear to be associated with zones of shearing, and locally brecciation is developed. Alteration assemblages are generally developed in country rock adjacent to vein systems. Mineralization within the hydrothermal veins is often spectacular, and reflects a hydrothermal assemblage of Fe-Mo-(W)-Cu-Zn-Pb-U-F-Ba, with minor enrichments in Co, Ag, Bi, Te, and Au. Gossan zones are always associated with the hydrothermal veins, which suggests that other gossan zones distributed throughout the Round Pond area are the result of hydrothermal activity, and may be closely related to vein systems not presently exposed. Primarily three types of mineralization are recognized as hydrothermal veins: massive and stockwork sulphides, mineralized fluorite veins, and quartz-molybdenite veins. A crude paragenetic sequence is developed from early massive sulphides, to later crosscutting mineralized fluorite and quartz veins.

a) Mineralization within massive and stockwork sulphide zones is dominated by pyrite, pyrrhotite, magnetite, chalcopyrite, with minor molybdenite, fluorite, and barite. Scheelite has also been identified, and generally occurs as discrete grains (<20 um) in pyrite. The pyritiferous sulphides also host a variety of Bi, Ag, Pb tellurides, and minor silver sulphides. Geochemical analyses also revealed significant enrichment in Co, reflecting the substitution of Co for Fe in pyrite. Analysis for Au within massive sulphides indicate anomalous background values for the mineralization in the Round Pond area. In view of these anomalous values, and the occurrence of various Bi, Ag, Pb tellurides, the potential exists for significant Au mineralization.

b) Fluorite veins are found as fracture fillings and slightly discordant veins within massive sulphide and rusty siliceous zones. Veins consist of finely crystalline, deep purple fluorite (with local quartz and adularia) hosting pyrite, phrrhotite, molybdenite and minor chalcopyrite.

All of these fluorite veins have significant uranium mineralization, with enrichments in Zn, Pb, and Ag. The uranium mineralization occurs as pitchblende in the form of either small individual grains, or as rims on zircons (Fig. 49.5), and is easily observed under the microscope as metamict patches in fluorite. A unique fluorite-amphibole vein was also observed as the contact of the metabasalt and rhyolite. The vein is 10-15 cm wide and consists of large (10 cm in length) euhedral hornblende crystals with fluorite and biotite. The vein is highly radioactive (>5000 ppm U), and contains chalcopyrite, molybdenite, galena, and sphalerite, with significant Ag enrichment.

c) Quartz-molybdenite veins have provided some of the most spectacular molybdenite mineralization in the Round Pond area. The veins are generally 2-10 cm wide, and appear to crosscut earlier hydrothermal mineralization. The veins consist of quartz with "booklets" of molybdenite, minor pyrite and chalcopyrite. The molybdenite "booklets" are generally concentrated at the vein margins, with finer, randomly orientated flakes permeating the country rock, or occurring as concentrations along fracture planes.

6) Linear radioactive zones

Linear radioactive zones represent a different mineralizing style from the Mo-base metal-U-F mineralization. The radioactive zones occur primarily east of Falls Lake, and are known as showings #16, 17 and 18 (Piloski, 1955). Two other important showings also occur, one northwest of Falls Lake, the other southeast of Round Pond. Except for the showing northwest of Falls Lake, the radioactive zones are hosted in meta-rhyolites. The 2-5 m wide zones can be traced up to several hundred metres in length and are quite distinctive, appearing red to pink as a result of hematization. At showings 16 and 17, the mineralization is concentrated at the contact of a porphyroblastic amphibolite with the rhyolite. The uranium mineralization occurs as discrete grains of pitchblende, or as intergrowths with sphene (Gandhi, 1978), that are disseminated throughout the hematized zones, or concentrated with black amphiboles (hornblende) in veinlets and fracture fillings. Significant sphalerite mineralization, with minor chalcopyrite, galena, pyrite, and anomalous Ag values are typically associated. Apatite and minor fluorite are associated with the mineralization, and may indicate that phosphate (and possibly fluorine) complexes were involved in the transport metals in mineralizing fluids.

The showing northwest of Falls Lake appears to be slightly different from the other radioactive zones. Although characterized by the same red hematized alteration and uranium mineralization, it also exhibits characteristics more typical of the Mo-base metal-U-F mineralization. It is hosted within the volcanic conglomerate, and is dominated by Cu mineralization, with only minor sphalerite. Molybdenite, pyrite, galena, and fluorite also occur. More importantly however, the showing shows a significant enrichment in Ag and Au. A grey crumbly mineral that may be stromeyerite (Ag, Cu)S_2 is found in the showing. A similar ore mineral assemblage was reported by Beavan (1958) at showing #7-11, and suggests that a correlation between Cu-U and Au-Ag mineralization may exist within the Upper Aillik Group.

Alteration

Alteration associated with the mineralized hydrothermal veins is restricted to areas immediately adjacent to the veins. The alteration is dominated by calc-silicates, primarily diopside-hedenbergite, and andradite-grossularite. Abundant quartz, fluorite, calcite, and lesser sphene, epidote, actinolite, and biotite also occur. Scapolite porphyroblasts are often observed in nearby dykes, and locally, silicic, chloritic and sericitic alteration is developed. The alteration assemblage is typical of that observed in calcic-skarn type environments, and is very similar to altered mineralized limestone intercalations reported by Beavan (1958) and Wilton et al. (in press) south of Makkovik. An interesting feature of the calcic skarn type alteration observed in the Round Pond area, is that it occurs in a felsic volcanic conglomerate, that in unaltered samples contains 3.0 wt % Ca0 to values that range between 6.0 and 12.0. Associated with the increase in Ca, are slight enrichments in K, along with minor decreases in Na.

Alteration in the linear radioactive zones is dominated by the distinctive red hematization. Gandhi (1978) stated that these zones in the Round Pond area were enriched in Na_20 (>6.0 wt %), and depleted in K_20 (<0.1 wt %). Although major element analyses are not yet complete, the abundance of abitized phenocrysts reported by Gandhi has been observed. This enrichment of Na, and depletion of K has been reported for many of the U showings throughout the Aillik Group (White, 1976; Gandhi, 1978; Kontak, 1980; White and Martin, 1980; Gower et al., 1982).

Source of mineralization

The source of widespread U-Mo mineralization within the Upper Aillik Group of the Central Mineral Belt has generally been thought (Gandhi et al., 1969; Gandhi, 1978; Gower et al., 1982) to be the magma that formed the felsic volcanic rocks of the Upper Aillik Group (i.e. syngenetic with Upper Aillik volcanism). Wilton and Wardle (1986) and Wilton et al. (in press) indicated that Mo and U mineralization in the Makkovik region of the Upper Aillik group was probably related to post-tectonic granitoids. The mineralization in the Round Pond area is significantly different from most other mineral occurrences in the Upper Aillik Group (especially those inland in the Michelin Deposit area), and the evidence gathered throughout the course of this investigation clearly points to the small plugs of Monkey Hill Granite as the source of the Mo-base metal-U-F mineralization.

The hydrothermal veins, being discordant with regional trends, are post-tectonic, as are the granitic intrusions. Recent Pb isotope analyses of galena mineralization from Big Bight,

northeast of Round Pond, have indicated an age of mineralization of 1529 + 112/-56 Ma. This is clearly within the reasonable error limits of the age of granitic intrusions in the area (i.e. the Monkey Hill Granite at 1620±60 Ma).

The source of mineralization associated with the linear radioactive zones near Falls Lake is not as readily apparent. Uranium mineralization in other zones throughout the Aillik Group has generally been related to leaching of the felsic volcanic rocks by hydrothermal fluids (Gandhi, 1978; Gower et al., 1982). However, Wilton et al (in press) believed that the uranium mineralization farther north in the Makkovik area was the product of the post-tectonic granitoid intrusives. Certainly, the association of molybdenite and uranium in magmatic-hydrothermal veins (Fig. 49.6) suggests a common source, the Monkey Hill Granite. The granite, which is enriched in U, also contains rare molybdenite. The occurrence of a showing northwest of Falls Lake that exhibits characteristics of both linear radioactive zones and mineralized magmatic hydrothermal veins, and the presence of fluorite in the radioactive zones, suggests that the two types may be related to similar processes. Whether the ultimate source of mineralization at Falls Lake was U-rich granitic intrusions, or the felsic volcanics, remains to be resolved.

Genetic model for mineralization

Based on the features discussed in this report, an epigenetic magmatic-hydrothermal mineralization is envisaged (Fig. 49.7).

The deformed felsic volcanic rocks of the Upper Aillik Group were intruded by the post-tectonic Monkey Hill Granite during the last stages of the Hudsonian Orogeny. The intrusions in the Round Pond area are small, highly differentiated, eipzonal stocks, that represent the higher levels or apical portions of a larger granitic batholith at depth. These small stocks were favourable sites for the accumulation of oxidized, metal-bearing, volatile phases during differentiation and crystallization of the granite.

The emplacement of the granitic stocks and subsequent boiling of the volatile-rich phase produced structural weaknesses in favourable or incompetent lithologies (i.e. felsic volcanic conglomerate). The induced structural weakness produced fractures, and zones of brecciation and shearing that were concentrated adjacent to the contact of the granitic stock, and allowed the escape of the metal-bearing, volatile-rich phase as oxidized magmatic-hydrothermal fluids. The



Figure 49.5. A zircon crystal (grey) with a pitchblende core and rim (white) in a fluorite vein. Pitchblende also occurs as individual grains (white) associated with flakes of molybdenite (medium grey).



Figure 49.6. A flake of molybdenite (medium grey) in a fluorite vein with small inclusions of pitchblende (white), and zircon (drak grey). Pitchblende and galena also occur as small scattered grains throughout the photograph.

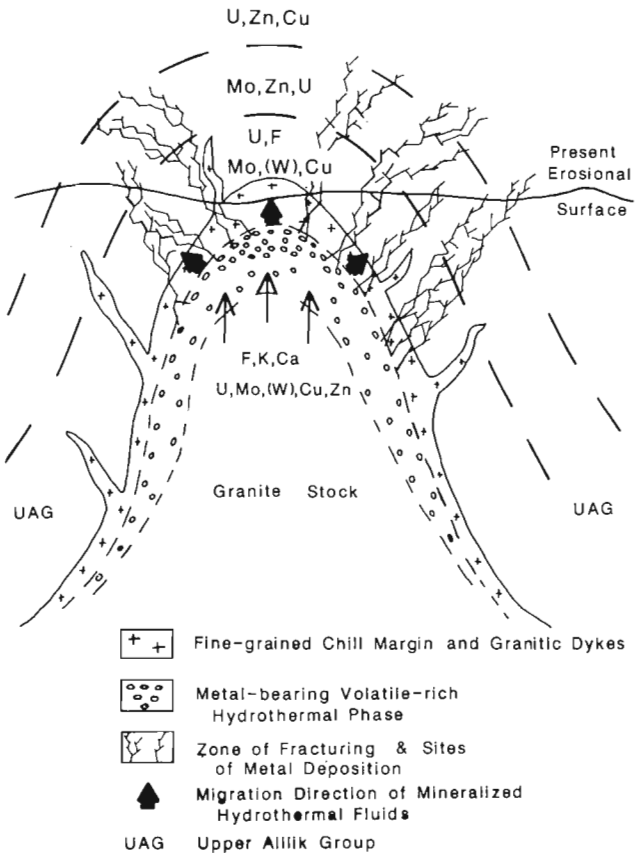


Figure 49.7. An idealized schematic diagram representing a genetic model for the Mo-(W)-base metal-U-F mineralization in the Round Pond area.

metals were probably transported within these fluids as various fluoride and phosphate complexes. The movement of these hot hydrothermal fluids through the cold country rock resulted in disequilibrium reactions which produced the associated calc-silicate alteration. The Ca necessary for these reactions would be in part supplied directly by the hydrothermal fluids, as well as by the Ca-bearing country rocks (i.e. the conglomerate).

Deposition of the metals as various sulphides occurred in response to increasing pH as a result of fluid-wall rock reactions, and the loss of volatiles during boiling of the hydrothermal fluids. In addition, the precipitation of fluorite (due to its lower solubility under low P-T conditions according to Bailey, 1977) and apatite would reduce the fluoride and phosphate activities as complexing agents (Romberger, 1984), and thus promote further metal deposition. Metal zonation outwards from the granite reflects the mobility of the various metals during the physio-chemical evolution of the hydrothermal fluid.

The linear radioactive zones in the southeastern portion of the map area may be directly related to the processes discussed above, or represent a much later redistribution of initially granite-related U and Zn, Cu mineralization by oxidized hydrothermal fluids generated during the Grenville Orogeny. The occurrence of apatite, and enriched P contents suggests that phosphate complexes were responsible for the mobilization and transport of metals in these zones.

Acknowledgments

This research work, undertaken as an MSc study by the first author at Memorial University, was financially supported by the Geological Survey of Canada through ERDA Agreement II-2 and through an NSERC Northern Supplement Grant to Wilton. We wish to acknowledge the logistical support of the Newfoundland Department of Mines and Energy from R.J. Wardle, A. Kerr, K. O'Quinn and W. Tuttle. We have benefited greatly from discussions with T. Birkett, P.L. Dean, B.J. Fryer, S.S. Gandhi, C.J. Gower, A. Kerr, L.M. MacKenzie, A.B. Ryan, D.F. Strong and R.J. Wardle. We are grateful to C. Pumphrey for able field assistance. Geochemical preparation and analyses were aided and/or completed by G. Andrews, C. Emerson, P. Moore, D. Press and G. Veinott of Memorial University.

The paper was critically reviewed by S.S. Gandhi and T. Birkett of the Geological Survey of Canada.

REFERENCES

Bailey, J.C.
1977: Fluorine in granitic rocks and melts: a Review; Chemical Geology, 19, p. 1-42.

Barua, M.C.
1969: Geology of uranium-molybdenite bearing rocks of the Aillik-Makkovik Bay area, Labrador; M.Sc. thesis, Queen's University, Kingston, Ontario, 76 p.

Beavan, A.P.
1958: The Labrador uranium area; Proceedings of the Geological Association of Canada, v. 10, p. 137-145.

Clark, A.M.S.
1970: A structural reinterpretation of the Aillik series, Labrador; M.Sc. thesis, Memorial University of Newfoundland, St. John's, 76 p.

Clark, A.M.S.
1973: A reinterpretation of the stratigraphy and deformation of the Aillik Group, Makkovik, Labrador; Ph.D. thesis, Memorial University of Newfoundland, St. John's, 346 p.

Cullers, R.L. and Graf, J.L.
1984: Rare earth elements in igneous rocks of the continental crust: Intermediate and silicic rocks – ore petrogenesis; in P. Henderson, ed., Rare Earth Element Geochemistry, Elsevier, New York, p. 237-274.

Daly, R.A.
1902: The geology of the northeast coast of Labrador; Bulletin of Comparative Zoology, Harvard, v. 38, Geological Series, v. 5, no. 5, p. 205-269.

Fryer, B.J.
1977: Rare earth evidence in iron formation for changing oxidation states; Geochimica et Cosmochemica Acta, v. 41, p. 361-367.

Gandhi, S.S.
1978: Geological setting and genetic aspects of uranium occurrences in the Kaipokok Bay–Big River area, Labrador; Economic Geology, v. 73, p. 1492-1522.

Gandhi, S.S.
1986: Uranium in Early Proterozoic Aillik Group, Labrador; in Uranium Deposits of Canada, ed. E.L. Evans; Canadian Institute of Mining and Metallury, Special Volume 33, p. 70-82.

Gandhi, S.S., Grasty, R.L. and Grieve, R.A.F.
1969: The geology and geochronology of the Makkovik Bay area, Labrador; Canadian Journal of Earth Sciences, v. 6, p. 1019-1034.

Gower, C.F., Flanagan, M.J., Kerr, A. and Bailey, D.G.
1982: Geology of the Kaipokok Bay–Big River area, Central Mineral Belt, Labrador; Newfoundland Department of Mines and Energy, Report 82-7, 77 p.

Hanson, G.N.
1980: Rare earth elements in petrogenetic studies of igneous systems; Annual Review Earth Planetary Science, v. 8, p. 371-406.

Henderson, P.
1984: General geochemical properties and abundances of the rare earth elements; in Rare Earth Element Geochemistry, ed. P. Henderson, Elsevier, Oxford, p. 1-31.

Kerr, A.
1986: Plutonic rocks of the eastern Central Mineral Belt: general geology and description of regional granitoid units; in Current Research, Newfoundland Department of Mines and Energy, Report 86-1, p. 89-100.

Kontak, D.J.
1980: Geology, geochronology and uranium mineralization in the Central Mineral Belt of Labrador, Canada; MSc. thesis, University of Alberta, Edmonton, 378 p.

Kranck, E.H.
1939: Bedrock geology of the seaboard region of Newfoundland and Labrador; Geological Survey of Newfoundland, Bulletin 19, 44 p.

Kranck, E.H.
1953: Bedrock geology of the seaboard of Labrador between Domino Run and Hopedale, Newfoundland; Geological Survey of Canada, Bulletin 26, 41 p.

Lieber, O.M.
1860: Notes on the geology of the coast of Labrador; Report of the United States Coast Survey for 1860.

Mutschler, F.E., Wright, E.G., Ludington, S. and Abbott, J.T.
1981: Granite molybdenite systems; Economic Geology, v. 76, p. 874-897.

Packard, A.S.
1891: The Labrador coast. New York, N.D.C. Hodges (publisher), 513 p.

Piloski, M.J.
1955: Geological report on the Aillik–Shoal Lake area; unpublished report, Brinex Ltd.

Piloski, M.J.
1960: Report on exploration in the Southwest Potash–Brinex joint venture area, Aillik Bay, Labrador; unpublished report, Brinex Ltd.

Romberger, S.B.
1984: Transport and deposition of uranium at temperatures up to 300°C: geological implications; in Uranium Geochemistry, Mineralogy, Geology, Exploration, and Resources, B. DeVivo, F. Ippolito, G. Capaldi, and P.R. Simpson, (ed.), Institute of Mining and Metallurgy, p. 12-17.

Sampson, C.J.
1966: The geology of the Round Pond–Cross Lake area, Labrador; Unpublished thesis, Imperial College of London, 65 p.

Stemprok, M.
1980: Differentiation of some elements by ore-bearing granites; Metallization Associated with Acid Volcanism, v. 3, p. 393-403.

Streckheisen, A.
1976: To each plutonic rock its proper name; Earth Science Review, 12, p. 1-33.

Taylor, S.R. and Gorton, M.P.
1977: Geochemical application of spark source mass spectrography — III element sensitivity, precision and accuracy; Geochimica Cosmochemica Acta, v. 29, p. 1243-1261.

Turekian, K.K. and Wedepohl, K.H.
1961: Distribution of the elements in the earth's crust; Geological Society of America Bulletin, v. 72, p. 175-192.

Wanless, R.K., Stevens, R.D., Lachance, G.R. and Delabio, R.N.
1970: Age determinations and geological studies, K-Ar isotopic ages, Report 9; Geological Survey of Canada, Paper 69-2A, p. 73-74.

White, M.V.W.
1976: A petrological study of acid volcanic rocks of the Aillik Series, Labrador; MSc. thesis, McGill University, Montreal, 92 p.

White, M.V.W. and Martin, R.F.
1980: The metasomatic changes that accompany uranium mineralization in the nonorogenic rhyolites of the upper Aillik Group, Labrador; Canadian Mineralogist, v. 18, p. 459-479.

Wilton, D.H.C. and Wardle, R.J.
(in press) Two contrasting granophile and non-granophile metallogenic styles in the early Proterozoic Upper Aillik Group, Central Mineral Belt, Labrador. Manuscript submitted to Min. Deposita.

Uranium, molybdenum and base metal sulphide mineralization: three different styles of ore formation in the Burnt Lake area, central Labrador[1]

DSS Contract 27ST.23233-5-0062

Leonard M. MacKenzie[2] and Derek H.C. Wilton[2]

MacKenzie, L.M. and Wilton, D.H.C., Uranium, molybdenum and base metal sulphide mineralization: three different styles of ore formation in the Burnt Lake area, central Labrador; in Current Research, Part A, Geological Survey of Canada, Paper 87-1A, p. 467-476, 1987.

Abstract

The Burnt Lake area is underlain by rocks of the Upper Aillik Group, which consists of siltstones and sandstones overlain by a mixed felsic volcanic assemblage of lapilli tuffs, ash flow tuffs, and varied porphyries (welded and nonwelded). The stratigraphically lower sedimentary rocks host the Emben uranium showings, while the Burnt Lake uranium showings are hosted by the felsic volcanic rocks. Near the Burnt Lake camp, the Upper Aillik Group is intruded by a high level, leucocratic, post-tectonic granite. Differentiation trends in geochemical data for this granite indicate vapour phase concentration towards the top of the pluton. Significant concentrations of molybdenite occur along the contact of this granite with meta-felsic volcanic rocks. The styles of uranium mineralization at the Emben and Burnt Lake showings are different, suggesting dissimilar ore-forming processes. There also appears to be a later base metal sulphide mineralization superimposed on the Burnt Lake showing.

Résumé

La région de Burnt Lake repose sur les roches du groupe d'Upper Aillik, qui se composent de siltones et de grès sous-jacents à un ensemble volcanique felsique mixte qui comprend des conglomérats volcaniques à lapillis, des tufs de cendres et divers porphyres lithifiés et non lithifiés. Les roches sédimentaires stratigraphiquement inférieures contiennent les venues d'uranium d'Emben, tandis que les venues d'uranium de Burnt Lake sont encaissées dans des roches volcaniques felsiques. Près du camp de Burnt Lake, le groupe d'Upper Aillik est recoupé par un granite leucocrate post-tectonique structuralement élevé. La différenciation géochimique de ce granite indique qu'il y a eu concentration de la phase vapeur vers le sommet du pluton. On trouve des concentrations élevées de molybdénite le long du contact entre le granite et les roches volcaniques felsiques métamorphiques. Les modes de minéralisation uranifère ne sont pas les mêmes à Emben et à Brunt Lake, ce qui porte à croire que les processus de formation des minerais étaient différents. Une minéralisation plus récente de sulfure et de métaux communs semble être superposée sur la venue de Burnt Lake.

[1]Contribution to the Canada–Newfoundland Mineral Development Agreement. Project carried by the Geological Survey of Canada, Mineral Resources Division, Project 770024

[2]Department of Earth Sciences, Memorial University of Newfoundland, St. John's, Newfoundland A1B 3X5

INTRODUCTION

The Burnt Lake area is located within the Central Mineral Belt (CMB) of Labrador approximately 30 km south of the village of Postville (Fig. 50.1). It is of considerable interest for uranium exploration and metallogeny. A metallogenic study was initiated in 1986 under a Federal–Provincial Mineral Development Agreement. An area of approximately 80 km^2 was mapped for this study during the 1986 field season. The project will be continued as an MSc. thesis at Memorial University of Newfoundland by the first author.

The Early Proterozoic supracrustal rocks of the Upper Aillik Group, which underlie the area, are dominated by felsic volcanic and volcaniclastic sedimentary rocks (Fig. 50.2). The Burnt Lake uranium showing occurs within felsic volcanic rocks. The Emben uranium showing, conversely, is hosted by sedimentary lithologies. The volcanic-sedimentary pile was intruded by a high level, peraluminous granitoid (the Burnt Lake Granite) which separates the Burnt Lake showing in the west from the Emben showing in the east. This granite contains high grade molybdenite mineralization near its western intrusive contact in the vicinity of the Burnt Lake showing.

PREVIOUS WORK

The Burnt Lake area has been intensively explored by Brinex Limited during the 1970s. The uranium occurrences of the area have been briefly described by Gandhi (1978; 1986) and Kontak (1980). The exploration reports, however, are confidential. Regional geology of the area has been described in more detail by Bailey (1979) and Gower et al. (1982). White and Martin (1980) studied the metasomatic alteration as related to mineralization from several showings in the region. C. Payette and R.F. Martin (personal communication, 1986) have studied glass inclusions from the area (both drill core and regional outcrop samples) in an attempt to define the primary chemical composition of the felsic volcanic rocks prior to metasomatic overprinting by the uranium bearing hydrothermal fluids.

GENERAL GEOLOGY

The geology of the Burnt Lake area (Fig. 50.2) is dominated by rhyolitic volcanic and sedimentary rocks of the Upper Aillik Group. The rocks are mainly pink to grey, porphyritic, subaerial tuffaceous rocks, with varying proportions of quartz and feldspar phenocrysts, that include welded and non-welded varieties. There are relatively minor amounts of non-porphyritic rhyolite, ash flow tuff, tuffaceous sandstones and siltstones, pyroclastic breccias and lappilli tuffs. The sedimentary rocks are well-bedded, tuffaceous sandstones and siltstones, which range in colour from buff, pale blue, grey, pink, green and maroon.

The sedimentary and volcanic sequence is folded and intruded by a large body of fine- to medium-grained, leucocratic quartz monzonite to granite called the Burnt Lake Granite. The age of this granite is about 1550±50 Ma (Bailey, 1979).

The Upper Aillik Group and Burnt Lake Granite were subsequently intruded by metadiabase and metadiorite dykes, and by younger northeast-trending, coarse grained gabbroic dykes of the Michael Gabbro Suite (ca. 1450 Ma).

Unit 1

Arkosic sandstone and minor tuffaceous constitute unit 1 at the base of the Upper Aillik Group in the study area (Gower et al., 1982). The unit has limited exposure east of Burnt Lake as heavy drift cover obscures the relationships with other units. The arkosic sandstone is predominantly pink to grey, and is composed of 80-90% potassium feldspar with variable amounts of quartz making up the remainder; accessory minerals include epidote, actinolite and opaques. The grains are well sorted and well rounded. In some outcrops, relict beds (1-2 cm thick) are outlined by the alignment of <1 mm thick mafic (up to 5% magnetite) bands. Intercalated with this

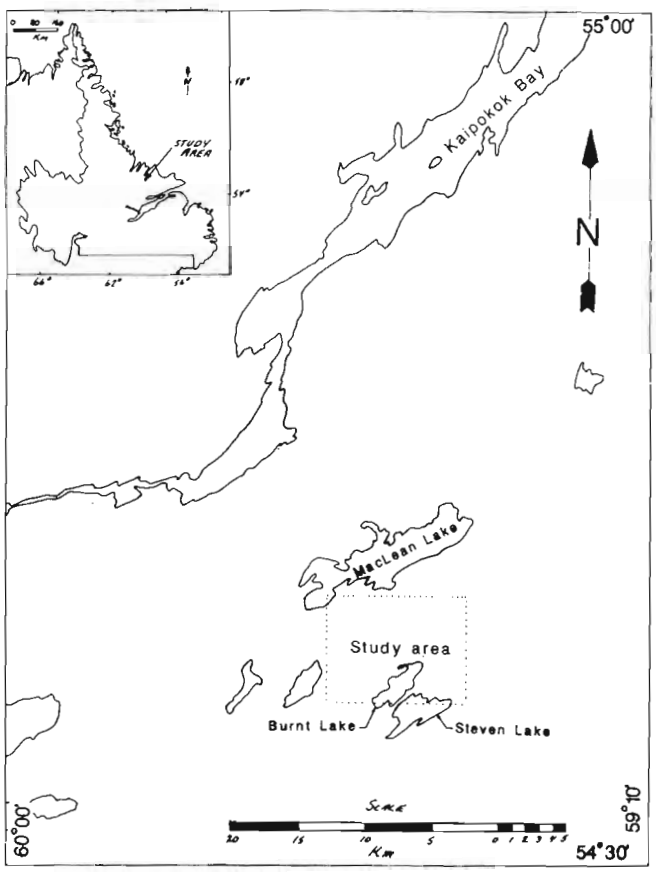


Figure 50.1 Location of the Burnt Lake map area.

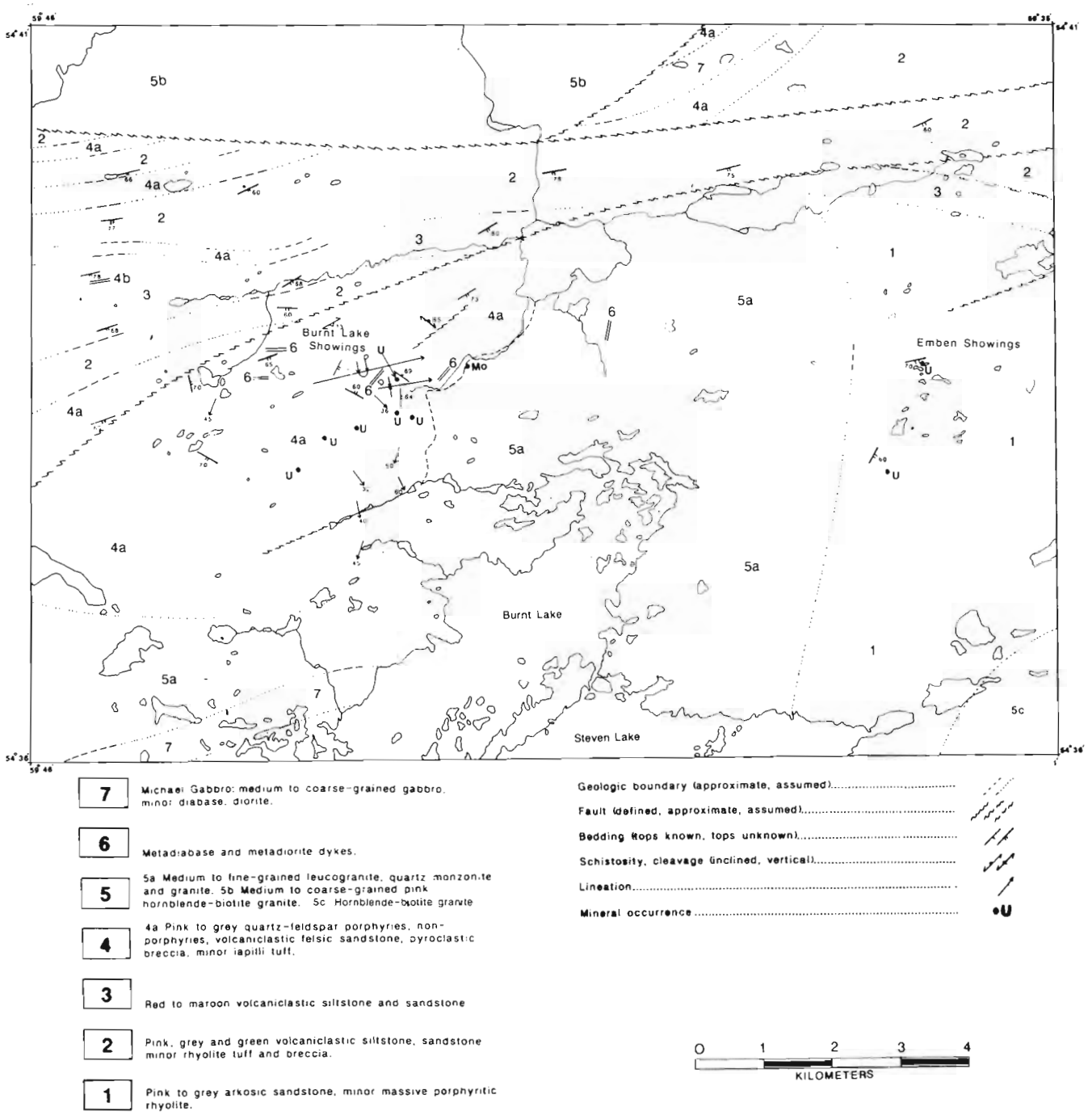


Figure 50.2 Geology and mineral location map of the Burnt Lake area, Labrador.

sedimentary unit are minor porphyritic tuffs; indicating the increasingly proximal nature of volcanism. This unit hosts high grade uranium mineralization in several locations, as the Emben showings.

Unit 2

The rocks in this unit are composed of well bedded, felsic volcaniclastic siltstone and sandstone in shades of pink, green and grey, possibly indicating changing depositional conditions. They are well exposed just south of Maclean Lake (Fig. 50.1) in a broad east trending belt. Its actual relationship with unit 1 is unknown, but it is assumed to overlie unit 1. Bedding and/or laminations are well preserved with a general east-west strike and southerly dip. Generally bedding is continuous, but in some places, crossbedding was observed. In thin

section the rock has a very fine grained quartzofeldspathic matrix; coarser layers have minor quartz and feldspar phenocrysts with a eutaxitic texture, and most grains are embayed and subrounded. Mafic minerals also define bedding in most cases. Accessory minerals include epidote and magnetite.

Unit 3

This unit forms a fault-disrupted east trending band across the map area. It consists of red to maroon volcaniclastic siltstone and sandstone. It conformably overlies unit 2 with similar bedding attitudes, and is probably the regressive equivalent of unit 2 (i.e. indicating very shallow water to terrestrial depositional conditions). In thin section, the rock has a very fine grained quartzofeldspathic matrix that is more deformed than unit 2; its texture approaches mylonite, with abundant calcite-rich veinlets. Bedding is defined by mafic-rich layers and coarser quartz and feldspar bands or layers.

Unit 4

This felsic volcanic unit is extensive in the western part of the area. It is the most important rock unit with respect to mineralization, yet is also the most difficult to unravel. Its outcrop pattern is generally of northeasterly trending linear ridges separated and overlain by abundant drift cover.

Unit 4 can be divided into several subunits, although an entirely satisfactory subdivision was not possible. Some contacts between the various subunits could be observed; transitions, however, were generally not documented. The dominant lithologies are pink to grey porphyries with a wide range of quartz and feldspar phenocryst ratios and grain sizes. Ash flow tuffs, both welded and non-welded, are common with crystal and lithic components. The quartz phenocrysts are generally blue, elliptical, and in the 1-4 mm size range. In thin section the quartz phenocrysts are recrystallized to a granoblastic texture. Some quartz grains are intensely corroded and show undulose extinction. The feldspar phenocrysts are usually subhedral with a rectangular shape (2-10 mm), although the lapilli tuffs have feldspar phenocrysts in the 1-2 cm range with minor quartz in a greenish matrix. The feldspar phenocrysts are orthoclase and plagioclase with varying secondary alterations. The matrices generally have granoblastic-polygonal textures composed of quartz and feldspar. Accessory minerals identified by SEM include ilmenite, sphene, zircon, magnetite, monazite and scheelite.

Unit 5a

This unit comprises the Burnt Lake Granite proper and has limited surface exposure in the area. The rock type is a fine- to medium-grained, pink to grey, muscovite-bearing leucogranite to quartz monzonite suite. In thin section the granites are composed of 20-30% quartz, 40-50% potassium feldspar and 20% plagioclase. The matrices are complex intergrowths of quartz and feldspar in an almost granular texture. The potassium feldspar is usually orthoclase with lesser microcline. The plagioclase is usually rimmed by another feldspar, and/or magnetite, and has irregular boundary contacts. Accessories include epidote, sphene, chlorite, ±tremolite. In general the mafic minerals (biotite and hornblende) are only minor constituents.

The intrusive contact with unit 4 is well exposed in the west and is quite sharp. The undeformed granite cuts metafelsic volcanic rocks that have a definite fabric without an obvious contact aureole, suggesting that the intrusion was high level. Pegmatite dykes (0.1 to 1 m wide) occur near the contact with the felsic volcanic rocks, suggestive of aqueous vapour phase accumulation at the contact. Bailey (1979), however, described the contact as a transitional pluton-hypabyssal volcanic relationship.

Unit 5b

This granitic phase outcrops in the northern section of the area in a steep cliff exposure. It is composed of a pink, medium- to coarse-grained, hornblende-biotite granite that is foliated and almost gneissic in places. This suggests that it may predate unit 5a. The rock is composed mainly of fractured plagioclase, with lesser potassium feldspar and quartz, that have all been recrystallized. Accessory minerals include epidote, sphene, zircon, pyrite and sphalerite.

Unit 5c

This distinctive granite outcrops in the southeastern corner of the map area. The rock is a grey, medium- to coarse-grained hornblende-biotite granite. This unit is much fresher looking than unit 5a with anhedral, twinned plagioclase (50% of the rock), microcline (20-25%) and interstitial quartz (10-15%). Besides hornblende and biotite, accessory minerals include epidote, sphene, calcite and magnetite.

Unit 6

Various metadiabase and metadiorite dykes, which cut all previous units, are grouped here as unit 6. Generally the dykes (10-20 m in width) have an easterly to northeasterly strike. Other mafic metamorphosed dykes include smaller (0.5 to 3 m wide) green coloured ones that have tight crenulation folds. In thin section these dykes are mainly composed of amphibole (riebeckite ?), biotite, plagiocalse and potassium feldspar. Quartz is a minor constituent.

Unit 7

Gabbroic dykes of this unit, are exposed in the northeast and southwest of the map area. They belong to the Michael Gabbro suite which is extensive south of the map area and has been dated at 1480 Ma (Fahrig and Larochelle, 1972). The rock is coarse grained gabbro with minor diabase and diorite components forming large east to northeasterly trending dykes.

GRANITE GEOCHEMISTRY

Major oxides were analyzed by atomic absorption methods; the trace elements by X-Ray Fluorescence on pressed whole rock powder pellets; and REE contents were determined by a thin film X-ray fluorescence technique (after Fryer, 1977). Major and trace element concentrations for selected Burnt Lake Granite samples are given in Table 50.1. REE data for the granite, felsic volcanic rocks and U-bearing units are listed in Table 50.2.

A wide variation in SiO_2 values from 62 to 77%, reflects successive fractionation within the granite and a crude SiO_2 zonation in which the SiO_2 content increases towards the western intrusive contact. The molybdenite mineralization located at and near this intrusive contact represents the most differentiated portion of the pluton. A thermogravitational-type model (e.g. Hildreth, 1981) for differentiation and elemental zonation may be applicable to the Burnt Lake Granite and associated mineralization. It is supported by correlation of REE and SiO_2 content, discussed below.

Al_2O_3 contents and total alkalis range from 12-15% and 8.5-9.5% respectively, however, there are two exceptions. Sample LM-134, from unit 5b in the northern part of the map area, and sample LM-151, from the northernmost extent of unit 5a, are low silica granites with higher Al_2O_3 and total alkalies. In general, they are chemically distinct from unit 5a.

All unit 5a granite samples are subalkaline and peraluminous, and become more differentiated towards the western, molybdenite mineralized intrusive contact with the Upper Aillik Group.

Chondrite-normalized REE patterns for the Burnt Lake Granite are illustrated in Figure 50.3. The patterns have LREE>HREE and a negative Eu anomaly. REE concentrations decrease with increasing SiO_2 (i.e. fractionation – sample LM-23 has 75.5% SiO_2; and LM-165 has 76.9% SiO_2). Also the patterns have a "saucer-shape" with increasing HREE from Dy to Yb. Such shapes have been interpreted by Taylor et al., (1981) to indicate the presence of F^- or $CO_3^=$ rich volatile phases in high level granitoids (the F^- or $CO_3^=$ ions supposedly complex and thus transport the HREE). This is plausible in the Burnt Lake Granite as there are demonstrated upper level volatile concentrations (shown by the pegmatite and molybdenite) in the contact zone and fluorite is also present in the vicinity of the contact.

MINERALIZATION

Metallic mineralization in the Burnt Lake area is diverse and the styles of uranium mineralization at the Burnt Lake and

Table 50.1. Geochemical data for the Burnt Lake Granites.

SAMPLE	GE01	GE02	LM23	LM34	LM151	LM165	LM166	LM167	LM168	LM174	LM134
SiO_2	72.00	72.00	75.50	74.90	63.50	76.90	72.60	76.20	75.20	68.60	61.90
TiO_2	0.28	0.28	0.16	0.08	1.12	0.08	0.20	0.08	0.16	0.24	0.92
Al_2O_3	14.20	14.30	13.40	13.50	19.20	12.60	14.10	12.70	13.20	15.40	15.10
Fe_2O_3	2.15	2.14	1.18	0.75	1.43	0.93	1.71	0.88	1.41	2.56	8.46
M_{no}	0.04	0.03	0.03	0.01	0.04	0.04	0.06	0.02	0.03	0.07	0.12
MgO	0.36	0.33	0.15	0.10	0.48	0.08	0.35	0.11	0.19	0.62	0.41
CaO	1.08	1.08	0.68	0.92	1.08	0.71	1.20	0.72	0.84	1.88	2.14
Na_2O	3.89	3.78	3.71	3.99	6.26	4.11	4.30	3.94	3.71	4.50	4.71
K_2O	5.01	5.57	5.02	4.60	6.29	4.16	4.69	4.74	5.14	4.64	5.32
P_2O_5	0.08	0.05	0.03	0.02	0.05	0.00	0.02	0.01	0.03	0.08	0.11
H_2O+	0.00	0.51	0.52	0.28	0.70	0.44	0.48	0.41	0.41	0.40	0.19
Total	99.55	100.07	100.38	99.15	99.15	100.05	99.71	99.81	100.32	98.99	99.38
PB	45	23	44	36	50	52	33	32	40	0	49
U	2	0	15	2	0	5	0	10	0	0	9
TH	34	15	29	32	43	58	22	45	33	128	42
RB	194	163	243	162	130	219	141	213	231	128	113
SR	122	118	81	110	242	38	229	89	95	346	171
Y	31	36	37	23	32	19	34	33	35	38	62
ZR	254	313	147	92	163	98	160	100	190	241	1748
NB	18	16	34	8	23	36	19	36	32	22	22
GA	20	18	23	21	21	20	18	22	22	21	20
ZN	31	34	15	0	11	0	22	0	20	28	89
CU	4	3	2	5	8	4	4	5	2	8	134
NI	0	0	0	0	0	0	26	0	0	0	0
LA	80	87	14	0	39	0	0	2	15	41	478
BA	718	842	489	427	1743	158	818	252	524	1190	596
V	1	2	0	0	23	0	4	0	0	23	16
CE	51	86	55	110	68	45	71	42	56	91	441
F	340	310	150	80	550	80	180	90	220	440	230

Table 50.2. Rare earth element data for the Burnt Lake Area.

EL(ppm)	LM14	LM23	LM32	LM37	LM60	W84-65A	W84-65A.1	W84-65B
YB	6.5	5.1	4.1	6.7	1.9	3.1	6.0	3.3
ER	6.9	4.0	4.5	7.2	2.7	3.7	11.2	6.5
DY	11.9	4.7	7.4	11.0	4.7	8.8	26.0	14.1
GD	9.3	4.0	8.5	11.4	6.6	10.5	32.8	15.8
EU	0.2	0.3	0.0	0.7	0.0	0.2	0.9	0.0
SM	10.6	3.4	11.7	15.0	10.5	16.2	40.6	20.5
ND	52.9	17.9	73.2	87.0	67.6	92.6	239.5	106.6
PR	11.7	4.1	16.9	19.1	16.2	19.7	55.4	24.3
CE	139.5	57.4	211.8	227.0	185.0	231.8	602.7	287.7
LA	62.1	23.3	107.9	107.2	89.8	108.6	292.6	118.7

EL(ppm)	W84-79	W84-79A	W84-79A.1	W84-79E	LM-165	LM-168
YB	10.3	10.9	10.0	14.4	2.9	4.2
ER	17.4	15.5	18.1	13.3	2.3	3.7
DY	48.4	29.3	39.0	20.8	3.0	5.2
GD	65.3	29.9	41.1	13.7	1.8	3.8
EU	2.0	3.9	2.2	0.2	0.0	0.3
SM	77.6	32.9	40.0	12.5	1.6	3.9
ND	290.7	164.2	173.7	39.8	7.0	18.2
PR	62.4	33.9	32.7	8.9	1.8	4.3
CE	480.5	320.3	287.2	95.8	21.4	63.8
LA	134.6	162.1	106.6	42.3	11.1	25.8

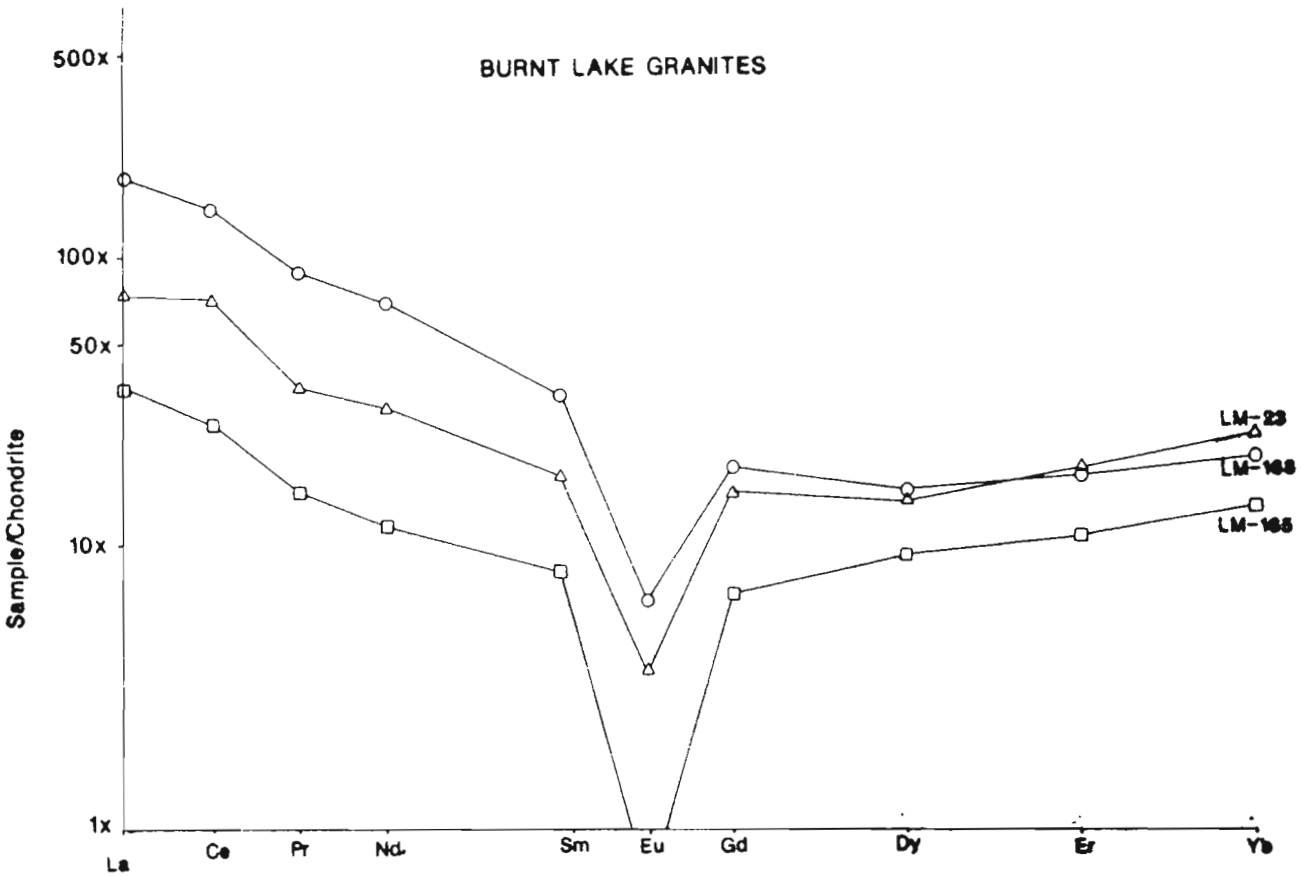


Figure 50.3 Chondrite-normalized (after Taylor and Gorton, 1977) REE patterns for the Burnt Lake Granite.

Emben showings are quite different. There also appears to have been two separate mineralizing events at Burnt Lake. The first event, which was much more predominant (and has been well documented in the literature by Bailey, 1979; Gandhi, 1978, 1986; Gower et al., 1982; Kontak, 1980, and White and Martin, 1980), produced uranium enrichments along with Na metasomatism, and Si and K depletions. The uranium, as suggested by Kontak (1980) and Gower et al. (1982), may have been leached from glasses in the felsic volcanic rocks by circulating hydrothermal fluids. The fluids themselves were predominantly meteoric but with a possible magmatic component. Precipitation of the dissolved uranium ions resulted from the oxidized hydrothermal fluids encountering relatively reduced country (now host) rock. Disseminated pyrite and magnetite are common in unmineralized country rock, whereas the mineralized zones are commonly associated with red hematitic alteration. The oxidation of magnetite to hematite would cause a drecrease in fO_2 of the hydrothermal fluids and promote precipitation of the "pitchblende" as discrete disseminated grains.

The other mineralizing event was accompanied by K metasomatism and a dramatic decrease in Na. Mineralization associated with this second event includes Pb-Zn-Cu sulphides and Ag, which formed minute stringers and veinlets. Uranium mineralization is also associated with these showings but may be remnant from the first event or may represent local remobilization during the second event.

The Emben showings are all characterized by intense Na enrichment (6-10% Na_20) and a K (0.05-0.2% K_20) depletion. Although Na metasomatism is a feature common to the Emben and Burnt Lake mineralization, there are differences in other aspects. The REE patterns are different between the two showings (Fig. 50.5, 50.6). The Burnt Lake showing has been radiometrically dated at 1726 Ma whereas the Emben showing has yielded a date of 1300 Ma (Gower et al., 1982). There is a close association between uranium and mafic dykes at the Emben, which is not the case at Burnt Lake. It appears that hydroxide or fluoride complexing was probably dominant in uranium transport at the Burnt Lake showing, but at the Emben showing, phosphate was probably the complexing agent (as suggested by the P contents of mineralized samples from the Emben Showing). The phosphate may have been derived from the mafic dykes. According to Romberger (1984), phosphate is an important uranium complexing agent at high temperatures and near neutral pHs.

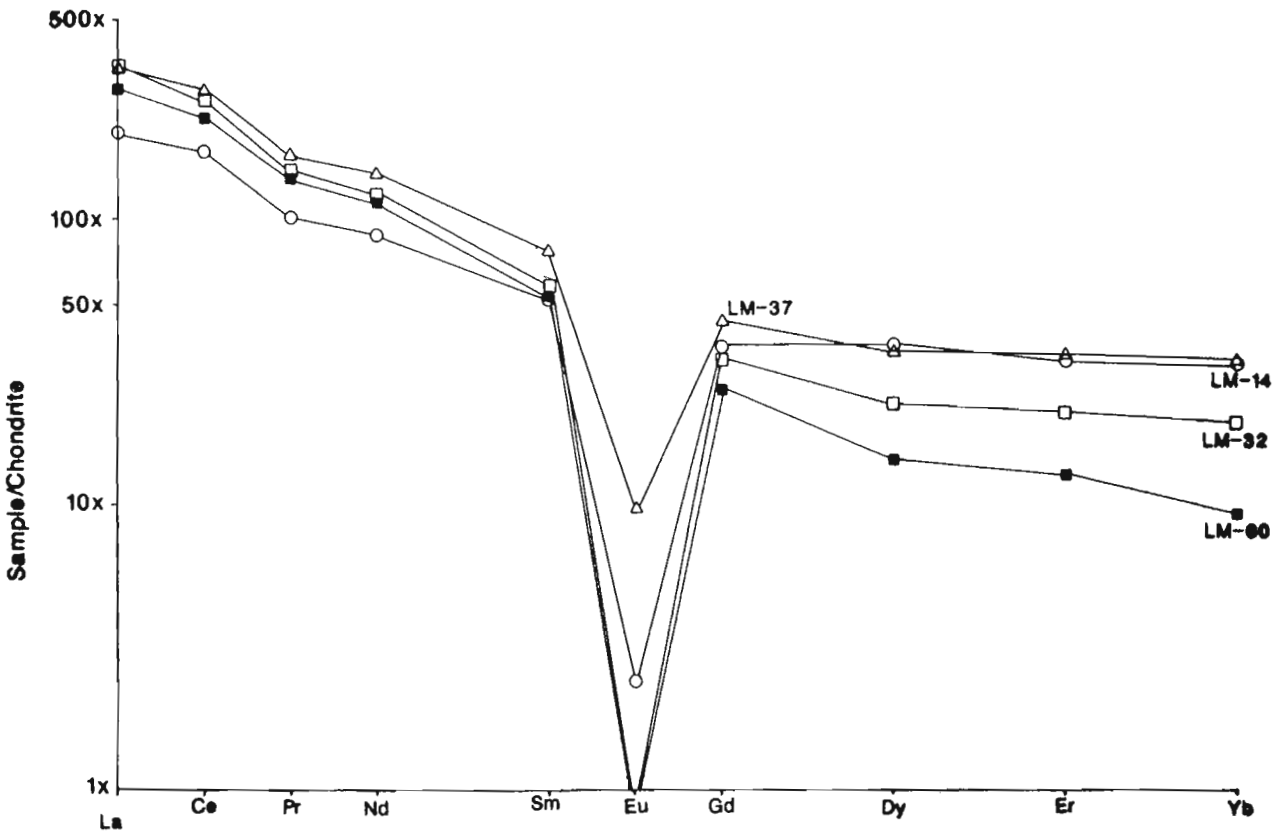


Figure 50.4 Chondrite-normalized REE patterns for non-mineralized felsic volcanic rocks of the Upper Aillik Group in the Burnt Lake area.

In general, unmineralized Upper Aillik Group felsic volcanic rocks have very enriched REE contents (up to ≈ 1000x chondrite elsewhere but only 20 to 400x near Burnt Lake; Fig. 50.4) and strong negative Eu anomalies. With respect to the uranium mineralized rocks at Burnt Lake (Fig. 50.5), REE patterns are the same (i.e. enriched and intense negative Eu anomalies) as those of the unmineralized host rocks. A similar relationship was shown by White and Martin (1980) for the Michelin deposit. The similarities in REE patterns suggest that the mineralizing fluids were chemically similar (with respect to REE contents) to the hosting felsic volcanic rocks or least had achieved a degree of equilibrium with these rocks. These considerations support the idea that syn- to slightly post-volcanic leaching produced the uranium mineralization.

In contrast, REE patterns for samples from the Emben showing (Fig. 50.6) are relatively flatter, yet enriched, with a much smaller negative Eu anomaly. Of the four samples plotted on this diagram, W84-79E, which has the biggest Eu depletion, contains the least U (82 ppm); whereas W84-79A, with the highest U concentration (10680 ppm), has a decreased Eu anomaly and also contains the greatest enrichments in REE (especially MREE). The other samples are intermediate (i.e. 79A has 129 ppm U; 79A1 has 1399 ppm U). These pattern types are reminiscent of those in the Makkovik area that were linked to granite-related, phosphate complex-bearing, hydrothermal fluids (MacDougall and Wilton, 1987; Wilton and Wardle, in press).

CONCLUSIONS

The Burnt Lake Granite is a high level granitoid which shows evidence of differentiation and the production of a molybdenum-bearing vapour phase. This granite, however, postdates the uranium mineralization at Burnt Lake. Unlike the uranium occurrences in the Round Pond and Makkovik areas, those at Burnt Lake appear to have been the products of syn- to post-volcanic leaching of volcanic glasses. The Emben showings on the other hand bear some resemblance (at least in terms of REE distributions) to the coastal showings, and were possibly produced by phosphate-bearing fluids of granitic origin. The second potassic-sulphide mineralizing event at Burnt Lake was also possibly derived from the vapour phase assemblages of the granitic magma. Future research is required to define the mineralizing sequences more completely.

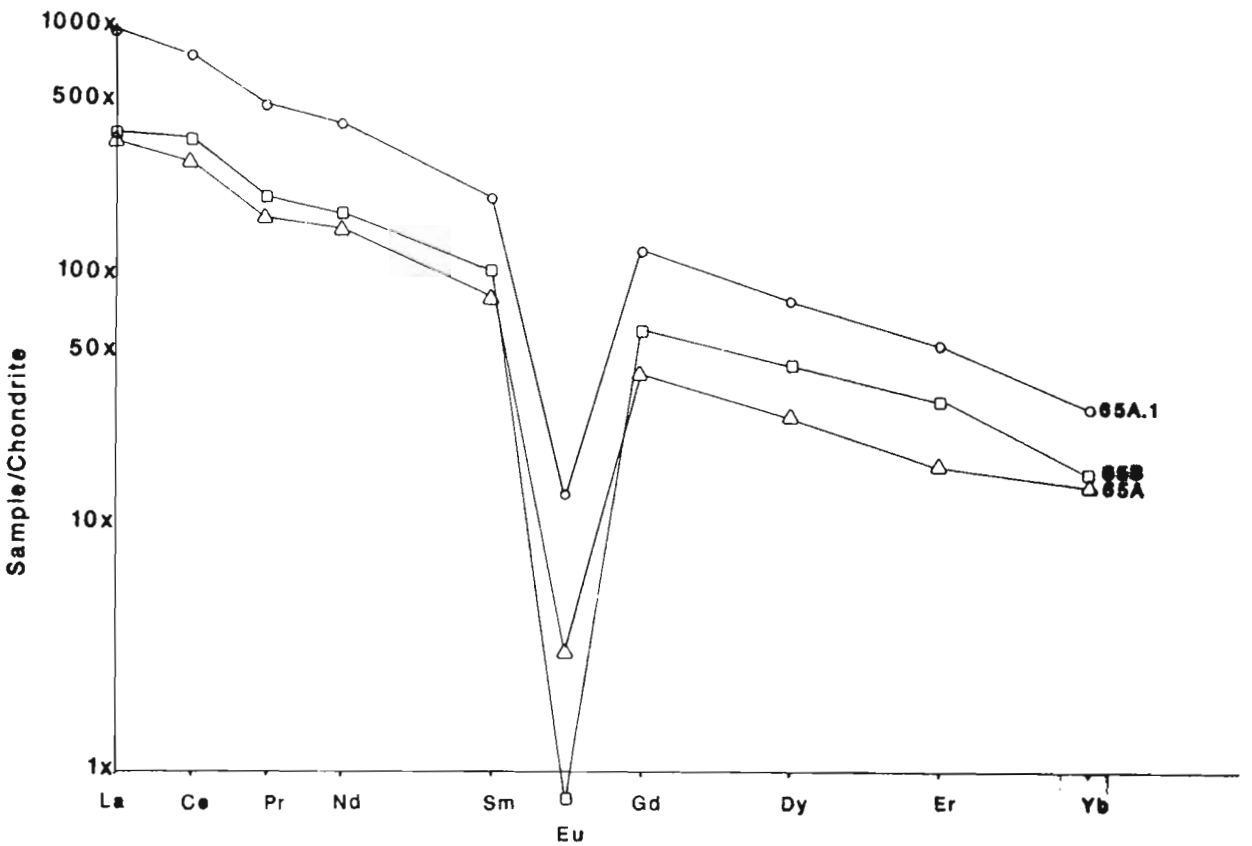


Figure 50.5 Chondrite-normalized REE patterns for uranium-bearing felsic volcanic rocks of the Upper Aillik Group at Burnt Lake.

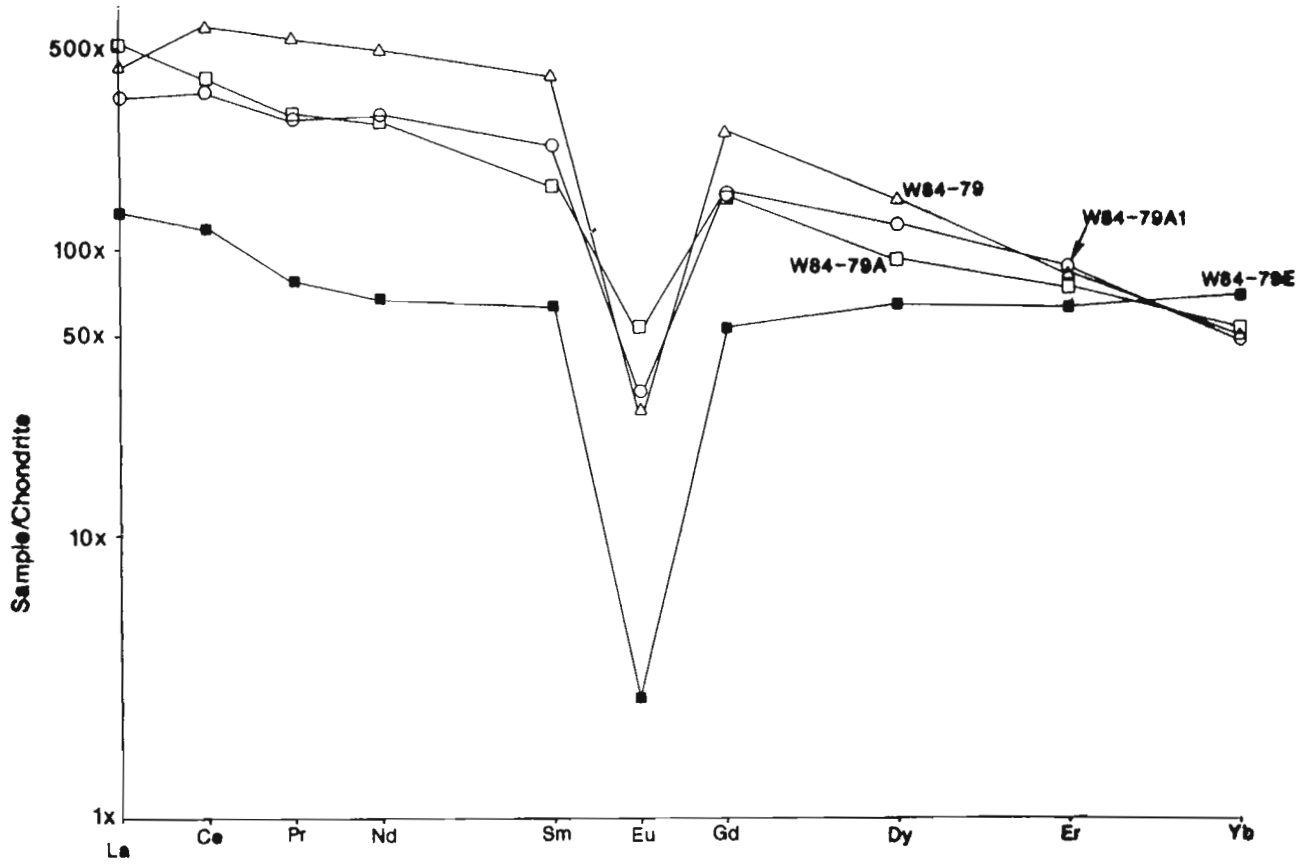


Figure 50.6 Chondrite-normalized REE patterns for samples from the Emben Showing (both mineralized and non-mineralized).

ACKNOWLEDGMENTS

Financial support for this project was provided by the Geological Survey of Canada through ERDA Agreement II-2 (Metallogeny of the Central Mineral Belt) and NSERC Northern Supplement grant to Wilton. Logistical support for the project was provided by the Newfoundland Department of Mines and Energy through R.J. Wardle, K. O'Quinn and W. Tuttle. We have benefited greatly from discussions with T. Birkett, B.J. Fryer, S.S. Gandhi, C.J. Gower, D. Kontak, C.S. MacDougall, R.F. Martin, C. Payette, A.B. Ryan, and R.J. Wardle. We are grateful to L. Fiander for able field assistance. Geochemical preparation and analyses were aided and/or completed by G. Andrews, C. Emerson, P. Moore, D. Press and G. Veinott.

The manuscript was critically read by S.S. Gandhi and T. Birkett of the Geological Survey of Canada.

REFERENCES

Bailey, D.G.
1979: Geology of the Walker-MacLean Lake area (13K/9, 13J/12) Central Mineral Belt, Labrador; Newfoundland Department of Mines and Energy, Report 78-3, 17 p.

Fahrig, W.F. and Larochelle, A.
1972: Paleomagnetism of the Michael Gabbro and possible evidence of the rotation of the Makkovik Subprovince; Canadian Journal of Earth Sciences, v. 9, p. 1287-1296.

Fryer, B.J.
1977: Rare earth evidence in iron formation for changing oxidation states; Geochimica et Cosmochemica Acta, v. 41, p. 361-367.

Gandhi, S.S.
1978: Geological setting and genetic aspects of uranium occurrences in the Kaipokok Bay – Big River area, Labrador; Economic Geology, v. 73, p. 1492-1522.

Gandhi, S.S.
1986: Uranium in Early Proterozoic Aillik Group, Labrador; Institute of Mining and Metallurgy, Special Volume 33, p. 70-82.

Gandhi, S.S., Grasty, R.L., and Grieve, R.A.F.
1969: The geology and geochronology of the Makkovik Bay area, Labrador; Canadian Journal of Earth Sciences, v. 6, p. 1019-1034.

Gower, C.F., Flanagan, M.J., Kerr, A., and Bailey, D.G.
1982: Geology of the Kaipokok Bay–Big River area, Central Mineral Belt, Labrador; Newfoundland Department of Mines and Energy, Report 82-7, 77 p.

Hildreth, W.
1981: Gradients in silicic magma chambers: Implications for lithospheric magmatism; Journal of Geophysical Research, v. 86, p. 10153-10192.

Kerr, A.
1986: Plutonic rocks of the eastern Central Mineral Belt; general geology and description of regional granitoid units; in Current Research, Newfoundland Department of Mines and Energy, Report 86-1, p. 89-100.

Kontak, D.J.
1980: Geology, geochronology and uranium mineralization in the Central Mineral Belt of Labrador, Canada; Unpublished MSc. thesis, University of Alberta, Edmonton, 378 p.

MacDougall, C.S. and Wilton, D.H.C.
1987: Middle Proterozoic granite-related mineralization in the Round Pond area, Labrador; in Current Research, Part A, Geological Survey of Canada, Paper 87-1A, report 49.

Romberger, S.B.
1984: Transport and deposition of uranium at temperatures up to 300°C: geological implications; in Uranium Geochemistry, Mineralogy, Geology, Exploration, and Resources, B. DeViro, F. Ippolito, G. Capaldi, and P.R. Simpson, ed., Institute of Mining and Metallurgy, p. 12-17.

Taylor, R.P., Strong, D.F., and Fryer, B.J.
1981: Volatile control of contrasting trace element distributions in peralkaline granitic and volcanic rocks; Contributions to Mineralogy and Petrology, v. 77, p. 267-271.

Taylor, S.R. and Gorton, M.P.
1977: Geochemical application of spark source mass spectrography – III element sensitivity, precision and accuracy; Geochimica et Cosmochemica Acta, v. 29, p. 1243-1261.

White, M.V.W. and Martin, R.F.
1980: The metasomatic changes that accompany uranium mineralization in the nonorogenic rhyolites of the upper Aillik Group, Labrador; Canadian Mineralogist, v. 18, p. 459-479.

Wilton, D.H.C. and Wardle, R.J.
in press: Two contrasting granophile and non-granophile metallogenic styles in the early Proterozoic Upper Aillik Group, Central Mineral Belt, Labrador; Submitted to Mineralia Deposita.

Advances in analytical methods based on atomic absorption spectrometry in the Geochemistry Laboratories of the Geological Survey of Canada

Project 580175

G.E.M. Hall, K.N. de Silva, J.C. Pelchat and J.E. Vaive
Mineral Resources Division

Hall, G.E.M., de Silva, K.N., Pelchat, J.C. and Vaive, J.E., Advances in analytical methods based on atomic absorption spectrometry in the Geochemistry Laboratories of the Geological Survey of Canada; in Current Research, Part A, Geological Survey of Canada, Paper 87-1A, p. 477-484, 1987.

Abstract

Research currently being conducted to expand the capabilities of atomic absorption spectrometric methods of analysis is described in three parts. The first concerns the development of a method to determine thallium, gallium and indium to levels at or below their average crustal abundances by graphite furnace atomization. The second area of investigation involves the analysis of biogeo chemical samples, predominantly ash material, for the elements gold, silver, platinum, palladium and rhodium down to the 2 - 10 ppb ($ng.g^{-1}$) range. The third, and more general, field of study concerns the application of flow injection analysis as a means of sample introduction and manipulation in order to automate efficiently such tasks as preconcentration and separation which will improve productivity greatly and minimize the quantities of reagents required.

Résumé

Le présent rapport décrit trois domaines de recherches en cours qui visent à élargir l'utilité des méthodes d'analyse par spectrométrie d'absorption atomique. La première partie porte sur la mise au point d'une méthode de dosage du thallium, du gallium et de l'indium par atomisation dans un four à graphite lorsque la teneur de ces éléments est égale ou inférieure à la teneur moyenne dans la croûte. La deuxième partie comprend l'analyse d'échantillons biogéochimiques, surtout de cendres, pour le dosage de l'or, de l'argent, du platine, du palladium et du rhodium à des teneurs variant de 2 à 10 ppb ($ng\ g^{-1}$). Le troisième domaine d'étude, plus général, concerne l'utilisation de l'analyse par injection pour l'introduction et la manipulation des échantillons, afin d'automatiser diverses tâches telles que la préconcentration et la séparation, et donc d'améliorer la productivité et de minimiser les quantités de réactifs utilisées.

PART 1: THE DETERMINATION OF THALLIUM, GALLIUM AND INDIUM

Introduction

The objective of this study is to determine the concentrations of the three elements, thallium (Tl), gallium (Ga) and indium (In), from the same sample digest of a geological material (rock, soil, or sediment) with determination limits equal to or less than the average crustal abundance levels. The approximate mean abundances of Ga, Tl and In are 19 $\mu g\ g^{-1}$, 1.3 $\mu g\ g^{-1}$ and 0.11 $\mu g\ g^{-1}$, respectively (Shaw, 1957). There are two methods of decomposition suitable for the determination of a suite of trace elements in common use today at the Geological Survey of Canada. One method, resulting in a solution to be analysed by inductively-coupled plasma emission spectrometry (ICP-ES), involves a mixed acid attack ($HF/HClO_4/HNO_3/HCl$) and fusion of any residue with $LiBO_2$. The second method involves a similar mixed acid attack but is carried out under pressure and it is assumed that if any residue remains it does not contain the elements of interest. This solution is routinely analyzed for lead, silver and cadmium by flame atomic absorption spectrometry (AAS), and, occasionally, for molybdenum by ICP-ES. In order to attain determination limits in the ppb (ng g^{-1}) range, graphite furnace – atomic absorption spectrometry (GF-AAS) is used as the analytical technique. The presence of numerous interferences, however, in this measurement step, necessitates separation of the analytes from the matrix elements. Solvent extraction of these elements as their halide complexes into methyl-isobutyl ketone (MIBK) provides an efficient and quantitative means of separation (Korkisch, 1969). Unfortunately, separate extractions must be carried out for the three elements for the following reasons. Firstly, Ga is quantitatively extracted from 4 M (or more concentrated) HCl into MIBK in the presence of a reducing agent, such as ascorbic acid, to prevent Fe (III) from co-extracting (Sukhoveeva et al., 1979). However, these conditions promote the reduction of Tl (III) to Tl (I) which does not extract into MIBK. Thus, Tl (III) must be extracted in the absence of a reducing agent and Fe is then back-extracted into 0.1 M HCl. Secondly, HBr is required in the extraction of In into MIBK as the extraction from HCl, at any concentration, is incomplete (Gawali and Shinde, 1976). Indium can also be extracted as its iodide complex into MIBK, in the presence of a reducing agent to prevent the co-extraction of Fe (III) (Hasegawa et al., 1972; Xiao-Quan et al., 1985).

Experimental

The details of the two decomposition methods used in this work are given below in Procedures A and B. Acids are used in their concentrated states unless specified otherwise. A portion (20 mL) of the solution thus derived is then evaporated to dryness, redissolved in 20 mL of 4 M HCl and the extractions performed as described schematically in Figure 51.1. The solvent, MIBK, is initially pre-equilibrated with either 4 M HCl or 2.5 M HCl/3 M HBr. The remaining solution from Procedure A or B is used to determine other trace elements directly by ICP-ES or flame AAS.

The instrumentation used for analysis is the Perkin-Elmer Model 5000 AA spectrometer equipped with the HGA-500 Graphite Furnace and the AS-1 Auto sampler. Operating conditions for the three elements are described in Table 51.1. Calibration is made with synthetic solutions also extracted under identical conditions. Palladium (10 μL of 10 $\mu g\ mL^{-1}$) is used as a matrix modifier as it was found that it enhanced the absorption signals at least ten-fold in the MIBK medium and allowed a higher charring temperature, probably through compound formation of an alloy (Xiao-Quan et al., 1985). Palladium is added in the MIBK medium, having been extracted as the iodide complex (Diamantatos, 1981). The "argon interrupt" mode during atomization is used throughout.

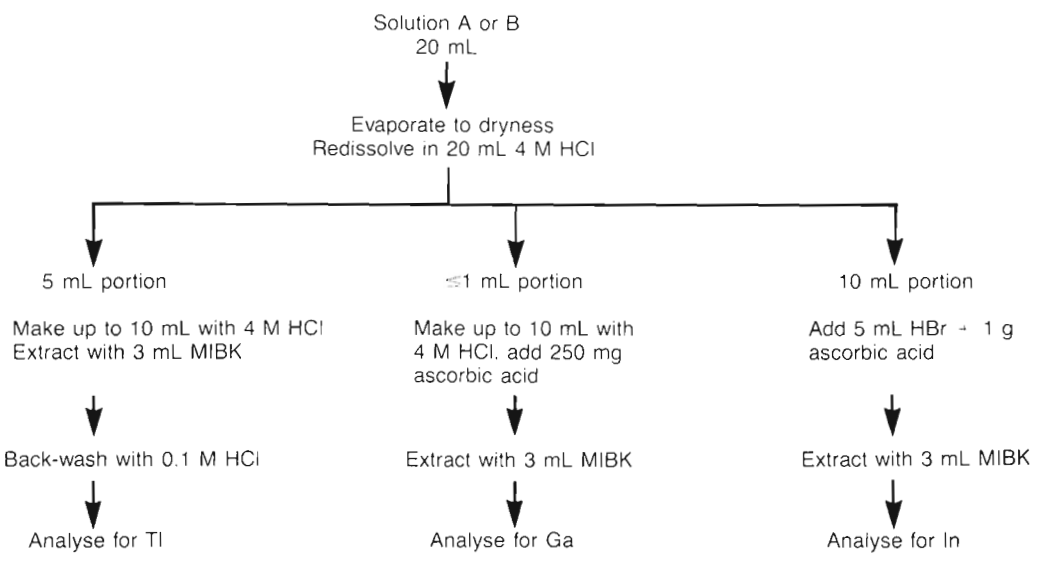


Figure 51.1. Sample extraction scheme for the determination of Tl, Ga and In.

Table 51.1 Operating conditions used in the determination of Tl, Ga, In by GF-AAS

Parameter	Tl	Ga	In
Injection volume/μL	25	25	25
Palladium volume/μL	10	10	10
Wavelength/nm	276.8	287.4	303.9
Drying temperature/°C	120	120	120
Ramp/holding time/s	10/20	10/20	10/20
Charring temperature/°C	700	1250	800
Ramp/holding time/s	10/10	10/10	10/10
Atomisation temperature/°C	2300	2500	2100
Ramp/holding time/s	0/5	0/5	0/5
Cleaning temperature/°C	2700	2700	2700
Ramp/holding time/s	1/2	1/2	1/2

PROCEDURE A

1. To a 1000 mg sample in a beaker, add 10 mL HNO_3 and 10 mL HF and evaporate to near dryness.
2. Add 10 mL HCl, 10 mL HF, 2 mL $HClO_4$. Evaporate to near dryness on a hot plate.
3. Add 10 mL HCl. Evaporate to dryness.
4. Add 10 mL HCl, 50 mL H_2O, 5 mL 0.8% EDTA. Warm.
5. Filter through #40 Whatman paper into a 100 mL beaker. Ignite paper and residue in a Pt crucible at 800°C and fuse the ash with 0.5 g $LiBO_2$ over a burner. Immerse the melt in the filtrate, add washings to filtrate and make up to volume (100 mL) with H_2O in a volumetric flask.

DILUTION FACTOR = 100

PROCEDURE B

1. To a 500 mg sample in a Teflon test-tube, add 2 mL HCl and heat for 20 minutes.
2. Add 2 mL HNO_3, 3 mL $HClO_4$ 5 mL HF. Cap the tube and heat for 1 hour, shaking twice.
3. After cooling, transfer all contents, with washing, to a teflon beaker and heat to incipient dryness.
4. Add 3 mL HNO_3, 1 mL HCl, 5 mL H_2O. Warm for 5 minutes with stirring.
5. Transfer, with washing, to a 25 x 150 mm text-tube and make up to volume (25 mL) with H_2O.

DILUTION FACTOR = 50

Results and discussion

The analysis of synthetic solutions, made by adding aliquots of standard calibration solutions in place of actual samples in step 1 of Procedures A and B, revealed that recovery for all three elements is greater than 95% using either decomposition. Combination of Procedure B and the extraction scheme shown in Figure 51.1 yields a determination limit of 10 ppb (0.01 $\mu g\ g^{-1}$) for each element. Contamination or significant 'blank' values by contribution from reagents was not encountered.

Shown in Table 51.2 are the results of the analyses of international reference materials for Tl and Ga from the United States Geological Survey (USGS), the Canadian Certified Reference Materials Project (CCRMP) and the Institute of Geophysical and Geochemical Prospecting, China (IGGE). The GSD-series (IGGE) was chosen in particular because they appear to be better characterised than other reference samples; there is a paucity of recommended or 'consensus' values in the literature for these elements and only the GSD-series of samples in Table 51.2 are indeed given 'recommended' values. At the time of writing, In had yet to be determined in these samples. It is evident that agreement with literature values for Tl and Ga is good and that either decomposition (A or B) can be chosen with equal reliability.

An evaluation of the precision of this method, using either decomposition procedure, can be made from the data shown in Tables 51.3 and 51.4. International reference materials as well as in-house control samples (NSH-1, CHRT, GNO1) were analysed from 4 to 14 times for Tl and Ga, mostly using the decomposition Procedure B. The precision, expressed as relative standard deviation, is 3 to 6% for Tl and 1 to 6% for Ga in the ranges 0.05 to 2 $\mu g\ g^{-1}$ and 5 to 20 $\mu g\ g^{-1}$, respectively. The precision obtained in the determination of Tl by either Procedure A or B appears to be similar, as evidenced by the in-house control samples (Table 51.3).

In conclusion, it has been demonstrated that the method described, namely solvent extraction combined with GF-AAS, is capable of producing precise and accurate results in the analysis of geological materials to levels at least a decade below average crustal abundances for Tl and Ga. Results for In will be forthcoming in the near future. Choice of decomposition procedure will be governed by the other analytical requests pertaining to that sample. Once digestion is complete, productivity is projected to be about 20 samples per day for all 3 elements.

REFERENCES

Abbey, S.
1983: Studies in "standard samples" of silicate rocks and minerals 1969-1982; Geological Survey of Canada, Paper 83-15, 114 p.

Diamantatos, A.
1981: A solvent-extraction scheme for the determination of platinum, palladium, rhodium, iridium and gold in platiniferous materials; Analytica Chimica Acta, v. 131, p. 53-62.

Gawali, S.B., and Shinde, V.M.
1976: Separation of gallium (III), indium (III), and thallium (III) by solvent extraction with 4-methyl-2-pentanol; Analytical Chemistry, v. 48, p. 62-64.

Table 51.2 Analyses of international reference materials by the proposed method for Tl and Ga

Sample	Tl/μg g^{-1}		Ga/μg g^{-1}	
	This method	Literature value	This method	Literature value
GSD-1 (stream sediment)	0.66 (B) 0.65 (A)	0.61±.14[a]	22.2 (B)	23±1.4[a]
GSD-2 (stream sediment)	1.89 (B) 1.93 (A)	1.9±0.5[a]	28.2 (B)	27.4±1.7[a]
GSD-3 (stream sediment)	0.48 (B) 0.51 (A)	0.58±.15[a]	16.2 (B)	15.9±1.2[a]
GSD-4 (stream sediment)	1.12 (B) 1.25 (A)	1.2±.2[a]	20.7 (B)	20.5±1.5[a]
GSD-5 (stream sediment)	1.23 (B) 1.24 (A)	1.16±.22[a]	20.2 (B)	20.3±1.2[a]
RGM-1 (rhyolite)	0.99 (A)	1.07±.11[b]	15.8 (A) 15.4 (B)	15?[c]
MAG-1 (marine mud)	0.85 (A)	0.79±.14[b]	21.0 (A) 20.9 (B)	21?[c]
QLO-1 (quartz latite)	0.21 (A) 0.20 (B)	0.23±.02[b]	17.1 (A) 17.4 (B)	18?[c]
AGV-1 (andesite)	0.29 (A)	0.27→0.38[d]	19.7 (A) 20.3 (B)	21[c]
BHVO-1 (basalt)	0.052 (A)	0.049[b]	21.2 (A) 20.9 (B)	21?[c]
SDC-1 (mica schist)	0.69 (A)	0.80±.10[b]	20.7 (A) 20.2 (B)	22?[c]
SY-2 (syenite)	1.58 (A) 1.51 (B)		28.5 (A)	28[c]
SY-3 (syenite)	1.49 (B) 1.48 (A)		28.7 (B)	26[c]

(A) Decomposition by Procedure A
(B) Decomposition by Procedure B
[a] Xuejing et al., 1985
[b] Simon et al., 1977
[c] Abbey, 1983
[d] Liem et al., 1984

Table 51.3 Study of the precision of the proposed method: thallium

Sample	Procedure	n	Mean/ μg g^{-1}	SD/ μg g^{-1}	RSD/ %
NSH-1[a] (carbonaceous, siliceous shale)	A	4	1.28	0.04	3.1
	B	4	1.29	0.05	3.8
GNO1[a] (composite outcrop)	A	4	1.51	0.08	5.2
	B	4	1.49	0.05	3.3
CHRT[a] (carbonaceous chert)	A	4	1.83	0.11	6.0
	B	4	1.98	0.12	6.1
GSD-1 (stream sediment)	B	4	0.67	0.03	4.4
GSD-2 (stream sediment)	B	3	1.85	0.07	3.8
BHVO-1 (basalt)	A	3	0.052	0.003	5.7
SDC-1 (mica schist)	A	3	0.69	0.02	2.8
STM-1 (syenite)	A	3	0.24	0.01	4.1

n Number of separate decompositions
SD Standard deviation
RSD Relative standard deviation
[a] Sample described in Hall and Vaive, 1986

Table 51.4 Study of the precision of the proposed method: gallium

Sample	Procedure	n	Mean/ μg g-1	SD/ μg g-1	RSD/ %
NSH-1[a] (carbonaceous, siliceous shale)	B	8	12.0	0.7	5.8
CHRT[a] (carbonaceous chert)	B	14	13.5	0.7	5.2
GNO1[a] (composite outcrop)	B	8	5.7	0.3	5.3
GSD-1 (stream sediment)	B	4	22.2	1.3	5.8
QLO-1 (quartz latite)	B	6	17.5	0.2	1.1
RGM-1 (rhyolite)	B	4	15.3	0.4	2.6
SDC-1 (mica schist)	B	4	20.2	0.7	3.5

n Number of separate decompositions
SD Standard deviation
RSD Relative standard deviation
[a] Sample described in Hall and Vaive, 1986

Hall, G.E.M., and Vaive, J.
1986: Analysis of in-house control reference samples by commercial laboratories using inductively-coupled plasma emission spectrometry; in Current Research, Part A, Geological Survey of Canada, Paper 86-1A, p. 71-79.

Hasegawa, Y., Takeuchi, H., and Sekine, H.
1972: The behaviour of indium (III) complexes in several distribution systems; Bulletin of the Chemical Society of Japan, v. 45, p. 1388-1394.

Korkish, J.
1969: Modern methods for the separation of rarer metal ions; Pergamon Press, p. 311-340.

Liem, I., Kaiser, G., and Sager, M.
1984: The determination of thallium in rocks and biological materials at ng g^{-1} levels by differential-pulse anodic stripping voltammetry and electrothermal atomic absorption spectrometry; Analytica Chimica Acta, v. 158, p. 179-197.

Shaw, D.M.
1957: The geochemistry of gallium, indium and thallium: a review; in Physics and Chemistry of the Earth, Pergamon Press, p. 164-211.

Simon, F.O., Campbell, E.Y., and Aruscavage, P.J.
1977: Thallium contents of 16 USGS standard rocks; Journal of Research, United States Geological Survey, v. 5, p. 579-581.

Sukhoveeva, L.N., Spivakov, B.Y., Karyakin, A.V., and Zolotov, Y.A.
1979: Atomic-absorption determination of gallium by means of a flame and a graphite furnace; Zhurnal Analiticheskoi Khimii, v. 34, p. 693-702.

Xiao-Quan, S., Zhe-Ming, N., and Zhi-Neng, Y.
1985: Determination of indium in minerals, river sediments and coal fly ash by electrothermal atomic absorption spectrometry with palladium as a matrix modifier; Analytica Chimica Acta, v. 171, p. 269-277.

Xuejing, X., Mingcai, Y., Lianzhong, L., and Huijun, S.
1985: Geochemical reference samples, drainage sediment GSD 1-8 from China; Geostandards Newsletter, v. IX, p. 83-160.

PART 2: ANALYSIS OF BIOGEOCHEMICAL SAMPLE MATERIAL FOR THE Pt-GROUP ELEMENTS, Au AND Ag

Introduction

The overall objective of this work is to design analytical procedures capable of achieving detection limits in the few ppb (ng g^{-1}) range for the determination of the Pt-group elements, given 1 - 2 g ash weight of plant material. Analysis of the same sample digest for Au and Ag is part of this goal. Currently, the elements Pd and Pt are most commonly determined on a 10 g ash weight by fire assay prior to directly-coupled or inductively-coupled plasma emission spectrometry (DCP- or ICP-ES) to limits of 2 and 10 ppb, respectively (Dunn, 1986). Neutron activation analysis (NAA) yields similar detection limits. A large weight of 50 g is necessary to determine all the Pt-group elements after a nickel sulphide fire assay; this is not practical since about 1500 g of dried leaf, 2500 g of dried twig, or 10000 g of dried conifer trunkwood would be required to produce such an ash weight. Gold alone can be determined down to 5 ppb on a 0.5 g weight by direct irradiation and instrumental NAA.

Following a review of the literature describing various analytical approaches, it was decided to begin the investigation by examining the effectiveness of separation of the elements Au, Ag, Pt, Pd and Rh using co-precipitation with tellurium after an acid digestion. The analytical technique to

be used initially was graphite furnace atomic absorption spectrometry (GF-AAS). However, upon successful development and application of the methodology, it is planned to change the measurement technique to ICP – mass spectrometry (ICP-MS) in order to improve production and lower detection limits further. Co-precipitation with Te as a means of separation from the matrix elements and concentration was appealing for several reasons. Firstly, Te is poorly soluble in aqueous or HCl solutions and hence only small quantities (several mg) would prove necessary. Secondly, much of the Te can be volatilised in the charring stage during analysis by GF-AAS and it does not create a significant interference in the atomisation stage. Thirdly, there are only a few other elements which form insoluble tellurides (Hg, Bi, Cu, Sn, Mo, Pb) and these are unlikely to be major consistuents of the ashed material.

Application of a similar method to the analysis of rocks has been described by Sighinolfi et al. (1984) and by Fryer and Kerrich (1978). The former reported results for all five metals (Ag, Au, Pt, Pd, Rh) on several international reference rocks, whereas the latter tabled results for Ag and Au only in in-house samples. McHugh (1983) determined Au in waters by GF-AAS after co-precipitation with Te and Elson and Chatt (1983) analyzed rocks by NAA after a similar co-precipitation. This is the first report, to the authors' knowledge, of this methodology applied to the analysis of ash material for these elements.

Experimental

The instrumentation used for analysis is the Perkin-Elmer Model 5000 AA spectrometer equipped with the HGA-500 Graphite Furnace and the AS-1 Auto sampler. Operating conditions for the five elements are described in Table 51.5. A cleaning cycle is required for Rh to eliminate a memory effect. Calibration is made with synthetic solutions taken through the identical procedure. Background correction (deuterium arc) and the "argon interrupt" mode are used throughout the analyses. Absorbance is read as peak height rather than peak area.

The major part of the investigation to date has involved the study of the decomposition, separation and final dissolution procedures, using synthetic solutions to estimate recovery. The proposed procedure is outlined below. Hydrofluoric acid is used to dissolve and volatilize silica, and aqua regia to actually dissolve the precious metals.

PROPOSED PROCEDURE

1. To a 2000 mg sample in a Teflon beaker, add 5 mL HF (concentrated) and 15 mL aqua regia ($HCl:HNO_3$ = 3:1). Evaporate to dryness.
2. Add 10 mL aqua regia, heat for 1 hour.
3. Transfer to a test-tube and centrifuge.
4. Decant solution into a beaker and evaporate to near dryness.
5. Add 5 mL HCl (concentrated), warm, and add 45 mL H_2O.
6. Add 5 mL of Te solution (1000 μg mL^{-1}, dissolved in 1.2 M HCl) and 5 mL of $SnCl_2$ solution (20 g $SnCl_2 \cdot 2 H_2O$ + 17 mL HCl, diluted to 100 mL with H_2O). Heat the solution to near boiling to coagulate the precipitate.
7. Add a further 2 mL $SnCl_2$ solution for complete reduction and continue heating (about 20 minutes).
8. Filter through a 0.45 μ filter paper (Millipore, type HAWP), washing with 1 M HCl.
9. Place the filter paper containing the precipitate into a glass beaker and add 5 mL aqua regia. Warm and remove filter paper, washing with 1 M HCl.
10. Evaporate to approximately 1 mL and transfer to a calibrated test-tube. Make up to the 10 mL mark with a dilute acid mixture (.2% HNO_3, .02% HCl).
11. Analyse by GF-AAS, calibrating with synthetic solutions taken through the same procedure. A matrix modifier is used in the determination of Au (dilution factor = 5).

Results and discussion

It was found that Te could not be completely removed in the charring step without, at times, encountering loss of analyte (especially Au). Since the presence of Te in the atomization stage suppressed the absorption signals for Au and, to a lesser extent, for Ag and Pt, matrix-matching of calibration standards is mandatory. Comparison of calibration curves constructed by synthetic standard solutions taken through the entire procedure and those simply matched in Te concentration revealed that better than 95% recovery is achieved for Ag, Pt, Rd and Rh; the recovery for Au, however, is about 90% and can indeed fall below this figure without proper care. If the aqua regia digest (in step 10) is allowed to evaporate to dryness rather than to about 1 mL, the recovery for Au can be as low at 75%; the weak acid mixture is obviously not

Table 51.5 Operating conditions used in the determination of Au, Ag, Pd, Pt, Rh by GF-AAS

Parameter	Au	Ag	Pd	Pt	Rh
Injection volume/μL	20	20	20	80	20
Wavelength/nm	242.8	338.3	247.6	265.9	343.5
Drying temperature/°C	130	130	130	130	
130 Ramp/holding time/s	15/20	15/20	15/20	20/40	15/20
Charring temperature/°C	840	500	950	1400	1100
Ramp/holding time/s	10/10	10/10	10/10	10/10	10/10
Atomisation temperature/°C	2500	2400	2600	2700	2600
Ramp/holding time/s	0/5	0/5	0/5	0/5	0/5
Cleaning temperature/°C	–	–	–	–	2700
Ramp/holding time/s					2/1

completely effective in resolubilising Au in that case. The variability in acid concentration created by evaporating down to 0.5 – 2 mL of aqua regia prior to making up to the 5 mL mark did not affect the sensitivity of measurement for any of the analytes.

Most interferences in the determination of these elements by GF-AAS have been reported to occur from the presence of alkali and alkaline earth elements (Slavin and Manning, 1982) and, therefore, do not present a problem here owing to the separation step. Investigation of mutual interferences (at 100-fold excess of the analyte) revealed that only Au is affected by the presence of the other four elements. This interference, enhancement in all cases, can be compensated for by adding 20 μL of a matrix modifier containing 400 ng L^{-1} Ag, Pt, Pd and Rh after automatic injection of analyte solution.

The determination limit for each element, defined as that concentration in a 2 g sample giving an absorbance signal of 0.01, is as follows: 2 ng g^{-1} for Ag, 5 ng g^{-1} for Au; 5 ng g^{-1} for Pd, 5 ng g^{-1} for Rh, and 10 ng g^{-1} for Pt. Contamination from reagents (especially Te and $SnCl_2$) and glassware is encountered only for Ag and care is required in changing batch numbers of such reagents. Results of three separate analyses on each of four different ash samples (twigs, leaves, trunk) are shown in Table 51.6. Rhodium was not found above the determination limit in any of these samples. These samples were collected over a known precious-metal occurrence and, hence, the concentrations are elevated. Reproducibility appears to be good, perhaps with the exception of Ag where dilution is required to reduce the concentration to be within the working range (<20 ng L^{-1}) and hence an error is introduced. Silver at these high levels would best be determined by the less sensitive technique of flame-AAS. At this time, comparative analyses by NAA are not available. Unfortunately, international reference materials reflecting biogeochemical types of sample matrix with certified values for these metals are not in existence. Hence, an evaluation of the accuracy of the proposed procedure is speculative at present.

Future work consists of obtaining independent analytical data to ascertain the accuracy of this methodology, analyzing more bulk control samples to better define the precision at various concentrations, and, finally, analyzing the same solutions by ICP-MS, with sample introduction by conventional nebulization and electrothermal vaporization.

REFERENCES

Dunn, C.E.
1986: Biogeochemistry as an aid to exploration for gold, platinum and palladium in the northern forests of Saskatchewan, Canada; Journal of Geochemical Exploration, v. 25, p. 21-40.

Elson, C.M., and Chatt, A.
1983: Determination of gold in silicate rocks and ores by coprecipitation with tellurium and neutron activation--spectrometry; Analytica Chimica Acta, v. 155, p. 305-310.

Fryer, B.J., and Kerrich, R.
1978: Determination of precious metals at ppb levels in rocks by a combined wet chemical and flameless atomic absorption method; Atomic Absorp tion Newsletter, v. 17, p. 4-6.

McHugh, J.B.
1983: Determination of gold in water in the nanogram range by electro thermal atomization after coprecipitation with tellurium; Atomic Spectroscopy, v. 4, p. 66-68.

Sighinolfi, G.P., Gorgoni, C., and Mohamed, A.H.
1984: Comprehensive analysis of precious metals in some geological standards by flameless AA spectroscopy; Geostandards Newsletter, v. 8, p. 25-29.

Slavin, W., and Manning, D.C.
1982: Graphite furnace interferences, a guide to the literature; Progress in Analytical Atomic Spectroscopy, v. 5, p. 243-340.

PART 3: SAMPLE INTRODUCTION METHODS BASED ON FLOW INJECTION ANALYSIS

Introduction

Sample introduction methods based on injection of small samples into a carrier stream and then into an atomic absorption spectrometer are currently being developed. In general terms, introduction of small amounts of sample into flowing streams, which are generally reagents, followed by analysis with an on-line detector, is known as flow injection analysis (FIA). The methods being developed are focused on system miniaturization with the following goals: increased efficiency, lower detection limits, system automation and considerable reduction in the amount of reagents required. The first paper describing FIA was published in 1975 (Ruzicka

Table 51.6 Analytical results for Au, Ag, Pd and Pt in four in-house ash samples (Three separate decompositions were performed for each sample)

Sample	Au/ng g^{-1}	Ag/ng g^{-1}	Pd/ng g^{-1}	Pt/ng g^{-1}
5001 – tree trunk	50; 62; 59	20,000; 15,000; 18,400	73; 87; 77	195; 215; 192
5001 – twig	210; 200; 212	6,500; 6,400; 8,200	427; 395; 435	800; 700; 700
8020C – twig	21; 15; 15	480; 450; 425	32; 32; 24	<10; <10; <10
8020C - leaves	53; 54; 70	1100; 1050; 1300	145; 155; 155	122; 110; 114

and Hansen, 1975) and there is now an annual international conference concerning this area of study. The reader is referred to a recent review by Ruzicka and Hansen (1986) published in a special issue of the journal, Analytica Chimica Acta, devoted solely to the topic of FIA.

Flame atomic absorption spectrometry is a widely used technique for the analysis of geological and environmental samples for trace metals. Although it is much less sensitive than the graphite furnace technique (GFAAS), the problems associated with interferences are generally less severe. Since it has the ability to continuously monitor the analyte in a liquid stream, it is more efficient than GFAAS and therefore more suitable for on-line combination of automated sample preparation/analysis schemes. However, in order to achieve the required detection limits, preconcentration of the analytes prior to the actual analysis becomes necessary. The following preconcentration/matrix separation methods are currently being developed at the GSC.

On-line preconcentration

Micro-columns made of chelating resins (e.g., Chelex-100) can be used to preconcentrate trace elements for subsequent elution of the analytes directly into the detector (Hartenstein et al., 1985). This will enable one to achieve much greater sensitivities and to remove interfering matrices. Preliminary results have shown that this technique has great promise for matrices such as natural waters, seawater or rock digests where analytes are generally present at very low levels in high salt matrices.

Automation of such a scheme will involve three basic steps: preconcentration, elution and rinsing/column conditioning. In order to achieve high preconcentration factors and, hence, very low detection limits, the amount of sample being used for preconcentration has to be as large as possible compared to the volume of eluent used for elution of the analyte from the column. As the flow rates through these micro-columns have practical limits, one has to come to a compromise between the sample throughput and the preconcentration factor. To circumvent this problem, a parallel multi-column system is being developed which would dramatically improve the sample throughput without sacrificing the enrichment factors. In this way, since the sample throughput will be limited only by the detection time, it is expected to achieve sample throughput rates in the order of 120 measurements/hour.

With the choice of suitable chelation chemistries, the above system can be extended for chemical speciation of trace metals in natural waters, etc. (Luque De Castro, 1986).

On-line solvent extraction

Solvent extraction is unavoidable in certain situations and extraction schemes which are commonly used in our laboratory are generally tedious and time consuming. Furthermore, a minimum volume of sample and reagents has to be used due to manual handling even in situations where only a few microliters of the extract are required for the final analysis. An automated on-line solvent extraction system is being developed to achieve much higher sample throughput, improved extraction efficiency and unattended operation. In addition, since the extractant used is only that amount required for the actual analysis, this should result in considerable reduction in the cost of reagents, typically by a factor of 100. Since the system has been designed using miniaturized Teflon components, problems associated with the use of bulk glassware, such as cross contamination, should be minimal.

FIA-hydride generation

Hydride generation – atomic absorption spectrometry (HG-AAS) is a highly sensitive technique for the determination of volatile hydride-forming elements such as As, Bi, Sb, Se, Te and Sn. Despite its high sensitivity, if the system is not designed properly, it can generate irreproducible signals.

A HG-AAS system has been developed using a microflow convergence technique in order to attain highly reproducible signals. Without any attempt to optimise the system, it has been possible to attain a detection limit of 0.2 ppb (in solution) for Sn. Besides the low detection capability, the above system has improved the sample throughput to more than 120 measurements/hour as opposed to about 30 measurements/hour with the conventional system. Since the present system uses considerably smaller flow rates, it will provide a considerable saving on the reagent usage, probably by a factor of 10.

The flame-heated quartz atomization cell in the detection system has been replaced by an electrically-heated cell which has made the temperature of the quartz cell much more stable on both a short and and long-term basis. This has resulted in very stable signals and baseline. With the current system, dispersion of the analyte appears to be governed by the volume of the quartz atomization cell which was previously designed for a flame-heated system. Optimum dimensions of the cell are being investigated and it is expected to reduce the sample/reagent flow rates even further with the same or better sensitivities.

REFERENCES

Hartenstein, S.D., Christian, G.D., and Ruzicka, J.
1985: Applications of an on-line preconcentrating flow injection analysis system for inductively coupled plasma atomic emission spectrometry; Canadian Journal of Spectroscopy, v. 30, p. 144-148.

Luque De Castro, M.D.
1986: Speciation studies by flow-injection analysis; Talanta, v. 33, p. 45-50.

Ruzicka, J. and Hansen, E.H.
1975: Flow injection analysis. Part 1. A new concept of fast continuous flow analysis; Analytical Chimica Acta, v. 78, p. 145-158.
1986: The first decade of flow injection analysis: from serial assay to diagnostic tool; Analytical Chimica Acta, v. 179, p. 1-58.

A preliminary investigation of the application of microwave radiation for the dissolution of geological materials

Projects 580175 and 690090

J.L. Bouvier and G.E.M. Hall
Mineral Resources Division

Bouvier, J.L. and Hall, G.E.M., A preliminary investigation of the application of microwave radiation for the dissolution of geological materials; in Current Research, Part A, Geological Survey of Canada, Paper 87-1A, p. 485-488, 1987.

Abstract

Microwave radiation is providing a new and efficient method by which to dissolve geological materials. Advantages include significant economies of time and amount of reagents required, minimal cross-contamination and loss by volatilization. A recently purchased microwave oven, specially designed to vent acid fumes has been used to decompose a suite of 27 Cu/Ni sulphide-enriched samples by an aqua regia – HF attack. Comparison of results of this initial study with the two lengthy procedures now used in the determination of major, minor and trace elements is shown for 16 elements. Only Ni and Si values appear low, by about 10% or less, and modifications to the procedure should rectify this problem. This preliminary investigation is most promising and examination of other types of matrices is planned.

Résumé

Une nouvelle méthode utilisant des micro-ondes permet de dissoudre des spécimens géologiques avec beaucoup d'efficacité. Cette méthode, entre autres avantages, permet d'économiser beaucoup de temps, diminue la quantité de réactifs nécessaire, et prévient la contamination d'un élément par un autre et la perte par volatilisation. La Division vient de se doter d'un four à micro-ondes spécialement conçu pour dissiper les vapeurs acides. On l'a utilisé pour décomposer une série de 27 échantillons enrichis en sulfures du Cu-Ni par attaque HF à l'eau régale. Les résultats obtenus pour 16 éléments à l'aide de cette technique ont été comparés à ceux de deux longues méthodes actuellement utilisées pour déterminer les éléments majeurs, accessoires et traces. Seules les valeurs de Ni et Si apparaissent sous-estimées, d'environ 10 % ou moins; les modifications apportées à la méthode devraient corriger ce problème. Cette étude initiale est des plus prometteuses, et on prévoit déjà d'examiner d'autres types de matrices.

Table 52.1 Results of analyses by ICP-ES: comparison of microwave dissolution vs conventional procedures*

Element (oxide)	Sample 31		Sample 10		Sample 11	
	Microwave procedure	conventional procedure	Microwave procedure	Conventional procedure	Microwave procedure	Conventional procedure
SiO_2/%	45.4	48.9, 48.5	40.5	43.3	39.4	42.5, 42.5
TiO_2/%	0.14	0.17, 0.17	0.16	0.20	0.17	0.24, 0.24
Al_2O_3/%	15.4	14.7, 14.7	14.5	14.0	13.1	12.5, 12.6
Fe_2O_3T/%	10.5	10.4, 10.7	17.6	17.4	19.7	19.7, 19.2
MnO/%	0.13	0.14, 0.14	0.12	0.12	0.12	0.12, 0.12
MgO/%	10.4	10.4, 10.7	9.30	9.32	9.40	9.43, 9.34
CaO/%	9.10	9.50, 9.60	9.50	9.43	9.10	9.27, 8.49
Na_2O/%	1.40	1.41, 1.36	0.99	0.94	1.20	1.13, 0.94
K_2O/%	0.74	0.77, 0.61	0.24	0.17	0.29	0.22, 0.22
Ba/ppm	100	110, 110	80	80	90	80, 80
Co/ppm	98	110, 120	260	280	320	370, 370
Cr/ppm	480	510, 580	100	100	110	110, 130
Cu/%	0.22	0.23, 0.24	0.27	0.26	0.24	0.24, 0.24
Ni/%	0.31	0.35, 0.36	0.39	0.42	0.47	0.52, 0.53
V/ppm	78	79, 86	81	81	83	86, 87
Zn/ppm	106	120, 130	68	74	70	88, 91
S/%	2.3		5.6		6.7	

*(Major elements reported as oxides by convention)

Element (oxide)	Sample 103		Sample 13		Sample 99		Sample 151	
	Microwave procedure	Conventional procedure	Microwave procedure	Conventional procedure	Microwave procedure	Conventional procedure	Microwave procedure	Conventional Procedure
SiO_2/%	22.4, 20.1	27.2	24.9	26.2	22.6, 24.9	27.9	9.50, 9.70	9.90
TiO_2/%	0.12, 0.11	0.13	0.07	0.08	0.08, 0.07	0.10	0.05, 0.06	0.06
Al_2O_3/%	6.38, 6.19	5.98	8.70	8.38	6.10, 6.41	6.10	1.06, 0.93	0.93
Fe_2O_3T/%	40.8, 40.2	40.8	38.9	40.3	37.5, 39.6	39.9	56.0, 61.7	59.5
MnO/%	0.08, 0.07	0.07	0.08	0.08	0.05, 0.05	0.05	0.07, 0.07	0.07
MgO/%	6.56, 6.50	6.70	6.30	6.42	5.67, 5.88	6.08	3.35, 3.41	3.59
CaO/%	4.01, 4.08	4.08	5.90	5.82	4.32, 4.45	4.57	1.96, 1.98	2.09
Na_2O/%	0.87, 0.84	0.80	0.72	0.58	0.90, 0.92	0.89	0.16, 0.14	0.15
K_2O/%	0.48, 0.49	0.34	0.19	0.15	0.37, 0.40	0.30	0.38, 0.37	0.10
Ba/ppm	100, 100	90	60	60	60, 70	70	60, 70	60
Co/ppm	800, 780	860	850	940	1100, 1100	1200	1400, 1300	1500
Cr/ppm	380, 380	360	73	87	360, 350	300	390, 360	410
Cu/%	0.40, 0.40	0.39	0.43	0.42	0.39, 0.39	0.39	1.4, 1.3	1.5
Ni/%	2.1, 2.1	2.4	1.5	1.6	2.4, 2.2	2.5	4.7, 4.4	4.9
V/ppm	80, 77	78	39	37	90, 87	89	22, 19	24
Zn/ppm	200, 340	230	93	110	210, 140	160	290, 270	320
S/%	19.4		19.8		20.3		31.4	

INTRODUCTION

Major advances in improved precision and accuracy have been made during the last decade in the analytical techniques of inductively-coupled plasma emission spectroscopy (ICP-ES) and flame and non-flame atomic absorption spectroscopy. These techniques, however, as well as the 'newcomer', ICP – mass spectroscopy, suffer from one important disadvantage: the sample must be brought into solution prior to elemental analysis. Solid-sample introduction is in its infancy, although the number of researchers in this field is increasing. Thus, the need to find an alternative dissolution technique to the conventional slow acid attack in open beakers or test-tubes on hot-plates or in heating-blocks has led investigators to examine the potential of the microwave oven.

The speed of dissolution is greatly enhanced using microwave radiation because energy is transferred to the sample by immediate absorption of radiation rather than through convection or conduction processes. Such intense internal heating causes rapid attack of sample surface layers and exposure to acid of new surfaces and, hence, hastens solubility. Most chemists studying decomposition procedures with microwave radiation are using closed Teflon digestion vessels since open work causes corrosion of equipment, possible cross-contamination, and volatilization losses. The use of elevated temperature and pressure increases the rate of reaction dramatically. The efficiency of the digestion, and, indeed, the safety of the procedure, is governed by critical control of this temperature and pressure. Kingston and Jassie (1986) have stressed the importance of understanding the fundamental parameters which control the reactions between the acids and the 2450 MHz microwave. They have computed the amount of power absorbed by each acid in single acid decompositions and then predicted the time and temperature necessary for a particular digestion. This is probably the first description of various procedures used where mathematic modelling rather than trial and error adjustment has led to optimization of conditions. This type of approach should be further applied to the multi-acid digestion situation. Teflon-PFA (perfluoralkoxy) material is commonly used to construct the sample-containing vessels as it has proved to be resistant to bulging and deformation which would lead to leakage.

The first report on the application of microwave radiation to the acid dissolution of geological samples (Matthes et al., 1983) described a modification of a conventional oven where any acid fumes generated were expelled to a fume-hood with a CO_2 gas flow (also used for cooling) through pre-drilled holes. To prevent uneven heating caused by the presence of hot spots, the samples were placed in polypropylene sealed bottles located in a rack on a moving carousel. Twelve samples could fit in the oven at once and a two-stage heating cycle was used: an initial 3 minute digestion in a mixture of HF-$HClO_4$-HNO_3 followed by a second 2 minute (sometimes longer) dissolution after boric acid (to complex excess F^-) had been added. Accurate and precise major element data were reported on three, previously certified, samples – a furnace slag, a feldspar, and an alloy.

Nadkarni (1984) studied the effectiveness of a 3 minute digestion at a 625 W power setting using a mixture of HF and aqua regia on, amongst other materials, two standard rocks (W-1 and BCR-1) and two standard sediments (IAEA SL-1 and NBS-1645). Of the 19 elements analyzed, agreement with recommended values was good for all except Cr, P, Mg and Ti where significantly lower results were obtained. An eight-fold reduction in digestion time was achieved by Smith et al. (1985) in changing from conventional methods to a 3 minute digestion at 477 W power (4 samples at once) in attacking Cu and Ni sulphide samples with a mixture of HF-HNO_3 and $KClO_3$. However, a residue of undissolved silica was found with some of the samples but this did not pose an immediate problem as it did not contain any traces of the analytes, Cu and Ni. Labrecque (1985) has described a dissolution procedure suitable for Pb, Cu and Ag concentrates where eighteen 300 mg samples are heated successively with HNO_3, HCl and H_2O at a microwave power/time combination of 240 W/3 minutes, 240 W/3 minutes, and 600 W/5 minutes, respectively. However, the maximum concentration of Pb reported was only about 1% and application of the above technique in this laboratory to samples where the main mineral constituent was galena was unsuccessful. Lamothe et al. (1986) reported accurate results on most of the elements analyzed in 51 geological reference materials where 12 samples (at once) of 100 mg each were digested with HF-HCl-HNO_3 for 2.5 minutes at 650 W power followed by a 10 minute cycle at 650 W power when boric acid, H_3BO_3, had been added. When Si was present as quartz, recovery was less than 50%, even with a finely ground sample of less than 325 mesh. Evaluation of the residues obtained in the dissolution of rocks revealed the main components to be quartz, corundum, chromite, zircon and rutile. The same refractory minerals, as well as cassiterite and magnetite, were found to be unattacked by this procedure when applied to ores and minerals. Furthermore, low recoveries were found for Pb and Ag in the Canadian reference materials, KC-1 and CPb, owing to the low solubilities of $PbSO_4$ and AgCl.

Thus, further research is required into the dissolution of refractory minerals and into preventing the precipitation of analytes once dissolved. This work has been initiated at the Geological Survey of Canada and is ongoing at Kidd Creek Mines, Timmins, Ontario (Labreque, personal communication, 1986) and at the National Bureau of Standards in Washington (Kingston, personal communication 1986). A bomb, recently manufactured to withstand 100 atmospheres pressure, may prove effective in overcoming some of these dissolution problems, thereby negating the need for present-day fusion attacks. We report, in this publication, our initial findings in carrying out an aqua regia – HF decomposition on a suite of Cu/Ni sulphide-rich samples using a microwave oven specially designed for laboratory applications. Analysis for major, minor and trace elements was conducted by ICP-ES and comparison made with conventional digestion procedures.

EXPERIMENTAL TECHNIQUES AND RESULTS

Equipment

The laboratory microwave oven used was the Model MDS-81 (CEM Corp., NC, U.S.A.), equipped with a 600 W magnetron of variable power in 1% increments. The Teflon – PFA digestion vessels were of 150 mL capacity and were manufactured by Savillex Corp., MN, U.S.A. The oven cavity was exhausted to a laboratory fume hood by a variable speed fan.

The ICP emission spectrometer used for analysis was the Jobin-Yvon Model 48 simultaneous instrument and major element corrections were made using coefficients previously established. All acids used were reagent grade and water was distilled, deionized.

Procedure

(1) Into each of 12 flasks, weigh a 500 mg sample. Add 6 mLs HNO_3 (concentrated) and 2 mLs HCl (concentrated). Cap, using the capping station.

(2) Heat at 80% power for 10 minutes.

(3) Cool in a water bath and add 7 mLs HF (concentrated). Cap.

(4) Heat at 80% power for 20 minutes.

(5) Cool, and add 27 mLs H_2O, 2.5 mLs of 0.8% EDTA and 3 g H_3BO_3. Cap.

(6) Heat at 80% power for 10 minutes.

(7) After cooling, transfer the contents to a calibrated 50 mL test tube and make up to volume with H_2O.

(8) Analyze the solution by ICP-ES (dilution factor = 100).

Results and discussion

Typical results obtained for the 27 Cu/Ni sulphide-rich samples analyzed are shown in Table 52.1, together with their S contents. Duplicate analyzes (separate decompositions), where made, are also given. An additional 0.5 g H_3BO_3 were added followed by a 10 minute heating cycle when a white, amorphous residue (CaF_2) was observed. In this manner, all solutions obtained were clear. Two separate decompositions are made in the conventional procedure: a lithium metaborate ($LiBO_2$) fusion after roasting (for sulphides) to determine major and minor elements, and an open HF-$HClO_4$-HNO_3-HCl attack with a $LiBO_2$ fusion of any remaining residue to determine the trace elements. Dilution factors are 500 and 100, respectively. Examination of the data reveals that agreement with conventional procedures is generally good for the 16 elements analyzed except for SiO_2, and, to a lesser extent, Ni. Contamination may have been the cause for the higher Zn values in the duplicate results for samples 103 and 99. It should be noted here that calibration strategies on the JY-48 are set up to analyse solutions obtained by the conventional procedures and, thus, there may be a shift in background occurring at certain wavelengths which is not being taken into account in this preliminary investigation. Hence, the authors conclude this to be the factor responsible for the lower Ni values. However, the low results obtained here for SiO_2 and also evidenced in the decompostion of in-house control samples (the Q-series) lead us to conclude that the digestion is not completely efficient for SiO_2 or it is partially lost as SiF_4. Changes in the procedure to improve recovery and precision are under investigation. The tremendous saving in time and cost of reagents incurred by eliminating the requirement for two separate decomposition procedures is particularly beneficial.

Future work will examine the effectiveness of microwave dissolution on various sulphide samples (galena, pyrite, molybdenite) with the objective of maintaining a small dilution factor ($\leq$100) so that determination of trace elements within these sulphide mineral samples by ICP-ES remains feasible with adequate limits of detection. The labour-intensive manipulations of placing samples in the microwave oven, adding reagents and so on, are ideally suited to the application of a robotics system. This is currently underway at Kidd Creek Mines and the National Bureau of Standards. Combination of robotics and microwave dissolution will realise many advantages over present day decomposition procedures, namely: enormous savings in time and costs of reagents, minimal cross-contamination and loss of elements through volatilization, reduced need for expensive fume hood systems, and increased safety in the laboratory.

REFERENCES

Kingston, H.M. and L.B. Jassie
1986: Microwave energy for acid decomposition at elevated temperatures and pressures using biological and botanical samples; Analytical Chemistry, v. 58, p. 2534-2541.

Labrecque, J.
1985: Microwave pressure dissolution system at Kidd Creek Mines: a review; 17th annual Canadian Mineral Analysts Conference, Sept. 17-20.

Lamothe, P.J., Fries, T.L. and Consul, J.J.
1986: Evaluation of a microwave oven system for the dissolution of geologic samples; Analytical Chemistry, v. 58, p. 1881-1886.

Nadkarni, R.A.
1984: Application of microwave oven sample dissolution in analysis; Analytical Chemistry, v. 56, p. 2233-2237.

Matthes, S.A., Farrell, R.F., and Mackie, A.J.
1983: A microwave system for the acid dissolution of metal and mineral samples; U.S. Department of the Interior, Technical Progress Report 120, pp 9.

Smith, F., Cousins, B., Bozic, J. and Flora, W.
1985: The acid dissolution of sulphide mineral samples under pressure in a microwave oven; Analytical Chimica Acta, v. 177, p. 243-245.

Metallogeny of the Woodstock area, New Brunswick[1]

DSS Contract 51SZ 23233-6-0080

R.D. Thomas[2] and C.F. Gleeson[2]

Thomas, R.D. and Gleeson, C.F., Metallogeny of the Woodstock area, New Brunswick; in Current Research, Part A, Geological Survey of Canada, Paper 87-1A, p. 489-498, 1987.

Abstract

The area is underlain mainly by Cambro-Ordovician quartzites with interbeds of slate, intruded by Devonian felsic stocks.

Sulphide mineralization is dominated by a porphyry copper deposit on Connel Mountain where 21 million tonnes grading 0.18% Cu have been outlined. The deposit is made up of disseminated and fracture filling chalcopyrite, pyrrhotite and pyrite in altered quartz diorite and granodiorite of the Gibson stock. The deposit is cored by a zone of phyllic alteration marked by strong sericitization, chloritization, silicification and sulphidation. Outside the core a zone of propylitic alteration hosts copper mineralization in quartz veins and stockworks in quartzite and granodiorite. Vein deposits of lead, in places containing sphalerite and chalcopyrite, are hosted in the sedimentary rocks outside the alteration zones.

Gold mineralization is most common in north-trending quartz veins in the propylitic zone. They are hosted in quartz-eye porphyry and granodiorite of the Gibson stock and in quartzite. Gold in lesser but anomalous quantities is also found in the porphyry copper zone on Connell Mountain.

Résumé

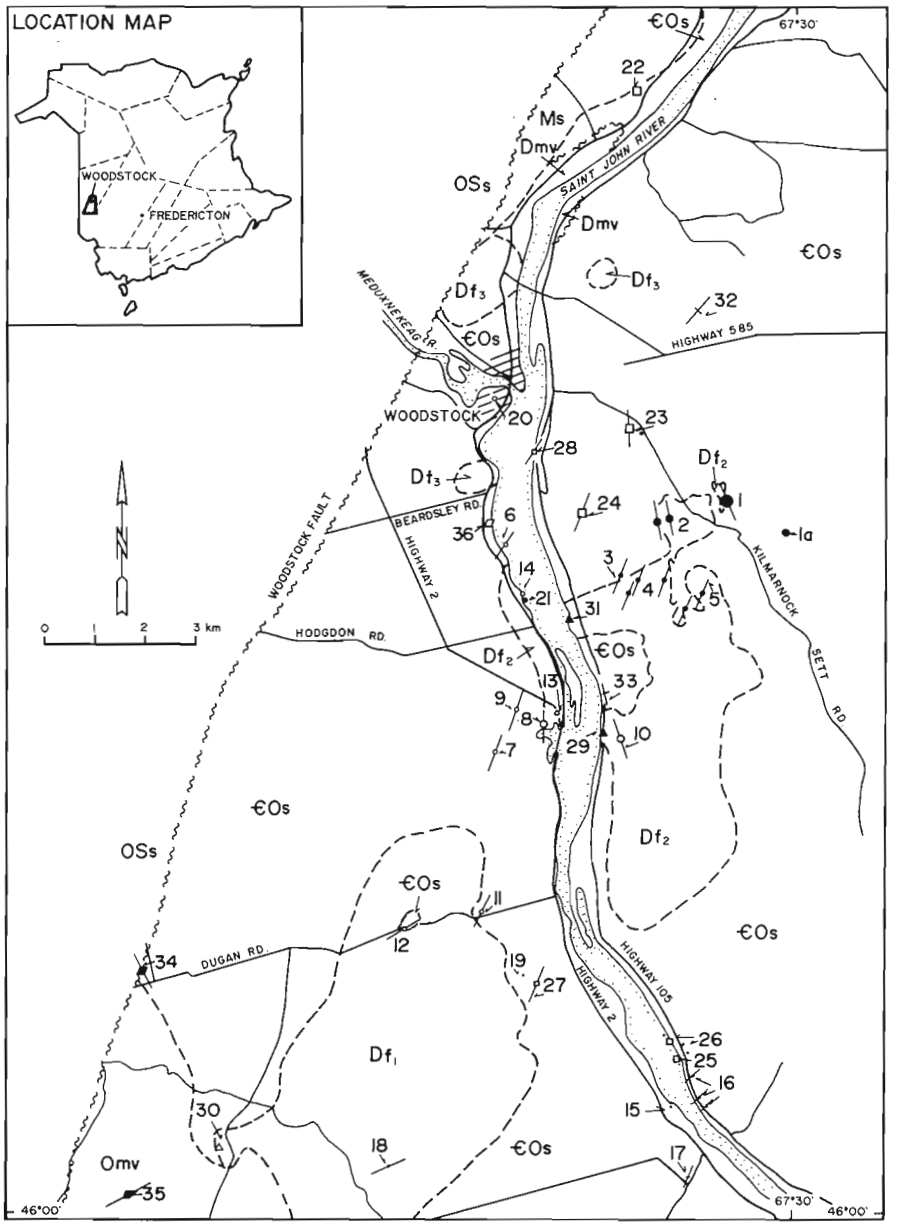
La région repose principalement sur des quartzites cambro-ordoviciennes à interstratifications de schiste ardoisier que recoupent de petits massifs intrusifs felsiques d'âge dévonien.

La minéralisation sulfurée prend la forme d'un gîte de porphyre cuprifère dans le mont Connell; les réserves y sont estimées à quelque 21 millions de tonnes d'une teneur de 0,18 % en Cu. Le gîte contient de la chalcopyrite, de la pyrrhotite et de la pyrite qui se présentent sous forme de minerais disséminés et de remplissages de fractures dans une diorite quartzique et une granodiorite altérées du massif intrusif de Gibson. Le noyau du gîte se compose d'une zone d'altération phylliteuse fortement marquée par des épisodes de séricitisation, chloritisation, silicification et sulfuration. À l'extérieur du noyau, une zone de propylitisation contient une minéralisation cuprifère dans les filons de quartz et les stockwerks de la quartzite et de la granodiorite. Les roches sédimentaires à l'extérieur des zones altérées contiennent des gisements filoniens plombifères qui, par endroits, renferment de la sphalérite et de la chalcopyrite.

Une minéralisation aurifère est très répandue dans les filons de quartz à orientation nord gisant dans la zone propylitisée. Ces filons sont encaissés dans le porphyre oeillée et la granodiorite du massif intrusif de Gibson et dans de la quartzite. La zone de porphyre cuprifère du mont Connell contient également des concentrations inférieures mais toutefois anormales d'or.

[1]Contribution to Canada – New Brunswick Mineral Devleopment Agreement 1984-1989. Project carried by Geological Survey of Canada, Mineral Resources Division

[2]C.F. Gleeson and Associates Ltd., Lakeshore Drive, R.R. 1, Iroquois, Ontario K0E 1K0



MISSISSIPPIAN

Ms Red clastic sediments

DEVONIAN

Df_3 Other granitic bodies

Df_2 Gibson Granite

Df_1 Benton Granite

LOWER DEVONIAN

Dmv Mafic flows and lapilli tuff

ORDOVICIAN and/or SILURIAN

OSs Undifferentiated sediments

ORDOVICIAN

Omv Mafic flows and tuffs

CAMBRIAN-ORDOVICIAN

€Os Grey clastic sediments

MINERAL OCCURRENCES (numbered according to Table 1)

- Porphyry copper (large, medium, small)
- Vein type and porphyry affiliate copper (large, medium, small, erratics)
- Vein-lead (medium, small)
- Fracture filling-copper
- Vein-Gold (vein,erratics)
- Barite veins
- Iron,Manganese (outcrop,erratics)

Note: line through symbol shows orientation of mineralized structure or vein

Figure 53.1. Mineral occurrences (identified in Table 53.1) of the Woodstock area (Geology modified after Venugopal 1979, 1981 and Lockhart 1971a, 1971b, Hamilton-Smith 1971)

INTRODUCTION

The Woodstock area, located 100km west of Fredericton, New Brunswick, has been actively explored for minerals since the mid 19th century. Initial interest in the area concerned the Silurian iron-manganese deposits at Jacksonville, to the northwest of Woodstock. These deposits, first described by Dr. C.T. Jackson as part of an assessment of the mineral potential of the State of Maine, were mined between 1848 and 1884, during which time approximately 63 600 tonnes (70000 tons) of ore were mined and smelted at Woodstock (Potter, 1983).

Base metals were mined from the Bulls Creek No.2 occurrence (8, in Fig. 53.1) for about four years. Mining was undertaken by the New Brunswick Mining Company which sank a shaft that struck ore in 1858 (Carleton Sentinel, 1858). The Bedell Farm copper occurrence was also explored at this time although there was no production. Prospecting and exploration in the area has continued to the present. A shaft was sunk at the Britton Mine (22) in 1891-1895 (Ingall, 1893, Selwyn, 1895), at the Dominion No. 1 (24) in 1907 and 1927 (Alcock, 1930) and at the Cobbler Sexton (10) in 1907 (Woodstock New Brunswick Press, 1909), but none of these prospects developed into producing mines.

Systematic exploration of the Woodstock area commenced in the early 1950s with the discovery of several mineral occurrences by A.A. Fraser and M.A. Briggs, (15, 25) and F.C. Tompkins (26). It culminated in 1968-1974 when much of the area was staked by A.W. Lockhart and explored by Phelps Dodge Corporation of Canada Ltd., Falconbridge Nickel Mines Ltd., Bethlehem Copper Corporation, and United Siscoe Mines. These programs resulted in the identification of a large porphyry copper system in which 21×10^6 t (23×10^6 tons) of protore grading 0.18% Cu and 0.9×10^6 t (1×10^6 tons) of supergene enriched ore grading 0.04-0.7% Cu were indicated (Venugopal, 1981).

Gold exploration in the area has been poorly documented. Quartz vein boulders with chalcopyrite and gold have been reported from the Oak Mountain area (30) (Anderson, 1968) and gold-bearing quartz veins are known to occur along the east side of the Saint John River near Upper Northampton (29, 31). There are no records of analyses or of exploration programs that would help determine the extent of gold occurrences at any of these locations. Gold assays of samples from the Cobbler Sexton, Dominion No. 1 and Wright Brook have been reported to contain up to 17.7g/t (Greer, 1938), 3g/t (Wright, 1939a) and 0.3g/t (Wright,1939b) respectively.

In 1985, the Geological Survey of Canada initiated an assessment of the mineral potential, particularly gold, of the central and southwest Miramichi Zone as part of the Canada-New Brunswick Mineral Development Agreement (Connell and Hattie, 1985). Geosleuth Mineral Exploration Services, Sussex, New Brunswick completed phase I of the program and identified the Woodstock area as warranting further investigation. The current project comprises phase II of the program.

TOPOGRAPHY AND DRAINAGE

The area lies within the Chaleur Uplands subdivision of the Atlantic Uplands division of the Appalachians physiographic region (Williams et al., 1972; Rampton and Paradis, 1981). The area is characterized by steep sided knobby hills, separated by broad valleys. Most peaks rise to over 200 m above sea level, with the highest point (284 m) in the area being Oak Mountain. The lowest point in the area is the Saint John River which is controlled at approximately 41 m by the Mactaquac Dam.

Drainage within the area is toward the Saint John River in a well developed bedrock controlled trellis pattern with stream segments oriented north, northeast or northwest. The Saint John River flows generally southwards across the area; in detail it is formed of southwest-, southeast- and south-trending reaches.

It should be noted that the Saint John River was raised approximately 10m in 1970 with the completion of Mactaquac Dam. This caused the flooding and submergence of many mineral occurrences that had been reported adjacent to the old course of the Saint John River.

PREVIOUS REGIONAL WORK

Brief comments have been made concerning various aspects of the geology and mineral occurrences of the Woodstock area in many reports by various authors. The first regional mapping of the geology was completed by Robb (1870). An appraisal of the economic potential of New Brunswick, including some discussion on the Woodstock mineral occurrences was completed by Bailey (1899).

Systematic mapping by Caley (1936) outlined the presence of three Devonian granite or syenite bodies intruded into pre-Silurian quartzites and slates. Caley reported on the iron deposits to the northwest of Woodstock but made no mention of the base metal occurrences in the area. The area was remapped by Anderson (1954, 1968) at the scale of 1:63 360 and by Venugopal (1979, 1981) at a scale of 1:25 000. The geology of the area has been compiled by van der Poll (1967), Hamilton-Smith (1971) and Fyffe (1982a). The mineral occurrence files of the New Brunswick Department of Natural Resources and Energy, Mineral Resources Division, prepared mainly by W.A. Take in 1972, contain the most complete compilation on mineral occurrences in the Woodstock area.

GENERAL GEOLOGY

The project area was restricted to the rocks of the Miramichi Anticlinorium (Rodgers, 1970), a tectonostratigraphic zone comprising Cambrian-Ordovician sediments, Ordovician mafic volcanics, Devonian felsic intrusions and minor areas of Devonian mafic volcanics and Mississippian sediments (Fig. 53.1). To the west, rocks of the Miramichi Anticlinorium are in contact withilurian rocks of the Matapedia Anticlinorium. The contact is marked by the Woodstock

Fault (Venugopal, 1979), a southwestward extension of the Catamaran Fault (Fyffe, 1982b).

Cambrian-Ordovician sedimentary rocks (COs) are a thick sequence of grey to greenish grey quartzites and slates and underlie much of the area. The quartzites are massive and fine grained, commonly in beds 10-20 cm thick but locally finely (2mm) laminated to coarsely (1.5m) bedded. Contacts are sharp with interbeds of slate units 1 mm to several metres thick. Venugopal (1981) observed cross-laminations, current ripples, load casts and flame structures in the quartzites . He also reported the composition of the quartzite as 40-60% quartz, 2-10% plagioclase and potassium feldspar, 1-5% rock (felsic volcanic) fragments and 20-40% matrix containing chlorite, muscovite, quartz, epidote and opaques. Common accessory minerals include zircon, tourmaline and apatite. He classified the rock as a quartz wacke.

Ordovician mafic volcanic rocks (Omv) (Pocomoonshine Volcanics) occur in the southwest part of the area and are composed of flows, tuffs and breccia (Venugopal, 1981). Included in this unit is a sequence of red slates and arenaceous slates that are the host of the Oak Mountain iron-manganese occurrence (35).

Devonian felsic intrusions (Df) occur as two large bodies known as the Benton stock (Df_1) in the southern part of the area and the Gibson stock (Df_2) in the central part of the area. Three smaller bodies of unknown affinity (Df_3) occur in the northern part of the area. The central part of the Benton Stock is pink, porphyritic quartz monzonite (Crocco, 1975), whereas the western portion toward Oak Mountain is grey, equigranular granodiorite. The Gibson stock is white to light pinkish grey, porphyritic to equigranular granodiorite, quartz monzonite and granite. The variability of texture and composition suggests to emplacement by multiple intrusions. The smaller bodies of felsic intrusives (Df_3) represented by few outcrops, are described by Venugopal (1981) as pinkish grey feldspar porphyry and feldspar-quartz porphyry. The two bodies to the north of Woodstock are epidotized, sericitized and chloritized; the one to the south is chloritized, sericitized and carbonatized.

Devonian mafic volcanic rocks, which occur only in the northern part of the area, are greyish, green porphyritic andesite flows of the Tobique Group (Venugopal, 1981). Mississippian sedimentary rocks which lie to the northwest are part of the Carlisle Formation, a sequence of red interstratified conglomerate, sandstone and shale (Venugopal, 1981).

Mafic dykes (not shown in Figure 53.1) are common throughout the area. Up to several metres wide, they trend northwesterly to northeasterly. They are dark grey, massive and fine grained to porphyritic. Commonly carbonatized, they appear to have chloritized adjacent host rocks. Generally considered to be Devonian, it is possible that two sets of dykes are present and that the later set is Triassic. Felsite dykes and breccia dykes occur within the area, particularly associated with the Gibson Stock. Both of the latter types of dykes are Devonian in age.

MINERAL OCCURRENCES

The main features of the mineral occurrences are outlined in Table 53.1; their locations are shown in Figure 53.1. Of the 36 occurrences tabulated, 26 were examined in the field. The remainder are covered by the flood waters of the Mactaquac Dam or occurring only in drillholes, the core from which has been lost.

Porphyry deposits – copper:

These deposits are concentrated in the northern part of the Gibson Stock where it intrudes quartzites. They were found by W. Lockhart (1976) in 1970 using soil geochemistry and on whose assessment reports (Lockhart 1971a, b; 1974) much of the ensuing descriptions are based. The main interest is on Connell Mountain (1) where some 21×10^6 t grading 0.18% copper have been outlined by trenching, diamond drilling and percussion drilling. Lockhart Anomaly 1a (Fig. 53.1) is probably an extension of occurrence 1. It has been prospected and percussion drilled but has not been completely evaluated (Lockhart 1974).

Greenish black to dark grey argillites, grey slates and quartzites, dipping steeply west and southwest comprise the sedimentary host rocks of the deposits. These have been brecciated and metamorphosed to meta-argillites and hornfels. Granodiorite to quartz diorite form the intrusive host rocks of the Connell Mountain area (1 and 1a) whereas quartz monzonite to granite host the other occurrences near Connell Mountain (2-5). The intrusive rocks generally orphyritic, but equigranular phases are common. Several Late Devonian, northeast trending, gabbroic and diabasic dykes, 1 m to 7 m wide transect most occurrences.

According to Lockhart (1974), phyllic alteration dominates and it restricted to the mineralized zone. This alteration is marked by moderate to strong sericitization of the feldspars, chloritization of mafic minerals silicification as numerous 1-2 cm quartz veinlets and stringers, bleaching and weak epidotization of the quartzites and moderate carbonatization as 1 cm calcite veins.

Primary Sulphide minerals are disseminated in the intrusive rocks and occur as fracture fillings in the intrusive and sedimentary rocks. Non-magnetic pyrrhotite is the dominant sulphide mineral. It is associated with and appears contemporaneous with chalcopyrite. Pyrite with associated chalcopyrite is mutually exclusive of pyrrhotite. It occurs as fracture fillings in the sedimentary rocks and may represent a second stage of sulphide mineralization. Trace amounts of molybdenite are reported from quartz veins and shear planes. Rare magnetite is reported from some drillholes primarily from Connell Mountain. Supergene enrichment has been identified to a depth of 15 m and is marked by the occurrence of thin coatings of tenorite, malachite, azurite and chalcocite on pyrite and chalcopyrite. The enrichment has tripled the copper content of the rock.

Preliminary analyses indicate a mean gold content of

15 ppb (7-21 ppb) for the intrusive rocks and 7 ppb for the quartzites from the Connell Mountain area. All four samples submitted from Connell Brook (2) contain less than 1 ppb Au. The slates from Monteith Farm (3) have 2 and 6 ppb Au in them. Three samples of quartz diorite from Smart Farm (4) contain 2, 21 and 32 ppb Au. One sample of quartzite from Upper Northampton Copper (5) contains 6 ppb Au whereas four other samples including sedimentary and intrusive rocks contain less than 1 ppb Au. Anomalous gold contents have been obtained from chloritized and silicified quartzites from Connell Mountain (32-290 ppb Au) and from chloritized granodiorite from Smart Farm (94 ppb Au). All of these samples have 5-10% pyrite in them. A coarse pyrite lens from Connell Mountain (1) contains 130 ppb Au and a gossan developed on a quartz vein contains 1300 ppb Au over a width of 50cm.

Vein type – and/or porphyry affiliated – Copper

Deposits in this group are characterized by chalcopyrite and pyrite in north- to northeast-trending quartz veins and stockworks. For the most part the host rocks are quartzite and granodiorite-quartz monzonite of the Gibson Stock, although the Bedell Farm occurrence (6) is reported to be in slates. The most mineralized occurrences (8 and 10) are near the west contact of the Gibson Stock, although the Dugan Road (11 and 12) and Hillman Copper (15) occurrences are spatially related to the Benton stock.

Silicification, chloritization, bleaching and /or hornfelsing are common alteration products in this group of occurrences. Carbonatization is present at Bulls Creek No.1 (7), Cobbler Sexton (10) and Dugan Road East (11). Epidotization andotassic alteration has occurred at Bulls Creek No. 2 (8). Interchange Copper (13) and Silvermaque (14).

Sulphide mineralization commonly consists of pyrite and chalcopyrite in quartz or quartz-calcite veins. The wall rocks commonly contain only pyrite except for Dugan Road East and West (11 and 12) the brecciated hornfels contains chalcopyrite and pyrite as fracture fillings. Pyrrhotite occurs at Bedell Farm (6) and Hillman Copper (15) while galena and sphalerite are present at Bulls Creek No. 2 (8) and Cobbler Sexton (10).

Preliminary gold analyses show up to 31 ppb Au at Bulls Creek No.1 (7), up to 1200 ppb Au at Bull Creek No.2 (8) and up to 650 ppb Au at Bulls Creek No. 3 (9). The anomalous samples (seven samples greater than 80 ppb Au) from the latter two occurrences are sulphide bearing quartz or quartz-carbonate veins, or associated wall rock. Unaltered quartzite and granodiorite contains less than 1 to 8 ppb Au (ten analyses). Visible gold was reported by R.W. Ells (Woodstock, New Brunswick Press, 1909) from the adit of the Cobbler Sexton occurrence (10) . Samples of mineralized quartz vein material from the waste pile contains 17 and 25 ppb Au. A quartz vein from one of the trenches contains 6-12ppb Au whereas the quartzite, wall rock has 7 ppb Au. Only one of eight samples submitted from Dugan Road East (11) has more than 1 ppb Au. This sample (55 ppb Au) consists of a 10 cm lens of massive pyrite filling a fracture in the hornfels. The Dugan Road West (12) occurrence appears to be low in gold (2 ppb) but a xenolith in the Benton stock some 60 m west of the occurrence contains 7 ppb Au.

Minor copper occurrences – fracture fillings

These occurrences are characterized by thin fracture fillings of chalcopyrite and pyrite in quartzite and at one location (18) in the Benton stock. Two of the occurrences, Woodstock Copper-Lead (20) and Wetmore Copper (21), are no longer accessible. The sulphide mineralization in this group of occurrences is accompanied by a significant increase in silicification as quartz stringers parallel to the main fractures and chloritization of wall rock immediately adjacent to the stringers.

Preliminary gold analyses indicate up to 10 ppb Au in a pyritized, silicified shear zone at Upper Northampton Copper (16), 4 ppb Au in a pyritized, vuggy quartz vein at Riceville Copper (17), and less than 1 ppb Au at Benton Copper (18).

Vein deposits – lead:

These are characterized by quartz-calcite veins in metasedimentary rocks. Two occurrences, Fraser and Briggs Pb-Zn-Cu (25) and Tompkins Prospect (26), lie beneath the waters of Mactaquac head pond. The sedimentary host rocks are commonly chloritized, carbonatized and bleached. Galena occurs as disseminations and on fractures within the quartz-calcite veins. Sphalerite where present is associated with galena. Chalcopyrite occurs both within the veins and on fractures in the wall rock adjacent to the vein. Pyrite is associated with galena and chalcopyrite and is also present on fractures and disseminated in the wall rock. Silver in the form of argentiferous galena occurs at the Britton Mine (22) and Dominion No. 1 (24).

Mineralized samples from the Britton Mine (22) contain lowold values of 1 ppb or less, and from Dominion No.1 (24) up to 13 ppb. Most samples from Wright Brook (23) are low in gold (less than 7 ppb). However, a sample of the sulphide-rich part of the quartz-calcite vein contains 220 ppb Au and a chip sample of 50 cm across the vein averages 91 ppb Au. The adjacent mineralized and highly silicified rock from the hanging wall and foot wall contain 32 ppb Au and 53 ppb Au respectively.

Gold occurrences:

All three of these mineralized zones are in quartz veins. Two are associated with the Gibson stock (29 and 31) and the third, Oak Mountain Gold (30), is at the southwest contact of the Benton stock.

Saint John River Gold (31) lies below the waters of the Mactaquac Headpond but it is probably similar to Upper Northampton Gold (29).

Upper Northampton Gold (29) consists of quartz veins (169°T/70°E) in a quartz eye porphyry phase of the Gibson

Table 53.1 Mineral Occurrences in the Woodstock Area

Ref. No. and Name	Metal	Host Rock	Alteration[1]	Mineralogy/ Style[2]	Dominant Structural Trends	Development/ Remarks
A. PORPHYRY-COPPER						
1. Connell Mountain (Lockhart Anom. 1)	Cu(Mo,Au)	quartz diorite quartzite	bl, sl, sr, ch, cr, sh, (pt, ep)	cp-fract. dissem., qv po-dissem py-fract, dissem. ch, tn, ml, az, sl, mg, mo	NW, N, NE	Trenches and drill holes; tonnage: protore 21×10^6 tons/0.18% Cu: Supergene 1×10^6 tons/0.04-0.7% Cu discovered by A.W. Lockhart 1970
1a. Connell Mountain (Lockhart Anom. 1a)	Cu	quartzite granodiorite	bl, sl, sr, ch, cr, sh, (ep)	py-fract, dissem. po-fract, dissem. cp-fract, dissem.	NE, NW	percussion drilling discovered by A.W. Lockhart, 1974
2. Connell Brook (Lockhart Anom. 3 and 4)	Cu	quartz diorite quartzite, slate	sl, sr, cl, py.	cp-fract. qv py-fract, qv (sp)	NE	trenches discovered by A.W. Lockhart 1970
3. Monteith Farm (Lockhart Anom. 5)	Cu	quartz diorite	sl, ch, sr, py.	cp-dissem, qv py-fract, qv	N, NNW	trenches discovery by A.W. Lochart 1970
4. Smart Farm (Lockhart Anom. 6, 7 and 9)	Cu (Mo)	hornblende granite/ granodiorite quartz diorite	ch, py, cr.	cp-qv, fract, diss. py-qv, fract, diss mo-qv (ch, ml)	NW	trenches discovered by A.W. Lockhart 1970
5. Upper Northampton Copper (Lockhart Anomalies 2 & 8)	Cu	quart diorite quartzite	sl, sh.	py-fract, diss, qv po-fract, diss, qv cp-diss, fract, qv	NE NW	trenches, percussion drilling diamond drilling discovered by A.W. Lockhart 1970
B. VEIN TYPE and/or PORPHYRY AFFILIATE-COPPER						
6. Bedell Farm	Cu (Ag)	slate	sl	cp-qv po-qv sp-qv	NE	trenches, pits, diamond drill hole; discovered circa, 1850
7. Bulls Creek No. 1 (Copper King)	Cu	quartzite	bl, ch, sl, cr.	cp-qv py-qv (ml, az)	NE	trenches, inclined shaft (125 ft.); discovered circa 1850
8. Bulls Creek No. 2 (N.B. Copper Mine)	Cu	granodiorite quartzite	sl, ch, ep, sr, cr, pt.	cp-qv py-qv (ml)	N	trenches, drill holes, shaft (120 ft), entrance (140 ft) drift; discovered circa 1850, production 1858-1862
9. Bulls Creek No. 3	Cu	quartzite	sl.	cp py (gn, sp?)	NE	trenches adit? discovered 1870
10. Cobbler-Sexton	Cu (Pb, Zn, Au)	granodiorite quartzite	sl, ch, cr.	cp-qv py-qv gn-qv sp-qv	160°T/65°E	adit (324 ft) shaft (20 ft), trenches diamond drill hole; discovered by John McClement and Edward Greer, 1907
11. Dugan Road East	Cu	quartzite	hr, py, sl, cr.	cp-fract, breccia, q-c vein py-fract, breccia, q-c vein	NNE	discovered by D.V. Venugopal, 1977
12. Dugan Road West	Cu	quartzite	hr, ch, sl.	cp-fract, q-ba vein py-fract, q-ba vein (mg)	NE	
13. Interchange Copper	Cu	quartzite	hr, bl, ch, py, pt, ep, sl.	cp-fract, qv py-fract, qv		diamond drill hole, discovered by Imperial Oil Enterprises Ltd, 1971
14. Silvermaque	Cu	quartz monzonite	sl, pt, ch, ep, py.	cp-qv py-qv		diamond drill hole, discovered by Imperial Oil Enterprises Ltd. 1971
15. Hillman Copper	Cu	quartzite		cp, po, py		diamond drill hole, discovered by A.A. Fraser and M.A. Briggs, 1953
C. FRACTURE FILLING-COPPER						
16. Lower Northampton Copper	Cu	Quartzite	sl, ch, sr, py.	cp-fract, pv-fract, qv	NE	road cut, discovered by F. Anderson, 1968
17. Riceville Copper	Cu	quartzite	sl, ch, py.	cp-fract, py-fract, qv	022°T/40°W	road cut, discovered by Chaleur Metals, 1958

Ref. No. and Name	Metal	Host Rock	Alteration[1]	Mineralogy/ Style[2]	Dominant Structural Trends	Development/ Remarks
18. Benton Copper	Cu	Benton granite	sl, py.	cp-fract, py-fract,	068°T/63°SE	road cut, discovered by D.V. Venugopal, 1977
19. Lilly Brook Cu-Mo (Johnstons Br.)	Cu, Mo	quartzite	sl, bl, ch.	cp-fract, py-fract,		float, discovered by D.V. Venugopal, 1977-1985
20. Woodstock Copper-Lead	Cu, Pb			cp, gn		infilled sewer trench, discovered circa 1896
21. Wetmore Copper	Cu	Gibson granite		cp		erratics on shore of Saint John River
D. VEIN-LEAD						
22. Britton Mine	Pb, Ag (Au?)	argillite slate	sl, cr.	gn-q-cv py-q-cv (cp, ml, Au?)		shaft (180 ft), drill hole discovered by Shaw and Britton, circa 1881
23. Wright Brook	Pb, Zn, Cu	quartzite	sl, ch, cr, bl.	gn-q-cv sp-q-cv cp-fract py-fract, q-cv, qv	175°T	pit, discovered prior to 1926
24. Dominion No. 1	Pb, Zn, Ag (Cu)	argillite quartzite	sl, ch, cr, bl.	gn-qv, diss. sp-qv, diss. py-qv, diss. cp-qv	020°T/70°W	shaft (60 ft) trenches, discovered by J. McClement and E.L. Greer 1907
25. Fraser and Briggs Pb-Zn-Cu	Pb, Zn, Cu	quartzite	sl.	gn, sp, cp, py		diamond drill hole, discovered by A.A. Fraser and M.A. Briggs, 1953
26. Tompkins Prospect	Zn, Pb, Cu, Ag	quartzite	sl.	sp, gn, cp		diamond drill hole, trenches, discovered by F.C. Tompkins, 1965
27. Lilly Brook Lead	Pb	quartzite	sl, ch, cr.	gn, py		outcrop, discovered prior to 1967
28. Grafton Lead	Pb, Cu	quartzite	sl, cr	gn-q-cv py-diss, qv cp-fract.	033°T/78°E	road cut; discovered by D.V. Venugopal, 1978 (py) & R.D. Thomas, 1986 (gn, cp)
E. VEIN-GOLD						
29. Upper Northampton	Au, Pb, Cu	quartz vein in quartz-eye porphyry	sl, cr.	gn-diss. in q-cv cp-diss. in qv py-diss. Au	169°T/70°E	road cut
30. Oak Mountain Au, Cu (Pb?)		quartz vein	sl, bl.	cp-qv gn-qv py-qv Au-qv		float-erratics
31. Saint John River	Au, Cu	Gibson granite	sl	cp-qv py-qv Au-qv		outcrop, discovered prior to 1907
F. VEIN-BARITE						
32. South Newbridge (Phillips Creek)	Ba, Pb	quartzite siltstone slate		ba-vein gn-diss. in ba-vein ml.	042°T	trench, discovered by H.A. Lee, 1958
33. Upper Northampton	Ba	quartzite	sl.	ba-vein py-diss. in wallrock	NNW	road cut
G. IRON AND MANGANESE						
34. Wickham	Mn, Fe	slate	sl.	hm, mn-fract.	NNE, EW, SSE	stripped outcrop
35. Oak Mountain	Fe, Mn	slate	sl.	hm-bedded mn-fract.	NNE	outcrop, discovery prior to 1884
36. Peabody Farm Iron	Fe	slate		hm		glacial erratics, discovered prior to 1898

(1) ABBREVIATIONS:
bl = bleaching, ch = chloritization, cr = carbonatization, ep = epidotization, hr = hornfels, pt = potassic, py = pyritization, sr = sericitization, sl = silicification, sh = sulphidation

(2) ABBREVIATIONS:
Au = gold, az = azurite, ba = barite, c = carbonate, ch = chalcocite, cp = chalcopyrite, gn = galena, hm = hematite, ml = malachite, mg = magnetite, mn = manganese, mo = molybdenite, py = pyrite, po = pyrrhotite, q = quartz, sl = selenite, sp = sphalerite, tn = tenorite, dissem = disseminated, fract = fracture filling, v = vein

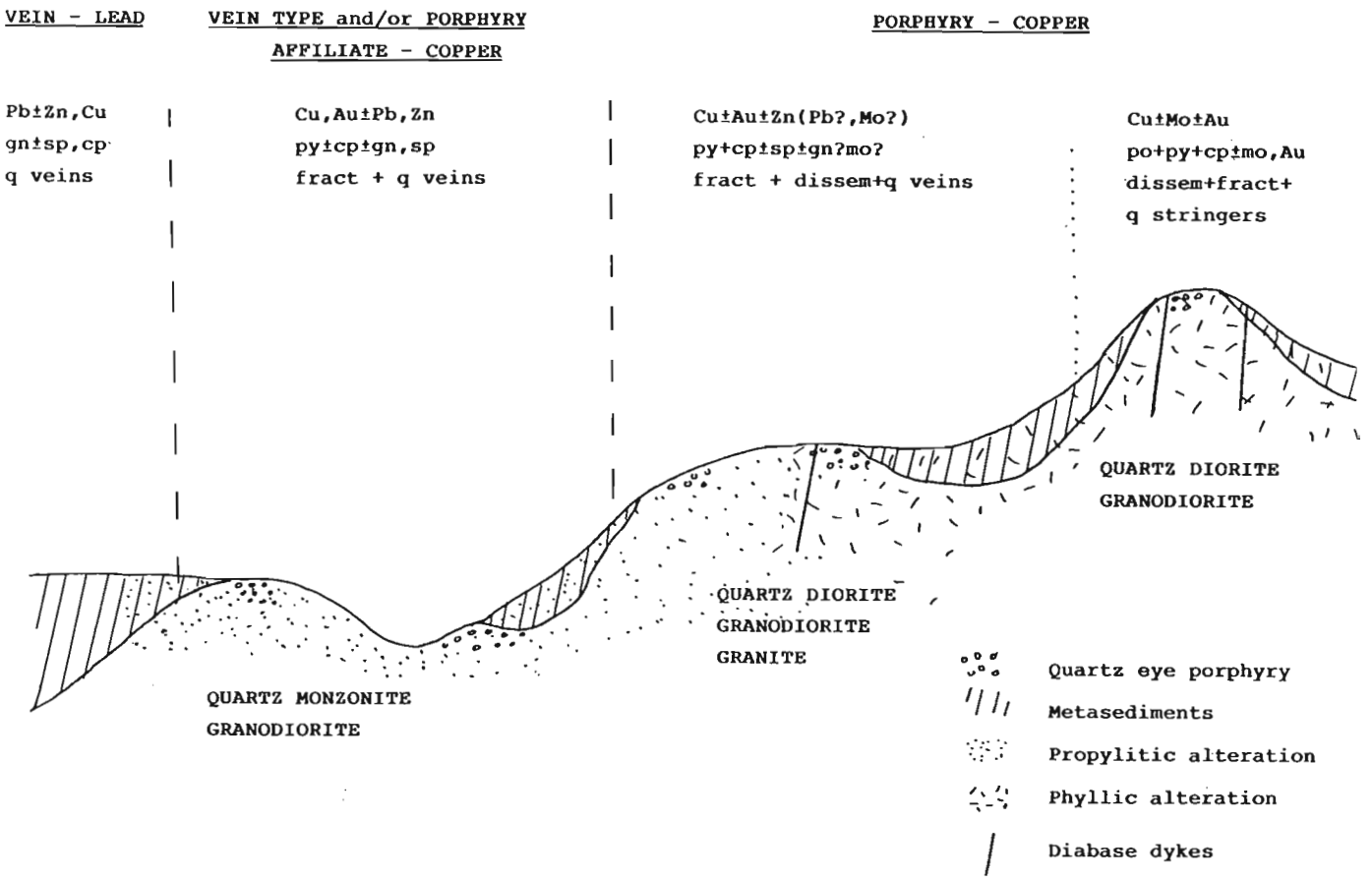


Figure 53.2. Schematic section of the Gibson stock and related mineralization. Abbreviations as in Table 53.1

stock. Galena, chalcopyrite and pyrite are present in the vein system and pyrite is disseminated in the quartz eye porphyry. A selected sample from the galena-rich portion of the vein contains 6000 ppb Au. Ten analyses of different splits from a bulk sample of the vein range from 62 ppb Au to 5200 ppb Au with a mean of 1349 ppb Au. The range of values attests to the inhomogeneity of gold distribution.

The Oak Mountain Gold occurrence is in limonite-stained, white, milky quartz vein boulders (Sabina, 1967) some of which contain chalcopyrite and appear to be hosted in quartzite. Gold values from some of the boulders vary from less than 1 to 180 ppb.

Barite occurrences:

There are three known veinccurrences of barite in the area, South Newbridge (32), Upper Northampton Barite (33) and Dugan Road West (12). The first is 30-50 cm wide by over 5 m long and contains galena and malachite, in fine grained quartzite, siltstone and shale (Richardson, 1959). The trench in which the vein was exposed has been partially back filled and now forms the course of a stream. A sample of float containing barite from the area south of the trench contains 15ppb Au. The second consists of two barite veins in the roadcut on Highway 105 near Upper Northampton (33). One vein is 1-2cm wide and is developed on fractures in quartzite. The second vein occurs as float and is associated with chalcopyrite- and galena-bearing quartz veins in quartz-feldspar porphyry. No gold analyses are available on these veins. The third occurrence of barite consists of quartz-barite veins in quartzite at the Dugan Road West copper occurrence (12). They contain low gold values (<1-2 ppb).

Iron and manganese:

A red hematitic slate unit some 60 m thick occurs southwest of Oak Mountain (35). Fractures in the slate contain manganese oxides and in places quartz veins. The slate appears to be intercalated with northeast trending Ordovician mafic tuffs and flows. The Wickam (34) occurrence consists of a north-northeast striking dark grey manganese oxide stained Cambro-Ordovician slate, in places cut by narrow (1cm) quartz veinlets.

The Peabody Farm occurrence (36) consists of hematitic slate float probably derived from similar Silurian strata up ice.

A sample from a quartz vein at the Oak Mountain occurrence (35) contains 43 ppb Au whereas the ferruginous slate contains less than 1 ppb Au. At the Wickham occurrence (34), gold in the slates ranges up to 8 ppb.

DISCUSSION

Many of the mineral occurrences of the Woodstock area are copper deposits related to the Gibson stock and are classed as porphyry or porphyry affiliate types. The style of mineralization and alteration fits the model proposed by Guilbert and Lowell (1974) for quartz monzonite-granodiorite intrusions in intermediate host rocks. A preliminary schematic section of the model as it would apply to the Gibson stock is shown in Figure 53.2. The alteration zones are not well developed around the stock mainly because the associated quartzites are relatively non-reactive. The alteration and sulphide mineralization indicate a zonation with Cu aqa Mo mineralization (1-5) marked by phyllic alteration central to the system. Peripheral quartz vein dominant Cu±Pb, Zn mineralization (6-10, 13, 14, 29) is in a zone of propylitic alteration. The outer propylitic shell also contains quartz vein-hosted Pb + Zn + Cu mineralization (22-28) in quartzite country rocks.

Preliminary results on gold indicate that it is concentrated in quartz veins (11-6600 ppb) particularly in the propylitic zone (8, 9, 10, 29, 31). However geochemically anomalous gold values (13-290 ppb) also occur in the mineralized host rocks of the Connell Mountain porphyry copper occurrence (1).

Many of the mineralized fractures and veins in and around the Gibson stock trend northerly as does the long axis of thentrusion. There is also a north-south alignment of the major drainages in the area. Therefore it is interesting to speculate that emplacement of the Gibson stock may have been controlled by pre-Devonian north-trending structures. Hollister et al. (1974) also have noted that in most Appalachian porphyry copper prospects mineralized fractures or joints most commonly trend northerly. According to them, the repetition of this trend from earliest Cambrian to the Devonian may imply a continuation of the regional tectonic stresses for that part of the Appalachian orogen where the deposits occur. Final remarks on the metallogeny of the district will have to await results from geochemical, petrographic and mineralographic studies now in progress.

ACKNOWLEDGMENTS

This project was financed by Department of Supply and Services contract number 51SZ-23233-6-0080. W.D. Sinclair, scientific authority for the project, provided much useful unpublished data from phase I, as well as helpful and stimulating discussions. Our thanks to A.W. Lockhart who provided useful background information concerning his involvement in development of the Connell Mountain area.

REFERENCES

Alcock, F.J.
1930: Zinc and lead deposits of Canada; Geological Survey of Canada, Economic Geology Report 8, 406 p.

Anderson, F.D.,
1954: Preliminary map, Woodstock, Carleton County, New Brunswick; Geological Survey of Canada, Paper 53-33, 3 p.

Anderson, F.D.
1968: Woodstock, Millville, and Coldstream maps-areas,Carleton and York Counties, New Brunswick; Geological Survey of Canada, Memoir 353, 69 p.

Bailey, L.W.,
1899: The mineral resources of the province of New Brunswick; Geological Survey of Canada,Annual Report, v. 10, pt. M, 41 p.

Caley, J.F.,
1936: Geology of Woodstock Area, Carleton and York Counties, New Brunswick; Geological Survey of Canada, Memoir 198, 21 p.

The Carleton Sentinel,
1858: New Brunswick Mining Company; The Carleton Sentinel, Feb. 6, 1858, v. X, no. 23, p 90.

Connell, M.D. and Hattie, D.W.,
1985: Metallogeny of central and southwest Miramichi Zone, New Brunswick; in: Tenth annual review of activities,project resumes 1985, S.A. Abbot, ed., New Brunswick Department of Forestry Mines and Energy, Mineral Resources Division; Information Circular 85-3, p. 71.

Crocco, P.E.,
1975: A summary report on granitic rocks of New Brunswick; New Brunswick Department of Natural Resources; Topical Report 75-6, 150 p.

Fyffe, L.R.,
1982a: Geology Woodstock, New Brunswick Department of Natural Resources, Map NR-4.

1982b: Taconic and Acadian structural trends in central and northern New Brunswick; Major structural zones and faults of the Northern Appalachians, P. St-Julien and J. Baaland ed, Geological Association of Canada, Special Paper 24, p. 124.

Greer, E.L.,
1938: Correspondance to Hon. Mr. Perie, November 18, 1938; unpublished manuscript, New Brunswick Department of Natural Resources; NTS Files.

Guilbert, J.M. and Lowell, J.D.,
1974: Variations in zoning patterns in porphyry copper deposits; The Canadian Institute of Mining and Metallurgical Bulletin; v. 67, no. 742, p. 99-109.

Hamilton-Smith, T.,
1971: Structural features of eastern Maine and western New Brunswick (21G, 21J, 21O); New Brunswick Department of Natural Resources, Mineral Resources Division, Map plate 80-3.

Ingall, E.D.,
1893: Division of Mineral Statistics and Mines; Geological

Hollister, V.F., Potter, R.R. and Barker, A.L.,
1974: Porphyry-type deposits of the Appalachian Orogen; Economic Geology, v. 69, p. 618-630.
Survey of Canada, Annual Report 1891, v. 5 pt II (1890-91), p. 8955.

Lockhart, A.W.,
1971a: Falconbridge Nickel Mines Limited, assessment work, report 5, Woodstock claim group, PN808,809, Carleton County, New Brunswick; Assessment Report 470235.

Lockhart, A.W.
1971b: Bulldozer trenching, Geological mapping and rock sampling of soil copper anomalies; Falconbridge Nickel Mines Limited, assessment work, report 7, Woodstock claim group, PN808-809, Carleton County, New Brunswick; Assessment Report 470237.

Lockhart, A.W.,
1974: Soil Geochemistry; Omni Mines Limited assessment work,report 8 Lockhart porphyry copper prospect, Woodstock, Carleton County, New Brunswick; Assessment Report 470244.

Lockhart, A.W.,
1976: Geochemical prospecting of an Appalachian porphyry copper deposit at Woodstock, New Brunswick; Journal Geochemical Exploration v. 6, p. 13-33.

Potter, R.R.,
1983: The Woodstock iron works, Carleton County, New Brunswick; Canadian Institute of Mining and Metallurgy Bulletin, v. 76, no. 853, p. 81-83

Rampton, V.N. and Paradis, S.,
1981: Quaternary geology of Woodstock Map area (21J), New Brunswick; New Brunswick Department of Natural Resources, Map Report 81-1, p. 2.

Richardson, P.W.,
1959: Moneta-Dome staking near Woodstock, New Brunswick; unpublished manuscript, NTS Files.

Robb, C.,
1870: Report on a part of New Brunswick; Geological Survey of Canada Report of Progress 1866-69 part VI, p. 173-210.

Rodgers, J.,
1970: The tectonics of the Appalachians; Wiley Interscience, New York, 271 p.

Sabina, A.P.,
1967: Rocks and minerals for the collector. Quebec and parts of New Brunswick; Geological Survey of Canada, Paper 66-51, p. 131-132.

Selwyn, A.R.C.,
1895: Summary report by the Director; Geological Survey of Canada Annual Report for 1892-93, v. 6, p. 80A

van der Poll, H.W.,
1967: Geology southern New Brunswick; New Brunswick Department of Natural Reosources, Mineral Resources Division, Map Plate 70-16.

Venugopal, D.V.,
1979: Geology of Debec Junction-Gibson Millstream-Temperance Vale-Meductic Region; map areas G-21,H-21, I-21 and H-22 (part of 21J/3, 21J/4, 21G/13, 21G/14), New Brunswick Department of Mines and Resources, Map Report 79-5.

Venugopal, D.V.,
1981: Geology of Hartland-Woodstock-Nortondale Region, Map areas H-19, H-20, I-20; New Brunswick Department of Mines and Natural Resources, Map Report 81-6.

Williams, H., Kennedy, M.J., and Neale, E.R.W.,
1972: The Appalachian structural province, in: Variations in tectonic styles in Canada, R.A. Price and R.J.W. Douglas eds, Geological Association of Canada, Special Paper 11, p. 181-261.

Woodstock, New Brunswick Press,
1909: Dominion No.1 has high class ore; Woodstock, New Brunswick Press, July 19, 1909.

Wright, J.D.,
1939a: Correspondance to Dr. W.J. Wright; unpublished manuscript, New Brunswick Department of Natural Resources, NTS Files.

Wright, W.J.,
1939b: Analyses, Wright Brook; Unpublished manuscript, New Brunswick Department of Natural Resources, NTS Files.

AUTHOR INDEX/INDEX DES AUTEURS

Anderson, R.G. 689
Andrew, K.P.E. 699
Anglin, C.D. 591
Annesley, I.R. 25

Banerjee, I. 337
Barr, S.M. 199, 263
Barrette, P.D. 515
Bégin, N.J. 619
Bell, K. 591
Bell, T. 101
Berger, G.W. 901
Bethune, K.M. 773
Blaise, B. 127
Bolduc, A.M. 43
Bornhold, B.D. 127
Bostock, H.H. 443
Bouvier, J.L. 485
Bowring, S.A. 699
Brooks, P.W. 331
Brown, D.A. 143

Calon, T. 435
Cameron, B.E.B. 925
Cameron, E.M. 281
Campbell, J.E.M. 643
Carrigan, W.J. 281
Clague, J.J. 177
Coderre, J.M. 815
Copper, P. 885
Corriveau, L. 897
Currie, K.L. 653, 663
Currie, L.D. 713

Dallimore, S.R. 913
David, J. 633
Davis, J.L. 913
Dennis, F.A.R. 643
de Silva, K.N. 477
de Vernal, A. 11
Dewing, K. 883
Digel, M.R. 429
Dyer, A. 101

Eckstrand, O.R. 835
Ernst, R.E. 673
Evans, S.G. 181, 929
Evenchick, C.A. 719
Evenson, E.B. 43

Fogarasi, S.L. 815
Franklin, J.M. 591
Frisch, T. 429

Gagné, R.M. 905
Gariépy, C. 633
Gibb, R.A. 815
Gibbins, S.F. 699
Gleeson, C.F. 489
Good, R.L. 905
Goodarzi, F. 317, 349, 353
Gorton, M. 897
Graves, M. 409
Grotzinger, J.P. 219

Hall, G.E.M. 477, 485
Hamilton, S.M. 451, 883
Hanmer, S.K. 563
Henderson, J.B. 783, 803
Hildebrand, R.S. 699
Hill, J.D. 415
Hill, J.R. 533
Hillaire-Marcel, C. 859
Hoffman, E. 591
Hood, P. 935
Hunter, J.A. 905

James, D.T. 803
Jefferson, C.W. 451
Jetté, H. 11
Jonasson, I.R. 591, 835
Judge, A.S. 191
Justino, M.F. 555

Kerr, D.E. 153
King, J.E. 515
Klassen, R.A. 43, 61, 101
Klassen, R.W. 111
Kostaschuk, R.A. 727
Kurfurst, P.J. 939

Labonté, M. 353
Laflèche, P.T. 191
Lambert, M.B. 605, 673
Lecheminant, A.N. 773
Lecheminant, G.M. 249
Leslie, R.V. 37
Lewis, C.F.M. 825
Lortie, G. 889
Loveridge, W.D. 783
Lucas, S.B. 619
Luternauer, J.L. 727, 901, 919

MacDougall, C.S. 457
Macfie, R.I. 681, 803
Machin, D.C. 305
Mackay, J.R. 37
Mackenzie, L.M. 467
Maclean, B. 847
Macnab, R. 865
Martin, R.F. 239
Matthews, J.V., Jr. 73, 165

McCormick, D.S. 219
McGrath, P.H. 803
McKenna, G.T. 919
McMartin, I. 89
Mortensen, J.K. 581
Mott, R.J. 165
Mucci, A. 17
Murphy, D.C. 735

Needham, T.W. 597

Orchard, M.J. 743
Osadetz, K.G. 331
Owen, J.V. 305, 643

Pagé, P. 17
Paktunc, A.D. 543
Parrott, D.R. 825
Payette, C. 239
Pelchat, J.C. 477
Pelechaty, S.M. 219
Pe-Piper, G. 573
Percival, J.A. 1
Piasecki, M.A.J. 391
Pilon, J.A. 191
Piper, D.J.W. 847
Praeg, D. 847
Procyshyn, E.L. 499
Pullan, S.E. 905

Raeside, R.P. 199
Rainbird, R.H. 53
Real, D. 763
Relf, C.D. 515
Ricketts, B.D. 369
Rivers, T. 435
Roberts, M.C. 757
Roddick, J.C. 773
Roddick, J.C.M. 375
Rogerson, R.J. 101
Ruzicka, V. 249

Sangster, A.L. 555
Schwarz, E.J. 423
Scott, D.J. 619
Sevigny, J.H. 751
Shilts, W.W. 159
Shor, A.N. 847
Simony, P.S. 713
Smith, S.L. 53, 159, 165
Snowdon, L.R. 331
Sobczak, L.W. 299
Sonnichsen, G.V. 877
Squires, G.C. 699
Stasiuk, L.D. 317, 349
St-Onge, D.A. 89
St-Onge, M.R. 619
Swinden, H.S. 381

Tella, S. 25
Teskey, D.J. 935
Tessier, A.C. 773
Thomas, M.D. 763, 815
Thomas, R.D. 489
Thompson, F.J. 61
Thompson, P.H. 783
Trettin, H.P. 357

Vaive, J.E. 477
van Berkel, J.T. 399
van Breemen, O. 783
van Gool, J. 435
van Staal, C.R. 605
Verhoef, J. 865
Vilks, G. 877
Vreeken, W.J. 111

Waldron, J.W.F. 409
Watkinson, D.H. 835
Weber, J.R. 299
Whalen, J.B. 209, 375
White, C.E. 199
Williams, E.J. 429
Williams, H.F.L. 757
Wilton, D.H.C. 457, 467
Woodside, J. 865
Wright, N. 423

Yaowanoiyothin, W. 199

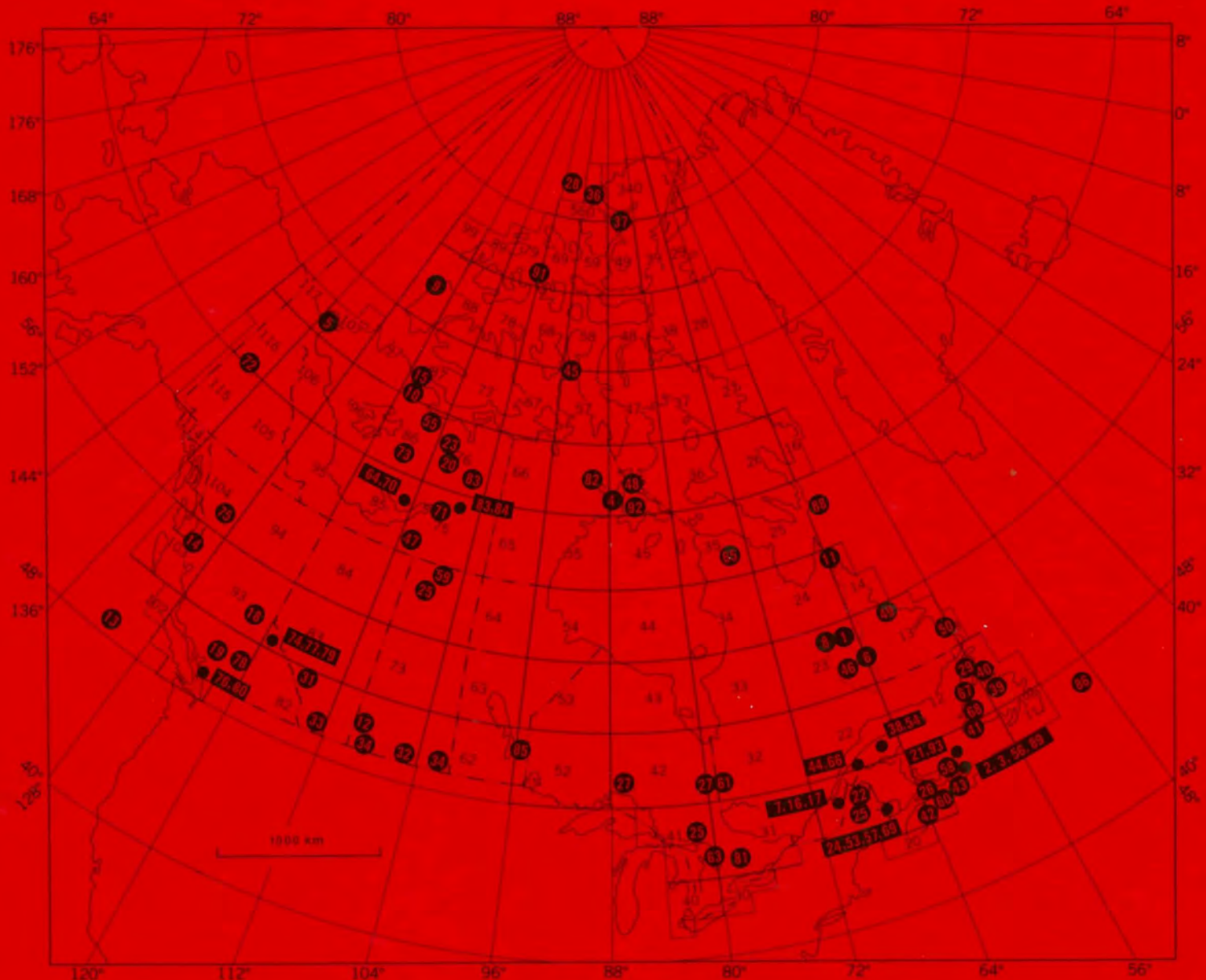
Zolnai, A.I. 323

NOTE TO CONTRIBUTORS

Submissions to the *Discussion* section of *Current Research* are welcome from both the staff of the Geological Survey and from the public. Discussions are limited to 6 double-spaced typewritten pages (about 1500 words) and are subject to review by the Chief Scientific Editor. Discussions are restricted to the scientific content of Geological Survey reports. General discussions concerning branch or government policy will not be accepted. Illustrations will be accepted only if, in the opinion of the editor, they are considered essential. In any case no redrafting will be undertaken and reproducible copy must accompany the original submissions. Discussion is limited to recent reports (not more than 2 years old) and may be in either English or French. Every effort is made to include both *Discussion* and *Reply* in the same issue. *Current Research* is published in January and July. Submissions should be sent to the Chief Scientific Editor, Geological Survey of Canada, 601 Booth Street, Ottawa, Canada, K1A 0E8.

AVIS AUX AUTEURS D'ARTICLES

Nous encourageons tant le personnel de la Commission géologique que le grand public à nous faire parvenir des articles destinés à la section *discussion* de la publication *Recherches en cours*. Le texte doit comprendre au plus six pages dactylographiées à double interligne (environ 1500 mots), texte qui peut faire l'objet d'un réexamen par le rédacteur en chef scientifique. Les discussions doivent se limiter au contenu scientifique des rapports de la Commission géologique. Les discussions générales sur la Direction ou les politiques gouvernementales ne seront pas acceptées. Les illustrations ne seront acceptées que dans la mesure où, selon l'opinion du rédacteur, elles seront considérées comme essentielles. Aucune retouche ne sera faite aux textes et dans tous les cas, une copie qui puisse être reproduite doit accompagner les textes originaux. Les discussions en français ou en anglais doivent se limiter aux rapports récents (au plus de 2 ans). On s'efforcera de faire coincider les articles destinés aux rubriques *discussions* et *reponses* dans le même numéro. La publication *Recherches en cours* paraît en janvier et en juillet. Les articles doivent être renvoyés au rédacteur en chef scientifique: Commission géologique du Canada, 601, rue Booth, Ottawa, Canada, K1A 0E8.



Energy, Mines and Resources Canada

Énergie, Mines et Ressources Canada

This document was produced
by scanning the original publication.

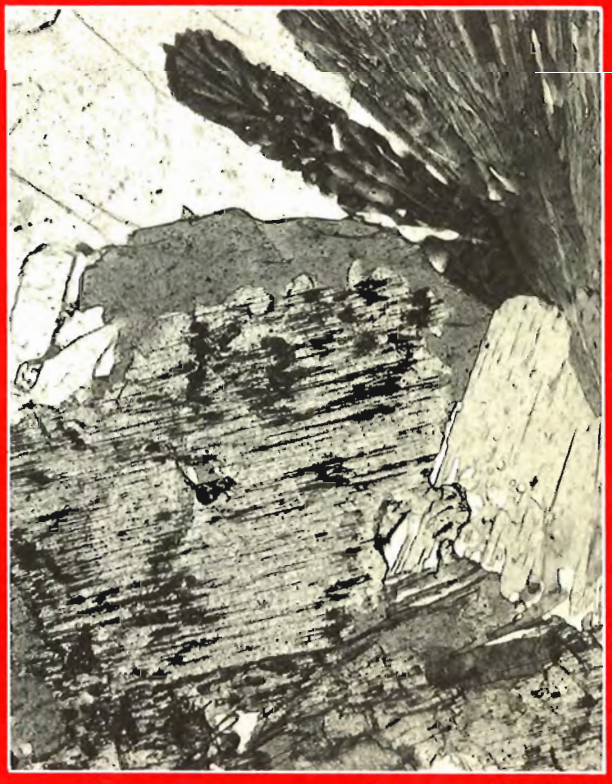
Ce document est le produit d'une
numérisation par balayage
de la publication originale.

Geological Survey of Canada
Commission géologique du Canada

PAPER
ÉTUDE 87-1A

CURRENT RESEARCH PART A
RECHERCHES EN COURS PARTIE A





(Pages 499-946)

Canada

1987

Notice to Librarians and Indexers

The Geological Survey's twice-yearly *Current Research* series contains many reports comparable in scope and subject matter to those appearing in scientific journals and other serials. All contributions to Current Research include an abstract and bibliographic citation. It is hoped that these will assist you in cataloguing and indexing these reports and that this will result in a still wider dissemination of the results of the Geological Survey's research activities.

Avis aux bibliothécaires et préparateurs d'index

La série *Recherches en cours* de la Commission géologique paraît deux fois par année; elle contient plusieurs rapports dont la portée et la nature sont comparables à ceux qui paraissent dans les revues scientifiques et autres périodiques. Tous les articles publiés dans les Recherches en cours sont accompagnés d'un résumé et d'une bibliographie, ce qui vous permettra, nous l'espérons, de cataloguer et d'indexer ces rapports, d'où une meilleure diffusion des résultats de recherche de la Commission géologique.



GEOLOGICAL SURVEY OF CANADA
PAPER 87-1A

COMMISSION GÉOLOGIQUE DU CANADA
ÉTUDE 87-1A

CURRENT RESEARCH
PART A

RECHERCHES EN COURS
PARTIE A

Issued in two sections/Publiée en deux volumes:
pages 1-498 and/et pages 499-946

1987

© Minister of Supply and Services Canada 1987

Available in Canada through

authorized bookstore agents
and other bookstores

or by mail from

Canadian Government Publishing Centre
Supply and Services Canada
Ottawa, Ontario, Canada K1A 0S9

and from

Geological Survey of Canada offices:

601 Booth Street
Ottawa, Canada K1A 0E8

3303-33rd Street N.W.,
Calgary, Alberta T2L 2A7

100 West Pender Street
Vancouver, British Columbia V6B 1R8

A deposit copy of this publication is also available
for reference in public libraries across Canada

Cat. No. M44-87/1AE Canada: $20.00
ISBN 0-660-53707-9 Other countries: $24.00

Price subject to change without notice

Sold in sets

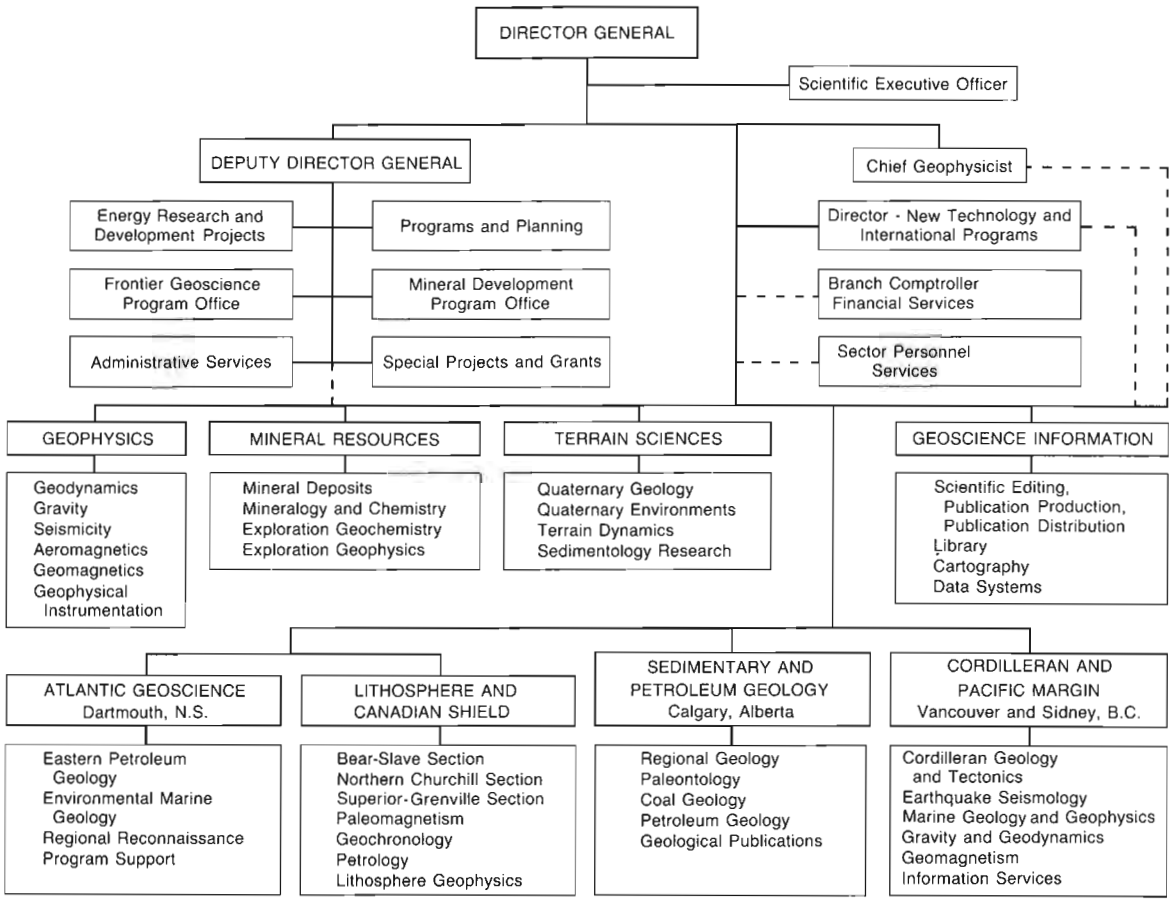
Cover/couverture

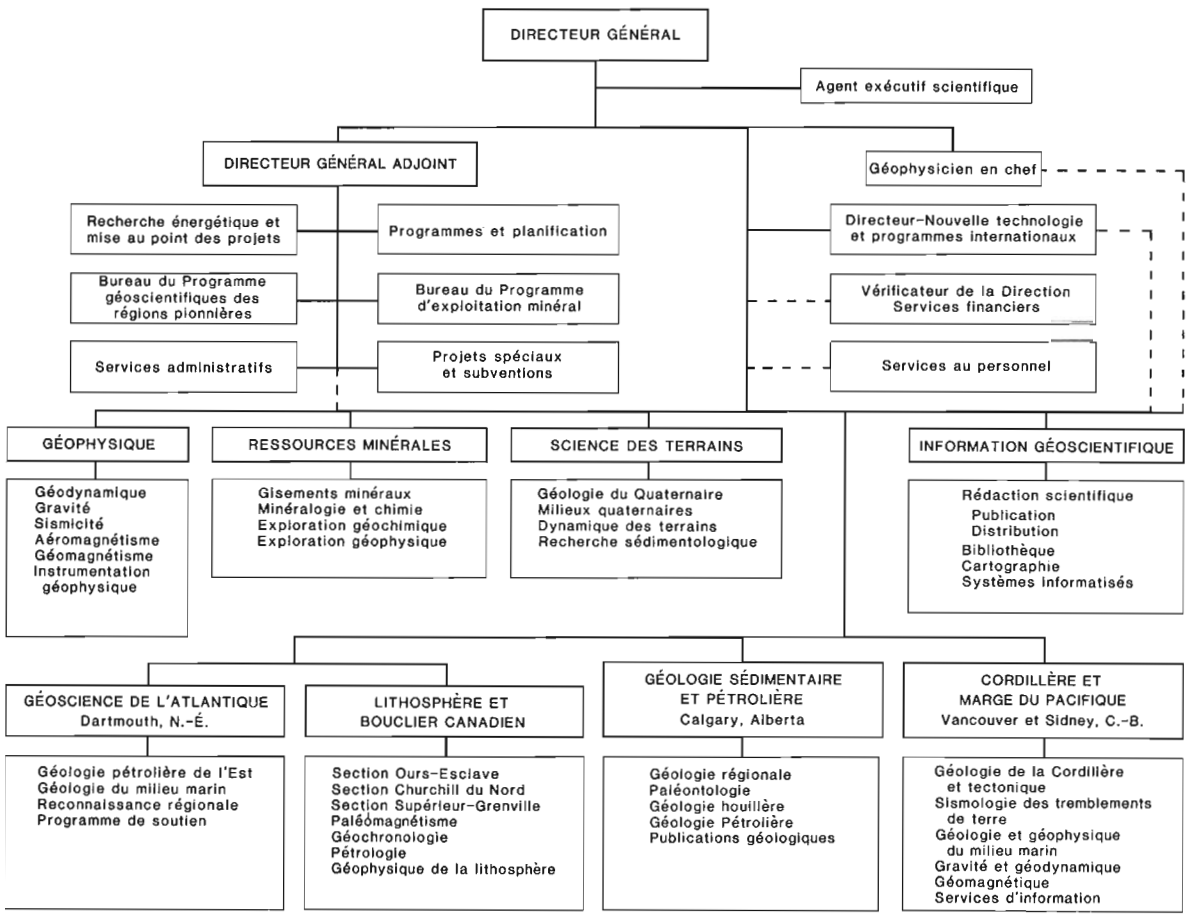
Left/gauche
Five-metre Zodiac inflatable boat used during seismic reflection survey. See report 91, p. 877-882 for details.

Le Zodiac, bateau gonflable de cinq mètres, utilisé au cours du levé de séismique réflexion. Voir le rapport 91, p. 877-882.

Right/droite
Photomicrograph of ferrodiorite showing orthopyroxene rimmed by amphibole and sieve-textured biotite. See report 82, p. 773-782 for details.

Photomicrographie d'une ferrodiorite montrant un orthopyroxène entouré d'une amphibole et d'une biotite de texture en tamis. Voir le rapport 82, p. 773-782 pour plus de détails.


DIRECTOR GENERAL
Scientific Executive Officer
DEPUTY DIRECTOR GENERAL
Chief Geophysicist
Energy Research and Development Projects
Programs and Planning
Director - New Technology and International Programs
Frontier Geoscience Program Office
Mineral Development Program Office
Branch Comptroller Financial Services
Administrative Services
Special Projects and Grants
Sector Personnel Services
GEOPHYSICS
MINERAL RESOURCES
TERRAIN SCIENCES
GEOSCIENCE INFORMATION
Geodynamics
Gravity
Seismicity
Aeromagnetics
Geomagnetics
Geophysical Instrumentation
Mineral Deposits
Mineralogy and Chemistry
Exploration Geochemistry
Exploration Geophysics
Quaternary Geology
Quaternary Environments
Terrain Dynamics
Sedimentology Research
Scientific Editing,
Publication Production,
Publication Distribution
Library
Cartography
Data Systems
ATLANTIC GEOSCIENCE
Dartmouth, N.S.
LITHOSPHERE AND CANADIAN SHIELD
SEDIMENTARY AND PETROLEUM GEOLOGY
Calgary, Alberta
CORDILLERAN AND PACIFIC MARGIN
Vancouver and Sidney, B.C.
Eastern Petroleum Geology
Environmental Marine Geology
Regional Reconnaissance
Program Support
Bear-Slave Section
Northern Churchill Section
Superior-Grenville Section
Paleomagnetism
Geochronology
Petrology
Lithosphere Geophysics
Regional Geology
Paleontology
Coal Geology
Petroleum Geology
Geological Publications
Cordilleran Geology and Tectonics
Earthquake Seismology
Marine Geology and Geophysics
Gravity and Geodynamics
Geomagnetism
Information Services


DIRECTEUR GÉNÉRAL
Agent exécutif scientifique
DIRECTEUR GÉNÉRAL ADJOINT
Géophysicien en chef
Recherche énergétique et mise au point des projets
Programmes et planification
Directeur–Nouvelle technologie et programmes internationaux
Bureau du Programme géoscientifiques des régions pionnières
Bureau du Programme d'exploitation minéral
Vérificateur de la Direction Services financiers
Services administratifs
Projets spéciaux et subventions
Services au personnel
GÉOPHYSIQUE
RESSOURCES MINÉRALES
SCIENCE DES TERRAINS
INFORMATION GÉOSCIENTIFIQUE
Géodynamique
Gravité
Sismicité
Aéromagnétisme
Géomagnétisme
Instrumentation géophysique
Gisements minéraux
Minéralogie et chimie
Exploration géochimique
Exploration géophysique
Géologie du Quaternaire
Milieux quaternaires
Dynamique des terrains
Recherche sédimentologique
Rédaction scientifique
Publication
Distribution
Bibliothèque
Cartographie
Systèmes informatisés
GÉOSCIENCE DE L'ATLANTIQUE
Dartmouth, N.-É.
LITHOSPHÈRE ET BOUCLIER CANADIEN
GÉOLOGIE SÉDIMENTAIRE ET PÉTROLIÈRE
Calgary, Alberta
CORDILLÈRE ET MARGE DU PACIFIQUE
Vancouver et Sidney, C.-B.
Géologie pétrolière de l'Est
Géologie du milieu marin
Reconnaissance régionale
Programme de soutien
Section Ours–Esclave
Section Churchill du Nord
Section Supérieur–Grenville
Paléomagnétisme
Géochronologie
Pétrologie
Géophysique de la lithosphère
Géologie régionale
Paléontologie
Géologie houillère
Géologie Pétrolière
Publications géologiques
Géologie de la Cordillère et tectonique
Sismologie des tremblements de terre
Géologie et géophysique du milieu marin
Gravité et géodynamique
Géomagnétique
Services d'information

Separates

A limited number of separates of the papers that appear in this volume are available by direct request to the individual authors. The addresses of the Geological Survey of Canada offices follow:

601 Booth Street,
OTTAWA, Ontario
K1A 0E8

Institute of Sedimentary and Petroleum Geology,
3303-3rd Street N.W.,
CALGARY, Alberta
T2L 2A7

Cordilleran and Pacific Margin Division,
100 West Pender Street,
VANCOUVER, B.C.
V6B 1R8

Pacific Geoscience Centre
P.O. Box 6000,
9860 Saanich Road,
SIDNEY, B.C.
V8L 4B2

Atlantic Geoscience Centre,
Bedford Institute of Oceanography,
P.O. Box 1006,
DARTMOUTH, N.S.
B2Y 4A2

When no location accompanies an author's name in the title of a paper, the Ottawa address should be used.

Tirés à part

On peut obtenir un nombre limité de "tirés à part" des articles qui paraissent dans cette publication en s'adressant directement à chaque auteur. Les adresses des différents bureaux de la Commission géologique du Canada sont les suivantes :

601, rue Booth
OTTAWA, Ontario
K1A 0E8

Institut de géologie sédimentaire et pétrolière
3303-3rd St. N.W.,
CALGARY, Alberta
T2L 2A7

Division de la Cordillère et marge du Pacifique
100 West Pender Street,
VANCOUVER, Colombie-Britannique
V6B 1R8

Centre géoscientifique du Pacific
B.P. 6000,
9860 Saanich Road,
SIDNEY, Colombie-Britannique
V8L 4B2

Centre géoscientifique de l'Atlantique
Institut océanographique de Bedford
B.P. 1006,
DARTMOUTH, Nouvelle-Ecosse
B2Y 4A2

Lorsque l'adresse de l'auteur ne figure pas sous le titre d'un document, on doit alors utiliser l'adresse d'Ottawa.

SCIENTIFIC AND TECHNICAL REPORTS
RAPPORTS SCIENTIFIQUES ET TECHNIQUES

ECONOMIC GEOLOGY/GÉOLOGIE ÉCONOMIQUE

J.J. CLAGUE: A placer gold exploration target in the Cariboo district, British Columbia 177

V. RUZICKA and G.M. LECHEMINANT: Uranium investigations in Canada, 1986 249

L.M. MACKENZIE and D.H.C. WILTON: Uranium, molybdenum and base metal sulphide mineralization: three different styles of ore formation in the Burnt Lake area, central Labrador 467

R.D. THOMAS and C.F. GLEESON: Metallogeny of the Woodstock area, New Brunswick 489

E.L. PROCYSHYN: Wall rock alteration mineral assemblages associated with the E-Zone ore bodies at Mines Gaspé, Murdochville, Quebec 499

A.D. PAKTUNC: Nickel, copper, platinum and palladium relations in Ni-Cu deposits of the St. Stephen intrusion, New Brunswick 543

I.R. JONASSON, O.R. ECKSTRAND, and D.H. WATKINSON: Preliminary investigations of the abundance of platinum, palladium and gold in some samples of Canadian copper-nickel ores 835

GEOCHEMISTRY/GÉOCHIMIE

B. BLAISE and B.D. BORNHOLD: Geochemistry of northern Juan de Fuca Ridge sediments, northeast Pacific 127

E.M. CAMERON and W.J. CARRIGAN: Oxygen fugacity of Archean felsic magmas: relationship to gold mineralization 281

G.E.M. HALL, K.N. DE SILVA, J.C. PELCHAT, and J.E. VAIVE: Advances in analytical methods based on atomic absorption spectrometry in the Geochemistry Laboratories of the Geological Survey of Canada 477

J.L. BOUVIER and G.E.M. HALL: A preliminary investigation of the application of microwave radiation for the dissolution of geological materials 485

C.D. ANGLIN, J.M. FRANKLIN, I.R. JONASSON, K. BELL, and E. HOFFMAN: Geochemistry of scheelites associated with Archean gold deposits: implications for their direct age determination 591

J. DAVID and C. GARIÉPY: Rare-earth element geochemistry of sedimentary sequences from the Lower St-Lawrence, Quebec Appalachians 633

GEOCHRONOLOGY/GÉOCHRONOLOGIE

J.B. WHALEN and J.C.M. RODDICK: K-Ar geochronology of the McGerrigle plutonic complex, Gaspésie Peninsula, Quebec 375

J.K. MORTENSEN: Preliminary U-Pb zircon ages for volcanic and plutonic rocks of the Noranda-Lac Abitibi area, Abitibi Subprovince, Quebec 581

O. VAN BREEMEN, J.B. HENDERSON, W.D. LOVERIDGE, and P.H. THOMPSON: U-Pb zircon and monazite geochronology and zircon morphology of granulites and granite from the Thelon Tectonic Zone, Healey Lake and Artillery Lake map areas, N.W.T. 783

GEOPHYSICS/GÉOPHYSIQUES

P.T. LAFLÈCHE, A.S. JUDGE, and J.A. PILON: Ground probing radar in the investigation of the competency of frozen tailings pond dams 191

L.W. SOBCZAK and J.R. WEBER: Gravity and bathymetry taken along seismic refraction lines from the Canadian Ice Island during 1985 and 1986 299

E.J. SCHWARZ and N. WRIGHT: Buried placers in Chaudière River sediments indicated by ground magnetometer survey, Eastern Townships, Quebec 423

D. REAL and M.D. THOMAS: Gravity models within the southern Central Metasedimentary Belt, Grenville Province, Ontario 763

J.M. CODERRE, M.D. THOMAS, R.A. GIBB, and S.L. FOGARASI: In situ density determinations by gravity measurements in the Underground Research Laboratory shaft, Lac du Bonnet granite batholith, Manitoba 815

MARINE GEOSCIENCE/ÉTUDES GÉOSCIENTIFIQUES DU MILIEU MARIN

A. DE VERNAL et H. JETTÉ: Analyses palynologiques de sédiments holocènes du lac Bras d'Or (carotte 85-036-016P), île du Cap-Breton, Nouvelle-Écosse 11

A. MUCCI and P. PAGÉ: The water chemistry of cruise 85-036 on Bras d'Or Lake, Cape Breton Island, Nova Scotia 17

R.A. KOSTASCHUK and J.L. LUTERNAUER: Large-scale sedimentary processes in a trained, high-energy, sand-rich estuary: Fraser River delta, British Columbia 727

C.F.M. LEWIS and D.R. PARROTT: Iceberg scouring rate studies, Grand Banks of Newfoundland 825

D. PRAEG, B. MACLEAN, D.J.W. PIPER, and A.N. SHOR: Study of iceberg scours across the continental shelf and slope off southeast Baffin Island using the **Sea MARC I** midrange sidescan sonar 847

C. HILLAIRE-MARCEL: Composition isotopique du carbone organique des carottes du forage 85-036-016 dans le lac Bras d'Or, île du Cap-Breton, Nouvelle-Écosse 859

R. MACNAB, J. VERHOEF, and J. WOODSIDE: Techniques for the display and editing of marine potential field data 865

G.V. SONNICHSEN and G. VILKS: A small boat seismic reflection survey of the Lougheed Island Basin–Cameron Island Rise–Desbarats Strait region of the Arctic Island channels using open water leads 877

G. LORTIE: Diatomées et évolution holocène du lac Bras d'Or, Nouvelle-Écosse: résultats préliminaires 889

PALEONTOLOGY/PALÉONTOLOGIE

F. GOODARZI and L.D. STASIUK: Graptolite preparation for reflected light microscopy – a technical note 317

M. LABONTÉ and F. GOODARZI: The relationship between dendographs and Pearson product-moment correlation coefficients 353

PETROLEUM GEOLOGY AND COAL/GÉOLOGIE PÉTROLIÈRE ET LE CHARBON

P.W. BROOKS, K.G. OSADETZ, and L.R. SNOWDON: Origin of compositional differences amongst oils from the Hummingbird Field (Paleozoic), southeast Saskatchewan 331

F. GOODARZI and L.D. STASIUK: Amorphous kerogen: bituminite in the Second White Speckled Shale, southern Saskatchewan 349

QUATERNARY GEOLOGY/GÉOLOGIE DU QUATERNAIRE

Mapping, geomorphological studies, and sedimentology/Cartographie, études géomorphologiques et sédimentologie

J.R. MACKAY and R.V. LESLIE: A simple probe for the measurement of frost heave within frozen ground in a permafrost environment 37

D.A. ST-ONGE and I. MCMARTIN: Morphosedimentary zones in the Bluenose Lake region, District of Mackenzie 89

T. BELL, R.J. ROGERSON, R.A. KLASSEN, and A. DYER: Acoustic survey and glacial history of Adams Lake, outer Nachvak Fiord, northern Labrador 101

R.W. KLASSEN and W.J. VREEKEN: The nature and chronological implications of surface tills and post-till sediments in the Cypress Lake area, Saskatchewan 111

D.E. KERR: Preliminary interpretation of the stratigraphy of the marine offlap sequence in the Clifton Point area, District of Mackenzie 153

S.G. EVANS: Surface displacement and massive toppling on the northeast ridge of Mount Currie, British Columbia 181

H.F.L. WILLIAMS and M.C. ROBERTS: Mid-Holocene paleosurfaces in vertical accretion deposits, Fraser River delta, British Columbia 757

Exploration technology and glacial dispersal studies/Techniques d'exploration et études de la dispersion glaciaire

A.M. BOLDUC, R.A. KLASSEN, and E.B. EVENSON: Cobble lithologies in eskers of central Labrador 43

S.L. SMITH and R.H. RAINBIRD: Soft-sediment deformation structures in overburden drill core, Quebec 53

R.A. KLASSEN and F.J. THOMPSON: Ice flow history and glacial dispersal in the Labrador Trough 61

S.L. SMITH and W.W. SHILTS: Quaternary stratigraphy of Noire River cores, Beauceville area, Quebec 159

Paleoenvironmental studies and geochronology/Étude des paléoenvironnements et géochronologie

J.V. MATTHEWS, JR.: Plant macrofossils from the Neogene Beaufort Formation on Banks and Meighen islands, District of Franklin 73

J.V. MATTHEWS, JR., S.L. SMITH, and R.J. MOTT: Plant macrofossils, pollen, and insect fossils of arctic affinity from Wisconsinan sediments in Chaudière Valley, southern Quebec 165

REGIONAL GEOLOGY/GÉOLOGIE RÉGIONALE

Appalachian region/Région des appalaches

S.M. BARR, R.P. RAESIDE, C.E. WHITE, and W. YAOWANOIYOTHIN: Geology of the northeastern and central Cape Breton Highlands, Nova Scotia 199

J.B. WHALEN: Geology of a northern portion of the Central Plutonic Belt, New Brunswick 209

C. PAYETTE and R.F. MARTIN: The Welsford igneous complex, southern New Brunswick: rift-related Acadian magmatism 239

S.M. BARR: Field relations, petrology and age of plutonic and associated metavolcanic and metasedimentary rocks, Fundy National Park area, New Brunswick 263

J.V. OWEN and D.C. MACHIN: Petrography and geochemistry of some mafic dykes in the Long Range Inlier, western Newfoundland 305

H.S. SWINDEN: Geology and mineral occurrences in the central and northern parts of the Roberts Arm Group, central Newfoundland 381

M.A.J. PIASECKI: Possible basement-cover relationships in the Fleur de Lys terrane, western Newfoundland 391

J.T. VAN BERKEL: Geology of the Dashwoods Pond, St. Fintan's and Main Gut map areas, southwest Newfoundland 399

J.W.F. WALDRON and M. GRAVES: Preliminary report on sedimentology of sandstones, slates, and bioclastic carbonate material in the Meguma Group, Mahone Bay, Nova Scotia 409

J.D. HILL: Geology of the Guysborough-Country Harbour area, Nova Scotia 415

J.R. HILL: A preliminary report on geology and on mineral occurrences in Precambrian carbonate rocks, Cape Breton Island, Nova Scotia 533

M.F. JUSTINO and A.L. SANGSTER: Geology in the vicinity of the Lime Hill zinc occurrence, southwestern Cape Breton Island, Nova Scotia 555

G. PE-PIPER: The Late Hydrynian Jeffers Group, western Cobequid Hills, Nova Scotia 573

J.V. OWEN, J.E.M. CAMPBELL, and F.A.R. DENNIS: Geology of the Lake Michel area, Long Range Inlier, western Newfoundland 643

K.L. CURRIE: A preliminary account of the geology of Harrys River map area, southern Long Range of Newfoundland 653

K.L. CURRIE: Late Precambrian igneous activity and its tectonic implications, Musquash-Loch Alva region, southern New Brunswick 663

Arctic Islands/Archipel Arctique

H.P. TRETTIN: Investigations of Paleozoic geology, northern Axel Heiberg and northwestern Ellesmere islands 357

B.D. RICKETTS: Preliminary structural cross-sections across Fosheim Peninsula and Axel Heiberg Island, Arctic Archipelago 369

Cordilleran region/Région de la Cordillère

D.A. BROWN: Hazelton-Bowser Lake Group stratigraphy and structure in the vicinity of the Silbak Premier Mine, northwestern British Columbia 143

R.G. ANDERSON: Plutonic rocks in the Dawson map area, Yukon Territory 689

L.D. CURRIE and P.S. SIMONY: Geology of the Alan Creek area, southeastern Cariboo Mountains, British Columbia 713

C.A. EVENCHICK: Stratigraphy and structure of the northeast margin of the Bowser Basin, Spatsizi map area, north-central British Columbia 719

D.C. MURPHY: Kaza Group, eastern Wells Gray Park, British Columbia 735

M.J. ORCHARD: Conodont biostratigraphy and correlation of the Harper Ranch Group (Devonian–Permian), Ashcroft map area, southern British Columbia 743

J.H. SEVIGNY: Field and stratigraphic relations of amphibolites in the late Proterozoic Horsethief Creek Group, northern Adams River area, British Columbia 751

Canadian Shield/Bouclier canadien

J.A. PERCIVAL: Geology of the Ashuanipi granulite complex in the Schefferville area, Quebec 1

S. TELLA and I.R. ANNESLEY: Precambrian geology of parts of Chesterfield Inlet map area, District of Keewatin 25

J.P. GROTZINGER, D.S. McCORMICK, and S.M. PELECHATY: Progress report on the stratigraphy, sedimentology, and significance of the Kimerot and Bear Creek groups, Kilohigok Basin, District of Mackenzie 219

T. FRISCH, M.R. DIGEL, and E.J. WILLIAMS: Precambrian Shield of the Boothia Uplift, southern Somerset Island and northern Boothia Peninsula, District of Franklin 429

J. VAN GOOL, T. CALON, and T. RIVERS: Preliminary report on the Grenville Front Tectonic Zone, Bruce Lake area, western Labrador

H.H. BOSTOCK: Geology of the south half of the Taltson Lake map area, District of Mackenzie 443

C.S. MACDOUGALL and D.H.C. WILTON: Middle Proterozoic granite-related mineralization in the Round Pond area, Labrador 457

J.E. KING, P.D. BARRETTE, and C.D. RELF: Contrasting styles of basement deformation and longitudinal extension in the metamorphic-internal zone of Wopmay Orogen, N.W.T. 515

T.W. NEEDHAM: Geological setting of two metagabbroic bodies, central Britt domain, southwestern Grenville Province, Ontario 597

M.B. LAMBERT and C.R. VAN STAAL: Archean granite-greenstone boundary relationships in the Beaulieu River volcanic belt, Slave Province, N.W.T. 605

M.R. ST-ONGE, S.B. LUCAS, D.J. SCOTT, and N.J. BÉGIN: Tectono-stratigraphy and structure of the Lac Watts–Lac Cross–Rivière Déception area, central Cape Smith Belt, northern Québec 619

M.B. LAMBERT and R.E. ERNST: Archean mafic dyke swarm, Beaulieu River volcanic belt, Slave Province, N.W.T. 673

R.I. MACFIE: The Clinton-Colden hornblende gabbro-anorthosite intrusion, Artillery Lake map area, District of Mackenzie 681

R.S. HILDEBRAND, S.A. BOWRING, K.P.E. ANDREW, S.F. GIBBINS, and G.C. SQUIRES: Geological investigations in Calder River map area, central Wopmay Orogen, District of Mackenzie 699

A.N. LECHEMINANT, J.C. RODDICK, A.C. TESSIER, and K.M. BETHUNE: Geology and U-Pb ages of early Proterozoic calc-alkaline plutons northwest of Water Bay, District of Keewatin 773

J.B. HENDERSON, P.H. MCGRATH, D.T. JAMES, and R.I. MACFIE: An integrated geological, gravity and magnetic study of the Artillery Lake area and the Thelon Tectonic Zone, District of Mackenzie 803

Interior Plains/Plaines Intérieures

I. BANERJEE: Interpretation of dipmeter logs of the Lower Cretaceous Cutbank Sandstone, Mannville Group, southern Alberta 337

STRATIGRAPHY/STRATIGRAPHIE

A.I. ZOLNAI: Structure and stratigraphy, Mount Bryant area, eastern Rocky Mountain Front Ranges, Alberta 323

C.W. JEFFERSON and S.M. HAMILTON: Structure and stratigraphy of the Paleozoic-Precambrian contact zone on White and Southampton islands, District of Keewatin 451

K. DEWING P. COPPER, and S. HAMILTON: Preliminary report on the stratigraphic position of oil shales in the Lower Paleozoic of Southampton Island, District of Keewatin 883

STRUCTURAL GEOLOGY/GÉOLOGIE STRUCTURALE

S.K. HANMER: Granulite facies mylonites: a brief structural reconnaissance north of Stony Rapids, northern Saskatchewan 563

SCIENTIFIC AND TECHNICAL NOTES
NOTES SCIENTIFIQUES ET TECHNIQUES

L. CORRIVEAU and M. GORTON: Potential economic significance of Precambrian potassic plutons in the Central Metasedimentary Belt, Grenville Province of western Quebec 897

G.W. BERGER and J.L. LUTERNAUER: Preliminary fieldwork for thermoluminescence dating studies at the Fraser River delta, British Columbia 901

S.E. PULLAN, J.A. HUNTER, R.M. GAGNÉ, and R.L. GOOD: Delineation of bedrock topography at Val Gagné, Ontario, using seismic reflection techniques 905

S.R. DALLIMORE and J.L. DAVIS: Ground probing radar investigations of massive ground ice and near surface geology in continuous permafrost 913

G.T. MCKENNA and J.L. LUTERNAUER: First documented large failure at the Fraser River delta front, British Columbia 919

B.E.B. CAMERON: Significance of Lower Jurassic hydrocarbon source rocks in the Cumshewa Inlet area, Queen Charlotte Islands, British Columbia 925

S.G. EVANS: A rock avalanche from the peak of Mount Meager, British Columbia 929

P. HOOD and D.J. TESKEY: Helicopter-borne aeromagnetic gradiometer surveys: a progress report 935

P.J. KURFURST: Cone penetration tests of the nearshore zone sediments off Richards Island, Northwest Territories 939

Author Index/Index des auteurs 945

Wall rock alteration mineral assemblages associated with the E-Zone ore bodies at Mines Gaspé, Murdochville, Quebec[1]

DSS Contract 03SQ.23233-4-446

Edward L. Procyshyn[2]

Procyshyn, E.L., Wall rock alteration mineral assemblages associated with the E-Zone ore bodies at Mines Gaspé, Murdochville, Quebec; in Current Research, Part A, Geological Survey of Canada, Paper 87-1A, p. 499-514, 1987.

Abstract

An extensive alteration aureole has been noted to surround the E_{32} ore body at Mines Gaspé, Murdochville, Quebec. The alteration assemblages and associated mineralization have been deposited from hydrothermal fluids that eventually crystallized quartz, calcite and fluorite. Quartz, K-feldspar, diopside, tremolite, phlogopite, chlorite and sphene are associated phases and define definite mineralogical subzones that envelope the ore body. The ore body was not deposited by a single event or fluid phase. By emphasizing the textural details within the various mineral assemblages, it has been possible to define a complex multiple infiltration history and evolving fluid characteristics.

Résumé

Une vaste auréole d'altération entoure le corps minéralisé E_{32} aux Mines Gaspé, à Murdochville, au Québec. Les assemblages produits par l'altération et la minéralisation associée proviennent de solutions hydrothermales qui sont également à l'origine de la cristallisation du quartz, de la calcite et de la fluorite. Les phases associées de quartz, de feldspath potassique, de diopside, de trémolite, de phlogopite, de chlorite et de sphène définissent des sous-zones minéralogiques précises qui entourent le corps minéralisé. Ce dernier n'a pas été formé au cours d'un événement unique ou par une seule phase fluide. L'examen des détails texturaux à l'intérieur des divers assemblages minéraux a permi de reconstituer l'histoire complexe des infiltrations polyphasées et de l'évolution des caractéristiques des solutions.

[1]Contribution to the Gaspé–Lower St. Lawrence Geoscience Program 1984-1988. Project carried by the Geological Survey of Canada, Mineral Resources Division, Project 850009

[2]Department of Geology, Concordia University, 1455 De Maisonneuve Blvd. W., Montreal, Quebec, H3G 3M8

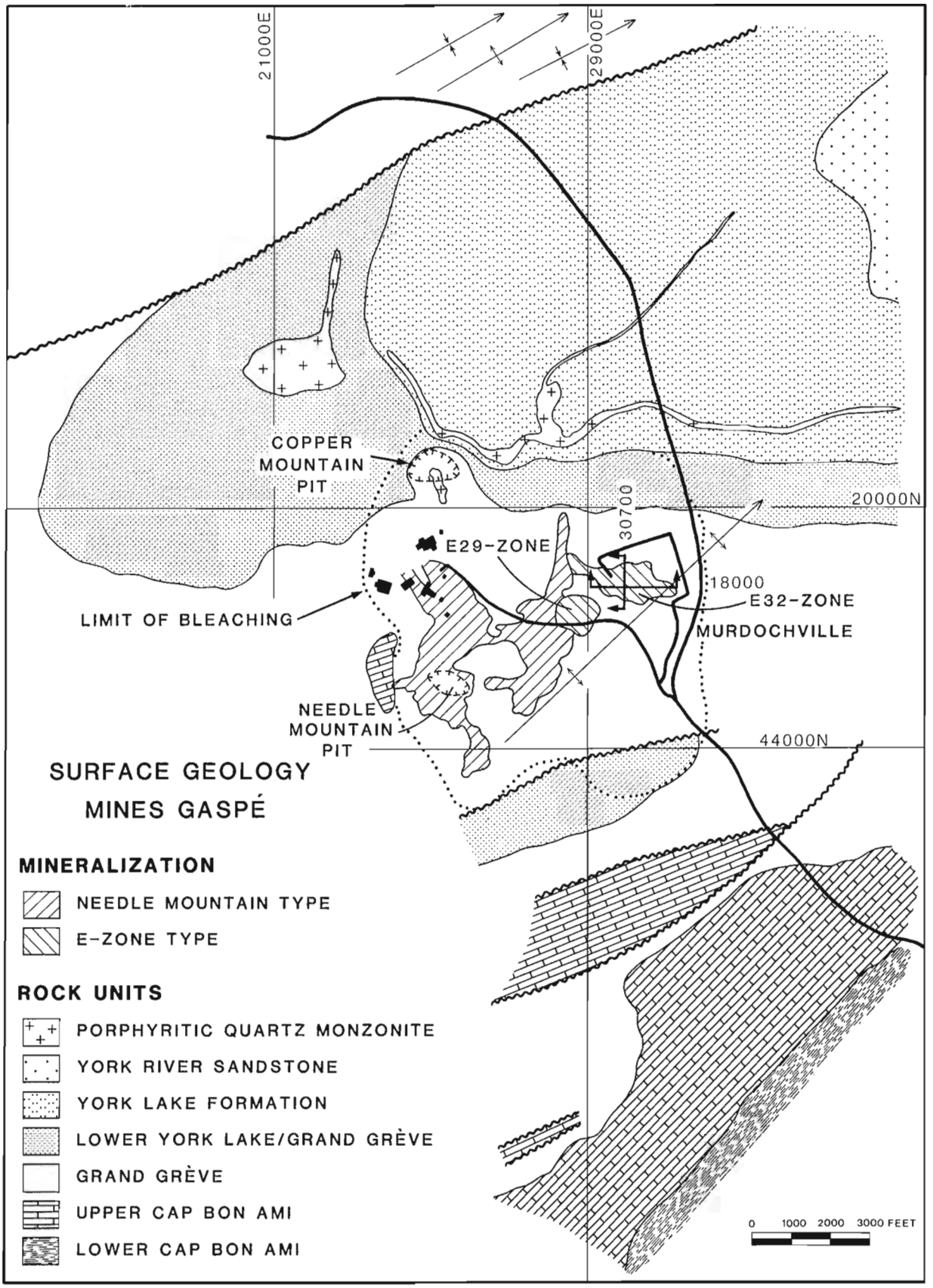


Figure 54.1. Surface geology, Mines Gaspé, showing the location of the ore zones as projected vertically to surface. Modified after Procyshyn (in press). (Published with permission from MERQ.).

INTRODUCTION

The copper deposits at Mines Gaspé, Murdochville are of two types: (1) the Needle Mountain type which consists of a stacked series of replacement skarn bodies containing disseminated chalcopyrite and pyrrhotite. Bornite is rare. Locally the skarns can contain up to 85% sulphide across widths up to 1 m. (2) the Copper Mountain type which is a typical porphyry Cu-Mo deposit and contains pyrite, chalcopyrite and molybdenite either disseminated or in quartz veins hosted within a highly crackled skarn rock that surrounds a small porphyritic quartz monzonite intrusion.

It is estimated that the Needle Mountain type of mineralization contained approximately 50 million tonnes of ore with an average grade of 1.4% Cu whereas the Copper Mountain type of mineralization contained approximately 200 million tonnes of ore with an average grade of 0.42% Cu. Because the cut-off grade is economically defined, it is difficult to estimate how many tonnes of total copper mineralization still exist in the area. The geological characteristics and genetic sources of these deposits have been described by Brummer (1966), Allcock (1982) and Shelton (1983).

In 1981, Mines Gaspé geologists discovered a new ore horizon and subsequently a "new" type of ore body that is located under the town of Murdochville. This new ore body is called E_{32}. It is estimated that this ore body contains 4.5 million tonnes of ore averaging 2.95% Cu and 0.49 oz./t Ag. Although this ore body is in part stratigraphically confined, unlike the Needle Mountain type of mineralization, it is not hosted within garnet-pyroxene bearing high temperature skarns. The host rock is a bleached porcellanite composed of calcite, tremolite and/or diopside. Within about 100 m of the ore body, the bleached porcellanite grades into dark calcareous mudstones and argillaceous calcilutites. The carbonate-rich interval, which hosts the E_{32} ore body, is located approximately 160 m below the C-Zone carbonate interval. The skarn ore bodies hosted by the C-Zone interval, collectively had contained the major portion the Needle Mountain type ore deposits.

In 1983, the Ministère de l'Energie et des Ressources, Québec (MERQ) undertook to map this new deposit and to revise, in more detail, the geological maps of the area (Fig. 54.1). In these studies, the particular objective was to define the nature of structures present in the vicinity of the ore deposits and to define their role in spatially localizing the ore. In 1984, the Geological Survey of Canada, in consultation with MERQ, undertook to provide additional support for laboratory-based petrogenetic studies of this deposit. Detailed petrographic, microprobe mineral analysis, S-O-C stable isotope analysis and fluid inclusion studies have thus been undertaken to help define the physiochemical conditions that have produced the recognizeable alteration patterns surrounding the E_{32} ore body and to demonstrate the extent to which these conditions have influenced the spatial localization of this deposit.

GEOLOGICAL SETTING

The E_{32} and Needle Mountain type of mineralization are localized on the northwest flank of a secondary shallowly plunging anticline (Procyshyn, 1985, in press). This anticline in turn rests on the south limb of a regional syncline (York Lake syncline) that plunges shallowly to the east. To date, all known ore deposits in the Murdochville area occur within pervasively bleached rocks that, in a rough way, asymmetrically surround the Copper Mountain quartz monzonite plug.

The E_{32} ore body occurs in the Lesseps facies (formerly the lower interval of the Cap Bon Ami Formation) within a carbonate rich interval approximately 160 m below the basal limestone unit (C-Zone L1 unit) that constitutes the basal member of the immediately overlying Shiphead Formation. A characteristic sequence of tuff marker horizons has been identified by geologists at Mines Gaspé within the otherwise lithologically monotonous calcareous mudstone/argillaceous calcilutite sequence of the Lesseps facies. Using these marker horizons, it has been possible to construct vertical sections of the E_{32} ore body (Procyshyn, 1984, 1985) from available diamond drilling data and geological map data that have recently been obtained for the drift development. The main ore body appears to have been localized in the axial region of a small anticlinal kink-style fold, associated with south-verging intrastratal slip and wedge faults (Fig. 54.2, 54.3). The mineralization is concentrated within two spatially distinct intervals:

(i) a lower thin sheet-like interval that closely parallels and immediately underlies a thin hornfels marker. In this report this is called the $E_{32\text{-}2}$ ore interval. More recently, the mine geologists refer to it as the E_{32}-200 ore zone.

(ii) a higher inverted pear-shaped body that is stratigraphically transgressive (Fig. 54.3) and structurally controlled (Fig. 54.2). In this report this is called the $E_{32\text{-}1}$ ore interval, whereas mine geologists prefer to call it the E_{32}-150 ore zone.

WALL ROCK ALTERATION AND NATURE OF ORE

The ore consists of very fine grained chalcopyrite and pyrrhotite deposited in varying amounts within peculiarly spotted rocks. At the fringes of the ore deposit, the sulphides are widely disseminated within bleached calcite-rich porcelanite. In the centre of the ore zone, the carbonate rocks become darker and sulphides locally replace up to 70% of the rock (Fig. 54.4). The replacement seems to be selective, leaving behind a palimpsest of the original decussate fabric commonly produced in its earlier history by tremolite and other mafic minerals set against a calcite rich matrix. The sulphides generally are very fine grained; but occasionally, where these sulphides have been cut by later structures, they have been recrystallized to produce a coarse grained annealed texture (Fig. 54.4B).

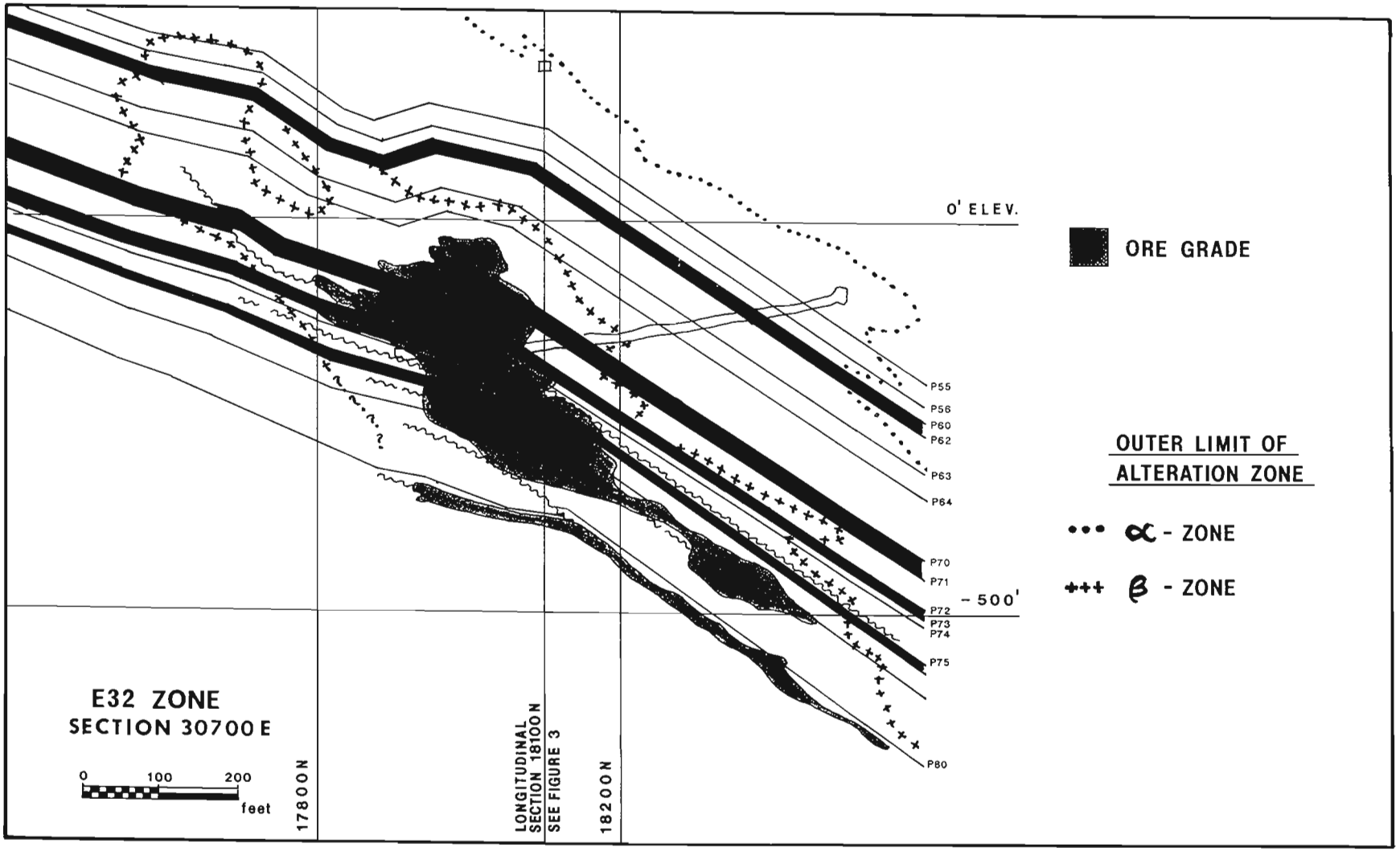


Figure 54.2. Cross section 30700E including drift 3100S modified after Procyshyn (in press). Published with permission from MERQ. Note that the ore is localized within the core of a kink-band fold overlying a ramp structure.

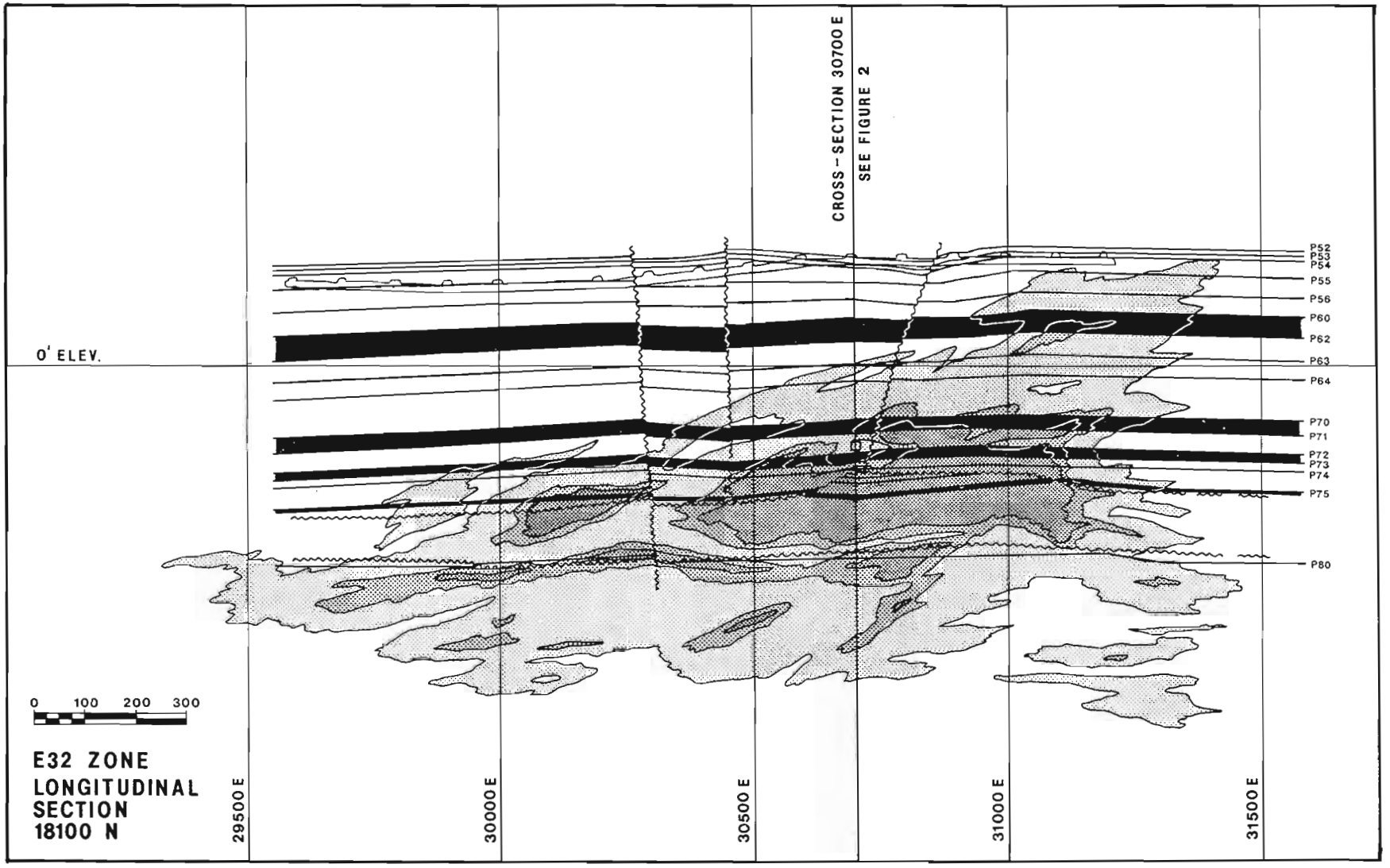


Figure 54.3. Longitudinal section 18100n containing drifts 2801 and 2802. This section clearly shows that the mineralization is stratigraphically transgressive. For legend, see Figure 54.2. Modified after Procyshyn (in press). Published with permission from MERQ.

The pervasive nature of the alteration patterns produced by metasomatism is impressive when viewed in the drifts adjacent to the ore body. It would appear that the metasomatic fluids soak through the rock at will and do not require structural channels to provide flow permeability (Fig. 54.5). However, despite the complex change of colour patterns produced by metasomatism, the preliminary chemical data that have been obtained by MERQ (Procyshyn, in preparation), indicate little or no change in FeO*, MgO, K_2O, $N_{a2}O$ or Al_2O_3 values and only a small increase in SiO_2 and a concommittant decrease in CaO as one approaches the core of the ore-body from its fringes.

In hand samples, a progressive alteration sequence can be recognized on the basis of changes in colour and in the nature of banding or spotting, and from crosscutting or superimposed relationships. Furthermore, two distinct styles and perhaps phases of alteration can be defined; an early bleaching phase which produces a massive fine grained light-coloured calc-silicate rock called porcellanite, and a later metasomatic-infiltration phase which produces darker coloured rocks that are often characterized by a spotted to beaded appearance. Further subdivisions of these alteration phases have been made at the microscopic level and are largely based on different mineral textures and assemblages. To simplify

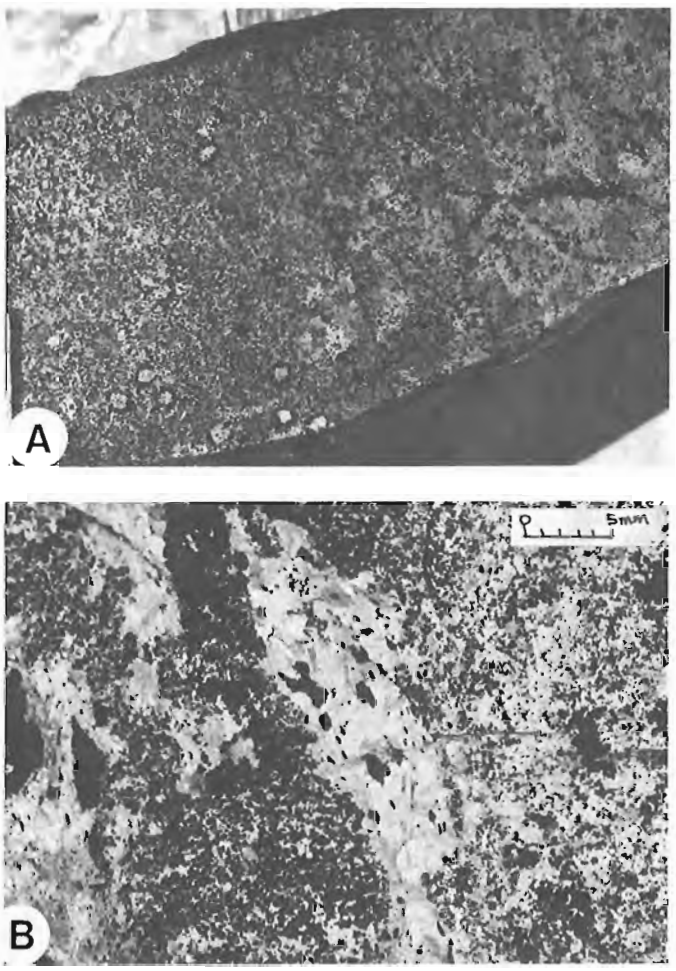


Figure 54.4. **A.** The sulphide-rich portions of the E_{32} ore body contain very fine grained chalcopyrite and pyrrhotite that pseudomorphically replaced the calcite rich matrix of the altered porcellanite and enclosed highly chloritized tremolite and phlogopite. Note that the decussate fabric of the original rock is still faithfully preserved. (3100S-140: polished hand sample-x2.) **B.** Locally portions of the "massive" sulphide appear to have been recrystallized to develop a coarser grain size and complex twinning fabric in the pyrrhotite. (3100S-140: polished hand sample.) GSC 204 224-I

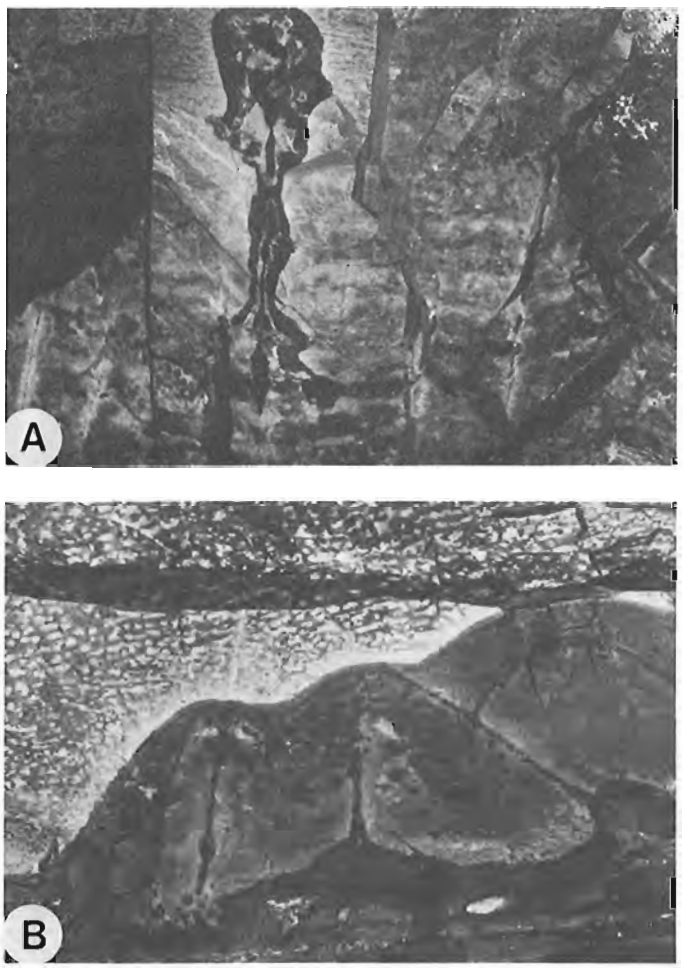


Figure 54.5. **A.** The rock adjacent to a hairline fracture is pervasively darkened by the infiltration of hydrothermal fluids flowing through the fracture. The photograph represents approximately 1.5 m of exposure in the drift. (With permission from MERQ.) **B.** The rock is pervasively altered by hydrothermal fluids flowing along bedding planes. The darker rock contains a mineral assemblage akin to that in the alteration zone bordering the E_{32} ore body. (With permission from MERQ.) GSC 204 224-H

the nomenclature, rocks produced by the earliest porcellanite-forming phase of alteration are assigned to the α-zone (distribution shown in Fig. 54.1) and those affected by metasomatic flooding and alteration are assigned to the β-zone. The subdivisions within the individual zones are denoted by a subscripted number following the letter α or β (see Table 54.1).

The alteration in the α-zone begins with a bleaching of the dark coloured sedimentary rocks to produce at first, irregular wispy light coloured patches which, with increasing alteration, coalesce to produce a massive white porcellanite. Adjacent to the E_{32} ore zone (30-50 m) within the β-zone, the porcellanite is altered and partially replaced by metasomatic fluids as they flow through the rock along the hairline fractures and the more permeable beds. With continued flow the fluids soak into the porcellanite adjacent to the permeable structures and progressively replace it. The replaced volume becomes more crystalline in appearance, slightly darker in colour and is composed dominantly of calcite and/or quartz and K-feldspar intergrowths (Fig. 54.6). Fluorite, which is

Table 54.1 Summary of characteristics of alteration zones

Zone	Field characteristics	Mineral assemblage	Sulfide occurrence	Distinguishing features
α_1	dark to med. grey	qtz-Cc-phl-Kfsp(?)	finely dissim.po	— Cc is very "dirty" and poorly crystallized — detrital qtz t:fsp readily visible
α_2*	dark to med. grey	qtz-Cc-tr-K-fsp	same as α_1	same as α_1
α_2	greenish to pale grey	qtz-Cc-tr-K-fsp-sph	occasional bleb but usually finely dissimated po	— rock completely recrystallized — calcite grains visible cores clean but margins indistinct — sphene forms clusters of tiny grains
α_3	light grey to white	qtz-Cc-siop-K-fsp-sph	sulphides (po) conc. in patches, & blebs. still very minor	— calcite clear and in polygonal aggregate — quartz-Cc concen. as irregular patches between dominantly diop-qtz-K-fsp areas — sphene grains large enough to be recognized but still in clusters
β_1	grey to brownish grey. Develops beaded to banded appearance.	— relict bands same as α_3 — margins to infiltration channels show tremolite replacing diop. — channels-Ce-qtz-phl-fluorite-po±py (also ±K-fsp±diop but altered	sulphides conc'd adjacent alteration margins and infiltration channels	— calcite in relict bands develops homotaxial polygonal aggregate. Clean — in alteration margin develops homotaxial poikiolitic xenoblasts — sphene forms individual large grains.
β_2	similar to β_1 but infiltration areas pale grey	— same as β_1 except phlogopite replaces diopside — epidote noted in channels always in association with opaques — clear pale green trem. needles in channels crossing qtz-Ce boundaries and enclosed.	same as β_1	same as β_1
β_3	pattern similar but infiltration channels darkened, relict beads and spots also darken	— similar to β_2 but massive phlog. in alteration margins	massive clots of po±cpy in infiltration and alteration margins	
β_4	Similar to β_3 but with appearance of white lace	— massive clots of fluorite-cpy±po and calcite in infiltration areas. — massive chlorite±phlogopite in replacement areas.	same as β_3, perhaps more cpy than po.	
α_1	β_4 rock develops a distinct green colour	— sulphides recrystallized to coarse grain size and anneal texture — diop. grains appear in granoblastic margin	same as β_4 but coarser grain size.	

usually accompanied by disseminated pyrrhotite, characteristically occurs within these calcite-rich areas. With increased intensity of "flooding", the matrix within the metasomatically replaced porcellanite progressively changes from a light grey to a white or faintly pinkish pale grey. Concommittantly, these "flood" areas more clearly define irregular channel-like areas. The unreplaced "relict" white porcellanite also shows a progressive change in form, developing at first a banded appearance which, with increased intensity of alteration changes to a beaded appearance, and finally to a spotted appearance. Immediately adjacent to the sulphide-rich core zone of $E_{32\text{-}1}$ ore zone, the matrix in the "flood" areas develops a dark colour. Almost all visible sulphide minerals (pyrrhotite, chalcopyrite) and definitely all fluorite occurrences, appear to be confined within the calcite-quartz rich "flood" matrix. Minor amounts of sulphides also occur as finely disseminated concentrations within the dark rims which generally envelope the spots or beaded layers adjacent to the infiltration channels.

ALTERATION MINERAL ASSEMBLAGES IN THE α-ZONE

Preliminary examination of thin sections indicates that a progressive sequence of mineralogical and textural changes can be identified in the porcellanite of the α-zone which hosts the $E_{32\text{-}1}$ ore body. Three alteration subzones are defined within this alteration aureole; their characteristics are summarized in Table 54.1 and their distribution is shown in Figure 54.3. Their mutual boundaries are defined on the first appearance of phlogopite (α_1-zone), disappearance of phlogopite and dominant presence of tremolite (α_2-zone) and the disappearance of tremolite and dominant presence of diopside (α_3-zone).

In the outermost part of the α-zone, even before the onset of bleaching, phlogopite and tremolite have been observed in the dark calcareous mudstones and calcilutites. Phlogopite normally is the first silicate mineral to crystallize. It first appears as pale brown wisps which contain acicular crystals that are barely visible even at the highest magnification (×900). The matrix at this stage, although crystalline, is clearly detrital in nature and "dirty" in appearance. With progressive alteration, the altered rocks become bleached to pale grey or white. Concommittantly, the phlogopite evolves into well developed books displaying frayed ends and the calcite in the matrix is progressively recrystallized to develop very small but microscopically visible individual grains which display clear centres and dark dirty poorly defined margins. Similarly, the detrital component is progressively recrystallized to form a quartz-feldspar polycrystalline mosaic that is irregularly dispersed between polycrystalline calcite patches. In hand sample, this bleached rock, now called porcellanite, is massive, white to pale grey and porcelain-like in appearance. The presence of the above mineral assemblages and textures is used to define the α_1-subzone.

Tremolite closely follows the appearance of phlogopite in space. At first, tremolite develops prismatic to acicular grain clusters which with increased degree of alteration, evolve to form bow-tie fascicular grain aggregates less than 10 μm wide. At this latter stage, the groundmass is almost totally recrystallized to form a very fine grained allotriomorphic

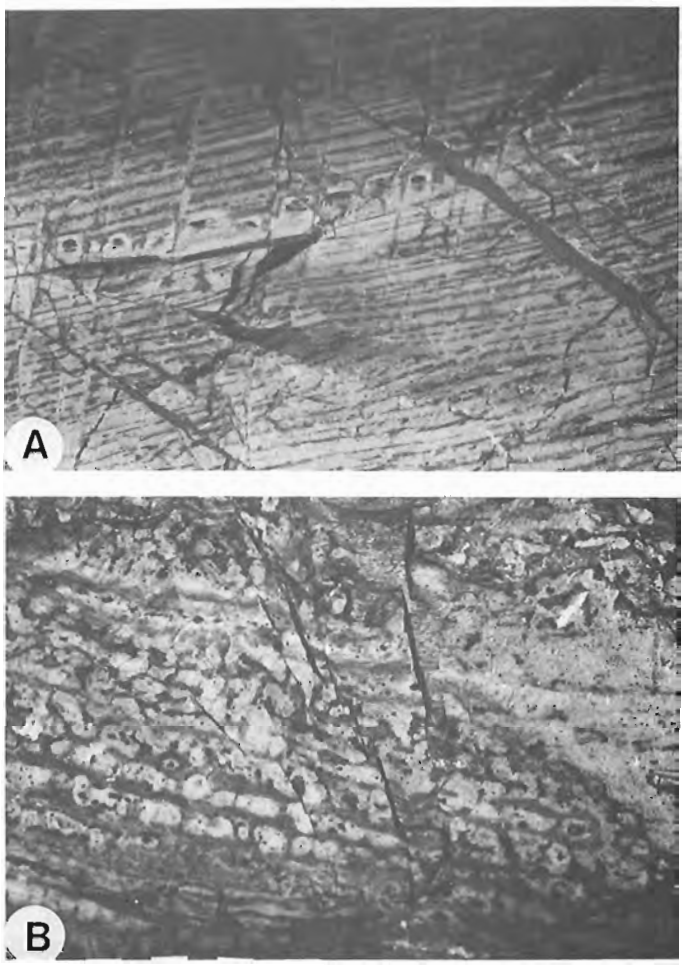


Figure 54.6. **A.** The earliest indications of pervasive flooding by hydrothermal/metasomatic fluids associated with the deposition of the E_{32} ore body is the appearance of darker calcite rich seams formed approximately parallel to bedding and which progressively replace the light coloured porcellanite. The relict white procellanite develops at first a banded appearance which with progressive alteration evolves to a beaded appearance shown here, and eventually to a spotted appearance as the relict porcellanite becomes isolated in the darker metasomatically altered rocks. The beaded alteration pattern shown here is typical of the α_1 subzone superimposed on the α_3 subzone. (With permission from MERQ.) **B.** The degree of alteration in this photograph is slightly higher than that shown in A. The porcellanite in contact with the infiltration assemblage, develops darker rims which contain finely disseminated pyrrhotite and phlogopite. This beaded to spotted pattern is typical of the β_2 subzone superimposed on α_3 subzone. (With permission from MERQ.) GSC 204 224-N

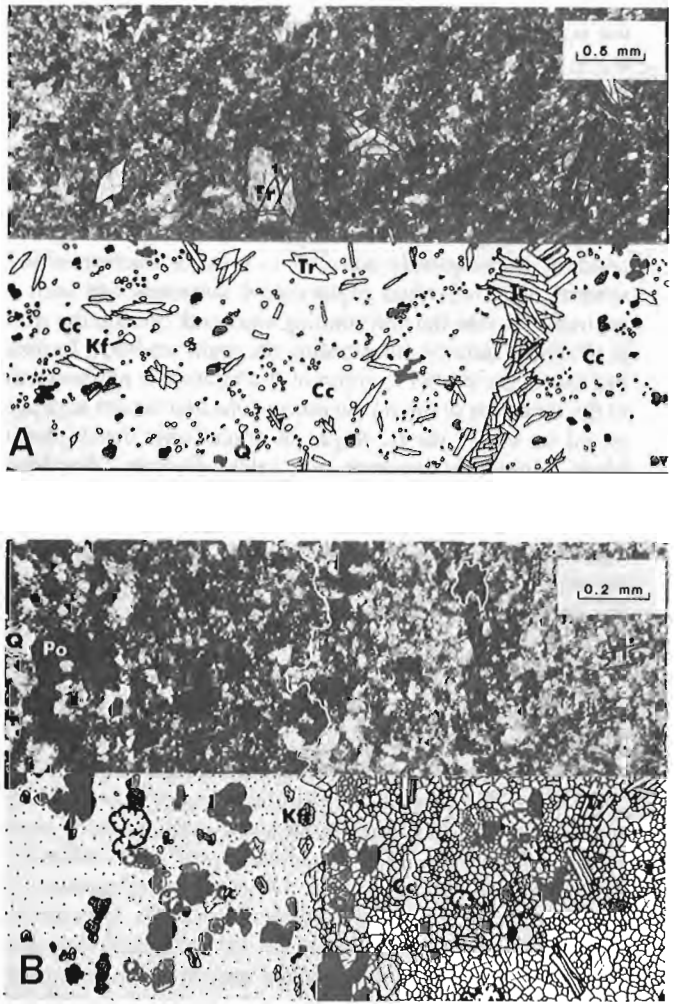


Figure 54.7. **A.** At the fringes of the bleach-zone, within black calcareous mudstone, idioblastic to subidioblastic acicular tremolite (Tr) grains commonly form fascicular aggregates set within a "dirty" groundmass composed of extremely fine grained calcite which contains numerous opaque inclusions. The groundmass also contains detrital quartz (Q) and K-feldspar (Kf) that are often concentrated in thin laminae to define a faint relict bedding. Occasional gash fractures are filled with well formed tremolite grains seen to protrude into the adjacent groundmass. This photograph represents the earliest form of the α_2 subzone. (Section 3400-195.) **B.** With increased alteration within the α_2 subzone, detrital quartz and K-feldspar are recrystallized to form allotriomorphic mosaics intergranular to calcite rich mosaics. In this figure, detrital quartz and K-feldspar, as well as the compositionally defined bedding (LHS vs. RHS) are only vaguely outlined. The more pyrrhotite rich argillaceous beds (LHS) contain a barely visible very fine grained crystalline matrix in which occasional crystals of quartz, feldspar, sphene and epidote (rare) and calcite may be recognized. The more calcareous beds (RHS) on the other hand, tend to be more coarsely crystalline, and contain finely bladed forms of tremolite (T_1), dusty aggregates of very fine sphene and patches of relatively clean, very fine grained anhedral calcite. (Section 3400-210.) GSC 204 224-M.

intergrowth of calcite, quartz and K-feldspar (Fig. 54.7). The tremolite rarely occurs in the presence of phlogopite, and when it does, the two minerals occur in distinct and separated areas. Only rarely have tremolite needles been observed to be superposed across phlogopite grains. In more advanced stages of alteration, the tremolite fibres evolve into larger compact grains up to 0.5 mm in size. At this stage of alteration, the calcite in the groundmass occurs as clear equigranular xenomorphic grains with irregular to sutured grain boundaries. All vestiges of even the coarsest detrital grains and bedding have now disappeared (Fig. 54.8A). This combination of textures and the dominant presence of tremolite in the alteration assemblage is used to define the α_2 subzone.

Diopside first appears as small (20-50 μm) anhedral clear grains within K-feldspar-quartz clusters. The first appearance of diopside is used to define the boundary between the α_2 and the α_3 subzones. In the α_3 subzone, diopside has never been observed to replace tremolite directly. With increasing alteration, the tremolite disappears within a few metres from the spot marking the first appearance of diopside. In the absence of tremolite, diopside occurs as subhedral blocky grains up to 0.5 mm in size, set on an inequigranular matrix composed of anhedral poikilitic quartz and K-feldspar. As recrystallization continues, individual subhedral diopside grains coalesce into clusters within which individual subhedral grains are separated by interstitial quartz and K-feldspar. With the appearance of blocky diopside, calcite begins to disappear. In these more highly altered rocks, calcite is a minor phase, and occurs as large clear poikilitic anhedral grains interstial to the quartz-feldspar-pyroxene patches (Fig. 54.8B). Occasionally within the α_3-subzone, the calcite also occurs concentrated in clot-like patches laced between the patches composed dominantly of calcsilicate minerals.

Although our data are spatially limited at this time, the above sequence of mineral subzones, in an approximate way, appears to surround the $E_{32\text{-}1}$ ore body (Fig. 54.3). Spatial distribution of these alteration zones and their textural features indicate that they were not produced by large scale infiltration of hydrothermal fluid phases. This is in contrast to the subsequent β-alteration patterns which are imprinted onto the porcellanite of the α-zone and which are described below.

ALTERATION MINERAL ASSEMBLAGES WITHIN THE β-ZONE

A somewhat different progressive alteration style is clearly overprinted on porcellanite of the α-zone. This alteration is associated with the infiltration of hydrothermal fluids and related metasomatic processes. At least four separate fluid infiltration events have been distinguished. Each event appears to have produced a characteristic style of alteration. Based on their general appearance in the drifts and drill core, they have been referred to in the field as (i) spotting calcite-fluorite infiltration – the β-zone, (ii) "pepper" infiltration – the δ-zone, (iii) "greening" infiltration that is generally cored by sphene, vesuvianite and salmon-pink hydrogrossularite –

the ϵ-zone, and finally (iv) garnet-clinopyroxene skarn "infiltration" – the ϕ-zone. All these fluid events preceded the Copper Mountain molybdenite-chalcopyrite-pyrite mineralizing event (Procyshyn, in preparation – MERQ).

At the present time, only the spotting alteration associated with the calcite-fluorite infiltration phase (β-zone) have been studied petrographically. This alteration pattern is found pervasively superimposed on the pre-existing porcellanites of the α_3 zone within the immediate vicinity (<50 m) of the $E_{32\text{-}1}$ ore zone. In other areas, in the presence of strong fracturing, an almost complete sequence of alteration zones similar to those that pervasively surround the ore body, commonly occurs telescoped adjacent to the borders of these fluid conduits. The size of the alteration envelope is variable and seems to depend on the size of the fracture or the bedding permeability, i.e. on the strength of fluid flow through the conduit. Consequently adjacent to a major fracture or vein system, the individual replacement subzones are seen to protrude far into the surrounding wall rock outside the main β-alteration aureole surrounding the main ore body. In these instances, the spatial location of β-alteration is not restricted to the core area of the α_3 alteration zone and occurs superimposed on α_2, or the α_1 stages of porcellanite development. More commonly however, the calcite-fluorite "flooding" along vein systems produces only thin selvages (<10 cm). Within these selvages a telescoped sequence of alteration assemblage is developed that closely resembles those observed in the β-alteration zone enveloping the $E_{32\text{-}1}$ ore body. However, these selvages only rarely appear to contain the "beaded" or "spotted" pattern that characterizes the β-alteration zone (Fig. 54.5, 54.6).



Figure 54.8. **A.** More advanced recrystallization in the α_2 subzone produces a coarsening of grain size and a development of "bow-tie" or fascicular aggregates of tremolite (Tr) superimposed on a more coarsely recrystallized matrix in which patches of fine-grained allotriomorphic calcite are laced with more silicate rich areas containing irregular clusters of quartz, K-feldspar, dusty clusters of very fine grained sphene (Sph) and/or pyrrhotite. All vestiges of detrital grains and bedding have now disappeared. (Section 3100E-38.) **B.** Within the α_3 subzone, the alteration assemblage is characterized by the appearance of subidioblastic diopside (Cpx) and finer-grained K-feldspar (Kf) both of which exhibit partially embayed grain contacts when set against calcite (Cc). The calcite in the matrix now develops an equigranular granoblastic texture. (Section 3400S-425B.) GSC 204 224-L

The spotted appearance in rocks occurring within the β-zone is produced by the preservation of relict beaded layers or spots of white porcellanite within the darker calcite rich "flood" areas that have more or less completely replaced the rock along "bedding" planes and along existing fractures and bedding boudinage. For convenience, these "flooded areas", are called infiltration channels. Observations of stained polished slabs and of thin sections, in all instances, indicate that the "flood" replacement areas, i.e. the infiltration channels, are considerably enriched in calcite and ubiquitously contain sulphides (po±cpy) and fluorite. The mineral assemblages contained within the infiltration channels, in part at least closely resemble those occurring within the core area of the ore deposit (Fig. 54.12) and therefore appear to have been produced by the same fluids responsible for the deposition of the ore.

In order to properly describe the β-zone mineral assemblages and textures, it is necessary to distinguish between relict "unreplaced" areas and "flood" replacement areas (i.e. infiltration channels): these in turn have to be distinguished from partially metasomatized reaction zones bordering the infiltration channel. The individual minerals present in each assemblage may therefore be one of three types: (i) relict mineral that had crystallized during an earlier phase of alteration and is now an inherited phase in the assemblage due to incomplete alteration; (ii) a prograde mineral that (a) grew directly within the infiltration fluid phase that later deposited calcite, quartz and/or fluorite to form the intergranular matrix to the infiltration channel; or (b) developed indirectly as a metasomatic replacement mineral in the reaction zone bordering the infiltration channel; or (iii) a late retrograde mineral that directly replaced the earlier prograde mineral during the waning metasomatic history of the infiltration hydrothermal fluids.

It is possible to separate the individual mineral types on the basis of their textural position and form. Minerals crystallized during a prograde phase of alteration rarely replace earlier "mafic" minerals (i.e. chlorite, phlogopite, tremolite or diopside) but instead nucleate as separate anhedral phases in the intergranular position within quartz-feldspar-rich patches. With increasing degree of fluid infiltration, these minerals develop a coarser grain size and a more blocky subhedral grain form. Prograde minerals which crystallized directly within the infiltration channels, almost always display euhedral form when set within or against quartz, K-feldspar, calcite and/or fluorite which subsequently crystallized within the "open" parts of the infiltration channel.

During the retrograde phase of metasomatic alteration, the earlier formed metamorphic minerals are degraded texturally to develop mortar-like textures prior to being replaced by lower grade phases. The mortar development begins at the margins and eventually extends into the interior of the grain. With increased alteration, these recrystallized granular mosaics of the earlier formed mineral, e.g. diopside now have only the vague form of the earlier large grain and now also contain small irregular patches of quartz and K-feldspar intergranular to the small dusty irregular pyroxene grains. These clusters, with increasing retrograde alteration are eventually directly replaced by later femic minerals, e.g. diopside by tremolite or chlorite. This contrasts with the prograde metasomatic crystallization of mafic minerals associated with later infiltration of hydrothermal fluids. In this latter instance, as with β-phase infiltration, the "new" mafic minerals are normally observed to nucleate within the intergranular areas of quartzo-feldspathic areas and never directly replace the earlier formed metamorphic mineral. In absence of these mortar textures within relict mafic phases, it becomes difficult to distinguish minerals developed during the retrograde replacement phases of the β-phase of alteration from those minerals developed during later (post β-phase) metasomatic phases that impose a lower grade assemblage on a previous relict mineralogy.

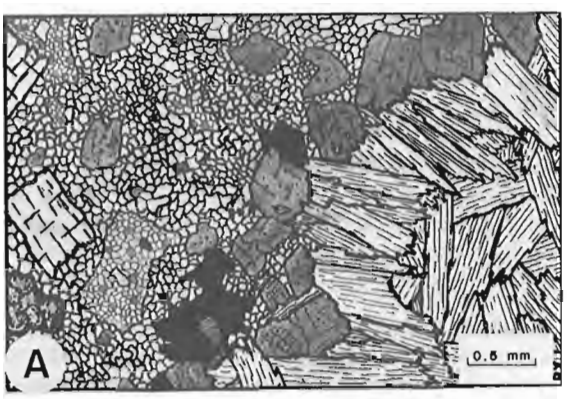
β-phase replacement envelopes, which indicate varying intensity of replacement, can also be seen at the thin-section scale. Consequently relict patches of α-assemblages become surrounded by and progressively replaced by β-zone assemblages. Occasionally unstable calcsilicate minerals, e.g. diopside in a β-phlogopite zone, are armoured from the reactant fluid and thus preserved as a relict phase. It is readily evident that within the β-zone of alteration, kinetic aspects control the mineral assemblages, the textures, and the degree to which the rocks have been altered.

Using the combination of new mineral development, texture, intensity of mineral replacement and the degree to which sphene and calcite have been recrystallized, it is possible to identify four mineral subzones within the β-alteration aureole that immediately surrounds the $E_{32\text{-}1}$ ore body; their main characteristics are given in Table 54.1. In order of their increasing "grade", these are called β_1, β_2, β_3 and β_4. Their respective boundaries are defined by the first appearance of: (i) metasomatic tremolite replacing diopside; (ii) phlogopite blades appearing within quartz-K-feldspar-calcite patches and in the presence of earlier tremolite; (iii) massive dark patches of discussate intergrowth of phlogopite appearing within calcite rich patches. Locally phlogopite also appears to replace calcite. Tremolite is generally absent in these zones; relict diopside being replaced by phlogopite however, is still locally present; (iv) massive fibrous mats of chlorite enclosing bladed phlogopite replacing calcite and diopside. The alteration subzone normally hosts or immediately envelopes the chalcopyrite rich portions of the $E_{32\text{-}1}$ ore zone.

In general, the β-alteration assemblage is superimposed on massive white, diopside-bearing, porcellanites of the α_3-zone. In these rocks, the first indication of β-zone alteration is the appearance of dark rimmed spots up to 15 mm in size. In thin section, the rim of a spot consists of a radial distribution of subidioblastic tremolite blades, which toward the centre of the spot develop a decussate fabric (Fig. 54.9A). The tremolite at the outer margin is surrounded by an irregular rim of large (0.5 mm) subidioblastic K-feldspar intergrown with irregular bleb-like grains of pyrrhotite which occurs concentrated at the outermost rim of the spot. The host porcellanite otherwise shows a complete absence of infiltration by calcite-depositing hydrothermal fluids. In thin section, the relict porcellanite consists of irregular patches composed of clear calcite, interlaced between granoblastic areas composed of quartz and K-feldspar that host well developed blocky diopside grains. The calcite infiltration "lace" is composed of a polycrystalline aggregate of clear poikilitic calcite grains that contain very small (2-15 μm) widely dispersed scalloped grains of quartz, K-feldspar, and less commonly irregular aggregates of sphene. Porphyroblastic grains of subhedral diopside (~15%), subhedral K-feldspar (~5%) and less commonly grain aggregates of anhedral sphene (~2%), occur embedded in the above calcite matrix. This texture and mineral assemblage is typical of the α_3 alteration zone.

In areas containing more advanced β_1-phase of alteration, the calcite-fluorite bearing "floods" appear as pale greyish white to pale pinkish white patches which spread irregularly into the white porcellanite along bedding planes and fractures, and progressively isolate the porcellanite into a beaded and/or spotted pattern. These "flood" or infiltration areas consist of an inequigranular saccaroidal poikiotopic mosaic of calcite within which there occur scattered clusters of highly embayed quartz and K-feldspar and less commonly highly corroded relicts of diopside grains. Fluorite is generally a minor mineral component in these flood zones and occurs widely dispersed as an intergranular phase to calcite. Locally however, fluorite also occurs in irregular clot-like concentrations. Characteristically prismatic to acicular euhedral tremolite grains are poikilitically enclosed within this infiltration assemblage.

In the β-phase of alteration, the areas of infiltration are darker in colour. The infiltration channels can be clearly identified at this stage because they are separated from the relict porcellanite by a dark rim (1-5 mm) which appears to define a metasomatic reaction "front" (Fig. 54.9B). These



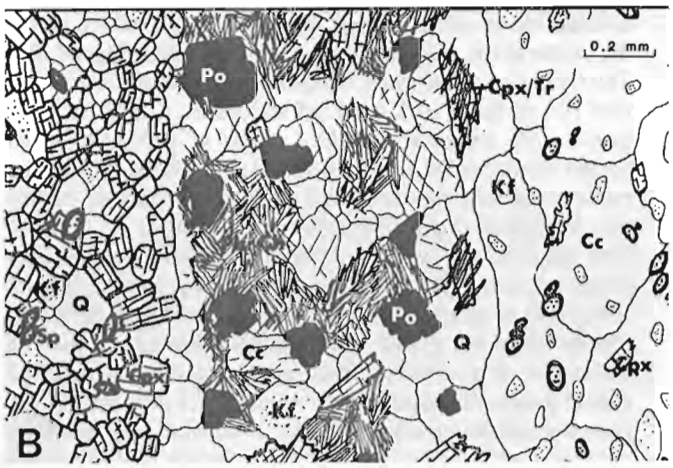


Figure 54.9. **A.** The appearance of dark tremolite spots up to 1.5 cm across, within massive white porcellanite herald the first appearance of the β_1 – alteration assemblage. In thin section, as shown here, the spot consists of subidioblastic tremolite (Tr) needles arranged in a radial fashion at the rim margin and in a more decussate fabric toward the spot interior. Large subidioblastic K-feldspar associated with irregular clusters of pyrrhotite develop a partial outer rim to the spot. The host porcellanite contains textures and mineral assemblages typical of the α_3 subzone. (Section 3400S-484.) **B.** In the β_2 subzone, the infiltration assemblage is more clearly differentiated from the relict assemblages. The infiltration assemblages on the right hand side (RHS) of this photograph consist of large, poikiliotopic calcite grains enclosing sphene, diopside (Cpx) and K-feldspar. A pronounced dark reaction envelope is developed between the infiltration and the relict phases. In the area adjacent to the relict porcellanite which typically contains α_3-subzone assemblages, the dark rim contains phlogopite clusters which are in part replaced by chlorite. Adjacent to the calcite rich side of the dark rim, the alteration assemblages consist of tremolite which appears to have replaced diopside and which itself becomes partially replaced by phlogopite near the centre of the alteration rim. Note the concentration of pyrrhotite within the reaction rim. GSC 204 224-K

dark rims are largely composed of chlorite, phlogopite, tremolite and occasional grains of diopside, which now are largely replaced by tremolite needles. Within these reaction envelopes, a distinct mineralogical zoning pattern is often observed. Phlogopite and chlorite are the dominant mafic phases at the outer boundary of the rim adjacent to the porcellanite. Tremolite, and particularly diopside now largely replaced by tremolite needles, occur on the inner boundary of the dark rim adjacent to the calcite-rich infiltration areas. Pyrrhotite, which commonly displays a pseudomorphic subhedral cubic form, is distinctly concentrated in these reaction rims. Large blocky grains of clear calcite and less commonly anhedral grains of K-feldspar also occur in minor amounts, interstial to the mafic minerals within the reaction rim. Away from the calcite rich side, tremolite itself becomes replaced by phlogopite. In the infiltration channel, the calcite occurs as large poikiliotopic grains which enclose much finer grained (10-20 μm) inclusions of diopside, sphene, K-feldspar and quartz with little or no replacement by phlogopite or tremolite. Elsewhere, although the "flood" zones are similar in form to that seen in the β_1 zone, it is now phlogopite, developing a bladed to platy rosette form, which forms the stable new mineral phase in the inequigranular calcite-fluorite matrix. In the β_2-zone, the calcite within the infiltration channels also changes form and begins to develop irregular polycrystalline patches composed of large (up to 3 mm in size) clear poikiliotopic grain mosaics that demonstrate complexly sutured boundaries.

In the drifts, and in the diamond drill core, zones β_1 and β_2 invariably interchange positions over a 30-50 m interval. It is thus difficult to define the exact map boundaries between these two alteration zones. The reasons for this are still unclear. This may be simply caused by inherent permeability differences that exist in the rock, which in combination with differences in flow volumes and residence time, affect the degree to which the host porcellanite interacts with the infiltrating fluid. It is interesting to note that outside the main β-alteration zone within the α_2 and the α_1 subzones, narrow (0.1 to 2 mm wide) lenticular calcite veins, which contain little or no quartz, commonly enclose clear euhedral grains of diopside. The diopside grains usually occur concentrated as rims along the wallrock of the vein. Minor sphene and K-feldspar also occur within these veins. The diopside, at the wall margin however, is often replaced by phlogopite that pervasively extends for some distance (0.5 to 15 mm) into the porcellanite (Fig. 54.10A).

Calcite-quartz veins containing tremolite in almost identical relationships to the above have also been noted. Alteration of the wall rock along tremolite-calcite filled fractures however, is limited to thinner selvages (~1 mm) whereas those containing diopside are, as a rule more pronounced. It can perhaps be argued that flow rates and residence time of the fluid in the rock will affect the activities of species such as Ca^{++} and SiO_4^{--}, involved in the wall rock reactions,

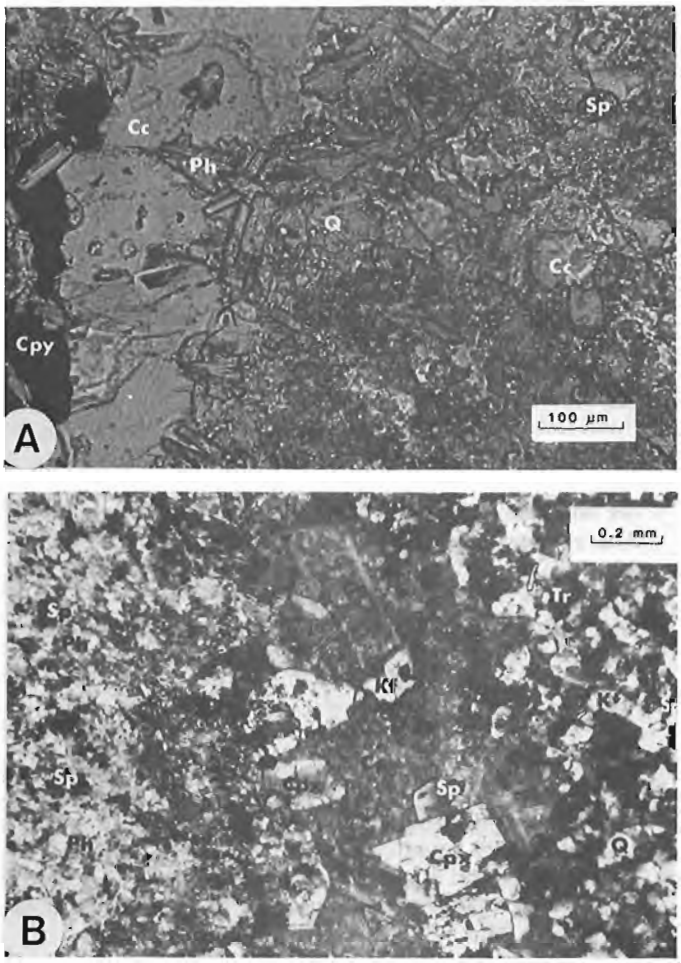


Figure 54.10. **A.** The β-alteration assemblage is often telescoped adjacent to calcite-quartz-fluorite filled veins cutting the porcellanite. The vein-infiltration assemblages consist of calcite and fluorite (high relief minerals) which carry chalcopyrite. Adjacent to the vein, blades and rosettes of phlogopite line the wall of the vein. The tremolite in the wall rock adjacent to the vein is now also almost completely recrystallized to phlogopite. The calcite in the wall rock adjacent to the veins occurs as large irregular clear grains which include clear quartz, feldspar, small clear grains of sphene (Sp) and more rarely diopside. This alteration assemblage is characteristic of the β_2 subzone. (Section 3100S-572.) **B.** Within the β_3-subzone, infiltration patches are composed of coarse homotaxial calcite (Cc) which contains smaller inclusions of euhedral diopside (Cpx) and irregular wisps and patches of pyrrhotite and chalcopyrite. Adjacent to the walls of the infiltration areas, the diopside is replaced by phlogopite (Ph) also containing irregular patches of sphene (Sp). This dark phlogopite also occurs interstitial to quartz-K-feldspar-tremolite in the porcellanite spots as shown on the right hand side of the photograph. This phlogopite appears to be replacing the calcite forming the matrix in the altered porcellanite. GSC 204 224-J

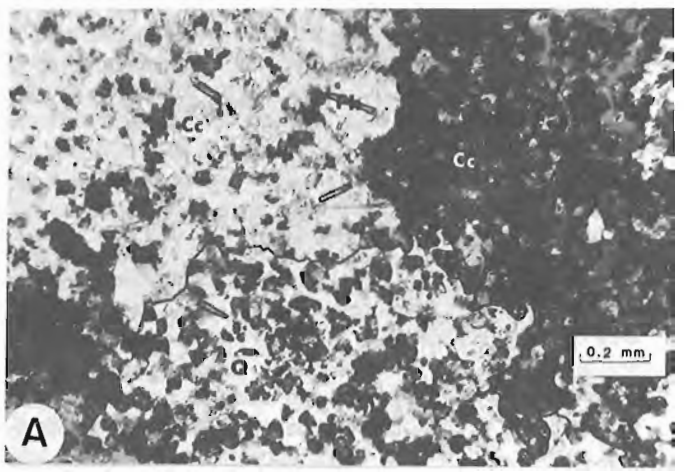
and thus the mineral sequences and assemblages that will be present in the reaction zones.

The β_3 and β_4 alteration zones are characterized by a pronounced darkening of the infiltration areas which locally form the major component (>70%) of the wall rock. At the hand sample scale, vague dark spots are enclosed by a lighter coloured matrix: this is opposite to the spotting relations observed within the β_2 and β_1 alteration zones. The darkening is produced by the respective appearance of phlogopite and chlorite mineral clusters within the poikiliotopic calcite matrix (Fig. 54.10B). The β_3 and β_4 alteration assemblages immediately (<30 m) envelope the chalcopyrite-rich portions of the $E_{32\text{-}1}$ ore body. Chalcopyrite and pyrrhotite locally form up to 80% of the rock volume within the core zone of this ore body. The boundary between β_3 and β_4 alteration zones is normally sharply defined; the boundary between the β_2 and β_3 alteration zones however, appears to be gradational but not alternatively mixed in nature.

Although the β-zone alteration has been seen to locally extend along well developed fractures outside the bleached area of α-zone alteration, it would appear from presently available data, that the β-alteration zone in general is peripheral to the $E_{32\text{-}1}$ ore body and forms an aureole approximately 30-50 m thick and centred within the α-zone alteration aureole. In addition to the appearance of chlorite, and new diopside, new tremolite and new phlogopite (i.e. diopside$_2$, tremolite$_2$, and phlogopite$_2$), the β-zone is also characterized by a noticeable change in the form of calcite and sphene. As noted earlier, the groundmass calcite changes from a granoblastic texture in the α_3-zone to large complexly sutured homotaxial grain clusters (0.3-0.5 mm) that poikiolitically enclose clean often euhedral tiny (10-20 μm) grains of quartz, K-feldspar, sphene, and diopside, or tremolite or phlogopite (Fig. 54.11A). Sphene now also occurs within the calcite-rich patches as large (2-3 mm) clear subhedral grains. Within the infiltration channel, fluorite, pyrrhotite and/or chalcopyrite are ubiquitously associated with calcite. Subhedral to euhedral grains of K-feldspar, and tremolite and less commonly diopside are also often observed within the infiltration channels. In the vicinity of the massive ore zone, both homotaxial quartz and calcite have been observed to form complexly interfingered but distinctly separated patches. Homotaxial quartz patches appear to occur most prominently immediately adjacent to the "massive" sulphide concentration within zone β_4. Similarly epidote/zoisite and rarely prehnite(?) are only observed in the vicinity of the "massive" ore zone often coating chalcopyrite in the presence of fluorite and calcite (Fig. 54.12).

The western portion of the $E_{32\text{-}1}$ ore body as noted in drill core, begins to develop a characteristic pistachio to olive green colour. Thin section examination of these samples indicates that the altered rock is enriched in pale green diopside and is relatively depleted in calcite. The groundmass mosaic develops a characteristic granoblastic texture. Except

for the tremolite-actinolite which is armoured and thus preserved within sulphide clots (Fig. 54.11B), all the tremolite normally present in this zone has now more or less disappeared. The sulphides have developed a coarser granularity and pyrrhotite, in particular, displays a prominent twinning like lamellae (Fig. 54.4B). All these textures suggest that part of the E_{32} deposit at least, is being thermally upgraded. This phase of alteration, designated as δ-zone (Table 54.1), has only recently been recognized in ore body and remain to be studied. In addition, the alteration phases in the E_{29} are now found to differ substantially from those found in the E_{32-1} ore zone.



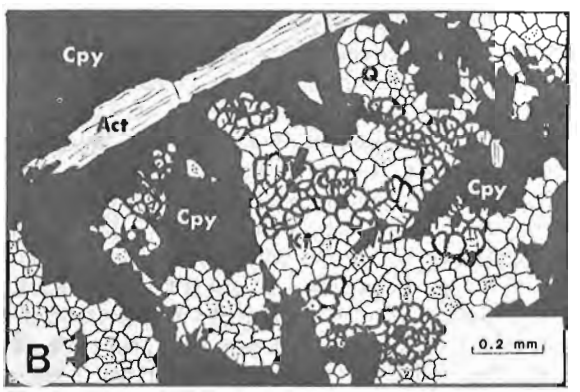


Figure 54.11. **A.** The β_3-alteration assemblages locally occur telescoped immediately adjacent to quartz-fluorite-calcite filled mariolite veins. The wall rock characteristically develops coarse poikiotopic calcite (Cc) and quartz (Q) which contains numerous inclusions of subhedral grains of quartz, feldspar, phlogopite and tremolite. (Section 2901-4A.) **B.** Within the "massive" sulphide zone of the ore body, chalcopyrite-pyrrhotite patches locally contain well developed actinolite (Act) crystals and granoblastic mosaic composed dominantly of K-feldspar-quartz and which appeared to have been armoured from the quartz-feldspar-phlogopite-chlorite matrix that normally surrounds the sulphide-rich areas. Within the granoblastic mosaic there also appear irregular clusters of pale green anhedral diopside grains. The sulphides also appear to be more coarsely crystalline in this area. These textures and mineralogical relationships suggest that locally along major structures, the ore may have undergone a later thermal event. (Section 118-305.) GSC 204 224-F

SUMMARY AND CONCLUSION

Petrographic examination of hand samples, drill core and polished thin sections substantiates the conclusion derived from underground mapping by MERQ that an extensive and complex alteration aureole surrounds the E_{32} ore body at Mines Gaspé. This alteration and associated mineralization appears to have been produced by widespread infiltration of fluids rich in fluorine and carbonate ions. By emphasizing the textural details within the various mineral assemblages, a complex multiple infiltration history is being deciphered. The ore body was not deposited by a single event or fluid phase. Alteration patterns indicate that permeability considerations, whether it be in the form of fractures, initial bedding, unsealing of earlier fluid channels, etc., strongly controlled the flux rate of fluids and heat passing through the rock and con-

Figure 54.12. **A.** Within the calcite-fluorite flood areas of the β_2 subzone, chalcopyrite-pyrrhotite specks and clots locally occur disseminated in the wall-rock. In detail as seen here, the sulphides occur intergranular to a decussate growth of tremolite. Elsewhere in absence of tremolite the sulphide spots are often surrounded by large poikiliotopic calcite patches. (Section 3100S-160.)

B. Another characteristic form of disseminated chalcopyrite-pyrrhotite specis in the β-zone is its cuspate association with fluorite which also encloses tremolite (acicular grains), sphene and epidote. (Section 3100S-160.)

C. Occasionally euhedral tremolite blades protrude from the fluorite rich patches which occur enclosed within chalcopyrite-pyrrhotite grains and which protrude into the sulphide grains themselves. (Section 2901-102.)

D. Locally in vicinity of permeable structures, at the fringes of the β-zone, pyrrhotite-chalcopyrite grains are contained within fluorite-calcite rich patches. The fluorite-calcite infiltration phases also host euderal grains of diopside. (Section 3100S-268.)

E. Within the α-zone, small gash structures often contain irregular pyrrhotite grains characteristically surrounded by large clean calcite grains as shown here. (Section 3100S-477.)

F. Chalcopyrite specks which locally appear within the α-zone, in detail are often surrounded by epidote as shown here. These specks of chalcopyrite within the α-zone are rare and are normally observed only in close proximity to larger mariolitie quartz calcite veins. (Section 3200S-505.) GSC 204 224-G

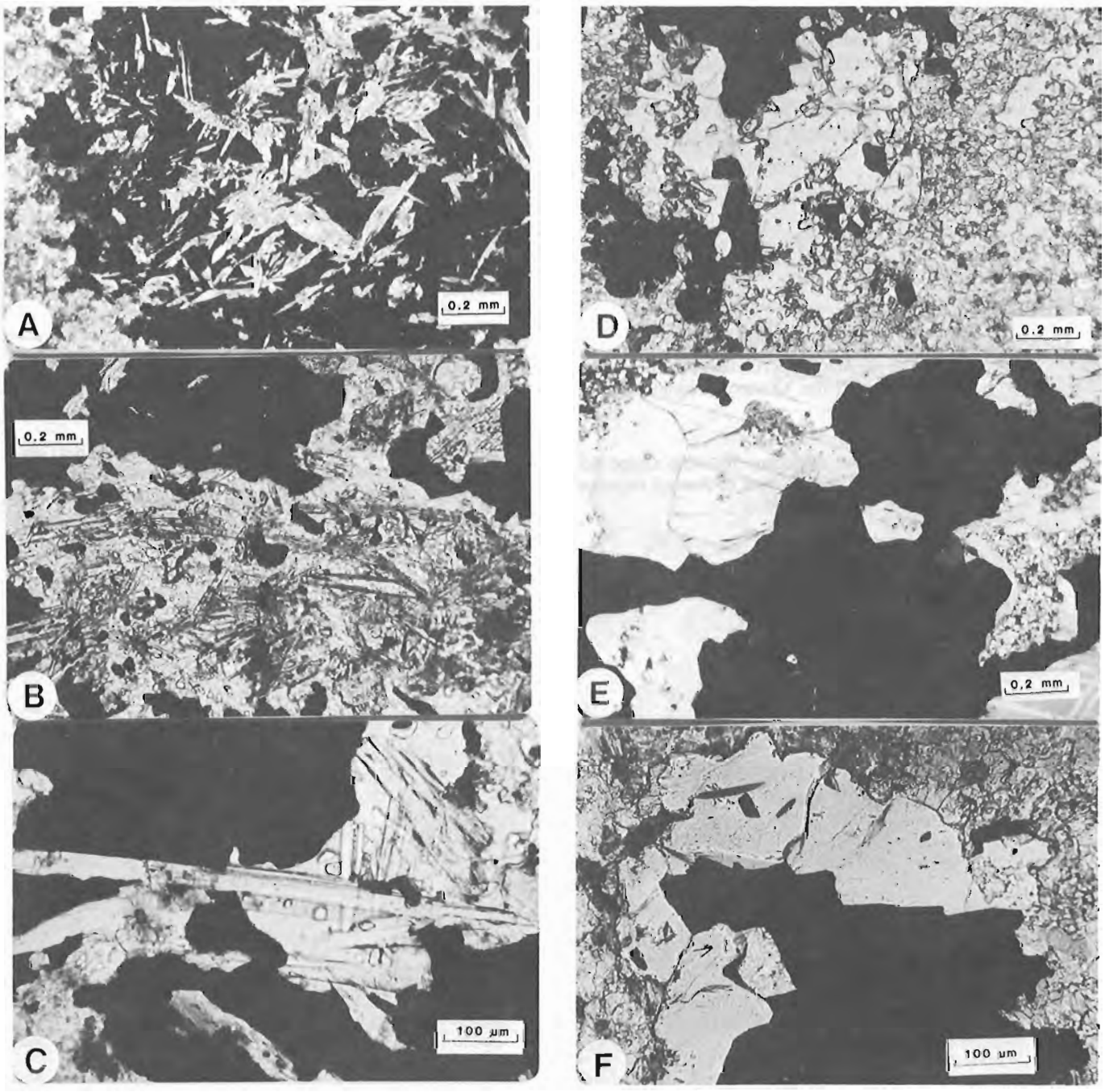


Figure 54.12

sequently the intensity of alteration and the degree to which the wall rock participated in buffering the fluid chemistry. Consequently there can be various combinations of overprinting relationships which can produce very different looking rock. Only now have the distinct infiltration phases been petrographically recognized. In the future I hope to describe the thermochemical characteristics of these different fluids.

ACKNOWLEDGMENTS

I thank the Ministère de l'Énergie et des Ressources for the use of unpublished data relevant to this report, and in particular Jules Cimon for the encouragement he has offered in the course of this study. I acknowledge the assistance and strong co-operation of Mines Gaspé personnel, in particular

R. Jean and C. Kloren for making available all their data and expertise concerning Mines Gaspé deposits. I also thank D. Sangster and F. Robert, Geological Survey of Canada, for their thoughtful discussion and criticism. I gratefully acknowledge the able assistance rendered to the completion of this report by M. Carter, P. Pelz, P. Shitahodo and D. Vlassopoulous.

REFERENCES

Allcock, J.B.
1982: Skarn and porphyry copper mineralization at Mines Gaspé, Murdochville, Quebec; Economic Geology, v. 77, p. 971-999.

Brummer, J.J.
1966: Northwest quarter of Holland Township, Gaspé North County; Quebec Department of Natural Resources, Geological Report 125, 85 p.

Procyshyn, E.L.
1984: Contrôles structuraux de la mineralisation et des teneurs de la Zone E à Mines Gaspé; Ministère de l'Énergie et des Ressources, Quebec, Travaux sur le Terrain 1984, DV 84-17, p. 22-25.
1985: Gîtologie des gisements métallifères aux Mines Gaspé; Ministère de l'Energie et des Ressources, Québec, Rapports d'Activité 85, DV 85-12, p. 16-17.
1986: Contrôles structuraux de la mineralisation et des teneurs de la Zone E à Mines Gaspé; Ministère de l'Energie et des Ressources, Quebec, Rapport Intermediaire, manuscript submitted.

Shelton, K.L.
1983: Composition and origin of ore forming fluids in a carbonate hosted porphyry copper and skarn deposit; a fluid inclusion and stable isotope study of Mines Gaspé, Quebec; Economic Geology, v. 78, p. 387-421.

Shelton, K.L. and Rye, D.M.
1982: Sulfur isotopic composition of ore from Mines Gaspé, Quebec; an example of sulfate-sulfide isotopic diseq-uilibrium ore forming fluids; Economic Geology, v. 17, p. 1688-1709.

Contrasting styles of basement deformation and longitudinal extension in the metamorphic-internal zone of Wopmay Orogen, N.W.T.

Project 850006

J.E. King, P.D. Barrette[1] and C.D. Relf[2]
Lithosphere and Canadian Shield Division

King, J.E., Barrette, P.D., and Relf, C.D., Contrasting styles of basement deformation and longitudinal extension in the metamorphic-internal zone of Wopmay Orogen, N.W.T.; in Current Research, Part A, Geological Survey of Canada, Paper 87-1A, p. 515-531, 1987.

Abstract

Archean basement in the metamorphic-internal zone of Wopmay Orogen is involved in orogenesis as faulted fragments at high structural levels and as large- scale, in places penetratively foliated, autochthonous folds at low structural levels. Strike-parallel lineations, pull-aparts and dextral shear zones that cannot be separated in time from east-west directed folding and thrusting may represent a history of dextral transpression.

Résumé

Des fragments faillés situés à des niveaux structuraux élevés ainsi que des grands plis autochtones, parfois feuilletés en profondeur et situés, eux, à de faibles niveaux structuraux, témoignent du fait que le socle archéen de la zone interne métamorphique de l'orogène de Wopmay aurait été touché par l'orogenèse. La formation de linéations parallèles à la direction, de structures formées par étirement et déchirement et de zones de cisaillement dextre impossibles à séparer chronologiquement des phases de plissement et de charriage à orientation est-ouest, pourrait correspondre à des épisodes de transpression dextre.

[1]Département de Mathématiques et de Statistiques, Université de Montréal, Montréal, Québec H3C 3J7
[2]Department of Earth Sciences, Memorial University of Newfoundland, St. John's, Newfoundland A1B 3X5

INTRODUCTION

The objective of field work in the summer of 1986 was to examine in detail different localities of Archean basement within the metamorphic-internal zone of the early Proterozoic Wopmay Orogen (McGlynn, 1970; Fraser et al., 1972; Hoffman, 1980) in order to understand more completely differing styles and processes of orogenic basement deformation. Specific points of interest included (Fig. 55.1): (1) the Kapvik structure (Easton, 1982), a fragment of Archean granite (Bowring and Van Schmus, personnel communication, 1986) previously interpreted by King (in press) to be at high structural levels and probably part of an undefined thrust system; (2) Archean granitoids adjacent to rift-facies units in the westernmost metamorphic-internal zone possibly within the northern extension of the Wopmay Fault Zone (King et al.,

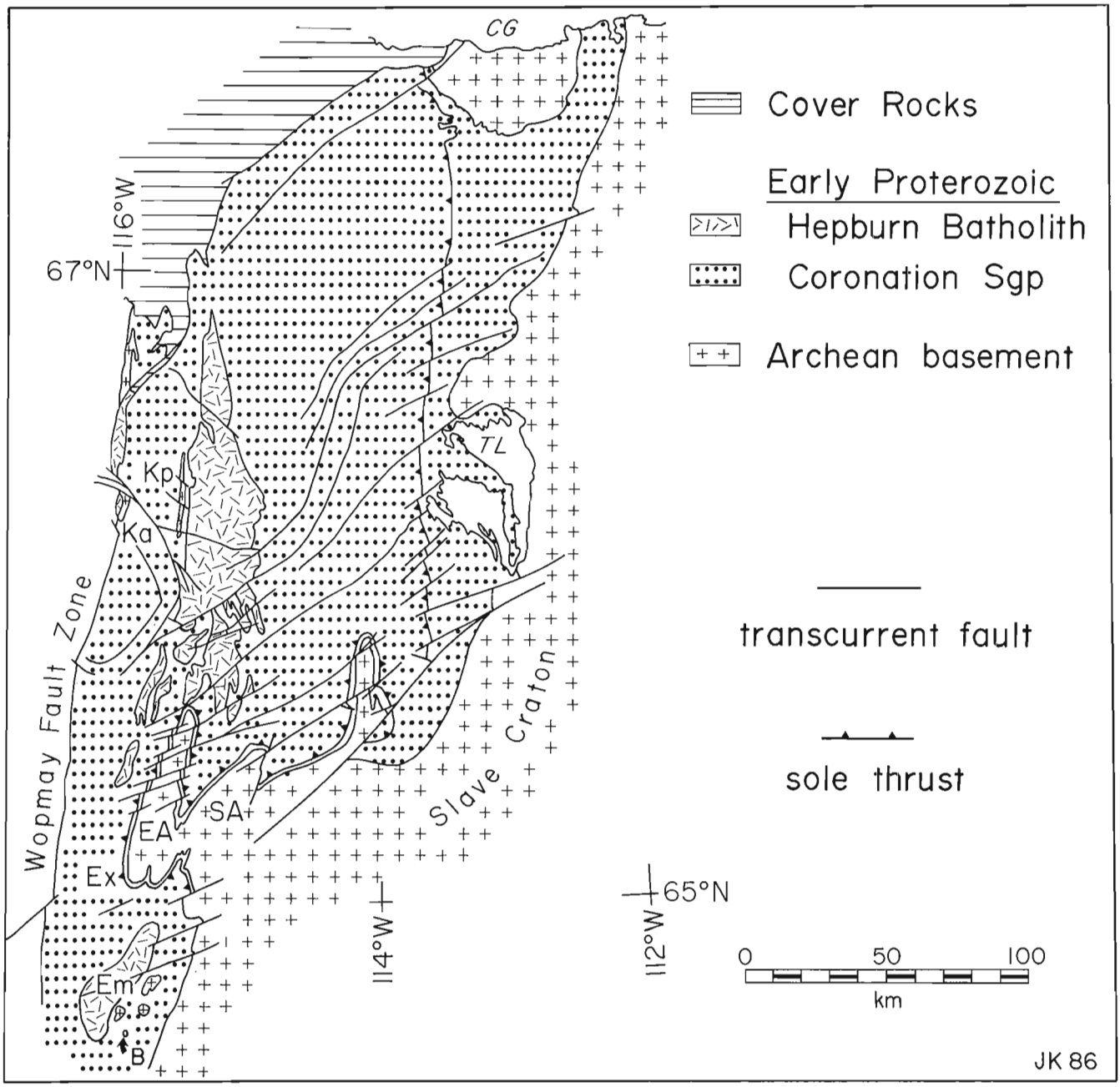


Figure 55.1. Simplified geological map of the northeastern part of Wopmay Orogen, showing location of study areas: Em – Emile River area; Ex – Exmouth Lake area; Ka – Kaiser Lake area; Kp – Kapvik Lake area. Abbreviations: B – Brownwater culmination; CG – Coronation Gulf; EA – Exmouth Antiform; SA – Scotstoun Antiform; Sgp – Supergroup; TL – Takujuq Lake. Modified from Hoffman and Bowring (1984) and Frith (1986).

1983; Hoffman, 1984a; King, 1985) (Kaiser Lake area); (3) the south end of the Exmouth Antiform, a large fold of autochthonous basement (St-Onge et al., 1984; King, 1985, in press) for which the processes of deformation were not well known; and (4) a set of basement-cored structural culminations near the Emile River that were previously interpreted as gneiss domes (in the sense of Eskola, 1949) (Frith, 1973; Frith et al., 1974; Frith and Leatherbarrow, 1975; Leatherbarrow, 1975). This work covered parts of N.T.S. map sheets 86 B, G, J and K.

KAPVIK AREA

Faulting of cover and basement

Previous work has established the lithologic assemblage of sediments and volcanics in the Kapvik Lake area (Easton, 1980, 1981, 1982; Hoffman, 1984b) to be part of the rift-fill units of the Akaitcho Group (Hoffman et al., 1978; Hoffman, 1981). The Okrark Fault was shown by Easton (1980) as an east-verging thrust and the Kapvik Granite (Easton, 1982) has a 2509±20 Ma U-Pb, zircon age (Bowring and Van Schmus, personal communication, 1986). Based on regional plunge projections, King (in press) has argued that the Kapvik Lake area represents high structural levels in the orogen. The current study has delineated four previously unrecognized faults between Sloan River and Hepburn Batholith, thus modifying understanding of the rift-facies stratigraphy, and has defined the relationship between the Kapvik granite and the adjacent rift-facies units (Fig. 55.2). The faults, including the Okrark Fault, are numbered 1 to 5 from west to east in Figure 55.2. The structural character of each fault and a brief description of the lithologic assemblage in each fault sheet is given below.

Fault 1 (Okrark Fault). This fault separates a thick package of orthoclase ± plagioclase ± quartz porphyritic rhyolite sills (Okrark sills) and thin screens of arkose (Easton, 1980, 1981, 1982), on the west, from a package of feldspathic sandstone, metagabbro and minor porphyritic rhyolites that have undergone at least two phases of isoclinal folding and some internal thrusting, on the east (Fig. 55.2). The sandstones and intrusive units are truncated by the Okrark Fault in the southwest part of the map area. The trace of the fault parallels the strike of schistosity within the Okrark Sills and its dip is inferred to likewise parallel that of schistosity. Easton (1980) has offered several arguments based on the stratigraphy and geochemistry of the rift-fill units and felsic sills that establish Okrark Fault as an east-verging thrust fault. The remarkable thickness of the Okrark Sills on the hanging wall of the fault may be the result of thrust imbrication although no direct evidence for this was found.

Fault 2. Between Okrark Fault and Fault 3, the attitudes of layering and cleavage define two domains, the western one dominantly west-dipping and the eastern one dominantly east dipping. The boundary zone between the two domains is sharp. Both domains contain polyphase, isoclinal folds that account for local variations in dip. Each domain has a distinctive lithologic assemblage; the western domain contains the assemblage in the footwall of the Okrark Fault, described above, while the eastern domain contains metabasalt, meta mafic tuffs, metagabbro, sandstone with minor pelite, rhyolitic porphyry and carbonate. If the boundary zone between domains is an anticlinorial hinge zone then it is surprisingly coincident with a major facies change. Alternatively, an interpretation of the boundary as a fault would account for both structural and stratigraphic changes. The dip of the fault surface could be either east or west, although arguments presented below (see section on fault 5) indicate a dip to the east.

Fault 3. East of the mixed stratigraphy and complex folds of the 'eastern' domain described above is a distinctive, longitudinally extensive unit of well layered metabasite (Fig. 55.2, 55.3) thought to be a metamorphosed volcaniclastic unit. The structural and stratigraphic complexity of the 'eastern' domain contrasts sharply with the simple, east-dipping volcaniclastic unit which appears to cut across the northern part of the 'eastern' domain. The contact between the 'eastern' domain and the volcaniclastic unit is interpreted to be a fault, possibly with a dip to the east, concordant with layering in the volcaniclastic unit.

Fault 4. East of the volcaniclastic unit, the Archean Kapvik granite is exposed in the core of an anticline (Kapvik Anticline) and is mantled on the west and southeast by a distinctive, unconformably overlying assemblage of sandstone, rusty micaceous sandstone, pelite and minor marble, granite-pebble conglomerate and metagabbro (Fig. 55.2, 55.4). The south end of the Kapvik granite is one of only two known localities where the sub-Akaitcho unconformity is exposed in Wopmay Orogen (see section on Kaiser lake area for the second locality). Kapvik Anticline is overturned to the west and plunges 10-15° south at its southern end. Plunges along the centre and north end of Kapvik Anticline are not well defined. The volcaniclastic unit does not fold around either the north or south end of Kapvik Anticline (Fig. 55.2 and regional pattern in Hoffman, 1984b) and thus is separated from the anticline by fault 4. If fault 4 dips to the east, parallel to the adjacent bedding-parallel foliation, then the occurrence of basement and basal units on the hanging wall and cover units on the footwall would indicate that it is a west-verging thrust fault.

Fault 5. The distinctive basal strata that mantle the western and southeastern flanks of the Kapvik granite are not present along most of the eastern flank. Either there is a significant facies change across the hinge zone of the Kapvik Anticline, or the basal strata are cut out by fault 5. Assuming that the fault dips 40-80° to the east, parallel to bedding-parallel foliation on its east and west sides (Fig. 55.2), the configuration of younger on older units would indicate that fault 5 has a normal, east-side-down component of displacement. Units east of fault 5 are similar to those between faults 2 and 3 but it is not known whether they are stratigraphically correlative.

The displacements on faults 1-5 have been interpreted above in terms of dip- slip displacement because of the position of the faults in the internal part of an east-directed

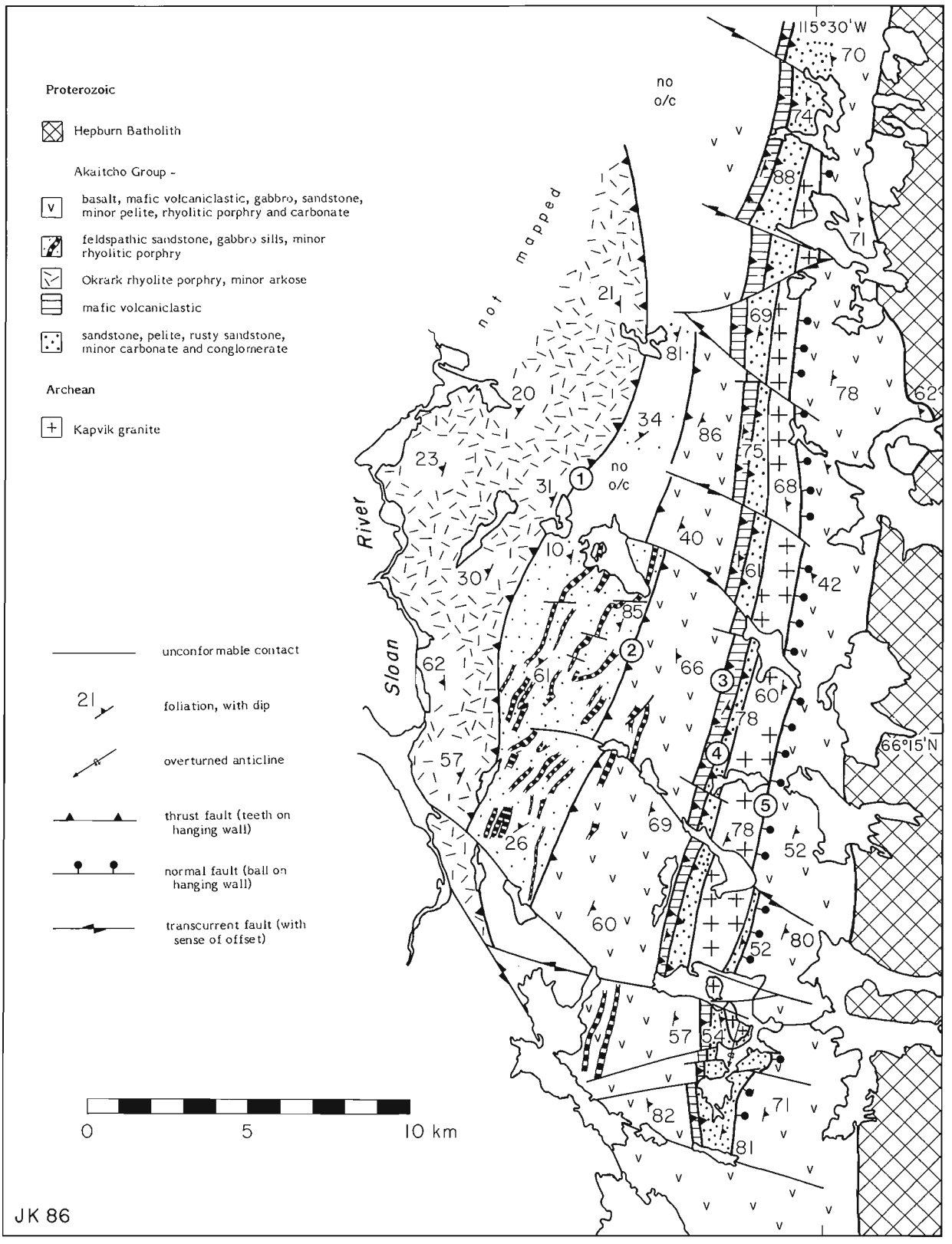


Figure 55.2. Simplified geological map of the Kapvik map area showing favoured interpretation of faults. Lithologies in legend not necessarily in chronological order. Faults: 1 – Okrark Fault; 2-5 – other faults discussed in text.

thrust-fold belt (Hoffman et al., 1978; Hoffman, 1980, 1984b; Tirrul, 1984). Evidence presented in the next section, however, for mesoscopic strike-slip shear zones allows the possibility that a component of displacement for faults 1-5 be strike-slip.

The Kapvik granite appears to be a thin fragment of Archean basement that has, together with its immediate cover units, been plucked from the autochthon and transported high into the thrust pile. As such it is a Type 1 crystalline thrust sheet (after Hatcher and Williams, 1986), similar in structural position to the Malton Gneiss of the Canadian Cordillera (Campbell, 1968; Simony et al., 1980; Oke and Simony, 1981; Monger et al., 1985). The basal strata are not of the transgressive-shelf facies characterized by orthoquartzite that mantle known autochthonous basement elsewhere in the orogen (St-Onge et al., 1984; King, in press), but rather are more similar to the mixed clastic units of the adjacent rift-facies Akaitcho Group. This suggests that the Kapvik granite was removed from the rift zone, perhaps as a 'chip' from a local topographic high. Easton (1981, 1982) and King (in press) have previously argued that basement to the Akaitcho Group was sialic. Penetrative deformation within the Kapvik granite is described in the next section.

Strike-parallel lineations, pull-aparts and shear zones

A pervasive mineral lineation, oriented within the associated foliation and parallel to the generally north-south structural grain of the orogen, characterizes the Kapvik Lake map area (Fig. 55.5, 55.6). Alignment of acicular amphiboles, elongate grain shapes of quartz and plagioclase, and streaks of recrystallized aggregates are the dominant linear elements. Very locally, pull-aparts of euhedral K-feldspar, with quartz fibers growing between fragments, record extension of up to 160%. The linear fabric is most obvious in the Okrark and other felsic porphyries where linear streaks of recrystallized matrix material are well developed and often occur as strain shadows about phenocrysts of euhedral quartz, plagioclase and K-feldspar and indicate that the strain was concentrated in the finer grained matrix. At all apparent intensities of finite strain the orientation and form of the mineral lineations are constant and the strain shadows symmetrical, suggesting that the penetrative deformation within the felsic sills was coaxial.

Most layered mafic units of the area are characterized by the development of symmetrical boudinage and pinch and swell structures although these are most pervasively and strongly developed within the well layered volcaniclastic unit (Figs. 55.3, 55.7). The boudins in the volcaniclastic unit are shaped like "flattened footballs" with the long axis oriented subhorizontally along the associated steeply dipping layering, the short axis normal to layering and the intermediate axis normal (near vertical) to these, thus recording a three dimensional strain. Dilational zones filled with quartz and feldspar, characterize the necks between 'points' of the footballs.

Spatially associated with the boudins are asymmetric pinch and swell structures that have either extensional shears or discrete planes of slip lying obliquely in the pinches. The shears correspond to an asymmetrical internal boudinage (Cobbold et al., 1971), more recently described as extensional crenulation cleavage (Platt and Vissers, 1980) and shear band foliation (White et al., 1980). The pinch and swell structures correspond to the Type 2B asymmetrical pull-aparts of Hanmer (1986). About 10% of the extensional shears observed had a dextral asymmetry; the asymmetry of the remaining 90% was indeterminate, mainly due to poor exposure. Sense of displacement on the discrete slip planes could not be determined. The occurrence of the asymmetrical extensional shears in association with boudinage and pinch and swell structures suggests a component of layer-parallel, dextral shear acted together with dominant layer-parallel extension. The extensional shears and, locally, the layer-parallel boundaries of symmetrical pinch and swell structures, are generally schistose, but may be mylonite zones (Fig. 55.8) up to 10 cm in width. Where mylonitic, the shears and boundaries contain a well developed, near horizontal mineral lineation. Syntectonic actinolite within these ductile deformation zones indicates that the zones formed within upper greenschist facies metamorphic conditions, indistinguishable from the metamorphic grade in the surrounding rock.

Three foliation-parallel shear zones were observed, one in a 10 cm-wide metasandstone on the east side of the Kapvik granite, one in a 50 cm-wide metasandstone on the west side of the Kapvik granite, and the third within a screen of feldspathic sandstone between Okrark sills. Kinematic indicators within the zones – sigmoidal deflection of the internal schistosity (Ramsay and Graham, 1970), C-S fabrics (Berthé et al., 1979), shear band foliations (Platt and Vissers, 1980; White et al., 1980) and Type 2B asymmetrical pull-aparts (Hanmer, 1986) – consistently indicate dextral transcurrent shear.

A broad zone of moderately well developed, steeply dipping, strike-parallel C-S fabrics with dextral asymmetry occurs along the southwestern margin of the otherwise only weakly foliated Kapvik granite (Fig. 55.9). The southward extension of the deformed zone is characterized by a very strongly developed north-south lineation that lies on a poorly developed biotite foliation.

Metagabbro bodies throughout the area are commonly transected by a braided array of schistose to mylonitic zones that trend generally north-south. Their outcrop pattern is very similar to the strain pattern produced by non-coaxial progressive, bulk, inhomogeneous shortening in isotropic materials (Bell, 1981). Near-horizontal, boundary-parallel lineations are the dominant fabric element in these zones, suggesting a history of north-south, strike slip flow.

The structural morphologies described above reflect a heterogeneous strain environment in which the maximum elongation, or flow direction, formed during coaxial and non-coaxial strains, is subparallel to the tectonic grain of the orogen. The heterogeneity of the finite strain pattern is a function of the differing mechanical properties characteristic of different units.



Figure 55.3. Compositionally well layered metabasite interpreted as a volcaniclastic unit. Note the well developed symmetrical boudins with quartz-feldspar in the dilated neck zones. Scale is in centimetres. GSC 204447-K.

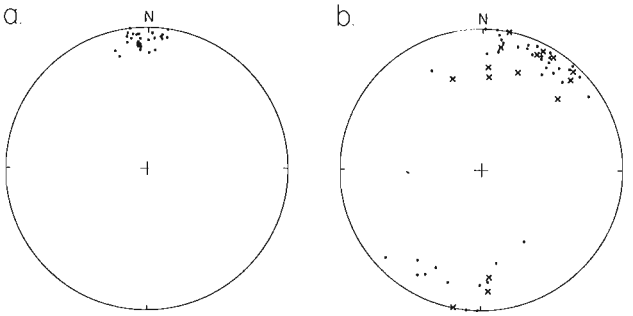


Figure 55.5. Stereonet showing linear elements in the Okrark sills (a) and in the mixed sediments and mafic and felsic units of the Akaitcho Group (b) in the Kapvik map area. The clockwise rotation of (b) relative to (a) is due to rotation during displacement on the set of left lateral transcurrent faults that transect the eastern part of the map area (Fig. 55.2). Symbols: dots – mineral and aggregate elongation, crosses – intersection lineation. Equal area projection.



Figure 55.4. Mixed autochthonous sediments (as) lying unconformably on Kapvik Granite (KG) at the hinge zone of Kapvik Anticline. Cliff is 10 m high. GSC 204447-F.



Figure 55.6. Shallow lineation defined by recrystalled quartz and plagioclase in streaks and pressure shadows around phenocrysts of K-feldspar in an Okrark porphry sill. GSC 204447-E.

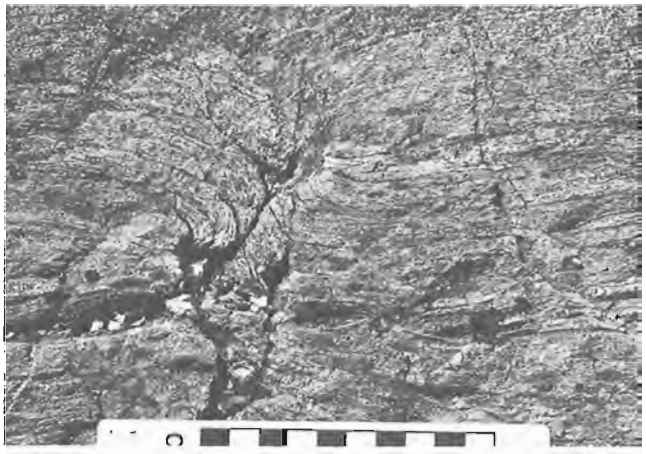


Figure 55.7. Symmetrical and dextrally asymmetrical, boudinage in the volcaniclastic unit. Note boudins within boudins. Scale is in centimetres. GSC 204447.

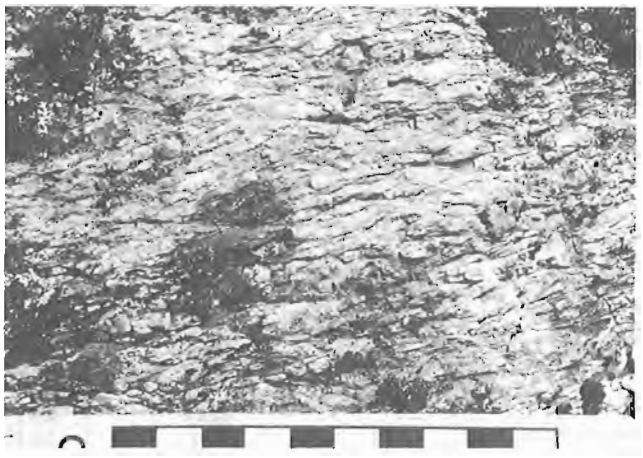


Figure 55.9. Steeply dipping C-S fabrics in the Kapvik granite showing a dextral sense of asymmetry. Scale is in centimetres. GSC 204447-Z.

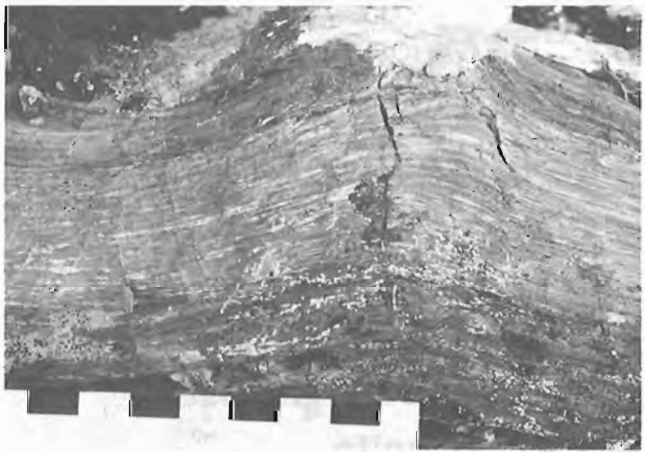


Figure 55.8. Mylonitized boundary of a pinch and swell structure in the volcaniclastic unit. GSC 204447-Y.

The relative timing of the east-west directed shortening (folding and thrusting), the north-south mineral lineations and the north-south dextral shear zones could not be unambiguously established. Field observations indicate that all these structural elements formed at upper greenschist facies conditions and no overprinting relationships were established, suggesting, but not proving, that these various structures may have developed synchronously. If so, they may reflect a history of oblique shortening that has been mainly accommodated by thrusting, folding and coaxial and non-coaxial, inhomogeneous shortening, with north-south finite extension, but also partially resolved into narrow, dextral wrench zones localized in highly anisotropic units (cf. Brun and Burg, 1982 and Ellis, 1986 for similar deformations in the Ibero-Armorican arc and the Canadian Cordillera, respectively). Similarly oblique shortening has been interpreted to have produced obliquely oriented, en echelon folds in the younger (1875-1870 Ma) Great Bear Magmatic Zone of the orogen (Hoffman and McGlynn, 1977; Hoffman, 1980; Hildebrand and Bowring, 1984; Hildebrand et al., 1986, in press), suggesting that dextral transpression, perhaps related to oblique plate convergence (Fitch, 1972) characterized successive phases of deformation in Wopmay Orogen.

KAISER LAKE AREA

Mixed granitic and amphibolitic gneisses, informally termed the Kaiser gneisses, are exposed in the core of a truncated antiform 12 km southwest of the Kapvik Lake map area (Kaiser Lake area) (Fig. 55.1, 55.10, cf. Hoffman, 1984b). The gneisses are unconformably overlain by high-grade metasediments and metavolcanics of the Akaitcho Group (Fig. 55.11). This locality is the second of only two known localities where the sub-Akaitcho basement is exposed. Because the base of the gneisses is not exposed it is not known whether they are allochthonous or autochthonous. Their position at high structural levels within the orogen (King, in press), however, suggests that they are allochthonous and are, like the Kapvik structure, a fragment of basement that has been transported together with a part of its cover. The Kaiser gneisses have not yet been dated but are very similar in appearance and structural setting to the gneiss complex that is infolded in the western part of the metamorphic internal zone near the Coppermine River (King et al., 1986) and that has been dated at about 2.9 Ga (U/Pb, zircon, M. Villeneuve, personal communication 1986).

The fold of gneiss and supracrustal units is truncated to the west by a fault zone that is characterized by ultramylonites and brittle faults (Fig. 55.10). East of the fault zone is a block of 2531±10 Ma Archean granite to tonalite (Bowring and Van Schmus, personal communication, 1986) that unconformably underlies the Great Bear Magmatic Zone (Bowring,

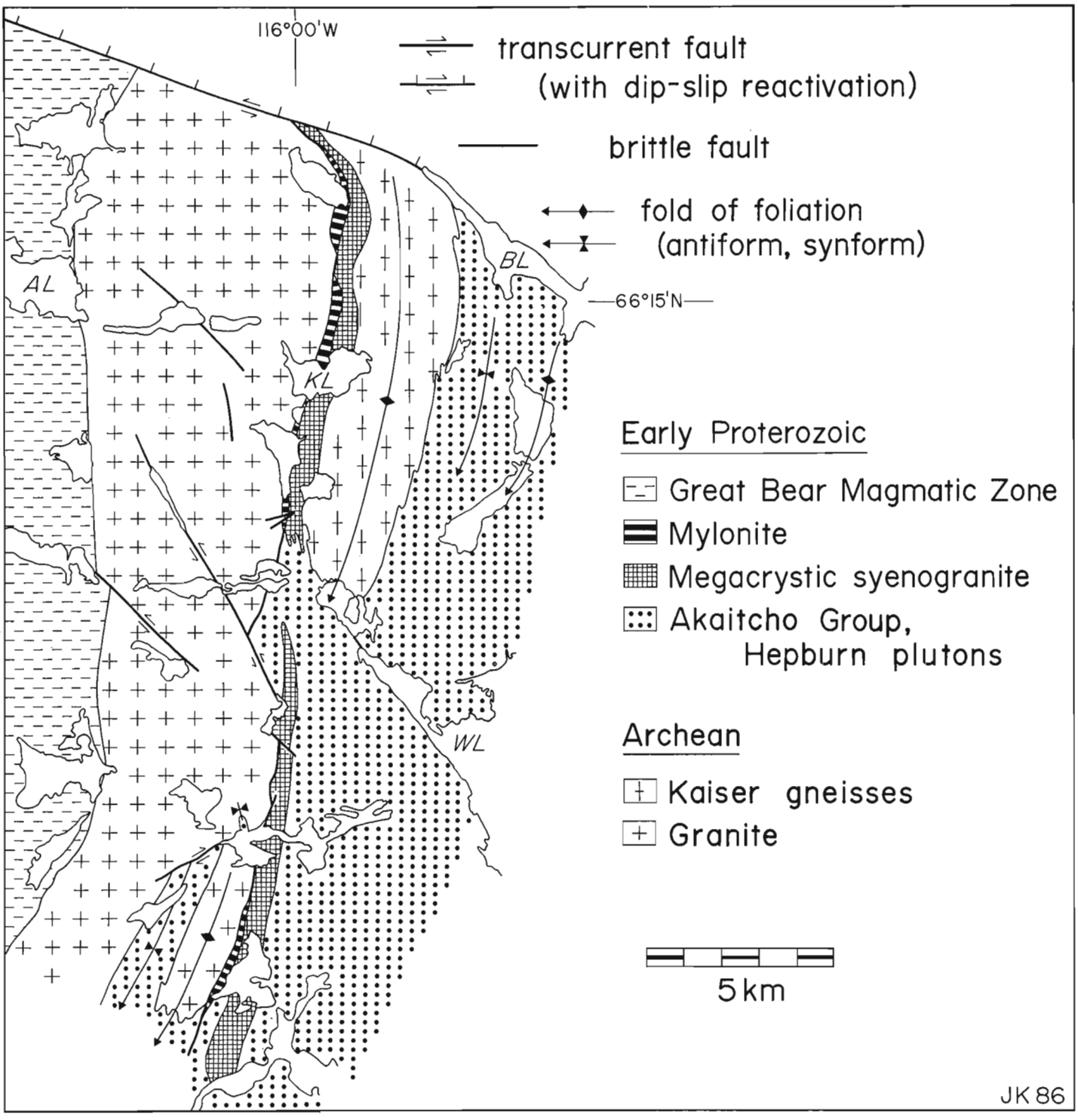


Figure 55.10. Simplified geological map of the Kaiser Lake area. Extension of some contacts is from Bowring (1982) and Hoffman (1984b). Bodies of water: AL – Adam Lake; BL – Belleau Lake; KL – Kaiser lake (informal name); WL – Wentzel Lake.

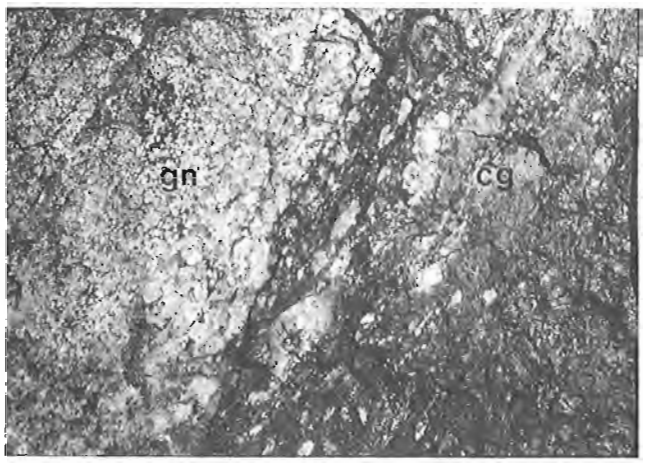


Figure 55.11. Basal conglomerate (cg) lying unconformably on (Archean?) granite gneiss (gn) in the Kaiser Lake area. Scale is in centimetres. GSC 204447-S.



Figure 55.12. Steeply dipping C-S fabrics in the K-feldspar megacrystic syenogranite adjacent to the pulled apart mylonite belt in the Kaiser lake area. Scale is in centimetres. GSC 204447-R.

1982). The ultramylonites, often intensely hydrothermally altered, occur as lozenges, up to 100 m wide and 1 km long, that are strung out along the fault zone. Between lozenges, the fault zone is characterized by intense hydrothermal alteration of the wall rock but no penetrative deformation related to the fault zone could be discerned. The map pattern suggests that the fault zone originated as a mylonite zone, of some unknown width, that has been subsequently disrupted along strike on more brittle faults.

The dominant protolith of the mylonite appears to be the Archean granite to the west. However, a younger pluton of K-feldspar megacrystic, biotite syenogranite that intrudes both the cover rocks and the gneiss complex (Fig. 55.10) is increasingly more strongly foliated to mylonitic with proximity to the fault zone and may therefore have contributed some material to the mylonites. This pluton has not yet been dated, but is very similar in composition and setting to a pluton 80 km to the south that yields a U-Pb (zircon) age of 1882 Ma (Bowring and Van Schmus, personnel communication, 1986). Very local, narrow, mylonitic and schistose shear zones are present in the cover units and basement gneiss complex east of the fault zone and may have been related to the main mylonite zone.

Within the ultramylonites the only fabric elements observed are a weakly developed, near horizontal mineral lineation contained in a steeply dipping foliation. The strained part of the younger megacrystic pluton near the fault zone does, however, contain well developed C-S fabrics (White et al., 1980) that indicate dextral displacement in its present orientation (Fig. 55.12).

This belt of mylonite lozenges and brittle faults is the northward extension of a belt of ultramylonites that itself is in the form of lozenges strung out along braided brittle faults, although the lozenges there are much larger (up to 20 km long and 1 km wide) (St-Onge et al., 1983a, 1984; Hoffman, 1984b; King, 1985). Kinematic indicators associated with the south part of the ultramylonite belt are, in their present orientation, similarly indicative of dextral transcurrent displacement. R.S. Hildebrand (personal communication, 1986) has however suggested that these mylonites have been rotated to their present position by later folding and may have originally been near horizontal. If such is the case, the kinematic indicators would be compatible with top-northward displacement.

EXMOUTH ANTIFORM

The Exmouth Antiform is the westernmost of three large scale, basement cored fold structures that are present at low structural levels of the metamorphic- internal zone of Wopmay Orogen (St-Onge et al., 1984) (Fig. 55.1). Regional mapping by St-Onge et al. (1984) identified the Archean (3.5 Ga, Bowring and Van Schmus, 1984) gneiss complex in the core of the antiform, and a retrograde Proterozoic schistosity within the gneisses near the basement-cover contact. However, since no Proterozoic structures were recognized within the main part of the basement gneisses, the processes by which the basement accommodated deformation during formation of the Exmouth Antiform were not defined. King (1985) argued, based on strain patterns in the cover rocks and a regional Type 1 interference pattern (Ramsay, 1967), that the Exmouth Antiform was a product of interference between regional scale NNE-trending Calderian (ca. 1885 Ma, Hoffman and Bowring, 1983, 1984; St-Onge et al., 1983b) folds and ENE-trending Tree River (Tirrul, 1984) cross folds. Proterozoic strain patterns identified throughout the southern half of the Exmouth Antiform this summer, described below, support the arguments of King (1985).

The southern half of the Calderian Exmouth Antiform is on the southern limb of a Tree River cross-arch and as such plunges moderately southwestward. The Archean gneissic layering within the core of the antiform is deformed by tight,

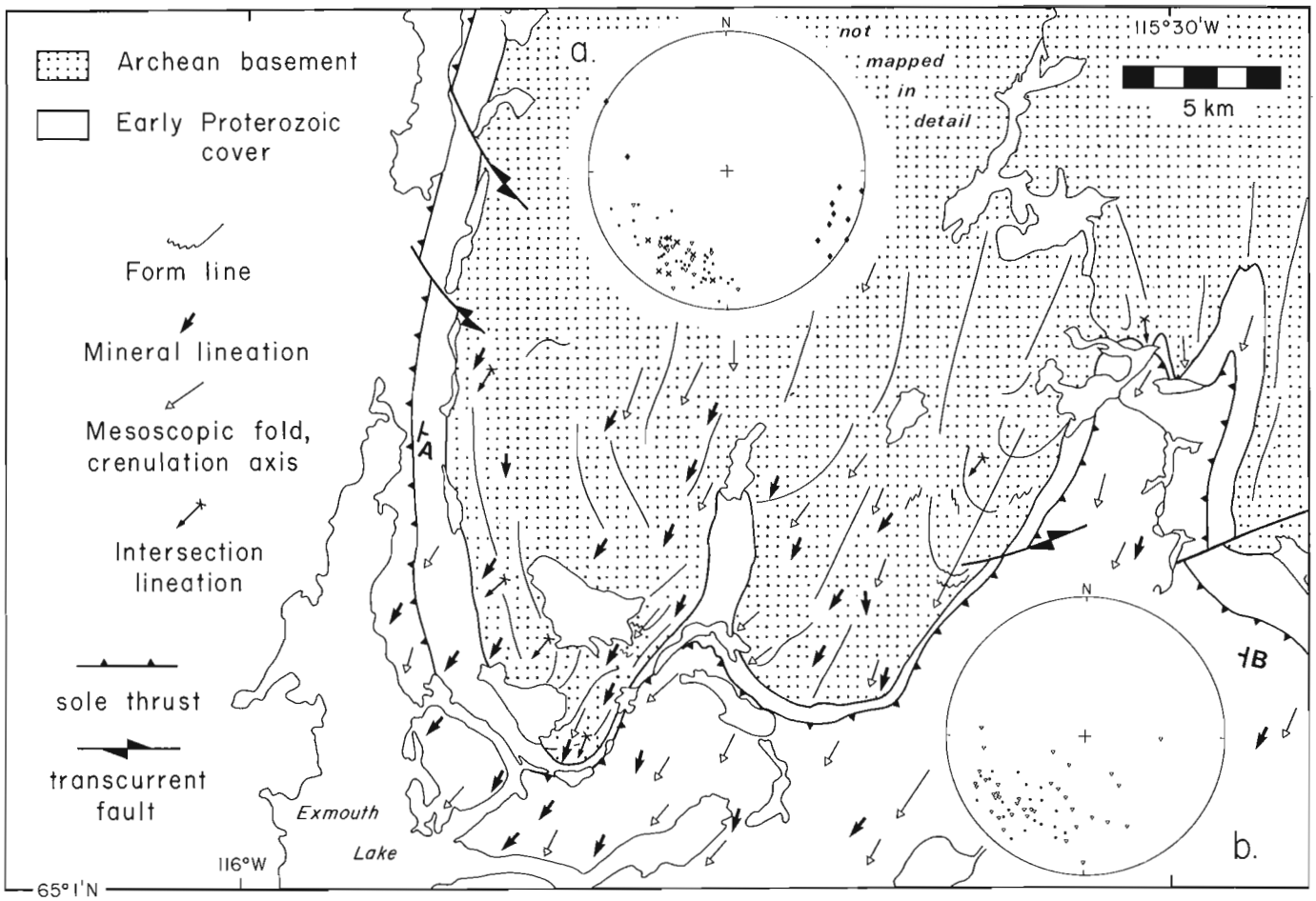


Figure 55.13. Simplified geological map of the south end of the Exmouth Antiform emphasizing structural elements in basement (based in part on field data of M.R. St-Onge and crew, 1983). For form lines in cover units see St-Onge et al. (1984). Only second generation folds are shown in the cover. Equal area stereonets show linear elements in (a) basement and (b) cover Symbols: dots- mineral lineations and streaking, x – intersections between Archean gneissic layering and Proterozoic cleavage; triangle – fold axes; stereonet of basement data includes poles to Proterozoic axial planar cleavage shown as diamonds). A-B is line of section for Figure 55.15.

upright, centimetre- to kilometre-scale folds that also plunge moderately southwestward (Figs. 55.13, 55.14). In the hinge zones of the folds, a steeply dipping, axial planar cleavage defined by the planar alignment of quartz and feldspar can be recognized (Fig. 55.14); on the limbs of the folds similar planar alignment of minerals occurs, but cannot be unambiguously distinguished from the earlier gniessic foliation. A pronounced lineation, defined by streaks of recrystallized quartz and feldspar, and occasionally by alignment of hornblende, coaxial with the axes of Proterozoic folds (including the main Exmouth Antiform) and the intersection between Archean gneissic layering and the later cleavage, occurs in the southern and western part of the basement core (Fig. 55.13). The pre-cross folding strain pattern of upright folds, steep cleavage, and coaxial lineations throughout the basement core is compatible with a history of horizontal, east-west shortening and layer-parallel (hinge-line) extension (cf. Watkinson, 1975) during Calderian deformation. The folds and lineations are coaxial with second generation, late metamorphic folds and lineations in Early Proterozoic cover rocks (Fig. 55.13, cf. St-Onge et al., 1984) suggesting that this phase of deformation in basement probably occurred during the late stages of Calderian deformation (although note caution of Williams, 1985). The strongly coaxial nature of the folds in the cover and basement also indicates that the pre-folding orientations of the layering in the basement (gneissic layering) and cover (transposed bedding and cleavage) were approximately parallel.

The angular relationships between gneissic layering in the Archean gneisses and the folded basement-cover interface show that the pre-folding attitude of the gniessic layering was inclined to the interface. On the east side of both lobes of the antiform, gneissic layering near the basement-cover interface

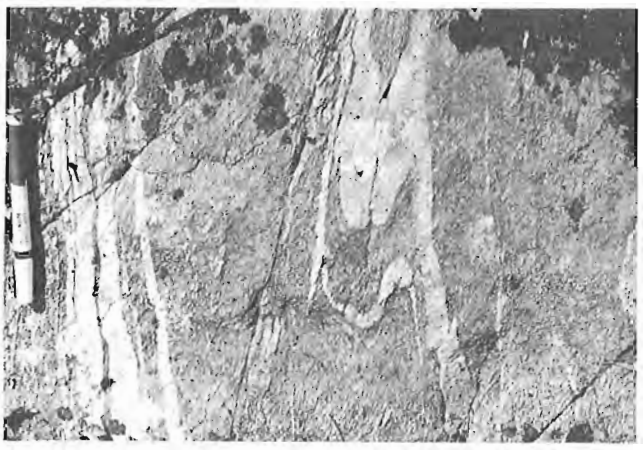


Figure 55.14. Proterozoic fold of Archean gneissic layering with associated axial planar cleavage from the south end of the Exmouth Antiform. Pen is 13.5 cm long. GSC 204447-U.

is drawn into macroscopic antiforms that are not expressed in the trace of the folded interface (Fig. 55.13). Elsewhere the layering is roughly parallel to the limbs and axial plane of the Exmouth Antiform. This pattern suggests that the gneissic layering originally dipped westward from the basement-cover interface (Fig. 55.15). Where the angular discordance was drawn into the east limbs of the fold lobes, it is modified, but is preserved; curvature of the layering records the folding of the originally obliquely inclined surface in this part of the fold. In the hinge zone the layering remains at an acute angle to the basement-cover interface but is not itself strongly curved; although it is probably modified. On the west limbs the original angular discordance is sufficiently modified to appear nearly parallel to the antiform limb and axial plane (cf. Ramsay, 1967 for similar folding patterns of obliquely inclined surfaces).

The interference pattern formed by polyphase folding in the cover rocks of the Exmouth Antiform (St-Onge et al., 1984) is the topic of a B.S. thesis by Steve Davies at McMaster University.

EMILE RIVER AREA

Archean basement outcrops in the cores of a set of domal culminations in the southern part of Wopmay Orogen, 10 km west of the main Slave (Archean) craton (Frith, 1973, 1986; Frith et al., 1974; Frith and Leatherbarrow, 1975; Leatherbarrow, 1975) (Figs. 55.1, 55.16). Previous workers (ibid) have interpreted these to be gneiss domes (in the sense of Eskola, 1949) that have probably been modified

by lateral compression. Alternatively, King (1985) has proposed that these structures are along-strike equivalents to the large-scale basement-cored antiforms that are exposed in a cross-antiform 40 km to the north (Fig. 55.1) and that gravity-driven, vertical tectonism was secondary in importance to lateral compression as a process of deformation. To

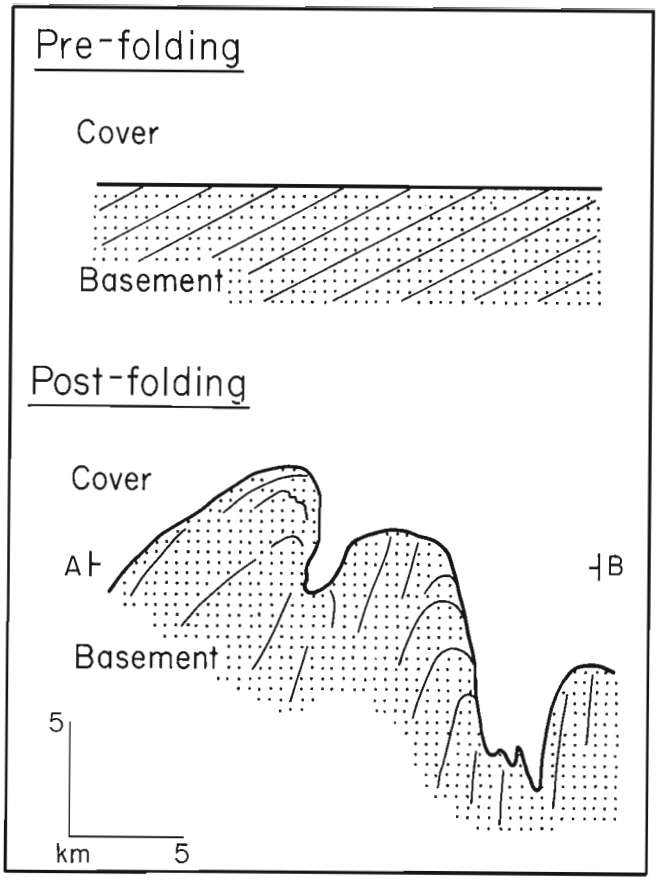


Figure 55.15. Cross sections showing modification of the attitude of Archean gneissic layering in the southern part of the Exmouth Antiform by Proterozoic folding. Post-folding cross section is a down-plunge projection modified from King (1985). Line of section A-B is shown in Figure 55.13.

test the two proposed models, the strain pattern associated with the well developed 'Brownwater' (Frith, 1986) and 'Sunken' (new informal name) culminations was examined in detail in 1986 (Fig. 55.16). In the course of this study, two other culminations, the 'Inbetween' and 'Baldeagle' culminations of Frith (1986) (Fig. 55.17) were examined at reconnaissance scale and a transect between the Brownwater culmination and the Slave Craton was investigated in order to understand more completely the structures preserved in the cover rocks.

The basement-cored culminations

The Brownwater and Sunken culminations of the Emile River area are first- order culminations in a spectacular Type 1 (Ramsay, 1967) interference pattern. Basins and domes occur at a variety of scales (Fig. 55.16) and are the result of an interference between two generations of upright folds, the early one (D_2) northerly, the later one (D_3) east-west in general orientation. Crenulations and, locally, intersection lineations associated with D_2 are observed to be folded about

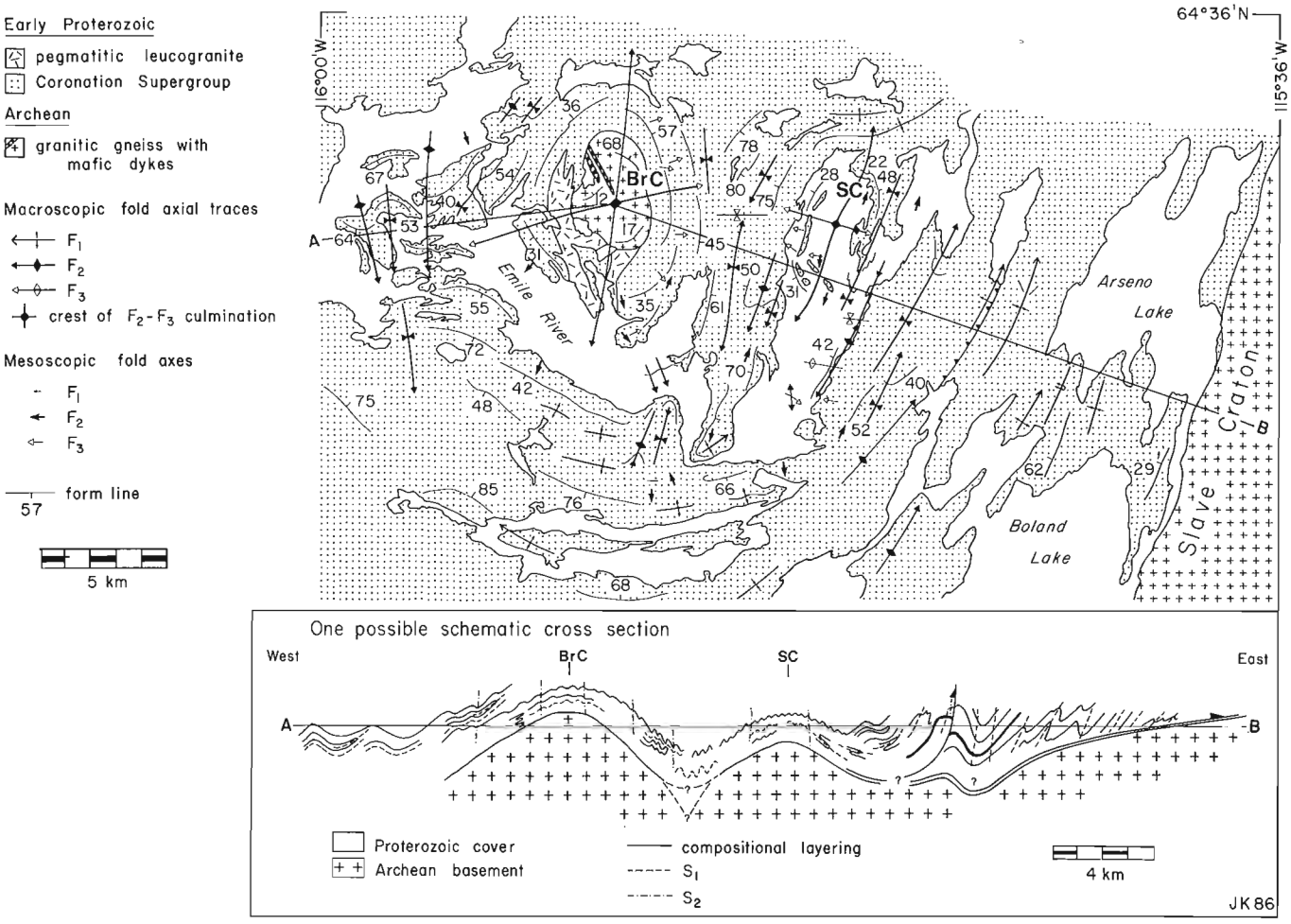


Figure 55.16. Simplified structural geological map of the Emile River area and one possible cross section. Data from the southernmost part of the area is from Frith (personal communication, 1986). The dip of the Slave Craton in the cross section is taken from the unconformity at Mattberry Lake, 30 km south of the present map area. Abbreviations: BrC - Brownwater culmination; SC - Sunken culmination.

F_3. All lineations observed were intersections or fold and crenulation axes. No evidence for a history of gravity-driven, vertically-directed tectonism was observed.

The Archean cores of the culminations comprise foliated to gneissic granitoids. In the Brownwater culmination granitic gneisses (dated at 2712±89 Ma) (Rb/Sr, Frith et al., 1974) intruded by metagabbro dykes form the basement core. A pegmatitic leucogranite intrudes both basement and cover near their interface (Fig. 55.16). This body is unique in the area and its genesis is not understood. A Rb-Sr date by Frith et al. (1977) of 1808±43 Ma on the pegmatitic leucogranitic is considered to be anomalously young (cf. Frith, 1986). Reconnaissance study of the Baldeagle and Inbetween culminations revealed several phases of foliated granitoids and granitic gneisses of which none have yet been dated. No Proterozoic fabrics were recognized within the Archean gneisses.

The nature of the basement-cover contact in the Emile River area could not be unambiguously defined. Neither the distinctive autochthonous Proterozoic sequence that mantles the basement-cored culminations to the north (cf. St-Onge et al., 1984), nor any evidence for a tectonic contact were recognized around the three domes examined; granulite facies metamorphism (Neilsen, 1978, 1986) (Fig. 55.17) and the younger granitic unit that intrudes along the contact serve to obscure primary relationships. Structural attitudes along a transect from the Brownwater culmination to the Slave Craton (Fig. 55.16), however, allow the possibility that the basement cores are the folded extensions of autochthonous Slave basement and that the culminations are analogous to the three basement- cored antiforms to the north. The map pattern and interpreted tectonic setting of the Emile River culminations are very similar to those of autochthonous basement rocks within the central part of the Scandinavian Caledonides (Gee, 1980).

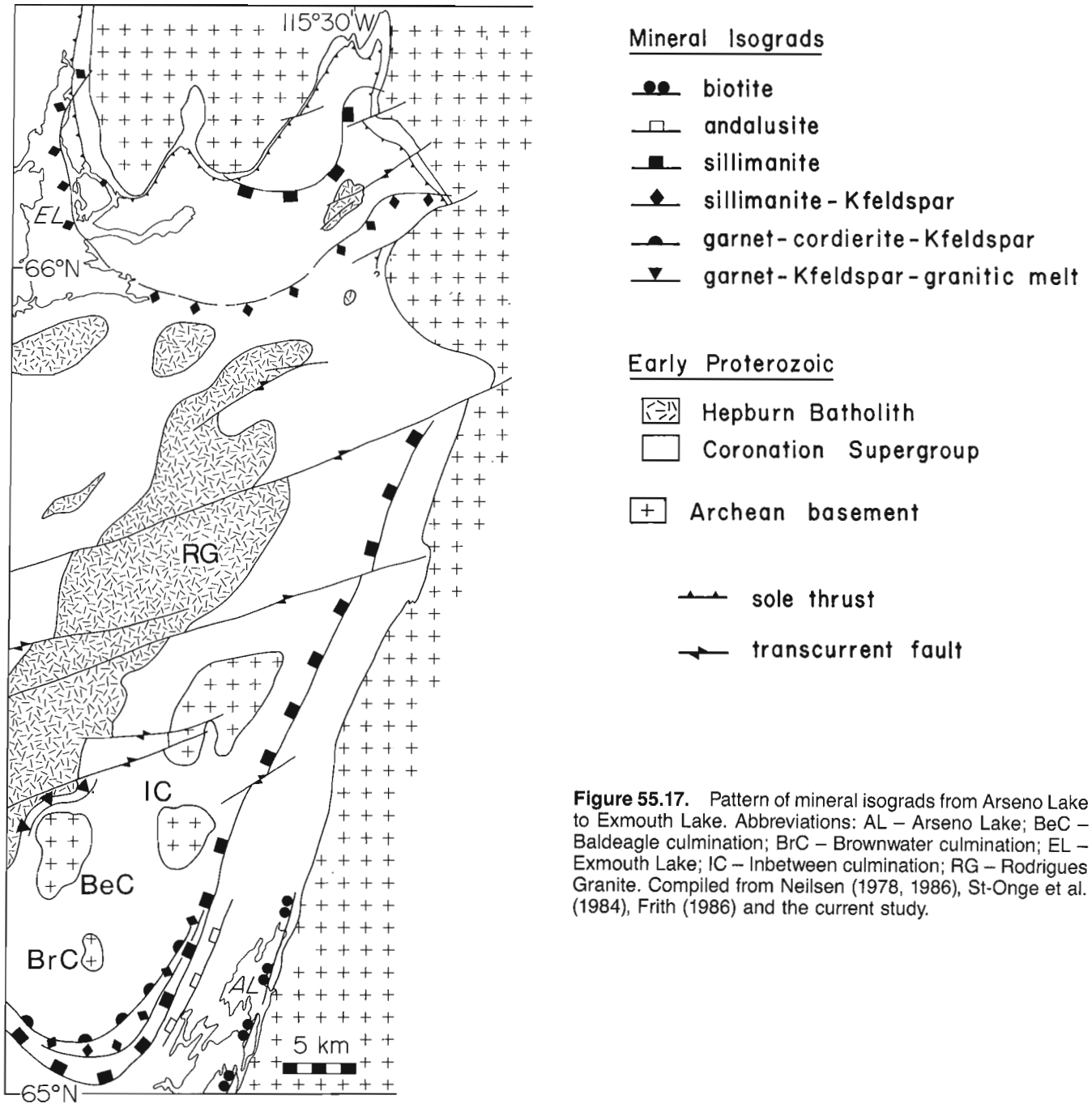


Figure 55.17. Pattern of mineral isograds from Arseno Lake to Exmouth Lake. Abbreviations: AL – Arseno Lake; BeC – Baldeagle culmination; BrC – Brownwater culmination; EL – Exmouth Lake; IC – Inbetween culmination; RG – Rodrigues Granite. Compiled from Neilsen (1978, 1986), St-Onge et al. (1984), Frith (1986) and the current study.

Cover rocks

In the Emile River area, early Proterozoic cover rocks consist predominantly of pelite and semipelite. Other stratigraphic units with a more restricted distribution are also present and show a change in character from east to west. Orthoquartzite, ferruginous dolomite and minor metagabbros occur within the imbricated sequence in the area of Arseno Lake (Fig. 55.16). West of Arseno Lake, minor units include ferruginous mafic schists, quartz-pebble and lithic conglomerates, grits and very minor dolomite. These units have been previously assigned to the Snare Group, a designation proposed by Lord (1942) for the metamorphosed and deformed, Proterozoic supracrustal rocks west of the Slave Craton. Recent work in the northern part of Wopmay Orogen, however, has established a well defined, early Proterozoic stratigraphy (Hoffman, 1981) with which the units in the Snare Group can be compared and perhaps correlated. The assemblage of pelites with minor quartzite and dolomite near Arseno Lake are similar to the slope-rise facies of the Odjick Formation.



Figure 55.18. F_1 and F_2 folds in the andalusite mineral zone of the Emile River area. Arrow points to hammer. GSC 204313-D

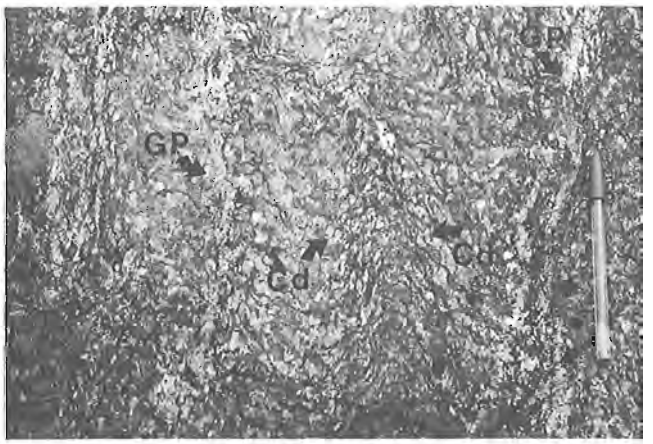


Figure 55.19. F_2 upright folds in which cordierite (Cd) is deformed and granitic melt pods (GP) are localized on the axial plane. GSC 204447-D

The pelites and semipelites with minor conglomerate, grit and dolomite are similar to units described by St-Onge et al. (1983a) and considered to be part of the easternmost rift-fill facies Akaitcho Group.

Neilsen (1978, 1986) has shown that the metamorphic grade in the Emile River area increases to the west and northwest although the heat source for metamorphism was not specified. Work this summer, however, delineated the highest grade isograd in the region, the biotite-out isograd (biotite + sillimanite + quartz" garnet + K-feldspar + liquid) (Thompson, 1982), adjacent to the Rodriques pluton, a K-feldspar megacrystic granite that is part of the syn-orogenic Hepburn Batholith (Hoffman et al., 1980; Frith, 1986) (Fig. 55.17). The apparent spatial relationship between isograd and pluton (more mapping is needed to establish this as a regionally valid relationship) suggests that the pluton is a local heat source for metamorphism. This interpretation is consistent with work in the northern part of Wopmay Orogen which shows that the regionally developed mineral isograds are related, in part, to heating by magmatic advection during emplacement of the Hepburn Batholith (St-Onge, 1981; St-Onge and King, in press). Although the attitudes of the isograd surfaces have not been determined in the Emile River area, the isograds are coextensive with inverted isograds beneath the Hepburn Batholith in the Exmouth Lake area (St-Onge et al., 1984; King, 1985: St-Onge and King, in press) (Fig. 55.18). This interpretation implies that in the Emile River area, Hepburn plutons were situated above the present erosion surface, with their southern termination accounting for the low-grade salient south of the Emile River (Fig. 55.17). The intrusions would therefore have been emplaced above relatively cool rocks and resulted in downward relaxation of isotherms into lower structural levels, including basement. St-Onge and King (in press) have argued for a synmetamorphic tectonic transport of the Hepburn Batholith and its associated thermal culmination in the northern part of Wopmay Orogen.

In the immediate vicinity of the basement-cored culminations, the cover rocks are involved in three generations of folds. The latter two are the north-south ($D2^{)}$ and east-west ($D3^{)}$ upright open folds whose interference produces the dome and basin pattern. The first generation folds are recumbent, isoclinal folds of compositional layering to which biotite, cordierite and granitic pods are axial planar. This early generation of folds is documented as far east (ie. down grade and toward the Slave Craton) as the andalusite mineral zone (Fig. 55.18). Farther east, only one generation of large scale folds was recognized. Near thrust faults the axial planar cleavage to these folds is intensely crenulated. The vergence of folds in the domain of single generation folds is consistently toward the east (Fig. 55.16).

The F_1 folds are everywhere synmetamorphic and are considered to be Calderian in age. In the high grade metamorphic zone, $F2^{n}$folds have *in situ* granitic melt pods localized in their axial planes but deform the cordierite porphyroblasts (Fig. 55.19). Only biotite is axial planar to F_2 folds in the sillimanite, andalusite, and biotite mineral zones. The axial planar granitic pods indicate that the second generation folds were developed while the core of the Calderian thermal culmination remained hot, although the periphery had already cooled to biotite-grade thermal conditions. Apophyses of the pegmatitic leucogranite in the Brownwater culmination both parallel and transect gneissic layering in the cover rocks but are folded by F_2 indicating that its intrusion occurred in the waning stages of Proterozoic metamorphism. No metamorphic mineral growth was observed to be associated with the F_3 folds. This observation and the east-west orientation of the $F3^{n}$folds in the Emile River area suggest that they are related to the Tree River cross-folding event that has been documented throughout Wopmay Orogen (St-Onge, 1984; Tirrul, 1984; King, in press), although the axial traces of the cross folds are 20 to 30° more southerly than those of the typical Tree River folds.

SUMMARY

Mapping in 1986 has shown that Archean basement in the metamorphic- internal zone of Wopmay Orogen is deformed in several contrasting styles. In the Kapvik structure is a basement-cored, fault bounded anticline which, together with a thin mantle of basal sediments, is tectonically inbricated with the surrounding metasediments and metavolcanics. The Kaiser Complex is also probably a transported fragment, likewise folded and carrying its associated cover. Proterozoic fabrics related to transport are not developed in these fragments. In contrast, basement in the Exmouth Lake and probably in the Emile River area remained autochthonous but was involved in large scale folds. Mesoscopic folds and a penetrative foliation related to the folding are well developed only in the Exmouth Antiform.

Synmetamorphic, strike-parallel lineations and pull-aparts in the Kapvik Lake area show that the maximum elongation during Calderian deformation there lies within the layering and is subparallel to the orogen. Locally developed shear zones, composite fabrics and asymmetrical pull-aparts suggest that there is a minor dextral shear strain associated with this extension. Because the structures related to east-west shortening (folds and faults) cannot be separated in time from those related to north-south extension and shear, it is possible that the strain pattern in the Kapvik Lake area records a history of coeval wrenching, folding and faulting during oblique shortening.

ACKNOWLEDGMENTS

We would like to thank Steve Davies for his capable assistance and independent mapping. Martin Irving is sincerely thanked for his remarkably efficient expediting services. This paper has benefitted from reviews by P. Hoffman, M. St-Onge and R. Tirrul.

REFERENCES

Bell, T.H.
1981: Foliation development – the contribution, geometry and significance of progressive, bulk inhomogeneous shortening; Tectonophysics, v. 75, p. 273-296.

Berthé D., Choukroune, P., and Jegouzo, P.
1979: Orthogneiss, mylonite and non-coaxial deformation of granites: the example of the South Armorican Shear Zone; Journal of Structural Geology, v. 1, p. 31-42.

Bowring, S.A.
1982: Preliminary geologic map of the Kamut and Adam Lake map area (86 K/9, 86 K/10); Department of Indian Affairs and Northern Development, Yellowknife, Economic Geology Series, 1:25,000 scale map.

Bowring, S.A. and Van Schmus, W.R.
1984: U-Pb zircon constraints on evolution of Wopmay Orogen, N.W.T.; Geological Association of Canada, Program with Abstrcts, v. 9, p. 47.

Brun, J.-P. and Burg, J.-P.
1982: Combined thrusting and wrenching in the Ibero-Armorican arc: a corner effect during continental collision; Earth and Planetary Science Letters, v. 61, p. 319-332.

Campbell, R.B.
1968: Canoe River (83D), British Columbia; Geological Survey of Canada, Map 15-1967.

Cobbold, P.R., Cosgrove, J.W., and Summers, J.M.
1971: Development of internal structures in deformed anisotropic rocks; Tectonophysics, v. 12, p. 23-53.

Easton, R.M.
1980: Stratigraphy and geochemistry of the Akaitcho Group, Hepburn Lake map area, District of Mackenzie: an initial rift succession in Wopmay Orogen (early Proterozoic); in Current Research, Part B, Geological Survey of Canada, Paper 80-1B, p. 47-57.
1981: Stratigraphy of the Akaitcho Group and the development of an early Proterozoic continental margin, Wopmay Orogen, Northwest Territories; in Proterozoic Basins of Canada, ed. F.H.A. Campbell, Geological Survey of Canada, Paper 81-10, p. 79-95.

Easton, R.M.
1982: Tectonic significance of the Akaitcho Group, Wopmay Orogen, Northwest Territories; Ph.D. thesis, Memorial University of Newfoundland, St. John's, Newfoundland, 432 p.

Ellis, M.A.
1986: Structural morphology and associated strain in the central Cordillera (British Columbia and Washington): Evidence of oblique tectonics; Geology, v. 14, p. 647-650.

Eskola, P.E.
1949: The problem of mantled gneiss domes; Geological Society of London Quarterly Journal, v. 104, p. 461-476.

Fitch, T.J.
1972: Plate convergence, transcurrent faults, and the internal deformation adjacent to southeast Asia and the western Pacific; Journal of Geophysical Research, v. 5, p. 2699-2709.

Fraser, J.A., Hoffman, P.F., Irvine, T.N., and Mursky, G.
1972: Bear Structural Province; in Variations in Tectonic Styles in Canada, ed. R.A. Price and R.J.W. Douglas; Geological Association of Canada, Special Paper 11, p. 183-185.

Frith, R.A.
1973: The geology of the Bear Slave boundary in the Indin Lake area, District of Mackenzie; in Report of Activities, Part A, Geological Survey of Canada, Paper 73-1A, p. 146-148.
1986: Precambrian geology of the Indin Lake map area, NTS 86B, District of Mackenzie; Geological Survey of Canada, Open File Report 1243, 81 p.

Frith, R.A. and Leatherbarrow, R.
1975: Preliminary report of the geology of the Arseno Lake map-area (86 B/12), District of Mackenzie; in Report of Activities, Part A, Geological Survey of Canada, Paper 75-1A, p. 317-321.

Frith, R.A., Frith, R., Helmstaedt, H., Hill, J., and Leatherbarrow, R.
1974: Geology of the Indin Lake area (86 B), District of Mackenzie; in Report of Activities, Part A, Geological Survey of Canada, Paper 74-1A, p. 165-171.

Frith, R., Frith, R.A., and Doig, R.
1977: The geochronology of the granitic rocks along the Bear-Slave Structural Province boundary, northwest Canadian Shield; Canadian Journal of Earth Sciences, v. 14, p. 1356-1373.

Gee, D.G.
1980: Basement-cover relationships in the central Scandinavian Caledonides; Geologiska Foreningens i Stockholm Forhandlingar, v. 102, p. 455-474.

Hanmer, S.
1986: Asymmetrical pull-aparts and foliation fish as kinematic indicators; Journal of Structural Geology, v. 8, p. 111-122.

Hatcher, R.D., Jr. and Williams, R.T.
1986: Mechanical model for single thrust sheets Part 1: Taxonomy of crystalline thrust sheets and their relationships to the mechanical behavior of orogenic belts; Geological Society of America Bulletin, v. 97, p. 975-985.

Hildebrand, R.S. and Bowring, S.A.
1984: Continental intra-arc depressions: a model for their origin with a Proterozoic example from Wopmay Orogen; Geology, v. 12, p. 73-77.

Hildebrand, R.S., Hoffman, P.F., and Bowring, S.A.
1986: Wopmay Orogen as an evolving continental arc: Magmatic response to contrasting stress regimes; Geological Association of Canada, Programme with Abstracts, v. 11, p. 81.

Hildebrand, R.S., Hoffman, P.F., and Bowring, S.A.
in press: Tectono-magmatic evolution of the 1.9 Ga Great Bear magmatic zone, Wopmay Orogen, northwestern Canada; Journal of Volcanology and Geothermal Research.

Hoffman, P.F.
1980: Wopmay Orogen: A Wilson Cycle of early Proterozoic age in the northwest of the Canadian Shield; in The Continental Crust and its Mineral Deposits, ed. D.W. Strangway; Geological Association of Canada, Special Paper 20, p. 523-549.
1981: Revision of stratigraphic nomenclature, foreland thrust-fold belt of Wopmay Orogen, District of Mackenzie; in Current Research, Part A, Geological Survey of Canada, Paper 81-1A, p. 247-250.
1984a: Wopmay Fault Zone and its role in evolution of Wopmay Orogen; Geological Association of Canada, Program with Abstracts, v. 9, p. 74.
1984b: Geology, northern internides of Wopmay Orogen, District of Mackenzie, Northwest Territories; Geological Survey of Canada, Map 1576A, scale 1:250000.

Hoffman, P.F. and Bowring, S.A.
1983: Extensive effects of three different collisions on the foreland of Wopmay Orogen, northwest Canadian Shield; Geological Association of Canada, Program with Abstracts, v. 8, p. A33.
1984: Short-lived 1.9 Ga continental margin and its destruction, Wopmay Orogen, northwest Canada; Geology, v. 12, p. 68-72.
1977: Great Bear Batholith: a volcano-plutonic depression, in Volcanic Regimes in Canada, ed. W.R.A. Baragar, L.C. Coleman, and J.M. Hall, Geological Association of Canada, Special Paper 16, p. 170-192.

Hoffman, P.F., St-Onge, M., Carmichael, D.M., and deBie, I.
1978: Geology of the Coronation Geosyncline (Aphebian), Hepburn Lake sheet (86J), Bear Province, District of Mackenzie; in Current Research, Part A, Geological Survey of Canada, Paper 78-1A, p. 147-151.

Hoffman, P.F., St-Onge, M.R., Easton, R.M., Grotzinger, J., and Schulze, D.W.
1980: Syntectonic plutonism in north-central Wopmay Orogen (early Proterozoic), Hepburn Lake map area (86J), District of Mackenzie; in Current Research, Part A, Geological Survey of Canada, Paper 80-1A, p. 171-177.

King, J.E.
1985: Structure of the metamorphic-internal zone, northern Wopmay Orogen, Northwest Territories, Canada; Ph.D. thesis, Queen's University, Kingston, Ontario, 209 p.
in press: The metamorphic internal zone of Wopmay Orogen (Early Proterozoic), Canada: 30 km of structural relief in composite section based on plunge projection; Tectonics, in press.

King, J.E., St-Onge, M.R., and Lalonde, A.E.
1983: Wopmay Fault Zone – a major mylonite and brittle fault belt, Internal Zone, Wopmay Orogen: Geological Association of Canada, Program with Abstracts, v. 8, p. A37.

King, J.E., Villneuve, M.E., Spethmann, D., and Wilcox, K.H.
1986: Geology of the northwestern metamorphic-interanl zone and an outlier of the eastern Great Bear Magmatic Zone of Wopmay Orogen, Big Bend area, District of Mackenzie; in Current Research, Part A, Geological Survey of Canada, Paper 86-1A, p. 21-33.

Leatherbarrow, R.W.
1975: Gneiss domes along the boundary between the Bear and Slave Structural Provinces (near Arseno Lake, N.W.T.); unpublished M.Sc. thesis, Carleton University, Ottawa, Ontario, 77 p.

Lord, C.S.
1942: Snare River and Ingray Lake map-areas; Geological Survey of Canada, Memoir 235, 55 p.

McGlynn, J.C.
1970: Bear Province; in Geology and Economic Minerals of Canada, ed. R.J.W. Douglas; Geological Survey of Canada, Economic Geology Report 1, p. 77-84.

Monger, J.W.H., Clowes, R.M., Price, R.A., Simony, P.S., Riddihough, M.R.P., and Woodsworth, G.J.
1985: B-2 Juan de Fuca plate to Alberta Plains transect; Geological Society of America DNAG Centennial Continent/Ocean Transect Number 7.

Nielsen, P.A.
1978: Metamorphism of the Arseno Lake area, Northwest Territories; in Metamorphism in the Canadian Shield, ed. J.A. Fraser and W.W. Heywood, Geological Survey of Canada, Paper 78-10, p. 115-122.

Nielsen, P.A.
1986: Metamorphism of the Arseno Lake area, N.W.T., Canada: an Abukuma facies series of Aphebian age; Canadian Journal of Earth Sciences, v. 23, p. 646-669.

Oke, C. and Simony, P.S.
1981: Basement gneisses of the western Rocky Mountains, Hugh Allan Creek area, British Columbia; in Current Research, Part A, Geological Survey of Canada, Paper 81-1A, p. 181-184.

Platt, J.P. and Vissers, R.L.
1980: Extensional structures in anisotropic rocks; Journal of Structural Geology, v. 2, p. 397-410.

Ramsay, J.G.
1967: Folding and fracturing of rocks; McGraw-Hill, New York, 568 p.

Ramsay, J.G. and Graham, R.H.
1970: Strain variation in shear belts. Canadian Journal of Earth Sciences, v. 7, p. 786-813.

St-Onge, M.R.
1981: "Normal" and "inverted" metamorphic isograds and their relations to syntectonic Proterozoic batholiths in the Wopmay Orogen, Northwest Territories, Canada; Tectonophysics, v. 76, p. 295-316.
1984: Geothermometry and geobarometry in pelitic rocks of north-central Wopmay Orogen (early Proterozoic), Northwest Territories, Canada; Geological Society of America Bulletin, v. 95, p. 196-208.

St-Onge, M.R. and King, J.E.
in press: Evolution of regional metamorphism during back-arc stretching and subsequent crustal shortening in the 1.9 Ga Wopmay Orogen, Canada; Philosophical Transactions of the Royal Society of London, Series A.

St-Onge, M.R., Lalonde, A.E., and King, J.E.
1983a: Geology, Redrock Lake and eastern Calder River map areas, District of Mackenzie: The central Wopmay Orogen (Early Proterozoic), Bear Province, and the western Archean Slave Province; in Current Research, Part A, Geological Survey of Canada, Paper 83-1A, p. 147-152.

St-Onge, M.R., King, J.E., and Lalonde, A.E.
1983b: The Calderian Orogeny of Wopmay Orogen, N.W.T.: Evolution of an early Proterozoic collision-generated metamorphic-plutonic zone; Geological Association of Canada, Program with Abstracts, v. 8, p. A66.

St-Onge, M.R., King, J.E., and Lalonde, A.E.
1984: Deformation and metamorphism of the Coronation Supergroup and its basement in the Hepburn Metamorphic-Plutonic Zone of Wopmay Orogen: Redrock Lake and the eastern portion of Calder River map areas, District of Mackenzie; in Current Research, Part A, Geological Survey of Canada, Paper 84-1A, p. 171-180.

Simony, P.S., Ghent, E.D., Craw, D., Mitchell, W., and Robbins, D.B.
1980: Structural and metamorphic evolution of the Shuswap Complex, southern Canoe River area, British Columbia, Cordilleran Metamorphic Core Complexes, ed. M.D. Crittendon, Jr., P.J. Coney, and G.H. Davis, Geological Society of America, Memoir 153, p. 445-462.

Thompson, A.B.
1982: Dehydration melting of pelitic rocks and the generation of H_2O- undersaturated granitic liquids; American Journal of Science, v. 282, p. 1567-1595.

Tirrul, R.
1984: Two contrasting styles of superimposed regional shortening in the externides of Wopmay Orogen; Geological Association of Canada, Program with Abstracts, v. 9, p. 111.

Watkinson, A.J.
1975: Multilayer folds initiated in bulk plane strain, with the axis of no change perpendicular to the layering; Tectonophysics, v. 28, p. T7-T11.

White, S.H., Burrows, S.E., Carreras, J., Shaw, N.D., and Humphreys, F.J.
1980: On mylonites in ductile shear zones; Journal of Structural Geology, v. 2, p. 175-187.

Williams, P.F.
1985: Multiply deformed terrains - problems of correlation; Journal of Structural Geology, v. 7, p. 269-280.

A preliminary report on geology and on mineral occurrences in Precambrian carbonate rocks, Cape Breton Island, Nova Scotia[1]

DSS Contract 34SZ.23233-6-0119

Johannes R. Hill[2]

Hill, J.R., A preliminary report on geology and on mineral occurrences in Precambrian carbonate rocks, Cape Breton Island, Nova Scotia; in Current Research, Part A, Geological Survey of Canada, Paper 87-1A, p. 533-542, 1987.

Abstract

A program involving geological mapping and lithogeochemical sampling of Precambrian carbonate units belonging to the George River Group and related formations was conducted over selected areas of Cape Breton Island, Nova Scotia, in 1986. The work was carried out both on a regional basis and locally within areas of known metallic and non-metallic mineralization in order to compile a geological and geochemical database for the economic evaluation and lithological metallogenic categorization of all metacarbonate rocks. Preliminary geological results have shown that carbonate sequences examined throughout Cape Breton may be placed into three distinct metamorphic-stratigraphic assemblages. Traditional concepts conferring stratigraphic equivalence to all metacarbonate rocks underlying Cape Breton Island, regardless of sedimentary association or metamorphic environment must therefore be re-evaluated. It is also apparent from the mineral deposits study that many of the carbonate-hosted metal occurrences cannot unequivocally be classed as contact metasomatic in origin. In fact, few deposits show evidence of intrusive-hosted mineralization and/or alteration phases; while many, especially the deposits at Lime Hill and Meat Cove and the Currie and Barachois River Fe occurrences, show some characteristics of sediment-hosted mineralization.

Résumé

Un programme de cartographie géologique et d'échantillonnage lithogéochimique des unités carbonatées précambriennes du groupe de George River et des formations associées a été entrepris en 1986 dans certaines parties de l'île du Cap-Breton, en Nouvelle-Écosse. Les travaux ont été effectués à l'échelle régionale et localement dans des régions dotées de minéralisations métalliques et non métalliques, afin de compiler une base de données géologiques et géochimiques susceptible d'aider à l'évaluation économique et à la classification lithologique et métallogénique de toutes les roches carbonatées d'origine métamorphique. Les données géolgiques provisoires permettent de classer les séquences carbonatées du Cap-Breton en trois ensembles métamorphiquement et stratigraphiquement distincts. Il faudra donc réexaminer l'hypothèse traditionnelle selon laquelle toutes les roches carbonatées d'origine métamorphique de l'île du Cap-Breton seraient stratigraphiquement équivalentes, peut importe leur association sédimentaire ou leur milieu métamorphique. L'étude des gîtes minéraux a également établi qu'un grand nombre des venues métalliques trouvées dans les roches carbonatées n'ont pas été formées par métasomatose de contact. En réalité, très peu de gîtes font voir des indices de minéralisation ou d'altération, on les deux, à l'intérieur de roches intrusives; par contre, de nombreux gîtes, notamment ceux de Lime Hill et de Meat Cove ainsi que les venues de fer de Currie et de Barachois River, présentent certaines caractéristiques d'une minéralisation en milieu sédimentaire.

[1]Contribution to the Canada–Nova Scotia Mineral Development Agreement 1984-1989. Project carried by Geological Survey of Canada, Project 860008

[2]Northwood Geoscience, 32 Nolan Ave., Ottawa, Ontario K1Y 3R3

INTRODUCTION

The first phase of a program dedicated to a study of the Precambrian carbonate rocks of Cape Breton Island was initiated during the 1986 summer field season. The project is designed to increase the awareness of the mineral industry to the resource potential of George River Group and related metacarbonate rocks of Cape Breton Island, and provide a database for mineral potential evaluations.

The scope of the project is two-fold: 1) to relate the major, minor and trace element geochemistry of the marbles to observed lithological and mineralogical components; and 2) to identify marble formations or environments of specific chemical composition which may be considered economically significant using statistical parameters.

This report summarizes the field relationships between the various carbonate terranes and the contained mineral occurrences.

STUDY AREAS AND PROCEDURES

Five areas of Cape Breton Island underlain by Precambrian carbonate rocks were examined during the period June to September, 1986 (see Fig. 56.1). Four areas are underlain by "classic" George River Group metasediments, as defined by Milligan (1970), including: a) the Boisdale Hills, characterized by approximately equivalent thicknesses of moderate to high metamorphic grade calcitic, dolomitic and silicious marbles and arenaceous sediments; b) the Craignish Hills, composed of crystalline limestones and dolomites to marbles, arenaceous and argillaceous metasedimentary rocks (quartzite, feldspathic sandstone, slate and phyllite) plus subdominant metavolcanics (massive andesitic and basaltic flows); c) North Mountain area, underlain by units similar to those found in the Craignish Hills, with the exception of the more highly metamorphosed marble and gneiss at Lime Hill and d) a narrow belt of dolomitic and calcitic marble in the Cape Dauphin-Kellys Cove (New Campbellton) area of southeastern Cape Breton Highlands. Detailed descriptions of all George River Group rock types found in southern Cape Breton Island have been summarized by Milligan (1970).

Metacarbonate units of inferred George River affiliation mapped by previous workers throughout the Cape Breton Highlands were also examined. The rocks consist predominantly of discontinuous interlayers of calcareous, dolomitic and silicious marbles within medium to high grade metamorphosed argillaceous and arenaceous sediments and intermixed (injection) granitoid rocks. Isolated marble outcrops in the Cape North area (mapped by Macdonald and Smith, 1980) and throughout the Pleasant Bay, Dingwall, Cape St. Lawrence and Cape North sheets (mapped by Neale, 1963a, b, 1964a, b) were examined. More continuous marble units in the southern Highlands including carbonates of the Ingonish River metasedimentary sequence in McMillan Flowage area (Raeside et al., 1984) were also described and sampled.

Carbonate-hosted mineral occurrences of both metallic and nonmetallic mineralization are common throughout the George River Group and equivalent units. A total of 11 metallic and 9 nonmetallic (industrial) mineral occurrences were examined and sampled during the 1986 program. Preliminary identification of metacarbonate-hosted mineral occurrences was obtained through use of the Mineral Occurrence Data Card file of the Nova Scotia Department of Mines and Energy, and through use of a computer-generated file containing all metallic and nonmetallic mineral occurrences in Nova Scotia compiled by Ponsford and Lyttle (1984) and Ponsford et al. (1985). Depending upon the degree of exposure and preservation of old excavations such as quarries, test pits or trenches, an attempt was made to map the areal extent of mineralization and define zonation patterns in individual deposits. In most cases, this proved to be difficult due to poor exposure and poor preservation of old workings. In many cases, old assessment reports or research papers containing descriptions of the showings were used to identify and delineate ore zone geometry and gangue assemblages. Sampling was carried out to determine elemental distributions in relation to lithological/mineralogical phases, to determine element associations in metallic mineral deposits and, in the case of bulk limestone or dolomite occurrences, to determine quality and consistency of product over larger areas.

GENERAL GEOLOGY

The George River Group is a loosely-defined series of interbedded carbonate and detrital sedimentary rocks associated with minor volcanic rocks of variable metamorphic grade, and probably Late Precambrian to pre-Middle Cambrian in age (Milligan, 1970). Weeks (1954, p. 8) stated that the name was probably first applied by Fletcher (1877) in the George River area to describe metamorphosed calcareous rocks interbedded with a succession of detritial metasedimentary and intrusive units. Weeks, however, favoured an Archean age for the group. He also alluded to problems in correlation between different areas underlain by George River rocks especially between the "type-section" at George River and the North Mountain and Eskasoni areas.

Metasedimentary rocks of the George River Group have been recognized throughout much of Cape Breton Island by two recurrent characteristic lithologies – arenite and carbonate. Within the areas examined, carbonate units vary from relatively pure crystalline limestone and dolostone of very low meta morphic grade, as in the Craignish Hills and North Mountain areas, to more highly metamorphosed calcareous, dolomitic and silicious (calc-silicate-bearing) marble of the Boisdale Hills and Lime Hill areas. Associated sedimentary rocks include quartzites, impure quartzites and feldspathic sandstones which stratigraphically bracket carbonate members. Argillaceous units are of more limited distribution and volcanic rocks (tuffs, pyroclastics and flows) which are common in the Craignish Hills and North Mountain areas but virtually absent in the Boisdale Hills.

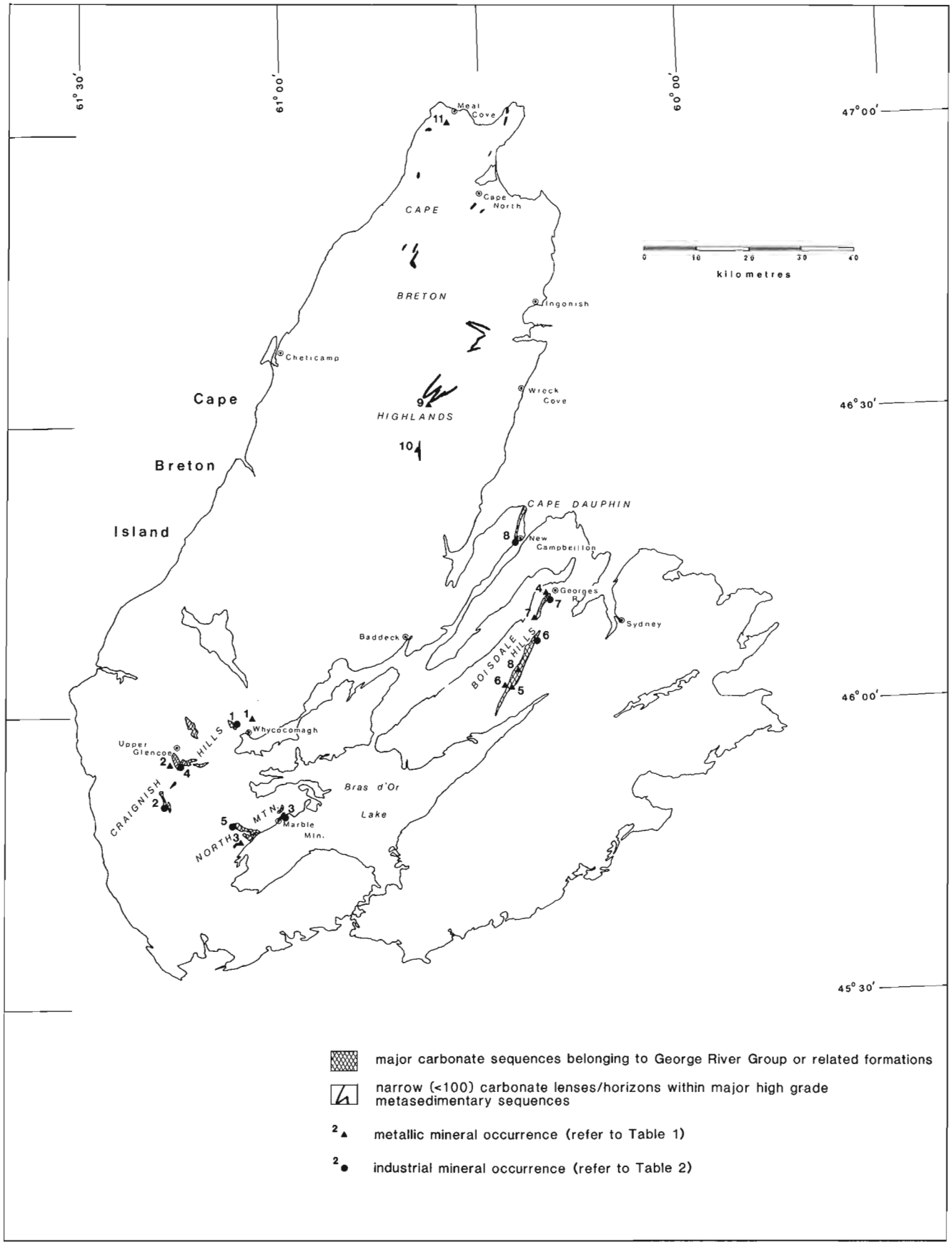


Figure 56.1. Distribution of Precambrian carbonate units in Cape Breton Island including the location of carbonate-hosted metallic and industrial mineral occurrences. The map shows only those formations and occurrences examined during the current study and geographic localities referred to in the report. (Geology from Keppie, 1979, and Raeside et al., 1984).

Throughout the Cape Breton Highlands, more highly metamorphosed and deformed carbonate-clastic metasedimentary rocks are less obviously related to the southern George River Group lithologies. In the Cape North area, Macdonald and Smith (1980) have tentatively correlated semipelitic and pelitic gneisses, marble and calc-silicate-bearing gneiss of the Cape North Group with the George River Group, even though arenaceous and calcareous facies represent a relatively minor component of the sequence. Similarly, Precambrian (?) metasedimentary rocks in southeastern Cape Breton Highlands, informally grouped into the Ingonish River metasedimentary sequence by Raeside et al. (1984), have been referred to by previous workers as George River equivalent (Murray, 1976; Keppie, 1979). In fact, carbonate lithologies here are greatly subordinate to pelitic, semipelitic and psammitic units and the equivalence of George River Group clastic-carbonate rocks (as identified in the southern half of Cape Breton Island) with the Ingonish River metasedimentary sequence is tenuous (Barr, et al., 1985).

CARBONATE LITHOLOGIES

A complex variety of lithologies has been recognized in George River Group and affiliated carbonate sequences throughout Cape Breton Island. Based on criteria such as chemical composition and intensity of metamorphism, most carbonate units fall into (or between) one of six basic lithological categories. They are:

1. cryptocrystalline limestone, apparently non-recrystallized
2. cryptocrystalline dolostone, apparently non-recrystallized
3. fine- to coarse-grained calcitic marble, obviously recrystallized
4. fine- to coarse-grained dolomitic marble, obviously recrystallized
5. siliceous (calcareous or dolomitic) marble bearing a wide variety of silicate minerals including micas and calc-silicates
6. skarns of either calcareous or dolomitic affinity containing greater than 40% calc-silicate minerals, and which may be characterized by contact metamorphic relationships.

Within each category variations in colour, grain size, texture and mineral assemblage can generate a complex series of discontinuous and poorly correlated carbonate members belonging to areally extensive carbonate sequences. The results of the lithogeochemical sampling program should clarify somewhat the relationship between macroscopic field categorization of carbonates and sedimentological or metamorphic variations.

Descriptions of the various lithological members which form mappable units plus general metamorphic and structural styles in each of the main study areas are discussed below. Detailed geological maps for the Craignish Hills, Boisdale Hills and North Mountain areas showing distribution of all George River Group rocks can be found in Milligan (1970).

CRAIGNISH HILLS

Carbonate rocks of the George River Group in the Craignish Hills are dominated by pure calcareous marble and crystalline to cryptocrystalline limestone. It is inferred, without the benefit of thin section examination, that metamorphic grade throughout the area is low.

The most widely distributed unit is a banded calcareous marble, light to dark grey, blue or green tinted, medium- to coarse-grained and equigranular. The lighter layers are composed of almost pure calcite grains, while the darker layers contain very fine grained argillaceous (micaceous) and/or carbonaceous material. The banding may reflect original compositional bedding or later metamorphic layering. Argillaceous marble units are characteristically more highly foliated than pure calcitic marbles. All marbles and limestones are highly fractured with calcite-filled veins pervasively crosscutting foliation. Sulphides are generally absent as accessory minerals.

The non-recrystallized limestone and dolostone beds appear to form relatively isolated units in the carbonate sequence, and are most commonly exposed at the upper and lower boundaries in contact with detrital sedimentary formations. Both limestones and dolostones are black to dark grey, massive, cryptocrystalline units, locally graphitic and perhaps argillaceous. The rocks are hard and fracture conchoidally but are pervasively cut by calcite- and/or dolomite-filled fractures. Their presence can be considered anomalous, as the relatively unmetamorphosed marble appears to be in conformable contact with obviously recrystallized calcareous sediments. The absence of metamorphic textures may be explained by differences in heat conductivity resulting from chemical variations in carbonate sedimentary rocks (especially H_2O content). Similar relationships can be observed in skarn environments of the southwestern United States, where calcareous sedimentary formations 1 to 2 km distant from the intrusive contact may contain, at apparently random stratigraphic intervals, units of recrystallized limestones/marbles within an otherwise completely unmetamorphosed calcareous sequence.

Pure dolomitic marbles are generally rare in the carbonate sequence of the Craignish Hills, forming isolated lenses perhaps 2 to 5 m thick. Dolomitic marbles occur either as light grey to buff, medium- to coarse-grained, sugary-textured, buff weathering units or as massive, blue-grey, very fine grained, highly fractured rock. Zones of dolomitization are commonly found within massive calcareous marble producing a brecciated texture and characteristic "lizard-skin" weathering pattern on outcrop surfaces.

Continuous stratigraphic sections of the carbonate sequences are rare but, where exposed, effectively illustrate the intimately interbedded nature of the marble and limestone members. For example, a 4 km stretch of East MacPhail

Brook in the Upper Glencoe area exposed a highly deformed and thinly interbedded section (of indeterminable stratigraphic thickness) composed of 1-2 m thick interbedded carbonaceous calcitic marble, argillaceous marble and banded calcitic marble; 3-4 m thick beds of pure buff-white calcitic marbles; and wider interbeds of black argillaceous limestone, calc-argillite and slate at the upper and lower boundaries of the carbonate sequence. However, outcrop density decreases drastically away from the stream valleys and mappable units become almost impossible to trace along strike so that geological mapping on a detailed scale becomes extremely frustrating.

North Mountain

Carbonate units in the George River Group in the North Mountain area east of Lime Hill include marble and limestone/dolostone units similar to the Craignish Hills formations. The Lime Hill area itself is underlain by serpentine, calc-silicate and sulphide-bearing marble as well as clean dolomite marble of medium to high metamorphic grade associated with high grade metasedimentary rocks and injection complexes. The low grade terrane is typified by the Kennedy's Big Brook (Campbell Brook) area. Here, a very pure, massive, calcitic marble, highly hematitic and pervasively cut by calcite and hematite-filled fractures, is dominant. Interbedded with this unit are numerous varieties of grey banded calcitic marbles, thinly foliated, micaceous, calcitic marbles and blue-grey, massive dolomitic marbles.

Cryptocrystalline, dark grey to black, massive limestones and dolostones similar to those found in the Craignish Hills, outcrop east of Kennedys Big Brook in a folded sequence of interbedded detrital sedimentary rocks. In the Marble Mountain area, a large block of crystalline calcitic and dolomitic marble is exposed in the pit and farther north in the MacAskills Lake area. Units in this area include fine- to coarse-grained, white to buff, massive calcitic to dolomitic marble which may display minor talc-serpentine alteration (as in the lower quarry at Marble Mountain) and light and dark grey calc-silicate minerals. Only locally is disseminated pyrite present.

In the Lime Hill area, it is immediately apparent that the carbonate and detrital sedimentary rocks have been affected by a much higher grade of metamorphism. This has led to the development of skarn lithologies including diopside and tremolite-bearing dolomitic marble, wollastonite-bearing calcitic marble and sulphide-bearing marble of economic interest. All display a retrograde talc-serpentine alteration overprint. The carbonate rocks are intermixed/interbedded in a highly complex structure with metapelitic gneisses and injection granitoid rocks suggesting that either: 1) the Lime Hill area represents an exposure of older Grenville-type basement upon which the younger George River sedimentary rocks (to the east) rest; or 2) the Lime Hill area represents a deeper stratigraphic level of the George River which has undergone more intense metamorphism due to burial and/or contact metamorphism (Justino and Sangster, 1987).

Boisdale Hills

Metacarbonate rocks of the George River Group exposed in Boisdale Hills display the same amount of lithological variability, but are of higher regional metamorphic grade, than carbonates in either the Craignish Hills or North Mountain areas. Varieties of grey banded calcareous to dolomitic marble dominate the sequence, interbedded with more massive, white to buff calcitic and dolomitic marble plus minor, very fine grained, blue-grey, massive dolomitic marble. All units are calc-silicate-bearing containing from 1-2% fine grained diopside in layers to 50% megacrystic tremolite porphyroblasts in a calcite groundmass. Many units display a high mica content, predominantly phlogopite and biotite, while disseminated, fine grained pyrite (trace to 1%) is ubiquitous throughout the carbonate sequence.

In most areas, especially the block of carbonate rocks west of George River, retrograde metamorphism has resulted in talc-serpentine-calcite alteration of higher grade calc-silicate minerals such as forsterite, diopside or tremolite. Nowhere is this more evident than in the Scotch Lake quarry at the north end of the Boisdale Hills where pervasive serpentinization has resulted in the almost total alteration of earlier calc-silicate minerals. All evidence therefore suggests that George River Group carbonate rocks in the Boisdale Hills area have undergone a higher intensity of metamorphism than in the Craignish Hills-North Mountain areas. The sequence is completely bounded in the west by younger intrusions. Locally, contact metamorphic assemblages are developed adjacent to the latter intrusions, including calc-silicate and sulphide and/or magnetite skarns. However, to call the entire carbonate sequence a skarn environment is incorrect. More accurately, high grade regional metamorphism could account for the presence of ubiquitous calc-silicate minerals and pyrite disseminated throughout most carbonate units.

Cape Dauphin–New Campbellton area

An almost continuous belt of George River carbonates plus minor meta sediments extends along a belt 7 km long by 300 m (average) wide from Cape Dauphin south to the dolomite quarry at New Campbellton (Kellys Cove). The sequence is fault-bounded on the west by a major Late Proterozoic granitoid batholith (Kellys Mountain granite) and on the east by apparently conformable petroliferous limestones and coal beds of Carboniferous age. Carbonate members of the George River Group consist of: 1) grey, banded to fissile calcitic marble which may be carbonaceous and micaceous; 2) green to pink, laminated calcitic marble with hematite, chlorite and epidote alteration; 3) buff to white, massive, crystalline very pure dolomitic marble ranging from a medium grained texture in the Cape Dauphin area to very fine grained in the quarry at Kellys Cove; and 4) black to dark grey, massive, cryptocrystalline limestone to argillaceous limestone.

The units appear to be of low metamorphic grade and nowhere is there evidence of contact metamorphism. The sequence can be most directly compared with George River carbonates of the Craignish Hill and North Mountain areas.

Cape Breton Highlands

Carbonate units throughout northern Cape Breton Highlands form narrow (100 m) lenses within medium- to high-grade metasediments including metapelite, metasemipelite, quartzite and quartz-feldspar-biotite gneiss. Minor metavolcanic units may also be associated with the carbonates. In the McMillan Flowage area, a tightly folded quartzite-carbonate horizon (part of the Ingonish River metasedimentary sequence) contains interbedded units of diopside and mica-bearing calcitic and dolomitic marble. The marble units are light grey to green to white, medium- to coarse-grained, highly foliated and thinly banded with pervasive serpentinitic alteration. Narrow (<5 m) sulphide and calc-silicate-bearing skarn horizons occur within the carbonate units, some of which may be highly mineralized.

Farther north in the Cape North area, carbonate lenses belonging to the Cape North Group range in width from 30 cm to 100 m. In almost all outcrops examined, the marble unit consists of a relatively pure calcitic or dolomitic middle member with calc-silcate-bearing marble in contact with bounding metasedimentary rocks. The pure marble units are usually white to buff, coarse grained, foliated, with biotite, phlogopite and graphite lenses. The calc-silicate units are green-grey foliated marbles containing variable amounts of calcite, dolomite, diopside, tremolite, biotite, phlogopite and pyrite. Serpentine alteration is pervasive in the calc-silicate-bearing marble.

The metamorphic grade of the enclosing metasediments reaches the silli manite zone of the amphibolite facies (Barr et al., 1985) which is the highest grade attained by any George River or affiliated rocks. This has led to the development of a monticellite-periclase-forsterite assemblage found in a metacarbonate roof pendent at Meat Cove, as compared with the forsterite-diopside-tremolite or diopside-tremolite-spinel assemblages most commonly found in the Boisdale Hills (Chatterjee, 1970).

CORRELATION OF PRECAMBRIAN CARBONATE UNITS

Detailed examination of selected Precambrian carbonate units covering a broad spectrum of sedimentary and metamorphic environments throughout Cape Breton Island, suggests that historical usage of George River Group as a lithostratigraphic unit to which all Precambrian to early Paleozoic carbonate-bearing sedimentary sequences are correlated, warrants revision. Based on field categorization alone, carbonate sequences examined to date may be placed into one of three distinct metamorphic-statigraphic assemblages. Carbonates underlying Craignish Hills, North Mountain (excluding the Lime Hill area) and the Cape Dauphin/Kellys Cove area are of low metamorphic grade forming thick, predominantly calcareous units associated with argillaceous and less commonly quartzitic metasedimentary rocks and metavolcanic rocks – an assemblage representative of basinal facies. The Boisdale Hills and Lime Hill areas are composed of silicious calcitic and dolomitic carbonate units which have undergone a much higher intensity of metamorphism, generating forsterite-diopside-tremolite or diopside-wollastonite assemblages. Associated lithologies are dominated by arenaceous metasedimentary rocks, including quartzite and feldspathic sandstone. The third category includes the narrow, discontinuous, calcitic to dolomitic and silicious marble layers and lenses of the Ingonish River metasedimentary sequence and Cape North Group associated with major thicknesses of moderate to high metamorphic grade (sillimanite zone) mica schists, quartz-feldspar-biotite gneisses and quartzites with very minor metavolcanic rocks. Carbonate forms a very minor lithofacies within extensive, high grade detrital metasedimentary sequences and, although the classic quartzite-carbonate association has locally been recognized as very narrow interbedded horizons, the correlation of this assemblage with George River Group rocks underlying Craignish Hills, for example, is not appropriate. The alternative is to consider the low metamorphic grade sedimentary-volcanogenic assemblages underlying Craignish Hills, North Mountain and Cape Dauphin/Kellys Cove as classic George River Group, representative of basinal, accreting continental margin sedimentation. The higher grade metasediments of Boisdale Hills, Lime Hill, and the Highlands may therefore be considered either: 1) older Grenville-type basement to the George River Group, 2) near shore facies sediments belonging to a deeper crustal section of George River equivalent formations, or 3) totally unrelated sedimentary sequences.

CARBONATE-HOSTED MINERAL DEPOSITS

Precambrian marbles of the George River Group and related sequences are host to a variety of metallic and industrial mineral occurrences of potential economic value. Historically, Fe-deposits such as those at the Currie Mine, MacPherson Mine and Upper Glencoe occurrence were actively investigated as potential sources of ore for the steel mills at Sydney, with minor amounts shipped during the late 1800s and early 1900s. More recently, increased activity in the base metals market led to the discovery of the Zn-deposits at Lime Hill and Meat Cove during the 1950's.

Of greater economic significance are the industrial mineral deposits of calcitic and dolomitic marble which once represented important sources of metallurgical grade dolomite and agricultural lime (e.g. Scotch Lake, Frenchvale and Marble Mountain quarries). Other minor operations involved recovery of filler-grade dolomite from the Churchview quarry near Whycocomagh, dimension stone from the Marble Mountain quarry and talc from the Frasers Mill area. Recently, high purity dolomitic marbles in the New Campbellton area have been recovered for potential metallurgical and agricultural application.

A summary and comparison of metallic and industrial mineral deposits examined during the 1986 field program follows. Emphasis is placed on deposit classification based on mineral assemblages and lithological relationships observed in the field without the benefit of geochemical data.

Metallic mineral occurrences

A summary of the basic metallogenic and mineralogical characteristics of eleven major metallic mineral showings hosted in Precambrian marbles throughout Cape Breton Island is outlined in Table 56.1. Much of the data are based on field observations by the author, but with additional data on mineral assemblages taken from various published reports.

The majority of the occurrences display characteristic skarn features including: a high grade calc-silicate mineral assemblage, a retrograde alteration overprint, spatially associated intrusions and massive, replacement-style mineralization. In comparison to Paleozoic skarn environments of the southwestern United States, however, the Paleozoic or older skarns of the George River Group display complex lithological and metallogenic relationships having undergone numerous phases of deformation and metamorphism. For example, it has proved extremely difficult to differentiate between prograde metamorphic assemblages resulting from regional events and high grade, contact metamorphic assemblages related to a single intrusive system. Only the Whycocomagh and McMillan Brook deposits display well developed endoskarn mineralization. In fact, it is apparent in many areas that prograde metamorphism, especially in the Boisdale Hills, is related to regional low pressure, high temperature metamorphism which produced assemblages dependent upon the original composition of the carbonates. It may be that a considerable temporal discontinuity exists between metamorphism and hydrothermal, retrograde alteration.

Three broad categories of skarn deposits based on dominant element association can be identified in the occurrences of Table 56.1. Most common are Fe-skarns in which magnetite and/or pyrite and pyrrhotite dominate but which also contain abundant Cu plus variable Zn, W, Mo, or Sn-bearing minerals. Of the seven Fe-skarns identified, only the Whycocomagh and McMillan Brook occurrences display intrusion-hosted mineralization characteristic of obvious contact metamorphic relationships. Although endoskarn mineralization appears to be absent, massive magnetite-pyrite-chalcopyrite at Upper Glencoe and at the Macdonald shafts appears to have formed by replacement of calc-silicate skarns in a marble xenolith surrounded by felsic intrusions. In contrast, massive magnetite/hematite at the Currie and Barachois River occurrences form lenses parallel to compositional layering or regional foliation, which may indicate recrystallization of sedimentary iron-formation. Another

Table 56.1. Summary of carbonate-hosted metallic mineral occurrences examined during 1986 field program.

#	Occurrence (Current) (classification)	Metals	Mode of mineralization	Host lithologies	Prograde assemblage	Alteration
1.	Whycocomagh (Fe-skarn)	Fe, Cu, W, Mo	endoexo-skarn replacement+ fracture-controlled mag, cpy, py, sch, moly, po	calcareous to dolomitic marbles, granodiorite to diorite intrusive	diopside-forsterite-garnet tremolite?	tremolite? talc-serpentine-chlorite chlorite-sericite
2.	Upper Glencoe (Fe-skarn)	Fe, Cu	skarn replacement mag, py, cpy, mal	calcareous marble xenolith in monzodiorite intrusion	diopside-forsterite?	talc-serpentine-epidote
3.	Lime Hill (Zn-skarn)	Zn, Fe, Cu, Pb, W (2.0 million tons @ 2.5% Zn)	banded disseminated sph, cpy, py, po, apy, sch; shear zone massive py	serpentinized dolomitic marble	forsterite-monticellite wollastonite	antigorite-talc-phlogopite antigorite-sericite
4.	Macdonald Shaft (Fe-skarn)	Fe, Cu	massive + vein-controlled py, mag, cpy, mal	siliceous calcitic marble	diopside-tremolite wollastonite?	talc-serpentine-chlorite
5.	Currie Mine (Fe-skarn)	Fe, Cu	massive, bedded? hematite, specularite; tr. mag, cpy	banded calcitic marble	phlogopite-diopside	talc-serpentine-sericite-chlorite
6.	Rear Boisdale (Zn-Pb-Ag skarn)	Fe, Zn, Pb Ag, Cu, W	massive replacement + stringer py, sph, gal moly?, po, cpy, apy	graphitic, micaceous calcareous marble	not apparent	talc-serpentine-chlorite
7.	Macpherson Mine (Fe-skarn)	Fe, Cu	fracture-controlled mag, py, cpy	serpentinitic calcitic dolomitic marble, diabase dyke	not apparent	talc-antigorite
8.	Frenchvale & Campbell Lake (?)	Pb, Cu	rare disseminated gal, cpy, py	micaceous dolomitic and calcitic marble	temolite-biotite	talc-serpentine-chlorite-sercite
9.	McMillan Brook (Fe-skarn)	Fe, Cu, Zn, Sn W, Mo	massive replacement + fractures py, cpy, po, bo, sph; endoskarn py, po, cpy, bo; disseminated Sn, W, Mo	siliceous calcitic and dolomitic marbles, quartz monzonite	forsterite monticellite diopside-forsterite (Chatterjee, 1977)	talc-tremolite antigorite
10.	Barachois River (Fe-skarn? or Fe-formation)	Fe, Cu	massive lense mag, py, bo (stratiform)	calcitic and dolomitic marbles, microdiorite	diopside-forsterite	talc-antigorite
11.	Meat Cove Pine Brook (Zn-skarn)	Zn, Fe, Cu, Pb (4.4 million tons) (@ 4% Zn)	massive replacement and banded disseminated sph, po; vein-controlled sph, gal, py; endoskarn py, bo cpy	Mg-skarn (siliceous dolomitic calcitic marble) hornblende syenite	forsterite-periclase-chondrodite-monticellite, diopside-spinel (Chatterjee, 1979)	talc-brucite-antigorite

questionable skarn environment is the fracture-controlled magnetite-serpentine mineralization examined at the Macpherson showing. Here, mineralization appears to be related to the emplacement of diabase dykes, and no high grade calc-silicate skarns are present in the host carbonate xenolith. The association of diabase dykes with many occurrences of carbonate-hosted mineralization in the Precambrian of Cape Breton Island requires further investigation.

The zinc deposits at Lime Hill (2 x 10^6 t @ 2.5% Zn; E.M.R., 1983) and Meat Cove (4.4 x 10^6 t @ 4.0% Zn; E.M.R., 1983) probably represent the most significant carbonate-hosted base metal occurrences found yet on Cape Breton Island. Sphalerite is the dominant mineral of economic importance in both deposits but minor Cu, Pb, Cd, and W-bearing minerals are also present. Mineralization, especially at Lime Hill, is unique in that banded, stratiform, disseminated sphalerite is associated with high grade Ca- and Mg-skarns overprinted by a retrograde hydrothermal alteration. Replacement sulphide textures can be observed only on a microscopic scale at Lime Hill, but are quite obvious at Meat Cove, indicating some degree of epigenetic mineralization, or recrystallization of sediment-hosted mineralization.

The third type of deposit examined in Precambrian marbles is represented by the Rear Boisdale Zn-Pb-Ag occurrence, where massive, replacement pyrite, sphalerite, galena, molybdenite and chalcopyrite pods and lenses formed in a micaceous, carbonaceous calcitic marble with only minor calc-silicate minerals. The lack of a well developed Ca- or Mg-skarn is again anomalous, however, results from the petrographic study may reveal a fine grained calc-silicate mineral assemblage in the groundmass of these rocks.

Industrial mineral occurrences

George River Group carbonates have historically been a major source of metallurgical grade dolomite marble and, to a lesser extent, agricultural lime and dimension stone. However, a much wider range of industrial minerals commonly associated with metamorphosed carbonate rocks and skarn environments can also be found. A number of these occurrences were examined and sampled during the 1986 field program and are listed in Table 56.2. Lithological descriptions of carbonate units associated with or forming the deposits are summarized. Production figures have been taken from

Table 56.2. Summary of industrial mineral occurrences examined during the 1986 field program.

#	Occurrence	Commodities	Lithological description	Production/usage
1.	Whycocomagh	dolomite	white to cream to blue, medium grained, massive, pure, dolomitic marble	2000 tons filler grade
2.	Glendale	graphite	black sooty, flakey to amorphous graphite layers, < 1 m wide in thinly laminated, black, carbonaceous limestone + cross-cutting carbonaceous shear zones	no production
3.	Marble Mtn.	calcareous to dolomitic marble	1. massive, green-buff, medium to coarse grained calcitic dolomitic marble 2. varieties of grey to blue, banded, medium grained, pure, calcitic marble (crystalline limestone) 3. sheared and highly foliated, multicoloured, fine grained calcitic marble 4. massive, grey-white, medium to coarse grained dolomitic marble with serpentine + epidote-filled fractures. 5. varieties of white, blue-white + pink-white, massive, pure calcitic marble	2.5 + million tons metallurgical and agricultural grade marbles, + dimension stone (1865 to 1921); ballast (recent?)
4.	Glencoe	calcareous and dolomitic marble	1. blue-black to white, very fine grained, massive dolomitic marble 2. varieties of grey, banded, fine to medium grained often micaceous or carbonaceous calcitic marbles 3. grey to white, massive, medium to coarse grained calcitic marble	no production 175 million tons total estimated reserves metallurgical grade marbles. 345 million tons total estimated reserves cement grade marbles (MacNeil, 1977)
5.	Campbell Brook	calcareous marble	varieties of banded to thinly laminated, pink to buff and grey to blue, calcitic, often micaceous, marbles; highly hematitic	no production
6.	Frenchvale	dolomite marble	1. massive, grey to green to black, medium to coarse grained dolomitic marble 2. varieties of grey/green and buff, banded, medium to coarse grained dolomitic marble, which may be highly micaceous, serpentinitic 3. biotite diorite 4. biotite granite	54,000 tons metallurgical grade marble (1964) ballast (current)
7.	Scotch Lake	dolomitic marble	1. massive, grey to white, medium to coarse grained dolomitic marble with variable talc-serpentine-calcite alteration forming greenish streaks and bands 2. diabase dykes	metallurgical grade marble; (1899 to 1954)
8.	New Campbellton	dolomitic and calcitic	pink-grey and green-cream, fine to very fine grained, massive dolomitic marble.	metallurgical and agricultural grade marble (current)
9.	Meat Cove	brucite	retrograde alteration of Mg-skarn, up to 15% disseminated brucite crystals	no production

the Nova Scotia Department of Mines, Mineral Occurrence Data Card file.

Chemical composition and mineralogical consistency are crucial in determining quality of bulk marble deposits where SiO_2, CaO, and MgO-content define metallurgical, agricultural or industrial (cement) grade marble. For filler grade calcitic or dolomitic marbles, mineralogical purity, consistency and colour (brightness) are most important. Major reserves of metallurgical and cement grade marble have been defined in the George River Group (eg. Glencoe area, New Campbellton) but only rarely have formations of high purity, white, dolomitic or calcitic marbles suitable for filler material been found (e.g. Whycocomagh). The potential exists for high-MgO dolomite as an ore of Mg metal at New Campbellton and, although of limited areal extent, similar potential exists for numerous small dolomitic units interbedded in carbonate sequences throughout Cape Breton. Bulk marble deposits also represent a source of dimension stone, for example, the dolomitic marbles of Cape Dauphin area. The Marble Mountain quarry appears to have been the only operation which produced cut marble for statuary and building stone, recovering up to six varieties of calcitic marbles.

Of the more specialized industrial minerals known to occur within Precambrian marble, wollastonite may have the greatest potential. The mineral has been identified in skarns at Lime Hill, possibly at the Macdonald occurrence, and at scattered localities throughout the Boisdale Hills not directly associated with metallic mineralization. Chemical purity of host carbonate sediments is a major factor in the formation of high grade deposits of calc-silicate minerals – a condition which is difficult to find in the thinly interbedded, highly deformed and highly metamorphosed marble of Cape Breton Island.

ACKNOWLEDGMENTS

The author acknowledges the capable geological assistance of A.R. Misner, Acadia University, Wolfville, during the 1986 field program. Technical discussions with numerous individuals on recent developments in Cape Breton geology were also appreciated. They include: A.L. Sangster, Geological Survey of Canada; S.M. Barr and R.P. Raeside, Acadia University; D.A. Murray and A.K. Chatterjee, Nova Scotia Department of Mines and Energy, Halifax; G.C. Milligan, Dartmouth, Nova Scotia; and H.R. Oldale, University College of Cape Breton, Sydney. Special thanks are extended to Jim Peers, Peers Management Associates Ltd., Sydney, for his logistical support during fieldwork in Cape Breton.

REFERENCES

Barr, S.M., Raeside, R.P., and Macdonald, A.S.
1985: Geology of the southeastern Cape Breton Highlands, Nova Scotia; in Current Research, Part B, Geological Survey of Canada, Paper 85-1B, p. 103-109.

Chatterjee, A.K.
1970: Mineralization: associated wall rock alteration; in G.C. Milligan, Geology of the George River Series, Cape Breton; Nova Scotia Dept. of Mines and Energy, Memoir 7, p. 79-90 (Chapt. IV).
1977: Copper-zinc deposit at McMillan Brook, Victoria County, Cape Breton Island; Nova Scotia Department of Mines and Energy, Report of Activities 1976, Report 77-1, p. 55-66.
1979: Geology of the Meat Cove zinc deposit, Cape Breton Island, Nova Scotia; Nova Scotia Deptartment of Mines and Energy, Paper 79-3, 27 p.

Energy Mines and Resources Canada
1983: Canadian mineral deposits not being mined in 1983; Energy Mines and Resources Canada, Mineral Bulletin Mr-198, 308 p..

Fletcher, M.
1877: Exploration and surveys in Cape Breton, Nova Scotia; Geological Survey of Canada, Report of Progress, 1875-76, p. 369-418.

Justino, M. and Sangster, A.L.
1987: Geology in the vicinity of the Lime Hill Zinc occurrence, Cape Breton Nova Scotia; in Current Research, Part A, Geological Survey of Canada, Paper 87-1A, report 58.

Keppie, D.J.
1979: Geological map of the Province of Nova Scotia; Nova Scotia Department of Mines and Energy, scale 1:500 000.

Macdonald, A.S. and Smith, D.K.
1980: Geology of Cape North area, northern Cape Breton Island, Nova Scotia; Nova Scotia Department of Mines and Energy, Paper 80-1, 60 p.

MacNeil, D.J.
1977: The Glencoe limestone and dolomite survey, Inverness County, Nova Scotia–preliminary report; Nova Scotia Department of Mines and Energy, Open File Report 329, 63 p.

Milligan, G.C.
1970: Geology of the George River Series, Cape Breton; Nova Scotia Department of Mines and Energy, Memoir 7, 111 p.

Murray, D.L.
1976: The structural relationship between the Fourchu Group and the George River Group in the Clyburn Brook – Ingonish River area, Cape Breton, Nova Scotia; Nova Scotia Department of Mines and Energy, Open File Report 140, 20 p.

Neale, E.R.W.
1963a: Geology, Pleasant Bay, Cape Breton Island, Nova Scotia; Geological Survey of Canada, Map 1119A (NTS 11K/15), scale 1″ = 1 mile.
1963b: Geology, Dingwall, Cape Breton Island, Nova Scotia; Geological Survey of Canada, Map 1124A (NTS 11K/16), scale 1″ = 1 mile.
1964a: Geology, Cape St. Lawrence, Nova Scotia; Geological Survey of Canada, Map 1149A (NTS 11N/02), scale 1″ = 1 mile.
1964b: Geology, Cape North, Nova Scotia; Geological Survey of Canada, Map 1150A (NTS 11N/01), scale 1″ = 1 mile.

Ponsford, M. and Lyttle, N.A.
1984: Metallic mineral occurrences map and data compilation, eastern Nova Scotia – map sheets 11F, 11G, 11J, 11K, 11N; Nova Scotia Department of Mines and Energy, Open File Report 600.

Ponsford, M., DeMont, G., and Lyttle, N.A.
1985: Industrial mineral occurrences map and data compilation, eastern Nova Scotia – map sheets 11F, 11G, 11J, 11K, 11N; Nova Scotia Department of Mines and Energy, Open File Report 607.

Raeside, R.P., Barr, S.M., and Jong, W.
1984: Geology of the Ingonish River – Wreck Cove area, Cape Breton Island, Nova Scotia; Nova Scotia Department of Mines and Energy, Report 84-1, pp. 249-258, (1 map).

Weeks, L.J.
1954: Southeast Cape Breton Island, Nova Scotia: Geological Survey of Canada, Memoir 277, 112 p. (incl. Map 1026A).

Nickel, copper, platinum and palladium relations in Ni-Cu deposits of the St Stephen intrusion, New Brunswick[1]

Project 840050

A. Doğan Paktunc
Mineral Resources Division

Paktunc, A.D., Nickel, copper, platinum and palladium relations in Ni-Cu deposits of the St Stephen intrusion, New Brunswick; in Current Research, Part A, Geological Survey of Canada, Paper 87-1A, p. 543-553, 1987.

Abstract

The St Stephen synorogenic intrusion contains numerous zones of significant Ni-Cu sulphide mineralization hosted by rocks varying in composition from gabbro to peridotite. Total reserves from the three most extensively explored zones are 1 000 000 tons at 1.05 % Ni and 0.53 % Cu. Mineralization consists of matrix, blebby, massive, and remobilized sulphides. Among these, the matrix and blebby varieties represent magmatic sulphides, whereas massive and remobilized types are believed to have formed by subsolidus mobilization of magmatic sulphides. Pyrrhotite is the dominant sulphide mineral. Pentlandite and chalcopyrite form only a minor portion of the total sulphide present. Maximum platinum and palladium abundances in 55 samples were 289 and 101 ppb respectively. Low metal (Ni and Cu) to sulphur ratios of the sulphides along with other chemical and textural evidence indicate that a large proportion of the sulphur present was derived from the country rock sediments. Contamination of the magma by certain components that are enriched in the country rock (e.g. SiO_2, Al_2O_3, K_2O) may have promoted the separation of the sulphides from the silicate magma.

Résumé

L'intrusion synorogénique de St. Stephen contient de nombreuses zones à forte minéralisation en sulfure de cuivre et de nickel dans des roches dont la composition varie du gabbro à la péridotite. Les réserves totales des trois zones les mieux explorées se chiffrent à 1 000 000 de tonnes d'un teneur de 1,05 % en Ni et de 0,53 % en Cu. La minéralisation se manifeste sous forme de sulfures dans la gangue, de bulles de sulfure, de sulfures massifs et de sulfures redistribués. Les deux premières variétés représentent des sulfures magmatiques, tandis que les deux dernières se seraient formées par migration à l'état de subsolidus de sulfures magmatiques. La pyrrhotite est le principal minéral sulfuré. La pentlandite et la chalcopyrite ne forment qu'une petite portion de l'ensemble des minéraux sulfurés. La teneur maximale en platine et en palladium de 55 échantillons est de 289 ppb et de 101 ppb, respectivement. Les faibles rapports de métal (Ni et Cu) à soufre de sulfures, ainsi que d'autres indices chimiques et texturaux, indiquent qu'une grande partie du soufre trouvé dans l'intrusion provenait des sédiments encaissants. La contamination du magma par certains composés sujets à l'enrichissement dans les roches encaissantes (p. ex., SiO_2, Al_2O_3, K_2O) pourrait avoir provoqué la séparation des sulfures du magma silicaté.

[1]Contribution to Canada-New Brunswick Mineral Development Agreement 1984-1989. Project funded by Geological Survey of Canada.

INTRODUCTION

The St Stephen intrusion underlies an area of approximately 24 km^2 in the southwestern corner of New Brunswick, and is one of many Devonian mafic-ultramafic intrusions in the Appalachian-Caledonian Orogen. The intrusion appears to have been emplaced synorogenically into the lower Ordovician Cookson Formation* sedimentary rocks during the Acadian Orogeny (Paktunc, 1986).

The intrusion hosts numerous zones of Ni-Cu mineralization, some of which have been known since 1870. They have been the subject of intermittent exploration and limited mining activities.

PETROLOGY

Three distinctive lithological units consisting of peridotitic, troctolitic and gabbroic cumulates have been outlined in the intrusion (Figure 57.1). Mineralogical, chemical and textural characteristics of the rock types are summarized in Table 57.1 and 57.2.

Peridotitic rocks occur in the north-central part of the intrusion. Poorly developed layering, which is marked by thin discontinuous anorthositic laminae, first appears near the transition of peridotitic rocks to picritic troctolite. Other than this, the rocks are massive. They display a weak north-northwesterly foliation which is believed to have developed during the Acadian Orogeny. Olivine is the only cumulus phase. Clinopyroxene in the form of large oikocrysts (<2 cm), plagioclase and sulphides form intercumulus phases.

* In a previous paper (Paktunc, 1986), an abandoned term, "Charlotte Group", was used for the sedimentary rocks around the intrusion. Cookson Formation (Ruitenberg and Ludman, 1978) is the appropriate name for it.

Troctolitic rocks consist of troctolite, picritic troctolite, and olivine gabbro. They are basically olivine-plagioclase and plagioclase-olivine cumulates. Picritic troctolites form a transitional rock type between the peridotitic and the troctolitic rock units. The transition appears to be gradational where observed and is marked by the appearance of plagioclase as a cumulus phase. Troctolites are medium- to coarse-grained plagioclase-olivine adcumulates. Olivine gabbros are plagioclase-olivine orthocumulates in which clinopyroxene forms coarse oikocrysts. Uncommonly, layers

Table 57.1 Mineral assemblage and textures of the rocks, St Stephen intrusion.

Rock	texture	mineral assemblage cumulus	intercumulus
Periodotite	mesocumulate	Ol, Chr	Cpx, Pla, Sul
Picritic troctolite	mesocumulate-adcumulate	Ol, Pla, Chr	Cpx
Troctolite	mesocumulate	Pla, Ol	Cpx
Olivine gabbro	orthocumulate	Pla, Ol	Cpx
Gabbro	Orthocumulate subophitic	Pla	Cpx
Anorthosite	mesocumulate	Pla	
Olivine gabbronorite	orthocumulate	Pla, Ol, Opx	Cpx
Norite	orthocumulate	Pla, Opx	Ilm

Chr, chromite; Cpx, clinopyroxene; Ilm, ilmenite; Ol, olivine; Opx, orthopyroxene; Pla, plagioclase; Sul, sulphide; Cumulus terminology after Irvine (1982).

Table 57.2 Summary of whole-rock and mineral chemistry.

	Rock	Ol 100*Mg/	Opx (Mg + Fe)	Cpx	Pla mole%
Peridotite	87.5(2.6)	80.3(4.1)	80.5(4.4)	86.7(2.1)	76.5(7.7)
Picritic troctolite	84	82			78.3(2.8)
Troctolite	75.7(3.3)	75.3(3.3)	78.3(5.0)	83.3(2.0)	72.8(9.1)
Olivine gabbro	71.4(3.4)	67.7(3.8)	70	78.8(3.7)	70.2(9.7)
Gabbro	67.8(8.1)			75.5(6.6)	64.7(11.2)
Anorthosite	67.0(6.2)	73		81	79.5(8.1)
Olivine gabbronorite	67	64.3(4.3)	72.0(3.6)	77.0(2.6)	61.8(9.4)
Norite	56		54.5(3.7)		60.3(13.3)

Number in parantheses indicate 1× standard deviation from mean values
An, anorthite; Chr, chromite; Cpx, clinopyroxene; Ol, olivine; Opx, orthopyroxene.

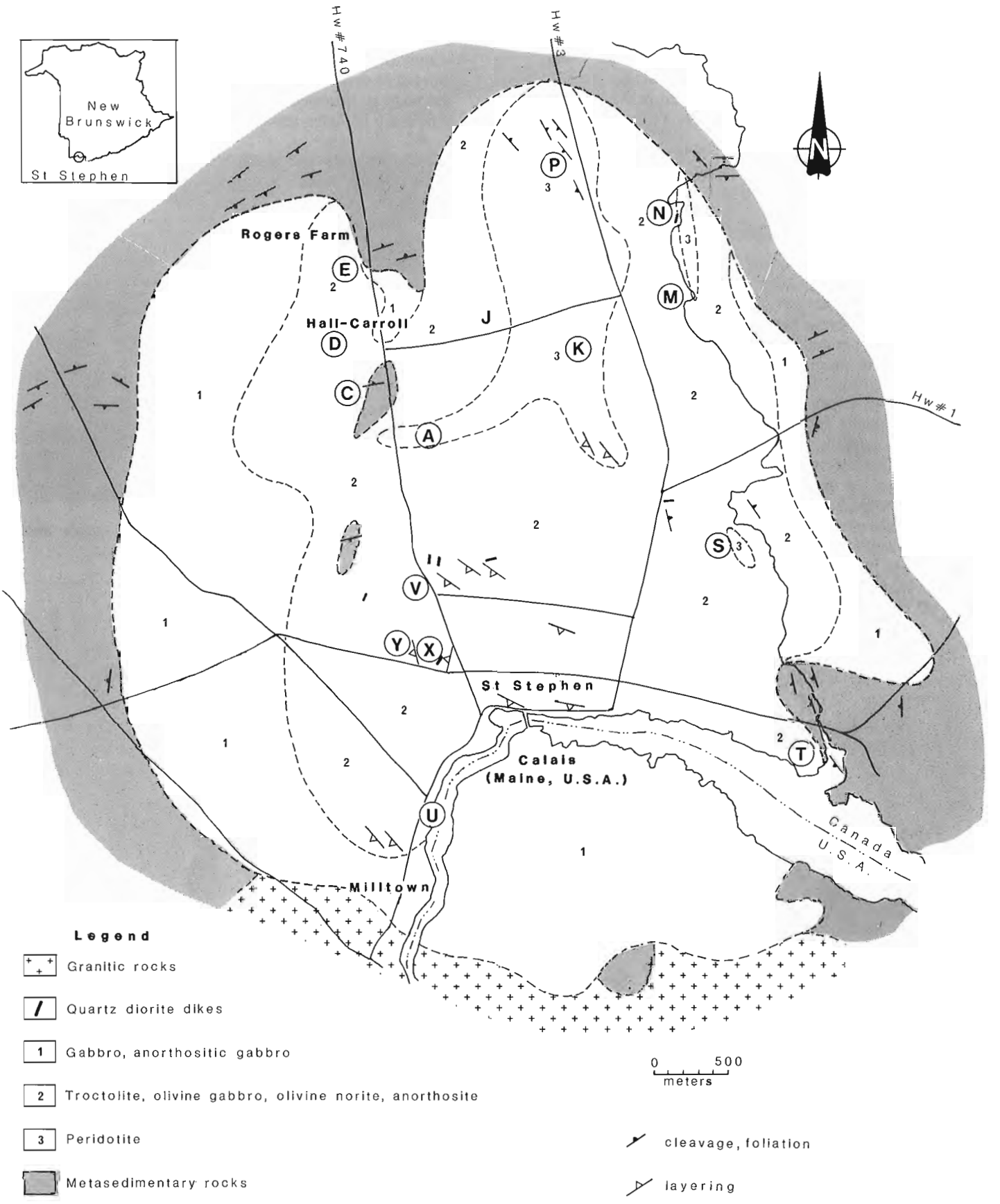


Figure 57.1. Geological map of the St Stephen intrusion; locations of ore zones and sulphide occurrences are indicated by letters.

several centimetres thick occur in the medium grained troctolites. The general attitude of the igneous layering and lamination observed in the troctolitic rocks of the intrusion is N40-50W/60-70 SW. Anorthosite, olivine gabbro-norite and norite form minor rock types included in the troctolitic unit and are described in Tables 57.1 & 57.2.

Gabbroic rocks which are mostly plagioclase orthocumulates appear to form a marginal unit in the intrusion. They are medium grained and massive.

MINERALIZATION

Ni-Cu mineralization has been classified into four types: matrix, blebby, massive and remobilized (Paktunc, 1986). Matrix sulphides are made up of a network of sulphides usually occupying the interstices between cumulus olivine crystals in peridotite and between cumulus olivine and plagioclase in picritic troctolite (Fig. 57.2). The amount of sulphide varies from 3 to 40% (by volume). Where the amount of sulphide is high, it forms an interconnected network. Blebby sulphides consist of subrounded to rounded blebs of sulphide surrounded by silicates (Fig. 57.3). The size of the blebs are usually 3 to 10 mm; however, sizes up to 4 cm across are not uncommon. Massive sulphide is the term used when the amount of sulphides is in excess of 60% by volume. Remobilized sulphide is a textural term used where solid state mobilization of sulphides is clear. The terms, "semi-massive" and "disseminated" were used to describe certain ore types in assessment files and company reports, and are retained here where data are quoted from these sources.

Sixteen mineralized zones have been identified within the intrusion (Fig. 57.1). Among them, the Rogers Farm, Hall-Carroll and "C" zones are the most extensively explored zones.

The Rogers Farm zone consists of two ore bodies (Fig. 57.4). The main ore body trends north-northeasterly, covers an area of 13 500 m^2 near the surface, and dips steeply extending to 90 m below surface (Fig. 57.5). It consists mainly of massive, semi-massive and blebby sulphides. The amount of sulphide blebs reaches 40% in places. The size of the body is estimated to be 340 000 tons at 1.05% Ni and 0.60% Cu (Boliden report, 1970). The other body which is

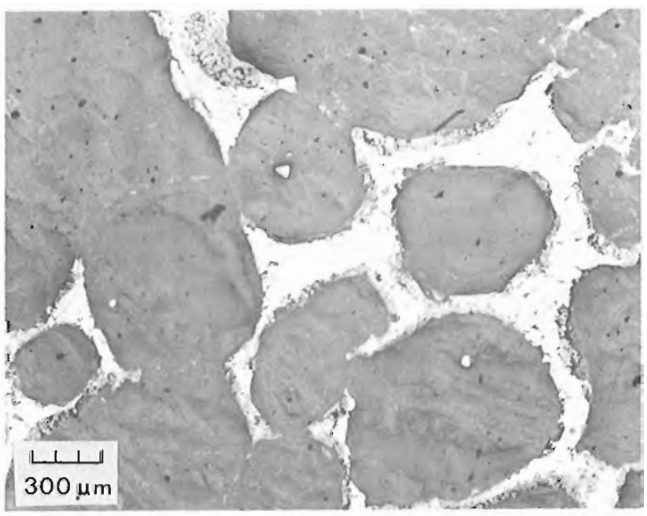


Figure 57.2. Matrix sulphide occupying interstices between cumulus olivine crystals in peridotite.

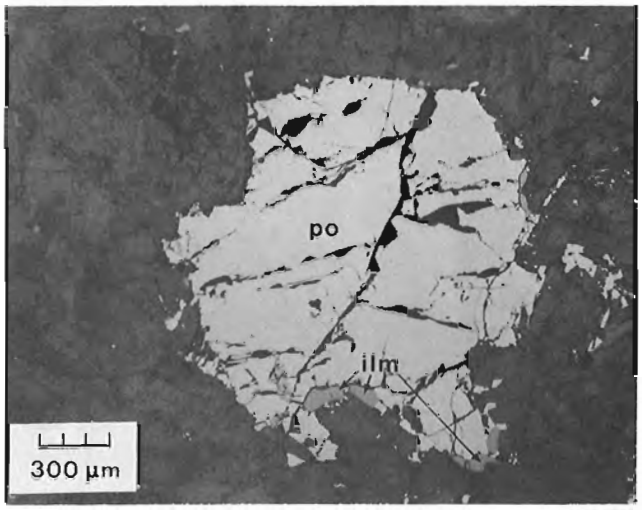


Figure 57.3. Photomicrograph showing a sulphide bleb. po: pyrrhotite; ilm: ilmenite.

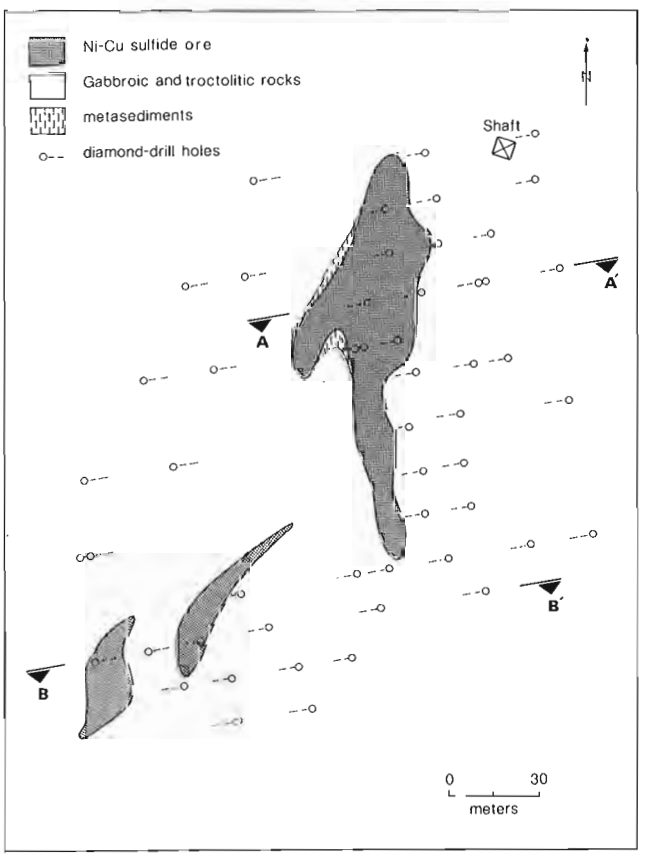


Figure 57.4. Simplified plan of the ore bodies in the Rogers Farm zone. Outline of the ore bodies at or near the surface drawn from the diamond-drill hole data.

disseminated to semi-massive in character lies to the southeast of the main body (Fig. 57.4). The lens-shaped body extends to at least 75 m below surface (Fig. 57.5) and appears to be connected to the main body at this depth. A report by Atlantic Nickel Mines indicates 49 000 tons of material grading 0.79% Ni and 0.36% Cu.

The Hall-Carroll zone occurs about 600 m southeast of the Rogers Farm zone. The lens-shaped body is continuous over 200 m along strike (Fig. 57.6). It is steeply dipping and extends to a depth of at least 150 m (Fig. 57.7). Its thickness ranges from 7 to 23 meters. The ore is largely massive to semi-massive in character. Estimated resource for the Hall-Carroll zone is 400 000 tons grading 0.94% Ni and 0.54% Cu (Atlantic Nickel report, 1969).

The "C" zone is located approximately 800 m south of the Hall-Carroll zone. It appears to lie adjacent to a large country rock inclusion which is believed to be a roof pendant.

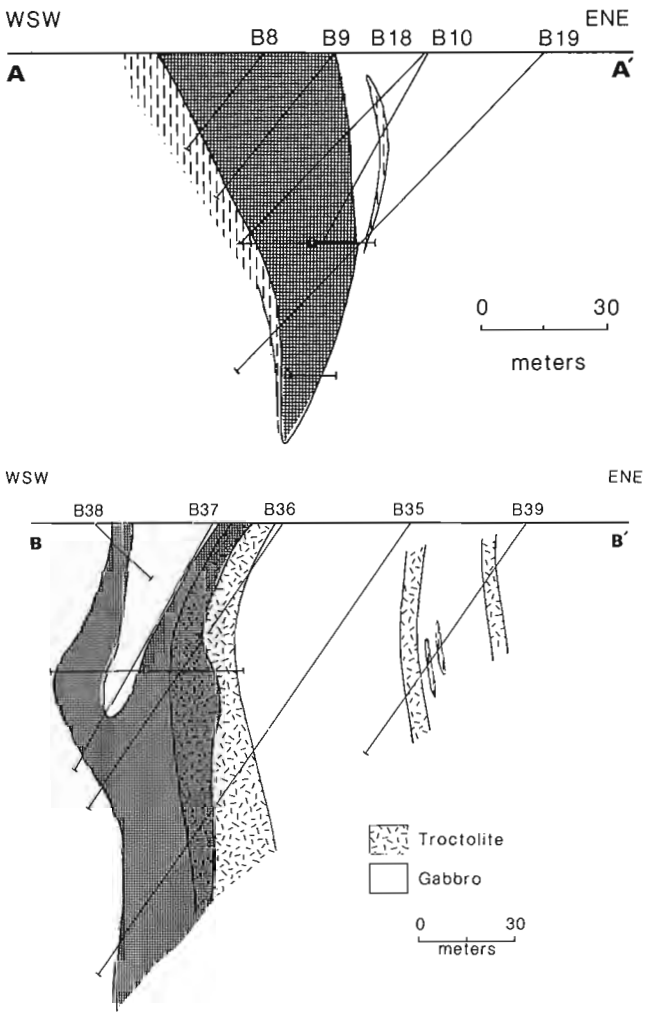


Figure 57.5. Cross-sections through the ore bodies of the Rogers Farm zone. Prepared from the diamond-drill hole logs of this study and those from the assessment files Location of sections is shown in Figure 57.4.

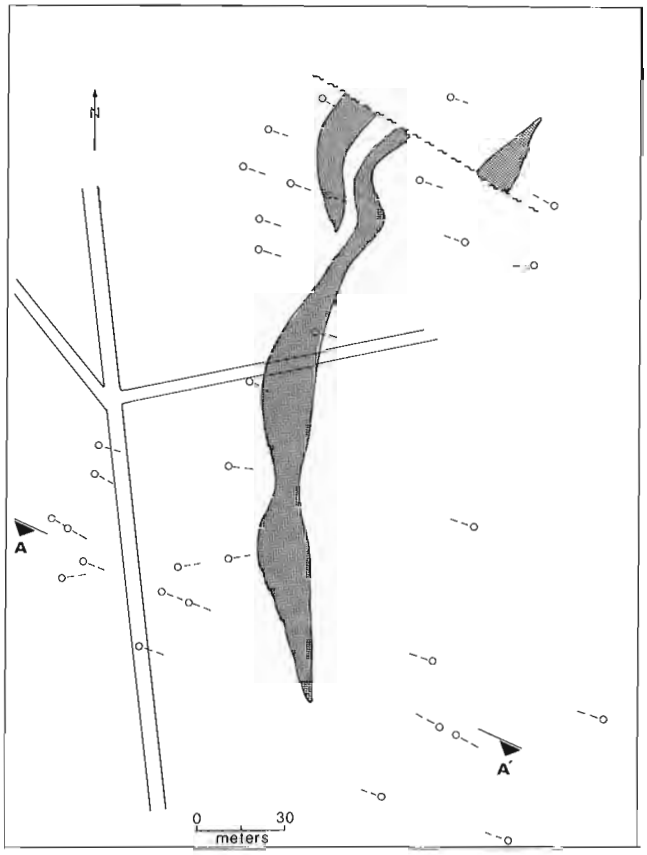


Figure 57.6. Plan of the Hall-Carroll ore body.

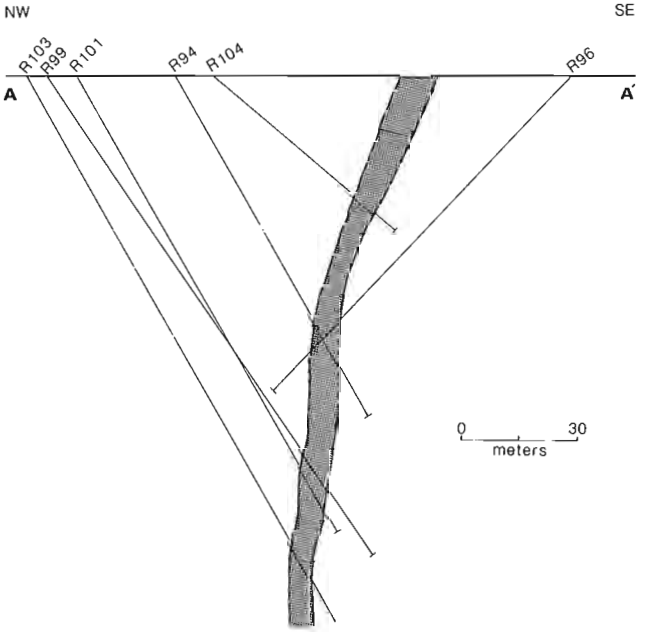


Figure 57.7. Sections through the Hall-Carroll ore body.

The "C" zone consists of four lens-shaped bodies which seem to show conformable character along the contact with the adjacent sedimentary roof pendant (Fig. 57.8). The two northern bodies seem to have a limited extension to a depth of 100 m below surface (Fig. 57.9). The two bodies to the south, on the other hand, extend to a minimum depth of 150 m. Resources estimated for this zone are 77 000 tons of high grade material at 1.30% Ni and 0.50% Cu.

The bodies in the Rogers Farm, Hall-Carroll and "C" zones appear to have been controlled by north-northeasterly structures. They are contained largely within olivine gabbro and gabbro. The rocks are variably altered and locally contain abundant fragments of sedimentary country rocks and intrusive rocks. The fragments are varied in size and angular or subangular. The nature of these fragments and their relations to mineralization are not clear. It is believed, however, that sulphides occurring as matrix to fragments are largely remobilized (Fig. 57.10). The sulphide to fragment ratio is quite variable and determines the massive or semi-massive nature of the ore.

The "A", "B", "K", "P", and "S" zones occur within the peridotite unit of the intrusion, and are largely of the matrix sulphide type. A limited number of holes also indicate the presence of narrow intersections of massive sulphides directly associated with matrix sulphides in these zones.

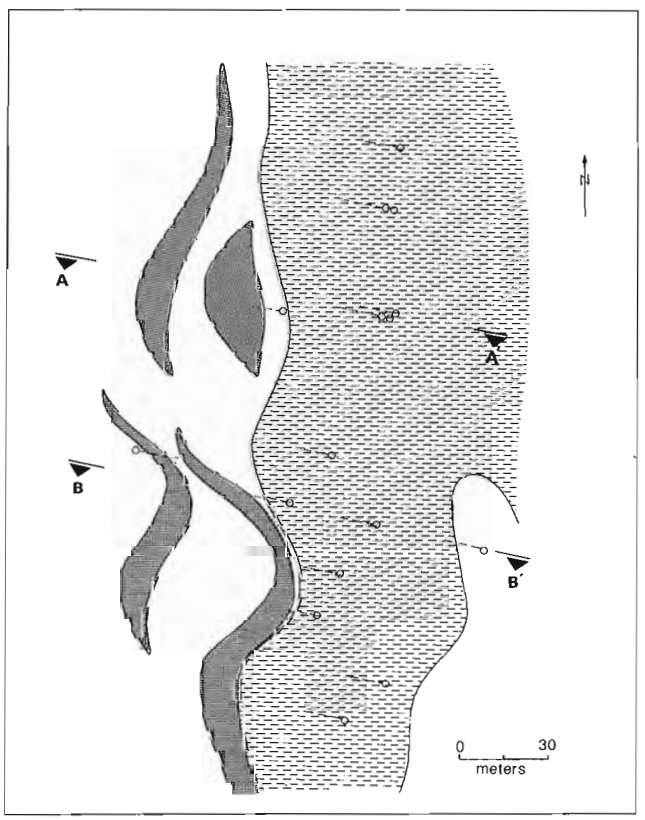


Figure 57.8. Plan of the "C" zone.

SULPHIDE MINERALS

The dominant sulphide mineral is pyrrhotite which is found in various forms and textures in almost every rock type. It contains up to 0.54% Ni. Pentlandite is found as euhedral to subhedral grains (Fig. 57.11) and as exsolution blebs in pyrrhotite in peridotitic and troctolitic rocks. The pentlandite is typically rich in Co, ranging from about 2 to 8%, and in the "K" zone Co content of pentlandite reaches 16% (Paktunc et al., 1986). Chalcopyrite is found as irregular grains and as thin veinlets associated with other sulphides. Abundances of sulphide minerals were calculated from the Ni, Cu and S

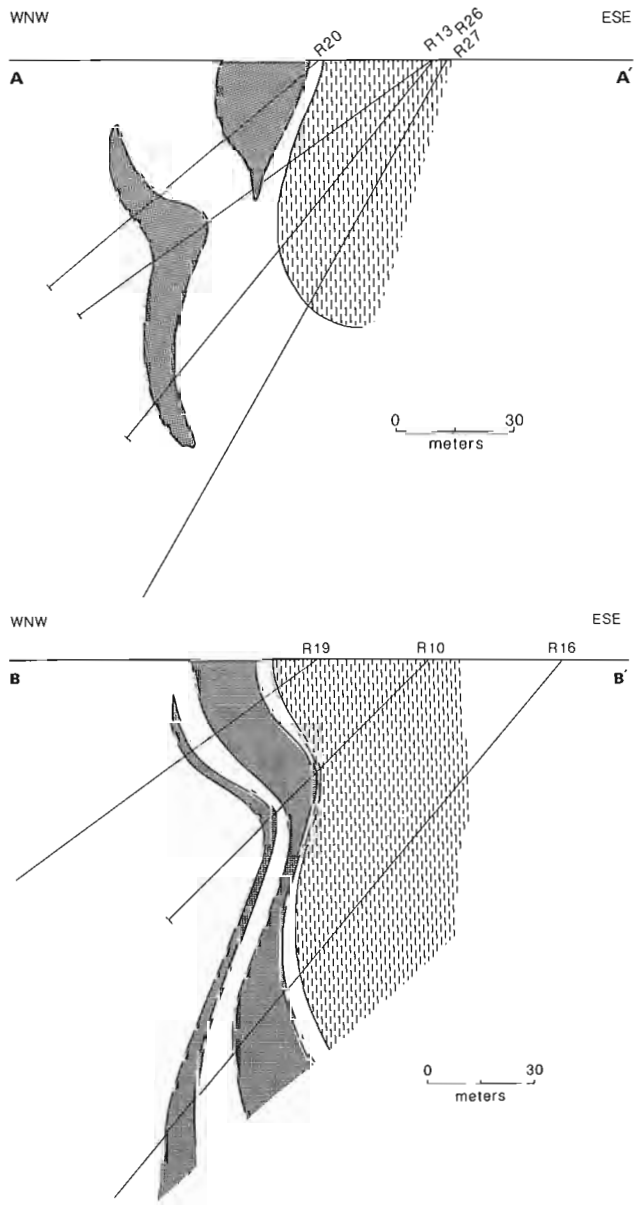


Figure 57.9. Sections through the ore bodies in the "C" zone. Location of sections is shown in Figure 57.8.

analyses. Pyrrhotite forms more than 90% (by weight) of the total sulphides, confirming visual modal (volume%) estimates of the sulphide phases.

GEOCHEMISTRY

Pt, Pd, and Au were analyzed by neutron activation or by direct current plasma techniques following fire-assay preconcentration (Hoffman et al., 1978). Ni and Cu analyses are by atomic absorption, direct current plasma or by neutron activation. S analyses are by X-ray fluorescence. Samples comprise large hand samples or 10 to 15 cm long drill core pieces.

On the basis of 454 Ni and Cu analyses, including the Atlantic Nickel and Boliden assays, the mineralized material at St Stephen has Ni contents ranging from 0.01 to 2.40% and Cu contents from 0.01 to 3.90% . Average Ni and Cu contents of the mineralized zones are given in Table 57.3. Due to the pyrrhotite-rich nature of the ores, metal (Ni + Cu) to sulphur ratios are expectedly very low (averaging 0.07). The Cu/(Cu + Ni) ratio seems to show a systematic variation with regard to the ore type. In most of the mineralized zones, this ratio increases from massive and matrix sulphides through semi-massive and blebby sulphides to disseminated and remobilized sulphides. This is also reflected in the overall average ratios (Fig. 57.12). Matrix sulphides occurring in the peridotite unit have markedly higher Ni/Cu ratios than the blebby type sulphides found in troctolite, olivine gabbro and

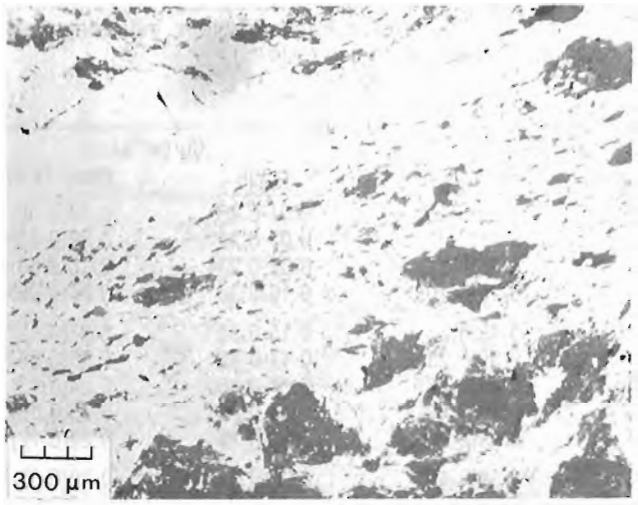


Figure 57.10. Photomicrograph of massive ore, containing mechanically incorporated rock fragments.

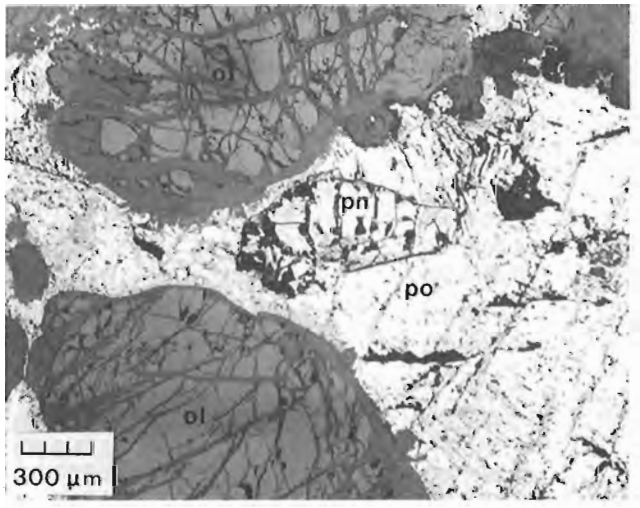


Figure 57.11. Photomicrograph showing an euhedral pentlandite grain (pn) in pyrrhotite (po). Ol: olivine.

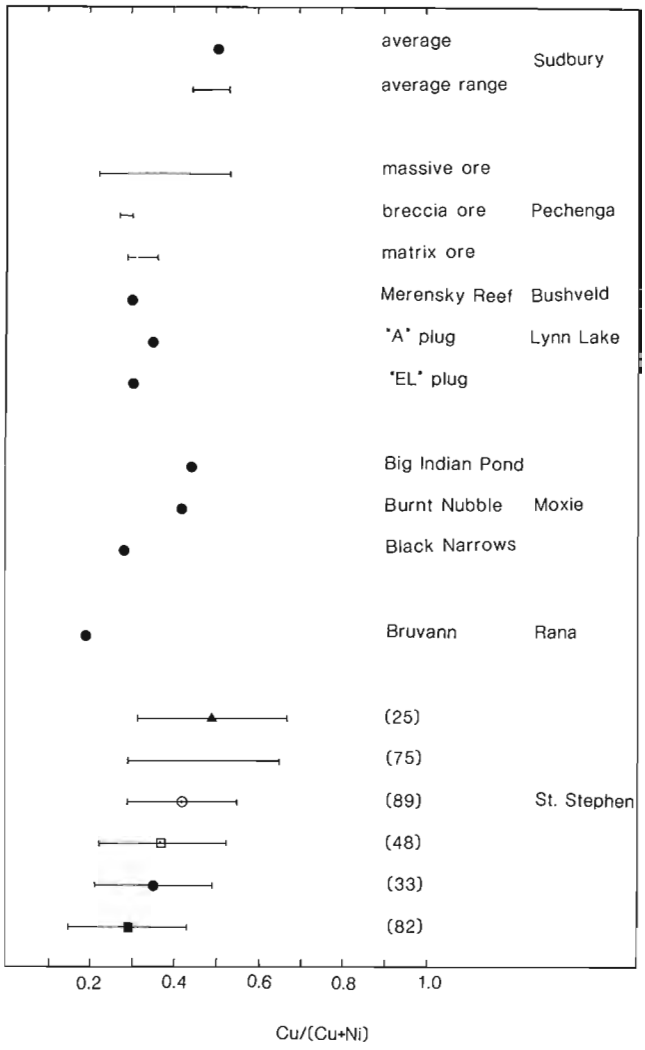


Figure 57.12. Cu/(Cu + Ni) ratios of various ore types compared to some tholeiite-related deposits. Numbers in parentheses indicate number of samples in average. Error bars represent 1 x standard deviation from mean. Symbols for the St Stephen ores: square, semi-massive ore; filled square, massive ore; circle, blebby sulphide; filled circle, matrix sulphide; triangle, remobilized sulphide; dot, disseminated sulphide. Data source: Sudbury (Pattison 1979, Cabri and Naldrett, 1984); Pechenga (Gorbunov, 1968); Rana (Boyd and Mathiesen 1979); Moxie (Thompson 1982); Lynn Lake (Pinsent 1980).

gabbro (Fig. 57.13). Such compositional dependence of sulphides on their host rocks is well known (Wilson and Anderson, 1959; Duke, 1979; Eckstrand, 1980; Naldrett, 1981). Gabbro-troctolite hosted massive ores from the "C", "D", Hall-Carroll, and Rogers Farm zones have higher Ni and Cu contents than those from peridotite hosted massive ores of the "A" and "B" zones (Fig. 57.13). Massive ores of the "C", "D", Hall-Carroll, and Rogers Farm zones are considered to be mobilized sulphides; therefore, the present host rock may not represent the composition of magma with which the contained sulphides equilibrated. The Ni and Cu depleted nature of the massive ores associated with the peridotites, however, is noteworthy because they show no evidence of having been remobilized. Another interesting point is that Ni and Cu abundances are about equal in various ore types of the "B" zone, even though the total amount of sulphide varies considerably. Thus the difference between ore types is determined mainly by the amount of pyrrhotite.

Overall, the St Stephen sulphides display similar Cu/(Cu + Ni) ratios to those associated with some tholeiitic

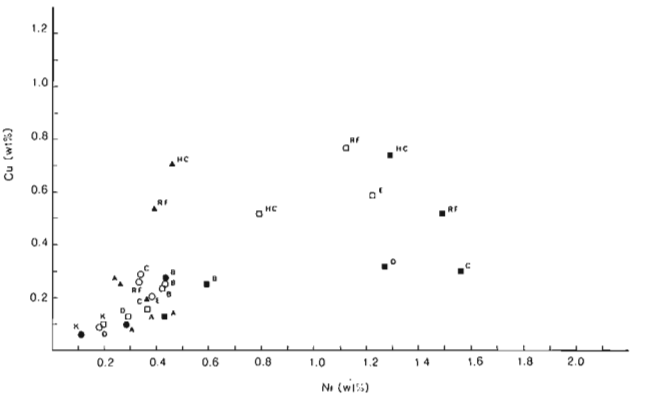


Figure 57.13. Ni vs Cu plot of sulphides representing various ore types from nine ore zones. Refer to Figure 57.12 for symbols. See Table 57.4 for standard deviations from the mean values. Note that some massive ore samples are significantly rich in Ni and extremely depleted in Cu. Also note the change in the Ni/Cu ratios of remobilized sulphides, indicating preferential mobilization of chalcopyrite.

Table 57.3 Ni and Cu contents of sulphides representing various ore zones.

Ore zone	Sulphide type	N	Ni (wt%) range	Ni (wt%) mean(s.d)	Cu (wt%) range	Cu (wt%) mean (s.d)
"A"	mx	22	0.04-0.78	0.28(0.19)	0.01-0.40	0.10(0.08)
	ms	10	0.03-1.10	0.43(0.27)	0.07-0.20	0.30(0.20)
	sm	7	0.07-0.75	0.36(0.21)	0.08-0.24	0.16(0.06)
	rm	4	0.14-0.40	0.26(0.10)	0.16-0.35	0.25(0.08)
"B"	mx	12	0.05-0.90	0.43(0.23)	0.15-0.55	0.27(0.10)
	ms	8	0.20-0.98	0.59(0.23)	0.17-0.42	0.25(0.08)
	sm	11	0.07-0.98	0.42(0.25)	0.07-0.55	0.24(0.13)
	bb	4	0.24-0.68	0.43(0.19)	0.20-0.29	0.25(0.03)
	ds	2	0.15-0.20	0.18(0.03)	0.12-0.35	0.24(0.12)
"C"	ms	3	0.95-1.90	1.56(0.43)	0.02-0.76	0.30(0.33)
	bb	10	0.15-1.10	0.34(0.28)	0.10-1.40	0.29(0.37)
	ds	28	0.03-1.47	0.37(0.30)	0.07-0.37	0.19(0.08)
"D"	ms	5	0.43-2.40	1.27(0.72)	0.15-0.57	0.32(0.15)
	sm	4	0.18-0.47	0.29(0.11)	0.10-0.15	0.13(0.02)
	bb	3	0.15-0.20	0.18(0.02)	0.07-0.12	0.09(0.02)
	ds	8	0.04-0.28	0.15(0.07)	0.03-0.12	0.08(0.03)
	rm	2	0.22-0.53	0.38(0.15)	0.20	
"E"	sm	5	0.76-1.64	1.22(0.36)	0.28-1.42	0.59(0.42)
	bb	3	0.12-0.69	0.38(0.23)	0.10-0.31	0.20(0.09)
	ds	5	0.14-0.52	0.43(0.26)	0.12-2.55	0.66(0.95)
Hall-Carroll	ms	21	0.45-1.75	1.29(0.36)	0.22-1.65	0.74(0.32)
	sm	12	0.47-1.70	0.79(0.36)	0.17-1.52	0.52(0.41)
	ds	22	0.05-0.43	0.20(0.11)	0.10-0.87	0.32(0.23)
	rm	6	0.12-0.80	0.46(0.25)	0.10-1.65	0.70(0.50)
"K"	mx	11	0.01-0.16	0.11(0.05)	0.01-0.10	0.06(0.04)
	sm	5	0.10-0.25	0.19(0.05)	0.06-0.15	0.10(0.03)
"N"	ds	4	0.08-0.30	0.19(0.08)	0.10-0.15	0.14(0.02)
Rogers Farm	ms	42	0.87-1.90	1.49(0.25)	0.06-0.90	0.52(0.26)
	sm	14	0.50-1.57	1.12(0.37)	0.20-3.90	0.77(0.90)
	bb	79	0.04-1.55	0.33(0.27)	0.03-2.00	0.26(0.31)
	ds	3	0.05-0.56	0.24(0.23)	0.03-1.31	0.58(0.54)
	rm	16	0.05-1.14	0.39(0.29)	0.10-3.86	0.54(0.89)

bb, blebby; ds, disseminated; ms, massive; mx, matrix; rm, rembolized; sm, semi-massive; Numbers in parantheses are standard deviations

intrusions (e.g. Lynn Lake, Manitoba; Pechenga, U.S.S.R; Fig. 57.12). The Burnt Nubble and the Big Indian Pond sulphide occurrences of the Moxie intrusion (Maine) are similar to St Stephen sulphides in their Cu/(Cu + Ni) ratios. The Black Narrows sulphide occurrence of the Moxie intrusion with higher Ni and Cu tenors, however, has lower Cu/(Cu + Ni) ratios. Another occurrence in a similar tectonic setting, the Bruvann deposit of the Rana intrusion (Norway) also has lower Cu/(Cu + Ni) ratios. An average Cu/(Cu + Ni) ratio of the Sudbury deposits, 0.5 (Pattison, 1979), and a range (0.44-0.53), given by Cabri and Naldrett (1984), are similar to the remobilized and disseminated ores of the St Stephen intrusion, but smaller than the massive and matrix sulphides.

Pt, Pd, and Au contents of fifty-five samples containing varying amounts of sulphides are presented in Table 57.4. Pt and Pd abundances in various ore types are shown graphically on Figure 57.14. It is seen that there is considerable scatter in the Pt and Pd abundances of the St Stephen sulphides. This scatter may be partly due to the remobilized nature of most of the sulphides. Remobilization, however, does not seem to alter one component preferentially over the other. Despite the scatter, blebby sulphides appear to be enriched in Pt and Pd compared to matrix sulphides. According to Naldrett and Cabri (1976) and Naldrett (1981), a negative correlation exists between the Pt/(Pt + Pd) and the Cu/(Cu + Ni) ratios of Ni-Cu sulphide deposits associated with tholeiitic magmas. The St Stephen sulphides do not

Table 57.4 Ni, Cu, Pt, Pd, Au and S analyses of the sulphide-bearing samples from the St Stephen intrusion

S. No	rock	Sul	Loc	Ni	Cu	Pt	Pd	Au	S
S05235	P	mx	A	0.16	0.05	15.0	2.0	22.0	4.54
S07570	T	mx	A	0.07	0.01	10.0	2.0	11.0	1.00
S17130	P	mx	A	0.32	0.04	15.0	4.0	17.0	9.08
R01462	P frg	rm	A	0.20	0.17	15.0	10.0	23.0	12.90
S17315	M alt	sm	A	0.75	0.24	30.0	61.0	26.0	12.30
S07470	P	mx	A	0.15	0.03	10.0	4.0	10.0	2.00
S07515	P	mx	A	0.04	0.03	10.0	2.0	3.0	1.00
S17640	P	mx	A	0.29	0.40	15.0	13.0	42.0	11.40
S07450	P	mx	A	0.07	0.02	20.0	4.0	7.0	2.00
S07555	T	mx,rm	A	0.14	0.16	10.0	6.0	4.0	7.00
8.317	OG	bb	B	0.68	0.29	na	na	na	13.20
26.362		ms	C	1.90	0.02	na	na	na	29.20
S10161	MS	ms	C	1.83	0.76	45.0	17.0	16.0	37.40
B53093	OG	bb	C	0.21	0.16	15.0	5.0	7.0	2.84
B58239	M frg	sm, rm	HC	1.34	0.33	45.0	7.0	22.0	28.40
30.170		sm	HC	1.70	0.38	na	na	na	26.40
B56090	OG	rm	HC	0.73	0.34	45.0	53.0	9.0	18.60
86.207	P	mx	K	0.12	0.03	na	na	na	19.20
86.194	MS	ms	K	0.30	0.03	na	na	na	31.50
HM2715	P	mx	K	0.03	0.01	10.0	2.0	16.0	1.00
HM2545	P	mx	K	0.09	0.01	5.0	5.0	10.0	5.00
R86140	P	mx	K	0.01	0.01	15.0	4.0	5.0	4.45
HM2720	P	mx	K	0.07	0.01	100.0	2.0	52.0	1.00
R85122		sm, rm	K	0.17	0.06	30.0	20.0	23.0	29.00
12.3	OGpeg	ds	N	0.00	0.00	41.0	8.0	10.0	0.01
A5.3	P	mx	P	0.22	0.18	40.0	8.0	41.0	0.66
B48283	MS	ms	RF	0.87	0.15	45.0	6.0	11.0	32.50
B48220	OG	bb	RF	0.21	1.65	114.0	30.0	34.0	8.85
B37204	MS	ms	RF	1.10	0.15	5.0	19.0	13.0	37.00
B37203	M alt	sm, rm	RF	0.51	3.90	5.0	67.0	20.0	21.00
B36254	M alt	rm	RF	0.12	3.86	188.0	24.0	63.0	7.70
B36327	M alt	bb, sm	RF	0.58	0.16	15.0	21.0	33.0	20.70
B35537	OG	bb	RF	0.49	0.38	5.0	24.0	23.0	15.00
112-3	G	sm	Rf	1.50	1.00	na	na	na	23.30
209-49		sm	RF	1.00	0.40	na	na	na	33.80
65-198	G		RF	0.91	0.29	na	na	na	29.00
65-199	OG	bb	RF	1.00	0.07	na	na	na	26.00
B35534		ms	RF	1.20	0.06	6.0	7.0	23.0	42.00
15.2	P	mx	S	0.17	0.03	5.0	8.0	13.0	8.00
20	T	bb	T	0.04	0.07	na	na	na	3.33
L14.1	MS	ms	U	0.22	0.15	5.0	42.0	9.0	41.00
D5.5	T	bb	X	0.01	nd	na	na	na	0.01

Pt, Pd and Au analyses in ppb; Cu, Ni and s analyses in wt%. Abbreviations: G: gabbro; M: mafic; MS: massive sulphide; N: norite; OG: olivine gabbro; P: peridotite; PT: picritic troctolite; T: troctolite; alt: altered; frg: fragments; peg: pegmatitic; na: not analyzed; nd: not detected; Refer to Table 57.3 for others.

seem to follow this relationship (Fig. 57.15). Some samples cluster near the one end of the tholeiitic trend, displaying dissimilarity to flood basalt-related deposits and, to a certain extent, to those of Sudbury on the one hand, and similarity to the Pechenga and Merensky (Bushveld) ores on the other. It appears that the variation in the Pt/(Pt + Pd) ratio of the St Stephen material is not dependent on the textural type. However, this may have been greatly complicated by mobilization. For example, some samples containing only minor amounts of remobilized sulphides show high Pt/(Pt + Pd) and/or Cu/(Cu + Ni) ratios.

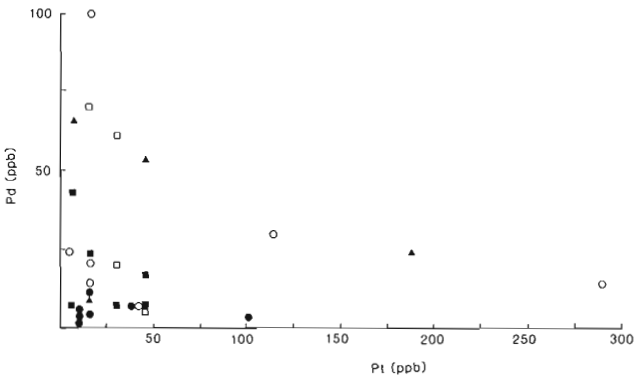


Figure 57.14. Pt vs Pd plot of sulphides representing various ore types. Refer to Figure 57.12 for symbols.

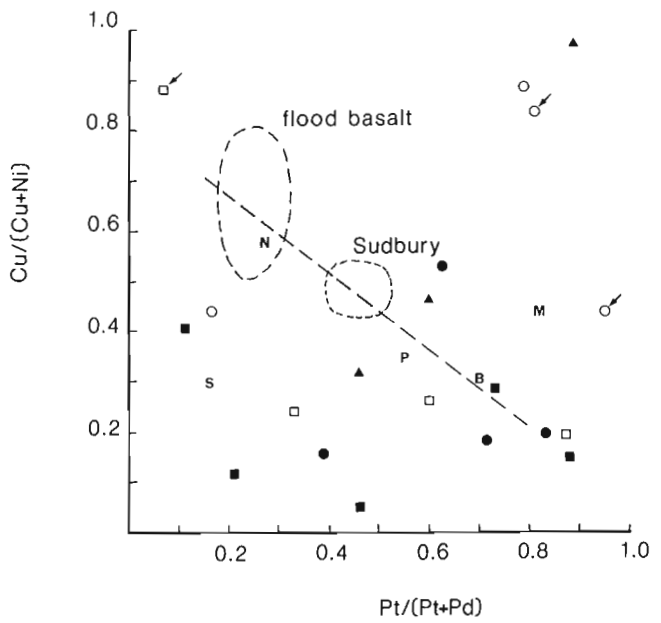


Figure 57.15. Pt/(Pt + Pd) vs Cu/(Cu + Ni) plot for sulphides representing various ore types. Refer to Figure 57.12 for symbols. Additional symbols: B, Merensky-Bushveld; M, Moxie; N, Noril'sk; P, Pechenga; S, Stillwater. Arrow-heads point to samples containing minor amounts of remobilized sulphides. Data from various other Ni-Cu sulphide deposits (Naldrett 1981, Cabri and Naldrett, 1984) and the tholeiitic trend (Naldrett and Cabri 1976) are shown for comparison.

ORIGIN OF SULPHUR

Low metal (Ni and Cu) to sulphur ratios and the pyrrhotite-rich nature of the sulphides suggest the possibility of addition of sulphur to the magma from an external source. The presence of abundant sedimentary rock fragments in the intrusion provide textural evidence that they have been incorporated into the magma (Paktunc, 1986). Localization of the "C" zone bodies near the sedimentary roof pendant (Fig. 57.10), and occurrence of the Rogers Farm and Hall-Carroll zones close to the margin of the intrusion suggest that the sulphides of the adjacent Cookson Formation were the source of sulphur. This interpretation is also supported by the sulphur isotope and the Se/S ratios of the sulphides (Paktunc et al., 1986).

If country rock assimilation took place, it would have had the effect of promoting the separation of sulphides from the basaltic magma by increasing oxygen fugacity, and SiO_2, Al_2O_3 and K_2O activities in addition to an increasing the sulphur fugacity.

Presence of matrix sulphides in the peridotitic rocks suggests early segregation of sulphides. Nickel depletion in olivines near the peridotite-picritic troctolite transition suggests that sulphide saturation was achieved following formation and accumulation of olivines. These sulphides with the exception of some from the "A" zone, represent the most likely example of mantle-derived sulphur or those that are the least modified by crustal contamination. Their low metal to sulphur ratios can be explained by an early segregation of olivine and sulphide. For example, segregation of an olivine-sulphide mixture with olivine/sulphide ratio of 10, can significantly deplete the magma in Ni and Cu (Duke, 1979). Blebby sulphides occurring in troctolitic and gabbroic rocks did not seem to segregate significantly following their formation as immiscible blebs. Alternatively, they might represent late segregation of sulphides. Following their solidification, sulphides were mobilized into low stress regimes such as shear zones and cleavage planes. This is especially apparent in the case of chalcopyrite which shows preferential mobilization. Subsolidus mobilization and redeposition of magmatic sulphides seem a reasonable explanation for the formation of massive and semi-massive ores containing abundant fragments. It is believed that the mobilization event corresponds to the Acadian orogenic deformation that affected the intrusion (Paktunc, 1986).

ACKNOWLEDGMENTS

The author is grateful to O.R. Eckstrand for helpful discussions throughout the project. Review of the manuscript by J.M. Duke, O.R. Eckstrand and W. D. Sinclair is acknowledged.

REFERENCES:

Boyd, R. and Mathiesen, C.O.
1979: The nickel mineralization of the Rana mafic intrusion, Nordland, Norway; Canadian Mineralogist, v. 17, p. 287-298.

Cabri, L.J. and Naldrett, A.J.
1984 The nature of the distribution and concentration of platinum-group elements in various geological environments; Proceedings of the 27th International Geological Congress, v. 10, p. 17-46. VNU Science Press.

Duke, J.M.
1979: Computer simulation of the fractionation of olivine and sulfide from mafic and ultramafic magmas; Canadian Mineralogist, v. 17, p. 507-514.

Eckstrand, O.R.
1980: Systematic Ni:Cu variations in nickel sulfide deposits; Geological Association of Canada-Mineralogical Association of Canada Joint Annual Meeting, Program with abstracts p. 20 (abstract).

Gorbunov, G.I.
1968: Geology and origin of the copper-nickel sulfide ore deposits of Pechenga (Petsamo); Nedra Press, Moscow, USSR (in Russian) 352 p.

Hoffman, E.L., Naldrett, A.J., van Loon, J.C., Hancock, R.G.V., and Manson, A.
1978: The determination of all the platinum-group elements and gold in rocks and ores by neutron activation analysis after preconcentration by a nickel sulphide fire-assay technique on large samples; Analytica Chimica Acta, v. 102, p. 157-166.

Irvine, T.N.
1982: Terminology for layered intrusions; Journal of Petrology, v. 23, p. 127-162.

Naldrett, A.J.
1981: Nickel sulfide deposits: classification, composition and genesis; Economic Geology, 75th Anniversary Volume, p.628-685.

Naldrett, A.J. and Cabri, L.J.
1976: Ultramafic and related mafic rocks: their classification and genesis with special reference to the concentration of nickel sulfides and platinum-group elements; Economic Geology, v. 71, p. 1131-1158.

Paktunc, A.D.
1986: St Stephen mafic-ultramafic intrusion and related nickel-copper deposits, New Brunswick. in Current Research, Part A Geological Survey of Canada, Paper 86-1A, p. 327-331

Paktunc, A.D., Eckstrand, O.R., and Simpson, P.R.,
1986: Nickel-copper deposits of the St Stephen intrusion: sulphur isotope and Se/S relations. Geological Association of Canada-Mineralogical Association of Canada. Joint Annual meeting, Ottawa, p. 111 (abstract).

Pattison, E.F.
1979: The Sudbury sublayer; Canadian Mineralogist, v.17, p. 257-274.

Pinsent, R.H.
1980: Nickel-copper mineralization in the Lynn Lake gabbro; Manitoba Department of Energy and Mines, Mineral Resources Division, Economic Geology Report ER79-3, 138 p.

Ruitenberg, A.A and Ludman, A.
1978: Stratigraphy and tectonic setting of early Paleozoic sedimentary rocks of the Wirral-Big Lake area, southwestern New Brunswick and southeastern Maine; Canadian Journal of Earth Science, v. 15, p. 22-32.

Thompson, J.F.H.
1982: The intrusion and crystallization of gabbros, central Maine and genesis of their associated sulfides; unpublished Ph. D thesis, University of Toronto, 353 p.

Wilson, H.D.B. and Anderson, D.T.
1959: The composition of Canadian sulfide ore deposits; Canadian Institute of Mining and Metallurgy, Bulletin, v. 62, p. 327-339.

Geology in the vicinity of the Lime Hill zinc occurrence, southwestern Cape Breton Island, Nova Scotia[1]

Project 860008

Mario F. Justino[2] and Alan L. Sangster
Mineral Resources Division

Justino, M.F. and Sangster, A.L., Geology in the vicinity of the Lime Hill zinc occurrence, southwestern Cape Breton Island, Nova Scotia; in Current Research, Part A, Geological Survey of Canada, Paper 87-1A, p. 555-561, 1987.

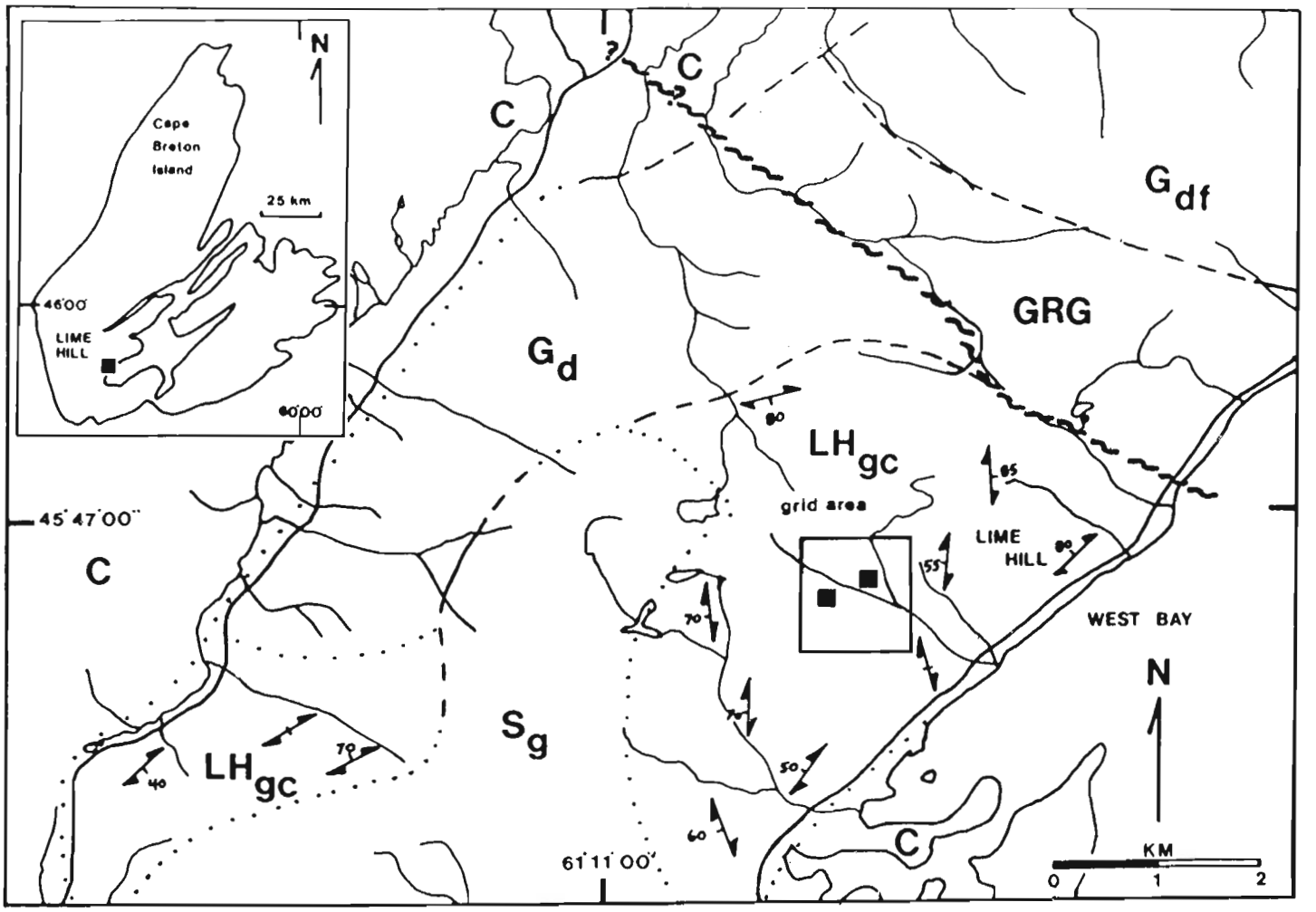
Abstract

Mapping at Lime Hill, Cape Breton, Nova Scotia has defined the presence of a gneissic complex which is distinct from adjacent, Hadrynian George River Group metasediments with which the Lime Hill rocks are normally correlated. The distinction is based on differences in metamorphic grade, texture, lithology, occurrence of intrusive phases and magnetic signature. The gneissic complex may be either an uplifted block of George River Group from a deeper structural level or a faulted-in segment of pre-George River basement of uncertain age.

Résumé

Les travaux de cartographie entrepris à Lime Hill, au Cap-Breton, en Nouvelle-Écosse, ont permis d'établir la présence d'un complexe gneissique distinct des métasédiments contingus du groupe hadrynien de George River avec lesquels les roches de Lime Hill sont normalement mises en corrélation. La distinction se fonde sur les différents degrés de métamorphisme, sur la texture, sur la lithologie, sur la présence de phases intrusives et sur la signature magnétique. Le complexe gneissique pourrait être un bloc du groupe de George River qui aurait été soulevé d'un niveau structural plus profond, ou encore, pourrait-il s'agir d'un segment de socle d'âge incertain mis en place par le mouvement d'une faille avant l'accumulation du groupe de George River.

[1]Contribution to the Canada-Nova Scotia Mineral Development Agreement, 1984-89. Project carried by Geological Survey of Canada.
[2]Department of Geology, Acadia University, Wolfville, Nova Scotia B0P 1X0



SYMBOLS

- Lime Hill Zn showing
- contact (defined, approximate, assumed)
- fault (approximate, assumed)
- gneissic layering (inclined, vertical)
- road

LEGEND

Carboniferous

- C sedimentary rocks of the Horton and Windsor Groups

Devonian (?) to Late Hadrynian (?) (ages unknown)

- Sg syenogranite
- Gd granodiorite
- Gdf granodiorite; weakly foliated

Precambrian (?)

- GRG George River Group; quartzite, slate, marble, metagraywacke, mafic metavol.
- LHgc Lime Hill gneissic complex; quartz-feld.-biot. gneiss (paragneiss), gneissic granite, marble (includes diorite).

Figure 58.1. Location map of Lime Hill in southwestern Cape Breton Island and geological map of area surrounding the Lime Hill zinc occurrence. The indicated grid area was mapped in detail (Fig. 58.2).

INTRODUCTION

The Lime Hill zinc showing, located in southwestern Cape Breton Island, Nova Scotia (Fig. 58.1), is an important sphalerite occurrence estimated to contain in excess of 2.0 million tons of ore grading 2.5% zinc (Chatterjee, 1977). The stratiform sphalerite mineralization is hosted by dolomitic marble. Previous workers have assigned the host rocks to the George River Group. In view of the stratigraphic implications of this type of mineralization, the objective of this study was to a) map in detail the immediate vicinity of the Lime Hill showing; b) characterize and define the extent of the country rocks which surround the mineralized marbles; and c) to determine if the mineralized carbonate rocks can be correlated with George River Group carbonates which outcrop in the region.

This study is based on field mapping and examination of a few thin sections. It is not a detailed petrographic study. The mineralization is currently the subject of a separate study by one of us (A.L.S.).

PREVIOUS WORK

The carbonate rocks of the Lime Hill showing were originally assigned to the George River Group by Fletcher (1881). This correlation was probably based on the presence of a belt of well exposed George River Group metasedimentary rocks, including abundant carbonate rocks, located approximately 3 km northeast of the Lime Hill showing. Subsequent workers, including Guernsey (1927), Kelly (1967), Milligan (1970) and Chatterjee (1980), have followed Fletcher's (1881) original assumption.

Guernsey (1927) recognized that the metasedimentary rocks at Lime Hill appeared to be more profoundly affected by intrusions than those of the George River Group that outcrop farther east. He mapped the rocks in the Lime Hill area as a mixed zone of highly metamorphosed, gneissic, George River Group metasedimentary rocks, intruded by a variety of dioritic to granitic bodies. Kelly (1967) showed the area of Lime Hill as dominantly granitoid units with numerous inclusions of George River Group. Chatterjee (1980) described the marbles in the vicinity of Lime Hill as roof pendants, of George River Group, in siliceous intrusions.

Since the late 1950s several exploration companies have mapped and extensively drilled the Lime Hill showing. Much of the core is still available and is currently stored at the Nova Scotia Department of Mines Core Library in Stellarton, Nova Scotia.

GEOLOGY OF THE LIME HILL ZINC OCCURRENCE

The area of the Lime Hill zinc showing was mapped in detail using a grid which covers an area of 1.3 km^2. The centre of the grid is located along the headwaters of MacCuspic's (McCuish) Brook at approximately 45°47'N; 61°09'W (Fig. 58.1). Numerous trenches within the grid are now overgrown; a few are still well exposed.

The geology exposed within the grid can be divided into two major lithological types: a metasedimentary suite of gneisses and marbles which are here referred to as the Lime Hill gneissic complex (Fig. 58.2), and a variety of mafic and granitic dykes and gneissic granite which intrude the metasedimentary suite.

Biotite-feldspar-quartz gneiss (unit 1)

Biotite-feldspar-quartz gneiss is the dominant rock type in the area of the grid. It is typically dark, fine-to medium-grained and well foliated with weak to moderately developed gneissic layering. Irregular, medium grained, thin, 2-10 mm, quartz-feldspar layers may form up to 10% of the rock. The foliation is highly contorted locally. The gneiss may be subdivided into two main types based on field appearance and mafic mineral content. One variety displays a whitish weathering surface and is quartz and feldspar-rich. The other type weathers a distinct rusty brown, is more biotite-rich and in places is weakly schistose. Both types of gneiss are composed of biotite, quartz, plagioclase (An $_{40\text{-}45}$), perthite, and minor amphibole and opaque minerals. Some samples contain cordierite, sillimanite, and garnet. In thin section the gneisses commonly display a granoblastic texture, and in places minor myrmekite is present. Alteration is weak, although some amphibole, cordierite and garnet have been moderately to extensively retrograded. Muscovite appears to be the most common retrograde product.

Abundant, dark green, mafic boudins occur in the more biotite-rich, rusty brown gneiss, usually where the latter outcrops in close proximity to marble. Some boudins are essentially very fine grained, extensively retrograded, amphibolite. These mafic boudins are commonly stretched and folded. Originally they may have been mafic calc-silicate layers and/or mafic dykes.

Carbonate rocks (unit 2)

The carbonate rocks of the grid area are coarsely recrystallized marbles. These can be subdivided into dolomitic marble, calcareous marble and serpentine marble. Thin calc-silicate layers occur sparsely in the marbles.

Dolomitic marble is commonly white with a pale buff weathered surface, medium to coarsely crystalline and massive. A weak foliation or layering is in places produced by disseminated serpentine or calc-silicate layers. This unit is composed of dolomite and minor, usually $< 5\%$, disseminated diopside or olivine, serpentine, phlogopite, $\pm$ pyrite. Dolomitic marble is the principal host for the sphalerite mineralization which occurs as thin, 1-5 cm, parallel bands of heavily disseminated sphalerite grains within the carbonate matrix.

Calcareous marble is only a minor component of the carbonate rocks in the grid area and commonly occurs as layers less than 20 m wide. Usually it is pale grey to dark bluish grey, medium grained, crystalline and locally exhibits well defined layering. It is composed essentially of calcite

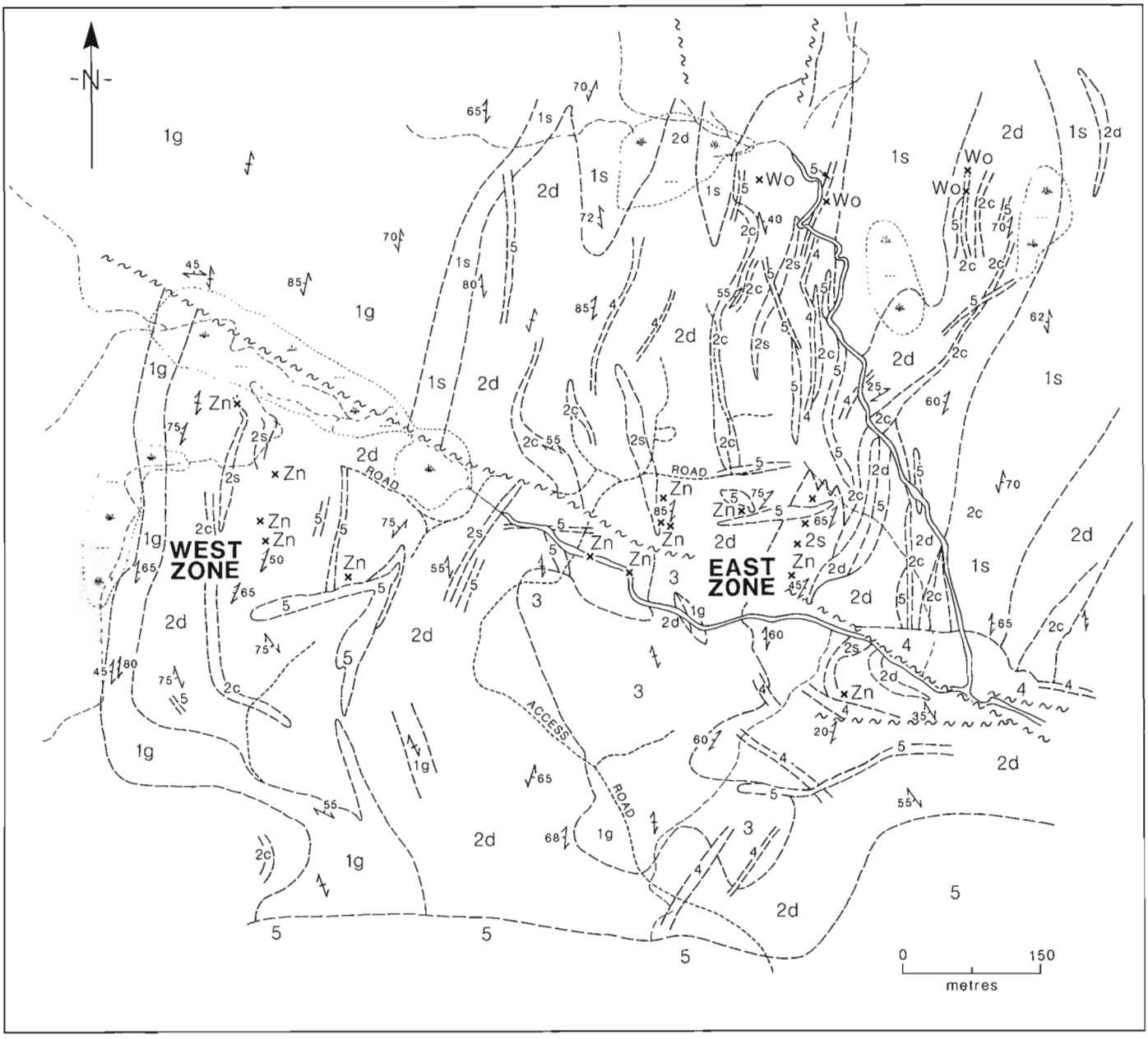


Figure 58.2. Geology of the Lime Hill Zn occurrence. Legend: 1. Biotite-quartz-feldspar gneiss (1 g) ± cordierite ± sillimanite ± garnet, (1s) more mica-rich; 2. Marble, (2a) calcareous marble, (2b) dolomitic marble, (2s) serpentine marble (<15% serpentine); 3. Granitic orthogneiss; 4. Foliated amphibolite dykes, includes some post-granite dyke diorite porphry; 5. Late granitic dykes of several ages, including white to pink biotite and/or amphibole-bearing syenite, granite, monzodiorite, leucogranite and sparse pegmatite; Wo = wollastonite; Zn = Sphalerite; $^{20}\!\!\nearrow$ = strike and dip of foliation; ~ ~ ~ = fault.

with minor amounts of diopside, phlogopite, serpentine % pyrite. There are sections of calcareous marble which contain thin layers or disseminated grains of fiberous white wollastonite. Chatterjee (1977) has identified scheelite from several drillhole sections associated with calcareous marble.

Although serpentine is a common mineral in the carbonate rocks of the map area, it is usually present in only minor amounts. The term serpentine marble is used here to defined a metamorphosed carbonate rock in which the serpentine content exceeds about 15%. Usually it occurs as thin layers in

clean marble, as thin zones surrounding fractures and as narrow aureoles beside some intrusive dykes. Wide sections of this rock type are uncommon. Serpentine marble is composed essentially of calcite, lesser dolomite and varying amounts of serpentine (> 15%), phlogopite, diopside, olivine ± pyrite. Serpentine appears to be principally derived from the retrograde alteration of diopside and olivine. Some serpentine marble appears to be spatially associated with the sphalerite mineralization, but the two are not always intimately associated.

Thin calc-silicate layers occur in the marbles. These are either pale green or white, commonly fine grained and massive to weakly layered. Some layers are essentially monomineralic diopside and, others contain varying amounts of diopside plagioclase and quartz. These calc-silicate layers for the most part appear to reflect original compositional variations. Some may have been derived by contact metasomatic processes.

Gneissic granite (unit 3)

A weakly foliated, medium grained gneissic granite intrudes and contains inclusions of the metasedimentary units. It is composed of plagioclase (andesine), quartz, biotite, perthitic microcline, amphibole and minor myrmekite. In thin section the texture is dominantly allotriomorphic. Amphibole is moderately to extensively altered to chlorite. Plagioclase has undergone weak to moderate sericitization. The foliation of the gneissic granite parallels the dominant foliation of the host metasedimentary rocks. Younger mafic and granitic dykes intrude the gneissic granite.

Granitoid intrusives (Unit 5)

The country rocks in the Lime Hill map area are intruded by a variety of tabular to irregular granitoid dykes. Most dykes exhibit a massive texture, but some are weakly to moderately lineated. They can be subdivided into at least seven varieties based on composition, texture, orientation and crosscutting relationships: white, medium-to coarse-grained, inequigranular, leucogranite; white to pink, poikiloblastic biotite granite; fine-to medium-grained, lineated biotite granite; dark pink, coarse grained, syenogranite; white, coarse grained, pegmatoidal, sphene- and diopside-bearing syenite to quartz syenite; and mesocratic hornblende-rich, equigranular, quartz diorite to quartz monzodiorite. Biotite granite forms well defined east-trending dykes that crosscut the marble-hosted sphalerite mineralization, north-trending dykes of lineated biotite granite and syenitic dykes. The pegmatoidal syenitic dykes appear to be restricted to the marbles. The details of dyke variability and composition are not shown on Figure 58.2 due to problems of scale.

Although poorly exposed, the aureoles surrounding these granitoid dykes appear to be restricted to within several centimetres of the contact. In the carbonate rocks the aureoles commonly consist of heavily disseminated pale green to yellow serpentine. Locally, massive green calc-silicates (diopside) surround and form inclusions in dykes of the coarse grained syenite.

Mafic dykes

Numerous mafic dykes occur in the map area. They vary in origin and age, but due to the difficulty in differentiating them in the field, they were mapped as a single unit. There are a number of thin, 1-2 m wide, mafic dykes or sills which parallel the country rock foliation. These are typically fine grained, dark greenish-black, hornblende-rich rocks. Some of these dykes are recrystallized amphibolite, rich in hornblende (60-70%), plagioclase, lesser quartz and minor biotite. Commonly, these dykes are intruded by an irregular stockwork of white, granitic material.

Large mafic dykes occur along the two branches of MacCuspic's Brook. Similar but smaller dykes occur sparsely in the map area. These dykes crosscut the country rock foliation and appear to parallel major fault zones. Typically, these are dark green, fine grained, locally porphyritic and consist of equal amounts of hornblende and lath-shaped plagioclase. The porphyritic variety contains medium grained, subheral to euhedral phenocrysts of both plagioclase and hornblende, in a fine grained matrix of the same composition.

Although poorly exposed away from major streams, dark greyish, mesocratic, fine grained microdiorite dykes are abundant along the major streams in the region.

METAMORPHISM

Cordierite is the most common metamorphic indicator mineral in the biotite- feldspar-quartz gneisses. Sillimanite and garnet are less common. The observed assemblages in the gneisses are indicative of at least medium grade metamorphism. In the marbles the most common metamorphic indicator minerals are diopside and olivine. Talc, tremolite, antigorite, monticellite, chondrodite, merwinite and spinel have been reported in the dolomitic marble (Chatterjee, 1980; p. 52). The presence of monticellite and merwinite indicate that a significant contact metamorphic event has affected these rocks. Wollastonite occurs at several locations in calcareous marble. Superimposed on the medium grade metamorphism is a low grade retrograde alteration. The biotite-feldspar-quartz gneiss is only weakly altered. The most common retrograde mineral is muscovite. In the marbles, diopside and olivine are moderately to extensively altered to serpentine. Phlogopite, on the other hand, tends to be unaffected. Chlorite alteration is common in some of the older mafic dykes.

Much of the retrograde alteration, and particularly the production of serpentine in the marbles, is believed to be related to aqueous fluid migration during the intrusion of the late granitic dykes.

STRUCTURE

The structure of the area is complex and not clearly understood. Scarcity of well developed fabric in the marbles makes these rocks difficult to interpret. The gneisses provide more useful information but not enough data are available for a detailed structural analysis. Figure 58.3 is a summary of the structural data measured within the grid area. At least three phases of folding have been recognized. Early folding produced mesoscopic, isoclinal, westward inclined to recumbent, shallow to gentle plunging, N- to NNE- trending folds. There is limited evidence for a second co-axial folding phase which refolded earlier minor folds into very tight isoclines. Open to tight, very steeply plunging, minor(?) folds appear to post-date the earlier fold phases.

The three most common fault trends are north-south, east-west and northwest-southeast. An apparent major fault, which trends at 290-310°, parallels the western tributary of MacCuspic's Brook. Fault zones appear to be the preferred sites for mafic dyke intrusion.

RELATION BETWEEN THE LIME HILL GNEISSIC COMPLEX AND THE GEORGE RIVER GROUP

Mapping outside the grid area has shown that the gneisses at the Lime Hill showing are more extensive than previously thought (Fig. 58.2). The gneissic complex which outcrops in the vicinity of Lime Hill covers an area of 15 km^2 and is bounded to the NE by George River Group metasedimentary rocks, to the north by massive biotite-amphibole granodiorite and to the west by coarse grained syenogranite. A similar belt of gneissic rocks is found on the other side of North Mountain, opposite Lime Hill, in the vicinity of Big Brook. These two isolated packages of gneissic rocks are separated by coarse grained syenogranite. Unlike the area of the grid, the remainder of the gneissic complex has few marble outcrops and is essentially composed of biotite-feldspar-quartz paragneiss of variable composition, granitic orthogneiss and a variety of felsic to mafic dykes. Along the major brooks on both sides of the grid area are numerous dykes of greyish, mesocratic fine grained, equigranular microdiorite to biotite granite.

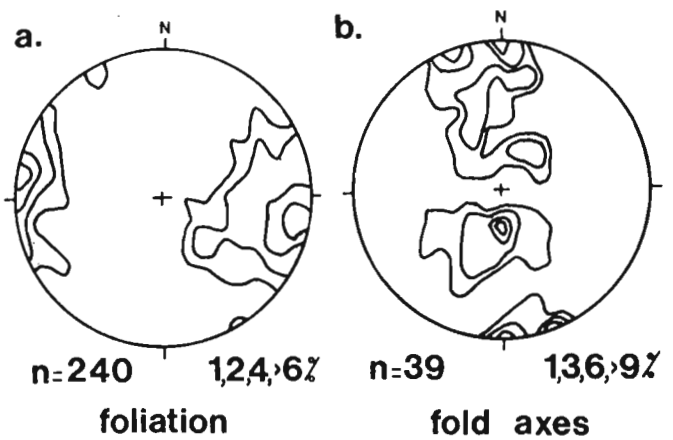


Figure 58.3. Summary of structural data within the grid area at the Lime Hill zinc occurrence; (a) is a plot of poles to foliations. (b) is a plot of fold axes. Contour intervals are indicated below the stereographic projections. n = number of data points.

Metasedimentary rocks assigned to the George River Group outcrop 3 km NE of the grid area. George River Group is a term used to describe a metasedimentary package, of probable late Precambrian age, comprised of quartzite, greywacke, slate, limestone, dolomite, minor mafic to intermediate volcanic rocks and their metamorphic equivalents (Milligan, 1970). This series of rocks is not well defined and its age, stratigraphy, structure, metamorphic history and basement rocks remain unresolved. Much of the confusion stems from the early mapping of Cape Breton Island in which all unfossiliferous metasedimentary rocks that contained crystalline limestone were included in the George River Group (Kelly, 1967).

The George River Group has been reported to include medium-to high-grade gneisses in the Cape Breton Highlands (Milligan, 1970). Recent mapping of the latter area has shown that previous correlations of these gneisses, as well as other metasedimentary units, with the George River Group is tenuous at best (Barr *et al.*, 1985).

The George River Group rocks exposed northeast of the Lime Hill area consist of very fine grained to crystalline limestone and dolomite or marble, metagreywacke, quartzite, slate to phyllites, and mafic metavolcanics. Metamorphic grade is in the greenschist facies. Although complexly folded, fine sedimentary layering is locally well preserved. Granodiorite plutons surround and contain inclusions of George River rocks; however, few intrusions occur within the George River package itself.

The gneissic complex and the George River Group are bounded by a major fault zone that trends at about 315°. The fault can be traced as a major topographic and aeromagnetic feature. Across their faulted contact, the George River Group and the Lime Hill gneissic complex exhibit sharp contrasts in metamorphic grade, texture, lithologies and intrusive phases (Table 58.1). Fine grained dolomitic marble or weakly recrystallized dolomite and finely layered slate of the George River Group contrasts sharply with coarse crystalline marble and rocks of the gneissic complex.

The absolute age relationship between these two sets of rocks is unknown. The gneissic complex could represent a deeper, more highly metamorphosed (perhaps by abundant intrusions), less carbonate-rich sequence of the George River Group stratigraphy. Alternatively, the gneissic complex may represent an uplifted, fault-bounded basement to the lower grade George River Group metasediments. In either case the Lime Hill gneissic complex is distinct from what is commonly referred to as the George River Group and the weight of evidence supports the interpretation that the gneisses are in fact basement to the George River.

Table 58.1 Contrasting characteristics of the Lime Hill gneissic complex and the George River Group

Characteristic	Gneissic Complex	George River Group
Metamorphic grade	Medium grade, locally transitional to high grade (?)	Low grade
	weak to moderately developed gneissic layering	Locally well preserved sedimentary layering
Lithologies	dominantly biot-feld-qtz paragneisses and minor marble	Abundant dolomite, limestone or marble, quartzite, slate, metagreywacke, minor mafic metavolcanics
Intrusive dykes	dioritic to granitic dykes	few intrusive dykes
Aeromagnetic	tight contours, high values	Open contours, low to moderate values

CONCLUSIONS

The Lime Hill zinc showing is an important base metal occurrence. The stratiform sphalerite mineralization is hosted by coarse crystalline dolomitic marble. The host rock dolomitic marble is part of the gneissic complex which includes abundant biotite-feldspar-quartz gneisses of apparent metasedimentary origin, orthogneiss and common intrusive dioritic to granitic dykes. Marble forms a minor part of the gneissic complex.

The rocks of the gneissic complex have been metamorphosed to at least medium grade and may possibly have reached high grade. Several phases of deformation have produced dominantly isoclinal gently to steeply plunging folds which have been shown to concentrate zinc mineralization (Sangster et al., 1985).

Previous correlations between the Lime Hill marbles and carbonates of the George River Group appear to be inappropriate. This has important implications for further exploration for carbonate-hosted base metal deposits similar to Lime Hill. George River Group carbonates do not appear to be host for such mineralization in the Lime Hill area.

Questions as to the extent of marble in the gneissic complex are unresolved. At the Lime Hill prospect, both the granite dykes and the gneissic rocks weather higher than the marble which is poorly exposed, and unrecognized zinc-bearing marble could be present elsewhere in the gneisses.

ACKNOWLEDGMENTS

We acknowledge, with thanks, discussions with Sandra M. Barr and Robert P. Raeside. Their comments improved an early version of this manuscript. We thank Mr. and Mrs. Robert Campbell of Malagawatch and Mr. and Mrs. MacDonald of Lime Hill for their warm and friendly hospitality during our stay in Cape Breton. W.A. (Sandy) Sears provided capable field assistance. We also thank Richard C.J. Edwards of Bluestack Resources Limited and C.W. Pegg, Consulting Geologist, for their interest and assistance in the project.

REFERENCES

Barr, S.M., Raeside, R.P., and MacDonald, A.S.
1985: Geology of the southeastern Cape Breton Highlands, Nova Scotia; in Current Research, Part B, Geological Survey of Canada, Paper 85-1B, p. 103-109.

Chatterjee, A.K.
1977: Tungsten mineralization in the carbonate rocks of the George River Group, Cape Breton Island, Nova Scotial; Nova Scotia Department of Mines, Paper 77-7.
1980: Mineralization and associated wall rock alteration in the George River Group, Cape Breton Island, Nova Scotia; unpublished Ph. D. thesis, Dalhousie University, Halifax, 197 p.

Fletcher, H.
1881: Report on Surveys in Richmond, Inverness, Guysborough, and Antigonish Counties, Nova Scotia; Geological Survey of Canada Report of Progress 1879-80, pt. F, 125 p.

Guernsey, T.D.
1928: The geology of North Mountain, Cape Breton Island; Geological Survey of Canada, Summary Report, 1927, Part C.

Kelly, D.G.
1967: Baddeck and Whycocomagh map-areas; Geological Survey of Canada, Memoir 351.

Milligan, G.C.
1970: Geology of the George River Series, Cape Breton; Province of Nova Scotia, Department of Mines, Memoir 7.

Sangster, A.L., Inglis, E.O., and Jones, K.
1985: Geology of the Number 9 Trench, Lime Hill prospect, Nova Scotia; in Program and summaries, ninth annual open house and review of activities; Nova Scotia Department of Mines and Energy, Information Circular no. 9, p. 133-134.

Granulite facies mylonites: a brief structural reconnaissance north of Stony Rapids, northern Saskatchewan

Project 830008

S.K. Hanmer
Lithosphere and Canadian Shield Division

Hanmer, S.K., Granulite facies mylonites: a brief structural reconnaissance north of Stony Rapids, northern Saskatchewan; in Current Research, Part A, Geological Survey of Canada, Paper 87-1A, p. 563-572. 1987.

Abstract

Brief reconnaissance in the Tantato domain, northern Saskatchewan, indicates the existence of extensive steeply dipping mafic to granitic granulite facies mylonites associated with a shallowly plunging extension lineation. The southern part of the Domain comprises a thick sheet of granulite facies mafic gneiss, whose internal concordant foliation dips gently southward with a dip-parallel extension lineation.

Résumé

Une brève étude de la structure du domaine Tantato, en Saskatchewan du Nord, a révélé l'existence d'une zone importante de mylonites, dont la composition passe du gabbro au granite, métamorphisées en faciès granulitique. Ces mylonites portent une linéation d'étirement sub-horizontale sur une foliation redressée. La partie méridionale du domaine comprend un lambeau pluri-kilométrique de gneiss mafique granulitique, dont la foliation, faiblement pentée vers le sud, porte une linéation d'étirement orientée selon la direction du pendage.

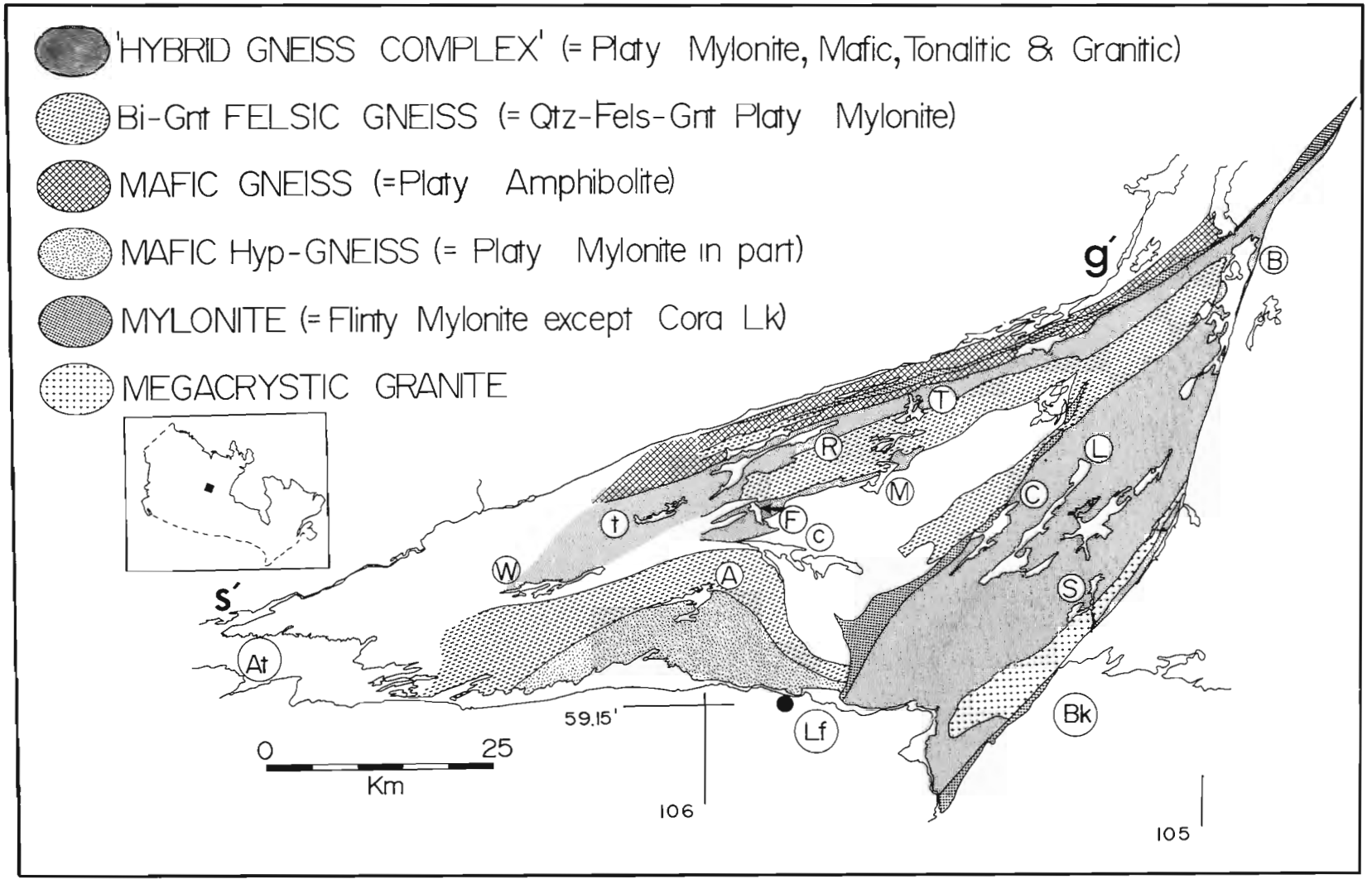


Figure 59.1. Geological sketch map of the main lithological subdivisions of the Tantato domain (after Colborne, 1962; Colborne and Rosenberger, 1963; Gilboy, 1980a,b). Captalized legend is after Gilboy. Legend in parentheses is a tentative extrapolation from structural reconnaissance on foot at Bompas (B) and Tantato (T) lakes and spot landings at Square (S), Lytle (L), Cora (C), Clut (c), Mary (M), Fenuick (F), Reeve (R), Turnbull (t), Wylie (W) and Axis (A) lakes plus Fond du Lac River (Lf). S'g' is Straight – Grease rivers. (At) is Lake Athabasca, (BK) is Black Lake. Dot is Stony Rapids. Inset is location map.

INTRODUCTION

A two week reconnaissance of the structural geology of the Tantato domain (Gilboy, 1980a; Gilboy and Ramaekers, 1981) in northern Saskatchewan has revealed the existence of extensive granulite facies mylonites (Fig. 59.1). The triangular shaped Tantato domain lies on the north side of the Athabasca Basin. It is separated in the west from the Dodge domain by the Grease and the Straight rivers and in the east from the Mudjatik domain by Black and Bompas lakes (Fig. 59.1: *see* Gilboy and Ramaekers, 1981). Pertinent previous work includes early 1:63 360 scale mapping by Johnston (1960, 1961, 1962, 1963, 1964), Colborne (1960, 1961, 1962), Colborne and Rosenberger (1963) and later mapping and compilation at 1:250 000 scale (Gilboy, 1980a). These workers recognized a narrow, fine grained, mylonite zone along the Straight and Grease rivers (Grease River shear zone) and a similar mylonite zone along the western shore of Black Lake (Black Lake shear zone) passing northwards along strike into an un-named fault. To the south, they recognized an extensive southward dipping sheet of "norite", which Gilboy (1980a) refered to as "hypersthene-bearing gneisses". These three elements comprise the geological boundaries of the Tantato domain.

My preliminary observations suggest that: (1) Much of the Tantato domain is underlain by steeply dipping granulite facies mylonite of mafic to quartzo-feldspathic composition. Foliation is vertical with a horizontal extension lineation in the west and steeply westward dipping with an oblique southwestward pitching lineation in the east. (2) The south margin of the Tantato domain comprises a shallowly southward dipping sheet of granulite facies mafic gneiss underlain by high grade ultramylonite. Mafic gneiss and ultramylonite both carry a south plunging extension lineation. (3) Shear sense criteria indicate penetrative dextral transcurrent shear in the west. A sinistral sense of shear is tentatively suggested by poorly developed and locally contradictory shear sense criteria in the east. (4) The Black Lake low grade mylonites appear continuous along the east side of the Tantato domain.

PREVIOUS WORK

To briefly summarize the above cited authors, the major lithological subdivisions of the triangular Tantato domain are as follows (Fig. 59.1).

(1) A "Hybrid Gneiss Complex" essentially composed of interlayered felsic and amphibolite gneiss of volcaniclastic origin, underlying the eastern and western parts of the area (*see* Fig. 59.3A-D, 59.4 and 59.5A-C).

(2) Felsic and mafic metavolcanics underlying the northwestern part of the area.

(3) A biotite – garnet felsic paragneiss forming a discontinuous "moat" inboard of 1 and 2 (*see* Fig. 59.3E-F).

(4) A "core" of metasediments (meta – arkose, greywacke and pelite).

(5) Norite underlying the north shore of Fond du Lac (*see* Fig. 59.5D).

Gilboy (1980a) gave non genetic names to 2 and 3, but clearly stated that the rocks of the Tantato domain appear to be largely volcaniclastic in origin (Gilboy and Ramaekers, 1981).

My reconnaissance, comprising foot traverses around Tantato and Bompas lakes supplemented by fixed wing supported visits to outcrops of the main lithological units previously mentioned, results in the following preliminary observations, presented in the form of extended legends to Figures 59.2A and 59.2B and as brief notes.

BOMPAS LAKE

Flinty mylonite: aphanitic, splinters readily, poorly developed fissility and lacking visible ribbon structure. Generally pinkish grey, apparently of granitic composition. Forms narrow zones, a few hundred metres wide.

Platy mylonite: fissile or slabby with good ribbon structure. Granitic composition. Forms narrow zone 500 m wide.

Platy amphibolite: fine fissile to slabby, very straight garnetiferous amphibolite with fine plagioclase – hornblende lamination. Contains concordant sheets of rarely garnetiferous quartz ribbon mylonite of leucogranite composition. From the size (several centimetres) of the relict porphyroclasts, these sheets are derived from pegmatites.

Straight "zebra" gneiss: (Fig. 59.3B) a straight gneiss (*see* Davidson et al., 1982) composed of rectilinear homogeneous amphibolite layers alternating with layers of tonalitic, granitic or nondescript quartz – feldspar – biotite material. Layers are centimetres to metres in thickness. Texturally the felsic layers are either sugary (i.e. granoblastic, no ribbons) or quartz ribbon mylonites to ultramylonites, with isolated 1 cm feldspar porphyroclasts set in the finer grained (500u) matrix (Fig. 59.3C). The accurately evocative term "zebra" was first used by Gilboy (1980a).

Platy quartz-feldspar-biotite gneiss: fissile or slabby, statistically homogeneous, fine grained straight gneiss. May be garnetiferous. May be well banded with amphibolite layers. May show feldspathic streaks, visibly derived by the smearing out of recrystallized centimetre size porphyroclasts. A similar structure occurs in the interlayered amphibolites.

Biotite-garnet gneiss: medium grained, straight banded with quartz-garnet to garnetite horizons, centimetres to 10s of centimetres in thickness. Often schistose. No aluminosilicates observed. Possible paragneiss.

Granitic gneiss: essentially a catch-all lithology for granitic gneisses and foliated granite which are clearly not mylonites. The easterly outcrops are cut by flinty mylonite. The westerly outcrops may be intrusive into the biotite – garnet gneiss. The central outcrops appear to be protolith to the platy (granitic) mylonite.

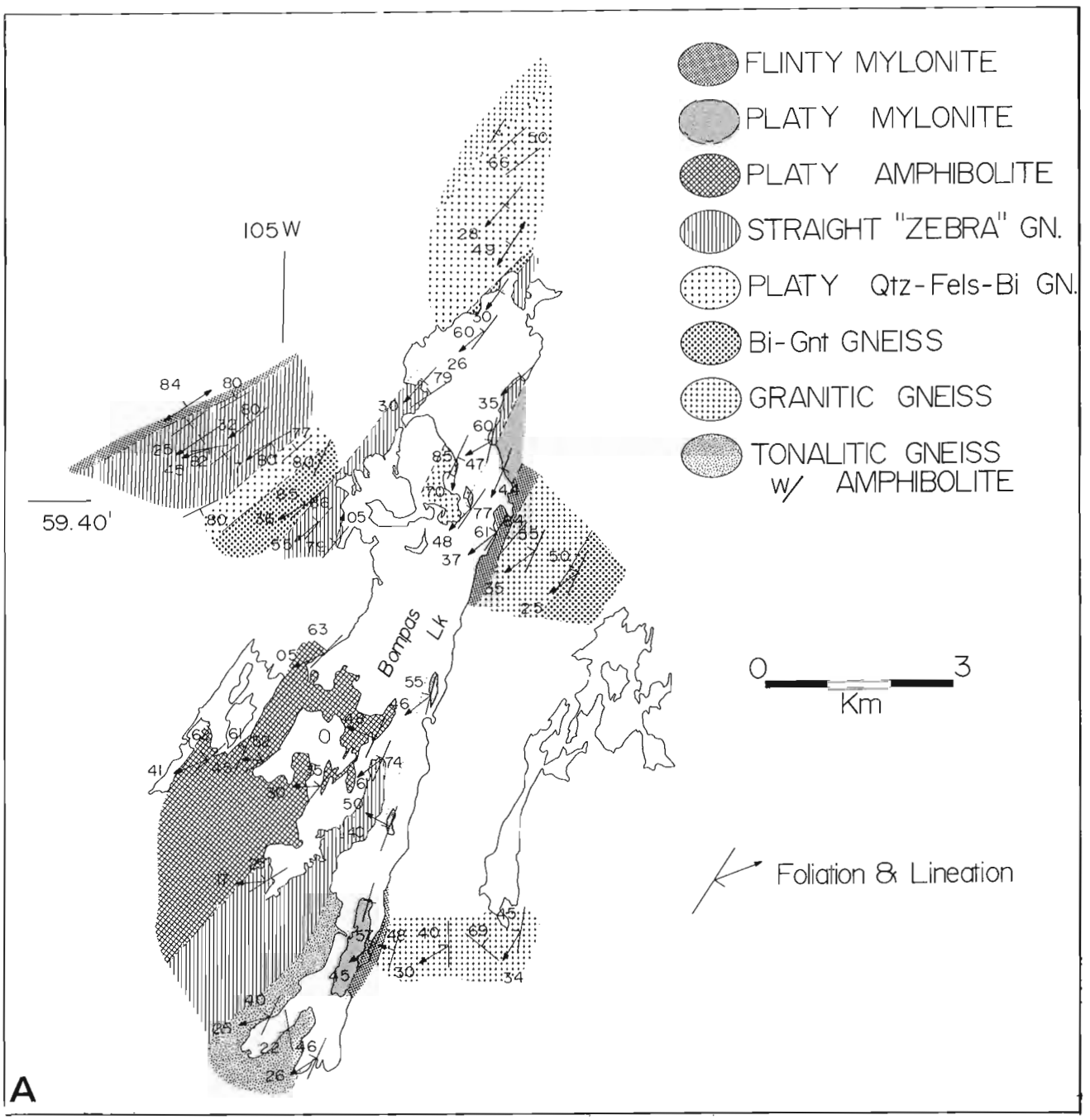
Tonalitic gneiss with amphibolite: coarse grained, well foliated tonalite with fat quartz leaves. The foliation is isoclinally folded and the folds are crosscut at a low angle by amphibolite sheets, several metres thick (Fig. 59.3A). Amphibolite

sheets are foliated and show streaked out feldspar megacrysts (ex-phenocrysts) concentrated in their centres. This irregular gneiss can be traced progressively into the adjacent straight gneiss.

TANTATO LAKE

As Bompas Lake except for the occurrence of:

Platy mafic mylonite: (Fig. 59.4) fine grained, thin polycrystalline monomineralic ribbons of ortho- or clinopyroxene and equally thin trains of cataclastically(?) drawn out garnet in a fine grained plagioclase matrix. This lithology is visibly derived by dynamic grain size reduction from meta-gabbro and -norite. Interlayered are abundant sheets, centimetres to metres thick, of tonalitic ribbon mylonite to ultramylonite and a bright green, very straight layered (centimetre thick) clinopyroxene amphibolite which occurs as concordant metric sheets within the tonalitic mylonite. Locally there are layers of pinkish grey ribbon ultramylonite of granitic composition.



Platy quartz-feldspar-garnet mylonite: (Fig. 59.3E-F) homogeneous, subtly layered platy ribbon mylonite to ultramylonite of quartz – feldspar – garnet composition. Feldspar porphyroclasts of several centimetres diameter are common. Quartz and feldspar in equal proportions. Garnet generally comprises 5 to 10% of the rock but locally thin (10s of cm) garnetite layers occur.

Meta-gabbro and meta-norite: (Fig. 59.4A-B) coarse (5 cm) grained, isotropic, generally preserving ophitic texture. The plagioclase generally forms a medium grained recrystallized matrix to both the pyroxenes and relict euhedral 2 cm plagioclase crystals. This coarse grained variety is cut by veins of micro-gabbro/norite. Long narrow inclusions of garnetite in the coarse grained facies are presumably xenoliths.

Other parts of the Tantato domain were visited by plane. The following preliminary observations were made and are presented in the context of the three sides and the centre of the triangular geometry of the Tantato Domain:

EAST SIDE

Square Lake: Near the southeastern limit of the "Hybrid Gneiss Complex" of authors. A well foliated medium grained leucogranite whose foliation is irregularly folded. The folds are cut by garnet amphibolite sheets up to 25 m thick, with both symmetrical and consistently asymmetrical plagioclase rims and tails. The sheets are heterogeneously extended, boudinaged and folded. In spite of this, if the consistently asymmetrical plagioclase tails on garnet observed in the horizontal plane are dragged pressure shadow structures, they suggest a sinistral transcurrent shear. Other mafic sheets of similar structural situation are homogeneous and garnet free. Do they comprise a separate suite? Is this assemblage a protolith to the straight gneiss along strike to the northeast?

Cora Lake: The flinty mylonite of authors is indeed a very fine grained mylonite. However, it clearly carries fresh garnet and both clinopyroxene and plagioclase polycrystalline monomineralic ribbons. This is ultramylonite derived from a coarse mafic parent rock such as a gabbro. Concordant intercalation of garnet amphibolite with centimetre size garnets results in a straight gneiss of bulk mafic composition, layered on a centimetre to decimetre scale.

WEST SIDE

Wiley and Turnbull lakes: Migmatitic gneiss of authors. A medium-fine grained, straight, platy, porphyroclastic, sugary textured garnet – biotite bearing quartzo-feldspathic gneiss.

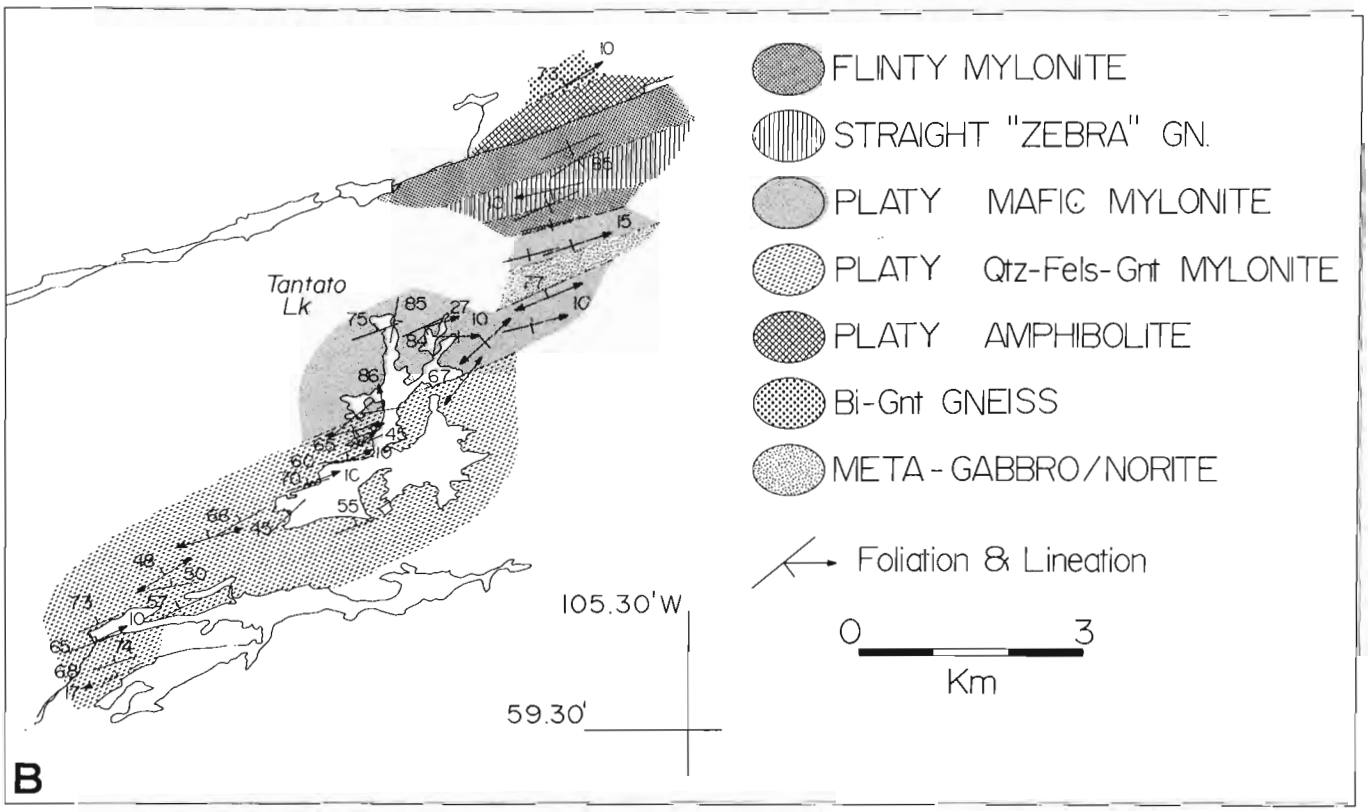


Figure 59.2. Details of foot and boat structural reconnaissance at Bompas Lake (A) and Tantato Lake (B). Extended legends given in text.

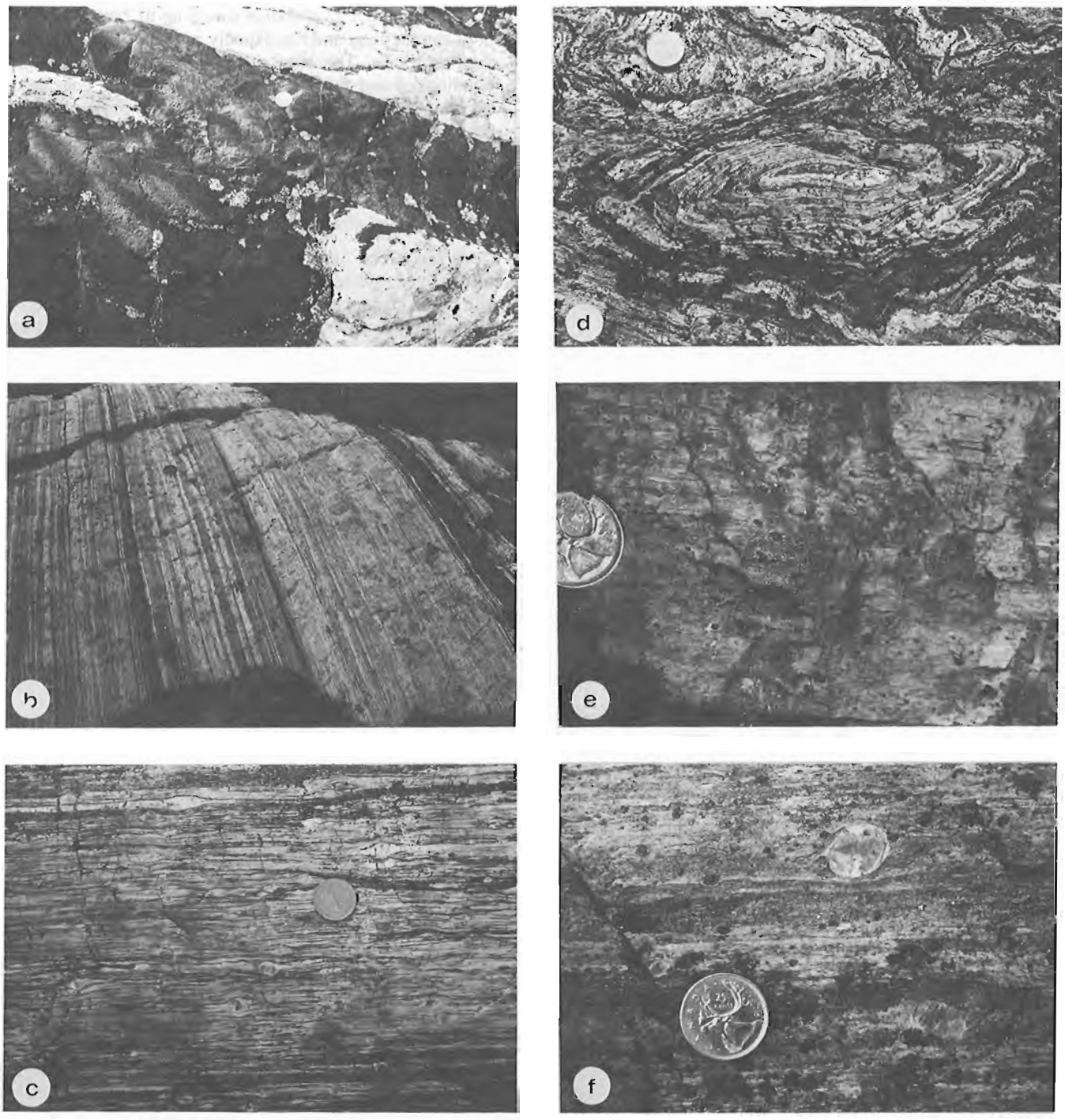


Figure 59.3. (A) White tonalitic gneiss with irregular-shaped mafic 'inclusion' crosscut by intruded amphibolite sheet. GSC 204337-R. (B) Deformed equivalent of A. The straightness of the ("zebra"-like) layering is clearly the result of transposition at high strain. GSC 204337-S. (C) Detail of the tonalitic component of B. Clearly a quartz ribbon mylonite derived from a once coarse grained rock. GSC 204337-T. (D) Further deformation of B. A sheath fold viewed along the extension lineation. GSC 204337-U. (E) Quartz-feldspar-garnet platy mylonite. Note long quartz ribbons and garnets (dark spots). GSC 204337-V. (F) As E, but with large isolated feldspar porphyroclasts. GSC 204337-W. Clearly derived from a once very coarse grained rock. A-D from Bompas Lake. E-F from Tantato Lake.

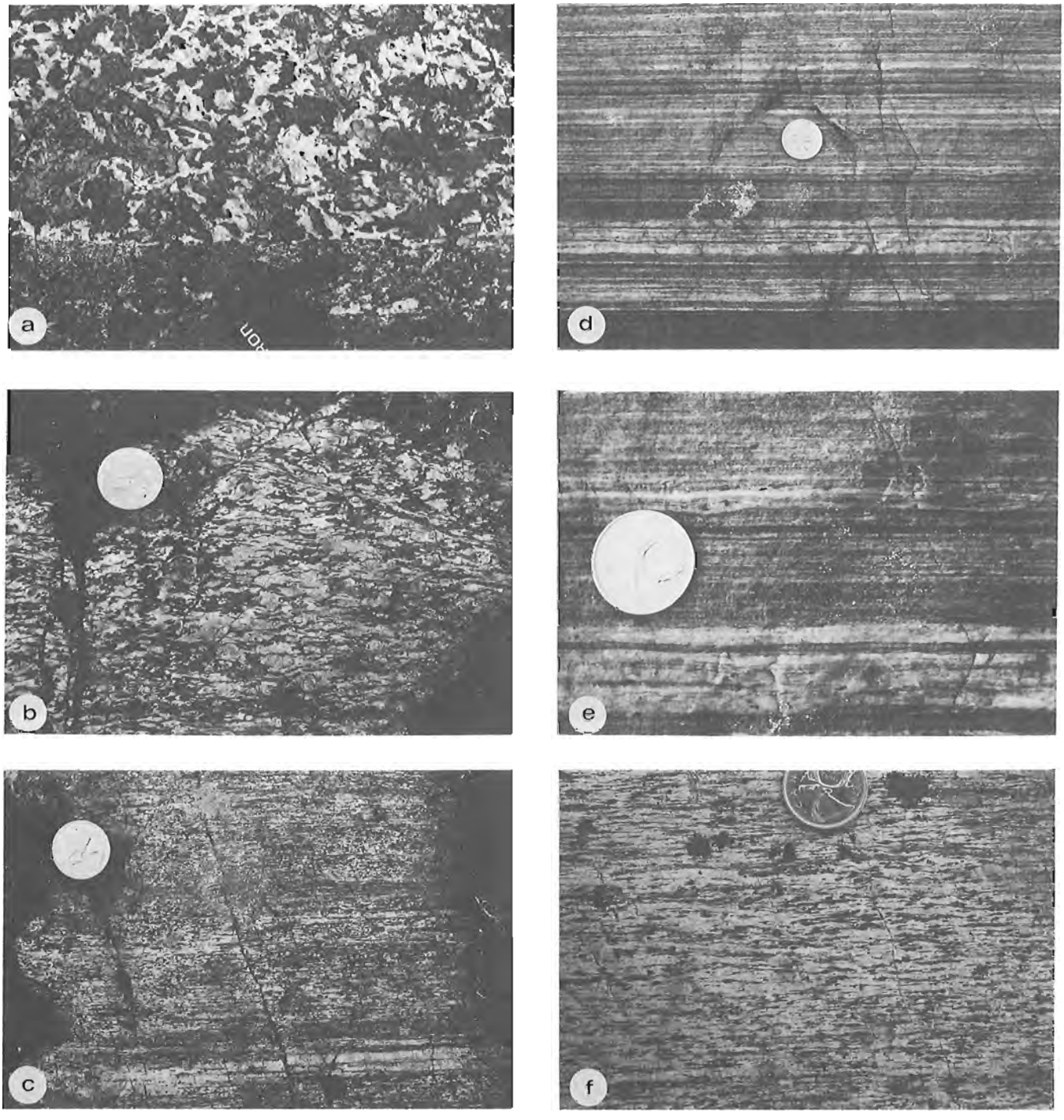


Figure 59.4. Progressive deformation of gabbro and norite, north Tantato Lake. (A) Isotropic meta-norite cut by sheet of meta-micronorite. Plagioclase matrix recrystallized. Note igneous texture preserved. GSC 204337-X. (B) Deformed meta-leucogabbro. GSC 204337-Y. (C) More deformed equivalent of (B) with thin sheets of tonalitic (white) composition (deformed veins; see Fig. 59.5). GSC 204337-Z. (D & E) Straight gneiss derived from C. Darker layers are mafic ortho- and clinopyroxene ribbon ultramylonite. Light layers are tonalitic quartz ribbon mylonite, see detail in E. GSC 204338 & GSC 204338-A. (F) Leucocratic mafic ultramylonite. Dark spots are garnet. Streaks are ortho- and clinopyroxene polycrystalline monomineralic ribbons. GSC 204338-B.

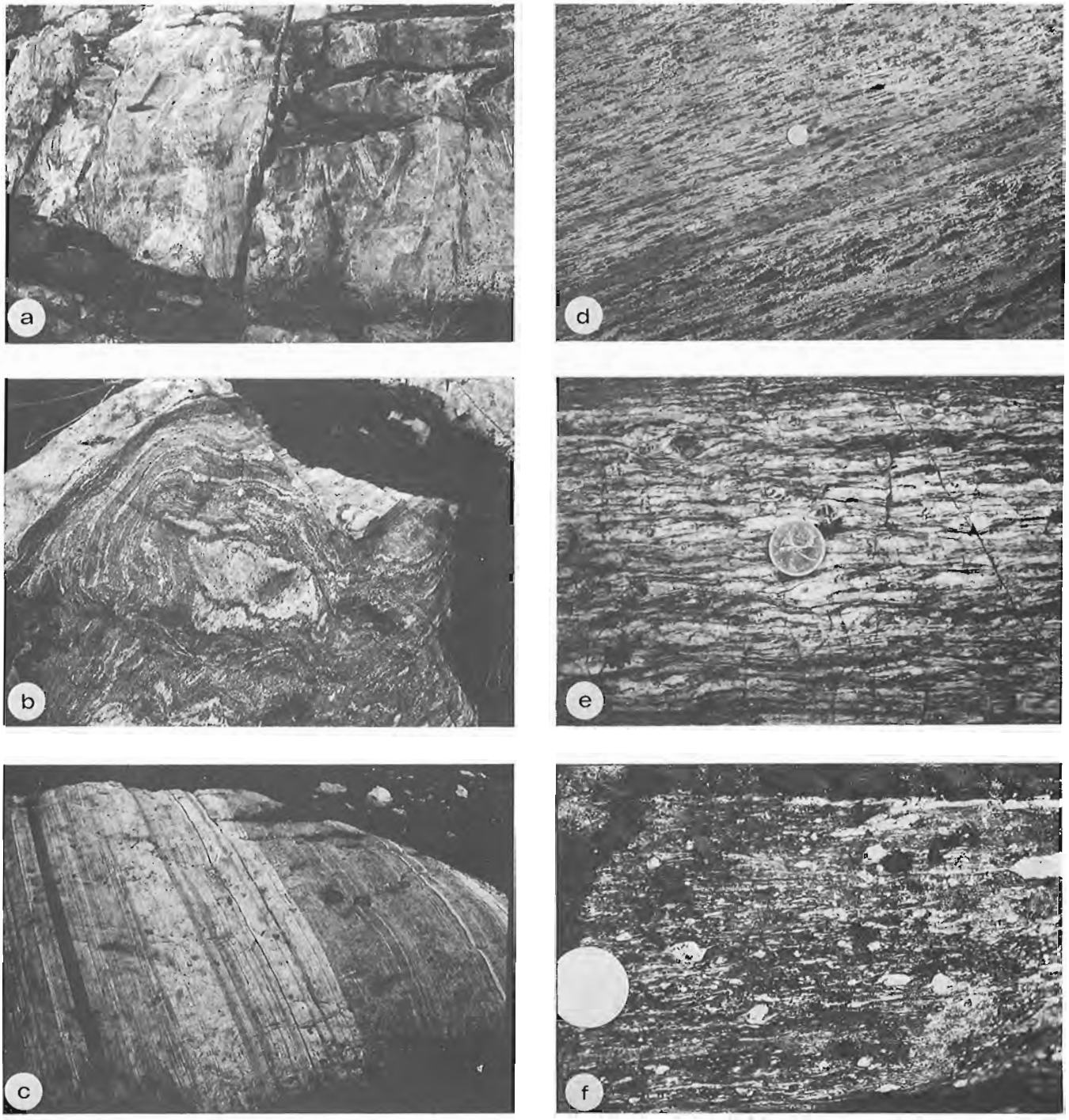


Figure 59.5. Transposition of a gneissic protolith, north Tantato Lake. (A) Folded (right) mafic gneiss (as Fig. 59.4 C-E?) crosscut by mafic dyke. Irregular, crosscutting (not shown) coarse tonalite sheets (left). GSC 204336-Y. (B) Sheath fold (tonalite rimmed by mafic gneiss) within the irregular gneiss of A. Pen parallel to extension lineation. GSC 204336-Z. (C) Transposed straight gneiss (ultramylonite) equivalent of A-B. Note dark amphibolite, light tonalite and intermediate grey mafic gneiss. GSC 204337-L. (D) Streaks of coarse garnet (lower right) and orthopyroxene in mafic hypersthene gneiss on north shore, Fond du Lac River. Light matrix is coarsely polycrystalline plagioclase. GSC 204337-O. (E & F) Shear sense indicators near Tantato Lake. Shear band foliation in quartz ribbon tonalitic mylonite in E and rotated winged feldspars in mafic mylonite in F. GSC 2043337-P & GSC 204337-Q.

The limpid, monocrystalline feldspar porphyroclasts lie isolated in the medium-fine platy matrix. Feldspathic streaks in the latter are deformed and recrystallized equivalents of the former. This rock is a sugary, platy ultramylonite.

Reeve Lake: Migmatitic gneiss of authors. Intercalated garnetiferous quartz ribbon tonalitic ultramylonite, platy plagioclase – clinopyroxene ribbon – garnet ultramylonite and ribbon ultramylonite of granitic composition. Very similar to the assemblage along strike underlying the northern half of Tantato Lake.

SOUTH SIDE

Fond du Lac; Norite of authors. (Fig. 59.5D) A coarse grained streaky plagioclase rock with steaks of orthopyroxene and streaks, clots and lenses of garnet all aligned in the foliation. Narrow (10 cm) veins of foliated very leucocratic plagioclase – orthopyroxene rock locally crosscut the streaky structure of the coarser grained host. Are such veins syntectonic? Relict igneous texture was not observed in either veins or host. A medium-coarse grained quartz – feldspar – garnet rock, compositionally similar to the platy quartz – feldspar – garnet mylonite at Tantato Lake is intercalated as mappable sheets with the mafic gneiss. It contains orthopyroxene streaks and thin (10-20 cm) concordant sheets of orthopyroxene-garnet bearing amphibolite.

Axis Lake: Norite of authors. A fine sugary plagioclase – clinopyroxene ribbon gneiss with rare pin-head size garnet. A mafic ultramylonite derived from a coarse mafic precursor.

Godfrey Bay: A prong on the south side of West Clut Lake, is underlain by an intercalation of very fine grained quartz – feldspar – garnet ultramylonite and medium-fine grained, faintly layered, well foliated, sugary plagioclase – clinopyroxene ribbon – garnet gneiss; a mafic ultramylonite very similar to that found at Tantato Lake.

CENTRE

Mary Lake: Meta-pelite or meta-arkose of authors. A medium grained quartz ribbon homoclastic protomylonite (*see* Hanmer and Lucas, 1985), apparently derived from a biotite megacrystic granite protolith, with trains of cataclastically(?) drawn out garnet.

Fenuick Lake: Garnet-hornblende gneiss of authors. A fine platy laminated plagioclase gneiss with feldspar porphyroclasts up to 2 cm and garnets, partially altered to hornblende, up to 1 cm in diameter. The lamination is essentially due to polycrystalline ribbons of plagioclase. The presence of porphyroclasts and ribbons of feldspar is strongly suggestive of derivation by mylonitization of a coarse grained mafic to intermediate precursor.

Clut Lakes: Meta-greywacke and meta-arkose of authors. The former is a fine, platy, streaky plagioclase-hornblende gneiss containing relicts of a coarse grained, locally igneous textured, mafic precursor of similar mineralogy. Feldspar porphyroclasts up to 2 cm diameter are common. Does this rock represent a more thoroughly hydrated equivalent of the Fenuick Lake material, or was it derived directly from plagioclase – hornblende meta-gabbro? The "meta-arkose" is a pink ribbon ultramylonite of granitic composition, carrying rare 1 cm feldspar porphyroclasts. It is interlayered with a grey medium grained plagioclase – hornblende rock with concordant strings of quartz – garnet ± plagioclase. This intercalation results in a straight "zebra" gneiss.

CONTEXT

The following is intended as a statement of the problem, not as a synthesis. The Tantato domain, 40 km across from Reeve Lake to Square Lake, contains a significant volume of mylonitic rocks, mylonitized at very high metamorphic grade. The triangular geometry of the Tantato domain is striking. First indications (i.e. a good assemblage of shear sense indicators (Fig. 59.5E-F): rotated winged feldspars (Hanmer, 1984), C&S fabrics (Berthé et al., 1979), shear band foliation (White et al., 1980)) are that the central part of the Domain has moved southwestward relative to the Dodge domain. On the east side, adjacent to the Mudjatik domain, both sinistral and dextral shear band foliations were observed. Sinistral shear bands would seem to be numerically dominant, but the number of observations is not statistically significant. In the less strained gneisses at Square Lake, plagioclase pressure shadows on garnets in upright NE-striking amphibolite sheets indicate a sinistral rotation. However, without regional coverage it remains to be demonstrated that these limited observations represent coeval deformation. Nevertheless, they raise the interesting possibility that the Tantato domain may have moved towards the SSW relative to the bounding Dodge and Mudjatik domains. The south side of the Tantato domain is in apparent structural discordance (i.e. overlies and truncates?) with the rest of the domain. However, the reconnaissance map pattern (Gilboy, 1980a) suggests that the eastern side gneisses may truncate those of the southern side. Once again there are no time constraints presently available. Nevertheless, it is tempting to envisage a dip-slip component of movement (either contractional or extensional) along the base of the shallow southward-dipping south side gneisses. Do the amphibolite facies mylonites at Fenuick and Clut lakes, lying beneath the south side mafic granulites, suggest inverted metamorphic zonation and northward directed overthrusting?

The low grade Straight River – Grease River and Black Lake – Bompas Lake mylonite zones rework the high grade mylonites and are later. At Bompas and Tantato lakes these mylonites are compositionally quite distinct (granitic) from the mylonites within the Tantato domain (mafic, tonalitic, garnetiferous quartzo-feldspathic).

At the broader scale, the Tantato domain lies at the apex of a large lozenge shaped area bounded by two positive aeromagnetic anomalies which pass under the Athabasca Basin into southern Saskatchewan (Geological Survey of Canada, 1982). Is the Tantato domain the confluence of two crustal scale shear zones? Are the shear zones coeval?

A detailed systematic structural mapping project is to be undertaken in the near future which will address some of the questions raised here.

ACKNOWLEDGMENTS

I was most ably assisted by Katherina Ross. Paul Hoffman and Marc St-Onge reviewed the manuscript.

REFERENCES

Berthe, D., Choukroune, P. and Jegouzo, P.
1979: Orthogneiss, mylonite and non coaxial deformation of granites: the example of the South Armorican shear zone; Journal of Structural Geology, v. 1, p. 31-42.

Colborne, G.L.
1960: The geology of the Clut Lakes area (west half), Saskatchewan; Saskatchewan Department of Mineral Resources, Report 43, 22 p.
1961: The geology of the Clut Lakes area (east half), Saskatchewan; Saskatchewan Department of Mineral Resources, Report 58, 31 p.
1962: The geology of the Wiley Lake area (east half), Saskatchewan; Saskatchewan Department of Mineral Resources, Report 69, 44 p.

Colborne, G.L. and Rosenberger, E.
1963: The geology of the Wiley Lake area (west half), Saskatchewan; Saskatchewan Department of Mineral Resources, Report 79, 29 p.

Davidson, A., Culshaw, N.G., and Nadeau, L.
1982: A tectono-metamorphic framework for part of the Grenville Province, Parry Sound region, Ontario; in Current Research, Part A, Geological Survey of Canada, Paper 82-1A, p. 175-190.

Geological Survey Of Canada
1982: Magnetic anomaly map, Lake Athabasca, no. 12-AM.

Gilboy, C.F.
1980a: Bedrock compilation geology: Stony Rapids area (NTS 74P); Saskatchewan Geological Survey, Preliminary Geological Map.
1980b: Reconnaissance bedrock geology: Chambeuil Lake East area (part of NTS 74P); Summary of Investigations 1980, Saskatchewan Geological Survey, p. 14-16.
1979: Reconnaissance bedrock geology, Stony Rapids North (part of NTS 74P); Summary of Investigations 1981, Saskatchewan Geological Survey, p. 12-18.

Gilboy, C.F. and Ramaekers, P.
1981: Compilation bedrock geology: Stony Rapids area (NTS 74P); Summary of Investigations 1981, Saskatchewan Geological Survey, p. 6-11.

Hanmer, S.
1984: The potential use of planar and elliptical structures as indicators of strain regime and kinematics of tectonic flow; in Current Research, Part B, Geological Survey of Canada, Paper 84-1B, p. 133-142.

Hanmer S. and Lucas, S.B.
1985: Anatomy of a ductile transcurrent shear: the Great Slave Lake Shear Zone, District of Mackenzie, NWT (preliminary report); in Current Research, Part B, Geological Survey of Canada, Paper 85-1B, p. 7-22.

Johnston, F.J.
1960: The geology of the Tantato Lake area, Saskatchewan; Saskatchewan Department of Mineral Resources, Report 44, 32 p.
1961: The geology of the Astrolabe Lake area (west half), Saskatchewan; Saskatchewan Department of Mineral Resources, Report 59, 26 p.
1962: The geology of the Chambeuil Lake area (west half), Saskatchewan; Saskatchewan Department of Mineral Resources, Report 68, 32 p.
1963: The geology of the Lytle Lake area (west half), Saskatchewan; Saskatchewan Department of Mineral Resources, Report 80, 20 p.
1964: The geology of the Lytle Lake area (east half), Saskatchewan; Saskatchewan Department of Mineral Resources, Report 90, 8 p.

White, S.H., Burrows, S.E., Carreras, J., Shaw, N.D., and Humphreys, F.J.
1980: On mylonites in ductile shear zones; Journal of Structural Geology, v. 2, p. 175-187.

The Late Hadrynian Jeffers Group, western Cobequid Hills, Nova Scotia[1]

DSS Contract 20ST.23233-6-0051

Georgia Pe-Piper[2]

Pe-Piper, G., The Late Hadrynian Jeffers Group, western Cobequid Hills, Nova Scotia; in Current Research, Part A, Geological Survey of Canada, Paper 87-1A, p. 573-580, 1987.

Abstract

Detailed mapping of the Late Hadrynian Jeffers Formation (Avalon Zone) has permitted its elevation to group status and subdivision into three formations: the Gilbert Hills, the Humming Brook and the Cranberry Lake. The volcanic Gilbert Hills Formation underlies and interfingers with deeper water argillite of the Humming Brook Formation and turbidite wacke and siltstone of the Cranberry Lake Formation. The Jeffers Group has a spatially inhomogeneous flat-lying cleavage, probably associated with thrust faults of Late Hadrynian age that were reactivited during the Acadian Orogeny. This thrusting, together with major strike slip faulting, has resulted in a complex distribution pattern for rocks of the Jeffers Group.

Résumé

La cartographie détaillée de la formation tardi-hadrynienne de Jeffers a permis de dorénavant compter cette dernière au nombre des «groupes» et de la subdiviser en trois formations, soit celles de Gilbert Hills, Humming Brook et Cranberry Lake. La formation volcanique de Gilbert Hills est non seulement sous-jacente, mais se mêle également, à l'argilite accumulée en eau plus profonde de la formation de Humming Brook et au wacke turbiditique et à l'aleurolite de la formation de Cranberry Lake. Le clivage horizontal et hétérogène dans l'espace du groupe de Jeffers est probablement associé aux failles de chevauchement tadir-hadryniennes qui ont été réactivées au cours de l'orgenèse acadienne. Le chevauchement, ainsi que combiné aux importants décrochements également observés, ont conféré aux roches du groupe de Jeffers un patron de répartition complexe.

[1]Contribution to the Canada–Nova Scotia Mineral Development Agreement 1984-89. Project carried by the Geological Survey of Canada, Lithosphere and Canadian Shield Division.

[2]Department of Geology, St. Mary's University, Halifax, N.S. B3H 3C3

INTRODUCTION

A series of Late Proterozoic and Paleozoic rocks outcrop north of the Cobequid Fault in the western Cobequid Hills of northern Nova Scotia (Fig. 60.1). The Cobequid Fault forms part of the Minas Geofracture (Keppie, 1982), marking the southern boundary of the Avalon zone. The principal rock units of the western part of the Cobequid Hills, in the area centred north of the town of Parrsboro (Fig. 60.2), are volcanic and sedimentary rocks of the Jeffers Formation (redefined below as the Jeffers Group), Late Hadrynian intrusions, shales of the Silurian Wilson Brook Formation, basalts and rhyolites of the Devono-Carboniferous Fountain Lake Group, and a series of Carboniferous plutons. Sedimentary rocks of the Cumberland Group (Carboniferous) onlap unconformably onto the northern margin of the Cobequid Hills (Fig. 60.1). South of the Cobequid Fault is a lowland region of Carboniferous and Triassic rocks.

The geology of the western Cobequid Hills has been recently reviewed by Donohoe and Wallace (1985) and Pe-Piper and Piper (in press). This paper summarizes the results of remapping the Jeffers Formation in the summer of 1986.

The Jeffers Formation was originally mapped by Donohoe and Wallace (1980, 1982) and defined in a type section in Jeffers Brook, north of Parrsboro, as a series of quartz metawackes and volcanic metawackes, metasiltstones, mafic volcanic rocks and minor marbles. Preliminary mapping of parts of the Jeffers Formation by Pe-Piper and Piper (1986), to support a geochemical study of the volcanic rocks, suggested that the formation was considerably more extensive and lithologically more variable than indicated by Donohoe and Wallace (1980, 1982) and that systematic remapping was required. This new work has shown that several mappable units can be distinguished within the Jeffers Formation. These mappable units (Fig. 60.2) are described below as new formations, necessitating the elevation of the Jeffers Formation to Group status.

Several major east-west trending faults (Fig. 60.2) cut the pre-Carboniferous rocks of the western Cobequid Hills (Pe-Piper and Piper, in press). The timing and sense of movement on these is poorly known and probably complex. The Cobequid Fault has a cataclastic zone several hundred metres wide and cuts large plutons of Carboniferous age, apparently with principally strike slip motion. The Kirkhill Fault appears to have been a strike slip fault at some time in its history, but the Carboniferous motion was probably mostly vertical. The Gilbert Mountain Fault (G.M.F., Fig. 60.2), separating the Jeffers Group from the Wilson Brook Formation, also shows predominantly vertical motion.

Between the Cobequid and Kirkhill faults, most of the exposed rocks are of Devono-Carboniferous age, and Jeffers Group rocks are rare. Most of the area between the Kirkhill and Gilbert Mountain faults consists of Jeffers Group and younger intrusions, with minor inliers of Fountain Lake Group. The Jeffers Group in this area includes thick quartz wackes previously mapped as Wilson Brook Formation by Donohoe and Wallace (1982); their identification as Jeffers Group is discussed by Pe-Piper and Piper (in press).

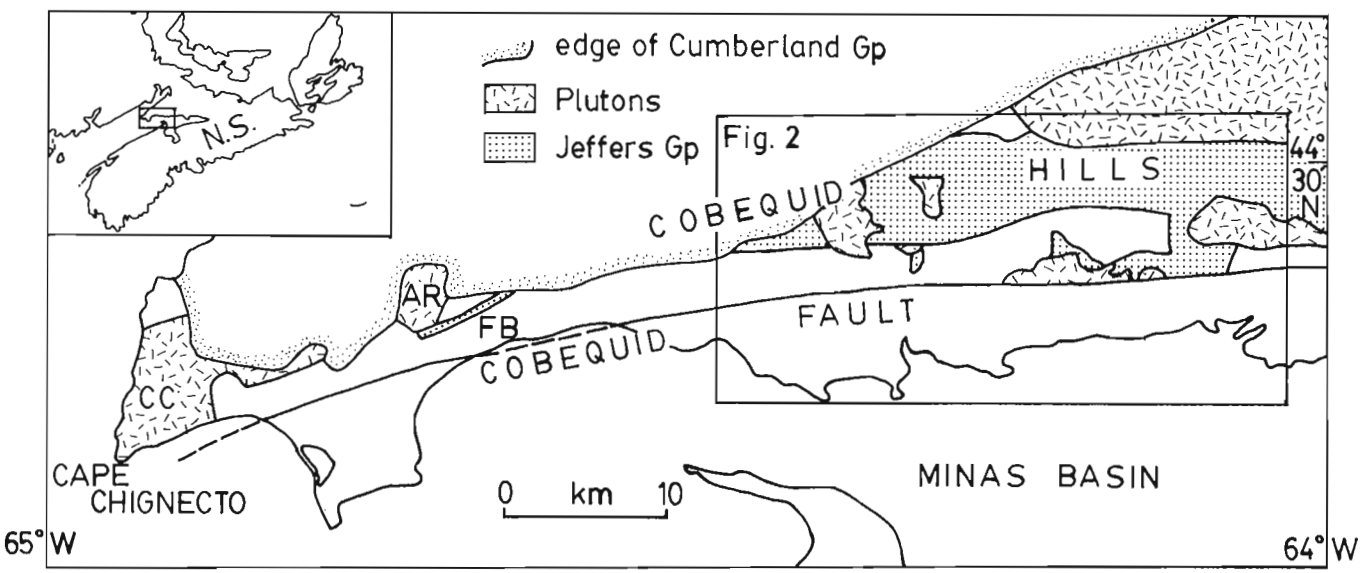


Figure 60.1. Location of the Jeffers Group and major plutons. Modified from Donohoe and Wallace (1982). FB = Fowler Brook Jeffers Group sections. CC = Cape Chignecto pluton. AR = Apple River pluton.

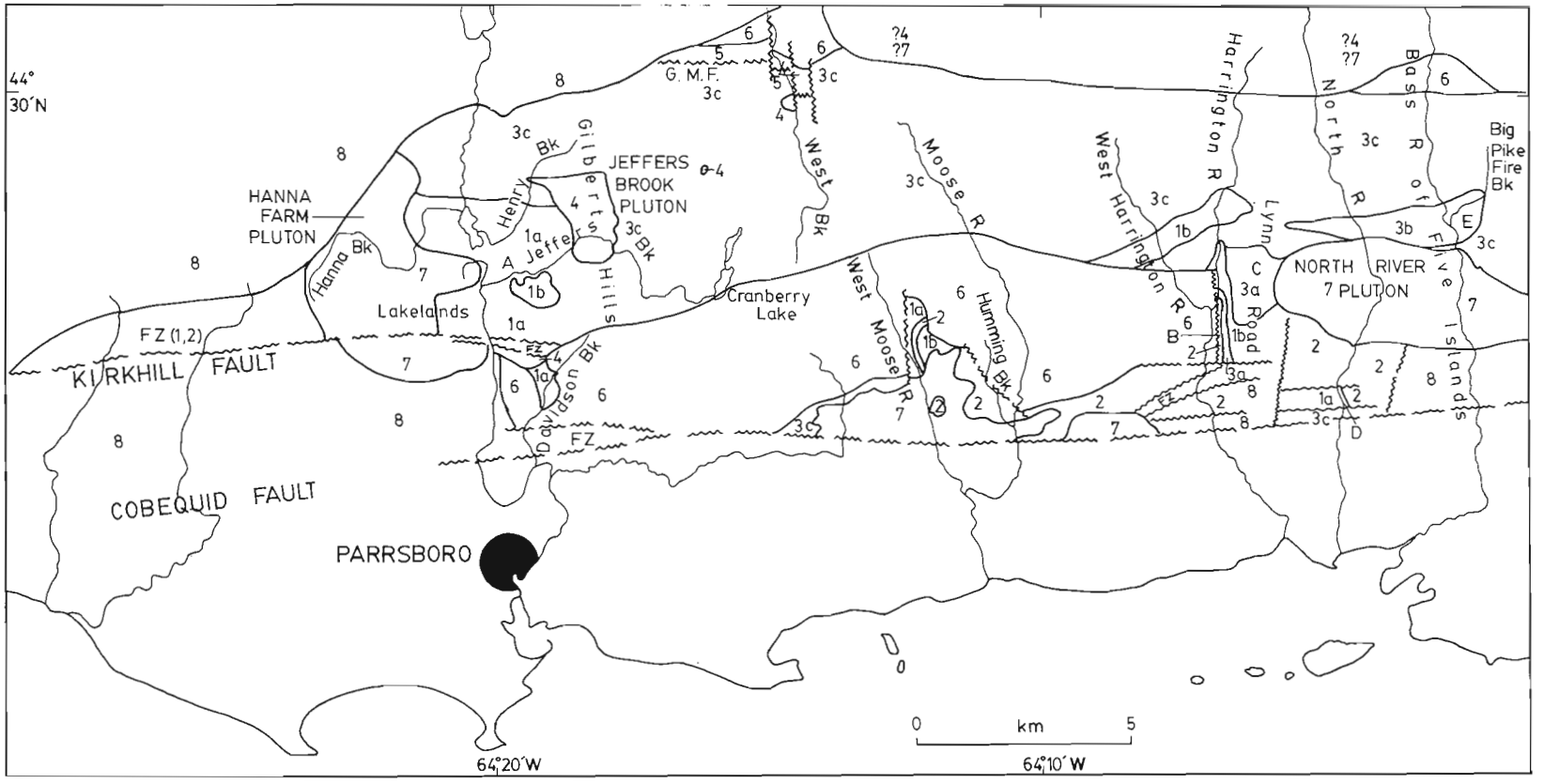


Figure 60.2. Preliminary map showing the Jeffers Group of the western Cobequid Hills.

1-3. Late Hadrynian Jeffers Group.
1 – Gilbert Hills Formation
  1a: Lakelands facies;
  1b: Harrington River facies.
2 – Humming Brook Formation
3 – Cranberry Lake Formation
  3a: Lynn Road facies;
  3b: Pike Fire Brook facies;
  3c: West Brook facies.
4 – Late Hadrynian plutons
5 – Wilson Brook Formation (Silurian)
6 – Fountain Lake Group
  (Devono-Carboniferous)
7 – Carboniferous plutons
8 – undivided Carboniferous sedimentary rocks
FZ – fault zone with a wide range of lithologies
G.M.F. – Gilbert Mountain Fault
A to E are sections illustrated in Figure 60.3.

STRUCTURE

Donohoe and Wallace (1982, 1985) recognized that the Jeffers Group has a distinctive shallow to moderately dipping foliation (S1), deformed by upright to inclined folds (F2), with both the S1 foliation and F2 folds cut by the Jeffers Brook pluton, which was radiometrically dated as latest Hadrynian. The new mapping has shown that the S1 foliation is spatially very variable; in places it is associated with intense flattening and stretching, with growth of chlorite-grade metamorphic minerals, whereas other parts of the group have only very weak, flat-lying penetrative cleavage and in places, no cleavage can be distinguished. Areas that are intensely cleaved are most common in the southern part of the study area, are typically a few tens to a few hundred metres thick and generally separate different stratigraphic units (Fig. 60.3). They probably indicate a thrust style of deformation.

The age of the flat-lying cleavage is only locally defined. At the eastern margin of the Jeffers Brook pluton Jeffers Group rocks with a very weak cleavage are cut by undeformed veins of coarse diorite. At the western margin of the pluton, highly cleaved Jeffers Group rocks are in fault contact with undeformed diorite. In the West River area, generally uncleaved Wilson Brook Formation (Silurian) shales are in fault

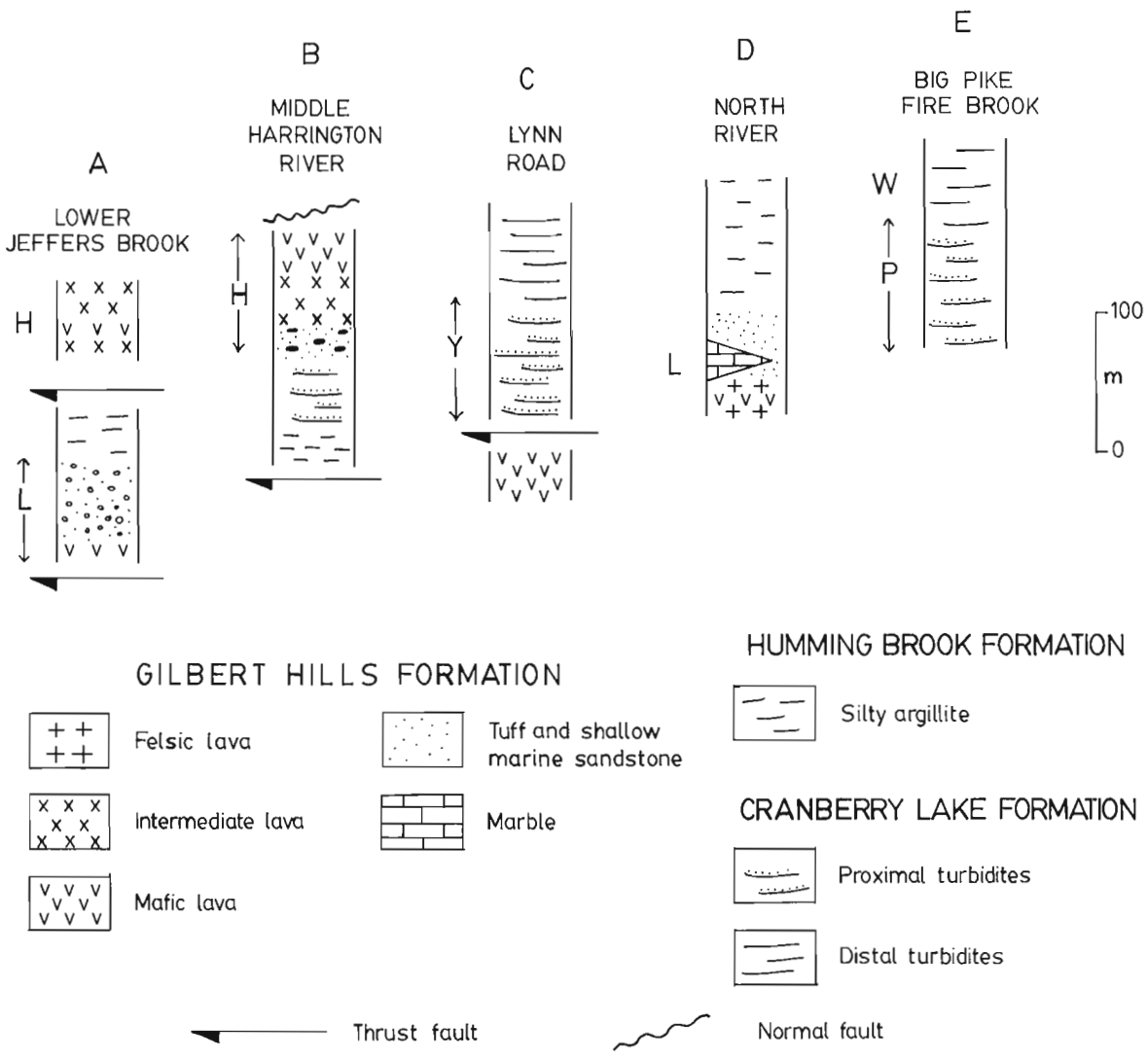


Figure 60.3. Schematic stratigraphic sections of the Jeffers Group. A: Lower Jeffers Brook, showing type section of the Lakelands facies (L) of Gilbert Hills Formation, with overlying Harrington River facies (H) in thrust contact. B: Middle Harrington River, showing type section of Harrington River facies (H) of Gilbert Hills Formation. C: Lynn Road, showing type section of Lynn Road facies (Y) of Cranberry Lake Group overlying highly sheared mafic volcanic rocks. D: North River, showing Lakelands facies (L) of Gilbert Hills Formation overlain by Humming Brook Formation. E: Big Pike Fire Brook, showing type section of Big Pike Fire Brook facies (P) of the Cranberry Lake Formation overlain by the West Brook facies (W).

contact with Jeffers Group that has a flat-lying cleavage. In several areas, cleaved Jeffers Group is cut by uncleaved rhyolite intrusions that are lithologically similar to the basal Wilson Brook Formation rhyolite extrusives mapped near Simpson Lake (east of the area shown in Fig. 60.2). In the West Moose River area, undeformed Fountain Lake Group rhyolite (Devono-Carboniferous) unconformably overlies intensely cleaved Jeffers Group. These observations all suggest a pre-Devonian and probably Late Hadrynian age for much of the flat-lying cleavage, as suggested by Donohoe and Wallace (1982, 1985).

West of Parrsboro, however, there is widespread evidence for a strong flat-lying foliation of Carboniferous age. The Cape Chignecto–Apple River plutonic complex (CC-AR in Fig. 60.1) is lithologically similar to other Carboniferous granites, and has yielded Carboniferous radiometric dates. The pluton and the nearby Fountain Lake Group and Rapid Brook Formation have been intensely deformed with the development of a strong, flat-lying stretching lineation and flat-lying sheared contacts between diorite and granite bodies. This deformation is probably related to Carboniferous thrusting in southwestern New Brunswick (Nance and Warner, 1986). Similar deformation of Carboniferous plutons can be recognized as far east as the Hanna Farm pluton northwest of Parrsboro; there is also local deformation within one kilometre of the Cobequid Fault farther east. It is therefore likely that some of the flat-lying deformation observed in the Jeffers Group is of Late Paleozoic age.

STRATIGRAPHY

The Jeffers Group comprises mafic, intermediate and acid volcanic rocks and interbedded volcaniclastic sediment. The volcanic rocks and immediately associated sediments are mapped as the Gilbert Hills Formation. The Humming Brook Formation comprises argillite and is developed in the southern part of the Cobequid Hills. The Cranberry Lake Formation is a thick sequence of greywacke and quartz wacke interbedded with and overlying the volcanic rocks. These formations are described below in approximate ascending order of age.

Gilbert Hills Formation

The Gilbert Hills Formation comprises lavas and pyroclastic rocks within the Jeffers Group. It is named for the Gilbert Hills, located within one of the areas in which volcanic rocks are best developed. The type section is in Jeffers Brook (Fig. 60.3), immediately west of the contact with the Jeffers Brook pluton (map reference 972354). Two facies are recognized within the formation, with different types of volcanic rocks and different stratigraphic position.

Lakelands facies

This facies consists predominantly of felsic volcanic rocks, and is defined in the type section of the Gilbert Hills Formation. It consists of a thin sequence of mafic lavas and possible pyroclastic rocks (which are highly sheared in the type section), overlain by several tens of metres of felsic pyroclastic rocks. The sequence passes up into silty agrillite.

Farther downstream in Jeffers Brook, the probable equivalent of the felsic pyroclastic sequence includes a felsic agglomerate several metres thick and rare rhyolite flows. An apparently correlative sequence of agglomerate and tuffs, local rhyolite flows and indistinctly bedded massive quartz sandstones (apparently derived from reworking of the pyroclastic rocks) occurs to the west and north in Hanna Brook and southern Henry Brook.

Highly deformed felsic rocks in Fowler Brook, in an inlier of Jeffers Group rocks 30 km west of Parrsboro (FB in Fig. 60.1), are assigned to this facies. Three other felsic pyroclastic sequences, with minor mafic rocks – in Davidson Brook, near the West Moose River, and in North River – are also assigned to this facies. The rocks in Davidson Brook are felsic tuffs and mafic volcanic rocks, cut by numerous hypabyssal intrusions and in fault contact with all other stratigraphic units. In the West Moose River area, felsic tuffs several tens of metres thick overlying highly sheared mafic rocks appear to be overlain by silty argillite of the Humming Brook Formation.

In North River, there is a sequence underlying the Humming Brook Formation that consists of felsic tuffs and less common basalt, together with quartz sandstones (apparently derived from reworking of the tuffs) and minor carbonates. The structural and mineralogical evolution of the carbonates is described by Boner (1985). The quartz sandstone appears to pass up abruptly into silty agrillite of the Humming Brook Formation. Carbonates are not known elsewhere in the stratigraphic section in the western Cobequid Hills, except for the Carboniferous Windsor Group south of the Cobequid Fault, so that highly deformed carbonate bodies in fault zones in the Bass River of Five Islands and south of Hanna Brook may also be part of the Lakelands facies.

Harrington River facies

The type section for this facies is located in the Harrington River (Fig. 60.3), north of the junction with the West Harrington River (map reference 125350). It consists of massive intermediate and mafic lavas and minor interbedded pyroclastics. Volcaniclastic lithic sandstones are interbedded with and underlie the volcanic rocks. In addition to the type section, the Harrington River facies is well exposed in the upper part of Harrington River, in Jeffers Brook (Fig. 60.3), and on the southern part of Lynn Road. The contacts of this facies of the Gilbert Hills Formation with other parts of the Jeffers Group are generally thrust faults, but in the type section the Harrington River facies conformably overlies rocks of the Lynn Road facies of the Cranberry Lake Formation (described below). The Harrington River facies differs from the Lakelands facies in the virtual absence of felsic volcanic rocks and the development of thick massive sequences of mafic and intermediate lavas. The Harrington River facies generally overlies the Cranberry

Lake Formation, whereas the Lakelands facies is overlain by the Humming Brook Formation.

In the type section, coarse turbidites of the Cranberry Lake Formation pass upwards into massive, poorly bedded, green lithic sandstones with rare large concretions. These are overlain by a series of light green intermediate lavas, which in turn are overlain by thick basalts. The entire sequence is many tens of metres thick. The top of the succession appears to be fault bounded.

In the northern part of the Harrington River, the Harrington River facies again appears to overlie sediments of the Cranberry Lake Formation. In this area, hypabyssal intrusions are extremely common, making up the greater proportion of the outcrops. Some rhyolite and minor intermediate to felsic tuffs are present within the succession.

In Jeffers Brook (Fig. 60.3), the base of the Harrington River facies is marked by a thrust fault, and the upper boundary is not exposed. The facies here consists of mafic and intermediate lavas, which locally overlie green lithic sandstones.

Humming Brook Formation

The type section for this formation is located in Humming Brook, a tributary of the West Moose River (map reference 074319). It consists of a thick sequence of isoclinally folded monotonous argillites with very fine silty laminae. There are also rare thin (<2 cm) beds of very fine sandstone or siltstone. The spacing of siltstone laminae generally appears random, but in a few localities graded laminated beds are visible, suggesting a turbidite origin. Total thickness of the formation is difficult to determine because of structural complexity, but is at least 100 m.

The Humming Brook Formation is well exposed in the Moose River area, in the lower Harrington River (where it is highly cleaved) and in North River and its tributaries south of the North River pluton. It is generally in fault contact with other formations within the Jeffers Group, but locally appears to overlie the Lakelands facies of the Gilbert Hills Formation, for example in North River, near West Moose River and in Jeffers Brook.

Cranberry Lake Formation

This is the most extensive lithotype within the Jeffers Group, comprising a sequence of greywackes and quartz wackes mostly or entirely of turbidite origin. The formation is best developed around Cranberry Lake, for which it is named. The total stratigraphic thickness is difficult to determine because of the likelihood of fault repetition of strata. The type section is defined on the Lynn Road (map reference 131345), where it consists principally of thin to thick bedded lithic and arkosic fine to coarse wackes, with interbedded argillite, with a thickness of at least 40 m. Three facies are distinguished within the Cranberry Lake Formation.

Lynn Road facies

The Lynn Road facies is defined at the type section of the Cranberry Lake Formation, and is also well developed in Harrington River. In the type section, the dominant lithology is medium to fine greywacke, typically in massive beds a few tens of centimetres thick with thin argillite partings. There are also rare thicker beds of silty argillite. Rare sole marks and crosslamination are visible: the crosslamination suggests current flow to the northwest. The coarsest rocks, near the base of the section, are arkosic wackes showing Bouma A and B divisions in beds up to one metre thick. Well bedded quartz wackes in beds 40 to 120 cm thick, with Bouma B and BC sequences, are also present.

Pike Fire Brook facies

The type section of this facies is in the lower part of Big Pike Fire Brook (map reference 181363), consisting of thick bedded quartz wackes with a "proximal turbidite" character, and minor interbedded argillite (Fig. 60.3). Similar thick bedded quartz wackes are exposed in nearby parts of the Bass River of Five Islands.

In the type section, the sequence maintains consistent dips over a stratigraphic thickness of at least 60 m. At the base, massive medium to fine quartz wackes up to 1.5 m thick interbedded with thin beds of argillite pass up into sequences of massive fine quartz wacke beds generally a few tens of centimetres thick. The quartz wackes show Bouma A or AB sequences, and amalgamated beds are present in places. Exceptionally, convolute bedding, sole marks and crosslamination are present.

West Brook facies

This facies, with a type section in West Brook (map reference 028383), consists principally of thin bedded fine grained greywacke turbidites interbedded with thin siltstone and argillite, with a sand/argillite ratio typically between 2:1 to 1:2. In the West Brook area, the facies is at least 40 m and more probably several hundreds of metres thick; thick sequences also occur in the upper parts of the Bass River of Five Islands, North River, Moose River, Jeffers Brook and Henry Brook. In the Henry Brook–Jeffers Brook area, the facies appears particularly siliceous. This facies is also well developed in fault slices in southern North River and southern Harrington River.

In general, the West Brook facies appears to occur stratigraphically higher and to be geographically more extensive than the other facies which appear to be of more limited extent lower in the section. The West Brook facies also shows more evidence for folding; the other facies generally occur in consistently upward-facing, gently dipping sequences.

STRATIGRAPHIC SYNTHESIS AND PALEOGEOGRAPHIC SETTING

No basement rocks to the Jeffers Group are seen in the

western Cobequid Hills. The stratigraphically oldest rocks, part of the Lakelands facies of the Gilbert Hills Formation, outcrop close to the Cobequid Fault. They consist of the top of a felsic volcanic sequence with minor mafic flows, together with sandstones derived from reworking of the volcanic rocks and minor carbonates. These rocks are overlain by thick silty argillite of the Humming Brook Formation, which is interpreted as a basin slope deposit. This silty argillite probably interfingers laterally and distally with coarse proximal turbidites of the Lynn Road facies of the Cranberry Lake Formation. The more northerly developments of the Lakelands facies of the Gilbert Hills Formation pass up into silicic turbidites of the West Brook facies of the Cranberry Lake Formation.

The intermediate and mafic volcanic rocks of the Harrington River facies of the Gilbert Hills Formation overlie turbidites of the Cranberry Lake Formation, and the transitional lithologies appear to represent shallow marine volcaniclastic or pyroclastic sediments. There is no evidence for the preservation of submarine extrusive rocks; the lavas are interpreted as subaerial flows.

The Jeffers Group thus represents sedimentation in a deep water basin, within which volcanic islands grew and then subsided. Paleocurrent data are sparse, but the general facies distribution suggests that more proximal basin sediments occur in the south and more distal sediments in the north.

HYPABYSSAL INTRUSIONS

Hypabyssal intrusions are widespread within the Jeffers Group. They are particularly common within and near the volcanic sequences of the Harrington River facies, suggesting that many of the hypabyssal intrusions may be genetically related to the Jeffers Group. Pe-Piper and Piper (in press) used the presence of a penetrative cleavage to attempt to distinguish between hypabyssal intrusions genetically related to the Jeffers Group volcanism and younger post-Hadrynian intrusions.

We now recognize that some of the flat-lying cleavage may be of "Acadian" age, so that the presence of a flat-lying cleavage is not necessarily evidence of a Hadrynian age. Only those hypabyssal intrusions with distinctive petrography and geochemistry that are regionally cleaved and always spatially associated with Jeffers Group volcanic sequences are identified as genetically part of the Jeffers Group and thus Hadrynian in age.

Probable Jeffers Group hypabyssal intrusions

1. Alkaline basalt sills and rare dykes. These are most abundant in the Harrington River area, but also occur in North River, Jeffers Brook and Lynn Road.

2. Feldspathic basaltic andesite sills, seen in the Lynn Road, Harrington River and Jeffers Brook sections.

3. Mafic porphyry with coarse plagioclase, occurring in thick sills south of Jeffers Brook and in the upper Harrington River.

4. Some cleaved mafic dykes may also be of the Late Hadrynian age.

5. Felsic dykes with prominent plagioclase phenocrysts which intrude rocks of the Lakelands facies in Davidson Brook.

Post-Jeffers hypabyssal intrusions

1. A series of cleaved mafic dykes striking northeast, many of which pass into sills and are associated with microgranite sills and dykes, are common in the Jeffers Brook section and were previously regarded as Late Hadrynian in age (Pe-Piper and Piper, in press). New mapping has shown clearly that these intrusions postdate the main thrusting in the Jeffers Brook section; their deformation is probably of "Acadian" age. Similar composite dykes of microgranite and diabase cut the Jeffers Brook pluton and are common in many other areas. Locally, the microgranites are extremely sheared, perhaps indicating that they were still warm and ductile when deformation occurred. These rocks probably represent feeders to the Fountain Lake Group.

2. A series of wide, north-striking mafic dykes, with ophitic texture and fresh clinopyroxenes, are particularly common east of the Jeffers Brook pluton.

3. Mafic dykes and sills cut many of the Carboniferous plutons; some of the diabase dykes cutting the Jeffers Group are probably related.

4. A distinctive suite of rhyolitic dykes, particularly common in the Henry Brook area, but also seen in the Lynn Road section, are lithologically very similar to rhyolite flows at the base of the Wilson Brook Formation in the Simpson Lake region (east of the study area).

MINERALIZATION

Mineralized samples have not yet been analyzed in detail, but some preliminary generalizations can be made. Specular hematite is widespread, associated with Carboniferous plutons and the Cobequid Fault. Barite mineralization also appears associated with the Cobequid Fault. Minor copper mineralization has been noted in the Hanna Farm pluton. Sphalerite and magnetite found in skarn in the Lakelands facies of the Gilbert Hills Formation in North River (Boner, 1985) are probably associated with the North River pluton.

No new observations have been made on mineralization associated with the Fountain Lake Group. Pyrite and possibly other sulphide mineralization appears common in the basal Silurian rhyolite in the Simpson Lake area and in related hypabyssal intrusions. Pyrite and other sulphides are also common in the Lakelands Member in the West Moose River area and east of the Jeffers Brook pluton.

ACKNOWLEDGMENTS

I thank F.W. Chandler for support and for visiting the field area; J.B. Murphy and J.W.F. Waldron for discussions in the

field; and D.J.W. Piper, D. Turner and G. Chinn for assistance in the field. Previous field work was supported by NSERC. Funding for this study through the Geological Survey of Canada is gratefully acknowledged. This manuscript was reviewed by F.W. Chandler and D.J.W. Piper.

REFERENCES

Boner, F.J.
1985: The geology of the North River area, Cobequid Highlands, Nova Scotia; unpublished B.Sc. (hons) thesis, St. Mary's University, Halifax, N.S., 83 p.

Donohoe, H.V., Jr. and Wallace, P.I.
1980: Structure and stratigraphy of the Cobequid Highlands, Nova Scotia; GAC–MAC joint annual meeting, Halifax, N.S., Field Trip Guidebook 19.
1982: Geological map of the Cobequid Highlands, Nova Scotia. Nova Scotia Department of Mines and Energy.
1985: Repeated orogeny, faulting and stratigraphy in the Cobequid Highlands, Avalon Terrain of northern Nova Scotia; GAC–MAC Joint Annual Meeting, Fredericton, N.B., Field Trip Guidebook 3, 77 p.

Keppie, J.D.
1982: The Minas Geofracture; in Major structural trends of the northern Appalachians, ed. P. St. Julien and J. Beland; Geological Association of Canada Special Paper 24, p. 265-280.

Nance, R.D. and Warner, J.B.
1986: Variscan tectonostratigraphy of the Mispec Group, southern New Brunswick: structural geometry and deformational history; in Current Research, Part A, Geological Survey of Canada, Paper 86-1A, p. 351-358.

Pe-Piper, G. and Piper, D.J.W.
1986: Detailed geological maps of part of the Western Cobequid Hills, Cumberland County, Nova Scotia. Nova Scotia Department of Mines and Energy Open File 86-018.
in press: The pre-Carboniferous rocks of the western Cobequid Hills, Avalon zone, Nova Scotia. Maritime Sediments and Atlantic Geology.

Preliminary U-Pb zircon ages for volcanic and plutonic rocks of the Noranda-Lac Abitibi area, Abitibi Subprovince, Quebec

Project 830006

J.K. Mortensen
Lithosphere and Canadian Shield Division

Mortensen, J.K., Preliminary U-Pb zircon ages for volcanic and plutonic rocks of the Noranda-Lac Abitibi area, Abitibi Subprovince, Quebec; in Current Research, Part A, Geological Survey of Canada, Paper 87-1A, p. 581-590, 1987.

Abstract

Preliminary U-Pb zircon ages are presented for volcanic and plutonic rocks from the Noranda-Lac Abitibi region in western Quebec. The uppermost rhyolite unit in the Blake River Group is dated at 2698 ± 1 Ma. The Flavrian Pluton has yielded a concordant age of 2701 ± 1.5 Ma, confirming its synvolcanic nature. Quartz-feldspar porphyry of the Hunter Mine Group is dated at 2730 ± 1.4 Ma, and rhyolitic flow rocks at Normetal appear to be of similar age. Three late- to post-tectonic plutons range in age from 2689 to 2694 Ma.

These results help place age constraints on both the depositional history and the timing of subsequent tectonism in this part of the Abitibi Subprovince.

Résumé

On présente des âges préliminaires à l'U-Pb par le zircon pour des roches volcaniques et plutoniques provenant de la région de Noranda-Lac-Abitibi de l'ouest du Québec. L'unité rhyolitique sommitale du groupe de Blake River a donné 2689±Ma. Le pluton de Flavrian a donné un âge concordant de 2701±1,5 Ma, ce qui confirme sa nature synvolcanique. Le porphyre quartzo-feldspathique du groupe de Hunter Mine a un âge de 2730±1,4 Ma, et les roches rhyolitiques d'écoulement de Normétal semblent avoir le même âge. Trois plutons tardi-tectoniques à post-tectoniques ont un âge qui varie entre 2689 ma et 2694 Ma.

Ces résultats permettent d'établir des limites chronologiques pour les événements de l'évolution sédimentaire et celle de la tectonique ultérieure dans cette partie de la sous-province d'Abitibi.

INTRODUCTION

The Abitibi Subprovince is the largest and best preserved Archean greenstone belt in the Canadian Shield, and as such, provides an ideal area in which to study the origin, tectonic evolution, and metallogeny of greenstone belts. A great number of detailed stratigraphic and structural investigations have been carried out in the Abitibi Subprovince, chiefly in and around the main mining camps. These, as well as more comprehensive studies of the belt as a whole, however, have been greatly hampered by a lack of precise age control on the supracrustal sequences and on plutonic rocks and possible basement gneisses.

Some indication of the age of the supracrustal assemblages has been obtained from Pb isotope studies of syngenetic sulphide deposits hosted within felsic volcanic portions of the stratigraphic sequences (e.g. Franklin et al., 1983; Thorpe, 1982; Thorpe et al., 1984). These ages are relatively imprecise, and somewhat model-dependent, however, and can therefore only be used in a general way to date the sequences. Similarly, Rb-Sr, Nd-Sm, and Pb-Pb isotopic systems are often disturbed, and/or do not offer sufficient precision to resolve individual, short-lived magmatic events in the evolution of the Abitibi Subprovince. U-Pb zircon (± baddeleyite, sphene) dating has proved to be the only technique capable of producing the minimum precision of ± 5 Ma required for this purpose.

The lack of age control is particularly evident in the eastern Abitibi Subprovince. Only a very small number of precise ages have been reported for plutonic rocks in this area, and none at all for the supracrustal sequences. Although precise ages have been obtained for several volcanic units in adjacent parts of eastern Ontario, the dated units can only be traced with confidence for a short distance into Quebec.

A regional U-Pb geochronological study of the eastern Abitibi Subprovince was initiated in 1985. A total of 41 samples of volcanic and plutonic rocks were collected, concentrating mainly on three main mining camps (Noranda, Chibougamau, and Matagami) where local stratigraphic relationships are reasonably well established. Nearly all of these samples have now been processed, and sufficient zircon (± baddeleyite, sphene) has been recovered for precise U-Pb dating from all but 5 samples. Zircon concentrates from 24 of the samples have been analyzed so far. For many of the samples, the analytical data are sufficiently unambiguous that preliminary ages can be assigned to the rocks, while for others more analyses are in progress to constrain crystallization ages.

Additional samples for U-Pb dating were collected in 1986 from the Noranda and Chibougamau areas, as well as from Joutel, Desmaraisville, and the area south of Kirkland Lake. The purpose of this work is to attempt to establish a regional chronostratigraphy for the eastern Abitibi Subprovince, and place absolute age constraints on the various stages of evolution of this belt.

In this contribution a number of new ages are presented for volcanic and plutonic rocks in the Noranda and Lac Abitibi areas of western Quebec. Because these ages are preliminary, and because in many cases additional fractions of zircon will be analyzed in order to reduce the associated errors, a complete listing of analytical data is not included here.

GEOLOGY OF THE NORANDA-LAC ABITIBI AREA

A generalized geological map of the Abitibi Subprovince in western Quebec and eastern Ontario is shown in Figure 61.1, along with all published precise age data. Also shown are localities sampled in the course of this study. Labelled localities in Figure 61.1 are discussed in the text.

The supracrustal sequence between the Kirkland Lake-Larder Lake Fault Zone (KLFZ) and Lac Abitibi (Fig. 61.1) has been divided into upper and lower supergroups (e.g. Dimroth et al., 1982; Jensen, 1985). The lower supergroup in this area is represented by the Hunter Mine Group, a thick sequence consisting largely of calc-alkaline felsic tuffs and breccias, with minor quartz-feldspar porphyry (Eakins, 1972; Gagnon, 1981a, b; Dimroth et al., 1982; Jensen, 1985). This unit surrounds the eastern end of Lac Abitibi, and passes through a facies change into sediementary strata of the Lois Formation farther east (Dimroth et al., 1982).

Most of the study area is underlain by volcanic rocks of the upper supergroup, which consists from base to top of 1) komatiitic flows of the Stoughton-Roquemaure Group; 2) tholeiitic basalts of the Kinojévis Group; and 3) mafic to felsic, tholeiitic and calc-alkaline flows and pyroclastic strata of the Blake River Group. The Blake River Group is considered by Dimroth et al. (1982) and others to represent a large central volcanic complex built on a mafic volcanic plain (Kinojévis Group). Some of the felsic centres farther east (e.g. Harricana II) are thought to occupy a similar stratigraphic position as does the Blake River Group, whereas other centres, such as the Destor and Val d'Or complexes, appear to be somewhat lower in the section, probably laterally equivalent to the Kinojévis Group. Lenticular sedimentary units such as the Kewagama Group occur locally within the upper supergroup.

Mafic and felsic volcanic rocks north of Lac Abitibi, including those in the vicinity of the Normetal Mine, have not been studied in detail, and their stratigraphic position is poorly known. They are tentatively correlated with the Hunter Mine Group and stratigraphically lower rocks that outcrop farther west.

Sedimentary rocks of the Pontiac and Cadillac groups, which occur along and to the south of the KLFZ (Fig. 61.1), both overlie and may be in part laterally equivalent to the Blake River Group (Dimroth et al., 1982). Fluvial and shallow marine clastic sediments with intercalated alkalic flows and tuffs occur along both the KLFZ and Destor-Porcupine Fault Zone (DPFZ; Fig. 61.1). These units, which inlcude the Timiskaming Group and the Duparquet and La Bruère formations, overlie all of the above formations, locally displaying a marked angular unconformity.

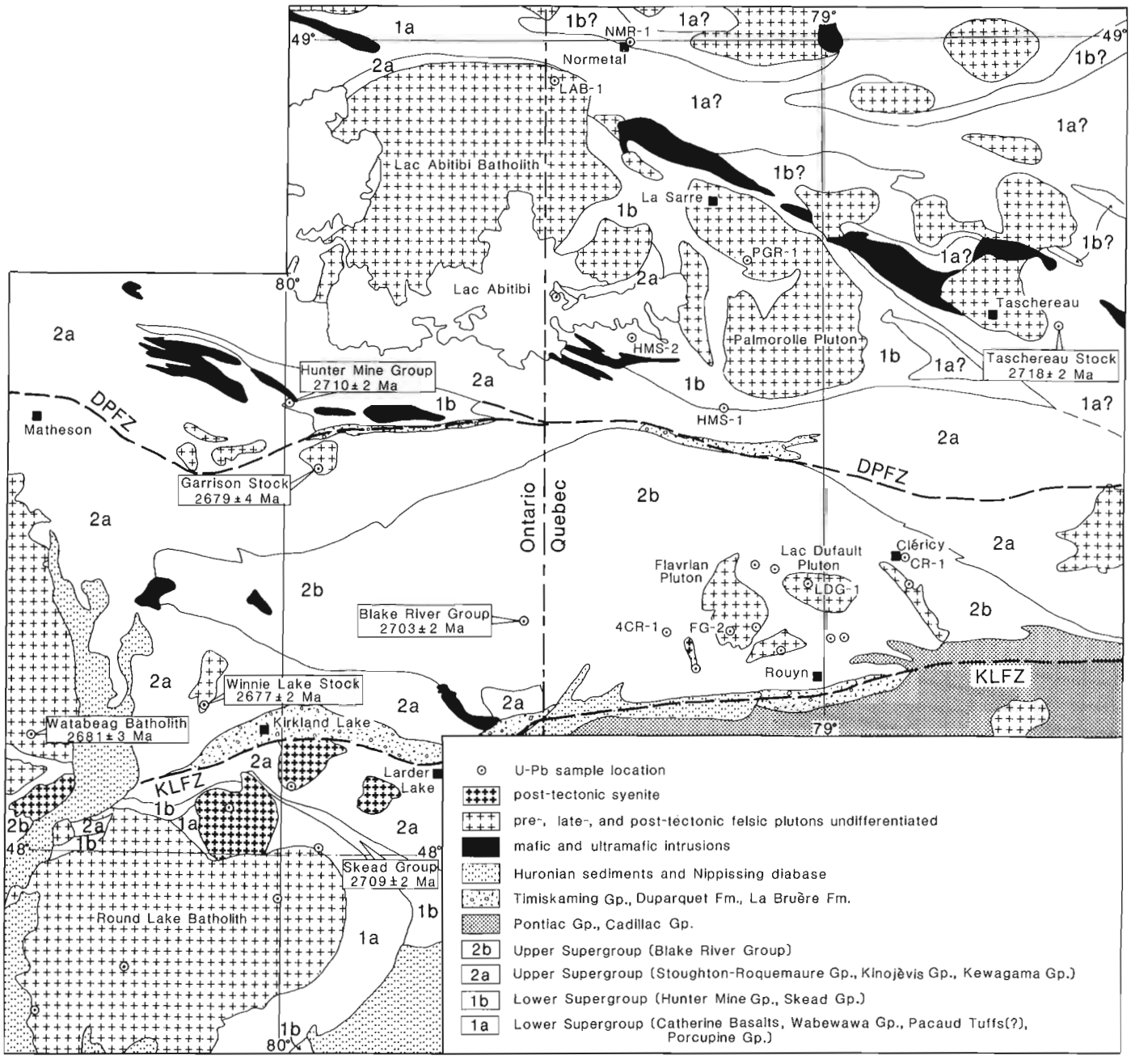


Figure 61.1. Geology of the Abitibi Subprovince in western Quebec and eastern Ontario (modified from MERQ-OGS, 1985). Also shown are all available U-Pb zircon ages and localities sampled in this study. Labelled localities are discussed in the text.

Several distinct plutonic events have affected the area. The age of emplacement of the various plutons can be established relative to the main deformation and metamorphism associated with the Kenoran Orogeny by examining overprinting relationships between Kenoran fabrics and metamorphic assemblages and contact aureoles surrounding individual intrusions. Thus the plutons shown in Figure 61.1 have been subdivided into pre-tectonic and late- or post-tectonic (e.g. Dimroth et al., 1983). It has been possible to demonstrate from field relationships and geochemical evidence that some of the intrusions, such as the Flavrian Pluton (Fig. 61.1), are approximately coeval and comagmatic with the surrounding volcanic rocks (e.g. Goldie, 1979; Paradis et al., 1983). There are two compositionally distinct suites of late- and post-tectonic plutons. The most abundant suite consists predominantly of tonalite, granodiorite, and quartz

monzonite, and includes such bodies as the Lac Dufault Pluton and Lac Abitibi Batholith (Fig. 61.1). Also present is a suite consisting mainly of medium- to coarse-grained syenite, which forms several small intrusions in the Noranada area, as well as a number of larger bodies south of the KLFZ.

PREVIOUS GEOCHRONOLOGICAL STUDIES

Although a considerable amount of K-Ar, Rb-Sr, and Nd-Sm data is available for rock units in the study area, only a small number of U-Pb zircon analyses have been carried out. The following summary is restricted to these U-Pb data.

Volcanic rocks of the lower supergroup have been dated in two localities. Dacitic tuffs of the Hunter Mine Group southwest of Lac Abitibi have yielded an age of 2710 ± 2 Ma (Nunes and Jensen, 1980). The Skead Group has been dated at 2709 ± 2 Ma by Nunes (personal communication, in Jensen, 1985). Several discordant zircon analyses for felsic volcanic rocks of the Blake River Group have been obtained by Krogh and Davis (1971) and R.K. Wanless (unpublished data). The only precise age for this sequence, however, is 2703 ± 2 Ma for quartz-feldspar porphyry and associated rhyolite from a locality near the Quebec-Ontario border (Nunes and Jensen, 1980).

Discordant zircon analyses from the Powell and Lac Dufault plutons have been reported by Krogh and Davis (1971, 1974). Their data are interpreted to indicate a minimum age for the Lac Dufault Pluton of 2701 Ma (Krogh, personal communication, in Nunes and Jensen, 1980). Three plutons of the late- to post-tectonic suite in eastern Ontario have yielded ages of 2677 ± 2 Ma, 2679 ± 2 Ma, and 2681 ± 3 Ma (Frarey and Krogh, 1986). The Taschereau Stock (Fig. 61.1), which was originally considered to be late- or post-tectonic, yielded an unusually old age of 2718 ± 2 Ma (Frarey and Krogh, 1986).

Gariépy et al. (1984) carried out single grain U-Pb analyses of detrital zircons from sedimentary rocks in the Pontiac Subprovince (Pontiac Group) immediately south of the area shown in Figure 61.1. Calculated $^{207}Pb/^{206}Pb$ ages for individual grains (minimum ages for exposed rock units in the provenance areas) ranged from 2535 to 2943 Ma. The exact relationship between the Pontiac Group and the Abitibi Subprovince strata to the north is equivocal, however, and the source region for Pontiac Group sediments has not been resolved. Thus the significance of the detrital zircon ages with respect to the Abitibi Subprovince remains uncertain.

ANALYTICAL TECHNIQUES

Zircon was separated from 25-30 kg samples using standard Wilfley table and heavy liquid techniques. Individual zircon populations were separated initially based on grain size and magnetic susceptibility, and final selection of grains for analysis was done using a high-magnetic-gradient "pin" described by Krogh (1982a), and grain clarity and mophological criteria. All zircons selected for analysis were carefully examined in transmitted light at high magnification for the presence of inherited zircon cores (no such cores were visible in any of the zircon fractions analyzed in this study). Most fractions were abraded to varying degrees (Krogh, 1982b). Separation and purification techniques for U and Pb are modified after Krogh (1973). Total procedural blanks for Pb ranged from 120 to 35 picograms, and U blanks averaged 10 picograms. Two separate ^{205}Pb spikes were used during the course of the study, one $^{205}Pb/^{235}U$ spike was prepared by Krogh and Davis (1975), and the other, a $^{205}Pb/^{233\text{-}235}U$ spike, was prepared by Parrish and Krogh (1986).

Pb was loaded on a single Re filament using the silica gel-phosphoric acid technique. U was loaded in water and run as the U^+ ion using a double Re filament assembly. Isotopic analyses were carried out on a Finnigan MAT 261 solid source mass spectrometer equipped with multiple collectors, secondary electron multiplier, and operating software modified to permit simultaneous measurement of all five Pb isotopes (Roddick et al., 1986). U was also analyzed using a static multicollection technique. Discordia line intercepts and associated errors were calculated using the line fitting technique of Davis (1982). In the case of concordant zircon analyses, the $^{207}Pb/^{206}Pb$ age is taken as the crystallization age of the rock. Errors assigned to these concordant analyses are calculated using a numerical error propogation technique. U and Th decay constants recommended by Steiger and Jäger (1977) were used for age calculations. All errors are quoted at the 2σ level.

ANALYTICAL RESULTS

In the Noranda area, felsic volcanic rocks of the Blake River Group have been subdivided into several cycles, which young to the east (Spence and de Rosen-Spence, 1975; Gélinas et al., 1984). Sample CR-1 was taken from the stratigraphically highest rhyolite unit (Cycle V of Spence and de Rosen-Spence, 1975; equivalent to Reneault cycle of Gélinas et al. (1984) approximately 1 km east of Clériсy (Fig. 61.1). The rock is a volcanic breccia, consisting mainly of fragments of quartz porphyry in a weakly foliated matrix. Four zircon analyses (Fig. 61.2) form a linear array of points with a calculated upper intercept (interpreted to represent the crystallization age of the rock) of $2697.9^{+1.3}/_{-0.7}$ Ma, and a lower intercept of 29.6 Ma.

The lowermost felsic volcanic unit recognized in the Noranda area (Cycle I of Spence and de Rosen-Spence, 1975; equivalent to the Duprat-Montbray cycle of Gélinas et al., 1984) was sampled immediately south of the Four Corners massive sulphide occurrence, approximately 2 km northeast of Lac Arnoux (sample 4CR-1, Fig. 61.1). The rock is a massive, quartz-phyric rhyolite flow. Four zircon analyses are all slightly discordant, and do not form a linear array (Fig. 61.3). The least discordant analysis yields the oldest $^{207}Pb/^{206}Pb$ age of 2698.7 Ma, which is interpreted as a minimum age for the rock.

The Flavrian Pluton is considered by Spence and de Rosen-Spence (1975) to intrude volcanic units at least as high

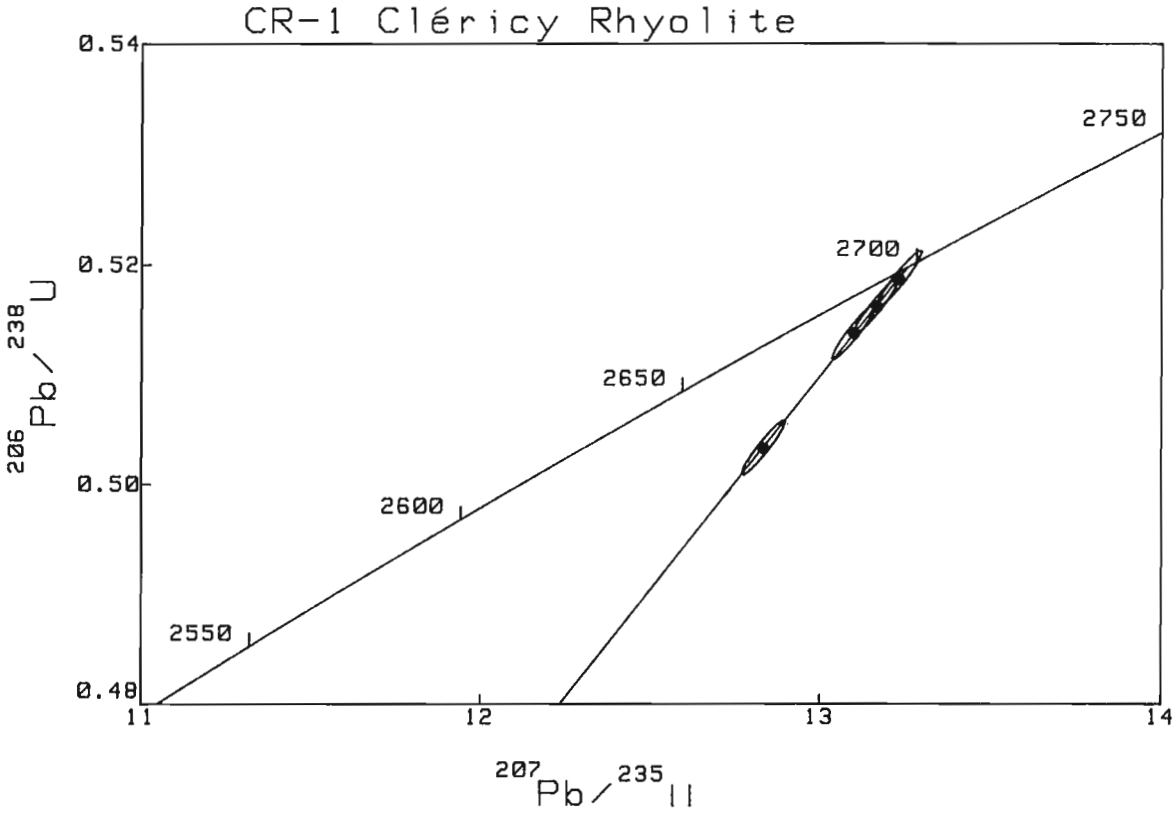


Figure 61.2. U-Pb concordia plot for zircon from Blake River Group rhyolite east of Cléricy (CR-1).

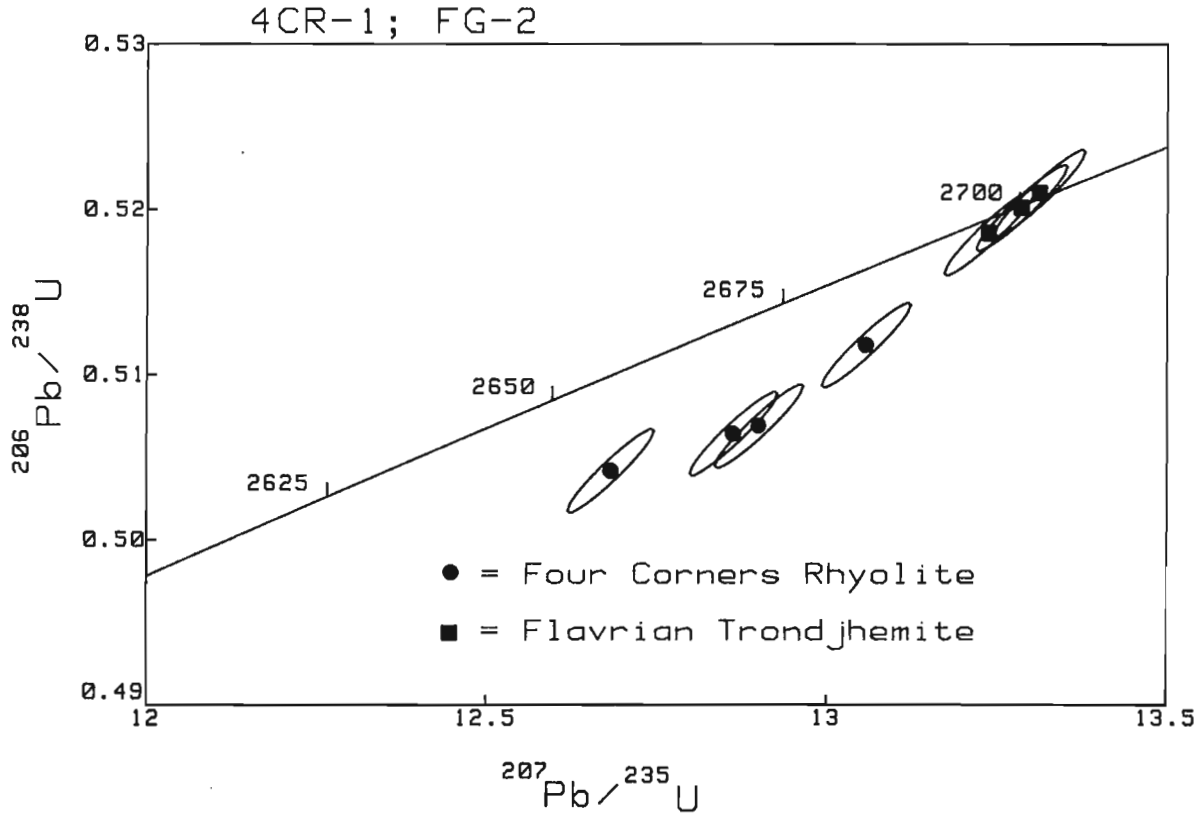


Figure 61.3. U-Pb concordia plot for zircon from Blake River Group rhyolite near the Four Corners massive sulphide occurrence (4CR-1), and from trondhjemite of the Flavrian Pluton (FG-2).

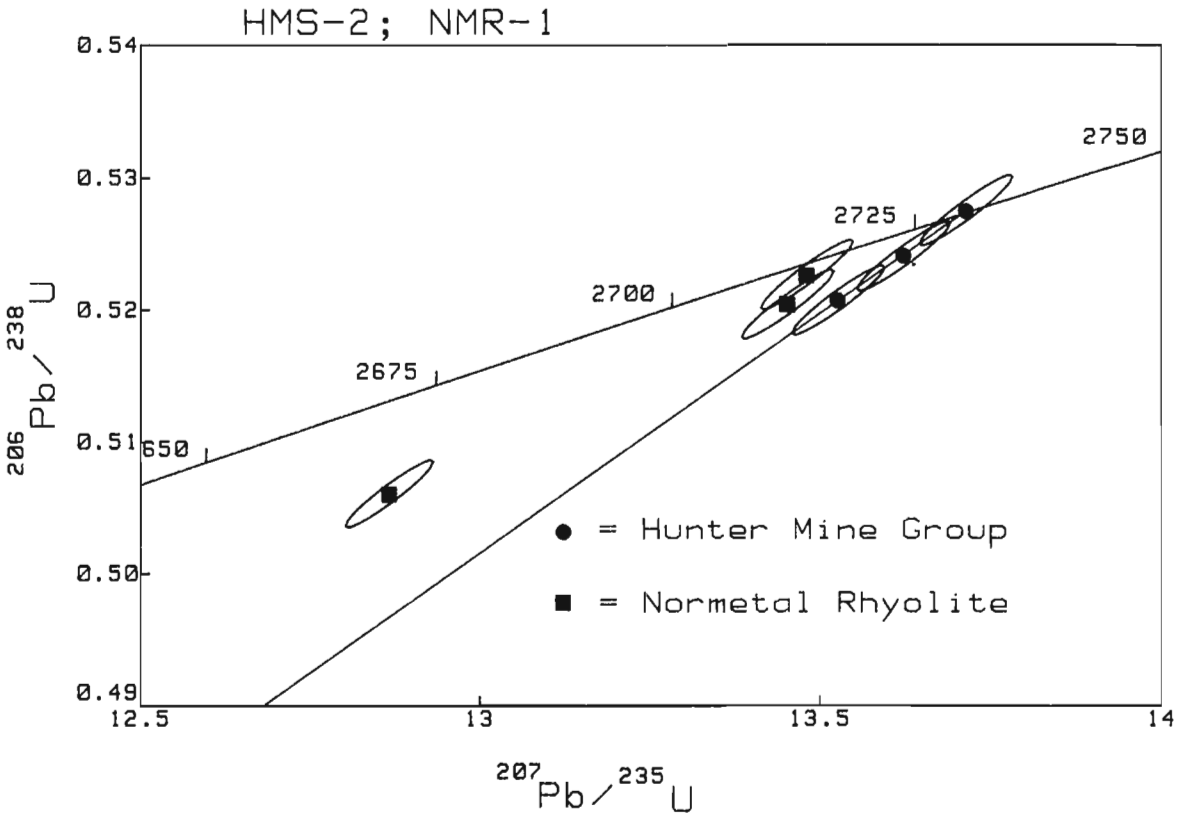


Figure 61.4. U-Pb concordia plot for zircon from porphyry of the Hunter Mine Group south of Lac Abitibi (HMS-2), and from rhyolite at Normetal (NMR-1).

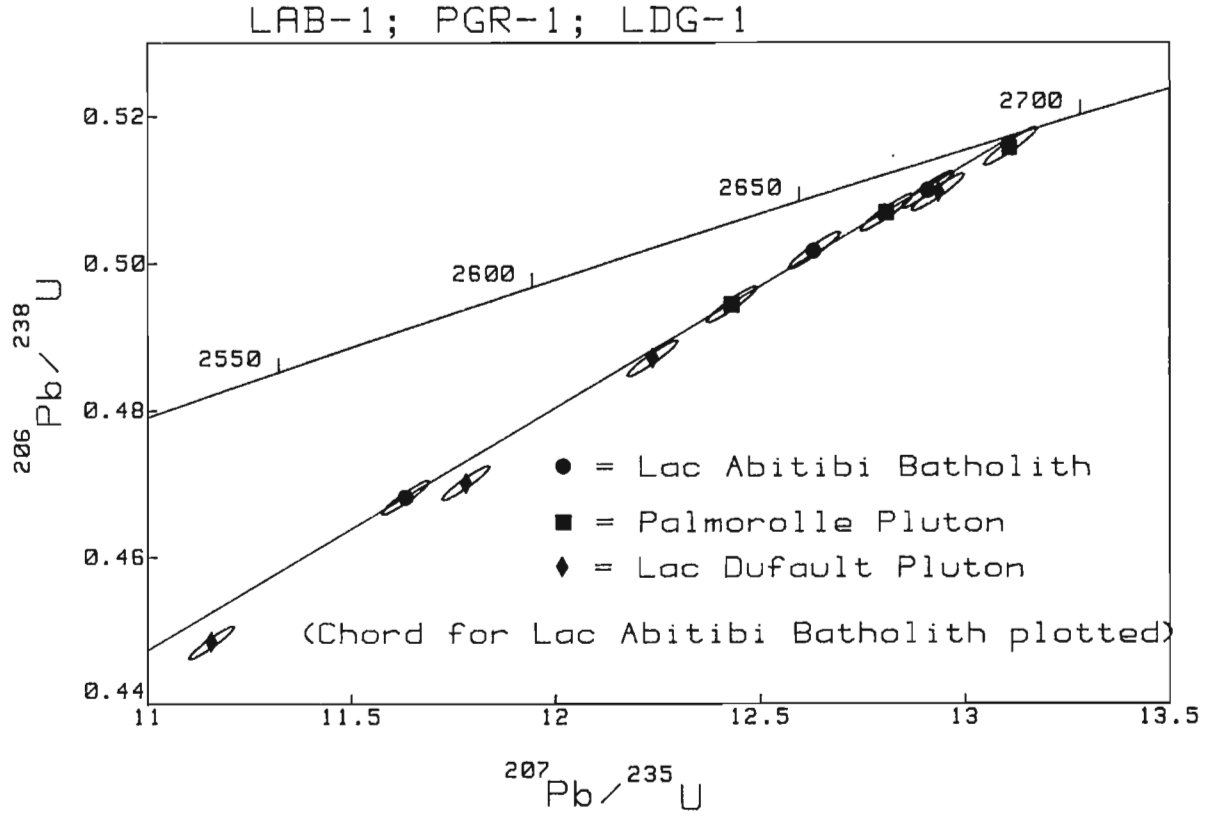


Figure 61.5. U-Pb concordia plot for zircon from the Lac Abitibi Batholith (LAB-1), Palmorolle Pluton (PGR-1), and Lac Dufault Pluton (LDG-1).

as their Cycle II in the stratigraphic sequence. Thus the emplacement of this body must post-date the deposition of the Four Corners rhyolite discussed above. A sample of massive trondhjemite of the Flavrian Pluton collected 5 km northwest of Evain (sample FG-2, Fig. 61.1) yielded abundant zircon. Three analyses lie on concordia (Fig. 61.3) and give statistically identical $^{207}Pb/^{206}Pb$ ages. The average $^{207}Pb/^{206}Pb$ age for these three analyses of 2700.5 ± 1.5 Ma is considered to be the crystallization age of the pluton. This is also a minimum age for the Four Corners rhyolite.

The Hunter Mine Group in the upper part of the lower supergroup was sampled at two localities. A sample of finely feldspar-phyric, flow-banded rhyolite about 4 km west of the type area for the unit (sample HMS-1, Fig. 61.1) yielded only a trace amount of zircon. A sample of massive quartz-feldspar porphyry from 2.5 km west of Couture on the south side of Lac Abitibi (sample HMS-2, Fig. 61.1), however, contained abundant high quality zircon. Three zircon fractions were analyzed (Fig. 61.4). One fraction is concordant, and the other fractions are very slightly discordant. The $^{207}Pb/^{206}Pb$ age for the concordant analysis (2730.0 ± 1.4 Ma) is interpreted to be the crystallization age of the rock.

A moderately foliated quartz-feldspar-phyric rhyolite flow on the northeast side of the Normetal townsite (sample NMR-1, Fig. 61.1) was collected for zircon dating. Three fractions of zircon have been analyzed so far. The analyses form a roughly linear array, ranging from 1.5 to 7.8% discordant (Fig. 61.4). The probability of fit to the calculated regression line, however, is very low (3%). The calculated upper intercept age ($2726.7^{+10.6}/_{-5.2}$ Ma) is probably close to the true crystallization age of the rock, and the oldest $^{207}Pb/^{206}Pb$ age obtained (2720.3 Ma) is a minimum age. These preliminary ages strongly suggest that the sequence of felsic volcanic rocks that hosts the Normetal massive sulphide deposit is correlative with the Hunter Mine Group farther south.

Preliminary ages have been obtained for three of the late- to post-tectonic plutons in the area. Three zircon fractions have been analyzed from a sample of porphyritic granodiorite from near the northeastern edge of the Lac Abitibi Batholith (sample LAB-1, Fig. 61.1). The analyses (Fig. 61.5) range from 1.9 to 12.4% discordant, and form a linear array with calculated upper and lower intercept ages of $2689.0^{+2.7}/_{-2.3}$ and 724.2 Ma, respectively. The upper intercept age is interpreted to date the intrusion of this phase of the batholith.

Zircon separated from hornblende granodiorite of the Palmorolle Pluton, which was sampled 2 km south of Colombourg (sample PGR-1, Fig. 61.1), was also analyzed. Three analyses range from 0.8 to 6.5% discordant, and define a discordia line with calculated intercept ages of $2693.8^{+4.0}/_{-2.7}$ and 871.0 Ma (Fig. 61.5). The upper intercept dates emplacement of the pluton.

Four fractions of zircon have been analyzed from biotite granodiorite of the Lac Dufault Pluton, sampled on Highway 101 approximately 1 km south of the Norbec Mine turnoff (sample LDG-1, Fig. 61.1). The analyses range from 2.2 to 16.8% discordant, and fit a discordia line with some scatter (probability of fit = 51.1%, Fig. 61.5). The calculated upper intercept age of $2694.4^{+8.2}/_{-6.8}$ Ma is interpreted to date the intrusion. A minimum age for the rock is given by the $^{207}Pb/^{206}Pb$ age of the least discordant point (2687.4 Ma). The calculated lower intercept of the discordia line is 611.2 Ma.

DISCUSSION

Results of the study obtained so far shed new light on the timing of magmatic and tectonic events in the eastern Abitibi Subprovince. According to the structural and stratigraphic interpretation of Hubert et al. (1984) and Gélinas et al. (1984), the rhyolite dated by Nunes and Jensen (1980) at 2703 ± 2 Ma is correlative with some of the oldest volcanic units in the Blake River Group in the Noranda area. This age, together with the results presented here, suggests that the entire volcanic sequence now exposed in the Noranda camp accumulated within 5 Ma, and certainly in less than 8 Ma. The data also confirm that the Flavrian Pluton is indeed synvolcanic, and is probably coeval with units at an intermediate level in the Noranda sequence.

The age of 2730.0 ± 1.4 Ma obtained for the Hunter Mine Group south of Lac Abitibi is considerably (20 Ma) older than that reported by Nunes and Jensen (1980) for a separate band mapped as Hunter Mine Group farther to the west. Nunes and Jensen (1980) stated that 2710 Ma is only a minimum age for the sample they studied, but that it is probably close to the true crystallization age. It is difficult to reconcile their data with an emplacement age of 2730 Ma, and it is therefore likely that two lithologically similar sequences of considerably different age are included in rocks presently mapped as Hunter Mine Group. Preliminary U-Pb data for felsic volcanic rocks in the Normetal area, and a minimum age of 2718 Ma for volcanic rocks intruded by the Taschereau Stock to the east, further suggest that the earlier phase of volcanism recorded in the Hunter Mine Group was quite widespread, at least in Quebec. Some revision of stratigraphic correlations in this part of the section in eastern Ontario may be required.

Ages reported here allow very tight constraints to be placed on the timing of Kenoran metamorphism and deformation. The youngest unit known to be strongly affected by the Kenoran Orogeny in this area is the rhyolite east of Cléricy. The age of emplacement of the adjacent Lac Dufault Pluton relative to Kenoran metamorphism is controversial; the contact aureole around this pluton is considered to be overprinted by Kenoran metamorphic mineral assemblages by Allen and Goldie (1979) and Dimroth et al. (1983), whereas de Rosen-Spence (1976) and Gélinas et al. (1984) concluded that the aureole is entirely post-tectonic. Dimroth et al. (1983), however, agreed that the Palmorolle Pluton to the north is syn- or post-tectonic and is surrounded by a contact aureole that overprints Kenoran fabrics and metamorphic assemblages. The bulk of Kenoran deformation and metamorphism in the Noranda area can therefore be bracketed between 2698 ± 1 and 2694 ± 4 Ma.

Davis et al. (1986) have suggested that the absence of an inherited zircon component in volcanic and plutonic rocks in the western Wabigoon Subprovince supports their contention that the greenstone belt evolved in an ensimatic environment. A similar argument can be made for the Noranda area, in spite of the fact the Gélinas et al. (1984) invoked partial melting of pre-existing crustal rocks to explain observed geochemical traits in some of the volcanic rocks in the area, and Gariepy and Allegre (1985) implied a similar crustal involvement in the genesis of the Lac Dufault Pluton.

It must be re-emphasized that the age data presented here are preliminary. Additional zircon analyses for these samples, now in progress, may change some of the ages reported here very slightly, and will certainly reduce the errors presently attached to some of these ages.

ACKNOWLEDGMENTS

I thank R.I. Thorpe and members of the staff of Corporation Falconbridge Copper (Noranda Division) for assistance in selecting sample localities and in collecting some of the samples. The paper benefited from reviews by R.I. Thorpe and W.D. Loveridge.

REFERENCES

Allen, J.M. and Goldie, R.
1979: Coexisting amphiboles from the Noranda area, Quebec: extension of the actinolite-hornblende miscibility to iron-rich bulk compositiions; American Mineralogist, v. 63, p. 205-209.

Davis, D.W.
1982: Optimum linear regression and error estimation applied to U-Pb data; Canadian Journal of Earth Sciences, v. 19, p. 2141-2145.

Davis, D.W., Edwards, G., and Sutcliffe, M.
1986: Geochronology of the western Wabigoon Subprovince and its boundaries: constraints on the origin of greenstone belts; Geological Association of Canada, Program with Abstracts, v. 11, p. 61-62.

de Rosen-Spence, A.F.
1976: Stratigraphy, development and petrogenesis of the central Noranda volcanic pile, Noranda, Quebec; Ph.D. thesis, University of Toronto, Toronto, Ontario, 166 p.

Dimroth, G., Imreh, L., Rocheleau, M., and Goulet, N.
1982: Evolution of the south-central part of the Archean Abitibi Belt, Quebec. Part I: stratigraphy and paleogeographic model; Canadian Jounral of Earth Sciences, v. 19, p. 1729-1758.

Dimroth, G., Imreh, L., Goulet, N., and Rocheleau, M.
1983: Evolution of the south-central part of the Archean Abitibi Belt, Quebec. Part III: plutonic and metamorphic evolution and geotectonic model; Canadian Journal of Earth Sciences, v. 20, p. 1374-1388.

Eakins, P.R.
1972: Canton de Roquemaure, Compté d'Abitibi-Ouest; Ministère des Richesses Naturelles, Rapport Géologique 150, 72 p.

Franklin, J.M., Roscoe, S.M., Loveridge, W.D., and Sangster, D.F.
1983: Lead isotope studies in Superior and Southern provinces; Geological Survey of Canada, Bulletin 351, 60 p.

Frarey, M.J. and Krogh, T.E.
1986: U-Pb zircon ages of late internal plutons of the Abitibi and eastern Wabigoon subprovinces, Ontario and Quebec; in Current Research, Part A, Geological Survey of Canada, Paper 86-1A, p. 43-48.

Gagnon, Y.
1981a: Lithogéochemie du complexe rhyolitique de la mine Hunter, Abitibi-Ouest; Ministère de l'Énergie et des Ressources, Québec, Rapport Préliminaire, DPV-789, 33 p.
1981b: Lithogéochemie de la partie orientale du complexe rhyolitique de la mine Hunter; Ministère de l'Énergie et des Ressources, Québec, Rapport Final, DPV-826, 30 p.

Gariépy, C. and Allègre, C.J.
1985: The lead isotope geochemistry and geochronology of late-kinematic intrusives from the Abitibi greenstone belt, and the implications for late Archeanb crustal evolution; Geochimica et Cosmochimica Acta, v. 49, p. 2371-2383.

Gariépy, C., Allègre, C.J., and Lajoie, J.
1984: U-Pb systematics in single zircons from the Pontiac sediments, Abitibi greenstone belt; Canadian Jounral of Earth Sciences, v. 21, p. 1296-1304.

Gélinas, L., Trudel, P., and Hubert, C.
1984: Chemostratigraphic division of the Blake River Group, Rouyn-Noranda area, Abitibi, Quebec; Canadian Journal of Earth Sciences, v. 21, p. 220-231.

Goldie, R.
1979: Consanguinous Archean intrusive and extrusive rocks, Noranda, Quebec: chemical similarities and differences; Precambrian Research, v. 9, p. 275-287.

Hubert, C., Trudel, P., and Gélinas, L.
1984: Archean wrench tectonics and structural evolution of the Blake River Group, Abitibi Belt, Quebec; Canadian Journal of Earth Sciences, v. 21, p. 1024-1032.

Jensen, L.S.
1985: Stratigraphy and petrogenesis of Archean metavolcanic sequences, southwestern Abitibi Subprovince, Ontario; Geological Association of Canada, Special Paper 28, p. 65-87.

Krogh, T.E.
1973: A low contamination method for hydrothermal dissolution of zircon and extraction of U and Pb for isotopic age determination; Geochimica et Cosmochimica Acta, v. 37, p. 485-494.
1982a: Improved accuracy of U-Pb dating by selection of more concordant fractions using a high gradient magnetic separation technique; Geochimica et Cosmochimica Acta, v. 46, p. 631-636.
1982b: Improved accuracy of U-Pb zircon ages by the creation of more concordant systems using an air abrasion technique; Geochimica et Cosmochimica Acta, v. 46, p. 637-649.

Krogh, T.E. and Davis, G.W.
1971: Zircon U-Pb ages of Archean metavolcanic rocks in the Canadian Shield; Carnegie Institution of Washington, Year Book, v. 70, p. 241-242.
1974: Alteration in zircons with discordant U-Pb ages; Carnegie Institution of Washington, Year Book, v. 73, p. 560-563.
1975: The production and preparation of ^{205}Pb for use as a tracer for isotope dilution analyses; Carnegie Institution of Washington, Year Book, v. 74, p. 416-417.

MERQ-OGS
1985: Lithostratigraphic map of the Abitibi Subprovince; Ministère de l'Énergie et des Ressources, Québec/ Ontario Geological Survey, DV 83-16.

Nunes, P.D. and Jensen, L.S.
1980: Geochronology of the Abitibi metavolcanic belt, Kirkland Lake area – progress report; Ontario Geological Survey, Miscellaneous Paper 92, p. 40-45.

Paradis, S., Ludden, J., and Gélinas, L.
1983: Le pluton de Flavrian: pétrologie, géochemie et sa relation avec les roches volcaniques du groupe de Blake River; Ministère de l'Énergie et des Ressources, Québec, DV-83-11, p. 143-146.

Parrish, R. and Krogh, T.E.
1986: Synthesis of purified ^{205}Pb for U-Pb geochronology: prelude to worldwide distribution; Terra Cognita, v. 6, p. 152.

Roddick, J.C., Loveridge, D.W., and Parrish, R.
1986: Precise U-Pb dating of sub-milligram quantities of zircon; Terra Cognita, v. 6, p. 152.

Spence, C.D. and de Rosen-Spence, A.F.
1975: The place of sulfide mineralization in the volcanic sequence at Noranda, Quebec; Economic Geology, v. 70, p. 90-101.

Steiger, R.H. and Jäger, E.
1977: Subcommission on geochronology: convention on the use of decay constants in geo- and cosmochronology; Earth and Planetary Science Letters, v. 36, p. 359-362.

Thorpe, R.I.
1982: Lead isotope evidence regarding Archean and Proterozoic metallogeny in Canada; Revista Brasileira de Geosciências, v. 12, p. 510-521.

Thorpe, R.I., Guha, J., Franklin, J.M., and Loveridge, W.D.
1984: Use of the Superior Province lead isotope framework in interpreting mineralization stages in the Chibougamau District; Canadian Institute of Mining and Metallurgy, Bulletin, Special Volume 34, p. 496-516.

Geochemistry of scheelites associated with Archean gold deposits: implications for their direct age determination[1]

Project 750098

C.D. Anglin, J.M. Franklin, I.R. Jonasson, K. Bell[2] and E. Hoffman[3]
Mineral Resources Division

Anglin, C.D., Franklin, J.M., Jonasson, I.R., Bell, K., and Hoffman, E., Geochemistry of scheelites associated with Archean gold deposits: implications for their direct age determination; in Current Research, Part A, Geological Survey of Canada, Paper 87-1A, p. 591-596, 1987.

Abstract

The trace element contents of scheelite samples from several gold deposits in the Canadian Shield have been determined by neutron activation analysis, in order to establish the feasibility of directly determining the time of emplacement of scheelite by isotopic methods. The initial data indicate that the trace element contents of scheelite within a single deposit or district are moderately homogeneous, but contents are distinctly different between districts. Strontium and rare earth element (REE) contents are sufficient to permit isotopic determinations. Positive europium anomalies indicate that the mineralizing fluids were reduced. Differences in REE and other trace element contents between districts indicate considerable variations in the sources of mineralizing fluids.

Résumé

La teneur en éléments en traces d'échantillons de scheelite tirés de plusieurs gîtes aurifères dans le Bouclier canadien a été déterminée par analyse de l'activation neutronique afin d'établir jusqu'à quel point les méthodes isotopiques peuvent servir à déterminer, de façon directe, l'âge de mise en place de la scheelite. Les données révèlent que la teneur en éléments en traces des échantillons de scheelite est plus ou moins homogène dans un même gisement ou district, mais qu'elle varie sensiblement d'un district à un autre. La teneur en strontium et en éléments des terres rares est suffisante pour permettre le dosage isotopique de ces éléments. La présence de teneurs positives anormales en europium montre que les fluides minéralisateurs étaient réduits. La variation, d'un district à un autre, de la teneur en éléments des terres rares et en éléments à l'état de traces indique que les fluides minéralisateurs provenaient de sources très différentes.

[1]Contribution to Canada–Ontario Mineral Development Agreement 1984-1989.
[2]Carleton University, Ottawa, Ontario K1S 5B6
[3]Nuclear Activation Services.

INTRODUCTION

During the past five years, most of the mineral exploration in Canada has been focused on finding new gold deposits. Spectacular discoveries at Hemlo, Ontario, and those in northern Quebec and the Northwest Territories, have done much to sustain the exploration industry. Coincident with this enhanced level of exploration, much of the focus for mineral deposits research in Canada has been directed towards obtaining a better understanding of the processes of gold mineralization. Direct determination of the age of gold mineralization is among the more significant problems that deserve attention, and the solution of which will provide Canada's industry with better guidelines and techniques for gold exploration.

The initial phase of this research has focused on understanding the relationships of deposits to their attendant structures, host lithologies and alteration mineral assemblages. Several fundamental questions remain regarding the mode of origin of the ore-bearing fluids, and the absolute age of mineralization and alteration. If the timing of gold emplacement can be shown to be related to specific magmatic or metamorphic events, then very specific geological criteria for these events can be documented, and new or better refined guidelines for exploration can be defined.

The lack of suitable minerals for dating has precluded the direct determination of the age of gold mineralization by conventional radiogenic isotope techniques. Although ages of certain specific minerals such as molybdenite may be determined by Re-Os methods, many mineral deposit types, including gold deposits, can be dated only indirectly. The age of host rocks has been established by the U-Pb (zircon) method (e.g. porphyritic intrusions that host gold deposits at Timmins and Geraldton, Ontario, Marmont, *in* Masliwec et al., 1985). The age of hydrothermal alteration associated with gold at the Hollinger Mine has been determined by the $^{40}Ar/^{39}Ar$ method (2617 +/− 5 Ma., Masliwec et al., 1985). Model ages determined on galena samples from a variety of gold deposits (Franklin and Thorpe, 1982) indicate younger ages for the deposits relative to their host rocks. These are subject to uncertainties in the calculation parameters for model ages, but some lead isochron age determinations (Franklin et al., 1983) yield ages that seem to fit with independently determined age constraints.

One way to determine the age of gold deposits directly is to obtain isotopic analyses for minerals that are known to be coeval with gold mineralization. Scheelite, a common constituent of gold-bearing veins, may be a suitable mineral for U/Pb, Sm/Nd, and/or Sr isotopic analysis. Boyle (1979) has noted the close association of scheelite with gold mineralization, and pointed out that scheelite "occurs in deposits of all ages from Precambrian to Tertiary". For this reason, a preliminary examination of the trace element and REE contents of scheelites from gold deposits has been undertaken to determine if the levels of REE, U and Sr would be sufficient for isotopic study.

To date we have collected more than 30 samples of scheelite from active or past producing gold mines, or gold prospects within known mining camps. Of these, 19 samples were analyzed for trace element and rare earth element (REE) contents. These include; the Beardmore-Geraldton area (Leitch Mine (2), Hard Rock Mine (1) and Little Long Lac Mine (1)), Lakehead Gold Mine (1), Pickle Crow (1), the Sigma Mine (4) and the Timmins area (one each from the Dome, Coniaurum, Hollinger, McIntyre and Preston Mines). All samples were associated spatially with gold; most contained abundant native gold. Preliminary petrographic investigations indicate that both scheelite and gold were formed during the same mineralizing event. Thus, compositional data from scheelite samples should yield significant information about the mineralizing fluid(s).

SAMPLE PREPARATION AND ANALYTICAL METHOD

The samples were crushed and sieved into two fractions: −100 + 200 and −200 mesh. The coarser fraction was purified by superpanning and heavy liquid techniques, followed by washing with acetone. Further purification was accomplished using a Frantz magnetic separator. Some of the samples remained variably contaminated with a maximum of 2% pyrite.

Preliminary analyses were made using the energy dispersive X-ray fluorescence method. These data indicated that measurable strontium and rare-earth elements are present in the scheelite samples tested.

The samples were then analyzed in the laboratories of Nuclear Activation Services for a selection of trace elements, including the REE. Approximately 0.5 g of sample material was accurately weighed and encapsulated in polyethylene vials. The sample vials and NBS 1632A reference standards were co-radiated for 45 minutes at a thermal neutron flux of $7 \times 10^{12} n.cm^{-2}s^{-1}$ in the rotating RIFLS facility of the McMaster University Nuclear Reactor. After an initial nine day decay period the samples were counted on a high purity 11% relative efficiency germanium detector with a resolution of 1.7 KeV at 1332 KeV. Data were reduced using a modified version of the TEABAGS computer program which corrects for inter-element interferences and production of rare earths from fission of uranium. Internal calibration was based on approximately 30 international standards and normalized to the neutron flux monitored by the flux wire. Additional standards were used for quality control. After a further 13 days decay to allow most of the activity from ^{187}W ($t_{1/2} = 23.9$ hours) to decay, the samples were recounted to improve the precision on determination of the long-lived radioisotopes.

^{165}Dy ($t_{1/2} = 2.33$ h) was determined by irradiating the samples and standards sequentially for 10 s at a thermal neutron flux of $7 \times 10^{12} n.cm^{-2}s^{-1}$ in the microprocessor automated RABBIT system. After a decay of 3600 s the

samples were counted and compared to international and internal (synthetic) Dy standards also irradiated in the batch.

RESULTS

The data (Tables 62.1 and 62.2) indicate that scheelite typically contains several tens of ppm of REE, very abundant strontium and, in some samples, uranium. Strontium may be an important isotopic tracer in establishing the source of fluids associated with the gold mineralization; uranium and its daughter elements may possibly be used to directly determine the age of the scheelite samples.

Table 62.1 Trace element content of Archean scheelites

Sample No.	Location	Cr	Fe	Ni	Zn	Sb	Mo	U	Th	Sr
85002	G-Hardrock	3.0	0.037	120	< 10	4.1	< 50	2.0	0.4	5700
85001	G-Leitch	< 4.0	0.037	< 70	110	2500.0	< 50	6.3	<0.4	6200
85015	G-Leitch	2.0	0.080	< 50	33	8.2	100	7.6	1.1	5300
85021	G-Little LL	25.0	0.020	< 60	< 8	< 1.2	46	< 5.0	3.2	>10000
85020	Lakehead	29.0	8.500	< 60	< 8	< 1.2	18	10.0	<2.0	>10000
85016	Pickle Crow	30.0	7.200	< 70	< 10	< 1.2	31	< 6.0	<2.2	< 100
85014	Sigma	3.8	1.010	220	140	17.0	10	0.1	<0.2	200
85011	Sigma	1.5	0.046	200	55	23.0	150	< 0.5	<0.5	200
85012	Sigma	1.5	0.010	330	70	2.7	60	0.2	<0.2	100
85013	Sigma	1.8	0.013	120	33	11.0	100	0.1	<0.3	200
85022	T-Coniaurum	<12.0	5.200	540	140	4.9	54	24.7	20.0	9000
85017	T-Dome	6.5	0.120	170	< 30	3.5	100	6.5	0.5	1300
85018	T-Hollinger	4.4	0.045	300	20	2.4	90	0.7	<0.3	1100
85019	T-McIntyre	< 2.0	0.050	520	20	5.1	100	0.1	<0.2	< 100
85003	T-Preston	2.1	0.037	270	< 50	23.0	< 50	1.6	0.5	700
5324	Yellowknife	<11.0	0.239	<150	< 5	9.7	< 2	972.0	4.1	>10000
5325	Yellowknife	<11.0	0.082	120	1600	24.0	< 2	417.0	27.0	< 100
5326	Yellowknife	<12.0	0.061	< 70	<160	< 1.2	< 2	439.0	49.0	8800
5327	Yellowknife	61.0	0.067	< 7	<150	3.2	91	41.5	45.0	< 100

T = Timmins G = Geraldton-Beardmore
Note: all values are reported as ppm, except Fe which is reported as percent.

Table 62.2 Rare earth element content of Archean scheelites

Sample No.	Location	La	Ce	Nd	Sm	Eu	Tb	Yb	Lu
85002	G-Hard Rock	8.9	44	39	20.20	19.00	6.5	2.78	0.20
85001	G-Leitch	20.0	16	10	3.71	6.00	1.2	6.30	0.27
85015	G-Leitch	4.1	9	8	2.45	6.67	1.2	1.74	0.17
85021	G-Little LL	3.1	10	<10	0.46	2.58	15.0	< .80	< .01
85020	Lakehead	1.9	< 4	< 3	0.42	1.80	5.2	1.20	< .01
85016	Pickle Crow	8.3	38	<10	3.61	8.70	1.3	5.20	< .24
85014	Sigma	9.9	36	45	37.00	34.00	30.0	13.00	0.90
85011	Sigma	7.8	38	48	27.70	37.00	16.0	6.30	0.82
85012	Sigma	9.6	57	68	40.00	47.00	16.0	11.00	1.18
85013	Sigma	7.2	11	5	9.10	15.00	8.6	14.00	1.18
85022	T-Coniaurum	27.8	84	17	3.91	87.30	2.4	15.30	1.38
85017	T-Dome	22.5	47	16	3.75	23.60	2.2	5.58	0.84
85018	T-Hollinger	28.0	81	38	15.00	50.00	4.7	6.59	0.43
85019	T-McIntyre	14.6	38	38	26.00	72.00	9.1	11.90	1.83
85003	T-Preston	23.0	100	45	12.70	31.00	5.5	12.00	1.14
5324	Yellowknife	218.0	226	195	52.30	34.60	1.5	3.70	< .01
5325	Yellowknife	26.2	150	38	27.10	22.90	22.2	2.00	< .01
5326	Yellowknife	77.4	210	70	30.70	< 0.19	21.6	0.54	< .01
5327	Yellowknife	10.3	39	<10	6.30	12.30	1.3	15.50	2.52

T = Timmins G = Geraldton-Beardmore

Note: all values are reported as ppm.

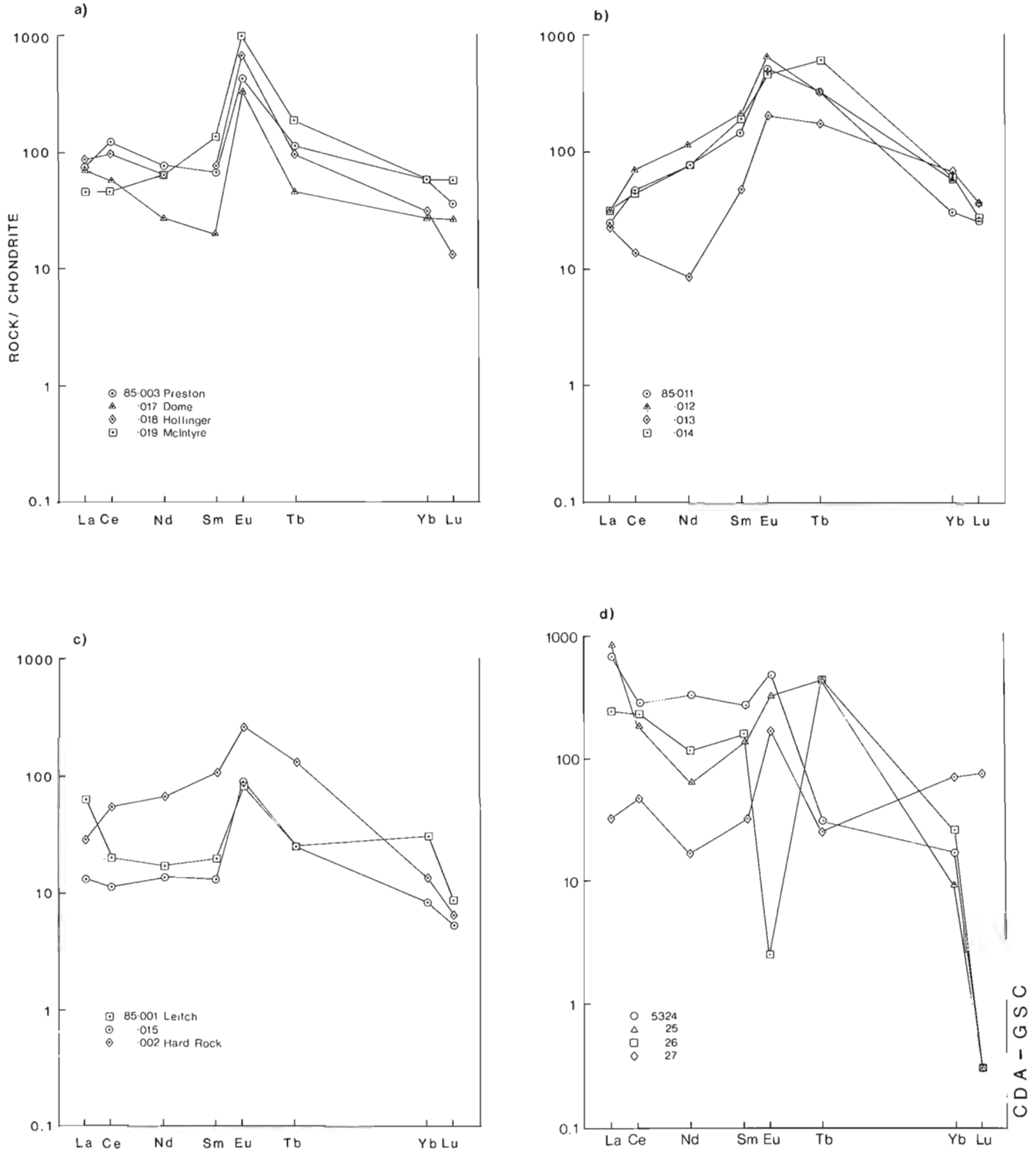


Figure 62.1. Rare earth element plots (chondrite normalized) for scheelites. a) Timmins; b) Sigma; c) Beardmore-Geraldton; d) Yellowknife.

DISCUSSION OF TRACE ELEMENT DATA

1) Strontium : The variation in content of strontium within scheelite samples for a single deposit, such as the Sigma Mine, is generally very restricted. There, the contents ranged between 100 and 200 ppm. Within each district, however, strontium contents are highly variable. Deposits in the Timmins district typically contain about 2400 ppm strontium, and those from Geraldton typically 7500 ppm. Yellowknife samples also have high and very variable Sr contents. The reasons for the differences in average strontium content between areas are not yet clear; groups of deposits with similar Sr contents (e.g. Geraldton and Yellowknife) are in very different geological settings (sedimentary rocks and porphyritic intrusions in the former area, basalt in the latter). Strontium has the same charge and similar ionic radius as calcium and likely substitutes for it in scheelite. The differences of several orders of magnitude in strontium contents of scheelite from different districts indicate that the mineralizing fluids contained different contents of strontium, and thus probably originated from different source rocks.

The contents of Sr in all cases are sufficient to permit determination of the initial $^{87}Sr/^{86}Sr$ ratios of the ore-forming fluids. Energy dispersive X-ray fluorescence analysis indicate that rubidium concentrations are less than 10 ppm (the detection limit for Rb). These ratios should have remained unaffected by radiogenic addition through time. Petrographic studies indicate that the scheelite samples have not been affected by later deformation or metamorphic effects, and thus the strontium isotopic composition should give a reliable indication of the primary fluid composition, and some indication of mantle versus crustal sources.

2) Rare earth elements: As with strontium, the REE contents within a single deposit or district are typically quite uniform, but significant variations exist among groups of deposits. For example, both the Geraldton and Sigma samples contain between 3 and 10 ppm (average of 9ppm) La, but the Timmins samples have 14 to 28 ppm (average 23 ppm) La. As with Sr, the REE contents of scheelite from Yellowknife are highly variable, and generally enriched over other deposits.

The chondrite-normalized REE patterns (Fig. 67.1) not only illustrate the relative REE contents, but also show two other features:

a) all samples have a significantly positive Eu anomaly. This is in contrast to data for scheelite samples from some other types of deposits, such as magmatic and skarn deposits, which have a distinctive negative or no Eu anomaly (Cottrant, 1981; Guion et al., 1985; Raimbault, 1985). Eu has two oxidation states, Eu^{2+} and Eu^{3+}; only Eu^{2+} normally substitutes for Ca^{2+}. A positive anomaly may therefore indicate that Eu was transported in the reduced state in the ore-forming fluid. The results of this study support similar conclusions based on the oxidation state of iron in the altered rocks associated with the Yellowknife gold deposits (Kerrich and Allison, 1978; Kerrich et al., 1977).

b) The REE patterns may be separated into two groups: 1) Samples from Timmins have relatively flat REE profiles, with the aforementioned distinctive positive Eu anomaly, and 2) samples from Sigma have a pattern with a broad positive hump in the intermediate REEs. The Geraldton-Beardmore samples show both types of profile. In both groups, the light and heavy rare earths (LREE and HREE) have approximately the same chondrite-normalized contents. Either the samples with the broad hump have incorporated the "middle" REE more efficiently than the other group, or else the REE compositions of the mineralizing fluids of each group were different. The approximate equality of the chondrite-normalized LREE and HREE indicates that the REE are partitioned more or less evenly into scheelite. Ionic radius and charge conditions which controlled the REE distribution in scheelite should be constant (with the exception of Eu), and thus different fluid compositions seem a more likely explanation of the differences in shape of the patterns. Possible temperature and pressure dependences of the REE partitioning need to be considered further, however.

From our preliminary data, it is clear that continued study of scheelite and other accessory minerals, will yield more information on the source of mineralizing fluids for gold deposits.

ACKNOWLEDGMENTS

Samples were obtained through the co-operation of mine geologists at many of the deposits mentioned above. Geologists at Pamour and Dome mines have offered advice on the project. François Robert provided the Sigma samples. Guy Darcy did the mineral separations, and preliminary chemical analyses were provided by G. Lachance of the Geological Survey of Canada. Comments by Bruce Taylor and Ralph Thorpe on earlier versions of the manuscript were most helpful.

REFERENCES

Boyle, R.W.
1979: The geochemistry of gold and its deposits, Geological Survey of Canada; Bulletin 280, 584 p.

Cottrant, J.
1983: Cristallochimie et Géochimie des Terres Rares dans la Scheelite. Application à Quelques Gisements Français. PhD thesis, L'Université Pierre et Marie Curie, Paris, France.

Franklin, J.M. and Thorpe, R.I.
1982: Comparative metallogeny of the Superior, Slave and Churchill Provinces; in Hutchinson et al., ed., Geological Association of Canada Special Paper 25, p 3-90.

Franklin, J.M., Roscoe, S.M., Loveridge, W.D., and Sangster, D.F.
1983: Lead isotope studies in Superior and Southern Provinces; Geological Survey of Canada, Bulletin 351, 60 p.

Guion, J.L., Towray, J.C., Toron, J.L., et Tullon, F.
1985: Détermination de l'état de valence prédominant de l'europium en solutions hydrothermales à partir des spectres de terres rares de couples scheelite-feldspath.

Application au de Montredon (Tarn); Bulletin de Minéralogie, No. 108, p. 851-853.

Kerrich, R. and Allison, I.
1978: Vein geometry and hydrostatics during Yellowknife mineralization; Canadian Journal of Earth Sciences, v. 15, p. 1653-1660.

Kerrich, R., Fyfe, W.S., and Allison, I.
1977: Iron reduction around gold-quartz veins, Yellowknife District, Northwest Territories, Canada; Economic Geology, v. 72, p. 657-663.

Masliwec, A., York, D., Kuybida, P. and Hall, C.M.
1985: The dating of Ontario's gold deposits: Grant 233; in V.G. Milne, ed., Geoscience Research Grant Program, Summary of Research 1984-1985: Ontario Geological Survey, Miscellaneous Paper 127, p. 223-228.

Raimbault
1985: Utilisation des spectres de terres rares des minéraux hydrothermaux (apatite, fluorine, scheelite, wolframite) pour la caractérisation des fluides minéralisateurs et l'identification des magmas sources et des processus évolutifs; Bulletin de Minéralogie, v. 108, p. 737-744.

Geological setting of two metagabbroic bodies, central Britt domain, southwestern Grenville Province, Ontario

Project 760061

T.W. Needham[1]
Lithosphere and Canadian Shield Division

Needham, T.W., Geological setting of two metagabbroic bodies, central Britt domain, southwestern Grenville Province, Ontario; in Current Research, Part A, Geological Survey of Canada, Paper 87-1A, p. 597-603, 1987.

Abstract

Detailed mapping in central Britt domain has established the geological setting of two metagabbroic bodies and a host of smaller metagabbro 'pods'. These mafic rocks are metamorphosed to upper amphibolite and possibly granulites facies. The core of the largest body contains rocks with relict olivine. Associated country rocks are metamorphosed and deformed to the extent that relict textures are rare and protoliths are for the most part obscure. Contacts with the metagabbro bodies are tectonic, or severely tectonically modified. Adjacent gneissic foliation strikes northwest and displays tight to isoclinal mesoscopic folds, locally giving rise to interference patterns. This tract of gneiss with its gabbroic pods is in the southwest limb of a major, gently southeast-plunging synform.

Résumé

Une cartographie détaillée dans le domaine central de Britt, a permis de démontrer le contexte géologique de deux petits massifs métagabbroïques et de plusieurs lentilles de nature semblable. Les roches gabbroïques ont été métamorphisées au faciès amphibolite supérieur et possiblement au faciès granulitique. Le centre du plus grand corps contient des reliquats d'olivine. Les roches encaissantes ont été métamorphisées et déformées au point où les textures résiduelles se font rares et les protolithes sont pour la plupart d'origines incertaines. Les contacts des corps métagabbroïques sont de nature tectonique ou fortement modifiés par tectonisme. La gneissosité sous-jacente est orientée vers le nord-ouest et met en évidence le plissement mésoscopique serré ou isoclinal résultant localement des formes d'interférence de plis. Ce terrain gneissique et ses corps de métagabbro se situent au côté sud-ouest d'un grand plis synforme qui plonge suivant inclination faible vers le sud-est.

[1]Department of Geology, Queen's University, Kingston, Ontario K7L 3N6

INTRODUCTION

The southwestern part of the Grenville Province in Ontario has been divided into a number of distinctive lithotectonic domains separated by broad, gradational zones of ductile shear (Davidson and Morgan, 1981; Davidson et al., 1982; Culshaw et al., 1983). It is envisaged that these domains represent stacked slices of crust which owe their tectonic setting to deep level, northwest-directed thrusting (Davidson, 1984).

The northwesternmost of these lithotectonic units, Britt domain, is composed of quartzofeldspathic gneisses among which can be recognized layered gneisses containing pelitic and rare quartz-rich and calc-silicate rocks of sedimentary origin, and orthogneisses derived from several types of plutonic rock. The orthogneisses, which yield ages between 1350 and 1500 Ma (van Breemen et al., in press), have been flattened and folded about southeast-plunging axes, giving rise to a prominent northwest-oriented structural grain for this domain. In general the rocks of Britt domain display upper amphibolite facies metamorphism, but isolated occurrences of hypersthene indicate that granulite facies was attained at least locally.

To the southeast, Britt domain is overridden by granulite facies rocks of Parry Sound domain. These two domains are separated by the Parry Sound shear zone (Nadeau, 1984), a broad, curvilinear belt of tectonized and mylonitized gneisses. Syntectonic pegmatites in the Parry Sound shear zone yield a Grenvillian age of 1160 Ma (van Breemen et al., in press).

Widely scattered among the gneissic rocks of Britt domain are several bodies of metagabbro; these are relatively equant in plan and rarely reach diameters exceeding 2 km. The bodies contain a number of mafic rock types, ranging in composition from ultramafic to anorthositic. Their states of preservation vary both from one body to another and within individual bodies. Two such metagabbro bodies are exposed on small islands at the southwest side of the southern tip of Shawanaga Island on the coast of Georgian Bay, approximately 35 km northwest of the town of Parry Sound (Fig. 63.1). They were chosen for detailed study because they are well exposed and contain occurrences of garnet-studded pyroxene-rich metagabbro, a rock found in several small mafic masses elsewhere in the Central Gneiss Belt; on account of its appearance, this rock type has been referred to as pseudo-eclogitic metagabbro (Culshaw et al., 1983). The study of these bodies, hereafter referred to as the Frederick Inlet metagabbros, will form the basis of a Master's thesis at Queen's University under the supervision of D.M. Carmichael. The aim of the project is to understand the metamorphic history of the metagabbro bodies and associated rocks, as a contribution toward understanding the metamorphic evolution of Britt domain as a whole. This report outlines the findings of detailed mapping undertaken in May and early June, 1986.

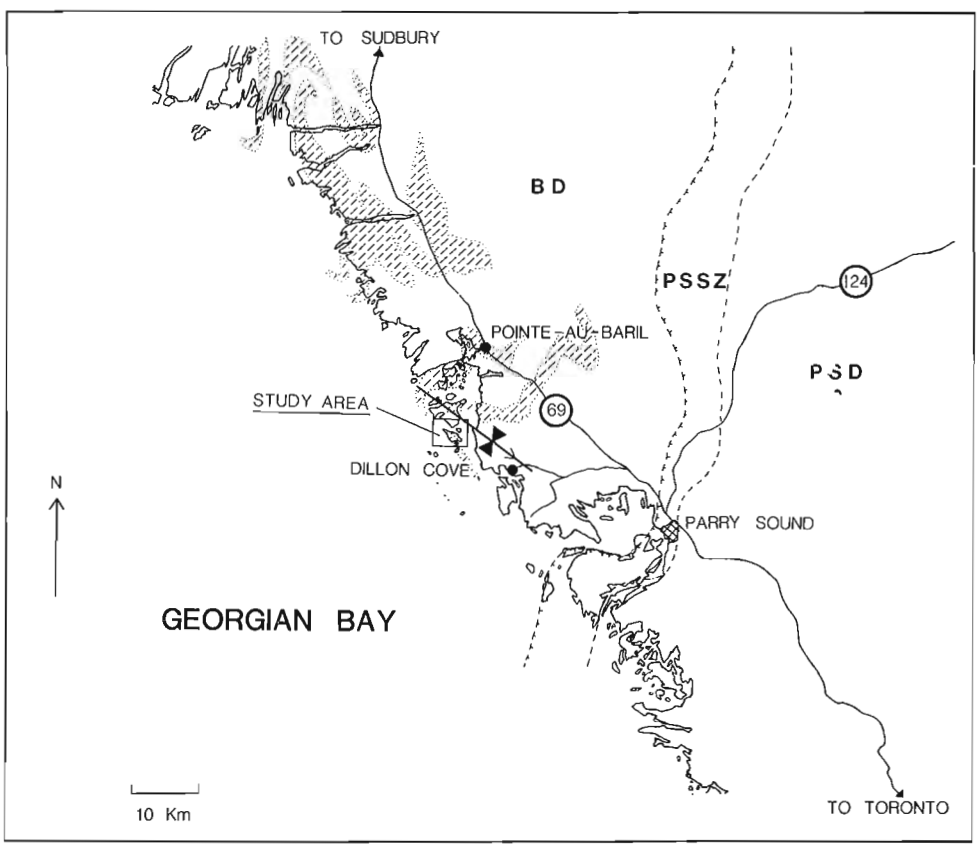


Figure 63.1. Map of the coast of Georgian Bay in the vicinity of Parry Sound showing the location of the study area and its geological setting. BD – Britt domain, PSSZ – Parry Sound shear zone, PSD – Parry Sound domain; hatched pattern denotes folded granitoid metaplutonic rocks.

ACKNOWLEDGMENTS

The author thanks Chris Robinson for his enthusiasm and help in the field, Dugald Carmichael for his advice and encouragement, Howard and Marion Coutes of Dillon Cove for the many courtesies they extended at base camp, and Tony Davidson for suggesting the project and for his support and untiring enthusiasm.

LOCAL GEOLOGICAL SETTING

The Frederick Inlet metagabbros comprise the two largest mafic masses that lie within the northwesterly structural grain formed by variably flattened quartzofeldspathic gneisses in the northeast-dipping limb of a major, southeast-plunging synform passing through Shawanaga Island (Fig. 63.1). Oval in plan, the larger, northwestern mass measures 1150 × 750 m and the smaller, 450 × 325 m (Fig. 63.2). Several smaller mafic bodies, and numerous pods too small to show at the scale of Figure 63.2, occur within the gneisses. They are generally composed of grey to buff-brown, fine grained, garnet-bearing amphibolite. They have foliated margins and may have massive cores showing relict igneous texture. The largest of the smaller bodies, 500 m east of the southeastern Frederick Inlet metagabbro (Fig. 63.2), differs in that it has a well preserved core of coronitic olivine gabbro, clearly similar to other coronites present throughout the Central Gneiss Belt (Davidson and Grant, 1986).

FREDERICK INLET METAGABBROS

The Frederick Inlet metagabbros are composed of a number of distinct rock types, each common to both bodies except for a massive, dense rock containing relict olivine which occurs only in the core of the northwestern body. The commonest rock type is fine grained, sugary metagabbro with a colour index close to 40. Plagioclase, clinopyroxene and hornblende are the dominant mineral phases; up to 10% pale pink garnet is present locally. Hornblende generally rims and partly replaces clinopyroxene. This rock exhibits a large variety of textures, ranging from homogeneous, equigranular or mottled to streaky and strongly foliated. In places it contains plagioclase-rich leucosomes ranging from millimetre-scale veinlets to centimetre-scale pods. Locally it grades into a mesocratic, buff-brown to dark grey, fine grained, sugary garnet-hornblende metagabbro. Usually massive, this rock becomes foliated only along the contacts with the gneissic country rocks. Its main minerals are hornblende, plagioclase and tiny red garnets; the rock has a metamorphic texture, though subophitic primary texture is mimicked in places.

Contained sporadically within the metagabbro are a number of buff to pinkish green, fine grained, sugary textured inclusions of garnet pyroxenite in many of which garnet dominates and clinopyroxene and minor plagioclase and biotite are interstitial. Such inclusions occupy up to 10% of the rock volume; the largest are of decimetric scale, but many appear to have broken apart to centimetre-sized pieces. The inclusions are subangular to subrounded, have either sharp or diffuse contacts and show no evidence of reaction with the host metagabbro. Where the host rock is flattened, foliation wraps the inclusions. The dominance of garnet and clinopyroxene suggests an affinity to eclogite, but the presence of plagioclase and the fact that the clinopyroxene is not an omphacitic variety (Davidson, personal communication, 1986) limits this rock to designation as 'pseudo-eclogite'.

A black to very dark green rock approaching ultramafic composition is a dominant phase in, though not exclusive to, the smaller, southwestern body. This rock ranges from fine- to coarse-grained, contains red garnet, clinopyroxene, hornblende and minor plagioclase. The garnets commonly form equant porphyroblasts and have narrow rims of plagioclase; as in the metagabbro phase already described, clinopyroxene is rimmed by hornblende. This rock type is generally massive, but locally exhibits well developed centimetre-scale layering defined by alternating concentrations of the individual constituent minerals. The layering shows no preferred orientation and cannot be traced from one outcrop to another. At two places in the northwestern body this rock type contains centimetre-scale xenoliths of the dominant metagabbro.

The core of the larger metagabbroic body contains a dense, black, fine- to medium-grained olivine metagabbro. This rock type can be recognized immediately in the field by its rounded, black, pitted surface. It contains plagioclase, clinopyroxene and relict olivine. Pale pink garnet and blue-green spinel occur locally. Texturally this unit is massive and homogeneous at outcrop scale. At one locality, a 10 m^2 area with polyhedral joints is present, the origin of which is uncertain. Inclusions of the metagabbro are also present in this rock.

Foliation has developed in the vicinity of the contact zones of the metagabbro bodies. It usually shows deflection into conformity with the adjacent contact. Isoclinal folds in the country rock gneisses are present in many places in the vicinity of the contacts. All exposed contacts are sharp and conformable with layering and foliation in the adjacent gneisses. No clear evidence of an intrusive relationship was observed; the contacts may thus have been intrusive but now severely modified, or be entirely tectonic.

COUNTRY ROCKS

All the metagabbroic bodies in the map area are in contact with light pink to grey, fine grained migmatitic gneiss. This rock generally has a sugary texture and contains pink quartzofeldspathic leucosomes. The leucosomes are well defined and demonstrate a large variation in strain; some leucosomes are highly attenuated whereas others show little evidence of deformation. The unit itself is structurally varied, ranging from well layered to well foliated and in places strongly lineated. Compositionally the pink, migmatitic gneisses range from granite to granodiorite, with mafic minerals consisting mainly of hornblende and biotite in varying proportions and together rarely exceeding 10% of the rock. The well developed layering in most of this rock suggests a sedimentary parentage, but absence of any primary features

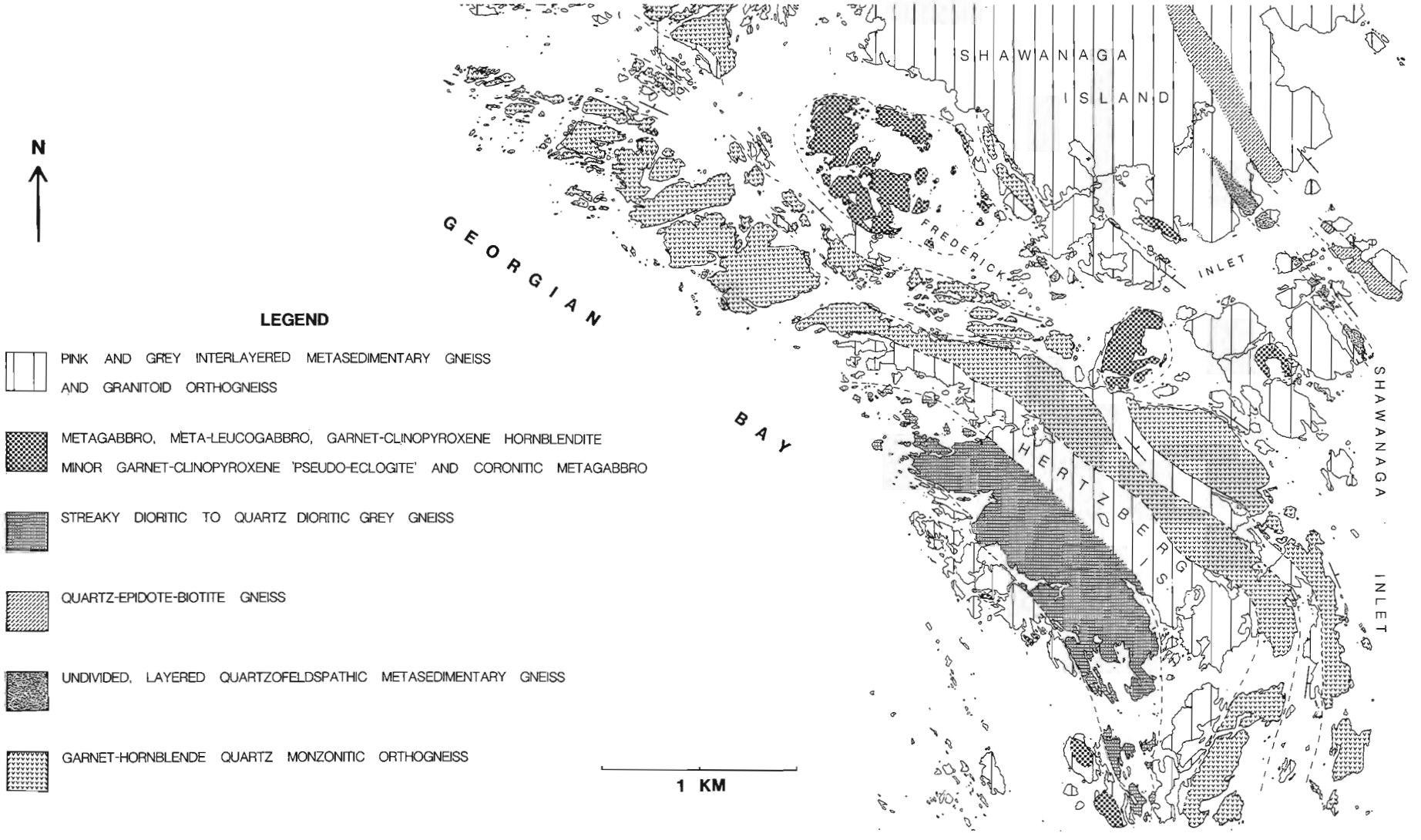


Figure 63.2. Geological setting of the Frederick Inlet metagabbros.

denies interpretation as to precursor. A number of deformed pegmatite and narrow metamafic dykes in the gneisses define tight to isoclinal folds. This demonstration of shortening is not at all apparent in the host rocks and may therefore indicate that migmatization post-dates an earlier deformation.

Immediately southwest of the Frederick Inlet metagabbros are two belts of a distinctive, highly attenuated quartz monzonite orthogneiss, separated by pink migmatitic gneiss. The orthogneiss units define the regional-scale synformal structure already mentioned. The rock is buff-brown, fine- to coarse-grained and compositionally homogeneous; it characteristically contains garnet along with hornblende, biotite, quartz and two feldspars. Distinctive are polycrystalline feldspar augen that in places have large, single crystal cores. Scattered sporadically throughout this unit are curious round, white, sugary inclusions of polycrystalline plagioclase surrounded by thin haloes of garnet. Foliation wraps these inclusions, suggested pre-tectonic origin. They may represent formerly large plagioclase megacrysts (xenocrysts?), now totally recrystallized.

The orthogneiss exhibits a strong planar and linear fabric, though locally this grades into patches or zones in which these elements are subdued and the average grain size is coarser. In these 'tectonically protected' patches, angular xenoliths of country rock migmatitic gneiss are present, strongly suggesting that the quartz monzonite precursor intruded already migmatitic gneiss. Evidence for such an intrusive relationship is rarely apparent at the contacts, however. There, foliation in the orthogneiss tends to intensify and grain size becomes markedly reduced. The megacrysts become totally recrystallized and are attenuated to thin, highly elongate polycrystalline streaks. At one locality a formerly coarse grained pegmatite has been reduced to fine grained mylonite, revealing the tectonic nature of the contact regions. The gneisses adjacent to the quartz monzonite orthogneiss commonly exhibit isoclinal folds.

At least two generations of centimetre-scale pegmatite veins cut the orthogneiss. The older generation is usually highly deformed, becoming boudined and folded. Such pegmatites may core either dextral or sinistral shears which occur thoughout the unit. The younger generation of pegmatite veins cut the country rock fabric elements and are themselves little deformed.

Southeast of the quartz monzonite orthogneiss units on Hertzberg Island, and separated from them by a belt of the pink, migmatitic gneiss, there occurs a grey to dark grey, fine grained, well foliated, streaky gneiss distinguished by its higher mafic content and the presence of garnet. Its streaky appearance is due to a strongly developed mineral aggregate lineation. Compositionally it is a quartz diorite with up to 60% mafic minerals consisting mostly of hornblende, biotite and garnet; clinopyroxene is present locally. The origin of this rock is not directly apparent.

Northeast of the Frederick Inlet metagabbro bodies an epidote-bearing quartz biotite gneiss occurs within the ubiquitous pink, migmatitic gneiss. This rock is grey to greenish grey, fine grained and sugary except for large quartz rods up to 10 cm in length, accentuated by differential weathering whereby the quartz rods form pencil-like ridges on the outcrop surfaces. Although only 200-300 m thick, this L-tectonite, here situated near the axial trace of the major synform, can be traced along strike for many kilometres to the southeast (Davidson, personal communication, 1986).

Scattered within the pink, migmatitic gneiss in the vicinity of Frederick Inlet are decametre-scale rafts of a homogeneous quartzofeldspathic gneiss, composed of several layers ranging from mafic-free, rusty to cream-white, granular gneiss to hornblende and biotite-bearing quartzofeldspathic gneiss. Differential weathering has produced grooves and ridges on outcrop surfaces that serve to accentuate intense intrafolial folding. These rocks are without obvious foliation and lineation.

The units outlined above were established on the basis of field observations; petrographic examination may modify somewhat their mineralogical descriptions.

STRUCTURE

As mentioned above, the Frederick Inlet metagabbros lie in the southwest limb of a southeast-plunging synform that is best defined by the two parallel units of quartz monzonite orthogneiss (Fig. 63.2). If these metaplutonic bodies were once roughly equant in dimension, their present folded surface form, measuring a few hundred metres wide by some 20 km along strike, is a good indication of the strain these rocks have experienced. The overall structural grain in the study area is northwest; foliation and layering dip moderately northeast. Lineations plunge shallowly either northwest or southeast. There is little deviation in attitude of the penetrative fabric elements from this orientation (Fig. 63.3).

Fold interference patterns are common in the study area, and are particularly apparent in the heterogeneous quartzofeldspathic gneisses, among which type 3 patterns (Ramsay, 1967) are readily discernible locally. Younger (F_2) fold axes are parallel to the axis of the major synform and lineation trend; some are doubly plunging. A steroplot of fold axes (Fig. 63.3C) shows definite northwest-southeast trends expressing the dominant F_2 orientation. The apparent scatter is likely due to the modification of F_1 fold axes by F_2 folding. The best examples of folding occur in the pink, migmatitic gneisses where rootless intrafolial folds, all with shallow northwest or southeast plunges, are clearly defined by transposed metamafic dykes. These folds are typically tight to isoclinal.

Extensional shears are prominent in the quartz monzonite orthogneiss. These centimetre-scale structures have steeply dipping shear planes and do not exceed more than a few metres in length. The strong foliation on the orthogneiss is deflected into the shear planes, indicating the sense of displacement and in places the amount, usually less than a metre. Cores of the shear zones commonly contain thick pegmatite dykes which are as discontinuous as the shears

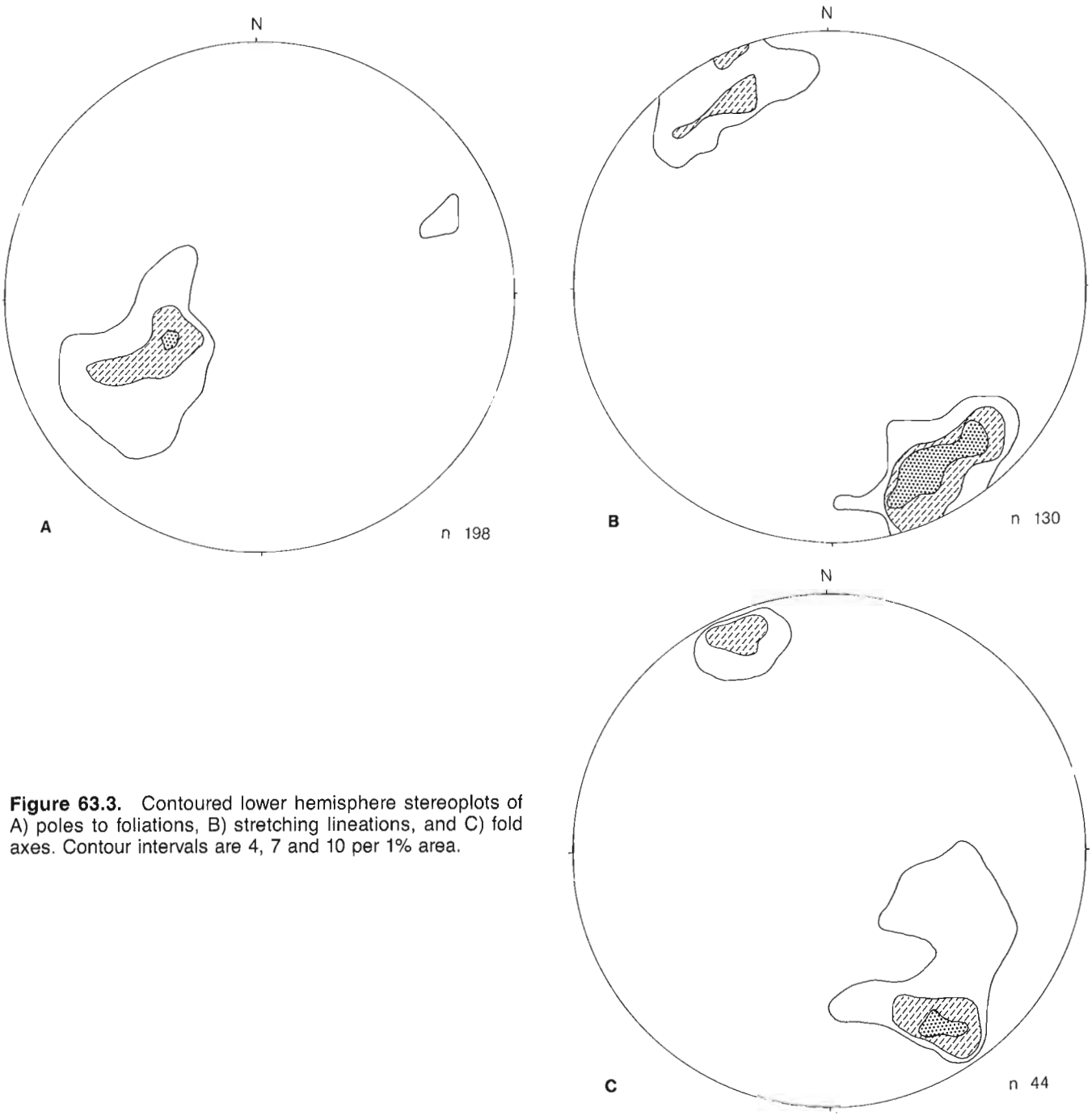


Figure 63.3. Contoured lower hemisphere stereoplots of A) poles to foliations, B) stretching lineations, and C) fold axes. Contour intervals are 4, 7 and 10 per 1% area.

themselves. Distinct from the small shears, a number of high strain zones are present in the quartz monzonite orthogneiss, marked by abrupt gradations from recognizably megacrystic orthogneiss to very fine grained rock of mylonitic aspect. These zones are only tens of metres thick and display very steep strain gradients. No kinematic sense was discernible in the field.

METAMORPHISM

Upper amphibolite facies appears to be the dominant grade of metamorphism throughout the map area, although there are no clearly diagnostic metamorphic mineral assemblages in the gneissic rocks. Sporadic occurrences of hypersthene observed in leucosomes in the orthogneiss, suggest that granulite facies was attained, at least locally. The metagabbro bodies themselves are thoroughly metamorphosed except for the cores of the coronitic gabbro body and of the largest Frederick Inlet metagabbro body, both of which contain relict olivine. These gabbroic rocks contain abundant metamorphic as well as primary clinopyroxene. Metamorphic garnet and hydrous minerals such as hornblende and biotite become prominent phases toward their margins.

The occurrence of subrounded to subangular inclusions of garnet-clinopyroxene rock, although 'pseudo-eclogite' rather than eclogite *sensu stricto*, may nevertheless indicate that these xenoliths were derived from a deep source and were carried to higher level during the emplacement of the gabbro. Their mineral assemblages may thus represent out-of-place metamorphism.

CONCLUSIONS

The Frederick Inlet metagabbro bodies occur at the same structural level within the regional layering of gneissic rocks with which they now have tectonic contacts. It is uncertain at present whether or not these bodies once formed part of a single mass or were originally two separate intrusive bodies. Keeping in mind the state of strain of the associated rocks, however, it may be suggested that these two bodies are megaboudins of a formerly single gabbroic mass.

The presence of inclusions of gabbro and leucogabbro in the more mafic phases of the metagabbro bodies indicates that these rocks have a complex magmatic history, either one of early crystallization at depth followed by incorporation of rafts in magma that then moved to higher level, or of different pulses of magma crystallized at the same, though not necessarily the present, level. Whatever the magmatic history, all the rocks are now metamorphosed and deformed such that primary minerals and most textures have been obliterated except for restricted zones in the cores of the bodies. Deformation is more severe in the quartz monzonite orthogneiss, whose extremely drawn out map pattern demonstrates the intensity of deformation experienced by these rocks.

The fact that the pink, migmatitic gneisses are homogeneous at outcrop scale and that only the transposed mafic dykes contained in this unit exhibit intense folding, strongly suggests that migmatization post-dates early deformation. It is also important to note that the quartz monzonite orthogneiss, slightly migmatized itself, likely post-dates migmatization in the country rock gneisses. These observations suggest that rocks exposed in this part of Britt domain, at least, experienced two phases of deformation and migmatization. It seems likely that the tectonic relationship of the metagabbro bodies to their country rocks was established during the second phase, to which is related the attenuation of the gneiss units and the formation of the major synformal fold.

REFERENCES

Culshaw, N.G., Davidson, A., and Nadeau, L.
1983: Structural subdivisions of the Grenville Province in the Parry Sound – Algonquin region, Ontario; in Current Research, Part B, Geological Survey of Canada, Paper 83-1B, p. 243-252.

Davidson, A.
1984: Identification of ductile shear zones in the southwestern Grenville Province of the Canadian Shield; in Precambrian Tectonic Illustrated, A. Kröner and R. Greiling (ed.); E. Schweizerbart'sche Verlagsbuchhandlung, Stuttgart, p. 263-279.

Davidson, A. and Grant, S.M.
1986: Reconnaissance geology of western and central Algonquin Park and detailed study of coronitic olivine metagabbro, Central Gneiss Belt, Grenville Province of Ontario; in Current Research, Part B, Geological Survey of Canada, Paper 86-1B, p. 837-848.

Davidson, A. and Morgan, W.C.
1981: Preliminary notes on the geology east of Georgian Bay, Grenville Structural Province, Ontario; in Current Research, Part A, Geological Survey of Canada, Paper 81-1A, p. 291-298.

Davidson, A., Culshaw, N.G., and Nadeau, L.
1982: A tectono-metamorphic framework for part of the Grenville Province, Ontario; in Current Research, Part A, Geological Survey of Canada, Paper 82-1A, p. 175-190.

Nadeau, L.
1984: Deformation of leucogabbro at Parry Sound, Ontario; unpublished M.Sc. thesis, Carleton University, Ottawa, Ontario.

Ramsay, J.G.
1967: Folding and Fracturing of Rocks; McGraw-Hill, New York, 555 p.

van Breemen, O., Davidson, A., Loveridge, W.D., and Sullivan, R.D.
— U-Pb zircon geochronology of Grenville tectonites, granulites and igneous precursors, Parry Sound, Ontario; in The Grenville Province, J.M. Moore, A. Davidson, and A.J. Baer (ed.), Geological Association of Canada, Special Paper 31 (in press).

Archean granite-greenstone boundary relationships in the Beaulieu River volcanic belt, Slave Province, N.W.T.

Project 730040

M.B. Lambert and C.R. van Staal
Lithosphere and Canadian Shield Division

Lambert, M.B. and van Staal, C.R., Archean granite-greenstone boundary relationships in the Beaulieu River volcanic belt, Slave Province, N.W.T.; in Current Research, Part A, Geological Survey of Canada, Paper 87-1A, p. 605-618, 1987.

Abstract

The geological relationships between Archean granite basement and greenstone cover shows the presence of a boundary zone characterized by relatively high strain and a mixed assemblage of basement and cover rocks. The cover rocks include a thin lens of ultramafic rocks, locally phyllonitic and serpentinized, that is continuous for at least 3 km. The structural history of basement and cover is complex. At least 3 and possibly 4 generations of folds can be distinguished. F_1 folds are accompanied by high strain and are interpreted to have developed as strongly overturned or recumbent folds prior to refolding by upright F_2 and F_3 folds. The style of F_1 folds and related deformation is compatible with the early progressive, thrust related deformation proposed by other workers although whether the cover rocks represent a dismembered Archean ophiolite is questionable.

Résumé

Les liens géologiques entre le socle granitique d'âge archéen et la couverture de schistes verts témoignent de l'existence d'une zone limite marquée par les effets de fortes contraintes et contenant un assemblage mélangé de roches du socle et de la couverture. Ces dernières se composent d'une mince lentille de roches ultramafiques qui, par endroits, affichent une nature phyllonitique et serpentinisée; cette lentille est continue sur une distance d'au moins 3 km. L'histoire structurale du socle rocheux et de la couverture est complexe. On y reconnaît au moins trois et peut-être même quatre générations de plis. Les plis F_1 sont associés a de fortes contraintes et auraient été des plis fortement déversés ou couchés avant d'avoir été déformés à nouveau par les plis droits F_2 et F_3. Le style du plissement F_1 et de la déformation associée serait compatible avec la déformation progressive plus ancienne liée au chevauchement, proposée par d'autres chercheurs, biens que l'hypothèse voulant que les roches de la couverture représentent une ophiolite archéenne démembrée soit douteuse.

INTRODUCTION

The Cameron River and Beaulieu River volcanic belts of Archean age lie in the southern part of the Slave Structural Province about 80 km northeast of Yellowknife, N.W.T. (Fig. 64.1). They are part of the Beaulieu Group (Lambert, in press) of the Yellowknife Supergroup (Henderson, 1970) which comprises thick sequences of volcanics generally overlain by greywacke-mudstone turbidites derived from a mixed felsic volcanic and granitic source. The Cameron-Beaulieu volcanic belts are deformed around basement terrane known as the Sleepy Dragon Complex (Henderson, 1985). Both basement and supracrustal rocks were intruded by extensive swarms of mafic dykes and later by a series of granitic to tonalitic plutons. Tectonic models proposed for the evolution of the Yellowknife Supergroup vary from ensialic rifts (McGlynn and Henderson, 1970) to back-arc basins (Folinsbee et. al., 1968; Helmsteadt and Padgham, 1986; Kusky, in press) to suggestions that granite-greenstone terranes are allochthonous and remnants of former accretionary complexes (Hoffman, 1986; Kusky, 1986b,in press).

Understanding the boundary relationships between the Sleepy Dragon Complex and the adjacent volcanic belts is a critical step toward testing these models. Following the 1:50 000 scale mapping of the Cameron-Beaulieu volcanic belts (Lambert, in press), investigations of the boundary zone along the northwestern side of the Beaulieu volcanic belt west of Amacher Lake (8 km northwest of Sunset Lake) were undertaken for 2 weeks during the 1986 field season to determine (1) structural relations between the volcanic belt and the Sleepy Dragon Complex, (2) history of deformation of the volcanic succession, and (3) to evaluate current hypotheses for the tectonic setting of the Cameron and Beaulieu volcanic belts.

The investigations led to the recognition of ultramafic rocks in the Beaulieu River volcanic belt which coincides with their discovery in volcanic belts near Cameron River and Point Lake (Kusky, 1986b, personal communication, 1986) and follows the first revelation of ultramafic compositions in the Slave Province, in the Hope Bay greenstone belt, by Gibbins and Hogarth (1986).

LITHOLOGICAL UNITS OF THE BOUNDARY ZONE

Units in the boundary zone include (1) granitoid gneisses of the Sleepy Dragon Complex, (2) ultramafic rocks, (3) Sunset Lake Basalt (including units of iron-formation and conglomerate), and (4) a swarm of diabasic and gabbroic dykes and sills metamorphosed into amphibolites (henceforth referred to as amphibolite dykes). All units trend northeasterly parallel to the general granite-greenstone boundary, referred to as the Amacher Shear Zone by Lambert (in press), and the general trend of the main foliation in the volcanic belt.

Sleepy Dragon Complex

The Sleepy Dragon Complex forms a rectangular block between the Cameron and Beaulieu River volcanic belts. It comprises a metamorphosed and deformed assemblage of mixed gneisses of dioritic, to granodioritic composition that are not formally subdivided. Some of its deformation predates deposition of the Yellowknife Supergroup (Henderson, 1985). The present detailed mapping includes only a small portion of the gneissic complex where it is in contact with the volcanic belt or is present as large lenticular bodies interleaved with the volcanic-dyke complex in the western part of the volcanic belt, referred to here as 'the boundary zone'. Granitoid rocks adjacent to the volcanic belt are intensely deformed by the Amacher shear zone, a 1-4 km wide zone of mylonites occurring along the eastern side of the Sleepy Dragon Complex (Lambert, in press).

In the northern part of Figure 64.1, two lenses of granitoid gneiss are present within the volcanic belt. The southern, 800 by 150 m, lens trends parallel to the boundary zone. The northern lens thins abruptly and tapers to a 40 by 300 m tongue that cuts obliquely across the volcanic belt to the northern end of Amacher Lake. Cataclasis is present along some of the exposed contacts between these granitoids and rocks of the volcanic belt.

The southernmost lens is bound to the east by iron-formation and to the west by conglomerate. Granitoids are intensely foliated all along the southern contact with iron-formation. This contact is commonly marked by 3-5 m wide band of gossan which locally also appears within the iron-formation. A thin band of iron-formation (Fig. 64.1) lies between the two granitoid lenses, which were probably separated by a dextral transcurrent fault (see below).

Ultramafic rocks and biotite schist

Ultramafic rocks were mapped for 3 km between the westernmost edge of the Beaulieu River volcanic belt and the Sleepy Dragon Complex where it is in contact with granitoid gneisses, locally mylonitic, of the Sleepy Dragon Complex. The ultramafite pinches and swells, has a maximum width of 60 m and tapers out southwards into biotite schist. The extent of the ultramafite in a northerly direction is not known. Contacts with overlying amphibolite dykes, dark green schistose mafic volcanics, mafic pillow lavas and granitoid gneisses are generally characterized by a strong foliation. Ultramafic rocks are typically characterized by pale brown to pale green weathering, smooth low relief and whale back outcrops in areas of poor or intermittent outcrop. In the northern part of the map area, the ultramafite is generally poorly exposed. It is commonly found as thin schistose smears on the western edges of volcanic bluffs that line a small northeasterly trending valley linking a series of lakes. The widest and best exposure of ultramafic rocks occurs on the eastern and southern shore of a small lake at reference locality A (Fig. 64.1). Figure 64.3 shows the complex relationships between amphibolite dyke, granitoid gneiss and the ultramafite . The ultramafite is largely a highly deformed serpentinite that shows a wide range of mineralogical and textural varieties from aphanitic serpentinite (mainly antigorite) with veins of chrysotile, fibrous actinolite, talc and chlorite schists, and relict coarse grained rocks. Some rocks

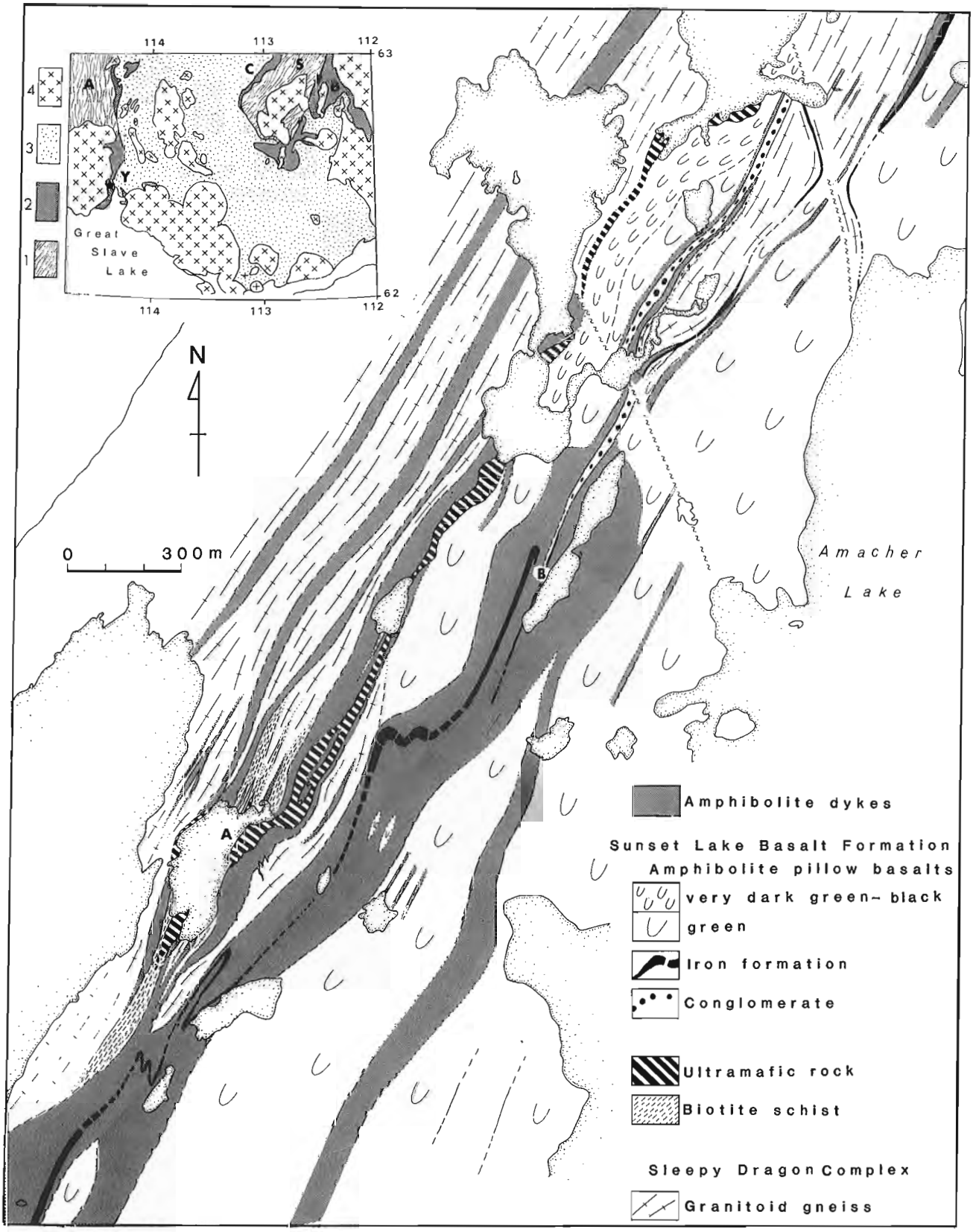


Figure 64.1. Geological map of the granite-greenstone boundary zone near Amacher Lake, Beaulieu River volcanic belt. Inset map shows geological setting of the southwestern part of the Slave Province generalized after Henderson (1985). 1 – Archean granitoid basement complexes: S, Sleepy Dragon Complex; A, Anton Complex. 2 – Volcanic belts, dominantly metabasalts with minor andesite, dacite, rhyolite: B, Beaulieu River volcanic belt; C, Cameron River volcanic belt; Y, Yellowknife volcanic belt. 3 – Burwash Formation; greywacke, mudstone-turbidites. 4 – Plutonic suites (undifferentiated). Black bar shows location of this figure and star locates the city of Yellowknife.

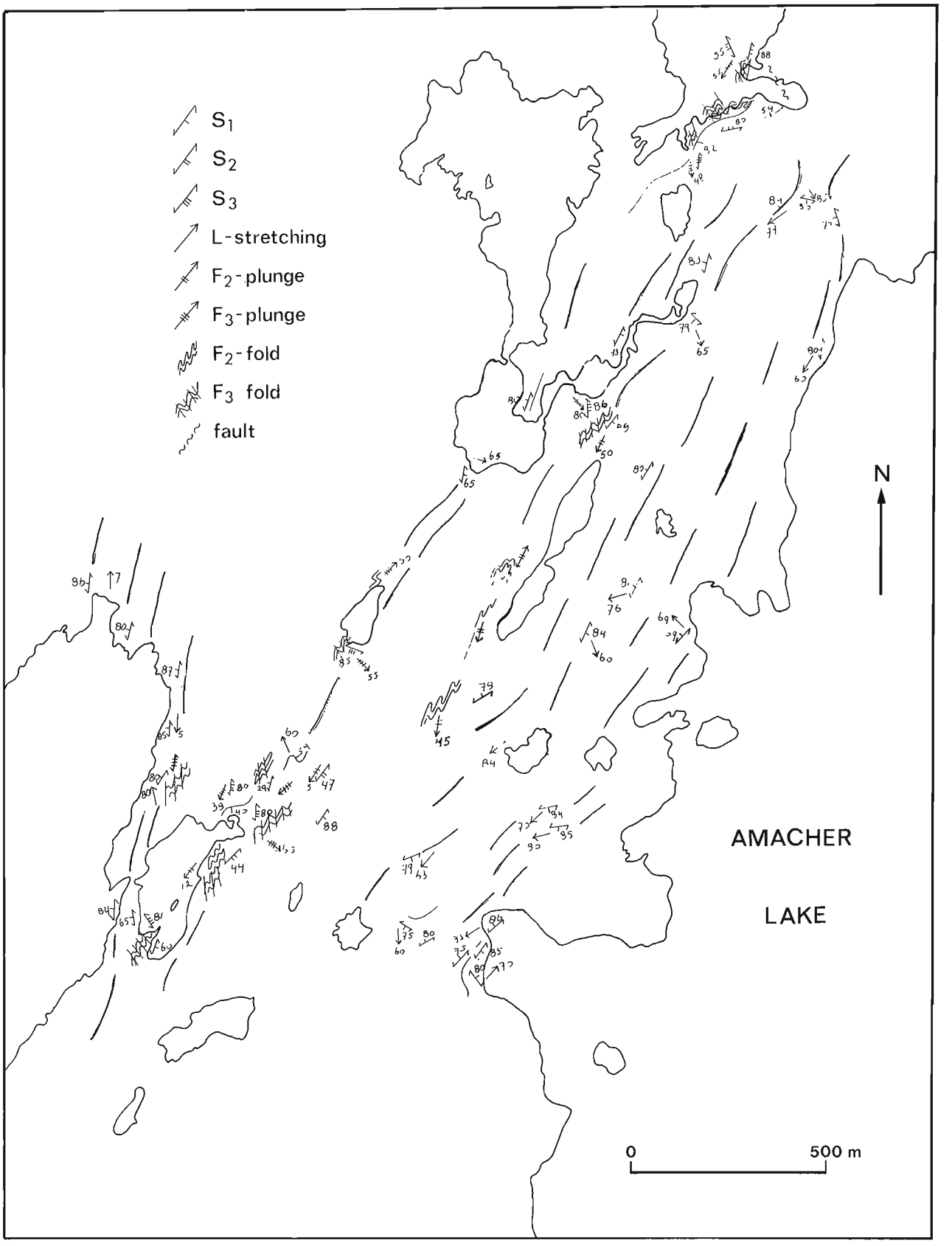


Figure 64.2. Structural map of the investigated area.

contain olivine, enstatite and amphibole (?anthophyllite). Zones of contrasting texture may represent primary igneous layering (see below).

Micaceous (mainly biotite) schists occur within but mainly as 20-50 m wide lenses immediately west and south of the ultramafite (Fig. 64.1).

Sunset Lake Basalt

Volcanic rocks in the map area belong to the lower part of the Sunset Lake Basalt formation (Lambert, in press) of the Beaulieu Group which makes up 70% of the Beaulieu River volcanic belt. The formation comprises dominantly pillow lavas, pillow breccias and associated hyaloclastite and minor layered volcaniclastic arenites (south of Amacher Lake), conglomerate and iron-formation, metamorphosed for the most part to amphibolite grade.

Pillows are everywhere deformed. The plane of flattening is invariably steeply dipping and is generally parallel to the trend of the volcanic belt. Some round to oval pillows that appear relatively undeformed in horizontal exposure are markedly elongated in vertical faces of outcrops. These elongated structures generally plunge steeply in the plane of foliation parallel to a stretching lineation (Fig. 64.4A). Typical dimensions of these pillows on horizontal surfaces range between 20 × 75 cm to 70 × 150 cm. In vertical exposures lengths are generally in the order of 300 cm.

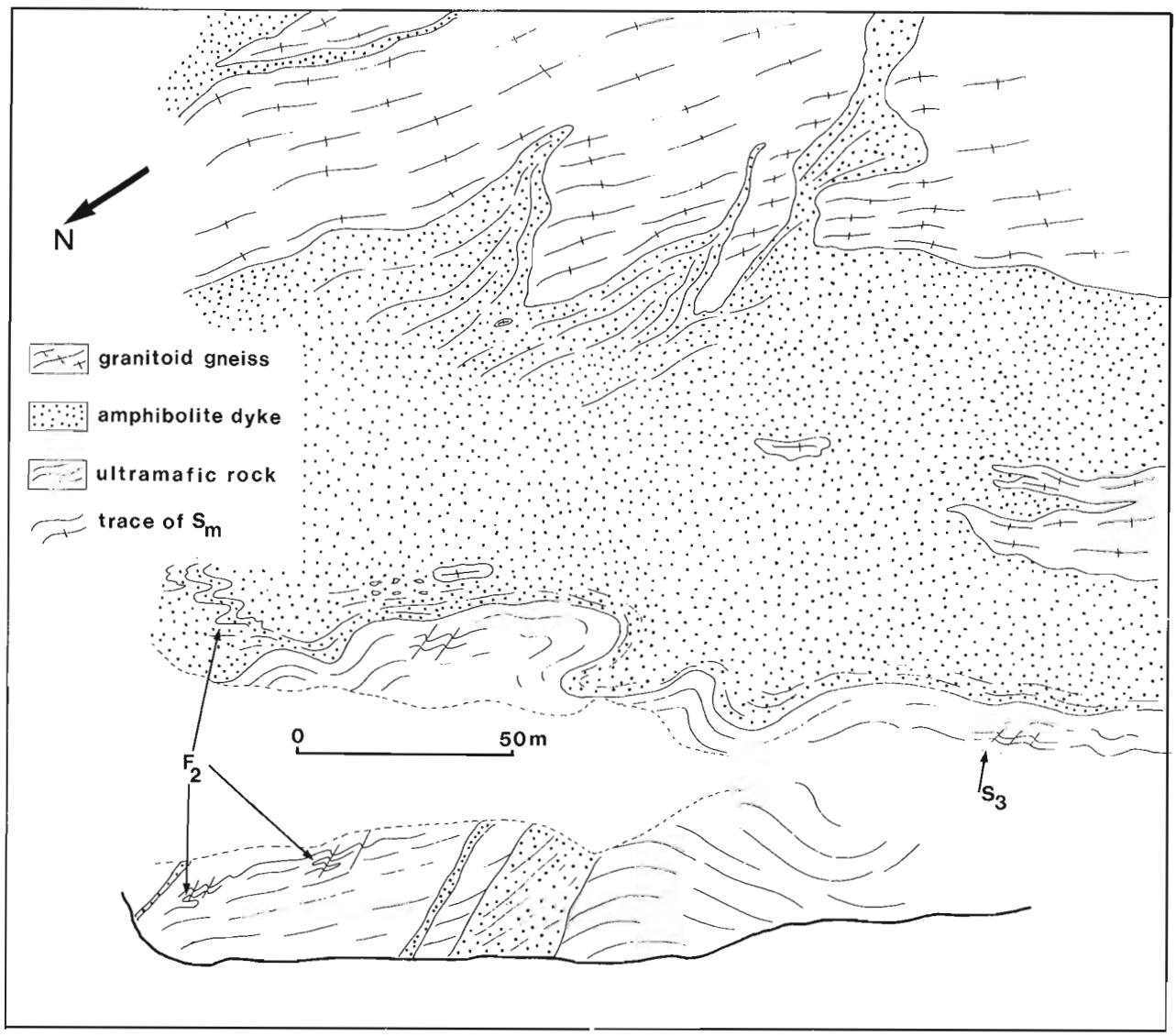


Figure 64.3. Detailed geological map showing relationships between ultramafic rock, amphibolite dyke and granitoid gneiss at reference locality A.

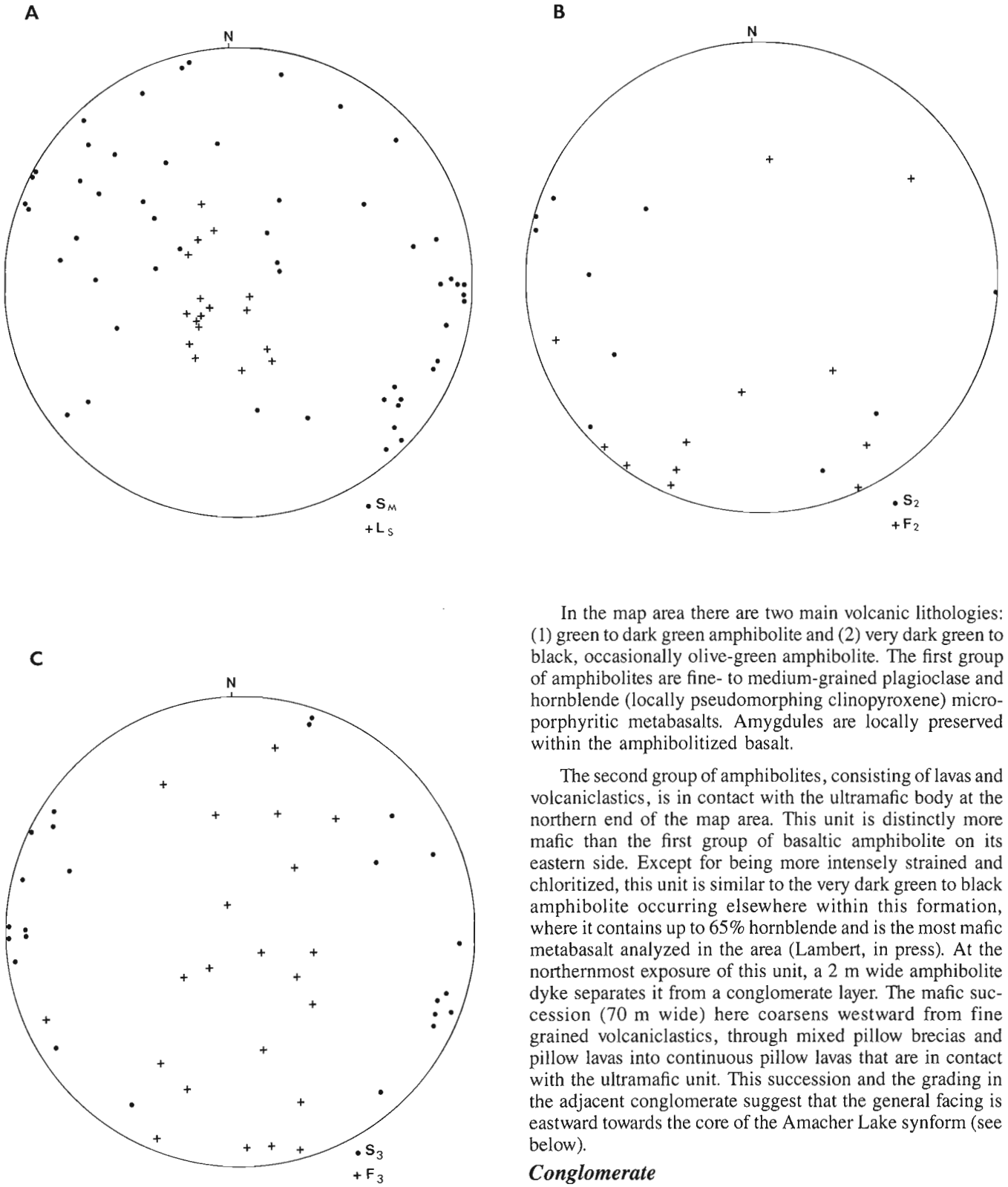


Figure 64.4. Lower hemisphere equal area projections of structural elements. A, plot of poles to the main foliation (S_0, S and S_1) and plunge of stretching lineations. B, plot of poles to S_2 and plunge of F_2 folds. C, plot of poles to S_3 and plunge of F_3 folds

In the map area there are two main volcanic lithologies: (1) green to dark green amphibolite and (2) very dark green to black, occasionally olive-green amphibolite. The first group of amphibolites are fine- to medium-grained plagioclase and hornblende (locally pseudomorphing clinopyroxene) microporphyritic metabasalts. Amygdules are locally preserved within the amphibolitized basalt.

The second group of amphibolites, consisting of lavas and volcaniclastics, is in contact with the ultramafic body at the northern end of the map area. This unit is distinctly more mafic than the first group of basaltic amphibolite on its eastern side. Except for being more intensely strained and chloritized, this unit is similar to the very dark green to black amphibolite occurring elsewhere within this formation, where it contains up to 65% hornblende and is the most mafic metabasalt analyzed in the area (Lambert, in press). At the northernmost exposure of this unit, a 2 m wide amphibolite dyke separates it from a conglomerate layer. The mafic succession (70 m wide) here coarsens westward from fine grained volcaniclastics, through mixed pillow brecias and pillow lavas into continuous pillow lavas that are in contact with the ultramafic unit. This succession and the grading in the adjacent conglomerate suggest that the general facing is eastward towards the core of the Amacher Lake synform (see below).

Conglomerate

Polymictic conglomerate forms a 1400 m long and up to 30 m wide unit, that is largely surrounded by a complex of mafic dykes. Near the central part a thin dyke splits the conglomerate longitudinally. Where the conglomerate is in contact with granitoid gneisses, the latter are cataclastically

deformed. This deformation and the presence of mafic dykes obscures the original contact relationships. Thus we cannot determine whether the conglomerate-granitoid contact is completely tectonic or a faulted unconformity.

This unit is a clast supported polymictic conglomerate comprising pebbles, cobbles and boulders in decreasing order of abundance of fine grained basaltic amphibolite, medium- to coarse-grained amphibolitic gabbro, vein quartz and granitoid gneiss. Clasts, which are flattened and elongated in a strongly foliated mafic rich matrix (Fig. 64.5), have variably oblate shapes with aspect ratios ranging from 6:6:1 to 12:6:1. Clasts are subangular (largest volcanic and gabbro fragments) to rounded (quartz and granitoid fragments) and have maximum sizes as follows: volcanic, 30×60 cm; metadiabase and gabbro, 20×40 cm; vein quartz, 4×10 cm; and granitoid, less than 10 cm. Largest clasts tend to be concentrated in crude layers and locally the outcrop shows a crude grading toward the east. In most places this is essentially a volcanic-gabbro conglomerate containing sparse (1-2 %) quartz and granite clasts.

The conglomerate is derived mainly from the enclosing volcanic pile and its related intrusives. The foliated granitoid clasts (Fig. 64.5), however, suggest proximity to a granitoid terrane that had a predepositional history of deformation (i.e. probably the Sleepy Dragon Complex).

Iron-formation

Banded iron-formation, sparse in the Cameron-Beaulieu volcanic belts, has been traced intermittently for 13 km near the western edge of the Beaulieu belt (Lambert, in press). In the central and southern part of the map area the iron formation is totally enclosed within an amphibolite dyke complex (Fig. 64.1). In one locality a thin sliver of iron-formation is in contact with volcanic conglomerate. The iron-formation, which is up to 22 m wide, is folded and perhaps split apart locally within the dyke complex. It may not be as continuous, therefore, as inferred in Figure 64.1. Contacts with surrounding amphibolite are both conformable and discordant with respect to compositional layering (Fig. 64.6A, B). In some places the abrupt termination of the iron-formation may be due to faulting or attenuation (see below).

Because of its well developed layering, the iron-formation shows some of the best evidence of polyphase deformational history within the volcanic belt. This layering is parallel to a strong, locally mylonitic, foliation in the surrounding volcanics and granitoid gneisses or schists.

The rock is a recrystallized chert-magnetite iron-formation comprising alternating white to grey quartzitic layers (less than 1 cm thick) interpreted as recrystallized chert and black to dark-green mafic layers (0.5-6 cm thick; averaging 1-3 cm). The latter consist mainly of quartz and magnetite that are locally accompanied by significant amounts of amphibole.

The iron-formation is interpreted as a single unit that has been folded, faulted and perhaps locally split apart by a complex mafic intrusion. The iron-formation may represent a local eruptive queiscence in the voluminous effusion of mafic lava that formed the Sunset Lake Basalt. It may also have been a plane of weakness in the volcanic pile which was the locus of dyke intrusion .

Dykes

North-northeast-trending mafic intrusives parallel the boundary zone and the trend of the lithological units. Although different generations of intrusives have not been distinguished, this units includes some early deformed intrusions as well as late dykes that cut across some major structures (granitoid lenses). "Amphibolite dyke" is used here as a loose term for all of the premetamorphic mafic dykes and sills. The northern end of a 6 km long by 300 m wide amphibolite dyke (Lambert, in press) intrudes or incorporates all units of the complex boundary zone. Although discordant relationships are locally preserved, the thin large intrusive complex may not have been a true dyke but rather a sill. This is a complex multiple intrusion made up of several intrusive units as indicated by internal zones of fining and chilling (the internal constitution of this dyke complex was not documented in detail).

Contacts with mafic volcanics locally are characterized by well developed foliations and/or lineations and are commonly the locus of gossans. Contacts with granitoid gneiss bodies are also obscured by deformation, so that chilling relations are difficult to establish. Although the dyke superficially appears massive and relatively undeformed, high strain is indicated by a pervasive foliation, fine grain size (reduced from presumed coarse grained size typical of large dykes elsewhere in this area) folded felsic veins and intensely



Figure 64.5. Detailed photograph of conglomerate. Note the openly, crenulated foliation in the granitoid clast below the lens cap. The main foliation in the mafic matrix is parallel to the axial planes of crenulations of the earlier foliation in the granitoid clast. The earlier foliation is interpreted as a predepositional structure considering the incompetency of the mafic clasts and matrix with respect to the granitoid clasts.

deformed migmatitic margins where locally the dyke has included swarms of granitoid inclusions. The folding of the enclosed iron-formation also suggests considerable deformation . Part of the dyke (Fig. 64.3) has intricate apophyses into granitoid gneiss on its east side, but its western margin with the ultramafic body is smooth and characterized by a well developed schistosity.

Thin undeformed and unmetamorphosed diabase dykes of north-northeasterly trend cut across the granitoid gneiss lenses in the northern part of the map area indicating that they are post major tectonic activity and may be related to Proterozoic dykes known throughout the general region (Henderson, 1985). Although some of the amphibolite dykes within the volcanic succession are probably closely related to volcanism, as has been established in other parts of the Cameron-Beaulieu belts (Lambert, in press), those in the Sleepy Dragon Complex may not be directly related to these volcanic belts.

Mineral occurrences

Gossans containing minerals such as pyrite, pyrrhotite, chalcopyrite and magnetite are common along contacts between mafic dykes and volcanics and also within the iron-formation where it is in contact with the southern granitoid lens. A line of gossans occurs in biotite schist and amphibolite immediately to the west of the ultramafic body.

STRUCTURAL GEOLOGY

Mesoscopic structure

Mesoscopic folds are generally rare in the mafic volcanic rocks. Nevertheless evidence for significant ductile deformation in the form of foliations and lineations is ubiquitous in these rocks. Folds are more common in the banded iron-formation, serpentinite and biotite schists (Fig. 64.7 and 64.8). Overprinting relationships demonstrate at least three generations of folds, designated as F_1, F_2 and F_3. In one

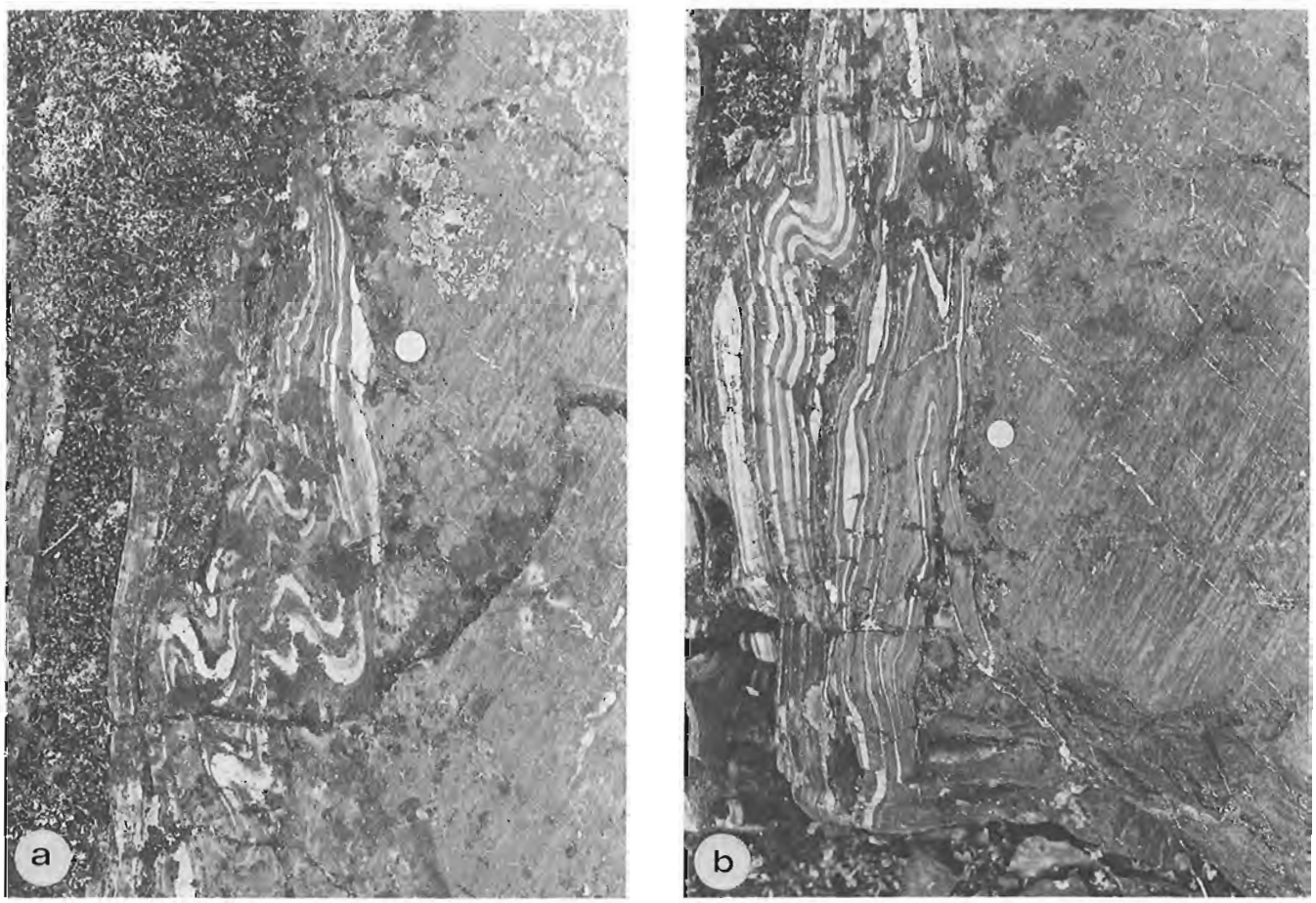


Figure 64.6 A, Preserved intrusive relationship between mafic dyke and iron-formation. B, Same mafic dyke as in A but note that dyke and iron-formation are both isoclinally folded in lower part of the photograph. These time relationships would not have been so clear without the folding. In fact, the dyke is only mildly foliated and one could easily have interpreted the timing of intrusion of the dyke in A as late syn- or post tight-isoclinal folding.

outcrop there is an indication of another generation of structures that overprints the F_3 folds.

F_1

First generation folds (F_1) generally are asymmetrical isoclines or even tighter structures (elasticas of Ramsay, 1967, p. 349). F_1 fold are most common in the banded iron-formation , where they fold a millimetre- to centimetre-scale compositional layering defined by oxide and silica rich layers. Fine millimetre-scale laminations are present within some of the individual layers. This layering probably represents bedding (S_0). Rare F_1 folded compositional layering in the serpentinite may represent relict igneous layering. F_1 folds are rare in the serpentinite and metabasalts, although evidence for F_1 related deformation in the form of a very strong, locally phyllonitic foliation (S_1) is ubiquitous. Locally this cleavage is axial planar to F_1 folds and is consistently folded by F_2 folds. F_2 or F_1 folded extensional veins filled by combinations of minerals like epidote, quartz and phyllosilicates are additional evidence for F_1 related deformation in the metabasalts. Monomineralic quartz veins are common in the biotite schists. They are locally folded by F_1 (Fig. 64.7B) together with a layering parallel foliation (S).

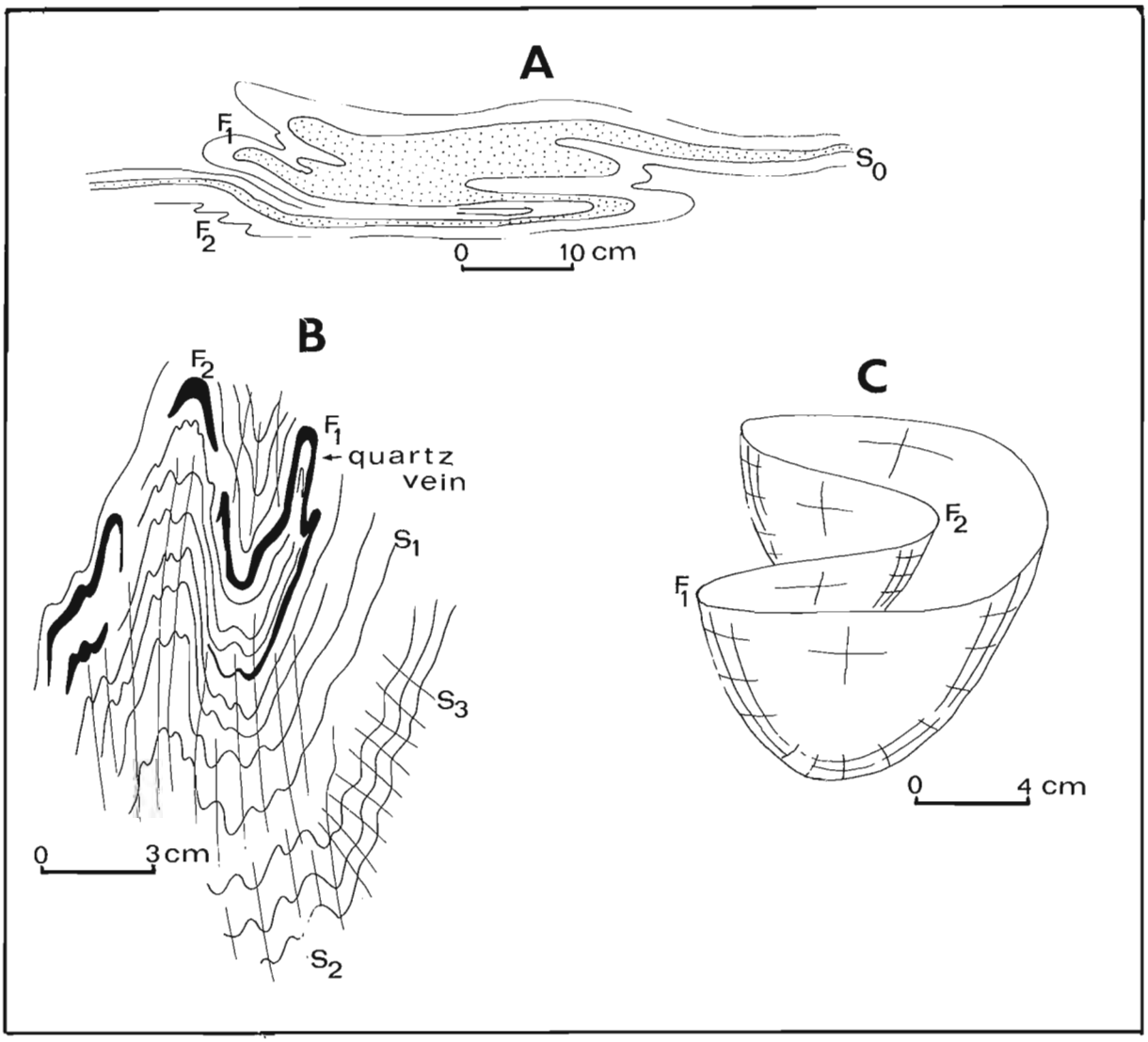


Figure 64.7. Sketches of overprinting relationships. A, F_1 fold in iron-formation with significant thickening in the hinge with respect to the limbs. B, Interference between F_1, F_2 and F_3 folds in biotite schist. F_1 folds are mainly defined by folded quartz veins, which suggest that some deformation preceded the formation of the F_1 folds. C, F_1 sheath fold in iron-formation that is refolded by F_2.

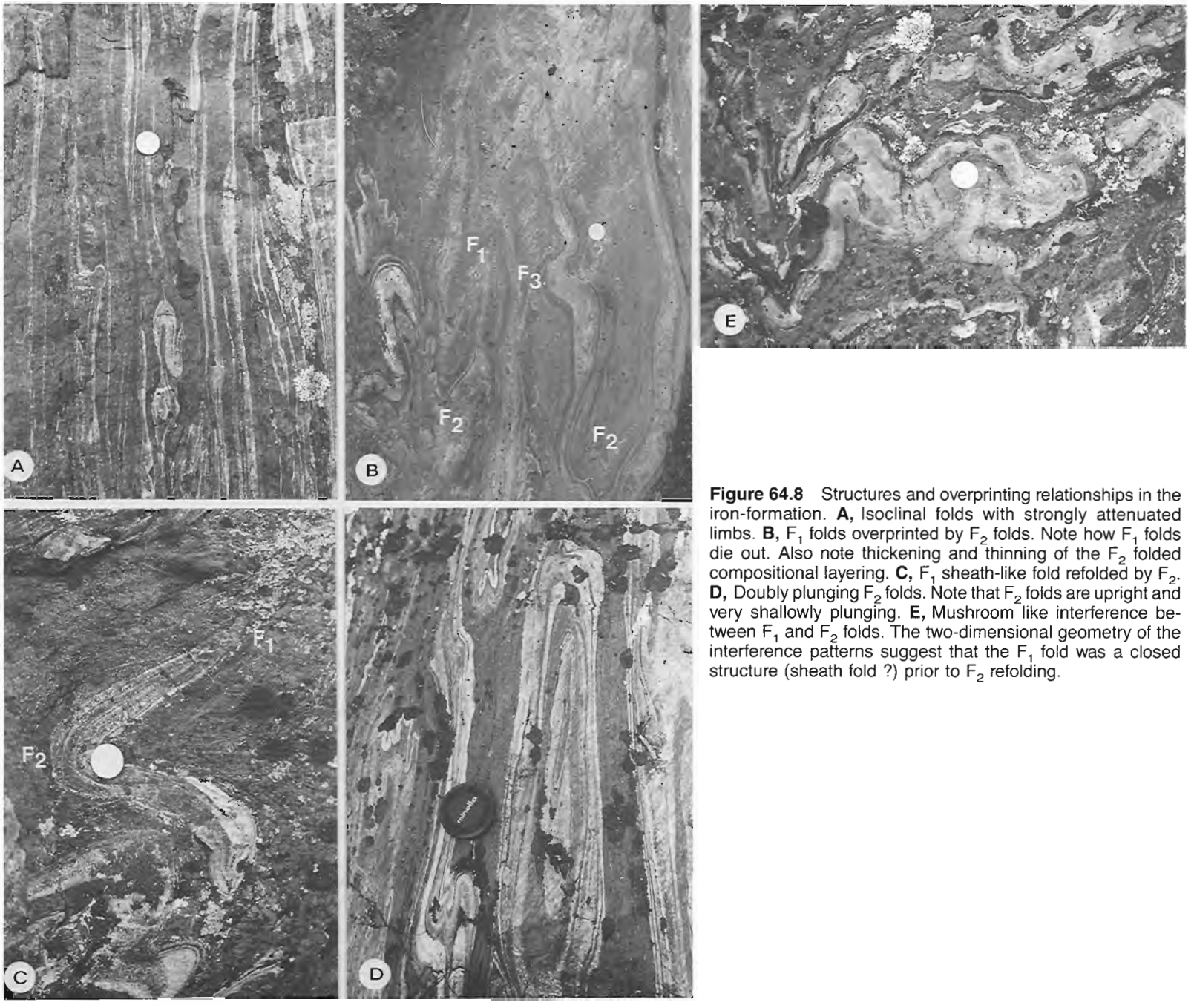


Figure 64.8 Structures and overprinting relationships in the iron-formation. **A,** Isoclinal folds with strongly attenuated limbs. **B,** F_1 folds overprinted by F_2 folds. Note how F_1 folds die out. Also note thickening and thinning of the F_2 folded compositional layering. **C,** F_1 sheath-like fold refolded by F_2. **D,** Doubly plunging F_2 folds. Note that F_2 folds are upright and very shallowly plunging. **E,** Mushroom like interference between F_1 and F_2 folds. The two-dimensional geometry of the interference patterns suggest that the F_1 fold was a closed structure (sheath fold ?) prior to F_2 refolding.

These features suggest that some deformation preceded the formation of the F_1 folds, assuming that the F_1 folded quartz veins are due to deformation induced mass transfer and the layering parallel folation is tectonic. We tentatively interpret all these structures (F_1, S, S_1 and extensional veins) as the result of one progressive deformation.

Locally F_1 folds display marked thinning (Fig. 64.7A and 64.8A) and boudinage along the long limbs to a stage that the folds become rootless (Fig. 64.8A). Transposition of layering is thus locally in an advanced stage, at least on a mesoscopic scale. Another characteristic of F_1 folds is their disharmonic nature. Most F_1 folds can be traced along the axial surface to a point where they die out.

F_1 folds vary in plunge, ranging from steep to moderately shallow. Locally where three-dimensional exposure is available at least some F_1 folds are markedly noncylindrical and closely resemble true sheath folds (Fig. 64.7C). T. Kusky (personal communication, 1986) found similar structures in the Cameron River area. The F_1 sheath folds are refolded by F_2 (Fig. 64.7C and 64.8C) and their noncylindrical shape is therefore not a product of dome and basin type interference between F_1 and F_2 folds. More likely the sheath-like shape is the product of a progressive deformation. A lineation of elongated quartz or aggregates parallel to the F_1 axis is locally observable in the silica-rich layers of the iron-formation. In the absence of thin sections, this lineation is tentatively correlated with a coaxial stretching lineation of plagioclase ribbons, amphibole needles, fibrous veins and elongated pillows in the surrounding metabasalts and gabbros. This generally steep (Fig. 64.4A) stretching lineation varies considerably in intensity and suggests that the F_1 related deformation was heterogeneous and concentrated in relatively narrow zones.

F_2

Second generation folds (F_2) are tight to isoclinal, generally asymmetrical, upright structures. Close to contact with the Sleepy Dragon Complex, however, F_2 folds are locally markedly overturned toward the west. A crenulation cleavage (S_2) axial planar to F_2 folds is present in F_2 folded biotite schists and serpentinite (Fig. 64.7B). F_2 folds plunge either in a northerly or more commonly a southerly direction (Fig. 64.4B). Locally, they are moderately doubly plunging structures (Fig. 64.8D). Exact measurements of the direction of plunge was commonly difficult or impossible because of the markedly magnetic character of the serpentinite, biotite schists and the iron-formation. Nevertheless, plunges were generally in the range between 10 and 50° (Fig. 64.8D). The tight or isoclinal, intrafolial character of F_2 folds causes transposition of all earlier foliations into parallelism with the F_2 axial planes. The regional foliation is therefore an S_2 transposition foliation, although it is for a large part made up of reoriented S_0, S and S_1. Overprinting between F_1 and F_2 folds predominantly give patterns generally taken as diagnostic of type 3 (coaxial refolding) interference (Ramsay, 1967, p. 53). However, Thiessen and Means (1980) have shown how this pattern can also be produced from certain sections through a mushroom type (type 2 of Ramsay, 1967) interference. Mushroom interference does indeed occur (Fig. 64.8E), so one could argue that all interference patterns in this area represent different cuts through type 2 patterns. Three-dimensional outcrops, however, demonstrate that, at least locally, type 3 patterns are present. Thus both type 2 and 3 interference patterns are present, indicating that F_1 plunges were probably quite variable prior to F_1 refolding, which is consistent with the closed, sheath-like F_1 folds observed in outcrop (Fig. 64.7B and 64.8C).

F_3

Third generation folds are represented by open to tight, asymmetrical structures generally with north-northwesterly trending axial planes. In strongly foliated rocks, such as the serpentinite, they are generally kinks or chevron folds with sharp angular hinges. Elsewhere, where more competent rocks such as amphibolites are involved, the folds can have rounded hinges. F_3 folds have an axial plane foliation which varies from a crenulation cleavage that fans around the hinge to a kink band boundary-like fracture cleavage. Locally there are abundant fractures that trend approximately parallel to S_3 (Fig. 64.9)

Striking is the dominantly Z-asymmetry (looking down plunge) of the F_3 folds. S-shaped F_3 folds were observed only in two outcrops. These can be explained as parasitic folds on the short limb of a larger order Z-shaped F_3 structures. F_3 folds occur most commonly in proximity to the boundary between the granitoid Sleepy Dragon Complex and the overlying greenstone belt (Fig. 64.2). F_3 fold axes show a large variation in plunge which roughly defines a girdle that approximately coincides with the average orientation of S_3 (Fig. 64.4C).

F_4

In one outcrop in the serpentinite, F_3 folds were transected by a younger cleavage (S_4) that is axial planar to open F_4 folds. The significance of this rare structure, which is similar in style to F_3 folds, is not certain.

Regional structure

The map area (Fig. 64.1) is interpreted by Lambert (in press) and Henderson (1985) to lie on the west limb of a large, N-trending, upright synformal structure, referred to here as the Amacher Lake synform. The postulation of the Amacher Lake synform, which is based on a few opposing facing directions, in pillow basalts, volcaniclastics and conglomerate from the east and west limbs of this structure, is compatible with the general dip of the main foliation (S and S_1) towards the east (Fig. 64.4A). Steeply west-dipping foliations are less common (Fig. 64.4A) and could be explained

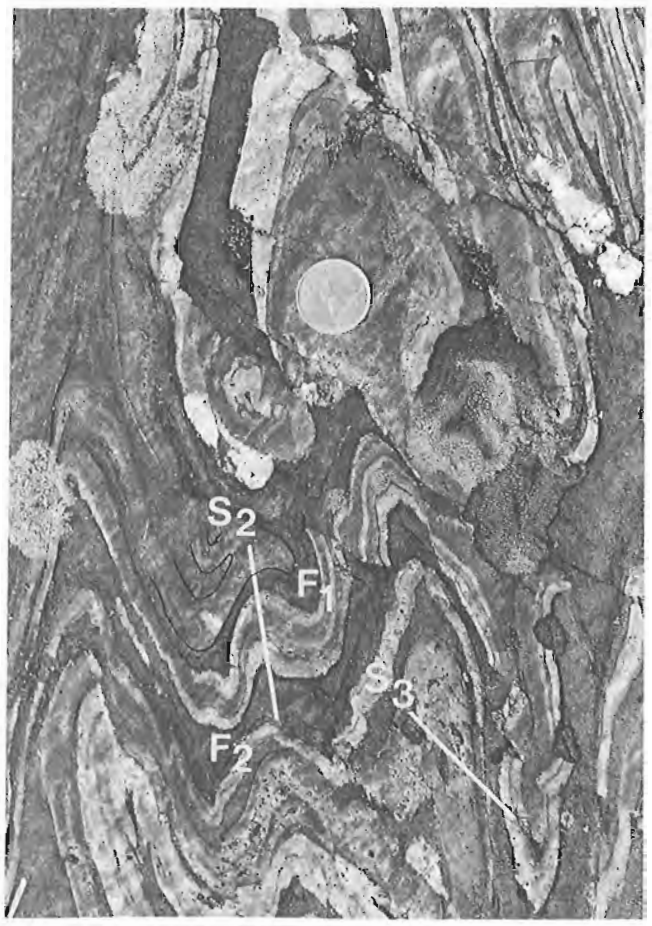


Figure 64.9. Hook-like interference pattern between F_1 and F_2 folds. Note the abundance of fractures, which show both sinistral and dextral offset. These fractures trend approximately parallel to the general orientation of S_3 in this part of the area.

as the result of smaller order folds related to the Amacher Lake synform. The existence of such folds is suggested by the outcrop pattern of the banded iron-formation, the only true marker horizon in this area. The interpretation of these folds should be treated with care, however, since the outcrop pattern is mainly based on joining discontinuous outcrops and the iron-formation is mainly surrounded by amphibolite dyke.

However, supporting evidence for the existence of at least some of these folds is provided by the style and asymmetry of the mesoscale F_2 folds. F_2 folds are generally tight, Z-shaped and gently southwards plunging on the long limbs of these interpretated structures, whereas more open and symmetrical F_2 folds occur close to, or in, the hinges. A few S-shaped folds have been observed on the short limbs, although the short limb of the best exposed of these structures, just west of reference locality B (Fig. 64.1) appears to be strongly attenuated and/or faulted. The predominantly gentle southerly plunge of the small scale F_2 folds as well the dominant Z-asymmetry suggest that the coplanar Amacher Lake synform, if it indeed exists, is probably also a southward plunging F_2 structure.

The contact between the Sleepy Dragon metamorphic complex and the Beaulieu River greenstone belt shows several Z-shaped steps on the 1:50 000 scale map of Lambert (in press). Similar steps are present in the area discussed in this paper as shown, for example, by the outcrop pattern of the serpentinite. These steps are open asymmetrical folds with N-NW-striking axial planes that redistribute S_1 and S_2 (Fig. 64.2, north margin). They are therefore interpreted as F_3 structures. Fyson (1975, 1980) recognized similar structures throughout the southern Slave Province and interpreted them as the result of regional, horizontal crustal shortening.

The outcrop pattern of the granitoid lenses in the northern part of the map area (Fig. 64.1; see also above) suggests the existence of a NW-striking, dextral transcurrent fault. Supporting evidence is the presence of cataclastically deformed rocks where this fault intersects the long lake northwest of Amacher Lake. Problematic is the geometry of the iron-formation (Fig. 64.1) in the vicinity of this fault, which suggests reversed drag. Reverse drag is a rare phenomena and mechanically not well understood (*see* also Hobbs et al., 1976 p. 306).

Timing of deformation

The main deformation in this area is Archean. Plutons of the unmetamorphosed Prosperous Lake Granite (dated at about 2520 Ma: Stockwell, 1962; Green et al., 1968; Green and Baadsgaard, 1971) which cut discordantly across the southwestern end of the Beaulieu River volcanic belt, the Sleepy Dragon Complex, and the Burwash sediments (Henderson, 1985; Lambert, in press) provide a minimum Archean age for the main F_1 and F_2 related deformation, and for tectonic activity along the Amacher shear zone. Perhaps more critical to dating deformation is the premetamorphic Amacher Granite (Henderson, 1985), considered to be a pre- or early-syndeformational pluton (Lambert, in press) which intruded at 2644 ± 14 Ma (Zircon age; J.B. Henderson and O. van Breemen, personal communication, 1986).

F_3 folds are similar in style and orientation to late minor folds with north to northwesterly trending axial planes that occur throughout the sediments and volcanic belts of the Yellowknife-Hearne Lake area (Henderson, 1985). The age of this late F_3-related deformation is poorly constrained at present and may even be post-Archean.

Northwesterly trending faults in the northern parts of the area may be related to regional faults, fresh unmetamorphosed diabase dykes and felsite dykes of this trend that transect the Sleepy Dragon Complex and the deformed volcanic belts and plutons. These faults clearly postdate the major regional structural patterns, and therefore may be Proterozoic similar to the dykes that mark them (Henderson, 1985).

DISCUSSION

Boundary zone between the Beaulieu River greenstone belt and the Sleepy Dragon Complex

Our mapping concentrated mainly on the boundary zone between the Sleepy Dragon metamorphic complex and the overlying metavolcanic and sedimentary rocks of the Beaulieu River greenstone belt. This boundary zone is characterized by discontinuous, elongated lenses of biotite schist, serpentinite, gneissic granitoids and basalt. The geometry and origin of this boundary zone is not well understood at this stage since our mapping is mainly based on a series of east-west traverses across the boundary zone, although the serpentinite was followed along strike for several kilometres. Moreover, geological relationships are further obscured by the presence of numerous gabbroic intrusives.

Detailed mapping showed that the isolated gneissic granitoid lens (Fig. 64.3) is intruded by gabbros and both are deformed by the earliest deformation recognized in the volcanic belt. Granitoid pebbles containing a foliation that is probably predepositonal are present in a narrow lens of conglomerate along the western side of the southern granitoid body (Fig. 64.1). Also, no intrusive relationships between the granitoids and the Beaulieu River supracrustals have been observed. These relationships suggest that the granitoid lenses either represent irregular-shaped basement highs or are slices of Sleepy Dragon material that were tectonically mixed with supracrustal material in the boundary zone.

Kusky (1986b) suggested that a similar boundary zone in the Cameron River greenstone belt represents a tectonic mélange, at least in part formed during ductile thrusting of oceanic crust over the top of the Sleepy Dragon Complex. We do not feel that the boundary zone investigated by us this summer represents a true mélange like the Franciscan, although deformation is more intense than in the central parts of the greenstone belt. The latter applies particularly to the serpentinite which has a strong F_1 related phyllonitic fabric.

Regional implications and discussion

Regional upright F_2 structures such as the Amacher Lake synform, have been described by Henderson (1985) from other parts of the Yellowknife-Hearne Lake area. These kilometre-scale folds are more or less symmetrical and gently doubly plunging structures (Henderson, 1985). Such structures are most simply explained by horizontal shortening of an earlier horizontal or shallow dipping layered sequence. This interpretation implies that S and S_1 were shallow dipping and F_1 folds strongly overturned or recumbent in this area prior to F_2 folding. Such an F_1 orientation is consistent with the overprinting patterns observed between F_1 and F_2 folds.

This structural history is compatible with the early F_1 related thrusting proposed by Kusky (1986a,b) in which Archean oceanic crust (greenstone belt) is emplaced on top of the Sleepy Dragon metamorphic complex, the boundary zone representing a major movement zone where rocks were highly strained and tectonically mixed. In this tectonic scenario, the asymmetry of the closed, sheath-like F_1 folds generated in S_0 and S are potential kinematic indicators. At this stage, however, we have several reservations towards Kusky's model. First, the work of Fyson (1975, 1980, 1982) suggests that the structural history of the Southern Slave Province may be more complicated than observed in the area discussed in this paper. Complications, not completely clear to us at this stage, are also indicated by the geometry of various structures in the Beaulieu River and Cameron River greenstone belts as shown on maps (Henderson, 1985; Lambert, in press).

Secondly, the presence of shallow plunging lineations and associated C-S fabrics in the zone of granitoids referred to as the Amacher Shear Zone by Lambert (in press) immediately west of the boundary zone (Fig. 64.1) indicate a dextral, strike parallel movement. These structures are more consistent with a dextral transcurrent motion than thrusting, provided the presently steep dip of the fault zone is not the result of subsequent deformation. However, the steep plunging stretching lineations in the more central part of the greenstone belt are not necessarily formed during the same period of deformation as the shallow plunging stretching lineations and are thus possibly related to a different movement picture. For instance, Lambert (in press) suggested that the Amacher Shear Zone was the site of relatively late transcurent strike-slip fault movement.

Thirdly, we are not convinced that the serpentinized ultramafic rocks mapped by Kusky (1986a,b) and by us in the boundary zones on both sides of the Sleepy Dragon Complex form part of a dismembered Archean ophiolite. For instance, the voluminous gabbroic part of ophiolite layer 3 has not been observed and the existence of a true sheeted dyke complex is still unclear.

ACKNOWLEDGMENTS

We are grateful to T.M. Kusky and W.S.F. Kidd for showing us some of their recent field results and for stimulating discussion during the first few days of our mapping in the boundary zone. We thank Rein Tirrul for critically reading the manuscript and Jack Fenton for field assistance.

REFERENCES

Folinsbee, R.E., Baadsgaard, H., Cumming, G.L., and Green, D.C.
1968: A very ancient island arc; American Geophysical Union, Geophysical Monograph 12, p. 441-448.

Fyson, W.K.
1975: Fabrics and deformation of Archean metasedimentary rocks, Ross Lake – Gordon Lake area, Slave Province, Northwest Territories; Canadian Journal of Earth Sciences, v. 12, p. 765-776.
1980: Fold fabrics and emplacement of an Archean granitoid pluton, Cleft Lake, Northwest Territories; Canadian Journal of Earth Sciences, v. 17, p. 325-332.
1982: Complex evolution of folds and cleavages in Archean rocks, Yellowknife, N.W.T.; Canadian Journal of Earth Sciences, v. 19, p. 878-893.

Green, D.C. and Baadsgaard, H.
1971: Temporal evolution and petrogenesis of an Archean crustal segment at Yellowknife, N.W.T., Canada; Journal of Petrology, v. 12, p. 177-217.

Green, D.C., Baadsgaard, H., and Cumming, G.L.
1968: Geochronology of the Yellowknife area, Northwest Territories, Canada; Canadian Journal of Earth Sciences, v. 5, p. 725-735.

Gibbins, W.A. and Hogarth, D.D.
1986: High magnesium or komatiitic peridotite from the Archean Hope Bay volcanic belt, Slave Province, Northwest Territories; Geological Association of Canada, Mineralogical Association of Canada, Canadian Geophysical Union, Joint Annual Meeting, Ottawa 1986, v. 11, p. 72.

Helmstaedt, H. and Padgham, W.A.
1986: A new look at the stratigraphy of the Yellowknife Supergroup at Yellowknife, N.W.T. – implications of the age of gold-bearing shear zones and Archean basin evolution; Canadian Journal of Earth Sciences, v. 23, p. 454-475.

Henderson, J.B.
1970: Stratigraphy of the Archean Yellowknife Supergroup, Yellowknife Bay-Prosperous Lake area, District of Mackenzie; Geological Survey of Canada, Paper 70-26, 12 p.
1981: Archean basin evolution in the Slave Province, Canada; in Precambrian Plate Tectonics, A. Kroner (ed.); Elsevier Scientific Publishing Company, Amsterdam.
1985: Geology of the Yellowknife-Hearne Lake area, District of Mackenzie: a segment across an Archean basin; Geological Survey of Canada, Memoir 414.

Henderson, J.F.
1938: Beaulieu River area, Northwest Territories; Geological Survey of Canada, Paper 38-1.

Hobbs, B.E., Means, W.D., and Williams, P.F.
1976: An Outline of Structural Geology: John Wiley & Sons, 571 p.

Hoffman, P.F.
1986: Crustal accretion in a 2.7-2.5 Ga "granite-greenstone" terrane, Slave Province, NWT: a prograding trench-arc system?; in Geological Association of Canada, Mineralogical Association of Canada, Canadian Geophysical Union, Joint Annual Meeting, Ottawa 1986, Program with Abstracts, v. 11, p. 82.

Kusky, T.M.
1986a: Basement-cover relationships in the Cameron River greenstone belt, Northwest Territories, Canada Geological Society of America, Abstract with Programs, Northeastern Section, p. 28.
1986b: Ultramafic rocks and melange units suggest an ophiolitic origin for Slave Province greenstone belts; 6th Annual Canadian Tectonics Group Meeting, Program with Abstracts.
– Are greenstones belts in the Slave Province, N.W.T., allochthonous?; in Workshop on the Tectonic Evolution of Greenstone Belts, Lunar and Planetary Institute, Houston (in press)

Lambert, M.B.
1977: Anatomy of a greenstone belt, Slave Province, Northwest Territories; Geological Association of Canada, Special Paper 16, p. 331-340.
– Cameron River and Beaulieu River Archean volcanic belts, District of Mackenzie, N.W.T.; Geological Survey of Canada, Bulletin 349 (in press).

McGlynn, J.C. and Henderson, J.B.
1970: Archean volcanism and sedimentation in the Slave Structural Province; in Symposium on Basins and Geosynclines of the Canadian Shield, A.J. Baer (ed.); Geological Survey of Canada, Paper 70-40, p. 31-44.

Ramsay, J.G.
1967: Folding and Fracturing of Rocks; McGraw Hill, 568p.

Stockwell, C.H.
1962: Interpretation of potassium-argon isotopic age GSC 60-49; in Age Determinations by the Geological Survey of Canada, Report 2, Isotopic Ages, J.A. Lowdon (ed.); Geological Survey of Canada, Paper 61-17, p. 29.

Thiessen, R.L. and Means, W.D.
1980: Classification of fold interference patterns: a reexamination; Journal of Structural Geology, v. 2, p. 311-316.

Tectono-stratigraphy and structure of the Lac Watts – Lac Cross – Rivière Déception area, central Cape Smith Belt, northern Québec

Project 850003

M.R. St-Onge, S.B. Lucas[1], D.J. Scott[2], and N.J. Bégin[2]
Lithosphere and Canadian Shield Division

St-Onge, M.R., Lucas, S.B., Scott, D.J., and Bégin, N.J., Tectono-stratigraphy and structure of the Lac Watts – Lac Cross – Rivière Déception area, central Cape Smith Belt, northern Québec; in Current Research, Part A, Geological Survey of Canada, Paper 87-1A, p. 619-632, 1987.

Abstract

In the 1.9 Ga Cape Smith Belt, thrust sheets of metasediments and metavolcanics (Povungnituk Group), pillowed basalts (Chukotat Group) and metaperidotites, metapyroxenites and layered metagabbros (Lac Watts intrusive suite) are separated by south-verging D1 thrust faults. The mafic and ultramafic units of the Lac Watts intrusive suite occur in a series of regionally extensive, kilometre-scale thick thrust sheets which distinguish the complex from the relatively thin gabbro-peridotite sills emplaced in the Povungnituk and Chukotat groups. Possible interpretations for the origin of the Lac Watts suite include a Bushveld-type layered intrusion or the layered cumulates and peridotites of an ophiolite suite. Two distinct sets of D1 thrust faults can be recognized: (1) pre-thermal peak regular stacking sequence thrusts and (2) pre- to post-thermal peak out-of-sequence thrust faults. A syn-thermal peak basal shear zone developed during D1 deformation locally contains imbricates of mylonitic Archean basement gneiss interleaved with Povungnituk Group thrust sheets along the north margin of the thrust-fold belt. Two post-thrusting episodes of basement and cover folding, late metamorphic east-west D2 folds and post-metamorphic north-south D3 cross folds, provide the necessary structural relief for the study of D1 mesoscopic and macroscopic structures.

Résumé

Dans la zone de Cap Smith d'âge 1,9 Ga, trois nappes de charriage, constituées de roches métasédimentaires et métavolcaniques (groupe de Povungnituk), de basaltes en coussins (groupe de Chukotat) ainsi que de métapéridotites, tétapyroxénites et métagabbros stratifiés (série intrusive de Lac-Watts), sont séparées par des chevauchements de type D1 orientés vers le sud. Les unités mafiques et ultramafiques de la série intrusive de Lac-Watts se trouvent dans une série de nappes de charriage régionales d'une puissance de 1 km environ qui séparent le complexe des filons-couches relativement peu épais de gabbro-péridotite dans les groupes de Povungnituk et de Chukotat. Il est possible que la série de Lac-Watts provient d'une intrusion stratifiée de type Bushveld ou de cumulats et de périodites stratifiés appartenant à une série ophiolitique. On peut reconnaître deux ensembles distincts de chevauchements de type D1 : 1) des faiiles inverses en succession régulière correspondant au maximum préthermique et 2) des chevauchements désordonnés correspondant au maximum pré-thermique à post-thermique. Une zone de cisaillement de base correspondant au maximum synthermique s'est formée pendant la déformation de type D1 et renferme par endroits des structures imbriquées constituées de gneiss mylonitique du socle archéen intercalé avec des nappes de charriage du groupe de Povungnituk le long de la marge nord de la zone constituée de pli-failles. Deux épisodes post-chevauchement, de plissement du socle et de la couverture, plus de type D2 tardi-métamorphiques de direction est-ouest, et plis transversaux de type D3 post-métamorphiques de direction nord-sud, fournissent le relief structural nécessaire à l'étude des structures mésoscopiques et macroscopiques de type D1.

[1]Department of Geological Sciences, Brown University, Providence, Rhode Island, U.S.A. 02912
[2]Department of Geological Sciences, Queen's University, Kingston, Ontario K7L 3N6

INTRODUCTION

The 1.9 Ga (R. Parrish, pers. com. 1986) Cape Smith Belt is a multiply-deformed thrust-fold belt (Hynes and Francis, 1982; Lamothe et al., 1984; Hoffman, 1985) preserved near the north margin of the late Archean Superior craton. The eastern half of the thrust-fold belt is exposed in a west-plunging oblique section displaying over 15 km of structural relief (St-Onge et al., 1986). Systematic regional mapping, during the summer of 1986, in the Lac Watts – Lac Cross – Rivière Déception area allowed identification of major tectono-stratigraphic units and documentation of their structural and metamorphic histories at relatively high structural levels. These results complement the tectono-stratigraphic, structural and metamorphic relationships established at relatively deep structural levels in the Wakeham Bay area by St-Onge et al. (1986). The two map areas will be linked during the summer of 1987 by regional mapping at intermediate structural levels to provide complete coverage and documentation of the exposed oblique section.

Summary of results

The highlights of eleven weeks of fieldwork in the central Cape Smith Belt map area (Fig. 65.1) are summarized as follows:

1. Povungnituk Group (Bergeron, 1959) metasediments and metavolcanics and Chukotat Group pillowed basalts occur as regionally extensive, distinct tectono-stratigraphic packages bounded by south-verging D1 thrust faults.
2. The Chukotat Group is devoid of sediment, and everywhere occurs in thrust faulted contact with Povungnituk Group units.
3. The Lac Watts intrusive suite consists of metaperidotites, metapyroxenites and metagabbros occurring in thrust-bound sheets interleaved with Povungnituk Group thrust packages. The kilometre-scale thickness of individual intrusive suite thrust sheets as well as the centimetre-scale cyclic layering in metagabbro suggests that the suite represents an imbricated, very large mafic-ultramafic body. Possible analogues include a Bushveld-type layered intrusion or the layered cumulates and peridotite of an ophiolite suite.
4. The distinct tectono-stratigraphic packages of the Povungnituk and Chukotat groups and Lac Watts intrusive suite are separated by D1 thrust faults characterized by narrow high strain zones. The attitudes of frontal thrust ramps in the southern (external) part of the thrust belt, and the sense of shear from shear bands associated with syn-thermal peak thrusts in the northern (internal) region are consistent with all thrusts verging southward.
5. D1 thrust faults can be grouped into two distinct sets: (1) pre-thermal peak, regular (piggy-back) stacking sequence thrusts (Boyer and Elliott, 1982); and (2) pre- to post-thermal peak, out-of-sequence thrust faults (Butler, 1982; Searle, 1985; Platt, 1986).
6. Imbricates of mylonitic Archean tonalite gneiss interleaved with Povungnituk Group thrust sheets occur in the Rivière Déception area within the syn-thermal peak basal shear zone (St-Onge et al., 1986).
7. Syntectonic tonalite plutons in the Lac Watts – Rivière Déception area are restricted to the hangingwall of a late out-of-sequence D1 thrust fault. They intrude both Povungnituk Group metavolcanics and thrust sheets of the Lac Watts intrusive suite.
8. The final map pattern and the spectacular structural relief in the thrust-fold belt is the result of a regional type 1 fold interference pattern (Ramsay, 1967). Two post-thrusting episodes of basement and cover folding produced late metamorphic east-west D2 folds and post-metamorphic north-south D3 folds.
9. In the Lac Cross area, late oblique-slip faults with a significant west-side-down normal slip component result in the east-west map scale repetition of distinct D1 fold closures and faults.

TECTONO-STRATIGRAPHIC UNITS

The regional-scale mapping in the Lac Watts – Lac Cross – Rivière Déception area has documented that units of the Povungnituk Group, Chukotat Group and Lac Watts intrusive suite occur as distinct D1 thrust packages. As a result, primary relationships between these tectono-stratigraphic groups are indeterminable. However, on the basis of a geochemical study of metabasalts across the map area, Hynes and Francis (1982) and Francis et al. (1983) concluded that the chemical evolution recorded between Povungnituk Group Fe- and Ti-rich continental tholeiites, Chukotat Group komatiitic basalts and Chukotat Group low-Ti tholeiites with MORB affinities reflects magma evolution in an epicontinental rift which ultimately formed oceanic crust.

Povungnituk Group

The lower part of the Povungnituk Group (Bergeron, 1959) in the map area (Fig. 65.1) consists predominantly of rusty, finely-laminated, biotite-rich semipelites which locally grade into thin (2-10 m) successions of micaceous sandstone. These clastic metasediments are locally carbonate-rich. Metabasites and meta-mafic sediment are also present, both as individual beds intercalated with the clastic sediment and as more extensive, kilometre-scale mafic volcanic centres. The Povungnituk Group metasediments and associated metavolcanic rocks are found in thrust sheets within the northern margin imbricate zone (Fig. 65.1), in a thrust sheet south of Lac Watts (H, Fig. 65.1) and in two thrust sheets near Lac Cross (C and E, Fig. 65.1). East of the area outlined in Figure 65.1, clastic sediments occurring within a fault-bound lozenge ("horse", in terminology of Boyer and Elliott, 1982) along a thrust fault within the Chukotat volcanics (separating thrust sheets F and G, Fig. 65.1) are correlated with the

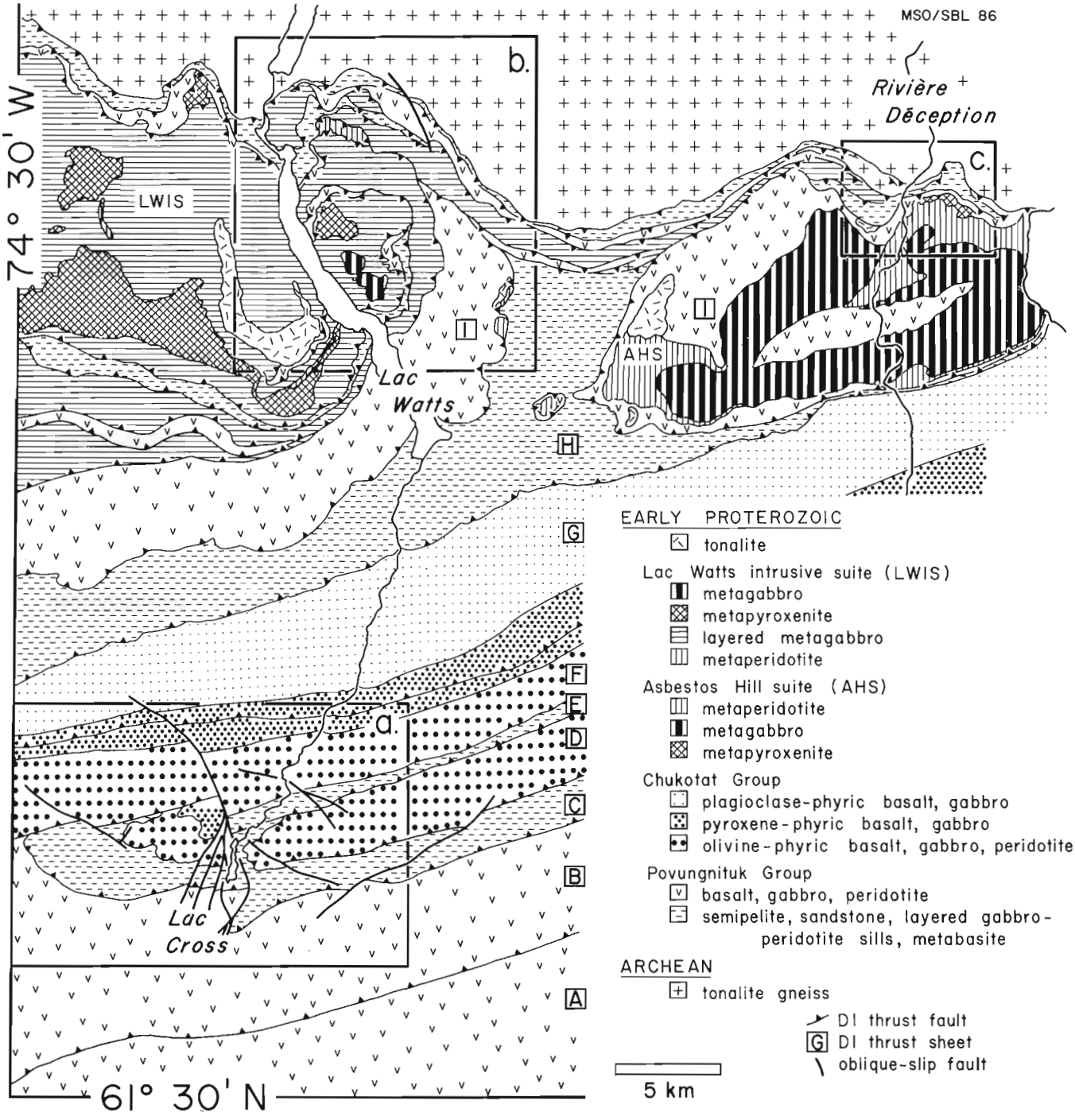


Figure 65.1. Geological map of the eastern Cape Smith Belt, Lac Watts – Lac Cross – Rivière Déception area. Descriptions of early Proterozoic units are given in text. Outlined areas "a", "b" and "c" correspond to areas in Figure 65.5, 65.6 and 65.17.

lithologically similar Povungnituk Group sediments observed on both the north and south margins of the belt. The lozenge contains a spectacular polymictic conglomerate and local arkosic sandstone beds. The conglomerate is poorly sorted, with subangular to subrounded clasts of tonalite gneiss, quartz, metabasalt and argillite forming a clast-supported framework filled with a matrix of biotite and chlorite (Fig. 65.2).

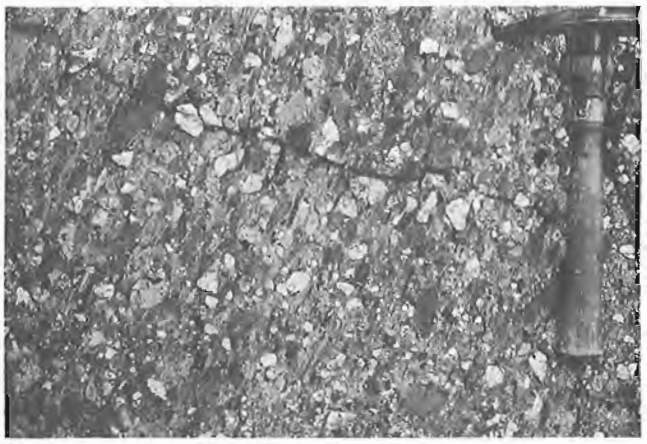


Figure 65.2. Povungnituk Group polymictic conglomerate with pebbles of tonalite gneiss, metabasite, argillite and quartz. Length of hammer is 34 cm. GSC 204234



Figure 65.3. Peridotite at base of layered peridotite-gabbro sill dipping to the north (left) and emplaced in Povungnituk Group metasediments. Peridotite unit is 200 m thick and shows well developed columnar jointing. GSC 204234-A



Figure 65.4. Plagioclase cumulate layering in gabbro above peridotite of Figure 65.3. Gabbro thickness in layered sill is 205 m. Length of pen is 15 cm. GSC 204234

The clastic metasediments in the Lac Cross thrust sheets are host to numerous layered peridotite-gabbro sills. These sills generally represent simple, in situ differentiated cooling units, with multiple magma influxes documented for only the largest sills. The maximum measured thickness of a layered sill in the Lac Cross area is 500 m. The base of the sills is commonly characterized by a pyroxenite chilled border phase overlain by columnar jointed peridotite (Fig. 65.3). The thicker sills show a layered gabbroic upper sequence above the peridotite, with cyclic plagioclase cumulate layering (Fig. 65.4), ferrogabbro and quartz ferrogabbro zones and in places a granophyric upper intrusive contact.

The upper part of the Povungnituk Group (Bergeron, 1959) consists of interlayered pillow basalt lavas, massive basalt flows and numerous gabbro sills for which Hynes and Francis (1982) reported Fe- and Ti-rich tholeiitic compositions. Minor amounts of rhyolite attest to the bimodal nature of the Povungnituk volcanism. Rare semipelite and fine grained sandstone are preserved between the flows.

Thick sequences of Povungnituk Group metabasites are preserved in two thrust sheets south of Lac Cross (A and B, Fig. 65.1) and in another thrust sheet originally extending from the southern half of Lac Watts to the Rivière Déception area (I, Fig. 65.1). Thrust sheet I is host to a large mafic-ultramafic sill complex, termed the Asbestos Hill suite (Fig. 65.1), dominated by gabbro displaying several differentiated intrusive units. Povungnituk Group metabasites are also found in relatively thin (50-500 m) thrust sheets in the northern margin imbricate zone.

Chukotat Group

The Chukotat Group (Bergeron, 1959), in contrast to the upper part of the Povungnituk Group, is devoid of sediments and consists of pillowed and massive basalt flows and relatively thin (5-100 m thick) mafic and layered mafic-ultramafic sills. The volcanic rocks range in composition from highly magnesian (komatiitic) basalts to low-Ti, tholeiitic basalts with affinities to modern MORBs (Hynes and Francis, 1982). The Chukotat Group in the map area is preserved in three thrust sheets between Lac Cross and Lac Watts (D, F, G, Fig. 65.1). Primary textures and volcanic structures, such as variolitic pillow margins, ropy lava, pillow lava and flowtop breccia are well preserved within the Chukotat Group. Three distinct pillow basalt types can be recognized based on the presence of a dominant pseudomorphed phenocryst type (Francis and Hynes, 1979; Hynes and Francis, 1982; Francis et al., 1983). As a result, olivine-phyric, pyroxene-phyric and plagioclase-phyric pillowed basalts were mapped (Fig. 65.1).

In the vicinity of Lac Cross (Fig. 65.5), olivine-phyric pillow basalts of the Chukotat Group are juxtaposed against underlying clastic metasediments of the lower part of the Povungnituk Group and associated layered peridotite-gabbro sills. The contact is characterized by a narrow (1-5 m) schistose zone in metabasites in which primary volcanic features are progressively destroyed, indicating accumulation of high strains. In addition, a map-scale discordance exists between Chukotat Group lavas and underlying Povungnituk Group metasediments and sills, such that the layered sills are cut-off against the overlying Chukotat Group pillowed metabasalts (Fig. 65.5). The presence of the high strain zone in the

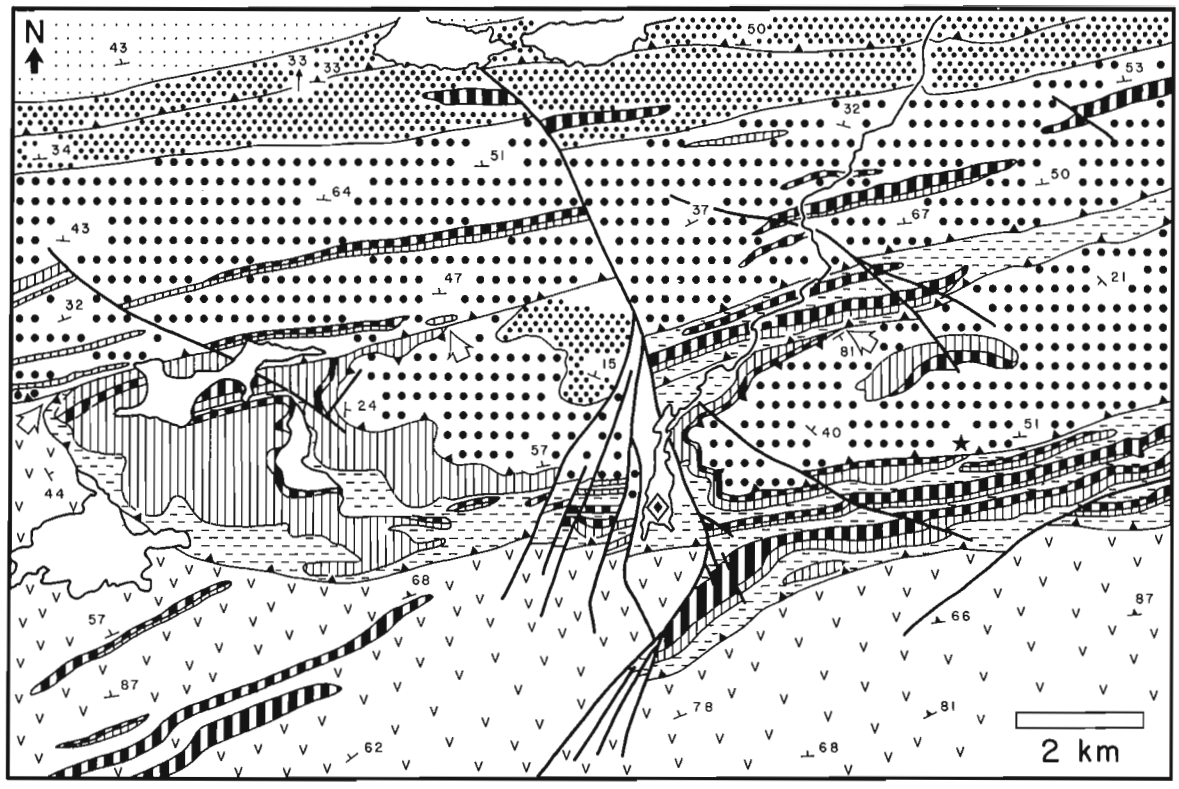


Figure 65.5. Geological map for area "a" outlined in Figure 65.1. East-plunging D1 Lac Cross syncline closure is repeated by a set of oblique-slip (west-side-down) faults. Open arrows refer to cut-offs of early regular sequence thrusts by later out-of-sequence thrust. Star refers to layered sill cut-off on footwall of thrust D.

basalts at the contact, and truncation of layered sills against the overlying basalts strongly suggest that a fault separates the Povungnituk and Chukotat groups. The fault, by analogy with the other regional faults, is interpreted as a thrust.

Lac Watts intrusive suite

Around the northern half of Lac Watts (Fig. 65.1, 65.6) a series of extensive, kilometre-scale thick imbricates of metaperidotite, metapyroxenite and layered metagabbro are interleaved with thrust sheets of both lower and upper Povungnituk Group units. The imbricates of metaperidotite, metapyroxenite and metagabbro are tentatively interpreted as consanguineous and are collectively named the Lac Watts intrusive suite (LWIS). Individual LWIS thrust sheets vary in thickness from 100 m to greater than several kilometres and the structurally highest LWIS thrust sheet (Fig. 65.1, 65.6) occupies the core of the large east-trending D2 synclinorium in the Lac Watts area (Fig. 65.7).

LWIS metaperidotites weather greenish grey, tan or reddish brown and often show centimetre- to metre-scale

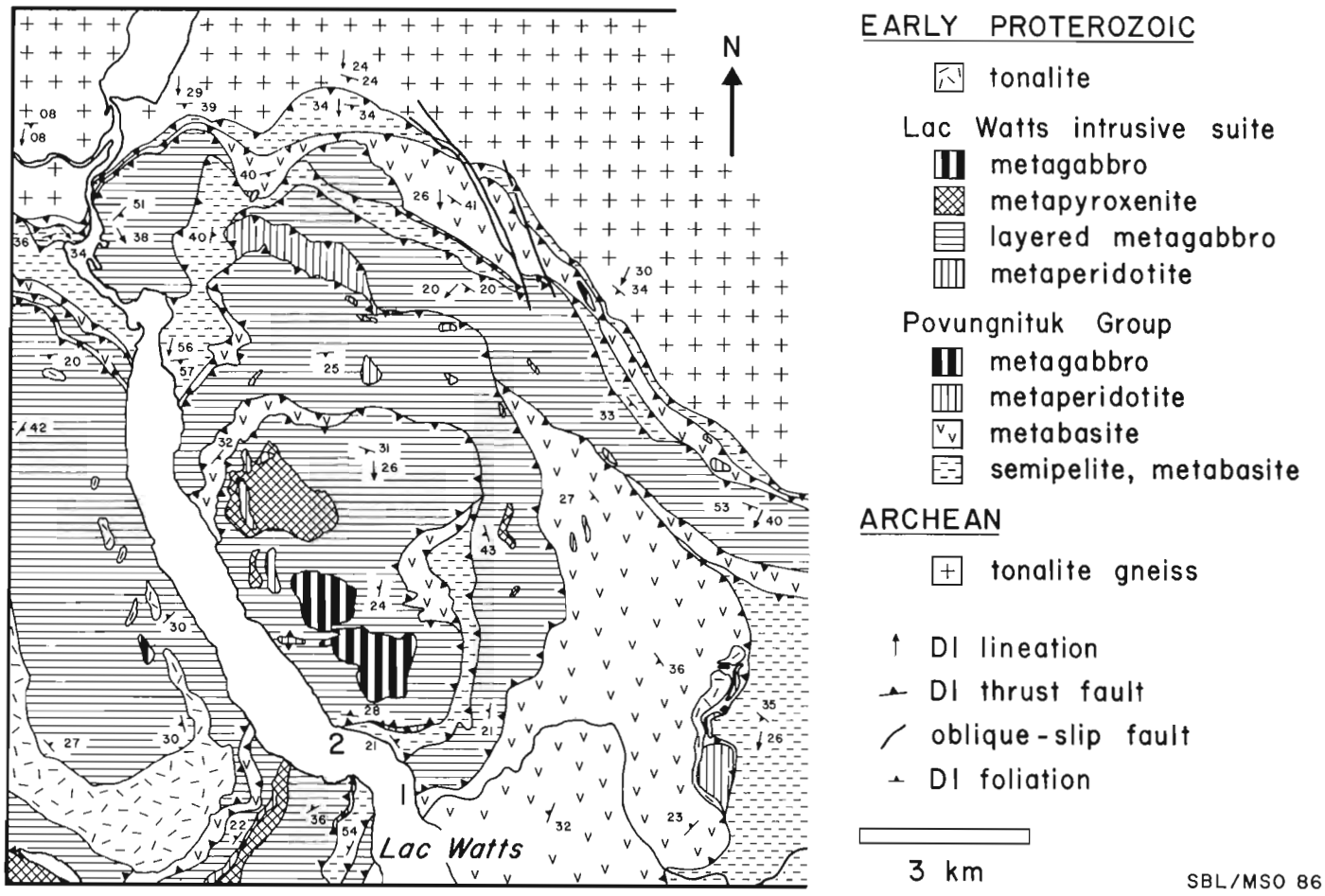


Figure 65.6. Geological map for area "b" outlined in Figure 65.1. Thrust fault bounded units of the Lac Watts intrusive suite (LWIS) are preserved in the core of the large east-west D2 synclinorium centred on Lac Watts (*see* Fig. 65.7). Out-of-sequence thrust faults numbered 1 and 2 are discussed in text.

layering defined by subtle colour changes and differential weathering. These changes are attributed to modal variations in the general metamorphic assemblage tremolite (-actinolite) - serpentine-talc-magnetite, which are in turn interpreted to reflect modal variations in the original igneous mineral assemblage. Up to 8 cycles showing a systematic increase in layer thickness from 2 cm to 2-3 m can be measured locally. Metaperidotite bodies occur in two different settings: as fault-bound lozenges (horses) at the base of thrust sheets of LWIS layered metagabbro, and as intrusions into both metagabbro and metapyroxenite of the LWIS. The largest metaperidotite body, northeast of the north end of Lac Watts, is a 500 m thick fault-bound lens incorporated into the overlying metagabbro thrust sheet and transported above a major D1 thrust fault. Margins of the fault-bound lenses of metaperidotite are characterized by the loss of primary layering during the development of high strain schistose zones, often with either an actinolite schist or a talc-magnetite schist as the final product.

LWIS metapyroxenite forms large tabular bodies intrusive into the layered metagabbroic sequence (Fig. 65.1) or metre-thick layers in the layered metagabbro which are commonly boudined (Fig. 65.8). The large tabular bodies have long dimensions that vary from three to over ten kilometres. The local presence of layered metagabbro xenoliths in the metapyroxenite at the margins of the large bodies clearly documents their intrusive relationship with the metagabbro. In the relatively low strain interiors of these bodies the assemblage hornblende-biotite-relict pyroxene prevails, with a coarse, several centimetre grain size and primary cumulate textures visible locally. Within the layered gabbroic sequence, individual pyroxenite layers have been either penetratively strained to form a hornblende-biotite schist or have been boudined to form low strain blocks wrapped by schistose hornblende-biotite margins (Fig. 65.8). Garnet is present in the metapyroxenite near the north margin of the belt.

The layered metagabbros form the most volumetrically

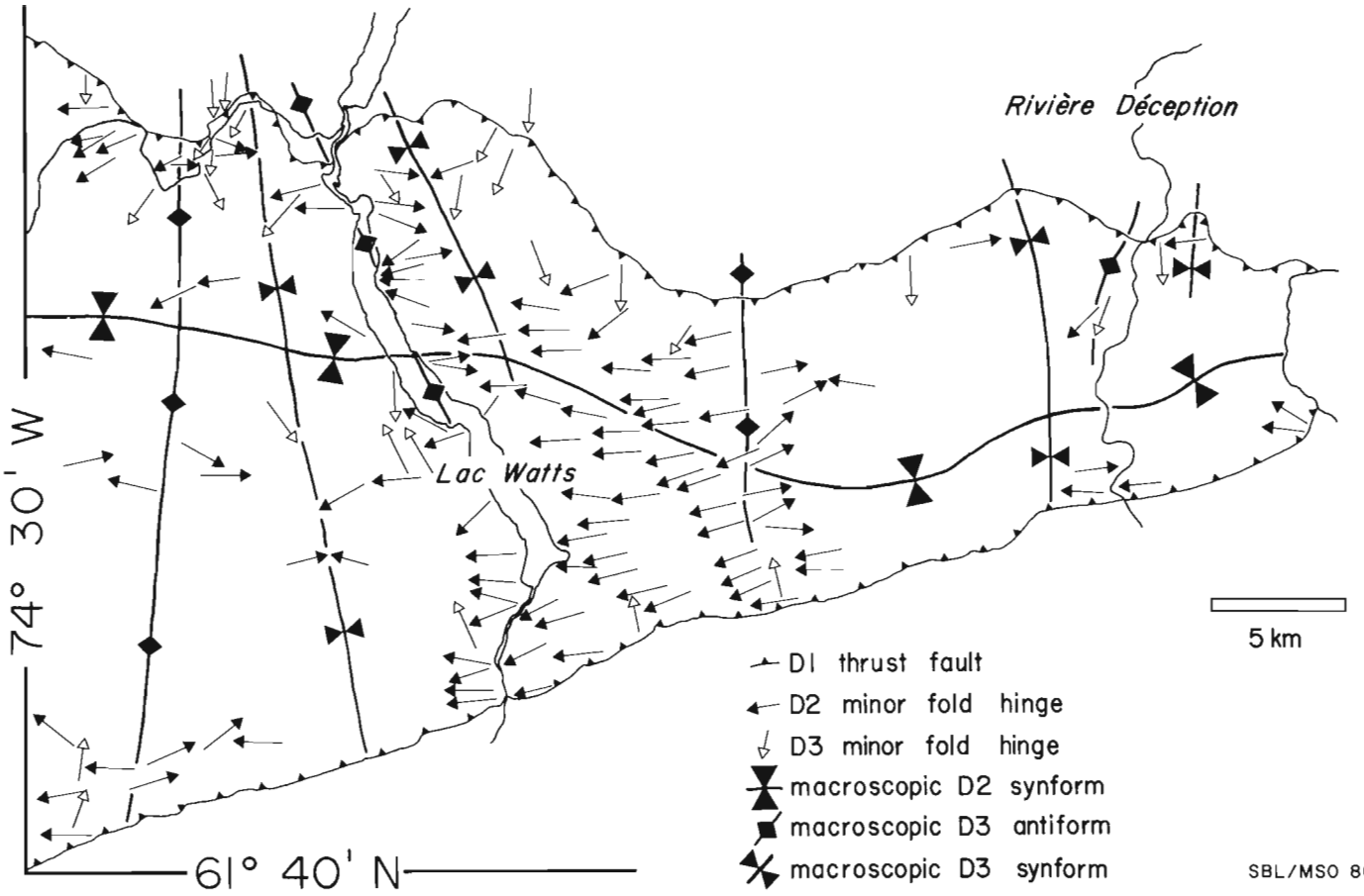


Figure 65.7. Mesoscopic and macroscopic D2 and D3 fold hinge compilation north of out-of-sequence thrust H (*see* Fig. 65.1).

important unit of the LWIS. The metagabbros occur only as fault-bound thrust sheets ranging in thickness from 100 m to several kilometres, and invariably display a syn-metamorphic penetrative foliation parallel to layering (see below). Layering in the metagabbros is typically well developed and characterized by centimetre- to tens of metres-scale layer thicknesses (Fig. 65.8). The layers are formed by variations in modal abundances of the two end-member mineral assemblages: hornblende (-actinotite), which forms black metapyroxenite layers; and plagioclase, which forms striking white meta-anorthosite layers. The two mineral assemblages possibly represent primary pyroxene-plagioclase cumulate layering. Sequences of repeated pyroxenite-gabbro-anorthositic gabbro-anorthosite cycles are common. Lateral continuity of any given layer increases with thickness but rarely exceeds 10-15 m for 1-2 m thick layers.

Individual lithologies within the LWIS are broadly similar to those in the layered sills emplaced into both the Povungnituk and Chukotat groups. However, several important differences exist. The LWIS layered metagabbros are characterized by compositional cycles repeated over hundreds of metres within individual thrust sheets. Metaperidotite thrust lozenges also display repeated compositional layering cycles. Individual thrust sheets of LWIS units are generally on the order of kilometres thick and represent only incomplete sections of the pre-deformation LWIS protolith. Finally, the LWIS units invariably occur in fault-bound thrust slices, without associated sedimentary or volcanic host-units. Consideration of these fundamental scale differences between LWIS units and the relatively thin layered sills intrusive into the Povungnituk and Chukotat Group units suggests that the LWIS had a different origin.

The repetition of cyclic units in the metaperidotites is similar in scale to that of the ultramafic zone of the Stillwater Complex or Muskox Intrusion (Jackson, 1970). Similarly, the layered metagabbros may represent deformed examples of layered gabbros like those in the Stillwater Complex (Jackson, 1961) or Skaergaard Intrusion (McBirney and Noyes, 1979). Therefore, it is possible that the LWIS represents an imbricated, transported and metamorphosed large layered intrusion.

Alternatively the LWIS may represent the lower part of an ophiolite suite (Moores, 1982) dismembered and interleaved

with continental rift margin deposits during tectonic transport. Fault-bound metaperidotite bodies in this interpretation would represent tectonic lenses of mantle or layer 3 peridotite, whereas the metagabbros would represent layer 3 cumulates. The stratigraphically higher components of the ophiolite suite, such as the isotropic gabbros, sheeted dyke complex and pillow lavas, would have been eroded from the top of the exposed metagabbroic thrust sheets in the map area. It is possible that the sheeted dykes and overlying pillow basalts of the ophiolitic sequence still exist at higher structural levels to the west where pillow basalts overlying layered metagabbros have been reported (C. Picard, personal communication, 1986).

Tonalite plutons

Thrust sheet I (Fig. 65.1) hosts several tonalite plutons that clearly intrude the Povungnituk Group metabasites, the metaperidotite of the Asbestos Hill suite and LWIS units. The plutons consist of grey- to white-weathering, massive to locally foliated biotite-muscovite tonalite. West of Lac Watts, garnet is a common accessory mineral phase. A discussion of the timing of pluton emplacement is given in the section on out-of-sequence thrusts.

D1 STRUCTURES

D1 structures in the map area consist of 1) pre-thermal peak regular stacking sequence thrust faults, 2) pre- to post-thermal peak out-of-sequence thrust faults and 3) a layer-parallel pre- to post-thermal peak schistosity to mylonitic foliation, typically containing a stretching lineation.

Regular sequence thrusts

The pre-thermal peak, regular sequence thrust faults can be readily mapped in the Cape Smith Belt based on structural repetitions of distinct tectono-stratigraphic units (St-Onge et al., 1986) and by recognition of discrete, laterally continuous high strain zones. Regular stacking sequence thrust faults represent the dominant structures accommodating north-south shortening south of thrust H (thrust faults discussed in text are identified by thrust sheet carried on the hangingwall and labelled in Fig. 65.1). Examples of regular sequence thrusts from this area include the faults B, C, D and G in Figure 65.1. For these thrusts, the stacking sequence is either unknown or may be interpreted to have proceeded in a "piggy-back" manner (see below). The thrust faults form a thrust system (Boyer and Elliott, 1982) at relatively high structural levels that appears similar to the system of thrusts rooting on the basal décollement documented at lower structural levels in the Wakeham Bay area (St-Onge et al., 1986).

At the high structural levels in the Lac Cross area, D1 deformation in the metavolcanic thrust sheets (A, B, D, F, G in Fig. 65.1) is restricted to 1-10 m thick high-strain zones adjacent to the bounding thrust faults. These high-strain zones have been traced for tens of kilometres along strike, rarely bifurcating to enclose horses of exotic units such as the Povungnituk Group polymictic conglomerate (Fig. 65.2). Spectacular strain gradients are developed grading into the high strain zones, in which all pre-existing primary structures, such as pillows in a basalt flow (Fig. 65.9) are progressively deformed until they are no longer discernible (Fig. 65.10). The ultimate product in the high strain zones is an aphanitic, extremely well foliated and lineated, platy mafic mylonite. Locally the hangingwall and footwall shear zones anastomose, enclosing low strain pods elongate parallel to the down-dip stretching lineation. Basalt flow pillows deformed in the high strain zones record a prolate strain with the pillows elongated approximately parallel to the mineral stretching lineation and aspect ratios in the cleavage plane reaching 10:1 (from initial ratios of at most 5:1).

The map-scale syncline at Lac Cross (Fig. 65.5) is an isolated fold structure bounded structurally above and below by homoclinal north-dipping thrust panels. The syncline must be of D1 age because it folds D1 thrust faults but is itself truncated by an out-of-sequence D1 thrust fault (Fig. 65.5). The fact that the syncline is an isolated fold and not related to a train of folds continuing to the south indicates that it was probably generated by movement of thrust sheets B, C, D (Fig. 65.1) over a ramp in fault B (fault bend fold of Suppe, 1983). Folding of the two thrust faults in the Lac Cross syncline above the inferred ramp suggests that regular sequence thrusting proceeded in a foreland propagating (piggyback) fashion (Boyer and Elliott, 1982). The north-dipping orientation of the inferred frontal ramp is consistent with the southward movement sense concluded for thrust faults in the Wakeham Bay area by St-Onge et al. (1986).

Out-of-sequence thrusts

Out-of-sequence thrust faults (Butler, 1982; Searle, 1985; Platt, 1986) have been mapped at all structural levels and all metamorphic grades in the Lac Watts – Lac Cross – Rivière Déception map area. Out-of-sequence thrusts are faults that develop in the hangingwall of an older thrust (Butler, 1982). These faults were recognized using several criteria: (1) thrust faults cutting down section in the transport direction; (2) truncation of footwall structures (e.g. folds, imbricates) by the thrust fault; (3) elimination of stratigraphic section in footwall units; and (4) development of a distinct syn- or post-thermal peak metamorphic assemblage in the high strain zone associated with individual thrusts. Examples of out-of-sequence faults from the map area include faults E, H and I on Figure 65.1. A relative chronology of out-of-sequence fault movement can be determined relative to the peak thermal metamorphic conditions by examining the assemblages associated with the syn-metamorphic foliation adjacent to the faults. While the regular sequence thrusts (except the basal décollement) probably all predate the thermal peak, as documented by Lucas and St-Onge (1986) for the deeper structural levels of the Wakeham Bay area, the out-of-sequence thrusts span the thermal peak. As a result, hangingwall and footwall structures directly related to out-of-sequence fault movement vary widely, reflecting changing physical conditions at the time of individual fault movement.

A narrow (1-5 m wide) high strain zone is developed in Chukotat Group metavolcanics on the footwall of the out-of-sequence thrust fault E. This fault truncates the north limb of the Lac Cross syncline and two earlier formed imbricates (C and D; Fig. 65.1). Microscopic examination of high strain zone metabasites is required to determine unequivocally the timing of fault movement, but the limited width of the footwall deformation zone suggests that the out-of-sequence fault may be pre-thermal peak in age.

The out-of-sequence fault H (Fig. 65.1) which is characterized by a chlorite-rich schistose zone is responsible for exposing deeper structural levels and higher grade rocks in the hangingwall, including the LWIS imbricates, than the regular sequence thrusted Chukotat and Povungnituk group rocks on the footwall. The hangingwall rocks record a complex D1 deformation history initiating with regular sequence thrusting followed by syn-metamorphic penetrative ductile strain of thrust sheets (see next section) and movement of discrete, syn-metamorphic, out-of-sequence faults, and culminating with post-thermal peak, out-of-sequence thrusting on several faults including fault H (Fig. 65.1).

Syn-peak metamorphic movement on an out-of-sequence fault (1, Fig. 65.6) imbricating the previously emplaced LWIS thrust sheets is demonstrable by examination of the syntectonic mineral assemblages and by comparison of the relative bulk strain recorded in layered metagabbros adjacent to the hangingwall with that in LWIS metagabbros hundreds of metres away from the fault. LWIS metagabbros distant from the fault experienced the bulk strain accumulated by all rocks in the hangingwall of thrust H during development of the syn-metamorphic foliation (Fig. 65.11). In contrast, the layered metagabbros in the 100 m thick thrust slice on the hangingwall of thrust 1 (Fig. 65.6) are straightened gneisses (in the sense of Davidson et al., 1982) in which heterogeneities in the foliation due to boudinage of layers have been reduced or eliminated concurrent with hornblende growth (Fig. 65.12). A top-to-the-south sense of shear for out-of-sequence fault 1 (Fig. 65.6) is demonstrated by the consistent attitude of shear bands (Platt and Vissers, 1980; White et al., 1980) deflecting the syn-metamorphic foliation (Fig. 65.13).

The development of a retrograde high strain shear zone adjacent to another thrust (2, Fig. 65.6), transporting previously imbricated LWIS units to a higher structural position, suggests that the fault is a post-thermal peak out-of-sequence structure. The retrograde shear zone is a 2-5 m wide, laterally continuous feature in which the syn-metamorphic fabric in layered metagabbro has experienced extreme ductile degradation. Foliated anorthosite layers have been boudinaged in a schistose actinolite-chlorite retrograde matrix (Fig. 65.14). A second out-of-sequence fault that was potentially active post-thermal peak is thrust I (Fig. 65.1), which carries tonalite plutons on its hangingwall not found in the footwall sequence, and truncates footwall imbricates. Since the plutons crosscut early, regular sequence thrusts and the syn-thermal peak foliation but are themselves locally foliated or mylonitized adjacent to the thrust, thrusting probably followed tonalite pluton emplacement and thus postdated peak thermal conditions. The final out-of-sequence fault to move in the map area was most likely fault H (Fig. 65.1) which has a well developed chlorite-bearing shear zone. It appears that fault H cuts off fault I, which carries the tonalite plutons, as it cuts up section in its hangingwall east of the map area.

Basal shear zone and Archean basement imbrication

All rock units north of thrust fault H (Fig. 65.1), except the most competent mafic-ultramafic intrusive lithologies, are characterized by a well developed, penetrative syn-metamorphic foliation and associated stretching lineation. The D1 fabrics overprint and reorient structures associated with pre-thermal peak regular sequence and out-of-sequence thrusts, and are intensified where associated with syn- or post-thermal peak out-of-sequence thrusts. Lucas and St-Onge (1986) suggested that the penetrative ductile strain overprint of earlier formed thrust structures in the Wakeham Bay area was the result of a progressive broadening, during thermal relaxation following tectonic thickening, of the zone accommodating slip on the basal décollement. The syn-metamorphic zone of continuous ductile strain was termed the basal shear zone by St-Onge et al. (1986).

Lucas and St-Onge (1986) proposed six criteria for the recognition of the basal shear zone in both cover units and Archean basement: (1) demonstrable or inferred strain-induced grain size reduction; (2) presence of a stretching lineation; (3) parallelism of all planar features (e.g. bedding, foliation, quartz veins); (4) presence of non-coaxial flow indicators; (5) boudinaged competent bodies (e.g. mafic-ultramafic sills); and (6) rotation of fold axes toward the stretching direction (sheath fold development). Applying these criteria, the basal shear zone in the map area extends from out-of-sequence thrust H (Fig. 65.1) north to include all of the cover thrust sheets and at least 100 m (structural thickness) of reworked Archean tonalite gneiss. Within this area, only the large (wider than 10 m) pyroxenite and peridotite bodies do not show a penetrative D1 syn-metamorphic fabric. D1 deformation features within these bodies are heterogeneously distributed; their margins are generally marked by thin (0.5-2 m) shear zones with strain increasing toward the contact, whereas their interiors deform along a three-dimensional network of narrow shears, often only several centimetres wide. The asbestos ore in the Asbestos Hill suite peridotite (Fig. 65.1) probably developed along such a network of shears during D1 syn-metamorphic ductile deformation.

The basal shear zone in the Lac Watts – Rivière Déception area is generally characterized by the presence of thermal-peak metamorphic assemblages growing in the D1 foliation. However, basal shear zone bulk shear at post-thermal peak conditions is indicated locally by dynamically recrystallized actinolite tails adjacent to host hornblende porphyroclasts in LWIS metagabbro (Fig. 65.15). A steeply raking (down-dip) stretching lineation is commonly developed in most lithologies within the Lac Watts – Rivière Déception area basal shear zone. The lineation is defined in quartz- and feldspar-rich rocks by quartz and/or feldspar smearing

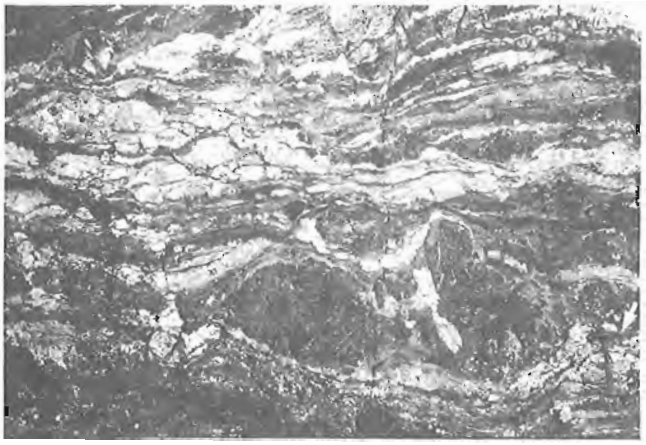


Figure 65.8. Sheared and boudined layered metagabbro from the Lac Watts intrusive suite. Disaggregated white layers are plagioclase-rich; dark layers contain hornblende-actinolite-plagioclase. Two large boudins in lower centre-right of photograph are metapyroxenite. Arrow points to hammer 34 cm long. GSC 204233-S



Figure 65.9. Low-strain, pyroxene-phyric pillow basalt from the Chukotat Group. Length of hammer is 34 cm. GSC 204233-X



Figure 65.10. Deformed Chukotat Group pyroxene-phyric pillow basalt in footwall of D1 regular sequence thrust fault G. Arrow points to 15 cm long pen. GSC 204233-Y

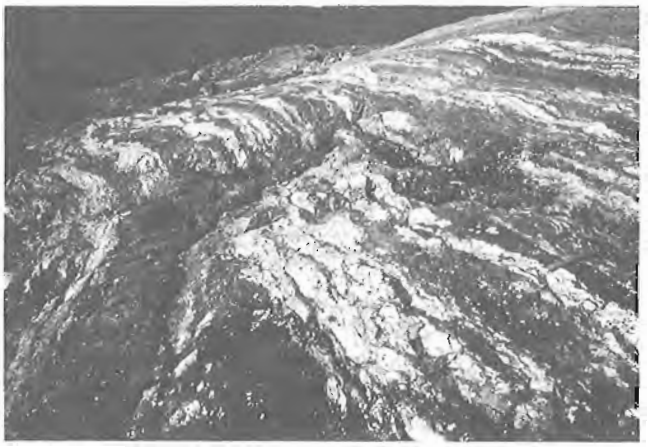


Figure 65.11. Sheared layered metagabbro from Lac Watts intrusive suite showing disaggregation of plagioclase-rich layers. Length of hammer is 34 cm. GSC 204233-T

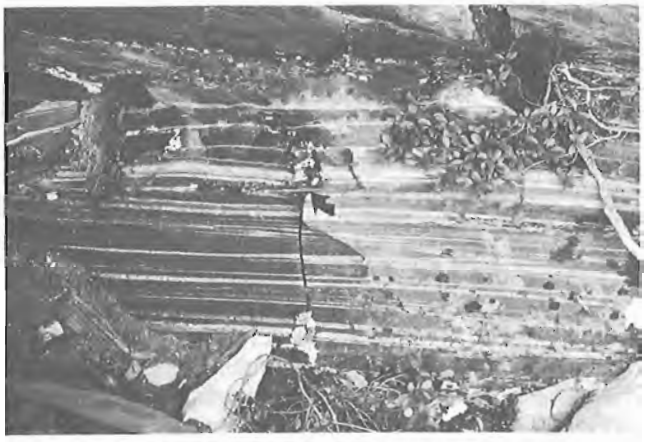


Figure 65.12. Straight gneiss derived from ductile high-strain zone in LWIS metagabbro. Arrow points to 15 cm long pen. GSC 204233-U



Figure 65.13. Shear bands developed in high strain zone related to out-of-sequence thrust and indicating top-side-to-south displacement. Length of pen is 15 cm and points north. C – high strain foliation; C′ – shear band. GSC 204233-V

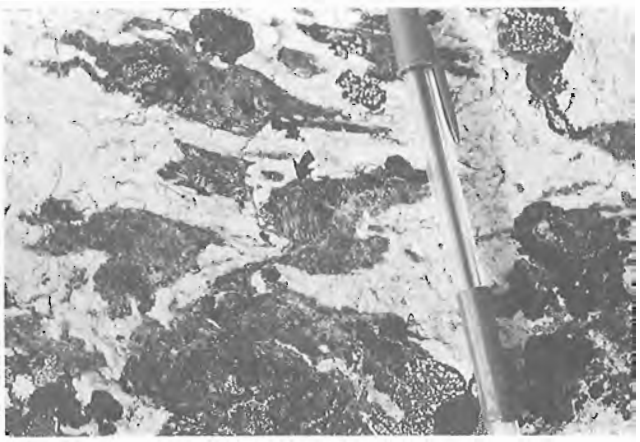


Figure 65.15. Hornblende porphyroclasts (arrow) with actinolite tails documenting continued D1 deformation past metamorphic thermal peak. Length of pen shown is 13.5 cm. GSC 204233-R



Figure 65.14. Tectonic schist along trace of late out-of-sequence thrust. White tectonic blocks are plagioclase-rich and are derived from overlying layered metagabbro unit. Long dimension of larger plagioclase-rich block is 75 cm. GSC 204233-W



Figure 65.16. D1 stretching lineation defined by quartz smearing in foliation plane of metasandstone. Length of pen is 15 cm. GSC 204233-P

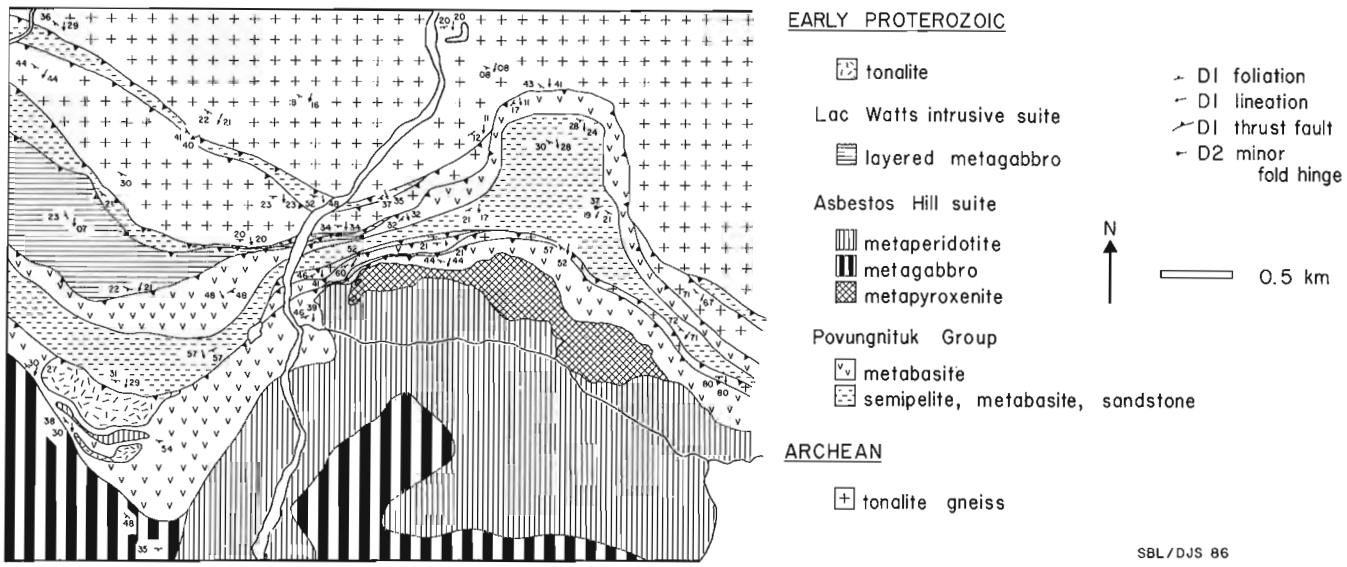


Figure 65.17. Geological map for area "c" outlined in Figure 65.1 showing Archean basement-Proterozoic cover imbrication. North-south river on map is Rivière Déception.

(Fig. 65.16), and in metabasites by plagioclase smearing and alignment of amphibole crystals.

Kinematic indicators are developed locally in the basal shear zone and indicate the D1 bulk shear deformation. These indicators include: (1) shear bands (Platt and Vissers, 1980; White et al., 1980) in LWIS metagabbro and reworked Archean tonalite gneisses; (2) C/S fabrics (Berthé et al., 1979) in reworked Archean gneisses; and (3) rare asymmetric folds of bedding in metasediments with an axial planar D1 fabric and a consistent south-verging asymmetry. Given that the sense of asymmetry of the kinematic indicators can only be determined in the plane parallel to the stretching lineation and perpendicular to the foliation (XZ plane of the finite strain ellipsoid), it is concluded that the finite extension closely parallels the transport direction for D1 deformation.

Archean basement tonalite gneisses along the north margin of the map area exhibit two distinct styles of involvement in the D1 deformation: (1) development of a protomylonitic to mylonitic foliation during syn-metamorphic basal shear zone bulk shear; (2) imbrication of basement gneisses and early Proterozoic units. In contrast to very limited basement involvement (3 m) related to basal shear zone deformation in the Wakeham Bay area of the Cape Smith Belt (St-Onge et al., 1986), more than 100 m of Archean tonalite gneiss was reworked by ductile processes beneath the imbricated cover units in the Lac Watts – Rivière Déception area. The syn-metamorphic high strain deformation in the basement is recognized by the presence of a protomylonitic to mylonitic foliation and stretching lineation parallel to those in the cover units, and by the growth of the hydrous assemblage muscovite-biotite in the D1 foliation. Strain related to D1 bulk shear in the basement gneisses increases toward the basement-cover contact where the basement gneisses are reduced to schistose mylonites. Increasing strain toward the basement-cover contact is consistent with this being the active basal décollement during basal shear zone development. Low strain pods of tonalite and coarse grained granitic pegmatite veins intruding previously deformed Archean gneiss act as excellent monitors of the intensity of D1 ductile deformation. Progressive strain-induced grain size reduction of the tonalite and ductile disaggregation of the pegmatites via recrystallization-accommodated dislocation creep (Tullis and Yund, 1985) in the feldspars illustrate the strain gradient and the amphibolite-grade deformation processes associated with the basement involvement in the basal shear zone.

Basement imbricates interleaved with Povungnituk Group and LWIS thrust sheets were mapped in the Rivière Déception area (Fig. 65.17). Individual basement thrust sheets range in thickness from 10 m to several hundred metres, and occur at several structural levels within the northern margin imbricate zone (Fig. 65.17). Although basement gneisses possess a penetrative D1 foliation in all the thrust slices, strain gradients are preserved towards the top and bottom contacts of each thrust sheet. This suggests that basement imbrication occurred during basal shear zone development.

LATE METAMORPHIC D2 STRUCTURES

D2 structures developed in the Lac Watts – Rivière Déception area include mesoscopic east-trending folds of the D1 foliation and map-scale east-trending folds of basement and cover units, D1 thrust faults and thermal peak mineral isograds. Although the mesoscopic D2 folds are approximately coaxial

with the map-scale D2 folds (Fig. 65.7), they do not appear to have developed coincidentally with the large scale folds. The mesoscopic folds generally have a marked limb asymmetry which maps out into distinct domains as noted by St-Onge et al. (1986) for the Wakeham Bay area. However, the limb asymmetry domains for the mesoscopic folds bear no relation to the position of the map-scale D2 fold hinge in the Lac Watts – Rivière Déception area, as was also noted by St-Onge et al. (1986) for the Wakeham Bay area. A plausible explanation for this is that the observed map-scale D2 folds overprint earlier developed mesoscopic folds.

At map-scale, D2 folding produced a large, 10 to 20 km wide synclinorium north of the late out-of-sequence thrust fault H (Fig. 65.1, 65.7). The map trace of the synclinorium axis is folded by north-trending D3 folds. Open upright D2 folds with 100-900 m wavelengths are developed in the core of the larger fold, and appear to be related to the first order, map-scale fold.

The D2 mesoscopic folds have chevron morphologies in lithologies with D1 platy minerals (metabasites and semipelites) and rounded profiles approaching a parallel geometry in those with dominantly quartz and feldspar (sandstones and mylonitized Archean basement gneisses). The D2 minor folds, as noted by St-Onge et al. (1986) are non-cylindrical and disharmonic and occur in fold trains continuous for tens of metres.

Crenulation microfolds are associated with the mesoscopic D2 folds in phyllosilicate- and amphibole-rich lithologies, clearly developed as parisitic folds to the outcrop-scale D2 structures. Commonly a spaced pressure solution crenulation cleavage is developed along steep microfold limbs, and rarely biotite, chlorite and muscovite are found growing axial planar to the D2 mesoscopic folds. These observations confirm those of St-Onge et al. (1986) that D2 mesoscopic folding (at least) occurred as a late metamorphic event during the uplift and erosion of the D1 thrust belt (St-Onge and Lucas, 1986).

D3 STRUCTURES

D3 structures in the map area include northerly trending macroscopic cross folds of both basement and cover and approximately coaxial, mesoscopic folds of the D1 foliation. The macroscopic D3 cross folds occur in a fold train with wavelengths of 5 to 15 km with the fold hinges well constrained by the reversal in plunge azimuths of the D2 mesoscopic fold hinges (Fig. 65.7). The superposition of macroscopic D2 and D3 folds has produced a map scale type 1 fold interference pattern (Ramsay, 1967) in the Lac Watts – Rivière Déception area (Fig. 65.7).

The mesoscopic D3 cross folds have morphologies very similar to the mesoscopic D2 folds described in the previous section. The folds commonly show a marked limb asymmetry. Similar to the D2 folds, the mesoscopic D3 fold asymmetries cannot be related systematically to the macroscopic fold geometry. The rare overprinting of D3 mesoscopic cross folds on D2 mesoscopic folds suggests that the D3 fold set developed in domains on an outcrop scale that were exclusive of D2 mesoscopic folds. This domainal development of D2 and D3 minor folds probably reflects the localization of minor folds (D2 or D3) in areas of suitable D1 foliation orientation, and the difficulty for relatively low strain, open D3 folds to refold rocks with D2 mesoscopic folds about an orthogonal axis. In contrast with the D2 folds, no pressure solution cleavage or new mineral growth is associated with the development of the D3 cross folds. The lack of a D3 fabric suggests that D3 cross folding took place at relatively low temperatures in a post-metamorphic regime, and that it represents a relatively low strain deformation.

LAC CROSS OBLIQUE-SLIP FAULTS

In the vicinity of Lac Cross, late brittle faults crosscut and offset all previously described D1 and D2 structures (Fig. 65.5). The faults are characterized by curvilinear traces and seem to terminate in sprays of short fault segments. Although they are probably oblique-slip faults, the west-side down component of displacement is the most striking at map-scale. This is documented by the repetition of the closure of Povungnituk Group sediments, layered peridotite-gabbro sills and overlying Chukotat Group pillow basalts in a major east-plunging D1 syncline (Fig. 65.5).

ACKNOWLEDGMENTS

We are grateful to Janien Schwarz for her culinary and camp preservation skills that kept us going during 6 weeks of summer and 5 weeks of winter. We thank Daniel Lamothe (MER-Québec) for continued assistance in the field and Herb Helmstaedt (Queen's University), Dugald Carmichael (Queen's University) and Tim Byrne (Brown University) for lively discussions on the outcrops. Falconbridge Ltd. and Delaware Resources Ltd. are gratefully acknowledged for subcontracting their Jet Ranger. Tony Davidson, Paul Hoffman and Rein Tirrul critically read and improved an earlier version of the manuscript.

REFERENCES

Bergeron, R.
1959: Povungnituk Range area, New Québec; Québec Department of Mines, Preliminary Report 392, p. 9.

Berthé, D., Choukroune, P., and Jegovzo, P.
1979: Orthogneiss, mylonite and non coaxial deformation of granites: the example of the South Armorican Shear Zone; Journal of Structural Geology, v. 1, p. 31-42.

Boyer, S.E. and Elliott, D.
1982: Thrust systems; American Association of Petroleum Geologists, Bulletin, v. 66, p. 1196-1230.

Butler, R.W.H.
1982: The terminology of structures in thrust belts; Journal of Structural Geology, v. 4, p. 239.

Davidson, A., Culshaw, N.G., and Nadeau, L.
1982: A tectono-metamorphic framework for part of the Grenville Province, Parry Sound region, Ontario; in Current Research, Part A, Geological Survey of Canada, Paper 82-1A, p. 175-190.

Francis, D.M. and Hynes, A.J.
1979: Komatiite-derived tholeiites in the Proterozoic of New Quebec; Earth and Planetary Science Letters, v. 44, p. 473-481.

Francis, D.M., Ludden, J., and Hynes, A.J.
1983: Magma evolution in a Proterozoic rifting environment; Journal of Petrology, v. 24, Part 4, p. 556-582.

Hoffman, P.F.
1985: Is the Cape Smith Belt (northern Quebec) a klippe?; Canadian Journal of Earth Sciences, v. 22, p. 1361-1369.

Hynes, A.J. and Francis, D.M.
1982: A transect of the early Proterozoic Cape Smith foldbelt, New Quebec; Tectonophysics, v. 88, p. 23-59.

Jackson, E.D.
1961: Primary textures and mineral associations in the ultramafic zone of the Stillwater Complex, Montana; U.S. Geological Survey Professional Paper 358, 106 p.
1970: The cyclic unit in layered intrusion – a comparison of repetitive stratigraphy in the ultramafic parts of the Stillwater, Muskox, Great Dyke and Bushveld complexes; in Symposium on the Bushveld Igneous Complex and other Layered Intrusions, D.J.L. Visser and G. von Gruenewaldt, (ed.); Geological Society of South Africa, Special Publication 1, p. 391-424.

Lamothe, D., Picard, C., and Moorhead, J.
1984: Région du Lac Beauparlant, Bande de Cap Smith-Maricourt, Nouveau Québec; Ministère de l'Énergie et des Ressources du Québec, DP 84-39, échelle 1:50 000.

Lucas, S.B. and St-Onge, M.R.
1986: Structural and thermal evolution of the basal shear zone in the early Proterozoic Cape Smith thrust-fold belt, Quebec; in Program with Abstracts, Geological Association of Canada, v. 11, p. 96.

McBirney, A.R. and Noyes, R.M.
1979: Crystallization and layering of the Skaergaard Intrusion; Journal of Petrology, v. 20, p. 487-554.

Moores, E.M.
1982: Origin and emplacement of ophiolites; Reviews of Geophysics and Space Physics, v. 20, no. 4, p. 735-760.

Platt, J.P.
1986: Dynamics of orogenic wedges and the uplift of high-pressure metamorphic rocks; Geological Society of America, Bulletin, v. 97, p. 1037-1053.

Platt, J.P. and Vissers, R.L.M.
1980: Extensional structures in anisotropic rocks; Journal of Structural Geology, v. 2, p. 397-410.

Ramsay, J.G.
1967: Folding and Fracturing of Rocks; McGraw-Hill, New York, 555 p.

Searle, M.P.
1985: Sequence of thrusting and origin of culminations in the northern and central Oman Mountains; Journal of Structural Geology, v. 7, p. 129-143.

St-Onge, M.R. and Lucas, S.B.
1986: Eastern Cape Smith Belt: imbrication, syn-metamorphic deformation and uplift of an early Proterozoic thrust-fold belt in northern Quebec; in Program with Abstracts, Geological Association of Canada, v. 11, p. 132.

St-Onge, M.R., Lucas, S.B., Scott, D.J., and Bégin, N.J.
1986: Eastern Cape Smith Belt: an early Proterozoic thrust-fold belt and basal shear zone exposed in oblique section, Wakeham Bay and cratère du Nouveau Québec map areas, northern Quebec; in Current Research, Part A, Geological Survey of Canada, Paper 86-1A, p. 1-14.

Suppe, J.
1983: Geometry and kinematics of fault-bend folding; American Journal of Sciences, v. 283, p. 648-721.

Tullis, J. and Yund, R.A.
1985: Dynamic recrystallization of feldspar: a mechanism for ductile shear zone formation; Geology, v. 13, p. 238-241.

White, S.H., Burrows, S.E., Carreras, J., Shaw, N.D., and Humphreys, F.J.
1980: On mylonites in ductile shear zones; Journal of Structural Geology, v. 2, p. 175-187.

Rare-earth element geochemistry of sedimentary sequences from the Lower St-Lawrence, Quebec Appalachians[1]

Project 840023

Jean David[2] and Clément Gariépy[3]

David, J. and Gariépy, C., Rare-earth element geochemistry of sedimentary sequences from the Lower St-Lawrence, Quebec Appalachians; in Current Research, Part A, Geological Survey of Canada, Paper 87-1A, p. 633-642, 1987.

Abstract

In this paper, we report on the trace and rare-earth element geochemistry of five sedimentary sequences from the Lower St-Lawrence area of the Appalachians. These are the Cambro-Ordovician Trinité Group, the Caradocian to Llandoverian Cabano Formation, the Llandoverian Lac Raymond Formation and the upper Silurian (Ludlow) Robitaille and St-Leon formations.

The geochemical analyses were completed on fine grained sedimentary rocks (mudstone and shale) which make up the bulk of these sequences. The results show that the Trinité Group was northerly derived from a mature cratonic source area. The Cabano Formation yields a geochemical composition indicating that it was derived from uplifted, Taconic age, sediments and volcanics. In contrast the overlying Lac Raymond was derived from the dissection of a volcanic arc located to the southeast. Finally, the Robitaille and St-Léon Formations were deposited in coastal basins and mostly derived from exposed lower to middle Silurian rocks.

Résumé

Ce rapport fait état des résultats de l'analyse géochimique d'éléments traces et de terres-rares, effectuées sur cinq unités sédimentaires de la région du Bas-St-Laurent. Les roches les plus anciennes sont celles du groupe de Trinité, d'âge cambro-ordovicien. Les autres strates sont d'âge silurien; la formation de Cabano débute à l'Ordovicien moyen et s'étend jusqu'au Silurien inférieur (Llandovery), la formation de Lac-Raymond est d'âge du Llandovery supérieur. Les formations de Robitaille et de St-Léon sont considérées comme étant du Ludlow.

Les analyses géochimiques ont été effectuées sur des sédiments à granulométrie fine, des mudstones et des shales. Ce type de roches représentent une composante importante des strates de cette région. Le group de Trinité est dérivé du nord, à partir d'une source cratonique mature. La formation de Cabano provient de l'érosion d'un empilement émergé et constitué de roches sédimentaires et volcaniques d'âge Taconique. Par contre, la formation de Lac-Raymond a une composition chimique dérivée de la dissection d'un arc volcanique situé au sud-est. Finalement, les formations de Robitaille et de St-Léon, constituées de sédiments de séquences marines de faible profondeur d'eau, ont été dérivées des roches sous-jacentes, dont l'âge varie du Silurien inférieur à moyen.

[1]Contribution to the Canada Economic Development Plan for Gaspé and Lower St-Lawrence, Mineral Program 1983-1988. Project carried by Geological Survey of Canada, Lithosphere and Canadian Shield Division

[2]Département de Géologie, Université de Montréal, C.P. 6128, Succ. "A", Montréal, Québec H3C 3J7

[3]Département des Sciences de la Terre, Université du Québec à Montréal, C.P. 8888, Succ. "A", Montréal, Québec H3C 3P8

INTRODUCTION

Trace and rare-earth element (REE) geochemistry has proved to be an essential tool to model the chemical structure of our planet, and to decipher the origin and the mode of evolution of igneous rocks (Pearce and Cann, 1973; Frey et al., 1974; Schilling, 1975; Winchester and Floyd, 1977, amongst others). The cited authors have shown that the composition of an igneous rock series is closely related to its tectonic environment through factors such as the source composition, the degree of partial melting and the fractional crystallization history of the magma.

This approach has been similarly applied to sedimentary rock piles in order to constrain the chemical composition of the continental crust (Nance and Taylor, 1976, 1977; Taylor and McLennan, 1980a, b; McLennan and Taylor, 1982). Meanwhile, several studies have shown that fine grained sediments, especially mudstones and shales, average out the chemical composition of their source areas (Taylor and McLennan, 1985), offering thus an opportunity to document the geochemical evolution of sedimentary provenances with time. Such studies have been especially successful in Archean terranes (Jenner et al., 1981; McLennan et al., 1984; Lajoie and Ludden, 1984) as there were, at that time, sharp lithological contrasts between the different rock sequences exposed at the surface.

In comparison, REE geochemistry of Phanerozoic sediments (Cullers et al., 1974; Nance and Taylor, 1976; Chaudhuri and Cullers, 1979; Bathia and Taylor, 1981; Basu et al., 1982; Bathia, 1985) have been more difficult to interpret. On one hand, the continental segments are involved in successive orogenic events and the crust tends to differentiate; on the other hand, sedimentary recycling, which accompanies orogenesis buffers the bulk composition of the continental crust (Taylor and McLennan, 1985). Consequently, the bulk composition of the continents, and thus that of the sedimentary record at the regional scale, appears to be relatively constant in post-Archean times (Taylor and McLennan, 1985; Allègre and Rousseau, 1984).

In this paper, we report on the trace and rare-earth element geochemistry of Ordovician and Silurian sedimentary rocks from the Lower St-Lawrence area. As expected, these rocks show a fairly uniform composition, similar in several aspects to other Phanerozoic sedimentary rocks of the world. Nevertheless, we will show that there are small, but significant variations of key elements within the Lower St-Lawrence sedimentary pile that help constrain the past tectonic framework of the area during Silurian times.

STRATIGRAPHIC OUTLINE

The terrigenous units considered in this paper are located within the central portion of the Quebec Appalachians, close to the boundaries with the province of New Brunswick and the state of Maine (Fig. 66.1). This area comprises the Trinité Group and the Cabano, Lac Raymond, Robitaille and St-Léon formations which have been initially mapped and described by Lajoie et al. (1968) and partly revised by David et al. (1985). An outline of the features pertinent to this study follows.

Age relationships

The Trinité Group (Fig. 66.1) is part of the sedimentary pile which accumulated before the so-called Taconic "orogeny"; it is not fossiliferous and could either be of Cambrian or of lower Ordovician age. The other formations are younger and only show structural features characteristic of the Acadian episode of deformation. The oldest unit is the Cabano Formation, deposited from middle Ordovician (Caradoc) to lower Silurian (Llandoverian A_4-B_3) times. The Cabano Formation is conformably overlain by the Pointe Aux Trembles Formation, a volcanic unit showing all the geochemical characteristics of calc-alkaline lavas from volcanic arcs (David and Gariépy, 1986). The Cabano Formation is also conformably overlain by the Lac Raymond Formation, which is the lateral equivalent of the Pointe Aux Trembles Formation, but is mainly composed of terrigenous rocks deposited during Llandoverian (C_1-C_5) times. In the southeastern sector of the studied area (Fig. 66.1) both the Lac Raymond and the Pointe Aux Trembles formations are paraconformably overlain by upper Silurian (Ludlow) strata belonging at the base to the Robitaille Formation and higher up in the sequence to the St-Léon Formation. To the northwest the Robitaille and St-Léon formations discordantly lie on Cambro-Ordovician (Taconic) sequences.

Petrographic features

The oldest rocks of the Trinité Group are found in the central part of the area (Fig. 66.1). Although the internal stratigraphy of the unit is poorly known, two facies have been recognized. The most prominent facies is a fine grained assemblage of black and dark green phyllites interstratified with thin beds of calcareous siltstones or very fine grained sandstones. The latter are mostly made of quartz (>80%) and altered feldspars set in a chloritic matrix (Lespérance and Greiner, 1969). The sedimentary structures are restricted to the coarsest materials and consist of parallel laminations or small ripples. Locally, the facies comprises a few beds of intraclastic calcareous conglomerates and some beds of calcisiltite. The second, less abundant facies is made of interbedded black slates and fine grained limestones (rarely conglomeratic) accumulated in beds less than 20 cm thick. Because of the intensity of the deformation, the stratigraphic relations between these two facies are indistinct and the sedimentary environment of the Trinité Group is unknown.

The sedimentological characteristics of the Cabano Formation have been previously summarized by David et al. (1985). The Cabano sediments comprise two distinct facies: the most abundant facies is defined by a close association of mudstones with siltstones/sandstones, whereas the second facies is found as lenticular horizons of conglomerates/sandstones. The syngenetic structures preserved in the rocks are those characteristic of subaqueous turbidites deposited in a

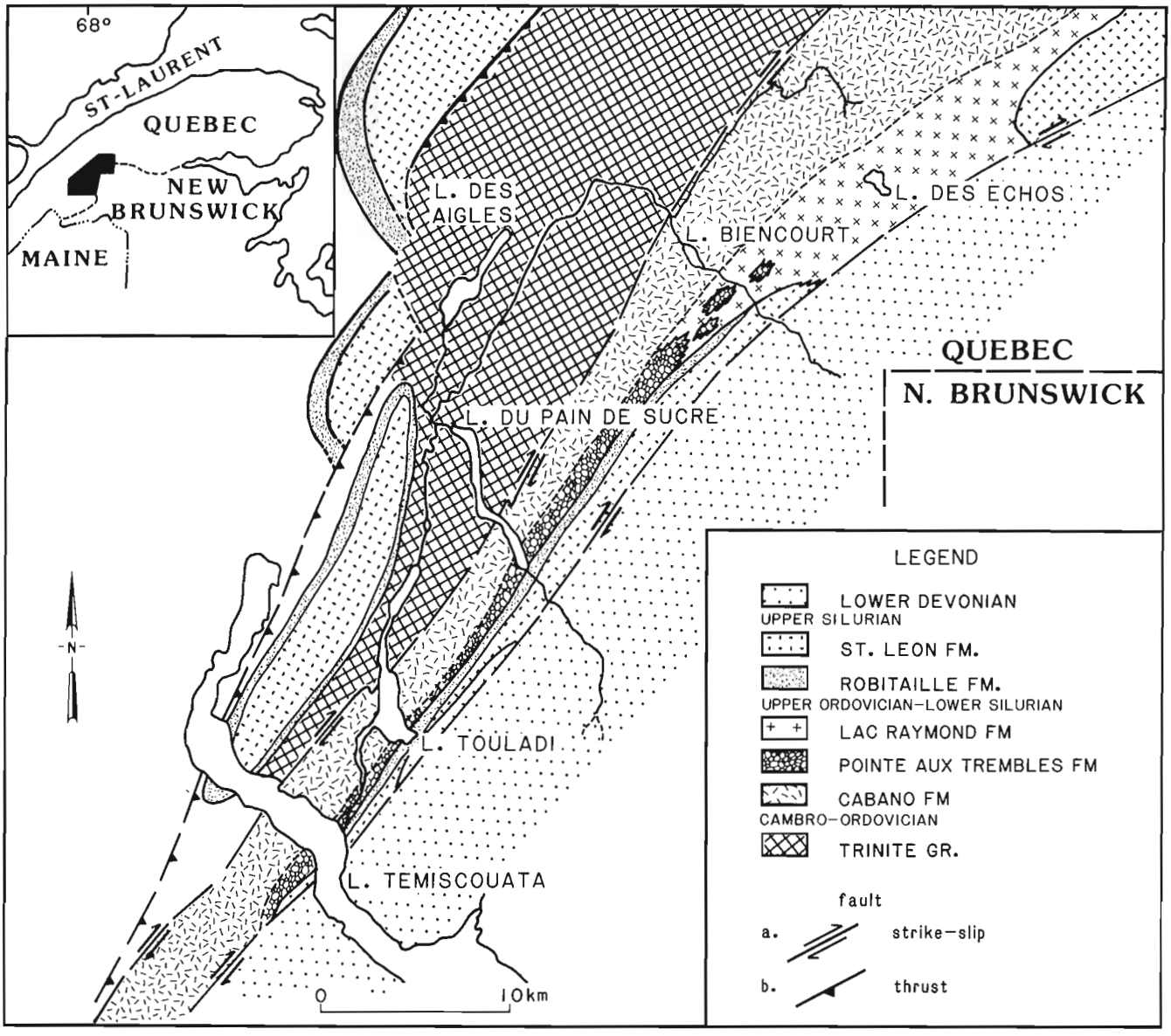


Figure 66.1. Generalized geological map of the area showing the location of the Cambro-Ordovician and Silurian formations (modified from Lajoie et al., 1968).

relatively deep basin. The composition of the sandstones which are lithic or subfeldspathic wackes, averages 53% quartz, 42% feldspars (mostly plagioclase). The rock fragments are essentially sedimentary-derived except for the occurrence, in trace amounts, of volcanic rock fragments. Traces of chromite have also been found in a few samples, but the distribution of this mineral is erratic.

The strata which accumulated during the late portion of the lower Silurian are exposed in the Pointe aux Trembles and Lac Raymond formations. The former comprises calc-alkaline volcaniclastics, debris flows, volcanic sandstones, crystal tuffs, lithic tuffs and a few andesitic lava flows (David and Gariépy, 1986). The bulk of the Pointe aux Trembles Formation accumulated in a subaqueous environment, with the exception of the uppermost portion which shows evidences of shallow water and even subaerial environments.

The Lac Raymond Formation comprises mostly mudstones and very thin beds of crystal tuff interstratified with siltstones and fine grained sandstones. A single lens of epiclastic conglomerate outcrops at the base of the formation. Petrographic observations of the lithic wackes and the siltstones show that these are made, on average, of 30% quartz, 20% calcic plagioclase, 23% rock fragments and 5% accessory minerals set in a matrix of quartz and phyllosilicates

(muscovite, sericite and chlorite). The rock fragments are, in order of abundance: cherts, volcanics, siltstones, slates and sandstones, granitoids and fossils. The accessory minerals include muscovite, clinopyroxenes, zircons and sulphides. From field evidences, the Lac Raymond Formation was apparently deposited in a relatively deep marine environment very similar to that of the Cabano Formation. However, this is poorly understood with respect to the upper section of the Pointe aux Trembles which is subaerial.

The Robitaille and St-Léon formations were not mapped in detail but petrographic descriptions are available from the work of Lespérance and Greiner (1969) and Lajoie (1971). The Robitaille Formation is made of characteristic red siltstones associated with rare mudstone, sandstone and conglomerate beds. The latter are arenites and quartz wackes typically showing quartz abundances in excess of 80% with 5 to 7% rock fragments mostly of sedimentary derivation. Accessory minerals include micas, zircon, tourmaline, rutile and iron oxides. Lajoie (1971) concluded that the Robitaille Formation was deposited in a coastal-type environment (high energy, marine, shallow water) based on the following observations: (1) types of fossils; (2) maturity of the sandstones; (3) presence of planar crossbeds.

The overlying St-Léon Formation, which stretches eastward over a considerable distance, comprises grey-green calcareous siltstones and sandstones, interbedded with dark grey shales. In the Rimouski area, the upper portion of the unit is characterized by a coarse grained facies made of conglomerates and sandstones. The mineralogical composition of the rocks is highly variable along strike and wackes, quartz arenites, feldspathic arenites and arkosic arenites have been reported (Lajoie et al., 1968). Both plagioclase and microcline are present in the sandstones as well as clastic fragments of siltstone, chert, quartz sandstone and volcanics. Lajoie (1971) considered that the St-Léon accumulated in a marine, shallow water basin environment similar to that of the Robitaille Formation.

ANALYTICAL TECHNIQUES AND SAMPLING

The trace and REE analyses were deliberately carried out on the fine (pelitic component of the units described above. Several arguments motivate the selection of that type of material. Firstly, Cullers et al. (1979) have shown that mechanical fractionation of the REE occurs during the deposition of coarser grained sediments: for example, in a sandstone the heavy minerals (zircon, sphene, apatite, etc.), which contain the bulk of the REE, are preferentially segregated along certain lamination planes. In comparison, the REE are more evenly distributed in finer sediments. Secondly, the bulk of the REE in clastic sedimentary rocks is present in the $<2\mu$ fraction (Taylor and McLennan, 1985); therefore pelitic samples offer the possibility of carrying out more precise analyses. Finally, pelitic clastic rocks are the most abundant material (generally >50%) in all the studied units and offer a better opportunity (1) to assess adequately the chemical variations present in a specific unit and (2) to compare the different units at the regional scale.

Pelitic sample were reduced to centimetre-sized fragments and only the freshest pieces, free of alteration surfaces, were powdered in an agate mortar. All the trace and REE determinations were completed by instrumental neutron activation analysis using the semi-absolute method of Bergerioux et al. (1979). The samples were irradiated using the SLOWPOKE II reactor (École Polytechnique) at a flux of $10^{12} n*cm^{2}*^{-1}$ and counted over a period of one month at the Université de Montréal using LEPS and Ge(Li) detectors. Replicate analyses of a pelite sample (Table 66.1) show that the overall precision is better than 5% (1σ) for all elements except for Tb, Lu and Sb (10%).

GEOCHEMISTRY

Geochemical hypothesis

Our objective was to use geochemical data to assess the compositional evolution of the different units described above. It is based on the hypothesis put forward by several authors (*see* Taylor and McLennan, 1985) that the REE and a few selected trace elements of fine grained terrigenous clastic sediments are not fractionated during weathering, transportation, deposition, diagenesis, and subsequent metamorphic episodes. This hypothesis has been verified in several studies (Taylor and McLennan, 1985) and, for example, there are marked changes in average REE distribution between Archean and post-Archean sediments. Nonetheless, REE geochemistry of shales may not be a panacea and, under special physico-chemical circumstances, it is possible that the REE of a given unit did not preserve a direct relationship with their abundances at the source area. Consequently, we will show that the trace and REE behaviour in the studied units is coherent, and compatible with Taylor and McLennan's hypothesis. Then, we will discuss the sedimentological implications of the data set.

Results

The average chemical composition of the different formations is listed in Table 66.2 together with classical reference composites which will be used for comparison purposes. Individual analyses are illustrated in Figures 66.2 to 66.4.

There are several geochemical features common to all the units:

1) All the units are enriched in light/heavy REE yielding $(La/Yb)_N$ ratios in the range 7.8 to 14.2.

2) All the units display large negative europium anomalies ($Eu/Eu* = 0.59$ to 0.68). The magnitude of the Eu anomalies is comparable to that of the post-Archean average shale (PAAS) and North-American shale composite (NASC); such values are considered to be a representative feature of the upper continental crust.

3) All the units show a significant internal dispersion that is considerably larger than the analytical precision evaluated from replicate analyses of a mudstone sample (see Table 66.1). The internal dispersion cannot be ascribed to sample heterogeneity and must be a primary characteristic of the units.

In our opinion, the latter is a key observation to interpret the geochemical evolution of the sedimentary units. An approach based on averaging the composition of the different samples to represent a particular unit, will erase the distribution trends which may vary from unit to unit. An example of that argument is illustrated in the Th vs. La diagram of Figure 66.2. Although, the Trinité Group and the Lac Raymond Formation yield similar average contents of La (36 and 32 ppm respectively) and Th (9 and 10 ppm), the diagram shows that the Trinité Group is significantly more heterogeneous in terms of its La and Th abundances.

Table 66.1 Duplicate (n = 4) analyses from Cabano Formation sample Pel-06, reference material; mudstone.

	$\bar{X}$	σ
La	38.8	0.4
Ce	66.1	2.4
Nd	27.5	0.5
Sm	5.6	0.1
Eu	1.03	0.02
Tb	0.53	0.14
Yb	1.9	0.06
Lu	0.31	0.03
Sc	12.9	0.2
Cr	103.4	1.9
Co	13.9	0.3
Rb	134.8	2.9
Cs	4.5	0.2
Ba	617.2	17.2
Hf	5.3	0.1
Ta	0.65	0.03
Th	8.4	0.2
U	2.9	0.05

Table 66.2 Average abundances and mean standard deviation of pelites from the studied formations and from reference composites (in ppm).

	TRINITE Gr N = 9		CABANO Fm N = 17		LAC RAYMOND Fm N = 13		ROBITAILLE Fm N = 3		ST-LEON Fm N = 3						
	X	σ	X	σ	X	σ	X	σ	X	σ	NASC	PAAS	AAS	PUC	CANSHD
La	35.9	13.2	41.3	4.9	31.6	9.0	41.6	9.7	39.9	4.0	32	38.0	12.6	30	32
Ce	63.4	17.7	73.1	10.7	56.4	16.6	75.5	19.3	73.5	9.0	73	80	26.8	64	65
Nd	24.9	8.2	29.6	6.8	22.7	7.7	30.6	8.3	28.9	2.5	33	32	13.0	26	26
Sm	4.9	1.3	6.3	1.9	5.0	1.2	6.9	2.3	6.0	0.6	5.7	5.6	2.8	4.5	4.5
Eu	0.86	0.18	1.15	0.32	1.00	0.20	1.22	0.19	1.21	0.27	1.24	1.10	0.90	0.88	0.94
Tb	0.54	0.11	0.83	0.37	0.70	0.15	0.85	0.14	0.73	0.21	0.85	0.77	0.48	0.64	0.48
Yb	1.6	0.3	2.4	0.4	2.7	0.4	2.6	0.7	2.5	0.5	3.1	2.8	1.8	2.2	1.5
Lu	0.25	0.05	0.38	0.08	0.40	0.06	0.41	0.09	0.40	0.06	0.48	0.50	0.28	0.32	0.23
Sc	13.5	3.1	15.0	2.8	17.7	4.1	16.2	3.3	18.2	1.4	–	–	25	10	7
Cr	89.9	25.7	99.8	22.6	85.1	18.5	86.1	8.1	90.9	9.2	–	–	140	35	35
Co	15.1	6.7	15.6	3.2	14.6	5.1	15.4	3.8	20.8	2.8	–	–	30	10	12
Na	8545	2401	9103	1267	12325	2343	8001	5214	9951	6239	–	–	23000	28200	25671
Rb	112.3	37.1	146.4	15.2	119.8	32.3	167.0	42.5	170.3	29.0	–	–	25	110	110
Cs	5.6	2.9	6.3	1.7	4.4	1.2	8.0	1.4	5.8	0.6	–	–	–	3.7	0.7
Ba	579.3	129.0	782.6	428.2	457.5	116.3	706.3	301.6	640.3	145.5	–	–	240	700	1070
Hf	3.1	1.1	5.1	1.1	5.9	1.1	5.3	0.5	6.3	2.5	–	–	3.0	5.8	5.8
Ta	0.6	0.2	0.8	0.1	0.7	0.1	0.9	0.3	0.8	0.2	–	–	–	–	–
Th	8.8	3.1	11.0	1.9	10.2	1.8	11.6	3.9	12.1	3.2	–	–	2.9	10.5	10
U	1.7	0.8	2.9	0.7	2.5	0.3	2.4	0.3	2.5	0.6	–	–	0.8	2.5	2.5
La/Th	3.8	0.5	3.1	0.7	4.2	0.6	3.7	0.3	3.4	0.5	–	–	4.3	2.8	3.2
Th/U	5.7	1.6	3.9	1.3	4.1	0.6	5.1	2.5	4.9	0.5	–	–	3.9	4.2	4.0
La/Ybn	14.2	4.5	11.5	1.4	7.8	1.6	10.4	0.4	10.7	1.4	6.8	9.2	4.8	9.0	14.1
La/Sm	7.2	1.2	6.8	1.1	6.3	1.0	6.1	0.6	6.6	0.6	5.6	6.8	4.5	6.7	4.2
Eu/Eu*	0.65	0.07	0.63	0.05	0.64	0.06	0.59	0.05	0.68	0.03	0.70	0.66	0.98	0.65	0.80
Sc/Cr	0.15	0.02	0.16	0.04	0.21	0.02	0.19	0.06	0.20	0.06	–	–	0.18	0.28	0.20

NASC = North American shale composite (Haskin and Paster, 1979)
PAAS = Post-Archean average Australian shale (Nance and Taylor, 1976)
AAS = average Archean sedimentary rocks (Australia) (Taylor and McLennan, 1980a)
PUC = present upper crust, calculated to be 20% lower than PAAS
CANSHD = average chemical composition of the Canadian Precambrian Shield (Shaw et al., 1967; 1976)

La/Ybn = ratio normalized to chondrite values of Taylor and Gorton (1977)
Eu/Eu* = Eu* is the theoretical values for no depletion nor enrichment in comparison with Sm and Nd

Figure 66.2 also shows a good correlation between La and Th, indicating a similar behaviour during the sedimentary processes. This correlation corresponds to a La/Th ratio in the range of 3 to 4 which is slightly higher than the most recent value for average sedimentary rocks, which is given at 2.8 +/− 0.2 by Taylor and McLennan (1985).

Several other element pairs show coherent geochemical variations in the studied rocks (Fig. 66.3).

1) Uranium and hafnium, which are both incorporated in zircon, are positively correlated (Fig. 66.3A) except for a few U-rich samples from the Cabano Formation.

2) The heavy rare-earth ytterbium, which is also incorporated in zircon, similarly shows a good correlation with Hf (Fig. 66.3B); note that the Trinité Group systematically stands out as being poorer in the "zircon component".

3) Lanthanum and tantalum are positively correlated (Fig. 66.3C). The diagram also illustrates the dispersion of the Trinité samples and shows that the Cabano rocks have higher La and Ta contents than the Lac Raymond samples.

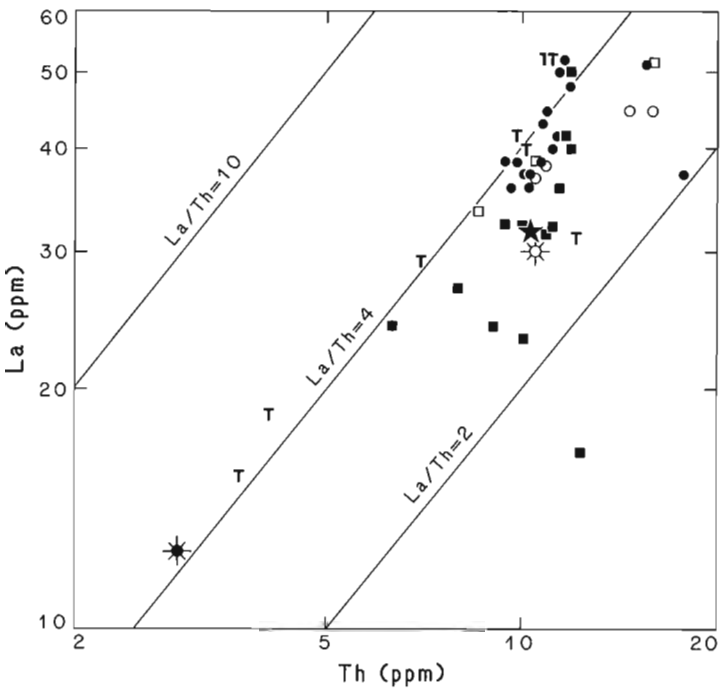
4) Figure 66.3D displays a positive correlation between Sc and Cr. In crustal systems, these are both compatible elements, with Sc being more compatible than Cr (Bathia and Crook, 1986), which are normally included in mafic mineral phases. Consequently, these will indicate the amount of mafic component present at the source area. Note that for a given Cr content, Lac Raymond samples systematically yield higher Sc abundances.

5) Scandium is also positively correlated with ytterbium (Fig. 66.3E) and, as a general rule, the mafic component seems more abundant in those rocks which have the highest heavy REE content.

6) Finally, the alkali element rubidium also displays a coherent behaviour (Fig. 66.3F). This is surprising and it shows, in contrast to what we were expecting, that Rb is not added to the sediment from seawater during diagenesis.

In summary, several elements showed a coherent behaviour during sedimentation of the Lower St-Lawrence series. However, element abundances may be affected by secondary processes such as a gain or loss of water and CO_2 during diagenesis and metamorphism. Consequently, we will use element ratios, which are insensitive to secondary gain/loss of elements, to confirm that the geochemical characteristics of the units are a primary feature of their provenance (Fig. 66.4A, B).

On a "fractionation" (La/Yb) versus "enrichment" (La) diagram (Fig. 66.4A) three of the studied units are clearly distinguished. The Trinité Group exhibits the most fractionated character and a large spread of its La/Yb ratios in the range 12 to 33 (Fig. 66.4A). In comparison, the Cabano rocks



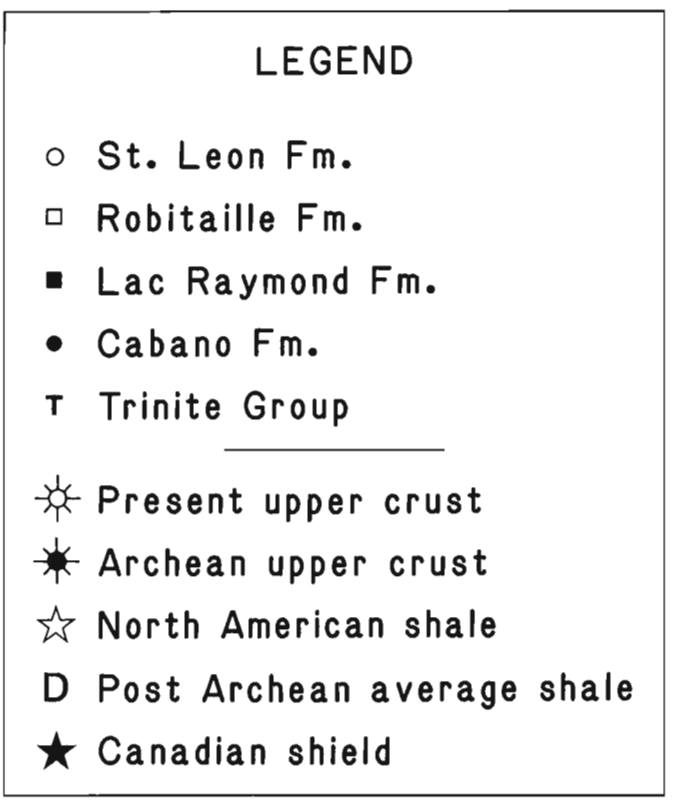


Figure 66.2. Th versus La diagram.

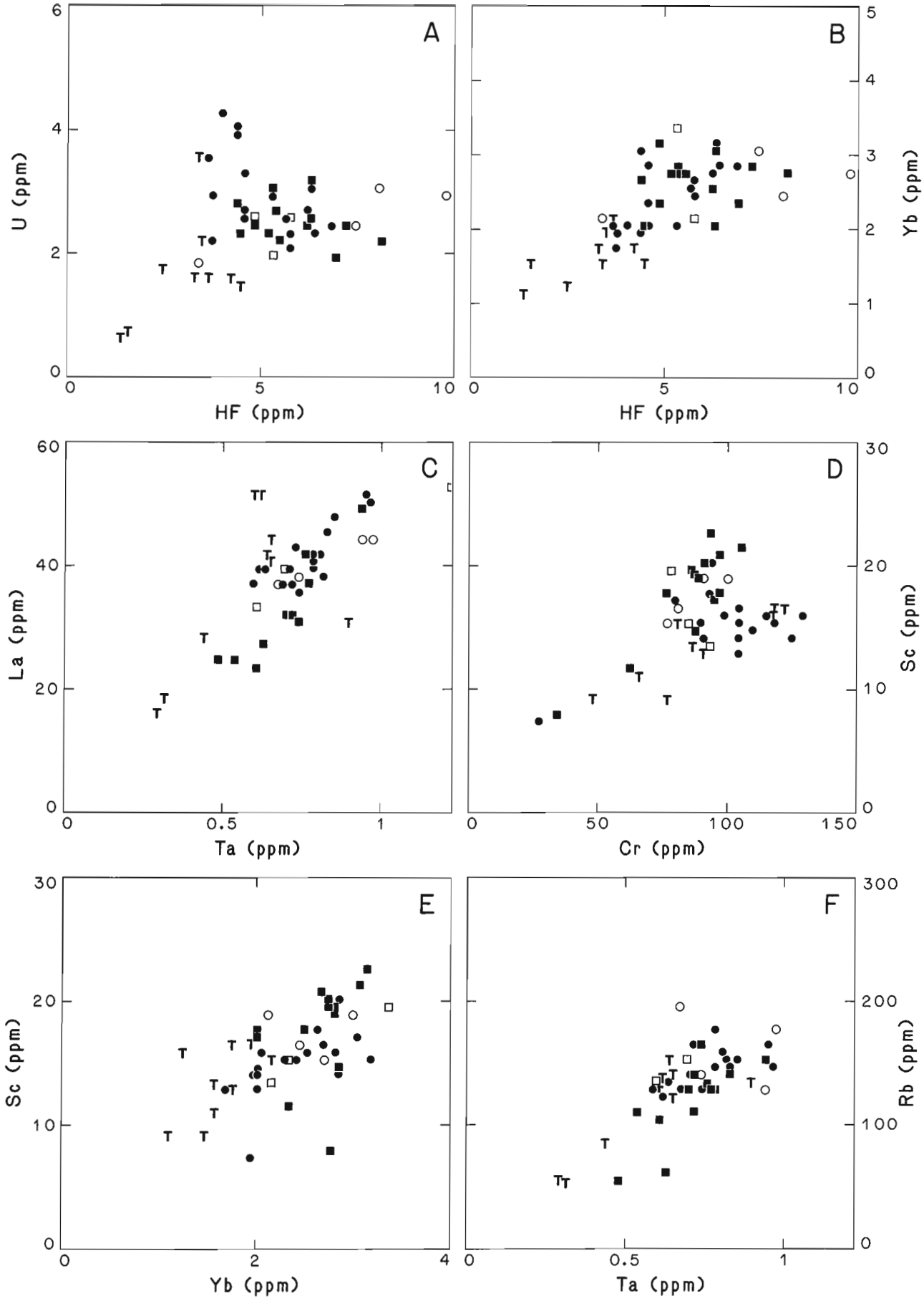


Figure 66.3. Selected trace element diagrams showing the coherent behaviour of the elements during sedimentary processes. See Figure 66.2 for symbol identification.

have a restricted compositional field both in terms of La abundances and of La/Yb ratios. The Lac Raymond samples are the most "primitive" yielding both the lowest La contents and La/Yb ratios (8 to 17). In addition, the Lac Raymond Formation is the closest in composition to different shale composites that are thought to be representative of the present day upper crust. Finally, the Robitaille and the St-Léon formations yield compositions almost identical to those of the Cabano pelites.

Figure 66.4B is a plot of the Sc/Cr ratio against the La/Yb ratio which is used to evaluate the amount of mafic component present in the shales. In crustal recycling processes, Sc is generally more compatible than Cr (Bathia and Crook, 1986). Once again, the Trinité samples are the most evolved, displaying the lowest Sc/Cr ratios, whilst the Lac Raymond pelites exhibit the highest amount of mafic component (Fig. 66.4A). Accordingly, the Robitaille and St-Léon pelites are similar to the Cabano samples which are intermediate between the Trinité Group and the Lac Raymond Formation.

DISCUSSION AND CONCLUSION

The Trinité Group is part of a thick pile of Cambro-Ordovician sediments found in the Lower St-Lawrence region. Several studies (Hubert et al., 1970; Lajoie et al., 1974; Johnson and Walker, 1979) have shown that this pile was derived from source areas located to the north, relative to their present-day position, and this source area must have been made of Grenvillian or older terranes. Although the Trinité Group may not be representative of the entire Cambro-Ordovician pile, it is very similar to other Cambrian sediments from the Eastern Townships or Beauce (H. Desbiens, personal communication, 1986) such as the Armagh, Rosaire, Oak Hill and Caldwell groups. These rocks are geochemically the most fractionated, showing that they were derived from crustal segments which underwent several episodes of recycling (orogeneses). In this respect, it is totally compatible with the interpretation of a source area located in a mature cratonic terrane such as the Grenville Province. Furthermore, examination of Figures 66.4A and 66.4B reveals that one of the reference composites is notably different from the others. This is the Canadian Shield composite, defined by Shaw et al. (1967), which shows a higher La/Yb ratio than the other composites that were, for the most part, defined in studies of Australian shales. It is likely that the Canadian Shield has, on average, a slightly different composition. The fact that the Trinité (and Cabano) samples have a geochemical composition closer to that of the Canadian Shield composite is not, in our opinion, fortuitous and it substantiates our conclusion that the Cambro-Ordovician sedimentary sequences are derived from a mature cratonic source.

The middle Ordovician to lower Silurian Cabano Formation belongs to a thick pile of Siluro-Devonian sediments which accumulated after the Taconic episode of deformation. Field evidence shows that the lower part of the Cabano pile is most likely synorogenic whilst the upper part is post-orogenic. Analysis of the sedimentary structures coupled with the presence of coarse grained strata indicate derivation from a high relief area located to the northwest. The geochemical signature is less fractionated than in the Trinité Group and accordingly, cannot be directly derived from either a mature craton or from the pre-Taconic sedimentary pile. However, the latter is not only made of terrigenous sediments but also contains a significant amount of mafic volcanic

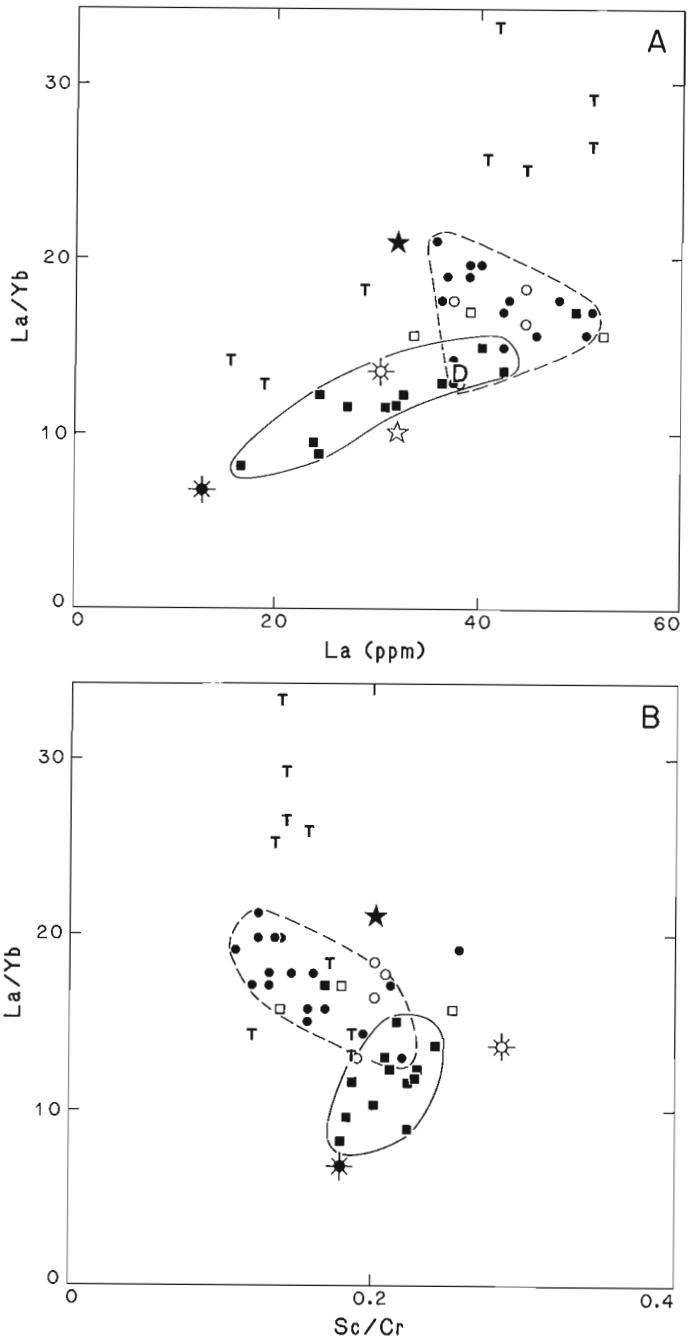


Figure 66.4. Trace element diagrams based on the use of element ratios. See Figure 66.2 for symbol identification.

rocks. The latter are well exposed in the Oak Hill and Caldwell groups (St-Julien and Hubert, 1975) and were outpoured during the initial opening of the Atlantic Ocean (Gariépy, 1978). Although no volcanic remnants are presently exposed in the area located immediately to the northwest of the Cabano Formation, rift-related Cambrian volcanics are present in the southeastern Quebec Appalachians as well as in the Newfoundland Appalachians (Williams, 1979). We do not know of any argument that would justify their absence in the Gaspé sector. As a matter of fact, the existence of laterally continuous zones is probably the most prominent feature of Paleozoic orogens like the Appalachians (see for example St-Julien and Béland, 1982). The Cabano rocks do record the presence of a mafic component and we feel that the most straightforward interpretation is to derive them from the Cambro-Ordovician prism of sediments and volcanics which was uplifted during the Taconic episode of deformation.

From its sedimentological characteristics, the Lac Raymond Formation must also be derived from a high relief area, shedding coarse grained material to the sedimentary basin. The Lac Raymond rocks are geochemically the most primitive of the area, recording a high proportion of mafic material (Fig. 66.4A). This formation is also the lateral equivalent of calc-alkaline volcanics which were, for the most part, outpoured under water. As there is no evidence of Silurian igneous activity, such as dykes or high-level intrusives, to the west of the Pointe aux Trembles Formation, the volcanic arc must have been located farther to the east or to the southeast. This volcanic arc is, in our opinion, the only source having a sufficiently large component of mafic rocks to produce the Lac Raymond Formation. Consequently, the latter corresponds to a major change in the paleogeography of the Lower St-Lawrence: in early Silurian times, the uplifted wedge of Taconic sediments was probably levelled and the sediments were shed from an emerged volcanic arc located to the east or the southeast of the sedimentary basin.

Finally, the upper Silurian Robitaille and St-Léon formations cannot be discriminated, using geochemical criteria, from the Cabano and part of the Lac Raymond sequence. As the Robitaille and St-Léon strata are shallow water features, paraconformably lying on the lower Silurian units, one can imagine that they are locally derived, either from the underlying units or from middle Silurian sequences now completely eroded.

ACKNOWLEDGMENTS

We thank K.L. Currie and the Geological Survey of Canada for proposing and supporting the project during several summers. We are also grateful to J. Ludden for providing access to his laboratory facilities, to G. Gauthier for his constant technical help, and to R. Lapointe and D. Surprenant for drafting the figures. Financial support has been provided to the first author through NSERC grants accorded to J. Lajoie and P.J. Lespérance.

REFERENCES

Allègre, C.J. and Rousseau, D.
1984: The growth of the continent through geological time studied by Nd isotope analysis of shales; Earth and Planetary Science Letters, v. 67, p. 19-34.

Basu, A., Blanchard, D.P., and Brannon, J.C.
1982: Rare earth elements in the sedimentary cycle: a pilot study of the first lag; Sedimentology, v. 29, p. 737-742.

Bathia, M.R.
1985: Rare earth element geochemistry of Australian Paleozoic graywackes and mudrocks: provenance and tectonic control; Sedimentary Geology, v. 45, p. 97-113.

Bathia, M.R. and Crook, A.W.
1986: Trace element characteristics of graywackes and tectonic setting discrimination of sedimentary basins; Contributions to Mineralogy and Petrology, v. 92, p. 181-193.

Bathia, M.R. and Taylor, S.R.
1981: Trace-element geochemistry and sedimentary provinces: a study from the Tasman Geosyncline, Australia; Chemical Geology, v. 33, p. 115-125.

Bergerioux, C., Kennedy, G., and Zikovsky, L.
1979: Use of the semi-absolute method in neutron activation analysis; Journal of Radioanalytical Chemistry, v. 50, p. 229-234.

Chaudhuri, S. and Cullers, R.L.
1979: The distribution of rare earth elements in deeply buried Gulf Coast sediments; Chemical Geology, v. 24, p. 327-328.

Cullers, R.L., Yeh, L., Chaudhuri, S., and Guidotti, C.V.
1974: Rare earth elements in Silurian pelitic schists from N.W. Maine; Geochimica et Cosmochimica Acta, v. 38, p. 389-400.

Cullers, R., Chaudhuri, S., Kilbane, N., and Koch, R.
1979: Rare-earths in size fractions and sedimentary rocks of Pennsylvanian-Permian age from the mid-continent of the U.S.A.; Geochimica et Cosmochimica Acta, v. 43, p. 1285-1301.

David, J. and Gariépy, C.
1986: Geochemistry of the Lower Silurian Pointe aux Trembles and Lac Raymond formations, central Quebec Appalachians: a preliminary report; in Current Research, Part B, Geological Survey of Canada, Paper 86-1B, p. 131-140.

David, J., Chabot, N., Marcotte, C., Lajoie, J., and Lespérance, P.J.
1985: Stratigraphy and sedimentology of the Cabano, Pointe aux Trembles, and Lac Raymond formations, Témiscouata and Rimouski counties, Quebec; in Current Research, Part B, Geological Survey of Canada, Paper 85-1B, p. 491-497.

Frey, F.A., Bryan, W.B., and Thompson, G.
1974: Atlantic ocean floor: geochemistry and petrology of basalts from Legs 2 and 3 of the Deep-Sea Drilling

Project; Journal of Geophysical Research, v. 79, p. 5507-5527.

Gariépy, C.
1978: Stratigraphie et Géochimie des laves cambriennes (?) du Groupe de Caldwell dans la Région de Lac Etchemin, Appalaches du Québec; M.Sc. thesis, Université de Montréal.

Haskin, L.A. and Paster, T.P.
1979: Geochemistry and mineralogy of the rare earths; in Handbook of Physical Chemistry of the Rare Earths, v. 3, chap. 21, North-Holland.

Hubert, C., Lajoie, J., and Léonard, M.A.
1970: Deep sea sediments in the Lower Paleozoic Quebec Supergroup; in Flysch sedimentology in North America, J. Lajoie (ed.), Geological Association of Canada, Special Paper 7, p. 103-125.

Jenner, G.A., Fryer, B.J., and McLennan, S.M.
1981: Geochemistry of the Archean Yellowknife Supergroup; Geochimica et Cosmochimica Acta, v. 45, p. 1111-1129.

Johnson, B.A. and Walker, R.G.
1979: Paleocurrents and depositional environments of the deep-water conglomerates in the Cambro-Ordovician Cap-Enragé Formation, Gaspé, Québec; Canadian Journal of Earth Sciences, v. 16, p. 1375-1387.

Lajoie, J.
1971: Région des Lacs Primes et Des Baies, Comté de Rimouski; Ministère des Richesses Naturelles du Québec, Rapport Géologique 139.

Lajoie, J., Lespérance, P.J., and Béland, J.
1968: Silurian stratigraphy and paleogeography of Matapédia-Témiscouata region, Québec; American Association of Petroleum Geologist, Bulletin, v. 52, p. 615-640.

Lajoie, J. and Ludden, J.
1984: Petrology of the Archean Pontiac and Kewagama sediments and implications for the stratigraphy of the southern Abitibi belt; Canadian Journal of Earth Sciences, v. 21, p. 1305-1314.

Lajoie, J., Héroux, Y., and Mathey, B.
1974: The Precambrian Shield and the Lower Paleozoic Shelf: the unstable provenance of the Lower Paleozoic flysch sandstones and conglomerates of the Appalachians between Beaumont and Bic, Québec; Canadian Journal of Earth Sciences, v. 11, p. 951-963.

Lespérance, P.J. and Greiner, H.R.
1969: Région de Squatek-Cabano, Comtés de Rimouski, Rivière-du-Loup et Témiscouata; Ministère des Richesses Naturelles du Québec, Rapport géologique 128.

McLennan, S.M. and Taylor, S.R.
1982: Geochemical constraints on the growth of the continental crust; Journal of Geology, v. 90, p. 347-361.

McLennan, S.M., Taylor, S.R., and McGregor, V.R.
1984: Geochemistry of Archean sedimentary rocks from West Greenland; Geochimica et Cosmochimica Acta, v. 48, p. 1-13.

Nance, W.B. and Taylor, S.R.
1976: Rare earth element patterns and crustal evolution – I. Australian post-Archean sedimentary rocks; Geochimica et Cosmochimica Acta, v. 40, p. 1539-1551.
1977: Rare earth elements and crustal evolution – II. Archean sedimentary rocks from Kalggorlie, Australia; Geochimica et Cosmochimica Acta, v. 41, p. 225-231.

Pearce, J.A. and Cann, J.R.
1973: Tectonic setting of basic volcanic rocks determined using trace element analyses; Earth and Planetary Science Letters, v. 19, p. 290-300.

Schilling, J.G.
1975: Rare-earth variations across "normal segments" of the Reykjanes Ridge, 60′-53′N, Mid-Atlantic Ridge, 29′S and East Pacific Rise, 2′-19′S, and evidence on the composition of the underlying Low-Velocity Layer; Journal of Geophysical Research, v. 80, p. 1459-1473.

Shaw, D.M., Reilly, G.A., Muysson, J.R., Pattenden, G.E., and Campbell, F.E.
1967: An estimate of the chemical composition of the Canadian Precambrian Shield; Canadian Journal of Earth Sciences, v. 4, p. 829-854.

Shaw, D.M., Dostal, J., and Keays, R.R.
1976: Additional estimates of continental surface Precambrian Shield composition in Canada; Geochimica et Cosmochimica Acta, v. 40, p. 73-83.

St-Julien, P. and Hubert, C.
1975: Evolution of the Taconian Orogen in the Quebec Appalachians; American Journal of Science, v. 275A, p. 337-362.

St-Julien, P. and Béland, J.
1982: Major structural zones and faults of the northern Appalachians; Geological Association of Canada, Special Paper 24, 280 p.

Taylor, S.R. and Gorton, M.P.
1977: Geochemical application of spark source mass spectrometry – III element sensitivity, precision, and accuracy; Geochimica et Cosmochimica Acta, v. 41, p. 1375-1380.

Taylor, S.R. and McLennan, S.M.
1980a: The rare earth element evidence in Precambrian sedimentary rocks: implications for crustal evolution; in Precambrian Plate Tectonics, A. Kroner (ed.); Elsevier, p. 527-548.
1980b: The composition and evolution of the continental crust: rare earth element evidence from sedimentary rocks; Royal Society of London, Transactions, v. A301, p. 381-399.
1985: The Continental Crust: its Composition and Evolution; Blackwell Scientific Publications, 312 p.

Williams, H.
1979: Appalachian Orogen in Canada; Canadian Journal of Earth Sciences, v. 16, p. 792-807.

Winchester, J.A. and Floyd, P.A.
1977: Geochemical discrimination of different magma series and the differentiation products using immobile elements; Chemical Geology, v. 20, p. 325-343.

Geology of the Lake Michel area, Long Range Inlier, western Newfoundland[1]

Project 840024

J. Victor Owen[2], Janet E.M. Campbell[3], and Frank A.R. Dennis[3]

Owen, J.V., Campbell, J.E.M., and Dennis, F.A.R., Geology of the Lake Michel area, Long Range Inlier, western Newfoundland; in Current Research, Part A, Geological Survey of Canada, Paper 87-1A, p. 643-652, 1987.

Abstract

Proterozoic rocks comprise a gneiss complex intruded by Grenvillian granitic plutons. The gneiss complex contains diverse amphibolite to granulite facies quartzofeldspathic gneisses, amphibolite and subordinate paragneiss. Metasedimentary rocks include massive to layered quartzite, pelitic gneiss and associated rocks. Migmatitic biotite ± garnet ± sillimanite ± orthopyroxene ± graphite-bearing pelitic gneiss, typically intercalated with quartzite, forms part of an assemblage of rocks including banded hornblende ± biotite ± orthopyroxene-bearing dioritic gneiss and/or biotite ± garnate ± pyroxene-bearing tonalitic gneiss. The protolith of quartzofeldspathic gneiss remains equivocal. Gneisses were folded about north-west-plunging (F1?-) axes prior to emplacement of the ca. 1042 Ma Lake Michel pluton which consists of megacrystic and non-megacrystic biotite ± hornblende granitic to granodioritic rocks. These foliated granitoid rocks are cut by the ca. 605 Ma mafic dykes of the Long Range swarm, and unconformably overlain by conglomerates and arenites of the Lower Cambrian Bradore Formation. The décollement postulated to separate inlier from platform either terminates or passes west of the Bradore in this area.

Résumé

Des roches du Protérozoïque comprennent un complexe gneissique pénétré par des plutons granitiques du Grenvillien. Le complexe gneissique est constitué de divers gneiss quartzofeldspathiques à faciès d'amphibolites à granulites, d'amphibolite et de paragneiss secondaire. Les roches métasédimentaires sont constituées de quartzite massif à stratifié, de gneiss pélitique et de roches connexes. Les gneiss pélitiques, migmatiques, riches en biotite ± grenat ± sillimanite ± orthopyroxène ± graphite, et typiquement intercalés avec des quartzites, constituent une partie d'un ensemble de roches comprenant des gneiss dioritiques, rubanés, riches en hornblende ± biotite ± orthopyroxène et des gneiss tonalitiques, riches en biotite ± grenat ± pyroxène. Le protolite des gneiss quartzofeldspathiques reste douteux. Les gneiss se sont plissés autour d'axes (de type F1?), plongeant vers le nord-ouest, avant l'emplacement il y a environ 1042 Ma, du pluton de Lake Michel constitué de roches granitiques à granodioritiques, porphyroïdes et non porphyroïdes à biotite ± hornblende. Ces roches granitoïdes foliées sont traversées par des dykes mafiques (environ 605 Ma) du système de Long Range et sont recouvertes en discordance par des conglomérats et des arénites de la formation de Bradore du Cambrien inférieur. Le décollement possible qui a permis le séparation de la fenêtre de la plate-forme pourrait soit s'arrêter soit passer à l'ouest de la formation de Bradore dans cette région.

[1]Contribution to Canada-Newfoundland Mineral Development Agreement 1984-1989. Project carried by Geological Survey of Canada, Lithosphere and Canadian Shield Division.

[2]Department of Mines and Energy, 95 Bonaventure Avenue, St. John's Newfoundland A1C 5T7

[3]Department of Geology, Acadia University, Wolfville, Nova Scotia B0P 1X0

INTRODUCTION

This report summarizes field data collected in 1986 during 1:100 000 scale mapping in the Lake Michel area (comprising all of NTS 12I/2, 3, 7, 8, and parts of 12I/4, 5-6, 9, and 10) of the northern Long Range Mountains of western Newfoundland. This mapping project completes the reconnaissance-scale investigation of the Precambrian Long Range Inlier initiated by Bostock (1983) and continued by Erdmer (1984, 1986a,b), and Owen (1986a,b).

The Long Range Inlier consists of Proterozoic quartzofeldspathic gneisses and mafic to felsic intrusive rocks flanked by Lower Paleozoic rocks of the Appalachian orogen. It is the largest Precambrian inlier in the Appalachians; it may represent either an in situ massif of the Grenville Province, or a slice of Grenvillian rocks displaced toward the foreland during Paleozoic tectonism.

The Lake Michel area is situated some 120 km north-northeast of Deer Lake. This area is underlain mainly by Precambrian rocks, forming the north-central portion of the Long Range Inlier (Fig. 67.1). The eastern contact with Paleozoic supracrustal rocks is not exposed in this area; however the western margin of the central part of the inlier is separated from the Cambro-Ordovician platform to the west by east-dipping thrusts or high-angle faults of unknown kinematic significance (Schuchert and Dunbar, 1934; Oxley, 1953; Nelson, 1955; Erdmer, 1986a,b; Williams et al., 1985; Cawood and Williams, 1986).

Preliminary isotopic dating of crystalline rocks of the inlier suggests that the area underwent granulite facies metamorphism at about 1250 Ma (U-Pb, zircon, Erdmer, 1986a) and was intruded by mafic plutonic rocks, and by voluminous granitic-granodioritic bodies of Grenvillian age (ca. 1042 Ma, U-Pb, zircon, Erdmer, 1986a; 1130 ± 30 Ma, Rb-Sr, whole rock, Pringle et al., 1971). The gneisses in the southern part of the inlier were deformed about a W- to NW-trending regional schistosity developed after the emplacement of the Grenvillian rocks (Owen, 1986a) and prior to the emplacement of mafic dykes assigned (Owen and Machin, 1987) to the ca. 605 Ma (Stukas and Reynolds, 1974) Long Range swarm (Strong and Williams, 1972; Strong, 1974). Owen and Erdmer (1986) estimated peak metamorphic conditions of ca. 800 ± 50°C and ≥6 kbar from high grade mineral assemblages preserved where the granulites lack the regional, overprinting schistosity. The Long Range dykes have also been polymetamorphosed, but typically have well preserved primary igneous textures. Owen and Machin (1987) suggested that the Long Range dykes in the southern part of the inlier were metamorphosed at low pressures soon after emplacement, and attributed a locally superimposed, higher-pressure, amphibolite-facies imprint to burial of parts of the inlier by Cambro-Ordovician rocks thrust westward during the Taconic Orogeny.

A greenschist facies overprint is locally evident in the Long Range dykes and their host rocks, U-Pb (sphene) dates of ca. 400 Ma for both Grenvillian and Acadian granites (Erdmer, 1986a) and a degassing event at ca. 380 Ma (Stukas and Reynolds, 1974) suggest that greenschist facies metamorphism in the area is Acadian. Orogenesis in the Long Range Inlier thus spans a period of at least 850 Ma.

LITHOLOGY

Rock units mappable at 1:100 000 scale within the inlier may be subdivided into four "groupings" according to their lithology and inferred age relative to major tectono-metamorphic and/or intrusive events. These are: (A) early- or pre-Grenvillian gneissic rocks; (B) Grenvillian (or younger) felsic plutonic rocks; (C) mafic dykes of the Long Range swarm, and (D) undeformed conglomerates and arenites of inferred Lower Paleozoic age.

A. Gneissic rocks

Eight types of gneissic rocks have been distinguished on the geological sketch map of the Lake Michel area presented in Figure 67.2. All but one (dioritic gneiss and amphibolite) are quartz-bearing, leucocratic to mesocratic rocks.

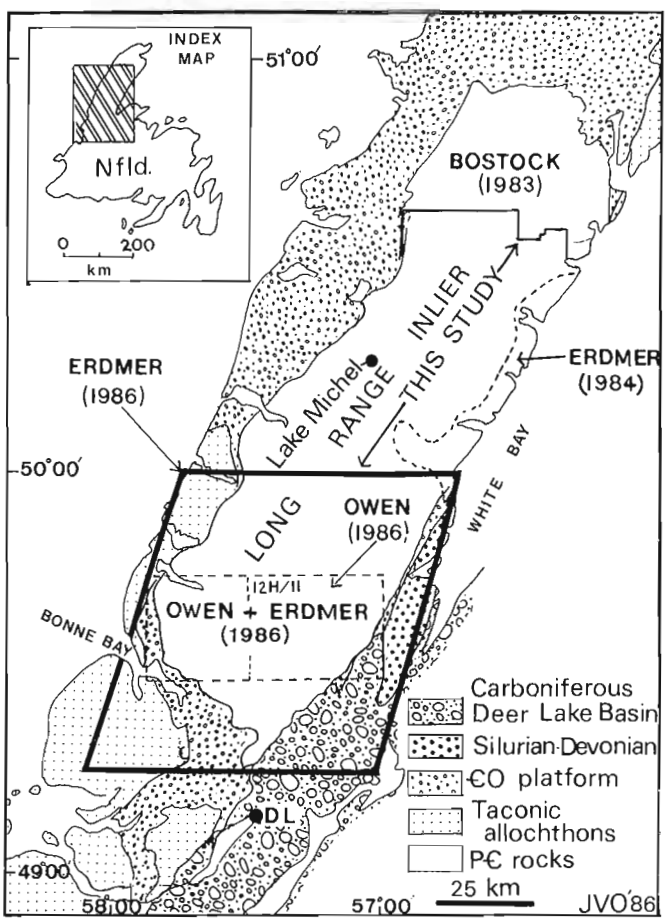


Figure 67.1. Regional geological setting of the Lake Michel area, showing previously mapped areas of the Long Range Inlier. DL-Deer Lake.

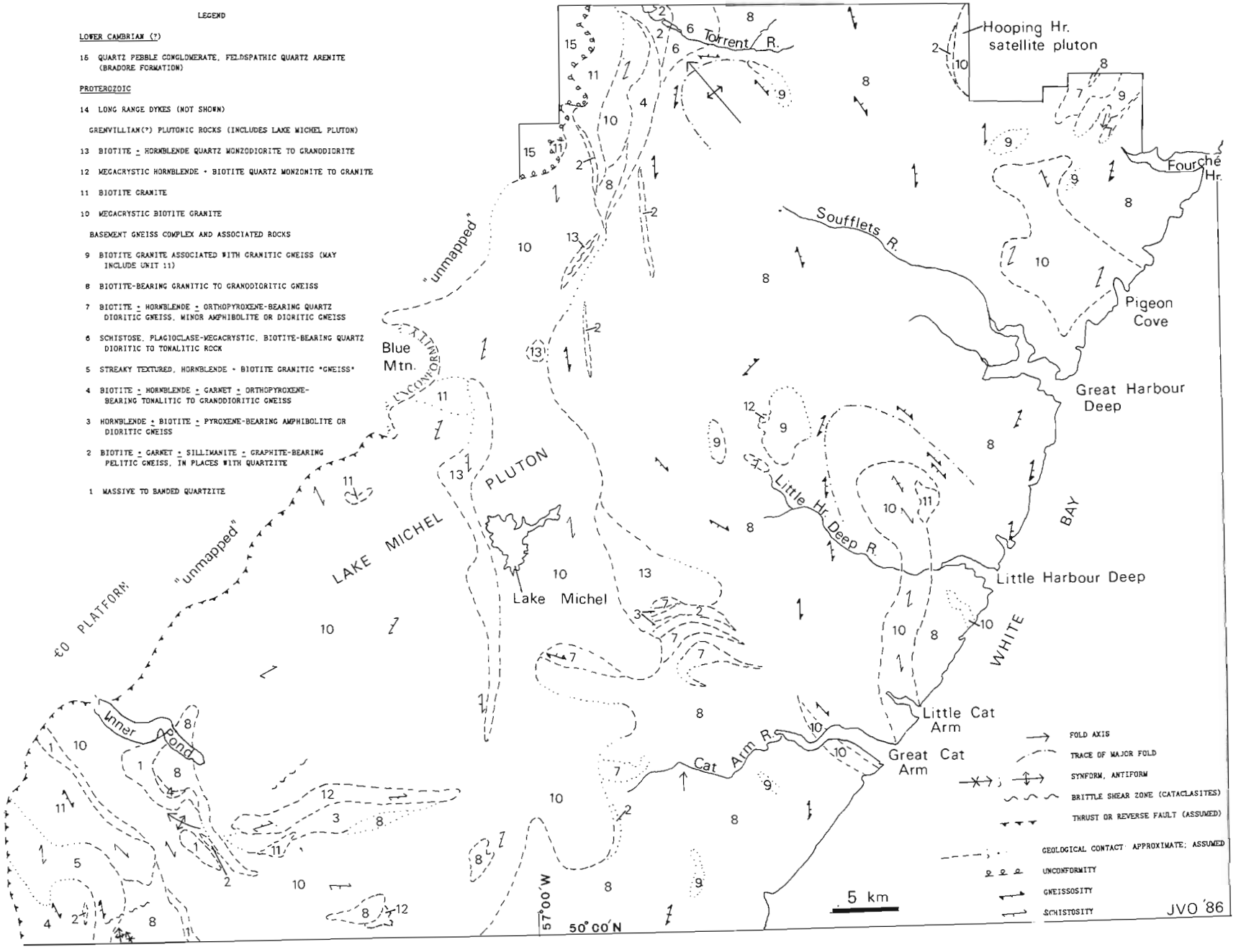


Figure 67.2. Geological sketch map of the Lake Michel area, incorporating some data from Erdmer (1984) along the west coast of White Bay.

Two types of metasedimentary rocks have been recognized. Unit 1 consists of massive to banded, white to grey, medium grained quartzite, which forms discontinuous bands up to about 1 km in width enclosed by quartzofeldspathic gneiss of uncertain (and diverse protolith, or intruded by granitic rocks of presumed Grenvillian age. Layering in the quartzites is developed on a millimetre- to metre-scale and is defined by colour banding, contrasting grain size, and/or by variations in the ratio of quartz to feldspar, Fe oxide, and/or biotite. Erdmer (1984) described a narrow band of quartz-rich gneiss, quartzite, and biotite schist extending northward from Little Harbour Deep along the coast of White Bay. Since only granitic gneiss was noted immediately inland along this coastal section in the present study, these rocks are omitted in Figure 67.2, although supracrustal rocks (of units 1 and 2?) may be exposed in shoreline exposures in this area.

Pelitic rocks are grouped as unit 2. These are biotite ± garnet ± sillimanite ± orthopyroxene ± hercynite ± graphite-bearing migmatitic gneisses (Fig. 67.3) which form narrow (typically <1 km) bands within more homogeneous quartzofeldspathic gneiss, or as enclaves within granite. Quartzite is a common constituent of several of the pelitic sequences (Fig. 67.4). A noteworthy feature of all the occurrences of pelitic gneiss is the local presence of sillimanite + K feldspar, indicating that the second sillimanite isograd was surpassed during regional metamorphism throughout the map area.

The remaining leuco- to mesocratic gneisses in the map area are quartzofeldspathic rocks of uncertain origin. Bostock (1983) inferred a sedimentary protolith for most of the gneisses to the north of the Lake Michel area, citing as evidence the widespread occurrence of "thin bands and remnants of quart-rich gneiss and pelitic schist" (Bostock, 1983, p. 8). Alternatively, Owen (1986) and Owen and Erdmer (1986) proposed that the relatively homogeneous nature of tonalitic to granitic gneisses in the Silver Mountain area (12H/11), in the south-central part of the inlier (Fig. 67.1) is indicative of an igneous protolith. We similarly infer igneous protoliths for most of the quartzofeldspathic gneisses in the Lake Michel area, however some units may be derived from diverse supracrustal protoliths, particularly rocks spatially associated with pelites and quartzite. For example, layered dioritic gneiss in the pelite-quartzite sequence enclosed in the north part of Lake Michel pluton, and in the pelites to the south of Inner Pond, is inferred to be derived from a supracrustal protolith. Since this layered dioritic gneiss forms bands up to a few tens of metres wide, it is not distinguished as a separate unit in Figure 67.2. By comparison, hornblende-bearing amphibolite (unit 3) is relatively homogeneous, forms bands in quartzofeldspathic gneiss ranging from a few centimetres to several hundred metres in width, and locally preserves a subophitic texture, demonstrating a mafic igneous protolith for some of the mafic rocks included in this unit.

The paragneiss sequences along Torrent River and to the south of Inner Pond are associated with biotite ± hornblende ± garnet ± orthopyroxene-bearing tonalitic to granodioritic (locally quartz dioritic) gneiss (unit 4). Unit 4 is locally migmatitic; tonalitic gneiss immediately to the south of Inner Pond contains diffuse, orthopyroxene-bearing leucocratic segregations in a homogeneous, biotite-bearing paleosome (Fig. 67.5). Even where the tonalitic gneiss has a well defined gneissic banding, it is characterized by a granoblastic texture, a feature characteristic of gneissic rocks throughout the map area.

Northeast of the granoblastic tonalitic gneiss (unit 4) near Inner Pond is a 2 km wide band of buff coloured, medium grained hornblende + biotite bearing granitic "gneiss" (unit 5). This is not a banded gneiss. Rather, it is a homogeneous granitoid rock, characterized by a flecked or streaked appearance imparted by 5-10 mm long, ovoid aggregates of hornblende + biotite, which weather recessively, giving the rock a pitted appearance on the altered surface (Fig. 67.6). Unit 5 is included as part of the basement gneiss complex due to the local presence of pyroxene and garnet in texturally-similar granitoid rocks along the western part of the unit. This interpretation is being tested by isotopic dating.

Unit 6 is a grey, homogeneous, schistose, biotite-bearing quartz dioritic to tonalitic rock studded with 5-10 mm plagioclase megacrysts. This unit flanks the eastern margin of the Torrent River pelites exposed within the map area. The homogeneity of the rock, together with the apparent absence of both quartzite and aluminosilicates, suggests an igneous protolith.

Unit 7 is a grey to green-grey, biotite quartz dioritic gneiss which in places is interlayered with amphibolite. The quartz dioritic gneiss flanks the paragneiss (unit 2) north of Cat Arm River where it locally contains orthopyroxene and hornblende. Northwest of Fourché Harbour, unit 7 is exposed as 1 km wide bands within biotite granitic gneiss (unit 8); both gneissic units are cut by medium grained biotite granite (unit 9) and associated granitic pegmatite.

Unit 8 comprises a variety of grey to rose, medium grained, granitic to granodioritic gneisses and associated foliated biotite granite. This is the dominant gneissic unit within the map area (Fig. 67.2). Further subdivision of the granitic gneiss is not possible at the scale of mapping. Biotite is the typical mafic mineral in the granitic gneiss, although hornblende and garnet are rare accessory minerals. The granitoid rocks assigned to unit 8 are texturally diverse. Typically, the granitic gneiss is a granoblastic rock marked by an indistinct gneissose fabric. Migmatitic textures locally developed in the gneiss categorize certain members of the unit as either metatexites, with biotite-seamed leucocratic veins, or as diatexites. The diatexites resemble schlieric granites, consisting chiefly of massive to foliated, medium grained biotite granite with diffuse, wispy, biotite-rich schlieren. At least some of these granites are anatectic bodies of local derivation, generated during regional, high grade metamorphism. Other medium grained granites lack a schlieric fabric and cut the granitic gneiss. These granites (unit 9) are interpreted to postdate high grade metamorphism of the basement gneiss complex.

B. Grenvillian felsic plutonic rocks

The largest Grenvillian granitic pluton of the Long Range Inlier is almost entirely contained within the present map area. Originally outlined by Baird (1960) and Clifford and Baird (1962), and termed the Portland Creek Pond pluton by Pringle et al. (1971), this pluton was renamed the Lake Michel pluton by Bostock (1983). Megacrystic granite from the north and central parts of the Lake Michel pluton give a combined Rb-Sr (whole rock) age of 1130 ± 90 Ma (Pringle et al., 1971). Biotite separated from two samples of megacrystic granite yield K-Ar ages of 821 ± 21 and 859 ± 21 Ma (Pringle et al., 1971). Zircon separated from megacrystic granite from the south part of the pluton has yielded a U-Pb age of 1042 $+22/-11$ Ma (Erdmer, 1986a).

Four members of the Lake Michel pluton have been recognized. All are massive to foliated granitoid rocks. The most abundant rock type is K-feldspar megacrystic biotite granite (unit 10), as in other, smaller plutons in the northern part of the inlier (Bostock, 1983). The megacrystic granite of the Lake Michel pluton is mesoscopically indistinguishable from that present in other plutons. Unit 10 is well foliated, with oriented, tabular to lens-shaped, salmon pink K-feldspar megacrysts generally 1-3 cm in length (locally up to 5 cm), constituting about 5-25% of the rock (Fig. 67.7). Greenish plagioclase has also been observed as a megacrystic phase, locally forming crystals up to 3 cm. The megacrystic granite contains about 5% biotite, and in places is extensively epidotized.

Megacrystic granite in the northern part of the Lake Michel pluton is cut by narrow (≤1 m) dykes of grey to rose, fine to medium grained biotite granite. The dykes cut the foliation in the megacrystic granite, and locally contain a schistosity parallel to their margins, which is cut by massive granitic pegmatite. The granitic dykes are correlated with grey to rose, medium grained biotite granite (unit 11) flanking the megacrystic granite farther to the west and southwest. The relationship between the medium grained biotite granites of units 9 and 11 is unknown; it is possible that granite cutting the basement gneiss complex was emplaced contemporaneously with biotite granite spatially associated with the Lake Michel pluton (i.e. unit 11). Biotite granite (unit 11) of the Lake Michel pluton is a homogeneous, variably foliated rock. Although biotite is the principal mafic mineral in the rock, accessory hornblende has been observed. Medium grained biotite granite is also present along the northeastern flank of the megacrystic granite pluton north of Little Cat Arm, informally named here the Little Cat Arm pluton.

The remaining two members of the Lake Michel pluton include diverse, biotite ± hornblende-bearing granitoid rocks. The ages of these units are unknown. Unit 12 is a grey to rose, coarsely megacrystic, hornblende + biotite quartz monzonite to granite occurring in a narrow, 17 km long, east-trending band in the southern part of the Lake Michel pluton and in a smaller body farther to the south. A small intrusion of unit 12 also occurs to the east of the Lake Michel pluton. K-feldspar megacrysts range from 1-5 cm in diameter, and typically constitute approximately 20-40% of the rock (Fig. 67.8). Where the megacrysts are more abundant (up to aboiut 60%), the rock is better described as being coarse grained rather than megacrystic. The rock is mesocratic, generally with 8-15% hornblende + biotite. Both mafic minerals occur with quartz, plagioclase, and minor K-feldspar in the groundmass. Sphene is a conspicuous accessory mineral in some samples.

Unit 13 is medium grained, grey to rose, biotite ± hornblende quartz monzodiorite to granodiorite (locally granite) occurring as a narrow, 27 km long, north-trending body in the centre of the Lake Michel pluton, and as smaller bodies near and along the eastern part of the pluton. It contains approximately 8-10% mafic minerals (Fig. 67.9). Plagioclase is generally saussuritized, and quartz commonly has a bluish cast.

C. Long Range dykes

Mafic dykes of the ca. 605 Ma (Stukas and Reynolds, 1974) Long Range swarm (unit 14) are a conspicuous feature of the eastern half of the map area. They are not depicted in Figure 67.2; however, the dykes are common east of a line extending southwest from the Hooping Harbour satellite pluton (Fig. 67.2). They form prominent ridges in this area. Individual dykes can be traced for 5 km or more. They range from about 5 m to 50 m or more in width. Although most are rectiplanar or slightly curved, some dykes show angular, S-shaped "kinks", dextrally offsetting the dyke by 100-300 m. The dykes do not appear to be folded, the consistent shape of the "kink" suggests that the offsets are primary features (i.e. outlines of extensional fractures developed prior to or during dyke emplacement.

The Long Range dykes in the study area locally preserve primary igneous textures and mineralogy. They have well developed chilled margins, and the medium-grained interiors have a subophitic texture defined by plagioclase laths partly enclosed in clinopyroxene (in places pseudomorphed by amphibole). Some dykes are plagioclase-phyric. The dykes near White Bay are recrystallized, and in places carry a penetrative schistosity. Bostock (1983) and Erdmer (1986a) reported that the Long Range dykes in the easternmost part of the inlier show a significant greenschist facies imprint.

D. Conglomerate and arenaceous rocks

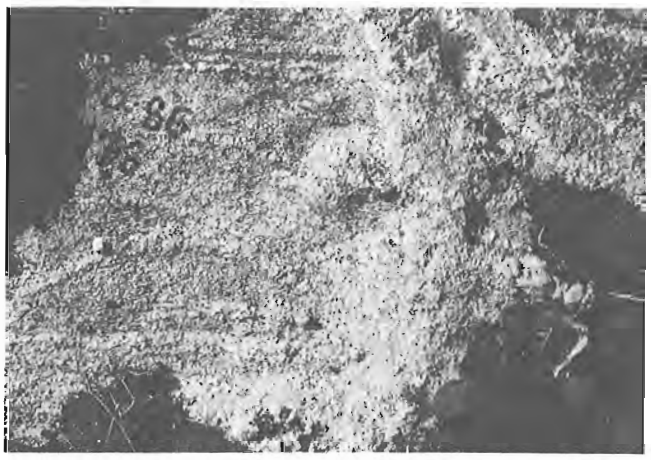
Flat-lying, undeformed conglomerate and feldspathic quartz arenite (unit 15) unconformably overlie granite of the Lake Michel pluton in the northwestern part of the map area. The conglomerate forms the basal unit. It is a poorly bedded, quartz pebble conglomerate, containing rounded clasts up to about 3 cm in diameter, and rare, thin, sandy interbeds. It underlies red to beige feldspathic quartz arenite containing conspicuous salmon-pink feldspar clasts. The feldspathic quartz arenites are well bedded on a centimetre-scale; crossbedding is locally evident (Fig. 67.10). Unit 15 is correlated with the Bradore Formation, a sequence of arkoses and conglomerate (Schuchert and Dunbar, 1934) of pre-late Early



67.3



67.4



67.5



67.6



67.7

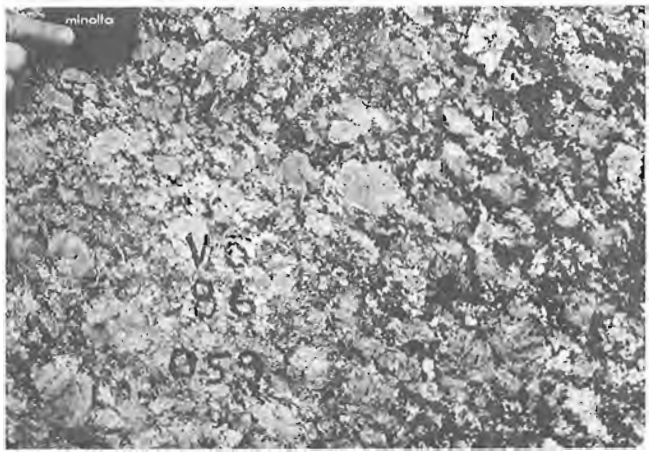
Figure 67.3. Migmatitic pelitic gneiss (unit 2) south of Inner Pond, with large garnet porphyroblasts in diffuse leucocratic segregations.

Figure 67.4. Folded quartzite with thin, sillimanite-rich pelitic bands (unit 2), from the supracrustal sequence north of Cat Arm River. The quartzite has a strong axial planar fabric. Knife is 13 cm long.

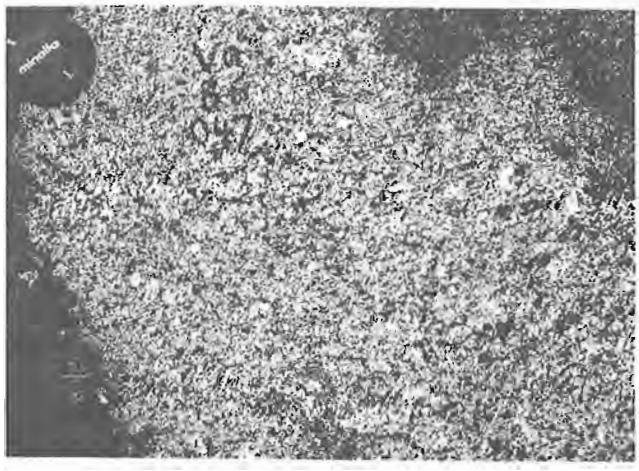
Figure 67.5. Migmatitic tonalitic gneiss (unit 4) with diffuse, orthopyroxene-bearing leucocratic segregations in a biotite-bearing paleosome. South of Inner Pond.

Figure 67.6. Homogeneous, streaky-textured hornblende + biotite granitic "gneiss" (unit 5) south of Inner Pond.

Figure 67.7. Foliated megacrystic biotite granite (unit 10) at Lake Michel.



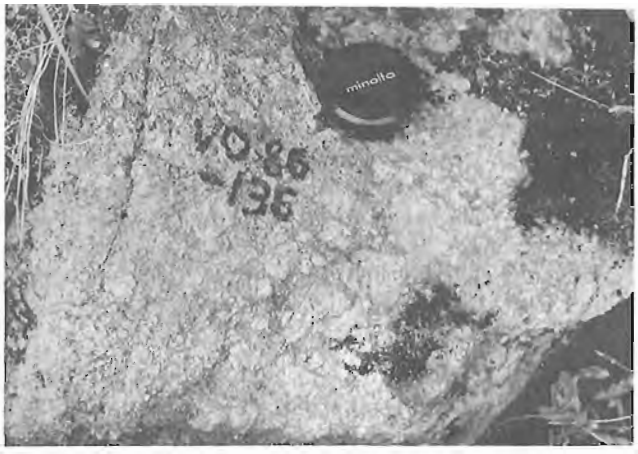
67.8



67.9



67.10



67.11



67.12

Figure 67.8. Megacrystic hornblende + biotite quartz monzonite (unit 12) southeast of Inner Pond. Some K-feldspar megacrysts have a pale feldspathic rim (rapakivi texture?).

Figure 67.9. Massive, biotite ± hornblende quartz monzodiorite (unit 13) of the Lake Michel pluton. Southwest of Lake Michel.

Figure 67.10. Crossbedded feldspathic quartz arenite of the Bradore Formation (unit 16), viewed from the south. Northwest corner of map area.

Figure 67.11. Cataclastic hornblende + biotite granitic "gneiss" (unit 5), south of Inner Pond.

Figure 67.12. Recrystallized granodioritic dykes cutting fabric (parallels knife) in granitic gneiss (unit 8), northeast of Lake Michel.

Cambrian age (Bostock, 1983). Bostock (1983) has described a nearly continuous belt of the Bradore Formation along the northern and northernwestern flank of the Long Range Inlier. Similar rocks have been described as far south as Blue Mountain (Nelson, 1955).

STRUCTURE

The regional distribution of crystalline rocks in the Lake Michel area outlines at least two fold sets. Large scale, NW-plunging folds (F1?) with wavelengths up to about 15 km deform gneissic rocks in the western part of the inlier. The age of these folds is uncertain. The N- to NE-trending orientation of schistose fabrics in the Lake Michel pluton suggests that the NW-plunging folds predate the emplacement of the Grenvillian plutonic rocks. Other observations suggest that some megacrystic granite bodies predate the major NW-trending folds. The northern end of the Little Cat Arm pluton (Fig. 67.2) is centred in a major, NW-trending fold developed in granitic gneiss. Insufficient data are available to assess the plunge direction of this fold. Both the southwestern and northeastern limbs of the fold dip toward the northeast, although some southwest dipping S-planes have been noted locally (Fig. 67.2). This structure may be either a southeast-plunging synform, or a northwest-plunging antiform. Northwest-trending schistose fabrics in the Little Cat Arm granite approximately coincide with the axial surface of the fold, implying that this structure developed after emplacement of the granite.

The NW-trending fold enveloping the Little Cat Arm granite is atypical of folds in the eastern part of the inlier. Folds in this area are relatively small scale, N- or S-plunging structures seen to deform earlier folds outlined by gneissic fabrics in both ortho- and paragneiss. The older fold set trends west to northwest, and is tentatively correlated with the major, NW-plunging folds in the western part of the map area. The younger, N-S trending folds (F2?) locally have a well developed, steeply dipping, axial planar fabric (see Fig. 67.4). This schistosity overprints compositional banding in gneissic rocks. It parallels on a regional scale the schistosity in foliated intrusive rocks near White Bay. S-planes developed in the megacrystic granite near Pigeon Cove trend north to north-northwest, and include mylonitic fabrics showing marked strain gradients (inferred from variable, and abrupt, degrees of grain size reduction and fabric development) in the eastern part of the intrusion.

The N- to NNE-trending axial planar schistosity of the F2(?) folds appears to be cut by the ca. 605 Ma Long Range mafic dykes, and is thus inferred to be a late Grenvillian structure. Dykes of the Long Range swarm for the most part are undeformed, but show evidence of static, amphibolite to greenschist facies recrystallization which overprints primary igneous textures. Rare examples of dynamic recrystallization of the dykes have also been noted. A Long Range dyke 10 km northwest of Great Cat Arm shows evidence of high strain along its northwestern margin. The centre of this dyke is medium grained, with a subophitic texture pseudomorphed by actinolite rimmed by hornblende. The steeply dipping schistose fabric along the northwestern margin of the dyke is defined by hornblende and/or actinolite and sphene, which coexist with albite, andesine, epidote, ± biotite ± chlorite. In addition to this penetrative fabric, the strained margin of the dyke contains a non-penetrative shear band foliation. These features are tentatively interpreted to indicate recrystallization of the dyke under greenschist facies to epidote amphibolite or lower amphibole facies conditions during an episode of local, simple shear deformation. Greenschist facies metamorphism of the dyke is interpreted to be Acadian; the age and regional significance of the higher grade metamorphic and structural imprint evident in the dyke is uncertain.

The youngest(?) structural features in the map area are cataclasite zones which are developed locally in both the basement gneiss complex and in the Lake Michel pluton. Their age relative to the Long Range dykes is unknown. The width of the cataclasite zones is variable, from a few millimetres to at least a few tens of metres. The cataclasites form rubbly fracture zones which contain angular, brecciated rock fragments (Fig. 67.11), in places with anastamosing pseudotachylite veins. The cataclasite zones are interpreted to coincide with late, high level, brittle faults which probably developed during Paleozoic uplift of the inlier (Erdmer, 1986a). Their relation to the sole thrust postulated to underlie part of the Long Range Inlier (e.g. Cawood and Williams, 1986, among others) is unknown since no major fault has been recognized within the map area. Since undeformed conglomerates and arenites of the Bradore Formation unconformably overlie the inlier in the northwest part of the map area, the postulated sole thrust is either discontinuous, or veers to the west of the exposed crystalline rocks.

METAMORPHISM

Evidence of at least four periods of metamorphism has been noted. Metamorphism in this area includes an early, high grade event before the emplacement and deformation of Grenvillian granitic plutons, and partial (and local) recrystallization of the Long Range dykes. Evidence for the high grade event, and for metamorphism and deformation of the Grenvillian granites (and their host rocks) is widely preserved in the inlier; however, recognition of the thermal aureoles of the Grenvillian granites is hampered by (1) the paucity of rocks of suitable bulk compositions to develop a range of metamorphic indicator minerals, and (2) the subsequent recrystallization of the granites and their host rocks.

Granulite facies mineral assemblages are widespread in gneissic rocks, particularly in the western part of the map area. Orthopyroxene characteristically occurs as porphyroblasts in leucocratic segregations (Fig. 67.5), or as equigranular crystals in homogeneous, non-migmatitic gneisses. It is a common constituent of tonalitic-granodioritic gneiss (unit 4), and is also observed locally in dioritic gneiss (unit 3), in quartz dioritic gneiss (unit 7), and in the pelitic rocks north of Cat Arm River. Orthopyroxene locally coexists with garnet, biotite and(or) clinopyroxene in the ortho(?)gneisses.

Gneissic rocks east of the Lake Michel pluton preserve amphibolite facies assemblages (e.g. hornblende ± biotite in mafic enclaves in granitic gneiss). However, orthopyroxene occurs in quartz dioritic gneiss, and in garnet + biotite + graphite-bearing semi-pelitic gneiss intercalated with sillimanite + K-feldspar + biotite ± garnet-bearing pelites north of Cat Arm River, suggesting that much of the inlier underwent regional, granulite facies metamorphism (see Owen, 1986a; Owen and Erdmer, 1986).

The large volume of granitic rock of Grenvillian age (units 9-13) suggest that these plutons influenced the regional distribution of metamorphic assemblages. For reasons noted above, however, recognition of the extent of the thermal aureoles associated with these plutons is difficult. To the north of the present map area, Bostock (1983) noted the local presence of andalusite in pelites intruded by megacrystic granite, and on this basis concluded that the host gneisses within the thermal aureoles of the Grenvillian plutons were retrogressed under low pressure (Abukuma type) conditions. In contrast, Underschultz (1986) attributed the second-generation sillimanite observed in pelites along the southeastern margin of the Lake Michel pluton (Fig. 67.2) to an overprinting of earlier pelitic mineral assemblages including rutilated biotite, almandine, and calcic plagioclase. While acknowledging the difficulty in correlating specific textural occurrences of sillimanite with different metamorphic events, the apparent absence of andalusite at this locality, together with the stability of sillimanite here and elsewhere may imply that the Lake Michel pluton was emplaced at a deeper crustal level than Grenvillian granitic plutons farther to the north.

The Long Range Inlier was subjected to regional metamorphism following the emplacement of Grenvillian plutonic rocks. The granites (i.e. units 10 to 13) have a well defined, variably oriented tectonic fabric which predates emplacement of the Long Range dykes. The schistose fabric in the granitoid rocks is defined by feldspar megacrysts and groundmass biotite, or by amphibole and biotite, with or without epidote. Schistose fabrics (S2?) in the eastern part of the map area paralleling this foliation overprint the gneissosity in the host rocks of the granites. The schistose fabric in orthogneiss (e.g. units 7 and 8) is defined by biotite oblique to the gneissosity, however, key mineral assemblages which would permit concise definition of the metamorphic grade associated with the development of this fabric have not yet been identified.

Many of the gneisses in the map area have a granoblastic texture. This is attributed to a late (post-plutonic) thermal event which annealed both the gneisses and diverse intrusive rocks. This interpretation is supported by the local occurrence of massive, granoblastic, metafelsic to metamafic dykes which cut both the gneissic fabrics in the basement complex (Fig. 67.12) and the schistose fabrics pervasively developed in the Lake Michel pluton.

Mesoscopic examination of the Long Range dykes in the map area indicates that they are recrystallized in the east, and locally contain a tectonic fabric. The deformed Long Range dyke described above contains a greenschist facies mineralogy, and shows evidence of an epidote amphibolite or lower amphibolite facies overprint. Mafic dykes from the southern part of the inlier also show evidence of polyphase metamorphism (Owen and Erdmer, 1986; Owen and Machin, 1987), but the greenschist facies imprint in these dykes appears to be the youngest event. This may signify regional differences in the grade and/or timing of Paleozoic metamorphism within the inlier.

Cataclasite zones interpreted to be late (Paleozoic?), high level fault breccias are developed on a millimetre to decametre scale in the western part of the map area. Narrow (1 mm) cataclastic bands transecting some samples of foliated megacrystic biotite granite (unit 10) and pelitic gneiss (unit 2) contain angular mineral fragments set in a very fine grained, green (low Ti) biotite-rich matrix. Similar green biotite fringes brown biotite outside of the cataclasite bands, indicating that relatively low grade mineral assemblages associated with Paleozoic(?) uplift may be developed in both massive or foliated rocks away from fault zones. It may thus be impossible in the general case to distinguish the (retrograde) mineral assemblages associated with late faulting from those resulting from the deformation of Grenvillian granites, and subsequent recrystallization of the Long Range dykes.

ACKNOWLEDGMENTS

We thank Sharon Baillie, Kim Bellefontaine, and Steve Orr for their enthusiastic and capable assistance in the field. Viking Helicopters and Newfoundland-Labrador Air Transport provided reliable logistical support. The manuscript has benefitted from critical reviews by Ken Currie and Philippe Erdmer.

REFERENCES

Baird, D.M.
1960: Sandy Lake (West Half) map area; Geological Survey of Canada, Map 47-1959.

Bostock, H.H.
1983: Precambrian rocks of the Strait of Belle Isle area; in Geology of the Strait of Belle Isle, northwestern insular Newfoundland, southern Labrador, and adjacent Quebec; Geological Survey of Canada, Memoir 400, 1 p. 1-73.

Clifford, P.M. and Baird, D.M.
1962: Great Northern Peninsula of Newfoundland-Grenville inlier; Canadian Mining and Metallurgical Bulletin, no. 599, p. 150-157 and 276, 277.

Cawood, P.A. and Williams, H.
1986: Northern extremity of the Humber Arm Allochthon in the Portland Creek area, western Newfoundland, and relationships to nearby groups; in Current Research, Part A, Geological Survey of Canada, Paper 86-1A, p. 675-682.

Erdmer, P.

1984: Summary of field work in the northern Long Range Mountains, western Newfoundland; in Current Research, Part A, Geological Survey of Canada, Paper 84-1A, p. 521-530.

1986a: Geology of the Long Range Inlier in the Sandy Lake map area, western Newfoundland; in Current Research, Part B, Geological Survey of Canada, Paper 86-1B, p. 19-27.

1986b: Geology of the Long Range Inlier in the Sandy Lake map area, western Newfoundland; Geological Survey of Canada, Open File 1310.

Nelson, S.J.

1955: Geology of Portland Creek, Port Saunders area, west coast, Geological Survey of Newfoundland, Report 7, 58 p.

Owen, J.V.

1986a: Geology of the Silver Mountain area, western Newfoundland; in Current Research, Part A, Geological Survey of Canada, Paper 86-1A, p. 515-522.

1986b: Geology of the Silver Mountain area, western Newfoundland; Geological Survey of Canada, Open File 1279.

Owen, J.V. and Erdmer, P.

1986: Precambrian and Paleozoic metamorphism in the Long Range Inlier, western Newfoundland; in Current Research, Part B, Geological Survey of Canada, Paper 86-1B, p. 29-38.

Owen, J.V. and Machin, D.C.

1987: The petrography and geochemistry of some mafic dykes in the Long Range Inlier, western Newfoundland; in Current Research, Part A, Geological Survey of Canada, Paper 87-1A report 29.

Oxley, P.

1953: Geology of the Parsons Pond – St. Pauls area, west coast; Geological Survey of Newfoundland, Report 5, 53 p.

Pringle, I.R., Miller, J.A., and Warrell, D.M.

1971: Radiometric age determinations from the Long Range Mountains, Newfoundland; Canadian Journal of Earth Sciences, v. 8, p. 1325-1330.

Schuchert, C. and Dunbar, C.O.

1934: Stratigraphy of western Newfoundland; Geological Society of America, Memoir 1, 123 p.

Streckeisen, A.

1976: To each plutonic rock its proper name; Earth-Science Reviews, v. 13, p. 1-33.

Strong, D.F.

1974: Plateau lavas and diabase dikes of northwestern Newfoundland; Geological Magazine, v. 111, p. 501-514.

Strong, D.F. and Williams, H.

1972: Early Paleozoic flood basalts of northwestern Newfoundland: their petrology and tectonic significance; Proceedings of the Geological Association of Canada, v. 24, p. 43-53.

Stukas, W.R. and Reynolds, P.H.

1974: $^{40}Ar/^{39}Ar$ dating of the Long Range dykes of Newfoundland; Earth and Planetary Science Letters, v. 22, p. 256-266.

Underschultz, J.

1986: Geology of a supracrustal slice in the Long Range Inlier, Cat Arm Dam area, western Newfoundland; University of Alberta, Department of Geology, B.Sc. Honours report, 30 p.

Williams, H., James, N.P., and Stevens, R.K.

1985: Humbar Arm Allocththon and nearby groups between Bonne Bay and Portland Creek, western Newfoundland; in Current Research, Part A, Geological Survey of Canada, Paper 85-1A, p. 399-406.

Williams, H. and Stevens, R.K.

1969: Geology of Belle Isle – northern extremity of the deformed Appalachian miogeosynclinal belt; Canadian Journal of Earth Sciences, v. 6, p. 1145-1157.

A preliminary account of the geology of Harrys River map area, southern Long Range of Newfoundland

Project 850017

K.L. Currie
Lithosphere and Canadian Shield Division

Currie, K.L., A preliminary account of the geology of Harrys River map area, southern Long Range of Newfoundland; in Current Research, Part A, Geological Survey of Canada, Paper 87-1A, p. 653-662, 1987.

Abstract

The Harrys River area exhibits granulitic gneiss and anorthosite of Grenvillian affinities (Disappointment Hill and Steel Mountain complexes) veneered by metamorphosed shelf-type sediments. The granulite-grade rocks pass gradationally into amphibolite-grade gneiss and then into a granite gneiss complex with cores of massive peralkaline granite (Tulks Pond complex). These rocks are separated by the major Grand Lake fault from the classic passive margin and allochthon sequences of western Newfoundland, and by a brittle shear zone from partially subaerial Ordovician volcanic rocks (Glover Group).

East of the Grand Lake fault rocks younger than the amphibolite-grade gneiss complex exhibit a single period of progressive deformation and metamorphism developed during thrusting which gradually changed transport direction from westward to north-northwest. Metamorphism reached amphibolite grade, and very large scale doming possibly accompanied late metamorphism. Brittle shear zones appear to be late features of little significance. Major movement took place on older, ductile shear zones. Relations between metamorphism and deformation show that the thrusting must be younger than that which formed the Humber Arm allochthon. The region appears to display the roots of alkali granite complexes.

Résumé

La région de la rivière Harrys montre un gneiss et une anorthosite granulitiques ayant des affinités avec des formations de Grenvillien (complexes de Dissapointment Hill et de Steel Mountain), ils sont recouverts d'un placage de sédiments métamorphisés de type du plateau continental. Les roches à faciès de granulites passent progressivement à des gneiss à faciès d'amphibolites puis à un complexe granito-gneiss avec des noyaux de granite massif alcalin (complexe de Tulks Pond). L'importante faille de Grand Lake sépare ces roches de la marge classique, passive et des séquences allochtones de l'ouest de Terre-Neuve et une zone de cisaillement fragile les sépare des roches volcaniques partiellement subaériennes de l'Ordovicien (groupe de Glover).

À l'est de la faille de Grand Lake, des roches plus jeunes que le complexe gneissique à faciès des amphibolites montrent une seule période de déformation et de méthamorphisme progressive ayant eu lieu pendant la poussée qui a progressivement changé la direction de transport de l'ouest vers le nord-nord-ouest. Le métamorphisme a atteint le faciès des amphibolites et a probablement été accompagné à sa phase finale par la formation de dômes à très grande échelle. Les zones de cisaillement fragile semblent être des caractéristiques tardives de faible importance. Un mouvement important s'est produit sur des zones de disaillement ductile plus anciennes. Les relations entre le métamorphisme et la déformation montrent que la poussée doit-être plus récente que celle qui a donné naissance à l'allochtone de Humber Arm. La région semble montrer les racines des complexes granitiques alcalins.

INTRODUCTION

Current paradigms for interpreting the geology of western Newfoundland envisage a block of the Precambrian Grenville province veneered by a passive margin sequence of Late Proterozoic to Early Ordovician age which was telescoped by westerly directed thrusting in early to middle Ordovician time, culminating in the emplacement of allochthons of oceanic material (Williams, 1979). The spectacular allochthons have been mapped in detail by Williams (1985), Williams and Cawood (1986), and Williams and Smyth, (1983), but the details of the collapse of the underlying passive margin, and the degree of basement involvement, if any, remain obscure. The northwestern flank of the Long Range Mountains exhibits a broad range of metamorphic and igneous rocks of presumed Precambrian age (Kennedy et al., 1979) as well as passive margin sedimentary rocks and deformed granites of possible Silurian age (Whalen and Currie, 1984). This region forms a critical testing ground for theories of both early and late Paleozoic deformation in Newfoundland. The Harrys River area (12B/9e) around the southern end of Grand Lake forms an easily accessible part of this region, and was the subject of theses by Kennedy (1981), Martineau (1980) and Knapp (1982).

GENERAL GEOLOGY

The Harrys River area lies on the western flank of the southern Long Range Mountains, a deeply dissected peneplane with average summit elevations of 500-600 m. In the Harrys River area dissection has produced isolated flat-topped hills with precipitous sides separated by broad wooded valleys which merge westward into boggy lowland. The valleys have been extensively cut over for pulpwood, and are now in various stages of regrowth. Access to the region is generally very good by means of an extensive network of woods roads, but many of these roads are in varying states of decay. Outcrop is unevenly distributed. Large exposures occur on some hill tops, in major creek valleys, and along Grand Lake, but hill sides between 150 and 350 m elevations are virtually devoid of outcrop except where road building operations have caused major slope wash. A thick blanket of stratified sand and gravel fills the western end of Grand Lake to a depth of tens of metres. Glacial material is entirely derived from the east, a fact used to advantage in mapping the eastern boundary of rock units.

The bedrock geology of the Harry's River area (Fig. 68.1) can be divided into six major units. (1) West of the Grand Lake fault only sedimentary rocks occur, mainly carbonates with intensely deformed phyllite along the fault. (2) A south central zone consists of anorthosite with marginal mafic rocks (Steel Mountain complex) and probably related granulitic gneiss and charnockite (Disappointment Hill complex). (3) A composite gneiss, characterized by intricate mixtures of granitoid gneiss, variously deformed and metamorphosed biotite-hornblende gneiss and amphibolite, and weakly deformed granitoid rocks outcrops in the central part of the area. (4) Parts of the composite gneiss were incorporated into a strongly lineated, generally granitoid complex which contains late massive, leucocratic peralkaline phases. (5) A series of metasedimentary rocks ranging from conglomerate and quartzite through pelitic schist to marble rests unconformably on the composite gneiss, has been strongly metamorphosed and intruded by the lineated granite, and stacked in thrust sheets about the same time as intrusion. (6) The most eastern exposures consist of salic and mafic volcanic rocks and hypabyssal correlatives (Glover Group) intruded by and hybridized with granite. The age of sedimentary rocks west of the Grand Lake fault is generally accepted to be Cambrian and/or Ordovician (Williams 1985), while the age of the Glover Group is Early Ordovician (Arenig, Knapp 1982). The age of other units is not established.

The structure of the Harrys River area is dominated by large faults and high strain zones. The Grand Lake and Long Range faults are major structures with long, complex movement histories. Much of the region between these faults forms a high strain zone which underwent metamorphism and intrusion during and after straining.

DESCRIPTION OF FORMATIONS

The Disappointment Hill complex (map unit P_1) forms the oldest rocks, granulitic gneisses in various stages of retrogression intruded by orthopyroxene- bearing granitoid rocks. On Disappointment Hill the gneiss exhibits granoblastic texture, compositional layering, and orthopyroxene in both salic and mafic varieties. The rocks are medium grained (0.5-1.0 mm) and lack small-scale structure, although mapping of foliation suggests open folding on a scale of hundreds of metres. These are the only rocks so far discovered in the southern Long Range which resemble the granulitic gneisses of the northern Long Range discussed by Erdmer (1986) and Owen (1986). South of Caribou Brook the gneisses are extensively retrograded and consist mainly of biotite gneiss with a distinctive fine granoblastic texture and homogeneous character. Both pristine and retrograded gneisses are intruded by an orthopyroxene-bearing granite which contains green feldspar and weathers to honey-yellow shades. On the crest of Disappointment Hill the rock is spectacularly megacrystic with irregular masses of feldspar up to 5 cm across. South of Caribou Brook the rocks usually contain biotite, but the colour, texture, and relict pyroxene remain distinctive. Although the charnockite cuts the granulitic gneiss, outcrops of the Disappointment Hill complex have a very homogeneous appearance and gneiss and charnockite appear to form a single unit.

On the steep western slopes of Disappointment Hill this charnockite is involved in a high-strain zone across which there is gradation to granitoid gneiss of unit OS. No relations have been found with the Steel Mountain complex (units P_2 and P_3), but the map pattern strongly suggests the Disappointment Hill complex and the Steel Mountain complex are related. The granulitic gneiss is the only rock so far discovered which could form a reasonable host for the Steel Mountain complex.

The Steel Mountain complex (units P_2 and P_3), a very large anorthositic complex (van Berkel et al., 1986), has its

northern termination in the Harrys River area. The main body consists principally of coarse white to lilac anorthosite. Spectacular pegmatite and cumulate layering textures are locally preserved, even where mafic minerals exhibit corona texture, but much of the anorthosite exhibits a range of cataclastic textures from granulation through brecciation to ductile deformation producing thinly layered anorthosite schist with biotitic parting planes. In addition to the main body, two satellite masses occur west of Tulks Pond. These satellite plutons contain a much higher proportion of mafic rocks, mainly coarse pyroxene and pyroxene-hornblende gabbro and pyroxenite, with well preserved graded layering. Bands of white to grey granular anorthosite up to 200 m wide also occur.

The Steel Mountain complex has proved difficult to fix in relative age. West of Tulks Pond the satellite pluton has been much affected by deformation and metasomatism which has converted the mafic rocks to distinctive hornblende-biotite schist with flattened plagioclase porphyroclasts. These schists form an integral part of the composite gneiss complex (unit P_4). In the extreme southwestern corner of the area calc-silicates of unit CH_1 appear to rest unconformably on anorthosite. The general character of the Steel Mountain complex suggests a mid-Proterozoic age similar to that of other massif anorthosites (Emslie, 1978).

The composite gneiss complex (unit P_4) consists mainly of varying proportions of amphibolite of several types, a white, granoblastic granitoid of trondjhemitic affinity, and hornblende biotite granite with numerous enclaves, schliers and partings of hornblende-biotite schist. Thin bands of garnetiferous biotite gneiss and quartzite were observed in a few outcrops. Typically the complex consists of layers 10 to 100 m thick of relatively homogeneous amphibolite or hornblende-biotite gneiss, commonly schistose and strongly lineated, containing large, brassy, poikilitic biotite flakes in the foliation. Between the layers sinuous to ptygmatic lenticles of white granite occur. Where biotite gneiss or strongly feldspathic amphibolitic layers occur they are always strongly migmatized in lit-par-lit fashion. North of Goose Hill a second period of migmatization has produced spectacular ellipsoidal masses of pink leucogranite which cut the older migmatitic host. The lithologies of the composite gneiss complex strongly suggest an extended and complex history involving two or more periods of dyking and at least two periods of migmatization.

A characteristic feature of the composite gneiss is mesoscale folding ranging from open, near concentric cylindrical folds, to very complex curviplanar folds. The folds appear to exhibit no consistency in style or orientation, and no axial plane cleavage. These observations suggest an origin by flowage rather than flexural slip. Where cleavage is recognizable, it consistently strikes north northeast, dips steeply, commonly cuts gneissosity at a large angle, and has no obvious relation to the folds. This late cleavage results from a low grade overprint which has affected all minerals, breaking down hornblende and straining and recrystallizing quartz and feldspars to fine grained mosaics. This cleavage contains new biotite south of Grand Lake and chlorite +/− biotite north of Grand Lake. North of Grand Lake the cleavage is locally strong enough to partially transpose the foliation, producing spectacular examples of younger deformation overprinting older (Fig. 68.2).

The age of the composite gneiss complex is uncertain. If the young deformation is Paleozoic, the early deformation and migmatization could be Grenvillian. All that can be stated with certainty is that the composite gneiss is younger than the Steel Mountain complex, satellites of which are incorporated into the composite gneiss, and older than the granite gneiss of the Tulks Pond complex (unit OS) which incorporates elements of the composite gneiss.

A metasedimentary complex comprising units CH_1 and CH_2 consists of a lower quartzite and conglomerate dominated unit and an upper unit dominated by pelitic schist and marble. This sequence has been variously termed the Loon Pond Group south of Grand Lake (Martineau, 1980), the Keystone schist on Glover Island (Knapp, 1982), and given formational names north of Grand Lake (Kennedy, 1981). The stratigraphic sections in all three regions are very similar or identical. The base of the sequence is exposed at three localities on the south shore of Grand Lake. Biotite-muscovite schist rests on composite gneiss with a sharp, but roughly conformable contact interpreted to be a slightly tectonized unconformity. Above a narrow (about 1 m) basal interval of mica schist, the lower part of the complex (unit CH_1) consists mainly of quartzite varying from flaggy with micaceous parting to quartzite and mica schist interbedded on a scale of a few centimetre. This interval contains a characteristic but discontinuous bed of conglomerate with rounded quartz cobbles and clasts of white, granular hornblende granite derived from the composite gneiss. The upper margin of the lower unit is marked by a distinctive massive granular calc-silicate band up to 10 m thick, commonly associated with an amphibolite of about equal thickness. The top of the lower unit is commonly marked by a thrust fault, or by an intercalation of strongly foliated biotite-muscovite granite. The upper unit of the complex (unit CH_2) consists of pelitic schist and marble. The base consists of relatively massive and homogeneous pelitic schist overlain by pelitic and carbonate units interlayered on a scale of a few mm, with some thicker carbonate beds up to a m, while the top of the sequence appears to be a massive marble unit more than 10 m thick.

South of Grand Lake the metamorphic grade of the metasedimentary complex is high. Pelitic beds contain biotite + muscovite + garnet + staurolite(+ kyanite), where the kyanite is now represented by muscovite pseudomorphs ("shimmer aggregate"). Calcareous units contain tremolite + diopside + quartz. The conglomerate lenses have been pervasively granitized. Two periods of metamorphism can be readily distinguished. The first was pre- to syn-tectonic, as demonstrated by wrapping of the minerals in the cleavage. The second period was post-tectonic and produced spectacular euhedral garnets and pegmatitic patches of calc-silicates. Both periods of metamorphism appear to be of the same grade, and it seems reasonable to suppose that deformation took place during an extended period of metamorphism.

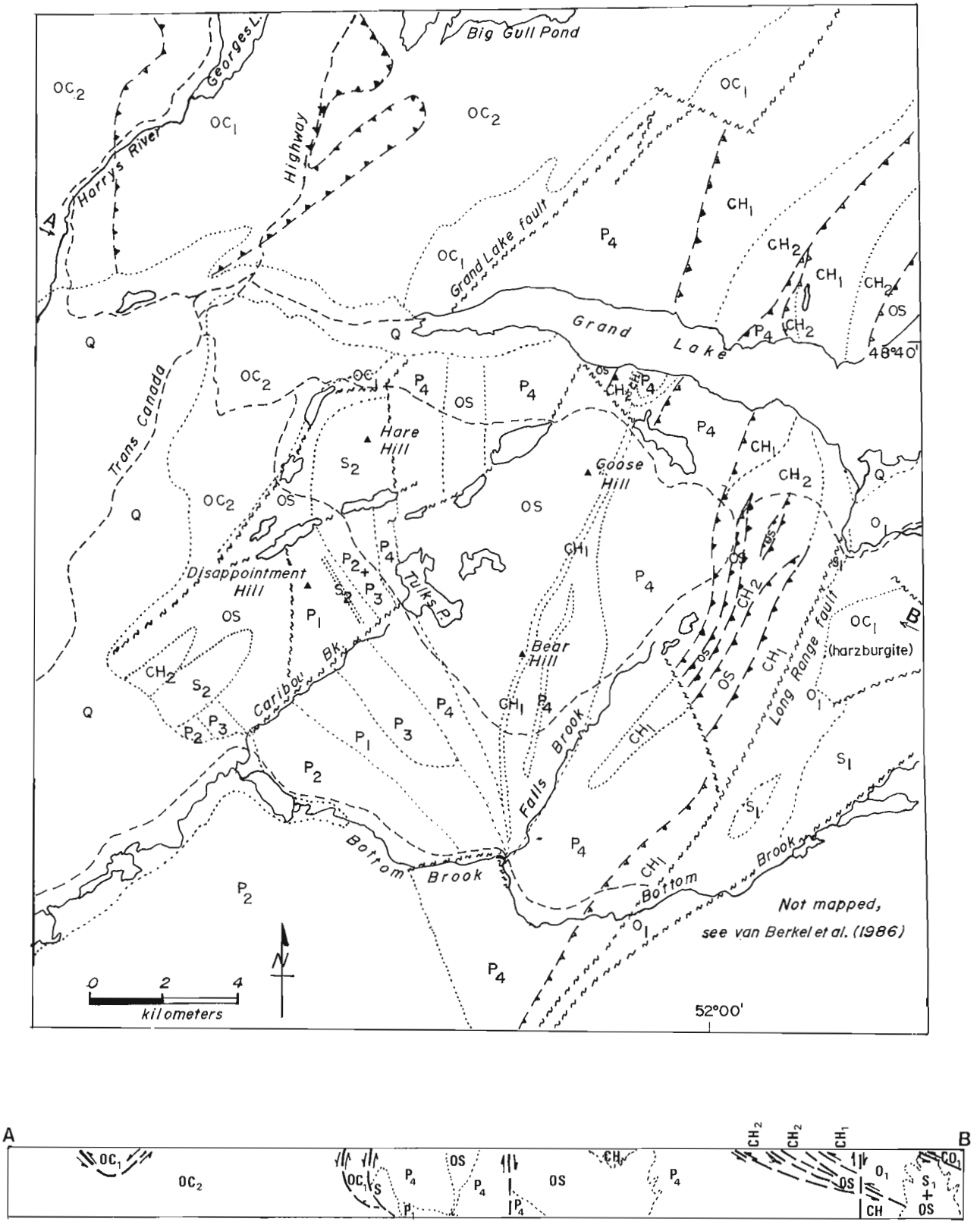


Figure 68.1. Geology of the Harrys River area.

LEGEND

Q_t glacial deposits; easterly derived cobbles and boulders in silty matrix, minor bedded sand and gravel

----- great unconformity -----

S_2 red to pink amphibole and aegirine granite, massive and coarse-grained to pegmatitic; (h) Hare Hill granite one feldspar granite; (g) Goose Hill one feldspar granite; (b) Bear Ridge two-feldspar amphibole-biotite granite; (d) biotite and biotite-muscovite granite, commonly foliated

----- gradational to OS_1, other relations unknown -----

S_1 pale pink chloritized amphibole leucogranite and brecciated granite; agmatite and hybrid rocks

----- intrudes O_1, other relations unknown -----

OS TULKS POND COMPLEX; Lineated, foliated granitic gneiss with up to 15% of biotite amphibole schist in concordant layers and schliers. Contains massive to fine granoblastic granite layers. (a) amphibole series, amphibole commonly in polycrystalline spindles, (q) quartz series, contains large quartz "studs", minor quartzite and biotite-garnet granite, (b) biotite series, mesocratic microcline-porphyritic granite gneiss (m) mafic schist and gneiss, tectonized mafic dykes

----- gradational to S_2 and P_4 -----

O_1 GLOVER GROUP; intermediate to acid volcanic rocks; chlorite actinolite schist, porphyritic rhyolite and porphyry, gabbroic and dioritic sills, minor red chert

----- tectonic contact -----

OC_2 grey to buff, finely recrystallized limestone and dolostone; original fine rhythmites preserved in tectonic inclusions, but mainly strongly tectonized

----- tectonic contacts -----

OC_1 olive to black shale and pelitic schist; phyllite with large pyrite crystals; (s) serpentinite, ultramafics

----- tectonic contacts -----

CH_2 finely banded pelitic and semi-pelitic schist with thin marble and quartzite beds, marble

----- gradational contact -----

CH_1 semi-pelitic schist with abundant quartzite beds, quartzite, deformed conglomerate, calc-silicate gneiss, amphibolite

----- tectonized unconformity -----

P_4 composite gneiss complex; biotite+/-amphibole schist and gneiss, amphibolite, granoblastic trondjhemite and trondjhemitic gneiss, heterogeneous migmatite; shows plastic small folds, later cleavage associated with retrogression

----- gradational contact -----

P_3 STEEL MOUNTAIN COMPLEX (units P_2 and P_3 gabbro, norite, pyroxenite, hornblende schist

----- interfingering contact, probably igneous -----

P_2 anorthosite, gabbroic anorthosite, anorthositic gabbro. Pale lilac to white, local preserved igneous texture, but generally strongly cataclastic

----- relations unknown -----

P_1 DISAPPOINTMENT HILL COMPLEX: salic to intermediate ortho-pyroxene-bearing gneiss and retrograded biotitic equivalents; orthopyroxene granite, locally megacrystic

geological contact — major road

fault, high angle — fault, thrust, teeth on thrust block

Geology by K.L. Currie, J.T. van Berkel and M.A.J. Piasecki, 1985 and 1986, and J.C. Martin, 1985. Geology northwest of Grand Lake partly after Williams (1985).

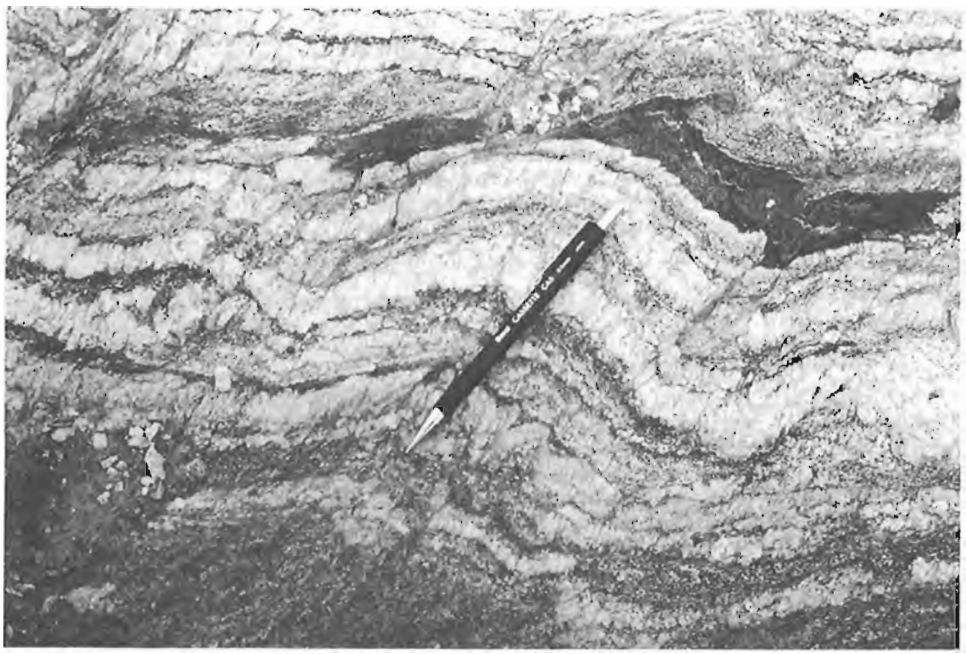


Figure 68.2. Composite gneiss (unit P_4) cut by prominent younger cleavage. The migmatic layering is broken into "tablet structure" by cleavage parallel to the panel. Locality is north of Grand Lake. GSC 204243-Q

North of Grand Lake the grade of metamorphism is generally very much lower, not exceeding biotite-chlorite-muscovite. This may indicate some tectonic break along Grand Lake, but the nature of this break, if any, is not presently understood. Both north and south of Grand Lake exposure of the metasedimentary rocks is controlled by a sequence of gently east-dipping imbricated thrust faults.

The relative age of the metasedimentary complex is well fixed, since it unconformably overlies the composite gneiss, and is intruded by the Tulks Pond granite complex. The absolute age is less certain. Williams (1985) considered the rocks correlative to, or slightly older than the Cambrian(?) rocks west of the Grand Lake fault. This hypothesis seems plausible, but there are other possibilities which are noted in the Discussion.

West of the Grand Lake fault, olive to black shale, pelitic schist and phyllite, (map unit OC_1) occur in a narrow belt along the trace of the fault. One belt extends from the vicinity of Hare Hill to the north edge of the map area. A Y-shaped belt of similar phyllite occurs along the Trans Canada Highway. The rocks vary from thin bedded (<1 mm) graded grey siltstone and shale, preserved only in tectonic inclusions, through intricately small folded and cleaved rocks to intensely sheared schist which spalls off in silver dollar sized pieces, to a chloritic schist. The most characteristic and ubiquitous unit is an olive coloured phyllite with large pyrite cubes spaced about 3-5 cm apart. Serpentinite blocks or pods occur in this unit at its southern tip and possibly also north of Grand Lake (Kennedy, 1982). North of Grand Lake the phyllite contains within it horses of carbonate (unit OC_2) and thinly banded quartz mica schist (unit CH_2) up to 200 m or more in largest dimension.

Correlation of these tectonites presents a major problem. Kennedy (1982) correlated the western belt with allochthonous middle Ordovician rocks of the Humber Arm allochthon, while he erected the Cambrian (?) Grand Lake Brook Group for the eastern belt. Williams (1985) rather arbitrarily separated the western belt from the contiguous Humber Arm allochthon and placed it in the autochthonous Cape Cormorant Formation, where he admitted that it fitted poorly. His compilation of the Grand Lake Brook Group followed that of Kennedy (1982). Recently Williams and Cawood (1986) reconsidered this problem and returned the western belt to the Humber Arm allochthon, noting that relations between allochthonous and autochthonous rocks had been considerably complicated by later deformation. Williams and Cawood (1986) did not consider the position of the Grand Lake Brook Group, but I was unable to find any lithologic reason to distinguish it from the western belt. The most distinctive lithology, the pyrite-rich olive phyllite, occurs in both belts. The eastern belt locally is clearly a tectonic melange, a feature also shared by the western belt (Williams and Cawood, 1986). I therefore suggest that the two belts are correlative, and the term Grand Lake Brook Group is superfluous.

The carbonate rocks west of the Grand Lake fault (unit OC_2) are strongly tectonized and completely recrystallized except for the extreme northwestern corner of the mapped area, and small tectonic inclusions, which suggest that much of the unit originally consisted of pale olive rhythmites with limestone and dolostone interbedded on a millimetre scale. Most of the unit has been converted to a fine grey marble in which the thin dolomite layers have been boudined and intricately folded. Some outcrops have been converted to

a marble gneiss, with thin, platy layering and large calcite porphyroblasts.

The Glover Group (unit O_1) outcrops south of Grand Lake and east of a major brittle shear zone. The rocks consist of uniform, fine grained grey green intermediate igneous material which could be either intrusive or extrusive, salic pyroclastics with preserved shards and fragments, and ignimbrites with well developed fiamme. Small amounts of red chert occur locally. The group contains abundant thin gabbroic sills, and less abundant pink porphyry dykes and sills, both interpreted to be sub-volcanic equivalents of the volcanics. Amphibolite and chloritized amphibolite are common around younger intrusions. Paleontological data indicating a Early Ordovician (Arenig) age for the Glover Group were presented by Knapp (1982).

The Tulks Pond complex (unit OS) forms one of the most characteristic units in the Harrys River area, a heterogeneous but generally granitoid complex characterized by L-S fabric, and granitization and metasomatic phenomena. In typical exposures south of Tulks Pond the complex comprises leucocratic, pale pink granitoid rocks with polycrystalline spindles of mafic minerals up to 2 cm long and several millimetres in diameter. Several subunits can be recognized depending on the nature and distribution of these spindles. Where they consist of fine grained amphibole, amphibole + garnet or amphibole + aegirine, the rock resembles the Hare Hill and Goose Hill granites to which it passes gradationally. This material passes, by increase in fine grained biotite, to a biotite-bearing phase which grades to the composite gneiss complex, schliers of which are found throughout the Tulks Pond complex. A highly distinctive variant of the complex contains large quartz crystals which stand up prominently on weathered surfaces, and may comprise up to 60% of the volume. This material is associated with quartzite and garnetiferous quartz-mica schist in a narrow belt which can be traced continuously for nearly 20 km. The Tulks Pond complex consistently contains 5-15% of mafic schliers and transposed dykes, most of which have been converted to biotitic schists. Near Goose Hill the dykes are slightly better preserved and the rocks appear to be a spectacular zone of mixing of salic and mafic rocks with visible disintegration of the mafic schliers into xenocrysts, generally rimmed, in the salic matrix.

The Tulks Pond complex exhibits a very strong and pervasive lineation defined by the polycrystalline mafic clots, but planar structures are locally also significant. The attitude of both lineation and foliation is strikingly consistent, with the lineation plunging 35-75° toward 160°, and the planar structure dipping 70-90° toward 070 to 090°.

Massive, or near massive, granitoid rocks in the Harrys River area have been divided into two units. Unit S_1 includes all granitoid rocks east of the Tulks Pond complex, while unit S_2 comprises the massive granite within the Tulks Pond complex and the body in the southwest corner of the area.

Large granite bodies within the Glover Group consist of coarse grained chloritized amphibole leucogranite with many schliers of chloritized amphibolitic material, presumably derived from the surroundings. Contacts appear to be sheeted, or even migmatitic. These coarse, deep-seated bodies cannot be confused with the distinctive, high-level porphyry dykes which cut the Glover Group and are thought to be related to it. One of the coarse granites is brecciated by a brittle deformation zone associated with the Long Range fault, demonstrating the young age of the brittle deformation.

Granites within the metasedimentary sequence typically form strongly foliated sheets and commonly contain a low tenor of muscovite, although biotite granites are also abundant. The contacts with the sedimentary rocks are gradational where granite is emplaced in the conglomerate of unit CH_1, but sharp and intrusive where granite contacts unit CH_2. The granite sheets range from 10 to 50 m in thickness, and were emplaced during the process of deformation, as shown by their strong foliation and undeformed skarn aureoles.

Massive, coarse alkaline to peralkaline leucogranite (unit S_2) occurs in four masses within the mapped area, three of which fall within the Tulks Pond complex. All of these bodies are very homogeneous, one-feldspar rocks with intersertal poikilitic mafics, but they differ considerably between each other. The Hare Hill body is pink, due to minor iron staining, and contains aegirine with possible relicts of enigmatite. The Goose Hill body is white and the mafics, probably originally alkali amphibole, have been pseudomorphously replaced by ilmenite. The Bear Hill body and the southwestern body appear substantially less alkaline, but are also one feldspar granites. Both are biotite-amphibole granites, but the Bear Hill body is a white granite with large, prominent quartz crystals, while the southwestern body is a pink granite which is near equigranular but distinctly foliated. In all cases the granites appear to pass continuously into surrounding strongly lineated and/or foliated rocks.

STRUCTURE

Faults and ductile shear zones dominate the structure of the Harrys River area. Recognizable folds occur only on a small scale and within certain units. The composite gneiss complex exhibits complex mesoscopic interference folds of diverse style which appear mainly due to plastic flow of the matrix. The carbonates west of the Grand Lake fault exhibit intricate mesoscopic folding of boudined dolostone beds, again probably due to flow of the matrix marble. The metasedimentary rocks east of the Grand Lake fault exhibit well developed small-scale folding. Such folds affect both compositional banding thought to represent bedding and at least one period of cleavage. These folds are tight to isoclinal, dip east at moderate angles (40-60°) and plunge gently south-southeast. They are thought to be related to westward thrusting which is well documented in this sequence. These folds occur in large numbers up to about 10 m amplitude, but outcrop is too poor to document similar larger scale folds in the thrust slices. No folds were mapped in the Glover Group, although Knapp (1982) mentioned the presence of folds in this unit.

Ductile shear zones occur in a large variety of sizes, styles and orientations. West of the Grand Lake fault strain is concentrated in narrow zones of brittle deformation. The

boundary between shale and carbonate is always marked by intense deformation and shearing of the shale. Dubious kinematic indicators in the shale (drag folds) suggest the carbonate consistently moved up with respect to the shale. Late northwest-trending faults in the carbonates are marked by reddening and brecciation. Sparse kinematic indicators suggest dextral or north side up motion.

The Grand Lake fault appears to be a vertical to steeply west-dipping major structure with a long and complex movement history. A preliminary study by M.A.J. Piasecki found evidence of dextral, sinistral and vertical motions, as well as traces of an older ductile deformation regime predating the late brittle motion. In plan the fault has a markedly sinuous trace. North of Grand Lake it appears to be offset dextrally by late northwest trending faults. The Grand Lake fault separates low grade metasedimentary rocks to the west from crystalline rocks to the east. Understanding the movement history of this fault is critical to understanding the geological history of western Newfoundland.

Between the Grand Lake fault and the Long Range fault the rocks fall into two structural domains, a western domain of crystalline rocks (anorthosite, granite) and an eastern domain of metasedimentary rocks. The structural history of the two domains appears to be similar, namely thrusting from southeast to northwest at elevated temperatures. The crystalline rocks, with the exception of the Tulks Pond complex, are dominated by a multitude of fine grained, laminated high strain rocks which transpose older foliations. The oldest foliations strike north-northwest, while younger ones strike progressively more northeasterly with decreasing age until they trend east, or even east-southeast. The rocks within the zones, which vary in width from 10 m to several hundred metres are mylonitic or blastomylonitic. Within the Tulks Pond complex these mylonitic zones are rare, but lineation is very strong and consistent, indicating the movement direction. The consistency of direction indicates this must be a relatively late movement direction, which is consistent with the north-northwest direction of transport indicated.

The metasedimentary rocks exhibit a spectacular, basement-involved stack of thrust slices. East of Falls Brook the bounding thrusts are well exposed, and the stratigraphy is repeated at least four times by thrusting. The basement-involved nature of this thrusting can be seen in the continuous exposure along Grand Lake where slices of the composite gneiss complex separate repetitions of the metasedimentary seqeunce in two places. A similar relation can be inferred north of the lake. The dip of the thrust slices appears to vary directly with the competence of the rocks involved. In the marbles and mica schists dips as low as 10° are common, while in the quartzite-schist sequence dips are commonly 30-50°, and in the crystalline rocks dips are 50-70°. As noted in the description of formations, thrusting took place during amphibolite facies metamorphism and granite intrusion.

South of Grand Lake the thrust complex terminates abruptly against a large shatter zone which separates metasedimentary rocks from metavolcanic rocks of the Glover Group. This zone does not appear to be a fundamental break in the geology since the same zone north of Grand Lake passes through the thrust complex. On Glover Island, Knapp (1982) argued that the Glover Group rested unconformably on correlatives of the metasedimentary rocks (Keystone schist). The fundamental break between the low grade rocks of western Newfoundland and the high grade rocks of the southern Long Range (van Berkel et al., 1986) appears to lie in Bottom Brook, and is associated with a large ultramafic mass south of Little Grand Lake. The nature of this break is not presently well understood, but is presumably a major fault.

DISCUSSION

Remapping of the Harrys River area confirms some aspects of large scale modelling of western Newfoundland, but raises serious problems for current models. If the youngest granites are assumed to be Silurian, as suggested by Whalen and Currie (1984) then the Harrys River area demonstrates large scale westward thrusting of passive margin sedimentary rocks and the underlying crystalline basement. Before examining the implications of this thrusting, it must be pointed out that a Silurian age for the peralkaline granites is by no means established. A more or less plausible case could be made for any of (a) a Grenvillian age (compare Williams, 1979), (b) a late Precambrian age (compare Williams et al., 1985), or (3) a Devonian age, as was long assumed for the similar Topsails intrusions (Williams, 1979). Determination of the age of the Hare Hill and related granites is clearly critical since this granite dates the end of the major deformation. This dating is now in hand. Following the arguments of Whalen and Currie (1984), I shall tentatively assume a Silurian age and examine the consequences.

The simplest model for the area would to be to correlate sedimentary rocks west and east of the Grand Lake Fault, as was done by Williams (1985). However such a correlation has some rather surprising consequences. Emplacement of the Humber Arm allochthon over the authochthonous or para-autochthonous sequences west of the Grand Lake fault is well constrained in terms of timing and mechanism (see Williams, 1985 for references). The allochthon exposes progressively deeper slices upward, culminating in the uppermost ophiolitic slices, and the lower slices are unmetamorphosed. Palinspastic reconstruction therefore requires that before and during thrusting which emplaced the Humber Arm allochthon the passive margin sequence was not metamorphosed. Therefore if the sedimentary rocks on opposite sides of the Grand Lake fault are correlative, the thrusting east of the fault must be younger than the emplacement of the Humber Arm allochthon, since it took place during metamorphism. This argument holds regardless of the timing of emplacement of the allochthon. However if the Hare Hill granite is Silurian, then a late Ordovician-Silurian deformation would fit well with recent isotopic measurements in the Topsails terrane (Whalen personal communication) and southern Newfoundland (O'Brien et al., 1986) which suggest major deformation at this time. A model proposed by Dewey and Shackleton (1984) may accomodate both an Arenig-Caradoc movement history for the Humber Arm allochthon and a late Ordovician-Silurian thrusting farther east. Their cartoons show two periods of thrusting, but the mechanics

requiring this are not explained. They require a late period of thrusting to explain the widespread occurrence of remnants of ophiolites, a feature prominent in southwestern Newfoundland (van Berkel et al., 1986).

The observed fold and thrust belt also clearly demonstrates major basement involvement. The basement involved appears to be Grenvillian in lithology and structural style, but it differs from the retrograded granulites of the northern Long Range. The latter lithologies may be represented by the granulitic gneisses of the Disappointment Hill complex which appear to be tectonically incorporated into the younger composite gneiss. These relations would be compatible with the northern Long Range being a deeper seated portion of the Grenville block from which all, or most, of the composite gneiss equivalent has been removed by erosion. The basement involved, synmetamorphic character of the thrusting implies that distinction between basement and cover will become progressively more difficult to the east where metamorphic grades are higher, and the intershuffling of basement and cover presumably more complex. This accords well with the uncertain presence of basement southeast of the mapped area (van Berkel et al., 1986) compared to the strong geophysical indications of basement (Keen et al., 1985).

The Harrys River area offers some interesting clues to the origin of peralkaline granite. Although other examples of syntectonic peralkaline rocks are known, the present examples appear to be the first where peralkaline granite can both be tied to a particular phase of deformation, and observed to grade laterally into sub-alkaline rocks. Field relations are compatible with derivation from a granulite facies crustal parent, and subsequent mechanical interaction with diverse wall rocks, as hypothesized by Whalen (personal communication).

The presence of ignimbrites in the Glover Group demonstrates that at least parts of this group were deposited subaerially. No evidence was found of deep-water deposition in the material examined, although Knapp (1982) supposed it to be a volcanic arc built on ocean floor (ophiolite). The field evidence observed in the Glover Group and the presumably correlative Buchans Group suggest generally ensialic, shallow water to emergent conditions. The ophiolitic fragments do not require a major ocean, but could be the products of local rifting of a generally continental crust.

Finally, I draw attention to the progressive swing in the direction of tectonic transport with time. The early transport direction, as shown by the thrust sheets, was from east to west, but with time the direction progressively shifted toward the north, reaching 340° during emplacement of the peralkaline granites, and 010° in late, brittle structures such as those in Little Grand Lake. This change needs to be explained in large scale modelling of the region.

ACKNOWLEDGMENTS

The portions of the map north of Grand Lake and south of Bottom Brook have been compiled largely from work by J.T. van Berkel. I also wish to acknowledge many discussions of the geology with J.T. van Berkel, as well as invaluable logistic assistance. Mapping of the Goose Hill region was a cooperative effort with M.A.J. Piasecki. I also wish to acknowledge the advice on structural problems and basement-cover relations offered by M.A.J. Piasecki. The Corner Brook Pulp and Paper Company kindly gave permission to use private roads, and gave access to company maps.

REFERENCES

Dewey, J.F. and Shackleton, R.M.
1984: A model for the evolution of the Grampian tract in the early Caledonides and Appalachians; Nature v. 312, no. 5990, p. 115-121.

Emslie, R.F.
1978: Anorthosite massifs, rapakivi granites and late Proterozoic rifting of North America. Precambrian Research v. 7, p. 61-98.

Erdmer, P.
1986: Geology of the Long Range inlier in Sandy Lake map-area, western Newfoundland; in Current Research, Part B, Geological Survey of Canada, Paper 86-1B, p. 19-27.

Kennedy, D.P.
1981: Geology of the Corner Brook Lake area, western Newfoundland; M.Sc. thesis, Memorial University of Newfoundland, Saint John's, 337 p.

Kennedy, D.P., Knapp, D.A., and Martineau, Y.A.
1979: Stratigraphy, structure and regional correlation of rocks at Grand Lake, western Newfoundland; in Current Research, Part A, Geological Survey of Canada, Paper 79-1A, p. 317-325.
Knapp, D.A.
1982:Ophiolite emplacement along the Baie Verte-Brompton line at Glover Island, western Newfoundland; Ph.D. thesis, Memorial University of Newfoundland, Saint John's, 337 p.

Keen, C.E., Keen, M.J., Nichols, B., Reid, I., Stockmal, G.S., Colman-Sadd, S.P., O'Brien, S.J., Miller, H., Quinlon, G., Williams, H., and Wright, W.J.
1986: Deep seismic reflection profile across the northern Appalachians; Geology (Boulder) v. 14, p. 141-145.

Martineau, Y.A.
1980: The relationships among rock groups between the Grand Lake Thrust and Cabot Fault, western Newfoundland; M.Sc. thesis, Memorial University of Newfoundland, Saint John's, 150 p.

O'Brien, S.J., Dickson, W.L., and Blackwood, R.F.
1986: Geology of the central portion of the Hermitage flexure area, Newfoundland; Newfoundland Department of Mines and Energy, Mineral Development Division Report 86-1, p. 189-208.

Owen, J.V.
1986: Geology of the Silver Mountain area, western Newfoundland; in Current Research, Part A, Geological Survey of Canada, Paper 86-1A, p. 515-522.

van Berkel, J.T., Johnston, H.P., and Currie, K.L.
1986: A preliminary report on the geology of the southern Long Range, southwest Newfoundland; in Current Research, Part B, Geological Survey of Canada, Paper 86-1B, p. 157-170.

Whalen, J.B. and Currie, K.L.
1983: The Topsails igneous terrane of western Newfoundland; in Current Research, Part A, Geological Survey of Canada, Paper 83-1A, p. 15-23.
1984: Peralkaline granite near Hare Hill, south of Grand Lake Newfoundland; in Current Research, Part A, Geological Survey of Canada, Paper 84-1A, p. 181-184.

Williams, H.
1979: Appalachian orogen in Canada; Canadian Journal of Earth Sciences, v. 16, p. 792-807
1985: Geology, Stephenville map-area, Newfoundland (north half); Geological Survey of Canada; Map 1579A.

Williams, H. and Cawood, P.A.
1986: Relationships along the eastern margin of the Humber Arm Allochthon between Georges Lake and Corner Brook, western Newfoundland; in Current Research, Part A, Geological Survey of Canada, Paper 86-1A, p. 759-765.

Williams, H. and Smyth, W.R.
1983: Geology of the Hare Bay allochthon; Geological Survey of Canada, Memoir 400, part 3.

Williams, H., Gillespie, R.T., and van Breemen, O.
1985: A late Precambrian rift-related igneous suite in western Newfoundland; Canadian Journal of Earth Sciences, v. 22, p. 1727-1735.

Late Precambrian igneous activity and its tectonic implications, Musquash-Loch Alva region, southern New Brunswick

Project 730044

K.L. Currie
Lithosphere and Canadian Shield Division

Currie, K.L., Late Precambrian igneous activity and its tectonic implications, Musquash-Loch Alva region, southern New Brunswick; in Current Research, Part A, Geological Survey of Canada, Paper 87-1A, p. 663-671, 1987.

Abstract

Late Precambrian igneous rocks in the Musquash-Loch Alva region comprise flanking zones of high level plagioclase porphyry plutons and correlative felsic volcanics (Coldbrook Group) about a central zone of deeper seated plutons (Golden Grove suite). These plutons are characterized by composition, texture, character of inclusions and presence of mixing phenomena. Northern and central zones of plutons are separated by a sheeted dyke complex (Kingston complex) bounded on both sides by major mylonite zones (Belleisle fault zone, Pocologan mylonite) which developed during active magmatic activity. The mylonite zones show evidence of dextral motion, but correlation of plutons on opposite sides of the dyke complex shows that net displacement did not exceed 2 km. The mylonite zone is truncated by a post-Silurian, pre-Late Devonian fault (Wheaton Brook fault) which bounds the Precambrian rocks to the south, and is itself truncated by the Late Devonian Mount Douglas pluton.

Résumé

Les roches ignées du Précambrien inférieur se trouvant dans la région de Musquash-Loch Alva comprennent des zones latérales constituées de plutons porphyriques à plagioclases, proches de la surface et des roches volcaniques, felsiques correspondantes (groupe de Coldbrook), entourant une zone centrale de plutons profonds (série de Golden Grove). Ces plutons sont caractérisés par la composition, la texture, le caractère des inclusions et la présence de phénomènes de mélanges. Les zones nord et centrale des plutons sont séparées par un complexe de dykes stratifiés (complexe de Kingston) flanqué des deux côtés par des zones importantes, mylonitiques (zone faillée de Belleisle, mylonite de Pocologan) qui se sont formées pendant une importants activité magmatique. Les zones mylonitiques montrent la preuve d'un mouvement dextre, mais la corrélation des plutons du côté opposé au complexe de dykes indique que le déplacement net n'a pas dépassé deux kilomètres. La zone mylonitique est tronquée par une faille du post-Silurian, Dévonien pré-supérieur (faille de Wheaton Brook) qui borde les roches Précambriennes au sud et qui est elle-même tronquée par le pluton de Mont Douglas du Dévonien supérieur.

INTRODUCTION

The region around Saint John, New Brunswick forms part of a distinctive terrane characterized by Middle Proterozoic or older basement and cover (Brookville gneiss and Green Head Group), voluminous Late Proterozoic igneous activity (Coldbrook Group of volcanic rocks and cogenetic plutons of the Golden Grove suite, sheeted dykes of the Kingston complex), a Cambro-Ordovician sedimentary section with an Acado-Baltic fauna (Saint John Group), and a deformed middle to upper Carboniferous clastic sedimentary sequence. North of the Long Reach (Fig. 69.1) this terrane abuts a contrasting terrane along the brittle Wheaton Brook fault (Currie, 1984). The terrane north of the Wheaton Brook fault lacks recognizable Precambrian rocks and is dominated by Silurian sedimentary rocks and Silurian to Devonian igneous rocks.

In the Musquash-Loch Alva region the Late Devonian Mount Douglas pluton appears to truncate the Wheaton Brook fault (Fig. 69.1). However a zone of strong ductile deformation (Belleisle fault zone) passes south of the Mount Douglas pluton through igneous rocks of uncertain age (Hay, 1968; Brown and Helmstaedt, 1970; Leger and Williams, 1986). If these rocks are of Devonian age, as supposed by McCutcheon and Ruitenberg (1984) then all deformation in this zone must be of Devonian or younger age, and the Saint John terrane along the Bay of Fundy is truncated by the Belleisle fault zone. However if the rocks are Late Proterozoic, as suggested by their lithology and alteration, then the deformation could be much older than the Wheaton Brook fault, and the Saint John terrane would be truncated by the Mount Douglas pluton. Resolution of these possibilities requires careful examination and evaluation of the igneous rocks of the Musquash-Loch Alva region.

GENERAL GEOLOGY

Various parts of the region of interest have been mapped by Alcock (1959), MacKenzie (1964), Hay (1968), Ruitenberg et al. (1979), and McCutcheon and Ruitenberg (1984). All of these maps contain useful information, but none divide the igneous rocks in a manner useful for correlation, and there are some rather drastic discrepancies in the definition and disposition of units. In this report, the rocks have been divided into five major zones (Fig. 69.1), which may be enumerated from north to south as follows: (1) Silurian supracrustal rocks (Jones Creek and Long Reach Formations) intruded by the Mount Douglas pluton, a Late Devonian biotite granite with a narrow dioritic margin; (2) a narrow belt of granite and high level porphyry plutons of unknown age with intervening volcanic and sedimentary screens; (3) the Kingston complex, a bimodal dyke complex bounded on both sides by spectacular mylonite zones; (4) a zone of deep-seated granitoid plutons ranging from diorite to aplitic leucogranite and including major amounts of mixed or hybrid material; and (5) a zone of high-level leucogranites grading to cognate rhyolite and dacite unconformably overlain by deformed Carboniferous rocks. Zones 4 and 5 are unconformably overlain by conglomerates of the Triassic Lepreau Formation.

DESCRIPTION OF FORMATIONS

The *Brookville gneiss* (unit Ab; Wardle, 1978, Currie et al., 1981), a variably migmatized and metasomatized hornblende-biotite tonalite gneiss which forms basement in the city of Saint John, occurs only in a small area of the southeast corner of Figure 69.1. This occurrence was described by Currie (1984). No trace of the Brookville gneiss occurs within the central belt of plutons.

The *Green Head Group* (unit Hgh), a platformal sequence of marble, quartzite and minor pelite, which overlies the Brookville gneiss (Currie et al., 1981) occurs as narrow belts in the southeast part of the mapped area, which were described previously (Currie, 1984). No further occurrences of Green Head Group have been found west of Musquash Harbour or north of Martinon. However a slice within the Kingston complex southeast of the Nerepis River consists of medium grained, granoblastic white marble with strong slaty cleavage containing phlogopite. This may be a fault slice of Green Head Group.

The *Martinon Formation* (unit Hm) which unconformably overlies the Green Head Group south of Martinon (Currie, 1984), consists mainly of very massive, brownish black siltstone and sandstone of turbiditic origin (Wardle, 1978) with minor amounts of cherty siltstone and thin carbonate interbeds, and with abundant sills or intercalations of basalt and dacite to rhyolite. Much of the Martinon Formation has been hornfelsed to a featureless brown, flinty rock. East of the Mount Douglas pluton such rocks come in contact with the lithologically similar Silurian Jones Creek Formation. The two units can be distinguished by the massive, featureless character of the Martinon compared to the bedded slaty character of the Jones Creek, particularly skarn beds, and an almost 90 degree divergence in strike. The Martinon Formation appears to be a lateral equivalent of the lower part of the Coldbrook Group. A small area south of Little Dipper Harbour, formerly mapped as Green Head Group (Alcock, 1959) is here included with the Martinon Formation since it seems clearly to form part of the volcanic package in this region. Much of the Martinon Formation occurs as screens separating granitoid plutons.

The *Coldbrook Group* (unit Hc) consists of acid to intermediate volcanic rocks and very minor sedimentary rocks. The detailed stratigraphy of the Coldbrook Group in the Saint John region is poorly known, but in the mapped area the rocks can be divided into two major types, namely pink to purple rhyolite and quartz-feldspar porphyry, and greenish fragmental rocks associated with red laharic breccia and minor grey rhyolite. The pink unit tends to be very massive and dense. Quartz phenocrysts, commonly hexagonal, are ubiquitous and pink feldspar phenocrysts occur in about half the outcrops. In a few places the rocks exhibit fiamme (Round Meadow cove) or flow banding and clearly represent densely welded ignimbrites. However much of the unit appears featureless and could be hypabyssal rather than volcanic. In places there appears to be a continuous transition from porphyry to felsite and aplite plutons. The fragmental rocks range

from grey rhyolite with disseminated chlorite fragments through various types of tuff and pyroclastic rocks to laharic breccias with a fragment content up to 40 per cent in a dark silty matrix. The fragmental rocks seem very susceptible to deformation and alteration, and commonly occur as indeterminate grey-green, sheared material.

The Coldbrook Group in the Chance Harbour-Dipper Harbour region was formerly mapped as part of the Carboniferous Mispec Group (Alcock, 1959; Rast and Currie, 1976; Rast et al., 1978), but the revised stratigraphy of the Mispec Group (Currie and Nance, 1983, Caudill and Nance, 1986), observation of a major unconformity between the Mispec Group and the volcanics, extensive chemical comparisons of the various volcanics, and a preliminary Pb-U age on zircon of about 550 Ma from the sub-volcanic Musquash pluton (P.A. Hunt, personal communication) demonstrates that these volcanics are part of the Coldbrook Group. Older maps show a belt of Coldbrook Group in the northern part of the area (Alcock, 1959, Ruitenberg et al., 1979), but remapping showed this region to be composed entirely of dykes of the Kingston complex and their cataclastic equivalents.

The Golden Grove suite (units Hp, Hd, Hg, He) was defined by Hayes and Howell (1937) to include the Late Proterozoic plutonic rocks of the Saint John area, and I have extended the terminology westward to cover similar rocks. Most earlier maps either lumped all plutonic rocks together (Alcock, 1959, Dickson, 1985) or split them on the basis of age determinations now thought to be unreliable (Ruitenberg et al., 1979). I found the following four-fold division to be helpful: (1) medium grained, hypidiomorphic plagioclase-hornblende rocks with colour indices ranging from 15-50 (unit Hd, Lepreau, Talbot Road, Red Bridge plutons); (2) massive, coarse grained granodiorite to granite, commonly with quartz phenocrysts (unit Hg Hansen Stream, Ragged Falls, Loch Alva, East Branch, Ludgate Lake, Henderson Lake plutons); (3) red, fine to medium grained granoblastic granite to granodiorite with large amounts of pink felsite and plagioclase porphyry (unit He Harvey Hill, Musquash, Rocky Lake, Lingley plutons); (4) a hybrid pluton in which all the above varieties occur as schliers, screens, blocks and hybrid-looking rocks suggesting magma mixing (unit Hp Prince of Wales pluton). This classification follows closely that of Belyea (1944) which has been unjustly neglected.

Using this simple classification, individual plutons can be easily mapped by physical characteristics such as proportion and character of inclusions. In the central belt of plutons, all examples appear to be deep-seated, with the possible exception of Harvey Hill. Contact relations vary from migmatized screens in the east to gradational without dykes or felsite in the west. The Harvey Hill pluton is finer grained than the others and contains discrete inclusions of the surrounding bodies. It could be significantly younger than the other plutons. The Prince of Wales pluton is heterogeneous on every scale. It includes spectacular megascopic examples of mixing and hybridization, as well as numerous screens of more homogeneous material. Some of these screens might be considered as plutons in more detailed work, but at the 1:50 000 scale used in this study, the very heterogeneity supplies a diagnostic criterion.

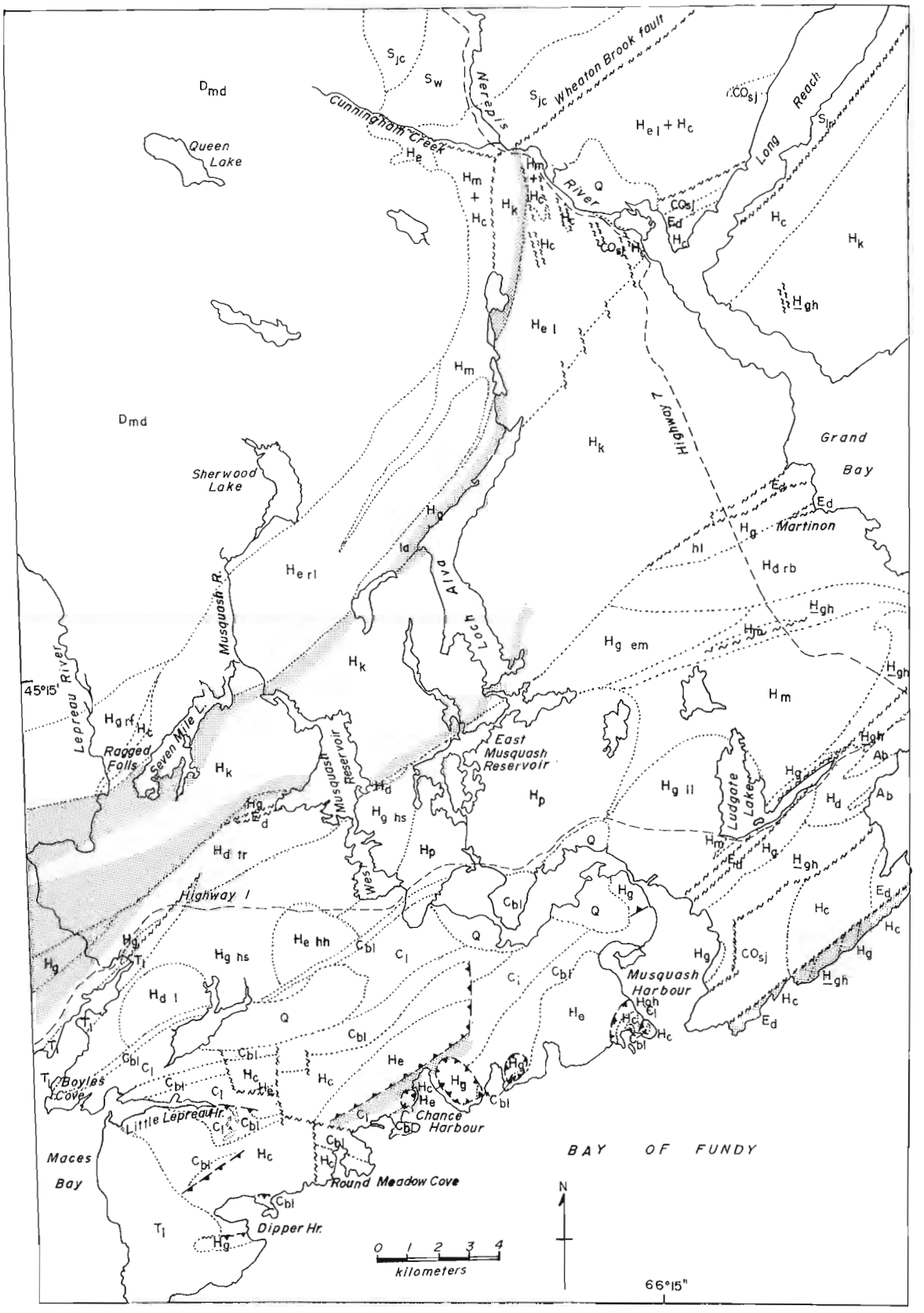
Plutons in the northern and southern zones are of high-level type compared to the central belt. Grain size is generally fine to medium, with many felsitic and aplitic patches, and the plutonic rocks grade within tens of metres to porphyries, and to igneous breccias and volcanics. Screens of sedimentary or volcanic rocks separate plutons, and are commonly dyked and incorporated in igneous breccias. Plutons of the northern and southern belts strongly resemble one another in their plagioclase porphyritic character and the association of textures.

The Coldbrook Group, Golden Grove suite and Kingston complex (unit Hk) share a pervasive epidote-chlorite alteration which is not found in younger igneous rocks. Even apparently fresh rocks contain chlorite and epidote on fractures, and the amount of epidote and chlorite seems to be controlled by the composition of the host. Completely unaltered rocks cannot be found. The alteration sufficiently changes the appearance of the rocks toward grey and green shades that considerable caution is necessary in mapping the plutonic rocks.

The Kingston complex (unit Hk, O'Brien, 1976, Currie 1984, 1986a) consists of salic and mafic dykes which in typical exposures alternate. Dyke widths vary from 20 cm to 50 m, but vary only slightly within single exposures. Either mafic or salic dykes may predominate over widths up to 400 m in ratios as high as 9:1, and at the southern end of Loch Alva mafic dykes predominate over a width of nearly a km. Dyke contacts are of three types; mutually chilled, intrusive, or sheared. Mutually chilled contacts form more than 75 per cent of exposed contacts, while intrusive contacts (both salic into mafic and vice versa) occur in about 20 per cent of cases, and sheared contacts occur in less than 5 per cent of observed cases. Shearing is always parallel to dyke walls, although the trend of dykes varies through nearly 90° across the region. Trend changes are quite abrupt near West Musquash Reservoir and in the Loch Alva area.

Mafic dyke lithologies vary from medium grained hornblende-plagioclase rocks, locally with large ovoid or irregular plagioclase which may be relict phenocrysts, to fine grained amphibole-rich rocks with nebulous micro-pegmatitic schliers. Most of the mafic dykes show a fining of grain size toward the margins, but true chilled margins are absent. Salic dykes consist mainly of pale buff weathering felsite which commonly contains plagioclase phenocrysts. In some dykes this lithology appears as a marginal phase while the core is distinctly coarser grained and granitoid.

The Kingston complex is bounded on both sides by major mylonite zones which follow approximately, but not exactly, the boundaries of the complex. North of the complex a porphyry pluton south of Ragged Falls exhibits a strong cleavage parallel to the mylonite zone over a width of about 100 m. South of the Kingston complex the southwestern extremity of the Talbot Road pluton is spectacularly


Dmd
Sjc
Sw
Nerepis
Sjc Wheaton Brook fault
Cunningham Creek
Queen Lake
He
Hm + Hc
Hk
Hc
Hel + Hc
COsj
Long Reach
Slr
River
Ed
Hgh
Hel
Hm
Dmd
Sherwood Lake
Hg
Id
Alma Loch
Hk
Highway 7
Grand Bay
Martinon
hl
Hd rb
Herl
Musquash R.
Hgh
Hg em
Hm
45°15'
Lepreau River
Hgrl
Ragged Falls
Seven Mile L.
Musquash Reservoir
East Musquash Reservoir
Hd
Hg hs
Hp
Hg ll
Ludgate Lakes
Ab
Hd tr
Highway 1
Wes
Q
Cbl
Cl
Hg
Tl
He hh
Musquash Harbour
Hd l
Boyles Cove
Little Lepreau Hr.
Chance Harbour
Maces Bay
Round Meadow Cove
Dipper Hr.
BAY OF FUNDY
N
0 1 2 3 4
kilometers
66°15"

LEGEND

QUATERNARY

Qg till, boulder clay; (s) stratified sand and gravel

----- unconformity -----

TRIASSIC

Tl LEPREAU FORMATION; chocolate-brown massive conglomerate, cross-stratified sandstone, red siltstone and shale

----- unconformity -----

CARBONIFEROUS

MISPEC GROUP (units Cl and Cbl)

Cl LANCASTER FORMATION: grey sandstone (lithic arenite) with quartz pebble beds and black, fossiliferous shale-siltstone beds. Mainly Westphalian A-C in age

----- gradational contact -----

Cbl BALLS LAKE FORMATION: Red polymict conglomerate, shale and sandstone; red to green limestone, black cryptalgal laminite; pink to green altered and silicified siltstone. Rocks of Visean to Westphalian age.

----- unconformity on unit Pc -----

Ck KENNEBECASIS FORMATION: red-brown massive conglomerate and cross-stratified sandstone. Basal grey to black siltstone and sandstone. Rocks of Fammenian to post-Visean age

----- unconformity -----

DEVONIAN OR MISSISSIPPIAN

Dmd MOUNT DOUGLAS PLUTON: red to pink coarse leucocratic biotite granite, commonly quartz porphyritic, rapakivi granite; biotite-plagioclase porphyry

----- intrusive contact (to unit Sw and Sjc) -----

SILURIAN

Sw WELSFORD PLUTON: riebeckite granite and syenite, porphyry

----- intrusive contact (to unit Sjc) -----

Sjc JONES CREEK FORMATION: thinly laminated grey green to black shale, siltstone and clcareous shale; hornfels

----- gradational contact -----

Slr LONG REACH FORMATION: plagioclase-porphyritic basalt flows minor calcareous siltstone and chert

----- tectonic contact -----

CAMBRO-ORDOVICIAN

Csj SAINT JOHN GROUP: grey green sandstone and siltstone, capped by black shale. Basal red to green sandstone with thin tuffaceous beds

----- disconformity -----

EOCAMBRIAN

Ed red feldspathic sandstone, siltstone, tuff; (b) vesicular basalt flows and sills; red sandstone, conglomerate with porphyry cobbles

----- disconformity? -----

HADRYNIAN

(age relations between the Coldbrook Group, Kingston complex and Golden Grove suite are uncertain. All are thought to be approximately coeval)

Hk KINGSTON COMPLEX: sheeted dyke complex of diorite and felsite dykes; (b) mafic dykes predominant

----- relations uncertain, probably gradational -----

GOLDEN GROVE SUITE (units He, Hg, Hd, Hp)

He red felsite, granoblastic epidote alaskite, plagioclase and quartz-plagioclase porphyry; (hh) Harvey Hill pluton, (l) Lingley pluton, (rl) Rocky Lakes pluton

----- intrusive to gradational contact -----

Hg pink to grey, coarse chloritized hornblende and biotite-hornblende granite to granodiorite, leucogranite. (hs) Hansen Stream pluton (10 cm rounded diffuse mafic inclusions); (l) Ludgate Lake pluton; (la) Loch Alva pluton; (em) East Musquash pluton; (rf) Ragged Falls pluton

----- intrusive to gradational contact -----

Hd coarse-grained hornblende plgioclase rocks, variously chloritized and epidotized; diorite, tonalite minor granodiorite; (l) Lepreau pluton, (tr) Talbot Road pluton; (rb) Red Bridge pluton

----- gradational contact -----

Hp hybrid rocks, strongly schliered and dyked mixtures of He, Hg and Hd with minor Hk. Prince of Wales pluton

----- relations uncertain -----

Hc COLDBROOK GROUP; acid to intermediate volcanic rocks; massive pink rhyolite, ignimbrites, quartz-feldspar porphyry; grey to green pyroclastics, red laharic breccia, agglomerate, minor conglomerate; undifferentiated grey-green volcanic rocks

----- interfingering contact -----

Hm MARTINON FORMATION: grey to black turbiditic sandstone and siltstone; proximal debris flow with marble clasts; rhythmically banded cherty siltstone; hornfels with sills of basalt

----- unconformity -----

HELIKIAN?

Hgh GREEN HEAD GROUP: grey to buff marble, locally stromatolitic; olive to grey fine-grained quartzite; black pelitic schist

----- mobilized unconformity -----

APHEBIAN?

Ab BROOKVILLE GNEISS; biotite+/-hornblende tonalitic gneiss, agmatite, migmatite; commonly severely chloritized

contact, approximate, assumed fault, high angle

thrust fault mylonite zone

Geology by K.L. Currie 1985, 1986, with additions from McCutcheon and Ruitenberg 1984, Hay 1968, MacKenzie 1964 and unpublished work by R.H. Grant.

Figure 69.1. Geology of the Musquash-Loch Alva.

mylonitized, the deformation dying out southward over a width of 200 m. This zone also contains remnants of a mylonitized salic pluton too deformed for certain identification. Both the mylonite zones consist of a marginal zone of fissile schists in which the salic-mafic alternation can be discerned, and a central core of uniform, flinty rock banded on a scale of a few millimetres. The cataclastic zones decrease in width from almost 3 km on the western margin of the mapped area to less than 200 m on Loch Alva. Like the dykes, the mylonite zones show marked changes in trend. The northern zone has been traced to within a few hundred metres of the Wheaton Brook fault where it is badly broken up and altered by brittle deformation assumed related to the Wheaton Brook fault. The southern zone disappears in a zone of poor outcrop east of Loch Alva. It may also be truncated by younger brittle deformation, since the southern boundary of the dyke complex in this region appears to follow a system of late, northeast-trending brittle faults.

A number of observations suggest that the mylonite zones are similar in age to the dyke complex, and probably to the major plutons. (1) The mylonite zone contains distinctive augen schists with plagioclase augen developed from the "blotchy" mafic dykes noted above, but is cut by lithologically similar dykes. (2) The dyke complex cuts bounding granitoid plutons, for example the Loch Alva pluton, but is deflected by and included in the Lingley pluton. (3) Mylonite and dyke complex are both pervasively epidotized and chloritized. Lower Silurian basalt of the Long Reach Formation shows no such alteration, even though it locally occurs as a slice within the Kingston complex. (4) Epidotized granite cobbles occur within conglomerates of the lowermost Cambrian Ratcliffe Brook Formation. These observations strongly suggest that emplacement of major plutons, emplacement of the dyke complex, mylonitization and epidote/chlorite alteration were all closely related Late Proterozoic events.

Eocambrian rocks (unit Ed) of the redbed-basalt sequence (Currie, 1984) occur in the southeastern corner of the mapped area, as described by Currie (1984). A number of fault slivers of red sandstone and conglomerates have also been assigned to this unit. These conglomerates were previously mapped as Carboniferous, or even Triassic, but several observations argue against such a young age. (1) The conglomerates are essentially monomict, containing only fragments of fine grained, porphyritic salic igneous rocks. This contrasts strongly with the polymict character of known Carboniferous and Triassic conglomerates, particularly the abundance of quartz fragments. (2) The dips of the conglomerates are vertical or very steep, and the occurrences appear to be fault bounded on all sides. Younger conglomerates commonly exhibit moderate to gentle dips and are bounded, at least on one side, by unconformities. (3) The conglomerates contain partially epidotized salic rocks, whereas in Carboniferous and younger conglomerates alteration of the salic rocks is complete. I tentatively suggest these fault slivers of conglomerate developed in small local grabens along the edges of major Late Proterozoic deformation zones. If this explanation is correct, the slight degree of alteration and metamorphism of the conglomerates shows that Phanerozoic metamorphism north of Highway 1 is entirely negligible.

The Cambro-Ordovician Saint John Group (unit COsj) of grey green to black sandstone and shale outcrops east of Musquash Harbour, as described by Currie (1984) and in two small fault slivers within the Lingley pluton. The latter occurrence is of particular interest since it not only defines the northwestern limit of the Saint John Group, but also shows that the Lingley pluton must be older than the unmetamorphosed sedimentary rocks, and demonstrates an important north-northwest-trending faulting.

The Lower Silurian (Llandovery) Long Reach Formation (unit Slr) consists mainly of plagioclase porphyritic basalt, commonly vesicular, with intercalations of siltstone and calcareous siltstone (Berry and Boucot, 1970). Along the Long Reach the formation forms a fault bounded sliver separated from the younger (Pridolian) Jones Creek Formation (unit Sjc) by Late Precambrian rocks and the Wheaton Brook fault. Along Cunningham Creek, however, black slaty siltstone apparently part of the Jones Creek Formation contains numerous 15-30 cm sills of basalt. In this region the Long Reach and Jones Creek formations appear to be interbedded. The contact of Silurian rocks with older rocks in this region has not been observed, but close to the assumed contact the rocks are extensively shattered, so that a major fault has been assumed.

The *Welsford complex* (unit Sw) consists of coarse peralkaline (riebeckite +/− aegirine) granite with porphyritic phases and a marginal red felsite phase which passes into correlative salic volcanics (McCutcheon and Ruitenberg, 1984, Currie, 1984). Payette and Martin (1987) showed that the volcanics equivalent to the Welsford complex are interbedded with the Jones Creek Formation. The complex is therefore of Silurian age.

The *Mount Douglas pluton* (unit Dmd) consists mainly of coarse pink biotite granite with distinctive large amoeboid quartz grains. Commonly large potash feldspar grains are rimmed and partially replaced by plagioclase, which may also rim quartz and biotite. The Mount Douglas pluton contains various porphyritic, generally plagioclase porphyritic, and aplitic phases which appear to form screens and dykes. These phases locally show gradational boundaries with the main phase. Aplitic lenticles pass to phenocryst/xenocryst choked margins, which pass by coarsening of the matrix to coarse granite. Along the Lepreau River the pluton exhibits a narrow (<100 m) marginal phase of biotite diorite which is veined by the other phases, and appears to be the source of the rare mafic inclusions within the main body of the pluton. Good exposures of the contact with the country rocks occur east of Lepreau River. The pluton dykes and agmatizes its surroundings and contains large rafts of the host felsite. Dykes down to 15 cm width exhibit the characteristic rapakivi texture. The Mount Douglas pluton gave a Rb-Sr isochron age of 345 +/− 15 Ma with an initial Sr ratio of 0.707 (Fyffe et al., 1981). Given the uncertainty, I interpret this to be a late Devonian age. The pluton contains a high

concentration of lithophile elements (Ruitenberg and Fyffe, 1982) and gives a marked anomaly on airborne radiometric maps (Shives, 1986). Emplacement was essentially post-tectonic and no tectonic deformation or fabric has been noted. The Mount Douglas pluton is presently being studied in detail by M.J. McLeod, New Brunswick Department of Forests, Mines and Energy.

The Carboniferous section within the mapped area consists of red siltstone, sandstone and conglomerate of the *Balls Lake Formation* (unit Cbl) and grey to black lithic arenite of the *Lancaster Formation* (unit Cl) (Currie and Nance, 1983; Caudill and Nance, 1986). The Balls Lake Formation locally exhibits a basal carbonate member, either in the form of a caliche horizon, or as a thin black to red limestone which has yielded Visean fossils (McCutcheon, 1984). McCutcheon (1984) grouped these carbonate occurrences into the Parleeville Formation, but in view of the small size and scattered nature of the occurrences I have included them in the Balls Lake. The unconformity between the Balls Lake and the Coldbrook Group outcrops in several places. In all cases the underlying rocks were strongly weathered and fractured prior to deposition of the Balls Lake. The top of the Balls Lake Formation is marked by several metres of very fine grained, pink silicified siltstone, which was incorrectly identified as rhyolite by several earlier workers including Currie and Nance (1983). The typical pale grey lithic arenite of the Lancaster Formation rests conformably on this material. The Lancaster Formation tends to be virtually massive except for quartz pebble conglomerate beds and black, fossiliferous siltstone-shale beds.

The Triassic *Lepreau Formation* (unit Tl) occurs in two areas along Maces Bay. A basal unconformity is exposed in the southeast corner of Dipper Harbour, south of Little Lepreau Harbour, at Boyles Cove and on the north side of the Lepreau River. The map pattern suggests that the occurrence on Lepreau River is bounded on the northwest side by a normal fault, but otherwise the formation appears to be entirely bounded by an unconformity, contrary to earlier mapping. The base of the conglomerate consists of large, angular, locally derived debris. Toward the southwest dips steepen abruptly across step-like features and red siltstone and sandstone become major lithologies. These relations suggest faulting of the underlying basement during deposition.

Quaternary deposits are varied and extensive in this region, to such an extent that they totally obscure the bedrock over considerable areas. In general the deposits are either stratified sand and gravel, or a boulder-mud mixture which locally overrides the stratified deposits.

STRUCTURE

The Musquash-Loch Alva region falls into five zones of contrasting structure. In the northern zone, dominated by the massive Mount Douglas and Welsford plutons, the Silurian supracrustal rocks generally face north and dip vertically to steeply southward, consistent with the essentially vertical isoclinal folding reported by McCutcheon (1981). The brittle Wheaton Brook fault bounds this zone. East of the Nerepis River the fault appears essentially planar, but west of the river the fault not only changes strike, but is stepped along a swarm of north- to northwest-trending minor faults. Similar stepped patterns occur farther south on the north side of the Henderson Lake pluton and along the north shore of Kennebecasis Bay (A. Leger, personal communication).

South of the Mount Douglas pluton a lunate zone of granitoid plutons separates the Mount Douglas pluton from the Kingston complex. Rather equivocal evidence suggests that this curvature is an original feature, and not controlled by the emplacement of the Mount Douglas pluton. (1) The curvature extends several kilometres from the pluton without obvious evidence of associated fracturing. (2) The Kingston complex, a very large body, exhibits similar curvature. (3) The chlorite-epidote alteration of the country rocks is unaffected in the curved portion. If curvature were due to emplacement of the Mount Douglas pluton, it would be expected that some overprinting of this assemblage would be observed. On these admittedly slender grounds, I conclude that the curvature is essentially primary, and possibly controls the shape of the southern margin of the Mount Douglas pluton.

The central zone consists essentially of the Kingston complex, bounded on both sides by spectacular mylonite zones. The mylonite zone bounding the north side of the Kingston complex has been studied by Leger and Williams (1986), who abundant S-C and C-C′ fabrics indicating major dextral movement. They considered the deformation to have taken place at temperatures in the vicinity of 450°C, compatible with the observed greenschist grade metamorphism of the Kingston complex. Leger and Williams (1986) assigned the deformation to the Acadian orogeny, mainly on the grounds that the associated cleavage has an "Acadian trend". Since the associated cleavage varies in strike by 90° within the mapped area, and since evidence for Acadian deformation is rare to non-existent in the Avalonian terrane around Saint John (Currie, 1986b), the age of deformation is here assumed to be Late Precambrian rather than Silurian-Devonian for reasons summarized under the description of units. Leger and Williams (1986) figured but did not describe the mylonite zone bounding the south side of the Kingston complex. My observations indicate that this zone is very similar to that on the north side of the complex, including the presence of S-C and C-C′ fabrics, Z folds with steep to vertical plunges, and other evidence of dextral movement. On the west side of the mapped area the two mylonite zones are separated by less than 1 km of less deformed material, and it seems probable that they merge to the west into the Pocologan mylonite zone of Rast and Currie (1976) and Rast and Dickson (1982).

A zone of granitoid plutons lies to the south of the mylonite zones. The plutons exhibit relatively little deformation, possibly due to their massive character. The northern fringe of the Talbot Road pluton has been involved in mylonitization, and the Henderson Lake pluton exhibits a complex series of stepped small brittle faults, possibly related to

the end of the southern mylonite zone. However most of the plutons exhibit only very local cataclasis and reddening along irregular fractures. The southern margin of the plutons is shown on older maps as a fault between granitoid rocks and Carboniferous sediments (Alcock, 1959, Dickson, 1985), but there seems to be little positive evidence for this fault. At its southwestern end at Boyles Cove the contact is clearly an unconformity.

The most southerly zone displays folded Carboniferous rocks sitting unconformably on volcanic and plutonic rocks of Late Precambrian age. The structure of this zone has been studied in detail by N. Rast and co-workers, whose conclusions have been modified by Currie and Nance (1983) and Currie (1984, 1986a). The structure is dominated by major dextral transcurrent faulting of Late Carboniferous and younger age, with a master fault located just offshore in the Bay of Fundy. As a result of curvature of this fault, the area along the shore exhibits a combination of high-angle transverse movement and low-angle thrusting from the south-southwest. The contrast in mechanical competence between the sediments and volcanics has produced a complex synclinorium in the Carboniferous rocks in which the crystalline core to the central anticline has been faulted upward as an essentially undeformed block. The spectacular, but small, thrust allochthons along the Fundy shore form festoons around the end of small scale splays from the hidden master fault.

DISCUSSION

Although this year's mapping does not complete coverage of the west end of the Saint John terrane, it does complete coverage of some of the most characteristic units, namely the volcanics of the Coldbrook Group and the Cambro-Ordovician sedimentary rocks of the Saint John Group. It therefore seems appropriate to consider current understanding of the nature and boundaries of this terrane. The stratigraphy and structure of the Avalonian rocks have recently been reviewed (Currie, 1986b). The following remarks therefore treat mainly the boundaries of the terrane, and its relation to surrounding terranes.

It now seems well established that the southern margin of the terrane lies on a major dextral fault which moved in Late Carboniferous and more recent time. The terrane to the southeast is not definitely known because the junction is covered by water and Triassic sedimentary rocks, but it seems likely that it is the Meguma terrane of southern Nova Scotia.

The northern boundary in the eastern part of the mapped area lies along the Wheaton Brook fault. The movement on this fault is unknown. Leger and Williams (1986) followed McCutcheon (1981) in supposing it to be high angle reverse, but McCutcheon (1981) described this movement as "postulated". The present study found no reliable kinematic indicators in the breccia zone accompanying this fault. The fault is clearly truncated by the Mount Douglas pluton, and must therefore be older than the southern boundary of the Saint John terrane. McCutcheon (1981) describes the movement as Acadian, which is plausible but unproved. Indeed the collapse of evidence for Acadian orogeny is one of the most striking features of the current investigations. The Saint John terrane contains no proved or probable major folding, metamorphism or salic magmatism of Silurian or Devonian age. The obvious contrast with the terrane to the north makes evident the importance of fixing the age, sense and scale of motions on the Wheaton Brook fault.

It is now evident, as pointed out by Rast and Currie (1976) that the Bellisle mylonite zone does not truncate the Saint John terrane, but lies within it. The mylonite-forming event must therefore pertain to the late Precambrian history, prior to the juxtaposition of the Saint John terrane with central New Brunswick. I point out that the dextral nature of the zone is compatible with the rifting-closing model previously proposed for the Kingston complex (Currie, 1986a), if the closing is slightly oblique. Since observed kinematic indicators such as S-C fabrics and z folds are formed, or rather reformed, at a very late stage, they may indicate only a relatively small total displacement, as indicated by matching of plutons across the zones.

Finally, attention must be drawn to the major northwest-trending features which seem to mark internal boundaries within the Saint John terrane. Leger and Williams (1986) proposed such a feature running south from Loch Alva to Musquash Harbour. However a much more significant feature runs down the Nerepis River and through Grand Bay, then abruptly changes direction to cross the foot of Ludgate Lake and end at the head of Musquash Harbour. Along this strong lineament the following major changes occur (1) the Green Head Group, Brookville gneiss and Martinon Formation are truncated. (2) The series of red conglomerate fault slivers is truncated. (3) The orientation of fault slivers changes from northeast to the east to northwest to the west. (4) The proportion of plutonic rocks increases abruptly, and basaltic compositions virtually disappear. (5) Bouguer gravity anomalies go from positive (0-10 mGal) to the east to strongly negative (-20 to -40 mGal) to the west (fragmentary data compiled by Chandra et al., 1982). The last two points suggest that this Nerepis-Grand Bay line must represent a contact between two quite different crustal blocks juxtaposed before the Late Precambrian magmatism, but later reactivated. The nature and significance of these crustal blocks is not presently understood, but hopefully detailed geochemical studies of the igneous rocks will help to unravel remaining problems in the Saint John terrane.

REFERENCES

Alcock, F.J.
1959: Geology of the Musquash map-area, New Brunswick; Geological Survey of Canada, Map 1084A.

Belyea, H.R.
1944: Plutonic rocks of the Musquash area, New Brunswick, part 1; Acadian Naturalist, v. 1, p. 87-102.

Berry, W.B.N. and Boucot, A.J.
1970: Correlation of the North American Silurian rocks; Geological Society of America, Special Paper 102, 289 p.

Brown, R.L. and Helmstaedt, H.
1970: Deformation history of part of the Lubec-Bellisle zone of southern New Brunswick; Canadian Journal of Earth Sciences, v. 7, p. 748-767.

Caudill, M.R. and Nance, R.D.
1986: Variscan tectonostratigraphy of the Mispec Group, southern New Brunswick: stratigraphy and depositional setting; in Current Research, Part A, Geological Survey of Canada, Paper 86-1A, p. 343-350.

Chandra, J., Chandra, S., Wallace, J., and Williams, D.
1982: Bouguer gravity map of Saint John; New Brunswick Department of Natural Resources, Mineral Resources Division Plate 82-34.

Currie, K.L.
1984: A reconsideration of some geological relations near Saint John, New Brunswick; in Current Research, Part A, Geological Survey of Canada, Paper 84-1A, p. 193-201.
1986a: The boundaries of the Avalon tectonostratigraphic zone, Musquash-Loch Alva region, southern New Brunswick; in Current Research, Part A, Geological Survey of Canada, Paper 86-1A, p. 333-341.
1986b: The stratigraphy and structure of the Avalonian terrane around Saint John, New Brunswick; Maritime Sediments and Atlantic Geology v. 22, no. 3.

Currie, K.L. and Nance, R.D.
1983: A reconsideration of the Carboniferous rocks of Saint John, New Brunswick; in Current Research, Part A, Geological Survey of Canada, Paper 83-1A, p. 29-36.

Currie, K.L., Nance, R.D., Pajari, G.E., and Pickerill, R.K.
1981: A reconsideration of the pre-Carboniferous geology of Saint John, New Brunswick; in Current Research, Part A, Geological Survey of Canada, Paper 81-1A, p. 23-30.

Dickson, L.W.
1985: Igneous rocks between Saint John and Negro Harbour, southwestern New Brunswick; Ph.D. thesis, University of New Brunswick, Fredericton.

Fyffe, L.R., Pajari, G.E., and Cherry, M.E.
1981: The Acadian plutonic rocks of New Brunswick; Maritime Sediments and Atlantic Geology, v. 17, p. 23-26.

Hay, P.W.
1968: Geology of the Saint George-Seven Mile Lake area, southwestern New Brunswick; New Brunswick Department of Natural Resources, Mineral Resources Branch Map Series 68-1.

Hayes, A.O., and Howell, B.F.
1937: Geology of Saint John, New Brunswick; Geological Society of America, Special Paper 5, 146 p.

Leger, A. and Williams, P.F.
1986: Transcurrent faulting history of southern New Brunswick; in Current Research, Part A, Geological Survey of Canada, Paper 86-1B, p. 111-120.

MacKenzie, G.S.
1964: Geology, Saint John, New Brunswick; Geological Survey of Canada Map 1113A.

McCutcheon, S.R.
1981: Revised stratigraphy of the Long Reach area, southern New Brunswick: evidence for major northwest-directed Acadian thrusting; Canadian Journal of Earth Sciences, v. 18, p. 646-656.
1984: Geology of the gold-bearing rocks in the Lorneville-Lepreau area; New Brunswick Department of Natural Resources, Mineral Resources Division Information Circular 84-2.

McCutcheon, S.R. and Ruitenberg, A.A.
1984: Geology, Saint John, New Brunswick; New Brunswick Department of Natural Resources, Mineral Resources Division Plate 84-17.

O'Brien, B.H.
1976: The geology of parts of the Coldbrook Group, southern New Brunswick; M.Sc. thesis, University of New Brunswick, Fredericton.

Payette, C. and Martin, R.F.
1987: The Welsford igneous complex, southern New Brunswick, rift-related Acadian volcanism; in Current Research, Part A, Geological Survey of Canada, Paper 87-1A, report 24.

Rast, N. and Currie, K.L.
1976: On the position of the Variscan front in southern New Brunswick and its relation to Precambrian basement; Canadian Journal of Earth Sciences, v. 13, p. 194-196.

Rast, N., and Dickson, W.L.
1982: The Pocologan mylonite zone; Geological Association of Canada, Special Paper 24, p. 249-261.

Rast, N. and Grant, R.H.
1973: Trans-Atlantic correlation of the Variscan-Appalachian orogeny; American Journal of Science, v. 273, p. 572-579.

Rast, N., Grant, R.H., Parker, J.S.D., and Teng, H.C.
1978: The Carboniferous deformed rocks west of Saint John, New Brunswick. in Guidebook for field trips in southeastern Maine and southwestern New Brunswick; A. Ludman, Geological Bulletin 6, p. 162-173. Queens College Press, Flushing, New York.

Ruitenberg, A.A., and Fyffe, L.R.
1982: Mineral deposits associated with granitoid intrusions and related sub-volcanic stocks in New Brunswick, and their relation to Appalachian tectonic evolution; Canadian Institute of Mining Bulletin, June, p. 1-15.

Ruitenberg, A.A., Giles, R.S., Venugopal, D.V., Buttimer, S.M., McCutcheon, S.R., and Chandra, J.
1979: Geology and mineral resources, Caledonia area; New Brunswick Department of Natural Resources, Mineral Resources Branch Memoir 1, 213 p.

Shives, R.
1986: Airborne gamma-ray spectrometric survey, % K, Saint John, west half; Geological Survey of Canada, Map 35721(8)G.

Wardle, R.J.
1978: The stratigraphy and tectonics of the Greenhead Group; its relation to Hadrynian and Paleozoic rocks, southern New Brunswick; Ph.D. thesis, University of New Brunswick, Fredericton.

Archean mafic dyke swarm, Beaulieu River volcanic belt, Slave Province, N.W.T.

Project 730040

M.B. Lambert and R.E. Ernst[1]
Lithosphere and Canadian Shield Division

Lambert, M.B. and Ernst, R.E., Archean mafic dyke swarm, Beaulieu River volcanic belt, Slave Province, N.W.T.; in Current Research, Part A, Geological Survey of Canada, Paper 87-1A, p. 673-679, 1987.

Abstract

A 2.5 km wide NNW-trending amphibolite dyke swarm along the NE margin of the Beaulieu River volcanic belt comprises approximately 60% amphibolite dykes separated by screens of foliated granitic gneiss. Most dykes are multiple intrusions as defined by internal chilled contacts. A 100-200 m shear zone separates the dyke-granitoid complex from the volcanic belt (also containing amphibolite dykes). No dykes have been traced across the shear zone. The Meander Lake Plutonic Suite intrudes the dyke swarm along its eastern margin.

This swarm differs from sheeted dykes of ophiolite complexes in that granitic screens are abundant throughout the swarm and there are no extensive or continuous areas of 100% dykes.

The shear zone may be a major tectonic boundary along which the volcanic belt and the dyke-granitoid complex have been juxtaposed.

Résumé

Un système de dykes amphibolitiques de direction NNW et de 2,5 km de large longe la marge NE de la zone volcanique de Beaulieu River et comprend environ 60 % de dykes amphibolitiques séparés par des écrans de gneiss granitique folié. La plupart des dykes forment des intrusions multiples, définies par des contacts internes refroidis. Une zone de cisaillement de 100 à 200 m sépare le complexe dykes-granitoïdes de la zone de roches volcaniques (qui renferme aussi des dykes amphibolitiques). On n'a pas observé de dykes qui traversent la zone de cisaillement. La série plutonique de Meander Lake pénètre le système de dykes le long de sa marge orientale.

Ce système de dykes diffère des dykes stratifiés des complexes ophiolitiques en ce sens que les écrans granitiques sont abondants dans tout le système et on ne voit nulle part de grandes étendues ou des étendues continues constituées uniquement de dykes.

La zone de cisaillement peut être une limite importante tectonique le long de laquelle la zone volcanique et le complexe dykes-granitoïdes ont été juxtaposés.

[1]Department of Geology, Carleton University and Ottawa-Carleton Centre for Geoscience Studies, Ottawa, Ontario

INTRODUCTION

Dense swarms of mafic dykes are a common feature of Archean greenstone belts and adjacent granitoid terranes that border the Yellowknife Supergroup in the southern Slave Province. Early mappers outlined the impressive swarms near the Cameron River (Henderson, 1941; Baragar, 1966) and mapped in detail the complex swarm in the Yellowknife volcanic belt (Henderson and Brown, 1966). Recent work extends mapping of dyke swarms in the northern part of the Yellowknife belt (Helmsteadt and Padgham, 1986) and provides more precise documentation of relationships of swarms in volanic belts and granitoid basement in the Cameron River and Beaulieu River volcanic belts (Lambert, 1982; in press). Although dykes and sills in the volcanic belts are intimately related to development of the volcanic piles (Lambert, 1982; in press), those in adjacent granitic basement of the Sleepy Dragon Complex may not be directly related to the adjacent volcanic belts (Lambert, in press; Kusky, in press) nor to the dykes they contain as previously interpreted (Baragar, 1966: Lambert, 1977, 1982). Helmstaedt and Padgham (1986) and Helmstaedt et al. (1986) suggested that the dyke swarm in the Yellowknife belt could be part of an ophiolite assemblage.

The densest swarm of mafic dykes in these belts occurs along the northeast side of the Beaulieu River volcanic belt. Following the mapping of the Cameron River and Beaulieu River volcanic belts at a scale of 1:50 000 (Lambert, in press) this swarm was chosen as a site for a detailed study to document the precise internal constitution of these dyke swarms; determine whether grain size variations and chilled contacts (such as would result from multiple intrusion) have survived an amphibolite grade metamorphism; determine relationships with the volcanic belts and adjacent granitic terrane; collect a representative suite of samples from the swarm for chemical and petrographic comparison with volcanic rocks and dykes elsewhere in the Cameron River and Beaulieu River volcanic belts; and to compare this swarm with sheeted dykes of well known ophiolite complexes.

DYKE SWARM

This north-northwesterly trending swarm which is about 2.5 km wide and at least 20 km long, tapers out southward but continues northward beyond the limits of Figure 70.1 (inset map). Most of the swarm occurs between a major shear zone on its west side and the Meander Lake Plutonic Complex (Henderson, 1985) to the east. A major north-northeast trending sinistral transcurrent fault, traceable for 30 km through the volcanic belt (Lambert, in press; Henderson, 1985) displaces the dyke swarm 800 m along the east side of Step'nduck lake (local name). The dyke swarm comprises a multitude of diabasic to gabbroic dykes metamorphosed to amphibolite grade (hereafter referred to as amphibolite dykes) separated by screens of granitic gneiss (grey weathering, sheared and foliated granodiorite to granite), volcanic flows, and minor dykes of felsite, pink granite and 'fresh' diabase. Figure 70.1 shows a detailed transect across this swarm at Step'nduck lake.

In the volcanic-dyke terrane adjacent to the shear zone pillows are highly "flattened", elongated bodies containing penetrative foliation and local zones of intense shearing parallel to the shear zone. Amphibolite dykes are rare where the volcanic succession comprises andesite to dacite flows (west central part of Fig. 70.1) but are abundant where flows are basaltic (southern corner of Fig. 70.1 and Lambert, in press).

Meander Lake Plutonic Suite

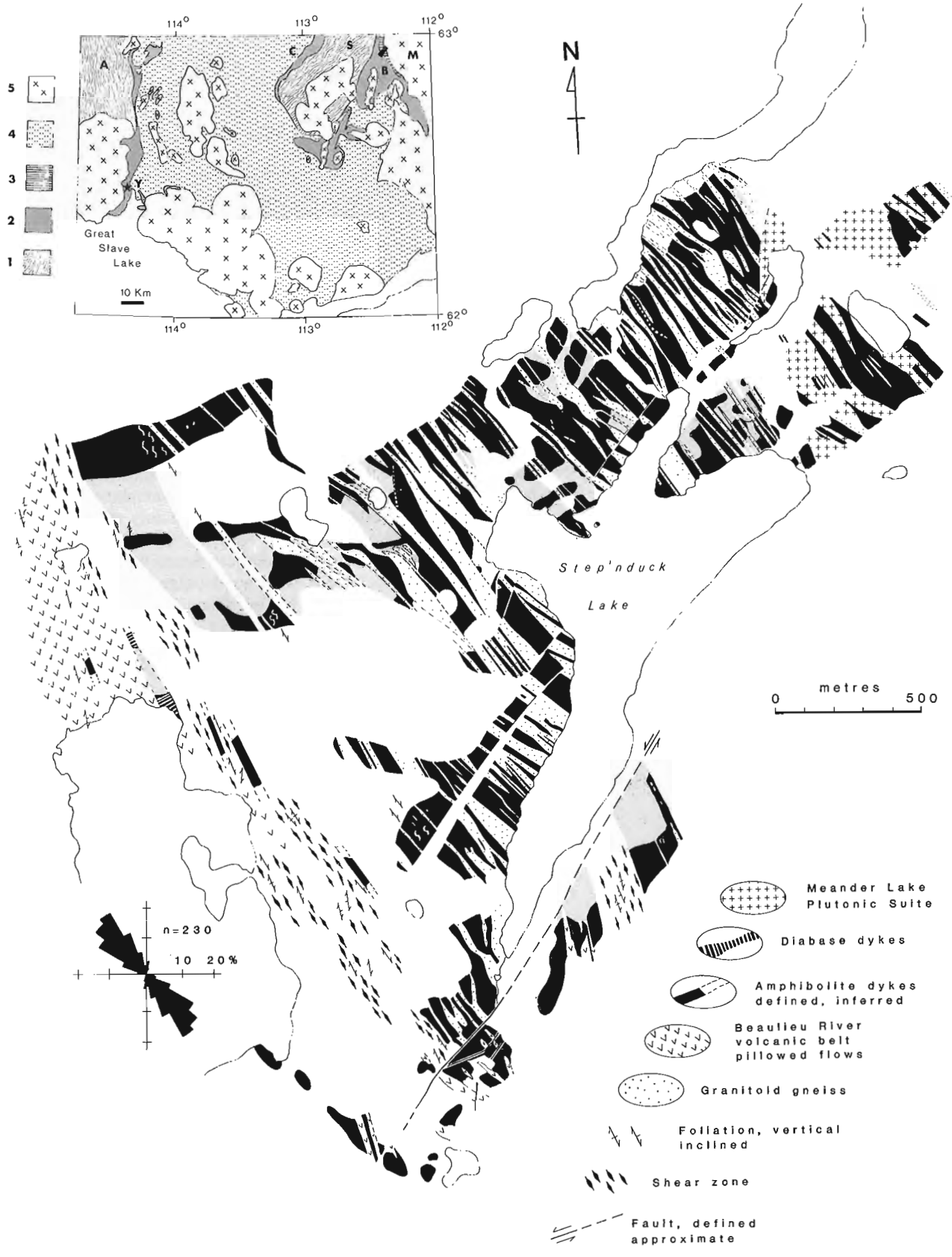
The Meander Lake Plutonic Suite (an extensive complex of granitic plutons and irregular areas containing abundant inclusions of Yellowknife Supergroup rocks, along the eastern side of the Yellowknife basin; Henderson, 1985) intrudes the eastern side of the dyke swarm. In contrast to the highly foliated granites that form screens in the dyke swarm, granites of the Meander Lake suite are generally, pink weathering, massive, medium- to coarse-grained biotite and biotite-muscovite quartz monzonite to granite. In the northeastern corner of the map area a pluton of the Meander Lake suite cuts obliquely across the northwesterly trend of the dyke swarm and across internal contacts in multiple dyke intrusions, and includes large (ca. 50 to 200 m) screens of amphibolite dykes and associated granite gneiss. This relationship is complicated by rare younger mafic dykes (not distinguished from amphibolite dykes in Fig. 70.1) that intrude Meander Lake plutons. These dykes are dark grey to rusty brown weathering 'fresh' dykes that cut cleanly through the granite and do not have foliated contacts. These may be related to presumed Proterozoic dykes known throughout this area (Henderson, 1985).

Dykes

Size, distribution and contact relations

Widths of dykes range from a few centimetres to 35 m (the largest single dyke) and average dykes are less than 10-15 m wide. Most 'dykes' in Figure 70.1 are in fact multiple intrusions as indicated by numerous internal chill contacts and small dykes that intrude larger dykes (Fig. 70.3). The largest multiple intrusion is about 300 m but most zones are less than 100 m wide. Both sides of all dykes can be accounted for within zones of multiple injection where outcrop exposure is continuous. Hence the concept of chilling bias across a dyke swarm as applied to sheeted dykes of ophiolite complexes (Kidd and Cann, 1974) is not relevent here.

Figure 70.1. Detailed map of a portion of the mafic dyke swarm along the northeast side of the Beaulieu River volcanic belt. Inset map shows geological setting of the southwestern part of the Slave Province generalized after Henderson (1985). 1 – Archean granitoid basement complexes: S, Sleepy Dragon Complex; A -Anton Complex. 2 – Volcanic belts, dominantly metabasalts with minor andesite, dacite, rhyolite: B, Beaulieu River volcanic belt; C, Cameron River volcanic belt; Y, Yellowknife volcanic belt. 3 – Mafic dyke swarm. 4 – Burwash Formation; greywacke, mudstone turbidites. 5 – Plutonic suites (undifferentiated). Star locates Yellowknife and black bar shows location of detailed map. Rose diagram shows distribution of 230 measured trends of dyke contacts.


114°
113°
112°
63°
62°
A
C
S
M
B
Y
5
4
3
2
1
Great
Slave
Lake
10 Km
N
Step'nduck
Lake
metres
0
500
n=230
10 20%
Meander Lake
Plutonic Suite
Diabase dykes
Amphibolite dykes
defined, inferred
Beaulieu River
volcanic belt
pillowed flows
Granitoid gneiss
Foliation, vertical
inclined
Shear zone
Fault, defined
approximate

Because of lithological similarity, individual dykes generally are difficult to trace with certainty for long distances. Multiple intrusion groups, however, between distinctive large granitic screens, have been traced for about 1 km, and distribution of rare but distinct lithologies (such as plagioclase phyric rocks) along trend of dykes for distances of 2 km; this suggests that dykes may have considerable lateral continuity.

Boundary relationships

Shear zone

The north-northwesterly trending shear zone along the west side of the dyke swarm is a belt of intensely sheared amphibolite, 100-200 m wide, in which the identity of the parent lithology (i.e. dyke or mafic volcanic rocks) cannot be recognized. The amphibolite has fine penetratative foliation and slaty cleavage commonly containing quartz veins. The attitude of foliation in sheared rocks is steep (85-90°). Horizontal surfaces show abundant evidence for a dextral sense of shear (asymmetric folds, rotated clasts, c-s shear bands).

The first recognizable parent lithologies northeast of the shear zone are invariably dyke rocks with inclusions or screens of granitic gneiss (the dyke-granitoid complex) and southwest of the zone are pillow lavas containing dykes (volcanic-dyke terrane). The most intense shearing seems to be localized in the dyke-granitoid complex since augen of granitic material are locally found in the shear zone. No dykes have been traced across this shear zone.

Shearing persists outside of the intensely sheared zone. Rocks are strongly foliated for up to 400 m into the dyke-granitoid complex and for at least 300 m into the volcanic-dyke terrane.

The dyke-granitoid complex within ca. 600 m of the shear zone is distinctly different from the complex farther northeast. Granitic screens have been deformed and are generally present only as isolated pods and slivers within massive to strongly foliated amphibolite dykes. At one location (southeast of Step'nduck lake) a former granitic screen has been boudinaged, broken and strung out into a train of inclusions aligned within the plane of foliation. Foliation in the amphibolite dykes is nearly vertical and trends north to northwesterly. This shearing has caused grain size reduction and locally produced fine grained schistose rocks from medium- to coarse-grained amphibolite. Locally, the foliation, granitic screens and internal chill contacts of multiply intruded dykes are folded and their axial traces parallel the main shear zone.

To the northeast of this zone of shearing (i.e. greater than 400 m away from the shear zone) amphibolite dykes tend to be unfoliated, massive rocks that only show development of foliation at contacts with the granitic screens and along occasionally discrete shear zones within dykes. However, even massive looking amphibolite dykes experienced some strain as indicated by occasional folded aplitic or quartz veins (dextral sense of movement is common).

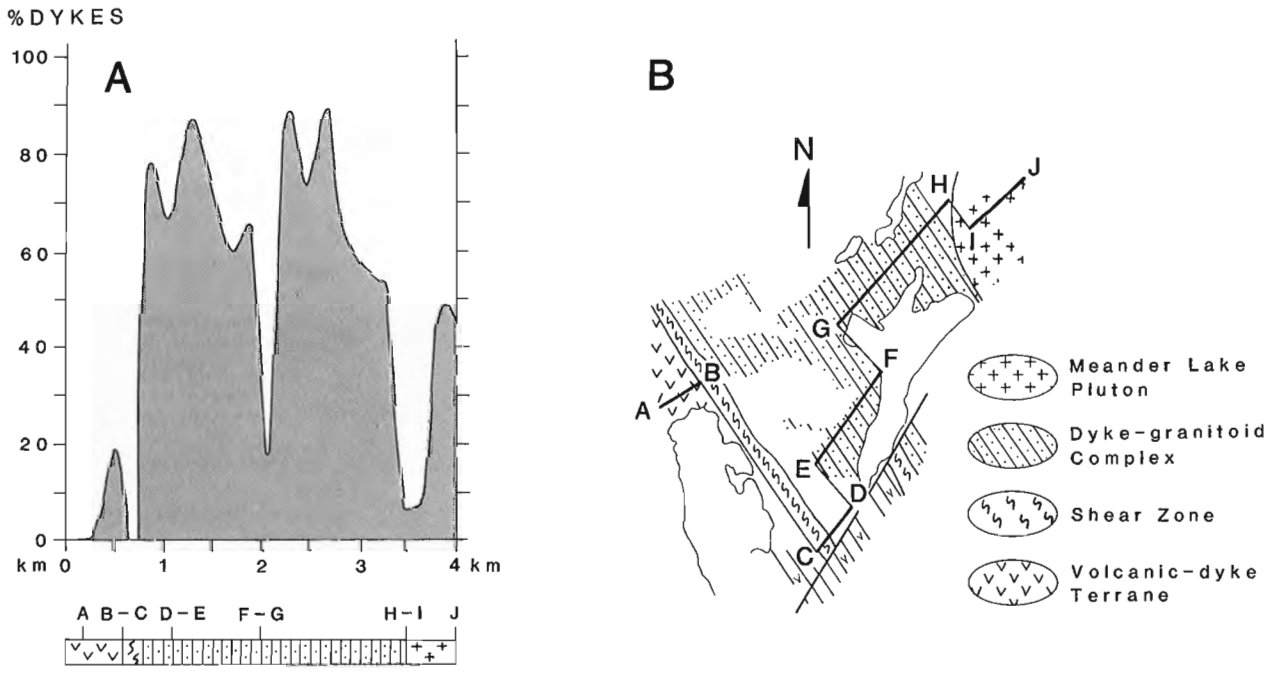


Figure 70.2. A, Percentage of dykes measured over 200 m intervals along section lines A to J. Horizontal bar represents lithologies along section shown in B, a generalized map of Figure 70.1.

Dykes have a strong northwesterly trend (Fig. 70.1, rose diagram) and contacts are dominantly vertical, rarely in ranges of 65-85° and only one small dyke with shallow (21°) dip.

Within a particular multiple intrusion internal dyke-dyke contacts of large dykes are regular and trend parallel to one another whereas smaller (centimetre to metre sized dykes) commonly undulate or weave through the intrusion but in the same general trend as the swarm (Fig. 70.4). No distinct set of dykes cuts across the main swarm.

In spite of the amphibolite grade of metamorphism relict primary textures, patterns of changing grain size and chilled contacts are distinguished (with variable degrees of difficulty) such that the multiplicity of intrusions has been documented for a large section across the swarm. Large dykes have coarse- to medium-grained centres, fine grain size within a metre of the contact, and chill selvages (very fine grained to aphanitic amphibolite) against older dykes or country rock. Where dykes were emplaced side-by-side contacts are doubly chilled. Chill relationships, however, may vary along strike from doubly chilled to one-sided chill against a very fine grained adjacent dyke margin. Amphibolite dykes invariably chill against screens of granitic gneiss and volcanics.

Granitic screens

Screens are present throughout the swarm and account for ca. 40% of the zone of dyking (Fig. 70.2). Screens are almost entirely light grey weathering, foliated granitic gneiss except for west of the shear zone where they are volcanic rocks. They range in size from thin slivers up to bodies 50-100 m wide and 1000 m long. They are fairly evenly distributed throughout the dyke swarm except within 400 m of the shear zone where they decrease in size and abundance.

Screens may taper out gradually, end as a train of slivers or angular to subrounded inclusions, end abruptly with blunt rounded to angular terminations or finger out.

Foliation in the gneissic screens is generally shallow (dips are commonly between 10-35°) in contrast to the vertical dykes that cut through them.

In sheared rocks within or near the shear zone granitic screens and their relicts may be folded or boudinaged and broken and reduced to swarms of lenticular augen down to a few centimetres across.

This multitude of screens represents the granitic host through which the dyke swarm intruded. The shear foliation in the gneiss is clearly unrelated to emplacement of the dyke swarm and to subsequent shearing events. The granite has had a pre-intrusion tectonic history similar to granitic gneisses of the Sleepy Dragon Complex to the west and may represent hitherto unrecognized Archean sialic basement.

Dyke lithology and relative chronology

Six main types of dykes are represented in the dyke swarm: (1) aphyric fine- to coarse-grained amphibolite, (2) plagioclase phyric amphibolite, (3) aphanitic dark green and grey amphibolite, (4) rusty brown weathering diabase, (5) felsite and (6) pink granite.

Most of the dykes in the map area belong to the first type, aphyric dark greenish grey weathering, fine-to medium grained and occasionally coarse grained amphibolite dykes. Weathered surfaces accentuate relict gabbroic textures in medium-and coarse-grained rocks and diabasic textures in fine grained rocks. Sheared dykes are schistose. The dykes have been completely recrystallized to an assemblage of hornblende-plagioclase-quartz-epidote and calcite. The amphibole is typically a poikiloblastic, blue-green hornblende

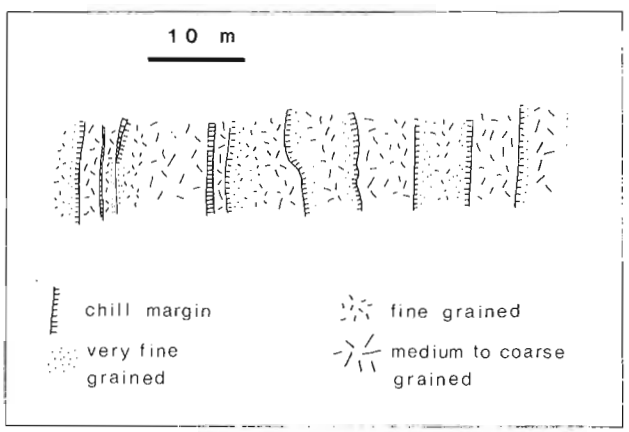


Figure 70.3. Chilling relationships and textural patterns of a multiple intrusion in amphibolite near the west-central shore of Step'nduck lake.

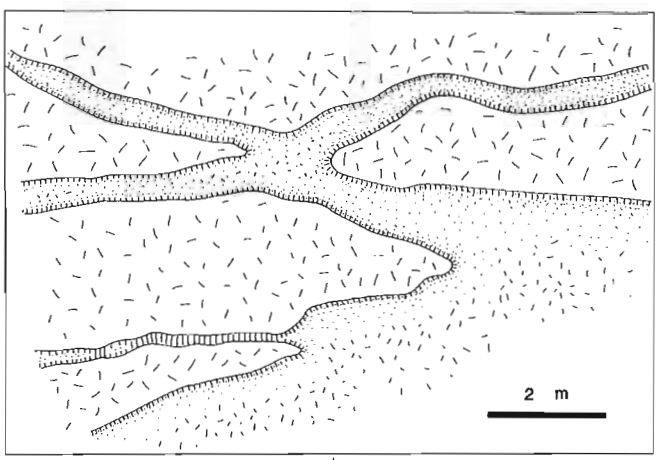


Figure 70.4. Thin apophyses of amphibolite undulating through an older amphibolite dyke. Patterns as for Figure 70.3 amphibolite dyke.

that encloses minute grains of crystalloblastic plagioclase and quartz and in some cases, calcite and epidote. Relicts of primary plagioclase are fine crystalloblastic felsic aggregates whose outlines define elongate to stubby lath forms.

An uncommon but distinctive lithology amongst the amphibolite swarm is plagioclase phyric dykes that appear intermittantly about 400 m and 1100 m east of the shear zone. Dykes are 3 to 15 m wide and contain euhedral to subhedral plagioclase phenocrysts (saussuritized), 5 to 50 mm across, and glomeroporphyritic clusters that make up 15-30% of the rock. Phenocrysts are concentrated in the centre of some dykes.

Dark green very fine grained to aphanitic dykes and dyklets are a late phase of the amphibolite dykes. These are narrow dykes, generally 10-30 cm wide that undulate across or along internal boundaries of larger dykes locally bifurcating and sprouting irregular apophyses.

Rusty brown weathering diabase dykes clearly postdate the main amphibolite swarm. These are 'fresh' undeformed units that intrude along or cut the amphibolite swarm at low angles, follow foliation and trend of pillow flattening in volcanic rocks immediately west of the shear zone and intrude the Meander Lake Plutonic Suite and have rare occurrence in the dyke-granitoid complex. They make sharp nonfoliated contacts with host rocks. One dyke (on the west side of Fig. 70.1) is continuous for 4 km in volcanic rocks along the west side of the shear zone (Lambert, in press). These rocks are unusually fresh compared to amphibolite intrusions. A dyke just west of the shear zone, for example, is a hornblende diabase containing brown to blue-green(on rims) hornblende that rarely preserves patches of clinopyroxene in their cores. Euhedral to subhedral laths of plagioclase have normal to oscillatory zoning with cores of labradorite and rims of andesine. Quartz forms anhedral grains or granophyre that occupies angular areas between plagioclase and pyroxene.

Felsic dykes are rare in the swarm. They are nonfoliated pale grey aphanitic felsite and massive pink fine grained granite, that intrude amphibolite dykes and granite gneiss. Some grade into fine grained pink granitic dykes similar to plutons of the Meander Lake suite whereas others are small bodies isolated in the amphibolite swarm.

Except for what can be determined in local multiple intrusion units and the late dark green dykes no general sequence of emplacement of the amphibolite dykes within the swarm has been determined. Consistent northwesterly trend of the vast majority of dykes and the numerous subparallel internal contacts suggest that they represent a series of penecontemporaneous injections.

The diabases which postdate metamorphism and deformation that affected the volcanic belt and amphibolite dyke swarm and also cut granitic plutons are probably post Archean and possibly related to the MacKenzie dyke swarm.

Felsic dykes, which are clearly younger than the amphibolite dyke swarm, could be related in part to intrusions of the Meander Lake Plutonic Suite or to a northwesterly set of post deformational dykes that intrude volcanic belts, Sleepy Dragon gneiss terrane and plutons of the region (Lambert, in press).

CONCLUSIONS

Detailed mapping across a segment of the dyke swarm leads to the following tentative conclusions.

1. The dyke swarm probably represents a major period of multiple injection of voluminous mafic magma into granitic gneiss that had a previoius history of deformation (possibly Archean basement?).
2. Most "dykes" between granitic screens are multiple intrusions.
3. Unlike sheeted dykes of ophiolite complexes, there is no extensive or continuous areas of 100% dykes and no transition to plutonic gabbros (although some dykes are in part gabbroic textured): granitic screens are abundant throughout the dyke complex on the east side of the shear zone and volcanic screens on the west side.
4. Density of dykes here , as in the swarm at the Cameron River Volcanic belt, is not much greater than that of some high standing volcanic complexes such as in Hawaii (Walker, 1986).
5. If at least some of the mafic magma represented by this dyke swarm erupted at the surface, then it is likely that the granitic gneiss through which the dykes intruded may be hitherto unrecognized Archean basement (no radiometric dates have yet been obtained from this unit).
6. The dyke swarm represents 1800 m of extension over a distance of 3000 m in a granitic gneiss terrane (i.e. 60% extension).
7. Areas of the dyke-granitoid complex in the northeastern portion of the map area are interpreted as large xenoliths within the Meander Lake Plutonic Suite.
8. A major shear zone separates the dyke-granitoid complex from the Beaulieu River volcanic belt. No dykes have been traced across this shear zone. This may be a major tectonic boundary at which the volcanic belt and dyke-granitoid terrane have been tectonically juxtaposed: a situation similar to that along the east side of the Cameron River volcanic belt (Lambert, in press; Kusky, in press).
9. The dyke-granite complex may be a tectonic slice of continental crust and its contained dyke swarm and the dykes of the main swarm may not be related to the adjacent Beaulieu River volcanic suite nor the dykes it contains.

ACKNOWLEDGMENTS

We thank Jack Fenton for cheerful and capable assistance during fieldwork and W.R.A. Baragar for reviewing the manuscript.

REFERENCES

Baragar, W.R.A.

1966: Geochemistry of the Yellowknife volcanic rocks; Canadian Journal of Earth Sciences, v. 3, p. 9-30.

Helmstaedt, H. and Padgham, W.A.

1986: A new look at the stratigraphy of the Yellowknife Supergroup at Yellowknife, N.W.T. – implications of the age of gold-bearing shear zones and Archean basin evolution; Canadian Journal of Earth Sciences, v. 23, p. 454-475.

Helmstaedt, H., Padgham, W.A., and Brophy, J.A.

1986: Multiple dikes in Lower Kam Group, Yellowknife greenstone belt: evidence for Archean sea-floor spreading?; Geology, v. 14, p. 562-566.

Henderson, J.B.

1985: Geology of the Yellowknife-Hearne Lake area, District of Mackenzie: a segment across an Archean basin; Geological Survey of Canada, Memoir 414.

Henderson, J.F.

1941: Gordon Lake south, District of Mackenzie, N.W.T.; Geological Survey of Canada, Map 645A.

Henderson, J.F. and Brown, I.C.

1966: Geology and structure of the Yellowknife greenstone belt, District of Mackenzie; Geological Survey of Canada, Bulletin 141, 87 p.

Kidd, R.G.W. and Cann, J.R.,

1974: Chilling statistics indicate an ocean-floor spreading origin for the Troodos Complex, Cyprus: Earth and Planetary Science Letters, v. 24, p. 151-155.

Kusky, T.M.

Are greenstones belts in the Slave Province, N.W.T., allochthonous?; in Workshop on the Tectonic Evolution of Greenstone Belts, Lunar and Planetary Institute, Houston (in press).

Lambert, M.B.

1977: Anatomy of a greenstone belt, Slave Province, Northwest Territories; Geological Association of Canada, Special Paper 16, p. 331-340.

1982: Synvolcanic intrusions in the Cameron River Volcanic Belt, District of Mackenzie; in Current Research, Part A, Geological Survey of Canada, Paper 82-1A, p. 165-167.

– Cameron River and Beaulieu River Archean volcanic belts, District of Mackenzie, N.W.T.; Geological Survey of Canada, Bulletin 349 (in press).

Walker, G.P.L.

1986: Koolau Dike Complex, Oahu: intensity and origin of a sheeted-dike complex high in a Hawaiian volcanic edifice: Geology, v. 14, p. 310-313.

The Clinton-Colden hornblende gabbro-anorthosite intrusion, Artillery Lake map area, District of Mackenzie

Project 840005

R.I. Macfie[1]
Lithosphere and Canadian Shield Division

Macfie, R.I., The Clinton-Colden hornblende gabbro-anorthosite intrusion, Artillery Lake map area, District of Mackenzie; in Current Research, Part A, Geological Survey of Canada, Paper 87-1A, p. 681-687, 1987.

Abstract

The Clinton-Colden hornblende gabbro-anorthosite occurs in the eastern Slave Province near the boundary with the Churchill Province. It intrudes mafic to felsic volcanic rocks of the Yellowknife Supergroup, and is intruded by diorites and granitoid rocks of presumed Archean age. It is irregularly zoned, grading from hornblende gabbro to anorthosite, with common hornblendite segregations. It typically consists of medium- to course-grained labradorite phenocrysts enclosed by large hornblende oikocrysts. Pyroxene does not occur. Minor dykes of pure anorthosite are common. Deuteric processes have resulted in albitization and growth of secondary amphibole. Most rocks have been affected by a long history of activity along the Thelon Tectonic Zone, which has produced dominantly north-northeast-trending shear zones and foliations.

The intrusion may represent a subvolcanic magma chamber. A sheet of similar hornblende gabbro to anorthosite occurs at the base of a mafic volcanic pile 10 km south.

Résumé

Le pluton de gabbro-anorthosite à hornblende de Clinton-Colden se trouve dans la province des Esclaves à proximité de la limite de la province de Churchill. Il pénètre des roches volcaniques mafiques à felsiques du super groupe de Yellowknife et est pénétré par des diorites et des roches granitoïdes probablement d'âge archéen. Il présente un rubanement irrégulier, et passe progressivement d'un gabbro à hornblende à une anorthosite, avec des ségrégations communes de hornblendite. Il est constitué d'une façon typique de phénocristaux moyens à grossiers de labradorite dont l'hôte est constitué de cristaux de hornblende. Le pyroxène est absent. Des dykes secondaires d'anorthosite pure sont communs. Des processus deutériques ont donné naissance à l'albitisation et à la croissance d'amphibole secondaire. La plupart des roches ont été déformées à la suite d'une longue activité suivant la zone tectonique de Thelon qui a donné naissance à des zones de cisaillement et à des foliations de direction principale nord-nord-est.

L'intrusion peut représenter une chambre magmatique subvolcanique. Une intercalation de gabbro à anorthosite à hornblende similaire se trouve à la base d'un amas de roches volcaniques mafiques à 10 km au sud.

[1]Ottawa-Carleton Centre for Geoscience Studies

INTRODUCTION

The Clinton-Colden hornblende gabbro-anorthosite intrusion (CHGA) lies in the southeastern part of the Slave Province near the boundary with the Churchill Province (Fig. 71.1). It was first recognized in 1984 during 1:250 000 scale mapping of the Artillery Lake map area (NTS 75 0, Henderson and Macfie, 1985). In 1986, mapping of the body was carried out at 1:14 000 to determine its petrogenetic significance, in particular the possibility of a genetic relationship between the intrusion and adjacent volcanic rocks of the Archean Yellowknife Supergroup.

REGIONAL GEOLOGICAL SETTING

The intrusion occurs approximately 30 km west of the western margin of the Thelon Tectonic Zone (Thompson and Henderson, 1983), the boundary between the Slave and Churchill structural provinces (Fig. 71.1). Within this 30 km zone a transition occurs from typical Slave Province geology (Yellowknife Supergroup supracrustal rocks intruded by lobate granitoid plutons) to the flattened heterogeneous rocks of the northeast-trending Thelon Tectonic Zone. The geology in the vicinity of the intrusion consists of weakly foliated intrusive rocks of varied composition and Yellowknife supracrustal rocks ranging in metamorphic grade from greenschist to amphibolite facies. The intrusions are of presumed Archean age and consist of granodiorite, biotite-muscovite granite, and diorite to gabbro plutons. In general, the geology of the region is typical of the Slave Province. However, structural and metamorphic effects related to the Thelon Tectonic Zone are apparent. Results of recent field work on the geology in the vicinity of the intrusion, and the nature and effects of the Thelon Tectonic Zone in this region, were presented by Henderson et al. (1987), Henderson and Macfie (1985, 1986), Henderson et al. (1982) and James (1985, 1986).

The CHGA intrudes volcanic rocks of the Yellowknife Supergroup to the northeast (Henderson and Macfie, 1985). To the south and east the CHGA is itself intruded by a body of heterogeneous dioritic rock. Both are in turn cut by a more extensive unit of Archean granitoid rock which varies from tonalite to granodiorite.

A similar occurrence of hornblende gabbro and anorthosite is found 10 km to the south, east of Ptarmigan Lake (Fig. 71.1), where a sheet of gabbro 9 km long and 5 km wide occurs at the base of a major mafic volcanic sequence (Henderson and Macfie, 1986). The hornblende gabbro is very poorly exposed and contact relations are unknown, but at a number of locations it is identical in all respects to the CHGA.

YELLOWKNIFE SUPERGROUP

The CHGA intrudes the southeast end of a belt of Yellowknife Supergroup metavolcanic and metasedimentary rocks which extends 40 km along the north side of Clinton-Colden Lake. Volcanic rocks within the belt are predominantly intermediate to mafic, and metamorphic grade ranges from greenschist to amphibolite facies (Henderson and Macfie, 1985; Henderson et al., 1982).

In the vicinity of the intrusion the volcanic rocks consist of pillowed and massive flows, breccias and finer volcaniclastic units (Henderson and Macfie, 1985). Significant felsic volcanic rocks are present. Units of volcanogenic metasediment, one of which is 500 m in width, make up less than 10% of the pile. Volcanic structures and top directions have commonly been obscured by later deformation. Mafic to felsic, massive and porphyritic feeder sills and dykes are very common in the volcanic sequence. A 3 m wide irregular intrusion of anorthosite, consisting of pure plagioclase, intrudes the volcanic rocks approximately 1 km north of the contact with the CHGA.

On the southeastern margin of the CHGA there occurs a 2 km wide unit of heterogeneous fine grained amphibolites and porphyritic dykes (Fig. 71.2). This unit is tentatively interpreted as deformed and metamorphosed volcanic rocks on the basis of their heterogeneous layered nature, the occurrence of porphyritic dykes identical to dykes in better preserved volcanic rocks, and the presence of schistose carbonate-rich layers which appear to be metasediments. It is strongly injected and agmatized by a variety of granodiorite, tonalite and diorite veins, dykes and sheets. Dykes of CHGA material cut the unit, and one can be followed from the main anorthosite body into the amphibolite unit.

Basement to the supracrustal rocks was not recognized as they are everywhere in contact with younger intrusive rocks.

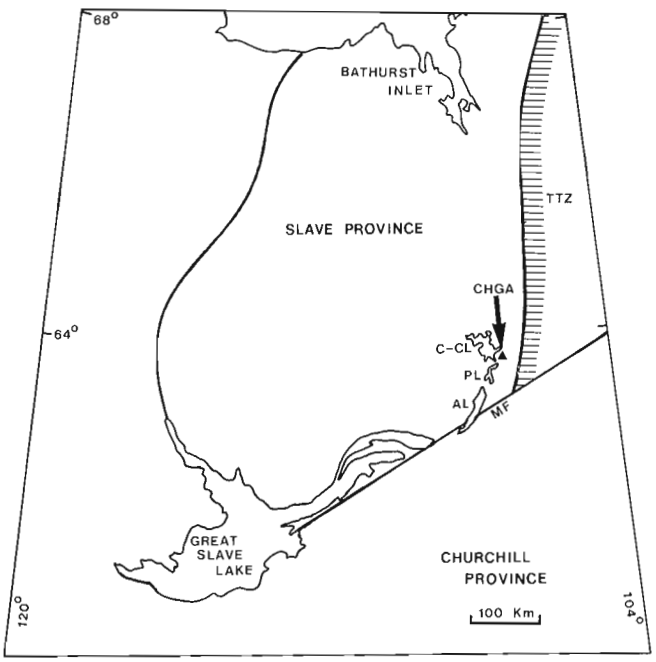


Figure 71.1. Location of the Clinton-Colden hornblende gabbro-anorthosite intrusion (CHGA). C-CL = Clinton-Colden Lake, PL = Ptarmigan Lake, AL = Artillery Lake, MF = McDonald Fault, TTZ = Thelon Tectonic Zone.

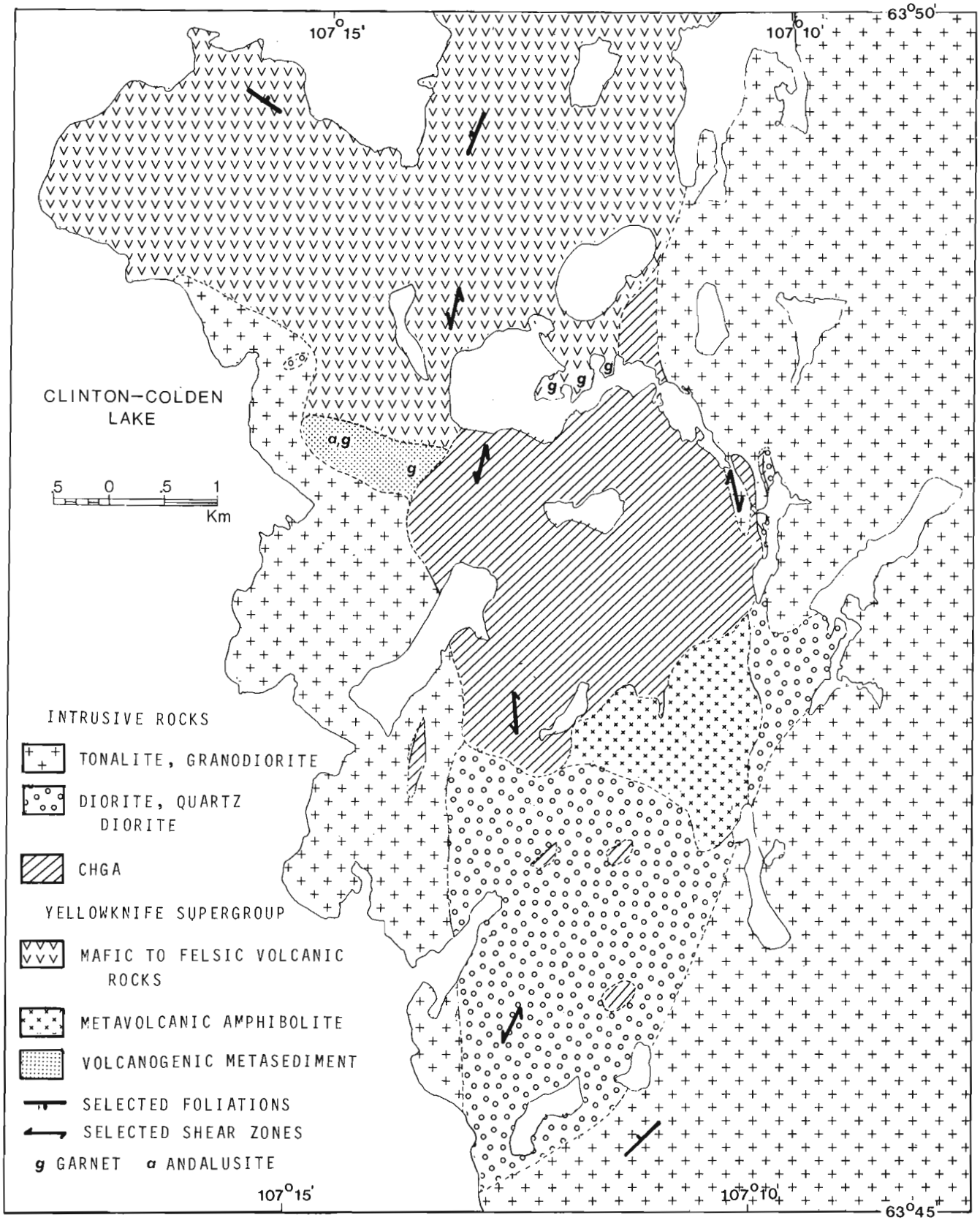


Figure 71.2. Generalized geology of the Clinton-Colden hornblende gabbro-anorthosite and vicinity.

CLINTON-COLDEN HORNBLENDE GABBRO-ANORTHOSITE INTRUSION

The intrusion is an elliptical body 4 km in length and 3 km in width (Fig. 71.2). Exposure is generally poor, although local areas of good outcrop exist. Contact relationships are apparent in most places.

Compositional variation

The CHGA consists of approximately 40% hornblende gabbro, 40% leucogabbro and 20% anorthosite. Compositional variation is a function of the percentage of interstitial hornblende in the rock. On a local scale variation is generally gradational and irregular (Fig. 71.3), and metre-scale zones of gabbro and anorthosite occur in all areas. Highly leucocratic zones are usually volumetrically minor, but several outcrop areas, up to 50 m wide, consist entirely of anorthosite to leucoanorthosite. These leucocratic zones may represent large anorthosite layers or dykes, as the largest such area does not appear to be transitional to gabbro. Small anorthosite and monomineralic anorthosite dykes, centimetres to metres wide, do occur in most areas.

Large-scale compositional variation across the pluton does exist, but it is less obvious than the small-scale variation, in part because of poor exposure. It consists of a subtle variation in average hornblende content in different sectors of the pluton, with leucogabbro dominating in the southeast, while in the north, sulphide- and magnetite-rich mafic gabbro is more common. The variation does not appear to represent simple layering, since zones are not traceable across the pluton.

A chilled margin may occur near the northern contact with volcanic rocks, where mafic-rich material dominates volumetrically, but compositional heterogeneity and the presence of leucocratic material suggest that the situation is complicated. The actual contact is not exposed in this area. In the southeast, where an intrusive contact with the heterogeneous amphibolitic unit is well exposed, a mafic chilled margin does not occur.

Mineralogy

Hornblende is dark green, and commonly occurs as large (often 10-20 cm in diameter) unrecrystallized oikocrysts enclosing euhedral labradorite phenocrysts up to 5 cm in length. Labradorite phenocrysts occasionally contain inclusions of hornblende oriented parallel to crystal faces (Fig. 71.4). Pyroxence has not been observed.

In nearly all cases plagioclase was the first major phase to crystallize, followed by interstitial hornblende. Irregular centimetre- to metre-scale hornblendite segregations occur within zones of leucogabbro and anorthosite (Fig. 71.5), perhaps representing concentration due to filter pressing. Centimetre-scale hornblendite veins also occur. Hornblendite segregations and mafic-rich gabbro zones are typically magnetite- and sulphide-rich, with pyrite constituting up to 5% of the rock.

Deuteric alteration

Plagioclase is extensively sericitized, although relatively fresh plagioclase is locally preserved. Hornblende is partly to completely altered to secondary amphibole in some samples. The presence of ubiquitous cross-cutting sets of millimetre-scale plagioclase veins (Fig. 71.6), which probably represent the filling of tension fractures developed during cooling, suggest that much of the alteration is deuteric. Fractures may

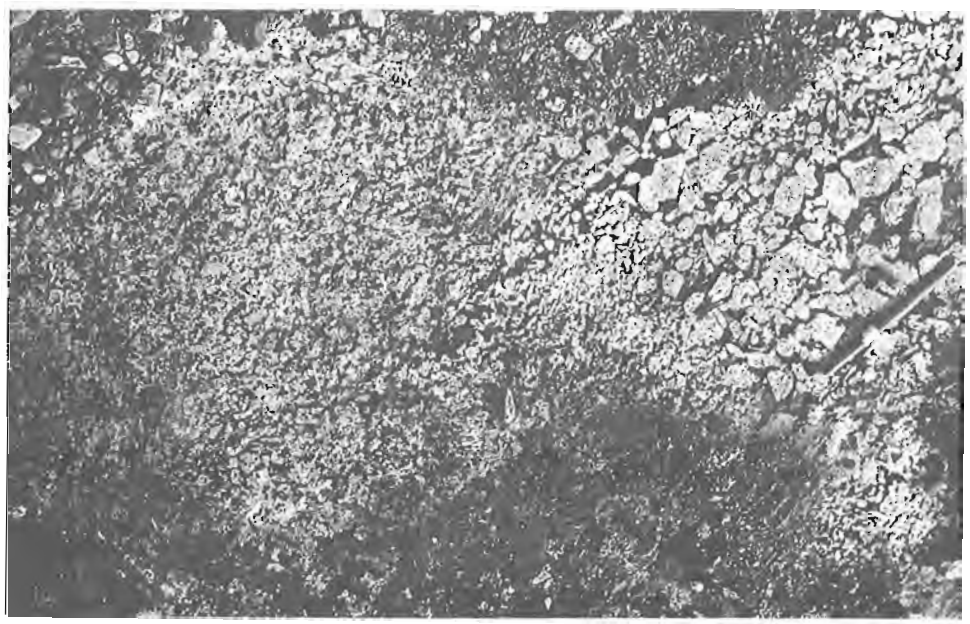


Figure 71.3. Textural variation in hornblende leucogabbro. Pen is 14 cm in length.

have served as channelways for albitizing and volatile-rich fluids responsible for plagioclase and amphibole recrystallization. A similar process has been suggested by Kamineni (1986) for the East Bull Lake anorthosite-gabbro complex. Centimetre-scale pods of fine grained epidote, plagioclase and bleached plagioclase and hornblende may also be products of deuteric processes.

DIORITE-QUARTZ DIORITE INTRUSION

An irregular but extensive body of dioritic rock, which consists of approximately 60% diorite, 35% quartz diorite and 5% mafic diorite or gabbro, lies to the south and east of the CHGA (Fig. 71.2). Unlike the CHGA, it appears to consist of multiple phases which are usually cross-cutting. These vary chiefly in grain size and in quartz content, which ranges from <1% to 10%. Such variation typically occurs on a scale of metres. Individual phases are homogeneous, with subtle to distinct cross-cutting contacts. This body is characterized in the field by a consistent colour index and dark-green amphibole. It is distinguishable from rocks of the CHGA on the basis of its consistent fine to medium grained equigranular texture, homogeneity of individual phases, and, above all, the presence of visible quartz. The main diorite body contains abundant inclusions of material derived from the CHGA, which is cut by diorite dykes. The diorite-quartz diorite has not undergone the extensive deuteric alteration which has



Figure 71.5. Mafic segregation (hornblende) in medium grained anorthosite.



Figure 71.4. Large plagioclase phenocrysts enclosed in coarse intercumulus hornblende. Plagioclase crystals contain hornblende inclusions oriented parallel to crystal faces.

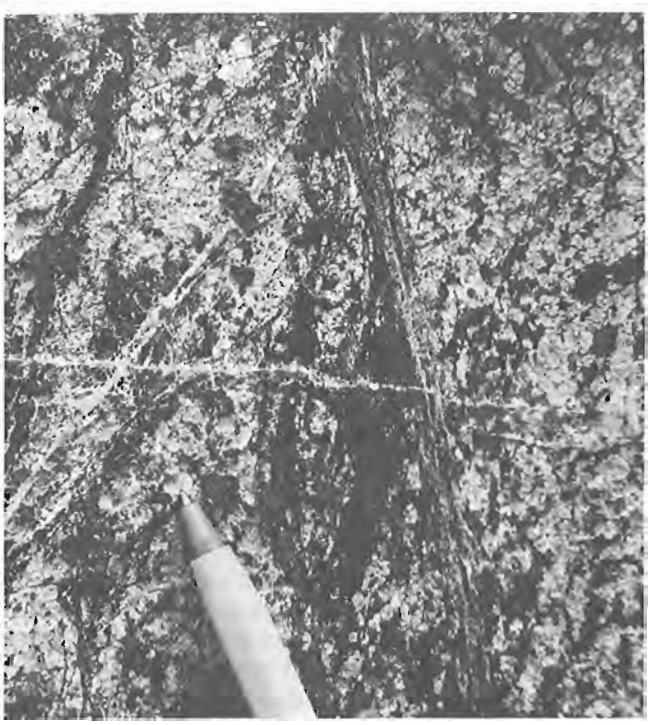


Figure 71.6. Albite and amphibole veinlets and a minor shear zone occurring in hornblende leucogabbro.

affected the CHGA. In particular, plagioclase-filled fracture sets and pods of altered and bleached rock, which are common in the CHGA, are absent in the diorite.

GRANITOID ROCKS

Much of the area adjacent to the CHGA is underlain by medium grained, equigranular granodiorite to tonalite, with minor granite (Fig. 71.2). In most places it contains approximately 10% biotite. Hornblende is commonly present, and locally makes up 20% of the rock. This unit appears to represent a single variable intrusion. Sharp contacts between phases have not been observed, except in the case of a sheet of cross-cutting coarse grained biotite granodiorite.

MAFIC DYKES

All of the above units are cut by 20-60 m thick foliated mafic dykes which trend approximately 090°. Two younger unfoliated dykes of the northwest-trending, 1200 Ma Mackenzie swarm occur in the area.

STRUCTURAL GEOLOGY

Apart from the Mackenzie dykes, all of the rocks of this area have undergone episodes of deformation which have produced dominantly north trending shear zones and foliations.

The oldest rocks in the area, those of the Yellowknife Supergroup, are flattened and are cut by ductile to cataclastic shear zones which trend northwest to northeast. The CHGA is cut by isolated and anastomosing centimetre- to metre-wide dominantly north-northeast-trending shears, which involve 5-10% of the pluton. Lineations are shallow-plunging, typically to the north. The pluton is otherwise undeformed. Most shears are ductile, but locally cataclastic deformation is apparent. The diorite-quartz diorite body is similarly deformed, though to a lesser degree. The granodiorite-tonalite unit shows a weak north-northeast-trending foliation. Rare metre-wide zones of greater deformation, occasionally mylonitic, also occur in this unit.

The general north-northeast trend of deformation features in this area suggests that they were produced during activity along the Thelon Tectonic Zone. Furthermore, there are indications of a long continuous, or punctuated, history of deformation. Older units bear the imprint of greater amounts of stress than do younger ones. Most noticeably, the granodiorite-tonalite unit is weakly foliated to undeformed, whereas volcanic rocks are strongly deformed and the CHGA is cut by abundant minor shears. Weakly foliated east-west dykes clearly truncate shear zones developed within the CHGA. One such dyke is foliated where it occurs in foliated granodiorite but is undeformed where it passes through the CHGA, though it cuts well developed shear zones in the latter. Evidently the CHGA shielded the dyke from late stress which produced a weak foliation in the granodiorite. Further evidence in support of long or repeated activity along the Thelon Tectonic Zone is summarized by Henderson et al. (1987).

The fact that the Mackenzie diabase dykes (Fahrig and West, 1986) are undeformed in this area indicates that deformation has ceased by 1200 Ma.

METAMORPHISM

In this area Yellowknife Supergroup rocks have been metamorphosed to amphibolite facies, as is apparent from the presence of abundant hornblende. East-west mafic dykes also show evidence of recrystallization. Contact metamorphic effects adjacent to the CHGA are apparent at several locations in the form of abundant garnet occurring in amphibolite, and at another in the form of andalusite and garnet which occur in volcanogenic metasediment (Fig. 71.2). Garnet and andalusite are observed only within 800 m of the contact with the CHGA.

Mackenzie diabase dykes have not been metamorphosed.

DISCUSSION

If the CHGA represents a sub-volcanic magma chamber intruding the volcanic pile in the Clinton-Colden Lake area, affinity between the intrusion and nearby mafic volcanic rocks may be geochemically demonstrable. Analysis of trace and rare earth element data from the package as a whole should cast light upon the nature of the magma source and upon the tectonic environment in which the rocks were produced. The evolution of the Slave Province and the origin of the Yellowknife Supergroup continue to be debated (e.g. Henderson, 1981; Padgham, 1985; Hoffman, 1986), and a major goal of this project is to determine whether a sialic rift environment (Henderson, 1981) or an oceanic arc environment (Folinsbee et al., 1968; Hoffman, 1986) best accounts for the chemical composition of these rocks.

The hornblende gabbro intrusion at Ptarmigan Lake may represent a second such sub-volcanic magma chamber, or a sill or dyke feeding the CHGA. Alternatively, the CHGA and the Ptarmigan Lake intrusion may be portions of a dyke which coincidentally intrudes older rocks of the Yellowknife Supergroup.

The rocks of the diorite-quartz diorite and granodiorite-tonalite units are also of interest with regard to the evolution of this part of the Slave Province. The presence of these presumed Archean intermediate and felsic intrusive phases may be of importance given the felsic components of the volcanic pile in this area (Henderson and Macfie, 1985).

Other Archean intrusions containing hornblende-bearing gabbro to anorthosite are known. For example, the Tessiuyakh gabbro complex of Labrador contains abundant green hornblende in pyroxene hornblendite, hornblende gabbro and anorthosite (Wiener, 1981). The Fiskenaesset anorthosite complex of west Greenland, which intrudes metavolcanic amphibolites, contains intercumulus hornblende in leucogabbro and anorthosite (Weaver et al., 1981). The CHGA contains more hornblende than do these bodies, and, unlike many other gabbroic intrusions (e.g. the East Bull Lake anorthosite gabbro complex, Kamenini, 1986), contains

abundant magmatic, rather than deuteric or younger, amphibole. It was volatile rich, and may be the product of a late stage of a fractionation process which is more fully represented in larger complexes. In any case, the origin of Archean plagioclase-rich intrusions is not well understood, and the CHGA presents an opportunity to study one such body in association with an Archean greenstone belt.

ACKNOWLEDGMENTS

The enthusiastic assistance of Natasha Wodicka (who mapped the volcanic rocks of the area as part of a B.Sc. thesis at the University of Ottawa) and Simon Leclair is gratefully acknowledged. J.B. Henderson provided useful advice, and A.E. Lalonde was of invaluable assistance during a visit in the field. Martin Irving supplied excellent expediting service. Critical review of this report was provided by J.B. Henderson, W.F. Fahrig and A.E. Lalonde.

REFERENCES

Fahrig, W.F. and West, T.D.
1986: Diabase dyke swarms of the Canadian Shield; Geological Survey of Canada, Map 1627A.

Folinsbee, R.E., Baadsgaard, H., Cumming, G.L. and Green, G.L.
1968: A very ancient island arc; American Geophysical Union, Geophysical Monograph 12, p. 441-448.

Henderson, J.B.
1981: Archean basin evolution in the Slave Province, Canada; in Precambrian Plate Tectonics, ed. A. Kroner; Elsevier, Amsterdam, p. 213-235.

Henderson, J.B., McGrath, P.H., James, D.T. and Macfie, R.I.
1987: The Artillery Lake map area and the Thelon Tectonic Zone – an integrated geological, Bouger gravity and magnetic study; in Current Research, Part A, Geological Survey of Canada, Paper 87-1A.

Henderson, J.B., Thompson, P.H. and James, D.T.
1982: The Healey Lake map area and the Thelon Front problem, District of Mackenzie; in Current Research, Part A, Geological Survey of Canada, Paper 82-1A, p. 191-195.

Henderson, J.B. and Macfie, R.I.
1985: The northern Artillery Lake map area: a transect across the Thelon Front, District of Mackenzie; in Current Research, Part A, Geological Survey of Canada, Paper 85-1A, p. 441-448.
1986: Artillery Lake map area, District of Mackenzie: a transect across the Thelon Front; in Current Research, Part A, Geological Survey of Canada, Paper 86-1A, p. 411-416.

Hoffman, P.F.
1986: Crustal accretion in a 2.7 Ga "granite-greenstone" terrane, Slave Province, NWT: a prograding trench-arc system; in GAC-MAC-CGU Program with Abstracts, v. 11, p. 82 (abstract).

James, D.T.
1985: Geology of the Moraine Lake area and the Thelon Front, District of Mackenzie; in Current Research, Part A, Geological Survey of Canada, Paper 85-1A, p. 191-195.
1986: Geology of the Moraine Lake area, District of Mackenzie; Part 2: a transect across part of the Thelon Tectonic Zone; in Current Research, Part A, Geological Survey of Canada, Paper 86-1A, p. 417-421.

Kamineni, D.C.
1986: A petrochemical study of calcic amphiboles from the East Bull Lake anorthosite-gabbro layered complex, District of Algoma, Ontario; Contribution to Mineralogy and Petrology, v. 93, p. 471-481.

Padgham, W.A.
1985: Observations and speculations on supracrustal successions in the Slave structural province; in Evolution of Archean Supracrustal Sequences, ed. L.D. Ayres, P.C. Thurston, K.D. Card and W. Weber; Geological Assocation of Canada, Special Paper #28, p. 133-151.

Thompson, P.H. and Henderson, J.B.
1983: Polymetamorphism in the Healey Lake map area – implications for the Thelon Tectonic Zone; in Current Activities Forum 1983, Program with Abstracts, p. 2-3 (abstract).

Weaver, B.L., Tarney, J. and Windley, B.
1981: Geochemistry and petrogenesis of the Fiskenaesset anorthosite complex, southern West Greenland: nature of the parent magma; Geochimica et Cosmochimica Acta, v. 45, p. 711-725.

Wiener, R.W.
1981: Tectonic setting, rock chemistry, and metamorphism of an Archean gabbro-anorthosite complex, Tessiuyakh Bay, Labrador; Canadian Journal of Earth Sciences, v. 18, p. 1409-1421.

Plutonic rocks in the Dawson map area, Yukon Territory

Project 840046

R. G. Anderson
Cordilleran and Pacific Margin Division, Vancouver

Anderson, R.G., Plutonic rocks in the Dawson map area, Yukon Territory; in Current Research, Part A, Geological Survey of Canada, Paper 87-1A, p. 689-697, 1987.

Abstract

Tombstone, Mt. Brenner and Antimony plutons in the Dawson map area comprise a crudely bimodal compositional suite. Mafic and basic or intermediate phases (hornblende clinopyroxenite, hornblende diorite, tinguaite, and biotite monzonite), quartz-poor felsic phases (hornblende and/or biotite alkali-feldspar syenite) and siliceous felsic phases (hornblende-biotite monzogranite) sequentially intrude Visean to Jurassic metasedimentary country rock and are post-tectonic.

In the Tombstone pluton, at least two phases of alkali-feldspar syenite intrusion occur. Uranium-base metal vein mineralization in tinguaite accompanies intrusion of the younger, more resistant, fluorite-bearing syenite phase.

Résumé

Les plutons de Tombstone, de Mont Brenner et d'Antimony de la région couverte par la carte de Dawson renferment une série de composition grossièrement bimodale. Des phases mafiques et basiques ou neutres (clinopyroxénite à hornblende, diorite à hornblende, tinguaïte, et monzonite à biotite), des phases felsiques pauvres en quartz (syénite à hornblende et à biotite ou les deux à la fois à feldspaths sodi-potassiques) et des phases felsiques siliceuses (granite monzonitique à hornblende-biotite) ont pénétré d'une manière séquentielle les roches encaissantes métasédimentaires allant du Viséen au Jurassique et sont post-tectoniques.

Dans le pluton de Tombstone, il existe au moins deux phases d'intrusion de syénite à feldspaths sodi-potassiques. La minéralisation de la veine en uranium-métaux communs, à l'intérieur de la tinguaïte, accompagne l'intrusion de la phase à syénite plus jeune, plus résistante et riche en fluorine.

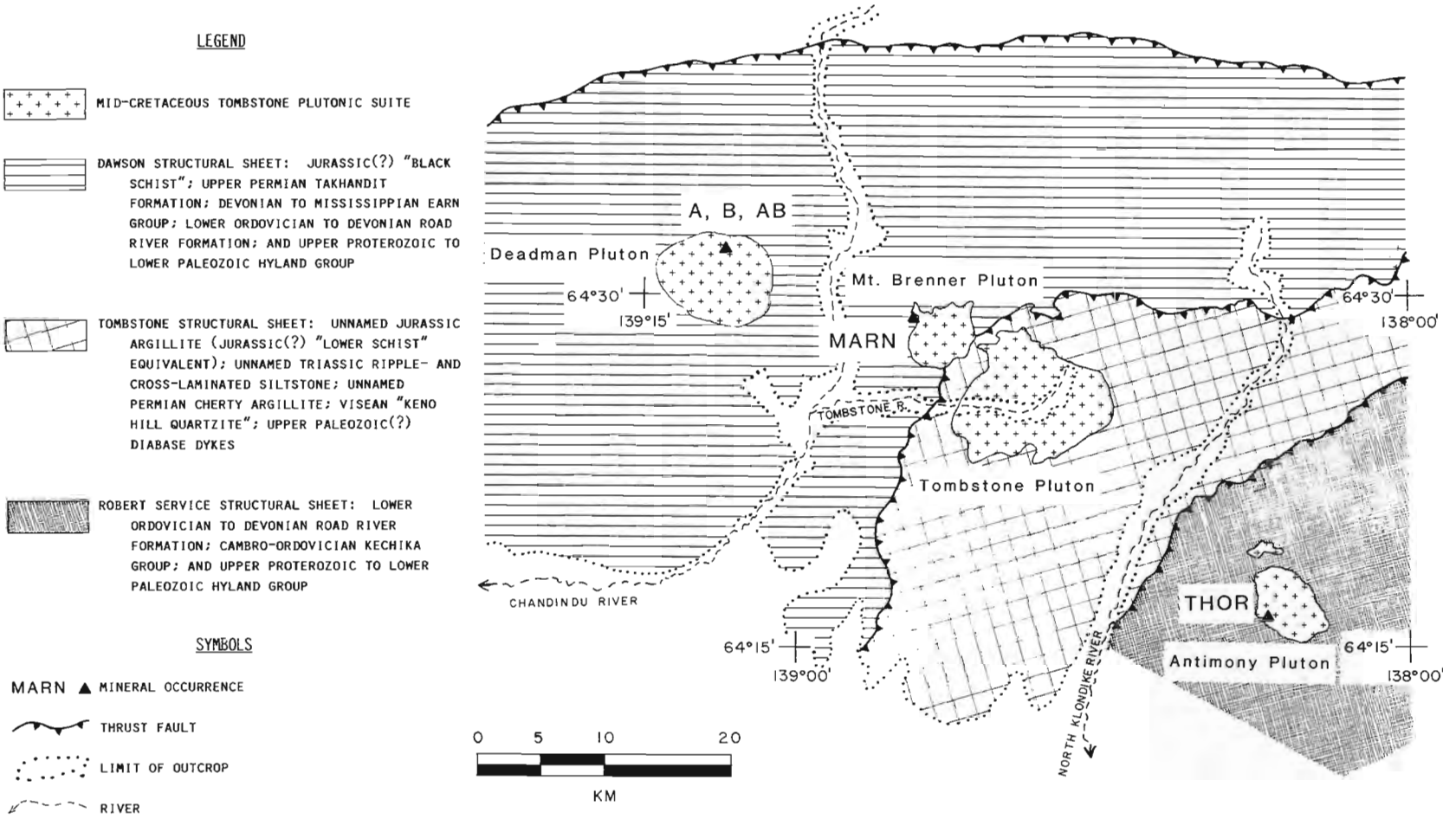


Figure 72.1. Location of the Deadman's Gulch, Tombstone, Mount Brenner and Antimony plutons of the Tombstone plutonic suite.

INTRODUCTION

Vein, skarn and disseminated F-U-Th-Sb-W-Sn-Mo-Ag-Au-base-metal occurrences within and around intrusions of the Tombstone plutonic suite have long been known and extensively sought after (Cockfield, 1919; Tempelman-Kluit, 1970, 1981; Green, 1972; Olade and Goodfellow, 1978; Sinclair et al., 1975; Morin et al., 1977, 1978; Emond, 1985).

Mapping and sampling of the Tombstone plutonic suite began in 1986 in collaboration with R.I. Thompson's revision of the regional geology of Dawson map area (116 B and C) (Project 800022; Thompson and Roots, 1982; Roots, 1983; Blaise and Mercier, 1984). Reconnaissance work in the Tombstone, Mt. Brenner and Antimony plutons (Fig. 72.1) was expedited by earlier, excellent mapping and geochemical work (Tempelman-Kluit, 1965, 1969, 1970, 1981; Lambert, 1966; Green, 1972; Olade and Goodfellow, 1978).

Details of the Tombstone intrusions' plutonic style (intrusive relations, geochronometry, and complementary mineralogical, geochemical and isotopic compositions) are relevant, not only as guides to the known granophile mineral potential, but also in comparisons with classic A-type granitoids (Collins et al., 1982; Anderson, 1985).

REGIONAL GEOLOGY

Rocks in the Dawson map area are the northwest extension of the foreland fold and thrust belt. Shallow water carbonate and clastic rocks having passive margin affinities and ranging in age from mid-Proterozoic to Jurassic have been telescoped northwards more than 100 km. The passive margin succession consists of five major time-stratigraphic sequences: Wernecke Supergroup (middle Proterozoic); Pinguicula Group (Middle Proterozoic?); Harper Group (Late Proterozoic); Lower Paleozoic shelf and off-shelf carbonates and clastics; and upper Paleozoic through Jurassic shelf and off-shelf carbonates and clastics. Each sequence was separated by a period of extension. Presumably, by Mesozoic time the crust had been substantially thinned. Tombstone plutonic suite intruded into and/or was generated from this thinned crust.

Country rock for the Tombstone and Mount Brenner plutons comprises rusty, contact metamorphosed equivalents of the Lower Carboniferous, grey to dark grey weathering, orthoquartzite and minor black slate of the "Keno Hill Quartzite" (Tempelman-Kluit, 1970; R.I. Thompson, personal communication, April, 1986). Upper Permian Takhandit Formation limestone hosts the MARN Cu-Ag skarn along the northwest margin of the Mount Brenner pluton. Chert and black shale of the Ordovician Road River Formation and black graphitic and phyllitic slate of the Jurassic(?) "Lower Schist" are also intruded by the Mount Brenner pluton (Fig. 72.5).

A thick, dark grey, inward-coarsening, hornblende diabase sill clearly intrudes and metamorphoses the "Keno Hill uartzite" near the southwestern margin of the Tombstone pluton (Figs. 72.5, 72.8a). The sill is intruded by antirapakivi-textured alkali-feldspar-porphyry syenite and appears fresher than the orange to brown weathering diorite and gabbro of Green's (1972) unit 20. Its position along the plutonic margin, intrusive relations, association with syenite porphyry apophyses and freshness suggest the diabase is not Paleozoic but may be related to the Tombstone pluton and is not thrust onto the "Keno Hill Quartzite". Similar dykes restrict Cu-Au skarns on the MARN property along pluton northwestern margin at Mount Brenner pluton.

The Antimony pluton intrudes Late Proterozoic to Eocambrian "grit unit" coarse clastics and Cambro-Ordovician Kechika Group calcareous slate and slaty limestone (Green, 1972; Tempelman-Kluit, 1981).

The Tombstone plutonic suite intruded rocks occupying the three extensive structural sheets northeast of the Tintina Trench, north to south: Dawson, Tombstone and Robert Service sheets. The intrusions crosscut some Mesozoic thrust faults and are considered post-tectonic. Deformation of coeval (Cenomanian) strata of the Monster Formation to the northwest (Ricketts, in press) suggests that postintrusion deformation has displaced the plutons from their source.

GEOLOGY OF THE PLUTONS

Plutons in the Dawson map area are circular to subcircular stocks (20-90 km^2) underlain predominately by massive to trachytoid, medium- to coarse-grained alkali-feldspar syenite. Hornblende clinopyroxenite, hornblende diorite, biotite monzonite and hornblende-biotite monzogranite are petrologically important but subordinate phases. Rocks of intermediate composition (e.g., monzodiorite, granodiorite) are rare and the suite is crudely bimodal. Mafic, geochemically basic to intermediate phases (hornblende clinopyroxenite, hornblende diorite, tinguaite, and biotite monzonite) are subordinate to quartz-poor salic (hornblende and/or biotite alkali-feldspar syenite) and siliceous felsic phases.

An economically important variety of the basic end member is tinguaite (feldspathoid syenite) in the Tombstone and Deadman's Gulch plutons (Morin et al., 1977). White, coarse, equant pseudoleucite (nepheline-alkali-feldspar intergrowth) phenocrysts in a dark grey, fine grained matrix characterize the rock (Fig. 72.2a; Tempelman-Kluit, 1969, 1970). In the Tombstone pluton, disseminated U mineralization, anomalously high F contents, and anomalous radioactivity is associated with the tinguaite (Morin et al., 1977; Olade and Goodfellow, 1978); U and Th mineralization are associated with the multiphase Deadman's Gulch pluton (Morin et al., 1977). Locally, the tinguaite is thinly layered and contains "dropstones" of coarsely porphyritic tinguaite which disrupt layering (Fig. 72.2b). Vein U mineralization in the tinguaite (Olade and Goodfellow, 1978) is probably associated with a specific period of alkali-feldspar syenite intrusion in the Tombstone batholith.

A biotite-clinopyroxene marginal phase is common to the Mount Brenner and Antimony plutons (Fig. 72.3). Cu-Au skarn at the MARN property on northwest margin of Mount Brenner pluton occurs near marginal phase aegerine-augite monzonite and garnetiferous biotite diorite and crosscutting radioactive porphyritic syenite, pyroxenite and biotite lamprophyre dykes (Tempelman-Kluit, 1981). However, it is

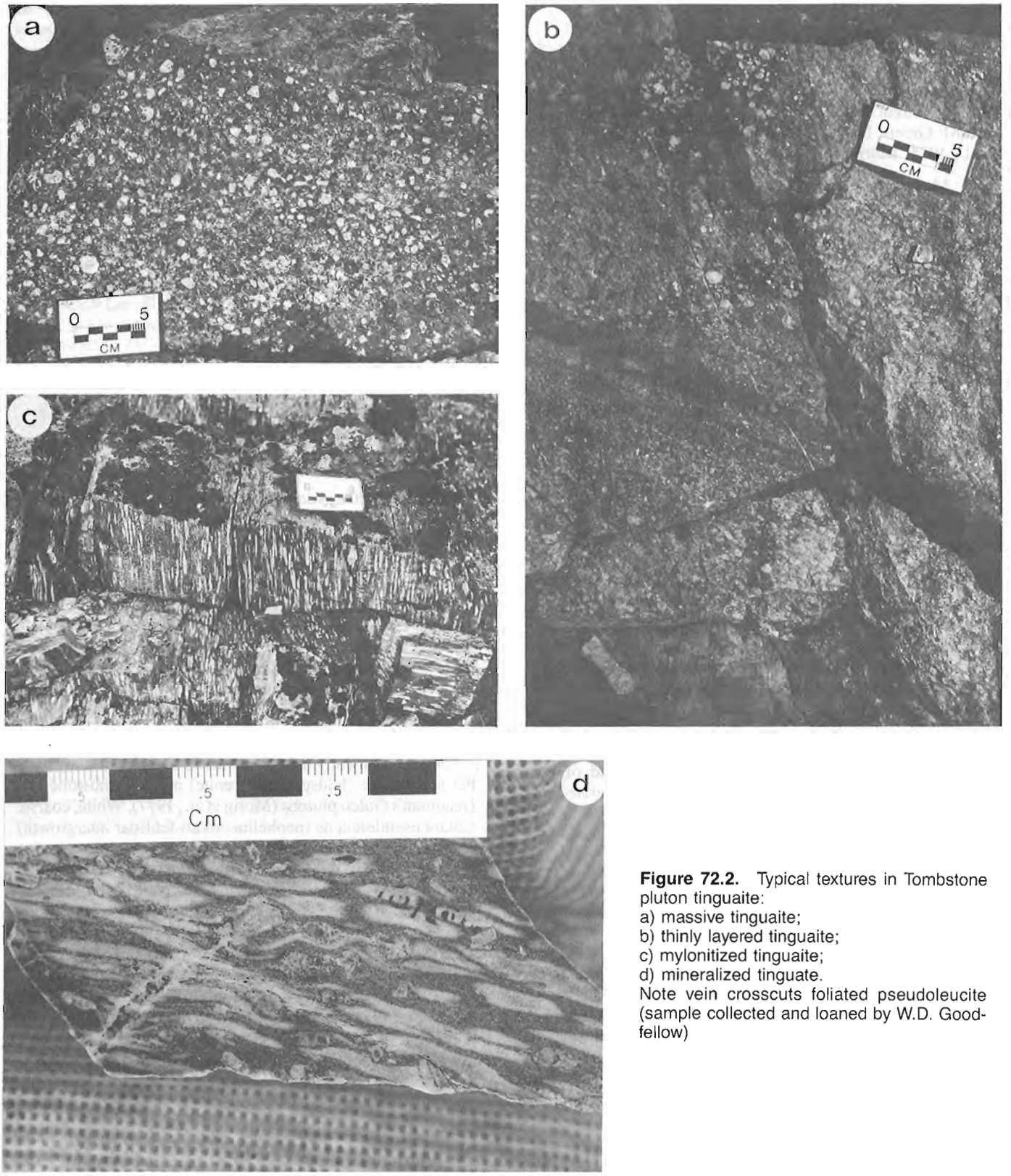


Figure 72.2. Typical textures in Tombstone pluton tinguaite:
a) massive tinguaite;
b) thinly layered tinguaite;
c) mylonitized tinguaite;
d) mineralized tinguate.
Note vein crosscuts foliated pseudoleucite (sample collected and loaned by W.D. Goodfellow)

confined by subparallel, locally thick, northwest-trending diorite sills (Emond, 1985). Gold veins along the northwestern (THOR property) and eastern margins of the Antimony pluton occur near its marginal biotite-clinopyroxene monzonite phase (Tempelman-Kluit, 1981).

Alkali feldspar syenite is the most texturally heterogeneous phase; medium- and coarse-grained, equigranular and megacrystic and porphyritic varieties occur. Alkali feldspar outlines foliation and lineation trends which mimic plutonic margins and concentric distribution of phases (Lambert, 1966). The fabric suggests intrusion of the plutons as nearly consolidated diapirs. Alkali feldspar syenite and monzogranite are inclusion-free and leucocratic (Fig. 72.4). Hornblende and biotite, euhedral in mafic and siliceous compositions, are distinctly interstitial with respect to euhedral feldspar grains in alkali-feldspar syenite.

In general, phases were intruded in a mafic to felsic sequence radially inward from and concentric with the pluton margins (Lambert, 1966; Tempelman-Kluit, 1970; see Figure 72.5). Dykes are rare or absent and are mostly fine grained, aplitic alkali-feldspar syenite or granite.

Alkali feldspar syenite intruded before and after tinguaite intrusion in southwestern Tombstone pluton (southwest of Tombstone Mountain). The younger syenite intrusion appears to control vein U and vuggy Cu mineralization (Figure 72.5). Older alkali-feldspar syenite is recessive and forms small, castellate outcrops along the southwestern pluton margin (Fig. 72.6). The compositionally similar but more resistant younger alkali-feldspar syenite forms the imposing landscape for which the Tombstone Mountains are renowned. It is distinguished by rare but widespread titanite (sphene) and purple or pink fluorite accessory minerals (Fig. 72.7). At the contact with the older alkali-feldspar syenite, tinguaite is fine grained and aphanitic. The older alkali-feldspar syenite locally contains pseudoleucite "porphyroblasts" and alkali-feldspar phryic syenite dykes. Within several tens of metres of the contact, pseudoleucite phenocrysts first appear and increase in size and abundance away from the contact. About one-half kilometre from the contact with the younger alkali-feldspar syenite, the tinguaite becomes a L-S tectonite within a series of discrete, easterly-trending shear zones which parallel the contact (Fig. 72.2c). Common, massive, fine-grained alkali-feldspar syenite apophyses crosscut the mylonitized tinguaite at the contact (Fig. 72.8b). Vein-uranium mineralization in the tinguaite also crosscuts the tinguaite's foliation (Olade and Goodfellow, 1978, Plate 1; see also Fig. 72.2d). Miarolitic cavities in the younger alkali-feldspar syenite near the tinguaite contact contain chalcopyrite and arsenopyrite.

Three lines of evidence favour the association of the younger alkali-feldspar syenite phase with vein-U mineralization. Deformation of the tinguaite is restricted to its northern contact with the younger alkali-feldspar syenite. Geometry, timing and structural setting of vein U mineralization and the younger alkali-feldspar syenite with respect to the deformed tinguaite are similar. Olade and Goodfellow (1978) noted the metallogenetic significance of correlated high U and F contents in the tinguaite and the transport of U in fluorine-rich melts. Deformed tinguaite near contacts with intrusive fluorite-bearing syenite would be a prime exploration target for U mineralization.

AGE

The Jurassic(?) "Lower Schist" country rock provides the only stratigraphic limit on the oldest age of the Tombstone plutonic suite. Concordant mid-Cretaceous isotopic ages are indicated for hornblende (82 ± 13 Ma) and biotite (93 ± 5 Ma) from quartz monzonite in the northeastern part of Tombstone pluton (Wanless et al., 1968, p. 54; Tempelman-Kluit, 1970, p. 41, 98).

DISCUSSION

The Tombstone intrusions exhibit a unique plutonic style and metallogenesis compared with other coeval, mid-Cretaceous granitoids of the Selwyn Plutonic Suite northeast of the Tintina Trench (Anderson, 1983, 1985; Pigage and Anderson, 1985).

Although both suites are post-tectonic, the history of the crust into which they were emplaced or generated differs. Tombstone intrusions were emplaced into crust which had undergone at least two of the four extensional episodes envisaged for the creation of the Cordilleran miogeocline (Thompson et al., in press).

Plutonism in the Selwyn mountains postdated effects of the extensive arc-continent collision seen in the southeastern Yukon (Tempelman-Kluit, 1979; Anderson et al., 1983). Selwyn Plutonic Suite granitoids intruded miogeoclinal rocks for which there is evidence only for the last (370-180 Ma) extensional event (S. Gordey, personal communication, 1986). Anvil batholith plutonism was syn- to post-tectonic with Buchan-type regional metamorphism and the second phase of deformation (Pigage and Anderson, 1985).

If the sparse geochronometry approximate the intrusion age of the Tombstone plutonic suite at about 90 Ma, this event represents the latest occurrence in the cyclical 200 million year extensional history in the Dawson map area since about 800 Ma. Protracted crustal extension must have had an important effect on the heat source for melting, protolith melted, and resultant bimodal composition of the plutons.

Tombstone plutonic suite alkali-feldspar syenite is alkali-feldspar-rich and crudely bimodal compared to the homogeneous monzogranite and granodiorite of the Selwyn Plutonic Suite. It is equally leucocratic but is predominantly hornblende- and linopyroxene-bearing and contains titanite (sphene), uncommon magnetite and fluorite as widespread accessory minerals. Two-mica monzogranite containing peraluminous accessory minerals is not recognized in the Tombstone plutonic suite.

Disseminated, vein and skarn occurrences within and around intrusions of the Tombstone plutonic suite, which

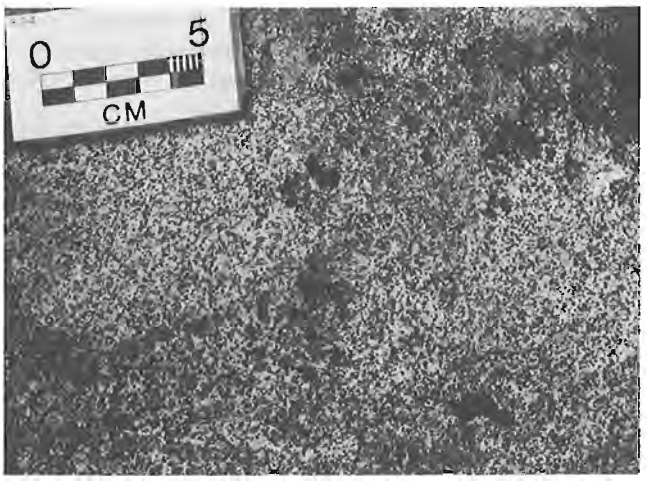


Figure 72.3. Biotite-clinopyroxene monzonite phase of Antimony pluton.



Figure 72.4. Hornblende-biotite monzogranite in eastern Tombstone pluton.

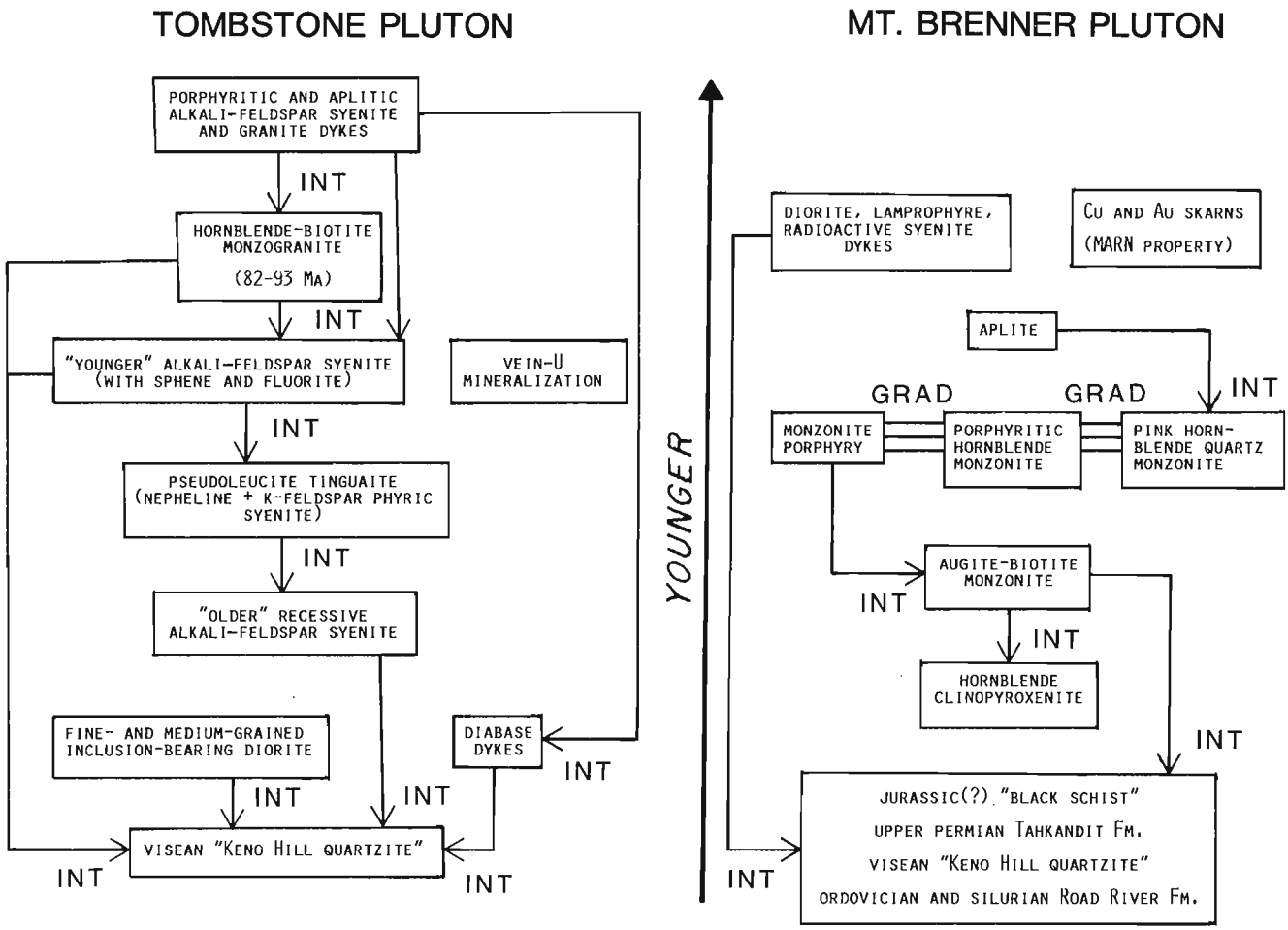


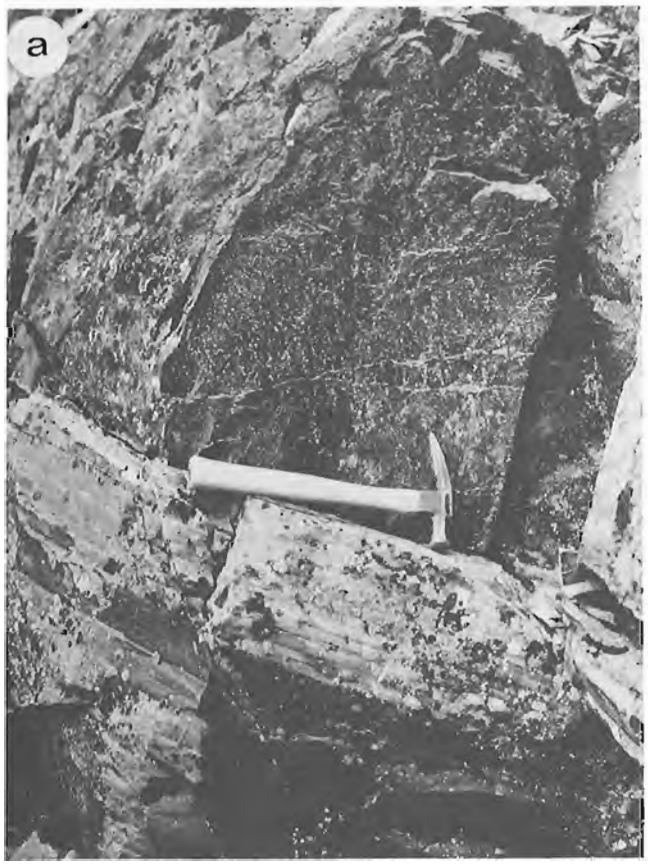
Figure 72.5. Intrusive relations for the Mt. Brenner and Tombstone plutons. Abbreviations are: "GRAD" = gradational contact; "INT" = sharp, intrusive contact.



Figure 72.6. Castellate outcrops of recessive, older alkali-feldspar syenite southwest of Tombstone Mountain. Figure gives 1.8 m scale.



Figure 72.7. Fluorite (F)-bearing, younger alkali-feldspar syenite at eastern margin of Tombstone pluton. Note interstitial biotite.



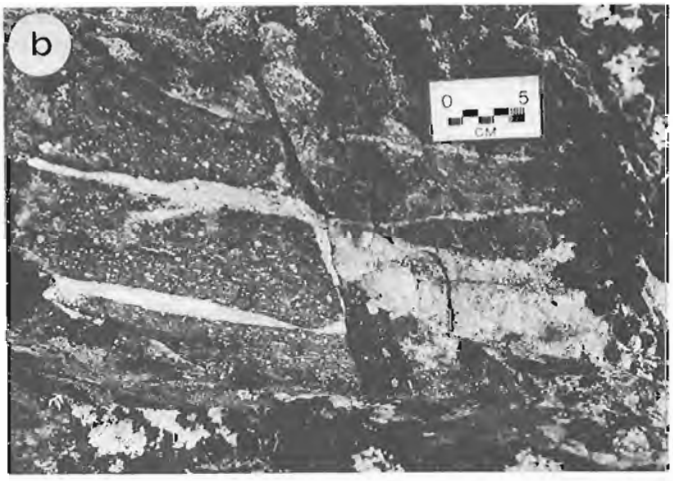


Figure 72.8. Intrusive relations in Tombstone pluton: a) intrusive contact of diabase sill (above hammer) and compositionally layered quartzite; b) apophyses of younger alkali-feldspar syenite in deformed tinguaite.

contain F, U, Th, Sb, W, Sn, Mo, Ag, Au and base metals, are unlike the important W-Cu (Pb-Zn-Mo) skarn deposits associated with peraluminous phases of the Selwyn Plutonic Suite (Dick and Hodgson, 1982; Anderson, 1983).

Selwyn Plutonic Suite plutons similar to but more siliceous than the Tombstone plutonic suite are the Emerald Lake pluton (Smit et al., 1985) and O'Grady batholith (Anderson, 1983). They comprise extensive, alkali-feldspar-megacrystic granite and quartz syenite phases, and are associated with Cu-Mo-Bi-W-Au-Sb-bearing veins, vugs and skarns.

Tectonic setting, composition, and associated mineralization of the Tombstone plutonic suite is closely similar to classic A-type plutonism described by Collins et al. (1982) and represents the closest Cordilleran analog to this series (Anderson, 1985; in press).

CONCLUSIONS

Crudely bimodal, extensive salic or felsic (alkali-feldspar syenite and monzogranite) and minor basic (clinopyroxenite, tinguaite, monzonite) phases constitute subcircular, granitic diapirs of the Tombstone plutonic suite. Vein-type-U mineralization in deformed tinguaite of the Tombstone pluton accompanies intrusion of a younger, fluorite-bearing alkali-feldspar syenite.

ACKNOWLEDGMENTS

The impetus for this study arose from compilations for the Decade of North America volume on the Canadian Cordillera and was achieved through the cooperation of R.I. Thompson (Project 820020) and logistical support from D. Morrow's field camp (Project 850031). M. Andrews provided cheerful, energetic and conscientious assistance in the field. Constructive comments by R.I. Thompson improved the manuscript.

REFERENCES

Anderson, R.G.

1983: Selwyn plutonic suite and its relationship to tungsten skarn mineralization, southeastern Yukon and District of Mackenzie; in Current Research, Part B, Geological Survey of Canada, Paper 83-1B, p. 151-163.

1985: An overview of some Mesozoic and Tertiary plutonic suites and their associated mineralization in the northern Cordillera; (extended abstract) in R.P. Taylor and D.F. Strong (editors), Granite-related Mineral Deposits, Geology, Petrogenesis, and Tectonic Setting, Extended Abstracts of Papers prescuted at C.I.M. Conference on Granite Related Mineral Deposits, Sept. 15-17, C.I.M. Geology Division, p. 1-20.

in press: An overview of some Mesozoic and Tertiary plutonic suites and their associated mineralization in the northern Cordillera; in R.P. Taylor and D.F. Strong (editors), Recent Advances in the Geology of Granite-related Mineral Deposits, Canadian Institute of Mining and Metallurgy, Special Volume 39.

Anderson, R.G., Armstrong, R.L., Parrish, R., and Bowman, J.R.

1983: Potential of SE Selwyn plutonic suite for W-skarn deposits; (abstract), Geological Association of Canada, Program with Abstracts, v. 8, p. A2.

Blaise, B. and Mercier, E.

1984: La sedimentation au Precambrien superieur et au Paleozoique inferieur sur la marge de la plate-forme du Mackenzie (Monts Ogilvie), Territoire du Yukon; in Current Research, Geological Survey of Canada, Paper 84-1B, p. 85-92.

Cockfield, W.E.

1919: The silver-lead deposits of the Twelvemile area, Yukon; Geological Survey of Canada, Summary Report, 1918, Part B, p. 15B-17B.

Collins, W.J., Beams, S.D., White, A.J.R., and Chappell, B.W.

1982: Nature and origin of A-type granites with particular reference to southeastern Australia; Contributions to Mineralogy and Petrology, v. 80, p. 189-200.

Dick, L.A. and Hodgson, C.J.

1982: The MacTung W-Cu(Zn) contact metasomatic and related deposits of the northeastern Canadian ordillera; Economic Geology, v. 77, no. 4, p. 845-867.

Emond, D.

1985: MARN property; Department of Indian and Northern Affairs, Yukon Exploration and Geology 1983, p. 278-279.

Green, L.H.

1972: Geology of Nash Creek, Larsen Creek and Dawson map-areas, Yukon Territory; Geological Survey of Canada, Memoir 364, 157 p.

Lambert, M.R.

1966: Geology of the Mount Brenner stock near Dawson City, Yukon Territory; unpubl. M.Sc. thesis, University of British Columbia, 64 p.

Morin, J.A., Marchand, M., Craig, D.B., and Debicki, R.L.

1978: Mineral Industry Report, 1977, Yukon Territory, Department of Indian and Northern Affairs, EGS 1978-9, p. 53-55.

Morin, J.A., Sinclair, D., Craig, D.B., and Marchand, M.,

1977: Mineral Industry Report, 1976, Yukon Territory, Department of Indian and Northern Affairs, EGS 1977-1, p. 140-143.

Olade, M.A. and Goodfellow, W.D.

1978: Lithogeochemistry and hydrogeochemistry of uranium and associated elements in the Tombstone batholith, Yukon, Canada; in Proceedings of the 7th International Geochemical Symposium, Golden, Colorado, ed. by J.R. Watterson and T.K. Theobold, Association of Exploration Geochemists, p. 407-428.

Pigage, L.C. and Anderson, R.G.

1985: The Anvil plutonic suite, Faro, Yukon Territory; Canadian Journal of Earth Sciences, v. 22, p. 1204-1216.

Ricketts, B.D.

in press: The Monster Formation: A coastal fan system of Late Cretaceous age, Yukon; Geological Survey of Canada, Paper 86-14.

Roots, C.F.
1983: Mount Harper complex, Yukon: early Paleozoic volcanism at the margin of the Mackenzie Platform; in Current Research, Part A, Geological Survey of Canada, Paper 83-1A, p. 423-427.

Sinclair, W.D., Maloney, J.M., and Craig, D.B.
1975: Mineral Industry Report, 1974, Yukon Territory, Department of Indian and Northern Affairs, EGS 1975-9, p. 73.

Smit, H., Armstrong, R.L., and van der Heyden, P.
1985: Petrology, chemistry and radiogenic isotope (K-Ar, Rb-Sr and U-Pb) study of the Emerald Lake pluton, eastern Yukon Territory; in Current Research, Part B, Geological Survey of Canada, Paper 85-1B, p. 347-359.

Tempelman-Kluit, D.J.
1965: Tombstone River (116 B/7) map-area; in Report of Activities, Field, 1964; Geological Survey of Canada, Paper 65-1, p. 35-36
1969: A re-examination of pseudoleucite from Spotted Fawn Creek, west-central Yukon; Canadian Journal of Earth Sciences, v. 6, p. 55-62.
1970: Stratigraphy and structure of the "Keno Hill Quartzite" in Tombstone River-Upper Klondike River map-areas, Yukon Territory (116 B/7, B/8); Geological Survey of Canada, Bulletin 180, 102 p.
1979: Transported cataclastite, ophiolite and granodiorite in Yukon: Evidence of arc-continent collision; Geological Survey of Canada, Paper 79-14, 27 p.
1981: MARN property; Yukon Geology and Exploration 1979-80, Department of INdian and Northern Affairs, p. 287-288.

Thompson, R.I. and Eisbacher, G.H.
1984: Late Proterozoic rift assemblages, northern Canadian Cordillera; (abstract), Geological Society of America, Abstracts with Programs, v. 16, no. 5, p. 336.

Thompson, R.I., Mercier, E., and Roots, C.F.
in press: Extension and its influence on Canadian Cordilleran passive-margin evolution; in M.P. Coward,, J.F. Dewey, and P.L. Hancock, (eds.), Continental Extensional Tectonics, Geological Society of London, Special Publication.

Thompson, R.I. and Roots, C.F.
1982: Ogilvie Mountains project, Yukon; Part A: A new regional mapping program; in Current Research, Part A, Geological Survey of Canada, Paper 82-1A, p. 403-414.

Wanless, R.K., Stevens, R.D., Lachance, G.R., and Edmonds, C.M.
1968: Age determinations and geological studies, K-Ar isotopic ages, Report 8; Geological Survey of Canada, Paper 67-2, Part A, p. 54.

Geological investigations in Calder River map area, central Wopmay Orogen, District of Mackenzie

Project 860002

R.S. Hildebrand, S.A. Bowring[1], K.P.E. Andrew[2], S.F. Gibbins[3], and G.C. Squires[4]
Lithosphere and Canadian Shield Division

Hildebrand, R.S., Bowring, S.A., Andrew, K.P.E., Gibbins, S.F., and Squires, G.C., Geological investigations in Calder River map area, central Wopmay Orogen, District of Mackenzie; in Current Research, Part A, Geological Survey of Canada, Paper 87-1A, p. 699-711, 1987.

Abstract

Rocks along the eastern Great Bear magmatic zone unconformably overlie 1.90 Ga granite and inferred Archean granite, both of which are locally mylonitized. Preliminary analysis of kinematic indicators within the mylonites suggests northward directed top over bottom movement between 1.90 Ga, the age of the granite that is deformed, and 1.875 Ga, the age of a tuff intercalated with sedimentary rocks that unconformably overlie the mylonites. Rocks of the Great Bear magmatic zone and its basement were folded just prior to, or during transcurrent faulting. When the folds are restored, the mylonitic rocks extend over a width of about 20 km orthogonal to transport direction, suggesting that the zone was never steeply dipping but more likely a nearly horizontal sheet. Stubby westward-thinning wedges of conglomerate within basal Great Bear sections indicate minor west-side down faulting during sedimentation and volcanism. Pre-folding plutonic rocks of the Great Bear zone typically progress from intermediate to siliceous with respect to time. A major unresolved problem is whether Archean granitoids of the Wompay fault zone were once part of Slave Craton or formed part of Hottah terrane.

Résumé

Les roches bordant l'est de la zone magmatique du Grand lac de l'Ours, recouvrent en discordance un granite de 1,90 Ga et un granite archéen hypothétique; tous deux sont localement mylonitisés. L'analyse préliminaire des indicateurs cinématiques présents dans les mylonites suggère qu'il y a eu un mouvement vers le nord des couches supérieures entre 1,90 Ga, l'âge du granite déformé, et 1,875 Ga, l'âge d'un tuf intercalé avec des roches sédimentaires recouvrant les mylonites en discordance. Les roches de la zone magmatique du Grand lac de l'Ours et du soubassement de cette zone ont été plissées immédiatement avant, ou durant l'apparition des failles de décrochement. Lorsque les plis sont reconstitués, on voit que les roches mylonitiques occupaient une largeur d'environ 20 km perpendiculairement à la direction de transport, ce qui suggère que cette zone n'a jamais été fortement inclinée, mais formait plus probablement une nappe subhorizontale. Les prismes courts et épais de conglomérat s'amincissant vers l'ouest, à l'intérieur des coupes de terrain basales du Grand lac de l'Ours, indiquent que durant les étapes de sédimentation et de volcanisme, a eu lieu un faillage normal, avec affraissement du compartiment ouest. Les roches plutoniques de la zone du Grand lac de l'Ours antérieures au faillage, passent en général de façon graduelle d'un type intermédiaire à un type siliceux, selon une progression ascendante. Un important problème encore non résolu est de savoir si les granitoïdes archéens de la zone faillée de Wopmay faisaient autrefois partie du Craton du Grand lac des Esclaves, ou du terrain exotique (terrane) de Hottah.

[1]Department of Earth and Planetary Sciences, Washington University, St. Louis, Missouri, 66130, USA
[2]Department of Geological Sciences, University of British Columbia, Vancouver, British Columbia, V6T 2B4
[3]Department of Geology, Carleton University, Ottawa, Ontario, K1S 5B6
[4]Department of Earth Sciences, Memorial University of Newfoundland, St. John's, Newfoundland, A1B 3X5

INTRODUCTION

The Calder River map area (86F) straddles three major tectonic zones of Wopmay Orogen, from east to west: Hepburn metamorphic-plutonic zone, Wopmay fault zone and Great Bear magmatic zone, about three quarters of the area being occupied by rocks of the Great Bear magmatic zone (Fig. 73.1). In recent years, St-Onge et al. (1982, 1983, 1984) mapped the adjoining area to the east (86G); Hildebrand et al. (1983, 1984; Hildebrand and Roots, 1985) mapped the area to the west (86E); and Bowring (unpublished data) mapped much of the area immediately west of the Wopmay fault zone within the Calder River area. Lord and Parsons (1947) and McGlynn (1974, 1976) mapped the Calder River area itself and recognized several distinct packages of rocks; however, their mapping was of insufficient detail to mesh the complex volcanic, sedimentological, plutonic, and tectonic history with that from the recent, more detailed, studies of adjoining areas. Thus, this project concerned mainly with the geology west of the Hepburn metamorphic-plutonic zone, will complete the central transect of Wopmay Orogen.

This progress report summarizes the results of: (1) geological mapping carried out by SAB and assistants during the 1983 field season; (2) geological mapping by RSH, SAB, KPEA, SFG and GCS during the 1986 field season; and (3) geochronology done by SAB during the fall of 1986. Although this work has yielded a considerable body of data, at the same time it has generated new questions, many of which remain unanswered. We highlight the following main points.

1) In the northern half of the map area the boundary between the Great Bear magmatic zone and the Wopmay fault zone is an unconformity. Rocks of the Great Bear magmatic zone unconformably overlie both mylonitized and non-mylonitized granitic rocks of inferred Archean age.

2) Mylonites of the Wopmay fault zone and rocks of the eastern Great Bear magmatic zone were folded about north-south axes prior to, or during, transcurrent faulting.

3) Rocks of 1.90 Ga occur beneath the eastern Great Bear magmatic zone just west of the Wopmay fault zone and are in apparent fault contact with inferred Archean granites of the Wopmay fault zone beneath a major syncline of Dumas Group, the easternmost supracrustal sequence of the Great Bear magmatic zone. This implies that the majority of movement on the brittle faults that characterize the Wopmay fault zone predates the Dumas Group.

4) Mylonites, perhaps related to those of the Wopmay fault zone, occur several kilometres west, within the Great Bear magmatic zone, where they affect the 1.90 Ga basement.

5) The 7-10 km east-west extent of the mylonites, and the fact that they are folded, both suggest that they formed a near horizontal to gently dipping, sheet or braided system when the Dumas Group was deposited on them.

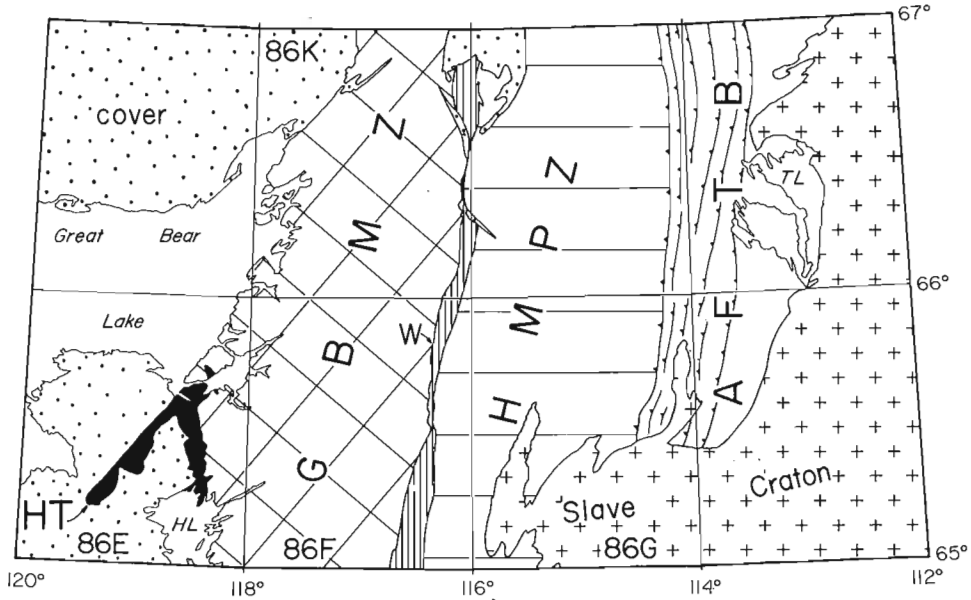


Figure 73.1. Tectonic sketch map of central Wopmay Orogen showing location of Calder River map area (86F).

HT = Hottah terrane;
GBMZ = Great Bear magmatic zone;
W = Wopmay fault zone;
HMPZ = Hepburn metamorphic-plutonic zone;
AFTB = Asiak fold-thrust belt;
HL = Hottah Lake;
TL = Takijuq Lake.

6) Preliminary analysis of kinematic indicators within the mylonites suggest northward-directed top over bottom movement.

7) Because granitic rocks of about 1.90 Ga are mylonitized and the mylonites of the Wopmay fault zone are unconformably overlain by supracrustal rocks of the Great Bear magmatic zone, recently dated at 1.875 Ga, the age of mylonitization is constrained to be between about 1.90-1.875 Ga, if the mylonites are coeval. However, the significance and origin of the mylonites are problematic; they may or may not be related to the Calderian orogeny, the deformational event responsible for the dominant north-south folds, east-vergent thrusts, and metamorphism that characterizes most of eastern Wopmay Orogen.

8) The U-Pb zircon age of 1.875 Ga determined from a welded tuff within the lower Dumas Group indicates that it is approximately coeval with andesitic stratovolcanoes and ash-flow calderas of the LaBine Group, interpreted to represent the main arc front then located near the western margin of the Great Bear magmatic zone.

9) Westward-thinning wedges of talus breccia within the Dumas Group, comprising blocks and cobbles of Archean granite and cryptalgal-laminated dolomite blocks derived from stratigraphically lower parts of the group suggest that some west-side-down faulting occurred while the Dumas Group was accumulating.

10) Plutonic rocks of the Great Bear zone generally have systematic compositional variations ranging from intermediate to siliceous with respect to time. One mapped complex contains multiple intrusions, each pulse of which intruded an older more intermediate phase and was progressively more siliceous.

11) The northeast-trending right-lateral transcurrent faults splay and appear to die out as they enter the north-trending strip of Dumas metasedimentary rocks. Since the belt of metasedimentary rocks and the Wompay fault zone, taken together, constitute a boundary between domains of northeast-trending right-lateral faults to the west and northwest-trending left-lateral faults to the east across which few strike-slip faults extend and because there has been considerable north-south extension on both sides of the belt, the north-south extension within the belt is penetrative at the map scale. It may be expressed visually at the outcrop scale by common boudinage of bedding.

12) A large triangular shaped magnetic low, bounded on the northwest by a large transcurrent fault and to the east by the north-south Dumas belt, that occurs in the north-central part of the map area apparently is caused by quartzofeldspathic gneisses and intensely epidotized granitoids not typical of the Great Bear magmatic zone. This suggests that the "triangle-zone" provides a window through the Great Bear magmatic zone into its basement. Similar magnetic lows characterize the southeast sides of several other major faults located farther south suggesting that additional exposures of basement may outcrop in those areas.

ACKNOWLEDGMENTS

We thank Fleur E.L. Harvey-Kelly for capable assistance in the field; Ron Gerow and the entire crew at Latham Island Airways for keeping us in the air and on the water when and where we wanted; and Martin Irving for succour. Discussions in the field with Simon Hanmer, Janet King and John Grotzinger were beneficial. Bob Smith and Charlie Bacon, both with the Branch of Igneous and Geothermal Processes, U.S. Geological Survey, spent a week with us examining plutonic and volcanic rocks: their ideas and thoughts on the outcrops were insightful and pointed. SAB thanks W.A. Padgham for his generous support of field and laboratory work. Lastly, we thank Simon Hanmer and Paul Hoffman for reviewing the manuscript.

WOPMAY FAULT ZONE

Wopmay fault zone (Hoffman, 1972, 1984; Easton, 1981; King et al., 1983; King, 1985) is a 7-18 km wide, north-trending belt of lenticular brittle-fault bounded blocks. Individual blocks within the area mapped during 1983 and 1986 (Fig. 73.2 and 73.3) include: inferred Archean and other undated granitoids, in places mylonitized; metasedimentary and metavolcanic rocks of the Grant Group (Easton, 1982), locally unconformably overlying undated granitoids; and mylonites derived from metasedimentary rocks of unknown age.

Archean rocks (?)

A long linear belt of inferred Archean granitoid rocks occurs within the Wopmay fault zone (Fig. 73.3). Although the granitic rocks have not been dated directly, granitic rocks to the north, along strike and continuous with those discussed here, yield U-Pb ages close to 2.5 Ga (Bowring and Van Schmus, in press). The granitoid rocks are mainly equigranular to potassium feldspar porphyritic biotite granite and subsidiary hornblende-biotite granodiorite, in places foliated. The belt is widest at the northern edge of the map area and narrows southward until it pinches out at about 65° 40′ north latitude. Wherever we observed the eastern boundary of the granitic belt it passed, with material continuity, into ultramylonite. The transition zone ranges from a few centimetres to about 15 cm wide. The foliation within the mylonites immediately adjacent to the isotropic granitoids dips steeply eastward and contains a subhorizontal stretching lineation. Preliminary field analysis of kinematic indicators, such as rotated feldspar porphyroclasts, shear band foliation, and deflection of planar structure into the shear zone, consistently indicate sinistral sense of shear. The western boundary of the belt is a sharp contact with medasedimentary rocks of the Dumas Group: it is excellently exposed in several places and, as in the Sloan River map area, is an unconformity (Hoffman and McGlynn, 1977; Bowring, 1982). Both the unconformity at the base and the bedding within the metasedimentary rocks dip steeply to the west or are vertical. Therefore, the granitoid rocks are interpreted to occupy the core of an anticline of post-Dumas Group age (Fig. 73.3).

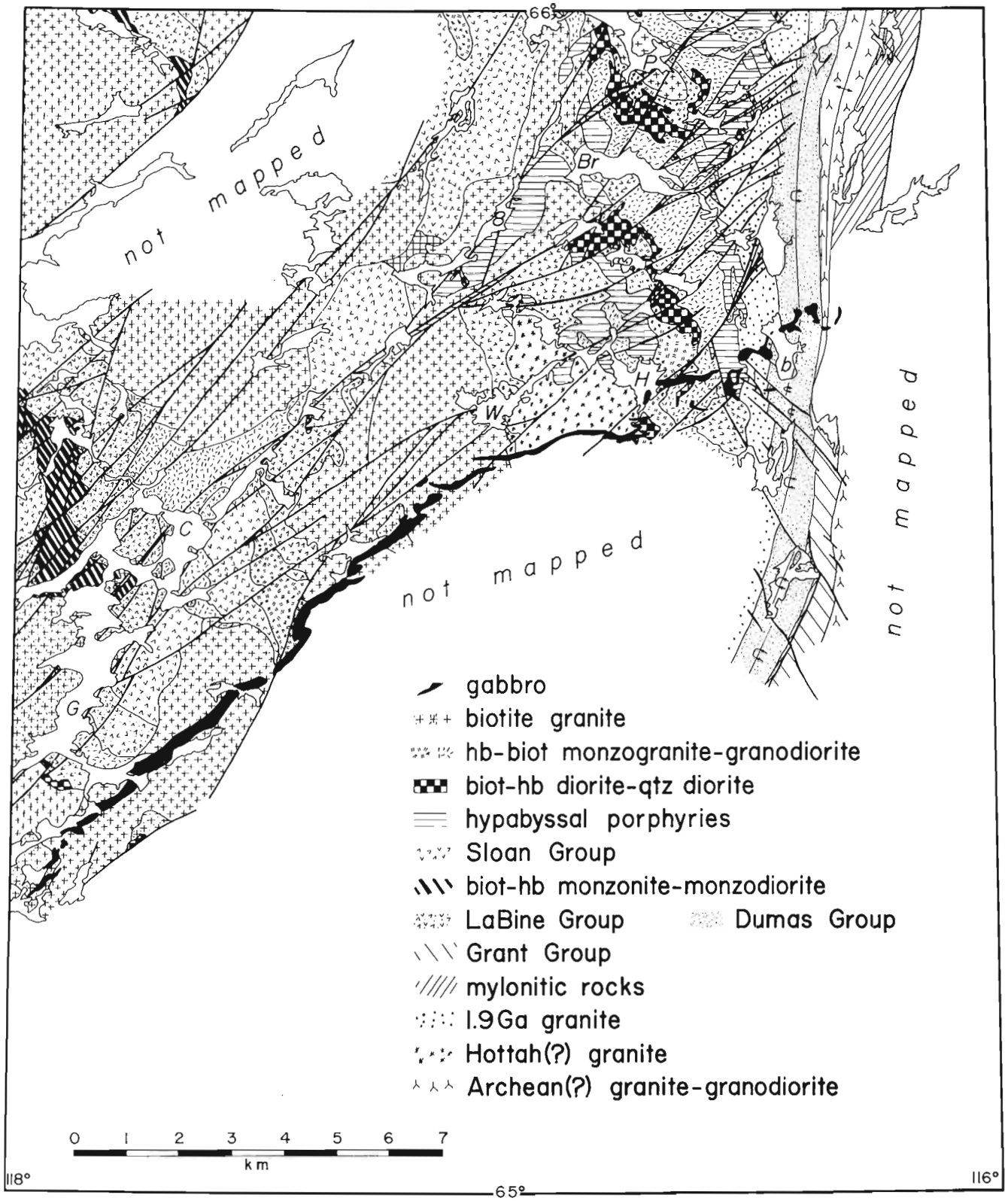


Figure 73.2. Geological sketch map of Calder River map area showing distribution of major rock units mapped to date.

C = Clut Lake;
G = Grouard Lake;
W = Wiley Lake;
H = Hansen Lake;
8 = Lake 837;
Br = Breadner Lake;
P = Handley Page Lake;
S = Smokey Lake;
b = Brain Damage Lake.

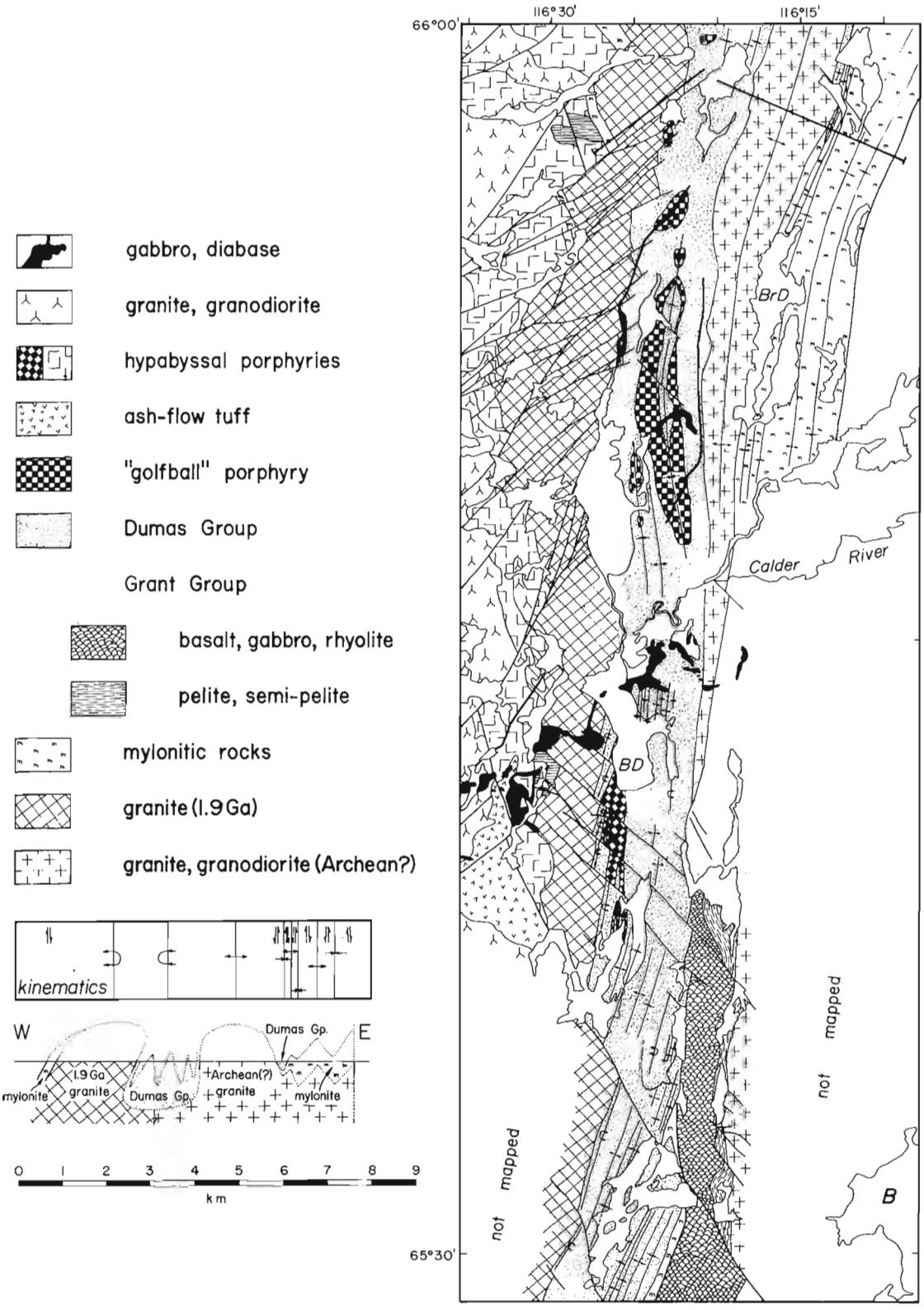


Figure 73.3. Geological sketch map of the northeastern part of Calder River map area showing the distribution of units in and adjacent to the Wopmay fault zone. The cross-section, constructed along the heavy lines in the northernpart of the map, is to scale but schematic. The plan view diagram of fold axes and sense of shear as deduced from kinematic indicators shows the consistent northward-directed top over bottom movement. B = Bishop Lake; Brd = Broken Dish Lake; BD = Brain Damage Lake; S = Smokey Lake.

Mylonitic rocks

One of the major rock types of the Wopmay fault zone is mylonite. The mylonites are derived from a variety of granitoids, some possibly Archean, as above, and others of unknown age, ranging in composition from syenogranite to quartz diorite as well as from metasedimentary rocks of unknown affinity. The zone containing the mylonitic rocks lies between the above mentioned anticline of inferred Archean granite on the west and a northward-trending brittle fault to the east: a width of about 3-4 km (Fig. 73.3). Within this belt the strain is extremely heterogeneous comprising ultramylonitic zones ranging from 1 km to 1 cm in width derived from less strained, but everywhere foliated and lineated, rocks.

Both the mylonitic rocks and the granitic rocks described above are tightly folded about north-trending axes. Fold wavelengths are on the order of 1-2 km. Dips of foliation on the fold limbs are typically steep, ranging from 65-85° with tight axial zones: they are large chevron-like folds. The mylonites have near horizontal mineral lineations. Kinematic indicators within the mylonites are consistently dextral on westward-dipping fold limbs and sinistral on fold limbs that dip eastward (Fig. 73.3). This indicates a sense of northward top-over-bottom movement when the effects of folding are removed.

Infolded remnants comprising volcanic and sedimentary rocks of the Dumas Group (Fig. 73.3) clearly indicate that the mylonites were folded after deposition of the supracrustal rocks, because bedding in the sedimentary rocks parallels the foliation in the mylonites. The unconformity between the supracrustal rocks and the mylonitic rocks is well exposed in several places northwest of Broken Dish Lake (Fig. 73.3).

Another zone of mylonitic rocks, mapped by SAB in 1983, occurs west of Bishop Lake (Fig. 73.3) and is in fault contact with the Grant Group on the east and unconformably overlain by sedimentary rocks of the Dumas Group to the west. This zone is less than a kilometre or so wide and is exclusively derived from granitoid rocks. The major protolith is a coarsely potassium feldspar porphyritic biotite syenogranite. Here, as in the mylonite belt to the north, the strain is heterogeneous and varies from ultramylonite to moderately foliated and lineated granite. Foliation within the zone dips steeply westward as does bedding in the overlying supracrustal rocks. Mineral lineations are nearly horizontal with kinematic indicators suggesting a dextral sense of shear. Because the spatial and temporal relationships, as well as the sense of shear, of the mylonites within this zone are similar to those of the more northerly belt, the two are considered to have originally been part of the same shear zone or shear system.

Grant Group

This group of rocks, mainly basalts, pelites and psammites, in places lying unconformably upon undated granitic basement, is another principal fault-bounded package of rocks within the Wopmay fault zone (Easton, 1982; King, 1985). It is amply described by those workers and is therefore not described in further detail here.

1.90 GA GRANITE AND HOTTAH TERRANE

Other than a few siliceous porphyries intruding the Akaitcho Group and Archean granitoids forming basement to both the Akaitcho and Grant groups, no plutons older than those of the Hepburn batholith were previously known near the eastern side of the Great Bear magmatic zone except for a small area of deformed granite, dated at 1.938 Ga, in the northeastern Sloan River map area (Bowring and Van Schmus, in press). During the 1986 field season we recognized a large pluton that is unconformably overlain by the Dumas Group in the Calder River map area.

The pluton, mapped during the field season and dated this fall, is a north-trending body coarsely potassium feldspar porphyritic biotite syenogranite. It is unconformably overlain by sedimentary rocks of the Dumas Group along the western side of the main overturned syncline shown in Figure 73.3, and zircons from a sample collected during the 1986 field season have yielded a preliminary U-Pb age of about 1.90 Ga. The granite is characterized by 2-6 cm size potassium feldspar phenocrysts, common in eastern exposures and decreasing in abundance westward, and anhedral quartz phenocrysts to 1 cm, and subhedral-euhedral plagioclase to 5 mm. The rock contains a conspicuous foliation, defined by biotite, that is best developed near the unconformity. In the northern part of the map area, north of the Calder River, the westernmost parts of the body are mylonitized (Fig. 73.3). The foliation within the mylonites dips westward at about 60°, has a subhorizontal stretching lineation, and preliminary examination of kinematic indicators suggests a dextral sense of shear. The mylonites and the granite are intruded by porphyries and granitoid plutons of unknown age. The westward dip of the mylonites suggests that the granite occupies the core of an anticline with its eastern limb overturned (Fig. 73.3). Because the sense of shear is compatible with the mylonites of the Wopmay fault zone they are considered to represent different parts of the same shear zone/system. If so, then the mylonites are exposed over an east-west distance of about 8 km, when separation on younger transurrent faults is restored, and since the mylonites are tightly folded their original east-west extent must have been considerably greater – perhaps 20 km or more. The fact that they are folded, coupled with the concordance between bedding in the Dumas Group and foliation in the mylonites, plus the consistent sense of north-directed top-over-bottom movement when the effect of the late folds is removed, suggest that prior to deposition of the Dumas Group the mylonites formed one nearly horizontal sheet. Since the zone was probably in excess of 20 km wide it is unlikely to have been a steeply dipping planar surface when the Dumas Group was deposited upon it.

The occurrence of the 1.90 Ga granite and the inferred Archean granitoids along the western and eastern sides, respectively, of the Dumas syncline for a distance of about

30 km suggests that the contact is not intrusive for it is far too linear. The contact is more likely to be a brittle fault similar to those of the Wopmay fault zone east of the Dumas syncline (King et al., 1983). If this interpretation is correct, the movement on the fault predates deposition of the Dumas Group.

Rock units suspected to be part of Hottah terrane occur farther to the west, mainly in the area around Wiley Lake (Fig. 73.2). In that area bodies of biotite-quartzofeldspathic gneiss, too small to represent on the map, occur along the northwestern margin of a large monzogranite pluton. A somewhat larger body of strongly epidotized granite occurs just to the northwest and, although not yet dated, is possibly of Hottah age. Whatever its age, it is one of the most altered granitoid rocks known anywhere within the Great Bear zone or Hottah terrane. Several other plutonic bodies, ranging from porphyritic hypabyssal intrusions to larger holocrystalline plutons in the same area are of unknown age.

GREAT BEAR MAGMATIC ZONE

The Great Bear magmatic zone comprises thick sequences of sedimentary and calc-alkaline volcanic rocks (MacTavish Supergroup), generally divided into 3 groups (Hoffman, 1978), from east to west: Dumas, Sloan, and LaBine. The supracrustal rocks are intruded by granitoid plutons whose compositions overlap those of the volcanic rocks. The LaBine Group clearly underlies the Sloan Group in the western part of the zone but age relations between the Sloan and Dumas groups have been equivocal: is the Dumas Group younger than the Sloan Group (Hoffman and McGlynn, 1977) or coeval with the LaBine Group (Hildebrand et al., in press)?

Dumas Group

In the Calder River map area, strata correlative with the lower part of the Dumas Group as defined by Hoffman (1978) in the Sloan River map area to the north, occur predominantly in a long, narrow overturned syncline along the western side of the Wopmay fault zone where they unconformably overlie rocks of inferred Archean age (Fig. 73.2 and 73.3) to the east and the 1.90 Ga granite to the west. On the east side of the syncline, as mentioned earlier, the unconformity dips steeply westward or is vertical; this contrasts with exposures on the Sloan River map area to the north where it dips at about 30-40° to the west. The western contact of the main Dumas belt is also an unconformity and there a coarsely porphyritic biotite granite of Hottah terrane is beveled to a near planar surface. Bedding in the overlying sedimentary rocks is concordant with the contact for at least 30 km along strike. The group was also found within the Wopmay fault zone where it occurs as synclinal remnants unconformably overlying granitic and mylonitic rocks (Fig. 73.3). In those areas bedding in the group parallels the foliation within the granites and mylonites. In the Calder River area the Dumas Group is metamorphosed to greenschist grade, which contrasts with the regional subgreenschist grade of the group in the east-central part of the Sloan River map area.

Within the major overturned syncline, rocks of the Dumas Group are tightly to isoclinally folded. The folds are generally upright although overturned folds have steeply inclined axial planes. Typical of the sedimentary rocks within the entire belt is an intense cleavage that parallels bedding on the fold limbs. Bedding within axial zones is incipiently transported (Fig. 73.4).

Wherever the unconformity was mapped, a basal conglomerate and/or regolith is absent to poorly developed. Along the eastern side of the main overturned syncline, rocks above the unconformity comprise medium- to coarse-grained mostly subangular to subrounded sandstone containing about 10-15% feldspar. The sandstone occurs as thin lenses up to 3 m thick where it is best developed in paleotopographic lows eroded into the Archean basement. Along strike variations appear to relate to the basement rock type – specifically to grain size; that is, where it is coarse grained granite the sandstone contains angular chips and subrounded granules of potassium feldspar, yet where the basement rock type is ultramylonite the rock immediately overlying the unconformity is finer grained than elsewhere and contains few, if any, grains larger than medium sand-size. Bedding within the unit is poorly developed but appears to consist of low angle cross stratification and some ripple cross stratification. This unit, interpreted as transgressive strandline sands, is gradational upward into a locally occurring dolomite unit.

Along the western side of the belt there are local lenses and lag deposits of pebbly sandstone clearly derived from the underlying granite. The sandstone is arkosic and stratification is predominantly low angle crossbedding. The arkose is only a few metres thick and is overlain by a succession of intercalated carbonate and siltstone beds. Individual beds are 1 to 5 cm in thickness and there are sparse horizons of slump



Figure 73.4. Axial zone of overturned fold showing incipient transposition along steeply dipping cleavage planes. The photograph was taken looking south, down the plunge of the fold, the overturned limb is to the right (west). Pen in extreme upper right of outcrop for scale. GSC 204400-R.

folds. Overlying the interbedded units are sandstones composed of almost only plagioclase grains and mafic debris, now metamorphosed to assemblages of albite, chlorite, and actinolite. Relict through crossbedding is well preserved in sets up to 20 cm thick.

The dolomite unit, found only along the eastern side of the belt, comprises about 1.5 m of laminated, brown, medium grained, ferroan(?) dolomite with wavy to irregular stratiform stromatolites, minor units containing microdigitate or digitate stromatolites with up to a few millimetres of synoptic relief, and rare tufted stromatolites. Platy oncolites, draped by layers of cryptalgal tufa are present but rare, as are sand-filled mudcracks and prism cracks. The dolomite unit, interpreted to represent carbonate tidal flats, contains several laminae of medium grained sandstone near the top and is overlain by a major mudstone-siltstone unit.

Abruptly overlying the carbonate unit is at least 40 m of finely to thickly interlaminated mudstone and siltstone containing lenses of conglomerate and minor thin beds (1-4 cm) of sandstone. Within the mudstone-siltstone some beds are size-graded. Although this unit is strongly cleaved, there is no evidence for desiccation in the form of mudcracks or mudchips; therefore, this unit is interpreted to have accumulated during rapid subsidence and to represent a distal shelf or basinal mudstone facies.

In the northern part of the map area there are several local conglomeratic lenses intercalated with the mudstone-siltstone sequence (Fig. 73.5). They are 3-15 m thick and contain clasts up to 1 m in diameter. The rock is clast-supported, has a sandy matrix, and contains subrounded to subangular clasts of granitoid rocks similar to those beneath the unconformity, angular blocks of stromatolitic dolomite, and minor sandstone clasts probably derived from stratigraphically lower units. The conglomerate units are not present in sections 2 km to the west. This, coupled with the occurrence of older lithologies in the conglomerate and the abrupt drowning of the tidal-flat carbonates by thick section of muds, suggests west-side-down normal faulting just to the west of the present outcrop belt during deposition of the mudstone. The conglomerates probably represent debris shed from the west-facing fault scarps along which granitoid basement was exposed.

Numerous beds of tuffaceous rocks occur interbedded with the mudstone-siltstone sequence in the central part of the syncline of Dumas Group. The tuffs, thin units that are mostly less than 20 m thick, vary from simple cooling units of ash-flow tuff containing 10-25% phenocrysts to reworked tuffs containing in excess of 50% broken crystals. They typically pinch out along strike and appear to fill shallow paleotopographic depressions. A recently completed U-Pb zircon age from one of the welded tuffs in this sequence indicates emplacement at 1.875 Ga, the same age as rocks of the LaBine Group. Thus, it appears that the Dumas Group represents material deposited cratonward of the main Great Bear arc front as represented by the LaBine Group.

The mudstone-siltstone sequence is cut by a distinctive quartz-plagioclase-potassium feldspar porphyritic intrusion, informally referred to as the "golfball" porphyry because the potassium feldspar phenocrysts are round and about the size of golfballs. The porphyry is similar to those mapped in the Sloan River map area by Hoffman (1978, 1984) and Bowring (1982). In that area the porphyries are sheet-like bodies (1.864 Ga, Bowring and Van Schmus, in press) that occur in the cores of anticlines, but in the Calder River map area they occur in the cores of synclines (Fig. 73.3). This suggests a slightly deeper level of erosion in the latter area and is in keeping with the higher metamorphic grade there.

The "golfball" porphyry and the mudstone-siltstone sequence are unconformably overlain by several metres of conglomerate and sandstone. The unconformity was first recognized during the 1983 field season by SAB and an unconformity also occurs above the "golfball" porphyry in the Sloan River map area (Bowring, 1982). In the Calder River area where the unconformity occurs on the porphyry there is typically a conglomerate containing almost exclusively porphyry debris of various grain size from sand to cobbles. Where the porphyry is absent it is difficult to recognize the unconformity because units above and below it are similar in composition and are roughly concordant with one another.

The synclinal remnants of Dumas Group that occur within the Wopmay fault zone have a different stratigraphy than sections of the group farther west. They comprise a basal arkosic sand and/or pebbly conglomerate overlain by amygdaloidal basalt flows, cut by brick-red siliceous porphyries. This stratigraphy is similar to that found in the Sloan River map area above the erosional surface cut into the "golfball" porphyry. The lack of the thick section of mudstones and siltstones characteristic of the Dumas Group beneath the unconformity suggests that the sections preserved in the Wompay fault zone represent the "upper" Dumas Group, and that the basin in which the thick mudstone-siltstone sequence accumulated was, at least in part, fault bounded on its eastern



Figure 73.5. Clast-supported granitic conglomerate of the Dumas Group. Pen in left centre for scale. GSC 204400-P.

side and that the margin lay between the two preserved synclines. This is consistent with sedimentological evidence for west-side-down faulting during the deposition of the lower Dumas Group as discussed earlier.

LaBine Group

Rocks of the LaBine Group are the oldest rocks of the western Great Bear magmatic zone. They unconformably overlie rocks of the Bell Island Group (Reichenbach, 1986) and lie unconformably beneath tuffs of the Sloan Group. Most of the LaBine Group in the Calder River map area was described in detail by Hildebrand (1984a,b); however, new exposures of the group were found along the east side of Grouard Lake (Fig. 73.2). The rocks placed within the LaBine Group are: intensely altered mafic-intermediate lavas, tuffs, and associated sedimentary rocks, have correlated with Camsell River Andesite; and densely welded, lithic and crystal-rich, intermediate ash-flow tuff assigned to White Eagle Tuff. Complete descriptions of the units are found in Hildebrand (1984a).

In the Grouard Lake area the upper part of the LaBine Group is a several kilometre thick section of simple cooling units of ash-flow tuff informally termed the "younger ash-flow tuffs" (Hildebrand, 1984a). During the 1986 field season we recognized that they are correlative with tuffs of the Sloan Group and, therefore, are shown on the current map as Sloan Group (Fig. 73.2).

Sloan Group

In the Calder River map area rocks mapped as Sloan Group consist almost entirely of densely welded ash-flow tuffs. Most of the tuffs are probably of intermediate composition as they contain 25-40% phenocrysts of plagioclase, quartz, ferromagnesian minerals, and potassium feldspar phenocrysts. There is a remarkable paucity of sedimentary rocks intercalated with the ash-flow tuffs; consequently, it is extremely difficult to define individual stratigraphic units. Where it is possible to map individual units, the Sloan Group comprises sequences, many kilometres thick, of simple cooling units that probably represent outflow facies sheets erupted from unknown sources. The great thicknesses of the sequences suggests that they may represent material deposited in older calderas. Other units of densely welded, crystal-rich intermediate ash-flow tuff are in excess of 1 km thick. They probably represent intercauldron facies tuff ponded within calderas during subsidence.

Granitic rocks

Granitic rocks make up a sizable proportion of the Great Bear magmatic zone mapped during 1986. There are two main assemblages of granitic rocks within the zone separated from one another in time by a period of oblique folding: a prefolding supersuite comprising intermediate to siliceous rocks and a postfolding suite comprising dominantly siliceous bodies and dyke swarms (see Hildebrand et al., in press). The folds within the Great Bear zone generally have gently plunging axes that trend northwest, except along the eastern and western margins of the zone where they trend north. The prefolding granites are identified by their general concordance with stratigraphy and their dominant northwest trend while plutons of the post-folding suite are discordant with respect to both stratigraphy and folds. In general, the folded plutons are more intermediate in composition and contain more hornblende than their post-folding counterparts, which are dominantly biotite syenogranites (Hoffman and McGlynn, 1977; Hildebrand et al., in press).

Prefolding supersuite

The oldest rocks of the Great Bear zone mapped during the current project are intermediate in composition. They occur most commonly as remnants along the contacts between younger granites. A few other bodies occur as enclaves up to several kilometres across in younger granodiorites and monzogranites. In the northern part of the area are much larger bodies, some 10 km or more across. At least one of the large bodies forms part of a typical zoned plutonic complex.

The intermediate bodies vary considerably in composition, individual bodies comprising clinopyroxene-biotite-hornblende bearing diorite, quartz diorite, monzodiorite, and quartz monzodiorite. Although some renmants are fairly uniform in composition, others are quite heterogeneous and internal variations that span this entire range are common; in fact, one body grades from biotite-hornblende monzodiorite to biotite syenogranite over a 100 m interval.

A 100-200 m wide body of pyroxenite occurs with a small swarm of mafic dykes east of Handley Page Lake. The pyroxenite occupies the central portion of an irregular-shaped gabbro body. This body and the dykes crosscut apparently folded plutonic rocks of the area but the age of those rocks is unknown.

The largest and most common granitoid plutons of the prefolding suite are hornblende-biotite monzogranites and granodiorites. They are mostly seriate textured rocks containing 15-30% ferromagnesian minerals. Potassium feldspar phenocrysts are common in many bodies but are absent in others. At least one of the bodies is sheet-like. It occurs west of Handley Page Lake (Fig. 73.2) and has eastward dipping upper and lower contacts parallel to eutaxitic foliation in the ash-flow tuffs that it intrudes. As the body is exposed over a horizontal distance of 2 km and the dip of contacts and bedding is 30°, the pluton is about 1 km thick. It appears to be the southernmost part of the Torrie pluton (Hoffman and McGlynn, 1977), one of the two largest folded plutons mapped to date in the Great Bear magmatic zone.

Perhaps the most interesting plutonic complex mapped during the 1986 field season is a zoned intrusive complex at Handley Page Lake (Fig. 73.6). It comprises three distinct phases, from oldest to youngest and from margin to core: (1) clinopyroxene-biotite-hornblende diorite and quartz diorite with local zones of clinopyroxenite, (2) hornblende-biotite monzogranite and granodiorite, and (3) potassium feldspar porphyritic biotite syenogranite. Contacts between

each successive phase are sharp and the complex appears similar in composition and intrusive history to the Tuolomne intrusive series (Bateman and Chappell, 1979) of the Sierra Nevada batholith. A detailed petrological and chemical study of the complex will form part of a Bsc. thesis by SFG at Carleton University.

Numerous porphyritic intrusive bodies occur throughout the mapped area. The largest occurs along the western side of the 1.90 Ga granite just west of the main Dumas syncline, where it intrudes mylonites derived from the granite (Fig. 73.3). The body is coarsely porphyritic containing potassium feldspar phenocrysts to 4 cm, anhedral quartz blobs up to 2 cm, and plagioclase to 5 mm. It weathers brick red and ranges from weakly foliated to nondeformed. Several similar bodies that strike northwest occur north of Handley Page Lake and another large unit of porphyry occurs along the eastern side of Lake 837 (Fig. 73.2).

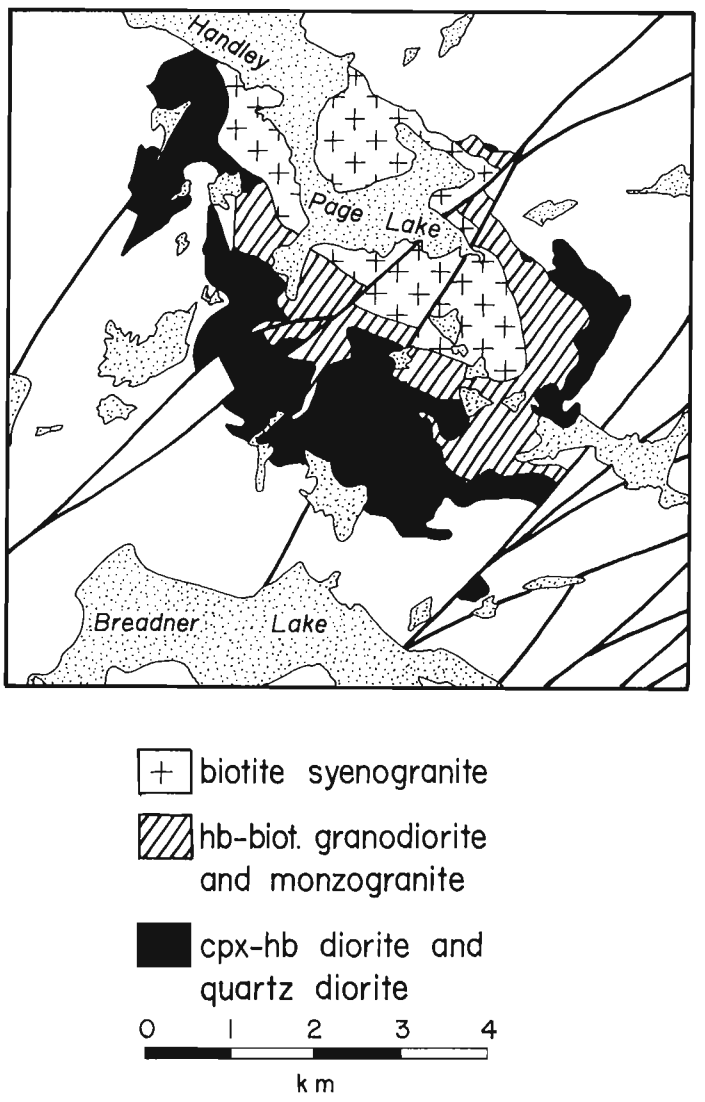


Figure 73.6. Geological sketch map showing the distribution of major rock types in the Handley Page intrusive complex.

Postfolding suite

This suite comprises mainly biotite syenogranite plutons which postdate the main period of folding within the Great Bear zone. The bodies crosscut fold axes and are ovoid to irregular-shaped plutons greater than 15-20 km in diameter (Fig. 73.2). They are typically potassium feldspar porphyritic. Sharp external contacts and little compositional variation with individual bodies are the rule. Miarolitic cavities and pegmatites are relatively common near the margins of some bodies.

Dyke swarms

Two major dyke swarms were mapped during the 1986 field season. Both appear to postdate folding as they cut plutons of the biotite syenogranite suite. They are cut by the transcurrent faults. Therefore, they are about the same age as the Grouard porphyry dykes of Hildebrand (1984a). One of the swarms occurs to the east of Lake 837 and the other occurs east of Hansen Lake (Fig. 73.2).

Dykes of the former swarm are generally brick-red weathering and contain variable quantities of biotite, hornblende, plagioclase, quartz, and potassium feldspar phenocrysts in an aphanitic to finely phaneritic groundmass. They trend north-northeast (Fig. 73.7). The other dyke swarm extends from Smokey Lake (Fig. 73.3) to southeast of Hansen Lake with the greatest concentration just east of Hansen Lake. This swarm is a bimodal suite consisting of brick-red siliceous dykes with phenocryst assemblages similar to dykes east of Lake 837 and dark-brown to black weathering hornblende-plagioclase porphyritic dykes that are probably intermediate to mafic in composition. The swarm trends northeast except in the southern region of extent where orientations swing sharply to the east (Fig. 73.8). The siliceous dykes are concentrated east of Hansen Lake and do not occur north of the Calder River. The siliceous dykes are older of the two: the intermediate-mafic dykes typically intrude the contact between the siliceous dykes and their wall rocks. Adjacent to their margins the intermediate-mafic dykes are commonly black, flinty, nearly aphyric but become progressively more coarsely crystalline and more porphyritic towards their interiors. They commonly contain potassium feldspar xenocrysts rimmed by a white weathering feldspar, probably albite, and quartz xenocrysts armoured by a ferromanesian mineral, probably clinopyroxene. Although the quartz shows a reaction relationship with the melt the groundmass typically contains 5-10% modal quartz.

Transcurrent faults

Abundant northeast-trending transcurrent faults, typical of the Great Bear magmatic zone (see Hildebrand et al., in press and references therein), were mapped during the field season. Most exhibit right lateral separation but a lack of piercing

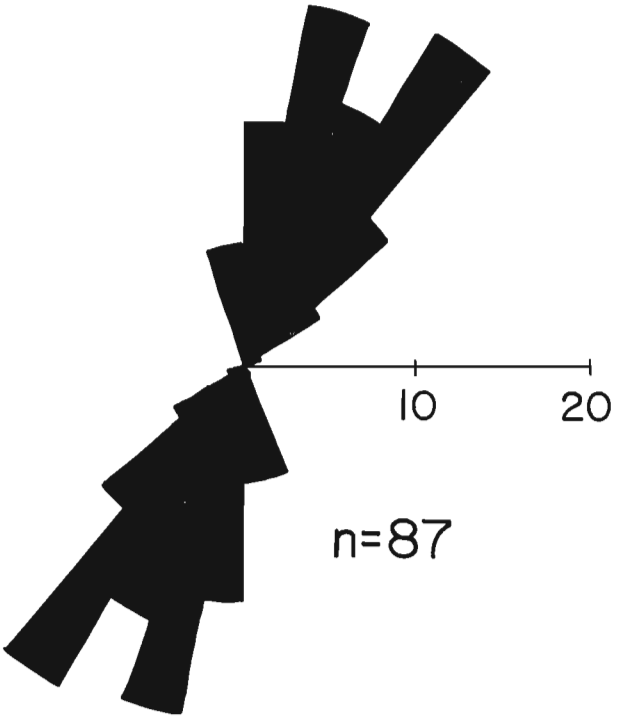


Figure 73.7. Rose diagram of siliceous dykes east of Lake 837.

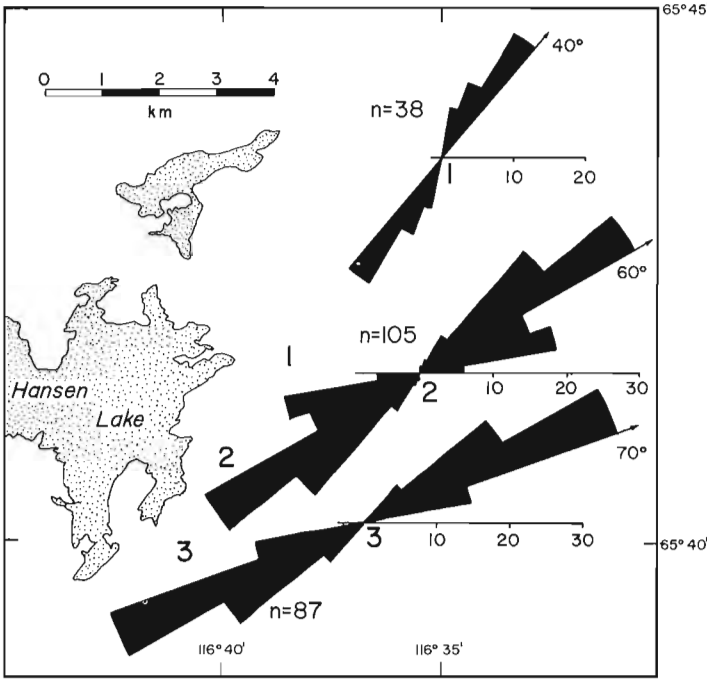


Figure 73.8. Rose diagrams of bimodal dyke swarm east of Hansen Lake. The numbers 1, 2 and 3 refer to the approximate locations for each of the rose diagrams. Note the progressive change in orientation from north to south.

points precludes any estimation of true displacement. The majority of the faults splay as they approach the synclinal Dumas belt and die out: they do not offset the eastern unconformity between the Dumas Group and the Archean granites. Although some northwest-trending, left-lateral faults, characteristic of the area east of the Dumas Group (Hoffman, 1984), cross the Dumas belt, for the most part it, and/or its basement (the zone of north-south oriented folds affecting the rocks in the vicinity of the Wopmay fault zone is here informally termed the "folded zone") forms a domain boundary between northeast-trending right-lateral faults to the west and northwest-trending left-lateral faults to the east. Because the faults are present on either side of the folded zone but do not in general cut it, there is a compatibility problem; that is, rocks within the folded zone must have extended in a north-south direction but deformation must be penetrative at the map scale. On the outcrop scale the only observed feature compatible with such deformation is pervasive boudinage of bedding (Fig. 73.9) indicating significant north-south extension but the age of the boudinage is unknown.

Triangle zones

Along the southeast side of the major transcurrent fault passing just east of Lake 837 is a triangular-shaped zone $36 \times 60 \times 53$ km that appears on aeromagnetic maps as a magnetic low relative to the "normal" magnetic signature of the Great Bear magmatic zone. Rocks of the region known to have relatively low magnetic susceptibility include Archean basement, Coronation Supergroup, Hepburn intrusive suite, Hottah terrane, and post-folding granites of the Great Bear zone. To date we have mapped only the northern half of the triangle zone but much of the area includes rocks that do not resemble the suite of post-folding granites of the Great Bear zone; therefore, they maybe predate the Great Bear magmatic zone. If so, then the triangle zone provides a "window" through the eastern Great Bear zone into its basement. Similar magnetic lows occur farther south on the southeastern sides of several of the largest transcurrent faults that cut the zone at regular intervals of about 20 km suggesting that additional exposures of basement to the Great Bear zone may be found in those areas.

YOUNGER GABBRO

There are three major diabase-gabbro assemblages known to occur in the Calder River map area: north-trending diabase dykes found mostly in the central to eastern parts of the sheet; northwest-trending diabase dykes of Cleaver diabase (Hildebrand, 1984b); and a large northeast-trending gabbro sheet, that dips northwestward and extends from Hottah Lake in the southwest to the Wopmay fault zone in the northeast (Fig. 73.2). Age relations between the two diabase dyke swarms were not observed but the gabbro still clearly cuts dykes of Cleaver diabase.



Figure 73.9. Arkosic sandstone of the Dumas Group. Note the boudinage formed in the more competent layers. GSC 204400-U.



Figure 73.10. Oblique aerial photograph, looking west over the floodplain of the Calder River where it crosses the Dumas syncline. GSC 204400-T.

ECONOMIC GEOLOGY

Mineralized zones proved to be scarce in the area mapped during 1986. Mineralized quartz veins were, however, found southwest of Wiley Lake in a transcurrent fault zone. One of the veins, 15 cm thick, contains a 2.5 cm central zone of pyrite, chalcopyrite, sphalerite, and bornite. The other, 20 cm thick, has margins of amethyst and a 10 cm core of honey-coloured sphalerite mantled by dark brown sphalerite.

Although no evidence for mineralization was seen, the pyroxenite bodies northeast of Handley Page Lake might be potential sources of platinum-group metals, but unless the bodies expand considerably at depth the tonnage would almost certainly make any deposit subeconomic.

QUATERNARY AND RECENT GEOLOGY

Although the area is generally free of extensive Quaternary cover there are numerous eskers that trend approximately east. A large field of boulders several kilometres across occurs at the east end of Handley Page Lake along the Calder River. Sets of raised beaches occur in the western part of the map area and may be related to ancient Lake McConnell (Craig, 1965). The Calder River has a well developed floodplain where it crosses the Dumas syncline (Fig. 73.3). There, the river is a typical meandering river with spectacular point bars and oxbow lakes (Fig. 73.10).

DISCUSSION

The occurrence of 1.90 Ga granitic rocks along the eastern side of the Great Bear magmatic zone, coupled with their close proximity to Archean granitoids of unknown affinity has some potentially interesting implications for the development of Wopmay Orogen. Based on similarities in age, lithology and geochemistry, Reichenbach (1985, 1986) suggested that volcanic rocks of the Akaitcho, Grant, and Bell Island groups are coeval and were erupted within the same basin – the Grant and Akaitcho Groups deposited unconformably upon Archean basement and the Bell Island Group deposited unconformably upon pre-1.900 Ga Proterozoic basement (Hottah terrane). This, coupled with data suggesting that Hottah terrane represents a magmatic arc (Hildebrand and Roots, 1985), led to a model in which the Coronation Supergroup originated within a marginal basin, with the Bell Island Group deposited on the western side of the basin and the Grant-Akaitcho assemblage deposited on the eastern side (Reichenbach, 1986; Hildebrand et al., in press). This model implies that Hottah terrane was contiguous to Slave Craton just prior to 1.90 Ga; however, a major unknown is whether the Hottah arc developed upon Archean crust of the western Slave Province or whether it developed on different basement that had earlier been accreted to Slave Craton. Thus, the close proximity of undated, but probably Archean, rocks known to unconformably lie beneath Akaitcho and Grant groups, and possible Hottah terrane, occurring in the triangle zone, brings up the question of whether or not Akaitcho, Grant, and Bell Island groups and their respective basements ever formed a coherent block, and if so did it extend to form a marginal basin on stretched Slave Craton, or is the entire assemblage exotic with respect to the craton and central and upper parts of the Coronation Supergroup? At present this question remains unanswered but additional mapping and geochronology, both to the north and south, may discover the answer.

REFERENCES

Bateman, P.C. and Chappell, B.W.
1979: Crystallization, fractionation and solidification of the Tuolomne Intrusive Series, Yosemite National Park, California; Geological Society of America, Bulletin, v. 90, p. 465-482.

Bowring, S.A.
1982: Preliminary geologic map of the Kamut and Adam

Lakes map areas (86K/9, 86K/8); Department of Indian Affairs and Northern Development, Yellowknife, Economic Geology Series Map.

Bowring, S.A. and Van Schmus, W.R.
– U-Pb zircon geochronology of the early Proterozoic Wopmay Orogen, NWT, Canada: an example of rapid crustal evolution; Tectonics (in press).

Craig, B.G.
1965: Glacial Lake McConnell, and the surficial geology of parts of Slave River and Redstone River map areas, District of Mackenzie; Geological Survey of Canada, Bulletin 122.

Easton, R.M.
1981: Geology of Grant Lake and Four Corners map areas, Wopmay Orogen, District of Mackenzie; in Current Research, Part B, Geological Survey of Canada, Paper 81-1B, p. 83-94.
1982: Tectonic significance of the Akaitcho Group, Wopmay Orogen, Northwest Territories, Canada; unpublished Ph.D. dissertation, Memorial University of Newfoundland, St. John's, Nfld, 432 p.

Hildebrand, R.S.
1984a: Geology of the Rainy Lake-White Eagle Falls area, District of Mackenzie – Early Proterozoic cauldrons, stratovolcanoes, and subvolcanic plutons; Geological Survey of Canada, Paper 83-20, 42 p,
1984b: Geology, Rainy Lake-White Eagle Falls, District of Mackenzie, Northwest Territories; Geological Survey of Canada, Map 1589A.

Hildebrand, R.S. and Roots, C.F.
1985: Geology of the Rivière Grandin map area (Hottah terrane and western Great Bear magmatic zone), District of Mackenzie: in Current Research, Part A, Geological Survey of Canada, Paper 85-1A, p. 373-383.

Hildebrand, R.S., Hoffman, P.F., and Bowring, S.A.
– Tectonomagmatic evolution of the 1.9 Ga Great Bear magmatic zone, Wopmay Orogen, northwestern Canada; Journal of Volcanology and Geothermal Research. (in press)

Hildebrand, R.S., Bowring, S.A., Steer, M.E., and Van Schmus, W.R.
1983: Geology and U-Pb geochronology of parts of the Leith Peninsula and Rivière Canadian map areas, District of Mackenzie: in Current Research, Part A, Geological Survey of Canada, Paper 83-1A, p. 329-342.

Hildebrand, R.S., Annesley, I.R., Bardoux, M.V., Davis, W.J., Heon, D., Reichenbach, I.G., and Van Nostrand, T.
1984: Geology of the early Proterozoic rocks in parts of the Leith Peninsula map area, District of Mackenzie: in Current Research, Part A, Geological Survey of Canada, Paper 84-1A, p. 217-221.

Hoffman, P.F.
1972: Cross-section of the Coronation Geosyncline (Aphebian), Tree River to Great Bear Lake, District of Mackenzie (86J,K,O,P): in Report of Activities, Part A, Geological Survey of Canada, Paper 72-1A, p. 119-125.
1978: Geology of the Sloan River map area (86K), District of Mackenzie: Geological Survey of Canada, Open File 535 (map).
1984: Wopmay Fault Zone and its role in the evolution of Wopmay Orogen; Geological Association of Canada, Programs with Abstracts, v. 9, p. 74.

Hoffman, P.F. and McGlynn, J.C.
1977: Great Bear Batholith: volcano-plutonic depression; in Volcanic Regimes in Canada, W.R.A. Baragar, L.L. Coleman, and J.M. Hall (ed.); Geological Association of Canada, Special Paper 16, p. 170-192.

King, J.E.
1985: Structure of the metamorphic-internal zone, northern Wopmay Orogen, Northwest Territories, Canada; unpublished Ph.D. dissertation, Queen's University, Kingston, Ontario, p. 000-000.

King, J.E., St-Onge, M.R., and Lalonde, A.E.
1983: Wopmay Fault Zone – a major mylonite and brittle fault belt, Internal Zone, Wopmay Orogen; Geological Association of Canada, Programs with Abstracts, v. 8, p. 37.

Lord, C.S. and Parsons, W.H.
1947: The Camsell River map area; Geological Survey of Canada, Map 1014A.

McGlynn, J.C.
1974: Geology of the Calder River map area (68F), District of Mackenzie; in Report of Activities, Part A, Geological Survey of Canada, Paper 74-1A, p. 000-000.
1976: Geology of the Calder River (86F) and Leith Peninsula (86E) map areas, District of Mackenzie; in Current Research, Part A, Geological Survey of Canada, Paper 76-1A, p. 359-361.

Reichenbach, I.R.
1985: Stratigraphy and structure of the early Proterozoic Bell Island Group, District of Mackenzie; in Current Research, Part B, Geological Survey of Canada, Paper 85-1B, p. 151-160.
1986: The Bell Island Group: implications for the evolution of Wopmay Orogen; unpublished M.Sc. thesis, Carleton University, Ottawa, Ontario, 115 p.

St-Onge, M.R., King, J.E., and Lalonde, A.E.
1982: Geology of the central Wopmay Orogen (early Proterozoic), Bear Province, District of Mackenzie: Redrock Lake and the eastern portion of Calder River map areas, in Current Research, Part A, Geological Survey of Canada, Paper 82-1A, p. 99-108.
1984: Deformation and metamorphism of the Coronation Supergroup and its basement in the Hepburn Metamorphic-Plutonic Zone of Wopmay Orogen: Redrock Lake and the eastern portion of Calder River map areas, District of Mackenzie: in Current Research, Part A, Geological Survey of Canada, Paper 84-1A, p. 171-180.

St-Onge, M.R., Lalonde, A.E., and King, J.E.
1983: Geology, Redrock Lake and eastern Calder River map areas, District of Mackenzie: the central Wopmay Orogen (early Proterozoic), Bear Province, and the western Archean Slave Province, in Current Research, Part A, Geological Survey of Canada, Paper 83-1A, p. 147-152.

Geology of the Allan Creek area, southeastern Cariboo Mountains, British Columbia

EMR Research Agreement 138-04-86

Lisel D. Currie[1] and P.S. Simony[1]
Cordilleran and Pacific Margin Division

Currie, L.D. and Simony, P.S., Geology of the Allan Creek area, southeastern Cariboo Mountains, British Columbia; in Current Research, Part A, Geological Survey of Canada, Paper 87-1A, p. 713-718, 1987.

Abstract

A steep postmetamorphic normal fault separates kyanite-staurolite grade, migmatite in the north from garnet- to kyanite-grade, migmatite-free rocks in the south. A right-side-up succession south of the normal fault appears to be continuous, with rocks to the south. Middle Marble equivalents underlie Lower Kaza equivalents and metamorphic grade increases from garnet- to kyanite-grade toward the north. North of the normal fault an overturned sequence contains a thrust that placed Lower Kaza over Horsethief Creek strata. Overturning of this sequence predates phase-two deformation.

600 MPa must have prevailed north of the normal fault. The pressure difference across the normal fault is near 100 MPa, suggesting an offset of about 4 km. Consequently, offset on the Albreda River Fault may be less than that on the North Thompson River Fault.

Résumé

Une faille normale à fort pendange, post-métamorphique, sépare des migmatites à faciès de cyanite-staurolite au nord des migamtites-roches libres à faciès de grenat à cyanite au sud. Au sud de la faille normale, une succession en position normale semble être continue avec des roches au sud. Des équivalents du Marble moyen sont sous-jacents à des équivalents du Kaza inférieur et le degré de métamorphisme augmente: il passe du faciès de grenat au faciès de cyanite vers le nord. Au nord de la faille normale, une séquence renversée est associée à une faille inverse qui ramène les couches du Kaza inférieur au-dessus des couches de Horsethief Creek. Le renversement de cette séquence s'est effectué avant la déformation de la phase deux.

Au nord de la faille normale, la pression a dû être de 600 MPa. La différence de pression à travers la faille normale est de l'ordre de 100 MPa, laissant supposer un décrochement d'environ 4 km. Par conséquent, le décrochement de la faille d'Albreda River pourrait être plus petit que celui de la faille de North Thompson River.

[1]Department of Geology and Geophysics, University of Calgary, Calgary, Alberta T2N 1N4

INTRODUCTION

Metasedimentary rocks have been correlated from the Purcell and Selkirk mountains into the Monashee and Cariboo mountains (Poulton and Simony, 1980; Brown et al., 1978; Pell and Simony, 1984; Struik, 1986). Fieldwork conducted in the Cariboo mountains during summer 1986, at a scale of 1:24 000, carried the detailed work northward into the area north of the North Thompson River, south of Camp Creek and east of Adolf Creek (Fig. 74.1, 74.2). The area was previously mapped at a scale of 1:250 000 by Campbell (1968) who placed the rocks in the late Proterozoic Kaza Group.

STRATIGRAPHY

In the field area two packages of mappable stratigraphic units are separated by a postmetamorphic fault (Fig. 74.2, 74.3). The southern package is composed of four units: a marble at the base; a semipelite unit; a phyllite unit; and a calcareous unit. The marble outcrops only in the southwest corner of the study area (Fig. 74.2). In addition to pure white marbles, semipelites (psammites with greater than 5% biotite) and micaceous and psammitic carbonates are present within this unit.

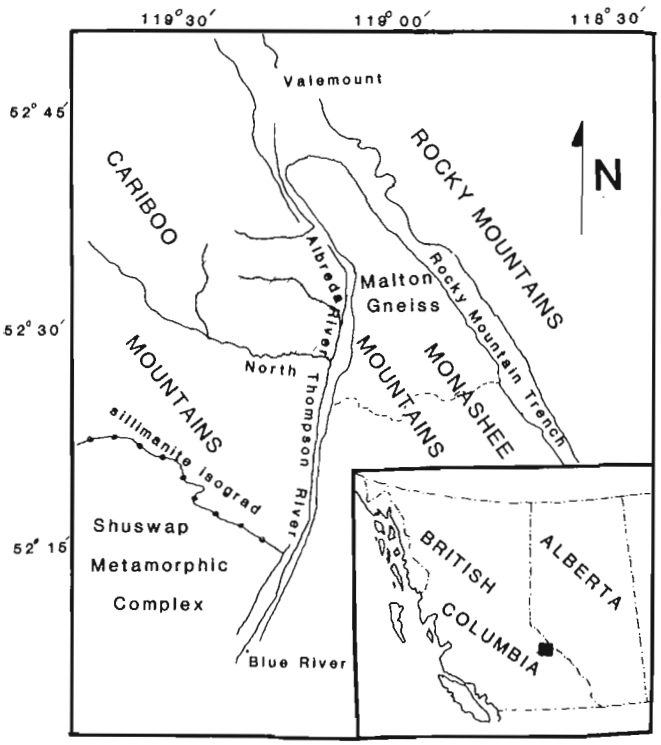


Figure 74.1. Location map for the Allan Creek area and relevent adjacent geological features. Ruled pattern shows the location of the study area.

The marble unit is overlain by a clastic unit of well-layered, platy semipelites. The layers are generally 5 to 20 cm thick and are separated by thin (millimetre scale) biotite schist partings (Fig. 74.4).

Above the semipelite is a unit dominated by black graphitic phyllites, and characterized by tight isoclinal folds and quartz veins which are also tightly folded. Minor carbonate and semipelite layers are infolded with phyllites. Although carbonate layers are more common near the top of this unit, the boundary between the phyllite unit and the overlying calcareous unit is abrupt and therefore easily mapped.

The calcareous unit is composed of psammitic and micaceous carbonate layers which are generally 0.5-1 m thick. Black phyllitic layers, and less commonly, semipelite layers are interbedded with the carbonate layers. Throughout the unit carbonate-dominated sequences, 3-10 m thick, alternate with slightly thinner phyllite-dominated sequences. A few 10 m thick semipelite layers outline the large scale structures within this unit, as shown in Figure 74.3.

Four stratigraphic units characterize the sedimentary package exposed north of the postmetamorphic fault, as displayed in Figure 74.2. The unit immediately north of the fault is dominated by black biotite-muscovite schist, semipelite and granule conglomerates (grits). It is followed to the north by a unit characterized by silvery muscovite schist. Farther north these two units structurally overlie a pelitic schist unit that in turn overlies a semipelite-amphibolite unit (Fig. 74.2, 74.3).

The black schist clastic unit, which is the southernmost unit of the northern package, is characterized by alternating, 3-10 m thick sequences of clastic rocks and sequences dominated by black, graphitic, biotite-muscovite schists. The clastic sequences are composed of granule conglomerates, semipelites, and minor schists. The schists, which resemble layers seen in the phyllite unit of the southern package, dominate the black schist sequences. Hornblende-rich amphibolites, calc-silicates, and leucocratic quartz-garnet-hornblende granofelses, similar to those described by de Vries (1971), form layers that make up less than 1% of this unit.

Next to the north is the muscovite schist clastic unit. It can be distinguished from the previous clastic unit by the replacement of black, graphitic, biotite-muscovite schist by light coloured biotite-muscovite schist, and the lack of hornblende-rich amphibolites and quartz-garnet-hornblende granofelses.

The pelitic schist underlies the muscovite-schist clastic unit and is primarily composed of biotite-muscovite schist and muscovite schist, which resemble schists seen in the overlying clastic unit.

The northernmost unit is characterized by platy semipelite layers (5-20 cm thick) that are interlayered with biotite or garnet-biotite partings (up to 3 cm thick), or hornblende or

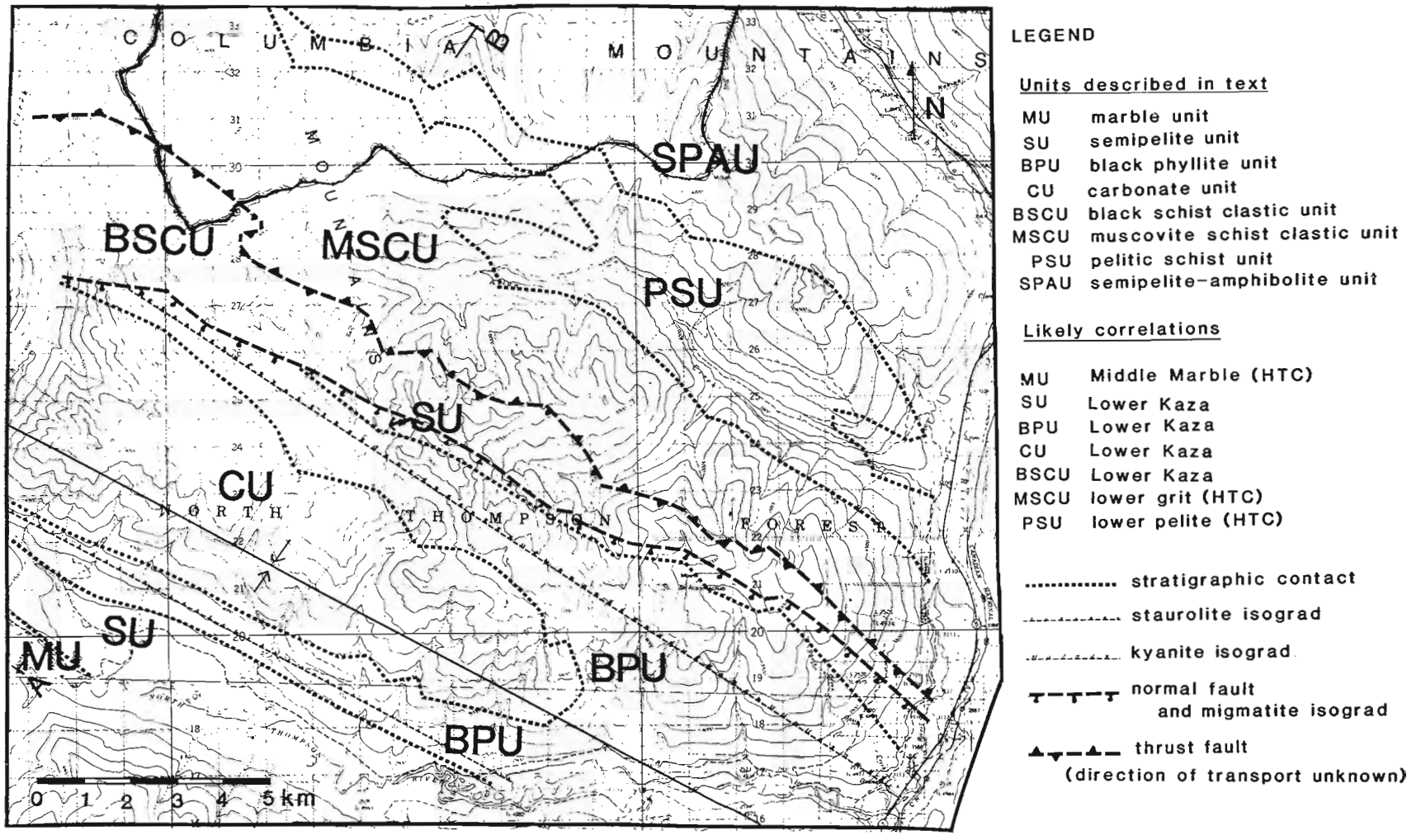


Figure 74.2. Geological map of the Allan Creek area. Likely correlations are presented in the legend.

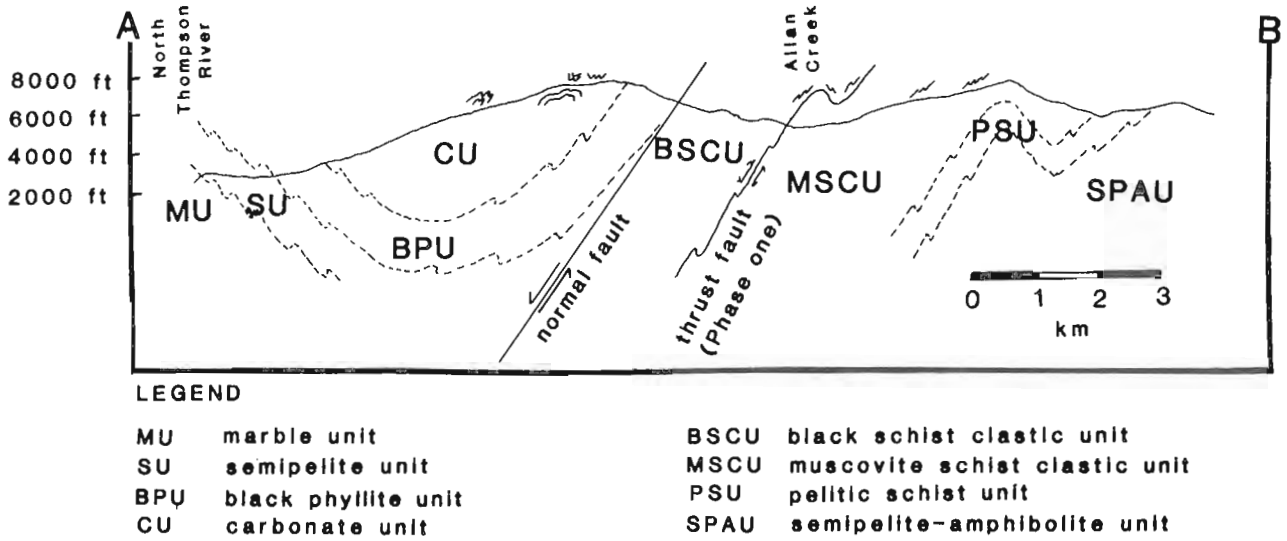


Figure 74.3. Cross-section A-B, showing the location of the late normal fault that separates two sedimentary packages and the phase-one thrust fault.

hornblende-garnet amphibolite layers (up to 30 cm thick). To the northeast the biotitic partings become thinner and the amphibolite layers become thicker (1-2 m thick), but are less common. Pelite dominated sequences (3-10 m thick) alternate with semipelite and granule conglomerate dominated sequences, resulting in strata which resemble the muscovite schist clastic unit.

Stratigraphic units which occur south of the normal fault appear to be continuous with, and therefore have been correlated with, stratigraphic divisions in the area south of the North Thompson River that have been described by Pell and Simony (1984). The marble unit is correlated with the Middle Marble division, the overlying semipelite unit with the Lower Kaza, and the black phyllite and carbonate units are thought to be a facies of the Lower Kaza (Fig. 74.2).

Immediately north of the postmetamorphic fault, rocks of the black schist clastic unit are thought to belong to the Lower Kaza Group, based on the presence of quartz-garnet-hornblende granofelses, hornblende amphibolites and granule conglomerates. he stratigraphic units to the north resemble rocks exposed in the Monashee Mountains and are correlated with divisions of the Horsethief Creek Group. The muscovite-schist clastic unit is correlated with the lower grit division of the Horsethief Creek Group, the schist unit is correlated with the lower pelite division, and the semipelite-amphibolite unit is correlated with the Semipelite-Amphibolite division.

If these correlations are correct, the Horsethief Creek strata must be overturned and in fault contact with the overlying Lower Kaza Group rocks (black schist clastic unit). Upside-down grading sequences (fining downwards) in granule conglomerates of the Lower Kaza suggest that this unit is also overturned, although the fine grained nature of many of the rocks, the high metamorphic grade and the presence of small scale folds prevent this interpretation from being unambiguous.

STRUCTURE

At least three phases of deformation can be documented within the study area. Structures which represent the first phase include: mesoscopic isoclinal folds in which the alignment of biotite flakes defines an axial plane schistosity; a large fold structure responsible for overturning the northern package prior to the development of subsequent folds; and a thrust which carries rocks belonging to the lower grit division of the Horsethief Creek Group, over Lower Kaza rocks (Fig. 74.2). The direction of transport on the thrust fault is, however, unknown.

Tight to isoclinal, northeast-verging mesoscopic phase-two folds, with shallowly plunging, east-southeast-trending fold axes, are common throughout the area (Figs. 74.3, 74.5). A large synform, located south of Allan Creek (Figs. 74.2, 74.3), is interpreted to be a phase-two structure, based on its fold-axis orientation and the vergence of the associated mesoscopic folds. In the north, phase-two folds are superimposed on the previously overturned northern package, including the phase-one thrust fault.

Mesoscopic evidence for later phases of deformation is present in the form of open folds, crenulations, and minor faults. On a larger scale, a postmetamorphic, south dipping, normal fault within the Allan Creek area juxtaposes two package of Lower Kaza strata (Fig. 74.2, 74.3). Two major normal faults occur near the study area. Southeast of the area the west-side-down North Thompson River Fault juxtaposes

the Malton Gneiss and late Proterozoic stratigraphy (Campbell, 1968; Pell nd Simony, 1984). Farther north, east of the study area, a fault follows the Albreda River valley, and is therefore called the Albreda River Fault (Fig. 74.1).

METAMORPHISM

Throughout the area metamorphism is garnet-grade or higher and increases toward the north. The location of the metamorphic isograds is shown in Figure 74.2. Isograds are subparallel with the regional structures, however, the pattern of metamorphic zones is complicated by a postmetamorphic normal fault. South of the fault, metamorphic grade increases from garnet-grade in the south, through staurolite- to kyanite-grade. North of the fault migmatites, kyanite and staurolite coexist.

In schistose rocks migmatite forms small lenses (50 × 100 mm) of quartz and feldspar, which lie in the plane of the foliation. In psammitic rocks quartzofeldspathic migmatite layers (less than 1 cm thick) are parallel with the regional foliation. As metamorphic grade increases, the lenses become larger (up to 30 × 100 cm) and the layers become thicker and more abundant, resulting in a gneiss-like fabric.

Isograds located south of the normal fault can be aligned with isograds mapped by Pell (1984) south of the North Thompson River. North of the normal fault, the presence of migmatite in kyanite- and staurolite-grade rocks suggests that the rocks have experienced pressures greater than 600 MPa (cf. Raeside, 1982) and may be similar to migmatite-bearing kyanite-grade rocks east of the Albreda Fault described by Morrison (1982).

CONCLUSIONS

Tentative stratigraphic correlations suggest that, in the Allan Creek area of the southern Cariboo Mountains, Horsethief Creek strata were thrust over Lower Kaza rocks, and the duplicated sequence, now exposed in the northern half of the

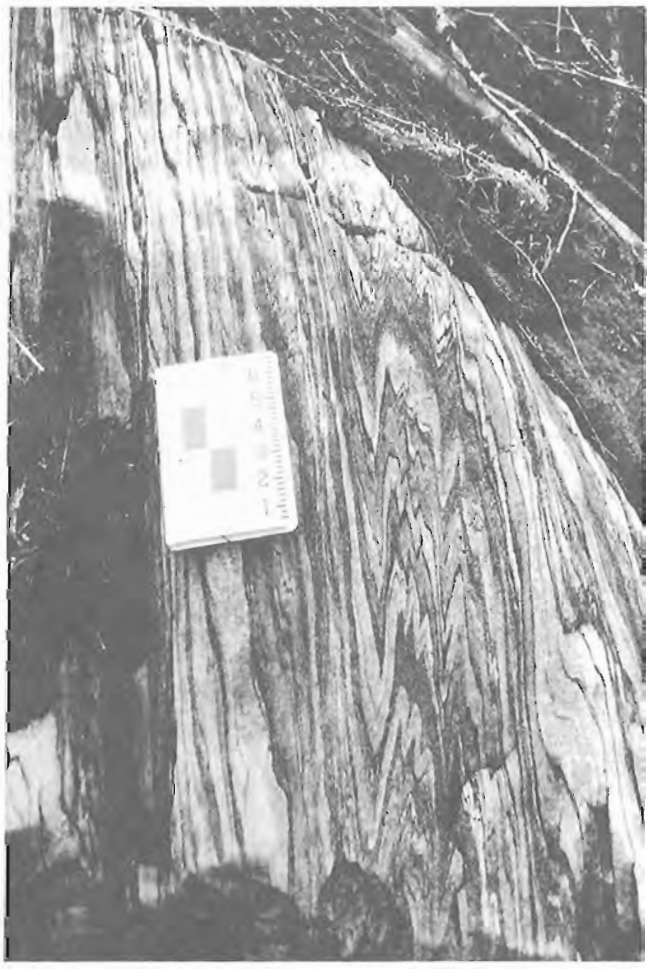


Figure 74.4. Slightly oblique view of folds in the semipelite unit.



Figure 74.5. View to the southeast of northeast-verging folds in the muscovite schist clastic unit.

Allen Creek area, was overturned during phase-one deformation. Phase-two structures refold the phase-one thrust and form a large scale, north-verging synform in the right-way-up sequence south of the normal fault. The synform is part of a fan structure mapped by Campbell (1968) and Pell (1984).

A postmetamorphic normal fault juxtaposes the right-way-up Lower Kaza rocks of the south with the overturned Horsethief Creek and Lower Kaza strata to the north. Since minimum pressures of 600 Mpa are estimated for the rocks north of the fault, and pressures of 470 MPa (Pell, 1984) have been estimated for rocks that may be continuous with rocks south of the fault, he pressure difference across the fault may be of the order of 100 MPa. This corresponds to an offset of approximately 4 km, assuming a density of 2.8 g/cm3 for the overlying material. An offset of approximately 4 km has been determined for the North Thompson River fault by Pell (1984). The similarity of mineral assemblages and migmatite west and east of the Albreda River Fault suggests that movement on the Albreda River Fault is less (perhaps 1 km less) than on the North Thompson River Fault. This is consistent with the 4 km-downward displacement of the block south of the Allan Creek normal fault and west of the North Thompson River Fault.

REFERENCES

Brown, R.L., Tippet, C.R., and Lane, L.S.
1978: Stratigraphy, facies changes and correlations in the northern Selkirk Mountains, southern Canadian Cordillera; Canadian Journal of Earth Science, v. 15, p. 1129-1140.

Campbell, R.B.
1968: Geology of the Canoe River, British Columbia; Geological Survey of Canada, Map 15-1967.

de Vries, C.D.S.
1971: Metamorphism and structure of the Esplanade Range, British Columbia; unpublished M.Sc. thesis, University of Calgary, Calgary, Alberta.

Morrison, M.L.
1982: Structure and petrology of the Malton Gneiss Complex; unpublished Ph.D. thesis, University of Calgary, Calgary, Alberta.

Pell, J.
1984: Stratigraphy, structure and metamorphism of Hadrynian strata in the southeastern Cariboo Mountains, British Columbia; unpublished PhD thesis, University of Calgary, Calgary, Alberta.

Pell, J. and Simony, P.S.
1984: Stratigraphy of the Hadrynian Kaza Group between the Azure and North Thompson Rivers, Cariboo Mountains, British Columbia; in Current Research, Part A, Geological Survey of Canada, Paper 84-1A, p. 95-98.

Poulton, T.P. and Simony, P.S.
1980: Stratigraphy, sedimentology and regional correlation of the Horsethief Creek Group (Hadrynian, Late Precambrian) in the northern Purcell and Selkirk Mountains, British Columbia; Canadian Journal of Earth Science, v. 17, p. 1708-1724.

Raeside, R.P.
1982: Structure, metamorphism and migmatization of the Scrip Range, Mica Creek, British Columbia; unpublished Ph.D. thesis, University of Calgary, Calgary, Alberta.

Struik, L.C.
1986: Imbricated terranes of the Cariboo gold belt with correlations and implications for tectonics in southeastern British Columbia; Canadian Journal of Earth Science, v. 23, p. 1047-1061.

Stratigraphy and structure of the northeast margin of the Bowser Basin, Spatsizi map area, north-central British Columbia

Project 770016

C.A. Evenchick
Cordilleran and Pacific Margin Division, Vancouver

Evenchick, C.A., Stratigraphy and structure of the northeast margin of the Bowser Basin, Spatsizi map area, north-central British Columbia; in Current Research, Part A, Geological Survey of Canada, Paper 87-1A, p. 719-726, 1987.

Abstract

Tight folding and related thrust faulting along the boundary of Bowser and Sustut basins accommodated a great amount of northeasterly shortening of the Jurassic and Cretaceous strata. A thrust fault, which places Lower Jurassic volcanic rocks on middle Cretaceous nonmarine strata, indicates significant tectonic burial of rocks which are a potential source for hydrocarbons. Different structural levels of the contractional deformation are exposed in blocks bounded by steeply dipping, dip-slip faults. Some of the dip-slip faults were active after a post-Kimmeridgian/pre-Albian phase of contractional deformation and prior to Late Cretaceous contractional deformation.

Elements of stratigraphy in the northernmost part of Bowser Basin can be roughly correlated with those near thelappan anthracite coal deposits. An Upper Jurassic(?) shallow marine to nonmarine succession that overlies the Ashman Formation (marine) in the north, may correlate with the lower part of the coal-bearing sequence farther south.

Résumé

Les plis serrés et le chevauchement associé qu'on retrouve le long de la limite des bassins de Bowser et de Sustut sont accompagnés d'un raccourcissement important vers le nord-est des strates jurassiques et crétacées. Une chevauchement qui ramène des roches volcaniques du Jurassique inférieur sur des roches non marines du Crétacé moyen indique un enfouissement tectonique important de roches qui constituent une source possible d'hydrocarbures. Différents niveaux structuraux de la déformation par contraction sont exposés dans des blocs limités par des failles transversales d'effondrement à fort pendage. Certaines failles ont été actives après la phase de déformation par contraction du post-Kimméridgien/pré-Albien et avant la déformation par contraction du Crétacé supérieur.

Il est plus ou moins possible de corréler des éléments de stratigraphie de la partie la plus septentrionnale du bassin de Bowser avec ceux qui sont à proximité des gisements d'anthracite dur de Klappan. Il est possible de corréler une succession marine à non marine peu profonde du Jurassique supérieur (?), qui repose sur la formation d'Ashman (marine) au nord, avec la partie inférieure de la séquence riche en charbon plus au sud.

INTRODUCTION

In summer 1986, mapping at 1:50 000 scale continued in Spatsizi map area (Fig. 75.1). The project was begun in 1985 to gain a better understanding of the structural style and tectonic setting of the northeastern margin of Bowser Basin (Evenchick, 1986).

The Bowser Basin contains Middle to Upper Jurassic marine and nonmarine clastic sediments (Bowser Lake Group) that overlie Lower Jurassic volcanic rocks of the Hazelton Group (Cold Fish volcanics), and fine grained, in part volcanogenic(?) sediments of the Spatsizi Group. It is bounded to the northeast by Cretaceous, mainly nonmarine sediments of Sustut Basin (Sustut Group). Northeast-verging folds and thrust faults that involve strata of the Bowser and Sustut basins, and their basement, have accommodated major northeasterly contraction. Steeply dipping dip-slip faults were active prior to deposition of the Sustut Group and after contractional deformation of the lower part of the Sustut Group.

A synthesis of the stratigraphy and its relationship to regional tectonics was described by Evenchick (1986). This report addresses: stratigraphy of Bowser Lake Group at the northeasternmost part of Bowser Basin, and possible correlation with the stratigraphy in the vicinity of the Klappan coal deposits to the south; and structure in the east-central part of the area and its implications for regional structure, stratigraphy, and timing of deformation.

STRATIGRAPHY OF THE BOWSER LAKE GROUP

The term Bowser Lake Group was first used by Tipper and Richards (1976) for Upper Jurassic marine strata in the southern Bowser Basin. It was applied to Middle and Upper Jurassic strata in the northern part of the basin by Gabrielse and Tipper (1984).

The base of the Bowser Lake Group is largely dark grey to black marine shale and siltstone, but in the extreme northeastern part of the basin coarse conglomerate lenses occur with the siltstone. Ammonites indicate a Bathonian to Callovian age (Gabrielse and Tipper, 1984, and personal communication, 1986). The shale sequence is overlain by a coarsening-up clastic sequence, and the youngest sediments known (Oxfordian-Kimmeridgian-Tipper, personal communication, 1986) are coarse, massive, chert-pebble to cobble conglomerate.

The Bowser Lake Group is most complete in a plunging anticline-syncline pair between the culmination of Cold Fish

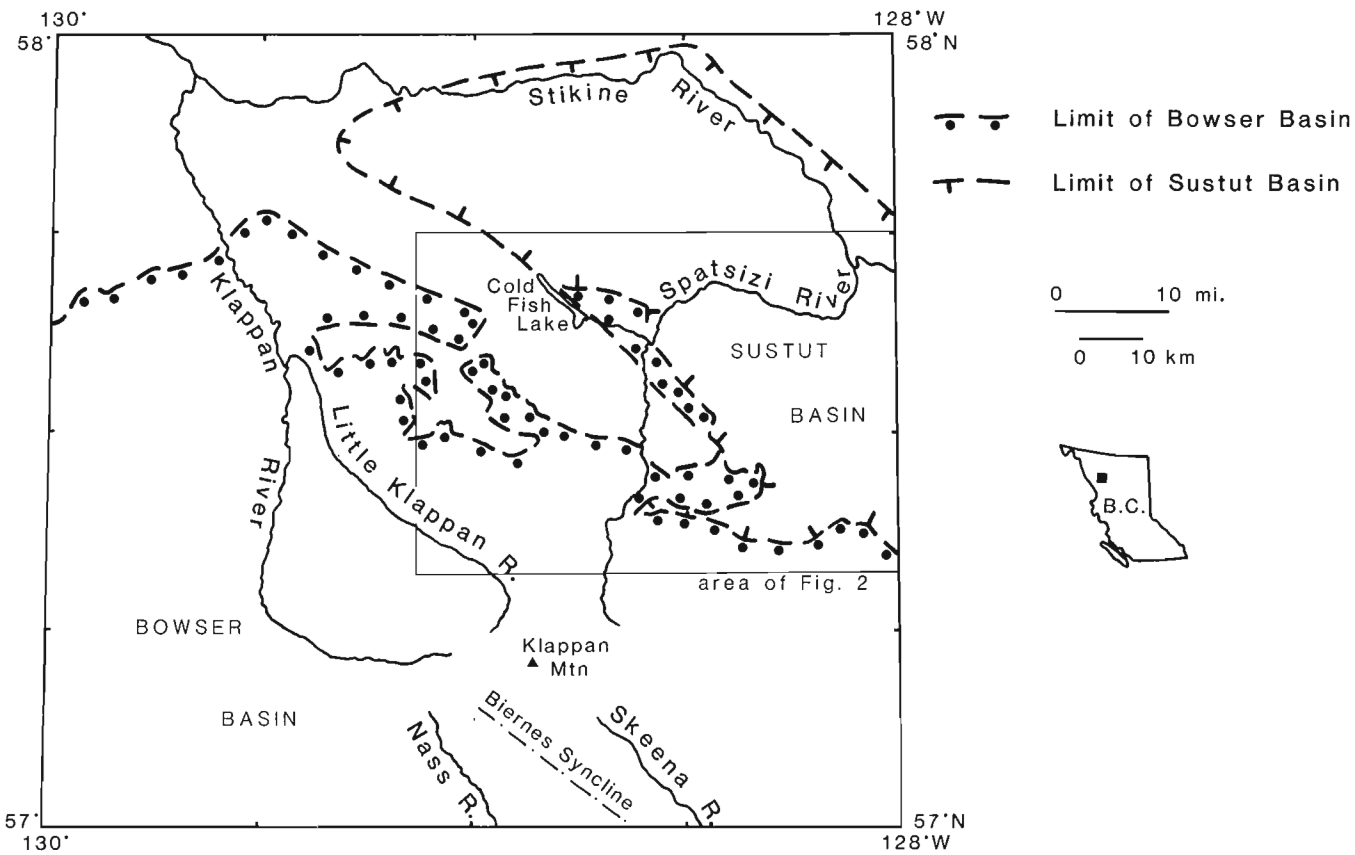
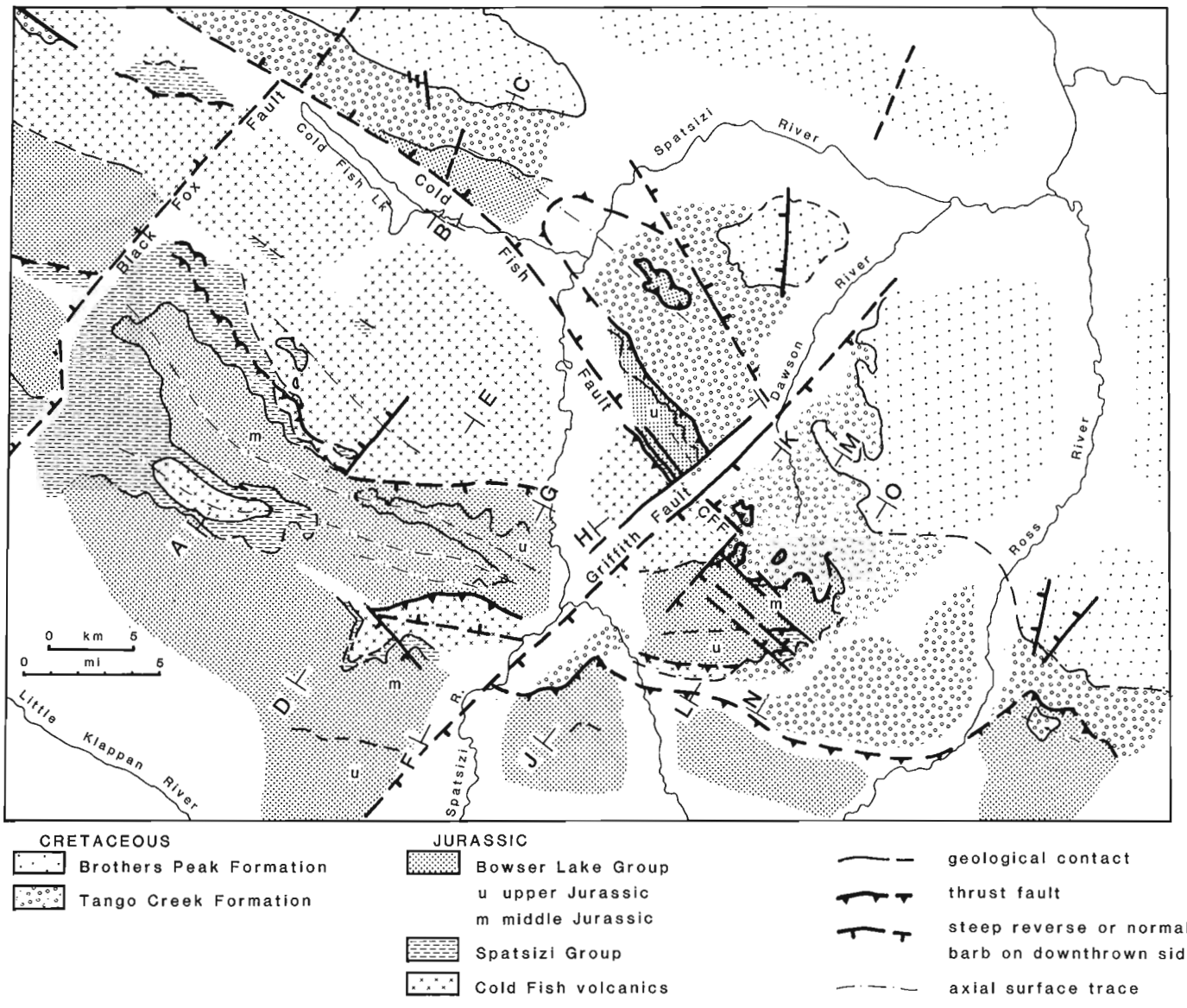


Figure 75.1 Map showing regional geological and geographic features of Spatsizi map area and the location of the study area.

volcanics at the Joan Lake Anticline and the core of a syncline west of the Spatsizi River valley (Fig. 75.2, 75.6 between sections DE and FG). The volcanics in the Joan Lake Anticline are overlain by sediments of the Spatsizi Group which thin to the northeast, and are overlain by the Bowser Lake Group. The base of the Bowser Lake Group is black siltstone. About 30 m above the base is a massive conglomerate member about 20 m thick that is locally made up of coalescing lenses. The conglomerate is overlain by thick, black and grey siltstone (Fig. 75.3), and then by siltstone with coalescing lenses of conglomerate on the north limb of the syncline, less common lenses on the south limb, and rare lenses to the southeast. The sequence of dominantly siltstone with varying amounts of chert-pebble conglomerate is about 1500 m thick. It is overlain gradationally by a unit of siltstone interbedded with intervals about 10 to 15 m thick of massive, medium grained, very well sorted, chert sandstone (Fig. 51.4). Chert-pebble conglomerate is rare and the unit has marine and nonmarine fossils. The sandstone/siltstone interval is 50 to 100 m thick. It is overlain by a rusty weathering sequence characterized by thick, massive, chert-pebble to cobble conglomerate (Fig. 75.5). Interbeds of siltstone and sandstone occur from 20 m above the base to the highest exposed beds. They comprise about 15% of the unit, and are generally less than 1 m thick. The thickest is near the top of the unit and is 15 m thick. The sandstone interbeds have abundant, coalified plant remains up to 15 cm long; one calcareous sandstone interval near the highest exposed strata



CRETACEOUS
Brothers Peak Formation
Tango Creek Formation

JURASSIC
Bowser Lake Group
u upper Jurassic
m middle Jurassic
Spatsizi Group
Cold Fish volcanics

geological contact
thrust fault
steep reverse or normal fault, barb on downthrown side
axial surface trace

Figure 75.2 Geological map of the study area.



Figure 75.3 View south to siltstone of the Ashman Formation.



Figure 75.4 View northwest to the interbedded siltstone and sandstone unit above the Ashman Formation. The dashed black line marks the base of the conglomeratic unit that overlies the siltstone/sandstone unit.

has pelecypods, ammonites, and belemnites. The age of these beds based on the ammonite fauna is Oxfordian/Kimmeridgian (Tipper, personal communication, 1986).

Four kilometres to the south, Pliensbachian Cold Fish volcanics are in fault contact with the Bowser Lake Group (Fig. 75.2, 75.6), and are overlain by 100 m of Spatsizi Group. At the base of the Bowser Lake Group, black siltstone with one member of resistant conglomerate about 30 m thick occurs 10 to 20 m above the base. The conglomerate is overlain by a thick (at least 1000 m), folded black siltstone sequence with less than 5% sandstone and no conglomerate. Six kilometres southwest of the base of the Bowser Lake Group contact, the sequence is overlain by siltstone interbedded with white weathering massive sandstone (Fig. 2). Two kilometres farther southwest, and across anticlinal and synclinal closures, the sequence is overlain by very rusty weathering, massive, well sorted, sandstone interbedded with black siltstone, rare conglomerate, and coal. Marine and nonmarine fossils are present. Similar lithologies have been described by Koo (1986) and Moffat (1985) in this area and south of Klappan Mtn., in the Biernes Syncline (Fig. 75.2).

From the transect described above, and two days spent in the Biernes Syncline, the following conclusions can be made.

A dark grey to black siltstone and shale unit (Fig. 75.3) with middle Jurassic marine fossils and varying amounts of chert-pebble conglomerate lenses can be mapped regionally. The term Ashman Formation (defined by Tipper and Richards, 1976) has been applied to this sequence by Gabrielse and Tipper (1984). Overlying the Ashman Formation is a unit of siltstone interbedded with sandstone (Fig. 75.4) that is distinct from overlying massive pebble conglomerate in the north, and sandstone interbedded with siltstone, conglomerate, and coal in the south. Along trend to the northwest, a similar sequence of Ashman Formation overlain by sandstone and siltstone, then by pebble conglomerate with Oxfordian/Kimmeridgian fossils occurs in the northwest corner of the Bowser Basin (Tipper, personal communication, 1986).

The Ashman Formation is lithologically similar to the part of the Jackson unit below the top 100 m as described by Bustin and Moffat (1983). Fossils from 100 m below the top of the Jackson unit are pre-Oxfordian (C. Stelck, *in* Bustin and Moffat, 1983) and are consistent with the Bathonian/Callovian age assigned to the Ashman Formation by Gabrielse and Tipper (1984). The overlying sandstone/siltstone unit in the north may be equivalent to the upper Jackson unit, which has similar lithologies and Oxfordian ammonites (P. Smith, *in* Bustin and Moffat, 1983). The upper conglomerate (with abundantlant debris) in the north may represent channels feeding a thick prograding deltaic sequence farther south, which is represented by part of the coal-bearing Currier and younger units in the Biernes Syncline (Fig. 1 and see Moffat, 1985). An Upper Jurassic age for plant fossils in the Currier unit (Rouse, in Bustin and Moffat, 1983) supports the correlation. The age of the youngest coal-bearing strata in the Biernes Syncline is unknown; they may have no time-equivalent in the north, due to either erosion, or to burial by thrust sheets.



Figure 75.5 View northwest to a syncline of massive chert-pebble conglomerate at the top of the Bowser Lake Group. The dashed black line marks the base of the unit.

According to Bustin and Moffat (1983) and Koo (1986), in the Biernes Syncline the thick sequence of siltstone with sandstone, abundant plant fossils, minor conglomerate and coal is overlain by a massive conglomeratic sequence with minor sandstone and siltstone, informally named the Devils Claw unit by Bustin and Moffat (1983). Palynology on samples from the sequence yielded an Albian age (Moffat, 1985). However, rocks of the same age in the Sustut Basin (the basal Tango Creek Formation) are sandstone and siltstone with abundant, coarse detrital muscovite that is expected to be easilyransported throughout the depositional system. An Albian age for the Devils Claw unit presents an enigma because the rocks in the Biernes Syncline bear no resemblance to Albian rocks of the Sustut Basin 35 km to the northeast. Possibly a northwest-trending arch was present in Albian time between the Sustut Basin and the area that eventually became the Biernes Sycnline. This explanation is consistent with latest Jurassic to early Cretaceous deformation inferred from a structural analysis of the region.

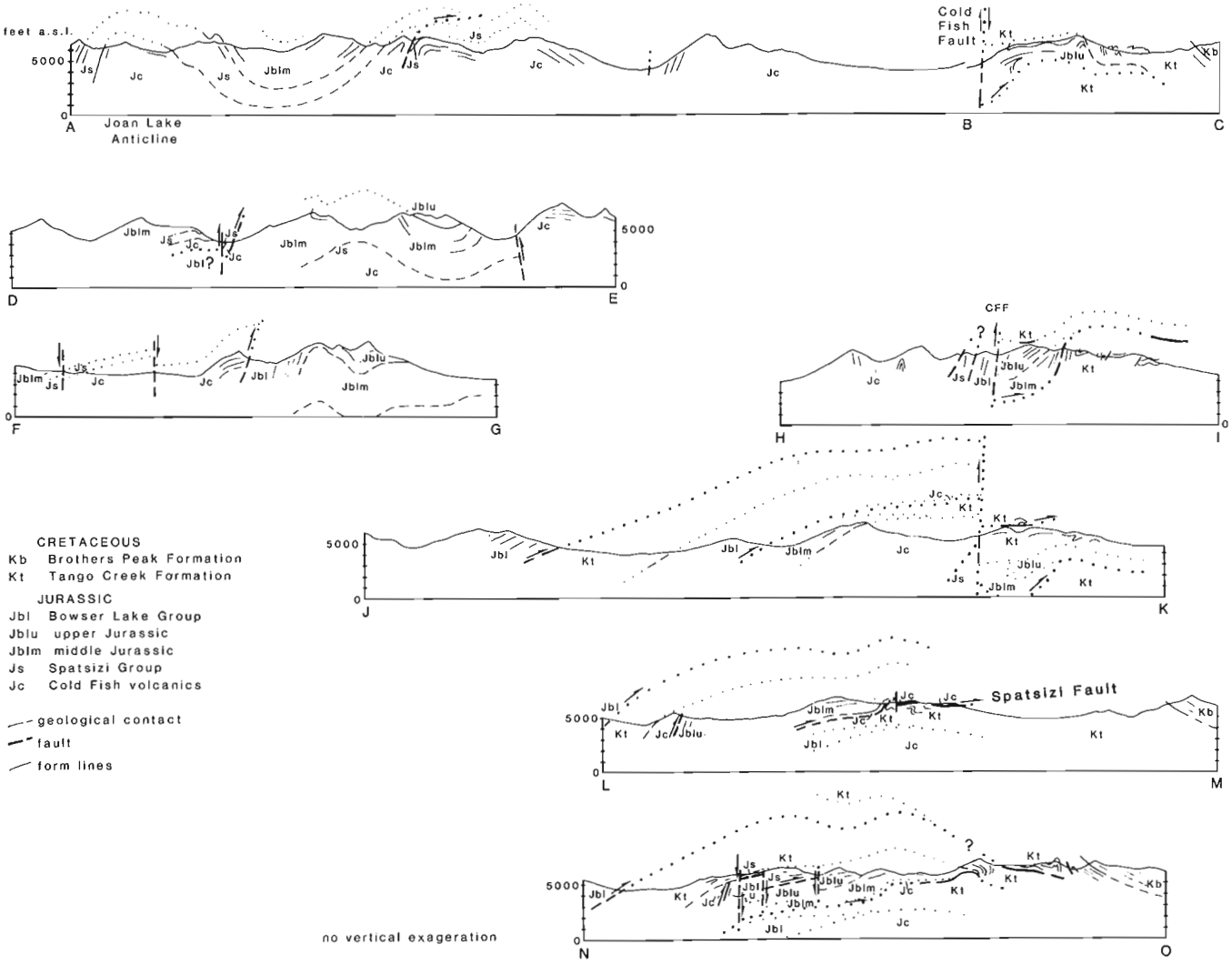


Figure 75.6 Schematic cross-sections of the study area. The locations of the sections are shown in Figure 75.2.

STRUCTURE

The focus of this contribution is on interpretation of the distribution of map units and map-scale structures. Strata involved in major northeasterly-verging contractional deformation at the northern boundary of the Bowser and Sustut basins are: Pliensbachian Cold Fish volcanics, Toarcian to Bajocian Spatsizi Group, Bathonian to Kimmeridgian Bowser Lake Group, and Albian to Santonian(?) Tango Creek Formation of the Sustut Group. High angle dip-slip faults divide the region into blocks in which the contractional structures can be traced coherently along trend and plunge. The structural geometry in the area between two dip-slip faults, the Black Fox and Griffith faults (Evenchick, 1986, Fig. 75.6, sections ABC, DE, FG) is relatively straightforward. Locating those structures on the southeast side of Griffith Fault is not straightforward, in part because of the complexity of the contractional structures. The structure of the two areas is tentativly linked by attempting to match structures in a block-faulted area immediately southeast of the Griffith Fault (Fig. 75.6, section JK) with those in section HI, which can in turn be related along plunge to those in section BC.

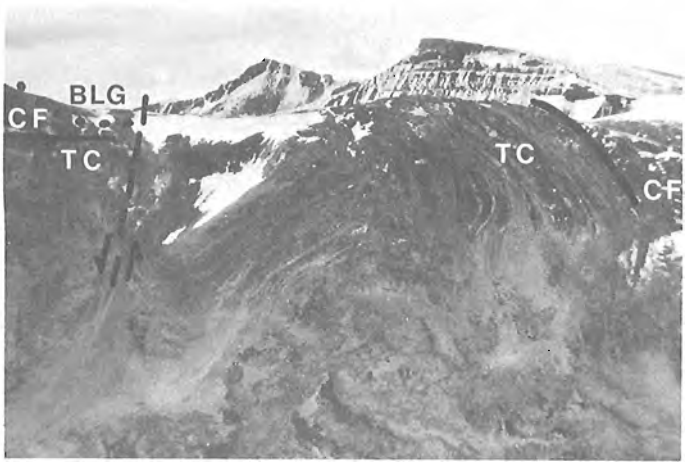


Figure 75.7 View southeast to the Spatsizi fault where it outcrops in section LM. The fault is marked by a solid black line, the dashed line is a dip-slip fault that cuts the Spatsizi fault. Cold Fish volcanics CF; Bowser Lake Group BLG; Tango Creek Formation TC.

NORTHWEST OF GRIFFITH FAULT

The Cold Fish volcanics, Spatsizi Group, and Bowser Lake Group are folded into a gently southeasterly plunging upright anticline-syncline pair that tightens to the southeast and has a curved axial surface trace. Although the core of the Joan Lake Anticline appears to be doubly plunging, the disappearance of volcanics to the northwest is probably an expression of thicker Spatsizi Group preserved beneath the Bowser/Spatsizi unconformity. The adjacent syncline outlined by the contact between the Spatsizi and Bowser Lake groups does not plunge to the northwest. The north contact of the Spatsizi Group with the volcanics is a folded and faulted unconformity (Fig. 75.6, section AB). In section DE the contact is a reverse fault that forms the south boundary of a block of uplifted volcanics. In section FG the volcanics are in steep fault contact with the Bowser Lake Group. The fault is either the ramp of a thrust fault, or is a reverse fault. High angle faults south of the thrust(?) fault offset contacts several hundred metres.

SOUTHEAST OF GRIFFITH FAULT

The most significant newly identified thrust fault puts Cold Fish volcanics on Tango Creek Formation (Fig. 75.6, section LM), and is herein informally named the Spatsizi fault. The Spatsizi fault is gently dipping where the volcanic rocks occur as two klippen on the top of a ridge of folded Tango Creek Formation. The volcanics are in steep fault (ramp) contact with the Tango Creek Formation 200 m south of the southmost klippe, and are overlain by the Bowser Lake Group (Fig. 75.7). In places the volcanics in the hanging wall of the fault are absent or are only 1-2 m thick and interleaved with the Bowser Lake Group. The Spatsizi fault can be followed downplunge southeast to section NO, where the Bowser Lake Group, low on the hillside, lies structurally on the Tango Creek Formation (Fig. 75.8). Near the top of the same ridge, the Bowser Lake Group is unconformably overlain by the Tango Creek Formation (Fig. 75.8). To the northeast, the unconformity is interpreted to be folded and cut by a hanging wall ramp as the Spatsizi fault cuts up-section (Fig. 75.6, section NO). The fault dips northeast because it is on the northeast limb of an anticlinal warp that postdates all contractional structures. The Tango/Bowser unconformity that outcrops in section NO can be traced to the southwest several kilometres. Where the unconformity crosses a small gully

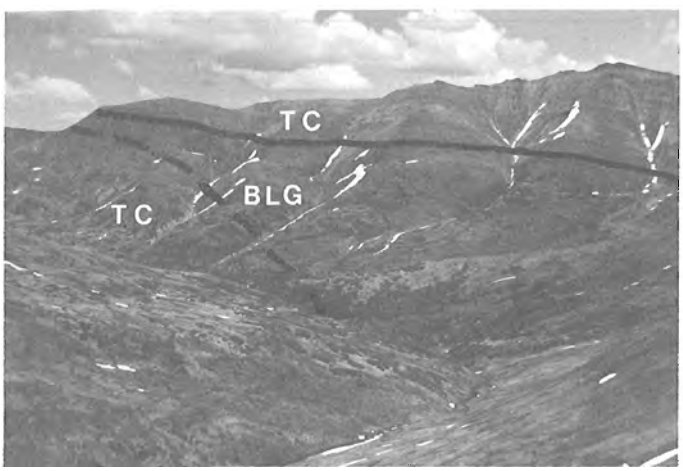


Figure 75.8 View southeast to the relationships illustrated in section NO. The Tango Creek Formation lies unconformably on Bowser Lake Group, which is thrust over the Tango Creek Formation. The solid line is the unconformity, and the dashed line is the Spatsizi fault.

3 km southwest of the right side of Figure 75.8, the underlying rock is siltstone of the Spatsizi Group. The Spatsizi Group has a structural thickness of 500 m from ridge top to valley bottom, and is inferred to be thrust on the Bowser Lake Group on slopes to the north. Another 1.5 km southwest, the Spatsizi Group beneath the unconformity abruptly has a structural thickness of 100 m, and is structurally above the Bowser Lake Group. Less than 1 km to the southwest, the Tango Creek Formation is dropped against the Spatsizi Group by a northwest-trending high angle fault, and below the unconformity is conglomerate of the upper Bowser Lake Group in steep fault contact with volcanics (Fig. 75.6, section NO). The presence of different units, and abrupt changes in thickness of units unconformably below the Tango Creek Formation is interpreted to be a result of pre-Albian deformation. The thrust fault that places Spatsizi Group on the Bowser Lake Group is offset by high angle faults that are overlapped by the Tango Creek Formation, and therefore the high angle faults, and the thrust fault are pre-Albian. The distribution of various map units in the valley north of the unconformity suggests that the steep faults are northwest-trending. The geometry of units could be accounted for if the Cold Fish volcanics and Spatsizi Group were thrust onto the upper Bowser Lake Group. The thrust fault was folded, and as a result the hanging wall ramp of volcanics on the Bowser Lake Group is steeply dipping as in section NO, and the fault is gently dipping where the Spatsizi Group overlies the Bowser Lake Group. The thrust fault was cut by two northwest-trending high angle faults that dropped it down to the northeast. Following erosion, basal Tango Creek Formation (Albian) was deposited on a block-faulted terrane. Tango Creek rocks were then overridden by a thrust fault that carried the Cold Fish volcanics, and a block-faulted terrane of pre-Albian strata that is unconformably overlain by Tango Creek Formation. The presence of pre-Albian block faults poses a major problem for structural analysis because the same post-Albian thrust fault need not have a predictable footwall or hanging wall pre-Albian stratigraphy along trend. The problem is compounded where pre- and post-Albian thrust faults must be identified across post-Albian high angle faults. Downplunge to the southeast of section NO (southeast of Ross River), a thrust fault with Bowser Lake Group in the hanging wall and Tango Creek Formation in the footwall, is shown schematically as the structure above the Spatsizi fault in section NO.

In section JK a thick (valley bottom to peak top) section of volcanics occurs only 1 km northwest of the part of section LM where the Spatsizi fault occurs near the valley bottom and has only 1 m of volcanics in the hanging wall. The volcanics in section JK are also bounded to the northwest by a thick section of Tango Creek Formation. The absence of the Spatsizi fault along trend in section JK requires that between sections LM and JK a northeast-trending high angle fault has a minimum of 1000 m of southeast-side-down displacement. The minimum displacement is inferred by assuming pre-Albian uplift which resulted in erosion of much of the Bowser Lake Group. Support for erosion of the Bowser Lake Group is the presence of Tango Creek Formation on volcanics in the northwest corner of Figure 75.2, indicating significant pre-Albian uplift of a northwest-trending belt bounded to the northeast by a major northeast-side-down fault (Cold Fish Fault). Erosion ofhe Bowser Lake Group below the Tango unconformity is shown schematically in sections LM and NO. The Cold Fish Fault puts thick volcanics against thick Tango Creek in section JK. It is inferred to have had at least 2000 m of post-Albian northeast-side-down displacement. The structure below the Tango Creek Formation northeast of the Cold Fish Fault in section JK is entirely inferred from southeast-side-down displacement of the structure in HI, along the Griffith Fault. The Tango Creek Formation is interpreted to unconformably overlie folded Bowser Lake Group in sections HI and BC (Evenchick, 1986). Below the unconformity in section BC, a thrust fault that places Bowser Lake Group on Tango Creek Formation is the downplunge projection of a folded thrust fault in section HI (*see* Evenchick, 1986).

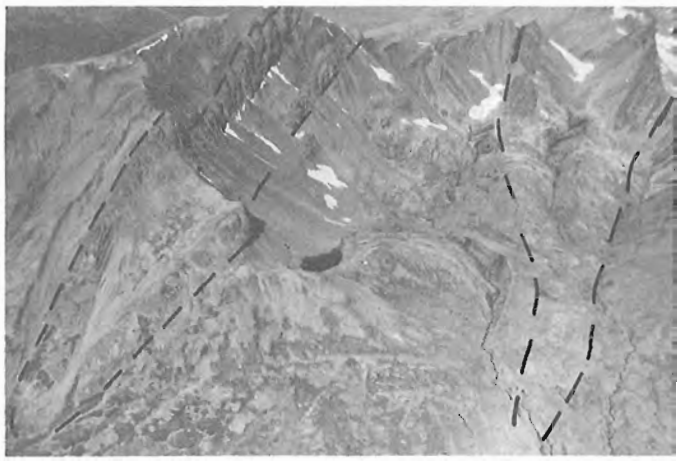


Figure 75.9 View northwest to folded coal-bearing upper Jurassic rocks between Little Klappan and Spatsizi rivers as shown on Figure 75.2. The dashed black line marks the base of the same resistant member.

CONCLUSIONS

Mapping of structures at the boundary of the Bowser and Sustut basins has provided the first direct evidence for involvement of the Lower Jurassic Cold Fish volcanics in major contractional deformation, and as a result indicates that thrust faults sole into a decollement in or below the basement to the Bowser Basin. The amount of shortening represented by both structures between faults, and the overlap of faults, is at least 50% (Fig. 75.6, 75.9, and Fig. 78.7 in Evenchick, 1986). The interpretation of pre-Albian block faults that offset a thrust fault is the most direct evidence for more than one pulse of contractional deformation.

Analysis of the structure involves restoration of northeast-verging folds and faults, and stratigraphy, across: 1) pre-Albian dip-slip faults which resulted in erosion and preservation of different pre-Albian stratigrpahy at the same structural level; 2) post-Albian dip-slip faults.

REFERENCES

Bustin, R.M. and Moffat, I.
1983: Groundhog coalfield, central British Columbia: reconnaissance stratigraphy and structure; Bulletin of Canadian Petroleum Geology, v. 31, p.231-245.

Evenchick, C.A.
1986: Structural style of the northeast margin of the Bowser Basin, Spatsizi map area, north-central British Columbia; in Current Research, Part B, Geological Survey of Canada, Paper 86-1B, p.733-739.

Gabrielse, H. and Tipper, H.W.
1984: Bedrock geology of Spatsizi map area (104 H); Geological Survey of Canada, Open File 1005.

Koo, J.
1986: Geology of the Klappan coalfield in northwestern British Columbia (104H/2,3,6,7); British Columbia Ministry of Energy, Mines and Petroleum Resources, Geological Fieldwork, 1985, Paper 1986-1, p.225-228.

Moffat, I.W.
1985: The nature and timing of deformational events and organic and inorganic metamorphism in the northern Grounghog coalfield: implications for the tectonic history of the Bowser Basin; unpublished Ph.D. thesis, University of British Columbia, 205 p.

Tipper, H.W. and Richards, T.A.
1976: Jurassic stratigraphy and history of north-central British Columbia; Geological Survey of Canada, Bulletin 270, 73 p.

Large-scale sedimentary processes in a trained, high-energy, sand-rich estuary: Fraser River delta, British Columbia

Project 790006

R.A. Kostaschuk[1] and J.L. Luternauer
Cordilleran and Pacific Margin Division, Vancouver

Kostaschuk, R.A. and Luternauer, J.L., Large-scale sedimentary processes in a trained, high-energy, sand-rich estuary: Fraser River delta, British Columbia; in Current Research, Part A, Geological Survey of Canada, Paper 87-1A, p. 727-734, 1987.

Abstract

The large-scale sedimentary processes in a high-energy, sand-rich, salt-wedge estuary of the Fraser River were examined from a series of channel cross-sectional profiles. The results indicate that erosion and deposition result primarily from variations in river discharge and secondarily from channel shape. Net erosion occurs as river discharge rises and deposition as discharge falls. Persistent deposition, most pronounced when river discharge is high, is dominant at the river mouth where the salt wedge is restricted to at low tide. Sedimentation near a large bend and in an artificially-maintained straight reach of the channel mimics that in meandering rivers. A localized zone of intense scouring and filling appears to be associated with a decrease in width and increase in depth of the channel.

Résumé

On a étudié les processus sédimentaires à grande échelle dans l'estuaire du fleuve Fraser à haute énergie, riche en sable, renfermant des biseaux de dépôts salins en examinant une série de profils transversaux des chenaux. Les résultats indiquent que l'érosion et la sédimentation ont principalement comme origine les variations des débits du fleuve et secondairement la forme des chenaux. L'érosion nette se produit lorsque le débit du fleuve augmente et la sédimentation lorsque le débit baisse. La sédimentation persistante, marquée surtout lorsque le débit du fleuve est élevé, est importante dans l'estuaire à l'endroit où le biseau de dépôts salins est restreint à la laisse de basse mer. La sédimentation à proximité d'un grand coude et dans un bief droit du chenal, maintenu artificiellement, ressemble à celle des rivières à méandres. Une zone localisée où l'érosion et la sédimentation sont intenses semble être associée au rétrécissement et à l'approfondissement du chenal.

[1]Department of Geography, University of Guelph, Guelph, Ontario N1G 2W1

INTRODUCTION

An estuary is "a semi-enclosed coastal body of water which has a free connection with the open sea and within which sea water is measurably diluted with fresh water derived from land drainage" (Pritchard, 1967). In estuaries with a well developed saline water intrusion (salt wedge) below fresh water flow sedimentary processes are dominated by river flow (Postma, 1980). Although sediment transport and accumulation mechanisms in this setting are reasonably well documented (e.g. Nichols and Biggs, 1985, p. 128), large variations in erosion and deposition are not. This preliminary examination of such large-scale variations in the outer main channel of the Fraser River delta (Fig. 75.1), a trained, high-energy, sand-rich, salt wedge estuary (Hodgins et al., 1977; Milliman, 1980) is one facet of a broader investigation of the sediment budget of the Fraser River (Kostaschuk et al., 1986). The study will aid in assessing the impact of river dredging and training on sediment supply to, and therefore the stability, of the delta front. A companion report by McKenna and Luternauer (1987) first documents a slope failure off the main channel.

SETTING

The Fraser River, the largest on the Pacific coast of Canada, originates in the Rocky Mountains and drains a 223 000 km2 area of British Columbia into the Strait of Georgia. Conditions within the river are characterized in autumn and early spring by low water and low sediment discharge, in late spring-early summer by a freshet period with high water and high sediment discharge, and in late summer by relatively high water and low sediment discharge (Milliman, 1980). Most of the sediment load is transported during the late spring-early summer freshet (op. cit.).

Superimposed on this fluvial regime is a strong tidal effect. Mixed semi-diurnal tides in the Fraser River estuary have maximum ranges at the river mouth which approach 5 m. Tidal range decreases both upstream and with increasing discharge (Ages and Woolard, 1976, p. 1). The tide, in concert with river discharge, controls the position of the salt wedge (Hodgins et al., 1977) which in turn affects the mechanisms and rates of sediment transport in the estuary (Kostaschuk et al., 1986).

METHODS

Ten channel cross-sections 500 m long were surveyed 4 or 5 times between 24 April and 17 September, 1985 (Fig. 76.2) by Public Works Canada. Lines were run from the Steveston Jetty and online navigation was accomplished using visual aids. Deviations from the line did not exceed 2.0 m. Distances from the jetty were measured with a Vyner RF4K Rangefinder which has a listed accuracy of ± 1.0 m. A Raytheon DE 719 fathometer, listed accurate to 0.5%, was used for depth sounding. Profiles were reduced to local low water datum with reference to measured water levels.

A number of sources of error are inherent in these surveys. Depth measurements are dependent on fathometer accuracy. The listed accuracy of the Raytheon 719 would result in an error of only 5 cm in 10 m of water. Actual error, however, will be somewhat larger because of variations in echo speed resulting from changing water salinity. More serious is the error introduced by migrating bedforms which have mean heights in the 0.5-1.0 m range. These sources of error allow us to compare only general and large-scale changes between temporally successive sections.

Public Works Canada and Sceptre-Reidel-Dawson Ltd. undertook channel dredging at various times during the study period. Dredging is designed to maintain a minimum channel depth of 8.1 m in the Sand Heads and Steveston Bend areas and 8.5 m in the Steveston area. Dredging records for the study area and period were obtained and tabulated (Table 76.1).

RESULTS

Bed elevation changes between temporally successive profiles were determined by measuring the vertical differences at 10 m horizontal intervals across the channel (Fig. 76.3-76.6).

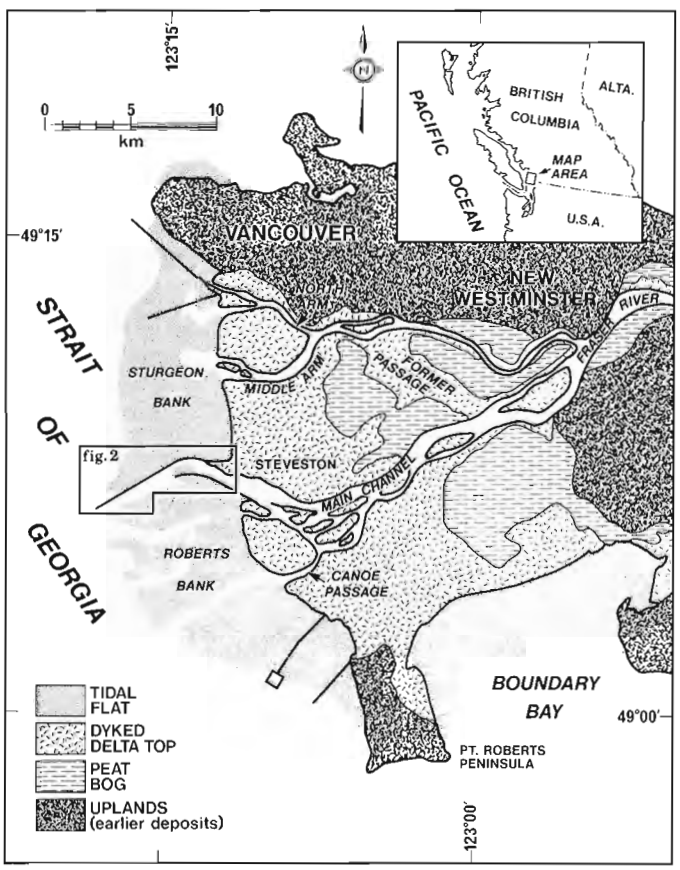


Figure 76.1. Location of the study area.

Table 76.1 Summary of dredging by Public Works Canada and Scepter-Reidel-Dawson Ltd., in the study area between April and September. Distances are measured in a upstream direction with Sand Heads as zero.

Dates Month	Days	Reach Dredged (km)	Volume Dredged (m^3)	Sections Affected
April	08-21	2.8 → 3.8	110,429	4, 5
	29-30	−1.0 → 1.9	35,703	1, 2
May	01-05	−1.0 → 1.9	30,963	1, 2
	06-26	−1.0 → 1.0	133,838	1, 2
June	10-30	−1.0 → 0.9	92,884	1
	17-30	5.0 → 7.4	35,088	6,7,8
July	08-14	−1.0 → 0.9	60,890	1
	12-25	−1.0 → 0.9	8,256	1
August	12-31	5.0 → 7.4	94,949	6,7,8
	02-29	5.0 → 7.4	100,107	6,7,8
September	23-30	7.5 → 10.9	30,960	9, 10
August 16-September 16		7.5 → 10.5	406,000	9, 10

In the subsequent description an increase in bed elevation is referred to as deposition and a decrease as erosion. Dredging records (Table 76.1) indicate where deposition has occurred. Possible downstream erosion or deposition triggered by upstream dredging has not been distinguished from that produced by what are considered the dominant processes.

Bed elevation changes measured by us and from dredging records indicate that the main spatial and temporal patterns of erosion and deposition within the channel can be summarized as follows:

(1) Net channel erosion between April and June and net deposition between June and September (Fig. 76.3-76.6).

(2) Persistent deposition between April and September (Fig. 76.3-76.6) at Sand Heads (sections 1, 2).

(3) Pronounced deposition on the north side of the channel and erosion on the south side between April and July (Fig. 76.3-76.5) in the reach between Sand Heads and Steveston Bend (sections 3 and 4), with minor deposition between July and September (Fig. 76.6).

(4) Intense erosion (6 m) on the north side of the channel and deposition on the south side between May and July (Fig. 76.3-76.5) at Steveston Bend (sections 5, 6, 7) with deposition on the north side of the channel between July and September (Fig. 76.6).

(5) Continuous deposition across the channel immediately upstream of Steveston Bend (section 8) between May and September (Fig. 76.3-76.6).

(6) Intense erosion (5 m) in the centre of the channel immediately downstream of Steveston (section 9) between April and May (Fig. 76.3), followed by intense deposition (4 m) between May and July (Fig. 76.4, 76.5) and limited deposition between July and September (Fig. 76.6).

(7) Deposition in the centre and south side of the channel etween April and July (Fig. 76.3-76.5) at Steveston (section 10), with deposition across the channel between July and September (Fig. 76.6).

DISCUSSION

Discharge variations

Mean daily discharges for the Fraser River at Hope, 160 km upstream of Sand Heads, for 1985 are summarized on Figure 76.7. This represents a fairly typical annual hydrograph, with low flows in March, a steep rising limb that peaks in late May and early June and a gentle recessional limb from June to September. The 1985 freshet peak of 9770 $m^3.s^{-1}$ on May 28 is very similar to the average freshet peak of 9600 $m^3.s^{-1}$ (Tamburi and Hay, 1978). Although actual discharges in the study area will lag behind and be larger than those at at Hope (Ward, 1976), the Hope values provide a useful indication of discharge fluctuations over the season.

The floor of sand-bed rivers usually are eroded during rising discharges with deposition occurring as discharge falls (Leopold et al., 1964). Net patterns of erosion and deposition in the Fraser follow this pattern. Most rivers, however, display considerable local variability in this overall trend. Exceptions to the rule in the Fraser estuary include the continuous deposition at Sand Heads and spatial variability caused by channel shape.

The continuous deposition in the Sand Heads area appears to be related to the position of the salt wedge at low tide. Kostaschuk et al. (1986) found that during 1985 freshet discharges, at high tide, a prominent salt wedge was apparent in the channel between Steveston and Sand Heads and suspended sediment loads were low. At low tide the salt wedge was situated near Sand Heads and suspended loads in the

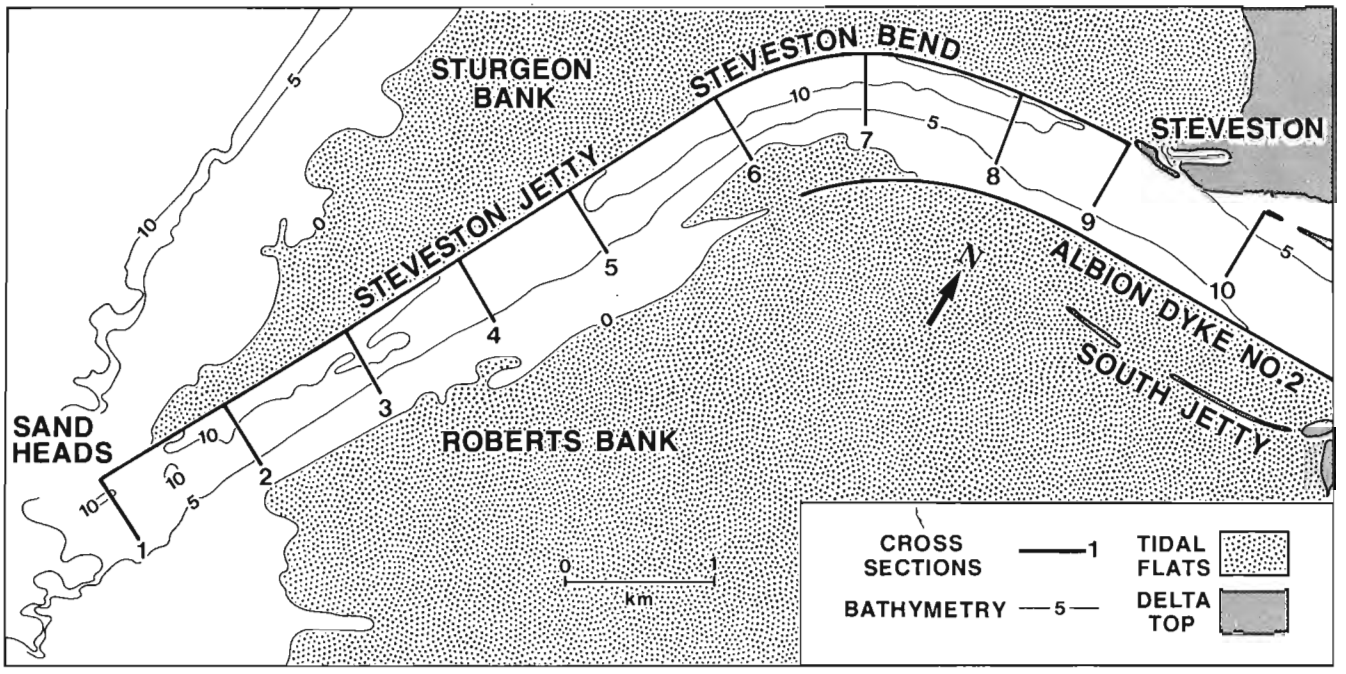


Figure 76.2. Location of cross-sections within the study area. Bathymetry is based on a 1985 edition of the Canadian Hydrographic Service Chart 3490.

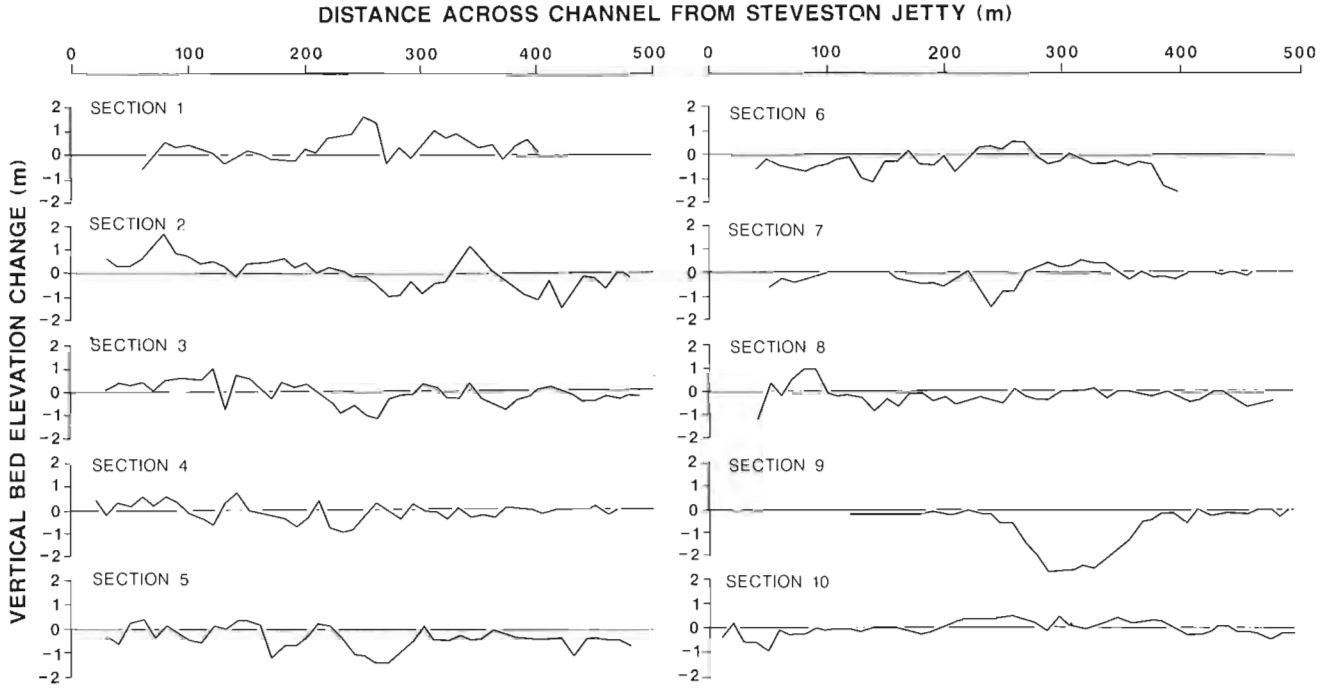


Figure 76.3. Vertical bed-elevation changes between 24 April and 4 June (sections 1 and 2) and 24 April – 24 May (sections 3-10).

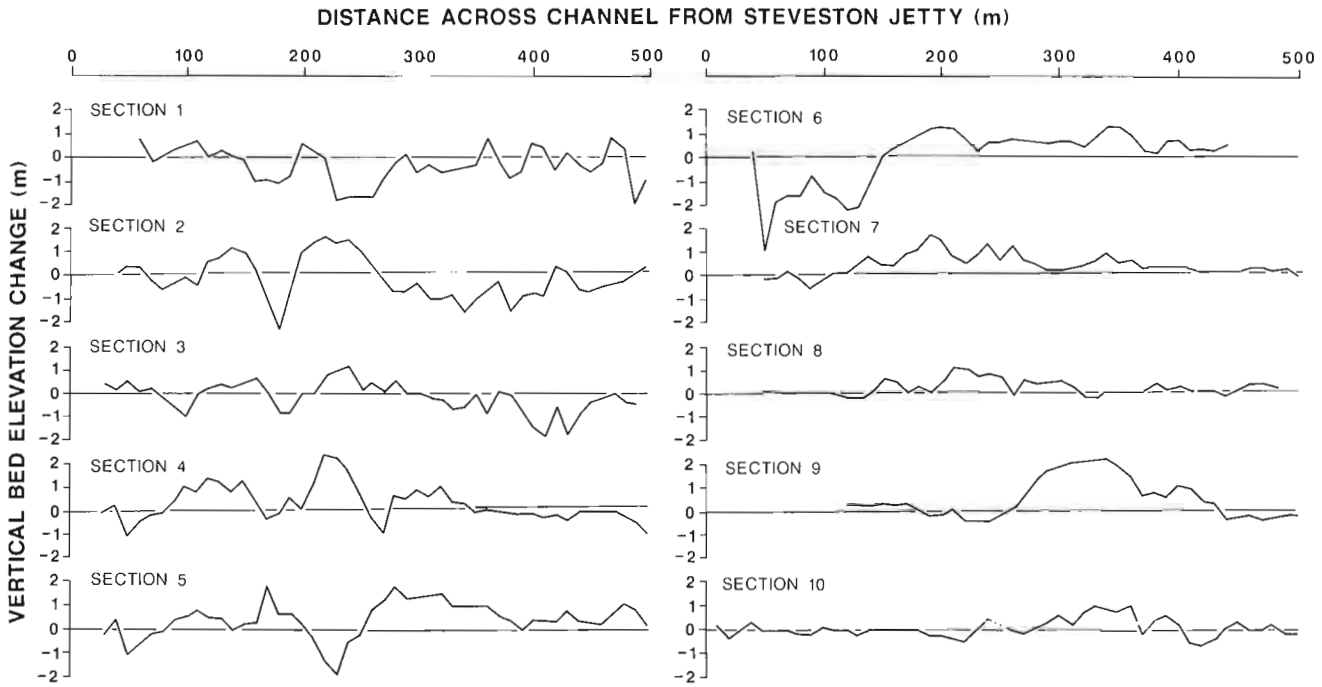


Figure 76.4. Vertical bed-elevation changes between 4 June and 13 June (sections 1 and 2) and 24 May to 13 June (sections 3, 5-10).

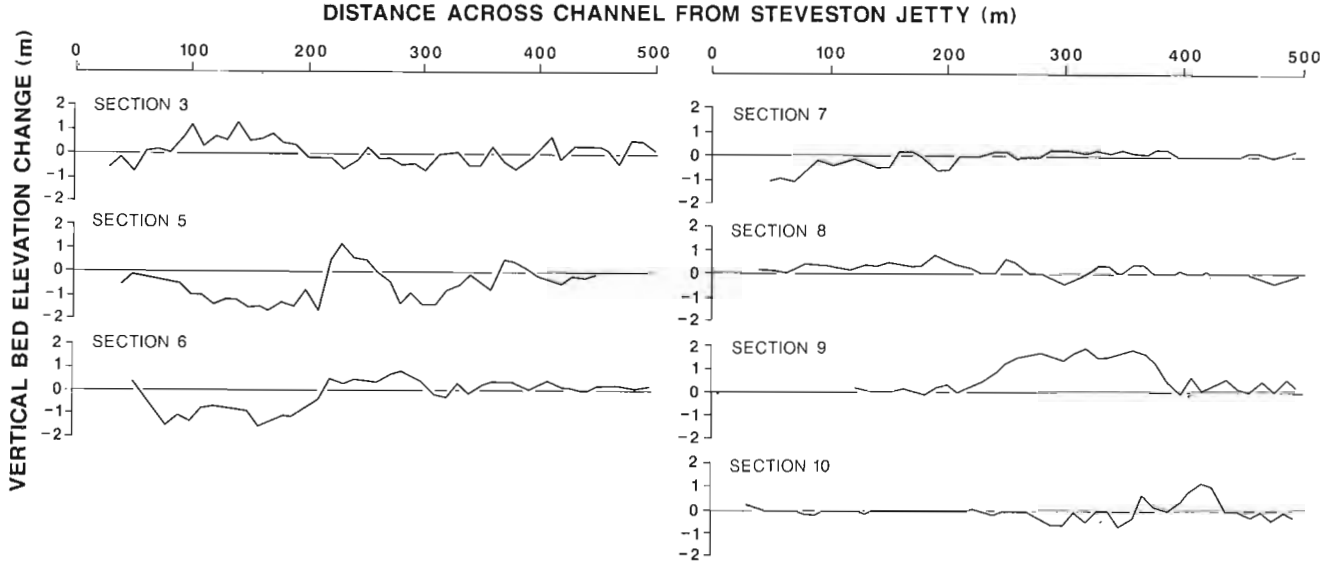


Figure 76.5. Vertical bed-elevation changes between 13 June and 25 July (sections 3, 5-10).

channel upstream of Sand Heads were high. The highest loads were measured when discharge was highest and tidal height was at a minimum.

Deposition in salt wedge estuaries is commonly associated with the position of the landward tip of the wedge (Nichols and Biggs, 1985). Material transported as bed load is deposited because the river is no longer in contact with the bed as it flows over the wedge. Much of the coarser suspended load is also deposited near the tip of the wedge as current speeds fall and there is mixing between fresh and salt water. When the tide is high, little salt-wedge-related deposition occurs in the outer channel, even at high discharge, because suspended loads are small. When tides are low and sediment

loads are high, considerable deposition takes place in the Sand Heads area where the tip of the salt wedge is situated.

Channel morphology

Upstream of Steveston the Fraser River has a meandering pattern in plan (Fig. 76.1). At the turn of the century, prior to the construction of training structures on the channel, the Steveston to Sand Heads reach also displayed a meandering form with a bend situated in a similar position to the present Steveston Bend (Clague et al., 1983, Fig. 4). In addition, here was a second bend trending in the opposite direction and cutting back across the location of the present channel north of Sand Heads (Fig. 76.8). Construction of the Steveston Jetty (1911-1932) and the Albion Dyke has maintained the first 'natural' bend in the channel but has removed the second, replacing it with a straight reach. This has important implications for the patterns of erosion and deposition in the area.

Meandering rivers have a characteristic pattern of sedimentation associated with them. Erosion occurs on the outside of the bend with deposition on the point bar on the inside of the bend and on the riffle between bends (Knighton, 1984, p. 132). This model explains the pattern of erosion and deposition at Steveston Bend. In an uncontrolled bend, erosion on the concave bank and deposition on the convex would result in lateral migration of the channel. Steveston Jetty prevents lateral movement and erosion is restricted to a narrow portion of the bed adjacent to the jetty. Long term deposition on the inside of the bend is indicated by the development of a large, sandy, intertidal shoal (Fig. 76.2). The temporal pattern of erosion at Steveston Bend differs from the general pattern outlined earlier. There, erosion is most prominent even as discharges are falling, between May and July. It appears that, on the outside of the bend, the morphological influence takes precedence over the hydrological and currents are sufficiently localized to allow erosion to continue even as discharges are falling.

The meandering river model also provides a possible explanation for deposition on the north side of the channel and erosion on the south side in the straight reach between Sand Heads and Steveston Bend. It may reflect incipient formation of a new meander bend similar in position to the one present prior to construction of the jetties (Fig. 76.8). If this is indeed the case, it has important implications for maintenance of the navigation channel in that dredging might be designed to take advantage of the natural pattern of scour in the reach.

The extremely localized nature of intense scour and fill at section 9 upstream of Steveston Bend, a pattern which was not apparent at sections 8 and 10, is difficult to account for. Between sections 10 and 9, the width of the Fraser decreases from 770 to 720 m and its mean depth increases from 7.2 to 8.9 m. Between sections 9 and 8 the width increases slightly from 720 to 740 m and the mean depth decreases from 8.9 to 8.5 m. Section 9 is thus somewhat narrower and deeper than areas immediately upstream and downstream; similar sections in other rivers have experienced similar patterns of scour and fill (Knighton, 1984).

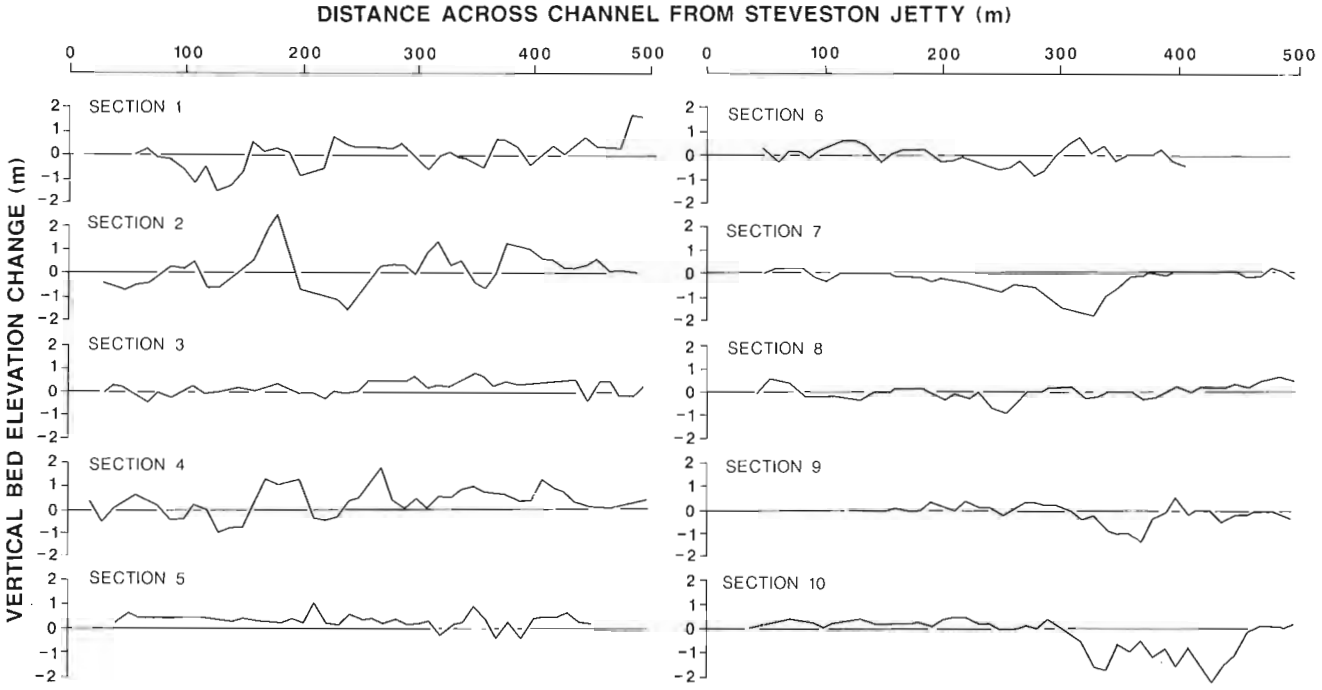


Figure 76.6. Vertical bed-elevation changes between 13 June and 17 September (sections 1, 2 and 4) and 25 July and 17 September (sections 3, 5-10).

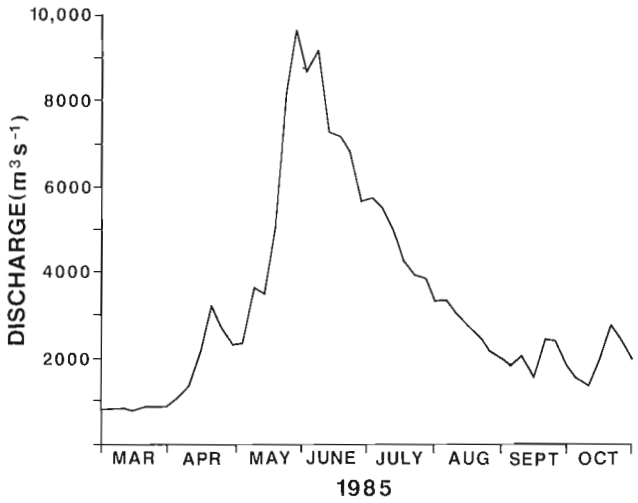


Figure 76.7. Variations in Fraser River discharge for April – October, 1985 (source: Water Survey of Canada, 1986).

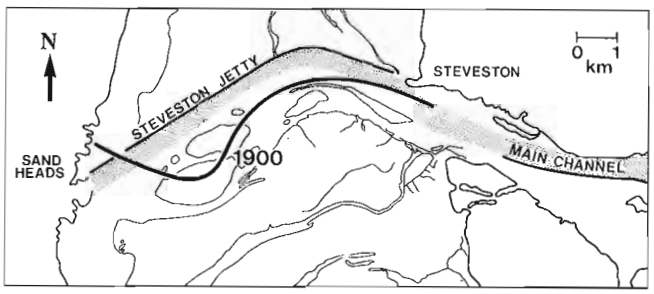


Figure 76.8. Position of the present channel and the channel thalweg in 1900 prior to construction of Steveston Jetty (*from* Clague et al., 1983).

CONCLUSIONS

The following conclusions can be drawn about large-scale sedimentary processes in the outer Main Channel of the Fraser River.

(1) Patterns of erosion and deposition are river-dominated and can be explained largely by variations in discharge and channel cross-sectional shape.

2) The channel undergoes general erosion between April and early June when river discharge is rising and net deposition between June and September when discharge is falling.

(3) Persistent deposition, most pronounced when discharges are high, occurs in the Sand Heads area at the low-tide limit of the salt wedge.

(4) Depositional/erosional patterns at Steveston Bend mimic those of meandering river bends.

(5) Erosion on the south side of the channel and deposition on the north side of the artificially maintained straight reach between Steveston Bend and Sand Heads may reflect incipient formation of a new meander bend.

(6) The intense scouring and filling of a small area upstream of Steveston bend probably occurs because the channel there is narrower and deeper.

ACKNOWLEDGMENTS

Financial support for this research was provided by a Natural Sciences and Engineering Research Council Postdoctoral Fellowship to Kostaschuk, and Luternauer's Geological Survey of Canada Project 790006. Special thanks are due M.A. Church (Department of Geography, University of British Columbia) for logistical (NSERC Operating Grant 677950) and technical support. Finally, we are indebted to R. Richardson and his crew at the Steveston B.C. office of Public Works Canada for their assistance in the survey program.

REFERENCES

Ages, A. and Woolard A.
1976: The tides in the Fraser Estuary; Pacific Marine Science Report 76-5, Institute of Ocean Sciences, Patricia Bay, Sidney, B.C., 100 p.

Clague, J.J., Luternauer, J.L., and Hebda, R.J.
1983: Sedimentary environments and post-glacial history of the Fraser delta and Lower Fraser Valley, British Columbia; Canadian Journal of Earth Sciences v. 20, p. 1314-1326.

Dyer, K.R.
1972: Sedimentation in estuaries; in The Estuarine Environment, R.S.R. Barnes, and J. Green, (ed.), Applied Sciences Publications, London. p. 10-31.

Hodgins, D.O., Osborn, T.R., and Quick, M.C.
1977: Numerical model of stratified estuary flows; Journal of the Waterways, Port, Coastal and Ocean Division, American Society of Civil Engineers, W.W.I., p. 25-41.

Knighton, D.
1984: Fluvial Forms and Processes; Edwin Arnold, London, 218 p.

Kostaschuk, R.A., Luternauer, J.L., and Millard, T.H.
1986: Sediment transport during the 1985 freshet in the outer Main Channel of the Fraser River Estuary, British Columbia Current Research, Part A, Geological Survey of Canada, Paper 86-1A, p. 565-570.

Leopold, L.B., Wolman, M.G., and Miller, J.P.
1964: Fluvial processes in geomorphology; W.H. Freeman, San Francisco.

McKenna, G.T. and Luternauer, J.L.
1987: First documented large failure at the Fraser River delta front, British Columbia in Current Research, Part A, Geological Survey of Canada, Paper 87-1A, note.

Milliman, J.O.
1980: Sedimentation in the Fraser River and its estuary, British Columbia; Estuarine and Coastal Marine Science, v. 10, p. 609-633.

Nichols, M.M. and Biggs, R.B.
1985: Estuaries; in Coast Sedimentary Environments, R.A. Davis, (ed.), Springer-Verlag, New York, p. 77-186.

Postma, H.
1980: Sediment transport and sedimentation; in Chemistry and Biogeochemistry of Estuaries, E. Olausson, and I. Cato, (ed.), Wiley, Chichester, p. 153-186.

Pritchard, D.W.
1967: Observations of circulation in coastal plain stuaries; in Estuaries, G.H. Lauff, (ed.), American Association for the Advancement of Science, Publication 83, Washington, D.C., p. 3-5.

Tamburi, A. and Hay, D.
1978: An introduction to river mechanics and the Lower Fraser River; Canada Department of Public Works, Pacific Region, Marine Civil Engineering Section, Vancouver, 72 p.

Ward, P.R.B.
1976: Seasonal salinity changes in the Fraser Estuary, British Columbia; Canadian Journal of Civil Engineering, v. 3, p. 342-348.

Water Survey of Canada
1986: Surface water data, British Columbia, 1985; Inland Waters Directorate, Waters Resources Branch, Environment Canada, Ottawa, Canada.

Kaza Group, eastern Wells Gray Park, British Columbia

EMR Contract 23254-6-0220

Donald C. Murphy[1]
Cordilleran and Pacific Margin Division

Murphy, D.C., Kaza Group, eastern Wells Gray Park, British Columbia; in Current Research, Part A, Geological Survey of Canada, Paper 87-1A, p. 735-742, 1987.

Abstract

A distinctive quartzite and phyllite unit in the Kaza Group of eastern Wells Gray Park is nearly identical to a unit located 70 km to the north near Castle Creek, establishing it as an important regional marker. The basal phyllitic quartzite is metamorphosed quartz siltstone, probably deposited as base cut-out turbidites. It passes upward into thinly interbedded phyllitic quartzite and grey phyllite inferred to be 'distal' turbidites and then into basinal graphitic phyllite.

Data from the north-northwest-trending segment of the Knutson Creek fault imply oblique slip (dextral-normal). This segment is interpreted as a transtensional link between west-northwest–trending strike-slip segments of the fault.

Several observations shed doubt on the location of the Pleasant Valley thrust in the Slide Mountain area. If the rocks underlying the presently mapped thrust surface are indeed younger than those overlying it, then these observations are inconsequential; however, it is an unlikely location for the fault.

Résumé

Une unité caractéristique de quartzite et de phylliet du groupe de Kaza dans l'est du parc Wells Gray est presque identique à une unité située à 70 km au nord, à proximité du ruisseau castle; ce phénomène en fait ainsi un important horizon repère régional. L'unité de quartzite phylliteux de base se compose d'un microgrès quartzeux de nature métamorphique tout probablement mis en place sous forme de turbidites de base entaillées. L'unité passe vers le haut à un quartzite phylliteux finement interstratifié avec une phyllite grise, que l'on considère toutes deux être des turbidites «distales», puis à une phyllite graphiteuse de bassin.

Les données provenant du segment de direction nord nord-ouest de la faille de Knutson Creek laisse supposer l'action d'un glissement oblique (dextre-normal). On interprète ce segment comme un lien de transtension entre des segments à rejet horizontal de direction ouest nord-ouest de la faille.

Plusieurs observations laissent planer un doute sur l'emplacement du charriage de Pleasant Valley dans la région du mont Slide. Si les roches sous-jacentes à la surface de charriage actuellement portée sur carte sont en effet plus jeunes que celles qui la recouvrent, alors ces observations sont sans importance; il s'agit toutefois d'un endroit improbable pour être l'emplacement de la faille.

[1]Department of Geological Sciences, University of British Columbia, Vancouver, B.C. V6T 2B4

INTRODUCTION

As defined by Pell and Simony (1984), the top of the middle Kaza Group in eastern Wells Gray Provincial Park, southern Cariboo Mountains, is a persistent and distinctive phyllite and quartzite unit. A similar unit was recognized in the Castle Creek area of the east-central Cariboo Mountains by Murphy and Rees (1983) and in the Miette Group in the Cushing Creek area (Rocky Mountain Main Ranges) by Carey and Simony (1984; Fig. 77.1). Carey and Simony (1985) and Murphy (1986) subsequently used this unit as a basis for regional correlation with the Kaza Group of the southern Cariboo Mountains, and in the latter case, local subdivision of the Kaza Group.

The occurrences of the distinctive unit mapped by Pell and Simony (1984) in Wells Gray Park were visited in 1986 in order to: (1) verify correlation with the similar unit in the Castle Creek area, (2) gather sedimentological data to determine the depositional environment of this unit, and (3) use this unit as a structural marker to clarify the structural geometry of the area along the eastern boundary of Wells Gray Park, especially with reference to the Pleasant Valley thrust and dextral (oblique transpressive) faults mapped by Struik (1985, 1986).

MIDDLE KAZA GROUP MARKER, WELLS GRAY PROVINCIAL PARK

Occurrences of the marker unit at the top of the middle Kaza Group were examined between St. Julien and Stormking creeks (Fig. 77.2), where it is approximately 350 m thick. The basal 250 m is composed of finely laminated, locally graded, green biotite-chlorite-garnet-quartz-calcite (+actinolite at higher metamorphic grade) phyllitic quartzite (metamorphosed quartz siltstone) with thin (up to 30 cm), laterally persistent, cross laminated, commonly contorted, tan to brown weathering calcareous quartzite (metamorphosed fine grained calcareous quartz sandstone or siltstone) and chloritic phyllite. This unit grades upward into a raphitic and locally pyritic phyllite with thin brown, recessive phyllitic marble and 3 - 5 m thick beds of white quartzite (metamorphosed quartz sandstone). The abundance of white quartzite within the graphitic phyllite increases to the southeast.

Comparison with Castle Creek marker

The middle Kaza marker in Wells Gray Park is virtually indistinguishable from its proposed equivalent in the Castle Creek area. In the Park, the marker is thicker and at higher metamorphic grade (garnet to kyanite zones vs. muscovite-chlorite to biotite zone), but both units exhibit the same distinctive composition and suite of sedimentary structures. There is little doubt that the Castle Creek and Wells Gray markers are one and the same unit.

One notable difference between the two areas is the abundance of white quartzite in the upper phyllitic portion of the unit. In the Castle Creek area, quartzite is restricted to one 75 cm thick bed. It is coarse grained, calcareous, and has marble and phyllite intraclasts. In contrast, in the Knutson Creek area (Fig. 77.2), up to three 3 - 5 m thick beds of fine grained (up to 1 mm), relatively well sorted, white quartzite were observed. They are generally massive but locally exhibit contorted bedding and have intraclasts of marble and phyllite.

Another difference is that graded bedding is apparently more common in the Wells Gray area. Grading is indicated by the upward increase in mica and porphyroblast (garnet, biotite and actinolite) contents. Graded beds are not obvious in the marker at Castle Creek; however, the Castle Creek area is within muscovite – chlorite and biotite zones and grading may have not been metamorphically enhanced to the extent seen in the Wells Gray area.

Depositional environments

In Wells Gray Park, the basal phyllitic quartzite consists primarily of laterally continuous, base cut-out turbidites (Tbc(e), Tbcd(e), Tcd(e), Tb(e), Tc(e)) with less common base-complete turbidites (Tab(e), Tabc(e)). Base cut-out turbidites are locally deposited on low-angle truncation surfaces. Rare channels with up to 20 cm of relief occur and are usually filled with base-complete turbidites.

The laterally persistent, well-sorted, fine grained, quartzose, and calcareous phyllitic quartzite is a significant departure from the discontinuous, coarse grained, and poorly sorted quartzofeldspathic turbidites of the underlying middle Kaza Group. The fine grain size, predominance of base cut-out turbidites, and lateral persistence of individual beds suggest a more 'distal', unchannelled setting relative to underlying rocks.

Above the basal phyllitic quartzite are several metres of alternating laterally continuous decimetre-scale beds of very fine grained calcareous phyllitic quartzite and grey phyllite. Individual fine grained quartzite beds are graded at their bases with plane laminated (Tabe) and, less commonly, cross laminated (Tabce) tops. The quartzite-phyllite (siltstone-shale) ratio of this portion of the marker decreases, and the graphite content increases, upward into the overlying graphitic phyllite. These transitional beds resemble classic distal turbidites and are inferred to have been deposited in a transition zone between where turbiditic sedimentation predominated and where basinal background sedimentation predominated. If a turbidite fan model is appropriate, these sediments would be considered outer fan sediments.

The upper graphitic phyllite is interpreted as the background sediment of the basinal environment into which Kaza turbidites were deposited. The specific environment of deposition of the graphitic phyllite is not known; characterization of this environment is necessary for an understanding of the depositional and tectonic settings of the Kaza turbidite system. Marble and quartzite within the phyllite are inferred to be turbidites, although definitive data in support of this interpretation are lacking.

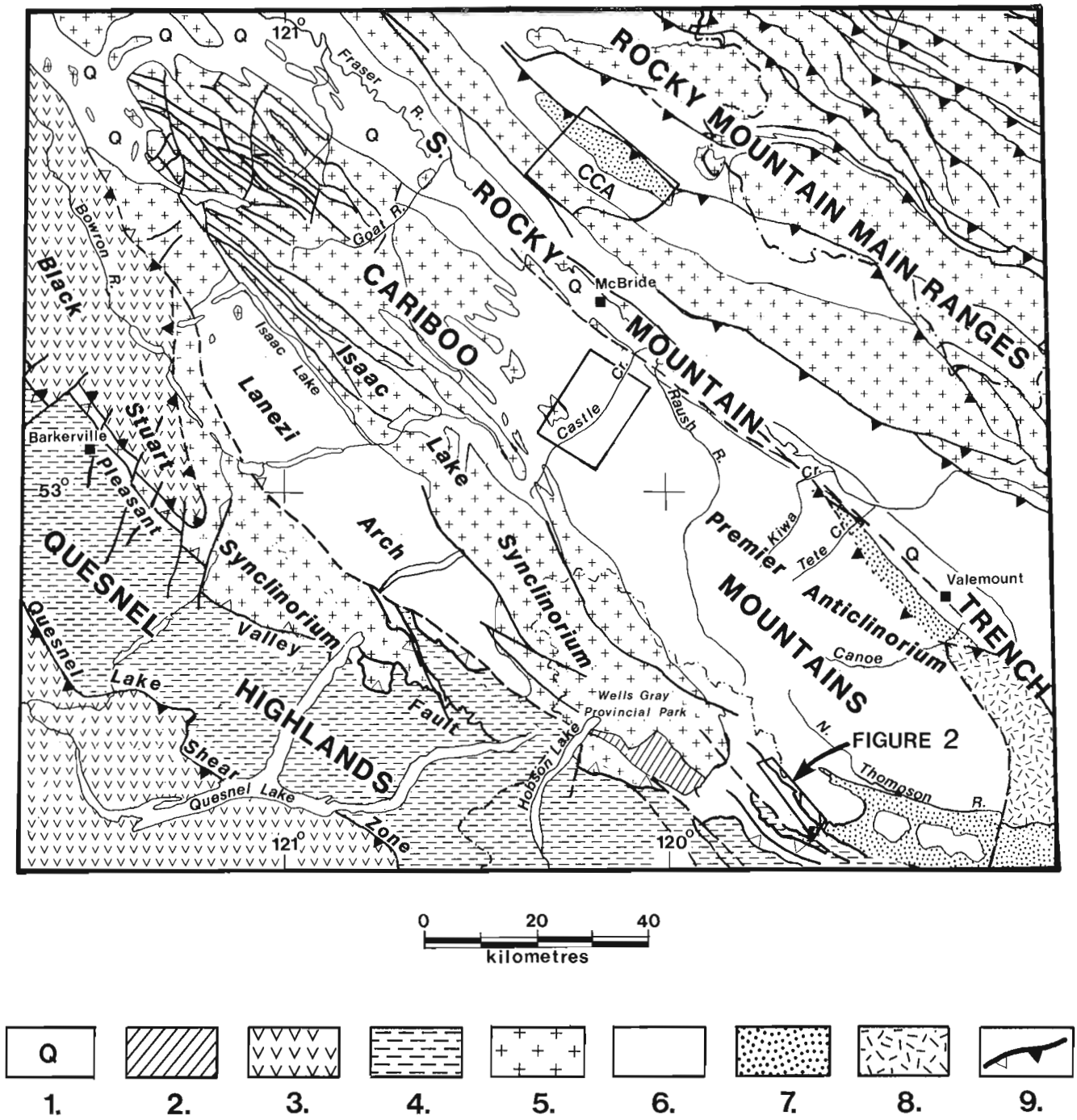


Figure 77.1. Regional geological map locating the Wells Gray area with respect to areas and features described in text. 1, Quaternary sediments, 2, mid-Jurassic Hobson pluton, 3, Paleozoic to Middle Jurassic Quesnel and Slide Mountain terranes of Struik (1984), 4, Proterozoic to upper Paleozoic Snowshoe Group (Barkerville terrane of Struik, 1984), 5, Proterozoic to early Paleozoic Cariboo Group (upper Miette Group in Rocky Mountains) and younger rocks, 6, Proterozoic Kaza Group (middle Miette Group in Rocky Mountains), 7, Proterozoic(?) Horsethief Creek Group (lower Miette Group in Rocky Mountains; inferred by Struik (1986) to be part of Barkerville terrane, 8, Malton gneiss, 9, fault, open triangles indicate SW-verging thrust fault, closed triangles indicate NE- or E-verging thrust fault; unadorned, strike-slip or normal fault. CCA, Cushing Creek area. Compiled from Wheeler et al. (1972), Struik (1985, 1986), and Pell (1984).

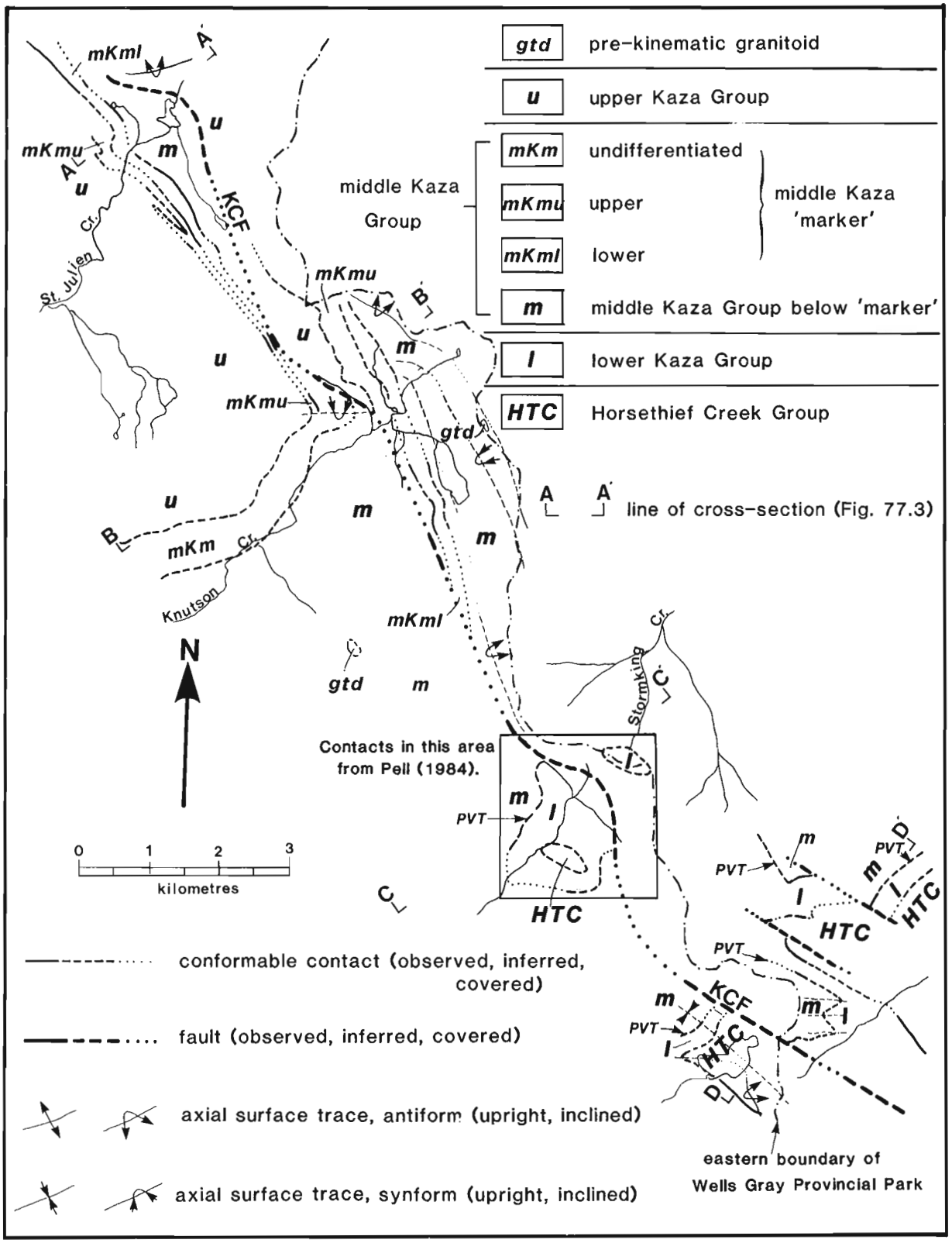


Figure 77.2. Geology of eastern Wells Gray Provincial Park between St. Julien Creek and Slide Mountain. KCF = Knutson Creek fault, PVT = location of the Pleasant Valley thrust proposed by Struik (1986)

The regionally extensive transition from coarse grained Kaza turbidites through the basal phyllitic quartzite of the marker to the basinal graphitic phyllite is most simply attributed to regional transgression. This conclusion differs from that of Murphy (1986) who interpreted he Castle Creek marker as a clastic shelf deposit, implying regional regression. In light of the association of graded beds with the distinctive plane and cross laminated beds common to both localities, this interpretation is being reconsidered.

STRUCTURAL GEOMETRY

Kaza and underlying Horsethief Creek Group rock in eastern Wells Gray Park are deformed by three sets of penetrative structures and cut by late northwest-trending faults, the most important of which is the Knutson Creek fault (KCF, Fig. 77.2; Pell, 1984; Struik, 1985). The structural geometry of this area is dominated by synmetamorphic, southwestwardly verging regional-scale folds (Pell, 1984). In the southern part of the area, these folds deform the surface identified by Struik (1986) as the Pleasant Valley thrust (PVT, Fig. 77.2); this surface was examined in several localities in the Slide Mountain area and, for reasons outlined below, is considered to be an unlikely candidate for a major fault.

Folding and mesoscopic fabrics

The earliest (D_n) and most significant structures, mappable from outcrop to regional (1:250 000) scale, are northwest-trending, primarily northwest-plunging, southwest-verging folds (Pell and Simony, 1982, 1984). These folds range from open to tight at all scales, with steeply dipping to overturned short (southwest-facing) limbs and gently northeast- or southwest-dipping long limbs (Fig. 77.3).

Middle and upper Kaza Group stratigraphy in the northern part of the area outline a major southwest-verging D_n anticline-syncline pair. Southwest of the KCF, the syncline is well defined by the middle Kaza marker which passes westwardly from a steep to overturned orientation with northeast-verging second-order D_n folds into a gently dipping orientation with symmetrical and southwest-verging folds (Fig. 77.2; Fig. 77.3, cross-section B-B′). Northeast of the KCF, the marker occurs on the steep to overturned, northeastern limb of this syncline; stratigraphically underlying middle Kaza Group rocks to the northeast define the neighboring D_n anticline (Fig. 77.2; Fig. 77.3, cross-sections A-A′ and B-B′).

In the southern part of the area, northeast of the KCF, marbles of the lower Kaza and upper Horsethief Creek groups outline a major southwest-verging D_n anticline-syncline pair (Fig. 77.2; Fig. 77.3, cross-section D-D′). Southwest of the KCF, the same stratigraphic units pass through near-recumbent folds whose axial surfaces are folded by an upright synform. Preliminary data suggest that the near recumbent folds are D_n structures.

D_n folds are associated with a prominent penetrative foliation (S_n) defined mesoscopically by the preferred orientation of matrix micas and the dimensional-preferred orientation of quartz-rich and mica-rich domains. As thin sections have not yet been prepared, it is not known whether this fabric is the earliest fabric in the rock. S_n is generally overgrown by randomly oriented prograde porphyroblasts. Thus, S_n and associated folds formed during regional metamorphism, but deformation ended before quenching of prograde mineral assemblages.

S_0, S_n, and prograde porphyroblasts are deformed by two sets of postmetamorphic structures. Where S_n is gently dipping, D_{n+1} crenulations occur; where S_n is more steeply dipping, D_{n+1} crenulations are rare but S_n is observed to be wrapped around porphyroblasts. The latter relationship is attributed to D_{n+1} rotation of S_n, causing it to tighten around porphyroblasts.

D_{n+2} structures consist of steeply dipping northeast-trending crenulations of S_n. The relationship between D_{n+1} and D_{n+2} is not clear; crosscutting relationships are not well displayed.

Macroscopic postmetamorphic structures are locally important. In the southernmost part of the area, the axial surface traces of D_n folds on both sides of the KCF are folded by D_{n+1} folds (Fig. 77.2; Fig. 77.3, cross-section D-D′). Southwest of the KCF, the axial surface trace of a near recumbent D_n antiform is folded into an open synform. The axial surface trace of the synform can be traced to the northwest where it crosses the middle Kaza marker west of the axial surface trace of the D_n syncline described above. The overall synformal shape outlined by the middle Kaza marker northwest of Knutson Creek is therefore a composite of both D_n and D_{n+1} deformation.

Macroscopic D_{n+1} structures have not been defined. The plunges of the lineation generated by the intersection of S_0 and S_n (L_{0xn}) and the hinges of D_n folds (F_n) vary from over 30°NW to 5°SE. D_{n+2} crenulations are suitably oriented to affect the orientation of these linear elements; however, the relationship between variations in plunge of D_n linear elements and macroscopic D_{n+2} deformation remains to be proven.

Northwest-trending faults

Northwest-trending faults were identified in this area by both Pell (1984) and Struik (1985). Three such faults were encountered: the northeast-dipping Knutson Creek fault (Struik, 1985), which extends the length of the area examined, and two sub vertical faults which were traced for relatively short distances and not examined in detail.

Knutson Creek fault

The KCF was first recognized by Pell and Simony (1982) in the Slide Mountain area and interpreted as a postmetamorphic, northeast-side-down normal fault. Struik (1985), citing dextral strike separation of two-dimensional features, reinterpreted the KCF as a dextral strike-slip fault with a possible component of transpression.

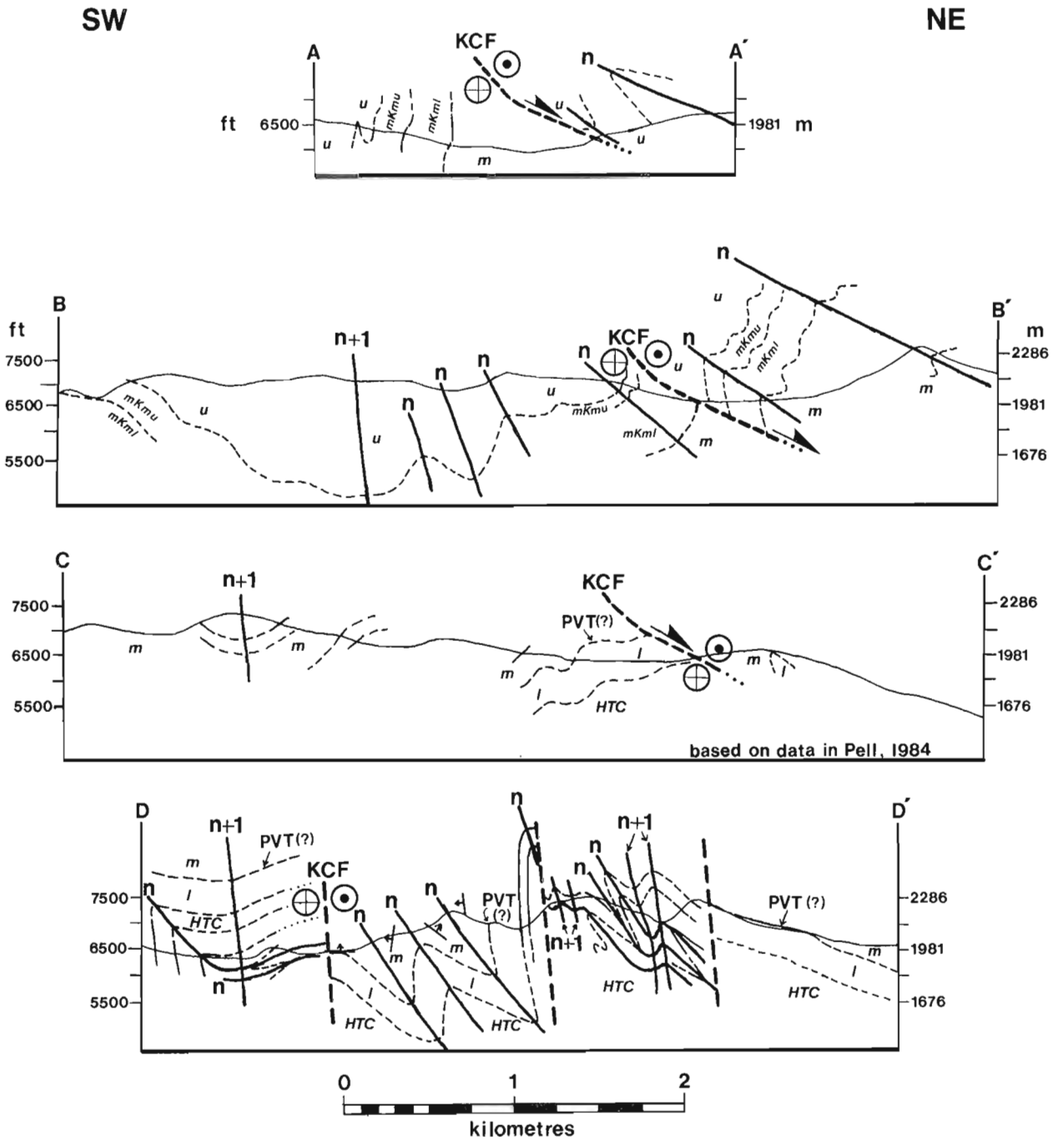


Figure 77.3. Cross-sections illustrating structural geometry of Kaza and Horsethief Creek groups, eastern Wells Gray Provincial Park. Lines of cross-sections indicated in Figure 77.2. n, n + 1 refer to axial surfaces of D_n and D_{n+1} folds, respectively. Dashed lines withing HTC are traces of individual marbles.

Geometric and kinematic data were collected during this study to constrain the nature of the displacement on the KCF. The location of the KCF can be determined within a few metres in several locations in the headwaters of Knutson Creek and in the divides between Knutson and St. Julien creeks and Knutson Creek and the next southwest-flowing drainage to the southeast. Structure contours of the fault strike at 324°; calculated dips steepen upward slightly from 34°NE between 1829 m (6000 ft) and 2134 m (7000 ft) to 44°NE above 2134 m. Structure contours project easily and accurately into the St. Julien Creek area but problems arise in extending them to the southeast. Struik (1985) traced the fault into a more northwestwardly rending subvertical orientation, requiring changes in both strike and dip.

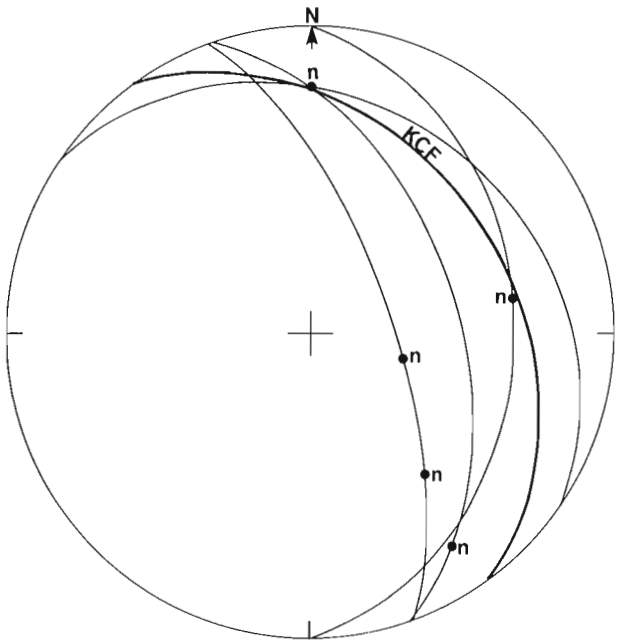


Figure 77.4. Equal area stereoplot of orientations of second-order faults (great circles) and associated slip linears (dots)

Kinematic data were collected from second-order faults which are well exposed in the northwest tributary of Knutson Creek. Although the main zone of dislocation of the KCF is generally narrow, second-order faults with centimetre to metre scale offsets of bedding, metamorphosed lamprophyric and basaltic dykes, and kyanite-bearing quartz veins are common in both hanging and footwalls near the fault. These faults are generally more northwardly striking and more steeply dipping than the KCF. Near the KCF, they offset, and are offset by, second-order faults sub parallel to the KCF, implying kinship (see Fig. 39.2 of Struik, 1985).

Although second-order faults are common, slip linears are rare. These include quartz and calcite fibres and striations which are too fine to determine if they are constructive (fibres) or destructive (scratches or grooves). Of the few observed, ESE trends and down-dip hangingwall displacement are most common, implying ESE extension (Fig. 77.4). Although not conclusive, this would suggest that the KCF has dextral oblique displacement with dextral and normal components.

The range of magnitudes of the dextral and normal components may be approximated by considering a fault plane map showing the offset basal contact of the middle Kaza marker and the range of net slip vectors (Fig. 77.5). This construction yields a dextral component ranging from 260 m to 2.05 km (strike-slip), and a normal component ranging from 0 to 350 m.

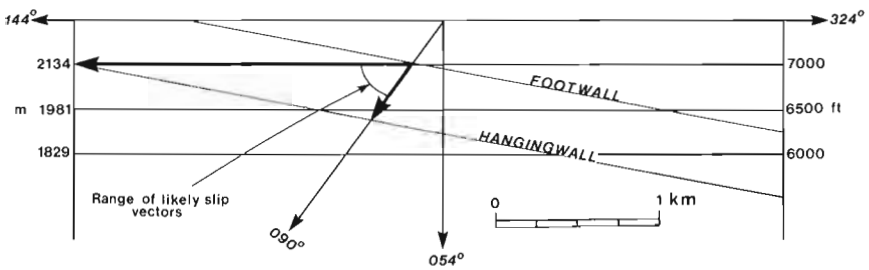
Kinematic data from the southeastward continuation of the KCF are not available. In the Slide Mountain area, the fault strikes more westwardly and is near vertical. If the range of slip vectors determined for the more northwardly trending, moderately dipping segment of the fault is approximately correct, the more westwardly trending, near vertical segment of the fault may be of a more purely trike-slip nature. As such, the gently dipping segment of the fault may be a transtensional link between more westwardly trending strike-slip faults.

The KCF is clearly postmetamorphic (Struik, 1985). Although the distribution of metamorphic minerals is not known in sufficient detail to document offset of mineral isograds, prograde garnet porphyroblasts are chloritized in the vicinity of the fault. In addition, the fault itself is marked by chlorite-carbonate alteration in several localities.

Pleasant Valley thrust

The middle Kaza marker is not affected by the Pleasant Valley thrust in this area and logistical considerations prevented tracking the marker into it. However, the surface mapped by Struik (1986) as the Pleasant Valley thrust was visited in the Slide Mountain area. There, Struik located the fault above a brown-weathering micaceous marble (described as mylonitic) at the base of the middle Kaza Group. In support of this placement, Struik cited the apparent Paleozoic age of underlying rocks, the apparent mylonitic texture of the marble, and truncation of strata above and below it.

Several observations argue against the presence of a major thrust fault at this locality. First, finely laminated (millimetre scale) sandy turbidites are found in a 1 m thick bed of phyllite immediately overlying the marble. Neither these



Likely displacement ranges from 430 m (dextral-oblique) to 2.05 km (dextral-strike).

Figure 77.5. Fault plane map of Knutson Creek Fault illustrating the range of likely slip vectors and the resulting range of displacement. Offset feature (hanging and footwall cutoffs) is the base of the middle Kaza marker.

turbidites nor the phyllite show any indication of being within a metre of a fault with several tens of kilometres of displacement. Secondly, channels locally cut downward into the phyllite to within 0.5 m of the contact with the marble. The channels are filled with very coarse grained quartzite (metamorphosed quartzofeldspathic pebbly sandstone) including intraclasts of carbonate which are virtually indistinguishable from the underlying marble. The contact with the marble is however, never observed to be breached by a channel. Thirdly, although highly strained, cross lamination and gradededding are both preserved in the marble, making it highly unlikely that it is mylonitic. Fourthly, immediately underlying the marble are coarse grained, commonly calcareous quartzites with clasts of bluish quartz and feldspar and intraclasts of carbonate and phyllite that are virtually indistinguishable from overlying Kaza clastic rocks. Fifthly, the contact is cut by a pre-D_n metalamprophyre of unknown age.

All of the above observations cast doubt on, but do not negate, the presence of a major thrust fault along this contact. Clearly, if the underlying rocks are Paleozoic, then a fault must exist and the above observations are of no consequence. However, on the basis of field observations alone, it is an unlikely location for a fault. More work is necessary to determine the trajectory of the Pleasant Valley thrust in this area.

CONCLUSIONS

1. The quartzite and graphitic phyllite marker described by Pell and Simony (1984) in eastern Wells Gray Park is almost undoubtedly the same marker unit observed in the Castle Creek area 70 km to the north, confirming correlations based on this unit.
2. The basal metasiltstone portion of the marker consists primarily of laterally persistent base-cut-out (Tbc(e), Tcd(e), Tbcd(e)) turbidites and, less commonly, Tab(e) and Tac(e) turbidites.
3. The upward transition from coarse grained, poorly sorted Kaza turbidites, through the basal siltstone of the marker to the upper basinal graphitic phyllite of the marker implies an overall progradation of distal facies over more proximal facies. The nature of the Kaza basinal facies is not known.
4. The structural geometry of eastern Wells Gray Park results from the superimposition of three sets of regionally extensive structures and late northwest-trending faults.
5. The Knutson Creek Fault is a dextral oblique-slip fault with both normal and dextral strike-slip components. Its orientation and sense of slip implies that it is a transtensional link between more westerly trending strike-slip faults.
6. Several observations cast doubt, but do not negate, the location of the Pleasant Valley thrust where mapped in the Slide Mountain area. More work is necessary to constrain the location of the fault in this area.

ACKNOWLEDGMENTS

Permission to work in Wells Gray Park was provided by the B.C. Ministry of Lands, Parks, and Housing. I thank Tom Bell of the Kamloops office for expediting our Parks Use Permit. Bert Struik of the GSC and David McMullin of U.B.C. read, and improved, an early draft of this report. Finally, I thank Len Gal for assistance in the field.

REFERENCES

Carey, A. and Simony, P.S.
1984: Structure and stratigraphy of the late Proterozoic Miette Group, Cushing Creek area, Rocky Mountains, British Columbia; in Current Research, Part A, Geological Survey of Canada, Paper 84-1A, p. 425-428.
1985: Stratigraphy, sedimentology, and structure of Late Proterozoic Miette Group, Cushing Creek Area, B.C.; Bulletin of Canadian Petroleum Geology v. 33, p. 184-203.

Murphy, D.C.
1986: Stratigraphy and structure of the east-central Cariboo Mountains, British Columbia and Implications for the geological evolution of the southeastern Canadian Cordillera; unpublished Ph.D thesis, Carleton University, 187 p.

Murphy, D.C. and Rees, C.J.
1983: Structural transition and stratigraphy in the Cariboo Mountains, British Columbia; in Current Research, Part A, Geological Survey of Canada, Paper 83-1A, p. 245-252.

Pell, J.
1984: Stratigraphy, structure, and metamorphism of Hadrynian strata in southeast Cariboo Mountains, British Columbia; unpublished Ph.D thesis, University of Calgary, 185 p.

Pell, J. and Simony, P.S.
1982: Hadrynian Horsethief Creek/Kaza Group correlations in the southern Cariboo Mountains, British Columbia; in Current Research, Part A, Geological Survey of Canada, Paper 82-1A, p. 305-308.
1984: Stratigraphy of the Hadrynian Kaza Group between the Azure and North Thompson rivers, Cariboo Mountains, British Columbia; in Current Research, Part A, Geological Survey of Canada, Paper 84-1A, p. 95-98.

Struik, L.C.
1984: Stratigraphy of Quesnel terrane near Dragon Lake, Quesnel Lake map-area, central British Columbia; in Current Research, Part A, Geological Survey of Canada, Paper 84-1A, p. 113-116.
1985: Dextral strike-slip through Wells Gray Provincial Park, British Columbia; in Current Research, Part A, Geological Survey of Canada, Paper 85-1A, p. 305-309.
1986: A regional east-dipping thrust places Hadrynian on to probable Paleozoic rocks in Cariboo Mountains, British Columbia; in Current Research, Part A, Geological Survey of Canada, Paper 86-1A, p. 589-594.

Wheeler, J.O., Campbell, R.B., Reesor, J.E., and Mountjoy, E.W.
1972: Structural style of the southern Candian Cordillera; Guidebook X01 - A01, 24th International Geological Congress, Montreal, Canada.

Conodont biostratigraphy and correlation of the Harper Ranch Group (Devonian – Permian), Ashcroft map area, southern British Columbia

Project 810028

M.J. Orchard
Cordilleran and Pacific Margin Division, Vancouver

Orchard, M.J., Conodont biostratigraphy and correlation of the Harper Ranch Group (Devonian – Permian), Ashcroft map area, southern British Columbia; in Current Research, Part A, Geological Survey of Canada, Paper 87-1A, p. 743-749, 1987.

Abstract

Conodonts from the Harper Ranch Group (Ashcroft map area), the Paleozoic basement of the Quesnel Terrane, are Late Devonian, Early Carboniferous and Early to ?Late Permian. The late Famennian Harper Mountain fauna represents a shallow water biofacies and occurs in a thin, plant-bearing clastic unit known from a single locality; the fauna is unique in the Canadian western Cordillera. The late Visean – early Namurian (late Mississippian) Pinantan Lake fauna occurs in siliceous limestones that have been reported to contain Pennsylvanian foraminiferids. This fauna is widespread both in the map area and elsewhere: it is correlated with units throughout British Columbia and the Yukon. Permian conodonts from Harper Ranch are divisible into five faunal assemblages that are tentatively regarded as ranging from late Sakmarian through early Guadalupian: elements of four of these occur elsewhere in the western Cordillera, particularly in the Stikine Terrane.

Résumé

Les conodontes du groupe de Harper Ranch (région cartographique d'Ashcroft), socle paléozoïque du terrain de Quesnel, appartiennent au Dévonien supérieur, au Carbonifère inférieur et au Permien inférieur à supérieur(?). La faune de Harper Mountain du Famennien supérieur représente un biofaciès d'eau peu profonde et se manifeste à l'intérieur d'une mince unité clastique, riche en plantes, connue dans un seul endroit; cette faune est unique dans la Cordillère canadienne de l'Ouest. La faune de Pinantan Lake dont l'âge varie du Viséen supérieur-au Namurien inférieur (Mississippien supérieur) se manifeste dans des calcaires siliceux qui renfermeraient des foraminiféridés du Pennsylvanien. Cette faune est répandue à la fois dans la région cartographique et ailleurs: elle correspond à des unités répandues dans toute la Colombie-Britannique et le Yukon. Les conodontes permiens de Harper Ranch se divisent en cinq ensembles fauniques que l'on place provisoirement entre le Sakmarien supérieur et le Guadalupien inférieur. On trouve des éléments de quatre de ces cinq ensembles ailleurs dans la Cordillère de l'Ouest, particulièrement dans le terrain de Stikine.

INTRODUCTION

This report summarizes the nature, age and correlation of conodont faunas from the Harper Ranch Group (Sada and Danner, 1976; Smith, 1979; Monger and McMillan, 1984), the Paleozoic basement of the Quesnel Terrane ("Quesnellia"), which underlies the Intermontane belt of southern British Columbia (NTS 92I). As presently conceived, the group includes limestone, argillite, siltstone, local coarser clastics, volcaniclastics and minor chert (Monger and McMillan, 1984). Formal definition and subdivision of the group has been hampered by poor outcrop and limited age control. Conodont sampling was carried out initially in conjunction with regional mapping of the Ashcroft map area (op. cit.). The conodont work has continued in order to both elucidate stratigraphic relationships and to characterize the conodont faunas of Quesnellia in a comparative study of paleontological signatures of juxtaposed Cordilleran terranes. To date, conodont faunas of Late Devonian (Famennian), Early Carboniferous (late Visean – early Namurian), and Early to ?Late Permian (Sakmarian?, Arstinskian, Guadalupian?) age are known (Plate 78.1). These are here described and compared with faunas elsewhere in the Cordillera.

LATE DEVONIAN HARPER MOUNTAIN FAUNA

Devonian strata occur at a single location on the north side of Harper Mountain (Fig. 78.1, A; GSC loc. nos. C-116075 through C-116083) where a roadcut exposes less than 30 m of plant-bearing siltstone, argillite, minor conglomerate, and a single 20 cm bed of fossiliferous bioclastic limestone. The latter contains brachiopods, gastropods, crinoids, ichthyoliths and a conodont fauna representative of the Devonian shallow water *"Icriodus" – Polygnathus* biofacies. The fauna is dominated by forms corresponding to *"Icriodus" costatus darbyensis* Klapper Morphotype 2 of Sandberg and Dreesen, many of which have strong connecting ridges, implying high energy conditions (Sandberg and Dreesen, 1984, p. 165). The remainder of the fauna comprises generally fragmented *Polygnathus* spp., including *P.* ex gr. *inornatus, P. delicatulus,* and *P. communis,* plus *Bispathodus stabilis,* and *Apatognathus varians varians.*

In terms of the shallow water zonation proposed by Sandberg and Dreesen (1984), *"Icriodus" costatus darbyensis* Morphotype 2 is indicative of the late Famennian Middle to Upper *"Icriodus" costatus* Zone. This is equivalent to all but the lowest part of the *expansa* Zone and to much of the succeeding *praesulcata* Zone of the standard (pelagic facies) zonation. The absence of typical *I. raymondi* suggests that the fauna is no older than the Upper *"Icriodus" costatus* Zone, that is equivalent to the Upper *expansa* through Middle *praesulcata* zones, although *praesulcata* Zone occurrences of the species are rare (Sandberg and Dreesen, 1984, p. 165). An upper limit is also provided by *Apatognathus varian varians*, which ranges from within the *marginifera* Zone (emmended) to high in the *expansa* or low in the *praesulcata* zones (Nicoll, 1980, p. 151). The known range of the polygnathids is compatable with this age too (Ziegler and Sandberg, 1984, p. 182). Therefore, in spite of the absence of diagnostic representatives of the pelagic *Palmatolepis* biofacies, the age of the Harper Mountain fauna can be reasonably constrained as Upper *expansa* – Lower *praesulcata* zones, with the emphasis on the former zone. This is consistent with the age of the brachiopods, determined as late Famennian by W. Norris (GSC, Calgary – personal communication, 1985).

Icriodus costatus darbyensis, although restricted environmentally, is geographically widespread. The species has previously been described from the American midwest (Wyoming, Colorado), Belgium and the U.S.S.R. (Sandberg and Dreesen, 1984, p. 165; Barskov et al., 1984). In addition, conodont faunules listed by Kuz'min et al. (1983) from Kazakhstan and by Wang and Ziegler (1982) from South China also appear to contain most, if not all of the elements of the Harper Mountain fauna. Few conodont faunas of this age have been systematically described from Canada, although Mound (1968, p. 458, 459) listed condodonts, including *Apatognathus varians,* from the Famennian Wabamun Group of the Alberta subsurface, regarded as equivalent to the Palliser Group of the Rocky Mountains. The brachiopods from Harper Mountain are also known from both these units (Norris, personal communication, 1985). The conodont fauna is unknown elsewhere in the Canadian Western Cordillera.

EARLY CARBONIFEROUS PINANTAN LAKE FAUNA

Fossil corals, brachiopods, foraminiferids and algae of Carboniferous age have been recorded from the Harper Ranch beds. Skinner and Wilde (1966) listed several foraminiferid faunas that they regarded as "probably Morrowan" (Early Pennsylvanian), and Sada and Danner (1974) later summarized eleven foraminiferid collections from the area and concluded that these were of late Mississippian (?one), Early Pennsylvanian (eight) and Middle Pennsylvanian (two) age. Smith (1979) made collections of fossils, including brachiopods, of probable late Mississippian age (Dutro, *in* Smith, 1979, p. 16; Fig. 78.1, no. 22).

Several of these Carboniferous localities have been sampled for conodonts. Those from the South Thompson No. 1 locality (Fig. 78.1, no. 23; GSC loc. nos. C-87091, C-116072/3) of Sada and Danner (1974), in which a foraminiferid faunule of Early Pennsylvanian age was reported, include *Vogelgnathus campbelli* and poorly preserved species of *?Gnathodus, Hindeodus* and *?Kladognathus*. Richer faunules containing each of these taxa are better known from an undescribed locality on the south sidef Pinantan Lake (Fig. 78.1, B; GSC loc. nos. C-118404/5, C-118812/5), where a roadcut exposes flaggy to massive, siliceous limestones interbedded with argillite. Some of these beds contain small silicified corals and large articulated crinoid stems, up to 1 cm in diameter and 10 cm in length. A suite of samples taken from these strata contain *Gnathodus bilineatus* with

less common *Gnathodus? homopunctatus*. In addition, *Vogelgnathus campbelli, Hindeodus* sp., *Kladognathus* sp., and *Idioprioniodus* sp. have been found in samples from the western end of the outcrop, whereas beds at the eastern end have yielded *Cavusgnathus* sp.

Gnathodus bilineatus is particularly widespread and is the index fossil of several zones established in Europe, North America and Asia: the species is restricted to upper Visean and lower Namurian strata in Europe and to the upper Mississippian in the United States. *Vogelgnathus campbelli* is also a cosmopolitan species. It occurs throughout the Visean in England (Higgins, 1975; Metcalfe, 1981), as high as the lower Namurian in Spain (Higgins and Wagner-Gentis, 1982), and within lower Chesterian rocks in the Illinois Basin (Norby and Rexroad, 1985); the species is also known from Japan, Sumatra and eastern Canada. Metcalfe (1980) also records *Vogelgnathus campbelli* in the Panching Limestone

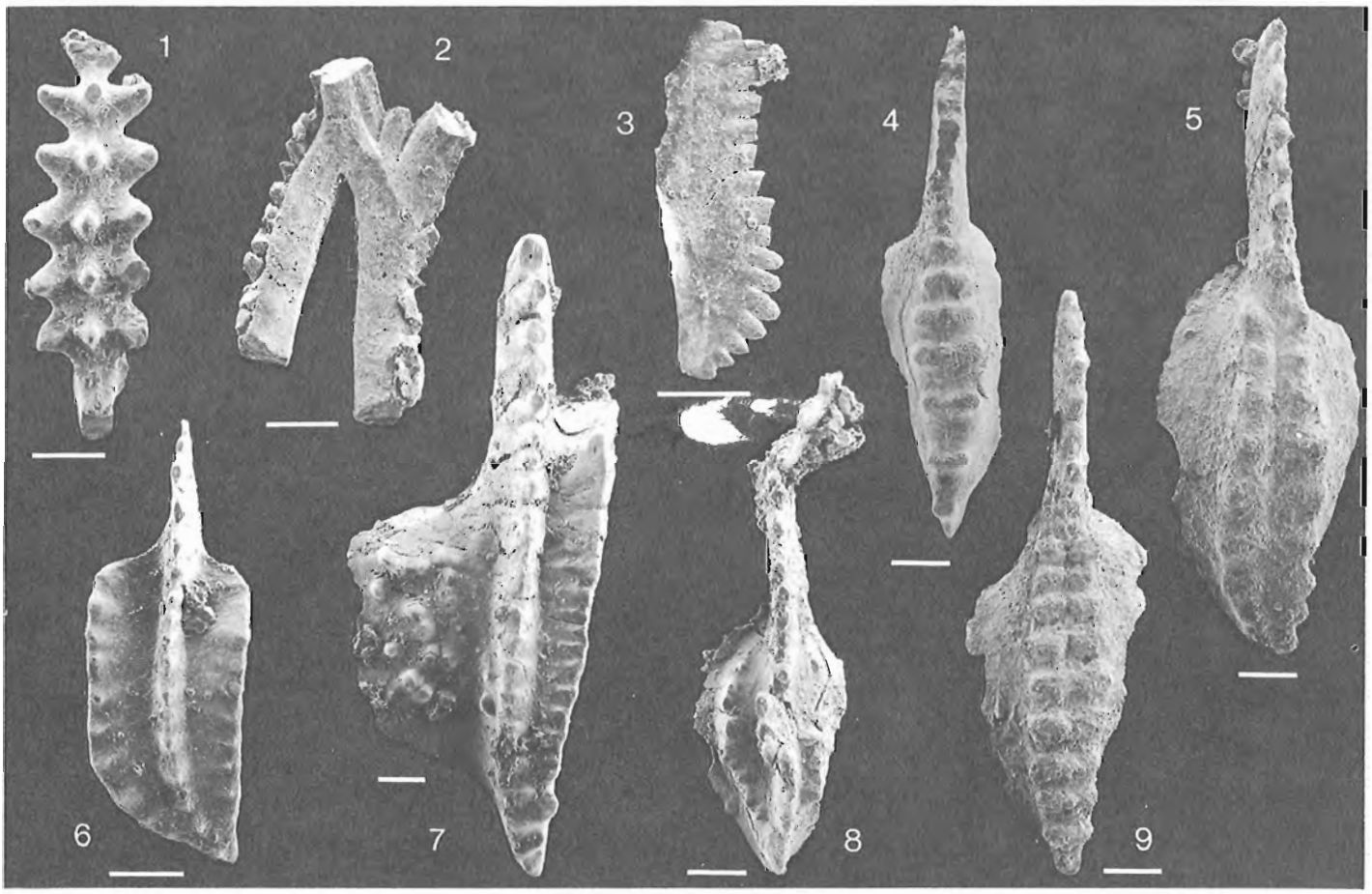


Plate 78.1. Devonian (Fig. 1,2,6), Carboniferous (Fig. 3,7,8) and Permian (Fig. 4,5,9) conodonts from the Harper Ranch Group. All figures are upper views of Pa elements, unless stated otherwise. Bar scales represent 100 microns.

Figure 1. *Icriodus costatus darbyensis* Klapper morphotype 2 Sandberg and Dreesen. GSC 81061, x100. GSC loc. no. C-116079.

Figure 2. *Apatognathus varians varians* Branson & Mehl. GSC 81062, x100. GSC loc. no. C-116079. Posterior view of M element.

Figure 3. *Vogelgnathus campbelli* (Rexroad). GSC 81063, x120. GSC loc. no. C-118813. Lateral view.

Figure 4. *Sweetognathus whitei* (Rhodes). GSC 81064, x80. GSC loc. no. C-116069.

Figure 5. *Neostreptognathodus* ex gr. *sulcoplicatus* (Youngquist, Hawley and Miller). GSC 81065, x80. GSC loc. no. C-116061.

Figure 6. *Polygnathus* sp. GSC 81066, x100. GSC loc. no. C-087380.

Figure 7. *Gnathodus bilineatus* (Roundy). GSC 81067, x60. GSC loc. no. C-118812.

Figure 8. *Gnathodus? homopunctatus* Ziegler. GSC 81068, x80. GSC loc. no. C-118814.

Figure 9. *Neostreptognathodus clarki* Kozur. GSC 81069, x80. GSC loc. no. C-118862.

of west Malaysia in association with Upper Carboniferous *Declinognathodus*, however, this record may be referable to the younger *Vogelgnathus* n. sp. of Norby and Rexroad (1985). *Cavusgnathus* is restricted to Mississippian rocks in North America, and equivalents elsewhere.

Gnathodus homopunctatus is common in Europe where it appears as early as the base of the Visean in Belgium (Conil et al., 1976), and extends as high as lower Namurian strata in northern England (Higgins, 1975). The species has been reported from three units in North America: the Skunk Spring Limestone of the Chainman Shale in Utah (Sandberg et al.,980; Tynan, 1980), the Peratrovich Formation of SE Alaska (Faulhaber, 1977) and the Denmar Formation of Virginia in the southern Appalachians (Chaplin, 1984); within each of these, the faunal associates are very similar to those in the Pinantan Lake fauna. The association of *Gnathodus bilineatus, G. homopunctatus* and *Vogelgnathus campbelli* is also reported from the Serpukhovian of the Moscow Basin (Barskov et al., 1979). In total, the Pinantan Lake fauna is regarded as late Visean to early Namurian (late Mississippian).

Additional Carboniferous conodont faunules are known from the Harper Ranch Group both within and outside the area shown in Figure 78.1. These are along the northern margin of the South Thompson River (HR23-24 in Monger and McMillan, 1984 and Fig. 78.1), on the south side of

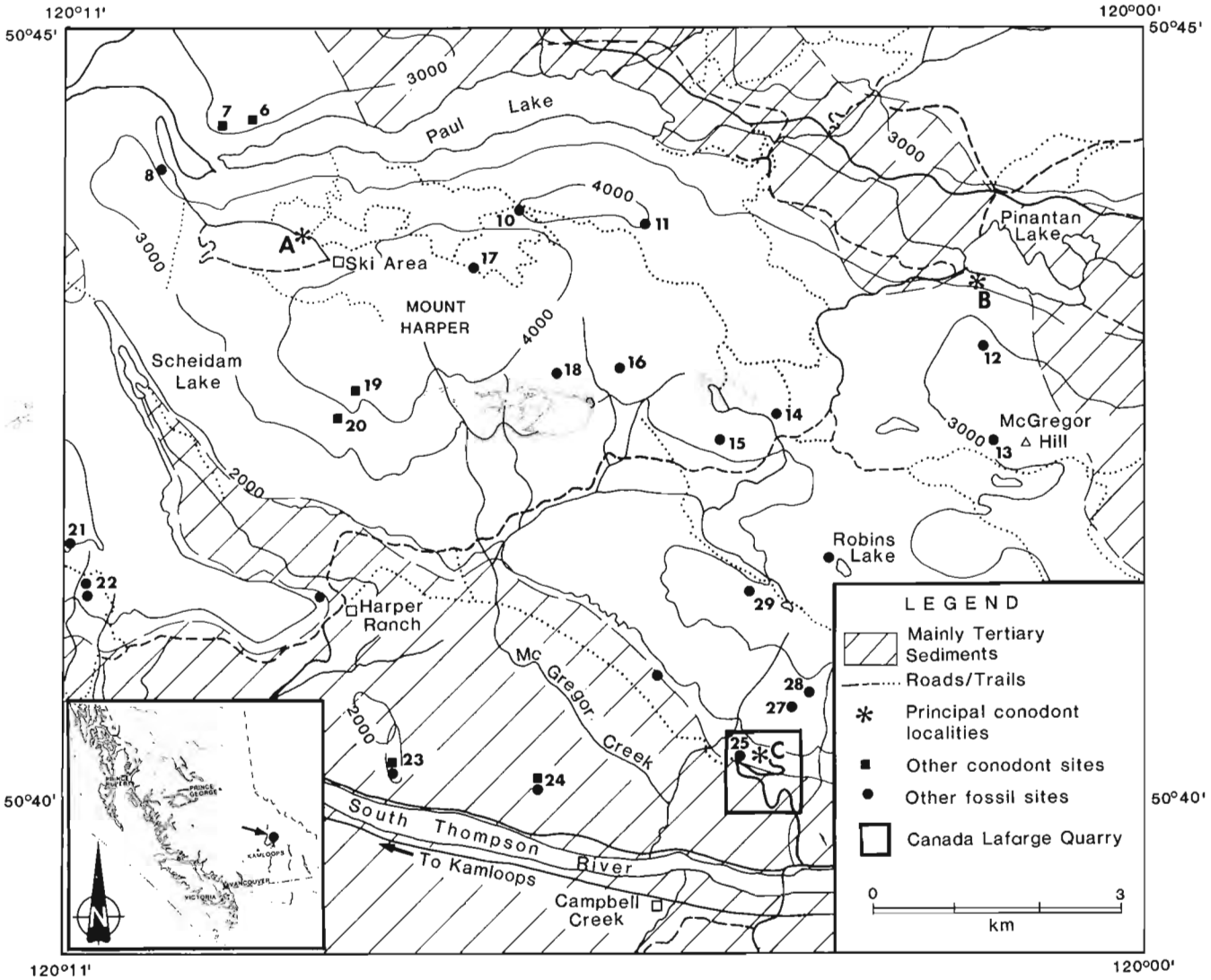


Figure 78.1. Fossil localities in the Harper Ranch Group based in part on Monger and McMillan (1984), supplemented by Sada and Danner (1976) and Smith (1979). Numbered localities correspond to those in Monger and McMillan (1984), who include citation of GSC locality numbers; additional GSC locality numbers, when available, are mentioned in text.

Mount Harper (HR19-20, op. cit.), at the northwest end of Paul Lake (HR6-7, op. cit.), and about 10 km to the northwest in the Dome Hills (HR1,3, op. cit.). Further localities occur on the flanks of Canada Lafarge Quarry and in strata mapped as undifferentiated, metamorphosed Paleozoic and Mesozoic rocks by Monger and McMillan (1984, PM2-3 occur 7km N and 20 km NNW of Fig. 78.1). The limestones at these several localities are sometimes interbedded with argillite and chert, as at Pinantan Lake, and appear in situ, but often they appear disrupted and occur as isolated limestone outcrops within an area of Triassic? volcaniclastics or Quaternary drift. Each of the above localities has yielded conodonts that are known within the Pinantan Lake fauna and may be directly correlated with that sequence. Preserved remnants of Carboniferous limestones within the Harper Ranch Group therefore attest to a widespread episode of upper Visean – lower Namurian (late Mississippian) carbonate sedimentation in northeastern Ashcroft area. There is, as yet, no conodontvidence for carbonate rocks of Late Carboniferous age in the area. The age attributed to at least some of the 'Pennsylvanian' foraminiferids from the Harper Ranch Group is therefore regarded as suspect; W.R. Danner (personal communication, 1986) also now views the Pennsylvanian ages as in need of revision.

Gnathodus? homopunctatus has not been reported from elsewhere in Canada, but both *Vogelgnathus campbelli* and *Gnathodus bilineatus* occur within the Etherington Formation of the Canadian Rocky Mountains (Baxter and von Bitter, 1984, p. 262) and they are also known from several units within the Canadian Western Cordillera, including part of the Eagle Bay Formation in Seymour Arm map area (Kootenay Terrane), and the Keno Hill Quartzite and correlative units in the Selwyn Basin, Yukon Territory. On the basis of the occurrence of *Gnathodus bilineatus*, the Pinantan Lake fauna is broadly correlative with the Blind Creek Formation (Penticton map area – Quesnel Terrane), parts of the Chilliwack Group (Hope map area – Chilliwack Terrane), the Ducie limestone (Prince Rupert map area – Alexander Terrane; Woodsworth and Orchard, 1985), an unnamed unit in Iskut map area (Stikine Terrane), the Englishmans Group (Teslin map area – Dorsey Terrane) and, in part, chert of the Antler and Fennel formations (Slide Mountain Terrane; Orchard, in press). The Nizi Formation (McDame map area) is also correlated on the basis of foraminiferid ages (Mamet and Gabrielse, 1969).

PERMIAN HARPER RANCH FAUNA

Well bedded to massive fossiliferous limestones of Permian age outcrop over a wide area between the South Thompson River and Harper Mountain, immediately to the east of Harper Ranch. Permian faunas of diverse age and character have been recorded therein: Miller and Warren (1933) and Miller and Crockford (1936) reported ammonoids of probable early Guadalupian age from a locality within the "upper" part of the Harper Ranch sequence; Thompson and Verville (1950) described Leonardian or slightly younger fusulinid faunas from several localities; Skinner and Wilde (1966) described additional foraminiferid faunas of Wolfcampian and early Guadalupian age; Sada and Danner (1976) described Wolfcampian *Pseudoschwagerina* (Fig. 78.1, no. 15); and Nelson and Nelson (1985) described a waagenophyllid coral, brachiopods and rare trilobites associated with Guadalupian fusulinids.

I earlier summarized the initial results of conodont sampling in the quarry of Canada Lafarge (Orchard, 1984b). Nine conodont collections made near the top of the multi-tiered quarry (Fig. 78.1, C) included *Sweetognathus* spp. and *Neogondolella bisselli*, in part associated with common *Adetognathus* and uncommon *Diplognathodus, Ellisonia* and *Hindeodus*. New collections from lower terraces within the quarry have duplicated these faunas, but immediately to the west and north of the quarry, younger faunas dominated by *Neostreptognathodus*, and more evolved *Neogondolella* have also been recovered. Five conodont faunal assemblages are now recognized in the Permian outcrop. These will be described more fully in a paper presently in progress. The faunas are:

1. The *Adetognathus* fauna
2. The *Sweetognathus whitei* fauna
3. The *Neostreptognathodus clarki* fauna
4. The *Neostreptognathodus* ex gr. *sulcoplicatus* fauna
5. The *Neogondolella* ex gr. *idahoensis* fauna

The *Adetognathus* fauna (fauna 1) was described by Orchard (1984a). It comprises abundant *A. paralautus* accompanied by relatively primitive sweetognathids and *Neogondolella bisselli*, and is tentatively regarded as late Sakmarian (= Wolfcampian). Fauna 2 comprises the restricted *Sweetognathus whitei – Neogondolella bisselli* association discussed by Orchard (1984b), now judged to be early Artinskian (= Leonardian).

A traverse sampled for conodonts by P. Forster (bachelors thesis, .B.C.) in 1985 revealed a new association (fauna 3) comprising an overlap of *Sweetognathus* and *Neostreptognathodus*. This fauna, now discovered in several other localities nearby, includes *Neostreptognathodus clarki*, a species described from the "late Artinskian" of the Russian Cisural (Movshovich, 1984).

Fauna 4, characterized by abundant *Neostreptognathodus*, has not been found within the quarry but is common and widespread in the surrounding area. Several late Early Permian species are identified, including forms close to *N. sulcoplicatus*.

The youngest fauna (5) known from Harper Ranch is composed entirely of *Neogondolella* showing affinity to late Leonardian *N. idahoensis* and its early Guadalupian derivatives. This fauna was first recovered from the locality that produced the fauna described by Nelson and Nelson (1985).

Several of the species known from the Permian Harper Ranch beds are known elsewhere in the Canadian Cordillera. Faunas 1 and 2 are present in the Chilliwack Group, and a variation on Fauna 2 appears also in the Sugar limestone of

the Cariboo belt (Orchard and Struik, 1985). Other occurrences are noted by Orchard (1984b, p. 209). Records of *Sweetogathus* from the Cache Creek Terrane are younger than those from Quesnellia and the only Permian conodont that the two terranes are currently known to have in common is the cosmopolitan *Neogondolella bisselli*, which occurs in limestone olistoliths of the Cache Creek Melange Unit (Orchard, 1984a); in my view the provenance of these olistoliths is undetermined – they may be derived from Quesnellia. *Neostreptognathodus* is known from the scattered occurrences in the Yukon but occurs most commonly in unnamed Permian strata of the Stikine Terrane in central and northern British Columbia. Permian (in addition to Early Carboniferous), conodonts from that area show great affinity with those of Quesnellia.

REFERENCES

Barskov, I.S., Alekseev, A.S., and Goreva, N.V.
1979: Carboniferous conodonts of Moscow Vicinities; in Palaeontological Characteristics of the Main Subdivisions of the Carboniferous, Meyen et al. (ed,); Proceedings of the VIII – ICC (1975), Compte Rendu, v. 3, p. 239-246.

Barskov, I.S., Simakov, K.V., Alekseev, A.S., Bogoslovsky, B.I., Byvsheva, T.V., Gagiev, L.N., Kononova, L.N., Kochetkova, N.M., Kusina, L.F., and Reitlinger, E.A.
1984: Devonian – Carboniferous transitional deposits of the Berchogur section, Mugodzary, USSR; Courier Forschungsinstitut Senckenberg, no. 67, p. 207-230.

Baxter, S. and von Bitter, P.H.
1984: Conodont succession in the Mississippian of southern Canada; in P.K. Sutherland, and W.L. Manger, (ed.); Proceedings of the IX – ICC (1979), Compte Rendu, v. 2, p. 253-264.

Chaplin, J.R.
1984: Conodont biostratigraphy of Lower Carboniferous strata in the southern Appalachians; in P.K. Sutherland, and W.L. Manger, (ed.); Proceedings of the IX – ICC (1979), Compte Rendu, v. 2, p. 265-281.

Conil, R., Groessens, E., and Pirlet, H.
1976: Nouvelle charte stratigaphique du Dinantien type de la Belgique; Société géologique du nord (France), Annales, v. 96, p. 363-371.

Faulhaber, J.J.
1977: Late Mississippian (late Osagian through Chesterian) conodonts from the Peratrovich Formation, southeastern Alaska; unpublished M.Sc. thesis, Department of Geology, University of Oregon, Eugene, 174 p.

Higgins A.C.
1975: Conodont zonation of the late Visean-early Westphalian strata of the south and central Pennines of northern England; Geological Survey of Great Britain, Bulletin 53, 90 p.

Higgins, A.C. and Wagner-Gentis, C.H.T.
1982: Conodonts, goniatites and biostratigraphy of the earlier Carboniferous from the Cantabrian Mountains, Spain; Palaeontology, v. 25, p.313-350.

Kuz'min, A.V., Barskov, I.S., and Kononova, L.I.
1983: Conodonts of the Famennian and Tournaisian of Atasu mining district, Central Kazakhstan; Doklady Akademii Nauk SSSR, 270(3), p. 672-674.

Mamet, B.L. and Gabrielse, H.
1969: Foraminiferal zonation and stratigraphy of the type section of the Nizi Formation (Carboniferous System, Chesteran Stage), British Columbia; Geological Survey of Canada, Paper 69-16, 19 p.

Metcalfe, I.
1980: Upper Carboniferous conodont faunas of the Panching Limestone, Pahang, West Malaysia; Palaeontology, v. 23, p. 297-314.
1981: Conodont zonation and correlation of the Dinantian and early Namurian strata of the Craven Lowlands of northern England; Institute of Geological Sciences Report 80/10, 70 p.

Miller, A.K. and Crockford, M.B.
1936: Permian Cephalopods from British Columbia; Royal Society of Canada, Transactions, v. 30, p. 23-28.

Miller, A.K. and Warren, P.S.
1933: A *Propinacoceras* from North America; American Journal of Science, v. 26, p. 295-299.

Monger, J.W.H. and McMillan, W.
1984: Bedrock geology of Ashcroft (92I) map area; Geological Survey of Canada, Open File 980.

Mound, M.C.
1968: Upper Devonian conodonts from southern Alberta; Journal of Paleontology, v. 42, p. 444-524.

Movshovich, E.V.
1984: Conodonts; in Main features of the Stratigraphy of the Permian System of the USSR; G.V. Kotlyar, and D.L. Stepanov, (ed.), All-Union Geological Research Institute, Trudy, New Series, v. 286, p. 263-270.

Nelson, S.J. and Nelson, E.R.
1985: Allochthonous Permian micro- and macrofauna, Kamloops area, British Columbia; Canadian Journal of Earth Sciences, v. 22, p. 442-451.

Nicoll, R.S.
1980: The multielement genus *Apatognathus* from the Late Devonian of the Canning Basin, Western Australia; Alcheringa, v. 4, p. 133-152.

Norby, R.D. and Rexroad, C.B.
1985: *Vogelgnathus*, a new Mississippian conodont genus; State of Indiana Department of Natural Resources, Geological Survey Occasional Paper 50, 14 p.

Orchard, M.J.
1984a: Pennsylvanian, Permian and Triassic Conodonts from the Cache Creek Group, Cache Creek, Southern British Columbia; in Current Research, Part B, Geological Survey of Canada, Paper 84-1B, p. 197-206.
1984b: Early Permian conodonts from the Harper Ranch Beds, Kamloops area, southern British Columbia; in Current Research, Part B, Geological Survey of Canada, Paper 84-1B, p. 207-215.
– Conodonts from Western Canadian chert: their nature, distribution and stratigraphic application; in Conodonts, Investigative Techniques and Applications, R.L. Austin (ed.); Proceedings of the Fourth European

Conodont Symposium (ECOS IV); Ellis – Horwood, Chichester, England (in press).

Orchard, M.J. and Struik, L.C.
1985: Conodonts and stratigraphy of upper Paleozoic limestones in Cariboo gold belt, east-central British Columbia; Canadian Journal of Earth Sciences, v. 22, p. 538-552.

Sada, K. and Danner, W.R.
1974: Early and Middle Pennsylvanian fusulinids from southern British Columbia, Canada and northwestern Washington, U.S.A.; Transactions and Proceedings of the Palaeontological Society of Japan, New Series, No. 93, p. 249-265.
1976: *Pseudoschwagerina* from the Harper Ranch Area near Kamloops, British Columbia, Canada; Commemoration Volume of the founding of the Faculty of Integrated Arts and Sciences, Hiroshima University, p. 213-228.

Sandberg, C.A. and Dreesen, R.
1984: Late Devonian icriodontid biofacies models and alternate shallow-water conodont zonation; Geological Society of America, Special Paper 196, p. 143-177.

Sandberg, C.A., Poole, F.G., Gutschick, R.C.
1980: Devonian and Mississippian stratigraphy and conodont zonation of Pilot and Chainman shales, Confusion Range, Utah; in Paleozoic Paleogeography of the West-central United States, T.D. Fouch and E.R. Magathan (ed); Rocky Mountain Paleogeography Symposium 1, p. 71-79.

Skinner, J.W. and Wilde, G.L.
1966: A new Permian fusulinid from southern British Columbia, Canada; Academy of Sciences of the U.S.S.R., Problems of Micropaleontology, No. 10, p. 105-108.

Smith, R.B.
1979: Geology of the Harper Ranch Group (Carboniferous-Permian) and Nicola Group (Upper Triassic) northeast of Kamloops, British Columbia; unpublished M.Sc. thesis, University of British Columbia.

Thompson, M.L. and Verville, G.J.
1950: Cache Creek fusulinids from Kamloops, British Columbia; Contributions to the Cushman Foundation for Foraminiferal Research, v. 1, p. 67-70.

Tynan, M.C.
1980: Conodont biostratigraphy of the Mississippian Chainman Formation, western Millard County, Utah; Journal of Paleontology, v. 54, p. 1282-1309.

Wang, C-Y and Ziegler, W.
1982: On the Devonian – Carboniferous boundary in South China based on conodonts; Geologica et Palaeontologica, v. 16, p. 151-162.

Woodsworth, G.J. and Orchard, M.J.
1985: Upper Paleozoic to lower Mesozoic strata and their conodonts, western Coast Plutonic Complex, British Columbia; Canadian Journal of Earth Sciences, v. 22, p. 1329-1344.

Ziegler, W. and Sandberg, C.A.
1984: *Palmatolepis*-based revision of upper part of standard Late evonian conodont zonation; Geological Society of America, Special Paper 196, p. 179-193.

Field and stratigraphic relations of amphibolites in the late Proterozoic Horsethief Creek Group, northern Adams River area, British Columbia

EMR Research Agreement 138-04-86

J. H. Sevigny[1]
Cordilleran and Pacific Margin Division

Sevigny, J.H., Field and stratigraphic relations of amphibolites in the late Proterozoic Horsethief Creek Group, northern Adams River area, British Columbia; in Current Research, Part A, Geological Survey of Canada, Paper 87-1A, p. 751-756, 1987.

Abstract

Metabasalts of the late Proterozoic Horsethief Creek Group, in the northern Adams River area, British Columbia are subdivided into three groups, including those representing; (1) sills and transposed dykes, (2) flows and tuffs, and (3) reworked tuffaceous material. This subdivision is based on field and stratigraphic relations, petrological observations, and major and trace element geochemistry. Geochemical data indicate that basalts evolved as a suite of high-iron tholeiites as evidenced by the marked iron and titanium enrichment and the systematic behaviour of immobile, incompatible elements during igneous differentiation. A suite of mineralogically distinct amphibolites has been produced by upper amphibolite facies metamorphism of variably fractionated basalts. Integrated geological and geochemical evidence suggests a model of synchronous, shallow water deposition of clastic rock, flows, and tuffs and, subsequent to and/or coeval with deposition, injection of sills and dykes in a crustally thinned tectonic setting along the western margin of North America during the late Proterozoic.

Résumé

Des métabasaltes du groupe de Horsethief Creek du Protérozoïque supérieur, de la région nord de la rivière Adams en Colombie-Britannique, sont répartis en trois groupes, notamment: 1) filons-couches et dykes transposés, 2) écoulements et tufs, et 3) matériaux tufacés remaniés. Cette répartition est fondée sur des relations observées sur le terrain et des liens stratigraphiques, des observation pétrologiques ainsi que sur la géochimie d'éléments importants et d'éléments à l'état de traces. Les données géochimiques indiquent que les basaltes se sont différenciés et ont donné une série de tholéiites riches en fer comme le montre l'enrichissement en fer et en titane marqué et le comportement systématique d'éléments immobiles et incompatibles pendant l'étape responsable de la différenciation ignée. Une série d'amphibolites, distinctes minéralogiquement, a été produite par un métamorphisme à faciès des amphibolites supérieur à partir de basaltes variablement fractionnés. Les données géologiques et géochimiques intégrées semblent indiquer un modèle de sédimentation synchrone et en eau peu profonde de roches clastiques, d'écoulements et de tufs ainsi que d'une injection postérieur ou contemporaine à la sédimentation, ou les deux, de filons-couches et de dykes dans un ensemble tectonique à croûte mince le long de la marge ouest de l'Amérique du Nord pendant le protérozoïque supérieur.

[1]Department of Geology and Geophysics, University of Calgary, Calgary, Alberta T2N 1N4

INTRODUCTION

The late Proterozoic Horsethief Creek Group (HCG) underlies much of the Shuswap Metamorphic Complex in southeastern British Columbia, and consists of a 3-6 km thick sequence of predominately coarse- to fine-grained clastic rock with lesser marble, amphibolite, and calc-silicate (Poulton and Simony, 1980; Raeside and Simony, 1983). Stratigraphic and sedimento-logical analysis (Poulton and Simony, 1980) suggests that the HCG represents a rifted continental margin sequence and this sequence is in many ways similar to an Atlantic-type margin sequence (eg., Schlee, 1980). Mapping during the 1985 and 1986 field seasons, in the northern Adams River area, has shown that the semipelite-amphibolite division and the lower section of the upper clastic division of the HCG are composed largely of amphibolite.

On the basis of field and stratigraphic relations, petrological observations, and whole-rock major and trace element geochemistry, amphibolites have been subdivided into three groups and the objective of this paper is a documentation of this subdivision as seen in the northern Adams River area. Geochemical data, will be summarized here as it serves to substantiate subdivision based on geological relations.

PREVIOUS WORK ON AMPHIBOLITES IN THE HORSETHIEF CREEK GROUP

Previous workers have shown that amphibolite is a persistent and locally abundant lithological component in the HCG, being most abundant in the semipelite-amphibolite division. Examination of the literature reveals that amphibolite exhibits more than one mode of occurrence. Amphibolite in the HCG is not well understood and the following review of previous work, along strike from south to north, demonstrates this.

The summary is concerned primarily with the semipelite-amphibolite division which is bounded on its lower and upper margins by the lower marble and middle marble, respectively. This characteristic stratigraphic package has been traced from the northern Purcell Mountains (Poulton and Simony, 1980) to the southern Cariboo Mountains (Pell and Simony, 1981), some 200 km along strike. Figure 79.1 displays geographic features referred to in the text.

To the south, in the Rogers Pass area of the southeastern Selkirk Mountains, Poulton and Simony (1980) reported mineralogically homogeneous amphibolite sheets with sharp contacts and suggested either an extrusive or intrusive origin for the amphibolite. West of the Purcell Mountains, in the Revelstoke area, Ghent et al. (1977) performed reconnaissance geochemistry on amphibolite boudins and concluded that the protobasalts were tholeiitic and chemically similar to diabase sills. In the northern Selkirk Mountains, Brown et al. (1978) noted that some amphibolite sheets have discordant, intrusive contacts. Simony et al. (1980) interpreted a 300 m thick garnet amphibolite body in the Mica Dam area as a sill-like mafic intrusion. In the Monashee Mountains, Raeside and Simony (1983) noted abundant amphibolite lenses and layers which, in places, comprise up to 60% of the semipelite-amphibolite division. Lastly, to the north, in the southern Cariboo Mountains, Pell and Simony (1981) documented amphibolite in the semipelite-amphibolite, although amphibolite is much less abundant there than in the Monashee Mountains. Thus, the literature suggests that amphibolite is present in a variety of geological occurrences in the HCG.

STRUCTURAL AND METAMORPHIC RELATIONS IN THE NORTHERN ADAMS RIVER AREA

The northern Adams River area (Fig. 79.1) lies along the northeastern margin of the Shuswap Metamorphic Complex (see Sevigny and Ghent, 1986, Fig. 72.1) which may be characterized as a multiply deformed, high grade terrane consisting of late Proterozoic metasedimentary and metavolcanic rocks. Geological relations in this area of the Shuswap Complex were discussed by Campbell (1968), Ghent et al. (1979, 1982, 1983), Raeside and Simony (1983), Doucet et al. (1985), and Sevigny and Ghent (1986). Documentation of amphibolite occurrences through contact relations and original mineralogy is complicated by the fact that the protobasalts were completely recrystallized during metamorphism and, possibly, structurally transposed during folding.

Stratigraphic relations in the HCG observed by the author in the Adams River area concur with the findings of Raeside and Simony (1983) in the adjacent Soards River area. The

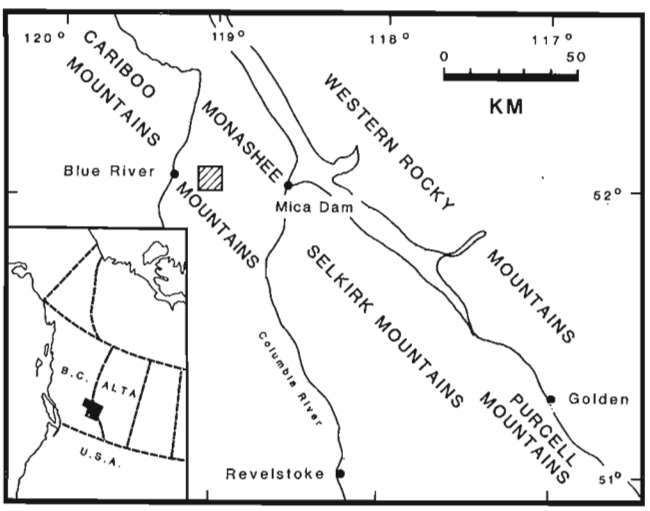


Figure 79.1. Location of geographic features in southeastern British Columbia referred to in the text. The location of the study area is shown by a ruled box west of Mica Dam in the Monashee Mountains (modified from Poulton and Simony, 1980).

majority of amphibolite occurs in the semipelite-amphibolite division, although the lower section of the upper clastic division contains considerable amphibolite. Of note, however, is the lack of amphibolite in the lower pelite division. Only the rare amphibolite boudin has been found in two seasons of mapping well exposed lower pelite.

The abundance of amphibolite in the sedimentary section above the lower pelite argues for a coeval, volcanic mode of occurrence, rather that emplacement solely by dykes and sills.

Three major phases of folding were recognized by Simony et al. (1980) and Raeside and Simony (1983) in rocks of the HCG in the northeastern Shuswap Metamorphic Complex. The first folding episode produced west-verging recumbent structures which were refolded by tight, northeast-verging structures to produce a southwest-dipping stack of folds on which third phase folds were imprinted. As discussed below, the transposition of basalt dykes, for example, was possible during the second phase of folding due to the PT and kinematic conditions that prevailed.

Metamorphic grade reaches a culmination in the northern Adams River area and ranges from sillimanite-muscovite to K-feldspar-sillimanite zone, with temperature and pressure reaching 680°C and 740 MPa (Sevigny and Ghent, 1986). Metamorphism was largely synkinematic as evidenced by the well developed axial planar foliation and elongate, sillimanite lineation coaxial with F 2 fold axes.

A qualitative estimate of PT conditions during F 2 , which permits some speculation regarding the possibility of transposition during folding of discordant structures such as dykes, can be made by incorporating Holdaway's (1971) Al_2SiO_5 phase diagram and two observations; the first being the coaxial nature of the sillimanite lineation and F 2 fold axes, and the second knowing that kyanite gives way to sillimanite immediately to the north (*see* Sevigny and Ghent, 1986, Fig. 72.1). It can be shown that PT conditions during F 2 folding can be bracketed between 500°C, 400 MPa and, 680°C, 450-720 MPa. Furthermore, by using a density of 2.8 g/cm^3 and assuming P total = P lithostatic, a pressure range of 400-720 MPa represents a depth range of 15-27 km. Thus, it is safe to conclude, in a qualitative sense, that transposition of basalt dykes or other discordant structures was highly probable due to the kinematic and PT conditions that accompanied the second phase of folding. Structural evidence is seen in the stretching of fold limbs, boudinage, and isoclinal folding.

AMPHIBOLITE OF THE HORSETHIEF CREEK GROUP

On the basis of field and stratigraphic relations, petrological observations, and whole-rock geochemical analyses, amphibolite has been subdivided into; (1) sills and transposed dykes, (2) flows and tuffs, and (3) reworked tuffaceous material.

Group 1 – sills and transposed dykes

The assignment of amphibolite to a group representing sills and transposed dykes is based primarily on geometric considerations as these may not be differentiated by field relations alone. Smaller, flattened and elongate boudins (*see* Ghent et al., 1977, Fig. 2) are believed to represent earlier discordant dykes which have been subsequently rotated into the foliation. A large body of geochemically fractionated amphibolite in the Nagle Creek area is likely a metamorphosed sill (*see* Knitter, 1979).

Sills occur as planar bodies, up to 250 m thick, with sharp contacts with the country rock. These bodies, although highly attenuated and dismembered, are traceable for many kilometres along strike. Petrographic examination reveals that, internally, sills are mineralogically heterogeneous. Sill margins may lack garnet and ilmenite, although invariably contain biotite. Internally, however, garnet is a common phase, as is ilmenite, while biotite is rare. Sulphides usually occur in sill interiors. These mineralogical trends can be correlated with geochemical data as shown below.

With the exception of Brown et al. (1978), no other workers have documented dykes or other discordant bodies of amphibolite. Amphibolite boudins up to 30 m long and up to 10 m wide have been noted by Raeside and Simony (1983). Boudins which are approximately 12 m long and 5 m wide are common in the northern Adams River area. Boudins studied by Ghent et al. (1977) likely belong to Group 1 of this study.

The mineralogy of boudins is variable and somewhat enigmatic. Most boudins contain garnet and ilmenite and characteristically have margins enriched in biotite. A few boudins studied lack garnet.

Group 2 – flows and tuffs

This group comprises the majority of amphibolite mapped in the study area. A massive, 200 m thick flow, interbedded with the middle marble, was mapped in two well exposed localities. A package of amphibolite with minor semipelite and psammite, which is composed largely of amphibolite of tuffaceous origin, occurs in the basal one-third of the semipelite-amphibolite division. This characteristic, tuffaceous-rich package has been traced for over 10 kms along strike.

Amphibolite of tuffaceous origin occurs as thin (1-30 cm), ontinuous, planar layers intercalated with marble (Fig. 79.2), and both psammmite and semipelite (Fig. 79.3). Both gradational and sharp contacts have been observed. However, contacts with coarse clastic rock are generally, mildly irregular. Tuffaceous amphibolites commonly contain garnet porphyroblasts, in places up to 2.5 cm across (Fig. 79.3). Biotite is ubiquitous in these amphibolite layers. Geochemical analyses have not been performed on this suite of rocks due to the possibility of clastic impurities and the high probability of elemental mobility during metmorphism.

Amphibolites interpreted to represent metamorphosed flows occur within stratigraphic proximity to the middle marble, near the top of the semipelite-amphibolite division and at the base of the upper clastic division. Flows range up to 200 m thick, are mineralogically and chemically homogeneous, and display an interbedded relationship with the middle marble. At one locality, amphibolite is in stratigraphic contact with marble (Fig. 79.4) which contains up to 40% thinly interbedded amphibolite, interpreted to represent metatuff (*see* Fig. 79.2). At another locality, 12 km to the west, the middle marble is interbedded with discontinuous lenses and layers of marble. A few blocks of marble were observed. Thin, clinopyroxene-bearing layers in the amphibolite are coplanar with marble layers and are interpreted to represent calcareous basalt. Clinopyroxene-bearing layers exhibit irregular contacts with amphibolite and are coplanar with the fabric of the underlying clastic rock. Unlike sills of similar thickness, flows are mineralogically homogeneous and, therefore, differentiation as evidenced by a heterogeneous mineralogy is lacking. Garnet is not present and ilmenite may or not be present in flows.

Group 3 – reworked tuffs

Amphibolite of this group occurs in clastic rocks associated with amphibolite layers and is recognized by the gradational nature of bulk compositional variations on the scale of a thin section. Typically, reworked tuffs are evident by the occurrence of hornblende-bearing semipelite. In thin section, mafic layers of hornblende + garnet + clinopyroxene + scapolite alternate with pelitic, garnet + biotite layers. Electron microprobe analyses of garnets reveals that hornblende layers contain garnet with 27-42 mol % grossular, typical of garnet in amphibolite, whereas pelitic layers contain garnet of significantly greater almandine and lesser grossular content. Aside from geothermometry and geobarometry, little attention has been paid to this group.

GEOCHEMISTRY OF AMPHIBOLITES

This section aims (1) to substantiate the above subdivision using a geochemical argument as the geological evidence alone is not conclusive, and (2) to suggest that amphibolites represent basalts derived from a source or sources of relatively unfractionated basalt which has undergone differentiation to a high-iron tholeiitic suite.

Samples from Group 1 and flows of Group 2 have been selected for geochemical analyses. In Fig. 79.5 are plotted the immobile, incompatible elements Zr, Y, Nb, trace element V, and minor oxide TiO_2 vs. total iron (FeO *) for amphibolites. Examination of Fig. 79.5 reveals: (1) all elements vary in a covariant, systematic manner with respect to FeO * , (2) FeO * and TiO_2 exhibit significant enrichment, and (3) the mineralogy of amphibolites, which can be correlated with occurrence, varies as a function of differentiation. The systematic and linear fashion of enrichment of the incompatible elements Zr, Nb, Y, and Ti with increasing FeO * suggests that HCG amphibolites may represent a comagmatic suite, derived from a single source, and related by a process of



Figure 79.2. Intercalated light marble and layers of dark metatuff. Vertical scale approximately 10 m.

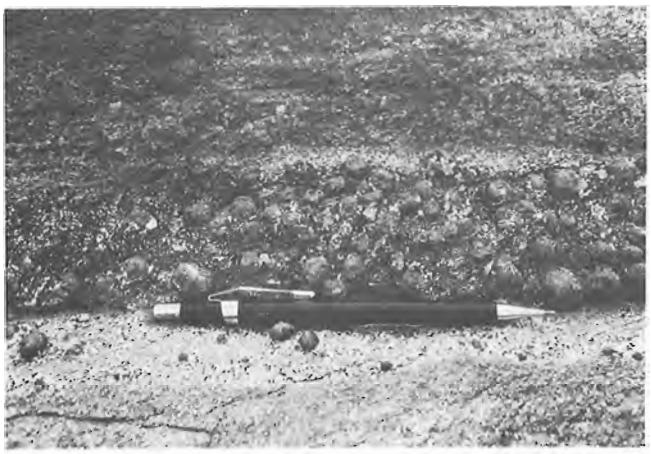


Figure 79.3. Gradational contact between light psammite and darker, garnet amphibolite. Note the occurrence of a few garnet porphyroblasts in psammite near amphibolite contact, and the lack of garnet in amphibolite away from psammite.



Figure 79.4. Contact between dark flow and coloured marble. Marble at this locality is approximately 20 m above Figure 79.2. Vertical scale approximately 50 m. Arrow shows the location of person in the snowfield.

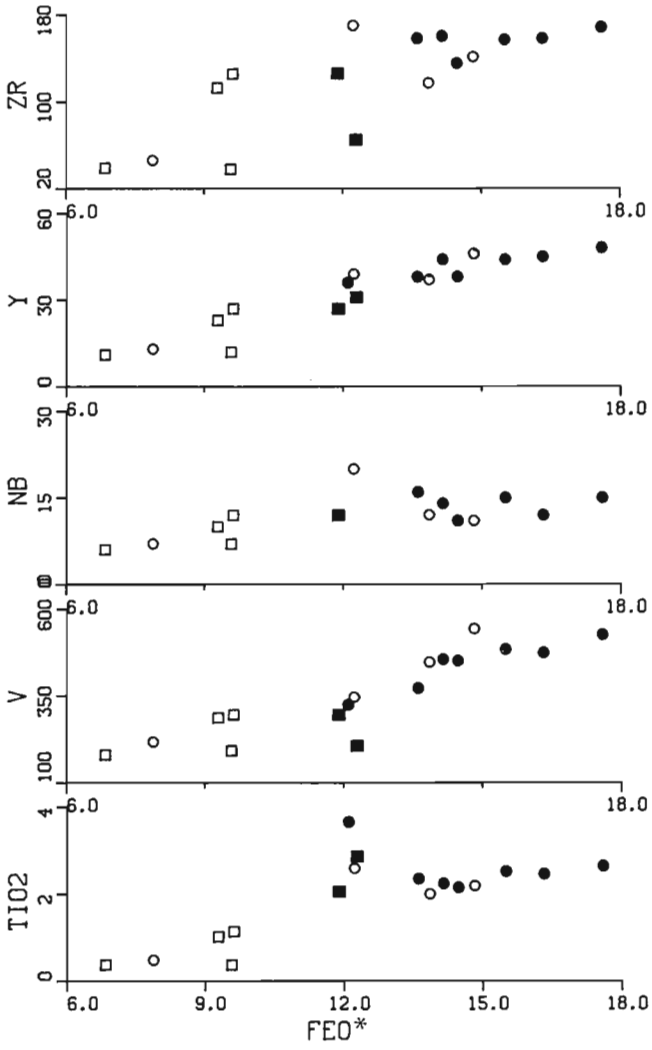


Figure 79.5. Incompatable elements Zr, Y, Nb, trace element V, and minor element TiO_2 vs. total iron (FeO *). Circles = amphibolite (hornblende + plagioclase + quartz + sphene + ilmenite), squares = biotite-bearing amphibolite. Filled symbols = garnet-bearing amphibolite, open symbols = amphibolites lacking garnet.

igneous differentiation. On the other hand, however, variable incompatible element ratios (ie. Zr/Y, Y/Nb, Zr/Nb, and Ti/Zr) argue for derivation from more than one source. Enrichment of FeO * and TiO_2 suggests that amphibolites of the HCG represent a suite of tholeiites related by a high-iron trend. Metabasaltic flows which lack garnet and contain biotite (open squares in Fig. 79.5) represent relatively unfractionated to moderately fractionated basalt, whereas sills (closed circles in Fig. 79.5) are highly fractionated. Subdivision based on geochemical data is consistent with geological evidence.

An inconsistency exists concerning the stage of fractionation evident in amphibolites which should be relatively undifferentiated. That is, amphibolites interpreted on geological grounds to represent dykes and tuffs generally contain garnet; however garnet occurs in amphibolites with FeO * greater than about 12 wt. %. An iron content of 12 wt. % is not attained until moderate stages of fractionation are reached. Possible explanations to this problem include; (1) some dykes and tuffs may actually represent basalts which were in an advanced stage of fractionation, (2) multiple episodes of intrusion may have occurred, and (3) deposition of tuffs in a clastic enviroment may have modified the original chemistry of basalt thus allowing garnet to crystallize during metamorphism.

IMPLICATIONS OF AMPHIBOLITE IN THE HORSETHIEF CREEK GROUP

The findings of this study are consistent with the sedimentological analysis of Poulton and Simony (1980) in suggesting that the HCG represents a rifted continential margin sequence. The occurrence of flows and tuffs, in places intercalated with marble and psammite, implies a model of shallow water deposition within close proximity to a volcanic source. The decrease in amphibolite to both the north and south suggests the paleo-volcanic centre was in the northern Adams River area.

ACKNOWLEDGMENTS

Jacky Vader and Jay Timmerman are thanked for their invaluable assistance in the field. Pat Michael provided technical advice during XRF analyses. This manuscript was reviewed by P.S. Simony and Lisel Currie.

REFERENCES

Brown, R.L, Tippet, C.R., and Lane, L.S.
1978: Stratigraphy, facies changes, and correlations in the Selkirk Mountains, southern Canadian Cordillera; Canadian Journal of Earth Sciences, v. 15, p. 1129-1140.

Campbell, R.B.
1968: Canoe River, British Columbia; Geological Survey of Canada, Map 15-1967.

Doucet, P., Ghent. E.D., and Simony, P.S.
1985: Metamorphism in the Monashee Mountains east of Blue River, British Columbia; in Current Research, Part A, Geological Survey of Canada, Paper 85-1A, p. 69-71.

Ghent, E.D., Nicholls, J., Stout, M.Z., and Rottenfusser, B.
1977: Clinopyroxene amphibolite boudins from Three Valley Gap, British Columbia; Canadian Mineralogist, v. 15, p. 269-282.

Ghent, E.D., Robbins, D.B., and Stout, M.Z.
1979: Geothermometry, geobarometry, and fluid compositions of metamorphosed calc-silicates and pelites, Mica Creek, British Columbia; American Mineralogist, v. 64, p. 874-885.

Ghent, E.D., Knitter, C.C., Raeside, R.P., and Stout, M.Z.
1982: Geothermometry and geobarometry of pelitic rocks, upper kyanite and sillimanite zones, Mica Creek, British Columbia; Canadian Mineralogist, v. 20, p. 295-305.

Ghent, E.D., Stout, M.Z., and Raeside, R.P.
1983: Plagioclase-clinopyroxene-garnet-quartz equilibria and the geobarometry and geothermometry of garnet amphibolites from Mica Creek, British Columbia; Canadian Journal of Earth Sciences, v. 20, p. 699-706.

Holdaway, M.J.
1971: Stability of andalusite and the aluminum silicate phase diagram; American Journal of Science, v. 271, p. 97-131.

Knitter, C.C.
1979: Metamorphism and structure of the Soards Creek area, British Columbia; unpublished M. Sc. thesis, University of Calgary, Alberta.

Pell, J. and Simony, P.S.
1981: Stratigraphy, structure, and metamorphism in the southern Cariboo Mountains, British Columbia; in Current Research, Part A, Geological Survey of Canada, Paper 81-1A, p. 227-230.

Poulton, T.P. and Simony, P.S.
1980: Stratigraphy, sedimentology, and regional correlation of the Horsethief Creek Group (Hadrynian, Late Precambrian) in the northern Purcell and Selkirk Mountains, British Columbia; Canadian Journal of Earth Sciences, v. 17, p. 1708-1724.

Raeside, R.P. and Simony, P.S.
1983: Stratigraphy and deformational history of the Scrip Nappe, Monashee Mountains, British Columbia; Canadian Journal of Earth Sciences, v. 20, p. 639-650.

Schlee, J.S.
1980: A comparison of two Atlantic-type contential margins; Geological Survey of America, Professional Paper 1167, p. 1-21.

Sevigny, J.H. and Ghent, E.D.
1986: Metamorphism in the northern Adams River area, north-eastern Shuswap Metamorphic Complex, Monashee Complex, British Columbia; in Current Research, Part B, Geological Survey of Canada, Paper 86-1B, p. 693- 698.

Simony, P.S., Ghent, E.D., Craw, D., Mitchell, W., and Robbins, D.B.
1980: Structural and metamorphic evolution of northeast flank of Shuswap Complex, southern Canoe River area, British Columbia; Geological Society of America, Memoir 153, p. 445-461.

Mid-Holocene paleosurfaces in vertical accretion deposits, Fraser River delta, British Columbia

EMR Research Agreement 275-04-84
and Project 790006

Harry F.L. Williams[1] and Michael C. Roberts[1]
Cordilleran and Pacific Margin Division

Williams, H.F.L. and Roberts, M.C., Mid-Holocene paleosurfaces in vertical accretion deposits, Fraser River delta, British Columbia; in Current Research, Part A, Geological Survey of Canada, Paper 87-1A, p. 757-761, 1987.

Abstract

A sequence of drill cores extending from the eastern Fraser River Delta into the western section of the floodplain of the Fraser River has provided stratigraphic evidence establishing the presence of two distinct paleosurfaces in the silty topset beds of the delta. The upper paleosurface, marked by a peat, is tentatively assigned an age of 5700 BP while the lower paleosurface (a tephra bed) is probably 6600 BP.

The combination of the two surfaces within the topset beds and radiocarbon dating control has established that the topsets vertically accreted in response to a rise in sea level during middle Holocene time (7700 to 4700 BP).

Résumé

Une série de carottes de forage prises dans la région allant de l'est du delta du fleuve Fraser jusqu'à la section ouest de la plaine d'inondation du fleuve a fourni la preuve stratigraphique qui permet d'établir la présence de deux paléosurfaces distinctes dans les couches sommitales limoneuses du delta. La mise en place de la paléosurface supérieur caractérisée par une couche de tourbe, date probablement d'il y a 5700 ans, alors que celle de la paléosurface inférieure (une couche de téphra) a probablement en lieu il y a 6600 ans.

La combinaison de ces deux surfaces à l'intérieur des couches sommitales et la datation au carbone radioactif ont permis d'établir que les couches sommitales se sont accrues verticalement à la suite d'une remontée du niveau marin pendant l'Holocène moyen (soit il y a 4700 à 7700 ans).

[1]Department of Geography, Simon Fraser University, Burnaby, B.C. V5A 1S6

INTRODUCTION

A preliminary interpretation of drill cores from Lulu Island, in the eastern section of the Fraser delta, indicates that vertical accretion of the deltaic topsets (floodplain and tidal flats) kept pace with the ca. 12 m rise in sea level which occurred between ca. 7700 BP and ca. 4700 BP (Clague et al., 1982; Williams, 1986; Fig. 80.1).

The term 'base-level-controlled vertical accretion deposits' is proposed for these sediments on the basis that they apparently formed in response to, and at pace with, the change in base level of the Fraser delta, brought about by the relative rise in sea level during middle Holocene time.

Further drilling on eastern Lulu Island and the adjoining Fraser Valley (Fig. 80.2), has revealed two extensive, well defined paleosurfaces in the silty topset beds. The existence of these two surfaces supports the hypothesis that the vertical accretion deposits grew in concordance with the rise of sea level.

METHODS

As part of an ongoing research program on the structure and evolution of the Fraser delta, a series of vibra-cores were obtained from eastern Lulu Island and the adjoining Fraser River floodplain (Fig. 80.2).

Field logging of cores involved the visual assessment of grain size, organic matter content and sedimentary structures. Tephra layers, where present, were collected for later laboratory identification. Wood fragments and samples of buried peat layers were also collected for 14C dating.

The vibra-core logs were used in conjunction with drillhole records provided by the B.C. Ministry of Transportation and Highways to construct a stratigraphic section from Pitt Meadows in the western Fraser Valley and along the east-west axis of Lulu Island. It is assumed that this axis parallels the direction of progradation of this part of the Fraser delta.

STRATIGRAPHY

A stratigraphic section across the delta and the western end of the Fraser floodplain is shown in Figure 80.3. A composite stratigraphic column of the delta in the eastern Lulu Island area is presented in Figure 80.4. The composite section shows the typical sequence found in the eastern delta: the middle unit (unit 2) is a 12 m thick organic-rich, horizontally bedded silt. Within this unit there are two marker horizons: a peat bed and a tephra bed. The buried peat bed up to 50 cm thick, in many cases containing horizontal laminations and having gradational contacts above and below, was found in 13 locations (Fig. 80.3). A tephra layer, up to 2 cm thick, was found extensively in the subsurface (15 locations). The tephra is relatively clean and has sharp contacts with the enclosing silts (Fig. 80.5), suggesting that it was probably deposited in a subaerial environment. The source of this tephra has yet to be confirmed, but given its stratigraphic location and associated radiocarbon dating, the tephra is probably of Mt. Mazama origin.

Overlying unit 2 is a peat (unit 1) ranging up to 4 m in thickness. The thickness of the peat reflects the amount of peat harvesting carried out in a particular area and the original domed shape of the peat bog (Hebda, 1977). The base of the peat has been dated at 4700 BP (Styan, 1981). Underlying unit 2 are the intertidal silts and sands of unit 3.

PALEOSURFACES

The peat and tephra beds are so extensive in the subsurface that they are evidence of paleosurfaces within the silt unit of the Fraser delta. The paleosurfaces are found at depths of about -2.5 m for the peat bed, and at about -5.5 m for the tephra (Fig. 80.3).

On the basis of a ^{14}C date of 5580 ± 70 BP (GSC-4238) from site D-23, at a depth of 5.19 m (-2.19 m below sea level), the -2.5 m paleosurface has been given the tentative age of 5700 BP. The -5.5 m paleosurface is assumed to have an age of 6600 BP on the assumption that the tephra is of Mt. Mazama origin.

DISCUSSION

It is proposed that the two paleosurfaces represent former subaerially exposed surfaces formed during the vertical accretion of the deltaic topset beds and adjoining floodplain of the Fraser River.

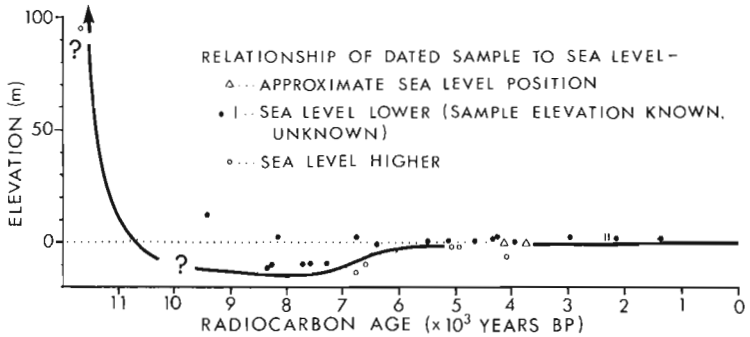


Figure 80.1. Fraser delta sea level curve (after Clague et al., 1982)

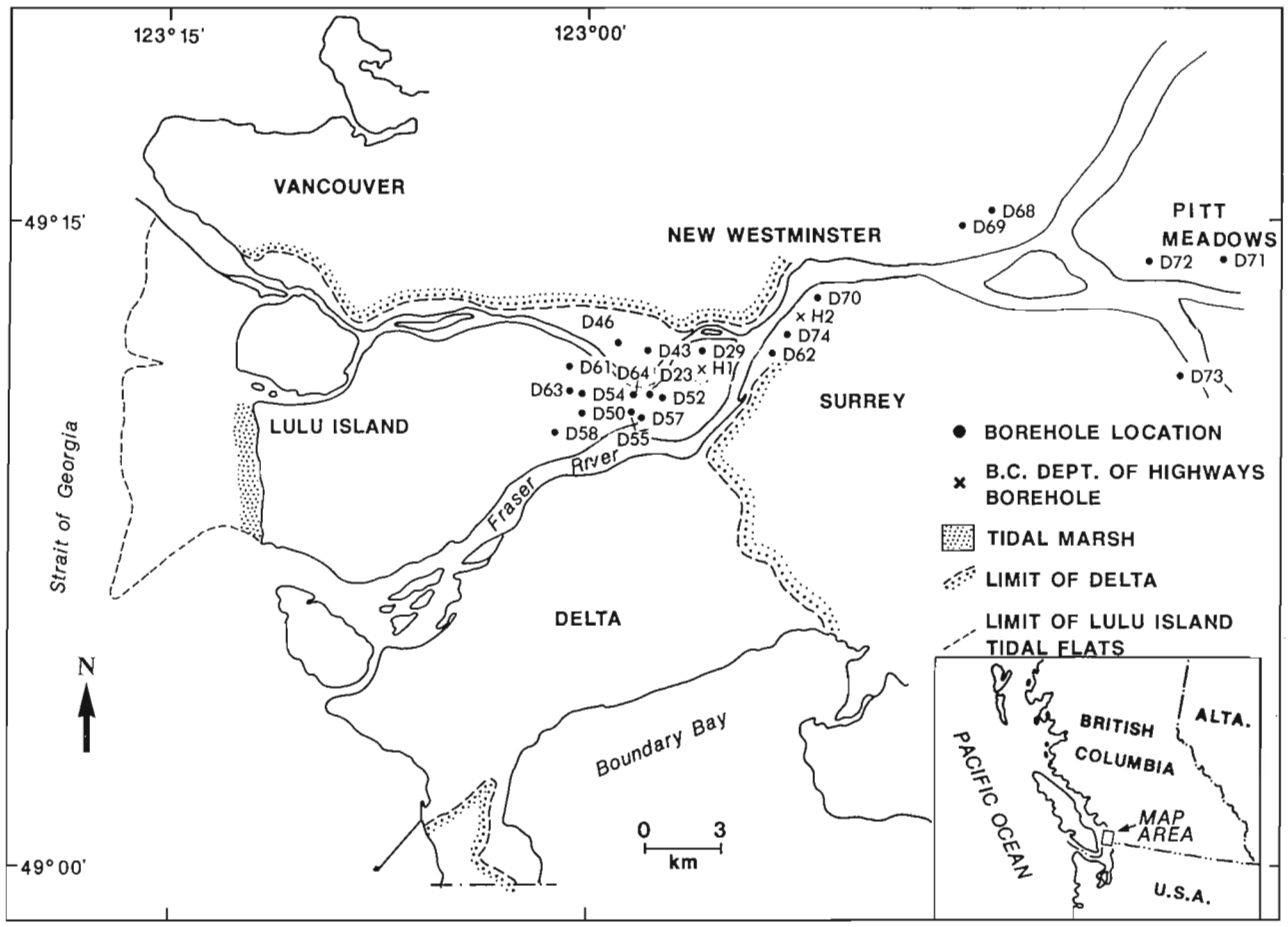


Figure 80.2. Drill site locations: Lulu Island and the western Fraser River valley.

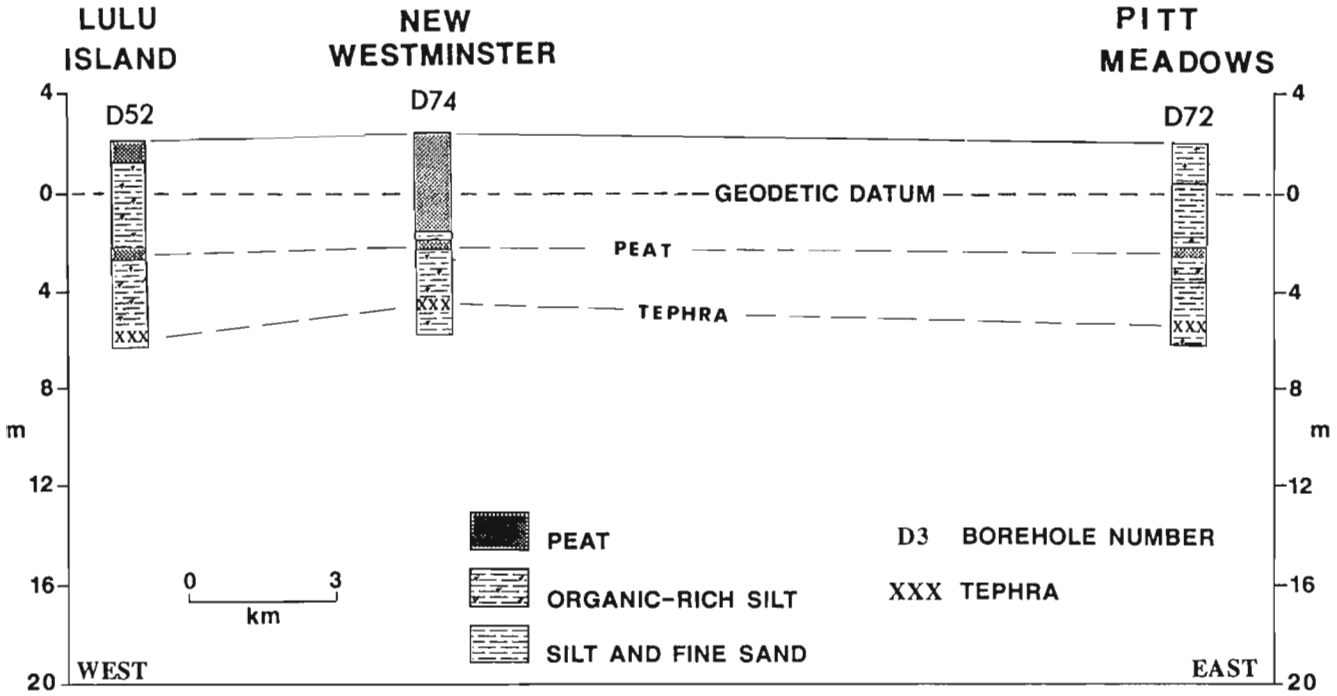


Figure 80.3. East-west stratigraphic section, Lulu Island and western Fraser River valley.

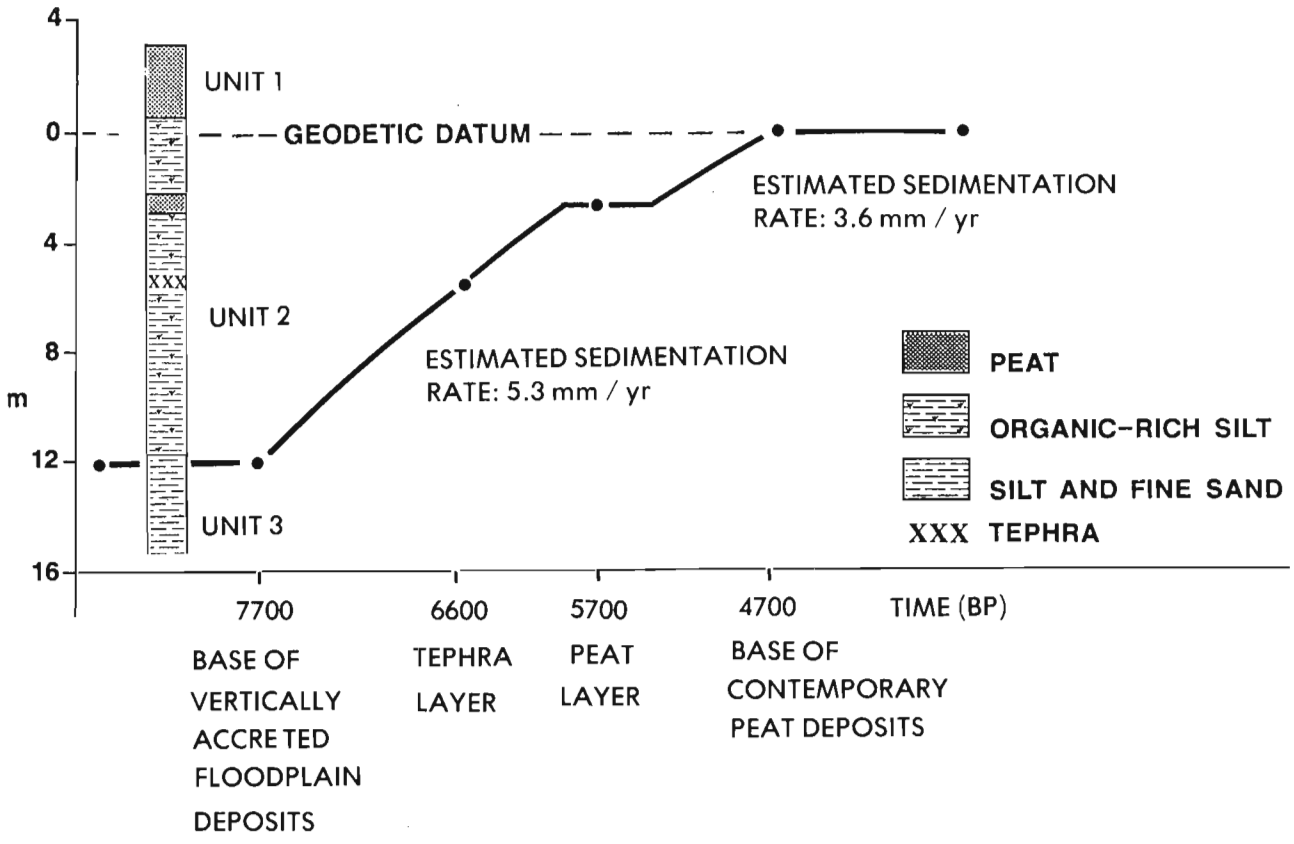


Figure 80.4. Composite stratigraphic column and sea level curve for eastern Lulu Island.

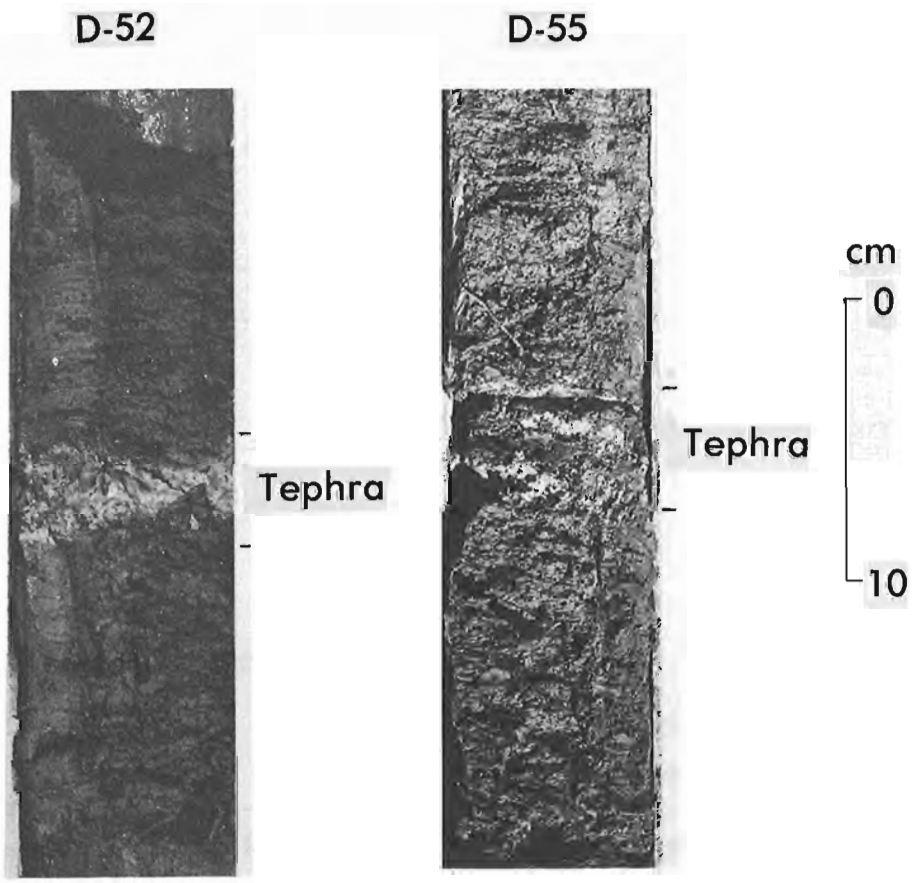


Figure 80.5. A core sample showing a tephra bed at drill sites D-52 and D-55.

The lack of peat throughout the lower part of unit 2 (Fig. 80.4) suggests sea level rose steadily at first, matched by deposition of organic-rich silts, but not allowing time for peat development. The tephra layer was deposited during this period.

The peat layer marking the −2.5 m paleosurface suggests a stillstand in sea level occurred at about 5700 BP, exposing this surface to subaerial conditions for a sufficient period of time for peat deposits to form. After the stillstand, sea level presumably continued rising, attaining its present level at about 4700 BP (Fig. 80.4).

On the basis of these proposals, a sea-level curve has been constructed for the Fraser delta area, covering the period 7700 BP to 4700 BP. Estimates of the sedimentation rates of the vertically accreted topset deposits have been incorporated into Figure 80.4.

Four peat samples from different locations of the −2.5 m paleosurface are awaiting ^{14}C dating. Studies are currently underway to determine the identification of the tephra samples by X-ray fluorescence signatures as well as by stratigraphic position.

CONCLUSIONS

1. The discovery of two extensive, formerly subaerial paleosurfaces, beneath present sea level within the topset beds of the Fraser delta, supports the hypothesis that vertical accretion of these beds kept pace with rising sea level during mid-Holocene time.
2. The continuity of the stratigraphy eastwards into the Fraser River valley shows that vertical accretion also occurred on the Fraser River floodplain, at least as far east as Pitt Meadows.
3. The presence of a buried peat layer within the deltaic topsets, suggests that a stillstand of sea level occurred at approximately 5700 BP, and was of sufficient duration to allow peat accumulation.

ACKNOWLEDGMENTS

We thank J.J. Clague and J.L. Luternauer for their advice and suggestions as this work progressed. The drilling crew of B. Morningstar, W. Ophoff, N. Hori and H. Jol are thanked for their willing efforts. Part of this research was funded by a Geological Society of America dissertation grant to H. Williams.

REFERENCES

Clague, J.J., Harper, J.R., Hebda, R.J., and Howes, D.E.
1982: Late Quaternary sea levels and crustal movements, British Columbia; Canadian Journal of Earth Sciences, v. 19, p. 452-462.

Hebda, R.J.
1977: The paleoecology of a raised bog and associated deltaic sediments of the Fraser River delta; unpublished Ph.D. dissertation, University of British Columbia, Vancouver, B.C., 202 p.

Styan, W.B.
1981: The sedimentology, petrography and geochemistry of some Fraser Delta peat deposits; unpublished M.Sc. thesis, University of British Columbia, Vancouver, B.C., 188 p.

Williams, H.F.L.
1986: Depositional facies and evolution of Lulu Island topset deposits, Fraser Delta, British Columbia; in Current Research, Part A, Geological Survey of Canada, Paper 86-1A, p. 559-564.

Gravity models within the southern Central Metasedimentary Belt, Grenville Province, Ontario

Project 6.4.3.13

D. Real[1] and M.D. Thomas
Lithosphere and Canadian Shield Division

Real, D. and Thomas, M.D., Gravity models within the southern Central Metasedimentary Belt, Grenville Province, Ontario; in Current Research, Part A, Geological Survey of Canada, Paper 87-1A, p. 763-772, 1987.

Abstract

Detailed gravity surveys in the southern Central Metasedimentary Belt (CMB) have provided a clearer picture of anomalies associated with certain plutonic intrusions and metavolcanic belts. The improved gravity database has been used to model quantitatively upper crustal structure. Felsic intrusions may be divided into two categories based on their depth extent. Relatively thick intrusions (2.4 to 4.2 km) include the Weslemkoon, Elzevir, Northbrook and Mazinaw Lake bodies. Thin intrusions (0.2 to 1 km) include the Cross Lake, Mellon Lake, Addington and Deloro bodies. Metavolcanics and gabbroic intrusions are modelled as having maximum depths of 3.4 and 2.6 km, respectively. It is apparent that structures within the uppermost 4 km of the crust can account for most, if not all, of the gravity variations within much of the southern CMB. This suggests that the underlying crust is laterally homogeneous and this may be significant in evaluating models proposed for the development of the CMB.

Résumé

Des études gravimétriques détaillées, exécutées dans le sud de la zone métasédimentaire centrale (ZMC), ont permis de fournir une image plus nette des anomalies associés à certaines intrusions plutoniques et à certaines zones métavolcaniques. La base de données gravimétriques améliorée sevir à élaborer des modèles quantitatifs de la structure supérieure de la croûte. On peut diviser les instrusions felsiques en deux catégories, selon leur profondeur. Les intrusions relativement épaisses (2,4 à 4,2 km) comprennent les massifs de Weslemkoon, d'Elzevir, de Northbrook et de Mazinaw Lake. Les instrusions peu épaisses (0,2 à 1 km) comprennent les massifs de Cross Lake, de Mellon Lake, d'Addington et de Deloro. On a élaboré des modèles des intrusions métavolcaniques et gabbroïques, avec des profondeurs maximales de 3,4 km et de 2,6 km respectivement. Il semble que les structures se trouvant dans les 4 km supérieurs de la croûte peuvent expliquer la plupart, si ce n'est l'ensemble, des variations gravimétriques dans la majeure partie du sud de la ZMC. Cela semble indiquer que la croûte sous-jacente est latéralement homogène, phénomène qui pourrait s'avérer important pour l'évaluation des modèles proposés pour la formation de la ZMC.

[1]Department of Geology, University of Ottawa, Ottawa, Ontario K1N 6N5

INTRODUCTION

The Central Metasedimentary Belt (CMB; Fig. 81.1) is a lithotectonic domain within the Grenville Province characterized by supracrustal rocks that include marble, quartzite, calc-silicates, paragneiss, amphibolite and metavolcanics ranging in age from about 1300 to 1200 Ma (Baer, 1976). The supracrustal rocks form the Grenville Supergroup. These are widely intruded by granitic, granodioritic, syenitic, dioritic and gabbroic intrusions emplaced approximately 1250 to 1000 Ma ago (Bell and Blenkinsop, 1980).

Various models have been proposed to explain the development of the CMB. Brown et al. (1975) proposed that the CMB marks the site of an ancient island arc, development of which was terminated by continental collision around 1050 Ma ago. The CMB is thought to be underlain by a collision zone. Baer (1976) suggested that the supracrustal rocks of the CMB were deposited in a northeast-trending aulacogen, the western margin of which coincides with a major lineament (Bancroft-Renfrew lineament) associated with a line of nepheline syenites. Bartlett et al. (1984) noted that a common interpretation of the early history of the CMB is that it represents a carbonate platform deposited at a cratonic margin. Recent work in the adjacent Central Gneiss Belt (CGB) to the northwest (Davidson et al., 1982; Culshaw et al., 1983) indicated that the CGB contains a series of crustal slices bounded by tectonite zones dipping gently to the southeast. Davidson et al. (1982) suggested that the slices were stacked by repeated northwestward ductile thrusting driven by Himalaya-type collision, a picture consistent with the collision event proposed by Brown et al. (1975).

Culshaw et al. (1983) concluded that the northwest boundary of the CMB is also tectonic and probably the locus of northwestward thrusting. The investigations of Hanmer and Ciesielski (1984) support this view, and these and continuing studies (e.g. van Breemen and Hanmer, 1986) indicate that a zone of highly strained gneisses and tectonic mélanges, several tens of kilometres in width, straddles the boundary between the CMB and CGB (Fig. 81.1); it is referred to as the CMB boundary zone (CMBBZ).

The western flank of a regional positive Bouguer gravity anomaly associated with the CMB is marked by a belt of relatively steep gradients that lies near or in part coincides with the western boundary of the CMB (Fig. 81.1). In the Bancroft area this belt, henceforth referred to as the western boundary gradient belt (WBGB), correlates closely with the CMBBZ, suggesting a possible causal relationship. This correlation provides an opportunity to study the CMBBZ using gravity, perhaps permitting definition of the geometry of the tectonite zones along which thrusting may have taken place. Furthermore, within the CMB itself felsic intrusions and metavolcanic belts show good correlation with gravity anomalies and are therefore amenable to quantitative modelling. The proximity of one of the intrusions to the CMBBZ, the Weslemkoon, suggested that an estimate of its depth could provide an idea of the minimum depth to any underlying tectonite zone that might dip under the CMB. With these objectives in mind detailed gravity measurements at 2 to 3 km intervals were made along selected traverses crossing the regional belt of steep gradients (WBGB) and a number of plutonic and metavolcanic bodies (Fig. 81.2, 81.3) within the CMB. This report describes the interpretation of profiles within the CMB.

GEOLOGY

A geology map of the area simplified from an unpublished map compiled for the Geological Survey of Canada by S. Marincak is shown in Figure 81.2. The Grenville Supergroup is represented by mainly mafic and intermediate metavolcanics (Hermon Group) and overlying clastic and carbonate metasedimentary rocks of the Mayo Group (Connelly, 1985). Lumbers (1967) estimated the minimum combined thickness of these groups to be about 8.2 km in this area; the base of the supracrustal sequence is not observed. Baer (1976) estimated that the supergroup rocks were deposited during the interval between 1300 and 1200 Ma. However, according to Bell and Blenkinsop (1980), volcanism commenced about 1250 Ma ago and terminated around 1100 Ma ago. Mafic and intermediate volcanic rocks occur in generally narrow belts marginal to the plutonic rocks, being most wide near the larger Weslemkoon and Elzevir plutons. The Flinton

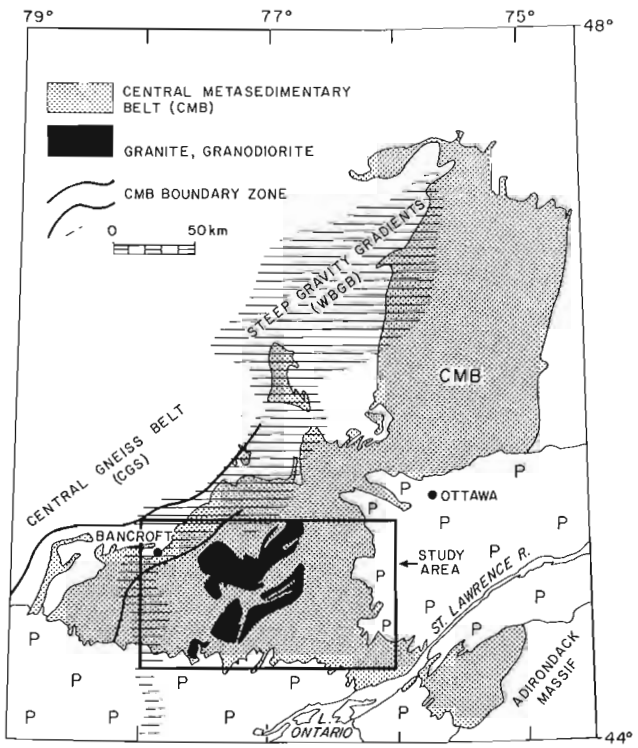


Figure 81.1. Location of study area within the Central Metasedimentary Belt. The belt of steep gravity gradients (WBGB = western boundary gradient belt) marks the western flank of a regional positive gravity anomaly. P, Paleozoic sediments. Position of CMB boundary zone from van Breemen and Hanmer (1986).

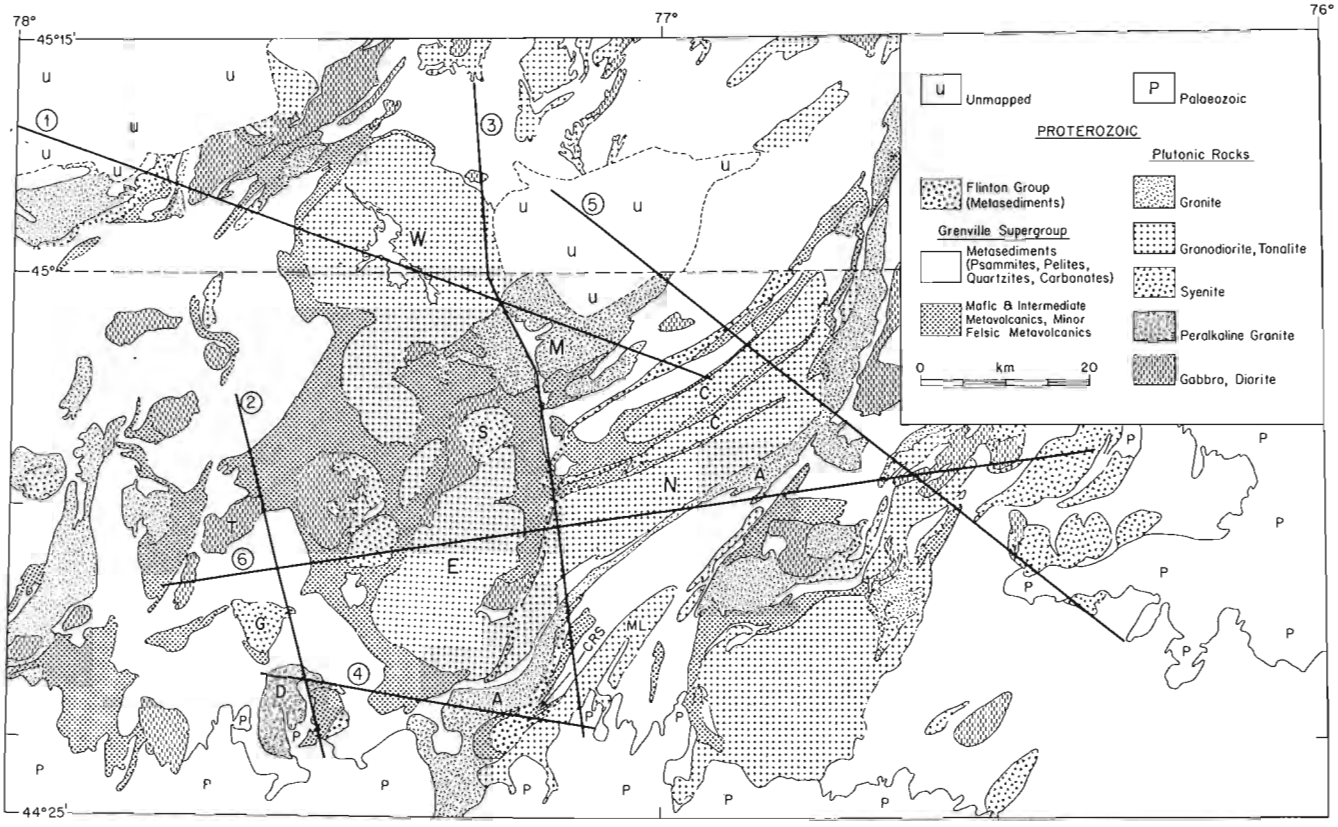


Figure 81.2. Map of study area based on an unpublished compilation of the geology of the Central Metasedimentary Belt undertaken by the Geological Survey of Canada (S. Marincak, compiler). Lines of gravity profiles interpreted in Figures 81.4 and 81.5 are indicated. Legend for intrusions: A, Addington granite; C, Cross Lake granodiorite; D, Deloro granite; E, Elzevir granodiorite; G, Gawley Creek syenite; M, Mazinaw Lake granite; ML, Mellon Lake granodiorite; N, Northbrook granodiorite; S, Skootamatta syenite; T, Tudor gabbro; W, Weslemkoon granodiorite.

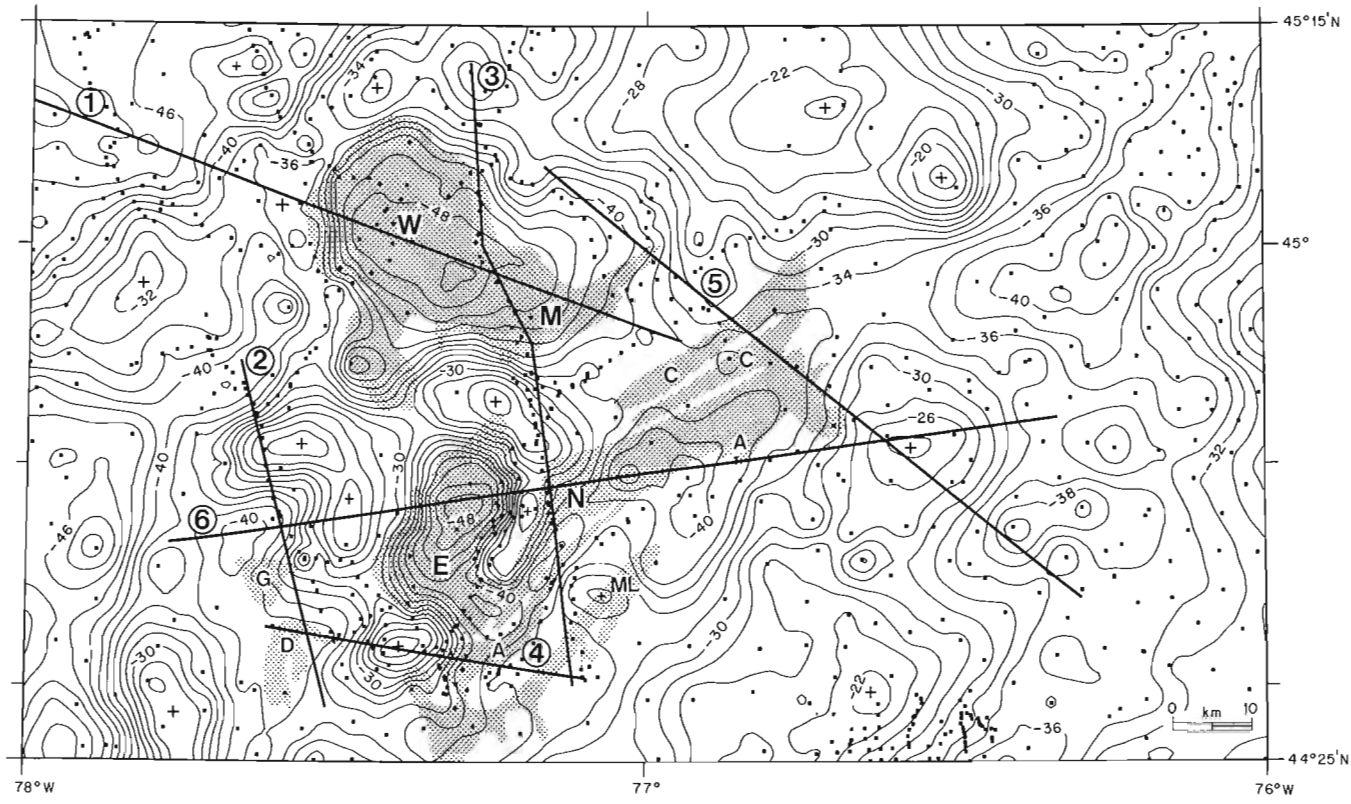


Figure 81.3. Bouguer gravity anomaly map contoured at 2 mGal intervals; gravity station distribution is indicated. Closed contours with plus signs indicate positive anomalies. Positions of felsic intrusions are superposed. Legend for intrusions is the same as that in Figure 81.2. Interpreted profiles (1-6) in Figures 81.4 and 81.5 are indicated.

Group of metasediments, which has a very limited distribution, unconformably overlies the Grenville Supergroup.

The Grenville Supergroup is intruded by three distinct plutonic suites, which in order of decreasing age are: a biotite-tonalite-granodiorite suite, a granite suite and a diorite-syenite suite; intrusion spanned the interval 1250 to 1000 Ma (Connelly, 1985). According to Pride and Moore (1983) plutonic rocks make up over 50% of the outcrop area in this region. The tonalite-granodiorite suite includes the Weslemkoon, Elzevir, Northbrook, Mellon Lake and Cross Lake intrusions (Fig. 81.2). The Weslemkoon and Elzevir are the largest and have a circular to oval geometry typical of many plutons. Connelly (1985) has suggested that the Elzevir intrusion was emplaced as a diapir, and Pride and Moore (1983) viewed it as the core of a north-south dome. The Northbrook, Mellon Lake and Cross Lake bodies differ in being elongated in a northeast direction parallel to the prevailing structural grain. The Cross Lake intrusion comprises two sheets folded into an anticlinal structure, the axis of which runs through the northern sheet (Kamilli, 1974). The Northbrook body runs along the southern flank of the Cross Lake structure and is separated from the Mellon Lake intrusion by another fold structure, the Clare River structure (Chappell, 1978); a sheet-like geometry is probable for these two intrusions also. The granite suite is represented by the Mazinaw Lake and Addington granites; the former is not completely mapped in detail (Fig. 81.2), whereas the Addington granite forms a narrow outcrop conforming to the regional structure and underlies the Clare River structure (Chappell, 1978). The diorite-syenite suite is represented by small bodies such as the Skootamatta and Gawley Creek syenites. The Deloro granite, a peralkaline granite, forms another small body.

ROCK DENSITIES

Rock densities were determined on a total of 346 samples collected throughout the study area, principally at roadside outcrops along the routes of the detailed gravity traverses. The rocks were assigned to one of the following categories: Flinton metasediments, carbonate metasediments, clastic metasediments, felsic metavolcanics, mafic-intermediate metavolcanics, gabbro, syenite, granite and granodiorite, and mean densities were estimated. For the latter two categories, mean densities were calculated also for specific plutonic bodies: Weslemkoon and Elzevir granodiorites, and Mazinaw Lake, Addington and Deloro granites. Contouring of the densities within the large northern lobe of the Weslemkoon batholith revealed that densities decrease from about 2.70 g/cm^3 at the margin to 2.62 g/cm^3 near the centre; the overall mean density is 2.66 g/cm^3.

It is estimated that carbonate and clastic metasediments of the Grenville Supergroup, with mean densities of 2.73 and 2.77 g/cm^3, respectively, have roughly equal distribution. Accordingly, a mean density of 2.75 g/cm^3 was adopted for the clastic and carbonate metasediments and is used as a background density against which other mean densities are compared for the purpose of gravity modelling. For example, the denser gabbroic bodies with a mean density of 2.94 g/cm^3 have a positive contrast of 0.19 g/cm^3 against the background. A summary of density data is provided in Table 81.1.

GRAVITY SURVEYS

Before the current investigation, the gravity field of the CMB within the study area (Fig. 81.3) was defined by regional stations with variable spacing ranging from 2.5 to 12.5 km.

Table 81.1 Summary of rock densities

Rock type	No. samples	Mean density (g/cm^3)	Standard deviation (g/cm^3)	Density contrast (g/cm^3)
Flinton Group				
Metasediments	17	2.80	0.10	+0.05
Grenville Supergroup				
Carbonate metasediments	55	2.73	0.05	0*
Clastic metasediments	90	2.77	0.10	0*
Mafic and intermediate metavolcanics	53	2.93	0.10	+0.18
Felsic metavolcanics	10	2.72	0.08	−0.03
Plutonic Rocks				
Granodiorite (all)	61	2.68	0.03	−0.07
Weslemkoon granodiorite	23	2.66	0.03	−0.09
Elzevir granodiorite	4	2.69	0.03	−0.06
Northbrook granodiorite				−0.07**
Cross Lake granodiorite				−0.07**
Granite (all)	45	2.63	0.03	−0.12
Addington granite	9	2.64	0.03	−0.11
Deloro granite	6	2.62	0.01	−0.13
Mazinaw Lake granite	8	2.62	0.02	−0.13
Syenite	3	2.66	0.03	−0.09
Gabbro	11	2.94	0.07	+0.19

* A density of 2.75 g/cm^3 has been adopted for the carbonate and clastic metasediments and this is the background density for gravity modelling.

** Values based on mean density of all granodiorite samples.

Note – A density of 2.75 g/cm^3 has been assumed for Paleozoic sediments.

In order to obtain a more detailed picture of the field, a survey was conducted in 1983. Measurements were made at intervals ranging mainly from 2 to 3 km along a number of road traverses crossing the WBGB and plutonic and volcanic bodies within the southern CMB. The standard error in the Bouguer anomalies is estimated to be about ±1 mGal and does not include terrain effects, which have not been computed. Station distribution is shown in Figure 81.3.

GRAVITY FIELD

A Bouguer gravity anomaly map contoured at an interval of 2 mGal is shown in Figure 81.3; several intrusive bodies discussed in the section on interpretation of gravity profiles are superposed on this map. There is a pronounced association between gravity anomalies and geology as would be expected from the variations in density listed in Table 81.1. The prevailing northeast trend of structure is reflected in the trends of the gravity contours, particularly in the eastern half of the area. As noted previously, the metasediments of the Grenville Supergroup are regarded as the country or background rocks whose density (2.75 g/cm^3) is used as a datum for comparing the densities of other rock units. It is evident that units with lower densities are characterized by anomalies that are negative with respect to the general level of the gravity field over the metasediments (estimated to be −36 mGal), and denser units are characterized by relatively positive anomalies.

The most pronounced negative anomalies are associated with the Weslemkoon-Mazinaw Lake and Elzevir bodies for which amplitudes (relative to the −36 mGal background) attain −14 and −12 mGal respectively. A negative anomaly of −7 mGal occurs near the centre of the Northbrook granodiorite and a small −3 mGal anomaly coincides with the Deloro granite, though the lack of stations makes this anomaly poorly defined. The Cross Lake, Mellon Lake and Addington intrusions generally do not have detailed coverage and distinct related anomalies are not obvious; gravity values associated with these bodies lie very close to the regional background.

Prominent positive anomalies are associated primarily with metavolcanic and gabbroic rocks on the north, west and south sides of the Elzevir intrusion; amplitudes reach values of about +14 mGal. Another large anomaly, +12 mGal amplitude, occurs on the eastern margin of the area and is likely related to a gabbroic body.

In the extreme northwest corner of the area, approximately northwest of the −38 mGal contour, a belt of steep gradients represents part of the WBGB; it is particularly steep between the −38 and −46 mGal contours.

INTERPRETATION OF GRAVITY PROFILES

Quantitative modelling of the gravity field has been carried out along 6 profiles indicated in Figures 81.2 (geology) and 81.3 (Bouguer map). Profiles 1 to 4 were selected as close as possible to the lines of detailed gravity traverses and are nearly perpendicular to geological boundaries. Profiles 5 and 6 cross areas where gravity coverage is relatively thin and models for these are accordingly less well-controlled. Modelling was accomplished using an interactive program initially developed as a 2D program by Wells (1979), but later modified to a 2.5D version by P.H. McGrath of the Geological Survey of Canada. This program allows a finite strike length to be assigned to the modelled bodies permitting more accurate determination of the dimensions of the models. Constraints for modelling were provided by the surface geological boundaries and the density contrasts listed in Table 81.1. In spite of such constraints, the gravity profiles retain a measure of ambiguity, and models other than those presented are possible. Attitudes of boundaries, therefore, are subject to varying degrees of change. In addition any variation of density with depth will influence depth estimates.

The modelled sections are shown in Figures 81.4 and 81.5; these figures also illustrate the observed Bouguer anomaly and the surface geology. The model curve is not shown, but in all cases generally matches the observed curve within ±1 mGal which is considered to be the standard error of Bouguer anomalies, terrain effects excluded.

Profile 1 (Fig. 81.4)

Profile 1 runs WNW-ESE across the Weslemkoon granodiorite and the Mazinaw Lake granite. These intrusions are associated with a major gravity low of approximately −14 mGal amplitude that reaches a minimum over the Weslemkoon body. The latter is modelled as a rectangular prism reaching a maximum depth of 4 km. The mean density of the intrusion is 2.66 g/cm^3, but densities in the central part of the northern lobe are up to 0.04 g/cm^3 less dense, and densities near the margin are as much as 0.04 g/cm^3 more dense. This pattern of densities is probably a reflection of a poorly defined compositional zoning (Lumbers, 1967). Sodic granite and granodiorite are concentrated near the western and central parts of the lobe and are partly surrounded by a zone rich in tonalite; elsewhere trondhjemite predominates. Therefore, a central unit with a density of 2.64 g/cm^3 has been modelled. It is sheet-like with a maximum thickness of 0.5 km, and is equated with the sodic granite phase which may be younger than other phases (Lumbers, 1967). Alternatively, rather than being a discrete unit it may grade imperceptibly into the main mass of the intrusion, in keeping with an idea that diffusion of alkalis has played a role in the formation of the sodic granite and associated granodiorites (Hodgson, 1965).

A steep contact has been modelled between the Weslemkoon body and adjacent Mazinaw Lake granite. The granite attains a maximum depth of 2.4 km, its floor being roughly 1.5 km above that of the Weslemkoon intrusion. The bottom of the Mazinaw Lake granite steps up to a depth of 1 km to the eastsoutheast where the intrusion thins dramatically to only a few hundred metres under its southeastern margin. In the same area a sheet-like inclusion of metasediments is present in the granite.

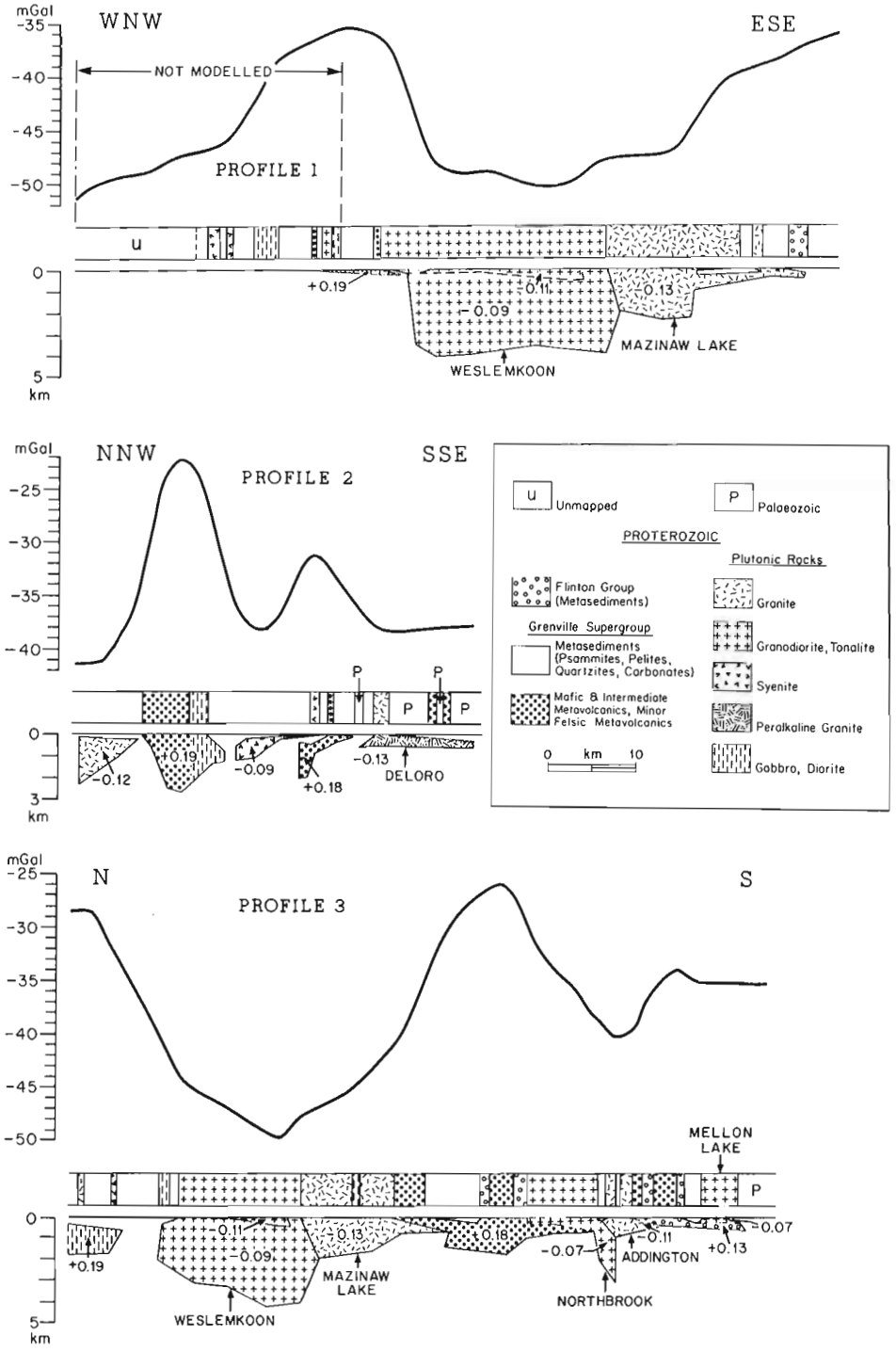


Figure 81.4. Observed gravity profiles, surface geology and gravity models for Profiles 1, 2 and 3 (see Fig. 81.2 and 81.3 for location). Density contrasts are indicated in units of g/cm^3. Model anomaly (not shown) matches observed profile within ±1 mGal.

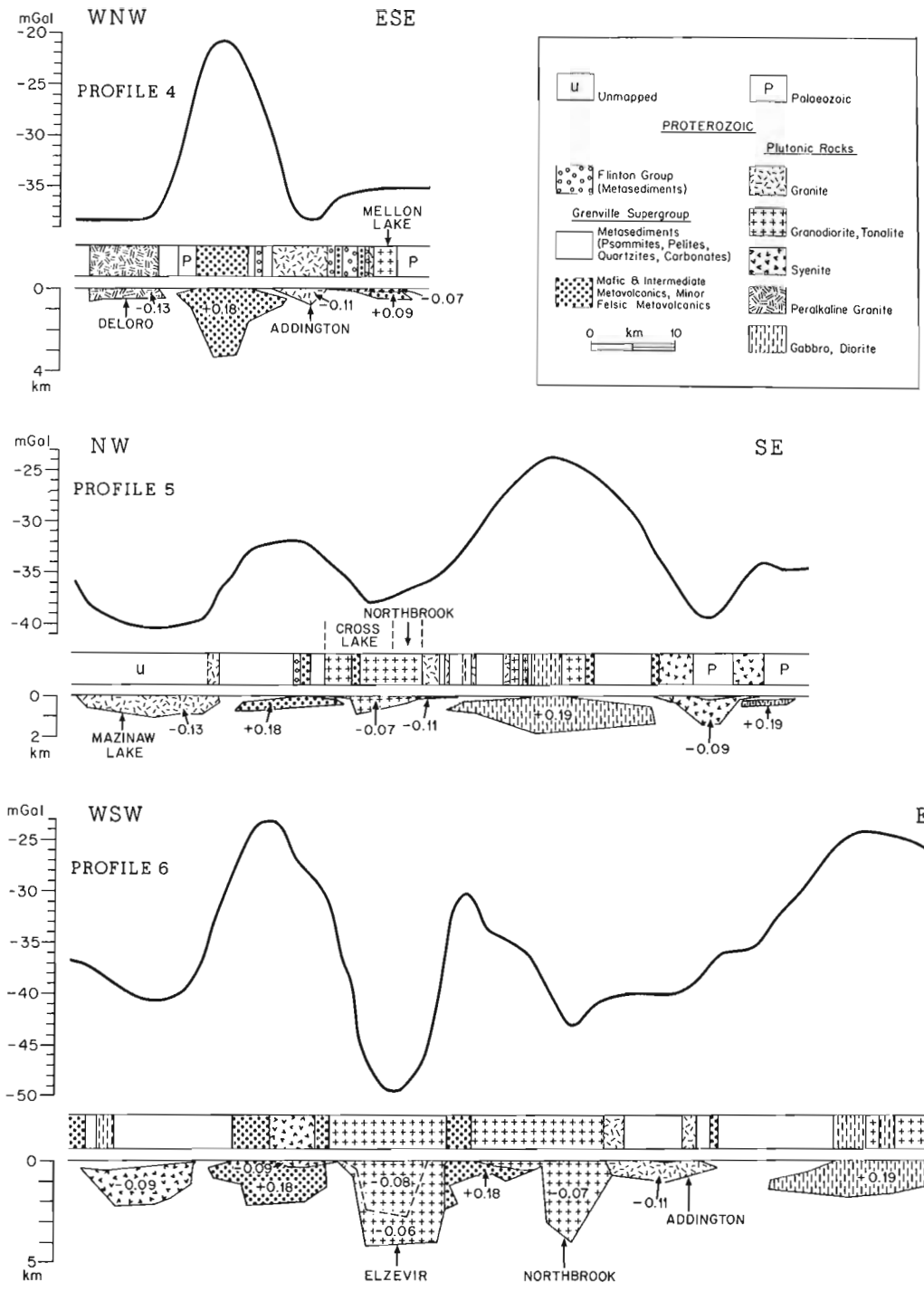


Figure 81.5. Observed gravity profiles, surface geology and gravity models for Profiles 4, 5 and 6 (see Fig. 81.2 and 81.3 for location). Density contrasts are indicated in units of g/cm^3. Model anomaly (not shown) matches observed profile within ±1 mGal.

Profile 2 (Fig. 81.4)

Profile 2 is located just west of the Weslemkoon and Elzevir intrusions and runs approximately NNW-SSE. At its north end it crosses mafic-intermediate metavolcanics and gabbro (Tudor gabbro) and these units are reflected in a large positive anomaly attaining an amplitude of about +14 mGal with respect to the background field. Because the densities of these two types of geological unit differ by only 0.01 g/cm^3, it is not meaningful to model them separately. They are, therefore, treated as one unit. A roughly bowl-shaped body reaching a depth of 2.6 km is modelled. A subsidiary high (amplitude about +5 mGal) coincides with a thin strip of metavolcanics. The gravity model suggests that these rocks extend to a depth of 2 km as a monoclinal sheet.

The Deloro granite is modelled as a thin slab with a maximum thickness of 0.5 km that thins southward under Paleozoic sediments. A subsurface granite attaining a depth of 2.3 km is assumed to cause a gravity low (amplitude about −5 mGal) at the north end of the profile. The central gravity low, amplitude −2 mGal, is tentatively interpreted as a shallowly buried body of syenite, based on the presence of the Gawley Creek syenite on the surface about 6 km south of the low. The buried syenite is about 1 km thick and is shown as extending to the surface outcrop as a sheet-like apophysis, although such a connection is not necessarily demanded by the gravity data.

Profile 3 (Fig. 81.4)

Profile 3 runs roughly N-S crossing successively the eastern part of the Weslemkoon granodiorite, the Mazinaw Lake granite, the Northbrook granodiorite, the Addington granite and the Mellon Lake granodiorite. As for Profile 1, the Weslemkoon intrusion is modelled with steeply-dipping sides and a variable density. It reaches a maximum depth of 4.2 km and thins to 2 km at its northern boundary. The contact with the Mazinaw Lake granite dips steeply to the south, and again there is a step up from the floor of the Weslemkoon granodiorite to the floor of the Mazinaw Lake granite which is at a depth of just under 2 km. The latter granite thins to a feather-edge southward beneath mafic-intermediate metavolcanics. These same metavolcanics are modelled as part of a fairly large body, maximum thickness 1.7 km, that reaches the surface farther south under the peak of the central positive anomaly. A subsurface gabbro reaching a maximum depth of 1.7 km is assumed to cause the gravity high (amplitude about +8 mGal) at the north end of the profile.

The Northbrook granodiorite is modelled as a boomerang-shaped body with a pointed root reaching a depth of 3 km under its southern margin. Where it outcrops, it has a maximum depth of only 0.6 km. The Addington granite also is modelled as having limited depth extent, attaining just 0.9 km. A density unit of combined Flinton metasediments and mafic-intermediate metavolcanics has been modelled as a very thin sheet (0.2 to 0.4 km thick) that extends southward under an even thinner sheet (less than 0.2 km) of Mellon Lake granodiorite. Between the Northbrook and Mellon Lake granodiorites the gravity station distribution is comparatively thin and hence the gravity field is somewhat smoothed. This and the small size of the bodies dictate that the models in this section of the profile must be regarded as preliminary.

Profile 4 (Fig. 81.5)

Profile 4 extends from the Deloro granite to the Mellon Lake granodiorite trending WNW-ESE. The gravity field is relatively flat, except for a +15 mGal amplitude gravity high over a mafic-intermediate metavolcanic unit. This unit is modelled as a somewhat bowl-shaped body with a maximum depth of 3.4 km. The Deloro granite is again interpreted as a flat slab reaching a general depth of only 0.5 km. The Addington granite is modelled as an inverted triangle, maximum depth 0.8 km. A density unit of combined Flinton metasediments and mafic-intermediate metavolcanics has been modelled as extending from the surface to underlie a very thin slab of Mellon Lake granodiorite which is only 0.16 km thick.

Profile 5 (Fig. 81.5)

Profile 5 extends NW-SE across the eastern part of the area where a northeast-trending structural grain is strongly developed, and where the geology is extremely variable. The most pronounced anomaly (about +12 mGal) is apparently related to gabbro that has limited surface outcrop, but which is modelled as a fairly extensive subsurface slab having a maximum thickness of 2.2 km. A subsidiary high in the northwestern half of the profile is attributed to a largely buried, flat-lying sheet of mafic-intermediate metavolcanics 0.5 km thick.

The Mazinaw Lake granite, with a depth of 2.4 km in Profile 1 to the southwest, is here modelled with a maximum thickness of about 1 km. The Cross Lake granodiorite, described by Kamilli (1974) as a series of sheet-like bodies, is modelled in a single unit with the Northbrook granodiorite as a thin intrusion that extends to about 0.8 km below the surface. At the southeast end of the profile a syenite associated with a small (amplitude about −3.5 mGal) negative anomaly is modelled as a bowl-shaped body reaching a depth of 1.3 km. In general, the bodies along this profile are shallower than to the west and, with the exception of gabbro and syenite, extend to depths of less than 1 km.

Profile 6 (Fig. 81.5)

Profile 6 runs WSW-ENE across the Elzevir and Northbrook granodiorites. The Elzevir intrusion is associated with a pronounced negative anomaly, approximately −13.5 mGal amplitude, that is flanked by strong positive anomalies on the west (about +13 mGal amplitude) and east (about +6 mGal amplitude) related to mafic-intermediate metavolcanics. The latter are modelled as bodies extending to depths of about 2 km.

The Elzevir intrusion was modelled, initially, to be about 15 km thick using a single density of 2.69 g/cm^3 based on

only 4 samples. In view of the much smaller depths modelled for other intrusions the 15 km value was considered to be unrealistically high. The neighbouring Weslemkoon granodiorite exhibits a decrease in density from its margin towards its centre; this is modelled in terms of a central subunit 0.02 g/cm^3 less dense than the rest of the body (Fig. 81.4). A similar density model was assumed, therefore, for the Elzevir intrusion, although most of the intrusion is described as homogeneous (Pride and Moore, 1983). This approach produces a body with a maximum depth of 4.2 km and steep, generally inward-dipping sides. It may be argued that the similarity of this depth to that of the Weslemkoon intrusion supports the somewhat arbitrary choice of densities and the model itself. However, the model must be regarded as tentative pending more detailed density studies, and the possibility of deeper models should not be ruled out.

The Northbrook granodiorite, associated with a maximum anomaly of approximately −7 mGal amplitude, attains a maximum depth of 4 km under the eastern half of its outcrop, but the western half is modelled as a thin wedge, maximum thickness 0.5 km overlying buried metavolcanics. The Addington granite is modelled as a synclinal sheet 1 km thick that lies on strike with the Clare River structure. A buried syenite roughly 2 km thick, discussed in the section on Profile 2, is interpreted to produce an approximately −5 mGal amplitude anomaly at the west end of the profile. A gabbro slab attaining a maximum thickness of 1.7 km is the apparent cause of a positive anomaly, about +12 mGal amplitude, near the extreme east end of the profile.

DISCUSSION

Gravity modelling within the southern CMB indicates that the surface geological units extend no deeper than about 4 km, although the Elzevir intrusion may prove to be an exception when detailed density information becomes available. The maximum depth extents computed are listed in Table 81.2. The felsic intrusive bodies all have tabular or sheet-like geometries but may be assigned to two categories based on maximum thickness. The first category includes the Weslemkoon, Elzevir and Northbrook granodiorites and Mazinaw Lake granite (2.4 to 4.2 km thick) and the second includes the Cross Lake and Mellon Lake granodiorites and the Addington and Deloro granites (0.2 to 1 km thick). It is noted that the thicker group of intrusions occurs in the western half of the region where a prevailing structural grain is not readily apparent, and where the intrusions have roughly circular to oval shapes typical of plutonic bodies. The thinner group of intrusions occurs in the eastern half of the region where a northeastward structural grain, partly controlled by folding, is strongly developed and where intrusions are elongated and narrow. One exception to the general rule is the Northbrook granodiorite which, although located in the eastern region and which in part is apparently sheet-like (Profile 6), locally attains a depth of 4 km. Gabbroic bodies extend no deeper than 2.6 km and mafic-intermediate volcanics no deeper than 3.4 km.

Table 81.2 Maximum depth extent of lithological units estimated by gravity modelling

Lithological unit	Maximum depth extent (km)
Intermediate-mafic metavolcanics	3.4
Gabbro	2.6
Weslemkoon granodiorite	4.2
Elzevir granodiorite	4.2
Northbrook granodiorite	4.0
Cross Lake granodiorite	0.8
Mellon Lake granodiorite	0.2
Mazinaw Lake granite	2.4
Addington granite	1.0
Deloro granite	0.5
Unnamed granite (Profile 2)	2.3
Syenite	2.0

Apparently, most of the Grenville Supergroup rocks and intrusions in the southern CMB are confined to the uppermost 4 km of the crust and the geological units observed at the surface account for most, if not all, of the gravity variations within the CMB. This implies that lateral density variations below a depth of 4 km are relatively insignificant. Caution must be observed when translating density structure into geological structure, but one possible conclusion to draw from these observations is that below a depth of about 4 km the major structures of the CMB and underlying crust are probably near-horizontal. One such structure might consist of Grenville Supergroup metasediments. What is the significance of this picture to the theories advanced for the origin of the CMB?

In view of the thin structural skin indicated by the gravity work, the island arc proposal (Brown et al., 1975) is, perhaps, the least attractive. Brown et al. suggested that the granodioritic intrusions were generated at depth by partial melting of a subducted slab. Yet now they are restricted to relatively thin surface bodies. Furthermore, island arcs involved in geologically-recent collisions include examples (e.g. Cretaceous Kohistan complex in the Himalayas) where internal structure is steeply folded and inclined for tens of kilometres deep into the crust (Coward et al., 1982; Bard, 1983). In contrast, gravity modelling suggests that the crust underlying the CMB is laterally homogeneous. Such disparities could be explained by the presence of thin-skinned tectonics, in which case the island arc hypothesis would not be unreasonable. It is possible that thin-skinned tectonics is present in the form of a subhorizontal décollement underlying the 4 km thick surface skin. The CMB could, therefore, be largely allochthonous. However, an observation that challenges the idea of an allochthon is the correlation of a regional positive gravity anomaly with the CMB. This suggests a spatial link between the crust underlying the CMB and the CMB itself. Such a relationship may be more compatible with the aulacogen model of Baer (1976) and cratonic margin model of Bartlett et al. (1984) or even a back-arc model. All of these models, together with the island arc model, will be evaluated in greater detail in ongoing studies.

On the question of thin-skinned tectonics, the identification of southeastward dipping tectonite zones in the CMBBZ (Culshaw et al., 1983; Hanmer and Ciesielski, 1984) suggests that structural discontinuities are present under the CMB. If the bottom of the Weslemkoon granodiorite at 4.2 km is taken as the minimum depth of a tectonite zone that links with the CMBBZ, then based on the position of the eastern margin of the CMBBZ it is possible to estimate the minimum dip of such a zone. Unfortunately, the position of the eastern boundary is still uncertain (S.K. Hanmer, personal communication, 1986). If limits of 10 and 20 km are adopted for the distance between the Weslemkoon intrusion and the boundary, the corresponding dips of tectonite zones below the CMB are 22° and 12°, respectively. Even the lower dip of 12° is too high to be consistent with the idea of the 4 km thick skin being controlled by a tectonite zone dipping from the CMBBZ, unless the latter becomes progressively more gently dipping at depth.

This preliminary gravity investigation has raised some interesting possibilities regarding structure and tectonic evolution of the CMB, a clearer understanding of which requires further study of the various geological and geophysical relationships.

ACKNOWLEDGMENTS

We thank L. Petrie for assistance with the detailed gravity survey and W. Miles and C. Willis for processing the data. Thanks are due also to J.M. Coderre, R.A. Gibb and A.G. Green for reviewing the manuscript.

REFERENCES

Baer, A.J.
1976: The Grenville Province in Helikian times: a possible model of evolution; Royal Society of London, Philosophical Transactions, v. A280, p. 499-515.

Bard, J.P.
1983: Metamorphism of an obducted island arc: example of the Kohistan sequence (Pakistan) in the Himalayan collided range; Earth and Planetary Science Letters, v. 65, p. 133-144.

Bartlett, J.R., Brock, B.S., Moore, J.M. (Jr.), and Thivierge, R.H.
1984: Grenville Traverse A, cross-sections of parts of the Central Metasedimentary Belt, Field Trip 9A/10A, GAC-MAC Joint Annual Meeting, London, Ontario.

Bell, K. and Blenkinsop, J.
1980: Whole-rock Rb-Sr studies in the Grenville Province of southeastern Ontario and western Quebec – a summary report; in Current Research, Part C, Geological Survey of Canada, Paper 80-1C, p. 152-154.

Brown, R.L., Chappell, J.F., Moore, J.M. (Jr.), and Thompson, P.H.
1975: An ensimatic island arc and ocean closure in the Grenville Province of southeastern Ontario, Canada; Geoscience Canada, v. 2, p. 141-144.

Chappell, J.F.
1978: The Clare River structure and its tectonic setting; unpublished Ph.D. thesis, Carleton University, Ottawa, 184 p.

Connelly, J.N.
1985: The Elzevir batholith: emplacement history with respect to the Grenville Supergroup and Flinton Group, southeastern Ontario; in Current Research, Part B, Geological Survey of Canada, Paper 85-1B, p. 161-167.

Coward, M.P., Jan, M.Q., Rex, D., Tarney, J., Thirlwall, M., and Windley, B.F.
1982: Structural evolution of a crustal section in the western Himalaya; Nature, v. 295, p. 22-24.

Culshaw, N.G., Davidson, A., and Nadeau, L.
1983: Structural subdivisions of the Grenville Province in the Parry Sound-Algonquin region, Ontario; in Current Research, Part B, Geological Survey of Canada, Paper 83-1B, p. 243-252.

Davidson, A., Culshaw, N.G., and Nadeau, L.
1982: A tectono-metamorphic framework for part of the Grenville Province, Parry Sound region, Ontario; in Current Research, Part A, Geological Survey of Canada, Paper 82-1A, p. 175-190.

Hanmer, S.K. and Ciesielski, A.
1984: A structural reconnaissance of the northwest boundary of the Central Metasedimentary Belt, Grenville Province, Ontario and Quebec; in Current Research, Part B, Geological Survey of Canada, Paper 84-1B, p. 121-131.

Hodgson, C.J.
1965: Petrology of the Weslemkoon batholith, southeastern Ontario; unpublished M.A.Sc. thesis, University of Toronto, Toronto, Ontario.

Kamilli, D.C.
1974: Progressive metamorphism of the Cross Lake granodiorite, Ontario, Canada; Geological Society of America, Bulletin, v. 85, p. 1755-1762.

Lumbers, S.B.
1967: Stratigraphy, plutonism, and metamorphism in the Ottawa River remnant in the Bancroft-Madoc area of the Grenville Province of southeastern Ontario, Canada; unpublished Ph.D. thesis, Princeton University, Princeton, N.J., 331 p.

Pride, C. and Moore, J.M. (Jr.)
1983: Petrogenesis of the Elzevir batholith and related trondhjemitic intrusions in the Grenville Province of Eastern Ontario, Canada; Contributions to Mineralogy and Petrology, v. 82, p. 187-194.

van Breemen, O. and Hanmer, S.
1986: Zircon morphology and U-Pb geochronology in active shear zones: studies on syntectonic intrusions along the northwest boundary of the Central Metasedimentary Belt, Grenville Province, Ontario; in Current Research, Part B, Geological Survey of Canada, Paper 86-1B, p. 775-784.

Wells, I.
1979: MAGRAV users guide – a computer program to create two-dimensional gravity and/or magnetic models; Geological Survey of Canada, Open File 597.

Geology and U-Pb ages of early Proterozoic calc-alkaline plutons northwest of Wager Bay, District of Keewatin

Projects 820004, 850004

A.N. LeCheminant, J.C. Roddick, A.C. Tessier[1] and K.M. Bethune[2]
Lithosphere and Canadian Shield Division

LeCheminant, A.N., Roddick, J.C., Tessier, A.C., and Bethune, K.M., Geology and U-Pb ages of early Proterozoic calc-alkaline plutons northwest of Wager Bay, District of Keewatin; in Current Research, Part A, Geological Survey of Canada, Paper 87-1A, p. 773-782, 1987.

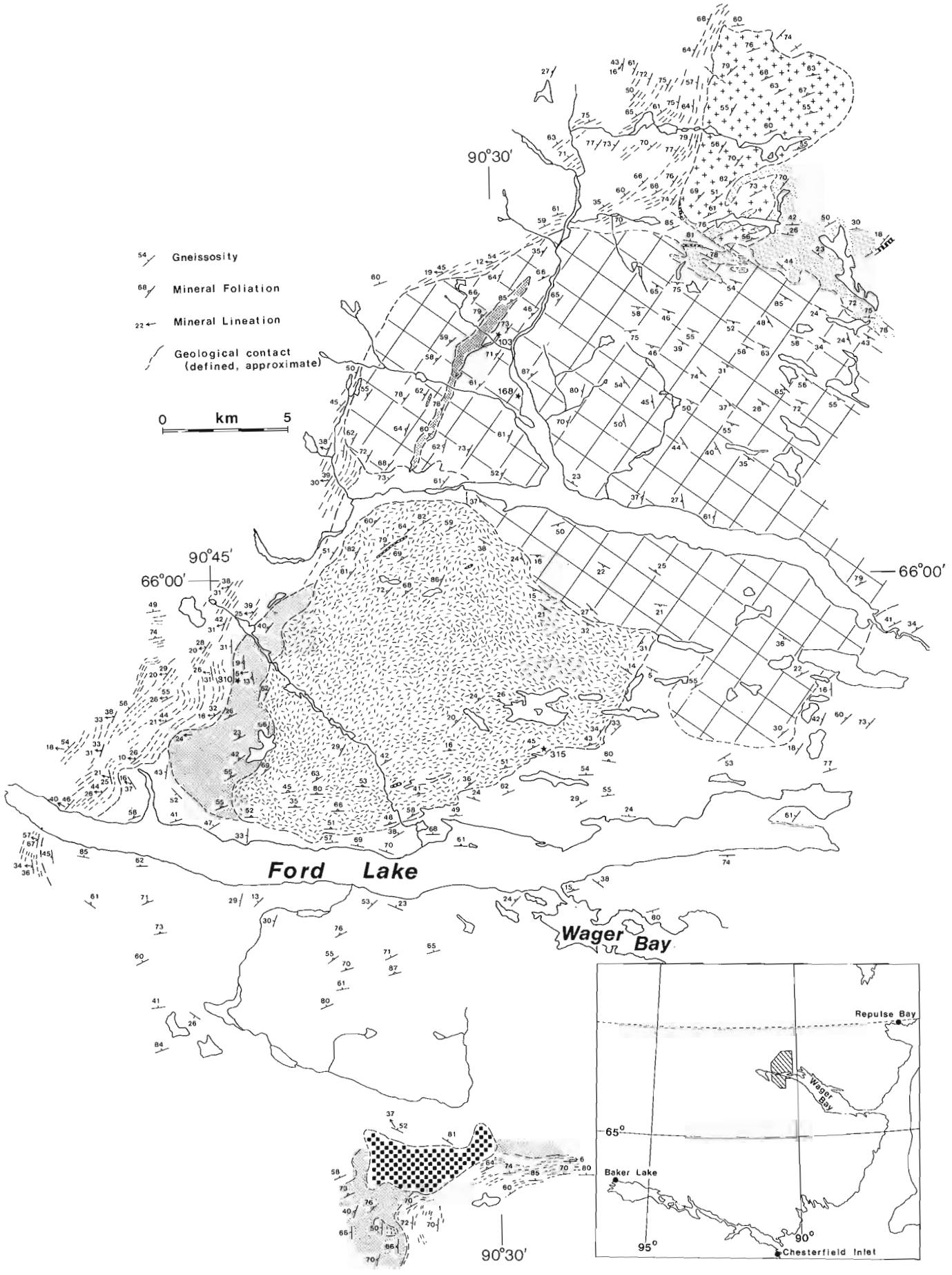
Abstract

A northeast-trending belt of I-type calc-alkaline plutons is well exposed in the region northwest of Wager Bay. The plutonic suite comprises large intrusions of hornblende-biotite granite/granodiorite with smaller bodies of monzodiorite, diorite and gabbro. The Ford Lake batholith is a 400 km² composite intrusion of coarse grained megacrystic granite/granodiorite enriched in K, Rb, Ba, Th and LREE. U-Pb zircon analyses provide precise crystallization ages of 1823 ±3 Ma and 1826 +4/−3 Ma for two plutons of the batholith emplaced into banded granitoid gneiss and (?)Penrhyn Group psammitic gneiss, calc-silicate and marble. The batholith probably intruded during late stages of regional metamorphism as part of a major episode of magma production within a continental magmatic arc.

Résumé

Une zone de direction nord-est, constituée de plutons calcaro-alcalins de type I, est bien exposée dans la région nord-ouest de la baie Wager. La série plutonique comprend d'importantes intrusions de granite et granodiorite à hornblende et biotite, accompagnées de plus petits massifs de diorite monzonitique, de diorite et de gabbro. Le batholite de Ford Lake représente une intrusion composite de 400 km² constituée de granite et granodiorite à mégacristaux grossiers et enrichie de K, Rb, Ba, Th et d'éléments de terres rares légers. L'analyse des zircons effectuée à l'aide de la méthode U-Pb à établi des âges précis de cristallisation, soit 1823 ± 3 Ma et 1826 +4/−3 Ma pour deux plutons du batholite mis en place dans un gneiss granitoïde rubané et un gneiss psammitique du groupe de Penrhyn(?), dans des roches calcaro-silicatées et dans du marbre. La mise en place du batholite date probablement des phases tardives du métamorphisme régional, correspondant à un épisode principal de production magmatique à l'intérieur d'un arc continental magmatique.

[1]École Polytechnique, Départment de Génie Minéral, Montréal, P.Q. H3C 3A7
[2]Department of Geological Sciences, Queens University, Kingston, Ontario K7L 3N6.


Gneissosity
Mineral Foliation
Mineral Lineation
Geological contact (defined, approximate)
0 km 5
90°30′
90°45′
66°00′
66°00′
Ford Lake
Wager Bay
Repulse Bay
Wager Bay
65°
Baker Lake
95°
90°
Chesterfield Inlet
90°30′

INTRODUCTION AND GEOLOGICAL SETTING

Coarse grained plutons ranging in composition from gabbro to granite are exposed in steep, rocky fiord country at the head of Wager Bay and around Ford Lake. Five weeks work in 1986 continued the mapping of the Ford Lake batholith (Henderson et al., 1986) and delimited several additional plutons separate from the main batholith (Fig. 82.1). The plutons comprise a calc-alkaline intrusive suite consisting of megacrystic hornblende-biotite granite/granodiorite with subordinate monzodiorite, diorite and gabbro.

The intrusive rocks make up part of a major belt of early Proterozoic granite and granodiorite plutons extending more than 300 km from west of Wager Bay northeast to Committee Bay (Heywood, 1961, 1967). The belt consists of more than a dozen large composite intrusions, with magnetite-rich intermediate to mafic plutons typically associated with K-Th-U-enriched granites. The southernmost intrusive rocks of the belt are mylonitized by ductile dextral transcurrent shear along the east-trending Wager Bay Shear Zone (Henderson et al., 1986). The present mapping provides a transect just to the north of the shear zone across one of the best-exposed parts of the plutonic belt. Intrusive ages have not previously been constrained by U-Pb zircon work. Results reported in this paper for samples collected in 1985 provide precise crystallization ages for two plutons in the Ford Lake batholith.

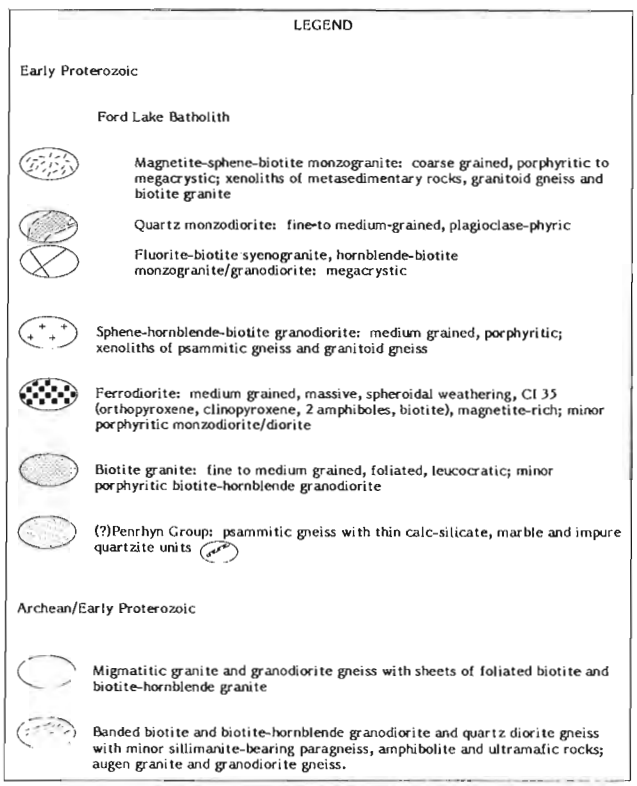


Figure 82.1. Simplified geological map of the region around Ford Lake and the northwestern end of Wager Bay.

GNEISSIC COUNTRY ROCKS

Gneisses older than the plutonic suite are subdivided into three lithological packages: (1) banded grey biotite and biotite-hornblende granodiorite and quartz diorite gneiss with enclaves of supracrustal rocks and subordinate augen granite and granodiorite gneiss; (2) weakly foliated, migmatitic granite and granodiorite gneiss with sheets of foliated leucocratic granite; and (3) calc-silicate gneiss, marble, psammitic gneiss and impure quartzite.

Banded and migmatitic gneisses

Banded grey granodiorite/quartz diorite gneiss comprises a distinctive unit along the west side of the plutonic belt (Fig. 82.1). Along its entire mapped length the gneiss has southwesterly foliation trends, typically with moderate northwesterly dips. The unit contains discontinuous lenses and pods of amphibolite and ultramafic rocks and minor thin bands of supracrustal rocks including sillimanite-rich paragneiss and schist. A relatively homogeneous K-feldspar augen gneiss with up to 1% magnetite also occurs along the west side of the plutonic belt. The augen gneiss forms discrete bodies within the banded gneiss although contacts are typically conformable and gradational. The homogeneity of the augen gneiss and the presence of abundant simple twinning in microcline augen indicates these rocks probably are of igneous origin and their distribution suggests they were intrusive into the supracrustal-bearing banded gneiss.

A separate unit of well foliated intermediate composition banded gneiss with southeasterly to easterly trending foliation extends along the south contact of the ferrodiorite pluton (Fig. 82.1). The white weathering gneiss contains a scattering of amphibolite pods, rare ultramafic rocks and boudinaged quartz-rich pegmatites.

An extensive area of migmatitic pink and grey granite and granodiorite gneiss occurs north and south of Ford Lake. The gneiss is compositionally heterogeneous and difficult to subdivide. It comprises an older grey granodiorite/tonalite component, amphibolite boudins and amphibolite agmatite zones (remnants of dykes?), nebulitic granitic gneiss and several generations of aplite, granite and pegmatite dykes. In rare cases, a foliated biotite-rich mafic dyke swarm can be used to separate different generations of granitic dykes which otherwise would appear to be coeval. The migmatitic gneiss was also intruded by irregular bodies of pink biotite and biotite-hornblende granite. These granites range from large concordant sheets of foliated weakly radioactive granite to massive or weakly foliated porphyritic granite with much higher radiometric response. The younger porphyritic biotite granite plutons that have been mapped separately from the migmatitic gneiss are discussed more fully in a subsequent section.

(?)Penrhyn Group

Deformed metasedimentary rocks dominated by psammites are cut by two of the major plutons in the northeast part of the

map area (Fig. 82.1). The metasedimentary assemblages are in apparent concordant contact with granitoid gneiss presumed to be basement to the metasediments. Along the basement contact a discontinuous sequence no more than 100 m thick forms a distinctive succession consisting of: (1) garnet-rich, locally sulphide-bearing, amphibolitic schist and gneiss; (2) coarse biotite quartzite; and (3) diopside-bearing calc-silicate gneiss and marble. This basal succession is followed by a thicker sequence of fine-to-medium grained thinly banded psammitic gneiss. Lenticular bedding, crossbedding and graded beds are locally preserved in the fine grained microcline-rich clastic rocks. The carbonate-psammite assemblages appear to be shallow marine deposits derived from a granitoid source. Structure in the metasedimentary rocks is dominated by shallow plunging tight to isoclinal folds. Structural, lithological and stratigraphic relationships strongly suggest that the metasedimentary rocks are correlative with the Early Proterozoic Penrhyn Group exposed to the northeast on Melville Peninsula (Heywood, 1967; Henderson, 1983).

Henderson et al. (1986) reported numerous metasedimentary enclaves in the southern monzogranite pluton of the Ford Lake batholith. Lithologically, these xenoliths are identical to Penrhyn Group rocks. Psammite xenoliths also characterize the northeastern contact zone of the Ford Lake batholith and are abundant throughout the granodiorite pluton to the north. Near external contacts of these plutons the adjacent metasedimentary rocks are cut by numerous undeformed dykes and sills of porphyritic granite and pegmatite. Poikiloblastic growth of amphibole in the contact rocks gives the psammites a distinctive spotted appearance which is also characteristic of many of the metasedimentary xenoliths in the plutons.

EARLY PROTEROZOIC PLUTONS

Two suites of early Proterozoic plutons are recognized on the basis of mapping to date in the Ford Lake area. An older suite of fine- to medium-grained leucocratic granites is intruded by coarser grained rocks of the compositionally more diverse calc-alkaline suite. The finer grained granites typically are poorly exposed and do not have a well defined aeromagnetic expression. For this reason, these bodies could only be locally subdivided from older granite sheets in the migmatitic gneiss unit. A pluton of porphyritic biotite granite separates the western banded gneiss unit from the megacrystic Ford Lake batholith (Fig. 82.1). A chemical analysis of this granite is presented in Table 82.1 for comparison to rocks of the megacrystic suite. South of Ford Lake similar granites were intruded by a ferrodiorite pluton. The southern granite is not completely mapped and it apparently extends northeast and southwest of the present mapping limit. The pluton is a weakly foliated leucocratic biotite granite that contains large rafts of granitoid gneiss and amphibolite. The granite is locally cut by irregular dykes and small bodies of coarser grained porphyritic hornblende-biotite granodiorite. On the basis of homogeneity, weak deformation and high radioelement content the leucocratic biotite granite plutons are thought to be only slightly older than the coarser grained plutonic suite.

The coarser grained plutonic suite consists of the megacrystic Ford Lake batholith, a pluton of ferrodiorite to the south and a pluton of porphyritic granodiorite to the north. Since the relative age of intrusion is not known the plutons are discussed on the basis of composition from mafic to felsic.

Ferrodiorite

A pluton of massive, spheroidal weathering ferrodiorite (Fig. 82.2A) is responsible for a 080° trending, 4000 gamma aeromagnetic anomaly south of Ford Lake (Geological Survey of Canada, 1974). The position and shape of the anomaly which is about 50% larger than the 8 km^2 surface area of the pluton (Fig. 82.1), suggests the pluton dips to the north.

Table 82.1 Representative major element, trace element and rare earth element analyses of Ford Lake batholith rocks. Trace element and rare earth element abundances in ppm.

Sample number	85LAA 310-1	85LAA 168-1	85LAA 103-1	85LAA 315-1
Map Unit	Biotite granite	Biotite syenogranite	Quartz monzodiorite	Sphene-biotite monzogranite
SiO_2	74.6	72.3	61.8	66.7
TiO_2	0.21	0.29	1.23	0.97
Al_2O_3	13.7	14.1	15.1	13.9
Fe_2O_3	0.7	0.4	2.2	2.3
FeO	0.9	1.7	5.4	3.3
MnO	0.03	0.03	0.12	0.08
MgO	0.4	0.4	1.3	1.4
CaO	1.00	1.47	4.69	2.66
BaO	0.07	0.13	0.25	0.12
Na_2O	3.2	3.1	3.0	3.2
K_2O	5.38	5.86	3.71	4.46
P_2O_5	0.05	0.09	0.83	0.46
$H_2O(T)$	0.2	0.5	0.6	0.7
CO_2	0.1	0.3	0.2	0.1
S	0.00	0.01	0.04	0.03
Total	99.91	100.68	100.47	100.38
Rb	240	310	100	230
Sr	130	230	560	290
Zr	200	300	760	450
As	1	120	3	88
Mo	0	9	5	1
Nb	13	29	43	34
Th	44	58	0	42
Be	2.3	2.3	4.2	2.6
Co	3	2	11	42
Cr	7	5	8	12
Ni	21	31	63	36
Cu	3	3	11	14
Zn	27	49	170	86
V	11	5	35	40
Y	28	32	61	61
La	63	170	180	140
Ce	120	290	370	270
Nd	51	100	190	130
Sm	7.7	14	28	20
Eu	0.7	1.9	6.0	2.5
Gd	6.1	8.5	19	15
Dy	5.3	6.2	13	12
Yb	2.1	2.4	4.4	4.4

Analytical techniques: major elements measured by XRF wavelength dispersive system on fused discs; H_2O, CO_2 and S by infrared absorptiometry; 1st set of trace elements by XRF energy dispersive system; 2nd set of trace elements by ICP trace methods; Y and rare earth elements by ICP preconcentration method. All analyses done at the Geological Survey of Canada.

Along the northern contact a discontinuous (?) upper border phase of porphyritic hornblende-plagioclase monzodiorite/diorite up to 500 m wide separates ferrodiorite from granitoid gneiss. Elsewhere, within the pluton the medium grained ferrodiorite is homogeneous except for amphibole-rich zones near external contacts and adjacent to one large enclave of gneiss. Small irregular aplite and pegmatite dykes, thin amphibole veinlets, and a few quartz or quartz-pyrrhotite veins cut the ferrodiorite. Rare gossans are due to minor pyrrhotite associated with magnetite-ilmenite rich pods.



Figure 82.2A. Spheroidal weathering ferrodiorite south of Ford Lake. GSC 204465.

Mineralogically the ferrodiorite is transitional to gabbro. Plagioclases are normally zoned in the range from about An_{48} to An_{41}. Early mafic minerals are iron-rich pyroxenes (hypersthene and augite) and a colourless amphibole. These phases are typically rimmed by green amphibole and may be overgrown by sieve-textured red-brown titaniferous biotite (Fig. 82.2B). Accessory minerals are quartz, perthitic orthoclase, magnetite, ilmenite, pyrrhotite, apatite and zircon. Zircon forms unusual anhedral skeletal grains with interstitial quartz. Myrmekite occurs along plagioclase grain boundaries. Plagioclase and iron-rich pyroxenes are clouded by minute rods and blebs of opaques, probably magnetite. Plagioclase grain boundaries are clear of inclusions for about 20-30 microns, otherwise the distribution of inclusions is quite uniform (Fig. 82.2C). Pyroxenes have coarser opaque inclusions with a more irregular distribution. Orthopyroxene also contains coarse blebby lamellae of clinopyroxene. Opaque inclusions, pyroxene exsolution lamellae and rimming of early mafic minerals by more hydrous phases record details of the late crystallization and cooling history of the pluton. Inclusions in plagioclase probably formed by exsolution; the clear rims are the result of diffusion near grain boundaries (Armbrustmacher and Banks, 1974; Harlow and Klimentidis, 1980).

Sphene-hornblende-biotite granodiorite

A pluton of medium- to coarse-grained plagioclase-phyric granodiorite is responsible for a triangular-shaped 1000 gamma aeromagnetic anomaly north of the Ford Lake batholith (Geological Survey of Canada, 1977). The external contacts of the homogeneous 30 km^2 pluton closely match the aeromagnetic anomaly. Internal foliation, defined by alignment of plagioclase phenocrysts and biotite, trends



Figure 82.2B. Photomicrograph of ferrodiorite: orthopyroxene rimmed by amphibole and sieve-textured biotite.

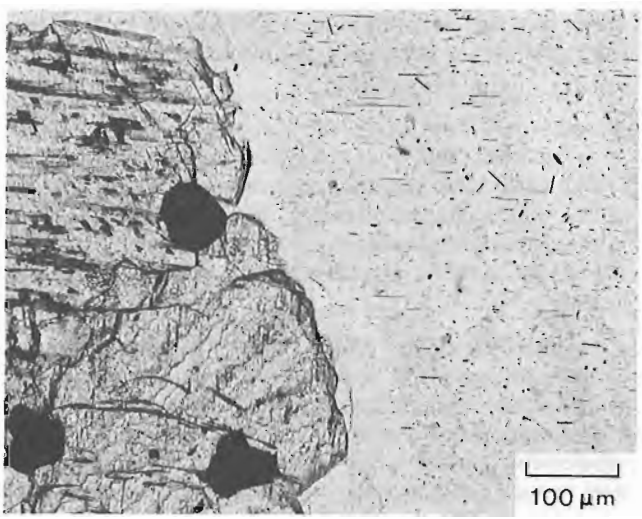


Figure 82.2C. Photomicrograph of ferrodiorite: plagioclase clouded by minute rods and blebs of opaques. Note plagioclase is clear of inclusions adjacent to pyroxene.

southwesterly with moderate to steep northwesterly dips. Xenoliths of (?)Penrhyn Group psammites, present throughout the pluton, are aligned parallel to the mineral foliation. The western contact of the pluton is subparallel to foliation in the granodiorite and in the adjacent gneiss. The northern contact is more complex and irregular. Gneissosity is sharply truncated and gneiss xenoliths are more common. However, no indication of contact metamorphism of the gneiss or marginal chilling of granodiorite was noted. Along the southeast contact (?)Penrhyn Group psammitic gneiss is interleaved with sheets of granodiorite. Foliation in both units is subparallel although psammite xenoliths clearly show an earlier foliation and granoblastic growth of amphibole.

The northeast corner of the pluton was intruded by a small elliptical body (300 × 200 m) of massive medium grained diorite. The body has a finer grained amphibole-rich margin and a deeply weathered diorite core similar to the ferrodiorite south of Ford Lake. The granodiorite pluton is also cut by several dykes of porphyritic biotite granite up to 20 m wide and minor pegmatite dykes and veins.

The granodiorite contains subhedral to euhedral plagioclase phenocrysts to 1.5 cm set in a medium grained matrix of quartz, plagioclase, microcline and ferromagnesian minerals (biotite 15-20%, hornblende 2-4%, sphene 1-3% and opaques 1%). Minor accessory minerals are apatite, zircon and allanite. Alteration is restricted to small amounts of sericite, carbonate and epidote. Plagioclase contains minute opaque rods identical to those in plagioclase of the southern ferrodiorite pluton.

Ford Lake batholith

The Ford Lake batholith comprises three major units of megacrystic granite to granodiorite and several small bodies of finer gained more mafic rocks (Henderson et al., 1986). In 1986 mapping continued northeast of the Y-shaped lake (Fig. 82.1 and Fig. 82.3A). The northern and northeastern contacts of the batholith were defined and the known area of the batholith has been extended to more than 400 km^2.

The southernmost pluton in the batholith is a homogeneous 140 km^2 body of porphyritic to megacrystic monzogranite. This pluton contains numerous xenoliths of (?)Penrhyn Group psammitic gneiss with several large rafts of calc-silicate gneiss and marble. Mineralogically the pluton is characterized by tabular microcline megacrysts to 5 cm in length and a mafic assemblage of magnetite, sphene and biotite.

Henderson et al. (1986) divided the coarser grained megacrystic pluton to the north of the monzogranite into a fluorite-biotite syenogranite central unit and a hornblende-biotite monzogranite/granodiorite western border phase. This subdivision is not shown in Figure 82.1 since internal variation in rock types proved to be more gradational in northeastern parts of the pluton. The dominant rock type northeast of the Y-shaped lake is a hornblende-biotite monzogranite with abundant microcline megacrysts (Fig. 82.3B and Fig. 82.3C). Foliation in the central part of the pluton is weak



Figure 82.3A. View looking west along the Y-shaped lake, Ford Lake batholith. Hills of megacrystic granite have a maximum relief of about 500 m. GSC 204465-C.



Figure 82.3B. Foliated megacrystic granite cut by a narrow dyke of fine grained biotite granodiorite. Note truncation of microcline megacrysts and absence of shear along the contact. Penknife is 5.8 cm long. GSC 203943-Z.

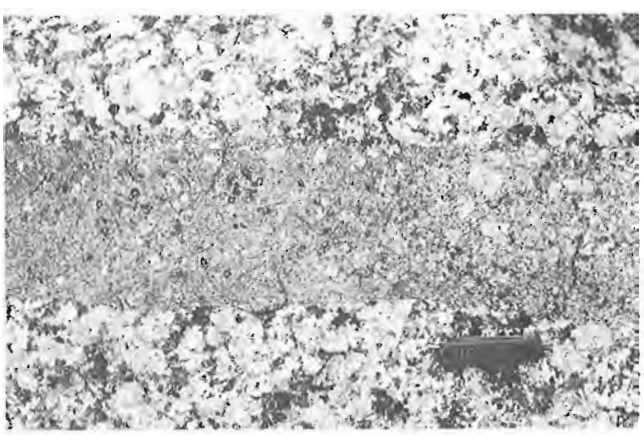


Figure 82.3C. Coarse grained megacrystic granite cut by a biotite granodiorite dyke containing local concentrations of microcline megacrysts aligned parallel to dyke contacts. GSC 204465-A.

and variable but towards the northeastern contact a southeasterly trending inwardly-dipping foliation is observed. A steep northeasterly trending fracture cleavage parallel to one of the major fracture sets in the pluton locally obscures the primary foliation. Metasedimentary xenoliths are abundant only near the external contact of the pluton with (?)Penrhyn Group paragneiss. This contact is very complex and has been extensively intruded by several generations of porphyritic granite and pegmatite dykes and sills. The megacrystic granite is slightly finer grained, less homogeneous and more mafic-rich near the contact.

Whole-rock geochemistry of three rocks from different units in the Ford Lake batholith plus a biotite granite from the older plutonic suite is reported in Table 82.1. The available chemical analyses are sufficient only to indicate the general geochemical character of the plutons. Batholith rocks are high in $K2^{O}$, Rb, BaO, Th, La, and Ce. REE analyses define LREE enriched patterns with weak to moderate negative Eu anomalies. Total REE abundances are high with La 440-570 and Yb 12-21 times chondrite values. La/Yb ratios range from 21-47. The biotite granite has an REE pattern similar to the batholith granites but contains less than half the total REE abundance.

U-Pb geochronology

Zircons were concentrated from two 25-30 kg samples taken from plutons in the Ford Lake batholith. Sample locations are indicated in Figure 82.1 and chemical analyses are listed in Table 82.1. For each sample, individual zircon populations were initially separated on the basis of grain size and magnetic susceptibility. Grains selected for analysis were hand picked to isolate the most euhedral, optically homogeneous, fracture-free and inclusion-free crystals. Zircons with anhedral cores were eliminated. Most fractions were abraded to remove the more altered outer parts of the grains (Krogh, 1982).

Separation and purification techniques for U and Pb are modified after Krogh (1973). Total procedural blanks for Pb ranged from 40 to 60 picograms, and U blanks averaged 50 picograms. A $^{205}Pb/^{233-235}U$ spike prepared by Parrish and Krogh (1986) was used in the analyses. Pb was loaded on a single Re filament using the silica gel phosphoric acid technique. U was loaded in water and run as the U + ion using a double Re filament assembly. Isotopic analyses were carried out on a Finnigan MAT 261 solid source mass spectrometer equipped with multiple collectors, secondary electron multiplier, and operating software designed for simultaneous measurement of all five Pb isotopes (Roddick et al., 1986). U was also analyzed using a static multicollection technique. Discordia line intercepts and associated errors were calculated using the line fitting technique of Davis (1982), with errors assigned to individual analyses using a numerical error propagation technique. U and Th decay constants recommended by Steiger and Jager (1977) were used for age calculations. All errors are quoted at the 2 sigma level.

Both samples contain euhedral to subhedral zircon crystals with minor inclusions and fractures; cores are present in a small percentage of grains. Pale yellow zircons in 85LAA 315 have length to width ratios form 1:1 to 3:1. Clear to amber zircons in 85LAA 168 have ratios from 2:1 to 5:1. Complete analytical results are shown in Table 82.2.

Two abraded zircon size fractions from the megacrystic syenogranite (85LAA 168) gave similar results with about 3% discordance (Fig. 82.4). Their U content (342, 384 ppm) is much lower than the 1612 ppm U in the more discordant (10%) unabraded fraction. This difference and the high U content suggest late stage zircon growth in a U-rich environment. Regression of the three data points defines an upper intercept age of $1826 +4/-3$ Ma and a lower intercept age of 483 ± 137 Ma. The upper intercept age is interpreted as the crystallization age of the syenogranite.

Four zircon fractions were analyzed from the southern monzogranite pluton. One fraction is almost concordant, two show approximately 3% discordance and the fourth is 10% discordant (Fig. 82.4). All fractions are relatively low in U (84-165 ppm) and, in contrast to the syenogranite, the unabraded fraction is not the most discordant nor does it have significantly higher U content than abraded fractions. The four fractions define a linear array with upper and lower intercept ages of 1823 ± 3 Ma and 189 ± 81 Ma, respectively. The upper intercept age is taken to be the age of intrusion of the monzogranite pluton. The age is not significantly different from that of the syenogranite.

DISCUSSION

Henderson et al. (1986) suggested that the megacrystic Ford Lake batholith is similar to I-type calc-alkaline plutons associated with plate margin igneous activity. Plutons north and south of the Ford Lake batholith mapped in 1986 extend the known compositional range of the plutonic suite to include more intermediate and basic rocks. The Ford Lake batholith and the northern granodiorite intrude (?)Penrhyn Group metasedimentary rocks which were deposited in a shallow marine environment on continental basement. These characteristics indicate that a likely tectonic setting for the plutonic belt is a continental magmatic arc.

Base metal content in Ford Lake batholith rocks is low (Table 82.1). Granites are enriched in thorium and rare earth elements and the arsenic content (88 and 120 ppm) of megacrystic granite appears anomalous. A few disseminated molybdenite grains were noted in batholith rocks. Along Ford Lake minor chalcopyrite and malachite were found in migmatitic granite gneiss, and molybdenite (rosettes to 4 cm) and chalcopyrite occur in crosscutting granite and pegmatite dykes.

The calc-alkaline plutons were probably emplaced during late stages of regional metamorphism when country rocks were still hot. Evidence indicative of slow cooling in hot country rocks includes: (1) lack of contact aureoles; (2) absence of chill margins on all but mafic intrusions; (3) segmented dykes that apparantly were emplaced before complete crystallization of the host pluton; and (4) exsolution

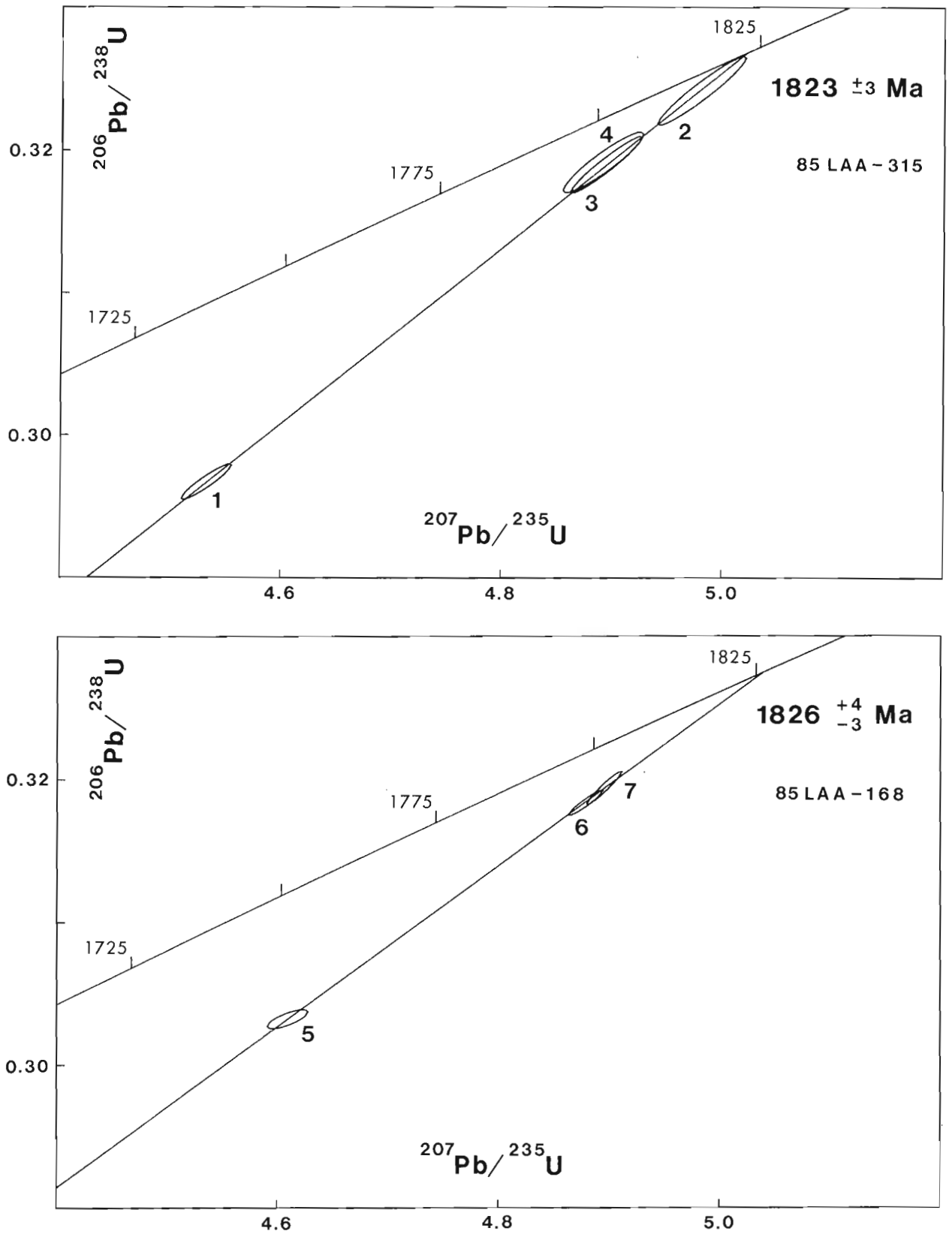


Figure 82.4. Isotope ratio plots for zircons from two plutons in the Ford Lake batholith.

Table 82.2 U-Pb zircon data – Ford Lake batholith.

No.	Sample size fraction[a]	Wt.[b] (mg)	U (ppm)	Pb_{rad} (ppm)	$\frac{206Pb}{204Pb}$[c]	Atomic abundance $\frac{206Pb}{204Pb}$	$\frac{206Pb}{207Pb}$	$\frac{206Pb}{208Pb}$ = 100[d]	$\frac{206Pb}{238U}$[e]	$\frac{207Pb}{235U}$[e]	$\frac{207Pb}{206Pb}$ Age (Ma)
				A. Magnetite-sphene-biotite monzogranite (85LAA-315-1)							
1	+149 M0,A	.044	148	49	983	.0523	11.79	20.72	.2967 ± .21	4.533 ± .25	1812.6
2	-149+105 M0,A	.020	165	56	644	.0683	12.07	13.40	.3242 ± .37	4.981 ± .40	1822.9
3	-105+74 M0	.025	165	58	860	.0500	11.81	18.33	.3190 ± .31	4.894 ± .33	1820.4
4	+74 NM0,A	.045	84	32	545	.1058	12.55	29.51	.3192 ± .33	4.892 ± .37	1818.4
				B. Fluorite-biotite syenogranite (85LAA-168-1)							
5	+74 NM0	.075	1612	507	865	.1140	12.57	13.44	.3032 ± .11	4.610 ± .20	1803.8
6	+74 NM0,A	.068	342	113	3199	.0228	11.43	10.68	.3183 ± .14	4.880 ± .16	1818.6
7	-74 NM0,A	.036	384	127	2760	.0220	11.42	10.28	.3194 ± .16	4.896 ± .18	1818.9

a NM,M, - nonmagnetic, magnetic at indicated degree of side tilt of Frantz isodynamic separator at 1.6 A and forward 15° slope; 74, 105, 149 - size in microns; A - abraded.

b Weight measured to ± .005 mg.

c Corrected for fractionation and spike Pb.

d Corrected for fractionation, spike and blank Pb; blank U.

e Correlated for fractionation, spike, blank and common Pb; error estimates are one standard error of mean in %.

textures. Exsolution of opaque inclusions within plagioclase crystals in both the ferrodiorite pluton and the northern granodiorite probably occurred during slow subsolidus cooling. There is no strong evidence for post-emplacement metamorphism or deformation as a cause for the exsolution and the inclusion patterns do not indicate they were trapped during crystal growth. Less compelling evidence for slow cooling is provided by the absence of rapakivi mantles on microcline megacrysts. Rapakivi mantles can form as a result of rapid, dendritic growth from a magma (Cherry and Trembath, 1978; Hibbard, 1981). Their absence suggests that no significant undercooling occurred during crystallization of the Ford Lake plutons.

Vernon (1986) concluded that all K-feldspar megacrysts in granitoid rocks and their enclaves are phenocrysts, not porphyroblasts. Evidence from the Ford Lake batholith clearly supports a primary igneous origin for the microcline megacrysts. This is indicated by their euhedral shape, abundant simple twins, zonally arranged inclusions, planar orientation parallel to pluton margins and rare examples of crude layering. The substantial barium content of batholith rocks (0.12-0.25% BaO) suggests the megacrysts have high Ba content and study of Ba zoning in megacrysts should reveal details of the magma dynamics of individual plutons (Long and Luth, 1979, 1986; Mehnert and Büsch, 1985). Megacrysts occur in most of the minor intrusions within the Ford Lake batholith but are not present in any of the numerous metasedimentary xenoliths. Small dykes within the plutons may truncate the megacrysts (Fig. 82.3B) or incorporate them as single crystals or crystal clusters aligned parallel to the dyke contacts (Fig. 82.3C).

U-Pb zircon analyses provide precise ages of 1823±3 Ma and 1826 +4/−3 Ma for the emplacement of two plutons of the Ford Lake batholith into (?)Penrhyn Group psammitic gneiss. Henderson (1983) demonstrated that Penrhyn Group rocks from the Foxe Fold Belt in Melville Peninsula show a postkinematic thermal culmination (about 700°C and 5 kb) that occurred at 1804±16 Ma (Rb-Sr isochron). The Ford Lake batholith was probably intruded under similar postkinematic P-T conditions as part of a major episode of magma production within a continental magmatic arc.

The Ford Lake batholith U-Pb results show no indication of inheritance of an older Pb component despite identification of cores in some zircon grains in the bulk fractions. Although zircons with cores were removed by handpicking, the results contrast markedly with our attempts to precisely date 1.76-1.9 Ga granite plutons southwest of the Wager Bay Shear Zone. Inheritance of an older, typically Archean, Pb component is invariably detected in the southern plutons despite careful grain selection. This contrast suggests that source regions for early Proterozoic magma generation north and south of the Wager Bay Shear Zone may be significantly different.

ACKNOWLEDGMENTS

The Polar Continental Shelf Project furnished rotary-wing support. We thank Jim Aspinall (pilot) and Orest Anhell

(engineer) for efficient camp moves. W. Spirito and S. Hamilton assisted ably and enthusiastically during the latter part of the field season. Co-ordination of base camp logistics by C.W. Jefferson and J.R. Henderson is gratefully acknowledged. M.N. Henderson and R. Theriault assisted with zircon sample preparation and G.M. LeCheminant provided preliminary microprobe data.

REFERENCES

Armbrustmacher, T.J. and Banks, N.G.
1974: Clouded plagioclase in metadolerite dikes, southeastern Bighorn Mountains, Wyoming; American Mineralogist, v. 59, p. 656-665.

Cherry, M.E. and Trembath, L.T.
1978: The pressure quench formation of rapakivi texture. Contributions to Mineralogy and Petrology, v. 68, p. 1-6.

Davis, D.W.
1982: Optimum linear regression and error estimation applied to U-Pb data; Canadian Journal of Earth Sciences, v. 19, p. 2141-2145.

Geological Survey of Canada
1974: Geophysical series (Aeromagnetic), Map 7629G, Wager Bay, scale 1:250 000.
1977: Geophysical series (Aeromagnetic), Map 7651G, Walker Lake, scale 1:250 000.

Harlow, G.E. and Klimentidis, R.
1980: Clouding of pyroxene and plagioclase in eucrites: implications for post-crystallization processing, Proceedings of the 11th Lunar and Planetary Science Conference, p. 1131-1143.

Henderson, J.R.
1983: Structure and metamorphism of the Aphebian Penrhyn Group and its Archean basement complex in the Lyon Inlet area, Melville Peninsula, District of Franklin; Geological Survey of Canada, Bulletin 324, 50 p.

Henderson, J.R., LeCheminant, A.N., Jefferson, C.W., Coe, K., and Henderson, M.N.
1986: Preliminary account of the geology around Wager Bay, District of Keewatin; in Current Research, Part A, Geological Survey of Canada, Paper 86-1A, p. 159-176.

Heywood, W.W.
1961: Geological notes, northern District of Keewatin; Geological Survey of Canada, Paper 61-18, 9 p.
1967: Geological notes, northeastern District of Keewatin and southern Melville Peninsula, District of Franklin, Northwest Territories (Parts of 46, 47, 56, 57); Geological Survey of Canada, Paper 66-40, 20 p.

Hibbard, M.J.
1981: The magma mixing origin of mantled feldspars, Contributions to Mineralogy and Petrology, v. 76, p. 158-170.

Krogh, T.E.
1973: A low contamination method for hydrothermal dissolution of zircon and extraction of U and Pb for isotope age determination; Geochimica et Cosmochimica Acta, v. 37, p. 485-494.
1982: Improved accuracy of U-Pb zircon ages by the creation of more concordant systems using an air abrasion technique; Geochimica et Cosmochimica Acta, v. 46, p. 637-649.

Long, P.E. and Luth, W.C.
1979: Petrogenesis of microcline megacrysts from Precambrian granitic rocks of the Dixon-Penasco area, northern New Mexico, New Mexico Geological Society, Guidebook 30, p. 145-163.
1986: Origin of K-feldspar megacrysts in granitic rocks: implications of a partitioning model for barium, American Mineralogist, v. 71, p. 367-375.

Mehnert, K.R. and Büsch, W.
1985: The formation of K-feldspar megacrysts in granite, migmatites and augengneisses, Neues Jahrbuch fuer Mineralogie, Abhandlungen, v. 151, p. 229-259.

Parrish, R. and Krogh, T.E.
1986: Synthesis of purified ^{205}Pb for U-Pb geochronology: prelude to worldwide distribution; Terra Cognita, v. 6, p. 152.

Roddick, J.C., Loveridge, D.W., and Parrish, R.
1986: Precise U-Pb dating of sub-milligram quantities of zircon; Terra Cognita, v. 6, p. 152.

Steiger, R.H. and Jager, E.
1977: Subcommission of geochronology: convention on the use of decay constants in geo- and cosmochronology; Earth and Planetary Science Letters, v. 36, p. 359-362.

Vernon, R.H.
1986: K-feldspar megacrysts in granites – phenocrysts, not porphyroblasts, Earth-Science Reviews, v. 23, p. 1-63.

U-Pb zircon and monazite geochronology and zircon morphology of granulites and granite from the Thelon Tectonic Zone, Healey Lake and Artillery Lake map areas, N.W.T.

Project 830006

O. van Breemen, J.B. Henderson, W.D. Loveridge, and P.H. Thompson
Lithosphere and Canadian Shield Division

van Breemen, O., Henderson, J.B., Loveridge, W.D., and Thompson, P.H., U-Pb zircon and monazite geochronology and zircon morphology of granulites and granite from the Thelon Tectonic Zone, Healey Lake and Artillery Lake map areas, N.W.T.; in Current Research, Part A, Geological Survey of Canada, Paper 87-1A, p. 783-801, 1987.

Abstract

Monazite from the Hanbury granite yields a 1920 ± 4 Ma U-Pb age interpreted to date emplacement. Zircon cores, some apparently of sedimentary origin, with an older age indicate a significant crustal component in this late tectonic granite.

A 1950±4 Ma U-Pb age on monazite from a mylonite containing unaltered partly comminuted hypersthene provides a younger limit for high grade metamorphism and intense deformation. Zircons from the same rock contain partly resorbed cores of probable igneous origin and mantles featuring discordant internal zonation. Growth of the metamorphic mantles appears to have been syn-shearing. An almost concordant cluster of ca. 1990 Ma U-Pb zircon ages is interpreted to predate granulite facies metamorphism but postdate crystallization of the igneous cores. A similar age of granulite facies metamorphism is indicated by U-Pb zircon ages from a hypersthene-gabbro. Zircons from a tonalite granulite gneiss are also consistent with a ca. 2000 Ma granulite event but contain older cores which record an earlier Aphebian event.

Résumé

L'analyse au moyen de la méthode U-Pb de la monazite du granite de Hanbury donne un âge de 1920 ± 4 Ma, qu'on suppose être la date de la mise en place. Des noyaux de zircon, certains apparemment d'origine sédimentaire, et d'âge plus ancien, témoignent de la présence d'une importante composante crustale dans ce granite tectonique tardif.

L'âge ainsi déterminé de 1950 ± 4 Ma de la monazite tirée d'une mylonite renfermant de l'hypersthène inaltéré partiellement pulvérisé, attribue une limite plus récente aux épisodes de métamorphisme élevé et de déformation intense. Les zircons de la même roche renferment des noyaux partiellement resorbés d'origine probablement ignée et des enveloppes caractérisées par une zonation interne discordante. La croissance des enveloppes métamorphiques semble avoir été contemporaine à l'épisode de cisaillement. Un groupe presque concordant dont l'âge de 1990 Ma environ, déterminé à partir de l'analyse des zircons à l'aide de la méthode U-Pb, est interprété comme ayant précédé le métamorphisme à faciès des granulites, mais ayant suivi la cristallisation des noyaux ignés. La même méthode de détermination d'âge, appliquée à un gabbro à hypersthène, attribue un âge similaire à l'épisode de métamorphisme à faciès des granulites. Les zircons provenant d'un gneiss à tonalite et à granulite correspondent aussi à un métamorphisme à faciès des granulites vieux de 2000 Ma environ, mais renferment des noyaux plus anciens qui enregistrent un événement aphébien encore plus ancien.

INTRODUCTION

The Thelon Tectonic Zone of the northwestern Churchill Structural Province separates the main part of the Churchill from the Slave Province to the west, a craton that has been only minimally deformed since the close of the Archean (Wright, 1957, 1967; Fraser, 1964; Thompson and Henderson, 1983). The zone is on the order of 75 to 100 km wide and can be traced over a distance of more than 800 km. The curvilinear structural style and generally low to intermediate metamorphic grade of the Slave contrasts with the strongly linear pattern and high metamorphic grade of the Thelon Tectonic Zone. The western boundary of the zone also corresponds with pronounced change in the aeromagnetic anomaly pattern in the region and, in the central part of the zone between the Bathurst and McDonald faults, a major paired gravity anomaly is present whose locus of inflection closely corresponds to the Thelon Front — the boundary between the Slave and the Thelon Tectonic Zone (TTZ). This has led Gibb and Thomas (1977) and Gibb (1978) to propose that the front represents a Proterozoic cryptic suture between two collided cratons. West of the front, Henderson and Thompson (1981) suggested that the change to a linear pattern of high grade gneisses and migmatites typical of the Thelon Tectonic Zone is Archean and older than a basic dyke swarm that, in turn, predates a major crustal overthrust invoked by Thompson and Henderson (1983) to explain a Proterozoic metamorphic overprint on dykes and Archean rocks west of the Thelon Tectonic Zone.

The western boundary of the Thelon Tectonic Zone and the adjacent Slave Province has been an area of concentration of regional mapping over the last few years (Frith, 1982; Henderson and Thompson, 1980, 1981; Henderson et al., 1982; Thompson and Ashton, 1984; Thompson et al., 1985, 1986; Henderson and Macfie, 1985, 1986) as well as more detailed studies (e.g., James, 1985, 1986). As part of this ongoing program geochronological studies have been undertaken in various parts of the region in an attempt to separate in time the complex series of events that took place to form the Thelon Tectonic Zone. This is the first of what is expected to be a series of reports on the geochronology of the region, and is concerned with the severely deformed and highly metamorphosed gneisses and deformed plutons of the Thelon Tectonic Zone immediately east of the Slave Province between the McDonald and Bathurst faults.

In Figure 83.1 the Thelon Front is considered to occur within (Henderson and Thompson, 1981) or immediately east of (James, 1985, 1986) the north- northeasterly trending 'straight zone' of mylonitized, migmatitic Archean Yellowknife Supergroup supracrustal rocks that bisect the southeast quadrant of the area. West of this zone, Archean geochronological data, mainly U-Pb zircon determinations, include part of the presumed granitoid gneissic basement block at about 2715 Ma, Yellowknife volcanic rocks extruded at about 2691 Ma and a series of intrusive plutons ranging in age between 2630 and 2530 Ma (van Breemen et al., 1986). The Yellowknife supracrustal rocks have been metamorphosed in the Archean with biotite-chlorite assemblages (greenschist) more common in the west, through cordierite-andalusite and sillimanite schists to kyanite-bearing sillimanite migmatites of the upper amphibolite facies which occur in a relatively narrow zone including and west of the straight zone. In addition a Proterozoic greenschist to lower amphibolite intermediate pressure facies has been superimposed on both Archean metamorphic assemblages and post Archean mafic dykes. A sharp change in Rb-Sr biotite dates from Archean ages in the west to about 1730 Ma in the east corresponds closely to the amphibolitization isograd in the Proterozoic dykes (van Breemen, 1986).

THELON TECTONIC ZONE

A complex heterogeneous assemblage of strongly deformed granitoid gneisses and migmatitic supracrustal rocks occur east of the straight zone (Henderson et al., 1982; James, 1955, 1986; Henderson and Macfie, 1985, 1986). Rock units within the zone consist of pink and grey strongly foliated to layered migmatitic granitoids, coarse augen gneisses, mafic gneisses, rusty quartzofeldspathic gneisses, foliated leucogranites and diatexites that grade into supracrustal migmatites. The migmatitic supracrustal rocks consist of either biotite-rich or amphibolite-rich layered migmatite and become increasingly abundant to the south. Although they are similar in some respects to the migmatitic Yellowknife Supergroup rocks to the west of the straight zone, their relationship to these rocks remains to be determined. The rocks units have a strong north-northeasterly trend that is particularly strongly developed in the northern part of the zone west of Moraine Lake due to the development of a series of mylonitic ductile shear zones that are particularly abundant in that part of the zone. Much of the terrane is at granulite grade in the northern part of the zone but the granulite grade zone appears to narrow to the south with amphibolite facies rocks occurring both east and west of a central granulite core.

Preliminary study of the complex gneissic package suggests that the main phase migmatization and formation of granulite facies assemblages has been overprinted by an event that caused widespread development of corona textures, particularly in relatively mafic layers of the granulite gneiss, and a high strain event evident to varying degrees in most compositions. In one sample, main phase granulite facies metamorphic layering is cut by the steep foliation formed during high strain, and clinopyroxene coronas in mafic layers outline a preferred orientation parallel to the mylonitic fabric in felsic layers. In other rocks, development of coronas and grain size reduction combine to produce a mortar texture. Mineral assemblages indicate the later event occurred under at least middle amphibolite facies conditions. James (1986) suggested that it is possible there are two granulite facies metamorphisms. Widespread, though not pervasive, alteration of primary and corona pyroxenes to colourless or blue-green amphibole is related to later hydration under low metamorphic grade. The extent to which these stages in the metamorphic history represent a discrete tectonometamorphic events or phases of a single event remains to be determined.

The presence of polymetamorphosed migmatitic Yellowknife Supergroup adjacent to the upper amphibolite and granulite facies gneisses along the eastern border of the straight zone led Henderson and Thompson (1982) to correlate tentatively the corona-forming and high strain events with the Proterozoic overprinting documented to the west and the main phase migmatitization/granulite facies assemblages with the late Archean metamorphism.

Two samples of granulite grade gneiss were collected at Moraine Lake (Fig. 83.1) for U-Pb geochronology, the northern sample from a sheared felsic layer, and the southern sample from a more mafic phase of the rather heterogeneous, well layered quartz-feldspar-biotite-hornblende-orthopyroxene gneisses. A third sample for zircon was collected from a metamorphosed orthopyroxene-bearing mafic sill that had intruded migmatitic granitoid gneisses that occur within the granulite zone on the Hanbury River. The fourth sample was collected from an elongate well foliated biotite-poor pluton that was emplaced in migmatitic supracrustal rocks east of the granulite zone, also on the Hanbury River.

ZIRCON MORPHOLOGICAL CRITERIA

Before the U-Pb zircon isotopic results are presented and discussed, criteria of zircon morphology are set out which are critical for the interpretation of the environment of growth and isotope systematics.

Zircon typically forms as a liquidus phase in magmas of granitic to tonalitic composition (Poldervaart, 1956). Bipyramidal prisms with euhedral internal zoning are characteristic of unimpeded growth in a liquid, as are long needle-shaped inclusions (Silver, 1969). A detailed classification of igneous type relates number and arrangement of euhedral crystal facets to variables of Al/alkaline ratio and temperature of crystallization (Pupin and Turco, 1972a, b; Pupin, 1980). Poldervaart (1956) and Spotts (1962) contrasted the euhedral zircons of granitoid melts with the irregular morphology of zircons from basic igneous rocks and interpreted the latter in terms of impeded late stage growth in the interstices between the major minerals. In this case internal zoning may be both concordant and discordant to the outer perimeter of the crystal (van Breemen et al., 1986a, Plate IIC).

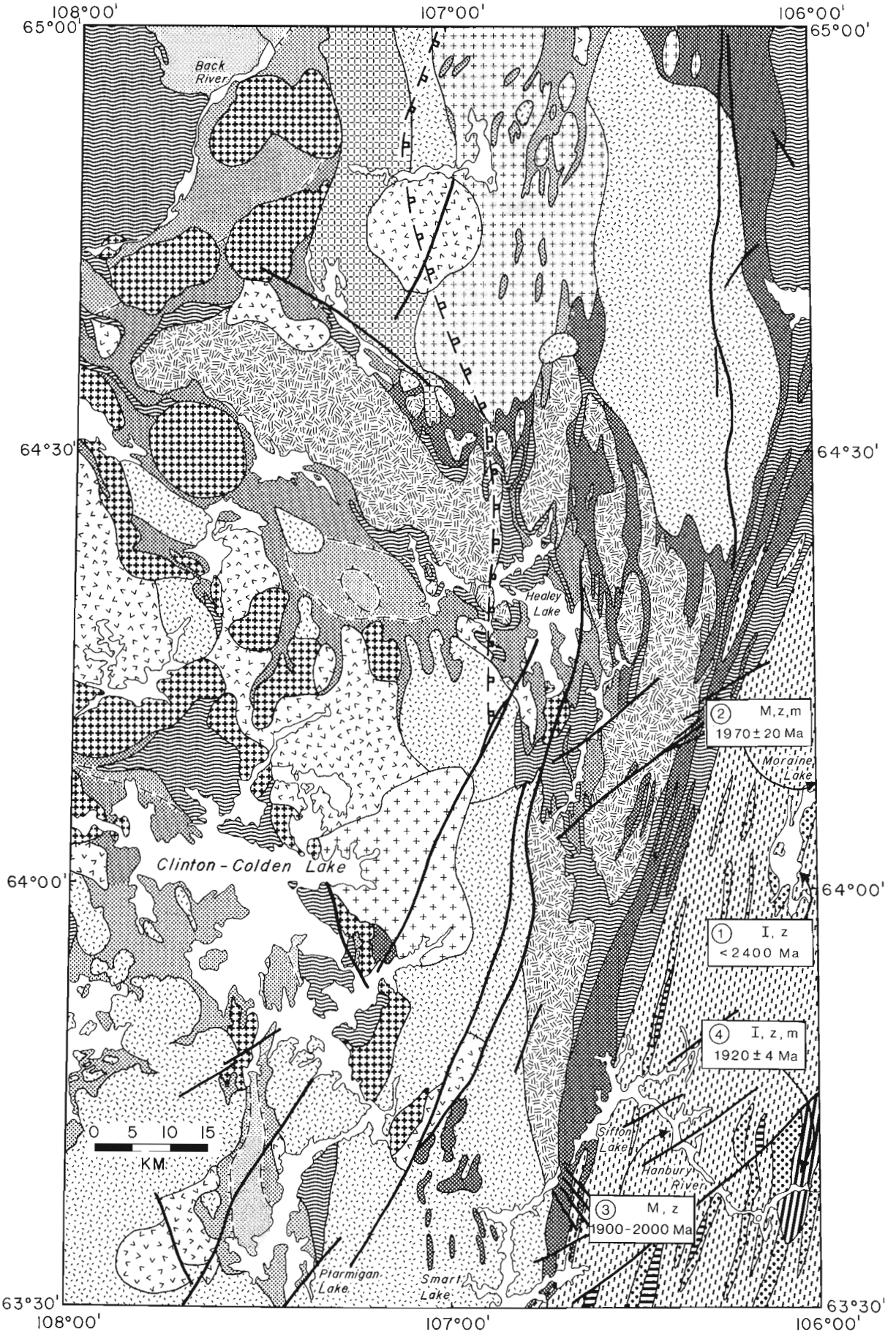
Irregular, broken zircons also form as a result of sedimentary processes (Poldervaart, 1955). In such cases internal zonation may not follow the outer perimeter although, fracture planes often parallel facets (F.W. Chandler, personal communication, 1986). The more common form of abraded sedimentary zircon is spherical or ovoid, with discordant internal zonation. Degree of rounding in sedimentary zircons does not appear to be a reliable indicator of distance travelled (Poldervaart, 1955) but could be an indicator of environment of deposition (Chandler, 1984).

Rounded forms have also been attributed to processes of chemical corrosion (Pidgeon and Aftalion, 1972). However, if such corrosion is extensive it is likely to form embayments which ultimately lead to smooth but highly irregular shapes (Spotts, 1962; van Breemen and Parrish, 1986).

Irregular and discordant internal zonation has been documented in zircons from granite magmas which crystallized in shear zones of the Grenville Province (van Breemen and Hanmer, 1986). Both features of the internal zonation have been interpreted in terms of impingement of growing zircon with rotating major minerals in a dynamic 'filter press' of melt and crystals. During this process zonal discordance was accomplished by a) partial resorption of previously deposited layers, b) discordant growth abutting straight edges of grains which change position and/or c) breakage of the zircon even as it grows. Embayments into euhedrally zoned central cores were probably caused by dissolution reabsorbtion by melt. While central zonation was euhedral prismatic, irregular zonation of the mantles led to ovoid grain boundaries featuring both crystal facets and irregularities. In some cases, adjacent zircons are overgrown by a common mantle producing apparent twins by docking of crystals (synneusis).

Multi-faceted spherical and ovoid zircons have been documented in numerous instances from eclogite and granulite facies rocks (Hoppe, 1966; Pidgeon and Bowes, 1972; Gebauer and Grunenfelder, 1979; Peucat et al., 1982; Percival and Krogh, 1982; van Breemen et al., 1982, 1986; Heaman et al., 1986). The high order, randomly multi-faceted forms with pits grooves, ridges and other small scale surficial irregularities (van Breemen et al., 1986a; plate ID) have been interpreted in terms of metamorphic growth in a solid medium. Development of many facets would appear to be related to resistance to crystal growth and or diffusion of zirconium through the surrounding medium. In this regard it is of interest that on the morphological classification of Pupin (1980) the simplest bipyramid form (eight faces) was grown in a hydrothermal solution (Caruba et al., 1975) while the simplest bipyramid prism (twelve facets) was the highest temperature form found in the least viscous, peralkaline, magma.

Although metamorphic reactions involving breakdown of zirconium-bearing minerals would provide a source of metamorphic zircon, there is little reliable data concerning the release of zirconium during granulite facies metamorphism. A recent study of Zr partitioning between igneous phenocrysts and groundmass showed Zr concentrations at circa 3 ppm for orthopyroxene, generally less than 1 ppm for plagioclase and in the tens of ppm (5-200 ppm) for clinopyroxene, hornblende and garnet (Fujimaki et al., 1984). Barr et al. (in press) documented extensive zircon overgrowths in metamorphosed alkaline syenite where clinopyroxene, likely to contain abundant Zr in such rock, had broken down to hornblende under amphibolite facies conditions. However, a recent study across a tectonic boundary between amphibolite and granulite facies rocks in the Grenville Province of Ontario (van Breemen et al., 1986) provided an unambiguous example of the general observation that, in metaplutonic rocks, metamorphic overgrowths on primary igneous zircon are rare in amphibolite facies terranes but common in granulite facies terranes. Less is known concerning metamorphic zircon growth in metasediments. Evidence for significant growth of authigenic and low grade metamorphic zircon (Saxena, 1966) was disputed by Marshall (1967) while Gastil et al. (1967) concluded that metadetrital zircons refacet only at near-melting conditions.


108°00'
107°00'
106°00'
65°00'
64°30'
64°00'
63°30'
Back River
Healey Lake
Clinton-Colden Lake
Moraine Lake
Ptarmigan Lake
Smart Lake
Orion Lake
Hanbury River
0 5 10 15
KM
② M,z,m
1970±20 Ma
① I, z
<2400 Ma
④ I, z, m
1920±4 Ma
③ M, z
1900-2000 Ma

WEST OF STRAIGHT ZONE

Granitoid rocks, undivided

Granite, granodiorite, muscovite-biotite, massive to strongly foliated, also pegmatite

Granite, megacrystic biotite (muscovite), massive to weakly foliated

Granite, granodiorite, tonalite undivided, biotite, minor to rare muscovite, foliated, metasedimentary inclusions locally abundant

Quartz tonalite, biotite, massive to weakly foliated, coarse quartz masses

Tonalite, granodiorite, quartz diorite, biotite-hornblende massive

Yellowknife Supergroup

Metagreywacke pelite and high grade equivalents, (a) biotite zone, (b) cordierite zone, (c) sillimanite zone (not defined south of 64°00') (d) migmatite zone

a b c d

Metavolcanic rocks, mafic to felsic, greenschist to amphibolite grade

Granitoid gneisses, heterogeneous assemblage of complexly deformed granite to diorite gneisses to plutonic units to to granitoid migmatite

EAST OF STRAIGHT ZONE

Granite, granodiorite, biotite, strongly foliated

Undivided foliated granitoid rocks, granitoid gneisses in part at granulite grade

High Grade Supracrustal Rocks

Migmatitic metasediments, with younger granitic sheets and intrusions

Migmatitic amphibolite, with younger granitic sheets and intrusions

Geological contact, defined or assumed

Fault or shear zone

Archean metamorphic isograd

Proterozoic metamorphic isograd (amphibolitization of diabase dykes)

Geochronological data

I Igneous age

M Metamorphic age

z Zircon

m Monazite

Figure 83.1. Geology of the Healey Lake and northern half of the Artillery Lake map sheets showing localities of samples investigated from the Thelon Zone. The main U-Pb age results are summarized at sample localities: M, metamorphic age; I igneous age; Z, zircon age; M, monazite age.

Similarly Peucat et al. (1985) documented overgrowth on detrital zircons from the migmatitic gneiss zone but not the sillimanite zone. Their drawing illustrating the zircon overgrowths from the migmatitic gneiss shows low order pyramidal facets more characteristic of igneous than metamorphic rocks.

With the approach of partial melting processes other than mineral transformation may be operative, such as 1) zircon dissolution and redeposition depending on the basicity or (Na + K + 2 Ca)/(Al + Si) of local melts (Watson and Harrison, 1983), 2) metasomatism between neosome and paleosome and 3) upward migration of fluids from deeper levels, probably channelled along shear zones.

It is also possible that zirconium in the form of fluorocarbonate complexes (Romberger, 1978; Skippen and Tromsdorff, 1986; Skippen personal communication, 1986) is mobilized during dewatering processes of granulite facies metamorphism. It is important to determine to what extent such CO_2-H_2O fluids are pervasive (Kreulen, 1980) or channelled (Valley and O'Neill, 1984).

Metamorphic overgrowths on igneous zircons from granulite facies meta-igneous rock result in ovoid to rounded prismatic forms (van Breemen et al., 1986). In the latter study from the Grenville Province, igneous and metamorphic zircon could be clearly distinguished in polished and etched grain mounts of zircons. Euhedral zoning of the igneous cores showed that these did not recrystallize during the metamorphism. U-Pb concordia diagrams for variously abraded populations of different aspect ratio showed mixing lines between older igneous and younger metamorphic zircon.

Metamorphic zircon growth may be preceded by radiogenic Pb loss during prograde metamorphism, so that on a U-Pb concordia diagram the position of data points along a chord joining primary and metamorphic ages may not simply reflect the relative proportion of igneous and metamorphic zircon, but also the degree of episodic Pb loss from the primary igneous zircon. Paradoxically zircons may suffer Pb loss during an initial low grade event but fail to record a late high grade event (e.g. Peucat et al., 1985). It would appear that the greater degree of Pb loss occurs during 300-350°C prograde metamorphism and fluid activity annealing zircon with a high level of time cumulative lattice damage by U decay (Pidgeon et al., 1973; Krogh and Davis, 1973; Gebauer and Grunenfelder, 1976). Cumulative lattice damage can result in recent Pb loss but the effect is reduced if metamict outer zircon is removed by the air abrasion technique (Krogh, 1982). Conversely, cases have been documented where the U-Pb zircon systematics have survived eclogite facies metamorphism (Gebauer and Grunenfelder, 1979; Peucat et al., 1982), granulite facies metamorphism (van Breemen et al., 1982, 1986), and melting (Pidgeon and Aftalion, 1978). Recent ion probe analyses on xenocrystic zircons in basalts yield distinct ages for cores and rims (Compston et al., 1986) confirming that rates of solid diffusion are extremely slow. Interpretation of U-Pb zircon ages as dating uplift and cooling (Mattinson, 1978; Percival and Krogh, 1983) can be considered only in cases of extremely slow regional cooling (c.f. Dodson, 1973).

Techniques of zircon separation, documentation and isotope dilution analysis are similar to those described in van Breemen et al. (1986). Analytical uncertainities (2σ) are 0.5% for the $^{206}Pb/^{238}U$ and $^{207}Pb/^{235}U$ ratios and 0.1% or 0.15% for the $^{207}Pb/^{206}Pb$ ratios. U-Pb isotope data are presented in Table 83.1 and isotope ratios have been plotted on corcordia diagrams Fig. 83.2 and 83.3.

CASE HISTORIES

Tonalitic granulite gneiss (sample 1)

The outcrop from which this sample was taken is characterized by well-defined gneissic layering several centimetres to several metres thick with alternation of dark-weathering mafic (40%) and pink-weathering (60%) granitic compositions. Widespread grain-size reduction and straightness of layering can be attributed to a high strain event, but migmatization that is older than the deformation, and primary compositional variations related to sedimentary, volcanic, or plutonic processes are also important factors in formation of these gneisses.

This sample is a brown-weathering, fine grained, thin-layered, tonalitic, granulite gneiss. Anhedral grains of orthopyroxene, hornblende and, less commonly, clinopyroxene occur in an even-grained, somewhat coarser, matrix of plagioclase and quartz and fine grained biotite, clinopyroxene, amphibole and opaque phases. Accessory apatite and zircon are present. The rock is characterized by a distinctive mortar texture with seams of relatively fine grained quartz, plagioclase, biotite, clinopyroxene and amphibole separating all the larger grains (Fig. 83.4A). Some plagioclase grains are 2-5 mm across. Orthopyroxene is pleochroic pale pink to pale green. Larger clinopyroxene grains have dark inclusion-rich cores. Clear clinopyroxene aggregates partially rim many, though not all, orthopyroxene and hornblende grains and appear to be replacing biotite. In most cases, orthopyroxene is separated from adjacent plagioclase by reaction rims of variable mineralogy. Splays of euhedral biotite contrast with a deformed coarser grained variety. Small amphibole grains sporadically present along rims of orthopyroxene and clinopyroxene are more actinolitic in composition than the yellow-green to green hornblende that predates the deformation. Bent cleavage and twin planes or undulatory extinction in orthopyroxene, plagioclase, and quartz, and the larger clinopyroxene grains are further evidence of the strain associated with development of the mortar texture.

Texture and mineral assemblages record only three of the stages in the history of this rock. A granulite facies event during which two pyroxenes, hornblende and plagioclase were stable, followed or was synchronous with migmatization. Later deformation occurred under lower temperature and/or higher pressure conditions compatible with the growth of clinopyroxene rims and development of montar textures in the stability field of biotite. Alteration of pyroxenes to fine grained amphibole is associated with the latest, lowest grade stage of mineral growth.

Zircons consist of rounded prisms with multiple high order facets. Polished sections etched with HF acid show that

the overall morphology is composite with euhedral to subhedral cores and overgrowths that give a rounded appearance to the prisms (Fig. 83.5A, B). Many zircons show low U (light colour in photo) outer and high U inner (metamict zircon leached out by acid) mantles when compared to the core as seen in Figure 83.5A. However, many zircons also show a greater degree of complexity with one or more zones of high U in an outer mantle of igneous but locally discordant zoning (Fig. 83.5B). This type of zoning with limited corrosion also contributes to more equidimensional shapes. However, even in the outermost high U mantles zoning outlines simple pyramids indicative of a liquid medium (Fig. 83.5A). For comparative purposes the reader is referred to Figure 83.5C which features zoning in a metamorphic zircon from the Grenville Province.

Of five hand picked fractions of zircon (Table 83.1), one consisted of most elongate prismatic grains and the remaining four were different sized grains of round or oval shape. The prismatic and two of the rounded fractions were abraded. Isotope ratios plot in an array subparallel to the concordia between 2200 and 2100 Ma.

A surprising feature of the distribution of data points is that the coarsest prismatic and abraded fraction (1a) yields the youngest $^{207}Pb/^{206}Pb$ age. Abrasion products in this case suggest breakage of prisms and rounding of ends which may have concentrated high U inner mantle. In both the ovoid fractions there has been a shift towards older ages after abrasion, with the greater shift occurring in the finer fraction. Of all the zircons, the finest unabraded fraction is the most discordant if interpreted in terms of recent Pb loss. Yet in both the rounded size fractions abrasion produced an increase in U content from ca. 150 to 400 ppm.

The data can be interpreted in terms of an array between a primary igneous age(s) older than 2200 Ma and a metamorphic event younger than 2100 Ma. Slight recent Pb loss is likely to account for at least some of the scatter of data points. The extent to which the measured age range represents on the one hand a mixing of old and new zircon and on the other prograde Pb loss (Gebauer and Grunenfelder, 1976) is difficult to determine. It is likely that the older multi-faceted low U rims represent new metamorphic zircon. The inner high U zones may in part represent a migmatitic stage of the same

Table 83.1 U-Pb isotopic data on zircon and monazite

Sample Size fraction (in microns)	Weight (mg)	U (ppm)	Pb* (ppm)	Measured $^{206}Pb/^{204}Pb$	Isotopic abundance, $^{206}Pb = 1000$ ^{204}Pb	 ^{207}Pb	 ^{208}Pb	 $^{206}Pb/^{238}U$	 $^{207}Pb/^{235}U$	$^{207}Pb/^{206}Pb$ Age (Ma)
1. Tonalitic granulite gneiss										
a, +177, N-1°, A	4.49	244.5	103.3	10213	0.078	132.4	149.9	0.38388	6.9535	2116.4
b, -177+149, N-1°, R	5.99	133.5	55.8	8227	0.067	134.5	126.2	0.38655	7.1203	2145.8
c, -177+149, N-1°, R,A	1.44	395.2	166.5	24768	0.020	133.7	130.5	0.38748	7.1524	2149.4
d, -105+74, N-1°, R	5.58	166.8	69.6	9167	0.096	135.7	124.6	0.38633	7.1607	2156.6
e, -105+74, N-1°, R, A	0.42	389.5	169.3	6289	0.078	139.2	124.8	0.40086	7.6343	2203.8
2. Mylonitic granitic granulite gneiss										
a, +105, N-1°, A	2.96	436.4	187.0	53612	0.006	113.6	258.2	0.36039	6.1022	1997.4
b, +105, N-1°, R	1.57	885.1	328.3	36004	0.018	122.8	84.3	0.35753	6.0406	1993.5
c, -105+74, N-1°, R	2.17	685.2	250.0	63839	0.005	122.5	63.6	0.35783	6.0413	1992.2
d, -74+62, N-1°, R	1.65	863.5	314.9	44354	0.006	122.5	63.2	0.35776	6.0403	1992.3
e, -105+74, N-1°, R	2.17	686.0	250.9	18287	0.024	122.6	64.2	0.35882	6.0480	1989.3
f, monazite	2.10	1399	4941	9182	0.015	119.9	10484	0.35103	5.7926	1951.4
3. Hypersthene metagabbro										
a,	0.99	262.5	112.5	5844	0.027	120.5	322.3	0.34525	5.7196	1958.4
b,	1.14	177.1	73.2	6036	0.002	119.0	291.5	0.34046	5.5829	1940.2
4. Hanbury granite										
a, +105, N-1°	0.84	660.5	222.0	1052	0.888	131.0	115.8	0.32427	5.3258	1943.0
b, +105, N-2°, A	0.21	1751.8	598.9	1971	0.397	126.8	102.9	0.32825	5.4981	1978.1
c, -105+74, N-1°	0.93	1526.3	478.4	1892	0.409	123.8	101.2	0.30227	4.9317	1931.1
d, -105+74, N-1°, R	0.92	1050.5	359.2	1891	0.499	125.0	104.5	0.32966	5.3792	1931.4
e, coarse, A	0.31	215.4	76.9	2865	0.103	122.4	82.2	0.34598	5.7719	1970.9
f, fine, A	1.55	1089.7	391.5	4868	0.197	122.4	114.2	0.34030	5.6200	1952.9
g, monazite	0.60	1085	3483	12425	0.035	118.0	9752	0.34075	5.5194	1918.2
h, monazite	0.33	3000	9473	22318	0.024	117.9	9459	0.34444	5.5860	1920.4

* Radiogenic Lead
R, ovoid grains
A, abraded
N, non-magnetic at given angle
M, magnetic at given angle

event although the above data (Table 83.1) suggest that most of the high U zircon is older than 2200 Ma. It is also possible that there are more than one age of primary igneous zircon.

The data do not support the hypothesis that sample 1 is reworked Slave craton. Age results west of the Thelon Tectonic Zone in the Healey lake map area indicate that Archean rocks are no younger than 2600 Ma (van Breemen et al., 1986). In the Thelon Tectonic zone of the Tinney Hills – Overby Lake map area to the north (Thompson et al., 1985), Archean (pink) gneiss contains slightly discordant zircons with consistent $^{207}Pb/^{206}Pb$ ages of ca. 2600 Ma (unpublished data). A chord drawn through 2600 and 2000 Ma (Fig. 83.2) intersects three out of five zircons from sample 1. Even though the U concentrations of these zircons and nearly concordant 2600 Ma zircons to the north are now similar, sample 1 zircons have undergone an 80% episodic Pb loss in the second event. Furthermore, a chord through the remaining more concordant data points 1a and 1e yields upper and lower intercept ages of 2410 and 2015 Ma. Assuming a metamorphic age of ca. 2000 Ma (see below) the data indicate that the average age of primary igneous zircon is less than 2400 Ma.

Mylonitic granitic granulite gneiss (sample 2)

This sample is from a well-layered outcrop that is more compositionally variable than the rocks at locality 1. The proportion of felsic layers is lower and they commonly contain garnet. Sillimanite-potassium feldspar-garnet-biotite is present in the sequence seven hundred metres farther west. Strain is heterogeneous across the outcrop with mylonitic zones such as this sample adjacent to less strained tonalitic layers very similar to sample 1 with respect to mineralogy and the development of coronas associated with a mortar texture.

Sample 2 is a very fine grained, homogeneous to thin-layered, quartzofeldspathic gneiss with a granodioritic composition and a mylonitic texture (Fig. 83.4B). Quartz and alkali-feldspar, both perthitic and homogeneous, are predominant; plagioclase is an essential mineral, and less than five percent of the rock is made up of orthopyroxene and opaque minerals. Accessory biotite, blue-green amphibole, zircon and apatite are also present. Tiny augen (<.5 mm) of quartz, plagioclase and microperthite are scattered through a finer grained ground mass (.01-.05 mm) of quartz, two feldspars and discontinuous streaks of small grains of

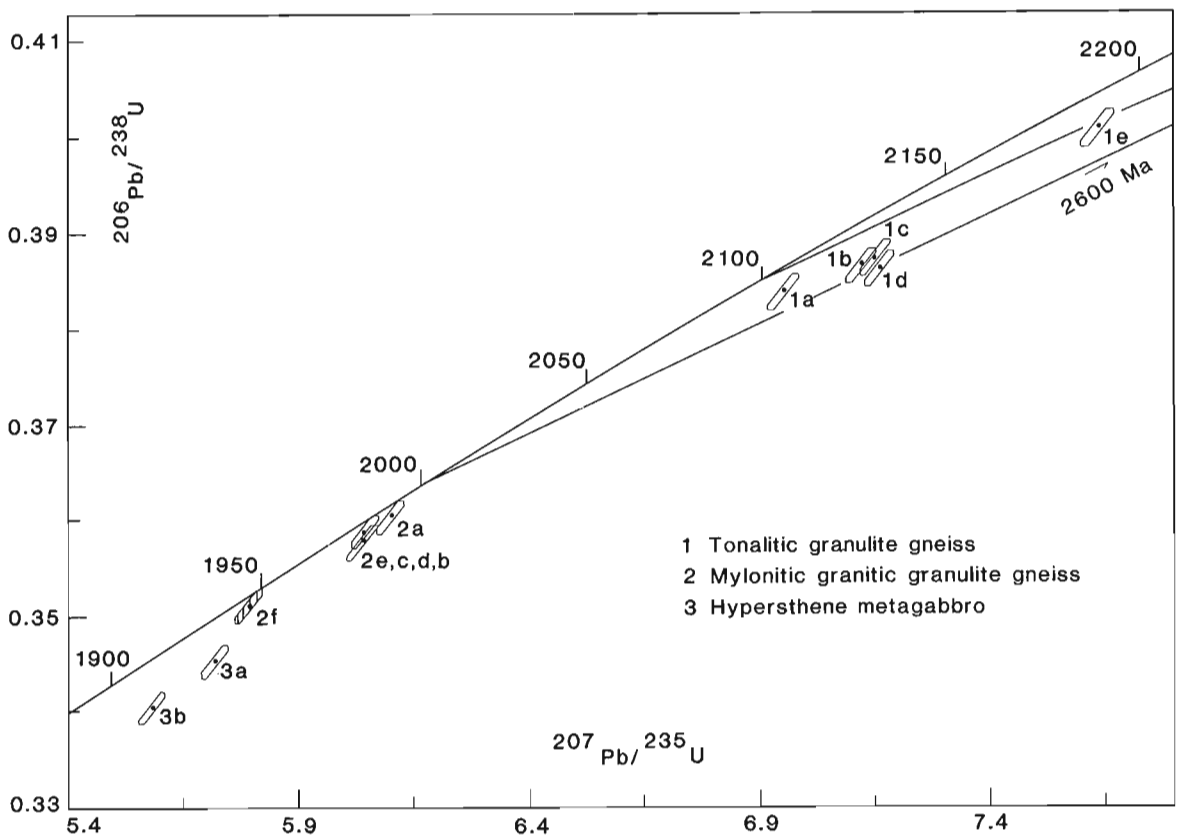


Figure 83.2. Isotope ratio plot for zircons (open error boxes) and monazite (patterned error box) from 1. tonalitic granulite gneiss, Moraine Lake, 2. mylonitic granitic granulite gneiss, Moraine Lake, and 3. hypersthene metagabbro. Numbers and letters with data points correspond to those on Table 83.1.

orthopyroxene and opaque phases that parallel the foliation. Although these streaks appear to be broken and dispersed parts of larger grains, the matrix surrounding these grains has completely recrystallized with widespread development of equilibrium grain boundary relations. Corona textures are not a feature of this rock. Most of the orthopyroxene grains are quite fresh with alteration and growth of biotite and/or blue-green amphibole limited to narrow zones at the grain boundaries. Biotite, though rare, occurs as clear sub-to-euhedral platelets. Locally it appears to be a pull-apart feature between two small orthopyroxene grains. Plagioclase is sodium-rich and concentrated in the finer grained portions of the sample. Several of the well-rounded zircons exhibit complex internal zoning and a tendency to develop asymmetrical outer rims that are elongated in the foliation.

The extreme grain size reduction that produced the well-foliated nature of the rock in thin section postdates the crystallization/recrystallization of a relatively coarse grained granulite facies orthopyroxene-quartz-K-feldspar-plagioclase-opaque assemblage. The high strain must have occurred at relatively high temperatures and/or very low water pressures in order for the orthopyroxene to be so well preserved. Grade was lower and water pressure higher at some time when the biotite and amphibole formed.

Zircons are mostly equidimensional but feature irregular faceting which differs from the typical metamorphic high order faceting which tends towards a spherical shape (van Breemen et al., 1986a; Plate 1D). Semi-planar surfaces have pronounced ridges, and broad valleys and dips, which often contain gangue, indicative of morphological control by surrounding minerals. The morphology is distinct from the faceted ovoid and bean shaped forms with smooth depressions characterizing zircons from granite magma emplaced in a shear zone (van Breemen et al., 1986; Fig 83.5) and from the highly irregular, smoothly embayed shapes of strongly resorbed zircons in granite deformed in a shear zone (van Breemen and Parrish, 1986).

Polished and etched sections show a threefold history (Fig. 83.5E,F,G). Internal cores have been variably affected by resorption (and possibly breakage Fig. 83.5G), with strongly resorbed cores showing irregular forms with smooth embayments (Fig. 83.5E,F). These cores have regular igneous internal zoning and euhedral to subhedral outlines, where not resorbed (Fig. 83.5G).

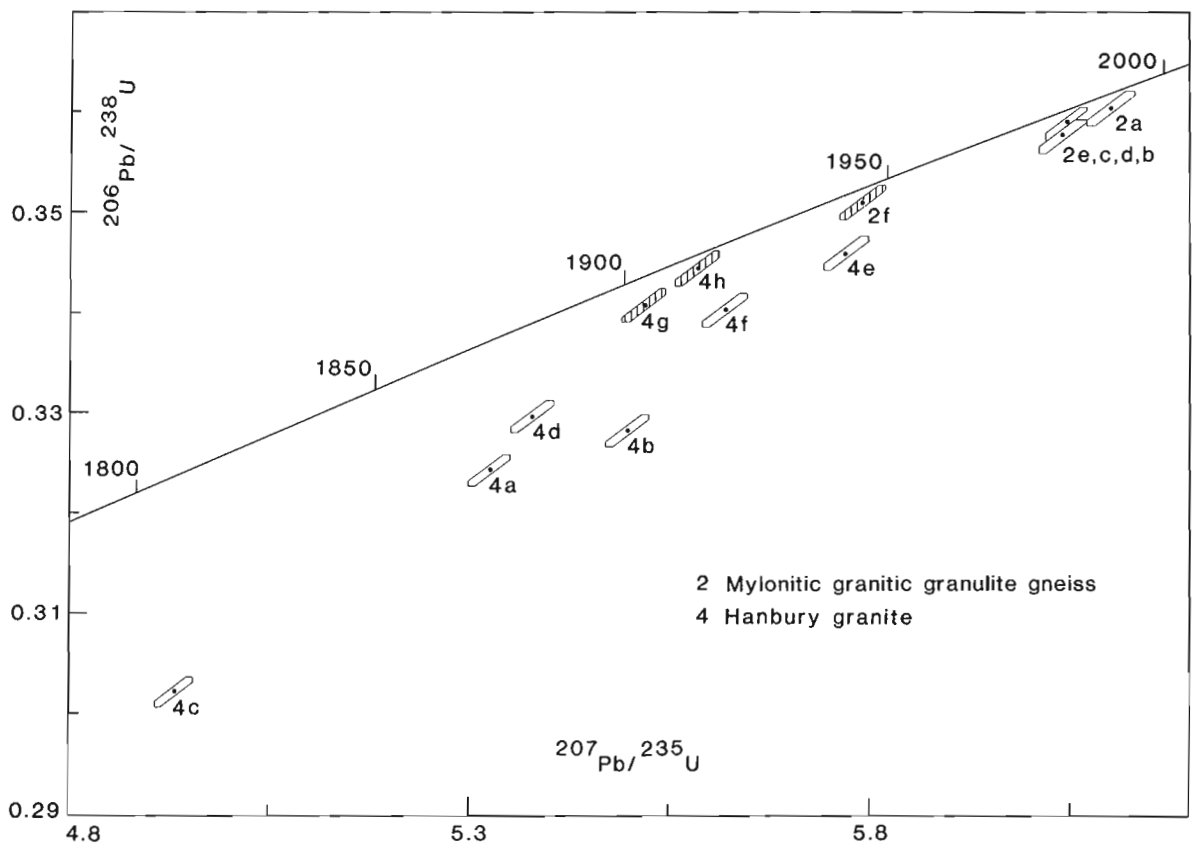
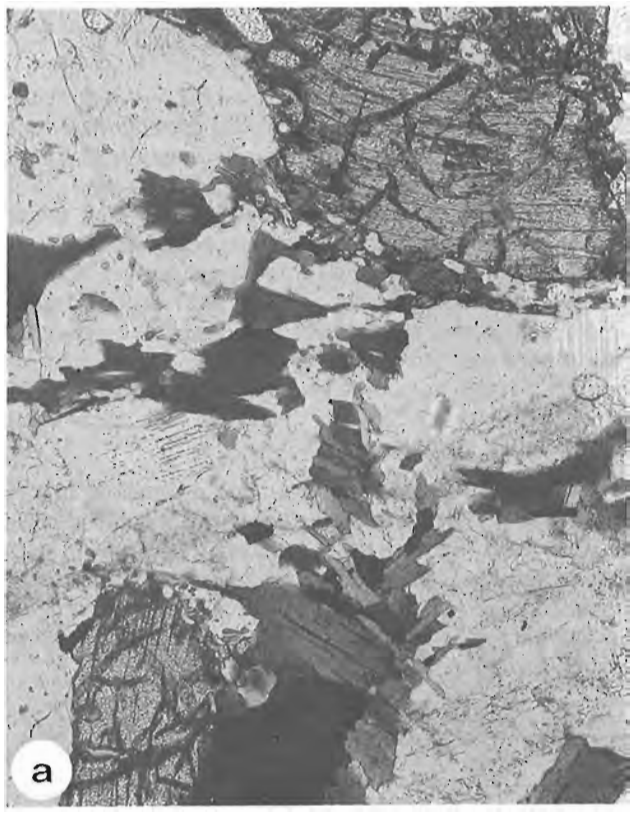


Figure 83.3. Isotope ratio plot for zircons (open error boxes) and monazites (patterned error boxes) from 2, mylonitic granitic granulite gneiss Moraine Lake and 4, the Hanbury Granite. Numbers and letters with datapoints correspond to those of Table 83.1.





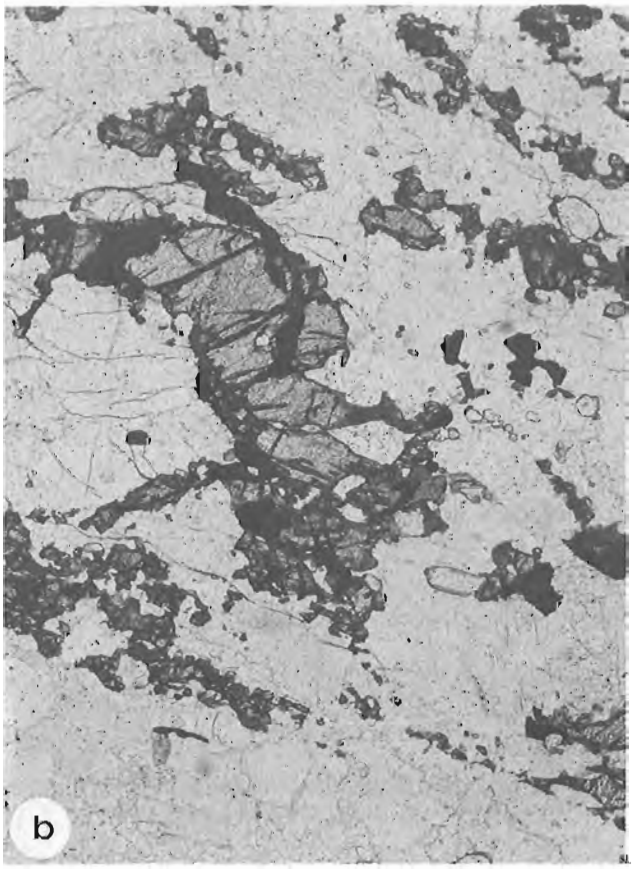


Figure 83.4. Photomicrographs of textural relationships seen in thin section using cross polarized transmitted light.
A. Bent orthopyroxene grain (0.75 mm) and relatively coarse plagioclase surrounded by fine grained mineral aggregates in tonalitic granulite gneiss (sample 1). Clinopyroxene, biotite and hornblende separate orthopyroxene from plagioclase.
B. Mylonitic texture from sample 2 bends around a grain of orthopyroxene (0.25 mm) that has broken into several subgrains. The pyroxene is partially rimmed by hornblende.
C. A rounded elongate zircon (0.045 mm) surrounded by plagioclase augen (0.45 mm) which in turn is rimmed by very fine grained quartz and feldspar (sample 2).

Inner mantles have been deeply excavated by the acid etch reflecting high U content. Weak etches bring out a discordant and irregular zoning which with stronger etching can be seen to continue into the outer mantle characterized by a lower U content. Yet the boundaries between the high U inner mantles and low U outer mantles are generally sharp with excavated molds showing an inner mantle morphology (Fig. 83.5E) similar to the outer mantle morphology.

Boundaries between inner mantles and cores are always sharp. There is clearly no transitional stage of zircon growth between cores and mantle, nor was there a separate metamorphic growth stage between these two events (Fig. 83.5G). It is not possible to determine whether core and mantle growth were separated by a distinct phase of chemical corrosion or if local reduction of the core occurred during the development of discordant relationships in the mantle (Fig. 83.5F).

The almost straight discordant zoning of the mantles of zircons from this mylonitic gneiss is similar to zoning in zircons from granites emplaced into shear zones (van Breemen and Hanmer, 1986). Even synneusis "twins" can be found. However, the textural evidence for a magmatic stage in the mantles as seen in the shear zone granite which contain, euhedral centres; transitions in the mantle where minor reversals between regular and irregular zoning occur, and, in some cases, euhedral zoning which can be traced into irregular zoning is absent from sample 2 zircons.

Given the mylonitic fabric of the rock it is possible that the mantles grew in a solid state mylonite from fluids channelled between rotating cores and surrounding grains, dissolving and redepositing zircon. The lack of retrogression of hypersthene indicates such fluids were not rich in H_2O and/or temperature was high enough that hypersthene was stable. A shear zone would be a natural conduit for migrating H_2O-CO_2 fluids capable of mobilizing zirconium and uranium in complex form (Skippen, personal communication, 1986). Variations in zircon/uranium concentration could reflect a transient flux depleting the granulite faces lower crust (Heier, 1973; Moorbath et al., 1969).

As explained above, however, there is no textural evidence that growth of hypersthene coincides with shearing, only that it was not retrograded during grain size reduction. Zircon is abundant with at least 20 grains visible in each thin section. Most grains are larger than the recrystallized groundmass. However a number of zircons featuring clearly distinguishable cores and mantles occur within larger feldspars (<.5 mm) which may be relicts of the coarser assemblage (Fig. 83.4C) coeval with hypersthene. Such textures do not provide conclusive evidence of paragenesis. However, all etched zircons show mantles with discordant zoning indicating metamorphic mantles are not younger than the high grade metamorphic assemblage.

Five zircon fractions were analyzed of which two consisted of unabraded equidimensional grains and one of abraded prismatic grains (Table 83.1). The data points are clustered near the concordia with a 1997 Ma $^{207}Pb/^{206}Pb$ age for the abraded fraction compared with an average 1992 Ma $^{207}Pb/^{206}Pb$ age for the unabraded fractions (Fig. 83.2). The degree of concordance or lack of recent Pb loss is remarkable in view of U concentrations ranging up to 885 ppm, which presumably reflect the inner metamict mantles. A U-Pb monazite analysis yields an almost concordant data point (Fig. 83.2) with a $^{207}Pb/^{206}Pb$ age of 1951±4 Ma.

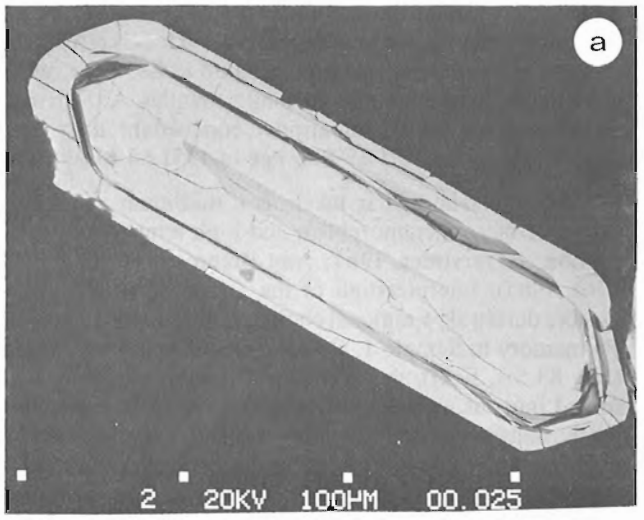
The monazite age is taken as a minimum age for the granulite faces metamorphism and high temperature deformation (Overstreet, 1967; van Breemen et al., 1982; Cliff, 1985). Interpretation of the zircon ages in terms of closure during slow regional cooling is not supported by older Pb memory in Sample 1. On the basis of inner morphology (Fig. 83.5E, F, G), the Pb^{207}/Pb^{206} zircon model ages are mixed igneous/metamorphic ages providing an upper limit for the metamorphism. The inner mantles cannot be part of an older metamorphic event because the average age is strongly weighted by their high U and Pb content. This case study provides evidence for a prograde Aphebian metamorphic event and shearing which may or may not have been intermittent.

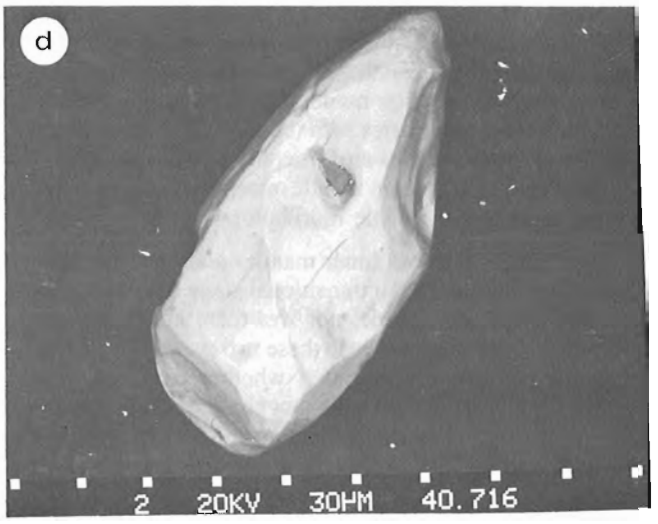
The age of the igneous cores has to be older than 2000 Ma. However, in view of the substantial proportion of cores seen in the more prismatic grains and almost 50 per cent reduction of U in abraded fraction 2a (compare with 1c and d) it is not considered probable that the cores are of Archean age.

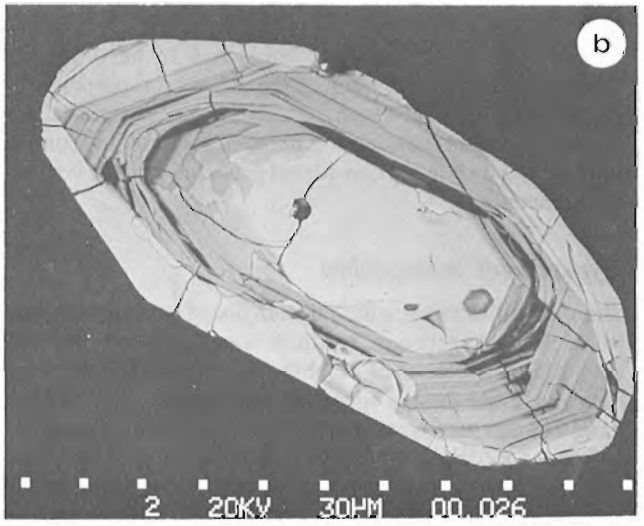
Hypersthene metagabbro

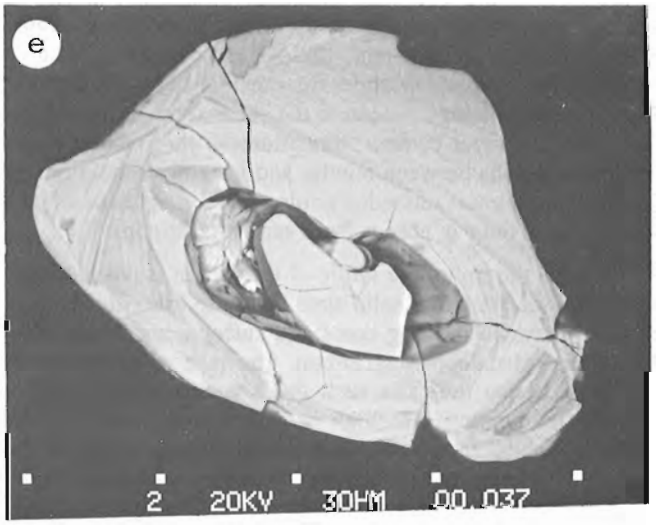
The metagabbro was collected from one of several dark green to black, homogeneous, medium coarse grained, well foliated, elongate blocks of amphibolite a few centimetres to a metre or more in size separated by strongly foliated white granitoid that locally veins the ends of the blocks. The amphibolite occurs in a well layered sequence of granulite grade gneisses ranging in composition from pink and grey granitoid gneisses commonly with coarse garnet to dark, mafic-rich gneisses of probable supracrustal origin. The metagabbro is interpreted as a mafic sill emplaced in the gneissic sequence at some time prior to granulite grade metamorphism.

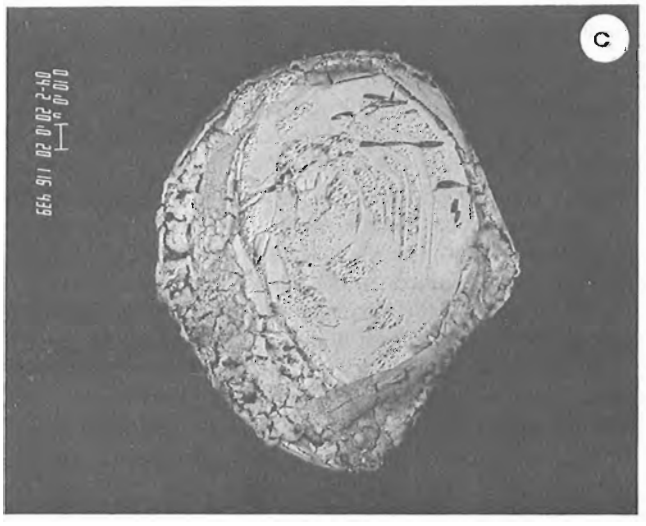
This fine grained, weakly foliated, black-weathering, mafic meta-igneous rock is made up of poikiloblasts (2-4 mm) of clinopyroxene and orthopyroxene and aggregates of plagioclase in a finer grained matrix of hornblende, two pyroxenes and plagioclase. Quartz, opaques, and apatite are accessory constituents. Laths, of unaltered biotite are scattered through one thin section but rare in a second. Twinning is prominent in the mainly unaltered plagioclase. Dusty "cores" and clear rims are typical of the grains in aggregates of plagioclase whose shape may be irregular or subhedral. Two types of colourless clinopyroxene and faintly pleochroic orthopyroxene are present. Relatively coarse grained subhedral clinopyroxene grains full of inclusions of biotite, hornblende, and opaque minerals contrast with the anhedral inclusion-free grains in the matrix. Clinopyroxene in some cases appears to have engulfed orthopyroxene. Green-brown to yellow-green hornblende is overgrown by both pyroxenes and is present in the matrix or even grained

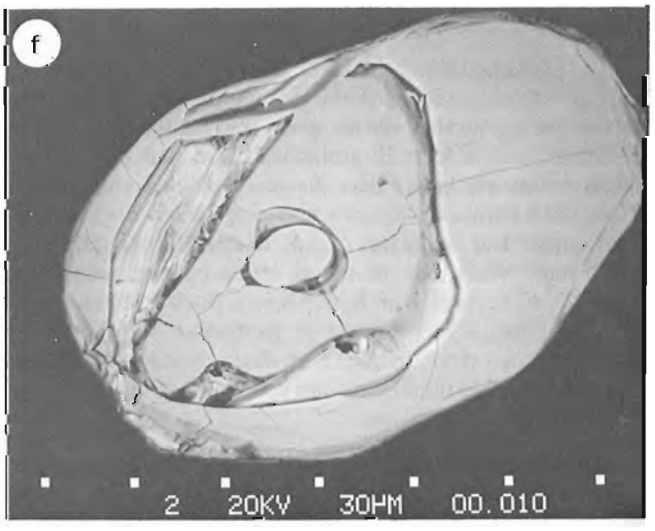

a
2 20KV 100PM 00.025

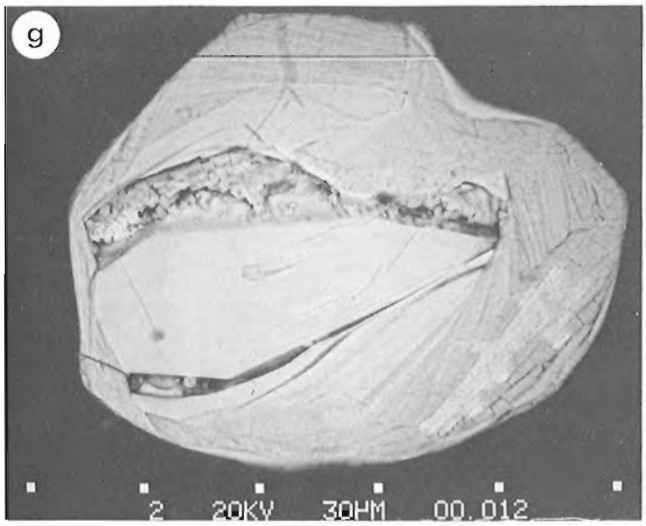

d
2 20KV 30PM 40.716

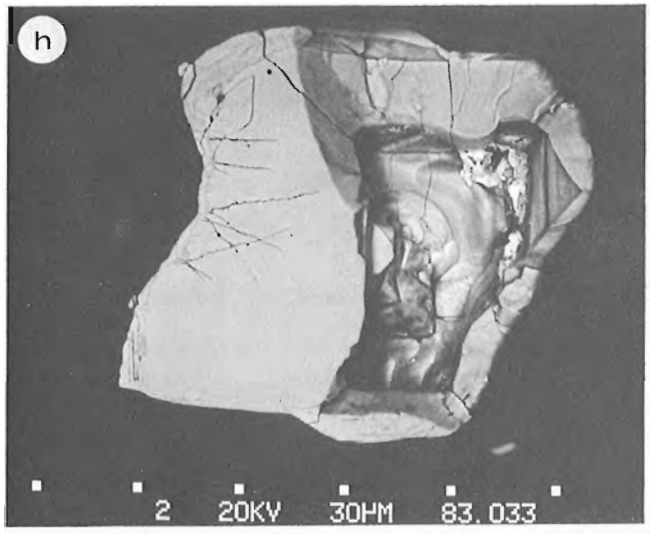

b
2 20KV 30PM 00.026


e
2 20KV 30PM 00.037


c


f
2 20KV 30PM 00.010





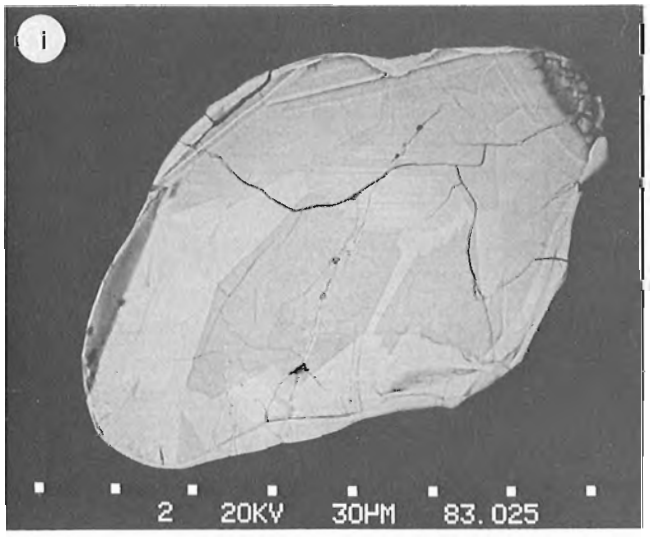


Figure 83.5. Scanning election microscope images of a zircon grain and polished and etched (HF) sections. All images are taken in the backscattered electron mode.

A. Zircon section from the tonalitic granulite gneiss (sample 1) shows a euhedral igneous core of which one pyramid has been rounded by resorption. A thin dark, high U inner mantle, where metamict zircon has been leached out by the etching HF acid, shows some discordant and some igneous zoning even where it follows a rounded termination. An outer mantle of low U zircon reflects the inner morphology, but also has multiple facets, partly obscured by contact with teflon of the mounting disc.

B. A narrow zone of partly discordant high U zircon surrounds an inner prismatic core. A broad mantle of more regular igneous zoning continues to near the edge where it is followed by a thin rim of multifaceted low U zircon (sample 1).

C. Section of a metamorphic zircon from a granulite in the Grenville Province of Ontario (van Breemen et al., 1986, sample 8, Algonquin domain). This multi-faceted, equidimensional grain has a mantle of strongly etched zircon (high in U, more metamict) containing a lower U centre in which concentric multi- faceted zoning is interpreted to reflect growth during metamorphism. The image provides a comparison with internal zoning in zircons from granulite facies rocks from the Thelon Tectonic Zone.

D. An irregular grain from the mylonitic granulite gneiss (sample 2) features multiple facets, narrow ridges, broad valleys and dips of which one contains gangue.

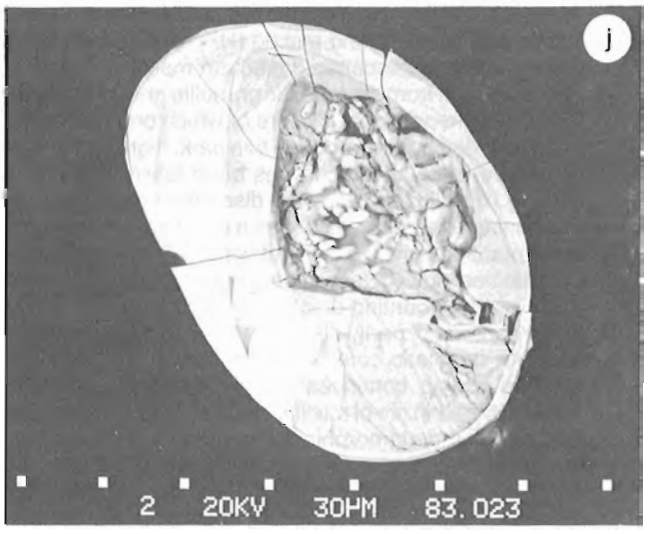
E. Section of an irregular grain features a strongly resorbed, scallop shaped core. An inner mantle of strongly leached high U zircon shows irregular mold of multi-faceted zircon with embayment, similar to outer perimeters. Outer mantle shows dramatic planar discordance which has been interpreted in terms of interference with rotating major minerals during mylonitization (sample 2).

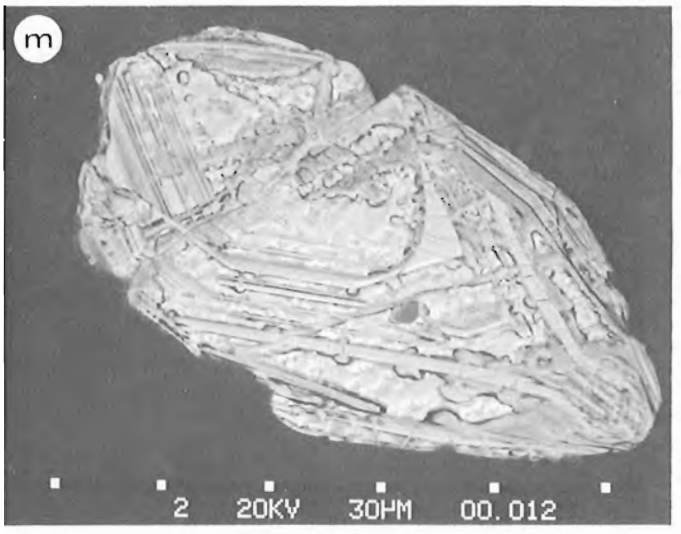
F. A more weakly etched section shows discordances in the inner high U mantle. Note rounding and embayment of core and how some of the discordance of the inner mantle is linked to resorption of the core (sample 2).

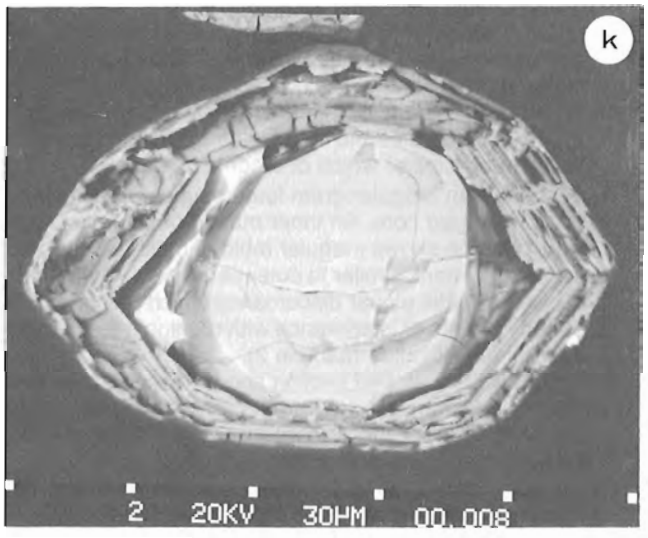
G. Euhedral zoning of a prismatic igneous core has been sharply terminated by two straight edges (breakage?). The sharply faceted euhedral outline of the core show that 1) there was no transitional growth stage between core and mantle 2) there was no metamorphic zircon growth prior to growth of the inner mantle and 3) core dissolution was localized (sample 2).

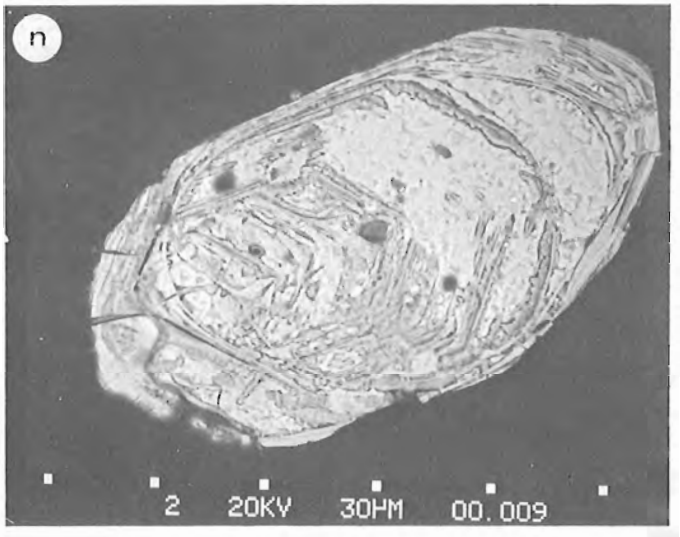
H. Zircon from hypersthene meta-gabbro (sample 3) shows high U core and low U mantle. There must have been a dramatic contrast between state of metamictization of rim and core as the former is barely etched while the latter has been completely excavated. The irregular prismatic core devoid of recognizable prisms is characteristic of late zircon crystallization in basic igneous rocks (Poldervaart, 1956).

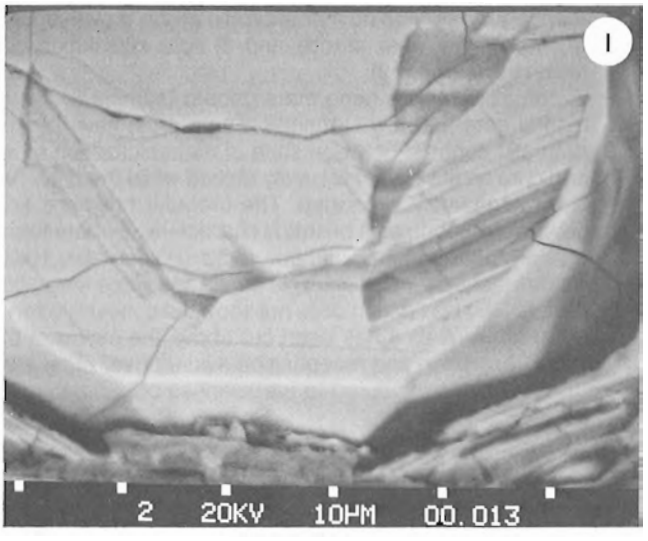
I. Mantles feature random multiple facets and some resorption (sample 3). This section does not show the concentric zonation of figure A as it has been cut above the centre of the grain. Resorption and redeposition evident near outer margin may have contributed to irregularities of perimeter.

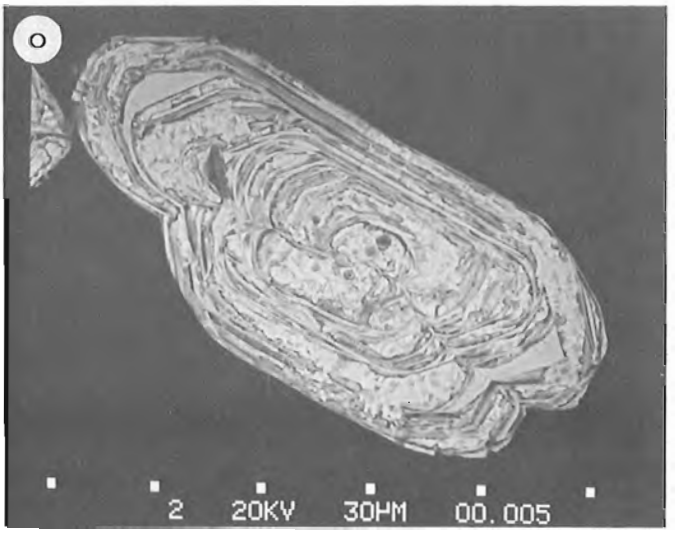

j
2 20KV 30HM 83.023


m
2 20KV 30HM 00.012


k
2 20KV 30HM 00.008


n
2 20KV 30HM 00.009


l
2 20KV 10HM 00.013


o
2 20KV 30HM 00.005

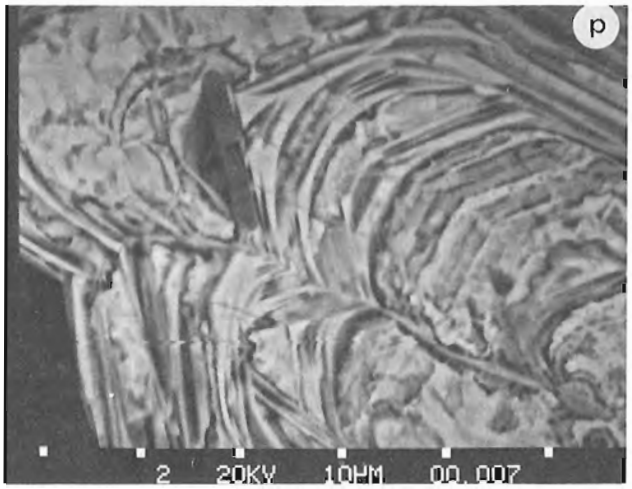


Figure 83.5. (continued)

J. An ovoid grain features excavated core and weak mantle zoning which nearest centre shows pronounced resorption. The image also shows how slight resorption of outer facets can enhance the effect of rounding.

K. Zircons from the Hanbury granite (sample 4) contain abundant cores which are distinct in having regular igneous zoning and lower U concentration. An almost round core is surrounded by a thin but continuous rim of low U zircon with high order facets. This rim is surrounded by high U zircon which is largely excavated but retains one ridge which conforms to the mostly regularly zoned igneous outer zircon.

L. A close-up of the margin of the core shows a smoothly curved perimeter strongly discordant to inner zoning and a straight perimeter parallel to some of the zoning. Numerous well preserved facets of the thin low U rim stand in strong contrast to simple igneous zoning of mantle and core (sample 4 same grain as K).

M. Many zircons from the Hanbury granite show discordances and other igneous zonal irregularities testifying to growth interference by other crystals. Of particular interest is the rounded feature near the centre which developed synchronous with continuous zoning in another part of the same crystal (sample 4).

N. Rounded features interrupting igneous zoning are typified here and are indeed a regular occurrence in zircons from this granite. Where this rounding interrupts zonal faceting of a pyramid it tends to be well developed. Even where the discordance is transverse to the prismatic zoning, embayment is limited. In this case continued growth and mild resorption generates a convex curve which is followed by simple pyramidal zoning with the opposite sense to that of the centre (sample 4).

O. A twin which probably started by synneusis (docking) of two small nuclei shows repeated but independant rounding of pyramids (sample 4).

P. A close-up of twinned pyramids shows repeated mild rounding of low order facets which clearly cannot have been caused by impingement with surrounding crystals as these would have disturbed zoning of the adjacent pyramid.

aggregates surrounding these minerals. Locally, colourless amphibole (cummingtonite?) has replaced both pyroxenes in patches or narrow zones.

The metamorphic history of this rock can be divided into three stages. Growth of the relatively coarse clinopyroxene and orthopyroxene poikiloblasts in rock composed of hornblende, biotite and plagioclase (hornblende gabbro?) was followed by crystallization of the two pyroxene aggregate in the matrix around the poikiloblast and, locally, alteration of both coarse and fine-grained pyroxenes to colourless amphibole and opaque phases. The presence of metamorphic orthopyroxene in the country rock indicates that at least one of the stages of pyroxene growth occurred during a regional granulite facies event. The late hydration suggests greenschist facies.

Zircons from this metamorphic basic igneous rock were sparse and only two fractions were analyzed. The two fractions yield U concentrations in the order of 200 ppm and $^{207}Pb/^{206}Pb$ model ages of 1958 Ma and 1940 Ma (Table 83.1; Fig. 83.2). The moderate discordance can be explained in terms of both inheritance and recent Pb loss.

A twofold zircon crystallization history is clearly indicated in polished and etched sections in that most of the etched grains consist of ovoid to irregular mantles surrounding prismatic to irregular molds of presumably metamict zircon which has been leached out as a result of high U content (Fig. 83.5H). The shape of the core is similiar to the irregular prisms of zircon with poorly developed pyramids in basic magma (Poldervaart, 1956).

Zircon mantles are randomly multi-faceted (Fig. 83.5I) and are interpreted to have grown during metamorphism. Evidence for resorption and redeposition in embayment near the outer rim (Fig. 83.5I) or the internal zoning (Fig. 83.5J) also suggests the action of fluids. There is, however, little resemblance to the strikingly angular discordance of zircons from sample 2.

The isotopic evidence provide further support for a granulite facies metamorphic event which is younger than 2000 Ma. If the cores are igneous, the significant proportion of core to rim material and the much higher U content of the cores suggests that this basic intrusion was not emplaced in the Archean.

Hanbury granite (sample 4)

The Hanbury granite is a strongly deformed pink to grey weathering even grained to locally inequigranular, typically biotite-poor granodiorite. It is emplaced in migmatitic biotite-rich metasediments, inclusions of which are commonly present throughout much of the body. Contact relations with the country rock are diffuse. Thin veins to narrow sills of similar pink foliated granite are commonly associated with similar migmatitic metasediments to the south. The pink

K-feldspar bearing granodiorite is considered a distinct phase unrelated to the white, quartz-plagioclase leucosome of the metasedimentary migmatites they intrude.

Sample 4 is a pinkish-grey weathering, fine grained, moderately foliated, biotite granodiorite. Plagioclase and microperthitic microcline grains range from 0.25 to 2 mm but most grains are less than 1 mm. Polycrystalline quartz lenticles 4-5 mm long define the foliation along with biotite and seams of relatively fine grained quartz and two feldspars. Locally chloritized biotite is pleochroic ranging to an unusually dark brown. Colour index of the rock is 10 to 15. Secondary white mica occurs with epidote as a very fine grained alteration of plagioclase and, less commonly, as coarser irregular patches. Plagioclase is often myrmekitic where it is in contact with K-feldspar. The foliated granoblastic texture with evidence of recrystallization of plagioclase and stability of biotite suggests medium grades of metamorphism accompanied the deformation. The variable intensity of grain size reduction, predominance of irregular grain boundaries and later alteration of plagioclase and biotite have resulted in a texture suggestive of disequilibrium and of deformation that either continued while conditions changed to those of the greenschist facies or that occurred during a later greenschist facies event.

Uranium concentrations in zircons from the Hanbury granite were extremely high, (660-1750 ppm; Table 83.1). The zircons are brownish-translucent in transmitted light but frequently contain clear cores. Strong abrasion of one fraction (4e) reduced U concentrations to 215 ppm, increased the concordance, and increased the $^{207}Pb/^{206}Pb$ age to 1970 Ma. In view of the combined effects of recent lead loss and xenocrystic Pb inheritance it is not possible to accurately determine the age of emplacement from the zircon isotope data alone. However, two monazite analyses yield slightly discordant data points with $^{207}Pb/^{206}Pb$ ages of 1920 and 1918 Ma. As these ages are consistent with the distribution of U/Pb data points (Fig. 83.3), they are taken to be the time of syntectonic granite crystallization.

Polished and etched sections reveal a great variety of zircon morphology. Numerous cores have generally lower U concentrations and regular igneous zoning which is distinct from the igneous zoning in the overgrowths. Some of the cores show evidence of a complex previous history, followed by rounding which could be attributed to processes of sedimentary abrasion (Poldervaart, 1955) or slight igneous resorption. Textural features that support sedimentary rounding include the following: a) cores show a distinctive style of zoning that is truncated by the rounded perimeter; b) rounding is only interrupted along some straight zoning; c) absence of embayments; d) the immediately adjacent thin, faceted rim is continuous (Fig. 83.5K, L). These thin high order rims of low U zircon (Fig. 83.5K,L) which if not simply conforming to the shape of the core could be interpreted as due to metamorphic growth. These rims are followed by high U igneous zircon (Fig. 83.5K).

The main igneous population shows some irregular zoning with discordances (Fig. 83.5M) and ovoid patterns (Fig. 83.5N,O,P). By comparison with zircons from a granite in a shear zone (van Breemen and Hanmer, 1986) irregularities and discordances may be caused by impingement with major minerals during zircon growth. Discordances and rounding are interpreted to be of igneous origin as these coincide and alternate with more euhedral zoning (Fig. 83.5M,N). The rounding has not resulted from impingement with other grains as can be seen from adjoining areas of rounded twins (Fig. 83.5O, P). Rather it would seem that zircon growth may have been interrupted by local changes in magma composition.

Fig. 83.5N shows well developed rounding at one end of a prism and a shallow embayment where euhedral zoning has been cut off (broken?). This embayment has been overgrown by new zircon in the form of a pyramid that was subsequently corroded to a rounded form producing at one stage an entirely oval shape. Perhaps corrosion in a viscous granite magma is less condusive to the development of embayments than corrosion by solutions.

There can be no doubt that the abundant cores with, distinct zoning, lower U content, and older isotopic signature, reveal a significant crustal component in the Hanbury granite. Together with tentative evidence for a stage of metamorphic zircon growth, for repeatedly changing conditions of zircon growth and corrosion and for some dynamic interference with major minerals the zircons indicate melting and/or assimilation in a syntectonic environment which is consistent with the foliation and tectonic setting of this granite.

DISCUSSION

The geological context of the samples used for this study involves a complex as yet poorly understood combination of igneous, metamorphic and deformation events. Henderson et al. (1982) and Henderson and Thompson (1982) indicated that Archean rocks were continuous across the western boundary of the Thelon Tectonic Zone in the Healey Lake map area and correlated the granulite facies metamorphism with the Archean migmatite-forming event west of the zone. They proposed that the corona-forming event and high strain in the straight zone were Proterozoic and related to the event which produced the Proterozoic metamorphic overprint in the Slave Province. In view of the limited quantity of U-Pb zircon data presented here and the tentative value of some of the interpretation the presence of Archean rocks reactivated in the Thelon Tectonic Zone during the Proterozoic cannot be ruled out. On the other hand, the only data pointing to a major older component (sample 1) indicate precursor ages (average?) in the range 2200-2400 Ma. The new isotope data document major metamorphic deformational and magmatic events in the Thelon Tectonic Zone between 2000 and 1900 Ma which juxtaposed granulite facies gneisses against polymetamorphosed Yellowknife Supergroup that did not surpass lower amphibolite facies grade in the Proterozoic. If all the granulite facies rocks lack an Archean component and represent newly formed Proterozoic crust the orthopyroxene zone boundary marks a major tectonic break that could correspond to the suture proposed by Gibb and Thomas (1977).

In the mylonitic granulitic gneiss, inner high U zircon mantles and outer lower U mantles, have been bracketed between 1990 and 1950 Ma. There is a striking resemblance between the numerous angular discordances in these mylonitic zircons and zircons from granites emplaced into shear zones (van Breemen et al., 1986). The absence of metamorphic growth around internal igneous cores provides evidence against earlier granulite facies metamorphism. The exciting possibility that zircons in mylonites may record the fluxing of fluids of changing composition during prograde upper amphibolite and granulite facies metamorphism should be pursued with work on trace elements and inclusions in zircons.

Zircons from the 1920±4 Ma foliated Hanbury granite possess the greatest textural variation. Cores can be unambiguously identified by isotope signature and distinct zoning. Zircon zoning formed during the melt phase of the Hanbury granite shows some discordance which may be attributed to interference with surrounding crystals but also to chemical corrosion independent of grain impingement (Fig. 83.5P). This corrosion has been attributed to changing composition of magma which caused only minor embayment. When corrosion is mild but recurrent, remarkably concentric oval zoning with cryptic discordances develops (Fig. 83.5O,P). In light of this evidence one could predict that if variably corrosive magma were channelled past zircons rolling in a crystal mush there would be a greater tendency for the development of discordances (cf. van Breemen and Hanmer, 1986).

In spite of the evidence for rounding by magmatic corrosion, rounded equidimensional cores with striking discordance of internal zoning but thin continuous, faceted overgrowth have been interpreted in terms of a sedimentary provenance. The cores combined with textural evidence for changing magmatic properties and impingement of growing zircons with other crystals may help to characterize syntectonic granites.

ACKNOWLEDGMENTS

Scanning electron photomicrographs were taken by D.A. Walker and S.V.T. Thompson. Authors thank colleagues in the Lithosphere and Precambrian Shield Division for critically reading the manuscript. Detailed comments by J.A. Percival were particularly helpful.

REFERENCES

Barr, S.M., Raeside, R.P., and van Breemen, O.
— Grenvillian basement in the northern Cape Breton Highlands, Nova Scotia; Canadian Journal of Earth Sciences (in press).

Caruba, R., Baumer, A. and Turco, G.
1975: Nouvelles synthèses hydrothermal du zircon: substitutions isomorphiques; relation morphology milieu de croissance; Geochimica et Cosmochimica Acta, v. 39, p. 11-26.

Chandler, F.W.
1984: Sedimentary setting of an Early Proterozoic copper occurrence in the Cobalt Group, Ontario: a preliminary assessment; in Current Research, Part A, Geological Survey of Canada, Paper 84-1A, p. 185-192.

Cliff, R.A.
1985: Isotope dating in metamorphic belts; Journal of the Geological Society of London, v. 142, p. 97-110.

Compston, W., Williams, I.S., Campbell, I.H., and Gresham, J.J.
1986: Zircon xenocrysts from the Kambalda volcanics: age constraints and direct evidence for older continental crust below the Kambalda-Norseman greenstones; Earth and Planetary Science Letters, v. 76, p. 299-311.

Dodson, M.H.
1973: Closure temperature in cooling geochronological and petrological systems; Contribution to Mineralogy and Petrology, v. 40, p. 259-274.

Fraser, J.A.
1964: Geological notes on northeastern District of Mackenzie, N.W.T.; Geological Survey of Canada, Paper 63-40 (Map 45-1963).

Frith, R.A.
1982: Second preliminary report on the geology of the Beechey Lake-Duggan Lake map areas, District of Mackenzie, N.W.T.; in Current Research, Part A, Geological Survey of Canada, Paper 82-1A, p. 203-211.

Fujimaki, H., Tatsumoto, M., and Aoki, K.
1984: Partition coefficients of Hf, Zr and REE between phenocrysts and groundmasses; Proceedings of the Fourteenth Lunar and Planetary Science Conference, Part 2, Journal of Geophysical Research, v. 89, p. B662-B672.

Gastil, R.G., De Lisle, M., and Morgan,
1967: Some effects of progressive metamorphism on zircons; Geological Society of America Bulletin, v. 78, p. 879-906.

Gebauer, D. and Grunefelder, M.
1976: U-Pb zircon and Rb-Sr whole rock dating of low grade metasediments: Montagne Noire; Contributions to Mineralogy and Petrology, v. 59, p. 13-32.
1979: U-Pb zircon and Rb-Sr mineral dating of eclogites and their country rocks, Munchberg gneiss massif, NE Bavaria; Earth and Planetary Science Letters, v. 42, p. 35-44.

Gibb, R.A.
1978: Slave-Churchill collison tectonics; Nature, v. 271, p. 50-52.

Gibb, R.A. and Thomas, M.D.
1977: The Thelon Front: a cryptic suture in the Canadian Shield?; Tectonophysics, v. 38, p. 211-222.

Heaman, L., Machado, N., and Krogh, T.
1986: Preliminary U-Pb zircon results from the Pikwitonei granulite terrain, Manitoba, (abstract), GAC, MAC, CGU. Program with abstracts, v. 11, p. 79.

Heier, K.S.
1973: Geochemistry of granulite facies rocks and problems of their origin; Philosophical Transactions of the Royal Society of London. A, v. 273, p. 429-442.

Henderson, J.B. and Macfie, R.I.
1985: The northern Artillery Lake map area District of Mackenzie: a transect across the Thelon Front; in Current Research, Part A, Geological Survey of Canada, Paper 85-1A, p. 441-448.
1986: Artillery Lake map area, District of Mackenzie; a transect across the Thelon Front; in Current Research, Part A, Geological Survey of Canada, Paper 86-1A, p. 411-416.

Henderson, J.B. and Thompson, P.H.
1980: The Healey Lake map area (Northern part) and the enigmatic Thelon Front, District of Mackenzie; in Current Research Part A, Geological Survey of Canada, Paper 80-1A, p. 165-169.
1981: The Healey Lake map area and the Thelon Front problem, District of Mackenzie; in Current Research, Part A, Geological Survey of Canada, Paper 81-1A, p. 175-180.
1982: Geology of Healey Lake map area (1:125,000 scale map and marginal notes): Geological Survey of Canada Open File 860.

Henderson, J.B., Thompson, P.H., and James, D.T.
1982: The Healey Lake map area and the Thelon Front problem, District of Mackenzie; in Current Research, Part A, Geological Survey of Canada, Paper 82-1A, p. 191-195.

Hoppe, G.
1966: Zirkone aus Granuliten; Ber. deutch Ges. geol. Wiss. B Mineral. Lagerstattenforsch, v. 11, p. 47-81.

James, D.T.
1985: Geology of the Moraine Lake area and the Thelon Front, District of Mackenzie; in Current Research, Part A, Geological Survey of Canada, Paper 85-1A, p. 449-454.
1986: The geology of the Moraine Lake area, District of Mackenzie, part 2; a transect across part of the Thelon Tectonic Zone; in Current Research, Part A, Geological Survey of Canada, Paper 86-1A, p. 417-421.

Kreulen, R.
1980: Co_2-rich fluids during regional metamorphism on Naxos (Greece): carbon isotopes and luid inclusions; American Journal of Science, v. 280, p. 745-771.

Krogh, T.E.
1982: Improved accuracy of U-Pb zircon ages by the creation of more concordant systems using air abrasion technique; Geochimica et Cosmichimica Acta, v. 46, p. 637-649.

Krogh, T.E. and Davis, G.L.
1973: The effect of regional metamorphism on U-Pb systems in zircon and a comparison with Rb-Sr systems in the same whole rock and its constituent minerals; Carnegie Institute of Washington, Yearbook 72, p. 601-610.

Marshall, B.
1967: The present status of zircon; Sedimentology, v. 9, p. 119-136.

Mattinson, J.M.
1978: Age, origin, and thermal histories of some plutonic rocks from the Salinian block of California; Contributions to Mineralogy and Petrology, v. 67, p. 233-245.

Moorbath, S., Welke, H., and Gale, N.H.
1969: The significance of lead isotope studies in ancient, high grade metamorphic basement complexes, as exemplified by the Lewisian rocks of northwest Scotland; Earth and Planetary Science letter, v. 6, p. 245-256.

Overstreet, W.C.
1967: The geologic occurrence of monazite; U.S. Geological Survey Professional Paper 530, 294 p.

Percival, J.A. and Krogh, T.E.
1983: U-Pb zircon geochronology of the Kapuskasing structural zone and vicinity in the Chapleau-Foleyet area, Ontario; Canadian Journal of Earth Sciences, v. 20, p. 830-843.

Peucat, J.J., Vidal, P.W., Godard, G., and Postaire, B.
1982: Precambrian U-Pb zircon ages in ecologite and garnet pyroxenite from south Brittany (France): an old oceanic crust in the Western European Hercynian belt; Earth and Planetary Science Letters, v. 60, p. 70-78.

Peucat, J.J., Tisserant, D., Caby, R., and Clauer, N.
1985: Resistance of zircons to U-Pb resetting in a prograde metamorphic sequence of Caledonian age in East Greenland; Canadian Journal of Earth Sciences, v. 22, p. 330-338.

Pidgeon, R.T. and Aftalion, M.
1972: The geochronological significance of discordant U-Pb ages of oval-shaped zircons from a Lewisian gneiss from Harris, Outer Hebrides; Earth and Planetary Science Letters, v. 17, p. 269-274.
1978: Cogenetic and inherited zircon U-Pb systems in granites: Palaeozoic granites of Scotland, in Crustal Evolution in Northwestern Britain and adjacent regions, Geological Journal Special Paper 10, p. 183-220.

Pidgeon, R.T. and Bowes, D.R.
1972: Zircon U-Pb ages of granulites from the central region of the Lewisian, northwestern Scotland; Geological Magazine, v. 109, p. 247-258.

Pidgeon, R.T., O'Neill, R.J., and Silver, L.T.
1973: Observations on the crystallinity and the U-Pb system of a metamict Ceylon zircon under experimental hydrothermal conditions; Fort Schr. Mineral., v. 50, p. 118.

Poldervaart, A.
1955: Zircons in rocks.1. Sedimentary rocks; American Journal of Science, v. 253, p. 433-461.
1956: Zircons in rocks. 2. Igneous rocks; American Journal of Science, v. 254, p. 521-554.

Pupin, J.P.
1980: Zircon and Granite Petrology; Contributions to Mineralogy and Petrology, v. 73, p. 207-220.

Pupin, J.P. and Turco, G.
1972a: Une typologie originale du zircon accessoire; Bull. Soc. Fr. Mineral. Crystallogr., v. 95, p. 348-359.
1972b: Application des données morphologiques due zircon accessoire en pétrologie endogène; C.R. Acad Si. Paris, v. 275(D), p. 799-802.

Saxena, S.K.
1966: Evolution of zircons in sedimentary and metamorphic rocks; Sedimentology, v. 6; p. 493-502.

Silver, L.T.
1969: A geochronological investigation of the anorthosite complex, Adirondack Mountains, New York; in Origin of Anorthosite and Related Rocks, ed. Y.W. Isachsen; New York State Museum and Science Service, Memoir 18, p. 233-251.

Skippen, G.B. and Tromsdorff, V.
1986: Hydrothermal systems in high-grade metasomatic rocks; (abstract) GAC, MAC, CGU, Program with Abstracts, v. 11, p. 128.

Spotts, J.H.
1962: Zircon and other accessory minerals in the Coast Range Batholith, California; Geological Society of America Bulletin, v. 73, p. 1221-1240.

Thompson, P.H. and Ashton, K.
1984: Preliminary report on the geology of the Tinney Hills-Overby Lake (west half) map area, District of Mackenzie: a look at the Thelon Tectonic Zone northeast of the Bathurst Fault; in Current Research, Part A, Geological Survey of Canada, Paper 84-1A, p. 415-423.

Thompson, P.H. and Henderson, J.B.
1983: Polymetamorphism in the Healey Lake map area implications for the Thelon Tectonic Zone; in Current Activities Forum 1983, Program with Abstracts, p. 2-3 (abstract).

Thompson, P.H., Culshaw, N., Thompson, D., and Buchanan, R.
1985: Geology across the western boundary of the Thelon Tectonic Zone in the Tinney Hills-Overby Lake area (west half), District of Mackenzie; in Current Research, Part A, Geological Survey of Canada, Paper 85-1A, p. 555-602.

Thompson, P.H., Culshaw, N., Buchanan, J.R., and Manojlovic, P.
1986: Geology of the Slave Province and Thelon Tectonic Zone in the Tinney Hills-Overby Lake (west half) map area, District of Mackenzie; in Current Research, Part A, Geological Survey of Canada, Paper 86-1A, p. 275-289.

Valley, J.W. and O'Neil, J.R.
1984: Fluid heterogeneity during granulite facies metamorphism in the Adrondacks: Stable isotope evidence; Contributions to Mineralogy and Petrology, v. 85, p. 158-173.

van Breemen, O., Aftalion, M., Bowes, D.R., Dudek, A., Misar, Z., Povondra, P., and Vrana, S.
1982: Geochronological studies of the Bohemian massif, Czechoslovakia, and their significance in the evolution of Central Europe; Transactions of the Royal Society of Edinburgh, Earth Science, v. 73, p. 89-108.

van Breemen, O. and Hanmer, S.
1986: Zircon morphology and U-Pb geochronology in active shear zones: studies on syntectonic intrusions along the northwest boundary of the Central Metasedimentary Belt, Grenville Province, Ontario; in Current Research, Part B, Geological Survey of Canada, Paper 86-1B, p. 775-784.

van Breemen, O. and Parrish, R.R.
1986: Zircons record ancient geological processes; GEOS, v. 15, p. 18-21.

van Breemen, O., Davidson, A., Loveridge, W.D., and Sullivan, R.W.
1986a: U-Pb zircon geochronology of Grenville tectonites, granulites and igneous precursors, Parry Sound, Ontario; in New Perspectives on the Grenville Problem, ed. J.M. Moore, A. Davidson and A.J. Baer; Geological Association of Canada, Special Paper.

van Breemen, O., Henderson, J.B., Loveridge, W.D., and Thompson, P.H.
1986b: Archean-Aphebian geochronology along the Thelon Tectonic Zone Healey Lake area, NWT (abstract), GAC, MAC, CGU, Program with Abstracts, v. 11, p. 139.

Watson, E.B. and Harrison, T.M.
1983: Zircon saturation revisited: temperature and composition effects in a variety of crustal magma types; Earth and Planetary Science Letters, v. 64, p. 295-304.

Wright, G.M.
1957: Geological notes on the eastern District of Mackenzie, Northwest Territories; Geological Survey of Canada, Paper 56-10.
1967: Geology of the southeastern barren grounds, parts of the Districts of Mackenzie and Keewatin (Operations Keewatin, Baker, Thelon); Geological Survey of Canada, Memoir 350.

An integrated geological, gravity and magnetic study of the Artillery Lake area and the Thelon Tectonic Zone, District of Mackenzie

Project 840005

J.B. Henderson, P.H. McGrath, D.T. James[1] and R.I. Macfie[2]
Lithosphere and Canadian Shield Division

Henderson, J.B., McGrath, P.H., James, D.T., and Macfie, R.I., An integrated geological, gravity and magnetic study of the Artillery Lake area and the Thelon Tectonic Zone, District of Mackenzie in Current Research, Part A, Geological Survey of Canada, Paper 87-1A, p. 803-814, 1987.

Abstract

The geology of the area on the boundary between the Slave and Churchill provinces changes from the curvilinear structural style and low to intermediate Archean metamorphic grade of the Slave to the linear structural pattern of the Thelon Tectonic Zone of the northwestern Churchill with its abundant mylonitic zones and very high metamorphic grade imposed during the early Proterozoic. A sample of the central Thelon Tectonic Zone translated 70 km into the area along the McDonald fault occurs in the southern part of the area. The boundary of the eastern Slave is marked by an abrupt change in the aeromagnetic pattern. There is also a major paired Bouguer gravity anomaly whose line of inflection corresponds, at least in part, to the boundary. There is little correspondence between surface rock density and the gravity pattern but a direct correspondence between the aeromagnetic anomaly pattern and surface rock magnetic susceptibility.

Résumé

La géologie de la région de la limite entre les provinces des Esclaves et de Churchill varie du style structural curviligne caractérisé par un métamorphisme archéen de degré faible à moyen dans la province des Esclaves au style structural linéaire dans la zone tectonique de Thelon du nord-ouest de la province de Churchill, remarquable par ses zones mylonitiques abondantes et son degré de métamorphisme très élevé datant du Protérozoïque inférieur. Un échantillon du centre de la zone tectonique de Thelon charrié sur 70 km dans la zone, le long de la faille de McDonald, se trouve dans la partie sud de la région. La limite de l'est de la province des Esclaves est marquée par un changement brusque du profil aéromagnétique. Il existe en outre une importante anomalie de Bouguer double dont la ligne d'inflexion correspond en partie à cette limite. La corrélation entre la densité des roches de surface et le profil gravimétrique est faible, mais il existe une corrélation directe entre le profil de l'anomalie aéromagnétique et la susceptibilité magnétique des roches de surface.

[1]Department of Geological Sciences, Queens University, Kingston, Ontario K7L 3N6
[2]Ottawa-Carleton Geoscience Centre, University of Ottawa, Ottawa, Ontario K1N 6N5

INTRODUCTION

The Artillery Lake map area is divided diagonally by the north-northeasterly trending Thelon Front. The front separates the Slave Structural Province, characterized by curvilinear structural trends, relatively massive plutonic bodies and mainly low to intermediate metamorphic grade metasediments and metavolcanics of the Archean Yellowknife Supergroup, and the Thelon Tectonic Zone of the northwestern Churchill Structural Province where linear trends, strongly foliated granitoids and high metamorphic grade gneisses and schists occur. Pronounced geophysical expressions of the boundary in this area are an abrupt change in the magnetic anomaly pattern and a major paired Bouguer gravity anomaly. The southeastern quarter of the area is transected by the McDonald Fault along the south side of which dextral transcurrent movement of about 70 km (Thomas et al., 1976) has translated a segment of the central Thelon Tectonic Zone westward into the area. Thus, within the map area, the transition from the Slave Province to the western part of the Thelon Tectonic Zone and a sample of the central part of the Thelon Tectonic Zone can be seen.

The past field season, the last of three, marks the completion of the geological mapping of the area at 1:250 000 scale (Fig. 84.1). The project is part of an ongoing series concerned with the examination of this major tectonic feature of the northwestern Canadian Shield that was first recognized by Wright (1957, 1967) and Fraser (1964). These include the investigations of Thompson et al. (1986) in the northern sector, the work of Frith (1982) and Henderson et al. (1982) in the central sector between the Bathurst and McDonald faults and that of Bostock (1987) in the south, all at 1:250 000 scale. As well, more detailed investigations including structural, metamorphic, geophysical, geochronological and sedimentological studies are currently ongoing at several localities within, or adjacent to, the Thelon Tectonic Zone (eg. James, 1985, 1986; Hanmer and Connelly, 1986; van Breemen et al., 1987; McGrath and Henderson, 1985; Tirrul, 1985; Grotzinger and Gall, 1986).

The Artillery Lake area was originally mapped at 1:1 000 000 scale as part of Operation Thelon (Wright, 1957,1967). The eastern half of the area was subsequently mapped at 1:250 000 scale by Fraser (1972). Gandhi (1984, 1985) recently studied the geology and mineral deposits in the immediate vicinity of Artillery Lake itself. Previous reports on the current mapping project were concerned with the northern and central parts of the area (Henderson and Macfie, 1985, 1986). Geological mapping during the past field season was concentrated on the southern half of the area but also included work in the less accessible parts of the northern half. In addition, a major detailed gravity survey was done (P.H.M.) over the large paired gravity anomaly situated between and east of the Bathurst and McDonald faults, whose line of inflection in part coincides with the western boundary of the Thelon Tectonic Zone. Geochronological and geochemical collections were made by O. van Breemen from most of the units in the area together with detailed outcrop examinations of each site in an attempt to appreciate the relationship of the various lithological phases sampled, particularly in the Thelon Tectonic Zone where it is rarely possible to understand all aspects of this very complex geology at the regional mapping scale. Macfie (1987) undertook detailed mapping of an unusual hornblende gabbro-anorthosite as part of his M.Sc. thesis.

GENERAL GEOLOGY

Three northerly trending, fault-bounded lithostructural domains have previously been recognized in the northern part of the area (Fig. 84.1). The western domain whose geology is characteristic of the Slave Province is separated from the eastern domain that consists of the high grade severely deformed rocks of the Thelon Tectonic Zone by a narrow central domain that is transitional in character. These three domains continue southward to the McDonald Fault where they are truncated. A fourth domain lies south of the fault and represents a segment of the central Thelon Tectonic Zone that has been translated into the area along the fault. The discussion of the geology that follows is based on these four domains.

Western domain

The western domain is typical of the main part of the Slave Province and underlies the west-northwestern third of the area. The eastern boundary of the domain extends from the southwest corner of the map area, northeasterly along the west side of Artillery Lake immediately south of Ptarmigan Lake, and north out of the area at about 107°W. The boundary is mainly a series of faults of somewhat varied trend that are not continuous. The contrast in structural style from the massive plutonic rocks of the western domain to the foliated granitoid rocks of the central domain is particularly evident east of Artillery Lake where the fault zone is several kilometres wide and contains rocks having protomylonitic to mylonitic textures. At the domain boundary east of Clinton-Colden Lake there is a distinct change in the magnetic levelhat corresponds closely with a mapped fault. Both the fault and magnetic change terminate east of the south end of Ptarmigan Lake.

The northern part of the domain is dominated by Archean metasediments and, to a lesser extent, intermediate to mafic metavolcanics of the Yellowknife Supergroup that are part of a major northwest-trending zone of supracrustal rocks that extend over 100 km into the central part of the Slave Province. The metasediments are greywacke-mudstone turbidites similar to those seen throughout the Slave Province. The mafic to intermediate volcanics are primarily part of a single edifice that extends more than 60 km along the northwest side of Clinton-Colden Lake, if the volcanics east of Ptarmigan Lake and separated from the main body by a granodiorite intrusion are included. Pillowed and massive flows are common but there are also abundant volcanic breccia and finer grained volcaniclastic units, commonly with carbonate matrix. The lower pressure type regional metamorphism is mainly amphibolite facies (cordierite-andalusite-staurolite in pelitic rocks) but there are large areas at greenschist facies in the central

part of the supracrustal terrane (Fig. 84.1). Most of the volcanics on the large island in Clinton-Colden Lake are at greenschist grade.

The southern part of the domain is underlain by a plutonic complex dominated by a massive, coarsely megacrystic, biotite-rich granite with a trace of muscovite. Also present are plutons of biotite-muscovite granite, a dioritic to tonalitic suite and a granodiorite suite that bears a remarkable resemblance in composition, texture and plutonic style to the Defeatlutonic Suite at Yellowknife (Henderson, 1985). Furthermore the two-mica granite is similar to the Prosperous Granite at Yellowknife, even to the local rare occurrence of spodumene-bearing pegmatite. A small body of hornblende gabbro-anorthosite occurs at the east end of Clinton-Colden Lake and east of the volcanics at Ptarmigan Lake. The main body was mapped in detail by Macfie (1987). The plutonic rocks are for the most part massive although a weak to moderate foliation is developed towards the eastern boundary of the domain.

Unconformably overlying the Archean rocks in the immediate area of Artillery Lake is a gently to moderately dipping dolomite unit that is pale yellow-brown to orange weathering, locally stromatolitic and in places contains minor lenses of fine, well rounded, quartz pebble conglomerate. The dolomite is typically brecciated on a wide range of scales and commonly contains irregular quartz veins. This unit has been described and named the Artillery Lake formation by Gandhi (1984, 1985). He also reported outcrops of interbedded grey and red shales and dolomite exposed over a strike length of 1.5 km on the southeast shore of Artillery Lake. Although outcrops of the shale are few, the abundance of glacially transported boulders of this unit on the west side of Artillery Lake suggests the lake may well be underlain by a significant proportion of this lithology. The southeasternmost exposure of the dolomite is in fault contact with the adjacent Archean rocks. The main trend of the formation is expressed by the chain of islands in the lake and whose existence may be due to the presence of another similar trending fault in the lake. The carbonates on the islands occur commonly in broad openolds whose trends are not always parallel to the trend of the formation as a whole. Gandhi (1984, 1985) reported and described Pb-Zn-Cu mineralized carbonate veins that occur most commonly at the unconformity and also within the formation. It has been suggested that the Artillery Lake formation is correlative with the Union Island Group of the East Arm of Great Slave Lake (P.F. Hoffman, personal communication, 1985; S.S. Gandhi, personal communication, 1986).

Central domain

The central domain is a transitional zone intermediate between the western and eastern domains and includes at least some of the lithological and/or structural characteristics of both. It is up to 30 km wide at its central part and narrows to about 15 km where it is truncated on the south by the McDonald Fault. The western boundary is the previously discussed faults that separate it from the western domain. The eastern boundary is the 'straight zone'.

The 'straight zone' is the impressive zone of mainly porphyroclastic migmatitic metasediments and amphibolitic rocks that can be traced from the Artillery Lake area north into the Healey Lake area (Henderson et al., 1982) over a distance of at least 90 km with a trend that does not deviate from 020°. This zone has been considered the best candidate for the Thelon Front or the western edge of the Thelon Tectonic Zone in this region (Thompson and Henderson, 1983; Henderson et al., 1982; James, 1985, 1986). At Sifton Lake the porphyroclastic straight zone deviates into a more southerly direction from its normal 020° trend, becomes much thinner and is split by long narrow units of foliated granitoid. At Smart Lake it becomes involved with a series of dextral splays off the McDonald Fault that translates it back to the southwest again before it disappears at the McDonald Fault south of Ford Lake at a point more or less on line with the 020° trend of the straight part of the zone. Throughout its length it consists of porphyroclastic metasedimentary migmatites that are considered to be part of the Yellowknife Supergroup, because in the northern Healey Lake area similar rocks continuous with the straight zone open out into one of the largest Yellowknife Supergroup terranes in the Slave Province.

The central domain is dominated by granitoid rocks although between Douglas Lake and Smart Lake large areas are underlain by biotite-sillimanite-garnet metasedimentary migmatites with varied proportions of leucosome (in places grading to diatexite) that are considered to be the high grade equivalent of Yellowknife metasediments. The concentration of metasedimentary migmatites in this part of the domain probably represents a continuation of the zone of greenschist to amphibolite facies Yellowknife rocks extending from Ptarmigan and Clinton-Colden lakes northwest into the central Slave Province. There are other, generally small, areas of migmatitic metasediments in the domain that are not shown in Figure 84.1.

The granitoid rocks are a heterogeneous assemblage ranging from recrystallized, thinly layered quartzofeldspathic gneisses, granitoid migmatites and moderately to strongly foliated plutonic bodies that vary in composition from mafic tonalite to granite. Some of the granitoid units are the more deformed equivalents of plutonic bodies recognized in the western domain. These include the two-mica granite and the megacrystic, biotite-rich (minor muscovite) granite east and west of Artillery Lake. Other bodies are similar toranitoid units in the eastern domain. Rock units lithologically similar to the black and pink megacrystic granite north of Deville Lake occur in the eastern domain, and the pink and grey migmatitic granodioritic body north of Smart Lake is similar in many respects to the dominantly granitoid unit immediately east of the straight zone (Fig. 84.1).

The rocks of the domain are moderately to strongly foliated throughout with, in general, the terrane in the southern part of the domain being much more deformed than the northern part. Trends are typically north-northeasterly with steep dips, although there can be wide variations. In the south there are zones of shearing with porphyroclastic zones similar in many respects to that of the straight zone. The most prominent of these is the several kilometre wide

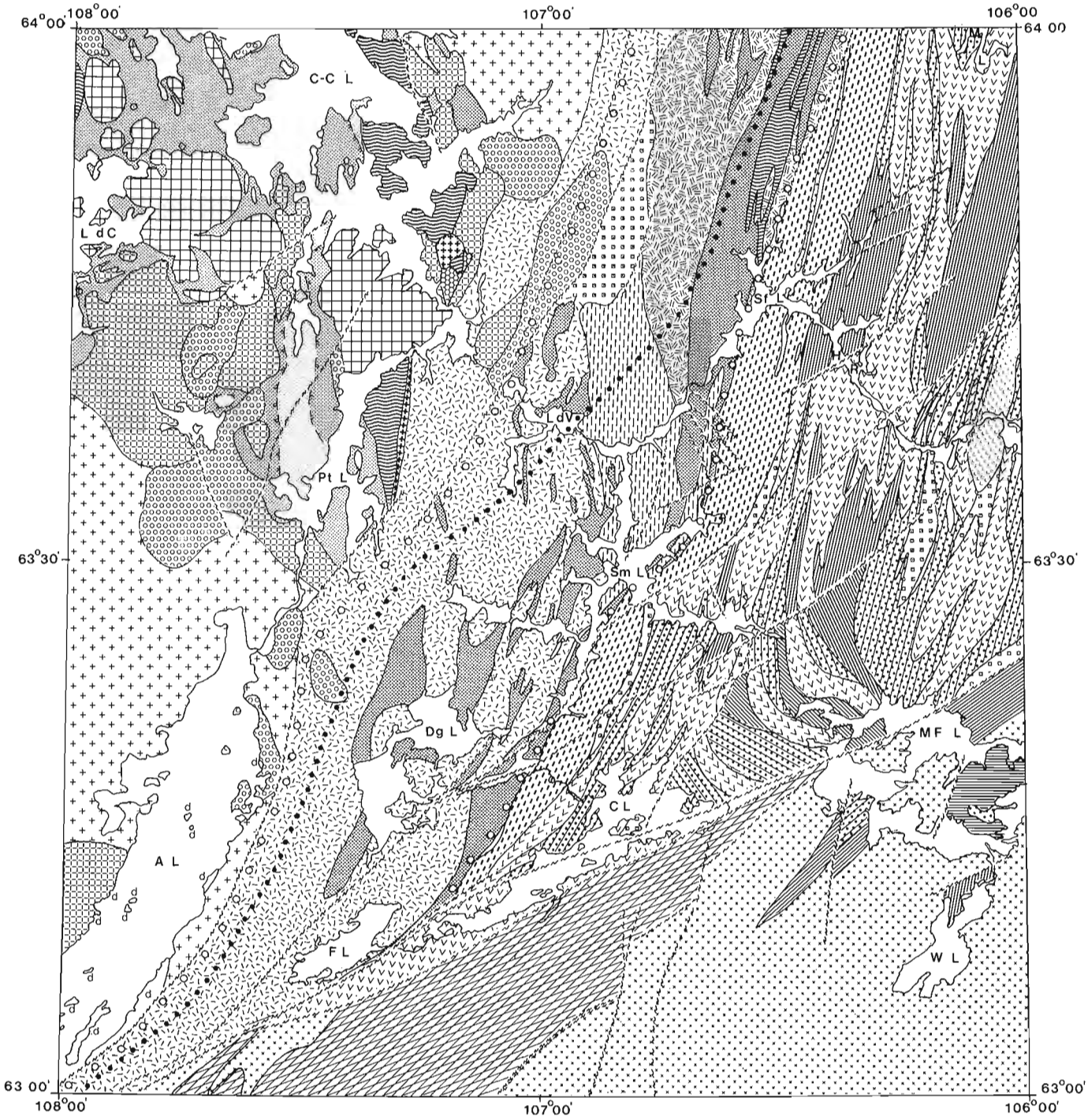
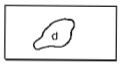


Figure 84.1 Generalized geology of the Artillery Lake area

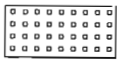
protomylonitic to mylonitic zone that marks the boundary of the domain east of Artillery Lake.

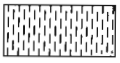
On the basis of the domain's lithological characteristics, it has strong affinities with the Slave Province of the western domain. However, most of the units that it shares in common with the Slave Province are much more strongly deformed and more highly metamorphosed in the central domain. This would suggest that the domain represents part of the Slave Province that is presently exposed at a deeper structural level than the immediately adjacent Slave Province proper.

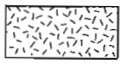
WESTERN AND CENTRAL DOMAINS

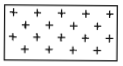


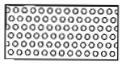
DOLOMITE, ARTILLERY LAKE FORMATION, EARLY PROTEROZOIC

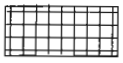

GRANODIORITE, GRANITE, PINK AND BLACK, MEGACRYSTIC, BIOTITE, MODERATELY TO STRONGLY FOLIATED

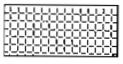

GRANITOID MIGMATITE; PINK AND GREY, BIOTITE-HORNBLENDE, MODERATELY FOLIATED

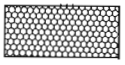

FOLIATED GRANITOIDS TO GRANITIC GNEISSES UNDIVIDED;

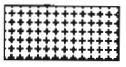

GRANITE, GRANODIORITE; BIOTITE (MUSCOVITE) MEGACRYSTIC, MASSIVE


GRANITE; BIOTITE- MUSCOVITE, MASSIVE

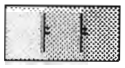

GRANODIORITE; BIOTITE (HORNBLENDE), MASSIVE


TONALITE, DIORITE; HORNBLENDE-BIOTITE, MASSIVE


QUARTZ DIORITE, DIORITE;


ANORTHOSITIC GABBRO, ANORTHOSITE

YELLOWKNIFE SUPERGROUP


METAGREYWACKE, PELITE AND HIGH GRADE EQUIVALENTS; (A) GREENSCHIST FACIES (B) AMPHIBOLITE FACIES (C) MIGMATITE


MAFIC TO INTERMEDIATE METAVOLCANIC ROCKS GREENSCHIST TO AMPHIBOLITE GRADE


GRANITOID GNEISSES; HETEROGENEOUS COMPOSITION, RECRYSTALIZED IN PART, IN PART POSSIBLY OLDER THAN YELLOWKNIFE


GEOLOGICAL CONTACT; DEFINED OR ASSUMED

FAULT, SHEAR ZONE

METAMORPHIC ISOGRAD

DOMAIN BOUNDARIES

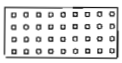
LINE OF INFLECTION BETWEEN POSITIVE AND NEGATIVE REGIONAL PAIRED GRAVITY ANOMALY



KILOMETERS

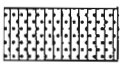
EASTERN DOMAIN

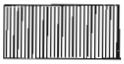

GRANITE, GRANODIORITE; BIOTITE, STRONGLY FOLIATED


GRANODIORITE, GRANITE; PINK AND BLACK, MEGACRYSTIC, BIOTITE, MODERATELY TO STRONGLY FOLIATED

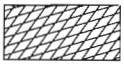

GRANITOID MIGMATITE; BIOTITE-HORNBLENDE, PINK AND GREY, STRONGLY FOLIATED

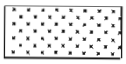

GRANITOID GNEISSES TO FOLIATED GRANITOIDS UNDIVIDED, SOME SUPRACRUSTAL GNEISSES

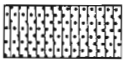

MIGMATITIC METASEDIMENTARY GNEISSES; WITH YOUNGER GRANITIC SHEETS AND INTRUSIONS

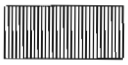

MIGMATITIC AMPHIBOLITE TO QUARTZOFELDSPATHIC AMPHIBOLE BEARING SUPRACRUSTAL GNEISS; WITH GRANITIC SHEETS AND INTRUSIONS

SOUTHERN DOMAIN


GRANODIORITE, GRANITE;BIOTITE, MEGACRYSTIC TO PORPHYROCLASTIC, FOLIATED


GRANITOID GNEISSES TO FOLIATED GRANITOIDS UNDIVIDED, SOME SUPRACRUSTAL GNEISSES


MIGMATITIC METASEDIMENTARY GNEISSES; WITH YOUNGER GRANITIC SHEETS AND INTRUSIONS


MIGMATITIC AMPHIBOLITE TO AMPHIBOLITIC GNEISS; WITH GRANITIC SHEETS AND INTRUSIONS

LAKE SYMBOLS

A L	ARTILLERY LAKE
C L	CAMPBELL LAKE
C-C L	CLINTON-COLDEN LAKE
Dg L	DOUGLAS LAKE
F L	FORD LAKE
H R	HANBURY RIVER
L dC	LAC DE CHARLOIT
L dV	LAC DEVILLE
M L	MORAINE LAKE
M F L	MARY FRANCES LAKE
Pt L	PTARMIGAN LAKE
Sf L	SIFTON LAKE
Sm L	SMART LAKE
W L	WILLIAMS LAKE

Another important aspect of this domain is its relationship to the paired gravity anomaly. The anomaly consists of a large negative component between the Bathurst and McDonald faults and a flanking positive component to the east that apparently extends across the faults (Fig 84.2). It has been noted that the line of inflection between the two parts of the anomaly corresponds in part to the boundary between the central domain and the Thelon Tectonic Zone, ie part of the straight zone (Henderson et al., 1982; Henderson and Macfie, 1985, 1986). However, near the point at which the straight zone ceases to be straight and swings into a more southerly trend, the line of inflection between the positive and negative anomalies swings towards the southwest. It follows that direction to just south of Ptarmigan Lake where it becomes parallel and close to the several kilometre wide shear zone that marks the western boundary of the domain (Fig 84.1).

Eastern domain

The eastern domain, part of the Thelon Tectonic Zone, is the most deformed, contains the highest grade metamorphic rocks, and is the most lithologically distinctive of the three northern domains. Its western boundary is the previously discussed straight zone and it is truncated on the south by the McDonald Fault.

The domain consists of both layered granitoid gneiss and strongly foliated granitoids together with rocks of supracrustal origin in more or less equal proportions. The supracrustal gneisses predominate in the south and the rocks of granitoid origin are more abundant in the north. It is noted, however, that everywhere the supracrustal gneisses have a varied proportion of granitoid components, and similarly in the granitoid terranes there are commonly supracrustal gneisses present to some degree.

The supracrustal gneisses have been subdivided into biotite-rich and amphibole-rich units. They are commonly rusty weathering and show the dark to medium olive green on the fresh surface characteristic of rocks at granulite grade. The biotite-rich rocks are typically migmatitic gneisses with a high proportion of white plagioclase-quartz leucosome and biotite-rich paleosome that also commonly contains garnet, amphibole, clinopyroxene and orthopyroxene. Sillimanite is rare but pink granitoid layers injected at all scales are widespread. These mainly homogeneous migmatites are interpreted as metasediments. The amphibole-bearing gneisses are much more heterogeneous varying from dark amphibolites, amphibolitic gneisses and amphibolitic migmatites through to quartzofeldspathic amphibole-bearing rocks and, like the metasedimentary gneisses, commonly have an injected granitoid component. Quartz-rich rocks are present locally and, in the large unit of amphibolitic supracrustal gneisses south of Moraine Lake, a zone of discontinuous lenses and layers of marble at roughly the same structural position in the unit can be traced over a distance of 15 km northward out of the area to where they had previously been noted by James (1986). The biotite-rich and amphibole-rich supracrustal gneisses are completely gradational with each other, so that in many of the units shown in Figure 84.1, both may well be present. Some of the more pelitic biotite-rich metasedimentary migmatites bear a strong resemblance to the Yellowknife migmatites of the central domain and the Healey Lake area to the north. Thus, they were previously considered to be correlative with the Yellowknife Supergroup of the Slave Province (Fraser, 1972; Henderson and Macfie, 1985). James (1985,1986), however, differentiated between supracrustal gneisses similar to the Yellowknife and others that were more heterogeneous. Following James, no attempt is now being made to correlate these supracrustal gneisses with the Yellowknife Supergroup of the Slave Province. To date the age of deposition of these supracrustal rocks is not known. At many localities, particularly in the north, these migmatitic gneisses have been metamorphosed at granulite grade. The age of granulite grade metamorphism has been determined to be between 1990 and 1950 Ma (U-Pb, zircon and monazite, van Breemen et al., 1987). The supracrustal gneisses have also been intruded by the Hanbury granite which has been dated at about 1920 Ma (U-Pb, zircon and monazite, van Breemen et al., 1987). These dates represent minimum ages for the deposition of the supracrustal rocks.

The strongly deformed granitoid gneisses and foliated granitoids that constitute somewhat more than half the eastern domain are a heterogeneous assemblage of phases that vary greatly in composition and texture. In most cases these cannot be presented adequately on the scale of Figure 84.1 and, to some degree, at even very detailed scales. Some units, however, are sufficiently homogeneous that they can be readily separated. These include long narrow bodies of pink and black megacrystic granite to granodiorite that commonly have a strong positive magnetic response and serve as useful marker horizons in the domain. The largest body of this lithology occurs in the northern central domain. The Hanbury granite, a strongly foliated, even-grained, fairly homogeneous, biotite-poor granodiorite, is mapped as a single pluton on the east border of the area. Equivalents of it occur throughout the eastern part of the domain as thin, layer parallel, sheets intruding the older gneisses. Neither appear to have been metamorphosed to granulite grade. Along the west border of the domain a relatively homogeneous unit has been identified that, where least deformed, can be seen to be a pink and grey granitoid migmatite; it consists of a grey, relatively finer grained biotite and/or hornblende-moderate granodiorite to tonalite with wispy lenses to layers of pink, mafic-poor, coarser grained granite leucosome. Where mylonitized, which is commonly the case, the rock becomes pink and grey, layered, with porphytoclasts of grey feldspar and black hornblende. This lithology occurs also throughout the undivided granitoid terrane to the east and bears certain similarities to the migmatitic granitoid in the central domain north of Smart Lake. The only geochronological data from the domain include a zircon – monazite date from the Hanbury granite at 1920 Ma (van Breemen et al., 1987). In addition rocks at two localities from the undifferentiated granitoid gneiss terrane at Moraine Lake, but north of the present map area, were determined to have an age of granulite grade metamorphism of between 1990 Ma and 1950 Ma with one of the samples having a precursor age of about 2400 Ma (van Breemen et al., 1987).

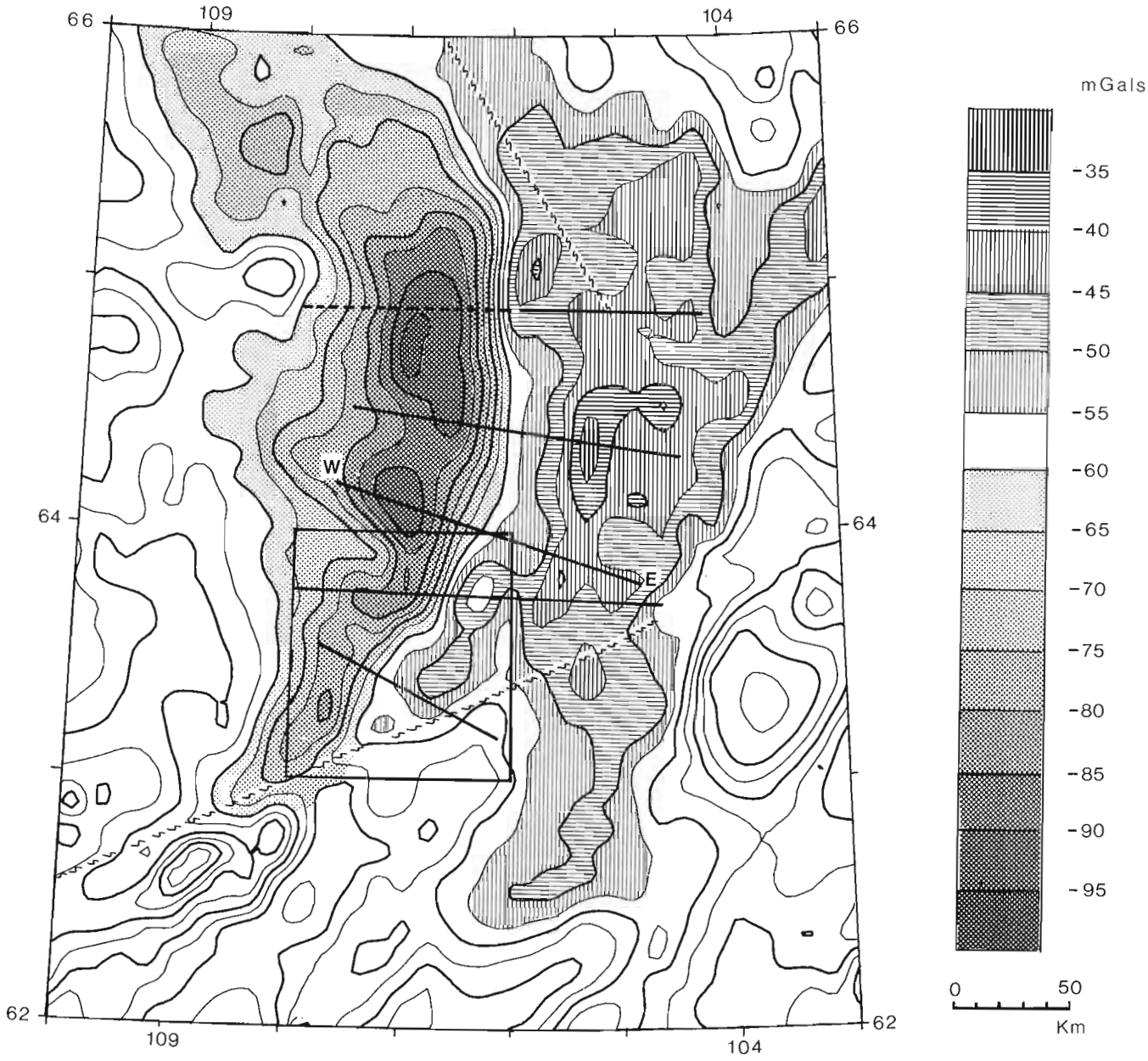


Figure 84.2 Bouguer gravity map with selected contour intervals shaded to enhance the expression of the negative-positive paired anomaly which occurs between the Bathurst (northwest-trending) and McDonald (southwest-trending) faults near the boundary of the Slave Province and the Thelon Tectonic Zone. The map was derived from gravimeter observations spaced at 8 to 10 km intervals. The solid black lines represent the positions of gravity profiles surveyed in 1986 using a 2 km station spacing; surface density and magnetic susceptibility observations were also made. The dashed line south of 65°N between 108°W and 106°W was surveyed as part of the regional survey at approximately 5 km station spacing and was later interpreted by Gibb and Thomas (1977). The square in the south-central part of the figure illustrates the boundary of the Artillery Lake map area. The survey results for profile WE are illustrated in Figure 84.3.

Throughout the domain the rocks are strongly but variably deformed. In the north the structure is straight and steep and there are abundant north-northeasterly trending mylonite zones. Throughout the region kinematic indicators on the whole indicate a dextral sense of movement in the domain. To the south, however, mylonitic zones become fewer and the structural trends more varied.

The eastern domain can be divided into a series of subdomains bounded by shear zones. The most prominent break can be seen north of Campbell Lake where the northwesterly structure of the gneisses coming out of Mary Frances Lake is abruptly truncated by the north-northeasterly trending gneisses to the west. This break can be traced across the series of splays off the McDonald Fault to the boundary between the dominantly granitoid gneiss terrane and amphibolitic gneiss terrane south of Moraine Lake. There is a slight discordance there as well as a series of small dioritic to anorthositic pods along the boundary. A second possible break separates the pink and grey granitoid migmatites east of the straight zone from the more heterogeneous granitoid and supracrustal gneisses to the east. A third break may be present north of Mary Frances Lake where it is most clearly expressed by the aeromagnetic anomaly pattern. East of the apparent break there is an abrupt change in the average magnetic intensity level and degree of local magnetic relief, although there does not appear to be any change in the lithological units. The break can be followed north to the large splay off the McDonald Fault where it is offset about 12km to the east boundary of the area. The break continues due north within a kilometre or so of the boundary beyond the area, truncating the amphibolite gneisses that strike into it at an angle of about 20°. This subdomain is also coincident with a minor low within the regional scale high of the paired gravity anomaly of the region. One feature that all of these apparent breaks have in common is the occurrence of the previously mentioned long narrow bodies of pink and black megacrystic granite-granodiorite, to such an extent that there must be a causal relationship. As these granitoids postdate the granulite grade metamorphism, the dating of this unit should provide another datum in the long complex history of the terrane.

Southern domain

The southern domain occupies the southeastern quarter of the area and is an exotic terrane in that it is out of context with the other three domains that are truncated by it, having been translated from the east a distance of about 70 km along the McDonald Fault (Thomas et al., 1976).

The most prominent feature of the domain is the large homogeneous body of foliated megacrystic to porphyroclastic granodiorite that occurs southwest of Campbell Lake. The nature of its contact with the other largely granitoid gneisses and foliated granitoids to the west is not known due to poor exposure, but its contact with similar and as yet undivided granitoid gneisses and foliated plutons to the east is a major, commonly finely-layered to 'glassy' mylonite up to several kilometres wide. The body has a relatively high magnetic expression. It was used as a magnetic marker by Thomas et al. (1976), who pointed out its possible correlation with the Thelon magnetic zone east of the area, in their determination of the amount of displacement on the McDonald Fault (*see* also Geological Survey of Canada, 1981, 1983).

The main part of the domain is underlain largely by undifferentiated granitoid gneisses and foliated to massive granitoids of varied composition. Amphibolite gneisses and biotite-rich gneisses of presumed supracrustal origin are present locally but are typically minor relative to the granitoid rocks that occur as large sheets that are predominant at most scales. Several wide zones of ultramylonite occur in this mainly granitoid terrane in addition to the major mylonite zone that marks the boundary ofhe megacrystic granodiorite. Several of these occur southeast of Williams Lake where they have a northeasterly trend. In general, these heterogeneous gneisses and granitoids have a northeasterly trend but in detail they are highly varied. Dips vary from vertical to flat.

Migmatitic amphibolite-rich and biotite-garnet-rich supracrustal gneisses occur in the vicinity of Mary Frances Lake. They are in most respects very similar to the supracrustal gneisses of the eastern domain and like them typically have a significant proportion of injected sheets of granitoid in addition to the leucosome.

GRAVITY AND MAGNETIC ANOMALIES

Paired Bouguer gravity anomaly

One of the most prominent expressions of the boundary between the Slave and Churchill provinces is the large paired negative-positive anomaly in the Bouguer gravity field. The negative component is located over the eastern Slave Province between the Bathurst and McDonald faults, whereas the adjacent positive component lies to the east and is centred approximately along a line joining the eastern extremities of the two faults (Fig. 84.2).

Paired anomalies such as this are characteristic of regions where crust of differing thickness and/or density have been juxtaposed (Gibb and Thomas, 1976; Gibb et al., 1983). Gibb and Thomas (1977), on the basis of the regional gravity data (Hornal and Boyd, 1972) which were collected at 8 to 10 km spacing and a single more detailed line at 5 km spacing, interpreted the anomaly as indicating a boundary zone between two collided plates.

To define the gravity anomaly associated with the Thelon Tectonic Zone, 334 additional gravimeter measurments were collected at a 2 km interval along four profiles across the paired anomaly during the 1986 field season. In addition the profile interpreted by Gibb and Thomas (1977) was extended 75 km to the east using a 2 km sampling interval. In order to cover most parts of the paired anomaly, the survey went beyond the Artillery Lake area, and included the Healey Lake area to the north (*see* Henderson et al., 1982 for geological data) and the west half of both the Baillie River map area and the Hanbury map area for which the only geological data

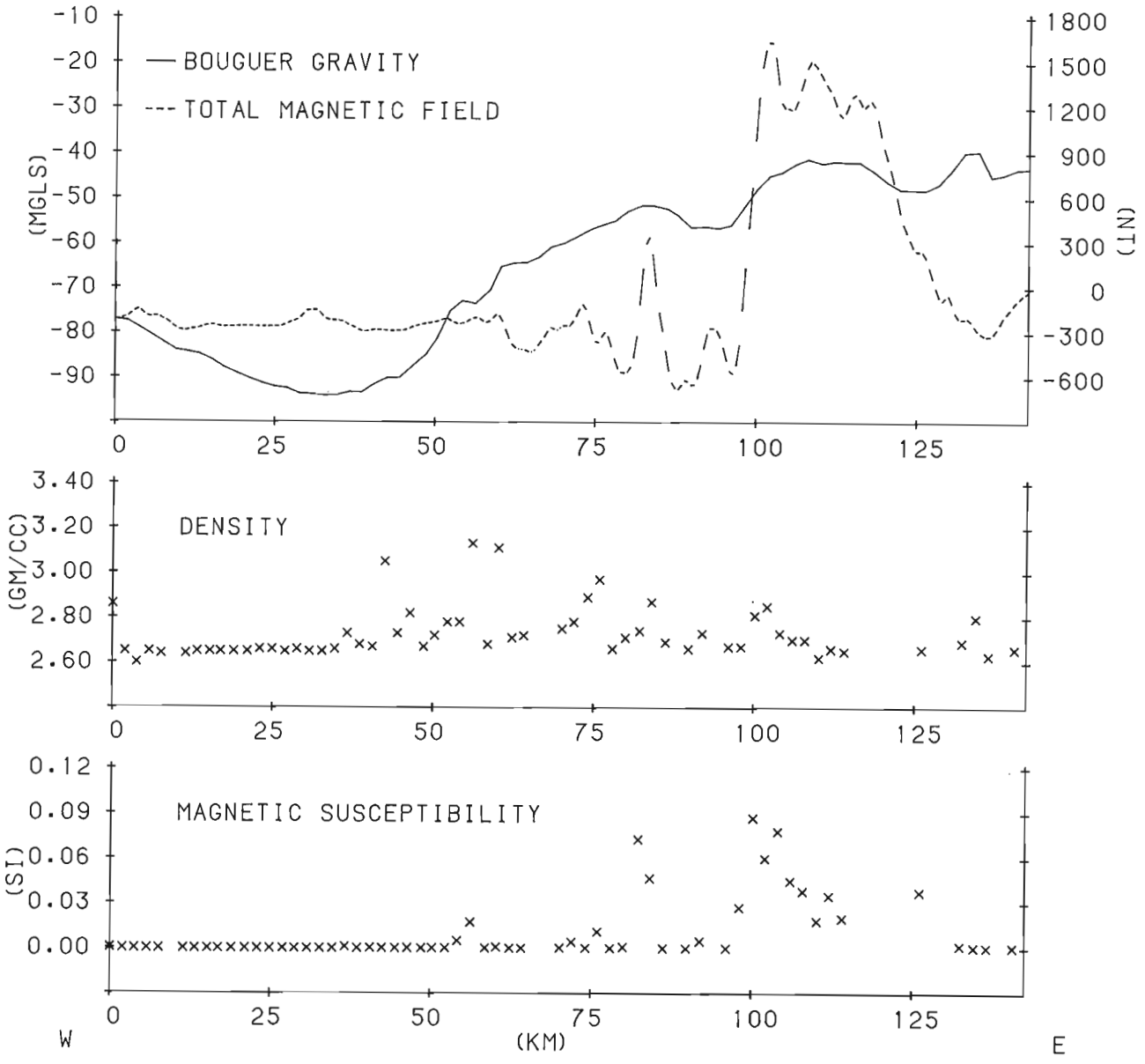


Figure 84.3 Profiles along WE (Fig. 84.2) of observed Bouguer gravity anomaly (solid line), total magnetic field (dashed line), surface density and magnetic suseptibility. The Bouguer gravity data illustrate a paired negative-positive anomaly, the overall extent of which is greater than the 142 km length of the profile. Such paired negative-positive gravity anomalies occur typically at the boundary between crustal blocks of contrasting thickness and/or density. The inflection point between the negative-positive pair lies between 50 and 75 km of the profile, indicating a major change in density, and hence suggesting that the boundary between the Slave Province and the Thelon Tectonic Zone may also lie within these limits. Superimposed on the smoothly varying paired anomaly are smaller anomalies. The relative minimums between 95-100 km and 124-130 km appear to correlate with the western and eastern boundaries of the body producing the large Thelon magnetic anomaly. Note also the poor correlation between variations in surface density and Bouguer gravity, and the good correlation between variations in magnetic susceptibility and the total magnetic field.

available are from the original 1:000 000 scale helicopter reconnaissance survey of Wright (1957, 1967).

A LaCoste-Romberg gravimeter was utilized for the survey. Subsiduary base stations, which were tied to the gravity base station in the terminal building at the Yellowknife airport, were established at Smart Lake campsite (63°30.75′ N, 106°50.77′ W), and at Healey Lake (64°20.84′ N, 106°51.91′W). The elevation of each gravimeter observation was determined using barometric altimeters which were tied to known elevations of nearby lakes. Standard corrections were applied to the gravimeter and altimeter observations. In addition, at each gravimeter site which occurred on or near an outcrop, a bedrock sample was collected for density determination, and several magnetic susceptibility observations were collected at random locations using a hand-held susceptibility meter manufactured by Geoinstruments of Finland.

The resultant data for profile WE (Fig. 84.2) are illustrated in Figure 84.3. The negative-positive paired Bouguer anomaly is immediately apparent with relative extrema of −94 mGal at 33 km along the profile and −40 mGal at 139 km. The overall extent of the paired gravity anomaly is greater than the 142 km length of the observed profile which in itself suggests the causative feature is extensive. The negative anomaly is a smoothly varying curve perhaps representing relatively uniform crust. The positive anomaly, on the other hand, is a composite of long and short wavelength anomalies signifying a segment of crust of differing character from that to the west with smaller anomalies caused by local density inhomogeneities, e.g. the local negative between 95-100 km. The short wavelength anomalies may reflect the segmentation of the area by north northeasterly trending transcurrent faults such as those seen in the eastern domain of the Artillery Lake area.

The density data (Fig. 84.3) do not correlate well in general with the Bouguer gravity field. For example, densities east of 100 km associated with the positive Bouguer anomaly are not significantly different from those west of 40 km associated with the negative anomaly. Similarly, there is little difference between the densities of the granulite grade gneisses (62-96 km) and the lower metamorphic grade amphibolitic rocks of the western Slave Province (42-62 km). Hence the large paired negative-positive Bouguer anomaly cannot be explained in terms of surface density contrasts, but rather is due to large scale differences between the crust underlying the Slave and Churchill provinces.

The position of the boundary between crustal segments differing in thickness and/or density is problematic. Since the paired anomaly is not a simple curve it is difficult to define the location of the boundary. As a first approximation it seems reasonable to assume that it lies close to the inflection point between 50 and 75 km on the profile. The most prominent geological feature that could be correlated with the boundary is the straight zone (62-66 km). However, as shown in Figure 84.1, and discussed previously, the trace of the maximum gradient between the negative-positive paired anomaly (roughly the −70 mGal contour) does not follow the straight zone along its entire length, but deviates to the north in the Healey Lake area along a mapped fault (Henderson et al., 1982), and to the southwest in the Artillery Lake area where it steps across to another fault zone just east of Artillery Lake itself. A complete understanding of these relationships and their significance to the boundary zone between the Slave and Churchill provinces awaits modelling of the gravity data and a more comprehensive interpretation of the other geoscience data.

Magnetic anomalies

The aeromagnetic anomaly pattern in the region of the boundary zone, like the Bouguer gravity anomaly pattern undergoes a major change in character. The data were digitized at a 500 m interval from the aeromagnetic maps published by the Geological Survey of Canada. The contribution of the Earth's core magnetic field has been subtracted from the digitized data using the appropriate International Geomagnetic Reference Field model for 1966. The data were then upward continued from the 305 m survey elevation to 1000 m in order to enhance the larger scale anomalies relative to local anomalies, e.g., dyke anomalies. The average values of the magnetic susceptibility observations collected during the ground survey are shown in the lower part of Figure 84.3. There is a good correlation between areas of high magnetic susceptibility and high magnetic field. For example, the magnetic high anomaly at 82 km is caused by a granulite grade granitoid gneiss with a large magnetic susceptibility. Because of the good correspondence between the aeromagnetic and magnetic susceptibility data it can be inferred that, unlike the Bouguer gravity data, the magnetic anomaly variations reflect near surface magnetic sources. The area between 0 and 62 km is composed in general of weakly magnetic rocks of the eastern Slave Province and the profile shows little relief. The region between 62 and 96 km contains moderately magnetic rocks related to granulite grade terrane whose western limit is marked by a small negative anomaly (62-66 km) over the straight zone. The region between 96 and 125 km transects an extensive and large amplitude NNE trending magnetic anomaly informally known as the Thelon magnetic anomaly. Although covered by overburden in the east, large average magnetic susceptibilities were measured on the western side of the vertically and very strongly foliated NNE trending originally megacrystic granitoid that underlies the anomaly. The megacrystic granitoid gneiss is also reflected in the Bouguer gravity data as a local high separating two small negative anomalies occurring at its eastern and western margins.

DISCUSSION

The completion of the mapping of the Artillery Lake area has given yet another perspective on the nature and significance of the boundary between the Slave Province and the Thelon Tectonic Zone. This is seen in the development of a distinct intermediate domain between the Slave Province and the Thelon Tectonic Zone, which is not seen in the Healey Lake area to the north. The central domain has closer affinities with the Slave Province and would appear to be a sharply defined,

moderately to strongly deformed deeper structural level of the Slave Province with clearly recognizable lithological units common to both the central and western domains. It is interesting to note that the original position proposed by Wright (1957, 1967) for the Thelon Front, the boundary between the Slave and Churchill Provinces is very close to the western boundary of the central domain, and indeed that is the first major regional scale change in structural style and metamorphic grade east of the relatively homogeneous structural style of the Slave Province proper. With respect to lithology and structure, the major break remains between the central and eastern domains as delineated by the through going 'straight zone', even though the feature curves somewhat in the southern two thirds of the area. On the whole the eastern domain would appear to have little in common with those to the west with the exception of granitoid migmatite and some intrusive units whose significance has yet to be determined.

To the north in the southern Healey Lake area and northern Artillery Lake area the western boundary of the Thelon Tectonic Zone is expressed in the Bouguer gravity field as a paired negative-positive anomaly which is typical of juxtaposed blocks of different crustal thickness and/or average density. With the appearance southward of the central domain in the Artillery Lake area, the locus of inflection between the anomalies steps across from the eastern to western side of the domain, and the magnitude of the negative anomaly in that region decreases significantly, perhaps further supporting the previously discussed suggestion that the domain represents an uplifted and , as a result, thinner crustal segment of the Slave Province.

A poor correlation exists between Bouguer gravity and surface density data suggesting the cause of the gravity anomaly is related to large scale crustal differences between the Slave and Churchill. A good correlation exists between variations in the magnetic field and surface susceptability measurements, hence the aeromagnetic maps for the area are useful in support of the surface mapping of lithology and structure. A good example of this is the expression of the low angle structural discordances, particularly in the eastern domain that are not always apparent from ground observations.

The new gravity data are compatible with the previous interpretation of Gibb and Thomas (1977) and Gibb (1978) that the boundary represents the collision of two continental plates. However, it is interesting to note that although the boundary between the Slave and the Thelon Tectonic Zone extends from at least the Arctic coast (eg Thompson et al., 1986) to possibly south of Great Slave Lake, the paired anomaly only occurs between the Bathurst and McDonald faults. As suggested by Gibb (1978) a genetic relationship may exist between the anomaly and the faults. These faults and their related splays offset the rocks of the Thelon Tectonic Zone. Geochronological data from the Thelon Tectonic Zone to date indicate a granulite grade event within the zone between about 1970 Ma and 1950 Ma (van Breemen et al., 1987). On the evidence of the internal textures of the zircons dated, it also represents a time of deformation. There is some evidence of a precursor event tentatively between 2200 and 2400 Ma. The deformed Hanbury granite of the eastern domain is about 50 Ma younger than the granulite grade metamorphism. Although the McDonald and Bathurst fault systems have not as yet been precisely dated, faults related to the McDonald Fault cut the Compton laccoliths of the East Arm of Great Slave Lake which were emplaced at about 1865 Ma (Bowring et al., 1984). Thus the anomaly, although large, may represent a somewhat localized event relatively late in the Proterozoic history of the zone. Further geochronological study of the other collected units of the zone, modelling of the geophysical data, and analysis of the geological data will contribute greatly to our understanding of what appears to be a long history of this zone.

ACKNOWLEDGMENTS

The fieldwork this year was greatly aided by the enthusiastic assistance and good company of Melanie Haggart, Stuart Miller, Owen Steele and Natasha Wodicka, geological assistants, and Martha Macfie, cook. Martin Irving of the GSC provided superior expediting services using the facilities of the Geology Division, Indian and Northern Affairs, Canada, at Yellowknife. We also acknowledge the Geophysics Division (GSC) for the use of the gravimeter, for computer processing of the resultant field data and the Gravity Data Centre of that Division for providing the contour data for Figure 84.2. We also thank David Halliday whose guidance and assistance in gravity survey techniques were vital to the success of the survey. Reference elevations along the survey lines were supplied by the Topographic Surveys Division of the Surveys and Mapping Branch. Finally we thank Gerald Dionne , helicopter pilot-engineer of Frontier Helicopters Ltd., whose care and attention resulted in no time lost, and whose special interest in the gravity survey resulted in our achieving much more than could normally be expected in the limited time available. This report has benefited from the critical reviews of A. Green, M.D. Thomas and P.H. Thompson.

REFERENCES

Bostock, H.H.
1987: Geology of the Taltson Lake area, south half, District of Mackenzie; in Current Research, Part A, Geological Survey of Canada Paper 87-1A, report 47.

Bowring, S.A., Van Schmus, W.R., and Hoffman, P.F.
1984: U-Pb zircon ages from Athapuscow Aulaucogen, East Arm of Great Slave Lake, NWT, Canada; Canadian Journal of Earth Sciences, v. 21, p. 1315-1324.

Fraser, J.A.
1964: Geological notes on northeastern District of Mackenzie, Northwest Territories; Geological Survey of Canada, Paper 63-40.
1972: Artillery Lake map area, District of Mackenzie; Geological Survey of Canada, Paper 71-38, 17p.

Frith, R.A.
1982: Second preliminary report on the geology of the Beechey Lake- Duggan Lake map area, District of Mackenzie, Northwest Territories; in Current

Research, Part A, Geological Survey of Canada, Paper 82-1A, p. 203-211.

Gandhi, S.S.

1984: Galena-sphalerite-chalcopyrite veins in Aphebian dolomite and Archean basement at Artillery Lake, Northwest Territories; in Current Research, Part B, Geological Survey of Canada, Paper 84-1B, p. 33-40.

1985: Geology of the Artillery Pb-Zn-Cu district, Northwest Territories; in Current Research, Part A, Geological Survey of Canada, Paper 85-1A, p. 359-363.

Geological Survey of Canada

1981: Lockhart River, Northwest Territories, Magnetic Anomaly Map; Geological Survey of Canada, Map 1566 A, 1:1 000 000 scale.

1983: Thelon River, Northwest Terrritories, Magnetic Anomaly Map; Geological Survey of Canada, Map NQ-12-13-14-AM, 1:000 000 scale.

Gibb, R.A.

1978: Slave-Churchill collision tectonics; Nature, v. 271, p. 50-52.

Gibb, R.A. and Thomas, M.D.

1976: Gravity signature of fossil plate boundaries on the Canadian Shield; Nature v. 262, p. 199-200.

1977: The Thelon Front: a cryptic suture in the Canadian Shield?; Tectonophysics, v. 38, p. 211-222.

Gibb, R.A., Thomas, M.D., Lapointe, P.L., and Mukhopadhyay, M.

1983: Geophysics of proposed Proterozoic sutures in Canada; Precambrian Research, v. 19, p. 349-384.

Grotzinger, J.P. and Gall Q.

1986: Preliminary investigations of Early Proterozoic Western River and Burnside River formations: evidence for foredeep origin of Kilohigok Basin, District of Mackenzie; in Current Research, Part A, Geological Survey of Canada, Paper 86-1A, p.95-106.

Hanmer S. and Connelly, J.N.

1986: Mechanical role of the syntectonic LaLoche Batholith in the Great Slave Lake Shear Zone, District of Mackenzie, NWT; in Current Research, Part B, Geological Survey of Canada, Paper 86-1B, p. 811-826.

Henderson J.B.

1985: Geology of the Yellowknife-Hearne Lake area, District of Mackenzie: a segment across an Archean basin; Geological Survey of Canada, Memoir 414, 135 p.

Henderson J.B. and Mafie R.I.

1985: The northern Artillery Lake map area: a transect across the Thelon Front, District of Mackenzie; in Current Research, Part A, Geological Survey of Canada, Paper 85-1A, p. 441-448.

1986: Artillery Lake map area, District of Mackenzie: a transect across the Thelon Front; in Current Research Part A, Geological Survey of Canada, Paper 86-1A, p.411-416.

Henderson J.B., Thompson, P.H., and James, D.T.

1982: The Healey Lake map area and the Thelon Front Problem, District of Mackenzie; in Current Research, Part A, Geological Survey of Canada, Paper 82-1A, p. 191-195.

Hornal, R.W. and Boyd, J.B.

1972: Gravity measurements in the Slave and Bear structural provinces, Northwest Territories; Gravity Map Series, Earth Physics Branch, no. 89-95.

James, D.T.

1985: Geology of the Moraine Lake area and the Thelon Front, District of Mackenzie; in Current Research Part A, Geological Survey of Canada, Paper 85-1A, p. 449-454.

1986: Geology of the Moraine Lake area, District of Mackenzie: a transect across the Thelon Tectonic Zone; in Current Research Part A, Geological Survey of Canada, Paper 86-1A, p. 417-421.

Macfie, R.I.

1987: The Clinton-Colden hornblende gabbro-anorthosite intrusion, Artillery Lake map area, District of Mackenzie; in Current Research, Part A, Geological Survey of Canada, Paper 87-1A, report 71.

McGrath, P.H. and Henderson, J.B.

1985: Reconnaissance ground magnetic and VLF profile data in the vicinity of the Thelon Front, Artillery Lake map area, District of Mackenzie; in Current Research, Part A, Geological Survey of Canada, Paper 85-1A, p. 455-462.

Thomas, M.D., Gibb, R.A., and Quince, J.R.

1976: New evidence from offset aeromagnetic anomaliesor transcurrent faulting associated with the Bathurst and McDonald faults, Northwest Territories; Canadian Journal of Earth Sciences , v. 13, p. 1244-1250

Thompson, P.H. and Henderson, J.B.

1983: Polymetamorphism in the Healey Lake area – implications for the Thelon Tectonic Zone; in Current Activities Forum 1983, Program with Abstracts, Geological Survey of Canada, Paper 86-1A, p. 275-289.

Thompson, P.H., Culshaw, N., Buchannan, J.R., and Manojlovic P.

1986: Geology of the Slave Province and Thelon Tectonic Zone in the Tinney Hills-Overby Lake (west half) map area, District of Mackenzie; in Current Research, Part A, Geological Survey of Canada, Paper 86-1A, p. 275-289.

Tirrul, R.

1985: Nappes in the Kilohigok Basin and their relation to the Thelon Tectonic Zone, District of Mackenzie; in Current Research, Part A, Geological Survey of Canada, Paper 85-1A, p. 407-420.

van Breemen, O., Henderson, J.B., Loveridge, W.D., and Thompson, P.H.

1987: U-Pb zircon and monazite geochronology and zircon morphology of granulites and granite from the Thelon Tectonic Zone, Healey Lake and Artillery Lake map areas, N.W.T.; Current Research, Part A, Geological Survey of Canada, Paper 87-1A, report 83.

Wright, G.M.

1957: Geological notes on eastern District of Mackenzie, Northwest Territories; Geological Survey of Canada, Paper 56-10.

1967: Geology of the southeastern barren grounds, parts of the District of Mackenzie and District of Keewatin (Operations Keewatin, Baker and Thelon); Geological Survey of Canada, Memoir 350, 91 p.

In situ density determinations by gravity measurements in the Underground Research Laboratory shaft, Lac du Bonnet granite batholith, Manitoba.

Project 6.4.1.08

J.M. Coderre, M.D. Thomas, R.A. Gibb, and S.L. Fogarasi
Geophysics Division

Coderre, J.M., Thomas, M.D., Gibb, R.A. and Fogarasi, S.L., In situ density determinations by gravity measurements in the Underground Research Laboratory shaft, Lac du Bonnet granite batholith, Manitoba; in Current Research, Part A, Geological Survey of Canada, Paper 87-1A, p. 815-824, 1987.

Abstract

A vertical gravity survey in a shaft penetrating the Lac du Bonnet granite batholith has provided estimates of in situ density for 21 intervals (equivalent to infinite horizontal slabs) of the granite between depths of 15 and 230 m. The weighted mean density and standard deviation for all 21 intervals is 2.61 ± 0.03 g/cm³, which compares with a mean density and standard deviation of 2.63 ± 0.02 g/cm³ obtained for 47 core samples using the conventional laboratory method of measuring density. At the 95% confidence level, these means are statistically different. The lower in situ density suggests that voids are present throughout the rock mass. Based on the difference of 0.02 g/cm³ in the means of the densities obtained by the two techniques, an overall porosity of 1.1% is estimated on the assumption that the voids are dry and 1.7% if they are completely water-filled. The influence of porosity is also reflected in the mean in situ densities of each of the three granitic lithologies penetrated, but weakly in two of them. There is a general correlation between low in situ densities and areas of high fracturing, indicating that fractures are probably the main form of void.

Résumé

Un levé gravimétrique vertical effectué dans un puits traversant le batholite granitique de Lac du Bonnet a permis d'établir des estimations de la masse spécifique in situ de 21 intervalles (équivalents à des dalles horizontales infinies) du granite enfouis entre 15 et 230 m de profondeur. La masse spécifique moyenne pondérée et l'écart type correspondant aux 21 intervalles est de 2,61 ± 0,03 g/cm³, valeur que l'on peut comparer à la masse spécifique moyenne et écart type de 2,63 ± 0,02 g/cm³ obtenue pour 47 échantillons de carottes à l'aide de la méthode classique de laboratoire qui permet de mesurer la masse spécifique. Lorsque le coefficient de confiance est de 95 %, ces moyennes sont statistiquement différentes. La plus faible masse spécifique in situ semble indiquer qu'il existe des vides dans toute la masse rocheuse. D'après la différence de 0,02 g/cm³ entre les moyennes des masses spécifiques obtenues selon les deux techniques, on a estimé que la porosité générale est de 1,1 %, en supposant que les vides sont secs, et de 1,7 % en supposant qu'il s'agisse de vides complètement remplis d'eau. L'influence de la porosité se reflète aussi dans la moyenne des masses spécifiques in situ de chacune des trois lithologies granitiques pénétrées, mais reste tout de même faible dans deux de ces dernières. Il existe une corrélation générale entre les faibles masses spécifiques in situ et les zones à forte fracturation, indiquant ainsi tout probablement que les vides prénnent principalement la forme de fractures.

INTRODUCTION

As part of the Nuclear Fuel Waste Management Program, Atomic Energy of Canada Limited is constructing an Underground Research Laboratory (URL) within the Precambrian Lac du Bonnet granite batholith in Manitoba (Fig. 85.1). The sinking of the URL shaft afforded an opportunity to conduct a variety of geological, hydrogeological and geophysical studies during the excavation. A vertical gravity traverse was undertaken in the shaft to examine the bulk homogeneity of the rock mass by estimating the in situ density of successive horizontal layers. This traverse is one element of a broader gravity study planned to include a surface survey (completed) and surveys in the underground galleries when they are excavated.

The density of igneous rock is primarily a function of mineral composition but it is also affected by the presence of voids. Anomalously low densities might, therefore, indicate zones of fracturing, which may be significant in terms of groundwater flow. In situ densities computed from the gravity measurements are compared with densities determined from hand samples of rock collected at the surface and from core obtained from nearby drillholes, and with fracture and lithological logs of the shaft walls. On the basis of these comparisons, it is possible to estimate bulk porosity of the granite at the URL site and to identify intervals of relatively high porosity.

SURFACE GEOLOGY

The Lac du Bonnet granite batholith is located in the Archean Superior Province of the Canadian Shield in southeastern Manitoba (Fig. 85.1). It is primarily a pink porphyritic granite-granodiorite of fairly consistent composition and texture throughout (McCrank, 1985). In general it is described as a massive, medium- to coarse-grained rock consisting of phenocrysts of plagioclase, microcline and quartz set in a fine-grained matrix of the same mineralogy. Biotite is also present in quantities ranging from 0 to 10% and has been used to subdivide the batholith into biotite-rich (> 5%) and biotite-poor (< 5%) units.

Four lithological units are recognized at the URL site (Fig. 85.2). The site is underlain predominantly by pink porphyritic to sub-porphyritic biotite-poor granite with phenocrysts of potash feldspar and plagioclase set in a medium to fine-grained quartz and feldspar matrix. Grey porphyritic granite, a xenolithic pink porphyritic granite with inclusions of tonalite, amphibolite, and metasedimentary rocks, and a mixed coarse- and fine-grained granite are also present (Stone et al., 1984).

Pegmatite and aplite dykes and low- and steeply-dipping mesoscopic fractures have been mapped on the surface of the batholith. The dykes are the oldest filled fractures exposed at the surface of the URL. They are uniform in abundance and the majority dip vertically and strike north-northeast. Dykes range in length from 5 to 80 m and have a median length of 22 m. These dykes are crosscut by younger fractures containing no magmatic filling materials. Low-dipping (< 40°) and steeply-dipping (> 60°) fractures are the most abundant and have mean lengths of 17.5 m and 14 m, respectively. Stone et al. (1984) concluded that the majority of fractures exposed at the surface of the URL formed shortly after emplacement of the batholith as the magma cooled.

SURFACE GRAVITY SURVEY

The results of the surface survey demonstrate that large anomalous masses which could influence the in situ density determinations are not present. The survey consisted of 191 gravity measurements in an area surrounding the shaft headframe (Fig. 85.1). The central 123 stations were spaced 20 m apart on a regular grid, while the outer 68 were located on a 40 m grid. The station locations and elevations were surveyed using a tape and a level and rod; the elevation accuracy is estimated to be ± 3 cm and horizontal positions are estimated to be accurate to within ± 10 cm. The gravity survey was conducted by two observers, one operating a Worden gravimeter (No. 754) and the other operating a LaCoste and Romberg gravimeter (No. G278). The data were reduced to a common vertical datum (sea level) using an uniform density of 2.67 g/cm^3. Terrain corrections were not computed because the terrain is relatively flat; a terrain correction computed at the headframe is only 0.02 mGal. The standard error in Bouguer anomaly due to errors in the gravity observation, horizontal position and elevation is estimated to be ± 0.05 mGal.

A plot of the Bouguer anomaly field superposed on the local geology is shown in Figure 85.2. Over most of the URL site, the variation in the gravity anomaly is very small, being less than 0.25 mGal. This area coincides mainly with pink porphyritic granite, and the gravity field reflects its homogeneity at and near the surface. Anomalous masses that could influence the in situ density values significantly are, therefore, not present. Small positive anomalies of about 0.70 mGal in the south half of the area apparently are related to the grey granite.

GEOLOGY OF THE SHAFT

Six principal lithological domains have been mapped within the shaft by Everitt and Brown (1985a) (Fig. 85.3). The domains represent three pairs of the same lithology, with slight variations being present in each. The lithologies correspond to those mapped at the surface, with the exception of the mixed granite which does not appear in the shaft. Domains 1 and 5 (Fig. 85.3) consist of medium- to coarse-grained gneissic pink porphyritic granite. The upper domain differs from the lower in that it includes some xenolithic pink porphyritic granite. Domains 2 and 4 are classified as xenolithic granites containing fragments of amphibolite, mafic metavolcanics and felsic granitoids in a matrix of pink porphyritic granite. Domains 3 and 6 consist of medium to coarse-grained grey granite. The upper domain is essentially structureless, while the lower section is more heterogeneous, containing various leucocratic segregations, and pegmatitic and porphyritic areas.

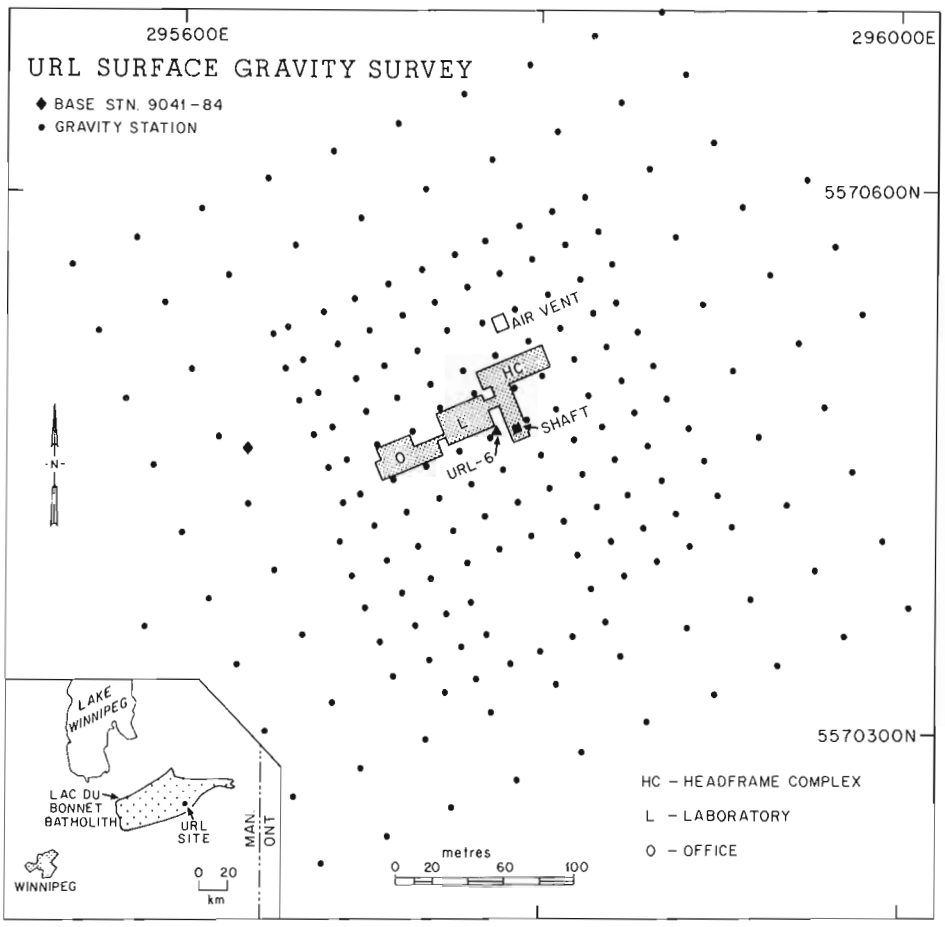


Figure 85.1. Surface gravity station locations in the vicinity of the URL shaft. General location map is shown inset.

Detailed fracture mapping within the shaft has identified both steeply-dipping (> 60°) and low-dipping (< 40°) fractures (Everitt and Brown, 1985b). The orientation and relative abundance of the steeply-dipping fractures change across fracture domain boundaries, which coincide with the lithological domain boundaries (Fig. 85.3). The fracture domain above and including fracture zone No.3 is more complex than those below this level. This may be a result of surface influences, such as the development of sheeting and intra-block fractures (Everitt and Brown, 1985a). The major low- intermediate-dip No. 3 fracture zone and the splay of No. 2 zone are intersected by the URL shaft between depths of 98 to 118 m and 203 to 217 m, respectively (Brown et al., 1984). Both zones dip southeast between 15° and 28°, these attitudes being strongly controlled by the local foliation.

VERTICAL GRAVITY SURVEY

Two gravity traverses were completed to a depth of 230 m in the URL shaft. The first traverse originated at a depth of 15 m and continued down to 230 m, while the second traverse began at the 230 m level and continued back up to the 15 m level. Twenty-two stations were occupied at an average interval of 10.2 m (Fig. 85.4). The intervals ranged between 7.5 m and 12.5 m (see 'dz' in Table 85.1). The first and last observations were read at an arbitrary base station, timber set No. 6, while the measurements further down the shaft were also made on timber sets located around the inside perimeter of the shaft walls. All measurements were made at the same position on each timber, 2.7 m east of the northwest corner of the shaft with a LaCoste and Romberg gravimeter (No. G255). The observer, recorder and cage operator stood on top of the elevator cage while travelling slowly along the shaft; this enabled easy access to each timber for accurate positioning of the gravimeter.

CALCULATION OF INTERVAL DENSITIES

The following method of determining in situ densities has been given in detail by Gibb and Thomas (1980). Two gravity values in a vertical line, such as a mine shaft or a borehole, are required for calculation of in situ rock density. The difference in gravity (dg) corrected for the difference in the effects of surface terrain and subsurface voids (dT) over a vertical interval (dz) is given by:

$$dg + dT = (F - 4\pi G\rho)dz + dc \quad (1)$$

where F (= 0.3086 mGal/m) is the assumed "normal" free-air vertical gradient of gravity, G [= 6.6732×10^{-8} cgs

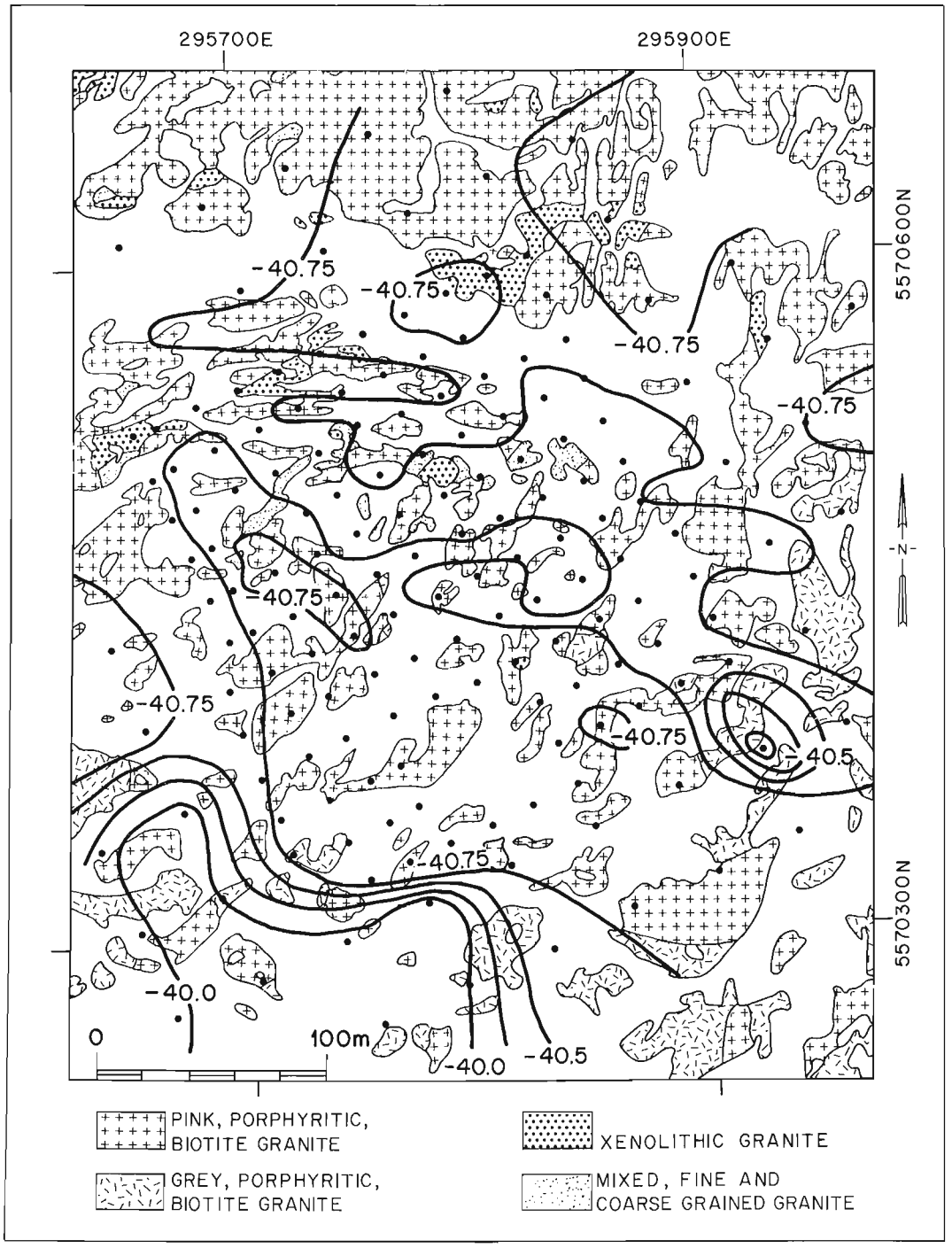


Figure 85.2. Bouguer anomaly contours (interval = 0.25 mGal) and station locations superposed over local surface geology (Stone et al., 1984) at the URL site. Blank areas are covered by surficial deposits.

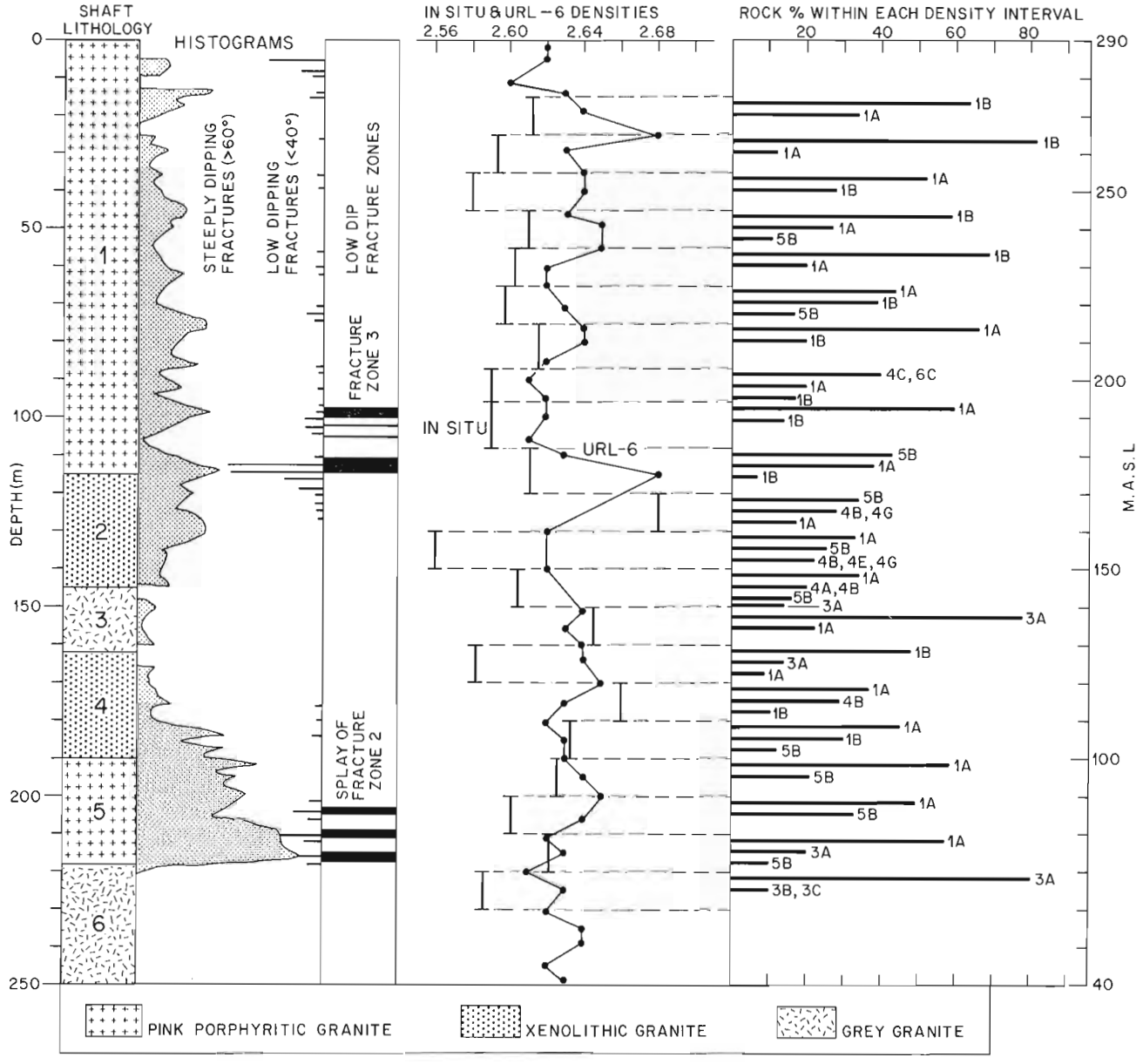


Figure 85.3. Shaft lithology (6 domains), fracture histograms (relative number of fractures per 2 m interval) of steeply- and low-dipping fractures (Everitt and Brown, 1985b), in situ interval densities (vertical bars), URL-6 core sample densities (dots) and percentages of rock type within each interval. Densities are in units of g/cm^3. 1A – pink porphyritic granite (biotite < 10%), 1B – pink porphyritic granite (biotite > 10%), 3A – normal grey granite, 3B – leuco-grey granite, 3C – pegmatitic grey granite, 4A – tonalite xenoliths, 4B – amphibolite xenoliths, 4C – biotitic metapelite xenoliths, 4E – quartzose iron formation xenoliths, 4G – calcareous diopside xenoliths, 5B – coarse-grained porphyroblastic sills and dykes, 6C – coarse-grained segregations, lenses and masses. M.A.S.L. = metres above sea level.

Table 85.1 Computation of interval densities for the URL shaft.

Timber set	M.A.S.L.	Depth	Grav1	Grav2	Avg.	Total(T)	dz	dg-avg	dT	Timber set	dg/dz	dT/dz	4*pi*G*p	Dens	Depth
6	274.7500	15.1500	4.2400	4.2400	4.2400	0.0040				6					15.1500
							10.0100	0.9250	-0.0277		0.0924	-0.0028	0.2190	2.6123	
10	264.7400	25.1600	5.1600	5.1700	5.1650	-0.0237				10					25.1600
							9.9900	0.9350	-0.0233		0.0936	-0.0023	0.2173	2.5930	
14	254.7500	35.1500	6.1000	6.1000	6.1000	-0.0470				14					35.1500
							10.0100	0.9450	-0.0211		0.0944	-0.0021	0.2163	2.5806	
18	244.7400	45.1600	7.0500	7.0400	7.0450	-0.0681				18					45.1600
							9.9700	0.9150	-0.0191		0.0918	-0.0019	0.2187	2.6097	
22	234.7700	55.1300	7.9700	7.9500	7.9600	-0.0872				22					55.1300
							9.9800	0.9200	-0.0179		0.0922	-0.0018	0.2182	2.6034	
26	224.7900	65.1100	8.8900	8.8700	8.8800	-0.1051				26					65.1100
							10.0000	0.9250	-0.0162		0.0925	-0.0016	0.2177	2.5975	
30	214.7900	75.1100	9.8200	9.7900	9.8050	-0.1213				30					75.1100
							12.4900	1.1350	-0.0188		0.0909	-0.0014	0.2192	2.6148	
35	202.3000	87.6000	10.9600	10.9200	10.9400	-0.1393				35					87.6000
							7.5000	0.6950	-0.0089		0.0927	-0.0012	0.2171	2.5904	
38	194.8000	95.1000	11.6600	11.6100	11.6350	-0.1482				38					95.1000
							12.5000	1.1500	-0.0068		0.0920	-0.0005	0.2171	2.5907	
43	182.3000	107.6000	12.8000	12.7700	12.7850	-0.1550				43					107.6000
							12.5100	1.0850	0.0369		0.0867	0.0029	0.2189	2.6118	
48	169.7900	120.1100	13.9000	13.8400	13.8700	-0.1181				48					120.1100
							10.0000	1.0650	-0.2245		0.1065	-0.0225	0.2246	2.6790	
52	159.7900	130.1100	14.9600	14.9100	14.9350	-0.3426				52					130.1100
							9.9700	0.8700	0.0671		0.0873	0.0067	0.2146	2.5604	
56	149.8200	140.0800	15.8400	15.7700	15.8050	-0.2755				56					140.0800
							9.9500	0.8750	0.0233		0.0879	0.0023	0.2183	2.6047	
60	139.8700	150.0300	16.7000	16.6600	16.6800	-0.2522				60					150.0300
							10.0000	0.8700	-0.0089		0.0870	-0.0001	0.2217	2.6449	
64	129.8700	160.0300	17.5500	17.5500	17.5500	-0.2531				64					160.0300
							10.0200	0.9300	-0.0065		0.0928	-0.0006	0.2164	2.5822	
68	119.8500	170.0500	18.5000	18.4600	18.4800	-0.2596				68					170.0500
							10.0000	0.8650	-0.0074		0.0865	-0.0007	0.2228	2.6586	
72	109.8500	180.0500	19.3600	19.3300	19.3450	-0.2670				72					180.0500
							10.0000	0.8850	-0.0065		0.0885	-0.0007	0.2207	2.6337	
76	99.8500	190.0500	20.2300	20.2300	20.2300	-0.2735				76					190.0500
							10.0100	0.8900	-0.0040		0.0889	-0.0004	0.2201	2.6258	
80	89.8400	200.0600	21.1400	21.1000	21.1200	-0.2775				80					200.0600
							10.0100	0.9050	0.0014		0.0904	0.0001	0.2181	2.6015	
84	79.8300	210.0700	22.0400	22.0100	22.0250	-0.2761				84					210.0700
							10.0000	0.8700	0.0100		0.0870	0.0018	0.2198	2.6224	
88	69.8300	220.0700	22.9200	22.8700	22.8950	-0.2581				88					220.0700
							10.0000	0.8400	0.0789		0.0840	0.0079	0.2167	2.5855	
92	59.8300	230.0700	23.7500	23.7200	23.7350	-0.1792				92					230.0700

GRAV1,2 - measured gravity value at each stn. (mGal); 1 down shaft, 2 up shaft (corrected for earth tide and instrument drift)

M.A.S.L. - meters above sea level

Avg - average of grav1 and grav2

Total(T) - shaft, chamber & terrain corrections at each stn. (mGal)

dz - vertical distance between stns. (m)

dg-avg - change in gravity between stns. (mGal)

dT - change in corrections between stns. (mGal)

4*pi*G*p = 4 * pi * grav. constant * density
= free air vert. gradient - dg/dz - dT/dz

Dens - calculated density (g/cm3) between stns.

Average weighted density (g/cm3)
from 15 to 230 m 2.6097 +/- 0.0271

Average depth interval (m)
10.2343 +/- 1.0658

Table 85.2 Void and terrain corrections (mGal) for each shaft stn.

Timber set	Depth (m)	Shaft	Mid chamber	Lower chamber	Terrain	Total (T)
6	15.15	0.01	0.00	0.00	-0.01	0.00
10	25.16	0.01	0.00	0.00	-0.03	-0.02
14	35.15	0.01	0.00	0.00	-0.05	-0.05
18	45.16	0.00	0.00	0.00	-0.07	-0.07
22	55.13	0.00	0.00	0.00	-0.09	-0.09
26	65.11	0.00	0.00	0.00	-0.11	-0.11
30	75.11	0.00	0.00	0.00	-0.13	-0.12
35	87.60	0.00	0.01	0.00	-0.15	-0.14
38	95.10	0.00	0.01	0.00	-0.16	-0.15
43	107.60	0.00	0.02	0.00	-0.18	-0.16
48	120.11	0.00	0.08	0.00	-0.20	-0.12
52	130.11	0.00	-0.14	0.00	-0.21	-0.34
56	140.08	-0.00	-0.06	0.00	-0.22	-0.28
60	150.03	-0.00	-0.02	0.00	-0.24	-0.25
64	160.03	-0.00	-0.01	0.01	-0.25	-0.25
68	170.05	-0.00	-0.01	0.01	-0.26	-0.26
72	180.05	-0.00	-0.00	0.01	-0.27	-0.27
76	190.05	-0.00	-0.00	0.01	-0.28	-0.27
80	200.06	-0.00	-0.00	0.02	-0.29	-0.28
84	210.07	-0.00	-0.00	0.03	-0.30	-0.28
88	220.07	-0.01	-0.00	0.06	-0.31	-0.26
92	230.07	-0.01	-0.00	0.15	-0.32	-0.18

Table 85.3 Granite densities from the Lac du Bonnet batholith

Area	Hole	Core length (m)	No. of samples	Mean density +/-S.D. (mGal)	Source
Core measurements					
WNRE	WN-1	475	131	2.63 +/- .01	Coderre (1983)
	WN-2	152	32	2.63 +/- .01	Coderre (1983)
	WN-4	928	285	2.64 +/- .01	Coderre (1983)
URL	URL-2	945	188	2.63 +/- .04	Drury
	URL-3	478	13	2.63 +/- .01	Drury
	URL-5	300	49	2.63 +/- .01	Tomsons
	URL-6	401	77	2.64 +/- .02	Tomsons
Surface measurements					
Batholith			154	2.61 +/- .02	Coderre (1983)
In-situ measurements					
URL shaft			21	2.61 +/- .03	This study

units (Nettleton, 1976)] is the gravitational constant, and $4\pi G\rho dz$ is the correction for the positive downward attraction ($2\pi G\rho dz$) of the intervening infinite slab of rock of mean density ρ and thickness dz on the upper station, and the negative upward attraction ($-2\pi G\rho dz$) of the slab on the lower station. A correction dc accounts for the effect of departures from the Bouguer concept of essentially horizontal layering (Smith, 1950).

At station k, T_k is the sum of the corrections for surface terrain and subsurface voids (the shaft and the mid and lower chambers in the case of the URL – see Fig. 85.4), and $dT = T_{k+1} - T_k$. For all subsurface stations n:

$$T_k = t_j - t_k^1 - v_k + v_k^1 \; (k = 1,2 \ldots ,n) \qquad (2)$$

where t and t^1 are corrections for topographic features above and below the surface elevation datum, respectively, and v is the void correction. At subsurface stations, t is positive and t^1 is negative. The correction v for a void above a station is negative, and the correction v^1 for one below is positive.

Terrain corrections were calculated out to zone L (outer radius 14.75 km) using the Bible template method (see 'terrain' column in Table 85.2) (Bible, 1962). The corrections are negative values because the surface datum is elevated with respect to the surrounding terrain. A density of 2.61 g/cm^3 was used in the computations, based on the mean density of 154 representative surface samples from the Lac du Bonnet batholith. These corrections are the most significant at most depths.

All void corrections were computed using a mean density of 2.63 g/cm^3, the mean density of core rock from drillholes in the vicinity of the shaft. A void correction for the rectangular shaft was calculated using an exact expression for the gravitational attraction of a right rectangular prism (Nagy, 1966). This correction is significant only at the extremities of the shaft, whereas most of the gravitational effects above and below a station tend to cancel each other (see 'shaft' column in Table 85.2). The gravity effects of the mid and lower chambers were calculated using a number of prisms to approximate their shapes (Fig. 85.4). The corrections for these chambers are significant only for the gravity stations within approximately 30 m of the void. The total effect at each station of the two chamber voids can be seen in Table 85.2.

The quantities ρ, dT and dc are all related to the subsurface vertical gravity gradient dg/dz rather than to gravity at a point (McCulloh, 1967). Thus, equation (1) rewritten in the form used in borehole gravimetry,

$$\rho = \frac{1}{4\pi G}\left(F - \frac{dg}{dz} - \frac{dT}{dz}\right) \qquad (3)$$

was used for the calculation of in situ densities in Table 85.1. The term dc/dz, required where lithological layering is not horizontal, is omitted from equation (3) because the shaft penetrates a single, non-layered, grossly homogeneous granitic formation.

The vertical gravity gradient dg/dz and the gradient due to the combined terrain and void correction dT/dz are listed in Table 85.1. From these gradients the in situ interval densities for the batholith were calculated. The densities range from 2.56 g/cm^3 to 2.68 g/cm^3, with the weighted mean density and its standard deviation for the total section being 2.61 ± 0.03 g/cm^3.

DENSITY DETERMINATIONS OF ROCK SAMPLES

Density measurements were made on 154 rock samples collected from surface localities throughout the batholith and on 775 core samples from seven drillholes (Table 85.3). Samples were weighed first in air and then in water and the density calculated from these weights. These determinations probably fall between the dry density (dry pores) and saturation density (water-filled pores) determinations, because a certain amount of water may be present in inter-grain pores. The granitic surface samples were collected and identified by D. Stone (AECL); they yielded a mean density of 2.61 ± 0.02 g/cm^3. Core samples from four drillholes at the URL site were measured by M. Drury of the Geological Survey of Canada (GSC) and D. Tomsons (AECL); these holes are all located within 675 m of the shaft. The mean density of 188 samples of URL-2 core is 2.63± 0.04 g/cm^3, and that of 13 samples of URL-3 core is 2.63 ± 0.01 g/cm^3. Core samples from URL-5 and URL-6, respectively numbering 49 and 77, have mean densities of 2.63 ± 0.01 and 2.64 ± 0.02 g/cm^3. Density measurements were made also on core samples from three drill holes at the Whiteshell Nuclear Research Establishment (WNRE). This area is located within the batholith, 10 km south of the URL site. A mean density of 2.63 ± 0.01 g/cm^3 was determined from 131 samples within drillhole WN-1, and 32 and 285 samples within holes WN-2 and WN-4 have mean densities of 2.63 ± 0.01 and 2.64 ± 0.01 g/cm^3, respectively.

Drillhole URL-6 is the closest to the shaft, 10 m to the west (Fig. 85.1). There is good correlation between the lithology of the shaft walls and that of the core rock from this drillhole (Everitt and Brown, 1985b). The URL-6 core sampled to the depth of the shaft has a mean density of 2.63 ± 0.02 g/cm^3. This density should best represent that of the shaft rocks. The densities of URL-6 samples are plotted in Figure 85.3.

The pink porphyritic granite samples of the URL-6 core, numbering 30, have a mean density of 2.63 ± 0.02 g/cm^3. Nine xenolithic granite samples have a mean density of 2.64 ± 0.02 g/cm^3 and eight grey granite samples have a mean density of 2.63 ± 0.01 g/cm^3. These mean densities are compared with the in situ mean densities in the next section.

DISCUSSION OF RESULTS

In situ density measurements using the gravity method yield information on the bulk density of a rock formation which include the effects of any air-filled or fluid-filled cavities or pore space in the determined value. For the purpose of research into groundwater flow at URL it is important to know the locations and volumes of such voids. However, in order to

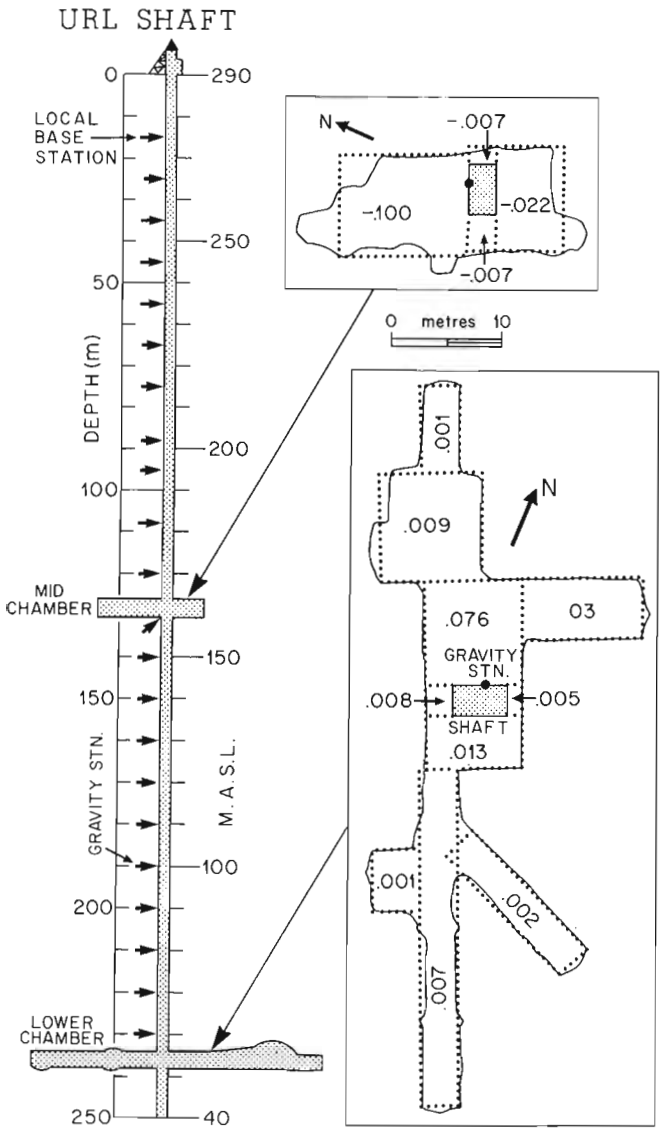


Figure 85.4. Cross section of URL shaft showing locations of gravity stations. Plans of the mid chamber at the 130 m level and the lower chamber at the 238 m level show right rectangular prisms (dotted) used to approximate the form of the voids. The corrections (mGal) are indicated for individual prisms. The mid chamber's gravity station is at the 130 m level (the floor of the void). M.A.S.L. = metres above sea level.

arrive at any conclusion based on the in situ densities presented, it is necessary to separate effects of variation in lithology from those of voids.

The in situ densities calculated through all lithologies within the shaft range from 2.56 g/cm^3 to 2.68 g/cm^3 and have a mean of 2.61 ± 0.03 g/cm^3. This value equals the mean density of 154 samples obtained regionally from the surface of the batholith. However, measurements of core and surface samples from four igneous formations at other AECL research areas show that the mean density of surface samples is 0.03 g/cm^3 less than that of the core samples of the same lithology and formation (see Table 85.4). It is believed that this difference is due primarily to surface weathering. Surface densities, therefore, tend to be lower than actual rock densities. For this reason, the densities of the core are more representative and are used for comparison with the in situ densities.

The 47 URL-6 core densities to the depth of the base of the shaft range from 2.60 g/cm^3 to 2.68 g/cm^3, and have a mean of 2.63 ± 0.02 g/cm^3. The mean in situ density for 21 intervals is 2.61 ± 0.03 g/cm^3. It is shown that these means are statistically different by comparing confidence intervals for the means calculated at the 95% confidence level (Student's t-distribution). The difference is most likely due to the presence of fractures, joints, cleavage, and other penetrative structures within the 230 m section of rock penetrated by the experiment. The general picture of a lower in situ density is observed at the scale of individual intervals for all three types of granite in the shaft; 16 of 21 intervals conform to this pattern. Four interval densities are higher, but three of these correlate with the xenolithic granite and may be explained by the presence of dense mafic xenoliths. An idea of the relative abundance of voids with depth may be obtained by comparing the in situ mean densities with those of URL-6 core samples within each of the three lithological units.

The pink porphyritic granite is the most extensive rock type within the shaft. The mean in situ density of this unit is 2.60 ± 0.01 g/cm^3; 12 individual in situ densities were used for this calculation. In comparison, the mean density of the 30 core samples of the same lithology is 2.63 ± 0.02 g/cm^3. At the 95% confidence level these two means are statistically different. The 0.03 g/cm^3 difference between the in situ and URL-6 mean densities is the largest of the three units, therefore the pink granite, apparently, has the greatest abundance of voids. The fracture log (Fig. 85.3) shows that both low- and steeply-dipping fractures are generally most common within this unit, and thus it is concluded that most of the voids take the form of fractures. The nine in situ densities in the upper pink granite domain (No. 1) have a mean which is 0.02 g/cm^3 lower than that of in situ densities in the lower domain (No. 5). This decrease is most likely due to the increased complexity and frequency of steeply- and low-dipping fractures at and above fracture zone No. 3 (Everitt and Brown, 1985a). The mean density of URL-6 core above and including fracture zone No. 3 does not differ from that of the pink porphyritic granite core from the lower domain, confirming that factors other than lithology influence the in situ densities.

Three individual pink porphyritic granite in situ densities are equal to or less than the overall mean density of 2.61 ± 0.02 g/cm^3 minus one standard deviation (i.e. 2.59 g/cm^3). These low densities probably reflect intervals where fracturing is most intense. The lowermost in situ density interval (between depths of 95 and 108 m) contains fractures of zone No. 3 (Fig. 85.3), and it is probable that this low-dipping fracture zone is responsible also for the low density in the interval (88 to 95 m) above. The third low in situ value, for the interval between 35 and 45 m, is the lowest (2.58 g/cm^3) and

Table 85.4 Difference between surface and core densities for samples of the same lithology and formation.

Area	Rock Type	No. of Samples, n Surface Density (g/cm^3)	No. of Samples, n Core Density (g/cm^3)	Difference, Core-Surface
Atikokan	granite	n = 66, 2.63	n = 1076, 2.66	0.03
Chalk River	orthogneiss	n = 122, 2.69	n = 565, 2.74	0.05
Lac du Bonnet	granite	n = 154, 2.61	n = 775, 2.63	0.02
East Bull Lake	gabbro	n = 251, 2.93	n = 378, 2.90	−0.03
	amphibolite	n = 380, 2.94	n = 189, 2.99	0.05
	diabase	n = 196, 2.95	n = 40, 3.04	0.09
	anorthosite	n = 83, 2.85	n = 437, 2.86	0.01
	gabbroic anorthosite	n = 72, 2.86	n = 72, 2.89	0.03

correlates with a moderate amount of steeply-dipping fractures (Fig. 85.3); more intense fracturing near the shaft is indicated.

The mean in situ density of the xenolithic granite is 2.62 ± 0.04 g/cm^3; only five individual densities were used for this calculation. The nine URL-6 core samples within this unit have a mean of 2.64 ± 0.02 g/cm^3. At the 95% confidence level these two means are statistically the same; however, the lower in situ value is consistent with the pattern observed for the pink porphyritic granite, and to be expected for bulk in situ densities, because they are influenced by large-scale voids. The difference of 0.02 g/cm^3 is, therefore, taken as an indicator that voids may be present within this unit; on the basis of the fracture log (Fig. 85.3) these voids are interpreted to be mainly fractures. The lower difference of 0.02 g/cm^3, compared with the 0.03 g/cm^3 value for the pink porphyritic granite, indicates that fracturing may not be as extensive within the xenolithic granite. The fracture log suggests that low-dipping fractures are less extensive in the xenolithic granite, and this may be the main factor contributing to the lower difference. There is no difference between the mean in situ densities or the mean core densities for the upper (No. 2) and lower (No. 4) domains; it is concluded, therefore, that the fractures have an equivalent effect within both domains. Several interval densities are greater than the core densities and this is attributed to the overriding effect of xenoliths.

The values of two consecutive interval densities within domain No. 2 are difficult to explain. An interval density of 2.68 g/cm^3 was calculated between the depths of 120 m and 130 m. This relatively high value may be due simply to the presence of dense xenolithic material. Within this interval a 10 m thick mafic xenolith has been mapped within the URL core and 28% of the shaft walls consist of inclusions of amphibolite and calcareous diopside (Fig. 85.3). A low interval density of 2.56 g/cm^3 has been calculated between depths of 130 m and 140 m. Although there are some steeply-dipping fractures within this interval, which could account for the low value, any such effect would likely be counteracted by mafic xenoliths which form 22% of the shaft walls. The fact that the highest and lowest density in the shaft occur in successive intervals suggests that small errors in the calculation of the void corrections for the mid chamber may contribute to these extreme values. The mid chamber is located between a depth of 126 and 130 m. A gravity reading within 3 m of a void measuring 3.5 m × 2.6 m × 3.5 m will be affected by only 0.01 mGal, whereas the in situ density of a 10 m interval containing the void will change by 0.02 g/cm^3. It is difficult to precisely estimate the effect of voids when approximating their shape, and small errors of the order of ± 0.01 mGal are, therefore, entirely possible.

The mean in situ density of the grey granite, calculated from one density in each of the upper (No. 3) and lower (No. 6) domains, is 2.62 ± 0.03 g/cm^3, statistically the same as the mean density of 2.63 ± 0.01 g/cm^3 measured for eight core samples. The lower in situ density value is consistent with the pattern observed in the other two granitic units.

CONCLUSIONS

The mean in situ density of the uppermost 230 m of the Lac du Bonnet granitic batholith determined from gravity measurements within the URL shaft is 2.61 ± 0.03 g/cm^3; this compares with a mean core density of 2.63 ± 0.02 g/cm^3 and is statistically different from it at the 95% confidence level. The lower in situ density is attributed to the presence of voids (fractures, joints, etc.) throughout the formation. The presence of fracturing throughout the shaft and correlations between several individual intervals of relatively low in situ densities and areas of increased fracturing of the shaft walls lead to the conclusion that fractures are the principal type of void in the granite. Intervals of anomalously low densities, where no or few fractures have been mapped, may indicate hidden or blind fractures that do not intersect the shaft walls.

Katsube (1981) has estimated that core samples from the Lac du Bonnet granite batholith contain 0.2 to 0.4% con-

necting pores and, in some cases, 0.2 to 0.6% blind pores. These estimates do not include porosity contained in major fractures or joints. The difference between in situ densities and core densities provides a means of estimating the porosity of such structures. It was noted previously that densities of rock samples discussed in this study are intermediate between dry and saturated values. In order to estimate bulk porosity, it is necessary to know the grain density of the core. The latter may be estimated on the basis of the core density (2.63 g/cm^3) obtained in this study providing the porosity of the core is known. A value of 0.3% for the core porosity is assumed based on the range of values given by Katsube (1981). Using this value, a grain density of 2.64 g/cm^3 is estimated on the assumption that pores were dry when the laboratory measurements of density were made, and a value 0.003 g/cm^3 lower is estimated on the assumption that they were filled with water. Bulk porosities were then calculated on the basis of the difference between the in situ and core grain densities. The bulk porosity is estimated to be 1.1% for the case where the voids are dry and 1.7% for the case where they are assumed to be completely water-filled.

This pattern of lower in situ densities and, therefore, the influence of porosity is observed in all three types of granite penetrated. The pink porphyritic granite, present mainly in the upper 115 m of the shaft, has the greatest difference between in situ and core densities (0.03 g/cm^3), and this implies a porosity of 1.4% for the case of dry pores or 2.1% for water-filled pores. It is concluded that fracturing is most widespread within this 115 m interval.

ACKNOWLEDGMENTS

The density experiment was facilitated by the cooperation and support of the management and staff at the URL. We thank R. Everitt, A. Holloway, and G. Simmons for their assistance and for providing technical data. We thank also A. Brown for providing and describing the detailed geological maps of the shaft walls, and A.G. Green, R.A.F. Grieve and J.R. Weber (all from the GSC) for critically reading earlier versions of the manuscript. Finally, we thank A. Rafeek for drafting and D. George and I. Wilkes for initial word-processing.

REFERENCES

Bible, J.L.
1962: Terrain correction tables for gravity; Geophysics, v. 27, p. 715-718.

Brown, A., Everitt, R., and Bloomer, S.
1984: Interim report on low- intermediate-dip fracture zones; Atomic Energy of Canada Limited, Internal Memorandum (unpublished).

Coderre, J.M.
1983: Rock density determinations, gravity anomalies, and geology of the Atikokan and East Bull Lake plutons, Ontario and the Lac du Bonnet pluton, Manitoba; University of Waterloo, 2A Work Term Report (unpublished).

Everitt, R.A., and Brown, A.
1985a: Interim report on lithology and fracture domains in the URL shaft; Atomic Energy of Canada Limited, Internal Memorandum, URL-EXP-008 No. 9 (unpublished).
1985b: Subsurface geology of the Underground Research Laboratory; An overview of recent developments; Proceedings of the 20th Information Meeting of the Canadian Nuclear Fuel Waste Management Program, v. 1, Atomic Energy of Canada Limited, Technical Report TR-375.

Gibb, R.A. and Thomas, M.D.
1980: Density determinations of basic volcanic rocks of the Yellowknife supergroup by gravity measurements in mine shafts – Yellowknife, Northwest Territories; Geophysics, v. 45, p. 18-31.

Katsube, T.J.
1981: Pore stuctures and pore parameters that control the radionuclide transport in crystalline rocks; Proceedings of the Technical Program, International Powder and Bulk Solids Handling and Processing, Meeting held at Rosemont, Illinois, May, 1981, p. 394-409.

McCrank, G.F.D.
1985: A geological survey of the Lac du Bonnet batholith, Manitoba; Atomic Energy of Canada Limited, Report AECL-7816.

McCulloh, T.H.
1967: Mass properties of sedimentary rocks and gravimetric effects of petroleum and natural gas reserves; Geological Survey, Professional Paper 528-A.

Nagy, D.
1966: The gravitational attraction of a right rectangular prism; Geophysics, v. 31, p. 362-371.

Nettleton, L.L.
1976: Gravity and Magnetics in Oil Prospecting; McGraw-Hill Book Co., Inc., New York.

Smith, N.J.
1950: The case for gravity data from boreholes; Geophysics, v. 15, p. 605-636.

Stone, D., Kamineni, D.C., and Brown, A.
1984: Geology and fracture characteristics of the Underground Research Laboratory lease near Lac du Bonnet, Manitoba; Atomic Energy of Canada Limited, Technical Record TR-243.

Iceberg scouring rate studies, Grand Banks of Newfoundland

Projects 790018, 830056

C.F.M. Lewis and D.R. Parrott
Atlantic Geoscience Centre, Dartmouth

Lewis, C.F.M. and Parrott, D.R., Iceberg scouring rate studies, Grand Banks of Newfoundland; in Current Research, Part A, Geological Survey of Canada, Paper 87-1A, p. 825-833, 1987.

Abstract

Icebergs from Greenland and eastern Arctic Canada presently drift onto the Grand Banks of Newfoundland at an average rate of about 400 per year. Some with deep keels scour the seabed. The scouring rates are being investigated by determining the age of this scour population, by calculating its formation rate from iceberg flux and draught information, by relating scour degradation rates to scour formation rates and by repetitive mapping of the seabed over known periods. Preliminary estimates of scouring frequency based on the foregoing estimates are diverse.

A feasibility study of remapping individual survey lines to obtain iceberg scouring rate information was successfully undertaken. Holocene and relict iceberg scours and gravel-sand boundaries were shown to have undergone little or no change over 6 years. The available evidence suggests that iceberg scouring rates on Grand Bank are low, particularly in relation to the more northerly shelves of eastern Canada.

Résumé

Les icebergs du Groenland et de l'est de l'Arctique du Canada dérivent actuellement vers les Grands bancs de Terre-Neuve à un rythme moyen d'environ 400 par an. Certains, avec une quille profonde, affouillent le fond marin. On étudie les vitesses d'affouillement en déterminant l'âge de cette population de cicatrices d'affouillement, en calculant leur vitesse de formation à partir de renseignements sur le flux et le tirant d'eau, en comparant les vitesses d'érosion par affouillement aux vitesses de formation de cicatrices d'affouillement et en dressent de nouvelles cartes du fond marin à intervalles réguliers. Les estimations préliminaires de la fréquence d'affouillement fondées sur les estimations ainsi établies sont diverses.

Une étude de faisabilité portant sur la réalisation de nouveaux travaux de cartographie des lignes de levé individuelles en vue d'obtenir des renseignements sur l'affouillement par les icebergs a été entreprise avec succès. On a démontré que des cicatrices d'affouillement holocènes et résiduelles laissées par des icebergs ainsi que des limites de gravier et de sable n'ont que peu ou pas changé pendant six années. Toutes les preuves à date semblent indiquer que les vitesses d'affouillement par les icebergs sur le Grand banc sont faibles, particulièrement par rapport à la région des plateaux continentaux les plus septentrionaux de l'Est du Canada.

INTRODUCTION

Arctic icebergs, carried southward by the Labrador current, drift onto the Grand Banks of Newfoundland at a mean annual rate of about 400 per year (Ebbesmeyer et al, 1980; Robe, 1980; Mobil Oil Canada, Ltd., 1985). Some of the deeper draught icebergs contact and disrupt the seabed, creating iceberg scours up to 10 m deep. In considering the significance of iceberg scouring as a sediment mixing agent, or as a hazard to seabed structures, it is necessary to determine how frequently they contact and penetrate the seabed.

Data concerning the distribution, abundance and character of iceberg scours have been compiled from sidescan sonar and high resolution seismic reflection profiles collected by industry and government since 1977 (d'Apollonia and Lewis, 1981; King and Gillespie, 1986; Schoenthaler, 1986). Despite our knowledge of the distribution and character of iceberg scours, little information presently exists in which we can place confidence concerning the age or rate of formation of scour marks on Grand Bank. Four distinct types of investigation into the question of iceberg scouring rates are currently being pursued:

1) Determination of the inception of the present period of iceberg scouring using geological methods.
2) Direct calculation of grounding rates using historical information for iceberg flux and draught distribution.
3) Evaluation of the rate of scour degradation as an indicator of the rate of scour formation.
4) Repetitive mapping of the seabed over known periods to determine new scour additions and other seabed changes.

INCEPTION OF ICEBERG SCOURING

Data from Grand Bank reveal a low-density, relatively young population of iceberg furrows and pits on the seabed to about 180 m water depth (Fig. 86.1) that is attributed to the Holocene iceberg flux (Fader and King, 1981; Lewis and Barrie, 1981). This low-density scour population implies a relatively low scouring rate, in contrast to the dense crosscut scour populations that characterize Labrador and northern shelves. A dense scour population also occurs on parts of Grand Bank below the Late Wisconsinan low stand of sea level at about 100 m present water depth (Fader and King 1981), but this is interpreted to be relict and thus irrelevant to modern iceberg scouring rates.

Ideas concerning the age of the low-density scour population, based on regional geological considerations and computer modelling results, vary from the Late Wisconsinan marine transgression about 10-15 ka (Fader and King, 1981), to the close of the climatic optimum about 3 ka (d'Apollonia and Lewis, 1986).

In order to refine our understanding of the age of the most recent iceberg incursion on Grand Bank, evidence of ice history (ice-rafted sediment) is being sought in continuous sediment sections on the adjacent northeast Newfoundland Shelf. On the shallow Grand Bank sediment accumulation is

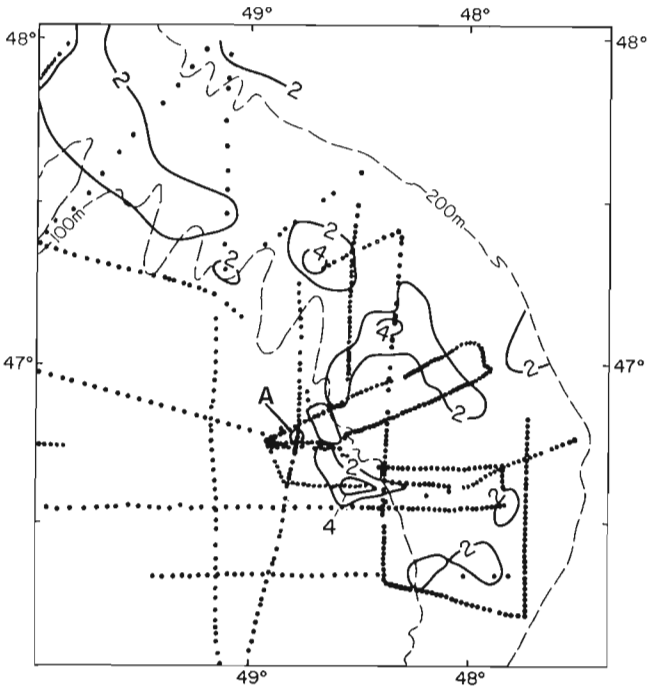


Figure 86.1. Mapped density of inferred Late Holocene iceberg scour marks on northeastern Grand Bank (scours/km^2) based on sidescan sonogram analysis at locations indicated by dots.

limited, and sediments are predominantly redistributed in bedforms (Barrie et al., 1984; Amos and King, 1984). The relatively deep and hydrodynamically quiet Northeast Newfoundland Shelf contains areas of relatively continuous sediment accumulation that record depositional conditions with time (Piper et al., 1978; Dale, 1979; Mudie and Guilbault, 1982; Scott et al., 1984). Three such areas (Notre Dame Channel at 50.89°N 53.30°W, southern NE Newfoundland Shelf at 48.90°N 51.82°W, and outer NE Newfoundland Shelf at 50.12°N 51.22°W) have been cored (Vilks, 1984) and evaluations of their ice history commissioned (Miller et al., 1985; M.P. Segall, personal communication, 1986).

Preliminary results from these paleontological and sedimentological studies suggest that ice-rafted sediments are common in the Late Wisconsinan to Early Holocene, rare in the Mid Holocene, and evident again in the Late Holocene. Assuming that the presence of abundant ice-rafted sediment correlates with the presence of icebergs, these results suggest that Grand Bank is a marginal iceberg zone, at times free of ice, that experiences intermittent iceberg incursions. The first of these events could reflect local Late Wisconsinan-Early Holocene glacier margins, while the second may relate to distant Greenland glacier margins during the Late Holocene. The latter iceberg flux, which extends to the present, would presumably have been aided by the intensification about 2.5 ka BP of the cold inner Labrador Current flowing southward along the eastern Canadian continental margin, as indicated by recent paleo-oceanographic interpretations based on

foraminiferal, dinoflagellate and pollen evidence (Scott et al., 1984). Thus the relatively young,low-density iceberg scour population documented on Grand Bank (Fig. 86.1) may date from the latest iceberg incursion about 2.5 ka BP.

Average, long term scouring rates for Grand Bank localities can be obtained from the ratio of seabed scour concentration (areal density) to the inferred scour population age, 2.5 ka. For example, long term scouring rates of about 0.4 scours/km^2/ka are indicated for the Hibernia region (location A on Fig. 86.1) and of 1.6 scours/km^2/ka for zones of greater scour density on the northern margin of Grand Bank in the 140- to 160-m range of water depths. These estimates assume that the observed scour densities constitute a complete record of the accumulated Late Holocene scour population. This assumption may not hold for areas of high bottom current stress such as shallow banks where scours may be obliterated by redistribution of surface sediment (Amos and Barrie, 1985; Barrie et al., 1984; Gaskill et al., 1985).

CALCULATION OF ICEBERG GROUNDING RATES

A simple box model for iceberg grounding (d'Apollonia and Lewis, 1986) has been used to calculate scouring rates in 9.3 × 9.3 km cells on northern Grand Bank. The model calculates the spatial distribution and mean frequency of iceberg groundings based on information about long-term mean iceberg flux, iceberg draught distribution, and the interaction of these parameters with local bathymetry. A unidirectional southward flux is assumed, but the grounding criteria, principally the range of iceberg draughts that are permitted to ground, may be adjusted to allow for looping iceberg trajectories and multiple scouring events by individual icebergs. This model has been calibrated recently by comparison with observed iceberg groundings from the Makkovik region of Labrador (S.J. d'Apollonia, personal communication, 1986), where grounding events have been interpreted from the behaviour of icebergs monitored by radars during exploratory drilling operations between 1973 and 1982 (El-Tahan et al., 1985; Woodworth-Lynas et al., 1985). The parameters derived from the Makkovik model results were then applied to determine scouring frequencies for the seabed of northern Grand Bank.

The resulting contours of scour frequency on northern Grand Bank are illustrated in Figure 86.2 using a baseline draught distribution with a modal depth of 25 m. The highest frequencies (>1/km^2/ka) occur in the area of the shelf edge, where icebergs are carried around the bank by the Labrador Current. Scour frequencies decrease southward on the bank where icebergs are less frequent; they also decrease in deeper water where fewer iceberg keels are able to touch the seabottom. These values are sensitive to the assumed draught distributions. For example, using a second distribution with a mode of 95 m, based on actual iceberg draughts measured north of Grand Bank (Mobil Oil Canada, Ltd., 1985), the model yields scour frequencies approximately 10 times greater. However the areal distribution of scour frequencies remains similar.

SCOUR DEGRADATION RATES

On ice-scoured seabeds subject to sediment input or sediment redistribution, ice scours may be degraded or eroded with time by current winnowing, bioturbation, sedimentary infilling or by rescouring. When these processes are well established the observed scour population may reflect an equilibrium between the rates of scour obliteration and scour formation. Thus by determining one rate the other may be predicted. This idea was first applied to sea ice scouring in the Beaufort Sea (Lewis, 1978). More recently Gaskill et al. (1985) used a non-deterministic numerical model to illustrate the modification of an initial scour depth distribution and its transformation with time as ice scouring and infilling (sedimentation) proceeded. They further derived relationships between the observed scour depth distribution and the scour frequency for a given rate of scour infilling. By applying assumed sedimentation rates for Grand Bank, they estimated scouring rates of 0.009 scours/km^2/ka for the Hibernia region (location A on Fig. 86.1) and 0.1 scours/km^2/ka for two deeper water locations centred at 120 and 180 m on the northeastern margin of Grand Bank.

Amos and Barrie (1985) derived scour frequency as a function of the rate of megaripple migration and the numbers of scours which crosscut megaripple fields. These considerations yielded example scour frequencies in the range of 0.5 to 6 scours/km^2/ka for the Hibernia field area.

Recently completed estimates of bedload sediment transport (about 0.1 m^3/m/a) for the Hibernia region (Barrie et al., 1986) suggested that an average-sized scour, approximately 1 m deep and 30 m wide would be infilled in 300 a and that a scour frequency of about 3.3 scours/km^2/ka would be required to maintain the observed scour density of about 1 scour/km^2 (Fig. 86.1) within the Hibernia region (J.V. Barrie, personal communication, 1986). This calculation assumes the scours are predominantly oriented perpendicular to the direction of sediment transport. For other orientations scour infilling would require more time and the derived scouring frequency would be less.

The concept of scour degradation as an indicator of scour formation frequency is interesting, but present estimates of scouring frequency using the concept are diverse, and indicate the need for a better understanding of sediment mobility and deposition on Grand Bank. At present the mechanisms, theory, and available data concerning the infilling of seabed depressions are under review to evaluate these methods for the estimation of iceberg scouring frequency.

REMAPPING THE SEABED

Remapping of the seabed has established rates of sea-ice scouring in the Beaufort Sea (Lewis, 1978; Shearer and Stirbys, 1986), and is being considered for evaluation of iceberg scour rates on the eastern Canadian continental shelf. Large-area repetitive surveys are anticipated in order to document the few new scours expected on Grand Bank.

A less expensive method of obtaining scour frequency information is to remap individual existing sidescan sonar

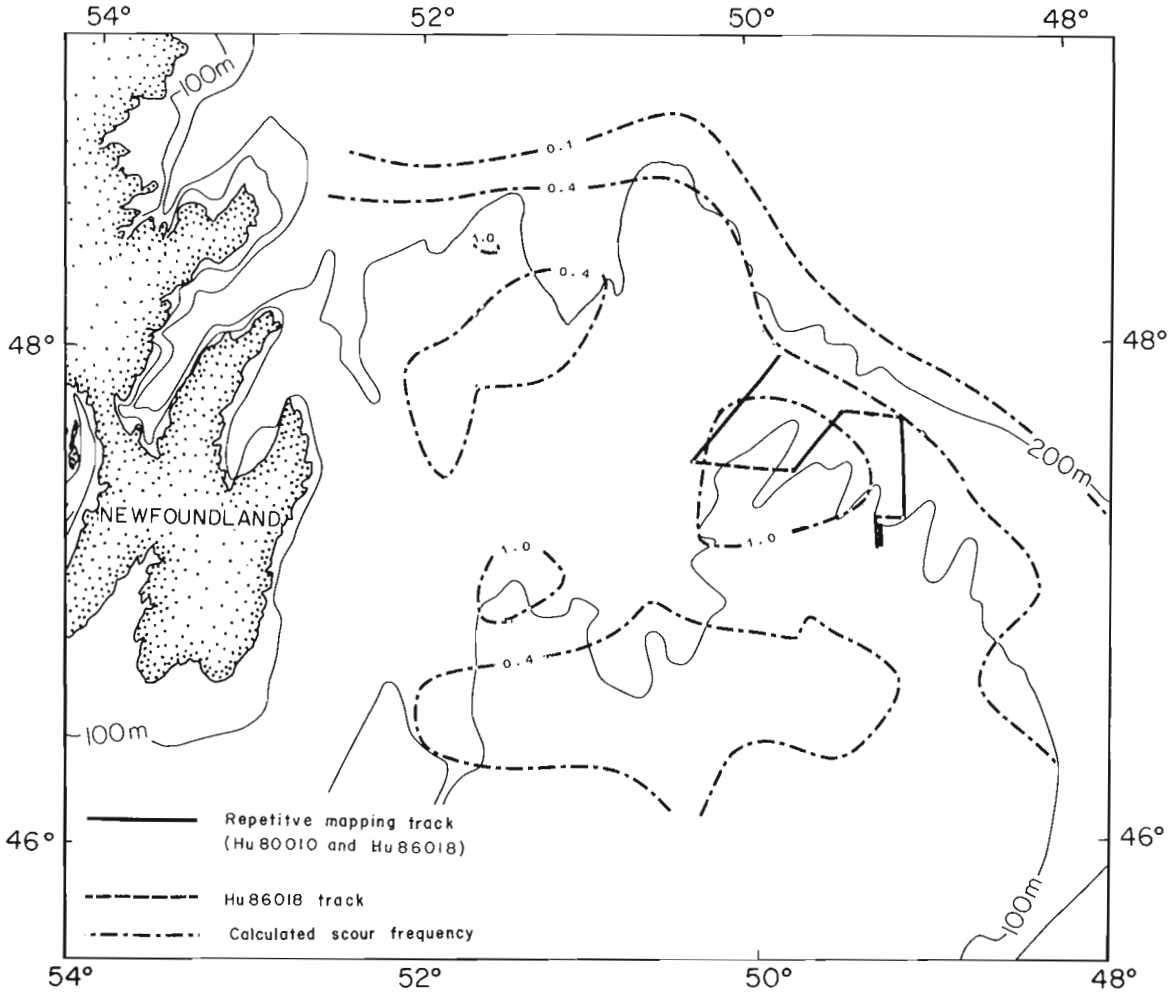


Figure 86.2. Map of northern Grand Bank showing location of remapping study and contours of calculated scouring frequency (scours/km²/ka).

lines of regional coverage. Although a suitable set of lines, totalling over 3000 km, exists from surveys conducted by both the Atlantic Geoscience Centre and the offshore oil industry since 1977, it was not certain that any of these lines could be rerun with sufficient accuracy to permit re-identification of existing seabed features and identification of new scours. A feasibility study was therefore implemented July 2-14, 1986, on cruise Hn 86-018 (Parrott and Lewis, 1986), to test a procedure for re-surveying existing lines. The area chosen for the feasibility study was northeastern Grand Bank, in water depths of 80-200 m. Surficial sediments in the study area consist of mainly sands and gravels (Fader and King, 1981).

Survey technique

The primary tool used for the field investigations was the Bedford Institute of Oceanography (BIO) 70 kHz sidescan sonar. This sidescan, with a nominal swath of 1500 m (1-s firing rate), was towed at 9-11 km/hr. Sidescan sonar data collected with this system on previous cruises to northeastern Grand Bank in 1980 and 1983 (Fader, 1980, Vilks, 1984) formed the basis for comparison with data collected in 1986 (Parrott and Lewis, 1986). In addition, Huntec Deep Towed Seismic (DTS) high-resolution subbottom profiles were collected to provide information on the depths and morphology of the iceberg scours. A Klein 100 kHz sidescan sonar, operated at 0.3 s sweep (225 m range each side), provided higher resolution sidescan sonar images.

Navigation for all the surveys under consideration in this report was provided either by LORAN-C, or by the BIONAV system (Wells et al., 1980). The BIONAV system calculates the ship's position by integrating data from LORAN-C, transit satellite, ship's gyrocompass and doppler sonar. Accuracy for the BIONAV system on northeastern Grand Bank is within about 120 m.

Survey lines were selected to coincide with previous ship's tracks and were rerun in the same direction using identical survey equipment under similar operating conditions. These procedures ensured that the scale and direction

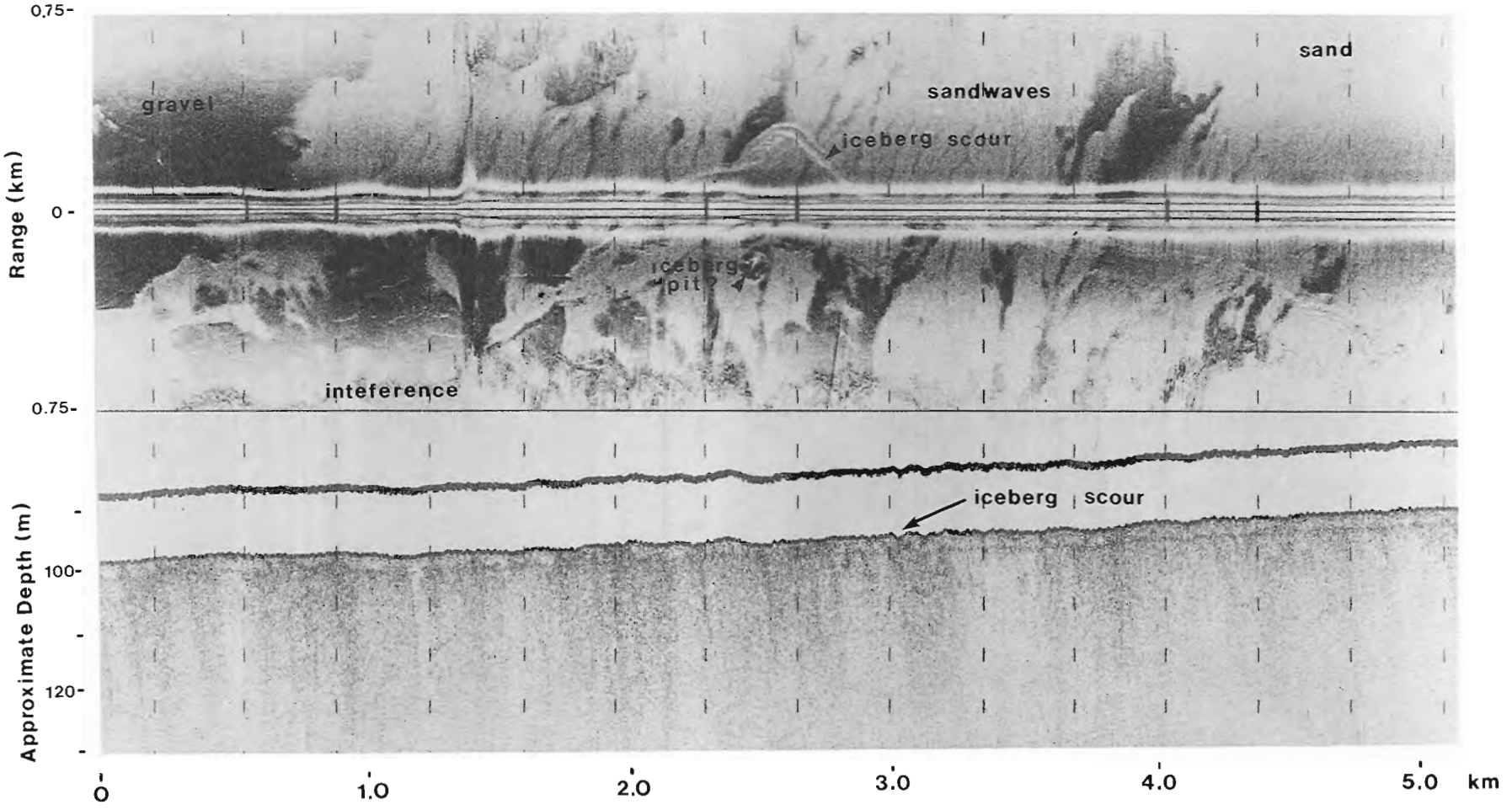
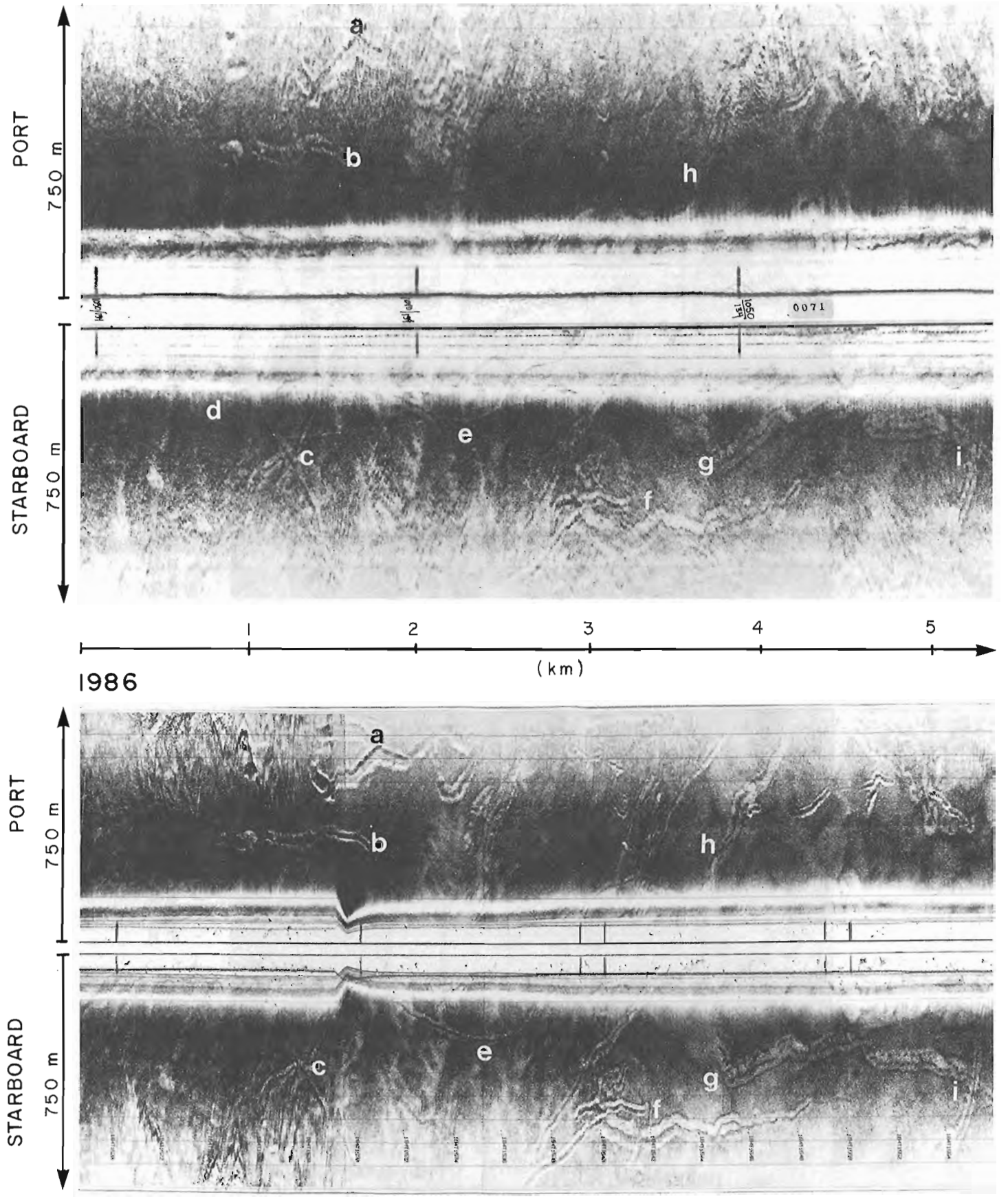


Figure 86.3. Scale-corrected BIO 70 kHz sidescan sonogram and Huntec high resolution subbottom profile collected over a scour formed in 1983, located 40 km northwest of Hibernia.


1980
PORT
750 m
STARBOARD
750 m
a
b
h
d
c
e
g
f
i
0071
1
2
3
4
5
(km)
1986
PORT
750 m
STARBOARD
750 m
a
b
h
c
e
g
f
i

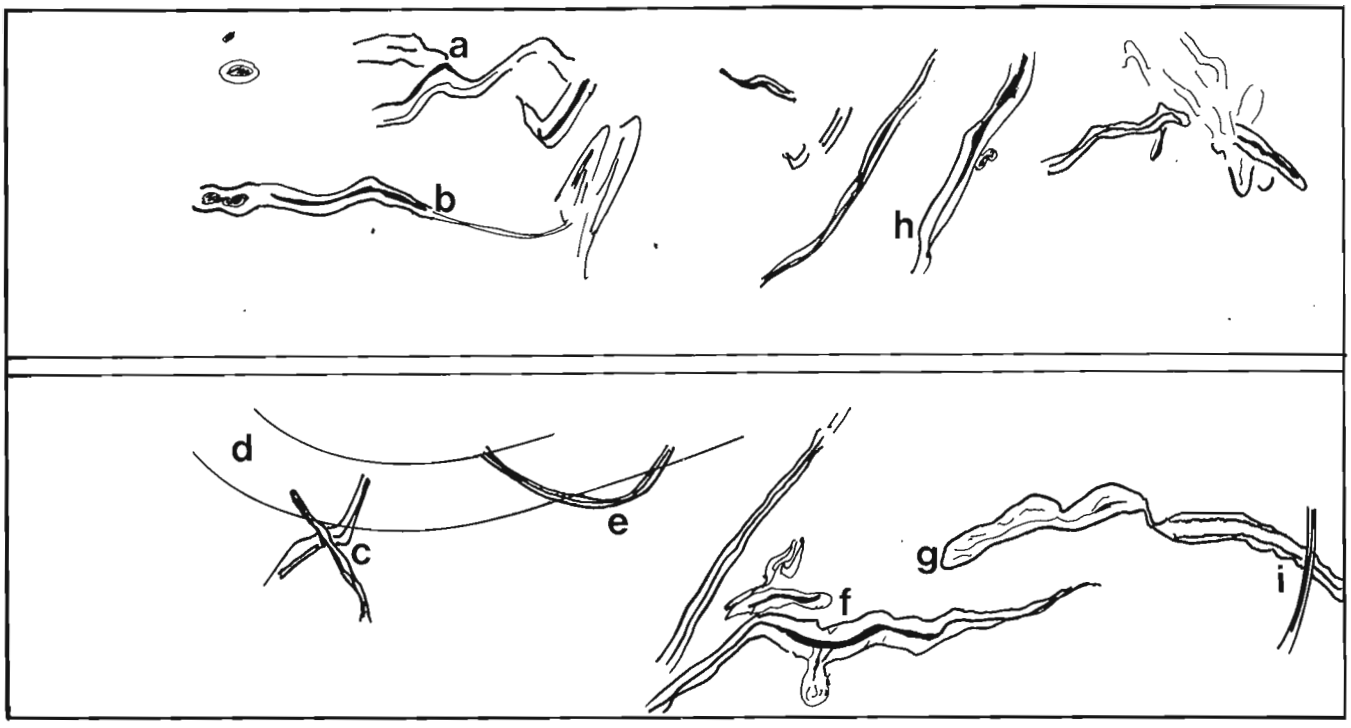


Figure 86.4. Comparison of seabed over 6 years based on BIO 70 kHz sidescan sonograms; upper sonogram collected 1980 (Fader 1980), middle sonogram collected 1986, and an interpretative drawing based on the 1980 sonogram. This record is located 120 km northwest of Hibernia in 110 to 130 m water depth.

of insonification ("illumination") for both the newly and previously collected images were nearly identical, thereby enhancing their comparison. These criteria are supported by repetitive mapping experience on the Labrador Shelf (Woodworth-Lynas and Barrie, 1985).

The BIO sidescan sonar data were displayed on a conventional 45.7-cm wet paper recorder, as had been done in previous years, to facilitate comparison with previous records. This display results in an aspect ratio of about 1:2 for the paper rates and ship's speeds used. An additional EPC Labs model 4800 three channel graphic recorder was introduced for the 1986 survey that also presented the two channels of sidescan sonar data in a scale corrected (but not slant range corrected) format. This unit provides microprocessor control of both paper advance rate and swath display width so that data can be presented at a scale of 1:15,000 with an aspect ratio of 1:1. The third channel of the recorder was used to display the seabed profile using the internal hydrophone data of the Huntec DTS system. An example of this display (Fig. 86.3) illustrates a scour formed by an iceberg grounding event in 1983 about 40 km northwest of the Hibernia region (L. Schoenthaler and J. Ransom, Mobil Oil Canada, Ltd., personal communications 1983 and 1986). This combined display provides a means of quickly comparing sidescan sonar data with the subbottom profile to determine the depth and morphology of features identified on the sidescan sonograms. It was found that, even though the records were not corrected for the layback of the different towfish, this display removed much of the ambiguity previously found in relating features identified on sidescan sonograms with corresponding features on subbottom profiles.

Results and discussion

About 130 km of line were successfully re-surveyed. The records were examined to identify features recognized on data from previous surveys, and offsets were calculated between correlative features of the different surveys. Preliminary examination of the records indicates that the lines were rerun with a mean offset of about 90 m.

A comparative example of 1986 and 1980 sonograms is given in Figure 86.4. Scours, and groups of scours, are identified on the sonograms and interpretative line drawing, as features a to c and e to i. Each of the scours identified in the 1980 survey were recognized in the 1986 re-survey of the area. There seems to be little change in the character of the scour marks over the 6-year period between surveys. Note that while there has been insufficient sediment mobility to significantly affect the appearance of the larger iceberg scours, a set of trawl marks identified in the 1980 survey (feature d) is no longer visible on the 1986 records. A set of new trawl marks was observed on another record.

In general, seabed features such as Holocene or relict iceberg scour marks and gravel-sand boundaries were easily

correlated between the 1986 records and previous data. A comparison of the lines suggests that all features have persisted with little or no change for at least 6 years. Although it would be desirable to extend the survey for greater precision in determining iceberg scouring rates, the present results are consistent with the idea that modern iceberg scouring is a relatively infrequent occurrence on Grand Bank.

SUMMARY

Four approaches are being taken to determine or to constrain estimates of the rates of iceberg scouring on Grand Bank: (1) the age of inception of the present iceberg incursion and its associated scour population, (2) calculation of scour frequency from iceberg flux and draught information, (3) scour degradation rates in relation to scour formation, and (4) seabed remapping.

Preliminary results suggest that Grand Bank is a marginal iceberg zone, in which the present iceberg incursion (and associated scouring) may have begun with strengthening of the cold inner branch of the Labrador Current about 2500 years ago. This implies a scouring rate of about 0.4 scours/km^2/ka for the Hibernia region.

Estimates of iceberg scouring rates based on the second and third approaches are diverse, for example, ranging from 0.009 to 6 scours/km^2/ka for the Hibernia region of Grand Bank. Future work is needed to increase our understanding of the scouring process, to improve simulation of scouring events, and to acquire better information for modelling in order to rationalize and converge the estimates of iceberg scouring frequency and scour depth distribution.

Remapping of individual regional sidescan sonar lines was successfully tested on the northeastern margin of Grand Bank. Modern and relict iceberg scours as well as gravel-sand boundaries were shown to persist for up to 6 years with little or no change; only small features such as fishing trawl marks appeared to degrade significantly.

Though diverse, the present results from all study approaches are consistent with the idea that modern iceberg scouring is a relatively infrequent occurrence on Grand Bank.

ACKNOWLEDGMENTS

We thank the Captain and staff of *CSS Hudson* and the Program Support Subdivision of the Atlantic Geoscience Centre for their assistance in acquiring, processing and archiving data for this study. D. Mosher and R.O. Miller kindly assisted with the preparation of the manuscript and G.B. Fader and D. Praeg provided critical discussion. We appreciate support and input from colleagues G. Vilks (AGC), A.L. Miller and D.B. Scott of the Centre for Marine Geology at Dalhousie University, J.V. Barrie, M.P. Segall and W.T. Collins of the Centre for Cold Ocean Resources Engineering, at Memorial University of Newfoundland, and H. Gaskill of Geonautics Ltd. The ideas in this paper have benefited from discussions with members of the Seabottom Ice Scour Committee of the Environmental Studies Revolving Funds, Ottawa. This is a contribution of Offshore Geotechnics Program 63201 of the federal Panel on Energy Research and Development.

REFERENCES

Amos, C.L. and King, E.L.
1984: Bedforms of the Canadian eastern seaboard: a comparison with global occurrences; Marine Geology, v. 57, p. 167-208.

Amos, C.L. and J.V. Barrie
1985: The frequency of ice scouring of the northeastern Grand Banks of Newfoundland using the interrelationship of scours and bedform migration; in Workshop on Ice Scouring, 15-19 February 1982: R. Pilkington, R. (ed.); National Research Council of Canada, Technical Memorandum No. 136, p. 220-221.

d'Apollonia, S.J. and Lewis, C.F.M.
1981: Iceberg scour data maps for the Grand Banks of Newfoundland between 46°N and 48°N.; Geological Survey of Canada, Open File 819. 13p.
1986: Numerical model for calculating long-term spatial distribution and mean frequency of iceberg-grounding events; in 1986. Ice Scour and Seabed Engineering: C.F.M. Lewis, D.R. Parrott, P.G. Simpkin, and J.T. Buckley, (ed); Environmental Studies Revolving Funds Report No. 049. Ottawa. 310p.

Barrie, J.V., Collins, W.T., Segall, M.P., and Lewis, C.F.M.
1986: Holocene development and sediment transport on the northeastern Grand Banks of Newfoundland; Contract Report, C-CORE, Memorial University of Newfoundland, Geological Survey of Canada, Open File 1396. 155 p.

Barrie, J.V., Lewis, C.F.M., Fader, G.B., and King, L.H.
1984: Seabed processes on the northeastern Grand Banks of Newfoundland; modern reworking of relict sediments; Marine Geology, v. 57, p. 209-227.

Dale, C.T.
1979: A study of high resolution seismology and sedimentology on the offshore Late Quaternary sediments northeast of Newfoundland; unpublished M.S. thesis, Dalhousie University, Halifax, Nova Scotia, 181 p.

Ebbesmeyer, C.C., Okuba, A., and Helseth, J.M.
1980: Description of iceberg probability between Baffin Bay and the Grand Banks using a stochastic model; Deep Sea Research, v. 27a: 975-986.

El-Tahan, M., El-Tahan, H., Courage, D., and Mi[illegible]er, P.
1985: Documentation of iceberg groundings; Environmental Studies Revolving Funds, Report No. 007, Ottawa, 162 p.

Fader, G.B.
1980: Cruise report No. 80-010 CSS HUDSON, April 21 – May 20, 1980; Internal Report, Atlantic Geoscience Centre, Geological Survey of Canada, Bedford Institute of Oceanography, Dartmouth. 5p.

Fader, G.B. and King, L.H.
1981: A reconnaissance of the surficial geology of Grand Banks of Newfoundland; in Current Research, Part A, Geological Survey of Canada, Paper 81A-1A, p. 45-56

Gaskill, H., Nicks, L., and Ross, D.
1985: A non-deterministic model of populations of iceberg scour depths; Cold Regions Science and Technology, v. 11: p. 107-122.

King, E. and Gillespie, R.
1986: Regional distribution and variability of iceberg scour on the eastern Canadian continental shelf; in Ice Scour and Seabed Engineering: C.F.M. Lewis, D.R. Parrott, P.G. Simpkin, and J.T. Buckley, (ed). Environmental Studies Revolving Funds Report No. 049. Ottawa. 310 p.

Lewis, C.F.M.
1978: The frequency and magnitude of drift-ice groundings from ice-scour tracks in the Canadian Beaufort Sea; Proceedings on Port and Ocean Engineering Under Arctic Conditions, Memorial University of Newfoundland, St. John's, Sept 26-30, 1977. pp 568-579.

Lewis, C.F.M. and Barrie, J.V.
1981: Geological evidence of iceberg groundings and related seafloor processes in the Hibernia discovery area of Grand Bank, Newfoundland; in Proceedings of the Symposium on Production and Transportation Systems for the Hibernia Discovery, W.E. Russell and D.B. Muggeridge (ed.); Newfoundland and Labrador Petroleum Directorate, St. John's, Newfoundland, pp 146-147.

Miller, A.L., Scott, D.B., and Smith, D.
1985: Post-glacial paleo-oceanography, northeast Newfoundland Shelf; Technical report No. 4, Centre for Marine Geology, Dalhousie University and Geological Survey of Canada, Open File 1194, 34 p.

Mobil Oil Canada Ltd.
1985: Hibernia development project environmental impact statement; v. IIIa Biophysical Assessment; Mobil Oil Canada Ltd., St. John's, Newfoundland, 258 p.

Mudie, P.J. and Guilbault, J.-P.
1982: Ecostratigraphic and paleomagnetic studies of late Quaternary sediments on the northeast Newfoundland Shelf; in Current Research, Part B, Geological Survey of Canada, Paper, 82-1B, p. 107-116.

Parrott, D.R. and Lewis, C.F.M. (ed.).
1986: Cruise Report Hudson 86-018, Grand Banks of Newfoundland and Flemish Pass, July 2-14, 1986; Atlantic Geoscience Centre, Geological Survey of Canada, Open File Report, Dartmouth.

Piper, D.J.W., Mudie, P.J., Aksu, A.E., and Hill, P.R.
1978: Late Quaternary sedimentation, 50 N, north-east Newfoundland Shelf; Geographie Physique et Quaternaire, v. 32, no. 4, p. 321-332.

Robe, R.Q.
1980: Iceberg drift and deterioration; in Dynamics of Snow and Ice Masses, S.C. Colbeck (ed.); Academic Press, New York, pp. 211-259.

Schoenthaler, L.
1986: Grand Banks ice-scour catalogue; in 1986. Ice Scour and Seabed Engineering, C.F.M. Lewis, D.R. Parrott, P.G. Simpkin, and J.T. Buckley, (ed); Environmental Studies Revolving Funds Report No. 049. Ottawa. 310 p.

Scott, D.B., Mudie, P.J., Vilks, G., and Younger, D.C.
1984: Latest Pleistocene-Holocene paleoceanographic trends on the continental margin of eastern Canada: foraminiferal, dinoflagellate and pollen evidence; Marine Micropaleontology, v. 9, p. 181-218.

Shearer, J. and Stirbys, A.
1986: Towards repetitive mapping of ice scour in the Beaufort Sea; in 1986. Ice Scour and Seabed Engineering, C.F.M. Lewis, D.R. Parrott, P.G. Simpkin, and J.T. Buckley, (ed.): Environmental Studies Revolving Funds Report No. 049. Ottawa. 310 p.

Vilks, G.
1984: Report of Cruise No. 83033; Internal Report, Atlantic Geoscience Centre, Geological Survey of Canada, Bedford Institute of Oceanography, Dartmouth, 51p.

Wells, D., Grant S., and McKeown, D.
1980: Accuracy of the Bedford Institute of Oceanography Integrated Navigation System (BIONAV); Proceedings of the 19th Canadian Hydrographic Conference, Halifax, N.S., March 20, 1980. p. 43-51

Woodworth-Lynas, C.M.T., Simms, A., and Rendell, C.M.
1985: Iceberg grounding and scouring on the Labrador continental shelf; Cold Regions Science and Technology 10: p. 163-186.

Woodworth-Lynas, C.M.T. and Barrie, J.V.
1985: Iceberg scouring frequencies and scour degradation on Canada's eastern shelf areas using sidescan sonar mosaic techniques; 8th International Conference on Port and Ocean Engineering under Arctic Conditions, Narssarssuaq, Greenland, Sept. 7-14, 1985. Vol. 8, p. 419-442.

Preliminary investigations of the abundance of platinum, palladium and gold in some samples of Canadian copper-nickel ores

Project 740107

I.R. Jonasson, O.R. Eckstrand, and D.H. Watkinson[1]
Mineral Resources Division

Jonasson, I.R., Eckstrand, O.R., and Watkinson, J.H., Preliminary investigations of the abundance of platinum, palladium and gold in some samples of Canadian copper-nickel ores; in Current Research, Part A, Geological Survey of Canada, Paper 87-1A, p. 835-846, 1987.

Abstract

Tables of analytical data for twenty-four elements, including gold, platinum and palladium are presented for some fifty occurrences of copper-nickel ore in Canada. Some preliminary observations are offered on abundances of the precious metals.

Résumé

On a regroupé dans des tableaux des résultats d'analyses de trente-quatre éléments, y compris, l'or, le platine et le palladium; ces tableaux donnent aussi les résultats de cinquante venues de minerai cupro-nikèlifère au Canada. Certaines observations préliminaires donnent des reseignements sur l'abondance de métaux précieux.

[1]Geology Department, Carleton University, Ottawa, Ontario K1S 5B6

INTRODUCTION

Samples of Cu-Ni ore from some fifty occurrences were selected from GSC (O.R.E.) collections for this geochemical reconnaissance study. These represent well-known mines and other deposits in the Sudbury and Thompson districts as well as other mines and deposits from 5 provinces and 2 territories of Canada.

Analysis of the results is not complete, and more detailed studies in part initiated by the results of this reconnaissance are in progress. However, in view of current interest in platinum group elements (PGE) and gold within the Canadian mining industry, the raw data sets are presented essentially without interpretation in this preliminary report.

The samples were originally collected as character samples of the kinds of sulphide-bearing rocks present in those deposits. They are, therefore, not necessarily accurately representative of the associated orebodies, but are considered to be indicative of the broad chemical character of the zones of mineralization.

All samples were crushed, ground and subjected to heavy liquid separation of sulphides (pyrite, pyrrhotite, pentlandite, chalcopyrite, etc.) and oxides (mainly magnetite) from the silicate matrix. Further separation into constituent minerals was not attempted because of their fine grained nature and complex intergrowth textures. The concentrates were then milled to pass a 250 mesh screen.

After dissolution with strong aqua regia, all prepared concentrate samples were analyzed for the following elements: Cu, Ni, Fe, Zn, Pb, Ag, Mn, Co, Bi, and Hg. Elemental determinations were made by conventional atomic absorption methods utilizing background correction. Chromium values were derived by a partial (nitric acid) leach of sulphides only, and should be regarded as minimum levels since the contribution from iron oxides remains unknown.

Other elements, As, Sb, Mo, Se, Te were determined on a third split by a variety of colorimetric techniques following total decomposition. U was determined by neutron activation analysis; S by a combustion-titration method and Au, Pt and Pd were analyzed by carbon-rod atomic absorption spectrometry following fire-assay preparation of lead beads (Bondar-Clegg and Co., Ottawa).

RESULTS AND DISCUSSION

Analytical data are presented in Tables 87.1 to 87.4. Mean values have been calculated for all deposits represented by at least three samples. It is important to keep in mind that all values represent heavy mineral concentrates. Sulphur content may be used as a rough guide to the amount of sulphide.

The data show many significant chemical differences between the heavy mineral concentrates of various deposits. Perhaps some of the most interesting of these are the highly variable concentration levels of Pt and Pd in different deposits. It is quite clear for instance that the Trebor, Rottenstone, Wellgreen and Gordon Lake deposits have anomalously high concentrations of Pt and Pd. These are in sharp contrast to the relatively low Pt and Pd values in deposits such as St. Stephen, Lynn Lake, Pipe 2, Moak Lake and Renzy. In addition to the between-deposits differences in Pt and Pd, some deposits show great within-deposit variations of these elements. A prominent example is the Pt content of the Shebandowan deposits. As regards the relative proportions of Pt and Pd, it is common that Pt and Pd are roughly equal in mafic-hosted deposits (Table 87.4) whereas Pd greatly exceeds Pt in most of the ultramafic-hosted deposits (Table 87.2).

Gold shows a trend to greater abundances as the total (Pt + Pd) increases. Often, high precious metal levels are accompanied by unusual values for As, Sb, Te, and Bi in particular. Mineralogical studies in progress on whole-rock samples from some of the deposits provide supporting evidence for these observations. For example, minerals bearing Ag, Pd, Te and Bi were sought and recognized at the Rottenstone Lake deposit. Studies such as these demonstrate the usefulness of trace element analyses in directing attention to those elements which commonly form mineral assemblages with certain of the platinum group metals.

Many other interesting and probably significant chemical differences between deposits could be pointed out. This chemical reconnaissance obviously provides abundant scope for recognition of many elemental associations and trends, with the prospect of relating these to geological features and modes of genesis of the deposits.

Table 87.1 Ultramafic-hosted Ni-Cu deposits. Base metals in heavy mineral concentrates.

	As	Sb	Mo	Hg	Pt ppb	Pd ppb	Au ppb	$\frac{Pt}{Pt + Pd}$	Se	Te	Bi	U	Sample
1. RENZY MINE QUEBEC	1	1	10	0.08	10	180	20	0.053	57	30	3	0.05	141
	1	1	5	0.15	5	210	700	0.023	54	20	3	0.00	147
	1	1	3	0.81	5	135	40	0.036	36	8	3	0.05	148
	1	1	3	1.43	5	140	15	0.034	21	2	3	0.00	151
	1	1	10	0.13	25	150	35	0.143	42	0	3	0.00	152
	1	1	3	0.22	10	100	740	0.091	42	0	3	0.27	161
	1	1	3	0.07	0	-	25	-	27	2	3	0.00	830
	1	1	3	0.66	10	125	30	0.074	42	19	3	0.00	832
	1	1	10	0.41	-	-	40	-	42	0	3	0.00	837
Mean Values	-	-	-	0.44	9	149	180	0.057	39	9	-	-	
2. TREBOR (KANICHEE) MINE TEMAGAMI ONT.	1	1	5	0.31	-	-	2245	-	24	39	3	0.00	27
	42	1	3	0.30	585	2500	2000	0.190	-	54	3	0.00	29A
	6	1	3	0.29	660	705	130	0.484	30	33	3	0.00	29B
	1	1	3	0.24	1505	3305	1350	0.313	95	18	3	0.00	29D
	1	1	3	0.10	2720	2120	220	0.562	57	0	3	0.00	29E
	4	1	3	0.31	2410	7455	2200	0.244	80	0	3	0.05	29F
Mean Values	8	-	-	0.26	1576	3217	1357	0.329	57	22	-	-	
3. MARBRIDGE MINE, QUE.	1	1	5	0.09	390	920	50	0.298	4	0	3	0.00	8A
	1	1	3	0.11	230	625	5	0.269	7	1	3	0.05	8B
	1	1	3	0.15	-	-	100	-	-	0	3	0.10	8D
	1	1	5	0.11	215	840	40	0.204	3	0	3	0.00	8E
	2	1	5	0.11	30	105	10	0.222	4	0	3	0.00	8F
	1	1	7	0.20	-	-	600	-	57	0	3	0.00	11
Mean Values	-	-	-	0.13	216	623	134	0.257	15	0	-	-	-
4. SOTHMAN MINES, ONT.	1	1	5	0.23	450	1520	205	0.228	4	28	3	0.05	198A
5. TEXMONT (FATIMA) MINES, ONT.	-	-	5	0.46	-	-	-	-	-	-	-	0.00	85
	53	1	5	0.41	-	-	125	-	-	-	-	0.00	90
	63	1	10	0.18	-	-	340	-	27	0	3	0.00	97
	58	1	3	0.17	30	1120	160	0.026	20	32	3	0.00	204
	-	-	3	0.45	-	-	220	-	6	-	-	0.00	159
Mean Values	58	-	-	0.33	-	-	211	-	18	16	-	-	-
6. ALEXO MINES, ONT.	1	1	3	0.31	660	1640	180	0.287	9	40	3	0.00	26A
	1	1	10	0.16	230	550	35	0.295	4	23	3	0.05	26C
	5	1	3	0.51	575	1600	185	0.264	10	38	3	0.00	168
Mean Values	-	-	-	0.33	488	1263	133	0.279	7	34	-	-	
7. EXPO-UNGAVA, QUE.	1	1	3	0.27	-	-	-	-	-	-	-	0.08	38
	1	1	-	0.33	-	-	-	-	-	-	-	0.80	43
	1	1	5	0.49	875	3420	10	0.204	33	0	3	0.00	45
	1	1	5	0.51	670	380	80	0.638	84	6	3	0.00	47
Mean Values	-	-	-	0.40	772	1900	45	0.289	59	3	-	-	
8. LAKEMOUNT PROPERTY, WAWA, ONT.	1	1	9	0.11	5	6560	35	0.001	27	40	3	0.00	36
9. SHEBANDOWAN MINE, ONT.	1	1	3	*1.17	3500	9190	540	0.276	10	0	3	0.00	95
	1	1	3	0.13	20	440	20	0.043	8	0	3	0.00	96
	84	1	3	0.17	370	1580	100	0.190	39	0	3	0.00	97
	1	1	3	0.15	350	980	90	0.263	54	0	3	0.05	98
	1	1	5	0.11	5	1135	155	0.004	63	2	3	0.00	80A
	1	1	3	0.13	0	960	135	0	57	1	3	0.00	80B
	1	1	5	0.13	25	1245	125	0.020	34	0	3	0.00	80C
Mean Values	-	-	-	0.14	610	2219	171	0.216	38	1	-	-	

Table 87.1 (cont.)

	As	Sb	Mo	Hg	Pt ppb	Pd ppb	Au ppb	$\frac{Pt}{Pt + Pd}$	Se	Te	Bi	U	Sample
10. LUCKY BOY CLAIMS, MANITOBA	-	-	3	0.26	-	-	90	-	6	4	3	0.00	869
	1	1	3	0.19			60		6	4	3	0.00	885
11. DUMBARTON MINE, MANITOBA	11	1	5	0.10	260	625	35	0.294	36	8	3	0.00	467
	1	1	5	0.21	255	1760	80	0.127	63	9	3	0.00	468
	3	1	5	0.16	90	1280	25	0.066	-	0	3	0.05	469
	3	1	5	0.08	0	500	40	0	33	0	3	0.08	470
	1	1	3	0.06	0	465	25	0	48	0	3	0.00	537
Mean Values	4	-	5	0.12	121	926	41	0.116	45	3	-	-	
12. NORPAX MINE, ONT.	1	1	23	0.41	70	3320	620	0.021	100	0	3	3.75	542
13. GORDON LAKE MINE, ONTARIO	1	1	5	0.94	510	4000	35	0.113	3	39	3	0.05	351
	3	1	3	2.32	-	-	75	-	45	38	3	0.00	464
	1	1	10	0.35	1820	4770	10	0.276	65	16	3	0.00	345B
Mean Values	-	-	-	1.20	1165	4385	40	0.210	38	31	-	-	
14. RANKIN MINE, NWT	32	18	3	0.57	730	1560	120	0.319	42	37	3	0.00	713B
	67	56	3	0.57	950	5420	735	0.149	45	64	3	0.00	713C
Mean Values	50	37	-	0.57	640	3490	428	0.155	44	51	-	-	
15. FERGUSON LAKE, NWT	2	1	10	0.67	0	15	750	0	30	27	3	1.63	736A
	1	1	3	0.08	110	1080	20	0.092	7	22	3	0.05	736B
16. SOAB NORTH MINE THOMPSON, MANITOBA	856	1	10	2.17	1820	2060	125	0.469	13	0	19	0.00	407
	662	1	5	5.93	-	-	425	-	12	30	26	0.03	411
	*3	1	3	0.39	0	425	20	0	12	31	7	0.25	413
	466	1	3	5.06	20	1315	120	0.015	12	0	13	0.05	408A
	636	1	10	1.46	890	1340	110	0.399	20	0	13	0.00	409A
	554	1	5	0.41	30	2880	550	0.010	14	41	14	0.00	409C
Mean Values	624	-	-	2.57	552	1604	225	0.256	14	17	15	-	
17. PIPE NO. 2 MINE THOMPSON, MANITOBA	55	1	10	0.35	0	15	20	0	12	4	3	0.00	388
	13	1	18	0.14	25	75	20	0.250	15	1	3	0.05	389
	52	1	15	0.21	5	150	30	0.032	10	0	3	0.00	396
	15	1	15	0.15	35	85	10	0.292	10	21	3	0.00	327A
	14	1	10	0.15	5	140	5	0.034	14	27	3	0.13	327B
Mean Values	30	-	14	0.20	14	93	17	0.131	12	11	-	-	
18. THOMPSON NO. 1 MINE MANITOBA	4	1	35	0.33	0	200	15	0	-	0	3	0.75	315
	30	1	10	0.21	0	805	15	0	12	14	3	0.00	316A
Mean Values	17	-	22	0.27	0	503	15	0	-	7	-	-	
19. BIRCHTREE MINE THOMPSON, MANITOBA	776	1	25	0.46	35	120	30	0.226	6	55	3	0.40	376
	10	1	10	0.35	5	20	10	0.200	12	22	3	0.00	377
	6	198	15	0.28	*2100	*14000	*1765	0.130	12	16	3	0.20	382
	480	1	20	1.33	0	500	20	0	5	0	3	0.05	383
	-	-	-	0.16	-	-	-	-	-	-	-	52.0	384
Mean Values	318	-	18	0.52	13	213	20	0.058	9	23	-	-	

Table 87.1 (cont.)

	As	Sb	Mo	Hg	Pt ppb	Pd ppb	Au ppb	$\frac{Pt}{Pt + Pd}$	Se	Te	Bi	U	Sample
20. MOAK LAKE MINE THOMPSON, MANITOBA	7	1	15	0.27	5	40	30	0.111	10	0	3	1.63	305A
	3	1	5	1.38	0	35	20	0	9	9	3	1.15	305B
	5	1	10	5.32	25	245	10	0.093	-	0	3	0.13	305C
Mean Values	5	-	10	2.32	10	107	20	0.085	10	3	-	0.97	
21. MYSTERY LAKE THOMPSON, MANITOBA	12	1	15	3.45	-	-	-	-	4	0	3	0.08	302B
22. CLAM LAKE, SASK. (CANADIAN BONANZA)	1	1	5	0.06	-	-	30	-	14	-	3	0.00	112
23. NEMEIBEN LAKE, SASK.	1	1	3	0.05	-	-	60	-	7	0	3	0.00	105
	1	1	5	0.03	0	880	20	0	30	29	3	0.00	87A
	1	1	3	0.06	0	1020	40	0	38	4	3	0.00	87B
Mean Values	-	-	-	0.05	0	950	40	0	25	11	-	-	
24. ROTTENSTONE MINE, SASK.	1	1	3	0.90	3530	4820	230	0.423	88	0	3	0.00	58B
	-	-	3	0.14	17790	6060	280	0.746	56	1	3	0.00	59
	1	1	3	0.06	12190	6780	150	0.643	52	28	3	0.00	60
	1	1	5	0.23	15950	3660	1000	0.813	34	0	3	0.00	61
	1	1	3	0.03	-	-	12285	-	112	24	125	0.13	62
	1	1	3	0.08	16750	4060	405	0.805	24	15	3	0.00	65
	1	1	3	0.03	-	-	4650	-	6	34	95	0.00	66
	1	1	3	0.03	5530	7180	180	0.435	52	63	3	0.00	67
ROTTENSTONE ISLAND	15	2	5	0.90	1010	650	30	0.608	13	0	3	0.00	73
Mean Values	-	-	-	0.27	10390	4750	2134	0.686	49	18	-	-	
25. MUSKOX INTRUSION: EAST CONTACT, SPEERS LAKE, N.W.T.	1	2	5	0.17	0	80	45	0	33	0	3	0.00	690
	133	1	5	0.17	90	770	60	0.105	27	0	3	0.00	691
26. TURNAGAIN RIVER PROP., B.C.	1	1	10	0.32	0	-	60	-	85	53	3	0.00	546
	1	1	3	0.61	530	505	25	0.512	13	35	3	0.05	548
	1	1	5	0.21	-	-	10	-	16	0	3	0.00	557
	6	1	3	0.55	485	760	20	0.390	24	0	3	0.05	550A
	1	1	5	0.49	385	610	20	0.387	2	0	3	0.05	550B
	1	1	15	0.76	0	15	15	0	95	20	3	0.05	543
Mean Values	-	-	-	0.49	280	473	25	0.372	39	18	-	-	
27. GIANT MASCOT MINE, B.C.	1	1	5	0.75	-	-	10	-	49	0	3	0.05	615
	1	1	5	1.11	-	-	370	-	27	0	3	0.00	624
	1	1	10	0.33	-	-	5	-	-	0	3	0.00	657
	1	1	3	0.24	-	-	-	-	32	0	3	0.00	639A
	1	1	20	0.31	0	-	20	-	39	0	3	0.00	659A
	57	1	18	0.13	0	345	20	0	21	0	3	0.00	659B
Mean Values	-	-	10	0.48	-	-	85	-	34	0	-	-	
DETECTION LIMITS	1	1	3	0.01	5	5	5		1	1	3	0.005	

* not included in averages; values in ppm unless noted;
- indicates no data

Table 87.2 Ultramafic-hosted Ni-Cu deposits. Precious metals and other elements in heavy mineral concentrates.

	Zn	Cu%	Pb	Ag	Ni%	Mn	Fe%	Co	Cr	S%	Cu/Cu+Ni	Sample No.
1. RENZY MINE, QUEBEC	85	2.24	3	4	2.13	375	51.5	988	110	33.3	0.513	141
	129	4.00	3	6	2.06	328	46.5	981	470	31.5	0.660	147
	56	0.94	3	4	1.88	537	46.1	1000	268	26.7	0.333	148
	59	1.52	3	2	1.50	833	35.8	834	328	18.6	0.503	151
	78	1.82	3	3	2.25	105	48.8	1091	298	12.9	0.447	152
	333	*18.5	3	15	1.25	27	39.0	573	40	30.9	0.937	161
	34	0.63	3	2	1.76	303	44.9	1222	722	26.6	0.264	830
	73	3.65	3	5	1.84	223	38.7	1568	544	27.3	0.665	832
	135	0.81	3	2	1.52	1322	45.2	1424	*3254	15.3	0.348	837
Mean Values	109	1.95	-	4	1.80	417	38.5	1076	348	24.8	0.520	
2. TREBOR (KANICHEE) MINE TEMAGAMI, ONT.	224	2.55	20	13	1.73	1522	57.4	693	4500	-	0.596	27
	137	1.83	3	10	1.26	1028	74.7	537	3500	7.6	0.592	29A
	212	0.78	3	5	2.78	611	47.3	562	2812	18.1	0.219	29B —
	25	0.93	15	11	4.74	174	48.7	797	226	28.0	0.164	29D —
	16	0.07	3	4	4.54	200	57.4	1083	112	24.6	0.015	29E
	26	0.85	3	8	5.53	215	49.6	1067	100	26.0	0.133	29F
Mean Values	107	1.17	-	8	3.43	625	55.9	790	1875	20.9	0.254	
3. MARBRIDGE MINE, QUE.	56	1.26	3	3	2.65	71	35.2	1417	483	27.2	0.322	8A
	23	0.27	3	3	3.53	147	41.7	1500	38	34.9	0.071	8B
	51	0.10	3	1	1.47	215	52.2	685	776	16.7	0.064	8D
	26	1.44	3	6	3.86	105	46.1	1034	250	31.6	0.272	8E
	29	0.05	3	1	0.57	31	31.4	1167	262	29.6	0.081	8F
	27	0.03	3	2	*18.0	159	15.8	812	2188	27.0	0.002	11
Mean Values	35	0.53	-	3	2.42	121	37.1	1102	666	27.8	0.180	
4. SOTHMAN MINES, ONT.	79	0.47	3	2	7.25	248	45.8	1396	173	21.2	0.061	198A
5. TEXMONT (FATIMA) MINES ONT.	83	0.02	25	1	14.7	1311	28.6	4160	2314	-	0.001	85
	20	0.06	3	1	26.8	500	29.8	5920	1170	19.1	0.002	90
	22	0.01	3	1	24.1	725	29.8	5600	1189	18.1	0.000	97
	65	0.70	20	4	16.4	71	34.3	1688	250	29.7	0.041	204
	404	0.02	19	1	8.41	517	29.4	6553	388	26.7	0.002	159
Mean Values	118	0.16	-	-	18.1	625	30.4	4784	1062	23.4	0.009	
6. ALEXO MINE, ONT.	42	0.05	3	2	3.59	179	43.5	700	250	14.2	0.014	26A
	46	0.06	3	2	3.59	195	41.7	693	288	39.0	0.016	26C
	28	0.10	3	1	1.54	191	54.1	633	473	28.7	0.061	168
Mean Values	39	0.07	-	2	2.91	188	46.4	675	337	27.3	0.023	
7. EXPO-UNGAVA QUE.	88	1.78	3	3	1.96	500	49.6	1019	1938	12.1	0.476	38
	77	0.40	3	1	2.05	501	41.8	1011	2688	-	0.163	43
	51	1.52	3	4	3.26	116	51.1	1153	212	28.5	0.318	45
	162	2.55	3	6	1.98	94	52.2	804	238	29.9	0.563	47
Mean Values	95	1.56	-	4	2.31	303	48.7	997	1269	23.5	0.403	
8. LAKEMOUNT PROPERTY WAWA ONT.	13	0.50	3	2	7.11	15	37.1	956	50	30.3	0.066	36

Table 87.2 (cont.)

	Zn	Cu%	Pb	Ag	Ni%	Mn	Fe%	Co	Cr	S%	$\frac{Cu}{Cu+Ni}$	Sample No.
9. SHEBANDOWAN MINE ONT.	193	2.47	3	7	3.46	1000	54.8	430	*1338	14.8	0.417	95
	19	0.16	3	2	3.54	65	42.7	786	142	25.5	0.043	96
	109	3.49	20	26	0.89	300	46.7	1917	162	39.9	0.797	97
	57	2.38	3	6	3.53	59	60.0	1875	62	36.9	0.403	98
	60	2.07	3	4	3.73	65	40.6	871	30	32.5	0.357	80A
	69	2.43	3	4	4.00	105	40.0	975	62	33.4	0.378	80B
	68	2.38	3	4	4.14	80	40.0	1049	80	31.9	0.365	80C
Mean Values	82	2.20	-	8	3.33	239	46.3	1130	90	30.7	0.398	
10. LUCKY BOY CLAIMS	1310	0.51	42	18	0.98	1525	30.2	752	596	-	0.342	869
MANITOBA	2737	0.01	3	2	0.14	49	40.8	692	17	27.8	0.067	885
11. DUMBARTON MINE	12	0.04	3	3	2.15	25	38.6	2789	42	35.0	0.017	467
MANITOBA	113	3.17	7	4	3.00	106	40.0	1660	418	29.4	0.514	468
	30	0.25	3	3	3.38	56	40.6	1091	50	38.6	0.069	469
	7	0.01	7	1	1.84	9	39.0	880	17	32.3	0.005	470
	25	0.28	3	1	4.77	65	46.4	1358	17	26.5	0.055	537
Mean Values	37	0.75	-	-	3.03	52	40.9	1556	109	32.4	0.198	
12. NORPAX MINE ONT.	136	4.36	118	20	5.65	158	33.6	2130	25	24.1	0.436	542
13. GORDON LAKE MINE ONT.	30	0.23	3	3	3.62	412	43.0	799	1124	20.4	0.060	351
	56	1.94	3	1	3.08	329	37.2	739	436	17.5	0.386	464
	23	0.49	3	2	5.64	27	40.0	1045	70	27.6	0.080	345B
Mean Values	36	0.89	-	2	4.11	256	40.1	661	543	21.8	0.178	
14. RANKIN MINE N.W.T.	29	0.66	15	4	5.69	304	35.4	1058	615	22.3	0.104	713B
	44	1.39	40	4	6.75	256	40.9	1155	2127	26.3	0.171	713C
Mean Values	37	1.03	28	4	6.22	280	38.2	1106	1371	24.3	0.142	
15. FERGUSON LAKE N.W.T.	18900	23.00	10	100	0.26	30	30.0	660	100	30.7	0.989	736A
	53	0.27	20	1	0.76	216	37.8	1275	108	13.2	0.262	736B
16. SOAB NORTH MINE	12	0.10	3	10	13.1	66	39.3	1091	32	21.3	0.008	407
THOMPSON MANITOBA	39	0.06	8	1	11.3	196	35.1	929	148	25.0	0.005	411
	18	0.10	3	2	7.67	5	43.5	463	26	29.3	0.013	413
	57	0.39	17	4	9.38	447	39.3	846	102	29.9	0.040	408A
	36	0.18	12	3	12.2	85	37.9	988	40	16.4	0.015	409A
	18	0.55	38	1	15.6	82	34.4	1091	40	29.9	0.034	409C
Mean Values	30	0.23	14	4	11.5	147	38.3	901	65	25.3	0.020	
17. PIPE NO. 2 MINE	32	0.70	3	1	2.00	27	47.7	310	180	21.9	0.259	388
THOMPSON MANITOBA	22	0.12	3	1	2.78	53	57.4	479	188	30.1	*0.041	389
	27	0.14	3	5	2.75	89	48.2	716	268	26.7	0.048	396
	30	0.12	3	2	2.18	53	54.8	394	226	31.8	0.052	327A
	18	0.22	3	1	2.45	124	41.7	500	198	32.3	0.082	327B
Mean Values	26	0.26	-	-	2.43	69	50.0	480	212	28.6	0.097	
18. THOMPSON NO. 1 MINE	17	0.17	8	3	4.64	193	44.4	656	136	28.2	0.035	315
MANITOBA	14	0.05	3	3	3.69	89	46.5	410	32	30.2	0.013	316A
Mean Values	15	0.11	4	-	4.17	141	45.4	533	84	29.2	0.026	

Table 87.2 (cont.)

	Zn	Cu%	Pb	Ag	Ni%	Mn	Fe%	Co	Cr	S%	Cu/(Cu+Ni)	Sample No.
19. BIRCHTREE MINE THOMPSON, MANITOBA	32	0.03	17	3	2.00	144	42.4	621	822	21.5	0.015	376
	124	0.11	3	3	3.15	32	48.9	858	116	25.1	0.034	377
	23	0.35	30	3	11.3	246	38.6	2157	32	27.5	0.030	382
	152	0.21	17	5	6.25	102	48.9	953	364	20.2	0.033	383
	38	1.21	21	6	3.20	40	16.4	411	42	-	0.274	384
Mean Values	74	0.38	17	4	5.17	113	39.0	1000	275	23.6	0.068	
20. MOAK LAKE MINE THOMPSON MANITOBA	1148	0.08	20	4	0.90	147	43.5	58	32	25.4	0.081	305A
	1222	0.07	30	5	0.90	120	44.1	58	32	26.2	0.072	305B
	50	0.22	12	1	2.19	319	44.1	473	864	22.1	0.091	305C
Mean Values	807	0.12	21	3	1.33	195	43.9	196	309	24.6	0.083	
21. MYSTERY LAKE THOMPSON MANITOBA	25	0.04	17	1	1.88	347	33.8	585	372	18.3	0.021	302B
22. CLAM LAKE SASK. (CANADIAN BONANZA)	10	0.12	3	1	5.56	26	6.1	2429	17	26.5	0.021	112
23. NEMEIBEN LAKE, SASK.	12	0.54	3	1	1.49	124	27.7	284	150	4.1	0.266	105
	83	1.20	233	11	4.83	92	31.4	1986	33	32.7	0.199	87A
	84	1.43	193	9	5.56	175	32.2	2286	33	26.6	0.205	87B
Mean Values	60	1.06	143	7	3.96	130	30.4	1519	72	21.1	0.211	
24. ROTTENSTONE MINE, SASK.	409	2.59	3	15	7.18	477	39.9	1769	618	27.6	0.265	58B
	78	1.62	3	9	9.38	277	36.4	2429	167	21.3	0.147	59
	54	1.31	3	6	7.73	64	35.6	1827	67	26.8	0.145	60
	157	5.13	3	14	4.83	350	36.8	1193	788	-	0.515	61
	404	*18.4	13	82	4.02	571	20.4	664	150	19.3	0.821	62
	42	5.80	13	17	6.63	293	34.9	1741	303	25.4	0.467	65
	154	4.91	3	24	0.94	153	8.7	327	167	27.4	0.839	66
	57	2.70	13	8	9.55	105	29.0	2643	237	26.6	0.220	67
ROTTENSTONE ISLAND	21	0.98	3	2	2.73	25	39.1	1539	17	25.2	0.264	73
Mean Values	153	3.12	-	19	5.89	257	31.2	1570	279	25.0	0.346	
25. MUSKOX INTRUSION: EAST CONTACT. SPEERS LAKE NWT	18	0.58	3	3	3.18	38	50.6	1311	336	29.7	0.154	690
	263	2.88	25	4	1.85	230	43.1	1348	50	24.8	0.609	691
26. TURNAGAIN RIVER PROP. B.C.	43	0.29	40	2	3.29	234	49.7	1783	679	18.6	0.081	546
	51	0.50	3	1	1.62	1511	47.8	950	3114	8.1	0.236	548
	87	0.06	3	1	0.35	1128	43.1	798	4714	12.5	0.146	557
	84	0.29	3	1	2.71	1234	43.1	1058	830	11.9	0.097	550A
	54	0.21	3	1	2.07	1191	40.9	850	2714	10.5	0.092	550B
	25	0.12	30	2	2.59	392	50.2	1444	1232	24.2	0.044	543
Mean Values	57	0.25	-	-	2.11	948	45.8	1147	2213	14.3	0.106	
27. GIANT MASCOT MINE, B.C.	13	0.40	3	1	6.00	18	48.6	702	70	28.8	0.063	615
	73	2.29	3	6	9.25	38	42.5	1420	364	28.6	0.198	624
	9	0.17	3	1	10.0	16	45.3	1589	25	29.3	0.017	657
	19	0.82	3	3	4.15	20	45.3	564	70	-	0.165	639A
	20	1.16	3	1	2.59	23	49.7	786	136	30.4	0.309	659A
	132	0.87	20	3	5.08	77	59.2	1082	42	31.3	0.146	659B
Mean Values	44	0.95	-	-	6.18	32	48.4	1023	117	29.7	0.133	
DETECTION LIMITS	1	-	3	1	-	2	-	1	5	-	-	

* not included in averages; values in ppm unless noted
- indicates no data

Table 87.3 Mafic-hosted Ni-Cu deposits. Base metals in heavy mineral concentrates.

	Zn	Cu %	Pb	Ag	Ni %	Mn	Fe %	Co	Cr	S %	Cu/Cu+Ni	Sample Number
1. ROGERS FARM	394	0.76	6	3	1.13	886	39.1	933	50	24.9	0.402	807
ST. STEPHEN, N.B.	135	0.04	3	2	0.70	266	49.6	601	42	23.6	0.054	810
	47	0.08	3	2	1.44	139	50.5	933	199	29.5	0.053	817
	17	0.79	3	5	1.13	53	43.5	856	180	38.6	0.411	819
	70	0.80	13	4	0.67	293	34.5	692	117	22.2	0.544	821
	72	0.30	13	2	0.74	218	34.1	808	83	21.7	0.288	823
	73	1.13	19	4	0.74	444	34.1	762	150	21.3	0.604	931
Mean Values	115	0.56	9	3	0.94	328	40.8	798	116	26.0	0.373	
2. HALL-CAROLL ZONE	31	0.38	3	2	0.92	435	41.1	933	108	26.2	0.292	786A
ST. STEPHEN N.B.	20	0.41	3	2	0.88	243	44.9	766	150	26.5	0.318	786B
	52	1.42	3	3	0.90	303	40.8	1006	83	27.1	0.612	786C
	*531	0.70	3	3	0.84	656	44.9	913	75	20.0	0.455	786D
Mean Values	34	0.73	-	3	0.89	409	42.9	905	104	25.0	0.451	
3. GOODWIN LAKE	86	0.15	3	1	1.18	252	50.9	936	17	-	0.113	750
GABBRO, N.B.	14	0.16	3	2	0.60	29	44.3	1589	17	-	0.211	770
Mean Values	50	0.15	-	1	0.89	141	47.6	1262	17	-	0.144	
4. PLUG EAST OF GOODWIN LK.	63	0.51	3	2	2.10	537	32.8	1063	673	17.8	0.195	776
5. ERICKSON NO.1 ZONE UNGAVA	85	1.95	3	4	1.00	43	37.7	550	46	29.4	0.661	245
6. RHINO NO.1 ZONE UNGAVA	114	4.84	3	7	0.84	73	42.4	175	32	29.5	0.852	198
7. SCHINDLER LAKE UNGAVA	78	1.07	3	8	0.94	46	42.3	348	40	25.9	0.532	223
8. MACASSA PROPERTY												
LIMERICK TWP., ONT.	22	0.11	3	3	2.82	10	45.1	1372	50	28.9	0.038	626
9. MEILLEUR PROPERTY												
CALUMET ISLAND, QUE.	53	2.27	3	2	0.74	685	24.6	1135	17	22.0	0.754	113
10. NEWELL MEILLEUR PROPERTY												
CALUMET ISLAND, QUE.	29	1.58	3	2	0.98	252	34.5	1352	17	23.5	0.617	924A
11. ENGLISH-CANADIAN PROPERTY												
CALUMET ISLAND, QUE.	28	0.07	3	1	3.38	96	37.2	1539	33	17.1	0.020	117
12. NIMITZ PROSPECT												
BEST TWP., ONT.	787	4.30	3	11	1.43	392	44.7	564	48	28.4	0.750	668
13. DUMONT NICKEL	141	1.27	3	9	0.86	59	53.0	344	38	26.8	0.596	18A
DUVERNY TWP., QUE.	183	1.38	3	8	0.69	126	48.7	333	26	22.3	0.667	18B
Mean Values	162	1.33	-	8	0.78	93	50.9	339	32	24.6	0.630	
14. DUMONT NICKEL												
LAUNAY TWP., QUE.	107	0.06	10	1	2.28	540	38.4	1920	4200	-	0.026	443
15. MATTAGAMI LAKE MINE QUE.	566	0.77	185	14	2.10	604	37.2	772	100	26.1	0.268	868
16. CLARABELLE PIT SUDBURY	60	0.50	3	4	2.76	132	50.4	693	38	27.0	0.153	8
17. CREIGHTON MINE SUDBURY	73	4.26	3	9	1.64	202	27.7	651	58	20.6	0.722	42
18. FALCONBRIDGE MINE	607	18.7	3	43	1.64	183	41.7	457	50	30.3	0.919	15
NO.5 ZONE SUDBURY	115	1.05	3	4	2.93	142	53.9	856	76	30.2	0.264	17
19. MURRAY MINE SUDBURY	23	0.20	3	2	3.29	48	50.4	945	112	32.7	0.057	3
	224	4.00	20	13	3.19	65	46.7	778	126	33.7	0.556	4
	302	6.33	3	8	2.35	126	55.7	619	100	27.4	0.729	1A
Mean Values	183	3.51	9	7	2.94	80	50.9	781	113	31.3	0.544	

Table 87.3 (cont.)

	Zn	Cu %	Pb	Ag	Ni %	Mn	Fe %	Co	Cr	S %	Cu/Cu+Ni	Sample Number
20. LEVACK MINE SUDBURY	36	0.50	3	1	2.47	135	55.7	648	112	28.7	0.168	12
21. BOUNDARY MINE SUDBURY	181	1.99	3	4	4.27	80	46.7	797	38	32.7	0.318	23
22. STRATHCONA MINE	505	1.43	19	3	2.24	619	46.9	762	17	19.6	0.390	898
SUDBURY, ONT.	141	0.10	3	1	0.59	1153	35.6	367	375	9.0	0.145	899
Mean Values	323	0.77	11	2	1.42	886	41.3	564	196	14.0	0.352	
23. TEMAGAMI MINE, ONT.	37	3.03	3	2	0.87	26	39.9	1493	25	24.3	0.777	661
24. MORTIMER PROPERTY TEMAGAMI, ONT.	259	0.77	28	4	0.76	116	35.2	2245	17	28.6	0.503	674A
25. STRICKLAND SHOWING THUNDER BAY, ONT.	302	0.35	3	1	0.24	1114	42.8	350	238	-	0.593	585
26. GREAT LAKES NICKEL THUNDER BAY, ONT.	280	1.25	3	5	0.63	2364	41.8	322	586	-	0.665	62
27. EMO PROPERTY	21	0.25	3	1	1.66	67	47.8	743	90	27.8	0.131	608
WESTERN ONTARIO	23	0.57	3	1	2.24	59	40.3	1614	145	24.7	0.203	609
	16	0.10	3	1	2.82	27	48.6	1855	127	29.5	0.034	611
	54	1.85	3	0	1.49	160	47.3	1396	33	-	0.554	620
Mean Values	29	0.69	-	-	2.05	78	45.9	1402	99	27.3	0.252	
28. KENBRIDGE PROPERTY	39	0.65	3	2	6.82	56	44.2	1165	74	20.1	0.087	563
WESTERN ONTARIO	459	*8.00	3	5	6.00	35	43.1	850	68	31.6	0.571	564
	66	1.85	3	3	5.29	33	45.7	1493	118	31.2	0.259	576
	47	1.45	3	1	6.50	44	43.7	1262	70	31.2	0.182	580
Mean Values	153	1.32	-	3	6.15	42	44.6	1192	83	28.5	0.177	
29. LYNN LAKE MANITOBA	59	2.81	3	9	1.50	15	44.7	424	40	-	0.652	463
	18	0.09	3	4	1.75	24	46.5	716	28	18.0	0.049	450
	23	0.40	3	2	2.31	18	42.9	733	40	32.0	0.148	450B
	124	0.95	3	3	1.66	18	47.1	483	40	40.1	0.364	456C
Mean Values	56	1.06	-	4	1.81	19	45.3	589	37	30.0	0.369	
30. RIVETT LAKE, N.W.T.	39	0.80	3	3	4.62	285	44.6	1831	33	24.5	0.148	706A
(EAST OF YELLOWKNIFE)	142	3.32	10	13	4.85	352	38.3	1493	50	30.5	0.406	706B
31. WELLGREEN MINE, YUKON	244	1.45	10	4	2.35	*2565	45.3	997	868	14.3	0.382	526
	85	0.24	3	1	3.19	105	54.8	1125	180	35.5	0.070	533
	166	3.94	20	11	2.47	167	46.4	1396	345	27.4	0.615	536
	108	5.35	13	10	1.83	178	27.1	1222	17	21.5	0.745	121
	85	1.69	13	5	3.94	163	36.4	1327	200	26.4	0.300	129
	125	2.16	19	8	2.49	619	38.7	893	17	20.0	0.465	132
	148	2.35	13	6	1.66	247	32.2	833	20	20.7	0.586	143
	51	0.76	3	1	1.96	53	32.9	1308	67	21.5	0.279	147
	100	1.17	3	3	4.27	273	36.4	1524	67	25.4	0.215	158
Mean Values	124	2.12	11	5	2.68	226	38.9	1181	198	23.6	0.442	
32. E AND L PROPERTY, NICKEL MOUNTAIN, B.C.	396	2.45	10	3	3.41	512	45.8	964	80	28.4	0.418	487
DETECTION LIMITS	1	-	3	1	-	2	-	1	5	-	-	

Table 87.4 Mafic-hosted Ni-Cu deposits. Precious metals and other elements in heavy mineral concentrates.

	As	Sb	Mo	Hg	Ptppb	Pdppb	Auppb	Pt/(Pt+Pd)	Se	Te	Bi	U	Sample Number
1. ROGERS FARM	4	1	3	0.21	-	-	20	-	30	26	3	0.00	802
ST. STEPHEN, N.B.	1	1	5	0.20	-	-	15	-	9	14	3	0.05	810
	1	1	3	0.24	0	3	20	0	12	16	3	0.05	817
	1	1	3	0.23	0	0	15	-	12	19	3	0.00	819
	1	1	3	0.19	0	0	55	-	9	6	3	0.00	821
	3	1	3	0.15	-	-	15	-	9	10	3	0.00	823
	3	1	3	0.06	-	-	60	-	12	0	3	0.05	931
Mean Values	-	-	-	0.18	-	-	29	-	13	13	-	-	
2. HALL-CAROLL ZONE	-	1	5	0.15	0	0	25	-	9	0	3	0.00	786A
ST. STEPHEN, N.B.	2	1	5	0.17	0	15	15	0	9	0	3	0.00	786B
	21	1	5	0.22	0	20	65	0	12	0	3	0.00	786C
	3	1	25	0.28	0	3	30	0	12	0	3	0.00	786D
Mean Values	9	-	10	0.21	0	10	27	0	11	0	-	-	
3. GOODWIN LAKE GABBRO, N.B.	1	1	5	0.21	0	15	15	0	12	4	3	0.00	750
	1	1	3	0.08	0	10	10	0	6	2	3	0.00	770
Mean Values	-	-	-	0.15	0	13	13	0	9	3	-	-	
4. PLUG EAST OF GOODWIN LAKE, N.B.	1	1	15	0.38	-	-	30	0	12	0	3	0.00	776
5. ERICKSON NO.1 UNGAVA, QUE.	1	1	5	0.50	120	720	180	0.143	19	0	3	0.00	245
6. RHINO NO.1 ZONE UNGAVA, QUE.	1	1	5	0.22	190	765	370	0.199	41	0	3	0.00	198
7. SCHINDLER LAKE, UNGAVA, QUE.	1	1	15	0.73	5	295	145	0.017	7	0	3	0.25	223
8. MACASSA PROPERTY													
LIMERICK TWP., ONT.	2	1	10	0.34	-	-	115	-	30	0	3	0.05	626
9. MEILLEUR PROPERTY													
CALUMET ISLAND, QUE.	1	1	5	0.08	0	2125	25	0	26	0	3	0.00	113
10. NEWELL MEILLEUR PROPERTY													
CALUMET ISLAND, QUE.	1	1	3	0.17	0	860	25	0	38	0	3	0.00	924A
11. ENGLISH-CANADIAN PROPERTY													
CALUMET ISLAND, QUE.	61	1	3	0.05	10	90	100	0.100	28	0	3	0.00	117
12. NIMITZ PROSPECT													
BEST TWP., ONT.	1	1	3	0.52	0	285	20	0	27	0	3	0.18	668
13. DUMONT NICKEL	1	1	2	0.10	0	5	50	0	30	10	3	0.00	18A
DUVERNY TWP., QUE.	1	1	1	0.21	0	0	95	0	21	30	3	0.00	18B
Mean Values	-	-	-	0.15	0	3	73	0	25	20	-	-	
14. DUMONT NICKEL													
LAUNAY TWP., QUE.	-	-	-	0.28	-	-	-	-	-	-	-	0.00	443
15. MATTAGAMI LAKE MINE QUE.	36	1	3	0.41	10	110	245	0.083	39	15	3	0.00	868
16. CLARABELLE PIT SUDBURY	1	1	5	0.17	410	95	35	0.812	54	7	3	0.05	8
17. CREIGHTON MINE SUDBURY	2	1	5	0.24	-	-	65	-	36	0	3	0.00	42
18. FALCONBRIDGE MINE	1	1	3	0.52	10	100	20	0.091	85	22	3	0.00	15
NO.5 ZONE SUDBURY	258	1	5	0.19	490	455	515	0.519	85	21	3	0.00	17
19. MURRAY MINE SUDBURY	1	1	2	0.24	1630	455	5	0.782	42	20	3	0.15	3
	1	1	5	0.13	470	1880	35	0.200	100	4	3	0.00	4
	1	1	2	0.21	750	303	15	0.711	95	12	3	0.00	1A
Mean Values	-	-	3	0.19	950	1028	18	0.480	79	33	-	-	

Table 87.4 (cont.)

	As	Sb	Mo	Hg	Ptppb	Pdppb	Auppb	Pt/(Pt+Pd)	Se	Te	Bi	U	Sample Number
20. LEVACK MINE SUDBURY	1	1	4	0.24	490	380	25	0.563	-	0	3	0.00	12
21. BOUNDARY MINE SUDBURY	1	1	3	0.10	1115	530	35	0.678	80	36	3	0.00	23
22. STRATHCONA MINE	1	1	3	0.21	200	315	30	0.388	24	0	3	0.00	898
SUDBURY, ONT.	1	1	5	0.17	-	-	55	-	0	6	3	0.05	899
Mean Values	-	-	-	0.19	-	-	43	-	12	3	-	-	
23. TEMAGAMI MINE ONT.	158	1	3	0.63	10	260	55	0.037	27	0	3	0.00	661
24. MORTIMER PROPERTY													
TEMAGAMI, ONT.	16	1	5	0.20	0	10	325	0	36	9	3	0.05	674A
25. STRICKLAND SHOWING													
THUNDER BAY, ONT.	29	1	35	0.15	-	-	-	-	10	-	3	0.10	585
26. GREAT LAKES NICKEL													
THUNDER BAY, ONT.	6	1	5	19.5	-	-	-	-	-	0	3	0.00	62
27. EMO PROPERTY	1	1	5	0.12	-	-	25	-	45	18	3	0.00	608
WESTERN ONTARIO	1	1	5	0.13	0	150	20	0	45	21	3	0.00	609
	1	1	5	0.17	50	60	20	-	39	9	3	0.00	611
	1	1	10	0.34	-	-	130	-	-	-	3	0.00	620
Mean Values	-	-	-	0.19	25	105	50	0.192	43	16	-	-	
28. KENBRIDGE PROPERTY	1	1	3	0.90	190	220	15	0.463	100	28	3	0.00	563
WESTERN ONTARIO	1	1	5	0.21	70	185	25	0.275	60	36	3	0.00	564
	1	1	5	0.17	100	85	165	0.541	100	33	3	0.00	576
	1	1	3	0.37	110	250	60	0.306	90	26	3	0.00	580
Mean Values	-	-	-	0.41	118	185	66	0.389	88	31	-	-	
29. LYNN LAKE MANITOBA	1	1	3	0.20	-	-	40	-	-	40	3	0.00	463
	1	1	5	0.25	0	80	25	0	42	39	3	0.10	450A
	1	1	10	0.23	5	30	30	0.143	36	40	3	0.00	450B
	1	1	10	0.20	1085	25	275	0.977	33	34	3	0.00	456C
Mean Values	-	-	7	0.22	-	45	93	-	37	38	-	-	
30. RIVETT LAKE, N.W.T.	1	1	3	0.06	0	0	300	-	24	1	3	0.00	706A
EAST OF YELLOWKNIFE	1	1	3	0.26	0	60	4400	0	30	25	3	0.00	706B
31. WELLGREEN MINE	1	5	3	0.34	2950	3160	125	0.483	20	10	3	0.00	526
YUKON	1	1	6	0.44	1510	395	330	0.793	57	16	3	0.00	533
	1	1	3	0.52	1290	860	320	0.600	48	13	3	0.00	536
	1	1	5	0.65	-	-	265	-	44	0	3	0.00	121
	1	1	5	1.02	2190	1280	245	0.631	50	0	3	0.00	129
	1	1	3	0.31	2150	2440	570	0.468	84	0	3	0.00	132
	1	1	3	0.52	2430	2840	350	0.461	50	10	3	0.00	143
	1	1	3	0.39	630	660	50	0.488	38	15	3	0.00	147
	1	1	5	0.18	3350	2100	140	0.615	50	9	3	0.00	158
Mean Values	-	-	-	0.51	2063	1717	266	0.546	54	9	-	-	
32. E AND L PROPERTY													
NICKEL MOUNTAIN, B.C.	1	1	5	0.20	590	1840	940	0.243	102	0	3	0.00	487
DETECTION LIMITS	1	1	3	0.01	5	5	5		1	1	3	0.005	

Study of iceberg scours across the continental shelf and slope off southeast Baffin Island using the Sea MARC I midrange sidescan sonar

Project 760015

Dan Praeg, Brian MacLean, David J.W. Piper, and Alexander N. Shor[1]
Atlantic Geoscience Centre, Dartmouth

Praeg, D., MacLean, B., Piper, D.J.W., and Shor, A.N., Study of iceberg scours across the continental shelf and slope off southeast Baffin Island using the Sea MARC I midrange sidescan sonar; in Current Research, Part A, Geological Survey of Canada, Paper 87-1A, p. 847-857, 1987.

Abstract

The shelf and slope southeast of Baffin Island were examined along a 280 km long, 5 km swath width Sea MARC I survey line across water depths of 320 to 2100 m. Variations in the abundance, orientation, size and character of iceberg scours suggest division of the scoured seabed along the survey line into four zones: inner, central and outer shelf and upper continental slope. The maximum depth of iceberg scours occurs on the upper continental slope at about 715 m. All or most iceberg scours observed are relict and date from an episode of greater iceberg drafts, probably in the late Foxe or early Holocene. A gradual decrease in iceberg drafts through time is compatible with features observed along the upper slope to central shelf transect, while a contrast in character between scours of the inner and central shelf suggests a different history, possibly related to fluctuations in the sill depth of the inner shelf Resolution Basin.

Résumé

Le plateau continental et le talus continental du sud de l'île Baffin ont été étudiés suivant une ligne de levé constituée d'une bande de 280 km de long sur 5 km de large par Sea MARC I, par des profondeurs de 320 m à 2100 m. Les variations de l'abondance, de l'orientation, de la taille et du caractère des cicatrices d'affouillement par des icebergs laissent supposer une division du fond marin affouillé le long de la ligne de levé en quatre zones: plateau continental intérieur, central et extérieur et talus continental supérieur. La profondeur maximale des cicatrices d'affouillement par des icebergs se rencontre sur le talus continental supérieur à environ 715 m. Toutes les cicatrices d'affouillement par icebergs observées ou presque sont des résidus et datent d'un épisode de dérives plus importantes des icebergs, probablement du Foxe supérieur ou de l'Holocène inférieur. Une diminution progressive des dérives des icebergs à travers le temps est compatible avec des caractéristiques observées le long d'une coupe transversale allant du talus supérieur au plateau central, alors que le contraste des caractères observés entre des cicatrices d'affouillement du plateau intérieur et du plateau central laisse supposer une évolution différente, probablement liée à des fluctuations de la profondeur du seuil du bassin de Resolution du plateau intérieur.

[1]Lamont-Doherty Geological Observatory of Columbia University, Palisades, New York 10964, U.S.A.

INTRODUCTION

In 1984 the Atlantic Geoscience Centre examined selected areas of seabed offshore eastern Canada using the Sea MARC I midrange (5 km swath width) sidescan sonar system (Kosalos and Chayes, 1983). Preliminary results of this program from the Scotian and Labrador continental margins have been presented by Josenhans et al. (1986), Pereira et al., (1985), Piper et al. (1985a, b, in press), and Piper and Sparkes (in press). This paper discusses sidescan sonar imagery collected along a 280 km Sea MARC I survey line across the continental shelf and slope off southern Baffin Island, between water depths of 300 to 2000 m (Fig. 88.1).

Previous investigations of the area indicate the presence of numerous iceberg scours incised into the unconsolidated sediments of the continental shelf and upper continental slope (Woodworth-Lynas, 1983; Praeg et al., 1986a), and suggest the possibility of mass movement on the continental slope (Geonautics Ltd., 1982). A Sea MARC I survey was conducted in order to: (1) examine the type and distribution of iceberg scours, (2) determine the maximum depth of occurrence of iceberg scours on the upper continental slope, and (3) investigate continental slope features. The survey line crosses the sites of two exploratory wells on the continental shelf, Aquitaine et al. Hekja 0-71 (Klose et al., 1982) and Canterra Ralegh N-18; a third well, Esso H.B. Gjoa G-37 (Klose et al., 1982), is 65 km north of the survey line (Fig. 88.1).

DATA COLLECTION

The Sea MARC I survey line was collected during 18-21 September, 1984, over a period of 61 hours, as part of *CSS Hudson* cruise 84-035. The Sea MARC I system comprises a dual channel sidescan sonar with 27 and 30 kHz transducers, and a 4.5 kHz subbottom profiler (Kosalos and Chayes, 1983). The system is housed in a neutrally buoyant vehicle, which was towed up to 2500 m behind the ship, at elevations of about 300 m off the seabed. In addition to the Sea MARC I data, echograms were collected from the ship using towed 3.5 kHz and hull-mounted 12 kHz sources, and seismic reflection pro files were collected using a Bolt Associates 655 cm^3 (40 $inch^3$) airgun source with a single channel Nova Scotia Research Foundation hydrophone. Positioning of the data was by satellite navigation and rho-rho LORAN C, integrated by the BIONAV system (Wells and Grant, 1981). The Sea MARC I vehicle was positioned using a wire-out indicator and vehicle depth.

REGIONAL SETTING

The southeast Baffin Shelf is both broad and deep: it extends approximately 170 km from Loks Land to the shelf break at 450-550 m, and across most of this distance is deeper than 200 m (Fig. 88.1). The continental shelf slopes southeastward in gradients less than 1° toward a large bathymetric depression east of Hudson Strait, and contains an inner basin off the mouth of Frobisher Bay informally referred to as the Resolution basin by Praeg et al. (1986a). The adjacent continental slope descends seaward in gradients less than 2° to about 1500 m depth, beyond which gradients up to 20° and relief up to 180 m occur in association with a bathymetric protrusion of the continental slope (Fig. 1) informally referred to as the Gjoa Spur. The Sea MARC I survey line extends across the continental shelf for 140 km, from the northern margin of the Resolution basin to the shelf break at 460 m, and across the continental slope for another 140 km, crossing the southern tip of the Gjoa Spur (Fig. 88.1).

Surface currents in the area are dominated by the southward flowing Baffin Current, which originates in northern Baffin Bay and flows along the Baffin coast and across the southeast shelf at velocities up to 40 cm/s (Collin and Dunbar, 1964). The Baffin Current carries numerous icebergs across the Baffin Shelf, most of which are calved from glaciers of western Greenland (Murray, 1969). An average of 3500 icebergs cross the latitudes of the study area each year (Ebbesmeyer et al., 1980).

The continental shelf along the Sea MARC I survey line is underlain by gently seaward dipping Tertiary sedimentary strata (Grant, 1975; MacLean et al., 1977), which are separated by an angular unconformity from overlying unconsolidated sediments less than 10 m thick (Fig. 88.2). The unconsolidated Quaternary sediments of the southeast Baffin Shelf have been mapped and discussed by Praeg et al. (1986a). The shelf along the survey line is underlain by gravelly sandy muds mapped as Davis Strait Silt subunit B, which are characterized on high resolution seismic reflection profiles by a general lack of acoustic stratification, and by a rough surface morphology attributed to iceberg scours (Fig. 88.2). Subunit B is laterally equivalent to unscoured, acoustically stratified, gravelly sandy muds of Davis Strait Silt subunit A (Fig. 88.2), which are present in the floor of the Resolution basin below 500-550 m depth (Fig. 88.1, 88.2). In the Resolution basin Davis Strait Silt subunit A laterally interfingers with glacial till of the Baffin Shelf Drift, indicating partial time-equivalency, and is partly overlain by basinal muds of the Tiniktartuq Silt and Clay. The immediate seabed in the area of the survey line has been modified by both the southward flowing Baffin Current and by tidal currents originating from Frobisher Bay (Osterman, 1982), resulting in the formation of an extensive, thin (50 cm) surface veneer composed dominantly of sand and gravel (Praeg et al. 1986a).

SIDESCAN SONOGRAMS

Sea MARC I sidescan sonar data were digitally recorded, and processed in real time to produce orthorectified images with horizontal slant range corrections. These were later manually compiled at a scale of 1:40 000. Examples of the resulting seafloor imagery are presented below (Fig. 88.3-88.5). Reproductions of the original 1:40 000 scale sonograms, and accompanying interpretations, are available as Geological Survey of Canada Open File 1254 (Praeg et al., 1986b).

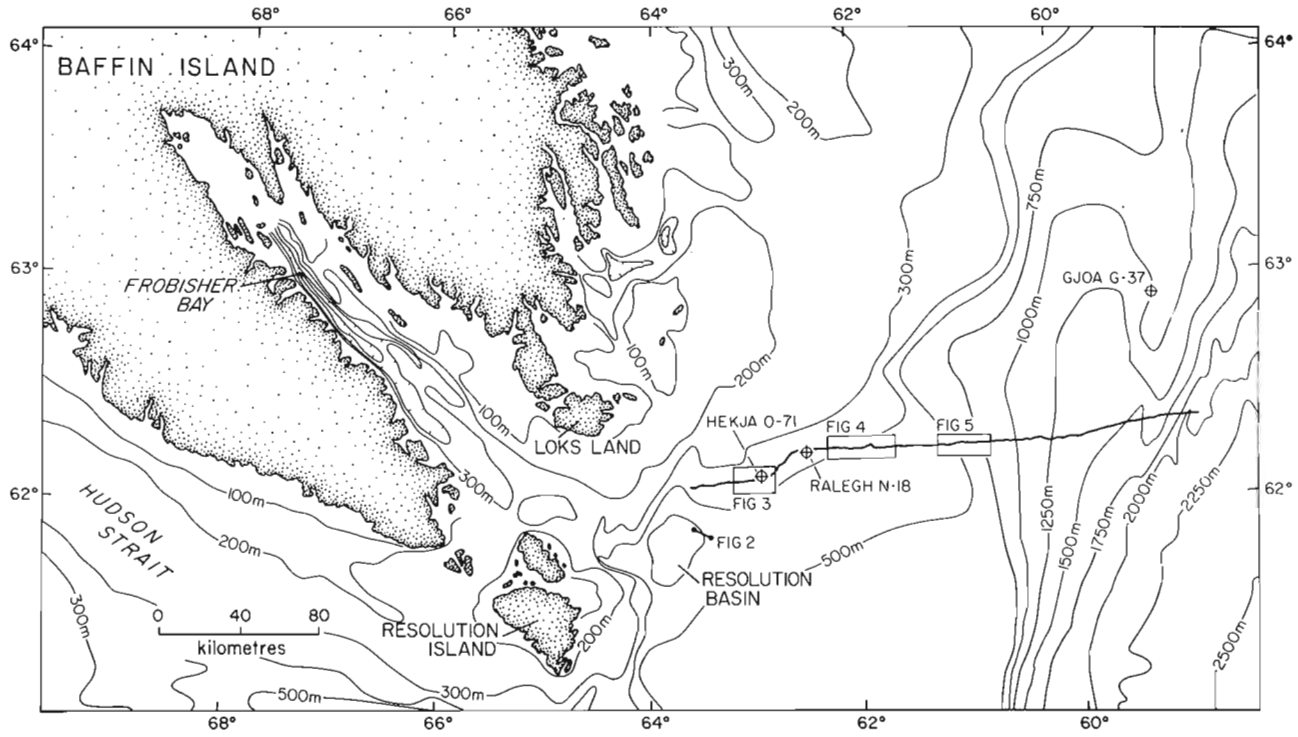


Figure 88.1. Index map of the continental shelf and slope off southeast Baffin Island, showing the Sea MARC I survey line and the location of Figures 88.2-88.6. The positions of three exploratory wells are also shown.

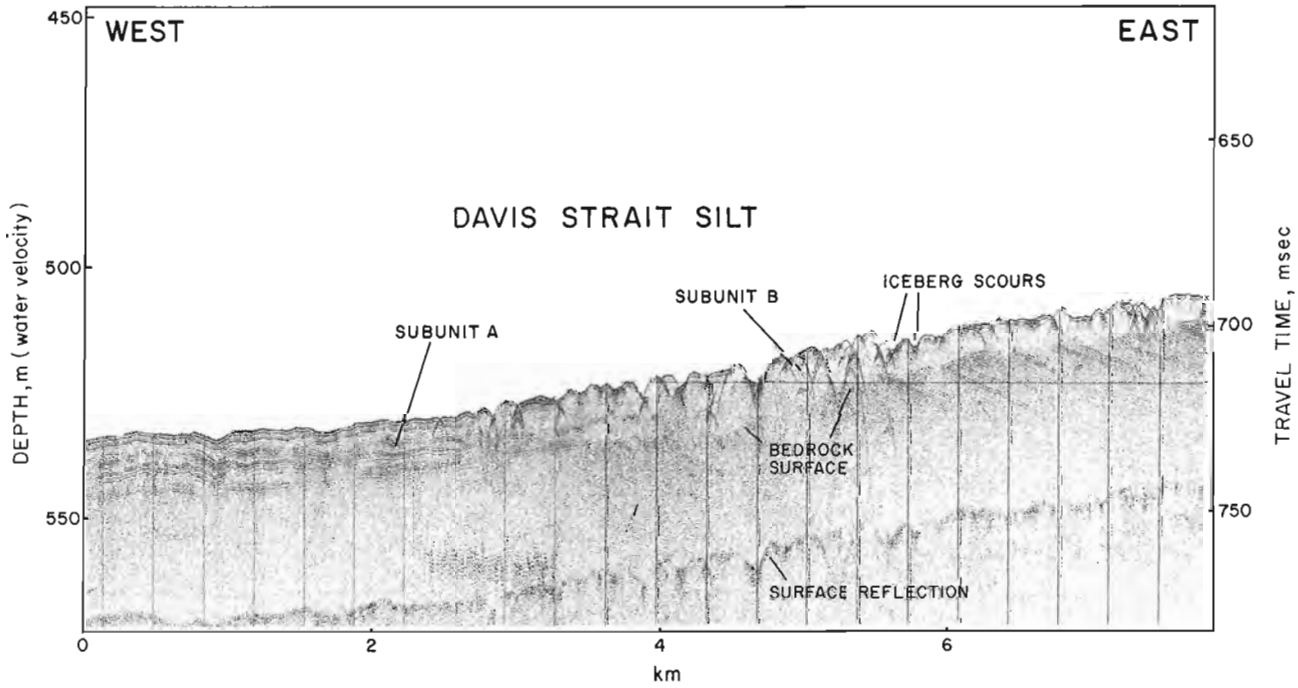


Figure 88.2. Huntec DTS high resolution seismic reflection profile from the Resolution basin (Fig. 88.1), illustrating lateral equivalency between stratified sediments of Davis Strait Silt subunit A and the acoustically unstratified, iceberg scoured sediments of subunit B. In deeper water southwest of the profile the conformable sediments of subunit A are overlain by basinal muds of the Tiniktartuq Silt and Clay. The unconsolidated sediments unconformably overlie gently seaward-dipping strata of semiconsolidated Tertiary sedimentary bedrock. From Praeg et al. (1986a).

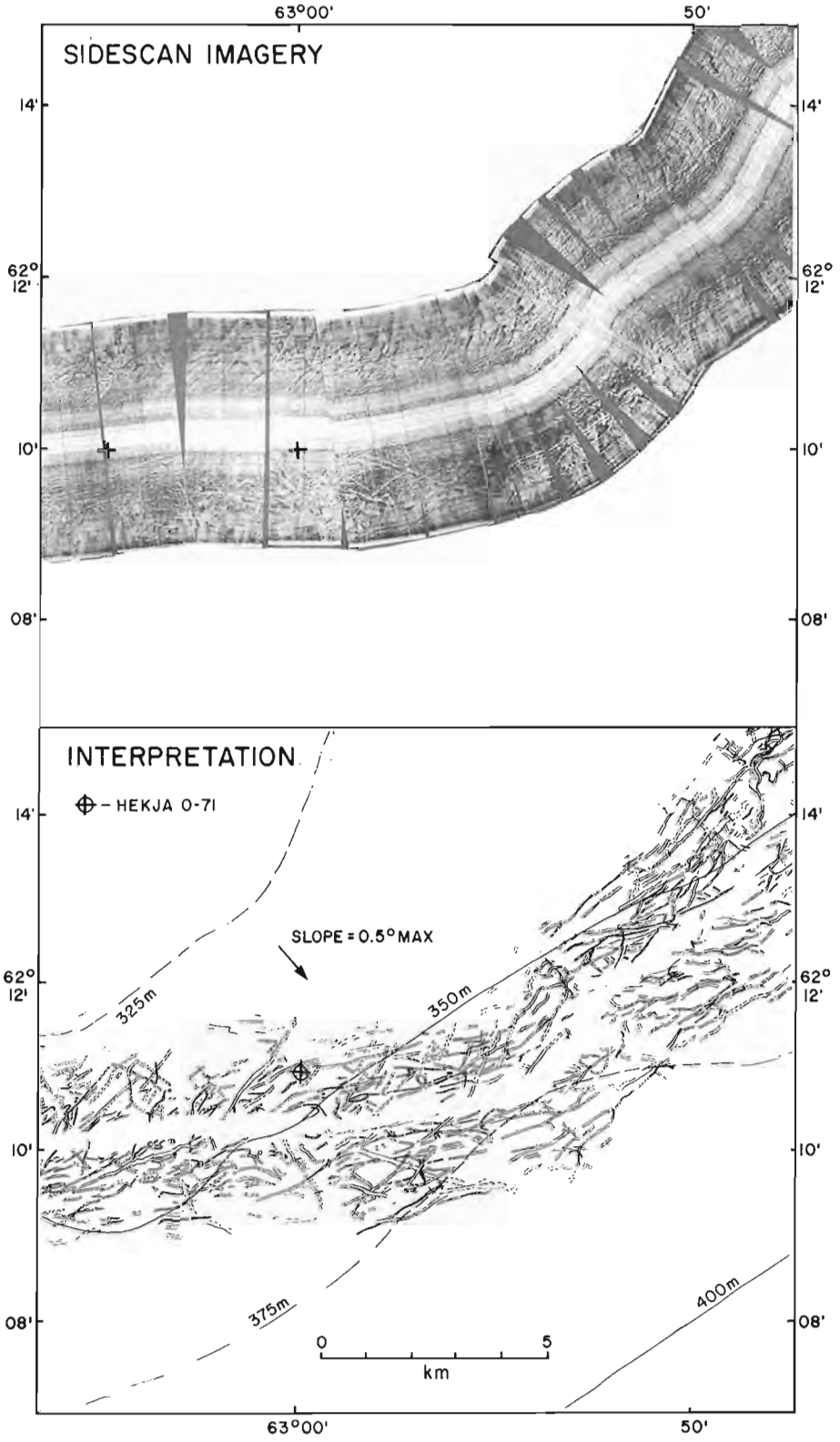


Figure 88.3. Sea MARC I sidescan sonogram and interpretation from the central shelf, in the area of the Hekja well site (Fig. 88.1). The sidescan imagery has been orthorectified, and so constitutes a 'true' picture of the seafloor. The darkness of the grey areas are proportional to the strength of the reflected acoustic energy, e.g. light areas represent weak returns. The outer kilometre of both sidescan channels are dominated by water column interference. Iceberg scours have affected the entire seabed, and are fairly consistently oriented parallel to the isobaths. Most scours are well defined.

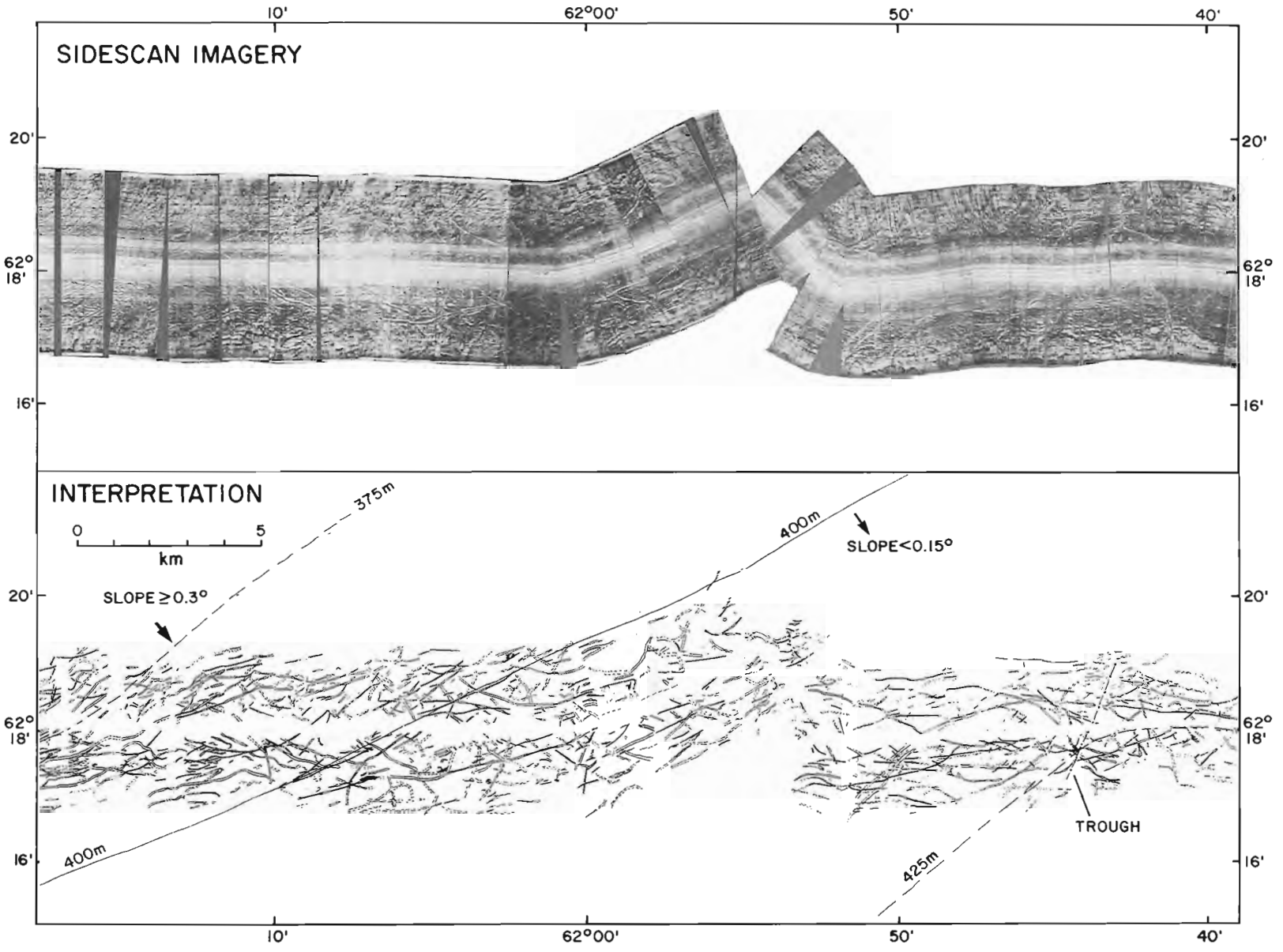


Figure 88.4. Sea MARC I sidescan sonogram and interpretation across the transition from the higher gradients of the central shelf to the lower gradients of the outer shelf (Fig. 88.1). Iceberg scours decrease in both abundance and consistency of orientation from west to east across the transition, which is marked by numerous subcircular low reflectivity patches interpreted as iceberg pits infilled with fine sediment. A large trough 150 m wide and 7 m deep, present to the east, appears to be an exceptionally large scour. See Figure 88.3 for information on sidescan interpretation, and see text for a detailed discussion of seabed features.

Sidescan interpretation

Iceberg scours have been previously reported across the study area (Woodworth-Lynas, 1983; Praeg et al., 1986a), and are recognized on the Sea MARC I imagery by their characteristic form, which ranges from linear (furrows: Harris, 1974) to equant (pits: Fader and King, 1981), and by their crosscutting relationships. Variations in scour abundance, size and orientation have been evaluated qualitatively. Abundance is assessed as proportion of seabed scoured (high, moderate, low). Size is measured directly from the sonograms (width) and echograms (depth), and is generally consistent enough within an area that representative values can be estimated. Orientation is assessed as consistency of the population about a particular direction. Scour orientations observed on sidescan imagery can have some dependence on the direction of sonification, i.e. scours parallel to the survey line can appear more prominent than those transverse to it (Todd, 1984). In the case of the Sea MARC I imagery, scours can generally be observed in numerous orientations in a given area, and apparent scour orientations vary in consistency and direction across the study area despite the generally fixed orientation of the survey line (Fig. 88.1). This suggests that any bias in apparent orientations is not significant, and that true relative variations are being portrayed.

Low reflectivity areas which are not acoustic shadows are observed on the continental shelf and slope, and are interpreted to indicate ponding of finer sediment within coarser, higher reflective areas of seabed. Reflectivity is a relative characteristic, so the actual texture of both finer and coarser sediments may vary across the area. Previous studies indicate that the immediate seabed of the continental shelf is composed primarily of sands and gravels (Praeg et al., 1986a), whereas finer sediments occur on the continental slope (see below). Low reflectivity areas include the troughs of many larger iceberg scours. Such scours often have poorly defined margins, in contrast to well defined or "fresh-looking" scours nearby. Low reflectivity troughs and/or poorly defined margins are interpreted to indicate infilling of scour troughs and/or degradation of berms due to bottom currents, a pattern of seabed modification previously recognized on both the southeast Baffin and Labrador Shelves (Praeg et al., 1986a; Josenhans and Barrie, 1982). Many well defined scours may also have been modified by bottom currents, which have produced an extensive sand and gravel veneer in the area, but at a scale or to a degree too small to be resolved by the Sea MARC I system.

Iceberg scours

Sea MARC I data indicate that the seabed of the continental shelf and upper continental slope is dominated by iceberg scours, which take the form of furrows and some pits. Qualitative assessment of variation in scour abundance, orientation, size and definition suggests that the scoured seabed along the survey line can be divided into four distinctive zones, which roughly conform to physiographic divisions: inner, central and outer shelf, and upper continental slope.

Central Shelf

The central part of the shelf along the survey line corresponds to the interval above about 375 m, up to 320 m, which contains seabed gradients of 0.2-0.5°; it includes both the Hekja and Ralegh well sites (Fig. 88.1). The abundance of iceberg scours is high across this interval and the entire seabed has been affected (Fig. 88.3). High resolution subbottom profiles available from the area (Geonautics Ltd., 1982) show that the characteristically acoustically unstratified sediments of Davis Strait Silt subunit B (Fig. 88.2) form the seabed. Iceberg furrow orientations are fairly consistent, showing a strong trend parallel to the local isobaths, although other orientations up to isobath-transverse are apparent (Fig. 88.3). Furrow lengths are difficult to assess due to a general orientation oblique to the survey line, but features at least 9 km long are observed. Furrows shorter than the width of the sonograms (5 km) also occur, and some iceberg pits. Furrows are generally up to 50 m wide and 3 m deep, but some exceptional features up to 100 m wide are recognized, for example southeast of the Hekja well site (Fig. 88.3). Most scours appear well defined or "fresh-looking" on the sonograms. However, some are poorly defined, often with low reflectivity troughs, and these are interpreted to reflect modification by currents. The well defined scours may also have been modified by currents, to a degree not resolved by the Sea MARC I system, and this is supported by local textural variability evident in bottom photographs and grab samples collected from the area of the Hekja well site.

Inner shelf

The inner part of the shelf along the survey line corresponds to the northern margin of the Resolution basin below about 375 m, to 400 m, which contains seabed gradients of 0-0.7°. In the deeper waters of the Resolution basin south of the Sea MARC I survey line, bottom profiles show an area of seabed unaffected by iceberg scouring below 500-550 m depth (Figs. 88.1, 88.2). Across the northern margin of the basin, the Sea MARC I imagery suggest moderate abundances of iceberg furrows and pits, which in general are poorly defined and of subdued relief (2 m) on bottom profiles. Furrows are difficult to trace laterally, but there appears to be little consistency in orientation. The scours are commonly associated with low reflectivity troughs, indicative of fine sediment infill, which increase in abundance downslope and grade into subcircular low reflectivity patches of ponded sediment. On the eastern flank of the basin above about 375 m, the Resolution basin scours are crosscut by well defined scours which have higher relief (up to 3 m) on bottom profiles, and which appear to be an extension of the well defined population observed on the central shelf. The contrasting poorly defined nature and subdued relief of the Resolution basin scours,

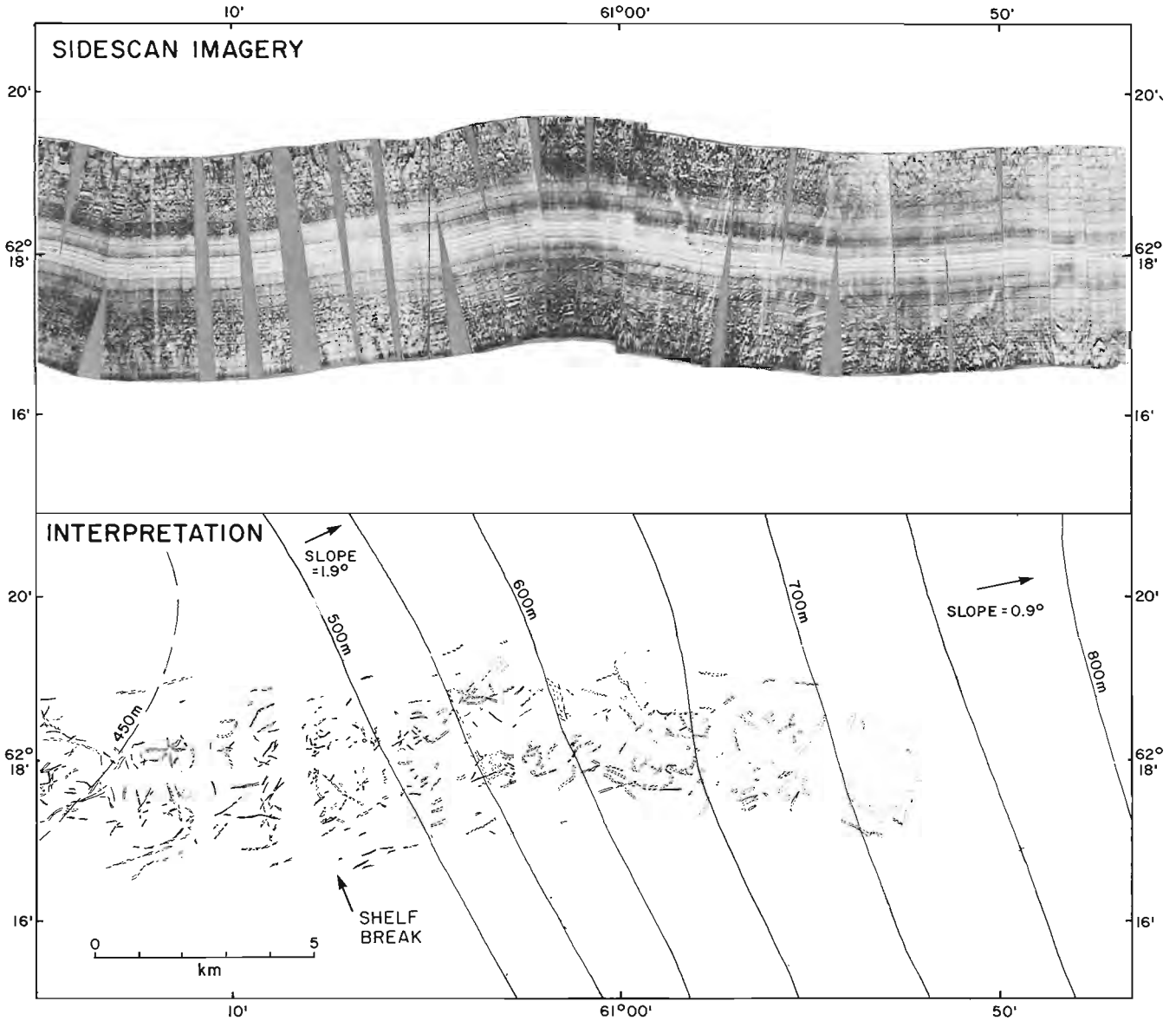


Figure 88.5. Sea MARC I sidescan sonogram and interpretation across the shelf break and upper continental slope (Fig. 88.1). The lower limit of iceberg scour is observed at about 715 m water depth, below which the seabed appears largely homogenous and subbottom profiles indicate a mud layer up to 5 m thick. Iceberg scours have not affected the entire seabed above 715 m, and are inconsistently oriented. Many scours are poorly defined and infilled by low reflectivity fine sediment. See Figure 88.3 for information on sidescan interpretation, and see text for discussion of seabed features.

along with the presence of ponded fine sediment, indicate modification of the inner shelf by currents to a significantly greater degree than observed on the central shelf.

Outer shelf

The outer part of the shelf along the survey line corresponds to a large area with gradients less than 0.1-0.2° extending from about 375 m to the slope break at 460 m (Fig. 88.1). The abundance of iceberg scours is moderate, and patches of apparently unscoured or partly scoured seabed are recognized (Fig. 88.4). These patches correspond to intervals of subsurface stratification on a high resolution subbottom profile along the survey line (Geonautics Ltd., 1982). Iceberg furrow orientations are inconsistent, varying from parallel to transverse to the gentle local gradients, although individual furrows tend to maintain a uniform orientation (Fig. 88.4). Furrow widths are generally up to 50 m, similar to those on the central shelf, but depths are slightly greater at up to 4 m; exceptional features up to 100 m wide and 8 m deep are also observed. A trough approximately 150 m wide and 7 m deep is present on the inner part of the outer shelf (Fig. 88.4). It appears to be an exceptionally large scour, rather than a topographic feature related to the subbottom bedrock surface, as a high resolution subbottom profile across the area (Geonautics Ltd., 1982) shows several large iceberg scours of comparable size and a fairly smooth bedrock surface. The transition from the central shelf to the lower gradients of the outer shelf is marked by an abundance of sub circular low reflectivity patches between water depths of about 370-410 m (Fig. 88.4). The patches are 50-150 m in diameter, and occur as isolated features or in some cases at the head of iceberg furrows. The features are interpreted as iceberg pits, or impact marks, which have been infilled by fine sediment. Many iceberg scours here and to seaward are poorly defined and have low reflectivity troughs, suggesting degradation and infilling due to currents. A grab sample located along the survey line in 400 m of water consists of sand and gravel, demonstrating the significance of current activity in this area (Praeg et al., 1986a).

Upper continental slope

Below the shelf break at approximately 460 m, iceberg scours decrease in abundance seaward across the relatively steep gradients (up to 2°) of the upper continental slope (Fig. 88.5). A high resolution subbottom profile along the survey line shows intervals of subsurface stratification, which abruptly become almost continuous below water depths of about 600 m (Geonautics Ltd., 1982). Iceberg furrow orientations are inconsistent across the upper continental slope, and some individual furrows display changes in orientation (Fig. 88.5). Furrows appear generally shorter than those on the continental shelf, and several pits are present. Furrow sizes are generally up to 50 m wide and 4 m deep, similar to the outer shelf; an exceptional feature at 670 m depth is approximately 100 m wide and 10 m deep. Iceberg scours are generally poorly defined, and low reflectivity troughs and patches suggestive of fine sediment infill increase in abundance in deeper water.

The lower limit of iceberg scours on the upper continental slope is recognized at approximately 715 m water depth on the Sea MARC I imagery, below which a largely featureless seabed occurs. On bottom profiles, this depth is the lower limit of hyperbolic reflections, which are associated with scour relief. Below this depth, subbottom profiles show an acoustically transparent layer up to 5 m thick, interpreted as a mud unit. It has a smooth upper surface, and an irregular basal surface dissimilar to iceberg scour relief.

DISCUSSION

Measurement of iceberg drafts in the Baffin Bay-Labrador Sea area, from both submersible and vertical sidescan sonar observations of several hundred icebergs, suggests present day maximum drafts of about 240 m (Wittman, in Murray, 1969; El-Tahan et al., 1985). Estimates of iceberg drafts from observations of thousands of apparently grounded (stationary) icebergs from drillrigs, shore-based radars, satellites and International Ice Patrol surveys suggest maximum drafts of approximately 300 m, although some uncertainty exists due to poor bathymetric control on many northern charts (El-Tahan et al., 1985). In the area of the Hekja well site (Fig. 88.1), one large iceberg observed during drilling was apparently grounded in water depths of 265 m (Geomarine Associates Ltd., 1980). These observations indicate that present-day iceberg drafts are generally less than 300 m, a depth which is shallower than any examined along the Sea MARC I survey line (Fig. 88.1), and much shallower than the maximum depth of iceberg scours observed on the upper continental slope at 715 m. The implication is that the 715 m maximum depth of iceberg scours dates from a time of greater iceberg drafts and/or lowered relative sea levels, and that most or all grounding features observed along the Sea MARC I survey line are relict. Andrews (1980) proposed a late Foxe (= late Wisconsinan) relative sea level lowstand of 80 m or more to account for the glacial stratigraphy of Baffin Island. However, glacial isostatic modelling has suggested relative sea levels 10 m higher than present during this same period (Quinlan, 1985). Clearly, even 80 m is insufficient to account for more than a part of the increased depth of scour, indicating that greater iceberg drafts were the dominant factor in generating a scour limit of 715 m.

Praeg et al. (1986) discussed the possibility of both syn- and post- depositional scouring in the development of Davis Strait Silt subunit B (Fig. 88.2). On the outer shelf, the coincidence of patches of unscoured or partly scoured seafloor (Fig. 88.4) with intervals of subsurface stratification in Davis Strait Silt subunit B, well above the lower limit of iceberg scours, indicates that reworking of seafloor sediments by iceberg scours was a post-depositional rather than a syn-depositional process. (The same may not apply to shallower areas, where shallower draft icebergs could have been grounding while the outer shelf remained unmodified.) Post-depositional scouring on the outer shelf implies a long period

during depositon of the Davis Strait Silt when icebergs were not grounding, due either to shallower iceberg drafts, or to a dearth of calving margins. Extrapolation of a radiocarbon date on a core of the Davis Strait Silt subunit A from the Resolution basin (Fig. 88.1) suggests that the Davis Strait Silt dates back to at least mid-Foxe time, ca. 35 000 BP (Praeg et al., 1986a). Davis Strait Silt subunit A is partly overlain in the Resolution basin and elsewhere by the Tiniktartuq Silt and Clay, which is considered to reflect a change in depositonal style on the southeast Baffin Shelf in the late Foxe or early Holocene (Praeg et al., 1986a). Thus the episode of greater iceberg drafts and lowered relative sea level associated with formation of the 715 m maximum depth of iceberg scours on the upper continental slope appears to date from a relatively discrete interval of time in the late Foxe or early Holocene.

The relict character of scours along the Sea MARC I survey line is corroborated by the evidence on the sidescan imagery for degradation and/or infilling of many scours due to currents. Scour modification is especially prominent on the inner shelf and upper continental slope (Fig. 88.5) and least evident on the central shelf (Fig. 88.3), although even here coarse seabed sediment textures attest to the influence of currents. Significant variation in the degree of scour modification observed in other areas has been used to distinguish scours or scour populations of different relative ages (Josenhans and Barrie, 1982; Fader and King, 1981; Pelletier and Shearer, 1972). On the northeastern margin of the Resolution basin, sidescan imagery and bottom profiles indicate an abrupt transition above about 375 m water depth, from poorly defined, infilled scours of subdued relief to well defined scours of hummocky relief. This transition suggests a clear distinction between older features of the inner shelf and younger features of the shallower central shelf. In contast, along the transect from the central shelf to the upper continental slope the increase in abundance of poorly defined and/or infilled scours is more gradual, and there is a slight increase in scour relief.

The central shelf is also distinguished from the outer shelf and upper continental slope by a greater abundance and more consistent orientation of iceberg scours (Fig. 88.3, 88.4). More numerous iceberg scours imply exposure to greater numbers of grounding icebergs than adjacent (deeper) areas, through a predominance of shallower draft icebergs and/or a longer period of exposure. Bottom gradients may also be a factor, as evidenced by the coincident increase in scour abundance and seabed gradients across the transition from the outer to the central shelf (Fig. 88.4); steeper gradients constitute targets for a broader range of iceberg drafts. Scour orientations, or trajectories of scouring icebergs, are controlled by factors including sediment type(s), gradients and currents. The coincident decrease in consistency of scour orientations and seabed gradients across the central to outer shelf transition (Fig. 88.4) suggests a potential control by gradients, but orientations remain inconsistent on the steeper gradients of the upper continental slope (Fig. 88.5) indicating the influence of other factors. These factors have obviously varied between the upper continental slope and central shelf, either contemporaneously or throughout the history of scouring.

Woodworth-Lynas (1983) analyzed iceberg scours from a mosaic of 1.5 km swath width sidescan sonograms located northwest of the Hekja well site (Fig. 88.1), in water depths of 280-290 m. He found that average scour width decreased with relative age, suggesting a decrease in iceberg size through time. A progressive decrease in iceberg drafts through time would be compatible with many of the scour characteristics recognized along the Sea MARC I central shelf to upper continental slope transect, such as the gradual increase in poorly defined and/or infilled scours and decrease in scour relief, and the greater abundance of scours in shallow water. The more consistent orientation of scours on the central shelf relative to the upper continental slope could reflect variations in conditions such as currents, either contemporaneously or as scouring progressed. On the inner shelf, however, the pronounced distinction between the subdued older scours of the Resolution basin, and the hummocky younger scours above about 375 m indicates that a gradual change in iceberg draft over time is not applicable for this area. The long period of degradation and sediment infilling implied for the older scours may reflect control on iceberg drafts accessible to the area by the effective sill depth of the Resolution Basin (Fig. 88.1), which would change with fluctuations in relative sea level. Alternatively, it could reflect changes in iceberg source, from local calving margins in the west to distant sources in the north.

Continental slope features

The mud layer observed on subbottom profiles below 715 m on the upper continental slope persists in thicknesses up to 5 m to the eastern edge of the Gjoa Spur at about 1500 m water depth (Fig. 88.1). Sea MARC I imagery is largely homogeneous across this interval, and no evidence for recent mass movement is observed on this part of the continental slope. Geonautics Ltd. (1982) identified a possible mass movement feature on the upper continental slope at 850 m depth from a high resolution subbottom profile, located along the Sea MARC I survey line. Examination of this profile shows that the feature is associated with a local change in gradient, which corresponds to two subcircular low reflectivity areas observed on Sea MARC I imagery at this depth. However, no evidence of downslope sediment dispersal is seen on the sidescan imagery, and the mud layer appears undisturbed on subbottom pro files.

Sea MARC I imagery across the Gjoa Spur in water depths of 1350-1550 m indicate the presence of wavy, slope-transverse lineations on both flanks of the spur, on gradients of about 4°. Similar slope-transverse lineations have been observed on Sea MARC I imagery from the Nova Scotia continental slope, where they are interpreted to reflect mass movement (Piper et al., 1985b). Areas of ponded sediments are also observed across the Gjoa Spur, in linear depressions on the crest and seaward flank.

SUMMARY

Qualitative evaluation of the variations in abundance, orientation, size and character of iceberg scours observed along the Sea MARC I survey line suggests division of the seabed into four zones: (1) inner shelf – associated with moderate abundances of poorly defined scours of subdued (2 m) relief, many of which are infilled; (2) central shelf – associated with high abundances of scours fairly consistently oriented approximately parallel to the isobaths, most of which are well defined and of hummocky (up to 3 m) relief; (3) outer shelf – associated with moderate abundances of inconsistently oriented scours generally up to 4 m in relief, some of which are poorly defined and/or infilled; (4) upper continental slope – associated with moderate to low abundances of inconsistently oriented scours generally up to 4 m in relief, which are poorly defined and show increasing evidence of infilling in deeper water. The lower limit of iceberg scours is observed on the upper continental slope at about 715 m. Most iceberg scours observed are relict, dating from an episode of greater iceberg drafts and possibly somewhat lowered relative sea levels, probably in the late Foxe or early Holocene. A gradual decrease in iceberg drafts during this episode is compatible with many of the scour characteristics observed along the upper continental slope to central shelf transect, but the sharp distinction between the scours of the central shelf and the subdued, older features of the inner shelf suggests a different control on scour characteristics in this area, possibly related to fluctuations in the sill depth of the Resolution basin.

No evidence for recent mass movement is observed on the gentle gradients of the continental slope west of the Gjoa Spur. However, slope transverse lineations may indicate mass movement on both flanks of the Gjoa Spur.

ACKNOWLEDGMENTS

The authors are grateful to Captain F.W. Mauger and the officers and crew of *CSS Hudson*, and to H.W. Josenhans, D.N. Chayes and other scientific staff from both the Atlantic Geoscience Centre and the Lamont-Doherty Geological Observatory, for their excellent co-operation and assistance while at sea. G.B. Fader, C.F.M. Lewis, and J.P.M. Syvitski reviewed the manuscript and provided helpful comments and suggestions.

REFERENCES

Andrews, J.T.
1980: Progress in relative sea level and ice sheet reconstructions, Baffin Island, N.W.T., for the last 125,000 years; in Earth Rheology, Isostasy and Eustasy, N.A. Morner, (ed.); John Wiley and Sons, New York, p. 175-200.

Collin, A.E. and Dunbar, M.J.
1964: Physical oceanography in Arctic Canada; Oceanography and Marine Biology, Annual Review, v. 2, p. 45-75.

Ebbesmeyer, C.E., Okubo, A., and Helseth, J.M.
1980: Description of iceberg probability between Baffin Bay and the Grand Banks using a stochastic model; Deep-Sea Research, v. 27A, p. 975-986.

El-Tahan, M., El-Tahan, H., Courage, D., and Mitten, P.
1985: Documentation of Iceberg Groundings; Environmental Studies Revolving Funds, Report No. 007, Ottawa, 162 p.

Fader, G.B. and King, L.H.
1981: A reconnaissance study of the surficial geology of the Grand Banks of Newfoundland; in Current Research, Part A, Geological Survey of Canada, Paper 81-1A, p. 45-56.

Geomarine Associates Ltd.
1980: Wellsite Survey Report, Aquitaine Company of Canada et al., Hekja A-72, Southeast Baffin Island, June 15-July 20, 1979. Project 79-15, Geomarine Associates Ltd., Halifax, Nova Scotia; Proprietary report to Aquitaine Company of Canada, Calgary, Alberta, 112 p., 11 encl.sheets, scales 1:10 000 and 1:5 000.

Geonautics Ltd.
1982: Final report of wellsite reconnaissance survey, 1982 Ralegh site, southeast Baffin Island; unpublished report to Canterra Energy Ltd., operator for the Baffin-Labrador Group of Companies. 56 p.

Grant, A.C.
1975: Geophysical results from the continental margin off southern Baffin Island; in Canada's Continental Margins and Offshore Petroleum Exploration, C.S. Yorath, E.R. Parker and H.R. Balkwill (ed.); Canadian Society of Petroleum Geologists, Memoir 4, p. 411-431.

Harris, I.McK.
1974: Iceberg marks on the Labrador Shelf; Geological Survey of Canada, Paper 74-30, p. 97-101.

Josenhans, H.W. and Barrie, J.V.
1982: Preliminary results of submersible observation on the Labrador Shelf; in Current Research, Part B, Geological Survey of Canada, Paper 82-1B, p. 269-276.

Josenhans, H.W., Zevenhuizen, J., and Klassen, R.A.
1986: The Quaternary geology of the Labrador Shelf; Canadian Journal of Earth Sciences, v. 23, p. 1190-1213.

Klose, G.W., Malterre, E., McMillan, N.J., and Zinkan, C.G.
1982: Petroleum exploration offshore southern Baffin Island, northern Labrador Sea, Canada; in Arctic Geology and Geophysics – Proceedings of the third International Symposium in Arctic Geology, A.F. Embry and H.R. Balkwill (ed.); Canadian Society of Petroleum Geologists, Memoir 8, p. 233-244.

Kosalos, J.G. and Chayes, D.N.
1983: A portable system for ocean bottom imaging and charting; in OCEANS 83 (Proceedings of the Third Working Symposium on Oceanographic Data Systems), p. 1-8.

MacLean, B., Jansa, L.F., Falconer, R.K.H., and Srivastava, S.P.
1977: Ordovician strata on the southern Baffin Island shelf revealed by shallow drilling; Canadian Journal of Earth Sciences, v. 14, p. 1925-1939.

Murray, J.E.
1969: The drift, deterioration and distribution of icebergs in the North Atlantic Ocean; in Ice Seminar; Canadian Institute of Mining and Metallurgy, Special Volume 10, p. 3-18.

Osterman, L.E.
1982: Late Quaternary history of southern Baffin Island, Canada: a study of foraminifera and sediments from Frobisher Bay; unpublished Ph.D. thesis, University of Colorado, Boulder, Colorado, 378 p.

Pelletier, B.R. and Shearer, J.M.
1972: Sea bottom scouring in the Beaufort Sea of the Arctic Ocean; in 24th International Geological Congress, Section 8, Marine Geology and Geophysics, p. 251-261.

Pereira, C.P.G., Piper, D.J.W., and Shor, A.N.
1985: Sea MARC I midrange sidescan sonar survey of Flemish Pass, east of the Grand Banks of Newfoundland; Geological Survey of Canada, Open File 938.

Piper, D.J.W., Shor, A.N., Farre, J.A., O'Connell, S., and Jacobi, R.
1985a: Sediment slides and turbidity currents on the Laurentian Fan: sidescan sonar investigations near the epicentre of the 1929 Grand Banks earthquake; Geology, v. 13, p. 538-541.

Piper. D.J.W., Farre, J.A., and Shor, A.N.
1985b: Late Quaternary slumps and debris flows on the Scotian Slope. Geological Society of America, Bulletin, v. 96, p. 1508-1517.

Piper, D.J.W., Shor, A.N., and Hughes-Clarke, J.
– The 1929 Grand Banks earthquake, slump and turbidity current; Geological Society of America, Special Paper (in press).

Piper, D.J.W. and Sparkes, R.
– Proglacial sediment instability features on the Scotian Slope at 63°W; Marine Geology (in press)

Praeg, D.B., MacLean, B., Hardy, I.A., and Mudie, P.J.
1986a: Quaternary geology of the southeast Baffin Island continental shelf; Geological Survey of Canada, Paper 85-14, 38 p.

Praeg, D.B., Shor, A.N., MacLean, B., and Piper, D.J.W.
1986b: Sea MARC I sidescan sonar survey line on the continental shelf and slope off southern Baffin Island, northwest Labrador Sea; Geological Survey of Canada, Open File /1254, 15 p., 18 encl. sheets, scales 1:40 000.

Quinlan, G.
1985: A numerical model of postglacial relative sea level change near Baffin Island; in Quaternary Environments: Eastern Canadian Arctic, Baffin Bay and West Greenland, J.T. Andrews (ed.); Allan and Unwin, Boston, Chapter 20, p. 560-584.

Todd, B.J.
1984: Iceberg scouring on Saglek Bank, Northern Labrador Shelf; unpublished M.Sc. thesis, Dalhousie University, Halifax, N.S., 176 p.

Wells, D.E. and Grant, S.T.
1981: An adaptable integrated navigation system: BIONAV; in Proceedings of Colloquium III on Petroleum Mapping and Surveys in the 80's; the Canadian Petroleum Association, Banff, Alberta.

Woodworth-Lynas, C.M.T.
1983: The relative age of ice scours using cross-cutting relationships; C-CORE, Technical Report 83-3, 54 p.

Composition isotopique du carbone organique des carottes du forage 85-036-016 dans le lac Bras d'Or, île du Cap-Breton, Nouvelle-Écosse

Project 0730072EP

Claude Hillaire-Marcel[1]
Centre géoscientifique de l'Atlantique

Hillaire-Marcel, C., Composition isotopique du carbone organique des carottes du forage 85-036-016 dans le lac Bras d'Or, île du Cap-Breton, Nouvelle-Écosse; dans Recherches en cours, Partie A, Commission géologique du Canada, Étude 87-1A, p. 859-864, 1987.

Résumé

La composition isotopique $\delta^{13}C$ de la matière organique sédimentaire a souvent servi à indiquer l'origine continentale ou marine de celle-ci. Ainsi, les sédiments post-glaciaires prelevés dans le bassin sud du lac Bras d'Or renferment de la matière organique dont la composition isotopique varie, dans l'ensemble, entre $-20,5\pm0,5$ ‰ et $-26\pm0,6$ ‰ (c. PDB), c'est-à-dire entre les pôles marin et continental déjà définis dans le golfe du Saint-Laurent. Depuis la déglaciation, le bassin du lac Bras d'Or a reçu, successivement, une sédimentation organique à dominante marine, puis continentale et à nouveau marine. Ces variations sont liées à l'évolution du niveau relatif de la mer dans cette région (phase d'émersion post-glaciaire suivie de la phase de submersion récente).

Abstract

The isotopic composition of sedimentary organic carbon depends on the origin (continental vs. marine) of the organic matter. In southern Lake Bras d'Or, the organic component of the postglacial sedimentary sequence shows $\delta^{13}C$ values ranging, as a whole, from -20.5 ± 0.5 to -26 ± 0.6‰ (vs. PDB), i.e., between values which characterize respectively the continental and marine organic matters in the Gulf of St. Lawrence. Three distinct sedimentary episodes occurred in Lake Bras d'Or since deglaciation as indicated by the succession of marine, then continental and finally marine organic matter in the sediments. These environmental changes occurred in relation to the regional relative sea level changes (postglacial emergence followed by the actual phase of submergence).

[1]GEOTOP et Département des Sciences de la Terre, Université du Québec à Montréal, C.P. 8888, succursale «A», Montréal (Québec), H3C 3P8

INTRODUCTION

Le rapport isotopique $^{13}C/^{12}C$ de la matière organique sédimentaire a souvent servi à déterminer l'origine marine ou continentale de celle-ci (Craig, 1953; Sackett, 1964; Smith et Epstein, 1971). Récemment, Tan et Strain (1979) ont mesuré des teneurs en ^{13}C (c. PDB) de l'ordre de -25 à -26 ‰ dans la matière organique des sédiments de surface du fjord du Saguenay et du haut estuaire du Saint-Laurent, comparativement à des valeurs de l'ordre de -22 ‰ dans le golfe du Saint-Laurent. Ils ont ainsi défini les deux pôles régionaux des mélanges de matières organiques continentale et marine.

Cet écart de composition isotopique selon le milieu d'origine de la matière organique est bien expliqué aujourd'hui (Deines, 1980). Dans les milieux continentaux septentrionaux, la plupart des plantes suivent le cycle photosynthétique de Calvin (Calvin et Bassham, 1962) qui s'accompagne d'un fractionnement isotopique $^{13}C/^{12}C$ de l'ordre de -18 à -20 ‰ (voir Bender, 1968 et 1971; Smith et Epstein, 1971, Troughton, 1972). Dans la mesure où la source de carbone, le CO_2 atmosphérique, présente une composition isotopique homogène (environ $-7,5$ ‰; voir Craig et Keeling, 1963), les produits biosynthétisés livrent des teneurs en ^{13}C, exprimées en unités δ, de l'ordre de -26 à -28 ‰ (Wickman, 1952; Craig, 1954; Troughton, 1972). À quelques unités δ près, cette composition isotopique se conserve dans la matière organique dérivée des premiers produits photosynthétisés, notamment dans la litière des sols et la matière organique détritique entraînée par le ruissellement.

Dans le milieu marin, le carbone organique authigène présente des compositions isotopiques moyennes de l'ordre de -20 à -23 ‰ (voir Williams, 1968; Cader et Parker, 1968; Jeffrey, 1969; Nissenbaum, 1974; Nissenbaum et Kaplan, 1972; etc.). Ces dernières, héritées de celles du plancton, varient d'un bassin à l'autre et, surtout, à proximité des continents, en fonction des apports plus où moins lointains de particules ou de produits solubles continentaux. Dans certains milieux particuliers, il n'est pas rare d'observer des proportions plus élevées de carbone lourd. Quoi qu'il en soit, les valeurs (environ -22 ‰) relevées par Tan et Strain (1979), dans le golfe du Saint-Laurent, peuvent être considérées comme représentatives du carbone organique «marin» caractéristique de la région.

Sur ces bases méthodologiques, il est intéressant d'analyser la composition isotopique de la fraction organique des sédiments du lac Bras d'Or (île du Cap-Breton, Nouvelle-Écosse), dans le cadre d'une étude multidisciplinaire destinée à préciser l'évolution du bassin depuis sa déglaciation il y a environ 11 000 ans; voir Mott et Grant, 1984), notamment en relation avec les variations du niveau relatif de la mer (voir de Vernal et coll., 1985). Les résultats préliminaires ci-présentés concernent un carotte de forage prélevée lors d'une mission en mer, sur le CSS Dawson, en novembre 1985.

LE FORAGE 86-036-016

Le choix de l'emplacement du forage, effectué dans la partie sud du lac Bras d'Or, dans la région de la baie East (fig. 89.1), était dicté par deux considérations. D'une part, les échosondages (Huntec) du bassin sud indiquaient la présence de deux unités sédimentaires distinctes (fig. 89.2) au dessus d'une surface réflichissante que l'on pouvait associer à la surface du till du Wisconsinien supérieur d'après les données stratigraphiques régionales (Grant, 1977; de Vernal et coll., 1986). L'unité basale présentait une stratification fine, bien visible sur les échogrammes, tandis que la couche de surface semblait plus massive. Le deuxième argument militant en faveur de ce site se trouvait être sa proximité aux coupes stratigraphiques de référence de la baie East (voir de Vernal et Mott, 1986).

Le carottage effectué par gravité a permis de recouvrer environ un mètre de sédiments tandis que le carottage effectué par carottier à piston en livrait environ 3,5 m. Le carottier n'a pu pénétrer au-delà d'un diamicton brun orangé très compact, contenant des éléments figurés striés, et présentant donc les caractéristiques lithologiques du till régional du Wisconsinien supérieur. À l'ouverture de la carotte prélevée par carottier à piston, la partie sommitale, soit une boue argileuse, noirâtre, homogène et apparemment riche en sulfures (odeur caractéristique), tranchait avec la partie basale, plus silteuse, brunâtre et présentant de fines interstratifications grises (voir de Vernal et Jetté 1987).

Un échantillonnage des carottes prélevées par gravité et par carottier à piston, à des intervalles de 20 cm, a été effectué aux fins d'analyse de la matière organique.

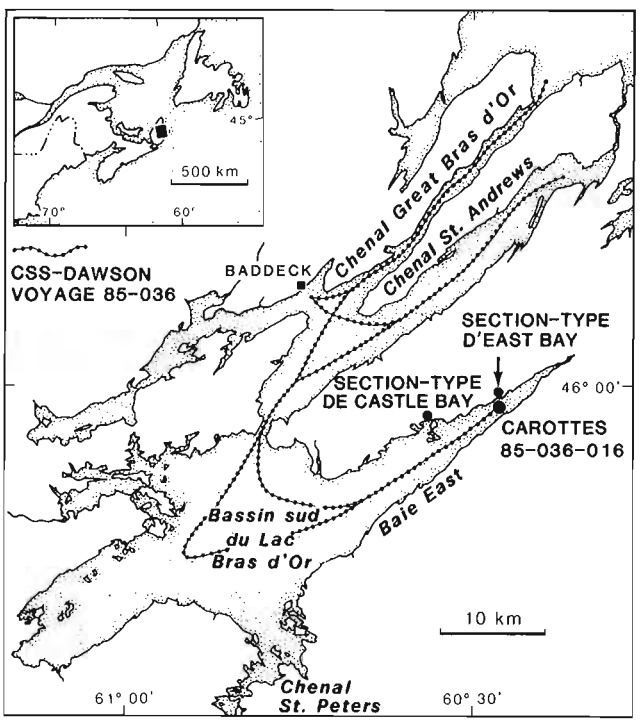


Figure 89.1. Le lac Bras d'Or; itinéraire du CSS Dawson et localisation des forages

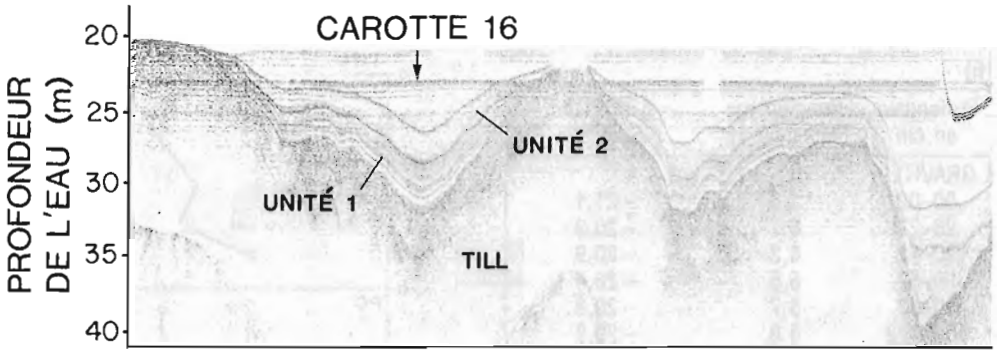


Figure 89.2. Échogramme Huntec du forage 85-036-016.

MÉTHODES ANALYTIQUES

Le dosage de la matière organique a été réalisé par titrage ($FeSO_4/K_2Cr_2O_7$; méthode Walkley-Black modifiée; voir De Kimpe, 1978). Les teneurs en pourcentage pondéral sont reportées sur le tableau 1.

L'oxydation du carbone organique, aux fins d'analyse isotopique, a été effectuée dans des tubes scellés, sous vide de 10^{-3} Torr, en présence d'oxyde de cuivre porté à 450°C. Les tubes ont ensuite été brisés dans une ligne à vide (10^{-3} Torr également); un double piégeage glace sèche-acétone et azote liquide a permis d'isoler le gaz carbonique dans des porte-échantillons. L'analyse isotopique a été réalisée dans un spectromètre de masse à triple collecteur SIRA-12, par rapport à l'étalon interne du GEOTOP (UQ-2). Les résultats (tab. 1), après corrections usuelles (voir Craig, 1957), sont exprimés en unités δ, soit en écart relatif pour mille, par rapport à l'etalon international PDB. La précision instrumentale est de ±0,05 ‰ (±2σ), la reproductibilité analytique, vérifiée régulièrement au laboratoire, est de l'ordre de ±0,1 ‰. Il faut cependant noter la nature peu homogène des sédiments pauvres en matière organique et contenant des macrorestes végétaux. Quelles que soient les précautions prises lors du prélèvement d'une partie aliquote, il est fréquent d'observer, dans de tels cas, des écarts de composition isotopique dépassant considérablement la déviation normale analytique. En ce qui a trait au forage 85-036-016, on a remarqué que les échantillons de la base de la carotte prélevée par carottier à piston présentent de telles anomalies.

RÉSULTATS

La matière organique totale représente 5 à 6 % en poids dans les premiers décimètres des carottes prélevées par gravité (TWC) et par carottier à piston (PC); ce pourcentage baisse ensuite à 3 à 4 %. En fonction de ceci, le recouvrement entre les deux carottes semble élevé: la diminution du pourcentage de matière organique observée entre 80 et 100 cm dans la carotte prélevée par gravité, apparaît entre 50 et 73 cm dans la carotte prélevée par carottier à piston. Environ 30 cm de sédiment de surface n'ont pas été recouvrés dans la seconde. Entre 240 et 260 cm (PC), le pourcentage de matière organique chute considérablement: il oscille entre environ 1,5 et 0,5 % au-dessous.

Les proportions de carbone lourd sont relativement homogènes. Ainsi, entre 0 et 155 cm (PC), elles s'établissent à $-20,5 \pm 0,5$ ‰, de 173 à 302 cm, elles diminuent à $-26 \pm 0,6$ ‰. Au-delà, les deux derniers échantillons, pauvres en matière organique, présentent une grande variabilité de composition isotopique de leur carbone organique: des analyses répétées sur des parties aliquotes ont livré des δ variant respectivement de $-19,9$ à $-12,4$ ‰ et de $-17,6$ à $-9,4$ ‰ (fig. 3).

DISCUSSION

La séquence sédimentaire analysée se divise clairement en trois unités, en ce qui concerne la composition isotopique du carbone organique. La plus récente correspond indubitablement à un milieu caractérisé par la présence d'une proportion importante de matière organique d'origine marine; la productivité biologique, démontrée par le pourcentage de matière organique, a été particulièrement importante pendant la phase d'accumulation des derniers 80 cm. Quoique le bassin actuel puisse être considéré comme légèrement saumâtre (voir Mucci et Pagé, 1987), les apports continentaux de matière organique y sont certainement restreints: il n'existe aucun réseau de drainage important sur l'île du Cap-Breton.

L'unité antérieure, par contre, correspond à une sédimentation organique de type continental, comme l'indiquent les basses teneurs en ^{13}C. Quoiqu'on ne puisse écarter la possibilité d'une pénétration faible ou occasionnelle, ou les deux, d'eau de mer pendant cet épisode, ce dernier peut être considéré comme lacustre, probablement d'eau douce, dans l'ensemble.

La base de la carotte prélevée par carottier à piston semble correspondre à un milieu de faible productivité biologique que l'on pourrait considérer comme «marin», compte tenu des proportions plus élevées de ^{13}C enregistrées dans la matière organique détritique. En se basant sur ces seuls résultats, il est impossible d'apporter plus de précisions dans le présent essai de reconstitution des paléoenvironnements du bassin.

Table 89.1. Pourcentage pondéral et composition isotopique ($\delta^{13}C$) de la matière organique du forage 85-036-016)

Numéro de l'échantillon	Profondeur en cm	Pourcentage MO (±0,1)	$\delta^{13}C$/PDB ±0,1 ‰
CAROTTE PAR GRAVITÉ			
UQC-36-01	00–02	3,8	−21,1
UQC-36-02	20–22	6,7	−20,3
UQC-36-03	40–42	6,2	−20,9
UQC-36-04	60–62	5,5	−20,4
UQC-36-05	80–82	5,7	−20,3
UQC-36-06	100–102	3,8	−20,2
CAROTTE PAR PISTON			
UQC-36-07	10–12	6,3	−20,4
UQC-36-08	30–32	6,2	−19,9
UQC-36-09	50–52	5,7	−20,2
UQC-36-10	73–75	4,0	−21,0
UQC-36-11	93–95	3,8	−19,6
UQC-36-12	113–115	3,2	−20,8
UQC-36-13	133–135	3,8	−21,4
UQC-36-14	153–155	3,6	−20,9
UQC-36-15	173–175	3,1	−25,4
UQC-36-16	193–195	3,8	−26,0
UQC-36-17	220–222	2,6	−26,8
UQC-36-18	240–242	2,4	−26,7
UQC-36-19	260–262	0,8	−25,6
UQC-36-20	280–282	1,6	−26,0
UQC-36-21	300–302	1,3	−25,2
UQC-36-22	320–322	1,2	−19,9 à −12,4*
UQC-36-23	340–342	0,7	−17,6 à −9,4**

*Dispersion sur 6 analyses/**Dispersion sur 5 analyses

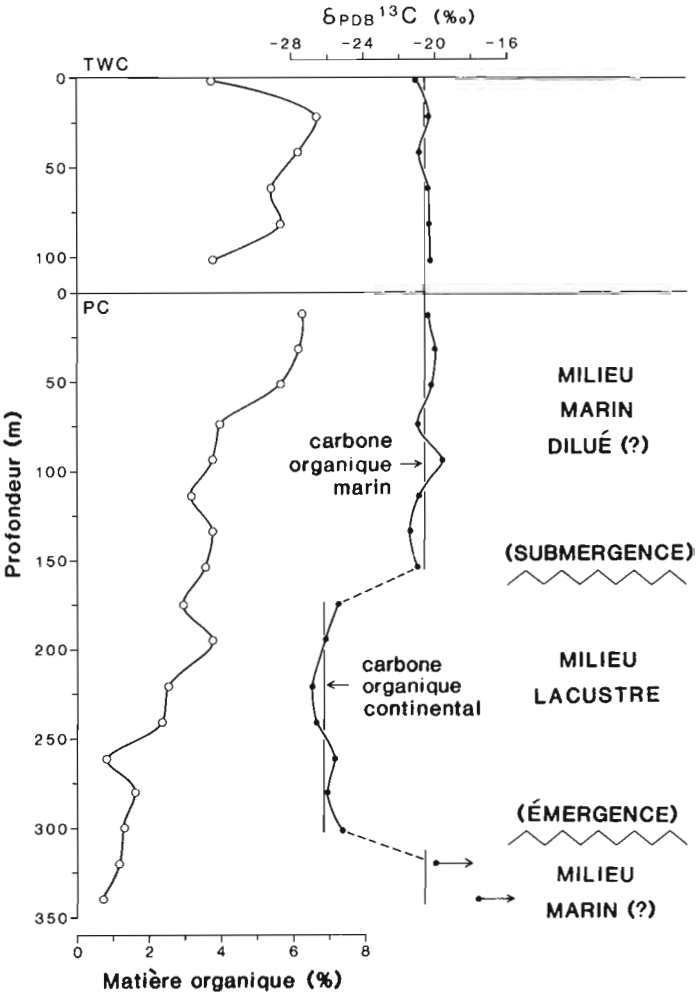


Figure 89.3. Profil du $\delta^{13}C$ et du pourcentage de la matière organique dans les carottes recueillies par gravité et par carottier à piston du forage 85-036-016: interprétation paléoenvironnementale.

Les corrélations palynologiques (de Vernal et Jetté, 1987) semblent indiquer que le début de la sédimentation post-glaciaire date d'il y a environ 9000 à 10 000 ans; on peut donc supposer que la déglaciation du bassin a été légèrement plus tardive que celle des hauteurs voisines (culots de glaces résiduels?). Quoi qu'il en soit, le retard au rajustement glacioisostatique post-glaciaire a très probablement permis l'instauration brève d'un milieu marin au cours de la période sédimentaire initiale. Très rapidement (de Vernal et Jetté, 1987), le niveau relatif de la mer a dû s'abaisser suffisemment pour permettre l'instauration d'un milieu lacustre. Enfin, la submersion régionale qui affecte l'ensemble de la Nouvelle-Écosse (Grant, 1980; Quinlan et Beaumont, 1981; de Vernal et coll., 1985), depuis une époque survenue il y a environ 5000 ans, a rétabli les communications entre le lac Bras d'Or et l'Atlantique, par-delà le seuil (environ −8m) du chenal Great Bras d'Or (fig. 89.1): le milieu marin saumâtre actuel daterait de cette époque.

CONCLUSIONS

Malgré les proportions relativement faibles de matière organique dans les sédiments holocènes du lac Bras d'Or, les teneurs en ^{13}C constituent, comme on pouvait s'y attendre, de bons repères paléoenvironnementaux. Elles permettent de reconstituer les grandes lignes de l'évolution post-glaciaire du bassin, d'abord brièvement ouvert sur la mer, puis à dominante lacustre, et enfin à nouveau marin saumâtre. Il faut bien sûr considérer cette évolution par rapport à celle du niveau marin relatif de la région. Les travaux ultérieurs sur les carottes du forage 86-036-016, ainsi que sur celles des autres forages de la même croisière, permettront d'établir une chronologie précise de ces changements du milieu et donc de reconstituer avec plus de précision cette évolution du niveau relatif de la mer. Par ailleurs, en ce qui concerne la composition isotopique de la matière organique, des analyses en cours sur la composition isotopique de l'hydrogène ($^{2}H/^{1}H$) permettront de mieux percevoir les changements de salinité dans le bassin. Le présent rapport représente donc simplement une étape préliminaire des travaux. En guise de conclusion partielle, il suffit de retenir que la composition isotopique du carbone organique permet de dresser des bilans, en termes de productivité et d'accumulation organique continentale ou marine, ou les deux, dans un milieu de transition d'eau douce

à eau salée, à défaut de servir d'indicateur très sensible des gradients de salinité. De ce point de vue, les études paléoécologiques (microflore et microfaune) sont indispensables.

REMERCIEMENTS

Cette étude préliminaire a été effectuée dans le cadre d'accords de coopération entre le Centre géoscientifique de l'Atlantique et l'Université du Québec. Je remercie sincèrement M.D. Piper (responsable scientifique de la mission en mer) et M.P.J. Mudie pour leur soutien, ainsi que les officiers et l'équipage du CSS Dawson pour leur collaboration. Les travaux analytiques ont été financés par le CRSNG (subvention A-9156) et le Fonds FCAR du Québec (Équipe 492); C. Guilmette et M.-A. Cloutier ont également apporté leur concours.

BIBLIOGRAPHIE

Bender, M.M.
1971: Variations in the $^{13}C/^{12}C$ ratios of plants in relation to the pathway of photosynthetic carbon dioxide fixation; Phytochemistry, v. 10, p. 1239-1244.

Bender, M.M
1968: Mass spectrometric studies of carbon-13 variations in corn and other grasses; Radiocarbon, v. 10, p. 468-472.

Calder, J.A. and Parker, P.L.
1968: Stable carbon isotope ratios as indices of petrochemical pollution of aquatic systems; Environmental Science Technology, v. 2, p. 535-539.

Calvin, M. and Bassham, J.A.
1962: The Photosynthesis of Carbon Compounds; Benjamin, New-York.

Craig, H.
1957: Isotopic standards for carbon and oxygen and correction factors for mass spectrometric analysis of carbon dioxide; Geochimica, Cosmochimica Acta, v. 12, p. 133-149.

Craig, H.
1954: Carbon-13 in plants and the relationship between carbon-13 and carbon-14 variations in nature; Journal of Geology, v. 62, p. 115-149.

Craig, H.
1953: The geochemistry of the stable carbon isotopes; Geochimica, Cosmochimica Acta, v. 3, p. 33-92.

Craig, H. and Keeling, C.D.
1963: The effects of N_2O on the measured isotopic composition of atmospheric CO_2; Geochimica, Cosmochimica Acta, v. 27, p. 547-551.

Deines, P.
1980: The isotopic composition of reduced organic carbon; in P. Fritz et J.-Ch. Fontes (editors), Handbook of Environmental Isotope Geochemistry, v. 1, The Terrestrial Environment, Elsevier, Amsterdam, p. 329-406.

de Kimpe, C.
1978: Manuel de méthodes d'échantillonnage et d'analyse des sols; J.A. McKeague (éditeur), Société canadienne des sciences du sol.

de Vernal, A. et Jetté, H.
1987: Étude palynostratigraphie d'une carotte holocène (85-036-016) du lac Bras d'Or, Nouvelle-Écosse; dans Recherches en cours, Partie A, Commission géologique du Canada, Étude 87-1A, nº 2.

de Vernal, A. et Mott, R.J.
1986: Palynostratigraphie et paléoenvironnements du Pléistocène supérieur dans la région du lac Bras d'Or, île du Cap-Breton, Nouvelle-Écosse; Journal canadien des sciences de la Terre, v. 23, p. 491-503.

de Vernal, A., Causse, C., Hillaire-Marcel, C., Mott, R.J. and Occhietti, S.
1986: Palynostratigraphy and Th/U ages of upper Pleistocene interglacial and interstadial deposits on Cape Breton Island, eastern Canada; Geology, v. 14, p. 554-557.

de Vernal, A., Lortie, G., Larouche, A., Scott, D.B. et Richard, P.J.H.
1985: Évolution d'un milieu littoral et remontée du niveau relatif de la mer à l'Holocène supérieur au nord de l'île du Cap-Breton, Nouvelle-Écosse; Journal canadien des sciences de la Terre, v. 22, p. 315-323.

Grant, R.J.
1980: Quaternary sea-level changes in Atlantic Canada as an indication of crustal delevelling; in Earth Rheology, Isostasy and Eustasy, N.A. Mörner (editor), J. Wiley & sons, New York, p. 201-214.

Grant, R.J.
1977: Glacial styles and ice limits, the Quarternary stratigraphic record and changes of land and ocean level in the Atlantic Provinces, Canada; Géographie physique et Quaternaire, v. 31, p. 247-260.

Jeffrey, L.M.
1969: Development of a method for isolation of gram quantities of dissolved organic matter from sea water and some chemical and isotopic characteristics of the isolated material; thèse de PhD, Texas A&M University, College Station, Texas.

Mott, R.J. and Grant, D.R.
1984: The Alleröd/Younger Dryas climatic oscillation in North America – fact or fiction; Sixth International Palynological Conference, Abstracts, p. 112.

Mucci, A. and Pagé, P.
1987: Bras d'Or Lake cruise Nº 85-036: the water chemistry; in Current Research, Part A, Geological Survey of Canada, Paper 87-1A, no. 3.

Nissenbaum, A.
1974: The organic geochemistry of marine and terrestrial humic substances: implications of carbon and hydrogen isotope studies; in B. Tissot and F. Bienner (editors), Advances in Organic Geochemistry 1973, Elsevier, Amsterdam, p. 39-52.

Nissenbaum, A. and Kaplan, I.R.
1972: Chemical and isotopic evidence for the in situ origin of marine humic substances; Limnology and Oceanography, v. 17, p. 570-582.

Quinlan, G. and Beaumont, C.
1981: A comparison of observed and theoretical postglacial sea level in Atlantic Canada; Canadian Journal of Earth Sciences, v. 18, p. 1146-1163.

Sackett, W.M.
1964: The depositional history and isotopic organic carbon composition of marine sediments; Marine Geology, v. 2, p. 173-185.

Smith, B.N. and Epstein, S.
1971: Two categories of C^{13}/C^{12} ratios for higher plants; Plant Physiology, v. 47, p. 380-384.

Tan, F.C. and Strain, P.M.
1979: Organic carbon isotope ratios in recent sediments in the St. Lawrence estuary and the gulf of St. Lawrence; Estuarine and Coastal Marine Science, v. 8, p. 213-225.

Troughton, J.H.
1972: Carbon isotope fractionation in plants; Proceedings of the eight Conference of Radiocarbon Dating, Royal Society of New Zealand, Wellington, v. 2, p. 39-57.

Wickman, F.E.
1952: Variations in the relative abundance of the carbon isotopes in plants; Geochimica, Cosmochimica Acta, v. 2, p. 243-254.

Williams, P.M.
1968: Stable carbon isotopes in the dissolved organic matter of the sea; Nature, v. 219, p. 152-153.

Techniques for the display and editing of marine potential field data

Projects 730081, 840056

Ron Macnab, Jacob Verhoef and John Woodside
Atlantic Geoscience Centre, Dartmouth

Macnab, R., Verhoef, J., and Woodside, J., Techniques for the display and editing of marine potential field data; in Current Research, Part A, Geological Survey of Canada, Paper 87-1A, p. 865-875, 1987.

Abstract

Efficient editing and production of potential field maps is facilitated with tools developed for enhancement and display of large data sets. These include software packages for gridding and contouring, construction of shadowgrams, and directional filters. The clean data bases that result from applications of these techniques are basic to high level geophysical interpretation.

Résumé

La préparation efficace et la production de cartes de champs potentiels sont facilitées grâce à des outils mis au point pour l'amélioration et l'affichage de grands ensembles de données. Ces ensembles comprennent des logiciels pour le tracé de quadrillage et de courbes de niveau, la construction d'ombrogrammes et de filtres directionnels. Les bases de données épurées obtenues après l'application de ces techniques représentent une interprétation géophysique de base à très élaborée.

INTRODUCTION

The Atlantic Geoscience Centre (AGC)has been compiling marine magnetic and gravity data collected by various EMR agencies off the east coast of Canada for over twenty five years (for an overview of offshore survey operations see e.g. Macnab, 1983; Miller et al., 1983; Macnab et al., 1985). The bulk of these data have recently undergone major overhaul and compilation, with a view to producing high quality regional maps and a clean data base for future reference and interpretation.

Our ability to handle large data sets has been increased by the acquisition of tools for display, manipulation, and editing. Using small and powerful micro-computers, we have streamlined many of the procedures that formerly consumed hours, and are now able to interact with our data in a manner impossible just a few years ago. A key component in this development has been the introduction of techniques for rapid graphical display, both in colour and in black and white. This is making it much easier to assess problems, and to correlate the information content of large geographic data sets.

THE DATA

The data consist of about 2.8 and 2.3 million observations of the magnetic and gravity fields, respectively. These observations consist of numerous discrete data sets collected on separate cruises ranging over the entire east coast offshore (Fig. 90.1). They represent data densities that range from isolated ships' reconnaissance tracks to closely spaced systematic surveys. There is overlap between many of the data sets, as in situations where systematic surveys have been carried out in areas crossed previously by reconnaissance tracks, or when certain areas have been resurveyed (sometimes after intervals of several years) at closer line spacings.

The quality of this data base is dependent on the accuracy of individual observations. The accuracy of the data is affected by a number of measurement, positioning, and processing errors. Obvious errors, like spikes are easily detectable. However, subtle inaccuracies in a large data set can better be dealt with through application of techniques like those described here.

Errors in the magnetic measurements are caused by short-term changes of the magnetic field (diurnal variations and storms), navigational inaccuracies, and failure or misapplication of the International Geomagnetic Reference Field (IGRF) to model adequately the long-term secular variation. Although the most current representations of the reference field (IAGA Division 1 Working Group 1, 1986) are considerably better than thelder ones (IAGA Division 1 Working Group 1, 1981), we found that there remains a small time-dependent factor (work in progress).

Major errors in gravity measurements arise from failure to properly account for ship's course and speed; these need to be observed accurately in order to calculate the Eotvos correction. Other problems arise from environmental and instrumental factors, e.g. accelerations introduced by ship's response to wave motion, slow changes in the mechanical or electrical characteristics of the gravimeter, etc. A third class of error arises from mis-ties to the land gravity reference network.

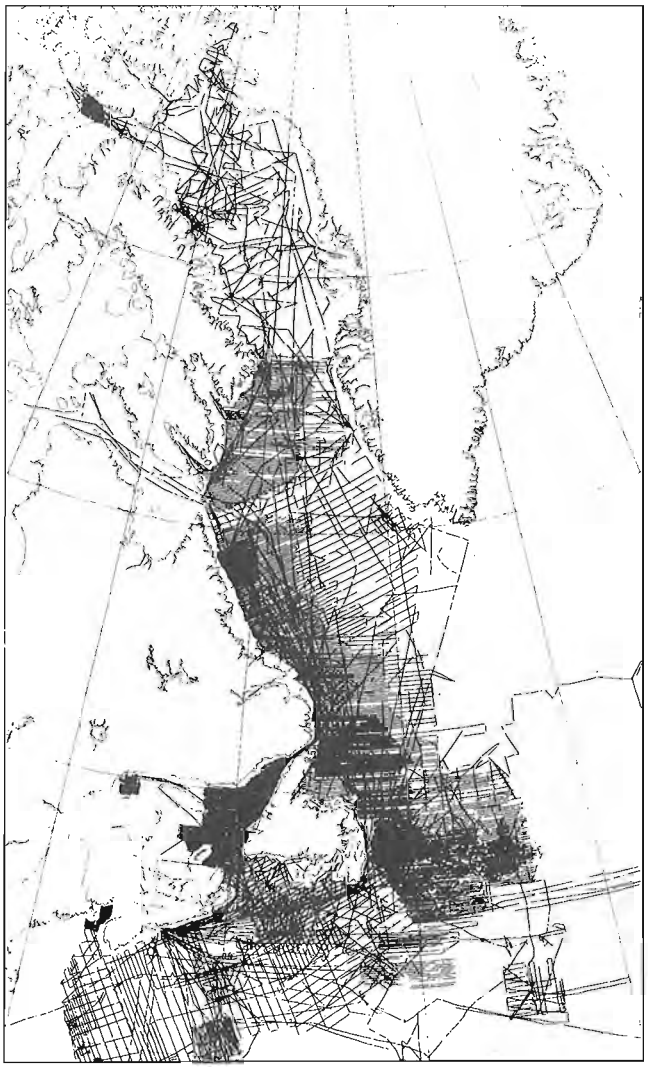


Figure 90.1. Track chart showing the coverage of magnetic and gravity measurements off Eastern Canada.

Whether in magnetics or gravity, the errors share a similar effect, which is to introduce disagreement between observations along intersecting or closely-spaced ships' tracks. Without automated techniques, the identification and correction of these problems can be a time-consuming and error-prone operation.

GRIDDING AND CONTOURING

The first step in data processing is to convert irregularly-spaced ship track data into observations distributed over a regular grid. For this, an automated gridding routine is

applied which is a combination of an adjustable digital filter with a weighting method (Slootweg, 1978, Verhoef et al., 1986). The method produces grid values that are unbiased by track-line geometry, and also diminishes the influence of residual positioning errors. It has the disadvantage that along-track details with wavelengths shorter than the mean track spacing are lost.

Computer contouring is accomplished in three steps:
1) generating a square grid over the area to be contoured;
2) estimating the mesh point values for this grid from the data point values;
3) drawing contour lines using the mesh point values.

The spatial filter used in the calculation of mesh point values from unevenly spaced data is a low-pass Butterworth filter of the first order, which reduces the short wavelength components in the data. The choice of the cut-off wavelength of this filter depends on the data point distribution and the expected spectral content of the variable to be contoured.

In general, marine survey operations yield sets of observation points with an irregular distribution: data points tend to be more closely spaced in along-track than in cross-track directions. Careful specification of filter constants should minimize the effects of this sort of data distribution, while predicting how much filtering will occur for any given wavelength.

If too low a cut-off wavelength is selected for the filter, the coherent structure of the resulting contour lines will be disturbed by irregularities in the data distribution. If on the other hand the cut-off wavelength is chosen too high, short wavelength detail will not appear in the contours. Thus an optimum value has to be established which will depend on the mean distance between tracks. If this mean distance varies largely over an area, the gridding can be done in subareas with different filter settings, and the resulting grid files merged by means of a simple averaging technique. However, in this case the resulting grid will be spectrally inhomogeneous.

Our current gridding procedure for the routine handling of track data uses as input the original time-sequential field observations, each tagged with latitude and longitude coordinates. The output consists of a grid file representing a matrix of mesh points separated by equal increments of latitude and longitude.

The grid file contains three quantities for each mesh point:
a) the summation of the values of the contributing data points multiplied by the weighting function;
b) the summation of the weight function;
c) the number of contributing data points.

Data points contribute to a grid value whenever the weight function, which is a function of the distance between the data point and the grid point, is higher than 0.3% of its maximum value. This maximum value occurs when data point and grid point coincide.

The gridding operation consists first of scanning and multiplying all data points by the appropriate weighting function for each grid point, with summations stored in the grid file as quantities a), b), and c) defined above. The value at each grid point is then calculated by dividing summation a) for that location by the corresponding total weight function b). If the number of data points contributing to one grid point is less than a set limit, a flag-value is stored indicating 'no data'.

Storing quantities a), b), and c) separately for each grid point makes it easy to update the grid file whenever new data are available, or to enter corrections for bad data. For instance, suppose that after contouring one observes several contour lines which are obviously disturbed by a series of erroneous values along a particular track. Eliminating these bad values is easily accomplished by re-running the gridding program on a synthetic track that matches the location of the bad track, but with signs reversed on all the offending data points. The weight functions are adjusted accordingly in the appropriate grid locations. Note that it is not necessary to re-grid the entire set of data to enter corrections for any given track segment.

The actual contour map is produced by drawing line segments within the elementary grid squares. The end points of these segments are found by linear interpolation between the mesh points. Other options are to display contours as changes in colour or line pattern. In this case the locations of the changes are also found by linear interpolation between the mesh points.

FILTER EFFECT OF THE GRIDDING AND CONTOURING PROCESS

A cut-off wavelength of 20 nautical miles appears to be the optimum for the total set of magnetic and gravity observations collected by AGC. This means that at 20 nautical miles from a mesh point the weights are 6 dB down (or approximately 70 %), decreasing further with increasing distance. In areas of smaller than average track spacing, this filter setting results in the loss of some detail.

This filter effect is illustrated in Figure 90.2, where the solid line represents observed magnetic anomalies along a short segment of ship's track. The dotted line shows the anomalies reconstituted from gridded values along the same track. The filter effect is clearly seen as an attenuation of the short wavelength anomalies. The effect is less pronounced for gravity observations, because the gravity field varies less over similar distances than the magnetic field.

Note tnat the dotted profile in Figure 90.2 displays a slight level shift. This might be the result of biases in the observed data, or it might be introduced from adjacent lines; the grid file contains influences from both sources.

The technique of comparing values observed along track with reconstituted grid values can also be applied to locate track segments that agree poorly with their neighbours. The average differences between observed and reconstituted values should yield random residuals for short wavelength anomalies over a number of points with no bias. However,

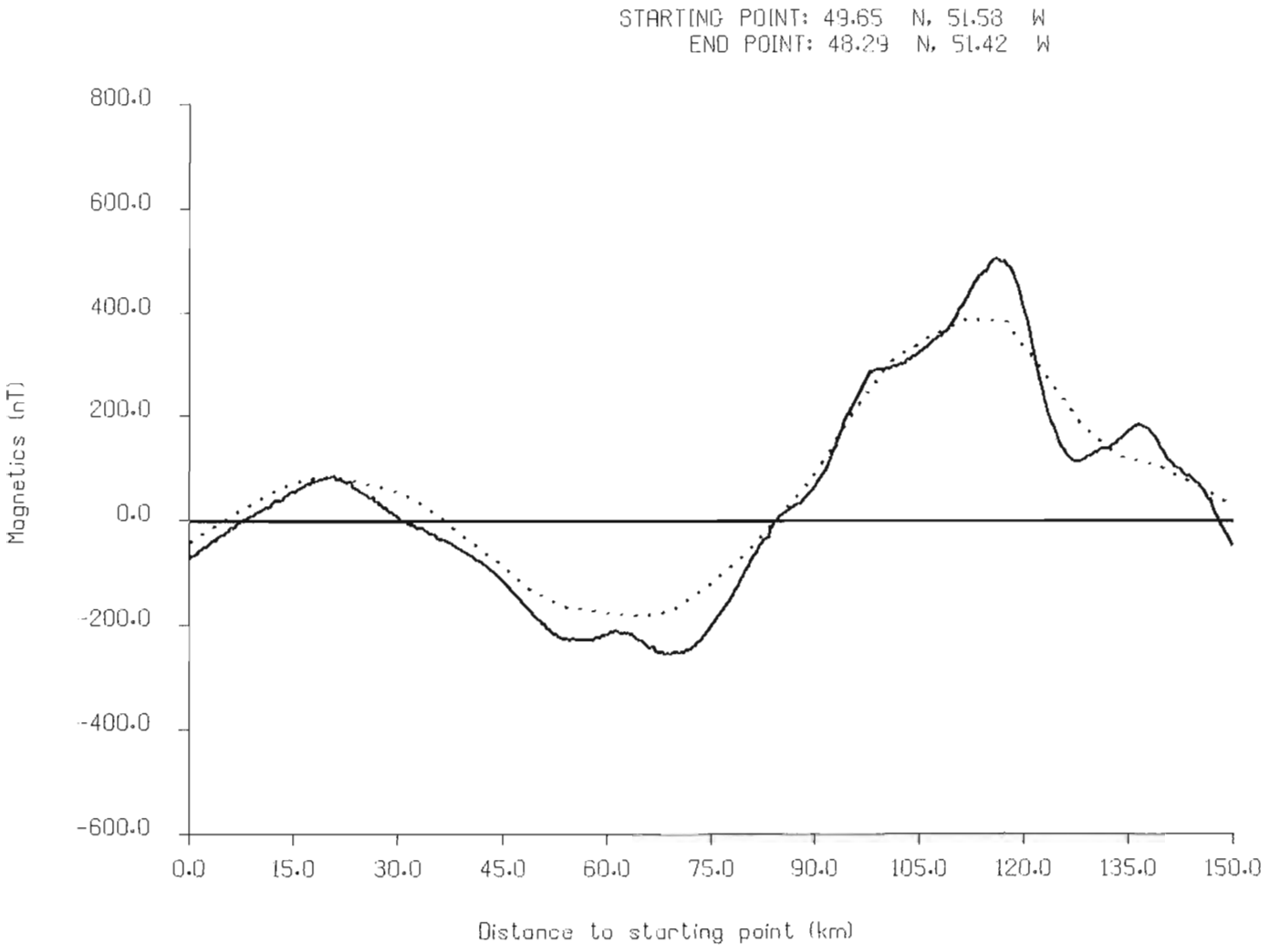


Figure 90.2. Filtering effect of the gridding routine. The continuous line represents the observed magnetic anomalies along a track of a 1979 cruise. The discontinuous line gives the anomalies along the same track, but now recalculated from the gridded values. The filter effect of the gridding, for which a Butterworth filter with a 20 nautical mile cut-off wavelength was used, is clearly seen as the attenuation of the short wavelength anomalies. The profile is located to the east of Newfoundland.

where a track segment agrees poorly with its neighbours, the residuals may be expected to have a consistent sign.

SHADOWGRAMS

Data presentation by way of a contour map has the disadvantage that features with amplitudes smaller than the contour interval may get lost. One solution is to present a three-dimensional view of the grid values. Another solution is to present slopes instead of values. The latter approach is easy to implement by calculating and plotting the directional derivative of the grid values. The direction of this derivative is user selectable, and depends on the slopes one wants to enhance (e.g. Verhoef et al., 1986).

The resulting plot suggests the shadows that would be obtained by shining light across the surface of the gridded data from a given direction. An advantage of this presentation is that one obtains a better resolution, due to the relative increase in power of the shorter wavelengths caused by the application of the directional derivative. Bad tracks are therefore more easily detected.

As an illustration of the method, we describe below a specific application of the shadowgram method to identify bad data in a subset of AGC data located northeast of Newfoundland.

Figure 90.3a is an anomaly map derived from marine magnetic observations. Clearly visible are the arcuate trends

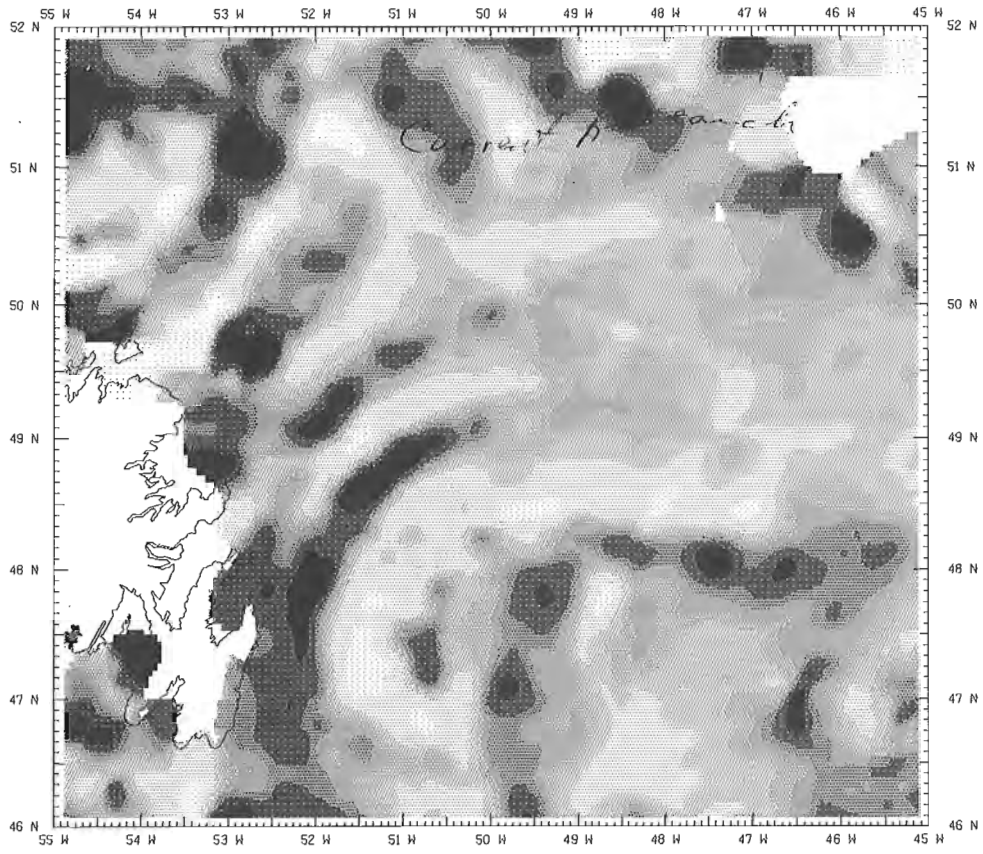


Figure 90.3a. Magnetic anomalies in an area to the northeast of Newfoundland. Clearly visible are the arcuate trends of the strong positive anomalies of the Avalon basement across the Grand Banks. The data include a 'bad track' which hardly shows.

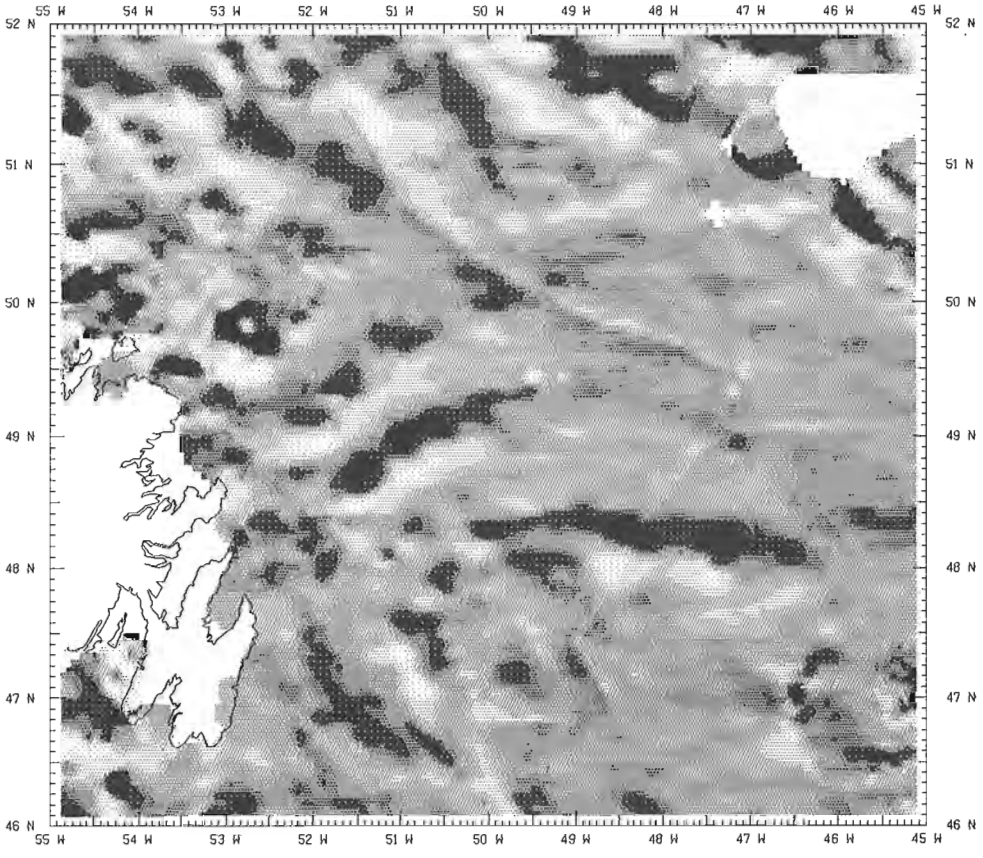


Figure 90.3b. Shadowgram of the magnetic anomalies of Figure 90.3a in the direction of 210°, i.e. 30° west of south. The values plotted are the slopes (unit is nT/km) of the anomalies. The 'bad track' showss the irregular zigzag feature tracking from the northern edge of the map to a point near the southern edge.

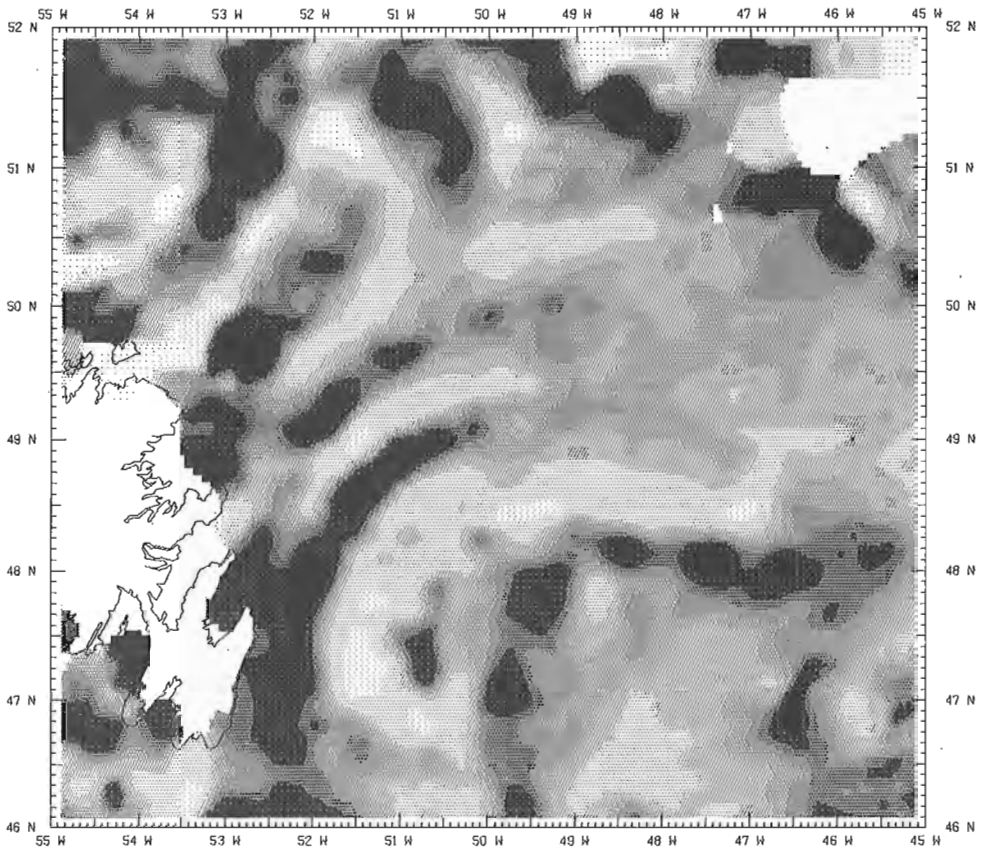


Figure 90.3c. Magnetic anomalies after correcting for the 'bad track'. The correction resulted only in some minor changes in the anomaly pattern.

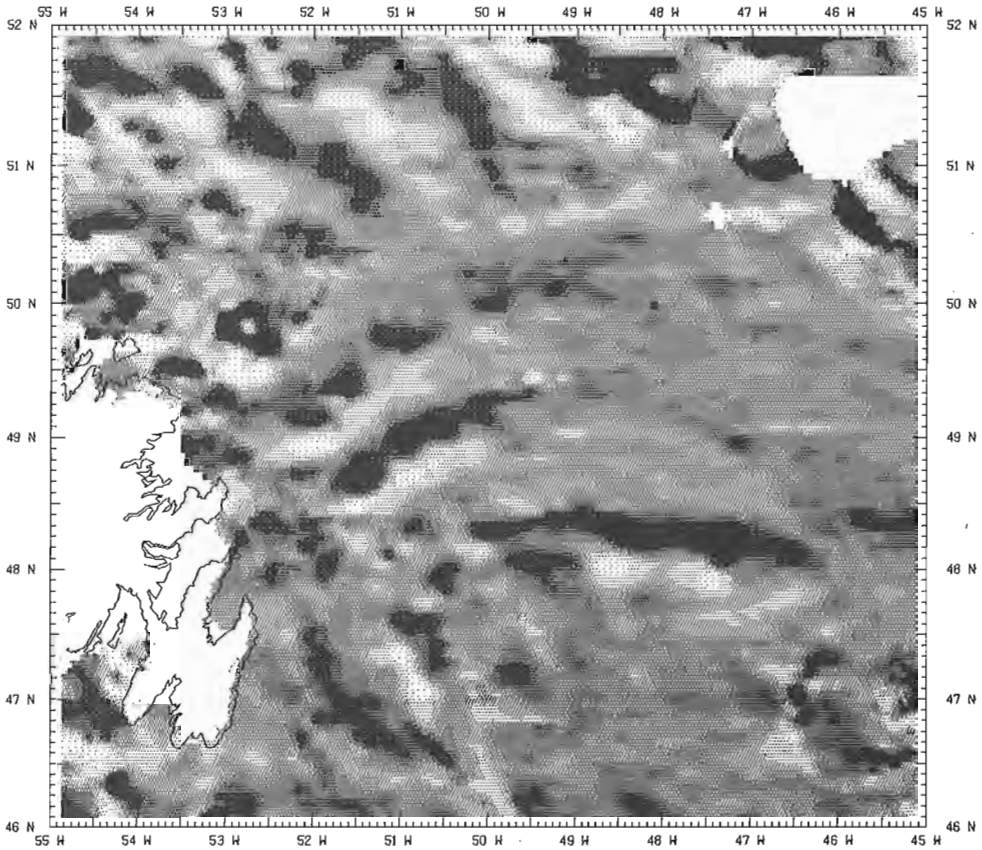


Figure 90.3d. Shadowgram of the corrected anomalies in the direction of 210°. The correction resulted in a significant change in the shadowgram. Note how the dominant lineation of Figure 90.3b has now disappeared.

of the Avalon basement across the Grand Banks and continuing into Orphan Basin (e.g. Haworth, 1980), where they decrease in amplitude. This map contains an erroneous track segment, although even a careful inspection of the contours does not reveal anything seriously amiss.

Figure 90.3b is a shadowgram of the same area, with the source of illumination at 210° (i.e. 30° west of south). Even a cursory glance suffices to detect an irregular zigzag feature tracking from the northern edge of the map to a point near the southern edge. An inspection of the ship tracks in the area shows that this feature indeed corresponds to an identifiable track segment.

The gridded data set can now be recalculated using a synthetic correction track as outlined above, to eliminate the effect of erroneous data. Figure 90.3c is the corrected magnetic anomaly field, which differs little from the uncorrected field. The corrected shadowgram in Figure 90.3d, however, clearly shows the improvement in the data set. The data base will likewise be cleaner following the correction.

The shadowgram technique was applied to the entire magnetic data set using various directions of illumination, in order to locate and identify erroneous track segments in different directions. Synthetic correction tracks were then fed into the gridding process to eliminate bad data. This resulted in the elimination of about 3% of the data set, and led to a significant improvement in the final magnetic anomaly map. This map will be published at 1:5 000 000 in a forthcoming Geology of Canada volume, together with corresponding maps of gravity, bathymetry and geology.

EDITING GRAVITY DATA FOR NESS MAPS

Editing of gravity data prior to publication as maps in the National Earth Science Series (NESS) is facilitated using some of the techniques described in this paper. Normally, someone must painstakingly examine all the posted values on each of twelve preliminary 1:250 000 scale maps which cover the area of a 1:1 000 000 NESS map. The search is for segments of data which are inconsistent with the surrounding data.

A series of graphical displays may be quickly and effectively used as an aid in finding erroneous data without the need to scan visually the entire set of posted values. Erroneous data show up, for example, on contour plots as "herring-bone" patterns where a track segment is shifted with respect to its neighbours or as "bull's eyes" when a spike is present. As noted above, they may be identified on shadowgrams as track-correlated bands, or by comparison of raw observed data with gridded values to determine if data are suspiciously different from the local field.

A systematic procedure is followed in the validation of data destined for the NESS maps. The criteria used are: line-to-line contourability of the data, consistency of crossover values, continuity between sheets, variability along north-south lines (where the Eotvos correction is notoriously difficult to determine), and compatibility of short unconnected track segments. A least squares adjustment of the gravity data optimizes crossover variations, and ensures that the data set is clear of drift and levelling variations. What remains to be done therefore is primarily the finding of data which have escaped this treatment, because they were not properly connected into the adjustment network. For each of the twelve subsets of a NESS sheet the data are plotted as shadowgrams and contours and compared automatically with filtered and gridded data. Visual checks of problem areas can then be made.

DIRECTIONAL FILTERING

Some parts of the magnetic data feature corrugations that are obviously due to level differences between adjacent and parallel ship tracks.

An example is shown in Figure 90.4a, which illustrates the magnetic anomaly field to the east of Nova Scotia. The East Coast Magnetic Anomaly (ECMA) is clearly visible as a strong positive feature running from about 41.5N/65W to 43.5N/59.5W, while a few subtle NNW-SSE lineations can be seen in the lower part of the map area. These lineations are more clearly visible in the shadowgram of Figure 90.4b, which has been constructed with a direction of illumination of 90°. An inspection of the track lines in Figure 90.1 indicates several track segments in the area with a similar spacing and orientation; the lineations in the magnetic field are obviously related to these tracks, and arerobably caused by levelling problems in the data.

One method for correcting levelling errors uses differences between tracks at crossovers. Data adjustments required to minimize these differences in a least squares sense are then used to adjust all the observations. This technique is well suited for adjusting gravity survey data, and has been applied to the gravity data using 21,813 crossovers (Earth Physics Branch, 1986). However, it is difficult to apply on observations of a time varying field like the magnetic field, when the period over which observations have been made is so long that time-dependent factors still remain after a first correction.

In the particular case of corrugations in the magnetic field, an effective approach involves the directional filtering technique.

From an examination of the shadowgram in Figure 90.4b and the track lines in Figure 90.1, it is obvious that the NNW-SSE lineations in the magnetic field will produce relatively high values in that direction of the power spectrum, with a wavelength determined by the track spacing. Figure 90.5 is the two-dimensional power spectrum of the data in this particular area, obtained by applying a 2D Fourier Transform to the gridded data.

In simple terms the power spectrum shows the variation of the square of the amplitude of the magnetic anomalies with their wavelength. In addition to the general decay of the power going from longer to shorter wavelengths, there is some local increase in the power along the direction of 55°.

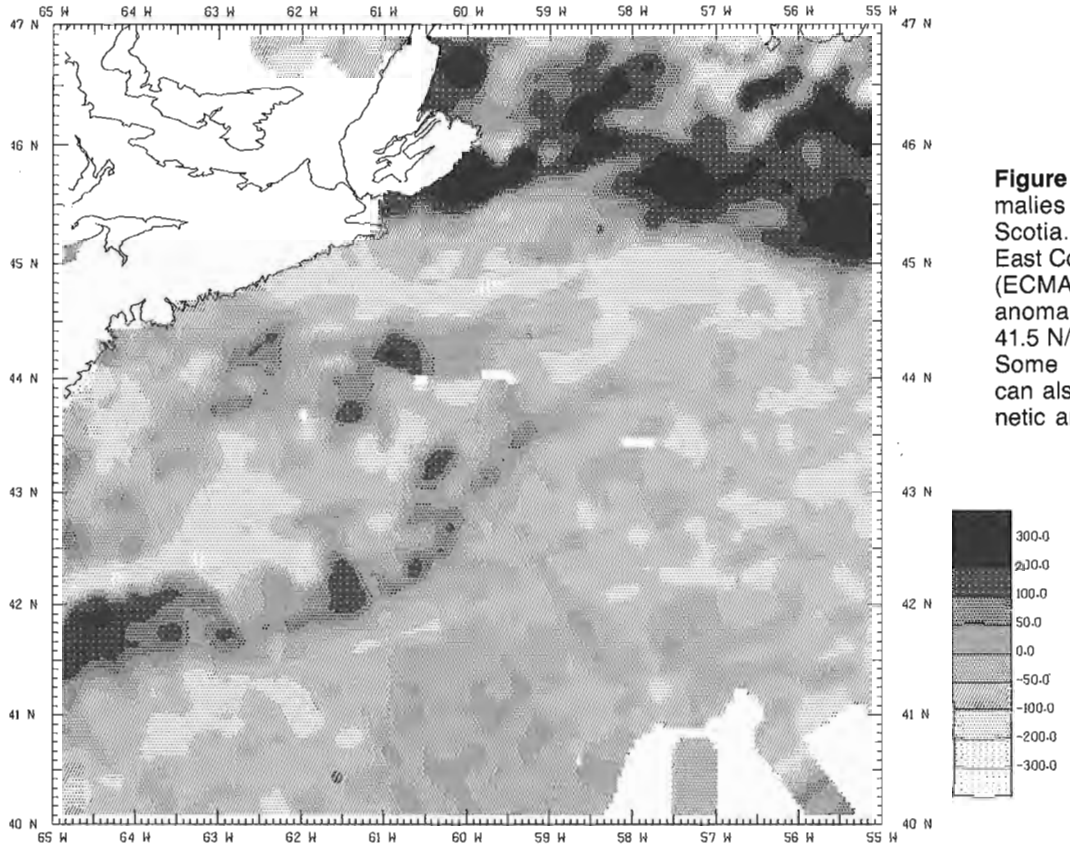


Figure 90.4a. Magnetic anomalies to the east of Nova Scotia. Clearly visible is the East Coast Magnetic Anomaly (ECMA) as a strong positive anomaly running from about 41.5 N/ 65 W to 43 N/ 59.5 W. Some NNW-SSE lineations can also be seen in the magnetic anomalies.

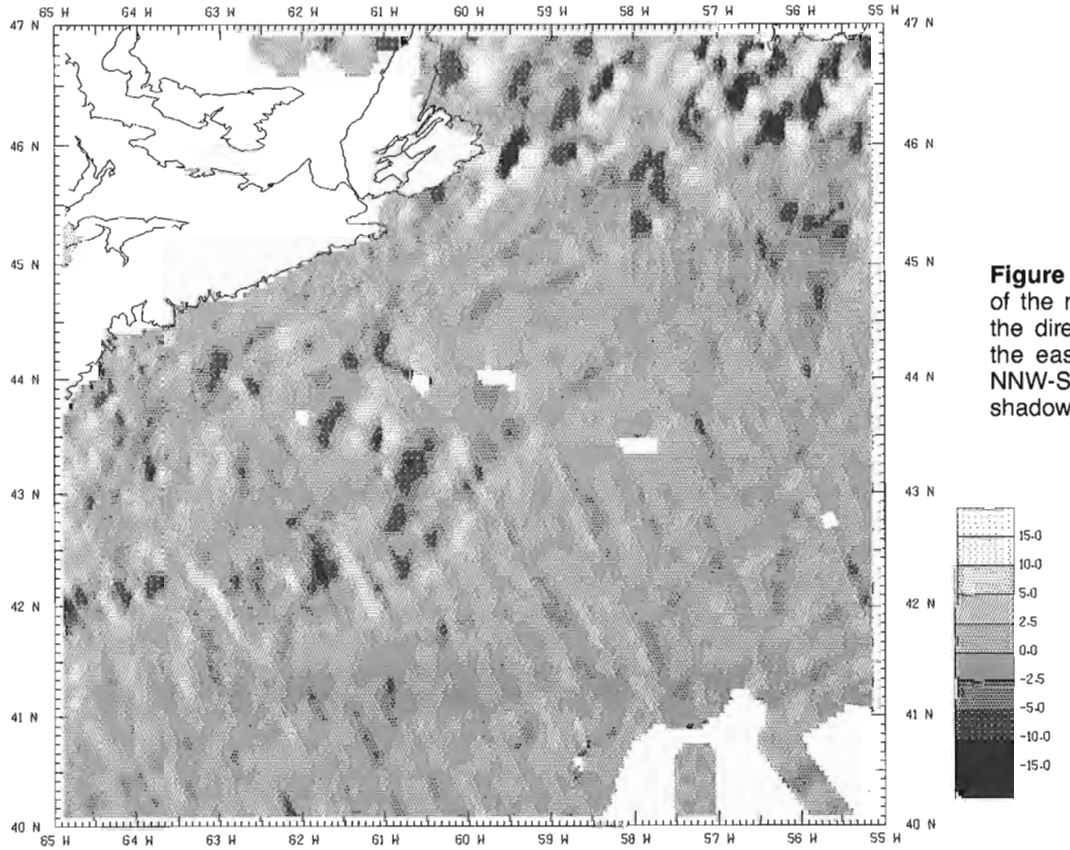


Figure 90.4b. Shadowgram of the magnetic anomalies in the direction of 90°, i.e. from the east. Note the dominant NNW-SSE lineations in the shadowgram.

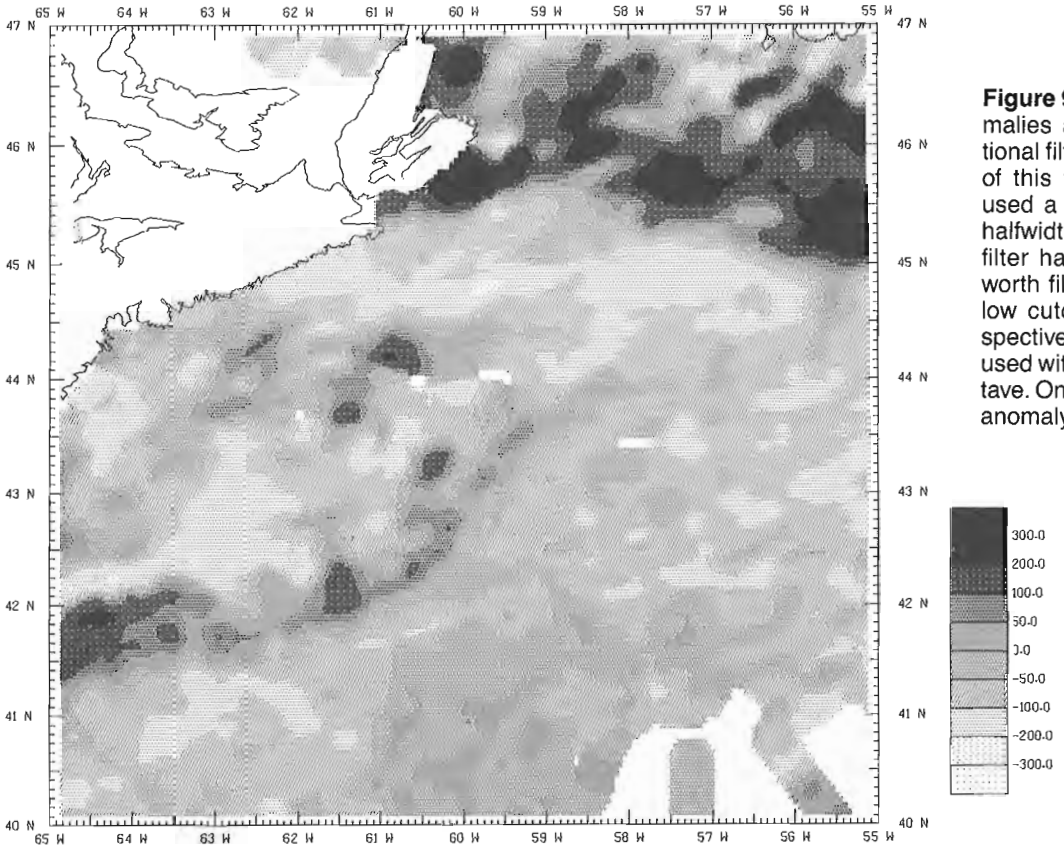


Figure 90.4c. Magnetic anomalies after applying a directional filter. The directional part of this filter is Gaussian; we used a direction of 55° and a halfwidth of 20°. In addition the filter has a bandpass Butterworth filter for which high and low cutoff wavelengths of respectively 18 and 65 km were used with a roll-off of 48 dB/octave. Only small changes in the anomaly pattern can be seen.

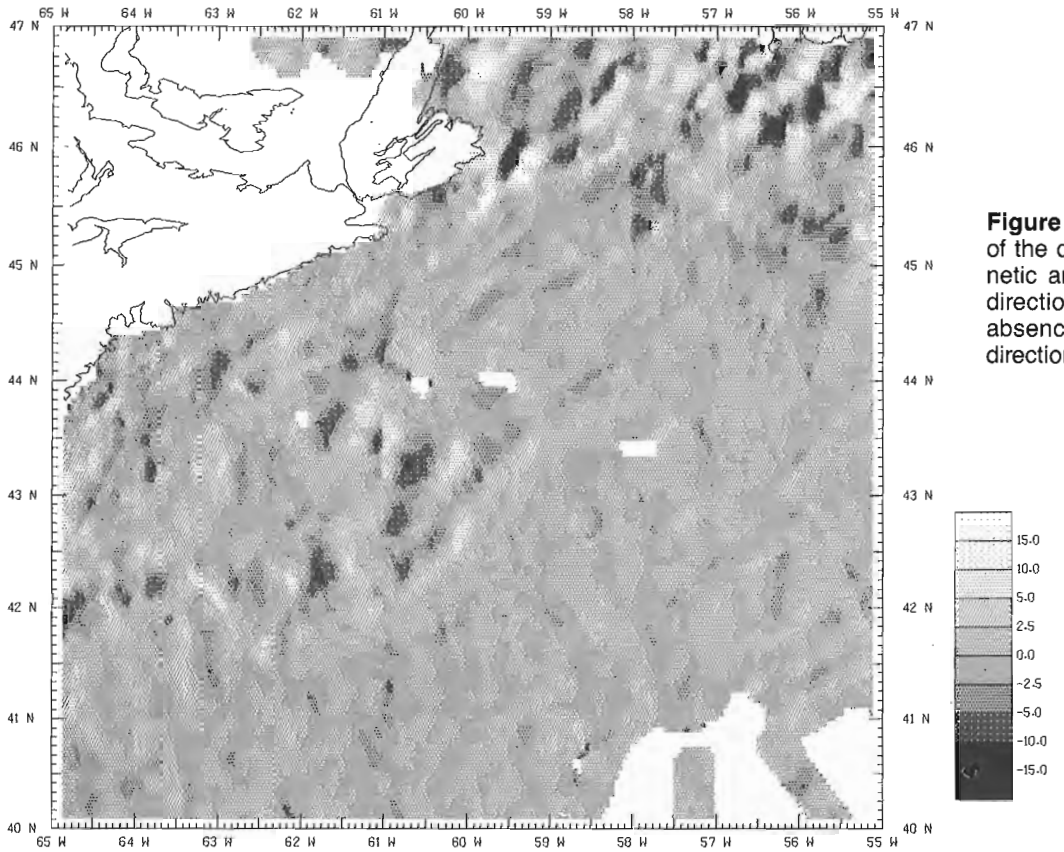


Figure 90.4d. Shadowgram of the directional filtered magnetic anomalies, again in the direction of 90°. Note the absence of the NNW-SSE directions.

This shows up as a series of small spots in the figure, extending from the centre along the 055-235 axis (see line indicated by arrows in Fig. 90.5).

The picture becomes clearer if we calculate the power spectrum at an azimuth of 55° (Fig. 90.6). The power in this direction and between wavelengths of 18 and 65 km is larger than the corresponding power in other directions. This indicates a relationship between lineations in the field, and the spacing and orientation of the tracks.

In order to isolate anomalous features in the power spectrum, it is possible to define a mean spectrum by averaging over the different directions, and then to look at the deviations

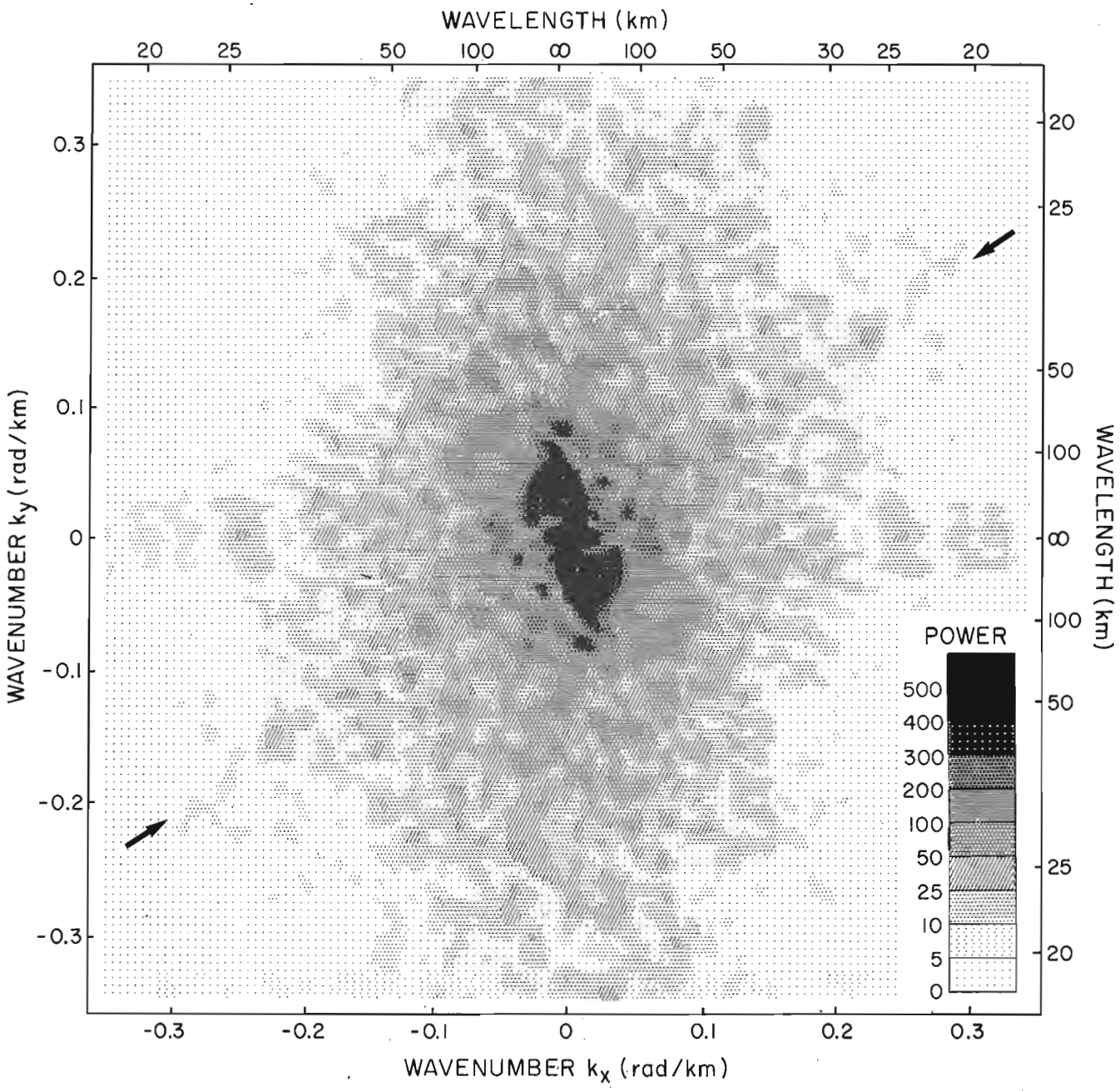


Figure 90.5. Two-dimensional power spectrum of the magnetic anomalies of Figure 90.4a. Before applying a 2-D Fourier Transform to the data, a best fitting plane was subtracted from the data and a cosine taper was applied. The wavenumber in the x-direction is shown along the horizontal axis, while the wavenumber in the y-direction runs along the vertical axis. As the input data were a real function the spectrum shows some symmetry: the first and third quadrant are the same, as are the second and fourth. For presentation purposes wavelengths of less than 18 km are not shown. The arrows gives the 055° direction.

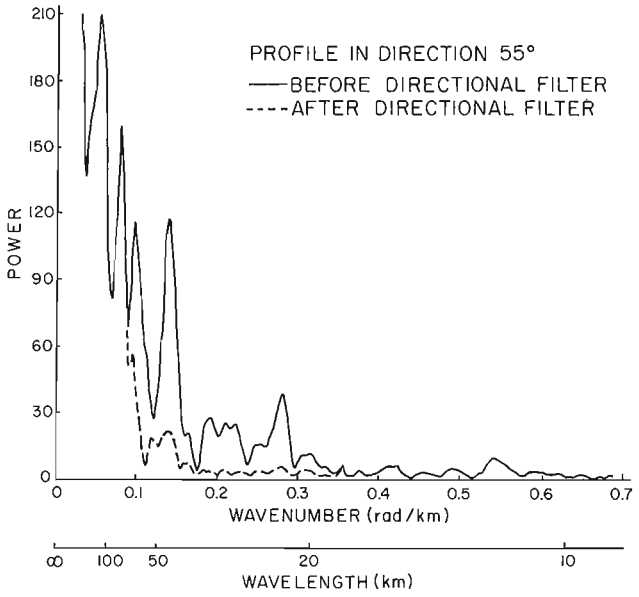


Figure 90.6. Power spectrum in the direction of 55°. The continuous line gives the power spectrum of the original anomalies. The dashed line gives the power spectrum in the same direction after applying a directional filter. Note the relatively high power between wavenumbers 0.36 and 0.12 in the original power spectrum, which was taken out by the directional filtering.

from these averages (e.g Simpson et al., 1986). However, the power spectrum of magnetic anomalies in general is not axially symmetric like that obtained from gravity anomalies; it has instead an elliptical shape due to the vectorial character of the magnetic anomalies.

To reduce the effect of mislevelling between tracks and hence to eliminate the lineations in the magnetic field, we reduce the power in the direction of 55° by applying a directional filter. The procedure we follow is to use a filter with a directional part which is Gaussian; the effective width of this filter is defined by a halfwidth specification. In addition to a directional component, the filter includes a Butterworth wavelength bandpass. We used cut-off wavelengths of 18 and 65 km for the bandpass filter, and a roll-off of 48 dB/octave.

The dotted line in Figure 90.6 shows the power in direction 055° after the directional filter has been applied. Figure 90.4c shows the magnetic anomalies in the area after applying the directional filter, with the corresponding shadowgram in Figure 90.4d. There has clearly been an improvement in the data set, especially in the NNW-SSE direction.

The method described above demonstrates how levelling problems can be eliminated by using a directional filter. However, the use of such a filter also eliminates genuine power in the specified direction. We are investigating different approaches to resolve this loss of information. One approach is to use the power in the direction of corrugation to define level corrections that are applied directly to observed data along selected tracks.

ACKNOWLEDGMENTS

The computer programs described and applied here were developed at the Marine Geophysical department of the Vening Meinesz Laboratorium at the Rijksuniversiteit at Utrecht, the Netherlands. The acquisition, processing and compilation of data would not have been possible without the active collaboration, at various stages, of a number of groups and individuals within the GSC (Geophysics Division) and in other departments (Canadian Hydrographic Service). Wayne Prime, Gordon Oakey, and Keh-Gong Shih were instrumental in wrestling large data sets into the excellent shape in which they are now. We thank B.D Loncarevic and F. Marillier for reviewing this paper.

REFERENCES

Earth Physics Branch
1986: Integration of Atlantic Geoscience Centre Marine Gravity Data into the National Gravity Data Base; Earth Physics Branch Open File 85-32, Joint Publication of Earth Physics Branch and Atlantic Geoscience Centre.

Haworth, R.T.
1980: Appalachian structural trends northeast of Newfoundland and their trans-Atlantic correlation, Tectonophysics, v. 64, p. 111-130.

IAGA Division 1 Working Group 1
1981: International Geomagnetic Reference Fields: DGRF 1965, DGRF 1970, DGRF 1975 and IGRF 1980, EOS, Transactions of the American Geophysical Union, v. 62, p. 1169.
1986: International Geomagnetic Reference Field Revision 1985, EOS, Transactions of the American Geophysical Union, v. 67, p. 523-524.

Macnab R.F.
1983: Multiparameter mapping off the east coast of Canada, in Current Research, Part A, Geological Survey of Canada, Paper 83-1A, p. 163-171.

Macnab R.F., Loncarevic B.D., Cooper R.V., Girouard P.R., Hughes M.D. and Shouzhi F.
1985: A regional marine multiparameter survey south of Newfoundland, in Current Research, Part B, Geological Survey of Canada, Paper 85-1B, p. 325-332.

Miller R.O., Macnab R.F., Amos C.L. and Fader G.B.
1983: Canadian East Coast multiparameter surveys, 1982, in Current Research, Part B, Geological Survey of Canada, Paper 83-1B, p. 331-334.

Simpson R.W., Jachens R.C., Blakely R.J. and Saltus R.W.
1986: A new isostatic residual map of the conterminous United States with a discussion on the significance of isostatic residual anomalies, Journal of Geophysical Research, v. 91, p. 8328-8372.

Slootweg A.P.
1978: Computer contouring with a digital filter; Marine Geophysical Researches, v. 3, p. 401-405.

Verhoef J, Collette B.J., Miles P.R., Searle R.C., Sibuet J-C. and Williams C.A.
1986: Magnetic anomalies in the northeast Atlantic Ocean; Marine Geophysical Researches, v. 8, p. 1-25.

A small boat seismic reflection survey of the Lougheed Island Basin – Cameron Island Rise – Desbarats Strait region of the Arctic Island channels using open water leads

Project 820050

G.V. Sonnichsen and G. Vilks
Atlantic Geoscience Centre, Dartmouth

Sonnichsen, G.V. and Vilks, G., A small boat seismic reflection survey of the Lougheed Island Basin – Cameron Island Rise – Desbarats Strait region of the Arctic Island channels using open water leads; in Current Research, Part A, Geological Survey of Canada, Paper 87-1A, p. 877-882, 1987.

Abstract

Lougheed Island Basin, Desbarats Strait, and Cameron Island Rise in the Arctic Island channels were geologically examined using helicopter-transported inflatable boats in open water leads through the near permanent ice cover. This experimental technique has allowed collection of the first continuous seismic reflection data in the region, as well as gravity cores and bottom photographs at four stations. Three stratigraphic units are identified from the seismic profiles: a lowermost unstratified sediment whose surface has irregular relief and variable thickness to 53 m., interpreted to be glacial drift; a localized stratified unit which reaches 10 m in thickness and overlies the drift; an uppermost ponded acoustically transparent mud which varies from 1 to 4 m in thickness and occurs in depths greater than 150 m.

Résumé

On a étudié la géologie du bassin de l'île Lougheed, du détroit de Desbarats et du massif de l'île Cameron dans les chenaux des îles arctiques à l'aide de bateaux gonflables transportés par hélicoptère dans des chenaux d'eau libre parcourant la couverture de glace presque permanente. Cette technique expérimentale a permis de collecter les premières données continues sur la sismique réflexion dans la région et a permis de prendre des carottes pour la gravimétrie et des photographies du fond dans quatre stations. On a pu identifier trois unités stratigraphiques grâce aux profils sismiques: un sédiment de base non stratifié dont la surface présente un relief irrégulier et qui a une puissance de 53 m a été interprété comme étant un sédiment fluvio-glaciaire; une unité stratifiée localisée qui atteint 10 m de puissance et qui recouvre l'unité précédente; une unité supérieure est constituée d'accumulation de boues acoustiquement transparentes dont la puissance varie entre 1 et 4 m et qui se trouve à des profondeurs supérieures à 150 m.

INTRODUCTION

From July 6 to August 12, 1986, the Atlantic Geoscience Centre conducted a marine seismic reflection and sampling program in the Lougheed Island Basin, Cameron Island Rise and Desbarats Strait area of the Arctic Island channels (Fig. 91.1). This project follows a 1985 through-ice sediment sampling project in the same area,. in which 78 cores and bottom sediment grabs were collected. These projects are part of a study of the geology of the Arctic Island channels supported by the Northern Oil and Gas Action Program (NOGAP) which is directed towards determining the composition, thickness, distribution, and geotechnics of the unconsolidated sediments, and identifying geological constraints to development.

The 1986 project was carried out from a basecamp on southern Lougheed Island (Fig. 91.1), with logistical and helicopter support organized through the Polar Continental Shelf Project. Continuous seismic reflection data were collected using helicopter-transportable systems deployed from five metre inflatable boats through open water leads (Fig. 91.2). The leads form seasonally in this area of near-permanent ice cover, which is normally inaccessible to conventional shipborne operations. One hundred and five line-kilometres of seismic reflection data were collected in eleven leads, and gravity cores and bottom photographs were taken at four locations.

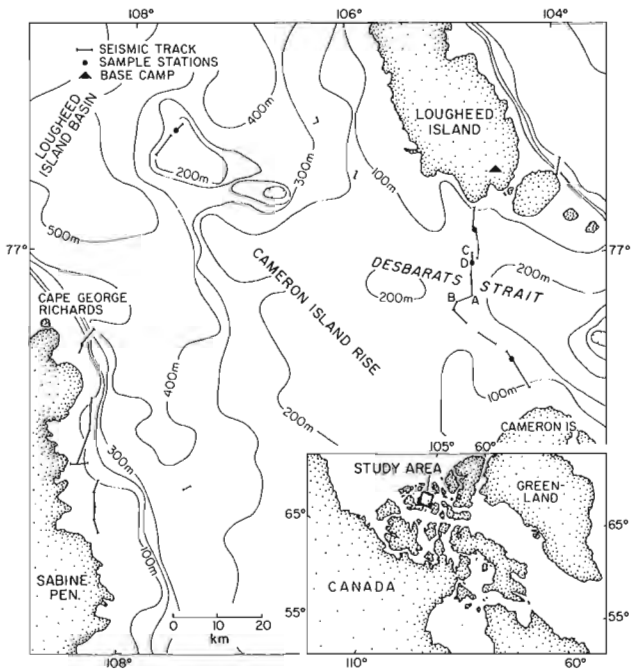


Figure 91.1. Index map of the 1986 field area, showing the location of the seismic reflection data and, sediment samples and bottom photographs collected, and of the base camp on Lougheed Island.

This paper discusses both the experimental technique used to collect seismic reflection data in the study area, and the subbottom information obtained during the survey.

METHODS

A large area of the Arctic Island channels is covered with a near-permanent ice cover, which precludes collection of continuous seismic reflection data using conventional shipborne methods. An alternative method was conceived which used the small cracks or leads which form in the ice cover during the summer thaw (Fig. 91.2). An aerial reconnaissance of the proposed study area undertaken in July, 1985, determined that the abundance and distribution of these leads was sufficient to allow regional collection of continuous seismic reflection data within the marine channels. As a result, an experimental program was carried out using the following methods:

Seismic profiling equipment was towed in the leads with a five metre Zodiac inflatable boat, fitted with a 15 horsepower outboard motor (Fig. 91.3). A JetRange 206L-1 helicopter was used to sling the boat and seismic equipment (Fig. 91.4) to a survey lead, while the remainder of the equipment, as well as survival gear, gasoline and 2-3 technicians were transported in a second flight. Communications between the Zodiac, helicopter, and the basecamp were by SBX-11 VHF radios.

Three lightweight and mobile acoustic profiling systems were operated along separate transects of the leads. Single channel seismic reflection profiles were obtained using the



Figure 91.2. Photograph of one of the eleven leads surveyed during the 1986 field program. Lead lengths varied from 1.5 to 20 km, while average width was from 6 to 10 m (above photo) and up to a maximum of 50 m. The photograph was collected at an approximate altitude of 100 m and the lead shown is 6 to 10 m wide.

Ferranti ORE Geopulse subbottom profiler. This system provided sufficient energy to penetrate the unconsolidated sediment section, as well as to obtain limited penetration into the underlying bedrock. In addition, both 3.5 kHz and 12 kHz subottom profilers were attached to the side of the boat by an aluminum frame, and the returned signal was processed through a Raytheon PTR transceiver and recorded on the EPC Model 1600 recorder.

Navigation for the program was provided by a Global Navigation System mounted in the helicopter, and a Magnavox MX 5102 satellite navigation receiver which was operated from the Zodiac during survey operations. In the latter part of the program, a replacement MX 4102 satellite receiver was used after the first receiver became unserviceable.

One hundred and five line kilometres of seismic reflection data were collected (Fig. 91.1), although the project was seriously constrained by both ice and weather conditions. 1986 was considered an unusually severe year, with lower than average temperatures delaying normal ice breakup by approximately a month. This resulted in fewer and smaller leads in the study area than were observed in 1985. Leads were also more discontinuous and irregular than expected, possibly due to the high concentration of multiyear ice frozen into the first-year ice matrix. On average, surveyed leads were 6.5 km long and the longest lead was 30 km long. In the latter part of the season, high winds began shifting the ice floes so that lead conditions became unstable and often unworkable.

Some smaller leads surveyed in the project had a distinct freshwater layer on top, often associated with a subsurface ice layer that affected both the acoustic signal and actual towing of the instruments. Seismic and sampling operations were halted on five days and hindered on many others because of poor weather and visibility. Six additional days were lost to the project when a hydraulic failure grounded the helicopter until a new part arrived.

The problems encountered in 1986 indicate improvements are necessary to the seismic equipment and transport techniques to allow more efficient use of the leads, especially in a severe ice year such as 1986. Despite this, the use of helicopter-transportable boats in open water leads has been shown to be a feasible method of obtaining continuous seismic reflection data in northern Canadian areas of persistent ice cover.

RESULTS

The seismic reflection profiles collected in the area (Fig. 91.1) provide information on the character and thickness of unconsolidated Quaternary sediments, as well as information on the underlying bedrock (Fig. 91.5). Data previously available on the surficial sediments in the survey area were limited to the upper 1.5 m observed in gravity cores (Marlow and Vilks, 1963; Maclean and Vilks, 1985). Profiles obtained with the Geopulse sparker system show unconsolidated sediments up to 53 m thick, and total subbottom penetrations up to a maximum of 60 m. Three stratigraphic units are recognized.

The lowermost unit is well-defined on the sparker seismic profiles, but was not penetrated on the 3.5 or 12 kHz records. It is unstratified (no coherent reflections) and has a characteristic surface morphology which varies from gently undulating to hummocky and irregular and which is independant of the relief of the underlying bedrock surface (Fig. 91.6). The unit rests unconformably on the bedrock surface and ranges in thickness form 7 to 53 m. On the profiles collected to the south of Lougheed Island, at least two such unstratified intervals can be distinguished. This unit is widespread and thins toward shore and over bathymetric highs.



Figure 91.3. One of two five-metre Zodiac inflatable boats used during the 1986 program, shown in a lead equipped for sparker seismic reflection profiling.



Figure 91.4. Photograph of a JetRanger 206L-1 helicopter slinging the Zodiac inflatable boat to a survey lead in the ice of the Arctic island channels. The outboard motor and acoustic and support equipment remained attached during transport to a new survey site.

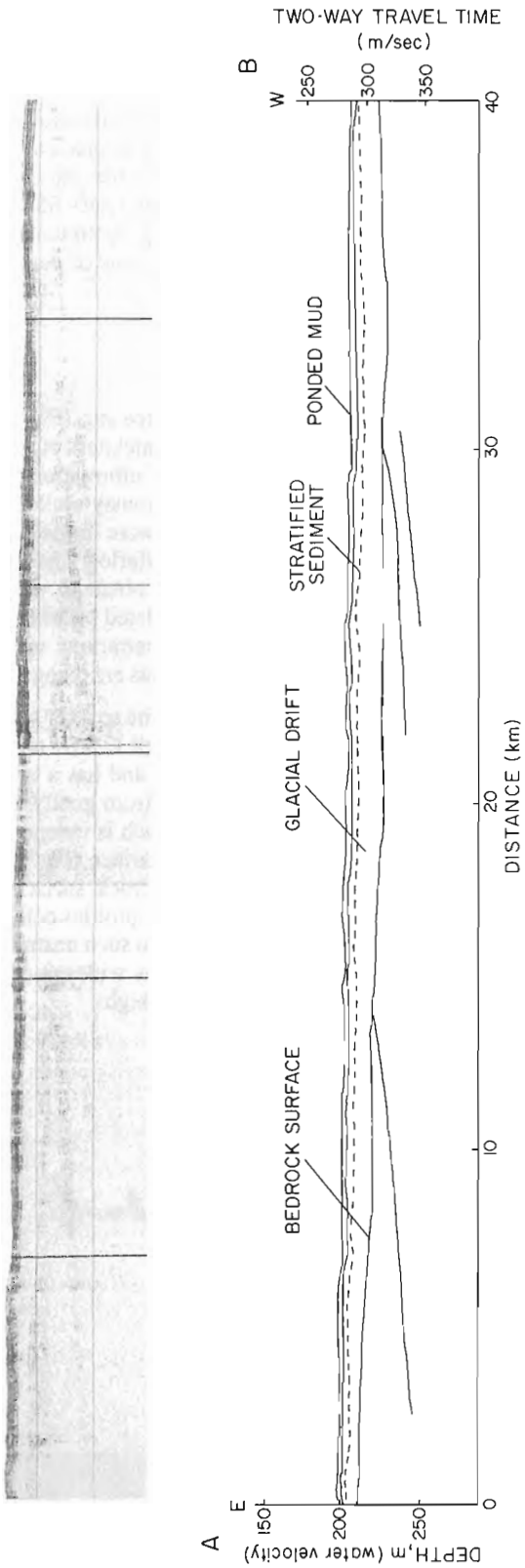


Figure 91.5. Geopulse sparker seismic reflection profile and composite interpretation derived from both the sparker and 12 kHz profiles, showing the unconsolidated sediment unconformably overlying the sedimentary bedrock.

The second unit directly overlies the first locally, mostly in depressions, and is recognized on 3.5 and 12 kHz profiles as a moderately transparent stratified unit of coherent reflections, with thicknesses of up to 10 m. Surface topography ranges from smooth to moderately hummocky with relief of 5 m. It is identified on profiles to the south and west of Lougheed Island in water depths from 130 to 240 m.

The uppermost unit is recognized on 12 kHz profiles as an unstratified and highly transparent unit up to four meters thick. The unit is observed in water depths greater than 150 m where it mantles underlying sediments or fills in bathymetric depressions. The transparent acoustic character of these sediments is consistent with the fine grained texture of sediment samples collected from this unit. Gravity cores collected from the this region typically contain 20-30 cm of brown unstratified silt and clay underlain by grey ryhthmically banded clayey sediments. These sediments are considered representative of the uppermost unit, and the sample distribution suggests that they are present throughout the region. In many places however, they may be too thin to be resolved by the 0.5 m resolution of the 12 kHz system.

Based on their seismic characteristics, the three stratigraphic units identified in the Arctic Island Channels are tentatively correlated to the stratigraphic sequence of glacial and post-glacial sediments recognized from much of offshore eastern Canada (King and Fader, 1986; Josenhans et al., 1986; Praeg et. al., 1986). The lowermost unit resembles sediments interpreted to be glacial till, while the second unit is similar to associated glacial marine sediments. The uppermost unit is acoustically and texturally similar to sediments interpreted as postglacial muds.

GLACIAL CHRONOLOGY

Land evidence from the adjacent Arctic Islands indicate the presence of glacial advances during the Quaternary. Hodgson (1981) recognized till deposits on Lougheed Island which he suggested may relate to pre-late Quaternary glacial advances. On the basis of glacial landforms and source erratics, he suggested a glacial movement from the southeast. Two hundred and fifty kilometres to the south, land evidence for the maximum extent of late-Quaternary grounded ice is seen in the Winter Harbour Moraine on Melville and Byam Martin Islands which has been dated at ca. 10 000 b.p. (Fyles, 1967; Hodgson and Vincent, 1984). The acoustic records from Lougheed Island Basin, Desbarats Strait and Cameron Island Rise show sediments which are interpreted to indicate the presence of at least one episode of grounded glacial ice and subsequent marine sedimentation. More extensive seismic data and lithologic and age control are needed to correlate the offshore drift deposits with either the younger tills on southern Melville or the older till on Lougheed Island.

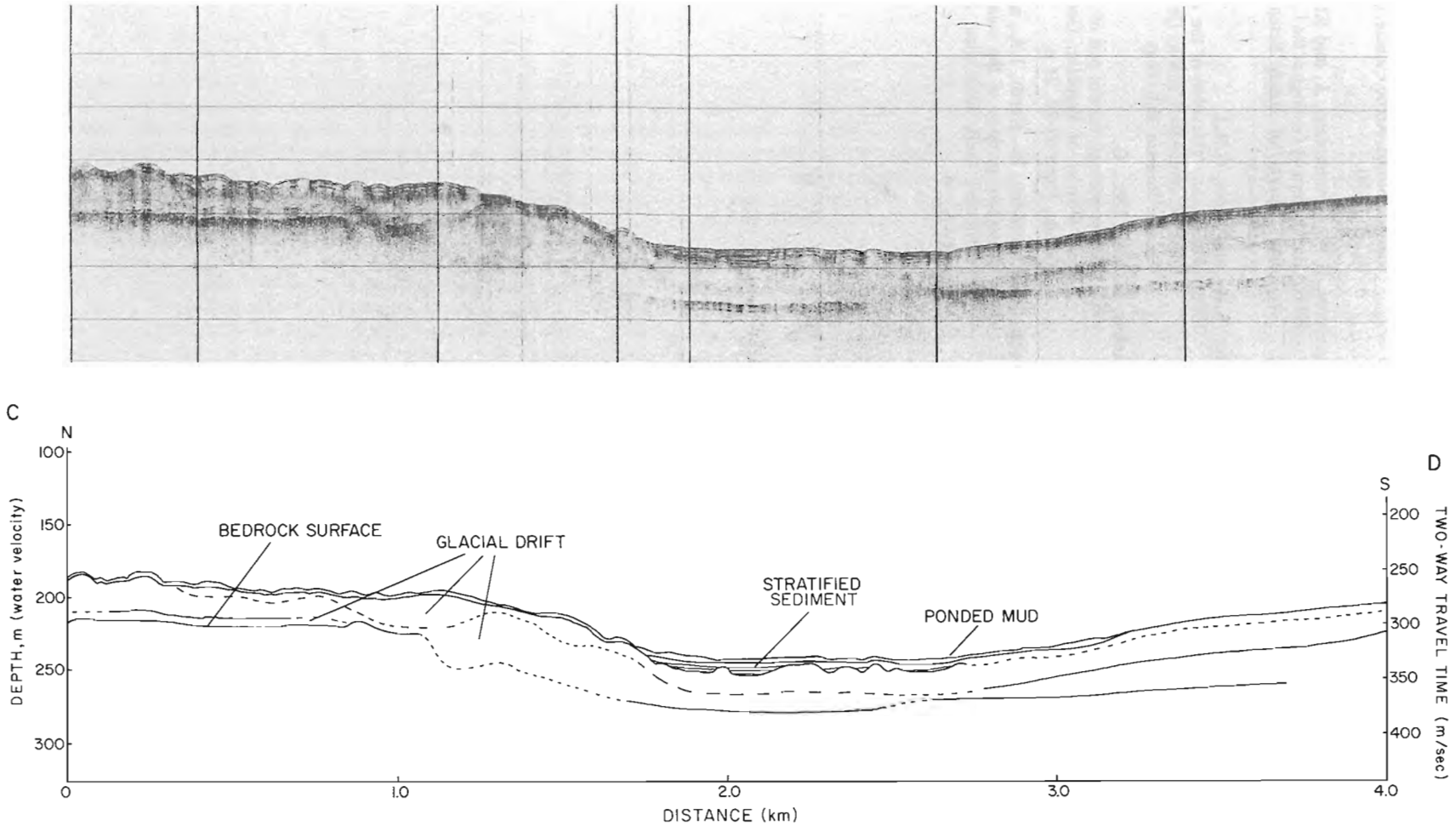


Figure 91.6. Sparker seismic reflection profile and composite interpretation derived from both the sparker and 12 kHz profiles, showing the three surficial units overlying the bedrock. Note the presence of three glacial drift units.

ACKNOWLEDGMENTS

Funding for this project was provided by the Northern Oil and Gas Action Program. Special thanks also are extended to G. Hobson, F. Hunt, B. Hough, of Polar Continental Shelf Project, and their staff; to Quazar Helicopter Ltd. pilots, E. Neil and R. Weibe; to E. Wolter of ISPG, and to A. Atkinson, F. Jodrey, J. Mooers, and A. Law of the Atlantic Geoscience Centre for their excellent field support. Thanks as well to B. Maclean for helpful comments and suggestions, and to G.B.J. Fader and D.B. Praeg for critically reading this paper.

REFERENCES

Fyles, J.G.
1967: Winter Harbour moraine, Melville Island. In "Report of Activities, Part A." Geological Survey of Canada Paper 69-1A, p. 194-195.

Hodgson, D.A.
1981: Surficial geology, Lougheed Island, northwest Arctic Archipelogo; in Current Research, Part C, Geological Survey of Canada, Paper 81-1C, p. 27-34.

Hodgson, D.A., and Vincent, J.S.
1984: A 10,000 year B.P. extensive ice shelf over Viscount Melville Sound, Arctic Canada; Quaternary Research 22, p. 18-30.

Josenhans, H.W., Zevenhuizen, J., and Klassen, R.A.
1986: The Quaternary Geology of the Labrador Shelf; Canadian Journal of Earth Sciences, v. 23, no. 8, p. 1190-1213.

King, L.H., and Fader, G.B.J.
1986: Wisconsinan glaciation of the Atlantic continental shelf of southeast Canada; Geological Survey of Canada, Bulletin 363, 72 p.

Marlow, J.I., and Vilks, G.
1963: Marine geology, eastern part of Prince Gustaf Adolf Sea, District of Franklin; Geological Survey of Canada, Paper 63-22, 23 p.

Praeg, D.B., MacLean, B., Hardy, I.A., and Mudie, P.J.
1986: Quaternary geology of the southeast Baffin Island continental shelf, Geological Survey of Canada, Paper 85-14.

Preliminary report on the stratigraphic position of oil shales in the Lower Paleozoic of Southampton Island, N.W.T.

Project 840003

K. Dewing[1], P. Copper[1], and S.M. Hamilton[1]
Mineral Resources Division

Dewing, K., Copper, P., and Hamilton, S.M., Preliminary report on the stratigraphic position of oil shales in the Lower Paleozoic of Southampton Island, N.W.T.; in Current Research, Part A, Geological Survey of Canada, Paper 87-1A, p. 883-888, 1987.

Abstract

Two black oil shales were examined on Southampton Island during fieldwork carried out in July 1986. The first, 3.5m thick, is part of the Boas River Shale unit and is exposed on the Boas River between the Bad Cache Rapids and Churchill River groups. It has an abundant Pseudogygites fauna indicating a Late Caradoc to Early Ashgill (Cobourg-Maysville) age. The second, exposed at 16 Mile Brook, is a discontinuous, 24cm thick black shale directly below the conformable contact between the Red Head Rapids and Severn River formations. The algal-laminated and algal-biothermal Red Head Rapids Formation is interpreted as a restricted hypersaline facies of the Early Silurian lower Sever River Formation.

Résumé

On a étudié deux schistes bitumineux noirs sur l'île Southampton pendant un levé effectué en juillet 1986. Le premier, de 3,5 m d'épaisseur, fait partie de l'unité de Boas River et affleure à la rivière Boas entre les groupes de Bad Cache Rapids et de Churchill River. On y trouve une faune abondante de Pseudogygites qui donne un âge qui s'étant du Caradocien supérieur au Ashgillien inférieur (Cobourg-Maysville). Le second, qui affleure au risseau 16 Mile, est un schiste noir discontinu, de 24 cm d'épaisseur, situé au-dessous du contact concordant entre les formations de Red Head Rapids et de Severn River. La formation de Red Head Rapids constituée d'algues laminées et d'un bioherme d'algues est interprété comme étant un faciès uniquement hypersalin appartenant à de la formation inférieure de Severn River du Silurien inférieur.

[1]Geology Department, Laurentian University, Sudbury, Ontario P3E 2C6

INTRODUCTION

The five Ordovician and Silurian formations on Southampton Island that are dealt with in this report were previously described on a reconnaissance scale by Sanford (in Heywood and Sanford, 1976). He mapped the extent of the Paleozoic sediments and described the lithology, stratigraphic position, age and depositional environment of the units. The rock units on Southampton Island were given the same names as those in the Hudson Bay Lowlands (Nelson 1963, 1964), due to their close lithological similarity. In ascending order these are: the Bad Cache Rapids Group, a highly fossiliferous limestone; the Boas River Shale, a petroliferous black shale informally named by Sanford (in Heywood and Sanford, 1976): the Churchill River Group, a highly fossiliferous limestone; the Red Head Rapids Formation, an algal-laminated and algal-biohermal dolomite; the Severn River Formation, a fossiliferous dolomite, and the Ekwan River and Attawapiskat formations (the last two not dealt with in this report).

Over the years controversy has arisen over the oil shale and the position of the Red Head Rapids Formation. Workers in the area have described one, two, or three oil shales in a variety of stratigraphic positions from the Middle Ordovician to the Silurian (see Nelson 1981, p. 1167, for a summary). The Red Head Rapids Formation has also been assigned a different age by different workers. Some place the formation in the Ordovician (Sanford in Heywood and Sanford, 1976), others in the Silurian (Nelson, 1981). The Boas River Shale similarly has been placed either in the Churchill River Group (Nelson, 1981) or at the top of the Bad Cache Group (Sanford, in Heywood and Sanford, 1976; and this paper).

Fieldwork was carried out on Southampton Island from 3-11 July, 1986. Three main areas were visited; the east side of Hansine Lake, the upper Cleveland River, and the upper Boas River near the Buttocks (Fig. 92.1). Stops were also made at 16 Mile Brook and at Coral Harvour. Logistical support was provided by the Polar Continental Shelf Project and the Geological Survey of Canada through C.W. Jefferson. This study is part of a mineral and energy resource appraisal for the Wager Bay-Southampton Island area jointly funded by Environment Canada, DIAND and EMR.

BAD CACHE RAPIDS GROUP

The Bad Cache Rapids Group on Southampton Island was divided by Sanford (in Heywood and Sanford, 1976) into two parts: the lower was described as 50 to 75ft of fossiliferous, algal-rich [*Receptaculites?*], anastomosing beds of limestones and recessive shales and the upper of uniformly bedded, microcrystalline limestones, weathering dark brownish grey. The lower few feet were noted as being sandy and conglomeratic. On White Island, northwest of Southampton Island, the base of the group is an 11m thick, fining-upward clastic sequence ranging from quartz arenites to calcareous shales (Jefferson and Hamilton, 1987). The Bad Cache Rapids Group there rests unconformably on Precambrain basement. The contact of the Bad Cache Rapids limestones with the overlying Boas River Shale was described by Sanford (in Heywood and Sanford, 1976) as gradational over 1 or 2 inches.

We examined Bad Cache Rapids strata at the Cleveland River and Boas River areas (Fig. 92.1). At the Cleveland River area the relatively barren upper Bad Cache Rapids and the richly fossiliferous lower Bad Cache Rapids limestones are both exposed, in linear outcrops flanking the Precambrian basement to the east, though not continuously. The lower units here, with a *Receptaculites-Maclurites* and diverse coral fauna of *Quepora*, *Saffordophyllum*, *Nyctopora* and *Calpoecia (Columnopora)* appear to indicate a late Blackriver to early Trenton age. On the east banks of the Boas River, directly upstream from the Boas River Shale, an upper 2.55m unit of thin- to medium-bedded, soft weathering argillaceous limestones carries a fauna of streptelasmid corals and brachiopods, including relatively large *Anazyga* and sowerbyellids which may represent the upper Bad Cache Rapids Group, which we believe may be of middle to late Trenton age (Middle Caradoc). No contact is exposed with the overlying Boas River Shale, about 300m downstream on the east bank. A second outcrop of Bad Cache Rapids Group. Similar corals occur in the lower outcrops of the Bad Cache Group as exposed in belts fringing the Precambrian basement 2 to 3km east of the Boas River, south The Buttocks. The age of the Bad Cache Formation based on this evidence is probably late Blackriver to Trenton (Middle to Late Caradoc). Barnes and Sinclair (in Heywood and Sanford, 1976) dated the Bad Cache Rapids faunas as post-Chazyan to early Upper Ordovician. There is assumed to be a partial age equivalence between the faunas found in the Bad Cache Group on Southampton Island and that at Silliman's Fossil Mount on Baffin Island (Miller, Youngquist and Collinson, 1954). We were unable to examine further Bad Cache Rapids outcrops exposed on the west bank of the Boas River due to high river levels.

BOAS RIVER SHALE

The Boas River Shale was found to outcrop at only one locality, on the west bank of the Boas River, about 3km downstream from The Buttocks and as scattered float and partly *in situ* debris on the opposite bank. The outcrop exposes a minimum of 3 to 3.5m of black, thin bedded, petroliferous oil shale. The base of the shale is underlain by 90cm of medium- to thick-bedded, hard, grey, fossiliferous micrite with a rich monospecific brachiopod fauna of *Cyclospira*, a diverse nautiloid fauna, numerous fragments of the trilobite *Pseudogygites*, rare graptolites and rare aulacerid stromatoporoids. The contact with the overlying Churchill River Group and the underlying Bad Cache strata is not exposed in the outcrop.

A sparse, low diversity fauna was found within the lower part of the oil shale. This included the trolobites *Pseudogygites hudsoni* Ludvigsen 1979 and *Isotelus*, graptolites, and ribbed nautiloids. The *Pseudogygites* identified by Ludvigsen (1979) was dated as probably of late Maysvillian age.

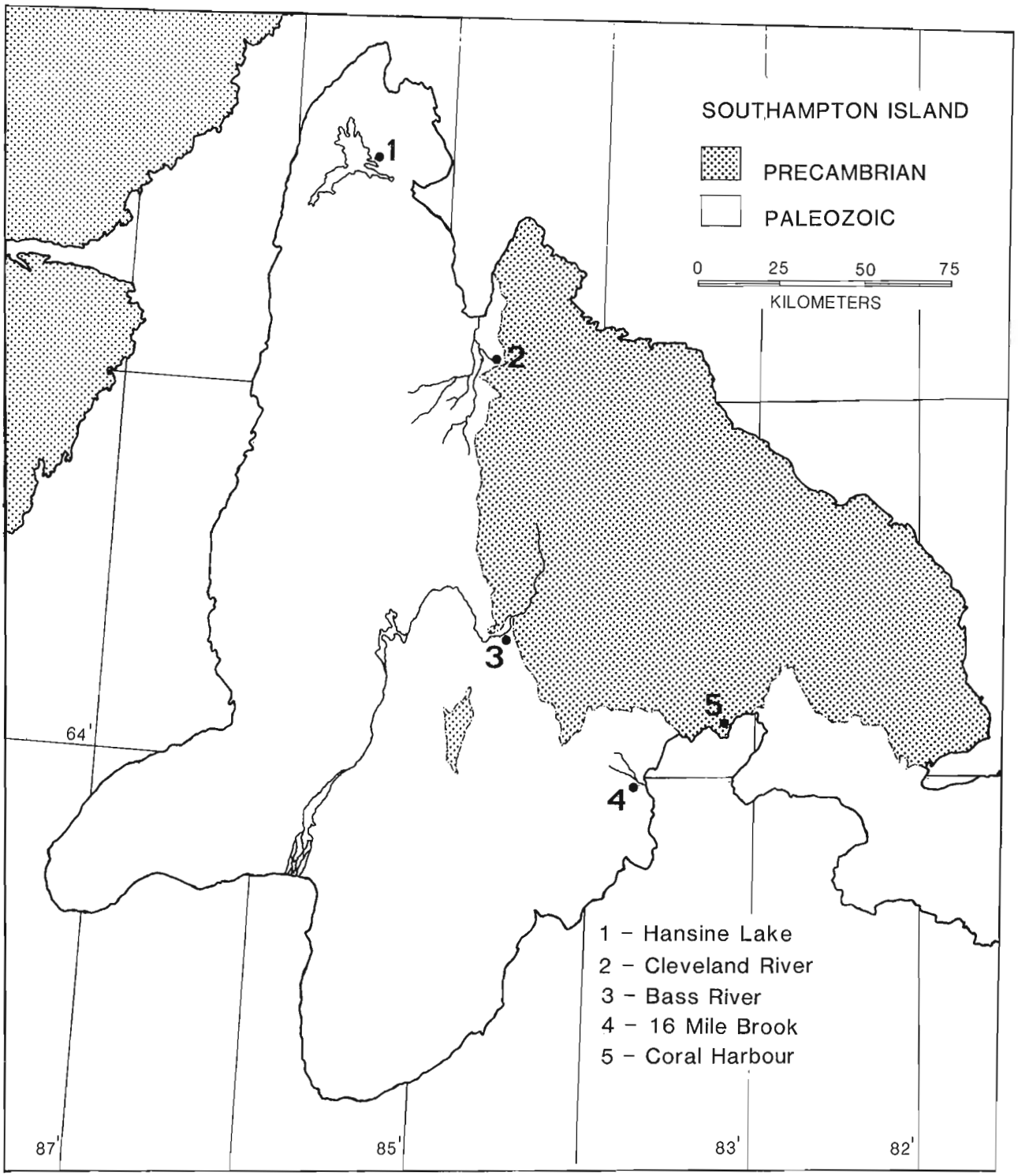


Figure 92.1 Southampton Island; location map.

The Boas River Shale is probably equivalent in age to the Collingwood shales (lower Whitby Formation) of Ontario, as suggested by Sanford (in Heywood and Sanford, 1976). Fossils found immediately underlying the shale in the transitional, medium- to thick-bedded, fetid micritic limestones included further *Pseudogygites*, nautiloids, shell lags of *Cyclospira*, rare aulacerid stromatoporoids and dendritic burrows. *Cyclospira* is a common brachiopod in the uppermost Cobourg Formation and possibly lowest Collingwood Shale (Low Whitby Formation) near Craigleith, Ontario. We consider these basal petroliferous limestones on the Boas River to be part of the Boas River Shale unit.

The substrate at the time of deposition of the oil shale was an anoxygenic mud. Sufficient oxygen was present to support a limited benthic fauna and shallow *Chondrites*-type burrows at the base of the formation, yet reducing conditions most have occurred within a few centimetres of the sediment-water interface to limit more extensive biological activity. Within the Boas River Shale diversity declines upwards, the richest fauna being found in the basal limestone units.

CHURCHILL RIVER GROUP

Poor outcrops of Churchill River strata in central and western Southampton Island limit our knowledge of their stratigraphy, upper and lower contacts, and fauna. Where these outcrop, they are grey weathering, brown, fine grained limestones. The formation is locally highly fossiliferous especially in the Hansine Lake area, with abundant tabulate corals and stromatoporoids. Near Hansine Lake, the fauna is rich and diverse enough to appear biostromal or biohermal. No contact between the overlying and underlying formations was observed in outcrop: most of the Churchill River strata occur as loose rubble.

The age of the Churchill River strata on Southampton Island is Late Ordovician (Ashgill: Richmondian, cf. Sanford, in Heywood and Sanford, 1976), based on megafaunas and conodont data (Barnes, in Heywood and Sanford, 1976). The *Paleofavosites*-rich coral beds of the Churchill River limestones at Hansine Lake suggest a high level within in the Ashgill (late Richmondian-Gamachian: i.e. Hirnantian). The depositional environment was an onshore, shallow, normal marine shelf.

RED HEAD RAPIDS FORMATION

The Red Head Rapids Formation consists of three units that were first described on Southampton Island by Sanford (in Heywood and Sanford, 1976). From bottom to top these units are composed of thin-bedded, fine grained, orange-brown weathering dolomite, overlain by a massive, thick-bedded, stromatolitic dolomite that weathers light grey. The third unit is biohermal, with the bioherms formed by stromatolites and thrombolites. Between the bioherms are algal-laminated dolomite beds, showing evidence of soft-sediment deformation. At the very top of the formation at 16 Mile Brook in southern Southampton Island, a minimum of 7m of the Red Head Rapids Formation is overlain by a local, thin (24 cm) black, petroliferous shale, capped conformably by the Severn River Formation. We observed no other direct contact between the overlying Severn River in underlying Churchill River strata. Nelson (1981) interpreted the limestones directly beneath the thin oil shale at 16 Mile Brooks as Churchill River strata, but included Heywood and Sanford's (1976) Red Head Rapids Formation in the Silurian. Macauley (1986) believed that the oil shales at 16 Mile Brook and the Boas River were of the same Ordovician age.

The Red Head Rapids Formation is here interpreted as a restricted, hypersaline facies of the lower Severn River Formation. At Hansine Lake it is possible to trace along a single horizon from stromatolitic and ostracode-rich Red Head Rapids Formation (unit 2), through algally laminated dolomites (unit 1) into increasingly fossiliferous Severn River Formation. This implies that at least part of the Red Head Rapids Formation is age equivalent to the lower Severn River Formation, the Severn River forming in the open marine, and the Red Head Rapids forming in a restricted, low intertidal lagoon or embayment. Sanford (personal communication, 1986) informed us that the Severn River may also include similarly restricted 'Red Head Rapids' facies higher in the succession.

The algal bioherms in the Red Head Rapids Formation occur directly beneath the contact with the Severn River facies. Individual bioherms are small (3-6m in diameter, less than 5m high) but commonly coalesce into larger structures. The cores of the bioherms are extensively recrystallized, vuggy limestones. Where structure can be seen, it appears that the bioherms were originally composed of thrombolites and stromatolites, including *Collenia*-type and *Gymnosolen*-type stromatolites. Flanking beds show evidence of extensive soft-sediment deformation. Algally laminated beds near bioherms show folding and minor faulting where they have slumped off the sides of the bioherms.

The thin black oil shale at the top of the formation is only locally present and does not form the extensive (50ft thick) beds described by Nelson and Johnson (1966). Sandford's view (in Heywood and Sanford, 1976) that the Red Head Formation undoubtedly includes the "oil shale interval" described by Nelson and Johnson (1966), appears to be correct. It pinches out and grades over several metres southwards into algal laminities which are similar to those that also occur directly below the shale at 16 Mile Brook. The shale was probably only locally deposited between the two formations. We have recovered a conodont fauna from the thin oil shale and this is presently under study.

The Red Head Rapids Formation is essentially devoid of fossils except for stromatolites and abundant peloids. Our age determination is based on the lithological gradation with the overlying more poorly fossiliferous Silurian Severn River Formation and the more abrupt change from the underlying richly fossiliferous, late Ordovician Churchill River strata at Hansine Lake.

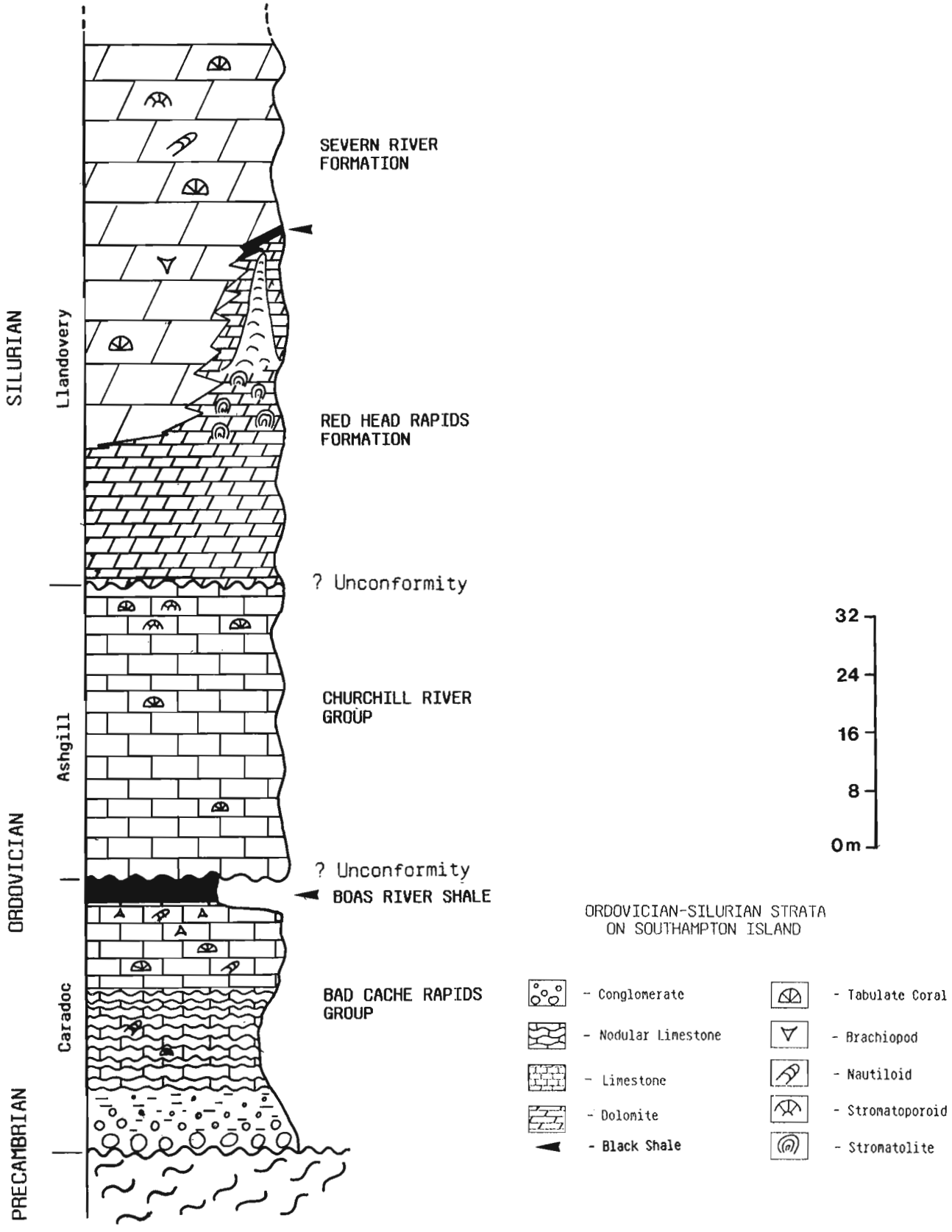


Figure 92.2 Ordovician – Silurian strata on Southampton Island.

SEVERN RIVER FORMATION

The Severn River Formation outcrops extensively as a yellow-brown dolomite on Southampton Island. Coarse grained, thick-bedded, massive to cross-bedded units alternate with fine grained, highly fossiliferous or barren beds. Where the unit is underlain by the Red Head Rapids, the contact is thought to be conformable. The Severn River is overlain by the Ekwan River Formation, not covered in this study. We have not observed a direct contact between the Severn River and the Churchill River Group below.

Fossils such as *Virgiana* indicate an early Silurian (Early to Middle Llandovery) age for the formation. Nautiloids and corals collected should refine the correlation of Sanford (in Heywood and Sanford, 1976) with the Severn River Formation in the Hudson Bay Lowlands. A locally abundant but low diversity and commonly dwarfed fauna of corals, brachiopods, stromatoporoids and nautiloids indicates an open to semirestricted, normal marine setting for the Severn River Formation. The widespread, thicker, cross-bedded units probably formed during periods of very high energy, e.g. widespread storms.

CONCLUSIONS

1. The 3.5m thick Boas River oil shale is of late Caradoc-early Ashgill (Cobourg-Maysville) age, roughly correlating with the Collingwood Shale of Ontario as stated by Sanford (in Heywood and Sanford, 1976). It overlies the Bad Cache Rapids Group conformably (Fig. 92.2).

2. A second oil shale, 24cm thick (the 'Sixteen Mile Brook Shale' of Nelson, 1981) occurs at the top of the Red Head Rapids Formation and is probably of earliest Silurian (Llandovery) age. This does not support the evidence for the coeval relationship of the Boas River and 16 Mile Brook oil shales determined by Nelson (1981; it should be noted that in Fig. 1 of Nelson the Boas River Shale is shown below the 16 Mile Brook Shale).

3. The Red Head Rapids Formation appears to grade into the Severn River Formation at the top and is interpreted as a partial facies equivalent of the Severn River Formation. The suggested early Silurian age of the Red Head Rapids Formation corroborates the conclusions of Nelson (1981).

REFERENCES

Heywood, W.W. and Sanford, B.V.
1976: Geology of Southampton, Coats, and Mansel Islands, District of Keewatin, Northwest Territories; Geological Survey of Canada Memoir 382, 35 p., Map 1404A.

Jefferson, C.W. and Hamilton, S.M.
1987: Structure and stratigraphy of the Paleozoic-Precambrian contact zone on White and Southampton islands, District of Keewatin, N.W.T.; in Current Research, Part A, Geological Survey of Canada, Paper 87-1A, report 48.

Ludvigsen, R.
1979: The Ordovician trilobite *Pseudogygites* Kobayashi in Eastern and Arctic North America; Royal Ontario Museum, Life Science Contribution, 120, 41 p.

Macauley, G.
1986: Geochemistry of the Ordovician Boas Oil Shale, Southampton Island, Northwest Territories; Geological Survey of Canada, Open File 1285, 15 p.

Miller, A.K., Youngquist, W., and Collinson, C.
1954: Ordovician cephalopod fauna of Baffin Island; Geological Society of America, Memoir 62, 234 p.

Nelson, S.J.
1963: Ordovician paleontology of the northern Hudson Bay Lowland; Geological Society of America, Memoir 90, 152 p.
1964: Ordovician stratigraphy of northern Hudson Bay Lowland; Geological Survey of Canada, Bulletin 108, 36 p.
1981: Stratigraphic position of Ordovician oil shales on Southhampton Island, Northwest Territories, Canada; American Association of Petroleum Geologists, Bulletin, v. 65(6), p. 1166-1175.

Nelson, S.J. and Johnson, R.D.
1966: Geology of Hudson Bay Basin; Bulletin of Canadian petroleum Geology 14(4), p. 520-578.
1976: Oil shales of Southampton Island, northern Hudson Bay; Bulletin of Canadian Petroleum Geology v. 24(1), p. 70-91.

Diatomées et évolution holocène du lac Bras d'Or, Nouvelle-Écosse: résultats préliminaires

Project 730072

Guy Lortie[1]
Centre géoscientifique de l'Atlantique

Lortie, G., Diatomées et évolution holocène du lac Bras d'Or, Nouvelle-Écosse: résultats préliminaires; dans Recherches en cours, Partie A, Commission géologique du Canada, Étude 87-1A, p. 889-896, 1987.

Résumé

Trois carottes prélevées au lac Bras d'Or ont été analysées en vue d'établir leur contenu diatomifère. La séquence la plus longue (019P) ne contient que des taxons d'origine marine. Les carottes 016P et 018P sont représentées par des argiles limoneuses organiques surmontant des graviers et cailloux; elles recouvrent probablement toute l'histoire post-glaciaire de la région. Trois zones générales correspondant à des changements de paléoenvironnements sont identifiées. La zone I, très pauvre en diatomées reflète sans doute un épisode marin initial. La zone II correspond à une phase lacustre représentée d'abord par une flore froide à Melosira teres, puis par un assemblage dulcicole plus diversifié dominé par Cyclotella bodanica. Après une brève transition saumâtre, la zone III à Thalassionema nitzschioides traduit finalement les conditions de baie profonde et salée qui prévalent aujourd'hui. Cette succession d'événements reflète la remontée régionale du niveau marin au cours de l'Holocène.

Abstract

Three cores have been collected in the Lake Bras d'Or area and analyzed for their diatom content. The longer 019P core shows only marine flora. In the shorter 016P and 018P cores, organic silty clay overlying pebbles and gravels, represents probably the entire postglacial local history. Three general diatom zones corresponding to environmental changes are observed. Zone one contains only very rare marine diatoms which imply possibly a marine environment. Zone II shows a cold lacustrine freshwater Melosira teres diatom flora followed by a more diversified assemblage dominated by Cyclotella bodanica. After a short brackish transition, a deep saline bay, about similar to actual conditions, is observed through the Thalassionema nitzschioides flora of zone III. This succession of events is related to the regional Holocene postglacial sea-level changes.

[1]Centre d'études nordiques, Université Laval, (Québec) G1K 7P4

INTRODUCTION

Localisées en marge de l'inlandsis des Laurentides du Wisconsinien supérieur, les provinces de l'Atlantique ont été davantage marquées par des complexes glaciaires régionaux que par l'extension de la calotte laurentidienne (voir Grant, 1977). Cette situation y a favorisé la conservation d'un certain nombre de séquences organiques discontinues dont l'âge se situe entre le Sanganomien et le Wisconsinien supérieur (Mott et Grant, 1985). Des analyses polliniques en ont démontré le caractère parfois interglaciaire (Prest et coll., 1976), le plus souvent interstadiaire, notamment dans les séquences pléistocènes importantes qui affleurent le long du littoral du lac Bras d'Or, dans l'île du Cap-Breton, en Nouvelle-Écosse (de Vernal et coll., 1986). Cette région a subi trois phases glaciaires, mais les corrélations stratigraphiques et l'interprétation de certaines unités organiques demeurent encore problématiques (Grant et King, 1984; Mott et Grant, 1985). Bien que des travaux assez abondants aient été consacrés à l'évolution transgressive du niveau marin dans les provinces de l'Atlantique au cours des derniers millénaires (p. ex. Quinlam et Beaumont, 1981, 1982) et à ses conséquences sur les milieux côtiers (Palmer, 1978; Scott et coll., 1981; de Vernal et coll., 1985; Brookes et coll., 1985), l'évolution postglaciaire de ce secteur demeure mal connue.

Le lac Bras d'Or (fig. 93.1) occupe une vaste dépression couvrant une superficie de près de 1060 km^2 dans la partie sud de l'île du Cap-Breton. Les chenaux Great Bras d'Or, Little Bras d'Or, et St. Peters mettent en contact cette mer intérieure avec les eaux de l'Atlantique. La profondeur maximale du premier, le plus influent, atteint 270 m, mais à son embouchure, elle ne fait guère plus de 10 m selon Vilks (1967) . Le deuxième montre une profondeur de 6 m à marée basse, tandis que le troisième se trouve pratiquement fermé à St. Peters. Les salinités enregistrées sont de l'ordre de 25 %, le lac Bras d'Or correspondant à une masse d'eau bien mélangée.

En novembre 1985, trois carottes (016P, 018P et 019P) ont été prélevées au lac Bras d'Or lors de l'expédition 85-036 du CSS Dawson (fig. 93.1). Un examen rapide de la flore des 69 échantillons transmis a rapidement mis en évidence des flores marines et dulcicoles dans le cas des carottes 018P et 016P tandis que les sédiments de la carotte 019P ne révélaient que des éléments marins. La présent rapport fait état des premières observations sur les flores de diatomées des carottes 016P et 018P, ainsi qu'une interprétation préliminaire des paléoenvironnements. Le même forage a également permis l'étude d'autres aspects géochimiques (Mucci et Pagé, 1987; Hillaire-Marcel, 1987) et polliniques (de Vernal et Jetté, 1987) de la région.

Matériel et méthodes

Les carottes 016P et 018P comprennent respectivement 346 cm et 312 cm de sédiments composés d'argiles limoneuses organiques de couleur brune surmontant un mince lit de graviers et cailloux; elles représentent probablement des séquences post-glaciaires entières. La carotte 019P ne couvre qu'une partie de l'Holocène, bien qu'elle comporte 733 cm de sédiments organo-terrigènes présentant parfois des alternances de lits organiques noirs et argileux gris foncés. Les échantillons utilisés pour l'analyse des diatomées ont été prélevés à un intervalle de 20 cm au laboratoire de l'Institut océanographique Bedford où les carottes sont entreposées. Les diatomées ont été nettoyées par oxydation à chaud au H_2O_2, rincées à l'eau distillée puis montées dans une résine à haut indice de réfraction (Naphrax, $n_d = 1{,}74$). Pour chaque échantillon, on a établi une liste taxonomique préliminaire des espèces présentes, puis dressé deux diagrammes (fig. 93.2 et 93.3) illustrant les taxons les plus fréquents et les plus caractéristiques. Malgré les limites évidentes de cette approche, les contrastes floristiques entre les espèces oligohalobes et méso-polyhalobes sont tels que ces diagrammes qualitatifs, même très sommaires, suffisent pour mettre en relief les grandes phases de l'évolution du lac Bras d'Or depuis la déglaciation. Sur les diagrammes, les espèces courantes sont indiquées par un X et les dominantes par un O.

RÉSULTATS

Ce premier examen sommaire des échantillons analysés a permis d'observer quelques 110 taxons où dominent les genres *Thalassiosira, Chaetoceros, Cyclotella, Thalassionema* et *Melosira*. Quelques-uns des éléments les plus représentatifs sont illustrés à la planche I. Pratiquement tous les échantillons comprennent un mélange variable de diatomées littorales et planctoniques. Chez les formes marines littorales couramment observées, on note *Cocconeis scutellum, Dimerogramma minor, Fragilaria fasciculata, Plagiogramma staurophorum* et quelques *Diploneis*, tandis que les éléments périphytiques dulcicoles sont représentés surtout par *Achnanthes minutissima et Cocconeis placentula*. Les taxons dominants, en autant que les observations qualitatives permettent d'en juger, sont cependant les espèces planctoniques *Melosira teres, Cyclotella bodanica, Cyclotella caspia* et *Thalassionema nitzschioides*. Cette dernière est une espèce néritique très largement répandue dans les eaux océaniques atlantiques, tandis que *C. caspia* est plutôt représentative de milieux côtiers moins salés. Bien qu'aucun taxon arctique n'ait été relevé, il est actuellement difficile d'affirmer que l'ensemble de la flore marine présente une origine uniquement atlantique. Quelques taxons ont été relevés sur l'ensemble des deux séquences, les deux plus largement répandus étant *Diploneis smithii,* espèce benthique, et *Cyclotella caspia*, espèce planctonique. Néanmoins, les assemblages sont bien caractérisés et il est possible de distinguer pour chaque séquence une zonation des diatomées.

Carotte 85-036-016P

Les 16 niveaux étudiés montrent trois zones très nettes (fig. 93.2). La zone I recouvre la base de la carotte jusqu'au niveau de 230 cm et ne comporte que de très rares fragments de diatomées et de spicules d'éponges. La zone II, comprise entre 230 et 180 cm, est caractérisée par une flore dulcicole assez variée, dominée par *Cyclotella bodanica*; parmi les éléments littoraux, on retrouve un certain nombre d'éléments épiphytes (*Epithemia adnata, Gomphonema* spp.) et quel-

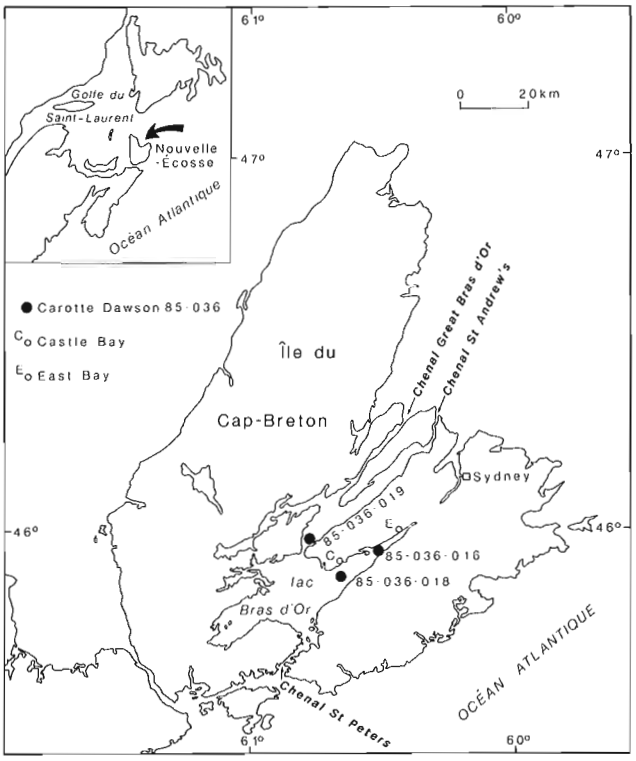


Figure 93.1. Localisation de la région à l'étude et des forages

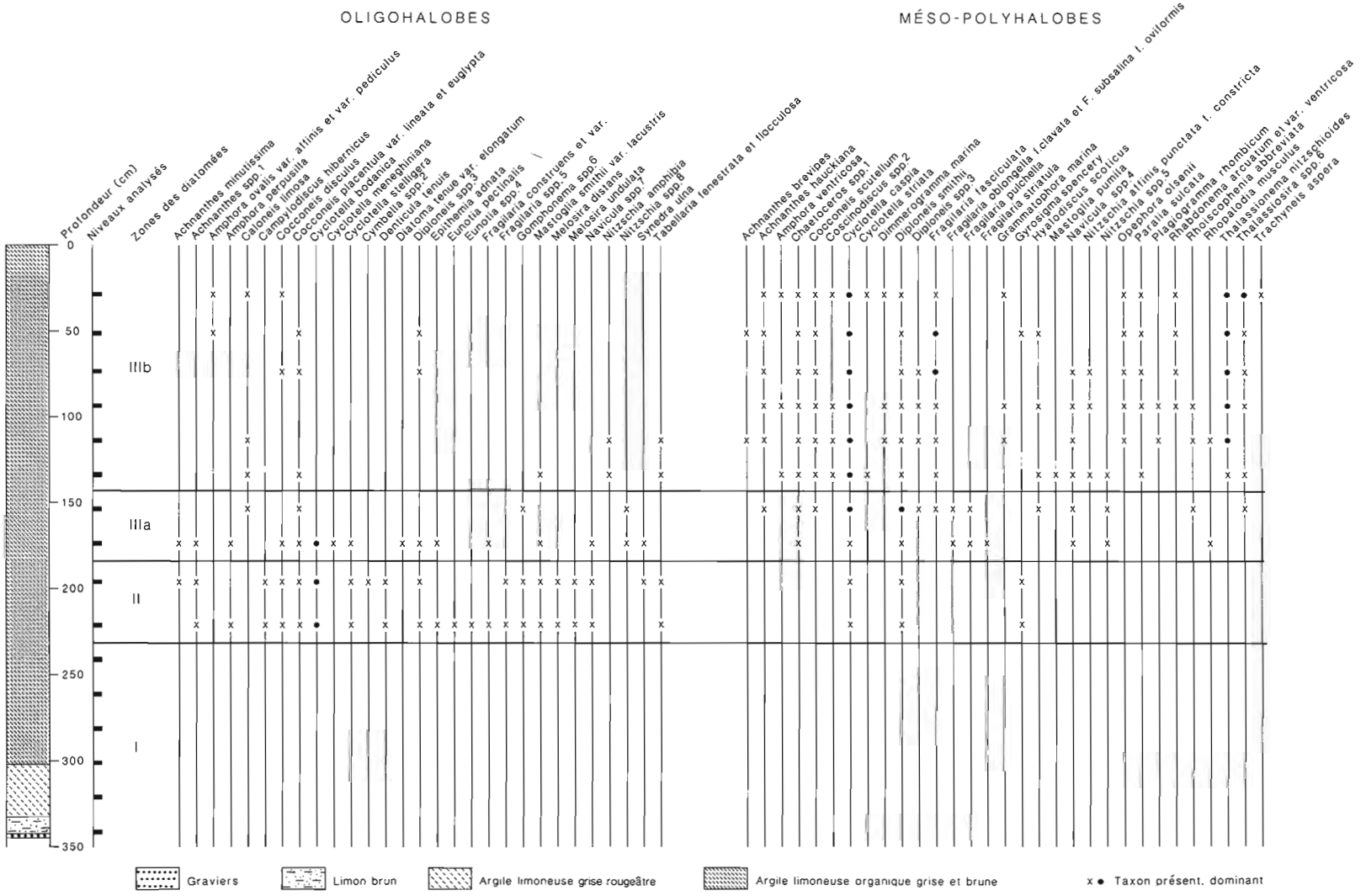
ques éléments benthiques rarements signalés, notamment *Campylodiscus hibernicus*. La dernière zone se distingue par l'arrivée contrastante des taxons de nature marine et saumâtre, et on peut y distinguer deux sous-zones: l'une (IIIa, de 180 à 160 cm) est marquée par l'incorporation à la flore d'eau douce précédente de quelques taxons planctoniques essentiellement saumâtres et souvent très tolérants, comme *Fragilaria pulchella* et *Cyclotella meneghianiana*, qu'accompagnent d'autres espèces d'origine marine, entre autres des *Chaetoceros* spp.; l'autre (IIIb) s'étend jusqu'au sommet et est caractérisée par une flore nettement plus marine, bien que ses éléments dominants, *T. nitzschioides, C. caspia*, et *Fragilaria fasciculata* soient capables de supporter des salinités aussi basses que 10-7 %. Cette dernière zone comporte également nombre de formes littorales, comme *Achnanthes hauckiana, Opephora olsenii* et plusieurs *Diploneis*. Les variations substantielles soup-çonnées de plusieurs de ces éléments altéreraient le rapport planctonique et littoral, mais en l'absence de comptages, on ne peut vérifier cette hypothèse.

Carotte 85-036-018P

Les trois zones observées dans la carotte 018P (fig. 93.3) sont définies par des flores très similaires à celles précédemment décrites, à l'exception de la deuxième. La première zone (346 à 180 cm), de nature essentiellement détritique, ne comprend que de rares spicules brisés et fragments de diatomées dont certaines ont pu être identifiées et attribuées à *Paralia sulcata*, une espèce marine littorale de nature cosmopolite et tolérante, au frustule robuste. La zone II comporte deux sous zones: la zone IIa (180 à 160 cm) se distingue par une flore dulcicole beaucoup plus abondante incluant des formes benthiques, comme *Campylodiscus hibernicus,* ou planctoniques, comme *Melosira teres*, qui en est sont taxon le plus typique. Cette deuxième zone fait place, entre 160 et 110 cm, à la sous-zone IIb composée d'une flore dulcicole à *Cyclotella bodanica* très semblable à celle décrite plus haut, avec le même mélange d'éléments littoraux et planctoniques. La dernière zone comporte une première sous-zone IIIa de transition (110 à 90 cm) où on observe également l'arrivée de quelques diatomées marines de nature planctonique, comme *Chaetoceros* spp., ou encore celle de formes très tolérantes ou légèrement saumâtres comme *Rhopalodia musculus*. Ce court épisode annonce la sous-zone IIIb que caractérise une flore marine à *T. nitzschioides* et *C. caspia*. Cette dernière espèce tend, apparemment, à être plus fréquente à la base, contrairement à la dernière zone de la carotte 016P.

PALÉOENVIRONNEMENTS ET CORRÉLATIONS

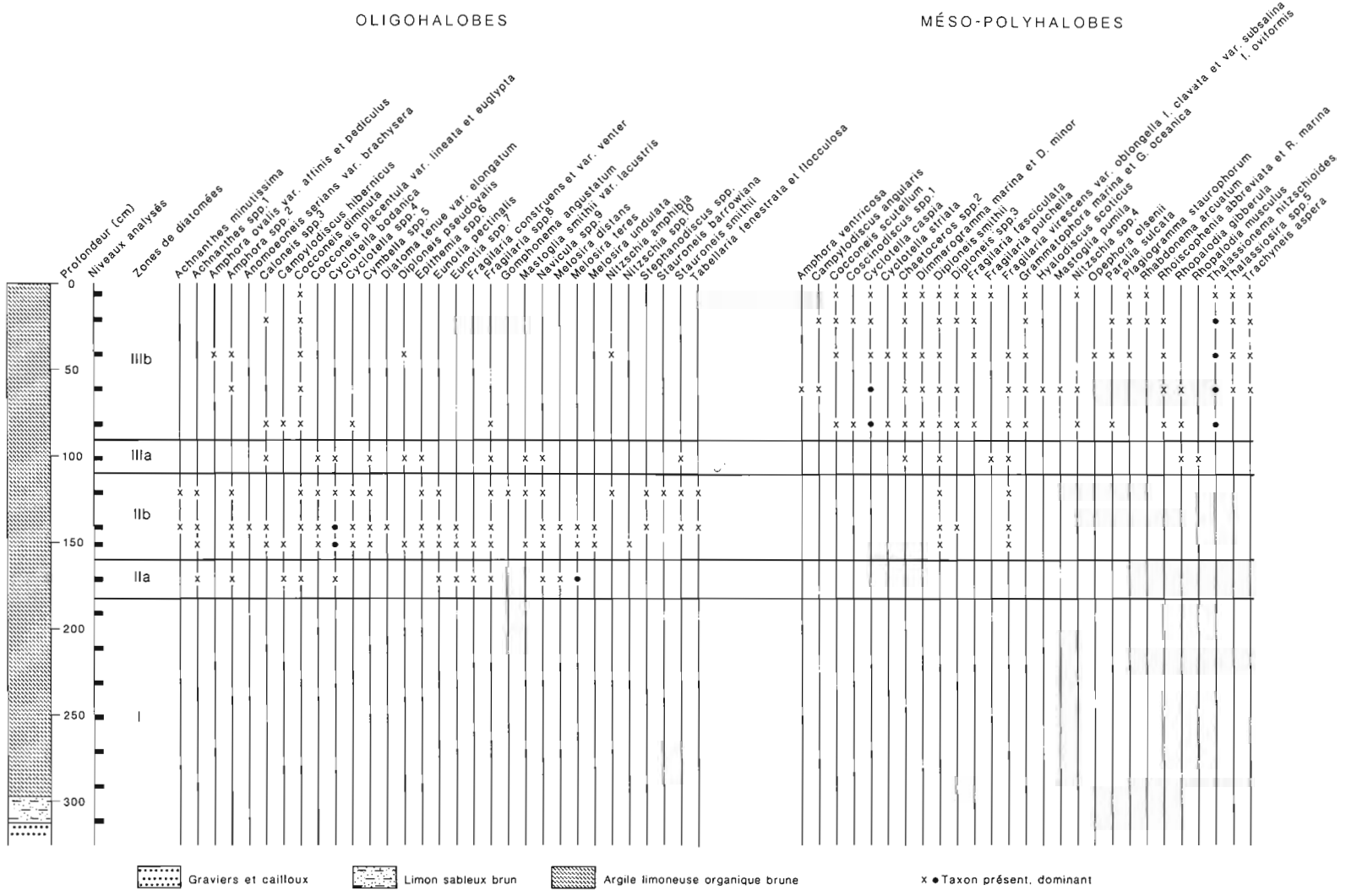
L'ensemble des zones distinguées dans les deux séquences étudiées présente une bonne corrélation stratigraphique, autant floristiquement que par l'importance des zones et sous-zones (fig. 93.4). La seule exception concerne la sous-zone à *M. teres* que l'on n'a pas retracée dans les sédiments de la carotte 016P. Cette sous-zone est cependant de peu d'ampleur, sans doute moins de 20 cm, et son absence est probablement liée aux écarts des intervalles de cette première analyse. À l'exception de la première zone, l'interprétation paléoenvironnementale globale des flores décrites ne pose guère de problèmes: elle correspond à un milieu lacustre qui a fait place à des conditions marines très similaires aux conditions actuelles. La zone I, quasi-stérile, correspond à un milieu aquatique très inhospitalier, avec un taux de sédimentation détritique très supérieur à la biomasse présente, certainement affectée par des conditions instables de turbulence, mélange et turbidité. Les rares diatomées identifiées sont des *P. sulcata*, phénomène qui semble indiquer la présence d'eaux peut-être marines, mais il est tout aussi possible qu'il s'agisse de quelques valves remaniées provenant des sédiments diatomifères interstadiaires présents à proximité (Lortie et coll., 1984). Dans un milieu très peu productif, marqué par une forte activité sédimentaire, l'incorporation de frustules allochtones est plausible et indétectable lorsqu'il s'agit de taxons cosmopolites comme *P. sulcata*. Par contre, à l'exception de *C. bodanica*, espèce très répandue dans ces formations anciennes voisines, les flores holocènes décrites dans le présent rapport diffèrent beaucoup des flores antérieures, ce qui indique un apport très négligeable de ces dernières aux flores modernes. D'autre part, si cette zone représente des conditions marines, il est probable qu'une zone de transition comportant un mélange de taxons plus tolérants existe. Les flores lacustres qui ont suivi ne montrent pas de telle transition à leur base, mais un échantillonnage plus serré devrait la révéler.



1.Achnanthes exigua var. heterovalva . A.lanceolata var.elliptica,A. linearis, 2. Cymbella microcephela , C. minuta, C. muelleri; 3. Diploneis af. pseudovalis, D. occulata; 4. Eunotia flexuosa, E. pectinalis ; 5. Fragilaria brevistriata, F. intermedia, F. virescens var. subsalina; 6. Gomphonema acuminatum, G. angustatum, G. bohemicum, G. intricatum, G. parvulum; 7. Navicula cocconeiformis, N. hungarica, N. minuscula, N. radiosa; 8. Nitzschia af. perminuta, N. tryblionella

1. Chaetoceros spp. (spores); 2. Coscinodiscus oculus-iridis, C. spp. 3. Diploneis dydima, D. splendida, D. stroemii; 4. Navicula abunda, N. digitoradiata, N. af. diplone-oides, N. forcipata, N. af. pseudoforcipata, N. tenera; 5. Nitzschia marginulata var. subconstricta, N. plana; 6. Thalassiosira af. aestivalis, T. decipiens, T. eccentrica, T. lacustris var. septentrionalis, T. oestrupii, T. spp.

Figure 93.2. Diagramme qualitatif des diatomées (carotte 85-036-016P)



1. Achnanthes calcar, A. clevei, A. lanceolata var. elliptica, A. exigua var. heterovalva; 2. Amphora bullatoides , A. perpusilla : 3. Caloneis bachmanii, C. limosa; 4. Cyclotella comta var. radiosa, C. meneghiniana, C. pseudostelligera; 5 Cymbella cymbiformis, C. delicatula , C. lunata, C. muelleri , C. sinuata; 6. Epithemia reicheltii, E. turgida; 7. Eunotia flexuosa, E. monodon var. maior; 8. Fragilaria brevistriata, F. lapponica, F. parasitica, F. pinnata; 9. Navicula cocconeiformis, N. pseudoscutiformis, N. jentzschii, N. radiosa, N. scutelloides, N. tuscula; 10. Nitzschia palea, N. perminuta.

1. Coscinodiscus spp.; 2. Chaetoceros spp. (spores); 3. Diploneis dydima, D. stroemii; 4. Nitzschia marginulata var. subconstricta, N. punctata var. constricta; 5. Thalassiosira af. aestivalis, T. decipiens, T. af. oestrupii, T. lacustris var. septentrionalis, T. spp.

Figure 93.3. Diagramme qualitatif des diamées (carotte 85-036-018P)

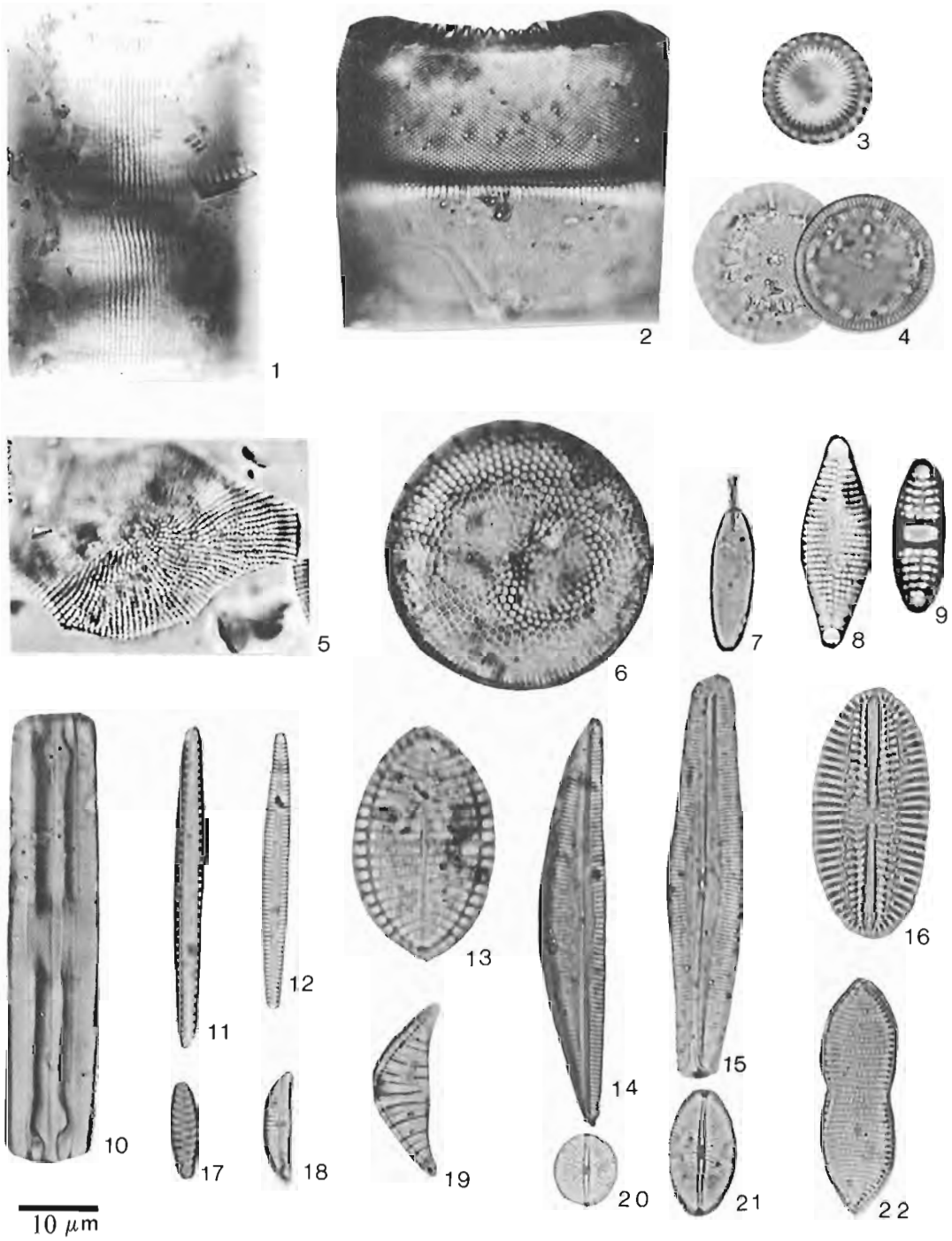


Planche 93.1

1. *Melosira undulata* (Ehr.) Kütz.
2. *Melosira teres* Brun
3. *Paralia sulcata* (Ehr.) Kütz.
4. *Thalassiosira nordenskioldii* Cleve
5. *Melosira undulata* (Ehr.) Kütz.
6. *Thalassiosira lacustris* var. *hyperborea* Grun.
7. *Chaetoceros* sp.
8. *Dimerogramma minor* var. *nana* (Greg.) Van Heurck
9. *Plagiogramma staurophorum* Hust.
10. *Grammatophora oceanica* var. *macilenta* (W. Smith) Grun.
11. *Thalassionema nitzschioides* (Grun.) Grun.
12. *Fragilaria fasciculata* (Agardh) Lange-Bertalot
13. *Cocconeis costata* Greg.
14. *Amphora ventricosa* Greg.
15. *Caloneis* af. *westii* (W. Smith) Hendey
16. *Diploneis smithii* (Bréb. ex-Schmith) Cleve
17. *Opephora olsenii* Møller
18. *Amphora perpusilla* (Grun.) Grun.
19. *Rhopalodia musculus* O. Muller
20. *Navicula pseudoscutiformis* Hust.
21. *Navicula cocconeiformis* Greg. ex Grev.
22. *Nitzschis punctata* fo. *constricta* Grun.

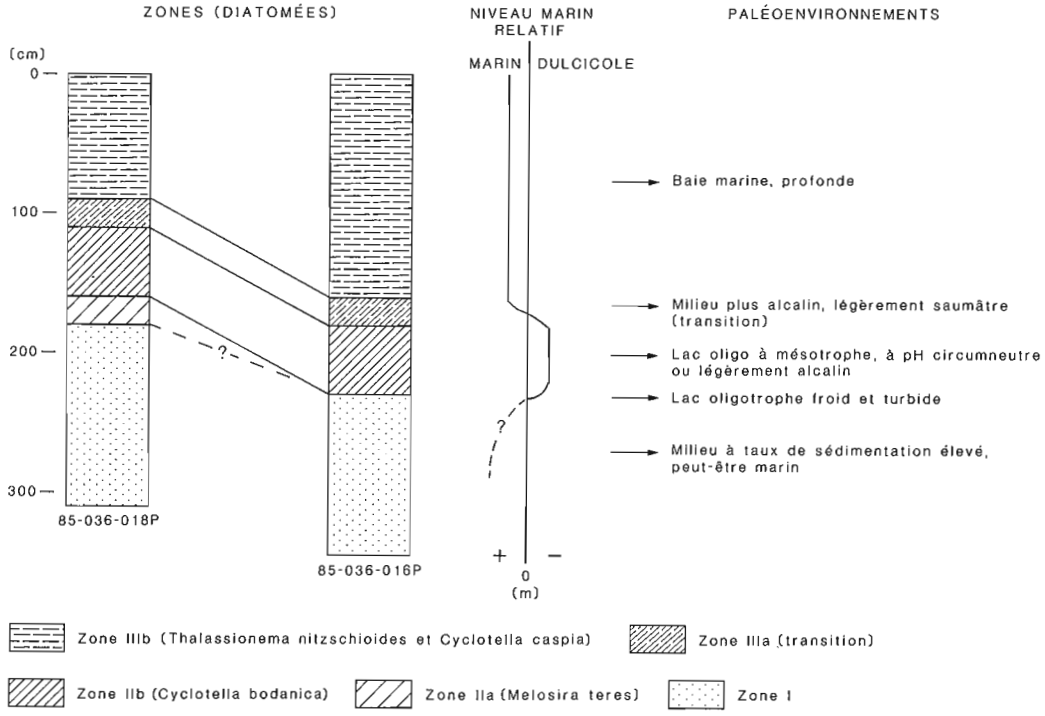


Figure 93.4. Corrélation stratigraphique des zones et interprétation des variations de milieux

Les conditions lacustres variables ont ensuite subsisté pendant une bonne partie de l'Holocène, à en juger par l'épaisseur des sédiments qui les représentent. La profondeur, ou encore la proximité, des rivages a probablement varié, mais l'intérêt peut-être le plus remarquable de cette phase lacustre réside dans la présence de *M. teres*, une forme planctonique apparemment circumpolaire qui caractérise la base de plusieurs séquences lacustres du sud du Québec et qui est corrélée aux assemblages polliniques de toundra (Lortie et Richard, 1986); elle apparaît ici dans les mêmes horizons polliniques (Jetté et de Vernal, comm. pers.). Ce taxon pourrait indiquer ici la présence d'eaux très froides, de versants encore peu stabilisés et d'une turbidité relativement forte, avant d'évoluer vers un trophisme plus marqué et des conditions plus normales.

La transgression marine postérieure apparaît progressivement avec une phase très légèrement saumâtre (sous-zone IIIa) avant de passer rapidement à des conditions de baie marine et profonde à peu près semblables à celles d'aujourd'hui. La transition saumâtre pourrait correspondre à de brèves incursions des hautes marées avant que le seuil ne soit franchi par les eaux de l'Atlantique (Hillaire-Marcel, 1987). Comme la sous-zone qui la représente est relativement importante, elle indique peut-être une remontée assez lente à cette époque. Compte tenu de la profondeur à l'entrée du chenal Great Bras d'Or, le niveau marin relatif minimum peut être estimé à environ 8 à 10 m sous son niveau actuel. Dans la carotte 016P, le début de la transgression est corrélé avec le déclin de *Tsuga*, survenu il y a entre 4000 et 5000 ans, ce qui permet de suggérer un taux de submersion de 16 à 20 cm par siècle (de Vernal et Jetté, 1987). À Port-aux-Port, au sud-ouest de Terre-Neuve, d'autres recherches (Brookes et coll., 1985) établissent ce bas niveau relatif minimum entre –11 et –14 m et le datent à 5800 ± 200 ans B.P., ce qui indique un taux de 19 à 24 cm par siècle. Les variations perceptibles de certains taxons, comme *C. caspia*, semblent indiquer des oscillations en termes de salinité ou encore de profondeur que seule une analyse plus approfondie pourra confirmer; l'ampleur de ces fluctuations est probablement plus marquée au fond de la baie, à l'endroit du sondage 016P.

CONCLUSIONS

Les trois zones de diatomées observées dans les carottes 85-016P et 018P marquent l'évolution du lac Bras d'Or depuis la déglaciation. Une première incursion, peut-être marine, a envahi le bassin. Isolé des eaux atlantiques par le relèvement glacioisostatique, une phase lacustre lui a succédée alors qu'une végétation de toundra caractérisait le paysage environnant. La transgression marine finale est associée à la remontée générale du niveau marin observée dans plusieurs secteurs des provinces de l'Atlantique (p.ex. Palmer, 1978; Scott et Medioli, 1980). Elle s'observe ici par de nets changements des flores de diatomées.

REMERCIEMENTS

L'auteur remercie MM. P. Mudie (Institut océanographique Bedford), A. de Vernal (UQAM, Montréal) et Mlle H. Jetté

(Commission géologique du Canada) qui ont effectué le sous-échantillonnage des carottes et transmis une description des sédiments ainsi qu'une première analyse pollinique des carottes 85-036-016P et 018P.

RÉFÉRENCES

Brookes, I.A., Scott, D.B. and McAndrews, J.H.
1985: Postglacial relative sea-level change, Port-au-Port area, west Newfoundland; Canadian Journal of Earth Sciences, vol. 22, p. 1039-1047.

de Vernal, A. Lortie, G., Larouche, A., Scott, D.B. et Richard P.J.H.
1985: Évolution d'un milieu littoral et remontée du niveau relatif de la mer à l'Holocène supérieur au nord de l'île du Cap-Breton, Nouvelle-Écosse; Journal canadien des Sciences de la Terre, v. 22, p. 315-323.

de Vernal, A. et Mott, R.
1986: Palynostratigraphie et paléoenvironnements du Wisconsinien supérieur dans la région du lac Bras d'Or, Nouvelle-Écosse; Journal canadien des sciences de la Terre, v. 23, p. 491-503.

de Vernal, A., Causse, C., Hillaire-Marcel, C. Mott, R. and Occhietti, S.
1986: Th/U Palynostratigraphy and ages of upper Pleistocene interglacial and interstadial deposits on Cape Breton Island, eastern Canada; Geology, vol. 14, no. 7, p. 554-561.

de Vernal, A. et Jetté, H.
1987: Analyses polliniques de sédiments holocènes du lac Bras d'Or (carotte 85-036-016P), île du Cap-Breton, Nouvelle-Écosse; dans Recherches en cours, Partie A, Commission géologique du Canada, Étude 87-1A, nº 2.

Grant, D.
1977: Glacial style and ice limits, the Quarternary stratigraphic record, and changes of land and ocean level in the Atlantic Provinces, Canada; Géographie physique et Quaternaire, vol. 31, p. 247-260.

Grant, D. and King, L.H.
1984: A dtratiographic framework for the Quaternary history of the Atlantic Provinces, Canada; Geological Survey of Canada, Paper 84-10 p. 173-192.

Hillaire-Marcel, C.
1987: Composition isotopique du carbone organique des carottes du forage 85-036-016 dans le lac Bras d'Or, île du Cap-Breton, Nouvelle-Écosse; dans Recherches en cours, Partie A, Commission géologique du Canada, Étude 87-1A, nº 89.

Lortie, G., de Vernal, A., Mott, R., et Occhietti, S.
1984: Sur des alternances de flores diatomifères marines et dulcicoles dans une séquence sédimentaire wisconsinienne au Lac Bras d'Or, Nouvelle-Écosse; ACFAS, Résumés, Ve Congrès, p. 35-37.

Lortie, G. and Richard, P.
1986: Late-glacial diatom and pollen stratigraphy from the lake Boucané, southeastern Québec; 8th International Diatom Symposium, Proceedings, p. 00

Mott, R. and Grant, D.
1985: Pre-late Wisconsinan paleoenvironments; Géographie physique et Quaternaire, vol. 39, p. 239-254.

Mucci, A. and Pagé, P.
1987: Bras d'Or Lake cruise No. 85-036: the water chemistry; in current Research, Part A, Geological Survey of Canada, Paper 87-1A, no. 3.

Palmer, A.J.M.
1978: Distom stratigraphy of Basin Head Harbour, Prince Edward Island; Nova Scotia Institute of Sciences, Proceedings, vol. 28, p. 201-215.

Prest, V.K., Terasmae, J., Matthews, J.V. and Lichti-Federovich, S.
1976: Late-Quaternary history of Magdalen Islands; Marine Sediments, vol. 12, p. 39-59.

Quinlam, G. and Beaumont, C.
1981: A comparaison of observed and theoretical postglacial relative sea level in Atlantic Canada; Canadian Journal of Earth Sciences, vol. 18, p. 1146-1163.

Quinlam, G. and Beaumont, C.
1982: The deglaciation of Atlantic Canada as reconstructed from the post-glacial relative sea-level record; Canadian Journal of Earth Sciences, vol. 19, p. 2232-2246.

Scott, D.B., and Mecholi, F.S.
1980: Quantitative studies of marsh foraminiferal distributions in Nova Scotia; implications for sea level studies; Cushman Foundation Foraminiferal Research, Special Publication, no. 17, 58 p.

Scott, D.B., Williamson, M.A. and Duffet, T.E.
1981: Marsh foraminifera of Prince Edward Island: their recent distribution and application for former sea-level studies; Maritime Sediments and Atlantic Geology, vol. 17, p. 98-129.

Vilks, G.
1967: Quantitative analysis of foraminifera in Bras d'Or Lakes, Geological Survey of Canada, Internal B.I.O. Report 67-1, 84p.

SCIENTIFIC AND TECHNICAL NOTES
NOTES SCIENTIFIQUES ET TECHNIQUES

Potential economic significance of Precambrian potassic plutons in the Central Metasedimentary Belt, Grenville Province of western Quebec

Project 760061

L. Corriveau[1] and M. Gorton[1]
Lithosphere and Canadian Shield Division

Corriveau, L. and Gorton, M., Potential economic significance of Precambrian potassic plutons in the Central Metasedimentary Belt, Grenville Province of western Quebec; in Current Research, Part A, Geological Survey of Canada, Paper 87-1A, p. 897-899, 1987.

Abstract

Late-tectonic potassic intrusions in the Mont-Laurier area of the Central Metasedimentary Belt have features of possible economic signifance that include occurrence of carbonatite and possibly lamproite dykes, skarns and presence of abundant apatite in some mafic and ultramafic rocks.

Résumé

Les plutons potassiques tardi-tectoniques de la région de Mont-Laurier dans la Zone métasédimentaire centrale presentent quelques points d'intérêts économiques. Ceux-ci comprennent la présence de dikes de carbonatite et possiblement de lamproïte, de skarns ainsi que l'abondance d'apatite dans certaines roches mafiques et ultramafiques.

[1]Department of Geology, University of Toronto, Toronto, Ontario M5S 1A1

INTRODUCTION

Potassic intrusions and associated dykes in the Mont-Laurier area, Central Metasedimentary Belt of the Grenville Province in Quebec, are both economically and academically significant. There are very few potassic intrusions documented in the world, and most of them have a limited variety of rock types. Those in the Mont-Laurier area, at least six, exhibit a complete spectrum of rock types ranging from micaceous pyroxenite to syenite (Corriveau, 1984, 1985). The recent discovery of diamond in potassic dykes (lamproite in northwest Australia and in Arkansas; Bergman, 1984), the abundance of apatite in some of the plutonic rocks and the association of the potassic intrusions with carbonatite and skarn substantiate their potential economic importance.

GEOLOGY

The Mont-Laurier area potassic intrusions (Fig. 1) consist of syenite, monzonite, diorite or melasyenite, biotite pyroxenite and minor nepheline syenite, quartz syenite and carbonatite. Fine grained lamprophyre and other mafic dykes occur abundantly throughout the plutons. Contact zones are characterized by heterogeneous syenites rich in clinopyroxene; adjacent country rocks are typically rich in calc-silicate minerals and include clinopyroxene-bearing quartzite; all these rocks are mineralogically similar in that they contain clinopyroxene, titanite, feldspar and minor scapolite and garnet.

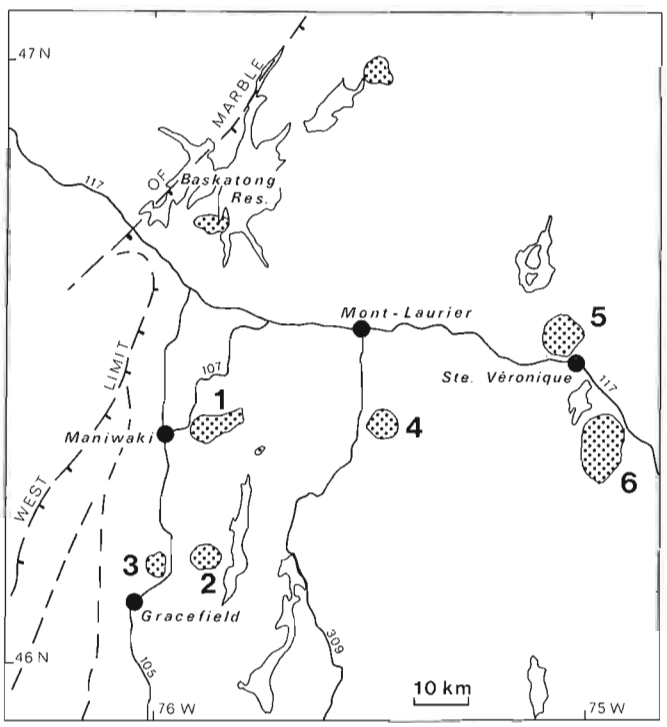


Figure 1. Location of potassic syenite plutons in the Mont-Laurier area. 1 – Kensington, 2 – Cameron, 3 – Gracefield, 4 – Lac Rouge, 5 – Ste. Véronique, 6 – Loranger.

Apatite

Apatite is associated with biotite-rich plutonic rocks and commonly constitutes 5 to 7 modal per cent of 1), pyroxenite, diorite and monzonite of the Kensington pluton, 2), syenite and rare pyroxenite or meladiorite of the Cameron, Gracefield and Lac Rouge plutons, and 3), pyroxenite and melasyenite of the Ste. Véronique pluton. Previous studies of apatite deposits appear to have been confined to the Ste. Véronique pluton.

Carbonatite

Two dykes of carbonatite (confirmed by trace element analyses; see below), a few decimetres thick, crosscut the eastern margin of the Gracefield pluton adjacent to country rock marble (46° 08′ 10″N, 76° 00′ 45″W). They contain calcite, apatite, clinopyroxene and K-feldspar. Metasomatic zones a few centimetres wide are associated with these dykes and consist of clinopyroxene and amphibole. Interstitial calcite between primary K-feldspar laths is common in Syenite I (Corriveau, 1985) of the Gracefield pluton. Calcite also occurs in rocks of the poorly exposed Lac Rouge pluton.

Skarn?

Marginal zones of heterogeneous syenite replete with diffuse masses rich in clinopyroxene surround the Kensington, Cameron, Gracefield and to a lesser extent the Lac Rouge plutons, and similar rocks exhibit crosscutting relationships in the Kensington and Ste. Véronique plutons. These marginal zones resemble endoskarns. They are locally crosscut or replaced by zoned veins containing varying proportions of clinopyroxene, amphibole, scapolite, spinel, biotite, titanite, calcite and pyrrhotite. Calc-silicate rocks and clinopyroxene-bearing quartzite are spatially associated with these contact zones and may prove to be exoskarns related to the emplacement of the potassic plutons in country rocks rich in marble.

Lamproite

Lamproite, a mafic igneous rock rich in potash and magnesia, has not been positively identified yet in the Mont-Laurier region, but only a small proportion of the abundant, fine grained, grey mafic dykes have been subjected to microscopical and geochemical study to date. Those that have are chemically and mineralogically similar to the plutonic rocks they intrude. Absence of olivine and presence of plagioclase in these dykes are more characteristic of lamprophyre than of lamproite. Occurrence of olivine, lack of plagioclase and the more potassic nature of the Ste. Véronique pluton together suggest that associated dykes may be a better prospect for identification of lamproite. A coarse grained olivine-biotite-clinopyroxene-orthopyroxene ultramafic rock is exposed for a few metres within diorite of the Kensington pluton. Field observations indicate that this rock postdates most coarse- to

medium-grained dykes. It contains a distinctive arrangement of unoriented, centimetre size biotite plates, apparently characteristic of olivine-bearing rocks (A.N. Lecheminant, personal communication, 1984). Boulders of similar rock were observed a few kilometres south of the Kensington pluton.

Zircon

Zircon is a common accessory phase in syenite of the Kensington and Lac Rouge plutons and in monzonite of the Loranger pluton. Baddeleyite (ZrO_2) occurs in the Lac Rouge syenite.

GEOCHEMICAL ASPECTS

Preliminary work by instrumental neutron activation at the Slowpoke II reactor, University of Toronto (Barnes and Gorton, 1984), and XRF analyses of major and trace elements at the same university indicate that the carbonatite is rich in REE (La – 464 ppm, Yb – 11 ppm) and Y (134 ppm), and poor in Nb (8 ppm), and that 3 wt. per cent P_2O_5 is fairly common in biotite pyroxenite, melasyenite and diorite. The calc-silicate rocks adjacent to the plutons and the contact syenites have low Au (0.1 ppb) and W (F1 ppm); Sn was not analyzed.

Geochemical analysis of the plutonic rocks and associated dykes, and microprobe analysis of their minerals are in progress and will document what already appears to be one of the most complete suites of potassic intrusions in the world. Petrogenetic modelling of the potassic suite of the Kensington pluton is anticipated. The presence of fine grained, mafic potassic dykes will allow comparison of this suite with lamprophyre and lamproite dykes The endo- and exoskarns associated with the western plutons will be documented, but it is not in the scope of the present study to detail their origin, temperature of formation and fluid evlution. Abundance of interstitial calcite in the plutonic syenite of the Gracefield pluton and the occurrence of carbonatite dykes within the pluton suggest a close relationship between these rock types. These rocks present a good opportunity for a detailed study addressing the possibility that carbonatite may originate by immiscibility from a felsic alkaline potassic magma.

SUMMARY

The economic potential of apatite in the potassic plutons of the Mont-Laurier area is not restricted to the Ste. Véronique pluton; it also occurs as an abundant accessory mineral in the Kensington, Cameron, Gracefield and Lac Rouge plutons. Further, the discovery of carbonatite dykes in the Gracefield pluton suggests that REE and trace element mineralization may be associated with these plutons. Skarn mineralization and the potential for the occurrence of diamond are far from being proven, but further research on this plutonic suite is clearly worth pursuing.

REFERENCES

Barnes, S.-J. and Gorton, M.
1984: Trace element analysis by neutron activation with a low flux reactor (Slowpoke II): results for international reference rocks; Geostandards Newsletter, v. 8, no. 1, p. 17-23.

Bergman, S.C.
1984: Lamproites and other potassium-rich igneous rocks: a review of their occurrence, mineralogy and geochemistry; in Proceedings of the Conference on Alkaline Igneous Rocks; Geological Society of London.

Corriveau, L.
1984: Account of field observations on rock units and structural features of the syenitic complexes of the Mont-Laurier area, Central Metasedimentary Belt of the Grenville Province; in Current Research, Part A, Geological Survey of Canada, Paper 84-1A, p. 303-306.
1985: Precambrian syenitic plutons, Central Metasedimentary Belt, Grenville Province of Quebec; in Current Research, Part A, Geological Survey of Canada, Paper 85-1A, p. 165-174.

Preliminary fieldwork for thermoluminescence dating studies at the Fraser River delta, British Columbia

Project 790006

G.W. Berger[1] and J.L. Luternauer
Cordilleran and Pacific Margin Division, Vancouver

Berger, G.W. and Luternauer, J.L., Preliminary fieldwork for thermoluminescence dating studies at the Fraser River delta, British Columbia in Current Research, Part A, Geological Survey of Canada, Paper 87-1A, p. 901-904, 1987.

Abstract

To answer fundamental questions about the "zeroing" assumptions of the thermoluminescence (TL) dating technique applied to waterlaid Quaternary sediments, we collected mineral grains in the water column at the Fraser River delta front by pumping suspensions into opaque containers on board a small research vessel. At the same time, the downwelling light in the visible spectrum was measured using a quanta spectrometer system. This first attempt to obtain such information for the study of TL in minerals has provided support for one of the assumptions of the TL dating technique applied to waterlaid sediments.

Résumé

Afin de répondre aux questions fondamentales sur les hypothèses concernant le point d'origine utilisé pour la méthode de datation par thermoluminescence (TL) appliquée aux sédiments quarternaires déposés en milieu aqueux, on a ramassé des grains minéraux dans la colonne d'eau du front du delta du fleuve Fraser en pompant des matières en suspension dans des contenants opaques se trouvant à bord d'un petit navire de recherche. On a mesuré, en même temps, on a mesuré par spectrométrie quantique la lumière de désexcitation dans le spectre visible. Cette première tentative d'obtenir de tels renseignements pour l'étude de la TL dans les minéraux a permis d'appuyer une des hypothèses liées à la datation par la TL appliquée aux sédiments déposés en milieu aqueux.

[1]Department of Geology, Western Washington University, Bellingham, WA, 98225, U.S.A.

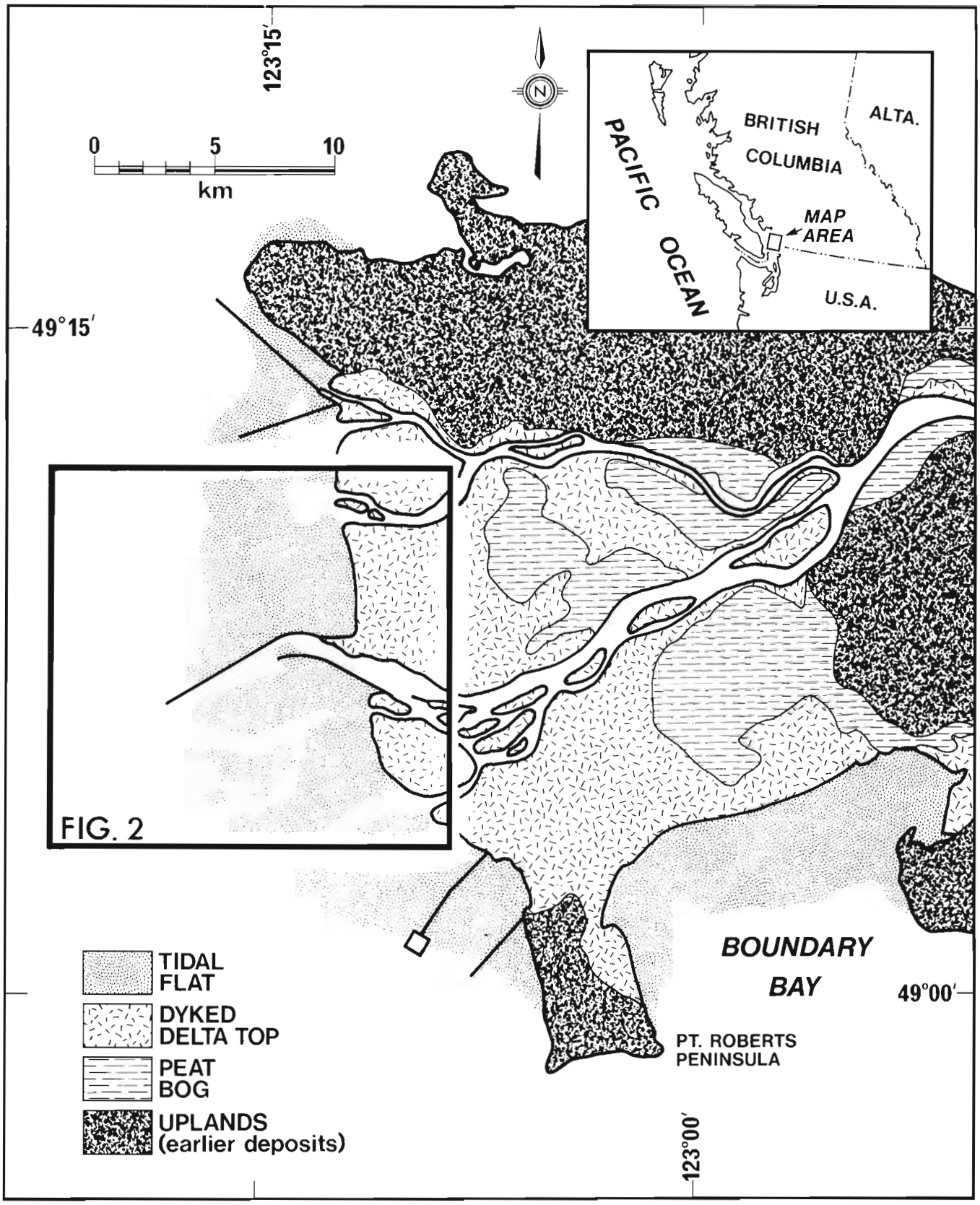


Figure 1. Quaternary deposits of the Fraser River delta area.

INTRODUCTION

The absolute deposition ages of many Quaternary deposits cannot be determined accurately. Some may not contain sufficient organics for C-14 dating; others may be older than the usual upper limit of the radiocarbon dating method, about 40 ka. The thermoluminescence (TL) dating technique (Aitken, 1985) has the potential to provide absolute deposition ages, from a few thousand to several hundred thousand years, for the detrital grains of feldspar and quartz in a wide variety of deposits. The principle underlying the technique is based on the fact that the luminescence emitted from a mineral heated in the laboratory is proportional to the number of electrons stored in traps formed by certain impurities and crystal defects. Natural ionizing radiation causes electrons to migrate into the traps. A TL apparent age involves two determinations, the luminescence and the rate of migration into the traps (the dose rate), and represents the time since the traps were last emptied. They can be emptied by heat or exposure to sunlight. In the case of detrital grains the event dated is the last exposure to sunlight, for minerals within a rock the event is the last cooling. Heating can 'completely' empty the traps (i.e. no thermoluminescence can be measured), but light causes a partial emptying that depends on such factors as the photon energy (wavelength), duration of exposure, mineral type and 'depth' of traps (the thermal activation energy of the traps).

Because waterlaid sediments are an important part of the uaternary record, it is desirable to know under what depositional conditions the TL of their detrital minerals is wholly reset or "zeroed". Previous laboratory studies (Berger, 1986) have shown that the "zeroing" of TL in waterlaid sediments can be far from complete. Not only is duration of suspension of grains important (2-10 m sized grains are usually selected) but also the spectral energy of the ambient light is critical. For example, TL is more readily "zeroed" by short wavelength visible light (blue) than by the lower energy visible light (e.g. yellow or orange). For this reason, if a laboratory light source is used that contains a greater fraction of the blue than did the natural, ambient light at deposition, then it is easy to obtain an erroneously large TL apparent age (Berger et al. 1984). This apparent anomaly arises because the laboratory light while having little effect on the TL of the primary sample causes a distinct lowering ('overbleaching') of the TL of the irradiated subsamples used in calculating the past dose. Fortunately, the reverse does not appear to be true – no error results if the laboratory (visible) light source is "redder" than the natural illumination.

In this context, a trial field program was initiated under the sponsorship of the U.S. National Science Foundation to collect mineral grains from the water column and to measure simultaneously the downwelling (the ambient light at the depth of the grains) spectral irradiance (light intensity vs. wavelength). It is known (e.g. Jerlov 1976) that scattering and absorption effects by suspended solid particles tend to "redden" the spectrum of sunlight in turbid water; however, the sampling project reported here is the first to relate direct, in situ optical measurements to TL studies.

FIELD TECHNIQUES

Sample collection and light measurements were conducted from on board the 28-foot launch REVISOR of the Canadian Hydrographic Service, outfitted with a davit, power winch, depth sounder and navigation aids. In 1986 two station areas were selected – one in the main channel of the Fraser River, and the other offshore in the sediment plume (Fig. 1,2). Stations were occupied at high tide in late July 1986. At each station suspended grains were recovered and downwelling light intensity was measured at different depths. The general equipment used for this purpose is shown schematically in Figure 3.

The spectral irradiance was measured on deck and under water by two separate quanta spectrometer systems, loaned by the Department of the Environment. These Techtum QSM-2500 systems, powered by mercury batteries, give the spectral distribution between 400 and about 730 nm (e.g. Adams and Flavelle 1978).

PRELIMINARY RESULTS

Problems were encountered with the transmissometer, but otherwise this pilot project was successful in obtaining useful spectral irradiance measurements and in recovering suspended ilts (60 L of water with suspended material were recovered at each depth). An example of the measured spectral distributions is shown in Figure 4, where a clear and dramatic difference between the downwelling irradiances is shown. This result justifies the practice (e.g., Berger, 1985) of blocking all all wavelengths below 550 nm in laboratory illuminations used for TL dating of waterlaid sediments.

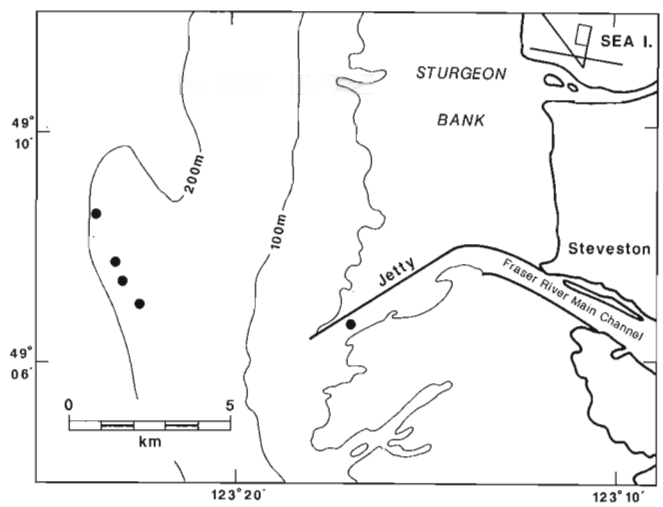


Figure 2. Two station areas occupied in the Fraser River delta area, south of Vancouver – one in the main channel near Sand Heads and the other about 7 km offshore in the sediment plume, near the 200 m depth contour. The offshore stations moved northwesterly in response to wind and currents.

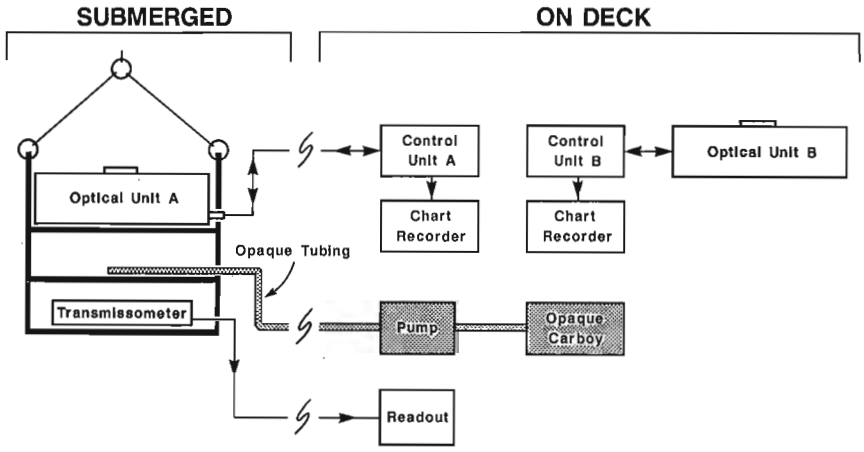


Figure 3. The basic equipment consisted of a frame-mounted (and weighted) package lowered to selected depths, and associated control and output devices on deck. Two spectrometer systems were used so that deck-level illumination could be recorded at the same time as the submerged illumination. Suspended grains were shielded from light during recovery and storage.

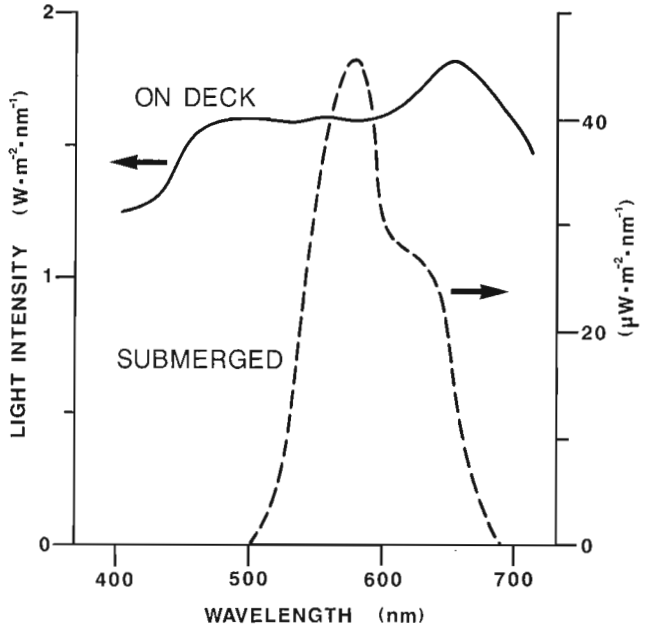


Figure 4. Downwelling spectral irradiance at the Sand Heads station. The illumination at a depth of 4 m is compared with that on deck.

CONCLUSIONS

The simple arrangement of instruments shown in Figure 3 enabled spectral measurements and sample recovery to be completed efficiently. Future studies of this sort could therefore readily assess the effects on spectral irradiance at depth of several variables, such as tidal conditions, time of day, and seasonal changes in input volume. However, the first order effects demonstrated in Figure 4 are expected to prevail, and to this extent this pilot project has provided very useful information that can be correlated directly with TL analyses of suspended grains. Results from this fundamental study will enable objective criteria to be applied to the selection and treatment of waterlaid sediments for dating by TL. This objectivity will provide more reliable TL ages, which can be expected to form the basis of absolute chronologies in applied studies of estuarine and continental shelf deposits. For example, knowledge of the development of the Fraser River delta could depend critically upon such absolute deposition ages.

ACKNOWLEDGMENTS

We thank several people for their generous donation of equipment and time. Foremost of these are M.A. Church (U.B.C.) and R.A. Kostachuck (U. of Guelph). Also, a debt of gratitude is owed to Gordon Allison and Brett Kelly for their cheerful and skillful assistance on the REVISOR, and to Bob MacDonald and Bill Hill of the Pacific Geoscience Centre for technical help. Finally, Greg Johnson and Alex Jogattka assisted in sample collection.

REFERENCES

Admas, W.A. and Flavelle, P.A.
1978: Low temperature adapted submersible spectrophotemeters for use in floating ice research; Scientific Series No. 82, Inland Waters Directorate, Environment Canada, 15 p.

Aitken, M.J.
1985: Thermoluminescence Dating; Academic Press, London/Orlando, 352 p.

Berger, G.W.
1985: Thermoluminescence dating applied to a thin winter varve of the late glacial South Thompson silt, south-central British Columbia; Canadian Journal of Earth Sciences, v. 22, p. 1736-1739.
1986: Dating Quaternary deposits by liminescence – recent advances; Geoscience Canada, v. 13, p. 15-21.

Berger, G.W., Huntley, D.J. and Stipp, J.J.
1984: Thermoluminescence studies on a C-14 dated marine core; Canadian Journal of Earth Sciences, v. 21, p. 1145-1150.

Jerlov, N.G.
1976: Marine Optics, second edition; Elsevier Scientific Publishing Co., New York, 231 p.

Delineation of bedrock topography at Val Gagné, Ontario, using seismic reflection techniques[1]

Project 850058

S.E. Pullan, J.A. Hunter, R.M. Gagné, and R.L. Good
Terrain Sciences Division

Pullan, S.E., Hunter, J.A., Gagné, R.M., and Good R.L., Delineation of bedrock topography at Val Gagné, Ontario, using seismic reflection techniques; in Current Research, Part A, Geological Survey of Canada, Paper 87-1A, p. 905-912, 1987.

Abstract

Optimum offset shallow seismic reflection sections from the Val Gagné, Ontario, test site show excellent agreement with available borehole logs. Bedrock topography and structure within the overburden, including the delineation of occurrences of till, were interpreted from the seismic profiles. The results of this survey indicate that the optimum offset shallow reflection technique could be a valuable tool in exploration programs in northern Ontario and Quebec where overburden drilling is used for gold prospecting. With the seismic information available prior to drilling, drillsites could be selected to sample thick pockets of till or specifically located in the glacial-lee of buried bedrock highs in order to maximize the useful returns of each borehole.

Résumé

Les profils de Val Gagné, en Ontario, obtenues au moyen d'une technique de sismique réflexion peu profonde à décalage optimal, concordent très bien avec les diagraphies disponibles. À partir de ces profils sismiques, on a reconstitué la topographie et la structure de la roche en place à l'intérieur du terrain de recouvrement et délimité les accumulations de till. Les résultats de ce sondage indiquent que la technique de sismique réflexion peu profonde à décalage optimal pourrait être un outil d'exploration précieux dans le nord de l'Ontario et du Québec, où la prospection des gisements d'or s'effectue par forage dans des sédiments meubles de recouvrement. Grâce aux données sismiques recueillies avant le forage, on pourrait ainsi choisir les lieux de forage de façon à pouvoir prélever des échantillons des épaisses accumulations de till ou, plus particulièrement, les établir sur le versant des élévations de roche en place orienté dans la direction de l'écoulement glaciaire, afin de tirer le maximum de chaque sondage.

[1]Contribution to Canada-Ontario Mineral Development Agreement 1985-1990. Project carried by Geological Survey of Canada.

INTRODUCTION

With the development of digital enhancement engineering seismographs and the concurrent proliferation of microcomputers over the last decade, it has become possible to apply seismic reflection techniques, well established since the 1930s in the oil industry, to shallow engineering or groundwater problems. The Terrain Geophysics Section of the Geological Survey of Canada has been developing shallow reflection methods and software to process the data since 1980 (Hunter et al., 1982a,b). The methods are now well established and have been tested in many areas of Canada (Hunter et al., 1984). This report describes a survey where this technique has been applied to a mining exploration problem to illustrate its potential usefulness in future exploration programs.

In the Matheson/Val Gagné area, east of Timmins, Ontario, gold prospecting has been inhibited by the thickness of the overburden. The area is covered by varying thicknesses of clay, silt, and/or sand, overlying pockets of till above the bedrock. The average depth to bedrock in 42 holes drilled in the area in 1984 by the Ontario Geological Survey (OGS) was 35 m (Jensen et al., 1985). The standard current exploration procedure is to drill and sample any tills that are encountered above bedrock. The samples are then assayed for gold content, and, if this is significant, drilling continues in the "up-ice" direction in search of the "mother lode". Under ideal conditions drillholes would be positioned in the glacial lee of buried bedrock highs where thick occurrences of till are likely to be found, but without any prior knowledge of the subsurface structure, much of the initial exploratory drilling is blind. It is estimated that as many as 25% of such drillholes encounter no till (R.B. Barlow, personal communication, 1986) if no geophysical definition of the subsurface is available.

Our initial work in the Val Gagné area in 1985 was done at the request of R.B. Barlow of the Ontario Geological Survey. Prior to our seismic surveying he had carried out airborne and ground electromagnetic (EM) field and interpretation work that had demonstrated the utility of these methods for indicating the presence of till pockets coincident with bedrock valleys. This then provided regional overburden drilling targets. Although the lateral extent of till pockets could be outlined by various imaging techniques applied to the EM data, resolving the vertical section (i.e., precise depths and thicknesses) through one-dimensional sounding interpretation methods requires much further research. He suggested that collaborative efforts, using seismic reflection methods together with EM methods, would allow the possibility of further advancing the electromagnetic interpretation problem, while at the same time demonstrating the capability of the seismic reflection method for resolving the complex vertical stratigraphy of the Quaternary sections in the area.

Seismic tests in 1985, at various sites selected on the basis of EM surveys conducted by OGS, proved the feasibility of this approach. In 1986 we applied the "optimum offset" reflection technique on a production basis at a test site near Val Gagné, Ontario. Data from this test site are presented below, along with corroborative drillhole data from recent OGS drilling programs (OGS, 1986).

METHOD

The "optimum offset" shallow seismic reflection profiling technique has been described by Hunter et al. (1984). Under optimum conditions this technique allows an accurate and detailed delineation of the overburden-bedrock contact and of the structure within the overburden, even when the subsurface structure is fairly complex. The resolution depends on the frequency of seismic energy that can be returned from the target reflector to the surface. We have found that the best conditions occur when the near-surface materials are fine grained and water saturated. Such conditions exist throughout the clay belts of northern Ontario, which are also ideal for geophysical surveying in that there is minimal surface topography and good road access. Thus the Val Gagné test site, which is located in the clay belt north of Matheson, Ontario is an excellent area for the application of the optimum offset technique.

Each trace on an optimum offset profile is obtained using a geophone to record the ground motion in response to seismic energy that is produced at a predetermined source-geophone offset. The final section consists of a series of such measurements made at a given geophone spacing.

Approximately 10 km of line has been shot at the Val Gagné test site, predominantly along roads (Figure 1). A source-geophone offset of 30 m and a geophone spacing of 2.5 m were used for Line 1 which was shot in 1985; Lines 100–600 were all recorded in 1986 with a source-geophone offset of 21 m and a geophone spacing of 3 m. The data were filtered in the field by high-frequency geophones (50 Hz for Line 1, 100 Hz for all other lines), and by the 300 Hz high pass analog filter on the seismograph. A 12-gauge "Buffalo gun" was used throughout the survey as the seismic source (Pullan and MacAulay, 1987). Shallow holes (1 m deep) were drilled in a ditch or at the edge of the roadway and filled with water before being used as shotholes.

The data were recorded on a Nimbus 1210F 12-channel engineering seismograph and stored in the field on a G724S digital tape recorder. The records were transferred daily to an Apple IIe microcomputer and stored on floppy disk. Preliminary processing and plotting were carried out with the Apple system in the field office (Norminton and Pullan, 1986). Final plotting and a detailed velocity analysis were completed after all the data were collected.

Processing of the data involved: 1) shifting traces in time to line up the first arrivals (refractions from the top of the water table); 2) digital filtering (300-800 Hz bandpass); and 3) the application of an automatic gain control and time-varying gain tapers.

Depth scales were calculated after an analysis of multichannel records which were recorded along with the optimum offset data. These records were used to obtain an estimate of average velocity as a function of depth; average

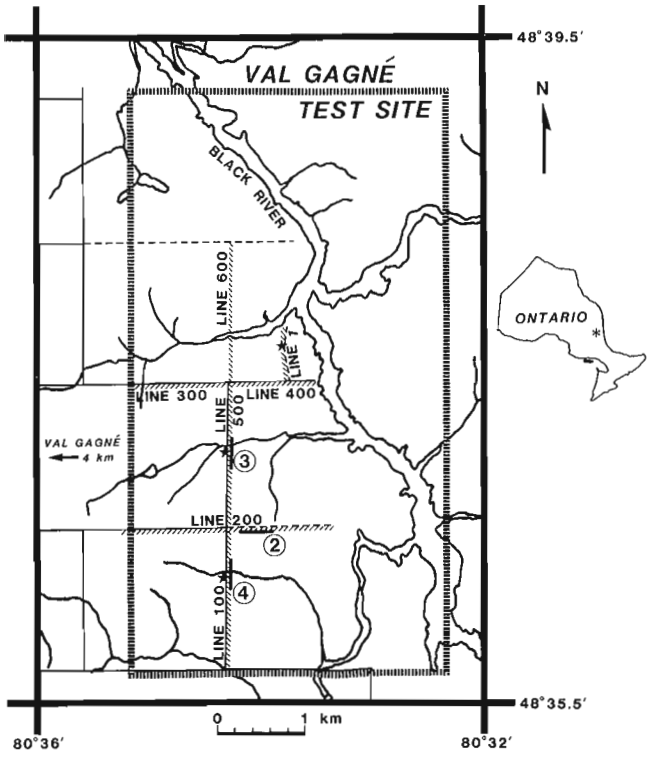


Figure 1. Map of the Val Gagné test site, indicating the location of seismic survey lines (hatched lines), drillholes (stars), and the sections shown in the following figures (solid lines related to circled numbers). Lines 100, 500, and 600 lie along the north-south baseline of the metric grid laid out for the test site; the east-west baseline is the southern limit of the site.

overburden velocities were in the range of 1500-1600 m/s. Depths are given with respect to the water table, as this is the datum on the seismic sections. Over most of the area, however, the water table is within 1 or 2 m of the surface and the depths given below are essentially those from ground surface.

The complete suite of shallow seismic reflection sections from the Val Gagné test site is available in Gagné et al. (in press).

RESULTS

Figure 2a is a 400 m section of the optimum offset profile along Line 200 which shows a buried bedrock valley. The section is reproduced in Figure 2b with interpretation lines superimposed. This section demonstrates the potential of the optimum offset shallow reflection method to map fairly rugged subsurface structure. This buried valley is 200 m wide, and the maximum relief on the bedrock surface is approximately 25 m. The steep sides of the valley are an indication that the survey line transects the valley at close to right angles, but additional east-west profiles would have to be shot to the north and south to define the strike and lateral extent of this feature.

Within the overburden, there are several reflectors which are almost flat lying. From the logs of nearby drillholes (see below), it is believed that the overburden is essentially a clay unit. The reflectors within this unit appear to be "draped" over the bedrock topography, that is, they dip gently towards the centre of the bedrock valley and are arched up over the bedrock highs. This is attributed to the dewatering and compaction of the clays after deposition. The draping effect can also be seen on the sections shown in the following figures, but it is more subtle because of the gentler bedrock topography.

There is no indication of any substantial thickness of till in this bedrock valley. Instead, we interpret there to be a remnant of till overlying bedrock on the west side of the section, and possibly another one on the east (Figure 2b). This interpretation is based on the seismic signature of till layers encountered in boreholes nearby (see below).

The depth scale for this and the following two figures was calculated using an average velocity of 1525 m/s. Velocity analyses of multichannel records in the area indicate this to be a reasonable velocity for the clay unit.

Figure 3 shows a 350 m section of the optimum offset profile along Line 100 centred on Sonic Drillhole 84-38 which was drilled by the Ontario Geological Survey in 1984 (Jensen et al., 1985; OGS, 1986). The bedrock dips gently to the north on this section, from a depth of approximately 30 m at 2300N to a depth of 35 m at 2600N. The overburden reflectors also dip gently to the north and again show the draping effect discussed in relation to Figure 2. According to the borehole log (OGS, 1986), the overburden consists of 9 m of massive clay above 23.5 m of varved clay. As the resolution in the upper 10 m of the seismic section is poor, due to the nonzero source-geophone offset and the resulting wide-angle reflections from shallow interfaces, it is not possible to resolve this contact on the section. The strong reflector on the seismic section at 28 ms corresponds to a significant increase in varve thickness which starts at a depth of 22 m. The clay ends at a depth of 32 m at a sharp contact with sandy till. The till is only 3 m thick and overlies diabase bedrock.

On the seismic section, the top of till is the major reflector with a weaker reflection from bedrock below it. The interpretation of this section in Figure 3b is based on this till/bedrock signature. We interpret there to be a continuous thin layer of till across this section north of 2300N. At the south end, a small bedrock high protrudes up into the clay unit. The till is believed to be thickest just north of 2500N where it fills a small hollow in the bedrock surface.

Figure 4 shows a 350 m section of Line 100 centred on OGS Sonic Drillhole 84 - 39 (Jensen et al., 1985; OGS, 1986). This section is only 1 km south of the section shown in Figure 3. Again, the borehole log indicates a predominantly clay overburden with a contact between massive and varved clay at a depth of 13 m. This interface is deep enough to be resolvable on the seismic section. The strong reflector within the overburden at a time of 30 ms is again attributed to a general increase in varve thickness which is logged at a depth of 24.4 m. The clay overlies a 1 m layer of till, below which there is 6.5 m of sand above argillaceous siltstone. The till

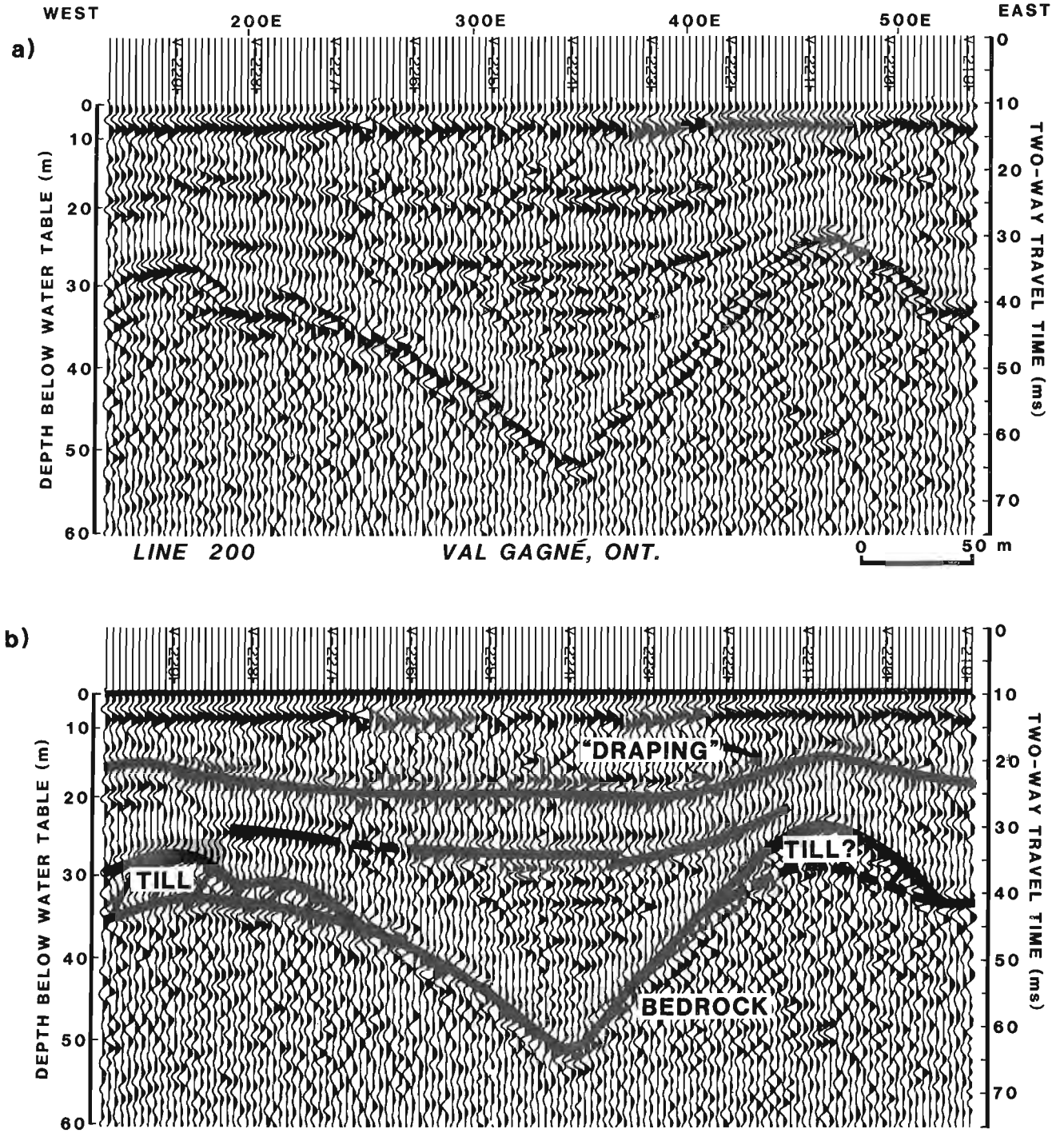


Figure 2.

a) Optimum offset seismic reflection section along Line 200 from 135E to 535E (i.e., with respect to the metric grid laid out for the test site).

b) An interpretation of Figure 2a, indicating bedrock topography, likely occurrences of till, and "draping" of overburden reflectors. See text.

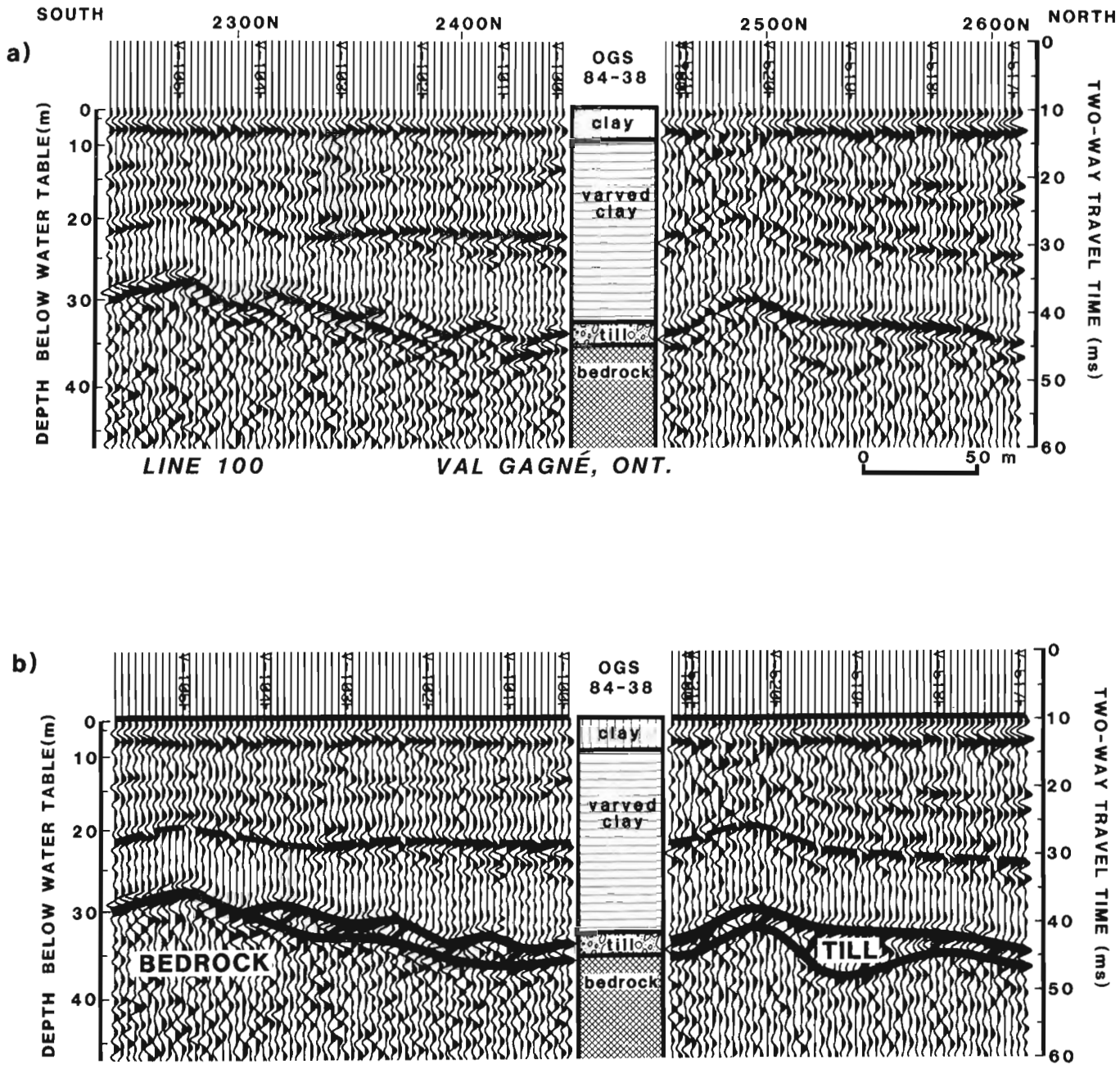


Figure 3.

a) Seismic reflection section along Line 100 from 224ON to 2610N. The section has been split at the site of OGS Sonic Drillhole 84-38, and a simplified drill log is shown there.

b) An interpretation of Figure 3a, outlining the likely extent and thickness of the till layer encountered in the borehole.

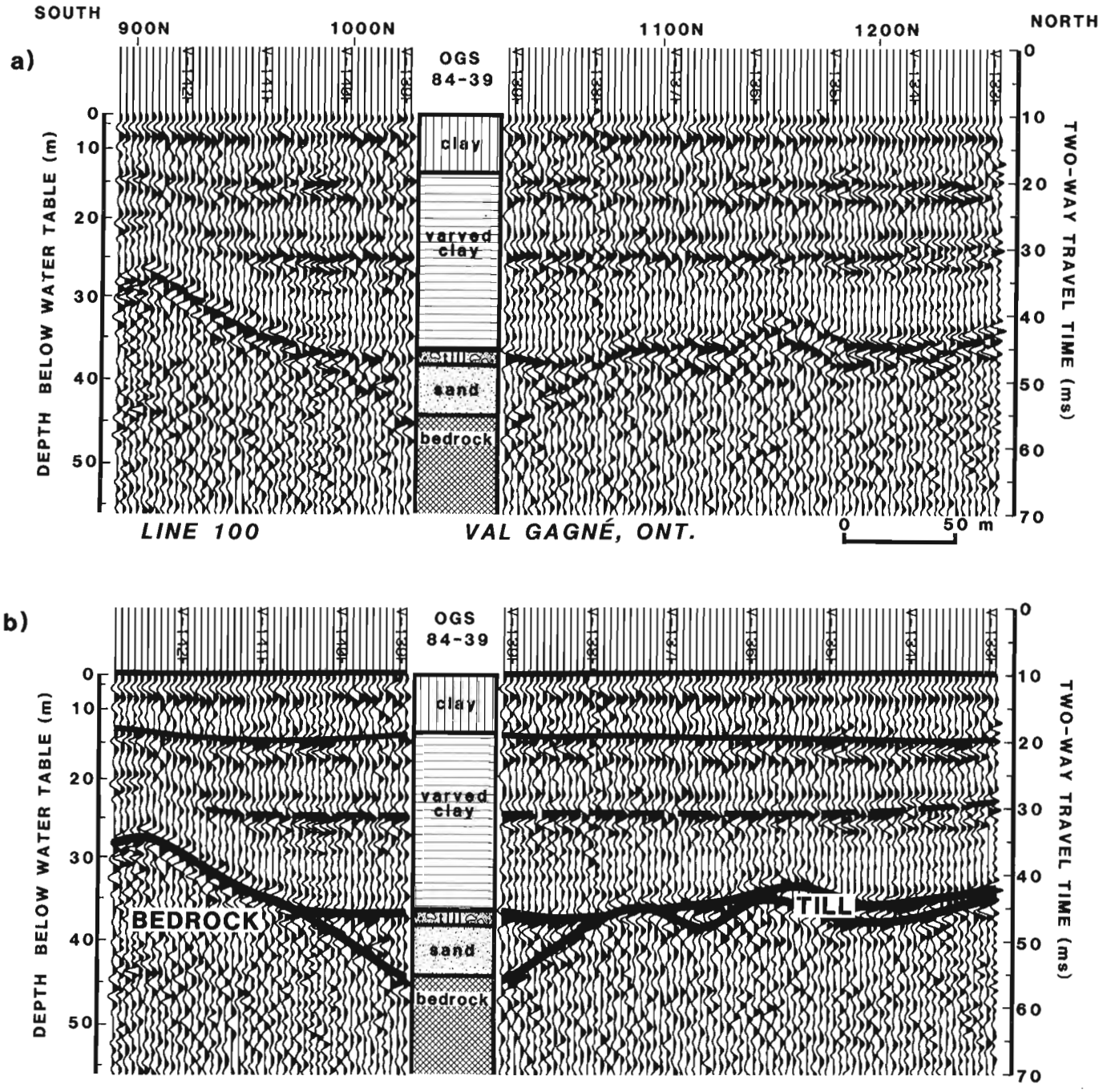


Figure 4.

a) Seismic reflection section along Line 100 from 890N to 1250N. A simplified drill log is shown at the location of OGS Sonic Drillhole 84-39.

b) An interpretation of Figure 4a, indicating the extension of lithological units north and south of the borehole, and likely occurrences of till.

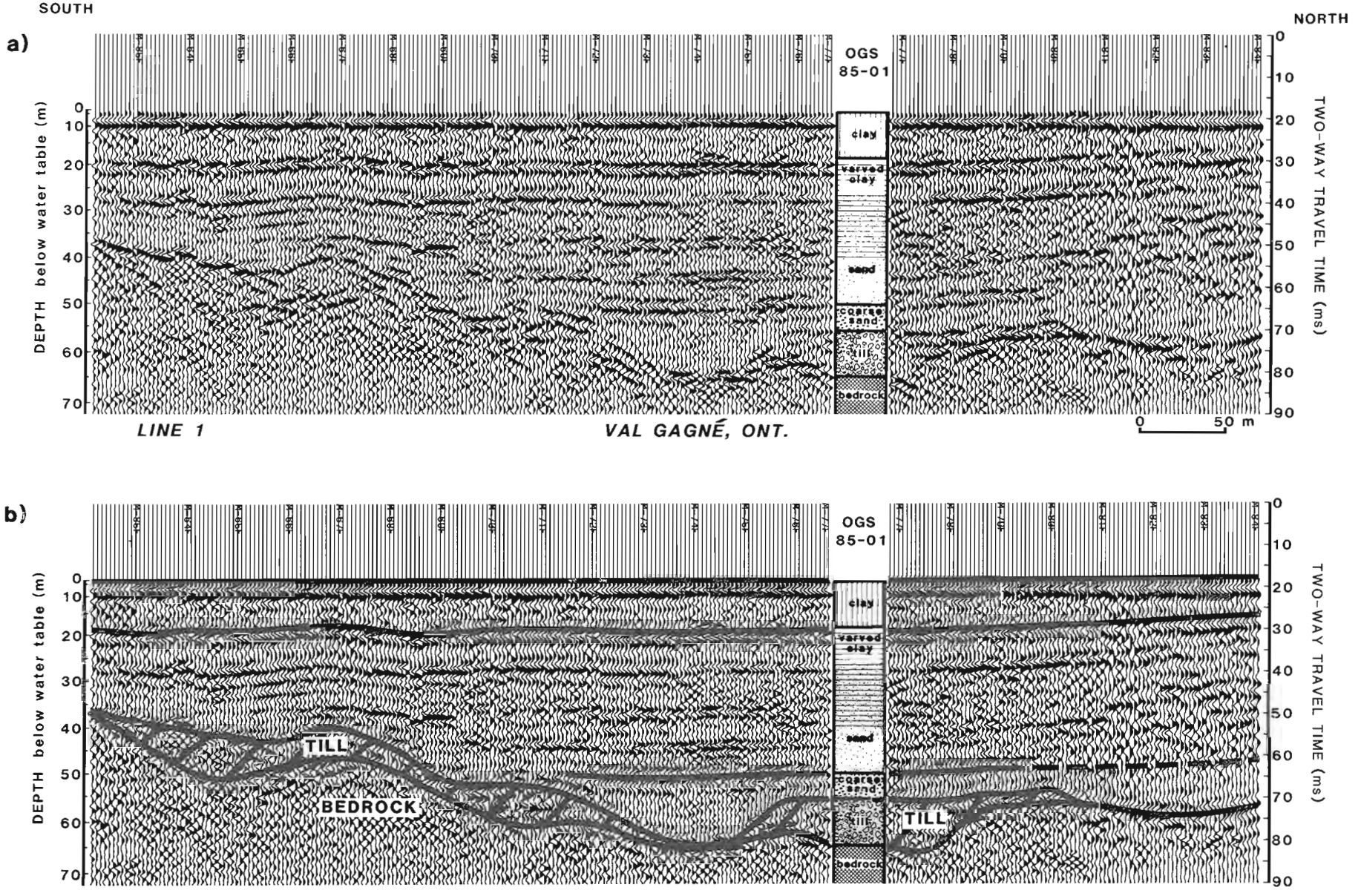


Figure 5.

a) Line 1 with a simplified drill log shown at the location of OGS Sonic Drillhole 85-0l.

b) An interpretation of Figure 5a, indicating the extension of lithological units north and south of the borehole, and likely occurrences of till.

layer is too thin to allow resolution of both the top of till and the top of sand on the section. The seismic profile indicates, however, that the sand fills a small hollow (50 m wide) in the bedrock surface (Figure 4b). Except for this pocket of sand and till, we interpret there to be only a thin layer of till, or sand and till, north of 1100N.

The most significant bedrock depression that has so far been discovered on the Val Gagné test site is along Line 1, shown in Figure 5. This section is 660 m in length, and bedrock varies from a depth of 37 m at the south end of the section to a depth of 65 m at the drillhole site (OGS Sonic Drillhole 85-01, R.B. Barlow personal communication, 1985). The essentially flat-lying overburden consists of clay grading into a thick sand unit. The contact between massive and varved clay occurs at a depth of 17 m and this interface is clearly visible on the seismic section at a time of approximately 30 ms. A small amount of fine sand first occurs at the bottom of the varves at a depth of 17 m, and this grades into a poorly layered sand from 40 to 50 m depth. The top of the sand is an indistinct boundary and is not easy to define on the seismic section; however, there is a weak reflector visible at a depth of approximately 40 m. Horizontal layering is clearly indicated throughout the clay/sand units with a small amount of draping visible.

At the drillhole, 15 m of sandy till overlies bedrock. This pocket of till was identified on the seismic section prior to drilling (R.B. Barlow, personal communication, 1985), and the drillhole site was selected specifically to sample this till. Figure 5b shows another major pocket of till south of the drillhole. This section clearly demonstrates the value of running seismic profiles prior to drilling; had 85-01 been drilled 100 m to the north of its location, only a minor occurrence of till would have been encountered in the hole.

DISCUSSION

The four short optimum offset seismic sections that have been presented above illustrate the potential benefit of this type of surveying, especially in combination with complementary electromagnetic techniques, to exploration programs in the clay belts of northern Ontario and Quebec. With some experience and drillhole control it is possible to delineate the subsurface bedrock topography, even when this is fairly rugged, to determine the structure and thickness of the overburden, and to define small occurrences of till overlying bedrock. Such information could greatly improve the success of overburden drilling, and it is hoped that these results will encourage further use of the optimum offset shallow reflection technique in this area.

REFERENCES

Gagné, R.M., Pullan, S.E., and Hunter, J.A.
: High resolution shallow seismic reflection profiles of the Val Gagné, Ontario test site; Geological Survey of Canada, Open File 1378. (in press)

Hunter, J.A., Burns, R.A., Gagné, R.M., Good, R.L., and MacAulay, H.A.
1982a: Mating the digital engineering seismograph with the small computer – some useful techniques; in Current Research, Part B, Geological Survey of Canada Paper 82-1B, p. 131-138.

Hunter, J.A., Burns, R.A., Good, R.L., MacAulay, H.A., and Gagné, R.M.
1982b: Optimum field techniques for bedrock reflection mapping with the multichannel engineering seismograph; in Current Research, Part B, Geological Survey of Canada, Paper 82-1B, p. 125-129.

Hunter, J.A., Pullan, S.E., Burns, R.A., Gagné, R.M., and Good, R.L.
1984: Shallow seismic reflection mapping of the overburden-bedrock interface with the engineering seismograph – some simple techniques; Geophysics, v. 49, p. 1381-1385.

Jensen, L.S., Baker, C.L., and Trowell, N.F.
1985: Preliminary results of bedrock samples from the sonic drilling program in the Matheson area, Cochrane District; Ontario Geological Survey, Map P. 2848, scale 1:100 000.

Norminton, E.J., and Pullan, S.E.
1986: Seismic reflection software for engineering seismographs; Geological Survey of Canada, Open File 1277.

Ontario Geological Survey
1986: Sonic drillholes 84-38 and 84-39, Taylor Township, District of Cochrane; Ontario Geological Survey, Map 80791, Geophysical/Geochemical Series, scale 1:100 000.

Pullan, S.E., and MacAulay, H.A.
1987: An in-hole shotgun source for engineering seismic surveys; Geophysics. (in press).

Ground probing radar investigations of massive ground ice and near surface geology in continuous permafrost

Project 850008

S.R. Dallimore and J.L. Davis[1]
Terrain Sciences Division

Dallimore, S.R. and Davis, J.L., Ground probing radar investigations of massive ground ice and near surface geology in continuous permafrost; in Current Research, Part A, Geological Survey of Canada, Paper 87-1A, p. 913-918, 1987.

Abstract

Field soundings using two new ground probing radar systems have been undertaken to map ground ice bodies and near surface geology at four sites on Richards Island, Northwest Territories and one site near Tuktoyaktuk, Northwest Territories. Preliminary correlation with borehole data indicates that the two radar systems are capable of mapping near surface soils to a depth of 10 m and in many areas to a depth of 30 m. At several locations where resistive materials such as ice or gravel occurred near the surface, reflections to 60 m depth were detected. Strong radar reflections were observed at the contacts between sediment and massive ice bodies even when the electromagnetic velocities of the sediment and the ice were similar.

Résumé

Des sondages ont été exécutés sur le terrain au moyen de deux nouveaux radars, pour lever des cartes des masses de glace souterraines et de la géologie de subsurface à quatre endroits dans l'île Richards et à un endroit près de Tuktoyaktuk, dans les Territoires du Nord-Ouest. Une corrélation préliminaire avec des données de diagraphies de sondage indique que les deux radars permettent de cartographier des sols de subsurface jusqu'à une profondeur de 10 m et, dans maintes régions, jusqu'à 30 m. À plusieurs endroits où des matériaux résistants comme de la glace ou du gravier se rencontrent à proximité de la surface, des échos ont été détectés jusqu'à 60 m de profondeur. Des échos puissants ont aussi été produits au contacts entre des sédiments et des corps de glace massifs, même lorsque les vitesses électromagnétiques des deux surfaces étaient comparables.

[1]A-Cubed Inc., 5566 Tomken Rd., Mississauga, Ontario L4W 1P4

INTRODUCTION

The detection and delineation of discrete bodies of ground ice are of particular interest to geotechnical engineers designing facilities such as buildings or pipelines and to surficial geologists attempting to interpret the origin or morphology of ice bodies. Geotechnical drilling has been used successfully in the past to determine ground ice distribution in near surface soils, but these data are often expensive to collect and problems occur in the interpretation of geological contacts between boreholes.

Ground-probing radar is a high resolution profiling technique capable of detecting electrical property variations in the ground. Since the electrical properties of most surficial materials are different, ground probing radar offers a means of detecting both geological contacts between different surficial materials and contacts between surficial materials and massive ground ice. Ground probing radar surveys are relatively inexpensive to run and thus they may provide a cost effective means to collect subsurface data and extend borehole information.

This report summarizes some of the results of field surveys undertaken to evaluate two newly developed ground probing radar systems for mapping buried ground ice bodies and subsurface geology at four sites on Richards Island, and one site on the Tuktoyaktuk Peninsula, Northwest Territories.

METHODOLOGY

Field work for the project was carried out in March and April 1986, when the active layer was frozen and snow cover provided easier access with the radar and drilling equipment. Field sites were selected to test radar effectiveness in a variety of terrains and geological conditions. Subsurface data for the radar investigations were obtained from boreholes drilled at specific sites along radar transects and from boreholes and geophyscial information already available from other studies.

The radar investigations were conducted by A-Cubed Inc. of Toronto with their pulseEKKO I and pulseEKKO II radar systems[1]. Field drilling was carried out under a separate contract in co-operation with an Indian and Northern Affairs study of granular deposits on Richards Island. Funding for the field studies was provided from the Office of Energy Research and Development.

RADAR TECHNIQUE

Ground probing radar is a high resolution geophysical technique, which is based on the measurement of the travel time of a transmitted electromagnetic signal which is reflected from various surfaces within the ground. If the velocity of propagation of the electromagnetic signal in the material is known, then the depth to the reflector can be determined.

The electrical properties of frozen ground are affected by changes in material type, phase of the water molecules, and the amount of unfrozen water. In general, radar is an effective tool for investigating frozen materials such as sands and gravels which are electrically resistive. Depth of signal penetration is limited in conductive materials such as clay and silt. A summary of the use of ground probing radar in permafrost is given by Annan and Davis (1976).

Early work with radar in permafrost areas was carried out by the Geological Survey of Canada in the mid 1970s. Field surveys at that time established that under certain conditions radar could be used for mapping buried bodies of ground ice (Davis et al., 1976). Technological advances, such as digital processing techniques and improved equipment sensitivity, have allowed significant design improvement since these initial studies.

Two radar systems with different system sensitivity and frequency were used in the study to map near surface soils in the 0-20 m depth range. The A-Cubed, pulseEKKO I radar, operating at a frequency of 100 MHz, was used for high resolution, continuous, near surface profiling. This system is an extensively modified Geophysical Survey System Inc. (GSSI) radar which was towed slowly on a toboggan behind a snowmobile. Figure 1 shows the field operation of the pulseEKKO I. The pulseEKKO II radar is a prototype digital radar system designed and constructed by A-Cubed Inc. for Energy, Mines and Resources, Canada. This radar operates at a lower frequency (30 MHz), providing greater depth penetration and increased system performance than the pulseEKKO I. The pulseEKKO II radar is operated in a step mode, with 4 m spacings used for most of the surveys reported here.

SURFICIAL GEOLOGY AND SITE SELECTION

Richards Island

Richards Island is situated in the continuous permafrost zone with permafrost thicknesses varying from 100 m to more than 700 m (Judge, 1986). Much of central Richards Island is covered by rolling moraine with local relief between 15 m and 30 m. To the southeast, particularly near Ya Ya Lake, a number of glaciofluvial ice contact ridges stand above the surrounding terrain. Other surficial materials include lacustrine deposits, colluvium, and pre-Wisconsinan sands (Rampton, in press). Massive ground ice has been reported from geotechnical investigations of granular materials associated with the ice contact features (Ripley, Klohn and Leonoff Int. Ltd., 1973) and from geophysical investigations of glaciofluvial outwash near Lousy Point (Rampton and Walcott, 1974).

[1]unpublished report "Mapping permafrost with the pulseEKKO I and II profilers" by A-Cubed Inc., 1986.



Figure 1. Field set-up for pulseEKKO ground probing radar survey.

Four sites were chosen for radar investigations on Richards Island; their locations are shown in Figure 2 and descriptions of each site is given below.

Lousy Point. The Lousy Point survey line begins on the west bank of the East Channel of Mackenzie River and runs about 7.5 km to the northwest, traversing a variety of surficial materials. The western part of this line was selected to overlap with a gravity survey carried out by the Geological Survey of Canada (GSC) in the mid 1970s (Rampton and Walcott, 1974).

Ya Ya Lake. The Ya Ya Lake survey lines were selected to study the effectiveness of the radar in delineating the subsurface geology of an ice contact ridge being investigated by Indian and Northern Affairs as a source of granular material. Previous drilling had shown the ridge to be underlain by massive ice. In total, 2.5 km of radar surveys were completed along two transects across the ice contact feature.

Illisarvik. Approximately 1.5 km of surveying was run along a pre-established grid at Illisarvik, an experimental, drained lake site located on northwestern Richards Island. This survey was undertaken in an attempt to delineate the freeze- back of the talik beneath the lake.

North Head. The North Head survey was conducted in the nearshore zone on the western side of Richards Island, to complement other studies of the geotechnical and geophyscial properties of the near surface soils (Kurfurst, 1986). Approximately 2 km of radar surveying along two lines were completed at North Head.

Tuktoyaktuk Peninsula

Involuted Hill. Radar surveys were also completed at Involuted Hill, located about 15 km northeast of Tuktoyaktuk. This site was studied in some detail in the mid 1970s by the GSC, at which time some of the first ground probing radar studies in permafrost were conducted. (Davis et al., 1976).

Previous drilling at Involuted Hill has shown it to be composed of a 5 to 10 m-thick cap of clay till underlain by a 10 to 15 m-thick massive ice body (J. Dugal, personal communication, 1986). The massive ice is underlain by brown sand.

PRELIMINARY RESULTS

The radar systems operated efficiently and produced reliable results under harsh operating conditions. The data from all the sites have been played back and reflector depths have been estimated using a simple one-layer model with an assumed velocity of 0.15 m/ns. Preliminary interpretation of the radar data has been carried out, and work is ongoing to correlate borehole and other subsurface data with the radar data.

The pulseEKKO I is a useful tool for providing a rapid survey of the near surface materials and identifying areas where further detailed radar studies would be of value. The pulseEKKO I usually detected reflectors in the 0 to 5 m depth range. Under exceptional conditions, with resistive materials, such as ice or frozen sand present near the surface, the pulseEKKO I was able to detect reflections to 30 m depth.

The pulseEKKO II was used mostly in areas of resistive materials, as identified by the pulseEKKO I, or in areas of particular geological interest. The pulseEKKO II detected reflections to 10 m depth and in many areas it detected reflectors to 30 m depth. At the Involuted Hill site, a very deep reflector, approximately 60 m below the surface, was detected in a survey run along a linear trough where massive ice occurred close to the surface.

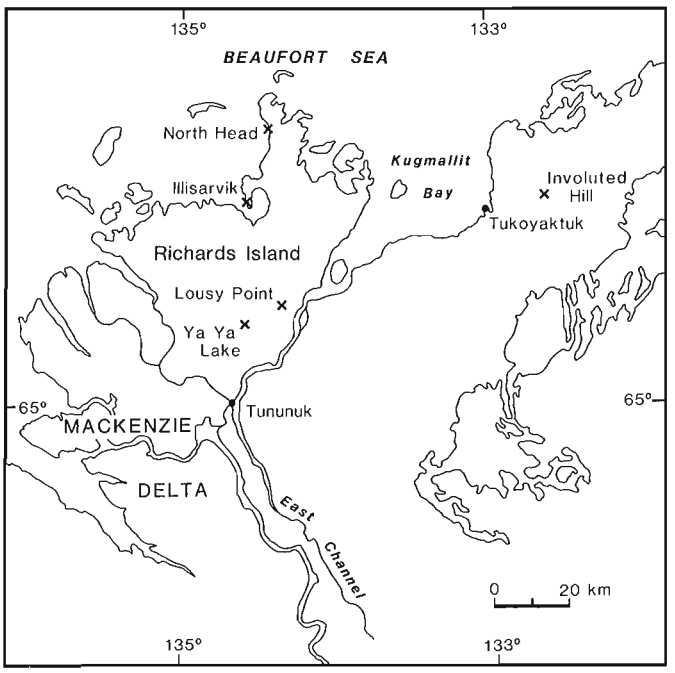


Figure 2. Location map showing sites of ground probing radar surveys.

Preliminary field drilling data indicate that the reflections shown in radar profiles can be due to contacts between different surficial materials or to reflections from interstratification within a particular surficial material. Strong reflections were found at contacts between massive ice bodies and the surrounding sediments, even when the electromagnetic velocity of the sediment was similar to that of ice, such as sand in contact with ice. Depth penetration in fine grained conductive materials such as clay had improved over earlier generation radar units but was still relatively limited. Some reflections however were detected with the pulseEKKO II radar at North Head where a conductive layer of sea water was present on top of unfrozen silt and sand.

Examples of data collected during the radar surveys is shown in Figures 3 and 4. These profiles show part of the Lousy Point line extending from a raised alluvial terrace in the east to an ice-cored glaciofluvial upland area to the west. The pulseEKKO I profile shown in Figure 3 indicates that near surface materials are relatively resistive, showing numerous reflectors in the upper 10 m of the ice cored ridge. Borehole SO-5 at chainage 0 + 737 m indicates that this zone is characterized by stratified sand, silt, and ice layers. The pulseEKKO II profile shown in Figure 4 reveals a number of deeper reflectors occurring at estimated depths of 10 to 30 m. Geology from Borehole SO-5 suggests that the undulating

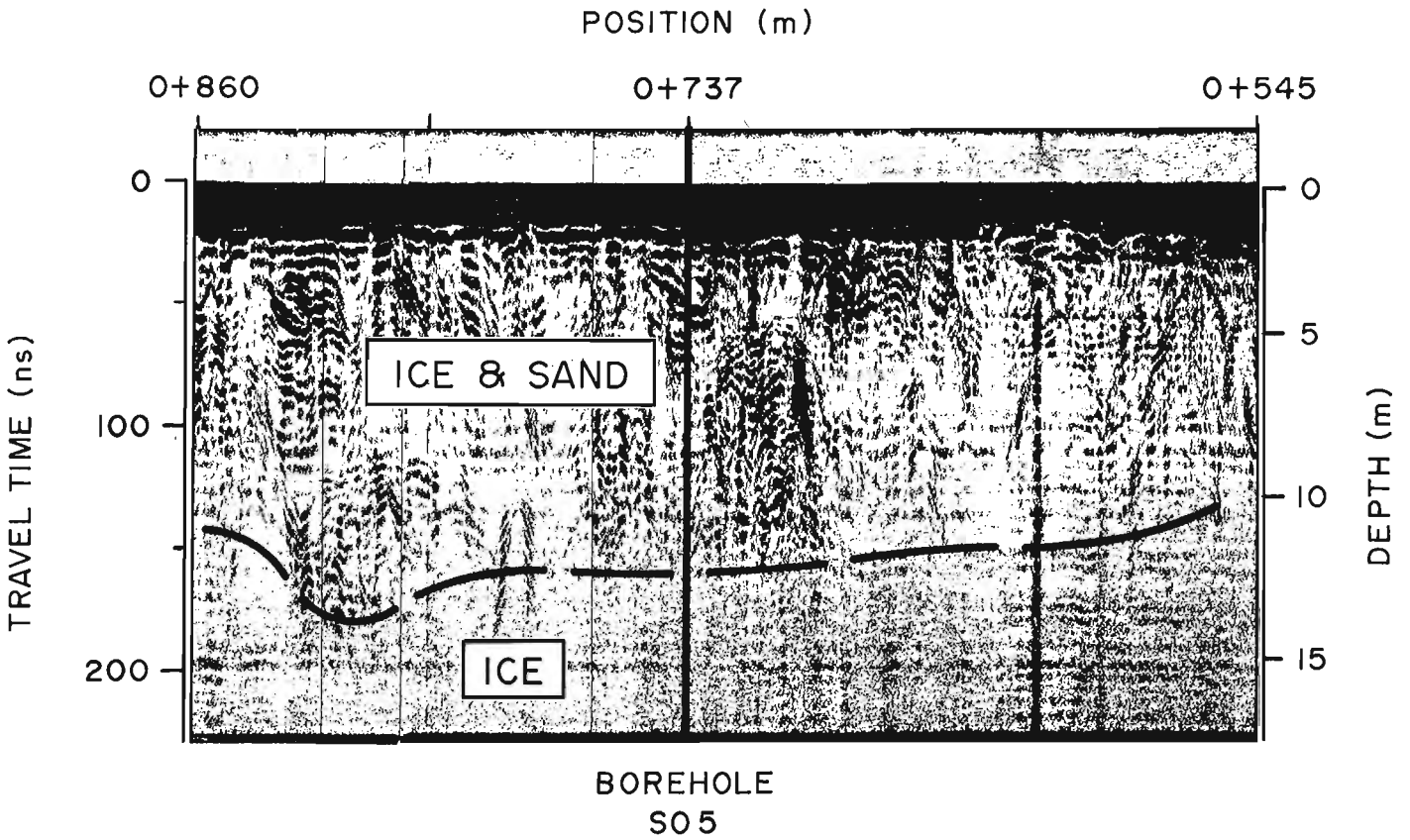


Figure 3. PulseEKKO I profile of a part of the Lousy Point survey line, showing stratified ice and sediment overlying massive ice.

reflector at 30 m depth running from 0 + 560 to 0 + 860 m is probably the lower contact between a massive ice body and underlying sands.

CONCLUSIONS

New generation ground probing radar instruments have been used successfully under harsh field conditions to map surficial materials and ground ice bodies at various sites on Richards Island and the Tuktoyaktuk Peninsula. The two instruments used were complementary for field operations. A continuous profiling, modified GSSI radar (pulseEKKO I0) was used to assess ground conditions rapidly near the surface and a prototype, low frequency, digital radar (pulseEKKO II) was used for deeper sounding. Preliminary correlation with subsurface data indicates that ground probing radar instruments used in the study can provide valuable subsurface information, delineating geological contacts between different surficial sediments and contacts between sediments and massive ground ice. Radar records can also provide an indication of the nature of stratification within a particular surficial material.

Further work is currently ongoing to correlate detailed borehole data, geotechnical information, and other geophysical information with the radar profiles. It is hoped that these studies will aid in determining the origin and morphology of the buried ice bodies found throughout central Richards Island and on Tuktoyaktuk Peninsula.

ACKNOWLEDGMENTS

Field work for this project would not have been possible without the assistance of the staff at Polar Continental Shelf Project base at Tuktoyaktuk. The authors also gratefully acknowledge the superior field assistance provided throughout the project by J.G. Bisson, F.M. Nixon, and S. Cosway.

The co-operation and logistical assistance provided by Indian and Northern Affairs and by the staff of EBA Engineering during the field drilling operations is also acknowledged.

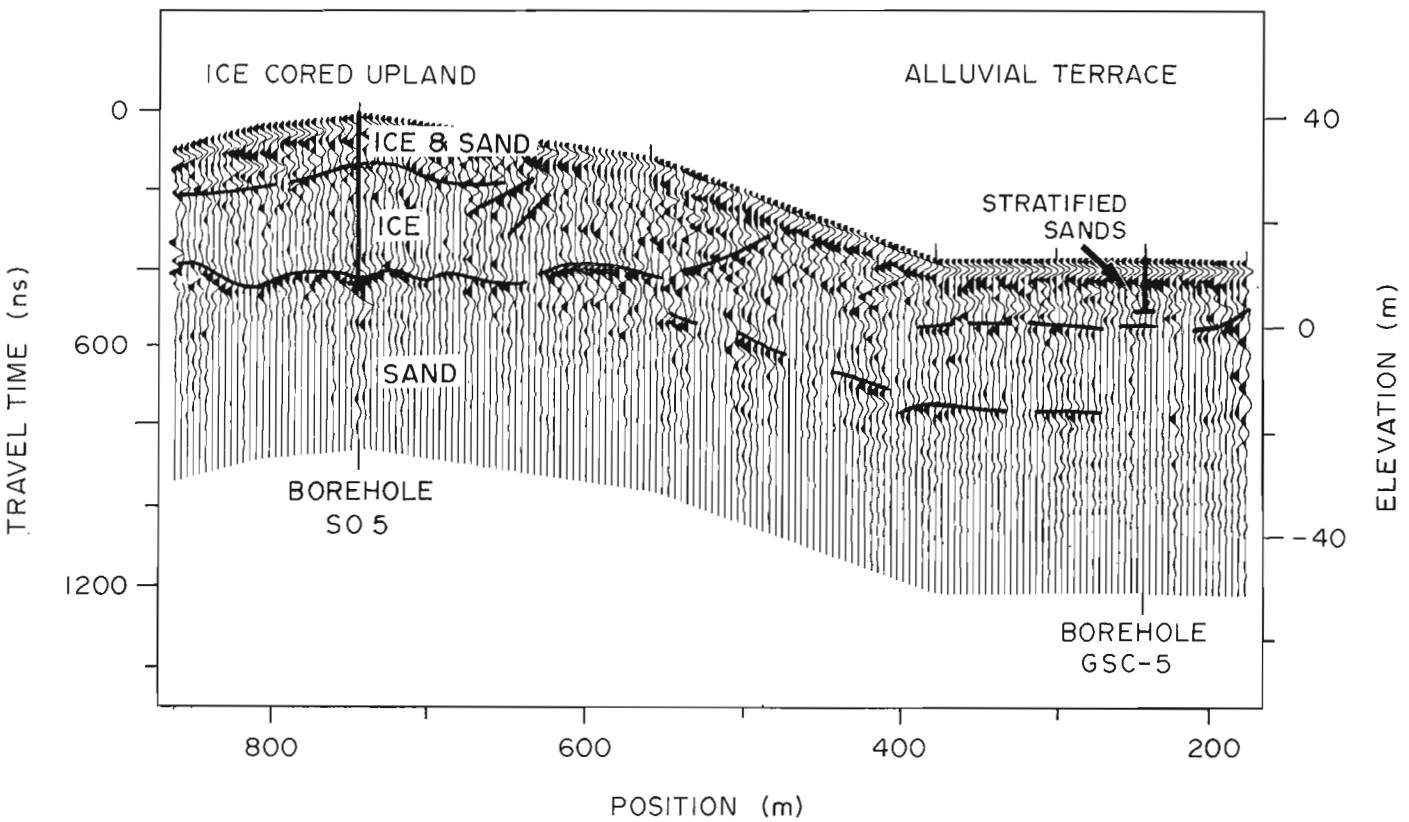


Figure 4. PulseEKKO II profile of Lousy Point line showing deeper reflections beneath ice-cored upland area.

REFERENCES

Annan, A.P. and Davis, J.L.
1976: Impulse radar sounding in permafrost; Radio Science, v. 11, no. 4, p. 383-394.

Davis, J.L., Scott, W.J., Morey, R.M., and Annan, A.P.
1976: Impulse radar experiments on permafrost near Tuktoyaktuk, Northwest Territories; Canadian Journal of Earth Sciences, v. 13, no. 11, p. 1584-1590.

Kurfurst, P.J. (compiler)
1986: Geotechnical investigations of the near-shore zone, North Head, Richards Island, N.W.T., Geological Survey of Canada, Open File 1376, 82 p.

Judge, A.S.
1986: Permafrost record and Quaternary history of the Mackenzie-Beaufort region: a geothermal perspective; in Correlation of Quaternary deposits and events around the margin of the Beaufort Sea; Geological Survey of Canada, Open File 1237, p. 41-46.

Rampton, V.N.
— Quaternary geology of the Tuktoyaktuk coastlands, Northwest Territories; Geological Survey of Canada, Memoir 423. (in press)

Rampton, V.N. and Walcott, S.
1974: Gravity profiles across ice-cored topography; Canadian Journal of Earth Sciences, v. 11, no. 1, p. 110-122.

Ripley, Klohn and Leonoff Int. Ltd.
1973: Granular materials inventory, Zone II: report to Department of Indian Affairs and Northern Development, Ottawa.

First documented large failure at the Fraser River delta front, British Columbia

Project 790006

G.T. McKenna[1] and J.L. Luternauer
Cordilleran and Pacific Margin Division, Vancouver

McKenna, G.T. and Luternauer, J.L., First documented large failure at the Fraser River delta front, British Columbia; in Current Research, Part A, Geological Survey of Canada, Paper 87-1A, p. 919-924, 1987.

Abstract

The first documented large failure at the delta front occurred at the mouth of the Main Channel of the Fraser River in July, 1985 and had a minimum volume of a million cubic metres. The failure scarp extended to within 100 metres of Sand Heads Lighthouse. The failure may have been triggered by rapid sediment loading at the end of the freshet combined with drawdown effects associated with large spring tides.

Résumé

La première grande rupture étudiée du front du delta qui s'est produite à l'embouchure du chenal principal du fleuve Fraser en juillet 1985 a déplacé un volume minimum d'un million de mètres cubes. L'escarpement causé par le glissement est arrivé à moins de 100 m du phare de Sand Heads. La rupture peut avoir été déclenchée par la charge rapide des sédiments à la fin de la crue, combinée aux effets d'abaissement de niveau associés aux grandes marées de printemps.

[1]Department of Geological Sciences (Geological Engineering), University of British Columbia, Vancouver, B.C. V6T 2B4

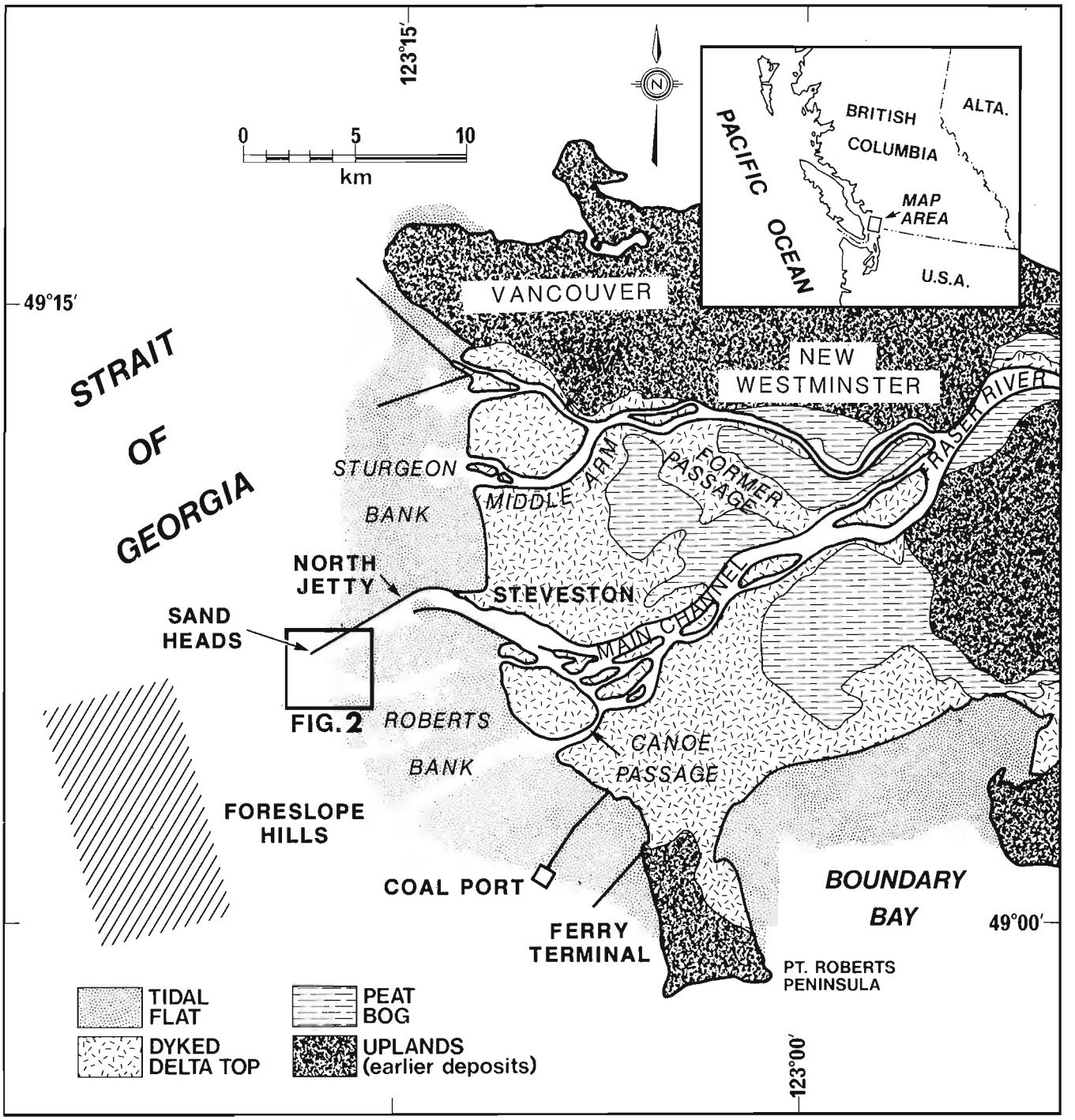


Figure 1. Index map.

INTRODUCTION

The Fraser River delta front (Fig. 1) is the site of numerous developments and much of the remainder of the delta surface is urbanized. Consequently, the stability of the delta has long been a concern (eg. Byrne, 1978; Luternauer and Finn, 1983). This paper presents the first documented evidence of a large failure on the delta front and explores some of the factors which may have triggered it.

GENERAL SETTING

The average thickness of the prograding delta has been estimated to be 120 m (Matthews and Shepard, 1962). Sandy tidal flats form most of the shelf between the shore face and the delta slope. The delta slope ranges from a maximum of approximately 23° (Scotton, 1977) to as little as 1-2° 2 km offshore (Matthews and Shepard, 1962). The effective angle of shearing resistance of the deltaic materials in about 35°

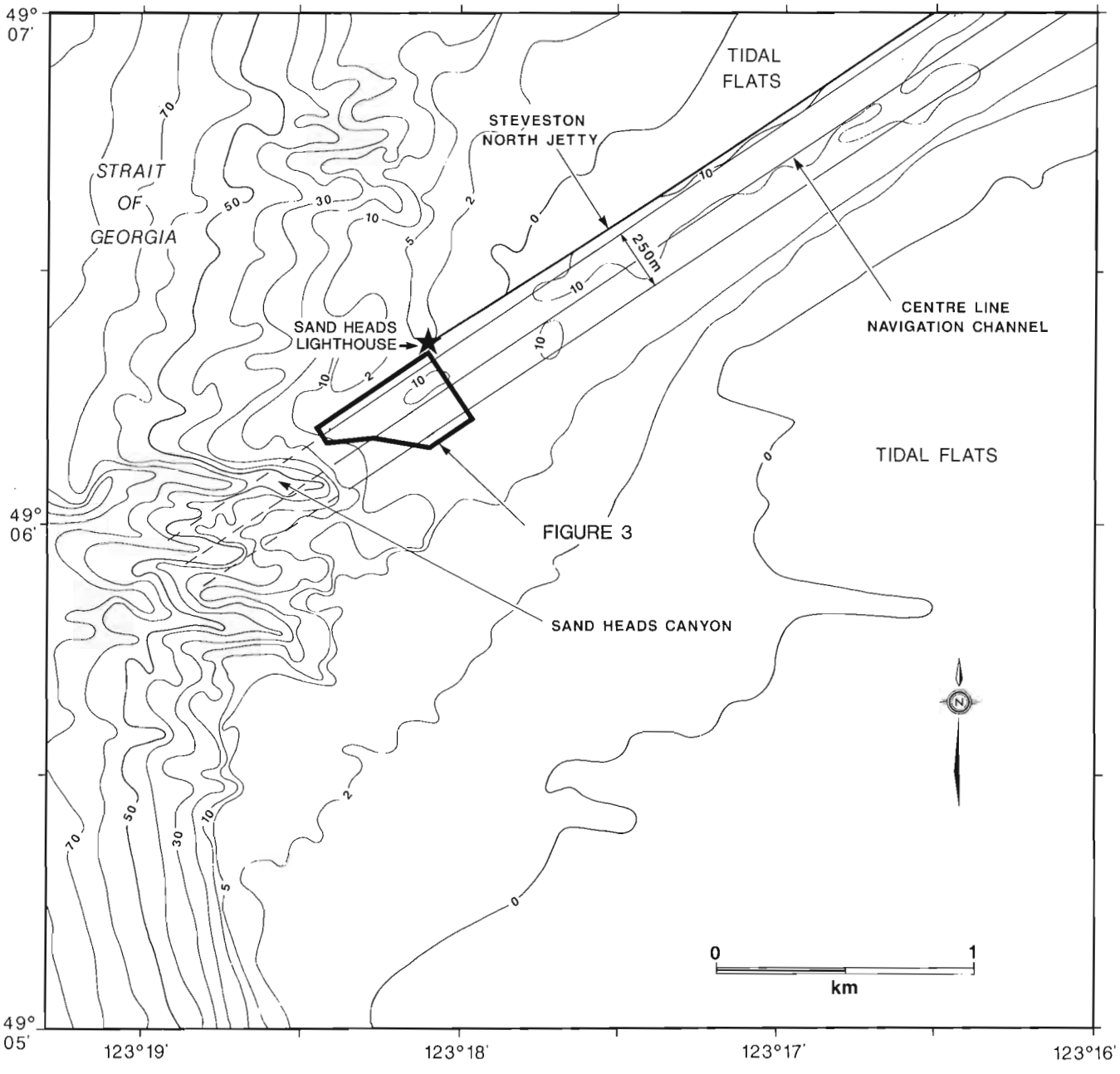


Figure 2. Morphology of the Fraser River delta foreslope off the Main Channel. Contours are in metres. Source: Canadian Hydrographic Service Chart 3490.

(Luternauer and Finn, 1983) suggesting that the slope of the delta front is controlled mainly by deposition rather than by erosion. Gullies and sand waves on the slope and an area of foreslope hills (approximately 10 km downslope from Sand Heads: *see* Fig. 1) are evidence of instability of the delta front (Luternauer and Finn, 1983; Hamilton and Luternauer, 1983).

Milliman (1980) reported that the mean annual discharge of the Fraser River is 2700 m^3/s of which 80% flows through the Main Channel. During the freshet (May to mid-July), flow averages greater than 4000 m^3/s and peaks between 5000 and 15 000 m^3/s. Approximately 80% of the 10-25 million tonnes of sediment discharged annually is carried during the freshet. Sand from Pleistocene glacial deposits, erosion of more indurated rocks, and bank erosion constitutes 50% of the annual sediment load. Training and deepening of the Main Channel by dredging (over 2 million tonnes/year) have increased the amount of sand carried in suspension by channellizing flow. Deposits on the Main Channel floor are mainly sand (Tywoniuk, 1972) and it is possible that the upper part of the sediment column affected by the failure described herein is similarly coarse grained.

Average wave height over the delta front is 0.6 m (Thompson, 1981). Hindcasting methods give a maximum significant wave height of only 2.7 m with a significant wave period of 8 s and a probable maximum wave height of 2.9 m. Tidal currents tend to follow bathymetric contours and are strong enough during spring tides (0.30 m/s) to carry sand-size material (Shepard and Milliman, 1978). The Strait of Georgia is an active tectonic region but no major earthquakes (i.e. greater than 5.0) have occurred in it since recording began (Rogers, 1982).

METHODS

Soundings of the mouth of the Fraser River at Sand Heads (Fig. 2) are performed by the Port and Waterways Engineering Survey Division of the Pacific Region of Public Works Canada to assist dredging activities. Surveys were carried out monthly between April and October, 1985. When major slope changes were noticed, the Geological Survey of Canada was informed by Public Works that a large submarine failure had probably occurred.

Soundings for 27 June and 11 July, 1985 (Public Works Canada, 1985a,b,c) were digitized and computer contoured (Fig. 3a,b). Differences in depth between these two surveys are presented (Fig. 3c) and a decrease in net volume of sediment was estimated by computing areas of various gridded profiles. Perspective views of the delta front off the Main Channel (Fig. 4) were prepared from additional soundings (Public Works Canada, 1978, 1985a,b,c) by W. Price at the Pacific Geoscience Centre on a CUBICOMP Model Maker 500 automated drafting system.

RESULTS

The net loss of sediment in the area outlined in Figure 3 is approximately a million cubic metres. The surveyed area of the failure scarp (Fig. 3b) shows the minimum aerial extent of the failure to be approximately 500 m long × 280 m wide with a maximum thickness of at least 28 m (Fig. 3b).

The head scarp of the failure (Fig. 3b) shows two small gullies on either side of a central region that has a fairly constant slope of 7-8° dipping approximately south. Maximum slope angle within the gullies is greater than 18°. The

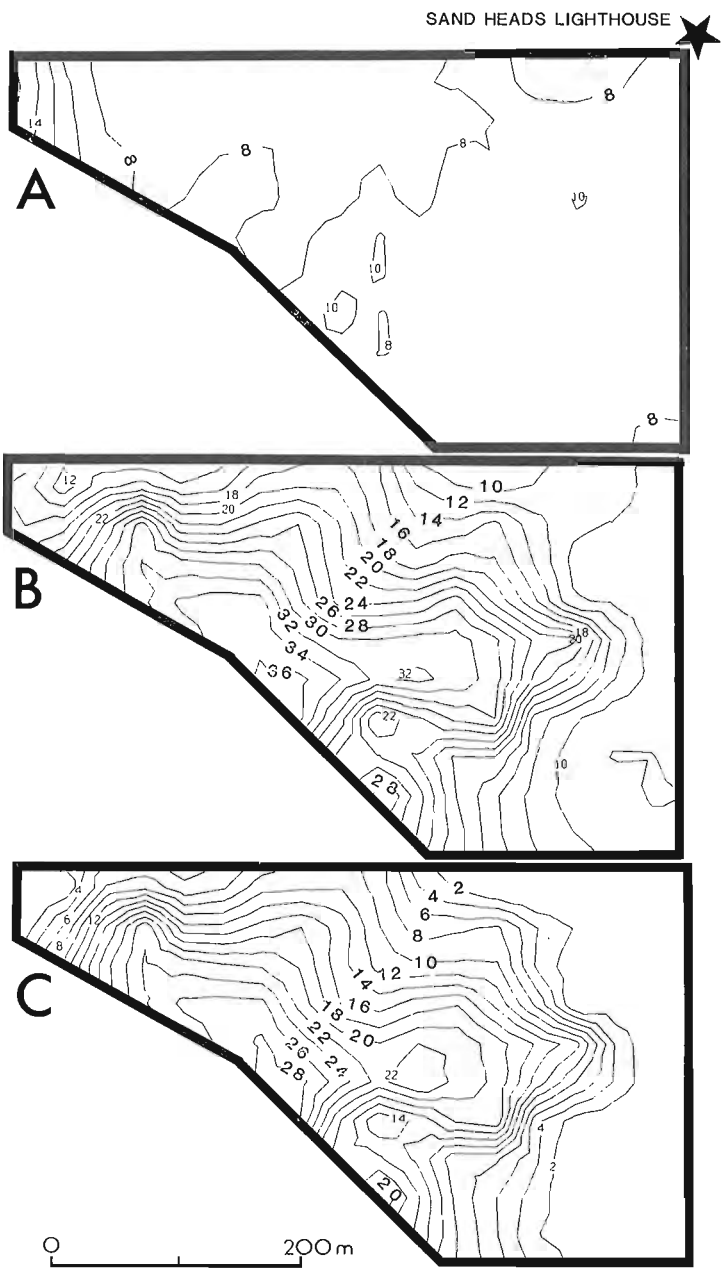


Figure 3. Soundings at the mouth of the Main Channel (2 m contours).
a. 27 June 1985 – before failure (410 sounding points contoured).
b. 11 July 1985 – after failure (78 sounding points contoured).
c. Net increase in depth between surveys.

shoreward extent of the head scarp lies within 100 m of the end of the Steveston North Jetty and Sand Heads Lighthouse. Comparison of the delta front surface in 1978 and 1985 (Fig. 4) offer graphic evidence of the greater instability of the area off the Main Channel as compared to adjacent parts of the slope.

DISCUSSION

Four categories of error that have to be considered in determining the volume and extent of the failure are: survey position, bathymetry, postfailure depositional and erosional changes between surveys, and limited aerial extent of survey. Errors in position and bathymetry are usually small and random and will tend to cancel each other out (U.S. Army Corps of Engineers, 1984). Since the failure occurred during the freshet, the scar was likely draped with some sediment before the second survey. This deposition would cause the true volume of the failure to be underestimated. The complex interaction of tidal and river processes makes the amount of deposition and erosion difficult to estimate but is likely insignificant compared to other uncertainties. The failure scar most likely continues downslope from the westward limit of the 11 July survey. If the failure is 280 m wide and the failure surface is 28 m below the seafloor and extends an additional 300 m past the limits of the survey, the estimate of the volume of the failure increases approximately 3-fold. This estimate, however, does not represent an upper limit.

If one looks at potential energy of the failure and uses the minimum estimate of a million cubic metres of sediment at 9 kN/m^3 and estimates that the sediment moved downslope an average of 100 m vertically, this represents a change in otential energy of 9×10^{11} Joules. If this energy release were to occur over a very short period of time it would likely cause a local tsunami. However, if the failure were to occur as a slow retrogressive grain flow over a period of hours then no measureable wave disturbance would occur. Hamilton (in press) reported that tide gauges at Point Atkinson and Steveston did not register the failure at Sand Heads.

Factors that may have triggered the failure include seismic activity, cyclic wave loading (Luternauer and Finn, 1983), rapid sediment loading, and/or drawdowns associated with large tidal ranges. Hamilton (in press) reported that there were "no local earthquakes of any consequence" in Georgia Strait during the first two weeks of July, 1985. Rapid sediment loading at the mouth occurs during the freshet and is caused by the retardation of flow of the channellized, sediment-laden river particularly where it comes in contact with the salt wedge (Kostaschuk and Luternauer, 1986). Spring tides greater than 4 m during the freshet result in large drawdowns further decreasing the stability of the sediments. These last two factors together probably initiated movement. It is possible that most severe loading occurs during less intense freshets as sand is more likely to be dumped at the mouth and not be jetted out into the Strait.

In order to understand the stability of the Fraser River delta front, more frequent, extensive and precise monitoring of the bathymetry of its slopes is necessary. Detailed surveys in areas of instability such as Sandheads Canyon would allow detection of smaller failures and documentation of larger failures. Since these failures are probably cyclical, better monitoring would also allow prediction of return period of

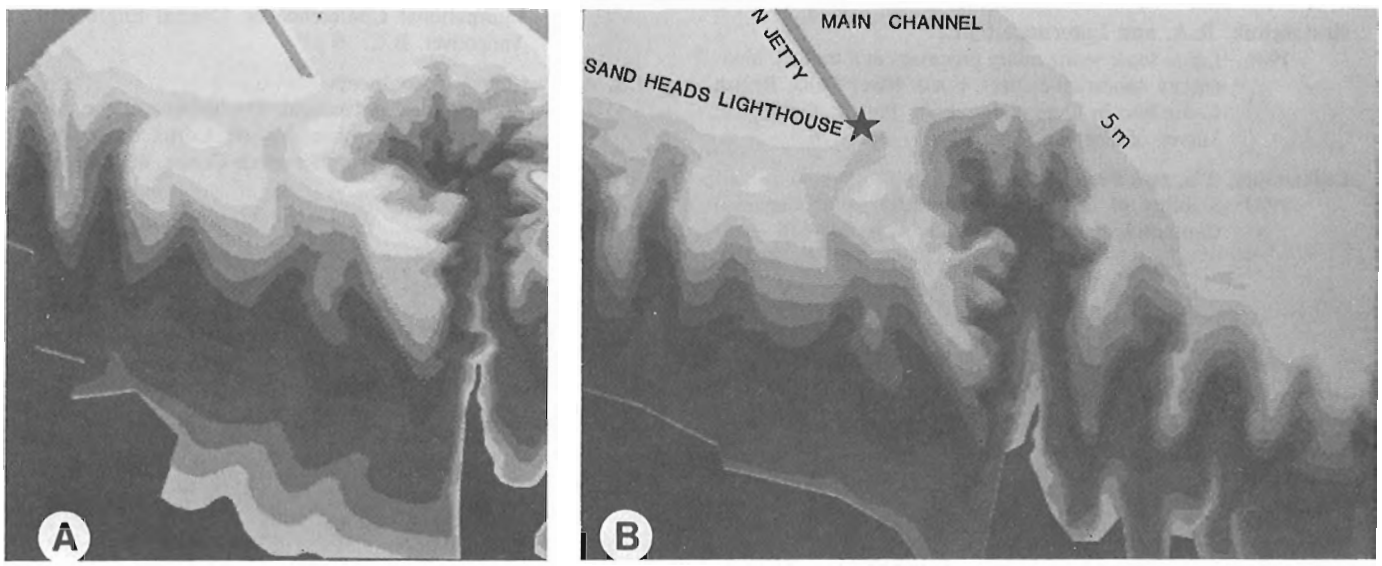


Figure 4. Computer generated oblique views of the slope off the Main Channel of the Fraser River delta. Five-metre shading contour.
a. May 1978. b. September 1985.

various sizes of failures. Often much larger failures are triggered by smaller initial failures due to the rapid unloading of the toe of a potential failure surface. Seemingly minor mass wasting on the delta front could lead to more catastrophic failures.

CONCLUSIONS

A large failure with a minimum volume of 1 million cubic metres occurred in 1985 between 27 June and 11 July, off the mouth of the Main Channel of the Fraser River. The failure scarp extended to within 100 m of Sand Heads Lighthouse. We suggest that sediment loading and tidal drawdown probably were the primary causes of the failure.

ACKNOWLEDGMENTS

We thank H. Wu, W. Williams and R. Richardson of the Pacific Region of Public works Canada for kindly making available the data upon which this report was based.

REFERENCES

Byrne, P.M.
1978: An evaluation of the liquefaction potential of the Fraser delta; Canadian Geotechnical Journal, v. 15, p. 32-46.

Hamilton, T.S.
– The foreslope hills of the Fraser delta: implication for tsunamis in Georgia Strait; Tsunami Journal. (in press)

Hamilton, T.S. and Luternauer, J.L.
1983: Evidence of seafloor instability in the south-central Strait of Georgia, B.C.: a preliminary compilation; in Current Research, Part A, Geological Survey of Canada, Paper 83-1A, p. 417-421.

Kostaschuk, R.A. and Luternauer, J.L.
1986: Large-scale sedimentary processes in a trained, high-energy, sand-rich estuary: Fraser River Delta, British Columbia; in Current Research, Part A, Geological Survey of Canada, Paper 87-1A, report 76.

Luternauer, J.L. and Finn, W.D.L.
1983: Stability of the Fraser River delta front; Canadian Geotechnical Journal v. 20, no. 4, p. 606-616.

Matthews, W.H. and Shepard, F.P.
1962: Sedimentation of Fraser River delta, British Columbia; American Association of Petroleum Geology, Bulletin 46, p. 1416-1438.

Milliman, J.D.
1980: Sedimentation in the Fraser River and its estuary, southwestern British Columbia (Canada); Estuarine and Coastal Marine Science, v. 10, p. 609-633.

Public Works Canada
1978: Chart soundings – Fraser River, FR3-51 – May.
1985a: Chart soundings – Fraser River, FR3-103 – June 27.
1985b: Chart soundings – Fraser River, FR3-105 – July 11.
1985c: Chart soundings – Fraser River, FR3-107 – Sept..

Rogers, G.C.
1982: Some comments on the seismicity of the northern Puget Sound-southern Vancouver Island region; in Earthquake Hazards of the Puget Sound Region Washington State, J.C. Yount (ed.), U.S. Geological Survey, Open File Report, 21 p.

Scotton, S.
1977: The outer banks of the Fraser River delta: engineering properties and stability considerations; unpublished M.A.Sc. Thesis, Department of Civil Engineering, University of British Columbia, Vancouver.

Shepard, F.P. and Milliman, J.D.
1978: Sea-floor currents on the foreset slope of the Fraser River delta, British Columbia (Canada); Marine eology, v. 28, p. 245-251.

Thompson, R.E.
1981: Oceanography of the British Columbia coast; Canadian Special Publication of Fisheries and Aquatic Sciences 56, 291 p.

Tywoniuk, N.
1972: Sediment budget of the lower Fraser River (estuary); Water Survey of Canada, Paper presented at 13th International Conference on Coastal Engineering, Vancouver, B.C., 6 p.

U.S. Army Corps of Engineers
1984: Shore protection manual; Department of the Army Waterways Experiment Station, Corps. of Engineers Coastal Engineering Research Centre, 4th ed., v. 1.

Significance of Lower Jurassic hydrocarbon source rocks in the Cumshewa Inlet area, Queen Charlotte Islands, British Columbia

Project 690075

B.E.B. Cameron
Cordilleran and Pacific Margin Division, Sidney, B.C.

Cameron, B.E.B., Significance of Lower Jurassic hydrocarbon source rocks in the Cumshewa Inlet area, Queen Charlotte Islands, British Columbia; in Current Research, Part A, Geological Survey of Canada, Paper 87-1A, p. 925-928, 1987.

Abstract

Newly discovered exposures of bituminous Lower Jurassic rocks in the Cumshewa Inlet suggest a regional continuation of these hydrocarbon source beds into the Hecate Strait area. The identification of these rocks as part of the Wrangellian tectono-stratigraphic terrane further suggests that the boundary between Wrangellia and Alexander terrane be placed much farther east in Hecate Strait than previously supposed. Much of Hecate Strait therefore can be considered as a potential oil province.

Résumé

Les affleurements nouvellement découverts de roches bitumineuses du Jurassique inférieur, dans la zone de l'inlet Cumshewa, suggèrent que ces lits qui constituent une source d'hydrocarbures, ont un prolongement régional dans la zone du détroit d'Hecate. Le fait que l'on ait identifié ces roches comme appartenant au terrane tectono-stratigraphique de Wrangellia, suggère que la limite entre le terrane de Wrangellia et celui d'Alexander pourrait être placée beaucoup plus à l'est dans le détroit d'Hecate qu'on ne l'avait supposé auparavant. Par conséquent, on peut considérer une grande partie du détroit d'Hecate comme une province pétrolifère potentielle.

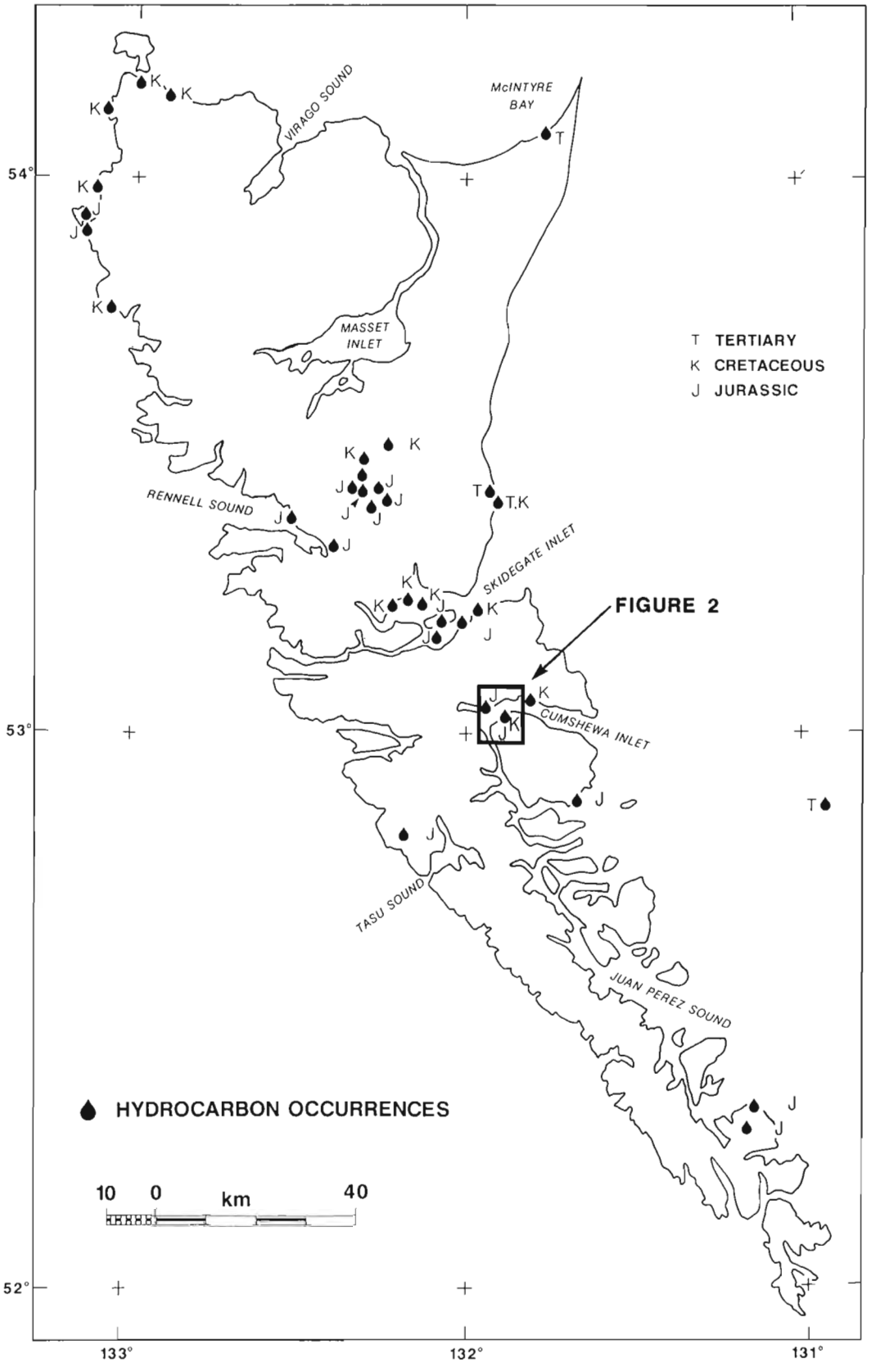


Figure 1. Distribution of hydrocarbon shows, Queen Charlotte Islands.

INTRODUCTION

During the field seasons of 1985 and 1986 significant new exposures of Lower Jurassic rocks were discovered in the Cumshewa Inlet area of the Queen Charlotte Islands. These rocks were previously mapped as Lower Cretaceous Longarm Formation (Sutherland Brown, 1968). Extensive collections of microfossils and ammonoids in addition to distinctive lithologies place them in the Lower Jurassic, Whiteaves, Fannin, Rennell Junction and Ghost Creek formations of the Maude Group. As outlined previously (Cameron and Tipper, 1981, 1985), most of these stratigraphic units are fetid and/or have bitumen or dead oil within them in other areas of the Queen Charlotte Islands. Parts of the Lower Jurassic in the Cumshewa Inlet area, especially the Ghost Creek Formation, are bituminous and fetid as well.

CUMSHEWA INLET AREA

On the north shore of Cumshewa Inlet, west of Dawson Cove (Fig. 2), Mesozoic rocks are represented by a series of fault-bounded slices of Triassic, Jurassic and Cretaceous age. Although exposures are discontinuous, a few observations can be made. In area A a Lower Jurassic section of the Maude Group consisting of 209 m of shale, sandstone and limestone was measured. The lower 72 m of this section are bituminous dark grey shale with minor sandstone and siltstone. The section is in fault contact with sandstone of the Cretaceous Haida Formation to the east and also in fault contact with intruded and highly folded limestone and shale of the Kunga Group to the west. Discontinuous and presumably fault-bounded slices of the Maude Group are exposed farther west on Gillatt Arm (area C), along with fragmentary exposures of the Kunga Group, Lower Cretaceous Longarm Formation and rocks of the Cretaceous Queen Charlotte Group. The Longarm Formation, previously mapped as occupying this whole area, is relatively poorly represented. One exposure of sandstones (area B, Fig. 2) probably assignable to the Longarm, rests with pronounced angular unconformity on rocks of the Kunga Group.

Further exposures of the Maude Group have been noted on the south shore of the Cumshewa Inlet, on the northwest

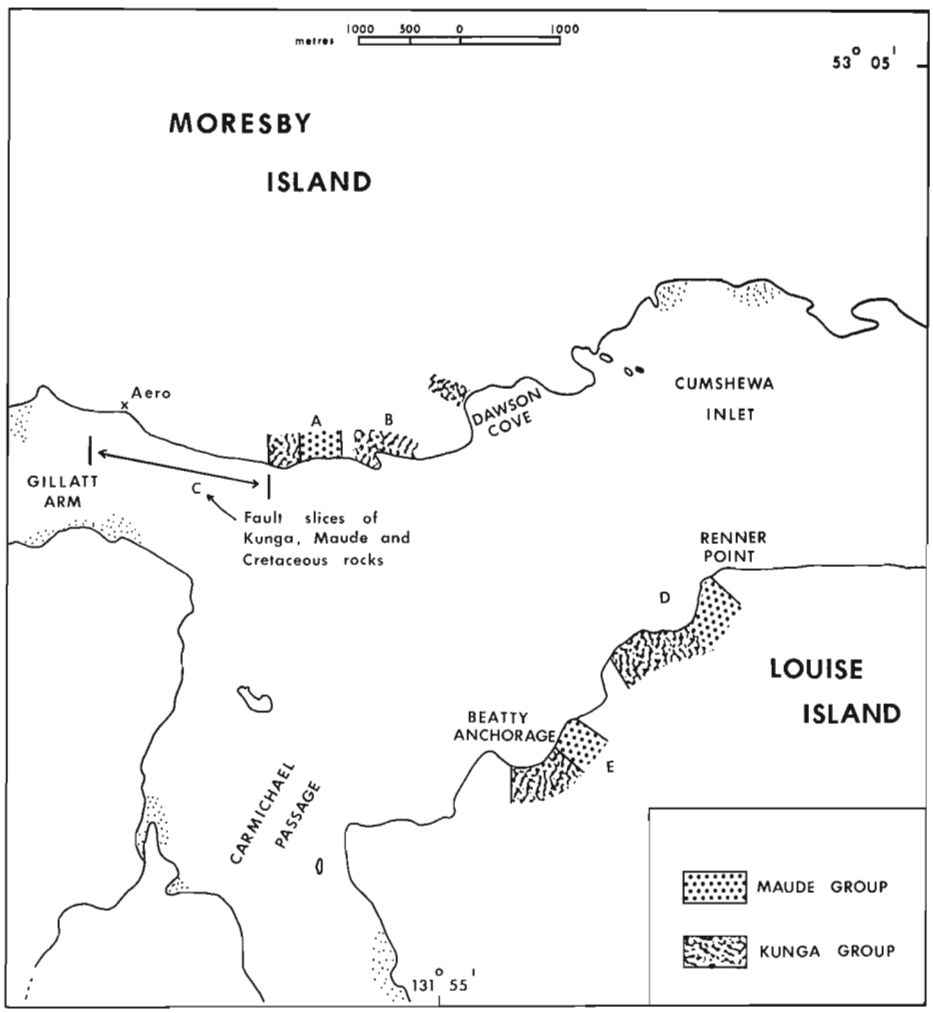


Figure 2. Jurassic outcrops, Cumshewa Inlet area.

shore of Louise Island where they were previously mapped as part of the ongarm Formation and part of the Kunga Group (Sutherland Brown, 1968). A section of the Maude Group (area D, Fig. 2), measured and described by H.W. Tipper (GSC) and P.L. Smith (UBC), consists of 131 m of limestone, sandstone, siltstone and shale assignable to the Fannin, Rennell Junction and Ghost Creek formations (personal communication, 1986). The basal 51 m of this section are composed of dark grey fetid siltstone and is underlain by rocks of the Kunga Group. Fault-bounded slices of the Maude Group are also present farther southwest, near Beatty anchorage (area E, Fig. 2).

REGIONAL DISTRIBUTION AND TECTONIC SIGNIFICANCE

As previously stated, oil stain and bitumen are common in rocks of the Lower Jurassic Sandilands and Ghost Creek formations. The regional distribution of known hydrocarbon shows is summarized in Figure 1. Also included in this diagram are areas from which Cretaceous rocks of the Queen Charlotte Group have shown oil stain or bitumen. Unlike the Lower Jurassic, however, shale and siltstone of the Queen Charlotte Group are, for the most part, not especially fetid or bituminous. It is suggested, therefore, that these Cretaceous shows are mainly attributable to escape oils from the Jurassic. Heavy oils and bitumen are also known from many outcrops of the Tertiary Masset volcanics (T.S. Hamilton, personal communication, 1986). Again, these shows are probably of Jurassic hydrocarbons.

The regional trend (Fig. 1) of hydrocarbon shows indicates an arcuate distribution from the northwest corner of the Queen Charlotte Islands to the southeast through Skidegate Inlet. The new discoveries in Cumshewa Inlet continue this trend to the southeast and imply continuation in this direction in subsurface through at least part of Hecate Strait. This trend would include the Shell Anglo Sockeye B-10 well (Fig. 3). The oil stain in the upper Tertiary rocks encountered in this well has been attributed to Jurassic escape oil (see Cameron and Tipper, 1985, p. 45). If it can be assumed that oil stain or bitumen observed in rocks of the Cretaceous and Tertiary are a reflection of Jurassic source beds in the subsurface, then perhaps the oil shows at Lawn Hill and in the surface of the Richfield et al. Tow Hill well (Fig. 3) give us a further indication of the subsurface distribution of these Jurassic rocks of the Kunga and Maude groups.

Jurassic rocks of the Kunga and Maude groups have been identified elsewhere (Yorath and Cameron, 1982) as an important part of the Wrangellian accretionary terrane. The tectono-stratigraphic boundary of this terrane and the adjacent Alexander terrane (Fig. 3) has been placed along the Sandspit fault system through the Queen Charlotte Islands and across southern Hecate Strait (Yorath and Chase, 1981). This boundary has been assumed to differentiate not only differing rock sequences but also which areas in Hecate Strait may be considered as gas prone (Alexander terrane to the north) or oil prone (Wrangellia to the south). If oil shows in the Tow Hill well (Fig. 3) and at Lawn Hill are truly reflective of Jurassic ydrocarbon source beds in subsurface, then they must also identify rocks of the Wrangellian terrane. In this case the boundary between these two tectono-stratigraphic terranes must be positioned much farther east, possibly towards the eastern side of Hecate Strait. In effect, this raises the possibility that a substantial part of northern Hecate Strait may in fact be oil prone, and not merely gas prone as previously supposed.

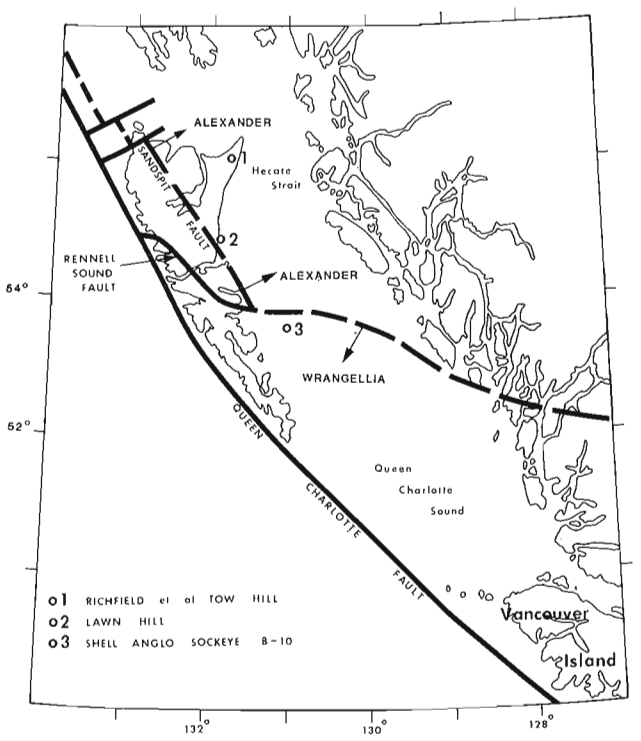


Figure 3. Suggested tectono-stratigraphic boundary between Alexander and Wrangellia (after Yorath and Chase, 1981).

REFERENCES

Cameron, B.E.B. and Tipper, H.W.

1981: Jurassic biostratigraphy, stratigraphy and related hydrocarbon occurrences of Queen Charlotte Islands, British Columbia; in Current Research, Part A, Geological Survey of Canada, Paper 81-1A, p. 209-212.

1985: Jurassic stratigraphy of the Queen Charlotte Islands, British Columbia; Geological Survey of Canada, Bulletin 365, 49 p.

Sutherland Brown, A.

1968: Geology of the Queen Charlotte Islands, British Columbia; British Columbia Department of Mines and Petroleum Resources, Bulletin 54.

Yorath, C.J. and Cameron, B.E.B.

1982: Oil off the west coast?; Department of Energy, Mines and Resources, GEOS, 11, p. 13-15.

Yorath, C.J. and Chase, R.L.

1981: Tectonic history of the Queen Charlotte Islands and adjacent areas – a model; Canadian Journal of Earth Sciences, v. 18, p. 1717-1739.

A rock avalanche from the peak of Mount Meager, British Columbia

Project 830016

S.G. Evans
Terrain Sciences Division

Evans, S.G., A rock avalanche from the peak of Mount Meager, British Columbia; in Current Research, Part A, Geological Survey of Canada, Paper 87-1A, p. 929-934, 1987.

Abstract

In March or April 1986 a rock avalanche occurred on the north peak of Mount Meager within the Mount Meager volcanic complex in the Coast Mountains of British Columbia. The detached rock mass of Pleistocene rhyodacite had an estimated volume of 0.5 $\times$ 10^6 m^3. The rock avalanche travelled over a glacier surface in the upper part of its track. Some of the debris reached Lillooet River, nearly 2000 m below the upper part of the detachment zone, and temporarily blocked it. The landslide is one of seventeen rock avalanches known to have occurred in the Cordillera since 1855.

Résumé

En mars ou en avril 1986, une avalanche de pierres s'est produite sur le sommet nord du mont Meager (2645 m), à l'intérieur du complexe volcanique du mont Meager, dans la chaîne Côtière de la Colombie-Britannique. La masse rocheuse détachée, constituée de rhyodacite du Pléistocène, avait un volume estimé de 0,5 $\times$ 10^6 m^3. L'avalanche de pierres a traversé une surface glaciaire dans la partie supérieure de son couloir. Des débris ont atteint la rivière Lillooet, située presque 2000 m sous la partie supérieure de la zone de décollement, et l'a bloquée temporairement. Le glissement de terrain représente une des dix-sept avalanches de pierres qui se sont produites dans la Cordillère depuis 1855.

INTRODUCTION

Mount Meager (50°37′53″N,123°30′13″W) is located within the Mount Meager volcanic complex in the Coast Mountains, about 160 km north of Vancouver, British Columbia (Fig. 1). The complex lies at the north end of the Garibaldi Volcanic Belt and consists for the most part of Pleistocene volcanic rocks which have been mapped in detail by Read (1978).

Several pre-historic rock avalanche deposits have been mapped on the northeastern flank of the complex (Read, 1978). Three rock avalanches are known to have occurred within the Mount Meager complex since 1931 (Patton, 1976) and numerous other rock avalanche deposits of unknown age are currently being studied. All these rock slope movements have involved Quaternary volcanic rocks.

In March or April 1986 part of the northern peak of Mount Meager (2645 m) collapsed (E. Talbot, personal communication, 1986) and the disintegrating rock mass travelled downslope as a rock avalanche, covering part of the glacier beneath (Fig. 20.2). This report is a preliminary description of the landslide based upon aerial reconnaissance observations made in August 1986 during a detailed study of landslides in the Garibaldi Volcanic Belt.

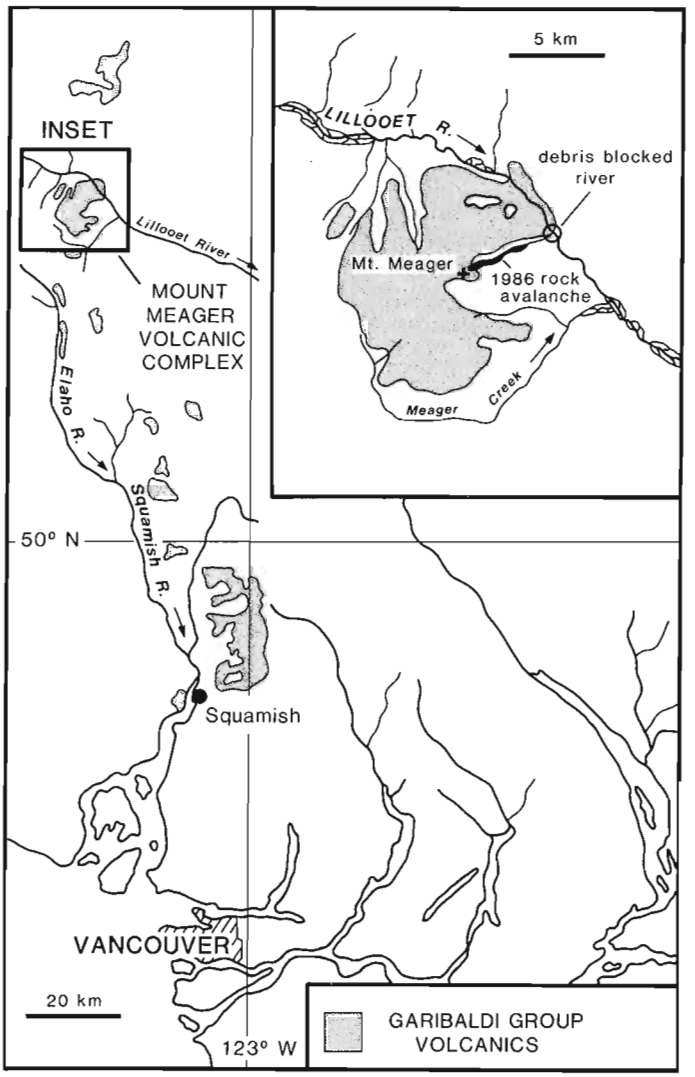


Figure 1. Position of Mount Meager Volcanic Complex in Garibaldi Volcanic Belt (geology after Tipper et al., 1981). Inset shows location of 1986 Mount Meager rock avalanche (geology after Woodsworth, 1977).



Figure 2. Oblique view of Mount Meager (2645 m), the detachment zone and the path of the 1986 rock avalanche. The height of the slope between the base of the detachment zone and the summit of Mount Meager is approximately 550 m. The slope consists of Pleistocene rhyodacite. Note the discontinuous cover of debris on the glacier, the bifurcation in the debris stream, and the ridges in the debris parallel to the direction of movement. 4-6-86

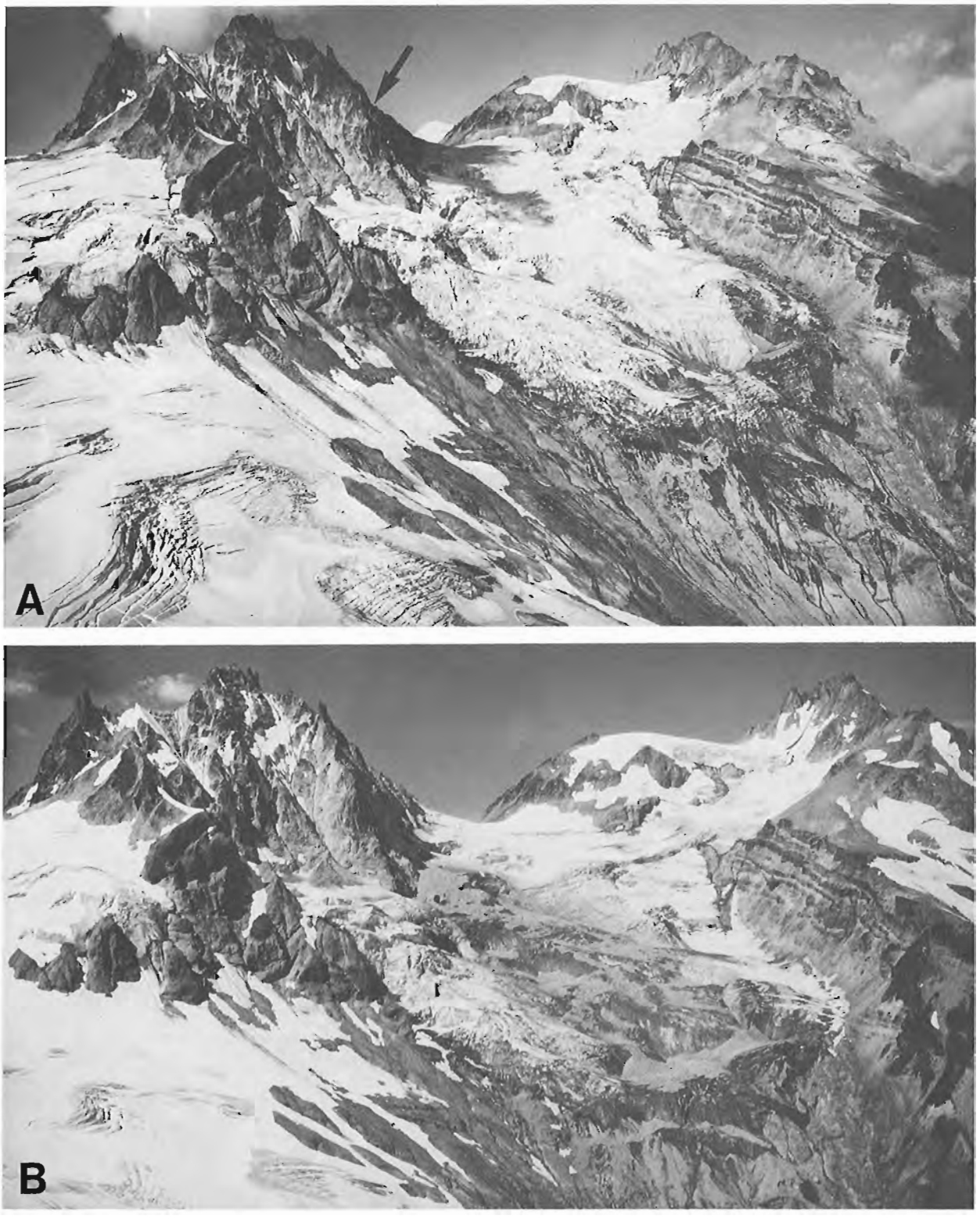


Figure 3. Comparative photographs taken before and after the rock avalanche showing the upper part of its track. Mount Meager (2645 m) is at left and Plinth Peak (2679 m) is at right. A, dating from August 1985, shows tension cracks in 1986 detachment zone (arrow). B, dating from August 1986, shows the detachment zone and debris on the surface of the glacier. 204246-X, 204247



Figure 4. View to west of steeply dipping flow layering in rhyodacite in vicinity of detachment zone. Note that the layering dips steeper than the slope. Contorted layering and closely jointed rock near the base of the slope (arrow) may have provided zone of weakness through which basal rupture took place. A is the upper part of the debris on the glacier surface. 204449-I

GEOLOGY AND MECHANICS OF DETACHMENT

The rock mass involved in the landslide became detached from between the 2100 and 2400 m[1] levels on Mount Meager which Read (1978) suggested is a dissected volcanic plug or lava dome. Comparison of Figure 3A, taken in August 1985 and Figure 3B, taken in August 1986, indicates the position of the detachment zone on the north face of Mount Meager. An estimate of the volume of the detached rock mass is difficult to make but it is probably in the order of 0.5-1.0 $\times$ $10^6 m^3$.

The peak of Mount Meager consists of grey rhyodacite of the Pleistocene Plinth Assemblage (Read, 1978). From the air, the structure of the rock mass in the vicinity of the detachment zone appears to be dominated by steeply dipping planar discontinuities which dip steeper than the slope face (Fig. 4). These were noted by Read (1978) who interpreted them to be steeply inclined flow layering. The detachment surface consists of a steep back surface, which is associated with the steeply dipping discontinuities noted above, and an irregular basal surface. Near the base of the slope the layering is contorted and the rhyodacite is heavily jointed (Fig. 4). These characteristics may have provided a weaker zone through which basal rupture took place either along an irregular surface defined by the discontinuities or through intact rock.

DEBRIS TRANSPORT AND DEPOSITION

Following detachment, the fragmenting rock mass hit the glacier surface and flowed downslope (Fig. 2). The initial 860 m of its travel between elevations 2130 m and 1780 m was on a highly crevassed glacier surface with an average slope of 25°. Much of the debris was deposited in this part of the track. On the glacier, the deposit averages approximately 400 m in width but is discontinuous in extent. Marked longitudinal flow lines are evident in the debris (Fig. 2). The thinning debris then split into two flows before joining up again and coming to rest in the creek channel between 1780 m and 1060 m. The angle between the end of the debris at 1060 m and the top of the detachment zone is 20°. Some debris travelled farther down the creek, below elevation 1060 m to Lilloet River (457 m), which is approximately 25 m wide at this location, and temporarily blocked it. It is unknown whether this latter phase of the movement was primary deposition from the rock avalanche itself or whether it involved secondary mobilization of the debris following cessation of initial movement.

FUTURE ROCK AVALANCHES FROM MOUNT MEAGER

Tension cracks were noted upslope from the detachment zone in the ridge that protrudes from the peak of Mount Meager (Fig. 4). An estimated 10 $\times$ $10^6 m^3$ could be involved in some future rock avalanche from the north slope of the peak of Mount Meager (Fig. 2) which would probably reach Lillooet River. In doing so it would dam Lillooet River and create the possibility of a dam break flood (Evans, 1986). Future rock avalanches from Mount Meager are therefore a ground failure hazard of considerable importance in the resource development of Lillooet River valley.

SIGNIFICANCE

According to unpublished project data, the 1986 Mount Meager rock avalanche is of considerable significance since it is:

(a) the fourth rock avalanche involving Quaternary volcanic rocks known to have occurred in the Mount Meager volcanic complex since 1931;
(b) the sixth rock avalanche involving Quaternary volcanic rocks known to have occurred in the Garibaldi Volcanic Belt since 1855;
(c) one of four rock avalanches to have occurred on slopes marginal to existing glaciers in the Coast Mountains since 1958;
(d) one of seventeen rock avalanches known to have occurred in the Canadian Cordillera since 1855.

It is also illustrative of rock slope movements in Quaternary Volcanic Centres which, as Evans (1984) note, is the most landslide prone geological environment in the southern Canadian Cordillera.

REFERENCES

Evans, S.G.
1984: The landslide response of tectonic assemblages in the southern Canadian Cordillera; Proceedings, IV International Symposium on Landslides, v. 1, p. 495-502.
1986: Landslide damming in the Cordillera of Western Canada; in Landslide Dams: Processes, Risk and Mitigation, R.L. Schuster (ed.), Geotechnical Special Publication No. 3, American Society of Civil Engineers, p. 111-130.

Patton, F.D.
1976: The Devastation Glacier Slide, Pemberton, B.C; Geological Association of Canada, Cordilleran Section, Program and Abstracts, p. 26-27.

Read, P.B.
1978: Geology, Meager Creek geothermal area; Geological Survey of Canada, Open File 603.

Tipper, H.W., Woodsworth, G.J., and Gabrielse, H.
1981: Tectonic assemblages map of the Canadian Cordillera and adjacent parts of the United States of America; Geological Survey of Canada, Map 1505A.

Woodsworth, G.J.
1977: Geology, Pemberton (92 J) map-area; Geological Survey of Canada, Open File 482.

[1]All elevations are considered approximate and estimated from the topographic base of Read's (1978) map.

Helicopter-borne aeromagnetic gradiometer surveys: a progress report[1]

Peter Hood and D.J. Teskey
Geophysics Division

Hood, P. and Teskey, D.J., Helicopter-borne aeromagnetic gradiometer surveys: a progress report, in Current Research, Part A, Geological Survey of Canada, Paper 87-1A, p. 935-938, 1987.

Abstract

For the past three years the GSC has been fostering the development of helicopter-borne aeromagnetic gradiometer survey systems through R and D and survey contracts to the Canadian airborne geophysical survey industry. A number of helicopter-borne aeromagnetic gradiometer systems have now been built by various Canadian airborne geophysical contractors. Most of these have now been field tested by surveys in the Gaspésie Peninsula of southeastern Quebec and in New Brunswick, Nova Scotia and Newfoundland with encouraging results.

Résumé

Au cours des trois dernières années la CGC a été amenée à la mise au point de systèmes de levés à gradiomètre aéromagnétique héliportés au moyen de contrats pour la recherche, le développement et les levés à l'industrie canadienne de levés géophysiques aéroportés. Un certain nombre de systèmes à gradiomètre aéromagnétique héliporté sont maintenant construits par des contracteurs canadiens spécialistes d'appareils géophysiques aéroportés. La plupart de ces systèmes ont été éprouvés lors de levés effectués en Gaspésie au sud-est du Québec, au Nouveau-Brunswick, en Nouvelle-Écosse et à Terre-Neuve; les résultats sont encourageants.

[1]Presented at the 56th Annual Meeting, SEG, Houston, 2-6 Nov., 1986.

INTRODUCTION

A national program of aeromagnetic surveying was commenced by the Geological Survey of Canada in 1947 and about 65% of Canada has now been covered. This coverage was obtained using essentially a common set of specifications, namely a 300 m flight elevation and a flight line spacing of 800 m, and the majority of the work was done under contract. In order to maintain its expertise and keep current in the aeromagnetic survey technique, the GSC has maintained an experimental group devoted to improving the state-of-the-aeromagnetic survey art. After the advent of optical absorption magnetometers with their much higher sensitivity, it was realized that airborne magnetic gradient measurements were feasible, and so in the period 1973-80, the development of an inboard vertical gradiometer for mineral exploration applications was undertaken.

Two optical absorption magnetometers separated by 2 m were installed in a twin fixed boom system on a Beechcraft B80 Queenair aircraft. Active 8 term magnetic compensation systems were used to nullify the effects of the aircraft itself and permit the full sensitivity of the magnetometers to be utilized. The later part of the program consisted of a series of experimental surveys in various parts of the country amounting to more than 100 000 line kilometres to demonstrate the efficacy of the technique both in geological mapping and mineral exploration programs.

What are the advantages of the vertical gradient data over total field data i.e. that obtained using a single sensor? The first is that the vertical gradient data have a superior resolution of anomalies produced by closely-spaced geological formations, because the resultant gradient anomalies have a shorter wavelength than the concomitant total field anomalies. The second advantage is that anomalies produced by near-surface features are enhanced with respect to those resulting from more deeply buried rock formations. The third advantage is a most important one to the geologist mapping the Canadian Precambrian Shield, namely that vertical contacts are directly delineated by the zero gradient contour value at high magnetic latitudes, so that the gradient technique may be considered to be a vertical contact mapper. The fourth important advantage is that the regional gradient of the main earth's field and any diurnal activity are automatically removed, and this permits the calculation of the total field data from the vertical gradient data. This is an important advantage in diurnally-active areas of northern Canada in close proximity to the auroral zone.

About 200 vertical gradient maps have now been produced as a result of the GSC experimental program. Much interest in the technique was stimulated by two particular surveys, a uranium-related survey in the eastern part of the Athabasca basin and a survey of the Val D'Or area of western Quebec, famous for its gold mines. The fact that the gold in the Val D'Or area is associated with diorite plugs having a magnetic expression led to the realization that the vertical gradiometer can be utilized as a direct prospecting tool. The geological fraternity in Canada also recognized that the resultant vertical gradient maps are in essence pseudo-geological maps, and this viewpoint was augmented by producing the maps using the newly introduced Applicon jet-ink plotter, in which the zero-gradient contour was made yellow so that geological contacts were directly delineated by the yellow lines between the red highs and blue/green gradient lows.

With the general acceptance of the technique in Canada, the GSC undertook a technology transfer program in 1981 so that airborne geophysical contractors could offer the service. The program has resulted in two companies, namely Kenting Earth Sciences Ltd. of Ottawa and Quester Surveys Ltd. of Toronto, equipping fixed-wing aircraft with inboard aeromagnetic gradiometer systems. Both companies have now received survey contracts from GSC and have demonstrated their ability to carry out such work.

One of the important conclusions of the gradiometer program is that national aeromagnetic surveys should be carried out in two phases in order to provide adequate coverage for multi-purpose usage. In the first phase, a regional aeromagnetic survey should be carried out at a sufficient height to permit a reasonably wide line spacing so that costs are not excessive. In the second phase, the areas of complex geology and/or interesting mineral possibilities should be reflown at a lower elevation and a closer line spacing; moreover vertical gradiometers should be utilized for the second survey phase because of their distinct advantages over total field i.e. single sensor systems which were earlier enunciated.

HELICOPTER-BORNE AEROMAGNETIC GRADIOMETER PROGRAM

There is a problem in carrying out Phase II aeromagnetic gradiometer surveys in areas of mountainous terrain. The Geological Survey of Canada utilized the technique of flying at constant barometric elevation to carry out regional total field aeromagnetic surveys of moutainous areas such as the Cordillera of British Columbia. However, this procedure does not yield useful results when flying vertical gradient surveys of rugged areas, because gradient surveys are much more sensitive to the separation between the sensors and the causative bodies than is the case for total field surveys. Gradiometer surveys must always be drape-flown. Accordingly, for the past three years the GSC has been fostering the development of helicopter-borne aeromagnetic gradiometer survey systems through R&D contracts to the Canadian airborne geophysical survey industry.

In 1983, two R&D contracts were issued by the Geological Survey of Canada to develop two helicopter-borne gradiometer systems. The successful companies that received funding were Geotech Ltd. of Markham, Ontario and

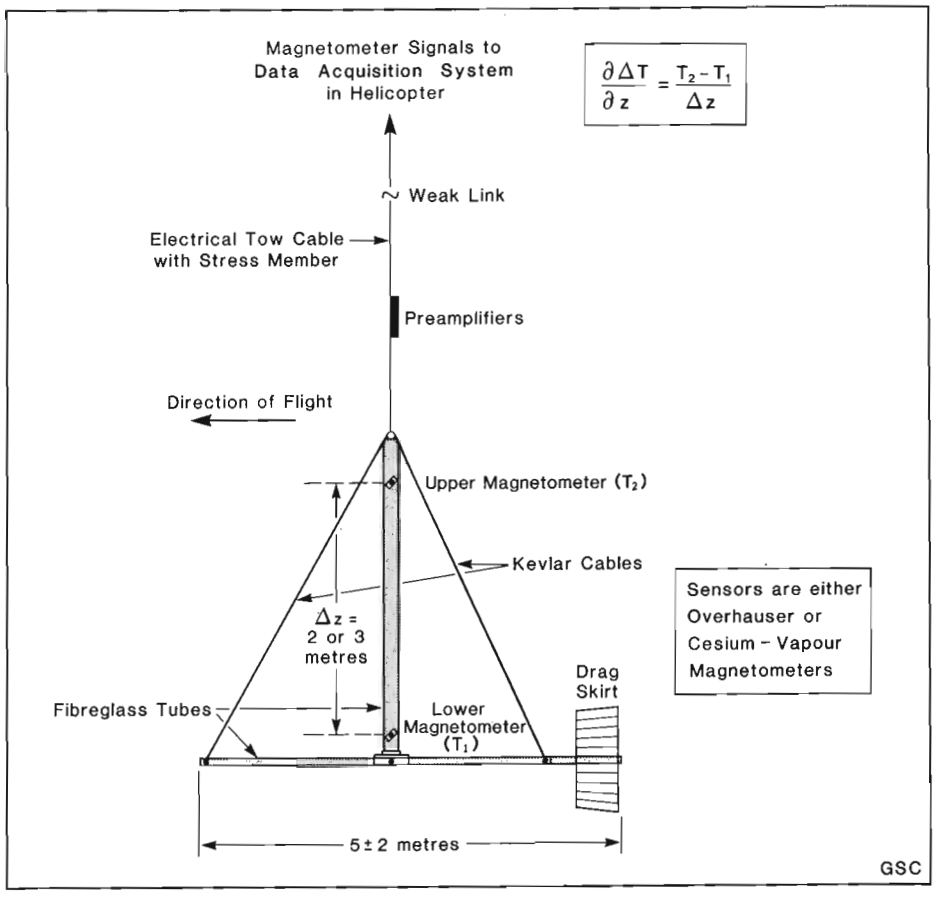


Figure 1. Typical helicopter-borne vertical gradiometer system for aeromagnetic surveying.

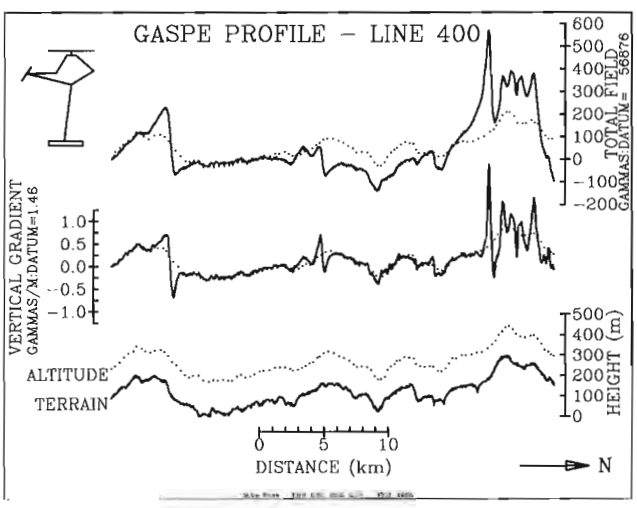


Figure 2. Helicopter-borne total field and vertical gradient profile from the 1984 survey in the Gaspésie Peninsula flown by Les Relevés Géophysiques of Quebec City.

Geophysical Surveys Inc. of Ste. Foy, Quebec. Geotech built a 3 m separation system using Overhauser magnetometers developed under a previous GSC-sponsored contract by Gem Systems Ltd. of Toronto. Two proton oscillators (GSM-11A) were installed in a mast-like structure above an EM bird with a 3 m separation. The noise envelope achieved was about 0.1 gamma for two readings per second for a single sensor and 0.033 gammas per metre for the gradient measurements.

The second helicopter-borne vertical gradiometer system was developed by Geophysical Surveys Inc. and utilized two V-200 Scintrex split-beam cesium-vapour magnetometers with a separation of 2 m mounted on a towed bird, permitting the vertical gradient to be measured twice a second with a sensitivity of 0.0005 gammas per metre. The total field and vertical gradient fourth-difference noise-levels of the system are respectively less than 0.02 gammas and 0.025 gammas/metre. The basic design of these and a number of other helicopter-borne gradiometer systems is summarized in Figure 1.

Both systems were first field tested in the relatively flat Carleton Place area previously flown by the GSC fixed-wing

system to ensure that repeatable results could be obtained. Then a survey of Mount Megantic, Quebec, some 700 m high, was carried out in March 1984 to ascertain whether the technique would produce useful results of areas of rugged terrain. The area had been previously surveyed in 1951-52 by a fixed-wing aeromagnetic survey flown by the Geological Survey of Canada. In general, the experimental surveys demonstrated the excellent repeatability of total field survey data, but in the fine detail there were many differences which are important to the mapping geologist. There is an even more striking comparison with the resultant vertical gradient colour interval map. This map showed that Mount Megantic consists of two concentric rings of magnetic rock extending about 270° in azimuth, which have significant magnetization and a central nonmagnetic core. This is confirmed by a comparison with the geological map which shows an outer ring of syenite, an innter ring of gabbro, and a central core of granite.



Figure 3. Vertical gradiometer boom system utilizing two cesium-vapour magnetometers with a 3 m separation: Aerodat Ltd., Mississauga, Ontario.

In 1984 a tender for the first contracted helicopter-borne vertical gradiometer work was issued for an area in the Gaspésie Peninsula of southeastern Quebec and the successful contractor was Geophysical Surveys Inc.

Figure 2 shows one of the resultant profiles oriented north-south, actually Line 400, flown by GSI across the Gaspésie Peninsula. At the bottom of the figure is the surface elevation and the altitude profile for the helicopter obtained from the barometric and radar altimeter readings. The central profile is the vertical gradient data and the upper profile is the total field data both with the altitude profile superimposed. The improved resolution of the vertical gradient data is readily apparent. It is also clear that the topographic feature at the north end of the profile is composed of more mafic material than the rocks underlying the lower elevation section to the south. It is clear even from this profile alone that the helicopter-borne gradiometer technique is a viable one for geological mapping programs and this is confirmed by the resultant contour maps. Moreover the results show a significant improvement in resolution over the older drape-flown survey.

Two other Canadian companies have developed helicopter-borne gradiometer systems. Aerodat Ltd. of Mississauga, Ontario, have fabricated a vertical gradiometer (Figure 3). The sensors are split-beam cesium-vapour magnetometers manufactured by Scintrex Ltd. and have a sensitivity of 0.005 gammas. A helicopter-borne gradiometer system is also being developed by Kenting Earth Sciences Ltd. of Ottawa using cesium-vapor magnetometers using a rather different design from that shown in Figure 1. The Kenting design consists of a rigidly mounted twin-boom system. Sander Geophysics Ltd. of Kanata, Ontario, have completed the development of a helicopter-borne vertical gradiometer system using Overhauser magnetometers of their own design. The sensor separation is 3 m and the 7 m long bird structure is towed by an Aerospatiale AS 350D Astar helicopter at the end of a 30 m cable. They have carried out their first contract survey for the Geological Survey of Canada in the Gaspésie Peninsula of eastern Quebec.

Helicopter-borne aeromagnetic gradiometer contracts have now been awarded for suveys in four eastern provinces, namely Newfoundland, Nova Scotia, New Brunswick and Quebec. It is clear that the helicopter-borne aeromagnetic gradiometer technique combined with VLF EM is an excellent geophysical tool to assist geological mapping programs in areas of rugged terrain.

Cone penetration tests of the nearshore zone sediments off Richards Island, Northwest Territories

Project 820038

P.J. Kurfurst
Terrain Sciences Division

Kurfurst, P.J., Cone penetration tests of the nearshore zone sediments off Richards Island, Northwest Territories; in Current Research, Part A, Geological Survey of Canada, Paper 87-1A, , p. 939-944, 1987.

Abstract

A "Hogentogler" electronic cone penetrometer system has been used to characterize unfrozen seabottom sediments and to determine their temperature regime in the nearshore zone in the southern Beaufort Sea. Typical sounding records, temperature profiles and their preliminary interpretation are presented.

Résumé

Un pénétromètre électronique à cône «Hogentogler» a été utilisé pour caractériser des sédiments non gelés du fond marin et pour déterminer leur régime de température dans la zone littorale du sud de la mer de Beaufort. On présente les enregistrements typiques de sondage, les profils de température et leur interprétation préliminaire.

INTRODUCTION

A multi-disciplinary program of detailed geotechnical investigations of the nearshore zone sediments was carried out off North Head, Richards Island, near Tuktoyaktuk, Northwest Territories. This program, undertaken in an area near proposed pipeline routes, was a continuation of investigations carried out by the Geological Survey of Canada in previous years (Kurfurst, 1984). The fieldwork, which was entirely financed by the Office of Energy Research and Development (OERD), was carried out in April 1986.

The major part of the field program consisted of the drilling, sampling, instrumenting and testing of seven boreholes drilled through the ice and water column to a depth of approximately 30 m below seabottom. The general location of the investigated area and the detailed location of the boreholes are shown in Figures 1 and 2, respectively.

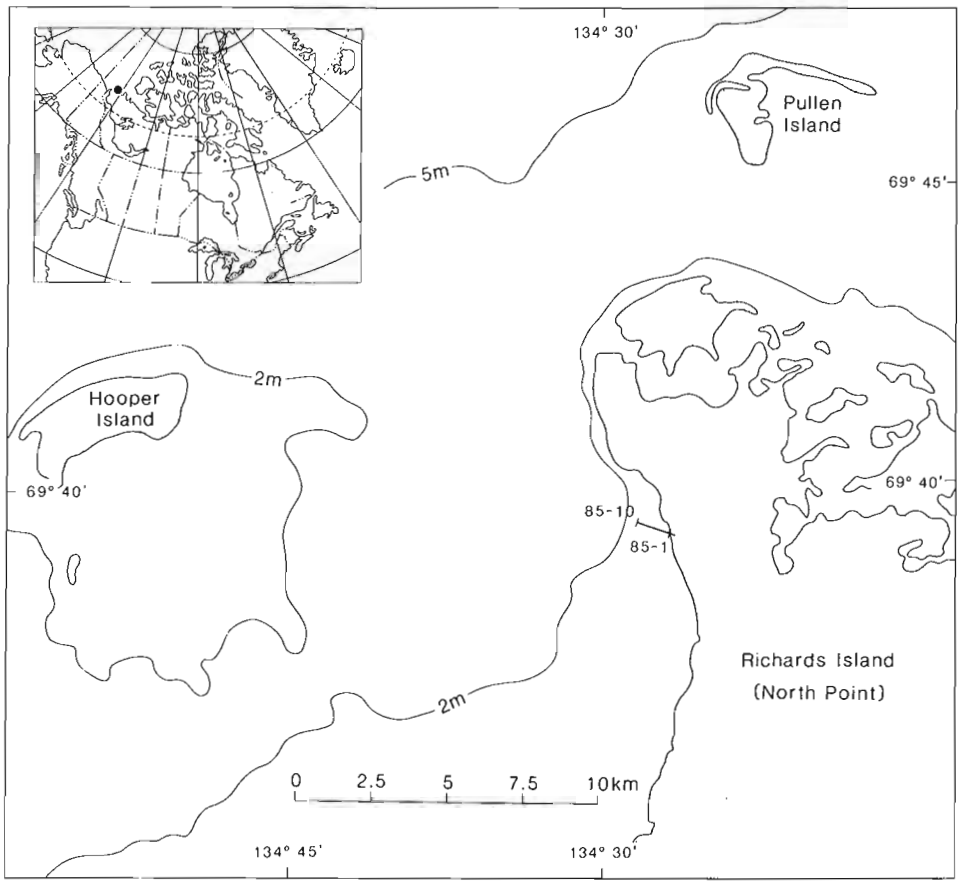


Figure 1. General location map.

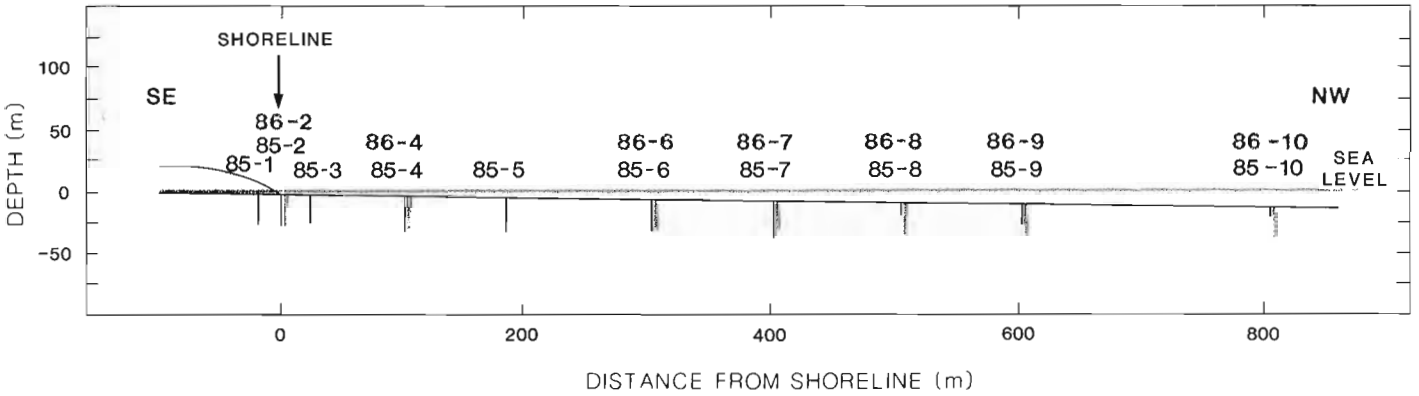
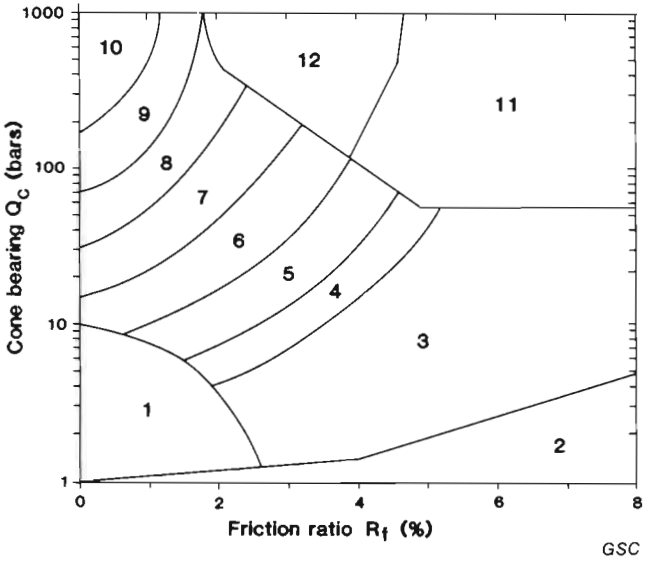


Figure 2. Detailed locations of boreholes drilled off North Head, Richards Island, Northwest Territories. Cone penetration tests were carried out near boreholes 86-8, 86-9, 86-10.



Zone	Q_c/N	Soil behaviour type
1	2	sensitive fine grained
2	1	organic material
3	1	clay
4	1.5	silty clay to clay
5	2	clayey silt to silty clay
6	2.5	sandy silt to clayey silt
7	3	silty sand to sandy silt
8	4	sand to silty sand
9	5	sand
10	6	gravelly sand to sand
11	1	very stiff fine grained (*)
12	2	sand to clayey sand (*)

(*) overconsolidated or cemented

Figure 3. Cone penetration test classification chart.

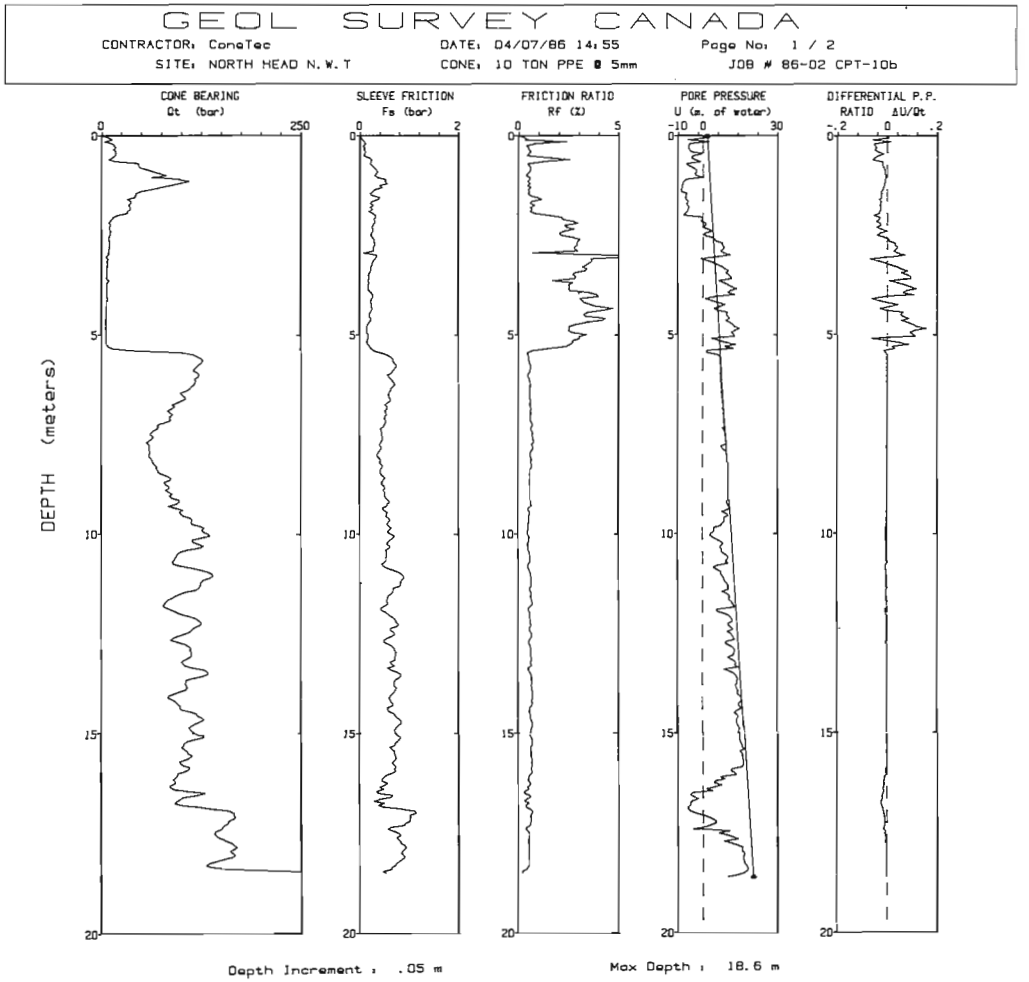


Figure 4. Example of cone penetration test data, borehole 86-10b.

ConeTec Investigations Ltd.

Site :ConeTec
On Site Loc:NORTH HEAD N.W.T
Comments :86-02 CPT-10b
Tot. Unit Wt. (avg) : 19 kN/m^3

CPT Date :04/07/86 14:55
Cone Used :10 TON PPE @ 5mm
Water table (meters) : 0

DEPTH (meters)	(feet)	Qc (avg) (bar)	Fs (avg) (bar)	Rf (avg) (%)	SIGV' (kPa)	SOIL BEHAVIOUR TYPE	Eq - Dr (%)	PHI deg.	SPT N	Su kPa
0.50	1.64	14.34	0.08	0.54	2.30	sandy silt to clayey silt	UNDFND	UNDFD	6	95.2
1.00	3.28	45.87	0.27	0.60	6.89	sand to silty sand	80-90	>48	11	UNDEFINED
1.50	4.92	72.94	0.38	0.52	11.48	sand to silty sand	80-90	>48	18	UNDEFINED
2.00	6.56	34.09	0.27	0.79	16.08	silty sand to sandy silt	60-70	44-46	11	UNDEFINED
2.55	8.37	11.24	0.27	2.38	20.90	clayey silt to silty clay	UNDFND	UNDFD	6	72.0
3.05	10.01	9.41	0.26	2.82	25.72	silty clay to clay	UNDFND	UNDFD	6	59.1
3.55	11.65	6.69	0.24	3.60	30.32	clay	UNDFND	UNDFD	7	40.4
4.05	13.29	6.75	0.19	2.79	34.91	silty clay to clay	UNDFND	UNDFD	4	40.1
4.55	14.93	6.22	0.23	3.68	39.50	clay	UNDFND	UNDFD	6	36.0
5.05	16.57	5.10	0.17	3.27	44.09	clay	UNDFND	UNDFD	5	27.9
5.55	18.21	31.26	0.25	0.80	48.69	silty sand to sandy silt	40-50	38-40	10	UNDEFINED
6.05	19.85	121.66	0.67	0.55	53.28	sand	80-90	44-46	24	UNDEFINED
6.55	21.49	111.95	0.64	0.57	57.87	sand	70-80	42-44	22	UNDEFINED
7.05	23.13	93.27	0.56	0.60	62.47	sand to silty sand	70-80	42-44	23	UNDEFINED
7.55	24.77	73.61	0.48	0.65	67.06	sand to silty sand	60-70	40-42	18	UNDEFINED
8.05	26.41	60.60	0.42	0.69	71.65	sand to silty sand	50-60	40-42	15	UNDEFINED
8.60	28.22	67.36	0.42	0.62	76.48	sand to silty sand	50-60	40-42	17	UNDEFINED
9.10	29.86	83.78	0.49	0.58	81.30	sand to silty sand	60-70	40-42	21	UNDEFINED
9.60	31.50	94.07	0.54	0.58	85.89	sand	60-70	40-42	19	UNDEFINED
10.10	33.14	119.81	0.59	0.49	90.49	sand	70-80	42-44	24	UNDEFINED
10.60	34.78	116.70	0.59	0.51	95.08	sand	70-80	40-42	23	UNDEFINED
11.10	36.42	106.68	0.59	0.55	99.67	sand	60-70	40-42	21	UNDEFINED
11.60	38.06	122.05	0.78	0.64	104.27	sand	70-80	40-42	24	UNDEFINED
12.10	39.70	86.42	0.53	0.61	108.86	sand to silty sand	60-70	40-42	22	UNDEFINED
12.60	41.34	116.30	0.70	0.60	113.45	sand	60-70	40-42	23	UNDEFINED
13.10	42.98	103.22	0.63	0.61	118.05	sand	60-70	40-42	21	UNDEFINED
13.60	44.62	114.71	0.69	0.60	122.64	sand	60-70	40-42	23	UNDEFINED
14.10	46.26	106.99	0.73	0.68	127.23	sand	60-70	40-42	21	UNDEFINED
14.60	47.90	97.32	0.62	0.64	131.82	sand to silty sand	60-70	38-40	24	UNDEFINED
15.10	49.54	118.61	0.76	0.64	136.42	sand	60-70	40-42	24	UNDEFINED
15.60	51.18	111.59	0.73	0.65	141.01	sand	60-70	40-42	22	UNDEFINED
16.10	52.82	105.77	0.71	0.67	145.60	sand	60-70	38-40	21	UNDEFINED
16.60	54.46	97.45	0.46	0.47	150.20	sand	60-70	38-40	19	UNDEFINED
17.10	56.10	121.17	0.65	0.54	154.79	sand	60-70	38-40	24	UNDEFINED
17.60	57.74	156.11	0.86	0.55	159.38	sand	70-80	40-42	31	UNDEFINED
18.10	59.38	159.53	0.85	0.53	163.98	sand	70-80	40-42	32	UNDEFINED
18.60	61.02	169.51	0.72	0.43	168.57	sand	70-80	40-42	34	UNDEFINED

Dr - All sands (Jamiolkowski et al. 1985) PHI - Robertson and Campanella 1983 Su: Nk= 15

**** Note: For interpretation purposes the PLOTTED CPT PROFILE should be used with the TABULATED OUTPUT from CPTINTR1 (v 3.02) ****

Figure 5. Example of a computer tabulation of cone penetration test data, borehole 86-10b.

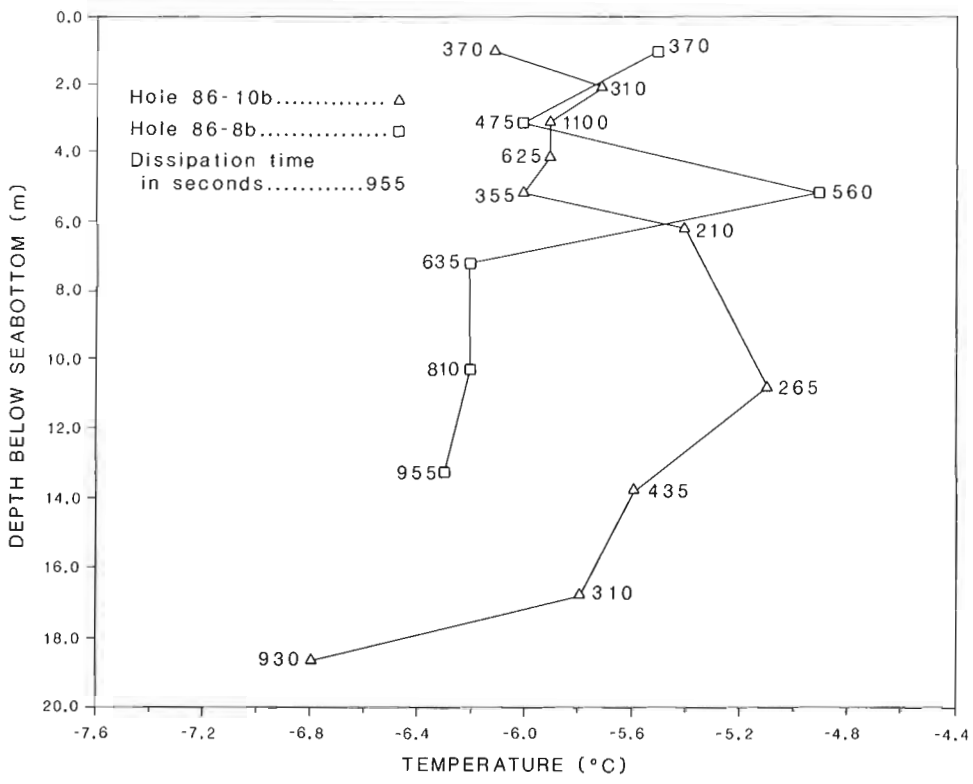


Figure 6. Cone penetration test, ambient ground temperature profiles, borehole 86-10b.

EQUIPMENT AND TECHNIQUE

The cone penetration testing was carried out by ConeTec Investigations Ltd. between April 4 and 8, 1986 as part of the drilling program (unpublished report to Geological Survey of Canada by Conetec Investigations Ltd., 1986, entitled "Presentation and interpretation of cone penetration data, North Head, Richards Island, N.W.T."). A "Hogentogler" electronic cone system and a 10 tonne compression type cone were used for all of the soundings. The following parameters were recorded at 5 cm intervals during each sounding: tip resistance, sleeve friction, dynamic pore pressure, temperature and cone inclination. Pore pressure dissipation was recorded at 5 second intervals during pauses in the penetration. A complete set of baseline readings was taken before and after each sounding to determine temperature shifts needed for data corections when required.

Cone penetration tests were usually carried out 3 to 5 m from the borehole location to avoid any disturbance which may have been caused by drilling. Prior to each sounding, a hole was augered through the ice and steel casing was installed to the seabottom to prevent buckling of the cone rods during penetration. The cone was pushed using the CME 750 drill rig used for conventional drilling, which had a downpressure capacity of 10 tonnes.

A total of five cone penetration tests were carried out to depths varying from 4 to 18 m below seabottom at locations near boreholes 86-8, 86-9, and 86-10. Table 1 presents a summary of the cone penetration tests performed.

The stratigraphic interpretation of the cone penetration test data is based on the relationship between cone bearing, Qc, and sleeve friction, F_s. The friction ratio, R_f (sleeve friction divided by cone bearing), is a calculated parameter which is used to infer soil behaviour type using the chart shown in Figure 3. Generally, cohesive soils have high friction ratios and low cone bearings, and cohensionless soils have low friction ratios and high cone bearings. Typical cone penetration test data are presented in graphical form in Figure 4. Computer tabulations of the data recorded and of the interpreted soil behaviour types, based on the cone penetration test soil behaviour chart (Fig. 3), are shown in Figure 5.

DATA INTERPRETATION

The interpreted results of the cone penetration test data suggest that the soils around holes 86-10a and 86-10b consist of

Table 1 Cone Penetration Tests Summary

Date	Hole No.	Penetration Below Seabottom (m)	Remarks
4/4/86	86-10a	6.2	Stopped on dense sand
5/4/86	86-9	4.1	Stopped on dense sand
6/4/86	86-8a	10.3	Stopped on dense sand
7/4/86	86-10b	18.6	Stopped on frozen ground
8/4/86	86-8b	13.2	Stopped on frozen ground
Total	5	52.4	

sandy silt to a depth of about 2 m and grade gradually into silty clay to a depth of about 5.5 m. The underlying deposits are interpreted as compact to dense sands to a depth of 18.6 m. The soil profiles around holes 86-9, 86-8a, and 86-8b are similar except for a thin layer of silty clay about 0.5 m thick encountered at a depth of about 6 m. These results agree well with drilling data which show similar soil types and indicate the presence of hard, dense sand in boreholes 86-9 and 86-10.

The silty clay displays relatively high shear strength which is in part due to slight overconsolidation. This evidence of overconsolidation is supported by the dynamic pore pressure response recorded during the sounding. The sand is also relatively dense which is also likely caused by overconsolidation.

The cone penetration tests were stopped either on contact with the dense sand layer or with frozen ground which the cone was unable to penetrate. The presence of frozen soils was confirmed by high positive pore pressures recorded.

Temperature measurements taken during cone penetration soundings vary significantly depending on the time allowed for heat dissipation. Penetration through cohesionless soils with high sleeve friction values generates a significant amount of heat that requires adequate time for its dissipation before true ambient temperatures are reached.

Temperature dissipation tests were carried out at varying depth intervals in holes 86-8b and 86-10b in an attempt to determine soil ambient temperatures. The results of these tests are presented graphically in Figure 6. The results indicate that the ambient soil temperature in both holes are within a range of 2°, varying between -4.8°C and -6.8°C, depending on depth and type of material encountered.

AUTHOR INDEX/INDEX DES AUTEURS

Anderson, R.G. 689
Andrew, K.P.E. 699
Anglin, C.D. 591
Annesley, I.R. 25

Banerjee, I. 337
Barr, S.M. 199, 263
Barrette, P.D. 515
Bégin, N.J. 619
Bell, K. 591
Bell, T. 101
Berger, G.W. 901
Bethune, K.M. 773
Blaise, B. 127
Bolduc, A.M. 43
Bornhold, B.D. 127
Bostock, H.H. 443
Bouvier, J.L. 485
Bowring, S.A. 699
Brooks, P.W. 331
Brown, D.A. 143

Calon, T. 435
Cameron, B.E.B. 925
Cameron, E.M. 281
Campbell, J.E.M. 643
Carrigan, W.J. 281
Clague, J.J. 177
Coderre, J.M. 815
Copper, P. 885
Corriveau, L. 897
Currie, K.L. 653, 663
Currie, L.D. 713

Dallimore, S.R. 913
David, J. 633
Davis, J.L. 913
Dennis, F.A.R. 643
de Silva, K.N. 477
de Vernal, A. 11
Dewing, K. 883
Digel, M.R. 429
Dyer, A. 101

Eckstrand, O.R. 835
Ernst, R.E. 673
Evans, S.G. 181, 929
Evenchick, C.A. 719
Evenson, E.B. 43

Fogarasi, S.L. 815
Franklin, J.M. 591
Frisch, T. 429

Gagné, R.M. 905
Gariépy, C. 633
Gibb, R.A. 815
Gibbins, S.F. 699
Gleeson, C.F. 489
Good, R.L. 905
Goodarzi, F. 317, 349, 353
Gorton, M. 897
Graves, M. 409
Grotzinger, J.P. 219

Hall, G.E.M. 477, 485
Hamilton, S.M. 451, 883
Hanmer, S.K. 563
Henderson, J.B. 783, 803
Hildebrand, R.S. 699
Hill, J.D. 415
Hill, J.R. 533
Hillaire-Marcel, C. 859
Hoffman, E. 591
Hood, P. 935
Hunter, J.A. 905

James, D.T. 803
Jefferson, C.W. 451
Jetté, H. 11
Jonasson, I.R. 591, 835
Judge, A.S. 191
Justino, M.F. 555

Kerr, D.E. 153
King, J.E. 515
Klassen, R.A. 43, 61, 101
Klassen, R.W. 111
Kostaschuk, R.A. 727
Kurfurst, P.J. 939

Labonté, M. 353
Laflèche, P.T. 191
Lambert, M.B. 605, 673
Lecheminant, A.N. 773
Lecheminant, G.M. 249
Leslie, R.V. 37
Lewis, C.F.M. 825
Lortie, G. 889
Loveridge, W.D. 783
Lucas, S.B. 619
Luternauer, J.L. 727, 901, 919

MacDougall, C.S. 457
Macfie, R.I. 681, 803
Machin, D.C. 305
Mackay, J.R. 37
Mackenzie, L.M. 467
Maclean, B. 847
Macnab, R. 865
Martin, R.F. 239
Matthews, J.V., Jr. 73, 165

McCormick, D.S. 219
McGrath, P.H. 803
McKenna, G.T. 919
McMartin, I. 89
Mortensen, J.K. 581
Mott, R.J. 165
Mucci, A. 17
Murphy, D.C. 735

Needham, T.W. 597

Orchard, M.J. 743
Osadetz, K.G. 331
Owen, J.V. 305, 643

Pagé, P. 17
Paktunc, A.D. 543
Parrott, D.R. 825
Payette, C. 239
Pelchat, J.C. 477
Pelechaty, S.M. 219
Pe-Piper, G. 573
Percival, J.A. 1
Piasecki, M.A.J. 391
Pilon, J.A. 191
Piper, D.J.W. 847
Praeg, D. 847
Procyshyn, E.L. 499
Pullan, S.E. 905

Raeside, R.P. 199
Rainbird, R.H. 53
Real, D. 763
Relf, C.D. 515
Ricketts, B.D. 369
Rivers, T. 435
Roberts, M.C. 757
Roddick, J.C. 773
Roddick, J.C.M. 375
Rogerson, R.J. 101
Ruzicka, V. 249

Sangster, A.L. 555
Schwarz, E.J. 423
Scott, D.J. 619
Sevigny, J.H. 751
Shilts, W.W. 159
Shor, A.N. 847
Simony, P.S. 713
Smith, S.L. 53, 159, 165
Snowdon, L.R. 331
Sobczak, L.W. 299
Sonnichsen, G.V. 877
Squires, G.C. 699
Stasiuk, L.D. 317, 349
St-Onge, D.A. 89
St-Onge, M.R. 619
Swinden, H.S. 381

Tella, S. 25
Teskey, D.J. 935
Tessier, A.C. 773
Thomas, M.D. 763, 815
Thomas, R.D. 489
Thompson, F.J. 61
Thompson, P.H. 783
Trettin, H.P. 357

Vaive, J.E. 477
van Berkel, J.T. 399
van Breemen, O. 783
van Gool, J. 435
van Staal, C.R. 605
Verhoef, J. 865
Vilks, G. 877
Vreeken, W.J. 111

Waldron, J.W.F. 409
Watkinson, D.H. 835
Weber, J.R. 299
Whalen, J.B. 209, 375
White, C.E. 199
Williams, E.J. 429
Williams, H.F.L. 757
Wilton, D.H.C. 457, 467
Woodside, J. 865
Wright, N. 423

Yaowanoiyothin, W. 199

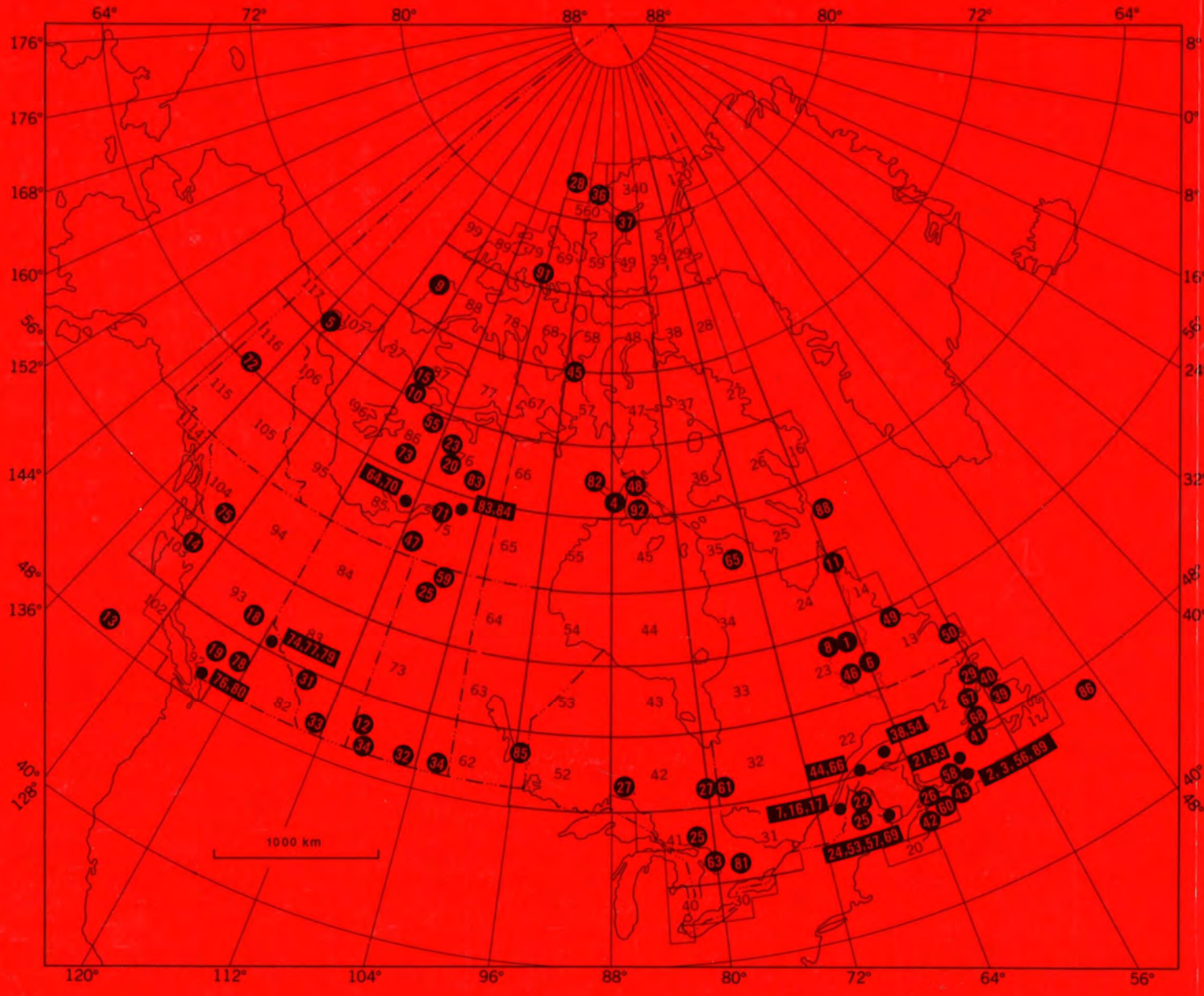
Zolnai, A.I. 323

NOTE TO CONTRIBUTORS

Submissions to the *Discussion* section of *Current Research* are welcome from both the staff of the Geological Survey and from the public. Discussions are limited to 6 double-spaced typewritten pages (about 1500 words) and are subject to review by the Chief Scientific Editor. Discussions are restricted to the scientific content of Geological Survey reports. General discussions concerning branch or government policy will not be accepted. Illustrations will be accepted only if, in the opinion of the editor, they are considered essential. In any case no redrafting will be undertaken and reproducible copy must accompany the original submissions. Discussion is limited to recent reports (not more than 2 years old) and may be in either English or French. Every effort is made to include both *Discussion* and *Reply* in the same issue. *Current Research* is published in January and July. Submissions should be sent to the Chief Scientific Editor, Geological Survey of Canada, 601 Booth Street, Ottawa, Canada, K1A 0E8.

AVIS AUX AUTEURS D'ARTICLES

Nous encourageons tant le personnel de la Commission géologique que le grand public à nous faire parvenir des articles destinés à la section *discussion* de la publication *Recherches en cours*. Le texte doit comprendre au plus six pages dactylographiées à double interligne (environ 1500 mots), texte qui peut faire l'objet d'un réexamen par le rédacteur en chef scientifique. Les discussions doivent se limiter au contenu scientifique des rapports de la Commission géologique. Les discussions générales sur la Direction ou les politiques gouvernementales ne seront pas acceptées. Les illustrations ne seront acceptées que dans la mesure où, selon l'opinion du rédacteur, elles seront considérées comme essentielles. Aucune retouche ne sera faite aux textes et dans tous les cas, une copie qui puisse être reproduite doit accompagner les textes originaux. Les discussions en français ou en anglais doivent se limiter aux rapports récents (au plus de 2 ans). On s'efforcera de faire coincider les articles destinés aux rubriques *discussions* et *reponses* dans le même numéro. La publication *Recherches en cours* paraît en janvier et en juillet. Les articles doivent être renvoyés au rédacteur en chef scientifique: Commission géologique du Canada, 601, rue Booth, Ottawa, Canada, K1A 0E8.



Energy, Mines and Resources Canada

Énergie, Mines et Ressources Canada